TRANSACTIONS

OF THE

AMERICAN SOCIETY

OF

CIVIL ENGINEERS

(INSTITUTED 1852)

VOLUME 121
1956

Edited by the Executive Secretary, under the direction of the Committee on Publications.

Reprints from this publication, which is copyrighted, may be made on condition that the full title of paper, name of author, and page reference (or paper number) are given.

NEW YORK
PUBLISHED BY THE SOCIETY

1956

Transp.
TA
1
.A526
v.121

Copyright 1956 by the AMERICAN SOCIETY OF CIVIL ENGINEERS

NOTE.—The Society is not responsible for any statement made or opinion expressed in its publications.

Transportation
Library
Gift
Direct
JAN 8 1957

PREFACE

With this volume, the *Transactions* of the Society have reached a total of 121 bound volumes, the first being issued in 1872. That first volume, published when the Society had 259 members and fellows, comprised a grouping of papers accumulated during the preceding twenty years (1852–1872). Thus, the *Transactions* constitute a technical record of the entire 104 years of the Society's existence.

The long span of years has given ample opportunity for changing patterns of thought and policy. In its early years the difference between the *Proceedings* and the *Transactions* was sometimes almost indistinguishable. The *Proceedings* then included advertising, a verbatim reporting of meetings, speech by speech, and the technical *Proceedings* papers. Later, the *Transactions* volume was more carefully collated and indexed, taking on a distinctive character of its own.

With the publication of *Civil Engineering* in 1930, *Proceedings* and *Transactions* were further improved because of the more rational distribution of different kinds of information among the several kinds of publications. Nevertheless, it was customary to expect that there were only a few papers in *Proceedings* that were not also included in the annual *Transactions* volume.

Volume 121 (1956) reflects an important change in publication policy inaugurated in July, 1953, with the presentation of *Proceedings Paper No. 200*, the first *Proceedings* paper to be produced by photo-lithography. This volume contains sixty-three titles, selected from a total of approximately 380 *Proceedings* papers. They must therefore be assumed as the very best of a large collection of good papers. Some of the papers excluded from this volume, or previous volumes, may be selected for subsequent volumes. Readers interested in *Proceedings* papers that are not now found in the *Transactions* are referred to the annual indexes published as *Proceedings*. Such indexes are *Proceedings Papers No. 582* and *No. 860*—the last "paper" published in December of each year.

THE COMMITTEE ON PUBLICATIONS

CONTENTS

No. Page

PREFACE III

ERRATA XIII

2783 DESIGN OF ALUMINUM ALLOY BEAM-COLUMNS

By Harry N. Hill, Ernest C. Hartmann, and John W. Clark 1

Discussion:

By Robert B. McCalley, Jr. 15

Herbert A. Sawyer, Jr. 16

Harry N. Hill, Ernest C. Hartmann, and John W. Clark 19

2784 ONE-WAY STREET SYSTEM IN SACRAMENTO, CALIF.

By D. Jackson Faustman 22

2785 STUDIES OF AIR ENTRAINMENT IN OPEN-CHANNEL FLOWS

By Lorenz G. Straub and Owen P. Lamb 30

2786 AN ENGINEERING APPROACH TO BLAST-RESISTANT DESIGN

By Nathan M. Newmark 45

Discussion:

By Stephen J. Fraenkel 62

Nathan M. Newmark 64

2787 FLOW EXPANSION AND PRESSURE RECOVERY IN FLUIDS

By Harald Tults 65

2788 HANDLING ATOMIC ENERGY INDUSTRY WASTES

By Joseph A. Lieberman and Arthur E. Gorman 85

2789 DEVELOPMENT OF AN INTERNATIONAL AIRPORT

By Earle M. Rader 96

2790 WIND LOADS ON GIRDER BRIDGES

By John M. Biggs, Saul Namyet, and Jiro Adachi 101

2791 SURVEYS AND MAPS FOR PIPELINES

By George E. MacDonald 121

Discussion:

By Norman O. Geuder 133

George E. MacDonald 134

2792 METROPOLITAN TRAFFIC AND TRANSPORTATION PLANNING

By Charles A. Blessing 135

No. PAGE

2793 UNSTEADY FLOW IN OPEN-TYPE PIPE IRRIGATION SYSTEMS
By Edward H. Taylor, Arthur F. Pillsbury, Thomas O. Ellis, and George A. Bekey 143

Discussion:
By ROBERT E. GLOVER 162
EDWARD H. TAYLOR, ARTHUR F. PILLSBURY, THOMAS O. ELLIS, AND GEORGE A. BEKEY 163

2794 PRIVATE ENTERPRISE CAN SATISFY THE PARKING DEMAND
By Charles T. McGavin 165

2795 THE EFFECT OF JET AIRCRAFT ON AIRPORT PAVEMENTS
By Gayle McFadden 172

2796 FACTORS INFLUENCING IRRIGATION IN HUMID AREAS
By Tyler H. Quackenbush 179

Discussion:
By ALFRED R. GOLZE 186

2797 VERTICAL SAND DRAINS FOR STABILIZING MUCK-PEAT SOILS
By J C Carpenter and Edward S. Barber 188

Discussion:
By HUBERT M. RAEDSCHELDERS 202

2798 ENGINEERING BIOTECHNOLOGY IN OCCUPATIONAL HEALTH
By Alvin F. Meyer, Jr. 205

2799 AN EXPERIMENTAL STUDY OF BUBBLES MOVING IN LIQUIDS
By William L. Haberman and Rose K. Morton 227

Discussion:
By JOHN A. ROBERSON, CHARLES L. BARKER, AND PAUL F. RUFF 251
WILLIAM L. HABERMAN AND ROSE K. MORTON 252

2800 THE DESIGN OF TWO STEAM ELECTRIC PLANTS
By Walter L. Dickey 253

2801 INCINERATION AND ALTERNATIVE REFUSE DISPOSAL PROCESSES
By Ralph Stone and Francis R. Bowerman 273

Discussion:
By GEORGE R. THOMPSON 299
WILLIAM A. XANTEN 300
SAMUEL A. GREELEY 304
RALPH STONE AND FRANCIS R. BOWERMAN 307

2802 MORNING-GLORY SHAFT SPILLWAYS: A SYMPOSIUM
PROTOTYPE BEHAVIOR
By Joseph N. Bradley 312

Discussion:
By BERNARD DONELAN 334
DONALD S. WALTER 334
FRED W. BLAISDELL 338
RODOLFO E. BALLESTER 340
JOHN WALLACE RIDLEY 342
JOSEPH N. BRADLEY 343

No. PAGE

DETERMINATION OF PRESSURE-CONTROLLED PROFILES
By William E. Wagner 345

Discussion:
By Maxwell W. White and Murray B. McPherson 369
Fred W. Blaisdell 374
Ibrahim M. Mostafa, Benoyendra Chanda, and Howard P. Johnson 375
William E. Wagner 380

PERFORMANCE TESTS ON PROTOTYPE AND MODEL
By Alvin J. Peterka 385

Discussion:
By Fred W. Blaisdell 406
Alvin J. Peterka 407

2803 MOMENTS AND DEFLECTIONS IN STEEL-GRID BRIDGE FLOORS
By Herbert J. Greenberg 410

Discussion:
By Kuang-Han Chu 426
Fu-Kuei Chang 428
Herbert J. Greenberg 432

2804 DESIGN OF GENERAL CARGO MARINE TERMINALS
By Frank W. Herring 433

2805 SIMILARITY OF DISTORTED RIVER MODELS WITH MOVABLE BEDS
By Hans A. Einstein and Ning Chien 440

Discussion:
By Thomas Blench 458
Hans A. Einstein and Ning Chien 459

2806 AN INFLUENCE-LINE ANALYSIS FOR SUSPENSION BRIDGES
By David J. Peery 463

Discussion:
By Nan-sze Sih 481
Jacob Karol 483
Harry M. Palmbaum 487
Vincenzo Franciosi 490
David J. Peery 501

2807 AERIAL SURVEYS FOR RESERVOIR PLANNING
By Francis J. Guscio 511

Discussion:
By Lewis A. Dickerson 518
Francis J. Guscio 519

2808 NUMERICAL ANALYSIS OF FRAMES WITH CURVED GIRDERS
By James Michalos 521

Discussion:
By William A. Conwell 540
James Michalos 541

No. PAGE

2809 INCREASING THE LOAD-CARRYING CAPACITIES OF SUBGRADES
By Charles M. Noble 544

Discussion:
By EUGENE Y. HUANG 550
CHARLES M. NOBLE 553

2810 PILE-LOADING TESTS, MORGANZA FLOODWAY CONTROL STRUCTURE
By Charles I. Mansur and John A. Focht, Jr. 555

Discussion:
By JOHN W. DUNHAM 577
LEROY D. GRAVES AND JAMES E. BINCKLEY 578
JAMES F. MCNULTY 581
CHARLES I. MANSUR AND JOHN A. FOCHT, JR. 584

2811 EXAMPLES OF TIMBER-STRUCTURE FAILURES
By Michael N. Salgo 588

Discussion:
By E. GEORGE STERN 601
RALPH H. GLOSS 601
MICHAEL N. SALGO 604

2812 A BRIEF FOR LIMIT DESIGN
By George C. Ernst 605

Discussion:
By ABDEL F. DIWAN 620
GEORGE C. ERNST 629

2813 A CONFORMAL AND WORLD-WIDE MILITARY GRID SYSTEM
By Floyd W. Hough 633

2814 ENGINEERING PROPERTIES OF EXPANSIVE CLAYS
By Wesley G. Holtz and Harold J. Gibbs 641

Discussion:
By RAYMOND F. DAWSON 664
WILLIAM T. ALTMEYER 666
EDWARD S. BARBER 669
LAWRENCE A. DUBOSE 674
WESLEY G. HOLTZ AND HAROLD J. GIBBS 676

2815 VERIFICATION OF THEORY FOR OBLIQUE STANDING WAVES
By Arthur T. Ippen and Donald R. F. Harleman 678

2816 SAFE LOADS ON DOG-LEG PILES
By James D. Parsons and Stanley D. Wilson 695

Discussion:
By A. E. CUMMINGS 717
JAMES D. PARSONS AND STANLEY D. WILSON 720

2817 AIRPORT STANDARDS
By John M. Kyle 722

No. PAGE

2818 ANALOG COMPUTERS APPLIED TO ELASTO-PLASTIC SYSTEMS
By Leo Schenker and Gunther Martin 728

Discussion:

By John S. Archer and Allen Lange 736

2819 RIVER SURVEYS IN UNMAPPED TERRITORY
By Gerard H. Matthes 739

Discussion:

By Frederic T. Mavis 753
T. H. F. Nevins 754
Chesley J. Posey 755
Edward Kuiper 755
Gerard H. Matthes 757

2820 NONUNIFORM TORSION OF PLATE GIRDERS
By Gerald G. Kubo, Bruce G. Johnston, and William J. Eney 759

Discussion:

By DeForest A. Matteson, Jr. 781
Gerald G. Kubo, Bruce G. Johnston, and William J. Eney 784

2821 LATERAL BUCKLING OF CANTILEVERED I-BEAMS UNDER UNIFORM LOAD
By Stanley Poley 786

2822 CORROSION AND CORROSION RESEARCH
By Thomas R. Camp 791

Discussion:

By Edward W. Moore 811
Thomas R. Camp 812

2823 CONTINUOUS PRESTRESSING
By Robert B. B. Moorman 814

Discussion:

By Abdel F. Diwan 826
Leopold J. Mensch 830
Robert B. B. Moorman 831

2824 THE PRESENT STATUS OF RESEARCH ON SEDIMENT TRANSPORT
By Ning Chien 833

Discussion:

By Thomas Blench 869
Jan M. Jordaan, Jr. 870
Joe M. Lara 871
Navinchandra L. Rupani and John B. Stall 874
Hsin-Kuan Liu 877
Ning Chien 881
Hans A. Einstein 883

2825 PITTSBURGH'S COMPREHENSIVE IMPROVEMENT PROGRAM
By Park H. Martin 885

No. Page

2826 ECONOMY AND SAFETY OF CONCRETE DAMS
By August E. Komendant 899

Discussion:
By Jaro J. Polivka 922
August E. Komendant 923

2827 EFFECT OF SAMPLE DISTURBANCE ON THE STRENGTH OF A CLAY
By Max L. Calhoon 925

Discussion:
By John H. Schmertmann 940
Max L. Calhoon 950

2828 THE BOX INLET DROP SPILLWAY AND ITS OUTLET
By Fred W. Blaisdell and Charles A. Donnelly 955

Discussion:
By Neal E. Minshall 987
Fred W. Blaisdell and Charles A. Donnelly 992

2829 THE OCTAGONAL-GIRDER FOUR-COLUMN SPACE FRAME
By Paul C. Disario, Jr., John S. Podolan, and Nicholas A. Weil 995

Discussion:
By Abdel F. Diwan 1022
Sidney Shore and Humberto Rincon 1028
Paul C. Disario, Jr., John S. Podolan, and Nicholas A. Weil 1033

2830 BEAM RESTRAINTS PROVIDED BY WALLS WITH OPENINGS
By Ibrahim A. Mohammed and Egor P. Popov 1034

2831 THE VIBRATIONS OF STEEL STACKS
By Walter L. Dickey and Glenn B. Woodruff 1054

Discussion:
By Richard Jenney 1071
George S. Vincent 1072
John N. Pirok 1075
Frederick B. Farquharson 1077
W. Watters Pagon 1082
Robert H. Sherlock 1084
Walter L. Dickey and Glenn B. Woodruff 1086

2832 RESONANT VIBRATION OF STEEL STACKS
By Ernest A. Dockstader, William F. Swiger, and Emory Ireland 1088

Discussion:
By Cedric Marsh 1110
Ernest A. Dockstader, William F. Swiger, and Emory Ireland 1110

2833 PIPELINE TRANSPORTATION IN THE UNITED STATES
By Eldon V. Hunt 1113

No. Page

2834 THICKNESSES OF CONCRETE PAVEMENTS FOR HIGHWAYS
By Joseph Herbert Moore 1125

Discussion:
By Lawrence A. Palmer 1143
Earl C. Sutherland 1144
Warner Harwood 1148
Albert de Neufville 1150
Joseph Herbert Moore 1151

2835 VIBRATION IN HYDROELECTRIC POWER PLANTS
By Samuel Judd 1153

2836 LATERAL BUCKLING OF ECCENTRICALLY LOADED I-COLUMNS
By Mario G. Salvadori 1163

2837 FUNDAMENTAL CONCEPTS OF RECTANGULAR SETTLING TANKS
By Alfred C. Ingersoll, Jack E. McKee, and Norman H. Brooks 1179

Discussion:
By Thomas R. Camp 1205
Henry L. Thackwell 1209
Alfred C. Ingersoll, Jack E. McKee, and Norman H. Brooks 1213

2838 A PHYSICAL APPROACH TO TURBULENT-BOUNDARY-LAYER PROBLEMS
By Donald Ross 1219

Discussion:
By William Douglas Baines 1241
James M. Robertson 1243
William J. Bauer 1250
Donald Ross 1252

2839 RESEARCH ON BOLTED CONNECTIONS
By William H. Munse 1255

2840 GRAPHIC DESIGN OF ALLUVIAL CHANNELS
By Ning Chien 1267

Discussion:
By Thomas Blench 1281
Emory W. Lane 1283
Ning Chien 1285

2841 MULTIPLE-SPAN GABLED FRAMES
By John D. Griffiths 1288

Discussion:
By Abdel F. Diwan 1308
John D. Griffiths 1315

2842 CONSTANT-SEGMENT METHOD FOR ANALYSIS OF NONUNIFORM MEMBERS
By Walter E. Hanson and Wallace F. Wiley 1317

Discussion:
By Thomas F. Hickerson 1331
Eugene J. Vayda 1332
Jaro J. Polivka 1334
Walter E. Hanson and Wallace F. Wiley 1335

No. PAGE

2843 SAFETY AND THE PROBABILITY OF STRUCTURAL FAILURE

By Alfred M. Freudenthal 1337

Discussion:

By ANTHONY CHIBARO 1376
LLOYD S. LAWRENCE 1377
JOSÉ M. CORSO 1381
OLIVER G. JULIAN 1386
AIDEN R. GIERASCH 1393
ALFRED M. FREUDENTHAL 1394

2844 OUR EXCITING PROFESSION: ADDRESS AT THE SUMMER CONVENTION, KNOXVILLE, TENN., JUNE 7, 1956

By Enoch R. Needles, President 1398

MEMOIRS OF DECEASED MEMBERS: ABSTRACTS 1411

SUBJECT INDEX 1437

AUTHOR INDEX 1479

ERRATA

Transactions, Vol. 120, 1955

Page 1267, running head, "Nizery and Brandeau on Stable Channels" should be "Nizery and Braudeau on Stable Channels."

Page 1612, lines 10 and 11, "Donald Q. Maejka" should be "Donald Q. Matejka."

Transactions, Vol. 121, 1956

Page 56, immediately following Eq. 7*a*, the expression $q_s = k/x_s$ should be changed to $q_s = k\, x_s$.

Page 58, line 7, the term q_c should be changed to q_s.

Page 74, Eqs. 3 and 5, the plus sign which follows the term α_1 should be changed to a minus sign.

AMERICAN SOCIETY OF CIVIL ENGINEERS
Founded November 5, 1852
TRANSACTIONS

Paper No. 2783

DESIGN OF ALUMINUM ALLOY BEAM-COLUMNS

BY HARRY N. HILL[1] AND ERNEST C. HARTMANN,[2] MEMBERS ASCE, AND JOHN W. CLARK,[3] J. M. ASCE

WITH DISCUSSION BY MESSRS. ROBERT B. MCCALLEY, JR.; HERBERT A. SAWYER, JR.; AND HARRY N. HILL, ERNEST C. HARTMANN, AND JOHN W. CLARK

SYNOPSIS

The procedures for determining the strength of a member as a column and as a beam separately are described. In order to design a beam-column the strength of the member under the combined loading can be determined from an appropriate interaction equation.

Several interaction equations are discussed by the authors. These equations are compared with the results of tests on eccentrically loaded columns. One of the equations is proposed for use in design because it gives the best agreement with tests, both for members that failed by buckling in the plane of the eccentricity and for those that failed by lateral, torsional buckling.

INTRODUCTION

Structural members are frequently designed to function simultaneously as columns and as beams. It is generally known that the presence of the one kind of loading will decrease the capacity of the member for the other kind of loading. In designing such a member, therefore, the allowable bending moment and end load should be reduced from the values that would be permissible if either occurred alone.

The first requisite in designing a "beam-column" is to determine, separately, the strength of the member as a column and its strength as a beam. The

---

NOTE.—Published, essentially as printed here, in October, 1953, as *Proceedings-Separate No. 300*. Positions and titles given are those in effect when the paper or discussion was approved for publication in *Transactions*.

[1] Chief, Eng. Design Div., Aluminum Research Labs., Aluminum Co. of America, New Kensington, Pa.

[2] Asst. Director, Aluminum Research Labs., Aluminum Co. of America, New Kensington, Pa.

[3] Research Engr., Eng. Design Div., Aluminum Research Labs., Aluminum Co. of America, New Kensington, Pa.

strength of the member under the combined loading can then be determined from an appropriate "interaction" equation.

This paper describes the methods of design for aluminum alloy columns, beams, and beam-columns evolved at the research laboratories with which the writers are associated after several years of work in this field. The design methods herein described have been incorporated in a handbook (1).[4]

Although these design procedures were devised specifically for aluminum alloys, the general principles involved should be equally applicable to other metals. There is, however, a fundamental difference between the approach adopted herein and the usual design specifications. The problem has been to derive design procedures which are applicable to a large number of different aluminum alloys, each in several different tempers, each having widely differing mechanical properties, and each being used in a wide range of fields of application. The procedures are therefore expressed in a form suitable for determining the strength of a member, in terms of the mechanical properties of the material of the member. They are not expressed in terms of allowable design stresses. The factor of safety to be applied in a specific design will be influenced greatly by the circumstances peculiar to the particular problem.

From general design methods such as those described in this paper, design specifications of the usual type (in terms of allowable stresses) can be derived for a specific material in a particular field of application. This has, in fact, been done for two of the aluminum alloys most commonly used in structural engineering (2)(3).

STRENGTH OF COLUMNS

The primary type of failure for a member under an axial compressive load, applied at the centroids of the end sections, involves bending of the member in the weakest direction. (Failure of torsionally weak members is considered beyond the scope of this paper.) If the maximum load a column is capable of supporting without buckling sideways does not introduce stresses in the member above the elastic limit of the material, the ultimate strength is expressed by the Euler formula:

$$f_C = \frac{\pi^2 E}{\left(\frac{k L}{r}\right)^2} \qquad (1)$$

in which f_C is the ultimate strength, in kips per square inch; E is the modulus of elasticity, in kips per square inch; r is the least radius of gyration of the cross section, in inches; L is the length of the column, in inches; and k is the end fixity factor.

The value of the fixity factor k will depend on how much the ends of the column are restrained from moving laterally and tipping in the direction of least stiffness. In selecting a value of k for a particular problem, it is sometimes helpful to visualize $k L$ as the effective length of the column—that is, the length between points of contraflexure when the column is in the deflected position attained just prior to failure. If the column is a member in a framed structure such as a truss, the choice of the k-value should be influenced by (*a*) the nature of the loading in the adjacent members and (*b*) the size of the adjacent members and the stiffness of the connections.

---

[4] Numerals in parentheses—thus: (1)—refer to corresponding items in the Bibliography (see Appendix)

If the ultimate strength computed from Eq. 1 exceeds the elastic limit of the material, the equation will provide too high an estimate of the strength of the column. Various methods have been used for calculating the strength of columns in the plastic stress region. A straight-line formula for column strength of aluminum alloys in the plastic range was proposed in 1938 (4) and was used in early editions (5) of the aforementioned handbook (1). Although this straight-line formula provides a good approximation of the column strength of the aluminum alloys for which it was derived, it was found to be less satisfactory for other alloys—particularly the artifically aged alloys such as 2014-T6 (formerly 14S-T6), 6061-T6 (formerly 61S-T6), and 7075-T6 (formerly 75S-T6) (6)—which are currently the most important alloys involved in structural design.

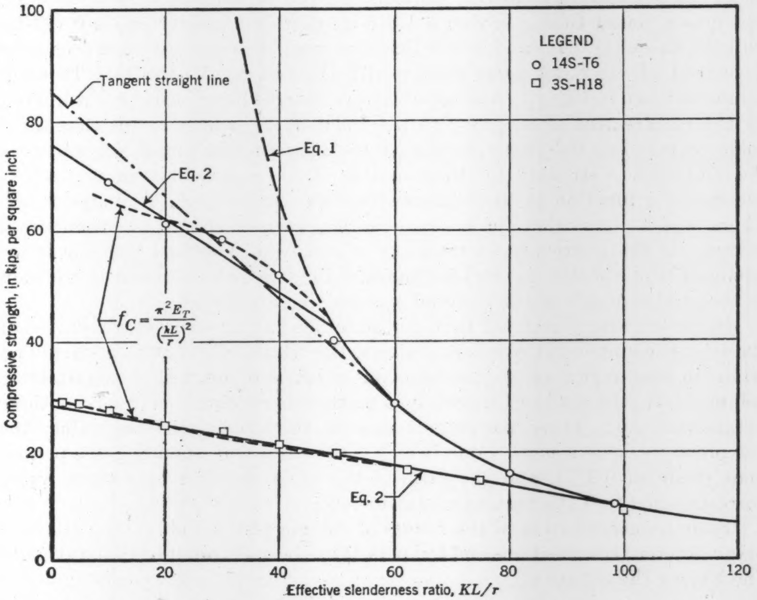

FIG. 1.—STRENGTH OF ALUMINUM ALLOY COLUMNS (SPECIMENS TESTED AS COLUMNS HAVING FLAT ENDS; $k = 0.5$)

Eq. 1 provides a close approximation of the ultimate strength of an axially loaded column in the plastic stress range if the elastic modulus E is replaced by the "tangent" modulus, E_T (4). The tangent modulus for a given stress value is simply the slope of the stress-strain curve at that stress. This "tangent-modulus method" for determining column strengths in the plastic stress range is used in the aircraft industry (7) and has also been used in specifications for aluminum alloy structures (2)(3).

It is a relatively simple matter to construct a column-strength curve by applying the tangent-modulus method to a specific stress-strain curve. It becomes cumbersome, however, to apply the method to a large number of aluminum alloys, involving many tempers of each alloy, ranging in yield strength from 4,000 lb per sq in. to more than 70,000 lb per sq in., and having marked differences in the shapes of their stress-strain diagrams. It was decided therefore to seek a generally applicable straight-line formula which would fit the data for all aluminum alloys more closely than that previously used.

Fig. 1 shows some typical column-strength curves and test results for aluminum alloys. The 2014-T6 specimens were of rolled and drawn 1-in.-diameter rod (8), and the 3003-H18 (formerly 3S-H18) specimens were of extruded and drawn round tubing having a 1.315-in. outside diameter and a 0.133-in. wall thickness (4). It can be seen that the straight line of the type originally developed (4) does not agree closely with the test results for 2014-T6 alloy columns shown in Fig. 1. Applicability of a straight line of this type is limited by the requirement of tangency to the Euler curve, which means that there could be only one independent variable for different alloys; this was taken as the compressive strength for the condition $k\,L/r = 0$. This value was expressed as a function of the compressive yield strength of the material (4). There was no provision for accommodating various shapes of stress-strain curves. If the restriction of tangency is removed, a second variable is introduced (slope of the line) and the shape of the stress-strain curve, in addition to the yield strength of the material, can be accommodated.

It has been demonstrated that, for materials having stress-strain curves of the type encountered in aluminum alloys, the relationship between stress and strain in that region of plastic behavior which is of interest in determining column strengths can be expressed by a mathematical equation involving three parameters (9). These parameters can be the elastic-modulus value, the compressive-yield-strength value (which is the stress corresponding to a permanent strain of 0.2%), and the ratio of the yield strength to a stress value corresponding to 0.1% permanent strain (10).

From an examination of the results of column tests on aluminum alloys of many different compositions and tempers, it has been determined that a straight line having the equation,

$$f_C = B - D\frac{k\,L}{r} \qquad \text{(2)}$$

agrees with test results about as closely as does the tangent-modulus column curve if the constants are defined as follows:

$$B = S_2\left[1 + \frac{\sqrt{10\,S_2}}{6}\left(\frac{S_2}{S_1} - 1\right)\right] \qquad \text{(3a)}$$

and

$$D = 0.5\sqrt{\frac{B^3}{E}\left(\frac{S_2}{S_1} - 1\right)} \qquad \text{(3b)}$$

in which S_2 is the stress at 0.2% permanent set, in kips per square inch (yield strength); S_1 is the stress at 0.1% permanent set, in kips per square inch

(British "proof stress"); and E is the modulus of elasticity, in kips per square inch.

In order to avoid straight lines that do not meet the Euler curve, the ratio S_2/S_1 is taken to be equal to 1.06 in Eqs. 3 if the actual ratio for the material in question exceeds this value. If the ratio S_2/S_1 is equal to 1.06, the straight line of Eq. 2 is tangent to the Euler curve. If the ratio S_2/S_1 were equal to unity (a condition not encountered in aluminum alloys), Eq. 2 would represent a horizontal line at a value of f_C equal to the yield strength. The straight lines that represent Eq. 2 in Fig. 1 were based on values of the ratio S_2/S_1 of 1.06 for the 3003-H18 alloy columns and 1.042 for the 2014-T6 alloy columns.

Values of the constants B and D of Eq. 2 have been listed elsewhere (1) with the mechanical properties for more than two-hundred classifications of alloy, temper, and product for wrought products and for more than fifty classifications of castings.

STRENGTH OF BEAMS

The problem of determining the strength of aluminum alloy beams of compact section, which are not subject to failure by lateral buckling, involves relating the stress in the member to the strength of the material.

For flanged members such as I-beams, channels, and plate girders—in which the resistance to bending is concentrated in the material in the flanges—the ultimate bending strength can be determined by substituting the tensile strength of the material for f in the equation:

$$f = \frac{Mc}{I} \quad \text{.......................... (4)}$$

in which f is the extreme fiber stress, in kips per square inch; M is the applied bending moment, in inch-kips; c is the distance from the neutral axis to the extreme fiber, in inches; and I is the moment of inertia of the cross section about its neutral axis, in inches^4.

The ultimate strength may be appreciably greater for beams of compact section having considerable material near the neutral axis than that indicated by substituting the tensile strength of the material in Eq. 4. Numerous tests on aluminum alloy beams have indicated that the maximum bending moment that such members can carry may be approximated by assuming that at failure both the tensile and compressive stresses over the whole cross section have reached a value equal to the tensile strength of the material. On this basis, form factors can be calculated for various cross sections. The ultimate strength of the beam can then be computed from Eq. 4 by substituting for f the tensile strength multiplied by the form factor for the cross section. The form factor for a solid rectangular section is 1.5 and for a solid round section, 1.7.

For I-sections, channels, and Z-sections that have equal flange areas and that fail by lateral buckling within the elastic stress range—

$$f_B = N \frac{\sqrt{E\, I_y\, G\, J}}{L} \frac{c}{I_x} \quad \text{.................... (5a)}$$

in which f_B is the critical bending stress, in kips per square inch; E is the modulus of elasticity, in kips per square inch; I_y is the moment of inertia of a beam about an axis parallel to the web, in inches^4; G is the modulus of elasticity in shear, in kips per square inch; J is the torsion constant, in inches^4; c is the distance from the neutral axis to the extreme fiber on the compression flange, in inches; I_x is the moment of inertia about an axis normal to the web, in inches^4; and N is a coefficient depending for its value on the nature and location of the applied load, the conditions of end restraint of the unsupported length L, and the relative importance of restraint against cross-sectional warping in the total resistance of the beam to twisting. (Lateral buckling involves both lateral bending and twisting.) Only cases of bending in one of the principal planes are considered in this paper.

Probably the most useful loading condition to assume for general design purposes is one which produces a uniform bending moment over the unsupported length, L; this is a close approximation to loading conditions frequently encountered. Lateral support is usually provided at points of load application. Eq. 5*a* for the case of uniform bending can be written as

$$f_B = \frac{\pi \sqrt{E\, I_y\, G\, J}}{k\, L} \sqrt{1 + \frac{\pi^2\, E\, C_s}{(k\, L)^2\, G\, J}\, \frac{c}{I_x}} \ldots\ldots\ldots\ldots (5b)$$

in which k is a factor representing lateral restraint at the end of the laterally unsupported length L, as for columns, and C_s is the torsion-bending constant of the cross section, in inches^6.

The torsion-bending constant C_s is the property of the cross section that measures its resistance to warping out of a plane when the member is twisted, in a manner similar to that in which the moment of inertia determines the bending stiffness (11). Formulas may be obtained for computing this constant for common structural cross sections (12), and tabulations of values of this and other common section elements are available (1) for a large variety of structural shapes.

If the ends of the laterally unsupported length of a simple beam are "fixed" ($k = 0.5$), Eq. 5*b* yields a satisfactory approximation of the critical stress (at the center of the unsupported length) for either distributed or concentrated loads applied at the neutral axis. If the ends of the laterally unsupported length are simply supported ($k = 1.0$), Eq. 5*b* yields results that are conservative for such loading conditions on simply supported beams. If a more precise calculation is desired for the buckling strength of beams under loading conditions other than uniform bending, use can be made of coefficients that are available for several different loading conditions (13).

The critical bending stress for a beam will be influenced by the location of the load relative to the neutral axis. Loading at the top flange (without lateral restraint) will result in buckling at a bending stress that is less than that for loads applied at the neutral axis. Conversely, the critical stress is increased by bottom-flange loading. The effect of loading at either the top or bottom flange can be approximated with reasonable accuracy by introducing the following multiplier terms into the appropriate equation for loading at the neutral axis:

$$f_{BB} = (f_B) \left[1 + \frac{2}{1.8 + \dfrac{k\, L}{a}}\right] \ldots\ldots\ldots\ldots (6a)$$

and

$$f_{BT} = \frac{f_B}{1 + \dfrac{2}{1.8 + \dfrac{k\,L}{a}}} \qquad \text{(6b)}$$

in which f_B is the critical bending stress for loading at the neutral axis, in kips per square inch (Eq. 5*b*); f_{BB} is the critical bending stress when the same loading is applied at the bottom flange, in kips per square inch; f_{BT} is the critical bending stress when the same loading is applied at the top flange, in kips per square inch; and $a = \sqrt{E\,C_s/G\,J}$. Other terms are as previously defined.

For I-beams with unequal flanges the critical stress under uniform bending can be expressed (14) as follows:

$$f_B = \frac{\pi^2 E\,I_y}{(k\,L)^2}\left\{e + \sqrt{e^2 + \frac{G\,J\,(k\,L)^2}{\pi^2 E\,I_y}\left[1 + \frac{\pi^2}{(k\,L)^2}\frac{E\,C_s}{G\,J}\right]}\right\}\frac{c}{I_x} \qquad \text{(7)}$$

in which *e* is the distance from the centroid to the shear center of the cross section, in inches (positive if the shear center lies between the centroid and the compression flange, otherwise negative).

Eqs. 5*a*, 5*b*, 6*a*, 6*b*, and 7 are applicable in cases of buckling within the elastic range of the material. In many instances, however, buckling occurs in the plastic range. To design against plastic buckling in a simple, conservative manner, use is made of the "equivalent-slenderness-ratio" method (5). The equivalent slenderness ratio is simply the slenderness ratio of a column that would buckle at the same stress as the beam in question. By equating the right-hand side of Eq. 1 to the right-hand side of the appropriate equation for the critical stress for a beam, one may solve for the radius of gyration, *r*. This value of *r* is termed an "equivalent radius of gyration" and is used with the proper effective length *k L* to form an equivalent slenderness ratio. The critical stress for buckling of the beam in the plastic stress range may then be obtained by substituting this equivalent slenderness ratio into Eq. 2. The equivalent radius of gyration for Eq. 5*b* is expressed by the equation:

$$r^2_e = \sqrt{I_y\,C_s\left[1 + \frac{(k\,L)^2}{\pi^2}\frac{G\,J}{E\,C_s}\right]}\,\frac{c}{I_x} \qquad \text{(8)}$$

This equivalent-slenderness-ratio method for solving the problem of the lateral buckling of beams in the plastic stress range—although not theoretically correct—yields results that are conservative but sufficiently accurate for design purposes.

LOCAL BUCKLING

Thus far in the paper, it has been assumed that failure of columns and beams would be of a general and not a local nature. There are, however, cases in which failure occurs or is initiated by local buckling. It is considered beyond the scope of this paper to discuss the kinds of local buckling that can influence the strength of a beam-column. Treatment of this subject can be found in many standard references (12)(15), and methods of design for aluminum alloy members are available (1)(2)(3). Buckling in the plastic stress range (1) is again treated simply and conservatively by the equivalent-slenderness-ratio method. It is well to remember that in some cases local buckling does not result in immediate and complete failure of the member.

STRENGTH OF BEAM-COLUMNS

In an early treatment of the design of aluminum alloy members under combined end load and bending (5), it was considered necessary to use two formulas because failure could occur in either of two ways—by bending in the plane of the applied bending moment or by lateral buckling. Since that time several experimental investigations have been conducted. The results of three of these investigations, which were undertaken to study the problem of the lateral buckling of beam-columns, have been published (16)(17). In a fourth investigation the behavior of beam-columns that fail by bending in the plane of the applied moment has been explored (18). The results of all these investigations, together with some previously conducted tests on eccentrically loaded tubular columns, have led to the recommendation of one simple equation, presented herein, for the design of all beam-columns regardless of the type of failures.

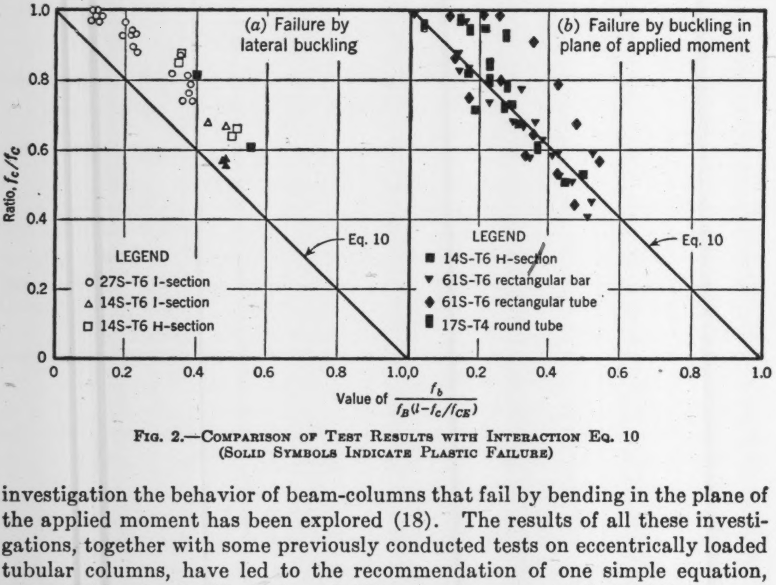

FIG. 2.—COMPARISON OF TEST RESULTS WITH INTERACTION EQ. 10 (SOLID SYMBOLS INDICATE PLASTIC FAILURE)

For problems involving combined loading, it is convenient to express the strength of a member in the form of an interaction equation that incorporates stress ratios (19). The simplest such equation for combined end load and bending is of the form:

$$\frac{f_c}{f_C} + \frac{f_b}{f_B} = 1 \quad \text{(9)}$$

in which f_c is the applied end load, in kips per square inch; f_C is the strength of the member under end load alone, in kips per square inch; f_b is the applied bending stress, in kips per square inch ($f_b = M_b\,c/I$); and f_B is the strength of the member under bending alone, in kips per square inch ($f_B = M_B\,c/I$).

This equation has been shown to be inadequate for the design of aluminum alloy beam-columns (16)(17)(18). The equation recommended for this purpose, based on the previously mentioned investigations, is

$$\frac{f_c}{f_C} + \frac{f_b}{f_B\left(1 - \dfrac{f_c}{f_{CE}}\right)} = 1 \qquad (10)$$

in which f_{CE} is the Euler critical load (Eq. 1) for buckling of the member in the direction of the applied bending moment, in kips per square inch. The use of such a simple equation to solve a complex problem entails some sacrifice in accuracy. It is thought, however, that Eq. 10 provides a reasonably accurate and sufficiently conservative basis for the design of aluminum alloy beam-columns. The extent to which the equation is supported by the test results can be seen in Fig. 2.

TABLE 1.—RESULTS OF TESTS ON ECCENTRICALLY LOADED COLUMN SPECIMENS OF ALUMINUM ALLOY 2017-T4 ROUND TUBES, 2-IN. OUTSIDE DIAMETER BY 0.083-IN. WALL THICKNESS[a]

Specimen No.	Slenderness ratio, L/r	Eccentricity, in inches	Average compressive stress at failure, in kips per square inch
6-102	150	0.024	4.39
12-102	150	0.141	4.17
13-102	150	0.263	3.82
14-102	150	0.377	3.60
5-54B	80	0.017	15.06
10-54A	80	0.137	12.51
10-54B	80	0.255	10.88
11-54A	80	0.435	9.78
4-27B	40	0.018	28.93
4-27C	40	0.117	24.80
4-27D	40	0.240	21.58
9-27A	40	0.427	18.18

[a] Data from an unpublished report by Marshall Holt, A. M. ASCE.

Fig. 2(*a*) shows the results of all the tests in which failure occurred by lateral buckling (17). Tests were made on I-section members in which bending was applied in the plane of the web. Bending moment was introduced by applying the end loads eccentrically. The ratios of the column strength of a specimen in the plane of the web to that normal to the plane of the web ranged between approximately 9 and approximately 0.9. Failure involved lateral buckling in both the elastic and plastic stress ranges.

In Fig. 2(*b*) have been plotted the results of tests in which the members failed by bending in the plane of the applied moment. The specimens were of four kinds: (*a*) An H-section, with bending in the plane of the web (17); (*b*) a solid rectangular section, with bending in the weak direction (18); (*c*) a hollow rectangular section (representative of members with material concentrated in flanges) with bending in the weak direction (16); and (*d*) hollow circular sections. The test results for the latter specimens are summarized in Table 1. The specimens listed in Table 1 were tested on platens having ball-bearing spherical seats and the centers of rotation in the bearing surfaces of the platens. The average compressive yield strength at 0.2% set, determined on specimens of the full cross section, was 38.53 kips per sq in. The average modulus of failure in bending (the maximum bending moment divided by the section modulus) was 64.0 kips per sq in. (20). Values of compressive strength for zero eccentricity, determined by plotting test values of the critical axial load against the corresponding critical bending moments and extending the curves through these points to the axis of zero bending moment, were 4.5 kips per sq in., 15.9 kips per sq in., and 30.1 kips per sq in. for specimens having slenderness ratios of 150, 80, and 40, respectively.

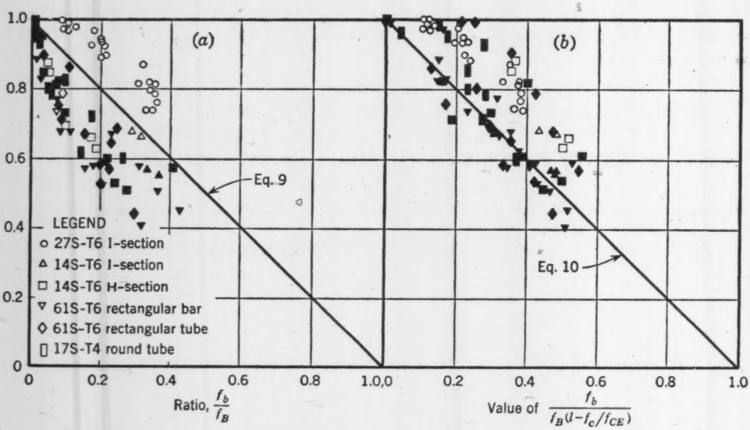

FIG. 3.—INTERACTION DIAGRAM FOR ALUMINUM ALLOY BEAM-COLUMNS, BOTH TYPES OF FAILURE (SOLID SYMBOLS INDICATE PLASTIC FAILURE)

COMPARISON OF INTERACTION EQUATIONS

Various interaction equations have been proposed or used for the design of members under combined end load and bending. It is not contended that all these equations have a rational theoretical basis; in fact, it is not required that an interaction equation be so based in order to be satisfactory. All that is required is that the equation provide a simple and reasonably accurate means for calculating the strength of such a member. In explaining the differences between the various equations, however, it is informative to consider the meaning of the relationships expressed by the equations.

The simple interaction relationship expressed by Eq. 9 is the basis for the treatment of the beam-column problem in a design specification for steel structures (21). The interaction relationship expressed by Eq. 9 has the following meaning: Failure occurs if the sum of the applied stresses ($f_c + f_b$) reaches a limiting value that varies from f_C (when $f_b = 0$) to f_B (when $f_c = 0$)—the variation of this sum with either of the ratios f_c/f_C or f_b/f_B being linear. That this equation is not in reasonable agreement with the results of tests on aluminum alloy beam-columns is shown in Fig. 3(*a*). Data are presented in Fig. 3 for I-sections and H-sections (17), rectangular bars and tubes (18), and round tubes (Table 1). The strength indicated by Eq. 9 ranges from 16% below the test results to 39% above them. In general, the use of this equation to predict the strength of the beam-columns tested would be decidedly unconservative.

The interaction equation proposed in this paper (Eq. 10) differs in meaning from the relationship expressed by Eq. 9 in this respect—the significant stress is considered to be $\left\{f_c + f_b\left[\frac{1}{1-(f_c/f_{CE})}\right]\right\}$ and not $f_c + f_b$. The multiplier applied to f_b is an approximate correction to take account of the fact that the bending stress at the center of the member is greater than the applied bending stress f_b because of the additional bending moment resulting from the end load and deflection of the member. The reasonably conservative agreement between Eq. 10 and the results of tests on aluminum alloy beam-columns has been shown in Fig. 2. In Fig. 3(*b*) all the test results, regardless of type of failure, have been plotted in comparison with this proposed interaction equation. The equation predicts strengths ranging from 18% below the test results to 10% above them.

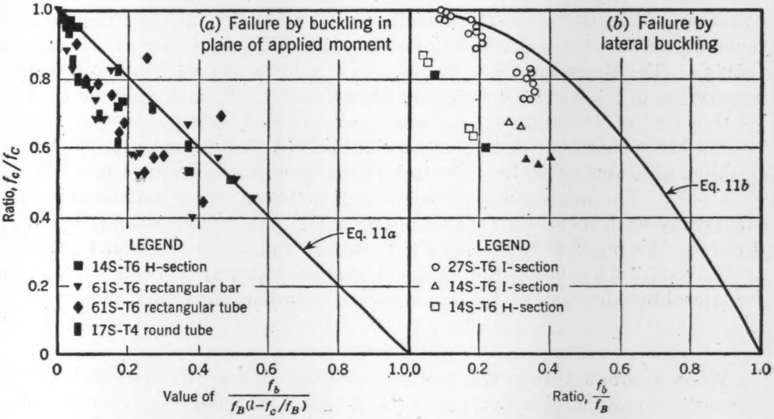

FIG. 4.—COMPARISON OF TEST RESULTS WITH INTERACTION EQS. 11
(SOLID SYMBOLS INDICATE PLASTIC FAILURE)

As previously stated, the original treatment of the design of aluminum alloy beam-columns (5) included two equations for the two general types of failure. Expressed in interaction form and in the terminology of this paper, these equations can be written as

$$\frac{f_c}{f_C} + \frac{f_b}{f_B\left(1 - \frac{f_c}{f_B}\right)} = 1 \qquad \text{(11a)}$$

and

$$\frac{f_c}{f_C} + \left(\frac{f_b}{f_B}\right)^2 = 1 \qquad (11b)$$

Eq. 11*a* was intended to apply to failure by bending in the plane of the applied moment, and Eq. 11*b* to failure by lateral buckling.

Eq. 11*a* was derived (22) by assuming that at failure the sum of the direct stress and bending stress is equal to f_B and by defining the maximum bending stress as $f_b \left[\frac{1}{1 - (f_c/f_C)}\right]$. In Fig. 4(*a*) this equation is compared with the test results from the aluminum alloy beam-columns that failed by instability in the plane of the applied moment (17)(18) (Table 1). It can be seen by comparing this plot with Fig. 2(*a*) that Eq. 11*a* is definitely inferior to Eq. 10 as a reasonable representation of the behavior of a beam-column. Eq. 11*a* predicts strengths ranging from 31% above the test results to 10% below them. This equation will be unconservative in the region of small (f_b/f_B)-values for long members because the actual maximum stress at failure may be considerably less than f_B. For short members, the equation may be found ultraconservative because use of the factor $1 - (f_c/f_C)$ rather than $1 - (f_c/f_{CE})$ overcompensates for the effect of deflection since f_C may be appreciably lower than f_{CE}.

Eq. 11*b* is based on the theoretical solution of S. Timoshenko for the lateral buckling of beams under axial load and equal bending moments applied at the ends (15). The inadequacy of this equation to represent satisfactorily the strength of such members (17) is shown in Fig. 4(*b*). This subject has been discussed in a previous publication (17), in which it was shown that Eq. 10 can be derived from a modification of the theoretical solution (11) of J. N. Goodier for lateral buckling failure by making certain simplifying assumptions.

CONCLUSION

When combined with the methods outlined herein for determining the strength of aluminum alloy columns and beams, the interaction relationship (Eq. 10) provides a reasonably accurate, simple means for calculating the strength of members subjected simultaneously to a compressive end load and bending. This conclusion is based on tests involving equal end moments. Additional investigational work is required in order to determine the limits of applicability of this interaction equation under such conditions as unequal end moments, end moments of opposite sign, and transverse loads with varying degrees of end restraint.

APPENDIX. BIBLIOGRAPHY ON BEAM-COLUMNS

(1) **"Alcoa Structural Handbook,"** Aluminum Co. of America, Pittsburgh, Pa., 1955.

(2) **"Specifications for Heavy Duty Structures of High-Strength Aluminum Alloy: Final Report of the Committee of the Structural Division on**

Design in Lightweight Structural Alloys," *Transactions,* ASCE, Vol. 117, 1952, p. 1253.

(3) **"Specifications for Structures of a Moderate Strength Aluminum Alloy of High Resistance to Corrosion: Progress Report of the Committee of the Structural Division on Design in Lightweight Structural Alloys,"** *Proceedings-Separate No. 132,* ASCE, May, 1952.

(4) **"Column Strength of Various Aluminum Alloys,"** by R. L. Templin, R. G. Sturm, E. C. Hartmann, and M. Holt, *Technical Paper No. 1,* Aluminum Research Labs., Aluminum Co. of America, Pittsburgh, Pa., 1938.

(5) **"Alcoa Structural Handbook,"** Aluminum Co. of America, Pittsburgh, Pa., 1938, 1940, 1945, 1948, and 1950.

(6) **"The Column Strength of Aluminum Alloy 75S-T Extruded Shapes,"** by M. Holt and J. R. Leary, *Technical Note No. 1004,* National Advisory Committee for Aeronautics, Washington, D. C., 1946.

(7) **"Strength of Metal Aircraft Elements,"** *ANC-5 Bulletin,* Subcommittee on Air Force-Navy-Civil Aircraft Design Criteria, Munitions Board Aircraft Committee, Washington, D. C., June, 1951.

(8) **"Column Strength of Aluminum Alloy 14S-T Extruded Shapes and Rod,"** by J. R. Leary and Marshall Holt, *Technical Note No. 1027,* National Advisory Committee for Aeronautics, Washington, D. C., 1946.

(9) **"Description of Stress-Strain Curves by Three Parameters,"** by Walter Ramberg and W. R. Osgood, *Technical Note No. 902,* National Advisory Committee for Aeronautics, Washington, D. C., 1943.

(10) **"Determination of Stress-Strain Relations from Offset Yield Strength Values,"** by H. N. Hill, *Technical Note No. 927,* National Advisory Committee for Aeronautics, Washington, D. C., 1944.

(11) **"Flexural-Torsional Buckling of Bars of Open Section,"** by J. N. Goodier, *Bulletin No. 28,* Cornell Univ. Eng. Experiment Station, Ithaca, N. Y., 1942. (*a*) Eq. 9.

(12) **"Buckling Strength of Metal Structures,"** by F. Bleich, McGraw-Hill Book Co., Inc., New York, N. Y., 1952.

(13) **"The Lateral Instability of Deep Rectangular Beams,"** by H. N. Hill, *Technical Note No. 601,* National Advisory Committee for Aeronautics, Washington, D. C., 1937.

(14) **"The Lateral Instability of Unsymmetrical I-Beams,"** by H. N. Hill, *Journal of the Aeronautical Sciences,* Vol. 9, 1942, p. 175.

(15) **"Theory of Elastic Stability,"** by S. Timoshenko, McGraw-Hill Book Co., Inc., New York, N. Y., 1936.

(16) **"Lateral Buckling of Eccentrically Loaded I-Section Columns,"** by H. N. Hill and J. W. Clark, *Transactions,* ASCE, Vol. 116, 1951, p. 1179.

(17) **"Lateral Buckling of Eccentrically Loaded I- and H-Section Columns,"** by H. N. Hill and J. W. Clark, *Proceedings,* First National Cong. of Applied Mechanics, ASME, 1952, p. 407.

(18) **"Eccentrically Loaded Aluminum Columns,"** by John W. Clark, *Transactions,* ASCE, Vol. 120, 1955, p. 1116.

(19) **"Stress Ratios,"** by F. R. Shanley and E. I. Ryder, *Aviation,* June, 1937, p. 28.

(20) **"Safe Beam Loading for Aluminum Tubes,"** by Marshall Holt, *Product Engineering*, January, 1943, p. 36.

(21) **"Steel Construction,"** AISC, 5th Ed., 1950, p. 284.

(22) **Discussion by E. C. Hartmann of "Rational Design of Steel Columns"** by D. H. Young, *Transactions*, ASCE, Vol. 101, 1936, p. 475.

(23) **"Contributions to the Theory of Combined Flexure and Torsion,"** by Robert B. McCalley, Jr., thesis presented to Cornell University, at Ithaca, N. Y., in 1952, in partial fulfilment of the requirements for the degree of Doctor of Philosophy.

(24) **"Theory of Bending, Torsion, and Buckling of Thin-Walled Members of Open Cross Section,"** by S. P. Timoshenko, *Journal*, Franklin Inst., May, 1945, p. 356.

(25) **Discussion by H. A. Sawyer of "Applied Column Theory,"** by F. R. Shanley, *Transactions*, ASCE, Vol. 115, 1950, p. 743, Eq. 71. (*a*) pp. 717 and 744, Figs. 15 and 23.

(26) **"Alcoa Structural Handbook,"** Aluminum Co. of America, Pittsburgh, Pa., 1945, p. 174.

(27) **"Strength of Tubing Under Combined Axial and Transverse Loading,"** by L. B. Tuckerman, S. N. Petrenko, and C. D. Johnson, *Technical Note No. 307*, National Advisory Committee for Aeronautics, Washington, D. C., June, 1929.

(28) **"Lateral Buckling of Channels and Z-Beams,"** by H. N. Hill, *Transactions*, ASCE, Vol. 119, 1954, p. 829.

DISCUSSION

Robert B. McCalley, Jr.,[5] J. M. ASCE.—Unsymmetrical cases occur often enough in practice so that a generalized form of Eq. 7 may be of interest. Eq. 7 applies to the case in which the constant bending moment lies in one of the principal planes of the cross section. In the general case, the x-axis and y-axis do not coincide with the principal axes. For a beam subject to a constant bending moment about the x-axis, the critical moment, M_{cr}, can be expressed (23) as

$$M_{cr} = \frac{\pi^2 E I_1 I_2}{I_x (k L)^2} \left[e \pm \sqrt{e^2 + \frac{G J I_x (k L)^2}{\pi^2 E I_1 I_2} \left(1 + \frac{\pi^2}{(k L)^2} \frac{E C_s}{G J} \right)} \right] \quad (12)$$

in which I_1 is the major moment of inertia, I_2 is the minor moment of inertia, and I_x is the moment of inertia about the x-axis.

However, the generalized definition of e is

$$e = y_t - y_s \quad (13)$$

in which y_t is the y-coordinate of a geometric point designated the "twist center" and y_s is the y-coordinate of the shear center. The twist center is the point about which a beam in pure torsion rotates. In symmetrical cases both the twist center and the shear center coincide with the centroid of the cross section. The twist-center coordinates (x_t, y_t) may be computed from

$$\left.\begin{aligned} x_t &= \frac{1}{2 I_1 I_2} \left(I_x \int \rho^2_a \, x \, dA - I_{xy} \int \rho^2_a \, y \, dA \right) + x_a \\ y_t &= \frac{1}{2 I_1 I_2} \left(I_y \int \rho^2_a \, y \, dA - I_{xy} \int \rho^2_a \, x \, dA \right) + y_a \end{aligned}\right\} \quad (14)$$

in which ρ_a is the radius vector from some convenient reference point (x_a, y_a) to a point (x, y) on the cross section and the integrations are performed over the whole area, A, of the cross section (23).

The critical stress f_B may then be determined from

$$f_B = \frac{M_{cr} (I_y y - I_{xy} x)}{I_1 I_2} \quad (15)$$

The x-coordinate and the y-coordinate of the extreme fiber must be chosen by inspection for the weakest case. In many instances, it may be convenient to eliminate the product term, $I_1 I_2$, in the foregoing equations by means of the identity:

$$I_1 I_2 = I_x I_y - I^2_{xy} \quad (16)$$

If the x-axis coincides with the major axis of the cross section, $I_x = I_1$, $I_y = I_2$, $I_{xy} = 0$, and Eq. 12 with Eq. 15 reduces to Eq. 7. Mr. Goodier (11) has previously called attention to the fact that the ± sign before the radical term indicates that the beam has one critical moment when bent downward but another when bent upward. The quantity e is equal to one half of Mr. Timoshenko's value (24) for β_1. The expression given by Mr. Timoshenko is referred to the principal axes of the section.

---

[5] Engr., Applied Physics Lab., The Johns Hopkins Univ., Silver Spring, Md.

HERBERT A. SAWYER, JR.,[6] M. ASCE.—Certain important refinements of present practice in designing beam-columns have been presented by Messrs. Hill, Hartmann, and Clark. These refinements apply not only to aluminum members, which were exclusively considered by the authors, but also to members of other structural materials.

The authors conclude from their evidence that the interaction equation, Eq. 10, yields a reasonably accurate, simple means for computing the strength of aluminum alloy beam-columns. The authors' justification of this equation for failures by bending in the plane of the applied bending moment was empirical, and therefore they state that additional investigation is needed to determine the limits of this equation's applicability to conditions differing from those of the cited tests. The cited tests were restricted as follows: All members were of aluminum alloy, applied bending was constant throughout the member lengths, and applied bending stresses were less than half of the ultimate bending modulus of the members ($f_b < f_B/2$).

The purpose of this discussion is to consider certain theoretical and experimental evidence on the use of this equation beyond these restrictions.

Theoretical Evidence.—The writer has previously derived (25) an expression for the strength of beam-columns similar to Eq. 10:

$$\frac{f_c}{f_{CO}} + \frac{f_b}{f_B\left(1 - \frac{f_c}{f'_{CE}}\right)}\left(1 + K\frac{f_c}{f'_{CE}}\right) = 1 \ldots\ldots\ldots\ldots (17)$$

in which f_{CO} is the strength per unit area of a short column and $f'_{CE} = \frac{\pi^2 E_t}{(L/r)^2}$ (in which E_t is the tangent modulus of the material at a stress of f_c, not f_C). The constant K depends on the distribution of the applied moments—that is, on the distribution of either initial eccentricities or initial moments from transverse loads. For triangular moment distribution, K is equal to approximately -0.18; for sinusoidal distribution, 0.00; for parabolic distribution, $+0.03$; for third-point trapezoidal distribution, $+0.05$ for quarter-point trapezoidal distribution, $+0.13$; and for rectangular distribution, approximately $+0.26$.

Eq. 17 was derived from the basic column equation, $f = P/A + M\,c/I$, using a generalized secant-formula type of derivation and assigning to "f" a sliding, limiting value varying from the short-column strength for concentric loadings to the modulus of bending (or rupture) for pure bending loadings. Of course, the main theoretical limitation of Eq. 17 is its inaccuracy beyond the elastic limit; the use of E_t instead of the elastic modulus somewhat reduces this inaccuracy. Another limitation of Eq. 17 is that it applies only to failures from bending in the plane of the applied moment. However, this is the case for which the authors presented only empirical justification for Eq. 10. The following comparison of Eqs. 10 and 17 is made to reveal certain theoretical justifications and limitations for this case of Eq. 10.

---

[6] Associate Prof. of Civ. Eng., Univ. of Connecticut, Storrs, Conn.

In Eq. 17 the factor containing K is significant in providing what the writer believes to be a fairly correct indication of the relative adjustments that should be made in the bending term of Eq. 10 to account for distributions of applied moment that are not of the rectangular shape considered in the paper. Choosing the most extreme case as an example—if the primary bending of a beam-column is caused by a single transverse load at the midlength (or out-of-lineness caused by a single short bend of the axis at the midlength), the primary moments would be triangular in distribution, and according to Eq. 17 the bending term of Eq. 10 should be multiplied by the factor:

$$\frac{1 - 0.18 \dfrac{f_c}{f'_{CE}}}{1 + 0.26 \dfrac{f_c}{f'_{CE}}}.$$

However, the importance of this factor should not be overestimated; it differs from unity significantly only when the term f_c/f'_{CE} is relatively large, but for large values of f_c the bending term of the interaction equation is relatively small and insignificant, and large percentage variations of this small term will have little effect on the allowable axial load. Therefore, for most design purposes the omission of this variation in Eq. 10 is justified, especially because this omission is always on the safe side.

The remaining differences between Eq. 10 and Eq. 17 are also more apparent than real. The term f'_{CE} differs from f_{CE} only for large values of f_c, but for such values the bending term of the interaction equation is relatively small. This difference tends to make Eq. 10 slightly less conservative than Eq. 17. The remaining difference, that between f_C and f_{CO}, vanishes for small values of L/r and is unimportant for small values of f_c, but for the larger values of L/r and f_c it becomes more significant, tending to make Eq. 10 more conservative than Eq. 17 in this range.

It may be concluded that, with the exception of the range just mentioned, Eq. 17 lends a sort of theoretical justification for Eq. 10, encouraging the expectation that Eq. 10 would apply for materials and loadings other than those of the cited tests.

Any designer attempting to use Eq. 10 (or Eq. 17) should note that the Euler-Engesser column equation which expresses the basic column strength differs from the usual design formulas because in it is neglected the effect of accidental eccentricity and heterogeneity. Also, the effect of accidental eccentricity was meticulously eliminated in the cited tests. Because such effects cannot be eliminated in practical construction, they always exist for both principal bending axes. The probable maximum accidental eccentricities must be predicted and the resulting stresses included in the term f_b. Provision for accidental eccentricities by increasing the factor of safety of the Euler-Engesser formula is not satisfactory because eccentricity and, hence, the percentage reduction in allowable load from eccentricity tend to be increased with an increase in column length. For example, a standard out-of-lineness tolerance for aluminum alloy tubing is 1/1,200 of its length (26).

Experimental Evidence.—The surest way to justify extension of the range of Eq. 10 is by comparison with test results. L. B. Tuckerman, S. N. Petrenko, and C. D. Johnson (27) have performed extensive tests on steel tubing and aluminum alloy tubing under combined axial loading and third-point transverse loads. Fig. 5 shows a comparison of these test results, Eq. 10, and Eq. 17 for tests of duralumin tubing. Eq. 10 conforms to these test results very well except for the largest values of L/r. This exception is predictable from the foregoing theoretical evidence. The writer believes that the disagreement for the case $L/r = 30$ may not be significant because the modulus of bending tends to increase for small values of L/r, and such increases were neglected in the report of these tests. Eq. 10 is on the side of safety for all values of L/r.

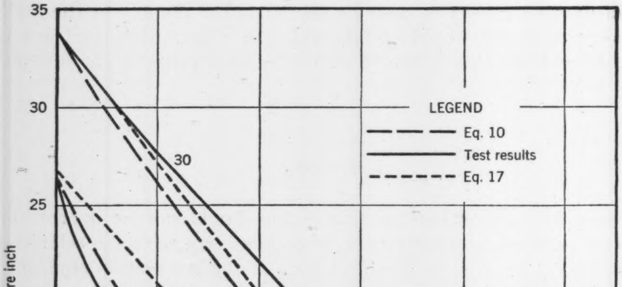

FIG. 5.—COMPARISON OF TESTS OF DURAL TUBING WITH EQS. 10 AND 17

Chrome-molybdenum steel tubing was used for the remaining tests by Messrs. Tuckerman, Petrenko, and Johnson. The writer has shown elsewhere

(25*a*) the remarkable agreement between Eq. 17 and these tests. Eq. 10 may also be compared with these test results, and such comparison shows close agreement for values of L/r between 30 and 70. As would be expected, Eq. 10 becomes conservative for greater values of L/r, the curve of Eq. 10 for $L/r = 90$ nearly coinciding with most of the experimental curve for $L/r = 100$, and the curve of Eq. 10 for $L/r = 120$ nearly coinciding with most of an extrapolated experimental curve for $L/r = 140$.

Conclusion.—It may be tentatively concluded on the basis of these comparisons with the theory and test data of Messrs. Tuckerman, Petrenko, and Johnson that Eq. 10 may be applied with safety to beam-columns (*a*) of certain metals other than aluminum, (*b*) which have applied bending moments resulting from transverse loads, and (*c*) which have applied bending stresses greater than half the bending modulus. Also, Eq. 10 is superior to Eq. 17 for general design purposes: It agrees somewhat better with the aluminum alloy test data of the paper; its variation is generally on the safe side; and, most important, it is suitable for failures by "lateral" buckling (buckling about a bending axis perpendicular to the bending axis for the applied moment).

If lateral buckling is neglected, tests of chrome-molybdenum-steel tubing and theoretical considerations would seem to indicate that Eq. 17 would prove more precise than Eq. 10 for materials such as mild steel, certain alloy steels, wood, and cast iron (with either sharp knees or somewhat uniform curvature in their stress-strain diagrams). However, on the basis of the present data, Eq. 10 seems to be more generally applicable and safe and is simple and suitable for design. Fig. 3(*a*) demonstrates the inadaquacy of the conventional interaction formula for beam-columns. Therefore, the authors have made a significant contribution to the art of structural design.

HARRY N. HILL[7] AND ERNEST C. HARTMANN,[8] MEMBERS, ASCE, and JOHN W. CLARK,[9] J. M. ASCE.—The discussers have made several interesting observations on the design of members for combined end loading and bending. Mr. McCalley's Eq. 12 expresses the critical bending moment for the general case in which both the cross section of the member and the condition of loading are unsymmetrical. Eq. 12 represents the same relationship as that derived by Mr. Goodier (11*a*), but Mr. McCalley has succeeded in stating the relationship in a manner that is particularly useful for design purposes. A special case that might be of interest is the case in which the cross section of the member is symmetrical but the loading is not; that is, the plane of the applied bending moment does not coincide with one of the principal axes. In this case, e is zero and Eq. 12 is reduced to

$$M_{cr} = \frac{\pi}{k\,L}\sqrt{\frac{E\,I_1\,I_2\,G\,J}{I_y}}\sqrt{1 + \frac{\pi^2}{(k\,L)^2}\frac{E\,C_s}{G\,J}} \quad \text{..........} \quad (18)$$

The value of the end fixity factor, k, in the foregoing equations always depends on the restraint against rotation of the end cross sections about the minor principal axis, even though in the case of unsymmetrical bending the minor principal axis is not in the plane of the applied bending moment. Thus, the ends of a beam may be "fixed" in the lateral direction (normal to the plane of the applied bending moment) yet not fixed in the direction that is of interest from the standpoint of determining k. This fact was demonstrated in a recent paper on the strength of aluminum alloy **Z**-beams subjected to pure bending moment (28).

---

[7] Chief, Eng. Design Div., Aluminum Research Labs., Aluminum Co. of America, New Kensington, Pa.

[8] Asst. Director, Aluminum Research Labs., Aluminum Co. of America, New Kensington, Pa.

[9] Research Engr., Eng. Design Div., Aluminum Research Labs., Aluminum Co. of America, New Kensington, Pa.

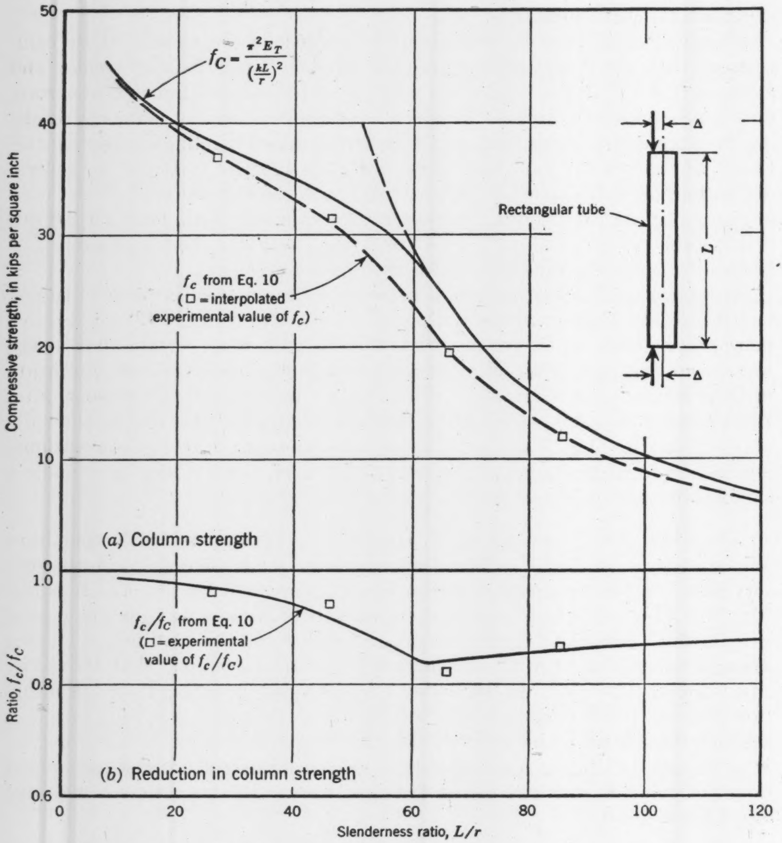

FIG. 6.—VARIATION IN COLUMN STRENGTH FOR 6061-T6 ALLOY RECTANGULAR TUBES, 3 IN. BY 2 IN. BY $\frac{1}{4}$-IN. WALL THICKNESS, $\frac{\Delta}{L} = \frac{1}{1,200}$

It is gratifying that Mr. Sawyer has furnished additional evidence in support of the use of Eq. 10 in the design of beam-columns. His theoretical analysis of Eqs. 10 and 17 supplements the writers' examination of interaction equations and their rational basis under the heading, "Comparison of Interaction Equations."

Mr. Sawyer has explained that the Euler-Engesser column formula does not include the effects of accidental eccentricity or heterogeneity, and he has concluded:

> "Provision for accidental eccentricities by increasing the factor of safety of the Euler-Engesser formula is not satisfactory because eccentricity and, hence, the percentage reduction in allowable load from eccentricity tend to be increased with an increase in column length."

It is true that initial crookedness tends to increase with increasing column length; however, it does not follow that the factor of safety resulting from the use of a formula for ideal columns decreases for the longer columns. As a matter of fact, if eccentricity is directly proportional to length, the minimum factor of safety provided by the use of a formula for ideal columns occurs in the general vicinity of the juncture between the elastic and inelastic parts of the curve relating strength to slenderness ratio.

The foregoing statement is illustrated in Fig. 6. The solid curve in Fig. 6(*a*) is the Euler-tangent-modulus column-strength curve for rectangular tubes of aluminum alloy 6061-T6, tested in a previously mentioned investigation (18). The lower, dashed curve in Fig. 6(*a*) represents the column strength computed from Eq. 10 for the same specimens loaded as pin-ended columns having a ratio of eccentricity, Δ, to length, L, of 1/1,200. None of the column specimens tested had a (Δ/L)-ratio of exactly 1/1,200. However, test values of column strength corresponding to this ratio of eccentricity to length were determined by interpolation from the test data. These interpolated test values are also plotted in Fig. 6(*a*).

Fig. 6(*b*) shows the ratio of column strength for a (Δ/L)-value of 1/1,200 to the strength of an ideal column determined from the curves and test points in Fig. 6(*a*). Both the computed curve and the test points in Fig. 6(*b*) illustrate the fact that the reduction in column strength caused by eccentricity does not necessarily increase with increasing length, even though the eccentricity itself does. Therefore, it does not appear unreasonable to design columns on the basis of formulas for ideal members, taking account of the effects of accidental eccentricity in the factors of safety.

AMERICAN SOCIETY OF CIVIL ENGINEERS

Founded November 5, 1852

TRANSACTIONS

Paper No. 2784

ONE-WAY STREET SYSTEM IN SACRAMENTO, CALIF.

By D. Jackson Faustman,[1] A. M. ASCE

Synopsis

The phenomenal increase in motor-vehicle transportation emphasizes the need for making the most efficient use of existing streets and highways. The one-way street offers an inexpensive, effective tool for better urban street use. The advantages of one-way streets include (*a*) increased traffic capacity, (*b*) relatively low cost, (*c*) reduction in accidents, (*d*) ease of accomplishment, (*e*) higher operating speeds, and (*f*) flexibility in meeting changing traffic patterns. These gains far outweigh the disadvantages of longer travel for some traffic, confusion to strangers, and a possible disruptive effect on certain types of business.

Over a period of seven years, Sacramento (Calif.) has installed ten pairs of one-way streets, a total of 35 miles at a cost of $200,000. The cost of a comparable widened two-way street system would have been in excess of $6,000,000.

Significant results have been achieved in traffic capacity, accident reduction, and speed of movement. Comparison of business indices reveals that the one-way street system has not unfavorably affected business activity. A number of major new business developments have occurred on the one-way street system. Community approval and acceptance have been overwhelming.

One-way streets are extremely valuable in improving traffic movement where warranted from engineering study. They are not a cure-all and should not be used without proper integration into a master street and highway plan.

Introduction

California is (as of 1955) facing a transportation crisis as are many other states in the United States because of the inability to provide a system of streets and highways adequate for the phenomenal increase in traffic movement. The problem is particularly acute in urban areas as it is there that traffic concentrations are the greatest and construction costs of the new

---

Note.—Published, essentially as printed here, in August, 1953, as *Proceedings-Separate No. 234.* Positions and titles given are those in effect when the paper was approved for publication in *Transactions.*

[1] City Traffic Engr., Sacramento, Calif.

facilities are the highest. Any method, therefore, of improving traffic conditions in urban areas quickly and inexpensively is deserving of close scrutiny.

The one-way street offers to the traffic engineer and highway engineer an exceedingly effective tool for facilitating traffic movement. Although it is not a panacea for all traffic ills and certainly should not be considered a final solution, it offers many advantages. These advantages include:

1. An increase in the carrying capacity of the street. A 50-ft street will accommodate from 45% to 60% more traffic with one-way traffic than with two-way operation.[2]
2. A relatively low cost. The cost of providing a one-way street system is only about 2% of the cost of providing a widened two-way street with the same traffic capacity.

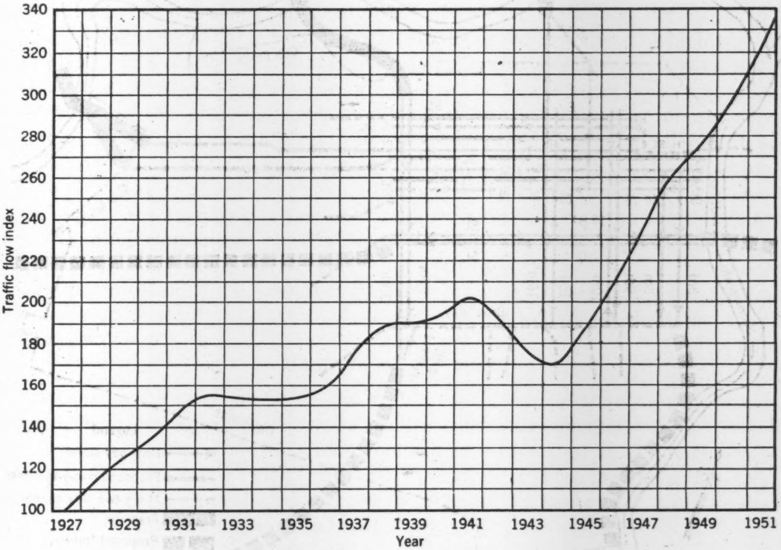

FIG. 1.—TRAFFIC TRENDS, SACRAMENTO, CALIF.

3. A reduction in most types of accidents as a result of basic changes in traffic patterns and conditions.
4. Speed and ease of accomplishment. A system of one-way streets can be placed in operation in less than one tenth the time required for a street-widening program.
5. Higher average operating speeds resulting from the elimination of opposing streams of traffic and turning conflicts and the more efficient operation of the traffic-signal system.
6. Flexibility in meeting changing traffic patterns.

---

[2] "Highway Capacity Manual," U. S. Bureau of Public Roads, Washington, D. C., 1950.

These gains far outweigh the disadvantages, which include longer travel for some traffic, confusion to the stranger, and a disruptive effect on certain types of businesses which are dependent on "drive-in" trade.

Experiences in Sacramento

The Sacramento one-way system affords a notable example of the results which can be achieved with such a system. Sacramento has a population (in 1955) of 157,000 with an additional 125,000 persons residing within a 7-mile radius. Automobile registration is unusually heavy—approximately 150,000 vehicles in Sacramento County. Thus, the per capita registration of vehicles is about 1 for every 1⅔ persons. Traffic movement has increased markedly since 1945, as shown in Fig. 1.

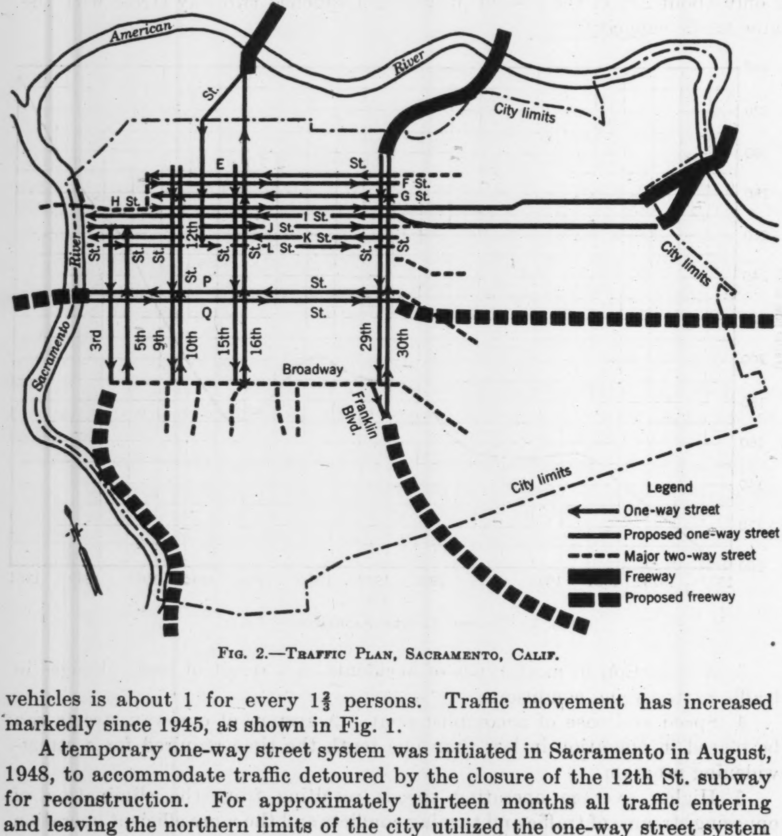
American River
City limits
E St.
F St.
G St.
H St.
I St.
J St.
K St.
L St.
P St.
Q St.
3rd St.
5th St.
9th St.
10th St.
12th St.
15th St.
16th St.
29th St.
30th St.
Broadway
Franklin Blvd.
Sacramento River
City limits
City limits
Legend
One-way street
Proposed one-way street
Major two-way street
Freeway
Proposed freeway

Fig. 2.—Traffic Plan, Sacramento, Calif.

A temporary one-way street system was initiated in Sacramento in August, 1948, to accommodate traffic detoured by the closure of the 12th St. subway for reconstruction. For approximately thirteen months all traffic entering and leaving the northern limits of the city utilized the one-way street system on 15th St. and 16th St. On completion of the subway and the reopening of 12th St., one-way traffic was abandoned. Traffic conditions on 16th St., as well as on many other city streets, had deteriorated so much that the public was clamoring for action; as a result, the city council, acting on the recommendations of the traffic engineer, adopted a comprehensive plan of one-way streets in April, 1950.[3] The plan was begun on a permanent basis during the summer of 1950 and was completed in December, 1953; the system is shown in Fig. 2. It consists of ten pairs of streets—a total of 35.5 miles. The cost was $200,000 of which about half was for additional traffic signals and the remainder for signing, striping, and other facilities. The cost of a somewhat comparable widened two-way street system would have been in excess of $6,000,000.

In designing the one-way street system, consideration was given to the use of one-way streets as a stop-gap measure pending the ultimate construction of freeways. It is noted in Fig. 2 that the system is integrated into the proposed system of freeways and major highways for the Sacramento area. This factor, coupled with a consideration of origin-destination patterns, street widths, geographical layout, and traffic trends, governed the development of the plan. The older areas of the city having a grid-street system were most easily adapted to one-way streets, whereas in the newer areas lack of parallel streets along the principal arteries ruled out any extensive use of one-way streets. As additional state and city highway funds become available, it is anticipated that the one-way streets will be replaced by freeways, either following the same alinement or placed so as to serve the same traffic. The one-way street, however, is not the final answer; a report prepared for the Joint Fact-Finding Committee on Highways for the California Legislature[4] notes that this one-way plan can be relied on only for ten years. Such a statement would not necessarily be true of a smaller community where traffic volumes in the foreseeable future will not be sufficiently heavy to overtax the capacity of the streets.

RESULTS OF STUDIES

Studies have been made of the results achieved by the one-way street system in Sacramento. The results are described subsequently.

Traffic Volumes.—Over-all traffic volumes have increased on all the one-way street pairs as compared with the former operation of these streets as two-way streets. The total over-all increase in average 24-hr traffic volume was (as of 1953) 35.2%, as shown in Table 1(*a*).

Accident Experience.—Comparison of the combined accident rate for all types of motor-vehicle accidents on the various pairs under one-way operation and two-way operation indicates an over-all reduction (as of 1953) of 37.1% under one-way operation, as shown in Table 1(*b*). The reduction in accidents on one-way streets is not just fortuitous but results from basic changes in traffic pattern and different conditions on a one-way street. Among the more important changes are (*a*) reduction in conflicting movements at intersections, (*b*) elimination of head-on collisions, (*c*) elimination of headlight glare, (*d*) increase in lane width, (*e*) elimination of trapping of pedestrians between opposing streams of traffic, and (*f*) improved signal timing giving smooth, continuous flow.

---

[3] "Improving Traffic Access into Central Business District," *City Traffic Engineer*, Sacramento, Calif. February, 1950.

[4] "California State Highways," Automotive Safety Foundation, Sacramento, Calif., 1952.

Speed and Delay.—Traffic movement under one-way operation as contrasted with two-way operation is considerably smoother and at higher average speeds.

Public reaction to the one-way street system indicates that the average driver is more concerned with the number of stops he has to make than with any other single consideration with respect to traffic. He enjoys being able to drive from one end of a one-way street to the other without a single stop. On a one-way street this is now possible at all times except during the evening rush hour or when double parking obstructs the free flow of traffic. This achievement is important quantitatively because approximately 90% of the total traffic is thus benefited.

The smooth, continuous flow is the result of a synchronized traffic-signal control system. The signal system imposes speed control along the arteries and, by bunching the traffic in compact groups, provides gaps for cross traffic and pedestrians at intersections not controlled by signals.

The results of speed and delays studies on 15th St. and 16th St. are offered herewith as typical of the improvement experienced in using a one-way street system. Speed and delay studies were made during both peak hours and off-peak hours. In making the studies the "floating-car method" was used. An observation vehicle was driven so as to "float" with traffic. Approximately two hundred and fifty runs were made under one-way and two-way operations and the results were as follows:

TABLE 1.—Comparison of Traffic Flow and Accidents

Street	(a) Average Traffic Flow, in Vehicles per 24-hr Period			(b) Accident Rate, in Number per Million Vehicle Miles		
	Two-way operation	One-way operation in 1952	Percentage change over two-way operation	Two-way operation	One-way operation in 1952	Percentage change over two-way operation
E and F..........	9,361	14,551	+ 55.5	20.4	13.3	−34.8
H and I..........	18,081	22,691	+ 25.5	26.1	14.5	−44.4
9th and 10th......	12,490	14,349	+ 14.9	28.9	24.1	−16.6
15th and 16th.....	27,828	30,454	+ 9.4	21.5	20.0	− 7.0
29th and 30th.....	2,724	13,424	+392.8	59.3	20.9	−64.8
12th............	19,321	25,934	+ 34.2	19.7	17.9	− 9.1
Over-all..........	89,805	121,402	+ 35.2	175.9	110.7	−37.1

	Average speed, in miles per hour during Peak hours	Other hours
Two-way operation	12.7	13.3
One-way operation..................	15.8	18.8
Percentage change................	+24.4	+41.4

It is emphasized that the data in the foregoing tabulation are average over-all speeds—that is, speeds computed by dividing the distance between certain fixed points by the total time required to drive between them. This average speed is not to be confused with speeds of individual vehicles passing a particular point; these are termed "spot speeds." A study of spot speeds at a given midblock location reveals the maximum speed reached by vehicles between intersections and, of course, in no way reflects the effect of cumulative delays. Such a spot-speed study is of value, however, in determining traffic violations.

There has been some criticism of excessive speeds on one-way streets; speed checks were made to determine spot speeds under one-way and two-way operation. The results are presented in Table 2. Table 2 indicates that spot speeds on one-way streets are not necessarily higher than they were when the same streets were two-way streets and that speeds are as high or higher on representative two-way streets throughout the city.

TABLE 2.—COMPARISON OF SPOT SPEEDS, IN MILES PER HOUR

Location		Average Speed		Pace		Maximum Observed Speed	
Street	Between	Two-way operation	One-way operation	Two-way operation	One-way operation	Two-way operation	One-way operation
9	U and V	23	24	22 to 28	24 to 30	32	32
16	F and G	21	23	18 to 24	22 to 28	30	32
T	24 and 25	23	...	22 to 28	...	36	...
F	24 and 25	...	24	...	24 to 30	...	34
Broadway	40 and 42	27	...	26 to 32	...	42	...
Capitol	23 and 24	26	...	24 to 30	...	36	...
Riverside	Swanston and Robertson	25	...	22 to 28	...	40	..

Effect on Business and Land Values.—Contrary to the popular claim by individual businesses or business groups, survey data indicate that one-way streets do not, on the whole, unfavorably affect the gross volume of business transacted.[5] Comparison of the business-volume index of the fourth quarter of 1948 and the first and second quarters of 1949 for all businesses in Sacramento County to that of businesses located on one-way streets in Sacramento discounts claims of business loss because of a change-over from two-way streets to one-way streets. In Table 3 the data indicate the changes in gross business between a nine-month period (fourth quarter of 1947 and first two quarters of 1948) when two-way traffic was in effect on 16th St. and a nine-month period (fourth quarter of 1948 and first two quarters of 1949) when one-way traffic was in effect on 16th St. This sales-tax comparison is shown in another way

TABLE 3.—CHANGES IN GROSS BUSINESS, IN PERCENTAGES

Enterprises	Sacramento County	Sacramento City one-way streets
Auto supply stores, garages, auto dealers, service stations, and tire shops	−4.6	−2.9
Eating and drinking establishments	−7.18	−3.98
All other businesses	−0.43	+8.6
All businesses	−1.30	+2.09

---

[5] "The One-Way Street, Its Effect on Retail Business," California Dept. of Highways and Public Works, Sacramento, Calif., March–April, 1953.

in Fig 3. It is to be observed that the trend of business on 16th St. closely parallels business activity throughout the county.

EFFECTS OF ONE-WAY STREETS

In an effort to determine the effect of one-way streets on land values, questionnaires were mailed in October, 1949, to the assessors of fifty-three cities comparable to or larger than Sacramento; it was asked what effect one-way streets had on valuation of abutting property. Of the forty-two cities having one-way street systems, two indicated an increase in assessed valuation, one a decrease, and the thirty-nine others, no effect. Of special interest is the reply of the city of Madison, Wis., in which it was stated that in the eight blocks bounded by one-way streets competition among the mercantile organizations to obtain locations in the area was quite severe and was increasing.

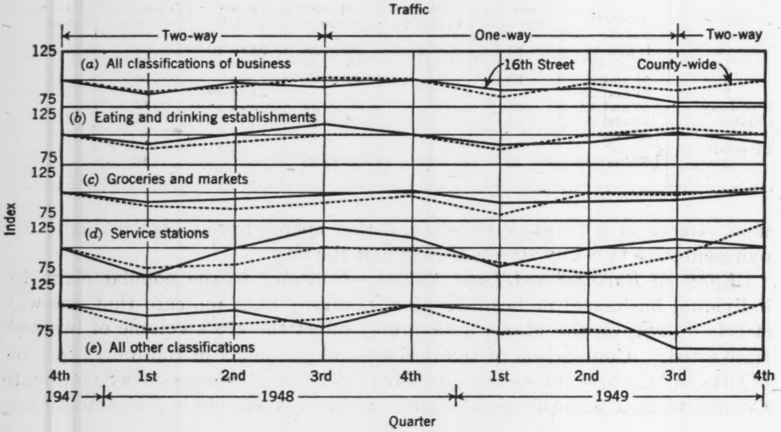

FIG. 3.—COMPARISON OF TAXABLE GROSS SALES

Of the forty-two cities reporting, at least twenty have had one-way streets for seven years or more (as of 1955). Of these twenty cities, eight have one-way streets in residential areas, none of which decreased in assessed valuation as a direct result of one-way streets. On the basis of reports received from the various cities it would appear that the advent of one-way streets has had little, if any, effect on the use of property bordering thereon, whether the property is used for business or for residential purposes. It is believed that this conclusion should be carefully studied before it is accepted as a general rule.

Judging from requests for information received from many cities throughout the United States, such as El Paso, Tex., Omaha, Nebr., Seattle, Wash., San Diego, Calif., and Fresno, Calif., one of the major factors to be overcome in installing a one-way street system is the fear of local business interests that the system will destroy business. In order to obtain additional data on the effect on business development, a study was made of new building construction and improvements on the Sacramento one-way street system. Records of the city assessor reveal that since the beginning of the one-way street operation a total of $2,730,000 has been spent on new construction and improvements on the streets (as of 1953). Of this amount, $1,300,000 was for retail stores, $1,000 for office buildings and commercial structures, $155,000 for gas stations and garages, and $275,000 for apartment buildings. It would appear that, if one-way streets were harmful to business and commercial activity, there would not have been developments such as these.

Public Acceptance and Approval.—The reaction of the community to the one-way street system appears to be one of overwhelming approval. The board of directors of the Sacramento Chamber of Commerce by letter commended the city council for the establishment of the system and later went on record as favoring the extension of the present system. The driving public has praised the system in personal letters addressed to the daily newspapers. The Citizens Committee on Truck Traffic, representing truckers and commercial interests, has asked that additional one-way streets be created. The board of directors of the Sacramento Retail Merchants Association has stated that many of those who were opposed to one-way streets before the system was tried have themselves become strong advocates of this method of handling traffic. This association has also advocated the extension of one-way streets to all streets in the central business district and has urged the city council to adopt their proposal.

Newspaper editorial comment has been strong and frequent in favor of one-way streets. An excerpt from an editorial[6] probably sums up the public approval and acceptance:

> "The overwhelming approval by the citizens of the one-way streets and the suggestions of the Merchants Association and the Chamber of Commerce to extend the plan all point to a feeling of civic wonderment as to how Sacramento ever got along without it."

CONCLUSIONS

All facts point strongly to the use of one-way streets where warranted and found indicated by appropriate engineering studies. One-way streets are not a cure-all and should never be used without proper integration into a master street and highway plan. It is important that the plan be "sold" to merchants and business groups—that they be given complete information as to the need for the system, the benefits to be had, and the cost of alternative plans. A sound one-way street plan, with public support, can result in a more efficient use of a congested street system.

---

[6] *Sacramento Bee*, October 25, 1950.

AMERICAN SOCIETY OF CIVIL ENGINEERS
Founded November 5, 1852
TRANSACTIONS

Paper No. 2785

STUDIES OF AIR ENTRAINMENT IN OPEN-CHANNEL FLOWS

By Lorenz G. Straub,[1] M. ASCE, and Owen P. Lamb[2]

Synopsis

The phenomenon of insufflation of air into water flowing at high velocities in open channels has long been of great interest to hydraulic engineers, but detailed experimental information regarding the occurrence and the investigation of the flow mechanism of air-water mixtures has been elusive because of an inadequacy of accurate observations made by means of customary instrumentation. New instruments for measuring velocities of mixed flows and the air concentration in such flows have been devised at the St. Anthony Falls Hydraulic Laboratory of the University of Minnesota, at Minneapolis, so that velocity traverses and air-entrainment traverses can now be made accurately for widely diverse flow conditions, both for velocities and percentages of air entrained.

This paper describes the results of experimental observations of self-aerated flows in an open channel for various slopes of from 15° to 45°. It is pointed out that customary open-channel flow relationships do not apply directly to air-entrained flows. For the range of conditions reported, actual velocities are shown to be greater than the velocities computed by hitherto proposed methods. The experiments reported are for the conditions of a smooth, painted-steel channel surface. The authors contemplate further studies with channels of differing roughness and greater slopes.

Introduction

The experimental investigation of self-aerated flows in flumes with steep gradients is a phase of the air-water mixture studies now in progress at the St. Anthony Falls (SAF) Hydraulic Laboratory of the University of Minnesota, at Minneapolis. These experiments are being conducted in a large laboratory facility (Fig. 1) especially designed and constructed to provide naturally

---

Note.—Published, essentially as printed here, in the *Proceedings* of the Minnesota International Hydraulics Convention, September 1–4, 1953, in Minneapolis, Minn. Positions and titles given are those in effect when the paper was approved for publication in *Transactions*.

[1] Director, St. Anthony Falls Hydr. Lab., and Head, Civ. Eng. Dept., Univ. of Minnesota, Minneapolis, Minn.

[2] FluiDyne Eng. Corp., Minneapolis, Minn.

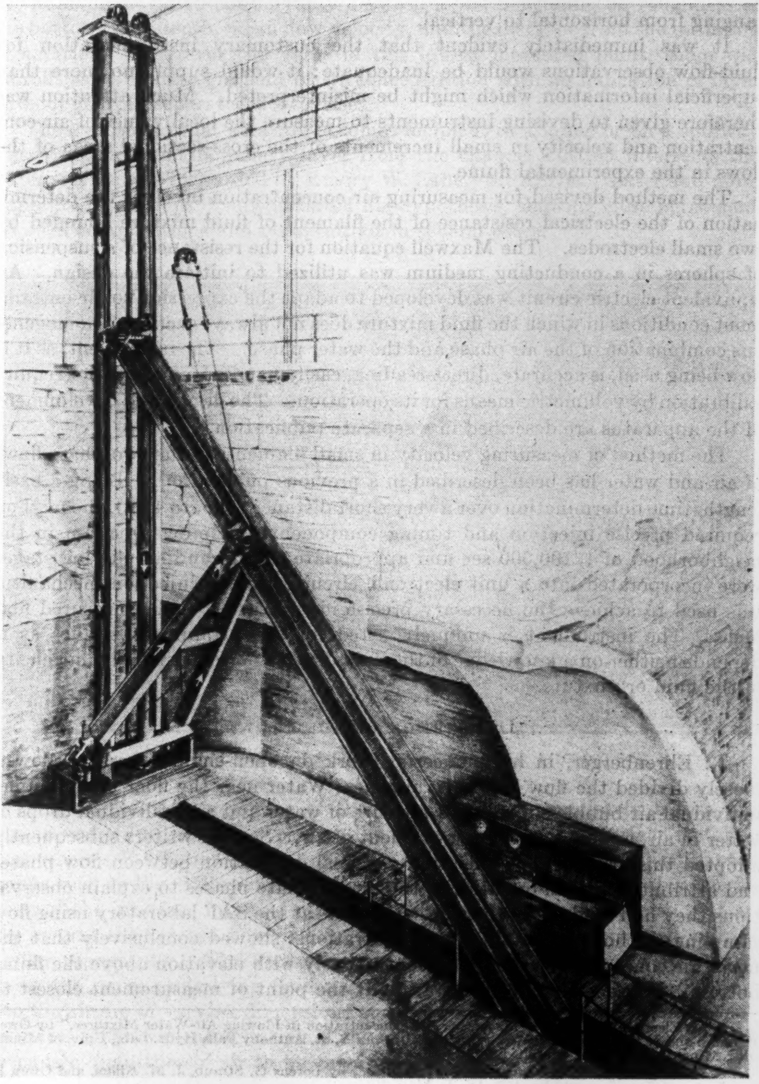

FIG. 1.—CHANNEL FOR AIR-ENTRAINMENT STUDY AT THE ST. ANTHONY FALLS HYDRAULIC LABORATORY

aerated flows through a considerable range of discharges and at all flume slopes ranging from horizontal to vertical.

It was immediately evident that the customary instrumentation for fluid-flow observations would be inadequate; it would supply no more than superficial information which might be misinterpreted. Much attention was therefore given to devising instruments to measure the local values of air concentration and velocity in small increments of the cross-sectional areas of the flows in the experimental flume.

The method devised for measuring air concentration involves the determination of the electrical resistance of the filament of fluid mixture bounded by two small electrodes. The Maxwell equation for the resistance of a suspension of spheres in a conducting medium was utilized to initiate the design. An equivalent electric circuit was developed to adapt the expression to air-entrainment conditions in which the fluid mixture does not always occur as a homogeneous combination of the air phase and the water phase. The instrument, as it is now being used, is accurate, direct-reading, easily handled, and does not require calibration by volumetric means for its operation. The design and development of the apparatus are described in a separate publication.[3]

The method of measuring velocity in small filaments of the two-phase flows of air and water has been described in a previous publication.[4] Being a basic length/time determination over a very short distance (3 in. to 4 in.), the method required precise injection and timing components. Timing precision in the neighborhood of 1/100,000 sec and appropriate pickup and amplifying stages were incorporated into a unit electronic circuit; a diesel injection mechanism was used to achieve the necessary precise identification of the measured filament. The instrument is uniquely fitted for air-entrainment studies as it depends neither on a knowledge of the fluid density nor on a strict homogeneity of the fluid or mixture.

DESCRIPTION OF THE FLOW

R. Ehrenberger, in his pioneering work on open-channel aerated flows,[5] loosely divided the flow into several zones: Water near the floor of the flume, individual air bubbles in water, a mixture of water and air, individual drops of water in air, and an overlying movement of air. Several writers subsequently adopted this arbitrary classification as a real delineation between flow phases and attributed special qualities to the intermediate phases to explain observations they had made. Earlier measurements at the SAF laboratory using flow sampling methods to obtain air concentrations[6] showed conclusively that the mean air concentration increased continuously with elevation above the flume bottom. The mean air concentration at the point of measurement closest to the flume floor varied considerably between flows, depending on roughness of the bottom, flow depth, mean flow velocity, and the distance from the initiation of aeration. Whatever the value of this lowest measured point, there was established a definite gradient of air concentration with no indication of layer flows or sharply separated flow phases.

---

[3] "An Electrical Method for Measuring Air Concentration in Flowing Air-Water Mixtures," by Owen P. Lamb and J. M. Killen, *Technical Paper No. 2*, Series B, St. Anthony Falls Hydr. Lab., Univ. of Minnesota, Minneapolis, Minn., March, 1950.

[4] "Velocity Measurements of Air-Water Mixtures," by Lorenz G. Straub, J. M. Killen, and Owen P. Lamb, *Proceedings-Separate No. 193*, ASCE, May, 1953.

[5] "Wasserbewegung in steilen Rinnen (Schusstennen) mit besonder Berucksichtigung der Selbstbelüftung," by R. Ehrenberger, *Österreichischer Ingenieur und Architektverein*, Nos. 15/16 and 17/18, 1926.

[6] "The High Velocity Flow of Water in a Small Rectangular Channel," by W. W. DeLapp, thesis presented in 1947 to the University of Minnesota, at Minneapolis, in partial fulfilment of the requirements for the degree of Doctor of Philosophy.

The hypothesis that aeration becomes incipient in a flume or on a spillway when the turbulent boundary layer from the channel bottom intersects the water surface was forwarded by Emory W. Lane,[7] M. ASCE. Later and more elaborate discussions[8,9] substantiated his hypothesis, showing close agreement between computations and observations in several cases.

STA. 44
STA. 43

FIG. 2.—SURFACE OF FULLY AERATED FLOW (EXPOSURE: 1/100,000 SEC)

A characteristic roughening of the water surface immediately before the appearance of "white water" can readily be seen in most free-surface installations where self-aeration occurs. Further observations with high-speed photographs such as Fig. 2 illustrate the persistence and magnification of this roughening of the interface into and during the highly aerated condition so that at any instant the aerated flow has the appearance of exceedingly rough and irregular topography. The depressions or open pockets of air at the interface above the dense underlying fluid and the spikes of water mixture projecting into the air are of varying dimensions and are spaced in seemingly random occurrence. This violent agitation of the interface between the mixture and the air causes quantities of air to be entrapped and broken into bubbles of a size that presents a balance between the work of agitation of the liquid and the surface energy of the resultant bubbles. Thus, the air bubbles in water are approximately spherical in shape and nearly the same general size for a particular set of flow conditions. This fact is illustrated in Fig. 3, which is a view through a transparent side wall into a partly aerated flow.

---

[7] "Entrainment of Air in Swiftly Flowing Water," by Emory W. Lane, *Civil Engineering*, February, 1939, pp. 89–91.

[8] "Air Entrainment on Spillway Faces," by G. H. Hickox, *ibid.*, December, 1945, pp. 562–563.

[9] "Study of Entrainment of Air by Flowing Water," by G. Halbronn, thesis presented in 1951 to the University of Grenoble, France, in partial fulfilment of the requirements for the degree of Doctor of Philosophy.

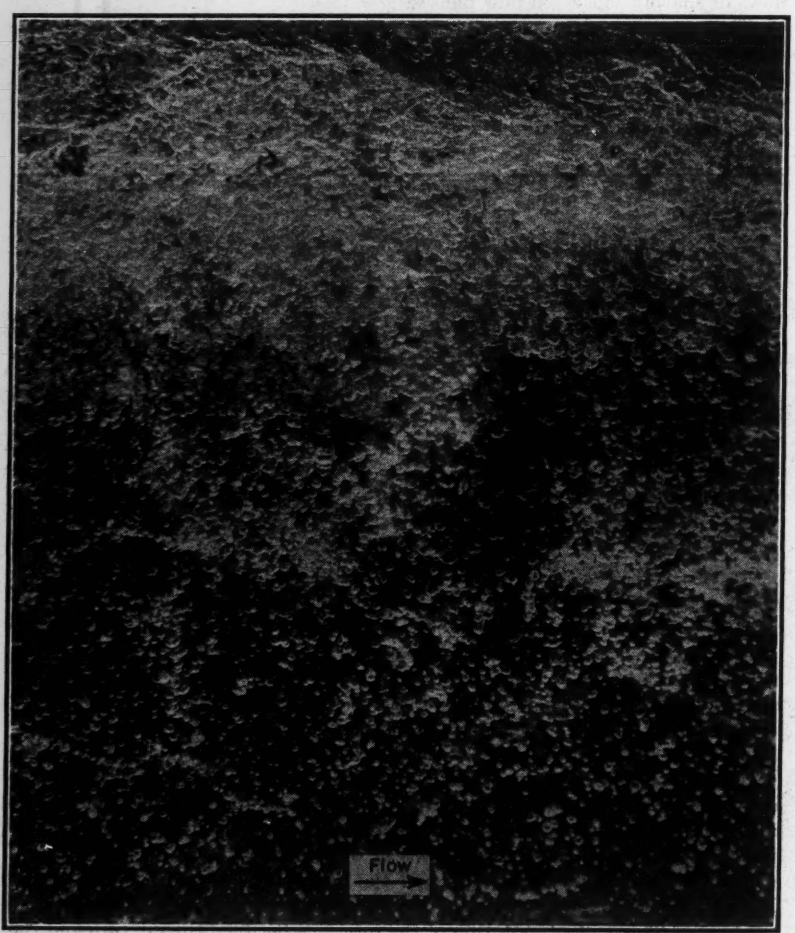

FIG. 3.—PROFILE OF PARTLY AERATED FLOW (EXPOSURE: 1/50,000 SEC)

Transport of bubbles farther into the flow by turbulence is counteracted by the buoyant force on each bubble so that a balanced condition is reached wherein as much air is buoyed out of the flow as is drawn into it. This insufflation balance can be compared to the suspended-load balance in a reach of a sediment-carrying stream in which neither aggradation not degradation occurs. When the flow has enveloped as many air bubbles as it can retain and when the rough surface topographies at adjoining sections along the channel have become statistically similar, the flow can be defined as having reached a condition of normal aeration for the particular section, slope, roughness, and discharge.

A portion of the discharge of water through a section in aerated flow consists of water droplets that have become detached from the stream and move through the air by virtue of their initial momentum. The force of gravity pulls them downward and they soon fall back into the flowing stream, with the result that, on the average, only a small percentage of the total water discharge flows as droplets at any slopes appreciably less than 90° with the horizontal. Air bubbles in the water tend to follow the turbulent fluctuations of the flow and to have the same mean velocity as the water enveloping them. There is not likely to be any appreciable "slip" in either the upstream or the downstream direction of these isolated bubbles in open-channel flows as compared to the bulk-flow velocities. Water droplets moving through the air, however, would have an appreciable velocity relative to the air, which tends to shorten their trajectories and, consequently, the time intervals spent as isolated droplets.

The roughened surface and the high flow velocities of the flow mixture tend to drag a considerable volume of air into motion above the flow. A velocity deficiency can be expected in the air-water mixture in the region of the roughened surface because of the drag necessary to sustain this air motion.

At relatively small flow depths, flows on steep gradients break into waves which appear to roll down the channel over a thin underlying stream of water. Bubbles are often entrapped into these wave fronts, and the "white water" has the appearance of regularly spaced bands or wave patterns moving down the slope. At slightly greater depths where a more general condition of aeration prevails, vestiges of these periodic waves can often be detected by their regularity as slightly higher stages immediately followed by pockets of greater air content. Formation of "roll waves"[10] without consideration of aeration is discussed in a recent summary of the problem which refers to preceding papers on the same subject.

The variety of differing and, in many cases, opposing opinions expressed by investigators of air-entrainment phenomena encountered in a survey of the literature[11] illustrates the many uncertainties that exist in this field. Distributions of density, of velocity, of water discharge, and of momentum flux in a cross section of aerated flows are of interest both for design purposes and ultimately for an understanding of the flows. Bulk increase of section by aeration, comparison of mean velocities with velocities in nonaerated flows, and the possibility of aeration are vital design considerations.

EXPERIMENTAL OBSERVATIONS

Experimental measurements described in this paper are largely restricted to velocity and air-concentration traverses in flows where normal aeration has been attained. Air concentration C is defined as the volume of air in a unit volume of air-water mixture. The concept of mixture is intended to embrace both the phase in which air bubbles are in the water and the condition where the unevenness of the surface contributes to the variation of density in planes parallel to the flume floor. The component directions x and y are taken positive in the downstream direction of the flow and the upward normal to the flume floor, respectively. The upper boundary of the flow has been arbitrarily defined as that value of y at which $C = 0.95$. This boundary envelops approximately from 98% to 99% of the total water discharge and can still be reliably measured with the concentration instrument. The velocity in the positive x-direction is labeled u and is the only velocity component measured with the SAF velocity meter. Direct velocity measurements can be obtained up to an elevation y that is approximately ½ in. smaller than $\bar{y}$.

---

[10] "Resistance Effects on Hydraulic Instability," by R. F. Dressler and F. V. Pohle, *Communications on Pure and Applied Mathematics*, Vol. VI, 1953, pp. 93–96.

[11] "Air Entrainment in Flowing Water," by Owen P. Lamb, *Project Report No. 19*, St. Anthony Falls Hydr. Lab., Univ. of Minnesota, Minneapolis, Minn., August, 1949.

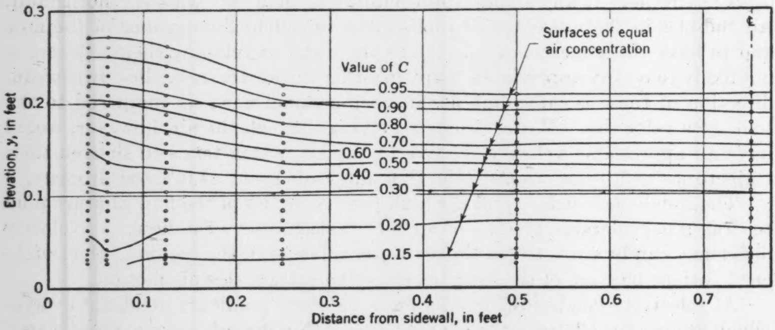

FIG. 4.—AIR CONCENTRATION DISTRIBUTION ACROSS SECTION OF FULLY AERATED FLOW

The summation $\sum_{y=0}^{y=\bar{y}} (1 - C)\Delta y$ is the total area occupied by water in a unit breadth of the flow cross section.

The summation $\sum_{y=0}^{y=\bar{y}} u(1 - C)\Delta y$ is the total water discharge q_w in a unit breadth of the flow cross section.

The mean velocity, $\bar{U}$, of the water through the section is obtained by dividing the second summation by the first—that is, by directly applying the equation of continuity to the measurements. The mean air concentration, $\bar{C}$, is equal to the summation $\sum_{y=0}^{y=\bar{y}} C\,\Delta y$ divided by $\bar{y}$ and is seen to depend in absolute value on the choice or definition of $\bar{y}$.

The total water discharge, Q'_w, in the 1.5-ft-wide flume is measured at metering stations in the supply pipes leading to the equipment. Discharge per unit width $q'_w = \frac{2}{3} Q'_w$ is used to compare with the integrated water discharge obtained with the instruments in the aerated flows and to act as a control on those measurements.

The inlet of the test flume is designed so as to present a uniform velocity profile to the jetted inflow at a controlled depth. Inlet velocity is adjusted until it is approximately the terminal velocity for the set slope and discharge. Thus, the flow aeration can be studied independently of large accelerative or decelerative effects, and a shorter flume with a greater flexibility and control can be utilized. Orientation of flume components was selected to provide identical inlet geometry throughout the 90° range of flume slopes. Until the present time (September, 1953), the equipment has been operated at flume slopes up to 45° with the natural gravity head of 50 ft available at the site, but with the completion of a pumped-supply system currently being installed, flows with jetted terminal velocities at flume angles approching 90° will also be tested.

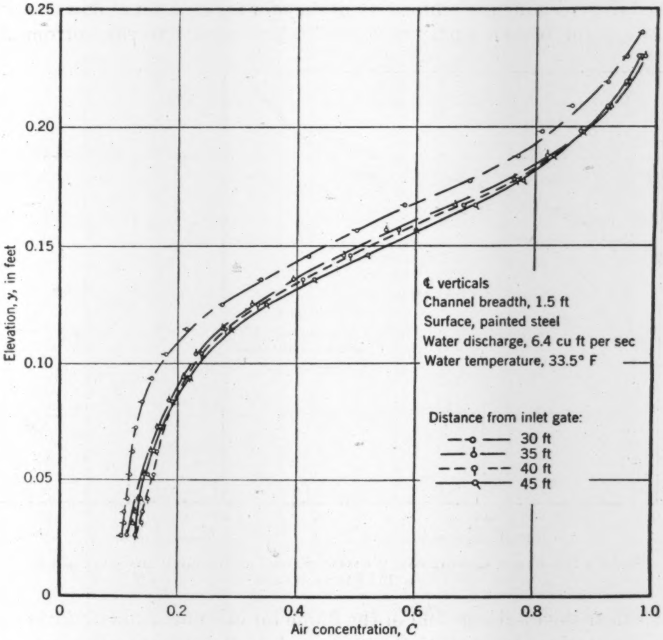

FIG. 5.—MEASURED AIR-CONCENTRATION VALUES AT VARIOUS DISTANCES FROM THE FLUME INLET GATE

The 1.5-ft breadth of flume is sufficiently large compared to the flow depths used to preserve a two-dimensional region of the flow several inches wide and symmetrical about the flume center line. Complete traverses across the entire cross section of the flume reveal no asymmetry about the center line for either nonaerated or aerated flow. Interpolated lines of equal air concentration drawn between measured values in normal aerated flow at a station 45 ft from the flume inlet are exhibited in Fig. 4. The 0.95 level of air concentration is considerably higher near the side wall than in the central region of the stream. This side-wall effect is especially noticeable before aeration begins in the central region; aeration at the sides is initiated by the turbulence from the side-wall boundary at the water surface and thus appears as "white water" sooner. The flat contours in the larger central region of the stream (Fig. 4) illustrate the two-dimensional character of that flow which remains uninfluenced by side-wall disturbances and is typical of the center-line region for all flows for which complete cross-sectional traverses were obtained. The remaining data presented in this paper were obtained in center-line vertical traverses of the stream.

Air-concentration vertical traverses at various distances from the inlet gate were used to determine the uniformity of the flow for each set of flow conditions. Fig. 5 is a graph of four such "verticals" taken normal to the bottom at 5-ft intervals near the discharge end of the flume for one flow value. Although the profiles for stations located 35 ft, 40 ft, and 45 ft from the inlet gate exhibit small differences, they are definitely closely grouped and, considering the measuring variation in the positioning and reading of the instrument, they cannot be considered as significantly different. On the other hand, the profile for station 30 is definitely different from the other three to an extent that is typical of changes occurring in the same increment of flume length either in flows with larger dicharges or at stations even closer to the inlet at which full normal aeration has not been established. For the test data here reported, a condition of normal aeration was substantially reached at station 45 but not at station 30. The remaining data presented in this paper were taken in the center-line "vertical" of the flows 45 ft from the inlet gate and are classified as fully aerated or partly aerated depending on their similarity to upstream profiles.

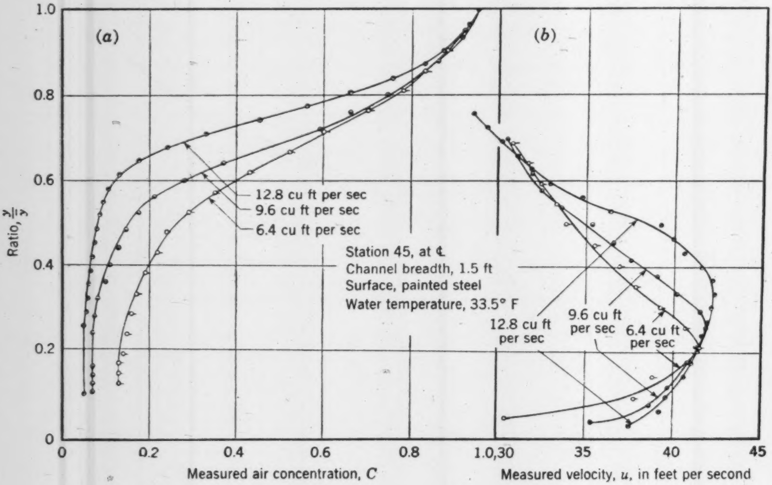

FIG. 6.—DISCHARGE COMPARISON, AERATED FLOWS AT VARIOUS DISCHARGES WITH A 15° FLUME ANGLE

Water discharges of 6.4 cu ft per sec, 9.6 cu ft per sec, and 12.8 cu ft per sec in the 1.5-ft-wide flume inclined 15° can be compared by means of the air-concentration profiles in Fig. 6(*a*) and the velocity profiles in Fig. 6(*b*). From Fig. 5 it was determined that the 6.4-cu-ft-per-sec flow had reached normal aeration, whereas respective data for the other flows indicated that the 9.6-cu-ft-per-sec flow was approaching normal aeration and that the 12.8-cu-ft-per-sec flow was definitely not normal but only partially aerated at station 45 where it had not yet reached a uniform or normal state.

Observations of these and many other flows with stroboscopic light and in some instances with high-speed photographs such as Fig. 7 indicate that the rapid increase in air-concentration gradient begins at an elevation above the flume floor corresponding to the lowest depressions or pockets of air. The air concentration below this elevation is due to the air bubbles in the water, some of which migrate far down into the stream even at low aerations.

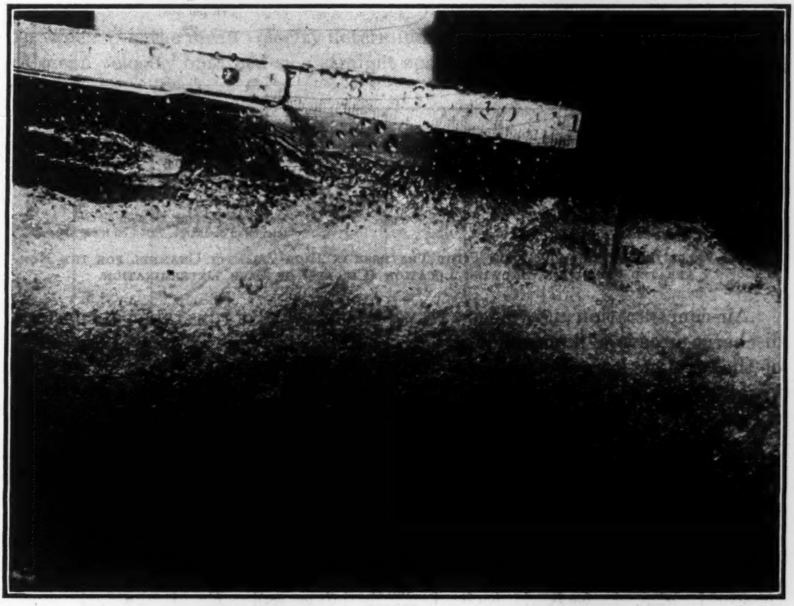

FIG. 7.—MEASURED VELOCITIES IN AERATED FLOWS AT VARIOUS DISCHARGES WITH A 15° FLUME ANGLE

Several uniform nonaerated flows were set at lower flume angles to form a basis of comparison for the values of mean velocity and for the distributions of discharge and momentum flux obtained with the aerated flows. Typical of these is the condition shown in Fig. 8, a nonaerated flow on the same painted-steel surface of the 1.5-ft-wide test flume as the aerated flows described herein.

The Manning n-values for the flume surface were determined from the basic pitot velocity measurements and are listed in Fig. 8. The n-value based on the hydraulic radius and the entire discharge was 0.0097; the n-value based on the two-dimensional discharge and the flow depth at the center line was 0.0106. The velocity distribution factor for the center-line vertical was 1.054.

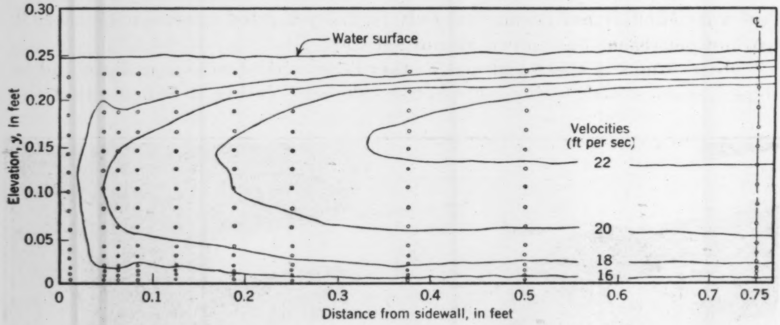

Station 45
Inlet opening, 0.25 ft
Water temperature, 34.5° F

Channel slope, 7.75
Measured discharge, 7.1 cu ft per sec
Integrated discharge, 7.044 cu ft per sec

FIG. 8.—VELOCITY DISTRIBUTION FROM PITOT TRAVERSE IN HIGH-VELOCITY CHANNEL FOR THE NON-AERATED CONDITION, SHOWING LOCATION (CIRCLES) OF EACH DETERMINATION

Air-concentration and velocity traverses of a series of runs taken at constant discharge on several flume angles are shown in Fig. 9. The reversal of curvature of the air-concentration gradient characteristic of all the data is evident in Fig. 9(a). The velocity profiles in Fig. 9(b) show the same sharp decline in velocity in the upper region of the flow which is characteristic of the various data obtained by direct measurement with the instruments. Table 1 indicates bulk and mean values of discharge, velocity, and air concentration for the flows of Figs. 6 and 9. The control imposed upon the flows and the agreement of the instrumental measurements may be judged by a comparison of the independently measured values of incoming water discharges in Table 1

TABLE 1.—FLOWS WITH NORMAL AND PARTIAL AERATION ON PAINTED-STEEL SURFACE

Flume angle, θ (degrees)	Defined upper boundary $\bar{y}$ (feet)	Measured water discharge, Q'_w (cu ft per sec)	Unit discharge, $q'_w = 2/3\ Q'_w$ (cu ft per sec)	Integrated water discharge, q_w (cu ft per sec)	Mean velocity, $\bar{U}$ (ft per sec)	Mean air concentration, $\bar{C}$	Kinetic energy disbribution factor, α	Aeration
7.5	0.2292	6.4	4.267	. . .		0.390		Normal
15	0.2188	6.4	4.267	4.60	35.38	0.406	1.045	Normal
22.5	0.2188	6.4	4.267	4.48	35.93	0.430	1.046	Normal
30	0.2135	6.4	4.267	4.31	36.25	0.443	1.042	Normal
37.5	0.2083	6.4	4.267	4.34	37.54	0.445	1.038	Normal
45	0.2032	6.4	4.267	4.27	39.79	0.472	1.035	Normal
15	0.2656	9.6	6.40	6.35	36.22	0.340	1.041	Partial
15	0.3229	12.8	8.53	8.59	36.34	0.268	1.038	Partial

with the water discharges integrated from the measurements of air concentration and velocity at station 45 where the flows had become highly aerated. The defined surface elevations listed were determined directly from the air-concentration verticals, and the mean values of air concentration and velocity were determined from the summations defining these values. The factor α listed in the table is the coefficient of the mean velocity head which gives the true measure of the kinetic energy of the flow. It is obtained from the following definition equation:

$$\alpha = \frac{\sum\limits_{y=0}^{y=\bar{y}} (1 - C)\, u^3 \,\Delta y}{(1 - \bar{C})\, \bar{U}^3\, \bar{y}}$$

in which $\bar{U}$ is the mean velocity determined in the manner previously proposed. A mean velocity obtained as a straight spatial average of the measured velocities could, when used in the foregoing expression, yield values of α less than unity, which values have no significance.

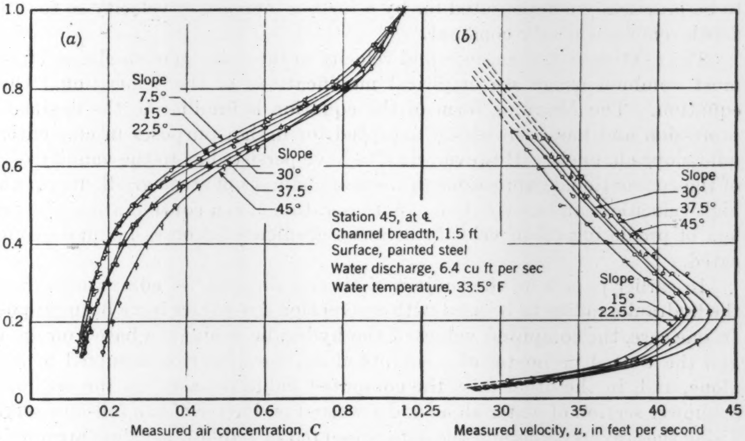

FIG. 9.—COMPARISON OF EFFECTS OF SEVERAL FLUME ANGLES ON FULLY AERATED FLOWS OF CONSTANT DISCHARGE

COMMENTS ON EXPERIMENTAL RESULTS

The values of mean air concentration listed in Table 1 depend on the choice or definition of the flow surface. However, by fixing the flow surface at a definite concentration level, the mean air-concentration values assume a relative importance among various runs for classifying bulking or aeration as they are related to significant variables such as slope, discharge, and roughness. An increase in mean air concentration with increasing flume angle is shown in Table 1 for a constant water discharge when the flows were established as having complete normal aeration. However, the spread of mean air-concentration values from 0.39 at a 7.5° flume angle to 0.472 at a 45° flume angle is quite small and suggests that the bulking of the flows is not particularly sensitive to slope changes alone. Because the runs at varying discharges were not all established as reaching a condition of normal aeration, the respective mean air-concentration values are not comparable on the basis of different discharges. A comparison of the slope and discharge for the nonaerated run of Fig. 8 with the slope and discharge of the normal aerated run on the 7.5° flume angle shows very little difference between the flow variables; however, a bulking of the flow equivalent to a mean air concentration of 0.39 and considerably higher velocities were measured in the aerated flow. This suggests possible critical flow criteria for the conditions at which aeration begins and requires further experimental study.

The defined flow depth $\bar{y}$ was changed very little by a change of slope for the various runs at constant discharge. Within the narrow range of the reported experiments, the tendency to increase the section by greater bulking appeared to be practically compensated for by a further increase in velocity so that flow depth remained nearly constant.

The relations between slope and velocity in the uniform open-channel flow in most common usage are empirical modifications of the semirational Chezy equation. The Manning form of the equation is familiar to the engineering profession and has been widely accepted for design purposes in conventional mild-slope channels. However, doubts have persisted as to the validity of any of the conventional expressions in cases of channels of steep gradients or where high velocities can be expected. With aeration also a consideration, the problem of predicting mean velocity at steep gradients becomes far more complicated.

In earlier papers on the subject of air entrainment,[12,13] computed values of the hydraulic radius to be used with conventional n-values have been proposed. In one case, the computed values of the hydraulic radius are based on an area and the wetted perimeter of a computed shallower section occupied by water alone, and, in the other case, the computed value is based on the area of the shallower section of water alone and a wetted perimeter of the full-flow section. Using these expressions and the data presented in Table 1, n-values are obtained by such assumptions which show no agreement with the n-value for uniform flow in the flume with no aeration. For the latter situation corresponding to flow in Fig. 8, for example, the n-value was 0.0106.

Combining the Manning equation for a unit breadth of channel with the equation of continuity, an expression for velocity in terms of discharge, slope, and roughness value is obtained:

$$V = \left(\frac{1.486}{n}\right)^{0.6} q^{0.4}{}_{w}\, S^{0.3}.$$

Using the measured value of $q_w = 4.267$ from Table 1 and $n = 0.0106$ derived in Fig. 8, the following values of mean velocity are obtained for flume angles from 15° to 45°:

---

[12] "Open Channel Flow at High Velocities," by L. Standish Hall, in "Entrainment of Air in Flowing Water: A Symposium," *Transactions*, ASCE, Vol. 108, 1943, pp. 1394 and 1494.

[13] "Second Progress Report on Studies of the Flow of Water in Open Channels with High Gradients," by V. L. Streeter, *Hydraulic Laboratory Report No. 40*, Bureau of Reclamation, U. S. Dept. of the Interior, Washington, D. C., October 13, 1938.

Flume slope, in degrees	Mean velocity, V (ft per sec), Manning formula	Measured mean velocity (from Table 1)
15	23.1	35.38
22.5	26	35.93
30	28.1	36.25
37.5	29.8	37.54
45	31.2	39.79

Thus, by comparing these computed mean velocities from the Manning formula with the measured $\bar{U}$-values from Table 1, it will be noted that in all cases the velocity computed by the assumption for unaerated flows is too low.

The importance of increase of section or of hydraulic radius because of aeration in explaining the high values of mean velocity must be minimized because, as can be seen from the velocity profiles in Figs. 6(*b*) and 9(*b*), any increase in section is more than offset by the upper-surface drag on the overlying air, which causes a decrease in velocity to less than the mean velocity throughout the added area.

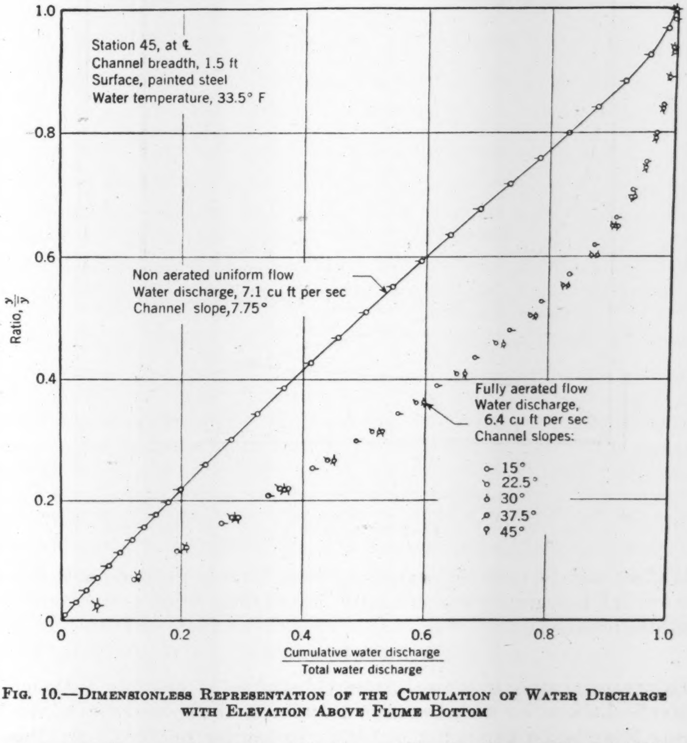

FIG. 10.—DIMENSIONLESS REPRESENTATION OF THE CUMULATION OF WATER DISCHARGE WITH ELEVATION ABOVE FLUME BOTTOM

Fig. 10 illustrates the difference between cumulative water discharges in the flow section for fully aerated and nonaerated flows. It will be observed that, for the test conditions recorded, nearly 90% of the water discharge is in the lower 0.6 of the depth in the case of the aerated flow.

Fig. 11 is a generalized diagram showing the curves of velocity and air concentration in aerated flow, modeled from the curves that were obtained by direct measurement. The position of the arbitrarily defined flow surface with respect to the entire flow field is indicated by the dotted line. The portion of the velocity curve above the defined surface refers to the moving air mass and not to the scattered water droplets that would be expected to have velocities closer to the velocities of the lower flow regions from which they were ejected. The general shape of these curves is believed to be characteristic of fully aerated flows although details of the profiles may vary with depth, roughness, and slope.

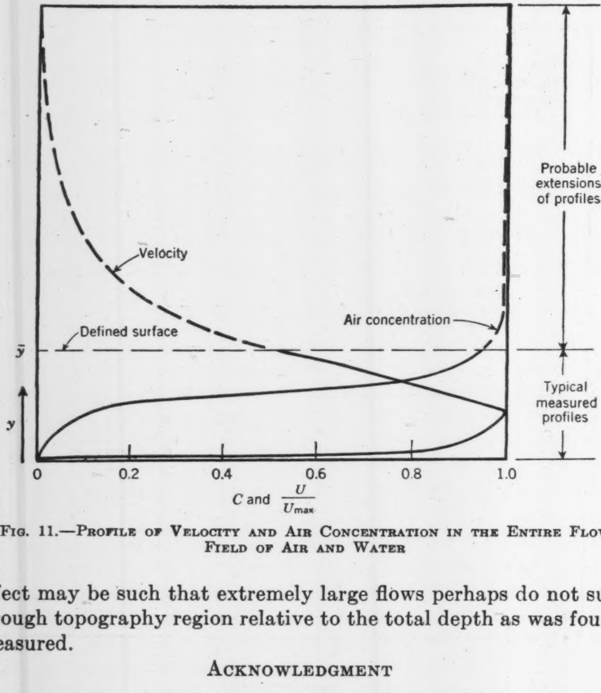

FIG. 11.—PROFILE OF VELOCITY AND AIR CONCENTRATION IN THE ENTIRE FLOW FIELD OF AIR AND WATER

Scale effect may be such that extremely large flows perhaps do not support as large a rough topography region relative to the total depth as was found in the flows measured.

ACKNOWLEDGMENT

Exploratory air-entrainment research studies at the St. Anthony Falls Hydraulic Laboratory were begun in 1939 under the sponsorship of the Engineering Foundation through the ASCE Committee on Hydraulic Research. Later and more comprehensive work has been undertaken in recent years under the sponsorship of the Office of Naval Research, United States Department of Defense.

AMERICAN SOCIETY OF CIVIL ENGINEERS
Founded November 5, 1852
TRANSACTIONS

Paper No. 2786

AN ENGINEERING APPROACH TO BLAST-RESISTANT DESIGN

By Nathan M. Newmark,[1] M. ASCE

With Discussion by Messrs. Stephen J. Fraenkel, and
Nathan M. Newmark

Synopsis

The problem of blast-resistant design is approached directly by means of reasonable simplifying assumptions. The resulting design procedure avoids time-consuming and misleading analysis. The author presents the procedure and the necessary mathematical relationships and explains their practical application.

Introduction

For the first time, a design procedure for blast loading is presented. Purposely the procedure is not readily useful to determine dynamic response or deflection. The field of structural dynamics is relatively new. It is therefore understandable that nearly all the previous study that has been made on the subject of the resistance of structures to atomic blast has been concerned primarily with the analysis of the response (that is, deflection) of a particular structure subjected to a given loading. This approach is mathematically very attractive, and the writer has contributed several methods of his own. However, there are two important reasons why the calculation of deflection of a given structure subjected to a given blast is not especially satisfactory from an engineering point of view:

(*a*) The structure to be designed does not yet exist; complication in the preliminary analysis lengthens the time it takes to select a reasonable structure for investigation. The real problem is the preliminary choice of the structure to be analyzed. If this can be done intelligently, further analysis may actually be unnecessary.

Note.—Published, essentially as printed here, in October, 1953, as *Proceedings-Separate No. 306*. Positions and titles given are those in effect when the paper or discussion was approved for publication in *Transactions*.

[1] Research Prof. of Structural Eng., Univ. of Illinois, Urbana, Ill.

(*b*) Even minor variations and uncertainties in the details of the blast loading or in the properties of the structure (such as yield point or stiffness) cause major changes in the computed deflections. This fact is not immediately evident from the usual detailed descriptions of analytical techniques suitable for dynamic analysis, but it can readily be demonstrated. Consequently, the customary type of analysis may be grossly misleading. The designer is concerned not with what actually will happen in specific circumstances but with what might happen under a range of circumstances, and with the probability of the occurrence of the phenomena in question.

For these reasons the writer presents without apology the relatively crude approximations in this paper as a means of quickly and simply arriving at a design. These procedures may be used equally well to determine the increased strength required for an existing building. For the preliminary design or strengthening of either a structural frame or of component parts such as wall covering panels, one needs to estimate (*a*) the natural period of vibration of the frame or component relative to the duration of the loading on the component, and (*b*) the ductility factor or the ratio of the desired limiting deflection (preferably for "collapse") to the yield-point deflection. Accurate values for these ratios are not required. Using these estimates, one readily determines from the approximate relations given herein the required "limit load" or yield resistance of the structure for a specified external pressure or size of bomb.

In other words, by this procedure one develops essentially an equivalent static loading (or resistance) for which the design must be made. Because this is a concept familiar to structural engineers in general the procedure can be followed easily in almost any engineering design office.

The inexperienced designer may have to revise his estimate of the basic parameters after a preliminary design is completed. This can be accomplished quickly and simply. Finally, after the design is completed, if it appears desirable, an analysis may be made by numerical procedures or other methods. In general, however, an accurate estimate of the deflection corresponding to the selected loading is neither necessary nor useful because the loading conditions and other pertinent parameters can never be accurately known.

BASIC CONSIDERATIONS

The designer must choose first the conditions governing the design. He may wish to make the structure adequate to resist the blast forces from the detonation of a bomb of specified size at a given radial distance and at a given height, or he may select several alternatives and insist that the structure be adequate for any of them. The designer may also select, merely as a standard criterion, a particular shape of blast pressure-time curve, with specified values of peak pressure and duration of the positive phase of the pressures.

The relations among these various blast parameters have been described in detail by the Atomic Energy Commission (AEC) (1)[2] and in papers by C. W. Lampson (2), the writer (3)(4), F. Reines (5), Walker Bleakney (6), and M. L. Merritt (7).

---

[2] Numerals in parentheses—thus (1)—refer to corresponding items in the list of references (see Appendix).

No real advantage is to be gained in designing for a particular size of bomb, detonated at a certain point, and involving definite but complicated loadings on the various faces of a building. There is, however, considerable advantage in considering a conventionalized blast loading so as to insure a uniform factor of safety against collapse in all parts of a given structure, or in all the structures in a region. This is the standard approach used in design for earthquake resistance (8) or for wind-load resistance.

The type of overpressure-time curve developed in a blast is shown in Fig. 1 by the solid curve labeled p_s. This curve can conveniently be replaced by a corresponding linear curve varying from a maximum pressure p_{so} to zero in a time t_s slightly less than t_o. For most structures it is convenient and not inaccurate to neglect the negative phase of the blast beyond t_o.

The next choice to be made is the type of structure—whether it is to be completely enclosed with a covering that resists the blast forces, and thereby shields the interior of the building, or whether it is to be essentially open, possibly covered with light, frangible siding that permits the blast to enter and pass through the structure. The forces acting on the structure and on its component parts differ greatly for these extreme types. The structure may also be intermediate in type with resistant covering having openings or windows which permit the blast to enter in part.

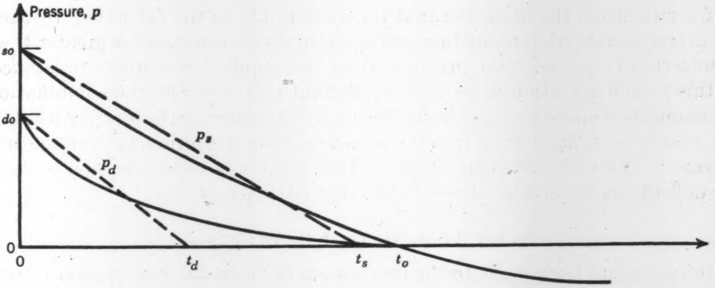

FIG. 1.—SIDE-ON OVERPRESSURE AND DRAG PRESSURE

Finally, the designer must make a decision as to what point in the range of the behavior of the structure he wishes to consider as the maximum permissible response for the other selected conditions. He may choose to have the structure remain elastic (but only rarely, because of the extremely heavy construction required), he may choose to permit the structure to deflect to the point of imminent collapse, or he may select some intermediate range. In most cases, design for collapse is reasonable because a factor of safety is already implied in the choice of the pressure curve for which the design is to be made. This choice has to be made independently for the different parts of the structure as the conditions are different for wall panels, structural framing members, and shear walls, for example.

The writer has avoided here the question of what constitutes "collapse"; this topic requires much discussion. However, collapse may be considered as the point of complete failure of the structure or component in general, in order not to overload the procedure with compounded factors of safety in too many hidden places.

When these various choices are made, the procedure leads to the computation of either the yield-point resistance required for the given overpressure or, alternatively, the peak overpressure that can be resisted by the given structure. The designer must recognize that factors beyond his control governing the blast pressure, duration, structural properties, and similar conditions may make his computed value uncertain by as much as 25%. However, nothing that he can do, particularly in refining his computations, can reduce this uncertainty. It is inherent in the problem. Only complete and accurate physical tests on the finished structure and accurate pressure measurements during the loading of the structure by blast can permit a more exact computation.

Therefore, a structure designed barely to resist collapse may suffer only slight plastic deformation, or conversely, in the extreme case of variation. Account may, where desired, be taken of this phenomenon in selecting the actual design in order to insure safety.

It is clear from the foregoing that the uncertainty in the deflection, reached by a given combination of loading and structural resistance, is far greater than the uncertainty in the blast pressure or in the required structural resistance. For this reason attention is focused throughout this paper on the combination of dynamic load and structural resistance required to produce failure. Although such failure is defined in terms of deflection, this definition is perforce not accurate. The procedure cannot be used with any degree of precision to compute deflections for given values of the other parameters.

Blast Loading on Structures

Reference has been made to the free stream or "side-on" overpressure curve (Fig. 1) which corresponds to the condition in which no structure or other object interferes with or causes diffraction of the shock wave in the blast. Accompanying this and dependent on it, there is a particle motion of the air which exerts a dynamic pressure or "drag" force on objects which interfere with the flow of air. It is convenient hereinafter to consider the drag pressure as corresponding to a drag coefficient of unity. It is also convenient, although not entirely accurate, to consider that the drag pressure p_d at any instant has the value it would have if the overpressure p_s at that time were a steady-state value. All pressures are to be expressed in units of pounds per square inch.

With these assumptions the value of p_d can be approximated by the relation:

$$p_d = \frac{0.025\, p_s^2}{0.07\, p_o + 0.01\, p_s} \approx 0.022\, p_s^2 \ldots\ldots\ldots\ldots\ldots (1)$$

in which p_o is the barometric pressure, usually 14.7 lb per sq in. at sea level. The approximate value holds for sea-level conditions. The relative values of p_d and p_s are shown as functions of time by the solid curves in Fig. 1. The drag pressure decreases more rapidly than the overpressure. In general, the drag pressure-time variation can be approximated by a straight line from the initial peak value p_{d_o} to zero at a time t_d which is approximately 0.5 t_s. Also, in general, t_s can be assumed to be approximately 0.75 t_o, in which t_o is the positive phase duration.

Diffraction-Type Structures.—When the shock wave from the blast encounters an obstacle such as the rectangular block in Fig. 2, the pressures on the block are related to but differ from the pressures in the curves of Fig. 1. Immediately upon striking the front wall the pressure in the shock is increased by a reflection, and the net reflected overpressure p_r is expressed by the relation:

$$\frac{p_r}{p_{so}} = 2 + \frac{6\, p_{so}}{7\, p_o + 6\, p_{so}} \qquad (2)$$

or without serious error, if p_{so} is less than 40 lb per sq in., and if p_o = 14.7 lb per sq in.,

$$p_r = p_{so}\left(2 + \frac{p_{so}}{20}\right) \qquad (3)$$

As the shock traverses the building, the pressures change. The high-pressure air trapped in front of the face of the building spills around and over the building permitting the pressure to decrease. The time for decrease to occur depends on the smaller of the two quantities H or $B/2$, designated by S, the least distance from the "stagnation" point on the front face of the structure to an edge. The quantity S is measured in feet. Several conventionalized relations have been published (9) for the net front-face pressure. The curve shown extending from p_r in Fig. 2 is a slightly amended representation of the results of the studies of Messrs. Bleakney (6) and Merritt (7). This curve indicates the pressure as decreasing to a value that is the sum of the side-on pressure plus a drag coefficient for the front face, c_f, multiplied by the drag pressure, in a time $3\,S/U$, in which U measured in feet per second is the velocity of propagation of a disturbance in the shocked air, but which is herein assumed for convenience to be the shock-front velocity as well. This velocity may be assumed, without introducing serious error in the results, to be 1,400 ft per sec. More accurate values can be determined from standard textbooks or from the AEC publication (1). The true value may range from 1,130 ft per sec to more than 2,000 ft per sec for strong shocks. However, the uncertainty in the other quantities

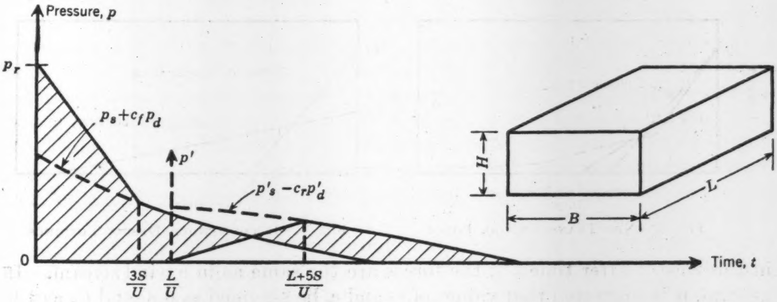

FIG. 2.—NET PRESSURES ON FRONT FACE AND REAR FACE

appearing in the relations in which U appears makes it unimportant to determine U precisely.

The shock reaches the rear face at a time L/U, later than that at which it strikes the front face, and the average pressure on the rear face, directed rearward, changes in an increment of time of approximately $5\,S/U$ to a value corresponding to the side-on pressure p'_s less the drag coefficient for the rear face, c_r, multiplied by the corresponding drag pressure p'_d. These quantities are shown in Fig. 2 with a prime to indicate that they are measured from a different origin in time L/U, later than the curves for the front face.

The difference between the forward pressure on the front face and the rearward pressure on the rear face is shown by the shaded area in Fig. 2 and by the solid curve in Fig. 3, until the time t'_1 when the net translational force on the building reaches zero. However, if L is small, the pressure on the rear face never gets larger than that on the front face, and the whole building experiences a forward drag. Because p'_d is very nearly the same as p_d if L/U is small compared with t_d, the net drag coefficient C_d is the sum of c_r and c_f. The dash-lined curve in Fig. 3 indicates the appearance of the net translational force in this case. After time t''_1, the forces are the same as in a wind stream. In general, it is suggested that values of c_f and c_r be assumed as 0.8, and C_d as 1.6, unless experimental values are available.

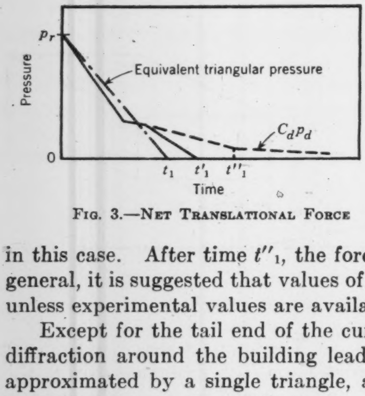

FIG. 3.—NET TRANSLATIONAL FORCE

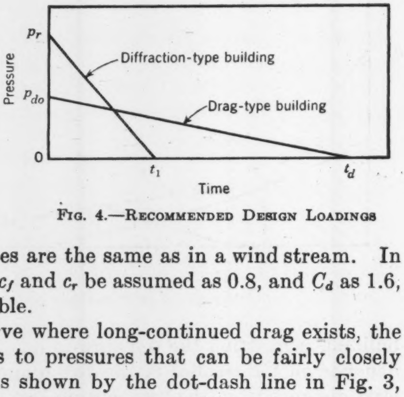

FIG. 4.—RECOMMENDED DESIGN LOADINGS

Except for the tail end of the curve where long-continued drag exists, the diffraction around the building leads to pressures that can be fairly closely approximated by a single triangle, as shown by the dot-dash line in Fig. 3, extending from p_r to zero in a time t_1, which is measured in seconds and expressed by

$$t_1 \approx \frac{L + 3\,S}{U + \frac{3\,S}{t_s}} \quad \text{(4)}$$

If L is less than S, the numerator is to be taken as $4\,S$, and if L is greater than $3\,S$, the numerator is to be taken as $6\,S$. In the denominator, if $3\,S/t_s$ is greater than $U/3$, the denominator is to be taken as $4\,U/3$.

For the pressure on a wall, the curve for the front wall of the building (Fig. 2) can be used. If the sloping line is extended down to the base line, a value of t_1 can be obtained. In general, this value will depend on the pressure level. No more refinement is usually necessary because maximum deflection in the wall panels of a building will usually occur so quickly that small changes in the pressure duration will not affect it. An approximate relation for the value of $t_1 = t_f$ for a front wall panel is the following:

$$t_f \approx \frac{6\,S}{U + \dfrac{3\,S}{t_s}} \qquad (5)$$

with the same limitations on the denominator as those applying to Eq. 4.

Because any wall may be exposed directly to a blast, the design conditions for all wall panels should be assumed the same. Also, the roof slab may be exposed to a force from a detonation above the roof so that it too is exposed to reflected pressures. However, if it is clear that the roof is never exposed to reflected pressure because of the location of the possible detonation, the value p_{so} can be used instead of p_r for the maximum roof pressure. Some data on the pressure to be expected on the roof for such a condition can be obtained from the report by Mr. Bleakney (6). As a crude approximation, however, one can assume the pressure to be approximately defined by a triangle having a maximum value p_{so} with a duration t_s.

For a completely closed structure, the walls and framing must be capable of resisting not only the crushing force from the positive overpressure, but also the differential bursting pressure in the negative phase of the blast. The minimum external pressure can drop below atmospheric pressure by approximately $\frac{1}{3}\,p_{so}$ but of course the minimum can never be less than absolute zero pressure.

Drag-Type Buildings.—For an open structure composed only of beams, columns, trusses, or other members with only small areas opposing the blast, each of the members receives an impulsive loading as the blast engulfs it and each member is then exposed to drag from the wind accompanying the blast. Because the blast is transmitted through the building in a finite time, the net translational force is increased in general until all or nearly all of the building is engulfed. However, the impulse from the diffraction around each member produces a "spike" on the net-force diagram as the blast reaches that particular member. Unless the building is extremely brittle and fails as a whole or in part without plastic deformation, it is reasonably accurate to consider the building as being subjected only to drag, neglecting the impulse spikes; but to compensate for this, one may assume that the whole building is engulfed at once. To neglect the impulse spike is not permissible, however, for an isolated narrow element such as a telephone pole. The pressures on such an element should be determined by the process indicated in Fig. 2.

This assumption leads to a net pressure on the projected area of each of the elements corresponding to the drag pressure multiplied by the drag coefficient for the individual members. The basic recommended pressure curves for use in design are shown in Fig. 4 for both diffraction-type buildings and drag-type buildings.

The drag coefficients to be used should take into account the shielding of certain elements by other elements placed a short distance away. However, if the distance between parallel elements is more than ten times their width, the shielding is probably negligible. It has been suggested (9) that one may use drag coefficients of approximately 2 for structural shapes, approximately 1.25

for box-shaped elements or for flat plates, and approximately 0.8 for cylinders. In the absence of better information these values can be used; although they are not accurate, they lead to reasonable results.

In Fig. 4, the value of p_{d_o} is obtained from Eq. 1 for the condition $p_s = p_{so}$.

Partly Open Buildings.—The problem of analyzing buildings with resistant walls but with openings in the walls is a difficult one. Any comprehensive treatment would be beyond the scope of this paper. However, the following approximate treatment is suggested.

When the area of the openings is more than about 50% of the area of the walls, one should consider the building as a drag-type building (9). The areas subjected to drag are then the net areas of the parts of the structure. The drag coefficient to be used can be taken to be 1.5. It has been suggested (9) that, if the area of the openings is less than 5% of the area of the walls, the building can be considered completely closed.

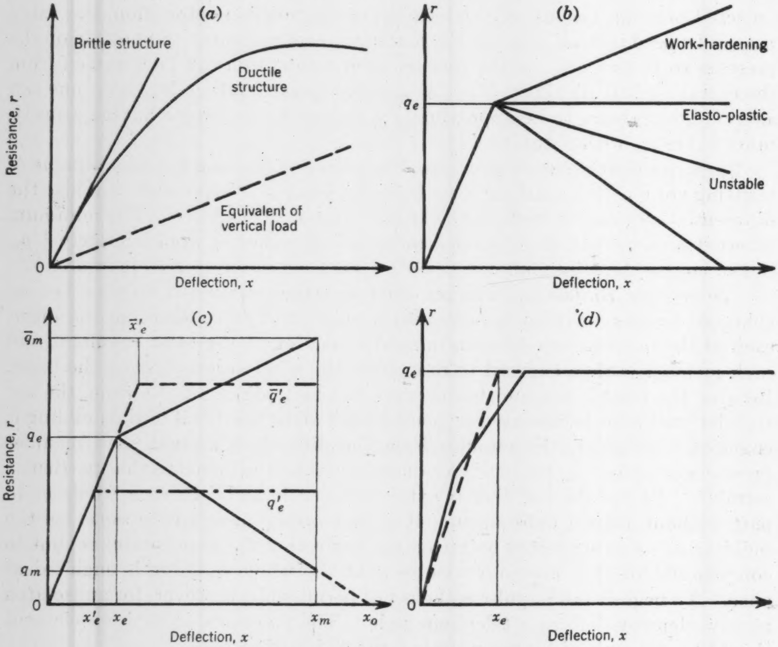

FIG. 5.—TYPICAL RESISTANCE–DEFLECTION RELATIONS

For intermediate conditions, the magnitude of the pressure passing through the opening must be considered. It is suggested, however, that, for lack of a better approach, a direct interpolation be made between diffraction loading and drag loading if the openings are more than 5% and less than 50% of the wall area—the interpolation to be made both for maximum force and for duration.

STRUCTURAL RESISTANCE

The relation between load and deformation, or between resistance and deflection of a structure or structural element, may take any one of a number of forms. It is convenient to define the structural resistance r in the same terms and in the same units as the external loading p. Then the relations between r and x may be indicated as in Fig. 5, in which x is either a particular deflection, an average deflection, or a parameter that defines all the deflections in terms of some mode shape.

In Fig. 5(*a*) there are shown curves of brittle and ductile resistance. The former is defined by the fact that failure occurs in or near the linear range of the load-deflection relationship.

When heavy dead loads or other large vertical forces in a structural frame deflect laterally, they produce moments and stresses in the frame. These reduce the ability of the frame to resist lateral load. The effect is proportional to the deflection and may be approximated on the resistance-deflection curve as shown by the dashed line in Fig. 5(*a*). The equivalent or effective resistance-deflection curve is the difference between the original curve and the dashed line. Consequently, the effective curve may have a net downward slope after yielding occurs and may even drop to zero resistance for a large enough deflection, at which point the structure would collapse physically of its own weight.

In Fig. 5(*b*) are shown conventionalized curves that represent the behavior of a variety of structures. The figure shows (*a*) a work-hardening relation in which the resistance increases with increasing deflection beyond the first yielding, (*b*) an elasto-plastic relation with an ideal plastic constant resistance after yielding, and (*c*) two unstable relations with decreasing resistance after yielding. These may arise as a result of the effect of vertical loading. The yield point, which is designated as q_e, is the same for all of these curves.

In Fig. 5(*c*) a work-hardening relation and an unstable relation are both represented by approximately equivalent elasto-plastic curves to give the same maximum deflection, at which the corresponding resistances are actually $\bar{q}_m$ and q_m. It is shown later that the equivalent curves can be stated in fairly convenient form, and therefore it is only necessary to consider in detail the behavior of idealized elasto-plastic structures in order to obtain a rational analysis of almost any structure.

Finally, in Fig. 5(*d*) there is shown a typical resistance-deflection relation for an element that yields in successive stages, as for example a fixed-end beam. In such a structure, the initial elastic relations apply up to the point where plastic behavior begins at the fixed end. Beyond this point, the structure behaves for additional load as if it were hinged at the end, and the slope of the load-deflection curve is correspondingly smaller than in the initial state. Finally, the beam yields also at the center and cannot carry a greater load. The limit resistance q_e is clearly defined; it is the maximum resisting capacity of the structure. However, it is less convenient in general to work with polygonal relations such as the one shown. Therefore, an equivalent elasto-plastic relation is used, as shown by the dashed curve, with the proper yield point q_e but with a fictitious yield deflection x_e, which is chosen so that the area under the equivalent curve is exactly the same as that under the original curve. In this way the work absorbed by the structure is unchanged.

REQUIRED RESISTANCE FOR ELASTO–PLASTIC STRUCTURES

The writer has standardized or conventionalized the problem to the point where there is a structure with an equivalent elasto-plastic resistance-deflection relation with a pulse loading having a maximum value p_{max} at time $t = 0$ and a duration t_1 or t_d. The yield resistance, q, is stated in the same terms as p_{max}.

The deflection has not been completely specified, nor does one need to specify it. One must only be sure that the maximum desired deflection or the collapse deflection x_m is measured in the same units and at the same point on the structure as the yield deflection at the knee of the curve, x_e. The ratio of the maximum to the yield deflection is defined as the ductility factor μ. For a completely brittle structure μ equals 1.0, for moderately brittle structures μ ranges from 3 to 5, for moderately ductile structures μ ranges from 10 to 30, and for very ductile structures μ is greater than 40.

Only one other quantity is needed to specify the essential characteristics of the structure or the component element. This quantity is the natural period of vibration, T. However, it is necessary to use the period corresponding to the stiffness of the equivalent elasto-plastic structure, as defined, for example, by the dashed line in Fig. 5(*d*) rather than as defined by the initial slope of the resistance curve. The equivalent curve is drawn so as to make the areas under the curves equal.

Standard procedures are available for the computation of the period of the structure in its initial elastic state, either analytically or by numerical means. Only an approximate value is required. For a single-degree-of-freedom structure having a mass m, the period is given by the relation:

$$T = 2\pi\sqrt{\frac{m\,x_e}{q_e}} \quad \text{......................} (6)$$

The effective period is obtained by use of the effective values of x_e and q_e in the equation.

If, however, the initial elastic period is known, the effective period is readily determined by multiplying the elastic period by the square root of the ratio of the effective yield-point deflection to the elastic deflection computed for the limit load q_e, using the initial elastic modulus of the structure.

With the simplifications outlined herein, the structure is essentially reduced to an equivalent simple one-degree-of-freedom system. Solutions of such systems have been obtained for several types of loading and for various types of resistance curves. A chart summarizing some of the results is presented in Fig. 6. This chart relates: (*a*) The ductility factor or the ratio of maximum deflection to yield deflection, (*b*) the ratio of the relative duration of the loading to the natural period of the structure, (*c*) the ratio of the structural resistance to the peak loading, and (*d*) the ratio of the time necessary to reach maximum deflection to the natural period. The first of these quantities is plotted as horizontal lines with a logarithmic spacing, the second as vertical lines also with a logarithmic spacing, the third as lines sloping generally upward to the right, and the fourth as dashed lines sloping generally downward to the right. If any two of the quantities are known, the other two can be obtained. For example, if $t_1/T = 2.0$ and $\mu = 20$, it is readily found that $q_e/p_{\max} = 0.6$ and $t_m/T = 1.7$.

Approximate equations for the items of interest appear subsequently in this paper.

Acceleration, Impulse, Momentum, and Energy

The relations governing the motion of a simple system can best be explored on a plot of the accelerations of the system as a function of time, as in Fig. 7. The accelerations produced by the external loading p are plotted as a triangle on the left-hand side of the figure. The negative accelerations produced by the resistance r are then shown as the curve of values increasing to a maximum and remaining constant after a time t_e. The part of the curve that is not known is the initial part of the resistance-time curve. This part can be determined by an iterative process, or it can be approximated quite readily as described in a paper by the writer (3).

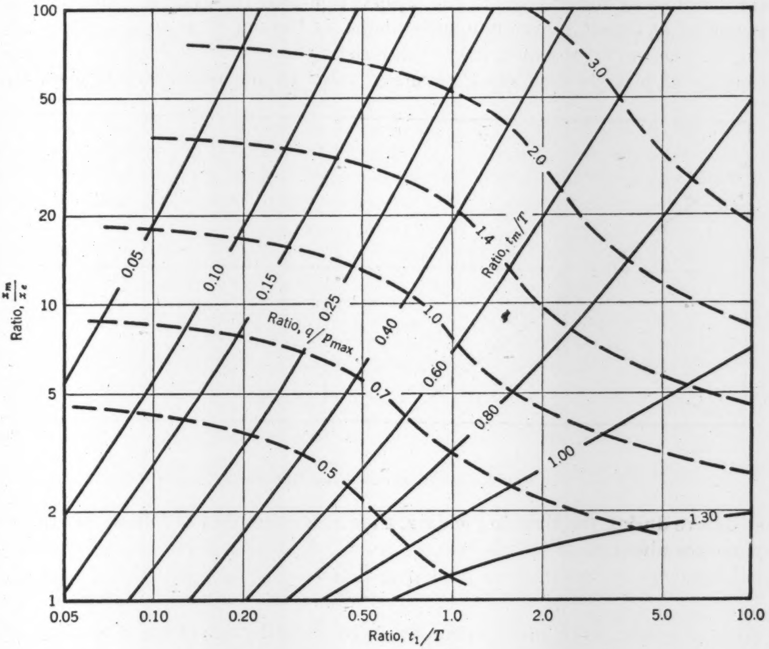

FIG. 6.—RESPONSE, PRESSURE, AND RESISTANCE RELATIONS FOR TRIANGULAR PULSE LOADING

The value of t_m is determined by the condition that the velocity at this time is zero. As a consequence, the net area between the curves must balance, or $A_1 + A_2 = A_3$.

This means also that in Fig. 7 the area under the pressure curve and the area under the resistance curve between the origin and the time of maximum displacement must balance. Furthermore, the moment of the couple formed by these equal areas is equal to the maximum displacement.

When t_1 is small, the shape of the load-time curve does not matter; so long as its impulse is constant, the maximum deflection and the time needed to reach it will be the same.

In order to take account of the speed of loading of the material, it is necessary to formulate an expression for the time required to reach yielding. This can be done by making use of the observation that the yield displacement x_e, occurring at time t_e, is the moment about t_e of the net areas to the left of t_e in Fig. 7. However, the moment of the resisting forces is small and can be neglected. If $\bar{p}$ is the "effective" average value of the pressure acting on the structure during the time to yielding, then x_e is computed as follows, by taking moments about t_e,

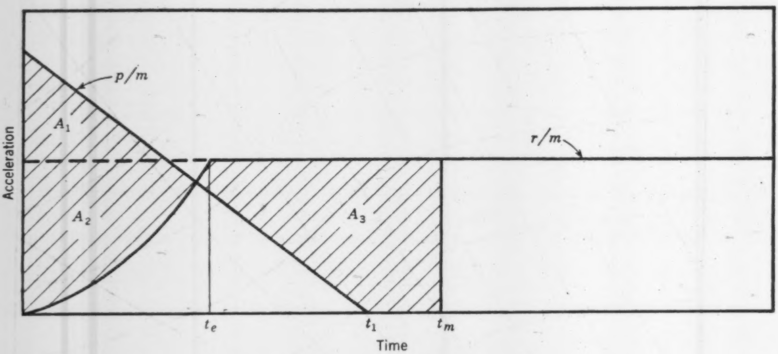

FIG. 7.—ACCELERATION-TIME RELATIONS

$$x_e = \frac{\bar{p}\, t_e^2}{2\, m} \quad \text{(7a)}$$

Since $q_e = k/x_e$, upon multiplying Eq. 7a by k and by use of Eq. 6 to eliminate m, one obtains the result,

$$q_e = 2\,\pi^2 \frac{\bar{p}\, t_e^2}{T^2} \quad \text{(7b)}$$

whence

$$\frac{t_e}{T} = 0.226 \sqrt{\frac{q_e}{\bar{p}}} \quad \text{(7c)}$$

Eq. 7c is valid if the duration t_1 of the pressure on the structure is greater than t_e, which is always the case for atomic bombs. If we designate the pressure on the structure at time t_e as p_e, then $\bar{p}$ is expressed by the equation:

$$\bar{p} = \frac{2\, p_{\max} + p_e}{3} \quad \text{(7d)}$$

In most cases it is sufficiently accurate to take $\overline{p} = p_{\max}$ because one is usually interested in the order of magnitude of t_e rather than in an accurate value.

For a complicated structure the parameters defining the structural properties are derived as follows: The distribution of blast pressure on the structure is considered as defining a pattern of loading. A static loading r is assumed to be applied to the structure in the same pattern. The deflection x is determined at the point which has the greatest or nearly the greatest deflection. Then a plot of r against x can be drawn, as in Fig. 5(*d*). From this plot one may choose the values of q_e and x_e as described previously.

The period of the structure in its initial elastic state can be computed by standard means, or it may be estimated. The effective period T is determined as described previously.

EMPIRICAL RELATIONS

If one considers the maximum work done by the pressure and by the resistance, one can see that these must be equal if the mass of the structure is initially at rest because the structure also stops temporarily at its position of maximum displacement. Also, if the pressure is applied very quickly as an impulse, the work done by the pressure is equal to the kinetic energy of motion of the structure after the external forces have ceased and before the internal resistances have developed.

From these concepts can be derived the following results:

If the pressure is of infinitely long duration, the external work done is equal to the internal energy absorbed at maximum deflection. Then,

$$p_{\max}\, x_m = q_e(x_m - 0.5\, x_e) \qquad (8a)$$

or

$$\frac{p_{\max}}{q_e} = 1 - \frac{0.5}{\mu} \qquad (8b)$$

On the other hand, if the pressure lasts a very short time, the positive impulse of the pressure is $0.5\, p_{\max}\, t_1$, and the initial kinetic energy of the mass is $0.25\, p^2_{\max}\, t^2_1/2\, m$. However, this energy is equal to the stored energy at maximum deflection, as before. Hence, with use of the relation,

$$m = \frac{m}{k}\frac{k\, x_e}{x_e} = \frac{q_e\, T^2}{4\, \pi^2\, x_e} \qquad (8c)$$

one can derive the result,

$$\frac{p_{\max}}{q_e} = \frac{(2\,\mu - 1)^{0.5}\, T}{\pi\, t_1} \qquad (8d)$$

Eq. 8*d* applies when t_1 is very small and Eq. 8*b* when t_1 is very large. Trials with various combinations of the equations led to the following generally applicable empirical result:

$$\frac{p_{\max}}{q_e} = \frac{T}{\pi\, t_1}\sqrt{2\,\mu - 1} + \frac{1 - \dfrac{1}{2\,\mu}}{1 + 0.7\,\dfrac{T}{t_1}} \qquad (9)$$

Eq. 9 is in error by less than 5% over the whole range of values of t_1 from zero to infinity and of μ from 1 to infinity. It can therefore be used instead of Fig. 6. From Eq. 9 one can readily determine q_e if $p_{\max}$ is known, and conversely.

Applying Eq. 9 and the relations between p_{so} and $p_{\max}$ (equal to p_{do} or p_r in Eqs. 1 and 3) and with the values of t_1 or t_d given, one can determine the required value of q_e for any overpressure directly, as soon as the drag coefficient and the value of μ and that of T are known or can be estimated for the structure.

It may be useful to have approximate expressions also for the time required for the structure to reach maximum deflection. These can be derived rather logically, but only the resulting empirical expressions are presented here:

If t_m is greater than t_1,

$$\frac{t_m}{t_1} = \frac{p_{\max}}{2\,q_e} + \frac{0.091\,\dfrac{T}{t_1} + 0.25}{(2\,\mu - 1)^{0.5}} \quad \text{(10)}$$

and for t_m less than t_1,

$$\frac{t_m}{t_1} = 2 - \left[\left(2 - \frac{1}{\mu}\right) - \frac{2\,(\mu - 1)}{\mu^2 + 100}\right]\frac{q}{p_{\max}} \quad \text{(11)}$$

These expressions are generally accurate within 10% or less. However, they do not yield exactly the same results when $t_m = t_1$; when these times are nearly equal it is not immediately clear which equation must be used.

Knowing the values of t_m, one can take account of other than triangular loading curves by selecting the closest triangular approximation to the actual loading curve in the region between zero and t_m. The loading beyond t_m does not matter.

Finally, expressions are required for the equivalent elasto-plastic resistance curves for use in cases such as that shown in Fig. 5(*c*).

For either of the types of resistance shown in Fig. 5(*c*) the following relations are applicable and are derived from considerations similar to those used in the derivation of Eq. 9. The symbol A designates the ratio of the area under the resistance curve up to the designated maximum deflection, $x_m = \mu\,x_e$, relative to the area in the elastic portion up to x_e. Then, for all cases of "work-hardening" or for those cases of "unstable" resistance functions in which the maximum deflection is less than some critical value of x_{cr}, the following relation applies:

$$\frac{p_{\max}}{q_e} = \frac{T}{\pi\,t_1}\sqrt{A} + \frac{\dfrac{A}{2\,\mu}}{1 + 0.7\,\dfrac{T}{t_1}} \quad \text{(12)}$$

For the unstable resistance function, the value of x_{cr} is expressed in terms of x_o, the deflection at zero resistance, as follows:

$$\frac{x_{cr}}{x_e} = \sqrt{\frac{x_o}{x_e}} = \gamma \quad \text{(13)}$$

For all values of deflection x_m greater than x_{cr} the quantity $A/2\mu$ in the numerator of the extreme right-hand term of Eq. 12 is replaced by $\gamma/(1+\gamma)$.

It is now possible to state the equivalent elasto-plastic resistance for the resistance functions in Fig. 5(*c*). For the work-hardening case the value of q'_e is so chosen as to preserve the area under the curve up to the maximum deflection. For the unstable case, the value of q'_e also preserves the area up to x_m if x_m is less than x_{cr}. For greater deflections the following approximate relation can be used:

$$q'_e \approx \frac{q_e + q_m}{2\left(1+\dfrac{t_1}{T}\right)} + \frac{\gamma\, q_e + q_m}{(1+\gamma)\left(1+\dfrac{T}{t_1}\right)} \qquad (14)$$

PROPERTIES OF MATERIALS

In making a preliminary design, an estimate must be made of the values of the ductility factor to be used. In general this factor is probably fairly small for wood structures, perhaps of the order of from 3 to 5. For steel structures, the factor is generally large, of the order of from 10 to 50, except in such instances as welded connections at low temperatures in which brittle fractures may be developed because of the speed of loading. For reinforced concrete the factor depends on the quantity of reinforcement, on the relative quantities of tensile and compressive steel, and on the way in which the compressive steel is tied together. Crushing of concrete in compression occurs at a fairly small strain value and causes a large reduction in moment-carrying capacity. Only limited data are available concerning the behavior of reinforced concrete beams up to the point of failure. From the results of test data obtained at the University of Illinois at Urbana, it appears that the following rules may be used for approximate preliminary estimates:

The maximum ductility factor for reinforced concrete beams is approximately

$$\mu = \frac{0.1\, A_c}{A_s - A'_s} \qquad (15)$$

in which A_c is the area of the concrete, A_s that of the tensile steel, and A'_s that of the compressive steel in the cross section. However, μ should not be taken greater than 30 for reinforced concrete, regardless of what Eq. 15 indicates. When A'_s is greater than A_s, the value 30 is also used.

For shear walls, the value of μ is likely to be quite small, much less than that for framed structures. Values of the order of from 5 to 10 seem to be as large as should be taken for such elements as shear walls and diaphragms.

The influence of the speed of loading on the yield point of mild steel should be considered. What this influence is, precisely, on steel members in a structure is difficult to evaluate. Factors of the order of from 20% to 30% greater than the static yield point seem reasonable, however, for members in the framing as do factors of from 30% to 50% greater for members in the wall or roof covering. Of course, these factors are to be applied generally to the average values and not to the minimum specified values.

CONCLUSIONS

In this paper is presented an approach that can be used in the preliminary design of structures to resist blast loadings from atomic bomb detonations. The procedure involves the selection of the required yield resistance of the structure against blast forces. This yield resistance may be as much as twice the peak blast force for a particularly brittle structure subjected to a very long load pulse or as little as 1/20 or less of the blast force for a ductile structure subjected to a short load pulse.

The duration of the pulse and the ductility of the structure must be considered in the solution of the problem. However, once the necessary yield resistance is determined, the remainder of the design is essentially like the ordinary routine for static loads.

After the preliminary design is made, more accurate values of the period of the structure and of its ductility factor can be computed. The procedure explained herein can be applied again to determine whether the strength of the structure is adequate. Usually, no more refined computation is necessary.

More detailed computations of structural response can be made, but these do not imply any more accurate results in so far as the design of the structure is concerned. More elaborate methods of analysis are available (3) (4) (10).

By way of illustration, one may consider the design load factors required for a typical building framework and for the wall covering resisting the same resultant pressure.

The period of the wall covering is likely to be of the order of 0.025 sec, whereas the period of the frame is likely to be of the order of 0.25 sec. There is assumed a duration of the blast force on both elements of the order of 0.25 sec. If the ductility factors for both elements are assumed to be 20, then from either Fig. 6 or Eq. 9 one finds that the required static resistance is approximately 0.4 times the peak pressure for the frame and 0.9 times the peak pressure for the wall panel. This example illustrates the general result that, for wall panel elements which usually have a short period, the static resistance required is approximately equal to the peak blast force, whereas for frame members it is considerably less. Therefore, for equal factors of safety these elements must be designed for very different yield loads. If they are designed for the same static equivalent load, the wall panels would be much weaker than the frame.

APPENDIX. REFERENCES ON DESIGN OF BLAST-RESISTANT BUILDINGS

(1) **"The Effects of Atomic Weapons,"** Atomic Energy Comm., U. S. Govt. Printing Office, Washington, D. C., June, 1950.

(2) **"The Blast and Radiation from an Atomic Bomb,"** by C. W. Lampson, *Proceedings*, Conference on Building in the Atomic Age, Massachusetts Inst. of Technology, Cambridge, Mass., June, 1952, pp. 4–10.

(3) **"Analysis and Design of Structures Subjected to Dynamic Loading,"** by Nathan M. Newmark, *ibid.*, pp. 34–47.

(4) **"Computation of Dynamic Structural Response in the Range Approaching Failure,"** by Nathan M. Newmark, *Proceedings*, Symposium on Earthquake and Blast Effects on Structures, Earthquake Eng. Research Inst. and Univ. of California, Los Angeles, Calif., June, 1952, pp. 114–129.

(5) **"The Air Blast Wave from a Nuclear Explosion,"** by F. Reines, *ibid.*, pp. 37–45.

(6) **"A Shock Tube Investigation of the Blast Loading of Structures,"** by Walker Bleakney, *ibid.*, pp. 46–73.

(7) **"Blast Loading of Idealized Structures Using High Explosives,"** by M. L. Merritt, *ibid.*, pp. 74–93.

(8) **"Lateral Forces of Earthquake and Wind,"** by the Joint Committee of the San Francisco Section, ASCE, and the Structural Eng. Assn. of Northern California, *Transactions*, ASCE, Vol. 117, 1952, pp. 716–780.

(9) **"A Simple Method for Evaluating Blast Effects on Buildings,"** Armour Research Foundation, Chicago, Ill., July, 1952 (revised edition, July, 1954).

(10) **"Methods of Analysis for Structures Subjected to Dynamic Loading,"** by Nathan M. Newmark, Report to Physical Vulnerability Div., Directorate of Intelligence, U. S. Air Force, November 17, 1949 (revised December 18, 1950).

DISCUSSION

Stephen J. Fraenkel.[3]—The writer welcomes the advent of this paper to the slowly but steadily increasing literature on structural dynamics. Aside from the appeal which this subject holds as a technical problem, recent newspaper headlines and stories are lending ample emphasis to the practical and immediate implications of this subject. This contribution to the sparse, unclassified literature existent in this field has the specific virtue of presenting the problem in terms of design rather than analysis. Although many procedures previously advocated, including those proposed by the writer, can be used on a trial-and-error basis for design purposes, they are not as conveniently or efficiently applicable to the design problem as the method proposed in the paper.

The writer will examine briefly the basic approach taken in the paper and compare it with earlier analysis procedures to determine what has made this transformation to the design approach possible. Expressed in its barest mathematical essentials, the problem of both analysis and design revolves around the solution of the following equation for a suitably simplified or idealized structure:

$$m\,\ddot{x} + r(x) = F(t) \qquad (16)$$

In the so-called analysis procedures, the value of the deflection x is sought as a function of time. The mass m, the building resistance r, and the external force F, which moves the building, are all known at the beginning of the problem. The method thus reduces to the solution of the foregoing differential equation. This solution may be difficult to obtain, depending on the complexity of the functions r and F. The paper departs from such an approach by recognizing the obvious fact that in the design of new structures the building resistance r is precisely the thing to be determined. Thus, r becomes the dependent variable, but, unfortunately, no explicit solution for r can be obtained from this differential equation for arbitrary forcing functions F. In order to overcome this difficulty the author simplifies F so that a closed-form solution of the differential equation can be obtained. Moreover, a specific value of the deflection x is selected which the resistance r will not permit to be exceeded. In this manner, through the selection of a fixed maximum deflection x and of a simple analytical forcing function F, the problem can be inverted from its usual formulation and the desired building resistance r can be solved for directly. In cases in which the actual forcing function F is too irregular to permit simple idealization, a crude approximation by the methods outlined in the paper will at least reduce the number of trials required by a more rigorous procedure. There is no doubt that the simplified approach advocated by the author should be of great help in many design activities.

The author has omitted the negative phase as a possible agent of destruction. The writer agrees with the legitimacy of this omission and offers two reasons in support of it which were not contained in the original paper. First, it is well known that the pressure and force associated with the negative phase are much smaller than those associated with the positive phase and are approximately of the order of one fifth of the latter. Damage to any structural system requires a certain threshold intensity of loading irrespective of duration, and computations would undoubtedly show that in most instances the pressure level during the negative phase would be below that required to do damage. Second, the direction and distribution of loading during the negative phase will be 180° opposite in direction to that encountered during the positive phase. The resistance of buildings is the same, however, for two diametrically opposite directions, and it is difficult to conceive therefore that a building not already damaged by the higher pressures in the positive phase will be damaged during the negative phase. If the forces exerted during the negative phase were not directly in line with those in the positive phase, one would be much less certain about the advisability of ignoring the effects of the negative phase.

---

[3] Director of Research and Development, Standard Ry. Equipment Mfg. Co., Chicago, Ill.

The author's paper, in common with several publications of the writer and of the writer's previous office, takes account of the vertical loads by adding them to the applied overturning moment. In this particular paper this effect is expressed as a reduction of the slope of the resistance displacement function. However, the two methods of recognizing this effect are entirely identical. There exists still another effect of the vertical load which is potentially of great importance in problems of this kind but because of its complexity it has thus far been ignored by nearly everyone. This effect concerns the changes in the resistance properties of the cross sections of the columns which is brought about by the simultaneous presence of direct forces and bending moments. Because both the forces and the moments are independent functions of time, enormous complexities would be introduced into procedures of this kind by considering this variation. There exists some evidence, however, that this effect may be fully as important as the inclusion of the vertical loads in the driving force, and future studies in this field should not ignore this effect without first providing adequate justification.

The author has classified buildings with openings constituting 50% or more of the front and rear walls as drag-type buildings. He does not mention possible restrictions that may have to be imposed on the dimensions of interior members lying in the path of a wave traveling through such a drag-type building. Several computations have been made as part of the preparation of a revised edition of a manual (9) in which quantitative limits of error are given which apply to the response predictions when interior framework of certain dimensions is present. These computations indicate a so-called "average" framework dimension commensurate with an acceptable maximum percentage error in the response prediction for a building of certain dimensions if this building is to be considered a drag-type building. This limitation must be superimposed on the minimum 50% wall-opening requirement stated in the paper. In most cases this limitation would not be restrictive from a practical point of view if one were not too punctilious about the expected accuracy.

Nathan M. Newmark,[4] M. ASCE.—Mr. Fraenkel has explained some of the more difficult aspects of design for dynamic loading.

Too often in structural engineering analysis and design procedures are confused. In many statical problems the confusion is not serious although it leads to wasted time and consequent inefficiency. However, computation of dynamic deflections of a structure is affected to such a major degree by uncertainties in the parameters defining the structure and loading that an accurate computation is an entirely academic task. In order to arrive at any solution of the practical engineering problem, one must decide beforehand which quantities are negligible and which are not. The writer has attempted to do this in his paper. Many items were omitted entirely from consideration because of their negligible influence on the result. It is hoped that the necessary condensation of the paper did not make some of the points too abstruse.

Because Mr. Fraenkel's remarks stem from his long association with dynamical problems and problems of structural behavior, his comments are greatly appreciated.

The further discussion presented by Mr. Fraenkel on the negative phase of blast loading adds to the value of the paper. Another reason why the negative phase can ordinarily be neglected is that the sequence of events in most cases involves a maximum response before the negative phase begins. For small bombs acting on structures with long periods of vibration this would not be true. In such cases the negative phase of the blast acts to reduce the effect of the loading, and this reduction is important enough to be considered. However, for most cases of engineering importance and for atomic bombs in general, either the negative phase of the blast occurs after the maximum response or the reduction in the response of the building produced by the negative phase is negligible.

The problem of vertical loads is important. The added vertical load produced by the vertical component of blast forces on the roof of a resistant building may affect the response. Some account of the added vertical load may be taken by consideration of an increased dead load equivalent to the added vertical force. Further studies of these points are necessary, however.

Another topic about which very little is known concerns buildings with moderate amounts of openings. Mr. Fraenkel's discussion and the studies to which he refers will be helpful in the consideration of this problem. However, major uncertainties still exist in the knowledge of the loading on structures with openings ranging from 10% to 50% of the frontal area.

The writer has had occasion to use the procedures described in the paper in several problems and has found that even for relatively complicated cases the simple procedures are sufficiently accurate for practical purposes. It is important to emphasize the fact that the procedure explained in the paper permits one to treat the problem of dynamic structural design from the point of view of an equivalent static load. The major innovation lies in the method of computing the equivalent static load and in the fact that the equivalent load is different for the different elements of a structure, being a function of easily definable structural parameters—such as the period of vibration, the permissible plastic or inelastic deflection, and the duration of the loading.

---

[4] Research Prof. of Structural Engr., Univ. of Illinois, Urbana, Ill.

AMERICAN SOCIETY OF CIVIL ENGINEERS
Founded November 5, 1852
TRANSACTIONS

Paper No. 2787

FLOW EXPANSION AND PRESSURE RECOVERY IN FLUIDS

By Harald Tults,[1] A. M. ASCE

Synopsis

To investigate the improvement of the pressure recovery in flow expansions, the separation phenomena were observed and the development of velocity profiles and pressure distribution were measured in a unilaterally expanding, two-dimensional, rectangular test canal. Two characteristic phases of the separation phenomena—"instant stop" and "separation start"—were measured and photographed.

The analysis of the data for pressure variations in both the longitudinal and transverse directions provides considerable information on the mechanics of flow separation. A simple analytical dependency is established between the angle of divergence and the rate of expansion at which the maximum pressure recovery in each section occurs. This dependency permits the prediction of the optimum divergence for any required rate of gradual expansion.

Experiments on the improvement of pressure recovery disclosed that the pressure efficiency can be improved considerably when the separation-endangered area is connected to a bypass which removes the retarded flow particles and carries them, in the direction of the pressure drop, back into the approach canal.

Notation

The letter symbols adopted for use in this paper are defined where they first appear, in the text or by illustration, and are arranged alphabetically in the Appendix.

Introduction

The conversion of kinetic energy to static energy is of great importance in hydraulic and aeronautical engineering. Unfortunately, the energy conversion in flow expansion is accompanied by an increase in energy losses and is strongly aggravated after the start of flow separation from the walls when the rate of divergence is too great. The separation of flow occurs when:

Note.—Published, essentially as printed here, in December, 1954, as *Proceedings-Separate No. 567*. Positions and titles given are those in effect when the paper was approved for publication in *Transactions*.

[1] Asst. Hydr. Engr., Pioneer Service and Eng. Co., Chicago, Ill.

1. The fluid, because of its inertia, cannot follow the abrupt boundary changes of the conduit.

2. The expanding flow is retarded by such locally acting counterforces as viscosity near the boundaries and gravity of the rising particles in the hydraulic jump. If the retarding viscous forces are not concentrated at boundaries but are evenly distributed over the entire section, as in seepage flow through porous soils, the flow in the expansion follows the potential pattern without separation.

3. Sometimes the separation may occur as a natural regulator of the energy balance. In flume intakes of a flow with too high a content of kinetic energy, as observed in front of regulated weirs during floods, the separation constricts the actual flow passage and destroys the excessive kinetic energy to conform to the conveyance capacity of the flume.

The theoretical treatment of separation problems by G. Hamel,[2] W. Tollmien,[3] H. Blasius,[4] and K. Pohlhausen[5] revealed that the capacity for laminar flow to expand and cause energy conversion is reduced with increasing Reynolds number, **R**. At $\mathbf{R} = 2{,}000$, the maximum divergence is 3°55′.

Engineering problems are concerned primarily with turbulent flows; even the possible laminar boundary layer becomes turbulent before the beginning of separation. Turbulent flow is able to undergo considerable expansion without visual evidence of separation. This characteristic of turbulent flow is attributed to the turbulent interchange of kinetic energy. A. A. Kalinske, M. ASCE, experimenting with energy loss in flow expansion, found[6] that the large-scale turbulence is more effective in energy interchange than the fine-grained turbulence and that the turbulent energy, which cannot be recovered, is only a fraction of the total energy lost in the expansion.

IMPROVEMENT OF PRESSURE RECOVERY

Among the methods used to improve pressure efficiency are (*a*) the increase of turbulence, (*b*) the deflection of kinetic energy into the separation area, and (*c*) the improved velocity distribution at the entrance to the expansion. All these methods help to delay the occurrence of separation.

(*a*) *Increase of Flow Turbulence.*—Artificially generated turbulence is not self-sustaining and thus differs from naturally established turbulence that is constantly engendered by shear forces. Consequently, artificially generated turbulence is subject to early viscous attrition and, therefore, should be utilized immediately.

The experiments by K. Andres[7] revealed that, when a whirl disk, perforated by three circular openings, was placed in front of a diffuser, it set the water into intensive large-scale whirling and improved the efficiency from 74% to 82%. However, a screen whose effective range—because of the small-scale turbulence—is comparatively short reduced the efficiency from 53% to 42%.

---

[2] "Spiralförmige Bewegungen Zäher Flüssigkeiten," by G. Hamel, *Jahresbericht der Deutschen Mathematiker Vereinigung*, Vol. 25, 1916, p. 34.

[3] "Grenzschichttheorie," by W. Tollmien, *Handbuch der Experimentalphysik*, Vol. IV, p. 241.

[4] "Die laminare Strömung in erweiterten Kanälen," by H. Blasius, *Zeitschrift für angewandte Mathematik und Physik*, Vol. 58, 1910, p. 90.

[5] "Zur näherungsweisen Integration der Differentialgleichungen der laminarer Reibungsschicht," by K. Pohlhausen, *ibid.*, Vol. 1, 1921, p. 252.

[6] "Conversion of Kinetic to Potential Energy in Flow Expansions," by A. A. Kalinske, *Transactions*, ASCE, Vol. 111, 1946, p. 355.

[7] "Versuche über die Umsetzung von Wassergeschwidigkeit in Druck," by K. Andres, *Forschungsarbeiten*, Verein Deutscher Ingenieure, No. 76, 1909.

The outflow from low-head hydraulic turbines has a very high kinetic energy. Recovery of that energy would be much less perfect if the large-scale turbulence generated by the vanes did not exist in the outflow. Because of this high-degree local turbulence a strong flow expansion and an efficient pressure recovery are feasible.

Another possible manner of intensifying the turbulent interchange of kinetic energy is by superimposition of a rotation upon the translation of flow, which obviously stimulates the turbulent activity near boundaries. Mr. Andres and H. Peters[8] created rotation by placing vanes in an approach canal of diffusers and obtained an improvement of from 15% to 20%. These experiments revealed that rotation is very effective. However, for the production of rotation, special guide vanes are necessary, which are often uneconomical to construct and are the cause of increased friction losses.

Existing rotation in turbine outflow may be most effective for pressure recovery in concentric-type draft tubes. In elbow-type draft tubes the direction of the rotation is partly opposite to the secondary motion in the form of a double spiral, inherent to elbow flow, and some of the tangential energy will be destroyed. The flattening of the elbow section in a draft tube aids in suppressing the inducement of secondary motion.

(*b*) *Deflection of Kinetic Energy.*—In hydraulic practice, deflectors are frequently used to guide kinetic energy to the endangered zones so as to help avoid separation. A typical example is the splitter in the bend of an elbow-type draft tube.

An improvement, considering the flow separation in a rotation-free expansion, can be obtained by secondary motion, which appears in its most intensive form in bends. The losses in bends are attributed to local flow expansions at the concave wall near the entrance and at the convex wall near the outlet. The experiments by H. Nippert[9] on flow losses in bends revealed that the most efficient bends had the most intensively developed secondary motion.

(*c*) *Improved Velocity Distribution in Entrance Section.*—An effective method of improving the diffuser performance is to set a nozzle or contraction in front of the expansion or to shorten the approach canal as much as possible. The high boundary velocity thus achieved or preserved helps to delay the occurrence of separation.

A. Riffart improved the efficiency about 17% by placing a nozzle in front of a diffuser.[10] J. M. Robertson, M. ASCE, and Donald Ross obtained[11] an increase of efficiency of from 5% to 7% by reducing the length-to-diameter ratio of the preceding straight pipe to cone from 10 to 3.

---

[8] "Conversion of Energy in Cross-Sectional Divergences under Different Conditions of Inflow," by H. Peters, *Ingenieur-Archiv*, Vol. II, 1931, p. 92. (Translated in *Technical Memorandum No. 737*, National Advisory Committee for Aeronautics, Washington, D. C., 1934).

[9] "Über den Strömungsverlust in gekrummten Kanälen," by H. Nippert, *Forschungsarbeiten*, Verein Deutscher Ingenieure, No. 320, 1929.

[10] "Versuche mit Verdichtungsdüsen," by A. Riffart, *ibid.*, No. 257, 1922.

[11] "Effect of Entrance Conditions on Diffuser Flow," by J. M. Robertson and Donald Ross, *Transactions*, ASCE, Vol. 118, 1953, p. 1068.

EXPERIMENTAL WORK

During the experimental work reported on herein, the greatest emphasis was placed on qualitative research to acquire the fundamental knowledge of internal mechanics of the separation occurrence. The experiments were performed with the simplest instruments available in the war-destroyed laboratory at the Technical University of Karlsruhe, Germany, during the years 1946–1948.

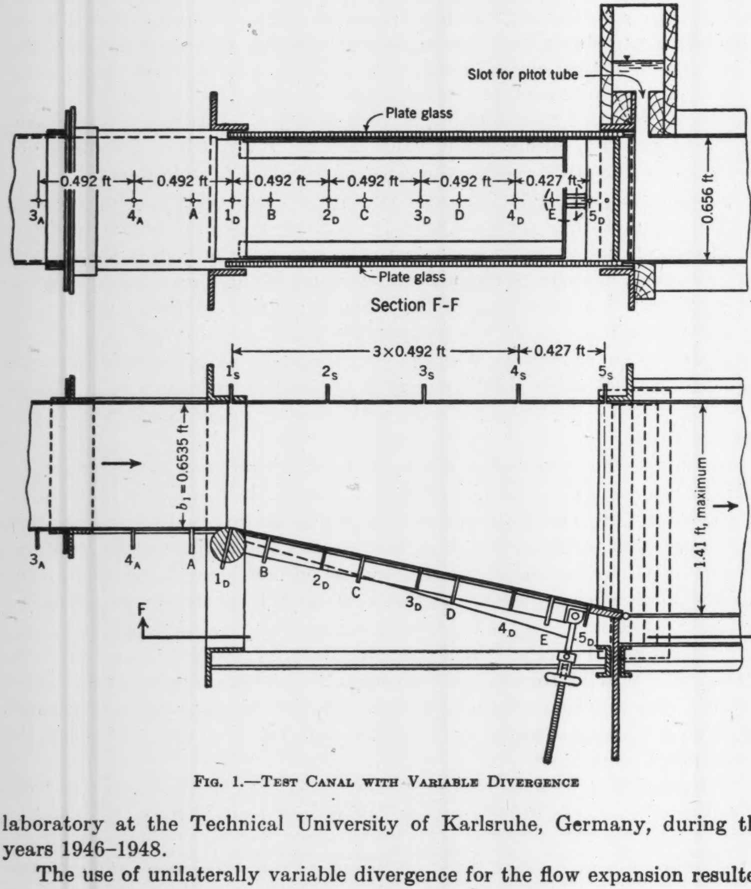
Slot for pitot tube
Plate glass
0.492 ft
0.492 ft
0.492 ft
0.492 ft
0.492 ft
0.427 ft
3A
4A
A
1D
B
2D
C
3D
D
4D
E
5D
0.656 ft
Plate glass
Section F-F
3×0.492 ft
0.427 ft
1S
2S
3S
4S
5S
b1=0.6535 ft
1.41 ft, maximum
3A
4A
A
1D
B
2D
C
3D
D
4D
E
5D
F
F

Fig. 1.—Test Canal with Variable Divergence

The use of unilaterally variable divergence for the flow expansion resulted in the following advantages:

1. The flow, especially after the onset of separation, was more stabilized, and it was possible to make more accurate measurements.

2. The measurements of static pressure could be accomplished conveniently at both walls, with pressure variation on the straight wall corresponding to pressure variation at the center line of a symmetrical expansion.

3. It was possible to investigate the improvement of pressure recovery in analogous transitions as in the horizontal leg of the elbow-type draft tube.

Test Facility.—The test canal (Fig. 1) consisted of a 29-ft-long straight approach canal of 0.654-ft by 0.656-ft cross section, a two-dimensional expansible test canal 2.85 ft long, and an outlet 4.5 ft long. The outlet canal had a movable wall which allowed for a maximum width of 1.41 ft. The bottom and the cover of the test canal were made of glass to enable visual observations. The angle of divergence could be increased from 0° to 20° by turning one sidewall on pivots. The transition curve had a radius of $\frac{15}{16}$ in.

The pressure variations along the walls were measured by fourteen wall piezometers: 1_A, 2_A, 3_A, and 4_A in the approach canal, 1_S, 2_S, 3_S, 4_S, and 5_S along the center line of the straight wall, and 1_D, 2_D, 3_D, 4_D, and 5_D along the diverging wall. The variations were recorded in glass tubes on a tube bank by verniers reading with an accuracy of 0.00033 ft (0.1 mm). To reduce measurement errors in fluctuating flow areas, as many as ten readings were made and the results were averaged. For visual observations, tubes of $\frac{1}{8}$-in. external diameter were inserted into the test canal through special guide tubes A, B, C, D, and E, and red aniline-dye solution was injected into the flowing water. The velocity was measured near the end of the expansion in the last piezometer section (5_S) by a differential vacuum pitot tube mounted on a cross-sliding carriage so that every filament of flow could be caught axially into the gaging tube.

The rate of flow was measured by use of a calibrated rectangular weir with a semicircular crest. The water for the experiments was supplied from a 1,400-cu-ft water tank with a constant surface level and was recirculated by a pump having a capacity of 2.8 cu ft per sec.

Velocity Distribution.—Using the pitot tube for velocity measurements does not give correct values in eddy-disturbed regions because of pulsations of flow and limited sensitivity; however, no other instruments were available at the time the tests were made.

The varying instantaneous velocity v can be divided into the temporal mean velocity $\bar{v}$ and the local velocity fluctuations v'. The relative fluctuation $v'/\bar{v}$ varies from a small value at the entrance to the expansion—where a turbulent uniform-flow pattern exists—to infinity at the separation point. It is clear that corrections of the pitot-tube indications are indispensable under such flow conditions. Unfortunately, coefficients for such corrections have not been established. R. Kröner[12] compared the rates of flow measured by a control weir and those evaluated from contour plans of velocities measured by pitot tube, and he found the latter to be from 5% to 10% higher.

The sensitivity of the pitot tube was limited by the least reading of the vernier—0.00033 ft—corresponding to a minimum measurable velocity of

---

[12] "Versuche über Strömungen in stark erweiterten Kanälen," by R. Kröner, *Forschungsarbeiten*, Verein Deutscher Ingenieure, No. 222, 1920.

0.14 ft per sec. As the gradient of the mean-velocity profile approached zero in the separation boundary, it was not possible to establish accurately the location of the separation points by using the pitot tube.

The pattern of variation of velocity profiles at divergences of 0°, 8°, 12°, 16°, and 20° in Fig. 2 is typical for flow expansion at different flow rates; in Fig. 2, V_1 is the mean velocity at the entrance, b_1 is the width of the entrance, and b is the width of the expanded section. The standard profile of uniform turbulent flow became more and more pointed with the increase of expansion. The reduction of velocity was strongest at the diverging wall where the separation occurred. The most important observation was that, after the occurrence of separation, the width of the forward flow remained almost constant. This maximum lateral extension of the forward flow represents the boundary of separation. Although the latter remained unchanged, the disturbances, as large-scale eddies intruded deeper into the forward flow, decelerated the adjacent flow filaments more and more. As a result, the maximum velocity and the velocity of flow in the opposite straight half of the conduit began to increase again. The curvature of the velocity profiles on the diverging side of the expansion became convex, exhibiting an inflection point characteristic of the separation profile.

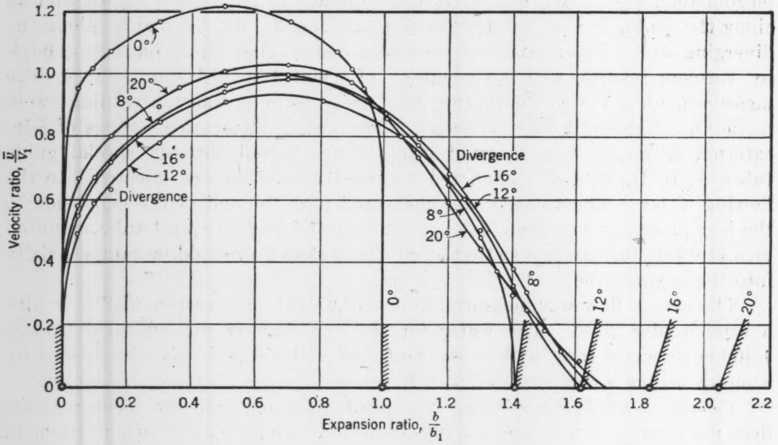

FIG. 2.—VELOCITY PROFILES

Pressure Variation.—Measurements of static pressure along the walls were made for rates of flow of 0.704 cu ft per sec, 1.407 cu ft per sec, and 2.110 cu ft per sec, corresponding to Reynolds numbers of 1×10^5, 2×10^5, and 3×10^5, respectively. The pressures were measured in reference to piezometer 2_A, 4.75 ft upstream from section 1. The pressure recovery itself was computed in reference to section 1, reduced by the friction loss established for the uniform flow.

The pressure variations are plotted in dimensionless form in Fig. 3 using the relationship:

$$\Delta \bar{p} = \frac{\Delta p}{\frac{V^2_1}{2\,g}} \qquad (1)$$

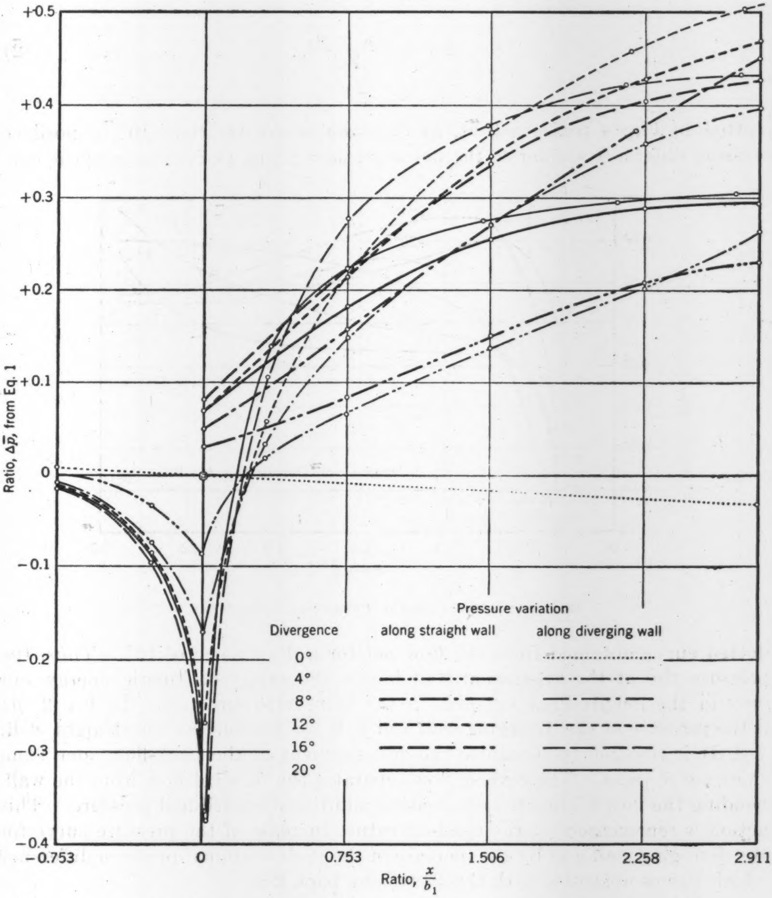

FIG. 3.—PRESSURE VARIATION ALONG THE WALLS

in which Δp is the pressure rise, measured from the beginning of the expansion and g is the gravitational acceleration. In Fig. 3, x is the horizontal distance from section 1.

The interpretation of the course of the conjugated curve pairs in Fig. 3, measured at the straight and at the diverging wall, permits the following conclusions to be drawn:

1. The pressure variations differ for each wall, especially at the entrance and outlet where the influence of the curvilinear transition flow predominates.
2. The cross-sectional pressure differences,

$$\Delta p' = \frac{p_D - p_s}{\dfrac{V^2_1}{2g}} \quad \ldots\ldots\ldots\ldots\ldots\ldots\ldots\ldots (2)$$

plotted in Fig. 4 indicate that, at divergences greater than 10°, a positive pressure difference similar to the potential flow exists, as demonstrated by the dotted curve obtained from the flow net for a divergence of 16°. Thus, the pressure rise at the separation wall blocks the suppy of kinetic energy not only in the longitudinal but also in the transverse direction. In Eq. 2, p_D is the pressure at the diverging wall and p_s is the pressure at the straight wall.

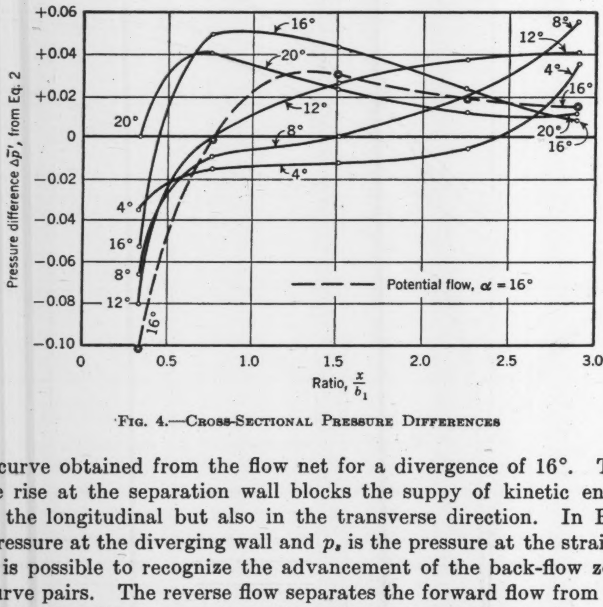

FIG. 4.—CROSS-SECTIONAL PRESSURE DIFFERENCES

3. It is possible to recognize the advancement of the back-flow zone from these curve pairs. The reverse flow separates the forward flow from the wall, bending the flow filaments and creating additional centrifugal pressure. This action is represented by the local-curvature increase of the pressure curve for the diverging wall and by the increase of the cross-sectional pressure difference which moves upstream with the advancing back flow.
4. The induced separation constricts the flow passage at the end of the canal. The flow filaments are straightened, and thus the cross-sectional pressure difference is reduced.

Furthermore, the variation of medium pressures were derived graphically for flows of 0.704 cu ft per sec, 1.407 cu ft per sec, and 2.110 cu ft per sec for

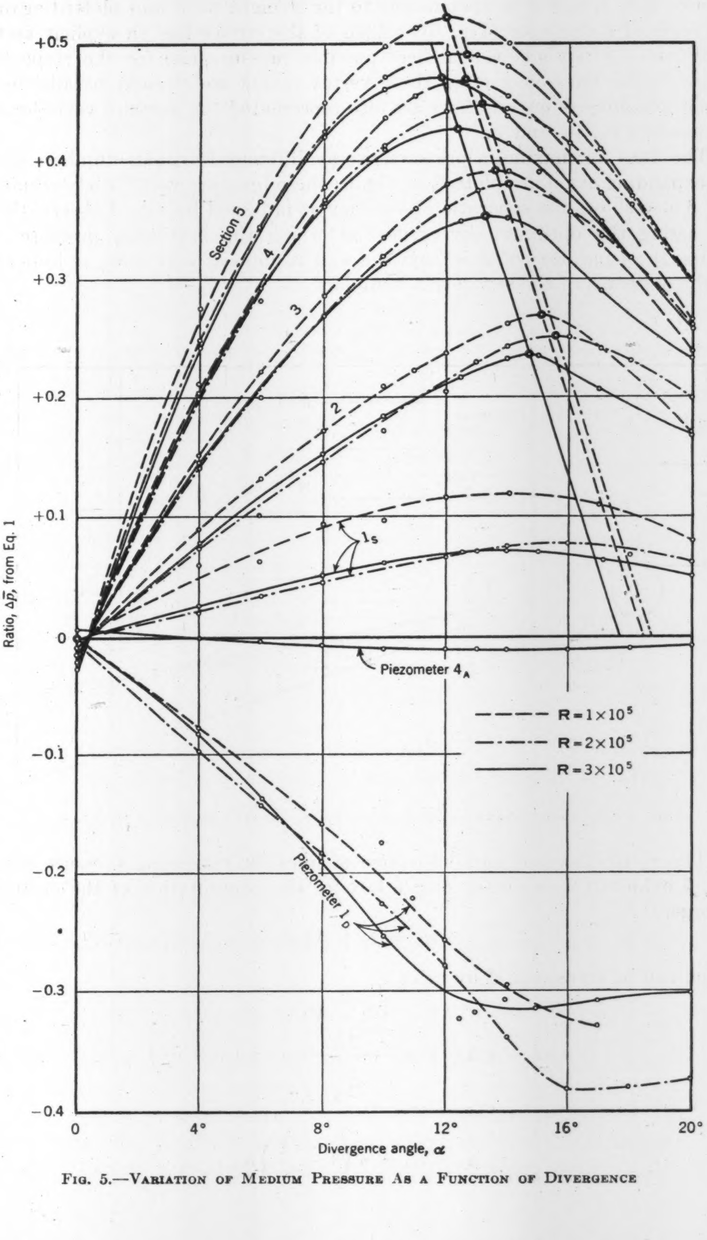

Fig. 5.—Variation of Medium Pressure As a Function of Divergence

sections 2, 3, 4, and 5 (perpendicular to the straight wall) and plotted against the angle of divergence (Fig. 5). Each of the curves has an explicit vertex point which represents the highest possible pressure rise for the respective section. The lines connecting these vertex points are straight parallel lines. In this assembly of curves there are also represented the pressure variations in piezometers 4_A, 1_B, and 1_S.

The lines for maximum pressure rise at different Reynolds numbers along the expanding canal are plotted in Fig. 6; these lines are very closely situated. Fig. 6 also shows the separation boundary as obtained by visual observations. Surpassing the optimum divergence, at which the maximum pressure rise occurs, the separation of flow from the wall is induced very soon, as indicated by the closeness of the separation boundary.

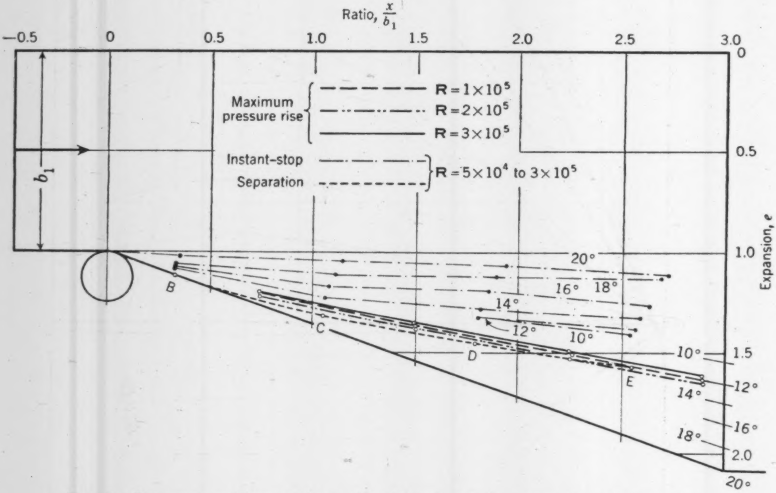

FIG. 6.—LOCATION OF INSTANT-STOP, BACK-FLOW, AND PRESSURE-RISE BOUNDARIES

The rectilinear and parallel course of lines for maximum pressure rise in Fig. 5 evidently indicates a simple law for the computation of the optimum divergence—

$$\alpha_0 = \alpha_1 + \Delta p\, \alpha_2 \qquad (3)$$

which can be transformed by using

$$\Delta p = \eta\, \Delta p_i = \eta \frac{\dfrac{V^2_1 - V^2}{2\,g}}{\dfrac{V^2_1}{2\,g}} = \eta \left(1 - \frac{1}{e^2}\right) \qquad (4)$$

to

$$\alpha_0 = \alpha_1 + \eta \left(1 - \frac{1}{e^2}\right) \alpha_2 \qquad (5)$$

In Eqs. 3 and 5, α_1 and α_2 are constant angles; Δp_i represents the dimensionless ideal pressure difference measured from the start of the expansion; η is the pressure efficiency; V is the mean velocity in the expanded section; and e represents the area ratio of the expanded section to the entrance section. The values of e and η for maximum pressure rise have been computed and are presented in Table 1.

TABLE 1.—EFFICIENCY FOR MAXIMUM PRESSURE RISE IN SECTIONS OF EXPANDED CANAL

Section	Distance, x, in feet	Optimum divergence, α_0, in degrees	Expanded width, b, in feet	Rate of expansion, $e = b/b_1$	Pressure rise, $\Delta \bar{p}$	EFFICIENCY	
						η	$\eta_{\text{aver.}}$
$Q = 0.705$ CU FT PER SEC, $\mathsf{R} = 1 \times 10^5$							
2	0.492	15.1	0.786	1.203	0.260	0.840	0.843
3	0.984	13.6	0.892	1.364	0.393	0.844	
4	1.476	12.6	0.984	1.505	0.469	0.840	
5	1.903	12.0	1.058	1.619	0.524	0.847	
$Q = 1.401$ CU FT PER SEC, $\mathsf{R} = 2 \times 10^5$							
2	0.492	15.6	0.791	1.210	0.254	0.788	0.785
3	0.984	14.2	0.899	1.376	0.381	0.802	
4	1.476	13.2	0.998	1.528	0.450	0.782	
5	1.903	12.6	1.081	1.653	0.492	0.769	
$Q = 2.110$ CU FT PER SEC, $\mathsf{R} = 3 \times 10^5$							
2	0.492	14.7	0.783	1.198	0.238	0.786	0.778
3	0.984	13.3	0.886	1.356	0.355	0.778	
4	1.476	12.4	0.978	1.497	0.432	0.780	
5	1.903	11.8	1.053	1.611	0.473	0.769	

As shown in Table 1, the efficiency for maximum pressure rise along the expanding canal for each **R**-value is almost constant. The deviations are not systematic, and therefore the use of the average efficiency for each **R** (that is, for each Q) is justified. Computing the angles α_1 and α_2, the equation for the maximum pressure rise (in the $\Delta\bar{p}$-coordinates and the α-coordinates) is

$$\alpha_0 = \alpha_1 - \eta \left(1 - \frac{1}{e^2}\right) 12.16° \ldots\ldots\ldots\ldots\ldots\ldots (6)$$

The value of α_2 is constant, but α_1 differs slightly for each **R**-value, as follows:

Value of **R**	Value of α_1	Value of η
1×10^5	18.3°	0.84
2×10^5	18.7°	0.79
3×10^5	17.6°	0.78

Eq. 6 makes it possible to compute the maximum divergence for the required rate of expansion; exceeding this maximum would not yield any rise of pressure, but rather a drop caused by increasing eddy losses.

The physical meaning for α_1 is the divergence for the rate of expansion, e, equal to one (that is, for the entrance section), at which the maximum pressure line meets the entrance section. As visual observations indicated, the separation point jumped to the entrance at a divergence of about 18°.

The other limit of divergence for e equal to infinity seems also to be a definite value determined by α_2 and η. Assuming that the efficiency of pressure recovery would not vary with the length of expansion, the maximum divergence for infinite expansion would be

$$\alpha_o = 17.6° - 0.78 \times 12.16° = 8.1°, \qquad \mathsf{R} = 1 \times 10^5 \ldots\ldots (7a)$$

$$\alpha_o = 18.7° - 0.79 \times 12.16° = 9.1°, \qquad \mathsf{R} = 2 \times 10^5 \ldots\ldots (7b)$$

and

$$\alpha_o = 18.4° - 0.84 \times 12.16° = 8.0°, \qquad \mathsf{R} = 3 \times 10^5 \ldots\ldots (7c)$$

Hunter Rouse, M. ASCE, has stated:[13]

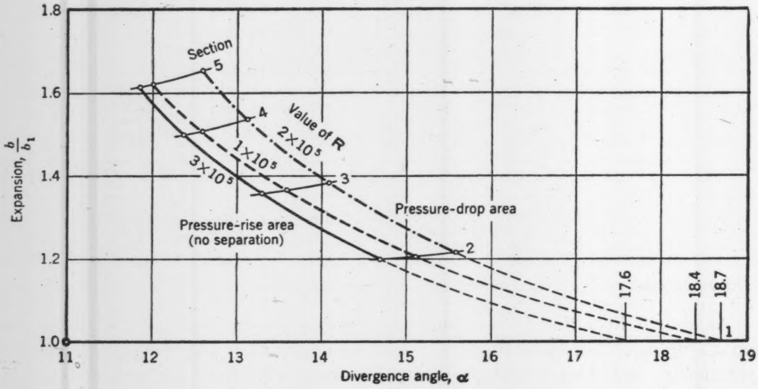

FIG. 7.—CURVES OF MAXIMUM PRESSURE RISE

> "In fact, when the deceleration is very gradual (i.e. for boundary inclinations less than perhaps 4°) the flow may be completely free from separation if the Reynolds number is sufficiently high (i.e. if the boundary layer is turbulent)."

The maximum divergences for infinite expansions, 8.1°, 9.1°, and 8°, computed by Eqs. 7, conform to this statement s the boundary inclinations of 4° in symmetric expansion correspond to the 8° unilateral expansion.

Using the data from Table 1, the curves for maximum pressure rise are plotted with the divergence and the expansion rate as coordinates in Fig. 7. Any expansion whose divergence angle and expansion rate are on the curve or in the area between curve and coordinates is separation-free. Furthermore, the results of pressure measurements for computing efficiency of pressure recovery were also used. In Fig. 8 there is presented the efficiency along the canal at **R** = 3×10^5. The efficiency of pressure recovery is maximum at the divergence of 8° and is essentially constant along the canal; it increases along the canal at smaller divergence and decreases at greater divergence. The manner in which pressure efficiencies vary with the divergence angle is illustrated for three different Reynolds numbers in Fig. 9. The maximum efficiency in a section occurs at a somewhat smaller divergence than the divergence that exhibits the highest pressure rise.

---

[13] "Engineering Hydraulics," by Hunter Rouse, John Wiley & Sons, Inc., New York, N. Y., 1951, p. 118.

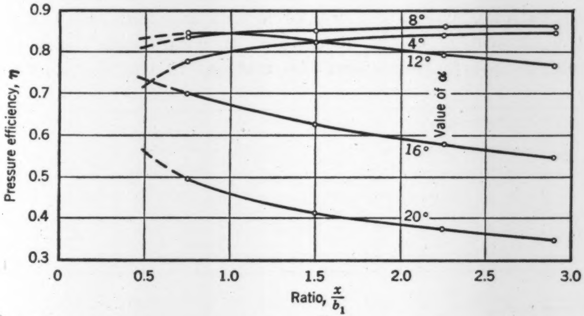

FIG. 8.—PRESSURE EFFICIENCY ALONG THE TEST CANAL WITH **R** EQUAL TO 3×10^5

The pressure efficiency, computed in the ordinary manner, is smaller than the true energy efficiency if the uneven velocity distribution is taken into account.

The true kinetic energy E_k in a flow section is

$$E_k = \int^A \frac{\gamma\, v^3}{2\, g}\, dA \ldots\ldots\ldots\ldots\ldots\ldots\ldots\ldots (8)$$

and the ratio C_e of the true kinetic energy to that based on the mean velocity is

$$C_e = \frac{1}{A}\int^A \left(\frac{v}{V}\right)^3 dA \ldots\ldots\ldots\ldots\ldots\ldots\ldots\ldots (9)$$

In Eq. 8, γ is the specific weight of the fluid and A is the section area.

For turbulent flow in a uniform conduit, C_e is close to unity; however, C_e exceeds unity in uneven velocity distributions such as in expanding flow. By graphical integration C_e-values have been computed from velocity contour plans at Q = 1.407 cu ft per sec (measured at cross section 5) to result in, for uniform flow, C_e = 1.13, and, for expanded flow with 12°30′, C_e = 1.51. With these ratios, the energy efficiency is 88%, which is appreciably higher than the pressure efficiency of 79%.

Some of this additional kinetic energy can be recovered as pressure in an outlet canal where the uneven velocity profile may resume the normal pattern of uniform flow. G. N. Patterson[14] has given the required length of duct following a cone, where the pressure continues to rise with two to six times the outlet diameter.

A practical application to recover such kinetic energy is used in well-designed draft tubes by contraction of the transition between the vertical and horizontal legs. As measurements indicate, such contraction does not only improve the velocity distribution but even yields a pressure rise instead of a drop as normally expected.

VISUAL STUDY

The observation of the movements of colored flow filaments has contributed much to the knowledge of the mechanics of separation. Such observation gives immediate information about the motions in the development of flow separation. In this study, the characteristic phases of separation were determined from flashlight photographs.

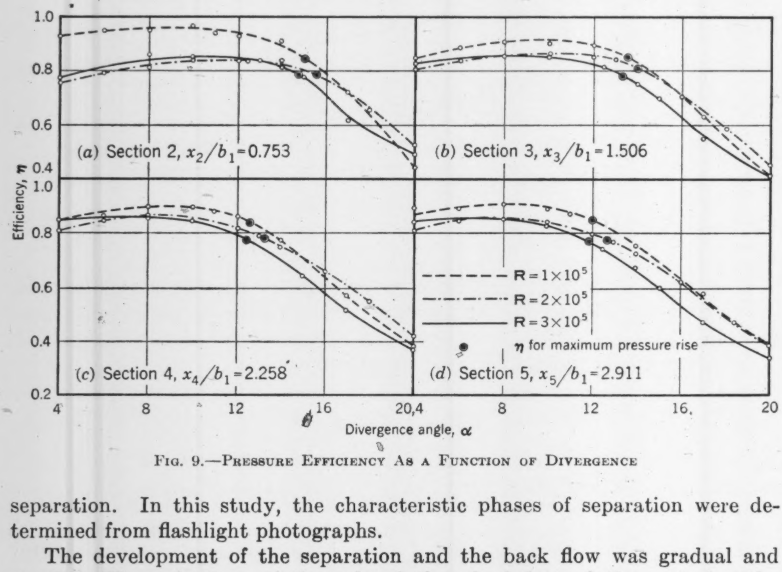

FIG. 9.—PRESSURE EFFICIENCY AS A FUNCTION OF DIVERGENCE

The development of the separation and the back flow was gradual and steady. The pulsations of the colored thread of dye solution entering the flow from tubes may be designated as "flickers" (change of velocity) and "flutters" (change of direction). The frequency of flickers decreased with increasing expansion, but the amplitudes of movements became higher and higher.

The first reliable marked phase of development of the flow to separation was an instantaneous stoppage of flow filaments with instantaneous velocity equal to zero. The interconnection line of all of these points along the expansion canal represents the "instant-stop boundary." The measurement of distances of instant-stop boundaries from the wall at different divergences made it possible to represent the intrusion of the disturbed region deeper into the forward flow.

---

[14] "Modern Diffuser Design," by G. N. Patterson, *Aircraft Engineering*, 1938, p. 267.

As the visual study revealed, the location of the instant-stop boundary is not affected appreciably by the rate of flow at the same angle of divergence. Fig. 6 shows the locations of instant-stop boundaries at increasing divergence from 10° to 20°.

The instant stops beyond the boundary turned into instant back-strokes whose duration and amplitude increased until a stage appeared, in which the colored filaments pendulated up and down, indicating that the temporal mean velocity $\bar{v}$ was equal to zero and thus the instantaneous velocity v was equal to local velocity fluctuations v'. This phase indicates the beginning of full separation and is designated as the "point of separation" on the wall and as "separation or back-flow boundary" between forward flow and back flow. It is of interest to note that the development phases appear in the same succession along the wall as in the cross section of a sufficiently expanded flow canal.

The separation from the wall began at the downstream section E with an expansion α equal to 12°30′ and moved upstream with increasing angle of divergence. The local minor separation behind the sharp-curved entrance transition did not extend itself with the increase of divergence. The flow always recontacted the wall downstream at a distance of approximately 1 in. from the end of the transition curve until the advancing back flow joined it abruptly when the divergence exceeded 18°.

No dependency of separation occurrence on the Reynolds number could be established by visual observations. The close invariability of the separation boundary, established by velocity measurements, was confirmed also by visual observations. The curves for occurrence of maximum pressure rise and the curve for separation are approximately parallel in their middle course because the maximum pressure rise takes place prior to the occurrence of separation. Further downstream, these curves intersect in front of the transition. Obviously, the occurrence of separation near the outlet is influenced by induced centrifugal pressure in the outlet transition while the pressure continues to rise because of the conversion of the uneven velocity profile to the normal one in the outlet canal.

The rate of expansion, e (Fig. 6) at which the separation occurs, is assumed to be a rational function of dimensionless distance x/b_1 from entrance section 1. The analytical equations for the occurrence of separation in the test canal are

$$e_{sep} = 1 + 0.3001\left(\frac{x}{b_1}\right) + 0.0493\left(\frac{x}{b_1}\right)^2 - 0.0776\left(\frac{x}{b_1}\right)^3 + 0.0176\left(\frac{x}{b_1}\right)^4 \quad ..(10)$$

and

$$\alpha_{sep} = \tan^{-1}\left[0.3001 + 0.0493\left(\frac{x}{b_1}\right) - 0.0776\left(\frac{x}{b_1}\right)^2 + 0.0176\left(\frac{x}{b_1}\right)^3\right] \quad ..(11)$$

Furthermore, the length and the duration of dye traces in the boundary layer after cutting off the inflow of dye solution were observed. The dye traces on the bright aluminum surface could be easily observed against the light. The adherent traces even floated laterally like flags in the wind and decreased from the upstream end toward the downstream end.

It was possible to record the length of dye traces up to 12 in. and duration up to 60 sec when the flow was slow with $\mathbf{R} = 5 \times 10^4$. The length and duration of dye traces were reduced by increasing the velocity as well as by increasing the divergence. No traces could be observed at the highest rate of flow ($Q = 2.11$ cu ft per sec).

Secondary Motion

The presence of a secondary motion was recognized by paths of air bubbles below the plate-glass cover and from flow-direction indicators on the bottom of the test canal. Both indicated that the flow direction near the cover and bottom had a greater angle to the straight wall than the angle of divergence.

In contour plans of velocity, the secondary motion caused inward pockets near the separation wall and outward pockets at the opposite wall. The course of the contour line for zero velocity displayed distinctly the accumulation of retarded flow particles in the center of the diverging wall.

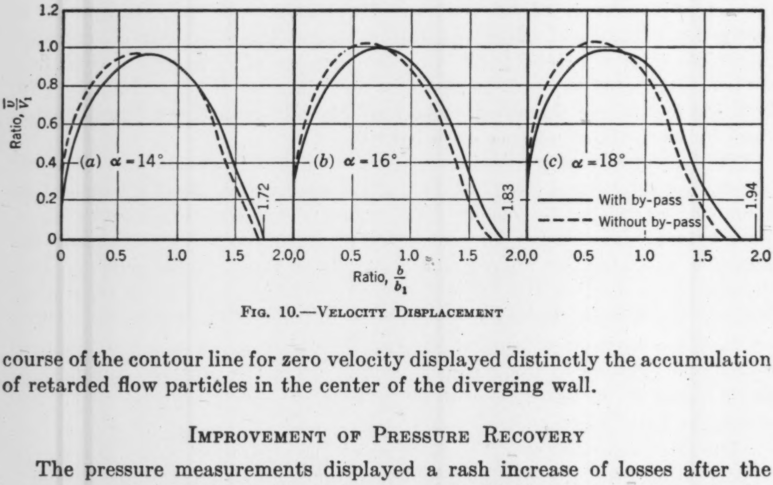

Fig. 10.—Velocity Displacement

Improvement of Pressure Recovery

The pressure measurements displayed a rash increase of losses after the occurrence of separation. Any reduction of the highly strained discontinuity zone between forward flow and back flow would be a very effectual method for the improvement of pressure conversion.

For that purpose three rows of openings were drilled into the diverging wall midway between piezometers 2_D and 3_D. Connecting these openings in the separation-endangered area with the approach canal by a bypass conduit, a flow in the direction of pressure drop was induced. This self-acting back flow drew off the retarded flow particles from the separation area and carried them into the approach canal.

At first, the entry into the approach canal was arranged on the shortest route in front of piezometer 1_D. The result was adverse because the entering fluid particles slowed down the boundary velocity and induced an early separation occurrence at a divergence about 3° smaller.

Connecting the bypass to the other side of the entrance section in front of piezometer 1_S, a marked improvement of pressure conversion was obtained. Figs. 10, 11, and 12 demonstrate the efficiency of the bypass manipulation. The curves are plotted from expansions with open and closed bypasses to obtain the comparative data of improvements as a result of the bypass action. Fig. 10 shows the displacements of velocity distribution at divergences of 14°, 16°, and 18°. Some of the kinetic energy of entering back-flow particles in the boundary layer was consumed by acceleration. As a result of the reduction of the velocity at the straight wall, the flow was deflected toward the separation area.

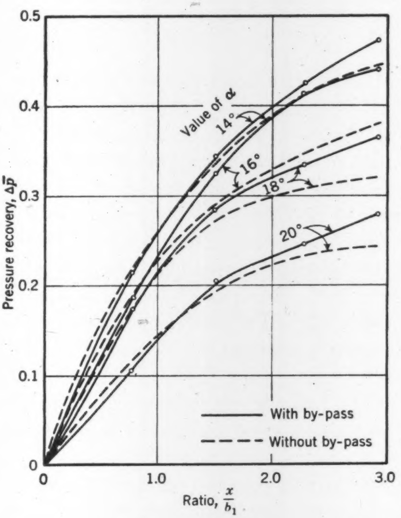

FIG. 11.—IMPROVEMENT OF PRESSURE RECOVERY

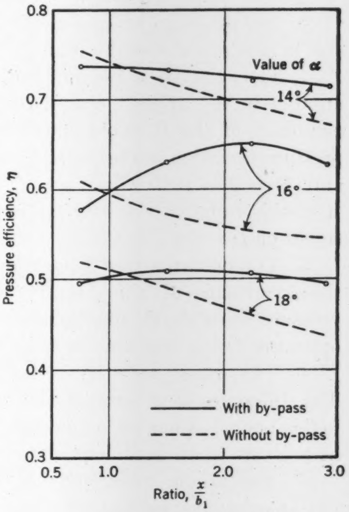

FIG. 12.—IMPROVEMENT OF PRESSURE EFFICIENCY

In Figs. 11 and 12 the pressure recovery and efficiency are plotted, respectively, as functions of x/b_1. The pressure recovery caused by the acceleration losses was reduced in the first part of the expansion in front of the draw-off openings. However, even the redistribution of kinetic energy downstream of the bypass not only effected a compensation of initial loss but even increased the pressure recovery considerably. The applied setup gave the best effect at a divergence of 16°, increasing the pressure recovery about 16% and the efficiency from 55% to 66%. The rate of draw-off was estimated by timing the passage of colored water through the bypass and was found to be only 5% of the total rate of flow.

CONCLUSIONS

The unilateral expansion created stabilized conditions for visual observations and measurements of the separation phenomena. The analysis of the test data allowed the following conclusions to be drawn:

1. The process of separation development is gradual and steady. The flow fluctuations at the diverging wall increase in amplitude but decrease in frequency.

2. It is possible to determine by visual observations two characteristic phases of separation: (*a*) The "instant-stop" boundary with instantaneous velocity equal to or greater than zero; and (*b*) the "separation or back-flow boundary" with temporal mean velocity equal to zero.

3. The same succession of phases of separation as along the wall exists also in sections across the flow.

4. The separation boundary did not vary with angle and with Reynolds number in the applied range; that itself is the principal condition for independency of the Reynolds number, yet the more accurate measurements of pressure variation in Fig. 5 displayed only a partial conformity for $\mathsf{R} = 2 \times 10^5$ and $\mathsf{R} = 3 \times 10^5$. Obviously, the boundary-layer pattern at the lowest Reynolds number was still laminar, as was revealed by observations of dye traces on the wall.

5. The occurrence of separation in any section is preceded very closely by the occurrence of a maximum pressure rise. For prediction of maximum pressure rise a simple quadratic relationship (Eq. 6) is established between the optimum divergence and the rate of expansion required.

6. The energy recovery is considerably higher than the pressure recovery. The difference is presumably highest at the fully developed separation profile before back flow begins. Some of this excessive kinetic energy can be recovered as pressure in an expedient outlet canal.

7. The minor separation, located behind the abrupt boundary change of entrance, could be avoided by flattening the transition curve. Any disturbance in that crucial section of entrance may decrease the boundary velocity and increase the expansion loss.

8. The pocket-like shape of the velocity contour lines near the separation wall revealed that the induced secondary motion is pushing the slackened flow particles toward the center of the wall and is capable of delaying the separation, at least in the corners of the conduit.

9. By connecting the separation-endangered area with a bypass conduit to the approach canal, it is possible to postpone the occurrence of separation and improve the pressure efficiency.

ACKNOWLEDGMENTS

This paper is based on a dissertation submitted in November, 1948, to the Technical University of Karlsruhe, in partial fulfilment of the requirements for the degree of Doctor of Engineering.

Paul Böss, director of the Institute of Hydraulics, provided advice and assistance during the investigation, and the Educational Fund of Estonians in Refuge made the financial contribution that enabled the construction of the test canal.

APPENDIX. NOTATION

The following symbols, adopted for use in this paper and for the guidance of discussers, conform essentially with "American Standard Letter Symbols for Hydraulics" (ASA Z10.2—1942) prepared by a committee of the American Standards Association with Society representation, and were approved by the Association in 1942:

A = area of the section of flow;

b = width of the expanded section;

b_1 = width of the entrance section;

C_e = coefficient of kinetic energy;

E = kinetic energy of flow in a section;

e = ratio of expansion = b/b_1;

e_{sep} = ratio of expansion at occurrence of separation;

g = gravitational acceleration;

p_D = pressure at diverging wall;

p_s = pressure at straight wall;

$\mathbf{R}$ = Reynolds number;

V = mean velocity in a section;

V_1 = mean velocity in entrance section;

v = instantaneous velocity = $\bar{v} + v'$;

  $\bar{v}$ = temporal mean velocity;

  v' = local velocity fluctuations;

x = distance in flow direction from section 1, parallel to the straight wall;

α_o = optimum divergence in degrees at which the maximum pressure rise in a section occurs;

α_1 = theoretical optimum divergence for the entrance section;

α_2 = a constant angle in degrees;

α_{sep} = angle of divergence for the occurrence of separation in a section;

γ = specific weight of the fluid;

Δp = pressure rise in expanding flow in reference to the entrance section:

$\Delta \bar{p}$ = dimensionless pressure rise in expanding flow $= \frac{\Delta p}{V^2_1/2\,g}$;

$\Delta \bar{p}'$ = dimensionless cross-sectional pressure difference $= \frac{p_D - p_s}{V^2_1/2\,g}$;

$\Delta \bar{p}_i$ = dimensionless ideal pressure rise in expanding flow $= \frac{V^2_1 - V^2}{V^2_1}$; and

η = pressure efficiency.

AMERICAN SOCIETY OF CIVIL ENGINEERS
Founded November 5, 1852
TRANSACTIONS

Paper No. 2788

HANDLING ATOMIC ENERGY INDUSTRY WASTES

BY JOSEPH A. LIEBERMAN[1] AND ARTHUR E. GORMAN,[2] M. ASCE

SYNOPSIS

The problems of waste treatment and disposal in the atomic energy industry are of unusual consequence. The health and welfare of people and the protection of natural resources may be involved to a much more serious extent than in the case of any other type of waste. The problems are augmented by the relative lack of current knowledge of adequate and economical methods and by the potentially rapid expansion of the industry.

INTRODUCTION

Industrial management in the United States has recognized that a liberal, farsighted policy in waste disposal and environmental sanitation has many advantages over the older "do-as-you-please" attitude that once was commonplace. Most industries that followed this policy now realize it was shortsighted, and those that continue to follow it are fast diminishing in number. Today there are such specialists as medical directors, industrial hygienists, sanitary engineers, chemical engineers, and biologists in industry conducting important research in waste disposal. These specialists hold important committee memberships in professional societies that are leading the way to a newer and mutually profitable relationship between industry and public agencies responsible for the health, safety, and welfare of the citizenry and the protection of natural resources. The purpose of this paper is to indicate some of the methods presently used in the handling and disposal of wastes in the atomic energy industry; it will also describe how waste disposal problems are being worked out both within and outside the industry and with the cooperation of public agencies, universities, and other industries.

NOTE.—Published, essentially as printed here, in March, 1954, as *Proceedings-Separate No. 422.* Positions and titles given are those in effect when the paper was approved for publication in *Transactions.*

[1] San. Engr., Div. of Eng., U. S. Atomic Energy Comm., Washington, D. C.

[2] San. Engr., Div. of Eng., U. S. Atomic Energy Comm., Washington, D. C.

Rapid Growth of the Atomic Energy Industry

The atomic energy industry with its unprecedented expansion program is, in fact, rather a late-comer in a well-integrated industrial, economic, and social community. This situation—in addition to the uniqueness of the industry's operations and its product, the lack of general knowledge of the industry's technology and terms, the secrecy which necessarily must be maintained, and the fact that, by an act of the Congress of the United States, the industry is under government control—places a more than ordinary responsibility on sponsors of the industry.

It is no simple task for a new industry to compress into a few years of research and development that which would normally take decades. The effort being made in the fields of waste disposal and environmental sanitation is to prevent, for this industry and the public, many of the difficulties which other industries have experienced and to do so without blocking progress while the industry is developing at an unprecedented rate.

Cooperation with Outside Agencies

The Atomic Energy Commission (AEC) has elected to evaluate and to solve its problems by enlisting the aid of experienced, well-established federal agencies that for many decades have been working on similar problems with other industries. In particular, these agencies are the Geological Survey (United States Department of the Interior) (USGS), the Weather Bureau (United States Department of Commerce), the Public Health Service (United States Department of Health, Education, and Welfare), the Corps of Engineers (United States Department of the Army), and the Bureau of Mines (United States Department of Commerce). Specialists from these groups are working on particular problems and in many areas. They are being indoctrinated in the various facets of the atomic energy industry. In turn, the staff of the AEC and its contractors are benefiting by the advice, experience, and continuing interest of these agencies. Much of the work is done under contract with the AEC. In some cases, however, the cooperating agencies have assigned engineers and scientists for service with the AEC or its contractors without reimbursement.

Research and development contracts in sanitary engineering have been made with a number of universities, private research institutions, and national laboratories serving the industry. The universities now working on such contracts include California (Berkeley), Harvard (Cambridge, Mass.), Illinois (Urbana), Johns Hopkins (Baltimore, Md.), New York (New York), Texas (Austin), the Massachusetts Institute of Technology (Cambridge), and Northwestern (Evanston).

The AEC follows the practice of conferring with those state officials who have the responsibility of preventing pollution of the atmosphere, ground waters, and surface waters in the disposal of wastes from industry. In several areas the commission participates through its staff and its contractors in advisory committees on which are represented federal, state, and local agencies. Usually the members of the committees are invited to visit the AEC production or research areas where they are informed of processes and waste disposal methods and are asked to submit criticisms and suggestions. Such advisory committees exist in relation to activities at the Hanford works (Washington), the Savannah River Plant (South Carolina), at the Knolls Atomic Power Laboratory near Schenectady, N. Y., and for the National Reactor Testing Station in Idaho. Visits to the Argonne National Laboratory (Illinois), Oak Ridge National Laboratory (Tennessee), and Brookhaven National Laboratory (New York) have been made by representatives of the Illinois, Tennessee, and New York state departments of health, respectively. The Ohio River Valley Water Sanitation Commission (ORVWSC) has been given information concerning nine major AEC projects in that valley. This information was supplemented by a visit to five of these plants by three security-cleared representatives of the ORVWSC.

DISPOSAL OF WASTES

Low-Level Wastes.—By far the largest volume of wastes from the atomic energy industry is low in radioactivity and toxicity. It is the practice to hold and monitor liquid wastes of this sort before they are released to the ground, to waterways, or to public sewers in order to be certain that their levels of activity are within prescribed limits of safety. Wastes that are produced in large volumes and whose levels of activity exceed safe limits present a real problem both in treatment and cost. Typical of such wastes are effluents from laundries handling garments contaminated by radioactivity, drainage from laboratory sinks in research areas where radioactive materials are used, wash water from decontamination processes, and water used in basins to shield operators from radioactive materials being stored or worked on.

Until more complete knowledge of the long-term effects of the release of atomic wastes is gained, a conservative policy has been adopted as to the degree of decontamination required. The principal methods now used in treating high-level wastes are evaporation and ion exchange. In the interest of economy, research is under way to find better and less expensive treatment systems than these for large volumes of low-level wastes. Such research has led, for example, to the design and construction of a modified trickling-filter sewage treatment plant at the National Reactor Testing Station. This plant handles both domestic sewage and radioactively contaminated laundry wastes. Work is also being done to evaluate the subsequent dilution factors in nature that may be used and thus reduce the degree of treatment required. Other industries use these dilution factors, and the indices for evaluating them in relation to many industrial wastes are reasonably understood by public officials who are responsible for protecting public health and national resources. Generally, less is known of dealing with radioactive wastes although, as research proceeds, some of the needed parameters are being established and recognized. The possibility of using biologic methods such as those used by sanitary engineers in treating domestic sewage and industrial wastes is being studied at several universities under AEC contract. At New York University the feasibility of using the trickling-filter process for decontaminating laundry wastes at the Knolls Atomic Power Laboratory is being investigated; the activated sludge process as a means of removing radioactivity from waste streams is under study at the University of California; the effect of radioactivity on anaerobic digestion of sewage sludges is the subject of research at the University of Illinois; at the University of Texas, studies are under way to determine the extent to which algae in streams or ponds could be used to take up radioactivity in low-level wastes.

The long half-life of certain radioactive materials makes it essential that the effect and probable ultimate fate of wastes from this industry be carefully appraised before they are released in any significant quantities into the ground, the air, surface waterways, or the sea. The importance of this time factor constitutes a significant difference between atomic energy wastes and these of most other industries. Chemical, biological, and bacterial contaminants, when released, are subject to substantial changes in nature, usually in hours or days, depending on the environment to which they are exposed. Ordinarily, with time these contaminants become progressively less obnoxious or hazardous, depending on their origin. By contrast, a radioactive waste will emit radioactivity for a definite period. In the case of long-lived elements, the prolonged period of hazard from radioactivity places a responsibility which cannot be dealt with lightly on one who disposes of such wastes.

The capacity of many inert materials and living things in nature to acquire and hold radioactivity is one of the most important factors in evaluating the capacity and limitation of various methods of disposal of low-level liquid wastes. The phenomenon is exceedingly important and needs to be more completely understood. Disposal on or into the ground through surface leaching pits, lagoons, cribs, or reverse wells must to a considerable degree be governed by the capacity of the upper soils to take up radioactivity prior to passage of the liquids downward to the water table.

The USGS is obtaining soil samples from all major AEC areas of operation and at many other places in the United States for purposes of classifying these soils as to their decontaminating properties and limitations. Further studies are being conducted at Yale University (New Haven, Conn.) and various AEC national laboratories. The objective is to learn more about these materials—particularly their physical structure and properties which may account for the ability to remove and perhaps fix radioactivity from water and waste streams. Resolving this problem will require much teamwork on the part of geologists, mineralogists, physical chemists, and nuclear physicists and chemists. When this phenomenon and its limitations are understood, the method can probably be applied to many water decontamination and waste disposal problems.

The direction and rate of movement of ground waters toward sources of downstream water supply must be carefully considered. The percentage of dilution of a contaminant released from a point source of discharge is governed by the characteristics of ground-water flow. Where this flow is laminar, as is usually the case in ground-water flow, the dilution may not be great. The contaminant may move in a ribbon-like manner expanding only little as it migrates. This fact must be considered when monitoring wells are used in evaluating the effectiveness of a waste disposal procedure. Failure to obtain evidence of contamination is no assurance that it does not exist or that the method of disposal followed has been effective. In the absence of correct information as to the geology of the area and the characteristics of the subsoils in retaining radioactivity, negative results could be misleading.

An important consideration when radioactive liquid wastes are discharged to surface waters is the ability of suspended matter and organisms in the water and at the stream bed to absorb radioactivity. Often when the contaminant is radioactive, the orthodox methods of stream surveying to evaluate the effects of organic pollution may not be adequate. In such a case the B.O.D. of the stream is of much less importance than the sediment loading, the characteristics of the sediment, and the conditions under which it is deposited and resuspended. Knowledge as to the sediments transported by a stream, its cross section, velocity, and physical flow characteristics is particularly important in an evaluation of the dilution or concentration factors of a stream or river.

High-Level Wastes.—The volume of wastes from atomic energy operations which are high in radioactivity are relatively small in comparison with low-level wastes. From the standpoint of total quantity of radioactivity, the major problem in treatment and disposal of radioactive wastes is associated with the chemical processing of spent fuel from a nuclear reactor in order to recover the unburned fuel. In most of the existing reactors there are solid fuel elements and fission of the uranium 235 results in retention of the fission products within the solid element. These fission products, which constitute the waste problem, are usually solids that go into solution when the whole element is dissolved for recovery purposes. The fuel elements are ordinarily cooled prior to dissolution to allow the short-lived activity to decay, thereby reducing the total quantity of radioactivity to be contended with in the recovery process. In the fuel element discharged from the reactor, the mass concentration of fission products will vary from 100 ppm to 1,000 ppm. During fuel-recovery processing, the fission-product concentration is reduced by dilution with water, and other solvents and solids.

Such wastes may be processed and stored under conditions having some parallel in other industries; however, the methods and facilities used, when applicable, require numerous extraordinary precautions and the use of special materials—all of which add substantially to the cost. Obviously, the value of the product as well as its hazardous properties have a direct relationship to the investment that can be made in a facility to store, treat, and dispose of a radioactive waste or a toxic waste. Regardless of value, however, the cost of treatment to render the waste harmless is properly a charge against the industry and must eventually be reflected in the cost of the product. Obviously, the solution of the cost problem lies in research and development—not in "cutting corners" and in exposing the industry to criticism and the citizenry to hazards. In some industries, as a result of research, profits have been realized from waste products, but this is the exception rather than the rule. A capricious attitude by industry in the disposal of long-lived radioactive wastes could seriously affect the national resources.

METHODS OF WASTE TREATMENT

Storage in Tanks.—At production plants, high-level and long-lived radioactive wastes have been and are being stored in underground tanks at costs ranging from 30¢ per gal to more than $2.00 per gal. Some of these wastes have a reclamation value, and research is being conducted to determine the feasibility of recovering important products contained in them. In the meantime, high-level wastes are being stored in tanks built of materials that will resist forces of corrosion from both within and without. It is expected that they will remain tightly sealed for many decades. Provision is made for monitoring so that the first evidence of leakage will be detected. The hazard of minute leaks could be minimized by intelligent preventive measures. If, however, the first leak were merely a portent of a generally defective condition of the container, a serious situation might follow. That is why great care is taken in selecting the location of a waste storage facility; why the geology of the area is carefully studied in advance of construction and thereafter; and why the downstream potentialities for affecting ground water are carefully appraised against the contingency of a slow leak or a serious accident that might conceivably release large volumes of waste to substrata.

So long as long-lived radioactive materials are stored underground—possibly for generations—there will be need for supervision over these wastes. Policies, procedures, and products may change, but these waste products cannot be forgotten or neglected.

Evaporation.—With high-level wastes containing more than 10^{-5} curies per liter and less than 10% solids, evaporation is effective in reducing the volume of "hot" material to be handled and in decontaminating the water which may be discharged to nature or recycled as process water. When the concentrate is stored as a liquid, the evaporation is carried to approximately 30% solids. At one installation, the concentration is carried to 50% solids or more. This concentrate will solidify when cooled in a suitable container. It is a relatively expensive process, however, with costs in the neighborhood of from 4¢ per gal to 8¢ per gal. The cutoff point at which some other less expensive process should be used must be selected with care. The high level of radioactivity in the residues of evaporators necessitates storage in containers that are shielded until sufficient decay takes place to permit safe handling for ultimate disposal. Using evaporation, the radioactivity in the water being discharged can be reduced by a factor of from 10^3 to 10^7 (decontamination factor of from 3 to 7) compared to the radioactivity of the feed.

Ion Exchange.—The use of ion-exchange materials is another means of decontaminating wastes of various levels of activity. It has limitations and presents the problem of ultimate disposal of the spent material. One of these limitations is that it is not very effective where dissolved solids in the waste stream exceed 500 ppm. Depending on the characteristic of the contamination and salt content, decontamination factors of from 1 to 4 are possible.

At some installations, ion exchange is used to decontaminate canal water (water used for shielding in fuel-element storage pits).

Co-Precipitation.—Co-precipitation processes in multiple cyles using coagulants are still a third method of decontamination. Usually the sludges that are formed are given further treatment and are partly dewatered for storage pending ultimate disposals. In wastes having less than 10^{-4} curies per liter or 10^{-5} curies per liter and more than 0.1% salt content, a coagulation-settling-filtration process quite similar to that used in a standard water treatment plant is probably more economical than evaporation or ion exchange. Decontamination factors of from 1 to 4 are possible. Because volume reductions depend on floc volume and not on the salt content of the waste, fairly substantial reductions are possible and may be as great as 500.

Crystallization.—Another waste treatment process that has been studied is crystallization. The process applies primarily to wastes having high salt concentration, when reuse of the salts is desirable. Series treatment may give decontamination factors up to 6 (10^6-fold reduction in radioactivity concentration). This method appears to be rather expensive and has not yet been applied on a production basis.

Ultimate Disposal of Radioactive Wastes

The ultimate disposal of radioactive wastes presents one of the more vexing problems of the industry. By ultimate disposal is generally meant the return to nature, and, more specifically, either land burial (or discharge into the ground) or sea disposal.

Land Burial.—Some of the aspects of discharge of radioactivity to the ground have been discussed previously. The writers believe that this method is being used successfully for certain wastes at several remote AEC installations. It is apparent that more knowledge of the fundamental factors involved—ion exchange, adsorption, and absorption—is required before much more extensive use is made of this method.

A burial ground near creviced or cavernous limestone, over a fault, or in gravelly soils through which seepage water would travel rapidly is obviously not satisfactory. The soil should preferably contain material that has the property of absorbing radioactivity. The capacity and limitations of the soil in this regard should be thoroughly evaluated, particularly with reference to the type of radioactive wastes to be released. Records should be kept as to the nature, location and activity, and prior shielding of all buried material. It is important that the depth of burial be planned so that cover will provide adequate shielding at the surface. Properly established burial grounds are restricted areas and are adequately fenced against unauthorized access for the lifetime of the radioactivity.

Consideration is being given to the policy and economic aspects of establishing designated burial grounds to serve several AEC areas. The selection and layout of the burial ground should be well planned with reference to its operation. The operation itself must be carefully supervised and monitored to prevent deleterious environmental effects.

Of specific interest with respect to ultimate disposal is the work being done at Brookhaven National Laboratory on the fixation of radioactive material on montmorillonite clay. Workers there have found that the exchange reaction between the clay and the radioactive ions can be made irreversible by heating the clay to about 800°C after it has taken up the radioactivity. Then the "hot" clay is buried in a naturally occurring bed of similar material. Because the clay itself is an end product of rock weathering, it is hoped that the radioactivity can be immobilized over periods approaching geologic time. The system's feasibility has been demonstrated on a bench scale, and a pilot plant for studying engineering and economics of the system is now being operated.

Sea Disposal.—To date, along the Atlantic and Pacific coasts, there has been occasional disposal of rather small quantities of radioactive wastes into the sea. This practice has been limited to materials that constituted special problems of burial on land, and the wastes have been dumped into deep water off the continental shelf. Usually the radioactive material is surrounded by cement and the shielded mass is contained in steel drums. Although ocean disposal has certain advantages, this method used in general practice in the ultimate disposal of high-level wastes needs a thorough evaluation before adoption. Recently a contract was negotiated with Johns Hopkins University to make such an evaluation, and the survey phase of the work has been completed. Oceanographers, geographers, biologists, and geologists with whom this problem has been discussed have presented some important questions that require much study. There is a feeling that, considering the limited current knowledge of the seas and their behavior and their potentialities as sources of food and minerals to serve future generations, the seeming advantages of sea disposal of long-lived radioactive wastes may be outweighed by its disadvantages. Another important fact is that once material is dumped into the sea essentially all control over it is relinquished.

SOLID WASTE DISPOSAL

Incineration.—Solid wastes may also be buried or disposed of at sea, but because of the bulk of certain combustible materials which have become radioactive, reduction of volume by incineration has been tried. Usually such materials include papers used as wipes or table covering in laboratories, contaminated clothing, carcasses of experimental animals, and materials for covering benches, floors, walls, sidings, and roofs. Studies at the Johns Hopkins University where wastes from use of radioactive isotopes were disposed of by burning in an ordinary institutional incinerator revealed that as much as 85% of the activity for certain isotopes such as P_{32} and Sr_{90} may be recovered in the ashes. Therefore, these ashes must be handled with care.

In order to assure complete protection of the environment, the bases of combustion should be decontaminated to a low level of radioactivity. This decontamination requires costly air cleaning facilities, including terminal filters of high efficiency. Experience with incinerators at the Argonne and Knolls national laboratories and at the Los Alamos Scientific Laboratory (New Mexico) has shown that the efficiency and operating cost of such units are items requiring much consideration. Present costs range up to 50¢ per lb of material burned. The Bureau of Mines, through its Combustion Research Laboratory at Pittsburgh, Pa., has made exhaustive studies of the problems involved in incineration of radioactive wastes. Its staff is developing an incinerator that shows much promise. This unit will be useful for general service at AEC production and research areas and at institutions using isotopes. It incorporates the use of tangential overfire air and also the use of molten caustic soda (solid at room temperature) as an ash fluxing system.

GASEOUS WASTES

When gaseous effluents are released to the air through high or low stacks, a sustained effort must be made to evaluate the atmospheric dilution that may be expected. The factor of dilution may vary widely during any day and seasonally, depending on the area. A careful study of the meteorology of the specific area and the region may present a pattern of conditions on the basis of which operations involving gaseous contaminants may be directed and controlled. With such data available the required degree of decontamination may be established within reasonable limits. Meteorological data are important in arriving at decisions as to the location and height of stacks, the location of the air intake with relation to the exhaust system, the spacing between buildings, and even the shape and configuration of buildings. Such data are also of great importance in the design of heating and ventilation systems, in cooling covers, in planning the sequence of construction work, in the storage of materials, in performance limitations due to weather conditions, and in evaluating work hazards that might be caused by unfavorable weather or extremes of weather.

Air cleaning within the atomic energy industry has received much attention and has progressed remarkably. Smokeless stacks used to release radioactive gases to elevations that will provide effective diffusion are common. From air-cooled reactors, large volumes of irradiated air may be discharged to the atmosphere. The hotter the temperature of the gaseous effluents, the greater will be their lifting power and subsequent dilution in the atmosphere.

As in the case of the USGS, the AEC has contracted with the Weather Bureau for assistance in evaluating the meteorological aspects of problems related to the release of gaseous effluents from its plants. In certain areas the prime contractor has elected to supplement this service and has staff meteorologists studying local problems. This is the case at the Savannah River Works, the Hanford Works, and at the Argonne National Laboratory. By having available data as to meteorological characteristics over an area, much can be done to lessen the cost of air cleaning facilities. For example, if a process that results in a highly contaminated effluent can be put into operation where natural atmospheric dilution factors are at maximum effectiveness, the degree of decontamination required may be relatively low in comparison with a process that must be in continuous operation. Periods of low wind velocities and prolonged inversion are critical, and, if they can be forecast and operations adjusted accordingly, much can be saved in the cost of air cleaning equipment.

Experience has shown that in processes requiring a high degree of air cleaning using such facilities as the Chemical Warfare Service or AEC filters it is correct practice to clean the incoming air and thus lessen the particulate load on the process air which later is to be decontaminated. In effluent cleaning, by filtration, roughing filters are a good investment in prolonging the service life of the more costly high efficiency units. An air filter has been commercially developed for use in the industry which has a collection efficiency of 99.95% with a test aerosol (di-octylphthalate) of $0.3\ \mu$ in diameter. One type using an asbestos and kraft paper filter is usable for air temperatures of 275°F or less. The cost of these units is about 5¢ per cu ft per min of capacity.

A newer one in which glass fibers are used has the same performance efficiencies and can treat gases at temperatures ranging from 550°F to 700°F.

Dust loading in the atmosphere is an important consideration in the selection of plant location and air cleaning equipment. Construction of roads and excavation for structures may disturb otherwise relatively stable soils, and care should be taken to minimize such disturbances. Data as to particle size both in the raw air and the process effluent are essential to the selection of efficient and economical air cleaning facilities. In the case of radioactive contamination, information as to distribution of particle sizes, mass, and activity is extremely important. In dealing with radioactive materials considerably more attention than that required in most industries must be given to small size particles even in the submicron range.

The behavior of contaminants of small size in the air, in air cleaning processes, and in the human body are not too clearly understood. This is the reason the AEC, on recommendation of its Stack Gas Working Group, sponsored the publication of a handbook.[3] This handbook includes selected reports on research conducted during World War II for the Office of Scientific Research, which were declassified especially for this handbook. A research contract on the behavior of aerosols has been in progress at the University of Illinois for nearly three years and has attracted much attention among research workers in air cleaning.

There is need of better and more uniform air sampling techniques and sampling paper to serve the industry. A research and development organization is working on the development of standards for filter papers to resolve this problem. A standard set of four or five filter papers to cover all sampling requirements appears likely.

The investment in air cleaning facilities at AEC plants is substantial. Early experience demonstrated that standard equipment was often not adequate to remove enough contaminated material to meet the strict standards that had been set up. To evaluate this situation and to assist those serving the industry to have more specific criteria on which to base specifications for air cleaning facilities, the School of Public Health of Harvard University, under AEC contract, has established an air cleaning laboratory in which valuable research and testing work has been conducted during the past three years. The staff of this laboratory has visited most AEC production and research areas and have made recommendations for improvements in air cleaning. In order that the results of their research may be made available to all concerned in air cleaning within the industry, the Harvard group has conducted two well-attended seminars on air cleaning and has prepared a handbook for general distribution.[4]

CONCLUSION

In conclusion, emphasis should be placed on the uniqueness of the environmental problems of the atomic energy industry, especially in so far as treatment and disposal of radioactive wastes are concerned. These problems require and are receiving special consideration. They provide the basis for much research sponsored by the AEC, its contractors, and national laboratories, by private research institutions, and by federal agencies. An organized effort is being made to cooperate with public officials interested in and concerned with these problems and to assist them in attaining a better understanding of the industry's policies, technology, and terms. It is confidently believed that this is an intelligent approach and that, as the uses of nuclear energy by private competitive industry expands, the newer problems which will surely arise can be solved with minimum risk to the population and to the nation's resources.

---

[3] "Handbook on Aerosols," U. S. Govt. Printing Office, Washington, D. C., 1950.

[4] "Handbook on Air Cleaning," U. S. Govt. Printing Office, Washington, D. C., 1952.

AMERICAN SOCIETY OF CIVIL ENGINEERS
Founded November 5, 1852
TRANSACTIONS

Paper No. 2789

DEVELOPMENT OF AN INTERNATIONAL AIRPORT

By Earle M. Rader,[1] M. ASCE

Synopsis

Although the solutions of the specific problems encountered at one international airport cannot be applied to another airport, there are presented herein some general rules and criteria for the development of a master plan. It is essential that the function of the airport be examined in relation to travel and the community. Furthermore, realistic appraisals must be made of future travel—including generated traffic. The terminal, which is the hub of the airport, must be planned to provide the traveler with all conveniences and services because it is the traveler that supports and maintains the airport; were it not for him, the entire project would vanish.

Introduction

It should be realized that (1) the same problems will not be encountered at every airport and (2) each airport cannot be developed by a predetermined pattern equally applicable in all situations. The development of an airport, like all other engineering projects, involves problems peculiar to that airport; the solution of these problems cannot necessarily be applied to all other airports. Nevertheless, wider knowledge of these problems, together with their solutions, will foster the acceptance of a design procedure flexible enough to permit the development of an airport in systematic increments. This development in increments is necessary to achieve economically the fundamental purposes of the development program and to maintain the proper interrelationship between the airport and surrounding community.

Functions of the Project

The first step in the analysis of a particular airport-development program might be the determination of the scope of the functions to be performed by the completed project. That is, one must determine the types of airfield activi-

---

Note.—Published, essentially as printed here, in February, 1954, as *Proceedings-Separate No. 406*. Positions and titles given are those in effect when the paper was approved for publication in *Transactions*.

[1] Senior Partner, Rader Eng. Co., Miami, Fla.

ties that are anticipated and the extent to which satellite functions are to be developed that will either complement the airfield activities or that will be auxiliary revenue producers which help finance the development.

The ensuing observations concern the problems encountered in the development of a large international airport. It is realized that there are engineering problems associated with smaller airports that may not appear in this category. However, these problems compose, to a large extent, a subject unto itself and should be examined separately.

It is no longer feasible to design an all-purpose airport where high-density air traffic is anticipated. Such a project would, of necessity, penalize and discourage all phases of aeronautical activity and could not adequately provide for the heterogeneous traffic encountered. It is therefore apparent that, before the actual design of an international airport can be begun, it is necessary to make comprehensive studies of the air-transportation market and to estimate the potential air traffic that can normally be expected. These studies are necessary for the determination of the size and complexity of the installation. The air-traffic studies should include forecasts sufficiently far into the future to determine air-installation criteria that will not become inadequate or obsolete during the life of the development bond issue. Cognizance not only of the air-transportation market but also of the trends in other forms of public transportation will be a prerequisite to the air-traffic study. Air-traffic forecasts have indicated, without exception, far less than the actual volume of air traffic subsequently encountered. Although many factors undoubtedly contributed to this unanticipated accelerated growth of air transportation, it is apparent that engineers have failed to realize fully the impact that dependable and economical air transportation has on the traveling public. The airlines generated a transportation market where none existed before, as did the railroads in their early days; the reduction in travel time made many trips feasible that would not previously have been considered. A comprehensive air-traffic study must also include a consideration of the "short-haul" passenger; unless adequate allowances are made for this type of passenger, the development and acceptance of helicopter service will generate an unexpected volume of air passengers for whom no facilities have been provided at large airports.

PLANNING THE AIRPORT

The number of air passengers and the volume of air cargo alone will not be sufficient data for planning a large airport. Advancement in aircraft design must be examined because, as the capacities of aircraft increase, there will be a corresponding decrease in plane movements for a given number of passengers. As the air-transportation market grows, there will be a crowding of schedules between large communities that can only be offset with larger aircraft. Commercial air transports are presently (1955) capable of carrying approximately 90 passengers, and it is not improbable that large aircraft will have capacities of 120 passengers or more in 1965. In addition to these larger aircraft, there are indications that the passenger-load factor will become substantially higher than has been accepted as normal. For these reasons the total number of plane movements at a given airport will not be as great as the passenger traffic may indicate, using accepted aircraft criteria. These larger aircraft will, however, require airfield facilities far superior in size and capacity to those in general use, and, in order to avoid allocating money for facilities that will not be required for some years, prudent airfield design will dictate that new facilities be constructed from plans easily susceptible to future expansion and alterations that will meet changing operational requirements.

In the attempt to correlate the air-traffic study with the design of future facilities, it is apparent that the peak-hour air traffic—rather than the average annual air traffic—will be the major factor limiting the growth of the airport. It is only logical to anticipate schedule saturation in the future; however, scheduled diversions cannot be used as an expedient for extending the capacity of the airport, as has sometimes been done previously. The peak-hour capacity of the airport should be determined with the knowledge that, although considerable progress has been made toward the perfection of electronic navigational aids and air-traffic control procedures, a runway can still safely handle no more than 40 landings and takeoffs per hour during unfavorable weather conditions, when all air traffic must be controlled. For planning purposes it should be considered doubtful that this number of operations can be attained under all conditions of mixed traffic; it more probably represents the maximum attainable. During visual-flight-rules weather the runway acceptance rate may approach 60 operations an hour, and, if two parallel runways are provided, the airport capacity can be increased to 120 operations during a peak hour. This additional runway will not appreciably increase the acceptance rate of the airport during instrument-flight-rules weather, and, should the airport be located in a region where instrument-flight-rules weather conditions prevail over extended periods, it would be foolhardy to estimate the airport capacity on the basis of the acceptance rate of dual runways. It is probable that future navigational and landing aids will permit the simultaneous operation of parallel runways during instrument-flight-rules weather; however, there are no indications that this will occur within the foreseeable future.

Area Plan.—In the master plan of a large international airport eventual air-traffic saturation should be anticipated, and an area plan for the future development of airports in the immediate vicinity should be suggested. The plan should be comprehensive enough to provide for facilities for the private aircraft owner, and the use of jet-propelled commercial aircraft should be foreseen as well as that of helicopter taxi service. At the same time the over-all plan should be flexible enough so that each factor can be adjusted according to its relative importance as time passes. In the area plan there must not only be considered air-navigation space and traffic patterns but also the interrelationship of the airport and the surrounding community. It is only normal to expect that communities will grow and eventually infringe on or encompass the boundaries of the airports, and therefore, in so far as weather conditions will permit, runways and approach zones should be oriented to take advantage of surrounding areas that are not susceptible to extensive development.

Noise Abatement

As the community begins to encompass the airport, the problem of controlling the noise of operating aircraft becomes more acute. Communities com-plain of the noises generated by large reciprocating aircraft engines; as the frequency of arriving and departing aircraft increases, together with the eventual introduction of jet-propelled aircraft into the transportation field, this problem may become so aggravated that the existence of the airport will be jeopardized. The seriousness of the problem can be appreciated when it is realized that the vast majority of complaints originate from the operation of reciprocating aircraft engines with sound intensities of approximately 100 decibels whereas a turbo-jet engine equipped with an afterburner may produce sound intensities approaching 140 decibels. These intensities are well above acceptable sound levels, and therefore every effort should be made to reduce ground run-up noises by including in the master plan any acoustical treatment that can be afforded by the proper arrangement of trees, shrubbery, and turf. Approach zones and traffic patterns should be arranged so that aircraft will not be required to fly over densely populated areas. It should not be concluded that a satisfactory solution to the noise problem can be obtained by the simple expedient of relocating airports or placing time limitations or restrictions on their use. Such solutions would not only be detrimental to the entire air-transportation industry but would also destroy progress made toward expediting the passengers between the airport and the community.

TERMINAL PLANNING

Terminal-site planning should be undertaken simultaneously with the airfield planning. Various surveys of air passengers and terminal visitors should be made in order to determine criteria for planning the future terminal site. These studies should be comprehensive enough to aid in the forecasting of future terminal visitors, the concession business that can be expected, the vehicular traffic in the terminal area, and the baggage and cargo to be handled through the terminal. The terminal should be designed so that future expansion is possible and various related facilities can be added as needed. All utilities serving the terminal area should be planned with future requirements in mind, even though it is probable that they will be constructed in stages. Because it is entirely probable that the terminal site will first be developed in units over a scattered area, it is important to plan the utilities so that they will serve small additional facilities when they are constructed in the future. Otherwise the cost of extending the utilities to a proposed facility may prohibit its construction on a self-amortizing basis.

In order that the traveling public may derive the maximum benefits afforded by air transportation it is necessary for the master plan to include a vehicular-traffic study on the approachs to the airport. Every effort should be made to make the airport more accessible to centers of population so that the time consumed traveling to the airport will be reduced sufficiently to make short-haul air trips feasible. If an express highway were provided for this purpose, it is possible that it would appeal not only to airport customers but to all cross-town traffic as well and therefore might easily be amortized during its life.

After the completion of the master plan and prior to initiating the construction program, the engineer will probably be required to make an economic survey of the existing and proposed air facilities. This survey will undoubtedly be used to substantiate the validity of a bond issue of sufficient magnitude to finance the proposed improvements. In many cases it will be found that the revenue derived from the completed project will not be sufficient to repay the bond issue and that additional money derived from taxation will be required. It will be to the advantage of all concerned and the duty of the engineer to recommend as many satellite revenue producers as can be justified. Discretion should be exercised in choosing these tenants so that the airport is not placed in a position of competing with private business in the community, thereby gaining the enmity of its citizens.

The international airport must have facilities in the terminal area for government agencies concerned with public health, immigration, and customs. Because these facilities are not revenue producers, it is necessary that the gross income derived from the operation of the terminal be great enough to offset this loss in revenue. These facilities may in some cases function in conjunction with a neighboring seaport and consequently require little terminal space. However, there are cases in which seaport facilities are subordinate to those at the airport, thus increasing the loss in net terminal revenue. It is therefore imperative that the functions of these agencies be precisely determined before the terminal-area design is initiated.

International air terminals will always be confronted with a language problem; provision should be made in the terminal design for a centrally located "international center" where foreign travelers may obtain information and assistance in accordance with their particular needs. In many cases the international passenger does not terminate his journey at his point of entry and may not have sufficient layover time to visit the surrounding community; in this case he may be seeking all types of additional services.

CONCLUSIONS

Although the master plan is chiefly concerned with the movement of aircraft and the development of the physical features of the airport, it is imperative that the air passenger be ever-present in the engineer's mind. In the final analysis it is the passenger who makes the whole project possible, and it is for him that the facilities are intended. He will require more consideration than has been afforded him in the past. As air transportation increases, he will come to accept as commonplace conveniences that once were luxuries. He has become accustomed to the easily accessible railroad and bus station that either provide or are adjacent to the necessities he may require while on his trip. These things are expected, and the passenger will therefore be hesitant to accept less from air transportation.

AMERICAN SOCIETY OF CIVIL ENGINEERS
Founded November 5, 1852
TRANSACTIONS

Paper No. 2790

WIND LOADS ON GIRDER BRIDGES

By JOHN M. BIGGS,[1] A. M. ASCE, SAUL NAMYET,[2]
AND JIRO ADACHI[3]

SYNOPSIS

This paper supplements the rather small fund of knowledge available for designing girder bridges to resist wind loads. The authors have made wind-tunnel studies of the effect of variation in the angles of attack, yaw, and roll. The paper includes a description of the models and the special measures necessary to circumvent blockage effects and to take into account other aerodynamic phenomena. Models of both railway bridges and highway bridges were studied, and results are compared with specifications of the American Railway Engineering Association and the American Association of State Highway Officials.

NOTATION

The letter symbols used in this paper are defined where they first appear, in the text or by illustrations, and are assembled for convenience of reference in the Appendix.

INTRODUCTION

Wind loads have been considered in the design of bridges for many years but even now few data are available on which to base the computation of these loads. This lack of information probably exists because (1) a completely satisfactory solution cannot be obtained analytically; (2) the facilities necessary for an experimental solution are not readily available to those most interested in the problem; and (3) for the majority of structures, wind loads are of secondary importance. With regard to the last fact, it may be noted that, in the case of the elevated highways that are becoming common in large cities, wind loads are of primary importance.

NOTE.—Published, essentially as printed here, in January, 1955, as *Proceedings-Separate No. 587*. Positions and titles given are those in effect when the paper was approved for publication in *Transactions*.

[1] Associate Prof. of Structural Eng., Massachusetts Inst. of Technology, Cambridge, Mass.

[2] Asst. Prof. of Structural Eng., Massachusetts Inst. of Technology, Cambridge, Mass.

[3] Structural Designer, Clarkson Eng. Co., Inc., Boston, Mass.; formerly Research Assistant, Massachusetts Inst. of Technology, Cambridge, Mass.

TABLE 1.—SECTION DIMENSIONS OF BRIDGE MODEL[a,b]

(a) RAILWAY-BRIDGE MODELS[a,b]

Section	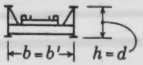			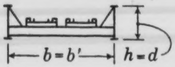	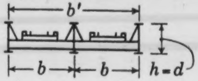			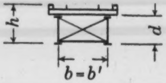			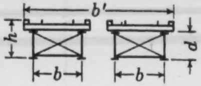		
Bridge Type	SINGLE-TRACK THROUGH			DOUBLE-TRACK THROUGH (2 GIRDERS)	DOUBLE-TRACK THROUGH (3 GIRDERS)			SINGLE-TRACK DECK			DOUBLE-TRACK DECK		
Model No.	1RTA	1RTB	1RTC	2RTB	3RTA	3RTB	3RTC	4RDA	4RDB	4RDC	5RDA	5RDB	5RDC
Elevation area[c]	0.312	0.625	0.937	0.625	0.312	0.625	0.937	0.375	0.687	1.104	0.375	0.687	1.104
Plan area[c]	0.681	0.799	0.847	1.220	1.285	1.495	1.565	0.509	0.541	0.570	1.02	1.09	1.15
h, in inches	1.50	3.00	4.50	3.00	1.50	3.00	4.50	2.00	3.50	5.00	2.00	3.50	5.00
b', in inches	5.50	6.62	6.62	12.12	11.00	13.25	13.25	2.81	2.81	2.81	8.81	8.81	8.81
d, in inches	1.50	3.00	4.50	3.00	1.50	3.00	4.50	1.50	3.00	4.50	1.50	3.00	4.50
b, in inches	5.50	6.62	6.62	12.12	5.50	6.62	6.62	2.81	2.81	2.81	2.81	2.81	2.81

(b) HIGHWAY-BRIDGE MODELS[a]

Section	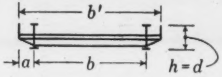		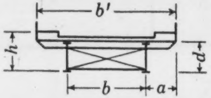			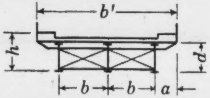			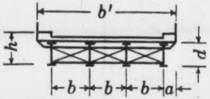		
Bridge Type	THROUGH		DECK (2 GIRDERS)			DECK (3 GIRDERS)			DECK (4 GIRDERS)		
Model No.	6HTB	6HTC	7HDA	7HDB	7HDC	8HDA	8HDB	8HDC	9HDA	9HDB	9HDC
Elevation area[c]	0.625	1.065	0.499	0.813	1.122	0.499	0.813	1.122	0.499	0.813	1.122
Plan area[c]	3.37	3.37	3.37	3.37	3.37	3.37	3.37	3.37	3.37	3.37	3.37
h, in inches	3.00	4.50	2.12	3.62	5.12	2.12	3.62	5.12	2.12	3.62	5.12
b', in inches	16.25	16.25	16.25	16.25	16.25	16.25	16.25	16.25	16.25	16.25	16.25
d, in inches	3.00	4.50	1.50	3.00	4.50	1.50	3.00	4.50	1.50	3.00	4.50
b, in inches	12.12	12.12	8.00	8.00	8.00	5.00	5.00	5.00	4.00	4.00	4.00
a, in inches	2.06	2.06	4.12	4.12	4.12	3.12	3.12	3.12	2.12	2.12	2.12

[a] All models 30 in. long. [b] All ties 4.12 in. long. [c] In square feet.

Of all the technical problems currently facing the structural engineer that of static wind loads is one which can be solved with relative ease. With a modest effort, loading coefficients can be obtained for all common bridge types in a form easily applied to design. For the more important structures where unusual structural forms are encountered, it is feasible to conduct wind-tunnel tests to determine the loads on that particular structure.

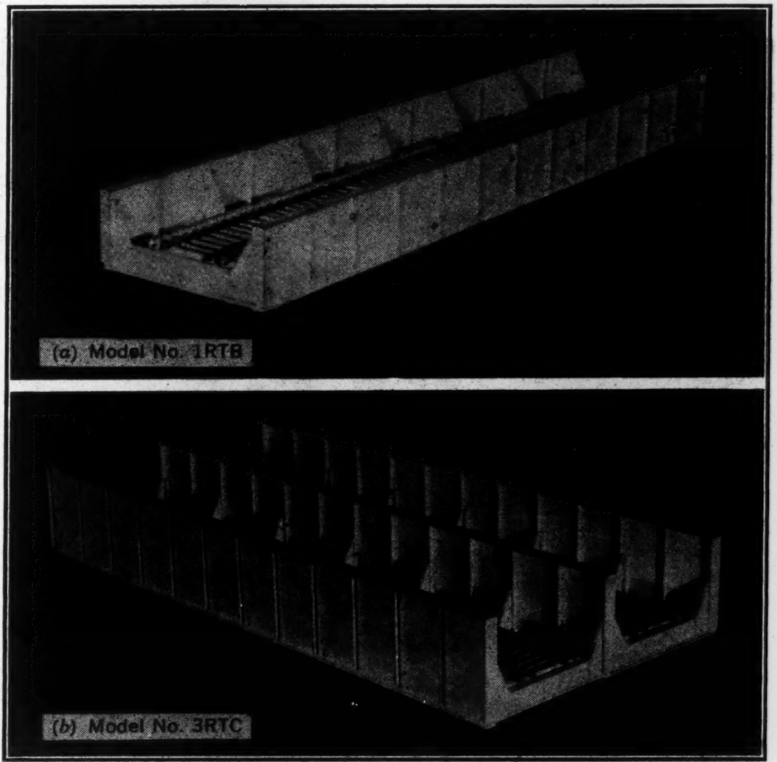

FIG. 1.—TYPICAL RAILWAY MODELS

The experimental program described in this paper is a continuation of earlier work on truss bridges which was previously reported.[4] Presented herein are wind-load data for several common types of railway and highway girder bridges. The railway types include single-track and double-track bridges of both through construction and deck construction. The highway types include through construction and deck construction with two, three, and four parallel girders. Because of the relatively small number of structural forms used in practice, the railway types tested represent the majority of railway bridges. However, there is a great variation in the form of highway bridges, and it was possible in this program to include only the more common types. It is hoped that future work will expand the data in this respect.

---

[4] "Wind Loads on Truss Bridges," by John M. Biggs, *Transactions*, ASCE, Vol. 119, 1954, p. 879.

All models were tested for various angles of attack (the angle between the wind directions and the horizontal plane). Also included are data which indicate the effect of angle of yaw (wind direction in the horizontal plane).

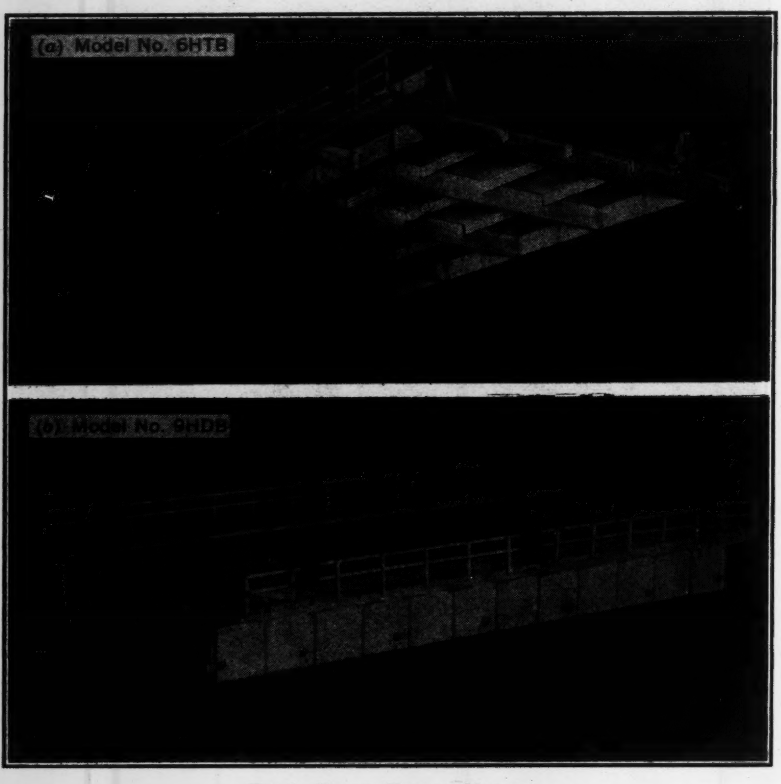

Fig. 2.—Typical Highway Models

Wind directions in the vertical plane containing the longitudinal axis of the bridge are also considered because the resulting forces are important in the design of bascule bridges.

Description of Models

Descriptions of the models are provided in Table 1, and photographs of a selected group are shown in Figs. 1 and 2. Five basic types of railway bridges and four types of highway bridges were included in the test program.

The wind-load characteristics of a bridge depend not only on the basic configuration or type but also on the proportions of the cross section. The most important variable within a particular configuration is the ratio of the girder depth to the other dimensions of the cross section. This parameter varies with the span of the bridge because the girder depth is, in general, a function of the span. In order to take into account the aerodynamic effect of the ratio of the girder depth to bridge width, each basic model type, with two exceptions, was tested with three different girder depths. Thus, data for a total of twenty-four models were obtained.

The tracks, ties, and floor systems of the railway bridge models were constructed to a scale of 1:32. The three girder depths used therefore correspond to 4 ft, 8 ft, and 12 ft at full scale. The scale of the highway models depends on the width of the roadway. If the roadway is 24 ft wide, the scale is approximately 1:25. At this scale the three girder depths correspond to approximately 3 ft, 6 ft, and 9 ft on the prototype scale.

The models were constructed of wood and contained as much detail as is necessary to reproduce aerodynamic characteristics of the prototypes (as shown in Figs. 1 and 2). In order to reduce the labor involved, the girders and floor systems were constructed separately so that the same set of girders could be used in all models. The girders consisted of three plates representing the web and flanges together with rectangular strips simulating stiffeners. In the railway models the track and ties were to scale, and the floor beams and stringers of the floor system were made of three rectangular pieces, also to scale. The roadways of the highway models were made of plywood slabs to which were glued rectangular strips representing stringers and floor beams. The bracing elements of all models were made of small rectangular strips.

The railings on the highway models were approximately to scale. The gaps in the railings which appear in the photographs were necessary to provide clearance for the mounting devices and they have had little effect on the total wind forces.

TEST PROCEDURES

All the tests described herein were conducted in the wind-tunnel facility at the Massachusetts Institute of Technology at Cambridge. The tunnel used is of the circulatory, nonpressured type having a test section 4.5 ft by 6 ft. The tunnel and its instrumentation are of conventional design. The maximum wind speed possible with the rather large models of this investigation was 80 miles per hr.

Wind-tunnel tests on models are useless unless the force coefficients produced are applicable to the prototype. In other words, for a given velocity, the ratio of the force on the model to that on the prototype must equal the scale squared. The parameter normally used to prove this similitude of the model and prototype is the Reynolds number R which is defined as $U\,D/\nu$, in which U is the wind velocity, ν is the kinematic viscosity of air, and D is a representative dimension of model or prototype. The minimum R for the tests of this investigation was 9.2 times 10^4 (computed for $U = 80$ miles per hr, $D = 1.5$ in., and $\nu = 1.6$ times 10^{-4} ft per sec^2). The maximum R that might be expected on a full-scale girder bridge is about 11 times 10^6 (computed for $U = 100$ miles per hr, and $D = 12$ ft).

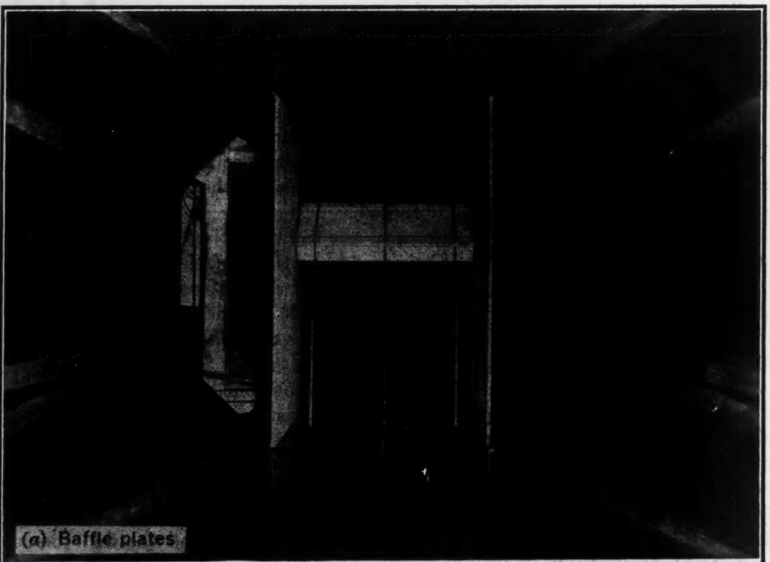

(a) Baffle plates

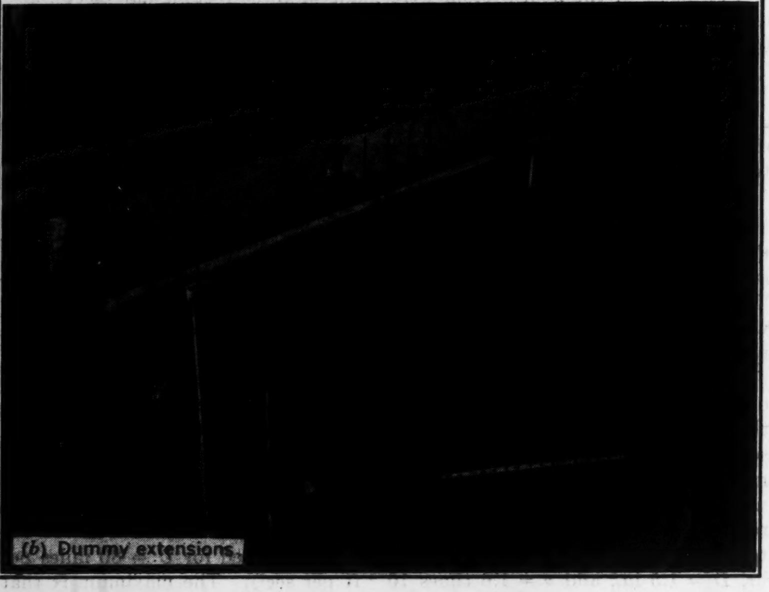

(b) Dummy extensions

FIG. 3.—METHODS FOR PREVENTING FLOW AROUND ENDS

A girder bridge is an assembly of sharp-edged objects and the Reynolds-number effect is essentially the same as that of these objects taken individually. For sharp-edged objects, such as a flat plate presented normal to the wind, the drag coefficient is a constant for all Reynolds numbers exceeding a critical value of approximately 10^3 and within the range significant for bridges. Because the **R** values computed for the model and prototype were both well above this critical value, it may be assumed that the force coefficients obtained for the model also applied to the prototype. In addition, the models were tested at velocities between 30 miles per hr and 80 miles per hour, and the drag coefficient did not change within this range. This fact indicates that the models were being tested at a Reynolds number above the critical value.

Another aerodynamic phenomenon that must be considered in wind-tunnel testing is the effect of aspect ratio which is defined as the ratio of the length to the depth of the model. It is well known that drag coefficients vary with aspect ratio, and in the case of flat plates the coefficient varies from approximately 1.2 to 2.0 as the aspect ratio increases from unity to infinity. For the case of actual girder bridges, the correct aspect ratio is not easily ascertained, but a value of infinity must be assumed. This assumption is probably correct for deck structures because the abutments effectively seal off the end of the structure. The actual condition is less certain for through bridges, but in most cases the depth-span ratio and the end conditions are probably such that the drag coefficient approaches that for an infinite aspect ratio. In any event, the most severe case must be assumed for design purposes.

All the models tested are considered to be sectional—that is, they represent only a portion of the span. In order to achieve an infinite aspect ratio in a wind tunnel, the flow of air around the ends of the model must be prevented. This flow might be prevented by one of several methods, but in this investigation only two were found practicable. The first of these involved the placement of two large baffle plates in the tunnel as shown in Fig 3(*a*). The models were inserted between the plates with the minimum practicable clearance on each side. The angle of attack was varied by rotating the model about the trunnion axis which is horizontal and perpendicular to the flow. The wind velocity was determined by means of Prandtl pressure tubes placed just forward of the opening between the baffle plates. These pressure measurements were calibrated and corrected for blockage effects as explained subsequently.

The second test method involved the use of dummy extensions to the models as shown in Fig. 3(*b*). The extensions were supported independently, and only the forces on the active model were measured. Thus, the end effects on the dummy extensions did not affect the data, and an infinite aspect ratio was attained. This second method had the disadvantage that extensions had to be constructed, but it had the advantage that yaw and roll angles could be considered by rotating the model and dummies about a vertical axis. This motion was provided by the turntable in the floor of the tunnel upon which both the model and dummies were mounted.

When large, blunt objects such as bridge models are tested in a wind tunnel, considerable error may be introduced as a result of the "blockage effect."

This error results from the fact that the large model causes an excessive disturbance in the normal flow pattern at the test section. The magnitude and distribution of the velocities between the model and the tunnel walls are not the same as would exist in the corresponding scaled space around the prototype. Normally the velocity pressure ($\rho U^2/2$) measured at points on the tunnel walls adjacent to the model is the free stream pressure, but this is not true when there is much blockage.

To circumvent this difficulty the velocity pressure must be measured at a point well forward of the disturbance caused by the model, and the measurements thus taken must be corrected according to the blockage introduced by the model. The necessary correction factors were obtained by placing in the tunnel flat plates of various widths for which the correct drag coefficient was known. When the drag force on each plate was measured, the effective velocity pressure for that plate could be computed using the known drag coefficient. The ratio of this effective velocity pressure to that given by the forward pressure tap is the blockage correction for that plate. Because it may be assumed that the blockage correction is a function of the total drag in the tunnel, the same correction applies to a model producing the same drag as the plate. By the use of several plate sizes a curve of blockage correction against total drag was produced, and this curve provided the corrections for the tests on bridge models.

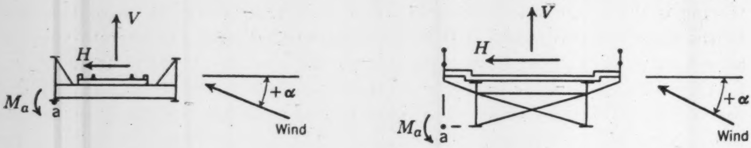

(*a*) Angle of attack

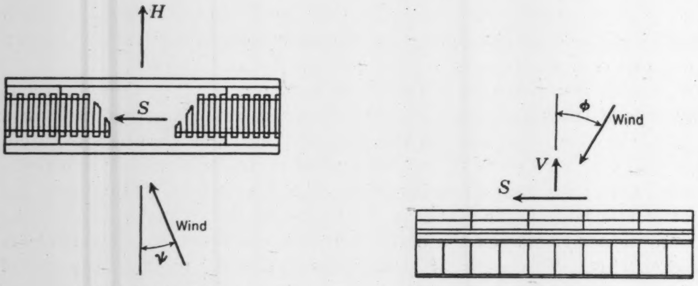

(*b*) Angle of yaw (plan view)

(*c*) Angle of roll (elevation view)

FIG. 4.—WIND DIRECTION ANGLES AND FORCE COMPONENTS

The same general procedure for determining the correction factors was used in both test methods previously described. Several of the models were tested by both methods, and the fact that the corrected values were in close agreement verifies the accuracy of the procedure followed.

TEST RESULTS

Wind direction angles and force components are defined in Fig. 4. The test data are presented in the form of dimensionless coefficients in Figs. 5 through 12.

The data for railway bridges when tested with varying angles of attack are plotted in Figs. 5, 6, 7, and 8 in terms of the coefficients C_H, C_V, and C_M. Similar data for highway bridges are shown in Figs. 9 and 10. Each figure contains the data for all the models of a particular type. The (d/b)-ratios

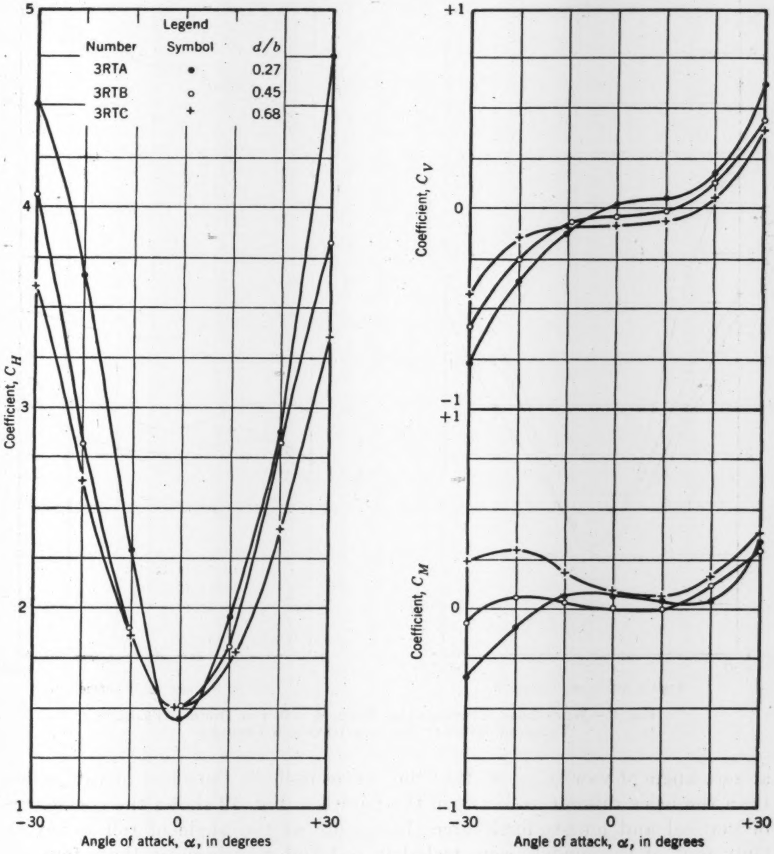

FIG. 5.—WIND-LOAD COEFFICIENTS, WHEN $\psi = 0$, FOR THROUGH RAILWAY BRIDGES HAVING 2 GIRDERS

are listed, and it is intended that for an actual structure this ratio be computed and the coefficients determined by interpolation.

The coefficients of transverse horizontal and longitudinal force for the models when the angle of yaw is varied are presented in Fig. 11. The transverse coefficient is plotted as a ratio of its value at a particular ψ-value to that at zero angle of yaw (C_{HO}) so that the curves indicate the effect of yaw rather than the basic differences between the models. Fig. 12 shows the coefficients of vertical and longitudinal force that apply as the angle of roll is varied. Only four of the models were tested in roll and yaw because these four are considered to be representative of all models.

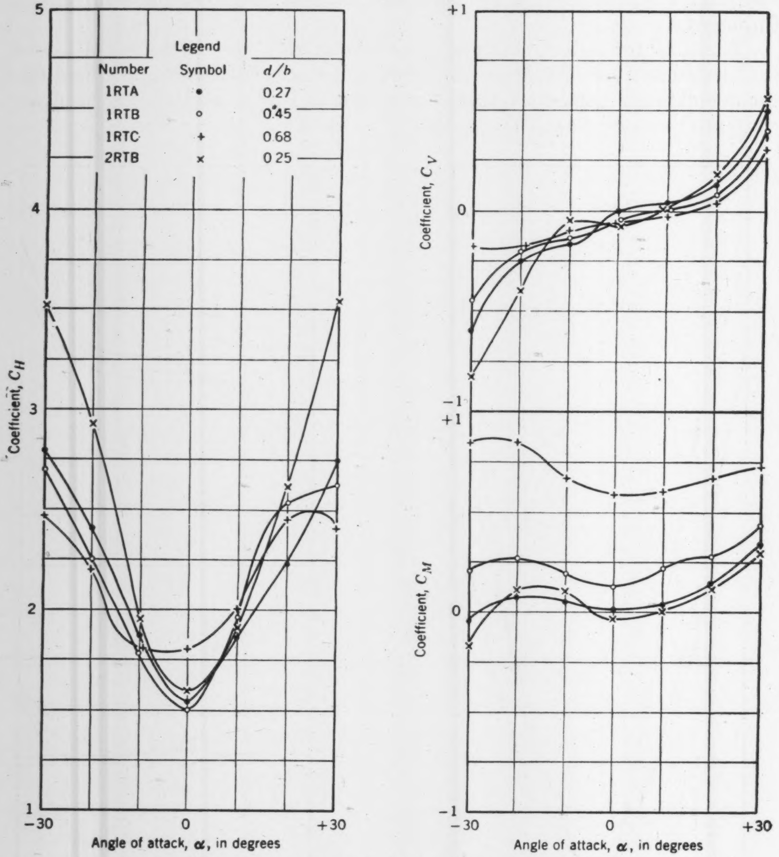

FIG. 6.—WIND-LOAD COEFFICIENTS, WHEN $\psi = 0$, FOR DOUBLE-TRACK THROUGH RAILWAY BRIDGES HAVING 3 GIRDERS

RESULTS—RAILWAY BRIDGES

In order to compute the maximum wind loads for design purposes it is necessary to decide what maximum angle of attack could occur at the site of the structure. This value is difficult to determine because very little information is available on the subject and the angle depends partly on the topography at the site. As may be observed in Figs. 5 through 10, the loads are very sensitive to changes in the angle of attack, and it is unfortunate that informa-

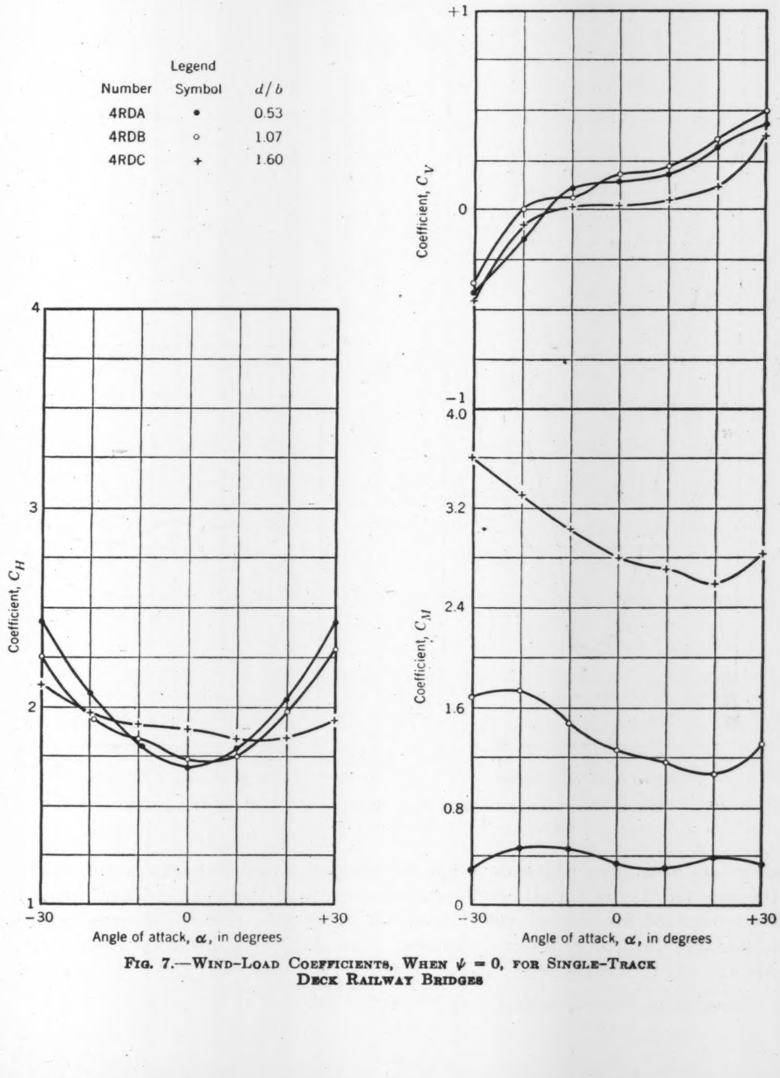

FIG. 7.—WIND-LOAD COEFFICIENTS, WHEN $\psi = 0$, FOR SINGLE-TRACK DECK RAILWAY BRIDGES

tion is not available on this subject. For the purpose of this paper it is assumed that the maximum possible angle of attack is ±15°.

Transverse Wind Forces.—The maximum transverse pressure, H/A_H, within the probable range of angle of attack (±15°) is given in Table 2 for each of the railway-bridge models tested. These pressures are based on the elevation area, A_H, which does not include the additional area presented by the leeward girder or other elements not seen in elevation. The pressures are computed for a wind velocity of 100 miles per hr which is considered a reasonable value for design purposes. The American Railway Engineering Association (AREA) specification[5] (1950) is 75 lb per sq ft (50 lb per sq ft on

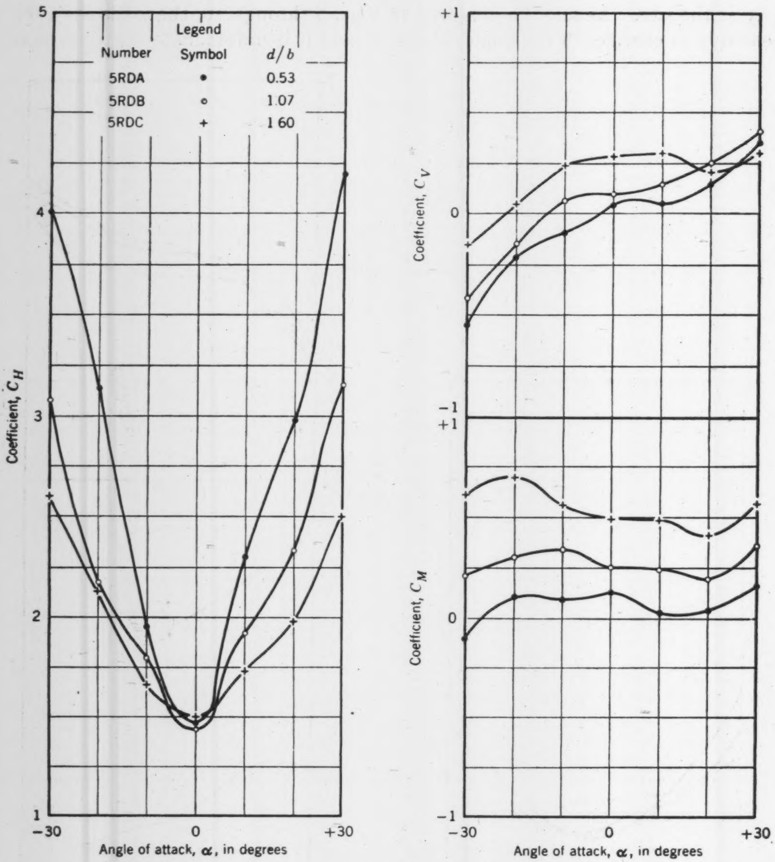

FIG. 8.—WIND-LOAD COEFFICIENTS, WHEN $\psi = 0$, FOR DOUBLE-TRACK DECK RAILWAY BRIDGES

---

[5] "Specifications for Steel Railway Bridges," A.R.E.A., 1950.

1½ times the elevation area), and it may be observed that in only one case (model 3RTA) is the experimental pressure as large as this value. The minimum design pressure indicated (model 5RDC) is only 63% of the maximum—a variation which is not provided for in the specification.

Comparison of models 1 and 3 reveals that the additional girder in model 3 has an appreciable effect on the maximum pressure for models having the shallow girders (A) but not for those having the other two girder depths (B and C). The same conclusion is reached by a comparison of models 4 and 5. This is probably due to the fact that, when the girders are deep relative to girder spacing, the windward girder creates a wake that completely envelops the leeward girders, thus preventing the development of drag forces on the latter.

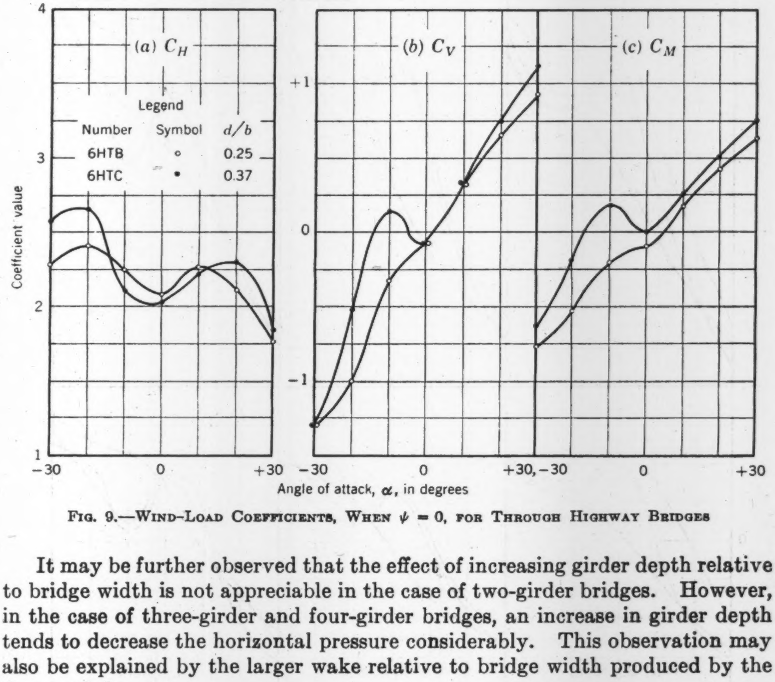

Fig. 9.—Wind-Load Coefficients, When $\psi = 0$, for Through Highway Bridges

It may be further observed that the effect of increasing girder depth relative to bridge width is not appreciable in the case of two-girder bridges. However, in the case of three-girder and four-girder bridges, an increase in girder depth tends to decrease the horizontal pressure considerably. This observation may also be explained by the larger wake relative to bridge width produced by the deeper girders.

As a matter of interest, the models were also tested at angles of attack greater than those reported herein. It was found that the maximum horizontal force on the railway models generally occurred at an angle of attack of approximately −40° and that the magnitude of this force was about 10% greater than that recorded at −30°.

Vertical Wind Forces.—Also given in Table 2 are the maximum upward pressures within the probable range of angle of attack. The maximum downward pressures are not considered significant for design purposes. In general,

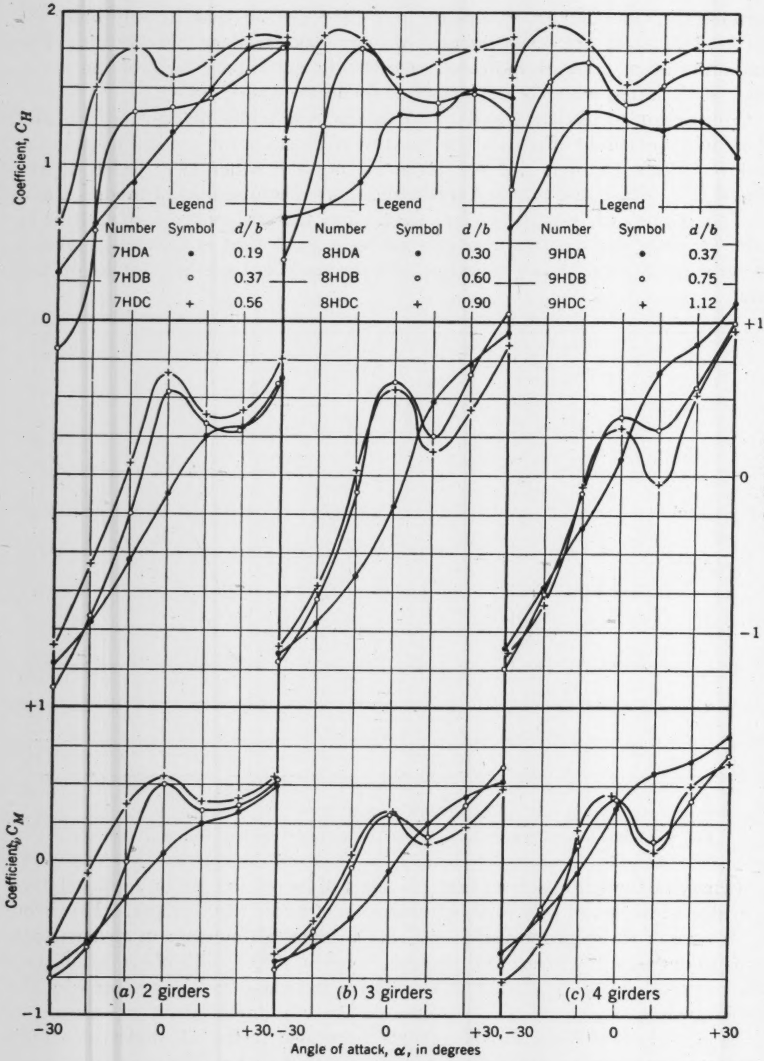

FIG. 10.—WIND-LOAD COEFFICIENTS, WHEN $\psi = 0$, FOR DECK HIGHWAY BRIDGES

deck structures are subjected to larger vertical pressures than are through bridges. The maximum pressure measured (model 5RDC) is 7.2 lb per sq ft, which is 15% of the maximum horizontal pressure. These results indicate that in the design of open-deck railway bridges, uplift wind pressures are not important.

Overturning Moments.—The maximum moment about point "a" of each model (Fig. 4) is recorded as M_a in Table. 2. In the absence of a specified vertical force, the designer usually assumes that the overturning moment results from the horizontal force alone and that this force acts at the middepth of the structure. A value thus computed (maximum $H \times h/2$) is shown in Table 2 for purposes of comparison with the experimental moment, M_a. The difference between these two quantities is due not so much to the presence of vertical pressures, which are small, but rather to a variation in the location

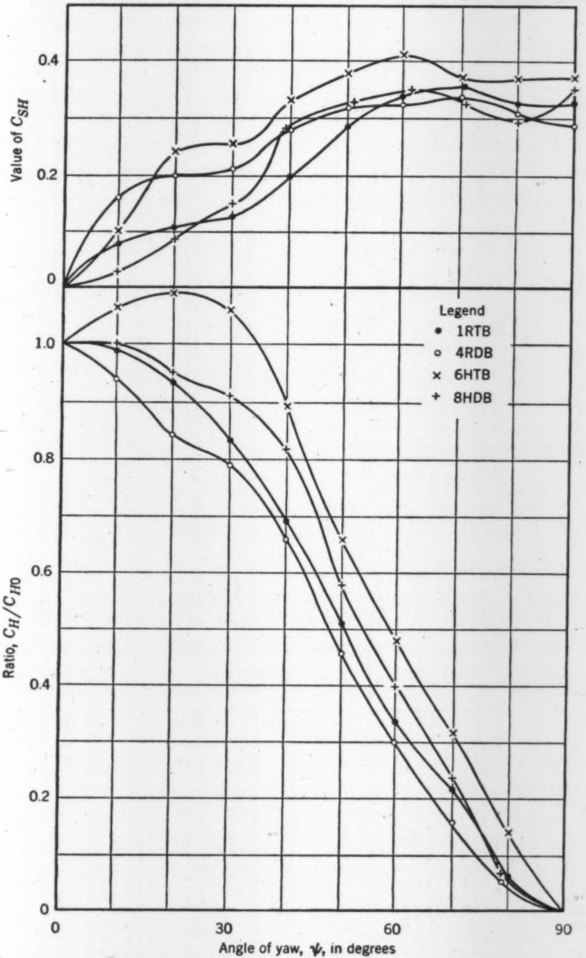

FIG. 11.—WIND-LOAD COEFFICIENTS, WHEN $\alpha = 0$, RELATED TO ANGLE OF YAW

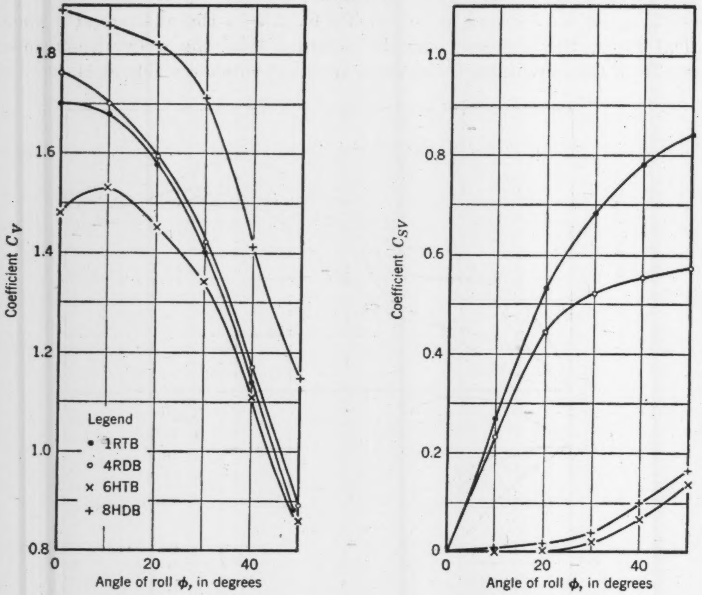

FIG. 12.—WIND-LOAD COEFFICIENTS RELATED TO ANGLE OF ROLL

TABLE 2.—RAILWAY BRIDGES—MAXIMUM WIND FORCES WITHIN THE POSSIBLE RANGE OF α-VALUES ($\pm 15°$)

Model No.	MAXIMUM TRANSVERSE PRESSURES				MAXIMUM UPWARD PRESSURES				MAXIMUM OVERTURNING MOMENT, M_e			
	Max C_H	α-value (degrees) for Max C_H	Max H/A_H (lb per sq ft) at 100 miles per hr	AREA specification (lb per sq ft)	Max C_V	α-value (degrees) for Max C_V	Max V/A_V (lb per sq ft) at 100 miles per hr	AREA specification	Max C_M	α-value (degrees) for Max C_M	M_e (lb-in.) at 100 miles per hr	Max $H(h/2)$ (lb-in.) at 100 miles per hr
1RTA	2.12	−15	54.2	75	0.08	+15	2.0	No Specification	0.09	+15	9	13
1RTB	2.37	+15	60.6	75	0.04	+15	1.0		0.27	+15	37	57
1RTC	2.28	+15	58.4	75	0	+15	0		0.75	−15	108	123
2RTB	2.45	−15	62.7	75	0.08	+15	2.0		0.13	−15	49	59
3RTA	2.93	−15	75.0	75	0.10	+15	2.6		0.06	−5	22	18
3RTB	2.30	−15	58.9	75	0.05	+15	1.3		0.05	−15	25	55
3RTC	2.19	−15	56.0	75	0	+15	0		0.27	−15	143	118
4RDA	1.93	−15	49.4	75	0.23	+15	5.9		0.49	−15	18	18
4RDB	1.88	−15	48.1	75	0.27	+15	6.9		1.64	−15	64	58
4RDC	1.93	−15	49.4	75	0.07	+15	1.8		3.14	−15	129	136
5RDA	2.67	+15	68.3	75	0.08	+15	2.0		0.12	0	28	26
5RDB	1.97	+15	50.5	75	0.21	+15	5.4		0.33	−10	81	61
5RDC	1.86	−15	47.6	75	0.28	+10	7.2		0.65	−15	169	132

of the resultant horizontal force. In the most severe case, the experimental moment exceeds the computed value of maximum $H \times h/2$ by 33% (model 5RDB). This difference is not serious because overturning moments are not particularly important in this type of bridge.

Effect of Yaw.—The results of the yaw tests are given in Fig. 11. For the two railway bridges tested in yaw, the maximum horizontal force coefficient occurs at $\psi = 0$. It may therefore be concluded that the results obtained for railway bridges in the angle-of-attack tests (Figs. 5 through 8) may be used directly without further consideration of the yaw effect.

Also shown in Fig. 11 is the longitudinal force coefficient, C_{SH}. The maximum value of this coefficient for the railway models is 0.36, which indicates that the maximum longitudinal force is not more than 20% of the maximum transverse force. It should be noted that this coefficient was obtained for models having dummy extensions on both ends as in Fig. 3(*b*) and should be considered to be applicable only to a center portion of the span. In some cases the effect of the exposed end of the structure might be appreciable.

TABLE 3.—HIGHWAY BRIDGES—MAXIMUM WIND FORCES WITHIN THE POSSIBLE RANGE OF α-VALUES (±15°)

Model No.	MAXIMUM TRANSVERSE PRESSURES				MAXIMUM UPWARD PRESSURES				COEFFICIENTS FOR MAXIMUM MOMENT	
	Max C_H	α-value (degrees) for Max C_H	Max H/A_H (lb per sq ft) at 100 miles per hr	AASHO specification (lb per sq ft)	Max C_V	α-value (degrees) for Max C_V	Max V/A_V (lb per sq ft) at 100 miles per hr	AASHO specification	Max $C_M(+)$	α-value (degrees) for Max C_M
6HTB	1.42	−15	36.3	75.0	0.50	+15	12.8	No Specification	0.33	+15
6HTC	1.36	−15	34.8	75.0	0.56	+15	14.3		0.41	+15
7HDA	1.65	+15	42.2	75.0	0.31	+15	7.9		0.28	+15
7HDB	1.50	+15	38.4	75.0	0.53	0	13.6		0.50	0
7HDC	1.76	+15	45.0	75.0	0.65	0	16.7		0.55	0
8HDA	1.42	+15	36.3	90.5	0.61	+15	15.6		0.34	+15
8HDB	1.75	−10	44.8	94.1	0.60	0	15.4		0.29	0
8HDC	1.87	−15	47.9	95.8	0.56	0	14.3		0.32	0
9HDA	1.36	−10	34.8	106.1	0.78	+15	20.0		0.61	+15
9HDB	1.68	−10	43.0	113.3	0.38	0	9.7		0.40	0
9HDC	1.87	−15	47.9	116.7	0.31	0	7.9		0.43	−5

Roll Tests.—The force coefficients for wind directions in the vertical plane through the bridge axis are shown in Fig. 12. These orientations are impossible on fixed spans but are important in the design of bascule bridges.

RESULTS—HIGHWAY BRIDGES

Transverse Wind Forces.—The maximum transverse pressures (H/A_H) for a wind velocity of 100 miles per hr are given in Table 3 for the highway-bridge models. These are the effective pressures on the elevation area, which does not include elements that are hidden in elevation. In Table 3 the experimental pressures are compared with those given by the American Association of State

Highway Officials (AASHO) specification[6] (1953) which requires that the effective area be taken as $1\frac{1}{2}$ times the elevation area plus $\frac{1}{2}$ the area of all girders in excess of two. Thus, the AASHO pressures given in Table 3 are equal to 50 lb per sq ft times the ratio of this effective area to the elevation area.

The experimental values do not indicate a significantly large variation in pressure with model type. However, the deck structures in general are subject to higher pressures than are the through structures, and the pressures tend to increase with girder depth. The specifications are apparently conservative. In no case is the experimental value (for 100 miles per hr) greater than 60% of the specified value. In one case (model 9HDA) the experimental pressure is only 33% of that given by the specification. Considering all models, the minimum wind velocity that would produce the pressure specified by the AASHO is 129 miles per hr. There is no general increase in transverse force as the number of girders is increased, and the specifications seem to be erroneous in this respect.

No tests were run on models of highway bridges having open-type decks. However, other investigators[7] have shown that such structures are subject to greater transverse pressures than are those having closed decks.

Vertical Wind Forces.—The maximum upward pressures acting on the plan area are given in Table 3. It may be observed that these pressures are of considerable magnitude. In the most severe case (model 9HDA) the vertical pressure is 58% of the transverse pressure. Taking into account the differences in plan and elevation areas, this indicates that the total upward force is 3.9 times the total transverse force. For design purposes, however, the upward force is significant only in so far as it affects the overturning moment.

Overturning Moments.—The results for the highway bridges (Figs. 9 and 10) reveal a striking similarity between the C_V-curve and the C_M-curve. This indicates that the overturning moment is caused almost entirely by the vertical force and that the moment due to the transverse force is small by comparison. Further investigation of the results reveals that the location of the resultant vertical force varies considerably and may lie anywhere within the windward half of the bridge width.

The maximum moment coefficients are given in Table 3. The magnitude of the moments indicated is not sufficient to cause overturning but may cause significant stresses in the two girders and their supports.

Effect of Yaw.—The results of the yaw tests shown in Fig. 11 indicate that for deck highway bridges the maximum transverse force occurs at $\psi = 0$. For through highway bridges the maximum occurs at $\psi = 20°$ and is 9% greater than that at $\psi = 0°$. This increase is not appreciable and probably does not occur at the angle of attack at which the maximum transverse force has been computed in Table 3.[8] It may therefore be concluded that the transverse-force coefficients (C_H) for highway bridges (Figs. 9 and 10) for the angle-of-attack tests may be used directly without modification for the effect of yaw.

---

[6] "Standard Specifications for Highway Bridges," A.A.S.H.O., 1953.

[7] "Aerodynamic Stability of Suspension Bridges," Pt. I, by F. B. Farquharson, Univ. of Washington Eng. Experiment Station, Seattle, Wash., June, 1949.

[8] "Investigation of Wind Forces on Highway Bridges," by G. S. Vincent, *Special Report No. 10*, Highway Research Board, National Research Council, Washington, D. C., 1953.

The maximum longitudinal-force coefficient (C_{SH}) for highway bridges shown in Fig. 11 is 0.41, which indicates that the maximum longitudinal force is not more than 30% of the maximum transverse force. The AASHO specifies a value of 25%.

Roll Tests.—The wind-load coefficients for wind directions in the vertical plane containing the longitudinal bridge axis are shown in Fig. 12. The through highway bridge is subjected to smaller forces normal to the deck because of the effect of the projecting girder flanges.

CONCLUSIONS

Railway Bridges.—(1) The type of structure has a considerable effect on the transverse wind pressure. The wind loads specified by the AREA are sufficiently large for the most severe case but variations with bridge type are not considered. (2) Vertical forces and overturning moments are not significant for open-deck railway bridges.

Highway Bridges.—(1) The AASHO specification is conservative with respect to transverse forces in all cases considered herein. (2) The presence of longitudinal girders in excess of two does not appreciably increase the wind loads. (3) Vertical forces and overturning moments on solid-deck highway bridges may be a significant design consideration.

APPENDIX

The following symbols, adopted for use in the paper and for the guidance of discussers, conform essentially with "American Standard Letter Symbols for Structural Analysis" (ASA Z10.8–1949), prepared by a committee of the American Standards Association with Society representation, and approved by the Association in 1949, and "Letter Symbols for Aeronautical Sciences" (ASA Y10.7–1954), prepared by a committee of the American Standards Association with Society representation, and approved by the Association in 1954:

A_H = the total projected area as seen in elevation;

A_V = the total projected area as seen in plan (in the case of railway bridges this includes track and ties as well as all structural elements seen in plan view);

b' = the width of the bridge (Table 1);

C_H, C_V, C_{SH}, C_{SV}, and C_M = dimensionless force coefficients;

D = representative dimension of the model or prototype;

$H = C_H A_H \rho \frac{U^2}{2}$ = the horizontal force acting transversely on the bridge;

h, d, and b = sectional dimensions as shown in Table 1;

$M_a = C_M A_V b' \rho \dfrac{U^2}{2}$ = the moment of the wind forces about an arbitrary point a (Fig. 4(a));

R = the Reynolds number;

$S = C_{SH} A_H \dfrac{U^2}{2}$ or $C_{SV} A_V \rho \dfrac{U^2}{2}$ = longitudinal force on the bridge;

$V = C_V A_V \rho \dfrac{U^2}{2}$ = the vertical force on the bridge, positive when upward;

α = angle of attack, the angle between the wind direction and the horizontal plane (Fig. 4(a)), positive when the wind is acting upward on the bridge;

ν = kinematic viscosity of air;

$\rho \dfrac{U^2}{2} = 0.00256\, U^2$ lb per sq in. (U in miles per hour);

ϕ = angle of roll, the angle of wind direction in the vertical plane containing the longitudinal axis of the bridge (Fig. 4(c)); and

ψ = angle of yaw, the angle of wind direction measured in the horizontal plane (Fig. 4(c)).

AMERICAN SOCIETY OF CIVIL ENGINEERS
Founded November 5, 1852
TRANSACTIONS

Paper No. 2791

SURVEYS AND MAPS FOR PIPELINES

By George E. MacDonald,[1] A. M. ASCE

With Discussion by Messrs. Norman O. Geuder, and
George E. MacDonald

Synopsis

Rapidity of pipeline construction is of sufficient importance to have induced significant changes in procedures used in pipeline surveys during recent years. The use of aerial photography has made possible great increases in the efficiency of pipeline layout, design, and construction.

Introduction

Since its inception, the petroleum industry has relied heavily on survey and mapping techniques. Exploring for new oil fields or gas fields and the development of unproven reserves have kept geological field parties constantly traversing and mapping the remote areas of the world. The development of the air-borne magnetometer was largely due to the exploratory requirements of the petroleum industry, and aerial photography has been a significant factor in reducing the mapping work formerly done by geologists.

As the petroleum industry expanded and developed, the need for economical transportation of its products to its markets led to the advent of long-range, "big inch" pipelines as a means of transportation. The subsequent increases in the use of the pipeline as an economical means of mass transportation has been a rapid modern-day revolution.

The office of Petroleum Administration for Defense (Washington, D. C.) estimates that about 163,000 miles of petroleum pipelines were in operation in the United States as of January 1, 1953, and an additional 10,000 miles were expected to be placed in operation during that year. The expansion of operating transmission pipelines by the natural gas industries has been no less rapid. The American Gas Association reports that from 1936 to 1951

Note.—Published, essentially as printed here, in January, 1954, as *Proceedings-Separate No. 393*. Positions and titles given are those in effect when the paper or discussion was approved for publication in *Transactions*.

[1] Vice-Pres., Lockwood, Kessler and Bartlett, Inc., Great Neck, N. Y.

the mileage of transmission lines operating in the United States was increased from 55,000 to 118,000.

Although the petroleum and natural gas industries are the undisputed "giants" of cross-country pipelines, the ultimate uses of pipelines as a means of mass transportation give wide range to the imagination.

Successful tests have already been made by a coal company on shipping coal by pipeline. The process is still in a development stage; the coal is finely crushed, immersed in water, and forced by pressure pumps through the pipeline. It was estimated that such a line from Cadiz, Ohio, to Lake Erie, a distance of more than 100 miles, might conceivably deliver coal for $1.00 per ton less than rail fare—the current rail rate being about $2.75 per ton.

Like railroads, airlines, and bus lines, long-distance pipelines are regulated by governmental bodies in the best interests of the public. For this reason, an application to the Federal Power Commission for a permit to construct a pipeline must be accompanied by a wealth of information regarding costs, design, and proposed rates.

In the regulating of permits, consideration is given such factors as a fair return to producers, the avoidance of injurious competition to established utilities, the meeting of present and future demands, the withdrawal rates from wells in accordance with sound conservation practice, evidence of long-term contracts with suppliers and distributors, and an assurance that the entire project is on a sound financial basis.

There may be several entrepreneurs competing for permission to construct a pipeline, and approval is usually given to the one most closely meeting the foregoing requirements with preference given to companies offering the lowest sales price to the public.

Meeting the requirements economically calls for skill and ingenuity on the part of planners and designers when it comes to choosing the most economical combination of pipe sizes, pumps, and compressors.

The entire development of the pipeline industry was, of course, based on the fundamental fact that the pipeline was the most economical means of transporting great volumes of fluid products. Such economic transportation not only depends on the operating costs of the system but also on the initial construction costs. Each of these factors affects the choice of a pipeline location, and consequently the location survey may be considered the most important of the several types of surveys attendant to pipeline construction.

Route Selection

The three prime requisites for the economic location of a pipeline are: (1) The choice of the shortest practicable route from end to end; (2) the avoidance of extreme differences in elevation; and (3) easy accessibility for both construction and maintenance.

Pipelines are first studied on small-scale maps showing all or a great part of the continent. On these maps a pipeline location is chosen, based on supply-and-demand studies, controlled by such major topographical features as mountain passes, feasible river crossings, the Great Lakes, and the Pre-Cambrian shield, and governed by national boundaries.

As regards route selection, there are some essential differences between pipelines and other transport facilities. The first is that all flow in a pipeline is one-way, as opposed to usual railroad, highway, and water routes. The second is that no "containers" such as railroad cars, highway trucks, or ships' holds are used. The latter must always be returned to the point of origin for new loads. Returning them empty is expensive. Hence, these carriers try to obtain revenue traffic on the return trip, even offering bargain rates to attract traffic. This practice, in turn, leads to influencing the choice of a route location by the need for interchange traffic. That is, it will often be considered desirable to deviate considerably from the most direct route if return or interchange traffic is so produced. Pipelines, on the contrary, have no need to deviate from the direct route. Therefore, the general rule for large pipelines is that the most direct route between suppliers and consumers is the best route. This choice will be tempered by location of mountain passes, feasibility of transportation of construction materials, and access for maintenance and operation.

Another important consideration for the pipeline locator is the comparative independence from any grade limitations, as compared with a railroad, highway, or canal. After the controlling elevations and length have been established, the mechanical engineering staff determines a hydraulic gradient that safely clears the control points. The pipeline locator has only to keep the grade below the hydraulic gradient. Minor terrain variations are of no significance except as construction problems. A pipeline can go over a hill; no expensive cuts or tunnels are involved. Hence, lengthening of the line in order to meet gradient requirements or to avoid excessive earthwork is unnecessary.

The selection of the general route of a pipeline is usually based on information provided by existing maps and statistics, supplemented by aerial and ground reconnaissance. Available sources include the Army Map Service, United States Department of the Army, which publishes maps with scales of from 1:1,000,000 to 1:25,000; the quad sheets of the Geological Survey, United States Department of the Interior (USGS), the USGS geological reports; the Production and Marketing Administration library of aerial photographs; state and county highway department maps; the charts of navigable streams of the Corps of Engineers, United States Department of the Army; the United States census reports on population; and the Federal Power Commission statistics on power consumption.

This first phase of the route selection serves only to determine the major obstacles that must either be contended with or avoided. The detailed study of all existing maps and charts in the vicinity of the contemplated pipeline route, combined with ground and air reconnaissance, enables the establishment of the general route.

Route Maps.—First, route maps are made up to show the area through which the pipeline will go. The set of route maps is compiled from existing state highway maps and is usually to a scale of 1 in. = 1 mile. This mapping is accomplished by a "lay-down" of the pertinent portions of the highway maps after each has been photographically reduced or enlarged to the desired scale. The entire assembly covering a strip approximately 15 miles wide is then photographically reproduced on a transparency. The purpose of these maps is to show the access roads, railroad network, and political and public land subdivisions in the vicinity. The proposed route is not placed on this set of route maps until the more detailed route selection is completed.

Location Surveys

As soon as the preliminary planning, source-and-market studies, general route selection, and financing have been completed and a charter and permission to construct have been obtained, the next step is the more detailed location of the proposed line.

Modern pipelines are characterized by astoundingly accelerated construction schedules in keeping with the general temperament of the petroleum and natural gas industries and of pipeliners in particular. Perhaps one of the foremost examples is the Lakehead Pipeline Extension under construction from Superior, Wis., to Sarnia, Ont., Canada—a distance of 630 miles. Mapping and surveys were begun in January, 1953, and were completed in July of that year; construction began in April, 1953, and was completed in November of the same year. The cost is of the order of $90,000,000. Included is a four-mile underwater crossing of the Straits of Mackinac, with a maximum depth of 240 ft. This is truly an astounding feat when it is considered that in this brief period surveys had to be made, special legislation passed, right of way acquired, pipe bought, manufactured, and delivered, construction contracts awarded, and the whole project coordinated for completion on schedule.

These accelerated construction schedules are inspired by sound financial reasoning. Money invested in a project must be paid for by interest charges. An uncompleted project is earning no income with which to amortize the investment and pay a profit to the stockholders.

The science and art of pipeline location have been evolving rapidly in the past ten years. After the general route had been chosen, it was typical in earlier procedure to provide a pipeline engineer with the available existing maps and to send him out to "flag" the route. He was fortunate if he had aerial photographs. By "flagging" is meant the selection of the most practicable places for the pipeline to cross roads and railroads. The object was for the locators to run the pipeline between the flags placed at these crossings. Although many thousands of miles of pipeline have been so located, use of the method had serious disadvantages. Little was known of the terrain between flags—whether it was favorable or difficult, or cheap or expensive. The right-of-way agent had little real information on property crossed by the line between roads. He was often unable to contact property owners and secure easement options before the arrival of the surveyors, thus complicating access for survey. Perhaps a more important fact is that, until actual completion of the survey, no one had a map of the complete line in any detail. This made realistic estimating almost impossible. Moreover, the pipeline maps had to be compiled from the surveyors' field notes. As a result, strip maps were seldom available for use in purchasing right of way or for construction planning—the times when such maps would have been of most use.

The first great improvement in location procedure was the use of a special set of aerial photographs of the route of the proposed pipeline. A typical scale would be 1 in. = $\frac{1}{4}$ mile, and the photographs would cover approximately $2\frac{1}{4}$ miles of width. Using these photographs, more precise control of the location was possible. The project's principal engineers could view and locate the entire route in the office. The resulting primary advantage was the choice of a location conforming to controlled standards of the pipeline engineers, rather than the heterogeneous ideas of different locators, each of whom covered from 30 to 50 miles of line.

Aerial photographs also furnish valuable preliminary information, including the probable length of line, area of clearing, comparative value of lands crossed (high-grade or low-grade farm land, pasture land, or waste land), and main and secondary access routes to the line. In addition, a competent photogeologist can aid the locator by outlining areas of rock outcrop and probable areas where ledge rock would be encountered above normal ditch level. When it is considered that the extra cost of rock excavation may be from $6 to $12 per lineal foot, or from $30,000 to $60,000 per mile, depending on pipe size and class of rock, the value of savings afforded by fullest use of aerial photographs is apparent.

Recent years have seen a considerable extension of pipeline construction through the northern United States and Canada. The severe winters introduce a complicating factor in the surveying and construction scheduling. Although surveys have been begun during the winter in order to meet construction schedules, they are usually frustrating and unsatisfactory operations. Days are short, cold is severe, snow is deep, travel is hindered and uncertain, and progress is slow and expensive. The snow conceals many terrain features that would normally influence location. If the locator is working from aerial photographs, the changed aspect of the country makes orientation difficult.

To overcome or eliminate some of these difficulties a new approach to the surveying and mapping problem of pipelines has recently been developed. Nevertheless, the land acquisition, field survey, and final route-mapping procedures still vary considerably in detail throughout the industry. The Lakehead Pipeline Extension, heretofore mentioned, is a good example of the application of most recent survey methods to the pipeline industry. This is a crude-oil line, 30 in. in diameter. Its owners took advantage of the lessons and experiences acquired throughout the industry and encompassed them into a positive procedure which produced a very efficient location survey.

After the general route selection, the recommended procedure can best be divided into five definite steps as follows:

1. *Aerial Photography.*—Photography of the general route is accomplished with a cartographic camera having a 6-in. focal length lens from an altitude of approximately 10,000 ft above mean terrain, producing a set of 9-in. by 9-in. contact prints showing a strip approximately 3 miles wide. The camera and altitude may be varied to yield a larger-scale photograph of congested or built-up areas if necessary. Generally, however, it has been found that a photographic scale of about 1 in. = 1,600 ft is suitable for pipeline work, and mapping at a scale of 1 in. = 1,000 ft is expedited.

2. *Study of Critical Area.*—The film is processed, and a detailed stereoscopic study of pairs of prints is made under Multiplex or Kelsh projectors. In this

study, experienced pipeline engineers locate exactly all difficult crossings such as rivers, canyons, or populated areas.

3. Stereocompilation.—Topographic mapping of the 2½-mile-wide strip of the entire route at a scale of 1 in. = 1,000 ft is begun in stereoplotting machines. Existing horizontal control is used in the development of these maps. In areas where there is no existing control, it must be established by field parties.

Normally, no contours are shown on these strip maps, but in extremely rugged terrain where there is a scarcity of planimetric detail relative contouring may be shown for field orientation purposes.

While the photographs are in these machines, pipeline locators are able to study especially difficult terrain in a three-dimensional view and select the detailed location between the control points previously selected. Geological interpretation of the photographs is also made at this time to determine areas where surface rock structures should be avoided. The topographic maps produced in the stereoplotting equipment show all planimetric detail in its true relationship. That is, houses, trees, pole lines, streams, ditches, fence lines, clearings, crop lines, highways, railroads, and similar features are truly located on the strip map prior to any field work.

On this same map the specific location is then projected so that, in essence, a complete set of "final" maps of the location survey can be delivered prior to any line stake-out.

If there is sufficient existing vertical control or if it can be economically established, an accurate profile of the selected route can also be made by the stereoplotting machines and placed on the strip maps.

4. Stake-Out Survey.—The stake-out in the field is then begun. As the line survey progresses, stakes are placed at even 200-ft stations along the center line, and all angle points are referenced so that the center line may be reestablished after the clearing and grading operations. All necessary property ties and astronomic observations are made to ensure the positive position of the center line. Because they have a full set of route maps, photographs, and detailed strip maps showing the proposed location, a minimum of decisions is left to the party chiefs.

5. Final Mapping.—Final mapping proceeds immediately after the survey notes are sent to the job-site drafting offices. This step includes the plotting of the field traverse on the original strip map and the stationing of all physical features crossed by the pipeline. At this time, the property lines of all parcels traversed are also plotted from the title search descriptions supplied by the right-of-way department.

The final strip map is scalable and shows all the background information previously described as well as the tract numbers or property owners' names and the roddage or acreage of easement taken across each piece of property.

The foregoing procedure has provided economies, not so much in the actual cost of survey as in the organization, planning, and administration of a pipeline project. Of these economies the following advantages are salient:

a. The detailed location is made by competent pipeline engineers in the office, with a three-dimensional view of the terrain in front of them. This enables them to select a route that will require a minimum of field revision and allows them to predetermine those areas that might require field location.

b. The stereocompilation of strip maps prior to the field stake-out provides a complete set of maps with which the right-of-way department can immediately begin to procure lands. This results in a substantial saving in time and money through narrowing the usual swath of options and abstracts normally secured by the right-of-way department.

c. The accurate projection of the selected route on the strip map provides a sound basis for the immediate obtaining of clearing permits from governmental agencies, such as those controlling any state forests and national forests involved.

d. With a two-man party sent out in advance of the center-line stake-out, all information for highway and railroad cross sectioning can be rapidly acquired, and permit drawings for such crossings can be completed and application made, far in advance of the survey.

e. The ground survey can be accomplished more efficiently because (1) all right-of-way permits have been obtained in advance, (2) trial survey lines are eliminated because the survey party need only follow the projected route, and (3) the survey can be scheduled for favorable weather without delaying office design or right-of-way acquisition.

f. The accurate planimetric map first produced can be used by the designers, right-of-way men, strip-map draftsmen, contractors, and field survey crews without the confusion attendant on the use of a miscellaneous collection of photographs, state and county maps, road maps, geological maps, and similar material.

LAND ACQUISITION

When the location of a pipeline has been projected, the surveyor must not only stake the line for the constructor's guidance but must also determine the properties crossed and the relation of the right of way to the land boundaries.

Pipeline companies, like other utility companies, must obtain permission and purchase the right to construct and maintain the line across government land or privately owned land. Obviously this right must be obtained prior to construction in order to eliminate subsequent costly litigation and damages for trespass and unlawful possession. To attain this right as quickly as possible, close coordination is maintained between the survey department and the right-of-way department.

Easements.—In the United States, a limited right to construct and operate a pipeline across properties is usually acquired in the form of an easement. Only those lands to be occupied by pump stations, tank farms, or other substantial permanent facilities are purchased in fee. The "floating easement" is most frequently used. As the name implies, the right of way is not definitely located or fixed within the property it affects but can be anywhere until fixed by the pipeline as constructed. Easements of this type, constituting a private agreement between the company and property owners, are acceptable to and registerable in the majority of land registry offices without an accompanying plat or right-of-way map. Obviously, this type of easement precludes the necessity of the surveyor obtaining accurate property ties prior to construction.

Few states have laws establishing precision, monumentation, and mapping standards for right-of-way surveys. It is left to the surveyor's judgment to decide on the survey precision and procedure which best serves the purpose with minimum expenditure of time and money. Usually, pipeline surveys are to the precision of 1:2,000 in rural areas and 1:5,000 or higher in urban areas.

With the knowledge of the approximate location of the pipeline, all available land subdivision maps of properties along the proposed route are obtained. These comprise: Plats of the original subdivision of public lands from the Bureau of Land Management (United States Department of the Interior) or state land offices; boundary maps of the state and federal forest lands from the state department of conservation; maps of Indian reservations from the Bureau of Indian Affairs (United States Department of the Interior); subdivision and individual property plats from the land registry offices; highway right-of-way maps from the state and county departments of highways; maps of utility and railroad rights of way from these companies; and tax maps and municipal street layout maps.

In the early days of pipeline location, right-of-way agents would accompany the survey crews and contact resident owners as the survey proceeded. Using information concerning property ownership thus gained and supplemented by searches in the land registry offices, entry permits and options were acquired. Lacking a predetermined line location, the agents could only negotiate for the rights a few parcels ahead of the line crew. By contrast, using modern aerial-photograph strip mosaics—usually to the scale of 1 in. = 1,000 ft and having the approximate route plotted thereon—property-outline maps can be prepared for use in right-of-way acquisition. In sectionalized country developed by farming, and even in the older sections of the United States where properties are irregularly shaped, the visual identification of boundary lines as evidenced by crop lines, tree lines, fences, and roads can be proved when compared with the deed description. The property-outline map developed from the mosaic enables time-consuming acquisition negotiations to be finished before field survey operations. The development of the planimetric map by photogrammetric methods eliminated the scale differences usually inherent in uncontrolled mosaics and further aided the identification and plotting of property outlines.

Property Ties.—As the field survey proceeds, the plus station of all physically evident property lines at the point of intersection with the line is determined, and the distance to the nearest property corner is measured. Unless specifically requested by the pipeline company, the right-of-way lines are not monumented. These property measurements are incorporated on the strip map with other topographic details along the line. Where properties are not physically evidenced by possession, the crossing location is computed. Strip maps normally plotted to the scale of 1 in. = 1,000 ft are made primarily for the use of the constructors and for the acquisition of right of way. They are not registered with the easement document.

Special Surveys.—Individual landowners often demand that the right of way be accurately located within their property. In the absence of conclusive monumentation evidence of the boundary line, a land surveyor re-establishes the line to eliminate possibility of encroachment and dispute.

Condemnation Surveys.—Continued owner opposition to the pipeline crossing occasionally occurs, forcing the company as a last resort to apply to the courts for condemnation. For this purpose, an accurate survey and plat are made by a licensed land surveyor; this is called a condemnation survey. Special surveys of this kind are necessarily more detailed and are performed with a precision commensurate with local conditions and standard practice.

Crossing Permits.—Pipeline crossings of highways, railroads, other utilities, and navigable streams or rivers also require special surveys and mapping in order to obtain permits prior to construction.

A profile of the ground surface and the location of fences, ditches, shoulders, edges and types of road pavement, railroad tracks, overhead and underground utilities, and the right-of-way lines of the facility crossed are determined along the center line of the proposed pipeline. Profile elevations are measured for a sufficient distance on each side of the crossing to enable the design of pipe bends to provide required depth and clearance of pipe beneath the facility crossed. The angle of crossing is measured, and the location of the crossing with respect to a railroad mile post, another intersecting highway, or a section line is determined. In the case of highway or railroad crossings, the level datum is assumed and normally need not refer to an established datum. Profile elevations of navigable streams under jurisdiction of the Corps of Engineers must refer to local mean low-water datum and indicate its relation to mean sea level datum.

The Corps of Engineers has established requirements indicating the information to be shown on the crossing application. This information includes a plan and profile, showing the diameter and thickness of the pipe and casing, depth of the pipe below river bottom and channel, direction of the current, the mean low-water line and the mean high-water line, the relation of the pipe to the properties on both sides and immediately adjacent to the river, the distance of the crossing from nearby bridges, location of shut-off valves, true bearing of the pipeline, and ties to existing horizontal-control monuments, plus right-of-way agreements showing the names of and the consent of the owners of these properties to the crossing of their lands. Maps of minor crossings are usually plotted on paper approximately 8½ in. by 11 in. in size and vary in scale depending on the over-all length of the crossing.

ACQUISITION VARIATIONS

It is interesting to note the range of land survey requirements for pipeline right of way, as established in Canada. Survey and mapping requirements are defined in the Dominion Land Act, the Official Surveys Act, and the Land Registry Act and are administered by the Surveyor General and the land registrars. The floating easement is not accepted for registration. In British Columbia, for example, an easement acceptable to the land registrar must contain a metes-and-bounds description accompanied by a right-of-way map delineating the strip to be taken and accurately locating its position within the property crossed.

Land survey accuracies are specified—they are of the order of 1:3,000 in undeveloped crown lands and 1:5,000 in urban and developed outlying areas.

Intersections of one side of the right of way with all property lines are marked by iron bars and marker posts. Both corner survey posts of a lot line are recovered, and the line between them is resurveyed to insure positive intersection with the pipeline right of way. Where property corner monumentation has been lost, the surveyor is required to re-establish the corner from adjoining property-survey posts.

The laws further require that right-of-way surveys and maps be made under the supervision and bear the signature of licensed provincial or dominion land surveyors.

Maps for registration are prepared in ink on tracing cloth to the scales of 1 in. = 400 ft for the rural areas and 1 in. = 200 ft for the urban areas or to larger scales as requested by the registrar. They show the boundary lines and dimensions of the properties crossed by the line; the width dimensions and true bearings of each of the courses of the right-of-way strip; the area of the right-of-way strip to be acquired in each property; the tie measurements to the property corners and the lot-line bearing; the monumentation set at changes of direction in the right of way and intersections with lot lines; the monumentation re-established at lost property corners; and the file numbers of registered maps pertaining to the properties crossed by the line.

The British Columbia pipeline right-of-way surveys under these high standards have proved to be from four to five times more costly than similar surveys in the United States.

CONSTRUCTION SURVEYS

Pipeline construction surveys are not as detailed and varied as those necessary for highways or railroads. The need for the majority of these surveys is eliminated because a pipeline can conform closely to the undulations of the existing terrain without adherence to predetermined grades. In addition, it can go around obstacles, if necessary, with a minimum radius of curvature as small as twenty-five pipe diameters.

This extreme flexibility makes the usual grade stake-out surveys unnecessary. Excepting crossings and places where the line is laid within or immediately adjacent to highways and streets, grading is largely left to the judgment of construction foremen. The primary purpose of grading is to smooth out irregularities in the ground surface and provide a working road for construction equipment and future maintenance access. The pipeline cannot be laid in fills because of the danger of washouts.

Not including the normal construction surveys at pump stations, tank farms, and other substantial installations, the construction surveys along a pipeline involve (1) establishing clearing limits by measuring from the staked center line to the edges of the clearing; (2) replacing alinement from the references set by the location surveys where stakes have been destroyed by farmers' cultivation or cleaning and grading operations; (3) furnishing line and grade as needed at crossings, at major highways, railroads, and rivers in order to build the pipeline as designed; (4) determining the horizontal and vertical curvatures of the excavated ditch for field pipe bending; and (5) making measurements for progress estimates of the volume of work performed as a basis for periodic payments to the contractors.

RECORD SURVEY

Frequently called an "inventory survey" or "completion survey," the data obtained by a survey of the completed line provide the physical inventory and location of materials, installations, and appurtenances—including the final route of the pipeline. Although the line is usually constructed as established by the location survey and construction plans, changes occasionally occur. During construction, engineers may discover places where it is economical to change the alinement to avoid underlying rock or swamps. Alinement revisions may also be made to by-pass certain properties or place the lines in a location more acceptable to the owner.

The purpose of the record survey is to determine the changes in location and deviations from the construction plans and to provide final maps and plans of the line as constructed.

The survey consists primarily of: (1) Rechaining of the line with the chain pulled tight along the surface of the ground or the top of the pipe, if exposed, and office conversion of partial stationing to continuous stationing. (This enables establishment of continuous mile-post markers in the field of maintenance and operations.); (2) determining the deflection angle at all side bends; (3) locating all appurtenances to the pipeline; (4) checking and recording deviations of these appurtenances from the construction plans; (5) locating changes of pipe wall thickness; (6) determining profile elevations, clearances and location of valves, vents, and casings and headers at crossings of highways, railroads, or rivers; and (7) locating rock cuts, culture, and wooded areas.

Record survey maps and plans serve as a guide to maintenance and operations purposes. In addition they constitute a substantiation of the construction costs and are submitted to the Interstate Commerce Commission (ICC) for consideration as a factor in determining the proposed rates.

One of the most extensive inventory surveys was made for the "Big Inch" and "Little Inch" pipelines built during World War II. The war emergency required that these lines be constructed and put into operation in the shortest possible time. As a result there were a great number of changes in alinement and construction. In order to save time the engineers had to make rapid decisions in the field. Such equipment as pumps, motors, and building materials specified for one pump station would be used at another site in order to expedite completion.

A complete resurvey in detail of the line and installations was made, and all maps and plans redrawn to be in agreement. This included all mechanical, electrical, structural, and architectural drawings.

CONCLUSIONS

Pipelines are conceived primarily as profit-making investments. Once the decision to construct has been made and money invested, the object is to complete construction and begin operating the pipelines on a paying basis. Speed of survey is indispensable.

The pipelines are first studied on small-scale maps showing all or a great part of the continent. Here, based on supply-and-demand studies and controlled by major topographical features, the general route of the pipeline is laid out. Use is then made of all maps of medium scale and small scale available from governmental sources, by means of which the route, with its minor alternates, can usually be narrowed down to a path approximately two miles wide. At this stage a field reconnaissance by automobile and light plane is usually made. If the engineer is satisfied as to the construction feasibility of the route, an aerial survey is the next step. From this point forward, methods may vary. The best practice is to compile planimetric strip maps from the aerial photographs. On these the route is projected with the aid of photographic interpretation, usually in pencil. Prints are distributed to all groups concerned: Engineering, legal, right of way, and survey. There is no such confusion as would attend the use of miscellaneous maps by the different departments. No matter what the season of the year, the right-of-way department can secure its easement options without waiting for surveys. In winter, survey activity can be concentrated on the detail surveys and plans, so-called "permit drawings," needed for the crossings of roads, railroads, canals, and rivers. When the weather improves, the surveyors may proceed to stake the center line and provide such monumentation as may be required. In the meantime, the engineering department has had the essential information length and location of the line, the elevation of control points, and, if needed, a profile of the route—necessary for the design of pipe sizes and for the location of pump stations or compressor stations and such auxiliaries as valve and scraper traps. As the center line is staked in the field, the exact location is plotted on the strip maps, and the preliminary pencilled route is removed. If the line is in an area where stringent legal requirements specify monumented title surveys tied to existing surveys as a prerequisite to registry of easements, these are made by licensed land surveyors following the staked center line.

Surveys and maps used in the location and construction of pipelines range from general area maps at a scale of 1:5,000,000 to title surveys at a scale of 1:1,200 and permit crossing drawings at a scale of perhaps 1:240. Use is made of the work of those long since deceased as well as those present, all combined with the efforts of promoters and constructors, to move gas and oil the thousands of miles from producing areas to consuming centers.

DISCUSSION

Norman O. Geuder,[2] A. M. ASCE.—Any transportation system—railroad, highway, or pipeline—can use the method described by the author to great advantage in the initial stages. Aerial photographs, when properly interpreted, provide a wealth of information that would take a great deal of time and money to acquire on the ground. Even in heavily forested areas such as are found in the Amaparí River basin in the Federal Territory of Amapá in Brazil, such features as small streams and the divides between them can be ascertained from a properly interpreted set of aerial photographs.

However, the accelerated survey schedules mentioned under the heading, "Location Surveys," can cause more expense than a slightly slower schedule. Although 630 miles of survey work in six months is very good progress, no choice of routes can be weighed during progress such as that. Possibly some savings have been overlooked. The operation with which the writer is associated had one such experience in which, by means of one month's delay to the location party (about 8% of the total time required for the entire survey and at a cost of approximately $10,000), they were able to save the owners $150,000 in construction costs plus a substantial portion of maintenance costs over the operational years. The accepted route ran for a distance of 6 km along the edge of the Amaparí River on side hills with slopes as steep as 70%. By a straight-line projection made in the office and based on the premise that a straight line is the shortest distance between two points as iterated by the author, it was possible to shorten the line, eliminate 5 km of riverside reverse curving with some side-hill cuts as deep as twenty meters, and reduce the soil quantities by approximately 20,000 cu m. With the accelerated surveying procedures described by the author, this saving could not have been made. Thus, the saving of time would have been more than cancelled by additional initial cost and continued higher operational costs.

Under the heading, "Land Acquisition: Easements," the author intimates that the states which have well-defined standards of precision, monumentation, and mapping cause unnecessary survey expense. The writer's experience with undefined easements and litigation over mistaken property lines indicates that proper monumentation of a line, easily discernible on the ground, will provide a saving for the owners over the years greater than the initial cost. These state laws, for the most part, were enacted at the suggestion of the men most experienced in the science of land surveying. An engineer who spends his early years in a survey crew for industries of various types does not acquire the real essence of land surveying as related to property ownership. The land surveyor who earns his livelihood at this profession has studied much more than the normal engineering-school curriculum offers; he has sometimes learned the need for precision the hard way. The individual working in an industrial survey crew is in a particular area for one survey only, and unprecise work will not cause him discomfort later. The writer sympathizes very strongly with the states that have these standards and would urge that they be adhered to even in those regions which do not require them as being good professional practice.

---

[2] Engenheiro de Escritório de Estrada de Ferro, Divisão de Construção, Indústria e Comércio de Minérios, Belém, Pará, Brasil.

In the author's conclusion, valid reasons for speed in surveys of this nature are advanced. Although rapid surveys will cause savings in interest costs and hasten the date when the profits begin to accrue, they can, unless carefully controlled, be overextended to the detriment of the project by the by-passing of long-term savings in exchange for small initial savings. A careful survey involving sufficient time to complete each section well in advance of any construction activity, although costing more initially, will usually save sufficient money and worries throughout the operational years to offset the extra initial expense advantageously.

GEORGE E. MACDONALD,[3] A. M. ASCE.—The interest evidenced by Mr. Geuder's discussion is appreciated, but some unwarranted inferences apparently have been drawn from the paper. Mr. Geuder's statement, "no choice of routes can be weighed during progress such as that," implies unfamiliarity with the thought processes concerning route location. Every line drawn, whether on a country-wide geographical map or a photogrammetric map to the scale 1 in. = 50 ft, is based on conscious or unconscious weighing of its location. Conscientious stereoscopic study of aerial photographs during route location involves weighing many factors, such as length of line, terrain types, river-crossing sites, value of property, and access for construction and maintenance, all leading to a general evaluation of the construction feasibility of the route. Granted that aerial photographs alone are deficient in quantitative values, inherent in their intelligent use is the weighing of many factors affecting the choice of route.

Mr. Geuder's point that careful, well-monumented right-of-way surveys are the best professional practice is not open to question. However, in rush construction programs, provided that the rights of the public and of the property owner are fully protected by accurate map presentation of the route and freely negotiated easements, it is desirable to postpone the right-of-way monumentation until after construction. This removes the stress of haste from the survey, reducing the probability of error, and has the important advantage of insuring that the monuments will not be disturbed by construction operations.

---

[3] Vice-Pres., Lockwood, Kessler and Bartlett, Inc., Great Neck, N. Y.

AMERICAN SOCIETY OF CIVIL ENGINEERS
Founded November 5, 1852
TRANSACTIONS

Paper No. 2792

METROPOLITAN TRAFFIC AND TRANSPORTATION PLANNING

By Charles A. Blessing,[1] M. ASCE

Synopsis

The broad problems of metropolitan transportation planning are outlined herein. A pattern is presented for coordinating the activities of the traffic engineer, the city planner, and others who have an influence or interest in the development of a comprehensive system. The effects of traffic congestion are examined and organizational plans that have been developed are presented. It is concluded that efficient and satisfactory planning can only be evolved by the cooperation of all interested parties.

Introduction

A survey conducted in 1950 by the American Institute of Public Opinion in the fourteen largest cities in the United States revealed that the residents consider traffic jams, with the attendant transportation and parking headaches, second only to the elimination of slums as the most serious domestic problem that they face. It is important to realize that this survey revealed not what the experts think but what the people feel about traffic problems.

It is unfortunately commonplace for advocates of one particular form of transportation or another to suggest that they alone have the solution to the problem. Arguments are continuous between the proponents of fixed-rail rapid transit and those who contend that modern expressways designed for rubber-tired vehicles offer the only hope for a sound solution to the urban-transportation problem. Others emphasize the importance of commuter railroads and cite the great progress made in the development of single-car diesel trains using existing or abandoned rights of way. Still others argue that rubber-tired rapid transit on the major thoroughfare system offers the greatest hope for an effective and economical solution.

Note.—Published, essentially as printed here, in January, 1955, as *Proceedings-Separate No. 602*. Positions and titles given are those in effect when the paper was approved for publication in *Transactions*.

[1] Director of City Planning, Detroit, Mich.

COORDINATED TRANSPORTATION

While these arguments continue unabated, traffic engineers, transportation experts, and city planners recognize that all too little attention has been given to coordinated transportation and the part that each mode of transportation can properly contribute to the over-all solution. In the light of the failure (as of 1955) to solve the metropolitan transportation problems by piecemeal approaches and in the face of the increasing severity of these problems, one is forced to accept as the first principle of sound urban traffic and transportation planning that such planning must be both metropolitan in breadth and comprehensive in scope. This planning must embrace in a single study all forms of transportation in metropolitan areas, including fixed-rail rapid transit, commuter railroads; expressways with or without fixed-rail transit facilities; major and secondary thoroughfares which serve as collectors and distributors for expressway traffic; terminal parking facilities; truck terminals; and a variety of facilities for interchange between the different forms of transportation.

Fortunately, the improvements in the techniques of traffic and transportation surveys have been rapid. Comprehensive travel studies showing passenger movement by transit, private vehicle, and taxi, as well as truck movements, have been made in ninety three of the larger cities in the United States and less intensive surveys have been made in hundreds of smaller cities. Although these origin and destination surveys have been largely standardized, refinement in the methods of traffic analysis is continuing. However, such surveys relate principally to the movement of vast and increasing quantities of traffic to, in, and through urban areas but cast little light on the effect of such traffic on the areas through which it moves.

The understandable preoccupation of traffic and transportation engineers with the efficient movement of traffic in urban areas has sometimes caused them to ignore the effects that their proposed solutions have had on cities generally and the failure of traffic palliatives in the face of fundamental urban deficiencies. Although the primary responsibility of the traffic engineer is to make provision for the efficient movement of traffic, he must increasingly share with the city planner the responsibility for making cities more healthful, safe, pleasant, and, in general, more satisfying places to live.

The broad objectives of any plan must be to provide for safe, convenient, and efficient movement of people and goods between all parts of the city and region and also to provide a transportation framework within which there can be developed the best possible environment in which to live, work, and play. Recognition by not only the city planner but also the traffic engineer of the fundamental and inherent conflicts between the efficient movement of people and goods and the achievement of safe, attractive, and stable urban neighborhoods is the first step in satisfactorily resolving these conflicts. Both the city planner and traffic engineer must recognize that there are inherent conflicts, and the consequent failure to resolve or minimize them in the process of building, redeveloping, or conserving cities is one of the major causes of some of the most serious shortcomings and problems with which cities are confronted.

Cities in the United States have substantially the same streets that they had at the beginning of the twentieth century, before the advent of the automobile. Adequate for the horse and buggy, the streets have become hopelessly overcrowded; they cannot serve the traffic. In order to bring about an effective solution to the traffic problem, one must first understand why the streets are inadaquate. The peace, quiet, and safety of most residential neighborhoods have been destroyed by a blanket of through traffic which moves daily over residential streets as well as major thoroughfares; family living has become almost impossible in many areas. Among the major factors causing deterioration of a residential area is the inability of families to find a safe and attractive neighborhood environment in these close-in central areas which are cut into narrow ribbons of housing by heavily traveled streets. Many central areas have become little more than funnels through which surge the daily ebb and flow of traffic from outlying areas to the heart of the city.

EFFECTS OF CONGESTION

If the city planner and the traffic engineer can agree that ever-increasing traffic congestion is one of the basic causes of the blight surrounding the core of every city, then perhaps they can together establish a sound basis for more effective correlation between transportation planning and land-use planning. One of the greatest needs in the improvement of cities is a clearer understanding of the relationship between these two types of planning. One need only consider the vast corrider areas of residential land through which traffic pours daily to the center of such cities as Chicago, Ill., or Detroit, Mich., for example, to appreciate the fact that there can be no hope of sound redevelopment nor even of conservation of such areas until the increasingly heavy volumes of through traffic are somehow eliminated from streets originally intended for neighborhood access only.

Cities recognize the basic nature of the conflict between street traffic and the protection and improvement of the residential, commercial, and industrial areas through which this traffic moves. Traffic congestion in urban centers is a major cause of the exodus of population and of commercial and industrial activity from the central areas of the cities to the suburbs. This exodus results basically from the fact that the street pattern of cities, having generally developed before the needs of the automobile were recognized or understood, is obsolete and inefficient.

Few attempts have been made to measure the loss to cities resulting from the stranglehold of traffic on the central areas or to determine what part of the total loss in central-area values may be ascribed to traffic problems as contrasted with other manifestations of urban deterioration. The assessed valuation of the downtown area of Detroit decreased 42% from $380,000,000 in 1930 to $220,000,000 in 1953. Traffic congestion is considered by many to be the principal problem in this downtown area.

The city planner must be concerned not only with the changes which have already occurred in the central cities but even more with those which may be expected to develop as traffic volume and traffic congestion continue to mount. The volume of automobile traffic in many cities has increased 5% or more in each of the years following the end of World War II. For the entire United States, estimates for 1963 indicate an increase from the 61,000,000 vehicles in

1955 to 68,000,000 vehicles, or approximately a 12% increase in an 8-year period. American cities must face the staggering problem of how to accommodate the contemplated increase in traffic with greater vision and determination than has been brought to bear on this problem in the past. This is true despite the tremendous progress made in the planning and construction of urban expressways in most large cities. It is anticipated that many of these expressways will reach a point of saturation soon after being opened for use. If this happens, how can long-range relief of traffic congestion on existing streets be expected when over-all traffic is expected to increase every year for many years in the future. What may be the situation in 20 years or 30 years?

Cooperation of Experts

The conclusion clearly is that all forces of metropolitan traffic and transportation must be analyzed together and in closer relationship to the land-use pattern of the entire urban area. The traffic engineer, the highway engineer, the transit expert, the railroad-transportation expert, the city planner, and the public-finance expert must work closely together, must pool their information more freely, and must go beyond their own limited fields. They must develop more effective cooperative working arrangements—they must together re-evaluate the entire problem of metropolitan traffic in terms of the movement of people and goods into, inside, and through the city and also the impact of various forms of traffic on the area through which it moves.

The city planner faces a basic problem of endeavoring to bring about a functionally better organized and otherwise more rational land-use pattern. He should seek better relationships between places of residence and places of work and better articulated and balanced distribution of industrial and commercial activities. Such changes in the established parts of cities will be difficult and slow of accomplishment. All the existing tools of sound city planning, zoning, and subdivision control will be needed. Urban redevelopment of those areas already too deteriorated to be maintained in their obsolete pattern is one of the most promising new tools with which to achieve basic improvements in cities. New programs of urban conservation will bring into sharp focus the problem of maintaining values in urban areas which are often obsolete in general city patterns but which can be conserved by methods short of complete clearance. Greater promise for new urban patterns lies in the intelligent direction of new urban growth in those outlying metropolitan areas which are undeveloped and unspoiled. The city planner's work requires a carefully balanced program giving direction to all three fields—redevelopment, conservation, and new growth.

In all these areas of city development, no single phase of the metropolitan traffic and transportation problem can be adequately studied unless it is related to the over-all problem. Expressways, rapid transit, local surface transit, major and secondary thoroughfares, commuter railroads, truck routes and terminals, and parking facilities—all must be analyzed as important and interrelated parts of the comprehensive metropolitan traffic and transportation system. Traffic engineers and city planners must join with finance experts in making careful cost analyses of all recommended expenditures for the relief of traffic congestion in relation to relative benefits to be received from the proposed improvements and extensions of competing forms of traffic. One of the most challenging problems faced by municipal governments is the determination of how much public revenue to assign for the improvement of the various competing types of transportation service.

The increasing complexity of the over-all metropolitan traffic problem has in most large cities led to the creation of a large number of single-purpose agencies, each established in response to the recognition of the need for solving a particular problem. Most or all of the following municipal and county agencies, departments, and commissions—each concerned with some particular phase of the planning and operations of the over-all traffic and transportation system—are common in the major metropolitan areas of the United States: Street-traffic commissions, departments of streets and traffic, street-railway departments, rapid-transit commissions, city-planning commissions, parking authorities, public-works departments, port authorities, bridge and tunnel authorities, departments of parks and boulevards, metropolitan-parkway authorities, truck-terminal committees, county-road commissions, and special origin and destination survey committees. Other agencies having jurisdiction are the budget bureaus, the expressway coordinators' offices, private bus companies, commuter railroads, and private transit companies. In the face of this multiplicity of agencies, it is hardly surprising that the efficient coordination of all forms of transportation has become an increasingly complex problem.

Subways have been built parallel to and near expressways which did not include fixed-rail transit facilities at a greater total cost for the two than if a single combined facility had been built. Expressways with downtown terminal parking have threatened the existence of transit systems. Commuter railroads, often with well-located rights of way, have curtailed or entirely eliminated service in the face of inroads from private automobiles and competing public transportation routes. Frequently both public and private commuter bus lines parallel commuter rail lines. How such costly and often wasteful competition can be avoided has become a problem of increasing urgency in many metropolitan areas.

It is not unusual for the city-planning authority or consultant to urge that the city-planning commission be recognized as the coordinating agency for all traffic and transportation planning. It has been a common occurrence for planning commissions with jurisdiction over all aspects of the comprehensive plan to surrender step-by-step major responsibility for traffic and transportation planning to special agencies created because of the failure of existing agencies to meet particular problems.

Most major cities have large, efficient, and well-established traffic-engineering departments with direct responsibility for traffic operations and for traffic planning, as well as street-traffic commissions charged with the responsibility for preparing a comprehensive city plan. One result of the multiplicity of agencies dealing with traffic problems has generally been the adoption of half-measures or palliatives which have, by taking care of extreme pressures, served to delay real transportation integration. Many of the traffic engineers' day-to-day techniques are relieving traffic pressures but are not solving the basic problem. Another result of the multiplicity of agencies concerned with traffic has been the dissipation of jurisdiction and authority so that it is difficult to place responsibility for a program of fully coordinated traffic improvements on any one body.

The only logical conclusion is that, if the over-all metropolitan traffic and transportation problem is ever to be grappled with effectively, some form of coordinated, metropolitan-wide approach to the problem must be developed. This approach must equally take into account the need for efficient movement of traffic and the effect of that traffic movement on the area through which it moves.

Transportation Plans

Many areas have conducted metropolitan origin and destination surveys as the basis for the preparation of comprehensive thoroughfare and expressway plans. Although coordinating committees have been established which include transit agencies as well as street-traffic agencies, it has not been uncommon for cities to separate the planning of thoroughfares and expressways from the planning of transit-system improvements. A notable exception is San Francisco, Calif., which, in 1948, prepared a broad transportation plan including a system of trafficways within the city, a comprehensive and balanced system of city-wide public transit, terminal facilities for interregional and suburban transit routes, recommendations for improved functional use of the city streets through modernized traffic control, and finally off-street parking facilities. This plan was based on data provided by a metropolitan traffic survey and on comprehensive land-use studies and other studies prepared by the city-planning commission.

The important achievement in the plan for San Francisco was the coordination of traffic and transportation studies with general city-planning studies of population, land use, economic resources, and public improvements. The organization for the transportation-planning job included the appointment of an administrative transportation council which in turn was served by a technical committee consisting of the director of public works, the manager of utilities, the deputy chief of police, and the director of planning. This committee was responsible for the preparation of a plan to be submitted to the administrative planning council and finally to the city-planning commission for consideration and adoption as the transportation section of the master plan. Coordination of staff studies was performed by the city engineer and the director of planning. A city-planning consultant was engaged to consider all aspects of the program from the over-all planning point of view, relating the sections of the transportation study to one another and to the land-use plan in order to coordinate transportation as a primary element of the master plan with the land-use and zoning plans. A transit and thoroughfare consultant was engaged to prepare detailed studies of transit, motorways, parking, the central-area problem, and interregional-transportation problems.

The comprehensive transportation plan for San Francisco is being supplemented (as of 1955) by a broad study of transportation problems throughout the area. This approach is cited as an illustration of the general type of coordinated organization which should be feasible for application to a metropolitan traffic and transportation planning program.

Such a metropolitan planning approach to the coordinated solution of traffic and transportation problems would be vastly improved under some form of consolidated or unified metropolitan organization. One of the most promising developments in metropolitan planning has been the establishment of the metropolitan council of Toronto, Ont., Canada, a body having jurisdiction over the central city and twelve surrounding suburbs. This council, established in 1953, has formed a metropolitan planning board which will prepare an official plan for the metropolitan area, the general scope of which will include land use, ways of communication, sanitation, greenbelts and park areas, and public transportation. The Toronto transit commission will be responsible for public transportation in the metropolitan area.

The metropolitan transportation plan in any major city will be unrealistic if it does not rest on a broad base of city and regional planning studies. On such studies must be based the metropolitan land-use plan, the population density and distribution plan, the neighborhood unit plan, the school and recreation facilities plan, the utilities plan, and the traffic and transportation plan.

Relationships between (*a*) types and capacities of traffic facilities and (*b*) population density and land-use patterns must be more specifically analyzed than has been done. Specific population densities required to permit economic construction and operation of different forms of transportation must be determined more carefully. More specific studies are needed on the extent to which traffic congestion and traffic hazards are contributing causes of blight. Research is needed to determine what traffic-improvement measures can be applied to the city's conservation areas to protect them from impending blight. Specific methods of measuring the harmful effect of through traffic on residential neighborhoods must be developed. Particular study must be given to the re-establishment of safe and attractive residential neighborhoods in the "corridor" areas through which great volumes of automobile traffic pour daily from suburb to downtown center. These are some of the many problems which neither city planner nor traffic engineer can solve by working alone.

Basic Problems

Many basic problems require the closest possible collaboration between city planners and traffic engineers working together on a technical committee of a metropolitan administrative transportation planning council. Such a committee is a basic element in any effective transportation planning study. Among the basic problems to be considered by such a technical committee are:

1. The over-all traffic demand for a specified period in the future based on (*a*) estimated future population density, (*b*) future patterns of industrial and commercial concentration, and (*c*) future patterns of major recreational facilities.

2. The assignment of a percentage of estimated future traffic demand to each of the competing types of transportation services.

3. The correlation of the thoroughfare plan with the residential-area plan so that the thoroughfare plan will define the pattern of neighborhoods and communities, with through traffic diverted around residential neighborhoods.

4. The correlation of the thoroughfare plan with the industrial and commercial land-use plan, with particular reference to community shopping centers and planned modern industrial districts.

5. The comparison of capacity and future demand on designated major thoroughfares as a basis for recommendations of thoroughfare improvements.

6. The assignment, on the basis of trends in transit volume and recommended capacity of major thoroughfares and expressways, of a percentage of the estimated future over-all traffic demand for surface and rapid transit.

7. The coordination of local-transit routes with major-thoroughfare plans and the coordination of express-transit routes with planned expressways and commuter-railroad routes. The recommendation for over-all local and express transit systems must be based on the relationship between the comprehensive plan for residential areas, projected population densities, and the need for transit service.

8. The determination of the feasibility of street closures in areas which are or will be subject to redevelopment and the selection of alternate routes.

9. The determination of street changes required in neighborhood-conservation plans and effect of these changes on estimated traffic requirements in the area.

10. The location of transfer points between automobiles and public-transit facilities and the determination of required parking facilities at these points.

11. The designation of specific truck routes and truck-terminal areas in relation to the commercial and industrial land-use plan.

12. The location and capacity of off-street parking facilities, both in the downtown area and in the outlying commercial and industrial centers.

Because these studies require analysis by the traffic engineer and the city planner, a joint staff would be most effective. Therefore, all phases of the metropolitan traffic and transportation planning problem would be brought together for review by a technical advisory committee which would in turn report to the metropolitan administrative transportation planning council.

CONCLUSIONS

Only through the careful collaboration of the proposed transportation planning group can the maximum benefit be derived from the information provided by a comprehensive metropolitan origin and destination traffic survey. The result of such a broad approach should be the ultimate creation of safe, convenient, and attractive cities and the provision of comfortable, fast, and economical transportation for all who live in cities.

AMERICAN SOCIETY OF CIVIL ENGINEERS
Founded November 5, 1852
TRANSACTIONS

Paper No. 2793

UNSTEADY FLOW IN OPEN-TYPE PIPE IRRIGATION SYSTEMS

By Edward H. Taylor,[1] A. M. ASCE, Arthur F. Pillsbury,[2] Thomas O. Ellis,[3] and George A. Bekey[4]

With Discussion by Messrs. Robert E. Glover; and Edward H. Taylor, Arthur F. Pillsbury, Thomas O. Ellis, and George A. Bekey

Synopsis

Severe "surging" has presented a serious operating difficulty in parts of the irrigation distribution system of the Coachella Valley County Water District in California. A model study of the mechanics of surge amplification is described, a mathematical analysis of the phenomenon is presented, and a practical method of control of surging is offered. The mathematical analysis was made with a differential analyzer, and the agreement between the theoretical results and the observed results was generally satisfactory.

Introduction

The Coachella Valley County Water District's irrigation distribution system in California delivers water to each arable 40-acre tract through a low-pressure, open-type pipe system. The static head is maintained at safe low levels by open stands in which overflow baffle walls are installed. The overflow stands are usually ½ mile apart, and the baffle walls serve to keep the head between the elevations of the overflow crest and the top of the stand. Part of a typical profile is shown schematically in Fig. 1.

When certain long, relatively flat laterals were placed in operation in 1950, severe "surging" was observed. In many cases the periodic rise and fall of the water surfaces in the stands was so severe that satisfactory deliveries could

---

Note.—Published, essentially as printed here, in December, 1953, as *Proceedings-Separate No. 369.* Positions and titles given are those in effect when the paper or discussion was approved for publication in *Transactions.*

[1] Associate Prof. of Eng., Dept. of Civ. Eng., Univ. of California, Los Angeles, Calif.

[2] Prof. of Irrig. and Eng., Dept. of Civ. Eng., Univ. of California, Los Angeles, Calif.

[3] Engr. Assistant, Univ. of California, Los Angeles, Calif.

[4] Junior Engr., Univ. of California, Los Angeles, Calif.

not be made. For half a minute there would be a big flush of water, commonly overflowing stands and then for another half minute there might be no flow.

J. H. Snyder, M. ASCE, and the two senior authors have made field studies of the Coachella system;[5,6,7,8] Howard G. Curtis, M. ASCE, also has reported on the problem.[9] The purpose of this work is to describe a later and more thorough series of model experiments in which the elevations of five fluctuating water surfaces were measured simultaneously as a function of time. A mathematical analysis is presented, and the results are compared with experimental observations. This analysis is of particular interest because it was performed with a mechanical differential analyzer.

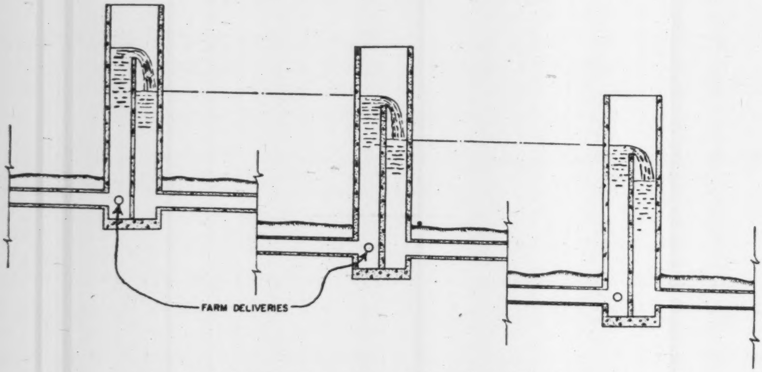

FIG. 1.—SCHEMATIC PROFILE OF AN OPEN-TYPE PIPE LATERAL

EXPERIMENTAL WORK

A model of part of a typical lateral was constructed on a scale of 1 to 12. Efforts were not made to simulate any particular lateral but simply to retain all essential hydraulic elements. A schematic diagram of the model is shown in Fig. 2, and Fig. 3 is a picture of the stands. Actually, the hypothetical prototype would consist of 5-ft (inside) diameter overflow stands spaced $\frac{1}{4}$ mile apart on a 24-in. (inside) diameter pipeline. The model stands have inside diameters of 5 in. and are plastic with $\frac{1}{4}$-in.-thick plastic baffles extending to a height of $21\frac{3}{4}$ in. above the center line of the pipe. The height of the stands is not necessarily to model scale. The 110-ft reach of pipe between each stand is 2 in. in diameter. The first 9 ft of pipe below each stand is clear plastic, and the remaining line is standard 2-in. galvanized pipe. There is a difference in

---

[5] "What Type Concrete Pipe Irrigation Distribution Systems?" by A. F. Pillsbury, *Western Construction*, Vol. 25, No. 9, 1950, pp. 90–92.

[6] "Improvement in Design and Installation of Plain Concrete Pipe Irrigation Systems," by A. F. Pillsbury, *Proceedings*, First Annual Convention, Am. Concrete Agri. Pipe Assn., Chicago, Ill., 1951.

[7] "Preliminary Notes on the Phenomenon of Surge as Observed in Open Type Irrigation Pipe Distribution Systems," by E. H. Taylor and A. F. Pillsbury, *Technical Progress Notes*, Dept. of Irrig. and Soils, Univ. of California, Los Angeles, Calif., 1952.

[8] "Hydraulic Characteristics of Pipe Systems for Irrigation Enterprises," by A. F. Pillsbury and E. H. Taylor, *Agricultural Engineering*, Vol. 34, 1953, p. 837.

[9] "The Bureau of Reclamation and Concrete Pipe," by Howard G. Curtis, *Proceedings*, First Annual Convention, Am. Concrete Agri. Pipe Assn., Chicago, Ill., 1951.

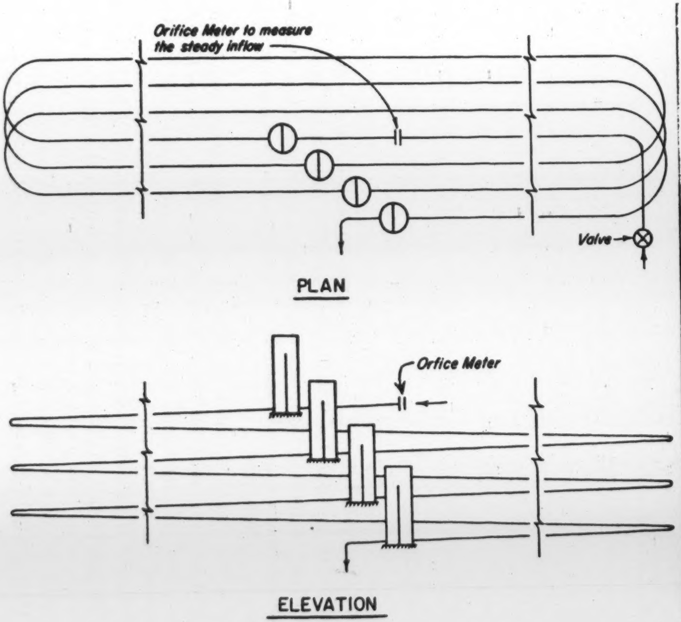
Orifice Meter to measure the steady inflow
Valve
PLAN
Orfice Meter
ELEVATION

Fig. 2.—Schematic Diagram of the Model

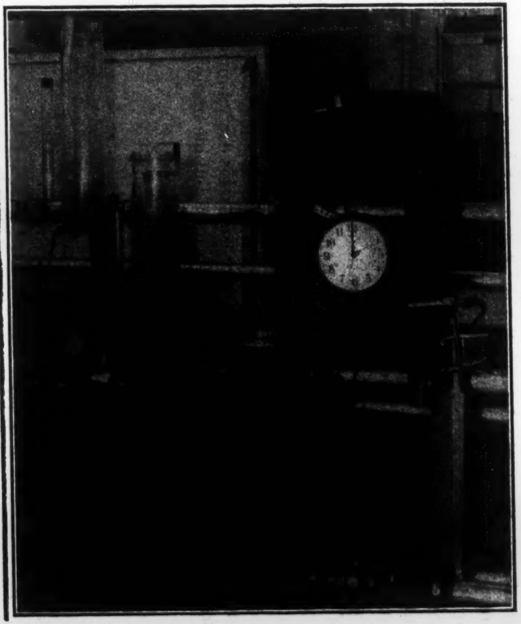

Fig. 3.—The Model Stands

elevation of approximately 1.4 in. between each of four stands; the three reaches of pipe are on a slope of approximately 0.013. The reaches of pipe were looped back on each other, as shown in Fig. 2, (*a*) to conserve space and (*b*) to locate all four stands together.

The notation used herein is shown in Fig. 4, in which the reaches appear in a straight line.

Preliminary Tests.—Qualitative observations were made during the early phases of the model study. These observations facilitated decisions as to the features of the problem most in need of analytical solution and permitted careful planning of the type and location of instruments.

It was found that, when the flow in the system is sufficient to allow the overfalling water to spring clear of the baffle crests, air is drawn into the pool on the downstream side of the stand. This air forms a bubble immediately below the stand, as indicated in Fig. 5. With high flows, the bubble may grow to a considerable size (beyond the 9-ft plastic section of pipe in the model), and air may sometimes be pumped through the reach. In all cases the bubble forms at the zone of separation and continues downstream to some point where it is broken in a hydraulic jump.

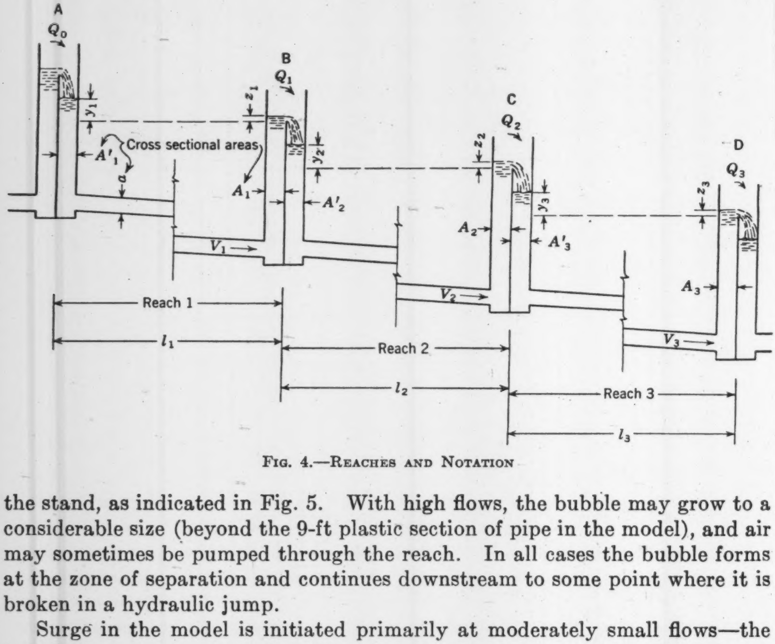

FIG. 4.—REACHES AND NOTATION

Surge in the model is initiated primarily at moderately small flows—the bubble forms, grows, and then blows back up the stand. As the bubble forms and grows, water is displaced; this results in a rise in the pool level and an acceleration of the flow in the pipe. As the acceleration continues, there is a greater discharge than there is water flowing into the pool. Consequently, the pool level begins to fall slightly. The pressure within the bubble is related to the pool level; when this level is lowered even slightly, the air begins to escape back through the pool. The storage space thus created receives water from the pool, the pool level drops further, and bubble pressure is further relieved—

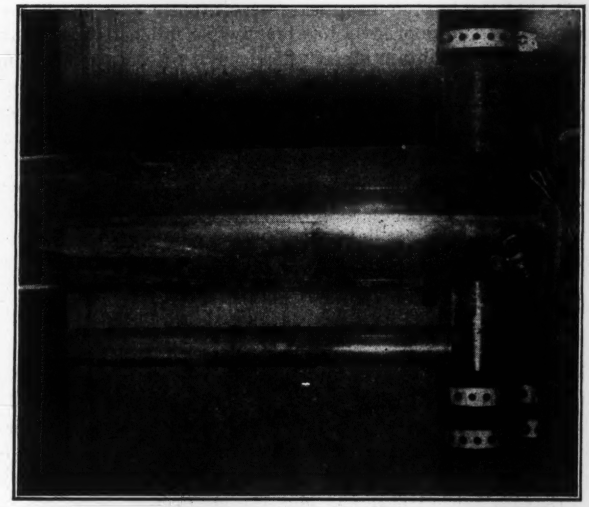

FIG 6.—VENTED OVERFLOW STAND

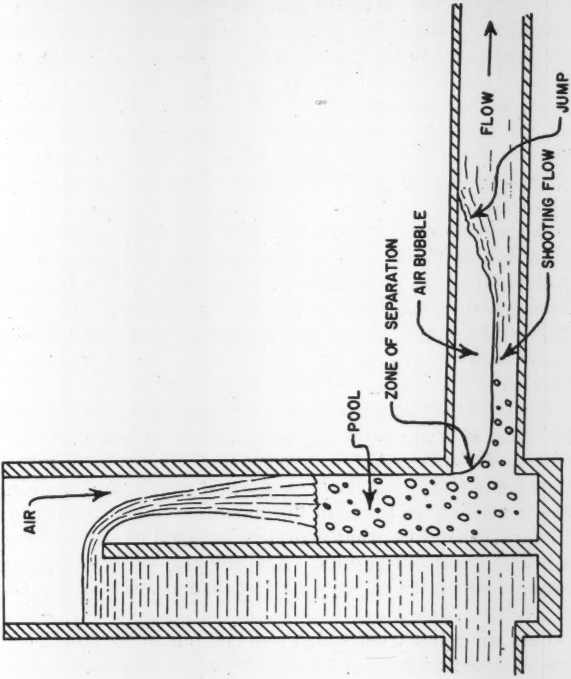
AIR
POOL
ZONE OF SEPARATION
AIR BUBBLE
SHOOTING FLOW
JUMP
FLOW

FIG. 5.—BUBBLE FORMATION

with the result that the bubble disappears very rapidly once the "blow-back" process is initiated. The pool level has meanwhile fallen to an elevation less than that necessary to maintain steady flow. With deceleration of flow, the pool level begins to rise, and the process of bubble formation and blow-back is repeated. In each stand in the system the same phenomenon may occur, with the result that the downstream stands would have a fluctuating component impressed on them from upstream.

It is essential to note that the part of a system comprised of the downstream side of stand A, the upstream side of stand B, and the connecting pipe resembles a large U-tube and has the oscillatory properties of such a tube. If friction could be disregarded, the natural frequency f of such a reach would be, in cycles per second,

$$f = \frac{1}{2\pi}\sqrt{\frac{a\,g}{A\,l}} \quad \text{(1)}$$

in which a is the pipe cross section, in square feet; A represents the half area of the stand, in square feet; l is the length of the connecting pipe, in feet; and g denotes the gravitational force per unit mass, in feet per second per second.

If stand A impresses a slightly fluctuating flow on stand B as a result of the bubble-making process, reach 2, comprising the downstream side of stand B and the upstream side of stand C plus the connecting pipe, reacts to the unsteady inflow in much the same way as a harmonic system reacts to a random excitation. That is, if the exciting influence contains components similar to the natural frequency of the reach, the reach will oscillate at its natural frequency. It may thus be expected that the flow over stand C will fluctuate more severely than that over stand B. Moreover, reach 2 will have "filtered out" most of the "randomness" of the excitation from reach 1, resulting in the application to reach 3 of a rhythmic pulse in resonance with the natural frequency of that reach. Reach 3, therefore, may be expected to be thrown into violent oscillation.

Preliminary observations substantiated this qualitative analysis. For rates of inflow which would cause periodic bubble formation it was noted that, whereas the elevation z_2 in stand B would fluctuate only a few thousandths of an inch, changes of from 8 in. to 10 in. were observed in the elevation z_3 in stand D. The level would drop below the baffle crest of this stand, and during part of the oscillatory cycle the flow in the pipe would actually be in the reverse direction.

It has been suggested[9] that the surge amplification could be eliminated by arranging the natural frequencies of successive reaches in such a way as to avoid resonance. However, practical considerations involved in the layout of a system often make this difficult. Operational problems with lids and gates which are used to accomplish the same purpose also render their use undesirable. It appeared logical, therefore, that complete removal of the exciting influence would bring about beneficial results. Accordingly, vents consisting of 1½-in. inside diameter, clear plastic tubes were installed below the stands, as shown in Fig. 6.

Smaller vents were first tried which reduced but did not entirely eliminate surge. From observation it would appear that the size used was barely ade-

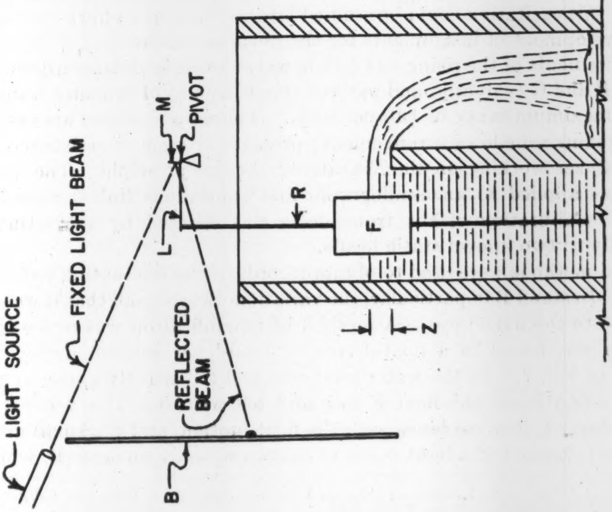
LIGHT SOURCE
FIXED LIGHT BEAM
REFLECTED BEAM
B
L
R
M
PIVOT
F
Z

Fig. 7.—Float-Driven Magnification System

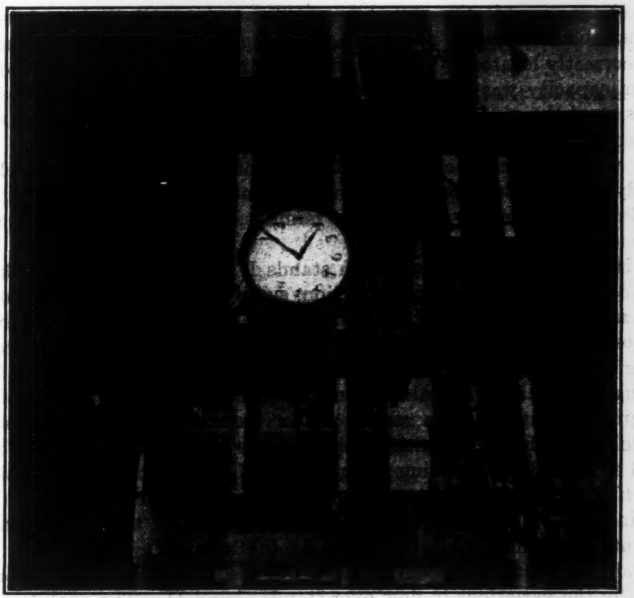

Fig. 8.—Photographic Record

quate to eliminate excitation completely. To remove excitation, vents should be as close to the stand as practical. The vents used were not adequate in size nor correctly located to remove all air during steady high flows, and thus maximum capacity was impaired. It might be desirable to have the vents the full size of the pipe for some distance above the pipe[10] and to provide a supplemental vent some distance downstream.

With vents of adequate size that fraction of the entrained air which had previously gathered in a bubble was released at a uniform rate through the vent. Surging dampened out in a few minutes, and steady flows were maintained.

It is interesting to note that, with stands B and C vented and with only stand A contributing to bubble formation, surge amplification was essentially as great as had been observed when bubbles had formed at stands B and C. It was possible to establish a perfectly steady flow with all stands vented and then plug the first vent and observe the growth of surge. Conversely, removal of the plug resulted in a gradual damping out of the oscillation. The possibility of changing instantly from a steady to an unsteady flow led to a simple technique by which the empirical characteristics of the model could be evaluated and expedited the planning of a program of quantitative investigation.

Quantitative Tests.—The problem of surge amplification was selected to be studied in detail. In this study attention was confined to reaches 2 and 3. The intent was to measure the temporal fluctuations in flow over stands B, C, and D and then to attempt, from knowledge of the flow over stand B, to predict analytically the variations in flow over stands C and D. The analytical predictions were then to be compared with the measured values. Admittedly, the ultimate causative agent—namely, the bubble excitation below stand A, is not considered. However, it was felt that, if the future should prove it desirable, this excitation could be studied later. Time and effort were devoted to the development of instruments for the purposes noted.

Measurements of the rising and falling water levels in the downstream parts of stands B and C (values y_2 and y_3) were made by use of pressure transducers having a maximum range of 1 lb per sq in. These instruments are essentially strain wires in a bellows arrangement; pressure is read as resistance with a strain analyzer working on the Wheatstone bridge principle. The amplified output was applied to an oscillograph, and continuous linked records were obtained. Calibration of the transducers was effected by subjecting them periodically to two known static heads.

Optical methods were used to obtain records of the fluctuating baffle heads, z_1 and z_2. In stand B in particular, the variation was so small that it was hardly discernible to the naked eye. A method of magnification was necessary, and a solution was found in a float-driven, optical-lever system, depicted schematically in Fig. 7. As the water level rose and fell slightly above and below the steady-flow level, the float F rose and fell with it. The vertical rod R tilted the lever L in accordance with the float motion, and the small mirror M caused the reflection of a light beam to move vertically on scale B, which was included in the periodic photography (Fig. 8). Magnification factors in the order of 100 were obtained, making it possible to detect water-level changes of the order of 0.0001 ft.

---

[10] "Analysis of Failure in Unreinforced Concrete Irrigation Pipe," by J. Roberson, *Bulletin No. 216*, State College of Washington, Pullman, Wash., 1952.

The overflow baffles were calibrated as weirs in steady flow, and relationships of the type

$$Q = C z^n \qquad (2)$$

were found empirically. This calibration had to be done with the system in steady flow; it should be noted that, had not the venting proved completely effective in producing steady flow, the calibrations could not have been made. This method worked well for recording the quantities z_1 and z_2 as their variations were relatively small. However, it could not be used in stand D because z_3-variations of from 8 in. to 10 in. would occur. A simple, extremely light float gage was devised for this stand with no magnification whatsoever and was included in the photography; however, it was not highly accurate.

The time variations of z_1, z_2, and z_3 were recorded photographically with a 35-mm motion-picture camera, exposures being made approximately every 2 sec; Fig. 8 shows one such exposure. Attention is directed to the light spots on the blackboard scales and to the float-gage indicator for z_3 in the lower right corner.

The experiment was performed as follows:

1. A steady flow was established with all vents open.
2. The recording oscillographs were started, calibrated, and synchronized with the clock in the photographs.
3. The motion-picture camera was started.
4. When the electric clock indicated one minute, the vent below stand A was plugged. At that moment unsteady flow was initiated.

Four runs of this type were made; the first run was most complete, and further work was concentrated on it.

In addition, four runs of a slightly different nature were performed. Run 7 was selected as having particular interest and is described herein. During the course of the experiment, it had been observed that vigorous surging would occur whenever a flow change was made, particularly if a sudden change was made from one steady value to a lower steady value; this was the case for run 7. A steady flow of 0.0107 cu ft per sec was established. At time equal to zero, this flow was quickly reduced to 0.0070 cu ft per sec; violent surges began and gradually died out. No vents were plugged during this run.

The experimental results of runs 1 and 7 are presented subsequently in Figs. 10 to 14 in which the theoretical results are also plotted for comparison.

THEORY

In the early qualitative stages of this study, the problem was thought to be an extremely complex phenomenon. So many different things appeared to be happening at once that a quantitative analysis seemed to be impractical. Actually, the analysis proved to be essentially simple in so far as the basic ideas were concerned.

In Fig. 4, reach 2 consists of the downstream side of stand B, the upstream side of stand C, and the connecting pipe. The principle of continuity requires that the flow into the downstream side of stand B less the flow out of it be equal to the rate at which water is accumulated in it—

$$Q_1 - a\,V_2 = A'_2\,\frac{dy_2}{dt}\ldots\ldots\ldots\ldots\ldots\ldots\ldots\ldots(3)$$

in which Q_1 is the fluctuating discharge over stand B—this quantity is taken as the given input to the system; V_2 represents the velocity in the connecting pipe; and y_2 is the elevation of the water surface in the downstream part of stand B above the baffle crest of stand C. The equation of continuity relating the pipe line and the upstream side of stand C is, similarly,

$$a\,V_2 - Q_2 = A_2\,\frac{dz_2}{dt}\ldots\ldots\ldots\ldots\ldots\ldots\ldots\ldots(4)$$

in which Q_2 is the fluctuating discharge over stand C—this quantity to be predicted from prior knowledge of Q_1—and z_2 represents the elevation of the water surface in the upstream side of stand C above the baffle crest. The dynamic equation of unsteady flow requires that the total driving head $(y_2 - z_2)$ less the friction head be proportional to the acceleration of the fluid column involved; that is,

$$y_2 - z_2 - h_{f2} = \frac{1}{g}\,\frac{dV_2}{dt}\ldots\ldots\ldots\ldots\ldots\ldots\ldots\ldots(5)$$

in which h_{f2} is the friction head in reach 2.

Eqs. 3, 4, and 5 are based on the following suppositions:

1. Water is completely incompressible. This implies that any pressure changes are transmitted instantly and that the column of water in the pipe line moves as a rigid plug; that is, for all values of t,

$$\frac{\partial V_2}{\partial x} = 0\ldots\ldots\ldots\ldots\ldots\ldots\ldots\ldots\ldots\ldots(6)$$

2. The inertia of the water in the stands may be negligible in comparison with that in the pipeline.
3. The water overpouring in stand B does not add more energy to the system than that expressed by y_2.

The following additional assumptions must be made:

a. The relationship between discharge and weir head, that is, between Q_1 and z_1, Q_2 and z_2, Q_3 and z_3, may be expressed in a form similar to Eq. 2, in which c and n are the same as those observed in steady flow.

b. The steady-flow values of friction head can be applied to unsteady flow.

Each baffle was carefully calibrated as a weir, and the empirical curves relating friction loss to pipe velocity in each reach were obtained.

Using the notations,

$$Q_2 = Q(z_2)\ldots\ldots\ldots\ldots\ldots\ldots\ldots\ldots\ldots(7a)$$

and

$$h_{f2} = h_f(V_2)\ldots\ldots\ldots\ldots\ldots\ldots\ldots\ldots\ldots(7b)$$

to emphasize these empirical functional relationships, Eqs. 4 and 5 become

$$a\,V_2 - Q(z_2) - A_2\frac{dz_2}{dt}\ldots\ldots\ldots\ldots\ldots\ldots(8a)$$

and

$$y_2 - z_2 - h_f(V_2) = \frac{l_2}{g}\frac{dV_2}{dt}\ldots\ldots\ldots\ldots\ldots\ldots(8b)$$

If the third reach is considered, the outflow $Q(z_2)$ of the second reach becomes the inflow to the third. Similar equations may be written for the third reach—

$$Q(z_2) - a\,V_3 = A'_3\frac{dy_3}{dt}\ldots\ldots\ldots\ldots\ldots\ldots(9a)$$

$$a\,V_3 - Q(z_3) = A_3\frac{dz_3}{dt}\ldots\ldots\ldots\ldots\ldots\ldots(9b)$$

and

$$y_3 - z_3 - h_f\,V_3 = \frac{l_3}{g}\frac{dV_3}{dt}\ldots\ldots\ldots\ldots\ldots\ldots(9c)$$

Eqs. 3, 8, and 9 are thus a set of simultaneous differential equations involving the six unknowns y_2, z_2, V_2, y_3, z_3, and V_3. No direct mathematical methods are available (as of 1955) for the solution because the equations are nonlinear. The nonlinearities occur partly because of the empirical functions $Q(z)$ and $h_f(V)$. Moreover, the cross-sectional areas of the upstream stands (A'_2 and A'_3) are not constant because during vigorous surging the water level periodically drops below the intersection of the stand and the pipe. The extreme upstream part of the pipe thus functions as part of the stand in providing storage capacity. The area A' is therefore a constant for values of y down to that of the intersection point and then increases very rapidly as the level is lowered further; therefore, the relationship between A' and the corresponding value of y had to be determined. A further complication was that the functions $Q(z)$ were zero for values of z equal to or less than zero.

A step-by-step numerical solution of these equations was first attempted. A run of 1-min duration was analyzed and compared with experimental data;[8] this procedure required 2 weeks. The results were sufficiently comparable to warrant making a long run and performing the computation on the differential analyzer of the College of Engineering, University of California, in Los Angeles.

SOLUTION BY DIFFERENTIAL ANALYZER

The mechanical differential analyzer[11,12] is a computer which solves differential equations by building a model or analog of them. Quantities are represented on this machine by angular positions of shafts, in revolutions or fractions thereof, from some zero position. The shafts in question are interconnected to the various basic components of the machine which perform the

---

[11] "A New Type of Differential Analyzer," by V. Bush and S. H. Caldwell, *Journal*, Franklin Inst., 1945, No. 240, pp. 255–326.

[12] "The Differential Analyzer of the University of California," by E. Janssen, College of Eng., Univ. of California, Los Angeles, 1947.

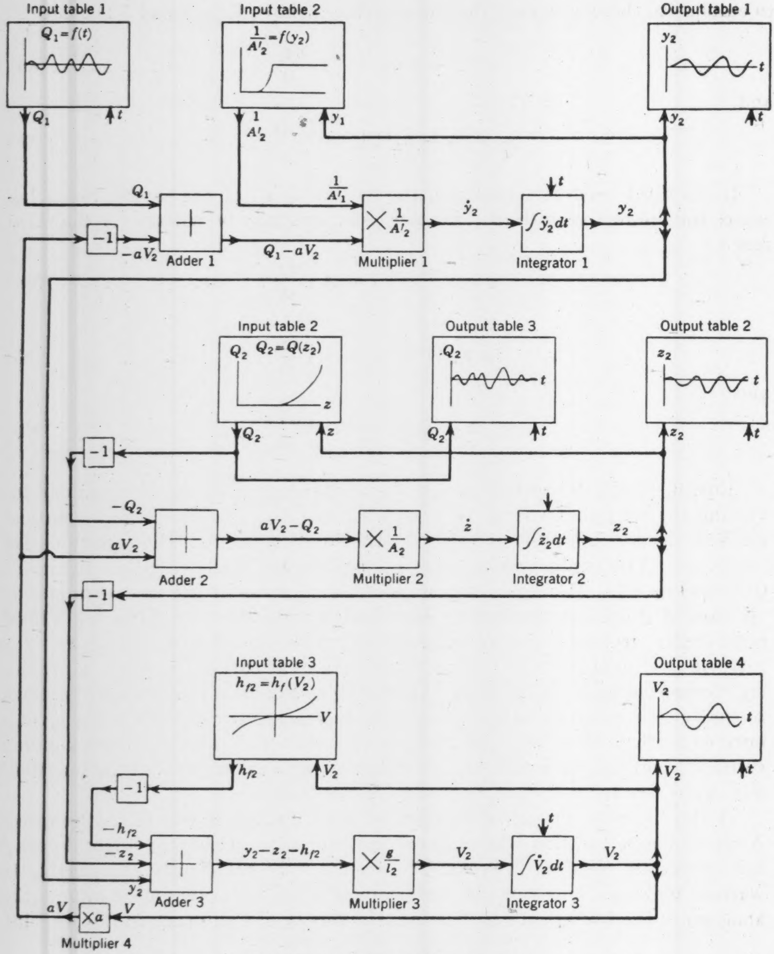
Input table 1
$Q_1 = f(t)$
Q_1
t
Input table 2
$\frac{1}{A'_2} = f(y_2)$
$\frac{1}{A'_2}$
y_1
Output table 1
y_2
t
y_2
t
Q_1
-1
$-aV_2$
Adder 1
$Q_1 - aV_2$
$\frac{1}{A'_1}$
$\times \frac{1}{A'_2}$
Multiplier 1
$\dot{y}_2$
t
$\int \dot{y}_2 dt$
Integrator 1
y_2
Input table 2
Q_2 $Q_2 = Q(z_2)$
z
Q_2
z
Output table 3
Q_2
t
Q_2
t
Output table 2
z_2
t
z_2
t
-1
$-Q_2$
aV_2
Adder 2
$aV_2 - Q_2$
$\times \frac{1}{A_2}$
Multiplier 2
$\dot{z}$
$\int \dot{z}_2 dt$
Integrator 2
z_2
-1
Input table 3
$h_{f2} = h_f(V_2)$
V
h_{f2}
V_2
Output table 4
V_2
t
V_2
t
-1
$-h_{f2}$
$-z_2$
y_2
Adder 3
$y_2 - z_2 - h_{f2}$
$\times \frac{g}{l_2}$
Multiplier 3
$\dot{V}_2$
t
$\int \dot{V}_2 dt$
Integrator 3
V_2
aV
$\times a$
V
Multiplier 4

FIG. 9.—DIFFERENTIAL ANALYZER

operations of addition and subtraction, multiplication and division, and integration. Addition and subtraction are accomplished by differential gears, whereas multiplication and division are performed by inserting appropriate gear ratios between the shafts on which the variables involved are represented. Integration is done by a wheel-and-disk integrator.[11]

The particular arrangement of adders, multipliers, and integrators is determined by the form of the differential equations to be solved. In the problem at hand, time was the independent variable and was represented by the number of revolutions of a certain shaft. Fig. 9 represents the interconnections among the various machine components necessary to solve the first three of the six differential equations. A particularly important feature of the differential analyzer is the ease with which arbitrary functions can be introduced by "input tables." For example, in Fig. 9, input table 1 is in the upper left corner. This table has a graph drawn to a definite scale showing the time variation of the influent quantity, Q_1. The revolutions of the time shaft move an indicator horizontally, by means of a lead screw, across the table from left to right. An operator, using a crank driving a vertical lead screw, keeps the indicator on the curve. The number of turns made by the operator is proportional to the quantity Q_1. The turns are delivered to a shaft which carries them to adder 1. Then the quantity $- a\,V_2$, which is simultaneously being generated, is also fed to this adder. The output of the adder is the left member of Eq. 3, and when it is multiplied by l/A'_2 the output of multiplier 1 is the derivative dy_2/dt or, more conveniently, $\dot{y}_2$; these revolutions go into integrator 1. As this quantity is the integrand, the number of turns representing it operate the lead screw in positioning the wheel on the disk while the time shaft is driving the disk. The number of turns of the integrator wheel is the integral,

$$\int \dot{y}_2\,dt = y_2 \qquad (10)$$

which is fed back to input table 2. The horizontal axis is driven by the y_2-shaft while a second operator follows, by hand crank, the variations in the quantity l/A'_2, which has been plotted on this table as a function of y_2. The revolutions of the y_2-shaft are also delivered to the vertical lead screw of output table 1. The time shaft drives the horizontal lead screw and moves a pen across the table from left to right while the y_2 lead screw plots the course of the variable y_2.

In Eq. 8*b*, y_2 is a variable; its shaft is connected to adder 3 which is also receiving $- z_2$ and $h_f(V_2)$, which are being generated simultaneously elsewhere in the system. The output of adder 3 is seen to represent the left member of Eq. 8*b*. The number of revolutions representing this quantity is reduced by a constant gear ratio representing $g/1$ in multiplier 3, and turns of this shaft represent the time derivative $\dot{V}_2$ in accordance with Eq. 8*b*. Integration with respect to time is accomplished as before in integrator 3, and the result is fed back to the horizontal lead screw of input table 3 where the friction head term is generated by an operator who follows the arbitrary function $h_f(V_2)$ with turns of the vertical lead screw. These turns are, as has been noted, delivered to adder 3 after going through a 1 to 1 gear ratio which changes the sign. Meanwhile, the revolutions of the V_2-shaft have undergone multiplication by a in multiplier 4 and a sign change and are fed back into adder 1, thus completing the circuit, for Eq. 3.

At the same time, the shaft revolutions representative of the quantity $a\,V_2$ are delivered to adder 2, which is also receiving $- Q_2$. Just as previously described, the left member of Eq. 8*a* is the output of adder 2, and subsequent multiplication and integration yield the quantity z_2 in accordance with Eq. 8*a*. Again, this is fed back to input table 2 as the abscissa while an

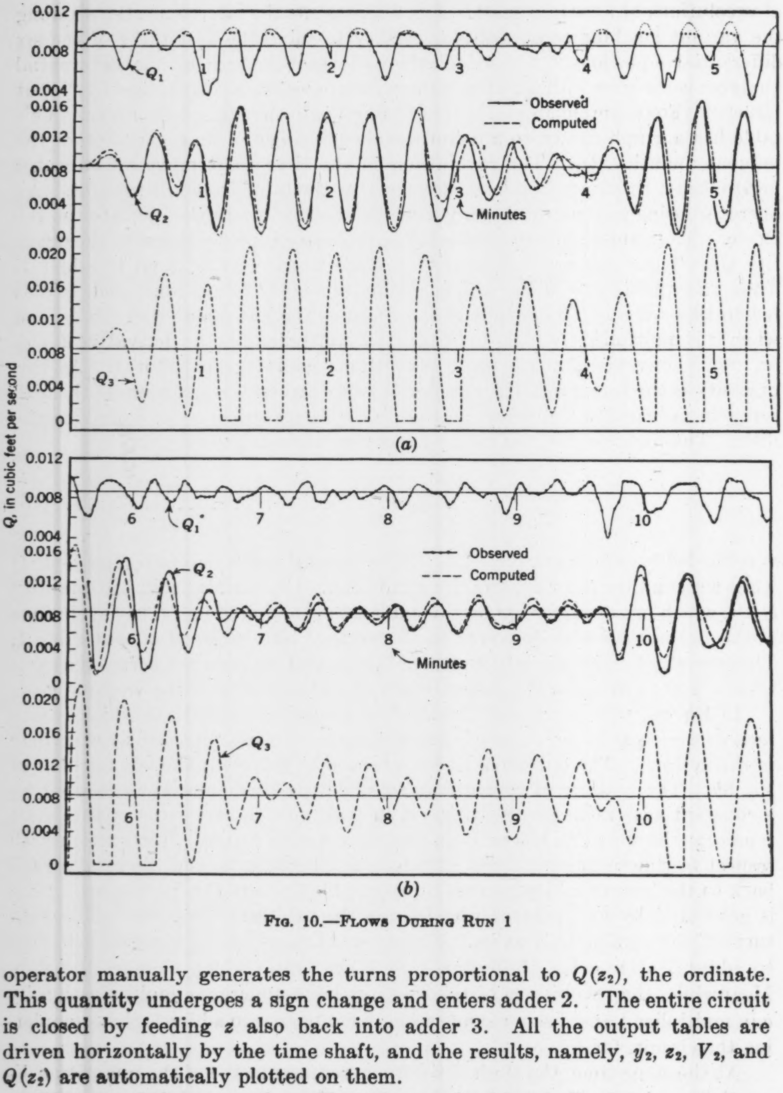

FIG. 10.—FLOWS DURING RUN 1

operator manually generates the turns proportional to $Q(z_2)$, the ordinate. This quantity undergoes a sign change and enters adder 2. The entire circuit is closed by feeding z also back into adder 3. All the output tables are driven horizontally by the time shaft, and the results, namely, y_2, z_2, V_2, and $Q(z_2)$ are automatically plotted on them.

The second three equations (Eqs. 9) are solved by similar interconnections among the elements of the differential analyzer. All subscripts are increased by one so that the outflow, Q_2, of the second reach becomes the inflow to the third.

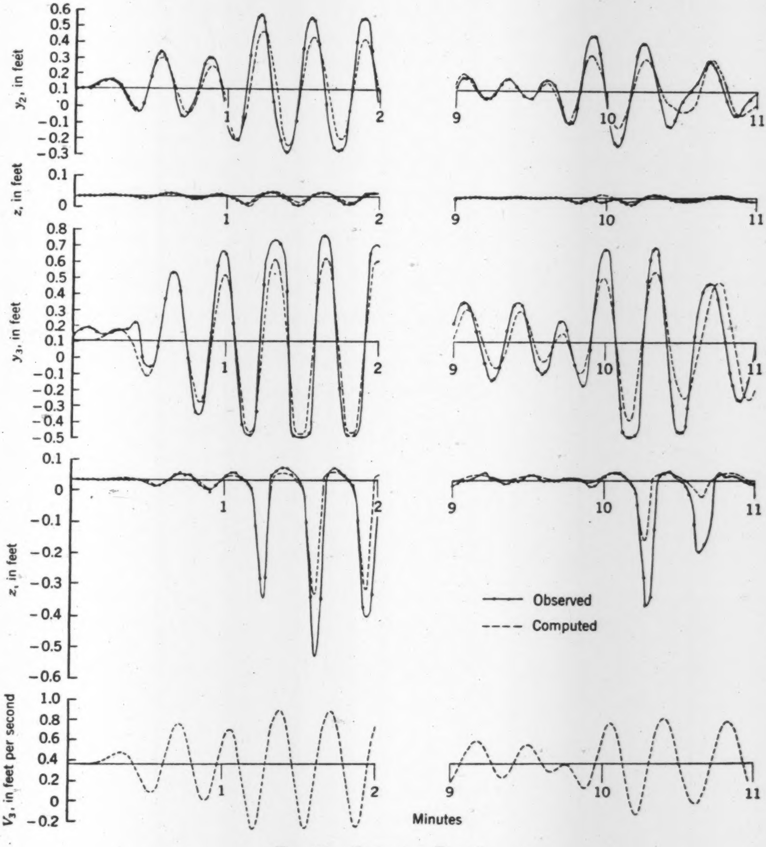

FIG. 11.—DATA FOR RUN 1

It is to be noted particularly that the analyzer connections form a completely closed loop. Although it may have been indicated that multiplication, integration, and such take place consecutively, actually these operations occur simultaneously.

RESULTS

In Fig. 10 are shown the values of Q_1, Q_2, and Q_3 for the entire eleven minutes of run 1; Q_1 is shown as observed and as used in table 1 for the input to the differential analyzer. The observed Q_2 is given as well as that computed by the differential analyzer, and Q_3 is given as computed. The values observed for z_3 were not believed to be of sufficient accuracy to warrant computation of Q_3 therefrom.

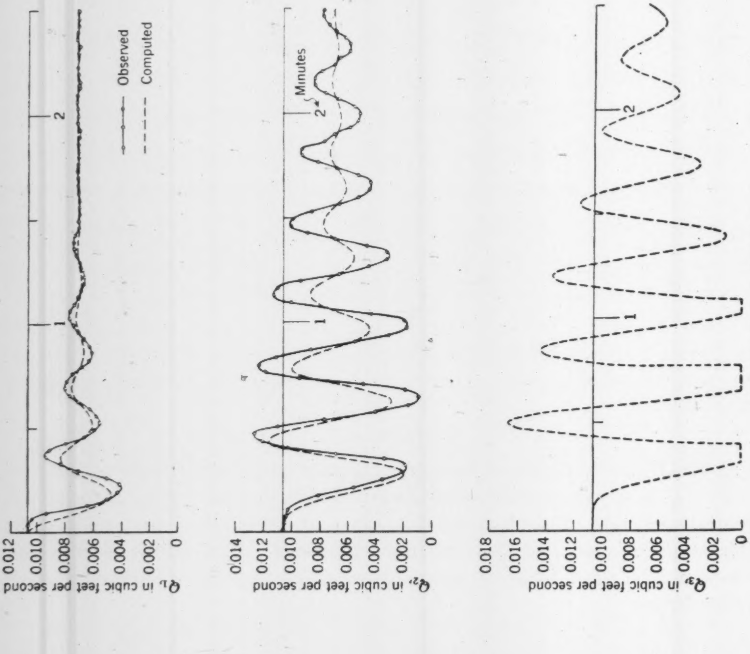

FIG. 12.—RUN 7, SOLUTION 2

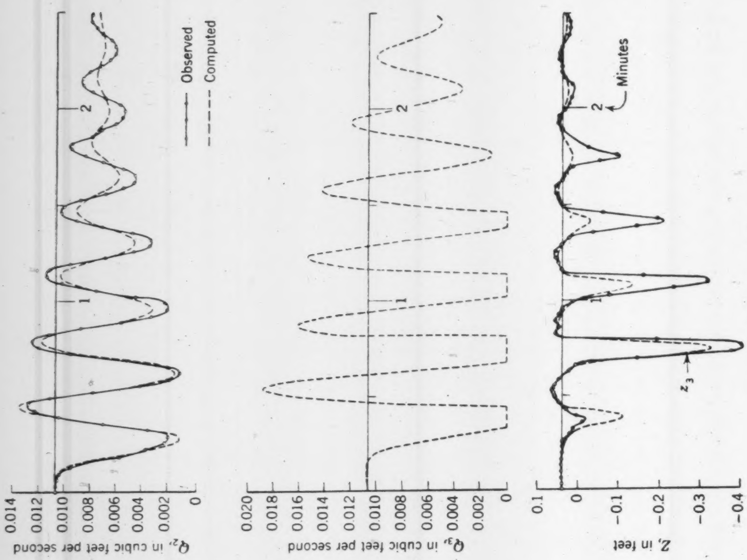

FIG. 13.—RUN 7, SOLUTION 3

Unfortunately, the optical system for measuring z_1 was so adjusted during run 1 that the knife edge of the lever L apparently hit the side of the groove in which the knife pivoted. This affected readings of approximately 0.010 cu ft per sec and higher, and therefore the arbitrary dotted-line correction was made.

The scales on which the various observed and computed values were plotted were found to vary slightly—only 4 sec to 5 sec in the total 11 min—but the variations were enough to make the observed and computed surges appear somewhat out of phase with each other. Rather than replotting the data, in preparing the charts the simple expedient was used of matching the curves at zero time in Fig. 10(*a*) and at the end of the run (11 min) in Fig. 10(*b*). Toward the right in Fig. 10(*a*) and toward the left in Fig. 10(*b*) the curves therefore appear slightly out of phase.

In the middle of the run there is a break in the experimental Q_2-curve. At that time a violent surge threw the rod R off the lever L of the optical system for measuring z_2. A few seconds elapsed before it could be put in order.

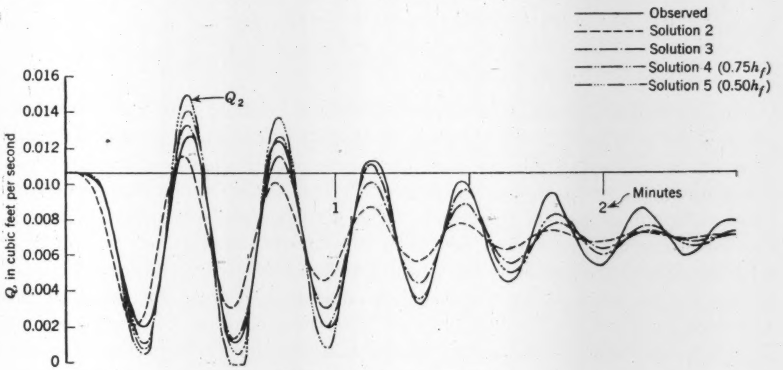

FIG. 14.—SURGES IN FLOW

Some of the other data of run 1, both computed and observed, are shown in Fig. 11. It was thought adequate to plot only the first 2 min and the last 2 min of the run for these data.

The values of Q for run 7 are shown in Fig. 12. In this run, at zero time Q_0 was reduced from 0.0107 cu ft per sec to 0.0070 cu ft per sec. Such a change invariably produces violent surging which gradually dies out; all vents in the model were open. The change in Q occurred above reach 1; therefore, the first stage of amplification is reach 1 instead of reach 2 as in run 1.

It was noted that the observed and computed data were somewhat out of phase for run 7. In order to see if this was caused by the time it actually took to change the flow in the model (the change was presumed to be instantaneous on the differential analyzer), another solution (solution 3) was attempted on the differential analyzer. In this solution (Fig. 13) the observed Q_1 was put on the input table rather than Q_0, indicating that the differences in phase were caused by the time it actually took to change the flow on the model. Also shown in Fig. 14 are Q_3 and z_3 for run 7 (solution 3).

For run 1 the observed surges were noted to be of somewhat greater amplitude that the computed surges, particularly for reach 3. This tendency was even more apparent in run 7, and, in addition, observed surging was more sustained that was computed. Less friction loss in the pipelines than determined for steady flow was a possible explanation. Values of friction loss for the pipeline in reach 2 as set up on the differential analyzer were therefore reduced 25% in solution 4 and 50% in solution 5. The Q_2-surges (Fig. 14) computed under these conditions were greater but not more sustained. It was therefore concluded that values assigned to pipe-friction loss were not the cause of differences between observed and computed surges.

It is probable that some differences in observed and computed values can be accounted for by inertia or the inaccuracy of the instruments. After careful review of the data, however, it has been concluded that differences that could be so explained were relatively minor.

There remain two original factors that may contribute to the differences:

1. Neglect of the inertia of the water in the stands.
2. Neglect of the energy periodically fed into a reach by the falling water from the preceding reach.

In addition to these factors, a fraction of the air entrained by the overfalling nappe bubbled directly back through the stand without ever reaching the pipe. This was a continuous process, and therefore a part of the storage volume was taken up by air under the water surface. The net effect was a decrease in the cross-sectional area A' of the stand. Had a correction been made for this, a smaller numerical value for A' would have been used in the analyzer solution, with the result that the computed amplitudes would have been larger. Because it was not known how to make such a correction, it is reasonable that the observed amplitudes were slightly larger than those computed. In this regard, it will be recalled that the ability of free-falling water to entrain air does not scale down. Hence, in constructing the model it was necessary to provide higher stands than strict model proportions would have dictated. Any inaccuracy in the theory caused by these suppositions would thus be of considerably less importance in a normal prototype than in this model.

Conclusions

1. In the model experiments surge was initiated below an overflow stand by the entrainment of air in the downpouring water, by the collection of that air in a bubble immediately downstream from the stand, and by the periodic blowing-back of that bubble into the stand.

2. This surge initiation can be completely eliminated by large vents placed immediately downstream of the stand.

3. Surge, initiated in an open-type pipe system, is amplified in subsequent reaches downstream, provided that the natural frequencies of succeeding reaches are close enough to the frequency occurring in the original reach. Fluctuations not in phase may cause amplification, but the surging will tend to die out, and surges not in phase will tend to be filtered out.

4. Venting provided to prevent surge initiation will have no significant effect on amplification of surge.

5. The theory presented provides a substantially accurate quantitative evaluation of surge amplification. Any tendency of observed amplification to exceed computed amplification can apparently be explained by the suppositions required for simplification of the theory. In prototypes, any differences between observed and computed surge should not be of appreciable magnitude.

6. Considerable work may be done to establish criteria by which surge difficulties in open-type systems can be minimized. However, such techniques generally add to the problems of regulating open-type systems. Therefore, it is recommended that systems which contain inherent oscillatory properties, as does the open-type system, be no longer built.

DISCUSSION

Robert E. Glover,[13] M. ASCE.—The comparison of the results of a model test with studies made with a differential analyzer contains much that is of value and interest. An observer's first experience with overflowing pipe stands is apt to be a very puzzling one because it appears that the water is running uphill in violation of hydraulic fundamentals. Only through analytical procedures can this peculiar behavior be explained. The analyses presented by the authors are of particular value because, by using the differential analyzer, they have been able to follow every important detail of the phenomena and to show that they are, after all, explainable on the basis of well-known laws. An inertia drive is the factor which forces the water levels temporarily above their normal running positions.

When surging of troublesome magnitude developed in the Coachella installation in 1950, a vigorous program of investigations was initiated by the Bureau of Reclamation, United States Department of the Interior (USBR). The Coachella distribution system serves an area which is approximately 25 miles long and 10 miles wide. Concrete pipes, with baffled pipe stands for pressure control, are used for conveying irrigation water in this area. Some of the lines on this system are from 6 miles to 8 miles long. The program included field studies, model studies, analytical researches, and electric-analog operation. These investigations led to the use of covers as an inexpensive and practical method of surge suppression, and much of the system is in use under this type of control. Other means of control were also studied; these included the use of gates, vents, and modifications of the pipe-stand arrangement to avoid air entrainment, but none of them proved to be as effective as the covers.

The air-driven auto-oscillation described by the authors is a persistent source of initiating oscillations. These oscillations are of small amplitude at the point of occurrence and would be of no significance if it were not for the amplifying tendencies of the succeeding pipe reaches. This amplifying tendency was discovered through analytical and experimental researches in the early part of the USBR's investigations. The capacity to amplify goes beyond mere resonance, although resonance is involved. It is remarkable that a simple hydraulic structure like a pipe stand should possess this capacity. The behavior of the stand is, however, closely analogous to that of an electronic vacuum tube, and it has the same capacity to feed energy into an oscillation. Amplifying factors of from 4 to 6 in each pipe reach are not unusual when the natural periods of succeeding reaches are similar and flow conditions are favorable.

The authors propose to control surging by the use of properly placed vent pipes. The purpose of these pipes is to permit the release of entrapped air and thereby to destroy the oscillations at their source. This treatment seems logical, and it is a fact that stable running could be produced in the USBR model by installing a vent in the first pipe reach. Field experience indicates, however, that surge control cannot usually be obtained in this way because the amplification tendencies remain and because there are other sources of initiating oscillations present in addition to those produced by air entrapment and release. It seems probable that a short line with no more than three or four pipe stands could be stabilized by vents, but in long lines the amplification factors run into almost astronomical figures and control by vents becomes impossible. For example, in a line 6 miles long with pipe stands at ¼-mile intervals, there would be twenty-four pipe reaches. If each reach had an amplification factor of 4, the over-all amplification possible for any initiating oscillation originating in the first reach would be 4^{23}. This is a tremendous amplification potential, which indicates that the line would be able to build the most minute initiating oscillation into a violent surge before the end of the line was reached. Field experience indicates that gusts of wind blowing over the tops of open pipe stands are quite capable of creating adequate initiating oscillations. The process of making and cutting off deliveries is also a source of initiating oscillations. The fact that these are of a temporary nature does not mitigate the severity of the surges they produce. There may be other unidentified sources of initiating oscillations, but, at any rate, field experience indicates that they are always present and that vents cannot control them.

---

[13] Research Engr., Bureau of Reclamation, U. S. Dept. of the Interior, Denver, Colo.

Auto-oscillation tendencies often remain even though vents are used because the best position for the vent varies with the flow. At velocities lower than those for which the vent placement is best adapted, a bubble may form between the vent and the pipe stand, whereas, at higher velocities, a bubble may form downstream from the vent. The auto-oscillation produced under these conditions is much weaker than it would be if the vent were absent, but with sufficient amplification downstream, it can initiate surges which acquire intolerable magnitudes.

The use of covers provides a means for grouping several reaches into a system which behaves as a unit but which has periods much different from those of the individual reaches. Not only can the number of oscillating systems in a pipeline be drastically reduced by this means, but the grouping can also be chosen to destroy or reduce the possibility of resonance. The covers therefore provide a powerful and positive method of surge control which is effective against disturbances arising from any source.

Edward H. Taylor,[14] A. M. ASCE, Arthur F. Pillsbury,[15] Thomas O. Ellis,[16] and George A. Bekey.[17]—The very able discussion by Mr. Glover is greatly appreciated, although the attempt, here and elsewhere,[18,19] to overemphasize the effect of covers and minimize the effect of vents is puzzling. Actually, those parts of the Coachella system where surging was a problem were made operable by a combination of covers and gates through the baffles. No mention was made by Mr. Glover of the operating difficulties of covers, such as (*a*) occasional occurrence of surge at certain flows regardless of covers, (*b*) the blowing off of the covers from time to time, or (*c*) the necessity to decrease the effectiveness of a given cover in order to obtain satisfactory delivery at that point. As for vents, model experiments would confirm that such field trials as were undertaken would not prove satisfactory. Until there are adequate field trials, the effectiveness of prototype vents must remain pure speculation.

---

[14] Associate Prof. of Eng., Dept. of Civ. Eng., Univ. of California, Los Angeles, Calif.

[15] Prof. of Irrig. and Eng., Dept. of Civ. Eng., Univ. of California, Los Angeles, Calif.

[16] Engr. Assistant, Univ. of California, Los Angeles, Calif.

[17] Junior Engr., Univ. of California, Los Angeles, Calif.

[18] "Surge Control of the Coachella Pipe Distribution System," by C. S. Hale, P. W. Terrell, Robert E. Glover, and W. P. Simmons, Jr., *Engineering Monograph No. 17*, Bureau of Reclamation, U. S. Dept. of the Interior, Denver, Colo., January, 1954.

[19] "Control of Surgings in Concrete Pipe Distribution Systems," by C. S. Hale, Robert E. Glover, P. W. Terrell, and W. P. Simmons, Jr., *Proceedings*, A.C.I., Vol. 50, No. 33, 1954, p. 573.

AMERICAN SOCIETY OF CIVIL ENGINEERS
Founded November 5, 1852
TRANSACTIONS

Paper No. 2794

PRIVATE ENTERPRISE CAN SATISFY THE PARKING DEMAND

By Charles T. McGavin[1]

Synopsis

The need for parking areas in cities is constantly increasing and can be filled either by a combination of commercial and merchant facilities or by municipal investment. The author presents data on off-street parking facilities and states the reasons for his conclusion that the municipality should cooperate in but not finance a parking program.

Introduction

The young and rapidly growing parking industry, representing more than a three-billion-dollar investment, stands on the very threshold of tremendous progress. It is managed by men skilled in their profession who are alert, progressive, resourceful, and acutely aware of their responsibilities to the motorist, to the taxpayers, and to the economic principles under which the United States has prospered. To understand this, it must be recognized that these skills and devotion to duty and principles have emerged from practical experience with the economic "facts of life." The purchase of valuable property (some of it worth more than a million dollars for a single piece), the gamble connected with signing of leases of 25-year and 50-year periods, and the necessity of meeting the payroll every Saturday night and paying the rent on the first of the month are vastly different from preparing plans, programs, or prospectuses, or making "guesstimates" of parking "demand."

In order to predict the future of this industry, it is advisable to study the past. There is an inscription on the Archives Building in Washington, D. C., which reads: "What is Past is Prologue." This idea has special application to the parking industry.

Evolution.—If the question of the role of private enterprise in parking were approached from the standpoint of the evolution of a typical American business, there would be a much clearer understanding and less difference of

---

Note.—Published, essentially as printed here, in January, 1955, as *Proceedings-Separate No. 599.* Positions and titles given are those in effect when the paper was approved for publication in *Transactions.*

[1] Executive Director, National Parking Assn., Washington, D. C.

opinion as to which way to achieve the desired end result most quickly and economically.

All business enterprises and industries experience first a "Topsy"-like growth and then, after a period of experimentation, the emergence of well-defined patterns of a planned development that adequately serves its market. The department-store idea, for example, had its beginning nearly 100 years ago and has since experienced dramatic evolutionary changes. In the writer's professional library there is a photograph of one of the largest department stores in a major American city, with a sign painted on the side of the building announcing that it has elevator service which is free to the public for business purposes only from 8 a.m. to 12 noon and from 1 p.m. to 6 p.m. This new service feature was introduced 50 years ago. The years since 1860 have brought a continuing flow of new concepts of service and operation in the department-store business. The same course of development is evident in the parking business although its evolution began later.

Evolution of Off-Street Parking

From 1920 to 1930.—The idea of off-street parking facilities had its real beginning about 1920. Parking lots were primarily only one facet of some other automotive service. The first parking garages designed as such came into existence about 1921. There was a substantial development of the multiple-floor garage in all major cities until 1930. However, about 1926 the pattern of financial failure began to emerge. Increasingly, projects failed to pay the bondholders, and well before the stockmarket failure in 1929 multiple-floor parking garages were financial failures because they were unable to operate successfully, using only 40% of their capacities.

Ground Hogs.—One of the greatest problems of the steam-heated garages was the motorist who would only patronize garages between Thanksgiving Day and St. Patrick's Day. These patrons were referred to as "ground hogs" because they would park indoors after the first snow flurry and leave after "Ground-Hog Day," the second of February. Garage management of that time could not solve the problems of operating on three months a year at full capacity and nine months at from 40% to 50% occupancy.

Parking Lots 1930–1939.—After 1930, banks and investment houses avoided further investments of this type. The period from 1930 to 1939 included almost no construction of multiple-floor parking garages. During this period, however, parking lots achieved a new and permanent status. They provided "breathing spaces" between buildings and helped to break up the dense, compact mass of building development. They realized a high rate of return on the property investment and successfully competed on the free market with other land uses. It is a fallacy to call these facilities "temporary."

Department-Store Parking Facilities.—Beginning in 1936, department stores recognized a relationship between convenient customer parking and the annual volume of sales. Some studies revealed that the patronage of customers who parked in store-provided facilities might be as great as $25,000 per parking stall per year. These studies formed the basis of a trend toward merchant-developed parking facilities which is now quite widely established.

New Generators of Parking Demand.—Although enlightened self-interest motivated the large merchants to recognize the business value of providing customer parking facilities, there was an increasing recognition among city-planning officials that in the development of new business structures the owners should be required, through zoning laws, to provide at their own expense adequate facilities to serve the parking requirements generated by the proposed structure. It was felt that such a zoning requirement would be economically feasible and would merely require, by law, that the owner do what he should do anyway as a matter of sound business. This trend has made outstanding progress since its beginning in 1937. Although a great number of cities now have such zoning laws, it is difficult to reconcile this zoning concept with the concept of parking as a municipal responsibility.

Municipal Parking, 1938.—In 1938 the American Society of Planning Officials and the International City Managers Association discovered that there was a well-established trend toward municipal parking facilities. Based on replies to 147 questionnaires from selected groups of cities in the different population brackets, it was found that one fourth of these cities had established municipal parking lots and additional cities were considering doing so. One third of the cities had established such facilities within the past 3 years; the idea of parking as a municipal responsibility can therefore be considered as beginning shortly before 1938.

The Federal Government and Public Parking.—At the Highway Research Board (National Research Council) meeting in 1940, the commissioner of public roads (United States Department of Commerce) announced that efforts to provide low-cost parking in cities had been feeble and ineffective and that, because American cities had done little or nothing to provide such facilities, the time had come to think of parking as an extension of the street system. The commissioner justified parking as a public responsibility on the grounds that accessibility to the downtown area was to the advantage of not only the motorist but also the property owner, the merchant, and the city itself. He declared:

> "This trend toward municipal operation is perhaps inevitable in view of the connection between parking and street facilities in the provision of highway transportation."

The philosophy of governmental subsidy, elimination of private-enterprise profits, and the use of special assessments, general obligation bonds, and revenue bonds to finance parking were specifically set forth.

This was followed by an issue of the magazine, *Public Roads,* in July, 1941, which was entirely devoted to parking—much of it dealing with the subject of legal aspects of municipally operated parking facilities.

Government Funds for Public Parking.—In November, 1941, the commissioner of public roads was authorized[2] to cooperate with the states in the location, development, and construction of off-street parking facilities and to consider such projects as highway projects. This act stipulated that funds available for expenditure

---

[2] **"Defense Highway Act," 55 stat. 765, November, 1941.**

> "* * * in accordance with the provision of the Federal Highway Act—are hereby also made available on the pro rata basis heretofore provided by law for the location, development, and construction of off-street parking facilities to serve the area where parking on such highway is prohibited."

The provisions of this act are still on the books 12 years later, although they have never been put into effect.

Research on Parking As a Public Responsibility.—During World War II, research work on parking as a municipal responsibility was conducted; this research resulted in the postwar unfolding of organized campaigns to plunge the municipalities into the parking business.

From the middle of 1945 to 1950, there was a succession of announced plans and programs based on the idea of parking as a public responsibility. Only now can one realistically appraise the practical results of these municipal programs and evaluate them objectively.

OFF-STREET PARKING CAPACITIES

The writer's preliminary study, based on available reports and surveys, reveals the following pattern of off-street capacity for downtown areas of cities in the following population brackets.

1,000,000 or More.—In 5 cities with populations exceeding one million there are approximately 250,000 off-street parking spaces in the downtown areas of which approximately 5% are municipally owned. Many municipally owned spaces are in the peripheral areas. Of the off-street capacity, 70% is provided in parking lots.

From 500,000 to 1,000,000.—In 13 cities having from one-half million to one million people, there are approximately 220,000 off-street parking spaces in the downtown areas of which about 10% are municipally owned. A large number of these municipal facilities are in the nature of fringe facilities, some are leased to private operators, and several are free parking lots. The writer would estimate the effective capacity in places where space is needed to serve the short-time parking clientele to be approximately 5%. Of the off-street facilities 60% is in the form of parking lots.

From 250,000 to 500,000.—In 23 cities of from one-quarter million to one-half million people, there are approximately 260,000 off-street parking spaces of which 4% are municipal parking facilities. Of the off-street parking capacity, 75% is provided in parking lots.

From 150,000 to 250,000.—In 23 cities within this population category, there are 130,000 off-street parking spaces in the downtown areas of which 4% are municipal parking facilities. Parking lots comprise 83% of the total off-street capacity.

From 100,000 to 150,000.—In 42 cities having populations of from 100,000 to 150,000 there are 135,000 off-street parking spaces in the downtown area of which 4% are municipally owned.

Average.—The over-all average for 106 cities of more than 100,000 population shows that 5% of the total off-street capacity is now provided by municipal parking.

From 50,000 to 100,000.—In the 126 cities of this population group, there are 245,000 off-street parking facilities in the downtown areas of which 10% are municipally owned. Parking lots comprise 85% of the total capacity. In this population bracket, the capacities for curb parking and off-street parking are nearly equal, averaging 2,000 spaces each per city in central business districts of the average city, and the congestion problem is not critical.

Summary.—The over-all situation for the 232 cities of more than 50,000 population is that municipal parking averages 675 spaces per city, counting only the cities having municipally owned facilities. Distributed over the entire 232 cities, the average would be about half that number. In all cities of more than 50,000 population, municipal parking represents approximately 6% of the total downtown capacity. Parking-lot capacity provides two thirds of the total off-street capacity.

TRANSIT INDUSTRY AND PARKING

The relationship of the transit industry to the general parking situation is an important one. Transit companies everywhere have contributed in large measure to the growth and development of valuable concentrated business areas; yet now, either through a calculated policy or through ignorance of where their best interests lie, cities are neglecting this industry. The transit service is being choked and forced to operate at much less than its capacity for service because of unjustified curb parking. Transit service has been given sympathetic words but has been harrassed and hampered by official acts or failure to act on matters which impede transit operations in congested areas. Curb lanes must be freed in order to improve traffic movement of the transit vehicle in congested areas. Abolition of curb parking, where needed, will speed transit service. This will encourage greater use of the mass transportation system and will relieve some of the pressure for additional parking. In many cities, surveys of occupancy and use of existing parking facilities reveal vacancies that are more than ample to contain all the cars forced from the curb; the writer has observed that curb-parking restrictions are invariably followed by the development of additional nearby off-street facilities when they are needed. There is no justification for using the parking problem as an excuse for congested traffic conditions. Traffic congestion will not be cleared until curb parking is prohibited. Traffic pressure brought about the abolition of diagonal parking in downtown streets 20 years ago when motor-vehicle registrations were 24,000,000. Now there are 58,000,000 vehicles on the streets and highways, and there is ample justification for the abolition of curb parking.

RELATIVE ADVANTAGES, MUNICIPAL AND PRIVATE PARKING

Private Enterprise.—From the foregoing data it is clear that, to date, private enterprise has supplied most of the parking space. Not quite 6% of parking is provided through municipal endeavor. This performance record of achievement by the parking operators of the nation has been in the best traditions of the private-enterprise system. There is every reason to believe that this splendid achievement will continue; indeed, the future of accelerated progress by private enterprise is very promising.

Parking requirements can be filled most quickly and most economically through private enterprise. This is certainly no revolutionary statement; its truth is evident. A private operator, by the very nature of his undertaking, must make a profit on his investment. Thus, land must be acquired as cheaply as possible; construction costs must be as low as is practical; and full advantage must be taken of improved construction techniques, improved layout and design, and improved operating techniques. If all current technological advances are to be combined with the progress that is being made in the field of parking management to create in effect a technological revolution in off-street parking, surely private enterprise will be responsible for the advance because they will be to the direct advantage of the private owner-operator. Indeed, this possibility of increasing profit is recognized as one of the strongest driving forces behind the development of improvements in any field.

Municipal Parking Costs.—Readily available figures on garage construction costs show that the cost of municipal parking is higher than the cost of private parking. Because the private operator cannot afford to lose money on his investment, his construction costs must not exceed $1,200 per car space. Some garages are designed that cost as little as $800 per car space at 1955 prices. Municipal costs may be as great as $2,500 per car space. Modernization of building codes would make lower construction cost possible.

The costs of properties acquired by city governments for parking are considerably greater than those acquired by private enterprise. There is a mistaken belief by many proponents of municipal parking that acquisition by condemnation is cheap. The reverse is true—the writer knows of one case when the proposed property had an assessed value of $40 per sq ft, but the owner could prove in court a market value of $115 per sq ft. It was not feasible for the city to condemn because on this basis the investment would be $6,000 per car space. However, the owner has proceeded to build a six-story parking structure on this site.

Mistaken Claims About Private Parking.—The claim that private enterprise cannot acquire property suitable for parking at the right locations is the principal argument in favor of condemnation. This claim is not correct. For example, in the writer's own city, private garages are being constructed on some of the city's most valuable commercial real estate. New developments in garage design have completely eliminated the need for large land parcels that cannot be acquired by purchase. That land which the private operator needs can be bought in the same skilful manner in which any other business organization acquires necessary real estate.

Another mistaken claim is that private enterprise cannot assure the permanence of parking facilities. This claim reveals a lack of knowledge of the competitive enterprise system. A parking facility that has proved to be a profitable investment and that produces a sizable income is as stable as any other kind of business. Parking use successfully competes with all other types of land use.

Provision of Parking Is Not a Municipal Responsibility

Parking cannot be considered an extension of the street system. Throughout the history of transportation—whether land, sea, or air—three basic components are essential: (1) The vehicle, (2) the roadway, and (3) the terminal facility. The highway component of automotive transportation is recognized as a matter of public undertaking, but it does not follow that the terminal facilities are an extension of the street system any more than the idea that the other component—the automotive industry—should be a government enterprise because it is also one of the three components comprising the automotive transportation system.

Parking provided by business organizations to serve their own customers or employees represents as much as one quarter of the total off-street capacity in some cities. This service will be abandoned in the face of municipal programs. Why should these organizations pay to fulfill the parking needs if the city will do this for them? How does one reconcile zoning ordinances requiring some property owners to provide for their own parking requirements if the municipality adopts a policy that provision of off-street parking is a public responsibility?

Under the economic system of the United States, parking facilities must compete successfully against other land uses. Subsidized municipal parking will reduce the yield of existing commercial parking and will eventually drive it out of business. A city, if it proceeds with a municipal parking program, must be prepared to absorb these losses. The city must also compensate for the progress lost by a halting of normal advances of private enterprise. Any more parking would have to be provided in addition to recouping the foregoing losses. Few city budgets could withstand this drain.

ARE SMALL SUBSIDIES POSSIBLE?

One of the most difficult questions to answer is: "Why not try a small amount of subsidizing?" While he was director of the Motor Vehicle Parking Agency in Washington, D. C., the writer tried to find a basis for teamwork between private enterprise and the government. After conscientious research, he came to the conclusion that this teamwork can only extend to cooperative efforts in surveys, fact gathering, guidance, and stimulation of private enterprise—that it must not include financial participation by the city government. If the city does more than act in an advisory capacity, such action becomes unwarranted encroachment in a field of private enterprise. In this matter the writer is in agreement with an opinion written by Justice Oxner of the South Carolina Supreme Court, in August, 1954, when a county was denied the right to compete with private enterprise:

> "We adhere to the concept of free enterprise entertained by our forefathers and the doctrine that government should not engage therein * * * This government was founded upon the idea of free enterprise, and under it has become the strongest nation in the world. It seems to us that governmental control and supervision of and participation in free enterprise under strained or liberal construction and application of social and economic ideology has gone far enough, if not too far, and should not be further extended."

As the title of this paper suggests, the parking problem presents itself as either a private or public responsibility. There is no middle road. It must be one or the other.

AMERICAN SOCIETY OF CIVIL ENGINEERS
Founded November 5, 1852
TRANSACTIONS

Paper No. 2795

THE EFFECT OF JET AIRCRAFT ON AIRPORT PAVEMENTS

By Gayle McFadden,[1] M. ASCE

Synopsis

The heat and blast of jet airplanes may damage an airport pavement unless it is properly designed and constructed. Spillage of fuel may also affect adversely an improperly built pavement. This paper describes tests determining the extent of these effects on bituminous concrete and portland cement concrete. In the light of the results, measures to guard against such damage are described.

Jet aircraft have now been in use for a sufficiently long time to enable engineers to analyze their effect on airfield pavement and to predict with reasonable assurance the behavior of pavements on which jet aircraft are used. However, a change in jet aircraft characteristics can produce a change in pavement behavior.

The effect of jet aircraft on airport pavements may be divided into two broad categories: (1) The effect of heat and blast and (2) the effect of fuel spillage.

The first category probably causes more concern because the degree of heat to which the pavement is subjected is directly related to the characteristics of the aircraft. It has been found from a study of the various aircraft in use that these characteristics vary with the type of aircraft to an appreciable extent. The distance from the exhaust nozzle of the propulsion unit to the area of exhaust impingement on pavements will vary considerably, depending on the type and size of the aircraft. Therefore, pavement surface temperatures induced by the same type of propulsion units will also vary greatly.

Herein described is the effect on pavement of only those aircraft for which the Corps of Engineers (United States Department of the Army) are presently (1953) being asked to design pavements. Army engineers have found that there is no serious damage to either portland cement concrete or bituminous pavements from heat and blast under the normal operating conditions of these

---

Note.—Published, essentially as printed here, in October, 1953, as *Proceedings-Separate No. 316*. Positions and titles given are those in effect when the paper was approved for publication in *Transactions*.

[1] Chief, Airfields Branch, Eng. Div. (Military Constr.), Office of the Chief of Engrs., U. S. Dept. of the Army, Washington, D. C.

aircraft. This finding will be amplified subsequently. Jet aircraft with characteristics different from those of aircraft now being designed, however, may be harmful to pavements.

The second category, the effect of fuel spillage, causes only slightly less concern. However, this effect also depends on those characteristics inherent in the design of the jet motor which control the quantity of normal spillage. In considering the effect of fuel spillage, one must also emphasize the significance of normal operating conditions. Under these conditions the Corps of Engineers do not find any significant damage either to the joint-sealing materials in concrete pavements or to the surface of bituminous pavements. This finding will also be explained in detail subsequently.

In order to be assured beyond any reasonable doubt as to the damage that might occur to pavements from the heat and blast of jet-engine exhausts, the Corps of Engineers initiated, in collaboration with the United States Air Force, a comprehensive study of this subject in the latter part of 1951. This study has been previously reported[3] in considerable detail and will only be summarized here.

This project was a part of a long-range, over-all study of the effect of current types of jet aircraft on airfield pavements and covered the phase of heat and blast effects on pavements. The testing was predicated on simulating normal jet-blast operation of each current type of jet aircraft being used by the Air Force. Eight types of jet aircraft were used. Only the latest models of each were used in the test. To ascertain that normal operating conditions would be simulated, a time-movement study was initiated. A representative number of Air Force bases occupied by jet aircraft were visited by a team of observers composed of Air Force and Corps of Engineers personnel. These observers timed the travel of the airplanes through the entire range of movement from the parking position through the take-off. The pilots of the planes were not informed that the observations were being made.

The time-movement studies showed that jet operations for all types of planes could be subdivided into the following groups: (1) A starting operation on the apron, (2) taxiing to the end of the runway, (3) a pretake-off check at the end of the runway, (4) take-off, (5) landing and taxiing to the parking place, and (6) a maintenance run-up on the apron. Only the starting operations on the apron, the pretake-off check at the end of the runway, and the maintenance run-up are critical from the standpoint of heat and blast because the airplanes are moving in the other operations and temperatures are not built up in the pavement. From an analysis of the data, normal time periods for the starting and pretake-off checks were selected. These normal times were approximately equal for single-engine, twin-engine, and four-engine planes. Therefore, single normal testing times could be established for each of the three types of planes. The time periods recorded for maintenance run-ups ranged from approximately 7 min to 36 min and followed no consistent pattern for the various air bases or planes. Because 80% of the observations indicated a duration of less than 14 min this was assigned as the normal test period for simulating maintenance run-up. In addition to the normal time periods, tests were made at periods 50% shorter and 50% longer than normal. The time-movement studies also yielded information on the percentage of power at which the engines were operating in each position. From these observations, a time schedule for the testing was established as is shown in Table 1.

---

[3] "The Corps of Engineers Approach to Pavements for Jets—Part I," by Charles R. Foster, *Proceedings*, Symposium on Airfield Pavements for Jet Aircraft, U. S. Naval Civ. Eng., Research and Evaluation Lab., Fort Hueneme, Calif., April 17 and 18, 1952.

The testing was accomplished on twenty-four specially constructed test panels. Twelve panels were of portland cement concrete and twelve of asphaltic concrete. They were constructed under carefully controlled conditions and followed closely the specifications of the Corps of Engineers for high-quality pavements for use by current types of aircraft. The purposes of the tests were (1) to obtain temperature data in pavements subjected to jet blast and (2) to observe the effect of the blast, if any, on the pavements. Thermocouples were installed in the panels in the form of a cross. They were placed at three elevations in each panel. Twenty nine were on the surface of the pavement, eight were at a 1-in. depth, and one was 2¼ in. below the surface.

TABLE 1.—SELECTED INTERVALS FOR JET–ENGINE OPERATIONS FOR TEMPERATURE MEASUREMENTS BASED ON DATA FROM TIME–MOVEMENT STUDIES

Type of plane	Starting				Pretake-Off				Maintenance			
	Percentage of total power	Time Period, in Minutes			Percentage of total power	Time Period, in Minutes			Percentage of total power	Time Period, in Minutes		
		−50 %	Normal	+50 %		−50 %	Normal	+50 %		−50 %	Normal	+50 %
Single engine	Idling to 60	1.75	3.5	5.25	Idling to 100	0.75	1.5	2.25	Idling to 100	7.0	14.0	21.0
Twin engine	Idling to 60	2.25	4.5	6.75	Idling to 100	0.75	1.5	2.25	Idling to 100	7.0	14.0	21.0
Four engine	Idling to 60	5.0	10.0	15.0	Idling to 100	1.25	2.50	3.75	Idling to 100	7.0	14.0	21.0

The jet aircraft were positioned so that the point of maximum heat would occur near the cross of the thermocouple pattern; they were operated in accordance with the selected time-power schedule. The temperatures produced in the pavements were automatically recorded. Measurements were noted at sufficiently frequent intervals to show the rate of temperature rise.

The results of these tests may be generally summarized as follows:

a. Maintenance run-ups developed the highest temperatures in the pavements, as might be expected because they involved the maximum exposure.

b. Temperatures developed in pretake-off run-ups were comparatively low, and those of starting run-ups were even lower.

c. The maximum temperature developed in the pavement by a fighter plane was 248°F, and this temperature occurred during a maintenance run-up 50% longer than the normal time period—involving a 21-min exposure, part of which was at 100% of that power.

d. The maximum temperature in the pavement produced by a bomber plane was 385°F. This temperature also occurred during maintenance run-up at a time period 50% longer than normal. It has been reported that this particular type of plane is now obsolete.

e. Only minor damage of asphaltic concrete pavements occurred from jet blast when the temperature reached 300°F. At lower temperatures there was no damage.

f. No rutting or detrimental behavior occurred when a plane equipped with tires inflated to 200 lb per sq in. was towed across the asphaltic concrete pavement at temperatures as high as 340°F.

g. Temperatures in portland cement concrete were generally from 30°F to 70°F less than those in asphaltic concrete.

h. Portland cement concrete pavements were not affected by the heat and blast although the joint seals were melted slightly in some instances and blown in the direction of the blast 5 in. or more.

Except in the joint-sealing material the investigations have not shown any deleterious results of fuel spillage on portland cement concrete pavements. This phase of the paper can therefore be devoted to its effect on asphaltic pavements.

The writer would find himself in a completely untenable position should he state that airplane fuel does not have a dissolving effect on asphalt. Having originated from the same parent stock, they have a natural affinity for each other. However, asphalt by itself does not constitute an asphaltic concrete pavement, nor do all so-called asphaltic concrete pavements prove acceptable as jet-fuel-resistant structures.

There are only two basic materials in common usage for the manufacture of pavements. These are cements—including portland cement, natural cement, slag cement, and others—and bituminous materials—including asphalt, tar, and similar substances. Engineers have not only structural but also economic responsibilities. Therefore, every effort should be made, both from an engineering and operational standpoint, to utilize available materials to the maximum extent. It is with this principle in mind that the Corps of Engineers have made exhaustive investigations in an endeavor to maintain a competitive field in pavement construction.

The effect of the spillage of airplane fuel on asphaltic pavements is a temporary softening of the surface. The depth to which this softening occurs is a function of the pavement structure. The length of time the softening remains depends on the volatility of the fuel and the ambient temperature. If left untouched, pavements softened by fuel spillage will usually return to normal hardness after the spilled fuel has evaporated. Pavements that are designed and constructed to produce a dense structure with the minimum of voids consistent with proper pavement performance will resist the infiltration of the fuel with resultant minimizing of the depth of softening. Pavements designed and constructed with a smooth close-textured surface will tend to disperse any spilled fuel rather than pocket it in surface voids and will thereby accelerate evaporation and reduce the chance of softening. Highly volatile fuels evaporate faster and permit the pavement to return to its original hardness sooner than do the less volatile fuels. These conclusions are the result of the inspection of hundreds of pavements either reported to have deteriorated or suspected of deterioration caused by the spillage of airplane fuel. The result of these inspections has definitely shown that for the majority of cases the reported damage has been relatively minor in character and in extent. Where the damage was reported as resulting from heat and blast, it was found that in most instances the pavement had been given a thin surface treatment or seal coat which had been entirely charred or melted and blown off. Damage reported from fuel spillage generally involved an area of small extent where continual dripping had softened the asphalt binder material and in some instances had stripped the aggregate of the binding agent. In either case, the area and extent of damage could generally have been considered in the category of normal maintenance and repaired at nominal cost.

The laboratory and field investigations may be summarized as follows:

1. An asphaltic concrete pavement, designed and constructed in conformance with current criteria of the Corps of Engineers, shows little or no deterioration when subject to spillage of fuel normal to the operation of the aircraft.
2. Conversely, a poorly designed and poorly constructed asphaltic concrete pavement shows appreciable damage.
3. Old, densely graded, hot-mix asphaltic concrete pavements are more resistant to the effect of spilled jet fuel than are newly constructed pavements of the same quality. This is probably because of the oxidation of the surface which reduces the volatile fraction at the surface to the extent that the in-place asphalt will not mix with the spilled fuel as readily as it would on a new pavement. Other factors are the smoothing action of traffic and the accumulated traffic film that fills surface voids and causes fuel to disperse instead of pocketing, thus retarding evaporation.
4. Thin surface treatments have not been found satisfactory for sealing porous pavements against fuel spillage and infiltration. No surface treatment has yet been found that can be considered a solution to the problem. This type of treatment is not resistant to jet blast or traffic abrasion. Concentrated jet blast will strip thin surface treatments from the pavement and leave areas vulnerable to infiltration. Furthermore, when punctured or cracked, the thin surface applications permit fuel to penetrate the porous pavement and the remaining seal prevents evaporation.

In an attempt to produce an asphaltic concrete pavement resistant to normal usage of jet aircraft, the Corps of Engineers have extended their investigations of the design and control of asphaltic concrete mixes and have produced a dense structure with a close-textured surface smooth and free from visible surface voids.

These asphaltic concrete mixes are designed and controlled by the Marshall method.[3,4] This method has four basic property requirements that must be satisfied. They involve stability, flow, voids in the total mix, and voids filled with asphalt. The optimum asphalt content is determined by averaging the

---

[3] "Investigation of the Design and Control of Asphalt Paving Mixtures," *Technical Memorandum No. 3-254*, Waterways Experiment Station, Vicksburg, Miss., May, 1948.

[4] "Symposium on Asphalt Paving Mixtures," *Research Report No. 7-B*, Highway Research Board, National Research Council, Washington, D. C., June, 1949.

asphalt contents required by these properties. The density and surface texture are obtained by careful control of the aggregate gradation. It has been found necessary to limit the voids in the total mix to from 3% to 5%, basing the design on 4%. This density can be obtained by conforming to a uniform grading of the aggregate from coarse to fine with proper consideration being given to the percentages of material passing the various screens so that the curve of maximum density is closely followed. It has also been found that the surface texture can be maintained within acceptable limits by controlling the percentage of aggregate passing the No. 10 sieve. In Table 2 is shown the gradation of two surface-course mixes that have proved acceptable both as to density and surface texture.

A surface course designed by the Marshall method and by using the gradations shown in Table 2 can be expected to yield a dense pavement with a close-textured surface with most aggregates. The asphalt contents for these gradations have been purposely omitted as the optimum content is determined by the Marshall method. Experience has shown, however, that with average aggregates the percentage by weight of asphalt will be between 5% and 6%. If porous or absorptive aggregates are used, the asphalt content can be expected to be from 2% to 3% higher.

TABLE 2.—BITUMINOUS SURFACE COURSES (CENTRAL HOT–PLANT MIX)

Sieve designations (square openings)	PERCENTAGE BY WEIGHT (PASSING)	
	1-in. sieve, maximum	¾-in. sieve, maximum
1 in.	100	
¾ in.	89–100	100
½ in.	78–90	86–100
⅜ in.	69–83	78–90
No. 4	55–70	60–73
No. 10	42–56	43–57
No. 20	30–43	29–43
No. 40	22–33	19–33
No. 80	14–22	10–20
No. 200	3–6	3–6

Experience has indicated that the Marshall properties to be expected from these gradations will be approximately as follows: (1) The stability will be from 1,500 lb to 2,500 lb, (2) the flow will be from 0.08 in. to 0.12 in., (3) the voids in the total mix will be from 3% to 5%, and (4) the voids filled with asphalt will be from 75% to 82%.

Porous or absorptive aggregates should be carefully considered in making the design computations. So much of the success of the pavement depends on the void ratio that an improper determination of the specific gravity of the aggregate will cause errors in the essential Marshall properties that will unbalance the design and produce a pavement in variance with that expected. The Marshall method specifies apparent specific gravity for normal computations, using aggregates having 0.5% or less water absorption. As the percentage of absorption increases, the error in computation increases when using this method of determining specific gravity. This is particularly true of aggregates having a high percentage of absorption, such as slag, sandstone, basalt, and similar aggregates.

The Corps of Engineers have nearly completed an investigation that has as its objective a method of determining the correct specific gravity of aggregates to be used in asphaltic concrete design based on the relative water-absorption characteristics. The specific gravity obtained by this method is termed "bulk impregnated specific gravity." Pending the completion of this study, a rule-of-thumb method is being used for determining the specific gravity of absorptive aggregates. This procedure involves a mean between the determination of bulk specific gravity and that of apparent specific gravity. The result approximates bulk, saturated, surface-dry specific gravity for most absorptive aggregates.

The design of an asphaltic concrete pavement is, of course, only part of the job. Its construction is equally important to success in producing a jet-resistant structure. The importance of maintaining the void ratio to assure against infiltration of fuel must again be emphasized. In construction, this can only be accomplished by proper rolling with proper equipment at the proper temperature and at the proper time. Density cannot be produced either by rolling a cold (or slightly warm) pavement or with equipment too light for the job. It is essential that complete control of the mixing and placing be maintained at all times with frequent sampling to see that the requirements are being met. The Corps of Engineers have recently introduced a multiple-wheeled, rubber-tired roller into their construction procedure in addition to the conventional 3-wheeled, 10-ton roller and 10-ton tandem roller. This rubber-tired roller can either follow the tandem rolling or can be used between the 3-wheeled roller and the tandem roller. It does not appreciably increase the density of the pavement structure but flattens surface irregularities and produces the close-textured surface required for use with jet airplanes.

CONCLUSIONS

1. The effects of jet aircraft on airfield pavements from heat and blast and from fuel spillage are directly related to the characteristics of the aircraft.

2. Portland cement concrete pavements are not affected by jet aircraft—except for the damage of the joint-sealing material. Certain joint-sealing materials manufactured as jet-resistant are affected by heat and blast but are quite resistant to fuel spillage. They are generally satisfactory for use with most jet aircraft.

3. Inspection of asphaltic pavements and investigations of the effect of jet aircraft on their performance indicate that (*a*) asphaltic concrete pavements, properly designed and carefully constructed of densely-graded, hot-mix material, resist satisfactorily the heat and blast and the fuel spillage of most airplanes under normal operating conditions; (*b*) old, densely-graded, hot-mix asphaltic concrete pavements are more resistant to jet-fuel spillage than newly constructed pavements; and (*c*) thin surface treatments are not satisfactory for sealing porous pavements against fuel spillage.

AMERICAN SOCIETY OF CIVIL ENGINEERS
Founded November 5, 1852
TRANSACTIONS

Paper No. 2796

FACTORS INFLUENCING IRRIGATION IN HUMID AREAS

By Tyler H. Quackenbush[1]

With Discussion by Mr. Alfred R. Golze

Synopsis

Irrigated agriculture in the eastern United States, if properly guided, offers one of the largest potentials available for increasing productivity of crop land and pasture land. Some of the data most urgently needed by the field engineer for a more adequate design for irrigation systems in the humid areas are those concerning water supply and its physical control, relationships between soil and moisture, irrigation-water requirements, methods of water application, and drainage. The need for more adequate water laws is emphasized.

Introduction

In order to maintain a prominent position in the world economy, the United States must conserve and use wisely its abundant natural resources. Probably the two most important of these resources are soil and water, both of which are involved in irrigation agriculture. The productive ability of thousands of acres of fertile land has been destroyed or severely damaged by the misuse of irrigation water. This has resulted in the somewhat illogical construction of irrigation systems and the development of new lands for irrigation, while at the same time there occurs the abandoning of many acres of formerly fertile soil, for which adequate irrigation water is available but which is unfit for cultivation because of the accumulation of alkali and the need for drainage.

There are approximately 26,000,000 acres of irrigated land in the United States (as of 1955) involving a capital investment of $1,868,300,000. However, the average efficiency of irrigation, from the point at which the water is diverted

---

Note.—Published, essentially as printed here, in July, 1954, as *Proceedings-Separate No. 462.* Positions and titles given are those in effect when the paper or discussion was approved for publication in *Transactions.*

[1] Irrig. Engr., Soil Conservation Service, U. S. Dept. of Agriculture, Washington, D. C.

into the main canal until it is stored in the root zone of the plant, is only 25%; 75% is wasted through ditch losses, coupled with deep percolation and surface runoff on the farm. Naturally, one cannot expect to achieve 100% efficiency, but there is ample room for improvement.

Progress is being made toward the conservation of land and water in the irrigated areas of the western United States. Organized research and an aggressive program by the water users themselves are the basic elements in the program to improve irrigation practices in these western states.

Advantage should be taken of the known mistakes made in the western states, and every effort should be made to avoid improper planning in the eastern United States. Improper methods should not be introduced and then supplanted; it is much easier to instruct a farmer who has never irrigated before in proper irrigation practices than it is to teach one who has been irrigating incorrectly for many years.

The census of 1950 reports that there were 157,000,000 persons in the United States—it is estimated that by 1975 the population will be 190,000,000. These estimates may, of course, be incorrect because the controlling social and economic factors involved do not lend themselves to precise computation. However, by even the most conservative forecasts of the population's growth, the agricultural capacity to produce must be increased substantially.

Irrigated agriculture in the eastern United States, if properly guided during its growth, offers one of the largest potentials available for increasing the productivity from the more or less fixed acreage of crop land and pasture land that is available.

The years of 1951, 1952, and 1953 have each produced widespread droughts throughout the "humid areas" of the eastern states. This fact, coupled with relatively high farm prices and the advent of light-weight portable pipe, has caused a phenomenal growth in irrigation agriculture in this area. This expansion of irrigation from west to east presents a number of problems of great interest to the engineer.

The 1940 census showed a total irrigated acreage in the 31 eastern states to be approximately 600,000 acres; the 1950 census shows 1,516,000 acres. This increase of 150% is all the more impressive because most of it occurred after the cessation of hostilities in World War II.

The Sprinkler Irrigation Association gives the following data on shipments of aluminum irrigation tubing, which are indicative of the rapid growth of sprinkler irrigation: In 1946—1,279,000 lb, and in 1954—32,000,000 lb.

To many persons, irrigation in the humid areas is thought to consist only of sprinkler irrigation. Sprinkler irrigation has played, and will continue to play, a very large part in the growth of irrigation agriculture in the eastern states. However, 1,360,000 acres are irrigated in the humid areas of Arkansas, Louisiana, and Florida, using gravity or surface methods—that is, methods in which the irrigation water flows over or is ponded on the surface of the ground. The irrigation of rice, which accounts for a large part of this acreage, presents many problems to the engineer interested in the conservation of soil and water. Engineers involved with irrigation should know well the limitations and the advantages of both surface and sprinkler irrigation. The ultimate solution is the proper use of both methods, using each where it is best adapted.

One of the most critical problems confronting the engineer responsible for the design and installation of irrigation systems in the humid areas of the United States is the lack of sound basic data on which to base the design. It is unfortunate that irrigation research and the collection of basic information have failed to keep abreast of the phenomenal growth of irrigation agriculture in the eastern states. Some organized research has been undertaken (as of 1955), but it will be some time before much usable information is made available to the engineer in the field. In the meantime, farmers will irrigate, and it is the responsibility of engineers to design and install their systems, based on the best information available.

Research and investigations to improve irrigation practices have been performed in the western states. From these studies and experience some basic irrigation principles have been learned that will apply in the eastern states as well. The basic principles of irrigation agriculture are generally the same, whether it be in a 50-in. rainfall belt or a 5-in. rainfall belt. The primary difference is in water management because of the variation in rainfall. This presents the problem of adapting established procedures to a different set of conditions in order to bridge the gap between the rapid installation of irrigation systems and the obtaining of results of local research.

Data Required

Water Supply and Its Physical Control.—A dependable water supply is essential to any irrigation system. Streams, lakes and ponds, and wells are the primary sources of supply. The tendency of most farmers in the humid areas to underestimate the water supply necessary for proper irrigation has brought about many unfortunate situations. Large investments have been made in irrigation systems and then it is discovered that the water supply is entirely inadequate for the proper functioning of the system. Where storage reservoirs are used, the field engineer is confronted with a difficult problem in estimating probable water yield. This applies particularly to small watersheds and small streams involved in the development of an individual farm-irrigation system. Additional data on the availability of ground water would be useful in many areas.

This problem of water supply is closely related to water laws and water rights. There is much additional work indicated in order to clarify this situation for the prospective water user.

Soil and Plant Moisture Relationships.—Irrigation agriculture involves water, soil, and plants; the ultimate effort is directed to the establishment of conditions for optimum crop production. A knowledge of interrelationships among water, soil, and plants is therefore essential. The soils must be classified with respect to their intake rates and water-holding capacities. The effect of tillage practices and crop rotations on these characteristics must be learned. Plant response to soil-moisture stress must be established. More data are needed on the relationships between moisture and fertilizers. Root-zone depths and moisture-extraction patterns are also needed for the various crops being irrigated.

Irrigation-Water Requirements.—Before a water supply can be provided or the system for conveying it determined, the quantities of water needed to meet crop requirements must be established. These requirements depend on many factors such as consumptive use by the plant, irrigation efficiency, quality of water, and method of delivery. The water supply and the distribution system must be designed to satisfy both the seasonal and maximum-use-period requirements.

H. F. Blaney, M. ASCE, and W. Criddle have developed[2] a method for estimating irrigation-water requirements. This method has been used in the humid areas with a reasonable degree of success. However, because this procedure was originally developed for use in the western states it has been necessary to modify various factors. Additional field measurements of consumptive use and irrigation efficiencies are needed, especially in so far as the "peak consumptive use" data are concerned.

Method of Water Application.—The primary concern of the irrigation farmer is how to get irrigation water into the storage space in the soil. This is a question of the physical application of the water. The method used must suit the crop, the soil, and the source of water. In addition, there must be (*a*) uniform distribution of water over the entire field and throughout the entire root zone; (*b*) maximum efficiency of water use—that is, minimum surface runoff, minimum deep percolation loss, and minimum evaporation; (*c*) minimum erosion; and (*d*) minimum labor and pumping costs.

Drainage.—Whenever irrigation is practiced there are certain excess water applications which are unavoidable. Drainage systems should be designed to handle excess rainfall plus surplus irrigation water. What are the basic requirements of drainage in areas where heavy rainfall may follow the application of irrigation water? To what degree should adequate drainage be a basic design factor for irrigation systems?

When these questions are answered, the field engineer will have much more reliable information on which to base his design. However, it should always be realized that, regardless of how good a design may be, the irrigation system will not operate successfully unless it is operated in accordance with the standards used in the original design. Many well-designed sprinkler irrigation systems have failed to do the job because they were not operated properly. Design engineers should be fully conscious of the fact that instruction in operation is essential to the success of a good design.

The old and widely used methods of irrigating when the crop changes color, when the leaves show some wilt, or at so-called critical stages of growth are not the complete answer to the proper operation of an irrigation system. The farmers must be shown that the procedures involved in successful irrigation are based primarily on the physical properties of the soil—its depth, its intake rate, its water-holding capacity—in addition to the growth characteristics of the plant. Engineers must emphasize the fact that the soil will primarily determine the answer to the two questions: "When do I irrigate?" and "How much do I put on?"

---

[2] "Determining Water Requirements in Irrigated Areas from Climatological and Irrigation Data," by H. F. Blaney and W. Criddle, *Technical Publication No. 96*, S.C.S., U. S. Dept. of Agriculture, Washington, D. C., August, 1950.

The widely accepted concept of using irrigation as an "insurance" against drought will do little toward increasing crop production. Many farmers have operated on this basis and invariably they encounter the old adage of "too little and too late." The irrigation is begun too late and, in order to cover the ground in a hurry, too little is applied. As a result, crops suffer and water is wasted; yields are increased very little over normal yields without irrigation. Therefore, the dividends received from the investment in equipment, labor, and water supply are much smaller than the system is able to produce.

Successful irrigation farmers have already accepted the fact that irrigation farming certainly involves a lot more than the application of water when crops begin to wilt. It should be the last step in a complete water-management program which includes control of soil erosion, removal of excess water, and the conservation and utilization of rainfall.

TABLE 1.—FORAGE YIELDS AND AMOUNTS OF RAINFALL AND IRRIGATION

Item	1950	1951	1952
Number of days[a]	126	125	137
Number of cuttings	6	7	8
Forage yields (over-dry basis), in pounds per day per acre			
"Normal" fertilization—rain only	14.3	20.0	27.9
—irrigated	18.7	27.0	42.0
"High" fertilization —rain only	44.9	55.6	55.2
—irrigated	48.4	60.6	61.6
"Mixed" fertilization —rain only	19.8	21.8	21.6
—irrigated	22.9	22.0	32.6
Rainfall, in inches	17.6	13.9	14.4
Rainfall, in inches per day	0.14	0.11	0.10
Rainfall plus irrigation, in inches	21.1	20.4	23.4
Rainfall plus irrigation, in inches per day	0.17	0.16	0.17
Number of irrigations	4	6	7

[a] From date of fertilizer application in spring to date of cutting in September. In 1950, May 9 to September 11; in 1951, May 17 to September 18; and in 1952, April 25 to September 9.

Studies[3] conducted at Ithaca, N. Y., by the United States Department of Agriculture and the Cornell University Agricultural Experiment Station in 1950, 1951, and 1952 showed a greater forage yield on nonirrigated "high fertilization" plots than on irrigated "normal fertilization" plots. This is an indication that proper management alone could increase yields more than irrigation coupled with poor management. The results of this study are shown in Table 1.

Does humid area irrigation pay? Tests conducted[4] cooperatively at Lewisburg, Tenn., by a United States Department of Agriculture dairy scientist and the Tennessee Agricultural Experiment Station have been reported on as follows:

> "During the two years of the test, the irrigated half of the pasture averaged 54 percent more milk production per acre and 38 percent more income above costs than the non-irrigated plot. This amounts to an increase in net return from the irrigated pasture average $115.53 per acre."

---

[3] "Irrigation Plus Good Management Increases Forage Yields," by George R. Free and Ernest A. Engdahl, *Farm Research*, Vol. XIX, No. 2, 1953.

[4] "Profit in Pasture Irrigation," *Agricultural Research*, Agri. Research Service, U. S. Dept. of Agriculture, Washington, D. C., Vol. 2, No. 6, 1953.

In studies on irrigation of pasture for beef-cattle production, conducted by the University of Illinois at Urbana,[5] it is reported:

> "During the five years of the tests, 6 irrigations were required annually and two inches of water were used for each one. Average annual costs for labor and gasoline were about $18.00 per acre. If the increase in gains is valued at 20 cents per 100 pounds, that would leave only $2.00 a year to cover such costs as depreciation and upkeep. But the depreciation on a $1,000 investment in equipment over a 10-year period at 3 percent compound interest would amount to about $27.00 an acre per year. With enough water, the same equipment could be used to irrigate four or five times as much land as the five acres included in these tests. That would reduce the fixed depreciation cost to about $6.00 an acre. But increased gains must be realized in order to pay the costs."

Such results are not necessarily conflicting after all the factors involved are analyzed, but the tendency of many people to assume "that irrigation in humid areas does or does not pay" based on short-time results has been rather misleading and confusing to the prospective irrigator.

Such experiments must be conducted over a period of years and must be specifically related to climate, soils, crops, and amounts and methods of applying irrigation water. It is logical to expect that varying results can and will be obtained from short-period studies as the differences in yield over nonirrigated crops may be small during years of high rainfall. Crop quality may be the deciding factor in many instances. It is not difficult to anticipate a reduction in yield on poorly drained soils. Similar studies to those conducted in Illinois and at Lewisburg have indicated some question concerning the feasibility of irrigating in humid areas unless adequate drainage is provided.

Generally speaking, the results of the many investigations that have been performed and the results being obtained by the thousands of farmers who have invested in irrigation systems seem to indicate that humid-area irrigation, when properly done, does pay good dividends through increased yields and better crop quality.

WATER LAWS

A serious obstacle in the path of future development of irrigation in the humid areas is the present (1955) status of the laws covering the use of water for irrigation. Nearly all the eastern states operate under the legal concept known as the riparian doctrine. According to this doctrine, every owner whose property touches a stream or lake has riparian rights. Riparian owners enjoy a right to have water flow by or through their lands undiminished in quantity except for use by upstream owners for domestic purposes.

Some states have adopted a modified riparian doctrine which permits the use of water for irrigation purposes, but even in most of these states there is no provision for rights of prior appropriation. A farmer who has been practicing irrigation for many years has no protection should his neighbors upstream follow his example and irrigate from the same water supply. Such action may deprive him of a large part of his water supply, but under the law he would not have established any priority in rights over these later users.

---

[5] "Pasture Irrigation at the Dixon Springs Station," *DS-46*, Univ. of Illinois, Urbana, Ill., September, 1953.

Some states are giving (as of 1955) serious consideration to the enactment of more adequate water laws to protect the irrigation farmer. South Carolina, Virginia, and Kentucky have adopted preliminary policy statements, each of which provides for authority to develop implementing legislation in succeeding years. Until adequate water laws are enacted in all the eastern states, the farmer who invests in an irrigation system is taking definite risks. As Raleigh Barlowe has stated:[6]

"(1) He is not always sure he has the right to take water for irrigation.
"(2) His operations may be stopped by injunction if his actions cause material damage to other riparian users.
"(3) He may lose much of his investment if upper riparian owners decide to irrigate from his already limited supply."

The use of wells and the storage of surface water before it reaches a well-defined stream, lake, or pond offer a lesser risk in most states. In many states, the rule of "reasonable use" covers the use of underground waters, and this water can be used for irrigation, providing there is no adverse effect on other users.

The riparian doctrine, strictly interpreted, is not compatible with irrigation. It is difficult, therefore, to visualize a real large-scale expansion of irrigation farming in the eastern states until each state clarifies the rights that irrigators have to the use of water for the irrigation of farm crops.

CONCLUSIONS

The problems confronted in the development of irrigation in the humid eastern United States is twofold. On the one hand there is the need for proper design of irrigation systems and their proper operation. On the other hand, there is the need for the development of water laws that are compatible with the needs of irrigation and, in addition, compatible with the growing needs for water by industry and municipalities. Engineers have a major part to play in the solution of both types of problems.

---

[6] "What Are Your Water Rights?" by Raleigh Barlowe, *American Fruitgrower*, June, 1953.

DISCUSSION

Alfred R. Golze,[7] M. ASCE.—Attention has been called to the apparent high inefficiency of irrigation systems measured by the percentage of available water utilized by crops. The engineer's part in reducing this water loss in gravity systems, and thereby increasing their efficiency, is limited to that part of the system that brings water to the farm. Once water reaches the farm, the responsibility shifts to the farmer. Records[8] of the Bureau of Reclamation, United States Department of the Interior (USBR), for example, show that system losses from the source of supply (reservior or stream diversion) to the farmer's turnout average from 30% to 40% on major projects operated by the USBR. These losses represent a combination of waste, seepage, and evaporation in gravity canal and lateral systems in the western states. The USBR has had in operation a lower cost canal-lining program designed to reduce losses from seepage. This program has made progress, and many canals have been lined with a variety of materials to test their efficiency as sealing devices. Concrete is still the principal sealing agent on the larger canals. The reduction or elimination of waste is a matter of operating water control under good management. There appears to be some relationship between the adequacy of water supply and water losses. Projects that have ample water supplies may be more liberal in running water through their systems so that water is wasted which, under drought conditions, would have undoubtedly been saved. The sprinkler irrigation systems in the humid areas operating with closed pipelines from their sources of supply are not subject to major losses such as in the open ditches of the western states. Sprinkler-system losses arise more in the operation stage, such as through overirrigation.

Mr. Quackenbush points out a number of problems involved in bringing irrigation into the humid parts of the United States. This expansion of irrigation and the problems involved are not going unnoticed by the press.[9]

The writer agrees with Mr. Quackenbush that the engineering experiences of the western states should be used in the eastern states. One of the greatest benefits the engineering profession can contribute to the solution of irrigation problems in the midwestern states and the eastern states is to apply its experience in the design and operation of systems in the western states. The lack of basic data on the behavior of soils under varying water tables and on the application of irrigation water in humid areas is a serious deficiency. If there are unpublished data on this matter, it would certainly be helpful if arrangements could be made for their publication. In the western states, drainage, for example, is usually a matter of handling return flows from irrigation during a period of little natural precipitation. In the midwestern and eastern states, maximum precipitation could occur at the same time the water table is high because of irrigation. There are possibilities of increasing the flood hazards if irrigation becomes widespread.

---

[7] Chief, Div. of Program Coordination and Finance, Bureau of Reclamation, U. S. Dept of the Interior, Washington, D. C.

[8] "1953 Crop Summary and Related Data—Federal Reclamation Projects," Bureau of Relcamation, U. S. Dept. of the Interior, Washington, D. C., 1954.

[9] "Pushbutton Rain: Sprinkler Irrigation Invades More Farms," by Winston C. Fournier, *Wall Street Journal*, September 2, 1954.

As the demand for irrigation increases in humid areas, it seems inevitable that there will be a banding together of farmers into districts or companies to finance the construction of facilities. Such facilities would provide a source of dependable water, not only for riparian use but for inland use. The engineering experience gained in the western states should be of considerable assistance when this point of development is reached.

Another experience that the western states can contribute to the eastern states, which Mr. Quackenbush cites, is the adjustment of state laws to control the legal use of water for irrigation purposes. The laws of nearly all western states have been modified during the past century to meet the changing needs of an irrigated agriculture. Whether substitution of the appropriation theory for the riparian theory will be the answer east of the 100th meridian remains to be seen. The formulation of irrigation districts or the bringing of irrigation activity into the existing soil conservation or drainage districts may be the solution. It is through local organizations such as these that farmers can obtain effective answers to their engineering, farm economics, and legal problems. Increasing pressure on the use of water supplies in areas subject to drought will probably be the incentive to the formulation of such districts or to the modification of existing ones, to secure such action as may be required.

The revision of a book[10] concerned with legal problems in the western states would be a valuable aid to the states in humid areas in solving the legal problems that will confront them as irrigated agriculture expands and as the uses of this limited resource increase.

---

[10] "Selected Problems in the Law of Water Rights in the West," by Wells A. Hutchins, U. S. Dept of Agriculture, Washington, D. C., 1942.

AMERICAN SOCIETY OF CIVIL ENGINEERS
Founded November 5, 1852
TRANSACTIONS

Paper No. 2797

VERTICAL SAND DRAINS FOR STABILIZING MUCK-PEAT SOILS

BY J C CARPENTER,[1] M. ASCE, AND EDWARD S. BARBER,[2] A. M. ASCE

WITH DISCUSSION BY MR. HUBERT M. RAEDSCHELDERS

SYNOPSIS

The use of vertical sand drains for consolidation of deep muck under highways is described. Its early history is reviewed, and recent applications are enumerated. The establishment of gaging apparatus for the control of construction progress is explained.

INTRODUCTION

When one speaks of drainage, one visualizes a fluid pulled downward out of a saturated mass that will become stable material if the fluid is removed. Gravity pulls the moisture out of the mass. This paper concerns a procedure in which the direction of flow is reversed and the water is pushed upward. Gravity does the work by pushing down on a superimposed load and squeezing the moisture out of saturated soils. An avenue of escape for the moisture is provided by installing vertical sand drains and a horizontal sand layer to conduct the water to the side of the embankment.

STABILIZATION WITH VERTICAL SAND DRAINS IN PUERTO RICO

Outside California, the sand-drain method of stabilization of soils to provide support for embankments was not widely used before 1941. At that time Puerto Rico was accelerating the construction on North Coast Highway No. 2 from San Juan to Borinquen Field (now Ramey Field), a vitally important 80-mile link in its militarily strategic highway network. As this route

---

NOTE.—Published, essentially as printed here, in November, 1953 as *Proceedings-Separate No. 351*. Positions and titles given are those in effect when the paper or discussion was approved for publication in *Transactions*.

[1] Superv. Highway Transport Research Engr., Coverdale & Colpitts, Cons. Engrs., New York, N. Y.

[2] Highway Engr., Bureau of Public Roads, U. S. Dept. of Commerce, Washington, D. C.

leaves San Juan, it crosses a marshy area between Fernandez Juncos Avenue and the Martin Peña Channel known as "El Fanguito" which means "Little Mud." The "Little Mud" extends 0.34 mile along the location of the road. The mud was from 25 ft to 50 ft deep, covered with water at high tide and so soft that at low tide barefoot boys sank ankle-deep. Projection of a four-lane highway across this quaking, custard-like foundation presented a serious problem.

The Puerto Rico Department of the Interior studied numerous schemes and prepared estimates of construction costs. Seven ideas seemed to be practicable. These ideas included building a timber trestle costing $187,000, excavating the muck and refilling with good material at a cost of $390,000, and constructing a concrete trestle costing $600,000. A. C. Clark, then district engineer for the Public Roads Administration in Puerto Rico, reviewed the project and suggested that the vertical sand-drain method used in California be included as an alternate plan. Plans were prepared and the cost of construction by this method was estimated at $103,200. Late in 1941 the project was advertised for bids, but because of some apprehension as to the success of the method, the advertisement was withdrawn before bids were received.

The plans were reviewed by the senior writer early in 1942 and, after some helpful correspondence with O. J. Porter, M. ASCE, they were revised in accordance with local conditions. One important change was in the diameter of the drains. The original plan proposed 30-in.-diameter sand columns to be placed by drilling a well with an auger or by driving a mandrel. In the supersaturated muck of El Fanguito it is impracticable to drill with an auger, and there was neither equipment nor material available on the island for a mandrel of this size. Steel pipe of 12-in. diameter was available and so the spacing of the drains was decreased and the 12-in.-diameter pipe was used.

The project was important in the war effort. The United States Navy had equipment and materials which could not, at that time, be furnished by civilian contractors. Capt. J. C. Gebhard, public works officer of the San Juan Naval Air Station, agreed to build the project if it were approved by the Bureau of Yards and Docks, United States Department of the Navy. The project was converted to access project number DA–WR1 and was promptly approved for construction. Work was begun in November, 1942. Comdr. J. G. Dodd, M. ASCE, was in charge of the navy contract work during its participation.

At this stage another important change in plans was approved. The contractors for the Navy could not support their equipment on the surface of the marsh. It was agreed that a tough clay blanket, no thicker than 2 ft, would be placed on the surface. It was understood that the sand columns must extend far enough above the top of this blanket so that no clay stratum would cut off the vertical drainage action.

The field superintendent for the Navy misunderstood instructions about the clay blanket and began placing a fill of rock-quarry waste. After approximately 200 ft of the right of way had been covered, a mud roll developed on the side of the embankment, a transmission tower began to move, and a 36-in.-diameter sewer was shoved out of line.

Filling was immediately suspended, and on its resumption the clay layer was successfully placed over the entire area.

The mandrel used was a 40-ft section of 12-in.-diameter steel pipe. To close the lower end of this pipe, concrete conical points 14 in. in diameter, with a 12-in.-diameter cylinder on top to fit the inside of the mandrel, were cast. The mandrel was driven with a steam hammer in 50-ft leads. Drains were spaced 11.8 ft transversely and 9.8 ft longitudinally. The area covered by the clay blanket was 90 ft wide for the length of 0.34 mile. An aggregate of 1,492 drains totaling 57,685 lin ft was placed at an average cost of $0.93 per ft. A wooden punch was driven through the clay blanket; the mandrel, with its concrete point, was placed in the hole and driven 40 ft or to refusal. The mandrel was filled with saturated sand which was heaped above the top of the driven mandrel; the mandrel was then withdrawn, leaving the concrete point and the column of sand in the muck. Fig. 1 shows the clay blanket and vertical sand drains with concrete points before the embankment load had been applied.

The method used in California provided for a 2-ft-thick blanket of sand on top of the drains to conduct the water to the sides of the fill. A settlement of from 15 ft to 20 ft below mean low water was anticipated, and it was believed there might be danger of slides if a heavy clay fill were placed on a 2-ft-thick sand blanket. As sand from the harbor bottom could be obtained at a reasonable cost it was decided that a sand fill would be placed for the full depth below the marsh surface and above the clay blanket.

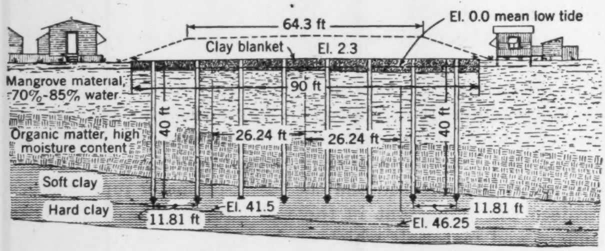

FIG. 1.—TYPICAL CROSS SECTION, EL FANGUITO MARSH (DIMENSIONS, IN FEET)

Between February and July, 1943, the Navy placed 44,000 cu yd of sand fill. The fill was 4 ft above the marsh level. Because of administrative changes in Navy operations, the work was suspended on July 13, 1943. Completion of the construction of the project became the responsibility of the Puerto Rico Department of the Interior on May 21, 1944. Recognizing the necessity for slow and careful application of the remaining sand fill, the department awarded three small contracts extending over the period from May, 1944, to July, 1945, and a final contract terminating the fill construction during December, 1945. These contracts covered the application of 77,000 cu yd of sand fill. After three months of traffic over the embankment had indicated little settlement, the surfacing—composed of sand-asphalt using emulsified asphalt on a water-bound base—was applied. Fig. 2 shows that the center elevation of the clay blanket sank to El.-4.0 m, approximately 14 ft below mean low tide. The cross section was developed from soundings into the clay by Mr. Antonsanti of Ponce.

During the operations performed by the Navy, their consulting engineers took undisturbed samples of the muck which were tested by E. K. Tan at Roosevelt Roads, Puerto Rico. It was found that the moisture content of the muck-peat ranged from 140% to 700% of its dry weight of approximately 20 lb per cu ft with an average of about 400%. The shear strength of the soil was negligible, the material failing of its own weight when unconfined. Model tests showed that the muck would consolidate twice as fast with vertical sand drains as without them. Mr. Tan predicted that the depth of sand fill required to provide stability would be between 10 ft and 19 ft. His predictions were close to the depth actually placed.

In May, 1943, during the Navy construction operations, a slip occurred on a section about 200 ft long at the center line of the fill near the Martin Peña end of the project (Fig. 3). The fill settled a foot in the eastbound lane, and there was movement in the other lane. Filling was stopped for a week at this time and then very slowly resumed. No additional faulting occurred during the construction period, but this area has been troublesome under traffic.

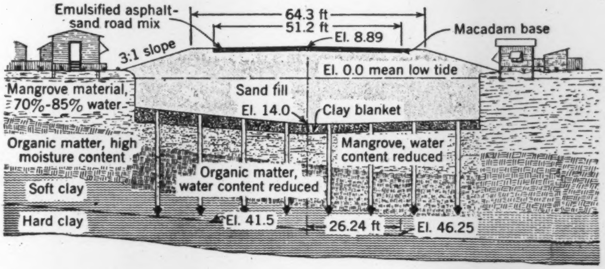
Emulsified asphalt-sand road mix
64.3 ft
51.2 ft
El. 8.89
Macadam base
3:1 slope
El. 0.0 mean low tide
Mangrove material, 70%-85% water
Sand fill
El. 14.0
Clay blanket
Organic matter, high moisture content
Mangrove, water content reduced
Organic matter, water content reduced
Soft clay
Hard clay
El. 41.5
26.24 ft
El. 46.25

FIG. 2.—TYPICAL CROSS SECTION, SHOWING PENETRATION OF CLAY AND SAND INTO MUCK

The rate of settlement was measured by observations on upright posts placed on settlement platforms installed at the top of the clay blanket at 50-ft intervals along the center line. Unfortunately, during the period when the work was suspended, the vertical posts were all carried away and it was not possible to reinstate them without considerable expense. However, measurements of the settlement at the top of the fill after heavy rolling provided a reasonably satisfactory comparative record of the rate of settlement. This record was supplemented by the borings made by Mr. Antonsanti.

An attempt was made to measure the pore pressure in the muck-peat soil. Six cylinders with standpipes attached were placed at varying depths at uniform intervals along the center line. Only one of these pressure cells showed any indication of high pressure. This one was near the site of the fault on the center line. The day before the slip occurred the water ran over the top of the standpipe approximately 4 ft above the elevation of the grade at that point.

Conducting this stabilization program involved considerable risk. Previous use of the method had not involved soils with such a high moisture content. Meager information was available on the characteristics of the soil to be treated, and the volume of water to be removed could not be accurately computed. Size and spacing of drains were arbitrarily determined; fortunately, this determination seemed adequate. The embankment has served satisfactorily, except at one place, for six years. On Cerra Street, paralleling this project along the harbor front, borings made through the surfacing showed that as much as 8 ft of macadam material had been placed at several locations.

The success of this project may be attributed to the slow rate of construction, to the use of a tough clay plate under the sand fill, and to the use of sand in the embankment above the clay blanket.

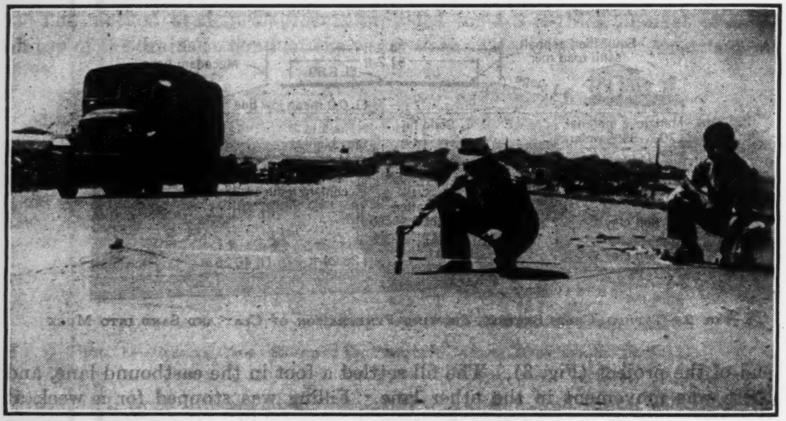

FIG. 3.—PAVEMENT DEPRESSION AT CENTER LINE WHERE A SLIP OCCURRED

EMBANKMENT CONSTRUCTION ON SOFT SUBSOIL

When a highway embankment is constructed, it tends to spread laterally and to consolidate its foundation. If the foundation is firm, the consolidation is small and the foundation develops strength enough to support the fill. However, on a soft soil, the lateral stresses from the fill displace the foundation. Several methods of treatment have been developed and successfully used. Four methods are briefly described.

1. Displacement of Soft Soil and Replacement with Acceptable Embankment Material.—Pre-excavation of the soft material and backfilling provides the firmest embankment but it is only economical for shallow depths (10 ft or less). For greater depths, blasting or jetting has been used to displace soft materials from under the center of the fill to obtain support from the firm material below and eliminate long-time settlement caused by consolidation. Granular fill is used so that its shape can be adjusted without cracking as the soft material is displaced. Large stones are not suitable because soft soil will destroy their aggregate stability by intrusion unless they are placed on a special blanket. Displacement is often difficult to control, especially for depths exceeding 10 ft to 20 ft. Much less fill will be required if all the material under the proposed embankment can be stabilized and kept under the fill.

2. Floating Embankment on Soft Soil.—If the foundation is almost strong enough, a stable condition may be obtained by reducing the overturning moment either by use of a reduced load resulting from less height or lighter material or by the addition of a balancing load. Where a meadow mat or constructed willow mattress controls the lateral stresses, the fill can often be floated on a soft foundation, although settlement due to consolidation must be anticipated. As the soil is being consolidated, it becomes stronger so that, if the fill is constructed slowly enough, moderately high fills can be built on initially very weak soils. The section of Puerto Rico Highway No. 2 between the Martin Peña Channel and Fort Buchanan was built on a natural mat of mangrove roots.

3. Drainage.—Time required for natural drainage of deep deposits (if this is practicable) is usually prohibitive unless special drainage is provided. Vertical sand drains reduce the time required for consolidation by shortening the distance the water squeezed from the soil must travel and by taking advantage of horizontal seams of more permeable material which are often present in soft foundations. Thin seams of weak clay sometimes occur in the subsoil of a generally strong material under an embankment. The weight of the embankment may cause the material above this weak clay to slide out laterally and let the fill down. Slow construction will usually provide adequate consolidation of thin clay seams in relatively permeable soil or of thin surface layers of clay if permeable material is used in the base of the fill.

4. Bridge Foundations.—Control of settlement and lateral thrust are especially important where utilities or structures are adjacent to the fill as in the case of fills at approaches to bridge abutments. If the soft layer is thin, replacement of that layer with granular fill may be possible. However, for deep soft strata the use of vertical sand drains may be indicated. A surcharge above the fill may be used to accelerate the final consolidation and to prestress the soil for the bridge load. When the required consolidation is realized, the extra fill may be used to flatten slopes. In volcanic soils or soils having a large percentage of organic material, secondary consolidation which is not accelerated by drainage may cause continued minor settlement.

Design Features for Vertical Sand Drains

The sand-drain system consists essentially of a sand blanket from 2 ft to 3 ft thick connected to vertical columns of sand from 12 in. to 30 in. in diameter. The theory of vertical sand drains is that channels filled with sand will allow the pressure of the fill to squeeze the moisture out of the muck, peat, soft clay, or other soil. The moisture will be forced up through the sand drains to the sand blanket and laterally through the blanket to the edges of the fill, as illustrated by Fig. 4. The sand blanket is extended beyond the sides of the fill so that drainage will not be blocked as the fill settles and forces the water upward and outward. In special cases, drainage may be directed downward into unsaturated material. Pumping from the drains may produce some consolidation by gravity drainage, but the force available is limited. For ideal conditions the required spacing of drains for a particular construction schedule can be computed from the results of shear and consolidation tests on undisturbed samples.[3] A center-to-center spacing of 10 ft is common, but a 15-ft spacing has been used where time for consolidation was not at a premium. A spacing of 5 ft has been used at bridge abutments where immediate construction was required. A square array is often used although a hexagonal array is more efficient. In Sweden, cardboard wicks have been used in clay with spacings of from 2 ft to 3 ft.

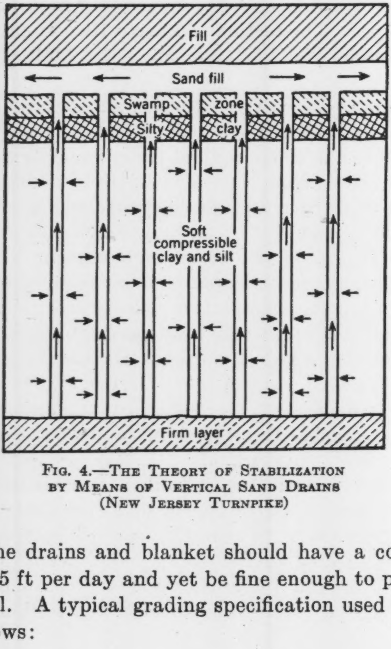

FIG. 4.—THE THEORY OF STABILIZATION BY MEANS OF VERTICAL SAND DRAINS (NEW JERSEY TURNPIKE)

The sand for the drains and blanket should have a coefficient of permeability of at least 15 ft per day and yet be fine enough to prevent intrusion of the surrounding soil. A typical grading specification used on the New Jersey Turnpike is as follows:

Sieve size, in inches	Percentage passing
2½	100
½	60–100

Of the material passing the No. 4 sieve, not more than 20% shall pass the No. 80 sieve and not more than 2% shall pass the No. 200 sieve.

---

[3] "Use of Direct Shear Tests in Highway Design," by Edward S. Barber, *Proceedings*, A.S.T.M., 1952.

For very wide fills permeability of the blanket may be augmented by the incorporation of drain pipes or gravel windrows.

CONSTRUCTION OF VERTICAL SAND DRAINS

If the natural surface will not support construction equipment, a working platform is required. This may be a clay blanket for very soft soil such as that found in El Fanguito, mats, ordinary fill, or an extra thick sand blanket. If the sand blanket is too loose, equipment may be used on about 3 ft of fill above the blanket.

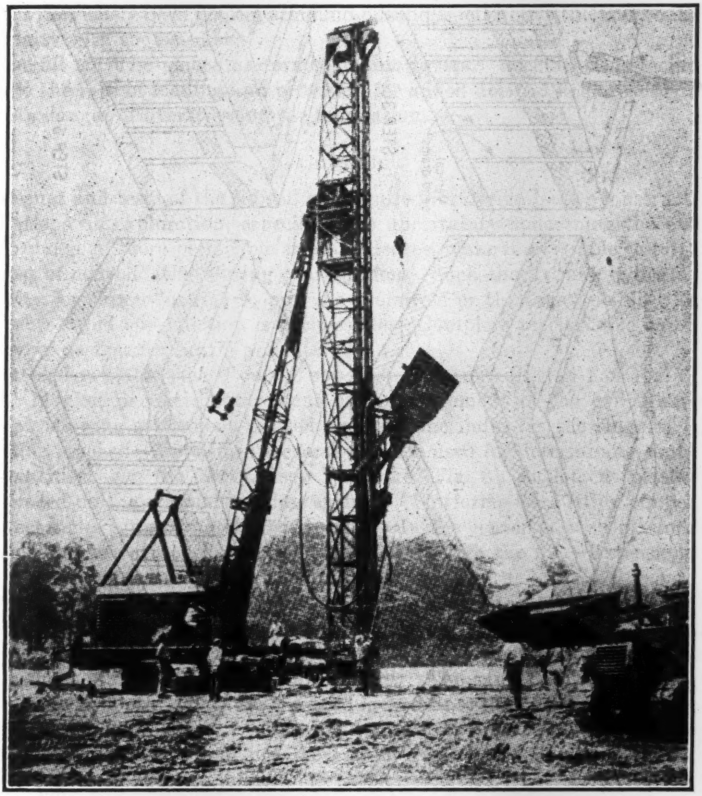

FIG. 5.—A TYPICAL SAND-DRAIN RIG (NEW JERSEY TURNPIKE)

The drains may be installed by any method that leaves clean sand in a continuous column from a firm base to the sand blanket. A frequently used method involves a mandrel or closed-end pipe driven or jetted down to penetrate hard layers. (For hard driving, smaller pipes have been driven

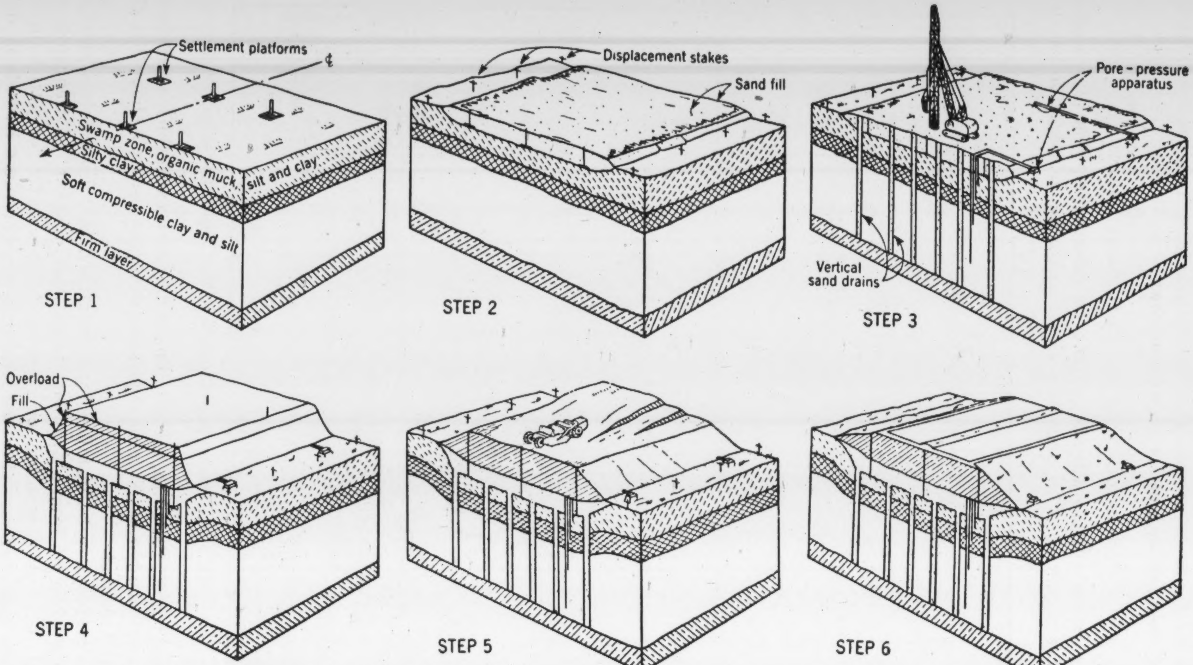
Settlement platforms
℄
Swamp zone, organic muck, silt and clay
Silty clay
Soft compressible clay and silt
Firm layer
STEP 1
Displacement stakes
Sand fill
STEP 2
Pore - pressure apparatus
Vertical sand drains
STEP 3
Overload
Fill
STEP 4
STEP 5
STEP 6

FIG. 6.—DIAGRAM SHOWING MEASURES FOR STUDYING CONSOLIDATION DURING CONSTRUCTION OF THE NEW JERSEY TURNPIKE (EXPLANATION IN TEXT)

or doubled-walled pipes used for jetting.) Jets should not be used in soft soil because they tend to smear over permeable layers and contaminate the sand with muddy water. The pipe is filled with sand by a skip hoist on the side as it is being driven (Fig. 5). On the New Jersey Turnpike, mandrels as long as 90 ft were driven with leads as high as 115 ft. When the required depth is reached, compressed air (or steam) is applied above the sand to prevent its rising as the pipe is pulled and to aid in pulling. If the blanket has not previously been placed, a mound of sand is left above the hole to insure continuity with the blanket.

The fill must be placed uniformly in thin layers. Specifications include a limit to the rate of loading and provision for added delay if field observations indicate danger of overstressing the foundation.

CONTROL

Borings and tests of the subsoil are required for design before construction. Limitations on exploration, especially the uncertainty concerning the extent and drainage of more permeable strata or lenses, make it advisable to test the progress of consolidation during construction. Such checks may indicate the necessity for slower loading to prevent overstress or they may possibly show that more rapid construction is permissible. Complete records also assist in improving designs for future projects.

Settlement plates placed on the subgrade, as shown in step 1 of Fig. 6, or on the blanket permit measurement of the settlement of the embankment. A graph showing settlement plotted against time indicates the stage of consolidation reached. Settlement records are also used for determining contract fill quantities. On the New Jersey Turnpike (Fig. 6), settlement platforms were placed on the original meadow surface. Platforms were either timber or steel rectangles approximately 3 ft square. In the center of each platform a vertical pipe was attached to extend upward through the fill. Extensions to this pipe were added as the fill was built up.

Displacement stakes placed in rows beyond the toe of fill indicate by outward movement overstress leading to lateral sliding (Fig. 6). For the New Jersey Turnpike, porous sand fill was placed on the meadow surface and displacement stakes were set outside the fill. The sand blanket was placed 3 ft or more in depth. Because the sand lacked fines to provide a satisfactory working surface for heavy equipment, contractors were allowed to deposit gravelly material containing not more than 15% fines on top of the sand blanket to form a working table.

Wellpoints (or water pipe), perforated at the lower end, are placed in holes drilled between the drains; they are surrounded by sand and the hole is sealed. After the pipe is filled with water, a pressure gage attached to the top indicates pore pressure. Because the pressure effective in developing the strength of the soil is the total pressure minus the pore pressure, an excessive pore pressure indicates insufficient effective pressure and therefore insufficient strength. The allowable pore pressure depends on the geometry of design and the soil characteristics but must generally be kept below 50% of the total pressure. In several cases where controls were inadequate, slides have occurred which destroyed the drains and necessitated reconstruction. Step 3 of Fig. 6 shows vertical sand drains that were installed on the New Jersey Turnpike through the clay, silt, peat, and muck subsoil materials. Some of the drains were 100 ft deep. Pore-pressure measuring devices were set at various depths. The mandrels used on this project were from 14 in. to 20 in. in diameter. Air pressure pushed the sand out of the bottom of the mandrel as it was withdrawn. The pore-pressure gages were read periodically, and control of the rate of loading the embankment was based on the differential readings. More than 100,000 pore-pressure readings were made on the New Jersey Turnpike.

On some projects the pore pressure is measured in vertical pipes extending up from well points or pressure cells. For a project built in California in 1933 and 1934,[4] standpipes were installed to measure hydrodynamic excess pressure. On a project in the Los Angeles (Calif.) area of the Terminal Island Freeway,[5] built in 1947, engineers used a pore-pressure apparatus involving a 10-in. by 2-in. well point at the bottom of a $\frac{3}{4}$-in.-diameter pipe driven to the depth at which they wished to know the pressure. The riser pipe is connected by two $\frac{3}{4}$-in.-diameter tubes to a gage and air cock on a post outside the fill area. Comparative readings of the gage indicate the variation in pore pressure. On a project completed in 1954 in Maine, pore-pressure readings were obtained using an apparatus consisting of a pressure cell set at an elevation in the muck

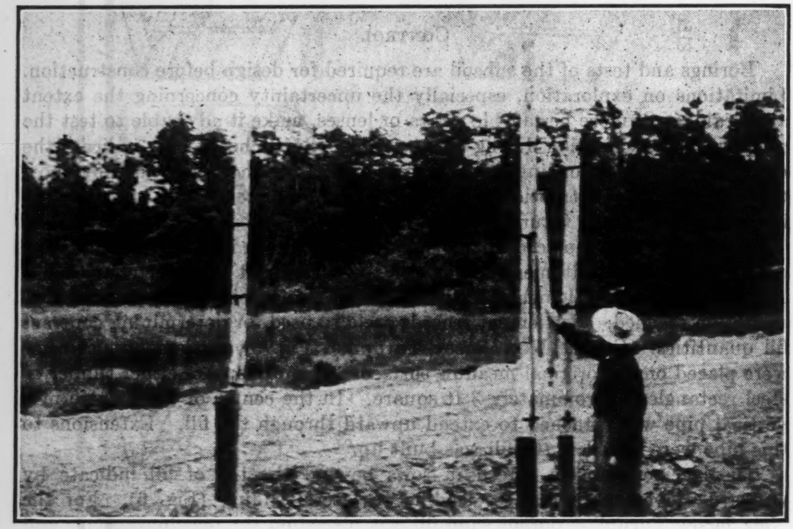

FIG. 7.—PORE-PRESSURE MEASUREMENT APPARATUS

soil where knowledge of pressures was desired. This cell was placed by driving a 4-in.-diameter pipe, cleaning out the cell and setting it, and then filling the area above the cell with sand, partly pulling the pipe, and sealing the top of the sand. From the cell, transparent plastic tubes extended upward above the fill. The three tubes shown in Fig. 7 were connected to pressure cells 14 ft, 24 ft, and 44 ft below the marsh surface. Elevations of water in the tubes were measured daily; placing of embankment material was suspended when excessive pressure was indicated by these gages.

---

[4] "Studies of Fill Construction Over Mud Flats Including a Description of Experimental Construction Using Vertical Sand Drains to Hasten Stabilization," by O. J. Porter, *Proceedings*, Eighteenth Annual Meeting, Highway Research Board, National Research Council, Washington, D. C., Vol. 18, 1938, p. 129.

[5] "Vertical Sand Drains Speed Consolidation of Soft Water-Bearing Soil," *Engineering News-Record*, March 6, 1947, p. 88.

It is customary to place an overload on the embankment area by filling above grade. After the sand drains have been placed, fill material is gradually placed and is compacted in thin layers. The pore-pressure gages, settlement platforms, and side-displacement stakes are watched. When any unusual movement is observed, the filling is stopped until conditions reach a state of equilibrium. After the fill reaches profile grade, from 2 ft to 8 ft of overload is placed and allowed to stay in place for at least three weeks before it is plowed off to the sides of the fill. Step 4 in Fig. 6 shows overload material on the New Jersey Turnpike. This overload material was placed in controlled increments, depending on the gain in strength of marsh material as determined by readings of field instruments and by soil laboratory tests.

When the time-settlement curves show a definite tendency to flatten out, it is known that the stabilization is nearing completion and the overload may be safely removed to widen the embankment and flatten the slopes.

The removal of the overload sometimes results in a slight rise in the embankment which may require from two weeks to four weeks for adjustment before paving is placed. Step 6 of Fig. 6 shows the final stabilized roadway with the surfacing in place. Pore-pressure devices and settlement platforms were left in place for future observation.

EXAMPLES OF THE USE OF VERTICAL SAND DRAINS

The Department of Soils Investigation, Highway Research Board, National Research Council, recognized the necessity for research in the treatment of subsoils for support of highway embankments and organized Project Committee No. 13 with Olaf L. Stokstad as chairman. The project was designated as a survey and treatment of marsh deposits. The use of vertical sand drains is particularly applicable in the treatment of marsh deposits, and Committee No. 13 is engaged in the accumulation of information on this process. There are several phases of the committee work that may be classified as research. The accumulation of all available important information on the treatment of marsh deposits, the correlation of this information, and its publication in a bibliography with brief abstracts of the texts are now under way.[6] Research is needed on the classification of the soils in marsh deposits so that the most economical method of treatment may be prescribed. The committee has this phase under study and expects to develop procedures as the study is continued. In the field of vertical sand drains there is a need for more comprehensive information on the types of soils to which the method is applicable and on the preliminary tests that must be made in order to be sure the method and design are economically correct. The size and spacing of drains, thickness of sand blanket, and other design features depend on the characteristics and extent of the material to be treated. The theory of design has been covered by soil scientists, among them the junior writer.[3] The application of this theory requires a comprehensive knowledge of the nature of the marsh deposits. As for the construction phase, there is a need for research on the use of pore-pressure devices to determine the best type to be used, for the collection and publication of information on the analyses of the readings obtained, and for the application of the results of these analyses to the control of the embankment construction. Other research phases may develop as the committee proceeds with its operation.

---

[6] "Survey and Treatment of Marsh Deposits," National Research Council, Highway Research Board, Washington, D. C., Bibliography, n. 15.

Outstanding construction projects on which vertical sand drains were used are listed herein and are briefly described. In 1934, the easterly fill approach to the San Francisco-Oakland Bay (California) Bridge was the site of a standpipe test to measure the nature and intensity of pressure developed by the application of a load to a saturated material. Vertical sand drains were not used on this project, but the information obtained from the experiment was used in the development of this California practice. The first application of vertical sand drains was on a portion of the Redwood Highway near Eureka (Calif.) near Beatriz Marsh. Here 84 drains 28-in. in diameter, averaging 42 ft deep and aggregating 3,530 lin ft, spaced 10 ft and 20 ft apart, were installed. Stabilization with vertical sand drains was successfully used on the East Bayshore Highway Approach to the San Francisco-Oakland Bay Bridge in 1936 and the Cuesta Grade Project in 1937.[4]

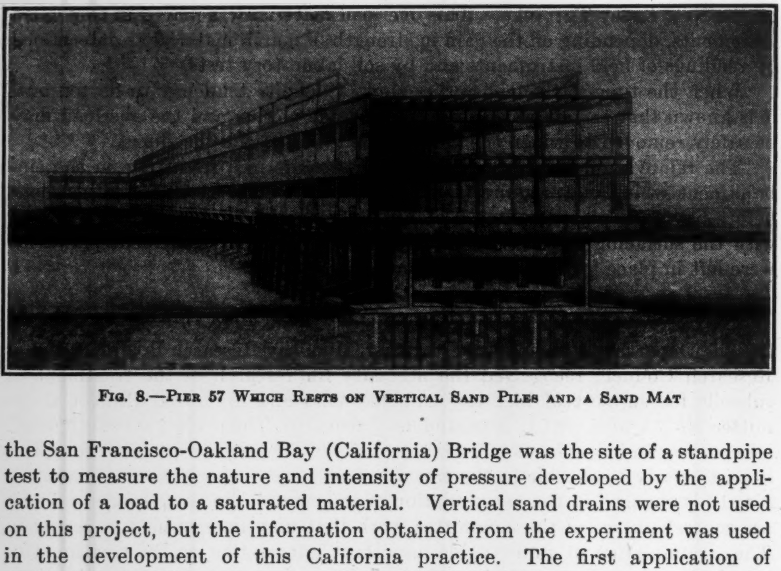

FIG. 8.—PIER 57 WHICH RESTS ON VERTICAL SAND PILES AND A SAND MAT

After the results of the test at Beatriz Marsh became available, the California State Highway Department began a program of applying this method to the stabilization of soft subsoils. In fourteen years the foundations on 22 projects, aggregating 1,108,807 lin ft of drains, had been treated.[7]

The use of vertical sand drains in the eastern part of the United States did not develop until the end of World War II. The Connecticut State Highway Department constructed a project at the Old Lyme Bridge[8] and has since developed a project on the new location of the highway crossing New Haven Harbor.

The State Highway Department of New Jersey has designed and supervised the construction of projects using vertical sand drains for stabilizing muck under Route 100 and on other marsh projects.[9]

The use of vertical sand drains on the El Fanguito project is described elsewhere.[10]

The largest project on which this method of stabilization has been used is the New Jersey Turnpike. Five million lineal feet, or approximately one thousand miles, of sand drains ranging in depth from 12 ft to 100 ft were used on this project.[11]

Vertical sand drains have been used for treatment of areas meant for types of construction other than highway. Examples are LaGuardia Airport (in New York, N. Y.),[12] Pier 57 (Fig. 8) in the Hudson River,[13] and railway embankment construction.[14] Pier 57 was constructed by the Department of Marine and Aviation in New York City.

Federal aid projects using vertical sand drains are under construction in California, New Jersey, Rhode Island, Connecticut, Washington, Hawaii, and Puerto Rico.

---

[7] "Sand Drains: Foundation Consolidation and Accelerating Settlement of Embankments," by Thomas E. Stanton, *California Highways and Public Works*, Sacramento, Calif., March–April, 1948, pp. 6–9 and pp. 38–40.

[8] "Sand Wells Speed Marsh Crossing," by Philip Keene, *Better Roads*, September, 1947, p. 27.

[9] "Making Sand Drains Stick in the Mud," *Engineering News-Record*, July 21, 1949, p. 42.

[10] "Sand Drains Stabilize Muck in Puerto Rico," by J C Carpenter, *ibid.*, July 22, 1948, p. 52.

[11] "Sand Drains Expedited Stabilization of Marsh Section," by O. J. Porter and L. C. Urquhart, *Civil Engineering*, January, 1952, p. 51.

[12] "Sand Drains for LaGuardia Field," *Engineering News-Record*, August 28, 1947, p. 291.

[13] "New York's Pier 57 Founded on Two 27,000-Ton Reinforced Concrete Boxes," by John M. Buckley and E. A. Verpillot, *Civil Engineering*, March, 1952, p. 361.

[14] "Sand Drains Reversed by Wellpoint System," by Byron J. Prugh, *Engineering News-Record*, June 5, 1952, p. 34.

DISCUSSION

Hubert M. Raedschelders[15].—The writer presents herein information on the use of vertical sand drains for stabilizing muck-peat soils in Europe. In the lowlands along the northwest coast of Europe, engineers have often had to build embankments for roads and railways on soft alluvial soils. Among the traditional methods of treatment, willow mattresses were widely used. Because the construction of concrete roads required a firm foundation and settlement after construction of the pavement had to be avoided, new methods were sought. In the north of Germany, soft material has been displaced by blasting. Charges of explosives buried in the soft soil under the center of the embankment material pushed the muck-peat soils laterally away until the embankment material was supported by the compact substratum. The acceleration of consolidation by means of vertical sand drains was adopted for the first time in Germany when a new road had to be built on glacial deposits in Schleswig-Holstein. Here 1,017 drains were installed, aggregating 20.604 lin ft. The vertical holes were constructed by the rotary jetting method. The result was very successful.[16]

In Belgium, the first application of vertical sand drains was on a part of the highway from Brussels to Ostend (the London-Istanbul Way) in 1952. The soil survey made by the National Geotechnical Institute of Belgium showed an alluvial deposit, approximately 33 ft deep, of an actual brook. The height of the fill was approximately 30 ft. Normal settlement due to consolidation computed by the hydrodynamic theory of consolidation of Karl Terzaghi, Hon. M. ASCE, is shown by curve 1, Fig. 9(*a*). In order to increase the rate of settlement the sand-drain system was adopted. A total of 1,034 drains with a center-to-center spacing of 10 ft was used in a hexagonal array. The vertical columns of sand 16 in. in diameter ranging in depth from 12 ft to 34 ft (total length 23.784 lin ft) were covered by a 3-ft-thick sand blanket.

For the construction and backfilling of the vertical holes, the driven-mandrel method has been used, and no difficulties were encountered. Instead of using the concrete point to close the lower end of the steel pipe, as described by the authors, Europeans have used a plug of sand and gravel compacted at the bottom of the open casing by a few firm blows of the driving hammer. The hitting of that plug by the special hammer was sufficient to drive the entire casing into the ground through the very soft alluvial clay. After reaching the permeable substratum, a few blows of the tamper with a simultaneous pulling up of the casing delivered the plug. The vertical sand drain was formed by gradually filling the casing during its lifting. This method saves the cost of the concrete point and produces at the same time a very permeable lower end for the sand column. The sand for the drains and blanket had a coefficient of permeability, k, of 0.28 ft per day compacted at a porosity of

---

[15] Director, National Geotechnical Inst. of Belgium, Gand, Belgium.

[16] "Vertikale Sanddrainagen als Mittel zur Beschleunigung von Setzungen und zur Sicherung von Strassendämmen in Gebieten mit organischen Bodenarten," by A. Dücker, *Strassen und Tiefbau, Strassenbau und Strassenbaustoffe*, Vol. 10, 1950.

40%. This permeability was thought to be sufficient, and at the same time the sand was fine enough to prevent the intrusion of the surrounding soil, the last condition being of more importance in this case.

The three-dimensional process of consolidation, also computed by means of the Terzaghi theory of consolidation, is represented by curve 2 in Fig. 9. The computation was made on the assumption that the bed of clay and peat was hydraulically isotropic. Because every sedimentary bed of clay is far more permeable in a horizontal direction than in a vertical direction, however, the filter wells were also computed assuming that $k_h = 10\, k_v$. The corresponding time-consolidation curve is also shown in Fig. 9 as curve 3. Curve 4 shows the graphically constructed time-consolidation curve for gradual application of the surcharge pressure.

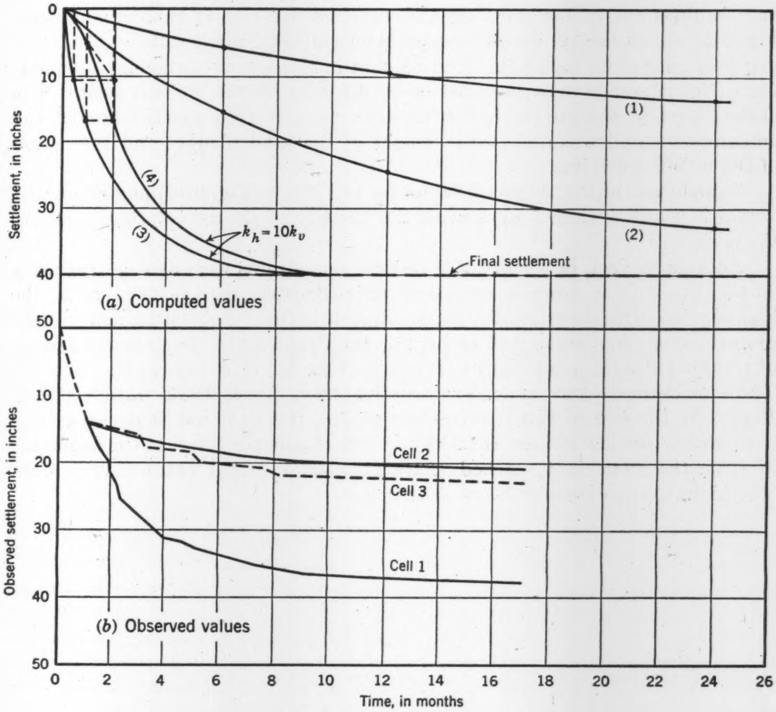

FIG. 9.—COMPUTED AND OBSERVED TIME-CONSOLIDATION RELATIONSHIPS

Because the project described was the first application of vertical sand drains in Belgium, special arrangements had been made to check the progress of consolidation during and after construction of the embankment. Settlement plates cause too much difficulty for the proper compaction of the fill material, and therefore settlement cells were used for the measuring. The cell operates on the principle that the level of liquids in two vessels connected by a tube will be the same. One of the two vessels consists of a small chamber welded to a square steel plate 12 in. on each side, placed in the embankment on the sand blanket. The chamber contains two orifices connected by means of reinforced rubber hoses to 1-in.-diameter steel tubes. Water is poured into one of the tubes until it overflows the upper orifice of the chamber and flows out through the other tube. The level of the water in a connected glass gage next to the inlet tube is the same as that of the upper orifice in the buried cell, and readings can be made during and after construction of the embankment. Fig. 9(*b*) shows the results of measurements on settlement cells. Cell No. 1 had been placed on top of the sand blanket in the center of the embankment. Cells No. 2 and 3 were installed near the toes of the embankment. The dashed part of the curves had been determined before construction of the embankment and was due to the weight of the sand blanket and the action of the mandrel driving.

Comparison of the observed values for cell No. 1 (Fig. 9(*b*)) and computed values in curve 4 (Fig. 9(*a*)) proves the validity of the assumptions made in the design.

Another project, in which 3,273 vertical sand drains were used, aggregating 93.435 lin ft, has been constructed near Brussels on the location of the highway to the Brussels-Melsbroek airport. The total settlement of the ground layers was computed to be 153 cm (60.24 in.). During the driving of the sand drains, a settlement of 25 cm (9.84 in.) in 4 months was noticed. The embankment was under construction from April, 1954, until October, 1954. At the end of this construction period, it was found that the ground had already settled 105 cm (31.34 in.). Three months later, at the beginning of 1955, the settlement reached 122 cm (40.03 in.) and became very slow. The highway was already in use at that date.

AMERICAN SOCIETY OF CIVIL ENGINEERS

Founded November 5, 1852

TRANSACTIONS

Paper No. 2798

ENGINEERING BIOTECHNOLOGY IN OCCUPATIONAL HEALTH

By Alvin F. Meyer, Jr.,[1] A. M. ASCE

Synopsis

The advance of technology during the twentieth century has produced machines and mechanical processes the capabilities of which exceed those of the men who operate them. Consequently, the problem of maintaining maximum productive effectiveness of the working population has become of major engineering significance. The author outlines the fundamentals of occupational health, physiology, and toxicology and explains the approach necessary to the solution of problems in engineering biotechnology. The basic procedure involved in the control of an occupational health hazard is explained, and the educational preparation required for this field of engineering is considered.

Introduction

It has become increasingly apparent that the attention of engineers should be focused on the fundamentals of engineering in relation to the control of occupational health hazards. This paper presents an appraisal of the problem and an introduction to the basic principles involved. It is intended not only for those concerned with the specialized aspects of sanitary and industrial hygiene engineering but for all engineers.

The importance of adverse factors in the working environment as sources of ill health was recognized as early as the Fourth Century, B.C., when Hippocrates first described lead poisoning. Recognition of the occupational origin of certain diseases was noted through the following years. However, during this period in which medicine was developing the philosophy of therapy of the individual as an entity, and in which engineering was undergoing the evolution of the technology which was to lead to the production of large modern centers of population, primary attention in so far as disease preventive measures was concerned was focused on those conditions relating to the

---

Note.—Published, essentially as printed here, in November, 1953, as *Proceedings-Separate No. 352*. Positions and titles given are those in effect when the paper was approved for publication in *Transactions*.

[1] Chief, Preventive Medicine Branch, Office of the Surgeon, Headquarters Strategic Air Command, Offutt Air Force Base, Omaha, Nebr.

biological origin of infection. The early concern of physicians with problems of occupational health is evidenced by the fact that in 1700 the first complete publication on occupational diseases was published by Bernadino Ramazzini (1).[2] The necessity for the inclusion of engineers and scientists in the public health team was recognized as early as 1850 in the Shattuck Report (2). Although in this report it was explained that the engineer member of the board should be competent in the planning and construction of public works in the best "architectural sanitary arrangements of public buildings, workshops," and other structures, it was not until 1869 that the Massachusetts State Board of Health included an engineer, and thirty-six years later, in 1886, before its organization included an engineering division, according to H. G. Baity, M. ASCE (3).

With the increasing understanding of the role of bacteria in the transmission of disease, the latter part of the nineteenth century and the early part of the twentieth saw the development to a high degree of the classic features of sanitary engineering, such as purification of water, sewage disposal, collection and disposal of waste, and control of insect and rodent vectors of disease. It was not recognized that engineers should have an intimate understanding of the physiological mechanisms involved except as a matter of transitory interest. It is doubtful that more than a few individuals fully realized the importance of engineering in the control of exposure of personnel to health hazards in their work environments. The development of industrial hygiene engineering is of fairly recent origin. It was not until 1913 that New York State included a mechanical engineer and chemist on the staff of the Medical Inspector of Factories (4). This was probably the first such use of engineering skills in an organized industrial health program.

The responsibilities of engineers concerning the effects of the projects conceived and directed by them on the community at large and on the individuals who utilize them have been recognized for many years. The code of practice of the Society that was adopted on January 18, 1927, states (5) as follows:

> "Part V.—Relations with the Public
>
> * * * * *
>
> "(5) He shall give consideration to the effect upon the community of every proposed project with which he is connected.
>
> * * * * *
>
> "(8) In addition to the safeguards required of them, Engineers shall recognize their broader obligation to provide amply for the safety, health, and comfort of the public in so far as affected by their operations."

The responsibility of engineers in safeguarding life and health is given legal status in the laws of the various states. The practice of engineering as defined in the model law (6) recommended by the Engineers Council for Professional Development (ECPD) and the National Society of Professional Engineers and which has been adopted by all forty-eight states is

> "* * * responsible professional service which may include consultation, investigation, evaluation, planning, designing, or supervision of construction in

---

[2] Numerals in parentheses—thus, (1)—refer to corresponding items in the Bibliography (see Appendix).

> connection with a public or private utility such as *structures, machines, equipment, processes, works or projects wherein the public welfare or the safeguarding of life, health and property* is concerned or involved when such professional service requires the application of engineering principles and the interpretation of engineering data."

The Canon of Ethics for Engineers adopted by the ECPD in October, 1947, reiterated (7) this philosophy in the following statement:

> "He will have due regard for the safety of life and health of the public and employees who may be affected by the work for which he is responsible."

Unfortunately, all too few engineers have been aware of the specialized nature of this problem. In order to achieve the necessary end of concern with safety and health protection, it is apparent that more than knowledge of the basic physical sciences is involved. The Shattuck Report is frequently cited as the origin of an integrated approach to public health. All too frequently, however, it is not emphasized that, to the end of preventive measures, engineers as well as members of the other professions involved must have an understanding of medical sciences. One of the basic approaches in industrial hygiene and occupational health involves the delineation of workers' responses to stresses in the form of finite relationships. This makes it possible to recognize and predict the effects of working conditions. On this basis, standards of human performance may be formulated from which industrial design and operation procedures can be developed to eliminate or minimize harmful effects and promote the health and well-being of workers (8). The requirement that engineers have a basic knowledge of physiology and anatomy is thus created. It is essential that a greater awareness be had by all engineers of the effects of their works on man, the user thereof. As technology becomes increasingly complex, the role of the sanitary and industrial hygiene engineer becomes of even greater importance in the protection of the health of the community and working population. All engineers, regardless of specialty, need to understand more about "human engineering" if they are to recognize their obligation to provide health, comfort, and safety.

Biotechnology and the Engineer

According to T. F. Hatch, sanitary engineering is concerned with the control of the human environment to the end that environmental stresses on man are maintained within acceptable limits in respect to health and well-being (9). This definition implies more than mere correction of deficiencies after they have occurred. In it is further recognized the concept pointed out previously that environmental stresses can be defined and specified and that, according to this specification, alterations to the environment may be designed. Engineers have frequently been criticized for tending to limit their activities and responsibilities to those areas in which problems can be solved by the laws of physical science alone. As a result of a lack of training in the principles and fundamentals of physiology and psychology, only functional requirements and the economics of production are generally considered (8).

The industrial potential of the United States has increased 700% since 1900. More than one half of this increase has occurred since 1942 (10).

Concurrent with this expansion of industrial potential, there has been a tremendous increase in exposures to hazardous or potentially hazardous conditions in every mode of life. Approximately sixty million persons in the United States are employed in various occupations (11). The chemical industry has grown tremendously and it now has the capability of synthesizing new chemicals for specific purposes. An example of this is the development of synthetic insecticides. In 1945 there were only a few insecticides in general use, and their toxicity was well understood. Today, there is in widespread use a host of materials which are potentially dangerous to human beings (11). The shelves of the average American home contain chemicals which afford serious dangers to health and well-being unless used intelligently.

It is obvious that in order to cope successfully with the problems created by the complexity of the modern environment (both living and working—be it in a large industrial plant, small workshop, or in the location of a self-employed operation) integrated knowledge of a wide variety of disciplines is required. The engineer must understand the physiological processes involved in the results of exposure to chemicals and other hazards in the environment if he is to assess the stresses created by the environment and translate them into appropriate designs and controls. A fundamental knowledge of physiology, psychology, anatomy, and the biological sciences is required if the engineer is to accomplish his mission (12). Adequate and economical environmental control measures for protection against hazards must be predicated on a knowledge of the mechanisms by which compounds are absorbed into the body, what effects are produced following absorption, how the compounds may be detoxified, where they are stored, and how they are eliminated. Both the long range and the immediate effects of exposure to any of the wide variety of abnormalities of environmental conditions that may be encountered should be fundamental considerations in the design of any structure or process.

As pointed out (13) by Mr. Hatch, human engineering is engineering design in relation to man's anatomical and physiological capabilities and limitations. He further indicates the excellent opportunities for engineers to function actively in the field of physiology and cites such contributions as the work in thermal physiology of the American Society of Heating and Ventilating Engineers. As long as the performance limits of man exceeded those of his machines or work environment, considerations inherent in engineering application within the definition of "human engineering" were probably of only minor significance. As machines are developed the performance of which exceeds man's capability, these considerations become of paramount importance. In the aviation industry in particular, this has become a matter of serious concern (14). When properly applied, the knowledge of the capabilities and limitations of man in conjunction with basic engineering knowledge can be utilized to determine the adequacy of the environment and man's ability to function within the environment or to synthesize solutions to the problem of his functioning therein.

FUNDAMENTAL CONCEPTS OF OCCUPATIONAL HEALTH

The purpose of any program of occupational health is to increase and maintain maximum productive effectiveness of the working population.

Productive effectiveness is in a sense a measure of individual productive ability. There is a definite interrelationship between general community health and the health of the working population. The engineer must concern himself not only with means of preventing disease and controlling hazards but also with means of improving the efficiency and comfort of the worker. The effect of plant waste or by-products on nearby areas must be taken into consideration.

It is estimated that the time lost annually in the United States due to illness and occupational conditions amounts to between 400 and 500 million man-days (15). In actuality, only a small percentage of the number of days lost in industry is due to conditions arising from the work environment. Although this percentage is small, it involves a considerable actual number of days lost which are more easily reduced by adequate controls than those caused by illness.

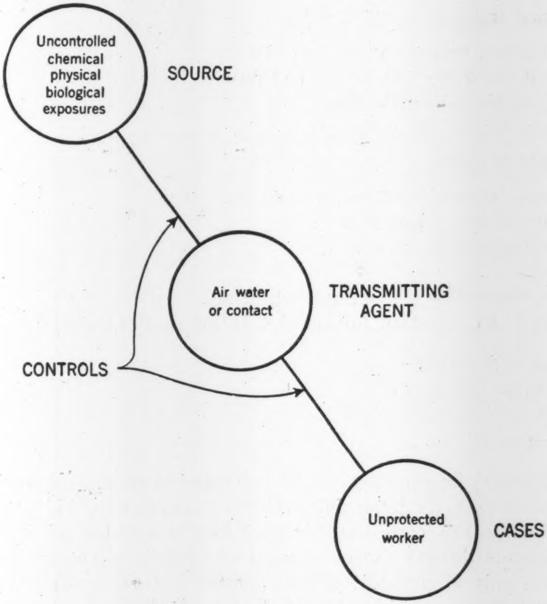

FIG. 1.—CONDITIONS FOR PRODUCTION OF OCCUPATIONAL DISEASES

In order for a case of occupational disease to be produced, there must exist three general conditions (Fig. 1). There must be an uncontrolled source of exposure to chemical, physical, or biological agents. This source must contaminate either air, food, or water or come in contact with an individual not protected against it. Occupational diseases are not communicable except for those of biological origin. The disease is acquired only through exposure to the offending material. Epidemics of occupational disease are the result of the exposure of large groups of unprotected persons to hazardous conditions at the same time. In the following sections of this paper are considered briefly some of the basic principles with regard to the sources of occupational diseases and the means of their control from an engineering viewpoint.

Chemical exposures consist of toxic or hazardous gases, mist, dust, fumes, vapors, and smokes. Physical hazards in the work environment include abnormalities of temperature, humidity, moisture, shock and vibration, deficiencies of illumination, and exposure to radiant energy and ionizing energy and noise. The biological agents of occupation disease include bacteria, fungi, pollens, and parasites. Toxic plants such as poison ivy are also included in this category. Among the sources of occupational disease are the following:

1. *Chemical Hazards.—*
   Toxic gases, vapors, mists, and fumes.
   Irritant gases, vapors, mists, and fumes.
   Toxic particulate materials.
   Irritant particulate materials.
2. *Physical Hazards.—*
   Abnormalities of temperature and humidity.
   Abnormalities of pressure.
   Defective illumination.
   Noise.
   Repeated motion, shock, and vibration.
   Exposure to radiation (ultraviolet, infrared, and ionizing).
3. *Biological Hazards.—*
   Infectious diseases.
   Fungi.
   Parasites.

As well as these, there exist problems of situational stress and worker fatigue. In addition to procedures determining whether or not an individual is physically capable of doing a job, consideration must be given to the job itself to insure that its demands do not exceed normal capabilities. Occupational fatigue may be the result of physical environmental factors, psychological factors, job requirements, or a combination of all three (16).

Occupational diseases are not restricted to production-line types of facilities. Approximately 99% of the working population of the United States is employed in plants and shops or in activities employing less than 1,000 workers (17). The employed agricultural population is exposed to a wide variety of hazards. Even the hobbyist such as the model airplane builder is exposed to dangers. One of the most glaring potentials of this type of hazard is the recommendation by many plastic model kit manufacturers that carbon tetrachloride be used as a solvent for bonding the component parts of the model. In several of these instructions no reference is made to the potential toxicity of the material by skin absorption although warnings such as "Do Not Breath the Fumes" may be provided. The staggering number of deaths from carbon monoxide poisoning due to faulty heating equipment illustrates the need for continous awareness of the dangers in the everyday living and working environment. The vast majority of large industries has become increasingly aware of the importance of an effective preventive and occupational medical program. Unfortunately, in the case of small plants and self-employed persons, this awareness has not been developed nor have official health agencies been able to devote the proper amount of time to this lack of awareness. Here again there is a challenge to the entire engineering profession to insure that processes and products developed contain inherent safeguards to the user. An estimate of the extent of some chemical exposures in the United States may be seen in Fig. 2, which is adapted from "Environment and Health" (11).

From the foregoing, it may be seen that there are two distinct aspects of the engineer's activities with regard to occupational health. First, there is the moral and legal responsibility of all engineers for including in basic designs consideration for the health, safety, and effective functioning of persons who are either exposed to, or must work with, the product, process, or structure involved. In this area of activity and interest the advice and assistance of specialists in engineering and applied science are essential.

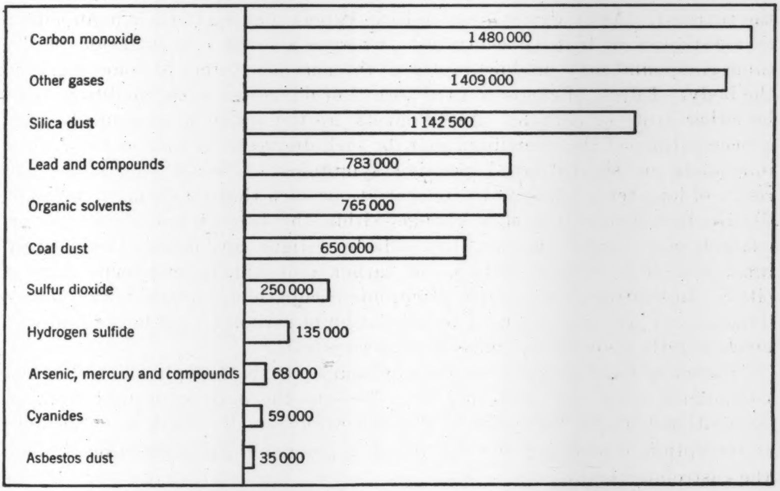

FIG. 2.—NUMBER OF WORKERS EXPOSED TO OCCUPATIONAL HAZARDS

Secondly, the specialized field of sanitary engineering involves the evaluation, detection, and control of adverse environmental factors in the occupational environment and the development of means of improving the environment so that man may better function therein. It includes provision of advice and assistance to engineering colleagues regarding the biotechnological aspects of their activities.

FUNDAMENTALS OF PHYSIOLOGY AND TOXICOLOGY

General.—Many physiological functions of the body may be considered in refined mathematical terms based on well-understood physical principles. Examples are the reactions to dust in the respiratory tract, the operation of the circulatory system, and the functions of the various membranes such as those in the kidney (13). According to R. N. Baillif and D. L. Kimmel (18), the structures which comprise the body should be understood first and then the manner in which the structures function. The main components are the skeletal, muscular, circulatory, digestive, respiratory, urogenital, endocrine, and central nervous systems. Included in the nervous system are the organs of vision, hearing, speech, and sensory perception. Any one or all these systems may be adversely affected by conditions arising from the work environment.

The cause-and-effect factors of chemical and physical exposures are related quantitatively and depend on the duration of exposure and concentration of the toxicant. As an example, some toxic vapors may exert their main action as anesthetics in high concentrations whereas a lower concentration of the same compound may produce injury to the nervous system or some organ of the body. Effects of exposure to abnormal or dangerous work conditions may be either acute or chronic. Acute effects are the result of exposure to high concentrations of the offending agent for such durations of time as to produce immediate or short-delayed positive symptoms. Chronic effects are the result of long-term exposure to concentrations such that no dramatic onset of disease is caused but a slow change within the body takes place. As an example of an acute exposure, the headache, fatigue, and nausea produced by inhalation of more than 400 ppm of carbon monoxide for two hours may be cited. In contrast, an example of chronic occupational disease is the kidney damage and jaundice produced by inhalation of carbon tetrachloride fumes at levels slightly above the permissible exposure level.

Portals of Entry.—There are three primary portals through which chemical compounds enter the body (Fig. 3). Perhaps the most important from an occupational health viewpoint is the respiratory tract. Next in importance is absorption of materials through the skin, and the third is ingestion through the gastrointestinal tract.

In the process of respiration the air is forced by atmospheric pressure on inspiration through the nose into the chamber of the nasal cavity where the nasal hairs and eddy currents cause the deposition of a considerable amount of dust. The air passes on through the pharynx making an abrupt change in direction which causes larger particles to be impinged on the walls of the nasal pharynx. These particles are subsequently removed either by expectoration or by swallowing. The air then passes through the upper respiratory tract into the alveoli of the lungs. In the adult, the respiratory tissue of the lung, which acts as an exchange between the blood and the air, presents a surface area of approximately 65 sq m. Such factors as the concentration of the toxicant in the air, solubility in blood tissues, length of exposure, the rate of breathing and rate of circulation, and whether the material is reacting with body tissue determine the accumulation of the gas or vapor in the body.

Determination of the effect of such accumulation must include consideration of whether any detoxification mechanisms take place, what the ultimate storage site within the body is, and the method and rate of elimination. A vapor relatively insoluble in blood plasma will saturate the body rapidly. On the other hand, if it is very soluble in blood, saturation will be slow. Because the arterial blood supply to the brain is large and a brief exposure to a high concentration of gas or vapor of low solubility produces rapid effects, this phenomenon has an important bearing on the effect of brief exposures to high concentrations of slightly soluble materials. Moderate concentrations may induce unconsciousness after a half hour or more of exposure and the effects will be somewhat prolonged, whereas concentrations which are sufficiently high to induce unconsciousness quickly may be recovered from shortly after removal from exposure.

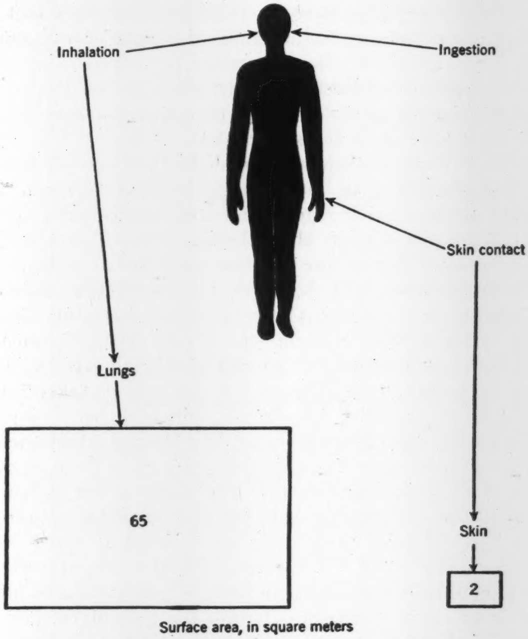

Fig. 3.—Portals of Entry of Toxic Materials

The absorption of particulate matter such as dust or fumes involves similar processes of accumulation, distribution, and elimination as do gases. However, this process is actually more complicated. Retention of particles is in direct proportion to the rate of respiration below 20 inhalations per min. It is directly proportional to the size of the particles or their aggregate density. Particles ranging in size from 0.25 micron to 16 microns show approximately

50% retention. Particles smaller than 0.1 micron are generally thought to be too small to be trapped in the alveoli of the lungs and are exhaled much the same as undissolved gas. Some dusts (from 5 microns to 20 microns in diameter) are impinged on the mucosa of the upper respiratory tract. Particles trapped along the bronchial tree are swept toward the pharynx by the ciliary action of the tracheal and bronchial membranes. Particles caught in the alveoli are probably absorbed through the wall or they may be engulfed by phagocytic cells and carried into the blood capillaries or enter the "lymphatics" where they will be concentrated in the nodes. Particles of silica of from 0.1 micron to 1 micron in diameter are among the most active and most dangerous. Similarly, particles of beryllium present a serious hazard. A fact frequently not recognized is one pertaining to materials which are only slightly volatile. Concentrations far in excess of those possible from partial pressure of the gaseous phase at room temperature may be encountered if the material is sprayed. A vapor harmless at ordinary temperatures may be extremely dangerous when atomized as an aerosol or mist.

The surface area of the average adult male body is approximately 2 sq m. It will be seen that the skin is an important portal of entry for those materials which may penetrate the intact skin. The absorption of chemicals through open lesions is much more rapid than through the unharmed skin. Most electrolytes in water do not penetrate the skin in significant amounts. Benzene (benzol, not to be confused with benzine), toluene, xylene, and chlorinated hydrocarbons can be absorbed to the extent that harmful effects may be produced. The salts of lead, tin, copper, arsenic, bismuth, antimony, and mercury are thought to penetrate by combination with fatty acid radicals of sweat. Dangerous amounts of hydrogen cyanide may be taken into the body through the skin from contaminated air. Materials or solutions of materials such as nitrobenzene, dinitrobenzene, nitrotoluene, dinitrotoluene, analine, dimethylanaline, and nitroglycerine are rapidly absorbed through skin contact. Dichloro-diphenyl-trichloroethane (DDT) and many other argicultural insectides may be absorbed through the skin when dissolved in a petroleum base.

The gastrointestinal tract may serve as a portal of entry secondary to inhalation, as previously noted. The eating of contaminated food or beverage or the placing of contaminated fingers or other objects in the mouth serves as a primary means of entry of intoxicants into the gastrointestinal tract. Although this mode of entry plays a minor role in absorption of most toxic materials, its significance cannot be overlooked. The importance of washing the hands prior to eating or smoking continues to be a principal preventive measure.

Mode of Action and Effects.—The mode of action of chemicals on the body may be classified by physiological considerations as outlined by Y. Henderson and H. W. Haggard (19). The five main classes are: (*a*) Irritants, (*b*) asphyxiants, (*c*) anesthetics and narcotics, (*d*) systemic poisons, and (*e*) particulate matter other than systemic poisons.

Irritant materials may be corrosive or vesicant in nature. The results of contacts with these materials may be mild irritation, a vesicle or a blister, of a third-degree burn resulting in actual scarring and destruction of the tissue.

Concentration is apparently of greater significance than time or duration of exposure.

Irritant materials may be divided into four major groups: Those that affect the upper respiratory tract, those that affect both the upper respiratory tract and pulmonary tissues, those that affect the terminal respiratory tree and alveoli, and those that produce a corrosive or irritant effect upon the skin. One of the most common examples of an irritant affecting the upper respiratory tract is acrolein which results mainly from the combustion of fuels and produces an irritation of the nose and eyes. Also known as allyl aldehyde, it has a disagreeable and strongly penetrating odor. Petroleum and petroleum products in themselves are toxic in varying degrees. Exposure to small concentrations for a few minutes will cause almost immediate irritation to mucous membranes, the conjunctiva of the eye, and the upper respiratory tract. Among the irritants which chiefly affect the upper respiratory tract and pulmonary tissues are bromine, chlorine, chlorine oxides, cyanogen bromide, cyanogen chloride, diethylsulfate and dimethylsulfate, fluorine, iodine, ozone, sulfur chloride, phosphorous trichloride, and phosphorous pentachloride. The effect of exposure to chlorine, which is a typical member of this group, is that of bronchitis, dryness of the conjunctiva, and occasionally painful irritation of the cornea. Symptoms such as headaches, vertigo, loss or weight, anemia, or premature senility are the result of chronic exposure to these materials. Arsenic trichloride, nitrogen dioxide, nitrogen tetraoxide, and phosgene are typical materials which affect the terminal respiratory tree and lungs. Gasoline is a common example of a primary skin irritant.

Asphyxiants may be divided into two principal groups—simple asphyxiants and chemical asphyxiants. Both groups of compounds exert their effects by interfering with the processes of oxidation in the tissues. Carbon dioxide, ethane, helium, hydrogen, methane, nitrogen, and nitrous oxide are examples of simple asphyxiants. They are physiologically inert gasses that act primarily by diluting atmospheric oxygen below the partial pressure required to maintain oxygen saturation of the blood sufficient for normal tissue respiration. Although included in the foregoing examples, methane and nitrous oxide may also be considered as belonging to the group of compounds of gaseous hydrocarbons which act as anesthetics. Frequently the toxic effects encountered on exposure to this group are caused by impurities normally found in commercially available products. Commercial ethylene has occasionally been directly contaminated with carbon monoxide. Acetylene used in welding contains from 10% to 14% of impurities, including phosgene, carbon disulfide, hydrogen sulfide, arsenic, carbon monoxide, and other hydrocarbons. Carbon dioxide is a simple asphyxiant. The release of carbon dioxide from automatic or manually operated fire extinguishing equipment in an enclosed space may result in asphyxiation of the occupants thereof through the replacement of the available oxygen supply.

Chemical asphyxiants either prevent the transportation of oxygen from the lungs through the blood stream or else interfere with normal oxidation in the tissue even though the blood itself is thoroughly oxygenated. Examples

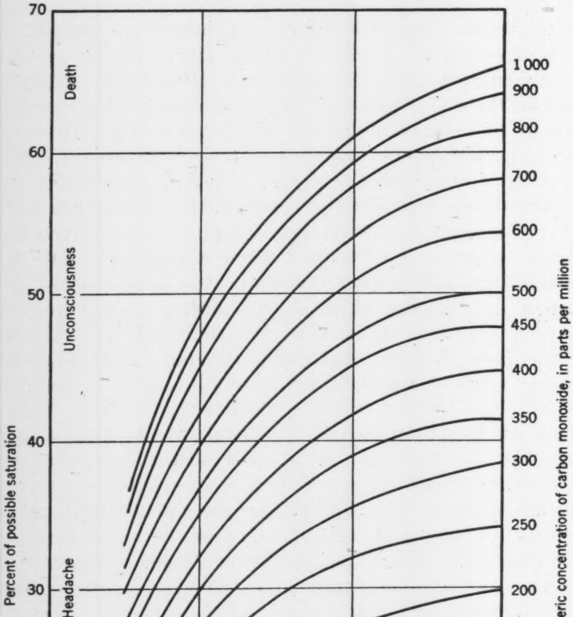

FIG. 4.—EFFECTS OF EXPOSURE TO CARBON MONOXIDE

of this type of material are carbon monoxide, cyanide compounds, aniline, and hydrogen sulfide.

One of the most common of this group of materials and one which presents one of the greatest hazards is carbon monoxide. The toxicity of this gas is a result of its affinity for hemoglobin, approximately 210 times that of oxygen. The carboxy hemoglobin which is formed does not rapidly absorb oxygen and hence interferes with the function of the blood in maintaining the flow of oxygen from the lungs to the tissue. The results of exposure to varying concentrations of carbon monoxide in the atmosphere are shown in Fig 4. Among the more serious consequences of exposure to low concentrations of carbon monoxide is the dulling of intellect and judgment without accompanying awareness of the situation. Reaction times are slowed down, and hearing and visual hallucinations may take place without warning.

Perhaps the largest group of chemicals used in homes and industry is halogenated hydrocarbons. For the most part, these materials have an anesthetic and narcotic effect. Common chloroform (trichloromethane) is a representative member of this family of chemicals. Carbon tetrachloride is widely used without awareness of its dangers. The toxic reactions which follow single exposures to high concentrations or the chronic results of prolonged exposure to moderate concentrations are primarily limited to effects on the kidneys and the liver. Initial acute intoxication is centered around the central nervous system. Early symptoms of exposure to these materials are dizziness, headaches, stupor, nausea, and vomiting.

The systemic poisons include those materials which cause organic injury to one or more of the visceral organs, the blood and blood-forming system, and the nervous system. This group also includes the toxic metals. Halogenated hydrocarbons cause damage to the visceral organs. Compounds such as benzene, phenols, and, to a lesser degree, toluene, xylene, and naphthalene are toxic because of their effects on the blood and blood-forming organs. The nerve poisons include carbon disulfide, methyl alcohol, thiophene, and some of the newer insecticides such as parathion. Toxic metals include lead, mercury, cadmium, antimony, and manganese. The extent of the absorption of these metals varies with the solubility and chemical reactivity of the compound, the number of particles distributed in the atmosphere, and the duration of exposure. Particulate matter other than the systemic poisons includes dusts, irritants, bacteria, and fungi. Silica, asbestos, and beryllium are among the principal causes of fibrosis of the lungs. Dusty operations such as grinding and bufing of resins and certain plastics may produce allergic reactions. Similarly, pollen dust and other organic dusts may produce serious problems. Toxic dusts include acids, alkaloids, fluorides, and chromates in particulate form. These substances frequently act only when dissolved, principally by perspiration or moisture on the skin or when in contact with mucous membranes.

Exposure (either chronic or acute) to physical agents produces tissue responses or organic responses which are frequently complex. The exact mechanism of these responses in many cases is obscure. In general, cell damage or destruction accompanied by systemic reaction occurs. As an example, exposure to ionizing radiation produces cell damage and destruction. If the exposure is sufficiently great, radiation sickness or death will follow. The effects of exposure to the various components of the electromagnetic spectrum should be understood by all personnel working in the field. Detailed information relative to exposures in various occupations and the symptoms of onset of occupational disease have been summarized (20).

CONCEPT OF THRESHOLD LIMIT VALUES

As previously explained, the degree of effect of exposure to hazards in the environment is related to the concentration of the contaminant, the duration of exposure thereto, and the rate of absorption and excretion by the body. The establishment of control measures for airborne chemical contaminants and, in fact, the design of ventilation systems for areas in which chemicals are utilized must be predicated on a knowledge of the maximum concentration of airborne chemicals which can be tolerated without ill health or discomfort. The contamination of workroom air may be determined rather precisely by using the laws of physics. A knowledge of the threshold limit value makes possible the determination of required ventilation rates. The term, "maximum allowable concentration," is gradually being replaced by "threshold limit value" (21). The committee on Threshold Limits of the American Conference of Governmental Industrial Hygienists compiles extensive lists of such limits. These values represent the concentration of gas, vapor, fume, or dust to which continuous exposure for long terms (eight hours a day, five days a week, and fifty weeks a year) during a normal working life of from thirty to forty years will not produce bodily discomfort or impairment of function. Many of the values applicable to man are derived from extrapolation of results of experi-

TABLE 1.—CLASSIFICATION OF CHEMICAL HAZARDS AND SERIOUSNESS OF EFFECT[a]

Hazard classification	Range of effects [b]
I. Materials producing vapors rapidly toxic or extremely irritating on exposure for a short time or to low concentrations.	Vapor (extremely) hazardous, (irritating) hazardous liquid and vapor (gas under pressure); vapor poisonous if inhaled, vapor may be fatal if inhaled.
II. Materials producing vapors hazardous at prolonged or repeated exposures or at exposure to high concentrations.	Vapor harmful. Causes irritation to eyes, nose and throat.
III. Gases and vapors physiologically inert.	Gases (vapors) reduce oxygen available for breathing; release of heavy gas (vapor) which may cause suffocation.
IV. Materialsi n dust form hazardous on inhalation or contact.	Hazardous (harmful) dust. Harmful if inhaled. Causes irritation of skin, nose, and throat.
V. Corrosive skin irritants.	Cause severe burns. Cause burns. May cause burns.
VI. Materials causing skin irritation after prolonged or repeated contact.	Cause skin irritation. May cause skin irritation.
VII. Materials toxic on skin absorption.	Hazardous solid (or liquid). Rapidly absorbed through skin. Absorbed through skin.
VIII. Materials toxic if swallowed.	Poisonous if swallowed. May be fatal if swallowed. Harmful if swallowed.

[a] See Bibliography reference (23*a*). [b] Words in parentheses may also be applied for certain materials.

ments on animals. All the values are subject to revision as more toxicological data become available.

It should be emphasized that there is a wide range in the individual response to various chemical exposures. It is obvious that, if the maximum allowable concentration for a particular material is 50 ppm, exposure to 55 ppm or 60 ppm for a short period of time will not have a deleterious effect. The threshold limit values should be utilized as guides to assist in defining generally safe working conditions (22). The same philosophy as is utilized in the development of threshold limit values for chemical exposures is also applicable in general to the permissible exposure for such hazards as ionizing radiation, noise, abnormalities of temperature and humidity, deficiencies of illumination, and shock and vibration.

In the development of permissible exposure limits (maximum allowable concentrations or threshold limit values) it is essential that the toxicity of the chemicals concerned be known. Toxicity data can be expressed in readily understood terms. As an example, an extremely toxic compound would be one of which one grain would probably be lethal to man. A relatively harmless material would be one which would require a quart or more to produce death. The range of toxicity is shown in the following tabulation:

Toxicity rating	Description		Probable lethal dose for man
1	Extremely toxic	•	1 grain
2	Highly toxic		1 teaspoon (4 cu cm)
3	Moderately toxic	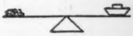	1 ounce
4	Slightly toxic		1 pint
5	Practically nontoxic		1 quart
6	Relatively harmless		More than 1 quart

Another classification of physiological responses according to F. T. Patty (16*a*) is as follows:

"a. Amount producing detectable or other degree of odor.
b. Amount producing detectable or other degree of irritation.
c. Maximum amount for repeated daily 8-hour exposure without injury.
d. Maximum amount for a single 8-hour exposure without serious disturbance.
e. Maximum amount for a single one-hour exposure without serious disturbance.
f. Amount dangerous to life within 4–8 hours.
g. Amount dangerous to life within one-half to one hour.
h. Amount causing death within a few minutes."

The Manufacturing Chemists' Association has developed a classification (23) for chemical hazards and the seriousness of effects as shown in Table 1. This association has prepared a handbook of warning labels (23) for all categories of hazardous chemicals which contains data on a large number of commonly used chemicals.

CONCEPTS OF ENGINEERING APPLICATION

As shown in Fig. 5, the basic procedure involved in the control of an occupational health hazard is the substitution of a less toxic or dangerous component or procedure for a hazardous one. When this is impossible, engineering control of occupational health hazards demands the design of protective devices. Under some circumstances, even properly designed processes constitute a hazard, or the nature of the work involved may preclude the development of integral safeguards. Under these conditions, personal protective devices must be utilized. When economy dictates or the nature of the work is such as to present special hazards, a combination of the three basic procedures must be applied. This principle of multiple barriers is utilized when dealing with extremely toxic processes. Regardless of whether one is dealing with the correction of existing hazards, the design of new work procedures or equipment, or the development of products, these general procedures (Fig. 5) should be followed.

It is cheaper to eliminate the requirement for costly protective or control measures by substituting less dangerous or less offending material, particularly if the operation in question is to be continued over a long period of time. In the case of chemical or physical hazards in the environment, consideration must be given not only to the work-process dangers but also to the control of waste products and attendant hazards of atmospheric or stream pollution. In the following consideration, chemical hazards are generally utilized as examples as they present the more common problems found among all occupations. The same principles apply to the control of physical hazards and to job or human engineering procedures. Frequently the very condition which creates the hazard is what makes the particular process or material useful, as in the case of ionizing radiation. Under these conditions elimination or substitution of less toxic or dangerous materials is impossible, and protective measures must be provided.

An example of the substitution of a less toxic or dangerous material for a hazardous one is the use of trichloroethylene instead of carbon tetrachloride as a cleaning solvent. The toxicity of trichloroethylene is approximately one half that of carbon tetrachloride. In addition, the material is much less readily absorbed through the skin. Although it is less toxic than carbon tetrachloride, appropriate ventilation methods must be utilized to protect personnel against the effects of inhalation of excessive concentrations of this vapor. Another example of substitution of a product is the use of freon as a refrigerant in place of methyl chloride in household refrigerators. A well-known example of elimination of a hazard is the use of nonsilica-bearing sands for sandblasting operations as a means of controlling silicosis.

As previously explained, even the substitution of a less toxic material for a dangerous one does not always eliminate completely the hazards; the substitute may be of such a nature as to require controls. If hazardous materials must be utilized, the process should be designed to expose personnel to the offending materials as little as possible. Consideration should first be given to isolating the process in a remote area if the danger warrants it. If isolation is impossible, complete inclosure or closed systems should be used. If the material is sufficiently dangerous, remote handling equipment with servomechanisms and television viewing may be required, as in the case of handling materials of extremely high levels of radioactivity. An entire field of remote-control engineering has been developed to deal with this problem (24).

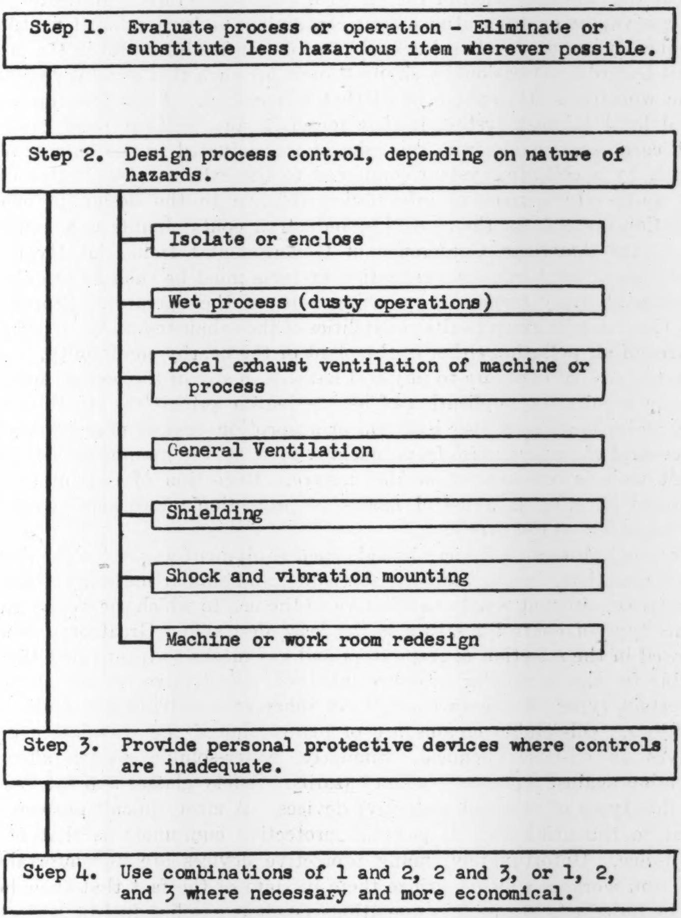
Step 1. Evaluate process or operation - Eliminate or substitute less hazardous item wherever possible.
Step 2. Design process control, depending on nature of hazards.
Isolate or enclose
Wet process (dusty operations)
Local exhaust ventilation of machine or process
General Ventilation
Shielding
Shock and vibration mounting
Machine or work room redesign
Step 3. Provide personal protective devices where controls are inadequate.
Step 4. Use combinations of 1 and 2, 2 and 3, or 1, 2, and 3 where necessary and more economical.

Fig. 5.—Engineering Control Principles

When the operation involves the creation of a dust hazard such as the grinding and buffing of lead or other metals, use of a wet process will materially reduce or eliminate the hazard. Another example of this type of control is the scraping of radium-painted instrument dials under oil or solvent so as to prevent the contamination of the air with radioactive dust. In dealing with toxic gas vapors or other atmospheric contaminants, local exhaust ventilation is frequently required. Local exhaust ventilation is also useful in the control of dust hazards. Occasionally circumstances are such that general ventilation of the workroom atmosphere is all that is required. A good example of a typical local exhaust system is that found in any well-equipped garage in which carbon monoxide from the exhaust is conducted to the outside of the building by a collector system connected to the exhaust pipes. One of the most up-to-date sources of information relative to the design of exhaust ventilation systems for the control of industrial contaminants is a handbook (25) of the American Conference of Governmental Industrial Hygienists. The design of local exhaust ventilation systems must be such as to draw the contaminant away from the breathing zone of the operator. Proper consideration must be given to the possibilities of the exhausted material becoming a source of air pollution either in the plant or the nearby community.

In the case of exposure to physical hazards, many of the control measures involved require the application of basic scientific principles. In the case of shock and vibration, proper isolation or absorption devices may be required. The control of impact noise from machine tools by the mounting of the tools on felt pads is one control of this nature. Reflection of radiant heat by aluminum sheeting is a useful means of protection of workers against the harmful effects of the exposure.

Personal protective devices include such equipment as respiratory devices, gloves, gauntlets, aprons, impermeable suits, and similar materials. Because protective equipment is only as effective as the use to which the wearer applies it, this type of control measure is the least desirable. Great care must be exercised in the selection of respirators and gas masks to insure that they are suitable for the particular exposure involved. Protective creams are useful for certain types of exposure but have inherent disadvantages under some conditions. Oil-soluble creams are of little value if the chemical exposure involves an oil-base chemical. Similarly, water-soluble creams afford no protection against aqueous-solution hazards. Safety glasses and safety shoes are other types of personal protective devices. A most difficult problem with regard to the utilization of personal protective equipment is that of user acceptance. Unfortunately, many protective devices are uncomfortable to wear, and workers will not utilize them in spite of the fact that their health may be impaired. In certain operations (such as gasoline fuel-tank cleaning) failure to utilize proper protective equipment may result in loss of life of the workers. The main burden of responsibility for the proper use of individual protective equipment lies with job supervisors. The writer has previously explained that it is possible to derive specifications for human performance under job stresses and thereby to develop adequate control measures. Utilizing an idea of R. N. McFarland (26), a method has been developed which is applicable not only to the design of specific job-hazard control measures but also to the hazards evaluation of existing processes or operations. In addition, this technique may be applied to any engineering works or design to insure that the human factors involved are recognized.

In using this method, a "pie diagram" is drawn with concentric circles showing varying degrees of environmental conditions beginning with "comfortable," then "acceptable," "uncomfortable," and "hazardous." The importance of the various environmental aspects of the condition under consideration is shown as sectors of the over-all circle, sized according to the degree of effect on the total operation. From a knowledge of the environmental factors, the parameters for the various environmental criteria can be shown on the chart. The environmental factors are thus presented pictorially. Requirements for for design that will account for human factors are easily visualized. The same procedure may be utilized in the evaluation of existing conditions by plotting on the chart the observed conditions. An example of this type of approach to human engineering problems is shown in Fig. 6 in which occupational environmental specification for a truck driver is shown as an example of the factors to which consideration

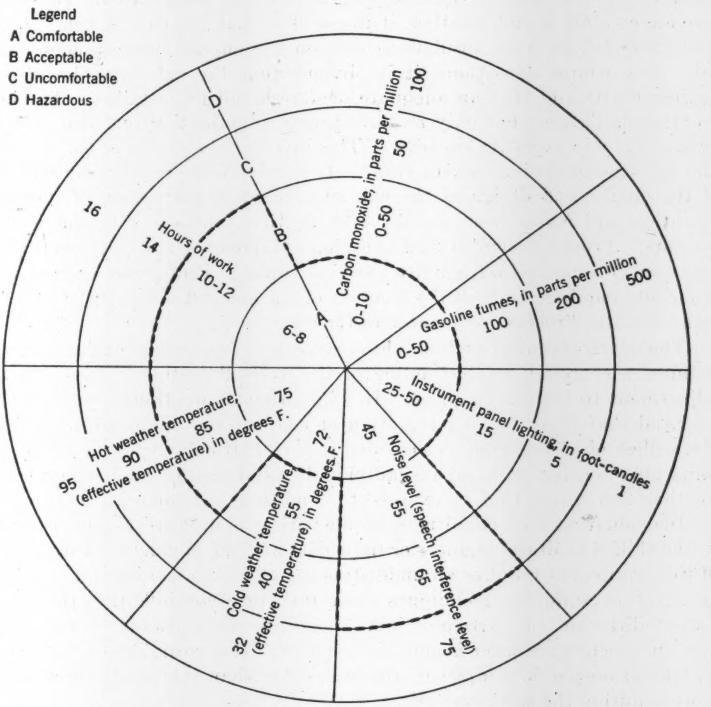
Legend
A Comfortable
B Acceptable
C Uncomfortable
D Hazardous
D
C
B
A
Carbon monoxide, in parts per million
0-10
0-50
50
100
Gasoline fumes, in parts per million
0-50
100
200
500
Instrument panel lighting, in foot-candles
25-50
15
5
1
Noise level (speech interference level)
45
55
65
75
Cold weather temperature (effective temperature) in degrees F.
72
55
40
32
Hot weather temperature, (effective temperature) in degrees F.
75
85
90
95
Hours of work
6-8
10-12
14
16

FIG. 6.—EXAMPLES OF AN OCCUPATIONAL ENVIRONMENTAL HEALTH SPECIFICATION

would be given in the design of a motor vehicle with regard to driver health, comfort, and safety of operation. One of the major causes of human failure is not subject to engineering correction but is related to good personnel management—namely, hours of work.

In determining the control measures and design factors of the vehicle cab and the vehicle itself, it was decided that a maximum trip of between 10 hr and 12 hr might be required. This is within the acceptable limits. A maximum concentration of carbon monoxide of 10 ppm would require a carefully designed vehicle exhaust system and proper cab ventilation. In order to provide comfort in hot weather, it is essential that the cab be ventilated and that there be adequate insulation between the engine compartment and the cab. For winter operations, it is obvious that the cab must be protected against drafts and that an adequate heater should be installed. The instrument-panel lighting not only requires proper illumination but also protection against glare in excessive contrast. This involves the design of the windshield and painting of the instrument panel. Control of noise requires soundproofing of the engine and design of the cab to preclude transmission of mechanical vibration and noises from the drive shaft, tires, and other mechanical components. Proper design of fuel-handling components and cab ventilation is necessary for protection against gasoline fumes. Protection against carbon monoxide requires study of the location of the exhaust with regard to possible leaks and the direction of air flow to the cab.

The development of such graphic occupational environmental specifications requires a thorough understanding of the over-all factors involved in man's adjustment to his environment. In evaluating occupational conditions, it is essential that there be an integration of medical and engineering techniques. Regardless of the safeguards provided in any particular work area, the possibility always exists that careless individuals will disregard the barriers provided for their safety and thus be exposed to conditions detrimental to their health.

In evaluating work conditions, a wide variety of instrumentation is available to the skilled sanitary engineer or industrial hygiene engineer. Intelligent use of this equipment requires an understanding of its limitations and capabilities. In addition, sampling techniques must take into consideration the exposure potentialities of the particular job. Readings must always be taken in the area in which the worker is actually exposed. It is meaningless, for example, to take atmospheric samples in any area other than the breathing zone of the worker during the work operation.

The joint efforts of physicians and engineers trained in the principles of occupational medicine and industrial health are essential to the proper evaluation of alleged cases of occupational illness. Results of environmental investigations should be an integral part of any case history dealing with an occupational disease.

Concepts of Training

All engineering students should receive at least one semester of "engineering physiology." The purpose of this course should be to acquaint the individual with various physiological processes of the body, its capabilities and limitations, and its anthropological specifications. A particular need exists for more emphasis on the fundamentals of elementary statistics in engineering education. Although all engineering courses include a large number of hours in laboratory work, little or no attention is given to the basic theory of statistical evaluation of the results of observations. Because human performance varies according to the laws of statistics, this knowledge is even more essential in the fields of sanitary engineering and industrial hygiene engineering. There has developed a growing awareness of the need for specialization (regardless of the basic engineering degree) in the engineering control of environmental occupational factors. Although notable steps have been made in developing special curricula in several educational institutions, much remains to be done to provide adequate training for the individual desiring to specialize in the broad fields of engineering related to environmental and occupational health. A well-rounded course at graduate level to qualify an individual in the broadest aspects of this area of activity will probably require a minimum of two years. There is a need for realization of the fact that, regardless of undergraduate specialty, all engineers should have training in basic sciences, basic engineering subjects, and general educational material in addition to the specialized phases of their particular branch of engineering. To the detailed engineering specialization training normally provided at graduate level, there should be added required training in biological and medical sciences which will equip the specialist in environmental health to function successfully as a member of the physician-engineer team of the future.

ACKNOWLEDGMENT

Lt. Col. John E. Boysen, Deputy Surgeon, Headquarters Air Materiel Command, contributed invaluable assistance in the preparation of the physiology and toxicology parts of this paper. In addition, his helpful advice and comments on the manuscript were sincerely appreciated by the writer.

The opinions expressed in this paper are those of the writer and do not purport to reflect the official policy of the United States Air Force.

APPENDIX. BIBLIOGRAPHY ON OCCUPATIONAL HEALTH

(1) **"Occupational Medicine and Industrial Hygiene,"** by Rutheford T. Johnston, The C. U. Mosby Co., St. Louis, Mo., 1948, pp. 18–19.

(2) **"Report of the Sanitary Commission of Massachusetts,"** by Lemuel Shattuck, et al, Harvard University Press, Cambridge, Mass., 1950 (facsimile edition).

(3) **"The Sanitary Engineer—His Training and Opportunity,"** by Herman G. Baity, *Journal*, Inter-American Association of Sanitary Engineering, Vol. IV, July, 1949, p. 2.

(4) **"Industrial Hygiene—Past, Present, and Future,"** by Phillip Drinker, *Industrial Medicine and Surgery*, Vol. 21, No. 6, 1952, pp. 288–291.

(5) **"Code of Practice,"** *Manual of Engineering Practice No. 1*, ASCE, 1927, pp. 6–7.

(6) **"A Model Law for the Registration of Professional Engineers,"** Engineers Council for Professional Development, New York, N. Y., 1945; reprinted 1946, p. 2.

(7) **"Canon of Ethics for Engineers,"** Nineteenth Annual Report, Engineers Council for Professional Development, New York, N. Y., 1951, p. 59.

(8) **"Report of the Panel on Environmental Hygiene,"** Ninth Annual Cong. on Industrial Health, Chicago, Ill., January 18–19, 1949.

(9) **"The Fitness of the Environment, Its Engineering Implications,"** by T. F. Hatch, presented at The American Public Health Assn. Meeting, Cleveland, Ohio, October 23, 1952.

(10) **"The Environmental Health Program of the U. S. Public Health Service,"** by Mark Hollis, *Archives of Industrial Medicine and Occupational Health,* Vol. 5, No. 6, 1952, pp. 580–586.

(11) **"Environment and Health,"** U. S. Govt. Printing Office, Washington, D. C., 1951, p. 89.

(12) **"USAF Physician-Engineer Team—An Evaluation of the Future,"** by J. E. Boysen and A. F. Meyer, *The Military Surgeon,* Vol. 3, No. 6, December, 1952, p. 407.

(13) **"Human Aspects of Engineering,"** by T. F. Hatch, *Journal,* ASME, May, 1949, pp. 406–408.

(14) **"Designing the Cockpit to the Man,"** by A. M. Mayo, *American Aviation,* Vol. 17, No. 3, July, 1953, p. 23.

(15) **"Industrial Health and Medical Programs,"** *U. S. Public Health Service Publication No. 15,* U. S. Govt. Printing Office, Washington, D. C., 1951, p. 96.

(16) **"Industrial Hygiene and Toxicology,"** by F. T. Patty, Vol. 1, Inter-Science Publishing Co., Chicago, Ill., 1948, pp. 45–104. (*a*) p. 193.

(17) **"Industrial Health and Medical Programs,"** *U. S. Public Health Service Publication No. 25,* U. S. Govt. Printing Office, Washington, D. C., pp. 38–43.

(18) **"Structure and Function of the Human Body,"** by Ralph N. Baillif and Donald L. Kimmel, Lippincott Co., Philadelphia, Pa., 1945, pp. 1–217.

(19) **"Noxious Gases,"** by Yandell Henderson and Howard W. Haggard, Reinhold Publishing Co., New York, N. Y., 1943, pp. 97–110.

(20) **"Occupational Hazards and Diagnostic Signs,"** *Bulletin No. 41,* U. S. Dept. of Labor, Govt. Printing Office, Washington, D. C., 1942.

(21) **"Preventive Medicine and Hygiene,"** by A. F. Maxey, Appleton, Century, and Crofts, New York, N. Y., 7th Ed., 1952, p. 1039.

(22) **"Report of the Committee on Threshold Limits,"** American Conference of Governmental Industrial Hygienists, Washington, D. C., 1948.

(23) **"Handbook of Warning Labels,"** *Manual L1,* Manufacturing Chemists Assn., Washington, D. C., 1952, pp. 1–86. (*a*) p. 18.

(24) **"Remote Control Engineering,"** by H. L. Hull, *Nucleonics,* Vol. 10, No. 11, 1952, pp. 34–35.

(25) **"Handbook on Industrial Ventilation,"** American Conference of Governmental Industrial Hygienists, Washington, D. C., 1952.

(26) **"Human Factors in Air Transportation,"** by Ross N. McFarland, McGraw-Hill Book Co., Inc., New York, N. Y., 1953, pp. 704–706.

AMERICAN SOCIETY OF CIVIL ENGINEERS
Founded November 5, 1852
TRANSACTIONS

Paper No. 2799

AN EXPERIMENTAL STUDY OF BUBBLES MOVING IN LIQUIDS

BY WILLIAM L. HABERMAN[1] AND ROSE K. MORTON[2]

WITH DISCUSSION BY MESSRS. JOHN A. ROBERSON, CHARLES L. BARKER, AND PAUL F. RUFF; AND WILLIAM L. HABERMAN AND ROSE K. MORTON

SYNOPSIS

In connection with other investigations at the David Taylor Model Basin in Washington, D. C., a fundamental study of the motion of bubbles was undertaken. As an initial step, experiments were conducted to determine the drag and shape of single air bubbles rising freely in various liquids.

The results of the experiments show that a complete description of the motion of air bubbles by use of three dimensionless parameters including the usual physical properties of the liquid (viscosity, surface tension, and density) is not possible. Three types of bubble shapes were observed in each liquid—spherical, ellipsoidal, and spherical cap. For a specific liquid the shape of the bubble was a function of its volume.

For tiny spherical bubbles, the drag coefficients coincide with those of corresponding rigid spheres. With an increase in bubble size, a decrease in the drag compared to that of rigid spheres occurs in some liquids. Thus, the drag curves of the spherical bubbles rising in various liquids lie between two limiting curves—namely, the drag curves of rigid spheres and fluid spheres. It was not possible to determine a criterion for the transition of the bubbles from rigid spheres to fluid spheres. Ellipsoidal bubbles occur at different ranges of Reynolds numbers for the various liquids. The drag coefficients of spherical-cap bubbles are independent of bubble size and have a constant value of 2.6.

For bubbles (of equivalent radius ranging from 0.03 cm to 0.30 cm) rising in tap water or water containing certain surface-active substances, experiments show an increase in drag compared to that of bubbles in pure water.

NOTE.—Published, essentially as printed here, in January, 1954, as *Proceedings-Separate No. 387.* Positions and titles given are those in effect when the paper or discussion was approved for publication in *Transactions.*

[1] Physicist, David Taylor Model Basin, U. S. Dept. of the Navy, Washington, D. C.

[2] Mathematician, David Taylor Model Basin, U. S. Dept. of the Navy, Washington, D. C.

Results of tests to determine the effect of the container walls on the velocity of rise are also presented, and the experimental apparatus is described.

NOTATION

The letter symbols adopted for use in this paper are defined where they first appear, in the illustrations or in the text, and are arranged alphabetically for convenience of reference in Appendix II.

INTRODUCTION

Detailed knowledge of the mechanism of bubble motion is of interest to the many fields of engineering that deal with the prediction of performance of equipment and of processes involving the motion of gaseous bodies. In general, the equation of motion of such bodies is

$$\text{Drag} + \text{Pressure Force} + \text{Weight} = (\text{Mass} + \text{Added Mass}) \times \text{Acceleration.}$$

This equation can be solved if the total mass of the bubble and all forces acting on it are known.

The drag of a bubble is, in general, a complicated function of its geometry, its velocity, and the physical properties of the medium. The shape that the bubble assumes is in turn a complex function of the hydrodynamic, viscous, and interfacial forces exerted. In addition, such effects as those of the container walls and bottom, the free surface of the liquid, and the adjacent bubbles may also have a strong influence on the drag of a bubble. Unfortunately, there is only meager information available on the drag of gas bubbles and almost no information on their added masses.

As an initial step to obtain information on the drag of gas bubbles, a study of single bubbles rising freely at their terminal velocity in various liquids was undertaken. For the case of motion at this constant velocity, the foregoing equation is reduced to

$$\text{Drag} + \text{Buoyant Force} + \text{Weight} = 0$$

because all forces acting on the bubble are in equilibrium. Specifically, the experiments described in this paper consisted of the determination of the terminal velocity, shape, and path of single air bubbles rising freely in various liquids, as a function of bubble size. The possible effect of the walls of the container on the velocity of rise was also investigated. Future studies of the effect of different pressure gradients on the drag and studies of apparent masses of gas bubbles are contemplated.

Theoretical solutions for the drag of bodies, applicable to gas bubbles, have been obtained for spheres moving slowly in an infinite medium.

Body	Equation	Investigator
Rigid sphere	$D = 6 \pi \mu r U$	G. G. Stokes (1)[3]
Fluid sphere	$D = 4 \pi \mu r U$	J. S. Hadamard, W. Rybczynski (1*a*)
	$D = 6 \pi \mu r U \dfrac{e + 2 r \mu}{e + 3 r \mu}$	J. Boussinesq (2)

---

[3] Numerals in parentheses—thus, (1)—refer to corresponding items in the bibliography (see Appendix I).

in which D is the drag of the sphere, μ the coefficient of dynamic viscosity of the liquid medium, r the radius of the sphere, U the terminal velocity of the sphere, and e the coefficient of surface viscosity. For fluid spheres (in contrast to rigid spheres) nonzero tangential velocities at the sphere interface are assumed. Messrs. Hadamard and Rybczynski assumed equality of the tangential velocities and stresses at the bubble-liquid interface, whereas Mr. Boussinesq included changes in the interfacial stresses resulting from "dynamic" surface tension. In the last of the foregoing equations, the factor $\dfrac{e + 2\,r\,\mu}{e + 3\,r\,\mu}$ approaches 1 as r approaches zero or as e becomes very large; it approaches 2/3 for $e \ll r\,\mu$—that is, for large r-values or for e-values approaching zero. Hence, for very small bubbles, the Boussinesq solution approaches the Stokes law as a limit, and the other limit is the Hadamard-Rybczynski solution.

A dimensional analysis of the motion of rising bubbles using eight physical variables—the velocity of the bubble, the acceleration due to gravity (g), the density of the liquid medium (ρ), the density of the bubble (ρ'), the length parameter of the bubble (l), the coefficient of dynamic viscosity of the liquid (μ) and of the gas (μ'), and the surface tension (σ)—yields

$$\left.\begin{aligned} &f_1\left(C_d, \mathsf{R}, \mathsf{W}, \frac{\mu}{\mu'}, \frac{\rho}{\rho'}\right) = 0 \\ \text{or}\qquad & \\ &f_2\left(C_d, \mathsf{R}, \mathsf{W}, \mathsf{R}', \frac{\rho}{\rho'}\right) = 0 \end{aligned}\right\}\cdots\cdots\cdots\cdots(1)$$

and so on. In Eq. 1 C_d is the drag coefficient, R the Reynolds number $\left(= \dfrac{2\,l\,U\,\rho}{\mu}\right)$, W the Weber number $\left(= \dfrac{2\,l\,U^2\,\rho}{\sigma}\right)$, R' the Reynolds number inside the bubble $\left(= \dfrac{2\,l\,U\,\rho'}{\mu'}\right)$, and M a dimensionless parameter $\left(= \dfrac{g\,\mu^4}{\rho\,\sigma^3}\right)$.

If the density and viscosity of the gas are considered negligible, the number of dimensionless groups are reduced to three:

$$\left.\begin{aligned} &f_3\,(C_d, \mathsf{R}, \mathsf{W}) = 0 \\ \text{or}\qquad & \\ &f_4\,(C_d, \mathsf{R}, M) = 0 \\ \text{or}\qquad & \\ &f_5\,(C_d, \mathsf{W}, M) = 0 \end{aligned}\right\}\cdots\cdots\cdots\cdots(2)$$

and so on. For bubbles, the most convenient length parameter is the equivalent radius (r_e), defined as $\sqrt[3]{\dfrac{\text{volume}}{(4/3)\,\pi}}$. The drag coefficient is thus $\dfrac{8}{3}\dfrac{g\,r_e}{U^2}$. For the Stokes and Hadamard-Rybczynski solutions the drag coefficients are, respectively,

$$\left.\begin{aligned} &C_d = \frac{24}{\mathsf{R}}\ \text{(rigid sphere)} \\ \text{and}\qquad & \\ &C_d = \frac{16}{\mathsf{R}}\ \text{(fluid sphere)} \end{aligned}\right\}\cdots\cdots\cdots\cdots(3)$$

For the special case in which only the velocity, the acceleration due to gravity, the density of the liquid, and the equivalent radius are considered, one dimensionless parameter is obtained—namely, C_d = constant. This solution will be shown to apply to the region of very large (spherical-cap) bubbles.

Previous experimental work on the rising motion of bubbles has been extensive. The investigations have, however, largely been restricted to bubbles rising in water. A bibliography of bubble motion, previously published (3), has been brought up to date in Appendix I.

EXPERIMENTATION

The terminal velocities of individual bubbles of various sizes rising in eight liquids were measured. The effect of the walls of the container on the bubble velocity was also determined. Details of the experimental apparatus and procedure, the generation of the bubbles, and the test liquids are described subsequently.

TABLE 1.—SUMMARY OF LIQUID PROPERTIES

Liquid	Temperature, in degrees Centigrade	Viscosity,[a] μ, in poises	Density,[b] ρ, in grams per cubic centimeter	Surface tension,[c] σ, in dynes per centimeter	$\frac{g\,\mu^4}{\rho\,\sigma^3}$
Water	19	0.0102	0.998	72.9	0.26×10^{-10}
Water	21	0.0098	0.998	72.6	0.24×10^{-10}
Cold water	6	0.0147	0.999	74.8	1.08×10^{-10}
Hot water	49	0.0056	0.989	68.1	0.307×10^{-11}
Glim solution	19	0.0103	1.000	32.8	2.78×10^{-10}
Mineral oil	27.5	0.580	0.866	20.7	1.45×10^{-2}
Varsol	28	0.0085	0.782	24.5	4.3×10^{-10}
Turpentine	23	0.0146	0.864	27.8	24.1×10^{-10}
Methyl alcohol	30	0.0052	0.782	21.8	$0.89 + 10^{-10}$
62% corn syrup and water	22	0.550	1.262	79.2	0.155×10^{-3}
68% corn syrup and water	21	1.090	1.288	79.9	0.212×10^{-2}
56% glycerine and water (T. Bryn)	18	0.0915	1.143	69.9	1.75×10^{-7}
42% glycerine and water (T. Bryn)	18	0.043	1.105	71.1	4.18×10^{-8}
13% ethyl alcohol and water (T. Bryn)	22	0.0176	0.977	43.5	1.17×10^{-8}
Olive oil (H. D. Arnold)	22	0.73	0.925	34.7	0.716×10^{-2}
Syrup (W. N. Bond and D. A. Newton)	17	180	1.48	91	0.92×10^{6}

[a] One poise equals 2.089×10^{-3} lb-sec per sq ft. [b] One gram per cubic centimeter equals 1.940 slugs per cu ft. [c] One dyne per cm equals 6.853×10^{-5} lb per ft.

Test Tanks and Liquids.—The tests were performed in three transparent-wall tanks; the large one was of 3-ft by 3-ft cross section and 5 ft high; the medium one, 1-ft by 1-ft cross section and 3½ ft high; and the small one was of 6-in. by 6-in. cross section and 2 ft high. Tests were also performed in an insert 6-in. by 6-in. in cross section and 20 in. high placed in the center of the medium tank.

Because the large tank was of sufficiently large dimensions no appreciable wall effect was expected. A few of the previous tests (4) made at the Taylor Model Basin (TMB) at Washington, D. C., originally conducted in a much larger tank, were repeated in the tank to observe any change in results. The medium tank was large enough to reduce wall effects yet small enough to allow the use of a variety of liquids. The small tank and insert provided an additional tank size. It was intended, if wall effect existed, to extrapolate the results obtained in the finite containers to the case of an infinite medium.

The eight test liquids were water (at three different temperatures), Varsol (heavy naphtha), methyl alcohol, water containing 0.42% (by volume) Glim (a nonionic, liquid detergent), turpentine, mineral oil, and two corn syrup-water mixtures. Turpentine was selected as one of the test liquids because it has, at room temperature, the same viscosity as cold water. One of the corn syrup mixtures had approximately the same viscosity as the mineral oil. The viscosities of the liquids were measured by means of ordinary and modified Ostwald viscosimeters. The accuracy of measurement of viscosity was $1\frac{1}{2}\%$ and $\frac{1}{2}\%$, respectively. The surface tension was determined by the capillary-rise method (the accuracy of measurement being 3%), and the specific gravity of the liquids was obtained by means of hydrometers (the accuracy of measurement being 1%). These physical properties were measured following each test; they are summarized in Table 1 together with those of liquids used by several other investigators (5) (6) (7).

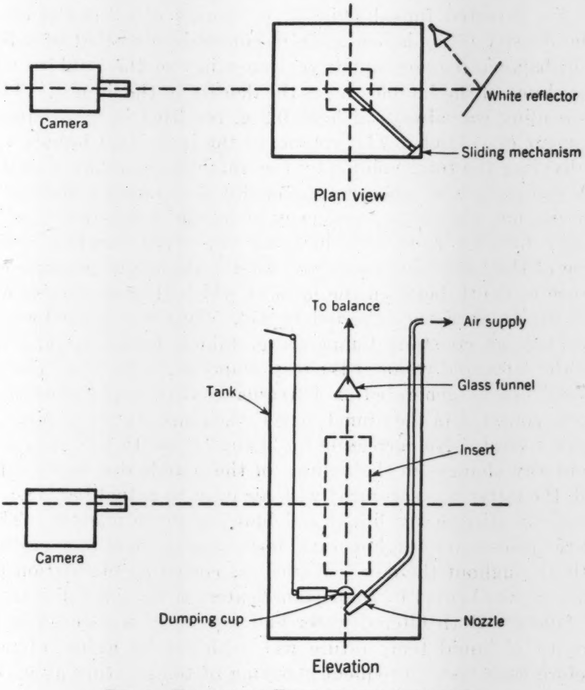

FIG. 1.—DIAGRAM OF EXPERIMENTAL APPARATUS

In Varsol and in water (at room temperature and hot), tests were conducted in all three tanks; tests using cold water and mineral oil were conducted in the medium tank and in the insert; for all other liquids, the tests were in the small tank only.

Test Procedure.—Small bubbles were generated by means of hypodermic needles and glass nozzles of various sizes. The larger bubbles were obtained by use of a dumping cup, which was inverted to release the air bubble. The nozzles and needles were connected to a brass tube which was fastened to a sliding mechanism (Fig. 1). This sliding mechanism allowed the tips of the various nozzles to be placed at the same position, eliminating the need for refocusing the camera after each change of nozzle. The air was supplied from a bottle of compressed air. A needle valve regulated the air flow so that bubbles were released at the desired intervals.

The bubble size was determined by "weighing" a sufficient number of bubbles in the inverted funnel (Fig. 1) by means of an analytical balance. Because the density of air is negligible in comparison to that of a liquid, the difference in balance reading equals the buoyancy of the bubbles (that is, it equals the volume of the bubbles times the density of the liquid). The change in balance reading was always at least 0.2 g, resulting in an accuracy of 1% in measurement of volume. The volume of the individual bubble was determined by dividing the total volume by the number of bubbles collected in the funnel. A comparison of photographs of different bubbles showed that the bubble size did not vary if the frequency of bubble generation remained constant. Large bubbles from the dumping cup were weighed individually. The volume of the bubble was adjusted for the change in pressure caused by the difference in depth between the level at which the rate of rise was determined and the level of the inverted funnel. This was done by use of the general gas law at constant temperature, taking into account the partial pressure of the saturated vapor at the test temperature (3) (4). Tiny spherical bubbles could not be generated at a frequency that would allow a sufficient number to be collected in the funnel; hence, their size was determined from the photographic record. No correction for change in depth was then needed.

To avoid any changes in the volume of the bubble due to air interchange with liquid, the latter was saturated with air prior to actual testing. This was accomplished by stirring the liquid and blowing air through it. The liquids for all but the cold-water and hot-water tests were at room temperature, which varied little throughout the day. Water was cooled by circulation through a water cooler; it was heated by immersion heaters or obtained directly from the hot-water faucet. Both filtered water and tap water were used in the tests.

Uniformity of liquid temperature was achieved by means of mechanical stirring before each test. Frequent checking of temperature at various locations inside the tank was done by means of immersion thermometers. In the process of stirring, small bubbles appeared in the liquid. The irregularity of motion of these small bubbles, which were still present after the stirring, served as an indication of residual turbulence in the liquid. In sufficient time, the motion of the small bubbles always became regular; thus, it was indicated that the residual turbulence, if still present, was not large enough to affect the motion of the bubbles. The actual test was not begun until all the small bubbles reached the surface of the liquid.

The rate of bubble flow was regulated by the needle valve so as to release bubbles with a minimum spacing of 24 in. This spacing reduced the effect of the wake created by the passage of a bubble on the motion of the following bubble. The same precaution was observed for the larger bubbles that were formed by dumping. An additional precaution was the rotation of the dumping cup at a steady speed in order to avoid splitting the bubble or forming satellites on release. The slow passage of the air through the brass tube inside the tank allowed the air to reach the temperature of the liquid. Contact of the air with the liquid at the nozzle tip or inside the dumping cup allowed saturation of the air with liquid vapor so that the air bubble could, in each instance, be assumed to be saturated with the vapor of the liquid in which it rose.

Motion Pictures and Their Evaluation.—The velocity, path, and shape of the bubbles were obtained from motion pictures made with a 35-mm camera using a special lens attachment to permit close-ups. Film speeds of 25 to 35 frames per second and back-lighting from a white reflector were used. For the first few tests, the film speed was determined by photographing a rotating clock dial; subsequently, a neon timing light with a 60-cycle voltage source was placed inside the camera. From the marks of the timing light on the film, the film speed was determined. The field of the camera ranged from 1.4 in. by 1.8 in. to 1.75 in. by 2.3 in., depending on the refractive index and horizontal depth of the liquid. A transparent scale photographed in the plane of the bubble provided the distance scale factor for the evaluation of displacement and size. The camera lens was placed at approximately the midpoint between the liquid level and the tank bottom for all tests. The camera was in each instance

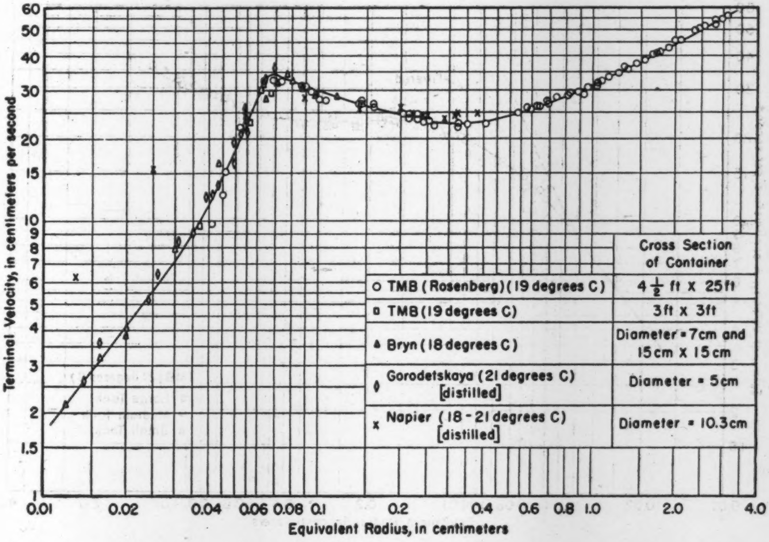

FIG. 2.—TERMINAL VELOCITY OF AIR BUBBLES IN FILTERED OR DISTILLED WATER AS A FUNCTION OF BUBBLE SIZE (1 CM = 0.3937 IN.)

located sufficiently far above the nozzle tip so that the bubbles reached their terminal velocity before passing in front of the lens.

Changes in bubble volume due to differences in liquid depth were minimized by making velocity measurements over a vertical displacement of less than 2½ in. The rate of rise of bubbles was determined by measuring the displacement of a bubble from a reference point on successive frames of the film by means of a Bausch and Lomb contour measuring projector using a magnification of twenty five. These displacements were then plotted against the frame number. A straight-line plot indicated that the velocity of the bubble remained constant as it passed the field of the camera. From the slope of the line, the frame speed, and the scale factor, the velocity of the bubble was computed.

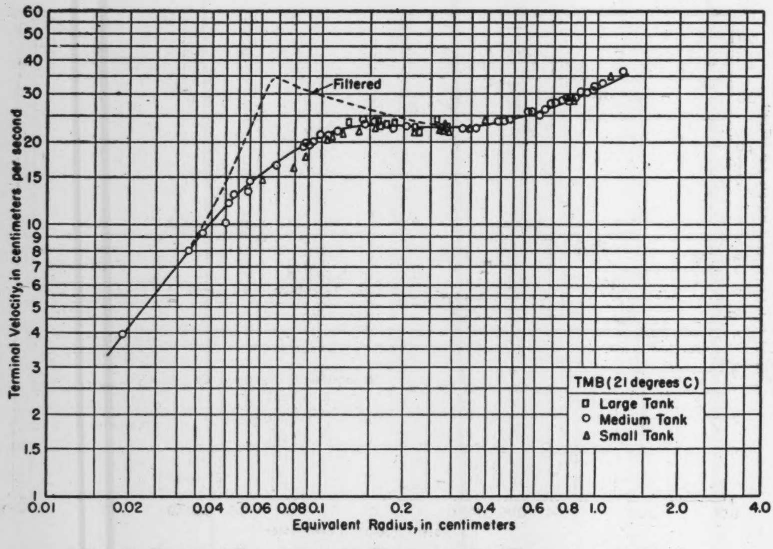

FIG. 3.—TERMINAL VELOCITY OF AIR BUBBLES IN TAP WATER AS A FUNCTION OF BUBBLE SIZE (1 CM = 0.3937 IN.)

RESULTS

Terminal Velocity of Bubbles.—The results of tests to determine the velocity of rise of gas bubbles in various liquids are most conveniently presented as a function of the equivalent radius of the bubble, defined as the radius of a sphere having the same volume as the bubble. Typical results are shown in Figs. 2 and 3 for bubbles in filtered water (including data obtained by other investigators) and for these in tap (unfiltered) water. A summary of all TMB velocity curves (except those for bubbles in tap water) and those obtained by T. Bryn is given in Fig. 4. A compilation of the properties of the liquids is given in Table 1. In general, the results as shown in Fig. 4 indicate that, for small (spherical) bubbles of particular volume, the viscosity of the liquid is the most important property determining the rate of rise. Very large bubbles (spherical "caps," described subsequently) rise independently of the properties of the liquid.

The results of tests to determine the effect of the container walls on the velocity of a bubble, conducted in tanks of different sizes with water, Varsol, and mineral oil showed within the limits of experimental accuracy the absence of a wall effect for the range of bubble sizes tested. The information in Figs.

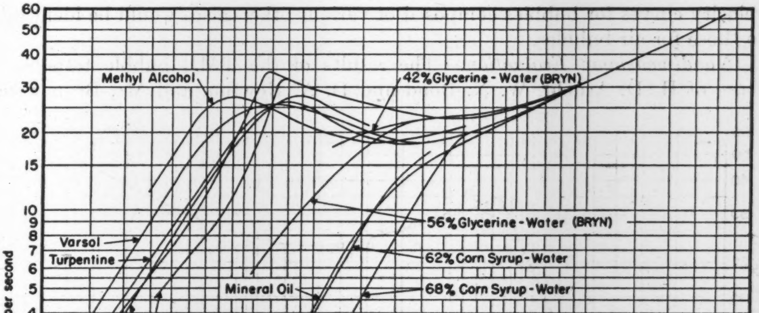

FIG. 4.—COMPARISON OF TERMINAL VELOCITIES OF AIR BUBBLES IN VARIOUS LIQUIDS

2 and 3 is typical of these results. Subsequent tests in the other liquids were made in the small tank only; its results may be applied to the case of an infinite medium.

No systematic investigation of the vertical proximity effect was made; vertical proximity effect is the effect of the wake created by the passage of a bubble on the motion of another bubble rising from below. Such effects were avoided in the experiments by spacing the bubbles sufficiently. However, the results of a few special observations indicate that proximity effects may be appreciable. For example, tests of bubbles having an equivalent radius of 0.17 cm and rising through mineral oil show an increase of 9% and 39% for spacings of 7.7 cm and 3.2 cm, respectively (1 cm = 0.3937 in.). The presence of the wake in the liquid results in higher velocities of rise of the bubble.

In Fig. 5 the rates of rise of air and oxygen bubbles in distilled water are compared. The latter were investigated by B. Stuke (8) and S. B. Zdonik (9). No significant change in the rate of rise of the bubbles with change in the gas composing them is indicated. It is therefore reasonable to assume that the velocity curves for bubbles composed of various other gases would be identical to those for air bubbles.

Nondimensional Evaluation.—The results of the TMB bubble tests and those of H. D. Arnold, W. N. Bond and D. A. Newton, and Mr. Bryn were plotted in terms of three dimensionless products. Fig. 6 presents the results in terms of the drag coefficient, Reynolds number, and the parameter *M*; Fig. 7 presents them in terms of the drag coefficient, the Weber number, and *M*. The results for tap water and for water containing Glim will be discussed subsequently. The curve for filtered or distilled water at a temperature of 19° C was drawn through points obtained from the experiments of Mr. Bryn and the TMB tests. Examination of Fig. 6 or Fig. 7 shows no systematic arrangement of the curves relative to the change in the parameter *M*, which is constant for a specific liquid. It can, therefore, be concluded that neither of the nondimensional sets presented nor any other complete set using the same six variables (velocity, acceleration due to gravity, density and viscosity of the

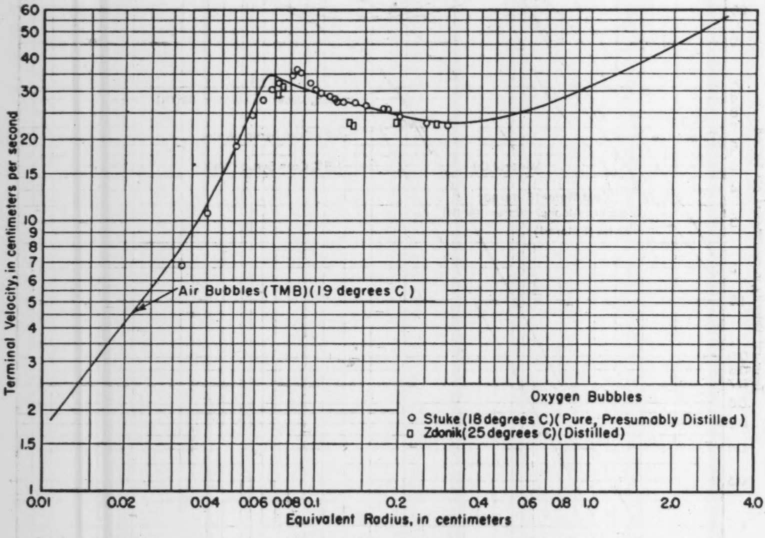

FIG. 5.—TERMINAL VELOCITY OF GAS BUBBLES IN DISTILLED WATER AS A FUNCTION OF BUBBLE SIZE (1 CM = 0.3937 IN.)

liquid, surface tension, and equivalent radius) is sufficient for the complete description of bubble motion.

The question thus arises whether bubble data could be correlated by using two additional dimensionless parameters—for example, the liquid-to-air ratios of viscosity and density or the Reynolds number inside the bubble and the density ratio. The results of the experiments do not permit conclusions regarding the importance of these parameters. The significance of the internal Reynolds number will be discussed briefly in subsequent sections.

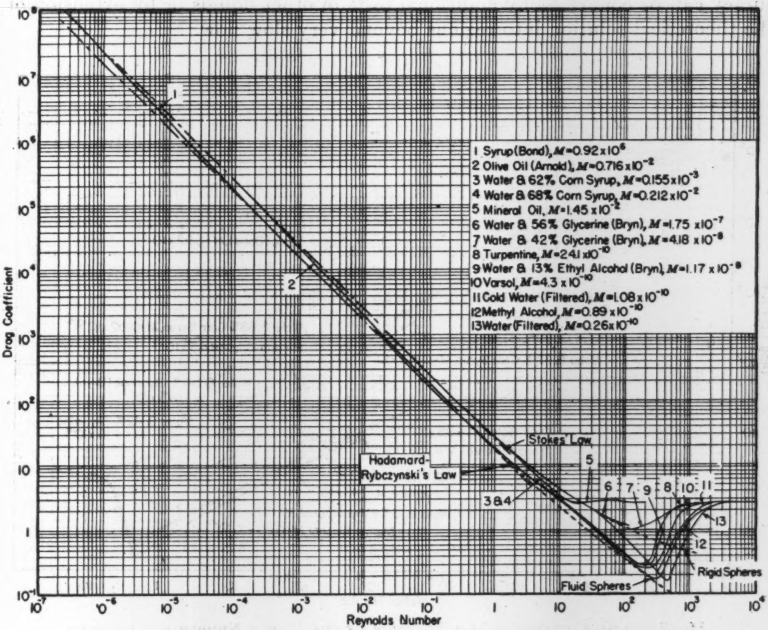

FIG. 6.—DRAG COEFFICIENT AS A FUNCTION OF THE REYNOLDS NUMBER FOR BUBBLES RISING AT THEIR TERMINAL VELOCITY IN VARIOUS LIQUIDS

Three types of bubble shapes were observed in the experiments. Small bubbles are spherical. Larger bubbles are flattened (ellipsoidal in shape), and the largest bubbles assume a spherical-cap shape. Of course, the volumes at which these transitions occur are different in different liquids. Photographs of typical bubble shapes are shown in Fig. 8. Some of the shapes shown in these photographs are instantaneous shapes; the shape of large bubbles does not remain constant during the ascent, except for those bubbles rising in a highly viscous medium such as mineral oil or corn syrup.

Table 2 shows the approximate extent of the three shape regions as a function of the Reynolds number for the various liquids tested at the Taylor

Model Basin. From Table 2 and Fig. 6—which also includes the drag curve for rigid spheres (10) and the lines for the Stokes law and the Hadamard-Rybczynski law—the following can be observed: The drag curves of the spherical bubbles in the various liquids lie between two limiting curves. The upper limit is the drag curve of rigid spheres, and the lower limit is the drag curve for fluid spheres. With a decreasing Reynolds number the rigid-sphere curve connects with the straight line of the Stokes law, and the fluid-sphere curve connects with the line of the Hadamard-Rybczynski law. The curve for the fluid sphere was obtained by drawing the lower envelope to the experimental curves; its accuracy can be confirmed by additional tests in other liquids or by extension of the theoretical solution into regions beyond very slow flow.

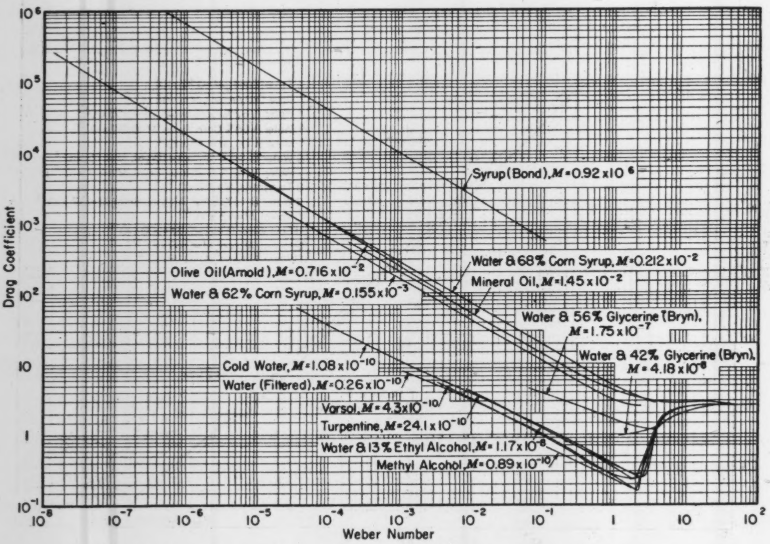

FIG. 7.—DRAG COEFFICIENT AS A FUNCTION OF THE WEBER NUMBER FOR BUBBLES RISING AT THEIR TERMINAL VELOCITY IN VARIOUS LIQUIDS

It will also be noted from Fig. 6 that the curve for bubbles in mineral oil, for example, follows the straight line of the Hadamard-Rybczynski law within a certain region of Reynolds numbers. This fact indicates that the boundary conditions assumed in the analytical solutions for fluid spheres are actually fulfilled and that circulation exists inside the bubble. The experimental curves also indicate an interesting aspect of the phenomenon of bubble motion—with a decreasing Reynolds number, the drag coefficient of the bubbles becomes equal to that of rigid spheres. The transition may occur at a Reynolds number of approximately 40 (as for filtered and distilled water) or may not occur until very low Reynolds numbers are reached—that is, well within the region of slow flow—as for olive oil (6) or very viscous syrup (5). Thus, from the experimental data available it appears certain that tiny air bubbles rising in any liquid follow the Stokes law.

For bubbles behaving like rigid bodies—indicating absence of motion inside the bubble—the internal Reynolds number (although nonvanishing) is of no significance in describing the rising motion of the bubbles. Likewise, the internal Reynolds number cannot be used to predict the transition point at which the drag of the bubbles becomes less than that of corresponding rigid spheres. Beyond this transition point, the internal Reynolds number might be important in describing the motion of the bubbles.

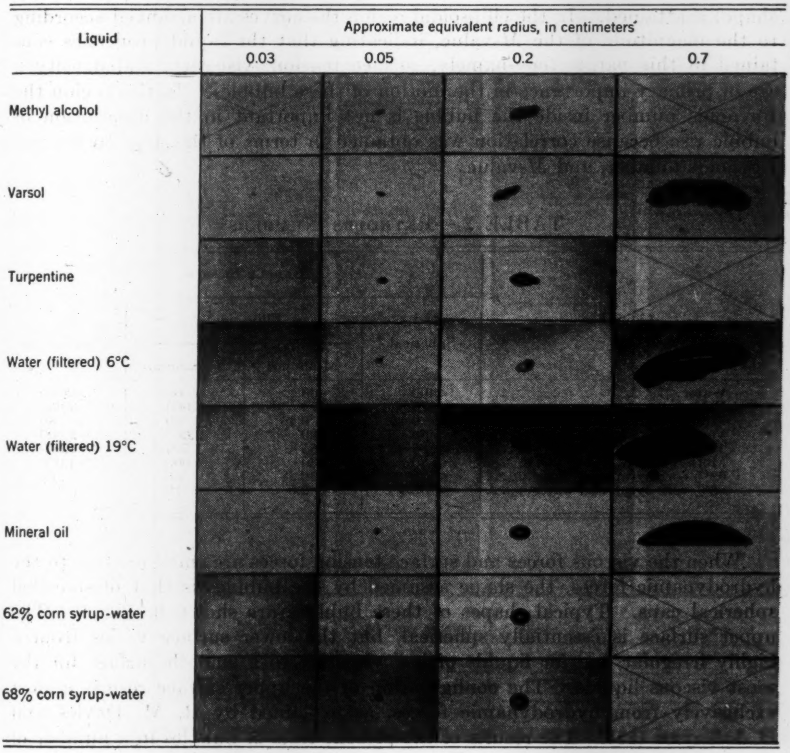
Liquid
Approximate equivalent radius, in centimeters
0.03
0.05
0.2
0.7
Methyl alcohol
Varsol
Turpentine
Water (filtered) 6°C
Water (filtered) 19°C
Mineral oil
62% corn syrup-water
68% corn syrup-water

FIG. 8.—TYPICAL SHAPES OF BUBBLES OF SEVERAL VOLUMES IN THE VARIOUS LIQUIDS

Surface tension tends to make the surface area of the bubble as small as possible. For a particular volume, the configuration of the minimum surface area is a sphere. This effect of surface tension is most pronounced for bubbles of small radii. For larger bubble sizes, the viscous and hydrodynamic forces become larger in comparison to the surface forces, and flattening of the bubble occurs. This flattening to an approximately oblate spheroid results in greater drag compared to a sphere of the same volume. Fig. 6 and Table 2 show that the region of ellipsoidal bubbles for the various liquids occurs at different ranges of the Reynolds number—that for liquids having a small *M*-value, a minimum drag coefficient is reached at Reynolds numbers of the order of 250, and that these minima occur near the transition from spherical to ellipsoidal shape. Such minima are not obtained for liquids of high *M*-value. The drag coefficients of bubbles in such liquids decrease with increasing Reynolds numbers until a constant value for the drag coefficient (that is, a spherical-cap shape) is attained. In the ellipsoidal region the curves are arranged according to the magnitude of the *M*-value, indicating that the liquid properties contained in this parameter—namely, surface tension, viscosity, and density—are of primary importance in the motion of these bubbles. In this region the Reynolds number inside the bubble is not important in the description of bubble rise because correlation was obtained in terms of the drag coefficient, Reynolds number, and *M*-value.

TABLE 2.—REYNOLDS NUMBERS

Liquid	Bubble Shapes			
	Spherical	Ellipsoidal		Spherical cap
		Minimum	Maximum	
Water	<400	400	5,000	>5,000
Cold water	<275	275	3,000	>3,000
Mineral oil	< 0.45	0.45	80	> 80
Varsol	< 80	80	2,000	>2,000
Turpentine	< 85	85	1,500	>1,500
Methyl alcohol	< 80	80	4,000	>4,000
62% corn syrup and water	< 0.28	0.28	60	> 60
68% corn syrup and water	< 2.5	2.5	110	> 110

When the viscous forces and surface tension forces are small relative to the hydrodynamic forces, the shape assumed by the bubbles is that of so-called spherical caps. Typical shapes of these bubbles are shown in Fig. 8. The upper surface is essentially spherical, but the lower surface varies from a highly irregular one for liquids of low viscosity to a smooth surface for the most viscous liquids. The configuration of the upper surface results almost exclusively from hydrodynamic forces, as explained by R. M. Davies and G. I. Taylor (11). The results of the present tests of bubbles in a number of liquids confirm the constant value of 2.6 for the drag coefficient obtained by previous investigators (4) (11). The velocity of spherical-cap bubbles of a particular size rising in any liquid can be determined from the value of the drag coefficient or directly from the velocity curve (Fig. 4). For $C_d = (8/3\, g\, r_e)/U^2 = 2.6$, one obtains for the rate of rise of spherical caps in all liquids—

$$U = 1.02 \sqrt{g\, r_e} \qquad (4)$$

Path of Rising Bubbles.—Fig. 9 shows typical paths and the corresponding shapes of bubbles in four liquids. Three types of motion of the bubbles were observed in the experiments: (*a*) Rectilinear motion, (*b*) motion in a helical path, and (*c*) rectilinear motion with rocking. The motion of spherical bubbles is either rectilinear or helical. For ellipsoidal and spherical-cap bubbles all three types of motion can occur. It appears that the type of motion may be predicted from the value of the Reynolds number at which the motion occurs. For Reynolds numbers less than approximately 300, the motion is rectilinear. With increase in the Reynolds number, spiraling begins and increases in amplitude and frequency until a maximum is reached. At Reynolds numbers of approximately 3,000, the spiraling disappears and only rectilinear motion with rocking is obtained. For bubbles rising in mineral oil and the corn-syrup mixtures, only rectilinear motion without rocking was observed. The maximum Reynolds number reached during those tests was 150.

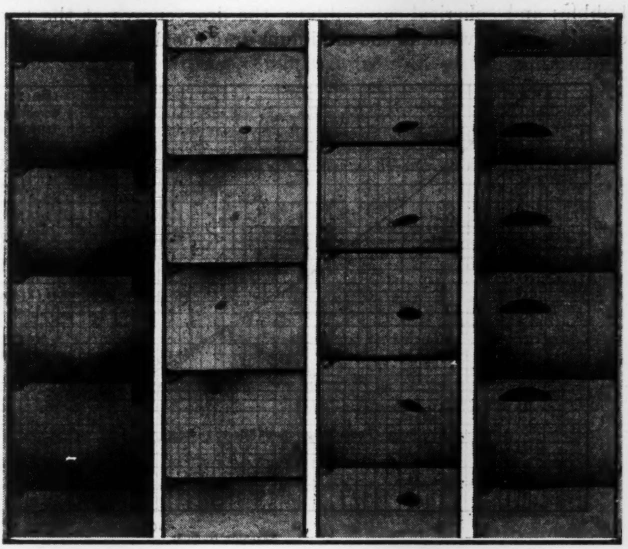

Liquid	Varsol	Cold water (filtered)	Methyl alcohol	Mineral oil
Equivalent radius (cm)	0.033	0.190	0.317	0.570
Velocity (cm/sec)	13.3	23.5	20.4	22.7
Reynolds number	81	628	1 960	42

FIG. 9.—TYPICAL PATHS OF BUBBLES RISING IN VARIOUS LIQUIDS

The helical path of the bubbles assumed either a clockwise or counterclockwise direction, depending on conditions of generation. The velocity of rise of these bubbles is not affected by the sense in which the bubble revolves. The major axis of ellipsoidal bubbles is always perpendicular to the direction of motion.

The oscillatory motion of bubbles is probably caused by the periodic shedding of vortices behind the bubble. Such vortex shedding has been observed experimentally for rigid spheres at the same magnitudes of Reynolds numbers as for bubbles (12).

Bubbles in Tap Water and Water Containing Surface-Active Substances.—The drag coefficients for air bubbles rising in tap water at two different temperatures are given in Fig. 10. A. Gorodetskaya's results for bubbles in tap water at room temperature (13) are also included. For comparison, the drag curves for bubbles in filtered and distilled water at room temperature and for rigid spheres are also shown. In the region of Reynolds numbers for spherical bubbles and spherical-cap bubbles, the drag curves at the two temperatures coincide. The value of the minimum drag coefficient of tap water is, however, greater than that of filtered water at the same temperature. In general, for Reynolds numbers up to approximately 300, the drag curves of bubbles in tap water follow closely the drag curve of rigid spheres. (The physical properties of tap water did not differ from those of filtered water.) Thus, the results of the experiments show that for bubbles (ranging in equivalent radius from 0.035 cm to 0.25 cm) an important consideration is whether the motion occurs in filtered (distilled) water or tap water.

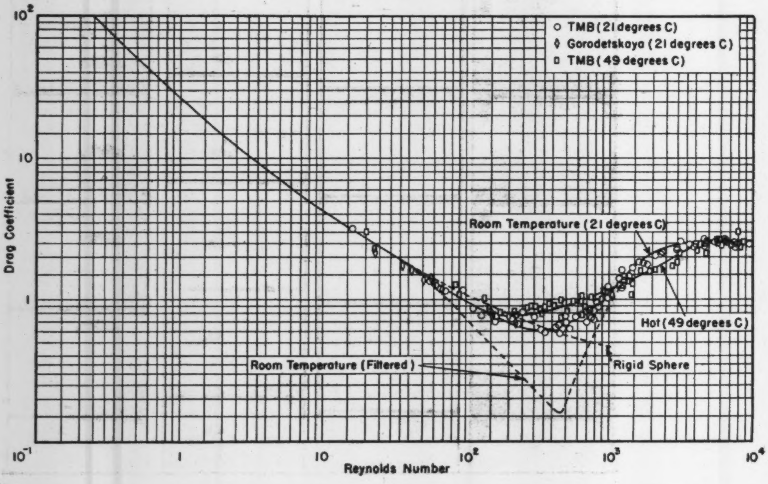

FIG. 10.—DRAG COEFFICIENT AS A FUNCTION OF THE REYNOLDS NUMBER FOR BUBBLES RISING AT THEIR TERMINAL VELOCITY IN TAP WATER

The fact that merely filtering the water produces a change in the drag of the bubbles indicates that the presence of minute particles causes this change. Most of these particles, which are known to exist in ordinary tap water, can be removed by filtering. Specifically, if such particles are present, a high concentration of them are found at the surface of the bubble. The particles at the surface would travel with the bubble—imparting, in effect, a rigid surface to the bubble. With increasing bubble velocities, the shear forces become large in comparison to the forces holding the particles in the bubble surface, and hence at a certain critical velocity a high concentration of particles cannot exist on the bubble surface.

The effect of surface-active substances on the rate of rise of air bubbles has previously been investigated by Miss Gorodetskaya (13), who added small concentrations of various alcohols to water and concluded that, beyond a certain critical concentration of the surface-active substance, the rate of rise of the air bubbles is not affected. Mr. Stuke (8) conducted experiments with oxygen bubbles rising in water containing small concentrations of caproic acid. The concentrations of the alcohols and the caproic acid were relatively small so that the decrease in the surface tension was only about 1 dyne per cm (6.853×10^{-5} lb per ft). The writers conducted tests in water containing Glim, a liquid detergent. The concentration of Glim (0.42% by volume) was high enough to decrease the surface tension by 40 dynes per cm. No measurable change in the viscosity and density of the test liquid due to the presence of Glim was noted (Table 1). This fact was also true for alcohol and caproic-acid solutions. Results from these experiments are presented in terms of the drag coefficient and the Reynolds number in Fig. 11.

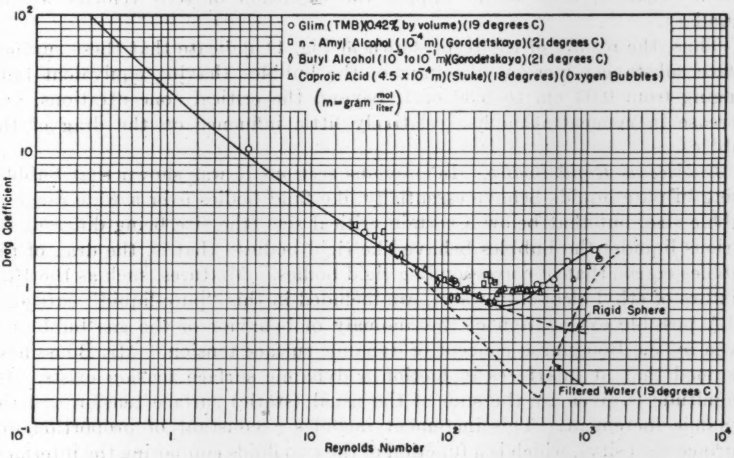

FIG. 11.—DRAG COEFFICIENT AS A FUNCTION OF THE REYNOLDS NUMBER FOR BUBBLES RISING AT THEIR TERMINAL VELOCITY IN WATER CONTAINING VARIOUS SURFACE-ACTIVE MATERIALS

The drag curve for bubbles in the Glim solution, as well as the experimental data recorded by other investigators for bubbles in water containing at least the critical concentration of the surface-active substance, follows the drag curve of rigid spheres to a Reynolds number of approximately 200. For concentrations below the critical concentration, the drag curve lies between that of pure water and the curve shown in Fig. 11 (8). In the region of Reynolds numbers ranging from 10 to 200, the drag curve for bubbles rising in a pure liquid having an M-value close to that of the Glim solution ($M = 2.78 \times 10^{-10}$) follows the drag curve of fluid spheres. Thus, the motion of bubbles in water containing surface-active materials cannot be compared with that of bubbles in pure liquids on the basis of the drag coefficient, Reynolds number, and M-value, even in the region of ellipsoidal bubbles. Although the range of bubble sizes did not extend fully into the region of spherical-cap bubbles, it is quite certain that the presence of surface-active substances will not alter their rate of rise, which was shown to be independent of all physical properties of the liquid.

The difference in behavior of the bubbles results from the surface conditions. A high concentration of molecules of the surface-active substance will be found at the surface of the bubble. As in the case of tap water, these molecules would travel with the bubble and impart, in effect, a "rigid" surface to the bubble—that is, they would impose the condition of zero velocity at the boundary.

Thus, the results of the tests shown in Fig. 11 indicate that these surface-active substances increase the drag of the bubbles (having equivalent radii ranging from 0.03 cm to 0.30 cm); beyond the critical concentrations, any increase in concentration has relatively little influence on the drag of the bubbles.

Bubbles as Rigid Bodies.—In previous sections it was shown that bubbles rising in pure liquids behave essentially like fluid bodies over a wide range of bubble size, but that below a certain critical size (the size being different for various liquids) the bubbles behave like rigid bodies—that is, the drag of the bubbles equals that of corresponding rigid bodies. Mixtures, such as the 13% mixture of ethyl alcohol in water, are included in this "pure-liquid" category.

A possible explanation of the anomaly of behavior of the gas bubbles is given by the Boussinesq concept of dynamic surface tension. Mr. Boussinesq assumed that at interfaces in motion a dynamic surface tension exists. Its magnitude is given by the sum of the usual (static) surface tension and the dynamic increment. This increment includes a constant of proportionality (surface viscosity), which is a function of the two fluids composing the interface. As mentioned in the "Introduction," for small bubbles the dynamic increment increases the drag value to that of corresponding rigid bodies. With increase in bubble size this effect becomes negligible, and the drag of the bubbles equals that of a fluid body. Therefore, for bubbles the transition region from "rigid" to fluid bodies would be different in the various liquids. There is, however, no experimental evidence that dynamic surface tension exists, as postulated by Mr. Boussinesq.

From a hydrodynamic point of view the reason for the transition of the behavior of bubbles to that of rigid bodies is not clear. The mere inclusion of surface tension as a pressure drop in the boundary conditions ($\Delta p = 2\,\sigma/r$) does not alter the analytical solution for fluid spheres. Hence, it appears that the presence of surface tension should have no effect on the motion of the bubble, except in maintaining the spherical shape. Thus, the anomalous behavior of the bubbles cannot be explained in terms of hydrodynamics but must be sought in terms of a surface phenomenon. If it could be shown analytically (even if only in the region of slow flow) that the equality of drag of corresponding rigid bodies and bubbles also implies equality of boundary conditions at the surface, the velocity on the entire surface of the bubble must vanish, as in the case of rigid bodies. The surface must then be able to hold molecules of the pure liquid, just as the surface of a bubble in a solution of tap water and a surface-active substance attracts and holds a high concentration of particles or molecules of the surface-active substance. The molecules at the surface would travel with the bubble and hence would, in effect, impart the same boundary conditions as a rigid surface. However, if the shear forces increase in comparison to the forces holding the molecules at the surface, "rigidity" at the surface cannot be maintained; circulation inside the bubble ensues, and the drag of the bubble becomes smaller compared with that of a rigid body.

Because it was not possible to correlate the results of the experiments on the motion of bubbles in the gravity pressure field in terms of nondimensional parameters, including the usual liquid properties (viscosity, surface tension, and density), further study of freely rising bubbles is necessary before the results obtained from such tests can be utilized, and before the more complicated behavior of bubbles in variable pressure gradients can be understood. An understanding of the reason for the transition of bubbles from fluid to rigid bodies as well as a criterion for this transition is particularly desirable because such a transition might be influenced by the magnitude of the pressure gradient. In the region of Reynolds numbers where the bubbles behave like rigid spheres, the pressure gradient probably has no effect on the drag coefficient.

SUMMARY

As the size of the bubbles was increased in the tests, a change in bubble shape from spherical to ellipsoidal to spherical cap was observed in all liquids. The volumes at which these transitions occurred, however, varied with the properties of the liquid. For spherical bubbles of given volume, the results show that the viscosity of the liquid is the most important property determining the rate of rise. In the case of ellipsoidal bubbles, the surface tension assumes greater importance. Spherical-cap bubbles rise independently of the properties of the liquid.

The results show that the motion of air bubbles rising at their terminal velocity in a gravity field cannot be described completely by use of dimensionless parameters including the usual liquid properties (viscosity, surface tension, and density), the equivalent radius of the bubble, the acceleration of gravity, and the terminal velocity.

The drag coefficients of tiny spherical bubbles coincide with those of rigid spheres of corresponding size. With increase in bubble size, a decrease in the drag as compared to that of rigid spheres occurs in some liquids. This change in the drag is caused by the development of circulation inside the bubble. The drag curves of the spherical bubbles rising in various liquids lie between two limiting curves—namely, the drag curves of rigid and fluid spheres. It was not possible to determine a criterion for the transition region of the behavior of the bubbles from rigid to fluid spheres.

Ellipsoidal bubbles occur at different ranges of Reynolds numbers for the various liquids. For liquids of low M-value (less than approximately 10^{-3}) a minimum in the drag curve is reached at Reynolds numbers of the order of 250. These minima occur near the transition from spherical to ellipsoidal shape. Such minima in the drag curve are not obtained for liquids of high M-value. For the liquids used, transition to spherical caps is completed at a Weber number of approximately twenty.

The drag coefficients of spherical-cap bubbles are independent of bubble size and have a constant value of 2.6. The rate of rise of these bubbles as a function of the equivalent radius is given by the experimentally determined relationship expressed in Eq. 4.

For bubbles (ranging in equivalent radius from 0.03 cm to 0.25 cm) rising in tap water, an increased drag compared to bubbles in clean (filtered or distilled) water was observed. The presence of certain surface-active substances in the water similarly increases the drag of bubbles (ranging in equivalent radius from 0.03 cm to 0.30 cm) as compared to bubbles in pure water. Beyond a certain critical concentration of these surface-active substances, an increase in concentration has relatively little influence on the drag of the bubbles.

Tests to determine the effect of the container walls on the velocity of rise indicate the absence of such effect for the range of bubble volumes and container sizes tested.

ACKNOWLEDGMENTS

The tests described in this paper were conducted at the David Taylor Model Basin, United States Department of the Navy, in Washington, D. C.

The writers wish to acknowledge the suggestions of Lawrence M. Kushner of the National Bureau of Standards regarding the explanation of the behavior of bubbles in tap water and water containing surface-active materials.

APPENDIX I. BIBLIOGRAPHY ON BUBBLE MOTION

(*a*) REFERENCES CITED IN TEXT

(1) **"Hydrodynamics,"** by Horace Lamb, Dover Publications, New York, N. Y., 1945, p. 598. (*a*) p. 600.

(2) **"Vitesse de la chute lente, devenue uniforme, d'une goutte liquide sphérique, dans un fluide visqueux de poids specifique moindre,"** by J. Boussinesq, *Comptes Rendus*, Vol. 156, 1913, p. 1124.

(3) **"An Experimental Investigation of the Drag and Shape of Air Bubbles Rising in Various Liquids,"** by William L. Haberman and Rose K. Morton, *Report No. 802*, David Taylor Model Basin, U. S. Dept. of the Navy, Washington, D. C., 1953.

(4) **"The Drag and Shape of Air Bubbles Moving in Liquids,"** by B. Rosenberg, *Report No. 727*, David Taylor Model Basin, U. S. Dept. of the Navy, Washington, D. C., 1950.

(5) **"Bubbles, Drops, and Stokes' Law,"** by W. N. Bond and D. A. Newton, *Philosophical Magazine*, Vol. 5, 1928, p. 794.

(6) **"Limitations Imposed by Slip and Inertia Terms Upon Stokes' Law for the Motion of Spheres Through Liquids,"** by H. D. Arnold, *ibid.*, Vol. 22, 1911, p. 755.

(7) **"Steiggeschwindigkeit von Luftblasen in Flüssigkeiten,"** by T. Bryn, *Forschung*, Vol. 4, No. 1, 1933 (*Translation No. 132*, David Taylor Model Basin, Washington, D. C., 1949).

(8) **"Das Verhalten der Oberfläche von sich in Flüssigkeiten bewegenden Gasblasen,"** by B. Stuke, *Naturwissenschaften*, Vol. 39, No. 14, 1952.

(9) **"Liquid Film Coefficient and the Mechanism of Bubble Absorption,"** by S. B. Zdonik, thesis presented to the Massachusetts Institute of Technology at Cambridge, in 1942, in partial fulfilment of the requirements for the degree of Master of Science.

(10) **"Modern Developments in Fluid Mechanics,"** edited by S. Goldstein, Oxford University Press, 1950, Vol. 1, p. 16.

(11) **"The Mechanics of Large Bubbles Rising Through Extended Liquids and Through Liquids in Tubes,"** by R. M. Davies and G. I. Taylor, *Proceedings*, Royal Soc. of London, Vol. 200, Series A, 1950, p. 375.

(12) **"Handbuch der Experimentalphysik,"** edited by Ludwig Schiller, Akademische Verlagsgesellschaft, Leipzig, 1932, Vol. IV, Pt. 2, p. 386.

√ (13) **"The Rate of Rise of Bubbles in Water and Aqueous Solutions at Great Reynolds Numbers,"** by A. Gorodetskaya, *Journal of Physical Chemistry*, (U.S.S.R.), Vol. 23, 1949, p. 71.

(*b*) ADDITIONAL REFERENCES

"The Motion of a Sphere in a Viscous Fluid," by H. S. Allen, *Philosophical Magazine*, Vol. 50, 1900, pp. 323–338 and 519–534.

"The Air-Bubble Viscometer," by G. Barr, *ibid.*, Vol. 1, Series 7, 1926, p. 395.

"Motion of an Air Bubble in a Liquid at Rest," by G. Benfratello—Pt. I. General Characteristics of the Phenomenon and Theoretical Investigations (Infinite Liquid), *L'Energia Elettrica*, February, 1953; Pt. II. Experimental Investigations (Liquid Practically Infinite), *ibid.*, August, 1953; and Pt. III. Experimental Investigations (Liquid in Small Vertical Tubes) and Conclusion, *ibid.*, July, 1954.

"Fluid Flow Patterns," by G. Birkhoff and T. E. Caywood, *Journal of Applied Physics*, July, 1949.

"Effect of the Frothing Agent on the Air Content in the Flotation Pulp," by A. S. Bogdanov, B. V. Kizevalter, and S. G. Mastova, *Bulletin*, Dept. of Technological Sciences, Academy of Sciences (U.S.S.R.), No. 3, 1950, p. 412.

"Propagation of Sound Through a Liquid Containing Bubbles," by E. L. Carstensen and L. L. Foldy, Pt. II, *OSRD No. 3872*, Section No. 6.1-sr 1130–1629, Office of Scientific Research and Development, Washington, D. C., June, 1944.

✓**"The Behaviour of Gas Bubbles in Relation to Mass Transfer,"** by P. D. Coppock and G. T. Meiklejohn, *Transactions*, Inst. of Chemical Engrs. (Great Britain), Vol. 29, 1951, No. 1, pp. 75–86.

"Studies for the Design of Gas Lift Pumps, Part I. The Formation and Characteristics of Gas Bubbles," by R. L. Datta, *Journal*, London Imperial College of Science and Technology, Vol. 4, 1948, p. 156.

"The Properties and Behaviour of Gas Bubbles Formed at a Circular Orifice," by R. L. Datta, D. H. Napier, and D. M. Newitt, *Transactions*, Inst. of Chemical Engrs. (Great Britain), Vol. 28, 1950, pp. 14–26.

"Ueber die Bewegung von Luftblasen in ruhenden und fliessendem Wasser," by R. Dubs, *Schweizerische Bauzeitung*, Vol. 97, No. 14, 1931, pp. 169–173, and No. 15, pp. 183–187.

"Stromung an einer Luftblase im senkrechten Rohr," by D. T. Dumitrescu, *Zeitschrift für Angewandte Mathematik und Mechanik*, Vol. 23, No. 3, 1943, pp. 139–149.

"Über die Aufstieggeschwindigkeit von Luftblasen im Wasser," by Felix M. Exner, *Physik Zeitschrift*, Vol. 28, 1927, pp. 825–829.

"Diffusion Mechanism in the Mixing of Fluids," by F. H. Garner, *Transactions*, Inst. of Chemical Engrs. (Great Britain), Vol. 28, 1950, pp. 88–96.

✓**"Circulation Inside Gas Bubbles,"** by F. H. Garner and D. Hammerton, *Chemical Engineering Science* (London), Vol. 3, 1954, p. 1.

"On the Motion of Long Air Bubbles in a Vertical Tube," by A. H. Gibson, *Philosophical Magazine*, Vol. 26, No. 156, 1913, pp. 952–965.

✓**"The Velocity of Ascension of Gas Bubbles in Water,"** by Herbert Göpfert, *Translation No. 341*, Dept. of Scientific Research and Experiment (Great Britain), April, 1946.

"Experiments on the Vertical Flow of Gas-Liquid Mixtures in Glass Pipes," by J. E. Gosline, *Transactions*, Am. Inst. of Mining and Metallurgical Engrs., Petroleum Div., Vol. 118, 1936, p. 56.

"On the Motion of a Cylindrical Bubble in a Tube and Its Application to the Measurement of the Surface Tension of a Liquid," by Sin-iti Hattori, Aeronautical Research Inst., Tokyo Imperial Univ., No. 115, 1935, pp. 163–195.

"Untersuchungen über die Strömungsvorgänge im Steigrohr eines Druckluft-Wasserhebers," by Kurt Hoefer, *Mitteilungen über Forschungsarbeiten*, Verein Deutscher Ingenieure, 1913, No. 138, pp. 1–12.

✓**"Investigations of Rise of Air Bubbles in Water at High Reynolds Numbers,"** by R. M. Ladyzhenskii, *Journal of Applied Chemistry* (U.S.S.R.), Vol. 27, 1954, p. 17.

"Disperse Gases III: Bubble Size and Time of Rise," by W. Luchsinger, *Kolloid-Zeitschrift*, Vol. 80, 1937, pp. 180–182. (*TMB Translation No. 115*, U. S. Dept. of the Navy, Washington, D. C., September, 1943.)

"The Motion of an Air Bubble Rising in Water," by Otogoro Miyagi, *Technical Reports*, Tohoku Imperial Univ. (Japan), Vol. 5, 1925, pp. 135–167.

"Measurement of Stream Velocity by Air Bubbles," by O. Miyagi, *Journal,* Soc. of Mech. Engrs. (Japan), July, 1929, Vol. 32, No. 147, pp. 305–313.

"Ascent of Air Bubbles in Air-Saturated Water," by D. H. Napier, *Report No. 10* (Gas Absorption Working Party), Dept. of Chemical Eng., Great Britain Imperial College, March, 1949.

"Velocity of Large Bubbles in Vertical Tubes," by Morrough P. O'Brien and James E. Gosline, *Industrial and Engineering Chemistry,* December, 1935, pp. 1436–1440.

"Studies on Absorption of Gas in Form of Bubbles," by Y. Oyama and K. Iwase, *Scientific Papers,* Inst. of Physics and Chemistry Research (Tokyo), January, 1939, pp. 131–157.

"Experiments on Air Lift Pumping," by J. S. Owens, *Engineering* (Great Britain), September, 1921, Vol. 112, pp. 458–461.

✓**"Studies on the Motion of Gas Bubbles in Liquids,"** by F. N. Peebles and J. J. Garber, *Chemical Engineering Progress,* Vol. 49, No. 2, 1953, p. 88.

"The Rate of Rise and Diffusion of Air Bubbles in Water," by C. L. Pekeris, *OSRD No. 976,* Section No. C4-sr 20-326, Office of Scientific Research and Development, Washington, D. C., October, 1942.

"The Rise of Gas Bubbles in Liquids," by F. Pickert, *Forschung (B),* Verein Deutscher Ingenieure, November–December, 1932, Vol. 3, pp. 308–309.

"Essentials of Fluid Dynamics," by Ludwig Prandtl, Hafner Publishing Co., New York, N. Y., 1952, p. 329.

✓**"Absorption of Small Gas Bubbles in Salt Water,"** by E. M. Redding, thesis presented, in 1942, to the Massachusetts Institute of Technology at Cambridge, in partial fulfilment of the requirements for the degree of Doctor of Science.

"The Rise of Air Bubbles in Lubricating Oils," by J. V. Robinson, *Journal of Physical and Colloid Chemistry,* March, 1947, No. 2, pp. 431–437.

"Ähnlichkeitstheorie der Bewegung der Flüsseigkeitsgasgemischen," by Ernst Schmidt, *Forschungsheft 365,* Verein Deutscher Ingenieure, 1934.

"The Rate of Absorption under Conditions of Bubbling," by K. N. Shabalin, S. F. Krylov, and V. I. Oborin, *Journal of Chemical Industry* (U.S.S.R.), Vol. 16, 1939, p. 10.

"Gasblasen in Flüssigkeiten Part II. Der Aufstieg von Gasblasen in Flüssigkeiten," by W. Siemes, *Chemie-Ingenieur-Technik,* Vol. 26, No. 11, 1954, p. 614.

"Die Bewegung von Gasblasen und Flüssigkeitstropfen," by B. Stuke, die Umschau in *Wissenschaft und Technik,* Vol. 54, No. 23, 1954, p. 715.

"The Rate of Rise of Large Volumes of Gas in Water," by H. N. V. Temperley and Ll. G. Chambers, *Report No. AUW/TRI 63/RF20,* Admiralty Undex Works, Undex 125 (Great Britain), January, 1945.

"Experimental Study of Air Lift Pumps and Application of Results to Design," by C. N. Ward and L. H. Kessler, Eng. Series, Univ. of Wisconsin, Madison, Wis., Series No. 1265, Vol. 9, No. 4, 1924.

"On the Rising Velocity of Air Bubbles in Water," by R. C. Worster, *Technical Note 1*, British Hydromechanics Research Assn. (London), July, 1948.

APPENDIX II. NOTATION

The following symbols, adopted for use in the paper and for the guidance of discussers, conform essentially with "American Standard Letter Symbols for Hydraulics" (ASA Z10.2-1942), prepared by a committee of the American Standards Association with Society representation, and approved by the Association in 1942:

C_d = drag coefficient = $(8/3)\, g\, r_e/U^2$;
D = drag of bubble;
e = coefficient of surface viscosity;
g = acceleration due to gravity;
l = length parameter of bubble;
M = dimensionless parameter = $\dfrac{g\, \mu^4}{\rho\, \sigma^3}$;
Δp = pressure drop across bubble surface due to surface tension = $\dfrac{2\,\sigma}{r}$;
r = radius of sphere;
r_e = equivalent radius of bubble—that is, radius of a sphere of equal volume;
R = Reynolds number = $\dfrac{2\, r_e\, U\, \rho}{\mu}$;
R' = Reynolds number inside bubble = $\dfrac{2\, r_e\, U\, \rho'}{\mu'}$;
U = terminal velocity;
W = Weber number = $\dfrac{2\, r_e\, U^2\, \rho}{\sigma}$;
μ = coefficient of dynamic viscosity of liquid medium;
μ' = coefficient of dynamic viscosity of gas;
ρ = density of liquid medium;
ρ' = density of gas; and
σ = surface tension.

DISCUSSION

JOHN A. ROBERSON,[4] CHARLES L. BARKER,[5] M. ASCE, AND PAUL F. RUFF,[6] J. M. ASCE.—The authors are to be complimented for their work concerning the movement of bubbles through liquids.

The writers have made studies of the movement of bubbles in a turbulent stream at The State College of Washington at Pullman. It is interesting to note the close agreement existing between the results reported by the authors and those observed by the writers.

The problem of determining the rise velocity of bubbles, although somewhat academic to many, may be of great importance—for example, in pipelines where air is mechanically entrained. In lines of this type small bubbles tend to coalesce and eventually form large air masses or "pockets." The removal of these air masses by pipe vents produces pressures that can be destructive. The problem of locating vents in a line for the removal of bubbles before they can form air masses has prompted the writers to make a study of bubble rise in a turbulent stream.

If U is the rise velocity, V the velocity of the water, and d the pipe diameter, the distance of travel, L, of a bubble in rising a distance d is

$$L = \frac{d}{U} V \qquad (5)$$

In determining vent location in pipelines, L in Eq. 5 is the distance the vent should be placed downstream from the point of entrance of the air bubbles into the pipeline and U is the minimum rise velocity of the bubbles.

Bubbles 0.25 in. in diameter or greater were studied by the writers. Messrs. Davies and Taylor (11) found the minimum rise velocity of bubbles of this size range in a stationary liquid to be 0.6 ft per sec. However, the problem with which the writers were concerned involved a turbulent liquid. An experimental apparatus was constructed of 5.5-in. lucite tubing to study the rise velocity of bubbles in a turbulent stream. The rise velocity, U, in a turbulent stream (Reynolds number = 50,000 to 300,000) determined by the writers agrees closely with the results obtained by Messrs. Davies and Taylor and by the authors. Precise comparison was not practical because of the variations above and below the mean rise velocity as a result of turbulence.

It was of interest to the writers to note that the data in Fig. 2 produce a smooth curve. The results presented by Messrs. Davies and Taylor and those of the writers produced a spread of points, especially for bubbles of relatively large diameter.

---

[4] Asst. Hydr. Engr., Div. of Industrial Research, and Instructor, Dept. of Civ. Eng., The State College of Washington, Pullman, Wash.

[5] Prof. of Hydr. Eng., The State College of Washington, Pullman, Wash.

[6] Junior Hydr. Engr., Div. of Industrial Research, and Instructor, Dept. of Civ. Eng., The State College of Washington, Pullman, Wash.

William L. Haberman[7] **and Rose K. Morton**[8].—The discussion by Messrs. Roberson, Barker, and Ruff deals with the upward and downstream motion of bubbles in horizontal pipes. The velocities of these bubbles are affected not only by the turbulence in the stream but also by the velocity distribution in the pipe and the proximity of the pipe walls. In addition, acceleration of the bubble in the downstream and upward directions occurs after release of the bubble. The velocities U and V of Eq. 5 are, therefore, average velocities. Because these effects are included in the experimentally determined rise velocities in pipes, scatter in the results is to be expected. For the same reason, these velocities should not be compared quantitatively with those obtained for bubbles rising freely in a large, quiet medium.

The discussers have commented on the absence of scatter in Fig. 2. It was observed during the experiments at the Taylor Model Basin that the velocities of large bubbles surrounded by smaller satellite bubbles differed somewhat from those of corresponding ones free of satellites. Hence, only the results for bubbles that were essentially free of satellites were included in the plot.

---

[7] Physicist, David Taylor Model Basin, U. S. Dept. of the Navy, Washington, D. C.

[8] Mathematician, David Taylor Model Basin, U. S. Dept. of the Navy, Washington, D. C.

AMERICAN SOCIETY OF CIVIL ENGINEERS
Founded November 5, 1852
TRANSACTIONS

Paper No. 2800

THE DESIGN OF TWO STEAM ELECTRIC PLANTS

By Walter L. Dickey,[1] M. ASCE

Synopsis

Two steam electric plants are examined from the standpoint of civil engineering design. The author describes the unusual hull-type foundations, the consideration of seismic factors, the grouted reinforced-brick masonry, turbine pedestals, wind vibration of the stacks, and the oil retaining rings or walls of prestressed concrete. These large plants generate an important percentage of the peak load of the system of which they are part.

Introduction

In this paper is described part of an expansion construction program consisting of an initial power plant to which have been added certain facilities, and a sister plant built to augment the earlier power-plant construction program.

As a result of the steam electric plant-construction program, by the end of 1952 approximately 60% of the system peak load of the Pacific Gas and Electric Company was to be generated by steam. In 1940 steam plants generated less than 25% of the system peak load. The number of kilowatt hours that will be generated by steam will, of course, depend on the amount of snow and rain in any particular year. In 1949 more than half the kilowatt hours produced by this company was developed in its steam plants, whereas in 1940 steam plants generated only 10% of the energy. From this comparison it can be seen that the system is not one supplied primarily by hydroelectric generating stations, but that steam plants are required not merely as a source of reserve to be used either in the event of transmission-line failure or for dry-year operation but also as the major part of the base load capacity. As such, the steam units must be capable of sustained operation at high efficiency.

The system serves an area of approximately 90,000 sq miles in northern and central California, an area having a population of 5,000,000. Along with other sections of the west coast, this area is experiencing an unusual growth

---

NOTE.—Published, essentially as printed here, in November, 1953, as *Proceedings-Separate No. 342*. Positions and titles given are those in effect when the paper was approved for publication in *Transactions*.

[1] Chief Civ. and Structural Engr., Power Div., Bechtel Corp., Engrs. and Constructors, San Francisco, Calif.

in population, in industry, and in the general level of business and agricultural activity. This growth is reflected in a rapidly increasing demand for electric power. Since the early 1930's the peak load on the system has been increasing steadily. During World War II the growth of the need was accelerated and after the war it continued to accelerate. The construction program lagged during the war and now must be expedited in order to meet the increased demand. It is gradually restoring adequate power margins and serving the rapidly growing needs of the area. Approximately 75% of the new capacity

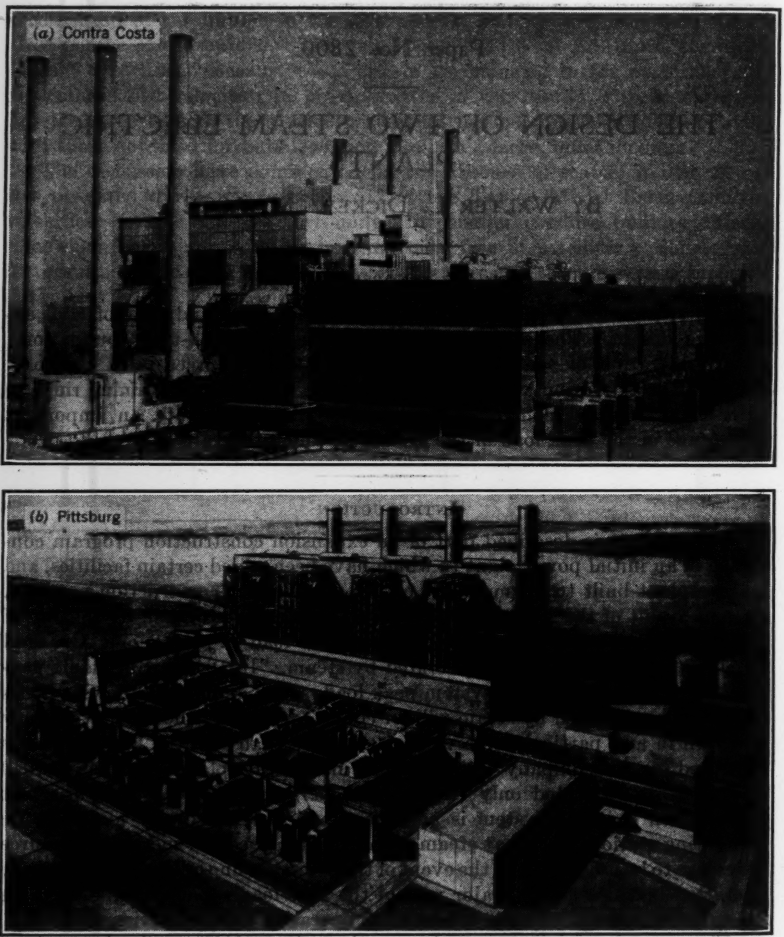

FIG. 1.—TWO STEAM ELECTRIC PLANTS

is accounted for by steam stations and 25% by hydroelectric developments. There are three basic reasons for the large proportion of steam generation: (1) Steam capacity additions were postponed by World War II. (2) Steam capacity is feasible because of the changing economic steam-hydro ratio. As the more favorable hydroelectric sites have already been developed, those remaining are more costly. The relative cost of steam electric plants has been reduced by technological developments in design. The over-all result has been a gradual shifting of the economic steam-hydro ratio from approximately 1:4 to approximately 1:1. (3) Additional steam capacity is required for the peak-load support of hydroelectric developments planned by the company for future construction.

The new Contra Costa steam electric station at Antioch, Calif., and others similarly planned at the same time, were designed for local and system use.

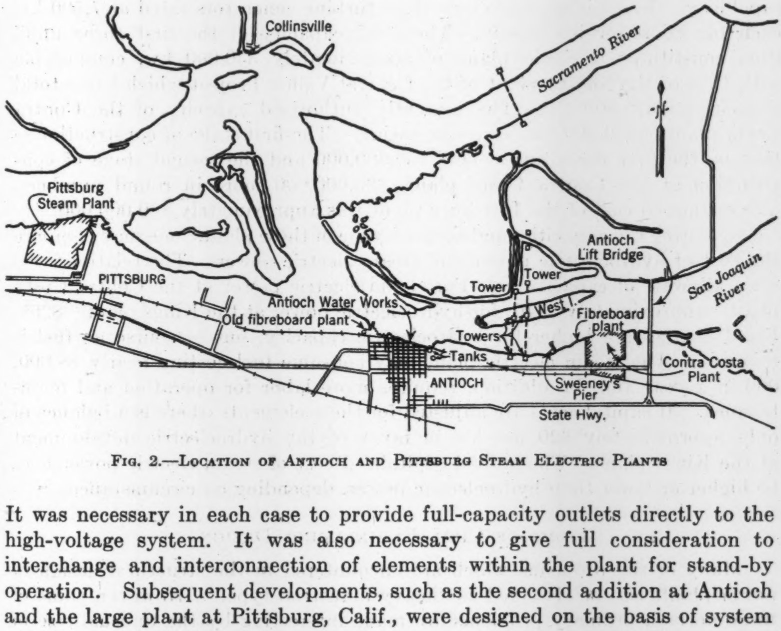
Collinsville
Sacramento River
N
Pittsburg Steam Plant
PITTSBURG
Antioch Lift Bridge
Tower
Tower
San Joaquin River
Antioch Water Works
West I.
Old fibreboard plant
Fibreboard plant
Towers
Tanks
Contra Costa Plant
ANTIOCH
Sweeney's Pier
State Hwy.

FIG. 2.—LOCATION OF ANTIOCH AND PITTSBURG STEAM ELECTRIC PLANTS

It was necessary in each case to provide full-capacity outlets directly to the high-voltage system. It was also necessary to give full consideration to interchange and interconnection of elements within the plant for stand-by operation. Subsequent developments, such as the second addition at Antioch and the large plant at Pittsburg, Calif., were designed on the basis of system security and interconnection; that is, it was not so important that any one plant be self-sufficient because the system could connect several relatively large plants. This made possible less interconnection and required fewer safety features and stand-by elements within each of the individual plants. Fig. 1 (*a*) shows the first stage of the Contra Costa plant nearly complete and the second stage (right, rear) under early construction. Fig. 1 (*b*) is an artist's presentation of the Pittsburg plant, showing its four "outdoor" 150,000-kw turbo-generator units.

The particular sites of the plants (Fig. 2) were chosen because adequate space and adequate water supplies were available, and the locations were favorable relative to load and transmission lines. The Antioch site is adjacent to the heavy industrial load along the lower San Joaquin River and is adequately served by interconnecting transmission lines that conduct hydroelectric power to the central California area. The site is served by a railroad, and docking facilities can be provided. Fuel can be satisfactorily delivered by interconnection with oil refinery pipelines. Fuel oil could also be delivered economically by barge or tankers, should such a requirement arise in the future.

Relatively little earth moving was required to make the site level and at a proper elevation to utilize low-head pumps for condenser circulating water, yet be safely above flood waters. The first three main turbine-generator units installed at the Contra Costa plant were rated at 110,000 kw each, maximum capability. In addition, there were three turbine generators rated at 7,500 kw each for house-service supply. The total capacity of the first three units thus constitutes a single plant of approximately 330,000 kw, comparable with that of the Shasta plant of the Central Valley Project which has a total capacity of 375,000 kw. The presently authorized capacity of the Contra Costa plant is 560,000 kw maximum rating. The first stage of construction—that is, the first three units—cost $50,000,000 and the second stage of construction at the Contra Costa plant, $30,000,000 more in round numbers. The estimated cost of the Pittsburg plant was approximately $80,000,000.

By noting the capacities and costs of some of these plants, one may compare the cost of hydroelectric power and steam electric power. The relative costs for a kilowatt of capacity are: For steam electric power at the Contra Costa plant—approximately $140; for hydroelectric power at the Kings plant—$260. Fixed charges are higher for hydroelectric capacity, but of course no fuel is required. The steam electric plant may consume fuel costing nearly $8,000,000 in a year and, in addition, requires more labor for operation and maintenance. If capital costs are adjusted for these elements, there is a balance of only approximately $20 per kw in favor of the hydroelectric development at the Kings plant. The annual capitalized cost of steam electric power may be higher or lower than hydroelectric power, depending on circumstances.

ITEMS OF CIVIL ENGINEERING DESIGN

Many of the problems which are encountered in the structural design of power plants can be classified as "heavy industrial type." However, some of these normal, ordinary problems are made interesting by the unusual size of the facility involved. For example, most industrial buildings normally contain bridge cranes, but a power-plant crane must lift and place a 200-ton weight very accurately in position. Also, the water heaters in the rear of the building are not ordinary water heaters; they are from 130 ft to 150 ft high, the equivalent of a ten-story or thirteen-story building. What is more important to structural engineers is that these water heaters weigh about 10,000 tons and impose individual column loads of approximately 3,000,000 lb.

Of the many interesting items, a few features will be examined in a general manner.

Foundation Design

There were many varied foundation problems in the construction of the initial and secondary extensions to the Contra Costa plant and also in the separate plant under construction at Pittsburg. The most interesting was probably the "bath-tub" foundation for the turbine bay, the first stage of construction at the Contra Costa plant. It is as indicated in Fig. 3. It was designed to carry the turbine foundation loads and building wall loads as a single foundation mat for the lateral distribution of loads. The elements included in the foundation construction are shown in Fig. 3(*a*) and include building foundation walls and intake tube, forebays or distributing tubes, discharge tubes, turbine foundations, and a water-storage area. These have been combined in the final design as shown in revised section, Fig. 3(*b*).

Advantage was taken of the fact that the vertical walls and basement floor slab were being designed and cast as an integral structure so that lateral loads would be resisted by rigid-frame action, thus permitting the use of a relatively thin foundation mat. It was felt by some engineers that the relatively thin slab might not be strong enough, although it could be proved by computation that the Vierendeel section as designed was the equivalent of a solid simple mat section 6 ft or 8 ft thick. Therefore, to demonstrate this point more clearly, a simple rubber model was made, merely for qualitative demonstration that the proposed structure was superior to a slab mat. One model simulated the solid mat and one the continuous box frame. As can be seen in Fig. 4, the deflections of the mat type of foundation were many times those in the model simulating the combined built-up girder structure that was proposed. Many analyses were made to verify the fact that the latter was a satisfactory foundation—it was checked for hogging and sagging as a ship's hull would necessarily be checked. These, too, were qualitative rather than precise quantitative analyses made to determine whether the foundation being provided met the standards of safety desirable for the construction of this important public utility.

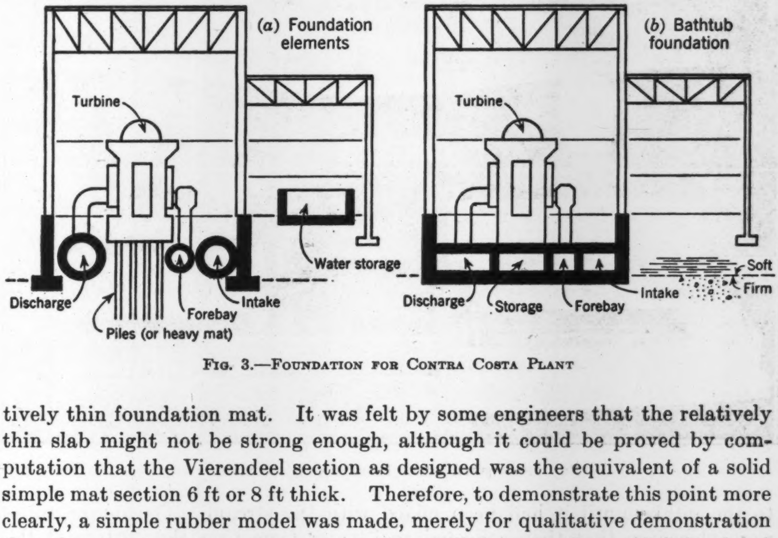

FIG. 3.—FOUNDATION FOR CONTRA COSTA PLANT

INTAKE TUBES

In order to provide adequate cooling water for the condensers in the turbine-generator units, approximately 400,000 gal per min of cooling water are required. This quantity of cooling water is required to maintain the high efficiency of the turbo-generator units by reducing the pressure on the discharge side.

Tidal influence is experienced in the stream at the site, and warm water discharged into the river either upstream or downstream of the intake might have flowed toward the intake and been recirculated. Because of the importance of maintaining cool water at the condenser, the intake and discharge points were placed far enough apart so that the backwash would not return to the intake until it had been mixed with the stream. The intake tubes were placed so that they collected cool water from near the bottom of the stream and discharged it in a thin layer overlying the surface of the river so that the possibility of mixing the warm discharge water with the cool intake water required for efficient operation was reduced. This arrangement at the Contra Costa plant has proved quite satisfactory. Investigation of the history of the stream contours at the Contra Costa site indicated that the stream bed adjacent to the site was relatively stable and that it would not be advisable to change the contours by dredging or other major operations. The designs of the inlet structures were, therefore, confined to such developments as would result in a minimum of change in the stream bed.

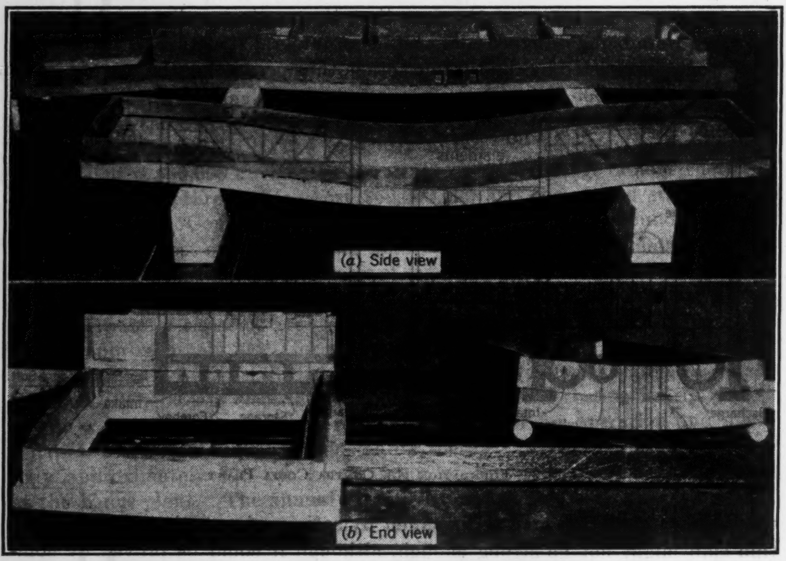
(a) Side view

(b) End view

FIG. 4.—RUBBER SCALE MODELS OF FOUNDATIONS

To reduce the height of the over-all intake structure, twin elements were placed side by side. It was originally planned that they extend from the shore in a temporary dredged trench to a point intercepting the deeper parts of the stream channel at a flow-line elevation of approximately 23 ft below the mean low-water elevation. To achieve this depth at a point of contact with the normal stream bed it was required that the tubes extend into the river 400 ft. It was also necessary that a coarse bar-rack structure be provided, with fine screening included, because of the concern felt by the Fish and Game Commission of the State of California that the small fish in this natural hatchery area might be killed.[2]

One of the complications of the intake-tube design is that provision must be made to permit dewatering of either or both of the tubes separately or simultaneously for inspection or any repairs that might be necessary. Because of these requirements for dewatering, thick-walled, heavy concrete tubes 12 ft in inside diameter were constructed. Another factor influencing this design choice was the fact that forms already fabricated for some tubes of this size were available in Los Angeles, and hence a considerable saving in form costs would be achieved. The end of each 100-ft section is supported on piles as are the gate structure and the transition section at the shore. The piles resist both downward and uplift forces.

SEISMIC CONSIDERATIONS

Special considerations were introduced into the design problem primarily because of the assumed magnitude of design lateral seismic force. The gravity loads were heavy, and the seismic coefficient, or assumed lateral seismic acceleration, was relatively high.

Although the factor from the 1946 "Uniform Building Code"[3] might have permitted a design factor of 8%, a factor of 20% was assumed for these plants because it is much more important that a plant such as this be undamaged and continue to operate without interruption after a disaster than it is for an ordinary industrial plant to do so.

Neither in the 1933 earthquake at Long Beach (Calif.) nor in the recent Tehachapi (Calif.) earthquake were the intensities of the earthquakes as great as that of the 1906 San Francisco (Calif.) earthquake—although at Long Beach accelerations of approximately 0.3 g were measured. A tank near Tehachapi designed with a 10% factor nearly collapsed during that earthquake. The diagonal tie rods bracing the tank were stretched so that the paint had spalled and they were sagging noticeably. An adjacent tank designed with a 20% factor suffered no distress or damage. This generalization serves to justify the 20% factor.

This lateral factor was not applied to all the design live loads because these assumed live loads do not represent loads that can be expected to exist in the plant at the time of a quake. The live-load occupancy in a power plant is relatively low and may be neglected. The high lateral factor was not applied to the piping loads in the plant because the piping is generally suspended from the structural frame by hangers; it does not impart lateral loads but tends to swing freely if there is lateral motion of the ground.

---

[2] "The Fish Rescue Project at the Pacific Gas and Electric Company's Contra Costa Steam Plant," by James E. Kerr, *Proceedings-Separate No. 264*, ASCE, September, 1953.

[3] "Uniform Building Code," Pacific Coast Building Officials Conference, Los Angeles, Calif., 1946.

Piping loads from long runs of pipe cannot be assumed as being applied laterally to the supports at a constant factor. It would be quite possible, for example, for the supports to move back and forth within the amplitude of the earthquake motion, but not impart great lateral amplitude or force to the central part of the pipe length; hence, the design lateral force assumed at supports would not be great.

The boiler support presented a unique problem. The tremendous weight of the drum and piping is suspended from the top of the frame approximately ten stories above the ground. It might be assumed—according to the local code recommendations—that 20% of the load supported at the top of the frame would be applied laterally at the top, indicating that there would be tremendous uplift forces and overturning moments applied at the base of the frame. However, the results are quite different. For example, if the entire weight is assumed to be suspended at the top by hangers, there would in effect be formed a perfect seismograph imparting almost no lateral force at the top.

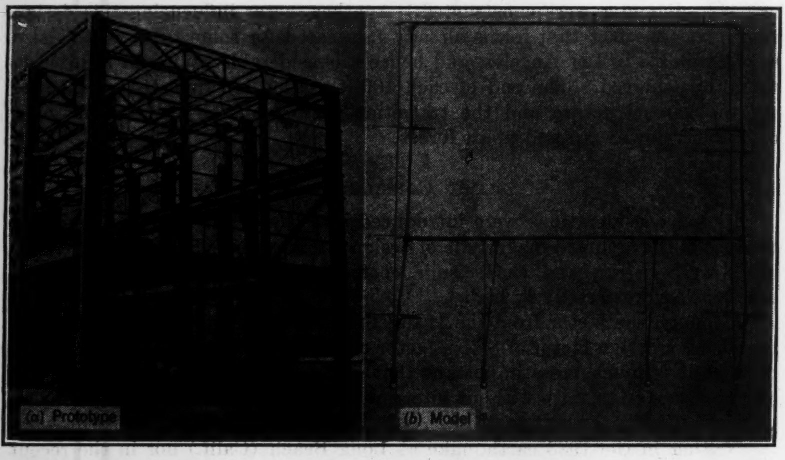
(a) Prototype
(b) Model

Fig. 5.—Turbine Hall Frame, Contra Costa Plant

Actually, however, there is in the boiler frame and structure a series of stops which prevents relative sidesway and a multiplicity of pipe connections that tie this otherwise free-swaying mass to the structure throughout the height of the frame. Therefore, the more rational assumption is that the lateral forces of each mass are applied at their centers of gravity

The basic design is relatively simple and conventional. Its simplicity is largely accounted for by the fact that the loads are so heavy that X-bracing was not required. The diagonals necessary to resist tension were so large that they had a sufficient slenderness ratio to carry compression also, so that a Warren-type bracing was used.

It was not possible to provide braces in the turbine hall extension of the Contra Costa plant; therefore, the columns, roof trusses, and floor beams were designed as a complete rigid frame, continuous in all joints and fixed at the base by the heavy foundation construction, as shown in Fig. 5(*a*). The simplified frame is shown more clearly in the photograph of the wire model of the frame bent, Fig. 5(*b*).

The model was used to check the necessary indeterminate frame computations for the many different loading conditions. It was made of brass wire designed so that the product of modulus of elasticity, E, times the moment of inertia, I, of the wire was proportional to that of the frame.

The principle used was the same as is used in the conventional Beggs Deformeter or Gottschaulk Continostat; that is, let the frame draw its own influence line of reactions. The technique has been simplified, however, so that little time and a small cost of equipment are involved. The material for this particular model cost $.97. A day was required to make the frame and draw the influence lines of all vertical, horizontal, and moment reactions. It was believed that the accuracy was as nearly within 10% as were the comparable mathematical computations.

The procedure is simple as well as effective: (*a*) Wires are calibrated by measuring the deflection caused by a standard pull. This gives a measure of $E\ I$. (*b*) The properly proportioned wires are soldered to the model, the scale of which is such that deflections are easily measured. (*c*) The model is deflected by displacement of the points of reactions. (*d*) The resulting influence lines are traced.

REINFORCED MASONRY CONSTRUCTION

The basic frame of the building at the Contra Costa plant is structural steel, providing lateral and vertical support for the concrete floors and lateral support for the masonry walls. The frame of the turbine bay and the adjacent bay is approximately as shown in Fig. 5. The walls span between these frames for a distance of 27 ft between columns, designed to resist heavy lateral earthquake loads. There are no steel beams incorporated in the masonry, the bond beam function being provided by the reinforcing placed in the masonry as part of the bricklayers' work.

This is one of the largest reinforced masonry buildings in this area—more than 1,000,000 of the large-size (jumbo) bricks were used. The 27-ft horizontal span of the walls is somewhat larger than normal, and the 80-ft height of the walls is considerably above average. The masonry is of grouted reinforced brickwork; a locally available common brick containing a dovetail key in one face was used. The outer and inner tiers of brick were laid and the reinforcing was placed; then the grout was poured in the space between the two tiers as the work progressed. Bond between this inner collar of reinforced grout, or concrete, and the masonry surfaces is provided not only by adhesion of the grout to the porous brick but also by the mechanical key provided on the back of the brick. This type of reinforced masonry was developed in southern California, an area which had suffered several serious earthquakes. It was developed primarily to provide a type of reinforced masonry that would be both structurally sound and economical. Details of this type of construction are shown in Figs. 6(*a*) and 6(*b*). This construction makes possible the utilization of the interior and exterior finishes as structural elements supporting the load—not merely contributing dead weight to be carried by an independent structural frame. It also provides an inexpensive type of wall in which structural glazed tile can be alternated with ordinary brick finish, as required in an occasional washroom or laboratories. Fig. 6(*c*) shows masonry chipped away to receive the new wall extension. The design stresses that were established as satisfactory maximums in these computations are as follows:

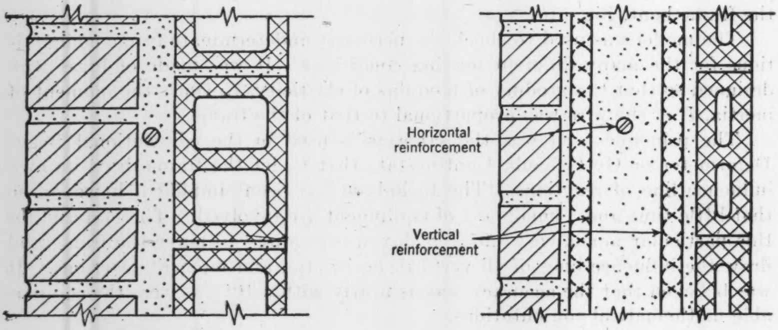

(*a*) Vertical wall section

(*b*) Vertical section at pilaster

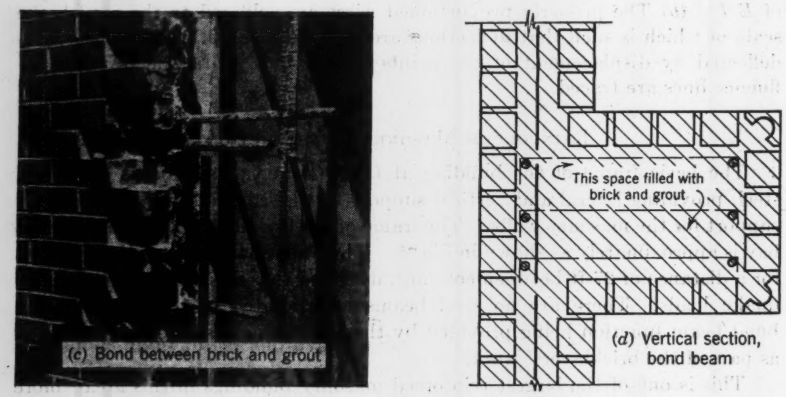

(*c*) Bond between brick and grout

(*d*) Vertical section, bond beam

FIG. 6.—GROUTED REINFORCED BRICK MASONRY

Type of stress	Stress, in pounds per square inch
Axial compression based on gross section	125
Flexural compression based on net section	250
Shear in joints	20
Shear in tile	20
Shear bond between grout and tile	30
Flexure in tile webs	75

Actual stresses due to the loadings were considerably less in all cases.

The reasons for the selection of this type of wall were: The favorable cost in comparison with that of concrete, the low maintenance costs, and the pleasing, dignified, and interesting appearance. One of its greater advantages is that there is a continuous, unbroken, vertical collar joint of grout that serves as an effective moisture barrier. There are no through headers or ties that would be potential passages for moisture penetration. Reinforced concrete bond beams were not used generally on this job because they would have required that the masonry crews stop and wait for the forming crews to place forms, for the concrete crews to place concrete, and for the forms to be stripped before masonry work could proceed. The starting and stopping and the coordination of these crews cause unpredictable delays which increase the intangible costs of construction. The typical bond beam construction was of masonry, as shown in Fig. 6(*d*). The strength of such walls—properly built—compares favorably with concrete structures. This fact may seem improbable to the engineer accustomed to concrete technology in which the high water-cement ratios so typical of proper masonry grout would certainly result in low-strength cylinders. However, three important factors are effective. First, the grout is really 6-sack or 7-sack concrete, and the water-cement ratio is approximately from 6 gal to 7 gal per sack. The second—and by far a more important factor to be noted—is that the grout is poured between two absorbent tiers of brick which promptly withdraw water from the grout, reducing the water-cement ratio to the no-slump value of from 3 gal to 4 gal per sack, which compares favorably with vacuum-processed concrete. The third factor is that, although some of this water migrates to the exterior of the wall and evaporates, some is retained and this, in effect, "wet cures" the grout. This grout, the strength of which is only between 1,500 lb per sq in. and 2,000 lb per sq in. when conventional wet cylinders are tested, was shown to have a strength of between 3,000 lb per sq in. and 6,000 lb per sq in. when tested under simulated job conditions.

Tests demonstrated qualitatively that the theory was correct. The grout would increase in strength as a result of decreased water-cement ratio and improved curing.

This reinforced grouted masonry was further utilized in walls of brick and glazed tile in various parts of the Pittsburg steam plant. In general, the interior walls were of brick, but in washrooms and laboratories the interior finish was of glazed structural clay tile. This made a composite brick-grout-tile wall in which the exterior finish and the interior finish served not merely as dead load but also as part of the structural element helping to support load and could be constructed by one crew without costly interruption or conflict. The section through the composite wall is as shown in Fig.6 (*b*). This design required rather complicated rigid-frame analyses on the cross section of the wall. To check the computations further, beams of the structural clay tile and brick were built and tested and were found to be considerably stronger than predicted by computations.

TURBINE PEDESTAL FOUNDATION DESIGN

The structural design of power plants involves considerable research and study. No part of the station is more important than the support for the turbines and generators, the "heart" of the plant. Although good engineering practice usually requires that structures be economically designed, more conservative consideration must be given to the turbo-generator supports, commonly called turbine pedestals, and to factors of safety. The support of these turbines is not only a static problem of supporting approximately 700 tons of equipment but also of guarding against the deflections and the probability of resonant vibrations that might occur in the structure. The stress considerations for the static loads are not unusual. However, the probability of vibrations makes it desirable that turbine pedestals be made of concrete rather than steel. Concrete has a better vibration damping factor than does the more resilient steel. These structures are usually rather large and of complicated shapes so that accurate computations are extremely difficult to make. Most of the rules governing the design are empirical, based on what the leading turbine-generator manufacturers have found to be good practice in the design of foundations. Therefore, designs are usually similar to those of foundations that have proved satisfactory. Some general rules to follow are that thin slabs or walls and cantilever brackets are to be avoided; generous haunches and large masses of concrete with respect to the size of the equipment to be handled are to be provided—for example, experience has indicated that concrete mass at least equal to 2½ times the weight of rotating parts should be provided. It is customary to limit the elastic deflections of the piers and girders to a maximum of 0.020 in. and to check further that the relationship between mechanical frequency and deflection is such that there is a minimum probability of the machine and the turbine pedestal being in tune. This limitation has been expressed by the General Electric Company as an equation: "The permissible frequency in cycles equals 187.7 divided by the square root of the deflection in inches." Therefore, for the following motor speeds, the following theoretical deflections for resonant vibrations should be avoided:

Speed, in revolutions per minute	Theoretical deflection for resonant vibration, in inches
1,200	0.025
1,500	0.015
1,800	0.011
3,000	0.004
3,600	0.0028

Although most available information concerning vibration and turbine pedestal foundations consists of equations of the rule-of-thumb type, there have been many papers on the subject published in German. The rule-of-thumb guides may be tempered by study of this foreign literature; J. G. Thon, M. ASCE, translated several German studies which were made on a more exact basis of analysis in order to assure the company further that these pedestals are soundly designed.

Evidence of the soundness of the design was indicated by the fact that, after the plant had been placed in operation there was less vibration noticed on the turbine pedestal than on the rest of the building floor—from which the pedestal was separated by a rubber strip.

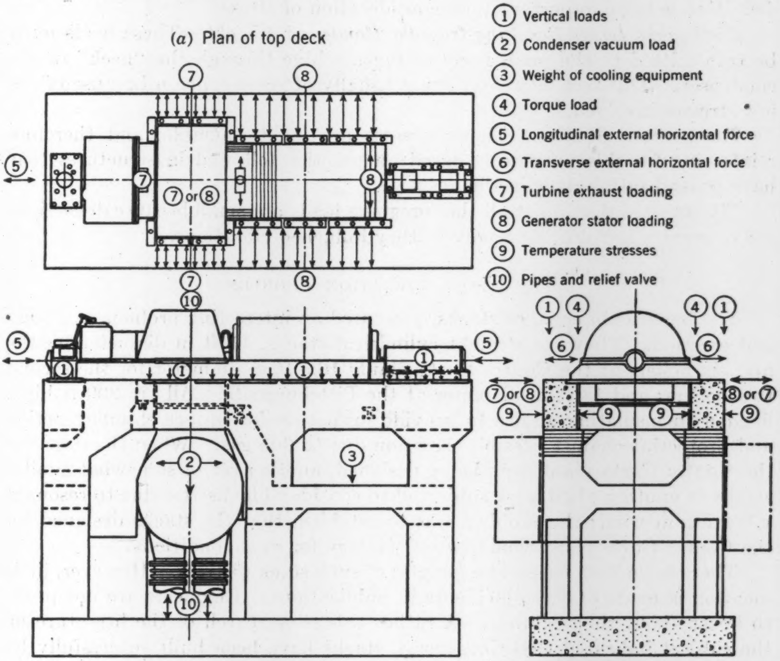
(a) Plan of top deck
① Vertical loads
② Condenser vacuum load
③ Weight of cooling equipment
④ Torque load
⑤ Longitudinal external horizontal force
⑥ Transverse external horizontal force
⑦ Turbine exhaust loading
⑧ Generator stator loading
⑨ Temperature stresses
⑩ Pipes and relief valve
⑦ or ⑧
⑦ or ⑧
⑧ or ⑦

(b) Elevation (c) Section through ℄ of exhaust

FIG. 7.—FOUNDATION LOADING DIAGRAM

The foundation design loads imposed by the turbine and generator are as follows and as shown in Fig. 7:

Vertical.—The vertical load is the total dead load of approximately 700 tons to which is added 35% of the dead load. This dead load is called "impact load;" it provides an additional factor of safety in the event of dynamic imbalance.

Steam Condenser Vacuum Load.—This load is determined by the method of mounting the condenser.

Torque Load.—This force is due to changes in load, acceleration, and similar factors and is approximately 7,000 times the number of kilowatts divided by the speed in revolutions per second. For a machine of the capacity used in these plants the torque load is approximately 1,000,000 lb; this load was used for design purposes.

External Horizontal Load.—It is assumed that horizontal loads, both transverse to and parallel to the longitudinal axis of the machine, are loads applied at the center of gravity of the shaft and that these loads equal between 20% and 25% of the weight of the machine. Guides are provided to resist such forces and to maintain the various parts of the turbine-generator unit in proper alinement. In this case also, maintenance of alinement or minimum deflection is more important than consideration of stress.

Earthquake Loads Resulting from the Condenser Weight.—These loads must be transmitted to the main body of the machine through the "neck" of the condenser. This fact, however, is not usually of great concern because of the low stresses involved.

Temperature Stresses.—These stresses are indeterminable, and therefore reinforcing for this purpose is based on practice followed in structures that have proved satisfactory in this respect.

The stresses that resist all the foregoing loads are small because deflections are of greater concern, especially as they influence vibrations.

THE STACK VIBRATION PROBLEM

The boiler chimneys, or stacks, presented an interesting problem in design and erection. They are straight cylindrical stacks, 11 ft in diameter for the first six boilers at the Contra Costa plant; 16.5 ft in diameter for the second two boilers; and 18 ft in diameter at the Pittsburg site. All are 200 ft high, lined with insulating gunite to provide insulation for proper chimney action and protection against possible corrosion due to flue gas. When the stacks at the Contra Costa plant were being designed, another set of somewhat similar stacks at another plant were subjected to considerable distress due to resonant vibration in wind; the problem was to establish that the stacks designed for the Contra Costa plant would be satisfactory for such conditions.

There have been frequent examples of such stack distress. However, little mention is made of these incidents in publications. Engineers are not prone to boast about their failures. A rather extensive search of the literature on the subject indicated that, in general, stacks have been built successfully by means of various devices, but there was very little research on stacks suffering distress, which may be of the type shown in Fig. 8. Fig. 8 shows a 12-ft-diameter steel stack that was subjected to wind of a velocity resulting in impulses approximately resonant with the period of the unlined stack. Failure was by buckling followed by tearing of the plate.

Wind, particularly when subject to uniform conditions so that steady laminar flow may exist, may "peel off" a cylindrical body alternately from one side and then the other, imparting a pulsating force perpendicular to the wind direction. The period of this pulsating, alternating force depends on the velocity of the wind and the diameter of the cylinder and is expressed by the equation:

$$f = \frac{S\,V}{d}$$

in which f is frequency, in cycles per second; V represents velocity, in feet per second; d denotes diameter, in feet; and S is the Strouhal number (approximately 0.20).

This phenomenon is known as von Kàrmàn vortices, shown in Fig. 9(*a*). If the frequency of these forces occurs at the natural period of the stack, the energy from each impulse will, of course, accumulate, just as a slight push on a child's swing at the proper time will cause energy to be accumulated until

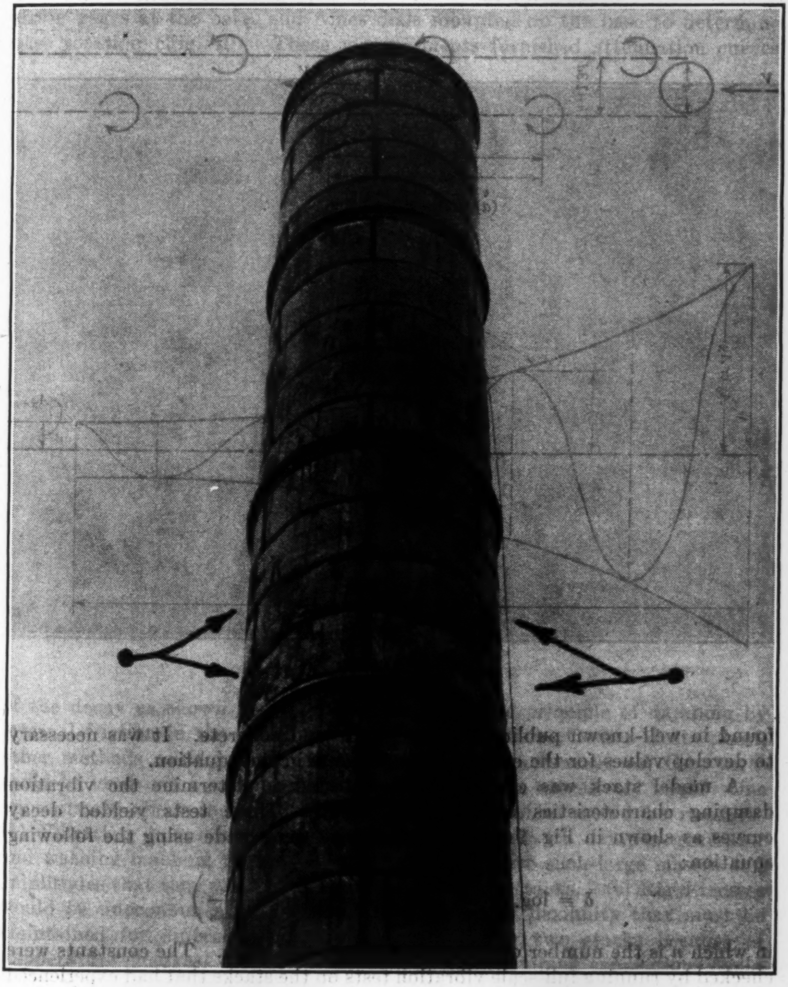

FIG. 8.—STACK FAILURE CAUSED BY WIND

it swings in relatively large amplitudes. Swinging will continue to increase in amplitude until damping is sufficient to dissipate the energy of each input. The damping is due to air friction, internal friction in the steel, internal friction in the lining if it exists, and dissipation of energy through base rotation or through friction on various attachments such as breeching connections.

Little basic information was available on the subject of this phenomenon, and the equations were not well established. There were some test data which established the damping coefficient due to internal friction in steel and in some materials such as aluminum and bakelite, but no authentic values were found in well-known publications for gunite and concrete. It was necessary to develop values for the exponential constants in the equation.

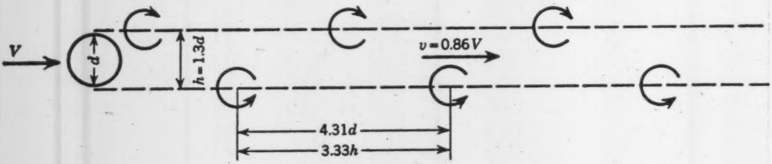

(a) Vortex trail

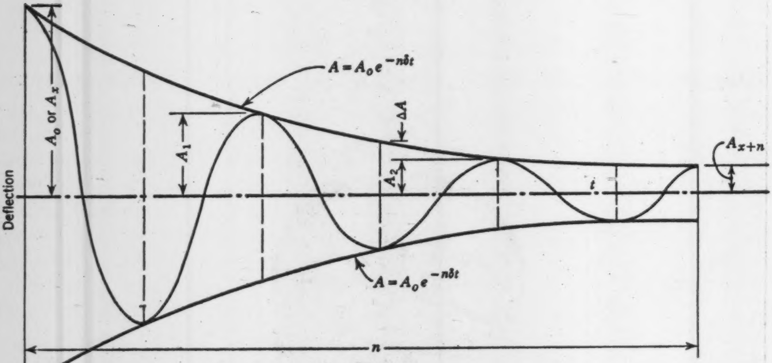

(b) Decay curve

FIG. 9.—STACK VIBRATION

A model stack was constructed and tested to determine the vibration damping characteristics of steel and gunite. These tests yielded decay curves as shown in Fig. 9(*b*). Computations were made using the following equation:

$$\delta = \log_e \frac{A_2}{A_1} \approx \frac{2\,\Delta A}{A_1 + A_2} = \frac{1}{n}\left(\log_e \frac{A_x}{A_{x+n}}\right)$$

in which n is the number of cycles between A_x and A_{x+n}. The constants were checked by running full-scale vibration tests on the stacks that had experienced the initial vibration distress. Also, computations were made regarding the Contra Costa stacks, and further vibration tests were made of those stacks, lined and unlined.

The final tests of the stacks at the Contra Costa plant consisted of placing rigging between the two stacks at the top and pulling them toward each other as one might twang a tuning fork. The stacks were pulled a foot out of line and released with a quick-release trip mechanism. Deflections were measured using a recording seismograph installed at the top of the stack, a pantograph recording needle on a scaffold approximately 60 ft above the base, electric strain gages at the base, and Ames dials mounted on the base to determine base rotation (Fig. 10). These measurements furnished attenuation curves of the decay as shown in Fig. 9(*b*). Although the principle of damping by internal friction in the lining material was used at the Contra Costa plant, other methods could have been used, such as the following: (*a*) Guy wires could be used but would not be very effective unless excessively large. One approximate check indicated that 3-in.-diameter cables would be required. (*b*) Vibration dampeners have been used successfully to dampen generator and washing machine vibrations but they would have such large masses and amplitudes that they would not be feasible on these stacks. (*c*) Rigid trusses would be uneconomical and difficult in view of the flexibility that must be maintained for differential expansion between any two stacks because of temperature changes. (*d*) Trussing with friction damping connections could

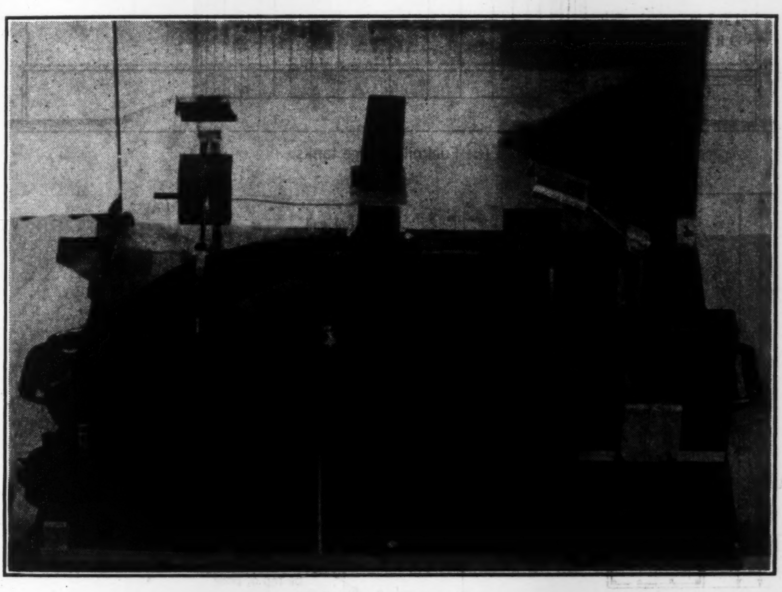

FIG. 10.—SEISMOGRAPH

be used. This method is expensive and would be subject to possible freezing of the moving parts and, hence, ineffective. (*e*) Miscellaneous methods might be devised to prevent the rhythmic formation of the vortices. Such methods are now the subject of a graduate research program at Stanford University (Stanford, Calif.).

The damping principle required the use of the test data previously mentioned. The design procedure in these stacks was more complicated than

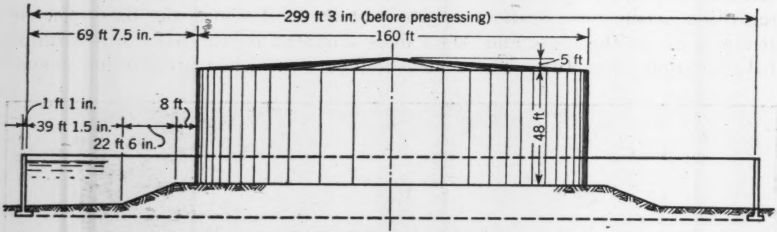
299 ft 3 in. (before prestressing)
69 ft 7.5 in.
160 ft
5 ft
1 ft 1 in.
8 ft
39 ft 1.5 in.
22 ft 6 in.
48 ft

(*a*) Fuel oil storage tanks

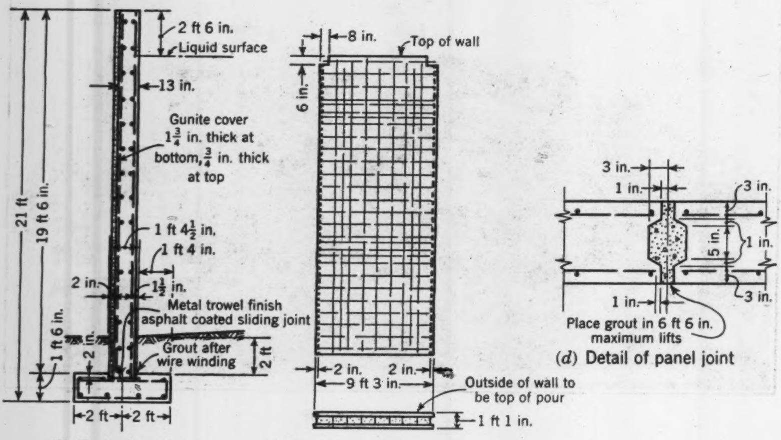
2 ft 6 in.
Liquid surface
13 in.
Gunite cover 1¾ in. thick at bottom, ¾ in. thick at top
21 ft
19 ft 6 in.
1 ft 4½ in.
1 ft 4 in.
2 in.
1½ in.
Metal trowel finish asphalt coated sliding joint
1 ft 6 in.
2 in.
Grout after wire winding
2 ft
2 ft
2 ft
8 in.
Top of wall
6 in.
2 in.
2 in.
9 ft 3 in.
Outside of wall to be top of pour
1 ft 1 in.
3 in.
1 in.
3 in.
5 in.
1 in.
1 in.
3 in.
Place grout in 6 ft 6 in. maximum lifts

(*b*) Typical section (*c*) Typical precast wall panel (*d*) Detail of panel joint

FIG. 11.—FUEL OIL RETAINING WALL

usual for simple stacks. The procedure consisted basically of the determination of (1) the period of the stacks as designed by conventional assumptions, (2) the corresponding resonant wind velocity, (3) the forces or energy imparted to these stacks by the wind, and (4) the amplitude at which the dissipation of energy by base rotation and internal stress friction would be as great as the energy input, beyond which point there will be no increase in amplitude. This procedure requires rather complicated computations, and for a simpler problem such as that presented when stacks are obviously conservatively designed or when stacks are shorter or smaller, this method of computation has been simplified.

Basically, the purpose of the simplified computation is to determine the period of the stack and the resonant wind velocity and to detail the stack in such a way that resonant vibration would not occur at a wind velocity of approximately 40 miles per hr. A simple assumption of a lateral force per impulse is made; a magnification factor of between 15 and 20 is assumed for unlined stacks and a factor of approximately 10 for lined stacks.

FUEL OIL RETAINING WALLS

Retaining walls were required around the fuel oil tanks to provide the customary capacity for retention of oil in the event of tank failure or fire. Because the conditions at the Pittsburg site were congested and because earth fill material was not economically available locally, it was found by a comparison of various types of retaining walls that the most economical, although somewhat unusual, solution would be to use circular rings of prestressed concrete. This usage is a method that has frequently been used on water-treatment tanks and other large concrete tanks such as sewage digesters. It utilizes high-strength steel wire capable of withstanding 175,000 lb per sq in. before permanently stretching. Although leakage was not a serious consideration in these large retention walls, the consideration of economy indicated that prestressing by high-strength wire would be the most desirable type of reinforcing and would also provide a wall free from shrinkage cracks.

FIG. 12.—WIRE STRESSING OPERATION

Another unusual development resulted from the economic investigation. Rather than pouring the circular rings as sectional segments poured in place or as a slip-form type of construction, the rings could be built up as a series of precast flat segments forming a multisided polygon. Because of the large diameter of these rings (300 ft), it was found that flat segments 23 ft 8 in. high by 9 ft 3 in. wide could be satisfactorily erected as "staves" and held in place by the wire wrapping. The resulting section of the wall is as shown in Fig. 11. The joints between the vertical staves were grout filled to provide proper bearing. Gunite protection was placed over the high-strength wire in order to provide protection. The thickness of the wall shown was necessary to resist the compression resulting from tension in the prestressing wires.

The design specified high-strength wires of approximately 200,000 lb per sq in., ultimate strength, to be placed with an initial tension of 140,000 lb per sq in. This initial tension would permit ample margin for decrease of stress due to shrinkage, plastic flow, and yield. The most economical method of placing the wire uniformly was a method involving the use of a carriage (Fig. 12) which traveled around the tank stressing the 0.162-in.-diameter wire by pulling it through a 0.144-in.-diameter die. The machine was supported by cables from a revolving rig on top of the tank and derived motive power from a chain drive. Fig. 12 shows the spreading of wires to miss sleeves and a wire splice at the lower right.

AMERICAN SOCIETY OF CIVIL ENGINEERS
Founded November 5, 1852
TRANSACTIONS

Paper No. 2801

INCINERATION AND ALTERNATIVE REFUSE DISPOSAL PROCESSES

By Ralph Stone[1] and Francis R. Bowerman,[2]
Associate Members, ASCE

With Discussion by Messrs. George R. Thompson; William A. Xanten; Samuel A. Greeley; and Ralph Stone and Francis R. Bowerman

Synopsis

Various refuse collection and disposal systems are studied in this paper. Incineration as a refuse treatment method is critically evaluated—historically, economically, and technically. The results of numerous refuse incineration studies are summarized, and a report is made of investigations on a system of high-rate incineration for optimum volume reduction. The thermodynamic considerations of incinerator design and operation are reviewed.

Introduction

The practicality of a particular refuse disposal system or systems is controlled by three basic factors:

1. The refuse disposal system should be sanitary and enable a nuisance-free elimination of the waste materials. Flies and other insects, rodents, pathogenic organisms, ground-water pollution, and air pollution are examples of health hazards resulting from inadequate refuse disposal.

2. Refuse handling and disposal should be functional and reasonably free from objectionable noise, odor, and effort, thereby obtaining the positive support of the residents in a community.

3. Refuse disposal should be economical within the limitations of high standards of sanitary and esthetic requirements. Fig. 1 represents a simplified comparison of various systems for the collection and disposal of wastes.

Note.—Published, essentially as printed here, in July, 1954, as *Proceedings-Separate No. 471.* Positions and titles given are those in effect when the paper or discussion was approved for publication in *Transactions.*

[1] Cons. Engr., Los Angeles, Calif.

[2] Div. Engr., Los Angeles County Sanitation Dists., Los Angeles, Calif.

INVESTIGATION

The writers were associated in 1951–1952 with the University of California Sanitary Engineering Research Project at Berkeley, studying municipal incineration. This and other investigations on incineration and alternative refuse disposal systems have been performed (1)[3] (2) (3) (4) (5) (6) (7) (8). The purpose of this paper is to present a critical evaluation of data on this subject based on: (*a*) A review of the literature, (*b*) a postal survey of cities utilizing incineration in the United States, (*c*) operational tests on two southern California municipal incinerators to determine the feasibility of high-rate burning, (*d*) field studies on the construction and operational features of numerous plants located throughout the United States, and (*e*) investigations of other systems of refuse disposal.

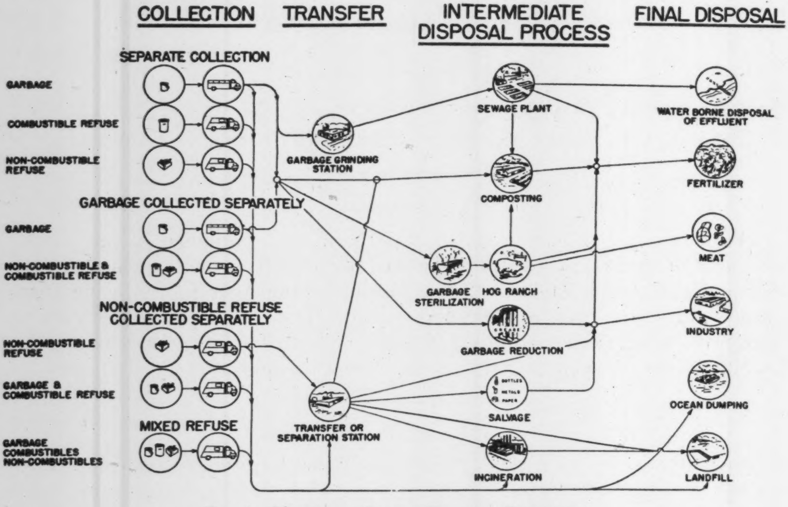
COLLECTION
TRANSFER
INTERMEDIATE DISPOSAL PROCESS
FINAL DISPOSAL
SEPARATE COLLECTION
GARBAGE
COMBUSTIBLE REFUSE
NON-COMBUSTIBLE REFUSE
GARBAGE COLLECTED SEPARATELY
GARBAGE
NON-COMBUSTIBLE & COMBUSTIBLE REFUSE
NON-COMBUSTIBLE REFUSE COLLECTED SEPARATELY
NON-COMBUSTIBLE REFUSE
GARBAGE & COMBUSTIBLE REFUSE
MIXED REFUSE
GARBAGE COMBUSTIBLES NON-COMBUSTIBLES
GARBAGE GRINDING STATION
TRANSFER OR SEPARATION STATION
SEWAGE PLANT
COMPOSTING
GARBAGE STERILIZATION
HOG RANCH
GARBAGE REDUCTION
BOTTLES
METALS
PAPER
SALVAGE
INCINERATION
WATER BORNE DISPOSAL OF EFFLUENT
FERTILIZER
MEAT
INDUSTRY
OCEAN DUMPING
LANDFILL

FIG. 1.—MUNICIPAL REFUSE DISPOSAL PROCESSES

FACTORS INFLUENCING THE QUANTITY OF REFUSE

The completeness and frequency of refuse collection influences the quantity and nature of waste materials. When all refuse is accepted for collection, maximum collections result. Similarly, semiweekly collections of garbage, combustible rubbish, and noncombustible rubbish result in a larger quantity of refuse collected than less frequent collection service. Back-yard pickup, alley pickup, or side-of-the-house pickup tend to produce greater quantities of refuse than does curb placement for collection. Climate, topography, the cultural, economic, and social status of the inhabitants of a community, as well as a community's basic industrial activities, all affect the quantity and nature of the refuse. Fig. 2 presents a graphic summary of quantities of refuse collected at Long Beach, Calif., Fort Worth, Tex., and Dallas, Tex. The information in Fig. 2(*d*) is from a book by Rudolph Hering and Samuel A. Greeley, Hon. M. ASCE (9). The type of collection vehicle used affects the density and, in some cases, the moisture content of the collected refuse. Collection vehicles that compact the refuse tend to make it more difficult to burn or salvage; closed collection vehicles protect rubbish from becoming wet during its collection.

---

[3] Numerals in parentheses—thus: (1)—refer to corresponding items in the Bibliography (see Appendix).

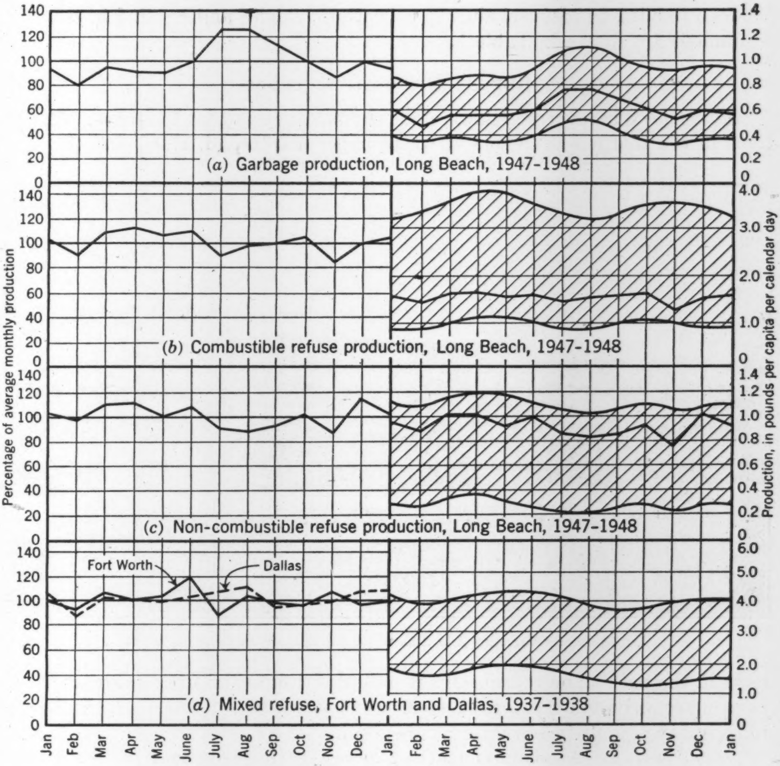

FIG. 2.—SEASONAL VARIATIONS IN REFUSE PRODUCTION

TRANSFER STATION

A flexible method for reducing the costs of transporting municipal refuse is the use of the transfer station. A transfer station should be located in or near the city, convenient to collection routes. The station may be either a simple elevated ramp or a depressed runway which provides the differential elevation for direct gravity discharge of refuse from the collection truck to a transfer truck or trailer. The transfer station may also, if necessary, be an elaborate structure, such as the one in Washington, D. C. (Fig. 3), which provides completely enclosed, dust-free, and odor-free transfer of garbage and ashes. Roll-type steel doors prevent the escape of dust and odors from the station; the interior is vented through activated-carbon filters.

After the refuse has been dumped into the large-capacity truck, trailer, or semitrailer, it can be hauled approximately fifteen or twenty miles before the combined cost of transferring, hauling, and landfilling may exceed the cost of disposal at a central location through incineration. Economic comparisons between hauling to disposal sites in collection vehicles and hauling in transfer equipment are shown in Table 1.

REFUSE DISPOSAL METHODS

Salvage.—Wherever possible, refuse should be reclaimed for reuse. Variations in the free market value of waste paper, cardboard, glass, and tin cans have in the past made refuse salvage a doubtful financial undertaking. However, many private operators successfully contract with cities, thereby directly reducing the quantity of refuse for disposal.

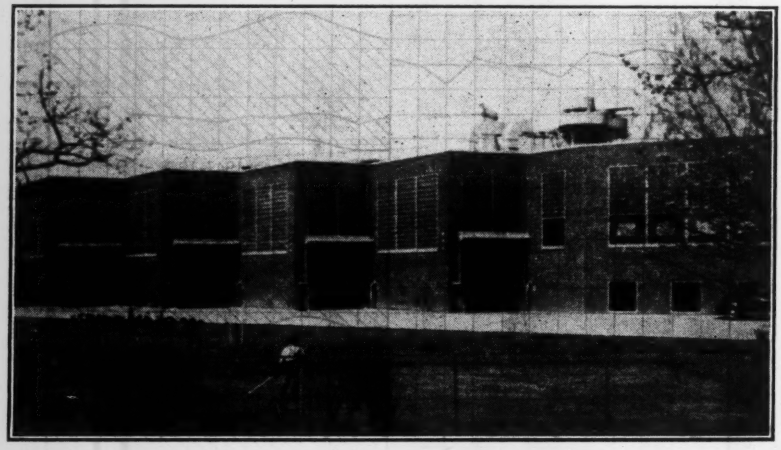

FIG. 3.—GARBAGE AND ASH TRANSFER STATION, WASHINGTON, D. C.

Hog Feeding.—A common method of raw-garbage disposal in the United States is hog feeding. American public health authorities have correctly opposed unrestricted feeding of raw garbage to animals because of the danger of transmission of trichinosis and vesicular exanthema. In England, and recently in the United States, the cooking of the garbage has proved to be a satisfactory method of preparing a homogenous and sanitary animal feed while still providing an economical means of disposing of garbage and conserving food values. Dessication of garbage is another possible method of sanitizing garbage and preparing an animal feed. The effects of boiling citrus peels or other typical American food wastes in preparing a sterile feed for animals remains to be determined.

Composting.—Composting of refuse is now practiced on a wide scale in the Netherlands and other countries. This process has had little utilization for disposal of municipal and industrial refuse in the United States. However, additional experimental work may develop its feasibility.

TABLE 1.—COMPARISON BETWEEN COSTS FOR STRAIGHT HAUL AND FOR TRANSFER AND HAUL

(*a*) COST OF ONE-WAY HAUL IN REFUSE COLLECTION TRUCKS[a]

City[b] designation	Time spent at landfill site (minutes)	Time traveling to landfill and return (minutes)	Round trip (miles)	Minutes per mile	Distance to disposal site (miles)	Cost for haul[c] (dollars)	Cost per ton[d] (dollars)
A	27	23	4.8	4.8	1	0.88	0.32
B	8	17	4.2	4.0	2	1.58	0.58
C	10	62	24	2.6	3	2.28	0.83
					4	2.89	1.05
Average	15	34	11	3.8	5	3.32	1.21
					10	4.73	1.72

[a] Assumptions: Average truck load equals 2.75 tons. Operation, maintenance and amortization of the collection truck, in dollars per hour 1.25
Labor (one driver), in dollars per hour 1.50
Labor (two swampers at $1.25 per hour each), in dollars per hour 2.50

Total, in dollars per hour 5.25
Total, in dollars per minute .... (0.0875)

[b] Hauling data is from three California cities. [c] At $0.0875 per minute; no charge is made for time at the disposal site as the collection truck must also dump at the transfer site when using the transfer method. [d] For a 2.75-ton load.

(*b*) COST OF ONE-WAY HAUL IN A TRANSFER TRUCK OR TRAILER[e]

Distance one way to disposal site (miles)	Time for round trip (minutes)	Cost for haul at $0.0667 per min (dollars)	Cost for 20-min dumping at site (dollars)	Total cost for hauling and dumping (dollars)	Unit cost for haul and dumping (dollars per ton)	Cost of transfer (dollars per ton)	Total cost (dollars per ton)
1	6	0.40	1.35	1.75	0.12	0.40	0.52
2	12	0.80	1.35	2.15	0.14	0.40	0.54
3	18	1.20	1.35	2.55	0.17	0.40	0.57
4	24	1.60	1.35	2.95	0.20	0.40	0.60
5	30	2.00	1.35	3.35	0.22	0.40	0.62
10	60	4.00	1.35	5.35	0.36	0.40	0.76
15	90	6.00	1.35	7.35	0.49	0.40	0.89
20	120	8.00	1.35	9.35	0.62	0.40	1.02

[e] Assumptions: Cost of operating and amortizing transfer stations equals $0.40 per ton. Average transfer-truck load or trailer load equals 15 tons. Operation, maintenance and amortization of equipment, in dollars per hour 2.50
Labor (one driver), in dollars per hour 1.50

Total, in dollars per hour 4.00
Total, in dollars per minute .... (0.0667)

Average travel time equals 3 min per mile, or 20 miles per hour. Average time spent at landfill site equals 20 min.

Garbage Reduction.—Reduction of garbage for salvage of fats has been tried in several cities including Minneapolis, Minn., Rochester, N. Y., Indianapolis, Ind., and Los Angeles. Over a long period of time, these reduction plants have proved financially unsatisfactory. In periods of high fat demand, such as during World War I, operations have been successful. Explosions are a frequent hazard at installations using solvent extractor units.

Land Disposal.—Refuse has been economically disposed of by burial in soil. Historically, use of an open dump, accompanied by burning, was a most obvious means of refuse disposal. The obnoxious odors from the smoldering refuse and the large population of rodents and insects supported by the dump were highly undesirable. More recently, in certain areas the use of controlled burning in which the refuse is carefully ignited, possibly with the use of auxiliary fuel and only when the wind is blowing from the right direction, has been resorted to. The remaining residue and partly burned refuse should be thoroughly wetted prior to ultimate landfill burial.

The controlled-burning dump has the advantage of conserving land burial area.

Sanitary Fill.—The sanitary fill is the most commonly used and satisfactory method of refuse disposal when considered from an economic, esthetic, or sanitary point of view. It can be operated as a fill and cover for ravines, swamps, tidelands, or gulleys, and for cut and cover on level land sites. One of the advantages of sanitary fill is that it is possible to reclaim waste lands for specialized use and to convert them economically to a positive asset. The conversion of refuse fills into parks and airport sites has been a popular feature in many American cities. The gradual settlement of the filled land results in foundation difficulties that demand careful engineering for heavy manufacturing buildings and similar structures; this settlement as well as the generation of noxious gases tends to limit the type of construction satisfactory for reclaimed land. Ashes from incinerators must also be disposed of to the land. Incineration is often considered a means of conserving the available land area by minimizing the volume of waste introduced into the receiving area. In part, burning can be thought of as a treatment method rather than a final disposal method. Where available low-cost land is situated adjacent to metropolitan areas, the sanitary landfill is accepted as an economical and satisfactory means of refuse disposal.

Water Disposal.—The dumping of refuse into water bodies has been a common practice among cities bordering on large bodies of water. New York, N. Y., Oakland, Calif., and San Francisco, Calif., for many years disposed of their refuse into the ocean. Refuse was carried by barges far out to sea before the wastes were dumped. However, in almost all instances, currents carried floatable refuse back to shore, causing nuisances. Furthermore, the cost of transferring refuse to the barges and transporting the refuse far from shore was considerable. The law courts have ruled and economics have proved that water dumping is generally an unacceptable disposal system.

Garbage Grinding.—Garbage grinding, either at the individual homes or in municipal grinding stations, is becoming commonplace. The ground garbage is handled as sewage in the water-carriage system and, because of the small particle size, is collected and disposed of by conventional sewage-treatment methods. The feasibility of economical water carriage of the other refuse components through grinding and discharge to the sewers remains an interesting item for future investigations.

Incineration.—Incineration can be described succinctly as the disposal of the gaseous combustion products and concommitant particulate matter to the atmosphere and the disposal of inert and unburned wastes to the land. Soluble minerals are dissolved by quenching water passing over the ashes or by contact with the ground water. The production of heat energy sustains and is a by-product of combustion.

HISTORICAL DEVELOPMENT OF INCINERATION

The British were the first to develop the high-temperature municipal incinerator and their experience is worthy of careful review (10). In 1874, at Nottingham, England, Alfred Fryer built the first plant designed specifically for disposing of municipal refuse. Mr. Fryer applied for patents on his incinerator, stating the operating principle involved as "charge, or supplying the refuse to the cells at the back and drawing out the clinker—the residuum—at the front." By 1900, more than forty municipal incinerators called "destructors" had been built in Great Britain. In that area the economies of utilization of clinker for construction material, the use of the available heat energy for a source of power, the relatively large Btu-content of the refuse, and the low cost of manual labor promoted the technical development of British incineration practice. At the turn of the twentieth century, incinerators were built with a secondary chamber in which boiler tubes were installed for heat transfer. In 1885, Charles Jones of Ealing, England, obtained a patent for eliminating smoke and odors by using secondary fires in the main flue prior to discharge of the gases through the stack. Subsequent experience demonstrated that the cost of operating the secondary fires was prohibitive, and a simpler solution for stack effluent quality control was to maintain high combustion temperatures in the range of 1250° F to 2200° F, thus enabling control of both odor and smoke and providing more efficient heat transfer. By 1920, the British had operated more than two hundred municipal plants; however, following World Wars I and II, the heat-energy content of the refuse and the value of power produced had so declined that there remain only two important power-generating incinerators operating in the British Isles—at Birmingham and Glasgow. Today, separation of the collected refuse is often necessary in order to remove excessive mineral inert matter so that a sufficient heat energy can be generated to burn the remaining refuse. Recently it was reported that in Great Britain there are thirty conventional-type incinerator plants and seventy separation incinerators. Most of these plants are used to handle very small tonnages. The first separation incinerator was built in 1919, and, with only three exceptions, every British incinerator constructed since that time has been designed as a separation type plant (1). Present-day British refuse disposal is largely achieved by "controlled tipping" (landfill).

The first continental plant was constructed at Hamburg, Germany, in 1896. It was an improved English type of destructor. Incineration has been little used in Europe and other parts of the world. There have been more municipal incinerators built in the United States than in any other country.

INCINERATION IN THE UNITED STATES

Historically, in the United States plentiful low-cost land has been readily available for dumping of refuse because of the dispersed nature of the populace.

Increased urban growth and the development of large municipalities encouraged more complex practices—exemplified by New York City's early barging and dumping of refuse into the Atlantic Ocean.

The first American incinerators were used for garbage disposal because this component of refuse provided the major source of disagreeable sanitary hazards, namely vermin and odor. The first garbage "crematories" were low-temperature burners that often produced both odors and fly ash. They were not economical and usually required auxiliary fuel. The first "crematory" was built in 1885 for the United States Army at Governor's Island in New York City. During the same year, the Rider Company built a municipal garbage crematory at Allegheny, Pa. In the following years Des Moines, Iowa, Elwood, Ind., and Minneapolis constructed plants of varying design, demonstrating such different features as water-jacketed, steel-lined burning chambers and hanging grates. When these plants did not maintain high combustion-gas temperatures, the operating problems were similar to those of the early garbage crematories.

By 1906, a high-temperature, British-type incinerator utilizing forced draft was built at Westmount, a suburb of Montreal, Que., Canada. Variations of the relatively efficient British-made destructors were applied in New York, Seattle, Wash., Milwaukee, Wis., Atlanta, Ga., San Francisco, and many other American cities. Although numerous types of mechanical refuse-charging devices were developed in England, Europe, and the United States, manual charging and stoking prevailed through the 1920's. The modern trend in the United States is toward mechanized charging and stoking and more efficient controls. In the United States the utilization of incineration by-products, namely waste heat and ashes, has never developed as a basic operational factor.

UNITED STATES INCINERATION SURVEY

The writers have undertaken a survey to determine the extent of municipal incineration experience in the United States. It is estimated that approximately 250 cities have in the past built municipal incinerators. Questionnaires were sent to 226 of these municipalities, and of this number 122 replied, using the survey form. Incineration is still used in 82 of the cities that answered, and 40 cities, or approximately one third of these answering, had abandoned their plants. Possibly many of the small communities that were questioned did not reply because they had abandoned their plants. Of the 106 cities described in the 1950 United States census as containing a population of 100,000 or greater, 69 cities are listed as having used municipal incineration at some time in their history. Of these, 53 replied to the survey questionnaire, indicating that 33 still utilized incineration (nine cities conserving part of the waste heat) and that the other twenty cities had abandoned their plants in favor of landfill. There are 17,452 incorporated cities in the United States with populations of 99,999 or less. Of the 122 communities that replied to the questionnaire, 82 still used their plants and 40 had abandoned them. Evidently, a much smaller percentage (1.3%) of the smaller cities have municipal incinerators (Fig. 4) than do the larger communities (65%).

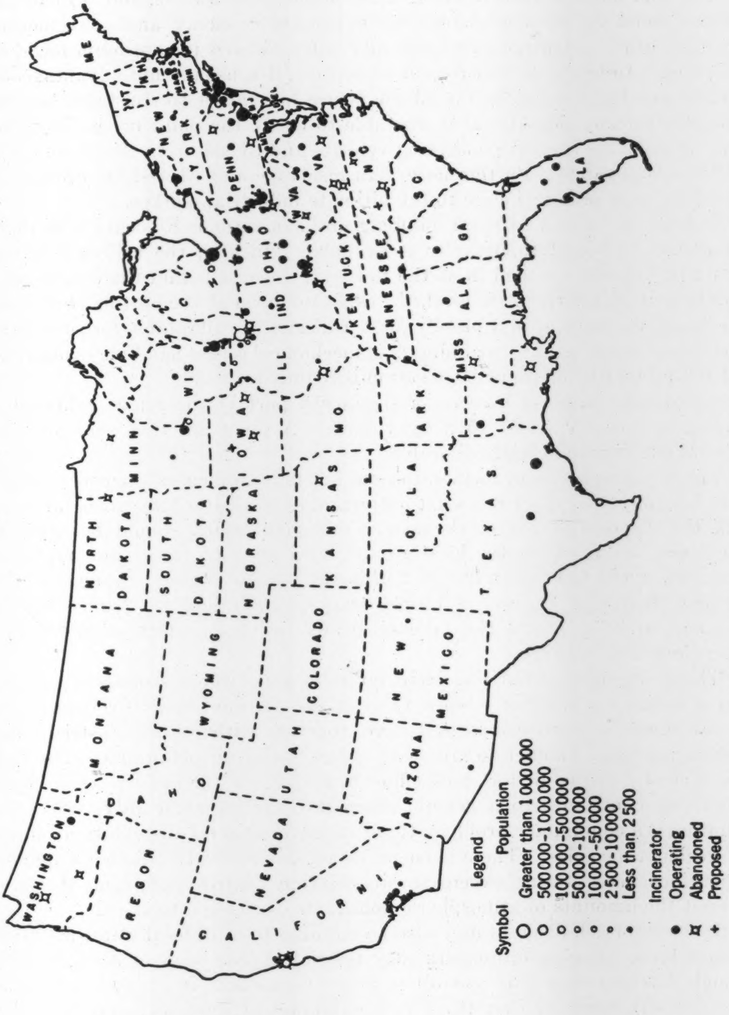
Symbol
Legend
Population
○ Greater than 1 000 000
○ 500 000-1 000 000
○ 100 000-500 000
○ 50 000-100 000
○ 10 000-50 000
○ 2 500-10 000
• Less than 2 500
Incinerator
● Operating
¤ Abandoned
+ Proposed
WASHINGTON
OREGON
CALIFORNIA
NEVADA
IDAHO
MONTANA
WYOMING
UTAH
ARIZONA
COLORADO
NEW MEXICO
NORTH DAKOTA
SOUTH DAKOTA
NEBRASKA
KANSAS
OKLA
TEXAS
MINN
IOWA
MO
ARK
LA
WIS
ILL
MISS
MICH
IND
KENTUCKY
TENNESSEE
ALA
OHIO
GA
FLA
SC
NC
VA
W VA
PENN
NEW YORK
VT
NH
ME
MASS
CONN
RI
NJ
DEL
MD

FIG. 4.—LOCATION OF EXISTING, ABANDONED, OR PROPOSED INCINERATORS IN THE UNITED STATES

LOCATION OF INCINERATORS

Generally accepted criteria for choosing an incinerator location have been: (*a*) The land must be readily available or municipally owned; and (*b*) hauling distance must be at a minimum for maximum economy and convenience. However, other important factors should be considered for optimum location of a plant. In the largest metropolitan centers, it is usually not advantageous to build one big incinerator for all the refuse but rather to construct smaller units strategically placed. It is desirable to locate the plant in an industrial area, where odors from the collecting vehicles and fly ash from the plant cause the least annoyance. Furthermore, refuse salvage and waste-heat utilization should be more practical close to the ultimate industrial market.

Another important factor in building an incinerator is to locate it so that, if possible, two-level topography is available. Ideally, the collected refuse should be directly dumped in at the top level, burned within the combustion chambers at an intermediate level, the ashes removed at the bottom elevation, and finally disposed of in a nearby pit. Hillsides are adaptable for such two-level construction. Thus, a minimum of mechanical refuse-handling equipment and ramp building or tunnel excavation is required.

Ash-residue disposal involves a significant part of the refuse collected—ranging between 5% and 45% by volume. A plant situated near an ash-disposal site is economically desirable.

The topography of an incinerator site not only influences the construction costs but may also affect the wind pattern; downdrafts in hilly areas interfere with the disposal of the stack gases. The plant stack should be between 100 ft and 200 ft above the local ground level so as to (*a*) obtain improved draft and avoid the possibility of flashbacks due to pressure changes in the burning chambers, (*b*) assure proper stack-gas dilution, (*c*) reduce fly-ash nuisance, and (*d*) utilize the psychologically beneficial effect on the public of an elevated discharge.

The desirability of building incinerators in areas where atmospheric pollution is already a problem is open to question. Atmospheric inversions may permit smoke concentrations that may, together with other industrial combustion products, blanket an area with objectionable air pollutants. The lack of sufficient diluting air for stack effluents may cause the incinerators in such regions to contribute to a general smog problem. Significantly, where air pollution is a community problem, there are governmental air-pollution control enforcement agencies. These agencies establish incinerator stack-gas quality regulations necessitating expensive air-pollution control equipment designed to limit the amounts of atmospheric pollutants discharged to the air.

Incinerator-ash disposal may also be required to meet local water-pollution control laws. Zoning ordinances may restrict the location of a plant. Although it is true that it is possible to place incinerators in expensive, totally-enclosed structures so that there is a minimum of nuisance, movements of heavy collection vehicles on the streets and some noises and odors cannot be avoided.

BY-PRODUCT HEAT

Most American refuse contains an average calorific content of between 3,500 Btu and 4,500 Btu per pound. This amount of heat energy will vaporize from 3 lb to 4 lb of water into steam. In practice, incinerators have been able to produce between 1½ lb and 2½ lb of steam per pound of refuse burned. In addition to supplying utilizable heat, refuse must first produce the heat energy required for (*a*) maintaining combustion gases and incinerator refractories at high temperatures, (*b*) vaporization of the moisture present in the refuse, (*c*) raising the temperature of freshly introduced refuse to the kindling point, and (*d*) preheating draft air.

BY-PRODUCT ASH

Ashes and clinker have been used to a limited extent in the United States for road building and light-weight concrete manufacture. Complete but uneconomical high-temperature burning is required in order to obtain an organic-free ash suitable for such use. Ashes have also been used for fertilizer, and fly ash from the secondary chamber may be used as an inert base in the preparation of insecticides and other powder-base industrial products. Tin cans, salvaged either before or after partial burning, constitute another waste product that is sometimes profitable in conjunction with normal plant operation. Altanta, Beverly Hills, Calif., Los Angeles, and Miami, Fla., are examples of cities where salvage is utilized.

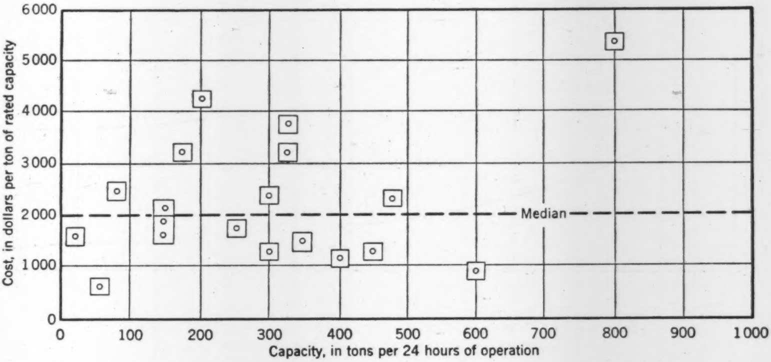

FIG. 5.—COST OF MUNICIPAL INCINERATOR CONSTRUCTION REDUCED TO 1950 LEVEL

Atlanta.—Burned tin cans from the incinerator are salvaged for use in local foundries.

Beverly Hills.—Cardboard cartons and paper are salvaged for paperboard processing. Cans and bottles are separated and salvaged.

Los Angeles.—Tin cans are processed by controlled burning for use in copper mining. Bottles and glass are salvaged for direct reuse or melted and remolded. More than thirty cities in the Los Angeles metropolitan area practice salvage.

Miami.—Burned tin cans from the incinerator are salvaged for foundry use.

COSTS

Typical costs of municipal incinerator construction and maintenance and operation charges are graphically summarized in Figs. 5 and 6, respectively.

In Fig. 5, each symbol represents the original construction cost of existing incinerators, reduced to the 1950 level by use of the *Engineering News-Record* building index. For Fig. 6, fixed charges are based on an initial construction cost of $2,000.00 per rated ton of capacity, amortized over 20 years at an interest rate of 3%. The current trend has been toward construction costs of greater than $2,000 to $4,000 per ton of rated 24-hr burning capacity. Incineration of refuse is a relatively expensive process, and even with economical installation the costs are generally more than $2.00 per ton of refuse burned. Costs as great as $4.00 or $5.00 per ton for burning refuse have been reported by city engineers maintaining complete and accurate records. Air-pollution control equipment may increase future incineration construction and operation costs.

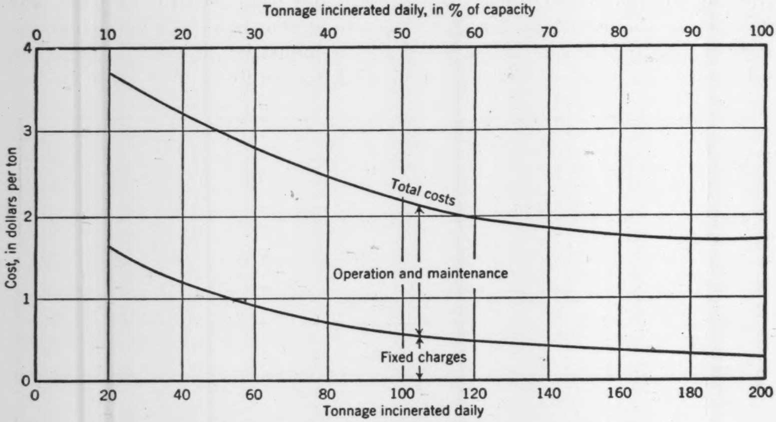

FIG. 6.—THE INFLUENCE OF PERCENTAGE UTILIZATION OF CAPACITY ON ESTIMATED COSTS FOR MUNICIPAL INCINERATION

INCINERATOR COMPONENTS OF CONTEMPORARY PLANTS

Weighing.—In large-capacity installations, it is desirable to use recording platform scales which operate semiautomatically and are able to weigh and record from sixty to seventy refuse trucks per hour with minimum standing time. The plant should accomodate a straight-line movement; that is, after the refuse is weighed, the truck should be driven forward to the dumping floor—avoiding, if possible, any necessity to back out so that it may return to the collection route rapidly. The weighmaster should keep careful weight records, classifying the loads whenever possible.

After weighing, the weighmaster should direct the truck driver to a dumping point so chosen that the heat energy of refuse charged to the incinerator furnace will be maintained as constant as possible, and the materials handling will be at a minimum.

Unloading.—Many incinerators operate from four hours to eight hours per day with refuse unloading in proximity or directly into the primary, or furnace, chamber. In such installations, no provision is made for storage of the unloaded refuse. This procedure is often unsatisfactory because the plant cannot be maintained in a clean, sanitary condition when refuse is piled on the dumping floor. On the other hand, where storage pits are used, considerable expense is introduced through the use of overhead monorail or bridge cranes to charge the refuse into the furnace. One disadvantage of directly charging the refuse from the collection truck into the primary chamber is that it is impossible to maintain continuous, small-volume charging. When using the batch process, the furnace is either underloaded or overloaded. At Pasadena, Calif., a small 80-cu-yd storage bin is emptied by an endless movable metal belt, approximately 15 ft. wide, which feeds refuse into the burning chamber efficiently and almost continuously.

Charging Inlet.—The charging gates in most modern plants may be operated hydraulically, pneumatically, or electrically. The charging inlet may vary in size from less than 4 ft by 6 ft to as much as 5 ft by 15 ft. Observations on many municipal incinerators indicate that the air introduced into the furnace through the charging gate during charging does not seriously deter the burning process because the fresh refuse requires additional oxygen and the differential gas pressure at the inlet is slight. Large inlets with wing-wall entrances are desirable so that tree stumps, boxes, and other refuse which would otherwise require considerable labor to reduce their size may be fed into the incinerator (Fig. 7).

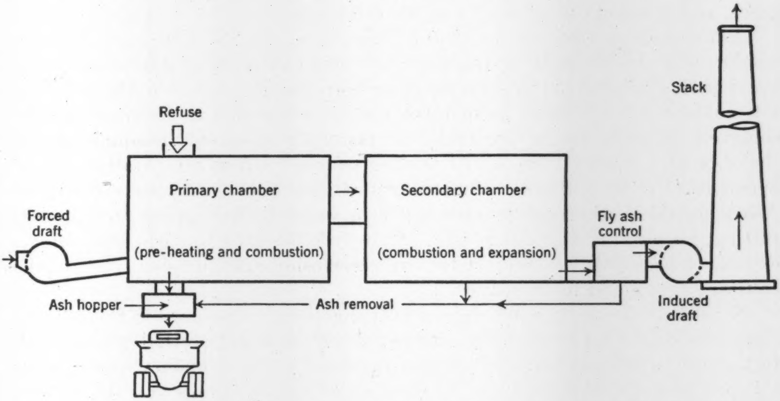

FIG. 7.—SCHEMATIC DRAWING OF AN INCINERATOR

Primary Chambers.—The primary burning chamber confines the combustion and enables drying and burning of refuse. An efficient plant will provide a maximum of predrying with the aid of the waste heat otherwise discharged to the atmosphere. For optimum burning, the furnace should allow both the continuous feed of refuse to the burning hearth and the removal of the remaining residue and ashes.

A common type of mechanically-stoked furnace utilizes a rotating rabble. Use of the rotary-kiln furnace is another method of reducing labor expense for stoking and ash disposal; unfortunately, it is an expensive structure to build. An additional type of modern primary chamber is the suspension grate, which provides two burning surfaces in the primary chamber. The suspended grate acts as a drying hearth where the fresh refuse is desiccated before being dropped to the burning grate and stoked for ash disposal. Traveling grates and movable pallets are types of continuous metallic belts adapted from coal-burning practice.

Forced draft is often provided by blowing in (*a*) air at atmospheric temperatures, (*b*) steam-heated air, (*c*) recuperator-heated air, or (*d*) partly recirculated combustion gases. The partial recirculation of heated gases has proved to be economical. Chamber and gas temperatures can be controlled with forced draft to implement high burning rates. When furnace temperatures are too high, additional cold air may be introduced to reduce the burning environment to the desired temperature; on the other hand, when primary burning-chamber temperatures are too low, auxiliary fuel, recirculated gases, and reduced forced draft may be necessary.

Ash storage may involve mechanical devices to collect the primary chamber residue and discharge it by gravity into some disposal system. As noted previously, conventional incinerator operation produces between 5% and 45% ash content by volume. Incinerator residue removal can be mechanically achieved through use of hydraulic or manually operated dumping grates, shaker grates, rotary kilns, and traveling pallets. Often comparatively large openings (4 ft by 8 ft) for easy removal of incinerator residue are desirable. Ashes should be thoroughly quenched in a water bath or spray to eliminate further burning at the dump site. Conveyer systems for ash removal are expensive to install, are subject to severe corrosion and abrasion, and require constant repair and maintenance.

Secondary Chambers.—When heat exchangers are introduced in the primary chambers they tend to cool the combustion environment so that it is difficult to maintain optimum burning. Other reasons for the secondary chamber are the promotion of the complete combustion of burning gases and the settling of fly ash. A crematory door for small animals and a fly-ash cleanout are usually provided in the secondary chamber. In incinerators operating at less than rated capacity it has been noted that the temperatures in the secondary chambers are usually from 100° F to 300° F lower than the temperatures in the primary or burning chamber; however, in incinerators operating at capacity or at greater than rated capacity, it has been noted that the gas temperatures in the secondary chamber are as much as 400° F higher than in the primary chamber.

FURTHER COMPONENTS

Blowers, fans, flues, particulate-matter control devices, and the stack are additional plant appurtenances. Because the primary and secondary chambers require a negative air-pressure head of from 1 in. to 4 in. of water for proper operation, it is necessary that the flues and stack be designed to permit correct gas flow. The negative air-pressure head enables the introduction of overfire air and underfire air into the burning chambers without flashback through the charging doors. Stacks are often used to produce the negative pressure head, although induced-draft fans are becoming increasingly common.

PARTICULATE MATTER AND STACK GASES

Particulate matter may be removed from the combustion gases through the medium of (*a*) baffle chambers, (*b*) gas-expansion chambers and sedimentation chambers, (*c*) complicated duct work, (*d*) cyclone precipitators, (*e*) dynamic centrifugal precipitators, (*f*) sonic glomerators in conjunction with cyclonic precipitators, (*g*) a wet chamber using a water bath or water spray, (*h*) bag filters made of steel or glass mesh, and (*i*) electrostatic precipitators. However, control of particulate matter is costly, and the finer particles are not completely removed by even the best processes. Tests of stack gases indicated that fly ash may represent as much as 1% by dry weight of the total ash produced. Large burning fly-ash particles may cause fires in the surrounding area in addition to settling out as an objectionable coating that litters the neighborhood and produces complaints from the citizenry.

Flues may transmit the burned gases to the stack with velocities of from 5 ft per sec to 25 ft per sec. In these flues there should be such instruments as thermocouples for temperature recorders, carbon dioxide recorders, and smoke recorders. Each component of the plant should have adequate automatic recording instruments so that maximum supervision of plant performance can be maintained. Carbon dioxide, it should be noted, is a reliable criterion of the air-to-fuel ratio and, in conjunction with the burning temperature, can be used as a general criterion for plant combustion efficiency. With high concentrations of CO_2, low air-to-fuel ratios prevail and high temperatures may exist, perhaps indicating the need for additional air in the primary chambers. When the inverse is true, excess air should be reduced.

An incinerator discharges small quantities of gases such as aldehydes, oxides of nitrogen, and sulfur dioxide. The presence of partly oxidized gases is a result of incomplete combustion. It is not reasonable to expect that complete oxidation will occur at all times in the burning process because chemical-thermodynamic reactions cannot practically be expected to go to completion during the time the gases are retained in the incinerator. The concentration of particulate matter and gases present in stack effluents can be reduced by blowing diluting air in at the base of the stack; however, this does not reduce the original weight of fly ash and combustion gases discharged into the air but merely represents dilution. A combination of carefully designed burning and expansion chambers, baffle walls, checker flues, and particulate-matter control systems is needed to maintain fly-ash and stack-gas quality within workable limits.

REFRACTORIES

Refractories are fire brick made from heat resistant clay and minerals. Refractories capable of withstanding extremely high temperatures and resisting thermal expansion and contractions contain a large percentage of alumina. The alumina-silica refractory may consist of between 15% and 90% of alumina; generally, the higher the content of alumina, the better the refractory quality and the greater the resistance of the refractory to thermal shock. Silica has the undesirable characteristic of a high coefficient of expansion between the temperatures of 200° F and 300° F. As a result of this expansion, considerable spalling will be present when high-silica refractories are used in the incinerator. Refractories can be purchased and installed either as bricks or as plastic. The bricks require masonry construction and the plastics are tamped in place using forms (Fig. 8). Bricks are burned in the manufacturer's kiln, but plastic refractory material consisting of essentially the same chemical composition as the brick is burned in place in the incinerator. The plastic refractory should be carefully burned-in to develop ceramic bond strength. Both constructions have been observed to be satisfactory. Plastic material can be readily used for repair of burned-out refractories. Continuous 24-hr high-temperature burning is more desirable for refractories than intermittant cooling and heating caused by 8-hr-per-day operation.

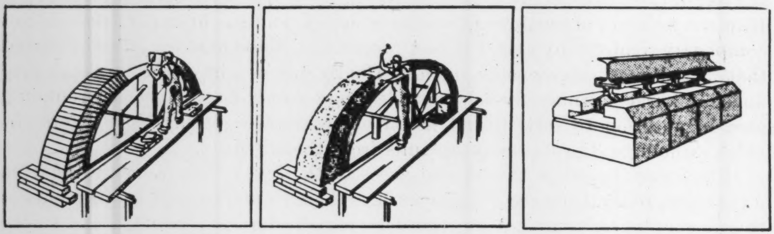

Arch-brick construction

Plastic-arch construction

Suspended, or flat-arch construction

(*a*) Ceiling construction

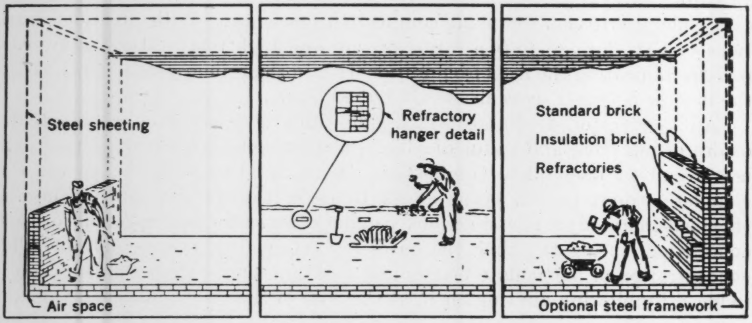

Troweled-brick construction

Plastic construction

Dipped-brick construction

(*b*) Refractory construction practices

Fig. 8

Laboratory Control

A simple laboratory for control tests is a necessity for any incinerator. Incineration should be a rigorous engineering activity rather than a confused art. Highly qualified engineering personnel capable of operating a control laboratory should be a mandatory personnel feature in the operation of future incinerators. Certainly an investment of from a half million dollars to five million dollars for an incineration plant justifies the work of able technical personnel and the use of advanced scientific controls.

RATING INCINERATOR CAPACITIES

Recent field tests on two mechanically-stoked municipal incinerators in southern California demonstrated some interesting possibilities for re-evaluating incinerator performance. Unfavorable economic comparison with cheaper landfills requires a revision in the approach to incineration to establish more realistic design criteria.

The primary reason for the incineration of combustible rubbish is the desire to reduce to a minimum the volume of material which must ultimately be buried. If garbage is to be disposed of, incineration is a method of eliminating the putrescible nature of the refuse. Incineration should be recognized as but one of several alternative steps in the treatment of refuse prior to ultimate disposal; it serves principally as a means of prolonging the use of landfills and permits a wider selection of land areas for final residue burial.

ASH QUALITY

Obviously, to produce an ash suitable for salvage requires that the rubbish be almost completely burned. This involves very high temperatures and prolonged periods of flame contact, dictating a need for relatively large, expensive structures. As most incinerator ashes are buried and not used, it is in the interest of economy to determine the optimum—not maximum—volume reduction to be achieved by burning.

VOLUME REDUCTION

The reduction in volume accomplished during the initial brief exposure to radiant heat and burning flame represents a significant volume reduction. During the first ten minutes of burning (excluding installations burning wet garbage and sewage sludge) a far greater volume reduction occurs than during the following ten-minute interval, with progressively less volume reduction during each subsequent ten-minute increment.

In a mechanically-stoked, primary burning chamber almost all the large-surface-area, low-density material such as loose paper, leaves, and readily volatile components in the refuse may be oxidized by flash burning. To burn thick tree branches and similar heavily insulated objects requires considerably longer contact time. To remove the final 5% of the unoxidized components may require a burning process fully as extensive as that required for oxidation of the first 95%. Hence, an incinerator that is forced to burn refuse to the point where less than 1% unoxidized material remains in the ash residue (a fairly common acceptance-test requirement) accomplishes relatively little volume reduction in the final burning stages.

APPEARANCE OF HIGH-RATE BURNED RESIDUE

Partly burned refuse requires more care in handling and disposal than does well-oxidized incinerator residue. Not only are the partly burned paper, tree limbs, and similar material unsightly and odorous, but because of the organic content they must be treated as though they constituted crude rubbish being disposed of at a landfill. However, if the residue is buried with the proper sanitary landfilling techniques, the ultimate result will be economical, sanitary, and esthetically acceptable. The less dense components having been eliminated, the remaining partly burned residue can be compacted so as to minimize subsequent settlement.

Appurtenances for ash storage and ash removal in an incinerator designed to achieve optimum volume reduction must be designed to handle the greatest volume of ashes produced and to discharge the larger objects in the residue so as to avoid clogging. Partly burned refuse must be thoroughly quenched to prevent the continued burning of the organic matter in transport and at the landfill.

TEMPERATURE OF COMBUSTION

The factor that governs the chamber temperature is the rate of heat release. When an incinerator is operated at less than design capacity, there may not be sufficient heat released to raise the temperatures of the refractory wall and the combustion gas to the range of between 1200° F and 2000° F; however, this does not mean that combustion is incomplete as long as released gases do not cool so quickly as to cease burning. Conversely, it is possible to "overload" an incinerator far beyond its design capacity without refractory temperatures rising beyond a reasonable limit. This condition may be accomplished by introducing air and rubbish so rapidly that large quantities of heat energy are used in raising the temperature of the refuse to the kindling point while the gases are vented through the incinerator stack.

DESIGN CONSIDERATIONS

To achieve the optimum rate of volume reduction, the raw refuse should be introduced continuously and exposed to flames or chamber temperatures sufficiently hot to dry and kindle it. Following initial burning, the refuse must be given sufficient grate area and adequate agitation with air so as to burn in turbulent suspension (11) and to avoid being smothered with new refuse; otherwise, the combustion process may be slowed down instead of accelerated. The partly burned, high-density residue should then be quickly removed from the primary burning chamber to prevent the clogging of grates as clogging reduces the inflow of under-grate air needed to sustain the rapid burning of loose and volatile combustibles in the freshly introduced refuse. Over-all incinerator burning temperatures in the range of 2000° F, although resulting in slag formation, obviously promote high combustion rates and should be attained when feasible.

Conveyor charging can approximate continuous feeding; rotary kilns or traveling grates provide maximum control over the length of the burning period.

PRINCIPLES OF COMBUSTION

In order to understand the fundamental operation of a refuse incinerator, it is desirable to review some of the basic requirements for self-sustained combustion of refuse in an incinerator.

Combustible Refuse.—Combustible refuse consists of such common organic compounds as grass, tree trimmings, paper, cartons, carpets, rags, rubber, garbage, petroleum products, ash from hard fuels, and similar wastes. Chemically, the wood and paper refuse is largely cellulose and lignin. The heat-energy value of the combustible materials can be determined accurately in a bomb calorimeter. When the particular heat value of the combustibles are known, an accurate prediction of the available heat energy can be made on the bases of percentage moisture and percentage of inert material present (Fig. 9). Representative calorimeter measurements of the heat energy of refuse samples are listed in Fig. 9. The percentage of inert matter is equal to the weight of inert matter divided by the weight of the raw sample and multiplied by 100.

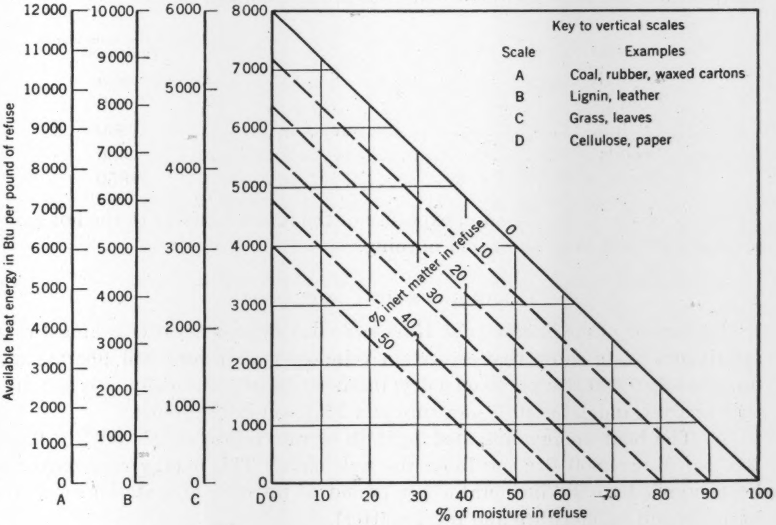

FIG. 9.—RELATIONSHIP BETWEEN HEAT ENERGY AND MOISTURE CONTENT AS A FUNCTION OF THE INERT MATTER IN THE RAW REFUSE

Similarly, the percentage of moisture is the ratio of the weight of water to the weight of raw refuse times 100.

Example Involving Fig. 9.—Calorimeter tests on a refuse sample show a dry, inert-free fuel value of 6,000 Btu per lb. Further analysis of the same sample indicates that 20% of the sample is inert matter and 30% is water. The point of intersection of the 30% moisture line and the 20% inert line is followed horizontally to the left where on scale C (based on 6,000 Btu per lb) is read the available heat energy: 3,000 Btu per lb.

Burning Process.—From physical and chemical analyses of the material to be burned, one can compute the weight and volume of ashes and gases which will result from combustion within the incinerator. Raw material should be introduced into the primary burning chamber with a minimum of handling. Cutting of the refuse increases the operating costs and should be avoided.

Refuse introduced into the primary chamber is exposed to hot burning gases and radiant heat emanating both from the refuse fire and the refractory walls. The refuse is dried and the excess moisture is evaporated; subsequently, the steam is drawn off with the combustion gases. The flame temperature of the burning refuse may be as high as 3000° F.

The greater the ratio of surface area exposed to the drying environment the more rapid will be the drying. The radiant heat from the refractories and the flame temperature of the burning refuse supplies the heat energy to the gases in the incinerator. The speed of drying is increased when make-up air is preheated and is moving rapidly. New burning surfaces burst into flame at the ignition-point temperature of the refuse material. The ignition-point temperatures for some common materials are as follows:

Material	Temperature, in degrees Fahrenheit
Asphalt	535
Coal gas	1100
Carbon	1300
Wood	350
Paper	350

Agitation of the raw refuse and exposure of the refuse surfaces to the hot gases promote quick drying and rapid burning.

THERMODYNAMIC COMPUTATIONS

Preliminary Computations for Mass and Heat Balances.—It is assumed that calorimeter tests show that a certain cellulose-type refuse will liberate approximately 9,600 Btu per lb on a dry, inert-free basis. Secondly, it is assumed that analysis indicates 40% moisture and 10% ash in the refuse:

A. The heat energy liberated by 1 lb of raw refuse equals 50% × 9,600 Btu per lb or 4,800 Btu per lb on the wet basis. This energy represents the heat supplied to the incinerator per pound of introduced material on a wet basis (including moisture and inert matter).

In the burning process, heat is expended through (*a*) the stack gases, (*b*) the refractories by conduction, and (*c*) the ashes. The moisture content of the refuse was experimentally determined to be 40%; therefore, 1 lb of raw refuse × 40% = 0.4 lb of water in the refuse. A relative humidity of 50% at 68° F is assumed in the air. There are approximately 40 grains of water per lb of this air. It is assumed that the oxygen in the air is chemically combined with the refuse and that this refuse is $C_6H_{10}O_5$ (cellulose).

B. The process may be stated:

$$C_6H_{10}O_5 + 6\,O_2 = 6\,CO_2 + 5\,H_2O + 4{,}800 \text{ Btu of energy (for } \tfrac{1}{2} \text{ lb of dry fuel)}$$

C. Molecular weights:

$$162 + 192 = 264 + 90$$
$$0.50 \text{ lb} + 0.59 \text{ lb} = 0.82 \text{ lb} + 0.28 \text{ lb.}$$

From this reaction it is determined that 0.59 lb of oxygen or 2.57 lb of air are needed to oxidize 0.50 lb of cellulose. Assuming that 200% excess air is used, 7.71 lb of air are blown into the primary chamber, per pound of refuse.

C. Moisture in the air equals 40 grains per lb of air, which when divided by 7,000 grains per lb of water and multiplied by 7.71 lb of air indicates that 0.04 lb of water are blown into the primary chamber, per pound of refuse.

D. The weight of water discharged in the stack gases is as follows:

Source	Weight of water, in pounds per pound of refuse
Refuse	0.40
Air supply	0.04
Formed through oxidation	0.28
Total	0.72

E. It is assumed that gas temperatures in the stack are maintained at 600° F by a heat exchanger or heat transfer which absorbs heat energy not used otherwise. These values are approximated as follows:

(*a*) The heat required to bring water to a boiling point is: $0.72 \times (212° \text{ F} - 60° \text{ F}) \times 1.0 = 110$ Btu (assuming the average specific heat to be 1.0).

(*b*) The approximate heat required to evaporate water to steam is: $0.72 \times 975 = 700$ Btu.

(*c*) The heat required to raise steam to 600° F is: $0.72 \times (600 - 212)\ 0.5 = 140$ Btu (assuming the specific heat of steam to be 0.5).

(*d*) The total heat needed to raise water to 600° F is approximately: $110 + 700 + 140 = 950$ Btu.

F. The specific heat of air, including CO_2, is assumed to equal 0.25. Then the heat needed to raise stack gases to 600° F will be:

(*a*) With 200% excess air, the total weight of gases is 7.71 lb of air minus 0.59 lb of oxygen plus 0.82 lb of carbon dioxide, which equals 7.94 lb. Thus, the heat required is: $7.94 \times (600 - 60) \times 0.25 = 1{,}072$ Btu.

(*b*) With 50% excess air, the total weight of gases is 3.85 lb of air minus 0.59 lb of oxygen plus 0.82 lb of carbon dioxide, which equals 4.90 lb. Thus, the heat required is $4.90 \times 600 \times 0.25 = 660$ Btu.

G. The heat loss due to incomplete combustion is, on the basis of the calorimeter tests and analysis of the refuse: $0.02 \times 0.5 \times 9{,}600 = 96$ Btu.

H. It is assumed that the average temperature in the ash and clinker is 500° F. The specific heat of the residue equals 0.20. The residue represents 12% of the original weight of the material. Therefore, the heat loss of the hot residue is: $0.12 \times 1 \times (500 - 60)\ 0.2 = 13$ Btu.

I. From incinerator tests, it is assumed that 5% of the heat from a pound of raw refuse is lost to refractories. This loss is $0.05 \times 4{,}800$ Btu, or 240 Btu.

Heat-Energy Balance.—The heat energy available per pound of raw refuse is 9,600 Btu × 0.5, or 4,800 Btu.

J. Summary:

Heat-energy uses	Energy, in Btu (200% excess air)
Moisture (600° F)	950
Gases (600° F)	1,072
Hot residue	13
Incomplete combustion	96
Other losses	240
Total	2,371

K. The excess waste-heat energy is the total energy available minus the total energy used, or: 4,800 − 2,371 = 2,429 Btu per lb of waste material. Thus, one can compute that 2,429 Btu are available for external heat utilization per pound of raw refuse introduced. It is possible to determine how much steam can be produced for generating power or other uses. Assume that approximately 1,200 Btu are needed to convert 1 lb of water to steam.

L. Water that could be converted to steam (assuming 100% efficiency) equals

$$\frac{\text{Excess waste heat, in Btu}}{\text{1,200 Btu per lb}} : \frac{2{,}416}{1{,}200} = 2.01 \text{ lb.}$$

Effect of Excess Air in Cooling the Primary Chamber.—The heat energy needed to raise the air temperature in the primary chamber to 1300° F can be computed as follows:

M. Using 200% excess air, 7.71 (1300 − 60) 0.25 = 2,390 Btu.

N. Using 50% excess air, 3.85 (1300 − 60) 0.25 = 1,190 Btu.

Primary-Chamber Temperatures.—To approximate the gas temperatures in the primary chamber the procedure in Table 2 may be followed.

O. The last column of Table 2 shows chamber temperatures for 200% excess air and for 50% excess air. After the approximate primary-chamber temperature is known, it is possible to recompute the energy balance for this condition. The mathematical summary of the heat energy used and the heat energy available should balance and be equal when the correct primary-chamber temperature has been used.

Heat Energy Required to Bring Refractories up to Operating Temperature.—Thermodynamic computations can be made to determine the heat energy required to raise the temperatures in the primary furnace to an operating temperature of 1300° F by means of the following equation:

P. Heat energy = specific heat × mean temperature increase × weight of furnace refractories.

Assuming a specific heat of 0.28, the mean temperature, in degrees Fahrenheit, is: 1300 − 60 = 1240. The average temperature increase, in degrees Fahrenheit, is: 1240/2 = 620. The refractory-wall thickness is 9 in. The volume of refractories in a primary chamber having a 1,000-ft surface area and a 9-in. thickness is 750 cu ft of refractory material. If this material weighs 140 lb per cu ft, the heat energy is: 0.28 × 620 × 750 × 140 = 18,000,000 Btu (heat energy from approximately 1.8 tons of raw refuse material).

Heat Energy Transferred by Refractories.—It is possible to compute the heat losses as a result of the transfer of heat through the refractory. For example, the heat losses as a result of the heat transfer in the primary chamber can be computed as follows:

TABLE 2.—COMPUTATION OF PRIMARY-CHAMBER TEMPERATURES

Gas	Weight[a]	Specific heat[b]	Weighted specific heat[b,c]	Average temperature increase[d,e]	Approximate primary-chamber temperature[d,f]
(a) 200% EXCESS AIR					
Air	7.12	0.25	1.78	1050	1650
CO_2	0.82	0.22	0.18		
H_2O	0.72	0.50	0.36		
Total			2.32		
(b) 50% EXCESS AIR					
Air	3.03	0.25	0.76	2180	2780
CO_2	0.82	0.22	0.18		
H_2O	0.72	0.50	0.36		
Total			1.30		

[a] In pounds per pound of refuse. [b] In British thermal units per pound per degree Fahrenheit. [c] The heat energy required to raise the products of combustion from 1 lb of refuse 1° F. [d] In degrees Fahrenheit. [e] Available waste-heat energy (item K) divided by total weighted specific heat. [f] The average temperature increase plus 600° F equals the approximate primary-chamber temperature.

Q. If the conductivity constant at 1300° F is 10 and if the temperature of the cold face is 150° F, the heat-transfer rate is: $10\,\frac{(1300 - 150)\,1{,}000}{9}$ $= 1{,}280{,}000$ Btu per hr (heat energy from approximately 250 lb of raw refuse material).

Cooling Effect of Raw Refuse Introduced into the Primary Chamber.—The introduction of raw refuse into an incinerator fire causes an initial cooling effect. The new fuel, before it can release any heat by its own combustion, must first be warmed to its ignition temperature. This temperature will usually vary between 500° F and 1300° F, depending on the characteristics of the refuse. A room temperature of 60° F and a furnace temperature of 1300° F are assumed. The specific heat of the refuse can be considered to be 0.25. The moisture in the refuse is 40%. If a 1-lb charge is fired, computations R, S, and T follow.

R. The heat needed to heat the refuse is: $0.6\,(1300 - 60)\,0.25 = 186$ Btu. The moisture in the refuse sample is:

Source of water	Weight of water, in pounds
Refuse	0.40
Air supply	0.04
Chemical reaction	0.28
Total	0.72

S. From item E, the heat required to bring the water to boiling and to evaporate it is: 110 + 700 = 810 Btu. To raise the steam to 1300° F, gas temperature requires 392 Btu (computed as in item E). Hence, 1,202 Btu are required to heat the water.

T. Raising the temperature of the refuse to 1300° F (combustion temperature) requires 1,202 Btu to heat moisture plus 186 Btu to heat dessicated refuse, or 1,388 Btu.

Mass Balance of Material Entering and Leaving Incinerator.—It is possible to apply the type of computations just shown (items A through T) to help design the various components of an incinerator. These computations can be checked for accuracy by computing the mass balance—the quantity of introduced materials should approximately equal the quantity of discharged materials.

Two hundred percent excess air and complete burning of organic refuse are assumed.

U. The following tabulations check the foregoing example.

Introduced material	Weight, in pounds
Inert material	0.10
Combustible refuse	0.50
H_2O in refuse	0.44
Dry air	7.71
H_2O in air	0.01
Total	8.76

Discharged material	Weight, in pounds
Ashes (grate and fly)	0.10
CO_2	0.82
Total H_2O	0.72
Other stack gases	7.12
Total	8.76

SUMMARY

1. Refuse disposal should be sanitary, convenient, and economical.

2. The quantity of refuse to be disposed of is influenced by the frequency and method of collection.

3. Transfer stations can be used to reduce the costs of transporting refuse.

4. Salvage, hog feeding, composting, garbage reduction, landfill, water disposal, and garbage grinding are alternative refuse disposal systems.

5. The British were the first to construct high-temperature destructor plants in the latter part of the nineteenth century. They developed the incinerator to produce by-products such as clinker for building materials and steam for heat and power. In recent years the British have found sanitary landfill more economical for most refuse disposal.

6. In the United States, incinerators were originally used to burn garbage. As the nation's population increased, incinerators were used by large cities to conserve the limited land-disposal sites.

7. Approximately 250 cities in the United States have used incinerators; the other municipalities are largely dependent on sanitary landfill.

8. Incinerators should be located to satisfy the following factors: (*a*) maximum economy of collection haul, (*b*) operation in an industrial area to reduce nuisances and promote refuse salvage, (*c*) two-level topography for minimum construction costs, (*d*) reduction of atmospheric pollution, and (*e*) convenient ash disposal.

9. American incinerators have made little use of by-products such as heat or clinker. Burned tin cans have been salvaged by some cities of the United States.

10. Incineration is a relatively costly refuse disposal process, involving from $2,000 to $5,000 per rated ton of 24-hr burning capacity for construction costs and ranging from $2 to $5 per ton of refuse burned as actual operating cost.

11. Incinerators in the United States tend to be increasingly mechanized as labor costs are increased.

12. Incinerator components include (*a*) a weighing station; (*b*) unloading and charging facilities; (*c*) a charging inlet; (*d*) primary drying and burning chambers with mechanical stokers, ash-disposal equipment, and induced and forced drafts; (*e*) a secondary chamber; and (*f*) flues, stacks, and particulate-matter and gas control devices.

13. Knowledge of the percentage of CO_2 concentration in the stack gases can be used as a means of controlling the air-to-fuel ratio.

14. The particulate-matter discharge from an incinerator stack can be controlled by settling, electrostatic precipitation, entrapment, filtering, and other such processes or devices.

15. Refractories are important elements in effective operation of an incinerator. Plastic refractory material can be used for repair of exposed surfaces.

16. Laboratory and other operating controls should be used in order to obtain optimum performance from expensive incineration plants.

17. High-rate burning using optimum volume reduction rather than complete oxidation may be desirable in order to reduce incineration costs.

18. High-rate burning does not completely burn large limbs and other well-insulated refuse. However, it does flash-burn low-density material, minimizing the volume of residue for land disposal. Special incineration design is required for successful high-rate burning and should include the following: Turbulent suspension of the introduced refuse, high-temperature burning, continuous feed of refuse and continuous removal of residue, thorough quenching of residue, and final sanitary land burial of the odorous residue.

19. The burning process in an incinerator includes drying the refuse, heating to the fire ignition point, and flame-burning in the presence of oxygen supplied by air.

20. Examples of thermodynamic computations for mass balance and heat-energy utilization are presented.

ACKNOWLEDGMENT

Harold B. Gotaas, M. ASCE, director of the University of California Sanitary Engineering Research Project, has cooperated in the preparation of

this paper. Albert F. Bush, A. M. ASCE, S. F. Mulford, Harvey F. Ludwig, M. ASCE, Percy H. McGauhey, M. ASCE, and L. M. K. Boelter—all of the University of California—and other engineers and officials have assisted in the development of the technical data.

APPENDIX. BIBLIOGRAPHY ON REFUSE DISPOSAL

(1) **"Municipal Incineration,"** *Technical Bulletin No. 5,* San. Eng. Research Project, Univ. of California, Berkeley, Calif., June, 1951.

(2) **"Incineration as a Municipal Waste Disposal Process,"** by Ralph Stone and H. B. Gotaas, *Wastes Engineering,* February, 1952.

(3) **"You're Burning Dollars in Your Incinerator,"** *Engineering News-Record,* March 20, 1952.

(4) **"The Shaoyang, China, Night-Soil Fertilizer Reclamation Plant,"** by Ralph Stone, *Sewage Works Journal,* November, 1949.

(5) **"Can Waste Heat from Refuse Incinerators be Employed Economically,"** by Francis R. Bowerman and H. B. Gotaas, *Civil Engineering,* May, 1952, p. 48.

(6) **"What Cities Use Incinerators—and Why?"** by Francis R. Bowerman and H. F. Ludwig, *The American City,* March, 1952.

(7) **"Problems in Municipal Refuse,"** by A M Rawn and Francis R. Bowerman, *Virginia Municipal Review,* May, 1953.

(8) **"Refuse Disposal Program for 27 Cities and County Area,"** by A M Rawn and Francis R. Bowerman, *Western City,* December, 1950.

(9) **"Collection and Disposal of Municipal Refuse,"** by Rudolph Hering and Samuel A. Greeley, McGraw-Hill Book Co., Inc., New York, N. Y., 1921.

(10) **"Municipal Refuse Disposal: An Investigation,"** by J. T. Fetherston, *Transactions,* ASCE, Vol. LX, 1908, p. 345.

(11) **"Turbulent Suspension Burning of Wet Wood, Bark, and Other Fuels,"** by Otto De Lorenzi, *Mechanical Engineering,* May, 1953, in "Technical Digest," p. 412.

(12) **"D. C. Refuse Transfer Station: A New Development in Large-Scale Odor and Dust Control Produces Nuisance-Free Refuse Handling Station,"** by William A. Xanten, *Engineering News-Record,* December 7, 1950.

(13) **Discussion by William A. Xanten of "Some Fundamental Considerations in the Design and Use of Incinerators in the Control of Atmospheric Contamination,"** by Richard C. Corey, *Air Pollution,* New York, N. Y., 1951.

(14) **"An Analysis of Refuse Collection and Sanitary Landfill Disposal,"** *Technical Bulletin No. 8,* San. Eng. Research Project, Univ. of California, Berkeley, Calif., December, 1952.

DISCUSSION

George R. Thompson,[4] M. ASCE.—The paper is comprehensive, and the subject matter well organized. The subject is a difficult one to treat satisfactorily because of the many variable interdependent factors involved. It would be more in order to suggest further study and elaboration of the subject than to offer critical comments on the paper. More statistical information from other sources would be helpful in evaluating generalized findings for specific cases.

Incineration is evaluated relative to basic factors—that is, history, economics, and technology. A fourth important factor is that of public acceptance of the entire system of collection and disposal.

Under the heading, "Factors Influencing the Quantity of Refuse," the authors state that back-yard pickup, alley pickup, or side-of-the-house pickup tend to produce greater quantities of refuse than does curb placement for collection. No reason is given for this apparently inconsistent statement. What becomes of the refuse that is not collected? A further statement that compaction of refuse makes it more difficult to burn is open to question as the compaction is usually of small degree and totally lost in handling the material at an incineration plant.

The introduction of the transfer station depends primarily on the length and cost of haul by the collection units directly to the disposal point as compared to the cost of additional handling to a transfer unit. If the collection units are relatively small and the haul is long, a transfer station may be needed. On the other hand, larger collection units hauling directly to the disposal point may prove more economical than the transfer station.

Salvage can undoubtedly best be performed by private contractors who are more aware of the fluctuating market value of salvage materials and who have established sales outlets. Generally, such an operation by a private enterprise having a profit motive is more successful than governmental operation.

The practice of hog feeding of municipal garbage is being abandoned—primarily because it spreads disease if not properly controlled. It can be used successfully only when cooking control is under direct supervision of a governmental agency.

Composting is still in the experimental stage. Michigan State College at East Lansing has a pilot plant and is studying the subject intensively. Its financial success depends on the ability to market the product in an area where the raw material is available. Because marketing of the product is involved, composting might properly be left to private enterprise.

Reduction methods usually are not profitable. The plant-odor nuisance, long hauls, and nonprofitable disposal of the end products have caused this method of disposal to be almost entirely eliminated.

Land-disposal sites within economic hauling distances of large cities are virtually nonexistent. Open burning is a nuisance, and the inclusion of garbage is unsanitary because of odor, rats, and flies.

---

[4] City Engr., Detroit, Mich.

Sanitary landfill disposal is satisfactory if an acceptable site within a reasonable length of haul is available and the operation is well conducted. Landfills are not suited to carrying superimposed loads of structures, roadways, or airport runways. Even when used for parks, special attention must be given to the growing of trees.

The sanitary fill may be used as a dump for ash from incinerators—indicating that incineration is a good method of conserving land available for dumps. It is unusual to consider incineration as part of the landfill process because a dump for incinerated ash is quite different from a dump for garbage and combustible refuse.

Fills in swamp areas—using water transportation, land transportation, or a combination of both—can serve the dual purpose of making valuable land and disposing of refuse. Care must be taken to select sites and methods which will not result in nuisance problems.

Garbage grinding at the point of food preparation is a rapidly growing, economical, sanitary, and convenient method of disposal. It is increasingly becoming the modern method of disposal. Savings to the municipalities will not be appreciably reflected until garbage collection by truck in a given area can be supplanted by grinding. Commercial grinding often effects great savings for food-processing companies because a collection service would otherwise have to be paid. The use of municipal grinding stations for raw garbage or wrapped garbage is still in the experimental stage but may be competitive with incineration. However, it does not provide a means for disposal of all other refuse.

The subject of incineration is ably treated at length from the viewpoints of historical development and practice including other considerations, such as design and thermodynamic computations. The location of incinerators and the problem of traffic to and from the plant are of the utmost importance from a public standpoint. Incineration is probably the most common method of disposal of garbage and combustible refuse in large cities of the United States. Even though the plants are carefully designed, efficiently operated, properly screened, and located where traffic concentration does not pass through residental neighborhoods, there is much local opposition to such plants in or near a residential area. Although they should be located at the center of load for the most economical hauling, this is of secondary consideration for their public acceptance.

The ideal incinerator is one that will take any rubbish—combustible or incombustible—together with garbage, wrapped or raw, and burn it economically, without nuisance. Such an incinerator eliminates the dual collection of garbage in one truck and other refuse in a second truck.

The paper is well written and illustrated. The foregoing constitute comments rather than criticisms. The authors are to be complimented on their work.

WILLIAM A. XANTEN,[5] M. ASCE.—The field of refuse disposal is one on which it is most difficult to generalize without subjecting the result to misinterpretation. Local conditions involving the area and population of a community, its physical and topographical characteristics, its climate, and many other factors must be given careful consideration and study before a practical and economical solution is reached. This is particularly true of large and densely populated cities in which the problem is vastly complicated by the absence of short-haul low ground for the final disposition of huge quantities of solid wastes and in which the methods utilized must of necessity be of a high sanitary standard in order to satisfy the requirements for nuisance-free performance. Nevertheless, Messrs. Stone and Bowerman have outlined the subject masterfully, and it is impossible to quarrel with most of their conclusions. This discussion will, therefore, be confined primarily to the phases of the report dealing with incineration and fly-ash control.

---

[5] Supt., Div. of Sanitation, Dist. of Columbia, Washington, D. C.

It is noted that the paper considers the relatively high cost of incineration from the standpoint of both capital outlay and operating costs. The picture in this respect is not as bleak as it seems. A most significant factor is the marked trend in the United States toward the increasing production of combustible rubbish and decreasing production of garbage and ashes. In the District of Columbia from 1930 to 1950 the per capita production of these three classes of refuse fluctuated as shown in Table 3.

TABLE 3.—FLUCTUATIONS IN REFUSE PRODUCTION IN WASHINGTON, D. C.

Year	Production, in cubic yards	Production, in cubic yards per capita	Production, in pounds per capita
(*a*) ASHES			
1930	154,056	0.32	417
1940	146,077	0.22	286
1950	127,406	0.16	208
(*b*) GARBAGE			
1930	189,278	0.39	390
1940	201,850	0.30	300
1950	183,670	0.23	230
(*c*) TRASH			
1930	295,790	0.61	135
1940	1,329,249	2.00	444
1950	3,174,151	3.95	880

With the unit weight of refuse being constantly reduced by the introduction of lighter and more combustible material, it is obvious that incinerator plants are handling much larger volumes of material. It would appear that, with the continuing use of frozen foods and the increasing installation of garbage grinders, this trend should continue. The point to be made is that substantial increases in plant efficiency have been required in order to hold costs of operation at present levels; these costs on a tonnage basis can hardly reflect the volumetric increase in work performance due to such marked changes in the quality of material handled.

Such changes also require incinerator design considerations notably different from those applicable to the situation in previous years. Although capital outlay costs on a per-ton basis show a trend upward, such unit costs are not necessarily comparable when radical improvements in design or more conservative ratings are applied in general to the essential plant facilities. The New York City Department of Sanitation reports that the use of preheaters for raising temperatures of the supplementary air systems has been discontinued in recent design, current experience having indicated that their infrequent use on excessively wet refuse does not warrant the over-all installation cost of about $250,000. In Washington, D. C., and Baltimore, Md., plants now under construction have been designed to accommodate, and are are equipped with, an extra crane (three instead of two) so as to avoid the operational slow-down involved in potential crane breakdowns and also to permit adequate crane-maintenance procedures. Installation of mechanical stoking units and sectionally supported walls, increases in pit capacities, provision of adequate combustion and suspension chambers, and design improvements have all tended to emphasize increasing plant efficiencies. Together with the increase in the construction-cost indices in the past decade, this change in emphasis represents a formidable surge toward higher unit costs for erecting incinerators. The surprising fact is that under the circumstances such costs have advanced so gradually and so nominally.

The problem of the method of disposal is sometimes one which of necessity must be solved by resorting to incineration. The cities of New York, Philadelphia, and Baltimore and many others of comparable size are rapidly finding it more and more difficult to locate and conserve areas suitable for landfilling purposes even for noncombustible refuse and incinerator residue within reasonable hauling distances. Since 1941 the controlled open-burning of combustible rubbish in excess of available incinerator capacity in the District of Columbia has been a method utilized as an alternative to sanitary landfilling for which areas were not available. During this period, in a 600,000-cu-yd landfill approximately 30,000,000 cu yd of rubbish have been incorporated. This could only be accomplished by an operation that involved (*a*) the maintenance of rigid separation requirements for rubbish, (*b*) the removal by magnets of all ferrous metals after burning, and (*c*) a well-controlled burning-and-quenching procedure. Despite the extreme care exercised, such a method involves the creation of a smoke nuisance that could only be tolerated pending the construction of additional incinerator capacity. The cost of this method of handling rubbish for disposal is approximately 20% of the cost of handling such material through a modern high-temperature incinerator. Nevertheless, the area utilized for this purpose is rapidly being filled, and no alternative place can even be considered; thus, the costlier but more satisfactory and relatively nuisance-free method of plant incineration has become an absolute requirement in the District of Columbia.

It should not be concluded from the foregoing that the sanitary-landfill method of disposal will not continue to be utilized as a most satisfactory and economical method for smaller communities or for larger communities where suitable and adequate acreages are readily available for long-range use. Nevertheless, the trend toward incineration in large cities will undoubtedly continue, and the collateral problems of strategic plant location, waste-heat utilization, and fly-ash control become increasingly important.

Inasmuch as the cost of refuse collection is seriously affected by the length of haul, the strategic location of incinerators or transfer stations is of paramount importance (12). Attempts to program general salvaging operations in connection with such plants are not conducive to nuisance-free performance. In order to further the acceptance of such installations in commercially zoned areas—and for that matter in areas adjacent to high-class residential areas—the primary consideration for the future would seem to be pleasing architectural treatment and careful plant maintenance. Plant capacities, although adapted to the over-all problem, should be limited to reasonable size.

In promising situations, the utilization of waste heat is a subject that would be weighed carefully from both the economic and practical viewpoint. The requirement of firm supply sometimes presents many objectionable operating problems to the refuse collection and disposal system. Local conditions with respect to existing power rates and potential demand for raw steam might, however, play the deciding role.

The subject of fly-ash control is of universal interest; Messrs. Stone and Bowerman have indulged in generalizations about this control that are not of much help to the designing engineer. It should be emphasized that the removal of particulate matter from incinerator stack gases presents a problem considerably different from that in boiler plants. Electrostatic or cyclonic precipitators have not demonstrated their effectiveness in dealing with the situation. The particles carried in the gases from the burning of cellulose materials lack density and are not spherical in shape. Such particles are difficult to ionize and have a tendency to scale when subjected to cyclonic precipitation devices. Temperature condition is another difficult factor to overcome. Common to all mechanical treatment processes is induced draft, which constitutes another element of maintenance cost and noise of operation to be avoided if possible.

Experience with stack discharges at the municipal rubbish incinerators of the District of Columbia would indicate that great improvements can be made in the design of combustion and suspension chambers; perhaps more emphasis should be given to this approach in an effort to produce combinations that would permit the operation of plants under natural draft. It is believed that satisfactory results can be achieved to the point of reducing stack discharges to approximately 0.4 lb per 1,000 lb of flue gases or even lower and that—by providing incinerators in which the design and capacity of the combustion and expansion chamber make possible the accomplishment of these results—adequate space will be provided to introduce experimental systems of handling the gases for further reduction, if required. The subject is covered in more detail by the writer (13).

This point of view is sustained by the City of New York as indicated in the following excerpt from a report by Casimer Rogus, director of engineering of the Department of Sanitation, to the American Public Works Association convention at New Orleans, La., in October, 1953:

> "Substantially sized expansion chambers (lined with firebrick) reduce air velocities from 15 f.p.s. in the preceding combustion chamber down to 5 f.p.s., all in the interest of completing the combustion but more

> particularly to settle out flyash. Because flyash, soot, fume, and odor emissions from incinerators have stirred public demands for improved air pollution control the City has expended considerable effort in investigating the merits of several types of dust removal systems. The high temperatures and large volumes of gases produced in incineration have negated economic installations of the conventional type dust removal systems such as cyclonic separators, mechanical filters, electric precipitators, water spray washers, or suitable combinations of these. Laboratory tests and research on pilot models of the prototype expansion chambers, by the Battelle Memorial Institute, hired for this purpose, developed the conclusion that expansion chambers of the present design, modified only through the installation of some relatively simple horizontal baffiles and skimmer plates would reduce the flyash emissions to about .56 lbs. per 1,000 lbs. of gas (corrected to 50% excess air). This value is well within the permissible limit of .85 lbs. specified by the New York Department of Air Pollution Control."

Little precise information is available regarding stack emissions from large municipal incinerators. Ringelmann-Chart measurements do not provide a satisfactory barometer of performance. Continuing research and actual field studies for the twofold purpose of providing (*a*) data for the establishment of proper criteria for regulatory agencies to apply to the local situation and (*b*), if at all possible, a simple method (similar to the Ringelmann-Chart method for oil-burning plants and coal-burning plants) for measuring performance for stack discharges from refuse incinerators.

Dealing with the fly-ash problem of incinerators by the installation of mechanical systems (either wet-type or dry-type) appears at the present time to be primarily experimental, and both the initial cost and the maintenance cost are unusually great. Based on the experiences of the District of Columbia and New York City in particular, in addition to those of other large municipalities where modern refuse incinerators either have been recently completed or are under construction, probably even more satisfactory results can be and will be achieved by the provision of more carefully designed combustion chambers, flues, and tall chimneys, by operation under natural draft, by the use of specially designed baffles, and by the application of operating procedures more conducive to nuisance-free performance than has been customary in the past.

Finally, it should be stated that the management and engineering problems involved in the economical and proper collection and disposal of refuse in large, densely populated communities are difficult and complex. It cannot be too strongly emphasized that they should be solved by engineering studies predicated on local conditions. Apparently there has been greater recognition of this fact in recent years, and the informative paper by Messrs. Stone and Bowerman accentuates the importance of this conclusion.

SAMUEL A. GREELEY,[6] HON. M. ASCE.—In presenting their paper Messrs. Stone and Bowerman have contributed significantly toward the solution of one of the more difficult problems in the field of sanitary engineering. The subject is so comprehensive that a competent discussion, which must necessarily be brief, cannot be written. Refuse disposal processes need careful consideration and application for each locality. Some comments follow which illustrate the need for an understanding of the relationship between general statements and their detailed application to specific problems.

---

[6] Partner, Greeley and Hansen, Engrs., Chicago, Ill.

It seems clear that refuse disposal will be different in different cities and in different parts of large cities and that this depends, in the first place, on what is meant by the term "refuse" and on the characteristics of the refuse for disposal. What, for instance, is the significance of the four subcaptions of Fig. 2? The writer's understanding is that mixed refuse is that resulting from a single collection and usually comprises garbage and combustible rubbish but sometimes includes noncombustible rubbish and ashes as well. The writer thinks the term "rubbish" or "trash" is used more often for the material referred to in Fig. 2 as combustible "refuse." Differences in the characteristics of refuse are important in studies relating to the application of disposal processes.

Item 3 in the "Summary" states that transfer stations can be used for reducing the costs of transporting refuse. This is generally true, but specifically for a particular locality the kind and cost of a transfer station, suitable to its location, is important. The one in Washington shown in Fig. 3 cost almost $1,000,000 in 1948. The local requirements may well demand a greater expenditure for transfer stations than has been made in the past and this in turn will affect the relative costs of disposal by landfill including the haul to the site, and of incineration.

Items 8, 9, and 10 of the "Summary" describe some general details of incineration plants. It is doubtful that two-level topography will greatly reduce construction costs for a crane-and-bin plant. The present availability of cranes that lift at relatively high speeds make level sites practicable and economical. Whereas some years ago crane lifts were limited to about 60 ft, this lift may be increased now to as much as 80 ft.

There has always been a hope that revenue could be obtained by the use or sale of by-products, but there have been few local situations in which salvage has proved worthwhile. In the writer's practice it has been difficult to obtain construction costs as low as $2,000 per ton of rated capacity. The range, in general, is from $3,000 to $4,000. In the writer's experience the total annual cost, including actual operating cost and debt service, is likely to range from $3.00 to $4.00 per ton of refuse burned.

Reference is made in the paper to the fact that the actual quantity burned does not often equal the rated capacity and that it will be wise to establish more realistic design criteria. This, of course, is true, but the application depends on how the rated capacity is determined. The writer thinks that an incinerator should be designed for an estimated maximum weekly quantity of refuse at a date perhaps twenty years in the future. On this basis and with the correct selection of furnace units, there will be opportunity during months of lower refuse quantities to accomplish much maintenance work. Reference to Fig. 6 indicates that the difference between the unit costs at approximately 85% of utilization is not much more than for use at rated capacity.

The thermodynamic computations are a helpful illustration. Such computations can be used to show the importance of the characteristics of the refuse.

Refuse having different characteristics may be illustrated as shown in Table 4.

In the writer's experience, refuse of which 40% is moisture and 10% is ash is not common, even for a mixture of garbage and combustible rubbish. Probably the percentage of ash and water will be somewhat greater. The composition in the column headed "Characteristics, based on the writer's data" (Table 4) is applicable to rubbish, although some of the time the percentage of ash might be somewhat lower. The writer usually considers somewhat greater heat losses than 7.0%. The tabulation shows the quantity of gaseous products of combustion amounting to 460 cu ft in accordance with the authors' computations and 580 cu ft per lb of refuse at 1650°F for the refuse assumed by the writer. This is a considerable difference when considering fly-ash removal facilities. A considerable range in characteristics should be used in the computations in order to cover changes in the refuse caused by weather and other conditions.

TABLE 4.—COMPARISON OF REFUSE

Item	Characteristics, based on the authors' data	Characteristics, based on the writer's data
(*a*) COMPOSITION OF REFUSE, IN PERCENTAGES BY WEIGHT		
Combustibles	50	60
Water	40	15
Ash	10	25
(*b*) COMPOSITION OF COMBUSTIBLES, IN PERCENTAGES BY WEIGHT		
Carbon	44.4	52
Hydrogen	6.2	6
Oxygen	49.4	40
Other elements	0	2
(*c*) HEATING VALUE OF COMBUSTIBLES, IN BTU PER POUND	9,600	9,600
(*d*) HEAT LOSSES BY CONDUCTION AND INCOMPLETE COMBUSTION, IN PERCENTAGE OF TOTAL	7	7
(*e*) GASEOUS PRODUCTS OF COMBUSTION, FOR 1 LB OF REFUSE (COMBUSTION-CHAMBER TEMPERATURE = 1650°F)		
Weight, in pounds	8.66	10.86
Volume, in cubic feet	460	580

The statement in item 15 of the "Summary" is important; the cost of construction, the operating cost, and the life of the furnace depend on the refractories used. The writer thinks that a suspended-arch construction for the roof and sectionally supported walls are likely to prove economical on a long-term basis.

Item 17 of the "Summary" is important because it seems unnecessary to limit the residual organic matter to very small amounts at considerable additional cost.

The writer has the impression from the paper that the authors believe that a competent study of a local situation will result in more frequent use of the sanitary fill method of disposal. The writer is in accord with this general objective but he has been somewhat surprised at the difficulty of accomplishing the simpler method of disposal. In large cities, a combination of methods for the disposal of garbage and rubbish is favorable if sites can be obtained. For both Chicago and for Cook County outside Chicago, the writer's firm has developed general plans that include loading or transfer stations, incinerators, and sanitary fills for refuse comprising mainly garbage and rubbish with some household ash.

In recent years there has been a growing demand for careful and competent engineering studies related to local refuse disposal conditions. The paper is a worthy contribution to this complex and difficult problem.

RALPH STONE[7] AND FRANCIS R. BOWERMAN,[8] ASSOCIATE MEMBERS, ASCE.—The writers greatly appreciate the comprehensive and valuable discussions presented. The subject matter as described by each reviewer will be discussed, and material common to the several discussions will be amplified.

Mr. Thompson has inquired regarding the influence of back-yard collection and alley collection in creating larger quantities of refuse than does curb placement. The information for the writers' statement was developed from data collected by the Sanitary Engineering Research Project, University of California (14). The principal reason that larger quantities are collected from back-yard pickup is believed to be the additional convenience of back-yard and side-of-the-house pickup. That is, such refuse as garden trimmings and leaves are often burned by the individual householder or paper contributed to salvage paper drives when the householder is required to haul the wastes to the curb in front of the residence.

Another question concerns the importance of compacted refuse in regard to the efficiency of burning at a municipal incinerator. It is noted that at incinerators where wet paper, leaves, and other combustibles have been compacted they form a blanket on the surface fire, thereby inhibiting the combustion within the primary burning chamber. Mr. Thompson correctly implies that, when refuse is processed or "fluffed" by special handling prior to burning in an incinerator, the influence of compaction is less important.

California's experience with the feeding of municipal garbage to hogs indicates that it is economical and practicable to sterilize garbage with steam so as to prepare a sanitary product that will not transmit diseases to hogs. Recent tests performed in California indicate that the presence of citrus peels in boiled garbage does not destroy its value for hog feeding, partly because the use of raw citrus produce has declined whereas the market for frozen and canned juices has developed. In any event, California citrus wastes do not now interfere with the sterilization of garbage for hog feeding. Garbage cooking, in fact, has increased the value of the waste for feed by breaking down the food products and making available additional nutrients. Garbage cooking is now similarly utilized in many other places. With respect to garbage, Mr. Thompson presents a useful yardstick for incinerator operation—namely, that an efficient plant will take any "rubbish, combustible and incombustible, together with garbage, wrapped or raw, and burn it economically, without nuisance."

---

[7] Cons. Engr., Los Angeles, Calif.

[8] Div. Engr., Los Angeles County Sanitation Dists., Los Angeles, Calif.

Mr. Xanten has emphasized the significance of fly-ash control in the design and operation of an incinerator. Fly-ash control and the discharge of noxious gases from the combustion system are highly technical subjects. Admittedly, one of the major disadvantages of incineration is that of discharging materials that pollute the atmosphere. In cities concerned with air-pollution problems, perhaps other refuse disposal systems should be used which do not contribute to the burden of the atmosphere. In this respect, composting, grinding of combustible rubbish to sewers, and sanitary landfill are obvious alternative systems.

Experience with fly-ash control indicates that well-designed incinerators, similar in engineering characteristics to Mr. Xanten's description, reduce fly ash and unburned gaseous emissions to a level of tolerance satisfactory to many communities. In particular, the use of fog nozzles to saturate a chamber wherein combustion products are treated appears to be effective in reducing atmospheric pollution. The cooling effect of the fine spray and the sweeping action of droplets assist the large fly-ash products to settle. A fog spray may provide greater interception of the ash particles than does a conventional water spray.

Particular attention should be directed to studies made for the City of New York at Battelle Memorial Institute in Columbus, Ohio, on the matter of fly-ash removal. By use of a scale model, internal baffles were designed to create "dead-spots" within the chambers and breeching; by use of such baffles, it was possible to reduce fly-ash discharge. Further study along these lines may yield designs which will eliminate much of the present conflict between incinerators and their environs. Of additional interest is the new incinerator at Milwaukee which utilizes combinations of water spraying and impingement baffles to reduce fly-ash discharge to acceptable levels. Unfortunately, not enough basic research in fly-ash control is being conducted. Mr. Xanten's additional information concerning the design of incinerator installations is a valuable contribution to the knowledge of the subject.

Mr. Greeley has presented interesting data concerning economic and technical problems involved in incineration. The writers have observed several instances in which two-level topography was used for plant construction, thus resulting in smaller, less expensive buildings and ramps. Two-level topography is of greater importance in direct-dump incinerators than in crane-and-bin plants; however, where two-level construction can be used, the operating expenses should be less in a crane-and-bin plant because a lower lift is required from the bin to the charging inlet of the incinerator.

The salvage of waste paper is an important industry in the United States and reduces the quantity of combustible rubbish subject to disposal. Although little revenue may be obtained from such salvage operations, the reduction in quantity of combustibles to be burned should provide significant savings to an operating installation.

Construction costs can be kept low if the plant superstructure can be reduced to a minimum. In localities where an attractive building is not required (such as in an industrial area) and also in temperate climates (such as prevail in the southwestern states of the United States), it is not necessary to use expensive enclosures. In such places, it is possible to construct incinerators at considerably less cost than in high-class residential areas where a noise-proof and dustless type with a high degree of air-pollution control is needed. The operating cost data presented by Mr. Greeley are approximately the same as those presented by the writers, when Mr. Greeley's estimate of from $3 to $4 per ton of refuse burned (based on a capital cost of from $3,000 to $4,000 per ton of rated capacity) is compared to the writers' lower capital-cost estimate of $2,000 per ton. Although some direct-dump incinerators are still being built for $2,000 per rated ton, the writers fully agree that today's market for crane-and-bin plants with devices for air-pollution control (such as spray chambers) is in the range of from $3,000 to $4,000, as suggested by Mr. Greeley.

The thermodynamic information presented by Mr. Greeley is valuable and representative of many eastern incinerator plants. In most areas of the western United States, gas and fuel oil are popular for heating homes. As a result, the typical refuse contains largely cellulose and relatively little ash. Also, because of the dispersed residential pattern of living in many California communities, much of the combustible rubbish is vegetation—such as garden trimmings, grass, and leaves. This helps explain the differences in the characteristics of hypothetical examples of refuse as described by the writers and those presented by Mr. Greeley.

In general, the discussers seem to be in agreement with the writers on the following significant points:

1. It is most important that each municipality make a careful engineering study to determine the nature and extent of local refuse disposal problems and to arrive at an engineering plan for an economical waste-handling system.
2. The cost of incineration is high, and economy requires careful operation and well-designed plants.
3. Air pollution in connection with incineration is an important deterrent to incinerator use. Further development of incinerator design, with particular reference to fly-ash and gaseous emissions, will have to be made to insure universally acceptable incinerator application.

The writers are indebted to the discussers for presenting valuable contributions to the storehouse of refuse disposal knowledge.

In conclusion, it may be of interest to compare the current economics of alternative municipal refuse disposal processes because costs are pertinent to the selection of refuse disposal systems. Although such cost data are incomplete, the following information is based on considerable experience and on actual cost studies. The future development of the several refuse disposal processes depends directly on improvements for reducing cost while providing increased convenience and sanitation. The asterisk indicates processes in which the higher costs are usually for small installations or for plants constructed to operate with a minimum of nuisance.

Refuse disposal process	Range of capital costs (dollars per ton of capacity per day)	Range of total operating costs, including amortization of capital cost (dollars per ton handled per day)
Incineration	1,500–6,000*	2.00–6.00*
Burning dump	Unsatisfactory for sanitary and aesthetic reasons	
Composting	100–5,000*	2.00–30.00
Hog feeding	300–1,000	Profit—1.00*
Garbage grinding	1,000–2,000	2.00–6.00*
Reduction of garbage	1,000–5,000	Profit—5.00
Salvage	0–1,000	Profit—1.00*
Sanitary landfill	250–1,000	0.40–1.50
Water disposal	Unsatisfactory for sanitary and aesthetic reasons	

AMERICAN SOCIETY OF CIVIL ENGINEERS
Founded November 5, 1852
TRANSACTIONS

Paper No. 2802

MORNING-GLORY SHAFT SPILLWAYS
A SYMPOSIUM

PAGE

Prototype Behavior
By Joseph N. Bradley, M. ASCE 312

Determination of Pressure-Controlled Profiles
By William E. Wagner, M. ASCE 345

Performance Tests on Prototype and Model
By Alvin J. Peterka, M. ASCE 385

PROTOTYPE BEHAVIOR

By Joseph N. Bradley,[1] M. ASCE

With Discussion by Messrs. Bernard Donelan, Donald S. Walter, Fred W. Blaisdell, Rodolfo E. Ballester, John Wallace Ridley, and Joseph N. Bradley

---

Synopsis

According to available records, the first morning-glory shaft spillway was completed in 1896, but the design did not come into general use until the latter part of the 1920's. Since then, approximately thirty spillways of this type have been completed or are under construction (as of 1955). As less than 30 years have elapsed since completion of the first spillway, it has not been until recently that a morning-glory spillway of any size has operated. Thus the spillway designer has been forced to rely entirely on theory and the results of model studies. Unfortunately, model studies do not solve all the problems involved, and therefore an investigation was begun in 1950 to collect information from spillways which have operated; the results of this investigation are presented herein.

Introduction

A morning-glory shaft spillway consists of (*a*) a collecting structure or morning-glory, (*b*) a vertical shaft or an inclined shaft, and (*c*) a horizontal tunnel. Usually a vertical rather than an inclined shaft is used, and this is connected to the horizontal tunnel through a sharp 90° bend; there are only two cases on record where inclined shafts have been used. In some cases a stilling basin is constructed at the downstream end of the horizontal tunnel whereas in other cases the horizontal tunnel discharges directly into the river.

The morning-glory spillway may operate with free flow, or, when designed properly, it can operate submerged. For free flow, the discharge characteristics are similar to those for a straight overflow-dam section; that is, an increase in discharge is proportional to the three-halves power of the head. When submerged, the flow characteristics change completely; an increase in discharge is proportional to the square root of the head. If, however, a part of the shaft flows full, the effective head will exceed the head measured above the crest of the morning-glory. After submerged flow commences, a further increase in head on the crest results in a very limited increase in discharge. Thus, if a morning-glory spillway is designed to operate submerged, an additional factor of safety is necessary to guard against the spillway capacity ever being exceeded.

Note.—Published, essentially as printed here, in April, 1954, as *Proceedings-Separate No. 431.* Positions and titles given are those in effect when the paper or discussion was approved for *Transactions.*

[1] Hydr. Engr., Bureau of Reclamation, U. S. Dept. of the Interior, Denver, Colo.

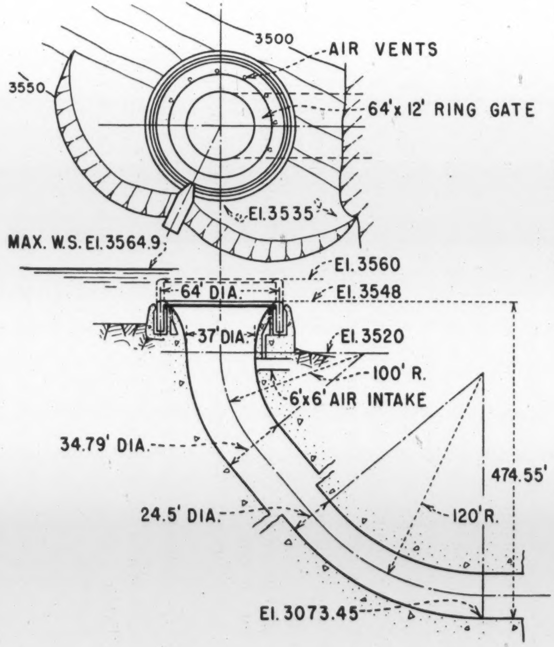
3500
AIR VENTS
3550
64'x 12' RING GATE
El. 3535
MAX. W.S. El. 3564.9
El. 3560
64' DIA.
El. 3548
37' DIA.
El. 3520
100' R.
6'x6' AIR INTAKE
34.79' DIA.
474.55'
24.5' DIA.
120' R.
El. 3073.45

Fig. 1.—Hungry Horse Dam Spillway

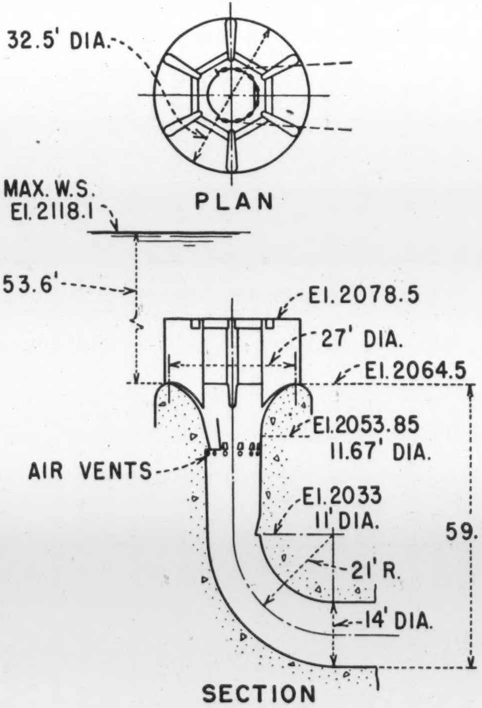
32.5' DIA.
PLAN
MAX. W.S.
El. 2118.1
53.6'
El. 2078.5
27' DIA.
El. 2064.5
El. 2053.85
11.67' DIA.
AIR VENTS
El. 2033
11' DIA.
59.5'
21' R.
14' DIA.
SECTION

Fig. 2.—Heart Butte Dam Spillway

The morning-glory spillway is attractive in that it can often be constructed at less cost than other types, and it is readily adapted to dams in narrow, steep canyons. Where a diversion tunnel is used to conduct the river around the site during construction, it can also later serve as a part of the spillway tunnel. When designed to operate submerged, this type of spillway is well adapted to flood-retention reservoirs where the downstream flow is to be limited.

The principal difficulty in design has been the fact that, until the 1920's, no morning-glory spillway of any size had operated. Thus, the designer has been faced with the task of designing solely on the basis of theory and model studies. From a hydraulic standpoint, this type of spillway is sound. The questionable factors are structural—namely, will the concrete or other material composing the curved surface of the vertical bend and the horizontal tunnel withstand the effects of the high-velocity water, will ice or debris present difficulties in operation, or will vibration or noise become objectionable?

For the design of the Hungry Horse Dam (Montana) spillway (Fig. 1), which features a total drop of 487 ft from headwater to invert of the horizontal tunnel, and the Heart Butte Dam (North Dakota) spillway (Fig. 2), which consists of a morning-glory designed for submerged flow with as much as 54 ft of head on the crest, the foregoing questions take on added significance. For example, erosion of the tunnel lining in the Hungry Horse Dam spillway at the very high velocities that are contemplated would produce intolerable difficulties both in operation and maintenance. Vibration in the Heart Butte Dam spillway, embedded directly in the earth dam, would also create a serious situation with respect to settlement of both the spillway tunnel and the earth embankment.

In an attempt partly to clarify some of the unanswered design problems in the light of prototype experience, questionnaires were sent out to persons connected with morning-glory shaft spillways. The texts of the questionnaires varied, but these four questions were common to all of them:

1. Has the spillway operated? If so, a log of operation would be appreciated.
2. Has erosion of the concrete been experienced in the shaft, the tunnel, or in the vicinity of the vertical elbow?
3. Has vibration or objectionable noise been noticeable in the structure during operation?
4. Has any difficulty been experienced with the passing of debris or ice?

The response and cooperation received in reply to this inquiry were excellent. In Table 1 there are listed the spillways investigated, their location, reference material where available, and the names of the correspondents contacted.

Basis for Investigation

The purpose of the prototype investigation was, first, to determine the merits or shortcomings of design practice with regard to morning-glory spillways and, second, to learn how the materials composing these structures withstand the forces imposed on them.

TABLE 1.—MORNING-GLORY SHAFT SPILLWAYS

Dam	Location	References to literature	References for correspondence
Owyhee	Owyhee Project—Idaho	"Floating Ring-Gate and Glory-Hole Spillway at Owyhee Dam," by L. G. Smith, *Reclamation Era*, August, 1940, p. 226. "Glory Hole Spillway," by A. P. Connor, *Power Plant Engineering*, November, 1933, p. 482. "Hydraulic Model Studies for the Morning-Glory Spillways at Owyhee and Gibson Dams," by F. C. Lowe, *Hydraulic Laboratory Report 159*, Bureau of Reclamation, U. S. Dept. of the Interior, Denver, Colo.	Regional Director, Bureau of Reclamation, Boise, Idaho
Gibson	Sun River Project—Montana	"Gibson Dam," by B. W. Steels, Dams and Control Works, Bureau of Reclamation, U. S. Dept. of the Interior, Washington, D. C., 1929, p. 79.	Regional Director, Bureau of Reclamation, Billings, Mont.
Sulak	Russia	"Engineering in Foreign Countries," *Engineering News-Record*, October 17, 1935, p. 546.	
Guernsey	North Platte Project—Nebraska	"Guernsey Dam," by W. H. Nalder, Dams and Control Works, Bureau of Reclamation, U. S. Dept. of the Interior, Washington, D. C., 1929, p. 55.	Regional Director, Bureau of Reclamation, Denver, Colo.
Davis Bridge	On Deerfield River near Whitingham, Vt.	"The Hydraulic Design of the Shaft Spillway for Davis Bridge Dam and Hydraulic Tests on Working Models," by Ford Kurtz, *Transactions*, ASCE, Vol. 88, 1925, p. 1.	H. M. Nelson, New England Power Service Co., 441 Stuart St., Boston 16, Mass.
Pleasant Hill	Mohican River near Perrysville, Ohio	"Hydraulic Model Studies for Pleasant Hill Dam," by George Barnes, Case School of Applied Science, Cleveland, Ohio, May, 1935.	Div. Engr., Ohio River Div., Corps of Engineers, U. S. Army, 536 U. S. Post Office Bldg., Cincinnati 1, Ohio
Kingsley	North Platte River near Ogallala, Nebr.	"Hydraulic Model Studies on Keystone Dam" (now Kingsley Dam) by George Barnes, Case School of Applied Science, Cleveland, Ohio, November, 1936.	Chf. Engr., Central Nebraska Public Power and Irrigation District, Hastings, Nebr.
Bouquet Canyon	Bouquet Creek, 50 miles from Los Angeles, Calif.	"Bouquet Canyon Reservoir and Dams," by H. A. Van Norman, *Civil Engineering*, August, 1934, p. 393.	Chf. Engr., Dept. of Water and Power, City of Los Angeles, Los Angeles 54, Calif.
Lady Bower	Derwent River in Derbyshire, England	"Model Results on the Ladybower Spillways," by G. H. Hill, *The Engineer*, London, November 3, 1939, p. 440.	G. H. Hill and Sons, 51 Mosley St., Manchester 2, England
Jubilee	Hong Kong	"Model Experiments on Bellmouth and Siphon-Bellmouth Overflow Spillways," by Geoffrey Morse Binnie, *Journal*, Inst. of C. E., London, November, 1938 and 1939, p. 65.	W. J. E. Binnie, Binnie, Deacon and Gourley, Artillery House, Artillery Row, Victoria St., Westminster, S. W., England

TABLE 1.—(*Continued*)

Dam	Location	References to literature	References for correspondence
Taf Fechan	Wales	"Bellmouth Weirs and Tunnel Outlets for Disposal of Flood Water," by W. J. E. Binnie, *Transactions*, Inst. of Water Engrs., London, England, 1937, p. 103.	W. J. E. Binnie, Binnie, Deacon and Gourley, Artillery House, Artillery Row, Victoria St., Westminster, S. W., England
Silent Valley	Ireland	"Bellmouth Weirs and Tunnel Outlets for Disposal of Flood Water," by W. J. E. Binnie, *Transactions*, Inst. of Water Engrs., 1937, p. 103.	W. J. E. Binnie, Binnie, Deacon and Gourley, Artillery House, Artillery Row, Victoria St., Westminster, S. W., England
Pontian Ketchil	Jahore, Singapore	"Bellmouth Weirs and Tunnel Outlets for Disposal of Flood Water," by W. J. E. Binnie, *Transactions*, Inst. of Water Engrs., 1937, p. 103.	W. J. E. Binnie, Binnie, Deacon and Gourley, Artillery House, Artillery Row, Victoria St., Westminster, S. W., England
Burnhope	Durham County, England	"Bellmouth Weirs and Tunnel Outlets for Disposal of Flood Water," by W. J. E. Binnie, *Transactions*, Inst. of Water Engrs., 1937, p. 103.	W. J. E. Binnie, Binnie, Deacon and Gourley, Artillery House, Artillery Row, Victoria St., Westminster, S. W., England
Manuherikia Falls Dam	New Zealand	"Bellmouth Weirs and Tunnel Outlets for Disposal of Flood Water," by W. J. E. Binnie, *Transactions*, Inst. of Water Engrs., 1937, p. 103.	J. W. Ridley, Hydro-electric Design Office, Ministry of Works, Wellington, New Zealand
Heart Butte	North Dakota	"Morning-Glory Shaft Spillways: Performance Tests of Prototype and Model," by A. J. Peterka, *Transactions*, ASCE, Vol. 121, 1956.	Regional Director, Bureau of Reclamation, Billings, Mont.
Hungry Horse	Montana		Regional Director, Bureau of Reclamation, Boise, Idaho
South Holston	South Holston River, Tennessee		Chf. Engr., Tennessee Valley Authority, Knoxville, Tenn.
Watauga	Watauga River, Tennessee	"Constructing the Watauga Project," by G. K. Leonard and Don H. Mattern, *Civil Engineering*, May, 1948, p. 21.	Chf. Engr., Tennessee Valley Authority, Knoxville, Tenn.
Akongtien	South Taiwan		Y. C. Chu, Engineer in Charge
Lumont	Philippine Islands		Filemon C. Rodriguez, General Manager, National Power Corp., Natividad Building, Manila, Republic of Philippines
La Regadera	Bogotá, Colombia		F. Wiesner Rozo, Superintendent, Acueducto Municipal de Bogotá, Bogotá, Colombia
Shade Hill	South Dakota	"Morning Glory Shaft Spillways-Performance Tests on Prototype and Model," by A. J. Peterka, *Technical Monograph No. 16*, Bureau of Reclamation, U. S. Dept. of the Interior, Denver, Colo., 1954.	Regional Director, Bureau of Reclamation, Billings, Mont.

An incident occurred in 1941 which caused much doubt in the minds of engineers concerning tunnel spillways. The Arizona spillway at Hoover Dam (Arizona-Nevada), which has a fall of approximately 570 ft, was first operated in August, 1941, until December, 1941. The average flow during the 4-month period was 13,500 cu ft per sec. The maximum flow was 38,000 cu ft per sec, which lasted for only a few hours. At the conclusion of operations, an eroded hole 115 ft long, 30 ft wide, and 45 ft below invert grade, was discovered immediately downstream from the vertical bend. The velocity in the horizontal tunnel was approximately 170 ft per sec. The spillway was designed for 200,000 cu ft per sec, so the average flow was only 7% of capacity.[2]

The Hoover Dam spillways are not of the morning-glory type, but the tunnel arrangement is similar to some morning-glory spillways. There are a number of theories as to what actually occurred at Hoover Dam but none is conclusive. Briefly, there was misalinement of the invert of the vertical bend and evidence of cavitation, and the large hole at the base of the inclined shaft was indicative of direct impact and scaling. The Hoover Dam incident has posed the question: If erosion can occur at the base of an inclined shaft, what can be expected in the case of a vertical shaft terminating in a sharp 90° bend?

INVESTIGATION

As far as it is possible to determine, there are (as of 1955) approximately thirty true morning-glory spillways either in existence or under construction; only those spillways which have operated will be considered herein. The first spillway of this type was built in 1896 and was designed by James Mansergh for the Blackton Reservoir in England. A second morning-glory spillway was constructed at the Front Reservoir in England in 1908. The remaining spillways have been constructed subsequent to 1926. With the general introduction of model studies in the United States and Europe in the 1920's, designers were able to take a more favorable attitude toward the morning-glory shaft spillway. It is interesting to note that model studies have been performed to aid in the design of almost all the morning-glory spillways dating back to 1926; unfortunately, model studies do not reveal all that is desired.

A record of the morning-glory shaft spillways which have operated is presented subsequently. These are cited in the order of their completion so that one can follow the evolution of design as well as learn of protype operation.

Davis Bridge Dam.—The first morning-glory spillway in the United States was constructed at the Davis Bridge Dam on the Deerfield River near Whitingham, Vt., completed about 1926. This spillway (Fig. 3) was designed for a maximum discharge of 27,000 cu ft per sec, a head on the crest of 8 ft, and a drop of 188 ft from reservoir to invert of horizontal tunnel. This structure has discharged a number of times for short periods. The maximum discharge occurred in the September hurricane flood of 1938 when the water reached 6 ft on the crest. The computed discharge at that time was approximately 19,400 cu ft per sec, or 72% of capacity. The spill during this flood exceeded

---

[2] "Experiences of the Bureau of Reclamation," by Jacob E. Warnock, *Transactions*, ASCE, Vol. 112, 1947, p. 55.

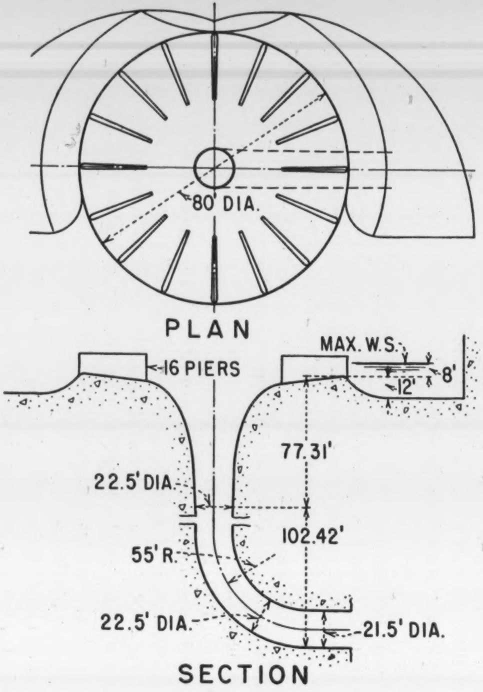
80' DIA.
PLAN
MAX. W.S.
8'
12'
16 PIERS
77.31'
22.5' DIA.
102.42'
55' R.
22.5' DIA.
21.5' DIA.
SECTION

FIG. 3.—DAVIS BRIDGE DAM SPILLWAY

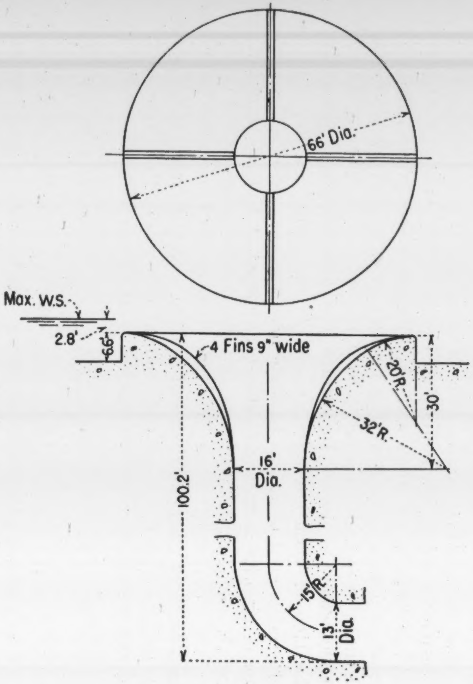
66' Dia.
Max. W.S.
2.8'
6.6'
4 Fins 9" wide
20'R.
32'R.
30'
16' Dia.
100.2'
15'R.
13' Dia.

FIG. 4.—TAF FECHAN DAM SPILLWAY

10,000 cu ft per sec for 15 hr. Inspection after the flood showed no appreciable erosion of the concrete in the horizontal part of the tunnel. An erosion pocket 3 ft wide by 6 ft long by 3 in. deep was apparent at the vertical bend, but it was not certain whether this was caused by erosion as a result of the velocity of the water or spalling caused by freezing and thawing of the concrete surfaces. In any event, the repairs were of a minor nature. All ice and debris which passed over the crest between the piers had readily gone through the spillway. Logs and trees 50 ft to 60 ft long were reported to have passed through the spillway at times. The spillway makes some noise when it is in operation, but this can be heard only a short distance from the dam, and vibration appears to be no problem. Sixteen piers on the crest act as an antivortex device.

Taf Fechan Dam.—A morning-glory spillway was completed at the Tef Fechan Dam in Wales in 1927. This spillway (Fig. 4) was designed for a maximum discharge of 3,000 cu ft per sec at a head of 2.8 ft on the crest; the drop is 103 ft. The long sweeping curves of this early design are very suggestive of the morning-glory flower. Correspondence with W. J. E. Binnie, who acted as consultant, indicated that no trouble has been experienced with this spillway and no unusual repairs have been required. It is interesting to note the presence of an antivortex device consisting of four small fins.

Gibson Dam.—The Gibson Dam spillway on the North Fork of the Sun River in Montana, a project of the Bureau of Reclamation, United States Department of the Interior (USBR), was completed in 1930. This structure (Fig. 5) was designed for a maximum discharge of 50,000 cu ft per sec at a head of 20 ft over the crest and a drop of 180 ft. As originally constructed, the spillway had a free crest, but the crest was later altered and six radial gates were installed (Fig. 6).

Prior to 1947, the spillway operated several times. Upon inspection of the tunnel, two areas approximately 2.5 ft by 1.5 ft by 2 in. deep prominently displayed erosion in the vertical bend. During the months of May and June, 1948, a total of 435,000 acre-ft of water flowed through the spillway. The peak flow was 13,100 cu ft per sec, or 26% of capacity. Water passing through the spillway at this time produced additional erosion of the areas cited previously. The areas had increased to 5 ft by 3 ft, exposing several reinforcing bars. The spillway again went into operation in 1949, 1950, and 1951, reaching discharges of 4,500 cu ft per sec, 7,500 cu ft per sec, and 6,000 cu ft per sec, respectively. The tunnel and vertical bend were inspected annually, and the rate at which erosion has occurred has been slow but progressive. Repairs to the extent of patching were scheduled for 1952. Because of the irregular surface of the vertical bend, produced by the rough formwork of this period, it would be unfair to fix the responsibility for this erosion on any one cause.

The invert of the horizontal tunnel also showed wear, but this probably occurred during diversion of the river at the time of construction. No ice has passed through the spillway, but large trees have passed through during flood season causing no apparent damage. Noise was reported to have been considerable, increasing with the discharge, but this was not particularly objec-

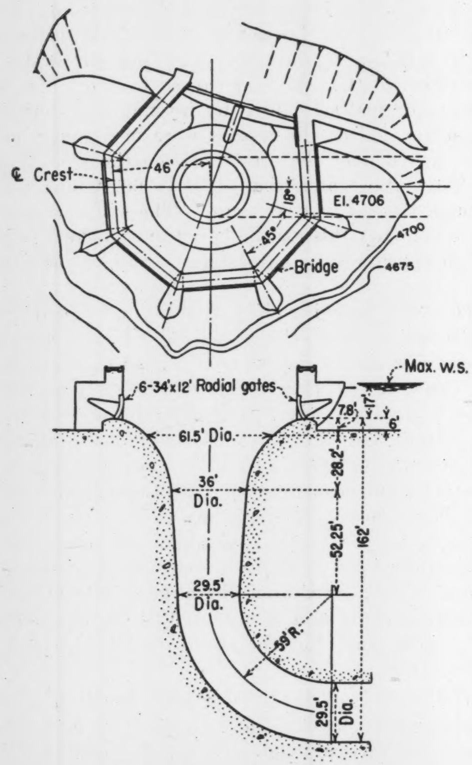
℄ Crest
46'
18'
El. 4706
45°
Bridge
4700
4675
Max. W.S.
6-34'x12' Radial gates
7.8'
1.7'
6'
61.5' Dia.
36' Dia.
28.2'
52.25'
162'
29.5' Dia.
59' R.
29.5' Dia.

FIG. 5.—GIBSON DAM SPILLWAY

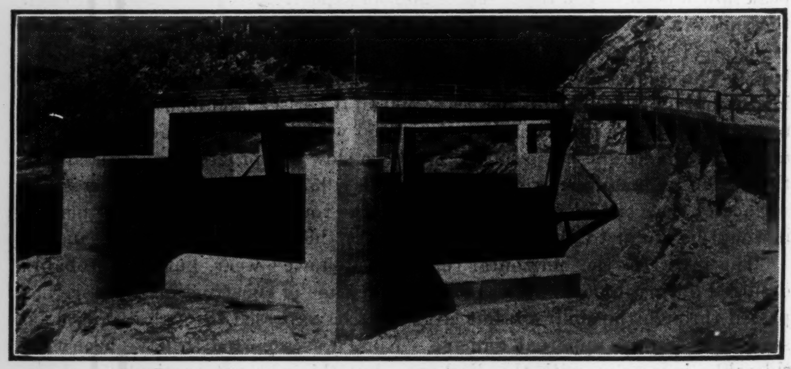

FIG. 6.—GIBSON DAM SPILLWAY GATE STRUCTURE

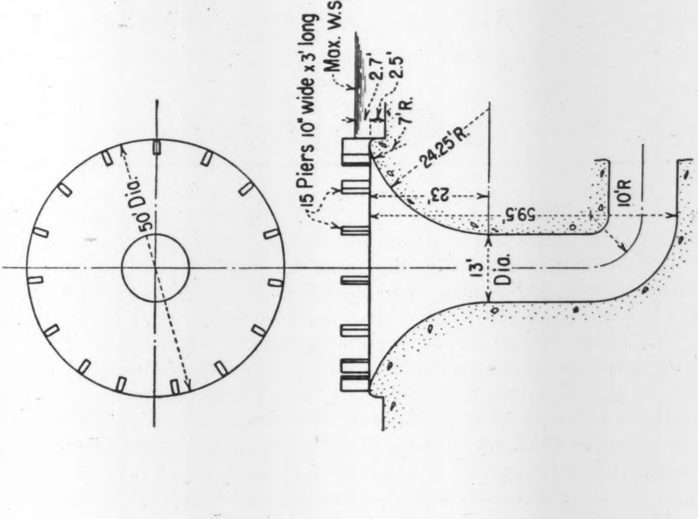
50' Dia.
15 Piers 10" wide x 3' long
Max. W.S.
2.7'
2.5'
7'R.
24.25'R.
23'
59.5'
10'R
13' Dia.

FIG. 7.—PONTIAN KETCHIL DAM SPILLWAY

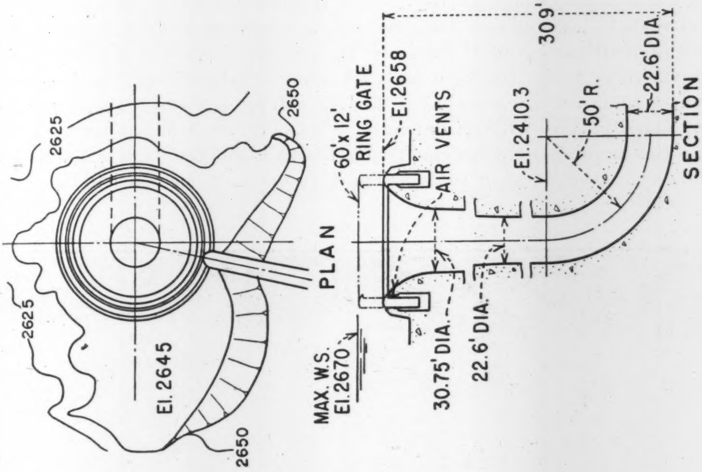
2625
2650
2625
2650
El. 2645
PLAN
MAX. W.S.
El. 2670
60'x 12'
RING GATE
El. 2658
AIR VENTS
30.75' DIA.
22.6' DIA.
El. 2410.3
50' R.
309'
22.6' DIA.
SECTION

FIG. 8.—OWYHEE DAM SPILLWAY

tionable. There was no noticeable vibration, and the radial gates and piers prevented vortex action. The radial gates have been quite satisfactory.

Pontian Ketchil Dam.—The Pontian Ketchil Dam in Singapore was completed in 1931. The spillway was designed for a discharge of 2,700 cu ft per sec, a head of 2.7 ft on the crest, and a fall of 60 ft (Fig. 7). Information indicates that this spillway has operated as expected, without objectionable erosion and without unusual repairs. The spillway is located in the Malayan forest where cyclonic storms of such intensity occur as to uproot large trees and carry them for considerable distances. Many of these trees have passed through the spillway without damage. An emergency spillway was provided in case the morning-glory became partly blocked, but the emergency spillway has not been needed (as of 1955). The antivortex device consists of 15 piers on the crest.

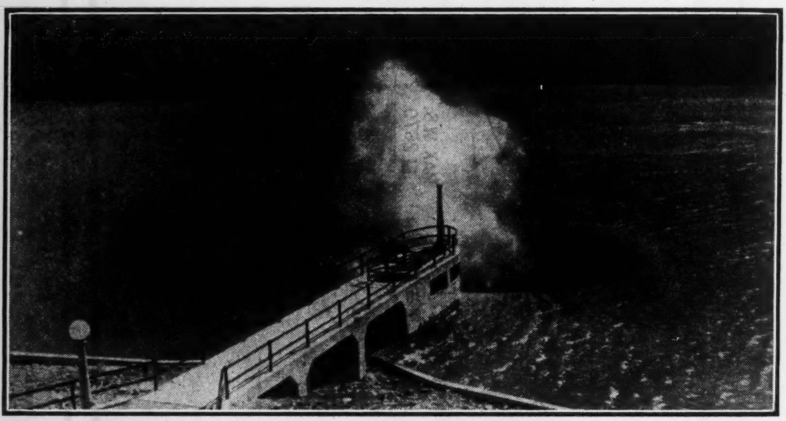

FIG. 9.—OWYHEE DAM SPILLWAY OPERATING WITH 1.5 FT OF HEAD ON THE CREST

Owyhee Dam.—The Owyhee Dam spillway in Idaho (Fig. 8), completed in 1932 by the USBR, was a daring design at the time. The capacity is 30,000 cu ft per sec, the maximum head on the crest for this discharge is 12 ft, and the water is dropped 320 ft through a vertical shaft. A flood occurred in 1936 in which 300,000 acre-ft of water were passed in 3 months. The maximum discharge recorded was 15,000 cu ft per sec, or one-half capacity. Subsequent to this flow, smaller discharges have passed through the spillway frequently. A flow of 6,600 cu ft per sec was recorded in 1951. The greatest flood occurred in 1952, when the spillway operated for more than a month. The maximum discharge through the spillway was 20,000 cu ft per sec, or 67% of capacity. Inspections of the spillway have been conducted frequently since the spillway first operated in 1936; the latest inspection was made after the 1952 flood. The spillway shaft appeared to be in excellent condition. The form board marks still appeared on the concrete surface. The visible part of

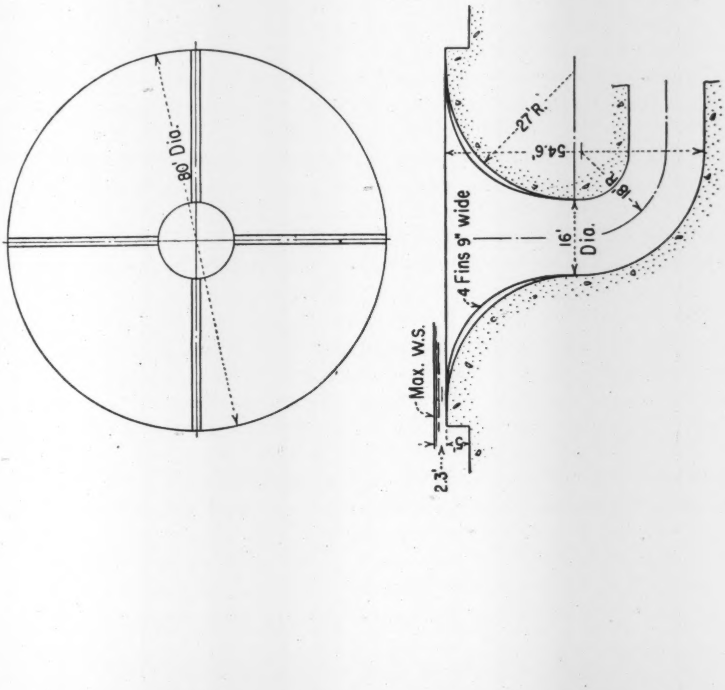
80' Dia.
Max. W.S.
2.3'
5'
4 Fins 9" wide
16' Dia.
18' R.
54.6'
27' R.

FIG. 10.—SILENT VALLEY DAM SPILLWAY

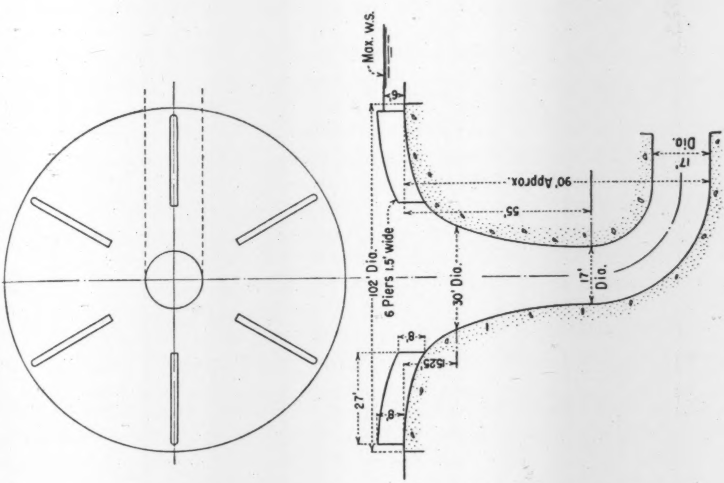
Max. W.S.
6'
102' Dia.
6 Piers 1.5' wide
30' Dia.
17' Dia.
55'
90' Approx.
17' Dia.
8'
8'
27'
15.25'

FIG. 11.—MANUHERIKIA FALLS DAM SPILLWAY

the invert of the vertical bend showed only slight surface wear, the maximum probably not exceeding ¼ in. in depth.

At the time of the inspection, 7 ft of water was standing in the tunnel so that it was impossible to inspect the lower part of the elbow except by probing. Probing with a piece of ½-in. pipe indicated no cavities or sign of excessive wear at the base of the vertical bend. As nearly as could be determined, the surface of the concrete in this area was not smooth, but the roughness probably did not exceed ½ in. in depth. The invert of the horizontal tunnel was also inspected by probing. No signs of excessive wear were found in this area, and the surface of the concrete appeared to be of about the same roughness as that observed near the base of the elbow. No evidence of vibration has been apparent during spillway operation, and the jet does not flutter even with the gate in a raised position. It is also of interest to note that a single pier controls the vortex action and also houses the ring-gate operating equipment.

As this spillway is unusual so far as size is concerned, a few of the operating characteristics will be cited. For heads of from 1 ft to 2 ft over the gate, the water falls in a solid sheet toward the center of the shaft, apparently entraining air faster than it can be released at the outlet end of the tunnel. This entrainment causes the pressure to increase until it is sufficient to "break back"; then air emerges with sufficient force to carry spray 50 ft or 60 ft above the level of the gate, as shown in Fig. 9. This phenomenon occurs sometimes as often as once every 5 min, depending on the tailwater elevation. For heads less than 1 ft on the crest, entrained air can apparently move back up the spillway shaft unhampered. For heads greater than 2 ft, the air pressure is not sufficient to break back and the air is forced through the outlet end of the tunnel, causing spray to be thrown high into the canyon. This action is directly related to the tailwater as a rather large tailwater depth causes a jump to form in the tunnel for most discharges.

The ring gate on the spillway and the controls have operated smoothly at all times. The ring gate was designed for automatic operation but it was learned that manual operation was preferable. A similar type of gate was incorporated on the spillway of the Hungry Horse Dam.

The Silent Valley Dam.—The spillway for the Silent Valley Dam in Ireland (Fig. 10) was designed for a capacity of 2,500 cu ft per sec, a head of 2.3 ft on the crest, and a fall of 55 ft. Apprehension that erosion might occur caused the designers to line the vertical bend with cast iron. The spillway has operated several times, as expected, without any unusual erosion or repairs.

Manuherikia Falls Dam.—The Manuherikia Falls Dam spillway in New Zealand (Fig. 11) is designed for 15,000 cu ft per sec, a fall of approximately 96 ft, and a head of 6 ft on the crest. This spillway has passed several small floods since its completion in 1935, aggregating about 2 ft of head on the crest, in addition to a moderately large flood in November, 1948. In 1948 the spillway passed a maximum flow of 5,000 cu ft per sec, representing one third of capacity. Erosion has occurred on the crest curve of the morning-glory at the construction joints. There are also signs of wear at the circumferential construction joints in the vertical shaft to approximately 25 ft below

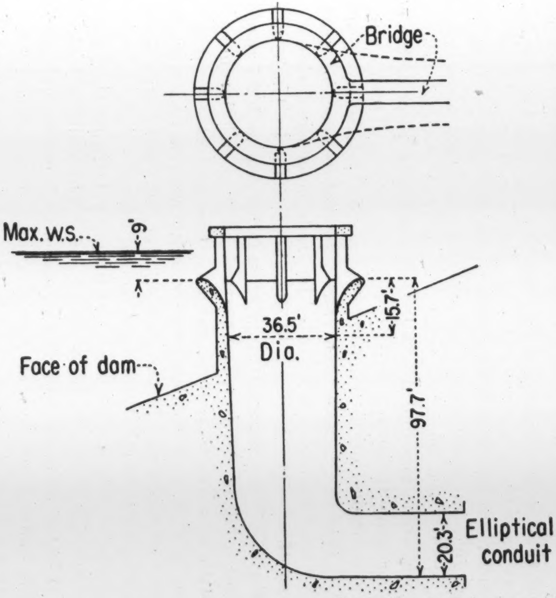
Bridge
Max. W.S.
9'
36.5'
Dia.
15.7'
Face of dam
97.7'
20.3'
Elliptical conduit

FIG. 12.—LA REGADERA DAM SPILLWAY

FIG. 13.—ENTRANCE, LA REGADERA DAM SPILLWAY

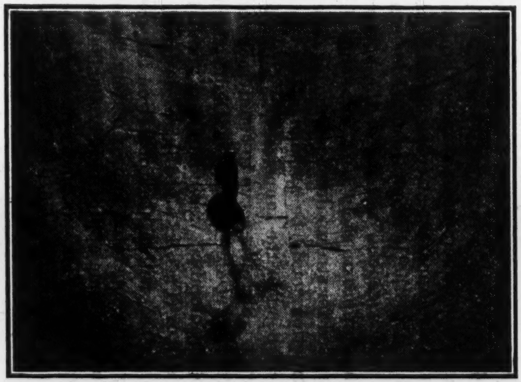

FIG. 14.—BEND AT BASE, LA REGADERA DAM SPILLWAY

crest level. At these joints some of the concrete has been eroded to a depth of 3 in. whereas a few patches on the surface show wear to a depth of approximately ¾ in. on areas up to 3 sq ft. Frost action may have caused some of the erosion, there being seepage through the rock surrounding the spillway. Wear is also apparent at construction joints (as much as 3 in.) at the vertical bend and in the horizontal tunnel for some 100 ft downstream. There has also been a general wearing of the bottom of the horizontal tunnel up to a depth of approximately 1 in., but some of this occurred while the tunnel was being used for stream diversion during dam construction. It is suggested that construction joints be avoided at the crest and also in the vicinity of the vertical bend in the tunnel. Very little debris or ice has passed through the spillway. Six piers serve to counteract vortex action.

Regadera Dam.—Regadera Dam, which forms a reservoir for the city of Bogotá, Colombia, was completed about 1935. The morning-glory spillway of this dam (Figs. 12 and 13) was designed for a maximum discharge of 15,000 cu ft per sec, with a head of 9 ft on the crest, and a total fall of 107 ft. This spillway has operated approximately 9 months out of every year since 1938. During this time approximately 800,000 acre-ft of water have passed through the spillway. The maximum discharge occurred in 1943 and was estimated to be approximately 5,670 cu ft per sec, or 38% of capacity. From November, 1938, to November, 1952, there were 78 days of operation in which the head over the crest exceeded 1.3 ft, and of the 78 days, the spillway operated 4 days with heads greater than 3.3 ft. There has been a general roughening of the surface at the base of the vertical bend, as can be seen in Fig. 14. The vertical shaft is in excellent condition, but the invert of the horizontal tunnel shows erosion to a depth of approximately 1 in. However, water from the outlet works flows through the horizontal part of the tunnel approximately 75% of the time. This could carry some abrasive material. In general, debris has passed through the spillway without difficulty. In 1943, however, some logs and debris lodged across the piers of the spillway, and it was necessary to lift this material out with cables. During one night of this flood, a great deal of vibration was noticeable and the noise was louder than usual. This could have been caused by debris blocking part of the spillway; no vibration has been reported before or since this incident.

Burnhope Dam.—The spillway at Burnhope Dam in Durham County, England (Fig. 15), has a capacity of 2,600 cu ft per sec, with 2.7 ft of head on the crest and a fall of 106 ft. The vertical bend in the Burnhope spillway was lined with cast iron to prevent erosion. One moderate flood of 1,440 cu ft per sec, or 55% of capacity, has been recorded with no undersirable operating conditions or damage. In this design, a curtain wall extends across the center of the spillway parallel to the horizontal tunnel.

Kingsley Dam.—The spillway for the Kingsley Dam on the North Platte River near Ogallala, Nebr., is shown in Fig. 16. The spillway is designed for a capacity of 54,000 cu ft per sec, with a head of 28 ft on the crest and a fall of 148 ft. This spillway has been in operation many times since 1947. During 1951, the gates were used to pass water for irrigation and power for almost the entire year. The maximum discharge has been approximately 4,500 cu ft per

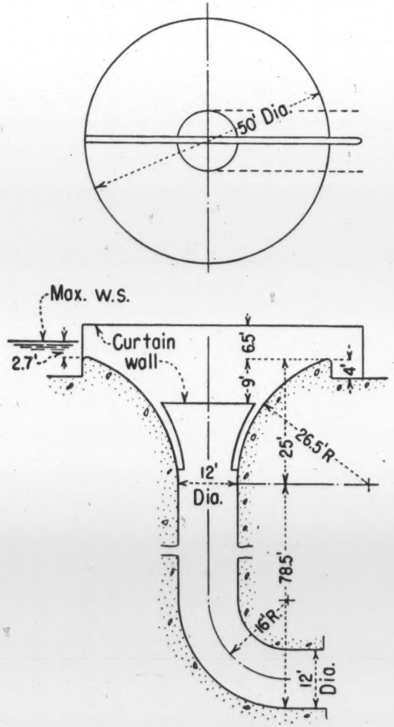
50' Dia.
Max. W.S.
2.7'
Curtain wall
6.5'
9'
4'
26.5'R
25'
12' Dia.
78.5'
16'R
12' Dia.

FIG. 15.—BURNHOPE DAM SPILLWAY

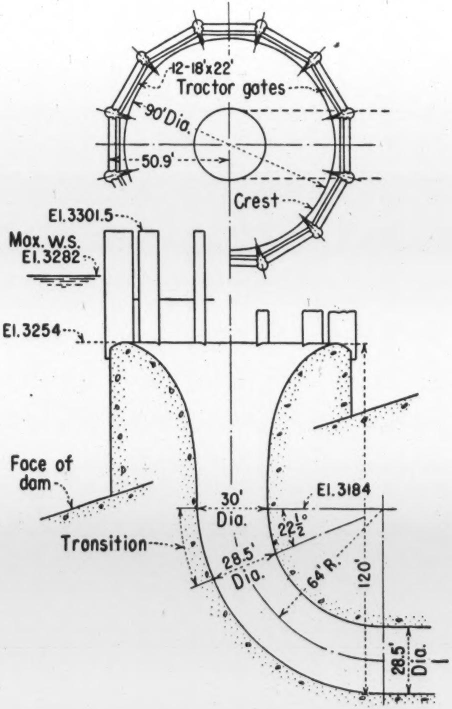
12-18'x22'
Tractor gates
90' Dia.
50.9'
Crest
El. 3301.5
Max. W.S. El. 3282
El. 3254
Face of dam
30' Dia.
El. 3184
22½°
Transition
28.5' Dia.
64'R.
120'
28.5' Dia.

FIG. 16.—KINGSLEY DAM SPILLWAY

sec, 8% of capacity. The vertical bend and tunnel show no perceptible wear, and there has been no opportunity to pass debris or ice through the spillway as the flow has always passed under the tractor gates. No difficulties have been encountered in connection with the operation of these high tractor gates.

Jubilee Dam.—The spillway at the Jubilee Dam, in Hong Kong (Fig. 17), has a capacity of 17,000 cu ft per sec, with a head of 9.4 ft on the crest and a drop of 245 ft. There was evidently some concern as to the advisability of dropping the water 245 ft into a vertical shaft, which is evidenced by the introduction of the inclined tunnel. The only information received on the Jubilee spillway is that the spillway operated as expected. Discharges have been small or moderate, and no erosion is reported. This is the first spillway in which special air venting was used in the shaft. A curtain of water tends to seal the tunnel at the entrance to the inclined shaft; thus, an air duct was provided in the inclined part of the tunnel. It is interesting to note that the curtain wall in this spillway is normal to the one on the Burnhope spillway.

Lady Bower Dam.—The Lady Bower Dam in Derby County, England, completed in 1944, utilizes two similar morning-glory spillways (Fig. 18). Each spillway is designed for a capacity of approximately 10,000 cu ft per sec, with a head of 6.5 ft on the crest and a fall of 128 ft. Several floods have passed over the spillways—in fact, three heavy storms occurred before the spillways were completed. The discharges through the spillways have been 1,240 cu ft per sec in 1947, 540 cu ft per sec in 1948, 310 cu ft per sec in 1949, 1,520 cu ft per sec in 1950, 1,460 cu ft per sec in 1951, and 2,310 cu ft per sec in 1952; it is assumed that these discharges should be divided between the two spillways. The tunnel and vertical bends on both spillways were inspected in 1951 and on several previous occasions. The only sign of erosion was at the inside of the vertical bend at about the midpoint. This involves an area of about a yard square and is little more than roughening of the concrete surface. The spillway has passed small quantities of ice, but the radial piers on the rim of the spillway prevent the passage of any large quantity particularly when the ice is thick. Only during the last stages of thaw does any ice go down the spillway. It has been noted that when the spillway is discharging heavily the cascade of broken water falling down the shaft acts as an air pump and produces an air current charged with spray, which discharges out the lower end of the tunnel in considerable volume. Contrary to expectations, the discharge is slightly greater for a given head with the stepped morning-glory than with a smooth one. The spillways have proved a highly efficient method of discharging overflow water from the reservoir and they are entirely reliable for that purpose.

Lumot Dam.—The spillway at the Lumot Dam in the Philippine Islands was completed in 1949; unfortunately, the drawings for this spillway are not available. The spillway is designed for a capacity of 7,060 cu ft per sec. The spillway operated intermittently from November 28, 1951, to March 1, 1952. The maximum discharge was 690 cu ft per sec, or approximately 10% of capacity. There has been no noticeable erosion throughout the tunnel lining. No debris has passed through the spillway, noise has been unnoticeable, and no vibration has been observed.

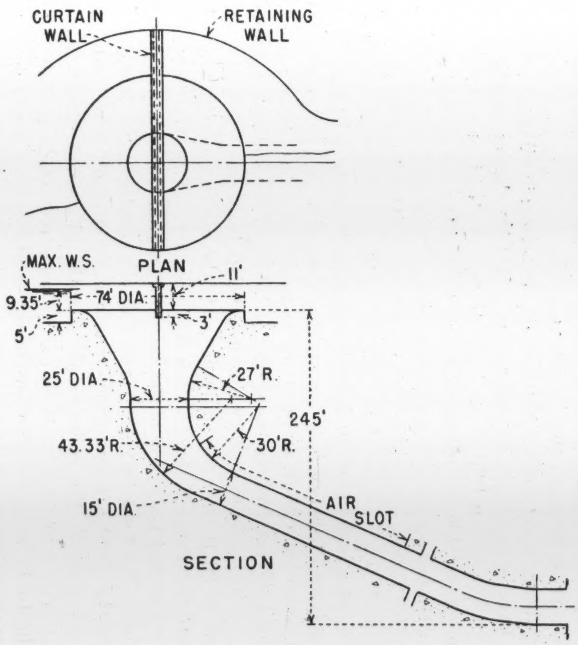
CURTAIN WALL
RETAINING WALL
PLAN
MAX. W.S.
11'
9.35'
74' DIA.
3'
5'
25' DIA.
27' R.
245'
43.33' R.
30' R.
15' DIA.
AIR SLOT
SECTION

Fig. 17.—Jubilee Dam Spillway

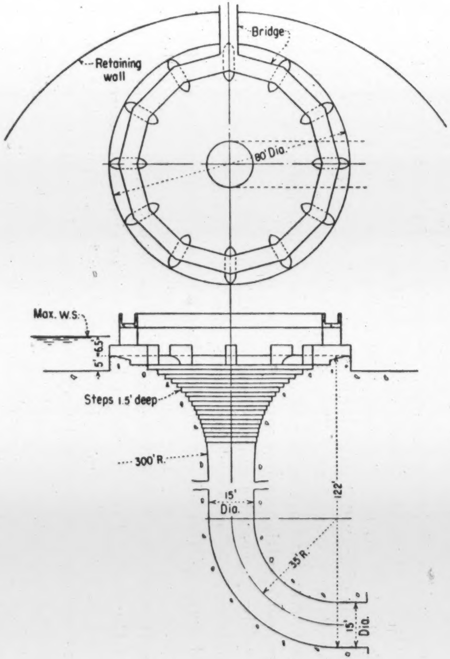
Bridge
Retaining wall
80' Dia.
Max. W.S.
5'-6.5'
Steps 1.5' deep
300' R.
15' Dia.
122'
35' R.
15' Dia.

Fig. 18.—Lady Bower Dam Spillway

Heart Butte Dam.—The Heart Butte Dam (Fig. 2) was constructed by the USBR and completed in 1949. The spillway is different from those previously cited in that it is designed to operate principally submerged. The capacity is 5,600 cu ft per sec for a head of 54 ft on the crest, and the water falls 113 ft to the invert of the horizontal tunnel. Free flow occurs for heads up to 6 ft, and submerged flow occurs for greater heads. Vortices form for heads of from 6 ft to 20 ft; for heads of from 20 ft to 54 ft, vortices are either small or nonexistent. The fixed piers on the crest serve to break the large vortex into a number of smaller ones, thus reducing fluctuations in discharge and resulting in improved flow conditions.

The spillway passed a major flood in 1950, less than a year after the dam was completed. It operated for approximately 1 month and passed 148,000 acre-ft of water. The maximum flow into the reservoir during the flood was 24,000 cu ft per sec, and the maximum discharge through the spillway was 3,800 cu ft per sec. An inspection after the flood showed erosion at two points in the vertical bend. In each case the eroded areas were about 8 in. in diameter and a maximum of 1 in. deep; casts have been made.[3] A second flood was experienced at the Heart Butte Reservoir in 1951. The spillway again operated for almost a month at a maximum discharge of approximately 3,000 cu ft per sec. Casts of the erosion in the vertical bend were again made after the second flood, and it was found that there was practically no difference in those taken in 1950 and 1951.

The spillway is not noisy and there is no noticeable vibration, but it has passed a large quantity of ice and debris. In 1950 the ice on the reservoir was 12 in. thick, and in 1951 it was 36 in. thick. As the flood occurred during a thaw much of this ice passed through the spillway, together with large timbers and debris.

Shade Hill Dam.—The Shade Hill Dam in South Dakota (Fig. 19), another USBR project, was completed in 1950. This is another retention reservoir, and the spillway is designed to operate submerged. The spillway is designed to pass more than 5,000 cu ft per sec, with a head of 40 ft on the crest. If the head increases above 25 ft, an emergency spillway will also go into operation. A flood filled the reservoir in the spring of 1951 and the spillway operated for 1½ months. The maximum flow through the spillway was 5,020 cu ft per sec for a head of 26 ft over the spillway crest whereas the maximum discharge flowing into the reservoir was 33,250 cu ft per sec. After the flood, plaster casts were made of the invert of the vertical bend but these showed no noticeable erosion. The tunnel and the vertical shaft were also in excellent condition.

During the flood a boom which was contrived of oil barrels and cables partly went through the spillway along with drift wood, timber, and ice, which was from 4 in. to 6 in. thick on the reservoir. A large dislodged tree some 18 in. to 20 in. in diameter, with roots and branches, was also observed going over the spillway. While operating submerged, a large vortex persisted over the spillway but there appeared to be no detrimental effect caused by it.

---

[3] "Morning-Glory Shaft Spillways: Performance Tests on Prototype and Model," by Alvin J. Peterka, *Transactions*, ASCE, Vol. 121, 1956, p. 385.

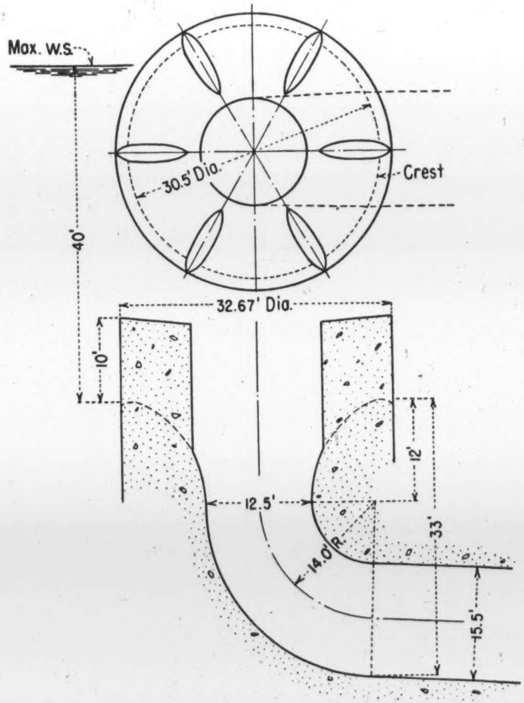
Max. W.S.
40'
30.5' Dia.
Crest
32.67' Dia.
10'
12'
12.5'
33'
14.0' R.
15.5'

FIG. 19.—SHADE HILL DAM SPILLWAY

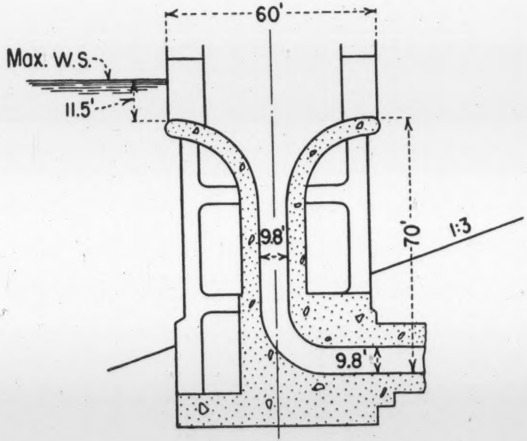
60'
Max. W.S.
11.5'
9.8'
70'
1:3
9.8'

FIG. 20.—AKONGTIEN DAM SPILLWAY

Akongtien Dam.—The Akongtien Dam in South Taiwan was completed in 1951. The spillway was designed for a maximum discharge of 3,250 cu ft per sec, with a head of 11.5 ft on the crest. The drop from headwater to invert of the horizontal tunnel is approximately 81 ft. The spillway discharged for approximately 5 days in 1953, with a maximum discharge of 1,000 cu ft per sec, or approximately one third of capacity. The volume of water passed was approximately 27,300 acre-ft. No erosion could be found in the shaft, vertical bend, or horizontal tunnel. This spillway operates submerged at about half capacity. Vibration was unnoticeable and noise was not objectionable. Very little debris passed over the spillway during the flood.

CONCLUSIONS

From the foregoing prototype information it can be noted that about half of the spillways that have operated have undergone a fair test. The results of the investigation are by no means conclusive but they are extremely encouraging. In summing up the foregoing, it can be said that in no case has erosion of a serious nature occurred in any of the spillways investigated. Of particular importance is the report from the Owyhee Dam which operated often, once at half capacity and once at two-thirds capacity. This is definitely the most adverse operating condition experienced with a morning-glory spillway dropping the water over 300 ft vertically, yet nothing but roughened surfaces has developed. There is good reason to believe that the erosion reported at the vertical bends on several of the spillways can be attributed to logs and objects falling down the shaft; to poor surface concrete which has been scaled off by the high-velocity water; or to spalling as a result of freezing and thawing. Vibration, noise, and vortex action have been found unobjectionable; it is possible, however, that unsymmetrical loading of the spillway with debris can produce vibration, as was surmised in the case of the Regadera spillway.

Several recommendations have been suggested in the correspondents' letters: Construction joints should be eliminated in the morning-glory part of spillways, as objectionable erosion was experienced in the case of the Manuherikia Falls Dam spillway. Several correspondents suggested that construction joints be eliminated in the vicinity of the vertical bend and that particular care be taken with formwork to eliminate offsets in this curved surface. Some went so far as to recommend grinding of the invert surface throughout the vertical bend.

Approximately one third of the spillways investigated showed considerable leakage at construction joints in the shaft and in the horizontal tunnel. This leakage is objectionable from the standpoint of frost action, inspection, and repairs. Also, large cavities can be formed around the tunnel lining where water has transported material through the construction joints. It was therefore suggested that rubber waterstops be considered in future designs.

The best method known for coping with erosion caused by high velocities in morning-glory spillways lies in maintaining smooth surfaces, outlawing misalinement, and eliminating construction joints in vertical bends. It stands to reason that a roughened surface is more susceptible to scaling, impact forces, and cavitation than a smooth one when exposed to high-velocity water.

On the basis of the foregoing, the designer should be able to view morning-glory spillway design with more confidence than has existed in the past.

ACKNOWLEDGMENTS

The following persons contributed the information on prototype operation: F. Kurtz, M. ASCE; H. M. Nelson, A.M. ASCE; G. E. Johnson, M. ASCE; A. C. Tilley; J. W. Ridley; and A. G. Park, M. ASCE (Wellington, New Zealand); H. Prescott Hill (Manchester, England); F. W. Rozo (Bogotá, Colombia); F. C. Rodriquez, A. M. ASCE (Manila, Philippine Islands); Y. C. Chu (South Taiwan); S. B. Morris, M. ASCE (Los Angeles, Calif.); Conrad P. Hardy, M. ASCE (Cincinnati, Ohio); C. E. Blae, M. ASCE (Knoxville, Tenn.); the associates of Mr. Binnie (Westminster, S. W. England); and the regional directors of the USBR at Billings, Mont., Denver, Colo., and Boise, Idaho. The assistance of D. C. Walter at Boise is greatly appreciated.

DISCUSSION

Bernard Donelan.[4]—The morning-glory spillway has been used at Kingsley Dam to discharge water a few months of every year since 1947. The spillway has never been operated as a flood-control structure as the reservoir has never reached the stage where it was necessary to discharge excessive water.

The statement by Mr. Bradley that no debris or ice has passed through the spillway because the flow has always passed under the tractor gates is correct. Also, no water has been discharged through the morning-glory spillway during extremely cold weather because the film of water between the tractor gates and the guides freezes the tractor gates to the guides and they cannot be moved. Therefore, the morning-glory spillway is not operated during the winter when an ice cap has formed on the reservoir.

The water in the morning-glory spillway discharge conduit is approximately 20 ft when the spillway is not in operation. A diver made a complete inspection of the part of the conduit under water in September, 1949, and found the surface of the concrete conduit to be in perfect condition with no signs of erosion or cavitation. The surface of the concrete above the water showed no wear.

The morning-glory spillway at the Kingsley Dam has only operated at a very small percentage of capacity; the tractor gates are all working perfectly. The spillway is operating with very little noise and no noticeable vibration.

Donald S. Walter.[5]—The material presented herein is a description of the Hungry Horse Project, with special emphasis on the initial operation of the spillway.

As mentioned by Mr. Bradley, the Hungry Horse spillway is a bold design of the morning-glory type. Hydraulic model studies of the spillway were made on a 1 to 36 scale model for the purpose of developing the hydraulic design. The morning-glory spillway with an adjustable ring-gate crest structure which discharges into a tapered and sloping tunnel presented unusual and difficult hydraulic problems. From a hydraulic standpoint, it was recommended that an open-channel entrance structure similar to the Hoover Dam spillways be utilized at the intake of the tunnel. However, structural limitations made the use of the morning-glory entrance more desirable.

The Hungry Horse reservoir was filled to capacity the first year following completion of the dam, when water began flowing over the spillway crest on July 9, 1954. Initial operating tests were performed on July 13, 1954, with releases through the spillway up to a maximum of 30,000 cu ft per sec. Although the spillway was designed to pass a flow of 53,000 cu ft per sec, combined releases from the reservoir had to be controlled so as not to cause the river to exceed the flood stage of 50,000 cu ft per sec at Columbia Falls, Mont.

---

[4] Resident Engr., Supt., Central Nebraska Public Power and Irrig. Dist., Hastings, Nebr.

[5] Regional Engr., Bureau of Reclamation, U. S. Dept. of the Interior, Boise, Idaho.

Hydrology.—Because the south fork of the Flathead River drains a high mountainous area of 1,640 sq miles bounded on the east by the Continental Divide and receives most of its precipitation through winter snowfall, the bulk of its floodwaters is discharged during April, May, and June, with the high-water peak usually arriving in May. There is a wide variation between the maximum and minimum yield, varying from 3,500,000 acre-ft to 1,400,000 acre-ft, with the average being 2,350,000 acre-ft per yr. In general, use of the spillway is required only when the reservoir is full in the spring and it is deemed advisable to draw down the reservoir level to reserve space for flood control.

Dam.—Hungry Horse Dam is a variable-thickness, concrete-arch dam 2,115 ft long at the crest with a maximum height of 564 ft. Containing 2,935,000 cu yd of concrete, it ranks fourth in the United States in volume, exceeded only by Grand Coulee (Washington), Shasta (California), and Hoover (Nevada) dams. The reservoir has a capacity of 3,468,000 acre-ft of which 2,982,000 acre-ft are active storage for power generation.

Outlet Works.—Three 96-in.-diameter outlet pipes are provided to regulate downstream water requirements and to permit rapid lowering of the reservoir for flood control. Discharge through the outlet pipes is controlled by hollow-jet valves in the valve house and ring-follower gates located in the foundation of the power plant. The maximum capacity of the outlet works is 14,400 cu ft per sec with full reservoir.

Power Plant.—The powerhouse is located at the toe of the dam in the original river channel and contains four main generating units. Each unit consists of a 75,000-kva generator driven by a 105,000-hp turbine. With full reservoir, each turbine requires a flow of slightly more than 2,000 cu ft per sec.

Spillway.—The outstanding hydraulic appurtenance of Hungry Horse Dam is the morning-glory spillway shown in Fig. 1. Located on the right abutment, the spillway consists of a concrete-lined tunnel with a 64-ft by 12-ft steel ring gate installed in the top of the morning-glory structure. The gate is a buoyant vessel that floats with 9 ft of freeboard in the water of the concrete gate chamber. The crest of the gate can be raised or lowered a distance of 12 ft by the operation of valves which balance the inflow and outflow of water in the gate chamber. An automatic control system maintains the water at any preset elevation, and manual control is provided for emergency operation. Air is supplied to the undernappe of the flow through the morning-glory by nine 8-in. pipes which terminate in a triangular-shaped air chamber encircling the structure. A 6-ft-square air-inlet tunnel opening to the atmosphere provides air for the air chamber and also to an opening in the crown of the tunnel just below the throat.

The throat or base of the converging section of the morning-glory is 37 ft in diameter, tapering to a diameter of 34.79 ft at the upstream end of the inclined tunnel. The incline has a total vertical drop of 341.3 ft and tapers to a diameter of 24.5 ft at the downstream end. A vertical bend connects the inclined tunnel to the nearly horizontal tunnel which continues to the outlet portal on a slope of 0.0019. The tunnel is 24.5 ft in diameter throughout the lower bend and for a distance of 219.25 ft downstream, then is transformed through a 166-ft-long transition section to a 31-ft-diameter horseshoe tunnel. The downstream end of the spillway floor is raised 13.5 ft by a long radius curve and forms a vertical deflector which raises the high-velocity jet above the river tailwater and allows the jet to drop into the river a safe distance from the structure. Thus, from the spillway crest to the invert of the tunnel at the outlet portal, the spillway discharge drops a vertical distance of 487 ft in a horizontal distance of 1,402.09 ft.

Precautions Taken During Construction.—In order to avoid, so far as possible, a recurrence of the erosion experienced in the Arizona spillway tunnel at Hoover Dam, several precautionary measures were taken during construction of the Hungry Horse spillway to assure accurate alinement, smooth concrete surfaces, and elimination of construction joints in the vertical curve and deflector sections. After placement of the tunnel lining, the surrounding rock was thoroughly grouted, using pressures varying between 125 lb per sq in. and 150 lb per sq in.

In the upper part of the inclined tunnel, all abrupt irregularities in the concrete lining were completely eliminated by grinding on a bevel of 1 to 50 ratio of height to length. For the remainder of the tunnel, abrupt irregularities were completely eliminated by grinding on a bevel of 1 to 100 ratio of height to length. A special finish was given to the concrete surface of the vertical curve below the center line of the tunnel. After removal of irregularities by grinding, the surface was thoroughly sandblasted so as to penetrate the small surface voids and completely etch the surface. When all loose materials were removed by washing, mortar was applied by hand-stoning with a fine-grit carborundum stone in sufficient quantity to produce a relatively thin mortar coating which barely covered the high points of the original surface. After the mortar had been water-cured for at least seven days, the surface was carefully smoothed by final grinding.

Special precautionary measures were taken during construction of the vertical bend and deflector sections of the spillway. The concrete in these sections was placed without construction joints and was cooled by pumping river water through tubing embedded in the concrete. The purpose was to repress the temperature rise as much as possible the first week after placement, so that the concrete in these critical sections of lining would not undergo large temperature variations, and therefore could be placed without construction joints and without the development of objectionable cracks.

Spillway Operation Tests.—In order to test the spillway and also to determine the extent of the river-channel improvement work that will be required below Hungry Horse Dam in the future, the spillway was initially placed in operation on July 13, 1954. The tests were conducted under the supervision of Louis Puls, A. M. ASCE, with actual operations being performed under the guidance of Charles Simmonds. Prior to beginning the spillway tests, the reservoir level was at El. 3560.5, resulting in 6 in. of water flowing over the crest of the 64-ft-diameter ring gate which was in the maximum raised position.

During the tests, observations were made at the spillway inlet or morning-glory and at the tailrace for the conditions shown in Table 2.

For each gate setting, the observations were made on (1) the elevation of the gate crest, (2) the elevation of the reservoir level, (3) the air intake velocity, (4) the elevation of the tailrace above the power-plant weir, (5) the elevation of the tailrace downstream from the power-plant weir, and (6) pressure readings in the morning-glory and the throat of the spillway tunnel.

TABLE 2.—FLOWS[a] AT HUNGRY HORSE DAM

Test	Reservoir release	Outlet works	Power plant	Total
1	2,000		8,100	10,100
2	5,000		8,100	13,100
3	10,000		8,100	18,100
4	10,000	3,000	8,100	21,100
5	10,000	6,000	8,100	24,100
6	15,000		8,100	23,100
7	20,000		8,100	28,100
8	30,000			30,000

[a] In cubic feet per second.

These readings and other pertinent data are being studied (1955) for comparison of the prototype behavior with the model. It is unfortunate that this information cannot be made available until after the study has been completed.

As the gate was slowly lowered, some spray emerged from the morning-glory opening when the head over the crest reached approximately 1 ft. However, as the head increased, the spray decreased in intensity, as in the case of the Owyhee Dam morning-glory spillway. It was noted that the minimum flow required in the tunnel to cause the flow to spring free of the deflector was between 1,000 cu ft per sec and 1,500 cu ft per sec.

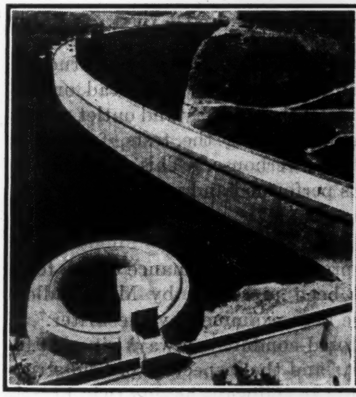

FIG. 21.—COMPLETED HUNGRY HORSE DAM SPILLWAY STRUCTURE

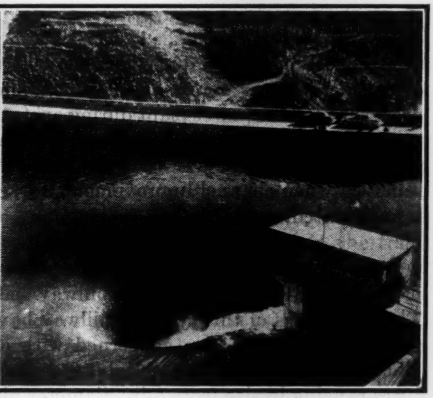

FIG. 22.—FLOW OF 30,000 CU FT PER SEC INTO SPILLWAY

In Fig. 21 there is shown the morning-glory structure prior to the time the reservoir was filled. Figs. 22, 23, and 24 show the flow characteristics of the spillway when the discharge reached 30,000 cu ft per sec. It is interesting to note that, during this high flow to the spillway, the velocity of air into the air-inlet tunnel was approximately 4,000 ft per min.

In order to observe tailrace conditions with both the spillway and outlet works in operation, two hollow-jet valves were opened to discharge approximately 3,000 cu ft per sec each, in combination with a release of 10,000 cu ft per sec from the spillway. Under these conditions, the water in the river was drawn down 20 ft below the level of the power-plant tailrace. This same condition existed during the model tests and resulted in the construction of a concrete weir across the river channel to assure adequate head on the draft tubes of the power plant during operation of the spillway and outlet works.

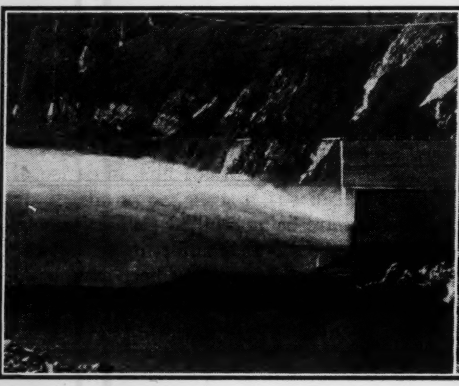

Fig. 23.—Spillway Jet at Deflector

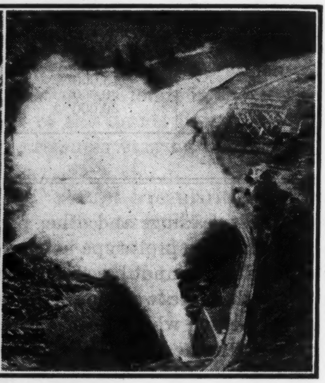

Fig. 24.—Overhead View of Discharge

Some erosion occurred in the river channel during the tests, forming a gravel bar 1,400 ft downstream from the powerhouse. This bar will be removed when channel improvement work is performed and no further erosion is anticipated.

Fred W. Blaisdell,[6] M. ASCE.—The prototype performance of one form of the closed-conduit type of spillway has been presented by Mr. Bradley. The hydraulics of this type of spillway have been examined by the writer.[7]

The writer has been concerned with closed-conduit spillways since 1940. This work has involved both laboratory tests and the inspection of field structures ranging in size from 8-in.-diameter pipes to spillways having twin barrels 6 ft square. These structures are small in comparison to morning-glory, closed-conduit spillways considered by Mr. Bradley, but because the Soil Conservation Service, United States Department of Agriculture (SCS), probably builds well over a thousand closed-conduit spillways each year, the statistical opportunity to observe the characteristics of these spillways is better than for the fewer large-size, morning-glory spillways.

---

[6] Project Supervisor, Agri. Research Service, U.S. Dept. of Agriculture, St. Anthony Falls Hydr. Lab., Minneapolis, Minn.

[7] "Hydraulic Fundamentals of Closed Conduit Spillways," by Fred W. Blaisdell, *Proceedings-Separate No. 354*, ASCE, Vol. 79, November, 1953.

The ability of the closed-conduit spillway to "knock the peak off" the flood hydrograph is an important attribute. The peak outflow of 3,800 cu ft per sec reported for the Heart Butte spillway is only 16% of the peak inflow. This large reduction in the peak flow is not uncommon for the closed-conduit spillway. The reduction of the peak outflow to only 3% of the peak inflow at the Shade Hill spillway reflects the effects of an excellent site.

It should be realized that the planned operation of closed-conduit spillways in the submerged range calls for engineering of the highest order because of the limited capacity inherent in this type of spillway. Not only the peak inflow to the reservoir is required; the complete inflow hydrograph is required so that the flood can be routed through the reservoir and sufficient volume of storage can be provided to care for the detained run-off; M. M. Culp, A.M. ASCE, has cited some of the factors involved.[8]

An emergency spillway, such as is used on the Pontian Ketchil and Shade Hill dams, is certainly a wise precaution. This precaution is more important when the spillway operates submerged than for unsubmerged operation when the discharge changes more rapidly with the head. For the small spillways built under the direction of the SCS, the emergency spillway is frequently lined with vegetation in the expectation that this type of spillway will be adequate for the infrequent peak flows—of short duration on these relatively small watersheds—which exceed the designed capacity of the closed-conduit spillway.

In contrast to the almost complete lack of trash difficulties reported by Mr. Bradley, trash is likely to clog the relatively small soil and water conservation spillways. Therefore, the emergency spillway is necessary to protect against overtopping of the dam from clogging. The writer has observed many types of trash racks under field conditions and has arrived at several opinions regarding these unattended racks: (1) All possible material should be permitted to pass through the spillway in order to delay clogging of the trash rack as long as possible. Therefore, the openings in the trash rack should be as large as feasible. (2) Trash racks should not be located on or close to the closed-conduit-spillway crest. The velocities at the crest are high, the trash packs tightly, and the rack soon becomes a dam rather than a strainer. (3) Timely maintenance is essential—something that often seems to be neglected. (4) The best trash rack for small closed-conduit spillways is (*a*) constructed of woven wire fencing, (*b*) located well away from the inlet so that packing of the trash is minimized, and (*c*) relatively long so that low velocities can be achieved.

Some device to inhibit vortex action should be used on all closed-conduit spillways. The writer has observed reductions in spillway capacity up to 44% as a result of vortex action, and A. M. Binnie and G. A. Hookings have reported[9] reductions up to 90% for plain-pipe entrances and up to 74% on models of bellmouth spillways. Of the vortex inhibiters tested by the writer, a dividing wall, such as is used on the Burnhope and Jubilee dams, has satisfactorily controlled vortex formation. The cross walls should be oriented with the approaching flow; it is not necessary that they be parallel to the axis of the discharge tunnel. An excellent picture of a vortex on a field structure was published by L. Standish Hall in 1942.[10] Uncovered piers, which are common on the spillways reported on by Mr. Bradley, have not been tested by the writer. However, a cover supported on three piers having a height about equal to the depth of initiation of submerged flow performed satisfactorily.

---

[8] "The Effect of Spillway Storage on the Design of Upstream Reservoirs," by M. M. Culp, *Agricultural Engineering*, Vol. 29, No. 8, 1948, pp. 344–346.

[9] "Laboratory Experiments on Whirlpools," by A. M. Binnie and G. A. Hookings, *Proceedings*, Royal Soc. of London, Series A, Vol. 194, 1948, pp. 398–415.

Tentatively, it is suggested that antivortex piers or walls be two shaft diameters high. This is somewhat higher than the 1.3 diameter height of the Heart Butte piers and the 0.8 diameter height of the Shade Hill piers. However, the vortex reported over the Shade Hill spillway is evidence that the piers may be a little low. Another uninvestigated factor that may govern the pier height is the shape of the entrance—the converging morning-glory entrance may require a smaller pier height than the straight entrances used by the writer in his tests. At a spillway tested at the Stillwater (Okla.) Outdoor Hydraulic Laboratory, small vortices were observed that increased in intensity as the total head decreased, resulting in some decrease in spillway capacity. Practically no vibration was detected in spite of the fact that sucking of air through the vortex was audible some distance away. W. O. Ree has stated (in an unpublished report made in 1954):

> "Vibration was noticed only during part-full flows when the straight inlet (culvert entrance) was 'gulping' air; and then it was felt just when standing on the head wall of the inlet structure. The feeling was not of vibration but of slight shocks due to the pulsations or surges of the flow."

When describing the Owyhee Dam, Mr. Bradley comments on spray caused by air entrainment. This air is suddenly released through the inlet at heads of from 1 to 2 ft on the gate and through the outlet at higher heads. Apparently Owyhee Dam is the only spillway having a submerged outlet. This is presumably the reason for the phenomena reported. The writer has observed many models in operation but has never observed the air blow-back if the outlet was not submerged. In fact, the air sucked in with the water up to the point where inlet submergence occurs always passed through the conduit without difficulty. Above the point of inlet submergence, only negligible quantities of air enter the spillway through small vortices, and this air passes through the spillway as a mixture.

Spillways of the closed-conduit type have unique flood-control characteristics that can be used advantageously in many cases. Their more frequent use attests to the fact that engineers are recognizing these advantages.

Rodolfo E. Ballester.[11]—The new San Roque Dam in Córdoba, Argentina, a multiple-purpose dam built to protect the city of Córdoba from floods, was first proposed in 1930.[12]

---

[10] "Drop Structures for Erosion Control," by L. Standish Hall, *Civil Engineering*, Vol. 12, 1942, pp. 247–250.

[11] Cons. Hydr. Engr., Buenos Aires, Argentina.

[12] "Dique San Roque," by R. E. Ballester, C. A. Volpi, and A. Suárez, *La Ingeniería*, Buenos Aires. August–October, 1930, pp. 298–320, 350–385, 394–427, and 463–492.

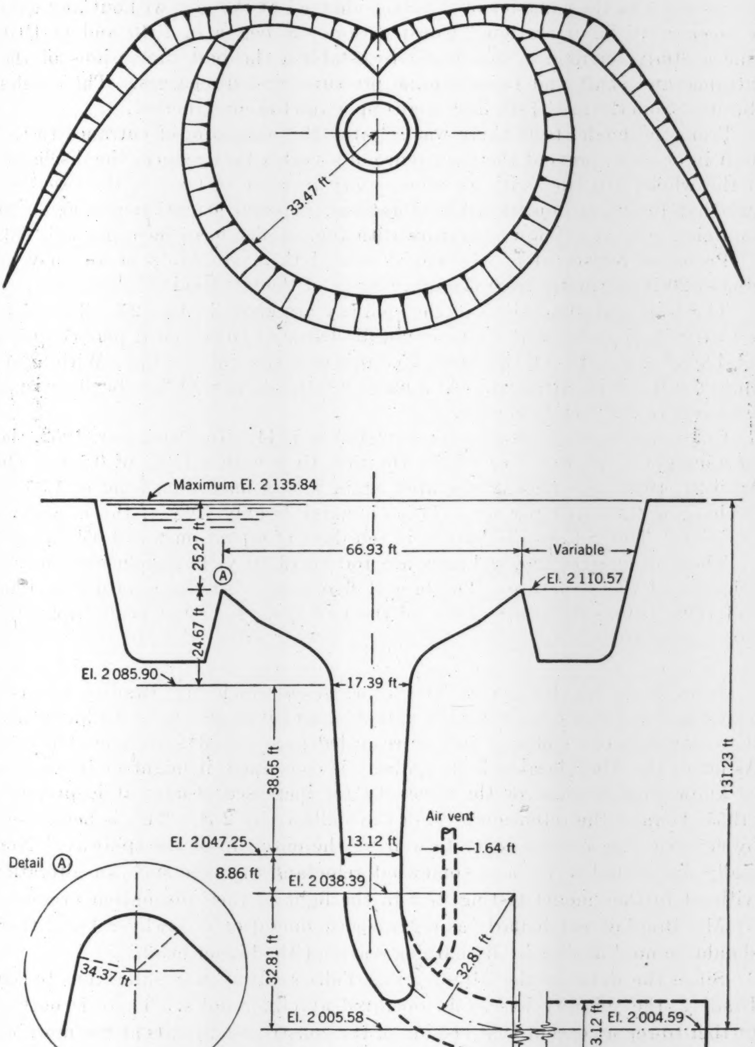
33.47 ft
Maximum El. 2 135.84
66.93 ft
Variable
25.27 ft
Ⓐ
El. 2 110.57
24.67 ft
El. 2 085.90
17.39 ft
38.65 ft
131.23 ft
Air vent
El. 2 047.25
13.12 ft
1.64 ft
Detail Ⓐ
8.86 ft
El. 2 038.39
34.37 ft
32.81 ft
32.81 ft
El. 2 005.58
El. 2 004.59
13.12 ft
436.35 ft

Fig. 25.—San Roque Dam Spillway

A morning-glory shaft spillway was designed to adjust the discharge from the reservoir to the capacity of the river channel at the city without any gate or mechanism for operation. Construction was begun in 1940 and at that time a study on models was made to establish the best dimensions of the entrance and shaft and to determine pressures and discharges. The results obtained from the model studies[13] were applied to the construction.

From the model tests there was selected the best form of entrance to the shaft in order to prevent the occurrence of a vortex that reduces the discharge of the whole structure with an unnecessary increase of level of the reservoir and that provokes objectionable vibrations. Special attention was given to obtaining submerged-flow operation with the smaller head over the weir sill.

Pressures registered on the model caused the installation of an air-vent pipe of 20-in. diameter from the inner curve of the 90° bend.

The principal dimensions of the spillway are given in Fig. 25. The shaft is 13.1 ft in diameter with a maximum discharge of 10,000 cu ft per sec and a total head of 131 ft. Of this head, 25.3 ft is over the spillway lip. With heads up to 6.0 ft, air is entrained. At a head of 6 ft, submerged flow begins with a discharge of 9,200 cu ft per sec.

Construction of the dam was completed in 1944. In December, 1952, the morning-glory spillway worked for the first time with a head of 0.5 ft. On April 24, 1954, the spillway operated again with a maximum head of 1.35 ft, discharging 920 cu ft per sec. This discharge is only 10% of the maximum capacity. The volume discharged in ten days of operation was 4,050 acre-ft.

These discharges and volumes are too small to yield conclusions on the behavior of the structure. The largest floods entering the reservoir in 1903 and 1923, before the construction of the new dam, have not been duplicated since (as of 1955).

JOHN WALLACE RIDLEY.[14]—The information which Mr. Bradley has collected and presented is extremely valuable, and it is gratifying to know that the morning-glory spillway can be regarded as a sound hydraulic structure. As far as the Manuherikia Falls spillway is concerned, it might be interesting to know that because of the necessity for increased storage it is proposed (1955) to raise the retention level of the spillway by 2 ft. This is being done by constructing a small concrete weir on the outer lip of the spillway. Normally one would have been somewhat reluctant to make such an alteration without further model testing, but in the light of the information presented by Mr. Bradley, particularly as regards gate operation at Owhyee Dam, there should be no difficulty in discharging water at the higher head.

Since the data on the Manuherikia Falls spillway was submitted to Mr. Bradley, the spillway has again operated at minor flows. There is nothing further to report except that erosion of the construction joints at the morning-glory crest is becoming progressively worse mainly because of frost action, and it will be necessary to repair these joints when the concrete weir is added.

---

[13] "Dique San Roque: Estudios con Modelos Reducidos del Pozo-vertedero," by R. J. Perazzo, *La Ingenierià*, Buenos Aires, October–November, 1941, pp. 1036 and 1114.

[14] Designing Engr., Ministry of Works, Wellington, New Zealand.

One point on which an expression of opinion might be worthwhile is the need for directing piers or vanes. Piers were included at Manuherikia because of the asymmetrical flow conditions shown by the model. However, it is apparent that many morning-glory structures have no guiding piers, and no adverse effects are evident. Owhyee Dam is a case in point where the spillway is asymmetrically placed with respect to topography and adjacent structures and yet its operation appears to be quite satisfactory; on the other hand, Davis Bridge Dam has sixteen guiding piers.

JOSEPH N. BRADLEY,[15] M. ASCE.—The writer is indebted to the discussers of the paper and is grateful for the additional information presented on morning-glory spillway operation. It was informative to learn from Mr. Donelan that an actual underwater inspection was made of the vertical bend and adjoining horizontal tunnel at Kingsley Dam. In the majority of cases inspection has been made by probing with poles or pipes.

Mr. Walter's presentation of the spillway operation at Hungry Horse Dam is of particular interest because this is the largest spillway of this type. The spillway operated for approximately two days. Attention is called to Mr. Walter's discussion concerning the precautions taken in construction of the spillway shaft and vertical bend regarding elimination of construction joints in the bend, elimination of offsets throughout by grinding, and the final sand blasting and finish treatment. It is anticipated that these precautionary measures will, in the long run, materially reduce maintenance costs.

Probing of the Hungry Horse tunnel and vertical bend showed no noticeable erosion of the concrete surfaces. Pressures measured in the throat section of the spillway during operation showed close agreement with those observed on the model; thus, air demand in the prototype is also comparable to that in the model. The lowest pressure measured was 8 ft of water below atmospheric pressure for a discharge of 30,000 cu ft per sec. A point of considerable interest was the action in the river channel downstream. Although the jet leaving the spillway, having an energy content approximating 1.5×10^6 hp, moved a considerable quantity of loose material in the river channel, it did not attack the banks (Figs. 23 and 24). The center line of the spillway was virtually alined with the center line of the river so the jet was aimed straight down the river. Were this not the case, there would certainly have been bank erosion. The erosion discernible on the left bank (Fig. 24) was caused by the jets from three 96-in. outlet valves which are not alined with the center line of the river. The erosion shown is the result of a single season of operation. The results obtained from these tests are invaluable to the profession; Mr. Puls and Mr. Walter are to be highly commended.

The comments of Mr. Blaisdell which relate his experiences with small closed-conduit spillway structures are most interesting. It is a significant fact that trash racks located in close proximity to a closed-conduit spillway usually present a hazard rather than a benefit. As Mr. Blaisdell states, trash collectors should be located well upstream in the lower velocities. Booms consisting of a single cable stretched across a river and floated on logs are used on a number of reservoirs of large dams to collect debris. These booms have proved to be effective but, of course, all trash collectors require systematic cleaning.

---

[15] Hydr. Engr., Bureau of Public Roads, U. S. Dept. of Commerce, Washington, D. C.

Although it cannot be stated with absolute certainty, it appears that vortex action observed on models and their prototypes is a linear relationship. Mr. Blaisdell's statement that the horizontal tunnel must be submerged for a morning-glory spillway to belch air from the inlet (Fig. 9) is not corroborated by Mr. Walter who states that the same phenomenon occurred for very small heads on the Hungry Horse spillway, which was free of submergence. The writer attributes the action to the fact that the spillway acts as a chimney through which a strong draft persists when water is not flowing. Very small discharges tend to neutralize or reverse the direction of air flow, resulting in the accumulation of small pressures in the shaft, intermittently permitting re-establishment of the updraft, which carries a small quantity of spray with it.

Appreciation is extended to Mr. Ballester for drawing attention to the spillway at the San Roque Dam on which information was lacking. This structure is interesting in that it is designed to operate submerged with as much as 25 ft of head on the crest. It should be noted that the design was verified or developed by model studies, which has been true of practically every morning-glory spillway constructed to date (1955). Mr. Blaisdell and Mr. Ridley will probably be interested in the absence of antivortex piers on the San Roque spillway, especially for submerged operation. Mr. Ballester does not explain the specific purpose of the 20-in. air pipe which connects to the upper part of the vertical bend. Is it logical to assume that admitting air at this point materially reduces the intensity of vortex action?

Mr. Ridley's cooperation in presenting further information on the Manuherikia Falls spillway is much appreciated. This is apparently the only spillway in which deterioration of the construction joints in the morning-glory and vertical shaft have been reported. Leakage from the reservoir is undoubtedly the principal cause of the difficulty. Mr. Blaisdell's remarks are pertinent to the question asked by Mr. Ridley regarding the value of guide piers on the crest of the spillway. For spillways that operate submerged piers are of definite value. They serve to convert the single large vortex into a number of smaller ones which are less objectionable. Piers, although desired, were not placed on the Owyhee or Hungry Horse spillway crests because of the complexity introduced by the ring gates. Model tests indicated that piers placed upstream from the ring gates were not sufficiently effective to justify their cost. Piers are of questionable value, however, on spillways operating free of submergence and at relatively low heads.

From the information gained from this prototype investigation it appears that the point has probably been reached where model studies can be dispensed with on the more common types of morning-glory spillway design. However, there still remains much to be learned regarding submerged operation, unusual approach conditions, subatmospheric crest pressures, and similar items.

DETERMINATION OF PRESSURE-CONTROLLED PROFILES

By William E. Wagner,[1] M. ASCE

With Discussion by Messrs. Maxwell W. White and Murray B. McPherson; Fred W. Blaisdell; Ibrahim M. Mostafa, Benoyendra Chanda, and Howard P. Johnson; and William E. Wagner

---

Synopsis

An extensive experimental study was conducted to determine the coefficients of discharge and to establish the shape of the nappe of water flowing over a sharp-crested circular weir for different approach depths and with pressures of varying magnitude beneath the nappe.

The studies were made on a sharp-crested weir approximately 20 in. in diameter, with heads ranging from 0.10 ft to 1.7 ft and with discharges of from 0.5 cu ft per sec to 11.5 cu ft per sec. Approach depths of 20 in., 3 in., and $1\frac{1}{2}$ in. below the weir crest were used. The effect of reducing the pressure on the lower surface of the nappe was also studied by removing air from the cavity under the nappe. Because the discharge coefficients and the profiles of the nappe are expressed as dimensionless ratios the results are in a convenient form for use in designing the overflow section of a morning-glory spillway. To demonstrate the practical use of the experimental data, the results of the study are compared with those of model studies on the morning-glory spillway for Hungry Horse Dam in Montana.

Introduction

With the increasing use of morning-glory shaft spillways, there has developed a general need for additional data to aid the hydraulic engineer in designing such a spillway for the many conditions encountered in the field. Some of the problems that must be solved concern the size and shape of the overflow section, the size of the shaft, the degree of curvature of the bend connecting the shaft with the horizontal tunnel, and the method of stilling the high-velocity flow before it enters the river channel below the dam. Each of these problems is important and requires careful consideration. The problem investigated herein is that of determining the size and shape of the overflow section that will pass the required quantity of water at the desired head and that will provide pressures on the morning-glory profile that are above the cavitation range. To find a solution to this design problem, a circular weir was constructed and tested in the Denver (Colo.) hydraulic laboratory of the Bureau of Reclamation, United

---

Note.—Published, essentially as printed here, in April, 1954, as *Proceedings-Separate No. 432*. Positions and titles given are those in effect when the paper or discussion was approved for publication in *Transactions*.

[1] Engr., Eng. Labs. Div., Bureau of Reclamation, U. S. Dept. of the Interior, Denver, Colo.

States Department of the Interior (USBR). The sharp-crested weir used in these studies was circular in plan and 20 in. in diameter. Because flow passing over a weir springs clear at the sharp edge, the lower trace of the nappe indicates the shape of the morning-glory surface for given conditions of head above the crest, approach depth, and pressure beneath the nappe.

Discharge coefficients and the shapes of the fully aerated upper and lower nappe surfaces were obtained for three approach depths—20 in., 3 in., and 1½ in. below the crest of the weir. The comparatively shallow depths of 3 in. and 1½ in. were chosen to assure a measurable effect on the discharge and nappe shapes. In addition, the effect on the nappe shape of reducing pressure by removing air from the space under the nappe was studied. The reduced-pressure studies were made for a negligible velocity of approach using the 20-in. approach depth. Data were taken only on an intermediate range of discharges where a stable jet could be maintained because at both higher and lower discharges pulsations in the nappe made measurement impossible.

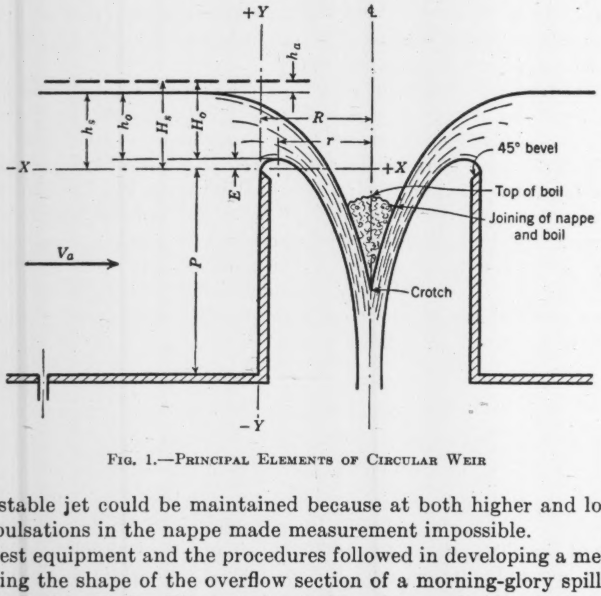

FIG. 1.—PRINCIPAL ELEMENTS OF CIRCULAR WEIR

The test equipment and the procedures followed in developing a method for determining the shape of the overflow section of a morning-glory spillway are subsequently described. The experimental results are then applied to a working model of the spillway for Hungry Horse Dam in Montana.

In Fig. 1, h_s is the observed head on the weir measured, in feet, 22 in. from the weir crest; V_a denotes the average velocity of approach, in feet per second, computed 22 in. from the weir crest; h_a is the average velocity head, in feet, and is equal to $V^2_a/2\,g$; H_s is equal to h_s plus h_a and is the total head, in feet, above the weir crest; E represents the maximum rise, in feet, of the lower-nappe surface above the sharp crest of the weir; h_o is the observed head, in feet, above the high point on the lower-nappe surface; H_o is equal to h_o plus h_a and is the total head, in feet, above the high point on the lower-nappe surface; R denotes the radius, in feet, of the sharp crest of the test weir; P is the depth, in feet, of the

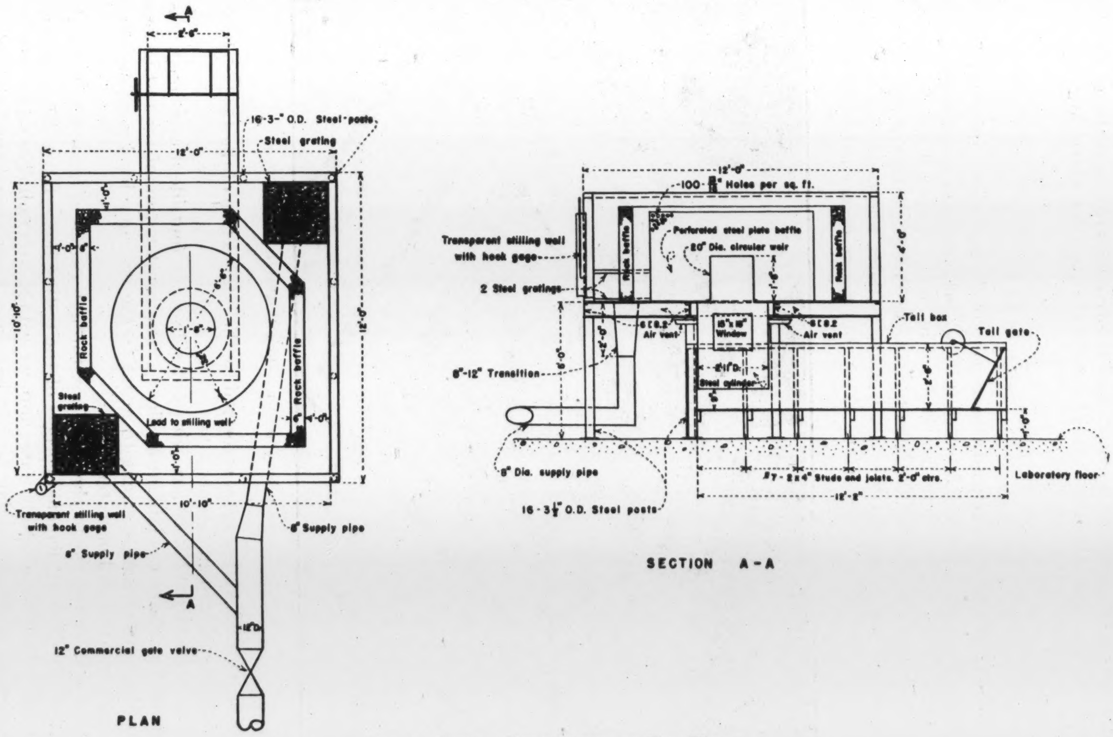
A
2'-6"
16-3-" O.D. Steel posts
Steel grating
12'-0"
1'-0"
1'-0" 6"
Rock baffle
6'-6"
1'-8"
10'-10"
12'-0"
Rock baffle
Steel grating
Lead to stilling well
6" 1'-0"
1'-0"
Transparent stilling well with hook gage
10'-10"
8" Supply pipe
8" Supply pipe
A
12" Commercial gate valve
12"
PLAN
12'-0"
100 - $\frac{3}{16}$" Holes per sq. ft.
Perforated steel plate baffle
20" Dia. circular weir
Transparent stilling well with hook gage
Rock baffle
Rock baffle
4'-0"
1'-6"
2 Steel gratings
6 [8.2 Air vent
15" x 16" Window
6 [8.2 Air vent
Tail box
Tail gate
6'-0"
2'-0"
8"-12" Transition
2'-11" D.
Steel cylinder
2'-6"
1'-0"
8" Dia. supply pipe
7 - 2 x 4" Studs and joists. 2'-0" ctrs.
12'-2"
Laboratory floor
16 - 3½" O.D. Steel posts
SECTION A-A

FIG. 2.—GENERAL ARRANGEMENT OF TEST WEIR

approach floor below the weir crest; X denotes the horizontal coordinate (origin at the weir crest, negative upstream and positive toward the center of the test weir), in feet; and Y is the vertical coordinate (positive above and negative below the crest of the weir), in feet.

TEST EQUIPMENT

The Test Weir.—The general arrangement of the test weir is shown in Figs. 2 and 3. The test weir was fabricated from a 20-in. length of seamless steel pipe having a 20-in. outside diameter with a ½-in. wall. A steel flange for bolting the test weir to the floor of the head box was welded to one end of the cylinder. The outside surface of the other end of the cylinder was machined to form a true circle, 1.6593 ft in diameter. A 45° bevel was then machined from the inner face until a knife edge was formed by the intersection of the 45° bevel and the outer machined surface.

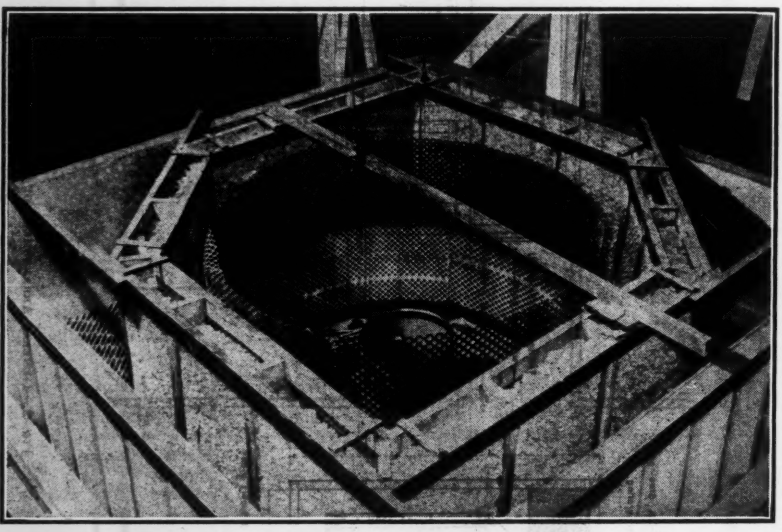

FIG. 3.—GENERAL VIEW OF HEAD BOX CONTAINING TEST WEIR

The head box, 12 ft square with 4-ft side walls (outside dimensions), was elevated 5 ft above the laboratory floor. The construction of the testing box and weir was sufficiently strong to maintain the weir in a level position when the head box was full of water.

Water was supplied to the head box through two 8-in. inlets which terminated in the floor at diagonal corners of the testing box. Several precautions were taken to assure that the water approached the weir radially and uniformly. A 6-in.-thick baffle containing ¾-in. to 1-in. gravel was placed approximately 1 ft from the side walls of the head box (Fig. 3). Two steel gratings were placed over each inlet to reduce the boil and distribute the inflowing water between the side walls of the head box and the gravel baffle. To quiet the flow further before it passed over the test weir, a perforated cylinder was placed between the gravel baffle and the weir. The perforated cylinder, 6½ ft in diameter and 4 ft high, was made from a 12-gage steel plate punched with one hundred $\frac{11}{16}$-in.-diameter holes per sq ft.

Discharge Measurements.—The discharge over the circular weir was measured with commercial venturi meters, the sizes of which were either 4 in., 6 in., 8 in., or 12 in., depending on the discharge required for the particular test. All the venturi meters were accurately calibrated in the laboratory by the use of a volumetric tank.

Water-Surface Gages.—The head, h_s, on the test weir was measured by a hook gage mounted in a stilling well at the side of the head box. A $\frac{3}{16}$-in.-inside-diameter rubber tube connected the stilling well to the head box at a point 22 in. from the sharp crest of the test weir.

Profiles of the upper water surface over the test weir were made with a point gage mounted on an aluminum channel. Sufficient readings were observed to establish a smooth curve describing the shape of the upper-nappe surface. The zero of these gages was checked before and after each set of runs.

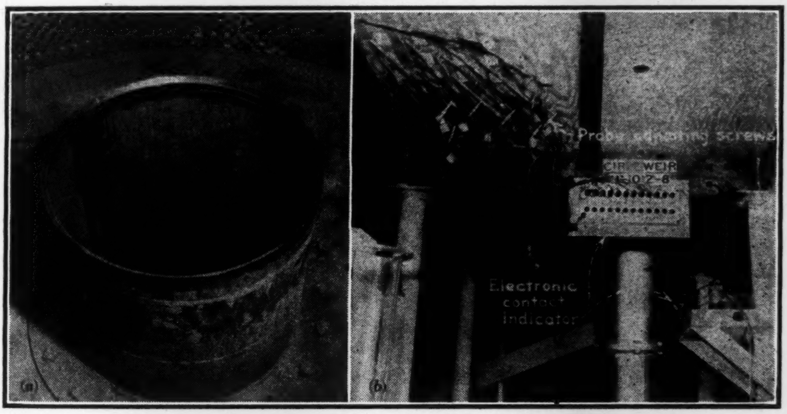

FIG. 4.—APPARATUS FOR OUTLINING LOWER-NAPPE SURFACE

To determine the shape of the lower-nappe surface, the profile was outlined by thirteen wire probes extending through the wall of the weir and spaced at various intervals below the crest of the test weir, as shown in Fig. 4(*a*). The end of each probe was positioned along the nappe by screwing the probe toward the sheet of water until contact was made with the lower-nappe surface. Contact of the probe with the nappe was indicated by a 6-volt bulb which lighted when the end of the probe touched the lower-nappe surface. Fig. 4(*b*) shows the probe-adjusting screws and the electronic contact indicator.

The coordinates of the points of each probe outlining the lower-nappe profile were measured with a specially designed point gage (Fig. 5). The gage consisted of a horizontal beam which rested on the crest of the test weir and a vertical bar mounted in a carriage which rode along the horizontal bar. The lower end of the vertical bar was fitted with a point for positioning the gage at the end of the wire probe. The point of the gage was positioned over the probe by moving the carriage horizontally along the beam and lowering the vertical bar until the point contacted the probe.

Altering the Velocity of Approach.—The test weir was constructed with its crest 20 in. from the floor of the head box; most of the data were obtained for this approach depth. However, to determine the effect of the velocity of approach on the coefficient of discharge and the nappe shapes, experiments also were made with approach depths of 3 in. and 1½ in. The approach depth, P, was changed by placing a horizontal false floor between the upstream face of the weir and the perforated cylinder (Fig. 6).

At an approach depth of 20 in., the velocity head, h_a, was less than 0.0005 ft for (H_s/R)-ratios under 0.60 and reached a maximum of 0.0007 ft for an (H_s/R)-ratio of 2.00. Therefore, the effect of velocity head was considered negligible for data obtained with the 20-in. approach depth. For the 3-in. approach depth, the velocity head varied from 0.001 ft to 0.004 ft and from 0.001 ft to 0.005 ft for the 1½-in. approach depth.

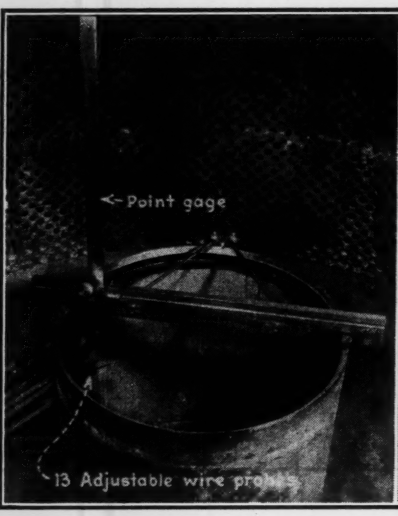

FIG. 5.—POINT GAGE FOR MEASURING PROBE COORDINATES

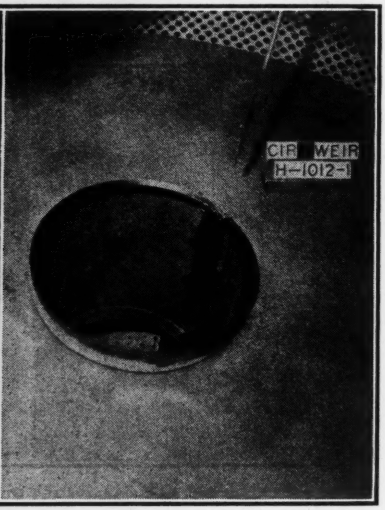

FIG. 6.—TEST WEIR WITH APPROACH DEPTH OF 3 IN.

Reducing the Pressure Under the Nappe.—To study the effect of subatmospheric pressures under the nappe, a sheet-metal cylinder—35 in. in diameter, 3 ft long, and flanged at one end—was bolted to the underside of the head box concentric with the test weir (Fig. 7). The lower end of the cylinder was approximately 9 in. from the floor of the tail box. The water surface in the tail box could be raised by a tail gate to submerge the end of the cylinder, thus sealing the air chamber between the falling jet and the cylinder walls. The jet, in falling, pumped some of the air from the chamber and reduced the pressure in the space beneath the nappe. Two vents, each 3 in. in diameter and equipped with gate valves, were placed in the wall of the cylinder. By controlling the air entering the chamber, a fairly stable pressure could be maintained under the nappe. For the lower pressures and discharges, it was found necessary to connect a vacuum line to the chamber to secure the desired pressure.

The pressure in the chamber was measured by a differential U-tube manometer filled with water. The legs of the manometer were tilted at a 45° angle to permit reading of the differential pressure to 0.001 ft.

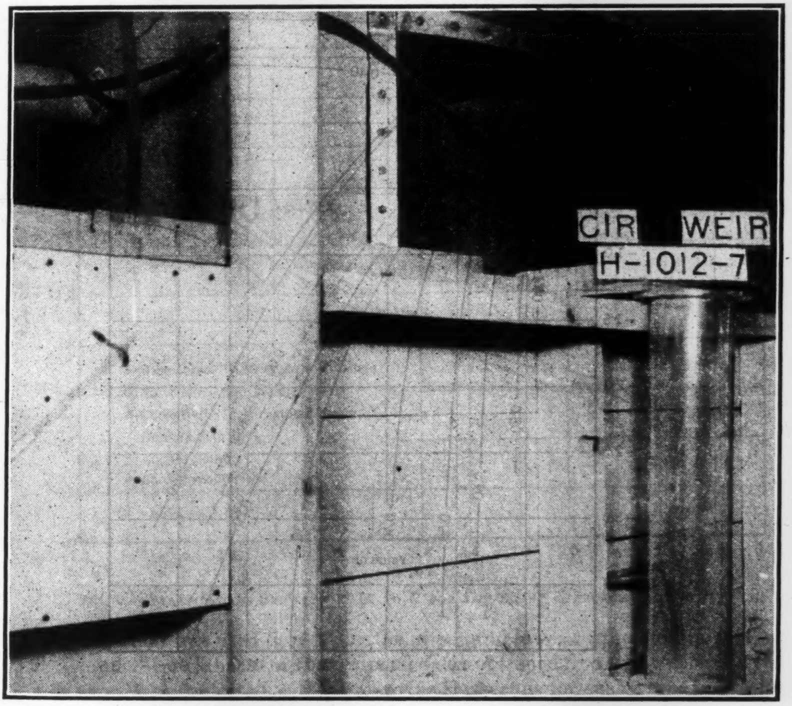

Fig. 7.—Tail Box and Cylinder for Reducing Pressure Under the Nappe

Interpretation of Results

Discharge Coefficient.—Flow over a circular weir can be classified as either free or submerged. For free flow, the discharge characteristics are similar to those of a rectangular weir—

$$Q = C\,L\,H_s^{3/2} \ldots\ldots\ldots\ldots\ldots\ldots (1)$$

in which Q is the flow, in cubic feet per second; C denotes a discharge coefficient; and L is the crest length, in feet. Thus, the theoretical discharge is proportional to the three-halves power of the head, H_s, on the weir.

When the discharge increases until the water surface is practically level above the weir, the weir becomes a re-entrant tube and the theoretical discharge follows the form,

$$Q = C_o A_o \sqrt{2\,g\,H_s} \ldots\ldots\ldots\ldots\ldots\ldots\ldots\ldots (2)$$

At tube flow, an increase in head results in a very limited increase in discharge as the theoretical discharge is then proportional to the square root of the head. For partial submergence, the discharge coefficient, C or C_o, changes more rapidly with head, and the discharge characteristics follow neither Eq. 1 nor Eq. 2.

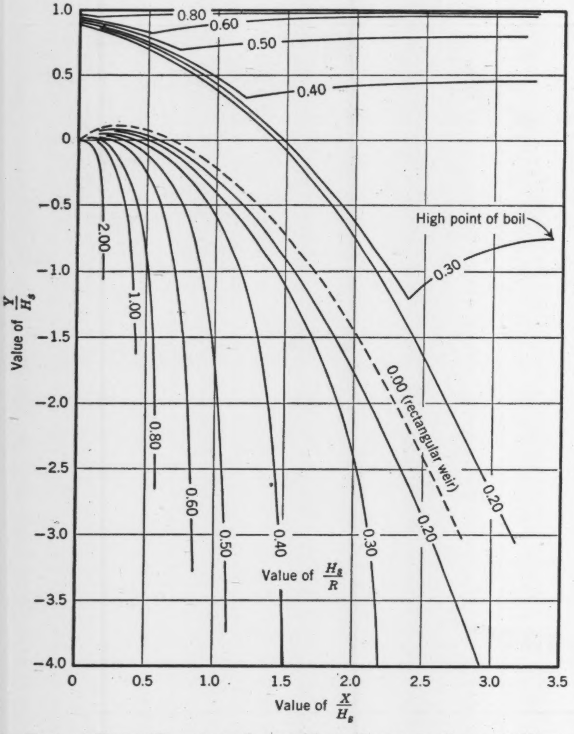

FIG. 8.—TYPICAL UPPER-NAPPE AND LOWER-NAPPE SURFACES (AERATED NAPPE AND NEGLIGIBLE VELOCITY OF APPROACH)

Because the point where weir flow ends and tube flow begins is difficult to define and in order to simplify the method of expressing the coefficient of discharge, Eq. 1 was used to compute the discharge coefficients throughout the range of testing. The weir formula was chosen because most morning-glory spillways are designed for free flow.

Nappe Profiles.—From the laws of similitude, it can be shown that the profiles of sheets of water flowing over any two sharp-crested, circular weirs with aerated nappes and negligible velocities of approach are similar if the respective ratios of the head, H_s, to the radius, R, of the weirs are the same. Thus, by expressing the X- and Y-coordinates of the nappe surfaces and the radius of the weir in terms of H_s, the results are in dimensionless form, and the nappe shape for any head and radius of weir can be determined. C. S. Camp and J. W. Howe,[2] found in their experiments on three weir arcs of different radii that

> "* * * nappe profiles plotted in terms of these dimensionless coordinates proved to be practically identical for runs having the same ratio of head to diameter of weir arc except in those runs in which the head was so low that the nappe adhered to the crest."

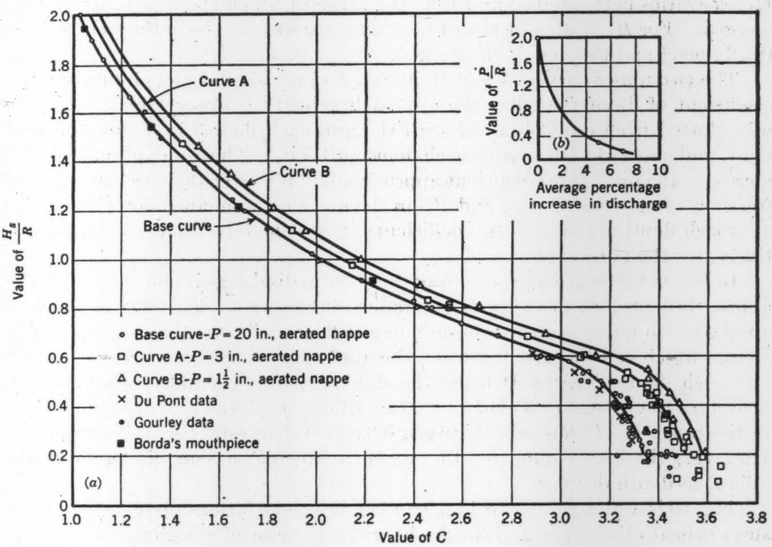

FIG. 9.—RELATIONSHIP BETWEEN H_s/R TO C FOR DIFFERENT APPROACH DEPTHS P

This method was used in plotting the upper and lower surfaces of the nappe. The X- and Y-coordinates of the nappe surfaces obtained from the test weir were divided by H_s and plotted with as many as three runs for each value of H_s/R; an average line was drawn through the points and Fig. 8 illustrates the shapes of the curves. The (X/H_s)-coordinates and the (Y/H_s)-coordinates are presented subsequently in Tables 1 through 6.

ANALYSIS OF RESULTS

Discharge Coefficients.—The relationship between the coefficient of discharge, C, and the dimensionless ratio, H_s/R, for three approach depths is plotted in Fig. 9(a). In each case, the lower surface of the nappe was open to the atmosphere and fully aerated. The lower curve, designated as the base curve, shows the discharge coefficient for (H_s/R)-ratios between 0.20 and 2.00

---

[2] "Tests of Circular Weirs," by C. S. Camp and J. W. Howe, *Civil Engineering*, Vol. 9, 1939, pp. 247–248.

with the approach floor 20 in. below the weir crest or with negligible velocity of approach.

Referring to Figs. 8 and 9(*a*), the flow apparently is free for (H_s/R)-ratios less than 0.45. In the range of free flow, the discharge coefficient decreases almost linearly from 3.34 to 3.20 between (H_s/R)-ratios of 0.20 and 0.45. These coefficients compare favorably with results obtained by other experimenters.[2,3,4]

As the (H_s/R)-ratio increases above 0.45, the weir becomes partly submerged and there is a sharp reduction in the coefficient of discharge. The largest change in coefficient for a relatively small increase in H_s/R occurs for (H_s/R)-ratios between 0.45 and 1.00, the range in which the weir is partly submerged. For H_s/R greater than 1.00, the water surface above the weir is practically level and the flow is submerged.

The two upper curves, A and B, in Fig. 9(*a*) are similar plots indicating the coefficient of discharge when the approach velocity is appreciable. Curve A was plotted from data obtained with the approach floor 3 in. below the weir crest, and curve B with an approach depth of 1.5 in. The 3-in. approach depth increased the discharge coefficient approximately 5% over the base curve in the free-flow range of discharges and 4% in the range of submerged flow; the 1.5-in. approach depth increased the coefficients approximately 7% and 8%, respectively, for the two ranges.

In Fig. 9(*b*) the average percentage increase in discharge is plotted against the approach depth, P, in terms of the radius of the weir. This curve, which is applicable to either free flow or submerged flow, indicates the increase in discharge which can be expected when the approach velocity is increased (or the approach depth decreased) using the discharge for negligible velocity of approach as the base. It is evident that additional experimental data are needed in the range of (P/R)-ratios between 0.3 and 1.0 to establish the curve fully. However, the curve indicates the approximate increase in discharge as the approach depth decreases.

Fig. 10 is a plot similar to Fig. 9 and shows the relationship of various pressures beneath the nappe and the discharge for the case of a negligible velocity of approach. Fig. 10(*a*) shows the discharge coefficient versus (H_s/R)-ratios for atmospheric pressure and for partial vacuums of 10%, 20%, 30%, 40%, and 50% under the nappe. The partial vacuums are expressed as ratios of the average vacuum—measured in feet of water in the air chamber beneath the nappe—to the head, H_s, on the weir. The solid lines indicate the part of the curve verified by experimental data, and the dotted lines indicate the estimated extension of the curves beyond the limits of the experiments.

Fig. 10(*b*) was plotted from the data contained in Fig. 10(*a*). The percentage increase in discharge above that indicated by the base curve was computed for (H_s/R)-ratios of 0.3, 0.4, and for 0.5 and 10% to 50% vacuums. The computed percentages for each of the five vacuums were averaged and plotted as shown in Fig. 10(*b*). Fig. 10(*b*) indicates the average increase in discharge for

---

[3] "Experiments on the Flow of Water Over Sharp-Edged Circular Weirs," by H. J. F. Gourley, *Proceedings*, Inst. of C. E., London, Vol. CLXXXIV, 1911, pp. 297–317.

[4] "Determination of the Under Nappe over a Sharp Crested Weir, Circular in Plan with Radial Approach," by R. B. duPont, thesis presented to Case School of Applied Science, Cleveland, Ohio, in 1937, in partial fulfilment of the requirements for the degree of Bachelor of Science in Civil Engineering.

different pressures beneath the nappe. The relationship is applicable only in the range of free flow as no tests with partial vacuums were made when the weir was flowing submerged. The curves in Fig. 10 should be used with reservation as they are based on meager experimental data.

The minimum value of the (H_s/R)-ratio, for which discharge coefficients are shown in Figs. 9 and 10, is 0.20. It was found that for runs with heads less than 0.15 ft the discharge coefficient was inconsistent and tended to increase as the head decreased. At low heads, surface tension of the water affects the flow characteristics by preventing the jet from springing clear at the sharp-edged crest of the weir. It is difficult to define the limits of this effect as the sharpness of the weir or a small quantity of oil can change its intensity. In summarizing the results of several experimenters, Mr. Howe showed[5] graphically that the discharge coefficient for a rectangular weir increases sharply for heads less than 0.20 ft, thus indicating the heads at which surface tension affects discharge. Therefore, the coefficients for the test weir are shown only for heads above the region of low flow.

Nappe Profiles.—Fig. 8 shows the general shapes of the upper and lower surfaces of the nappe expressed in terms of head with an aerated nappe and a negligible velocity of approach for representative (H_s/R)-ratios. Also included in Fig. 8 is the shape of the lower-nappe surface developed[6] by the USBR for the rectangular weir, which may be considered a circular weir having an infinite radius $(H_s/R = 0)$.

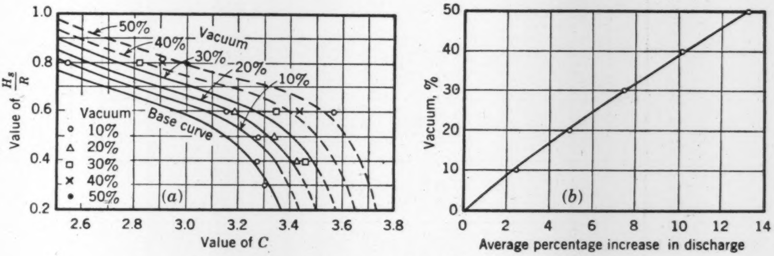

FIG. 10.—EFFECT OF VACUUM ON Q, H_s/R, AND C

Several attempts were made to obtain a profile for $H_s/R = 0.10$ (or a head of 0.083 ft on the test weir), but all the measured profiles for this head were comparatively flat near the weir crest and inconsistent with the other results, indicating that the nappe adhered to the weir crest. In Table 1 the coordinates for $H_s/R = 0.10$ are shown, but the profile was determined by interpolation between $H_s/R = 0.20$ and $H_s/R = 0$ rather than by actual nappe measurements on the test weir.

The lower-nappe traces expressed in dimensionless coordinates in Fig. 8 give a false impression as to the actual shape of the lower surface for different heads as the coordinates in terms of the head, H_s, become progressively less as

---

[5] "Engineering Hydraulics," edited by Hunter Rouse, John Wiley & Sons, Inc., New York, N. Y., 1950, p. 214.

[6] "Studies of Crests for Overfall Dams," *Bulletin No. 3*, Boulder Canyon Project Final Reports, Bureau of Reclamation, U. S. Dept. of the Interior, Denver, Colo., Pt. VI, 1948.

TABLE 1.—COORDINATES OF LOWER NAPPE SURFACE FOR NEGLIGIBLE APPROACH VELOCITY AND AERATED NAPPE

	$\frac{Y}{H_s}$														
$\frac{X}{H_s}$ \ $\frac{H_s}{R}$	0.00	*0.10	0.20	0.25	0.30	0.35	0.40	0.45	0.50	0.60	0.80	1.00	1.20	1.50	2.00
0.000	0.0000	0.0000	0.0000	0.0000	0.0000	0.0000	0.0000	0.0000	0.0000	0.0000	0.0000	0.0000	0.0000	0.0000	0.0000
.010	.0150	.0145	.0133	.0130	.0128	.0125	.0122	.0119	.0116	.0112	.0104	.0095	.0086	.0077	.0070
.020	.0280	.0265	.0250	.0243	.0236	.0231	.0225	.0220	.0213	.0202	.0180	.0159	.0140	.0115	.0090
.030	.0395	.0365	.0350	.0337	.0327	.0317	.0308	.0299	.0289	.0270	.0231	.0198	.0168	.0126	.0085
.040	.0490	.0460	.0435	.0417	.0403	.0389	.0377	.0363	.0351	.0324	.0268	.0220	.0176	.0117	.0050
.050	.0575	.0535	.0506	.0487	.0471	.0454	.0436	.0420	.0402	.0368	.0292	.0226	.0168	.0092	
.060	.0650	.0605	.0570	.0550	.0531	.0510	.0489	.0470	.0448	.0404	.0305	.0220	.0147	.0053	
.070	.0710	.0665	.0627	.0605	.0584	.0560	.0537	.0514	.0487	.0432	.0308	.0201	.0114	.0001	
.080	.0765	.0710	.0677	.0655	.0630	.0603	.0578	.0550	.0521	.0455	.0301	.0172	.0070		
.090	.0820	.0765	.0722	.0696	.0670	.0640	.0613	.0581	.0549	.0471	.0287	.0135	.0018		
.100	.0860	.0810	.0762	.0734	.0705	.0672	.0642	.0606	.0570	.0482	.0264	.0089			
.120	.0940	.0880	.0826	.0790	.0758	.0720	.0683	.0640	.0596	.0483	.0195				
.140	.1000	.0935	.0872	.0829	.0792	.0750	.0705	.0654	.0599	.0460	.0101				
.160	.1045	.0980	.0905	.0855	.0812	.0765	.0710	.0651	.0585	.0418					
.180	.1080	.1010	.0927	.0872	.0820	.0766	.0705	.0637	.0559	.0361					
.200	.1105	.1025	.0938	.0877	.0819	.0756	.0688	.0611	.0521	.0292					
.250	.1120	.1035	.0926	.0850	.0773	.0683	.0596	.0495	.0380	.0068					
.300	.1105	.1000	.0850	.0764	.0668	.0559	.0446	.0327	.0174						
.350	.1060	.0930	.0750	.0650	.0540	.0410	.0280	.0125							
.400	.0970	.0830	.0620	.0500	.0365	.0220	.0060								
.450	.0845	.0700	.0450	.0310	.0170	.000									
.500	.0700	.0520	.0250	.0100											
.550	.0520	.0320	.0020												
.600	.0320	.0080													
.650	.0090														

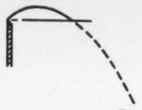

Note: The above tabulation is for that portion of the profile above the weir crest.

$\frac{Y}{H_s}$ \ $\frac{H_s}{R}$	$\frac{X}{H_s}$														
	0.00	0.10	0.20	0.25	0.30	0.35	0.40	0.45	0.50	0.60	0.80	1.00	1.20	1.50	2.00
0.000	0.668	0.615	0.554	0.520	0.487	0.450	0.413	0.376	0.334	0.262	0.158	0.116	0.093	0.070	0.048
-0.020	0.705	0.652	0.592	0.560	0.526	0.488	0.452	0.414	0.369	.293	.185	.145	.120	.096	.074
-0.040	0.742	0.688	0.627	0.596	0.563	0.524	0.487	0.448	0.400	.320	.212	.165	.140	.115	.088
-0.060	0.777	0.720	0.660	0.630	0.596	0.557	0.519	0.478	0.428	.342	.232	.182	.155	.129	.100
-0.080	0.808	0.752	0.692	0.662	0.628	0.589	0.549	0.506	0.454	.363	.250	.197	.169	.140	.110
-0.100	0.838	0.784	0.722	0.692	0.657	0.618	0.577	0.532	0.478	.381	.266	.210	.180	.150	.118
-0.150	0.913	0.857	0.793	0.762	0.725	0.686	0.641	0.589	0.531	.423	.299	.238	.204	.170	.132
-0.200	0.978	0.925	0.860	0.826	0.790	0.745	0.698	0.640	0.575	.459	.326	.260	.224	.184	.144
-0.250	1.040	0.985	0.919	0.883	0.847	0.801	0.750	0.683	0.613	.490	.348	.280	.239	.196	.153
-0.300	1.100	1.043	0.976	0.941	0.900	0.852	0.797	0.722	0.648	.518	.368	.296	.251	.206	.160
-0.400	1.207	1.150	1.079	1.041	1.000	0.944	0.880	0.791	0.706	.562	.400	.322	.271	.220	.168
-0.500	1.308	1.246	1.172	1.131	1.087	1.027	0.951	0.849	0.753	.598	.427	.342	.287	.232	.173
-0.600	1.397	1.335	1.260	1.215	1.167	1.102	1.012	0.898	0.793	.627	.449	.359	.300	.240	.179
-0.800	1.563	1.500	1.422	1.369	1.312	1.231	1.112	0.974	0.854	.673	.482	.384	.320	.253	.184
-1.000	1.713	1.646	1.564	1.508	1.440	1.337	1.189	1.030	0.899	.710	.508	.402	.332	.260	.188
-1.200	1.846	1.780	1.691	1.635	1.553	1.422	1.248	1.074	0.933	.739	.528	.417	.340	.266	
-1.400	1.970	1.903	1.808	1.748	1.653	1.492	1.293	1.108	0.963	.760	.542	.423	.344		
-1.600	2.085	2.020	1.918	1.855	1.742	1.548	1.330	1.133	0.988	.780	.553	.430			
-1.800	2.196	2.130	2.024	1.957	1.821	1.591	1.358	1.158	1.008	.797	.563	.433			
-2.000	2.302	2.234	2.126	2.053	1.891	1.630	1.381	1.180	1.025	.810	.572				
-2.500	2.557	2.475	2.354	2.266	2.027	1.701	1.430	1.221	1.059	.838	.588				
-3.000	2.778	2.700	2.559	2.428	2.119	1.748	1.468	1.252	1.086	.853					
-3.500		2.916	2.749	2.541	2.171	1.777	1.489	1.267	1.102						
-4.000		3.114	2.914	2.620	2.201	1.796	1.500	1.280							
-4.500		3.306	3.053	2.682	2.220	1.806	1.509								
-5.000		3.488	3.178	2.734	2.227	1.811									
-5.500		3.653	3.294	2.779	2.229										
-6.000		3.820	3.405	2.812	2.232										

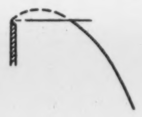

Note: The above tabulation is for that portion of the profile below the weir crest.

H_s increases. To illustrate the shape of the nappe as the head increases, typical lower-nappe traces expressed as true X- and Y-coordinates for several (H_s/R)-ratios are shown for the test weir in Fig. 11.

In the case of the rectangular weir, the lower-nappe traces spring farther from the weir crest as the head increases. This is not true, however, with the circular weir. In Fig. 11, it can be seen that for an increase in head or (H_s/R)-ratio the profile springs farther from the weir crest only in the region of the high point of the trace. Below the weir crest the traces cross, and the profile for the higher head falls inside those for the lower head. Therefore, if a morning-glory spillway is designed for the maximum head, it appears that subatmospheric pressures along the lower part of the trace will occur for heads less than maximum. To determine the extent of the subatmospheric pressures for different (H_s/R)-ratios was beyond the scope of these experiments. However, model tests on the morning-glory spillway at Hungry Horse Dam disclosed that any reduction in pressure for heads less than the design head could not be discerned on the model.[7]

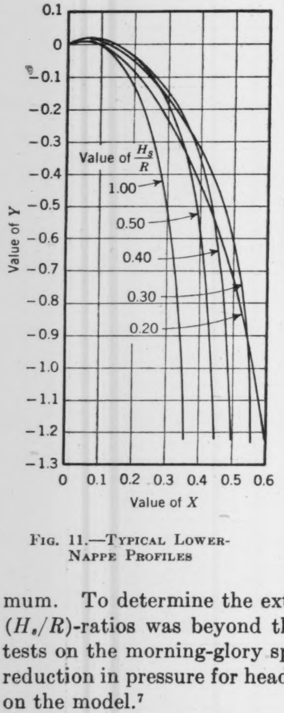

FIG. 11.—TYPICAL LOWER-NAPPE PROFILES

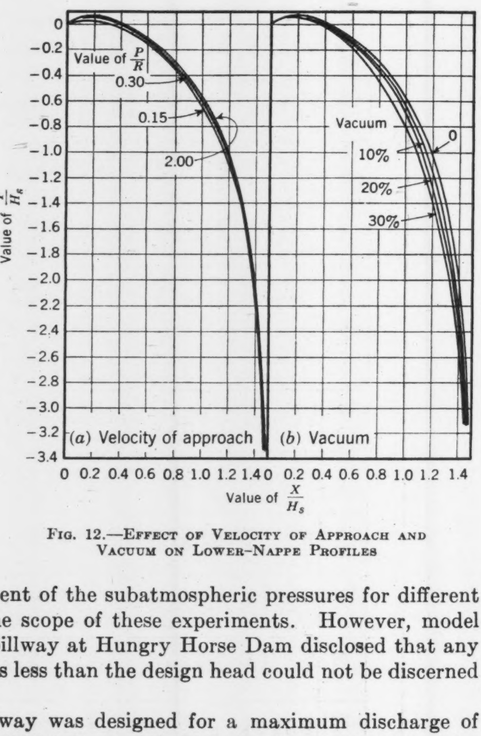

FIG. 12.—EFFECT OF VELOCITY OF APPROACH AND VACUUM ON LOWER-NAPPE PROFILES

Hungry Horse Dam spillway was designed for a maximum discharge of 53,000 cu ft per sec at a head of 16.9 ft, an (H_s/R)-ratio of approximately 0.50, and a 30% vacuum crest. Pressures observed on the model crest averaged approximately 5 ft, 3 ft, and 1.5 ft of water (prototype) below atmospheric for discharges of 50,000 cu ft per sec, 35,000 cu ft per sec, and 15,000 cu ft per sec, respectively. The observed absolute pressure at all piezometers along the spillway crest increased with each lower head or discharge. This example is inconclusive for the entire range of (H_s/R)-ratios but it indicates that spillway crests designed for (H_s/R)-ratios less than 0.50 will operate at approximately atmospheric pressure for discharges lower than the maximum.

---

[7] "Hydraulic Model Studies of the Morning-Glory Spillway for Hungry Horse Dam," by G. L. Beichley, *Hydraulic Laboratory Report No. Hyd.-355*, Bureau of Reclamation, U. S. Dept. of the Interior, Denver, Colo., April 23, 1954.

The (X/H_s)-coordinates and (Y/H_s)-coordinates of the lower-nappe surface for (H_s/R)-ratios from 0 to 2.0 with fully aerated nappe and negligible velocity of approach are presented in Table 1.

The effects of the velocity of approach on the lower-nappe surface are shown in Fig. 12(*a*), where the profiles for (P/R)-ratios of 2.0 (negligible approach velocity), 0.30, and 0.15 are plotted for an (H_s/R)-ratio of 0.40—which is typical of the profiles obtained for other (H_s/R)-ratios. As the approach velocity increases (or as P/R decreases), the contraction of the jet decreases and the nappe falls closer to the weir crest. A solid jet forms below the weir crest, and the lower-nappe profiles become similar in shape—the profile for the higher approach velocity falling slightly inside the profile for the lower velocity of approach. Below the point where a solid jet forms, the location of the lower-nappe surface is governed by the diameter of jet necessary to accommodate the discharge.

Lower-nappe shapes for an appreciable velocity of approach with a fully aerated nappe are presented in Table 2.

Fig. 12(*b*) shows the profiles for $H_s/R = 0.40$ with a partial vacuum under the nappe. In general, the profiles are similar in shape but not as flat near the crest as those obtained with a significant velocity of approach. As the pressure under the nappe is decreased, the profiles for a constant head fall progressively closer to the weir wall. That is, the diameter (or area) of the jet at any point along the profile becomes progressively greater as the pressure under the nappe is decreased.

The (X/H_s)-coordinates and (Y/H_s)-coordinates of the lower-nappe profile for a negligible velocity of approach and a partial vacuum under the nappe are given in Table 3.

Under-nappe profiles in dimensionless coordinates for a negligible approach velocity and an aerated nappe are presented in Table 4. The water surface is level for (H_s/R)-ratios greater than 1.0.

The effect on the upper-nappe profiles of lowered pressures beneath the nappe and increased velocity of approach was similar to that observed on the lower-nappe shapes. After passing the weir crest, the upper water surface fell progressively lower for each increasing vacuum beneath the jet, and when the approach velocity was increased a higher upper-nappe surface and boil were observed.

The (X/H_s)-coordinates and (Y/H_s)-coordinates of the upper water surface are given in Table 5 for an aerated nappe and approach depths of $P/R = 0.30$ and 0.15, and in Table 6 there are recorded similar upper-nappe shapes with a negligible approach velocity for vacuums of 10%, 20%, and 30% beneath the nappe.

Relationship of Rise and Discharge to Radius.—In these experiments, the discharge over the sharp-crested weir was computed in terms of H_s. In designing the overflow section of a morning-glory spillway, it is usually more convenient to begin the computations with H_o, the total head above the spillway

TABLE 2.—COORDINATES OF LOWER NAPPE SURFACE FOR AERATED NAPPE

	$\frac{Y}{H_s}$																	
	$\frac{P}{R}$ = 0.30									$\frac{P}{R}$ = 0.15								
$\frac{X}{H_s}$ \ $\frac{H_s}{R}$	0.20	0.25	0.30	0.35	0.40	0.45	0.50	0.60	0.80	0.20	0.25	0.30	0.35	0.40	0.45	0.50	0.60	0.80
0.000	0.0000	0.0000	0.0000	0.0000	0.0000	0.0000	0.0000	0.0000	0.0000	0.0000	0.0000	0.0000	0.0000	0.0000	0.0000	0.0000	0.0000	0.0000
.010	.0130	.0130	.0130	.0125	.0120	.0120	.0115	.0110	.0100	.0120	.0120	.0115	.0115	.0110	.0110	.0105	.0100	.0090
.020	.0245	.0242	.0240	.0235	.0225	.0210	.0195	.0180	.0170	.0210	.0200	.0195	.0190	.0185	.0180	.0170	.0160	.0140
.030	.0340	.0335	.0330	.0320	.0300	.0290	.0270	.0240	.0210	.0285	.0270	.0265	.0260	.0250	.0235	.0225	.0200	.0165
.040	.0415	.0411	.0390	.0380	.0365	.0350	.0320	.0285	.0240	.0345	.0335	.0325	.0310	.0300	.0285	.0265	.0230	.0170
.050	.0495	.0470	.0455	.0440	.0420	.0395	.0370	.0325	.0245	.0405	.0385	.0375	.0360	.0345	.0320	.0300	.0250	.0170
.060	.0560	.0530	.0505	.0490	.0460	.0440	.0405	.0350	.0250	.0450	.0430	.0420	.0400	.0380	.0355	.0330	.0265	.0165
.070	.0610	.0575	.0550	.0530	.0500	.0470	.0440	.0370	.0245	.0495	.0470	.0455	.0430	.0410	.0380	.0350	.0270	.0150
.080	.0660	.0620	.0590	.0565	.0530	.0500	.0460	.0385	.0235	.0525	.0500	.0485	.0460	.0435	.0400	.0365	.0270	.0130
.090	.0705	.0660	.0625	.0595	.0550	.0520	.0480	.0390	.0215	.0560	.0530	.0510	.0480	.0455	.0420	.0370	.0265	.0100
.100	.0740	.0690	.0660	.0620	.0575	.0540	.0500	.0395	.0190	.0590	.0560	.0535	.0500	.0465	.0425	.0375	.0255	.0065
.120	.0800	.0750	.0705	.0650	.0600	.0560	.0510	.0380	.0120	.0630	.0600	.0570	.0520	.0480	.0435	.0365	.0220	
.140	.0840	.0790	.0735	.0670	.0615	.0560	.0515	.0355	.0020	.0660	.0620	.0585	.0525	.0475	.0425	.0345	.0175	
.160	.0870	.0810	.0750	.0675	.0610	.0550	.0500	.0310		.0670	.0635	.0590	.0520	.0460	.0400	.0305	.0110	
.180	.0885	.0820	.0755	.0675	.0600	.0535	.0475	.0250		.0675	.0635	.0580	.0500	.0435	.0365	.0260	.0040	
.200	.0885	.0820	.0745	.0660	.0575	.0505	.0435	.0180		.0670	.0625	.0560	.0465	.0395	.0320	.0200		
.250	.0855	.0765	.0685	.0590	.0480	.0390	.0270			.0615	.0560	.0470	.0360	.0265	.0160	.0015		
.300	.0780	.0670	.0580	.0460	.0340	.0220	.0050			.0520	.0440	.0330	.0210	.0100				
.350	.0660	.0540	.0425	.0295	.0150					.0380	.0285	.0165	.0030					
.400	.0495	.0370	.0240	.0100						.0210	.0090							
.450	.0300	.0170	.0025							.0015								
.500	.0090	-.0060																
.550																		

Note: The above tabulation is for that portion of the profile above the crest.

$\frac{Y}{H_s}$ \ $\frac{H_s}{R}$	$\frac{X}{H_s}$																	
	0.20	0.25	0.30	0.35	0.40	0.45	0.50	0.60	0.80	0.20	0.25	0.30	0.35	0.40	0.45	0.50	0.60	0.80
-0.000	0.519	0.488	0.455	0.422	0.384	0.349	0.310	0.238	0.144	0.454	0.422	0.392	0.358	0.325	0.288	0.253	0.189	0.116
-0.020	0.560	0.528	0.495	0.462	0.423	0.387	0.345	.272	.174	0.499	0.467	0.437	0.404	0.369	0.330	0.292	.228	.149
-0.040	0.598	0.566	0.532	0.498	0.458	0.420	0.376	.300	.198	0.540	0.509	0.478	0.444	0.407	0.368	0.328	.259	.174
-0.060	0.632	0.601	0.567	0.532	0.491	0.451	0.406	.324	.220	0.579	0.547	0.516	0.482	0.443	0.402	0.358	.286	.195
-0.080	0.664	0.634	0.600	0.564	0.522	0.480	0.432	.348	.238	0.615	0.583	0.550	0.516	0.476	0.434	0.386	.310	.213
-0.100	0.693	0.664	0.631	0.594	0.552	0.508	0.456	.368	.254	0.650	0.616	0.584	0.547	0.506	0.462	0.412	.331	.228
-0.150	0.760	0.734	0.701	0.661	0.618	0.569	0.510	.412	.290	0.726	0.691	0.660	0.620	0.577	0.526	0.468	.376	.263
-0.200	0.831	0.799	0.763	0.723	0.677	0.622	0.558	.451	.317	0.795	0.760	0.729	0.685	0.639	0.580	0.516	.413	.293
-0.250	0.893	0.860	0.826	0.781	0.729	0.667	0.599	.483	.341	0.862	0.827	0.790	0.743	0.692	0.627	0.557	.445	.319
-0.300	0.953	0.918	0.880	0.832	0.779	0.708	0.634	.510	.362	0.922	0.883	0.843	0.797	0.741	0.671	0.594	.474	.342
-0.400	1.060	1.024	0.981	0.932	0.867	0.780	0.692	.556	.396	1.029	0.988	0.947	0.893	0.828	0.749	0.656	.523	.381
-0.500	1.156	1.119	1.072	1.020	0.938	0.841	0.745	.595	.424	1.128	1.086	1.040	0.980	0.902	0.816	0.710	.567	.413
-0.600	1.242	1.203	1.153	1.098	1.000	0.891	0.780	.627	.446	1.220	1.177	1.129	1.061	0.967	0.869	0.753	.601	.439
-0.800	1.403	1.359	1.301	1.227	1.101	0.970	0.845	.672	.478	1.380	1.337	1.285	1.202	1.080	0.953	0.827	.655	.473
-1.000	1.549	1.498	1.430	1.333	1.180	1.028	0.892	.707	.504	1.525	1.481	1.420	1.317	1.164	1.014	0.878	.696	.498
-1.200	1.680	1.622	1.543	1.419	1.240	1.070	0.930	.733	.524	1.659	1.610	1.537	1.411	1.228	1.059	0.917	.725	.517
-1.400	1.800	1.739	1.647	1.489	1.287	1.106	0.959	.757	.540	1.780	1.731	1.639	1.480	1.276	1.096	0.949	.750	.531
-1.600	1.912	1.849	1.740	1.546	1.323	1.131	0.983	.778	.551	1.897	1.843	1.729	1.533	1.316	1.123	0.973	.770	.544
-1.800	2.018	1.951	1.821	1.590	1.353	1.155	1.005	.797	.560	2.003	1.947	1.809	1.580	1.347	1.147	0.997	.787	.553
-2.000	2.120	2.049	1.892	1.627	1.380	1.175	1.022	.810	.569	2.104	2.042	1.879	1.619	1.372	1.167	1.013	.801	.560
-2.500	2.351	2.261	2.027	1.697	1.428	1.218	1.059	.837		2.340	2.251	2.017	1.690	1.423	1.210	1.049	.827	
-3.000	2.557	2.423	2.113	1.747	1.464	1.247	1.081	.852		2.550	2.414	2.105	1.738	1.457	1.240	1.073	.840	
-3.500	2.748	2.536	2.167	1.778	1.489	1.263	1.099			2.740	2.530	2.153	1.768	1.475	1.252	1.088		
-4.000	2.911	2.617	2.200	1.796	1.499	1.274				2.904	2.609	2.180	1.780	1.487	1.263			
-4.500	3.052	2.677	2.217	1.805	1.507					3.048	2.671	2.198	1.790	1.491				
-5.000	3.173	2.731	2.223	1.810						3.169	2.727	2.207	1.793					
-5.500	3.290	2.773	2.228							3.286	2.769	2.210						
-6.000	3.400	2.808								3.396	2.800							

Note: The above tabulation is for that portion of the profile below the crest.

TABLE 3.—COORDINATES OF LOWER NAPPE SURFACE FOR NEGLIGIBLE APPROACH VELOCITY

	$\frac{Y}{H_s}$												
	10-percent vacuum*					20-percent vacuum*				30-percent vacuum*			
$\frac{X}{H_s}$ \ $\frac{H_s}{R}$	0.30	0.40	0.50	0.60	0.80	0.40	0.50	0.60	0.80	0.40	0.50	0.60	0.80
0.000	0.0000	0.0000	0.0000	0.0000	0.0000	0.0000	0.0000	0.0000	0.0000	0.0000	0.0000	0.0000	0.0000
.010	.0135	.0135	.0130	.0130	.0112	.0132	.0130	.0128	.0110	.0130	.0127	.0125	.0107
.020	.0235	.0230	.0225	.0215	.0180	.0227	.0220	.0210	.0175	.0225	.0215	.0205	.0170
.030	.0325	.0310	.0295	.0285	.0230	.0300	.0290	.0280	.0225	.0295	.0280	.0275	.0220
.040	.0395	.0375	.0350	.0330	.0265	.0370	.0340	.0325	.0260	.0365	.0335	.0320	.0250
.050	.0460	.0435	.0400	.0370	.0285	.0430	.0395	.0365	.0280	.0420	.0390	.0360	.0275
.060	.0515	.0480	.0450	.0405	.0295	.0475	.0440	.0400	.0290	.0465	.0435	.0395	.0285
.070	.0560	.0520	.0480	.0430	.0300	.0510	.0470	.0425	.0295	.0505	.0465	.0420	.0285
.080	.0600	.0565	.0520	.0450	.0295	.0555	.0505	.0445	.0290	.0540	.0495	.0440	.0280
.090	.0635	.0590	.0540	.0460	.0280	.0580	.0530	.0450	.0270	.0565	.0520	.0445	.0260
.100	.0665	.0620	.0560	.0470	.0260	.0605	.0540	.0460	.0250	.0585	.0530	.0460	.0240
.120	.0705	.0655	.0580	.0475	.0190	.0640	.0565	.0460	.0180	.0620	.0545	.0450	.0175
.140	.0730	.0680	.0580	.0450	.0105	.0660	.0565	.0435	.0095	.0630	.0545	.0420	.0090
.160	.0740	.0680	.0570	.0410	-.0010	.0660	.0550	.0395	-.0020	.0630	.0530	.0380	-.0030
.180	.0740	.0670	.0540	.0360		.0640	.0520	.0340		.0610	.0500	.0320	
.200	.0730	.0650	.0500	.0290		.0620	.0480	.0260		.0580	.0450	.0245	
.250	.0670	.0550	.0360	.0040		.0500	.0320	.0020		.0455	.0290	-.0010	
.300	.0560	.0390	.0145			.0330	.0100			.0265	.0070		
.350	.0400	.0200	-.0125			.0120	-.0180			.0030	-.0225		
.400	.0200	-.0040				-.0140				-.0240			
.450	-.0045												

Note: The above tabulation is for that portion of the profile above the weir crest.

	$\frac{X}{H_s}$												
$\frac{Y}{H_s}$ \ $\frac{H_s}{R}$	0.30	0.40	0.50	0.60	0.80	0.40	0.50	0.60	0.80	0.40	0.50	0.60	0.80
0.000	0.442	0.393	0.328	0.257	0.158	0.374	0.319	0.253	0.157	0.356	0.313	0.248	0.155
-0.020	0.478	0.431	0.362	.288	.187	0.411	0.353	.284	.185	0.392	0.346	.279	.183
-0.040	0.512	0.465	0.392	.314	.210	0.444	0.383	.310	.208	0.425	0.375	.305	.205
-0.060	0.452	0.496	0.418	.338	.229	0.475	0.410	.333	.227	0.454	0.402	.328	.224
-0.080	0.572	0.525	0.444	.358	.247	0.504	0.434	.354	.244	0.482	0.426	.348	.240
-0.100	0.600	0.552	0.467	.377	.262	0.531	0.458	.372	.259	0.509	0.449	.367	.255
-0.150	0.663	0.613	0.519	.418	.295	0.592	0.508	.414	.291	0.567	0.498	.409	.287
-0.200	0.720	0.669	0.563	.454	.321	0.645	0.552	.449	.316	0.618	0.540	.443	.312
-0.250	0.773	0.718	0.601	.484	.343	0.692	0.589	.479	.339	0.664	0.577	.472	.333
-0.300	0.823	0.764	0.634	.511	.363	0.734	0.622	.506	.358	0.705	0.609	.498	.351
-0.400	0.913	0.843	0.690	.556	.395	0.813	0.678	.550	.389	0.779	0.664	.542	.381
-0.500	0.996	0.913	0.737	.593	.422	0.879	0.723	.587	.414	0.844	0.709	.578	.407
-0.600	1.068	0.973	0.779	.623	.442	0.938	0.763	.617	.435	0.900	0.749	.609	.427
-0.800	1.193	1.070	0.843	.670	.476	1.032	0.826	.663	.469	0.993	0.810	.656	.459
-1.000	1.303	1.144	0.889	.705	.501	1.108	0.873	.696	.493	1.071	0.860	.690	.483
-1.200	1.401	1.203	0.927	.732	.518	1.170	0.912	.723	.510	1.137	0.900	.716	.501
-1.400	1.492	1.253	0.955	.755	.533	1.223	0.943	.746	.525	1.193	0.931	.739	.516
-1.600	1.574	1.297	0.980	.773	.545	1.268	0.970	.765	.535	1.243	0.958	.757	.528
-1.800	1.649	1.331	1.000	.790	.555	1.307	0.991	.780	.546	1.287	0.980	.773	.538
-2.000	1.717	1.361	1.018	.803	.564	1.340	1.010	.795	.555	1.321	1.000	.785	.546
-2.500	1.865	1.420	1.053	.828	.579	1.408	1.046	.819	.571	1.389	1.039	.810	.564
-3.000	1.988	1.457	1.078	.848		1.450	1.070	.838		1.435	1.062	.830	
-3.500	2.088	1.482	1.093			1.473	1.083			1.467	1.077		
-4.000	2.158	1.498				1.490				1.483			
-4.500	2.205	1.508				1.500				1.492			
-5.000	2.228												
-5.500	2.230												
-6.000	2.231												

Note: The above tabulation is for that portion of the profile below the weir crest.

crest. To facilitate the interchange between H_s and H_o, the relationship of H_s/R to E/H_s for the three approach depths and the three vacuum crests is plotted in Figs. 13(*a*) and (13(*b*). The values of E/H_s which are equal to Y/H_s at the high point of the lower-nappe profile were obtained from Tables 1, 2, and 3. Because H_s is equal to H_o plus E (Fig. 1), the curves offer a method of determining H_o when H_s is known, or vice versa.

As the discharge equation for the circular weir, Eq. 1, involves three variables (C, L, or radius, and H_s), the procedure for determining the size of the overflow section for a morning-glory spillway by successive approximations is a long and tedious process. By expressing the discharge in terms of the dimensionless ratio H_s/R, the number of variables is reduced to two and work is minimized. From Eq. 1,

TABLE 4.—COORDINATES OF UPPER-NAPPE SURFACE FOR NEGLIGIBLE VELOCITY OF APPROACH AND AERATED NAPPE

	$\frac{Y}{H_s}$										
$\frac{X}{H_s}$ \ $\frac{H_s}{R}$	0.20	0.25	0.30	0.35	0.40	0.45	0.50	0.60	0.80	1.00	
-0.40	0.955	0.956	0.959	0.960	0.961	0.963	0.968	0.976	0.986	1.000	Level water surface for $\frac{H_s}{R} > 1.00$
-0.20	0.925	0.927	0.929	.930	.935	.936	.942	.958	.973	0.996	
0.00	0.880	0.886	0.892	.895	.900	.905	.920	.932	.955		
0.20	0.820	0.829	0.838	.845	.851	.861	.870	.900			
0.40	0.740	0.753	0.763	.772	.787	.801	.815	.855			
0.60	0.640	0.658	0.669	.684	.702	.726	.748				
0.80	0.518	0.540	0.556	.578	.600	.633					
1.00	0.372	0.402	0.420	.449	.475						
1.20	0.205	0.240	0.265	.300	.328						
1.40	0.013	0.051	0.081	.128							
1.60	-0.205	-0.160	-0.122	-.063							
1.80	-0.457	-0.400	-0.357								
2.00	-0.748	-0.678	-0.613								
2.20	-1.072	-0.981	-0.895								
2.40	-1.440	-1.315	-1.198								
2.60	-1.845	-1.670									
2.80	-2.268										
3.00	-2.685										
Point at which upper nappe surface joins boil											
X/H_s			2.410	1.711	1.208	0.810	0.725	0.510	0.120	-0.068	
Y/H_s			-1.210	-0.185	0.320	0.626	0.696	0.825	0.940	0.990	
High point of boil											
X/H_s				2.911	2.545	2.267	2.043	1.710	1.275	1.030	
Y/H_s				0.006	0.438	0.666	0.783	0.942	0.970	1.000	

$$Q = C\,(2\,\pi\,R)\,H^{3/2}_s = \frac{C\,2\,\pi}{\frac{H_s}{R}}\,H^{5/2}_s \ldots\ldots\ldots\ldots\ldots\ldots \quad (3)$$

Then,

$$\frac{H_s}{R} = 2\,\pi\left(C\,\frac{H^{5/2}_s}{Q}\right) \ldots\ldots\ldots\ldots\ldots\ldots\ldots \quad (4)$$

Values of $C\,H^{5/2}_s/Q$ for different (H_s/R)-ratios are plotted also in Figs. 13(*a*) and 13(*b*). When used in conjunction with the ratio E/H_s, the number of successive approximations required to determine C, R, or H_s is materially reduced.

TABLE 5.—COORDINATES OF UPPER-NAPPE SURFACE FOR AERATED NAPPE

	$\frac{Y}{H_s}$																	
	$\frac{P}{R}$ = 0.30									$\frac{P}{R}$ = 0.15								
$\frac{X}{H_s}$ \ $\frac{H_s}{R}$	0.20	0.25	0.30	0.35	0.40	0.45	0.50	0.60	0.80	0.20	0.25	0.30	0.35	0.40	0.45	0.50	0.60	0.80
-0.40	0.964	0.965	0.968	0.975	0.976	0.977	0.978	0.986	0.991	0.957	0.962	0.968	0.971	0.978	0.980	0.987	0.990	0.995
-0.20	0.929	0.934	0.936	.947	.949	.950	.954	.966	.981	0.917	0.924	.934	.942	.949	.955	.960	.970	.985
0.00	0.879	0.885	0.890	.901	.907	.911	.919	.938	.966	0.870	0.875	.887	.899	.909	.915	.922	.937	.970
0.20	0.813	0.818	0.829	.843	.853	.862	.871	.892	.944	0.800	0.810	.823	.836	.850	.860	.871	.894	.948
0.40	0.730	0.737	0.753	.772	.788	.798	.810	.836		0.715	0.727	.745	.759	.776	.792	.807	.841	
0.60	0.626	0.641	0.658	.683	.700	.715	.730			0.610	0.629	.648	.666	.686	.708	.735		
0.80	0.506	0.524	0.544	.574	.592	.611				0.490	0.511	.533	.556	.582	.612			
1.00	0.363	0.388	0.413	.442	.465					0.352	0.377	.398	.427	.465				
1.20	0.199	0.228	0.253	.292						0.187	0.216	.240	.277	.337				
1.40	0.005	0.042	0.071	.123						-0.007	0.028	.055	.106					
1.60	-0.223	-0.175	-0.135	-.070						-0.235	-0.190	-.155	-.081					
1.80	-0.482	-0.422	-0.368							-0.498	-0.437	-.388						
2.00	-0.772	-0.702	-0.625							-0.795	-0.710	-.648						
2.20	-1.083	-1.018	-0.910							-1.118	-1.023	-.903						
2.40	-1.415	-1.347	-1.235							-1.448	-1.350							
2.60	-1.767	-1.683								-1.800	-1.683							
2.80	-2.130	-2.018								-2.148	-2.035							
3.00	-2.500	-2.351								-2.522	-2.388							
Point at which upper nappe surface joins boil																		
X/H_s			2.410	1.733	1.096	0.938	0.714	0.420	0.315			2.222	1.723	1.260	0.948	0.732	0.420	0.344
Y/H_s			-1.253	-0.210	0.394	0.531	0.680	0.830	0.926			-0.932	-0.200	0.295	0.530	0.681	0.835	0.925
High point of boil																		
X/H_s			3.370	2.922	2.436	2.288		1.775	1.252				2.935	2.531	2.278	2.009	1.680	1.263
Y/H_s			-0.755	0.043	0.496	0.713		0.950	0.985				0.002	0.458	0.647	0.815	0.935	0.998

TABLE 6.—COORDINATES OF UPPER-NAPPE SURFACE FOR NEGLIGIBLE VELOCITY OF APPROACH

	$\frac{Y}{H_s}$												
	10-percent vacuum*					20-percent vacuum*				30-percent vacuum*			
$\frac{X}{H_s}$ \ $\frac{H_s}{R}$	0.30	0.40	0.50	0.60	0.80	0.40	0.50	0.60	0.80	0.40	0.50	0.60	0.80
-0.40	0.940	0.951	0.956	0.963	0.981	0.941	0.950	0.958	0.978	0.939	0.945	0.957	0.975
-0.20	.911	.927	.938	.940	.971	.911	.925	.931	.966	.908	.912	.929	.964
0.00	.865	.883	.897	.909	.960	.865	.886	.898	.957	.865	.870	.890	.952
0.20	.803	.825	.848	.873	.950	.808	.835	.860	.941	.803	.815	.843	
0.40	.725	.753	.783	.825		.735	.770	.808		.723	.742	.789	
0.60	.628	.662	.711			.641	.697			.622	.650	.724	
0.80	.508	.551				.522				.491			
1.00	.358	.413				.368				.325			
1.20	.170	.242				.173				.105			
1.40	-.062	-.053				-.070				-.163			
1.60	-.327					-.345				-.460			
1.80	-.629					-.638				-.783			
2.00	-.975												
2.20	-1.374												
2.40	-1.819												
2.60	-2.300												
Point at which upper nappe surface joins boil													
X/H_s	2.600	1.504	.721	.403	.300	1.808	.722	.418	.299	1.803	.735	.608	.152
Y/H_s	-2.300	-.043	.665	.821	.944	-.644	.647	.803	.931	-.790	.620	.722	.940

APPLICATION OF RESULTS

To illustrate the practical use of these experimental results in determining the profile of a morning-glory spillway, a comparison with the model studies for Hungry Horse Dam spillway will be made. Although the crest profile for Hungry Horse Dam spillway was determined from specific tests on the circular test weir, none of the Hungry Horse data was used in these experiments.

The first step in the computations is to determine the radius of the spring point, R, required to pass 53,000 cu ft per sec when the head, H_o, above the high point of the crest is 16.9 ft. Because the experimental data are in terms of head above the weir, H_s, it is necessary to assume a value of H_s as well as a coefficient, C. Assuming $H_s = 18.5$ ft and $C = 3.0$,

$$\frac{C\,H^{5/2}_s}{Q} = \frac{3.0(18.5)^{5/2}}{53{,}000} = 0.083.$$

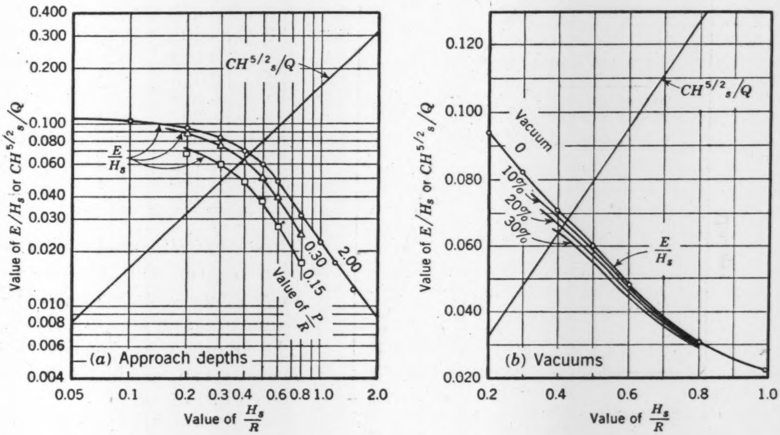

FIG. 13.—RELATIONSHIP OF H_s/R TO $C\,H^{5/2}_s/Q$ AND E/H_s FOR DIFFERENT APPROACH DEPTHS AND PRESSURES UNDER THE NAPPE

Entering this value into Fig. 13, $H_s/R = 0.52$ and $E/H_s = 0.053$ for a 30% vacuum crest. Then

$$E = 0.053(18.5) = 0.98 \text{ ft}$$

and

$$H_s = 16.9 + 0.98 = 17.88 \text{ ft}.$$

From Fig. 10, $C = 3.39$, which does not check the assumed value.

Using the new values of C and H_s, the process is repeated—

$$\frac{C\,H^{5/2}_s}{Q} = \frac{3.39(17.9)^{5/2}}{53{,}000} = 0.086.$$

From Fig. 13, $H_s/R = 0.53$ and $E/H_s = 0.052$. Therefore, $E = 0.93$ and $H_s = 17.83$ ft. From Fig. 10, $C = 3.38$, which checks sufficiently well with the trial values. Therefore,

$$R = \frac{17.83}{0.53} = 33.6 \text{ ft.}$$

The radius, R, and the head, H_s, above the weir have been established.

With the ratio, $H_s/R = 0.53$, it is possible to determine the shape of the overflow section. The (X/H_s)- and (Y/H_s)-coordinates for a 30% vacuum crest are given in Table 3 for (H_s/R)-values of 0.50 and 0.60. By interpolation, sufficient coordinates to describe the curve for $H_s/R = 0.53$ are obtained.

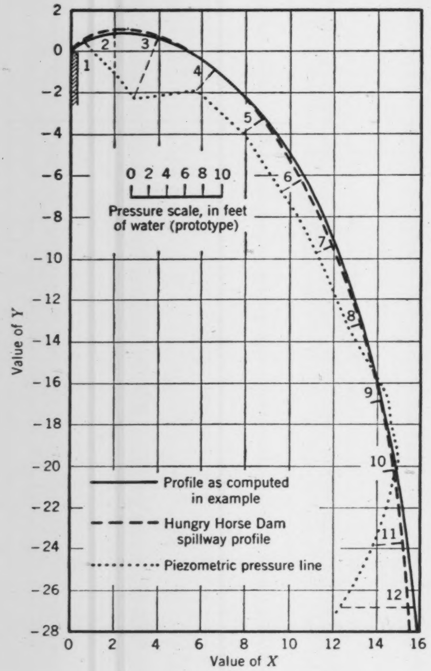

FIG. 14.—COMPARISON OF SPILLWAY PROFILES

TABLE 7.—COORDINATES FOR FIG. 14

$\frac{X}{H_s}$	$\frac{Y}{H_s}$	X	Y
0.050	0.038	0.89	0.68
0.070	0.045	1.25	0.80
0.100	0.051	1.78	0.91
0.200	0.039	3.56	0.70
0.293	0	5.22	0
0.424	−0.10	7.55	−1.70
0.545	−0.25	9.71	−4.45
0.627	−0.40	11.18	−7.12
0.707	−0.60	12.60	−10.69
0.764	−0.80	13.60	−14.25
0.809	−1.00	14.40	−17.81
0.845	−1.20	15.03	−21.39
0.873	−1.40	15.54	−24.95
0.898	−1.60	16.00	−28.50

These (X/H_s)- and (Y/H_s)-coordinates and the corresponding X-values and Y-values are presented in Table 7. The overflow section of the spillway can now be plotted as shown in Fig. 14.

Table 8 shows a comparison of the foregoing computations with those in the model studies of the Hungry Horse Dam spillway.

Col. 2, Table 8, shows the significant data from these experiments that were used in computing the example, and Col. 3 contains similar data used in the design of the Hungry Horse Dam spillway. It is noted that the experimental data show slightly lower values of H_s, E, and R than those used in the Hungry Horse design, which accounts for the higher coefficient of discharge, C, obtained with the experimental data.

Because the model was constructed using the spillway dimensions listed in Col. 3, the values of H_s, H_o, E, and R are identical in Cols. 3 and 4. The discharge obtained in the model is approximately 7% less than the design flow. This discrepancy can be explained as follows: (1) The spillway is designed with a 9-ft-wide pier placed over the rounded crest. In computing the discharge in Cols. 2 and 3, the reduced effective length of the crest (because of the pier) was not considered, which accounts for approximately half the 7% discrepancy. (2) The experimental data are based on the ideal situation where all the flow enters the spillway on radial lines. For the Hungry Horse Dam spillway approximately half the crest is located in an approach channel cut in the hillside, and only 50% to 60% of the flow approaches the crest on radial lines.

Whether the reduction in discharge caused by the nonradial approach conditions is greater or less than that indicated by the difference in the computed and model discharges cannot be determined from the available data.

A comparison of the two rounded crests is shown in Fig. 14 where the profile, as determined from these experiments, is plotted as a solid line and the Hungry Horse crest is denoted by a broken line. Also shown are the piezometric pressures in feet of water (prototype) observed on the model for a discharge corresponding to a prototype flow of 50,000 cu ft per sec. Pressures above atmospheric are indicated above and to the right of the profile, and subatmospheric pressures are shown below and to the left of the profile.

TABLE 8.—COMPARISON OF COMPUTATIONS AND MODEL STUDIES

Item (1)	Experimental data (2)	Hungry Horse Dam spillway, as designed (3)	Hungry Horse Dam spillway model results (4)
H_s, in feet	17.83	17.9	17.9
H_o, in feet	16.90	16.9	16.90
E, in feet	0.93	1.00	1.00
R, in feet	33.6	34.0	34.0
Q, in cubic feet per second	53,000	53,000	49,000
C	3.38	3.28	3.06
Vacuum crest, in feet	−5.3	−5.0	0.8 to −8.0
Crest shape	See Fig. 14	See Fig. 14	

The greatest deviation in the two profiles occurs in the region between piezometers 4 and 7 and at the lower end of the rounded crest between piezometers 11 and 12. The observed pressures on the model crest suggest the true shape of the overflow section for the design conditions by indicating where the curvature of the model crest profile should be adjusted to obtain a uniform pressure of approximately −5 ft of water along the spillway face. Lower pressures usually occur where the degree of curvature is too great.

To verify the magnitude and uniformity of the pressures on the computed profile would require tests on a model representing that particular crest shape. However, the observed pressures on the Hungry Horse model tend to confirm the fact that the observed and computed pressures should agree.

LIMITATIONS ON APPLICATION OF RESULTS

Certain limitations should be recognized when applying the experimental results to determine the coefficient of discharge and profile of a morning-glory spillway. The test data were obtained from a circular weir in which the water fell freely through the atmosphere or a partial vacuum. Thus, the upper-nappe surface was subject to atmospheric pressure in all tests, whereas the lower-nappe surface was subject to either atmospheric pressure or a partial vacuum depending on the test arrangement. Therefore, the head producing the discharge was the head above the weir plus the pressure under the nappe measured in feet of water below atmospheric pressure.

In the morning-glory spillway, the same conditions exist except that the space under the nappe is replaced by concrete. However, when a morning-glory spillway is designed for the submerged condition or with the top of the boil near the crest of the spillway, an additional head is acting on the spillway because of the siphonic action of the column of water in the shaft. This additional head, which does not exist in the circular weir because the jet is surrounded by air, causes a pressure reduction in the shaft and an increase in discharge over the spillway. Therefore, when a morning-glory spillway is designed for near-submerged conditions, similitude between the spillway and the circular weir no longer exists. If the shaft is designed to flow partly full, however, flows in a morning-glory spillway and a circular weir are similar.

In applying the experimental results from the circular weir to a morning-glory spillway, some method of maintaining the design pressure along the lower-nappe surface should be provided to restore similitude between the two flows. The design pressure may be maintained by several methods: (*a*) Design the spillway with a small (H_s/R)-ratio so that the shaft never flows full. (*b*) Place a constriction in the shaft at any point below the boil to maintain the design pressure under the nappe at the boil. (*c*) Provide air vents under the nappe at the boil to relieve the suction head caused by the shaft flowing full.

At the Hungry Horse Dam air was supplied to the lower-nappe surface by several air vents placed under the lip of the ring gate. In addition, a 6-ft by 6-ft air vent was placed in the crown of the vertical bend connecting the shaft with the inclined tunnel. Model tests on the Hungry Horse Dam spillway showed that pressures lower than those indicated in Fig. 14 were observed when the air vents were closed.

Additional research is required for the economical design of a submerged morning-glory spillway with a pressure-controlled profile. However, if the previously cited limitations are recognized and means are provided to deal with them, the results should prove helpful in designing a morning-glory spillway.

ACKNOWLEDGMENTS

The test weir was constructed and the tests performed in the hydraulic laboratory of the USBR in Denver. Many members of the laboratory staff made valuable contributions to the paper. Credit is due J. N. Bradley, M. ASCE, D. J. Hebert, and A. J. Peterka, M. ASCE, for their suggestions in formulating the testing program and in evaluating the experimental results.

It is also desired to acknowledge the assistance of T. J. Rhone, A.M. ASCE, G. L. Beichley, A. S. Reinhart, P. F. Enger, J.M. ASCE, J. V. Williamson, N. E. Smith, J.M. ASCE, R. E. Selleck, J.M. ASCE, and L. A. Browning, who assisted in preparing the equipment plans, collecting the test data, and tabulating the results.

DISCUSSION

Maxwell W. White[8] **and Murray B. McPherson**,[9] A.M. ASCE.—The characteristics of morning-glory shaft spillways in important structures are determined by a model test of the actual structure, by an application of principles arrived at by studies on model spillways, or by more fundamental studies on sharp-crested circular weirs. The "scaling up" of results from these model tests to prototype conditions requires that the scale effects (that is, the factors affecting flow over the model weir which are not present in the prototype) either be negligible or else be accounted for in the computation.

The results given for discharge coefficients by Mr. Wagner concern spillways designed for maximum heads from H_s/D (in which $D = 2\,R$) greater than 0.10 to past the submerged range. However, not many spillways have been designed to perform submerged. Of the eighteen morning-glory spillways for which details have been published[10] only four are designed to perform submerged, six for ratios of H_s/D between 0.10 and 0.20, and eight for ratios of H_s/D less than 0.10.

Tests were performed on sharp-edged circular weirs in the hydraulic laboratory of the Fritz Engineering Laboratory of Lehigh University (Bethlehem, Pa.) between 1949 and 1954.[11] These tests were intended to determine (*a*) the head-discharge relationship—that is, the relationship between the basic parameters, Q, H, and D, (*b*) the effect on this relationship of fluid properties such as surface tension and viscosity, particularly at small heads, and (*c*) the point at which weir flow changes to flow through a re-entrant tube. These results were compared with those of other investigators to extend the range and value of the results. A brief survey of the investigations and of the results obtained is presented herein. These results were not extended to pressure-controlled lower nappes as mentioned by Mr. Wagner, all tests being conducted with the lower nappe aerated at atmospheric pressure and with the nappe springing clear from the crest. The approach conditions were fixed for uniform radial flow.

From preliminary tests it was found, in agreement with Mr. Wagner, that when P was greater than D the effects of the velocity head and the ratio H_s/P on the discharge coefficient were negligible. Accordingly, this factor was eliminated from subsequent testing, P in all cases being greater than D.

With these variables eliminated, the remaining factors can be grouped into dimensionless parameters—

$$\frac{Q}{H_s^{1.50}\, D^{1.00}\, g^{0.50}} = \frac{C\,\pi}{g^{0.50}} \qquad (5)$$

$$\frac{H_s}{D} \qquad (6)$$

---

[8] Research Assistant, Lehigh Univ., Bethlehem, Pa.

[9] Associate Prof. of Civ. Eng., Lehigh Univ., Bethlehem, Pa.

[10] "Morning-Glory Shaft Spillways: Prototype Behavior," by Joseph N. Bradley, *Transactions*, ASCE, Vol. 121, 1956, p. 312.

[11] "Characteristics of Sharp-Crested Circular Weirs," by M. W. White, G. M. Brey, and R. G. Dittig, *Report No. A-1342*, Fritz Eng. Lab., Lehigh Univ., Bethlehem, Pa., April, 1954.

and

$$\frac{H^{1.50}_s\, g^{0.50}}{\nu} = \mathbf{R} \qquad (7)$$

in which **R** is a Reynolds number, and

$$\frac{\gamma\, H^{2.00}_s}{\sigma} = \mathbf{W} \qquad (8)$$

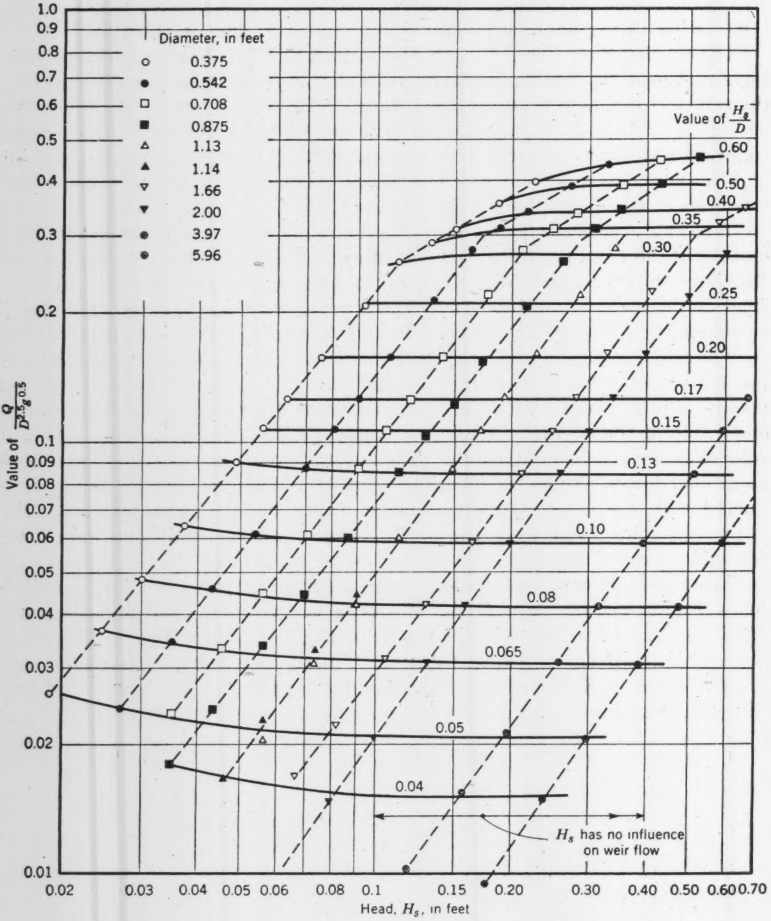

FIG. 15.—THE RELATIONSHIP BETWEEN $Q/(D^{2.5}\, g^{0.5})$ AND H_s FOR CONSTANT VALUES OF H_s/D

in which **W** is a Weber number and from which

$$\frac{Q}{H_s^{1.50}\, D^{1.00}\, g^{0.50}} = f\left(\frac{H_s}{D}, \frac{H_s^{1.50}\, g^{0.50}}{\nu}, \frac{\gamma\, H_s^{2.00}}{\sigma}\right) \ldots\ldots\ldots\ldots (9)$$

The parameter in Eq. 5 is a theoretical coefficient of discharge. Dimensional analysis shows that this coefficient is a function of (1) H_s/D, which expresses the contractive effect; (2) **R**, which expresses the effects of viscosity; and (3) **W**, which expresses the effects of surface tension.

In the tests at Lehigh University only water was used; therefore, the parameters **R** and **W** could not be varied independently because both are functions of fluid properties and head, H_s, only. The effects of the two factors could therefore not be presented generally for any fluid, nor could their individual effects be distinguished. For this reason the results presented herein apply only to water, and in the investigations the parameters **W** and **R** can be represented as a function of H_s only, for water.

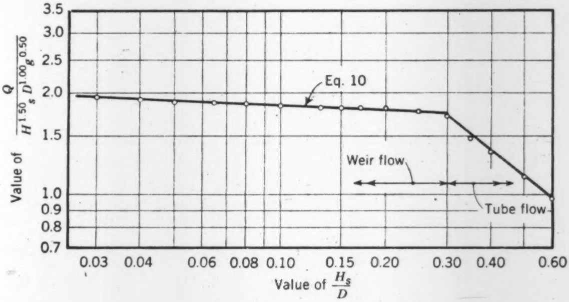

FIG. 16.—THE RELATIONSHIP BETWEEN $Q/(H_s^{1.50} D^{1.00} g^{0.50})$ AND H_s/D FOR THE REGION WHERE H_s HAS NO INFLUENCE

Within these limitations, the investigation was concerned with the effect on the coefficient of discharge of the head H_s and the effect of the ratio H_s/D.

The diameters used at Lehigh University were 0.375 ft, 0.542 ft, 0.708 ft, and 0.875 ft. Results of studies[2,3,4] were also used for weirs with diameters of 1.13 ft, 1.14 ft, 1.66 ft, 2.0 ft, 3.97 ft, and 5.96 ft. A summary of all the data is available.[11]

From all available experimental data, Fig. 15 was plotted. Fig. 15 shows the variation of $Q/(H_s^{1.5} D^{1.0} g^{0.5})$ with the head H_s for various constant values of H_s/D. For clarity, the ordinate has been plotted as $Q/(D^{2.5} g^{0.5})$ which—because curves are plotted for constant values of H_s/D—has only the effect of separating the curves.

Fig. 15 indicates that, when H_s is greater than approximately 0.10 ft, the value of $Q/(H_s^{1.5} D^{1.0} g^{0.5})$ remains constant for each value of H_s/D up to

$H_s/D \simeq 0.30$. That is, the relationship is independent of H_s for heads greater than 0.10 ft (corresponding to $\mathsf{R} = 16{,}600$ and $\mathsf{W} = 125$).

These values are more definite limits than Mr. Wagner has given for the minimum size of the weir that will eliminate scale effects. The inconsistencies in the discharge coefficient for low heads (mentioned by Mr. Wagner under the heading, "Analysis of Results: Discharge Coefficients") were not found in the Lehigh tests, probably because of the shorter time required to establish steady conditions. The tendency of the discharge coefficient to "increase as head decreased" was caused by surface tension or viscosity. The separate effects of surface tension and viscosity can be determined only by tests with various fluids flowing over the weir. Until such tests are completed these findings are applicable only to water.

Fig. 16 shows the relationship between $Q/(H^{1.5}_s\, D^{1.0}\, g^{0.5})$ and H_s/D for the range in which the former is independent of H_s. On a log-log graph, this relationship plots as a straight line in the range of H_s/D equal to from 0.03 to 0.30. The relationship is

$$\frac{Q}{H^{1.50}_s\, D^{1.00}\, g^{0.50}} = 1.66 \left(\frac{H_s}{D}\right)^{-0.04} \qquad (10)$$

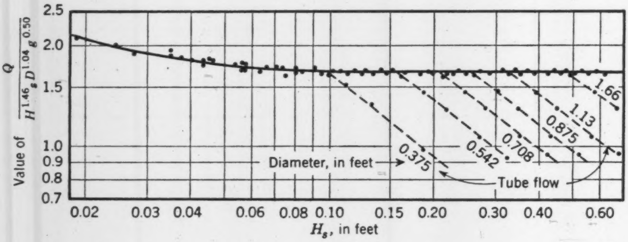

FIG. 17.—THE RELATIONSHIP BETWEEN $Q/(H^{1.46}_s\, D^{1.04}\, g^{0.50})$ AND H_s FOR WATER

or

$$Q = 1.66 \left(\frac{H_s}{D}\right)^{-0.04} \sqrt{g}\, D\, H^{1.50}_s \qquad (11)$$

That is,

$$C = \frac{1.66}{\pi} \left(\frac{H_s}{D}\right)^{-0.04} \sqrt{g} \qquad (12)$$

Eq. 12 is in very close agreement with the values given by Mr. Wagner (Fig. 9) for the more limited range of his tests. Eq. 12 can also be written as

$$Q = 1.66 \sqrt{g}\, D^{1.04}\, H^{1.46}_s \qquad (13)$$

In Fig. 17, the parameter $Q/(H^{1.46}_s\, D^{1.04}\, g^{0.5})$ is plotted against the depth H_s. After H_s exceeds approximately 0.10 ft, the value of the parameter is constant at 1.66. For heads less than 0.10 ft, the available results for all the weirs with heads as low as 0.02 ft fall on a smooth curve. In addition to indicating that the effects of surface tension or viscosity are correctly represented by Reynolds and Weber numbers involving the head only, Fig. 17 also shows the value of the discharge coefficient for any head below 0.10 ft when water is the fluid medium.

The point at which weir flow is "flooded out," the regime changing to flow through a re-entrant tube, was found in the Lehigh experiments to occur when H_s/D was approximately equal to 0.30 (the upper limit) above which weir flow cannot exist. However, if a vortex is formed, the flow diverges from weir flow at an earlier point. This is probably why Mr. Wagner and earlier investigators found the limit for free discharge to be lower than 0.30. The effect of vortex formation is to reduce the discharge for a given head,[12] as shown in Fig. 18 which is a discharge-head curve for an arbitrary 1-ft-diameter circular weir. If the vortex is eventually destroyed by the establishment of tube flow, the vortex causes a gradual transition between the two types of flow. When a vortex is suppressed by simple radial baffles, weir flow continues to the upper limit of $H_s/D \simeq 0.30$; most morning-glory spillways have radial baffles to prevent the formation of vortices.[10] No quantitative results have been obtained for the effect of a vortex in terms of the vortex strength.

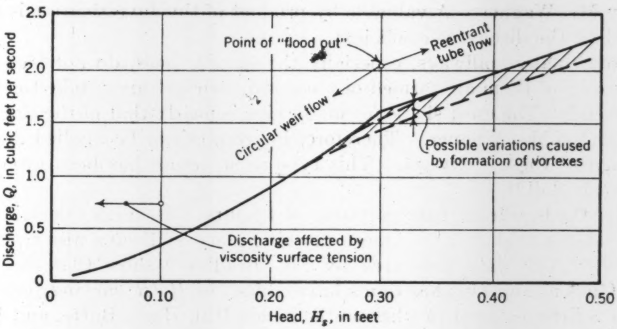

FIG. 18.—HEAD-DISCHARGE RELATIONSHIP FOR FLOW OVER A CIRCULAR WEIR HAVING A DIAMETER OF 1 FT

The conclusions from the Lehigh tests can be summarized as follows: For the flow of water over a sharp-edged circular weir with the following limitations —(*a*) radial approach conditions (no vortex), (*b*) *P* greater than weir diameter, and (*c*) aerated flow (that is, the lower nappe being at atmospheric pressure)— the relationship between the discharge, head over weir, and weir diameter (up to the point of "flood-out") can be expressed as

---

[12] "How the Vortex Affects Orifice Discharge," by C. J. Posey and H. Hsu, *Engineering News-Record*, March 9, 1950, p. 30.

$$Q = K \left(\frac{H_s}{D} \right)^{-0.04} \sqrt{g}\, D\, H_s^{1.50} \qquad (14)$$

or

$$Q = K \sqrt{g}\, D^{1.04}\, H_s^{1.46} \qquad (15)$$

The value of K is a function of the head over the weir H_s. If H_s exceeds 0.10 ft, K is constant and equals 1.66. If H_s is less than 0.10 ft, the value of K may be obtained from Fig. 17 for heads as low as 0.02 ft.

The upper limit at which weir flow changes in character to flow through a re-entrant tube is given by $H_s/D = 0.30$; the formation of a vortex causes the flow to deviate from true weir flow at a lower value of this ratio.

FRED W. BLAISDELL,[13] M. ASCE.—A most interesting presentation of experimental results of a determination of pressure-controlled profiles has been made by Mr. Wagner. A valuable by-product of this investigation is the data obtained on the discharge coefficient.

A great many spillways, especially the smaller ones, do not have shaped crests; many of them are formed of pipe, and their entrances take the shape of the pipe end. The crest shape for metal pipe is nearly that of the sharp-edged weir used by Mr. Wagner. Therefore, his results can be applied directly to the design of these spillways. This type of structure has been discussed by L. Standish Hall.[14]

Under the heading, "Interpretation of Results: Discharge Coefficient," Mr. Wagner states that " . . . most morning-glory spillways are designed for free flow." The data presented by Mr. Bradley [10] show that the Hungry Horse, Gibson, and Owyhee dams have values of H_s/R varying from a little above to a little below 0.45 whereas the Shade Hill, Heart Butte, and Kingsley dams have values of H_s/R greater than 1. Mr. Wagner (under the heading, "Analysis of Results") states that free flow exists for values of H_s/R less than 0.45 and submerged flow exists for values of H_s/R greater than 1.00. Therefore, it appears that a sufficient number of dams operate in the submerged-flow range (three of four dams completed in the United States since 1940) to make this statement open to question.

Because

$$C_o = \frac{2}{\sqrt{2\,g}} \frac{H_s}{R} C \qquad (16)$$

and as Mr. Wagner already has values of H_s/R and C, the determination of the values of C_o should be relatively easy. Such a determination would be a valuable addition to the paper, would permit the use of the coefficients in the orifice equation (which is theoretically correct for values of H_s/R exceeding 1.00), and would permit extrapolating beyond the range covered by Mr. Wagner's tests.

---

[13] Project Supervisor, Agri. Research Service, U. S. Dept. of Agriculture, St. Anthony Falls Hydr. Lab., Minneapolis, Minn.

[14] "Drop Structures for Erosion Control," by L. Standish Hall, *Civil Engineering*, Vol. 12, 1942, pp. 247–250.

It is unfortunate that no data were obtained for a zero depth of approach ($P/R = 0$). This depth exists in many smaller structures in which the vertical shaft or drop inlet is formed of pipe and the approach is level with the crest.

Tables 4 and 5 provide interesting verification of Mr. Wagner's statement, apparently derived from a study of Figs. 8 and 9, that the weir becomes partly submerged at values of H_s/R above 0.45. It is usually considered that the tailwater level will not affect the head on a weir unless the tailwater reaches a level above the weir crest exceeding the critical depth of flow d_c. Because $d_c = \frac{2}{3} H_s$, the value of Y/H_s is 0.667 when Y is equal to the critical depth. Tables 4 and 5 show that the value of H_s/R for $Y/H_s = 0.667$ at the point where the upper-nappe surface joins the boil is between 0.45 and 0.50. The value of H_s/R can be determined more precisely by plotting values of Y/H_s against H_s/R, which shows that $H_s/R = 0.47$ for $P/R = 2.00$, and 0.49 for $P/R = 0.30$ and 0.15 when $Y/H_s = 0.667$. These values closely confirm Mr. Wagner's value of 0.45.

For the free-flow part of the base curve in Fig. 9, a variable discharge coefficient is shown. It has been stated [2] that C is a constant equal to 3.28 (within 1%) for values of H_s/R between 0.16 and 0.40. Unfortunately, Mr. Camp and Mr. Howe do not give values of C_o so these comparisons are not possible.

IBRAHIM M. MOSTAFA,[15] J.M. ASCE, BENOYENDRA CHANDA,[16] AND HOWARD P. JOHNSON.[17]—The experimental results that Mr. Wagner has presented are of value because they can be used directly in the design of morning-glory spillways. Some interesting analytical and experimental comparisons can be made with these results. Although somewhat different geometry is used in part of the analysis, the comparisons made herein support the data presented by the author.

Dimensional analysis can be used to account for all the physical variables that affect flow over circular weirs. The variables pertinent to this case can be expressed as

$$Q = \phi\,(\mathbf{R}, P, H_s, h_p, g) \qquad (17)$$

and

$$Y = \phi\,(\mathbf{R}, P, H_s, h_p, X) \qquad (18)$$

in which h_p is the observed pressure in the air chamber under the nappe.

---

[15] Post-Doctoral Fellow, State Univ. of Iowa, Iowa City, Iowa.

[16] Graduate Student, State Univ. of Iowa, Iowa City, Iowa.

[17] Graduate Student, State Univ. of Iowa, Iowa City, Iowa.

Eqs. 17 and 18 can be put into the dimensionless forms,

$$C_d = \frac{Q}{\mathsf{R}\, H_s^{3/2} \sqrt{g}} \equiv \phi\left(\frac{p}{H_s}, \frac{H_s}{\mathsf{R}}, \frac{h_p}{H_s}\right) \qquad (19)$$

and

$$\frac{Y}{H_s} = \phi\left(\frac{p}{H_s}, \frac{H_s}{\mathsf{R}}, \frac{h_p}{H_s}, \frac{X}{H_s}\right) \qquad (20)$$

The coefficient of discharge C_d and the nappe profile will depend on the geometry of the weir and the pressure intensity below the nappe. The functional relationship indicated in Eqs. 19 and 20 can be determined experimentally.

If the weir is completely submerged and the depth of approach is infinite, a relationship for the coefficient of discharge can be derived analytically for the two-dimensional counterpart of the flow. Although this analytical approach has been developed for two-dimensional flow only, the results obtained can be applied with accuracy to three-dimensional flow.[18,19] A comparison with the results obtained in Fig. 9 for the range in which the weir is submerged and the velocity of approach is negligible is relevant to the author's purpose in presenting the study.

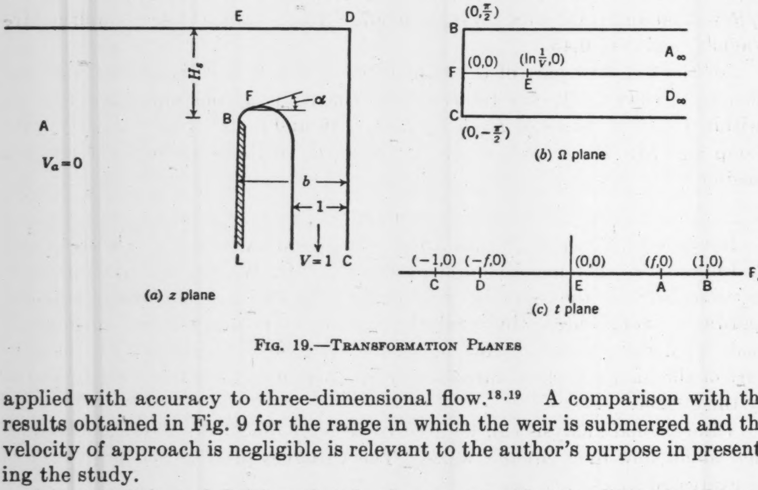

FIG. 19.—TRANSFORMATION PLANES

Fig. 19(*a*) is a definition sketch of a comparable two-dimensional case. Revolution of the boundary BL around DC would give the boundary of a circular weir. The free water surface above the weir, which is practically level when the flow is submerged, is represented by ED. The weir becomes an orifice when it is submerged, and the gravitational effect on the coefficient of contraction is known to be secondary; for this reason an ultimate width of

---

[18] "Characteristics of Irrotational Flow Through Axially Symmetric Orifices," by H. Rouse and A. Abul-Fetouh, *Transactions*, ASME, Vol. 17, 1950, p. 421.

[19] "Free-Streamline Analyses of Transition Flow and Jet Deflection," edited by John S. McNown and Chia-Shun Yih, *Studies in Engineering, Bulletin No. 35*, State Univ. of Iowa, Iowa City, Iowa, 1953.

the nappe can be assumed. By a series of mathematical transformations, the flow is transformed into a much simpler pattern. The three transformations used in the following analysis are shown in Fig. 19. For simplicity, the ultimate width of the nappe and the velocity of the free streamline have been taken as unity.

The flow is represented in the logarithmic hodograph (the Ω-plane) by the relationship,

$$\Omega = -\ln V + i\,\theta \ldots\ldots\ldots\ldots\ldots\ldots\ldots\ldots (21)$$

for which the flow region takes the form indicated in Fig. 19(*b*). The latter region is mapped on the upper half of the auxiliary *t*-plane. As indicated in Fig. 19(*c*), the values − 1, 0, and 1 are assigned to the points C, E, and B in the *t*-plane. The values of *t* for D and A can be denoted by − *f* and *f*, respectively.

The appropriate relationship between Ω and *t* is then obtained by the use of the Schwarz-Christoffel transformation—

$$\Omega = -\,i\tan^{-1}\left(\sqrt{\frac{t^2-1}{1-f^2}}\right) + i\,\frac{\pi}{2} \ldots\ldots\ldots\ldots\ldots (22)$$

The constants in the transformation were evaluated by substitution of the values of Ω and *t* for points E and F in the two planes.

The complex potential ω can be expressed in terms of *t* by the methods of elementary hydrodynamics—

$$\omega = \frac{1}{\pi}\left[\ln\,(t+1) - \ln\,(t-f)\right] \ldots\ldots\ldots\ldots\ldots\ldots (23)$$

Completion of the analyses involves the algebraic definition of the lower nappe as a function of the assigned value *f*. The relationship between the horizontal coordinate of the upper-nappe surface (*b*) and the head above the weir crest (H_s) can be expressed as

$$b - 1 = \frac{1}{\pi}\int_1^{-1}\left(\frac{1}{t-f} - \frac{1}{t+1}\right)\sqrt{\frac{t^2-1}{t^2-f^2}}\,dt \ldots\ldots\ldots (24)$$

and

$$H_s = \frac{\sqrt{1-f^2}}{\pi}\int_1^{-f}\left(\frac{1}{t-f} - \frac{1}{t+f}\right)\frac{dt}{\sqrt{t^2-f^2}} \ldots\ldots\ldots (25)$$

For any given value of *f*, Eqs. 24 and 25 can be solved for *b* and H_s. The integration in Eq. 24 can only be made numerically. In Eq. 25, the integrals are elementary and have been taken from tables; the result is

$$H_s = \frac{1}{\pi}\left(1 + \frac{1}{f} + \ln\frac{1}{f}\right) \ldots\ldots\ldots\ldots\ldots\ldots\ldots\ldots (26)$$

For the two-dimensional case, if there is no loss of energy, the coefficient of discharge C_d is simply $1/b$.

The computed results are compared with the author's observations on the basis of the assumption that the ratios H_s/b and H_s/R are identical. Values of C, in the form used by Mr. Wagner, have been plotted against H_s/b in Fig. 20, in which results from Fig. 9 are included. The analytically computed coefficients of discharge correspond remarkably well with the experimental coefficients for $H_s/R > 0.8$. For $H_s/R \geq 0.8$ the surface above the weir is practically horizontal, which is the condition assumed for the upper free surface in the analytical solution. The values of the coefficients of discharge C obtained from the test results are consistently slightly higher than those computed for any value of H_s/R. This may be partly explained by the fact that the latter were obtained for an infinite depth of approach.

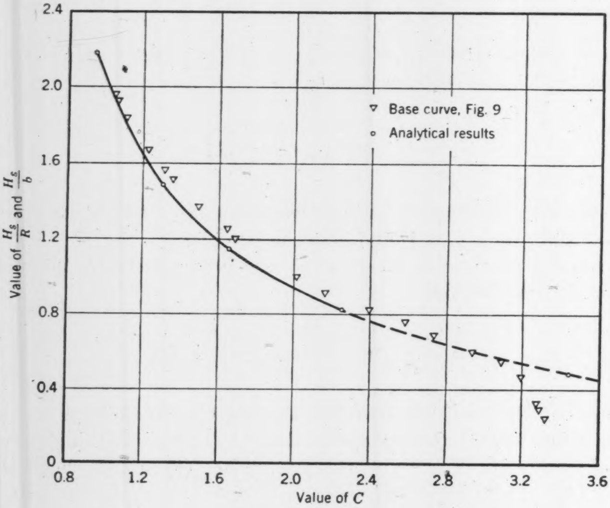

FIG. 20.—COMPARISON OF ANALYTICAL AND EXPERIMENTAL RESULTS

The profile of aerated nappe surfaces presented in Fig. 8 are almost exact reproductions of the profiles presented[20] by Mr. Camp. Fig. 21 shows the position of points selected from Mr. Camp's data and plotted on the profiles determined by Mr. Wagner. The earlier work was conducted using weir arcs with radii of 3 ft, 2 ft, and 1 ft having circular angles of 29°, 44°, and 97°, respectively.

---

[20] "Determination of Shape of Nappe and Coefficients of Discharge of a Vertical Sharp-Crested Weir, Circular in Plan, with Radially Inward Flow," by C. S. Camp, thesis presented to the State University of Iowa, at Iowa City, in 1937, in partial fulfilment of the requirements for the degree of Master of Science.

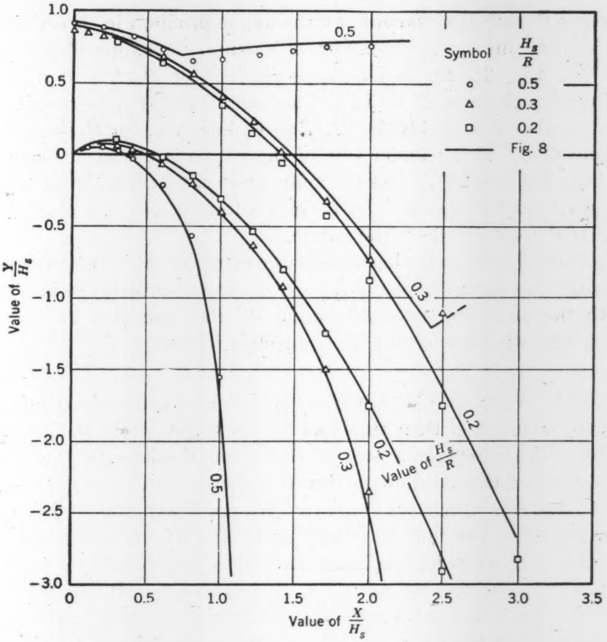

FIG. 21.—PROFILES OF AERATED NAPPE WITH NEGLIGIBLE VELOCITY OF APPROACH

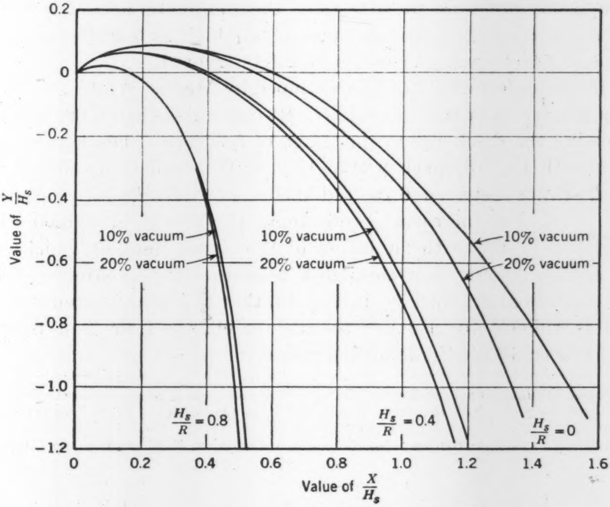

FIG. 22.—EFFECT OF VACUUM IN THE LOWER-NAPPE PROFILE

Regarding the effect of vacuum on the nappe profile, Fig. 22 reveals that, as the submergence increases, the effect of vacuum on nappe displacement diminishes. In Fig. 22, the lower-nappe profiles for $H_s/R = 0$ were secured from an investigation made[21] by L. A. Thorssen. The 10% increase in vacuum shifts the profile considerably for $H_s/R = 0$; however, for $H_s/R = 0.80$, only a slight movement of the under side of the nappe is observed for changes of vacuum from 10% to 20%. As the spillway becomes completely submerged, vacuum apparently acts as an increase in head and does not materially change the shape of the under side of the nappe.

It has been shown that the results presented by Mr. Wagner, which are well supported by earlier investigations of a similar nature, are in close agreement with the analyses presented herein for the case of a two-dimensional submerged weir when the depth of approach is infinite.

WILLIAM E. WAGNER,[22] M. ASCE.—Gratitude is expressed to the individuals who devoted so much of their time and energy to preparing their constructive discussions. The discussions are valuable contributions to the problem of properly designing the overflow section of a shaft spillway.

Figs. 15 and 17, which are supported by much experimental data, clearly define the region of low flow in which "scale effects" must be considered. It is interesting that weirs having heads as low as 0.10 ft may be used without surface tension or viscosity affecting the discharge. It should be noted, however, that these results were obtained in a laboratory under conditions where close control of the approach conditions, sharpness and cleanliness of the weir, and steadiness of flow were maintained. In general practice, where ideal conditions are difficult to attain, the minimum head for flow over a weir should be somewhat greater—possibly as high as 0.20 ft—to assure flow conditions in which scale effects can be safely ignored.

The discharge formula, Eq. 13, developed by Messrs. White and McPherson for heads greater than 0.10 ft and (H_s/R)-ratios less than 0.60, is convenient for expressing the discharge in the range of free flow. Discharge coefficients computed with Eq. 13 check within $1\frac{1}{2}$% of the coefficients shown in Fig. 9 for (H_s/R)-ratios between 0.20 and 0.50. For (H_s/R)-ratios greater than 0.50, the deviation increases—more than 4% for $H_s/R = 0.60$ (Fig. 23). This deviation leads to the question of the upper limit at which weir flow changes in character to flow through a re-entrant tube. Messrs. White and McPherson showed graphically, in Fig. 16, that this change occurs at $H_s/R = 0.60$. It is difficult to visualize the abrupt change from weir to tube flow indicated in Fig. 16 for the following reasons:

---

[21] "Effect of Vacuum on a Free Nappe," by L. A. Thorssen, thesis presented to the State University of Iowa at Iowa City, in 1946, in partial fulfilment of the requirements for the degree of Master of Science.

[22] Engr., Design and Construction Div., Bureau of Reclamation, U. S. Dept. of the Interior, Denver, Colo.

1. As noted by Mr. Blaisdell, the head on a weir is usually considered to be affected when the "tailwater reaches a level above the weir crest exceeding the critical depth of flow d_c," or when $Y/H_s = 0.667$. Table 4 shows that this tailwater (or boil height) is reached when H_s/R is between 0.45 and 0.50. When $H_s/R = 0.60$, $Y/H_s = 0.94$; the high point of the boil is at a level above the crest equal to 0.94 of the head. A backwater of this height surely affects the head upstream from the weir and causes a departure from true weir flow at some (H_s/R)-ratio less than 0.60; in Fig. 24 there is shown the operation of the circular weir when $H_s/R = 0.50$.

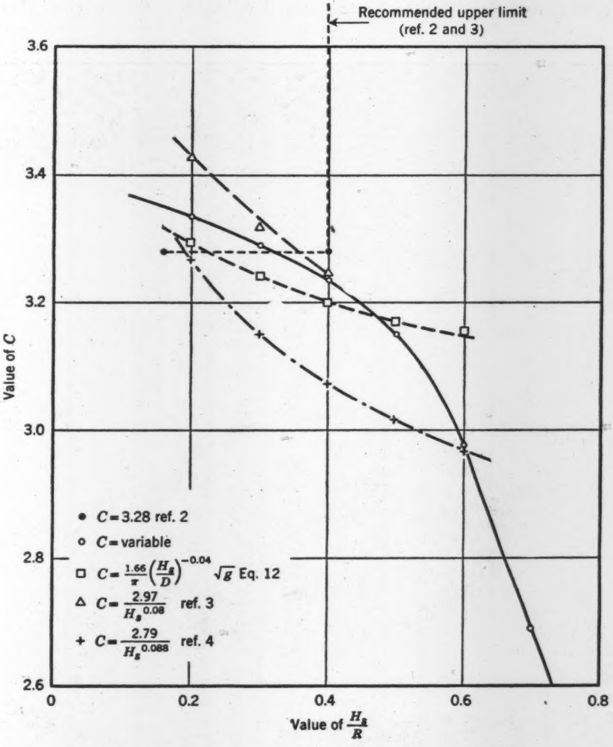

FIG. 23.—COMPARISON OF FREE-FLOW DISCHARGE COEFFICIENTS DETERMINED BY VARIOUS EXPERIMENTERS (NEGLIGIBLE VELOCITY OF APPROACH AND AERATED NAPPE)

2. In Fig. 25, some of the writer's original data are plotted on a graph similar to Fig. 16. Fig. 25 clearly indicates that a transition zone exists between tube flow and weir flow and supports the original conclusion that the

upper limit of weir flow is $H_s/R = 0.45$ and the lower limit of tube (or orifice) flow is $H_s/R = 1.00$. Unfortunately, actual calibration points of other experimenters are not available. However, the reports of Messrs. Camp and Howe[2] and H. J. F. Gourley[3] indicate a similar transition zone; they recommend an upper limit of $H_s/R = 0.40$ when using their formulas (Fig. 23).

The writer questions whether a vortex can form in the range of flows where H_s/R is less than 0.60 as suggested by Messrs. White and McPherson.

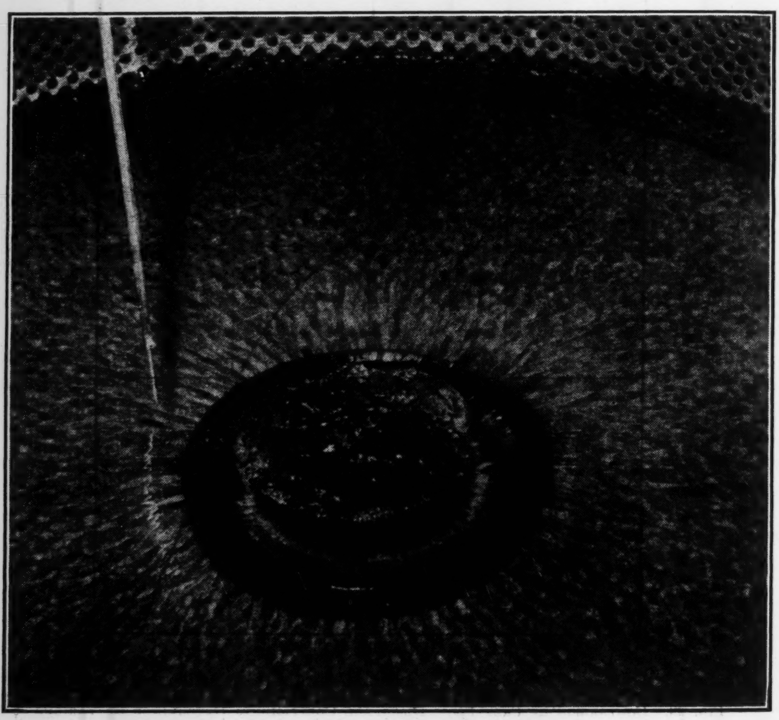

Fig. 24.—Flow When $H_s/R = 0.50$

At these flows, the velocity of the upper-nappe surface is comparatively high and well directed with a clear line of demarcation between the boil and the nappe, as shown in Fig. 24. Any vortex beginning to form in the nappe is carried immediately through the weir. Because of the turbulence within the boil it is unlikely that a vortex can be formed and maintained in this region. However, air may become entrained where the nappe joins the boil and perhaps may affect the weir discharge—it is questionable whether radial piers or baffles will prevent the entrainment of air. C. J. Posey, M. ASCE, and H. Hsu[12] found in their vortex studies that "with purely radial inflow the vortex is small and transitory; its effect on discharge is negligible."

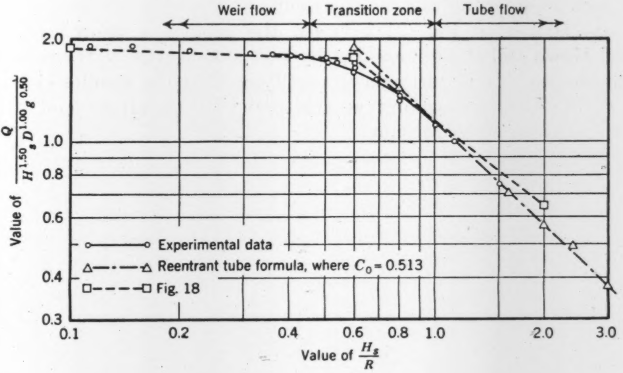

FIG. 25.—THE REGION WHERE WEIR FLOW CHANGES TO TUBE FLOW

Mr. Blaisdell questions the writer's statement that "most morning-glory spillways are designed for free flow." Messrs. White and McPherson, in their discussion, state:

> "Of the eighteen morning-glory spillways for which details have been published[10] only four are designed to perform submerged, six for ratios of H_s/D between 0.10 and 0.20, and eight for ratios of H_s/D less than 0.10."

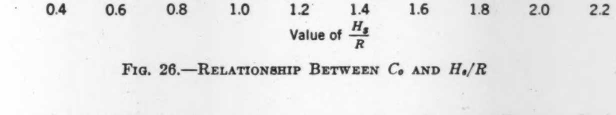

FIG. 26.—RELATIONSHIP BETWEEN C_o AND H_s/R

With more than 75% of the reported morning-glory spillways designed to operate in the free-flow range, the statement can hardly be questioned.

As suggested by Mr. Blaisdell, the discharge coefficient, C_o, is given in Fig. 26 for (H_s/R)-values between 0.4 and 2.0. For (H_s/R)-values greater than 1.00, the coefficient is practically constant at 0.51. This value checks very closely the coefficient of 0.52 commonly used for flow through a re-entrant tube. For comparison, the analytical results of Messrs. Mostafa, Chanda, and Johnson expressed in terms of C_o and H_s/R are also shown in Fig. 26. The two results compare remarkably well, considering the entirely different methods used in determining the coefficients.

The comparison in Fig. 21 between the profiles measured by Messrs. Camp and Howe and those measured by the writer supports the reliability of the nappe shapes. It is particularly gratifying that the profiles check in the vicinity of the weir springpoint as this region is important and extremely difficult to measure with accuracy.

PERFORMANCE TESTS ON PROTOTYPE AND MODEL

BY ALVIN J. PETERKA,[1] M. ASCE

WITH DISCUSSION BY MESSRS. FRED W. BLAISDELL, AND ALVIN J. PETERKA

SYNOPSIS

The performance of the model of the Heart Butte Dam (North Dakota) morning-glory spillway and outlet works is compared with the performance of the prototype structure. Certain elements of the prototype performance which could not be included in the model tests are also described. The results of the comparisons add further support to the premise that prototype performance can be predicted with accuracy from model tests.

INTRODUCTION

There is a general need for data which can be used to compare the performance of models and prototypes and thus extend the range of usefulness of models as aids to design. Prototype data are often difficult to obtain and when obtained they are usually not in the prototype range of heads or discharges, making direct comparisons difficult. The Heart Butte Dam (North Dakota) spillway, however, operated soon after its completion and almost immediately after the hydraulic model tests were made. With the model test data still "fresh" it was possible to obtain, on short notice, prototype data that could be compared with model tests.

A brief description is presented subsequently of the hydraulic model tests that were conducted on a 1:21.5 model to aid in the design of the structure and to yield data useful in operating the prototype structure. Following a report of the 1950 flood on the Heart River, which produced a discharge of 68% of the maximum anticipated outflow, the performance of the prototype structure is described.

Direct model-prototype comparisons are made of spillway performance and discharge for free and submerged conditions, spillway air demand, stilling-basin performance—including erosion downstream from the basin—and tailwater elevations in the excavated channel. Photographs and charts are used to illustrate the agreement found between model and prototype performance.

Certain aspects of the prototype performance which are beyond the scope of model tests are also cited, including the effect of ice completely covering the morning-glory spillway during submerged discharge, the erosion of the down-

---

NOTE.—Published, essentially as printed here, in April, 1954, as *Proceedings-Separate No. 433.* Positions and titles given are those in effect when the paper or discussion was approved for publication in *Transactions.*

[1] Hydr. Engr., Research, Eng. Labs. Branch, Design and Construction Div., Bureau of Reclamation, U. S. Dept. of the Interior, Denver, Colo.

stream riverbanks, and the effectiveness of the riprap used on the excavated channel banks. The results of an inspection of the spillway tunnel and structure following the 1950 and 1951 floods are also presented.

Description of Project

The Heart Butte Dam is located on the Heart River 60 miles west of Bismarck, N. Dak., and is a part of the Heart River unit of the Missouri River Basin Project. The dam is of compacted earth fill with a rock riprap cover, rises 135 ft above the Heart River stream bed, and is 1,860 ft long (Fig. 1). The dam is a combined irrigation and flood-control structure, with no power being developed. The reservoir at maximum water-surface elevation contains 392,500 acre-ft from a drainage area of 1,810 sq miles.

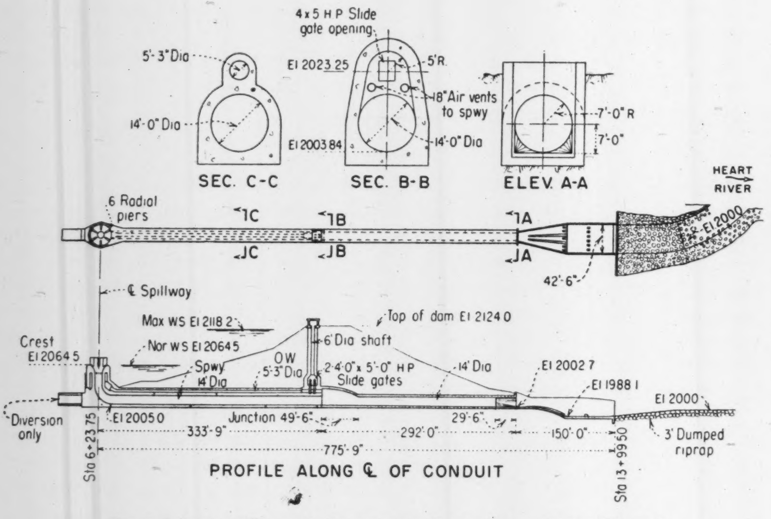
4x5 HP Slide gate opening
5'-3" Dia
El 2023.25
5'R.
18" Air vents to spwy
14'-0" Dia
El 2003.84
14'-0" Dia
7'-0" R
7'-0"
SEC. C-C
SEC. B-B
ELEV. A-A
HEART RIVER
6 Radial piers
C
B
A
El 2000
42'-6"
℄ Spillway
Max WS El 2118.2
Top of dam El 2124.0
Crest El 2064.5
Nor WS El 2064.5
6' Dia shaft
Spwy 14' Dia
OW 5'-3" Dia
2-4'-0" x 5'-0" HP Slide gates
14' Dia
El 2002.7
El 1988.1
El 2000
Diversion only
El 2005.0
Junction 49'-6"
29'-6"
333'-9"
292'-0"
150'-0"
775'-9"
3' Dumped riprap
Sta 6+23.75
Sta 13+99.50
PROFILE ALONG ℄ OF CONDUIT

Fig. 1.—General Plan and Sections for Spillway and Outlet Works

The flood-control spillway, located near the right abutment, consists of a morning-glory spillway having an outside diameter of 32 ft 6 in. and discharging into a vertical shaft 11 ft in diameter. The shaft is connected to a 90° vertical bend and nearly horizontal tunnel 14 ft in diameter and approximately 800 ft long (Fig. 2), which leads to the hydraulic-jump stilling basin (Fig. 1). The maximum vertical fall from headwater to stilling-basin floor is approximately 130 ft.

The morning-glory spillway at Heart Butte is unusual in that it is designed to operate throughout the range of free discharge, throughout the transition range between free and submerged discharge, and up to a submergence as great as 53.7 ft of water above the crest. The spillway crest is equipped with six equally spaced piers placed radially in plan; it does not have control gates of any kind. The outlet works, used primarily for release of irrigation water (Figs. 1 and 2), is an integral part of the spillway structure. The entrance to the outlet works encircles the vertical shaft of the spillway and discharges into a 5.25-ft-diameter tunnel located directly above the spillway tunnel. The smaller tunnel is controlled at its lower end by a 4-ft by 5-ft, high-pressure slide gate and discharges into the spillway tunnel, entering the larger tunnel from above through a specially designed junction section. The spillway tunnel carries the outlet-works discharge into the single stilling basin used for both spillway and outlet-works discharges (Fig. 1).

The capacity of the outlet works is 650 cu ft per sec with the reservoir elevation at the spillway crest level (El. 2064.50). The outlet works is closed when the spillway is in normal operation. The capacity of the spillway is 5,450 cu ft per sec at maximum reservoir elevation (El. 2118.2).

The feasibility of a combined spillway and outlet structure was determined, and the detailed shape and arrangement of the various parts of the structure were developed from hydraulic model tests on a 1 : 21.5 model.

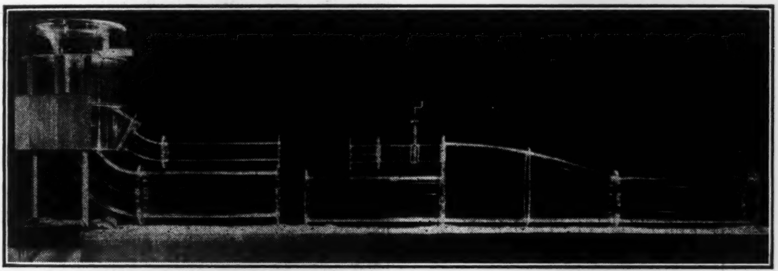

FIG. 2.—TRANSPARENT-PLASTIC MODEL OF THE SPILLWAY AND OUTLET WORKS

HYDRAULIC MODEL TESTS

The Model.—Tests were made on a 1:21.5 model of the discharge structures, including the spillway, the outlet-works intake structure, and the surrounding topography; these were constructed in the head box. The two tunnels including the outlet-works control gate, the 90° vertical bend, and the tunnel-junction section were built outside the head box. The stilling basin common to the spillway and outlet works and part of the down-river topography were constructed in the tail box. Much of the structure was modeled in transparent plastic to permit the observation of flow conditions throughout the structure (Fig. 2).

Spillway and Pier Tests.—Tests on a preliminary design of the morning-glory spillway indicated that the discharge capacity was larger than necessary. Consequently, the diameter of the vertical shaft was reduced from 14 ft to 11 ft, the spillway profile was reshaped to fit the vertical shaft, and a 90° vertical-transition bend was installed. The discharge capacity was then found to be approximately correct, according to the irrigation and flood-control requirements.

Vortices which formed in the model when the spillway was submerged were thoroughly investigated, experimentally and mathematically, and when it was found that the same vortices could form to scale in the prototype, attempts were made to eliminate them. Various arrangements of piers, dividing walls, and floating and fixed rafts were tested, and as a result six spillway-crest piers were recommended for use on the prototype (Fig. 3). It was found unnecessary to extend the piers as high as the maximum headwater elevation, a distance of 54 ft. Because vortex action diminished rapidly when the head on the crest approached 14 ft, it was necessary to extend the piers only to this height.

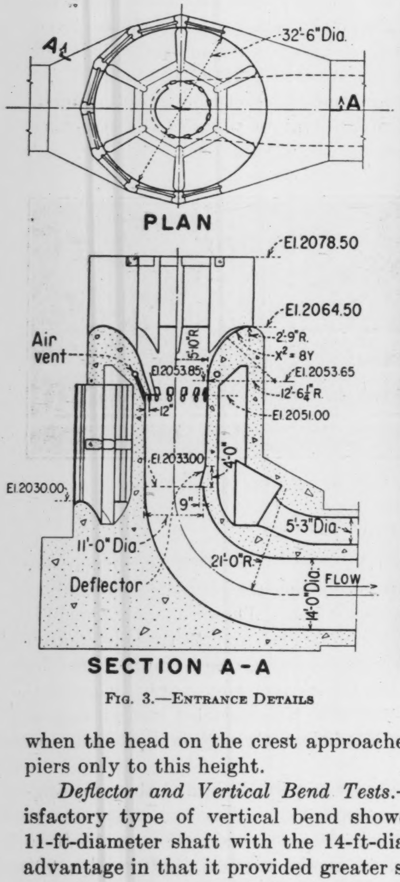
A
32'-6" Dia.
A
PLAN
El. 2078.50
El. 2064.50
Air vent
2'-9" R.
$X^2 = 8Y$
5'-10" R.
El. 2053.85
El. 2053.65
12'-6¼" R.
12"
El. 2051.00
El. 2033.00
4'-0"
El. 2030.00
9"
5'-3" Dia.
11'-0" Dia.
21'-0" R.
Deflector
FLOW
14'-0" Dia.
SECTION A-A

Fig. 3.—Entrance Details

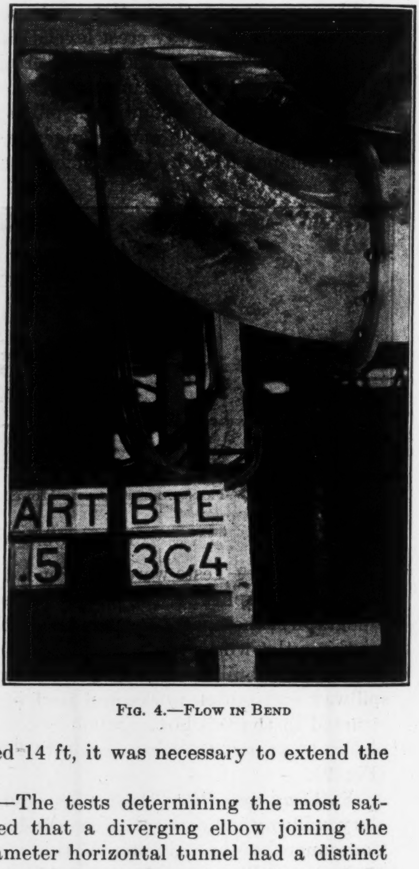
ART BTE
.5 3C4

Fig. 4.—Flow in Bend

Deflector and Vertical Bend Tests.—The tests determining the most satisfactory type of vertical bend showed that a diverging elbow joining the 11-ft-diameter shaft with the 14-ft-diameter horizontal tunnel had a distinct advantage in that it provided greater space between the water surface and the tunnel crown for ventilation in the vertical bend from the atmosphere at the tunnel outlet. However, with this arrangement in place, difficulty was encountered in preventing the horizontal tunnel from filling unexpectedly when the spillway and outlet works were both operating. Flow passing through the bend did not break cleanly from the crown of the bend. The flow tended to follow the crown through the bend, causing a change in the location of the flow control. When the control moved downstream the head on the system increased, causing a temporary increase in discharge which filled the tunnel. This resulted in negative pressures of considerable magnitude on the spillway face. After the tunnel filled, it was impossible to obtain open-channel flow again unless the head on the spillway was reduced considerably below the point where it had filled. Consequently, a small deflector was placed at the base of the vertical shaft on the downstream, or crown, side of the shaft (Fig. 3). The deflector (*a*) provided a positive control at the base of the vertical shaft and prevented the tunnel from filling, (*b*) had a stabilizing effect on smaller flows and provided a flat water surface on all flows passing into the vertical bend, and (*c*) provided a clear passage for air to circulate as far upstream as the base of the deflector. The thickness of the deflector at the base was varied in the model to determine the size necessary to meet exactly the discharge requirements at certain heads because precise tests had shown that the 11-ft-diameter vertical shaft was slightly too large. Spillway flow in the tunnel was found to be satisfactory after the structure had been modified as described. In Fig. 4 there is shown the flow entering, passing through, and leaving the vertical bend with the deflector in place; the surface of the flow entering the tunnel is smooth and flat.

Stilling-Basin Tests.—An effective energy-dissipating device was required in the stilling basin because of the friable nature of the material in the river channel and riverbanks; even moderate erosion tendencies and wave heights could not be tolerated. Consequently, it was felt that a hydraulic-jump basin would be necessary to provide good energy dissipation and a smooth water surface in the downstream channel. The first stilling-basin tests indicated that the main problem was concerned with spreading the high-velocity water (60 ft per sec) into a uniformly distributed sheet suitable for the formation of a jump. The first attempt to induce lateral spreading was by use of a sudden rise in the stilling-basin floor downstream from the tunnel portal. It was found that a hump sufficiently long to produce even a moderate spreading resulted in an extremely long stilling-basin structure. The problem was solved by discharging the flow on a horizontal floor 23 ft long after the flow had passed through a transition section at the end of the tunnel which began the spreading of the flow (Fig. 5). The flat floor induced more spreading before the flow dropped in its downward trajectory. Tests showed that this arrangement produced good lateral distribution of flow as far downstream as the trajectory curve and fairly good distribution beyond that. The addition of two low walls, placed so as to divide the basin approximately into thirds, produced excellent downstream distribution of flow and an efficient hydraulic jump in the basin. The walls, which varied from 3 ft to 4 ft high, did not extend upward through the flow for high discharges but produced the desired effect of distributing the flow from a 14-ft width at the tunnel portal to an ultimate 42.5-ft width in a horizontal distance of 75 ft.

Chute blocks and baffle piers were used to increase the fine-grain turbulence in the basin and thereby reduce the necessary length of the stilling basin. The shapes of the baffle piers, dividing wall noses, and trajectory curves were modified to provide atmospheric (or greater) pressures on critical areas as tests on preliminary designs had indicated that pressures as low as 18 ft of water below atmospheric pressure occurred downstream from sharp corners.

The performance of the stilling basin was evaluated from erosion tests made on a movable bed located downstream from the model basin and from wave-height observations made in the excavated tailrace channel. Erosion tests were made using a well-graded sand; 100% passed through a No. 4 sieve and 3% passed through a No. 50 sieve. These tests showed that erosion tendencies were less severe on the channel bottom than on the sloping banks. Wave action originating in the hydraulic jump combined with a slight surging action caused rapid decay of the banks. Every effort was made to keep the waves and surges to a minimum, but it was deemed necessary to riprap the banks of the prototype.

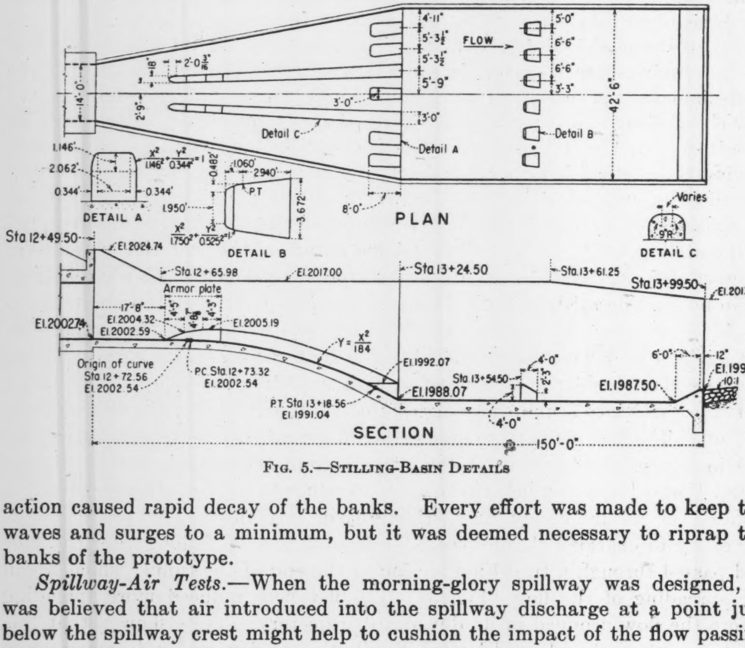

4'-11"
5'-3½"
5'-3½"
5'-9"
FLOW
5'-0"
6'-6"
6'-6"
3'-3"
42'-6"
14'-0"
18"
2'-0 3/16"
2'-9"
3'-0"
3'-0"
Detail C
Detail A
Detail B
1.146'
2.062'
0.344'
0.344'
$\frac{X^2}{1.146^2}+\frac{Y^2}{0.344^2}=1$
DETAIL A
0.482'
1.060'
2.940'
P.T
1.950'
3.672'
$\frac{X^2}{1.750^2}+\frac{Y^2}{0.525^2}=1$
DETAIL B
8'-0"
PLAN
Varies
9"R
DETAIL C
Sta 12+49.50
El. 2024.74
Sta. 12+65.98
El. 2017.00
Sta 13+24.50
Sta. 13+61.25
Sta 13+99.50
El. 2013.00
Armor plate
17'-8"
4'-5"
4'-6"
4'-3"
El. 2002.74
El. 2004.32
El. 2002.59
El. 2005.19
$Y=\frac{X^2}{184}$
Origin of curve
Sta 12+72.56
El. 2002.54
P.C. Sta 12+73.32
El. 2002.54
P.T. Sta 13+18.56
El. 1991.04
El. 1992.07
El. 1988.07
Sta 13+54.50
4'-0"
2'-3"
4'-0"
6'-0"
12"
El. 1987.50
El. 1990.50
10:1
SECTION
150'-0"

Fig. 5.—Stilling-Basin Details

Spillway-Air Tests.—When the morning-glory spillway was designed, it was believed that air introduced into the spillway discharge at a point just below the spillway crest might help to cushion the impact of the flow passing around the vertical bend. It was important that unnecessary impact and vibrations caused by the flowing water be eliminated because the entire structure was to be constructed on sand. Furthermore, if for any reason cavitation should occur in or near the vertical bend, the presence of the entrained air might reduce damage to the concrete tunnel lining. Laboratory tests have shown that even very small quantities of air introduced in the flow will delay cavitation damage.[2]

---

[2] "The Effect of Entrained Air on Cavitation Pitting," by Alvin J. Peterka, *Proceedings*, Minnesota International Hydraulics Convention, IAHR, ASCE, 1953.

Model tests on the many devices proposed to increase entrained air in the flow showed that only a relatively small quantity of air entered the flow regardless of the arrangement of the air-entraining devices. However, it was known that airflow in small hydraulic models is uncertain and that a greater percentage of air can be expected to enter a similar prototype structure. The increase to be expected in the prototype is not known and cannot be computed as the factors governing the entrainment of air are not generally known. After tests on many different model arrangements, it was finally decided to construct the prototype air vents shown in Fig. 3 and to provide measuring facilities in the prototype structure so that air-quantity determinations could be made. Fig. 4 shows the vertical bend discharging 3,750 cu ft per sec with air induced by the air deflectors entrained in the flow. To the unaided eye the air flow appeared continuous, but in the 1/15,000-sec exposure photograph the air is shown to enter in gusts; this was more clearly illustrated in the extremely slow motion pictures made of this condition.

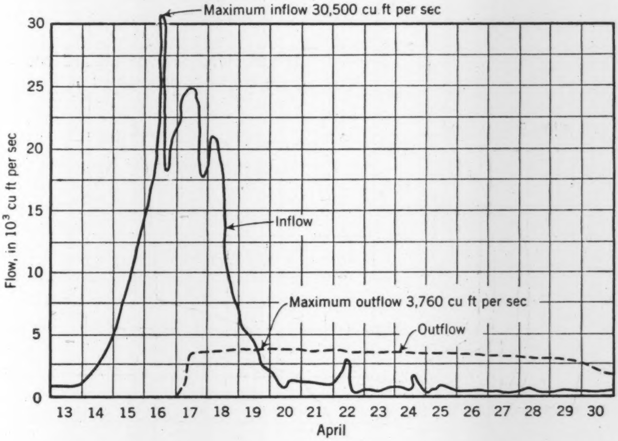

Fig. 6.—Flood Hydrographs for 1950

Description of 1950 Spring Flood

Preceding the heavy runoff in April, 1950, the weather had been cold and the ground was frozen and covered with snow. A stiff wind had blown the snow off the ridges, concentrating it on the slopes and in the valleys of the drainage area. The weather turned unseasonably warm, causing a fast melt and heavy runoff from the frozen terrain. On April 15, 1950, the temperature was 80°F, and the snow melt caused an increase in the inflow to the reservoir of from 5,000 cu ft per sec to 30,500 cu ft per sec on April 16 (Fig. 6). The high runoff and inflow continued through April 17 and most of April 18. The spillway went into operation on April 17, reaching a peak flow of 3,760 cu ft per sec on April 19, and continued without appreciable reduction in discharge through April 29—a period of more than twelve days. The maximum outflow discharge represented 68% of the anticipated maximum outflow, and the maximum reservoir elevation indicated that 38% of the flood storage had been utilized. Fig. 7 shows the hydraulic data in terms of the spillway elevations. At the time of maximum outflow the spillway crest was submerged 17.24 ft, making the reservoir elevation 3.24 ft over the tops of the spillway piers. The maximum height of fall from headwater to tailwater was 72 ft, and the energy entering the stilling basin was 31,000 hp.

The Heart River, on which the Heart Butte Dam is constructed, flows into the Missouri River at Mandan, N. Dak., about 6 miles from Bismarck.

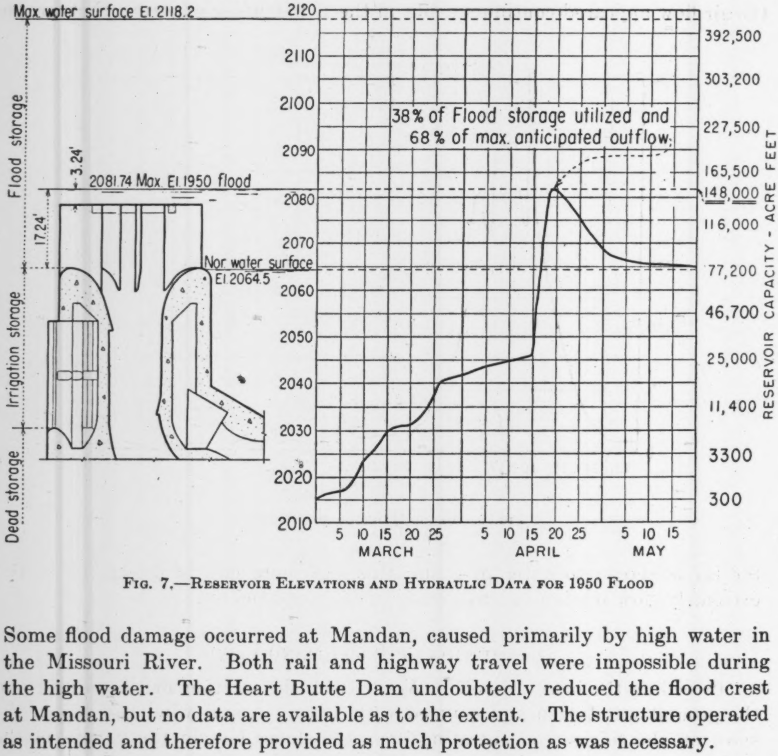

Fig. 7.—Reservoir Elevations and Hydraulic Data for 1950 Flood

Some flood damage occurred at Mandan, caused primarily by high water in the Missouri River. Both rail and highway travel were impossible during the high water. The Heart Butte Dam undoubtedly reduced the flood crest at Mandan, but no data are available as to the extent. The structure operated as intended and therefore provided as much protection as was necessary.

Model-Prototype Comparison Tests

It was recognized that model-prototype comparison data pertaining to the spillway discharge and the air demand would be particularly valuable and that comparisons of the erosion in the excavated channel, wave heights below the stilling basin, and profiles below the stilling basin would also be of interest. In the course of recording these data, other comparisons were made which included observations on vortex formation above the spillway and the computed and actual tailwater curves in the excavated channel and in the river. Water-surface profiles in the stilling basin and data on the riprap protection were also obtained.

Spillway Capacity.—During the 1950 runoff when the headwater was above the spillway crest, readings were taken each morning and afternoon on the headwater gage located in the gate-operating house (Fig. 7). Using the discharge-capacity curve obtained from the model tests on the morning-glory spillway (Fig. 8), an outflow hydrograph was prepared (Fig. 9). On April 17, 19, and 25, and May 1, the Geological Survey, United States Department of the Interior (USGS), made stream-gage measurements in the river downstream from the stilling basin to determine the discharge of the spillway. During these measurements, the irrigation outlet works were closed. The discharges determined by the USGS, designated by circles in Fig. 9, indicate the agreement between the model and prototype measurements. Differences were 4.6%, 1.1%, and 1.8% for the April 17, 19, and 25 determinations, respectively. For all practical purposes, these points indicate good agreement between model and prototype discharge characteristics. On May 1 the difference was 23.4%, indicating considerable disagreement; however, the measurements on April 17 and May 1 were not made under ideal conditions. The USGS notes for April 17 indicated that ice in the channel may have affected the measurements, and on May 1, when the greatest disagreement was found, that a wind was blowing which might have altered the relationship

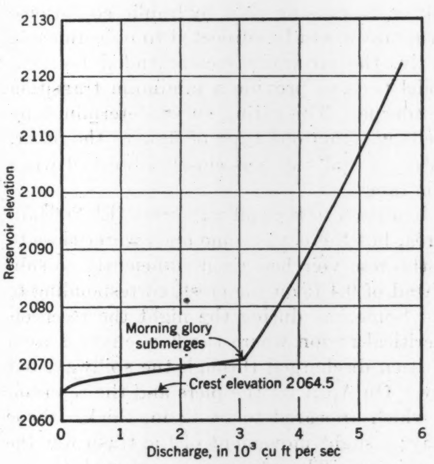

FIG. 8.—DISCHARGE CAPACITY OF SPILLWAY FROM MODEL STUDY

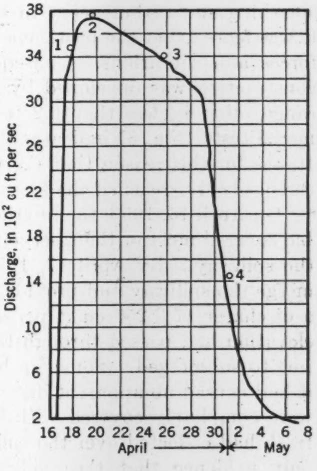

FIG. 9.—COMPARISON BETWEEN MODEL AND PROTOTYPE DISCHARGE

between the head on the crest and the headwater-gage reading. Another possible cause for the discrepancy might be the rapid fall in discharge during the measurements on May 1, as indicated in the hydrograph in Fig. 9. In general, however, the agreement between model and prototype discharges is excellent—particularly at the higher discharges—and it is believed that the rating curve obtained from the model adequately serves to determine discharges through the prototype morning-glory spillway.

Spillway Performance with Free and Submerged Discharges.—During the model tests it was noticed that for certain arrangements of the structure the transition from free flow to submerged flow and vice versa was accompanied by violent surging in the vertical shaft. In some cases the unstable flow condition existed over several feet of change in reservoir elevation. A mushroom-shaped column of water rose and fell in the shaft, causing excessive splashing and turbulence. In addition to causing poor hydraulic conditions, it was feared that the prototype structure would be subjected to objectionable forces and vibrations. Consequently, the structure recommended for field construction was developed by model tests to provide a minimum transition range—that is, less than 0.2 ft prototype. The rating curve determined by model tests (Fig. 8) indicates the change from one type of flow to the other. It was for this reason that the prototype spillway was closely observed when the headwater reached the transition range.

On April 16, 1950, the reservoir had risen to the spillway crest (El. 2064.5). Ice covered most of the reservoir area, but there was some open water close to the spillway. By April 17, 1950, the reservoir had risen sufficiently to submerge the spillway and provide a head of 9.4 ft on the crest, corresponding to a discharge of 3,250 cu ft per sec. Sometime during the night the reservoir elevation had passed through the critical region where the flow changes from free to submerged. Some ice had been discharged through the spillway, but it had caused no apparent difficulty. On April 18, the piers and the reservoir were completely covered with ice which appeared to be 12 in. thick. Some trash had collected over the spillway; a slight movement of the trash was the only evidence that the spillway existed. The reservoir continued to rise through April 19, but on April 20 it began to recede. On April 21, the reservoir was still approximately 1 ft above the piers. The ice was breaking up fast, and the wind was shifting it around the spillway area. Regardless of whether ice or water was over the spillway entrance, the operation was satisfactory, with no evidence of serious vortex action.

On April 26, with the reservoir at El. 2074 and the piers again visible, operation was also satisfactory. Water inside the pier structure was level with the reservoir, and only occasional light turbulence was visible. On April 28, the reservoir was down to El. 2071, or about 0.7 ft above the point where the flow changes from submerged to free discharge (Figs. 8 and 10). Fig. 10 indicates the mild condition inside the spillway; there was no pulsation or rising and falling of the "mushroom."

On April 29, the reservoir had fallen to 0.8 ft below the critical submergence point, and although the "mushroom" was lower in the shaft it was still stable with no evident rising and falling. Again the flow had passed through the critical range during the night when photographs and observations were impracticable. Indications are that the prototype was submerged at about the headwater elevation shown by the break on the curve in Fig. 8 and that the change occurred abruptly as indicated on the model curve. On April 30, the spillway was discharging freely (1,600 cu ft per sec) with the reservoir at El. 2068.6. No spray emerged from the morning-glory hole at this or lower heads as has been noted on some other morning-glory spillways.

Throughout the flow range there was no vibration noticeable in the structure. Several excursions into the outlet-works gate access well were made while the spillway was operating. Efforts were made to detect vibration by feeling the various parts of the structure; none could be detected. Also, there was no noise from the spillway that could be detected from the top of the dam or from the reservoir banks. The outlet-works gate was opened and closed on April 21, 1950; no noise or vibration was evident during this operation.

One year later the spillway again went into operation, reaching maximum reservoir El. 2075—about 7 ft less than occurred in 1950. On March 27, 1951, the reservoir was at El. 2070, about 0.2 ft below the submergence point. Again the operation was satisfactory. Despite the fact that on February 15, 1951, the ice in the reservoir was 36 in. thick, there was no visible difficulty caused by the ice.

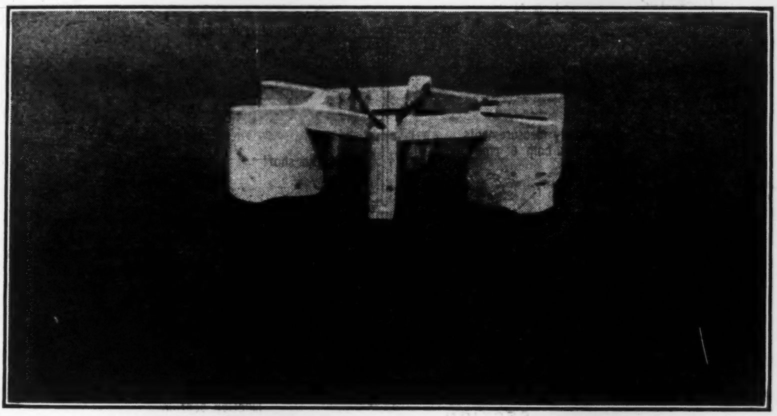

FIG. 10.—SPILLWAY ON APRIL 28, 1950

Spillway-Air Demand.—Measurements were made in the model to determine the quantity of air being entrained by the spillway discharge as it passed over the air-entraining deflectors located on the spillway face just below the spillway crest (Fig. 3). Air-flow measurements in the model were made using a $\frac{3}{8}$-in.-diameter sharp-edged orifice connected to a differential water manometer. All air entering the model passed through the orifice before entering the venting system. Because the differential was extremely small for the air quantity flowing in the model, a specially constructed gage was used which multiplied the actual differential so that more consistent readings could be obtained throughout a series of tests. The gage was calibrated to provide reasonably accurate air measurements, but consistency was considered more important than absolute accuracy.

At the time of prototype construction, pipe was extremely difficult to obtain on short notice. Because the model tests continued through most of the construction period, only a small quantity of pipe and special fittings could be provided for measuring stations in the prototype. Thus, the data obtained from the prototype are not sufficient to determine pressures in various parts of the venting system but do indicate the quantity of air flow in the prototype for various spillway discharges.

The air quantity flowing in the prototype vents was determined by measuring the air velocity with a hand-held anemometer in the 18-in.-diameter air-vent pipes. Air-velocity determinations were made in one of the vertical pipes contained in the wall of the gate-operating house and in one of the horizontal pipes just upstream from the point where it emerges into the tunnel-junction section (Fig. 11). Concurrent with the air-velocity measurements, pressure measurements were made in the other horizontal air vent using a U-tube water manometer. The pressure-measuring station is also shown in Fig. 11.

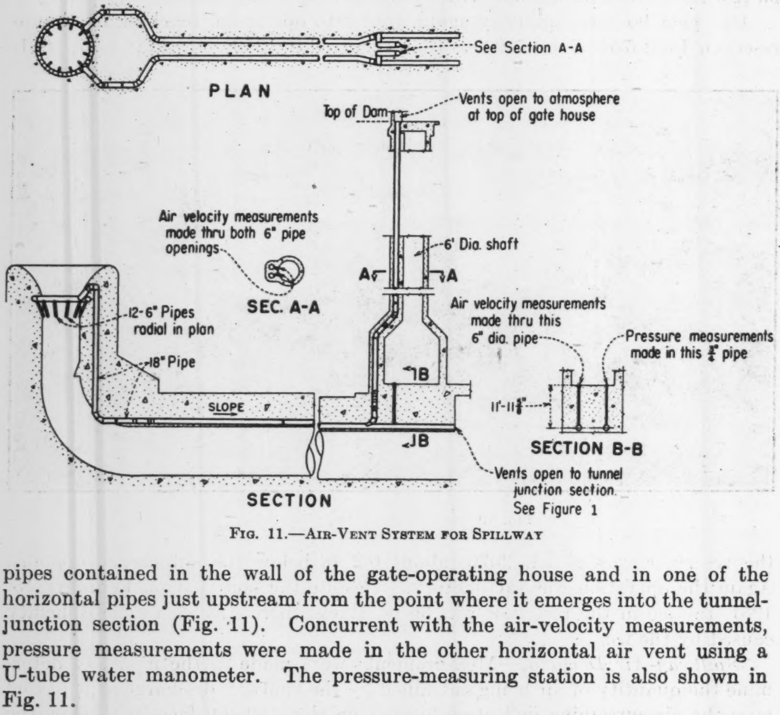
See Section A-A
PLAN
Top of Dam
Vents open to atmosphere at top of gate house
Air velocity measurements made thru both 6" pipe openings
SEC. A-A
6' Dia. shaft
A
A
12-6" Pipes radial in plan
18" Pipe
SLOPE
Air velocity measurements made thru this 6" dia. pipe
Pressure measurements made in this 3/4" pipe
B
B
11'-11 3/8"
SECTION B-B
SECTION
Vents open to tunnel junction section. See Figure 1

FIG. 11.—AIR-VENT SYSTEM FOR SPILLWAY

Air flow in the prototype was not smooth, as evidenced by the sound of the air flow and the difficulty experienced in holding the anemometer steady. There was chance for considerable error in any one anemometer measurement, and so several determinations were made for each flow in both the vertical and horizontal vent pipes. The anemometer recorded lineal feet of flow which, when divided by the elapsed time, gave the air velocity in feet per second. Each observation lasted about 2 min and sufficient readings were taken so that the average velocity of air flow was that occurring for a testing time of from 6 min to 12 min. Pressures measured in the U-tube also indicated that the air flow was not steady. Differentials varied from plus to minus, but average readings were relatively easy to obtain.

The results of the determinations of air quantity and pressure are shown in Fig. 12. The percentage of air entrained in the spillway discharge for both model and prototype showed a decrease as the discharge increased. In this respect the model predicted the performance of the prototype. The prototype, however, entrained approximately four times as much air as was predicted by the model. In this respect, also, the prototype performed as anticipated except that accurate predictions could not be made from the model tests to determine how much more air the prototype would entrain. When the model showed an air entrainment of 5.5% of the water discharge for 1,000 cu ft per sec of spillway discharge, the prototype showed 20.5%. For 3,600 cu ft per sec the model showed 1.9% and the prototype 7.7%.

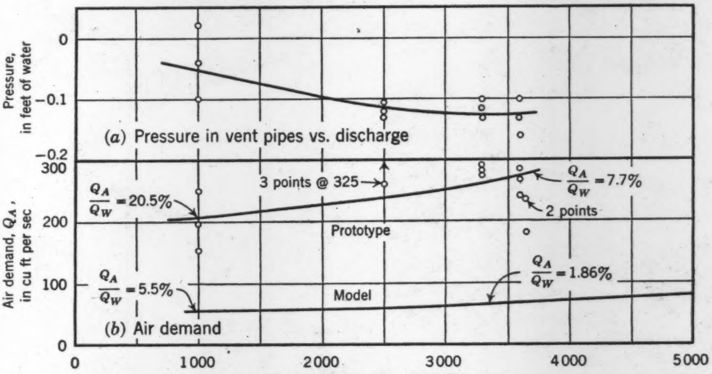

FIG. 12.—RELATIONSHIP BETWEEN SPILLWAY AIR DEMAND AND DISCHARGE

The points from which the curves in Fig. 12 were drawn are also shown. The prototype air-demand curve was not drawn through the points for 2,500 cu ft per sec because the pressure values, which were considered more reliable, indicated that the curve should be drawn below the velocity points. Moreover, the shape of the curve was then similar to the model curve, which was based on very consistent data. To support the validity of the shape and values of the prototype air-demand curve, computations of air flow were made using the measured pressures, assuming that both vent pipes carried equal quantities of air and using the usual losses for bends, friction, inlet, and similar items. The computed values were found to be in fair agreement with the curve values.

Performance of the Stilling Basin.—The performance of the stilling basin was satisfactory in every respect and, furthermore, it performed according to the predictions made from the model tests. A general view of the basin and surrounding area is shown in Fig. 13 when, on April 17, 1950, the outflow was 58% of capacity.

Water leaving the tunnel appeared to be well aerated and at the approximate depth indicated in the model studies. The entire basin contained extremely turbulent water (Fig. 14) and was long enough so that the full jump height was attained before the flow entered the excavated channel. A considerable quantity of spray was thrown into the air at times where the outflow from the tunnel plunged beneath the tail water, but most of the spray fell back into the basin. The small quantity of spray that fell adjacent to the basin caused no difficulty. Much of the time the flow entered the basin smoothly. Flow leaving the basin had a relatively quiet water surface with few measurable waves. There were long-period swells, however, with a maximum height of from 12 in. to 18 in. which were caused by pulsations in the stilling basin. The disturbances below the stilling basin were similar to those noted during the model tests.

FIG. 13.—OUTFLOW INTO RIVER WITH DISCHARGE OF 3,250 CU FT PER SEC

Water-surface profiles were measured in cubic feet per second, in the prototype for discharges of 3,700, 3,300, 2,350, and 1,050. These profiles are shown in Fig. 15 together with the profile obtained during the model tests for 5,600 cu ft per sec. Although no exact comparisons can be made, the prototype profiles seem to agree closely with the model profile. If differences do exist, they are probably caused by the greater air entrainment in the prototype —making the prototype profiles slightly higher than those in the model for the same discharge.

Erosion Downstream from the Stilling Basin.—Erosion tests in the model had indicated that the channel banks just downstream from the stilling basin would be subjected to greater erosion forces than the channel bottom and that rock riprap would be necessary in the prototype to prevent bank damage. The channel bottom was shown by the model tests to be relatively free from erosion tendencies, and no damaging erosion was expected there. As a precaution, however, because of the fine-textured friable material composing the channel, rock riprap was used in the prototype channel bottom. No riprap was used in the model tests.

Before the runoff in the spring of 1950, cross sections had been taken in the prototype channel on May 31, 1949. Following the 1950 runoff, cross sections were again taken on June 15, 1950. Cross sections for both dates at a station located just downstream from the end sill are shown in Fig. 16. These typical sections show the maximum erosion depth to be less than 12 in. Close to the end sill there is no significant erosion. Using all the cross sections taken (Figs. 16 and 17) computations made to determine the volume of material moved indicated that less than 20 cu yd of material was removed from the channel bottom during the entire runoff.

FIG. 14.—HYDRAULIC JUMP IN STILLING BASIN

Conversely, the channel banks, despite their riprap cover, were eroded to a greater degree. The riprap, however, had been placed in a thin layer and was not well graded as to size; in places the earth banks could be seen between the individual rocks. Swells were observed to rise over local areas and penetrate very easily into the large voids. When the water receded some of the earth was removed from behind the riprap. This was evidenced by the darker, earth-colored water which could be seen adjacent to the riprap. After several days of operation the riprap had slumped and the earth banks had caved. Despite the apparent damage to the banks, the riprap continued to provide protection against further cutting.

Damage to the bank was not caused primarily by waves of the ordinary variety as these were only a matter of inches in over-all height but rather by swells caused by surges in the hydraulic jump. The model stilling basin had been equipped with baffle piers and chute blocks to reduce the over-all length of the stilling basin and decrease its cost. It had been noted during these and other model tests that, when a hydraulic jump is reduced in length by the use of artificial devices such as baffle piers, the jump becomes more stable in most respects but exhibits a tendency to produce the swells previously noted. The swells are considered the lesser of the evils, however, and are not impossible to cope with. With a base layer of gravel and successive layers of larger and larger rock there probably would have been no damage.

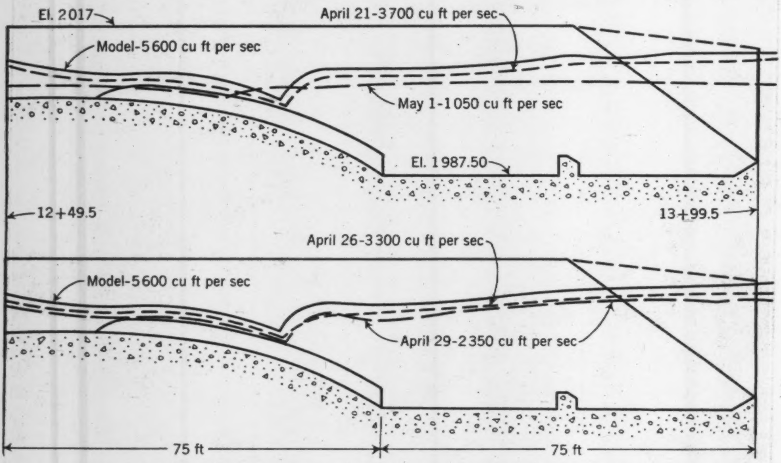

FIG. 15.—MODEL-PROTOTYPE COMPARISON OF STILLING-BASIN PROFILES

Tailwater Elevations.—The topography in the model extended only a short distance downstream from the stilling basin into the excavated channel and did not include any part of the Heart River. Tailwater elevations were set by an adjustable tail gate located at the end of the model—using a computed curve, tailwater elevation versus discharge, for the Heart River. The excavated channel was designed so that the expected tailwater elevation would be essentially the same as that expected in the river channel. The tailwater curve used in the model tests and shown in Fig. 18 was computed for a point located 200 ft downstream from the axis of the dam in the Heart River.

During the prototype operation it was readily apparent to the unaided eye that the tailwater elevation in the river was considerably lower than that in the excavated channel. Water entering the river from the channel had a steep surface slope and a much higher velocity than anticipated. Observations, however, were not sufficient to establish whether the tailwater in the channel was too high or that in the river too low. Consequently, levels were run to determine the tailwater elevation at four separated points for five different discharges. The location of these points and the tailwater elevation and discharge are shown in Fig. 18, plotted below the tailwater curve used in the model tests. These data show the computed tailwater curve to be 2.3 ft higher at 1,000 cu ft per sec and 4.1 ft higher at 3,600 cu ft per sec than the actual measured points in the Heart River. Tailwater elevations measured in the excavated channel more nearly coincided with the computed curve, but at 3,600 cu ft per sec the elevation at point C in Fig. 18 in a quiet area adjacent to the wing wall at the end of the apron was 1 ft below the computed curve. Elevations obtained from water-surface profiles taken along the basin center line agreed with the computed curve but only because they included the boil height at the end of the apron which was slightly higher than the adjacent tailwater.

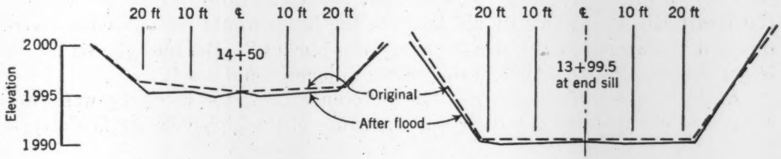
20 ft
10 ft
℄
10 ft
20 ft
2000
1995
1990
Elevation
14+50
Original
After flood
20 ft
10 ft
℄
10 ft
20 ft
13+99.5
at end sill

Fig. 16.—Erosion Below Stilling Basin

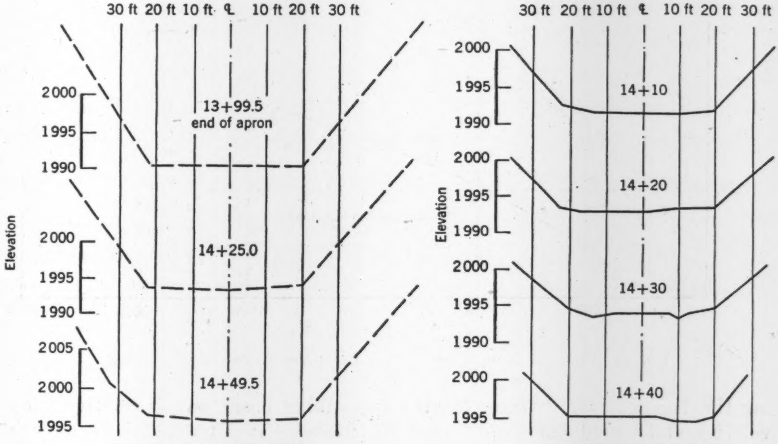
30 ft
20 ft
10 ft
℄
10 ft
20 ft
30 ft
Elevation
2000
1995
1990
13+99.5
end of apron
2000
1995
1990
14+25.0
2005
2000
1995
14+49.5
30 ft
20 ft
10 ft
℄
10 ft
20 ft
30 ft
Elevation
2000
1995
1990
14+10
2000
1995
1990
14+20
2000
1995
1990
14+30
2000
1995
14+40

Sections taken May 31, 1949 (original)

Sections taken June 15, 1950 (after flood)

Fig. 17.—Cross Sections Below Stilling Basin

The model stilling basin was tested to determine the reduction in tailwater possible before the jump was swept off the apron. In the model it was possible to lower the tailwater only from 3 ft to 4 ft before the jump was swept out for the maximum discharge of 5,600 cu ft per sec. As the tailwater elevation in the Heart River is 4.1 ft lower at a discharge of 3,600 cu ft per sec than the computed tailwater, it is imperative that the excavated channel be closely watched to prevent damage which might lower the tailwater to the level of the Heart River. If this should happen, the jump would undoubtedly sweep out and the apron would operate as a "flip bucket." Because the structure is not designed for this type of operation, damage could result.

Erosion in the Heart River.—The difference in water levels between the excavated channel and the river was the cause of the high-velocity flow entering the Heart River. Water leaving the stilling basin was of relatively low velocity and would not have caused ill effects as it entered the river. The 4-ft difference in elevation, however, caused an increase in velocity which proved to be sufficient to cause considerable damage to the unprotected downstream riverbank. Some damage was caused by the direct effects of the current flowing diagonally across the river and cutting into the far (left) bank. A great part of the damage, however, was caused by a large induced eddy in the river. This eddy caused an upstream current along the left bank which removed large quantities of material from areas considerably upstream of the point where the main flow impinged on the bank. Although the damage was considerable, it had no ill effects on the structure or its operation. Riprap placed in the eroded area will prove of value, however, as the damage will

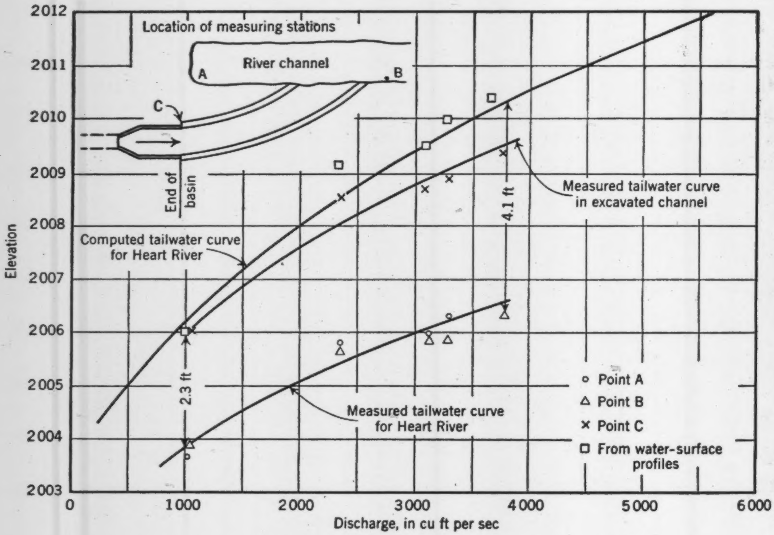

FIG. 18—COMPARISON OF MEASURED AND COMPUTED TAILWATER ELEVATION

become greater with each successive runoff and the end result is difficult to predict. A comparison of Figs. 13 and 19 shows the extent of the bank damage that occurred between the beginning of the runoff and May 5, 1950.

Inspection of Structure Following 1950 and 1951 Floods.—An inspection of the spillway conduit was made following the 1950 flood and again after the 1951 flood. Certain findings are of interest and are considered subsequently.

The conduit inspection in both instances revealed that the concrete was in excellent condition with the exception of four small areas located in the 90° bend. Following the 1950 flood, plaster casts were made of the two most prominent areas. The largest area is about the size of a man's hand and by actual measurement has a maximum depth of erosion of ¾ in. (Fig. 20). The smaller area shows a maximum depth of ½ in. The surface shown in Fig. 20 was molded in sponge rubber against the plaster casts made in the field and is therefore an exact replica of the tunnel surface following the 1950 flood.

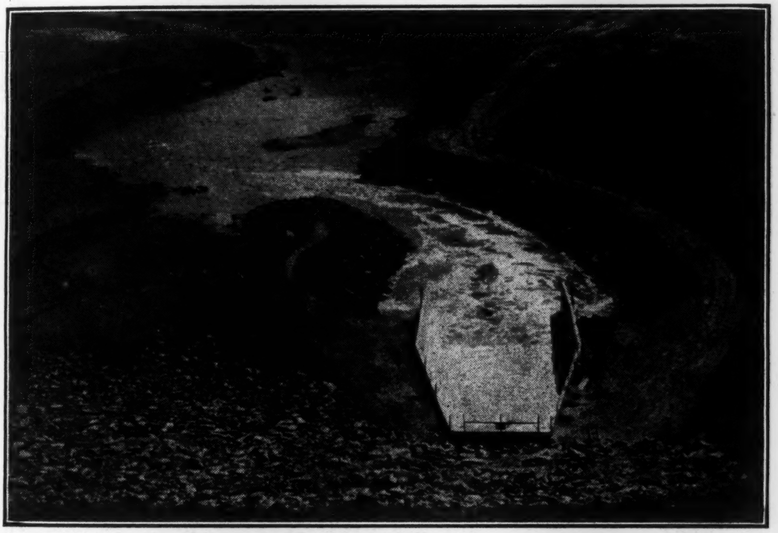

FIG. 19.—DOWNSTREAM BANK EROSION AFTER PASSING OF FLOOD

The eroded areas are located near the invert and near the bottom of the 90° bend. Construction timbers or ice falling into the shaft could have caused the surface damage shown by impact. Persons who have viewed the rubber casts have unanimously been of the opinion that the damage was not begun by cavitation.

Following the 1951 flood, these areas were again inspected. There did not appear to have been any marked change in these areas as a result of the 1951 spring floods, and no repairs were believed to be necessary.

Inspection of the riprap downstream from the stilling basin following the 1950 flood indicated that repairs would be advisable. The slumped

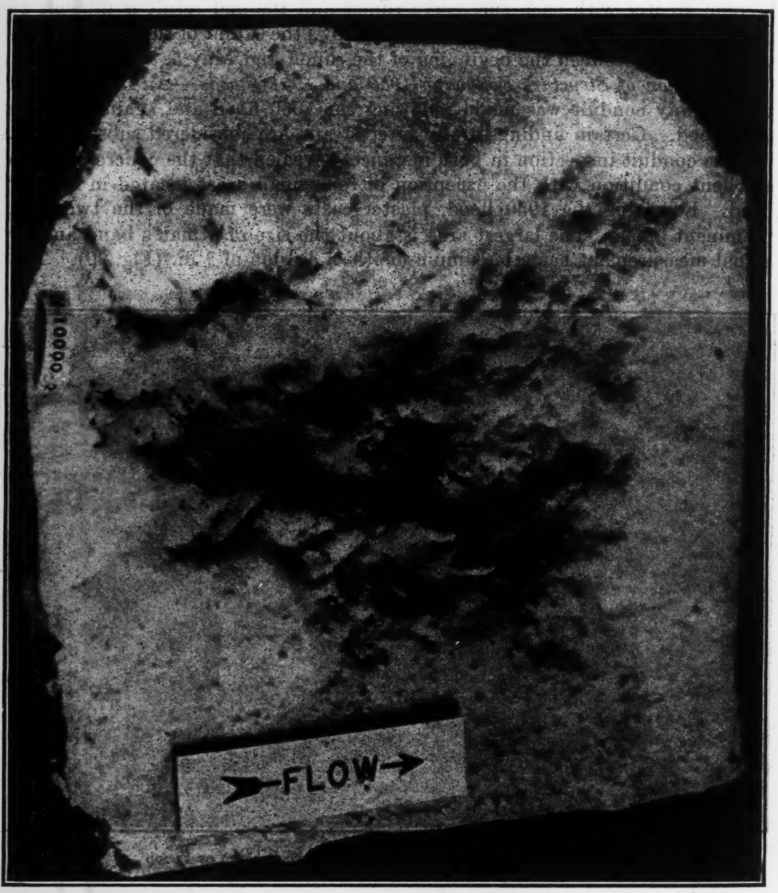

FIG. 20.—ERODED AREA IN BEND

riprap in the channel immediately downstream from the stilling-basin structure was repaired in May and June, 1950. Gravel backfill was placed on the slopes to bring them to grade, and rock was replaced over the gravel. The eroded section of riverbank just downstream from the end of the riprapped channel was sloped and covered with gravel and rock.

CONCLUSIONS

It is generally accepted that hydraulic models are useful as an aid in design and in predicting the general features of future prototype performance. The comparison of model and prototype performance made on the Heart

Butte morning-glory spillway supports this premise and in addition indicates that precise predictions of performance of untried or unusual features of a proposed structure are also possible.

Observations downstream from the structure showed that the computed and actual tailwater curves were quite different. To assure obtaining prototype performance equal to that predicted by the model, the curve should be determined with great care.

Observations of the prototype stilling basin indicated that the effect of insufflation of air caused only a reasonable increase in water-surface elevation in the basin, that splash was no greater than predicted by the model, and that, as expected, spray was more extensive. The basin performed in every way as predicted by the model.

The close agreement between model and prototype spillway-capacity curves, the similarity between submergence characteristics of the morning-glory spillways, the indications that vortex action was reduced by use of spillway piers, and the several other comparisons made suggest that a hydraulic model is indispensable in providing assurance that a proposed structure will give satisfactory performance at the lowest possible cost.

ACKNOWLEDGMENT

The 1950 runoff occurred without warning at a site located 700 miles from the Denver (Colo.) hydraulic laboratory of the Bureau of Reclamation, United States Department of the Interior (USBR). General flooding of a large area outside the area protected by the dam caused the road to the site to be flooded, and access to the project was difficult. Prototype test equipment was not available at the dam, and trained personnel were not available to make as many observations as might have been considered ideal. The USBR office in Bismarck did, however, perform an excellent job of supplying observers to record data during the runoff period. These observers supplied most of the data, photographs, and motion pictures of the spillway in operation. The Denver laboratory contributed to the program by outlining the tests to be made, supplying the equipment necessary to make measurements, and by collecting the data and making final comparisons. The USGS cooperated with the USBR Bismarck office in supplying men and equipment to make the river-gaging measurements.

The assistance of C. F. Burdg and B. L. Mendenhall in supplying observers and their wholehearted spirit of cooperation are acknowledged. W. J. Colson, Philip E. Ehrenhard, A. M. ASCE, and John Serungard assisted in obtaining photographs, motion pictures, and data.

DISCUSSION

Fred W. Blaisdell,[3] M. ASCE.—This comparison of the model and prototype performance of a spillway and its stilling basin is extremely interesting. Confidence in the use of model studies for the experimental design of morning-glory spillways cannot help but be strengthened as a result of this paper. For several years the writer has been concerned with the performance of this general type of structure; a few comments will be made on some of the points cited by Mr. Peterka.

If the tunnel had been 11 ft in diameter instead of 14 ft, it seems likely that it could have been expected to flow full instead of unexpectedly filling when the deflector was not used. It is implied in Fig. 1 that the tunnel dimensions were fixed by the diversion requirements—the tunnel subsequently being adapted for spillway use. This would, of course, have limited the laboratory staff in recommending changes in the tunnel size. The use of the deflector at the base of the vertical shaft provides a good solution to the problem as it exists. It also provides a definite point for the computation of the head on the spillway for the submerged condition. It is apparent from Mr. Peterka's comments that this point would have been difficult to determine accurately with the tunnel partly full and would have shifted from the vertical bend to the tunnel exit at times if the deflector had not been utilized.

It is the writer's experience that the use of some type of antivortex device is an absolute necessity if the spillway is to operate submerged. The antivortex device can be the pier type used on the Heart Butte Dam spillway, although other types are also effective. For other types of spillway entrance, such as a uniformly sized pipe on a small spillway, the antivortex piers might have to be somewhat higher than those at the Heart Butte Dam to prevent vortex formation.

Mr. Peterka notes that no spray was observed to emerge from the morning-glory hole. This may be because the tunnel outlet is not submerged; if the outlet were submerged, air could accumulate in the tunnel and eventually blow back through the inlet or be discharged violently through the outlet.

From Fig. 4, it appears that the tunnel flows about half full. If the tunnel had been full it would have been necessary to include conical fillets in the upper half of the tunnel exit as well as in the lower half.

It seems likely that the side-wall flare could have been begun at the upstream end of the transition, resulting in some shortening of the outlet. In this case the fillets would be segments of oblique cones rather than the segments of right cones used at Heart Butte. This arrangement has been used successfully by the writer.

The side-wall flare seems quite rapid—in fact, it is about twice the flare the writer would have thought acceptable.[4] One reason it is acceptable at Heart

---

[3] Project Supervisor, Agri. Research Service, U. S. Dept. of Agriculture, St. Anthony Falls Hydr. Lab., Minneapolis, Minn.

[4] "Flow Through Diverging Open-Channel Transitions at Supercritical Velocities," by Fred W. Blaisdell, SCS-TP-76, Soil Conservation Service, U.S. Dept. of Agriculture, Washington, D. C., April, 1949.

Butte is undoubtedly a result of the use of guide walls. This side-wall flare should not be used in other installations unless model tests are made to check the design.

A horizontal floor has also been used by the writer to help spread the flow. It is pressure on the floor that spreads the water, and there can be no pressure on the floor if the floor profile has the same shape as the trajectory of the free-falling stream. Therefore, there will be no pressure on the floor if the flow enters the trajectory curve at the point where the side-wall flare begins. Consequently, there can be no spreading unless a flat floor, similar to that at Heart Butte, is used.

The writer and his associates have checked the comment under the heading, "Model-Prototype Comparison Tests: Erosion Downstream from the Stilling Basin," that erosion is less severe on the channel bed than on the channel banks; this condition involves, of course, a well-designed stilling basin. It has also been found that a flaring wingwall, triangular in elevation, provides sufficient protection so that sand in back of the model wingwalls stands at its angle of repose. There is usually a local widening of the downstream channel near the stilling basin. Ordinarily it is felt that this widening can be tolerated and that riprap protection is not economically warranted. However, wave wash or beaching, mentioned by Mr. Peterka, is a problem, and some bank protection may be required in the vicinity of the water surface. Wave wash was apparently the major damage observed at Heart Butte, although there it was unsightly rather than dangerous to the safety of the structure.

One wonders, when the model tests have shown that no damaging erosion will occur in the channel bed, why riprap is used there. Is it a practice carried over from the time when less efficient stilling basins made the riprap necessary? If so, it is a wasteful practice.

The necessity for the best possible determination of the tailwater elevation is vividly brought out by Mr. Peterka; this elevation determines the elevation of the stilling-basin floor and assures the satisfactory performance of the stilling basin. The comments by Mr. Peterka relative to the large differences between the computed and observed tailwater elevations in the Heart River might be helpful to others faced with similar problems.

Frank evaluations such as are presented in the paper appear all too seldom despite their great value in engendering confidence in the good points of a design or design method and pointing out pitfalls to be avoided.

ALVIN J. PETERKA,[5] M. ASCE.—The comment by Mr. Blaisdell that confidence "in the use of model studies * * * cannot help but be strengthened" is of interest because similar tests on a companion structure, the Shade Hill Dam (South Dakota) morning-glory spillway, have been made since the paper was written (and are reported in this Symposium). Of particular interest in these tests[6] was the agreement between model and prototype discharges. A graph containing twelve instead of four field measurements showed remarkable agreement with Fig. 9. The average variation between model and prototype discharges was 2.7%, with maximum and minimum variations of 5.0% and 0.2%, respectively. These results strengthen the conclusion that the Heart Butte spillway model rating curve is accurate.

---

[5] Hydr. Engr., Bureau of Reclamation, U. S. Dept. of the Interior, Denver, Colo.

[6] "Spillway Tests Confirm Model Prototype Conformance," by A. J. Peterka, *Engineering Monograph No. 16*, Bureau of Reclamation, U. S. Dept. of the Interior, Denver, Colo., October, 1954.

Other comments by Mr. Blaisdell provide an opportunity to emphasize certain points which were not fully explained. In regard to the filling of the tunnel during the model tests, it should be made clear that the tunnel size was fixed before the model tests were begun. Consequently, no attempts were made to reduce the tunnel diameter during the tests. As Mr. Blaisdell notes, the use of a deflector at the base of the shaft, in addition to preventing filling of the horizontal tunnel, is a valuable addition to a structure of this type. The stabilizing effect of the deflector on both partial and maximum flows provides smoothness in operation which under most circumstances allows reduction in the tunnel diameter with an accompanying reduction in construction cost. The establishment of a positive control point should be the first consideration in the design of any hydraulic structure.

The use of spillway piers is discussed by Mr. Blaisdell; he states that other antivortex devices are also effective. The writer has been intimately connected with the hydraulic model tests on the Pleasant Hill (Ohio), Watuaga (Tennessee), South Holston (Tennessee), Heart Butte, Shade Hill, and Hungry Horse (Montana) morning-glory spillways and has firsthand knowledge of the tests on the Owyhee (Idaho) and Gibson (Montana) dams. In each case various other types of antivortex devices were tested, but spillway piers proved to be most effective even though in some cases prototype piers were not constructed. Because many other morning-glory spillways make use of piers in various shapes and forms it is the writer's opinion that spillway piers, in some form, offer the only known economical and practical solution to the vortex problem. In addition, piers often serve a second purpose as flow guides in unsymmetrical approaches when the spillway is discharging freely.

The spray above a morning-glory spillway in operation is, as Mr. Blaisdell notes, usually caused by the outlet being submerged to some degree. Spray may also be seen, however, when the outlet is free. Spray is sometimes caused by a ragged flow surface in the upper part of a spillway being torn apart by an updraft in the tunnel. At times tunnel spillways act as chimneys, producig an upward draft of air. At low spillway discharges or when the spillway first begins to operate, the air velocity is often sufficient to produce spray above the spillway.

The comments by Mr. Blaisdell on the stilling-basin side-wall flare are entirely correct. No attempt should be made to use such rapidly flaring walls without guide walls or other flow-spreading devices.

Mr. Blaisdell questions the use of riprap on the prototype channel bottom when the model tests show that serious erosion will not occur. There are two reasons for this use: First, the prototype channel consisted of very fine material having little if any more resistance to erosion than the sand used in the model.

With the greater forces in the prototype acting on a much lighter (considering the scale) material, it was feared that deeper erosion might occur in the prototype than was predicted by the model. As assurance against making expensive underwater repairs, riprap was recommended for use on the channel bottom. A second reason was the possibility of degradation of the channel bed. Experience has shown that clear water picks up fine material on entering the river channel. Degradation of this type has been found to be, in certain cases, as serious as erosion. It is hoped that the riprap will reduce channel degradation close to the structure.

AMERICAN SOCIETY OF CIVIL ENGINEERS
Founded November 5, 1852
TRANSACTIONS

Paper No. 2803

MOMENTS AND DEFLECTIONS IN STEEL-GRID BRIDGE FLOORS

BY HERBERT J. GREENBERG[1]

WITH DISCUSSION BY MESSRS. KUANG-HAN CHU, FU-KUEI CHANG, AND HERBERT J. GREENBERG

SYNOPSIS

Formulas are proposed for computing the maximum deflection and maximum negative edge-moment occurring in a steel-grid highway bridge floor under wheel loads. Separate equations are given for concrete-filled steel-grid floors and open-grid steel floors, respectively. These equations take into account the basic anisotropy of such floors as a variable and are designed to fit the data tabulated by K. C. Kuo who completely analyzed the problem.[2] For completeness, the results of Mr. Kuo's analysis are summarized, including the formulas he proposed for computing maximum positive bending moments in such floors. Graphs of the deflection and moment coefficients over the required ranges of span and the anisotropy variable are included.

It is proposed that the formulas presented in this paper be used as a basis for specifications used in designing steel-grid highway bridge floors.

INTRODUCTION

In a recent paper,[2] K. C. Kuo gave a complete solution of the problem of determining moments and deflections in both simple and one-way, continuous, anisotropic, rectangular slabs under central loads. All Mr. Kuo's original computations have been available to the writer in the preparation of this paper. Mr. Kuo applied this general theory to the problem of determining the moments and deflections in steel-grid highway bridge floors under wheel loads. This provided the first satisfactory analysis of steel-grid floors taking into account the basic anisotropy of such floors and thus extended the work of H. M.

NOTE.—Published, essentially as printed here in December, 1954, as *Proceedings-Separate No. 562*. Positions and titles given are those in effect when the paper or discussion was approved for publication in *Transactions*.

[1] Associate Prof. of Math., Carnegie Inst. of Technology, Pittsburgh, Pa.

[2] "Moments in Steel Grid Highway Bridge Floors," by K. C. Kuo, *Proceedings*, Convention Group Meetings, A.A.S.H.O., Omaha, Nebr., 1951.

Westergaard[3] who considered the case of long, isotropic, simple slabs under concentrated loads. Because of the restriction to isotropy, the Westergaard theory, although applicable to reinforced concrete slabs, is not applicable to steel-grid slabs which vary in degree of anisotropy over a wide range. Nevertheless, in the absence of a more complete analysis, the Westergaard equations were used as a basis for designing steel-grid floors.[4] On the basis of his extended analysis Mr. Kuo proposed new expressions to be used for design. These equations express the maximum positive bending moments under a standard loading as functions both of the span and a basic anisotropy parameter. The formulas are given for two separate ranges of the anisotropy parameter—one corresponding to concrete-filled, steel-grid floors and the other to open-grid floors.

For purposes of design, in addition to the maximum positive bending moment, information is required as to the maximum deflection and the maximum negative moment occurring over a support (which may, under some conditions, govern the design). Although Mr. Kuo tabulated the deflections and the negative edge-moments, he did not propose practical formulas to fit these data which could be used for specifications in design. (The theoretically obtained equations from which Mr. Kuo originally tabulated the deflections and moments were in the form of complicated infinite series and double infinite series unsuited for use as design formulas.) It is the primary purpose of the writer to supplement Mr. Kuo's paper by providing convenient equations for the deflections and negative edge-moments. These equations accurately fit Mr. Kuo's tabulated data as functions of span and the anisotropy parameter. Separate equations are provided for the ranges of the anisotropy parameter corresponding to concrete-filled, steel-grid floors and open-grid floors, respectively. The secondary purpose of this paper is to bring the results of Mr. Kuo's analysis to the attention of a wider audience and, by collecting his equations with the ones being proposed at present, provide a convenient reference of basic formulas for use in the design of steel-grid highway bridge floors. Graphs of the moment and deflection coefficients are included. The writer will first present a review of the results of Mr. Kuo's analysis.

Analysis of Steel–Grid Floors

Steel-grid floors may be treated as homogeneous, anisotropic, elastic, rectangular slabs having principal directions parallel to the edges. The stringers supporting the floor divide it into rectangular panels forming a one-way, continuous slab simply supported on rigid supports. Each panel may carry a load, and the problem is to determine the bending moments and deflection of the continuous slab under the given loads.

One panel of the continuous slab of span S and length b (Fig. 1) is considered with flexural rigidities D_x and D_y and twisting rigidity H. These elastic constants are defined by S. Timoshenko,[5] who has presented a derivation of the

---

[3] "Computation of Stresses in Bridge Slabs Due to Wheel Loads," by H. M. Westergaard, *Public Roads*, March, 1930.

[4] "AASHO Standard Specifications for Highway Bridges," A. A. S. H. O., 1949.

[5] "Theory of Plates and Shells," by S. Timoshenko, McGraw-Hill Book Co., Inc., New York, N. Y., 1940, Chapter V.

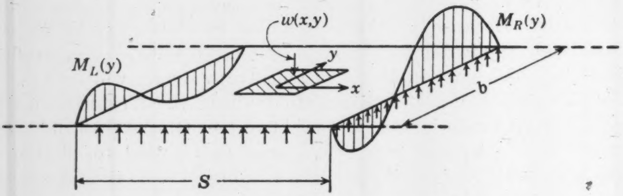
$w(x,y)$
$M_R(y)$
$M_L(y)$
y
x
b
S

FIG. 1.—PANEL OF A CONTINUOUS SLAB

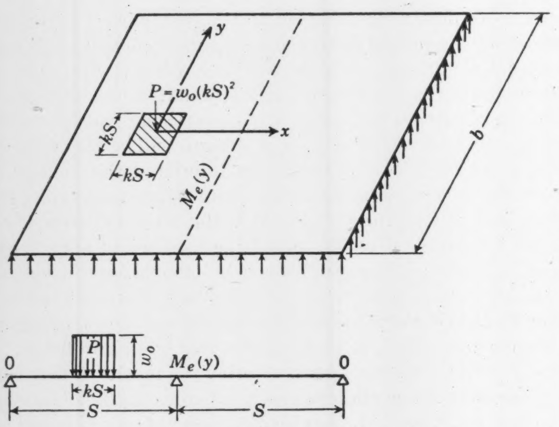
y
$P = w_o(kS)^2$
x
kS
kS
$M_e(y)$
b
P
w_o
0
$M_e(y)$
0
kS
S
S

FIG. 2.—CENTRALLY LOADED PANEL

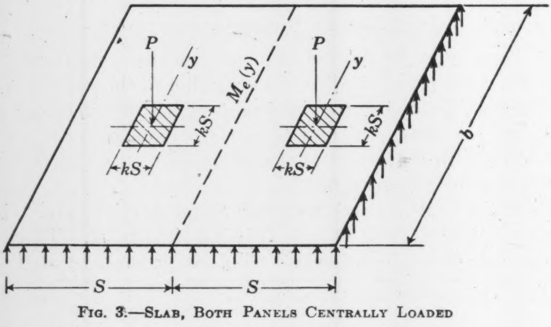
P
y
$M_e(y)$
P
y
kS
kS
kS
kS
b
S
S

FIG. 3.—SLAB, BOTH PANELS CENTRALLY LOADED

basic equations governing anisotropic slabs. For a grid, rigidities would be computed as blockwise averages. The deflection $\delta_e = \delta_e(x, y)$ at any point (x, y) in this panel can be determined by superposition as the sum of (1) the deflection $\delta = \delta(x, y)$ of the panel considered as a simple slab under the load distribution $w = w(x, y)$, which is actually being applied to this panel, and (2) the deflection $\delta' = \delta'(x, y)$ of the panel due solely to the edge moments $M_L\ (y)$ and $M_R\ (y)$, transmitted from the panels on the left and right of the given panel. Thus,

$$\delta_e = \delta + \delta' \ldots\ldots\ldots\ldots\ldots\ldots\ldots\ldots (1)$$

The deflection $\delta(x, y)$ of the panel treated as a simple slab under the applied loads $w(x, y)$ must satisfy the partial differential equation,[5]

$$D_x \frac{\partial^4 \delta}{\partial x^4} + 2\,H \frac{\partial^4 \delta}{\partial x^2\,\partial y^2} + D_y \frac{\partial^4 \delta}{\partial y^4} = w \ldots\ldots\ldots\ldots (2)$$

which is subject to the boundary conditions of zero deflection and moment. Following the Navier method[5] used also in the isotropic case by Mr. Westergaard,[3] the solution w is obtained as a double infinite series of trigonometric functions of the two variables x and y, chosen to satisfy the boundary conditions. The coefficients are determined by expanding the given load function w in a similar series and then substituting these series into Eq. 2 and solving for the coefficients of δ by equating coefficients of corresponding terms.

The deflection $\delta'(x, y)$ of the panel due solely to the transmitted edge moments $M_L(y)$ and $M_R(y)$ was obtained by Mr. Kuo as follows. A trigonometric series in y is assumed for each of the two functions $M_L(y)$ and $M_R(y)$ and indeed for the distribution of moment along any intermediate support separating two panels of the continuous slab. The moments along the simply supported edges of the two terminal slabs are zero. Assuming (*a*) the deflection δ of each panel treated as a simple slab to have been found as previously described and (*b*) the deflection δ' of each panel due to its edge-moments to be expressed in terms of these moments, the conditions of continuity of the slope of the slab across an intermediate support leads to an equation involving the edge-moments over three successive supports. This is a generalized three-moment equation for the one-way, continuous slab; from this equation the coefficients of the expansions of the edge-moment functions are determined. These in turn determine the deflection δ' and the total deflection δ_e is determined from Eq. 1.

By the foregoing procedure, in general terms, Mr. Kuo has found the deflection for an arbitrary panel in a one-way, continuous, anisotropic slab under arbitrary loading. He has then applied these results in determining the maximum moments and deflections in steel-grid bridge floors under wheel loads as follows (notation slightly revised).

The wheel load on a panel is represented by a uniform load over a square area in the center of a panel. This loading, except in extreme cases, produces maximum positive moments at the center of the panel. Assuming all panels of the continuous slab to be identical, the maximum positive bending moment occurs if the number of panels is two and if one of the panels is centrally loaded (Fig. 2). The uniform central load is given by $P = w_o\ (k\ S)^2$ in which w_o is the uniform load per unit area and $k\,S$ is the length of a side of the loaded square area expressed as a fraction k of the span S. Under this loading, the deflection δ of the unloaded panel treated as a simple slab is 0. The deflection δ of the loaded panel treated as a simple slab is found by the Navier method to be given by the double infinite series:

$$\delta = \frac{16\,w_o\,S^4}{\pi^6\,D_x} \sum_{m,n=1,3,\ldots}^{\infty} A_{mn} \cos\frac{m\,\pi\,x}{S} \cos\frac{n\,\pi\,y}{b} \qquad (3)$$

in which

$$A_{mn} = \frac{\sin\dfrac{m\,k\,\pi}{2}\quad \sin\dfrac{n\,S\,k\,\pi}{2\,b}}{m\,n\left[m^4 + 2\,m^2\,n^2\left(\dfrac{S}{b}\right)^2 s + n^4\left(\dfrac{S}{b}\right)^4 r\right]}$$

and in which the summation is a double summation extended over odd integral values of the indices m and n and the letters r and s stand for the rigidity ratios:

$$\left.\begin{aligned} r &= \frac{D_y}{D_x} \\ s &= \frac{H}{D_x} \end{aligned}\right\} \qquad (4)$$

They are measures of the anisotropy of the slab ($r = s = 1$ corresponding to the case of isotropy). The dimensionless deflection coefficient δ^* corresponding to δ (when evaluated at the center of the loaded panel) is defined as follows:

$$\delta^* = \frac{\delta\,D_x}{P\,S^2}\bigg\|_{(0,\,0)} = \frac{16}{\pi^6\,k^2} \sum_{m,n=1,3,\ldots}^{\infty} A_{mn} \qquad (5)$$

The bending moments at the center of the loaded panel corresponding to the deflection δ are given in terms of the second partial derivatives of δ as[5]

$$\left.\begin{aligned} M_x &= -\left(D_x \frac{\partial^2\delta}{\partial x^2} + D_1 \frac{\partial^2\delta}{\partial y^2}\right)\bigg|_{(0,\,0)} \\ &\text{and} \\ M_y &= -\left(D_y \frac{\partial^2\delta}{\partial y^2} + D_1 \frac{\partial^2\delta}{\partial x^2}\right)\bigg|_{(0,\,0)} \end{aligned}\right\} \qquad (6)$$

in which D_1 is an elastic constant.

From the continuity condition and the resulting three-moment equation are determined the coefficients in the series for the interior edge-moments,

$$M_e = \sum_{n=1}^{\infty} E_n \cos\frac{n\,\pi\,y}{b} \qquad (7)$$

to be given by

$$\frac{E_n}{P} = \frac{16\,\rho\,\theta_1}{\pi^5\,k^2}\,\frac{\cosh 2\,n\,\theta_1 - \cos 2\,n\,\theta_2}{\sin 2\,n\,\theta_2 - \rho\sinh 2\,n\,\theta_1}\quad T(k,\,n) \qquad (8)$$

in which

$$T(k, n) = \sum_{m=1,3,\dots}^{\infty} (-1)^{(m-1)/2}\, m\, n\, A_{mn} \dots\dots\dots\dots \tag{9}$$

and

$$\left.\begin{aligned} \theta_1 &= \frac{S\pi}{b}\left[\tfrac{1}{2}\left(\sqrt{r} + s\right)\right]^{\frac{1}{2}} \\ \theta_2 &= \frac{S\pi}{b}\left[\tfrac{1}{2}\left(\sqrt{r} - s\right)\right]^{\frac{1}{2}} \\ \rho &= \frac{\theta_2}{\theta_1} \end{aligned}\right\} \dots\dots\dots\dots \tag{10}$$

The contribution of continuity to the deflection of the loaded panel has then been shown by Mr. Kuo to be

$$\delta' = \frac{8\,P\,S^2}{\pi^5\,k^2\,D_x} \sum_{n=1,3,\dots}^{\infty} \left[A_n(x) - B_n(x)\right] T(k, n) \cos\frac{n\pi y}{b} \dots\dots \tag{11}$$

in which

$$\begin{aligned} A_n(x) &= \frac{1}{C_n} \sinh n\left(\xi x - \frac{\theta_1}{2}\right) \sin n\left(\eta x + \frac{3\,\theta_2}{2}\right) \\ B_n(x) &= \frac{1}{C_n} \sinh n\left(\xi x + \frac{3\,\theta_1}{2}\right) \sin n\left(\eta x - \frac{\theta_2}{2}\right) \\ C_n &= n^2\,\theta_1\left(\sin 2\,n\,\theta_2 - \rho \sinh 2\,n\,\theta_1\right) \end{aligned}$$

and $\xi = \theta_1/S$, $\eta = \theta_2/S$. The dimensionless deflection coefficient δ'^* corresponding to δ', when evaluated at the center of the loaded panel, is defined as

$$\delta'^* = \delta' \frac{D_x}{P\,S^2}\bigg|_{(0,\,0)} = -\frac{8}{\pi^5\,k^2} \sum_{n=1,3,\dots}^{\infty} \frac{1}{n}\, T(k, n)\, \phi(n\,\theta_1, \rho) \dots\dots \tag{12}$$

in which

$$\phi(\theta, \rho) = \frac{\sinh\dfrac{3\,\theta}{2} \sin\dfrac{\rho\,\theta}{2} - \sinh\dfrac{\theta}{2} \sin\dfrac{3\,\rho\,\theta}{2}}{\theta\left(\rho \sinh 2\,\theta - \sin 2\,\rho\,\theta\right)} \dots\dots\dots \tag{13}$$

The bending moments M'_x and M'_y at the center of the loaded panel, resulting from the continuity contribution δ' to the deflections, are expressed in terms of the second partial derivatives of δ' by equations exactly analogous to Eq. 6, with δ replaced by δ' (as given by Eq. 11) and M_x, M_y replaced by M'_x, M'_y.

The final three expressions for the total deflection and total bending moments are, by superposition, Eq. 1 and the following:

$$\left.\begin{aligned} M_{cx} &= M_x + M'_x \\ M_{cy} &= M_y + M'_y \end{aligned}\right\} \dots\dots\dots\dots \tag{14}$$

In terms of dimensionless quantities, the maximum deflection coefficient is given by

$$\delta^*_c = \delta^* + \delta'^* \dots\dots\dots\dots \tag{15}$$

in which δ^* is given by Eq. 5 and δ'^* by Eq. 12. The maximum positive bending-moment coefficients are simply M_{cx}/P and M_{cy}/P because the bending moments are actually bending moments per unit of length in the x-direction or y-direction.

The edge-moment M_e becomes a maximum when both panels are subjected to the square, centrally located load, $P = w_o\ (k\ S)^2$ (Fig. 3). This is twice the M_e-value for the case in which one panel is loaded and therefore can be directly obtained from Eq. 7. The coefficient of edge-moment, which is taken at the center of the edge to yield the maximum value, for the case of both panels loaded is given by

$$M^*_e = -\frac{32}{\pi^5 k^2} \sum_{n=1,3\ldots}^{\infty} \frac{1}{n}\, T(k, n)\, \Theta(n\,\theta_1, \rho) \ldots\ldots\ldots\ldots (16)$$

in which

$$\Theta(n\,\theta_1, \rho) = \frac{n\,\theta_1\,(\cosh 2\,n\,\theta_1 - \cos 2\,\rho\,n\,\theta_1)}{\sinh 2\,n\,\theta_1 - \dfrac{1}{\rho}\sin 2\,\rho\,n\,\theta_1} \ldots\ldots\ldots\ldots (17)$$

The coefficients of deflection and moments were tabulated by Mr. Kuo for the ranges $0.005 \leq r \leq 1$ and $0 \leq s/\sqrt{r} \leq 1$, in which the cases of interest for application to steel-grid slabs are covered. The values of the ratio S/b used ranged between 1/3 and 1; it was expected that, as in the isotropic case where the bending moment for $S/b = 1/3$ differs by only 1% from that for $S/b \rightarrow 0$, there would be little change in moment over the range $0 \leq S/b \leq 1/3$. The ratio k of the side of the central square load to the span was varied between 0.1 and 1. In order to have the span S appear explicitly rather than the dimensionless variable k, the loaded area representing the wheel load was assumed to be 15 in. square. Thus, $k\ S = 1.25$ ft, and the range of k from 0.1 to 1 corresponds to a range of span values of from 1.25 ft to 12.5 ft.

In general, it was found that the variation of the coefficients with the anisotropy parameter $s/\sqrt{r}$ which enters through the quantities defined in Eq. 10 was small. To eliminate the explicit dependence on this variable in the final proposed formulas, the value $s/\sqrt{r} = 1$ was chosen as representative for concrete-filled steel grids whereas for the open grids the value $s/\sqrt{r} = 0.05$ was selected as average.

For the concrete-filled, steel-grid floors the constant D_1 from Eq. 6 is assumed to be given approximately by $\mu\ D_x$, in which μ is the Poisson ratio of the slab and is assumed to be 0.15 for the computations. In Fig. 4, the solid lines show the variation of the bending-moment coefficient M_{cx}/P in the x-direction with span S for $r = 0.1, 0.2, 0.4, 0.7$, and 1.0 which covers the range of r for concrete-filled grid floors. The broken line shows the graph of M_{cx}/P against S from the formula given in the 1949 specifications of the American Association of State Highway Officials (AASHO).[6,7] Because this curve is for an isotropic slab it must be compared with the solid curve for $r = 1.0$. This comparison furnishes a check on Mr. Kuo's analysis against that of Mr. Westergaard and the agreement is seen to be close. The variation with anisotropy from the

---

[6] "AASHO Standard Specifications for Highway Bridges," A.A.S.H.O., 1949, Article 3.3.5(*b*).

[7] *Ibid.*, Article 3.3.2.

AASHO-specified curve is clearly shown. In Fig. 5 the moment coefficient M_{cy}/P in the y-direction is plotted against span for a range of values of r. The 1949 AASHO specifications do not refer to M_{cy}; however, Mr. Kuo points out that, even though M_{cy} is in general smaller than M_{cx}, the slab is usually weaker in the y-direction than in the x-direction—that is, D_y is smaller than D_x. Hence, it may be necessary to design for both M_{cy} and M_{cx}.

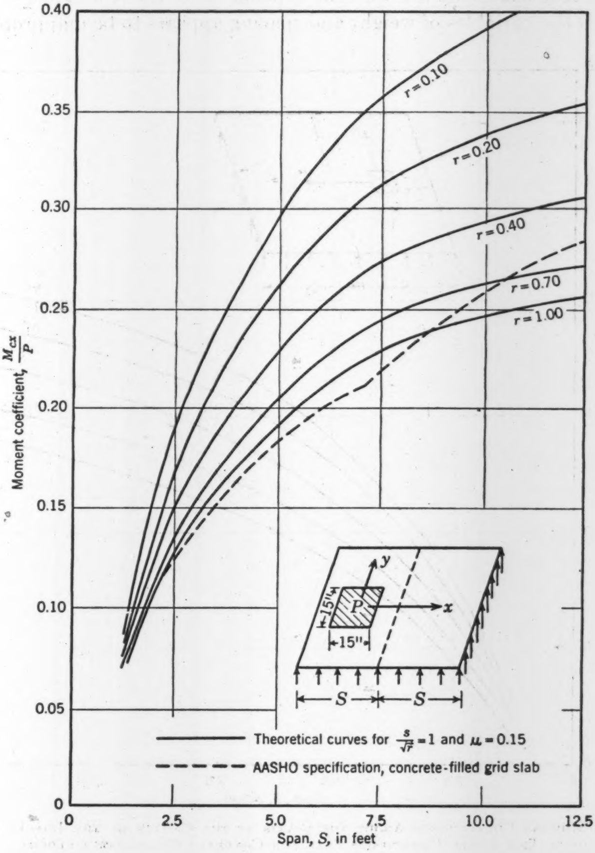

FIG. 4.—MOMENT COEFFICIENTS ABOUT THE x-AXIS AT THE CENTER OF THE LOADED PANEL OF A TWO-PANEL CONTINUOUS SLAB FOR CONCRETE-FILLED GRID FLOORS

For an open grid the value of the Poisson ratio may be considered to be approximately zero, and accordingly the value $D_1 = 0$ was used in Eq. 6. In Fig. 6 are compared the curves obtained for M_{cx}/P by Mr. Kuo with those from the 1949 AASHO specifications. The coefficient M_{cx}/P is shown plotted in solid lines against span S for $s/\sqrt{r} = 0$ and 0.1 and $r = 0.01$, 0.02, and 0.04—covering the range of values of these parameters which would occur in the typical open-grid slabs. The AASHO specifications[8] yield the straight dashed lines covering the usual design range of weight and spacing b_1 between main bars. Mr. Kuo has explained[2] that the dependence of the AASHO-specification formulas on the variables of weight and spacing appears to be inappropriate for the design problem because the theoretical curves for the coefficient M_{cx}/P are dependent on only the anisotropy parameters.

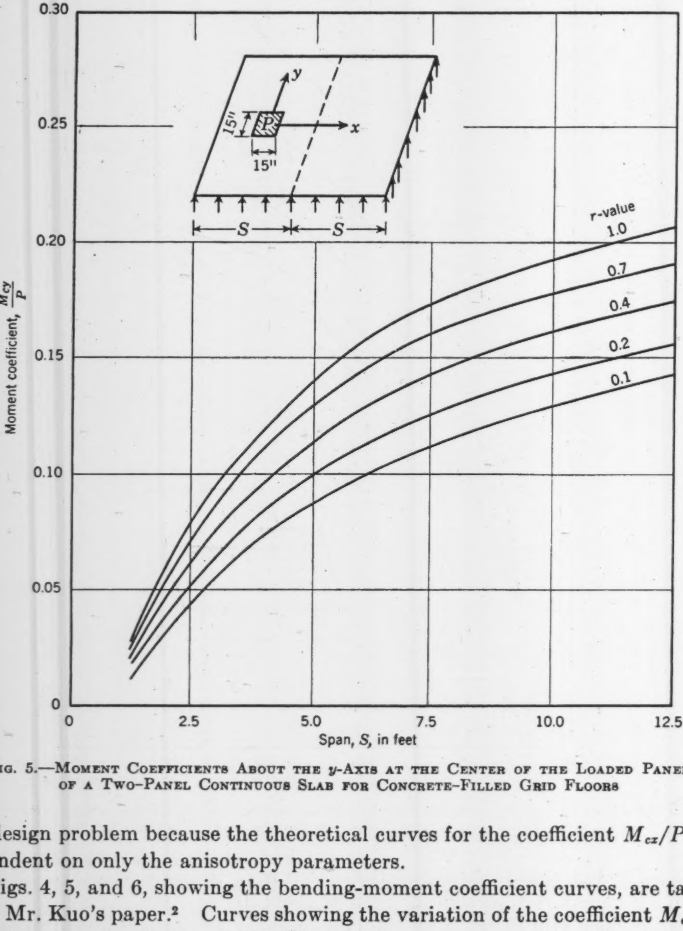

FIG. 5.—MOMENT COEFFICIENTS ABOUT THE y-AXIS AT THE CENTER OF THE LOADED PANEL OF A TWO-PANEL CONTINUOUS SLAB FOR CONCRETE-FILLED GRID FLOORS

Figs. 4, 5, and 6, showing the bending-moment coefficient curves, are taken from Mr. Kuo's paper.[2] Curves showing the variation of the coefficient M_{cy}/P for an open grid with k, r, and $s/\sqrt{r}$ have also been presented by Mr. Kuo in a series of charts which are not repeated here. In the next section the writer

---

[8] "AASHO Standard Specifications for Highway Bridges," A.A.S.H.O., 1949, Article 3.3.5(c).

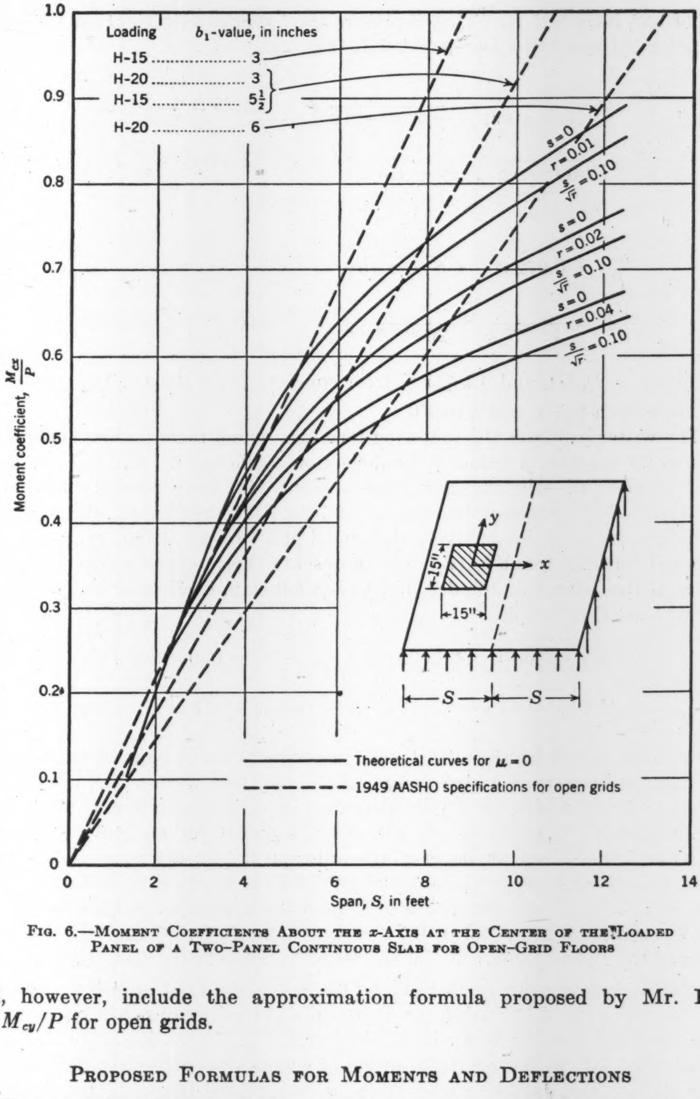

Fig. 6.—Moment Coefficients About the x-Axis at the Center of the Loaded Panel of a Two-Panel Continuous Slab for Open-Grid Floors

will, however, include the approximation formula proposed by Mr. Kuo for M_{cy}/P for open grids.

Proposed Formulas for Moments and Deflections

Concrete-Filled Steel-Grid Floors.—The following equations were proposed by Mr. Kuo as furnishing close approximations to the maximum positive values of the bending-moment coefficients M_{cx}/P and M_{cy}/P in a one-way continuous concrete-filled steel-grid slab under a wheel load P uniformly distributed over an area of 1.25 ft by 1.25 ft. They represent the moment coefficients at the center of the loaded panel of a two-panel slab (Fig. 2).

$$\left.\begin{aligned} \frac{M_{cx}}{P} &= \frac{S}{1.4\,(\log_{10} r)(S+2.5)+19} && (1.25\text{ ft} \leq S \leq 2.5\text{ ft}) \\ \frac{M_{cx}}{P} &= \frac{S}{2.6\,r^{0.28}\,(S+2)+7.5} && (2.5\text{ ft} \leq S \leq 12.5\text{ ft}) \end{aligned}\right\} \ldots (18)$$

and

$$\left.\begin{aligned} \frac{M_{cy}}{P} &= 0.072\,r^{0.21}\sqrt{S-1.15} && (1.25\text{ ft} \leq S \leq 4.0\text{ ft}) \\ \frac{M_{cy}}{P} &= \frac{S}{3\,r^{-0.09}\,S+20\,r^{-0.30}} && (4.0\text{ ft} \leq S \leq 12.5\text{ ft}) \end{aligned}\right\} \ldots\ldots (19)$$

in which $r = D_y/D_x$ and $0.1 \leq r \leq 1$ for concrete-filled slabs. The parameter $s/\sqrt{r}$ has been taken equal to 1.0.

The writer proposes the following formulas which furnish close approximations to the maximum value of the deflection coefficient δ^*_c and the maximum negative moment—the negative edge-moment M^*_e for a concrete-filled steel-grid slab. The proposed formula for δ^*_c (Eq. 20) represents the deflection coefficient at the center of the loaded panel of a two-panel slab (Fig. 2). The proposed formula for M^*_e (Eq. 21) represents the moment coefficient at the center of the intermediate edge in a two-panel slab, each panel subject to the central load P as in Fig. 3.

$$\delta^*_c = (0.015 - 0.008\,k) - (0.011 - 0.009\,k)\log_{10} r \ldots\ldots\ldots (20)$$

and

$$-M^*_e = (0.146 - 0.041\,k^{1.20}) - (0.036 - 0.034\,k^{1.51})\log_{10} r \ldots. (21)$$

in which for convenience the writer has used the variable k rather than span S, the relation between k and S being $k\,S = 1.25$ ft as before, if S is measured in feet. The formula for δ^*_c furnishes a close approximation to Mr. Kuo's data over the range $0.1 \leq r \leq 1.0$, $0.1 \leq k \leq 1.0$ (or equivalently 1.25 ft $\leq S \leq$ 12.5 ft)—the error being of the order of 2% for intermediate values of k and r and increasing to the order of 10% for the smallest spans where $k = 1$ or $S = 1.25$ ft. The formula for M^*_e furnishes a good approximation to Mr. Kuo's data for $0.2 \leq r \leq 1.0$, $0.1 \leq k \leq \frac{1}{2}$ (2.50 ft $\leq S \leq$ 12.5 ft), the error being of the order of 2%. As in Mr. Kuo's proposed formulas, the parameter ratio $s/\sqrt{r}$ has been assumed equal to 1.0 and so does not appear explicitly.

The variation of δ^*_c with k (or S) for different values of r over the range for concrete-filled slabs is shown in the curves of Fig. 7(*a*). Fig. 7(*b*) shows the variation of M^*_e with k (or S) for different r-values over the range for concrete-filled slabs. The data for these curves were obtained from Mr. Kuo's tabulations.[2]

Open-Grid Steel Floors.—The following formulas were proposed by Mr. Kuo to approximate the maximum positive values of the bending-moment coefficients, M_{cx}/P and M_{cy}/P, in a one-way continuous open-grid steel slab support-

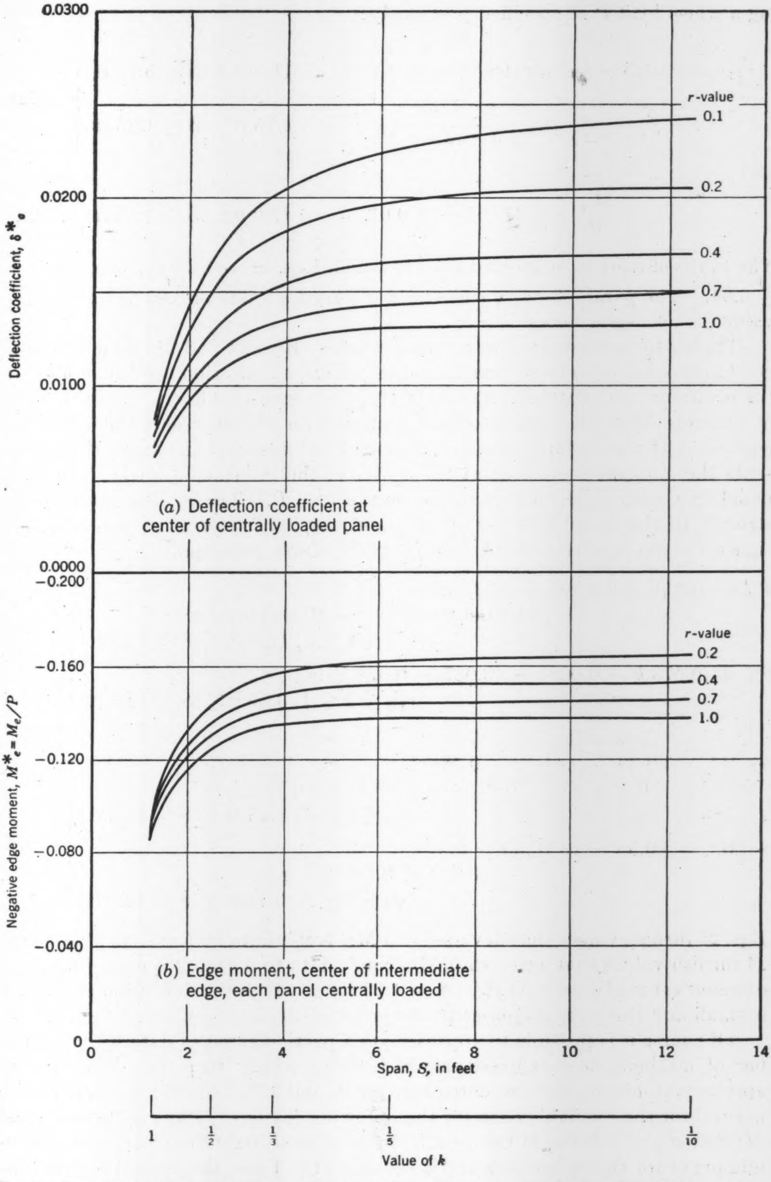

Fig. 7.—Deflection Coefficients and Negative Edge-Moments for a Two-Panel Continuous Slab over the Range of r-Values for a Concrete-Filled Grid Floor ($s/\sqrt{r} = 1.0$)

ing a wheel load P as specified previously:

$$\left.\begin{aligned} \frac{M_{cx}}{P} &= (0.325 - 0.7\sqrt{r})(S - 1) + 0.1 && (1.5\text{ ft} \leq S \leq 3.75\text{ ft}) \\ \frac{M_{cx}}{P} &= \frac{S}{0.25\,r^{-0.29}(S + 2) + 4.5} && (3.75\text{ ft} \leq S \leq 12.5\text{ ft}) \end{aligned}\right\} \quad ..(22)$$

and

$$\frac{M_{cy}}{P} = 0.37\,r^{0.38}\,S + 0.01 \qquad (2.0\text{ ft} \leq S \leq 12.5\text{ ft}) \quad ..(23)$$

The range of r for an open-grid floor to which Eqs. 22 and 23 apply is $0.01 \leq r \leq 0.04$. The parameter $s/\sqrt{r}$ has been assigned a value of 0.05 as an average value for open-grid floors.

The writer proposes the following formulas (Eqs. 24 and 25) which furnish good approximations to the maximum value of the deflection coefficient δ^*_c and the maximum negative edge-moment M^*_e for an open-grid floor. As in the case of concrete-filled steel-grid floors the equation for δ^*_c represents the deflection coefficient at the center of the loaded panel of a two-panel slab, and M^*_e represents the moment coefficient at the center of the intermediate edge in a two-panel slab, each panel subject to the central load P. The rigidity ratio r is restricted to the range $0.01 \leq r \leq 0.04$, and the parameter $s/\sqrt{r}$ has been assigned the average value 0.05, following Mr. Kuo's precedent:

$$\left.\begin{aligned} \delta^*_c = {} & (0.011 + 0.028\,k - 0.027\,k^2) \\ & - [0.019\,(1.20 - k)^{2.8} - 0.002]\log_{10} r \\ & \qquad (\tfrac{1}{3} \leq k \leq 1,\ 1.25\text{ ft} \leq S \leq 3.75\text{ ft}) \\ \delta^*_c = {} & (0.073\,k - 0.008) - (0.037 - 0.078\,k)\log_{10} r \\ & \qquad (\tfrac{1}{10} \leq k \leq \tfrac{1}{3},\ 3.75\text{ ft} \leq S \leq 12.5\text{ ft}) \end{aligned}\right\} \quad ..(24)$$

and

$$\left.\begin{aligned} -M^*_e = {} & [0.30 - 0.44\,(k - 0.33)^{2.8}] \\ & - [0.21\,(1 - k)^{3.3} - 0.003]\log_{10} r \\ & \qquad (\tfrac{1}{3} \leq k \leq 1,\ 1.25\text{ ft} \leq S \leq 3.75\text{ ft}) \\ -M^*_e = {} & [0.30 - 10\,(0.33 - k)^{4.6}] \\ & - (0.114 - 0.180\,k)\log_{10} r \\ & \qquad (\tfrac{1}{10} \leq k \leq \tfrac{1}{3},\ 3.75\text{ ft} \leq S \leq 12.5\text{ ft}) \end{aligned}\right\} \quad ..(25)$$

Eqs. 25 furnish values that deviate from Mr. Kuo's data by less than 2%. Eqs. 24 furnish values that agree with Mr. Kuo's data to within 2% except near the extreme value of $k = 1$ (that is, $S = 1.25$ ft) at which the deflection coefficient is small and the error increases to the order of 10%.

Of course it is possible to approximate a particular set of data by any number of mathematical expressions which differ widely in form. The type of approximation formulas presented here for δ^*_c and M^*_e, however, appeared quite natural for the available data for the following reasons. Plots relating δ^*_c and M^*_e to $\log_{10} r$ for different values of k appeared as straight lines on semi-logarithmic paper for the ranges of r and k considered. Thus, the desired approximation formulas were of the form: $A \log_{10} r + B$, in which A and B could be read as functions of k from the straight lines plotted. Where A and B were not sufficiently closely approximated by a linear function of k, either a quadratic function or a power law—that is, $A - A_o = (k - k_o)^p$, was used—the latter being conveniently obtained through the use of logarithmic paper.

The variation of δ^*_c with k (or S) for different values of r over the range for open-grid steel floors is shown in the curves of Fig. 8(*a*). Fig. 8(*b*) shows the variation of M^*_e with k (or S) for different r values over the range for open-grid steel floors. The data for these curves were taken from Mr. Kuo's tabulations.

Estimate of Rigidities

In order to apply Eqs. 18 through 25 to determine the coefficients M_{cx}/P, M_{cy}/P, δ^*_c, and M^*_e, it is only necessary to substitute in the equations the desired value of the span S, in feet, or the fraction $k = 1.25/S$, and the value of the rigidity ratio r for a particular floor. The estimation of the value of the rigidity ratio $r = D_y/D_x$ for practical design purposes was discussed by Mr. Kuo.[2] For the case of concrete-filled steel-grid floors he sets

$$\left.\begin{aligned} D_x &= \frac{E_c\, I_x}{b_1\,(1 - \mu^2)} \\ \text{and} \qquad D_y &= \frac{E_c\, I_y}{a_1\,(1 - \mu^2)} \end{aligned}\right\} \qquad (26)$$

in which b_1 is the spacing between the main bars of the grid (measured in the y-direction) and a_1 is the spacing between the cross bars (measured in the x-direction), E_c and μ are the modulus of elasticity and the Poisson ratio for concrete, and I_x and I_y are the sectional moments of inertia of an elementary block of size a_1 by b_1 of the grid as computed by the usual method of transformed sections used for reinforced concrete. For the case of open-grid steel floors, Mr. Kuo sets $\mu = 0$ to obtain

$$\left.\begin{aligned} D_x &= \frac{E\, I_x}{b_1} \\ \text{and} \qquad D_y &= \frac{E\, I_y}{a_1} \end{aligned}\right\} \qquad (27)$$

in which a_1 and b_1 are as defined, E is the modulus of elasticity for the steel, and I_x and I_y are the sectional moments of inertia of an elementary block of size a_1 by b_1 of the grid.

Having determined the coefficients, the actual moments and deflections can be obtained for a specified load P. In the case of the bending moments this is done by simply multiplying the coefficient by the load. In the case of the deflection,

$$\delta_c = \frac{P\, S^2}{D_x}\, \delta^*_c$$

in which D_x is determined by either Eq. 26 or Eq. 27.

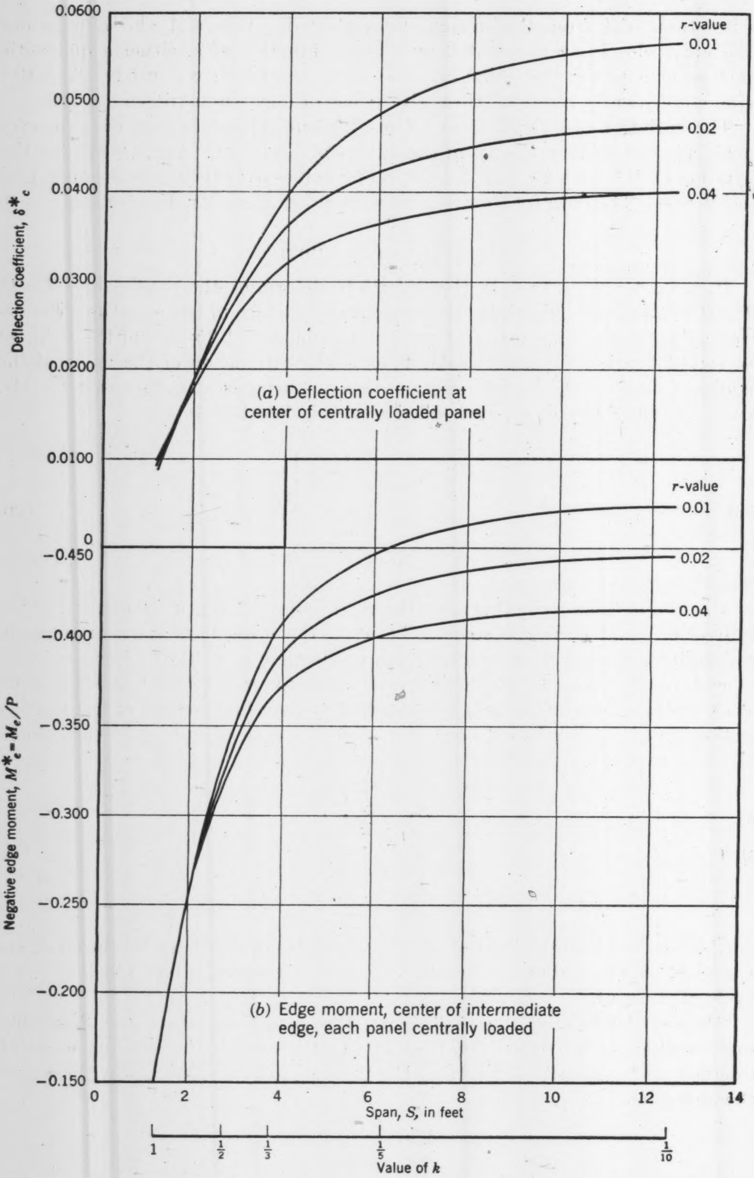

FIG. 8.—DEFLECTION COEFFICIENTS AND NEGATIVE EDGE-MOMENTS FOR A TWO-PANEL CONTINUOUS SLAB OVER THE RANGE OF r-VALUES FOR AN OPEN-GRID STEEL FLOOR ($s/\sqrt{r} = 0.05$)

CONCLUSION

Eqs. 18, 19, 22, and 23, which Mr. Kuo proposed as formulas for the determination of the maximum positive moments in concrete-filled grid and open-grid steel bridge floors under wheel loads, have been supplemented by Eqs. 20, 21, 24, and 25 for determining the maximum deflection and maximum negative moment in both types of floors. These proposed formulas are the first to take into account the dependence of the coefficients of moment and deflection on the anisotropy of the floor as measured by the ratio $r = D_y/D_x$ of the flexural rigidities in the two principal directions. These formulas are based on the results of the complete theoretical analysis of the deflection of an anisotropic, one-way, continuous, rectangular slab under concentrated loads made by Mr. Kuo.[9]

The theory and the equations presented can ultimately be verified only by correlation of the predicted results with the results of a properly designed experimental program. Subject to the results of such actual tests, it is proposed that these equations be used as a basis for the design of steel-grid highway bridge floors.

ACKNOWLEDGMENTS

The writer would like to thank Reliance Steel Products Company of McKeesport, Pa., which sponsored these investigations.

---

[9] "Moments in Steel Grid Highway Bridge Floors," by K. C. Kuo, *Proceedings*, Convention Group Meetings, A.A.S.H.O., Omaha, Nebr., 1951, Section 2.

DISCUSSION

Kuang–Han Chu,[10] A.M. ASCE.—Some valuable information for designing steel-grid bridge floors is presented in the paper. However, the approximate expressions seem to be too complicated for routine design use. The writer suggests the following equations for concrete-filled, steel-grid floors (Eqs. 28 to 32):

$$\frac{M_{cx}}{P} = \frac{0.2\,S}{0.6\,S + 2.5} \times \frac{1}{\sqrt[5]{r}} \qquad 2\text{ ft} \leq S \leq 7\text{ ft} \ldots\ldots\ldots\ldots (28)$$

$$\frac{M_{cx}}{P} = \frac{0.2\,S}{0.4\,S + 3.75} \times \frac{1}{\sqrt[5]{r}} \qquad S > 7\text{ ft} \ldots\ldots\ldots\ldots (29)$$

Eqs. 28 and 29 for the condition $r = 1$ are the same as those given in the AASHO specifications.

$$\frac{M_{cy}}{P} = 0.75\,\frac{M_{cx}}{P}\,\sqrt[3]{r} \ldots\ldots\ldots\ldots (30)$$

Eq. 30 is understood to be based on either Eq. 28 or Eq. 29, depending on the span length S.

$$\frac{M_e}{P} = 0.135\,\frac{1}{\sqrt[8]{r}} = \frac{M_{ef}}{P} \qquad S \geq 2.5\text{ ft} \ldots\ldots\ldots\ldots (31)$$

$$\frac{M_e}{P} = \left(\frac{M_{ef}}{P} - 0.05\right)\frac{S}{2.4} + 0.05 \qquad S < 2.5\text{ ft} \ldots\ldots\ldots\ldots (32)$$

The writer suggests the following equations for open steel-grid floors (Eqs. 33 to 36):

$$\frac{M_{cx}}{P} = \frac{0.2\,S}{1.70} \times \frac{1}{\sqrt[5]{100\,r}} \qquad S \leq 5\text{ ft} \ldots\ldots\ldots\ldots (33)$$

For the condition $r = 0.01$, Eq. 33 corresponds to the AASHO specification for an H-15 loading and a grid spacing b_1 equal to $2\frac{3}{4}$ in.—that is, $M_{cx}/P = 0.2\,S/(W + 2\,b_1)$ in which W equals 1 in. per ton of standard H or H-S trucks For H-15, if $b_1 = 2\frac{3}{4}$ in., $W + 2\,b_1 = 1.70$ ft.

$$\frac{M_{cx}}{P} = 0.2\left(\frac{S}{5} + 2\right)\frac{1}{\sqrt[5]{100\,r}} \qquad S > 5\text{ ft} \ldots\ldots\ldots\ldots (34)$$

$$\frac{M_e}{P} = 0.475\,\frac{1}{\sqrt[8]{100\,r}} = \frac{M_{eo}}{P} \qquad S \geq 4.5\text{ ft} \ldots\ldots\ldots\ldots (35)$$

$$\frac{M_e}{P} = \left(\frac{M_{eo}}{P} - 0.1\right)\frac{S}{4.5} + 0.1 \qquad S < 4.5\text{ ft} \ldots\ldots\ldots\ldots (36)$$

---

[10] Designer, D. B. Steinman, Cons. Engr., New York, N. Y.

TABLE 1.—FILLED STEEL–GRID FLOORS

$r=D_y/D_x$	Span, S, in feet	M_{cx}/P			M_{cy}/P			M_e/P		
		Fig. 4	Eq. 28	Eq. 29	Fig. 5	Eqs. 28, 30	Eqs. 29, 30	Fig. 7 (*b*)	Eq. 31	Eq. 32
1.0	1.5							0.100		1.101
	2.5	0.128	0.125		0.079	0.096		0.125	0.135	
	5.0	0.190	0.182		0.140	0.137		0.137	0.135	
	7.5	0.229	0.214	0.222	0.172	0.160	0.167	0.138	0.135	
	10.0	0.246	0.235	0.258	0.193	0.176	0.194	0.138	0.135	
	12.5	0.257	0.250	0.285	0.207	0.188	0.214	0.138	0.135	
0.7	1.5							0.103		0.105
	2.5	0.135	0.134		0.070	0.089		0.130	0.141	
	5.0	0.205	0.195		0.138	0.130		0.143	0.141	
	7.5	0.243	0.230	0.238	0.160	0.153	0.158	0.143	0.141	
	10.0	0.261	0.252	0.277	0.179	0.168	0.184	0.144	0.141	
	12.5	0.271	0.268	0.306	0.191	0.178	0.204	0.145	0.141	
0.4	1.5							0.107		0.111
	2.5	0.150	0.150		0.062	0.083		0.136	0.151	
	5.0	0.228	0.219		0.112	0.122		0.150	0.151	
	7.5	0.273	0.257	0.267	0.142	0.142	0.148	0.150	0.151	
	10.0	0.293	0.282	0.310	0.161	0.156	0.172	0.151	0.151	
	12.5	0.306	0.300	0.342	0.173	0.166	0.190	0.152	0.151	
0.2	1.5							0.110		0.119
	2.5	0.168	0.172		0.050	0.076		0.144	0.165	
	5.0	0.261	0.251		0.100	0.110		0.160	0.165	
	7.5	0.312	0.295	0.306	0.125	0.130	0.135	0.162	0.165	
	10.0	0.340	0.324	0.356	0.143	0.142	0.156	0.164	0.165	
	12.5	0.355	0.345	0.394	0.157	0.152	0.173	0.165	0.165	
0.1	1.5									
	2.5	0.190	0.199		0.044	0.069				
	5.0	0.295	0.289		0.085	0.101				
	7.5	0.359	0.340	0.353	0.110	0.118	0.123			
	10.0	0.392	0.374	0.410	0.129	0.130	0.143			
	12.5	0.415	0.399	0.470	0.143	0.139	0.164			

A comparison of the values thus obtained with those scaled from the author's curves is given in Tables 1 and 2.

Table 1 also lists values from Eq. 28 for $S > 7$ ft for comparison. The moments determined using Eq. 29 are greater than those given by Mr. Greenberg for $S > 8$ ft. However, it should be noted that the author's values are based on

TABLE 2.—OPEN STEEL–GRID FLOOR ($s/\sqrt{r}=0.05$)

$r=D_y/D_x$	M_{cx}/P				M_e/P			
	Span, S, in feet	Fig. 6	Eq. 33	Eq. 34	Span, S, in feet	Fig. 8 (*b*)	Eq. 35	Eq. 36
0.01	2.0	0.20	0.235		2.0	0.260		0.267
	4.0	0.47	0.470		4.0	0.410		0.433
	5.0	0.57	0.590	0.60	4.5	0.422	0.475	
	7.5	0.70		0.70	6.0	0.449	0.475	
	10.0	0.80		0.80	8.0	0.464	0.475	
	12.0	0.86		0.88	12.0	0.473	0.475	
0.02	2.0	0.20	0.204		2.0	0.260		0.250
	4.0	0.43	0.410		4.0	0.395		0.400
	5.0	0.51	0.515	0.522	4.5	0.403	0.436	
	7.5	0.62		0.610	6.0	0.425	0.436	
	10.0	0.70		0.695	8.0	0.440	0.436	
	12.0	0.75		0.765	12.0	0.446	0.436	
0.04	2.0	0.20	0.178		2.0	0.260		0.233
	4.0	0.39	0.356		4.0	0.375		0.366
	5.0	0.45	0.446	0.455	4.5	0.383	0.400	
	7.5	0.55		0.530	6.0	0.400	0.400	
	10.0	0.62		0.606	8.0	0.410	0.400	
	12.0	0.66		0.666	12.0	0.417	0.400	

a single load applied at midspan whereas for longer spans the writers of the AASHO formula (Eq. 29) may have taken account of the effect of more than one load on a span. In fact, it should be noted that Mr. Greenberg's data are subject to the following limitations: (1) The wheel load is assumed to be distributed over an area of 15 ft by 15 ft. (2) The analysis is made for continuous slabs of two equal spans only. (3) The slabs are on unyielding supports of zero width. (4) For maximum center moments, one wheel load only is applied at the center of one span. (5) For maximum edge-moments, both spans are loaded. One wheel load only is applied to each span and it is applied only at the center of the span. The wheel loads on both spans are of equal intensity.

Fu-Kuei Chang,[11] A. M. ASCE.—The formulas proposed by the author and Mr. Kuo for calculating moments and deflections in a steel-grid highway bridge floor are highly valuable because the anisotropic property of the floor has been taken into account. The actual problem of analyzing this kind of floor is

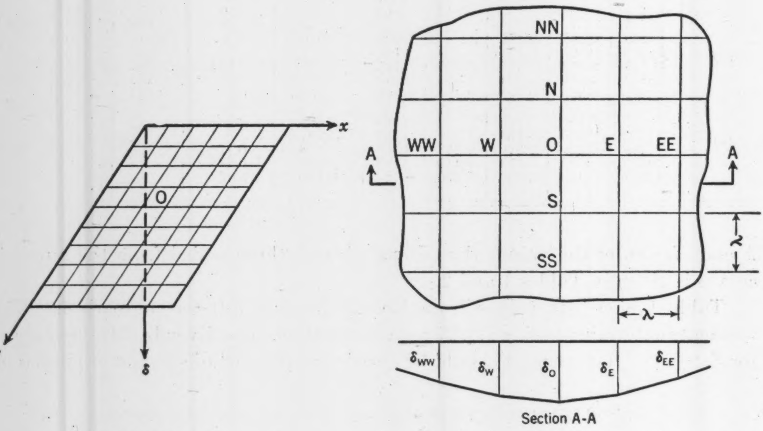

x
O
y
δ
NN
N
WW
W
O
E
EE
A
A
S
SS
λ
λ
δ_WW
δ_W
δ_O
δ_E
δ_EE
Section A-A

(a) Orientation

(b) Net

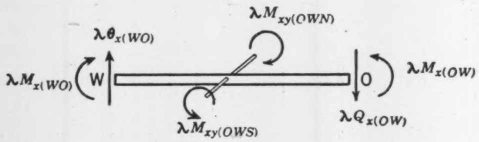

$\lambda M_{xy(OWN)}$
$\lambda \theta_{x(WO)}$
$\lambda M_{x(WO)}$
W
O
$\lambda M_{x(OW)}$
$\lambda M_{xy(OWS)}$
$\lambda Q_{x(OW)}$

(c) Bending of a bar

Fig. 9.—Difference Solution of an Anisotropic Plate

rather involved. It is a continuous anisotropic plate on elastic supports with partly restrained edges under concentrated or uniform loading. The author and Mr. Kuo assume rigid supports and a hinged edge condition. These assumptions are believed to be satisfactory for practical purposes; however, the proposed formulas for maximum moments are based on two continuous spans that correspond to the exterior spans, that part of the floor between the exterior stringer and the first interior stringer. These formulas are overconservative for interior spans (the part of the floor between interior stringers) which constitute a major part of the floor. Formulas applicable to an interior span are also desirable. In actual construction, the interior span length can be made larger than that of the exterior span if the same floor is used throughout.

---

[11] Designer, Ammann and Whitney, New York, N. Y.

The steel-grid floor as an anisotropic plate can also be solved by a numerical method. Eq. 2 can be replaced by a difference equation and the latter, in turn, can be replaced by a set of simultaneous equations. The whole problem will then be reduced to the solution of simultaneous equations.

It is assumed that the imaginary net shown in Fig. 9 behaves as an anisotropic plate. The value of $\partial^2\delta/\partial x^2$ at any net point—say, point "O"—can be evaluated approximately from the deflections (δ's) of its neighbor points.

$$\frac{\partial^2\delta}{\partial x^2} \approx \frac{\dfrac{\delta_E - \delta_O}{\lambda} - \dfrac{\delta_O - \delta_W}{\lambda}}{\lambda} = \frac{\delta_E - 2\,\delta_O + \delta_W}{\lambda^2} \qquad (37)$$

Similarly, the following expressions can be derived:

$$\left.\begin{aligned}
\frac{\partial^2\delta}{\partial y^2} &\approx \frac{\delta_S - 2\,\delta_O + \delta_N}{\lambda^2}\\
\frac{\partial^4\delta}{\partial x^4} &\approx \frac{\delta_{WW} - 4\,\delta_W + 6\,\delta_O - 4\,\delta_E + \delta_{EE}}{\lambda^4}\\
\frac{\partial^4\delta}{\partial y^4} &\approx \frac{\delta_{SS} - 4\,\delta_S + 6\,\delta_O - 4\,\delta_N + \delta_{NN}}{\lambda^4}\\
\frac{\partial^4\delta}{\partial x^2\partial y^2} &\approx \frac{4\,\delta_O - 2\,(\delta_N + \delta_S + \delta_E + \delta_W) + (\delta_{NW} + \delta_{NE} + \delta_{SW} + \delta_{SE})}{\lambda^4}
\end{aligned}\right\} \qquad (38)$$

By substituting these expressions into Eq. 2 the following difference equation at point O is obtained.

$$\begin{aligned}
w\,\lambda^4 = (6\,D_x + 6\,D_y + 8\,H)\,\delta_O - 4\,(D_y + H)(\delta_N + \delta_S)\\
- 4\,(D_x + H)(\delta_E + \delta_W) + 2\,H\,(\delta_{NW} + \delta_{SW} + \delta_{NE}\\
+ \delta_{SE}) + D_y\,(\delta_{NN} + \delta_{SS}) + D_x\,(\delta_{WW} + \delta_{EE}) \qquad (39)
\end{aligned}$$

At each net point, an equation similar to Eq. 39 can be obtained. The number of the linear equations equals the number of net points in the network. By solving these linear equations simultaneously the deflections at all the net points can be determined. If a finer net is used, the results will be more accurate.

The bending moments per unit length in both directions, M_x and M_y, can be determined from the deflections. For example, the bending moments at both ends of the bar OW in Fig. 9 are

$$\left.\begin{aligned} M_{x(OW)} &= -D_x\frac{\partial^2\delta}{\partial x^2} = -D_x\frac{\delta_E - 2\,\delta_O + \delta_W}{\lambda^2} \\ \text{and} \quad M_{x(WO)} &= -D_x\frac{\partial^2\delta}{\partial x^2} = -D_x\frac{\delta_O - 2\,\delta_W + \delta_{WW}}{\lambda^2} \end{aligned}\right\} \qquad (40)$$

Illustrative Example.—Let it be required to find the moments and deflections of a concrete-filled, steel-grid bridge floor, 9 ft wide, 12 ft long, and continuous over two spans (Fig. 10) which are caused by the application of two 1-kip loads at points 8 and 8′. Each load is distributed uniformly over an area 18 in. square. The ridigity D_x = 23,300 kip-in., D_y = 4,820 kip-in., and H = 14,360 kip-in.

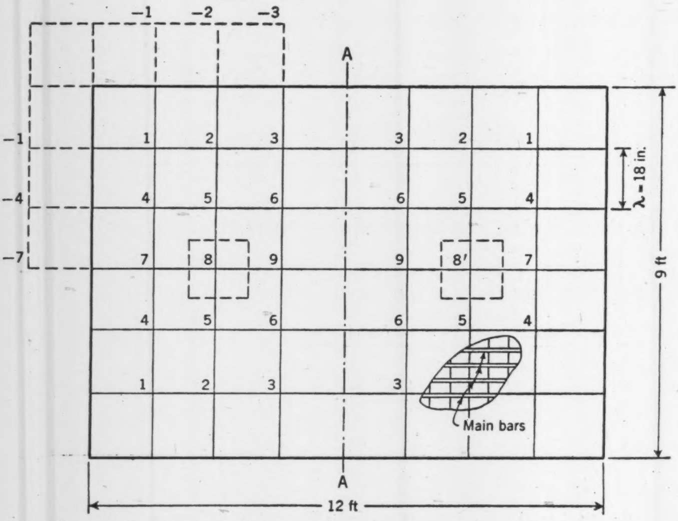

FIG. 10.—EXAMPLE

Because both the edge and load conditions are symmetrical about the midsupport A-A each half of the slab can be considered as fixed along A-A and simply supported along the other three sides. By the use of Eq. 39 the following nine simultaneous equations in which λ = 18 in. can be written:

$$
\left.\begin{array}{cl}
\text{Point} & \text{Equation} \\
1 & 0 = 283.62\,\delta_1 - 76.73\,\delta_4 - 150.65\,\delta_2 + 28.68\,\delta_5 \\
 & \qquad + 4.82\,(-\delta_1 + \delta_7) + 23.30\,(-\delta_1 + \delta_3) \\
2 & 0 = 283.62\,\delta_2 - 76.73\,\delta_5 - 150.65\,(\delta_3 + \delta_1) \\
 & \qquad + 28.68\,(\delta_4 + \delta_6) + 4.82\,(-\delta_2 + \delta_8) \\
3 & 0 = 283.62\,\delta_3 - 76.73\,\delta_6 - 150.65\,\delta_2 + 28.68\,\delta_5 \\
 & \qquad + 4.82\,(-\delta_3 + \delta_9) + 23.30\,(\delta_1 + \delta_3) \\
4 & 0 = 283.62\,\delta_4 - 76.73\,(\delta_1 + \delta_7) - 150.65\,\delta_5 + 28.68\,(\delta_2 + \delta_8) \\
 & \qquad + 4.82\,\delta_4 + 23.30\,(-\delta_4 + \delta_6) \\
5 & 0 = 283.62\,\delta_5 - 76.73\,(\delta_2 + \delta_8) - 150.65\,(\delta_6 + \delta_4) \\
 & \qquad + 28.68\,(\delta_1 + \delta_3 + \delta_7 + \delta_9) + 4.82\,\delta_5 \\
6 & 0 = 283.62\,\delta_6 - 76.73\,(\delta_3 + \delta_9) - 150.65\,\delta_5 + 28.68\,(\delta_2 + \delta_8) \\
 & \qquad + 4.82\,\delta_6 + 23.30\,(\delta_4 + \delta_6) \\
7 & 0 = 283.62\,\delta_7 - 76.73\,(\delta_4 + \delta_4) - 150.65\,\delta_8 + 28.68\,(\delta_5 + \delta_5) \\
 & \qquad + 4.82\,(\delta_1 + \delta_1) + 23.30\,(-\delta_7 + \delta_9) \\
8 & \dfrac{\lambda^2}{1{,}000} = 283.62\,\delta_8 - 76.73\,(\delta_5 + \delta_5) - 150.65\,(\delta_9 + \delta_7) \\
 & \qquad + 28.68\,(\delta_4 + \delta_6 + \delta_4 + \delta_6) + 4.82\,(\delta_2 + \delta_2) \\
9 & 0 = 283.62\,\delta_9 - 76.73\,(\delta_6 + \delta_6) - 150.65\,\delta_8 + 28.68\,(\delta_5 + \delta_5) \\
 & \qquad + 4.82\,(\delta_3 + \delta_3) + 23.30\,(\delta_7 + \delta_9)
\end{array}\right\}\ldots(41)
$$

In forming the equations for the points near the boundaries, imaginary deflections at points outside the boundaries are required. The imaginary deflections exterior to the slab are symmetrical with those in the floor about the fixed edge. For a simply supported edge, the corresponding deflections are equal in magnitude but have opposite signs. The general procedure in forming and solving similar simultaneous equations is to be found elsewhere as, for example, in the work[12] of V. P. Jensen, M. ASCE. The solutions, in inches, of Eqs. 41 are as follows:

$\delta_1 = 0.00055$

$\delta_2 = 0.00071$

$\delta_3 = 0.00032$

$\delta_4 = 0.00146$

$\delta_5 = 0.00201$

$\delta_6 = 0.00097$

$\delta_7 = 0.00259$

$\delta_8 = 0.00408$

$\delta_9 = 0.00191$

The maximum negative moment at support A-A ($-M_x$), the maximum positive moment at the center of the span (M_x), and the moment in the longitudinal direction (M_y) can be found by using equations similar to Eq. 40, from which $-M_x = -0.275$ in.-kips per in., $M_x = 0.263$ in.-kips per in., and $M_y = 0.062$ in.-kips per in.

---

[12] "Analysis of Skew Plates," by V. P. Jensen, *Bulletin No. 332*, Univ. of Illinois Eng. Experiment Station, Urbana, Ill., 1941.

HERBERT J. GREENBERG,[13] Mr. Chu's approximate equations have the advantage of being close in form to the AASHO formulas for the isotropic case in addition to being somewhat simpler for computation. The values furnished are in sufficiently close agreement with the tables given by Mr. Kuo in his paper. In reference to the limitations listed by the discusser, the following remarks should be added. The results of Mr. Kuo's analysis were originally presented in terms of the nondimensional parameter k which is the ratio of a side of a central square load to the span, S (Figs. 2 and 3). If the loaded area is assumed to be l inches on one side rather than 15 in., the corresponding expressions are obtained by changing S in the same proportion—that is, $(l/15)\ S$. Moreover, the exact assumption as to the shape of the loaded area—whether square, circular, or some other shape—does not significantly affect results except in extreme cases. Also, because the exact shape of the loaded area is unknown, there is little reason to choose one shape in preference to another except for purposes of mathematical simplicity. In connection with points (2) and (5), for the case of equal panels the maximum moments and deflections will occur in the case of two panels loaded as shown in Fig. 2 or in the case of edge moments as in Fig. 3. The case of more than one load for longer spans could be handled in special cases by superposition—or in any case by reverting to Mr. Kuo's general treatment, which is applicable to an arbitrary panel in a one-way continuous, anisotropic slab under arbitrary loading, and carrying out the numerical computations from the series solution.

As Mr. Chang remarks, the formulas are on the conservative side for interior spans. Additional computations based on Mr. Kuo's theoretical solution would furnish the desired information. The numerical difference solution suggested by Mr. Chang is always possible, but as usual the accuracy cannot be determined. It would seem preferable in these problems to proceed from an exact solution as based on Mr. Kuo's results even though the solution is not immediately in a useful numerical form.

In a letter, T. A. Koe has pointed out that the formula (Eq. 23) proposed by Mr. Kuo for the moment coefficient M_{cy}/P for the case of open-grid floors is not in close agreement with the tabulated values in his paper. This may be due to a typographical error in the formula, but it has not been possible to check this. The following approximate equation, however, has been found to furnish close agreement with the tabulated values:

$$\frac{M_{cy}}{P} = (0.0088\,S + 0.17)\,r^{(1.35/S)+0.24}$$

for the range $0.01 \leq r \leq 0.04$, $2.5\text{ ft} \leq S \leq 12.5\text{ ft}$.

---

[13] Associate Prof. of Math., Carnegie Inst. of Technology, Pittsburgh, Pa.

AMERICAN SOCIETY OF CIVIL ENGINEERS

Founded November 5, 1852

TRANSACTIONS

Paper No. 2804

DESIGN OF GENERAL CARGO MARINE TERMINALS

BY FRANK W. HERRING,[1] M. ASCE

SYNOPSIS

The design of a modern marine terminal is analyzed by studying its functions and basic form. Standards developed by The Port of New York Authority are included, and reference is made to two modern facilities in the harbors of New York, N. Y., and San Francisco, Calif.

INTRODUCTION

One of the most overworked words in present-day usage is "modern." Even more, the words "modern design" are the catchwords of every advertising copy writer. That these words are used so much can probably be ascribed to the fact that they lack an exact meaning. The artist, the engineer, the architect, the economist—each has his own idea of what constitutes "modern design."

"Modern design" for a general cargo marine terminal is judged strictly from a utilitarian point of view. Whether it is constructed wholly of prestressed concrete, whether it is pleasing to the eye, or even whether it is new—none of these features makes a cargo pier modern. A marine terminal can be said to be modern only when it is so constructed that it can efficiently and expeditiously (1) accommodate the latest developments in the water and land transportation systems that it serves and (2) provide for full use of the latest techniques in materials handling.

FUNCTIONS OF A GENERAL CARGO MARINE TERMINAL

A general cargo marine terminal is principally an interchange point for cargo moving via a combination of land and sea transportation routes. The transit shed, typically the only superstructure of consequence, is named for this interchange. Here cargo is received, sorted, consolidated, and generally processed for exchange between one form of transportation and another; it is not stored for an indefinite period.

NOTE.—Published, essentially as printed here, in February, 1955, as *Proceedings-Separate No. 615.* Positions and titles given are those in effect when the paper was approved for publication in *Transactions.*

[1] Chief, Planning Div., The Port of New York Authority, New York, N. Y.

There are two basic forms that a marine terminal can take—namely, the finger pier and the marginal wharf. The finger pier is a long, narrow structure jutting out into the water, perpendicular to the shore line. This type of construction is the most common in ports in the United States. In those ports where easily developed water frontage is at a premium, as it is on the island of Manhattan in New York Harbor, the finger pier is the type of pier most often used. With this type of construction, a given length of water front yields the maximum number of ship berths.

The second basic form of pier is the marginal wharf. This type is constructed parallel to the shore and is used where there is no shortage of easily developed water-front space or where the waterway adjacent to the pier is too restricted to permit the use of the finger pier.

Whether the finger pier or the marginal wharf form is used depends on the economic geography of the particular port. There is no intrinsic advantage in either type as far as modern design is concerned.

Factors Governing the Design of a Modern General Cargo Marine Terminal

It is a well-known fact that a certain number of piers in a port will always be of obsolete design. Marine structures are usually built for a long life, with amortization periods of forty years or more, and long before a pier has suffered any extensive physical deterioration it is likely to be obsolete. Fault can only be found when new piers are built with the design features that do not fit modern conditions.

Perhaps the best way to analyze the design requirements for a modern general cargo terminal is to begin by reviewing the changes that have taken place since 1900 in ocean and land transportation and in materials-handling techniques. If a pier is built to accommodate a horse and wagon, the pier certainly cannot be considered modern when the motor truck has long since taken the horse's place. Again, a pier cannot be considered modern if it is built to accommodate the cargo of a sailing ship.

One of the most revolutionary changes has been the development of the motor truck. In 1925, the motor truck was not an important element in the transportation system. In 1955, however, it is as important as the railroad in many ways. In the transportation of oceanborne cargo to and from piers, the motor truck is carrying as much as 50% of the cargo either for local delivery or long hauls. Moreover, it is still growing as a factor in the land transportation of freight having overseas origin or destination. Conversely, railroad freightage of cargos to and from marine terminals appears to be declining in relative importance.

Ranking in importance with this development of the motor truck is the development of labor-saving devices for cargo handling such as fork-lift trucks, small mobile cranes, and other equipment for use on the wharf. The baling hook, the hand truck, and the longshoreman's back muscles—even though they are still in use—are no longer the principal elements of the materials-handling system.

Ships too have undergone changes. Although there has not been any striking increase in the over-all size, the cubic capacity for a given size of ship has increased. A ship of a given length and draft is carrying as much as 100% more cargo in its hold than it did in the past. Ship speeds have also increased but not enough to affect the design of the general cargo terminal.

Another important change affecting the design of the cargo terminal has been the development of rapid communication methods. The importer can order goods by telegraphing anywhere in the world. The frequency of sailings, the speed of ships, the rapidity of communications, and the reliability of sailing schedules have made it unnecessary for the importing merchant to maintain large inventories. These conditions not only necessitate a different concept of merchandising but also a different concept in the design of the marine terminal.

Other changes have taken place since 1900, but those which have been enumerated are the principal elements affecting the construction and design of the modern cargo terminal. Each of the changes, in turn, has produced various offshoot developments which must also be considered in pier design. These developments affect and actually create the design criteria for the cargo pier.

DEVELOPMENT OF MODERN STANDARDS

The over-the-road truck is the most important single element to be considered in the design of a general cargo marine terminal.

If the terminal is of the finger-pier type, it is necessary to provide cargo and working space on the pier and an unimpeded roadway for truck egress and ingress. Even before cargo space is considered, therefore, the modern cargo terminal requires greater dimensions than the typical terminal designed a generation ago. If the construction is of the marginal-wharf type, provision must be made for truck "back-up" areas on the inshore side of the shed and loading platforms at the height of the truck tailgates to eliminate unnecessary lifting of cargo in the truck-loading operation.

The increasing use of over-the-road trucks also means that the general layout of the upland area must be carefully planned. There should be sufficient space and adequate traffic control for the waiting lines of trucks picking up or delivering cargo on the pier. The amount of space that is necessary for such waiting lines is minimized if the pier itself can assure quick loading or discharging.

The motor truck dimensions and the space required for maneuvering may be controlling factors in the spacing of columns and the vertical clearances of beams and doors.

The increasing use of the truck has also reduced the amount of cargo moved by rail and has thereby lessened the need for extensive rail facilities at the terminal. It is not that rail facilities may be ignored but rather that rail transportation is no longer the dominant method of moving cargo to and from a marine terminal. Furthermore, the diminishing use of railroads also means that there is a diminishing proportion of direct transfer from rail or lighter to ship. Cargo that once moved in this fashion without even temporary storage at the terminal must now be accommodated in the transit shed, increasing the required pier space further.

The great number of labor-saving devices that have been introduced into the handling of cargo constitutes the second major factor affecting pier design. The first and most notable of these devices is the fork-lift truck. Its introduction has revolutionized the entire system of handling general cargo. Instead of the individual handling of each item, cargo is assembled on pallets and carried from the side of the ship to the place of stowage on the pier and vice versa. With the use of fork-lift trucks, cargo can be stacked as high as 20 ft whereas before it could be piled only as high as the longshoreman could reach. This has a twofold effect on the design of the pier—namely, the overhead clearance requirement has been increased and the load-bearing capacity of the wharf must be greater. To provide fully for the use of the fork-lift truck the cargo pier must also have a smooth or at least an even deck surface, uninterrupted aisles, and adequate aprons.

The increased speed of communication has had a twofold effect on water-front facilities. The first has been the diminishing need for water-front warehouse space. Since 1940 there has been a steady decline in the use of warehouse space along the water front. The second effect has been on the typical size of the cargo shipment arriving at the pier. The custom of many merchants ordering small amounts of goods creates a situation in which a ship carries an enormous variety of items on its manifest, a far larger number for a given tonnage than characterized ocean shipping of the nineteenth century. The pier, therefore, must provide sufficient space to accommodate the sorting, separate stacking, and consolidation of these shipments. In other words, the space requirements have increased even on a per-ton basis.

CURRENT (1955) STANDARDS

Using the C-2 vessel as typical of the ships likely to be berthed at a pier and taking into consideration the developments described, minimum standards can be established for the controlling dimensions of the modern general cargo marine terminal. The ship berth should be at least 550 ft long and should have a depth of from 32 ft to 35 ft at mean low water. The slip between two adjacent piers should be at least 250 ft wide. If two or more ships are to be berthed at either of the piers, 300 ft or more are needed.

Making allowances for the foregoing factors, a minimum shed space of 90,000 sq ft is required for each ship berth. The apron of a pier should be at least 15 ft wide unless it includes rail tracks and, in this event, its width will depend on the number of tracks to be installed. The overhead clearance within the shed must be 20 ft, the floor loading capacity must be between 500 lb per sq ft and 600 lb per sq ft, and the doors must be of adequate height to accommodate over-the-road trucks and all the various cargo-handling devices used on the pier. In addition to these strategically important dimensions, the standard items of any construction—such as illumination, fire protection, and sanitation facilities—must also be provided in accordance with modern thinking in those fields.

The 90,000-sq-ft requirement for shed area for each ship berth can be explained as follows: Freight rates on oceanborne cargo are computed on the basis of "weight" tons and "measurement" tons. A long ton of cargo that can be stowed in less than 40 cu ft is known as "weight" cargo, and freight is charged per weight ton. The lighter commodities—those that occupy 40 cu ft or more per long ton—are referred to as "measurement" cargo, and freight is charged on a measurement ton basis of 40 cu ft to the ton. For example, the general cargo which is shipped through the Port of New York averages about 70 cu ft to the long ton; therefore, most of it is shipped as measurement cargo.

It has been found that the typical dry cargo ship calling at a New York terminal loads and discharges about 12,500 measurement tons. Half of this cargo is discharged from the ship, the other half is loaded. Because the ship must be discharged first and then loaded the transit shed must be designed to accommodate both inward and outward cargoes at the same time.

These 12,500 measurement tons occupy 500,000 cu ft, and this is the volume for which storage space must be provided within the shed. Most of this cargo can be placed on pallets and stacked three tiers high. These three tiers will be about 15 ft high, less 6 in. for each of the three pallets—or have a net height of approximately 13½ ft. The floor area requirement, therefore, would be 36,000 sq ft if all the stacks were full height, but some stacks will be short because of broken lots. To allow for the inevitable lost space, the 36,000 sq ft theoretically required are increased 25% to 45,000 sq ft. Another 45,000 sq ft will be required for working aisles, truck roadways, and truck loading areas. The total gross area requirement of 90,000 sq ft per ship berth has been adopted by The Port of New York Authority as the minimum for a modern general cargo berth and has been applied to the design of its new marine terminal facilities.

The stated area requirement includes provision for thirty truck berths, each 40 ft by 12 ft, for loading and unloading. That number is based on the assumption that the 12,500 measurement tons of cargo are delivered to or taken from the pier in five working days. It also assumes that half the cargo moves by truck and that the average truck load is 10 measurement tons. This amounts to 1,250 measurement tons a day, moving in 125 trucks. For an eight-hour day about 16 trucks must be handled every hour. Because it takes almost two hours to load or unload a truck, approximately 30 available truck spots for each berth are needed.

Obviously, the design of terminals cannot be standardized. There is ample reason for considerable variation, not only between ports but even between different areas within the same harbor.

The choice of finger pier or marginal wharf depends primarily on the geography of the available water front. Where the dominant movement of freight is by rail, trackage facilities will have to be given more prominence and motor vehicle roadways less. Although the 90,000-sq-ft area for the transit shed is valid for a terminal at which an entire ship load is to be handled, in the smaller ports where ships load and discharge only part of their cargos, or at some terminals within a major port, a proportionately smaller figure can be used.

MODERN DESIGN ILLUSTRATED

Several examples can be cited to illustrate the varieties of design that are possible while still meeting modern criteria. Among recent developments in New York are the Hoboken (N. J.)-Port Authority piers and the new terminals developed at Port Newark, N. J. On one of these projects a finger-type plan is used while on the other a marginal wharf. By a different approach, each has been designed to handle the new large ships and to accommodate trucks, freight cars, and lighters. Both projects called for single-deck transit sheds with 90,000 sq ft or more gross shedded area per berth, and the other standards cited in the foregoing have been applied in the design. The Port Authority's Pier C at Hoboken, a two-berth facility, is 700 ft long and 328 ft wide. This is probably one of the most spacious two-berth piers in the United States. One apron of this pier is 20 ft wide whereas the other, which includes one railraod track, measures 25 ft. The shed has a center well 500 ft long to accommodate two depressed railroad tracks and it also has a U-shaped, two-lane truck boulevard surrounding the center well to permit one-way truck movement.

The cargo pier development at Port Newark, on the other hand, follows the quay-type construction. There, a minimum length of 550 ft is allowed for a ship berth, and the apron measures 50 ft and carries two railroad tracks. The rear of each shed has a tailgate-high freight platform abutting on a 100-ft-wide paved roadway and two rail tracks laid flush with the surface.

The Hoboken and Port Newark facilities are both new and modern. On the other hand, several good examples of modernization can be cited whereby obsolete piers have been modified to conform to the needs of modern transport methods. In San Francisco Harbor, for example, two piers, 680 ft long and 203 ft wide, have been joined by a pile-supported platform which occupies what was formerly the 222-ft intervening slip. The center part of the platform, 150 ft wide, was designed as a depressed well for truck maneuvering and back-up and for rail track accommodation. The remainder of the slip width was utilized for pier and shed widening. The terminal now (1955) provides three generous berths, one on each side and a third across the end. The entire facility is leased to a navigation company which operates general cargo and passenger ships in the trans-Pacific service and has been in operation since January, 1952.

Other illustrations can be cited of modernization of older facilities so as to make provision for motor trucks, fork-lift trucks, and the other important developments in cargo handling.

SPECIALIZED CARGO FACILITIES

There are certain specific commodities which are transported along regular routes in sufficient quantities to justify specialized facilities designed for the handling of that commodity alone. Bulk liquids, such as petroleum products, can be pumped into and out of ships' tanks, bulk ores and grain can be gravity loaded into ships' holds through chutes and unloaded by giant 20-ton cranes, whereas stems of bananas can be unloaded by endless belts and other special machinery. Two especially interesting facilities in New York Harbor are the *Daily News* newsprint terminal in Brooklyn and the United Fruit Company's banana unloading terminal in Weehawken (N. J.).

At the newsprint terminal a permanent crew of 28 men operate a system of conveyor belts, hoists, and specially designed fork-lift trucks to handle rolls of newsprint moving to the terminal by ship, barge, and box car and from the terminal to the plant via truck. Longshoremen unload the ship and place the newsprint rolls on the conveyor system at shipside. All the newsprint requirements of the *Daily News*—about 1,000 tons—move through this facility each working day.

The Weehawken Interchange Terminal, as the banana unloading terminal is called, is designed to facilitate the rapid and safe transfer of stems of bananas from steamships to refrigerated cars and trucks. Four specially designed traveling cranes housing endless belt conveyors transfer the stems of bananas from ships' holds to an extensive system of horizontal belts called "curveyors," which run between strings of refrigerated cars and over-the-road trucks. A crew of 330 longshoremen can transfer a shipload of 60,000 stems of bananas from a ship to rail cars or to motor trucks in an eight-hour day.

Each of these facilities is new and modern; the newsprint terminal was completed in 1952 and the interchange terminal in 1953. Each was designed around a materials-handling system tailored to fit the specific needs of one industry.

CONCLUSION

A concept of modern general cargo terminal design has been presented. Whenever a terminal becomes a bottleneck to cargo movement it cannot be considered modern. Modernity consists simply of integrating the cargo pier into the system of handling cargo from and to the ocean-going vessel. In summary—the modern cargo terminal is one that is in functional harmony with modern transportation techniques and practices.

Even though criteria for a modern facility have been presented, it must be emphasized that terminal design cannot be standardized. The main purpose of the paper is to stress the factors of modern-transportation technology that should govern the design. It is hoped that transport technology will continue to advance and that terminal design will be correspondingly progressive.

AMERICAN SOCIETY OF CIVIL ENGINEERS
Founded November 5, 1852
TRANSACTIONS

Paper No. 2805

SIMILARITY OF DISTORTED RIVER MODELS WITH MOVABLE BEDS

BY HANS A. EINSTEIN,[1] M. ASCE, AND NING CHIEN,[2] A. M. ASCE

WITH DISCUSSION BY MESSRS. THOMAS BLENCH; AND HANS A. EINSTEIN AND NING CHIEN

SYNOPSIS

The similarity conditions for distorted river models with movable beds are derived from the theoretical and empirical equations which describe the hydraulics and the sediment transport in such rivers. A complete numerical example is used to demonstrate the method of application to a particular river.

INTRODUCTION

There are many problems in hydraulic engineering for which the basic equations are known but which are geometrically so complicated that the direct application of the equations is impossible. Many such problems can be solved by the use of models which duplicate this complicated geometry and in which the resulting flow patterns can be observed directly. Such models permit the prediction of the corresponding prototype flows quantitatively only if the exact laws of model similarity are known. The prediction of the model scales cannot be based on simple dimensional considerations if the model is distorted and the motion of a movable bed is involved. A different approach must be used to find compatible systems of model scales and distortions.

In 1944, there was published a short account[3] of methods for finding compatible systems of scales. It was proposed therein that model scales be derived from empirical working equations rather than from the underlying differential equations of motion. It was also noted that equations must be used which

---

NOTE.—Published, essentially as printed here, in December, 1954, as *Proceedings-Separate No. 566*. Positions and titles given are those in effect when the paper or discussion was approved for publication in *Transactions*.

[1] Prof. of Hydr. Eng., Univ. of California, Berkeley, Calif.

[2] Associate Prof. of Hydraulics, Tsing Hwa Univ., Peiping, China; formerly Asst. Research Engr., Inst. of Eng. Research, Univ. of California, Berkeley, Calif.

[3] Discussion by H. A. Einstein of "Conformity Between Model and Prototype: A Symposium," *Transactions*, ASCE, Vol. 109, 1944, p. 134.

are applicable in the same form to both model and prototype and which preferably have the form of power functions; this approach will be used herein. Many subsequent developments in the description of flow and sediment transport in alluvial rivers will be incorporated.

Before the conditions of similarity can be stated it is necessary to define the exact meaning of the term. Similarity may be said to exist if (*a*) to each point, time, and process in one scale which may be termed the prototype, a corresponding point, time, and process of the other scale, which may be termed the model, can be coordinated uniquely and (*b*) the ratios of corresponding physical magnitudes between model and prototype are constant for each type of physical magnitude. For an undistorted model this definition implies that all magnitudes of equal dimension must follow the same scale ratio and also that the various laws which interrelate the variables, parameters, and constants of the prototype must apply to the model as well. The results of the operation of such a hydraulic model may thus be transferred to the prototype by the use of the scale ratios. A distortion in the physical sense exists if there are two types of variables or parameters of equal dimension in the same problem which are physically sufficiently independent so that they can be given different scale ratios.

The application of distortions in engineering is not novel; examples can be found in presentations of flat sections and profiles. The desirability of such distortion in hydraulic models has become apparent to everyone who has tried to design a model of wide and shallow watercourses in which large horizontal dimensions call for a model scale which is much too small for application to the vertical direction. Such a small water depth would often cause laminar flow in the model which cannot be used to duplicate the turbulent prototype flow. Many laboratories have built models in which the vertical scale is much larger than the horizontal scale. It is impossible, however, to introduce only one distortion. This fact is apparent in the case of side slopes distorted in the same manner as vertical heights. The velocity scale must be chosen to satisfy the Froude condition and will satisfy the friction equation only if the roughness of the various boundaries is also properly distorted. It will be shown subsequently that in the case of a sediment-carrying stream still more distortions must be introduced to balance their effects in the various equations describing flow and sediment motion.

NOTATION

The letter symbols adopted for use in this paper are defined where they first appear, in the illustrations or in the text, and are arranged alphabetically, for convenience of reference, in the Appendix. The symbols with the subscripts p and M indicate quantities in prototype and model, respectively. The ratio of corresponding values in the two scales is denoted by the subscript r. The ratio of depth scales, for example, is defined as $h_r = h_p/h_M$.

DISTORTIONS

In this study several distortions are contemplated:

1. If the ratio of horizontal lengths L_r is independent of h_r, the model is vertically distorted.

2. If the grain-size ratio D_r is different from both L_r and h_r, a third length scale is introduced and with it a second distortion.

3. If the slope ratio S_r is chosen independent of L_r and h_r, the model is assumed to be tilted in addition to the other distortions.

4. If the ratio of effective densities of the sediment $(\rho_s - \rho_f)_r$ is assumed to be different from the ratio of the fluid densities ρ_{f_r} which is unity, there is a fourth distortion.

5. A fifth distortion is introduced if the hydraulic-time ratio t_{1r} for the time values involved in the determination of velocities and sediment rates is chosen different from the secimentation-time ratio t_{2r} of durations for individual flow conditions, indicating the speed at which flow-duration curves are duplicated.

6. A sixth distortion is a result of the impossibility of obtaining suspended-load rates in a model in the same scale at which the bed-load rates are reproduced; that is, the bed-load-rate ratio q_{Br} is different from the total-load-rate ratio q_{Tr}.

7. A seventh and last distortion permits the ratio of settling velocities V_{sr} of corresponding grains to be different from the ratio of corresponding flow velocities.

RELATIONSHIPS DESCRIBING ALLUVIAL FLOWS

As it has been noted previously, the flow and sediment description of the alluvial reaches to be studied in the model must be accomplished by identical formulas for model and prototype. These formulas can be transformed into relationships between the various ratios and thus represent conditions which must be satisfied when the various distortions are chosen. The individual relationships shall be cited using equations that have been presented elsewhere.[4] It is not believed that the choice of the equations in the exact form presented herein is a strong restriction to the generality of the method. Even if one prefers to substitute different formulas for the ones offered herein, it will be found that it is not possible to change the number of equations which must be satisfied in a particular problem. It is thus apparent that one must have the same number of conditions and, therefore, the same number of degrees of freedom in choosing the ratios. It will be found that the substitute equations will contain the same variables and that the entire difference will be a slightly changed set of exponents.

Friction Criterion.—It has been noted[4,5,6] that the flow in an alluvial channel cannot generally be described by one formula with universal constants but that it must be interpreted as a composite effect, the various parts of which follow different and independent laws. It can easily be shown that no distorted model is possible if the friction criterion is formulated as an identity—that is, if one stipulates that both the grain resistance (surface drag) and the bar resistance (shape resistance) must both be similar. Actually this is not necessary for over-all similarity as long as the total friction is similar. It is proposed, therefore, that the frictional similarity be based on the behavior of the entire section for which it assumes the form of a rating curve. As most rating curves approximate a straight line if the total discharge Q is plotted against the stages on a log-log chart, it is assumed that the prototype and the model channel can be described by an equation of the form,

---

[4] "The Bed-Load Function for Sediment Transportation in Open Channel Flows," by Hans A. Einstein, *Technical Bulletin No. 1026*, U. S. Dept. of Agriculture, Washington, D. C., September, 1950.

[5] "River Channel Roughness," by Hans A. Einstein and Nicholas L. Barbarossa, *Transactions*, ASCE, Vol. 117, 1952, pp. 1121–1146.

[6] "Linearity of Friction in Open Channels," by Hans A. Einstein and R. B. Banks, Association Internationale d'Hydrologie Scientifique, Assemblée Générale de Bruxelles, 1951, pp. 488–498.

$$V = \frac{C\sqrt{g}}{D^m} S^{1/2} h^{(1/2+m)} \dots\dots\dots\dots\dots\dots (1)$$

which is a generalized Manning equation. In Eq. 1, V represents flow velocity, C is a constant, g denotes gravitational acceleration, h is the hydraulic radius and is characteristic of a depth, and the superscript m is an unknown. Eq. 1 becomes identical to the Manning equation when $m = 1/6$ and if one uses[7] the relationship $n \sim D^{1/6}$, in which n is a friction factor. If it is assumed that the exponent m can be used to describe both the prototype and the model relationships, at least for the most important range of discharges, the equation between ratios can be written as

$$V^2{}_r\, S^{-1}{}_r\, h^{-1-2m}{}_r\, D^{2m}{}_r\, C^{-2}{}_r = \Delta_v \dots\dots\dots\dots\dots\dots (2)$$

The value of Δ_v is unity if the similarity between prototype and model is exactly satisfied but may indicate a small deviation from exact similarity if such a deviation is necessary for any practical reason.

Whereas V_r, S_r, h_r, and D_r are ratios which will recur in other equations, m and C_r are the exponent and the ratio of the constants in the generalized Eq. 1—

$$\frac{V}{\sqrt{R_T S g}} = C\left(\frac{R_T}{K_s}\right)^m \dots\dots\dots\dots\dots\dots (3)$$

in which R_T is the hydraulic radius of the total section with the bottom width as the wetted perimeter and K_s denotes the grain size of the bed which is representative in its grain roughness. If one can assume that the grain mixtures in the model are similar to those in the prototype, the ratio of the K_s-values equals that of the grain sizes D. The values of C must be determined individually for model and prototype, and the ratio must be found for a representative average channel section. The hydraulic radius R_T assumes the value,

$$R_T = \frac{A_T}{P_b} = \frac{A'_b + A''_b + A_W}{P_b} = \frac{R'_b P_b + R''_b P_b + R_W P_W}{P_b}$$
$$= R'_b + R''_b + \frac{R_W P_W}{P_b} \dots\dots\dots\dots\dots\dots (4)$$

In Eq. 4, A_T is the total cross-sectional area, P_b denotes the wetted perimeter of the bed, A'_b is the cross-sectional area pertaining to the grains, A''_b represents the cross-sectional area pertaining to the irregularities, A_W is that part of the cross section pertaining to the banks, R'_b denotes the hydraulic radius with respect to the grains, R''_b is the hydraulic radius for the channel irregularities, R_W represents the hydraulic radius with respect to the bank, and P_W is the wetted perimeter of the banks. The model values of C and m can only be determined by a trial-and-error method as they depend on the choice of the remaining scale ratios. This procedure will be explained in the example of the model of Big Sand Creek in Mississippi.[4]

---

[7] "Laws of Turbulent Flow in Open Channels," by G. H. Keulegan, *Report No. 1151*, U. S. National Bureau of Standards, U. S. Dept. of the Interior, Washington, D. C., 1938, p. 738.

Froude Criterion.—In open-channel flows, Froude's law is one of the principal criteria as it balances the gravitational forces against the inertia forces. Because the energy content of the flow can be divided into its kinetic and potential parts as velocity head and depth, both are correlated by

$$\frac{V^2}{2\,g} + h = \text{constant} \qquad (5)$$

Although in river channels the slope of the water surface is often very small, one must remember that it is the gravitational force which maintains the flow. Furthermore, any river-improvement plan usually involves certain river constrictions such as training walls, jetties, and groins along the banks. At the constricted sections and especially in the neighborhood of the structures, the elevation of the water surface may change rapidly. It is, therefore, advisable to include the Froude law as one of the criteria in designing river models because it assures similarity of flow and energy loss around structures and other channel irregularities.

There appears to be a possibility that the Froude criterion loses its significance in deep rivers when the Froude number is very low; that is, when $\mathsf{F} = V^2/(g\,D) \ll 1$. Velocity changes do not affect the depths materially in this case, and any possible energy losses are taken care of in the friction criterion. No experience exists (as of 1955), however, with models which eliminate entirely the Froude criterion.

The Froude law may be written in ratios as

$$V_r\, h^{-1/2}_r = \Delta_{\mathsf{F}} \qquad (6)$$

Again $\Delta_{\mathsf{F}} = 1$ indicates exact similarity, and a deviation from unity signifies a possible necessary deviation from the exact solution.

Sediment-Transport Criterion.—In order to have similar sediment-transport conditions near the bed it is, in general, necessary that both the intensity of transport Φ_* and the intensity of shear Ψ_* for the individual grain sizes be equal in model and prototype as these two quantities are not connected by a power-type equation. Only if the transport rates are restricted to a very narrow range of values is it possible to combine the two conditions. The equality of the values,

$$\Phi_* = \frac{i_B}{i_b}\,\frac{q_B}{g(\rho_s - \rho_f)}\left(\frac{\rho_f}{\rho_s - \rho_f}\right)^{1/2}\left(\frac{1}{g\,D^3}\right)^{1/2} \qquad (7)$$

is possible for all fractions of a mixture only if the two mixtures are similar so that the ratios of the i-values become equal to unity. In Eq. 7, i_B is that fraction of bed load in a given grain-size range and i_b denotes that fraction of bed material in a given grain-size range. With ρ_f equal in model and prototype, the equation of equal Φ_*-values can be written as

$$q_{Br}\,(\rho_s - \rho_f)^{-3/2}{}_r\, D^{-3/2}{}_r = 1 \ldots\ldots\ldots\ldots\ldots\ldots (8)$$

No deviation from Eq. 8 is usually desired.

Zero Sediment-Load Criterion.—The equality of Ψ_*-values in model and prototype is often interpreted as the condition of similar flow at the beginning of sediment motion. It can be expressed as equal Ψ_*-values—

$$\Psi_* = \frac{\rho_s - \rho_f}{\rho_f}\,\frac{D}{R_b\,S}\,\xi\,Y\left[\frac{\log_{10} 10.6}{\log_{10} 10.6\,\dfrac{X}{\Delta}}\right]^2 \ldots\ldots\ldots\ldots (9)$$

in which ξ is the "hiding factor" of the grains in the mixture, Y denotes the pressure correction for Ψ_* in the transition from smooth to rough friction along the bed, X is the characteristic grain size of the mixture, and Δ represents the apparent roughness diameter. In order to analyze the significance of all the corrections, one must realize that ξ is different for the various grain sizes of a mixture. For the larger sizes, both in model and prototype, ξ has the value of unity. For similarity, the ratio of ξ-values must be unity for all sizes. Because ξ is a function of D/X, D_r must equal X_r. It has been found[4] that (*a*) X is equal to 1.39 δ for Δ/δ less than 1.8, (*b*) X equals 0.77 Δ for Δ/δ greater than 1.8, and (*c*) Y is a function of (K_s/δ) with Δ equal to K_s/x and x a function of (K_s/δ). In the foregoing, δ is the thickness of the laminar sublayer and x is the parameter for transition from smooth to rough friction. With $(K_s)_r$ equal to D_r by definition, it can be seen that, in general, similarity will be possible only if δ_r is equal to D_r. This condition will permit some slight deviation, however, as it controls only some corrections. With δ_r equal to D_r, x_r is equal to unity and Δ_r equals D_r. Thus, in ratios, equality of corresponding Ψ_*-values is expressed by

$$(\rho_s - \rho_f)_r\, D_r\, \eta^{-1}{}_r\, h^{-1}{}_r\, S^{-1}{}_r = 1 \ldots\ldots\ldots\ldots\ldots\ldots (10)$$

in which η is the ratio of the hydraulic radius R'_b referred to the surface drag to the entire radius R_T. This correction must be introduced as R_{Tr} is equal to h_r but R'_{br} does not equal h_r.

Laminar-Sublayer Criterion.—As has been shown δ_r must usually equal D_r for similarity. This can be written, in ratios, as

$$D_r\, \eta^{1/2}{}_r\, h^{1/2}{}_r\, S^{1/2}{}_r = \Delta_\delta \ldots\ldots\ldots\ldots\ldots\ldots\ldots\ldots (11)$$

Again, a slight deviation of the value Δ_δ from unity can be permitted especially in cases in which the bulk of the bed is considerably coarser than δ and, therefore, not directly affected by its value. In the derivation of Eq. 11 it should be noted that δ is dependent on the surface drag only and thus must contain

$$u_* = \sqrt{R'_b\,S\,g} \ldots\ldots\ldots\ldots\ldots\ldots\ldots\ldots (12)$$

which has the ratio, $\eta^{1/2}{}_r\, h^{1/2}{}_r\, S^{1/2}{}_r$. In Eq. 12, u_* is the shear velocity with respect to the grain. The viscosity ν is assumed to be equal in model and prototype but can be introduced differently if necessary.

Additional Relationships Describing Alluvial Flows

By computing some characteristic flows in model and prototype the ratio of q_T to q_B, the average ratio of these ratios, q_{Tr}/q_{Br}, can be determined; it may be termed B. This value can be used to give a general relationship between the two load ratios—

$$q_{Br}\, q^{-1}{}_{Tr}\, B = 1 \ldots\ldots\ldots\ldots (13)$$

Hydraulic time t_1 may be defined as the time which a water particle takes to move with velocity V through a distance L—

$$V_r\, t_{1r}\, L^{-1}{}_r = 1 \ldots\ldots\ldots\ldots (14)$$

The time t_2 may indicate the duration of individual flows. Ratios of this time must be such that corresponding time intervals are required by corresponding sediment rates q_T to fill corresponding volumes. Expressed in ratios this equation can be written for the unit width as

TABLE 1.—Exponents for Model Laws for River Models with Sediment Motion[a]

Eq.	L_r	h_r	V_r	S_r	D_r	$(\rho_s-\rho_f)_r$	q_{Br}	q_{Tr}	t_{1r}	t_{2r}	B	C_r	η_r	Δ_V	Δ_F	Δ_δ	Δ_N	
2		$-1-2m$	2	−1	$2m$							−2		−1				=1
6		−1	2												−2			=1
8					−3	−3	2											=1
10		−1		−1	1	1							−1					=1
11		1		1	2								1			−2		=1
13							1	−1			1							=1
14	−1		1						1									=1
15	−1	−1				−1		1		1								=1
16	−1	−1		1													−1	=1

[a] The values of B, C_r, η_r, and m are determined from auxiliary computations. Values of Δ may be chosen to suit the conditions.

$$q_{Tr}\, t_{2r}\, L^{-1}{}_r\, h^{-1}{}_r\, (\rho_s - \rho_f)^{-1}{}_r = 1 \ldots\ldots\ldots\ldots (15)$$

assuming the porosity of the deposits to be equal in model and prototype; the sediment rates q_T are measured in weight under water. The time t_{2r} is the time scale at which the prototype hydrographs must be repeated in the model.

Independent ratios have been introduced in this study for length, height, and slope, implying that the model is not only vertically distorted but also tilted. Because the tilt is applied to the model during construction and because it is assumed to be proportional to the prototype slope, it can be applied only to flows which have, at all points, water-surface slopes and energy-line slopes which are constant with time. This condition is not fulfilled when the flow reverses direction, such as under the influence of the tide or in most overbank flows. In all such cases no additional tilt can be permitted—

$$S_r\, L_r\, h^{-1}{}_r = \Delta_N \ldots\ldots\ldots\ldots (16)$$

in which Δ_N is equal to unity when there is zero tilt. A small tilt is represented by a small deviation of Δ_N from unity.

SOLUTION OF THE SIMILARITY EQUATIONS

Table 1 gives the nine independent equations which have been introduced herein as products of powers of the various ratios equal to unity; the values in Table 1 are the exponents of the various ratios. There appear thirteen ratios (of which ten are free), the exponent m, and four Δ-values. The exponent m and the three last ratios must be determined by auxiliary computations (as shown in the subsequent problem), and the Δ-values can be chosen to suit the conditions.

Between the ten free ratios there are nine equations to be satisfied so that only one of the ten can be chosen freely if the Δ-values are held rigidly to unity or to some other fixed value. If some of the Δ-values are permitted to deviate from unity by a certain margin, it is possible to choose two or more of the free ratios within certain limits.

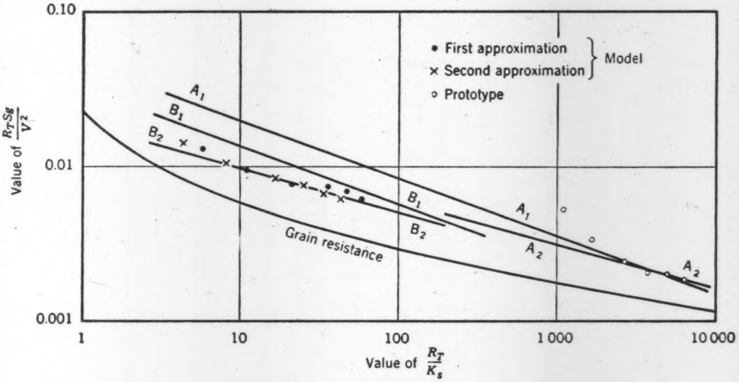

FIG. 1.—FRICTION CONDITION FOR BIG SAND CREEK IN MODEL AND PROTOTYPE

The nine equations are solved in Table 2 in three different ways—first, with the vertical scale h_r chosen freely, then with the horizontal scale L_r chosen, and finally, with the density of the model sediment chosen. One of the solutions will usually satisfy the particular need in designing the model. The exact solution is obtained with all Δ-values equal to unity. If some deviations of Δ from unity are accepted, it is possible to choose more than one scale arbitrarily. This is sometimes necessary when the size of the model is governed by the available space and the sediment density is determined by the availability of materials for the particular purpose. The design of a complete set of distorted model scales will be demonstrated subsequently on a fictitious model of Big Sand Creek, the channel of which was used previously as an example for a sediment-load computation.[4]

TABLE 2.—MODEL RATIOS FOR OPEN-CHANNEL FLOWS WITH SEDIMENT MOTION [a]

Symbol	h_r	L_r	$(\rho_s - \rho_f)_r$	C_r	η_r	B	Δ_F	Δ_δ	Δ_N	Δ_v
				(*a*) DEPTH RATIO, h_r, CHOSEN						
L_r	$\frac{4m+1}{m+1}$	…	…	$\frac{2}{m+1}$	$\frac{m}{m+1}$	…	$\frac{-2}{m+1}$	$\frac{-2m}{m+1}$	1	$\frac{1}{m+1}$
V_r	$\frac{1}{2}$	…	…	…	…	…	1	…	…	…
S_r	$\frac{-3m}{m+1}$	…	…	$\frac{-2}{m+1}$	$\frac{-m}{m+1}$	…	$\frac{2}{m+1}$	$\frac{2m}{m+1}$	…	$\frac{-1}{m+1}$
D_r	$\frac{2m-1}{2(m+1)}$	…	…	$\frac{1}{m+1}$	$\frac{-1}{2(m+1)}$	…	$\frac{-1}{m+1}$	$\frac{1}{m+1}$	…	$\frac{1}{2(m+1)}$
$(\rho_s - \rho_f)_r$	$\frac{3(1-2m)}{2(m+1)}$	…	…	$\frac{-3}{m+1}$	$\frac{3}{2(m+1)}$	…	$\frac{3}{m+1}$	$\frac{2m-1}{m+1}$	…	$\frac{-3}{2(m+1)}$
q_B	$\frac{3(1-2m)}{2(m+1)}$	…	…	$\frac{-3}{m+1}$	$\frac{3}{2(m+1)}$	…	$\frac{3}{m+1}$	$\frac{3m}{m+1}$	…	$\frac{-3}{2(m+1)}$
q_{Tr}	$\frac{3(1-2m)}{2(m+1)}$	…	…	$\frac{-3}{m+1}$	$\frac{3}{2(m+1)}$	1	$\frac{3}{m+1}$	$\frac{3m}{m+1}$	…	$\frac{-3}{2(m+1)}$
t_{1r}	$\frac{7m+1}{2(m+1)}$	…	…	$\frac{2}{m+1}$	$\frac{m}{m+1}$	…	$\frac{-(m+3)}{m+1}$	$\frac{-2m}{m+1}$	1	$\frac{1}{m+1}$
t_{2r}	$\frac{5m+2}{m+1}$	…	…	$\frac{2}{m+1}$	$\frac{m}{m+1}$	−1	$\frac{-2}{m+1}$	$\frac{-(3m+1)}{m+1}$	1	$\frac{1}{m+1}$
				(*b*) LENGTH RATIO, L_r, CHOSEN						
h_r	…	$\frac{m+1}{4m+1}$	…	$\frac{-2}{4m+1}$	$\frac{-m}{4m+1}$	…	$\frac{2}{4m+1}$	$\frac{2m}{4m+1}$	$\frac{-(m+1)}{4m+1}$	$\frac{-1}{4m+1}$
V_r	…	$\frac{m+1}{2(4m+1)}$	…	$\frac{-1}{4m+1}$	$\frac{-m}{2(4m+1)}$	…	$\frac{2(2m+1)}{4m+1}$	$\frac{m}{4m+1}$	$\frac{-(m+1)}{2(4m+1)}$	$\frac{-1}{2(4m+1)}$
S_r	…	$\frac{-3m}{4m+1}$	…	$\frac{-2}{4m+1}$	$\frac{-m}{4m+1}$	…	$\frac{2}{4m+1}$	$\frac{2m}{4m+1}$	$\frac{3m}{4m+1}$	$\frac{-1}{4m+1}$

D_r	...	$\frac{2m-1}{2(4m+1)}$	...	$\frac{2}{4m+1}$	$\frac{-(2m+1)}{2(4m+1)}$	...	$\frac{-2}{4m+1}$	$\frac{2m+1}{4m+1}$	$\frac{1-2m}{2(4m+1)}$	$\frac{1}{4m+1}$
$(\rho_s-\rho_f)_r$	...	$\frac{3(1-2m)}{2(4m+1)}$	...	$\frac{-6}{4m+1}$	$\frac{3(2m+1)}{2(4m+1)}$	...	$\frac{6}{4m+1}$	$\frac{2m-1}{4m+1}$	$\frac{3(2m-1)}{2(4m+1)}$	$\frac{-3}{4m+1}$
q_{Br}	...	$\frac{3(1-2m)}{2(4m+1)}$	...	$\frac{-6}{4m+1}$	$\frac{3(2m+1)}{2(4m+1)}$	...	$\frac{6}{4m+1}$	$\frac{6m}{4m+1}$	$\frac{3(2m-1)}{2(4m+1)}$	$\frac{-3}{4m+1}$
q_{Tr}	...	$\frac{3(1-2m)}{2(4m+1)}$	...	$\frac{-6}{4m+1}$	$\frac{3(2m+1)}{2(4m+1)}$	1	$\frac{6}{4m+1}$	$\frac{6m}{4m+1}$	$\frac{3(2m-1)}{2(4m+1)}$	$\frac{-3}{4m+1}$
t_{1r}	...	$\frac{7m+1}{2(4m+1)}$	...	$\frac{1}{4m+1}$	$\frac{m}{2(4m+1)}$	...	$\frac{-2(2m+1)}{4m+1}$	$\frac{-m}{4m+1}$	$\frac{m+1}{2(4m+1)}$	$\frac{1}{2(4m+1)}$
t_{2r}	...	$\frac{5m+2}{4m+1}$	...	$\frac{-2}{4m+1}$	$\frac{-m}{4m+1}$	−1	$\frac{2}{4m+1}$	$\frac{-(2m+1)}{4m+1}$	$\frac{-(m+1)}{4m+1}$	$\frac{-1}{4m+1}$
(c) SEDIMENT-DENSITY RATIO, $(\rho_s-\rho_f)_r$, CHOSEN										
L_r	...	...	$\frac{-2(4m+1)}{3(2m-1)}$	$\frac{-4}{2m-1}$	$\frac{2m+1}{2m-1}$	...	$\frac{4}{2m-1}$	$\frac{2}{3}$	1	$\frac{-2}{2m-1}$
h_r	...	...	$\frac{-2(m+1)}{3(2m-1)}$	$\frac{-2}{2m-1}$	$\frac{1}{2m-1}$	...	$\frac{2}{2m-1}$	$\frac{2}{3}$	...	$\frac{-1}{2m-1}$
V_r	...	...	$\frac{-(m+1)}{3(2m-1)}$	$\frac{-1}{2m-1}$	$\frac{1}{2(2m-1)}$	...	$\frac{2m}{2m-1}$	$\frac{1}{3}$	...	$\frac{-1}{2(2m-1)}$
S_r	...	...	$\frac{2m}{2m-1}$	$\frac{2}{2m-1}$	$\frac{-2m}{2m-1}$	...	$\frac{-2}{2m-1}$	...	...	$\frac{1}{2m-1}$
D_r	...	...	$-\frac{1}{3}$	...	...	...	...	$\frac{2}{3}$	...	...
q_{Br}	...	...	1	...	...	...	...	1	...	...
q_{Tr}	...	...	1	...	...	1	...	1	...	...
t_{1r}	...	...	$\frac{-(7m+1)}{3(2m-1)}$	$\frac{-3}{2m-1}$	$\frac{4m+1}{2(2m-1)}$	...	$\frac{2(2-m)}{2m-1}$	$\frac{1}{3}$	1	$\frac{-3}{2(2m-1)}$
t_{2r}	...	...	$\frac{-2(5m+2)}{3(2m-1)}$	$\frac{-6}{2m-1}$	$\frac{2(m+1)}{2m-1}$	−1	$\frac{6}{2m-1}$	$\frac{1}{3}$	1	$\frac{-3}{2m-1}$

[a] Solution with known effects of omitting Eqs. 2, 6, 11, and 16.

THE BIG SAND CREEK MODEL

The friction conditions in the Big Sand Creek prototype are summarized in Table 3[8] with $S = 0.001050$ and $D_{65} = K_s = 0.00115$ ft.

A similar hydraulic pattern for the model is obtained by trial and error. First, the length scale $L_r = 150$ is chosen on the basis of available room. Then the prototype friction is plotted in Fig. 1 as $(R_T\,S\,g)/V^2$ versus R_T/K_s (open-circle symbol) and the points for the higher discharges are approximated by the line $A_1 - A_1$ with the relationship,

TABLE 3.—FRICTION CONDITIONS, BIG SAND CREEK

R'_b, in feet	R''_b, in feet	R_J, in feet	V, in feet per second	η_p	$\frac{R_T S g}{V^2}$	$\frac{R_T}{K_s}$	$\frac{R'_b S g}{V^2}$	$\frac{R'_b}{K_s}$	Q, in cubic feet per second
0.50	0.86	1.30	2.92	0.384	0.00515	1,130	0.00198	435	409
1.00	0.76	1.92	4.44	0.520	0.00330	1,670	0.00172	870	1,110
2.00	0.50	3.06	6.63	0.653	0.00236	2,660	0.00154	1,740	3,710
3.00	0.30	4.40	8.40	0.682	0.00211	3,820	0.00144	2,610	9,160
4.00	0.14	5.73	9.92	0.698	0.00197	4,980	0.00137	3,480	19,850
5.00	0.07	7.04	11.30	0.711	0.00186	6,110	0.00132	4,350	35,700

$$\frac{V^2}{R_T\,S\,g} = 21.05\left(\frac{R_T}{K_s}\right)^{0.372} \quad \dots\dots\dots\dots\dots\dots (17)$$

Next, the model resistance is chosen to follow the line $B_1 - B_1$ with the equation,

$$\frac{V^2}{R_T\,S\,g} = 30.76\left(\frac{R_T}{K_s}\right)^{0.372} \quad \dots\dots\dots\dots\dots\dots (18)$$

TABLE 4.—FIRST APPROXIMATION

R'_b, in feet	u'_*, in feet per second	δ, in feet	$\frac{D_{65}}{\delta}$	x	Δ in feet	$\text{Log}_{10}\left(12.27\frac{R'_b}{\Delta}\right)$	V, in feet per second	Ψ'	$\frac{V}{u''_*}$
0.0134	0.0425	0.00289	1.22	1.59	0.00221	1.872	0.458	3.02	16.80
0.0268	0.0601	0.00204	1.72	1.46	0.00241	2.135	0.738	1.51	27.0
0.0536	0.0850	0.00145	2.44	1.27	0.00277	2.376	1.160	0.72	51.0
0.0805	0.1042	0.00118	2.98	1.18	0.00298	2.520	1.51	0.50	87.0
0.1072	0.1202	0.00102	3.44	1.14	0.00309	2.630	1.82	0.38	150
0.1342	0.1348	0.00091	3.86	1.10	0.00320	2.712	2.10	0.30	240

From the relationships given in Eqs. 17 and 18 one can find the values of C and m: $C_p = 4.595$, $C_m = 5.55$, $C_r = 0.827$, and $m = 0.186$. Assuming that $\eta\,r = 1$ and all Δ-values $= 1$,

$$\begin{aligned}
h_r &= L_r^{(m+1)/(4m+1)}\,C_r^{-2/(4m+1)}\,\eta_r^{-m/(4m+1)} \\
&= 150^{0.68} \times 0.827^{-1.147} = 37.3 \\
S_r &= L_r^{(-3m)/(4m+1)}\,C_r^{-2/(4m+1)}\,\eta_r^{-m/(4m+1)} \\
&= 150^{-0.32} \times 0.827^{-1.147} = 0.25 \\
D_r &= L_r^{(2m-1)/[2(4m+1)]}\,C_r^{2/(4m+1)}\,\eta_r^{-(2m+1)/[2(4m+1)]} \\
&= 150^{-0.18} \times 0.827^{1.147} = 0.326
\end{aligned}$$

---

[8] "The Bed-Load Function for Sediment Transportation on Open Channel Flows," by Hans A. Einstein, *Technical Bulletin No. 1026*, U. S. Dept. of Agriculture, Washington, D. C., September, 1950, p. 52, Table 6.

and

$$(\rho_s - \rho_f)_r = D^{-3}{}_r = 28.6.$$

From these ratios, the model values obtained are

$$S_M = \frac{0.00105}{0.25} = 0.0042$$

$$\rho_{SM} = 1.059 \text{ g per cu cm}$$

$$D_{35M} = 0.00288 \text{ ft}$$

and

$$D_{65M} = K_{SM} = 0.00352 \text{ ft.}$$

The model hydraulics of the first approximation is given in Table 4. The values of R'_b used in Table 4 correspond to those used in the prototype for $\eta_r\, h_r$ equal to 37.3. The values of the wall friction, of stage, and of R_T are determined by the trial-and-error method given in Table 5 and Fig. 2. First, the model bank roughness must be chosen. The prototype banks are rather rough, and it is assumed that the Manning formula applies in model and prototype. The wetted perimeter of the banks was assumed in the prototype computation[4] to equal twice the water depth. In order to make the wall friction an equivalent part of the total friction in model and prototype,

$$A_{W_r} = R_{W_r}\, P_{W_r} = L_r\, h_r \ldots\ldots\ldots\ldots\ldots\ldots (19)$$

OF MODEL HYDRAULICS

u''_*, in feet per second	R''_b, in feet	R_b, in feet	Stage, in feet	R_T, in feet	$\frac{R_T\, S\, g}{V^2}$	$\frac{R_T}{K_s}$	η_M	η_p	η_r
0.0273	0.0055	0.0189	4.010	0.020	0.0129	5.68	0.670	0.384	0.573
0.0273	0.0055	0.0323	4.034	0.0375	0.0093	10.64	0.714	0.520	0.730
0.0227	0.0038	0.0574	4.086	0.075	0.0076	21.3	0.716	0.653	0.911
0.0174	0.0022	0.0827	4.172	0.1240	0.0074	35.2	0.650	0.682	1.050
0.0121	0.0011	0.1083	4.260	0.1650	0.0068	46.4	0.650	0.698	1.073
0.0087	0.0006	0.1348	4.340	0.2000	0.0061	56.8	0.672	0.711	1.060

from which, for $P_{W_r} = h_r$, $R_{W_r} = L_r$. In the Manning equation for the banks,

$$V_r = \frac{1}{n_{W_r}} R^{2/3}{}_{W_r}\, S^{1/2}{}_r \ldots\ldots\ldots\ldots\ldots\ldots (20)$$

one obtains n_{W_r} by introducing previously determined values and $\Delta = 1$,

$$n_{W_r} = \frac{1}{V_r} R^{2/3}{}_{W_r}\, S^{1/2}{}_r = h^{-1/2}{}_r\, L^{2/3}{}_r \left(\frac{h_r}{L_r}\right)^{1/2} = L^{1/6}{}_r \ldots\ldots (21)$$

From the foregoing,

$$n_{W_r} = \sqrt[6]{150} = 2.305$$

$$n_{WM} = \frac{0.050}{2.305} = 0.0217$$

and

$$R_W = \left(\frac{V\, \eta_W}{1.486\, S^{1/2}} \right)^{3/2} = \frac{V^{3/2}}{9.34}$$

Fig. 2 gives, first, the curves of P_W, P_b, R_T, and A_T as functions of the stage, all derived from corresponding prototype curves and similarity scales (solid curves). For each computed value of R_b, values of A_T are determined from Table 5 for various fictitious values of the stage. These A_T-values for each R_b-value are connected by a dashed line. The intersection with the solid A_T-curve indicates the actual stage at which the R_b-value occurs. These values of R_T are used in Table 4 to determine η_r for the first approximation. Also, $R_T\, S\, g/V^2$ is computed and plotted in Fig. 1 against R_T/K_s. It may be seen in Fig. 1 that the first assumed line $B_1 - B_1$ was somewhat too high and too steep to describe the model points.

TABLE 5.—DETERMINATION OF HYDRAULIC RADIUS BY TRIAL AND ERROR

R_b, in feet	R_W, in feet	Stage, in feet	P_b, in feet	P_W, in feet	$P_b\,R_b$, in square feet	$P_W\,R_W$, in square feet	A_T, in square feet
0.0189	0.0332	4.000	0.50	...	0.00945	...	0.0095
		4.050	0.86	0.07	0.0162	0.0023	0.0185
		4.100	1.22	0.17	0.02285	0.00565	0.0285
0.0328	0.0672	4.000	0.50	...	0.01615	...	0.0162
		4.050	0.86	0.07	0.0278	0.0047	0.0325
		4.100	1.22	0.17	0.0394	0.0114	0.0508
0.0574	0.1340	4.050	0.86	0.07	0.0493	0.0094	0.0587
		4.100	1.22	0.17	0.0700	0.0228	0.0928
		4.150	1.57	0.27	0.0900	0.0362	0.1261
0.0827	0.1985	4.100	1.22	0.17	0.1010	0.0338	0.1348
		4.150	1.57	0.27	0.1300	0.0536	0.1836
		4.200	1.95	0.37	0.1612	0.0735	0.2347
0.1083	0.264	4.200	1.95	0.37	0.2110	0.0978	0.3088
		4.250	2.36	0.47	0.2560	0.1240	0.3800
		4.300	2.85	0.57	0.3085	0.1508	0.4593
0.1348	0.326	4.300	2.85	0.57	0.3840	0.186	0.570
		4.350	3.36	0.67	0.4530	0.218	0.671
		4.400	3.87	0.77	0.5220	0.251	0.773

A second approximation of a line $A_2 - A_2$ for the prototype and (parallel to it) $B_2 - B_2$ for the model was therefore tried. The line $A_2 - A_2$ does not cover the two smallest prototype discharges and is therefore not correct except at the larger flows. This is a minor defect, however, as most of the transport and bed changes occur at medium and high flows.

The second approximation is based on line $A_2 - A_2$ for the prototype friction—

$$\frac{V^2}{R_T\, S\, g} = 44.5 \left(\frac{R_T}{K_s} \right)^{0.290} \qquad \text{(22)}$$

and on $B_2 - B_2$ for the model friction—

$$\frac{V^2}{R_T\, S\, g} = 52.6 \left(\frac{R_T}{K_s} \right)^{0.290} \qquad \text{(23)}$$

From these one obtains, for $L_r = 150$, $C_p = 6.66$, $C_M = 7.25$, $C_r = 0.902$, $m = 0.145$, and $\eta_r = 1.0$. The same formulas used in the first approximation result in $h_r = 42.25$, $S_r = 0.282$, $D_r = 0.292$, $(\rho_s - \rho_f)_r = 40$, and $V_r = 6.5$. These values lead to the following model dimensions: $S_M = 0.00372$, $D_{65M} = 0.00394$ ft, $D_{35M} = 0.00322$ ft, and $\rho_{sM} = 1.041$ g per cu cm. A new computation of the hydraulics on this basis gives the points (crosses) of Fig. 1, which still follow Eq. 23 with sufficient accuracy. The values for the model and the ratios of prototype and model values are thus assumed to be usable together with η_r equal to unity and L_r equal to 150. So far, Eqs. 2, 6, 10, 11, and 16 have been used; Eq. 14 gives

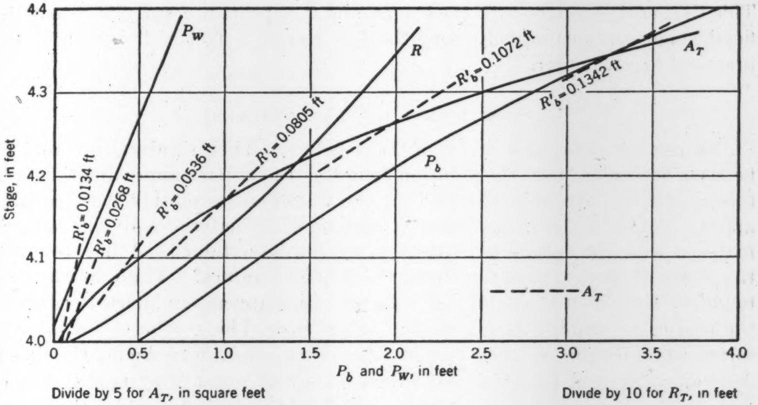

FIG. 2.—TRIAL-AND-ERROR SOLUTION FOR THE HYDRAULIC RADIUS

$$t_{1r} = L_r\, V^{-1}{}_r = 23.1$$

and Eq. 8 gives

$$q_{Br} = D^{3/2}{}_r\, (\rho_s - \rho_f)^{3/2}{}_r = 40.$$

TABLE 6.—DETERMINATION OF B–RATIOS

R'_{bp}, in feet	$(\Sigma i_T\, Q_T)_P$, in tons per day	$(\Sigma i_T\, q_T)_P$, in pounds under water per cubic foot per second	$(\Sigma i_T\, q_T)_M$, in pounds under water per cubic foot per second	Value of B	Value of t_{2r}	1 year duplicated in hours
0.5	700	0.9042	0.00173	1.36	4,650	1.89
1.0	3,790	0.420	0.00555	1.89	3,350	2.62
2.0	33,600	2.67	0.0184	3.63	1,745	5.02
3.0	156,000	9.11	0.0386	5.90	1,075	8.15
4.0	538,000	22.3	0.0685	8.15	778	11.28
5.0	1,433,000	46.2	0.1090	10.6	598	14.65

The value of q_{Tr} is determined from Eq. 13 which calls for the knowledge of the ratios B. These are determined in Table 6 which lists first the computed prototype total load $\Sigma i_T\, Q_T$ in tons per day.[9] In a table similar to that previously cited,[8] the corresponding model values have been computed and are given in the next column. The ratio of $(\Sigma i_B\, q_B)_p/(\Sigma i_B\, q_B)_M$ is equal to q_{B_r} as corresponding i_B-values are equal in prototype and model.

---

[9] "Conformity Between Model and Prototype: A Symposium," *Transactions*, ASCE, Vol. 109, 1944, p. 84, Table 8.

Eqs. 13 and 15 permit the determination of t_{2r} as

$$t_{2r} = L_r\, h_r\, (\rho_s - \rho_f)_r\, q^{-1}{}_{Br}\, B^{-1} = \frac{6{,}340}{B} \qquad (24)$$

This time scale changes with the stages, and it appears necessary to extend the flood stages proportionately over the low stages, a fact well known to the practical experimenter.

SIGNIFICANCE OF THE Δ-VALUES

No use has been made so far of the Δ-values. Their significance may best be seen beginning with the solution found as the second approximation. In this system a material is required for the model sediment that has a specific gravity of 1.041. Let it be assumed that no such material is available but a material with the specific gravity of 1.045 can be obtained. What would be the effect of such a deviation from the required values? This can easily be found by the choice of one of the Δ-values which appears to be least critical in the particular problem to absorb the deviations. The system of equations is solved again for the assumed values of L_r and $(\rho_s - \rho_f)_r$, introducing the chosen Δ as an additional variable. One then finds that an entirely new system of scales will result together with the magnitude of the deviation which the chosen Δ-value must undergo to satisfy the remaining equations.

CONCLUSIONS

It is likely that one has received the impression that all the complications involved in the method have no other effect than to make the system of similarities more and more unreliable. This is not true; what the method does is to show that a distorted river model is, at best, an acceptable compromise permitting the solution of certain problems which otherwise cannot be solved except by experimentation in the prototype, which under all conditions is more expensive. This method of designing a model has one great advantage over all other such methods: It permits the prediction of its reliability at least in a qualitative way; with respect to the choice of Δ-values it even gives such deviations quantitatively.

What are the most important reasons for the loss of similarity?

1. In the description of the channel friction the modified Manning formula cannot be expected to describe with equal *m*-values both model and prototype conditions over the entire range of discharges. It is necessary, therefore, to permit deviations in the friction relationship for the less important flow conditions. This fact is most important if a wide range of flow conditions exists in the problem area.

2. If flows must be considered in more than one channel, it is even more difficult to find a friction equation which describes all flows.

3. The total-load rates must be used to determine the time ratio t_2 for flow durations. Because the bed-load rates must be made similar to obtain similar bed configurations and as the ratio between bed-load rates and total-load rates changes with the stage, a sliding time scale appears to be necessary in many cases, especially if the range of discharges is wide. The determination of this scale is somewhat indeterminate if flow in more than one channel is important.

4. If the deposition of sediment in low-velocity areas—such as overbank areas or reservoirs—is an important phase of the problem under investigation, the wash load must be introduced into the model. Its characteristic is not given by the ability to be transported as bed load, however, but by its ability to remain in suspension permanently in the flow of the overbank areas.

Because of these difficulties it is absolutely necessary to verify the model and its scales. Such verification involves the reproduction of known prototype developments in the model by similar flows. Only if such a verification is possible and successful can the model be depended on for the prediction of future developments. It is common experience that the greatest difficulty in most model studies of this type is the gathering of the necessary prototype information for the construction, operation, and particularly the verification of the model. It is felt that this method of designing model scales shortens the time-consuming trial-and-error method of finding the proper model scales so much that more effort can be spent on reliable verification and determination of the basic river information.

ACKNOWLEDGMENT

This work represents results of research performed for the Corps of Engineers, United States Department of the Army, Missouri River Division, Omaha, Nebr., under contract with the University of California at Berkeley.

APPENDIX. NOTATION

The following symbols, adopted for use in the paper and for the guidance of discussers, conform essentially with "American Standard Letters Symbols for Hydraulics" (ASA Z10.2–1942), prepared by a committee of the American Standards Association, with Society representation, and approved by the Association in 1942:

A_T = total cross-sectional area:

- A_W = cross-sectional area pertaining to the banks;
- A'_b = cross-sectional area pertaining to the grains;
- A''_b = cross-sectional area pertaining to the irregularities;

B = ratio of q_{T_r} to q_{B_r};
C = constant in the generalized Manning equation;
D = grain size:
    D_{35} = grain size of which 35% is finer;
    D_{65} = grain size of which 65% is finer;
F = Froude number;
g = acceleration of gravity;
h = vertical lengths;
i_B = fraction of the bed load in a given grain-size range;
i_b = fraction of bed material in a given grain-size range;
i_T = fraction of total load in a given grain size;
K_s = grain size of the bed representative for its grain roughness;
L = horizontal length;
m = unknown superscript in the generalized Manning equation;
n = friction factor;
n_W = friction factor of the banks;
P = wetted perimeter:
    P_b = wetted perimeter of the bed;
    P_W = wetted perimeter of the banks;
Q = total discharge;
Q_{Tl} = total sediment load;
q_B = bed-load rate;
q_T = total-load rate;
R_T = hydraulic radius of the total section with the bottom width as the wetted perimeter:
    R_W = hydraulic radius with respect to the banks;
    R'_b = hydraulic radius with respect to the grains;
    R''_b = hydraulic radius with respect to the irregularities;
S = slope;
t_1 = hydraulic time;
t_2 = sedimentation time;
u'_* = shear velocity with respect to the grain;
u''_* = shear velocity for channel irregularities;
V = flow velocity;
V_s = settling velocity of the sediment;
X = characteristic grain size of the mixture;
x = transition parameter from smooth to rough;
Y = pressure correction in the transition from smooth to rough;
Δ = apparent roughness diameter;

δ = thickness of the laminar sublayer;
η = ratio of R_s to R_T;
ν = viscosity;
ξ = hiding factor of the grains in the mixture;
ρ_f = density of fluid;
ρ_s = density of sediment;
Φ_* = intensity of transport for the individual grain size;
Ψ_* = intensity of shear for the individual grain size; and
Ψ' = intensity of shear for the representative particle.

DISCUSSION

Thomas Blench,[10] M. ASCE.—River-model scales have been investigated from a study of bed-load transport in flumes; the writer has also examined this subject[11] by studying the self-adjustment of large canals and rivers. Superficially the results must appear quite different because of the large number of formulas required by the former method and the few required by the latter. However, if the mathematics is disregarded so that essential principles can be compared, the authors and the writer appear to have expressed identical views on all important dynamical matters, whether postulated or deduced.

The concordance of essential opinions, arrived at from quite opposite viewpoints, seems to necessitate some explanation of the superficial differences. Such an explanation can be developed from the regime theory.[12,13,14] A model maker can impose only three scales on a mobile-bed model; after they have been imposed all other scales will adjust themselves. Any three independent scales are imposable—as examples, (*a*) discharge, (*b*) side factor (implying tractive-force intensity in the side zone where there is no bed movement), and (*c*) bed factor (implying Froude number in terms of depth). Obviously, the discharge scale can be imposed directly. The side-factor scale can be imposed indirectly by computing directly imposable scales from it and imposing them. The bed-factor scale is imposed by using a suitable bed material, in suitable quantities, with a fluid of suitable nature; but, as the authors note and the writer has also stated,[11] there are circumstances under which only unity scale is permissible. To find how to produce a required bed factor with a given material requires a great deal of time for experiments.

Suppose that the model maker has so vast a knowledge of sediment-transport mechanics that he knows exactly how the bed factor depends on all its physical constituents. He can then dispense with the time necessary for experimentation and specify, from his knowledge, that a sand of (*a*) a definite median size, with (*b*) a definite dispersion of grain sizes about the median, and (*c*) a definite relative density should be used with (*d*) a certain charge (that is, ratio of weight per second of material to weight per second of water). Furthermore, the fluid should have a definite viscosity and suspended load. To be more exact, he should also specify angularity of grains, perhaps the ratio of grain size to water depth, and even the ratio of channel width to depth in cross-over sections; however, these factors would not be particularly important. Thus, for the one item, bed factor, one would have at least six, and perhaps nine, degrees of freedom which, added to the discharge and side factor, would give eleven degrees of freedom. The authors have specified most of these constituent parts of bed factor and so they have had to produce appropriate equations. The actual identification of the factors from the equations is difficult without some practice, and there seems no point in attempting it herein.

---

[10] Cons. Engr. and Prof. of Civ. Eng., Univ. of Alberta, Edmonton, Canada.

[11] "Scale Relations among Sand-Bed Rivers Including Models," by Thomas Blench, *Proceedings-Separate No. 667*, ASCE, April, 1955.

[12] "Regime Theory for Self-Formed Sediment-Bearing Channels," by Thomas Blench, *Transactions*, ASCE, Vol. 117, 1952, p. 383.

[13] "Practical Regime Theory Design of Artificial Channels with Self-Adjustable Boundaries," by Thomas Blench, submitted for ASCE convention at St. Louis, June, 1955.

[14] "Canals, Channels and Rivers," by T. Blench in "Civil Engineering Reference Book," Butterworths, London, 1951.

It is felt that there are two points concerning the authors' equations that deserve comment. The first is that the equations depend on the prior elimination of the effect of sides by a method that is thought to be dubious. The second is that, according to the regime theory, Eq. 1 contains D in an incorrect manner and m should be $\frac{1}{4}$. The incorrectness arises from the fact that according to the regime theory (from observed behavior of channels in the field) the linear dimension characterizing roughness should not be D, but a composite of the shear stress on the sides and the bed factor; D is implicit therein but would appear in the numerator rather than the denominator if made explicit—a paradox that used to worry river engineers before they found it was associated with dune movement. The writer has commented[15] that extrapolation of the authors' formulas to the design of large channels is not satisfactory; perhaps Eq. 1 is a principal cause, but regime analysis of flume data [16,17] seems to show that there is no existing information with the accuracy, range, or completeness to justify extrapolation beyond a very low limit.

HANS A. EINSTEIN,[18] M. ASCE, AND NING CHIEN,[19] A. M. ASCE.—It is regretted that comments have been voiced by only one engineer who is practically involved in the construction and interpretation of models in large laboratories. Are others not interested in this problem?

Mr. Blench formulated opinions on the proposed equations from the viewpoint of regime theory. Engineers may fast be getting tired of this steady dispute as to which of the two methods by which sediment-carrying channels are being computed should be used; an explanation of the basic differences between the two methods is desirable.

The regime theory was developed in India from field measurements in artificial canals of rather uniform character but having widely varying sizes. Three equations were developed which can be brought into a form that indicates that any one of three variables (average depth, average velocity, and channel width) are unique functions of the discharge. These functions were obtained by plotting canal data on log-log charts and by drawing the best-fitting straight lines through the points. This was easily accomplished because of the inherent regularity of the canal data which were obtained from canals that were all empty or running at design diacharge. A stage-discharge relationship as is known for rivers does not exist in these canals.

---

[15] Discussion by Thomas Blench of "Graphic Design of Alluvial Channels," by Ning Chien, *Transactions*, ASCE, Vol. 121, 1956.

[16] "Regime Formulas for Bed-Load Transport," by Thomas Blench, *Proceedings*, International Assn. for Hydr. Research, September, 1955.

[17] "Analysis of Bed-Load Data," by R. B. Erb, thesis presented to the University of Alberta at Edmonton, Canada, in 1955 in partial fulfilment of the requirements for the degree of Master of Science.

[18] Prof. of Hydr. Eng., Univ. of California, Berkeley, Calif.

[19] Associate Prof. of Hydraulics, Tsing Hwa Univ., Peiping, China; formerly Asst. Research Engr., Inst. of Eng. Research, Univ. of California, Berkeley, Calif.

The resulting relationships thus had the form:

$$\text{Variable} = \text{constant} \times Q^u$$

in which the variable is any one of these three variables, u is supposedly a universal constant in each equation, and the constant is supposed to be an unspecified function of sediment grade, sediment load, and some other factors. What is satisfactory for the Indian canal data (from which many results were excluded) is not applicable to American natural rivers. Fig. 3 presents, as an example, the channel width b in terms of the discharge Q for river sections[5] compared with the predictions of the regime theory.[20] It may be seen that not only is the constant in most cases wrong by a factor of three, but also the slopes of the various river curves differ among themselves and definitely differ from the regime prediction. It even appears questionable that a straight line can always be applied to describe river behavior. To discover if it can, the average velocity in the same stream sections was plotted against the average

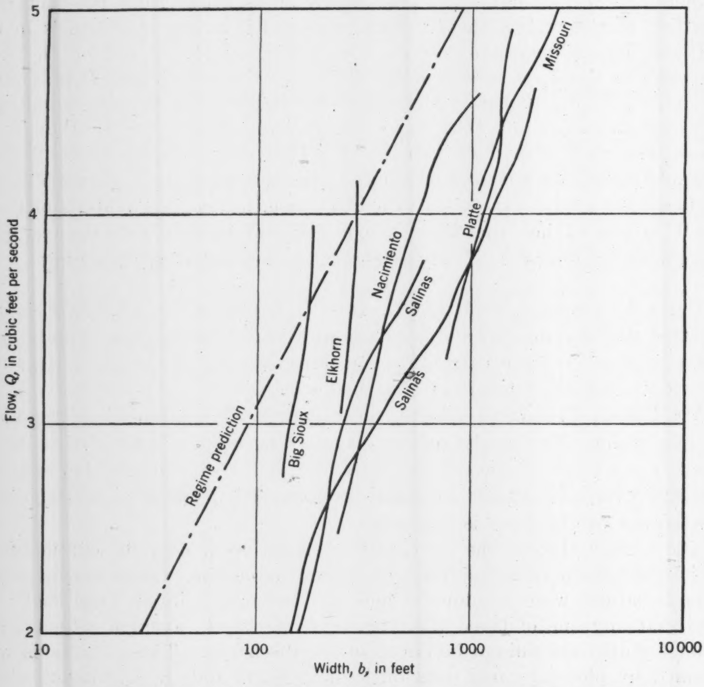

FIG. 3.—RELATIONSHIP BETWEEN FLOW AND WIDTH OF VARIOUS AMERICAN RIVERS

depth in Fig. 4. In Fig. 4 the deviations from the straight line are so pronounced that the senior writer's proposal[5] appears to be a distinct progress. Whereas the writers used, basically, the Manning equation, Mr. Blench uses the regime line. It is not possible, on the basis of Fig. 4, to understand the great superiority of the regime formula, particularly if one takes into account the facts that the constant of the Manning formula can be predicted, that of the regime formula must be guessed, and a further correction for bar resistance can be applied to the Manning formula whereas the regime formula does not need correction by "dubious" means.

---

[20] "Regime Flow in Incoherent Alluvium," by Gerald Lacey, *Publication No. 20*, Control Board of Irrig., Simla, India, July 18, 1939.

The bed-load function, however, gives the best possible description of the sediment and flow in model and prototype and compares the two by model

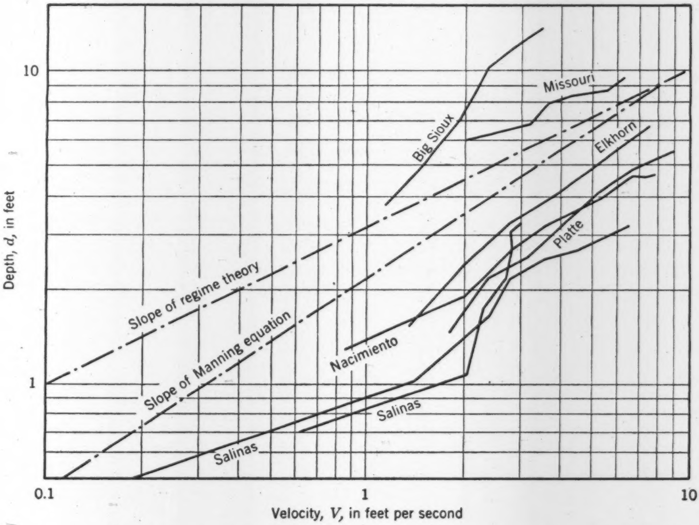

FIG. 4.—RELATIONSHIP BETWEEN DEPTH AND VELOCITY OF VARIOUS AMERICAN RIVERS

laws. Proponents of the regime theory cannot describe the alluvial river flow by hiding the sediment transport in the bed factors. Sediment transport is one of the most important parameters of the problem and should be studied as such.

Similarity is most easily established for power functions of the type used in the regime theory but it gives good results only if the flows actually follow the curves. The method in which relationships are approximated in both scales by power functions of equal exponent and by the ratio of the constants thus determined is an enlightened use of something similar to the regime theory. The differences between this and Mr. Blench's proposal are that one takes a known and calculated risk and that the deviation from the true similarity can be estimated.

An even more important method of applying similarity is through the use of general relationships between dimensionless variables. Such relationships are usually not only power relationships. When this is the case, the individual dimensionless parameters entering the equations must be made equal in model and prototype. This method is used in the paper—for example, in the case of Φ_* and Ψ_*—to derive the similarity conditions—for example, for the *f*-values—whereas the regime theory does not give the necessary relationships explicitly.

Once again, it is regretted that more engineers with the necessary model-prototype experience did not enter the discussion. Perhaps the future will see some efforts in proving or disproving the contention that model scales of such distorted models of alluvial rivers with movable model beds can be predicted and designed without much trial and error.

AMERICAN SOCIETY OF CIVIL ENGINEERS
Founded November 5, 1852
TRANSACTIONS

Paper No. 2806

AN INFLUENCE-LINE ANALYSIS FOR SUSPENSION BRIDGES

By David J. Peery,[1] M. ASCE

With Discussion by Messrs. Nan-sze Sih, Jacob Karol, Harry M. Palmbaum, Vincenzo Franciosi, and David J. Peery

Synopsis

Long-span suspension bridges cannot be analyzed by using the usual procedures for elastic structures. Because stresses and deflections are not proportional to loads it is not possible to superimpose various loading conditions or to use influence lines in the normal manner. It is customary to integrate the differential equation of the truss deflection curve, obtaining expressions in terms of exponential or hyperbolic functions. The equation for the cable-tension component H is implicit, containing the unknown H in the exponential or hyperbolic terms. This equation must be solved by trial for numerous loading conditions.

The differential equations for a suspension-bridge truss are shown herein to be identical with the equations for a beam in tension. A hypothetical tensile force is therefore assumed to act on the stiffening truss at all times. If the axial tensile force remains constant under all loading conditions, the bending moments, shears, and deflections are directly proportional to the transverse loads, and various loading conditions may be superimposed. Influence lines are readily computed as deflection curves of beams in tension. Influence lines for continuous trusses are drawn by superimposing deflection curves which restore continuity of slope at supports.

The ordinates of deflection curves may be readily tabulated in dimensionless form to cover the entire range of suspension-bridge proportions. From these tables, influence lines may be computed using a slide rule with no further reference to tables of exponential or hyperbolic functions. Two sets of influence lines, each corresponding to one constant value of the tensile force, are computed. Final bending moments are determined by linear interpolation.

Note.—Published, essentially as printed here, in December, 1954, as *Proceedings-Separate No. 558*. Positions and titles given are those in effect when the paper or discussion was approved for publication in *Transactions*.

[1] Prof. of Aeronautical Eng., Univ. of Michigan, Ann Arbor, Mich.

INTRODUCTION

Most engineering structures may be considered to be completely elastic. The structural deflections are small enough so that the moment arms of forces in the deflected structure may be assumed equal to the moment arms in the undeflected structure. These assumptions are not valid for the long-span suspension bridge in which the stiffening truss is erected in such a manner that it resists no dead-load stress at mean temperature. The high ratio of dead load to live load and the comparative flexibility of the structure are such that the change in moment arm of the cable tensile force must be considered in the analysis. The total dead-load and live-load cable force is displaced to produce a moment increment which has a strong effect on the live-load bending moment in the stiffening truss. The analysis procedure for suspension bridges which includes this effect is termed the "deflection theory" as distinguished from the "elastic theory" which follows usual structural design procedures.

The fundamental equations for the deflection theory were presented by Muller-Breslau in 1881 and developed by Josef Melan in 1888. The equations were extended to a three-span suspension bridge by L. S. Moisseiff and F. E. Turneaure during the design of the Manhattan Bridge (New York, N. Y.) in 1909. The deflection theory was further extended to structures of any number of spans with continuous or noncontinuous trusses by D. B. Steinman,[2] M. ASCE. In all these procedures the equation of the deflection curve is written in terms of exponential functions which contain the variable H in the exponent and which require trial solutions using several values for the exponent. The practical computations often require the use of six significant figures because similar large numbers must be subtracted.

It has been recognized since the early days of the deflection theory that the differential equations involved are not linear and that procedures of superposition and influence lines are not applicable in the normal manner. In the conventional deflection theory the differential equations are linearized over a small range by assuming that the exponential term containing H is constant during the integration. Exactly the same assumption is made in the influence-line procedure, but engineers have been reluctant to accept the use of influence lines in deflection-theory analysis.

The use of influence lines in deflection-theory analysis was correctly stated and demonstrated by T. Godard[3] in 1894. An extensive treatment of the deflection theory and the use of influence lines was published by Hans H. Rode,[4] in 1930. Mr. Rode used a linear interpolation between two influence lines computed for different values of H. Although Mr. Rode's paper attracted considerable attention by first introducing the effect of horizontal cable displacement, the influence-line procedure has not been generally accepted in practice by American engineers.

---

[2] "A Generalized Deflection Theory for Suspension Bridges," by D. B. Steinman, *Transactions*, ASCE, Vol. 100, 1935, p. 1133.

[3] "Recherches sur le calcul de la resistance de tabliers des ponts suspendus," by T. Godard, *Annales des Ponts et Chaussees*, 1894, Vol. 8, pp. 105–189.

[4] "New Deflection Theory," by Hans H. Rode, *Transactions*, Det Kongelige Norske Videnskabers Selskab, 1930, No. 3.

The practical usefulness of influence-line procedures has been demonstrated by Arne Selberg[5] and S. O. Asplund[6], M. ASCE. Mr. Selberg prepared dimensionless charts from which influence-line ordinates can be obtained for bridges of any proportions. Mr. Asplund prepared extensive dimensionless tables from which influence lines can be readily computed for bridges of any proportions.

The use of influence lines was extended to bridges with continuous trusses by Jacob Karol,[7] M. ASCE. The moments at the towers were determined by a procedure of moment distribution for analogous beams in tension, and dimensionless tables were compiled to facilitate analysis. Mr. Karol, in 1938, also questioned the trend toward more flexible stiffening trusses and warned of dangers from wind action.

The usual deflection theory has been used for half a century, and various simplifications and short cuts have been developed. Engineers are hesitant to adopt a new method of analysis until the computation procedure has been proved. The procedure will be explained in detail in this paper.

BEAM ANALOGY

The assumptions commonly used in deflection-theory analysis are retained. The initial cable curve is assumed parabolic, the moment of inertia of the stiffening truss is assumed constant in each span, and the dead load is assumed to produce no bending moment in the stiffening truss. Although other conditions may be readily considered,[4] the cable area will be assumed constant, and tower and suspender elongations will be neglected. The towers are assumed to resist no horizontal cable load.

The usual notation for suspension-bridge analysis will be used.[2] The notation for general dimensions of the structure is shown in Fig. 1. Because influence-line procedures are used, a single concentrated live load P is assumed at a distance k from the left end of each span.

The cable curve in each span is assumed parabolic, as defined in the following equations:

$$\left.\begin{aligned} y &= \frac{4fx}{l^2}(l - x) \\ &\text{or} \\ y_1 &= \frac{4f_1x_1}{l^2_1}(l_1 - x_1) \end{aligned}\right\} \qquad (1)$$

The suspenders are assumed to be closely spaced and to provide a uniform live-load distribution along the span and cable of $8\,fH/l^2$, in addition to a nonuniform distribution resulting from the deflections. The bending moment in the stiffening truss for any span is found from the conventional equation of the deflection theory:

$$M = M_o - H\,y - H_r\,\eta \qquad (2)$$

---

[5] "Design of Suspension Bridges," by Arne Selberg, *Transactions*, Det Kongelige Norske Videnskabers Selskab, 1945, No. 1.

[6] "On the Deflection Theory of Suspension Bridges," by S. O. Asplund, Orebro, Sweden, 1943.

[7] "A Partial Influence Line Procedure for Suspension Bridge Analysis by the Deflection Theory," by Jacob Karol, thesis presented in 1938 to the University of Illinois, at Urbana, in partial fulfilment of the requirements for the degree of Doctor of Philosophy.

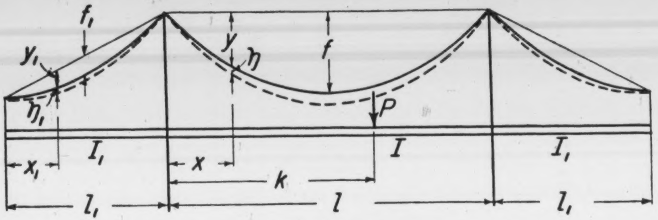
f_1
y_1
η_1
y
η
f
P
I_1
I
I_1
x_1
x
k
l_1
l
l_1

FIG. 1.—NOTATION DIAGRAM

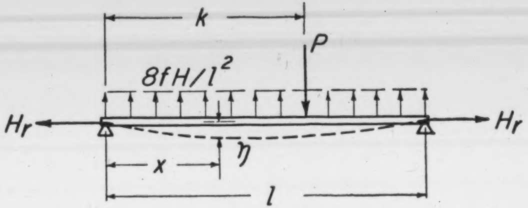
k
P
$8fH/l^2$
H_r
H_r
x
η
l

FIG. 2.—ANALOGOUS BEAM

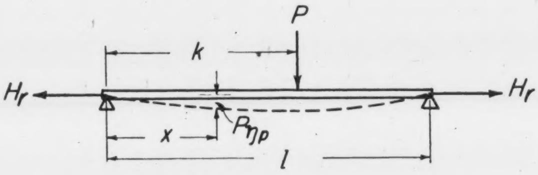
P
k
H_r
H_r
x
$P\eta_p$
l

(a) Loads and Deflections

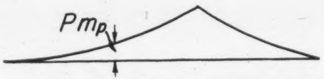

(b) Bending Moment

FIG. 3.—BEAM WITH LIVE LOAD

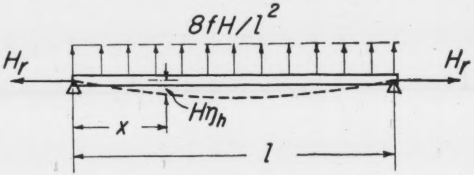
$8fH/l^2$
H_r
H_r
x
$H\eta_h$
l

(a) Loads and Deflections

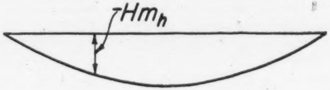

(b) Bending Moment

FIG. 4.—BEAM WITH SUSPENDER LOADS

The term M_o represents the simple-beam bending moment for the live load, P. The term $H\,y$ represents the simple-beam bending moment produced by the uniformly distributed suspender load of $8\,f\,H/l^2$, in which y represents the parabola defined in Eq. 1. The term H_r represents the sum of the dead-load horizontal cable-tension component H_w and the live-load horizontal cable-tension component H—

$$H_r = H_w + H \quad \text{(3)}$$

The moment $H_r\,\eta$ results from the vertical deflection η of the cable from its initial parabolic curve. This moment $H_r\eta$ represents the difference between the moments of the elastic theory and of the deflection theory and is transmitted to the stiffening truss by means of a nonuniform suspender load on the truss.

The beam shown in Fig. 2 resists an axial force H_r concurrently with the transverse concentrated load P and the uniformly distributed load $8\,f\,H/l^2$. The bending-moment equation for this beam is also expressed by Eq. 2 when y is defined by Eq. 1 and η is the vertical deflection at any point. The suspension-bridge structure is therefore directly analogous to the beam with an axial tension force H_r.

The procedure for superposition of various transverse loading conditions is firmly established for beams with axial loads.[8,9] If the axial force remains constant during application of each increment of transverse load, the final deflections, shears, and bending moments may be determined by superimposing the effects of all increments. The beam shown in Fig. 2 may therefore be analyzed by superimposing the values for the beams of Fig. 3 and Fig. 4. The bending moment, M, and the deflection, η, are expressed by the following equations:

$$M = P\,m_p + H\,m_h \quad \text{(4)}$$

$$\eta = P\,\eta_P + H\,\eta_h \quad \text{(5)}$$

The terms m_p and η_P represent bending moments and deflections of the beam (Fig. 3) for unit values of the transverse load P. The terms m_h and η_h represent bending moments and deflections of the beam (Fig. 4) for a unit value of H. The axial tension force H_r must be considered constant in order for the superposition procedure of Eqs. 4 and 5 to be valid.

In a suspension bridge the resultant cable-force component, $H_r = H_w + H$, varies with the live load and temperature conditions. If, however, the correct final value of H_r is assumed to act for each loading condition, several loads P may be combined to yield any desired live-load distribution. Further analysis will be made for a single load P in order to construct influence lines in the conventional manner.

SUSPENSION BRIDGES WITH SIMPLY SUPPORTED TRUSS SPANS

The suspension bridge in which the stiffening trusses are continuous over the supports is more difficult to analyze than the bridge in which the trusses are

---

[8] "Aircraft Structures," by David J. Peery, McGraw-Hill Book Co., Inc., New York, N. Y., 1950, p. 528.

[9] "Airplane Structures," by A. S. Niles and J. S. Newell, John Wiley & Sons, Inc., New York, N. Y., 3d Ed., 1943, Vol. II, p. 100.

simply supported. The equations and computations for the case of simple support will therefore be completed first, before considering the case of continuity. The equations for bending moment and deflection will first be derived for a beam in tension. These equations will be applicable to any span of a suspension bridge. If side spans are considered, subscripts may be added to the terms (l_1, f_1, x_1, and so on) of the equations (Fig. 1).

The bending moments and deflections for the beams shown in Figs. 3 and 4 are readily determined by integrating the common-beam equation:

$$\frac{d^2\eta}{dx^2} = -\frac{M}{E\,I} \quad \text{(6)}$$

The following abbreviation is customary in suspension-bridge analysis:

$$c^2 = \frac{H_r}{E\,I} = \frac{H_w + H}{E\,I} \quad \text{(7)}$$

For the beam shown in Fig. 3, the term containing H does not appear, and the following expressions are obtained from Eqs. 2, 6, and 7, after integrating and evaluating the constants of integration:

$$m_p = \frac{\sinh c(l-k)}{c \sinh c\,l} \sinh c\,x \qquad x < k \quad \text{(8)}$$

$$m_p = \frac{\sinh c\,k}{c \sinh c\,l} \sinh c(l-x) \qquad x > k \quad \text{(9)}$$

The bending moment at any point in the beam in Fig. 4 is determined in the same manner as for the beam in Fig. 3. The term M_o vanishes in Eq. 2, y is defined by Eq. 1, and H is assumed to have a unit value.

$$m_h = -\frac{8f}{c^2 l^2}\left(\tanh\frac{c\,l}{2}\sinh c\,x - \cosh c\,x + 1\right) \quad \text{(10)}$$

The deflection resulting from a unit value of H is expressed as follows:

$$\eta_h = \frac{8f}{E\,I\,c^4 l^2}\left(\tanh\frac{c\,l}{2}\sinh c\,x - \cosh c\,x + 1 - \frac{c^2 l^2 y}{8f}\right) \quad \text{(11)}$$

In many computations it is preferable to use exponential functions rather than hyperbolic functions. Eqs. 8, 9, 10, and 11 can be readily converted to equations containing exponential functions by substituting the relationships $2 \sinh z = e^z - e^{-z}$ and $2 \cosh z = e^z + e^{-z}$. The hyperbolic terms are most frequently used for beams in tension, and Eqs. 8, 9, 10, and 11 are derived elsewhere[9] with slightly different notation.

In conventional elastic structures the influence line for any redundant force is calculated as the deflection curve of the load line for a unit displacement of the redundant. The suspension bridge may also be considered as an elastic structure if H_r is assumed to have a constant value. The horizontal component H of the cable tension will be considered as the redundant force, and the influence line for H will be calculated as the deflection curve of a beam with axial tension H_r. The cable is assumed to be cut at the center line (Fig. 5) and a unit displacement applied to the cut ends. The truss deflections, η_h/D, represent ordinates of the influence line for H.

The values of the deflections η_h defined by Eq. 11 result from a unit value of H. These must be divided by D, the displacement of the redundant force H resulting from the unit value of H. The displacement D contains a term for cable stretch, $L_s/A\,E_c$, and a term for truss bending equal to the product of the suspender pull, $8\,f/l^2$, and the deflection, η_h, summed over all spans.

$$D = \frac{L_s}{A\,E_c} - \sum \frac{8\,f}{l^2} \int_0^l \eta_h\,dx \qquad (12)$$

The term $L_s/A\,E_c$ represents the horizontal component of the cable stretch for a unit H, evaluated between anchorages. The summation term includes all spans with proper values of f and l for the side spans. The equation of the influence line for H is

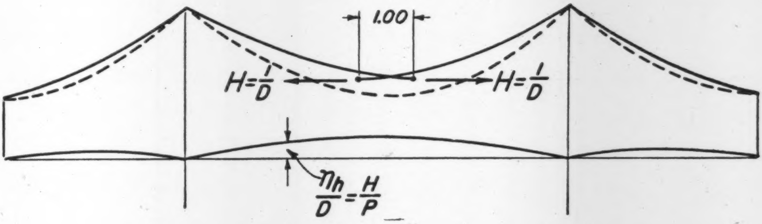

FIG. 5.—DEFLECTION CURVE REPRESENTING INFLUENCE LINE FOR H

$$\frac{H}{P}\text{ (influence line)} = -\frac{\eta_h}{D} \qquad (13)$$

in which η_h is obtained by substituting k for x in Eq. 11.

The bending moment at any section in the stiffening truss is expressed by Eq. 4. In order to determine bending-moment influence lines each term will be divided by P, and all terms will be considered as functions of k.

$$\frac{M}{P}\text{ (influence line)} = m_p\text{ (influence line)} + m_h\,\frac{H}{P}\text{ (influence line)} \qquad (14)$$

The term m_p is considered as a function of k, with x constant. The term m_h is constant because it does not contain k.

Temperature stresses are calculated independently and superimposed on other stress conditions. The horizontal cable-force component, H_t, resulting from a temperature change is determined as follows:

$$H_t = -\frac{\omega\,t\,L_t}{D} \qquad (15)$$

If the cable is cut at the center line, the cut ends would move a distance $\omega\, t\, L_t$ for a temperature change t and a temperature coefficient ω of the cable. The term D is defined by Eq. 12. The bending moment produced by a temperature change, M_t, is found from Eq. 4 for the condition $P = 0$.

$$M_t = H_t\, m_h \qquad (16)$$

NUMERICAL APPLICATION

A structure analyzed by Mr. Steinman[2] will be considered. The same structure will later be used for the continuous case. The dimensions are $l =$ 800 ft, $f = 84$ ft, $l_1 = 400$ ft, and $f_1 = 21$ ft. The truss stiffness is the same in all spans, $E\,I = E\,I_1 = 56{,}840{,}000$ ft²-kips. For the cable, $L_s = 2{,}075$ ft, $L_t = 1{,}998$ ft, $A = 87.8$ in.², and $E_c = 25{,}000$ kips per sq in. The loading per cable is 3,850 lb per ft dead load (w) and 1,300 lb per ft live load. The dead-load cable component, $H_w = w\,l^2/8\,f$, is 3,667 kips. Other values are: $t = \pm$ 60° F, $\omega = 0.0000065$, and $8\,f/l^2 = 8\,f_1/l^2_1 = 1/952.4$.

TABLE 1.—TRUSS MOMENTS AND DEFLECTIONS RESULTING FROM A UNIT VALUE OF H

$\frac{x}{l}$	$-\frac{m_h}{f}$ (Eq. 10)		$-\frac{\eta_h\, E\, I \times 10^4}{f\, l^2}$ (Eq. 11)			
	$c\,l = 6.0$	$c\,l = 7.0$	$c\,l = 3.0$	$c\,l = 3.5$	$c\,l = 6.0$	$c\,l = 7.0$
(1)	(2)	(3)	(4)	(5)	(6)	(7)
0	0	0	0	0	0	0
0.05	0.0573	0.0482	88.0	74.9	36.9	28.9
0.10	0.0995	0.0819	172.6	147.6	72.4	56.8
0.15	0.1307	0.1057	252.4	215.8	105.4	82.5
0.20	0.1536	0.1225	325.1	277.8	135.1	105.6
0.25	0.1703	0.1341	389.2	332.3	161.0	125.7
0.30	0.1822	0.1421	443.4	378.4	182.7	142.4
0.35	0.1906	0.1475	486.5	415.0	199.8	155.6
0.40	0.1961	0.1509	517.9	441.5	212.2	165.1
0.45	0.1991	0.1528	536.9	457.6	219.7	170.9
0.50	0.2001	0.1534	543.3	463.1	222.2	172.8
			AREA UNDER CURVES: $-\frac{E\,I \times 10^4}{f\, l^3} \int_0^l \eta_h\, dx$			
			349.1	297.9	143.9	112.2
			SLOPE AT SUPPORTS: $\left(\frac{d\eta_h}{dx}\right)_o \times \frac{E\,I}{f\,l} \times 10^4$			
			1,762	1,509	742.6	583.5

Two sets of influence lines will be constructed. One set, for $c\,l = 6.0$ and $c_1\,l_1 = 3.0$, corresponds approximately to the minimum value of H_r. The other set, for $c\,l = 7.0$ and $c_1\,l_1 = 3.5$, corresponds to a value of H_r somewhat less than the maximum value. Final bending moments will be determined by linear interpolation between values for the two sets of influence lines.

The influence lines for H will first be computed from Eqs. 12 and 13. Use of these equations requires determining η_h-values from Eq. 11. The values of η_h are shown in Table 1. The bending moments m_h resulting from a unit value of H are also shown in Table 1. The values shown in Table 1 are dimensionless and apply to any structure having an applicable value of $c\,l$. The values in the two bottom sections of Table 1 are obtained by integrating and differentiating Eq. 11 and will be used for computing D and for the later analysis of the continuous truss.

The value of D is determined from Eq. 12. The integrals of Eq. 12 are evaluated as follows for the side span, with $c\,l = 3.0$:

$$-\frac{8f_1}{l^2_1}\int_0^{l_1} \eta_h\,dx = \frac{8f_1}{l^2_1}\,\frac{f_1\,l^3_1}{E\,I_1 \times 10^4}\,(349.1) = 0.000867 \text{ ft per kip.}$$

For the main span, with $c\,l = 6.0$,

$$-\frac{8f}{l^2}\int_0^{l} \eta_h\,dx = \frac{8f}{l^2}\,\frac{f\,l^3}{E\,I \times 10^4}\,(143.9) = 0.011433 \text{ ft per kip.}$$

The cable term is $L_s/A\,E_c = 0.000945$ ft per kip and D is the sum of the integrated terms for the main span and two side spans:

$$D = 2(0.000867) + 0.011433 + 0.000945 = 0.014112 \text{ ft per kip.}$$

Similar computations are made for $c\,l = 7.00$ and $c_1\,l_1 = 3.50$:

$$D = 0.000945 + 2\,\frac{8f_1}{l^2_1}\,\frac{f_1\,l^3_1}{E\,I_1 \times 10^4}\,(297.9) + \frac{8f}{l^2}\,\frac{f\,l^3}{E\,I \times 10^4}\,(112.2) = 0.011342 \text{ ft per kip.}$$

The influence lines for H have been computed in Cols. 2 and 6, Table 2, using Eq. 13. The values of η_h are listed in dimensionless form in Table 1 and must be multiplied by $f\,l^2/(E\,I\,D \times 10^4)$ to determine the influence-line ordinates.

The influence lines for bending moment in the main span at a point $0.2\,l$ from the support have been computed in Table 2. Values of $-\,m_h/f$ for this point are given in Table 1 as 0.1536 for $c\,l = 6.0$ and 0.1225 for $c\,l = 7.0$. For $f = 84$ ft, the values of m_h are $-\,12.90$ ft and $-\,10.29$ ft, and these values are used as multipliers of the ordinates of the influence lines for H to obtain the values in Cols. 3 and 7, Table 2. Values of m_p are computed from Eqs. 8 and 9 and tabulated in Cols. 4 and 8. The final bending-moment influence lines are computed in Cols. 5 and 9 by adding values of m_p and $H\,m_h/P$ as specified in Eq. 14.

The temperature effects on H and M are computed from Eqs. 15 and 16. For $c\,l = 6.00$, $H_t = \mp\,55.2$ kips, $M_t = \pm\,55.2 \times 12.90 = \pm\,712$ ft-kips. For $c\,l = 7.00$, $H_t = \mp\,68.7$ kips, $M_t = \pm\,707$ ft-kips. The temperature effects are superimposed on the live-load effects.

The areas under the influence lines may be computed readily by using the Simpson rule. Comparison with areas determined by integration indicates five-place accuracy of the Simpson rule for the shapes of the influence lines. Values are shown in Table 3 for a live load extending over four tenths of the main span and for a temperature rise of 60° F. Calculations were also made by the customary deflection theory for comparison. The only error introduced by the influence-line procedure is produced by the linear interpolation. The deflection-theory computations were made for $c\,l = 6.70$. If influence lines are computed for this value, the final results are identical. The linear interpolation yields bending moments which are 0.2% greater than those computed

TABLE 2.—INFLUENCE LINES FOR H AND FOR BENDING MOMENT AT 0.2 l (TRUSSES SIMPLY SUPPORTED)

Procedure:
Col. 2 contains, for the side span, values in Col. 4 of Table 1 multiplied by 4.189×10^{-4}, and for the main span, values in Col. 6 of Table 1 multiplied by 67.02 by 10^{-4}.
Col. 3 contains values in Col. 2 of Table 2 (this table), multiplied by − 12.90.
Col. 4 contains values determined from Eqs. 8 and 9.
Col. 5 contains the sums of Col. 3 plus Col. 4 (Eq. 14).
Col. 6 contains, for the side span, values in Col. 5 of Table 1 multiplied by 5.212×10^{-4}, and for the main span, values in Col. 7 of Table 1 multiplied by 83.39×10^{-4}.
Col. 7 contains values in Col. 6 of Table 2 (this table), multiplied by − 10.29.
Col. 8 contains values determined from Eqs. 8 and 9.
Col. 9 contains the sums of Col. 7 plus Col. 8 (Eq. 14).

	$c_1 l_1 = 3.00$, $c\,l = 6.00$				$c_1 l_1 = 3.50$, $c\,l = 7.00$			
$\frac{k}{l}$ (1)	$\frac{H}{P}$ (2)	$H\,m_h/P$, in feet (3)	m_p, in feet (4)	M/P, in feet (5)	$\frac{H}{P}$ (6)	$H\,m_h/P$, in feet (7)	m_p, in feet (8)	M/P, in feet (9)
SIDE SPAN								
0	0	0	0	0	0	0	0	0
0.1	0.072	− 0.93	0	− 0.93	0.077	− 0.79	0	− 0.79
0.2	0.136	− 1.75	0	− 1.75	0.145	− 1.49	0	− 1.49
0.3	0.182	− 2.35	0	− 2.35	0.197	− 2.03	0	− 2.03
0.4	0.217	− 2.80	0	− 2.80	0.230	− 2.37	0	− 2.37
0.5	0.228	− 2.94	0	− 2.94	0.241	− 2.48	0	− 2.48
MAIN SPAN								
0	0	0	0	0	0	0	0	0
0.05	0.247	− 3.19	12.22	9.03	0.241	− 2.48	10.07	7.59
0.10	0.495	− 6.39	25.57	19.18	0.474	− 4.88	21.38	16.50
0.15	0.706	− 9.11	41.22	32.11	0.688	− 7.08	35.34	28.26
0.20	0.905	−11.67	60.62	48.95	0.881	− 9.07	53.67	44.60
0.25	1.079	−13.92	44.90	30.98	1.048	−10.78	37.82	27.04
0.30	1.224	−15.79	33.26	17.47	1.187	−12.21	26.65	14.44
0.35	1.339	−17.27	24.63	7.36	1.298	−13.36	18.78	5.42
0.40	1.422	−18.34	18.25	− 0.09	1.377	−14.17	13.23	− 0.94
0.45	1.472	−18.99	13.50	− 5.49	1.425	−14.66	9.32	− 5.34
0.50	1.489	−19.21	9.99	− 9.22	1.441	−14.83	6.57	− 8.26
0.55	1.472	−18.99	7.39	−11.60	1.425	−14.66	4.62	−10.04
0.60	1.422	−18.34	5.45	−12.89	1.377	−14.17	3.25	−10.92
0.65	1.339	−17.27	4.01	−13.26	1.298	−13.36	2.28	−11.08
0.70	1.224	−15.79	2.94	−12.85	1.187	−12.21	1.60	−10.61
0.75	1.079	−13.92	2.12	−11.80	1.048	−10.78	1.11	− 9.67
0.80	0.905	−11.67	1.50	−10.17	0.881	− 9.07	0.75	− 8.32
0.85	0.706	− 9.11	1.02	− 8.09	0.688	− 7.08	0.53	− 6.55
0.90	0.495	− 6.39	0.64	− 5.75	0.474	− 4.88	0.30	− 4.58
0.95	0.247	− 3.19	0.30	− 2.89	0.241	− 2.48	0.14	− 2.34
1.00	0	0	0	0	0	0	0	0

in the usual manner. The computations were carried out to five and six significant figures for the comparison, although values in Tables 1 and 2 were rounded off. Normally, slide-rule computations are adequate, except for computing m_h, η_h, and m_p from the hyperbolic functions.

TABLE 3.—COMPARISON OF RESULTS WITH VALUES DETERMINED USING THE DEFLECTION THEORY FOR SIMPLY SUPPORTED TRUSSES

Cause of Stress (1)	INFLUENCE-LINE SOLUTION: $c\,l = 6.00$ (2)	$c\,l = 7.00$ (3)	$c\,l = 6.70$, by interpolation (4)	Deflection-theory results for $c\,l = 6.70$ (5)	Percent error (6)
VALUES OF H, IN KIPS					
Live load on 0.4 of the span........	349.3	339.0			
Temperature change of +60° F.....	−55.2	−68.7			
Live load plus temperature.........	294.1	270.3	277.5	277.5	0
VALUES OF M, IN KIP-FEET					
Live load on 0.4 of the span........	8,477	7,339			
Temperature change of +60° F.....	712	707			
Live load plus temperature.........	9,189	8,046	8,389.5	8,371	0.2

The values of terms shown in Table 1 and the values of m_p/l may be tabulated for all bridge proportions. The writer[10] has prepared dimensionless tables for $c\,l = 0.5, 1.0, 1.5 \ldots 10.0$. The use of such tables eliminates the need of any other tables, and all further influence-line computations may be made by slide rule.

SUSPENSION BRIDGES WITH CONTINUOUS STIFFENING TRUSSES

The suspension bridge in which the stiffening trusses are continuous through the towers has additional redundancies. The truss bending moments at the towers, T_1 and T_2, must be sufficient to provide equal slopes of the truss deflection curves for spans adjacent to the towers. The effects of these moments may be superimposed on other effects when H_r is constant.

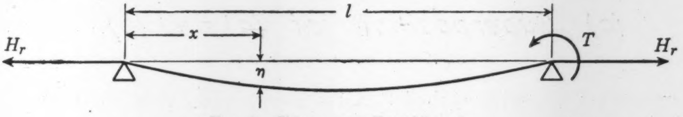

FIG. 6.—BEAM WITH END MOMENT

The effect of the end moment T shown in Fig. 6 is readily computed from the beam equations:

$$M = -E\,I\,\frac{d^2\eta}{dx^2} = \frac{T\,x}{l} - H_r\,\eta \ldots\ldots\ldots\ldots\ldots\ldots (17)$$

---

[10] "A Deflection Theory Analysis of Suspension Bridges by the Use of Influence Lines," by David J. Peery, thesis presented in 1941 to the University of Michigan, at Ann Arbor, in partial fulfilment of the requirements for the degree of Doctor of Philosophy

Integrating and substituting the boundary conditions, $M = \eta = 0$ when $x = 0$ and $M = T, \eta = 0$ when $x = l$, the following equations are obtained:

$$M = T\frac{\sinh c\,x}{\sinh c\,l} \qquad (18)$$

and

$$\eta = \frac{T}{H_r}\left(\frac{x}{l} - \frac{\sinh c\,x}{\sinh c\,l}\right) \qquad (19)$$

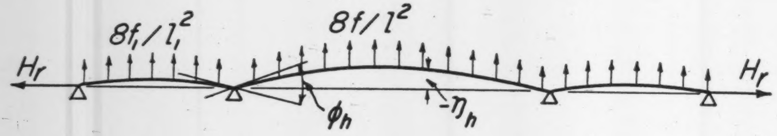

(a) Unit H, Simply Supported Spans

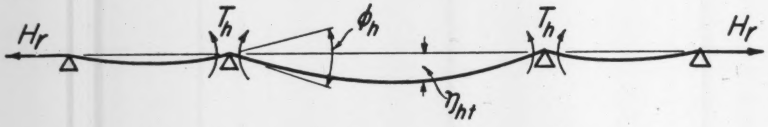

(b) Corrections for Continuity

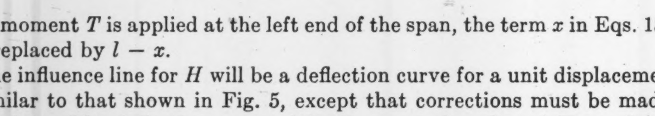

(c) Superposition of (a) and (b)

FIG. 7.—INFLUENCE LINE FOR H

If the moment T is applied at the left end of the span, the term x in Eqs. 18 and 19 is replaced by $l - x$.

The influence line for H will be a deflection curve for a unit displacement of H, similar to that shown in Fig. 5, except that corrections must be made for continuity. The deflections η_h resulting from a unit value of H are shown in Fig. 7(*a*) for simply supported spans. These values yield an angular discontinuity ϕ_h at each tower. The tower moments T_h (Fig. 7(*b*)) are sufficient to remove the angular discontinuity at the towers for the unit value of H and produce deflections η_{ht}. The influence line for H is obtained in Fig. 7(*c*) by superimposing deflections η_h and η_{ht} to yield deflections of the continuous beam for a unit H-value and by dividing by D_1, the displacement of the redundant, H, in

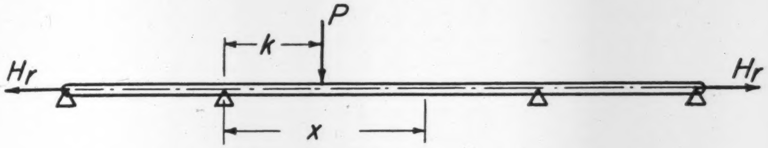

(a) Continuous Beam in Tension

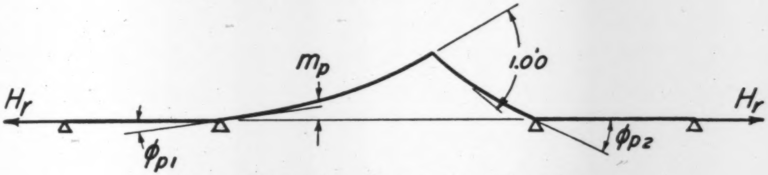
m_p
1.00
Hr
Hr
ϕ_{p1}
ϕ_{p2}

(b) Simple Beam in Tension

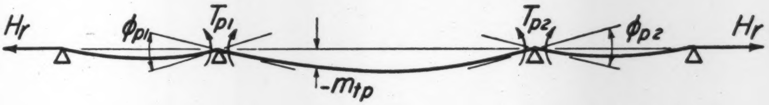
Hr
ϕ_{p1}
T_{p1}
T_{p2}
ϕ_{p2}
Hr
$-m_{tp}$

(c) Effects of Continuity

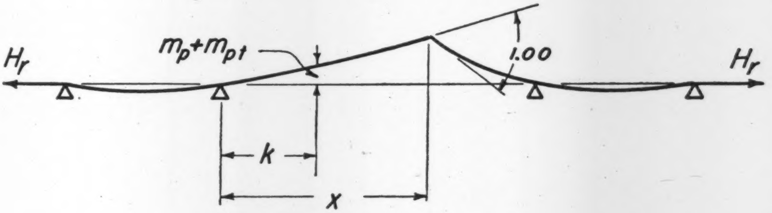
Hr
$m_p + m_{pt}$
1.00
Hr
k
x

(d) Superposition of (b) and (c)

FIG. 8.—INFLUENCE LINE FOR BEAM BENDING MOMENT

a continuous bridge for a unit H-value. The term D_1 is similar to the term D for the noncontinuous bridge (Eq. 12) but also includes the continuity effects η_{ht}.

$$D_1 = \frac{L_s}{A\,E_c} - \sum \frac{8f}{l^2} \int_0^l \eta_h \, dx - \sum \frac{8f}{l^2} \int_0^l \eta_{ht} \, dx \quad \ldots\ldots\ldots (20)$$

The influence line for H is determined from the following equation:

$$\frac{H}{P} \text{ (influence line)} = - \frac{\eta_h + \eta_{ht}}{D_1} \quad \ldots\ldots\ldots\ldots\ldots\ldots (21)$$

The influence line for the bending moment at any point in a continuous suspension bridge will be computed from the influence line for the bending moment in a continuous beam with axial tension H_r (Fig. 8(*a*)). The influence line for bending moment at distance x is a deflection curve for unit angular displacement at distance x, as shown in Fig. 8(*d*). The influence-line ordinates m_p for a noncontinuous beam were computed from Eqs. 8 and 9 and have slopes ϕ_{p1} and ϕ_{p2} at the towers (Fig. 8(*b*)). Tower moments, T_{p1} and T_{p2}, must be applied in order to remove the angular rotations (Fig. 8(*c*)). The deflections m_{tp} resulting from these moments are superimposed on the values of m_p in order to correct the influence lines for continuity effects. The final ordinates of the bending-moment influence line for the continuous beam in tension are $m_p + m_{tp}$ as shown in Fig. 8(*d*).

TABLE 4.—INFLUENCE LINE FOR *H* (TRUSSES CONTINUOUS OVER SUPPORTS)

Procedure:
Cols. 2, 7, and 8 contain values determined using Eq. 19.
Col. 3 contains values in Col. 2 multiplied by -0.935.
Col. 4 contains values in Col. 5 of Table 1 multiplied by 9.085×10^{-4}.
Col. 5 contains the sums of Col. 3 plus Col. 4.
Col. 9 contains the sums of Col. 7 plus Col. 8.
Col. 10 contains values in Col. 9 multiplied by -0.935.
Col. 11 contains values in Col. 7 of Table 1, multiplied by 145.6×10^{-4}.
Col. 12 contains the sums of Col. 10 plus Col. 11.

Description	SIDE SPAN, $cl = 3.50$					MAIN SPAN, $cl = 7.00$						
	$\frac{k}{l}$ (1)	$\frac{\eta}{T_1/H_r}$ (2)	$-\frac{\eta_{ht}}{D_1}$ (3)	$-\frac{\eta_h}{D_1}$ (4)	$\frac{H}{P}$ (5)	$\frac{k}{l}$ (6)	$\frac{\eta}{T_2/H_r}$ (7)	$\frac{\eta}{T_1/H_r}$ (8)	$\frac{\eta}{T/H_r}$ (9)	$-\frac{\eta_{ht}}{D_1}$ (10)	$-\frac{\eta_h}{D_1}$ (11)	$\frac{H}{P}$ (12)
$\frac{H}{P}$	0	0	0	0	0	0	0	0	0	0	0	0
	0.1	0.074	−0.073	0.134	0.061	0.05	0.049	0.245	0.294	−0.276	0.421	0.145
	0.2	0.154	−0.144	0.152	0.108	0.10	0.099	0.403	0.502	−0.470	0.825	0.355
	0.3	0.224	−0.210	0.344	0.134	0.15	0.148	0.500	0.648	−0.606	1.199	0.593
	0.4	0.285	−0.266	0.401	0.135	0.20	0.197	0.553	0.750	−0.702	1.536	0.834
	0.5	0.331	−0.310	0.421	0.111	0.25	0.245	0.576	0.821	−0.768	1.827	1.059
	0.6	0.357	−0.334	0.401	0.067	0.30	0.293	0.577	0.870	−0.814	2.071	1.257
	0.7	0.352	−0.330	0.344	0.014	0.35	0.339	0.564	0.903	−0.845	2.262	1.417
	0.8	0.305	−0.285	0.252	−0.033	0.40	0.385	0.539	0.924	−0.864	2.400	1.536
	0.9	0.196	−0.183	0.134	−0.049	0.45	0.429	0.507	0.936	−0.876	2.484	1.608
	1.0	0	0	0	0	0.50	0.470	0.470	0.940	−0.879	2.512	1.633
$\frac{\phi}{T/H_r}$		2.506					0.987	6.00	6.987			
$\frac{\text{Area}}{T l/H_r}$		0.2310					0.3574	0.3574	0.7148			

The final bending-moment influence line in a continuous suspension bridge is obtained by superimposing the cable effect, $H(m_h + m_{th})$, on the continuous-beam effect.

$$\frac{M}{P} \text{ (influence line)} = m_p + m_{tp} + (m_h + m_{th}) \frac{H}{P} \text{ (influence line)} \ldots (22)$$

This equation differs from Eq. 14 by the inclusion of continuity effects m_{tp} and m_{th}.

APPLICATIONS TO BRIDGES WITH CONTINUOUS STIFFENING TRUSSES

The structure which was previously analyzed as a bridge with simply supported spans will now be considered as having continuous spans. Computations will be shown for only one set of influence lines—for $c\,l = 7.00$ and $c_1\,l_1 = 3.50$. Similar computations for $c\,l = 6.00$ and $c_1\,l_1 = 3.00$ must be made, but only the results are included.

The deflections in the side span for a moment T_1 at the tower are computed from Eq. 19 and are shown in dimensionless form in Col. 2, Table 4. Similar computations for the main span are shown in Cols. 7 and 8 for moments at each tower. Deflections for equal moments $T = T_1 = T_2$ at the towers are computed in Col. 9 as the sum of terms in Cols. 7 and 8. The areas of these deflection curves and their slopes at the towers are shown at the bottoms of the columns.

The end moments T_h for a unit value of H will be evaluated by equating the angles at the towers. From Table 1,

$$\phi_h = 0.1509\,\frac{f_1\,l_1}{E\,I_1} + 0.07426\,\frac{f\,l}{E\,I} \quad \text{(23a)}$$

The tower moments T_h must produce an equal angular deflection, as obtained from Table 4.

$$\phi_h = 2.506\,\frac{T_h}{H_r\,l_1} + 6.987\,\frac{T_h}{H_r\,l} \quad \text{(23b)}$$

Equating the angles of Eqs. 23,

$$\frac{T_h}{H_r} = 0.006434\,\frac{f\,l^2}{E\,I} \quad \text{(24)}$$

The last term in Eq. 20 will be computed from this value of T_h/H_r and from the areas shown in Table 4, as follows:

$$-\sum \frac{8f}{l^2}\int_0^l \eta_{ht}\,dx = -\,2 \times \frac{8f_1}{l^2_1} \times 0.2310 \times \frac{T_h\,l_1}{H_r} - \frac{8f}{l^2} \times 0.7148\,\frac{T_h\,l}{H_r} = -\,0.004835 \quad \text{(25)}$$

The value of D_1 is determined by adding this term to the value of D previously computed for the noncontinuous structure: $D_1 = 0.011341 - 0.004835 = 6{,}506 \times 10^{-6}$ ft per kip. This value of D_1 and the value of T_h/H_r are used to compute values of η_{ht}/D_1 in Cols. 3 and 10 by multiplying the dimensionless values of Cols. 2 and 9 by $T_h/H_r\,D_1 = 0.9353$. The values of $-\,\eta_h/D_1$ shown in Cols. 4 and 11 were computed from Table 1 in the same manner as for the noncontinuous structure previously analyzed. The H-influence-line ordinates were obtained in Cols. 5 and 12 of Table 4 by summing the preceding columns.

The influence line for bending moment at $x = 0.2\,l$ has been computed in Table 5. The bending moment m_{th}, which is the continuity correction to the bending moment for a unit value of H, is determined from Eq. 18 by substituting T_h from Eq. 25. Because T_h acts at both ends of the main span, values of $x = 0.2\,l$ and $l - x = 0.8\,l$ must both be used.

$$m_{th} = T_h \frac{\sinh 0.2\,c\,l + \sinh 0.8\,c\,l}{\sinh c\,l} = 6.62 \text{ ft.}$$

TABLE 5.—INFLUENCE LINE FOR BENDING MOMENT AT 0.2 l (TRUSSES CONTINUOUS OVER SUPPORTS)

Procedure:

Col. 2 contains values in Col. 5 of Table 4, multiplied by − 3.67.
Col. 3 contains values in Col. 2 of Table 4, multiplied by (left span) − 18.03 and by (right span) 1.37.
Col. 4 contains the sums of Col. 2 plus Col. 3 of Table 5 (this table).
Col. 6 contains values in Col. 12 of Table 4 multiplied by − 3.67.
Col. 7 contains values determined by using Eqs. 8 and 9.
Col. 8 contains the values in Col. 8 of Table 4 multiplied by − 18.03.
Col. 9 contains the values in Col. 7 of Table 4 multiplied by 1.37.
Col. 10 contains the sums of Cols. 6, 7, 8, and 9, of Table 5 (this table).

Side Spans (m_p = 0)			
$\frac{k_1}{l_1}$ (1)	$\frac{H}{P}(m_h+m_{th})$, in feet (2)	m_{tp}, in feet (3)	$\frac{M}{P}$, in feet (4)
Left			
0	0	0	0
0.1	−0.22	−1.33	−1.55
0.2	−0.40	−2.78	−3.18
0.3	−0.49	−4.04	−4.53
0.4	−0.49	−5.14	−5.63
0.5	−0.41	−5.96	−6.37
0.6	−0.25	−6.47	−6.72
0.7	−0.05	−6.35	−6.40
0.8	+0.12	−5.50	−5.38
0.9	+0.18	−3.54	−3.36
1.0	0	0	0
Right			
0	0	0	0
0.1	+0.18	0.27	0.09
0.2	+0.12	0.42	0.30
0.3	−0.05	0.48	0.43
0.4	−0.25	0.49	0.24
0.5	−0.41	0.45	0.04
0.6	−0.49	0.39	−0.10
0.7	−0.49	0.31	−0.18
0.8	−0.40	0.21	−0.19
0.9	−0.22	0.10	−0.12
1.0	0	0	0

Main Span					
$\frac{k}{l}$ (5)	$\frac{H}{P}(m_h+m_{th})$, in feet (6)	m_p, in feet (7)	m_{tp1}, in feet (8)	m_{tp2}, in feet (9)	$\frac{M}{P}$, in feet (10)
0	0	0	0	0	0
0.05	−0.53	10.07	− 4.42	0.07	5.19
0.10	−1.30	21.38	− 7.28	0.13	12.93
0.15	−2.18	35.34	− 9.03	0.20	24.33
0.20	−3.06	53.67	− 9.98	0.27	40.90
0.25	−3.88	37.82	−10.39	0.34	23.89
0.30	−4.61	26.65	−10.41	0.40	12.03
0.35	−5.20	18.78	−10.16	0.46	3.88
0.40	−5.64	13.23	− 9.72	0.51	− 1.62
0.45	−5.90	9.32	− 9.15	0.59	− 5.14
0.50	−6.00	6.57	− 8.47	0.64	− 7.36
0.55	−5.90	4.62	− 7.74	0.70	− 8.32
0.60	−5.64	3.25	− 6.95	0.74	− 8.60
0.65	−5.20	2.28	− 6.13	0.77	− 8.28
0.70	−4.61	1.60	− 5.27	0.79	− 7.49
0.75	−3.88	1.11	− 4.42	0.79	− 6.40
0.80	−3.06	0.75	− 3.54	0.76	− 5.09
0.85	−2.18	0.53	− 2.66	0.69	− 3.62
0.90	−1.30	0.30	− 1.78	0.55	− 2.23
0.95	−0.53	0.14	− 0.89	0.34	− 0.94
1.0	0	0	0	0	0

The value of $m_h = -\ 10.29$ ft is the same as previously computed for the noncontinuous structure: $m_h + m_{th} = -\ 10.29 + 6.62 = -\ 3.67$ ft. This value represents the bending moment at $x = 0.2\,l$ in the continuous truss for a unit value of H. The values of $(H/P)\,(m_h + m_{th})$ are computed in Cols. 2 and 6 of Table 5 by multiplying the H-influence-line ordinates by -3.67.

Values of m_p as defined in Fig. 8(b) are tabulated in Col. 7, Table 5, and are the same as those in Col. 8, Table 2, for the noncontinuous structure. The angles ϕ_{p1} and ϕ_{p2} defined in Fig. 8(*b*) were computed by differentiating Eqs. 8 and 9 with $\phi_{p1} = 0.2466$ and $\phi_{p2} = 0.0035$. These angles must be equated to the angles produced by T_{p1} and T_{p2} obtained from Table 4.

$$\phi_{p1} = 2.506 \frac{T_{p1}}{H_r\, l_1} + 6.000 \frac{T_{p1}}{H_r\, l} + 0.987 \frac{T_{p2}}{H_r\, l} = 0.2466$$

and

$$\phi_{p2} = 2.506 \frac{T_{p2}}{H_r\, l_1} + 6.000 \frac{T_{p2}}{H_r\, l} + 0.987 \frac{T_{p1}}{H_r\, l} = 0.0035.$$

Solving these equations simultaneously yields $T_{p1} = 0.02254\ H_r\, l$ and $T_{p2} = -0.00171\ H_r\, l$. The values of m_{tp} in the side spans (Col. 3, Table 5) were determined by multiplying values in Col. 2, Table 4, by $-\ 0.02254\ l$ or $-\ 18.03$ for the left side span and $+\ 0.00171\ l$ or 1.37 for the right side span. The values of m_{tp} in the main span were computed separately for T_{p1} and T_{p2}. Col. 8, Table 4, was multiplied by $-\ 0.02254\ l$ to yield Col. 8, Table 5, and Col. 7, Table 4, was multiplied by $+\ 0.00171\ l$ to yield Col. 9, Table 5. The final bending-moment influence-line ordinates were obtained for the side spans in Col. 4 by combining Cols. 2 and 3. The influence-line ordinates for the main span are obtained in Col. 10 as the sum of ordinates in Cols. 6, 7, 8, and 9.

The temperature stresses may be computed in a manner similar to that for the simply supported structure.

$$H_t = \mp \frac{\omega\, t\, L_t}{D_1} = \mp \frac{0.0000065 \times 60 \times 1{,}998}{0.006506} = \mp\ 119.9 \text{ kips.}$$

The change in bending moment resulting from the temperature change has the following values at $x = 0.2\, l$: $M_t = H_t\, (m_h + m_{th}) = \pm\ 119.9 \times 3.67 = \pm$ 440 ft-kips.

The final values of H and M will be computed for the uniform live load extending from the left tower to $x = 0.41\ l$ of the main span in order to compare results with those of Mr. Steinman[2]. Another set of influence lines was computed for $c\, l = 6.00$, and areas were obtained by the Simpson rule. The final values for $c\, l = 6.632$ (used by Mr. Steinman) are interpolated. The final bending moment for $c\, l = 7.0$ is 6,570 ft-kips and for $c\, l = 6.0$ is 7,480 ft-kips. The interpolation yields a bending moment of 6,900 ft-kips as compared to 6,970 ft-kips computed by the deflection theory. A part of the error is probably computational.

CONCLUSIONS

Long-span suspension bridges may be readily analyzed by the use of influence lines. Two sets of influence lines are necessary, corresponding to different values of $c\, l$. A linear interpolation yields the desired accuracy. For each set of influence lines, $c\, l$ is assumed constant. This permits superposition of loads, bending moments, shears, and deflections. Any type of continuous or noncontinuous structure may be considered.

Influence lines for shear may be constructed in the same manner as the bending-moment influence lines. The influence line for shear in a simple beam in tension is determined by differentiating Eqs. 8 and 9. The shear effect of the cable is found by differentiating Eq. 10. The final influence line for shear in a noncontinuous bridge is then determined by multiplying the ordinates of the influence line for H by a constant and superimposing them on the influence line for a simple beam in tension. In a continuous structure the continuity effects are also superimposed.

The influence-line procedure has many advantages over more abstract mathematical procedures. The designer can visualize the shape of the influence lines as deflection curves of the structure and thus check each step of his work against gross errors. The work is facilitated by use of tabulated ordinates of deflection curves in dimensionless form.

ACKNOWLEDGMENTS

The preliminary copy of this paper was read by Mr. Steinman, C. H. Gronquist, M. ASCE, Mr. Selberg, and Mr. Karol. Their suggestions and encouragement are appreciated. The late A. A. Jakkula contributed to earlier work[10] on this problem.

DISCUSSION

Nan-sze Sih,[11] A. M. ASCE.—The author has used the concept of a fictitious beam in tension in his analysis of the suspension bridge by the deflection theory and the assumption of superposition. This results in the misleading idea of the function of the stiffening truss and the basic principle of the deflection theory because the deflection theory is also applicable to the suspension bridge without a stiffening truss. However, if η is replaced by $\eta_P + \eta_h$ in the basic equation (Eq. 2) (as defined by the author), the two following equations will result:

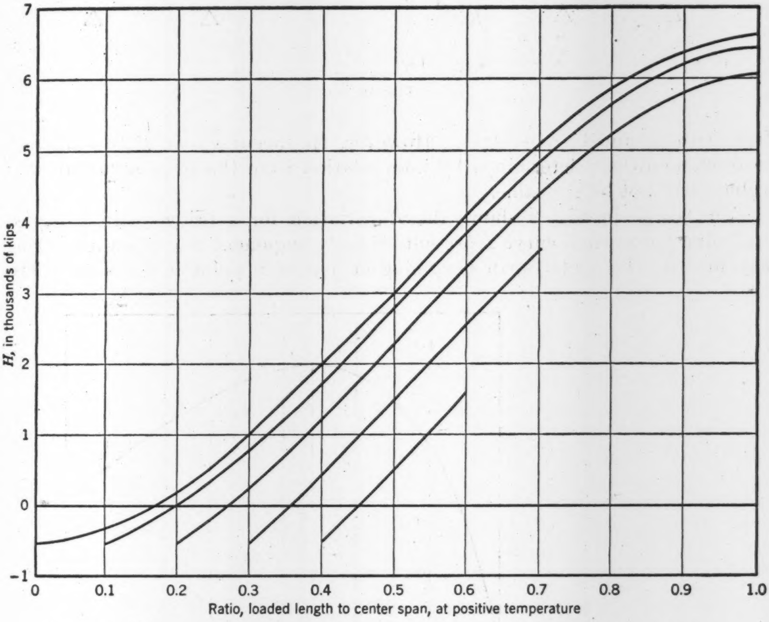

Fig. 9.—*H*-Variation Produced by an Advancing Live Load on the Center Span

$$E\,I\,\frac{d^2\eta_P}{dx^2} = M_o - (H_w + H)\,\eta_P$$

and

$$E\,I\,\frac{d^2\eta_h}{dx^2} = -\,H\,y - (H_w + H)\,\eta_h \qquad \text{.............. (26)}$$

in which y is assumed to be parabolic. Eqs. 26 are similar to the expression for the bending moment of a simple beam. All the results as presented by the author are also yielded by integration of Eqs. 26.

---

[11] Asst. Structural Engr., Ammann & Whitney, Cons. Engrs., New York, N. Y.

The same is true in the influence line of H for the cable which can also be determined using the work-and-energy concept, noting that $(8\,f/l^2) \int_0^l \eta_P\, dx = \eta_h$.

The convergence of the equation for H in the deflection theory is rapid so that usually a second trial will produce a sufficiently accurate result. This fact is also illustrated by the author in obtaining the H-value by interpolation from two assumed $(c\,l)$-values. However, the accuracy of H for different loading conditions determined by interpolation from the same assumed $(c\,l)$-values may not be the same.

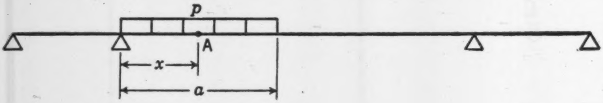

FIG. 10

The graph in Fig. 9 shows the H-variation for a bridge with a hinged stiffening truss; each curve represents the H-component due to an advancing live load on the center span beginning at a certain point in the span. The graph was made while computation was progressing; it was then used to predict other trial values and also served as a check on the consistency of the results. From Fig. 9 it can be seen that H varies almost linearly only within a certain range of loading.

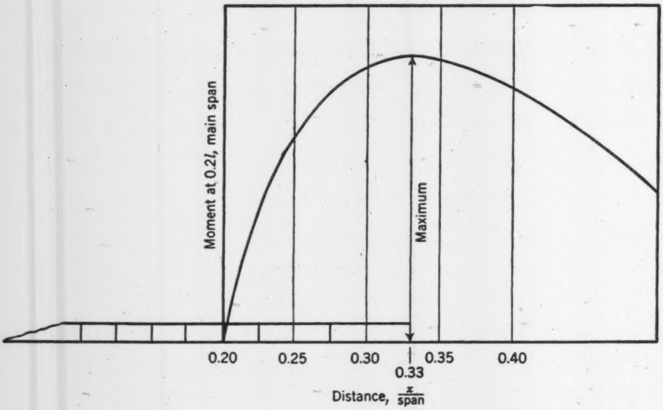

FIG. 11.—LOADING PRODUCING MAXIMUM MOMENT AT 0.2 L OF THE CENTER SPAN

The H-component for the cable is the only redundant in the analysis; after H is found, determination of the bending moment in the stiffening truss is rather simple. In using the deflection-theory equations, simplification can be made by omitting certain terms in the equation by inspection—for example, for the moment at point A under the loading as shown in Fig. 10,

$$\left.\begin{aligned} C_1 &= \frac{p}{2\,H\,c^2}\,\frac{e^{c(l-a)} + e^{-c(l-a)} - 2\,e^{-cl}}{e^{cl} - e^{-cl}} - \frac{8\,f}{l^2}\,\frac{1}{1 + e^{cl}}\,\frac{1}{c^2} \\ C_2 &= -\,C_1 + \frac{1}{c^2}\left(\frac{p}{H} - \frac{8\,f}{l^2}\right) \\ \text{and} \quad M_x &= -\,H\left[C_1\,e^{cx} + C_2\,e^{-cx} - \frac{1}{c^2}\left(\frac{p}{H} - \frac{8\,f}{l^2}\right)\right] \end{aligned}\right\} \ldots\ldots (27)$$

If a is small in comparison to span L, the equation for moment at A may be written as

$$M_x = -\,H\left[\frac{1}{c^2}\frac{1}{2}\frac{p}{H}\,e^{-c(a-x)} - \frac{1}{c^2}\left(\frac{p}{H} - \frac{8\,f}{l^2}\right)(1 - e^{-cx})\right] \ldots\ldots (28)$$

The values of e^{cx} can be interpolated from a table of values of e^{kcl}.

To find the maximum value of the moment at a point, moments are computed for different lengths and positions of loading, and a curve can be drawn to determine the loading producing the maximum moment—such as the one shown in Fig. 11.

Similar procedures can be used for all other analyses of the suspension bridge by the deflection theory—a fact which can simplify the analysis—and the effect of such simplification is always known. On the other hand, it would be helpful if the effect of the assumption of superposition as suggested by the author were illustrated by a few typical examples and if the effect of this assumption were expressed analytically.

JACOB KAROL,[12] M. ASCE.—The use of influence lines in the analysis of suspension bridges by the deflection theory is shown in this excellent paper to be both feasible and accurate. The procedure is similar to that used in the analysis of indeterminate structures and should be readily understood by bridge designers. The writer developed a similar procedure in his doctoral thesis,[7] except that a single influence line for cable tension was determined for a value of H based on the dead load plus one half the live load on all spans. For computing the maximum live-load moment or shear at a particular point, a loaded length was assumed and the value of H was determined. The moment or shear was then found by substitution in the basic equation of the deflection theory using the final value of $c\,l$. To facilitate analysis dimensionless tables for the slopes and deflections at the tenth points of the span and areas under the deflection curves were given in the thesis for integral values of $c\,l$ from 0 to 10, for concentrated and partial uniform loads, and for end moments. Stiffness and carry-over factors and fixed-end moments were also given for integral values of $c\,l$ from 0 to 10, making possible the use of moment distribution in computing the moments and shears in continuous stiffening trusses. For the same continuous structure analyzed by the author, the moments were generally within 1% of those determined by Mr. Steinman,[2] thus indicating that the use of a single influence line for H yields results accurate enough for final analysis.

---

[12] Prin. Design Engr., Howard, Needles, Tammen and Bergendoff, Kansas City, Mo.

With this in mind, it will now be shown that computation of only one set of influence lines is necessary in the author's procedure as well. Simple formulas will be presented for determining the necessary correction to the final values of $c\,l$.

The writer first considers the influence line for horizontal cable tension for the bridge with hinged stiffening trusses. It is assumed that this has been computed for $c\,l = 7.0$ in the main span and $c_1\,l_1 = 3.5$ in the side spans. If the influence line for H for another set of $(c\,l)$-values is assumed to be affinely related to the known curve, its ordinates will be directly proportional. Hence, it is only necessary to compute the ordinate at the center of the main span using Eq. 13 to determine this ratio. This statement is applicable to the cable tension due to live load only. For temperature stresses, the cable tension is inversely proportional to the D-values for the two sets of values for $c\,l$. Applying this method to the results in Table 3 for $c\,l = 6.0$ and $c_1\,l_1 = 3.0$, live load on 0.4 of the span, plus a temperature change of + 60°, produces

$$\begin{aligned} H \text{ (live load)} &= 339.0 \times 1.0333 = 350.3 \text{ kips} \\ H \text{ (temperature)} &= -\,68.7 \times 0.804 = -\,55.2 \text{ kips} \\ &\qquad\qquad\qquad\quad \overline{295.1 \text{ kips}} \end{aligned}$$

The author's computed H-value is 294.0 kips.

The cable tension for any value of $c\,l$ can also be determined directly using the elastic theory. Studies by the writer indicated that the cable tension due to live load on the main span is approximately

$$H = H_o \times \frac{K}{K + c\,l} \quad \text{.....................} \quad (29)$$

in which H_o is the cable tension from the elastic theory and $K = 57.5 \div (1 + p/w)$. Similarly, the cable tension due to temperature is

$$H_t = H_{ot} \times [1 + 0.1\,(c\,l)^2] \times \frac{K}{K + c\,l} \quad \text{............} \quad (30)$$

in which H_{ot} is the cable tension determined by using the elastic theory. For the loading previously specified, $H_o = 396.5$ kips, $H_{ot} = -\,13.7$ kips, and $K = 43.0$. Correcting this to the final value of $c\,l = 6.70$ for a live load on 0.4 of the span and for a temperature change of + 60°,

$$\begin{aligned} H &= 396.5 \times 0.865 = 343.0 \text{ kips} \\ H &= -\,13.7 \times 5.49 \times 0.865 = -\,65.0 \text{ kips} \\ &\qquad\qquad\qquad\qquad\quad \overline{278.0 \text{ kips}} \end{aligned}$$

Eqs. 29 and 30 can also be used to correct the cable tension from a known set of $(c\,l)$-values to another set of $(c\,l)$-values. Correcting the assumed known values for $c\,l = 7.00$ to the final value of $c\,l = 6.70$,

$$\begin{aligned} H &= 339.0 \times 1.006 = 341.0 \text{ kips} \\ H &= -68.7 \times 0.9305 \times 1.006 = -64.2 \text{ kips} \\ &\qquad\qquad\qquad\qquad\qquad\overline{276.8 \text{ kips}} \end{aligned}$$

This nearly checks the author's H-value in Table 3.

The writer will next consider the value of the moment at the 0.2 point in the main span for the specified loading. The influence line for moment for another set of $(c\,l)$-values is not affinely related to that for $c\,l = 7.0$ and $c_1\,l_1 = 3.5$; hence, another method of correction must be used.

It is assumed that the stiffening truss has zero deflection and moment at the end of the loaded length. Hence, the loaded segment is equivalent to a simple beam. The rate of change of moment for a particular span x uniformly loaded with the change in $c\,x$ is

$$\frac{dM}{d(c\,x)} = M\left(\frac{-2}{c\,x} + \frac{1 + \cosh 0.5\,c\,x}{\sinh c\,x}\right)\Delta(c\,x) \approx M\left(\frac{-2\,\Delta(c\,x)}{c\,x - 0.3 + \pi^2/c\,x}\right) \quad \text{..(31)}$$

For greater accuracy the average value of $c\,x$ should be used in Eq. 31. The correction is applied to the total moment due to live load and temperature.

The moment will be computed corresponding to the final value of $c\,l = 6.70$ because that will be the result used in design. For $c\,l = 7.00$, $c\,x = 2.80$. For $c\,l = 6.70$, $c\,x = 2.68$. The average value of $c\,x$ is 2.74, and the correction factor by Eq. 31 is $0.0397\,M$. Hence, the final moment is $M = 1.0397 \times 8{,}046 = 8{,}365$ ft-kips.

It is interesting to compute the final moments using the values for $c\,l = 6.00$ as known values. For $c\,l = 6.00$, $c\,x = 2.40$. The average value of $c\,x = 2.54$, and the correction factor by Eq. 27 is $-0.0913\,M$. Hence, the final moment is $M = 0.9087 \times 9{,}189 = 8{,}351$ ft-kips. Both results are in close agreement with the value of 8,371 ft-kips yielded by the deflection theory.

A similar correction formula can be written for shear. The rate of change of shear for a specified span x uniformly loaded with the change in $c\,x$ is

$$\frac{dV}{d(c\,x)} = V\left(\frac{-1}{c\,x} + \frac{1}{\sinh c\,x}\right)\Delta(c\,x) \approx V\left[\frac{-\Delta(c\,x)}{c\,x - 1 + (6.7/c\,x)}\right] \quad \text{..(32)}$$

It should be noted that the loaded length is used as the span for positive moment and shear, but the unloaded length should be used for negative moment and shear. The corrections for shear at intermediate points of the span on this basis are approximate but satisfactory because shear is not usually critical in the design of suspension bridges.

Correction formulas for cable tension for the moment and shear in continuous stiffening trusses would be more complicated than those developed here. However, because of the greater amount of computation involved in determining the influence lines, even an approximate method of correction would be desirable.

The influence line for horizontal cable tension for another set of $(c\,l)$-values may be assumed affinely related to that computed for $c\,l = 7.0$. If the live load extends from the left tower to $x = 0.41\,l$, $H = 350$ kips for $c\,l = 7.0$. For $c\,l = 6.0$ and $c_1\,l_1 = 3.0$, corrections will be made using Eqs. 29 and 30 even though they are applicable only to hinged stiffening trusses. Hence, the approximate cable tension for these $(c\,l)$-values is for live load on 0.41 of the span and for a temperature change of + 60°

$$\begin{aligned} H &= 350 \times 1.020 = 357.0 \text{ kips} \\ H &= -119.9 \times 0.780 \times 1.020 = -95.3 \text{ kips} \\ & \qquad\qquad\qquad\qquad\quad \overline{261.7 \text{ kips}} \end{aligned}$$

By interpolation, the value of H for $c\,l = 6.632$ is approximately 242 kips. Using this value of H the total cable tension is 3,909 kips, for which the computed value of $c\,l$ is 6.633. This is a close check on the accuracy of the proposed method despite the approximations involved.

The correction for the moment at a distance $0.2\,l$ on the main span is complicated by the fact that there is a negative moment at the left tower and a positive moment at the right tower for this loading so that the length to be used for the equivalent simple span is not apparent. It will arbitrarily be assumed as the loaded length, $0.41\,l$. For $c\,l = 7.00$, $c\,x = 2.87$. For the final value of $c\,l = 6.632$, $c\,x = 2.72$. The average value of $c\,x = 2.795$, and the correction factor from Eq. 31 is $0.0497\,M$. Hence, the final moment is $M = 1.0497 \times 6{,}570 = 6{,}896$ ft-kips. This is practically the same as the author's M-value of 6,900 ft-kips.

The designer must exercise judgment in estimating the equivalent length to be used for correcting the moments at other points in the span. Thus, for the negative moment at the tower, full load on the side span contributes about one half of the total moment. Hence, a correction based on the side span as the equivalent length should yield results that are accurate enough for design. If the influence lines are computed for a value of H corresponding to a load equal to the dead load plus one half the live load on all the spans, the corrections will usually be small and the errors necessarily smaller. The assumptions used in design, especially that of uniform moment of inertia, involve greater errors than does the foregoing correction procedure.

Some discussion of the equivalent uniform moment of inertia to be used in analysis is worthwhile because the stiffening girders or trusses for longer spans, at least, vary in section along the span. In computing the influence line for horizontal cable tension, the hanger loads are assumed to be uniformly distributed along the spans. Also, each span is deflected in a single loop. Hence, an equivalent uniform moment of inertia for each span which gives the same center deflection for uniform load as that computed for the actual stiffening member seems logical for this condition. For partial live load in the main span, that span deflects in two or three loops, and the equivalent moment of inertia may be different for each loop. Furthermore, the effect of web deflection is usually ignored in computing the equivalent moments of inertia. Web deflection for the single loops is approximately from 5% to 10% of the chord deflection. For the double and triple loops, it would be somewhat greater. However, the effect of ignoring both the web deflection and the variation in section is compensating, and therefore the computed values of moment and shear based on the uniform *I*-value are probably somewhat on the safe side. It should be apparent that computations by the deflection theory for an ideal but hypothetical uniform *I*-value do not yield the exact values of moment and shear at all sections in the actual structure.

The writer has developed a simple numerical procedure for analyzing suspension bridges by the deflection theory, taking into account the variation in *I* for both hinged and continuous trusses. For the continuous truss investigated by the author, it was found that the maximum negative moment at the tower increased about 10%. In the hinged truss, the maximum moment near the quarter point increased approximately 3%. These results were based on neglecting the effect of web deflection in computing the equivalent *I*-value.

It is hoped that Mr. Peery's dimensionless tables will be included in the closure because his method of analysis is predicated on their availability for ease and rapidity in computation.

HARRY M. PALMBAUM,[13] J. M. ASCE.—The author is to be commended for his clear explanation and derivation of the influence-line equations for a suspension bridge. However, only the equations for analyzing moment in the stiffening truss were developed. The writer intends to demonstrate how the same type of reasoning can be applied to shear in a simply supported stiffening truss.

To avoid the use of trial-and-error methods for determining the necessary loaded lengths of a bridge for maximum shear, values of loaded lengths can be obtained for two extreme values of stiffness. After the influence lines for shear at a distance *x* have been found for two values of stiffness, an approximation can be made for some intermediate stiffness. The approximation of straight-line interpolation is usual, but the shear values do not vary linearly. Although the work of producing the influence line is lengthy and tedious, most of the work, except for a few constants, can be re-used for any other bridge whose stiffness ranges between the available extremes.

The method of variation of the influence line for shear with stiffness is shown in Fig. 12. The physical meaning of Fig. 12 can be explained by an increase in temperature, causing an increase in cable sag with a corresponding decrease in bridge stiffness. At the lower stiffness value more of the span may be loaded for a maximum positive shear at distance *x*, and therefore the zero point for $c\,l = 13$, the minimum stiffness to be expected for a particular span, yields a longer critical loaded length than does the zero point for $c\,l = 13$.

Referring to the author's paper and using a "*v*" after the equation number to denote shear equations similar to the author's moment equations, the following equations result.

---

[13] Engr., Freyssinet Co., Inc., New York, N. Y.

By differentiating Eq. 8,

$$v_p = \frac{\sinh c\,(l - k)}{\sinh c\,l} \cosh c\,x \qquad x < k \ldots\ldots\ldots\ldots (8\,v\,a)$$

or in exponential form,

$$v_p = \frac{e^{2(cl-ck)} - 1}{2\,(e^{cl} - e^{-cl})\,e^{cl-ck}}\,(e^{cx} + e^{-cx}) \qquad x < k \ldots\ldots\ldots (8\,v\,b)$$

By differentiating Eq. 9,

$$v_p = \frac{-\sinh c\,k}{\sinh c\,l} \cosh c\,(l - x) \qquad x > k \ldots\ldots\ldots\ldots (9\,v\,a)$$

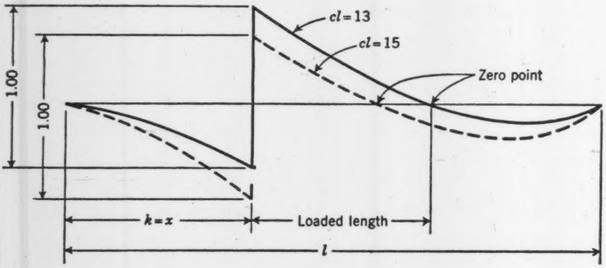

FIG. 12.—METHOD OF VARYING THE INFLUENCE LINE FOR SHEAR

or in exponential form,

$$v_p = \frac{e^{ck} - e^{-ck}}{2\,(e^{cl} - e^{-cl})}\,(e^{cl-cx} + e^{-cl+cx}) \qquad x > k \ldots\ldots\ldots (9\,v\,b)$$

The terms in Eqs. 8 v and 9 v are independent of physical characteristics and can, when tabulated, be re-used for any suspension bridge of equal stiffness. By differentiating Eq. 10,

$$-\,v_h\,\frac{l}{f} = \frac{8}{c\,l}\left(\tanh\frac{c\,l}{2}\cosh c\,x - \sinh c\,x\right) \ldots\ldots\ldots\ldots (10\,v\,a)$$

or in exponential form,

$$-\,v_h\,\frac{l}{f} = \frac{4}{c\,L\cosh\frac{c\,L}{2}}\,(e^{c(0.5l-x)} - e^{-c(0.5l-x)}) \ldots\ldots\ldots\ldots (10\,v\,b)$$

$$\eta_h\,\frac{E\,I}{f\,L^2} = \frac{8}{c^4\,l^4}\left(\tanh\frac{c'}{2}\sinh c\,x - \cosh c\,x + 1 - \frac{c^2\,l^2\,y}{8\,f}\right) \qquad (11\,v)$$

The terms in Eq. 11 v show that this factor or Eq. 13 v (which appears subsequently) can also be re-used in future influence-line computations of the same ($c\,l$)-value, provided the sag-length ratio is unchanged.

By substituting the value found in Eq. 11 for η_h in Eq. 12 and by integrating and transforming into exponential form, Eq. 12 v results.

$$D = \frac{l_s}{E_c\,A_c} + \sum \frac{8\,f\,l^2}{E\,I}\left(\frac{-8}{c^5\,l^5}\right)\left(\frac{e^{cl}-1}{e^{cl}+1}\,\frac{e^{cl}+e^{-cl}-2}{2} - \frac{e^{cl}-e^{-cl}}{2} + c\,l - \frac{c^3\,l^3}{12}\right) \quad \text{(12 } v\text{)}$$

Thus, for one bridge, D varies with $c\,L$ only, and therefore parts of this term can be re-used in future influence-line computations.

$$v_h\frac{H}{P} = \left(\frac{f^2\,l}{E\,I}\,\frac{1}{D}\right)\left(-\frac{v_h}{f}\,l\right)\left(\eta_h\,\frac{-E\,I}{f\,l^2}\right) \quad \text{(13 } v\text{)}$$

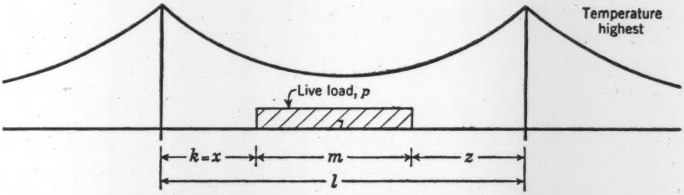

FIG. 13.—LOADING FOR MAXIMUM SHEAR, IN WHICH $z = l - (m + k)$ AND TEMPERATURE IS A MAXIMUM

In Eq. 13 v the term $f^2\,l/E\,I$ is constant for any one bridge and as such is independent of the ($c\,L$)-value. The term $1/D$ is a constant for one ($c\,L$)-value but for only one bridge. The term $\eta_h\,E\,I/(f\,l^2)$ occurs at distance k and is a constant factor in the influence line for any one value of stiffness.

By using a tabular form of solution for $-\,v_h\,l/f$, v_p and $\eta_h\,E\,I/(f\,l^2)$, the influence-line equation for shear, Eq. 14 v, can be developed.

$$\frac{V}{P}\text{ (influence line)} = v_p\text{ (influence line)} + v_h\,\frac{H}{P}\text{ (influence line)} \quad \text{(14 } v\text{)}$$

For maximum positive shear values in the main spans from the left end to near the center of the span, a partial loading can be used as shown in Fig. 13.

If the influence line is not used, several loaded lengths of span for each of twenty points along the span to be investigated are solved for shear, and a curve is plotted for each point showing the variation of shear at that point. An envelope of maximum positive shears is then drawn connecting the maximum value of shear determined at each of the twenty points along the span. Because of symmetry, the number of points can be halved to ten. However, at each one of the points a minimum of three complete results of shear must be determined.

When influence lines for shear corresponding to two stiffnesses are known, as well as the corresponding zero points, the trials for shear are eliminated.

For example, with a partial loading on the main span and the highest positive temperature, the assumed $(c\,l)$-value should be approximately 13.5 for a trial. By linear interpolation between the zero-point values for $c\,l = 13$ and $c\,l = 15$, trial lengths for m and z are obtained. Corresponding to the $(c\,l)$-value assumed is a value of H from Eq. 7. Using deflection-theory equations for this loaded length and temperature, a value of H is determined which will be somewhat different from the assumed value. Because the values of H converge rapidly it is a speedy process to solve for new values of c, $c\,l$, m, and z and find the third value for H. The second trial for H will usually be sufficient; maximum shear values at each point can be immediately solved and the envelope of maximum shears plotted very quickly.

Because the zero points of the influence lines for the longer spans can differ by as much as $2\frac{1}{2}\%$ of the length, it seems more reasonable not to use the areas under the influence line. By using the influence line, several trials for shear at each point are unnecessary, the shear variation due to partial loading is easily visualized, and the design time can be reduced. Furthermore, many of the computations for the influence line can be re-used as indicated for future similar work.

VINCENZO FRANCIOSI.[14]—The treatment by Mr. Peery is based on the identity of the equations relating the deflections to the bending moments in both (1) the suspension bridge and (2) the simple beam subjected to (*a*) an axial force equal to total horizontal tension H_r, (*b*) a uniformly distributed load equal to $-8\,f\,H/l^2$, and (*c*) the same concentrated loads as those acting on the suspension bridge.

From this consideration it would be possible to add algebraically the stresses producible by the component loadings of a combination of loadings and by a constant value of the total horizontal tension H_r, thereby producing the influence lines for the stresses. The principal meaning of influence lines is lost, however. In fact, the applied loads cause the horizontal tension to vary, and, hence, it is impossible to know which position of a given train of loads causes the stresses in a particular section of the beam to attain their greatest values. The use of these influence lines is then confined to the valuation of the stresses for a specified load condition, for which purpose it is more convenient simply to draw the influence line of the horizontal tension H; with the influence line known, it is an easy matter to determine the deflections and then the bending moments along the entire span of the stiffening truss.[15,16]

The possibility of adding the stresses due to the component loadings of a particular load has already been demonstrated by the writer with reference to

---

[14] Prof. of Bridge Construction, Univ. of Naples, Naples, Italy.

[15] "Lezioni di ponti," by G. Albenga, Vol. II, Unione Tipografica Editrice Torinese, 1930, p. 390.

[16] "Sul calcolo statico dei ponti ad arco sottile con trave irrigidente," by P. B. J. Gravina, *Giornale del Genio Civile*, Rome, May, 1949.

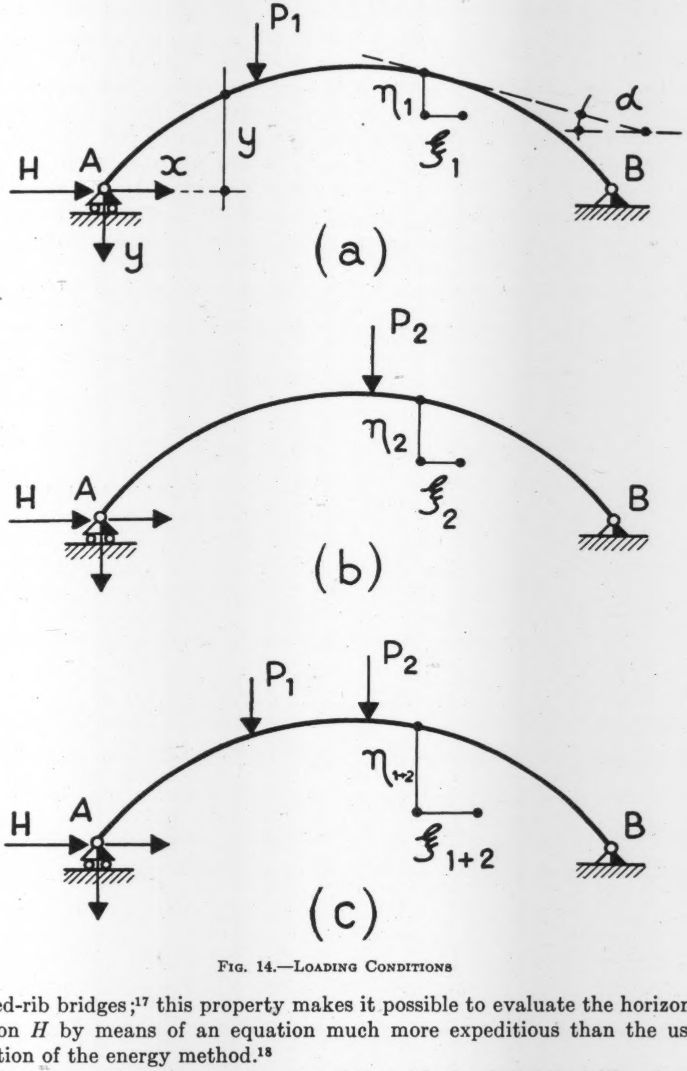

FIG. 14.—LOADING CONDITIONS

arched-rib bridges;[17] this property makes it possible to evaluate the horizontal tension H by means of an equation much more expeditious than the usual equation of the energy method.[18]

The forces acting on a structure are distinguished as being "axial" or "transverse" according to the manner in which they are influenced by the deformation

---

[17] "Il metodo della 'linea d'influenza del secondo ordine' per la ricerca della spinta addizionale nei ponti a travata irrigidente," by V. Franciosi, *La Ricerca*, Naples, 1951.

[18] "Mathematical Methods in Engineering," by Theodor Von Kármán, McGraw-Hill Book Co., Inc., New York, N. Y., 1940, p. 281.

—whether they cause additional stresses or not. The three loading conditions of the beam in Fig. 14 are considered: Transverse force P_1, transverse force P_2, and transverse force $P_1 + P_2$. The three load conditions are inclusive of the force H which is both transverse and axial—transverse because it causes moments $- H y$ (moments being considered positive if the bottom fibers are stretched), and axial because it causes moment $- H \eta$ (the deflections η being considered positive if directed downward). In this treatment, forces will always be considered transverse for the tensile and shearing stresses.

The deflections η_1 and η_2 are produced by P_1 and P_2, and η_{1+2} by $P_1 + P_2$ in the structure already deformed by H; the vertical and horizontal deflections are given by the following equations:

$$\left.\begin{aligned} E\,I \cos\alpha \frac{d^2 \eta_1}{dx^2} &= - M_1 - H \eta_1 \\ E\,I \sin\alpha \frac{d^2 \xi_1}{dx^2} &= - M_1 - H \eta_1 \end{aligned}\right\} \dots\dots\dots\dots (33)$$

$$\left.\begin{aligned} E\,I \cos\alpha \frac{d^2 \eta_2}{dx^2} &= - M_2 - H \eta_2 \\ E\,I \sin\alpha \frac{d^2 \xi_2}{dx^2} &= - M_2 - H \eta_2 \end{aligned}\right\} \dots\dots\dots\dots (34)$$

and

$$\left.\begin{aligned} E\,I \cos\alpha \frac{d^2 \eta_{1+2}}{dx^2} &= - M_1 - M_2 - H \eta_{1+2} \\ E\,I \sin\alpha \frac{d^2 \xi_{1+2}}{dx^2} &= - M_1 - M_2 - H \eta_{1+2} \end{aligned}\right\} \dots\dots\dots\dots (35)$$

in which M_1 and M_2 are the bending moments producible by P_1 and P_2 in the absence of H.

Adding Eqs. 33 and 34 yields

$$\left.\begin{aligned} E\,I \cos\alpha \frac{d^2 (\eta_1 + \eta_2)}{dx^2} &= - M_1 - M_2 - H (\eta_1 + \eta_2) \\ E\,I \sin\alpha \frac{d^2 (\xi_1 + \xi_2)}{dx^2} &= - M_1 - M_2 - H (\eta_1 + \eta_2) \end{aligned}\right\} \dots\dots (36)$$

By comparing Eqs. 35 and 36, one deduces that

$$\eta_{1+2} = \eta_1 + \eta_2$$

and

$$\xi_{1+2} = \xi_1 + \xi_2$$

which demonstrates the possibility of adding algebraically the effects due to the transverse forces, if the axial forces remain unaltered. Subject to the same limitation, the theorem of Betti is applicable:

$$P_1 \eta_{21} = P_2 \eta_{12} \dots\dots\dots\dots (37)$$

The two load conditions shown in Fig. 15 will be considered. The displacements η_1 and ξ_1 are due to the condition shown in Fig. 15(*a*), and η_2 and ξ_2, due to condition in Fig. 15(*b*). They are evaluated from the configuration corresponding to equilibrium under the dead load w and its corresponding horizontals tension H_w; hence, they are caused by the transverse forces, P and H (Fig. 15(*a*)), and H (Fig. 15(*b*)) in the presence of the axial force $H_w + H$, which is the same under both load conditions. Eq. 37 is valid and yields

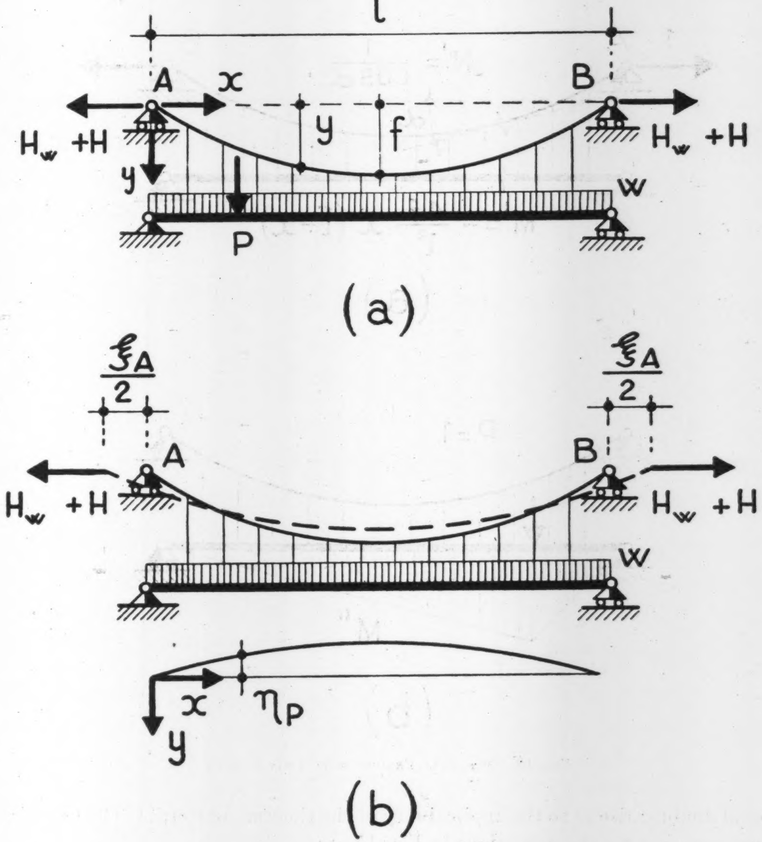

FIG. 15.—LOADS AND REACTIONS

$$H\,\xi_{2A} + P\,\eta_{2P} = H\,\xi_{1A} \quad \text{(38a)}$$

Alternatively, Eq. 38*a* can be derived in a direct way.

For that purpose, Fig. 16 shows the bending moments M' caused by two unit concentrations at A and B, respectively, equal but with opposite signs and the moments M'' caused in the same beam by a unit concentration directed along the line of action P.

Only bending moments are considered because the forces are distinguished by the writer as axial and transverse, and only in reference to the bending moments could doubts arise as to the applicability of the theorem of Betti. The bending moments causing the deflections in Fig. 15 are

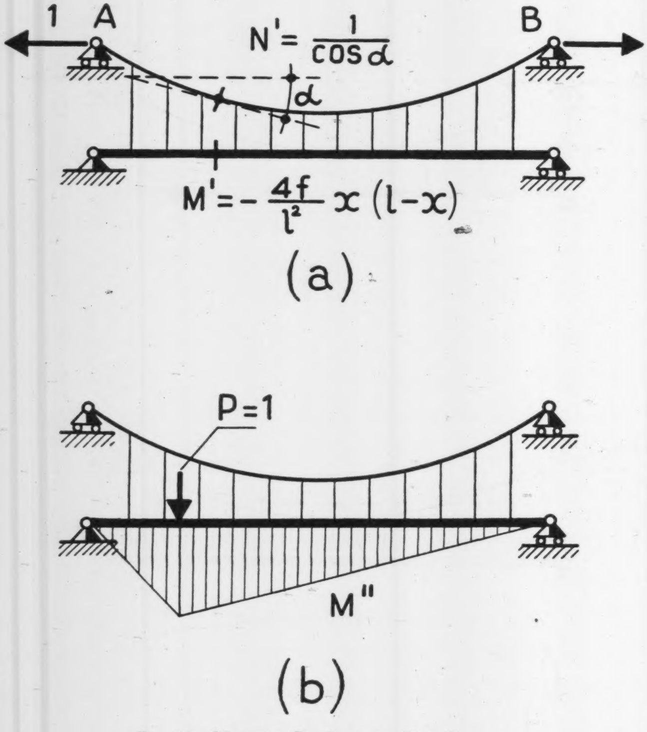

FIG. 16.—MOMENTS PRODUCED BY UNIT FORCES

$$M_1 = P\,M'' - H\,y - (H_w + H)\,\eta_1$$

and

$$M_2 = -\,H\,y - (H_w + H)\,\eta_2.$$

The principle of virtual work, applied to the equilibrated stresses of Fig. 16 and to the congruent displacements of Fig. 15, yields

$$\xi_{1A} = \frac{1}{E\,I}\int_0^l M_1\,M'\,dx = -\frac{P}{E\,I}\int_0^l M''\,y\,dx$$

$$+\frac{H}{E\,I}\int_0^l y^2\,dx + \frac{H_w + H}{E\,I}\int_0^l y\,\eta_1\,dx$$

$$\xi_{2A} = \frac{1}{E\,I}\int_0^l M_2\,M'\,dx = \frac{H}{E\,I}\int_0^l y^2\,dx + \frac{H_w + H}{E\,I}\int_0^l y\,\eta_2\,dx$$

$$\eta_{2P} = \frac{1}{E\,I}\int_0^l M_2\,M''\,dx = -\frac{H}{E\,I}\int_0^l M''\,y\,dx - \frac{H_w + H}{E\,I}\int_0^l M''\,\eta_2\,dx.$$

Eq. 38*a* can then be written

$$H^2\int_0^l y^2\,dx + H\,(H_w + H)\int_0^l y\,\eta_2\,dx - P\,H\int_0^l M''\,y\,dx$$

$$-\,P\,(H_w + H)\int_0^l M''\,\eta_2\,dx = -\,P\,H\int_0^l M''\,y\,dx$$

$$+\,H^2\int_0^l y^2\,dx + H\,(H_w + H)\int_0^l y\,\eta_1\,dx$$

and

$$H\int_0^l y\,\eta_2\,dx - P\int_0^l M''\,\eta_2\,dx = H\int_0^l y\,\eta_1\,dx$$

which can also be written as

$$\int_0^l M_{10}\,\eta_2\,dx = \int_0^l M_{20}\,\eta_1\,dx \dots\dots\dots\dots\dots\dots (38b)$$

in which M_{10} and M_{20} are the parts of first order of M_1 and M_2. The validity of Eq. 38*a* is then subordinate to the validity of Eq. 38*b*. Proof of Eq. 38*b* follows (derivatives being indicated by dots):

$$E\,I\,\ddot{\eta}_1 = -\,M_{10} + (H_w + H)\,\eta_1$$
$$E\,I\,\ddot{\eta}_2 = -\,M_{20} + (H_w + H)\,\eta_2.$$

By solving for M_{10} and M_{20} and introducing these values into Eq. 38*b*, one obtains

$$-\,E\,I\int_0^l \ddot{\eta}_1\,\eta_2\,dx + (H_w + H)\int_0^l \eta_1\,\eta_2\,dx$$

$$= -\,E\,I\int_0^l \ddot{\eta}_2\,\eta_1\,dx + (H_w + H)\int_0^l \eta_2\,\eta_1\,dx \,..\, (38c)$$

By integration,

$$\int_0^l \ddot{\eta}_1\,\eta_2\,dx = (\dot{\eta}_1\,\eta_2)_0^l - \int_0^l \dot{\eta}_1\,\dot{\eta}_2\,dx$$

$$= -\int_0^l \dot{\eta}_1\,\dot{\eta}_2\,dx$$

$$\int_0^l \ddot{\eta}_2\,\eta_1\,dx = -\int_0^l \dot{\eta}_2\,\dot{\eta}_1\,dx$$

and Eq. 38*c* can then be written as

$$E\,I \int_0^l \dot{\eta}_1\,\dot{\eta}_2\,dx + (H_w + H) \int_0^l \eta_1\,\eta_2\,dx$$

$$= E\,I \int_0^l \dot{\eta}_2\,\dot{\eta}_1\,dx + (H_w + H) \int_0^l \eta_2\,\eta_1\,dx$$

which is an identity. Eq. 38*c* is hence valid, and Eq. 38*a* also. If H in Fig. 15 is caused by P on the cable hinged in A and B, then $\xi_{1A} = 0$, and Eq. 38*a* can be written as

$$H\,\xi_A + P\,\eta_P = 0 \quad\text{.....................}\quad (39)$$

(The subscript 2 has been omitted for the sake of simplicity.)

From Eq. 39,

$$H = -\,P\,\frac{\eta_P}{\xi_A} \quad\text{.......................}\quad (40)$$

whereas for a distributed load p extending from abscissa a to abscissa b,

$$H = -\,\frac{1}{\xi_A}\int_a^b p\,\eta\,dx \quad\text{.....................}\quad (41)$$

Eq. 40, directly derived, is coincident with Eq. 13; it lends itself, as will be shown, to the determination of H through a procedure characterized by rapid convergence and based on the use of trigonometrical functions.

Eq. 41 assures that the diagram of η-values, to the scale in which $\xi_A = 1$, is the influence line of H. However, Eq. 41 is valid only if the horizontal tension $H_w + H$ is equal in both systems of Figs. 15(*a*) and 15(*b*). This means that, of the infinite number of lines $\eta(x)$ that can be drawn (each due to an assigned value of H), the only one which would be valid for a particular load condition must yield, through Eq. 41, the same value for H as that for which it has been drawn.

Because $M = -\,H\,y - (H_w + H)\,\eta$, it follows that

$$E\,I\,\frac{d^2\eta}{dx^2} = H\,y + (H_w + H)\,\eta \quad\text{.................}\quad (42)$$

If n represents the odd-numbered digits, and if

$$\eta(x) = \sum_{n=1,3}^{\infty} \eta_n \sin \frac{n \pi x}{l} \qquad (43a)$$

$$y(x) = \sum_{n=1,3}^{\infty} y_n \sin \frac{n \pi x}{l} \qquad (43b)$$

then, by Eq. 1 and the Fourier theorem, there results

$$y_n = \frac{2}{l} \int_0^l y \sin \frac{n \pi x}{l} \, dx = \frac{32 f}{n^3 \pi^3} \qquad (44)$$

By substituting the values from Eqs. 43*a* and 43*b* in Eq. 42 and by equating the coefficients of the sinusoids of the same order, there results

$$\eta_n = - \frac{32 H f}{n^3 \pi^3 \left(\frac{n^2 \pi^2 E I}{l^2} + H_w + H \right)} \qquad (45)$$

The displacement ξ_A is caused by the moments of first order,

$$M_o = - H y = - \frac{4 f H}{l^2} x (l - x) \qquad (46)$$

by the moments of second order,

$$M^{(2)} = - (H_w + H) \eta = - (H_w + H) \sum_{n=1,3}^{\infty} \eta_n \sin \frac{n \pi x}{l} \qquad (47)$$

and by the normal stresses,

$$N = \frac{H}{\cos \alpha} \qquad (48)$$

To obtain the values ξ_{A1}, ξ_{A2}, and ξ_{AN} connected to the stresses of Eqs. 46, 47, and 48, the principle of virtual work can be used. The writer refers to the system of equilibrated forces in Fig. 14(*a*) corresponding to the beam bending moments,

$$M' = - \frac{4 f}{l^2} x (l - x) \qquad (49)$$

and the cable normal stresses,

$$N' = \frac{1}{\cos \alpha} \qquad (50)$$

for the moments M' there are considered the relative rotations due to the moments M_o and $M^{(2)}$ and for the normal stresses N' the relative axial displacements due to the forces N.

$$\xi_{A1} = \frac{1}{E\,I}\int_0^l M_o\,M'\,dx = \frac{8\,H\,f^2\,l}{15\,E\,I}$$

$$\xi_{A2} = \frac{1}{E\,I}\int_0^l M^{(2)}\,M'\,dx = 16\,(H_w + H)\,\frac{f\,l}{E\,I\,\pi^3}\sum_{n=1,3}^{\infty}\frac{\eta_n}{n^3}$$

and

$$\xi_{AN} = \frac{1}{E\,A}\int_c N\,N'\,ds = \frac{H}{E\,A}\int_c \frac{ds}{\cos^2\alpha} = \frac{H}{E\,A}\int_0^l \frac{dx}{\cos^3\alpha} = \frac{H\,L_s}{E\,A}$$

in which A is the cross-sectional area of the cable. For a parabolic cable, the length $L_s = l + 8\,f^2/l$. Eq. 41 can be written conclusively:

$$H = -\frac{\sum_{n=1,3}^{\infty}\eta_n\,S_n}{\frac{8\,H\,f^2\,l}{15\,E\,I} + 16\,(H_w + H)\,\frac{f\,l}{E\,I\,\pi^3}\sum_{n=1,3}^{\infty}\frac{\eta_n}{n^3} + \frac{H\,L_s}{E\,A}} \quad\ldots\ldots\ (51)$$

in which

$$S_n = \int_a^b p\,\sin\frac{n\,\pi\,x}{l}\,dx.$$

In the presence of a temperature variation $\pm\,\Delta t$, Eq. 39 is modified[19] as follows:

$$H\,\xi_A + P\,\eta_P = \mp\int_c \frac{H}{\cos\alpha}\,\omega\,\Delta t\,ds = \mp\,H\,\omega\,\Delta t\int_0^l \frac{dx}{\cos^2\alpha} = \mp\,H\,\omega\,\Delta t\,L_t \ldots (52)$$

in which for a parabolic cable $L_t = l + 16\,f^2/3\,l$. In the generalized principle of Betti,[19] which is valid in the presence of displacements independent of the external forces (distortions) and which has the same limitations as does the classical principle of reciprocity, it is asserted that $L_{ab} = L_{ba}$—in which L_{ab} and L_{ba} are the "mutual works" done by the two systems of forces and distortions applied to the same structure. By mutual work L_{ab} is meant that work done by the external forces of system "a" for the displacements of system "b" and by the internal forces (stresses) of system "a" for the distortions of system "b." In the present case, the mutual work is (Fig. 14) $L_{12} = H\,\xi_A + P\,\eta_P$ and $L_{21} = \mp\int_c \frac{H}{\cos\alpha}\,\omega\,\Delta t\,ds$.

From Eq. 52 is obtained

$$H = -\frac{P\,\eta_P}{\xi_A \pm \omega\,\Delta t\,L_t} \quad\ldots\ldots\ldots\ldots\ldots\ldots\ (53)$$

That is, Eq. 51 is modified by adding the term $\omega\,\Delta t\,L_t$ to the denominator.

---

[19] "Sulle linee d'influenza di coazioni," by V. Franciosi, *L'Industria Italiana del Cemento*, Rome, March, 1950.

Use of Eq. 51 offers the advantage of determining H with as many significant digits as desired. In Mr. Peery's procedure the value to assume for H (Table 3) is determined by linear interpolation between the values computed on the basis of two values of $c\,l$, without the possibility of evaluating the error and bettering the approximation.

The errors made in computing the bending moments are therefore twofold; they can be reduced by computing H by means of Eq. 51 and by interpolating to determine only the moments with the exact value of H as a basis.

Eq. 51 can also be used in the study of arched-rib bridges, provided some modifications are introduced. In the expression for η_n (Eq. 45), the signs of H_w and H are changed so that

$$\eta_n = \frac{-\,32\,H\,f}{n^3\,\pi^3\left(\dfrac{n^2\,\pi^2\,\kappa}{l^2} - H_w - H\right)}$$

in which $\kappa = E_t\,I_t + E_a\,I_a \cos\alpha$, this expression being assumed constant.

The sign of the term $\omega\,\Delta t\,L_t$ in Eq. 53 also varies. The term A in Eq. 51 is replaced by the mean value A_m between the springing and the crown.

A numerical example involving an arched-rib bridge with the following characteristics is presented: $l = 141.73$ ft, $f = 17.06$ ft, $E = 29.87 \times 10^5$ lb per sq in., $A_m = 10.25$ sq ft, $I_a \cos\alpha\ 0.578$ ft^4, $I_t = 14.349$ ft^4, $\kappa = 641.2 \times 10^7$ lb-sq ft, $w = 4.1 \times 10^3$ lb per ft, $H_w = 603.3 \times 10^3$ lb, and $L_s = 158.16$ ft.

The load $p = 672$ lb per ft acts from the abscissa $x = 0$ to $x = l/2$. The first value assigned to H is the one producible by p in a three-hinged arch: $H = p\,l^2/16\,f = 49.45 \times 10^3$ lb. By taking into account only the first and second terms of Eq. 51, one obtains

$$S_n = \frac{l\,p}{n\,\pi}\left(\cos\frac{n\,\pi\,a}{l} - \cos\frac{n\,\pi\,b}{l}\right).$$

Also, $\eta_1 = -\,0.3490269$ ft, $\eta_3 = -\,0.0011637$ ft, $\xi_{A1} = 0.1696554$ ft, $\xi_{A2} = 0.0443367$ ft, $\xi_{AN} = 0.0017743$ ft, $\xi_A = 0.2157667$ ft, $S_1 = \dfrac{p\,l}{\pi} = 30{,}315.432$ lb, $S_3 = \dfrac{p\,l}{3\,\pi} = 10{,}105.9$ lb, and $H = 49{,}092$ lb.

By recomputing with the new value of H, one finds $\eta_1 = -\,0.3459932$ ft, $\eta_3 = -\,0.0011555$ ft, and $\xi_A = 0.2141178$ ft. Thus, H is found to equal 49,041 lb. Refining this result with another step, $\eta_1 = -\,0.3456283$ ft, $\eta_3 = -\,0.0011542$ ft, and $\xi_A = 0.2138852$ lb. Hence, $H = 49{,}044$ lb.

For the same case, using the classical equation of energy—(*a*) beginning with $H = 49{,}450$ lb, one finds $H = 4{,}903$ lb; (*b*) with $H = 48{,}263$ lb, one finds $H = 143{,}482$ lb, and (*c*) with $H = 49{,}044$ lb, one finds $H = 49{,}046$ lb.

The equation of energy does not prove convenient for a computation involving successive approximations because this iteration would diverge, and for the solution special procedures are necessary[20] together with the use of many digits. Instead, it is indicated by the developed example that Eq. 21 can be solved quickly by successive approximations, yielding at only the second step the technically exact result and requiring that only a few significant digits be determined. The error is 0.1% at the end of the first cycle and 0.005% at the end of the second one.

---

[20] "The Theory of the Suspension Bridge," by A. A. Jakkula, *Memoires*, Association Internationale des Ponts et Charpentes, 1935, p. 333.

The procedure already shown is easily extended to suspension bridges with continuous stiffening trusses. If $\bar{M}$ is the value of the moments due to the force H at the towers, Eq. 42 is written as $E\,I\,\frac{d^2\eta}{dx^2} = H\,y + (H_w + H)\,\eta - \bar{M}$, and $\bar{M} = \frac{4\,\bar{M}}{\pi}\sum_{n=1,3}^{\infty}\frac{1}{n}\sin\frac{n\,\pi\,x}{l}$. Eq. 45 is corrected to

$$\eta_n = -\frac{32\,H\,f - 4\,\bar{M}\,n^2\,\pi^2}{n^3\,\pi^3\left(n^2\,\pi^2\,\frac{E\,I}{l^2} + H_w + H\right)} \qquad \text{(54a)}$$

The η-values of the side span, with the origin of coordinates at the simply supported end, are

$$\eta_1 = \sum \eta_{1n}\sin\frac{n\,\pi\,x_1}{l_1}$$

The equation,

$$E_1\,I_1\,\frac{d^2\eta_1}{dx^2_1} = H\,y_1 + (H_w + H)\,\eta_1 - \bar{M}\,\frac{x_1}{l_1}$$

yields

$$\left.\begin{aligned} \eta_{1n} &= -\frac{32\,H\,f_1 - 2\,\bar{M}\,n^2\,\pi^2}{n^3\,\pi^3\left(n^2\,\pi^2\,\frac{E_1\,I_1}{l^2_1} + H_w + H\right)} \qquad n \text{ odd} \\ \eta_{1n} &= -\frac{2\,\bar{M}}{n\,\pi\left(n^2\,\pi^2\,\frac{E_1\,I_1}{l^2_1} + H_w + H\right)} \qquad n \text{ even} \end{aligned}\right\} \qquad \text{(54b)}$$

From the equation,

$$\left(\frac{d\eta_1}{dx_1}\right)_{x_1=l_1} = \left(\frac{d\eta}{dx}\right)_{x=0}$$

is found

$$\bar{M} = \frac{16}{\pi^2}\,H \times \frac{\frac{f_1}{l_1}\sum_{n=1,3}^{\infty}\frac{1}{n^2\left(n^2\,\pi^2\,\frac{E_1\,I_1}{l^2_1} + H_w + H\right)} + \frac{f}{l}\sum_{n=1,3}^{\infty}\frac{1}{n^2\left(n^2\,\pi^2\,\frac{E\,I}{l^2} + H_w + H\right)}}{\frac{1}{l_1}\sum_{n=1,2}^{\infty}\frac{1}{n^2\,\pi^2\,\frac{E_1\,I_1}{l^2_1} + H_w + H} + \frac{2}{l}\sum_{n=1,3}^{\infty}\frac{1}{n^2\,\pi^2\,\frac{E\,I}{l^2} + H_w + H}} \qquad \text{(55)}$$

Also,

$$\xi_{A1} = \frac{8}{15} H \left(\frac{f^2 l}{E I} + \frac{2 f^2_1 l_1}{E_1 I_1}\right) - \frac{2}{3} \bar{M} \left(\frac{f l}{E I} + \frac{f_1 l_1}{E_1 I_1}\right) \ldots\ldots (56a)$$

$$\xi_{A2} = 16 \, (H_w + H) \frac{f l}{E I \pi^3} \sum_{n=1,3}^{\infty} \frac{\eta_n}{n^3} + 32 \, (H_w + H) \frac{f_1 l_1}{E_1 I_1 \pi^3} \sum_{n=1,3}^{\infty} \frac{\eta_{1n}}{n^3} \ldots (56b)$$

and

$$\xi_{AN} = \frac{H L^*_s}{E A} \ldots\ldots\ldots\ldots\ldots\ldots\ldots\ldots\ldots\ldots (56c)$$

in which $L^*_s = \int_s \frac{dx}{\cos^3 \alpha}$. The load p_1 acts on the side span, and the load p on the central one. By expressing them with

$$p_1 = \sum p_{1n} \sin \frac{n \pi x_1}{l_1}$$

$$p = \sum p_n \sin \frac{n \pi x}{l}$$

Eq. 41 yields

$$H = - \frac{\frac{l}{2} \sum \eta_n p_n + \frac{l_1}{2} \sum \eta_{1n} p_{1n}}{\xi_{A1} + \xi_{A2} + \xi_{AN}} = - \frac{\sum \eta_n S_n + \sum \eta_{1n} S_{1n}}{\xi_{A1} + \xi_{A2} + \xi_{AN}} \ldots\ldots (57)$$

The procedure is begun by choosing an arbitrary value of H—for example, that producible in the structure statically determined by inserting hinges in the stiffening truss. Through Eq. 55 is obtained $\bar{M}$, and through Eqs. 54, η_n and η_{1n} (usually stopping at $n = 3$). Through Eqs. 56 is determined the value of ξ_A; and from Eq. 57, a better approximated value for H is thus obtained. From this value a new cycle for iteration of the procedure is begun.

DAVID J. PEERY,[21] M. ASCE.—The discussions include significant supplementary theory and substantiation of the writer's basic influence-line procedures. These contributions are appreciated. Most of the discussers treat the simpler case of the bridge with hinged stiffening trusses. The obvious questions concern the accuracy and the relative simplicity of the influence-line procedure as compared with the customary deflection theory.

Mr. Sih questions whether influence lines are applicable to unstiffened bridges and feels that they give a "misleading idea of the function of the stiffening truss." The influence lines shown in Fig. 17 include the complete range of values from $c\,l = 0$ (elastic theory) to $c\,l = \infty$ (unstiffened bridge). These influence lines are readily visualized as deflection curves, whereas the conventional long equations of exponential or hyperbolic terms do not present a simple physical picture.

Mr. Sih also questions the assumption of superposition. In reality, this assumption is identical with that used in all deflection-theory analysis, and

---

[21] Prof. of Aeronautical Eng., Univ. of Michigan, Ann Arbor, Mich.

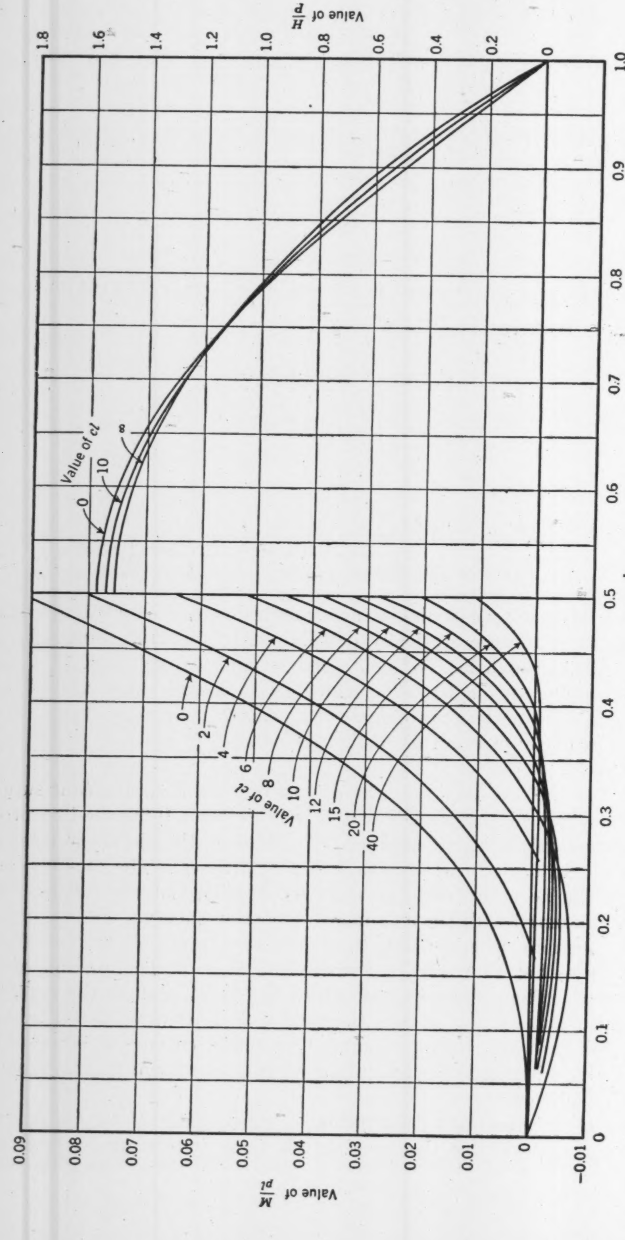

FIG. 17.—INFLUENCE LINES FOR M AT MIDSPAN AND FOR H (WITH $D = 1.25\ D_e$, $l = 10f$)

influence-line ordinates can be computed to any desired precision by successive corrections of the ($c\,l$)-values. The basic differential equation of the deflection theory, $\ddot{\eta} - c^2\,\eta = -\,M/E\,I$, is nonlinear because c is not constant. It is not feasible to integrate this nonlinear equation and therefore c is always assumed constant during integration, thus linearizing the differential equation. Superposition procedures apply for the solution of linear differential equations but not for nonlinear problems.

Mr. Karol presents simple equations for the variation of H, M, and V with $c\,l$. If these equations are used, it is necessary to compute influence lines for only one value of $c\,l$. Values can then be corrected to correspond to the true value of $c\,l$ for each particular loading. The computation work is obviously reduced from that required for two sets of influence lines.

Mr. Palmbaum extends the influence-line procedure to the computation of shears in the stiffening truss. This is an important contribution because two segments of the span may be loaded, and the influence lines provide the only convenient method for determining the correct loaded length.

Mr. Franciosi substantiates the writer's procedure for finding influence lines as deflection curves or by using the theorem of Betti. He proves the validity of this procedure for suspension bridges and arches, provided H_r remains constant. He also proposes a method of successive approximation which is applicable to arches or suspension bridges. The successive approximations would probably converge more slowly for suspension bridges than for arches because of the larger values of $c\,l$. The equations for M are also more sensitive to changes in $c\,l$ than are the equations for H.

Several of the discussers requested more design data and further examples of the computational procedure. Charts and tables will therefore be presented for bridges with simply supported tresses. Most bridges of this type are somewhat similar—most of the flexibility being contributed by the main span. The side spans are always considered as unloaded or as uniformly loaded for the entire span, hence influence lines are not required for the side spans. It will be assumed that 80% of the denominator D of the equations for H (Eqs. 12 and 13) is contributed by the main-span term, which will be designated as D_o, and the remaining 20% of D is contributed by the side-span term $2\,D_s$ and the cable-stretch term $L_s/(A\,E_c)$. This assumption is stated in the following equations which also define D_o and D_s:

$$D = D_o + 2\,D_s + \frac{L_s}{A\,E_c} \qquad \text{(58a)}$$

$$D \approx 1.25\,D_o \qquad \text{(58b)}$$

$$D_o = -\,\frac{8\,f}{l^2}\int_0^l \eta_h\,dx \qquad \text{(58c)}$$

and

$$D_s = -\,\frac{8\,f_1}{l^2_1}\int_0^{l_1} \eta_{h1}\,dx \qquad \text{(58d)}$$

The influence lines will be computed for bridges having these proportions. The final bending moments will then be corrected to the true ratios of D/D_o.

The value of D_o (or D_s) is determined by substituting η_h from Eq. 11 into Eq. 58c and integrating:

$$D_o = \frac{64 f^2 l}{E I c^2 l^2}\left(\frac{1}{12} - \frac{1}{c^2 l^2} + \frac{2 \tanh c l/2}{c^3 l^3}\right) \ldots\ldots\ldots\ldots (59)$$

TABLE 6.—VALUES OF D_o OR D_s

$c l$	$\frac{D_o E I}{f^2 l}$	$\frac{D_o H_r l}{f^2}$	$c l$	$\frac{D_o E I}{f^2 l}$	$\frac{D_o H_r l}{f^2}$	$c l$	$\frac{D_o E I}{f^2 l}$	$\frac{D_o H_r l}{f^2}$
(1)	(2)	(3)[a]	(1)	(2)	(3)	(1)	(2)	(3)
0	0.53333	0	5.5	0.13159	3.981	11	0.040501	4.901
1.0	0.48469	0.485	6.0	0.11514	4.145	12	0.034465	4.963
1.5	0.43451	0.978	6.5	0.10138	4.283	13	0.029662	5.013
2.0	0.37969	1.519	7.0	0.08979	4.400	14	0.025783	5.053
2.5	0.32678	2.042	7.5	0.07997	4.499	15	0.022608	5.087
3.0	0.27930	2.514	8.0	0.07161	4.583	16	0.019979	5.115
3.5	0.23831	2.919	8.5	0.06444	4.656	18	0.015919	5.158
4.0	0.20384	3.261	9.0	0.05826	4.719	20	0.012973	5.189
4.5	0.17514	3.547	9.5	0.05289	4.773	40	0.003310	5.295
5.0	0.15134	3.784	10.0	0.04821	4.821	∞	0	5.333

[a] Col. 3 equals Col. 2 times $c^2 l^2$.

For conversion to exponentials, $\tanh c l/2 = (e^{cl} - 1)/(e^{cl} + 1)$. Values of $D_o E I/(f^2 l)$ or $D_s E I_1/(f^2{}_1 l_1)$ are listed in Table 6 for various values of $c l$. These terms are also multiplied by $c^2 l^2$ in order to permit easy interpolation among the larger values of $c l$.

TABLE 7.—VALUES OF $\frac{H}{p l}$ FOR ADVANCING UNIFORM LOAD

($l = 10 f$ AND $D = 1.25 D_o$)[a]

k'/l	$c l = 5$	$c l = 10$	$c l = 15$	k'/l	$c l = 5$	$c l = 10$	$c l = 15$
0.02	0.0010	0.0011	0.0011	0.28	0.1842	0.1870	0.1887
0.04	0.0041	0.0042	0.0044	0.30	0.2090	0.2117	0.2134
0.06	0.0091	0.0095	0.0098	0.32	0.2350	0.2376	0.2392
0.08	0.0164	0.0168	0.0172	0.34	0.2620	0.2644	0.2659
0.10	0.0252	0.0261	0.0268	0.36	0.2897	0.2922	0.2933
0.12	0.0361	0.0373	0.0381	0.38	0.3182	0.3204	0.3215
0.14	0.0489	0.0504	0.0514	0.40	0.3476	0.3494	0.3504
0.16	0.0636	0.0652	0.0664	0.42	0.3774	0.3788	0.3797
0.18	0.0799	0.0818	0.0830	0.44	0.4075	0.4088	0.4095
0.20	0.0979	0.1000	0.1014	0.46	0.4381	0.4390	0.4395
0.22	0.1171	0.1197	0.1212	0.48	0.4688	0.4693	0.4697
0.24	0.1382	0.1408	0.1424	0.50	0.5000	0.5000	0.5000
0.26	0.1605	0.1633	0.1650	1.00	1.0000	1.0000	1.0000

[a] For other proportions, tabulated values should be multiplied by $1.25 \frac{D_o}{D} \times \frac{l}{10 f}$.

The influence line for H is obtained by substituting $D = 1.25 D_o$ and values of η_h from Eq. 11 into Eq. 13. The influence lines for the case of $l = 10 f$ are plotted in Fig. 17 for various values of $c l$. The influence lines are seen to have little variation in shape because the maximum ordinate varies from 1.5625 for $c l = 0$ to 1.5000 for $c l = \infty$, or only 4%. This confirms Mr. Karol's state-

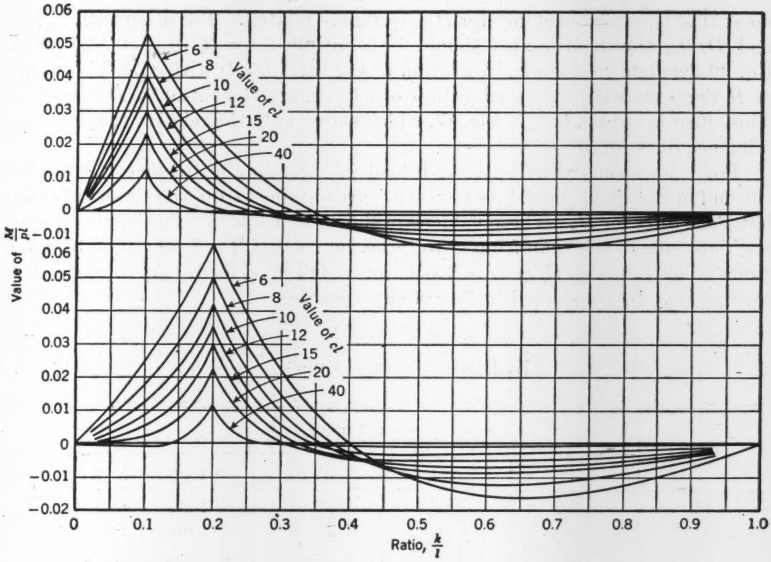

FIG. 18.—INFLUENCE LINES FOR M AT $0.1\,l$ AND AT $0.2\,l$ ($D = 1.25\ D_o$)

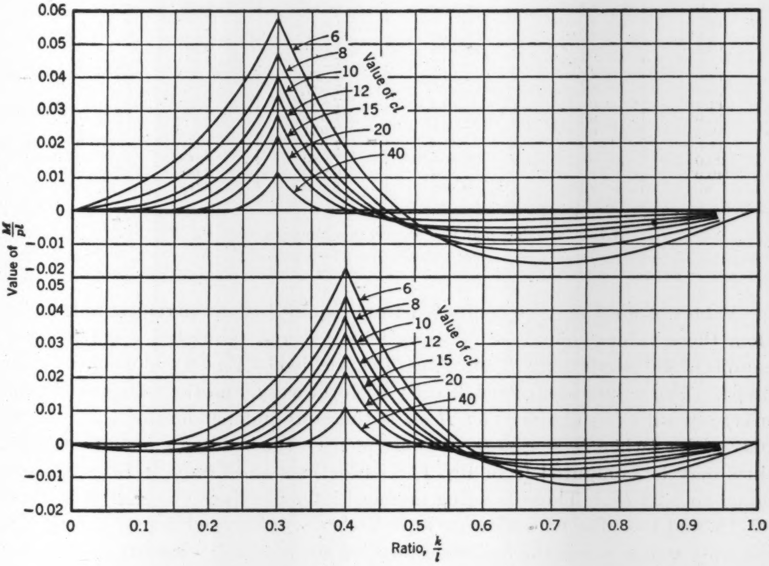

FIG. 19.—INFLUENCE LINES FOR M AT $0.3\,l$ AND AT $0.4\,l$ ($D = 1.25\ D_o$)

ment that the influence lines for H are affinely related. For other ratios of f/l and D/D_o, the H-ordinates should be multiplied by $(l/10\,f) \times 1.25\,D_o/D$. Eq. 29 depends on a typical variation of the ratio D_o/D with $c\,l$. The values of H decrease with increased values of $c\,l$ because the ratio D_o/D decreases. This effect is not evident in Fig. 17, which shows only the relative shapes of the influence lines for H.

For a uniformly distributed live load p, extending a distance k' from the left end of the span, the values of $H/(p\,l)$ are obtained from the areas under the influence lines for H. These values are shown in Table 7. For live loads over the right side of the span from k' to l, the values in Table 7 may be subtracted from 1.000 because $H/(p\,l) = 1.000$ for a full live load. Any partial live loading may be considered by use of superposition.

TABLE 8.—VALUES[a] OF $-\dfrac{c^2\,l^2\,m_h}{f}$

$c\,l$	VALUES OF x				
	$0.1\,l$	$0.2\,l$	$0.3\,l$	$0.4\,l$	$0.5\,l$
3.0	1.842	3.126	3.969	4.445	4.599
3.5	2.195	3.672	4.611	5.133	5.302
4.0	2.519	4.150	5.156	5.701	5.873
4.5	2.817	4.567	5.609	6.161	6.331
5.0	3.092	4.932	5.987	6.529	6.695
5.5	3.346	5.250	6.300	6.824	6.981
6.0	3.584	5.530	6.560	7.059	7.205
6.5	3.808	5.780	6.778	7.245	7.380
7.0	4.014	6.001	6.961	7.393	7.517
8.0	4.400	6.373	7.244	7.606	7.706
9.0	4.746	6.672	7.447	7.745	7.824
10.0	5.056	6.916	7.594	7.831	7.892
11.0	5.337	7.112	7.701	7.891	7.934
12.0	5.590	7.272	7.779	7.928	7.960
13.0	5.820	7.405	7.837	7.952	7.976
14.0	6.024	7.512	7.880	7.968	7.984
15.0	6.213	7.602	7.911	7.979	7.991
16.0	6.385	7.674	7.934	7.986	7.994
18.0	6.678	7.782	7.964	7.994	8.000
20.0	6.920	7.854	7.980	8.000	8.000
40.0	7.854	7.998	8.000	8.000	8.000
∞	8.000	8.000	8.000	8.000	8.000

[a] Tabular values may also be used to compute $\eta_h = (y - m_h)/H_r$.

Values of m_h/f may be computed from Eq. 10. For convenient interpolation, these values should be multiplied by $c^2\,l^2$ and tabulated. Table 8 is a sample of the tabulation. The values of m_p yielded by Eqs. 8 and 9 depend only on $c\,l$. The values of m_h vary directly with the sag f, and the values of H vary inversely with f. The product $H\,m_h$ is therefore independent of f and varies only with $c\,l$ when $D = 1.25\,D_o$. Consequently, the bending moment influence lines may be computed from Eq. 14 as functions of $c\,l$ only, if D is assumed equal to $1.25\,D_o$. These bending moment influence lines are plotted in Figs. 17, 18, and 19. For normal ratios of D/D_o, these influence lines are sufficiently accurate to determine the final load position for maximum positive or negative bending moment.

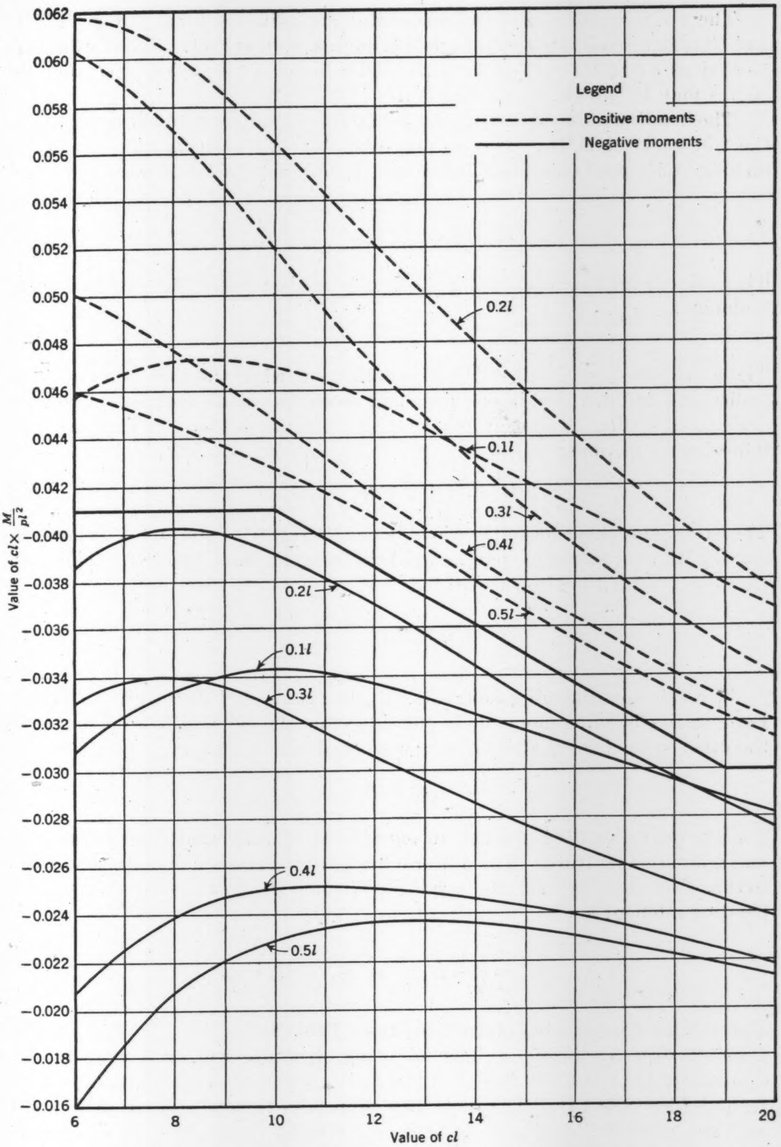

FIG. 20.—MAXIMUM POSITIVE AND NEGATIVE BENDING MOMENTS RESULTING FROM LIVE LOAD IN THE MAIN SPAN ($D = 1.25\ D_o$)

The positive and negative areas under the influence lines of Figs. 17, 18, and 19 may be computed by integration of Eqs. 8, 9, and 11. These values are plotted as $c\,l \times M/(p\,l^2)$ in Fig. 20. The factor $c\,l$ is included so that the curves may be plotted to a larger scale.

The bending moments computed for $D/D_o = 1.25$ must now be corrected to the true ratio of D/D_o. If the value from Table 7 is designated as H_o, the increment δH produces a bending-moment correction of $\delta H \times m_h$.

$$\delta H = H_o \left(\frac{1.25\,D_o}{D} - 1 \right) \frac{l}{10\,f} \qquad \text{(60)}$$

This value of δH may be added to H_t to correct the positive main-span bending moments.

$$M = (H_t + \delta H)\,m_h \qquad \text{(61)}$$

The maximum negative bending moments occur when the side spans are fully loaded. A full live load in one side span produces a cable component which is designated by H_s. The negative bending moments in the main span have the following corrections:

$$M = (2\,H_s + H_t + \delta H)\,m_h \qquad \text{(62)}$$

The cable component for full live load in one side span is determined by integratign Eq. 13 over one side span and substituting D_s from Eq. 58*d*. The value $H_w = w_1\,l^2{}_1/(8\,f_1)$ is also substituted.

$$H_s = H_w \frac{p}{w_1} \frac{D_s}{D} \qquad \text{(63)}$$

The side-span bending moments, M_s, are computed directly from Eq. 10. For negative bending moments in one side span, the value of H is computed for the other spans loaded at minimum temperature:

$$M = H\,m_h \qquad \text{(64)}$$

For a positive bending moment in one side span, only that span is loaded at maximum temperature. The uniform load, p, produces a moment proportional to the moment m_h by the ratio $-\,p\,l^2{}_1/(8\,f_1)$, or $-\,H_w\,p/w_1$. The total positive bending moment is

$$M = \left(-\,H_w \frac{p}{w_1} + H_s - H_t \right) m_h \qquad \text{(65)}$$

The values of m_h can be interpolated from Table 8.

Numerical Application.—The following structure will be analyzed. The dimensions are $l = 3{,}800$ ft, $l_1 = 1{,}800$ ft, $f = 350$ ft, $f_1 = 78.53$ ft, $L_s = 9{,}140$ ft, and $L_t = 8{,}482$ ft. The flexibility properties for one side are $E\,I = E\,I_1 = 1{,}884 \times 10^6$ ft²-kips, and $L_s/A\,E_c = 0.000880$ ft per kip. The load per cable is $w = w_1 = 4.7$ kips per ft and $p = 1.0$ kip per ft. The values of $t = \pm\,60°$ F, $\omega = 0.0000065$, and $H_w = w\,l^2/(8\,f) = 24{,}240$ kips are used.

TABLE 9.—Computation of Bending Moments

Procedure:

Line (1) was determined from Figs. 17, 18, and 19 (feet).
Line (2) was determined by multiplying values in Table 7 by 3,800 (kips).
Line (3) was determined as $-393 - 0.0573\, H_s$ (kips).
Line (4) was determined by multiplying values in Table 8 by $350/(14)^2$ (feet).
Line (5) contains positive values from Fig. 20 multiplied by $(3{,}800)^2/14$ (foot-kips).
Line (6) contains the product of values in Lines (3) and (4) (foot-kips).
Line (7) contains the sums of values in lines (5) and (6) (foot-kips).
Line (8) contains interpolated values (foot-kips).
Line (9) was determined by subtracting line (2) from 3,800 (kips).
Line (10) was determined as $1{,}101 - 0.0573\, H_s$ (kips).
Line (11) contains negative values from Fig. 20 multiplied by $(3{,}800)^2/14$ (foot-kips).
Line (12) contains the products of values in Lines (4) and (10) (foot-kips).
Line (13) contains the sums of values in lines (11) and (12) (foot-kips).
Line (14) contains interpolated values (foot-kips).
Line (15) was determined from Table 8.
Line (16) was determined as $5{,}180 \times f_1/(c^2_1\, l^2_1) \times$ Line (15) (foot-kips).
Line (17) was determined from Table 8.
Line (18) was determined as $4{,}640 \times f_1/(c^2_1\, l^2_1) \times$ line (17) (foot-kips).

Description	Point, x/l				
	0.1	0.2	0.3	0.4	0.5
Main Span, Positive Moment, $c\,l=14$					
(1) Load position	0–0.26 l	0–0.33 l	0.11 l–0.43 l	0.25 l–0.53 l	0.37 l–0.63 l
(2) H_s	625	944	1,375	1,490	1,468
(3) $H_t+\delta H$	−429	−447	−472	−478	−477
(4) m_h	−10.76	−13.42	−14.08	−14.22	−14.25
(5) M_t	44,600	49,400	44,100	40,100	39,100
(6) δM	4,600	6,000	6,700	6,800	6,800
(7) M	49,200	55,400	50,800	46,900	45,900
(8) M (Int.)	50,400	56,000	51,200	47,000	46,100
Main Span, Negative M, $c\,l=14$					
(9) H_s	3,175	2,856	2,425	2,310	2,332
(10) $2\,H_s+H_t+\delta H$	924	938	963	970	968
(11) M_t	−33,330	−35,400	−29,520	−25,400	−24,340
(12) δM	−9,940	−12,600	−13,560	−13,800	−13,800
(13) M	−43,270	−48,000	−43,080	−39,200	−38,140
(14) M (Int.)	−40,200	−44,300	−40,300	−37,100	−36,000
Side Span, Positive M, $c_1\,l_1=6.45$					
(15) $m_h \times c^2_1\, l^2_1/f_1$	3.786	5.755	6.756	7.226	7.363
(16) M (Eq. 64)	36,900	56,000	65,900	70,400	71,800
Side Span, Negative M, $c_1\,l_1=7.05$					
(17) $m_h \times c^2_1\, l^2_1/f_1$	4.033	6.023	6.975	7.404	7.532
(18) $M=H\,m_h$	−29,600	−44,200	−51,100	−54,300	−55,200

The main-span bending moments will be interpolated between computed values for $c\,l = 14$ and $c\,l = 15$, but only the computations for $c\,l = 14$ are shown. For $c\,l = 14$, $c_1\,l_1 = 14 \times 1{,}800/3{,}800 = 6.63$ and $H_r = c^2 E\, I =$ 25,570 kips. From Table 6, $D_o = 5.053\, f^2/(H_r\, l) = 0.006370$ and $D_s = 4.314 \times f^2_1/(H_r\, l_1) = 0.000578$. From Eq. 58*a*, $D = 0.008406$ ft per kip. The ratio D/D_o is 1.320. For a temperature change, $H_t = \pm\, \omega\, t\, L_t/D = \pm\, 393$ kips. For full live loads in the main span, $H = H_w \dfrac{p}{w} \dfrac{D_o}{D} = 3{,}908$ kips. For full live load in one side span, $H_s = H_w \frac{p}{w_1} \frac{D_s}{D} = 354$ kips. Maximum $H = 3{,}908 + 2 \times 354 + 393 = 5{,}009$ kips.

The bending moments have been computed in Table 9. The load positions were obtained from the influence lines. The main-span bending moments were first obtained from Fig. 20 which represents the positive and negative areas under the influence lines. These moments have been designated as M_i in lines 5 and 11 of Table 9. The moments were then corrected for the (D/D_o)-ratio and for temperature and side-span loads. The moments computed in lines 7 and 13 are for $c\,l = 14$. The moments shown in lines 8 and 14 were interpolated from similar computations for $c\,l = 15$. The side-span bending moments were computed for the correct values of $c_1\,l_1$ in lines 16 and 18.

Summary.—In the paper were presented methods for obtaining influence lines for suspension bridges with any number of spans and with hinged or continuous stiffening trusses. The procedure permits a direct determination of the critical loading conditions and consideration of any type of live-load distribution without the usual restriction of uniform loading. Influence lines are obtained by superimposing simple deflection curves, thus permitting a designer to detect gross errors. The customary long, abstract equations are avoided. Any desired degree of accuracy may be achieved by computing influence lines at small intervals of $c\,l$, although engineering accuracy may always be achieved with only two values of $c\,l$.

For two-hinged suspension bridges, influence-line procedures had previously been used by Messrs. Rode,[4] Selberg,[5] Asplund,[6] and Karol,[7] all of whom prepared tabular data. Similar charts and curves are readily prepared for continuous bridges because the equations (Eqs. 18 and 19) are simple. However, tables covering the complete range of values would be too voluminous for the purposes of the paper.

The influence lines constructed for $D = 1.25\ D_o$ appear adequate for most two-hinged bridges. For bridges of unusual proportions, the influence lines may be easily corrected to give the exact load position. Similar influence lines may be constructed for shear.

Acknowledgment.—The data used in the numerical application correspond to preliminary dimensions of the Mackinac Straits Bridge between Mackinaw City, Mich., and St. Ignace, Mich., and were provided by Mr. Steinman.

AMERICAN SOCIETY OF CIVIL ENGINEERS
Founded November 5, 1852
TRANSACTIONS

Paper No. 2807

AERIAL SURVEYS FOR RESERVOIR PLANNING

By Francis J. Guscio,[1] A. M. ASCE

With Discussion by Messrs. Lewis A. Dickerson, and Francis J. Guscio

Synopsis

Engineers who plan and design multipurpose reservoir projects know that the importance of securing dependable topographic maps cannot be overestimated. Topographic mapping of the extensive areas of such projects by the use of the transit and level or plane table and alidade is time-consuming and expensive. The speed, economy, and map accuracies obtained with photogrammetric methods make it essential to give full consideration to the utilization of aerial surveying in mapping reservoir projects for as many planning purposes as practicable.

Introduction

Preliminary planning for reservoir projects—namely, the selection of the dam sites, the determination of the drainage areas and reservoir levels, the computation of reservoir volumes and backwater curves, and the flood routing of past and possible future floods—has for many years been satisfactorily accomplished by assembling a composite map or maps of uniform scales from all available topographic-survey information and limited new field-survey data. This procedure has generally consisted of utilizing available quadrangle sheets prepared by federal agencies; the scales of these sheets have varied in the past from 1:125,000 with contour intervals of 100 ft to 1:24,000 with contour intervals of from 10 ft to 40 ft. These were supplemented by the use of mosaics made from available aerial photographs and additional contour information secured—if it was considered vital—by means of plane-table surveys using the minimum of horizontal and vertical controls. The volume and accuracy of available maps have been greatly increased during the past

---

Note.—Published, essentially as printed here, in February, 1954, as *Proceedings-Separate No. 407*. Positions and titles given are those in effect when the paper or discussion was approved for publication in *Transactions*.

[1] Prin. Engr., Chf. Master Planning Branch, Eng. Div., South Atlantic Div., Corps of Engrs., U. S. Dept. of the Army, Atlanta, Ga.

fifteen years by federal agency programs of mapping and remapping quadrangles. These have been made on a 1:24,000 scale from new aerial photographic data, translated by a multiplex aeroprojector into standard-accuracy topographic maps.

Although the latest of these 1:24,000-scale federal maps are of high quality, the scale is not large enough nor the contour interval small enough for use in planning and designing all the engineering and related features of multipurpose reservoir projects. After the site is fixed for the dam, which normally occupies a relatively small area of the whole reservoir project, topography information needed for the design of the dam and its appurtenant works can be secured accurately, economically, and with dispatch by conventional transit-and-level survey methods. However, the topographic information needed for planning the related features (usually called reservoir planning) is much more extensive and varied. The time required to make these surveys by conventional ground methods and to compile the various maps is so great and the cost is so enormous that much detail and topographic coverage are frequently sacrificed.

In 1951, after experiencing the problems and the high costs of surveying and mapping the reservoir areas of several projects of the Corps of Engineers (United States Department of the Army) in the South Atlantic Division to meet reservoir planning needs, it was decided to investigate the feasibility of aerial surveys and stereoscopic mapping in order to effect economies and to expedite that phase of project planning. It was recognized that, to accomplish these objectives, the resulting maps must be made at some uniform scale or scales, using photographs of only one series of aerial survey flights.

The most suitable scale at which to map the reservoir area must be determined by fully considering the uses that are to be made of the completed maps. These uses and the scales of maps previously used for such planning are described herein.

Land Acquisition

The planning of land acquisition for a reservoir project is a twofold problem—one part is the fixing of the boundary of the project or "taking line" that is required to operate the project for the purposes for which it is authorized to be constructed; the other is that of mapping the various tracts of land for real estate appraisal and purchase, either in fee title or easement estate. To resolve these problems, careful consideration must be given to the terrain and to the location and elevation of natural and cultural features. The more accurate the basic topographic maps, the simpler is the task of planning and accomplishing the land acquisition.

The first step toward establishing the reservoir taking line is the hydrological determination of significant reservoir flood-pool elevations below which the lands must be acquired. Depending entirely on terrain characteristics, several feet are frequently added to these elevations to allow for anticipated shore-line erosion and changed water-table effects. These elevations, when plotted on a contoured map of the reservoir, are connected by lines that form a sloped contour enclosing the land to be covered by the water surface of the reservoir in addition to any land areas along the reservoir shore that are expected to be physically changed by the reservoir during adverse flood conditions. This sloped contour is the basic guide line for land acquisition and has been most effectively used for this purpose when incorporated on reservoir topographic maps at a scale of 1:6,000 and on a controlled mosaic at a scale of 1:12,000. After the guide line for acquisition has been established and mapped, a tentative taking line is delineated that will satisfy the requirements of management and operation for project purposes and the administration of incidental permissible uses anticipated or planned for the reservoir.

The tentative taking line is projected on the reservoir topographic maps and aerial mosaics to show the lands traversed by the line. Work on obtaining ownership information and preparing property maps of the boundary tracts may then proceed while similar work is being done on tracts lying entirely within the reservoir taking line. These property maps, used for real estate appraisals and tract acquisitions, have been satisfactorily prepared by utilizing photographic prints of flight negatives and reproducible prints of topographic maps. The prints of these flight negatives are enlarged to a 1:6,000 scale, and the topographic maps show culture, grid, and control network, also on a 1:6,000 scale. After all property corners have been located and indicated on prints of the topographic map, the individual tract acreages and descriptions are determined therefrom. The tract boundaries are then delineated on the controlled-mosaic scale of 1:12,000. The final map required for land acquisition is a composite map traced from the aerial mosaic, showing the tracts, pertinent contours, grid system, and tract numbers, and containing a register indicating the tract number, name of owner, and the estate acquired in the reservoir lands.

Relocations

There are few if any multipurpose dam sites selected in the southeastern United States where the reservoirs formed by their construction will not inundate several railroads, highways, or county roads that must be relocated. Topography is frequently a determining factor in fixing the alinement of the longer relocations. Preliminary paper locations and ruling grades have been determined by using federal quadrangle maps of the 1:24,000 scale; however, these have seldom been available for planning multipurpose reservoirs unless specifically made for them. Frequently, the final alinement of either railroad or highway has been selected from topographic maps of a 1:6,000 scale and controlled mosaics of a 1:12,000 scale with only a check by field reconnaissance. The time required and the costs encountered in running alternate preliminary lines by use of transit and level are thereby saved. These larger-scale topographic maps are also used in the acquisition of right-of-way lands. Another important use of the topographic maps is for determining the drainage areas tributary to bridges and culverts on the relocated routes of railways and highways.

Special Reservoir Studies

The deposition in reservoirs of silt carried by tributary rivers and creeks is of special interest in the planning stage of a project because the storage capacity of a reservoir is gradually diminished by silting. Continuing post-construction measurements are made of volume and rate of silting, not only as a record of the changes in the reservoir but also for use as reference data in similar work elsewhere. The reservoir projects in the authorized program of the Corps of Engineers in the southeastern United States have large storage volumes by comparison with the estimated rates of deposition. These reservoirs are not expected to be functionally impaired by silting until long after their normal economic life spans. Silt ranges are selected in a reservoir and cross sections are surveyed before impoundment for comparison with future cross sections surveyed along the same ranges at time intervals sufficient to indicate the changes in silt accumulations. Dependable topographic maps at a scale of 1:24,000 or greater are especially useful in locating and selecting the smallest number of ranges that should be established to conduct the silting studies.

Riverbank or stream-bank erosion and channel changes which may occur below the dam as a result of water discharges during project operation are also a concern of the operating agency. Records of these changes are secured by comparing cross sections taken periodically after the completion of construction with cross sections surveyed before project operation and as indicated by the study of aerial mosaics flown at low altitudes during or before project construction.

RESERVOIR PREPARATION

Although there are a number of reservoirs that have been filled without having been previously prepared for inundation by the cleanup of floatable debris and the disposal of standing timber, there are valid reasons that fully justify some degree of cleanup and timber removal in most large multipurpose reservoirs, particularly those in the southern and southeastern United States.

Planning for reservoir clearing includes: (*a*) Consideration of the elimination of obstructions to navigation; (*b*) mosquito control to protect the resident population and visitors to the reservoir from malaria and other indigenous mosquito-borne diseases; (*c*) the prevention of interference with operation of or damage to project structures from floating debris; (*d*) provision for recreation, boating, fishing, and other public uses; (*e*) the preservation of scenic attractiveness and the conservation of fish and wildlife; and (*f*) the facilitation of operational maintenance and post-impoundment silt studies.

During the period of unlimited availability of cheap manpower and prior to the advent of the bulldozer rake and the portable power saw, land clearing for reservoirs was customarily performed by hand labor organized and hired locally or through small acreage contracts with landowners and small local operators. Except for making preliminary estimates of time and costs required to perform the clearing, there was little need for accurately mapping the work to be performed. Shortages of manpower and the development of heavy construction equipment during the latter part of the 1930's and in the early 1940's made it expedient to clear reservoir areas by contracting with private construction firms.

This change made it necessary to prepare representative plans, specifications, and estimates of the work involved. The reservoir topographic maps that had been prepared for preliminary planning purposes together with aerial mosaics were utilized for preparing the contract plans. Some clearing plans were simple tracings of the preliminary topographic maps with outlined areas of different clearing classifications, such as "light," "medium," and "heavy," drawn on the tracings as well as they could be determined from aerial photographs and field reconnaissance. It was soon learned that it is less expensive and easier to make field appraisals of the work involved when the limits of clearing which are usually contours are shown on the aerial mosaics. However, because the aerial mosaics made for preliminary planning purposes several years before the time of contract bidding were not truly representative of the tree cover during the project construction stages, long and careful field reconnoitering by the prospective contractors was necessary to make intelligent appraisals and offer firm bid prices.

It is readily appreciated, therefore, that reservoir clearing plans are most useful when up-to-date aerial mosaics and dependable contour information are available for use in their preparation. Cultural features, extent and type of tree cover, and clearing limits are adequately presented on aerial mosaics of a 1:12,000 scale. The most complete and least expensive plans are made when it is possible to use prints of aerial reservoir manuscript maps of a 1:12,000 scale that include both topography and planimetry with the photographic record.

The topographic maps are also used to locate potential mosquito-breeding areas where drainage by ditching will be required and areas where drift may be stranded or yarded for removal. The proximity of these areas and other parts of the reservoir to habitation is readily discernible on aerial mosaics. It is on the basis of this information that the reservoir mosquito-control plans and floatage-removal plans are formulated. For mosquito-control planning, the maps should include the topography of areas within approximately 1½ miles of the line delineating the maximum reservoir operating level, on a scale of 1:12,000, using a 10-ft contour interval with intermediate 5-ft contour intervals between the minimum operating level and maximum flood level if the slope of the terrain is less than 5%.

RESERVOIR DEVELOPMENT AND MANAGEMENT

Reservoirs and their fringe lands offer many potential collateral uses which, if not expertly planned in advance of impounding, can seldom be developed or managed for full resource utilization. The Congress of the United States has specifically authorized the Chief of Engineers, United States Army, to provide and to permit others to provide for the development of public park and recreational facilities on government reservoirs under the control of the Department of the Army when such facilities are not in conflict with primary project purposes.

The planning for collateral uses is accomplished by preparing a master plan for public-use development and recreational development, for conservation and preservation of the resources, and for reservoir management. The master plan includes consideration of reservoir area topography, accessibility, relationship to population centers, soil characteristics, vegetative cover, fish and wildlife habitat, significant historical and archeological sites and interests, forestry and agriculture, and grazing-land uses. This planning is seldom achieved without reservoir topographic maps and field reconnaissance.

Planning for development includes the preparation of a general development plan that zones the reservoir area for its many uses as well as layout plans of individual areas considered suitable and necessary for recreational and public-use developments. To complete the general development plan, site reconnaissance is required; this is greatly facilitated by dependable topographic maps and photographic aerial mosaics. A scale of 1:12,000 for both maps and mosaics is satisfactory for this use, although prints of manuscript maps of the same scale containing topography, photography, and planimetry would save both time and office work. The layout plans have been mapped on scales varying from 1:8,000 to 1:2,400—scales of 1:6,000 or 1:4,800 being the most commonly used. Contours are essential both above and below the normal operating reservoir water surface to meet the need for developing swimming beaches, piers, and boat-launching ramps in water areas and for siting buildings, roads, parking areas, and utilities on shore lands. A contour interval of 10 ft in steep terrain is adequate, but a maximum interval of 5 ft is needed where ground slopes are 5% or less.

The maps that are used for development planning are also valuable for managing and operating the reservoir for recreational and public use; for guiding post-impoundment site planning and site leasing; for facilities construction; for marking of boat channels and unsafe areas; and for aiding in fire control, erosion control, and mosquito control.

Aerial Surveys

Taking into consideration the many reservoir planning purposes which may be served by a single aerial survey and recognizing the speed, accuracy, and relatively low cost of aerially surveying large areas, specifications were prepared for aerial surveys and stereoscopic mapping of two major reservoir projects of the South Atlantic Division of the Corps of Engineers, and contracts were awarded for the work. The projects were either in the design stage or initial construction stage.

The following is a generalized outline of the maps and materials needed for reservoir planning purposes which the contractors were required to furnish:

a. Aerial photographs of the reservoir area, including negatives, prints, and indices.

b. Manuscript sheets covering 3 minutes of latitude and longitude at a compilation scale of 1:6,000.

c. Planimetric maps of the reservoir area with topography delineated by a 10-ft contour interval and an auxiliary 5-ft contour interval at strategic locations together with intermediate contours of significant flood-pool elevations and operating-pool elevations needed for land acquisition or reservoir clearing.

d. Separate transparent overlay of manuscript sheets showing all vegetation.

e. Two copies of completed maps reduced photographically to a 1:12,000 scale (one with vegetation and one without).

f. Bound volumes of prints of completed maps reduced photographically to a 1:12,000 scale.

g. Linen tracings of designated parts of the reservoir area as needed, at a scale of 1:6,000.

h. Prints or reproducible films of controlled mosaics at a scale of 1:12,000, with contours and without; also prints of mosaics, as needed, at a 1:24,000 scale.

i. Aerial photographs of the river below the dam for approximately 50 miles, at a scale of 1:4,800, prepared from low-altitude photography.

j. All map-compilation materials, including all horizontal and vertical control data, field-survey notes, computations, and other pertinent data.

One of these contracts—that of mapping the reservoir area of the Hartwell project on the Savannah River in Georgia and South Carolina—involved 770 sq miles of surveying and mapping and 360 sq miles of topography, all work to be completed in 15 months. The other, that of mapping the reservoir area of the Buford project on the Chattahoochee River in Georgia, involved 430 sq miles of surveying and mapping and 250 sq miles of topography—all work to be completed in 10 months. It is estimated that multipurpose aerial surveying of these reservoir areas executed in accord with the planning described herein will reduce over-all mapping costs by from 60% to 70% in comparison with costs that would be entailed if separate surveys were made for each purpose, as has frequently been done in the past.

CONCLUSIONS

It is no longer necessary in the planning of reservoirs to use inadequate maps prepared from uncontrolled aerial mosaics combined with topographic data secured by conventional ground-survey methods involving inconvenient delays and attendant high costs. During the past decade, advances in aerial surveying and photogrammetry have resulted in the speedy production of accurate and high-quality maps. Concurrently, experience gained by engineers in reservoir planning for multipurpose use has shown that the mapping needs for land acquisition, relocations, special reservoir studies, reservoir preparation, and reservoir development and management can be adequately served by uniform-scale maps. With these needs anticipated, suitable maps and information can be obtained by aerial surveys and stereoscopic mapping expeditiously enough to be used for reservoir planning purposes and at a substantial saving compared with ground surveys and conventional mapping methods.

DISCUSSION

Lewis A. Dickerson,[2] M. ASCE.—Mr. Guscio's paper ably describes a field of engineering to which aerial surveying has been applied with marked advantage. Particularly well presented is the need for advance planning to insure that the survey procedures produce suitable data for all the anticipated requirements with a minimum of cost and effort.

In the "Introduction," Mr. Guscio points out that the time spent and the cost involved in making reservoir planning surveys are so great that "much detail and topographic coverage are frequently sacrificed." The situation cited is common to surveys for many engineering projects; however, aerial photogrammetric surveys have done much to correct this. Even though the work may not always be accomplished for less cost by aerial methods, these methods almost always produce a better survey as a result of larger area coverage, more complete information obtained, and a uniform accuracy throughout. These factors have undoubtedly resulted in better and more economical engineering designs with attendant savings in construction costs which really should be credited to the aerial surveys.

In the first paragraph of the "Introduction," Mr. Guscio refers to the data from various topographic surveys assembled for preliminary planning purposes. He has been fortunate in having to secure only "limited new field-survey data." That would not be the case in the approximately 50% of the United States that has absolutely no topographic data in existence. In such areas, the aerial photogrammetric survey method becomes even more important because it is adaptable to almost any desired accuracy for preliminary planning purposes and the cost is low. With present-day equipment and methods it is possible to prepare preliminary maps in such areas without any additional field work. Such maps surpass in accuracy those older topographic maps of some parts of the United States and even closely approach some of the modern topographic maps. Progress is emphasized by the fact that such preliminary mapping only costs from $10.00 to $15.00 per sq mile.

The author states that the objective was to use only "one series of aerial survey flights." This is a desirable objective but it need not necessarily be adhered to in all cases. When there is only topographic mapping of the entire reservoir area, this rule should be adhered to because the highest accuracy requirement deemed necessary for the entire area to be mapped will govern the manner of flying. Should there be a requirement for mosaics, in addition to the topographic maps, economy may sometimes be realized by flying separate coverage for that purpose. In addition, some smaller parts of the area—for example, likely relocation areas or dam sites—may require higher accuracies in topographic mapping and should be photographed again at a lower altitude.

In making higher-accuracy surveys for areas such as dam sites, Mr. Guscio can anticipate increased applications of aerial survey methods to reservoir projects. Such methods are being applied successfully at scales as large as

---

[2] Partner, Sargent, Webster, Crenshaw & Folley, Architect-Engineer Associates, Watertown, N. Y.

1:240 and with contour intervals as small as 1 ft. The writer feels that the methods are applicable to the mapping of dam sites and the securing of design data required for relocations. The methods can even be used to determine the cross section along the established silt ranges with an accuracy consistent with that later achieved in sounding the depths to the the silt layer. Economy in these surveys requires thorough advance planning so that aerial photography and field surveys may be properly scheduled and accomplished simultaneously with similar operations for the larger reservoir area.

Mr. Guscio makes several references to the "controlled mosaic" that was prepared and used for many purposes. Such a mosaic made available no information or data not already supplied by the topographic maps and the individual aerial photographs from which the maps were prepared, although it made the photographic information available in a more convenient form for the varied uses to which it was put. The latter fact probably justified the cost involved in preparation of the mosaic. Although the paper does not indicate how well the mosaic was controlled, the writer believes that a highly accurate mosaic would not be justified on projects of the nature described.

Mr. Guscio indicates that the aerial photographs were of much value in determining the land-ownership lines after the topographic mapping was complete. It is pertinent to note that, when appropriate, ownership lines can be also located during mapping. Property corners, lines, or both, identified on the aerial photographs as a result of field work and deed-and-plat study, may be plotted into correct map position during the photogrammetric operation. The extra effort required for this operation is insignificant.

Francis J. Guscio,[3] A. M. ASCE.—Mr. Dickerson's discussion indicates general agreement with the use of aerial surveys for reservoir planning. In addition, he has advocated the adoption of aerial mapping of greater and lesser accuracies to use for more and less extensive site-planning purposes than outlined in the paper. The purpose of the paper was to emphasize the applicability of aerial surveys for reservoir-planning purposes as actually experienced by the writer and others responsible for reservoir planning, particularly when such surveys are properly timed and accomplished during a single series of flights with topography mapped on uniform scales so as to serve adequately the many planning purposes at a reasonable cost.

Mr. Dickerson refers to the use of aerial surveys in areas of the country where no topographic data are in existence, stating that in such areas aerial photogrammetric survey methods are of even more importance for preliminary planning purposes and can be secured at low costs. The importance is no doubt true but the costs would be "reasonable" rather than "low." That maps of such areas can be prepared with present-day equipment without any additional field work is not questioned; however, the accuracy and usefulness of such maps would not be dependable enough for reservoir planning as described in the paper. Mr. Dickerson's statement that such maps surpass in accuracy some older topographic maps and closely approach some modern topographic maps is questionable, and preliminary mapping costs of "from $10.00 to $15.00 per sq mile" may average one fiftieth of the cost of the maps needed for over-all reservoir planning.

---

[3] Prin. Engr., Chf. Master Planning Branch, Eng. Div., South Atlantic Div., Corps of Engrs., U. S Dept. of the Army, Atlanta, Ga.

Mr. Dickerson predicts the use of higher-accuracy surveys for mapping dam sites, planning relocations, and establishing silt ranges by aerial survey methods that are today successfully being used to produce maps at 1:240 scale with a 1-ft contour interval. Because the maps for dam sites and relocations need only be to a scale of from 1:600 to 1:1,200 with a 2-ft contour interval, his prediction is probably true, providing the costs of such surveys are not unreasonable as compared to the use of accepted ground-surveys methods. Because, for silt ranges, range monuments have to be set following the clearing of the ranges, the same ground-survey crew could probably obtain the necessary profile data more cheaply than it could be secured by aerial surveying.

Mr. Dickerson is correct in his statement that use of the controlled mosaics is justified on the basis of making the photographic information available in convenient form and that highly accurate mosaics would not be justified for reservoir planning. The accuracy of the mosaic required should correspond to the accuracy required and tolerated for producing the topographic data specified; scales and contour intervals are recommended in the paper. The controlled mosaics can be justified as to cost and accuracy for the purpose of land acquisition alone in the southeastern United States.

Regarding Mr. Dickerson's discussion of plotting ownership lines into correct map position during the photogrammetric operation rather than plotting them on the aerial photographs or controlled mosaics after completion, it is extremely doubtful that the extra effort required would be insignificant in the southeastern United States, although it may be practicable to follow this procedure in parts of the western United States where ownerships on regular land lines exist.

There exists a common field of agreement between the paper and the discussion that suitably accurate maps and information are obtainable by means of aerial surveys and stereoscopic mapping at reasonable costs for reservoir planning.

AMERICAN SOCIETY OF CIVIL ENGINEERS
Founded November 5, 1852
TRANSACTIONS

Paper No. 2808

NUMERICAL ANALYSIS OF FRAMES WITH CURVED GIRDERS

BY JAMES MICHALOS,[1] M. ASCE

WITH DISCUSSION BY MESSRS. WILLIAM A. CONWELL, AND JAMES MICHALOS

SYNOPSIS

An arithmetical procedure is presented for determining moments in continuous frames with curved girders. Values of the required properties for application of the procedure in the usual case of girders of circular-arc plan are included. Two numerical examples are worked out in detail.

INTRODUCTION

In keeping with modern trends in architecture and with clearance and space requirements, it seems likely that there will be an increasing use of frames with curved girders.

Some girders of circular-arc plan, such as that illustrated in Fig. 1(*a*), have been analyzed[2,3] by distributing moments about normal and tangential axes at the supports. Fig. 1(*b*) and Fig. 1(*c*) are plan views of frameworks in which the normal and tangential axes of the several members framing into a joint are not similar. Methods used for analyzing the structure in Fig. 1(*a*) are not applicable to the structures in Fig. 1(*b*) and Fig. 1(*c*).

In a previous paper[4] the writer presented a numerical procedure for determining moments in continuous frames whose members are straight but join at various angles in space. That procedure involves successive corrections to moments about arbitrarily chosen rectangular axes.

NOTE.—Published, essentially as printed here, in August, 1953, as *Proceedings-Separate No. 250*. Positions and titles given are those in effect when the paper or discussion was approved for publication in *Transactions*.

[1] Prof. of Structural Eng. and Chairman, Dept. of Civ. Eng., New York Univ., New York, N. Y.

[2] "Moment Distribution Applied to Flexure and Torsion," by Mervin B. Hogan, *Bulletin No. 26*, Univ. of Utah, Eng. Experiment Station, Salt Lake City, Utah, 1945.

[3] "Analysis of Continuous Circular Curved Beams," by Becla Velutini, *Proceedings*, A.C.I., Vol. 47, 1951, p. 217.

[4] "Numerical Analysis of Continuous Frames in Space," by James Michalos, *Transactions*, ASCE, Vol. 119, 1954, p. 565.

In this paper the same general idea is used, all moments and properties of the members being referenced to a pair of orthogonal axes in the plane of the frame. The members can have any curvature in plan, including segmental, but of particular concern is the common, circular-arc shape. Tables of the required properties of such shapes are included, as are numerical examples illustrating the procedure.

For open sections, such as I-beams and channels, it would be important to consider the effect of warping restraint when determining the torsion factor, J. However, such open sections would hardly be used for curved girders subjected to appreciable torques. For closed sections, as contemplated herein, the warping effects are considered secondary and are not included.

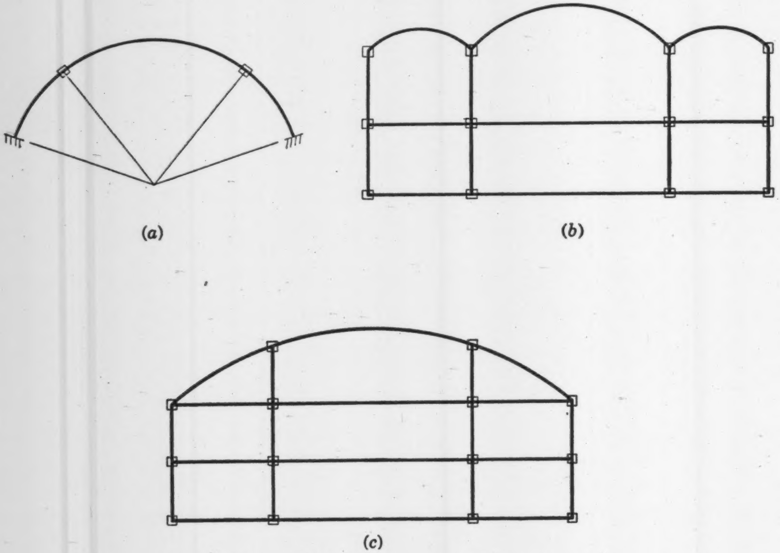
(a) (b)

(c)

Fig. 1.—Plan Views of Frames with Curved Members

Stiffnesses and Carry-Over Factors

In Fig. 2(*a*) a moment, M_{zB}, is applied about the z-axis at end B of a curved member lying in the xz-plane. This member is restrained against translation at ends A and B. If no rotation is permitted about the x-axis at end B and if no rotation is permitted about either the x-axis or z-axis at end A, the applied moment will induce moments about the x-axis at B and about the x-axis and z-axis at A. These moments are labeled M_{zB} $(C_{xz})_{B-B}$, M_{zB} $(C_{xz})_{B-A}$, and M_{zB} $(C_{zz})_{B-A}$. The terms $(C_{xz})_{B-B}$, $(C_{xz})_{B-A}$, and $(C_{zz})_{B-A}$ are called carry-over factors. The first subscript within a parenthesis designates the axis to which the carry-over is made, and the second subscript designates the axis about which the original moment was applied. The subscripts outside a parenthesis indicate the direction of carry-over.

TABLE 1.—Stiffnesses of Circular Segments

Angles (Fig. 3) in Degrees		$EI/GJ = 1$				$EI/GJ = 2$				$EI/GJ = 6$			
ϕ	η	$\frac{K_{zB}\,r}{EI}$	$\frac{K_{zA}\,r}{EI}$	$\frac{K_{zB}\,r}{EI}$	$\frac{K_{zA}\,r}{EI}$	$\frac{K_{zB}\,r}{EI}$	$\frac{K_{zA}\,r}{EI}$	$\frac{K_{zB}\,r}{EI}$	$\frac{K_{zA}\,r}{EI}$	$\frac{K_{zB}\,r}{EI}$	$\frac{K_{zA}\,r}{EI}$	$\frac{K_{zB}\,r}{EI}$	$\frac{K_{zA}\,r}{EI}$
15	82½	4.165	3.907	14.916	15.174	2.382	1.996	14.756	15.141	1.190	0.722	14.534	15.003
	67½	5.863	5.158	13.218	13.923	4.425	3.372	12.711	13.766	3.446	2.167	12.278	13.558
	52½	8.547	7.584	10.534	11.497	7.579	6.140	9.558	10.997	6.886	5.137	8.839	10.587
	37½	11.497	10.534	7.584	8.547	10.997	9.558	6.140	7.579	10.587	8.839	5.137	6.886
	22½	13.923	13.218	5.158	5.863	13.766	12.711	3.372	4.425	13.558	12.278	2.167	3.446
	7½	15.174	14.916	3.907	4.165	15.141	14.756	1.996	2.382	15.003	14.534	0.722	1.190
	− 7½	14.916	15.174	4.165	3.907	14.756	15.141	2.382	1.996	14.534	15.003	1.190	0.722
	−22½	13.218	13.923	5.863	5.158	12.711	13.766	4.425	3.372	12.278	13.558	3.446	2.167
	−37½	10.534	11.497	8.547	7.584	9.558	10.997	7.579	6.140	8.839	10.587	6.886	5.137
	−52½	7.584	8.547	11.497	10.534	6.140	7.579	10.997	9.558	5.137	6.886	10.587	8.839
	−67½	5.158	5.863	13.923	13.218	3.372	4.425	13.766	12.711	2.167	3.446	13.558	12.278
	−82½	3.907	4.165	15.174	14.916	1.996	2.382	15.141	14.756	0.722	1.190	15.003	14.534
30	75	2.577	2.081	6.938	7.433	1.853	1.123	6.638	7.368	1.347	0.476	6.255	7.126
	60	3.784	2.926	5.730	6.588	3.285	2.022	5.206	6.470	2.887	1.378	4.714	6.224
	45	5.253	4.262	4.262	5.253	4.975	3.516	3.516	4.975	4.672	2.929	2.929	4.672
	30	6.588	5.730	2.926	3.784	6.470	5.206	2.022	3.285	6.224	4.714	1.378	2.887
	15	7.433	6.938	2.081	2.577	7.368	6.638	1.123	1.853	7.126	6.255	0.476	1.347
	0	7.561	7.561	1.953	1.953	7.431	7.431	1.062	1.062	7.138	7.138	0.465	0.465
	−15	6.938	7.433	2.577	2.081	6.638	7.368	1.853	1.123	6.255	7.126	1.347	0.476
	−30	5.730	6.588	3.784	2.926	5.206	6.470	3.285	2.022	4.714	6.224	2.887	1.378
	−45	4.262	5.253	5.253	4.262	3.516	4.975	4.975	3.516	2.929	4.672	4.672	2.929
	−60	2.926	3.784	6.588	5.730	2.022	3.285	6.470	5.206	1.378	2.887	6.224	4.714
	−75	2.081	2.577	7.433	6.938	1.123	1.853	7.368	6.638	0.476	1.347	7.126	6.255
45	67½	2.207	1.524	4.097	4.789	1.876	0.878	3.703	4.700	1.581	0.423	3.234	4.392
	52½	3.159	2.213	3.155	4.101	2.954	1.591	2.625	3.987	2.684	1.102	2.131	3.713
	37½	4.101	3.155	2.213	3.159	3.987	2.625	1.591	2.954	3.712	2.131	1.102	2.684
	22½	4.789	4.097	1.524	2.207	4.700	3.703	0.878	1.876	4.392	3.234	0.423	1.581
	7½	5.041	4.750	1.273	1.527	4.901	4.540	0.678	1.043	4.539	4.115	0.276	0.700
	− 7½	4.750	5.041	1.527	1.273	4.540	4.901	1.043	0.678	4.115	4.539	0.700	0.276
	−22½	4.097	4.789	2.207	1.524	3.703	4.700	1.876	0.878	3.234	4.392	1.581	0.423
	−37½	3.155	4.101	3.159	2.213	2.625	3.987	2.954	1.591	2.120	3.712	2.684	1.102
	−52½	2.213	3.159	4.101	3.155	1.591	2.954	3.987	2.625	1.102	2.684	3.713	2.131
	−67½	1.524	2.207	4.789	4.097	0.878	1.876	4.700	3.703	0.423	1.581	4.392	3.234
60	60	2.114	1.279	2.591	3.426	1.946	0.781	2.155	3.320	1.706	0.404	1.681	2.983
	45	2.834	1.871	1.871	2.834	2.723	1.378	1.378	2.723	2.443	0.942	0.942	2.443
	30	3.426	2.591	1.279	2.114	3.320	2.155	0.781	1.946	2.983	1.681	0.404	1.706
	15	3.730	3.248	0.975	1.457	3.577	2.904	0.525	1.197	3.175	2.423	0.212	0.964
	0	3.664	3.664	1.040	1.040	3.425	3.425	0.677	0.677	2.971	2.971	0.417	0.417
	−15	3.248	3.730	1.457	0.975	2.904	3.577	1.197	0.525	2.423	3.175	0.964	0.212
	−30	2.591	3.426	2.114	1.279	2.155	3.320	1.946	0.781	1.681	2.983	1.706	0.404
	−45	1.871	2.834	2.834	1.871	1.378	2.723	2.723	1.378	0.942	2.443	2.443	0.942
	−60	1.279	2.114	3.426	2.591	0.781	1.946	3.320	2.155	0.404	1.706	2.983	1.681
75	52½	2.064	1.153	1.669	2.580	1.958	0.735	1.244	2.466	1.694	0.391	0.825	2.128
	37½	2.580	1.669	1.153	2.064	2.466	1.244	0.735	1.958	2.128	0.825	0.391	1.694
	22½	2.904	2.238	0.828	1.495	2.743	1.848	0.459	1.354	2.330	1.376	0.190	1.144
	7½	2.951	2.707	0.782	1.026	2.713	2.385	0.488	0.816	2.244	1.895	0.274	0.624
	− 7½	2.707	2.951	1.026	0.782	2.385	2.713	0.816	0.488	1.895	2.244	0.624	0.274
	−22½	2.238	2.904	1.495	0.828	1.848	2.743	1.354	0.459	1.376	2.330	1.144	0.190
	−37½	1.669	2.580	2.064	1.153	1.244	2.466	1.958	0.735	0.825	2.128	1.694	0.391
	−52½	1.153	2.064	2.580	1.699	0.735	1.958	2.466	1.244	0.391	1.694	2.128	0.825
90	45	2.000	1.080	1.080	2.000	1.884	0.708	0.708	1.884	1.562	0.377	0.377	1.562
	30	2.326	1.531	0.753	1.548	2.160	1.142	0.432	1.450	1.756	0.730	0.182	1.208
	15	2.442	1.983	0.637	1.096	2.205	1.617	0.387	0.975	1.741	1.148	0.199	0.791
	0	2.317	2.317	0.761	0.761	2.006	2.006	0.586	0.586	1.518	1.518	0.421	0.421
	−15	1.983	2.442	1.096	0.637	1.617	2.205	0.975	0.387	1.148	1.741	0.791	0.199
	−30	1.531	2.326	1.548	0.753	1.142	2.160	1.450	0.432	0.730	1.756	1.208	0.182
	−45	1.080	2.000	2.000	1.080	0.708	1.884	1.884	0.708	0.377	1.562	1.562	0.377
105	37½	1.892	1.033	0.715	1.574	1.728	0.687	0.422	1.463	1.347	0.361	0.181	1.167
	22½	2.052	1.423	0.555	1.184	1.819	1.056	0.332	1.094	1.371	0.649	0.156	0.878
	7½	2.012	1.782	0.596	0.826	1.710	1.430	0.441	0.720	1.133	0.969	0.296	0.550
	− 7½	1.782	2.012	0.826	0.596	1.430	1.710	0.720	0.441	0.969	1.133	0.550	0.296
	−22½	1.423	2.052	1.184	0.555	1.056	1.819	1.094	0.332	0.649	1.371	0.878	0.156
	−37½	1.033	1.892	1.574	0.715	0.687	1.728	1.463	0.422	0.361	1.347	1.167	0.181
120	30	1.738	0.997	0.511	1.252	1.512	0.666	0.303	1.149	1.091	0.343	0.133	0.881
	15	1.759	1.331	0.490	0.918	1.466	0.978	0.349	0.837	1.010	0.578	0.214	0.645
	0	1.610	1.610	0.639	0.639	1.271	1.271	0.544	0.544	0.823	0.823	0.402	0.402
	−15	1.331	1.759	0.918	0.490	0.978	1.466	0.837	0.349	0.578	1.010	0.645	0.214
	−30	0.997	1.738	1.252	0.511	0.666	1.512	1.149	0.303	0.343	1.091	0.881	0.133
135	22½	1.543	0.964	0.425	1.003	1.262	0.643	0.290	0.908	0.832	0.325	0.161	0.670
	7½	1.458	1.246	0.509	0.721	1.131	0.904	0.421	0.648	0.815	0.515	0.293	0.478
	− 7½	1.246	1.458	0.721	0.509	0.904	1.131	0.648	0.421	0.515	0.815	0.478	0.293
	−22½	0.964	1.543	1.003	0.425	0.643	1.262	0.908	0.290	0.325	0.832	0.670	0.161
150	15	1.319	0.931	0.420	0.808	1.005	0.618	0.335	0.722	0.599	0.305	0.216	0.510
	0	1.164	1.164	0.574	0.574	0.833	0.833	0.506	0.506	0.459	0.459	0.356	0.356
	−15	0.931	1.319	0.808	0.420	0.618	1.005	0.722	0.335	0.305	0.599	0.510	0.216
165	7½	1.083	0.894	0.466	0.655	0.765	0.589	0.401	0.576	0.408	0.285	0.267	0.390
	− 7½	0.894	1.083	0.655	0.466	0.589	0.765	0.576	0.401	0.285	0.408	0.390	0.267
180	0	0.854	0.854	0.535	0.535	0.558	0.558	0.462	0.462	0.265	0.265	0.298	0.298

In Fig. 2(*b*), Fig. 2(*c*), and Fig. 2(*d*) are shown the carry-over moments resulting from the application of moments M_{zA}, M_{xB}, and M_{xA}, respectively. All moments in Fig. 2 are positive and are shown as vectors. The right-hand screw rule should be used for sense of these positive moments.

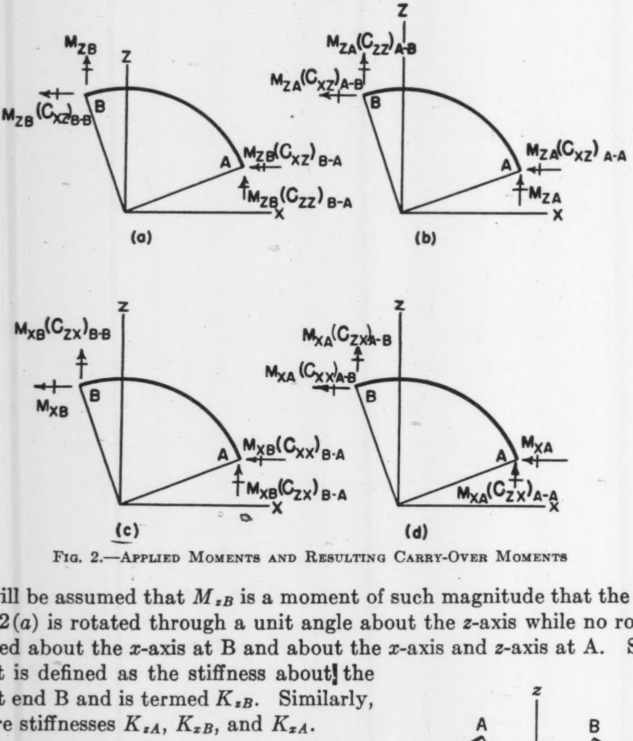

M_ZB
Z
M_ZB (C_XZ)_B-B
B
A
M_ZB (C_XZ) B-A
M_ZB (C_ZZ) B-A
X
(a)
Z
M_ZA (C_ZZ) A-B
M_ZA (C_XZ) A-B
B
A
M_ZA (C_XZ) A-A
M_ZA
X
(b)
Z
M_XB (C_ZX) B-B
M_XB
B
A
M_XB (C_XX) B-A
M_XB (C_ZX) B-A
X
(c)
Z
M_XA (C_ZX) A-B
M_XA (C_XX) A-B
B
A
M_XA
M_XA (C_ZX) A-A
X
(d)

FIG. 2.—APPLIED MOMENTS AND RESULTING CARRY-OVER MOMENTS

It will be assumed that M_{zB} is a moment of such magnitude that the end B in Fig. 2(*a*) is rotated through a unit angle about the *z*-axis while no rotation is allowed about the *x*-axis at B and about the *x*-axis and *z*-axis at A. Such a moment is defined as the stiffness about the *z*-axis at end B and is termed K_{zB}. Similarly, there are stiffnesses K_{zA}, K_{xB}, and K_{xA}.

Stiffnesses for circular segments of various lengths and orientations are presented in Table 1. Values are tabulated for three ratios of bending to torsional rigidity ($E\,I/G\,J$) along the segment. All values of stiffness given in Table 1 are in terms of $r/E\,I$, in which r is the radius of curvature (Fig. 3). The method by which these stiffness values were determined is explained at the end of this paper.

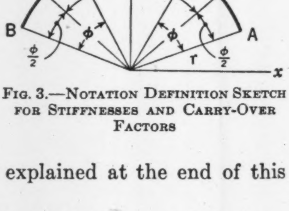

z
A
B
-η
η
B
A
φ
φ
φ/2
φ/2
r
x

FIG. 3.—NOTATION DEFINITION SKETCH FOR STIFFNESSES AND CARRY-OVER FACTORS

Curves can be drawn from the values given in Table 1; one set of these curves is shown in Fig. 4. Such curves enable one to interpolate between tabulated values and also between the three values of $E\,I/G\,J$ considered in making the tabulation. A study of Table 1 will show that the values of all four stiffnesses are related, and consequently all four stiffnesses can be read from one chart such as Fig. 4.

Carry-over factors are presented in Table 2. By tabulating carry-over factors in terms of the stiffnesses, only six, instead of twelve, sets of values are required for each value of the ratio of $E\,I$ to $G\,J$. This is because of the equalities resulting from reciprocal relationships. All values in Table 2 are also in terms of $r/E\,I$. Therefore, a carry-over factor can be obtained directly by dividing a value in Table 2 by the appropriate value from Table 1. The determination of the values in Table 2 is explained at the end of the paper.

For general use, curves should be drawn by means of the values in Table 2. Actually, only three sets of curves need be constructed for each value of the ratio of $E\,I$ to $G\,J$. For example, if a set of curves is drawn to determine the

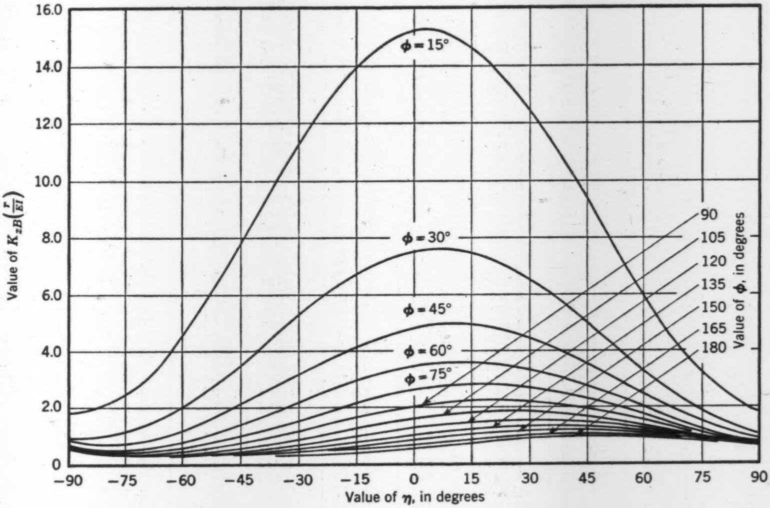

FIG. 4.—STIFFNESSES FOR CIRCULAR SEGMENTS, $\frac{E\,I}{G\,J} = 2$ (ANGLES DEFINED IN FIG. 3)

values of $(C_{zz})_{A-B}$, values of $(C_{zz})_{B-A}$ can be obtained from the same curves by changing the sign of the angle η.

Curves representing values of stiffnesses and carry-over factors (in terms of stiffnesses) have the shape of sine curves or cosine curves. As a result, any curve is adequately defined by only a few points. In Tables 1 and 2, values are limited to an angle η equal to $\pm 90°$, but, because the shape of the curve is known, they can be extended to include any value of η.

FIXED-END MOMENTS

In Fig. 5(*a*) positive bending and twisting moments are shown at the ends of member AB. Positive moments about the x-axis and z-axis at the ends of the same member are shown in Fig. 5(*b*). The latter moments are related to the

TABLE 2.—Carry-Over Factors, in Terms of Stiffnesses,

Angle, in Degrees		$EI/GJ = 1$						EI/GJ		
ϕ	η	$K_{zB}(C_{zz})_{B\text{-}A}(\tau/EI) = K_{zA}(C_{zz})_{A\text{-}B}(\tau/EI)$	$K_{zA}(C_{zz})_{A\text{-}B}(\tau/EI) = K_{zB}(C_{zz})_{B\text{-}A}(\tau/EI)$	$K_{zB}(C_{zz})_{B\text{-}A}(\tau/EI) = K_{zA}(C_{zz})_{A\text{-}B}(\tau/EI)$	$K_{zA}(C_{zz})_{A\text{-}B}(\tau/EI) = K_{zB}(C_{zz})_{B\text{-}A}(\tau/EI)$	$K_{zB}(C_{zz})_{B\text{-}B}(\tau/EI) = K_{zB}(C_{zz})_{B\text{-}B}(\tau/EI)$	$K_{zA}(C_{zz})_{A\text{-}A}(\tau/EI) = K_{zA}(C_{zz})_{A\text{-}A}(\tau/EI)$	$K_{zB}(C_{zz})_{B\text{-}A}(\tau/EI) = K_{zA}(C_{zz})_{A\text{-}B}(\tau/EI)$	$K_{zA}(C_{zz})_{A\text{-}B}(\tau/EI) = K_{zB}(C_{zz})_{B\text{-}A}(\tau/EI)$	$K_{zB}(C_{zz})_{B\text{-}A}(\tau/EI) = K_{zA}(C_{zz})_{A\text{-}B}(\tau/EI)$
(1)	(2)	(3)	(4)	(5)	(6)	(7)	(8)	(9)	(10)	(11)
15	82½	−3.647	7.405	−1.980	−0.982	−1.957	−0.993	−1.802	7.415	−1.980
	67½	−2.166	5.925	−4.544	−3.546	−4.383	−3.677	−0.567	6.179	−4.117
	52½	0.399	3.360	−6.025	−5.027	−5.634	−5.376	1.572	4.041	−5.353
	37½	3.360	0.399	−6.025	−5.027	−5.376	−5.634	4.041	1.572	−5.353
	22½	5.925	−2.166	−4.544	−3.546	−3.677	−4.383	6.179	−0.567	−4.117
	7½	7.405	−3.647	−1.980	−0.982	−0.993	−1.957	7.415	−1.802	−1.980
	− 7½	7.405	−3.647	0.982	1.980	1.957	0.993	7.415	−1.802	0.490
	−22½	5.925	−2.166	3.546	4.544	4.383	3.677	6.179	−0.567	2.629
	−37½	3.360	0.399	5.027	6.025	5.634	5.376	4.041	1.572	3.863
	−52½	0.399	3.360	5.027	6.025	5.376	5.634	1.572	4.041	3.863
	−67½	−2.166	5.925	3.546	4.544	3.677	4.383	−0.567	6.179	2.629
	−82½	−3.647	7.405	0.982	1.980	0.993	1.957	−1.802	7.415	0.490
30	75	−1.572	3.360	−1.919	−0.928	−1.831	−0.973	−0.743	3.376	−1.919
	60	−0.530	2.318	−2.961	−1.970	−2.676	−2.181	0.127	2.505	−2.789
	45	0.894	0.894	−3.343	−2.352	−2.804	−2.804	1.316	1.316	−3.108
	30	2.318	−0.530	−2.961	−1.970	−2.181	−2.676	2.505	0.127	−2.789
	15	3.360	−1.572	−1.919	−0.928	−0.973	−1.831	3.376	−0.743	−1.919
	0	3.741	−1.953	−0.495	0.495	0.495	−0.495	3.695	−1.062	−0.730
	−15	3.360	−1.572	0.928	1.919	1.831	0.973	3.376	−0.743	0.459
	−30	2.318	−0.530	1.970	2.961	2.676	2.181	2.505	0.127	1.330
	−45	0.894	0.894	2.352	3.343	2.804	2.804	1.316	1.316	1.648
	−60	−0.530	2.318	1.970	2.961	2.181	2.676	0.127	2.505	1.330
	−75	−1.572	3.360	0.928	1.919	0.973	1.831	−0.743	3.376	0.459
45	67½	−0.789	1.878	−1.812	−0.842	−1.624	−0.940	−0.330	1.899	−1.820
	52½	0.058	1.033	−2.309	−1.330	−1.884	−1.630	0.376	1.192	−2.228
	37½	1.033	0.058	−2.309	−1.330	−1.630	−1.884	1.192	0.376	−2.228
	22½	1.878	−0.789	−1.812	−0.842	−0.940	−1.624	1.899	−0.330	−1.820
	7½	2.365	−1.274	−0.977	0.002	0.003	−0.935	2.307	−0.738	−1.113
	− 7½	2.365	−1.274	−0.002	0.977	0.935	−0.003	2.307	−0.738	−0.273
	−22½	1.878	−0.789	0.842	1.812	1.624	0.940	1.899	−0.330	0.409
	−37½	1.033	0.058	1.330	2.309	1.884	1.630	1.192	0.376	0.818
	−52½	0.058	1.033	1.330	2.309	1.630	1.884	0.376	1.192	0.818
	−67½	−0.789	1.878	0.842	1.812	0.940	1.624	−0.330	1.899	0.409
60	60	−0.342	1.056	−1.692	−0.729	−1.377	−0.895	−0.091	1.081	−1.687
	45	0.357	0.357	−1.879	−0.916	−1.312	−1.312	0.495	0.495	−1.844
	30	1.056	−0.342	−1.692	−0.729	−0.895	−1.377	1.081	−0.091	−1.687
	15	1.567	−0.853	−1.181	−0.217	−0.239	−1.073	1.510	−0.520	−1.258
	0	1.754	−1.040	−0.482	0.482	0.482	−0.482	1.667	−0.677	−0.672
	−15	1.567	−0.853	0.217	1.181	1.073	0.239	1.510	−0.520	−0.087
	−30	1.056	−0.342	0.729	1.692	1.377	0.895	1.081	−0.091	0.342
	−45	0.357	0.357	0.916	1.879	1.312	1.312	0.495	0.495	0.499
	−60	−0.342	1.056	0.729	1.692	0.895	1.377	−0.091	1.081	0.342
75	52½	−0.053	0.518	−1.536	−0.593	−1.085	−0.841	0.067	0.546	−1.527
	37½	0.518	−0.053	−1.536	−0.593	−0.841	−1.085	0.546	0.067	−1.527
	22½	1.012	−0.547	−1.251	−0.308	−0.371	−1.038	0.961	−0.348	−1.287
	7½	1.298	−0.832	−0.757	0.186	0.198	−0.713	1.200	−0.587	−0.872
	− 7½	1.298	−0.832	−0.186	0.757	0.713	−0.198	1.200	−0.587	−0.393
	−22½	1.012	−0.547	0.308	1.251	1.038	0.371	0.961	−0.348	0.021
	−37½	0.518	−0.053	0.593	1.536	1.085	0.841	0.546	0.067	0.261
	−52½	−0.053	0.518	0.593	1.536	0.841	1.085	0.067	0.546	0.261
90	45	0.141	0.141	−1.362	−0.444	−0.777	−0.777	0.172	0.172	−1.345
	30	0.592	−0.311	−1.241	−0.322	−0.444	−0.903	0.550	−0.207	−1.244
	15	0.923	−0.641	−0.911	0.008	0.009	−0.786	0.828	−0.484	−0.966
	0	1.044	−0.761	−0.459	0.459	0.459	−0.459	0.929	−0.586	−0.588
	−15	0.923	−0.641	−0.008	0.911	0.786	−0.009	0.828	−0.484	−0.209
	−30	0.592	−0.311	0.323	1.241	0.903	0.444	0.550	−0.207	0.068
	−45	0.141	0.141	0.444	1.362	0.777	0.777	0.172	0.172	0.169
105	37½	0.264	−0.128	−1.177	−0.288	−0.478	−0.708	0.235	−0.093	−1.151
	22½	0.604	−0.468	−0.980	−0.091	−0.120	−0.748	0.519	−0.377	−0.987
	7½	0.801	−0.664	−0.641	0.248	0.270	−0.588	0.683	−0.541	−0.703
	− 7½	0.801	−0.664	−0.248	0.641	0.588	−0.270	0.683	−0.541	−0.375
	−22½	0.604	−0.468	0.091	0.980	0.748	0.120	0.519	−0.377	−0.091
	−37½	0.264	−0.128	0.288	1.177	0.708	0.478	0.235	−0.093	0.073

FOR CIRCULAR SEGMENTS (ANGLES DEFINED IN FIG. 3)

= 2			$EI/GJ = 6$						ANGLE, IN DEGREES	
$K_{zA}(C_{zz})_{A\text{-}B}(\tau/EI) = K_{zB}(C_{zz})_{B\text{-}A}(\tau/EI)$	$K_{zB}(C_{zz})_{B\text{-}B}(\tau/EI) = K_{zB}(C_{zz})_{B\text{-}B}(\tau/EI)$	$K_{zA}(C_{zz})_{A\text{-}A}(\tau/EI) = K_{zA}(C_{zz})_{A\text{-}A}(\tau/EI)$	$K_{zB}(C_{zz})_{B\text{-}A}(\tau/EI) = K_{zA}(C_{zz})_{A\text{-}B}(\tau/EI)$	$K_{zA}(C_{zz})_{A\text{-}B}(\tau/EI) = K_{zB}(C_{zz})_{B\text{-}A}(\tau/EI)$	$K_{zB}(C_{zz})_{B\text{-}A}(\tau/EI) = K_{zA}(C_{zz})_{A\text{-}B}(\tau/EI)$	$K_{zA}(C_{zz})_{A\text{-}B}(\tau/EI) = K_{zB}(C_{zz})_{B\text{-}A}(\tau/EI)$	$K_{zB}(C_{zz})_{B\text{-}B}(\tau/EI) = K_{zB}(C_{zz})_{B\text{-}B}(\tau/EI)$	$K_{zA}(C_{zz})_{A\text{-}A}(\tau/EI) = K_{zA}(C_{zz})_{A\text{-}A}(\tau/EI)$	η	ϕ
(12)	(13)	(14)	(15)	(16)	(17)	(18)	(19)	(20)	(21)	(22)
−0.490	−2.429	−0.990	−0.571	7.442	−1.978	−0.169	−2.725	−0.976	82½	15
−2.629	−5.196	−4.144	0.503	6.369	−3.838	−2.028	−5.696	−4.417	67½	
−3.863	−6.572	−6.187	2.362	4.509	−4.911	−3.102	−6.141	−6.672	52½	
−3.863	−6.187	−6.572	4.509	2.362	−4.911	−3.102	−6.672	−7.141	37½	
−2.629	−4.144	−5.196	6.369	−0.503	−3.838	−2.028	−4.417	−5.696	22½	
−0.490	−0.990	−2.429	7.442	−0.571	−1.978	−0.169	−0.976	−2.725	7½	
1.980	2.429	0.990	7.442	−0.571	0.169	1.978	2.725	0.976	− 7½	
4.117	5.196	4.144	6.369	−0.503	2.028	3.833	5.696	4.417	−22½	
5.353	6.572	6.187	4.509	2.362	3.102	4.911	7.141	6.672	−37½	
5.353	6.187	6.572	2.362	4.509	3.102	4.911	6.672	6.141	−52½	
4.117	4.144	5.196	0.503	6.369	2.028	3.838	4.417	5.696	−67½	
1.980	0.990	2.429	−0.571	7.442	0.169	1.978	0.976	2.725	−82½	
−0.459	−2.224	−0.960	−0.185	3.425	−1.914	−0.171	−2.423	−0.913	75	30
−1.330	−3.122	−2.393	0.578	2.663	−2.677	−0.933	−3.376	−2.454	60	
−1.648	−3.184	−3.184	1.620	1.620	−2.956	−1.213	−3.336	−3.336	45	
−1.330	−2.393	−3.122	2.663	0.578	−2.677	−0.933	−2.454	−3.336	30	
−0.459	−0.960	−2.224	3.425	−0.185	−1.914	−0.171	−0.913	−2.423	15	
0.730	0.730	−0.730	3.705	−0.465	−0.872	0.872	0.872	−0.872	0	
1.919	2.224	0.960	3.425	−0.185	0.171	1.914	2.423	0.913	−15	
2.789	3.122	2.393	2.663	0.578	0.933	2.677	3.336	2.454	−30	
3.108	3.184	3.184	1.620	1.620	1.213	2.956	3.336	3.336	−45	
2.789	2.393	3.122	0.578	2.663	0.933	2.677	2.454	3.376	−60	
1.919	0.960	2.224	−0.185	3.425	0.171	1.914	0.913	2.423	−75	
−0.409	−1.911	−0.914	−0.014	1.950	−1.801	−0.163	−1.984	−0.826	67½	45
−0.818	−2.112	−1.747	0.609	1.327	−2.160	−0.522	−2.131	−1.707	52½	
−0.818	−1.747	−2.112	1.328	0.609	−2.160	−0.522	−1.707	−2.131	37½	
−0.409	−0.914	−1.911	1.950	−0.014	−1.801	−0.163	−0.826	−1.984	22½	
0.273	0.164	−1.190	2.309	−0.373	−1.178	0.459	0.277	−1.305	7½	
1.113	1.190	−0.164	2.309	−0.373	−0.459	1.178	1.305	−0.277	− 7½	
1.820	1.911	0.914	1.950	−0.014	0.163	1.801	1.984	0.826	−22½	
2.228	2.112	1.747	1.328	0.609	0.522	2.160	2.131	1.707	−37½	
2.228	1.747	2.112	0.609	1.327	0.522	2.160	1.707	2.131	−52½	
1.820	0.914	1.911	−0.014	1.950	0.163	1.801	0.826	1.984	−67½	
−0.342	−1.526	−0.854	0.097	1.124	−1.641	−0.138	−1.482	−0.730	60	60
−0.499	−1.374	−1.374	0.611	0.611	−1.780	−0.276	−1.266	−1.266	45	
−0.342	−0.854	−1.526	1.124	0.097	−1.641	−0.138	−0.730	−1.482	30	
0.087	−0.105	−1.269	1.500	−0.279	−1.266	0.237	0.013	−1.289	15	
0.672	0.672	−0.672	1.638	−0.417	−0.752	0.752	0.752	−0.752	0	
1.258	1.269	0.105	1.500	−0.279	−0.237	1.266	1.289	−0.013	−15	
1.687	1.526	0.854	1.124	0.097	0.138	1.641	1.482	0.730	−30	
1.844	1.374	1.374	0.611	0.611	0.276	1.780	1.266	1.266	−45	
1.687	0.854	1.526	0.097	1.124	0.138	1.641	0.730	1.482	−60	
−0.261	−1.112	−0.785	0.171	0.584	−1.445	−0.097	−0.985	−0.636	52½	75
−0.261	−0.785	−1.112	0.584	0.171	−1.445	−0.097	−0.636	−0.985	37½	
−0.021	−0.247	−1.142	0.942	−0.187	−1.240	0.110	−0.116	−1.069	22½	
0.393	0.357	−0.865	1.148	−0.393	−0.881	0.468	0.435	−0.868	7½	
0.872	0.865	−0.357	1.148	−0.393	−0.468	0.881	0.868	−0.435	− 7½	
1.287	1.142	0.247	0.942	−0.187	−0.110	1.240	1.069	0.116	−22½	
1.527	1.112	0.785	0.584	0.171	0.097	1.445	0.985	0.636	−37½	
1.527	0.785	1.112	0.171	0.584	0.097	1.445	0.636	0.985	−52½	
−0.169	−0.710	−0.710	0.214	0.214	−1.228	−0.043	−0.548	−0.548	45	90
−0.068	−0.321	−0.909	0.533	−0.093	−1.144	0.138	−0.178	−0.771	30	
0.209	0.154	−0.864	0.765	−0.336	−0.910	0.274	0.240	−0.787	15	
0.588	0.588	−0.588	0.850	−0.421	−0.593	0.593	0.593	−0.593	0	
0.966	0.864	−0.154	0.765	−0.336	−0.274	0.910	0.787	−0.240	−15	
1.244	0.909	0.321	0.533	−0.093	−0.138	1.144	0.771	0.178	−30	
1.345	0.710	0.710	0.214	0.214	0.043	1.228	0.548	0.548	−45	
−0.073	−0.355	−0.634	0.231	−0.034	−0.874	−0.014	−0.205	−0.469	37½	105
0.091	0.019	−0.743	0.462	−0.265	−0.874	0.147	0.115	−0.607	22½	
0.375	0.388	−0.653	0.595	−0.398	−0.643	0.378	0.402	−0.584	7½	
0.703	0.653	−0.388	0.595	−0.398	−0.378	0.643	0.584	−0.402	− 7½	
0.987	0.743	−0.019	0.462	−0.265	−0.147	0.874	0.607	−0.115	−22½	
1.151	0.634	0.355	0.231	−0.034	0.014	0.874	0.469	0.205	−37½	

TABLE 2.—

ANGLE, IN DEGREES		$EI/GJ = 1$						EI/GJ		
ϕ	η	$K_{zB}(C_{zz})_{B\text{-}A}(\tau/EI) = K_{zA}(C_{zz})_{A\text{-}B}(\tau/EI)$	$K_{xA}(C_{xx})_{A\text{-}B}(\tau/EI) = K_{xB}(C_{xx})_{B\text{-}A}(\tau/EI)$	$K_{zB}(C_{zx})_{B\text{-}A}(\tau/EI) = K_{xA}(C_{xz})_{A\text{-}B}(\tau/EI)$	$K_{xA}(C_{xz})_{A\text{-}B}(\tau/EI) = K_{zB}(C_{zx})_{B\text{-}A}(\tau/EI)$	$K_{zB}(C_{zx})_{B\text{-}B}(\tau/EI) = K_{xB}(C_{xz})_{B\text{-}B}(\tau/EI)$	$K_{zA}(C_{zx})_{A\text{-}A}(\tau/EI) = K_{xA}(C_{xz})_{A\text{-}A}(\tau/EI)$	$K_{zB}(C_{zz})_{B\text{-}A}(\tau/EI) = K_{zA}(C_{zz})_{A\text{-}B}(\tau/EI)$	$K_{xA}(C_{xx})_{A\text{-}B}(\tau/EI) = K_{xB}(C_{xx})_{B\text{-}A}(\tau/EI)$	$K_{zB}(C_{zx})_{B\text{-}A}(\tau/EI) = K_{xA}(C_{xz})_{A\text{-}B}(\tau/EI)$
(1)	(2)	(3)	(4)	(5)	(6)	(7)	(8)	(9)	(10)	(11)
120	30	0.332	−0.315	−0.988	−0.133	−0.207	−0.635	0.263	−0.275	−0.955
	15	0.569	−0.552	−0.751	0.104	0.128	−0.613	0.460	−0.472	−0.758
	0	0.655	−0.639	−0.428	0.428	0.428	−0.428	0.532	−0.544	−0.488
	−15	0.569	−0.552	−0.104	0.751	0.613	−0.128	0.460	−0.472	−0.219
	−30	0.332	−0.315	0.133	0.988	0.635	0.207	0.263	−0.275	−0.022
135	22½	0.353	−0.438	−0.804	0.013	0.019	−0.559	0.262	−0.391	−0.764
	7½	0.497	−0.583	−0.554	0.264	0.296	−0.494	0.381	−0.510	−0.557
	− 7½	0.497	−0.583	−0.264	0.554	0.494	−0.296	0.381	−0.510	−0.318
	−22½	0.353	−0.438	−0.013	0.804	0.559	−0.019	0.262	−0.391	−0.111
150	15	0.335	−0.509	−0.632	0.144	0.189	−0.484	0.236	−0.453	−0.593
	0	0.400	−0.574	−0.388	0.388	0.388	−0.388	0.289	−0.506	−0.387
	−15	0.335	−0.509	−0.144	0.632	0.484	−0.189	0.236	−0.453	−0.188
165	7½	0.287	−0.538	−0.476	0.254	0.295	−0.410	0.191	−0.473	−0.428
	− 7½	0.287	−0.538	−0.254	0.476	0.410	−0.295	0.191	−0.473	−0.250
180	0	0.217	−0.535	−0.341	0.341	0.341	−0.341	0.134	−0.462	−0.294

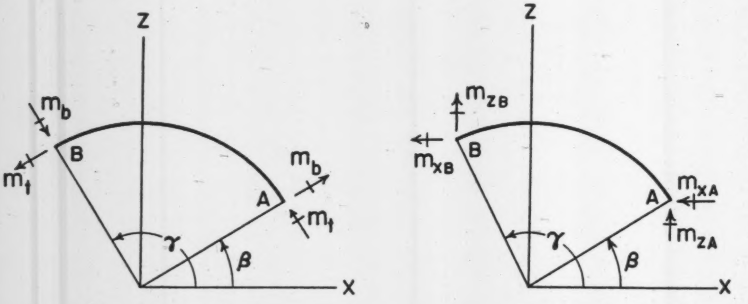

(a) Positive Bending and Twisting Moments.

(b) Positive Moments about the Assumed Rectangular Axes x and z.

FIG. 5.—POSITIVE MOMENTS AT ENDS OF A CIRCULAR SEGMENT

former as follows:

$$\left.\begin{aligned} m_{xA} &= m_t \sin\beta - m_b \cos\beta \\ m_{zA} &= m_t \cos\beta + m_b \sin\beta \\ m_{xB} &= m_t \sin\gamma + m_b \cos\gamma \\ m_{zB} &= m_t \cos\gamma - m_b \sin\gamma \end{aligned}\right\} \qquad (1)$$

Table 3 contains values of fixed-end moments resulting from a concentrated load *W* on members of circular-arc plan. The angles are defined in Fig. 6(*a*).

(Continued)

= 2			$EI/GJ = 6$						ANGLE, IN DEGREES	
$K_{zA}(C_{zz})_{A\text{-}B}(r/EI) = K_{zB}(C_{zz})_{B\text{-}A}(r/EI)$	$K_{zB}(C_{zz})_{B\text{-}B}(r/EI) = K_{zB}(C_{zz})_{B\text{-}B}(r/EI)$	$K_{zA}(C_{zz})_{A\text{-}A}(r/EI) = K_{zA}(C_{zz})_{A\text{-}A}(r/EI)$	$K_{zB}(C_{zz})_{B\text{-}A}(r/EI) = K_{zA}(C_{zz})_{A\text{-}B}(r/EI)$	$K_{zA}(C_{zz})_{A\text{-}B}(r/EI) = K_{zB}(C_{zz})_{B\text{-}A}(r/EI)$	$K_{zB}(C_{zz})_{B\text{-}A}(r/EI) = K_{zA}(C_{zz})_{A\text{-}B}(r/EI)$	$K_{zA}(C_{zz})_{A\text{-}B}(r/EI) = K_{zB}(C_{zz})_{B\text{-}A}(r/EI)$	$K_{zB}(C_{zz})_{B\text{-}B}(r/EI) = K_{zB}(C_{zz})_{B\ B}(r/EI)$	$K_{zA}(C_{zz})_{A\text{-}A}(r/EI) = K_{zA}(C_{zz})_{A\text{-}A}(r/EI)$	η	ϕ
(12)	(13)	(14)	(15)	(16)	(17)	(18)	(19)	(20)	(21)	(22)
0.022	−0.070	−0.559	0.226	−0.192	−0.661	0.069	0.034	−0.398	30	120
0.219	0.241	−0.605	0.379	−0.345	−0.641	0.222	0.269	−0.479	15	
0.488	0.488	−0.488	0.435	−0.402	−0.432	0.432	0.432	−0.432	0	
0.758	0.605	−0.241	0.379	−0.345	−0.222	0.641	0.479	−0.269	−15	
0.955	0.559	0.070	0.226	−0.192	−0.069	0.661	0.398	−0.034	−30	
0.111	0.132	−0.486	0.203	−0.281	−0.474	0.117	0.172	−0.336	22½	135
0.318	0.358	−0.487	0.336	−0.370	−0.493	0.270	0.350	−0.377	7½	
0.557	0.487	−0.358	0.336	−0.370	−0.270	0.493	0.377	−0.350	− 7½	
0.764	0.486	−0.132	0.203	−0.281	−0.117	0.474	0.336	−0.172	−22½	
0.188	0.254	−0.417	0.169	−0.319	−0.318	0.154	0.229	−0.280	15	150
0.387	0.387	−0.387	0.206	−0.356	−0.294	0.294	0.294	−0.294	0	
0.593	0.417	−0.254	0.169	−0.319	−0.154	0.318	0.280	−0.229	−15	
0.250	0.302	−0.353	0.127	−0.320	−0.193	0.178	0.227	−0.232	7½	165
0.428	0.353	−0.302	0.127	−0.320	−0.178	0.193	0.232	−0.227	− 7½	
0.294	0.294	−0.294	0.083	−0.298	−0.190	0.190	−0.190	−0.190	0	180

Because of the more economical presentation that results, the fixed-end moments tabulated are those about the bending and twisting axes. For use in the numerical procedure of this paper, these bending moments and twisting moments must be resolved into fixed-end moments about the x-axes and z-axes as indicated by Eqs. 1. The method by which the tabulated fixed-end bending and twisting moments were obtained is outlined at the end of this paper.

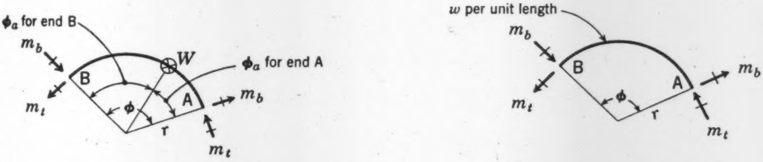

(*a*) Concentrated load (*b*) Uniformly distributed load

FIG. 6.—NOTATION DEFINITION SKETCH, FIXED-END MOMENTS

All values in Table 3 are in terms of the concentrated load, W, and the radius of curvature, r. If more than one concentrated load is on the member, the fixed-end moments due to each load can be superimposed. For general use, curves for m_b and m_t should be drawn by means of the tabulated values. Such curves for m_b, for a ratio of EI to GJ equal to 2, are shown in Fig. 7. These curves have the typical shape of influence lines for fixed-end moments.

Values for fixed-end bending moments and twisting moments resulting from a uniformly distributed load are listed in Table 4. Curves can be plotted for general use.

TABLE 3.—FIXED–END BENDING AND TWISTING MOMENTS PRODUCED BY A CONCENTRATED LOAD (ANGLES DEFINED IN FIG. 6)

ϕ_a/ϕ	$m_b(1/W\,r) \times 10^5$			$m_t(1/W\,r) \times 10^5$			$m_b(1/W\,r) \times 10^5$			$m_t(1/W\,r) \times 10^5$		
$EI/GJ =$	1	2	6	1	2	6	1	2	6	1	2	6
	$\phi = 15°$						$\phi = 105°$					
0.1	02123	02125	02128	00000	00000	00001	15610	15743	16091	00389	00485	00694
0.2	03364	03372	03373	00000	00001	00002	25673	25895	26949	01200	01413	02092
0.3	03860	03864	03877	00001	00001	00003	30384	30905	32147	02006	02468	03409
0.4	03782	03786	03799	00001	00002	00004	30461	30907	32099	02525	03084	04176
0.5	03286	03291	03308	00001	00002	00004	26671	27101	27887	02625	03184	04210
0.6	02527	02531	02551	00001	00002	00004	20395	20787	21045	02234	02771	03565
0.7	01657	01660	01672	00001	00001	00003	13375	13454	13313	01666	01985	02478
0.8	00836	00832	00845	00000	00000	00001	06684	06807	06384	00907	01143	01288
0.9	00237	00236	00237	00000	00000	00000	01832	01806	01656	00267	00311	00359
	$\phi = 30°$						$\phi = 120°$					
0.1	04268	04271	04294	00004	00005	00009	18046	18085	18609	00640	00767	01028
0.2	06763	06782	06851	00009	00013	00028	29928	30363	31393	01977	02354	03096
0.3	07794	07824	07932	00015	00022	00047	35616	36203	37561	03309	03908	05032
0.4	07654	07690	07820	00019	00031	00059	35716	36285	37476	04166	04898	06134
0.5	06655	06689	06810	00019	00028	00061	31365	31764	32411	04325	05017	06138
0.6	05115	05144	05236	00017	00022	00053	24085	24249	24248	03783	04341	05147
0.7	03357	03375	03438	00012	00018	00039	15620	15589	15134	02724	03090	03530
0.8	01704	01713	01743	00007	00010	00022	07747	07641	07118	01474	01650	01802
0.9	00473	00478	00487	00001	00003	00006	02101	02100	01775	00430	00470	00490
	$\phi = 45°$						$\phi = 135°$					
0.1	06432	06452	06522	00015	00021	00042	20529	20711	21163	00981	01135	01439
0.2	10257	10316	10515	00045	00064	00127	34313	34785	35951	03044	03490	04334
0.3	11865	11956	12261	00084	00106	00210	41028	41648	43076	05103	05795	07029
0.4	11685	11791	12138	00093	00133	00263	41222	41771	42917	06426	07224	08531
0.5	10180	10280	10602	00097	00139	00272	36168	36475	36920	06660	07402	08478
0.6	07832	07663	08157	00086	00122	00238	27672	27686	27359	05805	06369	07038
0.7	05139	05038	05338	00063	00089	00173	17829	17636	16827	04159	04498	04760
0.8	02605	02556	02692	00035	00049	00095	08758	08530	07746	02234	02376	02385
0.9	00730	00716	00749	00010	00015	00028	02345	02238	01895	00646	00673	00632
	$\phi = 60°$						$\phi = 150°$					
0.1	08644	08687	08821	00045	00063	00115	23050	23251	23742	01426	01595	01930
0.2	13874	13997	14374	00138	00192	00350	38792	39299	40512	04440	04917	05816
0.3	16130	16317	17356	00230	00319	00676	46555	47188	48659	07455	08166	09421
0.4	15944	16158	16783	00290	00401	00717	46804	47303	48381	09389	10162	11392
0.5	13920	14119	14673	00302	00417	00736	40969	41146	41380	09713	10373	11248
0.6	10719	10871	11270	00266	00367	00642	31176	31002	30354	08433	08871	09245
0.7	07030	07123	06866	00195	00267	00362	19914	19526	18380	06005	06210	06166
0.8	03558	03597	03672	00107	00147	00250	09664	09297	08268	03198	03241	03029
0.9	00994	01002	01010	00032	00044	00074	02547	02388	01953	00914	00904	00781
	$\phi = 75°$						$\phi = 165°$					
0.1	10909	10980	11188	00108	00145	00243	25595	25816	26337	01982	02153	02502
0.2	17642	17844	18416	00331	00444	00735	43323	43867	45144	06194	06651	07554
0.3	20629	20933	21767	00551	00736	01206	52114	52765	54276	10419	11052	12297
0.4	20472	20812	21710	00694	00923	01495	52345	52801	52897	13119	13730	14743
0.5	17914	18221	18962	00722	00958	01526	45631	45686	45754	13540	13958	14469
0.6	13801	14025	14491	00636	00840	01314	34466	34112	34108	11702	11857	11539
0.7	09041	09168	09376	00463	00609	00938	21775	21198	19779	08285	08219	07747
0.8	04562	04609	04639	00255	00333	00503	10407	09906	08681	04365	04233	03728
0.9	01268	01275	01256	00076	00099	00146	02688	02479	01974	01232	01161	00932
	$\phi = 90°$						$\phi = 180°$					
0.1	13230	13333	13614	00217	00282	00434	28150	28395	28942	02653	02809	03157
0.2	21574	21860	22616	00668	00862	01310	47852	48454	49794	08323	08706	09559
0.3	25380	25803	26869	01114	01430	02142	57607	58314	59890	14025	14476	25479
0.4	25287	25725	26824	01403	01791	02637	57710	58178	59222	17652	17950	18615
0.5	22171	22564	23388	01460	01853	02677	50000	50000	50000	18169	18169	18167
0.6	17079	17345	17783	01283	01619	02290	37396	36927	35883	15621	15323	14659
0.7	11166	11285	11384	00932	01168	01612	23295	22587	21011	10960	10509	09506
0.8	05611	05643	05552	00510	00634	00851	10926	10324	08985	05716	05333	04481
0.9	01550	01547	01474	00151	00186	00242	02752	02506	01959	01590	01433	01085

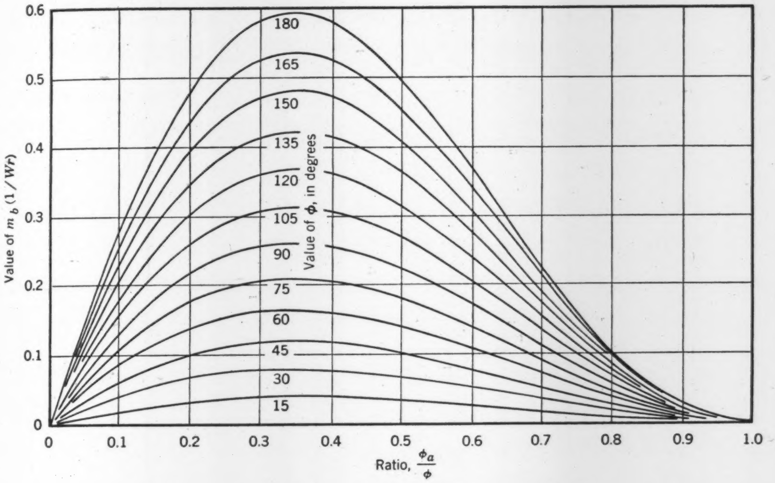

FIG. 7.—INFLUENCE LINES FOR FIXED-END BENDING MOMENTS, $\frac{E\,I}{G\,J} = 2$ (ANGLES DEFINED IN FIG. 6)

NUMERICAL EXAMPLES

A plan view of a frame containing curved members is shown in Fig. 8. The curved girders and straight beams are supported by columns at their intersections. The straight beams are considered fixed at one end. They could be framed into other members without affecting the numerical procedure

TABLE 4.—FIXED-END BENDING AND TWISTING MOMENTS DUE TO A UNIFORMLY DISTRIBUTED LOAD (ANGLE ϕ DEFINED IN FIG. 6)

ϕ	$m_b \frac{1}{w\,r^2}$			$m_t \frac{1}{w\,r^2}$		
	$\frac{E\,I}{G\,J}$					
	1	2	6	1	2	6
15	0.00573	0.00574	0.00576	0.00000	0.00000	0.00000
30	0.02315	0.02361	0.02521	0.00005	0.00012	0.00052
45	0.05292	0.05334	0.05469	0.00041	0.00058	0.00114
60	0.09601	0.09712	0.10022	0.00169	0.00233	0.00412
75	0.15358	0.15572	0.16088	0.00502	0.00666	0.01060
90	0.22676	0.23004	0.23790	0.01216	0.01543	0.02230
105	0.31643	0.32059	0.32822	0.02545	0.03087	0.04082
120	0.42301	0.42742	0.43458	0.04782	0.05546	0.06782
135	0.54624	0.55004	0.55557	0.08261	0.09180	0.10516
150	0.68502	0.68745	0.69057	0.13346	0.14253	0.15454
165	0.83729	0.83862	0.83913	0.20398	0.21028	0.21798
180	1.00000	1.00000	1.00000	0.29756	0.29756	0.29756

except that it would be necessary to distribute carry-over moments at those ends. The relative moments of inertia of members in Fig. 8 are as follows:

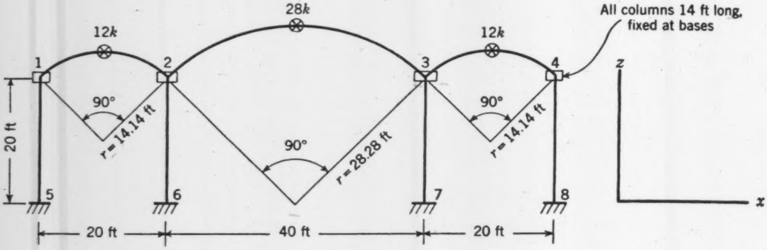
28k
12k
12k
All columns 14 ft long, fixed at bases
1
2
3
4
z
20 ft
90°
r=14.14 ft
90°
r=28.28 ft
90°
r=14.14 ft
5
6
7
8
x
20 ft
40 ft
20 ft

FIG. 8.—CONTINUOUS FRAME, $E\,I/G\,J = 1$ FOR ALL MEMBERS

Columns	I_x	I_z
1 and 4	1	3
2 and 3	2	6

Curved Girders	I
1–2 and 3–4	4
2–3	20

For all straight beams, $I = 3$. For all members, $E\,I/G\,J = 1$.

With these properties and the dimensions given in Fig. 8, the stiffnesses can be obtained from Table 1 for the curved members and from the expressions $4\,E\,I/L$ and $G\,J/L$ for the straight members. They are as follows:

For members 1–2 and 3–4,

$$K_{z1} = K_{z2} = 2.317\,\frac{E\,I}{r} = 2.317\,\frac{4\,E}{14.14} = 0.657\,E$$

and

$$K_{x1} = K_{x2} = 0.761\,\frac{E\,I}{r} = 0.761\,\frac{4\,E}{14.14} = 0.215\,E.$$

For member 2–3,

$$K_{z2} = K_{z3} = 2.317\,\frac{E\,I}{r} = 2.317\,\frac{20\,E}{28.28} = 1.642\,E$$

and

$$K_{x2} = K_{x3} = 0.761\,\frac{E\,I}{r} = 0.761\,\frac{20\,E}{28.28} = 0.539\,E.$$

For the straight beams,

$$K_x = \frac{4\,E\,I}{L} = 4\,E\,\frac{3}{20} = 0.600\,E$$

and

$$K_z = \frac{G\,J}{L} = \frac{E\,I}{L} = \frac{3\,E}{20} = 0.150\,E.$$

For columns 1 and 4,

$$K_x = \frac{4\,E\,I_x}{L} = 4\,E\,\frac{1}{14} = 0.285\,E$$

and

$$K_z = \frac{4\,E\,I_z}{L} = 4\,E\,\frac{3}{14} = 0.855\,E.$$

For columns 2 and 3,

$$K_x = \frac{4\,E\,I_x}{L} = 4\,E\,\frac{2}{14} = 0.570\,E$$

and

$$K_z = \frac{4\,E\,I_z}{L} = 4\,E\,\frac{6}{14} = 1.710\,E.$$

For convenience in distributing unbalanced moments at joints 1, 2, 3, and 4, distribution factors equal to $K_x/\Sigma K_x$ and $K_z/\Sigma K_z$ were determined for each member at each joint. For example, at joints 1 and 4, these factors were as shown in Table 5. Similarly, distribution factors were obtained for joints 2 and 3. All distribution factors ("Dist. Factors") are listed near the top of Table 6.

TABLE 5.—DETERMINATION OF DISTRIBUTION FACTORS AT JOINTS 1 AND 4

MEMBER	K_x	K_z	DISTRIBUTION FACTORS	
			x-axis	z-axis
1–2 (or 4–3)	0.215	0.657	0.195	0.395
1–5 (or 4–8)	0.600	0.150	0.546	0.090
Column	0.285	0.855	0.259	0.515
Totals	1.100	1.662	1.000	1.000

Carry-over factors were obtained by means of the values listed in Table 2. For example, for member 1–2, with ϕ equal to 90° and η equal to zero,

$$K_{z1}\,(C_{zz})_{1-2} = K_{z2}\,(C_{zz})_{2-1} = 1.044\,\frac{E\,I}{r}.$$

Then, dividing by K_{z1} and K_{z2}, respectively,

$$(C_{zz})_{1-2} = \frac{1.044\,\frac{E\,I}{r}}{2.317\,\frac{E\,I}{r}} = 0.452$$

and

$$(C_{zz})_{2-1} = \frac{1.044\,\frac{E\,I}{r}}{2.317\,\frac{E\,I}{r}} = 0.452.$$

Because the angles ϕ and η are the same for all three of the curved girders, the carry-over factors for all three are identical. The carry-over factors are listed near the top of Table 6.

The fixed-end moments (F.E.M.) listed in Table 6 were obtained by use of Table 3. For all girders the ratio of ϕ_a to ϕ is equal to 0.5, and therefore the fixed-end bending moment and the fixed-end twisting moment at each end are (from Table 3) $m_b = 0.22171\ W r$ and $m_t = 0.01460\ W r$. Substituting the appropriate values of W and r in the foregoing expressions, the moments m_b and m_t were found to be equal to 37.7 kip-ft and 2.5 kip-ft, respectively, for girders 1–2 and 3–4. For girder 2–3 these values were found to be 176.0 kip-ft and 11.6 kip-ft. Substituting these values in Eqs. 1, the fixed-end moments shown in Table 6 were obtained.

The columns and straight beams are not listed in Table 6 because it is not necessary to make intermediate distributions. Moments in these members are determined after the moments at the ends of the curved girders have been obtained.

All moments about the x-axis are listed in the left half of Table 6, and all moments about the z-axis in the right half. The unbalanced moments at each joint are distributed by multiplying by the appropriate distribution factors and are listed opposite "Dist." For example, the original unbalanced moment about the x-axis at joint 2 is equal to the algebraic sum of $-$ 24.9 kip-ft and $-$ 116.1 kip-ft, or $-$ 141.0 kip-ft. To balance this moment the distributions must be positive and are (in kip-feet):

$$0.112\ (141.0) = +\ 15.8 \text{ (to member 2–1)}$$

and

$$0.280\ (141.0) = +\ 39.5 \text{ (to member 2–3).}$$

The remainder of the unbalanced moment is resisted by the column and member 2–6 and will be accounted for subsequently.

The distributed moments are then multiplied by the appropriate carry-over factors and entered in Table 6 as carry-over moments. Carry-over moments due to moments about the x-axis are listed opposite the designation COM(x), and carry-over moments due to moments about the z-axis are listed opposite COM(z). To illustrate, the carry-over moments resulting from the initial distribution to the x-axis are considered. These moments are first multiplied by the upper line of carry-over factors, $(C_{xx})_{1-2}$ to $(C_{xx})_{4-3}$, and the results (in kip-feet) are listed in the left half of Table 6 opposite COM(x) as $-$ 15.8, * * *, $-$ 15.8. They are listed in the left-half part of the table because they are carry-over moments to the x-axis, and they are placed opposite COM(x) because they are due to moments about the x-axis. The moments distributed to the x-axis are next multiplied by the carry-over factors in the middle line, $(C_{zx})_{1-2}$ to $(C_{zx})_{4-3}$. The resulting products (in kip-feet), $-$ 9.5, * * *, + 9.5, represent carry-over moments to the z-axis due to moments about the x-axis, and consequently are placed in the right-hand part of the table, opposite the designation COM(x). Similarly, the use of the carry-over factors in the

TABLE 6.—ANALYSIS OF THE CONTINUOUS FRAME OF FIG. 8

Line	MOMENT	MOMENT ABOUT THE x-AXIS, IN KIP-FEET						MOMENT ABOUT THE z-AXIS, IN KIP-FEET					
	JOINT	1	2		3		4	1	2		3		4
	MEMBER	1–2	2–1	2–3	3–2	3–4	4–3	1–2	2–1	2–3	3–2	3–4	4–3
1	Factors: Dist.	0.195	0.112	0.280	0.280	0.112	0.195	0.395	0.158	0.394	0.394	0.158	0.395
2	Carry-Over	$(C_{xx})_{1-2} = -1.000$ $(C_{xx})_{1-2} = +0.601$ $(C_{xx})_{1-1} = +0.601$	$(C_{xx})_{2-1} = -1.000$ $(C_{xx})_{2-1} = -0.601$ $(C_{xx})_{2-2} = -0.601$	$(C_{xx})_{2-3} = -1.000$ $(C_{xx})_{2-3} = +0.601$ $(C_{xx})_{2-2} = +0.601$	$(C_{xx})_{3-2} = -1.000$ $(C_{xx})_{3-2} = -0.601$ $(C_{xx})_{3-3} = -0.601$	$(C_{xx})_{3-4} = -1.000$ $(C_{xx})_{3-4} = +0.601$ $(C_{xx})_{3-3} = +0.601$	$(C_{xx})_{4-3} = -1.000$ $(C_{xx})_{4-3} = -0.601$ $(C_{xx})_{4-4} = -0.601$	$(C_{zz})_{1-2} = +0.452$ $(C_{zz})_{1-2} = -0.198$ $(C_{zz})_{1-1} = +0.198$	$(C_{zz})_{2-1} = +0.452$ $(C_{zz})_{2-1} = +0.198$ $(C_{zz})_{2-2} = -0.198$	$(C_{zz})_{2-3} = +0.452$ $(C_{zz})_{2-3} = -0.198$ $(C_{zz})_{2-2} = +0.198$	$(C_{zz})_{3-2} = +0.452$ $(C_{zz})_{3-2} = +0.198$ $(C_{zz})_{3-3} = -0.198$	$(C_{zz})_{3-4} = +0.452$ $(C_{zz})_{3-4} = -0.198$ $(C_{zz})_{3-3} = +0.198$	$(C_{zz})_{4-3} = +0.452$ $(C_{zz})_{4-3} = +0.198$ $(C_{zz})_{4-4} = -0.198$
3	F.E.M.	−24.9	−24.9	−116.1	−116.1	−24.9	−24.9	−28.4	+28.4	−132.3	+132.3	−28.4	+28.4
4	Dist.	+ 4.8	+15.8	+ 39.5	+ 39.5	+15.8	+ 4.8	+11.2	+16.4	+ 40.9	− 40.9	−16.4	−11.2
5	COM (x)	−15.8	− 4.8	− 39.5	− 39.5	− 4.8	− 15.8	− 9.5 + 2.9	+ 2.9 − 9.5	− 23.8 + 23.8	+ 23.8 − 23.8	− 2.9 + 9.5	+ 9.5 − 2.9
6	COM (z)	+ 3.2 + 2.2	− 2.2 − 3.2	− 8.1 + 8.1	− 8.1 + 8.1	− 2.2 − 3.2	+ 3.2 + 2.2	+ 7.4	+ 5.1	− 18.5	+ 18.5	− 5.1	− 7.4
7	Dist.	+ 2.0	+ 5.6	+ 13.9	+ 13.9	+ 5.6	+ 2.0	− 0.3	+ 3.2	+ 7.8	− 7.8	− 3.2	+ 0.3
8	COM (x)	− 5.6	− 2.0	− 13.9	− 13.9	− 2.0	− 5.6	− 3.5 + 1.2	+ 1.2 − 3.5	− 8.3 + 8.3	+ 8.3 − 8.3	− 1.2 + 3.5	+ 3.5 − 1.2
9	COM (z)	+ 0.6 − 0.1	+ 0.1 − 0.6	− 1.6 + 1.6	− 1.6 + 1.6	+ 0.1 − 0.6	+ 0.6 − 0.1	+ 1.4	− 0.1	− 3.5	+ 3.5	+ 0.1	− 1.4
10	Dist.	+ 1.0	+ 1.8	+ 4.6	+ 4.6	+ 1.8	+ 1.0	+ 0.4	+ 0.9	+ 2.3	− 2.3	− 0.9	− 0.4
11	COM (x)	− 1.8	− 1.0	− 4.6	− 4.6	− 1.0	− 1.8	− 1.1 + 0.6	+ 0.6 − 1.1	− 2.8 + 2.8	+ 2.8 − 2.8	− 0.6 + 1.1	+ 1.1 − 0.6
12	COM (z)	+ 0.2 + 0.1	− 0.1 − 0.2	− 0.5 + 0.5	− 0.5 + 0.5	− 0.1 − 0.2	+ 0.2 + 0.1	+ 0.4	+ 0.2	− 1.0	+ 1.0	− 0.2	− 0.4
13	Dist.	+ 0.3	+ 0.7	+ 1.7	+ 1.7	+ 0.7	+ 0.3	0.0	+ 0.2	+ 0.5	− 0.5	− 0.2	0.0
14	COM (x)	− 0.7	− 0.3	− 1.7	− 1.7	− 0.3	− 0.7	− 0.4 + 0.2	+ 0.2 − 0.4	− 1.0 + 1.0	+ 1.0 − 1.0	− 0.2 + 0.4	+ 0.4 − 0.2
15	COM (z)	0.0 0.0	0.0 0.0	− 0.1 + 0.1	− 0.1 + 0.1	0.0 0.0	0.0 0.0	+ 0.1	0.0	− 0.2	+ 0.2	0.0	− 0.1
16	Dist.	+ 0.1	+ 0.1	+ 0.6	+ 0.6	+ 0.1	+ 0.1	0.0	+ 0.1	+ 0.2	− 0.2	− 0.1	0.0
17	Totals	−34.5	−15.3	−116.1	−116.1	−15.2	−34.4	−17.4	+44.8	−103.8	+103.8	−44.8	+17.4

lowest line results in the values (in kip-feet), + 2.9, * * *, − 2.9, placed in the right-hand part of the table, and also placed opposite COM(x).

The carry-over moments due to moments about the z-axis are then obtained as products of the carry-over factors and the distributed moments in the right-hand section of the table. These carry-over moments are all entered opposite COM(z).

The next step is to determine the new unbalanced moment at each joint and about each axis and to distribute it. For example, at joint 2 the unbalanced moment (in kip-feet) about the z-axis is $+ 2.9 - 9.5 + 5.1 - 23.8 + 23.8 - 18.5 = - 20.0$. This unbalanced moment is distributed:

$$0.158\ (20.0) = + 3.2 \text{ (to member 2–1)}$$

and

$$0.394\ (20.0) = + 7.8 \text{ (to member 2–3)}.$$

Four cycles of carry-over and distribution were considered adequate in Table 6. Because of the symmetrical case considered, the final end moments about the x-axis for member 2–3 are approaching the fixed-end moments, − 116.1 kip-ft, and are listed as such. Also, the sum of the final end moments about the x-axis for each of members 1–2 and 3–4 is converging to a moment equal to the sum of the fixed-end moments, or 49.8 kip-ft.

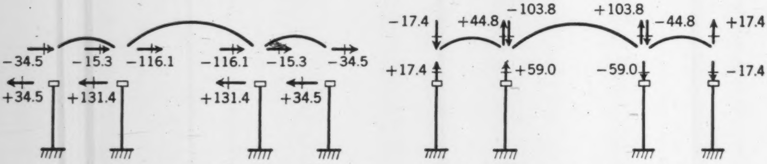

(*a*) Moments about the x-axis (*b*) Moments about the z-axis

FIG. 9.—FINAL END MOMENTS, IN KIP-FEET, IN THE FRAME OF FIG. 8

The moments about the x-axis or z-axis anywhere in the curved girders can now be found by computations of statics from the final end moments. Then, moments about the x-axis and the z-axis can be resolved into bending moments and twisting moments.

The final step is to determine the moments in the columns and connecting straight beams. The final end moments obtained in Table 6 are shown in Fig. 9. With these data, the moments in the individual columns and straight beams can be obtained by distribution of the moments acting on column and beam together. For example, the total moment to be distributed about the x-axis to column and beam at joints 2 and 3 is 15.3 kip-ft plus 116.1 kip-ft, or 131.4 kip-ft. This moment is distributed in proportion to the relative stiffnesses, 0.570 and 0.600, as follows:

$$\frac{0.570}{0.570 + 0.600}\ (131.4) = 64.0 \text{ (to top of column)}$$

and

$$\frac{0.600}{0.570 + 0.600}\ (131.4) = 67.4 \text{ (to the beam)}.$$

TABLE 7.—ANALYSIS OF CONTINUOUS CURVED GIRDER OF FIG. 10

Line	MOMENT	MOMENT ABOUT THE x-AXIS, IN KIP-FEET						MOMENT ABOUT THE z-AXIS, IN KIP-FEET					
	JOINT	1	2		3		4	1	2		3		4
	MEMBER	1–2	2–1	2–3	3–2	3–4	4–3	1–2	2–1	2–3	3–2	3–4	4–3
1	Factors: Dist.		0.839	0.161	0.161	0.839			0.591	0.409	0.409	0.591	
2	Carry-Over		$(C_{xx})_{2-1} = +0.375$ $(C_{zx})_{2-1} = +0.469$ $(C_{zx})_{2-2} = +0.906$	$(C_{xx})_{2-3} = -1.000$ $(C_{zx})_{2-3} = +0.995$ $(C_{zx})_{2-2} = +0.995$	$(C_{xx})_{3-2} = -1.000$ $(C_{zx})_{3-2} = -0.995$ $(C_{zx})_{3-3} = -0.995$	$(C_{xx})_{3-4} = +0.375$ $(C_{zx})_{3-4} = -0.469$ $(C_{zx})_{3-3} = -0.906$			$(C_{zz})_{2-1} = +0.265$ $(C_{xz})_{2-1} = +0.625$ $(C_{xz})_{2-2} = +0.640$	$(C_{zz})_{2-3} = +0.487$ $(C_{xz})_{2-3} = -0.197$ $(C_{xz})_{2-2} = +0.197$	$(C_{zz})_{3-2} = +0.487$ $(C_{xz})_{3-2} = +0.197$ $(C_{xz})_{3-3} = -0.197$	$(C_{zz})_{3-4} = +0.265$ $(C_{xz})_{3-4} = -0.625$ $(C_{xz})_{3-3} = -0.640$	
3	F.E.M.	− 8.16	+ 4.76	−37.24	−37.24	+ 4.76	− 8.16	− 4.76	+ 8.16	−68.10	+68.10	− 8.16	+ 4.76
4	Dist.		+27.26	+ 5.22	+ 5.22	+27.26			+35.44	+24.50	−24.50	−35.44	
5	COM (x)	+10.21		− 5.22	− 5.22		+10.21	+12.78	+24.73	− 5.20 + 5.20	+ 5.20 − 5.20	−24.73	−12.78
6	COM (z)	+22.15	+22.65	− 4.82 + 4.82	− 4.82 + 4.82	+22.65	+22.15	+ 9.38		−11.90	+11.90		− 9.38
7	Dist.		−14.62	− 2.81	− 2.81	−14.62			− 7.60	− 5.23	+ 5.23	+ 7.60	
8	COM (x)	− 5.50		+ 2.81	+ 2.81		− 5.50	− 6.86	−13.25	+ 2.80 − 2.80	− 2.80 + 2.80	+13.25	+ 6.86
9	COM (z)	− 4.75	− 4.86	+ 1.03 − 1.03	+ 1.03 − 1.03	− 4.86	− 4.75	− 2.01		+ 2.55	− 2.55		+ 2.01
10	Dist.		+ 1.72	+ 0.33	+ 0.33	+ 1.72			+ 6.33	+ 4.37	− 4.37	− 6.33	
11	COM (x)	+ 0.65		− 0.33	− 0.33		+ 0.65	+ 0.81	+ 1.56	− 0.33 + 0.33	+ 0.33 − 0.33	− 1.56	− 0.81
12	COM (z)	+ 3.96	+ 4.06	− 0.86 + 0.86	− 0.86 + 0.86	+ 4.06	+ 3.96	+ 1.68		− 2.13	+ 2.13		− 1.68
13	Dist.		− 3.13	− 0.60	− 0.60	− 3.13			+ 0.34	+ 0.23	− 0.23	− 0.34	
14	COM (x)	− 1.18		+ 0.60	+ 0.60		− 1.18	− 1.47	− 2.84	+ 0.60 − 0.60	− 0.60 + 0.60	+ 2.84	+ 1.47
15	COM (z)	+ 0.21	+ 0.22	− 0.05 + 0.05	− 0.05 + 0.05	+ 0.22	+ 0.21	+ 0.09		− 0.11	+ 0.11		− 0.09
16	Dist.		− 0.69	− 0.13	− 0.13	− 0.69			+ 1.75	+ 1.20	− 1.20	− 1.75	
17	COM (x)	− 0.26		+ 0.13	+ 0.13		− 0.26	− 0.32	− 0.63	+ 0.13 − 0.13	− 0.13 + 0.13	+ 0.63	+ 0.32
18	COM (z)	+ 1.09	+ 1.12	− 0.24 + 0.24	− 0.24 + 0.24	+ 1.12	+ 1.09	+ 0.46		− 0.58	+ 0.58		− 0.46
19	Dist.		− 1.05	− 0.20	− 0.20	− 1.05			+ 0.72	+ 0.49	− 0.49	− 0.72	
20	COM (x)	− 0.39		+ 0.20	+ 0.20		− 0.39	− 0.49	− 0.95	+ 0.20 − 0.20	− 0.20 + 0.20	+ 0.95	+ 0.49
21	COM (z)	+ 0.45	+ 0.46	− 0.10 + 0.10	− 0.10 + 0.10	+ 0.46	+ 0.45	+ 0.19		− 0.24	+ 0.24		− 0.19
22	Dist.		− 0.55	− 0.11	− 0.11	− 0.55			+ 0.70	+ 0.49	− 0.49	− 0.70	
23	Totals	+18.48	+37.24	−37.24	−37.24	+37.24	+18.48	+ 9.48	+54.46	−54.46	+54.46	−54.46	− 9.48

One half of 64.0 kip-ft is carried over to the far end of the column, and one half of 67.4 kip-ft is carried over to the far end of the beam.

The total moment to be distributed about the z-axis to column and beam at joints 2 and 3 is 59.0 kip-ft. The distribution, in kip-feet, is

$$\frac{1.710}{1.710 + 0.150}(59.0) = 54.2 \text{ (to top of column)}$$

and

$$\frac{0.150}{1.710 + 0.150}(59.0) = 4.8 \text{ (to the beam)}$$

in which 1.710 and 0.150 represent the relative stiffnesses (about the z-axis) of column and beam, respectively. One half of 54.2 kip-ft is carried over to the bottom of the column. However, because the moment of 4.8 kip-ft is a torsional moment, all of it is carried over to the far end of the beam.

A plan view of a curved girder, fixed at its ends and having two intermediate simple supports, is shown in Fig. 10. If columns and straight beams were framed into the supports, the numerical procedure would be no different except that moments would be distributed to more than two members at a joint.

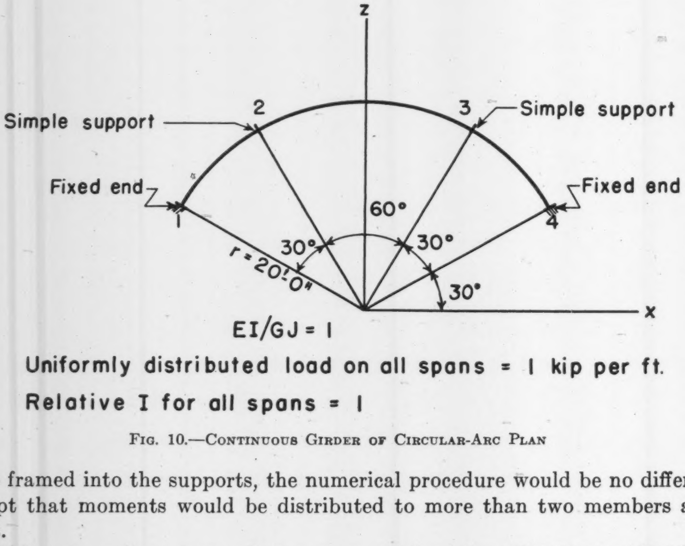
z
2
3
Simple support
Simple support
Fixed end
Fixed end
1
4
60°
30°
30°
30°
r = 20'-0"
x
EI/GJ = 1
Uniformly distributed load on all spans = 1 kip per ft.
Relative I for all spans = 1

FIG. 10.—CONTINUOUS GIRDER OF CIRCULAR-ARC PLAN

Stiffnesses and carry-over factors were obtained from Table 1 and Table 2. Fixed-end bending moments and twisting moments due to uniform load were obtained by means of Table 4, and they were resolved into fixed-end moments about the x-axis and z-axis.

Moments are distributed and carried over in Table 7 in the same manner as before, but there is no distribution to, and no carry-over from, the fixed ends. Because of symmetry about the z-axis in span 2–3, the final end moments about the x-axis at joints 2 and 3 will converge to the fixed-end moments of span 2–3, and are listed as such.

DETERMINATION OF STIFFNESSES, CARRY-OVER FACTORS, AND FIXED-END MOMENTS

The stiffnesses, carry-over factors, and fixed-end moments listed in Tables 1, 2, 3, and 4 were obtained by means of the shear-torsion analogy.[5] Symbolic expressions were written for each of the terms in the three equations of the analogy. The expressions were integrated to obtain general expressions for stiffnesses, carry-over factors, and fixed-end moments which were then evaluated for the cases listed in Tables 1, 2, 3, and 4.[6] From the resulting expressions, values of stiffness, carry-over factors, and fixed-end moments can be obtained for any ratio of $E I$ to $G J$.

For members of other than circular-arc plan and constant section, values of stiffness, carry-over factors, and fixed-end moments can be determined by numerical application of the shear-torsion analogy.[5]

CONCLUSION

A numerical procedure has been presented for the structural analysis of continuous frames containing curved girders and straight members. The procedure is applicable whether the straight beams are parallel to one of the adopted axes (as in Fig. 8) or not. If they are not parallel, stiffness and carry-over factors for the straight beams can be determined from a previous paper[4] by the writer. Moments are then distributed and carried over with respect to the adopted system of axes, as before.

---

[5] "Laterally Loaded Plane Structures and Structures Curved in Space," by Frank Baron and James P. Michalos, *Transactions*, ASCE, Vol. 117, 1952, p. 279.

[6] "Properties for Numerical Analysis of Frames with Curved Girders," by Timothy Chin, thesis fubmitted, in 1952, to Iowa State College at Ames, in partial fulfilment of the requirements for the degree os Master of Science.

DISCUSSION

William A. Conwell,[7] M. ASCE.—A wealth of data that will be of great value to structural engineers is included in the paper. It is the purpose of this discussion, after some general comments, to demonstrate the wide application of the information presented by Mr. Michalos.

Under the heading, "Stiffness and Carry-Over Factors," the author has not stated that, during the application of the moments, the ends of the curved girders are restrained against translation, although he obviously intends this. It is believed that the paper should be explicit on this point particularly in view of the current work[8] by L. E. Grinter, M. ASCE, and C. H. Tsao which deals with moment distribution where translation of the joints is permitted.

Although the author has devised excellent nomenclature for his work, the writer would prefer a slightly different expression for the carry-over factor. The author uses the first subscript inside the parentheses to indicate the axis to which the moment is carried; the second subscript is used to indicate the axis about which the moment is applied. Interchanging these two subscripts would make the subscripts inside the parentheses parallel with those outside. For instance, $(C_{xz})_{B-A}$ would then be the carry-over factor from the x-axis at B to the z-axis at A. The author, no doubt, has good reasons for using his nomenclature. It would be of value to know what led to its adoption.

The curves in Fig. 4 are a fine representation of tabular data. The additional curves to which the author refers under the heading, "Stiffnesses and Carry-Over Factors," may have sufficient value to be included in the closing discussion.

One of the most important facts stated in the paper is that the same procedures that engineers have used for straight beams may be followed for circular girders.[9] For instance, if one wishes to determine the fixed-end moment for a uniformly distributed load on a part of the span of a circular girder, the continuous girder shown in Fig. 11(*a*) may be initially solved with a false support at C beginning with the fixed-end moments of Table 4. After computing the reaction at C it is possible (from Table 3) to obtain the fixed-end moments for a load W at C, equal to and opposite in direction from the reaction (Fig. 11(*b*)). The superposition of Figs. 11(*a*) and 11(*b*) yields Fig. 9(*c*) which shows a circular girder partly loaded. It is recognized that Table 3 can be used to obtain this information by taking a series of positions for the load W. On occasions when, as stated under the heading, "Determination of Stiffnesses, Carry-Over Factors, and Fixed-End Moments," it is desired to consider shapes of girders other than circular for which data similar to the author's are not available, the procedure just outlined may result in a saving of time and effort.

---

[7] General Engr., Structural Eng. and Design Dept., Duquesne Light Co., Pittsburgh, Pa.

[8] "Joint Translation by Cantilever Moment Distribution," by L. E. Grinter and C. H. Tsao, *Transactions*, ASCE, Vol. 119, 1954, p. 1195.

[9] "Continuous Frames of Reinforced Concrete," by Hardy Cross and Newlin Dolbey Morgan, John Wiley & Sons, Inc., New York, N. Y., 1932.

In a consideration of the over-all problems of numerical analysis of frames, there comes to mind not only the fixed-end moments, stiffnesses, and carry-over factors mentioned by Mr. Michalos but also the effect of translations of the joints. In the treatment of circular girders, the problem could arise in analyzing the effect of settlement of a column or perhaps, in extreme cases, in providing for the axial deformation that might occur in a comparatively light column or hanger. Although the author does not specifically mention translations of joints, he has provided the data for computing this effect.

As with straight members, it is apparent that the effect of translations of the joints can be determined by introducing equal rotations at each end of a member. For instance, as shown in Fig. 12, if end A of a circular girder were to settle an amount Δ, the effect could be duplicated by adding the effects of rotations around the z-axis introduced at ends A and B and equal to Δ/r.

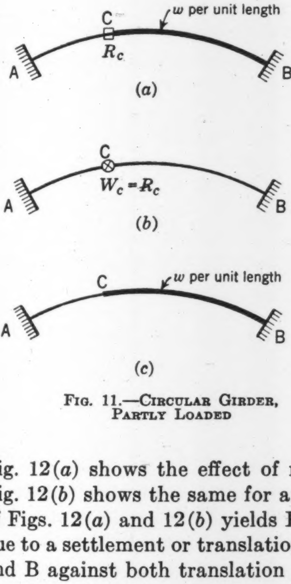
C
w per unit length
R_c
A
B
(a)
C
$W_c = R_c$
A
B
(b)
C
w per unit length
A
B
(c)

FIG. 11.—CIRCULAR GIRDER, PARTLY LOADED

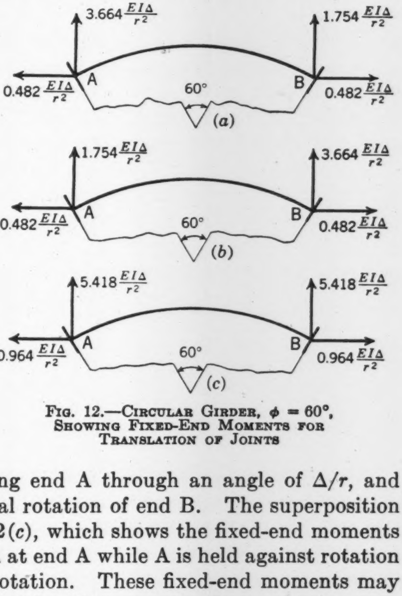
$3.664 \frac{EI\Delta}{r^2}$
$1.754 \frac{EI\Delta}{r^2}$
$0.482 \frac{EI\Delta}{r^2}$
A
60°
B
$0.482 \frac{EI\Delta}{r^2}$
(a)
$1.754 \frac{EI\Delta}{r^2}$
$3.664 \frac{EI\Delta}{r^2}$
$0.482 \frac{EI\Delta}{r^2}$
A
60°
B
$0.482 \frac{EI\Delta}{r^2}$
(b)
$5.418 \frac{EI\Delta}{r^2}$
$5.418 \frac{EI\Delta}{r^2}$
$0.964 \frac{EI\Delta}{r^2}$
A
60°
B
$0.964 \frac{EI\Delta}{r^2}$
(c)

FIG. 12.—CIRCULAR GIRDER, $\phi = 60°$, SHOWING FIXED-END MOMENTS FOR TRANSLATION OF JOINTS

Fig. 12(a) shows the effect of rotating end A through an angle of Δ/r, and Fig. 12(b) shows the same for an equal rotation of end B. The superposition of Figs. 12(a) and 12(b) yields Fig. 12(c), which shows the fixed-end moments due to a settlement or translation of Δ at end A while A is held against rotation and B against both translation and rotation. These fixed-end moments may be distributed like any others to determine the over-all effect on a structure of which member AB is a part.

The writer considers the paper to be of great value to the engineering profession.

JAMES MICHALOS,[10] M. ASCE.—Mr. Conwell's discussion has added to the value of the paper, and his kind comments are greatly appreciated.

An interchange of subscripts within the parentheses in the notation for carry-over may be desirable. The arrangement chosen seemed convenient, but this is largely a matter of preference. However, because the paper is related to another[4] and occasionally use of both may be necessary for an analysis, some additional remarks regarding notation are pertinent. In the earlier paper, a prime mark was used to indicate carry-over to the opposite end of a member. In the present paper it was necessary to use a more specific subscript designation, such as *A-B* and *B-A*, for carry-over factors.

---

[10] Prof. of Structural Eng. and Chairman, Dept. of Civ. Eng., New York Univ., New York, N. Y.

Tables or curves of properties are not available for other members than those of circular-arc plan and constant cross section, but, as stated in the paper, values of stiffnesses, carry-over factors, and fixed-end moments can be determined for any shape and variation in cross section by applying the shear-torsion analogy presented elsewhere.[5] In that paper it was shown that moments resulting from load applied normal to the plane of a structure fixed at its ends can be computed directly by a numerical procedure in a manner analogous to the computation of stresses due to direct shear and torsion in a strut. The procedure is illustrated in that paper.[11,12] The reader should observe the difference in sign conventions used in that paper and this one and should also observe that the y-axis of that paper is the z-axis of this one. With these differences accounted for, the fixed-end moments in an illustration[12] become $m_x = -8.79$ and $m_z = -15.01$ at A, and $m_x = -2.46$ and $m_z = +4.81$ at B.

When account is taken of the differences in axes and signs, the stiffness at an end A of a member AB, of which end A is the right-hand end, and the corresponding carry-over factors (in terms of the stiffness) can be computed as follows:

$$\left.\begin{aligned} K_{zA} &= \frac{1}{A'_z} + \frac{(x_c)^2{}_A}{J_y} \\ K_{zA}\ (C_{xz})_{A-A} &= -\frac{P'_x}{A'_x} + \frac{(x_c)_A\ (z_c)_A}{J_y} \\ K_{zA}\ (C_{xz})_{A-B} &= \frac{P'_x}{A'_x} - \frac{(x_c)_A\ (z_c)_B}{J_y} \\ K_{zA}\ (C_{zz})_{A-B} &= -\frac{1}{A'_z} - \frac{(x_c)_A\ (x_c)_B}{J_y} \end{aligned}\right\} \quad \ldots\ldots\ldots\ldots\ldots (2)$$

By interchanging all *A* and *B* subscripts in Eqs. 2, K_{zB} and the corresponding carry-over factors may be obtained. By substituting x for z and z for x in Eqs. 2, K_{xA} and the corresponding carry-over factors may be determined. The *A* and *B* subscripts and the z and x subscripts should be interchanged in order to obtain K_{xB}.

If symmetry exists, as in Fig. 7 of a previously mentioned paper,[12] or if all elements of the member are parallel to one or the other of the reference axes, as in Fig. 6 of that paper,[11] then both P'_x and P'_z are equal to zero, and A'_x and A'_z are equal, respectively, to A_x and A_z. As an example of the use of Eqs. 1, a stiffness and the corresponding carry-over factors (in terms of stiffness) will be obtained for the parabolic arch of variable section shown in Fig. 7. First, however, it is necessary that ends A and B of Fig. 7 be interchanged to conform to the nomenclature used in the paper now under discussion. Then, for end B (end A in Fig. 7),

---

[11] "Laterally Loaded Plane Structures and Structures Curved in Space," by Frank Baron and James P. Michalos, *Transactions*, ASCE, Vol. 117, 1952, pp. 294–295, Fig. 6.

[12] *Ibid.*, pp. 298–299, Fig. 7.

$$K_{zB} = \left[\frac{1}{84.38} + \frac{(-50)^2}{62{,}086}\right] E\,I = 0.0521\,E\,I,$$

$$K_{zB}\,(C_{zz})_{B-B} = \left[-\frac{0}{70.04} + \frac{(-50)(-9.42)}{62{,}086}\right] E\,I = 0.0076\,E\,I,$$

$$K_{zB}\,(C_{zz})_{B-A} = \left[\frac{0}{70.04} - \frac{(-50)(-9.42)}{62{,}086}\right] E\,I = -\,0.0076\,E\,I,$$

and

$$K_{zB}\,(C_{zz})_{B-A} = \left[-\frac{1}{84.38} - \frac{(-50)(50)}{62{,}086}\right] E\,I = 0.0285\,E\,I,$$

in which I is the moment of inertia about the z-axis at the crown.

Tables of fixed-end moments, stiffnesses, and carry-over factors for any shape can be prepared by writing general algebraic expressions for the various terms of the shear-torsion analogy. The tables for members of circular-arc plan were prepared in that manner.

Mr. Conwell outlines a straightforward procedure for obtaining fixed-end moments produced by a uniform load applied over part of a circular girder. Such values can also be obtained directly, as implied by Mr. Conwell, from influence lines. Influence lines for fixed-end bending moments are shown in Fig. 7. These were drawn by plotting values from Table 3. Influence lines for fixed-end twisting moments can be drawn in the same manner. To illustrate the method of obtaining fixed-end moments due to partial loading, a circular girder AB, whose central angle, ϕ, is equal to 90°, will be assumed. Its arc length is L. Furthermore, this girder will be considered to be subject to a uniformly distributed load, w per unit length of arc, over two thirds of its length beginning at end A. The fixed-end bending moment at A is equal to $w\,r\,L$ times the area under the curve in Fig. 7 marked $\phi = 90°$ between values of ϕ_a/ϕ equal to 0 and 0.667. The fixed-end bending moment at B is equal to $w\,r\,L$ times the area between the values of ϕ_a/ϕ equal to 0.333 and 1.000. Fixed-end twisting moments can then be found from similar curves, and those values can be combined with the fixed-end bending moments, as shown in Eqs. 1, to obtain fixed-end moments about the x-axis and z-axis.

The writer believes that the use of continuous girders curved in plan and the use of continuous frames with curved girders will increase. This will be true for bridges and elevated expressways as well as for buildings and foundation frameworks, such as the new Highbridge Interchange at the George Washington Bridge in New York.[13] The procedure presented in this paper readily yields a solution for even the most complicated cases.

---

[13] "Box Girder on Stilts," by Howard E. Reid and Phillips H. Lovering, *Engineering News-Record*, February 7, 1952, p. 28.

AMERICAN SOCIETY OF CIVIL ENGINEERS
Founded November 5, 1852
TRANSACTIONS

Paper No. 2809

INCREASING THE LOAD-CARRYING CAPACITIES OF SUBGRADES

BY CHARLES M. NOBLE,[1] M. ASCE

WITH DISCUSSION BY MESSRS. EUGENE Y. HUANG, AND CHARLES M. NOBLE

SYNOPSIS

The practice of strengthening pavement subgrades gradually by repairing depressed spots when necessary is incompatible with modern trends in rapidly increasing axle loads and traffic volumes. Adequate drainage, the use of granular material, and the development of heavy compaction equipment are the primary current solutions to the problem. These enable the construction of highways and airfields capable of bearing many repetitions of great anticipated loads with a minimum of repairing.

INTRODUCTION

The rapid increase in wheel loads and tire pressures have stimulated the development of improved techniques and equipment for strengthening subgrades in order to lay pavements with reasonable assurance against failure.

There has been a phenomenal increase in axle loads on highways and, equally important, the volume of truck traffic on highways has been increased enormously, thus bringing the repetitive-load problem to the fore. Tire pressures have been kept fairly constant, at 90 lb per sq in.

Airplane design has advanced rapidly until currently (1952) a wheel assemblage carrying 150,000 lb is utilized for the heavier planes; tire pressures have been increased to the point where 250 lb per sq in. has become an immediate possibility.

Thus, engineers are faced with the problem of heavier mass loads, often applied many times daily, and with loads of high unit intensity. These conditions require subgrades of high stability under all weather conditions.

NOTE.—Published, essentially as printed here, in September, 1954, as *Proceedings-Separate No. 505.* Positions and titles given are those in effect when the paper or discussion was approved for publication in *Transactions.*

[1] Chf. Engr., New Jersey Turnpike Authority, New Brunswick, N. J.

In New Jersey, the main highways carry more than 5,000 heavy trucks per day, and axle loads in excess of 40,000 lb have been weighed. A significant part of the daily truck traffic has axle loads in excess of 30,000 lb. The heavy repetitive load engenders a pumping action that flushes water from the suggrade to the surface causing a "quaking" that will destroy all but the heaviest pavements, whether of the rigid type or the flexible type. Observations show that the damage curve rises uniformly up to 200 applications per day; it then turns upward and, after 300 applications, it rises very steeply. Other states are experiencing similar problems to a varying degree dependent on the load laws and the volume of heavy traffic.

For more than a hundred years it has been recognized that subgrades must be well drained and must be kept dry regardless of weather conditions if they are expected to bear heavy wheel loads, particularly when these loads are applied frequently. The heavier and more frequent the load, the greater the depth to which stability is required in order to lower the unit stress to the capacity of the saturated soil. In climates subjected to freezing and thawing, the water table should be below the level of frost penetrations for all but the most porous soils. (Perma-frost conditions are not treated herein because they present specialized problems.)

Within the past thirty years, the principles of subgrade drainage have been neglected in many instances, particularly during the earlier years when loads were light and infrequent; more recently, it was believed that heavy-duty pavement could bridge and overcome deficiencies in the subgrade. As a consequence, engineers began to lose sight of the advantages and the necessity of providing positive subgrade drainage. Since World War II, with the upsurge in the volume of "weight" traffic, engineering practices have returned to first principles and greater attention is being paid to drainage.

Soils engineers have classified the various types of soils, and precise information is now available on the characteristics of the various classes of soils and which types are suited for use in embankments and subgrades.

Thus, the engineering tools are available for the adequate economic design of subgrades used in conjunction with a selected pavement design to meet the requirements of loading, frequency, soil, and climatic conditions.

Designs are used which provide the greatest over-all economy of pavement and subgrade while taking into consideration ultimate life and upkeep cost. Under conditions prevailing in the United States, designers must take into account the use of materials and methods which permit placement by large-capacity, heavy-duty, fast-moving machines incorporating low-cost local materials as much as is consistent with economy.

Illustrative of recent trends, the designs and methods utilized on a large eastern highway project will be reviewed.

The project is located in a humid area, with an average annual rainfall of 45.86 in., maximum summer temperatures ranging up to 100° F, and winter temperatures below 0° F, with frost penetration down to a depth of 4 ft. The ground-water table is high throughout the length of the project. The pavement was designed for 36,000-lb axle loads with unlimited repetitions and tire pressures of 90 lb per sq in.

Design work proceeded on the assumptions that the ground-water table had to be permanently lowered to a depth of 4 ft below the surface of the pavement, unsuitable soils had to be removed from within the roadway area, surface soils would be stripped before placing fills, cuts in unstable soils would be undergraded, and all fills and cuts within the roadway would be consolidated to specified densities at optimum moisture.

This procedure provided a stable foundation on which to place the subbase and subgrade layers composed of selected granular, frost-resistant, free-draining materials consolidated to specified densities at optimum moisture.

Grading specifications required cutting and removing all timber, brush, grain, grass, weeds, stumps, and rubbish for the full width of the cuts and embankments. Grubbing was required within all excavated areas for a depth of 12 in. below excavation lines and in embankment areas to 12 in. below the original ground surface.

After clearing, grubbing, and stripping had been completed, the ground surface for a depth of 12 in. upon which fills 5 ft or more in depth below the finished pavement were to be placed were compacted to 90% density (AASHO modified test) in cultivated areas and, for fills less than 5 ft deep, all ground areas were compacted to 90% density 12 in. deep. Cuts were compacted to 90% density between ditch lines for a depth of 12 in. below template grade, which was the surface on which the layers of subgrade materials were placed as hereinafter described.

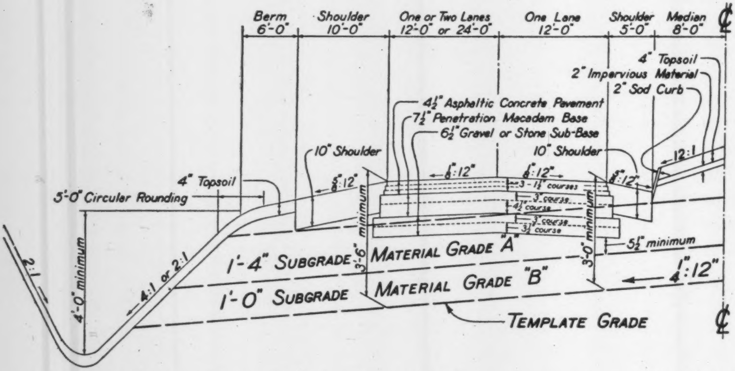
Berm 6'-0"
Shoulder 10'-0"
One or Two Lanes 12'-0" or 24'-0"
One Lane 12'-0"
Shoulder 5'-0"
Median 8'-0"
℄
4" Topsoil
2" Impervious Material
2" Sod Curb
4½" Asphaltic Concrete Pavement
7½" Penetration Macadam Base
6½" Gravel or Stone Sub-Base
10" Shoulder
10" Shoulder
12:1
4" Topsoil
5'-0" Circular Rounding
5/8":12"
1/8":12"
1/8":12"
5/8":12"
3 - 1½" courses
3" course
4½" course
3" course
3½" course
3'-6" minimum
3'-0" minimum
5½" minimum
1'-4" Subgrade
Material Grade "A"
1'-0" Subgrade
Material Grade "B"
1/4":12"
Template Grade
4'-0" minimum
2:1
4:1 or 2:1
℄

FIG. 1.—TYPICAL HALF SECTION, EXAGGERATED VERTICALLY

Embankment material was deposited in layers not to exceed 6 in. thick and compacted to 90% density, except that the material within 12 in. of template grade was compacted to 95% density. Material classified as A-6 or A-7 (classification system of the Bureau of Public Roads, United States Department of the Interior) was not permitted between vertical planes through the tops of the embankment slopes.

These requirements for excavation and embankment construction to template grade were calculated to provide a tested, stable, compacted foundation of suitable soil materials on which to place the special subgrade materials (Fig. 1).

The special subgrade was subdivided into grade A and grade B, the latter being placed first on the prepared template grade. This frost-resistant granular material, 12 in. thick, was required to have a plasticity index of not more than 6 and so graded that no more than 10% passed a 200-mesh sieve. It was required to have a California Bearing Ratio (CBR) of not less than 15% when compacted at 100% of maximum density. The bottom of this material was slightly above the elevation of the side ditches. The grade A material, 16 in. thick, placed on top of the grade B material, was also a pervious, free-draining, frost-resistant material classified as A-3 by the Bureau of Public Roads, having a plasticity index of not more than 3 and graded so that no more than 6% passed a 200-mesh sieve. When tested for bearing it had a CBR-value of not less than 20% when compacted to 100% of maximum density.

Frost-resistant material was defined as being a material of which not more than 10% passed a 200-mesh sieve and having not more than 5% of its particles less than 0.02 mm in size.

Material of grade A and grade B was placed in 6-in. layers and at optimum moisture was compacted to 95% (AASHO modified) maximum density.

This then was the foundation on which the subbase material and paving layers were placed. The side ditches, 4 ft deep below shoulder elevation, intercepted surface water and subsurface water flowing toward the roadway while the pervious A and B material of low capillarity permitted water which might flow upward beneath the roadways to percolate out laterally to the side ditches. In addition, many thousands of feet of pipe underdrainage were provided where wet spots were encountered in clay formations, at sags in the grade line, and at other locations where additional subsurface drainage was required.

The subbase material consisting of a 6½-in. depth of gravel or broken stone (maximum size 3 in., with not more than 5% passing the 200-mesh sieve) compacted to 95% density, was placed on the foundation after it had been reshaped by "boxing-out" to the pavement cross section. After the boxing out was completed and before the subbase was placed, the foundation was again compacted at optimum moisture to 95% density and prestressed by four passes (producing two complete coverages) of rubber-tired rollers having a tire load of not less than 25,000 lb. The recompaction of the foundation was not permitted more than 48 hours before placing subbase material; it was considered necessary because the foundation had lain open through the winter and had been subjected to frost action and heavy hauling, which had caused loosening of the upper portion.

The subbase material was surmounted by two layers of penetration macadam and three layers of hot-mix asphaltic concrete. Before the hot mix was placed, the surface of the macadam was, in addition to the standard rolling, subjected to four passes (providing two complete coverages) of rubber-tired rollers having a wheel load of not less than 25,000 lb.

This review of the make-up of the subgrade and associated drainage features of this project illustrates the trend in providing well-drained, high-load-carrying foundations and subgrades for modern pavements. The development of rapid-moving, heavy, mechanized construction equipment has made this development economically possible.

During the construction period of the project a number of practical observations were made which may be of interest. First, the design required that the template grade and each layer of the grade A and grade B material be sloped downward from the center line toward the side ditches for the purpose of shedding rainfall to the ditches and then to suitable outlets. Two contradictory things happened. In spite of the slope and due to the porosity and the small-sized gradation of the grade A and grade B materials, a considerable volume of rain water penetrated through to the underlying soil layers and, where such soil was partly composed of clayey or silty material, these underlying soils were softened and caused instability to depths of as much as 7 ft below the surface of the pavement.

On the other hand, in many areas considerable rain water ran off and washed granular material into the side ditches. It may be argued that these problems could be overcome by waterproofing the surface as a temporary measure until the pavement is placed. However, heavy hauling would have quickly destroyed a thin waterproofing film, and a thicker treatment would not only have been expensive but would have introduced difficulties when the foundation was "boxed out" for the subgrade material and pavement layers. This is not a serious problem as it is confined to the construction period only but it is worthy of consideration where foundations are constructed of finely graded granular materials such as are encountered in coastal areas of the United States. These sands are not only fine grained but are also of such gradation that they will become consolidated so densely that porosity will be reduced. Tests show that, when these sands are consolidated to 100% of density, water will flow through them only at a rate of from 0.2 ft per day to 1.00 ft per day.

Therefore, water will percolate downward in such materials and reach the underlying soil long before it can travel laterally the 60 ft required to reach the side ditch.

It had been thought that the use of heavy pneumatic wheels for consolidating and pretesting, without regard to tire pressure, would uncover all weak and unstable areas in the foundation and subgrade. It was found that unstable areas could indeed be detected if an inspector walked continuously behind the pneumatic rollers and immediately observed the minute traverse cracks that indicated subsurface instability. These small cracks disappeared shortly after the passage of the roller. In several instances, the cracks were not observed and the subgrade material was placed and consolidated. The contractor then operated a fleet of trucks with tires at pressures of 90 lb per sq in. hauling stone over the grade for the macadam courses. This large number of repetitions caused instability in the weak areas, and the unstable material had to be dug out and replaced. At several locations, instability developed after the top course of penetration macadam had been placed and, in a few cases, after the hot-mix asphaltic concrete had been laid. This experience indicates that consideration should be given to utilizing high tire pressures on pneumatic-tire rollers for consolidation.

It is evident that well-drained stable subgrades and foundations are necessary to a depth at which the underlying soil can support the distributed load at the required number of daily repetitions. Where ground water is present, this will require a determination of the load-carrying capacity of the soil in a saturated condition at the plane below the influence of the underdrainage or ditch system. Eventually the underlying soil may become sufficiently compacted by the constant passage of heavy loads so that excess water may be prevented from entering the soil. In the meantime, if the design is deficient, failures will develop, requiring repairs under traffic.

Engineers are familiar with the fact that many older roads constructed of granular materials successfully carry heavy loads for years when surfaced with relatively thin pavement, particularly when they are well drained and located on favorable soils. Some roads in the United States have been in continuous use and under maintenance for more than a century. During this period traffic has constantly hammered down and consolidated the roadbed. Often the road metal has been driven down into the soil several feet, and in the process weak areas in the subgrade were dug out by the maintenance forces and replaced with high-quality granular material of high stability. After many years of this "repair-as-it-fails" process, during many weather cycles the roadbed becomes stabilized and is capable of carrying heavy loads safely.

If it is desired to accomplish ultimate stability initially during a relatively short construction period, stable subgrade materials of known load-carrying capacity, water-reaction qualities, and resistance to frost must be utilized to the depths required by the underlying soil and the loads expected to be carried; they must be compacted with heavy construction equipment in order to achieve in a few months that stability which might take a century under a "fill-in-the-weak-places" program.

Subgrade design is an economic problem, the engineer selecting the design that is most economical under job conditions of climate, availability of local materials, traffic loads and frequency, and suitability of construction by heavy, fast-moving mechanical equipment. Because of the absence or growing scarcity of suitable, cheap, local materials, widespread research is resulting in the development of several interesting processes, materials, and chemical adaptations for stabilizing soil which may affect greatly the approach to subgrade design. Cement, bitumins, lime, fly ash, calcium chloride, chrome-lignin, and sodium silicate are all under investigation. More research, development by material and equipment manufacturers, and the construction of test projects are necessary before those tools will be fully available to the engineer on a competitive economic basis.

Meanwhile, drainage, granular materials, and heavy compaction equipment remain as the bulwark in increasing the load-carrying capacity of subgrades.

DISCUSSION

Eugene Y. Huang,[2] A. M. ASCE.—The importance of the role played by the subgrade of a highway or an airport pavement cannot be overemphasized. This is the element of a pavement structure that actually supports the weight of traffic regardless of whether the superimposed pavement is rigid or flexible. It is closely associated with the structure of the pavement. The integrity of a pavement cannot be preserved if the subgrade is insufficiently strong to support traffic loads without serious deformation occurring in either the pavement or subgrade. Many of the defects to which a pavement is susceptible may be attributed, directly or indirectly, to the subgrade on which the pave- is built. It is important, therefore, that appropriate attention be given to the subgrade in the design and construction of pavement structures.

Mr. Noble's paper reviewing the recent trends and methods of improving the load-carrying capacities of subgrades contains a great deal of useful information and should be of interest to those who are engaged in road or airport construction work when confronted with the problem of rapid, although not unanticipated, increase in the volume of traffic accompanied by increased wheel loads and increased percentages of heavy loads.

Recognizing the fact that the subgrade must withstand stresses due to traffic, it is obvious in deciding on the type and thickness of pavement to construct on any particular soil that primary consideration should be given to the strength of the stressed layer of soil under local conditions and to the weight and intensity of traffic using the paved structure. The basic objective of an engineer is to provide a structure having a pavement of sufficient thickness and strength to distribute the applied loads to the supporting subgrade without exceeding its bearing capacity.

There are two fundamental approaches to this problem. In the first it is assumed that the supporting subgrade in its natural environment must be accepted as it exists; the type and thickness of the pavement are taken as the items of control. An extreme of this idea is the questionable concept mentioned by Mr. Noble that "* * * heavy-duty pavement could bridge and overcome deficiencies in the subgrade." Accordingly, heavy-duty pavements with prohibitive thicknesses have been suggested for weak or poor subgrades.

The second approach focuses attention on the supporting subgrade and its associated conditions. The subgrade is to be designed or, if necessary, improved so that it will support a standard pavement section believed to be economically most feasible. This latter method emphasizes the importance of subgrade support for pavements. The functions of a pavement may be regarded as providing a smooth riding surface, resistant to the wear of traffic and the disintegrating influence of climate; shielding of the subgrade; and maintaining its ability to support applied loads. One well-known example of this practice is the Michigan method of design for flexible pavement in which the supporting foundation is designed to support a standard pavement section depending on the traffic volume to be carried.[3]

---

[2] Research Asst. Prof. of Civ. Eng., Univ. of Illinois, Urbana, Ill.

[3] "Thickness of Flexible Pavements," *Current Road Problems No. 8-R*, Highway Research Board, National Research Council, Washington, D. C., 1949, p. 15.

The writer does not intend to discuss further these methods of design here but merely wishes to point out that, whatever the design method may be, a subgrade properly prepared or improved to receive the load distributed from the pavement is generally highly advisable. To design a pavement bridging over a weak supporting subgrade may sometimes be desirable but in most instances is too expensive to be practical. It is generally agreed that designs should "* * * provide the greatest over-all economy of pavement and subgrade * * * taking into consideration ultimate life and upkeep cost" and that an "* * * adequate economic design of subgrades used in conjunction with a selected pavement design to meet the requirements of loading, frequency, soil, and climatic conditions" is sound engineering practice.

Among the various measures for improving the load-carrying capacities of subgrades, perhaps the most important is proper drainage and the protection of the subgrade from the detrimental influence of water. The strength of a subgrade material is usually measured in terms of its resistance to shear, which depends on two fundamental properties—cohesion and internal friction. The strength of almost any soil mixture will be decreased by the penetration of moisture into the voids because this causes rapid disintegration and excessive volume change which weakens the cohesion of the cohesive material and changes the mechanical arrangement of soil particles, thus lowering the internal friction of the granular fraction of a soil mass. Proper drainage is therefore essential in preserving a soil in a serviceable condition, not by changing the basic character of the soil but by maintaining its sources of shearing resistance. There are certain types of soil, however, which have low permeability and high capillarity and are not susceptible to ordinary drainage. In this case, other corrective measures should be adopted. In as much as granular material itself is permeable so that water drains through it readily and the removal of excess moisture is not difficult, it is often used to replace undesirable subgrade soil or to blanket weak subgrade sections. In the latter case, granular material not only permits better drainage conditions below the pavement but also provides for load distribution over the less stable heavy soils.

The writer wishes to submit some data regarding pavement performance at Willow Run Airport in Michigan as an example of the effect of a well-drained, granular subgrade material on the behavior of a concrete pavement. The airport is located in an area where an outwash or delta deposit of sand and some gravel has been laid over the clay till plain. The depth of sand and gravel deposits varies from 4 ft or 5 ft to as much as from 30 ft or 40 ft. The depth to the water table had varied from very deep to close to the surface during the wet period of the year but has been substantially lowered by the subdrainage system installed when the field was built. Table 1 shows the soil classification of typical subgrade material by three different methods in current use. It may be noted that the soil condition was close to ideal for airport construction.

The pavement at Willow Run Airport was built in three stages. The original field was built in 1941, and the pavement consisted of plain concrete having an 8-in., 6-in., 8-in. thickened-edge section. In 1942, the first extensions were added. This pavement was also plain concrete but was somewhat heavier, having a 10-in., 7-in., 10-in. thickened-edge section. Additional extensions were made in 1943, and this pavement too was a plain 8-in., 6-in., 8-in. thickened-edge section. In 1944, the existing airport pavement installations were evaluated, and the operating limit which was generally used to forecast the useful life of the runways or pavement areas was established. The flexural test results of test beams from all three construction projects showed that the modulus of rupture of the concrete in the 1941 construction was 945 lb per sq in.; in the 1942 construction, 825 lb per sq in.; and in the 1943 construction, 773 lb per sq in. Under the rating system of the U. S. Engineer Office of the War Department, the gross plane weight for "capacity operation," which was based on the maximum traffic that could possibly operate on an airfield for a period of approximately 20 years, was 52,000 lb for runways and 41,600 lb for the field. Under "limited operation," which was defined in general terms as a few operations a day for a period of 20 years (about 10% of "capacity operation") or the maximum traffic that could possibly operate for a period of from 2 years to 4 years, the rating was 100,000 lb for the runways and 80,000 lb for the field. The minumum rating for the field was controlled by the taxiways and aprons of the 1943 construction.

TABLE 1.—CLASSIFICATION OF SUBGRADE SOILS, WILLOW RUN AIRPORT, MICHIGAN

Method	Classification	Description
Civil Aeronautics Authority	E-1	Well-graded granular soil, stable under poor drainage conditions, and not subject to detrimental frost heaving.
Corps of Engineers	SP	Poorly graded sand, few or no fines.
Bureau of Public Roads (Highway Research Board modification)	A-3 A-1-b	Poorly graded sands, some gravels, few or no fines.

Data on the traffic and operations at Willow Run Airport have shown that the operating commercial airlines supply 80% of the aircraft movements at the field, military planes supply 4%, and civil aircraft, 16%. According to the studies made by Mr. Housel of the University of Michigan:

> "As of 1953 the gross weight of commercial planes using the field varied from 26,200 pounds for the lightest plane, a DC-3, to 132,000 pounds for the heaviest plane, a Stratocruiser, and the total airline traffic amounted to 135 scheduled operations. From analysis of the scheduled operations about 5% of the traffic exceeds the minumum field ratings by more than 200% and about 15% of the traffic is equal to or less than the field rating. As compared to the capacity for limited operations approximately 20% of the loads are greater than the limited capacity of 80,000 pounds, and approximately 5% of the traffic exceeds the limited operating capacity by approximately 65%."

From these figures it is obvious that the pavement in the airfield has been subjected to traffic and loading conditions far exceeding the nominal measures of operating capacity; however, as of the end of 1953, all of the pavement, as far as the serviceability was concerned, was relatively well preserved.

This is particularly indicated by the 1941 pavement built on good subgrades. In this case, the crackings of the pavement which were, more or less, indications of the pavement performance were almost negligible and consisted largely of single transverse cracks near the center of a slab 25 ft long; they did not constitute serious structural failure. The excellent performance of the pavement seems to be attributed largely to the excellent subgrade conditions, which include exceptionally stable soils and perfect drainage conditions with no necessity for providing for frost action. The evidence further indicates that a well-constructed plain concrete pavement of 8-in., 6-in., 8-in. thickened-edge section may be able to carry, without serious damage, heavy wheel loads and high intensity of traffic far in excess of those for which the pavement has been designed or rated, provided the pavement has been constructed on subgrades of high supporting capacity. It should be mentioned, however, that there were some critical areas where imperfections in the original construction combined with heavy loading and concentration of traffic produced progressive deterioration. It is nevertheless believed that the damage would have been even more serious under less favorable subgrade conditions.

As the author noted, the necessity for good drainage practice and adequate subgrade support was indeed recognized by engineers more than a hundred years ago. This idea was stated by John L. McAdam in a report to the President of the Board of Agriculture and was reprinted in 1824 in his book on the making and repairing of roads in Great Britain:[4]

> "* * * it is the native soil which really supports the weight of traffic: * * * while it is preserved in a dry state, it will carry any weight without sinking, * * * it does in fact carry the road and the carriages also; * * * this native soil must previously be made quite dry, and a covering impenetrable to rain, must then be placed over it, to preserve it in that state."

Although tremendous progress has been made in the field of highway and airport engineering since the days of Mr. McAdam, it is interesting to note that this basic principle is even now of great value to the construction of highways and airports just as was recognized by road engineers more than a hundred years ago.

Charles M. Noble,[5] M. ASCE.—Since the paper was written (1952), several manufacturers have begun to produce heavy rollers with 25,000-lb wheel loads, mounting pneumatic high-pressure tires. In the specifications for widening the New Jersey Turnpike a tire pressure of 140 lb per sq in. on such rollers is required. This modern tool will assist in securing properly compacted subgrades composed of granular materials.

The discussion by Mr. Huang is important in emphasizing the absolute necessity of providing adequate drainage that will permanently lower the ground-water table to an acceptable depth below the surface of the pavement. It is also worthy of note that granular subbases must extend to the ditch lines or to continuous longitudinal pipe underdrains, or else water will be trapped and prevented from flowing laterally out from under the pavement. This water may enter from below in cuts and may originate by penetration through the median of dual highways during wet weather.

---

[4] "Remarks on the Present System of Road Making," by John Loudon McAdam, Longmans, Hurst, Rees, Orme, Brown & Green, London, 1824, pp. 46–47.

[5] Chf. Engr., New Jersey Turnpike Authority, New Brunswick, N. J.

Boxed-out or trenched sections filled with granular subbase material may become reservoirs for water unless there is positive means for the water to escape.

The relative ease of compacting granular material to 95% density (AASHO modified test) raises the question of whether this density is sufficient to withstand, without distortion, heavy repetitious loads such as are experienced on densely traveled highway trunk routes. Recent studies indicate that granular soils should be compacted to approximately 105% of the AASHO modified test value. It is hoped the forthcoming Illinois test road will provide further information on this question so that specifications can reflect requirements that will assure subgrades free from subsequent compaction under traffic.

AMERICAN SOCIETY OF CIVIL ENGINEERS
Founded November 5, 1852
TRANSACTIONS

Paper No. 2810

PILE-LOADING TESTS, MORGANZA FLOODWAY CONTROL STRUCTURE

By Charles I. Mansur,[1] M. ASCE, and John A. Focht, Jr.,[2] A. M. ASCE

With Discussion by Messrs. John W. Dunham; Leroy D. Graves and James E. Binckley; James F. McNulty; and Charles I. Mansur and John A. Focht, Jr.

Synopsis

A comprehensive pile-testing program was performed at the site of the Morganza Floodway control structure to determine the size of pile required to support the design loads—both compression and tension—without any significant movement. As an 80-ft layer of very compressible clay overlies sand at the site of the structure, an attempt was made to determine the bearing capacity of only that part of the piles penetrating the sand. This capacity was determined by testing various sizes of compression piles in pairs. One pile of each pair was stopped above the top of the sand and was loaded to obtain the resistance developed by skin friction in the clay. A test on a second pile driven into the sand indicated the total supporting capacity of both the clay and sand. The difference in the capacities of these two piles was then assumed to be the tip capacity of the pile driven into sand. Tension tests were also made on a third pile of the same size which was driven into the sand. The sizes of the piles tested ranged from a tapered pile with an 8-in. tip to a 30-in. pipe pile. Details of the loading arrangement and test procedures are described.

From the results of the tests, a pile having a 20-in. diameter was selected to support the loads of 100 tons in compression and 25 tons in tension, with an ample factor of safety against both detrimental settlement and sudden plunging. It was found that the skin friction developed by both compression piles and tension piles in clay was approximately equal to the shear strength of the clay as indicated by unconfined compression tests. The bearing capacities of

---

Note.—Published, essentially as printed here, in November, 1953, as *Proceedings-Separate No. 324* Positions and titles given are those in effect when the paper or discussion was approved for publication in *Transactions*.

[1] Asst. Chief, Embankment and Foundation Branch, Soils Div., Waterways Experiment Station, Corps of Engrs., U. S. Dept. of the Army, Vicksburg, Miss.

[2] Associate Engr., Greer and McClelland, Houston, Tex.

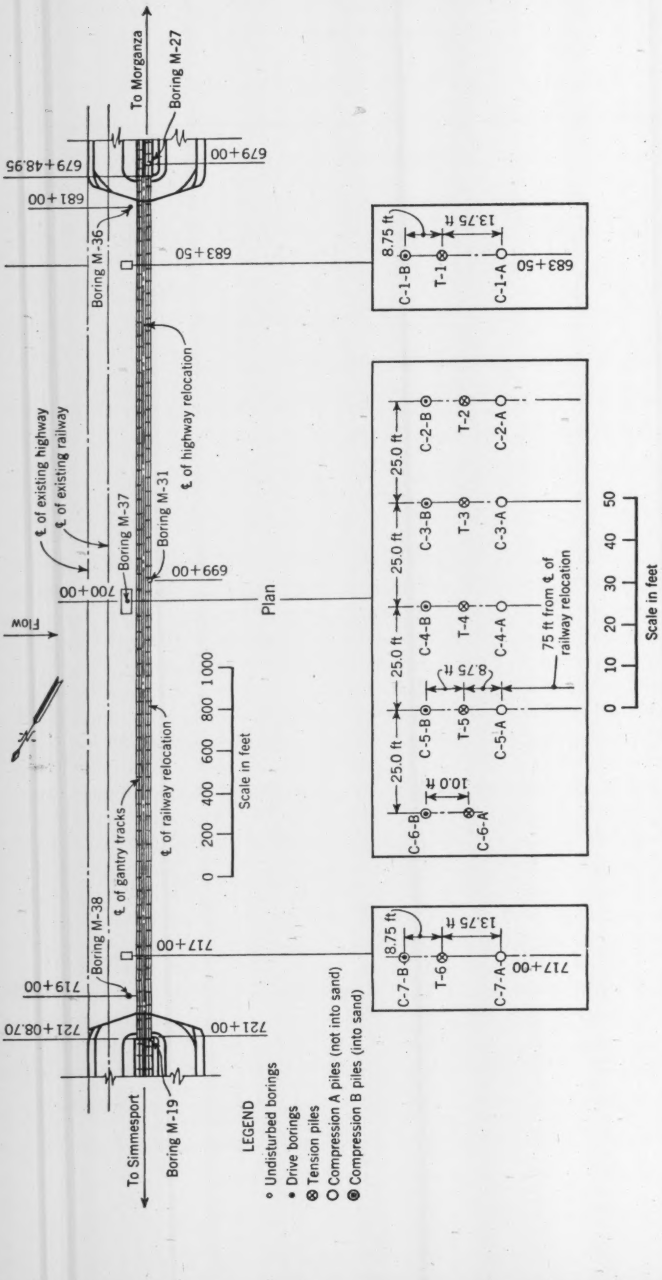
To Morganza
Boring M-27
679+48.95
679+00
681+00
Boring M-36
683+50
℄ of existing highway
℄ of existing railway
Boring M-37
Boring M-31
℄ of highway relocation
699+00
700+00
Flow
Plan
Scale in feet
0 200 400 600 800 1000
℄ of gantry tracks
℄ of railway relocation
Boring M-38
717+00
719+00
721+08.70
721+00
Boring M-19
To Simmesport
LEGEND
∘ Undisturbed borings
• Drive borings
⊗ Tension piles
○ Compression A piles (not into sand)
⊙ Compression B piles (into sand)
C-1-B
T-1
C-1-A
8.75 ft
13.75 ft
683+50
C-2-B
T-2
C-2-A
C-3-B
T-3
C-3-A
C-4-B
T-4
C-4-A
C-5-B
T-5
C-5-A
C-6-B
C-6-A
25.0 ft
25.0 ft
25.0 ft
25.0 ft
25.0 ft
8.75 ft
10.0 ft
75 ft from ℄ of railway relocation
C-7-B
T-6
C-7-A
8.75 ft
13.75 ft
717+00
0 10 20 30 40 50
Scale in feet

FIG. 1.—ARRANGEMENT OF TEST PILES

the parts of the piles in sand, as computed by several different methods, showed reasonable agreement with the pile-test results. The pile capacities computed by dynamic pile-driving formulas did not, in general, agree with the pile-test results.

INTRODUCTION

The soil conditions at the site of the Morganza Floodway control structure in Louisiana necessitated the use of long piles driven through soft clay into sand, the top of which was at a depth of approximately 80 ft. Because the pile foundation for the structure was required to support large loads in both compression and tension with little movement, it was decided to perform a series of pile-loading tests to determine the size of pile that would carry a design load of 100 tons without any significant settlement. There are presented herein the procedures used in making the pile tests, the types of piles tested, and the results and conclusions made. Comparisons are made between test results and values computed from various pile-capacity formulas and from pile-driving formulas.

Description of Structure.—The Morganza Floodway control structure is located approximately 3 miles northwest of Morganza, La. The structure consists of a gated weir for control of flood waters and a railroad and highway crossing of the floodway. The structure (Fig. 1), approximately 4,000 ft long, is connected to the guide levees of the floodway by embankments, which carry a highway and railroad and which serve as part of the main-line levee system of the Mississippi River. The pile foundation beneath the gated weir consists of precast concrete piles driven to sand on a batter of 2 on 1. There are twenty-seven piles beneath each pier—eleven battered upstream and sixteen downstream.

Foundation Conditions.—The soil conditions at the site consist of strata of predominantly highly plastic clays approximately 80 ft thick underlain by sand as shown by a typical boring log in Fig. 2. The clay strata have average water contents ranging from 42% to 60% and liquid limits ranging from 60% to 100%.

Consolidation tests on samples of clay taken from beneath the structure showed that the foundation is quite compressible and that piles driven to sand were necessary to support the structure. As evidence of this compressibility, 30-ft embankments near the structure have settled from 2½ ft to 5 ft.

Unconfined compression tests and unconsolidated, undrained, triaxial-compression tests on undisturbed samples taken from the clay strata beneath the structure indicated an over-all average cohesive shear strength of 660 lb per sq ft for the foundation clays. Six unconfined compression tests on remolded samples taken at varying depths beneath the structure showed an average remolded strength of 620 lb per sq ft. Thus, pile-driving operations were not expected to influence appreciably the shear strength of the foundation clays.

The sand underlying the clay strata is a uniformly graded fine sand composed of subrounded to subangular grains. Driving of a standard 1⅜-in. inside-diameter, split-spoon sampler with a 30-in. drop of a 140-lb hammer showed the sand to have an average driving resistance of 55 blows per ft. A typical driving record is shown in Fig. 2. The relative density of the sand was approximately 80%.

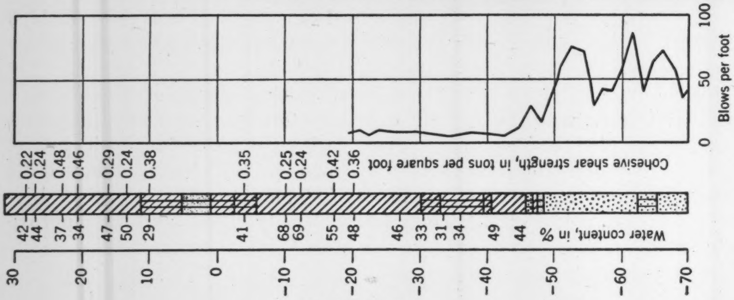

FIG. 2.—TYPICAL BORING LOG

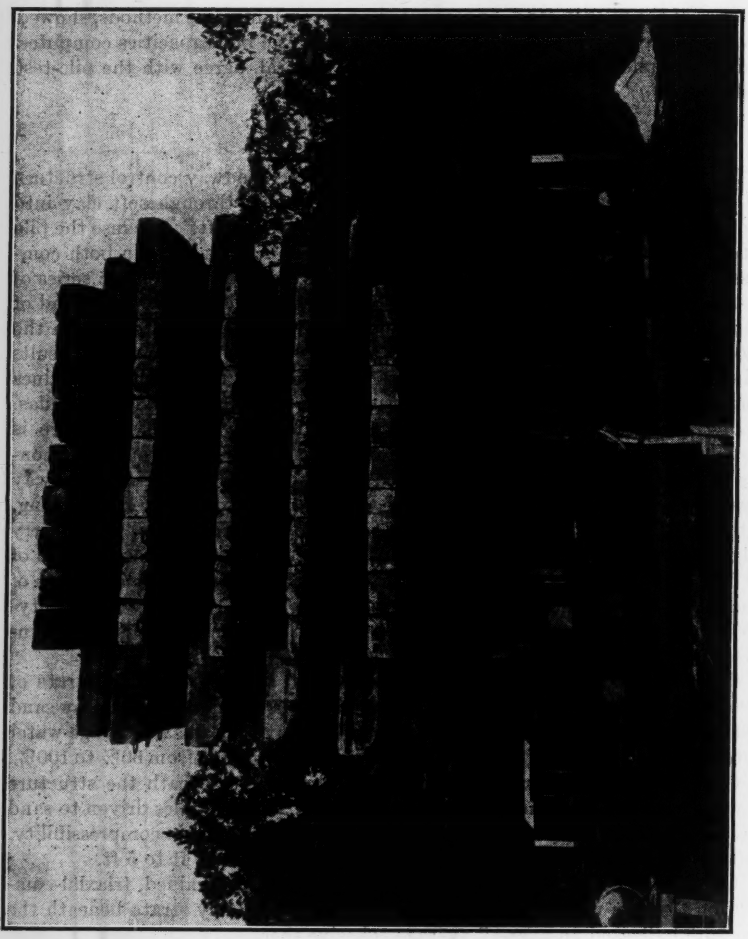

FIG. 3.—LOADING ARRANGEMENT FOR COMPRESSION PILES

Purpose of Tests.—The purpose of the pile-loading tests was to determine what size pile would be required to carry a 100-ton compression load and what tension load a pile of that size would carry. All test piles were driven vertically for ease of testing. Although the bearing capacity of the tips of vertical piles is probably somewhat greater than that of the batter piles, the difference probably is not more than 5% to 15%. Detailed reports of these loading tests have been published.[3,4]

GENERAL TEST PROCEDURES

Because the clay overlying the sand is quite compressible the compression tests were made in such a manner that the bearing capacity of the part of the piles driven into the sand could be evaluated. For the purpose of simplicity, that part of the pile driven into sand is termed the "tip"; the point and sides of the pile in sand are both included in this definition; both carry part of the load. To determine the bearing capacity of the tip it was necessary either to eliminate completely or to measure the frictional resistance developed along that part of the pile in the clay stratum. In these tests the resistance developed in the clay was determined by testing the piles in pairs. The frictional resistance in the clay stratum was determined from a pile driven to 5 ft above the top of the sand; the combined frictional resistance and tip capacity were determined from a pile driven into the sand. Piles driven to 5 ft above the sand are herein termed A piles, whereas piles driven into sand are termed B piles. The tension piles also were driven into sand. Because all piles beneath the structure were to be loaded in compression prior to any tension loading, all tension test piles were loaded with a normal "working" compression load prior to testing in tension. Holes were excavated at each test-pile location to eliminate any skin friction above the proposed base of the structure.

TABLE 1.—DESCRIPTION OF TEST PILES

Piles	Type	Diameter, in inches	Description
C-1, T-1	Cylindrical pipe	24	⅜-in. wall thickness, 1.9-ft-long conical point.
C-2, T-2	Fluted steel, tapered	...	No. 7 gage metal, 18-in. butt diameter, tapered 1 in. in 7 ft to 8-in.-diameter, hemispherical tip.
C-3, T-3	Fluted steel, constant section	12	No. 3 and No. 7 gage metal, 12-in. diameter, 9-in.-long conical point.
C-4, T-4	Cylindrical pipe	18	⅜-in. wall thickness, 1.5-ft-long conical point.
C-5, T-5	Cylindrical pipe	24	⅜-in. wall thickness, 1.9-ft-long conical point.
C-6	Cylindrical pipe	30	⅜-in. wall thickness, 2.4-ft-long conical point.
C-7	Precast concrete	...	22-in. square, point tapered to 8-in. square in 2 ft.
T-6	Cylindrical pipe	24	⅜-in. wall thickness, 1.9-ft-long conical point.

TYPES OF PILES AND DRIVING EQUIPMENT

The locations of the test piles along the structure are shown in Fig. 1; the piles are described in Table 1. A tension test (denoted by T) was conducted on each type of pile with the exception of the 30-in.-diameter pipe pile and the precast concrete pile.

---

[3] "Morganza Control Structure Pile Tests," Corps of Engrs., New Orleans, La., December, 1949.

[4] "Pile Loading Tests—Combined Morganza Floorway Control Structure," *Technical Memorandum No. 3-308*, Waterways Experiment Station, Vicksburg, Miss., January, 1950.

The piles were driven by a skid-mounted, whirly-type driver with 82-ft leads. A single-acting hammer delivering 30,225 ft-lb of energy was used to drive the 24-in. and 30-in. pipe piles and the 22-in.-square concrete piles. A single-acting hammer delivering 15,000 ft-lb of energy was used for driving all anchor piles, the fluted-steel piles, and the 18-in. pipe piles. All piles were filled with concrete a few days after driving. A period of from 4 weeks to 6 weeks elapsed after driving before any loads were applied to the piles.

COMPRESSION TEST PILES

Load Arrangement.—The test piles were loaded by jacking against concrete weights that were stacked on platforms over the test piles as shown in Fig. 3. The platforms were supported on rows of six timber piles on each side of the test pile. The weights were precast concrete slabs and rectangular blocks weighing approximately 3.5 tons and 5 tons, respectively. Hydraulic jacks mounted on fabricated steel pedestals placed on top of the test piles were used to apply the loads to the piles. Two of the jacks used were of 200-ton capacity, six of 100-ton capacity, and four of 60-ton capacity.

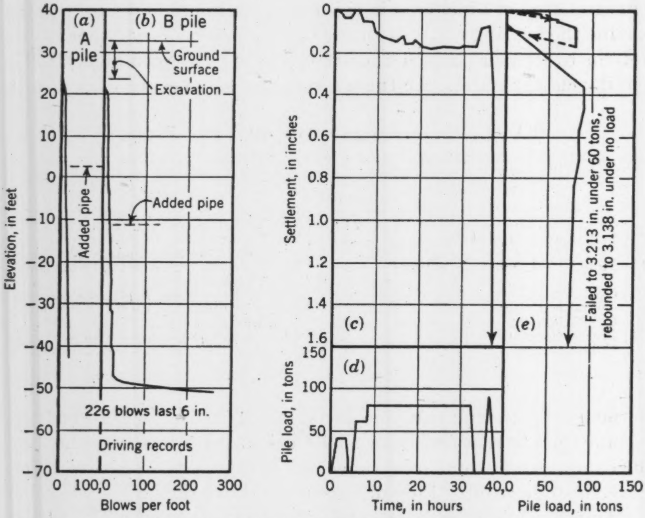

FIG. 4.—COMPRESSION TEST, C–4–A (DRIVEN LENGTH, 79.6 FT; LOADED LENGTH, 78.7 FT; IMBEDDED LENGTH, 67.1 FT; TIP AT EL. −43.6)

Loading Procedure.—The A piles, which were driven only into clay, were loaded and tested to failure before the B piles, which were driven into sand, were loaded. In general, loads were applied to the piles in 20-ton increments at a rate of $1\frac{1}{2}$ tons per min. Each increment was maintained until 80% of the estimated ultimate movement under that increment of load had taken place, but not for longer than 24 hr. Time-settlement curves were plotted during the tests to estimate the ultimate settlement under each increment of load. The

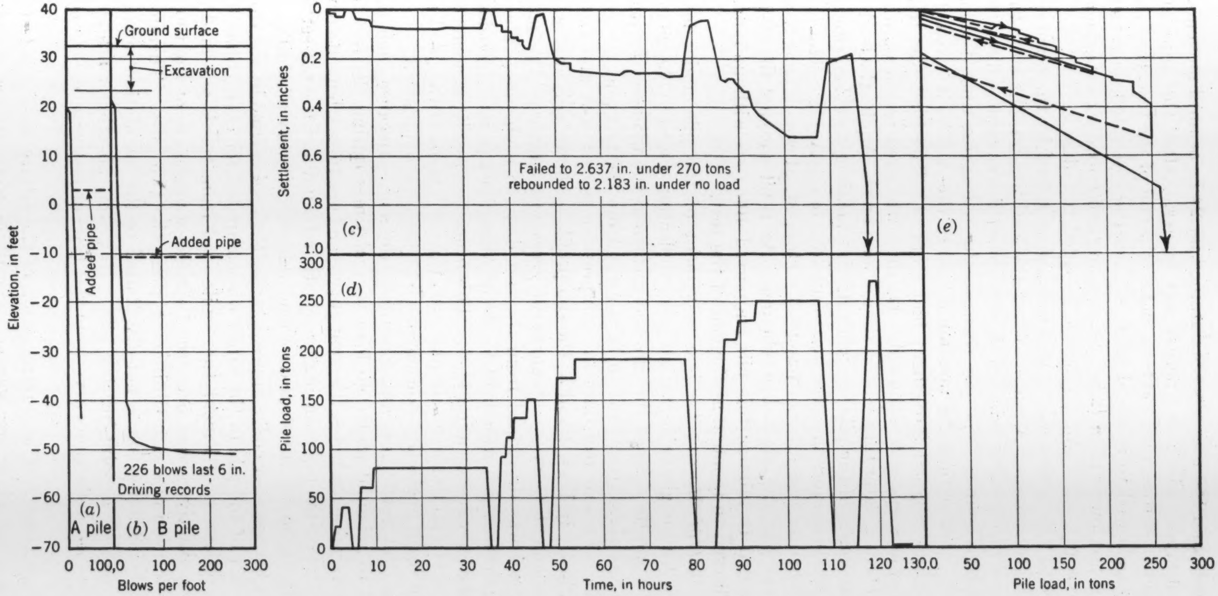

Fig. 5.—Compression Test, C-4-B (Driven Length, 95.8 Ft; Loaded Length,[f] 86.6 Ft; Imbedded Length, 75.0 Ft; Tip at El. −51.5)

loads of 80 tons and 160 tons were maintained for 24 hr or until movement had practically stopped, whichever period was longer. After the application of loads of 40 tons, 80 tons, and 160 tons and at the end of the test, the piles were unloaded and allowed to rebound until 80% of the estimated movement had occurred, but not longer than 12 hr. Unloading and reloading were done at the rate of 1½ tons per min. All A piles were loaded to failure.

The B piles, which were driven into sand, were loaded by the same schedule used for the corresponding A piles. When the load was 60 tons more than the maximum load of the corresponding A pile, the load was removed and the pile was allowed to rebound. The pile then was loaded again; when the load became 100 tons greater than the maximum load of the A pile, it was held constant until practically all movement had stopped. The load was removed, and the pile was allowed to rebound. Loading was then resumed; when the load was 160 tons greater than the maximum load on the A pile, the load was removed and rebound of the pile was permitted. Loading was then resumed up to a load of 200 tons more than the maximum load of the A pile. This load was maintained until movement had practically stopped, at which time it was removed and the pile was allowed to rebound. All B piles except the 30-in. pipe pile were loaded to failure; this pile supported 400 tons without failure. All piles were allowed to rebound at the end of the test.

Measurement of Movement.—The movement of the pile under load was measured with an engineer's level and dial deflection gages. The gages were mounted on opposite sides of the pile and measured the movement with reference to concrete slabs from 12 ft to 14 ft away from the test pile.

Test Data.—Typical test data for compression piles C-4-A and C-4-B are shown graphically in Figs. 4 and 5; the soil profile is shown only in Fig. 2.

Load-Settlement Curves.—A curve of gross movement of the pile head versus pile load was developed from the test data on each pile. The points representing loads which were held for 24 hr were given primary consideration in drawing the curves shown in Fig. 6. This procedure results in a curve which should represent (up to the maximum load) the movement of the pile head under sustained load, neglecting consolidation of the clay foundation.

Curves of Net Settlement and Elastic Settlement.—Because each test pile was allowed to rebound under no load several times during the test, it was possible to determine the net-settlement curves and elastic-settlement curves for each pile. The points representing the elastic rebound and the net settlement remaining after rebound are plotted for each rebound of every pile in Fig. 6.

Tip-Load Curves.—A curve approximating the load carried by the tip of the B pile (the part of the pile in the sand) was computed for each B pile by subtracting at any gross settlement the A-pile load from the B-pile load. This method is not exactly correct because at similar movements of the top of the pile the distribution of strain is different along the two piles. Therefore, the load carried by a friction pile is not distributed to the foundation in the same way as the load on a point-bearing pile. However, no other method of developing a tip-load deflection curve from this type of test was considered more accurate.

Pile-Failure Loads.—The determination of the failure load of a test pile is usually arbitrary. Therefore, various procedures were utilized to obtain a

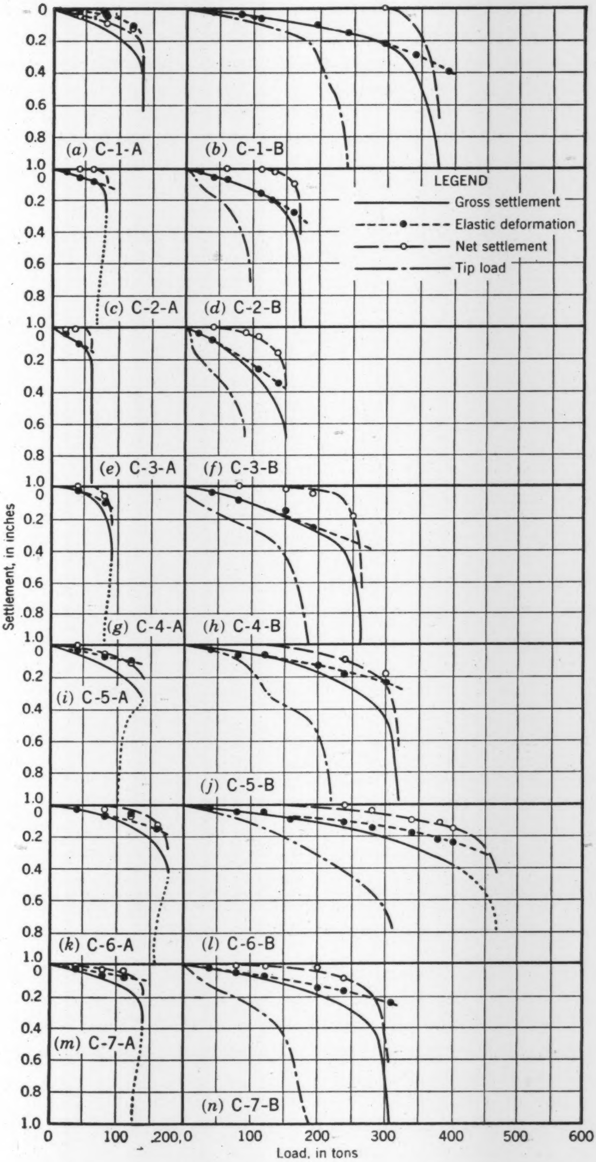

FIG. 6.—LOAD-SETTLEMENT CURVES

value for each pile. A failure load for each compression pile was determined as that load (*a*) which produced a net settlement of 0.25 in., (*b*) indicated by the intersection of tangent lines to the flatter part of the gross-settlement curve and to the steeper part of the same curve, (*c*) beyond which, by inspection, there was an increase in gross settlement disproportionate to the increase in load, (*d*) at which the slope of the net-settlement curve was four times the slope of the elastic deformation curve, and (*e*) beyond which, by inspection, there was an increase in net settlement disproportionate to the increase in load.

TABLE 2.—RESULTS OF THE VARIOUS METHODS OF DETERMINING THE FAILURE LOADS, IN TONS, OF COMPRESSION-TEST PILES

Pile	0.25-in. net settlement	Tangent intersection of gross-settlement curve	Inspection of gross-settlement curve	Slope of net-settlement curve 4 times slope of elastic-settlement curve	Inspection of net-settlement curve	Average of five methods	Inspection of tip-load curve for failure load	Corrected tip-failure load[a]	Adjusted tip-failure load[b]
C-1-A	134	131	125	132	130	130	...	...	...
C-1-B	357	360	320	347	330	343	...	176	160
Difference	223	229	195	215	200	213	185	...	...
C-2-A	80	78	78	76	73	77	...	...	...
C-2-B	169	170	145	164	155	162	...	74	62
Difference	89	92	67	88	82	85	80	...	...
C-3-A	60	57	56	57	55	57	...	...	...
C-3-B	149	143	145	148	140	145	...	85	101
Difference	89	86	89	91	85	88	90	...	...
C-4-A	89	78	80	85	75	81	...	...	...
C-4-B	254	258	230	240	240	244	...	159	173
Difference	165	180	150	155	165	163	165	...	...
C-5-A	139	135	137	185	136	136	...	...	...
C-5-B	304	307	305	302	300	304	...	171	163
Difference	165	172	168	167	164	168	185	...	...
C-6-A	174	173	165	160	160	166	...	...	...
C-6-B[c]	450	462	450	455	445	452	...	276	275
Difference	266	289	285	295	285	286	280	...	...
C-7-A	139	138	135	130	135	135	...	...	...
C-7-B	293	290	285	283	285	287	...	120	115
Difference	154	152	150	153	150	152	140	...	...

[a] Correction made to loads indicated by tip-load curves on the basis of greater length in clay of B piles than A piles. [b] Adjustment of corrected loads made to 5-ft penetration into sand and 85-ft depth of point using Eq. 1. [c] C-6-B was not loaded to failure; values indicated are based on estimated curves.

The results of the analysis of each test are given in Table 2 with the average of the five methods; the average of the five methods is used in subsequent analyses. The 30-in. pipe pile driven into sand (C-6-B) did not fail under a maximum load of 400 tons. However, a failure load was estimated for this pile by extrapolating the settlement-load curve.

Other procedures which have been suggested or are given in building codes for determining the failure load of a test pile were discarded after preliminary trials. The methods not utilized are intended primarily for use with tests on smaller piles under much lighter loads.

There are no significant differences in the values indicated for any pile by the five methods. If a pile test is not performed under a specific building code with a definite method established for determination of the failure load, it appears desirable, or at least helpful, to average the results indicated by several methods of analysis.

Average Bearing Capacity of Pile Tip.—Because the piling was designed so that the part of the pile in the sand would carry the design load, the average relationship of the bearing capacity of the pile tip to the diameter of the pile tip was determined. Two methods were utilized to compute the relationship. In the first, the difference between the average failure loads of the A and B compression piles, as listed in Table 2, was taken as the bearing capacity of the tip of the B piles. The second method utilized the tip-failure load determined by inspection of the tip-load curve. The capacity of the tip of each B pile determined by each of the two methods is tabulated in Table 2 and is plotted versus the tip diameter in Fig. 7. Both methods indicate an approximate straight-line relationship between the tip load and tip diameter. Because the penetration into sand of all piles was not the same a direct comparison was not possible with the approximately parabolic relationship between load and tip diameter

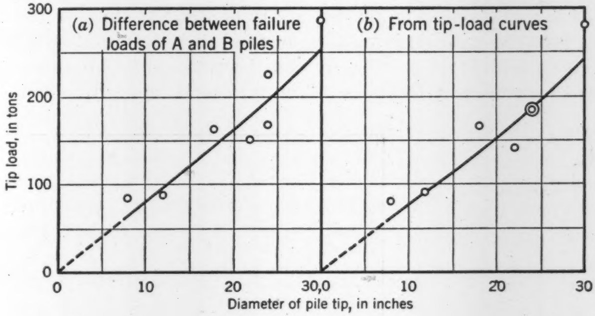

FIG. 7.—AVERAGE TIP-BEARING CAPACITY

TABLE 3.—SKIN FRICTION

Pile	Skin friction, in pounds per square foot
C-1-A	730
C-2-A	694
C-3-A	543
C-4-A	524
C-5-A	660
C-6-A	650
C-7-A	589
Avg.	630

TABLE 4.—INTERNAL FRICTION ANGLE OF SAND

Pile	VALUE OF ϕ, IN DEGREES, AS DETERMINED FROM				
	Eq. 1	Eq. 2	Eq. 3	Eq. 4	Eq. 5
C-1-B	29	32	22	30	34
C-2-B	36	39	27	37	41
C-3-B	36	36	30	37	38
C-4-B	34	35	28	36	37
C-5-B	29	31	23	30	32
C-6-B	30	32	24	31	33
C-7-B	18	27	14	20	28
Avg.	30	33	24	32	35

indicated by most bearing-capacity formulas for piles driven into sand foundations.

Average Skin Friction in Clay.—The skin friction developed by the compression piles stopped in clay above the sand at average failure loads was computed using the nominal diameter of the piles and the embedded length of the pile; the resulting values are presented in Table 3. The average value of 630 lb per sq ft agrees closely with the average shear strength of 660 lb per sq ft determined by shear-strength tests on undisturbed samples from the foundation borings.

Required Size of Pile.—The total capacity of a pile at this site (with respect to plunging into the ground) is the sum of the capacities developed in the clay by skin friction and those in sand by skin friction and point resistance. This capacity was measured by the piles driven into sand (type B). A pile of large circumference could be driven which would not penetrate the sand and yet would have an adequate total capacity. However, under the sustained load, such a pile would undergo considerable settlement as a result of consolidation within the clay. The load on a pile driven into sand will be initially carried largely by skin friction in the clay. However, because the clay at the site is quite compressible the clay tends to become relieved of almost all its supporting stress by consolidation within the clay strata. If the total load applied to the pile is greater than the capacity of the part of the pile in sand, the pile will not fail by plunging but will settle appreciably because of consolidation. Thus, to guard against detrimental settlements, the long-time capacity of the piles was taken as the capacity of the tip of the piles in sand. On the basis of the data shown in Fig. 7, a pile diameter of 20 in. was selected as being adequate to

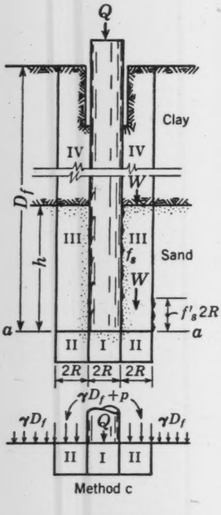

FIG. 8.—THEORETICAL BEARING CAPACITY

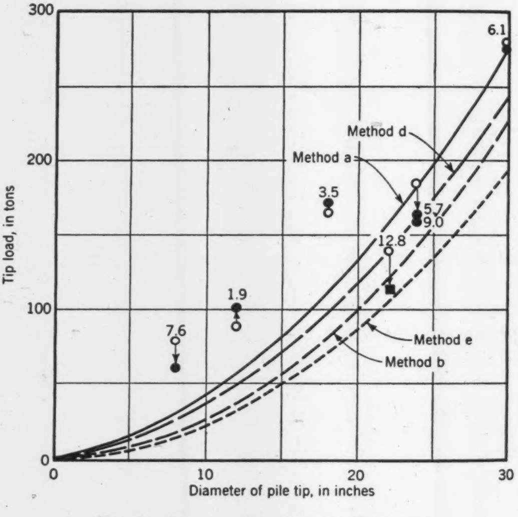

FIG. 9.—ADJUSTED TIP-BEARING CAPACITY

carry the design compression load of 100 tons, with a factor of safety of approximately 1.5 against detrimental settlement and a factor of safety of approximately 3.0 against failure by plunging. Octagonal piles with a minimum dimension of 20 in. were used for lengths up to 100 ft; 20-in. square piles were used where lengths greater than 100 ft were required.

Bearing-Capacity Formulas.—The results of the pile tests were utilized to compute the indicated angle of internal friction of the sand, using methods that have been suggested for computing the bearing capacity of piles or deep piers. The basic methods used were:

a. A bearing-capacity equation for cylindrical piers and piles,[5] suggested by Karl Terzaghi, Hon. M. ASCE, is as follows:

$$Q = \pi R^2(\gamma D_f N_q + 0.6 \gamma R N_\gamma) + 2 \pi R h f_s \quad \text{..........} \quad (1a)$$

in which Q, as shown in Fig. 8, is the total load on the pile at failure assuming that the clay carries no load; R denotes the pile radius; γ is the effective unit weight of the soil; D_f represents the depth of the pile point below the ground surface; N_q and N_γ are bearing-capacity factors; h is the penetration of the pile into the sand;

$$f_s = \gamma \left(D_f - \frac{h}{2} \right) \tan \phi \quad \text{..................} \quad (1b)$$

and ϕ is the angle of internal friction for the sand.

b. A modification of method *a*,

$$Q = \pi R^2(\gamma D_f N_q + 0.6 \gamma R N_\gamma) \quad \text{................} \quad (2)$$

c. An approach also suggested[5,6] by Mr. Terzaghi,

$$Q = \pi R^2 [(\gamma D_f + p) N_q + 0.6 \gamma R N_\gamma] + 2 \pi R h f_s \quad \text{......} \quad (3a)$$

in which

$$p = \frac{2 \pi R h f_s + 12 \pi R^2 f'_s}{8 \pi R^2} \quad \text{.................} \quad (3b)$$

and f'_s is the skin friction on the pile in the sand.

d. An equation developed by J. Jaky[7] for piles,

$$Q = \pi R^2 \gamma D_f \tan^2 \left(45 + \frac{\phi}{2} \right) e^{\pi \tan \phi} + 2 \pi R h f_s \quad \text{........} \quad (4)$$

e. A modification of method *d*,

$$Q = \pi R^2 \gamma D_f \tan^2 \left(45 + \frac{\phi}{2} \right) e^{\pi \tan \phi} \quad \text{.............} \quad (5)$$

---

[5] "Theoretical Soil Mechanics," by Karl Terzaghi, John Wiley & Sons, Inc., New York, N. Y., 1934, p. 134,

[6] Discussion by Karl Terzaghi of "Application of Soil Mechanics in Designing Building Foundations," by A. Casagrande and R. E. Fadum, *Transactions*, ASCE, Vol. 109, 1944, p. 430.

[7] "On the Bearing Capacity of Piles," by J. Jaky, *Proceedings*, Second International Conference on Soil Mechanics, Vol. I, Rotterdam, June, 1948, p. 102.

Other methods were used in preliminary analyses but were discarded because they indicated absurd values. The angle of internal friction of the sand was computed by each method for each compression pile driven into sand using the indicated capacity of the pile tip, less the skin friction in the clay below the tip of the A piles and the top of the sand, and the actual penetration of the pile in sand. To determine the depth of penetration of the pile into sand it was assumed from the nature of the pile-driving records that, when the driving resistance was 30 blows per ft, the top of the tapered point was at the upper surface of the sand.

The angle of internal friction of the sand necessary to give the corrected bearing capacity was obtained by a trial-and-error method using Eqs. 1 through 5.

Indicated Friction Angle of Sand.—The angle of internal friction of the sand computed from the corrected tip load carried by each B pile is listed in Table 4.

FIG. 10.—LOADING ARRANGEMENT FOR TENSION PILES

With the exception of method *c*, Eq. 2, the analyses show that the friction angle of the sand is usually between 30° and 35°—within the range of the friction angles usually obtained for this type of sand.

Summary.—The computed angle of internal friction of the sand is approximately the same, whether computed from method *b* or method *e*, neither of which account for skin friction in the sand, or from methods *a* and *d*, which assume skin friction of the sand against the pile. As it is believed that skin friction of the sand on the pile will carry some of the tip load, methods *a* and *d* appear to be the most logical for estimating the tip-bearing capacity of piles driven into sand.

A usual assumption for the shear strength of sand is $\phi = 30°$. Using this value, the bearing capacities of piles of various sizes driven 5 ft into sand with

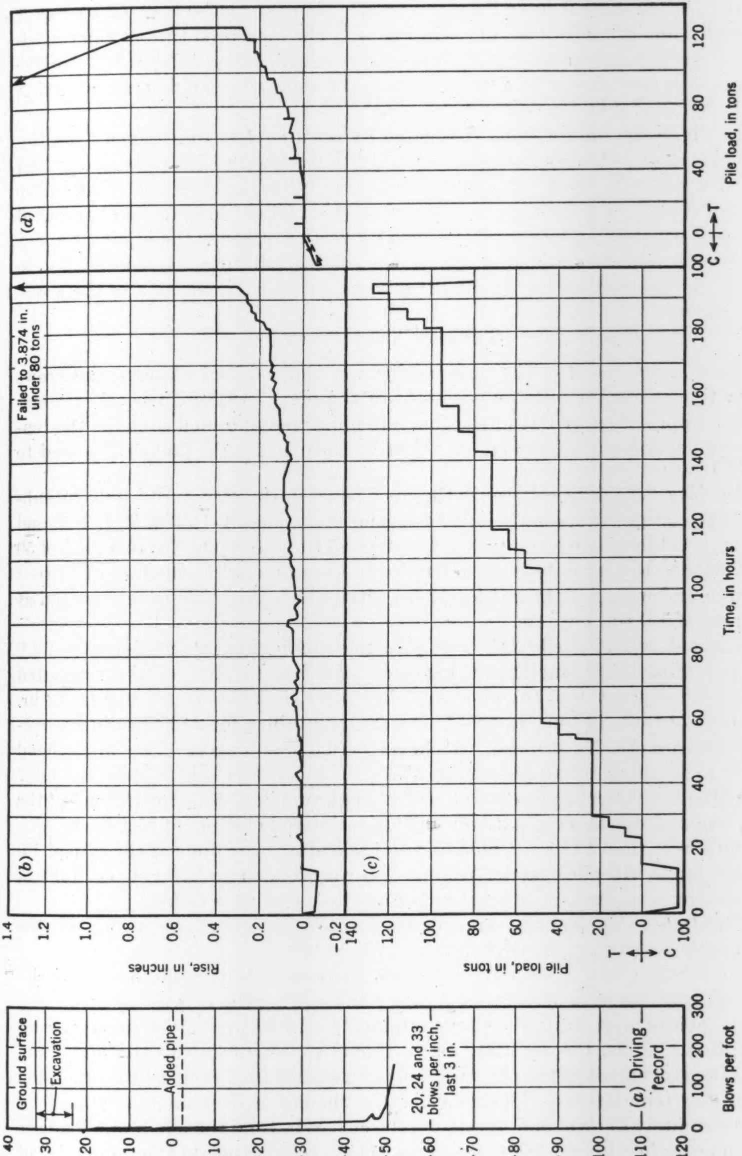

FIG. 11.—TENSION TEST, T-4 (DRIVEN LENGTH, 87.4 FT; LOADED LENGTH, 84.9 FT; IMBEDDED LENGTH, 74.9 FT; TIP AT EL. −51.4)

an overburden of 85 ft have been computed using the methods given by Eqs. 1 through 5 and are shown as curves in Fig. 9. The measured tip-bearing capacities of the piles, adjusted to the conditions assumed for computation of the curves, are also shown in Fig. 9. From the data presented it appears that methods *a* and *d* fit the test data reasonably well.

In Fig. 9 the failure loads (indicated by open circles) were taken from tip-load curves and then corrected for the additional length of B piles in clay and adjusted to a 5-ft penetration into sand and an 85-ft depth of the point on the basis of Eq. 1. The adjustment from the actual failure load to that computed for a 5-ft penetration into sand is shown by vertical arrows; the numbers above the circles indicate the actual penetration of the pile into the sand. Also in Fig. 9, the tip load for the 30-in. pile is based on an extrapolation of the gross-load curve.

TENSION TEST PILES

Load Arrangement.—The tension piles were loaded by jacking against rows of six timber anchor piles on each side of the pile. An 8-in. I-beam was embedded approximately 9 ft in the concrete filling the pile shell to make the tension connection shown in Fig. 10. Two 100-ton hydraulic jacks were used to apply load to the test piles.

Loading Procedure.—Because the piles beneath the structure would be subjected to compression load prior to a tension load, piles T-1, T-2, T-4, T-5, and T-6 were subjected to a compression load of 85 tons, and pile T-3 to a load of 50 tons prior to testing in tension. The loads were applied at the rate of 1½ tons per min and were maintained for 12 hr, after which the loads were removed at the rate of 1.0 ton per min.

The pull was applied to the test piles in 8-ton increments at the rate of 1.0 ton per min. Each increment was maintained until 80% of the estimated movement of the top of the pile had taken place, but for not more than 12 hr. Loads of 24 tons, 72 tons, and 96 tons were maintained for 24 hr or until movement had practically stopped, whichever period was longer. The 48-ton load was held for 48 hr on all piles except T-5; that load was held on pile T-5 for 7 days (168 hr). After application of certain loads on pile T-5 and at the end of the test, rebound was allowed until 80% of the estimated movement had occurred—but no longer than 12 hr. Unloading and reloading were done at the rate of 1.0 ton per min. All piles except T-5 and T-6 were loaded to failure; the limit of the loading equipment was reached before these two piles failed.

Test Data.—Typical test data for tension pile T-4 are shown in Fig. 11; the soil profile is the same as that shown in Fig. 2.

Load-Rise Curves.—A curve of gross movement of the pile head was developed from the test data on each pile. In drawing the curves shown in Fig. 12, the points representing loads maintained for 24 hr were given primary consideration. Thus, the resulting curve should represent (up to the maximum load) the movement of the pile head under sustained load (neglecting expansion of the clay foundation). The true shape of the curve after the maximum load is not definitely known, and, therefore, the curves beyond the maximum load are shown as dashed lines. No attempt was made to extrapolate the remainder of the curves for piles T-5 and T-6 which did not fail.

Pile-Failure Loads.—In studying the load-rise curves in Fig. 12, two different conditions of failure were considered. The first is that the rise of the piles during loading would be such as to have a detrimental effect on the structure. A gross rise of 0.25 in. was taken to be the limiting criterion for this condition; this rise was used to determine the allowable tension load. The second condition is the complete failure of the pile under load, causing a reduction in the capacity of the pile to carry the load. The failure load for the second condition was determined by an inspection of the gross-rise curves and net-rise curves for the load beyond which there was an increase in deflection disproportionate to the increase in load. The second condition was used to determine the average tension skin friction in the clay. The results of the analysis of each test are presented in Table 5.

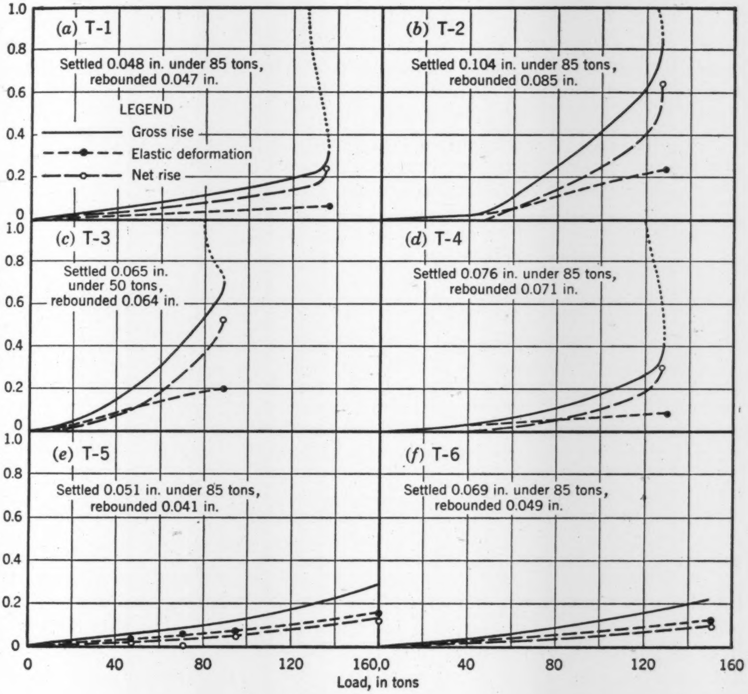

FIG. 12.—LOAD–RISE CURVES

Average Load Capacity.—Because the embedded lengths varied somewhat, the loads that produced a gross rise of 0.25 in. were corrected to an embedded length of 75 ft by assuming that the tension capacity was directly proportional to the length. These corrected values (Table 5) are total loads applied to the head of the pile. These loads are also plotted against the average pile diameter in Fig. 13. The tapered fluted-steel pile was plotted at a diameter of 13 in., the average of the tip and butt diameters, which were 8 in. and 18 in., respectively. The average line drawn through the points indicates that a 20-in.-diameter round pile 75 ft long can carry the design tension load of 25 tons with a factor of safety of approximately 4.5.

Average Skin Friction in Clay.—It is not possible to compute directly from the tension test data the skin friction that developed in the clay. The tension piles were driven into the sand, and the sand should have a materially different skin friction on the pile than the clay. The total force carried by the clay was computed by subtracting from the pile-failure load, determined by inspection of the net curve, the buoyant weight of the pile and the total force developed by friction in the sand, assuming a coefficient of earth pressure of 1.0 and an angle of internal friction of the sand of 30°. The unit skin friction in the clay was computed from this corrected failure load, using the embedded length in the clay and the nominal diameter of the pile; the resulting values are also presented in Table 5. For purposes of comparison, the skin friction determined from adjoining A compression piles is also shown in Table 5. Because piles T-5 and T-6 were not loaded to failure the skin-friction values listed for them were the values developed under the maximum load. The average skin friction shown in Table 5 was based on the data on piles T-1 through T-4. From the data in Table 5 it is concluded that the skin friction developed at failure by either a tension pile or a compression pile in the Morganza clay is fairly close to the average strength of the foundation clays, as indicated by unconfined and unconsolidated, undrained, triaxial-compression tests.

TABLE 5.—TENSION-FAILURE LOADS AND SKIN FRICTION

Pile	DETERMINATION OF FAILURE LOADS, IN TONS, FROM				Tension skin friction, in pounds per square foot	Compression skin friction, in pounds per square foot
	0.25-in. gross rise	Corrected gross rise[a]	Inspection of Curve of			
			Gross rise	Net rise		
T-1	133	139	134	134	608	730
T-2	80	75	125	122	829	694
T-3	53	52	88	87	706	543
T-4	117	117	125	125	639	523
T-5	150	141	200	200	651	659
T-7	167	134	160	160	350	588
	Average[b]				695	623
	Average of tension and compression tests				660	

[a] Load for 0.25-in. gross rise corrected to an embedded length of 75 ft. [b] Based on piles T-1 through T-4.

The fact that the tapered pile T-2 indicated the highest skin friction is not believed to be highly significant because the variations in skin friction indicated by the various types of piles could be caused by variations in soil strengths—not necessarily by characteristics of the piles. From the one test made it appears that at the site a pile with a small taper, such as 1 in. in 7 ft for piles C-2 and T-2, responds to loading in tension or compression in a manner similar to a pile of constant section with the same average diameter.

DYNAMIC PILE–DRIVING FORMULAS

The six dynamic pile-driving formulas that were used to compute the capacity of the compression piles driven into sand are as follows:

Engineering-News,[8] factor of safety of 6—

$$R = \frac{2\,W\,h}{s + 0.1} \quad \text{(6)}$$

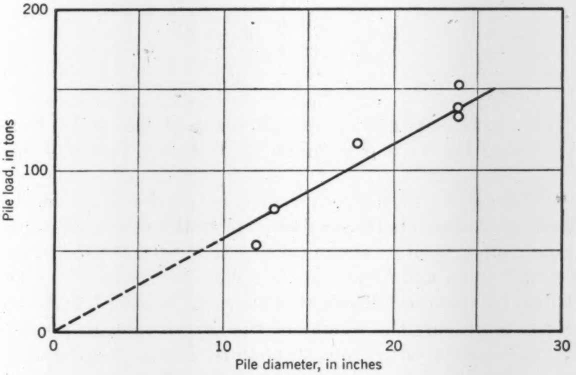

FIG. 13.—AVERAGE TENSION CAPACITY

Engineering-News (modification 1),[9] factor of safety of 6—

$$R = \frac{2\,W\,h}{s + 0.1\,\dfrac{P}{W}} \quad \text{(7)}$$

Engineering-News (modification 2),[10] factor of safety of 6—

$$R = \frac{2\,W\,h}{s + 0.3} \quad \text{(8)}$$

Eytelwein (modified),[9] factor of safety of 6—

$$R = \frac{2\,W\,h}{s + 0.3\,\dfrac{P}{W}} \quad \text{(9)}$$

---

[8] "Piles and Pile Driving," edited by A. M. Wellington, Engineering News Publishing Co., New York, N. Y., 1893.

[9] "Pile Foundations," by Robert D. Chellis, McGraw-Hill Book Co., Inc., New York, N. Y., 1951, p. 530.

[10] *Ibid.*, p. 531.

Canadian National Building Code,[11] factor of safety of 3—

$$R = \frac{3.6\, W\, h\, n}{s + \frac{1}{2} C} \quad \text{(10a)}$$

in which

$$n = \frac{W + 0.5\, e^2\, P}{W + P} \quad \text{(10b)}$$

and

$$C = \frac{3\, R}{A}\left(\frac{12\, L}{E} + 0.0001\right) \quad \text{(10c)}$$

Pacific Coast Uniform Building Code,[12] factor of safety of 1—

$$R_u = \frac{12\, W\, h\, \dfrac{W + K\, P}{W + P}}{s + \dfrac{12\, R_u\, L}{A\, E}} \quad \text{(11)}$$

in which K is a coefficient that equals 0.25 for steel piles and 0.10 for all other piles. When using Eq. 11 it is recommended[12] that a factor of safety of 4 be used.

In Eqs. 6 through 11, A is the average cross-sectional area of driven parts, in square inches; e represents the coefficient of restitution and is equal to 0.5 for a ram striking a steel anvil on steel or concrete piles or 0.4 for a ram striking a steel anvil containing a wood cushion; E is the modulus of elasticity of the pile material; h denotes the free-fall height of the ram, in feet; L is the length of the pile, in feet; P represents the weight of the driven pile, in pounds; R is the design carrying capacity of the pile, in pounds; R_u denotes the ultimate carrying capacity of the pile, in pounds; s is the set per blow, in inches; and W represents the weight of the falling mass, in pounds.

The Canadian National Building Code and the Pacific Coast Uniform Building Code are modifications of the Hiley formula.[13] It was not possible to use the later formula because the rebound of the pile during driving was not measured. The driving data of the piles stopped above the sand were not used to compute the indicated capacity by the driving formula. It is usually accepted that pile-driving formulas are meaningless for friction piles driven in clay.

Relationship of Formulas to Test Results.—The driving resistance for the last 3 in. of penetration was used in Eqs. 6 through 11 to compute the design capacity of each of the compression piles driven into sand. These values are given in Table 6, together with certain computed ratios of formula capacity to test capacities. It appears, in general, that the pile-driving formulas did not give capacities that checked with either the total capacity or tip capacity of the test piles at the site of the Morganza Floodway control structure. The only good agreement obtained was between the "ultimate capacity" computed from Eq.

---

[11] "Pile Foundations," by Robert D. Chellis, McGraw-Hill Book Co., Inc., New York, N. Y., 1951, p. 527.

[12] *Ibid.*, p. 529.

[13] "Pile Driving Calculations with Notes on Driving Forces and Ground Resistance," by A. Hiley, *The Structural Engineer*, July and August, 1930.

11 and the "ultimate tip-test capacity." With respect to the average ratios shown in Table 6, it should be noted that formulas resulting in ratios greater than 1 are on the radical side, whereas formulas resulting in ratios less than 1 are on the conservative side. The ultimate capacities indicated by Eqs. 6 through 9 were considerably more than both the total capacity of the pile and the capacity of the tip alone (ratios of 1.5 to 4.0). Eqs. 10 and 11 indicated conservative ultimate capacities; the ratio of code capacity to test capacity ranged from 0.4 to 1.0.

TABLE 6.—COMPARISON BETWEEN TEST RESULTS AND PILE-DRIVING FORMULAS

Pile (1)	Total ultimate test capacity[a] (2)	Design short-time (test) load[b] (3)	Ultimate tip-test capacity[c] (4)	Design long-time (test) load[d] (5)	DYNAMIC FORMULAS Eq. 6 (6)	Eq. 7 (7)	Eq. 8 (8)	Eq. 9 (9)	Eq. 10 (10)	Eq. 11 (11)
					DESIGN CAPACITIES[e]					
C-1-B	343	172	185	123	230	243	92	97	45	51
C-2-B	162	81	80	53	109	123	45	52	19	21
C-3-B	145	73	90	60	118	183	46	78	18	19
C-4-B	244	122	165	110	118	92	46	37	29	29
C-5-B	304	152	185	123	230	244	100	101	43	54
C-6-B	452	226	280	187	238	204	92	79	48	55
C-7-B	287	144	140	93	230	56	100	19	59	39
					AVERAGE RATIOS[f]					
Average ratio of design capacity and Col. 3					1.35	1.30	0.55	0.53	0.27	0.28
Average ratio of design capacity and Col. 5					1.80	1.69	0.74	0.69	0.36	0.36
Average ratio of ultimate capacity and Col. 2[g]					4.05	3.90	1.65	1.59	0.41	0.55
Average ratio of ultimate capacity and Col. 4[g]					7.20	6.76	2.96	2.76	0.72	0.96

[a] The total test capacity was taken from Table 2. [b] Total ultimate test capacity divided by 2.0; that is, the factor of safety against plunging under a short-time load is 2.0. [c] The ultimate tip-test capacity was determined by inspection of tip-load curves. [d] Ultimate tip-test capacity divided by 1.5; that is, the factor of safety against detrimental settlement under a long-time load is 1.5. [e] Formula capacities indicated by the pile-driving formulas are design loads based on the driving resistance for the last 3 in. of driving. [f] Average ratios were computed by averaging data for individual piles. [g] Ultimate capacity indicates design formula capacity times suggested factors of safety.

SUMMARY OF RESULTS

Piles with a minimum diameter of 20 in. were recommended for the foundation of the structure to carry a load of 100 tons with little or no settlement. Octagonal piles were used for lengths up to 100 ft, and square piles were used for lengths greater than 100 ft.

The skin friction that can be developed by a friction pile in the clay at this site is nearly the same in tension as it is in compression and is approximately equal to the average strength of the clay, as indicated by unconfined compression tests and unconsolidated, undrained, triaxial-compression tests on undisturbed samples of the clay.

The average angle of internal friction in the foundation sand into which the piles were driven is estimated from analysis of the pile-loading test data to be between 30° and 35°, which values are considered reasonable for this type of sand.

Methods *a* and *d* are believed to be the most reasonable theoretical methods of those considered for use in estimating the capacity of a pile tip driven into sand in that they allow for the frictional resistance of the sand along the side of the tip. All methods considered are rather empirical and, although useful for estimating purposes, they should not replace load tests. This is borne out by the scattered results and lack of complete agreement of the pile tests with the capacities indicated by theoretical methods.

In general, capacities of piles computed by the various dynamic pile-driving formulas did not check with the ultimate total test load or ultimate tip load, or the design total or tip loads.

Conclusions

Skin friction that can be developed by a friction pile in clay in the area near Morganza can be estimated satisfactorily by using the average strengths indicated by unconfined or unconsolidated, undrained, triaxial-compression tests on undisturbed samples of the clay.

A reasonable estimate of the bearing capacity of a pile driven into deep, relatively dense sands can be made by using method *a* or method *d* and an average angle of internal friction in the sand of 30°. The results obtained should be used only for estimating purposes.

The use of dynamic pile-driving formulas is not warranted for long, large-diameter piles that are to be heavily loaded.

Acknowledgments

The pile-loading tests described were performed under the general direction of the Engineering Division of the Mississippi River Commission, Corps of Engineers, United States Department of the Army. The testing program and interpretation of the test data were planned by the Soils Division of the Waterways Experiment Station in Vicksburg, Miss. The pile tests were performed by the New Orleans District of the Corps of Engineers.

DISCUSSION

John W. Dunham,[14] M. ASCE.—The type of information offered by the authors is the material of which the science of pile design must be built. The data on piles C-4-A, C-4-B, and T-4 are particularly valuable in this respect because of the detailed quantitative data on the piles, the soil, and the tests.

The question of what constitutes failure of a pile under test loading is important. A confusing ambiguity would be resolved if engineers could agree on a definition. It is believed that failure should be defined in terms of the movement of the pile head as that is the quantity that affects the behavior of the superstructure. The following criterion has been used by the writer to determine, from test results, whether or not a pile is satisfactory for the design load:

> For the test to be considered successful, the head of the pile must not settle more than 0.01 in. per ton under any increment of test load before the test load equals the design load, nor more than 0.02 in. per ton under any increment of load before the test load equals twice the design load.

That is, among other things, a test pile must carry at least twice its design load before the slope of the load-deflection curve becomes steeper than 0.02 in. per ton; that slope is a criterion of failure. The slope of the load-deflection curve for pile C-4-A exceeds this value at 90 tons; that for pile C-4-B exceeds it at 260 tons.

The writer concurs in the decision to discount the transient supporting value of the clay and feels that the design selected to carry the structure was proper. Although the propriety of the design is not questioned, certain interpretations of the data are of importance to the understanding of pile behavior and should be examined further.

The values of the angle of internal friction that were derived from the test results appear to be quite low. The resistance to the driving of the sample spoon, the pile-driving record, and the 80% relative density that was cited, all indicate a dense sand. The sand is further described (under the heading, "Introduction: Foundation Conditions") as a "uniformly graded fine sand composed of subrounded to subangular grains." Representative values of ϕ indicate[15] that the angle of internal friction for such a sand should be approximately 40°.

The load-deflection diagram for pile C-4-A (Fig. 4) shows the typical failure of a pile in clay. The total settlement under the last loading was approximately 3.13 in. or 0.035 in. per ton of load. The settlement was probably limited by the possible travel of the jack. It would be valuable to know what load was on the jack when the pile head stopped moving. This information would make it possible to estimate the value of sliding friction, which apparently was substantially less than that of static friction, through the clay.

---

[14] Supervising Structural Engr., Public Bldgs. Service, Washington, D. C.

[15] "Soil Mechanics in Engineering Practice," by Karl Terzaghi and R. B. Peck, John Wiley & Sons, Inc., New York, N. Y., 1948, p. 82.

The load-deflection diagram for pile C-4-B (Fig. 5) appears to show the same sort of failure even though the pile tip was in sand. The total settlement under the last loading was approximately 2.46 in. or 0.0095 in. per ton of load. It would be pertinent to know if the pile showed any signs of coming to rest under the final load and why the loading was not continued until a greater settlement was recorded.

The low value derived for ϕ, the shape of the load-deflection curve for pile C-4-B, the comparatively small total settlement of that pile, and the lower value indicated for sliding friction on pile C-4-A suggest the following possibilities:

1. The sharp break in the load-deflection diagram for pile C-4-B represents the beginning of the transition from static friction to sliding friction in the clay.
2. The transition preceded shear failure of the sand.
3. The settlement did not proceed far enough to produce a shear failure in the sand.

It is hoped that the authors can supply the additional information and that they will comment on the suggested possibilities. They have earned the gratitude of the profession for making available this information and their method of dealing with the problem.

LEROY D. GRAVES,[16] A.M. ASCE, AND JAMES E. BINCKLEY,[17] J.M. ASCE. —The type of data presented by Messrs. Mansur and Focht is sorely needed in soil mechanics. However, the computation methods presented as Eqs. 1 through 5 would not have predicted either the bearing capacity or pull-out resistance actually encountered in a series of test piles at the site of the sewage-treatment plant for South Bend, Ind.; these pile tests were made in May and June, 1953. The load-movement curves for these tests are presented in Figs. 14 and 15, and the boring logs for the site are presented in Fig. 16. The site is adjacent to the St. Joseph River, and the water table is at the ground surface.

The failure loads of the test piles determined by the five methods used by the writers are presented in Table 7(*a*). In Table 7(*b*), under the heading, "Eq. 1," there are listed the friction angles that would be necessary to produce the failure loads computed from Eq. 1, using an effective soil weight of 50 lb per cu ft; obviously, the soil could not have such friction angles. Reasoning that the driving of a pile could produce passive soil pressure on its side, a new computation was made using Eq. 1, with the modification that f_s was made equal to the average Rankine's passive pressure in the sandy soil multiplied by the tangent of ϕ. The friction angles required to produce the failure loads by this computation were reasonable, as shown in Table 7(*b*) under the heading, "Eq. 1 (modified)."

Comparison between the boring logs in Fig. 16 and the soil conditions at Morganza shows immediately why the reasonable ϕ-values in Table 4 were obtainable with Eq. 1 at the Morganza site but not at South Bend. The

---

[16] Associate Prof. of Civ. Eng., Univ. of Notre Dame, Notre Dame, Ind.

[17] Engr., North American Aircraft, Inc., Downey, Calif.

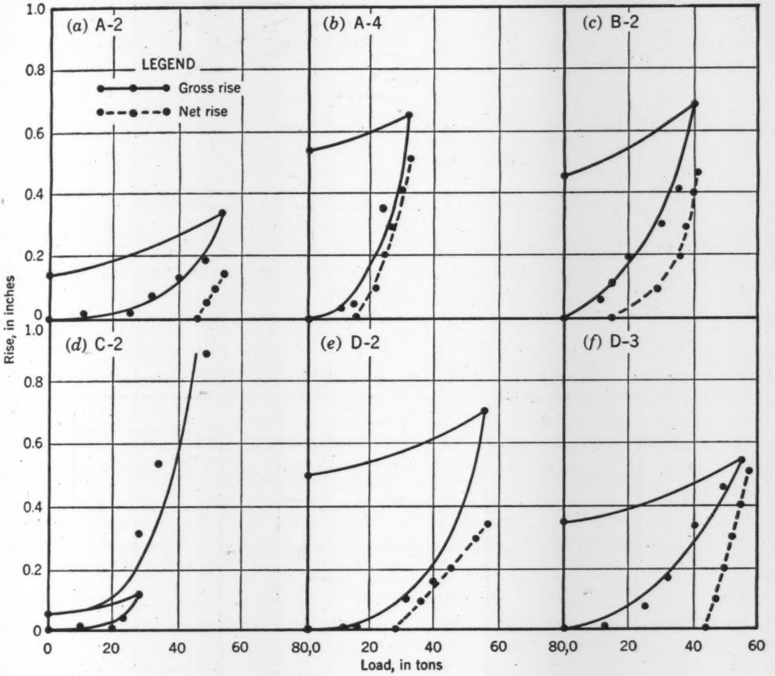

FIG. 14.—LOAD-RISE CURVES

TABLE 7.—TEST-PILE FAILURE LOADS, IN TONS, AND FRICTION ANGLES, IN DEGREES, FOR SOUTH BEND, IND.

Pile	Pile length, in feet	(a) FAILURE LOADS AS DETERMINED BY						(b) FRICTION ANGLES	
		0.25-in. net settlement	Tangent intersection of gross-settlement curve	Inspection of gross-settlement curve	Slope of net-settlement curve 4 times slope of elastic-settlement curve	Inspection of net-settlement curve	Average of five methods	Eq. 1	Eq. 1 (modified)
A-2[a,b]	34.83	...	45.5	45.0	47.4	47.2	46.3	45	23
A-4[a,c]	18	25.2	17.8	15.0	16.5	18.5	18.6	61	30
B-2[a,d]	31	36.8	33.4	35.0	38.5	32.9	35.3	49	25
C-2-1[e,f]	21.83	...	33.0	33.0	...	45.0	37.0	51	34
C-2-6[a,f]	21.83	...	29.3	28.0	...	...	28.7	64	32
D-2[a,g]	25	48.5	26.5	29.5	27.0	30.0	32.3	54	27
D-3-2[e,g]	28	...	51.0	41.0	71.0	95.5	64.6	52	32
D-3-3[a,g]	28	49.8	41.5	36.9	47.0	43.7	43.8	56	28
Average								54	29

[a] Tension test. [b] Concrete step taper, 10 in. by 14 in. [c] Concrete step taper, 10 in. by 12 in. [d] Wood, 8 in. by 12 in. [e] Compression test. [f] Wood, 8 in. by 10 in. [g] Concrete step taper, 10 in. by 13 in.

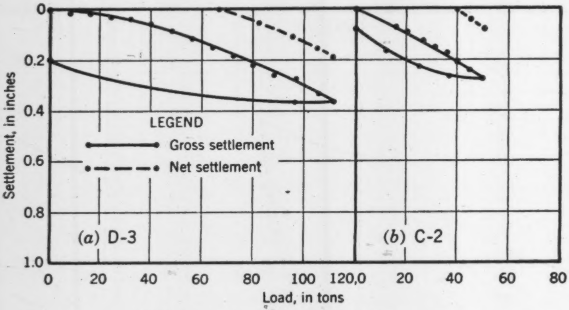

FIG. 15.—LOAD-SETTLEMENT CURVES

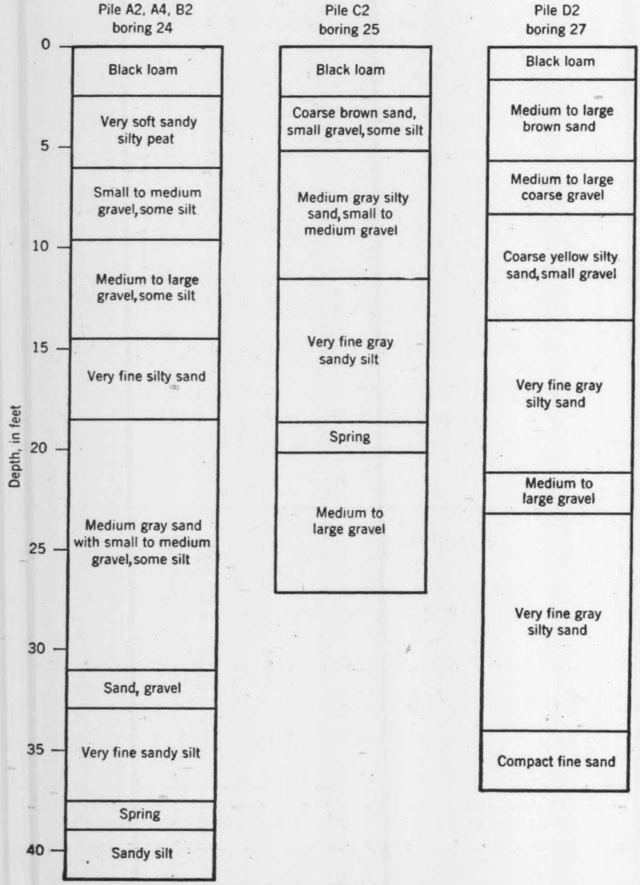
Pile A2, A4, B2
boring 24
Pile C2
boring 25
Pile D2
boring 27
Depth, in feet
0
5
10
15
20
25
30
35
40
Black loam
Very soft sandy silty peat
Small to medium gravel, some silt
Medium to large gravel, some silt
Very fine silty sand
Medium gray sand with small to medium gravel, some silt
Sand, gravel
Very fine sandy silt
Spring
Sandy silt
Black loam
Coarse brown sand, small gravel, some silt
Medium gray silty sand, small to medium gravel
Very fine gray sandy silt
Spring
Medium to large gravel
Black loam
Medium to large brown sand
Medium to large coarse gravel
Coarse yellow silty sand, small gravel
Very fine gray silty sand
Medium to large gravel
Very fine gray silty sand
Compact fine sand

FIG. 16.—BORING LOGS

shallow sand embedment at Morganza coupled with the 80-ft clay overburden made the point-bearing capacity of the pile a much larger part of the supporting power than the side friction in the sand; thus, the value of f_s had little effect. However, the South Bend site had only a little soft peaty overburden with most of the pile embedded in a sandy soil. This condition caused the side friction to be by far the larger part of the supporting power of the pile and, of course, all of its resistance to being lifted. Thus, f_s became the most important factor and could consequently be evaluated more accurately.

On the basis of the results of the South Bend tests, the statement in the "Conclusions" relative to the bearing capacity as determined from method *a* or method *d* might be revised to:

A reasonable estimate of the bearing capacity or pull-out resistance of a pile driven into sand may be made by using method *a* or method *d* using the ϕ-angle appropriate to that sand and assuming that the lateral pressure against the pile is Rankine's passive pressure for the sand.

Acknowledgments.—The South Bend pile-loading tests were performed under the supervision of Consoer, Townsend and Associates of Chicago. The pile tests were made by the Raymond Concrete Pile Company of New York, N. Y.

JAMES F. MCNULTY,[18] A. M. ASCE.—In computing the theoretical bearing capacity of a pile driven through clay into sand, the authors utilize Eq. 1*b* for ultimate skin friction on a pile in sand. The use of this equation is unjustified both theoretically and empirically. In a two-dimensional problem of plane strain, Coulomb's equation states that sliding will occur in an ideal sand when the shearing stress on any surface is equal to the product of the normal force and the tangent of the angle of internal friction; the three-dimensional problem has not been solved. Thus, Eq. 1*b* is theoretically unwarranted. Similarly, the use of $f_s = c$ for a clay is theoretically unjustified; its use, however, is prevalent because it often checks test data fairly accurately as in the case reported. If the authors are proposing the use of

$$f_s = \sigma \tan \phi \quad \text{(12)}$$

for empirical reasons, more evidence is required for its influence is negligible in this case.

It is believed that a somewhat sounder theoretical solution for the ultimate bearing capacity could be obtained by choosing ϕ and f_s (for sand) on the basis of the penetration value for the sand. This method results in the approximate values, $f_s = 2{,}000$ lb per sq ft and $\phi = 35°$.

In Table 8 there is indicated the percentage error involved in computing the theoretical capacity for the piles tested by the authors based on the following assumptions: (1) 65-ft imbedment of A piles in clay; (2) 70-ft imbedment of B and T piles in clay; (3) 5-ft imbedment of B and T piles in sand; (4) 10-ft surcharge; (5) f_s of 660 lb per sq ft for clay; (6) f_s of 2,000 lb per sq ft for sand; (7) $\phi = 35°$; and (8) point-bearing pressure in sand expressed as

---

[18] Structural Engr., National Advisory Comm. for Aeronautics, Langley Field, Va.

$A\gamma D_f N_q$ in which A is the point area, $\gamma = 50$ lb per cu ft, and the other omitted terms are negligible.

It should be noted that, although the errors are within estimating accuracy, it is because of the accuracy with which the skin-friction value of the clay has been approximated. As is revealed in Table 8, the percentage error for the piles in the clay stratum is under 10%; this is exceptional accuracy. Table 9(*a*) has been prepared to show the error associated with estimating the capacity of the pile in the sand stratum; the following assumptions are made: (1) Tip load failure is equal to the B-pile load failure less 70/65 of the A-pile load failure; and (2) theoretical tip failure is expressed by $A\,\gamma\,D_f\,N_q + 2\,\pi\,R\,h\,f_s$.

It is apparent that the estimates obtained are unreliable; analysis, however, does indicate a significant fact. Table 9(*a*) reveals that the theory gives accurate results for a pile diameter of 12 in., yields underestimations for diameters less than 12 in., and makes overestimations for diameters greater than 12 in.; that is, the unit failure point-bearing load is inversely affected by point area.

TABLE 8.—ERROR IN CAPACITIES

Pile	Theoretical capacity, in tons	Failure load from gross-settlement curve, in tons	Percentage error, plus or minus
C-1-A	130	125	4
C-1-B	438	320	37
T-1	170	130	31
C-2-A	72	78	8
C-2-B	117	145	19
T-2	87	120	27
C-3-A	65	56	14
C-3-B	152	145	5
T-3	85	85	0
C-4-A	97	80	21
C-4-B	278	230	21
T-4	128	125	2
C-5-A	130	137	5
C-5-B	438	305	44
T-5	170	>160	...
C-6-A	163	165	1
C-6-B	633	450	40
T-6	213	>150	...
C-7-A	152	135	13
C-7-B	487	285	70
Average, A piles			9
Average, B piles			34
Average, T piles			15
Average, all piles			20

Assuming f_s for sand to be equal to 2,000 lb per sq ft and subtracting its influence from the capacities in Table 9(*a*) results in the values listed in Table 9(*b*).

In Fig. 17 the failure loads from the test are shown to fall below the theoretical failure loads for the larger diameter piles. It is realized that insufficient test points are available to plot the test curve with certainty; however, there is an indication that Eq. 1*a*, used for estimating the capacity of shallow footings, could be utilized for estimating the point capacity of a pile if modified by a tip-area factor (α).

A formula for the tip capacity of long piles would then be

$$Q_p = \alpha\,A\,\gamma\,D_f\,N_q \ldots\ldots\ldots\ldots\ldots\ldots (13)$$

Values of α as functions of tip area could then be plotted. For example, Fig. 18 is based on the curves in Fig. 17. The equation for the straight part of this curve is

$$\alpha = 2.2 - 0.6 \log 144\,A \ldots\ldots\ldots\ldots\ldots\ldots (14)$$

TABLE 9.—ERROR IN TIP CAPACITIES OF PILES DRIVEN INTO SAND

Pile	(a) FRICTION FROM SAND STRATUM INCLUDED			(b) FRICTION FROM SAND STRATUM EXCLUDED		
	Theoretical tip capacity, in tons	Tip-failure load, in tons	Percentage error	Theoretical tip capacity, in tons	Tip-failure load, in tons	Percentage error
C-1-B	298	185	+ 61	268	155	+ 73
C-2-B	40	61	− 34	30	51	− 39
C-3-B	82	85	− 4	67	70	− 4
C-4-B	173	144	+ 20	150	121	+ 24
C-5-B	298	157	+ 90	268	127	+111
C-6-B	458	272	+ 68	420	234	+ 80
C-7-B	323	140	+131	286	103	+180

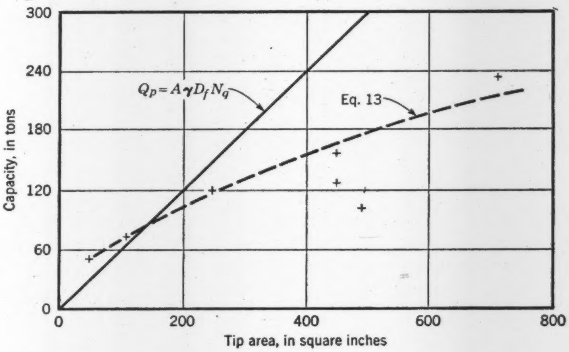

FIG. 17.—CORRELATION OF THEORETICAL AND TEST RESULTS

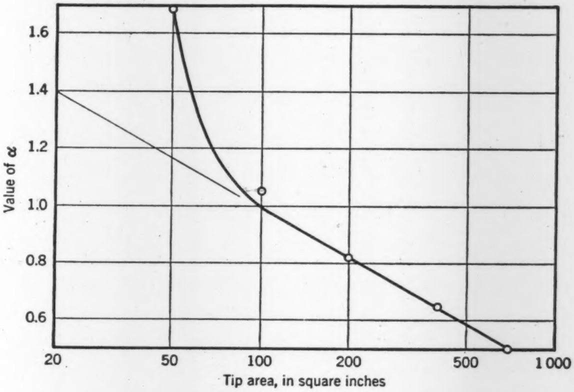

FIG. 18.—THE RELATIONSHIP BETWEEN α AND TIP AREA

Thus, the complete equation for estimating the capacity of a B pile would be

$$Q = 2\pi R(l f_s + h f'_s) + (2.2 - 0.6 \log 144 A) A \gamma D_f N_q \ldots\ldots (15)$$

in which l is the imbedment in clay, h denotes the imbedment in sand, and f'_s is the skin friction in sand.

There is (as of 1955) no satisfactory theoretical method available to estimate either the skin-friction value of a pile in sand or its point-bearing capacity. It is not known whether the refinement of α suggested herein is empirically sound. Hindering progress greatly is the paucity of joint soil and test results such as the authors' report. Messrs. Mansur and Focht are to be congratulated both for their concise, complete report and for the methods utilized in the testing. This is exactly the type of paper which is urgently needed; it should be used as a pattern for future testing and reporting.

CHARLES I. MANSUR,[19] M. ASCE, AND JOHN A. FOCHT, JR.,[20] A. M. ASCE.—The movement of the pile head is important in the interpretation of pile-loading tests and should be given consideration in the design of a structure and the pile foundation, as Mr. Dunham has emphasized. However, the question of what constitutes failure of a pile can be answered only in relation to the proposed structure and its desired characteristics. Usually considerable movement of the pile head will result from elastic deformation of the pile and the surrounding soil as the load is applied. Generally, this type of movement is not detrimental to a structure because it occurs as the weight of the structure is progressively increased during construction. Therefore, it is important to distinguish between complete failure of a pile and whether or not the movement of the pile head is more or less than an arbitrarily selected amount. Although deformation of the pile head is important in the design of a structure and some minor damage might occur if it were excessive, knowing the capacity of the pile from a failure standpoint appears to be of much greater importance.

The criterion to determine a design load proposed by Mr. Dunham is considered to be satisfactory for relatively short or lightly loaded piles, and this criterion was one of the procedures initially used for determining the failure load of a test pile; it was discarded after preliminary trials. For long piles that are heavily loaded, the elastic deformation of the pile and soil may be initially greater than 0.01 in. per ton of load, as with piles C-1-A, C-2-A, C-3-A, C-3-B, and C-5-A. According to Mr. Dunham's criterion, these piles would not be suitable to carry any load. Mr. Dunham suggests that the "slope of the load deflection curve" be a criterion of failure, but in determining a value of 90 tons for pile C-4-A and 260 tons for pile C-4-B he apparently selected the point at which the total movement became more than 0.02 in. per ton of load. Averaging the results indicated by several methods of analysis appears to be the most desirable procedure for determining the pile-failure load if the test is not performed under a specific building code.

The value of the angle of internal friction, ϕ, found in laboratory tests on undisturbed samples of similar sands in the Lower Mississippi Valley is approximately 35°. No triaxial tests were performed on undisturbed or remolded sand samples from the site of the pile tests. The high driving resistance of the standard split spoon in the sand at this location is believed to be caused, in part, by the depth of the sand. Extensive investigations of split-spoon driving resistance and cone-penetration resistance tests have indicated[21] that the penetration resistance is materially affected by physical dimensions (such as depth and water table) and by soil properties other than relative density and the angle of internal friction. It is doubtful that the value of ϕ is as high as 40°, as suggested by Mr. Dunham, but it may be more than the 30° that was indicated.

---

[19] Asst. Chief, Embankment & Foundation Branch, Soils Div., U. S. Waterways Experiment Station, Vicksburg, Miss.

[20] Associate Engr., Greer & McClelland, Houston, Tex.

No measurements were made to determine the sliding friction in the clay. It was noted during the tests that the load required to maintain motion of the piles decreased after reaching a maximum (for example, pile C-5-A and C-6-A). It is interesting to note that measurements of skin friction during dynamic driving of piles in another test-pile program in the same type of soil[22] indicated values comparable to the undisturbed, unconfined shear strength of the soil.

Mr. Dunham suggests that the settlement of the B piles was not sufficient to produce failure in the sand. However, the maximum settlement of pile C-4-B was approximately 15% of the pile diameter, which should be sufficient to produce failure. If the sharp break in the load-deflection diagram were the beginning of the transition from static to sliding friction—not failure in both the sand and clay—there should have been a second break in the curve resulting in an S-shape (similar to the tip-load curve for pile C-5-B in Fig. 6) when the movement of the pile tip became sufficient to develop load-carrying capacity in the sand. However, the settlement continued to increase at an increasing rate with increasing load after the sharp break. The tip-load curves in Fig. 6 are intended to illustrate the load being carried by the tip of the pile. These curves indicate that substantial loads were being carried by the sand and that failure did take place in the sand. Therefore, it is concluded that the sharp break in the load-settlement curve represents failure in both the clay and the sand.

Messrs. Graves and Binckley suggest, on the basis of pile-loading tests at South Bend, that the coefficient of lateral earth pressure on a pile in sand may be equal to the Rankine passive pressure rather than 1.0 as used in methods *a* and *d*. It has been learned (by correspondence) that Messrs. Graves and Binckley had used values of N'_q and N'_γ for "local" shear in computing the indicated friction angle given in Table 7—rather than N_q and N_γ for "general" shear as used in Fig. 8. It is the opinion of the writers that values of N_q and N_γ for general shear are more applicable for piles driven into sand and gravelly deposits than values for local shear. Although N'_q and N'_γ are sometimes used for computing the bearing capacity of footings founded in very loose sands, it is believed that vibration and displacement caused by driving a pile in a cohesionless deposit would make the soil in the vicinity of the pile so dense that values of N_q and N_γ are more appropriate for computing skin friction along a pile than values of N'_q and N'_γ. It is not considered appropriate to compare the data in Table 4 and Table 7 because different formulas were used in computing the data. Use of the Rankine passive pressure on a pile in computing the angles of internal friction listed in Table 4 would result in even smaller indicated values of ϕ by methods *a*, *c*, and *d*. The writers are of the opinion that the value of K to be used in computing the skin friction of piles founded in sand lies between 0.5 and 3.0; using $K = 1.0$, together with values of N_q and N_γ for general shear, is considered reasonable or slightly conservative.

---

[21] "Standard Penetration Tests, Reid-Bedford Sand, Mississippi River," *Potamology Investigation Report No. 5-5*, U. S. Waterways Experiment Station, Vicksburg, Miss., May, 1950.

[22] "Steel and Timber Pile Tests, West Atchafalaya Floodway, N.O.T. & M. Railway," *Bulletin No. 489*, Advance Report of Committee 8, A.R.E.A., September-October, 1950, p. 149.

Mr. McNulty objects to the use of Eq. 1*b* for skin friction in sand as being both theoretically and empirically unjustified. It was assumed in writing Eq. 1*b* that the coefficient of lateral earth pressure was 1.0. Theoretically, the frictional force of sand on concrete, wood, or steel should increase with increasing normal force. The use of ϕ as the angle of friction between soil and concrete is routine in earth-pressure computations for retaining walls when consideration is given to the friction between the soil and the wall. Therefore, Mr. McNulty's general objection appears unwarranted. In any case, Mr. McNulty and Messrs. Graves and Binckley are correct in noting that the influence of skin friction in sand was small in the Morganza tests.

Nevertheless, Mr. McNulty cannot obtain a "sounder theoretical solution * * * on the basis of the penetration value for the sand" as the correlation of ϕ and penetration resistance is not only empirical but one with a large possible error. The value of f_s equal to 2,000 lb per sq ft apparently is from a source[23] which is based on tests on short piles. It is stated therein: "In every sand the average skin friction per unit area of contact * * * increases with increasing depth." Thus, the skin friction to be expected at a considerable depth might be more than 2,000 lb per sq ft. The skin friction developed by sand at a depth of 85 ft, using ϕ equal to 30° and a lateral earth pressure equal to the Rankine passive pressure, is 7,350 lb per sq ft. For an earth pressure coefficient of 1.0, the value of f_s would be 2,450 lb per sq ft, which is only slightly different from Mr. McNulty's value of 2,000 lb per sq ft.

In the development of Tables 8 and 9, to show the percentage error involved in estimating the pile capacity, Mr. McNulty did not give any consideration to the actual variation in penetration. He thereby included in his tabulated error the potential error which would be involved in predicting the penetration into sand. If a curve such as is shown in Fig. 18 and the equation (Eq. 14) derived therefrom are to be developed, the actual penetration of each pile into sand should be utilized. Furthermore, as the skin friction in the sand may have been of somewhat greater value than that used by Mr. McNulty, the refinement suggested does not appear to be justified. It also appears that Mr. McNulty neglected to carry forward the algebraic sign of his computed percentage error in averaging the error.

Fig. 9, as well as Table 9, indicates that the potential error in estimating the bearing capacity of the pile tip is large and possibly unconservative for large-diameter piles. The close agreement for a 12-in. pile between Mr. Mc-

---

[23] "Soil Mechanics in Engineering Practice," by Karl Terzaghi and R. B. Peck, John Wiley & Sons, Inc., New York, N. Y., 1948, p. 461.

Nulty's theoretical computation and the test data is accounted for by the values of f_s and ϕ assumed in his computations. For other assumed values of f_s and ϕ, agreement between computations and test results will be indicated at other pile sizes. Fig. 9, which is based on the indicated value of ϕ equal to 30°, shows an underestimation by the theoretical analysis for piles less than 20 in. in diameter. The writers feel that the scatter of data is too wide to justify more than very general conclusions.

The writers disagree with Mr. McNulty that the use of the value of the cohesion of clay for the skin friction on piles is unjustified, particularly in soft clays. Mr. McNulty states that $f_s = c$ often checks test data; this empirical agreement is ample justification for its use.

AMERICAN SOCIETY OF CIVIL ENGINEERS
Founded November 5, 1852
TRANSACTIONS

Paper No. 2811

EXAMPLES OF TIMBER-STRUCTURE FAILURES

BY MICHAEL N. SALGO,[1] M. ASCE

WITH DISCUSSION BY MESSRS. E. GEORGE STERN, RALPH H. GLOSS, AND MICHAEL N. SALGO

SYNOPSIS

There is presented a brief history of timber structures with particular emphasis on their part in the construction program of World War II. A description of the common causes of failure in timber structures is followed by a presentation of examples of timber-structure failures. The selected examples are discussed in some detail with explanations offered as to probable causes of failure. It is concluded that timber structures that are properly designed, constructed, and maintained have their place in the construction field.

INTRODUCTION

During the accelerated construction program of World War II, wood construction experienced perhaps the greatest expansion in its history. Framing systems using split-ring connectors and shear plates were widely used, and timber construction became an accepted component in the field of engineered construction. During World War II, the Bureau of Yards and Docks, United States Department of the Navy, designed and built timber structures for almost all types of shore establishments. These included "lighter-than-air" (LTA) hangars; glued and laminated drill-hall structures; floating drydocks; and numerous long-span structures for varying uses, such as aircraft plants, shipyard shops, and fabricating plants. Hundreds of millions of dollars were expended in the construction and maintenance of long-span timber structures by the Bureau of Yards and Docks in this period. It is of significance to note that relatively few major structural failures occurred during this tremendous construction program despite the pioneering nature

---

NOTE.—Published, essentially as printed here, in November, 1954, as *Proceedings-Separate No. 544*. Positions and titles given are those in effect when the paper or discussion was approved for publication in *Transactions*.

[1] Prin. Assistant to Dist. Civ. Engr., Third Naval Dist., Headquarters, New York, N. Y.

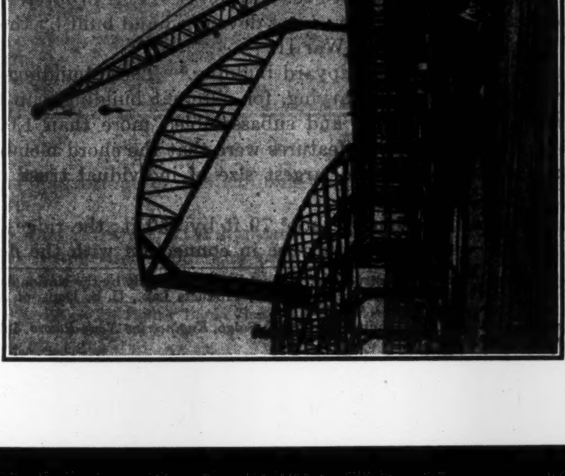

FIG. 1.—SHIPYARD SHOP BUILDING

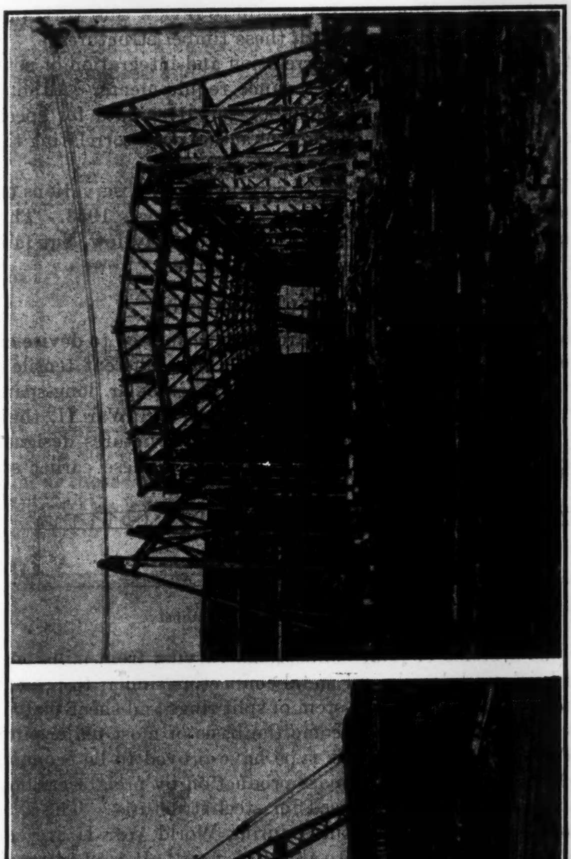

FIG. 2.—SHIPYARD SUBASSEMBLY SHOP

of many of the designs. However, it is useful to review this work and to take advantage of the experience gained with these timber structures.

The need has always existed for correlation and integration of new designs with practical construction and maintenance requirements. Although there is considerable literature available on laboratory test data for specific joint details, there has been a conspicuous lack of actual data correlating the results of tests and experiences with full-scale construction.

There will be presented subsequently certain actual observations of failures that occurred in timber structures from 1940 through 1953. The known failures of major timber structures have been relatively few, but failures did occur, and it is from these that lessons can be learned.

RESEARCH AND CONSTRUCTION

During the 1930's, considerable research was performed to devise connector systems which could economically develop the high inherent tensile strength of lumber.[2] Although the major and most spectacular long-span timber structures were built during and subsequent to World War II, there was a considerable number of unusual long-span timber structures designed, built, and standing before this time, mostly in Europe. These earlier structures included various systems of joint connections varying from mill construction to the use of hardwood dowels and metal connectors similar to present (1955) timber-connector systems. This system of split rings and shear plates evolved from a series of studies[2] and has become the basis of most major timber construction. Timber structures of this type have proved to be economical and subject to (*a*) standardization, (*b*) mass production by prefabrication, and (*c*) erection methods similar to those used for steel structures. The availability and use of long-span timber structures during World War II are considered to have been a major contribution to the war effort. It is of interest to note some typical examples of timber structures developed and built by the Bureau of Yards and Docks during World War II.

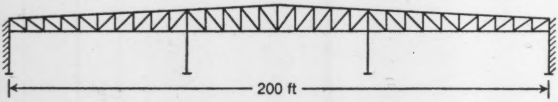

FIG. 3.—STANDARD WAREHOUSE BUILDING

Fig. 1 illustrates a standard shipyard building.[3] These buildings are 100 ft by 250 ft with a clear height varying, for different buildings, up to 25 ft. The buildings were prefabricated and subassembled more than 1,000 miles from their site. Other interesting features were that the chord members were glued and laminated and that the largest size of individual truss members was 4 in. by 6 in.

Fig. 2 illustrates a subassembly shop[3] 79 ft by 550 ft; the ridge height is 52 ft. The building was designed for use in connection with the destroyerescort construction program; an entire ship could be built at one time in this building. Doors 36 ft wide by 30 ft high were located in each bay to permit removal of the subassemblies, and two 5-ton bridge cranes were included within.

---

[2] "Modern Connectors for Timber Construction," Report Prepared Jointly by the National Committee on Wood Utilization, U. S. Dept. of Commerce and Forest Products Lab., U. S. Dept. of Agriculture, U. S. Govt. Printing Office, Washington, D. C., 1933.

[3] "Timber Rigid Frames," by C. G. Jennings and M. N. Salgo, *Engineering News-Record*, July 15, 1943.

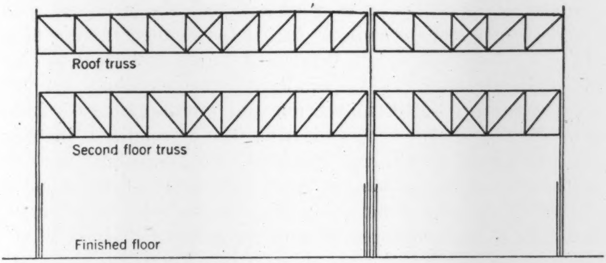

Fig. 4.—Shipyard Multistory Shop Building

Fig. 3 illustrates a standard 200-ft by 600-ft warehouse building. The structure has a 200-ft span with two intermediate supports; these dimensions are the same as those for a standard steel or reinforced concrete storage building.

Fig. 4 illustrates a multistory shop building. The lower floor was used as a shipfitters' shop whereas the second floor was used as a joiner shop. The lower floor had bridge cranes running on glued and laminated crane-runway girders.

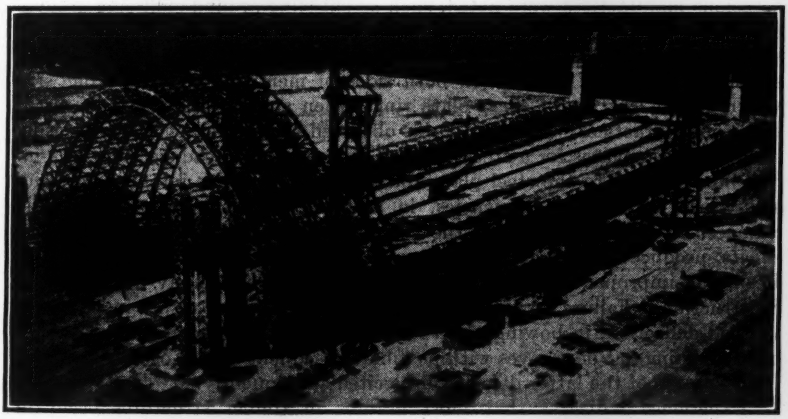

Fig. 5.—Standard LTA Hangar

Fig. 5 illustrates an LTA hangar.[4, 5] These hangars housed the airships that played such an important part in antisubmarine warfare during the early part of World War II. The hangar shell is 1,000 ft long and 176 ft high

---

[4] "Navy Develops All-Timber Blimp Hangars," by Arsham Amirikian, *Civil Engineering*, Vol. 13, 1943, p. 471.

[5] *Ibid.*, p. 525.

at the crown with an over-all width at ground level of 296 ft. These structures are among the largest timber structures ever built.

MAINTENANCE

As the many timber structures were erected, the need for establishing inspection and maintenance standards for timber-connector type trusses soon became evident. To this end, the Bureau of Yards and Docks prepared two publications[6, 7] in October, 1944. Similarly, two excellent articles[8, 9] contributed greatly toward better inspection and maintenance of timber structures. Some of the reasons necessitating the specialized inspection and maintenance pertained to design, material, workmanship, and conditions inherent in the system of framing in timber-connector type structures. Although most of the timber structures were designed by competent engineers, it was found that some structures were underdesigned because of the lack of design experience concerning the behavior of wood construction and in a few cases because of lack of competent engineering services. In many cases, particularly during the earlier war years, it was necessary under emergency conditions to use unseasoned and nonstructural material or unseasoned material of a lower grade than specified. Much of the lumber used received its drying while in place as structural framing. Also, the volume of construction increased so rapidly that it was practically impossible to have sufficient artisans properly trained and skilled in this comparatively new field. On many occasions malpractices were noted, such as chiseling around split-ring grooves to get a proper fit. Inaccurate drilling of holes and grooves, omission of split rings (this made erection easier but was not beneficial for structural strength), cutting of grooves on both sides of members when only one side was required, cutting of shear-plate rings when split rings were to be used, and similar practices. In 1952, it was observed that workmen were not using standard shear plates for a steel-to-wood connection; instead, sections of 4-in. pipe were welded to the steel plate and fitted into grooves intended for 4-in. split rings. All these deficiencies, in addition to problems of volumetric changes, flow in the wood, and the use of data that did not anticipate these effects, produced maintenance problems that were of appreciable significance. Results of improper maintenance manifest themselves in many ways in wood construction. Failure to tighten bolts periodically may result in excessive vertical deflection, in bowing and twisting of members, and in the split rings partly coming out of grooves with possible subsequent failure of the structure. One example of the latter defect will be cited subsequently.

Experience indicates that most failures in timber structures occur in individual truss members and do not result in the failure or collapse of the structure. There usually is an elastic or plastic readjustment among other framing members so that the stresses are redistributed to other members in the truss assembly.

---

[6] "Maintenance Procedure for Timber Trussed Structures," by O. C. Benson (Pt. 1 of Navdocks P-106), October, 1944.

[7] "Inspection, Maintenance and Repair of Timber Structures," by G. S. Friend (Pt. II of Navdocks P-106), October, 1944.

[8] "Timber Maintenance Methods," by Verne Ketchum, *Western Construction News*, January, 1945.

[9] "Are Timber Checks and Splits Serious?" by Verne Ketchum, Thornton K. May, and Frank J. Hanrahan, *Engineering News-Record*, July 27, 1944.

One of the factors causing the most failures noted in individual members occurred in unseasoned timbers where the slope of the grain was greater than that allowed for the lumber grade of the member. Such failures were observed in members of bracing systems and were particularly conspicuous when one timber of a double-timber member failed and the remaining timber showed no sign of distress.

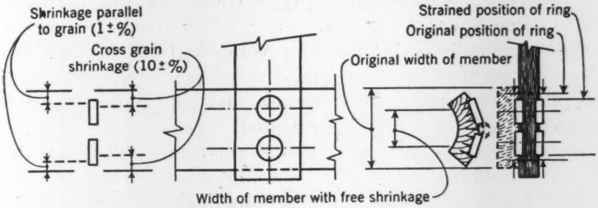
Shrinkage parallel to grain (1 ± %)
Cross grain shrinkage (10 ± %)
Strained position of ring
Original position of ring
Original width of member
Width of member with free shrinkage

FIG. 6.—EFFECT OF DIFFERENTIAL SHRINKAGE

One of the most important factors in timber-connector type trusses is the bolt-and-connector details in joints of trusses made with unseasoned timbers. The details should be arranged to minimize the effect of cross-grain shrinkage.

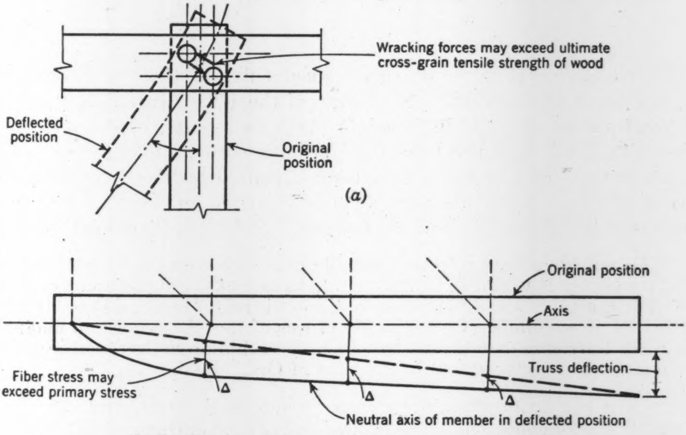
Wracking forces may exceed ultimate cross-grain tensile strength of wood
Deflected position
Original position
(a)
Original position
Axis
Truss deflection
Fiber stress may exceed primary stress
Δ
Δ
Δ
Neutral axis of member in deflected position

(b) Bending in members continuous over several panels

FIG. 7.—EFFECTS OF LARGE DEFORMATIONS

The importance of this factor is illustrated in Fig. 6. It is noted from Fig. 6 that:

a. Maximum stress conditions result from the use of unseasoned timbers.
b. Shrinkage parallel to the grain is practically zero.
c. The strength of timber parallel to the grain is high, which practically "fixes" rings in position.

d. Shrinkage perpendicular to the grain is relatively high.

e. The tensile strength perpendicular to the grain is weak.

f. As timber tends to shrink, the "fixed rings" produce substantial cross-grain tension stresses.

Experience with timber-connector type structures and particularly with parallel-chord trusses has been that deflections have been considerably in excess of those originally estimated from consideration of elastic strains. It has also been noted that in many cases "secondary stresses" resulting from elastic and plastic deformation of members and slip, plus stress deformation of ring connectors, cannot be safely neglected.

Fig. 7 illustrates the effects of large deformations. The joint detail (Fig. 7(*a*)) indicates wracking forces on the connectors that produce cross-grain tension. The bending stresses in continuous chord members caused by deflection of the trusses are illustrated in Fig. 7(*b*); the fiber stresses from this bending may at times exceed primary stresses. The complete analysis of complicated joints and "secondary stresses" may become extremely difficult and, at times, impracticable. One approach to this problem would be to investigate the effect of typical joint motions, to adopt standards for joint details, thus minimizing the effects of these motions, and to specify the use of reduced stresses for certain connector combinations. The use of suitable standards for joints and connections is advocated.[10]

FAILURES

LTA Hangars.—Perhaps the most spectacular of the timber structures developed are LTA hangars. The failure of the LTA hangars at Richmond, Fla., has been adequately discussed in previous reports. However, in connection with this failure, it is considered propitious to quote pertinent excerpts from a report before an annual meeting of Building Officials Conference of America, entitled "Joint Report on Investigation of Destruction During Hurricane of the Three LTA Hangars at the U. S. N.A.S. Richmond, Florida.":

> "Conclusions drawn from available evidence include: * * * Under the circumstances it would be unreasonable to expect the structures as designed to withstand the loading imposed and, since it might be considered unreasonable and uneconomical to design structures of this character and magnitude to meet hurricane conditions to which these buildings were subjected, the collapse may be considered in the 'Act of God' classification."

This was a case of structures properly designed, built, and maintained, but which failed when winds of unprecedented magnitude struck the area. Structures were designed for winds of 110 miles per hr whereas previous records had indicated a high of 87 miles per hr during a 5-min period and an extreme velocity (fastest mile) of 96 miles per hr for a 33-yr period. Actual winds at the time of failure were estimated to be at least 155 miles per hr as a 5-min average, 170 miles per hr as a 2-min average, 178 miles per hr for the fastest mile, and extreme gust velocities as high as 250 miles per hr—thus the "Act of God" classification. Attention is also invited to the fact that, exclusive of the Richmond hangars, the only factor used to determine whether the various LTA hangars were to remain in use was pure military necessity.

---

[10] "Draft of Proposed Recommended Specifications for the Design of Structural Timber Framing," Am. Inst. of Timber Construction, Washington, D. C., July, 1953.

Storehouse Building.—A failure that can be attributed to design occurred in a standard storehouse structure (200 ft by 600 ft) at an inland supply depot. Fig. 3 illustrates general framing of this structure. The 200-ft span had two interior supports and it was at the interior supports that actual failure occurred. The detail of the top-chord connection provided for the opposing ends of the chords to be attached to opposite sides of the top of the wide timber column. This arrangement caused high cross-grain tension stresses in the vertical members which caused splitting of the column and failure of the trusses. Fig. 8 further illustrates this failure.

At the time of the failure it was decided to have a complete inspection made of timber structures at the station. An engineering firm experienced in timber engineering accomplished this survey and inspection. Station personnel involved in maintenance of timber structures were assigned as observers and thus gained valuable experience. Revisions to the joint detail were made, and remedial work was accomplished by station forces.

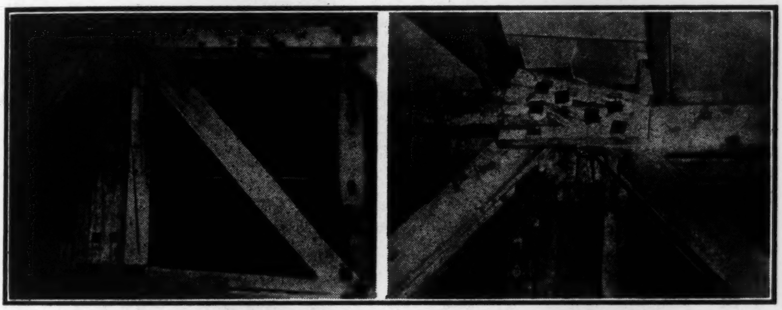

FIG. 8.—FAILURE IN STOREHOUSE BUILDING

Shipyard Shop.—As previously noted, experience with parallel-chord roof trusses has shown that actual deflections have been considerably in excess of predictions determined by use of existing design data. As a result there have been several cases where serious consequences have ensued.

In one case, in particular, this excessive deflection resulted in interference with operations of the bridge cranes in a shop. The question arose as how to restore the cranes to operation. Maintenance personnel, obviously inexperienced and unfamiliar with timber structures and without consulting the engineering staff of the shipyard, found a quick, easy answer—they cut off part of the ends of the web members that protruded below the bottom chord. This, of course, reduced the edge and end distance for all the cut web members in the trusses but provided the extra few inches needed for bridge-crane clearance. However, the trusses continued to deflect and, fortunately, the maintenance personnel referred the entire problem to the engineering staff. Further cutting of the end distances could have led to disastrous results.

Various schemes were used to keep the bridge cranes in temporary operation, such as removing all second-floor live loads. A major rehabilitation design using an ingenious system of steel-rod auxiliary framing was prepared by the public works design division. The structure has since been rehabilated to permit its full use in accordance with original design loading.

Aircraft Plant.—Early in World War II, considerable difficulties were encountered with timber trusses at one of the aircraft plants under construction. Numerous failures were experienced, and a report on conditions made by a firm of engineering consultants disclosed some interesting information. Two test trusses were set up using actual trusses scheduled to go into the structure.

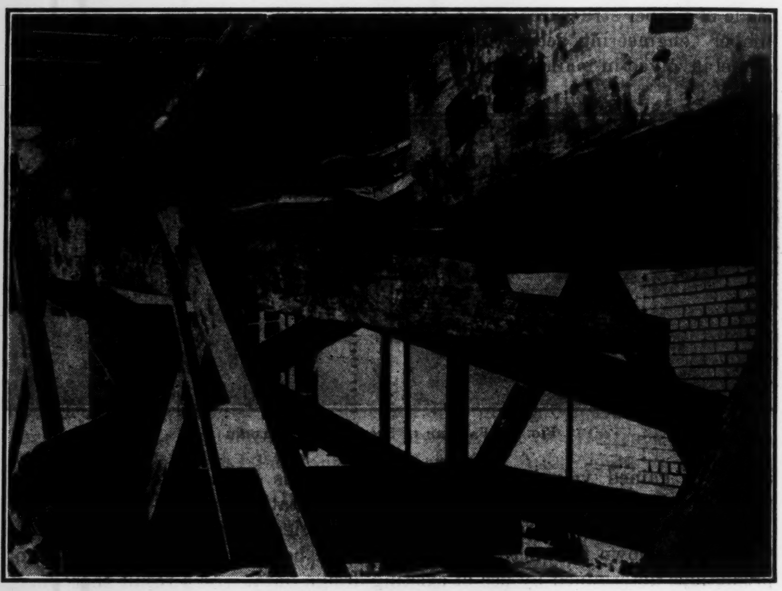

FIG. 9.—FAILURE IN TEST TRUSS

These trusses were considered to be better than the average of those being used. One of the trusses had the bolts tightened, whereas the other had the bolts slackened off one turn ($\frac{3}{32}$ in.). The truss with tightened bolts carried over two thirds more load than the truss with the slackened bolts. Fig. 9 showing the test trusses indicates some of the difficulties with unseasoned and inferior material, improper construction methods, and improper maintenance procedures.

Conclusions from this report were that failures were caused because bolt-tightening operations were not accomplished, inferior unseasoned material was used, and no precautions were taken to use this material judiciously so that

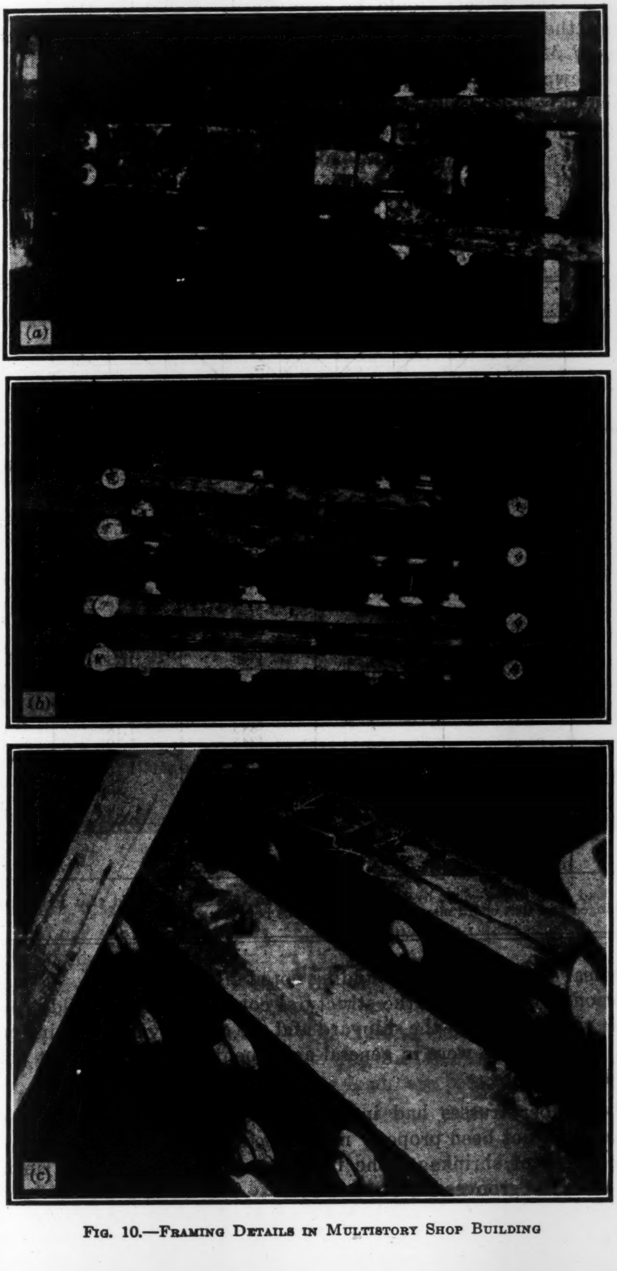

Fig. 10.—Framing Details in Multistory Shop Building

the effect of the defects would be minimized. Following the investigation and report, there were no further records of failures and unusual problems.

Shipyard Multistory Shop Building.—One of the most interesting failures from the viewpoint of the structural engineer concerns a shipyard multistory shop building. Fig. 4 illustrates the general framing arrangement for this building. Early in 1949, under conditions of no roof live load, practically no wind load, and no floor live loads, an upper roof truss collapsed. The second floor of this building was only in intermittent use at that time. Fig. 10 shows typical conditions in the building noted after the failure. Two separate investigations were made of the structural condition of this building—one by the public works officer of the shipyard and the other by a consulting engineering firm. The results were in general agreement; the more salient points are as follows:

TABLE 1.—DIRECT AND FLEXURAL STRESSES, IN POUNDS PER SQUARE INCH, FOR ACTUAL LOADS[a]

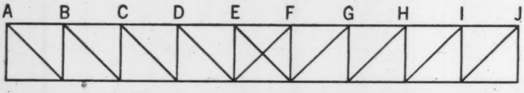

Member	Direct-Load Stresses		Flexural stresses	Total Stresses	
	Gross area	Net area		Gross area	Net area
AB	350	420			
			345	695	765
			345	954	1,085
BC	609	740			
			209	818	949
			209	986	1,139
CD	777	930			
			406	1,183	1,336
			406	1,259	1,516
DE	853	1,110			
			406	1,259	1,516
			406	1,256	1,424
EF	850	1,018			
			209	1,059	1,227
			209	1,052	1,219
FG	843	1,010			
			345	1,188	1,355
			345	1,100	1,338
GH	755	983			
			0	755	983
			0	582	688
HI	582	688			
			398	980	1,086
			398	728	792
IJ	330	394			

[a] Dead load = 58 lb per sq ft, live load = 40 lb per sq ft. It is assumed that web members and splices are hinged and that chord members are continuous between splices.

1. The timber trusses had in all probability been built of unseasoned lumber and had not been properly maintained. Figs. 10(*a*) and 10(*b*) clearly show the effect of shrinkage; the bolts became loose and the rings partly emerged from the grooves.

2. An analysis was made of the original design, taking into consideration secondary stresses caused by elastic, plastic, and shrinkage strains and various conditions of joint restraint in addition to primary stresses. In some cases the secondary stresses were computed to be as much as 300% of primary stresses. Table 1 shows representative results of the analysis for primary stresses.

3. The actual dead load of the roof was considerably in excess of the designed dead load. In addition, excessive deflections of the parallel-chord roof truss caused a "hollow" in the roof where there was a permanent additional dead load of water. The total constant permanent load was actually in excess of the designed dead load plus live load.

4. The design of the center splice was exceptionally weak. It was in this area that failure occurred. Fig. 10(*c*) shows conditions at the splice typical of the trusses that had not failed. The differential movement in individual chord members should be noted. Fig. 11 shows the truss that failed—the broken chord member and shifting at the splice.

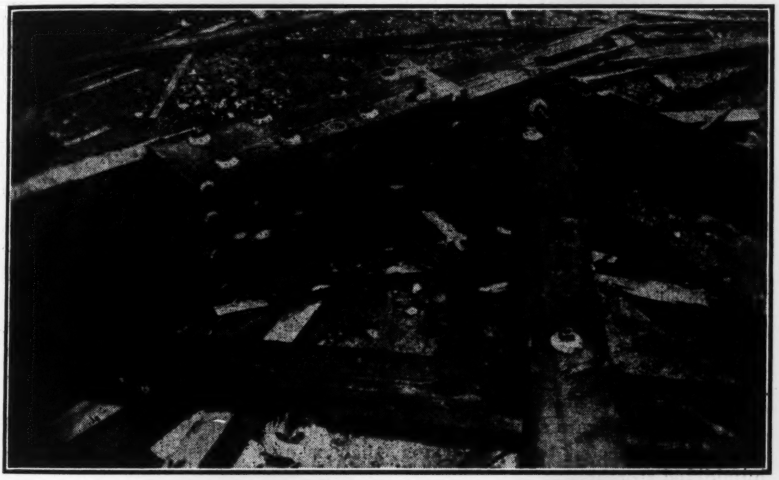

FIG. 11.—TRUSS THAT FAILED

This failure was actually caused by deficiencies in design, construction, and maintenance. However, on the basis of the reanalysis cited previously, repairs and extensive maintenance were accomplished. This building with an estimated value of $1,000,000 was rehabilitated for less than $40,000. However, the allowable second-floor live loads are somewhat less than those contemplated by the original design.

CONCLUSIONS

There have been presented examples of failures in timber structures, the causes of which have varied from the "Act of God" category to deficiencies in design, construction, and maintenance—and combinations thereof. A summary of conclusions based on this timber-structure experience follows:

a. Many of the difficulties encountered in parallel-chord roof trusses could have been eliminated or reduced by careful consideration of the bending stresses inherent in wood-framed structures caused by excessive deflections as a result of slip and strain in the connectors. Avoidance of the major part of the slip effects would have little effect on the construction costs and would encourage types of framing in which the slip would have a reduced effect; optimum framing would thus be achieved. Design of timber structures (particularly long-span, parallel-chord trusses) should, in addition to the usual analyses, include evaluation of secondary stresses resulting from movements of the connectors (slip and elastic deformation) and local stresses caused by eccentricities inherent in the framing system.

b. The effect of long-duration loads on the plastic yield of wood should be given further consideration in establishing the allowable design stresses. This could be done by reducing the allowable stresses for higher ratios of dead load to live load.

c. The timber bowstring truss, with or without timber connectors, has proved to be one of the most economical of roof-framing structures from both the initial cost and maintenance viewpoints. Failures and maintenance problems with bowstring trusses have been practically nonexistent.

d. If unseasoned lumber is to be used in trusses where the lumber will season in place, certain restrictions should be observed. One set of restrictions suggested for split-chord trusses or multiple-chord trusses other than bowstring would be that (1) no span shall exceed 75 ft; (2) the total length of unseasoned wood along the axis of a bolt for split-ring connections shall not exceed 13½ in., permitting 5-ft 3-in. nominal size members; (3) for all trusses in excess of 50 ft in span maintenance procedures shall be recommended on design plans; and (4) in truss joints with members in opposed grain arrangement, connectors shall be limited to a two-bolt pattern.

e. Particular care should be taken when unseasoned timber is to be used in trusses subjected to rapid drying, such as over ovens, boilers, or in dehumidified storehouses.

f. Maintenance and construction standards have been well established; there does exist an educational problem as there is a need for more widespread information. Articles [8, 9] on this subject are of considerable help. These articles are designed for reading by the engineers and artisans who are actually building and maintaining timber structures; more such articles are needed.

g. Most of the difficulties experienced with timber structures can be attributed to incomplete designs, the use of unseasoned and lower grades of lumber, and the lack of proper periodic bolt-tightening operations. Timber structures properly designed, constructed, and maintained have taken their place as major components in the construction program.

DISCUSSION

E. George Stern,[11] M. ASCE.—Reference has been made by Mr. Salgo to timber structures assembled with split-ring connectors and bolts. No details have been given as to the type of split-ring connector used.

Three types of split-ring connectors have been used in the United States. The original standard split-ring connector made of flat steel strips is still (1955) sold commercially. In 1939, the split-ring connector with inside bevels was introduced and, a few years later, the split-ring connector with inside and outside bevels was placed on the market, replacing its immediate predecessor.

Because of the apparent inherent advantages brought about by the use of bevelled split rings in comparison with flat split rings,[12] it is of interest to learn whether flat or bevelled split-ring connectors were used for the structures which showed joint failures. The bevelled split ring fits tightly into its precut groove. Consequently, both initial slip and joint deformation during load application can be minimized. This results in reduced truss deflection and smaller superimposed secondary stresses than encountered with use of flat-sided split rings.

In light of the importance of decreasing secondary stresses in structural assemblies, information on field experiences with flat-sided split-ring connectors versus bevelled split-ring connectors would be elucidating.

Ralph H. Gloss,[13] A. M. ASCE.—This review of wartime mistakes in timber construction serves as a helpful reminder of what can occur when designers, fabricators, contractors, and maintenance crews are literally forced to use a material with which they are not familiar or when they are in such a hurry that there is no time for proper application of what they do know.

The irony of the experience gained in World War II is that the mistakes and troubles were not a basic fault of the material and with few exceptions could have been avoided or certainly minimized; yet the limited number of unsatisfactory experiences of that period may have adversely affected some persons' opinions of timber construction. Others are undoubtedly influenced by lack of knowledge of the true cause of the trouble.

Each of the failures described by Mr. Salgo seems to have been avoidable, without need for any drastic change in design and construction practice with respect to truss type and method of framing or fastening. The paper, particularly some parts of the conclusions, can be construed as perhaps unintentionally placing the blame largely on truss types or fastening methods rather than on errors of design, fabrication, and maintenance.

The parallel-chord truss and flat truss with timber connectors were the popular trusses because of their adaptability to fast field fabrication, and unfortunately the troubles which resulted are therefore blamed by some on the truss type or on the fastening used rather than on the conditions of the times. It does not matter to some persons who have witnessed or learned of such troubles that they could and would have been avoided in normal times; just such troubles were avoided prior to World War II. The results would not have been substantially different if other truss types, such as the bowstring, had been used and subjected to the same abuses. With reference to the specific failures cited by Mr. Salgo, the general causes of failure would be likely to apply to any type of truss or else would certainly be avoidable.

---

[11] Research Prof., Virginia Polytechnic Inst., Blacksburg, Va.

[12] "A Study of Lumber and Plywood Joints with Metal Split-Ring Connectors," by E. George Stern, *Bulletin No. 53*, Pennsylvania State College Eng. Experiment Station, State College, Pa., 1940.

[13] Structural Engr., Timber Eng. Co., Washington, D. C.

The design inadequacy and cross-grain tension failure of the storehouse building would seem independent of truss type. At least one large warehouse project involved failure of bowstring trusses because of the same type of cross-grain tension; however, this occurred at eccentric web-member connections which are customarily used.

The deflection of the shipyard trusses was to be expected because of the unseasoned lumber. Ring grooves that have been cut grossly oversize for easy installation could account for some of the deflection. It is regrettable that sufficient design clearance was not provided so that the greater-than-expected deflection would not have hindered use of the building.

The test of aircraft plant trusses is of interest, and the better results of the tight trusses are in line with experience. The tight test truss, however, has no parallel in practice as seasonal variation in the moisture content of lumber causes all truss bolts to be slightly loose at some times during the year. In basic tests on which connector values are based, joints were used with bolts loosened ½ turn to minimize the unreliable friction present in a tight joint. It is not clear whether the test failures were caused by a joint or wood failure. It would be of interest to know whether adequate ratios of test to design loads were obtained even with the loosened joint truss.

The troubles occurring in the shipyard multistory building as a result of deficiency in design, construction, and maintenance would not seem to be restricted to flat trusses. The discussion of secondary stresses is of particular interest. It is recognized that secondary stresses do exist, but one may doubt the validity of most computations determining their magnitude as such computations involve too many critical assumptions with respect to joint fixity. The same elasticity, yield, or creep which permits more than expected deflection in unseasoned lumber trusses and thus theoretically causes large secondary stresses also acts to relieve the secondary stresses. If the overload or excessive deflection occurred quickly, a secondary stress analysis would have had more validity, but it is not felt to be applicable for a gradual increase in deflection, which is the usual case.

An interesting comparison to secondary stress computation for trusses is the theoretical computation of bending stress set up in one laminate of a curved laminated member as that laminate is bent to curvature. Theoretically, unit bending stresses of many thousands of pounds can be created by such bending, but there is adequate evidence that such stresses are quickly relieved. Similarly, an unseasoned beam in bending assumes a permanent set which, by the same reasoning as in the secondary-stress truss analysis, might be interpreted as setting up high secondary stresses, whereas the permanently set beam is just as strong as it was at first—perhaps stronger by reason of the seasoning.

The generally good experience with peacetime structures and with most wartime structures does not justify the author's concern over secondary stresses or eccentricities inherent in lapped joints (not confined to timber connectors). Although multiple or split-chord flat or pitched trusses are not as efficient as the bowstring truss for balanced loading, they are quite satisfactory when designed and built to accepted standards and need not be arbitrarily restricted in use.

In 1953 restrictions were proposed for trusses other than bowstring; they were similar to the restrictions reported by Mr. Salgo. However, the proposed restrictions were dropped after thorough consideration as being unnecessary and unrealistic.

Good performance of timber trusses is the result of proper design, fabrication, and maintenance where necessary; it is not restricted to any one type of truss, type of framing, or type of connection. When good practice is violated in any one of these three general fields of work, trouble may be expected—with other materials as well as with timber.

With respect to the restrictions offered under item *d* in the "Conclusions"—

1. Restriction of span is no cure for poor practice—larger spans can be just as satisfactory as smaller spans, or, conversely, smaller spans can be just as troublesome.

2. Length of wood on a bolt is a measure of need for tightening but not of adequacy. There is no evidence that joints with bolts or other fastenings are less in need of tightening than are those with timber connectors. The shrinkage for equal thickness is the same in a bowstring truss as in any other type of truss, and there would be the same general reduction in joint strength and increase in deflection for all truss types if joints were not tightened.

3. Inspection and maintenance are recommended for all types and spans of heavy trusses built of unseasoned lumber, including the bowstring truss. Freedom from maintenance is very little, if at all, related to span. No conclusive evidence has been offered that only a certain type of truss, system of framing, or type of fastening has a monopoly on freedom from maintenance; most trusses are maintenance-free except for possible bolt tightening. Any loose joint should be tightened, and any member structurally damaged by seasoning needs repair regardless of the type of truss in which it occurs.

4. As far as is known, no conclusive evidence is available to warrant restriction of the number of bolts with or without connectors in a joint, and there is little reason to suspect that bolts alone would be substantially different from connectors. The writer is familiar with data for bolts with connectors which indicate that three or four bolts with connectors are superior to two bolts with connectors. The same data indicate that recommended reductions in design loads for unseasoned lumber are adequate.

Michael N. Salgo,[14] M. ASCE.—Inquiry is made by Mr. Stern as to the type of split rings that were used in the structures cited. All the structures reported on had the standard split ring in use at that time—namely, the split ring with a bevelled inside face and flat outside face. In view of this, the desired information on field experiences with flat-sided versus bevelled split-ring connectors is not available from the writer.

Mr. Gloss is apparently of the opinion that the writer has placed the blame for failures encountered on truss types or fastening methods, rather than on the errors of design, fabrication, or maintenance; this was definitely not intended. On the contrary—particular care was taken to note the causes which were basically design, construction, and maintenance. Certain types of framing did have a higher incidence of failures than others and these were noted.

As Mr. Gloss indicates, the writer is of the opinion that the over-all performance of timber trusses during World War II was outstanding and that, as stated under the heading, "Research and Construction," "The availability and use of long-span timber structures during World War II are considered to have been a major contribution to the war effort." However, failures and difficulties did occur, and from these certain lessons can be learned.

One of the major sources of difficulties with parallel-chord trusses during World War II was the fact that actual deflections were considerably in excess of those which could have been predicted on the basis of available design data for deformation of split-ring joints under load. Subsequent design data increased the expected deflections for timber-connector type trusses. However, by this time, many timber-truss structures had been built which were cambered on the basis of the available design data. Results of this lack of information were manifested in a lack of clearance for bridge cranes, binding of large hanga doors, and similar difficulties. Where bowstring trusses were used, the effect of the deformation data was not as critical as in the parallel-chord trusses.

Mr. Gloss indicates particular interest in the matter of secondary stresses. Although recognizing the presence of the secondary stresses, he questions the validity of most computations determining their magnitude as such computations involve many critical assumptions. These assumptions are not necessarily as critical as Mr. Gloss indicates because the same assumptions that satisfactorily predict the total deflections (including creep effects) can also be used to predict member distress. Table 1 illustrates the results of such an analysis, which were subsequently used as the basis for necessary repairs and strengthening. However, these analyses are often quite difficult, time-consuming, and beyond the demands of ordinary design; for this reason, inclusion of certain limiting factors in building codes is justified.

There appears to be an honest difference of opinion concerning the proposed restrictions for trusses other than bowstring trusses where unseasoned lumber is used. To belabor this point further does not appear warranted. However, at the time this paper was prepared, the inclusion of the proposed restrictions was still pending (1953). A decision was subsequently made not to include the restrictions in the "Timber Construction Standards" of the American Institute of Timber Construction;[15] however, these restrictions are good practice, and the writer recommends their use.

---

[14] Prin. Assistant to Dist. Civ. Engr., Third Naval Dist. Headquarters, New York, N. Y.

[15] "Timber Construction Standards," Am. Inst. of Timber Construction, Washington, D. C., 1st Ed., 1954.

AMERICAN SOCIETY OF CIVIL ENGINEERS
Founded November 5, 1852
TRANSACTIONS

Paper No. 2812

A BRIEF FOR LIMIT DESIGN

BY GEORGE C. ERNST,[1] M. ASCE

WITH DISCUSSION BY MESSRS. ABDEL F. DIWAN, AND GEORGE C. ERNST

SYNOPSIS

The familiar concepts of slope and deflection are presented as a means of analyzing continuous beams and rigid frames for the evolution of plastic hinges and subsequent failure under static loadings. The presentation may be considered an argument in behalf of limit design in that the necessary relationship between load and deflection is demonstrated.

NOTATION

The letter symbols in this paper are defined where they first appear, in the text or by diagram, and are assembled alphabetically in the Appendix.

INTRODUCTION

Beyond the solely elastic state of stress, adjustments in slopes and deflections are necessary during the development of plastic hinges leading to the ultimate failure of a continuous beam or rigid frame. The necessary adjustments of slopes and deflections, consistent with static equilibrium, may be evaluated in such a manner as to reveal the position and evolution of the plastic hinges by the direct use of revised moment-area theorems, in which the angular yieldings of plastic hinges are included with a conversion to unit rotations (rates of change of slope) in place of $(M/E\,I)$-values (M denoting moment; E, Young's modulus; and I, the moment of inertia).

The conversion to unit rotations is accomplished by the substitution of a unit rotation diagram for an $(M/E\,I)$-diagram for computations of the elastic slopes and deflections that occur during the yielding of the plastic hinges. A

NOTE.—Published, essentially as printed here, in January, 1955, as *Proceedings-Separate No. 583.* Positions and titles given are those in effect when the paper or discussion was approved for publication in *Transactions.*

[1] Prof. and Chairman, Dept. of Civ. Eng., Univ. of Nebraska, Lincoln, Nebr.

unit rotation diagram, consistent with the type of loading, dimensions of the members, and properties of the materials, may be established for a structure because all sections, other than those yielding as plastic hinges, will be stressed below the free yield range. The basic shape of the unit rotation diagram will have the characteristics of a bending-moment diagram with all critical sections, consistent with static equilibrium, fully developed. Required bearing lengths and possibilities of localized failures, as well as the location and evolution of plastic hinges, may be established by the inclusion of the total angular yield of such hinges with the unit rotation diagram.

REVISED MOMENT–AREA THEOREMS

I.—The change in slope between any two points on the deflection curve of a flexural member is equal to the sum of the area of the unit rotation diagram and the angular yields of plastic hinges between the corresponding points thereon.

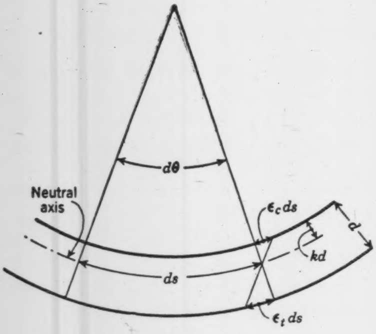

FIG. 1

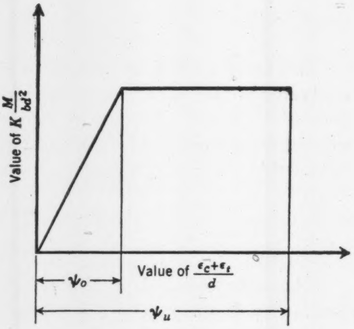

FIG. 2

II.—The departure of a point on the axis of an originally straight flexural member from the tangent to the deflection curve at another point is equal to the sum of the first or statical moment of the area of the unit rotation diagram and the first moments of the angular yields of plastic hinges between the corresponding points thereon, with respect to the point for which the deflection value is sought.

III.—The true slope at any point of a flexural member may be computed as the shear at the same point in a conjugate beam loaded with the unit rotation diagram combined with the angular yields of plastic hinges as concentrated loads located at their respective points of development.

IV.—The true deflection at any point of an originally straight flexural member, measured normally from its unloaded axis, is equal to the bending moment at the same point in a conjugate beam loaded with the unit rotation diagram combined with the angular yields of plastic hinges as concentrated loads located at their respective points of development.

CURVATURE PROPERTIES

A short length of a flexural member is shown in Fig. 1, for which the customary relationship between strain and rate of change of slope is expressed as

$$\left.\begin{aligned} d\theta &= \frac{\epsilon_c + \epsilon_t}{d}\, ds \\ \frac{d\theta}{ds} &= \psi = \frac{\epsilon_c + \epsilon_t}{d} \end{aligned}\right\} \qquad (1)$$

in which ϵ_c and ϵ_t are the maximum unit compressive and tensile strains, d is the depth of the member, and ψ is the angular rotation per unit length of member.

An idealized relationship between the unit rotation ψ and K $(M/b\,d^2)$ is illustrated in Fig. 2 in which the plastic range is included. The constant K is a function of the shape of the cross section, M is the bending moment, and b is the breadth of the section. A definite limit to the extent of plastic yield is shown, inasmuch as structural materials do not deform without limit. The maximum unit rotation must extend throughout a sufficient length of the flexural member to accumulate the required total angular change at a plastic hinge. In other words, the maximum total angle change at a specific section subjected to a constant moment is limited by the distance throughout which the maximum unit rotation extends.

Steel.—The plastic properties of structural steel in flexure have been subjected to extensive analytical and experimental research by others.[2,3,4] These studies have yielded broad basic principles for both design and analysis but have not provided a familiar approach to the more common types of indeterminate structures. Numerical values for Fig. 2 to be used with the methods of this paper as applied to steel construction may be obtained from the references cited.[2,3,4]

Reinforced Concrete.—For rectangular beams or T-beams of reinforced concrete which contain less than balanced reinforcement, $K = 1$. Expressions for unit rotation may be developed in the following manner for use with Fig. 2.

Equating the total compressive force to the total tensile force and neglecting the resistance of compression steel at the ultimate load,[5]

$$p\,f_s = k\,f_{av} \qquad (2)$$

in which p is the ratio of steel area to concrete area; f_s and f_{av} are steel stress and average concrete stress, respectively; and k is the ratio of distance between the extreme fiber and the neutral axis to the effective depth of the section.

Also, based on the assumption of the conservation of plane sections,

$$\frac{\epsilon_c}{\epsilon_t} = \frac{k}{1-k} \qquad (3)$$

---

[2] "Theory of Inelastic Bending with Reference to Limit Design," by Alexander Hrennikoff, *Transactions*, ASCE, Vol. 113, 1948, p. 213.

[3] "Recent Progress in the Plastic Methods of Structural Analysis. Pt. I," by P. S. Symonds and B. G. Neal, *Journal*, Franklin Inst., Vol. 252, 1951, p. 387.

[4] "Theory of Limit Design," by J. A. Van Den Brock, John Wiley & Sons, Inc., New York, N. Y., 1948.

[5] "Studies in Reinforced Concrete—Section V," by W. H. Glanville and F. G. Thomas, *Technical Paper No. 22*, Dept. of Scientific and Industrial Research, H. M. Stationery Office, London, 1939.

Solving Eqs. 2 and 3 to eliminate k,

$$\epsilon_c + \epsilon_t = \frac{\epsilon_c f_{av}}{p f_s} \qquad (4)$$

For sections on the verge of free yielding and having less than balanced reinforcement,

$$\psi_o d = \epsilon_c + \frac{f_{yp}}{E_s} = \frac{\epsilon_c f_{av}}{p f_{yp}} \qquad (5)$$

in which ψ_o is the unit rotation at the beginning of free yielding, f_{yp} is the yield point stress, and E_s is the modulus of elasticity of steel.

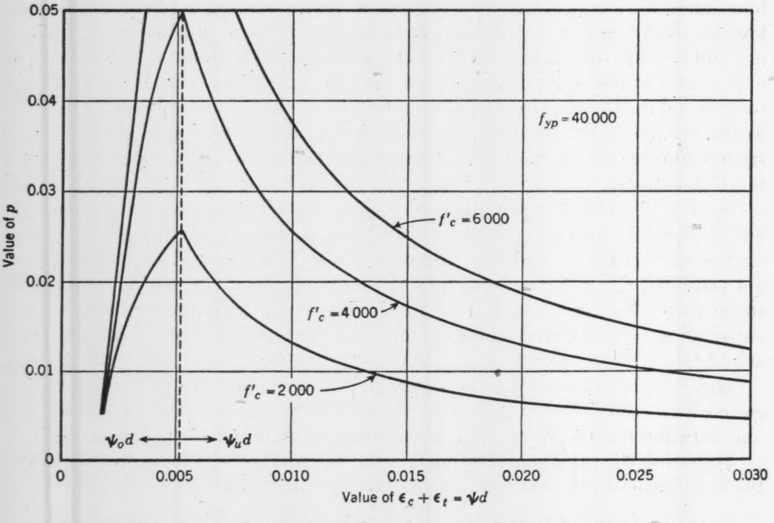

Fig. 3.—Values from Eqs. 5 and 6 (Stresses are in Pounds Per Square Inch)

Also, at the point of ultimate rotational yielding, using 0.0038 as the ultimate compressive deformation of all grades of concrete in flexure,[6]

$$\psi_u d = 0.0038 + \epsilon_t = \frac{0.0038 f_{av}}{p f_{yp}} \qquad (6)$$

in which ψ_u is the ultimate unit rotation.

Values from Eqs. 5 and 6 are plotted in Fig. 3, using the Ritter-Hognestad stress-strain curve[6] for concrete of three different grades with a grade of steel having a yield point of 40,000 lb per sq in. Numerical values taken from Fig. 3 must be divided by the effective depth, d, to determine the unit rotation.

---

[6] "A Study of Combined Bending and Axial Load in Reinforced Concrete Members," by E. Hognestad, *Bulletin No. 399*, Illinois Eng. Experiment Station, Urbana, Ill., 1951.

$M/b\,d^2$ may be determined from a plastic-theory equation[7] or from

$$\frac{M}{b\,d^2} = j\,p\,f_{yp} \qquad (7)$$

in which j is the ratio of the distance between the resultants of the compressive and tensile stresses to the effective depth. Values of j may be determined from Fig. 4.

DIAGRAMS OF UNIT ROTATION, SLOPE, AND DEFLECTION

The method proposed for determining deflections is essentially that presented many years ago for reinforced concrete beams.[8] The primary difference is in the extension of the method to include ultimate deflections and in the use of the revised moment-area theorems. Fig. 5 presents the basic procedure for analyzing a beam carrying concentrated loads at the third-points of the span, in which ψ_o represents the unit rotation of the beginning of free yield and ψ_u is the ultimate unit rotation.

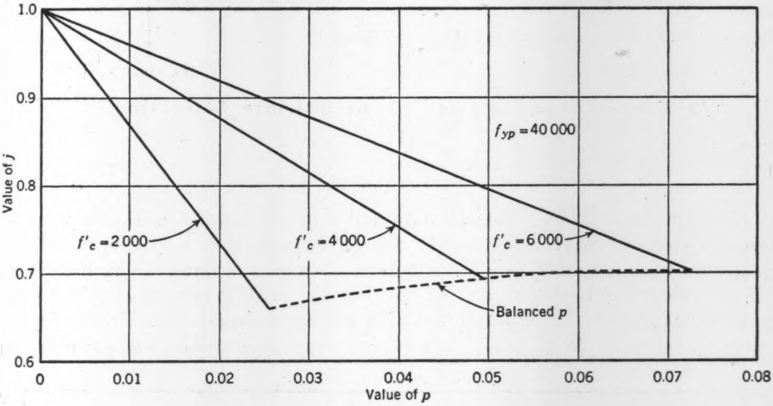

FIG. 4.—RELATIONSHIP BETWEEN j AND p (STRESSES ARE IN POUNDS PER SQUARE INCH)

Using a conjugate beam loaded with the unit rotation diagram, the following expressions for deflections, δ, are determined from Fig. 5:

$$\delta_o = \frac{23}{216}\,\psi_o\,L^2 \qquad (8)$$

and

$$\delta_u = \left(\frac{\psi_o}{27} + \frac{5}{72}\,\psi_u\right) L^2 \qquad (9)$$

---

[7] "Plastic Theory of Reinforced Concrete Design," by Charles S. Whitney, *Transactions*, ASCE, Vol. 107, 1942, p. 251.

[8] "Relation Between Deflection and Deformation in Reinforced Concrete Beams," by G. A. Maney, *Proceedings*, A.S.T.M., 1914, p. 310.

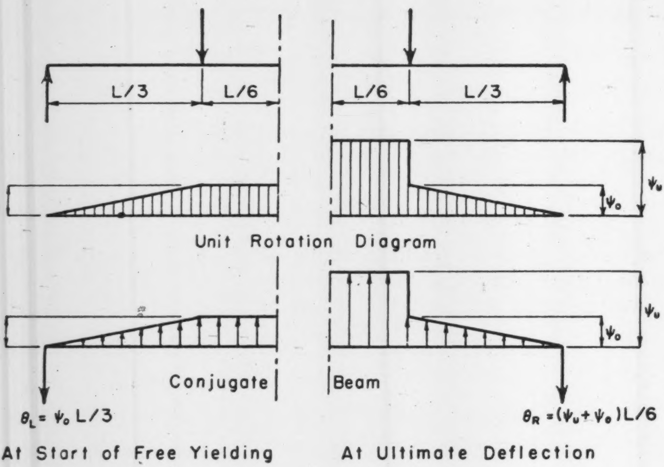
L/3
L/6
L/6
L/3
ψ_o
ψ_u
Unit Rotation Diagram
Conjugate
Beam
$\theta_L = \psi_o L/3$
$\theta_R = (\psi_u + \psi_o) L/6$
At Start of Free Yielding
At Ultimate Deflection

FIG. 5

THEORY COMPARED WITH TESTS

Experimental data on the ultimate deflection of beams, particularly reinforced concrete beams, is extremely meager because it is necessary that the deflection be known for which the deformation in the outer fibers has been fully developed in both tension and compression. Most reports of past beam tests do not provide such information with any degree of fidelity. However, an outstanding example of such information regarding reinforced concrete is

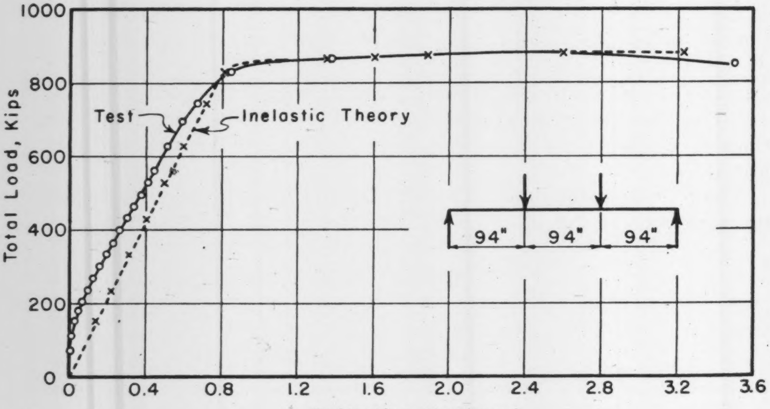

FIG. 6.—COMPARISON OF MEASURED AND COMPUTED DEFLECTIONS OF A PRECAST REINFORCED CONCRETE SLAB

provided by the report of a test of a full-size precast railway crossing slab, conducted in 1908 by A. N. Talbot[9] and for which it was reasonably evident that both concrete and steel had been fully developed without complications because of diagonal tension or bond. A comparison of measured and computed deflections are provided in Fig. 6, from which it may be noted that the agreement is quite close at ultimate value and does not deviate significantly at lesser values. The slab was selected for test from a large number of similar units fabricated by the Illinois Central Railroad for carrying railroad loading. The span was 23.5 ft, the effective depth 30.5 in., the breadth 6.25 ft, the steel ratio 0.0127, and the weight 33 tons. The beam was tested in the field, with loading continued until compression failure was visually impending in the concrete. The computed deflections shown in Fig. 6 were determined through the use of a curve of unidealized $M/b\,d^2$ against unit rotation. The ultimate deflection based on the idealized form of Fig. 2 is presented in Table 1, in which several other beams are listed.[10,11,12] The agreement between test values and computed deflections is quite close if one considers the experimental difficulties encountered in carrying a beam test to a true flexural ultimate deflection.

TABLE 1.—ULTIMATE DEFLECTIONS OF SEVERAL BEAMS

Source (complete references in footnotes to text) (1)	Beam number (2)	Span, L, in feet (3)	Breadth, b, in inches (4)	Depth, d, in inches (5)	Ratio, p (6)	Yield point steel stress, f'_s (lb per sq in.) (7)	Ultimate concrete stress, f'_c (lb per sq in.) (8)	Type of failure[a] (9)	DEFLECTIONS, IN INCHES	
									Measured (10)	Computed (11)
Univ. of Illinois Exp. Sta. Bull. No. 1	28	14	12	12	0.0152	57,500	1,800	C	1.35	1.35
Univ. of Illinois Exp. Sta. Bull. No. 1	29	10.7	12	6.5	0.0148	55,000	1,800	C	1.52	1.51
Univ. of Illinois Exp. Sta. Bull. No. 4	35	12	8	10	0.0148	33,000	1,500	T	1.60	1.17
Univ. of Illinois Exp. Sta. Bull. No. 4	37	12	8	10	0.0124	33,000	1,500	T	1.80	1.54
Univ. of Illinois Exp. Sta. Bull. No. 28	72	23.5	75	30.5	0.0127	52,000	4,000[b]	T	3.50	3.08
Technical Publ. No. 2, National Bureau of Standards	491	12	8	9.3	0.0172	37,900	1,589	T	1.12	1.26

[a] Compressive failure designated C, tensile failure designated T. [b] Estimated.

CONTINUOUS BEAMS

A two-span continuous beam with an unsymmetrically placed concentrated load on the right-hand span is shown in Fig. 7 (a). The location and magnitude of free plastic yielding are desired for the ultimate value of the concentrated load, with the steel ratio equal to 0.01 for both positive and negative moments, f'_c = 4,000 lb per sq in., f_{yp} = 40,000 lb per sq in., and d = 20 in. From Fig. 3, $\psi_e = 0.002/20 = 0.0001$ radian per in. and $\psi_u = 0.0256/20 = 0.00128$ radian per in.

---

[9] "A Test of Three Large Reinforced Concrete Beams," by A. N. Talbot, *Bulletin No. 28*, Illinois Eng. Experiment Station, Urbana, Ill., 1908.

[10] "Tests of Reinforced Concrete Beams," by A. N. Talbot,, *Bulletin No. 1*, Illinois Eng. Experiment Station, Urbana, Ill., 1904.

[11] "Tests of Reinforced Concrete Beams—Series of 1905," *Bulletin No. 4*, Illinois Eng. Experiment Station, Urbana, Ill., 1906.

[12] "The Strength of Reinforced Concrete Beams," by R. L. Humphrey and L. H. Losse, *Technical Publication No. 2*, National Bureau of Standards, Washington, D. C., 1912.

The unit rotation diagram is shown as a load on the conjugate beam in Fig. 7 (*c*); the critical sections at R2 and under the load are fully developed. Prior to solution, the location and magnitude of free plastic yielding is not known, but the adjustment to be made by yielding is determined as the deflection of the right end which is assumed to be unsupported. Yielding at R2 would adjust the right end downward, whereas yielding under the load would move the right end up, for maintaining the positions of the supports. The direction and location of the angular yielding, $\psi\lambda$, as shown in Fig. 7 (*c*), reflects the assumption of an upward adjustment at the right end and infers that free plastic yielding must occur under the load. It is evident that $\psi\lambda x$ will be negative and yielding will occur at R2 if the foregoing assumption is incorrect. In $\psi\lambda x$, λ is the distance throughout which ψ is distributed and x is the distance from the point of assumed deflection to the section of plastic yielding.

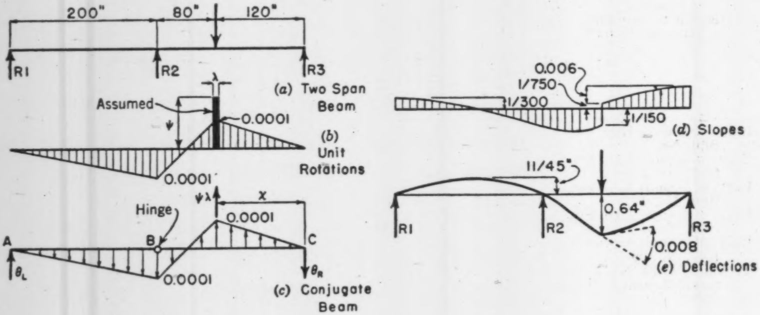

FIG. 7.—A TWO-SPAN BEAM, UNSYMMETRICALLY LOADED

For the conjugate beam, if $\Sigma M_B = 0$,

$$200\,\theta_L - \frac{(0.0001)(200)^2}{(2)(3)} = 0$$

and

$$\theta_L = \frac{1}{300}$$

If $\Sigma M_C = 0$,

$$\frac{4}{3} - \frac{8}{3} + \frac{1.12}{3} + \psi\lambda x = 0$$

and

$$\psi\lambda x = 0.96 \text{ in.}$$

The necessary adjustment in deflection at R3 is 0.96 in. in an upward direction. Because the section under the load is required to make this adjustment by plastic yielding, the position x is 120 in. from R3. The magnitude of the angular yielding is equal to $0.96/120 = 0.008$ radian under the load. With an ultimate limit of 0.00128 for ψ, the minimum length of beam throughout which the 0.008 radian must be accumulated in order to prevent premature failure of the section is 0.008/0.00128, or somewhat more than 6 in. The true slope diagram and deflection curve are shown in Figs. 7 (d) and 7 (e), respectively.

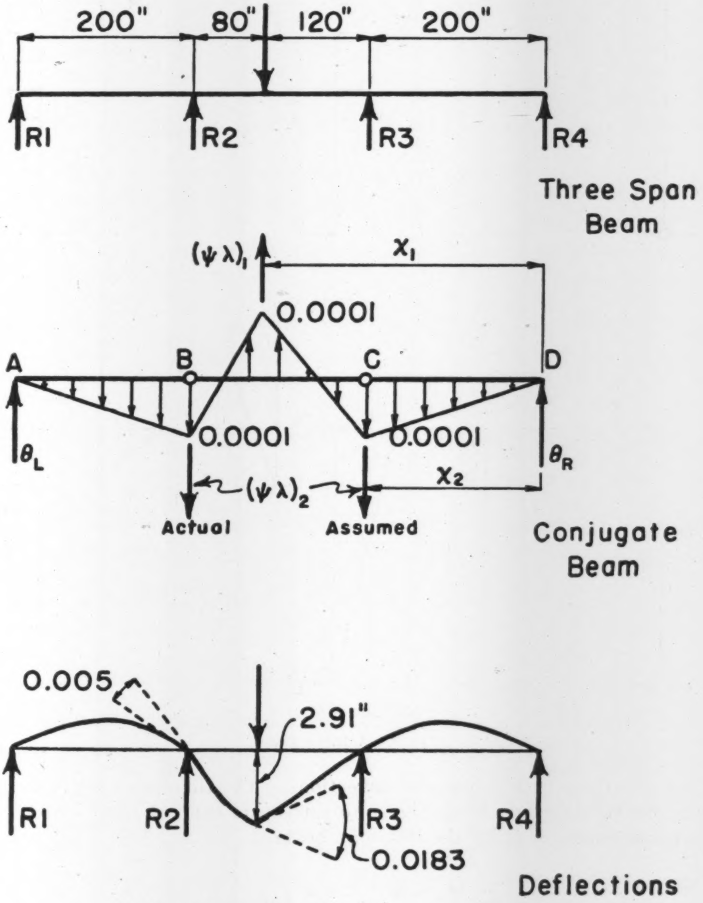
200"
80"
120"
200"
R1
R2
R3
R4
Three Span Beam
$(\psi\lambda)_1$
X_1
0.0001
A
B
C
D
0.0001
0.0001
θ_L
θ_R
$(\psi\lambda)_2$
X_2
Actual
Assumed
Conjugate Beam
0.005
2.91"
R1
R2
R3
R4
0.0183
Deflections

FIG. 8.—A THREE-SPAN BEAM, UNSYMMETRICALLY LOADED

If consecutive pairs of spans are analyzed in the foregoing manner, for a continuous beam of any number of spans the yielding sections at ultimate load may be determined through the relative magnitudes and directions of the re-

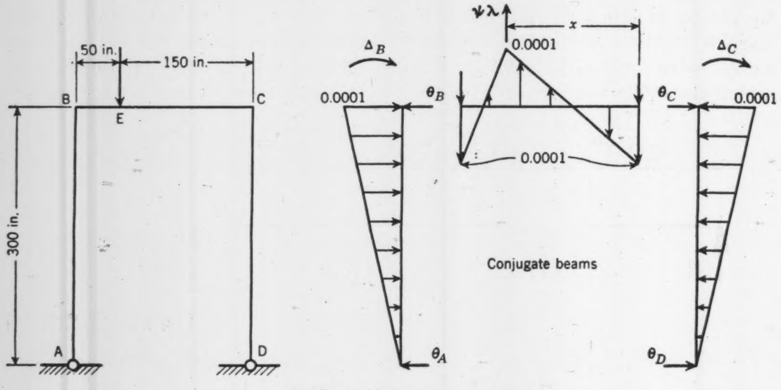
50 in.
150 in.
B
E
C
300 in.
A
D
$\psi\lambda$
x
0.0001
Δ_B
Δ_C
0.0001
θ_B
θ_C
0.0001
0.0001
Conjugate beams
θ_A
θ_D

(*a*) Free sidesway

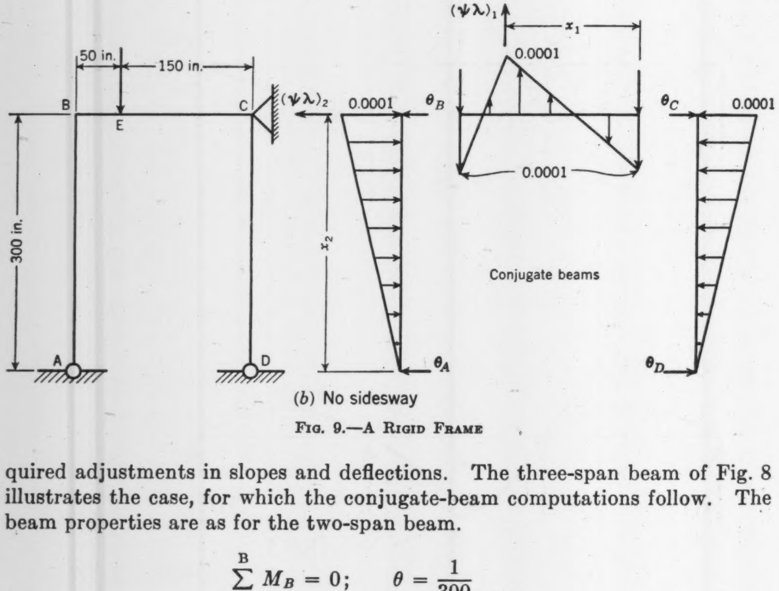
50 in.
150 in.
B
E
C
$(\psi\lambda)_2$
0.0001
θ_B
$(\psi\lambda)_1$
x_1
0.0001
θ_C
0.0001
0.0001
300 in.
x_2
Conjugate beams
A
D
θ_A
θ_D

(*b*) No sidesway

FIG. 9.—A RIGID FRAME

quired adjustments in slopes and deflections. The three-span beam of Fig. 8 illustrates the case, for which the conjugate-beam computations follow. The beam properties are as for the two-span beam.

$$\sum_{A}^{B} M_B = 0; \qquad \theta = \frac{1}{300}$$

$$\sum_{A}^{C} M_C = 0; \qquad (\psi\,\lambda\,x)_1 = 1.2 \text{ in.}$$

The value of 1.2 in. is an upward adjustment required at R3, which locates a yield under the load equal to 1.2/120 = 0.01 radian, which must be included as a concentrated load 120 in. to the left of point C on the conjugate beam in computing the value of $(\psi \lambda x)_2$ from

$$\sum_{A}^{D} M_D = 0; \qquad (\psi \lambda x)_2 = -\frac{2}{3} \text{ in.}$$

The direction of $(\psi \lambda x)_2$ was assumed incorrectly; therefore, the necessary adjustment at R4 is $\frac{2}{3}$ in. upward. This direction of adjustment can only occur through additional plastic yielding under the load combined with plastic yielding at R2. The angular movement of the length of beam from the load to θ_R, necessary for the adjustment of $\frac{2}{3}$ in. upward at R4, is $(\frac{2}{3}) \div 200 = 1/300$ radian. This movement causes the beam to drop $120(1/300) = 0.40$ in. under the load, thereby rotating the length of beam from R2 to the load through an angle of $0.40/80 = 0.005$ radian, which is the plastic angular yield required of the section at R2. The total plastic angular yield under the load is the sum of all angular yields accumulating at that section, or $0.0100 + 0.0033 + 0.0050 = 0.0183$ radian. This magnitude of yielding would require a minimum bearing length of 0.0183 divided by 0.00128, or more than 14 in., if local distress is to be avoided. The sequence of development of the yielding sections, as identified by relative magnitudes of yielding, may be noted to occur under the load first, followed by yielding at R2. A shorter solution, in which the full yield of 0.0183 under the load is determined in its entirety, is found by proceeding from D to A.

RIGID FRAMES

A two-hinged rectangular frame, supporting an unsymmetrically placed concentrated vertical load, is shown in Fig. 9. The steel ratios, f'_c, f_{yp}, and d are the same as for the beams. If the frame is free to sway sidewise, the solution using the conjugate-beam analysis will be

$$\sum_{B}^{A} M_A = 0; \qquad \Delta_B = 300\,\theta_B - 3$$

$$\sum_{C}^{D} M_D = 0; \qquad \Delta_C = 3 - 300\,\theta_C$$

$$\Delta_B = \Delta_C; \qquad 300\,\theta_B + 300\,\theta_C - 6 = 0$$

$$\Sigma\, V = 0; \qquad \theta_B + \theta_C - \psi \lambda = 0$$

$$\sum_{B}^{C} M_C = 0; \qquad 200\,\theta_B - \frac{1}{3} - 150\,\psi \lambda = 0$$

in which V denotes shear.

Solving the last three equations simultaneously, $\psi \lambda = 0.02$ radian, $\theta_B = \frac{1}{60}$ radian, and $\theta_C = \frac{1}{300}$ radian; therefore, $\Delta_B = \Delta_C = 2$ in.

If sidesway is prevented, the conjugate-beam analysis is

$$\sum_{D}^{C} M_C = 0; \qquad \theta_D = 0.005$$

$$\sum_{A}^{C} M_C = 0; \qquad \begin{cases} (\psi\,\lambda\,x)_1 & = 2\frac{1}{3}\text{ in.} \\ (\psi\,\lambda)_1|_{x_1} & = \frac{7}{150} = 0.0467\text{ radian} \end{cases}$$

$$\sum_{D}^{A} M_A = 0; \qquad \begin{cases} (\psi\,\lambda\,x)_2 & = -\,8\text{ in. (to the right of A)} \\ (\psi\,\lambda)_2|_B & = \frac{8}{300} = 0.0267\text{ radian.} \end{cases}$$

With the limit of 0.00128 radian per in. as the maximum value of ψ_u, it becomes evident that the length of member throughout which the value of 0.00128 must be distributed in order to develop fully the knee sections is not a rational possibility when sidesway is prevented, unless the load is divided into two concentrated loads approximately 3 ft apart or distributed by some other means. Inasmuch as there are no means by which distribution of any significant value can be assured at the knee, unless it is very carefully proportioned, the required length of 0.0267/0.00128 = 21 in. at B would probably prevent the full development of the material at C. Indeed, it is doubtful that the knees for full sidesway would be fully developed unless care was taken to assure a distribution of yielding at the load over a distance of 0.02/0.00128 = 15.6 in.

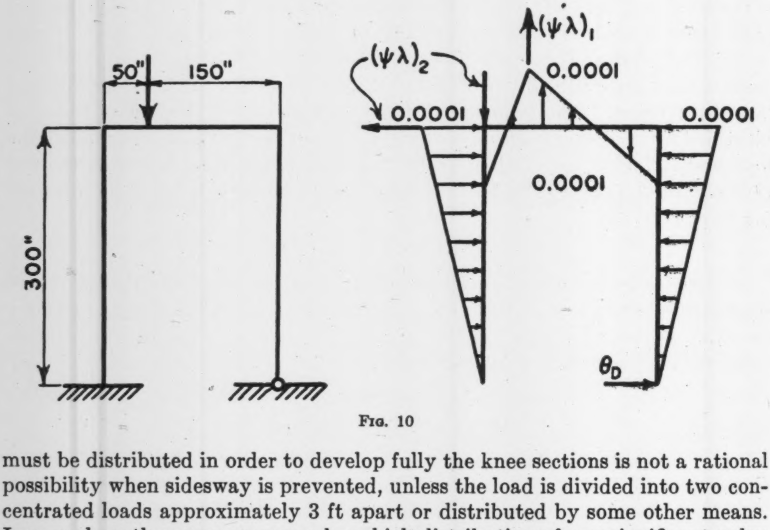

FIG. 10

The same frame, fixed at A and hinged at D, is illustrated in Fig. 10. For this frame, yielding develops first under the load and then at B; $\psi\,\lambda$ (at load) = 0.027 radian, and $\psi\,\lambda$ (at B) = 0.007 radian.

A general solution for the frame of Fig. 10 may be developed from Fig. 11, resulting in the following groups of equations expressing deformation of the bent as the load is increased from 0 to the ultimate value of 80,000 lb.

Prior to yielding,

$$15{,}000\,\psi_A - 37{,}500\,\psi_B - 52{,}500\,\psi_C + 30{,}000\,\psi_E = 0$$
$$90{,}000\,\psi_A - 103{,}750\,\psi_B - 11{,}250\,\psi_C + 35{,}000\,\psi_E = 0$$

and

$$\psi_A + \psi_B - \psi_C = 0.$$

With yielding at the load only,

$$15{,}000\,\psi_A - 37{,}500\,\psi_B - 52{,}500\,\psi_C + 300\,(\psi'\lambda)_E = -3$$
$$90{,}000\,\psi_A - 103{,}750\,\psi_B - 11{,}250\,\psi_C + 450\,(\psi'\lambda)_E = -3.5$$

and

$$\psi_A + \psi_B - \psi_C = 0.$$

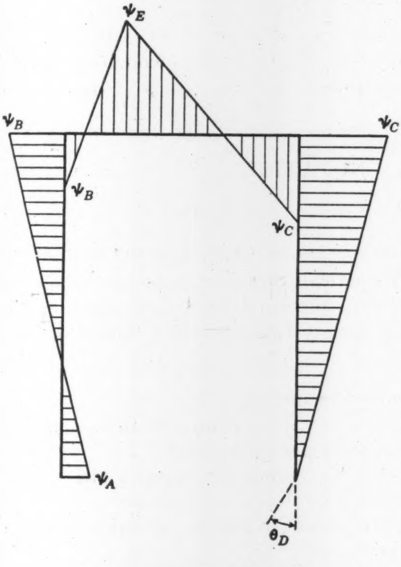

FIG. 11.—ELASTIC UNIT ROTATIONS OF THE FRAME OF FIG. 10

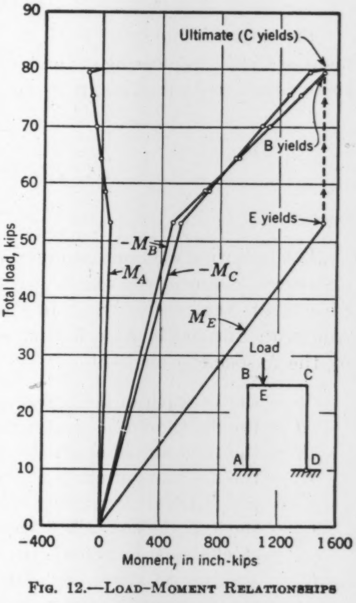

FIG. 12.—LOAD-MOMENT RELATIONSHIPS

With yielding at the load and at point B,

$$15{,}000\,\psi_A - 300\,(\psi'\lambda)_B - 52{,}500\,\psi_C + 300\,(\psi'\lambda)_E = 0.75$$
$$90{,}000\,\psi_A - 600\,(\psi'\lambda)_B - 11{,}250\,\psi_C + 400\,(\psi'\lambda)_E = 6.875$$

and

$$\psi_A - \psi_C = -0.0001.$$

The solution of these equations throughout the loading range from zero to the ultimate load is plotted in Fig. 12, from which it may be noted that, due to the requirements for maintaining static equilibrium, stresses in the knee having the greatest moment prior to initial yielding of any section were not developed as rapidly as in the other knee after the start of yielding at the load.

SUMMARY

It has been demonstrated that ultimate slopes and deflections may be determined in the same basic manner as elastic slopes and deflections through the use of the curvature properties of the cross sections in flexure.

Revised moment-area theorems are presented as a means for analyzing continuous beams and rigid frames to determine the magnitude and location of plastic yielding, the required length of distribution of such yielding, and the possibility of local failure prior to full development of all critical sections.

ACKNOWLEDGMENT

The writer is indebted to G. R. Swihart, assistant professor of the Department of Civil Engineering at the University of Nebraska at Lincoln for checking the continuous-beam and rigid-frame examples

---

APPENDIX. NOTATION

The following symbols, adopted for use in the paper, and for the guidance of discussers, conform essentially with "American Standard Letter Symbols for Structural Analysis" (ASA Z10.8 – 1949), prepared by a committee of the American Standards Association, with Society representation, and approved by the Association in 1949:

b = the breadth of a flexural member, in inches;

d = the depth of a flexural member, as measured from ϵ_c to ϵ_t, in inches;

E = the modulus of elasticity, in pounds per square inch;

E_s = the modulus of elasticity of steel, in pounds per square inch;

f'_c = the cylinder strength of concrete, in pounds per square inch;

f_{av} = the average concrete compressive stress, in pounds per square inch;

f_s = steel stress, in pounds per square inch;

f_{yp} = yield-point stress, in pounds per square inch;

I = the moment of inertia, in inches^4;

j = the ratio of the distance between the resultants of the compressive and tensile stresses to the effective depth for a reinforced concrete section;

K = a constant;

k = the ratio of the distance between the extreme fiber and the neutral axis to the effective depth of a reinforced concrete section;

L = span length, in inches;

M = bending moment, in inch-pounds;

p = steel ratio;

s = distance along the beam axis, in inches;

x = the distance to the yielding section, in inches;
ϵ_c = unit compressive strain, in inches per inch;
ϵ_t = unit tensile strain, in inches per inch;
θ = beam slope, in radians;
λ = the distance throughout which yielding is distributed, in inches;
$\psi = \frac{d\theta}{ds}$, or unit rotation, in radians per inch:
  ψ_o = unit rotation at the start of free yielding, in radians per inch; and
  ψ_u = the ultimate unit rotation, in radians per inch.

DISCUSSION

Abdel F. Diwan,[13] A.M. ASCE.—In connection with the theory of "limit design," it is usually assumed that the relation between the moment M acting at any section and the unit rotation ψ produced is that shown as Type 1 in Fig. 13. However, this relation is not suitable for producing any necessary plastic hinge unless the bending moment is constant throughout some length of the beam sufficient to accumulate the required rotation. In the case of a concentrated load where the bending moment reaches its maximum value at one section only, no plastic hinge can possibly develop because the length of the yielding part is theoretically zero. It is therefore necessary to consider as an idealized (M-ψ)-relationship the curve of Type 2 in Fig. 13, in which the plastic range begins at a moment M_o called the "yield moment" and continues with a slight increase in the bending moment until the ultimate value M_u is reached, with an ultimate unit rotation ψ_u at which point final collapse occurs. The plastic portion in the frame will then extend throughout the length where the moment exceeds the yield value M_o. However, this length may not be sufficient to accumulate the necessary plastic rotation at the section, in which case, at least theoretically, further plastic rotations at other sections cannot possibly be developed.

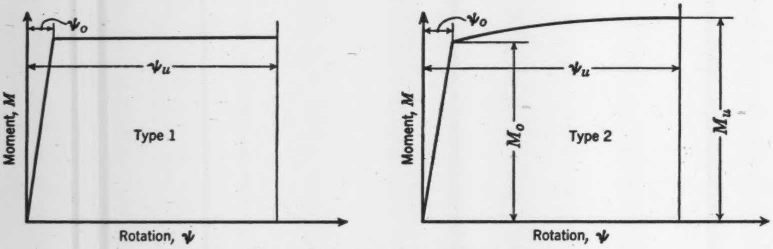

FIG. 13.—MOMENT-ROTATION RELATIONSHIPS

Such a distinction between the yield moment M_o and the ultimate moment M_u, although not necessary when considering the state of final collapse, is important when computing the slopes and deflections prior to that state. No such distinction is made by the author when using the unit rotation diagram in place of the ($M/E\,I$)-diagram.

Indeed, the use of the unit rotation diagram lacks most of the advantages of the ($M/E\,I$)-diagram and seems to have no merit. The ($M/E\,I$)-diagram possesses the following advantages:

1. The conditions of equilibrium at any joint are easily seen, especially when the members framing into the joint have different cross sections. The unit rotations there will not be equal and they will not all reach the yield value ψ_o.

---

[13] Structural Dept., Faculty of Eng., Alexandria Univ., Alexandria, Egypt.

2. The bending moment is allowed to reach the ultimate value M_u at the sections where the plastic hinges are developed whereas it reaches only the yield value M_o at the section on the verge of the plastic range. When using the unit rotation diagram, the author takes the same ψ_o-value for both types of sections.

3. The equilibrium conditions necessary to draw the bending-moment diagram produced by any loading system prior to final collapse are directly available, and the ultimate value of the loads may be readily computed.

Under the heading, "Revised Moment-Area Theorems," the following theorem may be added:

V.—The component of the translation at any point in the frame in any direction is equal to the sum of the moments at that point for all the elastic weights of the (M/EI)-diagram and the rotations at the end support and at the plastic hinge, all to one side of the point and all considered as forces acting parallel to the required direction of translation. The summation may start at any intermediate point provided the rotation and translation there are known and are appropriately included in the summation.

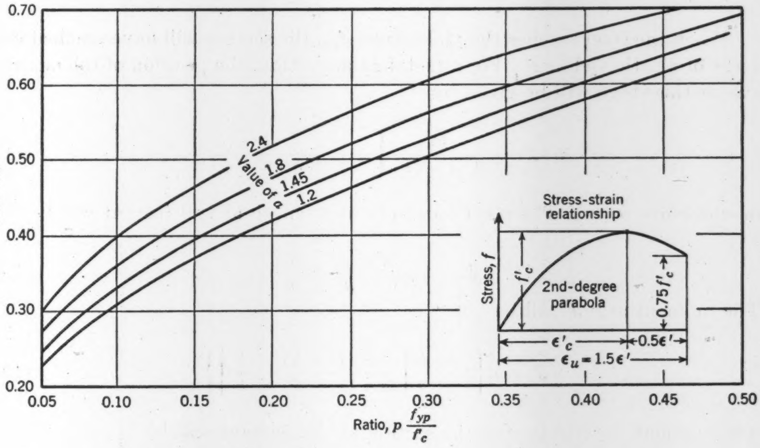

FIG. 14.—VALUES OF *k* FOR FOUR *a*-VALUES ($a = \epsilon'_c \div \epsilon'_s$; $\epsilon'_s = f_{yp} \div E_s$)

This theorem is essential for the analysis of the frames and makes it possible to arrive at the final solution without the need of solving several simultaneous equations as presented by the author. This is shown subsequently by several examples.

In general, the available conditions of static and elastic equilibrium will be sufficient to determine both the bending-moment diagram and the magnitudes of the plastic rotations, due to any type of loading on the frame prior to final collapse. By elastic equilibrium is meant the equilibrium of the elastic weights.

Plastic Properties of Reinforced Concrete Sections.—An idealized stress-strain relationship for concrete is shown in Fig. 14. The curve is assumed to be a second-degree parabola with a vertical axis at the maximum concrete stress f'_c corresponding to the strain ϵ'_c.

The ultimate strain ϵ_u is assumed to be 1.5 ϵ'_c when $f_u = 0.75\, f'_c$. Experiments show that the strain ϵ'_c does not vary much with variation in concrete mixes, and although the strain may be assumed constant, this is not necessary. With such an idealized curve the only variables governing the inelastic behavior of any concrete mix are f'_c and ϵ'_c.

For under-reinforced sections, the steel will reach the yield stress f_{yp} first, and the strain therein will be

$$\epsilon'_s = \frac{f_{yp}}{E_s} \qquad (10)$$

When the steel reaches the yield stress f_{yp}, the section will have reached the verge of plastic yielding. For a rectangular section, the position of the neutral axis at this stage will be given by

$$p\,\frac{f_{yp}}{f'_c} = \frac{k^2}{a\,(1-k)}\left[1 - \frac{k}{3\,a\,(1-k)}\right] \qquad (11)$$

in which $a = \epsilon'_c/\epsilon'_s$. The rotation ψ_o per unit length at this instant will be

$$\psi_o = \frac{\epsilon'_s}{d(1-k)} = \frac{C_3}{d} \qquad (12)$$

The moment arm J will be

$$J = d\left\{1 - \frac{k}{4}\left[\frac{4\,a\,(1-k) - k}{3\,a\,(1-k) - k}\right]\right\} \qquad (13)$$

The moment of resistance of the section at this instant will be

$$\left.\begin{aligned} M_o &= p\, f_{yp}\, b\, d\, J \\ \text{or} \qquad M_o &= C_2\, f'_c\, b\, d^2 \end{aligned}\right\} \qquad (14)$$

The moment M_o and the rotation ψ_o will be called the yield moment and yield rotation, respectively.

Prior to M_o, the relation between M and ψ may be assumed as linear, with a section stiffness $E\,I$ such that

$$E\,I = \frac{M_o}{\psi_o} = C_4\, f'_c\, b\, d^3 \qquad (15)$$

The constants k, C_2, C_3, and C_4 are given graphically in Figs. 14, 15, 16, and 17 for the values $a = 2.4$, 1.8, 1.45, and 1.20, respectively. For $\epsilon'_c = 0.0024$ and $E_s = 30 \times 10^3$ kips per sq in., these a-values will represent the cases in which f_{yp}, in kips per square inch, equals 30, 40, 50, and 60, respec-

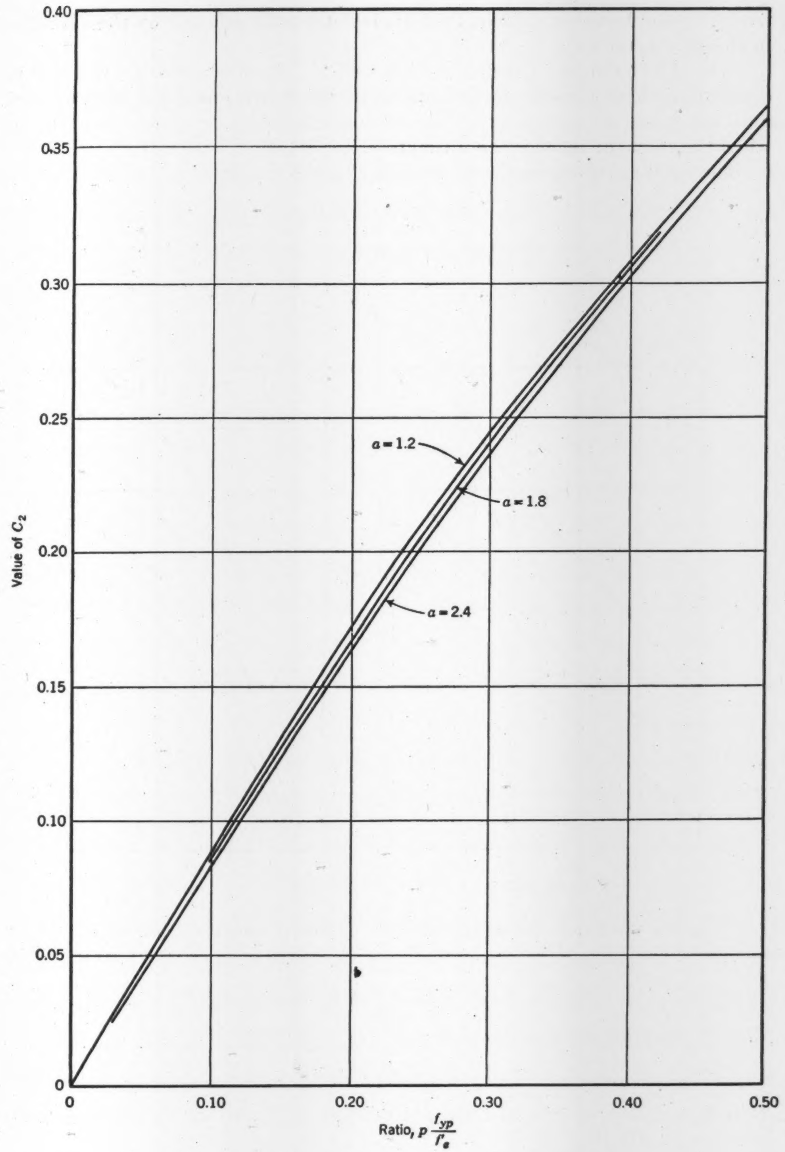

FIG. 15.—YIELD MOMENTS, M_e (EQ. 14)

tively. It can, however, be seen that M_o is not greatly affected by the variation in the parameter a.

When the moment on the section exceeds M_o, the steel stress f_{yp} will remain constant with an increase in moment while the neutral axis will shift upward until the stress distribution over the section will finally be as shown in Fig. 18 when the moment reaches the ultimate value M_u.

The total compression C and tension T will be

$$C = 0.75\, k\, b\, d\, f'_c \quad \text{(16a)}$$

and

$$T = p\, b\, d\, f_{yp} \quad \text{(16b)}$$

Thus,

$$k = \frac{4}{3}\, p\, \frac{f_{yp}}{f'_c} \quad \text{(17)}$$

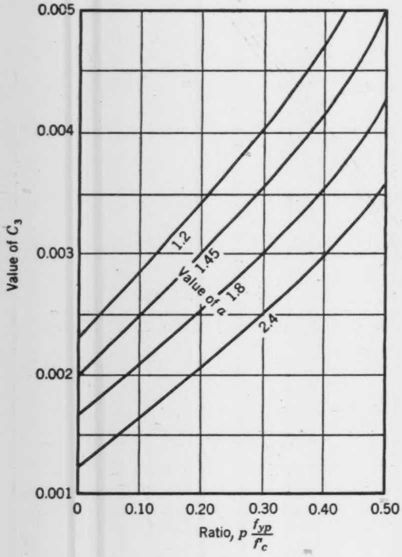

FIG. 16.—YIELD ROTATION, ψ_o (EQ. 12)

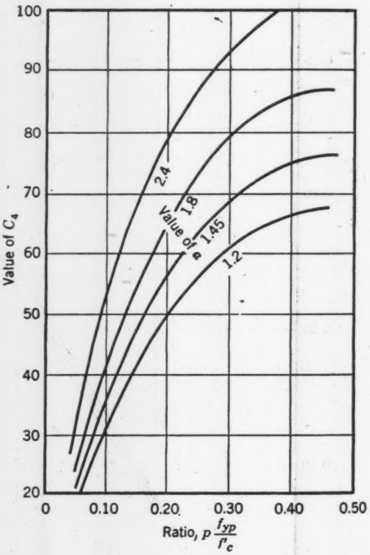

FIG. 17.—SECTION STIFFNESS, EI (EQ. 15)

and

$$J = (1 - 0.416\, k)\, d \quad \text{(18)}$$

The ultimate moment, M_u, will be

$$M_u = C_6\, f'_c\, b\, d^2 \quad \text{(19)}$$

It is seen that k, J, and M_u will not depend on the strain ϵ'_c. The ultimate rotation ψ_u will then be

$$\psi_u = \frac{1.125\, \epsilon'_c\, f'_c}{p\, f_{yp}\, d} = \frac{C_5}{d} \quad \text{(20)}$$

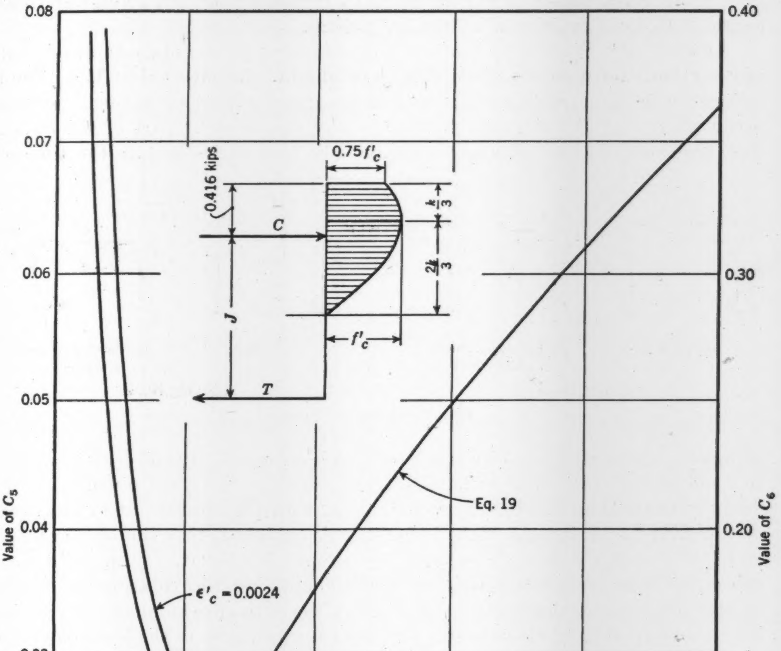

FIG. 18.—ULTIMATE VALUES OF ψ_u AND M_u (MOMENTS IN KIP-FEET)

Fig. 18 gives values of the constant C_6 for all values of ϵ'_c and values of constant C_5 for ϵ'_c-values of 0.0024 and 0.0020.

Analysis of a Single-Bay Frame.—For a yield or plastic hinge to develop at any section, the moment there should reach the ultimate value M_u. Total collapse will occur when four plastic hinges form whereas local collapse will occur when only three hinges develop in any one straight part of the frame. The positions of these plastic hinges for any case of loading at the time of collapse can be determined by trial[14] or by relaxation.[15] It is desired, however, to consider the state prior to final collapse when the last yield hinge is on the verge of developing but has not yet done so, with the moment at the location of this hinge reaching the yield value M_o. At which section the plastic hinge will last develop is best determined by proper judgment, taking into consideration that the elastic weights corresponding to the rotations ϕ at the plastic hinges must have the same sign as the ultimate moments M_u there. Any violation of this rule indicates a wrong assumption as to the location of the plastic hinge.

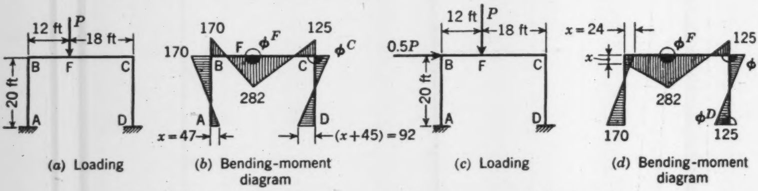

(*a*) Loading (*b*) Bending-moment diagram (*c*) Loading (*d*) Bending-moment diagram

Loading No. 1 Loading No. 2

FIG. 19.—LOADED FRAME

TABLE 2.—ANALYSIS OF THE BENT OF FIG. 19

Member	Section Properties					M_o (kip-feet)	M_u (kip-feet)	ψ_o (rad. per in.)	ψ_u (rad. per in.)
	b (in.)	d (in.)	p	EI (kip-feet^2)	L/EI (kip-feet)$^{-1}$				
AB	10	20	0.015	122,000	0.000164	170	183	0.000116	0.0009
BC	10	30	0.010	32×10^4	0.000094	264	282	0.000069	0.0009
CD	10	20	0.010	93,500	0.000214	117	125	0.000103	0.00135

For the frame in Fig. 19, $f'_c = 4.0$ kips per sq in., $\epsilon'_c = 0.0024$, $f_{yp} = 40$ kips per sq in., and $E_s = 30{,}000$ kips per sq in.; thus, $a = 1.80$.

The values EI, L/EI, M_o, M_u, ψ_o, and ψ_u for the three members AB, BC, and CD in feet and kip units are shown in Table 2.

In Fig. 19(*b*) it is assumed that plastic hinges are developed at F and C; thus the moment will reach the ultimate values there, whereas it only attains the yield value M_o at B. If $M^A = x$, then from statics, $M^D = x + 45$. Because the horizontal translations at B and C are equal, $(2x - 170)\,16.4 = [125 - 2(x + 45)]\,21.4$, from which $x = 47$. Therefore $M^A = 47$ ft-kips and $M^D = 92$ ft-kips.

---

[14] "Limit Design of Beams and Frames," by H. J. Greenberg and W. Prager, *Transactions*, ASCE, Vol. 117, 1952, p. 447.

[15] "Design of Frames by Relaxation of Yield-Hinges," by J. Morley English, *ibid.*, Vol. 119, 1954, p. 1143.

The unknown concentrated elastic weights at F and C corresponding to the rotations ϕ^F and ϕ^C are computed as follows:

$$\sum_A^C M^C = 0; \quad \phi^F = 0.0108 \text{ radian}$$

$$\sum_D^B M^B = 0; \quad \phi^C = 0.0038 \text{ radian.}$$

However, if the plastic hinge had been assumed at B instead of C, the rotation ϕ^F would have been -0.00397 radian. This assumption for the location of plastic hinges is found impossible because the negative value of ϕ^F is inconsistent with the sign of M_u.

Fig. 19(*d*) shows the assumed state prior to collapse under a second loading, with plastic hinges at F, C, and D, where the moments have reached the ultimate value M_u; the moment at A has just reached the yield value M_o. The only unknown moment is that at B which, by simple statics, is found to be 24.

For the plastic rotation ϕ^F, assuming all elastic weights to act vertically, $\sum_A^C M^C = 0$; therefore, $\phi^F = 0.00885$. Next, with all elastic weights acting horizontally, $\sum_A^D M^D = 0$; therefore, $\phi^C = 0.01120$.

Finally, assuming the elastic weights to act horizontally, and from the equality of the horizontal translations at B and C, $\sum_A^B M^B = \sum_D^C M^C$, from which it is determined that $\phi^D = 0.00425$ radian.

Multiple-Bay Frames.—The analysis may be extended to the case of continuous multiple-bay frames prior to total or local collapse. In Fig. 20, final collapse will be local in girder AB. However, because there will be no plastic hinge developed in bay EBCF prior to the state of final collapse, stresses in this part may be considered as remaining within the elastic range. The final solution can be simplified by reducing the continuous frame to a single-bay virtual system with EBCF replaced by an equivalent elastic system,[16,17] as shown in Fig. 20(*b*). The elastic constants for the equivalent symbolic system will be $\bar{S} = 0.0000185$, $\bar{y} = -4.7$ ft, and $I_z = 0.0038$ in.^{4}

Prior to collapse the bending-moment diagram will be as shown in Fig. 20(*c*), with the plastic hinges fully developing in member AB, at J and B, and with the moment at A reaching the yield value for column AD. If the mo-

---

[16] "Equivalent Elastic Systems in the Analysis of Continuous Structures," by L. Beaufoy and A. Diwan, *Concrtee and Construction Engineering*, 1950.

[17] Discussion by Abdel F. Diwan of "Multiple-Span Gabled Frames," by John D. Griffiths, *Transactions*, Vol. 121, 1956.

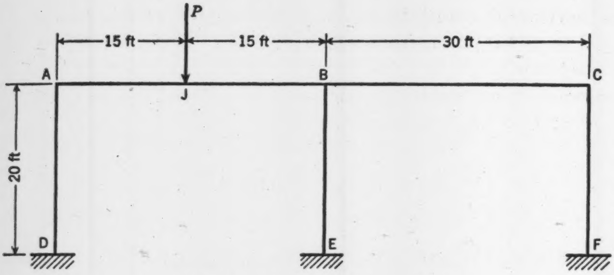
P
15 ft
15 ft
30 ft
A
B
C
J
20 ft
D
E
F

Column sections: 10 in.×20 in.; $p = 0.015$
Girder sections: 10 in.×30 in.; $p = 0.010$

(*a*) Frame

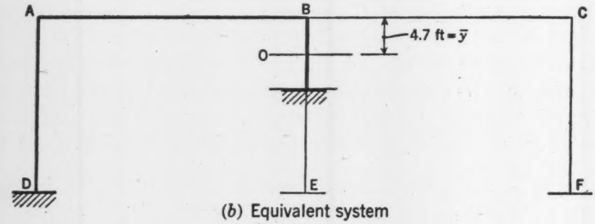
A
B
C
4.7 ft = ȳ
O
D
E
F

(*b*) Equivalent system

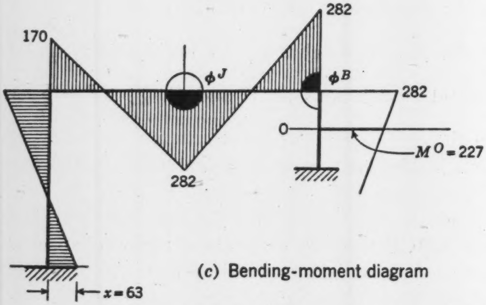
282
170
φ^J
φ^B
282
O
M^O = 227
282
x = 63

(*c*) Bending-moment diagram

FIG. 20.—MULTIPLE-BAY FRAME (MOMENTS IN KIP-FEET)

ment at D is equal to x, then by simple statics the moment at the centroid O of the symbolic system will be $(242 - 0.235\,x)$.

From the equality of the horizontal translations at A and B,

$$\Delta^A = \frac{20}{6}\,(170 - 2\,x)(0.000164)$$

and

$$\Delta^B = 4.7\,(0.235\,x - 242)\,(0.0000185) + \left(\frac{170 + x}{20}\right)(0.0038)$$

from which $x = 63$ kip-ft. Then $\sum_{D}^{B} M^{B} = 0$; therefore, $\phi^{J} = 0.01335$ radian. Likewise, $\sum_{O}^{A} M^{A} = 0$; therefore, $\phi^{B} = 0.00288$ radian.

George C. Ernst,[18] M. ASCE.—Mr. Diwan's discussion is based in its entirety on the rejection of the completely idealized relationship between M and ψ for conditions prior to collapse and on a questioning of the value of the unit rotation diagram.

With regard to the relationship between M and ψ, the true curve is a function of the steel ratio, local bond development and failure, steel properties in tension, and concrete properties in tension and compression. Prior to initial tensile cracking not exceeding a unit deformation in the concrete of approximately 0.0002, a reinforced concrete beam does not materially differ from a plain concrete beam in so far as slope and deflection relationships are concerned. Subsequent to tensile cracking, the tensile properties of the concrete have a gradually decreasing effect until local failure of bond occurs between cracks, thereby resulting in steel deformations conforming to $E_s = 30{,}000{,}000$ lb per sq in. over fairly large portions of the beam. Crack formation during the early stages of loading does not produce accumulated rotations as computed from $E_s = 30{,}000{,}000$ lb per sq in. as Mr. Diwan has assumed. From the development of yield in the steel at M_e to the ultimate moment M_u, the shape of the curve is dominated by the compression properties of the concrete and the steel ratio[19] for any given grade of steel. In general,

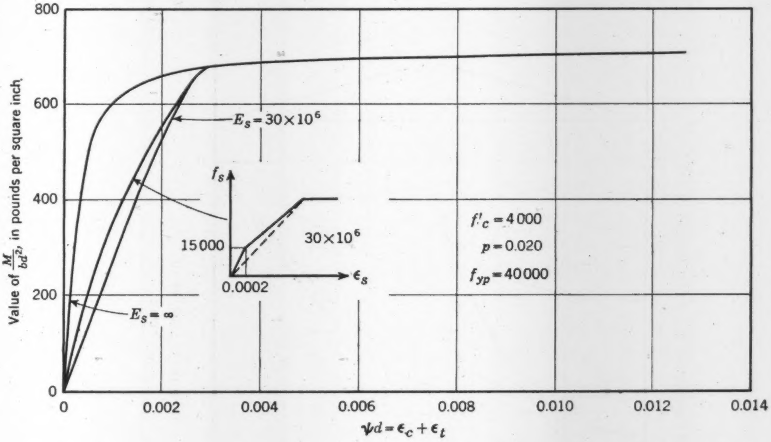

Fig. 21.—Unit Rotation As Affected by Reduction in Steel Strain Due to Concrete Cover

progressive local bond failure in the vicinity of tensile cracks begins at a unit deformation of approximately 0.0002 in the concrete and a steel stress at the crack of approximately 15,000 lb per sq in. In Fig. 21 the $(M\text{-}\psi)$-curves are compared for three different assumptions concerning the effective E_s-value, the intermediate assumption being most representative of the true variation. In Fig. 22 are compared the slopes and deflections for a simply supported beam with a concentrated load at midspan, for which the curvature from M_o to M_u in Mr. Diwan's Type 2 curve (Fig. 13) has been used with each of the three assumptions as to the effective E_s value. Obviously, the assumption of an infinite value of E_s merely expresses the upper limit of stiffness for the tensile face, and the value of 30,000,000 lb per sq in. for E_s expresses the lower limit up to yield.

---

[18] Prof. and Chairman, Dept. of Civ. Eng., Univ. of Nebraska, Lincoln, Nebr.

[19] "Inelastic Behavior of Reinforced Concrete Members," by Lawrence H. N. Lee, *Transactions*, ASCE, Vol. 120, 1955, p. 181.

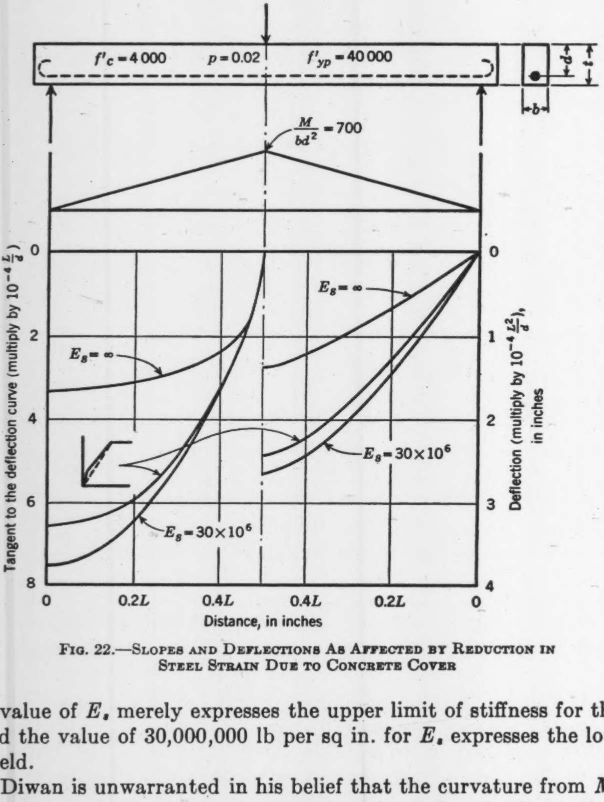

FIG. 22.—SLOPES AND DEFLECTIONS AS AFFECTED BY REDUCTION IN STEEL STRAIN DUE TO CONCRETE COVER

Mr. Diwan is unwarranted in his belief that the curvature from M_o to M_u will provide a realistic estimate of the length of the plastic portion in the vicinity of a "peaked" M_u for purposes of moment redistribution in a continuous structure. He has selected relatively favorable conditions for redistribution of moments in his examples. However, taking the values of M_o and M_u from his table, the difference in moment is about 7% of M_u for a decrease of 87% in unit rotation for AB and 6.4% corresponding to a 93% decrease for

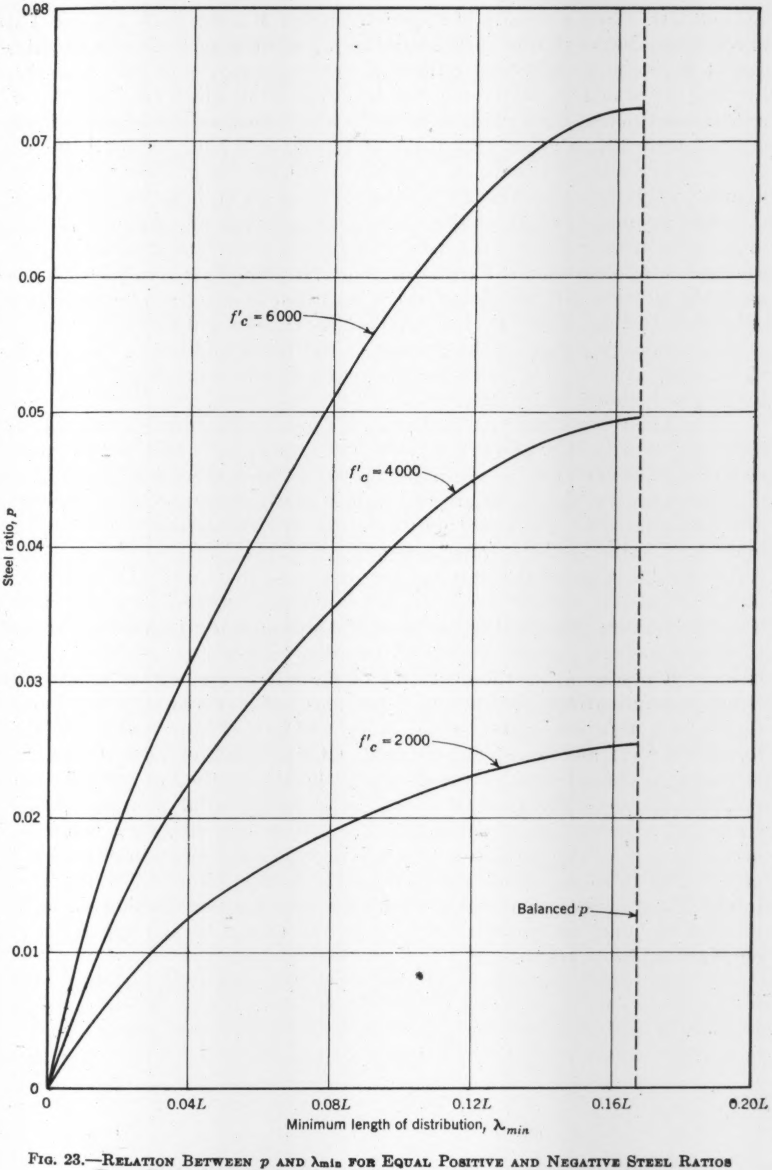

FIG. 23.—RELATION BETWEEN p AND λ_{min} FOR EQUAL POSITIVE AND NEGATIVE STEEL RATIOS (FIXED-ENDED BEAM UNDER UNIFORM LOAD, WITH f_{yp} = 40,000 LB PER SQ IN.)

BC and CD. In the vicinity of a linearly peaked M_u, therefore, 7% (for AB) or 6.4% (for BC or CD) of the distance to the point of zero moment on either side of M_u would be affected by the unit rotations between M_o and M_u. For Loading No. 2 of Fig. 19, the required length through which the angle $\psi_u - \psi_o$ must be accumulated to produce ϕ^C is 12.0 in., whereas the length actually affected from M_o to M_u is only 6.4% of 120 in. or 7.7 in. Apparently, Mr. Diwan is depending on some other unstated property to provide for the total required angle change. Fig. 23 illustrates the effect of variation in the steel ratio and concrete strength on the minimum length over which plastic rotation must occur at the supports of a fixed-ended beam under uniform load in order to assure complete moment redistribution. It should be recalled that ψ is markedly decreased if the steel ratio is increased or the concrete strength is reduced,[19] thereby reducing the total angle change available for moment redistribution by virtue of the portion of the beam affected by M_o to M_u. Contrarily, this in turn increases the required minimum length of plastic hinging as is shown in Fig. 23.

In summary, moment redistribution cannot significantly depend on the difference between Mr. Diwan's Type 1 and Type 2 curves (Fig. 13) but rather on the distribution of ψ_u as controlled by the distance throughout which steel yielding can occur due to length of bearing, width of column, shape of knee, and similar factors. The effect of these factors can be determined only through laboratory tests of full-sized members and structures.

As to the value of the unit rotation diagram, the $(M/E\,I)$-diagram is a unit rotation diagram based on a linear relationship between stress and strain. The $(M/E\,I)$-concept for those portions of a structure in which strains are less than first yielding was not presented because, for the purpose of the paper, it was felt best to avoid the obscuring of the purely geometrical relationship between deformations, slopes, and deflections. The writer does not believe that the unit rotation diagram, either in its basic form or converted to $(M/E\,I)$-form, will have any significant usage in ultimate-load, or limit design. Its usefulness is limited even for the so-called "elastic" method of analysis. The problem is essentially that of obtaining a fundamental understanding of structural response throughout the loading history of a structure, and a very necessary part of the problem is the experimental determination of the extent of distribution of unit rotations beyond the first yielding. The paper was intended to draw attention to this feature as well as the moment-slope-deflection relationship, and the writer is indebted to Mr. Diwan for the opportunity of emphasizing its importance.

AMERICAN SOCIETY OF CIVIL ENGINEERS
Founded November 5, 1852
TRANSACTIONS

Paper No. 2813

A CONFORMAL AND WORLD-WIDE MILITARY GRID SYSTEM

By Floyd W. Hough,[1] M. ASCE

Synopsis

Efficient fire control under battle conditions requires a plane-rectangular coordinate system with the property of conformality. In 1947, the United States Department of the Army adopted the Universal Transverse Mercator projection as most suitable for this purpose. Implementation involves the mass conversion of geodetic data and reduction to a common datum by the Army Map Service.

Introduction

It has become almost axiomatic that for military purposes some system of plane-rectangular coordinates, as opposed to geodetic coordinates, is essential for the efficient and rapid utilization of fire-control data under battle conditions. Speed and simplicity in the determination of accurate direction and distance between points and a quick method for clearly defining the location of a point for reference purposes are paramount considerations in the adoption of a suitable military projection and grid. The comparatively cumbersome computations required for direction and distance from geodetic coordinates have forced the military authorities of practically all nations to adopt the simpler system of plane-rectangular coordinates.

In 1917, when the United States became engaged in World War I, the need was recognized for a plane-rectangular system primarily for the use of the artillery. At that time, the United States Coast and Geodetic Survey (USCGS), with the aid of enlisted personnel from the United States Army, computed the polyconic grid tables for the 5′ intersections of latitude and longitude on the Clarke Spheroid of 1866.[2] This was the official military grid of the Army throughout World Wars I and II until 1947 when it was abandoned in favor of the military grid and reference system termed the Universal Transverse Mercator (UTM) system.

Note.—Published, essentially as printed here, in October, 1954, as *Proceedings-Separate No. 524.* Positions and titles given are those in effect when the paper was approved for publication in *Transactions.*

[1] Chief, Geodetic Div., Army Map Service, Washington, D. C.

[2] "Grid System for Progressive Maps in the United States," *Special Publication No. 59,* Coast and Geodetic Survey, U. S. Dept. of Commerce, Washington, D. C., 1919.

MAP PROJECTIONS

Conformality in a projection is the property otherwise termed "orthomorphic" which comes from the Greek word meaning "same shape." Thus, in a conformal projection, an area on the map retains the same shape as on the ground, the angles are correct, over reasonably limited areas, and the scale is equal in all directions from a point. In a nonconformal projection or nonorthomorphic projection, such as the polyconic projection, none of these three characteristics is present, resulting in an intolerable distortion in northerly-southerly directions, particularly in the case of artillery fire. Prior to the adoption of the UTM system in 1947, the United States was the only major country which used a nonconformal projection for military purposes.

A map projection is indicated by a mathematical representation of the latitude and longitude lines of a geometric figure of the spheroidal earth onto a plane surface. A grid is a regular system of parallel lines, equally spaced and at right angles to each other, superimposed on the projection. The true Mercator projection, in almost universal use by navigators, projects the features of the earth onto a cylinder tangent at the equator. The transverse Mercator projection is difficult to picture but is best described as the projection of a limited part of the earth's surface onto a cylinder at right angles to the true Mercator, or tangent to a meridian. The cylinder is then rolled out onto a plane and the grid superimposed on the projection.

The transverse Mercator projection is not new as such; it was invented by Karl F. Gauss early in the nineteenth century and is referred to by some as the Gauss projection. The transverse Mercator projection in 6° bands was proposed by the International Union of Geodesy and Geophysics in 1936 and was recommended to the Army in 1941 by the USCGS to replace the polyconic projection. Both Germany and Russia, at least, had been using the transverse Mercator projection for many years as their military projection and grid.

ADOPTION OF UTM SYSTEM BY THE ARMY

In 1944, an initial consultation of interested geodesists was held to consider the desirability of a new grid system. The basic consideration of a projection and grid system satisfactory for military purposes is that it must be conformal in order to preserve true shapes over reasonably large areas. Other desirable features are:

1. The grid system should have a minimum number of zones or junctions for the desired minumum accuracy without a necessity for the application of scale corrections.
2. One transformation table should suffice for the conversion of coordinates between adjacent zones for any one spheroid.
3. Only one table should be required for a spheroid throughout the entire system for the computation from geographic coordinates to grid coordinates, and only one table for the inverse computation.
4. The east-west span of the grid zone should be limited to the extent that the divergence of grid north from the meridian will not be troublesome, perhaps not exceeding 4° or 5°.

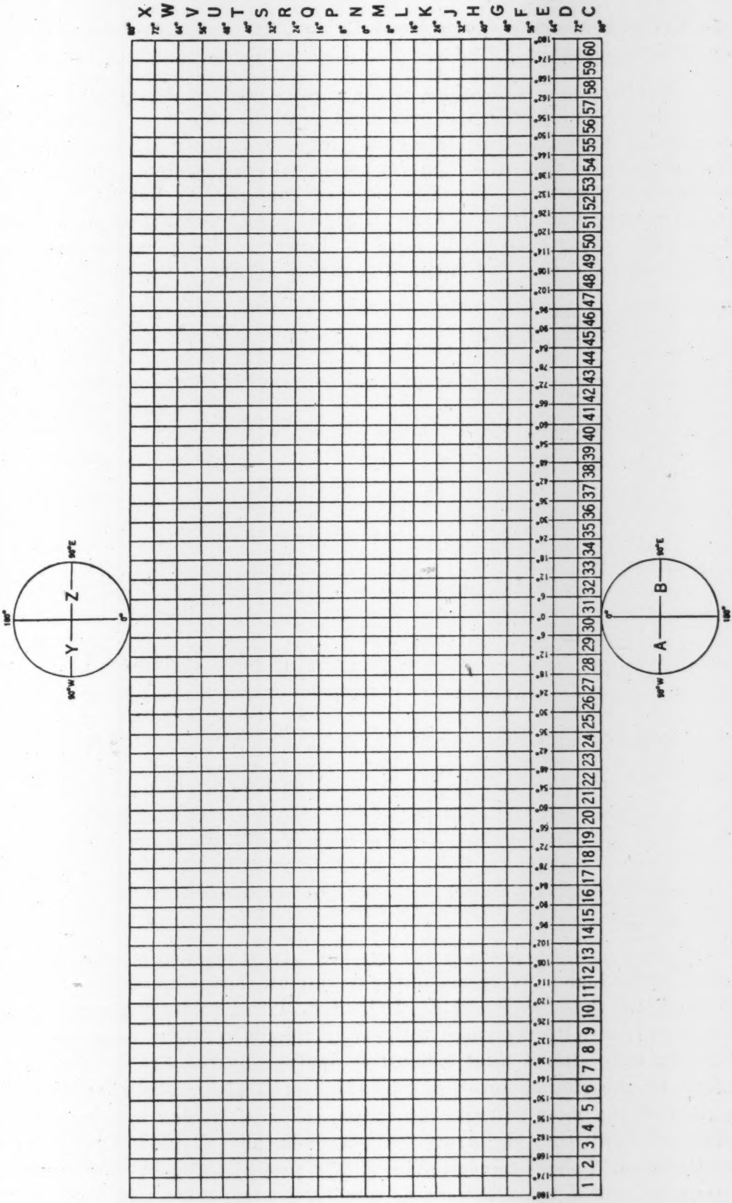
C D E F G H J K L M N P Q R S T U V W X
80° 72° 64° 56° 48° 40° 32° 24° 16° 8° 0° 8° 16° 24° 32° 40° 48° 56° 64° 72° 80°
1 2 3 4 5 6 7 8 9 10 11 12 13 14 15 16 17 18 19 20 21 22 23 24 25 26 27 28 29 30 31 32 33 34 35 36 37 38 39 40 41 42 43 44 45 46 47 48 49 50 51 52 53 54 55 56 57 58 59 60
180° 174° 168° 162° 156° 150° 144° 138° 132° 126° 120° 114° 108° 102° 96° 90° 84° 78° 72° 66° 60° 54° 48° 42° 36° 30° 24° 18° 12° 6° 0° 6° 12° 18° 24° 30° 36° 42° 48° 54° 60° 66° 72° 78° 84° 90° 96° 102° 108° 114° 120° 126° 132° 138° 144° 150° 156° 162° 168° 174° 180°
Y
Z
A
B
90°W
90°E
0°
180°

FIG. 1.—MAJOR ELEMENTS OF THE UTM REFERENCE SYSTEM

5. The grid should adapt itself readily to a unique map reference system for point designation.

In weighing the qualifications of the various conformal systems and considering that the projection and grid must be world wide in application while retaining the desired features, the choice, except for the polar areas, quickly narrowed down to two—the Lambert conformal conic system and the transverse Mercator system. The first satisfied conformality but could not be made to comply with items 2, 3, and 5 of the requirements; compliance with item 4 would cause it to fail in item 1. However, the transverse Mercator was conformal and could be modified to satisfy all five of the specified items.

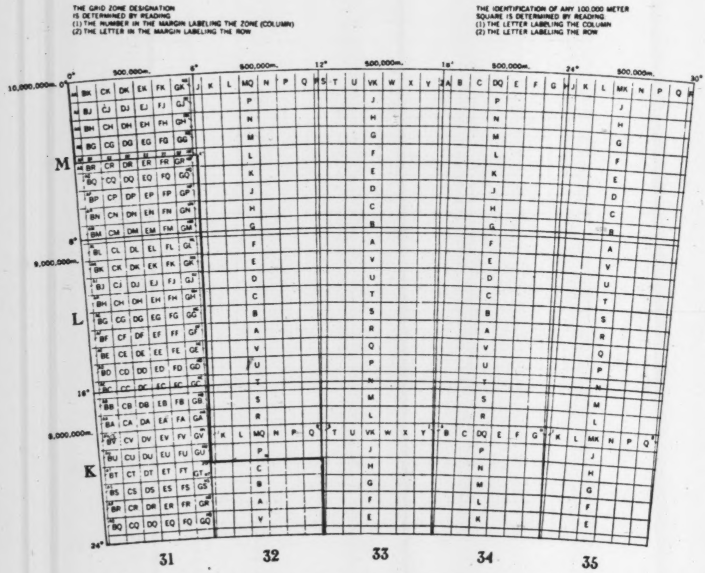
THE GRID ZONE DESIGNATION
IS DETERMINED BY READING
(1) THE NUMBER IN THE MARGIN LABELING THE ZONE (COLUMN)
(2) THE LETTER IN THE MARGIN LABELING THE ROW
THE IDENTIFICATION OF ANY 100,000 METER
SQUARE IS DETERMINED BY READING
(1) THE LETTER LABELING THE COLUMN
(2) THE LETTER LABELING THE ROW
0°
6°
12°
18°
24°
30°
500,000m.
500,000m.
500,000m.
500,000m.
500,000m.
10,000,000m. 0°
8°
9,000,000m.
16°
8,000,000m.
24°
M
L
K
31
32
33
34
35

Fig. 2.—Detailed Elements of a Representative Section of the UTM Reference System

For the polar caps, where the transverse Mercator projection is not practicable because of the high convergence of the meridians, there seemed to be only the one choice of the stereographic. Here item 4 had to be foregone and the relation to true north dispensed with except for general index purposes.

It was only after a most exhaustive analysis by the Army Map Service (AMS), by the ground forces, and by other units of the Army, of the entire question of the most suitable projection and grid, taking into account all factors involved, that the Army (in 1947) officially adopted the UTM and the Universal Polar Stereographic (UPS) projection, grid, and reference systems to replace the polyconic as rapidly as practicable. Included in the recommendations were several special provisions to be incorporated in the system, among which were a scale reduction of 1 part in 2,500 on the central meridian, an extent of coverage from 80° south latitude to 80° north latitude, the use of the metric system to replace the English system used in the polyconic projection, and a 1° overlap at all zone junctions. Subsequently, the the 1° overlap was modified to provide for a uniform 50 miles throughout, and a stereographic system was recommended for the polar caps.

Owing to the contemplated use of the new projection and grid systems by the Army in its world-wide mapping program and to the features incorporated therein, as well as to their possible adoption by other nations, it was thought appropriate to designate the systems as the Universal Transverse Mercator projection and the Universal Polar Stereographic projection, respectively. The AMS later devised the reference systems for point designation which are corollaries to and are based directly on these two systems. These reference systems are unique in their provision that no two points in the world can have the same designation.

In 1949, the Joint Chiefs of Staff, United States Department of Defense, directed that these systems be used by land, sea, and air forces in all combined military operations (Figs. 1, 2, and 3).

IMPLEMENTATION OF UTM SYSTEM

Immediately following the adoption of the system in 1947, the AMS proceeded to implement the directive as rapidly as its facilities would permit. At the same time, through correspondence and at various international conferences, it successfully presented the logic of this standardized system to many other countries. In this endeavor, it was greatly assisted by the fact that the International Union of Geodesy and Geophysics, with a membership of some forty-two nations (in 1953), had expressed the wish that countries preparing maps for parts of Africa adopt a projection system for the entire continent that was referred to one general system. This reference to Africa was further extended to all continents and countries by a resolution of the union at its Brussels (Belgium) meeting in 1951. The Commonwealth Survey Officers' Conference in London (England) also in 1951, reinforced the union action by a resolution recommending the UTM system for the countries of Africa. At the Ciudad Trujillo (Dominican Republic) session of the Commission on Cartography of the Pan-American Institute of Geography and History in October, 1952, that assembly recommended favorable consideration of the system to all countries of the Antilles, West Indies, and Central and South America.

The AMS is the United States depository for the geodetic data of the world and has the responsibility of processing it to usable form for the operational use of the military services. It has in its files the coordinates of approximately three million horizontal control stations of various countries. The computation of this mass of data to the new military grid is far advanced (as of 1955). It is only feasible through the use of the most modern mass computing facilities, including electronic digital equipment. The processing of geodetic data of the world to usable form for military purposes consists not only in the procurement, analysis, translation, and computations of such data, but in the preparation and printing of numerous trigonometric lists giving all necessary descriptive information on the control stations, including their UTM grid-coordinate positions and their elevations. Five thousand of these lists (in 1955) containing an average of one hundred and seventy points each have been printed.

In order to make most effective use of the standardized UTM projection and grid, it is highly desirable that the triangulation control of an entire continent be reduced to a single geodetic datum involving one figure of the earth, all based on a common least-squares adjustment. Examples of this are the first-order triangulation networks of North America and the adjustment of the first-order triangulation of Europe and northwest Africa. Continental adjustments of the major triangulation of Africa and that of South America are proposed at the AMS following the completion of the existing gap in the arc of the 30th meridian in Africa and the extensive operations of the Inter-American Geodetic Survey in South America. Eventually, through the intercontinental ties possible by methods utilizing solar eclipses and star occultations, geodesists envision a single geodetic datum for the entire globe. The determination of a new figure of the earth is therefore underway at the AMS. The service will make use of the extensive long arcs of triangulation,

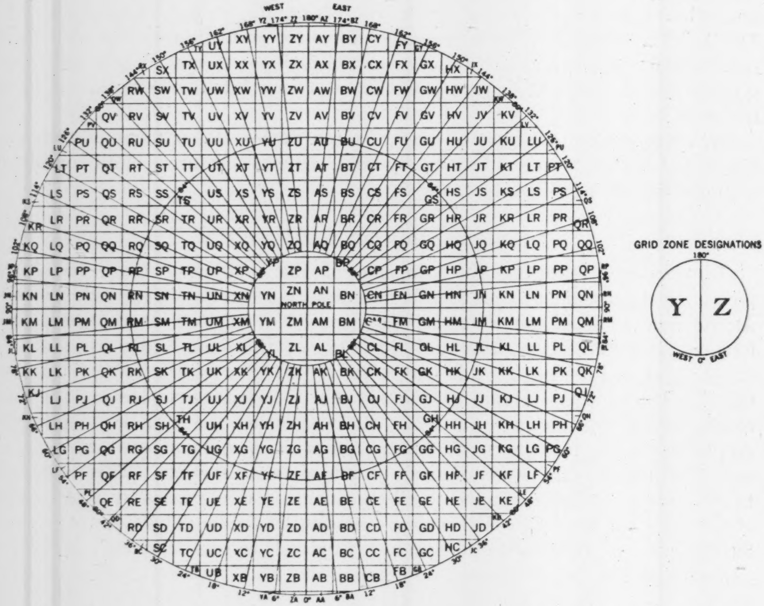

FIG. 3.—ELEMENTS OF THE UPS REFERENCE SYSTEM

astronomic stations, and gravity observations, throughout both hemispheres, which were not available when the Hayford international ellipsoid was computed in 1909. A world geodetic datum calls for the use of this greatly increased information in order to arrive at improved values for the parameters of the figure which best fit the geoid as a whole or, at least, a verification of the international ellipsoid.

Implementation of the UTM grid and reference system has involved and continues to require the reduction of masses of geodetic data to usable form and the preparation of trigonometric lists, as well as the conversion to the new grid of thousands of military topographic maps of various scales throughout the world. This conversion of existing map coverage to the new grid has been simultaneous in nearly all areas with the reduction of the numerous geodetic datums to different and fewer datums, often including a change in the previous ellipsoid. Therefore, in addition to the transformation of coordinates of geodetic control stations and their least-square adjustments to the new datums, it has been necessary to compute and tabulate UTM sheet-corner values for the thousands of map sheets previously cited. Electronic computing equipment has been used and is the answer to this problem also.

Fortunately, in changing the grid and even the geodetic datum on a map, it is not necessary to redraft the contours and other features as might be supposed at first. A far more economical plan was adopted whereby the original sheet lines were retained unaltered. It was necessary only to prepare a new grid plate using the computed and tabulated sheet-corner data. With the substitution of the new UTM grid plate, every feature on the map is automatically transferred to the new datum and grid. Where the sheet lines were originally on even minutes of latitude and longitude, this process results in odd values at the corners. This is not objectionable, however, because the latitude and longitude lines on the military map serve only as an index, whereas the plane UTM coordinates are used exclusively for military purposes.

Since 1951, the UTM grid-conversion program has been vigorously carried on by the AMS in cooperation and in collaboration with other interested countries; much remains to be done (as of 1955). The change-over from the old grid to the UTM system takes place on certain dates agreed upon internationally and by large area blocks, usually covering several countries at a time. This conversion date is predicated on the completion of map conversion of all scales, the publication of trigonometric lists, the substitition of UTM map stocks, and the accomplished distribution of these items to the appropriate military units. On the designated conversion date all previous maps and grids in the area automatically become obsolete.

An undue number of grid junctions is a well-recognized liability in an area of military operations. These junctions are especially difficult for the artillery when the method of transformation between adjacent zones is not uniform. One important area in which the UTM grid has contributed much to the reduction of troublesome grid junctions is in Europe, west of a meridian through Moscow (U.S.S.R.). The previous grid system consisted of twenty different zones with a total of forty junctions; on nearly all of these a different type of transformation was involved in passing from one zone to the adjacent zone.

With the substitution of the standard UTM system in this area, the zones were reduced to eight and the number of junctions to seven with identical transformation at all seven junctions. In addition, the twenty zones had required a separate computation table for nearly every zone whereas only one table was needed for any number of UTM zones on the same spheroid.

The UTM and the UPS systems were carefully designed to meet requirements of a suitable grid system for the world-wide military mapping program of the AMS and for general military operations of the Army. It was never intended, and the AMS has not so recommended, that these systems should replace the cadastral grids of any nation. The state plane coordinate systems are retained in the United States for cadastral purposes. It is a distinct advantage in cadastral as well as military surveys to avoid the necessity for the application of scale corrections to the measured lengths on the ground. Most cadastral grids, as they involve smaller areas, use narrower zones with more junctions—thus retaining a maximum scale correction of about 1 part in 10,000. A military grid system with world-wide coverage, on the other hand, demands the minimum number of different zones and junctions which will yield the required accuracy without scale corrections. The UTM system fully satisfies military requirements in this respect as its accuracy without scale corrections is 1 part in 2,500, or better, in all areas of latitude higher than 45°; in lower latitudes it slowly drops until it reaches 1 part in 1,000 at the equator, but this is only at the extreme edges of the zones in this region of lesser military importance. It must be emphasized, however, that, when the simple scale corrections are applied to ground measurements, the UTM system is fully as good as the original ground survey permits, even to the standard of first-order accuracy. For this reason, certain countries, preferring to use but one grid for all purposes, have adopted the UTM system for cadastral as well as military use. Because both cadastral grids and the UTM grid are conformal it is a simple matter at the AMS to receive the data in a cadastral system and transform them to the UTM system through the use of electronic computing equipment. The accuracy and feasibility of the UPS grid system in those land areas are comparable to the UTM system.

CONCLUSIONS

The extension of the UTM system to combined operations of the military services, its acceptance by the North Atlantic Treaty Organization and by various other countries as their official military grid system, the recommendation for its wide adoption for topographic mapping by such international organizations as the International Union of Geodesy and Geophysics, the Pan-American Institute of Geography and History, and the British Commonwealth Survey Officers' Conference, and, particularly, its acclaimed use during the military operations of Korea, all attest to the soundness in the design and the adaptability of the system. There is ample evidence that these grid systems, the UTM and the UPS, represent a distinct and important advance in military engineering in keeping with the wide technical progress of the age.

AMERICAN SOCIETY OF CIVIL ENGINEERS
Founded November 5, 1852
TRANSACTIONS

Paper No. 2814

ENGINEERING PROPERTIES OF EXPANSIVE CLAYS

By Wesley G. Holtz,[1] M. ASCE, and Harold J. Gibbs,[2] A. M. ASCE

With Discussion by Messrs. Raymond F. Dawson; William T. Altmeyer; Edward S. Barber; Lawrence A. DuBose; and Wesley G. Holtz and Harold J. Gibbs

Synopsis

Expansive clay soils have been encountered at the sites of structures throughout the western United States. Inasmuch as most of these structures are hydraulic, the normal difficulties encountered when expansive clays are present in the subgrade foundation are greatly magnified. As a result of some of the difficulties that have been experienced, considerable research testing has been undertaken so that expansive clays can be recognized and their potential swelling properties anticipated.

Such petrographic laboratory facilities as equipment for making microscopic examinations, x-ray diffraction determinations, and differential thermal analyses are quite valuable in determining the presence of objectionable clay minerals which may ultimately cause expansions. In addition, relatively simple tests that can be performed in the average soil mechanics laboratory yield excellent indices of expansion properties such as colloid content, plasticity index, and shrinkage limit.

Numerous actual expansion tests have been performed to determine the actual volume-change values and the uplift pressures that can be developed when the volume is maintained constant. The volume-change data have been correlated with the three foregoing index values. In addition to these laboratory tests, the load-expansion and stability characteristics of many soils have been studied, and methods of controlling expansion in remolded soils have been developed.

Note.—Published, essentially as printed here, in October, 1954, as *Proceedings-Separate No. 516*. Positions and titles given are those in effect when the paper or discussion was approved for publication in *Transactions*.

[1] Head, Earth Lab. Section, Bureau of Reclamation, U. S. Dept. of the Interior, Denver, Colo.

[2] Research Engr., Earth Lab. Section, Bureau of Reclamation, U. S. Dept. of the Interior, Denver, Colo.

Included in the paper is a study of several actual design and operation experiences including the uplift of the piers of the Malheur Siphon in Oregon, the cracking and uplift of concrete canal linings in the Central Valley area of California, instability of clay slopes in this area, remedial measures inaugurated on later work in this area, the use of belled-out piles to resist uplift at Wellton-Mohawk Pumping Plant No. 3 in Arizona, and bentonitic soils in the spillway subgrade of the proposed Tiber Dam in Montana.

INTRODUCTION

Expansive clay soils have been encountered in widespread locations throughout the western United States at the sites of structures built by the Bureau of Reclamation (USBR), United States Department of the Interior. The problems encountered with expansive soils when used for highway fills or subgrade foundations or when used for building foundations have frequently been described. However, this paper is believed to be one of the first in which are described the difficulties encountered with such soils when used as foundation materials for a variety of hydraulic structures. It is quite obvious that the height of uplift, the uplift pressures, and the loss of stability can be magnified greatly in hydraulic structures as compared with such nonhydraulic structures as buildings and roadways because of the presence of water which will eventually saturate the foundation soils. The types of structures in which the writers are primarily interested are canals and appurtenant structures, pumping plants, power plants, and dams and appurtenant structures.

The USBR first became actively interested in the destructive effects of expansive foundation soils in 1938 when considerable distress was noted in the piers and anchors of a large steel siphon across the Malheur River on the Owyhee Project in Oregon. Since that time other structures have shown distress caused by the destructive forces of expansive soils. A rather complete laboratory research program was initiated in order to secure basic data on these expansive soils so that their actions could be predicted and proper design and construction measures could be adopted to provide trouble-free structures.

In this paper are described the laboratory tests that were used to identify the expansive clay soils and study their engineering properties. In addition, some of the problems that developed when these soils were encountered will be discussed.

LABORATORY TESTS

Identification Tests.—There are a number of laboratory tests that are useful in identifying clay soils and estimating potential swelling properties. Detailed characteristics of the clay minerals can be described by tests which are quite technical, such as microscopic examination, x-ray diffraction, and differential thermal analysis. To the practicing engineer, facilities for such tests may not be available and there is the need for more simplified tests to identify expansive soil. Also, the engineer is interested in directly observing the effects of expansion for loadings and moisture conditions that simulate those in the actual structure.

The clay minerals of major importance to soils engineers are included in the montmorillonite, illite, and kaolinite groups. The montmorillonite clay minerals swell when wetted by water whereas the clay minerals of the other two groups do not swell, or swell considerably less. The amount of swelling to be anticipated from a soil containing montmorillonite clay minerals depends largely on the quantity of this mineral which is present and the kind and amount of exchangeable bases. Where petrographic laboratory facilities are available, microscopic, x-ray diffraction, and differential thermal analysis techniques are useful in determining whether expansions are likely. The tests are used to determine whether expansive material is present in a soil and—if so—the quantity and other information about the exchangeable bases. Each of these methods has its particular use. All three methods are desirable in a detailed investigation of fine-grained material because only by close coordination of the three methods can the mineralogical composition and the influence of texture and structure be determined. Brief descriptions of these detailed tests are as follows:

a. Microscopic examination permits direct observation of an enlarged image of the material. An identification depends on the fact that all materials reflect light to different degrees and that they possess somewhat definite optical properties which can be observed precisely in polarized light. Certain stains make possible easy identification of many clay minerals. The main purpose of the microscopic examination is to determine mineralogic composition, texture, and internal structure. For fracture surfaces and fragments, the stereoscopic microscope is used, usually at magnifications of from 10 to 200. This process permits the examination of gross structures and textural relationships and the identification of particles of gravel, coarse to medium sand, and organic remains. For examination in more detail and at higher magnification, thin sections are prepared. (Fragile soils require the impregnation with a suitable resin or plastic.) This process permits examination of any but the finest particles for identifying minerals and describing intimate details of internal structure and texture. It especially permits observations of the nature of voids and their interconnection, the grain-to-grain relationships, the binding materials, and the concretionary developments.

b. Analysis by x-ray diffraction supplements microscopic examination in identifying the finest fractions and in determining quantitatively the mineral constituents. The method depends on the manner in which the atomic structure of the compound diffracts x-rays of a certain wave length and it determines the arrangement of atoms within crystals. Amorphous substances such as volcanic glass, opal, allophane, and cliachite are not detected by x-ray, and minor constituents, representing approximately 10% or less, cannot be observed. Patterns of x-ray diffraction may be recorded on photographic film. Film patterns permit comparison with standard reference patterns for identification of mineral constituents. This method may frequently yield misleading results if interlayering exists within individual crystals, such as when montmorillonite and kaolinite, or illite and montmorillonite alternate at random in the same crystal. For reasons such as this, precise analysis of most soils is a special and time-consuming problem. Semiquantitative analysis, however, usually can be accomplished rapidly. Particularly in connection with expansive clay, the change in dimensions of the lattice can be observed when patterns are made at varying humidity conditions.

c. The differential thermal analysis also supplements the microscopic examination in identifying the finest fractions and their relative abundance. The method involves the differential measurement of heat absorbed or released by a material while it is being heated at a constant rate. It yields definite results only with crystalline substances because only crystalline compounds exhibit several characteristic levels of energy release or absorption during heating in the usual ranges from room temperature to 1100° C. Many types of equipment have been developed, but few are available commercially. An international committee is now trying to establish the requirements of a satisfactory instrument. This analysis is valuable because it reveals interlayering in clay minerals, which x-ray diffraction fails to do. Also, distinction between clay minerals containing differing exchangeable ions is possible. A soil sample containing ingredients that have great energy exchanges might have the minor energy exchanges of other constituents masked. Observations by microscopy are especially valuable for detection of these other constituents.

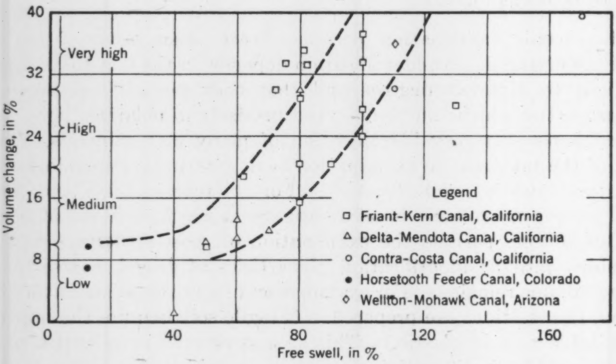

FIG. 1.—FREE SWELL RELATED TO VOLUME CHANGE (AIR-DRY TO SATURATED CONDITION UNDER A LOAD OF 1 LB PER SQ IN.)

In addition to the foregoing, more complex petrographic tests, there are other identification tests that may be performed in the average soil laboratory to determine possible expansive characteristics. The most simple of these is the free-swell test. This test is performed by slowly pouring 10 cu cm of dry soil passing the No. 40 sieve into a 100-cu cm graduate filled with water and noting the swelled volume of the soil after it comes to rest at the bottom. The free-swell value in percentage is determined by using the expression: [(final volume minus initial volume) ÷ initial volume] × 100. A good grade of high-swelling commercial bentonite will have a free-swell value of from 1,200% to 2,000%. Soils having free-swell values as low as 100% may exhibit considerable volume change when wetted under light loadings and should be viewed with caution whereas soils having free-swell values below 50% seldom exhibit appreciable volume changes, even under very light loadings.

It has not been possible to work out close correlations between free-swell values and actual total volume changes determined by controlled expansion tests conducted in laboratory consolidometers. However, general trends are apparent and, in many instances, the free-swell values will provide sufficiently accurate data for preliminary design. These trends are shown in Fig. 1, which is a plot of free swell against the total expansion of undisturbed soil specimens placed in laboratory consolidometers and expanded from air-dry to saturated conditions. These consolidometer tests will be explained in detail in subsequent paragraphs.

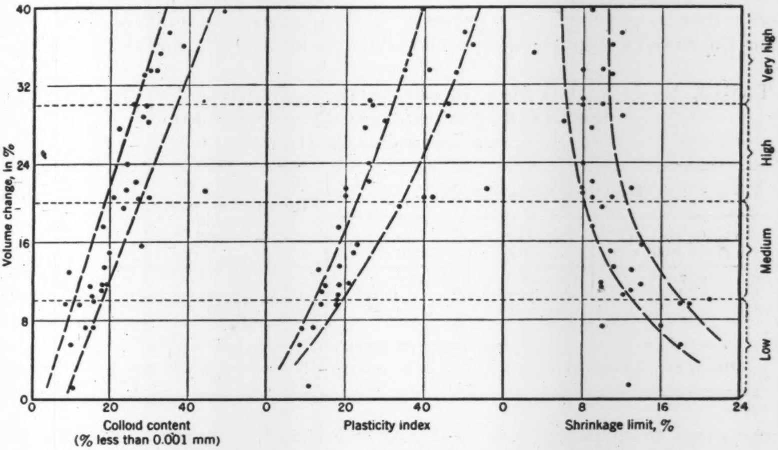

FIG. 2.—RELATION OF VOLUME CHANGE TO COLLOID CONTENT, PLASTICITY INDEX, AND SHRINKAGE LIMIT (AIR-DRY TO SATURATED CONDITION UNDER A LOAD OF 1 LB PER SQ IN.)

In searching further for simplified identifying tests, it was found that the colloid content of a soil and the Atterberg or consistency tests provide satisfactory indicators of the expansive characteristics of clays when considered together. This is true for the following reasons:

1. The colloid content, determined from the gradation test, indicates the amount of the colloidal-size fraction, which is the most active part of any soil material contributing to expansion.

2. The plasticity index, which demonstrates the magnitude of the range of moisture change possible while the soil retains a plastic condition, is related to expansion because the water in the voids and clay minerals occupies space, thus causing changes in moisture content to reflect volume change. High plasticity indices are indicative of active soils and, therefore, would be

necessary in order for a soil to change volume appreciably when going from the semi-solid phase to the liquid phase

3. The shrinkage limit which describes, indirectly, the minimum volume to which a soil will shrink upon drying and is an expression of percentage of water necessary to fill the void spaces when the soil is at minimum volume is valuable supplemental information to the foregoing data. A low shrinkage limit would show that a soil could begin volume change at a low moisture content.

Table 1 is based on actual expansion tests for 38 undisturbed soil samples, and the results of these tests are summarized in Fig. 2. The expansion tests from which the data on total volume change were obtained are discussed in subsequent paragraphs. In Fig. 2 the thin dashed lines were drawn on the basis of judgment so as to enclose most of the points and still keep the limits as narrow as possible. The values in Table 1 express the limits of these lines for the various degrees of expansion (low, medium, high, and very high) as compared to colloid content, plasticity index, and shrinkage limit. Because the data were obtained from undisturbed samples, with a variety of density conditions, the results of the measured total volume changes are somewhat irregular. More consistent and regular results could be expected from compacted specimens in which density conditions were controlled. However, the writers' interest at the time of testing was primarily in identifying the expansiveness of undisturbed soils because they represented the actual subgrade soils on which canal structures were to be placed. Although the initial or in-place density conditions varied, the range of variation in the Central Valley of California, where the samples were obtained, was not great. Therefore, the index data could be used to estimate expansiveness quickly in the field.

TABLE 1.—DATA FOR MAKING ESTIMATES OF PROBABLE VOLUME CHANGES FOR EXPANSIVE SOILS FROM DELTA–MENDOTA AND FRIANT–KERN CANALS (CALIFORNIA)

DATA FROM INDEX TESTS			Estimated probable expansion,[a] in % (dry to saturated)	Degree of expansion
Colloid content (% minus 0.001 mm)	Plasticity index	Shrinkage limit (%)		
>27	>32	<10	>30	Very high
18–37	23–45	6–12	20–30	High
12–27	12–34	8–18	10–20	Medium
<17	<20	>13	<10	Low

[a] Based on a vertical loading of 1.0 lb per sq in. in the one-dimensional consolidation testing machine.

Other tests that were investigated for the purpose of estimating expansive characteristics included the (1) percentage smaller than 0.005 mm, (2) liquid limit, (3) free swell, and (4) montmorillonite mineral content. However, from the standpoint of the soil mechanics engineer, it is believed that the three tests used provide a more simple and practical means of estimating the expansion characteristics.

Load-Expansion Tests.—The Load-expansion test which provides factual data for predicting the amounts of expansion is a form of the standard one-dimensional consolidation test. The testing equipment is similar to that used in most soil laboratories for consolidation studies. This equipment, called a consolidometer, is of the fixed-ring type. It accommodates a remolded or undisturbed specimen 4.25 in. in diameter and 1.25 in. deep. Porous stones are provided at each end of the specimen for drainage or saturation. The specimen container is placed on the weighing table of a platform scale, and the load is applied by a yoke actuated by a screw jack. The load imposed on the specimen is measured by the scale beam, and a dial gage is provided to measure the vertical movement (Fig. 3). Test specimens are cut from undisturbed samples and placed in the testing container with extreme precision. Water may be added to observe the effect of wetting on volume change. Fig. 3(*c*) shows the large volume changes caused by wetting the soils while they were under a loading equivalent to that of a canal lining.

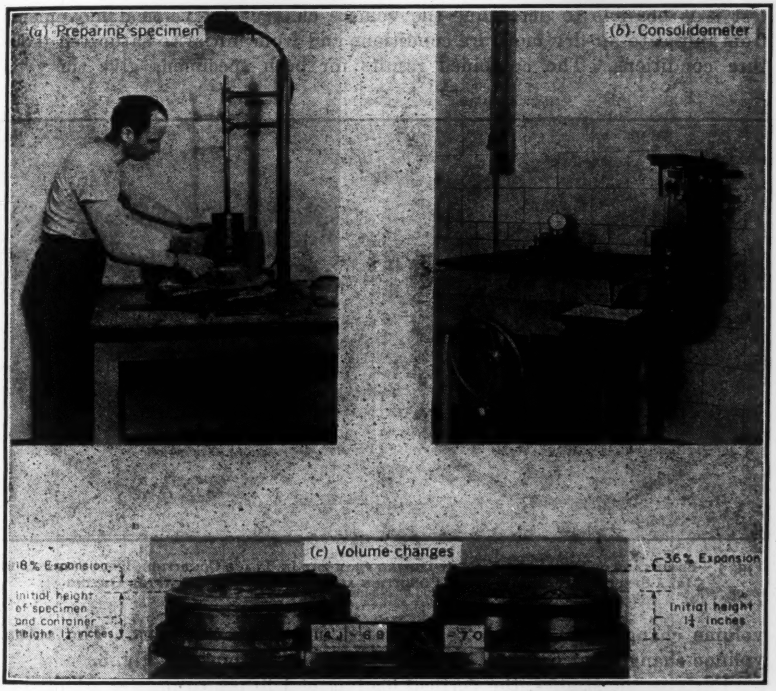
(*a*) Preparing specimen
(*b*) Consolidometer
(*c*) Volume changes
18% Expansion
initial height of specimen and container height 1¼ inches
(4J)-6.9
-7.0
36% Expansion
Initial height 1¼ inches

FIG. 3.—LABORATORY STUDIES OF EXPANSIVE CLAYS

The somewhat standard procedure that the USBR have adopted for testing the expansiveness of clays for concrete-lined canal subgrades requires two test specimens. These can be cut from undisturbed soil samples or remolded at desired moisture and density conditions from loose samples. After the specimens have been placed in the consolidometer ring and the original volume and moisture have been determined, they are allowed to dry in air to at least the shrinkage limit. The volume change at the air-dry condition is determined on the first specimen by a mercury displacement method. The second specimen is placed in the consolidometer under a vertical loading of 1 lb per sq in. (or any anticipated structure load) and is saturated. The vertical movement indicates the volume change. From the foregoing test it is possible to determine the volume change and vertical movements from initial to air-dry moisture conditions and from initial to saturated moisture conditions. The combined results for both specimens give the total volume change from air-dry to saturated moisture conditions. The actual volume change that occurred during typical tests is shown in Fig. 3.

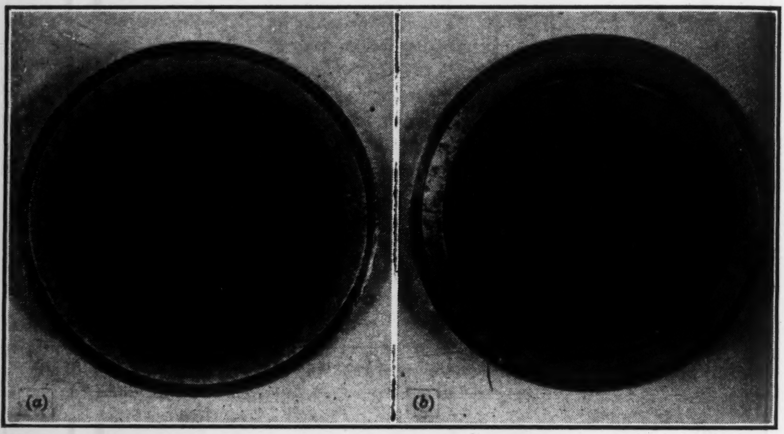

FIG. 4.—SHRINKAGE OF EXPANSIVE CLAY BY DRYING FROM THE IN-PLACE CONDITION, DEMONSTRATED BY (a) A SPECIMEN AT THE IN-PLACE CONDITION AND (b) SAMPLE 3T-103 AFTER DRYING

Early in the studies, the vertical loading of 1 lb per sq in. was adopted as the load to be applied while saturating the specimens because it represented the approximate loading on the subgrade of concrete canal linings which were then under study. Because of the data accumulated under this load condition, the correlative data contained in this paper between index or identification properties and actual expansive characteristics are based on the total volume change from the air-dry to the saturated condition under the loading of 1 lb per sq in.

Although the test just described was used primarily to indicate relative expansiveness of subgrade soils subjected to light loadings, other information can be secured by means of the one-dimensional consolidometer as job conditions require. In some instances third specimens are prepared and treated in the same manner as the second specimens, except that during the saturation period sufficient load is applied throughout the test to prevent vertical movement. By this process, the vertical uplift pressures may be determined. In other cases it has been desirable to make rather accurate predictions of the actual movement that might occur under various load conditions. This has been done by securing load-expansion data by means of the consolidometer test, varying the load conditions during the test. In these latter cases the sample was usually saturated directly from the initial placement condition while bearing a load to simulate field conditions.

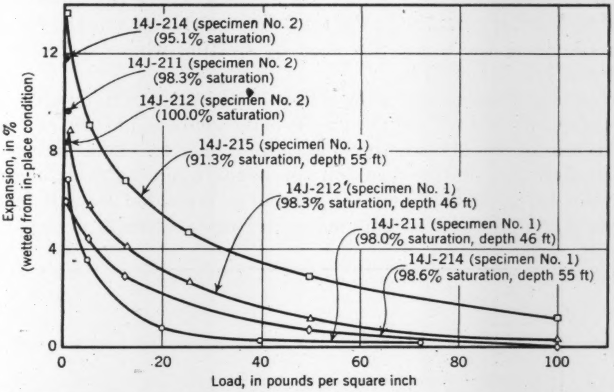

FIG. 5.—LOAD-EXPANSION STUDIES ON UNDISTURBED SAMPLES—WELLTON-MOHAWK PUMPING PLANT, ARIZONA

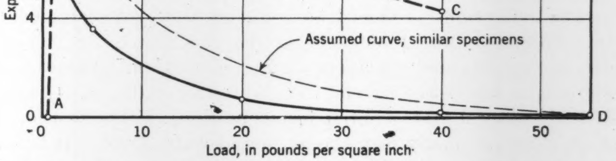

FIG. 6.—EFFECT OF SEQUENCE OF LOADING AND WETTING ON EXPANSION

As a matter of general interest, the maximum uplift pressure recorded for the expansive clays in the Central Valley of California was 147 lb per sq in. This pressure was that required to hold the vertical height constant while the specimen was saturated from an air-dry condition in the consolidometer. In this test some lateral movement of particles occurred as the cracks were being filled during expansion. It was felt that this test simulated the action that would occur under a structure placed on an air-dry expansive clay subgrade. Typical shrinkage of air-dry specimens is shown in Fig. 4. Shrinkage of the sample in Fig. 4(*b*) was 16.4% and the swelling above the initial condition, produced by wetting, was 7.6%; the total volume change was therefore 24.0%. For this specimen, the uplift produced by wetting while holding the height constant was 11.1 lb per sq in.

In some of the most interesting studies, the load-expansion characteristics were determined so that actual uplift movements could be computed for various types of canal structures and for concrete canal linings. These studies involved (*a*) undisturbed soil specimens where natural subgrade conditions were being studied and (*b*) specimens remolded to anticipated field conditions where compacted subgrades and embankments of expansive soil were being studied. Fig. 5 shows the results of some of the load-expansion tests conducted on undisturbed soil specimens taken from a pumping-plant foundation in Arizona. Specimen No. 1 of each sample was tested by (*a*) measuring the load required to restrain the sample during saturation and (*b*) measuring the expansions produced by reducing the load increments to 1 lb per sq in. Specimen No. 2 of each sample was tested by measuring the swelling of an unrestrained specimen during saturation. These soils, which were described as high-swelling clays were nearly saturated (from 91% to 100%) in their natural state (initial test condition) although they were obtained at an elevation many feet above ground-water level. It is interesting that although these clays had high initial saturation they expanded greatly as free water was made available to them and as the load conditions were varied. Also, if the specimens were first heavily loaded to permit no volume change during saturation, their expansions when loadings were reduced to zero were not as great as for specimens that were wetted under zero (or similar light) loadings.

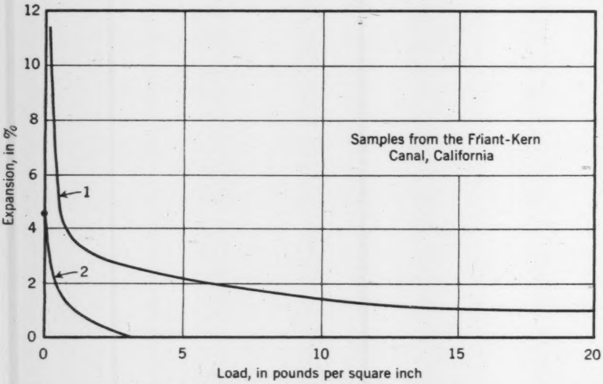

FIG. 7.—LOAD-EXPANSION DATA FOR SOILS THAT ARE CRITICAL WITH RESPECT TO LOADING

Fig. 6 shows the difference in load-expansion characteristics for a soil that was loaded before saturation (curve DE) and one that was saturated before loading (curve ABC). Specimen No. 1 was wetted under maximum uplift load, and then the load was reduced in increments. Specimen No. 2 was wetted under very light load and then loaded. Curve BD is the assumed curve for several similar specimens wetted while under their respective loadings. Thus, it becomes apparent that the test procedure is quite important if uplift is to be estimated accurately. If more accurate estimates of uplift are required—for example, on a thick layer of clay under a pumping plant—it is necessary to prepare several specimens for consolidometer tests. These specimens should then be loaded with the plant loading plus the weight of overlying material from the base of the plant to the elevation of the material they represent. The specimens should then be saturated under their respective loadings and the load-expansion data plotted from the uplift data obtained. One would then obtain a curve BD which would be intermediate between the load-expansion curves obtained for saturation before loading and for saturation under an initial load large enough to inhibit expansion. In many studies it is not practical to go into such detail and sufficient data may be obtained from two tests, as curves ABC and DE; curve BD then can be

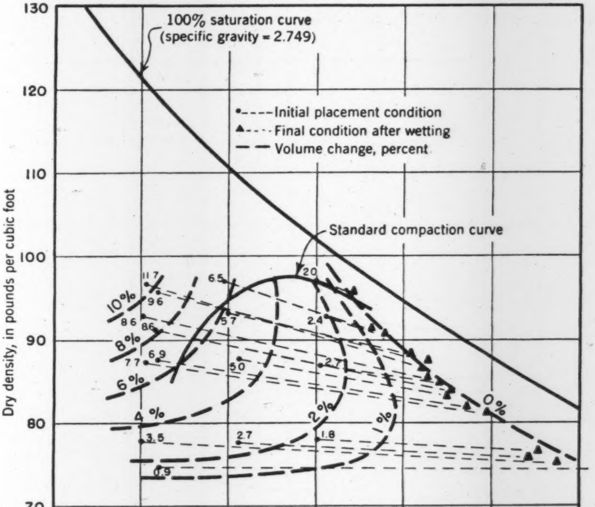

FIG. 8.—PERCENTAGE OF EXPANSION FOR VARIOUS PLACEMENT CONDITIONS FOR SOIL UNDER A LOAD OF 1 LB PER SQ IN.

drawn by use of judgment. Considerable judgment may be required, however, as the expansion may be critical with respect to loading as shown by Fig. 7. In this case, very light loads inhibited the swell considerably. The shape of curve DE in Fig. 6, however, generally indicates this fact. A few intermediate test points may be necessary for more detailed analysis of a BD-curve.

A control of expansions can be obtained by decreasing the density of the soil to near the expanded density which it will have when under the load conditions at which it will be saturated in a structure. Many times this can be accomplished in subsurface foundation soils by prewetting an area prior to construction. However, because of the time involved in saturating impervious clays of this nature, this method may not be practical and other design or construction measures must be adopted.

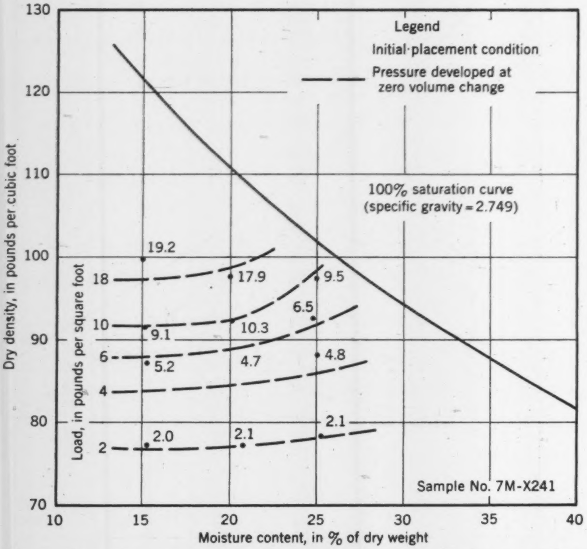

Fig. 9.—Total Uplift Pressure Caused by Wetting—for Various Placement Conditions

The control of expansion in compacted clay embankments or subgrades is considerably easier as density, and to some extent the moisture can be controlled to give more favorable conditions. To study closely the effect of various moisture and density conditions on expansion, several series of soil specimens compacted at a variety of moistures and densities were tested in the laboratory consolidometers. For each placement condition, duplicate specimens were prepared and tested to determine (1) the expansion under loadings of 1 lb per sq in. when saturated and (2) the uplift pressure or load required to restrain expansion. (These specimens were then allowed to expand by reducing the restraining load in increments.) In Figs. 8 and 9 are the results of these tests on "Porterville clays" from the Delta-Mendota

Canal in the Central Valley for canal embankment studies. Fig. 8 is a summary of the expansion data for specimens placed with moisture contents at approximately 15%, 20%, and 25% and densities in pounds per cubic foot of 77, 87, 92, and 97 for each moisture condition. The placement conditions are indicated for each specimen by circular points in Fig. 8. The percentage of expansion of initial volume is shown beside each point. The trend of expansion is shown by thin dotted lines drawn from these points to the triangular points that represent the final conditions of density and moisture content after expansion. The lines form a distinct fanning pattern, being steep for higher placement densities and flat for low placement densities. A heavy dashed line has been drawn through the triangular points to represent the placement conditions for zero expansion for a loading of 1 lb per sq in. A series of heavy dashed lines has been drawn to indicate placement conditions that would result in near equal expansions; each line is labeled to indicate the expansion anticipated. It can be seen from studying Fig. 8 that a combination of placement densities lower than those obtained by standard compaction and placement moistures near or higher than standard optimum are required to insure low expansion. It is evident that the reduction of density alone will not always provide the desired reduction in expansion for light loadings. Increased moisture provides increased expansion control, especially

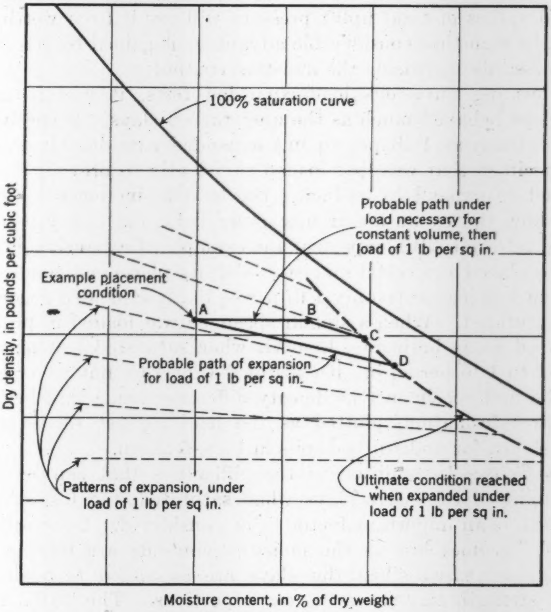
100% saturation curve
Probable path under load necessary for constant volume, then load of 1 lb per sq in.
Example placement condition
A
B
C
D
Probable path of expansion for load of 1 lb per sq in.
Patterns of expansion, under load of 1 lb per sq in.
Ultimate condition reached when expanded under load of 1 lb per sq in.
Dry density, in pounds per cubic foot
Moisture content, in % of dry weight

FIG. 10.—DEMONSTRATION OF EXPANSION TRENDS WITH RESPECT TO SEQUENCE OF LOADING AND SATURATING

in the higher expansion ranges; however, it is usually not possible to place these soils at high moisture contents because of construction difficulties. Therefore, a combination of moderately high moisture and low density control is most suitable.

Fig. 9 is also of interest in studying the effect of various placement densities and moistures on uplift pressures when the initial volume was held constant during the consolidometer test. In this illustration, the load, in pounds per square inch, necessary to hold the volume at no expansion is shown alongside each point of placement density and moisture. On the basis of these values, the heavy dashed lines were drawn to represent placement conditions for which equal values of total uplift pressure will result from wetting. In this case, it can be seen that considerable advantage is gained by reducing density without necessarily increasing the moisture content.

By performing numerous load-expansion tests, it was found that the remolded clays behaved much as the undisturbed clays. A specimen bearing a light load (such as 1 lb per sq in.) expanded considerably more than an identical specimen that was first loaded sufficiently to prevent expansion and then allowed to expand by reducing the load in increments. Fig. 10 was drawn to show the expansion trends under light and heavy loadings. The heavy lines, AD and ABC, represent the example of expansive characteristics of specimens placed at a certain moisture-density placement condition. When one specimen was loaded to only 1 lb per sq in., it expanded according to line AD when saturated. When a similar specimen was loaded to prevent expansion, it moved along horizontal line AB when saturated. When the loading was reduced to 1 lb per sq in., it expanded (line BC) but never expanded as much as the first specimen (the density difference being that between C and D). Similar information, plotted as the load against the expansion, was previously shown for undisturbed soils in Figs. 5 and 6.

Stability Tests.—In addition to the difficulties that can be encountered from the uplift of expansive clays when saturated, the loss of stability or shear strength is an important factor to be considered. Generally the shearing strength becomes less as the moisture contents are increased, and the densities are decreased when the clays are expanded through saturation. This loss of strength may assume large proportions. The USBR has not conducted basic research on this phase with expansive clays, but many data have been collected in the course of regular project work. The extreme loss of strength that may occur in an undisturbed expansive clay is clearly shown by average test results obtained on four specimens from a sample of very fat clay of class[3] CH, secured from the foundation area of Pumping Plant No. 3 of the Wellton-Mohawk canal system. The average consistency test results, in percentages, were: Liquid limit $L_w = 75$, plasticity index $I_w = 50$, shrinkage limit $S_w = 12$, and colloids $= 59$. This clay, which had a dry density of 103 lb per cu ft and was 93% saturated in its natural state, had an unconfined compressive strength of 155 lb per sq in. When saturated, under no loading, the material expanded to an average dry density of 85.7 lb per cu

---

[3] "Unified Soil Classification System," A Supplement to the Earth Manual, Bureau of Reclamation, U. S. Dept. of the Interior, Washington, D. C., March, 1953.

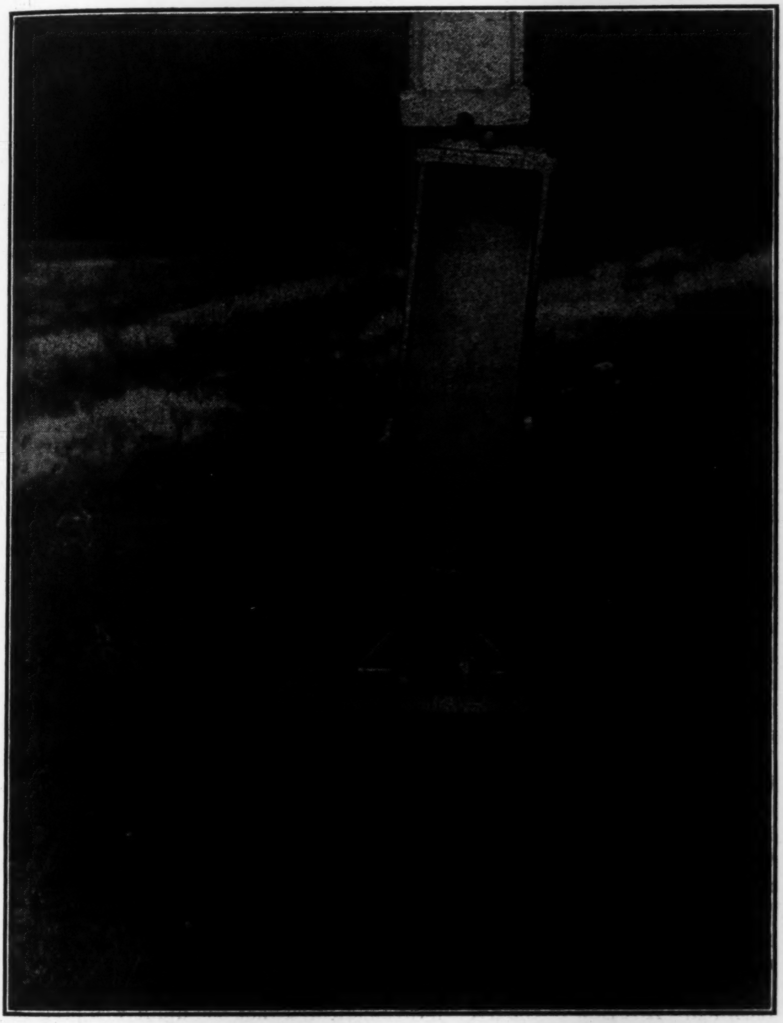

FIG. 11.—DISTRESS IN ROCKER SUPPORTS AT PIERS OF THE MALHEUR SIPHON, OREGON

ft at 99% saturation, and the unconfined compressive strength was reduced to practically zero.

The strength loss of compacted (remolded) Porterville clays from the Central Valley is illustrated by tests made on canal lining clays from the Friant-Kern canal system. At one location the clay, which was compacted to a maximum laboratory dry density of 94 lb per cu ft and was 70% saturated at optimum moisture (22%), had an unconfined compressive strength of 28 lb per sq in. Average test results were: $L_w = 57$ and $I_w = 37$. The classification[3] was CH. Upon saturation under a low loading, the density decreased to 91 lb per cu ft, the saturation increased to 94%, and the unconfined compressive strength was reduced to 4 lb per sq in. (These data are based on averages for four specimens.) Thus, it can be seen for these last data that—although the density change may be small—the strength can be materially reduced by wetting.

If these remolded clays are air-dried prior to saturation, further reductions in strength can be anticipated. For example, one set of specimens which were remolded at maximum laboratory density and optimum moisture showed a strength reduction to 4 lb per sq in. when saturated from the optimum moisture condition and to 1 lb per sq in. when saturated after air-drying. Numerous tests substantiate the trends of the foregoing examples, which are further discussed in subsequent paragraphs on field operations.

DESIGN AND OPERATION EXPERIENCES

The following paragraphs include some general discussions of several structures to which soil expansions were considered dangerous or became detrimental during operation, necessitating designs which would prevent subsequent trouble.

Malheur River Siphon.—The upward movement of the piers of the Malheur River Siphon, in the eastern part of Oregon, furnishes an interesting example of structural difficulties that can occur from foundation expansion.[4] This siphon consists of an 80-in.-diameter steel welded pipe 21,976 ft long and a 78-in.-diameter, precast reinforced concrete pipe 1,020 ft long at the inlet and outlet ends. The steel pipe lies entirely above ground and is supported on piers and anchors at maximum spans of 60 ft and 972 ft, respectively. The pipe is supported at each pier by two steel rockers which are set against bearing shoes on the pipe. One expansion joint was placed in the pipe between each pair of anchors to allow movements accompanying load and temperature. In the spring of 1938, within three years after construction, significant distress was noted at supports in the section of the siphon lying north of the river. This section represented approximately 10% of the total siphon length. Five surveys were made at intervals between 1938 and 1943. At certain piers the displacements were greater than the displacements for which the rockers were designed, the maximum being 0.45 ft. Maximum pier movements of 0.73 ft longitudinally, 0.58 ft laterally, and 1.07 ft upward were recorded. A review of the five surveys indicated that the uplift was progressive but at a declining rate.

A foundation investigation program was undertaken in 1943 so that remedial measures could be initiated. This program consisted of boring, sampling, and laboratory testing. The bedrock in the general vicinity is of the Idaho formation and in the immediate vicinity is composed predominantly

---

[4] "Foundation Displacements Along the Malheur River Siphon as Affected by Swelling Shales," by R. C. Mielenz and C. J. Okeson, *Economic Geology*, Vol. XLI, No. 3, May, 1946.

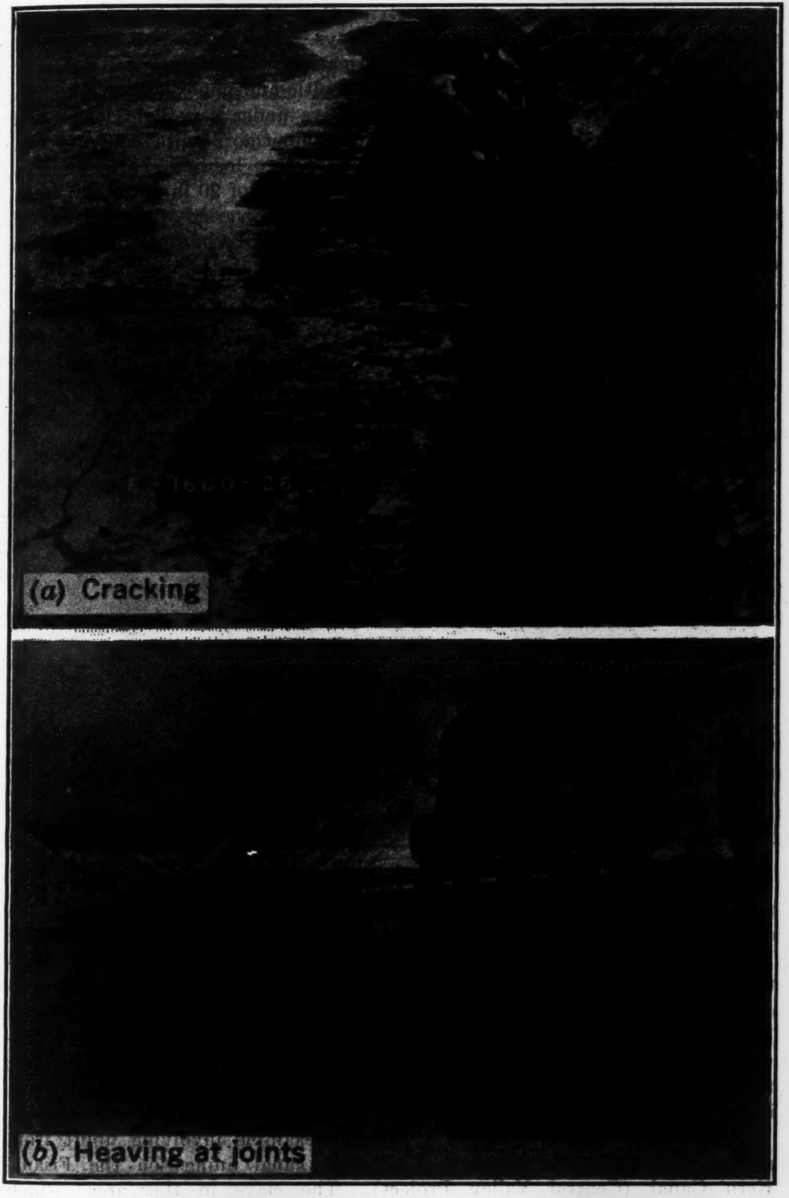
1600-26
(a) Cracking
(b) Heaving at joints

FIG. 12.—EFFECTS OF SEEPAGE INTO THE EXPANSIVE CLAY SUBGRADE, FRIANT–KERN CANAL (CALIFORNIA); HEAVING INDICATED BY DRY AREAS ALONG JOINTS

of shale. The material directly underlying the siphon consisted of sand and sandy silts, clayey silts, and lean-to-fat clays. The clayey soil represented weathered shale and claystone of the formation. Laboratory tests showed that the silty and sandy soils were nonbentonitic and nonexpansive, the lean clays slightly bentonitic and slightly expansive under very light loads, and the fat clays were highly bentonitic (high montmorillonite content) and moderately expansive (more than 10% under zero loading, 7.0% under a loading of 5 lb per sq in., and 0.1% under a loading of 20 lb per sq in. when saturated). The effect of expansion on the siphon varied with the natural water content of the soil, the depth of nonexpansive overburden soils, and the characteristics of the fat clays. It was found through the exploration work that the cause of expansion after construction was due to wetting of the expansive clays primarily by seepage waters from the canal above the siphon. However, some addition to the ground water was derived from nearby irrigation and precipitation. The measures to prevent further displacements included (1) lining 2,000 ft of the canal beyond the outlet of the siphon and 1,000 ft of a nearby lateral; (2) placing a compacted earth blanket and providing drainage gutters along critical parts of the siphon to prevent wetting from precipitation; and (3) the removal of certain agricultural lands from irrigation. Fig. 11 shows the distress in the rocker supports at the piers.

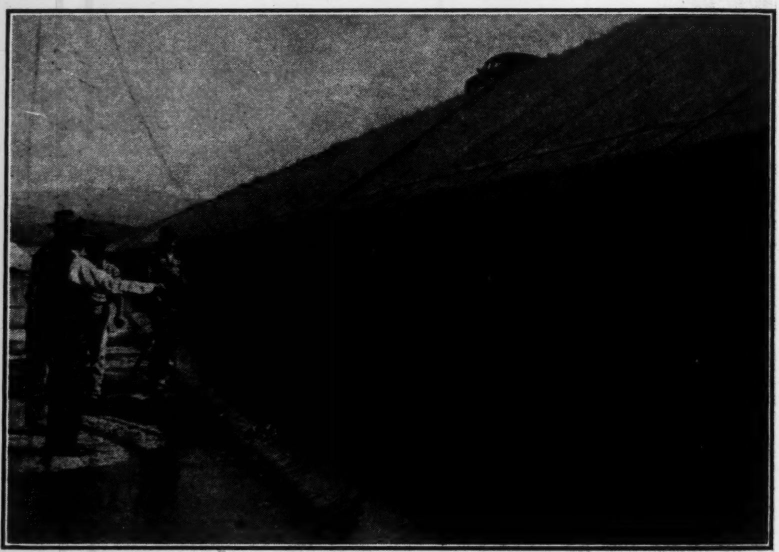

Fig. 13.—Disrupting of the Concrete Canal Lining by the Expansion of Subgrade Clays

Friant-Kern Canal.—Another interesting example involving uplift from expansive clays is the heaving of concrete canal linings on the Friant-Kern Canal (Central Valley Project). The clays in this area, which are locally known as "Porterville clays," contain appreciable proportions of the montmorillonite mineral, are very fine-grained, and are highly plastic when wetted. Some of the physical properties of these clays were discussed in previous paragraphs. In the construction of the Friant-Kern Canal, the expansive clays were encountered in several reaches along the canal and to varying depths below the surface. For economic reasons it was necessary to construct the fill section out of the clay soils existing along the canal line.

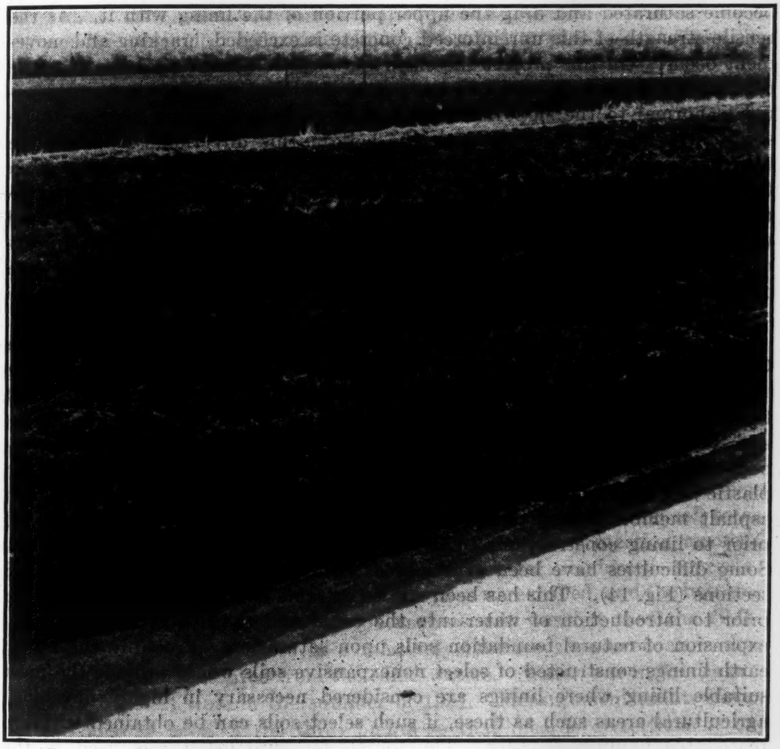

Fig. 14.—Typical Slide in Compacted Earth Lining of Expansive Clay Soil

Considerable distress has occurred at several locations along this canal when highly expansive subgrade clays were saturated by water seeping through joints and cracks in the lining. Distress first occurred in the bottom of the canal, evidenced by cracking of the lining at the toe of the slopes and heaving at the joints (Fig. 12). It has been found that expansions on the side slopes are not generally as critical as expansion of clays composing bottom subgrade materials because the slope linings are less restrained against movement than are bottom linings. However, there have been instances where some side heaving has occurred, necessitating replacement of lining panels (Fig. 13). Such failures are considered to be due to uplift forces rather than to slope instability.

There have also been instances at the Delta-Mendota Canal in California, in which longitudinal cracks of widths up to 1.5 in. have opened in the slope lining. Similar Porterville clays were used on this project to construct embankments on partial fill sections. The cracks are apparently caused by an uplift of the upper portions of the embankment which heave upward as they become saturated and drag the upper portion of the lining with it. As the tensile strength of this unreinforced concrete is exceeded, cracking and movement occur. On this project the clays were only slightly expansive at grade depths, and no bottom cracking has occurred. No side cracking from movements normal to the slope has occurred as the slope lining appears to be sufficiently flexible to move with the soil in this direction. A large-scale field test was made during construction to test the effect of expansiveness on the slope linings of this project. Highly expansive clays used in the embankment were saturated by artificial means, and elaborate measurements of all movements were taken. Although the slope lining underwent lateral movement, varying from zero at the toe of the slope to about 0.11 ft at the top, no cracking occurred; thus, it was concluded that the slope lining was flexible enough to withstand anticipated movements. This has generally been true.

Remedial measures contemplated for later construction on the Friant-Kern Canal consisted of (1) prewetting the subgrade soils prior to final trimming and lining; (2) the use of asphalt membranes under the concrete lining; (3) the use of a heavy earth lining (3-ft normal thickness) instead of concrete; and (4) controlled embankment-placing procedures. Difficulties were encountered when prewetting was attempted because the clays became so plastic and sticky that the trimming machine could not handle the soil. An asphalt membrane was placed on the subgrade for one reach of the canal prior to lining construction. This appears to have reduced major cracking. Some difficulties have been experienced with earth slides on the earth-lined sections (Fig. 14). This has been due to extreme cracking of the earth lining prior to introduction of water into the canal and the loss of strength from expansion of natural foundation soils upon saturation. Probably the use of earth linings constructed of select nonexpansive soils would provide the most suitable lining where linings are considered necessary in highly developed agricultural areas such as these, if such select soils can be obtained within a reasonable hauling distance. The fourth measure listed was used in the construction of equalizing reservoir embankments. For this plan the materials were placed at lower densities and higher moisture contents than those specified for normal soils. These embankments were placed as wet as the use of conventional compaction equipment would allow and at densities which, as indicated by laboratory tests, would provide minimum expansion when wetted and minimum consolidation if the soil were required to resist the water load prior to saturation. Thus, a minimum total movement was anticipated for the concrete lining.

Tiber Dam Spillway.—Field explorations showed that the foundation of the spillway site for the proposed Tiber Dam, near Chester, Mont., contained bentonitic layers or seams within the firm Colorado-shale bedrock. A testing program was conducted to study the consolidation or expansion and stability properties of these bentonitic soils. The average consistency test results, in percentages, were as follows: $L_w = 112$ to 245, $I_w = 78$ to 216, $S_w = 4$ to 15, colloids = 31 to 54, and montmorillonite material = 45 to 90. Of concern were the problems of (1) uplift from expansion when the clay is saturated under light loads; (2) settlement of the layers when under the heavy loads of the dam; and (3) the shearing strength of the saturated clays. Load-consolidation tests and triaxial-shear tests were made on several samples to answer these questions. Although the bentonitic soils were almost saturated in this natural state, it was found that appreciable expansion or uplift would occur when water was supplied to the soils under loads less than from 10 lb per sq in. to 15 lb per sq in. Consolidations of up to 13% were obtained under loadings of 220 lb per sq in. Shear values were difficult to determine because of nonuniformity of specimens, but apparent values of cohesion equal to 9 lb sq in. and $\tan \phi = 0.2$ were indicated. The results of the expansion tests indicate that removal of materials to a depth of 10 ft or 15 ft and replacement with nonexpansive soils would be required in critical areas of the spillway to assure against uplift.

Wellton-Mohawk Pumping Plants.—The investigations of the foundations of the Wellton-Mohawk pumping plants, near Yuma, Ariz., showed that a series of alternating strata of fat clay, silty clay, and silt existed at the proposed sites of Plants No. 2 and No. 3. It was found that the strata of fat clay were highly expansive. At Pumping Plant No. 2 the ground-water table was above foundation grade. Inasmuch as the expansive clays were saturated and the difference in load between the overburden at grade and the plant loadings was small, no uplift from the clays was anticipated. At the site of Plant No. 3 no ground water was encountered in holes extending to 35 ft below the foundation grade, and tests showed the soils to be expansive under loadings representing the plant loading plus the weight of the soil to a depth of about 20 ft below the grade line. To provide protection against uplift (particularly differential uplift) 25-in.-diameter reinforced concrete piles 20 ft long were specified. Holes for the piles were drilled, and the bottom of the holes were belled out to provide anchors. It was felt that the 20-ft length placed the pile anchors in a relatively inactive zone even after the foundation became saturated from the canal waters. Water was in this canal system for the first time in the summer of 1951. Measurement points have been provided at each of the three plants so that records of settlement or uplift can be made. Immediately after constructing the plant the average settlement was 0.035 ft. In 1955, four years after operation was begun, the average uplift was equal to the initial settlement and the base of the plant was at the original elevation. Thus, it appears that the foundation design was reasonable.

CONCLUSIONS

Expansive clay soils can produce detrimental uplifts to hydraulic structures placed on them. The expansiveness depends on the quantity of montmorillonite mineral present in the soil and the kind and amount of exchangeable bases.

Petrographic laboratory tests are useful in identifying expansive soils and in determining expansiveness by determining the amount and types of minerals present. The petrographic microscope, x-ray diffraction, and differential thermal analysis techniques are used for this purpose.

Common soil laboratory tests for such data as the colloid content, the plasticity index, and the shrinkage limit are also effective in determining the expansiveness of soils. A simple free-swell test provides a quick qualitative measure of expansiveness.

In contrast to the foregoing index tests for estimating potential expansiveness, the soil-laboratory consolidometer may be used to determine quantitative uplift values for anticipated load conditions. These tests are usually made by saturating undisturbed or remolded subgrade soil specimens under the load conditions anticipated for the structure. Load-expansion curves may thus be developed for a variety of load conditions. The expansions observed in similar soil specimens that are allowed to become saturated under variable load conditions (from zero to maximum uplift) and then brought to a common load condition are generally considerably different. Therefore, it is important to duplicate the anticipated field conditions of saturation and loading as closely as possible.

Because the volume change of a particular expansive clay soil when saturated under a specified loading is dependent on the moisture content and density at the time saturation is begun, it is possible to control the amount of expansion in compacted clay soils by increasing the moisture or decreasing the density, or both. The initial density and moisture conditions for expansion control can be computed from results of laboratory consolidometer tests.

The increased moisture and decreased density resulting from the expansion of montmorillonite clay soils have a tendency to reduce the shearing strength of these soils. Under light load conditions the cohesion of the soils can be reduced to almost zero on saturation, even though the soils may have fairly high cohesive strengths at moderate moisture conditions.

When hydraulic structures are to be constructed in areas where expansive clays exist, it is necessary to take special precautions against uplift unless the structure loads are sufficient to resist the uplift forces. Stability should also be checked. If structure loads are not sufficient to prevent expansion of the subgrade soils, the following measures may be adopted:

a. The natural subgrade expansive clays may be removed and replaced with nonexpansive soils to a depth sufficient to provide loadings that will resist uplift.

b. If the subgrade is a remolded expansive soil, the volume change may be controlled by compacting the soil at high moisture contents and low densities as predetermined through laboratory tests unless large periodic changes in moisture are anticipated. It may be necessary to check for consolidation during any presaturation period, however.

c. The saturation of the foundation soils may be prevented by shutting off all sources of water supply, although this may be difficult and impossible in some cases.

d. Piles anchored in an inactive zone below a structure provide reliable assurance against uplift if properly incorporated into the structure base.

It may be possible to control the expansions of montmorillonite clays by changing their exchangeable bases, as, for example, changing a sodium clay to a calcium clay. This, however, has not been attempted by the USBR in actual construction practice.

The soils laboratory can be of assistance to designers in identifying clay soils that can produce detrimental uplifts to their structures. By means of proper field explorations and laboratory tests any dangers can be recognized, quantitative uplift values determined, and recommendations for protective measures made.

DISCUSSION

Raymond F. Dawson,[5] M. ASCE.—Messrs. Holtz and Gibbs are to be congratulated for studying an important subject that has been neglected far too long. The expansive properties of clays and their effect on structures depend closely on climatic conditions, thus making it difficult to set any limit on the properties of soils in determining their swelling characteristics. Under conditions of uniformly distributed rainfall many clays may behave satisfactorily, but during long periods of dry weather the same clays will exhibit enormous expansive properties.

The authors have described several laboratory tests in identifying the expansive clays and have carefully explained the limitations of each of the tests. This information will be extremely valuable to the engineering profession because, in the past, various tests have been suggested to determine the expansive properties of clays whereas, in actuality, certain clays which have enormous swelling properties will not reveal this characteristic by a single test. The authors also point out the difficulties of making certain tests and the fact that these cannot be used as routine tests.

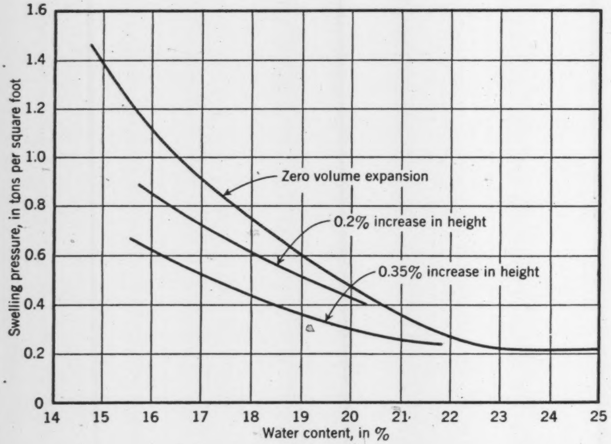

Fig. 15.—Relation of Swelling Pressure to Moisture Content

The free-swell test is very interesting and helpful. This should enable engineers to add another simple test to determine the possibilities of expansion in clay soils. It has occurred to the writer that perhaps, when making the free-swell test, it would be desirable to specify a time limit before taking the final reading. The writer has observed that after a few hours there has been considerably more swelling than at the time the material was poured into the water. Furthermore, although Messrs. Holtz and Gibbs suggest that free-swell values of less than 100% may not cause trouble and those having a free-swell value of less than 50% very seldom exhibit appreciable volume changes, several Texas clays with free-swell values in the range of 50% have caused considerable trouble through expansion. It is believed that this expansion is due to the combination of climatic conditions and the soil rather than to the actual free-swell characteristics of the soil. Therefore, whereas limits that are fairly high may be set for one area, in other sections having more severe climatic conditions lower values must be used. In the opinion of the writer, the free-swell test combined with the Atterberg test will provide the most satisfactory indicators for use on many projects. It is also believed that any attempt to set limits for these tests must include data on the climatic condition that exists in the area.

---

[5] Prof. of Civ. Eng. and Associate Director, Bureau of Eng. Research, The Univ. of Texas, Austin, Tex.

The load expansion tests are interesting and warrant further study, particularly in relation to the Skempton "activity" value for the soils. It is a well-established fact that, as expanding clays are permitted to swell, the resulting pressures are greatly reduced. Fig. 15 shows the swelling pressures that were developed at different moisture contents and at different precentages of expansion in a series of tests conducted at the University of Texas at Austin. The soil was a silty clay from the Taylor marls of central Texas and had a low "activity." Its physical characteristics were:

Physical characteristic	Value
Liquid limit	50
Plasticity index	31
Specific gravity	2.74
Activity	1.09

The optimum moisture at maximum dry density for the standard Proctor test was 18.5%.

Some cylinders were compacted at various moisture contents by the standard Proctor method, and three consolidation specimens were cut from each cylinder. For zero volume expansion, loads were added to the specimens to prevent swelling when water came in contact with the soil. For the other samples, the soil was permitted to expand a predetermined percentage after the water came in contact with the soil and was then loaded to prevent further expansion. When the specimens showed no further tendency to swell (from six to eight hours for a sample ¾ in. thick), the load required to restrain the soil was determined.

A study of Fig. 15 shows that a small percentage of expansion greatly reduced the swelling pressures. Also, an increase in the compacting moisture reduced the swelling. For this soil, with standard Proctor compaction and with moisture contents greater than 23%, there is a small but constant swelling pressure regardless of the expansion permitted. The chart also indicates that, to reduce the effect of swelling clays, the soils should be placed when well on the "wet side" of the density curve and should be permitted to expand slightly when absorbing moisture. It may not be possible to permit expansion of the soil for some structures, but if so one must expect the higher expansion pressures. The writer firmly believes that flexible structures which, like boxers, "roll with the punches" will be subject to much less damage due to swelling soils than will the more rigid structures.

A study of the swelling pressures of this soil when compacted at densities less than the standard Proctor density has not been successful because of the nonuniformity of the specimens.

The authors suggest prewetting as a method of controlling expansion. This offers possibilities, but how long must the soil be prewetted? In a housing project in Austin the soil under one of the houses was prewetted before construction. Trenches dug for the foundations were filled with water which was allowed to stand approximately six weeks. Then the water was pumped out, the foundations were placed on the wet soil, the trenches were again filled with water, and the soil was kept saturated thereafter. The house, like those constructed in the dry trenches, has continued to rise since construction. Some of these houses have been built for more than six years and are still rising. The question of how long the soil must be prewetted before this method will be successful has not yet been answered.

The authors describe some field experiences that will be valuable to engineers designing and building with materials of this type. They report a maximum upward movement of slightly more than 1 ft. In San Antonio, Tex., when a basement floor was placed on a slab on fill, the slab had actually risen 1.5 ft above the original grade.

The drilled and belled, cast-in-place piling that was used on the Wellton-Mohawk pumping plants has been used successfully in the Texas area for more than twenty years. A large truck-mounted earth auger is used to drill a vertical shaft to a depth below the line of seasonal moisture change, and a reaming attachment is used to bell out the bottom of the pile. This bell is essential to this type of construction because the expanding soil will often grip the pile and lift it. If a straight-shaft pile is used, it can easily be lifted; however, the bell offers great resistance to this vertical lifting. The writer knows of no underreamed piles, properly constructed and reinforced, that have been damaged by the vertical pressures due to the lifting of the piles. Nevertheless, there has been damage to this type of foundation when it has been placed on a hillside; there, creep has broken the piles and damaged structures. When construction on this type of soil is placed on hillsides, extreme care must be taken in order to obtain a satisfactory foundation.

Although only a limited number of thorough examinations have been made, it has been found that piers and columns are usually sheared off at a depth of from 4 ft to 6 ft below the surface of the ground where hillside creep has occurred. Perhaps in other areas this depth may be different from those the writer has observed.

William T. Altmeyer,[6] A. M. ASCE.—By coincidence the approach of the authors to the identification of expansive clays closely parallels experiments performed by the writer and other engineers in the writer's organization. Several of the authors' conclusions are substantiated by the results obtained in the tests by the writer and his collegues, and the writer will supplement the authors' paper with identification criteria he has found to be equally significant and valuable.

---

[6] Foundation Engr., Donald R. Warren Co., Cons. Engrs., Los Angeles, Calif.

In 1951, the tremendous increase in the construction of new homes in the Los Angeles (Calif.) area inevitably led to the development of marginal-type land where deep deposits of both residual and transported clays, known by the colloquial term "adobe," constituted the foundation medium. The federal loan guaranty agencies were besieged with complaints by the veteran owners concerning heaving foundations and "galloping" porches. Recommendations for establishing criteria for the identification of clay soils whose volume change with moisture variations was critical were urgently requested.

As Messrs. Holtz and Gibbs have explained, microscopic examination, x-ray diffraction analysis, and differential thermal analysis are useful in determining the amount and type of mineral present, particularly the highly expansive montmorillonite. These tests were rejected by the writer and his associates as being too time-consuming and requiring special expensive equipment and highly skilled techniques. They were of the opinion that the commonly used Atterberg limits could provide reliable indicators of the expansion to be expected for a given clay soil.

The criteria developed by the writer's firm includes the shrinkage limit, although within more narrow boundaries than those selected by the authors to represent indications of low, medium, high, and very high expansion. The range of shrinkage limits in the medium range (8–18) established by the authors (Table 1) overlaps their ranges of very high, high, and low. The criteria adopted by the writer's firm with respect to anticipated volume change as indicated by the shrinkage limit are as follows:

Shrinkage limit (%)	Volume change
<10	Critical
10–12	Marginal
>12	Noncritical

The authors specified a shrinkage limit of greater than 13 to denote a low degree of expansion (Table 1). A very high degree of expansion was indicated by a shrinkage limit of less than 10 which, by coincidence, the writer and his associates selected as indicative of a critical degree of volume change.

The percentage of colloids used by the authors was rejected for two reasons: First, the classification system used by the writer's company (the Uniform Soil Classification of the Corps of Engineers (United States Department of the Army)) does not depend on hydrometer analyses for its descriptions, and the percentage of colloids would require additional testing in the laboratory for questionable utility as evidenced by the wide overlapping of values reported by the authors. Secondly, the percentage of colloids is relatively meaningless unless it is also known whether the colloids represent minerals of the montmorillonite, kaolinite, or illite groups. The writer and his associates feel that other indices are more conclusive.

The writer is surprised that the authors did not use the percentage of linear shrinkage. They mentioned, under the heading, "Laboratory Tests:

Identification Tests," that the plasticity index demonstrates the range of moisture content possible in the plastic range and consequently indicates the volume change to be expected. Although there is no doubt that the foregoing relationship is correct, the writer and his colleagues believe that a more significant value is the percentage of linear shrinkage occurring when the moisture of a soil mass is reduced from an upper limit (commonly taken to be the field moisture equivalent) to the lower limit below which no volume change occurs (shrinkage limit). This conclusion is based on the fact that the soil in place will tend to shed water before the liquid limit is reached. The field moisture equivalent consequently represents a more realistic upper limit.

The following boundaries were established with respect to percentage of linear shrinkage:

Linear shrinkage (%)	Volume change
>8	Critical
5–8	Marginal
<5	Noncritical

It should be explained that the boundaries established were based on the results of a large number of laboratory tests performed on soils encountered in the greater Los Angeles area, and, as is the case with any set of arbitrary limits, borderline conditions and even contradictions will occasionally result. As frequently occurs in the practice of soil mechanics, the indices are relative rather than absolute.

Additional confirmation of the volume change to be anticipated was sought in the form of data on actual expansion under loads typical of residential construction. Remolded specimens of the soil under test were allowed to become saturated under a normal load of 650 lb per sq ft. This load is roughly equivalent to footing dead loads for single-story, wood-frame structures. As explained by the authors (Fig. 9), the expansion is greatly dependent on molding moistures and densities. The writer's company decided to test two specimens. One specimen was loaded at approximately 85% of maximum density and at a moisture content equal to the shrinkage limit and then allowed to become saturated under the previously mentioned restraining load. This test condition, it was felt, represented conditions in undisturbed soil. Because many homes in the Los Angeles area are built all or in part on compacted fill, a second expansion test was performed on a specimen remolded to 90% of maximum density and at optimum moisture content. Again the specimen was allowed to become saturated under a normal load of 650 lb per sq ft. This test represented the behavior of compacted fill under footings. The more critical of the two cases was then considered to govern design with respect to the following ranges:

Percentage of expansion	Volume change
>1.5	Critical
0.5–1.5	Marginal
<0.5	Noncritical

The expansion test was performed in a standard fixed-ring type of consolidometer. A remolded specimen approximately 2.5 in. in diameter and 1 in. high was loaded by means of a beam. The vertical expansion during saturation was measured by a dial indicator.

The value adopted for critical expansion (1.5%) is considerably smaller than that presented by the authors for very high expansion (30%) because of the difference in the restraining loads used in the expansion tests (650 lb per sq ft as compared to 144 lb per sq ft or 1.0 lb per sq in.). If the clay soil tested is in the marginal range, it is frequently recommended that special precautions be taken with lightly loaded flatwork such as porch slabs, garage slabs, and patios. These precautions would include the use of wire reinforcing mesh, nonexpansive backfill under raised porches, and the casting of garage slabs separate from the footings.

The anticipated expansion can be considerably reduced by avoiding overcompaction of expansive soils and by placing them at moisture contents as high as is practicable for proper operation of construction equipment. Engineers of the writer's organization have recommended ponding and saturating clay soils on which slabs will be cast to raise the in-place moistures to the upper limit of the moisture range that produces volume change. After the concrete has been poured capillary attraction and the presence of the slab will keep seasonal changes of moisture to a minimum, and consequently volume change of the foundation soil will be negligible.

Conclusions.—Commonly used soil laboratory tests such as those for the shrinkage limit and the percentage of linear shrinkage can be used as qualitative indices of the expansiveness of clay soils. Potential expansion can be measured quantitatively by saturating remolded specimens of soil in the consolidometer under restraining loads equivalent to anticipated footing loads.

Considerable variations in the amount of expansion can be produced by variations in molding moisture and density and through sample preparation methods. Further studies in standardizing the test procedures are being conducted by the writer.

EDWARD S. BARBER,[7] A.M. ASCE.—The properties of expansive clays are clearly illustrated in this paper. The following data supplement and, in general, agree with the authors' presentation.

Table 2, like Fig. 5, compares the expansion or swell of various compacted soils when immersed and unloaded gradually with the swell when immersed under the final load of 20 lb per sq ft. Table 3 shows the effect of various loads at the time of immersion for the A-6 clay. The first two columns correspond to the assumed curve in Fig. 6.

The effect of temporary prevention of movement decreases as the moisture at the time of compaction is increased, as shown in Table 4. This is because higher moisure contents produce a more uniform structure or arrangement of the soil particles, which reduces the opportunity for internal rearrangement of particles when the immersed soil is restrained from swelling.

Table 5 shows the expansion of duplicate samples immersed under a heavy load and then unloaded after various lengths of time. While the expansion

---

[7] Prin. Soils Engr., Tippetts-Abbett-McCarthy-Stratton, Guatemala City, Guatemala.

TABLE 2.—CUMULATIVE THICKNESS INCREASE, IN PERCENTAGES, FOR DIFFERENT SOILS[a] UNDER DIFFERENT LOADS

Soil	LOADS, IN KIPS PER SQUARE FOOT							
	8	4[b]	2[b]	1[b]	0.5[b]	0.2[b]	0.02[b]	0.02
A-1	−0.4	−0.3	−0.1	0.0	0.1	0.5	2.1	11.8
A-2	0.0	0.6	1.0	1.4	2.0	2.7	6.6	13.1
A-3	0.0	0.0	0.2	0.2	0.3	0.3	0.6	0.4
A-4	0.8	1.9	3.2	4.3	5.7	7.4	12.9	22.5
A-5	0.5	2.1	2.9	4.6	6.2	7.8	15.1	17.1
A-6	12.2	13.9	16.0	18.2	23.1	...	38.4	70.7
A-7	1.4	4.7	5.5	6.6	7.6	9.0	13.2	21.4
A-8	10.1	12.9	15.6	16.4	17.4	19.1	63.5	98.7

[a] Air-dry soil compacted under 500 kips per sq ft. [b] After swelling under previous load.

TABLE 3.—EFFECT, ON SWELL, OF LOAD AT TIME OF IMMERSION[a]

Load at time of immersion, in pounds per square foot	MAXIMUM THICKNESS INCREASE, IN %	
	Under immersion load	Under 20 pounds per square foot
8,000	12.2	38.4
4,000	16.1	33.8
2,000	19.3	34.0
1,000	27.7	42.7
500	30.1	43.5
200	40.5	51.8
20	70.7	70.7

[a] Air-dry A-6 soil compacted under 500 kips per sq ft.

TABLE 4.—EFFECT OF TEMPORARY RESTRAINT ON SWELLING OF CLAY[a]

Initial moisture content, in %	THICKNESS INCREASE AS WATER IS SORBED, IN %	
	Sample restrained 24 hours	Sample unrestrained
15	7.3	12.3
18	6.4	12.3
21	6.2	8.9
24	5.5	4.9

[a] Tuxedo clay mixed to various moisture contents and compacted to 103 lb per cu ft, allowed to sorb water under a load of 170 lb per sq ft,

TABLE 5.—EXPANSION OF A SOIL[a] AFTER SORPTION OF WATER UNDER COMPACTING LOAD

Thickness from Which Increase Was Measured	TIME BETWEEN WATER APPLICATION AND LOAD RELEASE					
	1 Minute	1 Hour	1 Day	1 Week	1 Month	1 Year
	Thickness Increase, in %, of Soil Under Load of 20 Lb Per Sq Ft					
(a) Initial Thickness	17	7	4	2	1	2
(b) Thickness at time of load release	17	17	15	16	17	19

[a] Air-dry Tuxedo clay loaded to 16 kips per sq ft, to which water was applied while loaded, and the load reduced to 20 lb per sq ft after various lengths of time.

from the initial thickness decreases as loading time is increased, the expansion from the time of load release is constant, indicating that the reduction of expansion by temporary restraint is due to reorientation of particles without a release of the elasticity stored by their compression and bending.

The effect of structure on expansion is also demonstrated by using different methods of compaction. In a typical case, tamping, which produces a more uniform structure, gave one third less expansion than static compaction for the same soil at the same moisture and density.

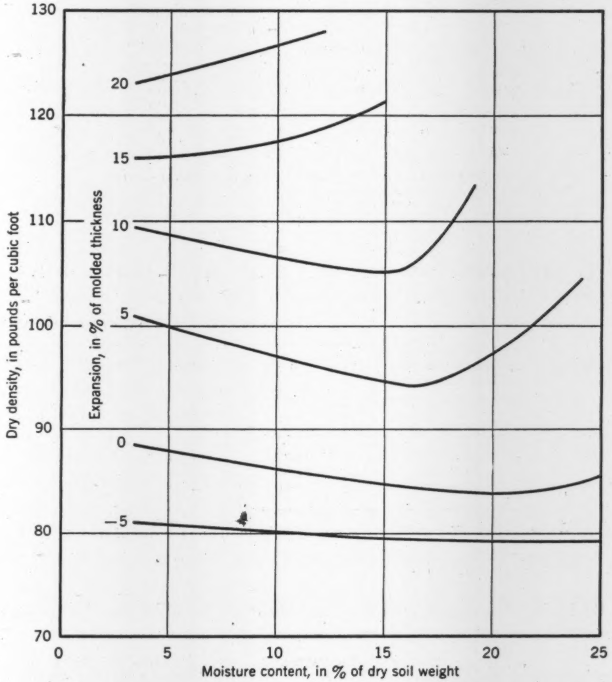

Fig. 16.—Expansion of Tuxedo Clay While Immersed Under 350 Lb per Sq Ft After Molding to Different Moistures and Densities

Fig. 16, showing the expansion under a load of 350 lb per sq ft after molding to various moistures and densities, is similar to Fig. 8. For the combination of low density and low moisture content in Fig. 16, the expansion is less for the dry soil because the initial soil contained hard lumps of clay as large as the No. 10 sieve size with a relatively uniform internal structure which predominates over the effect of the static load used in forming the samples.

In Table 6 is shown the reduction of the swelling pressure produced by an increase in permitted displacement. The first value is comparable to those shown in Fig. 8. In Table 7, similar effects of variations in moisture content and density on swelling pressure are shown in addition to the effect of the time allowed for rebound of the sample before setting it against the restraint. If sufficient time is not allowed for the rebound after compacting and before the restraint is applied, an increased pressure is recorded. The low reaction (50 lb) for the 20% moisture content at 118 lb per cu ft is due to the fact that water was squeezed from the sample into the mold during molding and reabsorbed during the time allowed for rebound.

TABLE 6.—THE EFFECT OF STRAIN ON THE SWELLING PRESSURE OF A CLAY[a]

DISPLACEMENT PERMITTED		Maximum pressure, in pounds, developed by sorption
In inches	In % thickness	
0.000	0.0	2,520
0.006	0.6	1,900
0.012	1.2	1,500
0.018	1.8	1,220
0.024	2.4	950

[a] Sample of Tuxedo clay compacted to 118 lb per cu ft at 10% moisture, 1 in. thick, 4 in. in diameter.

TABLE 7.—SWELLING PRESSURE OF A CLAY[a] AGAINST FIXED RESTRAINT

Density, in pounds per cubic foot	Time between compression and setting of restraint	MOISTURE CONTENT, IN PERCENTAGES			
		0	10	15	20
		Swelling Pressure, in Pounds			
118	5 min	2,970	2,510	2,120	1,070
118	24 hours	2,280	2,080	660	50
107	24 hours	640	610	370	210

[a] Tuxedo clay statically compressed, 4-in.-diameter specimen.

TABLE 8.—SWELLING PRESSURE AND EXPANSION OF TWO SOILS

Compacting load, in kips, on 4-in.-diam. specimen	SWELLING PRESSURE, IN POUNDS		SUBSEQUENT EXPANSION, IN %, UNDER A LOAD OF 20 LB PER SQ FT	
	Tuxedo clay	Organic silt	Tuxedo clay	Organic silt
1	20	20	1	3
10	620	250	12	7
20	1,280	580	18	11
40	3,280	1,140	26	14
60	4,520	1,700	30	18

Table 8 shows the increase of swelling pressure and expansion with increase of the compacting load. The maximum swelling pressure shown—4,520 lb—is 50 kips per sq ft or 360 lb per sq in.

Although there was lacking the arid climate contributing to several of the authors' field situations, important movements have been observed involving a marine clay (Tuxedo clay) in the coastal plain near the District of Columbia. The writer has investigated an apartment house that was badly cracked when a stairwell was lifted an inch by swelling clay. Several other structures have cracked due to drying of the same clay, especially when aided by the roots of trees. Fig. 17 shows a wall distorted by the shrinkage craters over the root systems of a row of trees. Fig. 18 shows similar settlement of an iron fence.

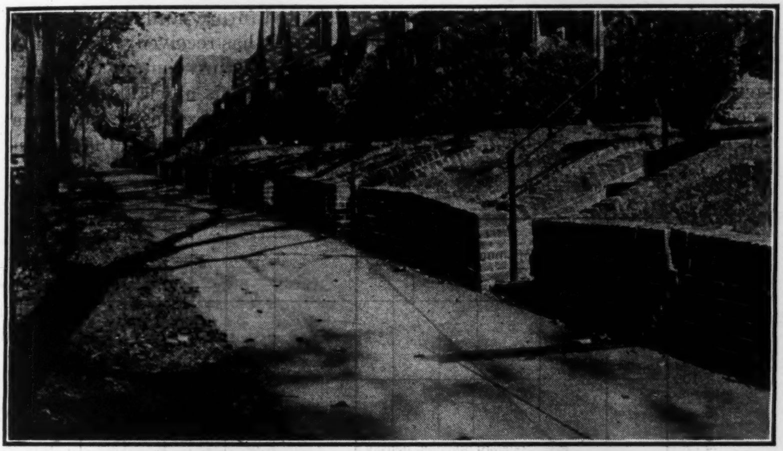

Fig. 17.—Distortion of a Wall Caused by a Row of Trees

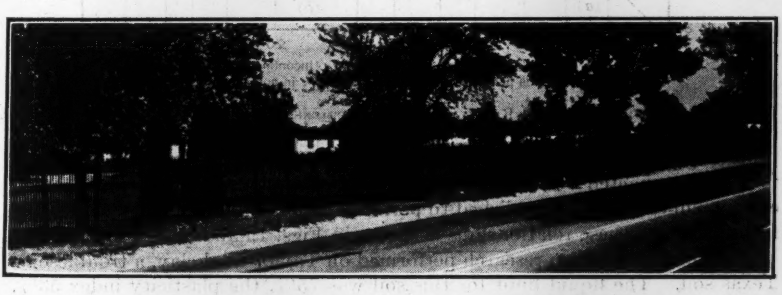

Fig. 18.—Settlement of a Fence Beside a Row of Trees

Lawrence A. DuBose,[8] A. M. ASCE.—After the comprehensive treatment of the expansive-clay problem by Messrs. Holtz and Gibbs, the soils engineer should have little difficulty in recognizing soils possessing this undesirable property. Although numerous papers have considered soils from the standpoint of density, moisture content, surcharge, volume change, and strength, seldom has an attempt been made to correlate these factors with expansive clays.

The design of compacted fills to meet anticipated future needs is a phase of soils engineering that deserves more emphasis than it has received. In normal fill construction the selection of a combination of moisture content and compaction effort necessary to produce a desired strength is a relatively simple procedure. In the southwestern United States, where expansive clays are not uncommon the swelling under low surcharges complicates the design problem. However, by performing volume-change tests and strength tests for soils compacted at several combinations of moisture content and applied energy, curves can be established to permit a rational fill design. One method for illustrating these relationships is shown in Figs. 19 and 20.

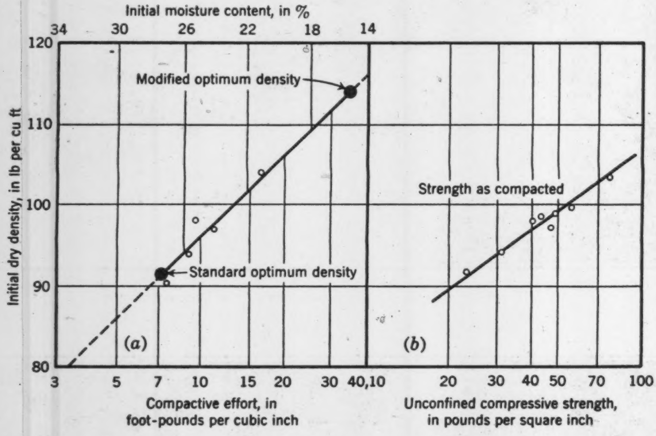

Fig. 19.—Strength and Density Relationship for Specimens Compacted at Optimum Conditions

These data are from research performed on Taylor marl clay, a troublesome Texas soil. The liquid limit for this soil was 75%, the plasticity index 53%, the shrinkage limit 12%, and the colloid content 40%. The research in this study included volume change and strength tests for specimens compacted to optimum conditions using efforts varying from one half to five times the standard AASHO compaction.

Fig. 19(*a*) illustrates the increase in optimum density for increased compaction, and Fig. 19(*b*) indicates the strength of specimens compacted to this condition. The small circles represent test data. The illustration can easily be extended to show similar relationships for samples compacted to specified percentages on the wet or dry side of the optimum condition. Strength tests can also be included for anticipated future moisture conditions.

---

[8] Asst. Prof. of Civ. Eng., Agri. and Mech. College of Texas, College Station, Tex.

The surcharge pressures required to prevent volume changes for Taylor marl specimens compacted to optimum conditions are shown in Fig. 20. This curve was established in essentially the same manner as described by Messrs. Holtz and Gibbs, using consolidometers. It was found that the use of 0.5-in.-thick rings reduced the testing time by more than 50% and yielded data comparable to the data found when using 1.25-in.-thick rings.

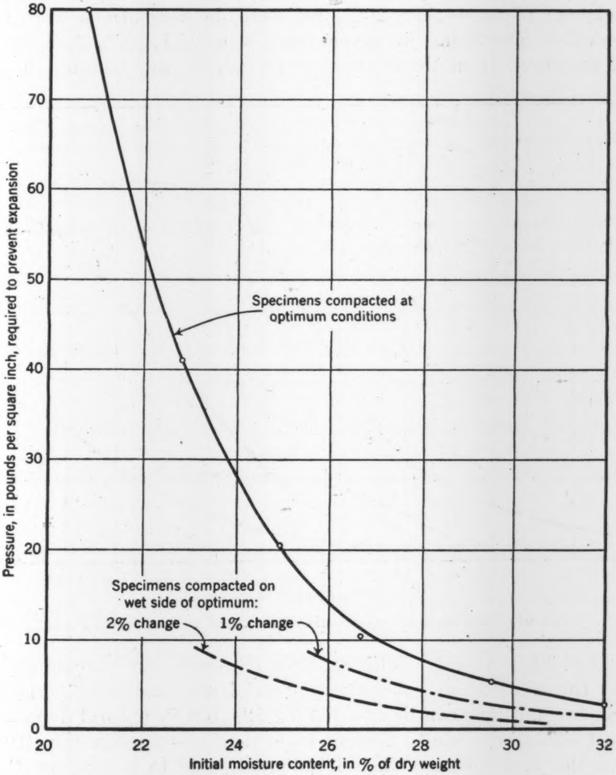

FIG. 20.—RELATION OF THE FACTORS INDICATED, NECESSARY TO RESULT IN ZERO VOLUME CHANGE

The curves in Figs. 19 and 20 may be used to select a moisture content and compactive effort that would both limit the volume changes and provide the necessary strengths. For high fills it might even be desirable to use several combinations as the surcharge decreases from the lower layers to the top of the fill.

Another interesting relationship found in the Taylor marl research was the influence of time on expansion. The data in Fig. 21 show that the selection of some time interval—for example, 4 days—may result in incorrect volume-change conclusions. One notes that the expansion is divided into "primary" and "secondary." For the specimens 0.5 in. thick and 1.25 in. thick, the primary expansion occurred in the first 4 days. For the 5-in.-thick specimens, only approximately 30% of the primary expansion occurred in the first 4 days. After specimen No. 2 had been permitted to swell for 55 days to yield a total volume change of more than 20%, moisture determinations were made at 1-in. intervals. The values in percentages were 25.1, 27.5, 30.2, 33.5, 35.0, and 38.2 measured from the bottom to the top of the sample. The initial moisture content was 15%. This example represents an extreme case, but it illustrates the tremendous expansion potential possible under certain conditions. Such conditions can be avoided for fills, but in natural deposits allowances must either be made to prevent movement or to design the structure to withstand the movement. When it is practicable to design for the latter case, the soils engineer needs a more definite procedure for determining the magnitudes of future heaving.

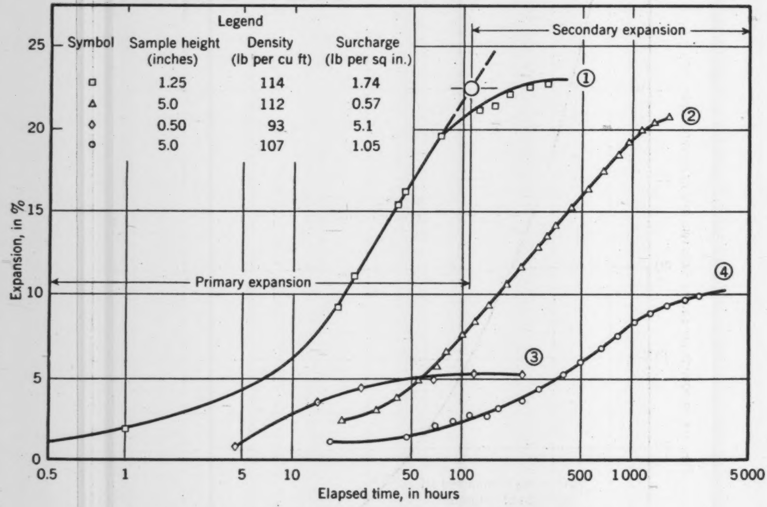

FIG. 21.—THE INFLUENCE OF SAMPLE THICKNESS ON EXPANSION TIME

WESLEY G. HOLTZ,[9] M. ASCE, AND HAROLD J. GIBBS,[10] A. M. ASCE.—Each discusser has contributed distinctly to the subject of engineering properties of expansive clays.

The writers agree with Mr. Dawson's comments that the Atterberg tests are more reliable indicators of expansion characteristics than is the free-swell test, and they wish to point out further that the free-swell tests were considered applicable only for indicating general trends by a simple procedure. Tests that are more closely controlled are of course better indicators. The index table presented in the paper is similar to the Skempton activity values in that both involve particle size and Atterberg constants; however, the Skempton activity value is arrived at through a graphical plot.

---

[9] Head, Earth Materials Lab., Bureau of Reclamation, U. S. Dept. of the Interior, Denver, Colo.

[10] Engr., Earth Materials Lab., Bureau of Reclamation, U. S. Dept. of the interior, Denver, Colo.

The writers also agree with Mr. Dawson that a slight relief of expansion movement greatly reduces the swelling pressures. This is shown by Fig. 9 for the case when expansive soil is compacted at variable densities and is measured for uplift pressure and by Fig. 5 which shows the amounts of expansion for various restraining loads.

Mr. Altmeyer indicates the similarity between his criterion based on the shrinkage limit and the part of the writers' criteria in which the shrinkage limit was used. The closeness of the independent conclusions is of interest to the writers. However, such similarity is believed to be factual rather than coincidental. It should be noted that Mr. Altmeyer's soil is also from the California area and thus may be similar to the soils from which much of the writers' data was obtained. Because soils from other areas may act differently, the writers felt that the index to expansion should be based on more than the shrinkage limit and, therefore, they also included the percentage of colloids and plasticity index as additional indicators that must be taken together. By viewing these items together, a fairly reliable evaluation of expansion can be made in spite of the overlapping of limits for individual items in Table 1.

The classification system referred to by Mr. Altmeyer is the same as that used by the writers. The "Unified Soil Classification" was sponsored jointly by the Corps of Engineers and the Bureau of Reclamation.[3]

Mr. Barber gives some interesting data comparing the expansion of soils of various classifications, such as the high expansion of an A-6 soil (United States Bureau of Public Roads classification) with other types. He also shows the same reduction of uplift pressure by the slight relief of expansion as did Mr. Dawson.

The writers agree with Mr. DuBose that placement conditions of expansive soil should vary as the surcharge decreases from lower layers to the top of the fill. Laboratory load-expansion tests would indicate this requirement. For a certain soil, expansion may have a time relationship, as Mr. DuBose has shown. The writers have observed distinctly different speeds of expansion for different soils. This is believed to be caused by differences in water affinity which in turn are affected by mineral and chemical characteristics and may vary greatly in different soils.

AMERICAN SOCIETY OF CIVIL ENGINEERS
Founded November 5, 1852
TRANSACTIONS

Paper No. 2815

VERIFICATION OF THEORY FOR OBLIQUE STANDING WAVES

By Arthur T. Ippen,[1] M. ASCE, and Donald R. F. Harleman,[2] J. M. ASCE

Synopsis

Changes in section or alinement of open channels flowing at supercritical velocities produce depth changes that may be abrupt or gradual depending on the type of wave produced. A series of experiments was undertaken to verify the hydrodynamic theory for both oblique hydraulic jumps and expansion waves with Froude numbers ranging from two to seven. The position of the standing waves caused by a wall deflection and the associated depth changes were observed and compared with existing theory. The average agreement was of the order of 2% for oblique jumps with a somewhat larger discrepancy for the expansions, depending on the magnitude of the wall deflection.

An analysis and experimental observations of the nature of the transition between undular and roller-type jumps are presented. It is shown that the transition occurs at a depth ratio of 2.

Introduction

The publication in 1949 of the symposium on high-velocity flow in open channels[3] made available to the engineering profession a unified treatment and general method of design for supercritical flow in hydraulic structures. Since that time, experimental information relating to oblique standing waves has been obtained in the hydrodynamics laboratory of the Massachusetts Institute of Technology at Cambridge. The experiments have served to verify much of the basic theory underlying the mechanics of supercritical flow as applied, for example, to the design of channel and spillway transitions, and their results are presented to further the broad acceptance of the principles involved. Such acceptance properly depends on adequate experimental confirmation of the

---

Note.—Published, essentially as printed here, in October, 1954, as *Proceedings-Separate No. 526*. Positions and titles given are those in effect when the paper was approved for publication in *Transactions*.

[1] Prof. of Hydraulics, Massachusetts Inst. of Technology, Cambridge, Mass.

[2] Asst. Prof. of Hydraulics, Massachusetts Inst. of Technology, Cambridge, Mass.

[3] "High-Velocity Flow in Open Channels: A Symposium," by Arthur T. Ippen, Robert T. Knapp, John H. Dawson, Hunter Rouse, B. V. Bhoota, and En-Yun Hsu, *Transactions*, ASCE, Vol. 116, 1951, p. 265.

basic theory. In addition, the experiments revealed some interesting correlations between oblique jumps and the general theory of irrotational translation waves.

The experimental work is divided into two phases, the first of which deals with the oblique hydraulic jump (also called the oblique shock wave by analogy to the supersonic case). This type of jump is produced when a vertical boundary is deflected inward to the flow as in the case of a channel contraction. This condition results in an abrupt depth increase along a jump front which is propagated from the point of boundary discontinuity and depends in magnitude on the angle of deflection. The limiting case of the oblique standing wave is the familiar hydraulic jump in which the front is normal to the direction of flow.

The second phase deals with the opposite situation of an expansion wave produced when a vertical boundary is deflected outward from the supercritical flow, as in a channel expansion. Because a negative hydraulic jump is physically impossible, this boundary condition must produce a gradual decrease in the depth of the flow as defined by lines of constant depth radiating from the boundary discontinuity. The extreme case of an expansion wave is represented by the abrupt termination of the side walls, with the channel bottom continuing at the same slope. This case has been investigated experimentally by Hunter Rouse, M. ASCE, B. V. Bhoota, A. M. ASCE, and En-Yun Hsu.[3]

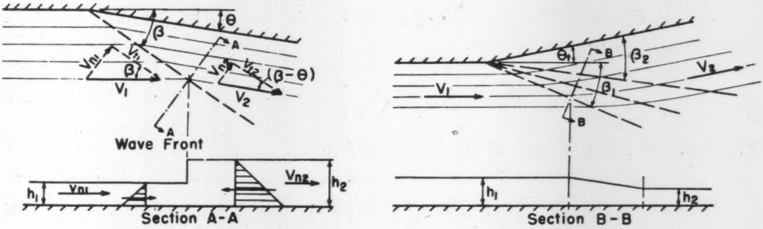

(a) Oblique Hydraulic Jump (b) Oblique Expansion Wave

Fig. 1.—Oblique Standing Waves

All the waves investigated were of the standing-wave type—that is, the wave fronts were stationary and the flow was steady.

Theoretical Background

The derivation of the fundamental relationships for both the oblique jump and expansion waves are presented in detail in the symposium previously cited;[3] therefore, only a summary of the theory is included in this paper. In addition, however, a detailed analytical investigation of the transition from the undular-type jump to the roller-type jump, which has not been described thus far, is presented herein.

Oblique Hydraulic Jump.—For purposes of definition, Fig. 1(*a*) shows the conditions to be investigated. If a boundary wall is deflected into a supercritical stream through an angle θ, an oblique hydraulic jump will occur as a standing wave at an angle β with respect to the original flow direction. The velocities and depths before and after the jump are designated V_1, V_2, and h_1, h_2, respectively, as shown in Fig. 1(*a*). Velocity components normal to the wave front are V_{n1} and V_{n2}. This analysis is concerned only with initial and final conditions of flow and is therefore independent of the character of the depth change taking place across the jump.

Application of the relationships involving steady-flow continuity (Eq. 1) and momentum (Eq. 2) in the direction normal to the wave front, together with Eq. 3, obtained from the geometry of the velocity-vector diagram (Fig. 1(*a*)), provides a total of three independent equations.

$$h_1 V_{n1} = h_2 V_{n2} \qquad (1)$$

$$\frac{g}{2}(h^2_2 - h^2_1) = h_1 V_{n1} (V_{n1} - V_{n2}) \qquad (2)$$

and

$$\frac{\tan \beta}{\tan (\beta - \theta)} = \frac{V_{n1}}{V_{n2}} \qquad (3)$$

$$(V_{t1} = V_{t2})$$

Solving Eq. 2 for V_{n1} and eliminating V_{n2} by Eq. 1, the familiar hydraulic jump relationship is obtained:

$$V_{n1} = \sqrt{g\,h_1}\sqrt{\frac{1}{2}\frac{h_2}{h_1}\left(1 + \frac{h_2}{h_1}\right)} \qquad (4a)$$

The Froude number normal to the jump front is thus

$$\mathbf{F}_{n1} = \sqrt{\frac{1}{2}\frac{h_2}{h_1}\left(1 + \frac{h_2}{h_1}\right)} \qquad (4b)$$

Because the actual flow velocity $V_1 = V_{n1}/\sin\beta$ and the initial Froude number $\mathbf{F}_1 = V_1/\sqrt{g\,h_1}$, Eq. 4*b* can also be written as follows:

$$\sin\beta = \frac{1}{\mathbf{F}_1}\sqrt{\frac{1}{2}\frac{h_2}{h_1}\left(1 + \frac{h_2}{h_1}\right)} \qquad (4c)$$

The characteristics of the oblique hydraulic jump are completely determined if any three of the six quantities, h_1, h_2, $\mathbf{F}_1$, $\mathbf{F}_2$, β, and θ, are specified as independent variables. In the practical application of oblique jump theory, it is usually convenient to consider the initial Froude number $\mathbf{F}_1$, the initial depth h_1, and the boundary deflection angle θ as the independent variables. With these known quantities, the wave angle β and the depth ratio h_2/h_1 may be determined.

Eq. 4*c* when solved for the depth ratio becomes

$$\frac{h_2}{h_1} = \tfrac{1}{2}\left(\sqrt{1 + 8\,\mathbf{F}^2_1 \sin^2\beta} - 1\right) \qquad (5)$$

Eqs. 1 and 3 can be combined to yield

$$\frac{h_2}{h_1} = \frac{\tan\beta}{\tan(\beta - \theta)} \qquad (6)$$

If Eqs. 5 and 6 are equated, a relationship involving F_1, θ, and β is obtained:

$$\tan\theta = \frac{\tan\beta\,(\sqrt{1 + 8\,\mathsf{F}^2_1 \sin^2\beta} - 3)}{2\tan^2\beta + \sqrt{1 + 8\,\mathsf{F}^2_1 \sin^2\beta} - 1} \qquad (7)$$

Inasmuch as Eq. 7 cannot be solved for β in terms of F_1 and θ, a plot of this equation is necessary for the solution of oblique jump problems. A comprehensive representation of all characteristics expressed by Eqs. 5, 6, and 7 is given in a four-quadrant graph.[4] The primary aim of the first phase of this investigation was the verification of Eqs. 5 and 7 over a wide range of Froude numbers and deflection angles.

Limiting Conditions for the Undular Jump.—During the course of the experimental work on the oblique jump, it was observed that, if the depth ratio was less than two, the jump was composed of a series of undulations whereas for larger depth ratios the characteristic "roller" was present. This fact has already been established by B. A. Bakhmeteff[5,6] in his early work on the special case of the normal hydraulic jump and has since been observed by other investigators. Because the experimental determination of the angle of the oblique jump, β, is one of the objects of this study, an analytical correlation of these two forms of the jump is necessary for the interpretation of the experimental data.

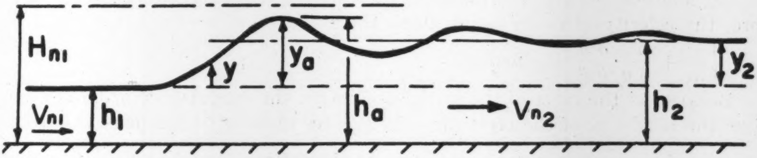

FIG. 2.—PROFILE OF TYPICAL UNDULAR JUMP

The propagation velocity, c, of a constant discharge translation wave of appreciable height and curvature moving in still, shallow water is, according to Boussinesq,[7]

$$c = \sqrt{g\,h_1}\left(1 + \frac{3}{4}\frac{y}{h_1} + \frac{h^2_1}{6\,y}\frac{\partial^2 y}{\partial x^2}\right) \qquad (8)$$

with the notation as shown in Fig. 2. This constant-discharge translation wave can be reduced to an oblique standing wave by superimposing on it any steady flow having an initial stream velocity V_1 with an component V_{n1} equal and opposite to c. This statement implies that the tangential components V_{t1} and V_{t2} of the velocity V_1 are equal because no momentum change takes place parallel to the wave front. Eq. 8 may then be written in terms of the ratio $V_{n1} \sqrt{g\, h_1} = \mathbf{F}_{n1}$ which is the initial Froude number normal to the wave front—

---

[4] "Mechanics of Supercritical Flow," by A. T. Ippen, *Transactions*, ASCE, Vol. 116, 1951, p. 287, Fig. 8.

[5] "Hydraulics of Open Channels," by B. A. Bakhmeteff, *Engineering Societies Monograph*, McGraw-Hill Book Co., Inc., New York, N. Y., 1932.

[6] "The Hydraulic Jump in Terms of Dynamic Similarity," by B. A. Bakhmeteff and A. E. Matzke, *Transactions*, ASCE, Vol. 101, 1936, p. 630.

[7] "Wave Motion," by G. H. Keulegan, in "Engineering Hydraulics," John Wiley & Sons, Inc., New York, N. Y., 1950, Chapter XI, p. 719.

$$\mathbf{F}_{n1} = 1 + \frac{3}{4}\frac{y}{h_1} + \frac{h^2{}_1}{6\, y}\frac{\partial^2 y}{\partial x^2} \qquad (9a)$$

The fact that Eq. 9*a* is the appropriate relationship for the undular hydraulic jump is demonstrated by the following observations:

(*a*) The undular jump is composed of a series of oscillations of decreasing amplitude about the equilibrium depth y_2. Because $\partial^2 y/\partial x^2 = 0$ when $y = y_2$, Eq. 9*a* becomes

$$\mathbf{F}_{n1} = 1 + \frac{3}{4}\frac{y_2}{h_1} \qquad (9b)$$

or because $y_2 = h_2 - h_1$,

$$\mathbf{F}_{n1} = \frac{1}{4}\left(1 + 3\frac{h_2}{h_1}\right) \qquad (9c)$$

If Eq. 9*c* is compared to the momentum analysis given by Eq. 4*b*, the results agree within 1% in the range of depth ratios from 1 to 2.

(*b*) The entire wave is stationary with respect to the oncoming flow. Therefore, the celerity of every point along the wave must be the same—that is, $1 + \frac{3}{4}\frac{y}{h_1} + \frac{h^2{}_1}{6\, y}\cdot\frac{\partial^2 y}{\partial x^2} = \text{constant.}$

Because at the crest of the initial oscillation the curvature $\partial^2 y/\partial x^2$ is negative, the height y_a of the crest must be greater than y_2 to compensate for the effect of the curvature term in Eq. 9*a*. It also follows that, because $\frac{\partial^2 y}{\partial x^2} = 0$ at the points of inflection of the oscillations, these points must all occur at the same height as the equilibrium surface for depth y_2.

The solitary wave is a special limiting case of the undulations at the front of a positive surge. G. H. Keulegan[8] has shown that these undulations are essentially cnoidal waves propagated without change of form and that the vertical distance between the center of gravity of such a wave and the original free surface is one third the maximum wave height. By equating the propagation velocity of the center of gravity of the wave to that of the wave train itself, Mr. Keulegan concludes that the height of the initial undulation y_a is three halves the height of the layer y_2. Therefore,

$$y_a = \tfrac{3}{2}\, y_2 = \tfrac{3}{2}\,(h_2 - h_1) \qquad (10)$$

Making use of the foregoing principles, the limiting conditions for the existence of an undular jump may be determined.

With the notation of Fig. 2, $h_a = y_a + h_1$, in which h_a is the height of the initial crest above the channel bottom. Eliminating y_a by means of Eq. 10,

$$h_a = \tfrac{3}{2}\, h_2 - \tfrac{1}{2}\, h_1 \qquad (11)$$

---

[8] "Mathematical Theory of Irrotational Translation Waves," by G. H. Keulegan and G. W. Patterson, *Journal of Research RP1273*, Bureau of Standards, U. S. Dept. of Commerce, Washington, D. C., Vol. 24, 1940.

It is apparent that the total height h_a of the first undulation plus the kinetic energy head at the crest cannot exceed the energy level of the flow immediately in front of the jump. In fact, h_a will be maximum when it is equal to the initial energy head. When this occurs, the particle velocity at the crest must be zero, and thus the crest is presumed to be inherently unstable. At this point, the front will change from the undulating to the roller-type front.

The initial energy head referred to the channel bottom is expressed by H_1, as follows:

$$H_1 = h_1 + \frac{V^2{}_1}{2\,g} = h_1 + \frac{V^2{}_{n1}}{2\,g} + \frac{V^2{}_{t1}}{2\,g} \quad \text{(12)}$$

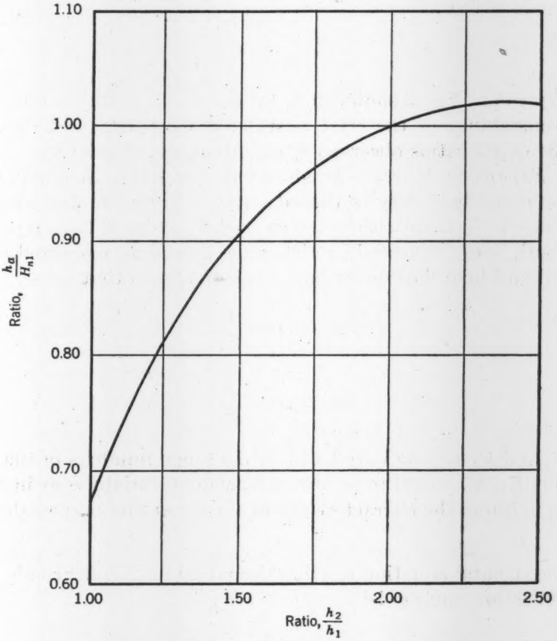

FIG. 3.—RATIO OF INITIAL CREST HEIGHT AND TOTAL ENERGY HEAD TO JUMP DEPTH RATIO

However, the initial energy head in the flow field containing the oblique standing wave can change only with changes in $V^2{}_n/2\,g$ and the depth because $V^2{}_t/2\,g$ is constant throughout the flow. Thus, H_{n1} alone represents that portion of the total energy head H_1 which is of significance with respect to the limiting properties of the wave front.

Therefore,

$$H_{n1} = H_1 - \frac{V^2{}_t}{2\,g} = h_1 + \frac{V^2{}_{n1}}{2\,g} \quad \text{(13)}$$

If Eq. 11 is divided by Eq. 13, the ratio of the height of the first crest to the initial energy level is obtained.

$$\frac{h_a}{H_{n1}} = \frac{\frac{3}{2}\frac{h_2}{h_1} - \frac{1}{2}}{1 + \frac{\mathsf{F}^2_{n1}}{2}} \qquad (14a)$$

The Froude number F_{n1} can be eliminated in terms of the depth ratio h_2/h_1 across the jump by the momentum equation 4*b*; therefore,

$$\frac{h_a}{H_{n1}} = \frac{6\frac{h_2}{h_1} - 2}{\left(\frac{h_2}{h_1}\right)^2 + \frac{h_2}{h_1} + 4} \qquad (14b)$$

A plot of Eq. 14*b* in Fig. 3 shows that, for $h_a/H_{n1} = 1$, the depth ratio is $h_2/h_1 = 2$. The instability of the crest postulated for $h_a/H_{n1} = 1$ thus is seen to occur for the depth ratios observed in experiments and practice.

Oblique Expansion Waves.—As shown in Fig. 1(*b*), an oblique expansion wave occurs if the boundary is turned outward from the flow at an angle θ_t. A gradual depth decrease occurs which is defined by a fan-shaped region of constant depth lines delineated by the angles β_1 and β_2, measured with respect to the initial and final flow directions, respectively, so that

$$\left.\begin{aligned} \beta_1 &= \sin^{-1}\frac{1}{\mathsf{F}_1} \\ \text{and}\quad \beta_2 &= \sin^{-1}\frac{1}{\mathsf{F}_2} \end{aligned}\right\} \qquad (15)$$

in which F_1 and F_2 are the initial and final Froude numbers of the flow.

Assuming F_1, h_1, and θ_t to be the independent variables, as in the analysis of the oblique jump, the characteristics of the expansion may be determined as follows:

The fundamental equation relating the initial and final Froude numbers to the total deflection angle θ_t is[3]

$$\theta_1 = \theta = \sqrt{3}\tan^{-1}\frac{\sqrt{3}}{\sqrt{\mathsf{F}^2 - 1}} - \tan^{-1}\frac{1}{\sqrt{\mathsf{F}^2 - 1}} \qquad (16)$$

in which

$$\theta = 0 \quad \text{when} \quad \mathsf{F} = \mathsf{F}_1$$

and

$$\theta = \theta_t \quad \text{when} \quad \mathsf{F} = \mathsf{F}_2$$

Thus, if F_1 and θ_t are given, F_2 can be determined from Eq. 16 or its graph,[9] and the angular region in which the depth change takes place is found from Eq. 15. Because the depth changes without perceptible energy dissipation, the depth at any point in the flow is uniquely related to the magnitude of the local Froude number. Equating the specific energy heads before and after the expansion,

---

[9] "Mechanics of Supercritical Flow," by A. T. Ippen, *Transactions*, ASCE, Vol. 116, 1951, p. 276, Fig. 3

$$h_1 + \frac{V^2_1}{2\,g} = h_2 + \frac{V^2_2}{2\,g}$$

and dividing through by h_1 and rearranging, the expression for the total depth change is obtained—

$$\frac{h_2}{h_1} = \frac{\mathbf{F}^2_1 + 2}{\mathbf{F}^2_2 + 2} \quad \text{(17)}$$

The second phase of the experimental work is concerned with the verification of the foregoing equations.

EXPERIMENTAL EQUIPMENT AND PROCEDURE

All the experimental investigations were conducted in the high-velocity channel in the hydrodynamics laboratory of the Massachusetts Institute of Technology. The rectangular channel is approximately 40 ft long, 4 ft wide, and 1 ft deep. The floor consists of ½-in.-thick plate glass, and the side walls are constructed of carefully alined aluminum plate. The entire channel can be set at any desired slope up to 8% by the push-button operation of an electrically driven spindle-type lifting mechanism. The magnitude of the slope is obtained by a calibrated revolution counter attached to the motor. Water from the main laboratory supply system enters the channel through a converging nozzle 4 ft wide, which can be set to admit water to the test section at any depth up to 4 in. Water depths are measured with a point gage attached to a dial indicator that can be read to the nearest 0.01 in., and velocities are measured by a Prandtl tube $\frac{3}{16}$ in. in diameter. A venturi meter in the supply line provides for measurement of the discharge.

The desired oblique jumps or flow-expansion zones were produced by a deflector vane approximately 7 ft long and 1 ft high located 15 ft downstream from the nozzle. The vane was arranged so that it could be fixed in various positions up to a maximum angle of $\theta = 21°$ in 3-degree increments. In the case of the oblique jumps, the hinge was placed 4 in. away from the channel wall so as to be independent of the side-wall boundary effects. Expansion waves were produced by the same vane with the hinge set 18 in. from the channel wall. A lead vane set parallel to the channel walls was used to determine the effect of a controlled side-wall boundary layer on the characteristics of the standing waves.

For each run, values of the three independent variables $\mathbf{F}_1$, h_1, and θ were chosen. The discharge and depth were chosen to give a desired nominal Froude number, and the slope of the flume was adjusted to produce uniform flow. The actual values of $\mathbf{F}_1$ and h_1 were then determined from pitot-tube traverses and point-gage traverses of the channel cross section with the deflector vane set at zero degrees.

Oblique Jump Experiments.—In the series of experiments dealing with oblique hydraulic jumps, a total of 52 runs was made with nine initial Froude numbers ranging from a minimum of 2.00 to a maximum of 7.00 at initial

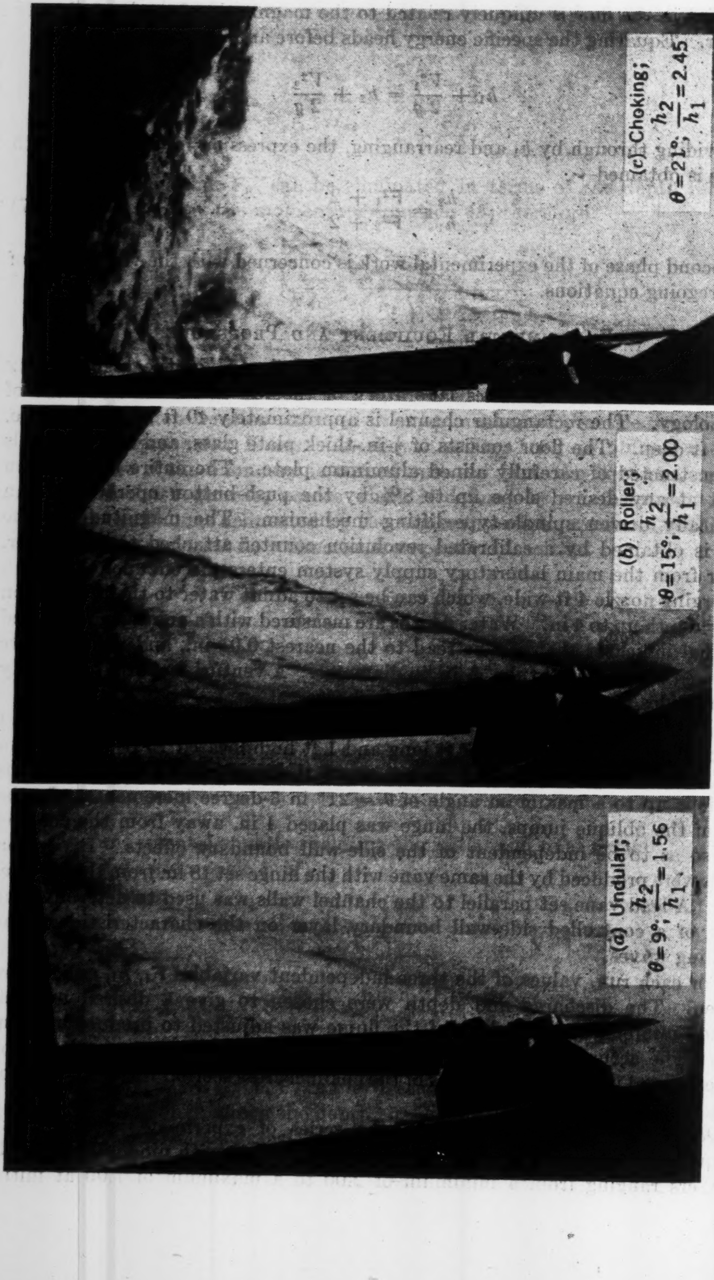

(a) Undular; $\theta = 9°;\ \frac{h_2}{h_1} = 1.56$

(b) Roller; $\theta = 15°;\ \frac{h_2}{h_1} = 2.00$

(c) Choking; $\theta = 21°;\ \frac{h_2}{h_1} = 2.45$

FIG. 4.—OBLIQUE HYDRAULIC JUMPS, $F_1 = 3.20$

depths of 0.90 in. and 1.50 in. Fig. 4 shows a series of three photographs of oblique standing waves looking downstream along the deflector vane. In Fig. 4(*a*), the deflection angle is 9° and the depth ratio across the jump is 1.56; the undular form of the wave is clearly shown by comparison with Fig. 4(*b*) at $\theta = 15°$ and a depth ratio of 2.00. In agreement with the analysis previously presented, the crest has become unstable and the jump front is much more abrupt because of the presence of a roller. The final photograph shows the limiting deflecting angle (in this case, $\theta = 21°$) imposed by the finite width of the channel. This so-called "choking" condition is produced when the reflection of the initial shock wave from the wall opposite the deflector vane strikes the downstream end of the vane. If the local Froude number at this point becomes less than unity, a normal hydraulic jump will gradually move upstream and come to rest near the leading edge of the deflector vane. For certain cases, it was possible to delay the formation of the normal jump by adding energy to the flow in the form of a jet of water introduced along the right-hand wall near the point at which the initial wave was reflected.

The experimental data required for the determination of the wave angle β and the corresponding depth ratio across the jump were obtained by taking depth profiles transversely across the flow, beginning at the deflector vane and extending to the opposite wall of the channel. These profiles were taken at 1-ft intervals downstream from the leading edge of the vane.

Expansion Zone Experiments.—In the series of experiments on the characteristics of expansion zones, a total of 27 runs was made at Froude numbers of 1.95 and 2.94 for initial depths of 0.90 in. and 1.50 in. The experimental procedure was the same as that used in the study of the oblique jumps.

EXPERIMENTAL RESULTS

Oblique Standing Waves.—For each experimental run with F_1, h_1, and θ determined in advance, the depth ratio h_2/h_1 and wave angle β were determined in the following manner:

A plot of the experimental data was made in which a plan view of the test section was represented, using the same longitudinal and transverse scales. The wave profiles were then plotted at their respective longitudinal stations; the actual depths were plotted to an exaggerated vertical scale independent of the longitudinal scale. The resulting plot gives a "perspective" view of the jump front while retaining all dimensions in true scale, the only restriction being that angles must be measured in the plane of the channel bottom. Two plots of this type are shown in Figs. 5 and 6 at Froude numbers of 2.08 for a 9° deflection angle and 4.18 for a 15° deflection angle. Fig. 5 illustrates a wave form characteristic of the undular jump, and Fig. 6 is typical of the roller-type jump at depth ratios larger than 2.

In the case of undular jumps, the depth h_2 is readily determined from the equilibrium depth and the points of inflection of the undulations as shown by the dashed line representing this depth in the profiles of Fig. 5. It has also been repeatedly observed that the height of the initial crest is $\frac{3}{2}$ $(h_2 - h_1)$ as was previously predicted. In the case of the roller-type jumps, the depth h_2 is less easily defined because of the intense surface disturbances near the front. In

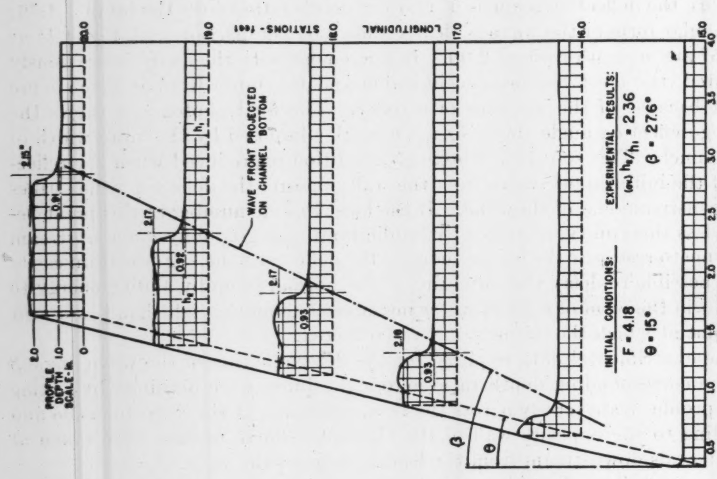
PROFILE DEPTH SCALE - in.
2.0
1.0
0
2.15"
0.91
2.17
0.92
2.17
0.93
2.18
0.93
h₁
h₂
WAVE FRONT PROJECTED ON CHANNEL BOTTOM
LONGITUDINAL STATIONS - feet
20.0
19.0
18.0
17.0
16.0
15.0
β
θ
INITIAL CONDITIONS:
F = 4.18
θ = 15°
EXPERIMENTAL RESULTS:
(av.) h₂/h₁ = 2.36
β = 27.6°
TRANSVERSE STATIONS - feet
0.5
1.0
1.5
2.0
2.5
3.0
3.5
4.0

FIG. 6.—CROSS SECTIONS OF REGULAR JUMP, LOOKING DOWNSTREAM

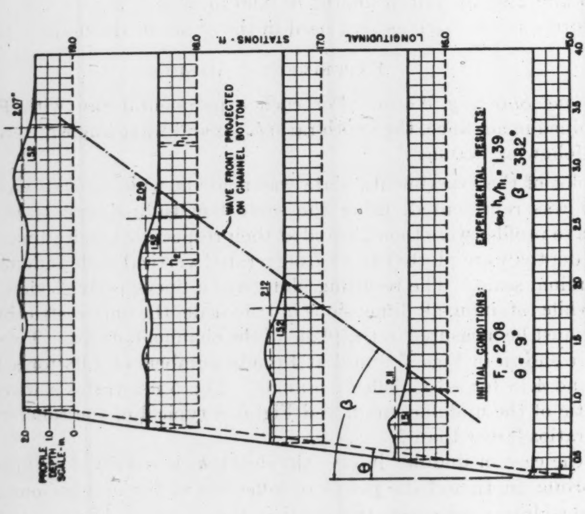
PROFILE DEPTH SCALE - in.
2.0
1.0
0
2.07"
1.52
2.09
1.52
2.12
1.52
2.11
1.51
h₁
h₂
WAVE FRONT PROJECTED ON CHANNEL BOTTOM
LONGITUDINAL STATIONS - ft.
19.0
18.0
17.0
16.0
15.0
β
θ
INITIAL CONDITIONS:
F₁ = 2.08
θ = 9°
EXPERIMENTAL RESULTS:
(av.) h₂/h₁ = 1.39
β = 38.2°
TRANSVERSE STATIONS - feet
0.5
1.0
1.5
2.0
2.5
3.0
3.5
4.0

FIG. 5.—CROSS SECTIONS OF UNDULAR JUMP, LOOKING DOWNSTREAM

this case, the depth at the deflector vane is used. The final value of h_2/h_1 for each run is the average of the individual ratios for the several transverse depth profiles.

The method for the experimental determination of the wave angle β is one that applies equally to undular jumps or roller-type jumps. The location of the wave front for a particular profile is approximated by a vertical line drawn so that the triangular areas (above and below the wave profile) formed by the horizontal depth lines h_1 and h_2 and the vertical line are equal. The intersection of this line with the channel bottom is marked for each profile, and a straight line is drawn through the points to determine the angle of the standing wave with respect to the oncoming flow. This somewhat arbitrary method has the advantage of not placing undue weight on any one measured point on the wave front; this feature is important in the case of the roller-type jumps in which depth measurements are difficult. This line from which the wave angle is measured may not pass exactly through the point of boundary discontinuity because of the finite thickness of the wave front.

TABLE 1.—OBSERVATIONS ON OBLIQUE STANDING WAVES

Run[a]	Deflection angle	Wave Angle β		Depth Ratio h_2/h_1		Wave Angle β		Depth Ratio h_2/h_1		Wave Angle β		Depth Ratio h_2/h_1	
		Experimental	Theoretical	Experimental	Theoretical	Experimental	Theoretical	Experimental	Theoretical	Experimental	Theoretical	Experimental	Theoretical
		(*a*) Run I; $\mathbf{F}_1 = 2.00$				(*d*) Run F; $\mathbf{F}_1 = 3.20$				(*g*) Run G; $\mathbf{F}_1 = 5.91$			
1	3°	33.4	33.2	1.12	1.12	21.8	20.8	1.18	1.18	12.4	12.2	1.26	1.34
2	6°	35.2	36.6	1.25	1.26	23.4	23.6	1.37	1.38	14.5	15.0	1.61	1.70
3	9°	39.0	40.3	1.39	1.40	26.2	26.5	1.56	1.58	17.4	17.6	2.02	2.10
4	12°	43.0	44.6	1.52	1.54	29.0	29.6	1.78	1.79	20.2	20.6	2.41	2.49
5	15°	...	...	...	...	32.4	32.8	2.00	2.00	23.1	23.6	2.94	2.90
6	18°	...	...	...	...	35.6	36.2	2.24	2.22	25.6	26.7	3.33	3.29
7	21°	...	...	...	...	39.0	39.8	2.45	2.44	...	...	...	...
		(*b*) Run D; $\mathbf{F}_1 = 2.08$				(*e*) Run C; $\mathbf{F}_1 = 3.80$				(*h*) Run H; $\mathbf{F}_1 = 6.30$			
1	3°	31.7	31.9	1.13	1.13	17.4	17.8	1.2	1.22	11.6	11.6	1.35	1.36
2	6°	33.8	35.1	1.26	1.26	19.8	20.4	1.43	1.45	14.1	14.2	1.74	1.75
3	9°	38.2	38.8	1.39	1.40	23.1	23.3	1.66	1.69	17.2	17.1	2.14	2.16
4	12°	41.6	42.8	1.55	1.55	26.4	26.4	1.89	1.94	19.6	20.0	2.58	2.59
5	15°	...	...	...	...	29.6	29.5	2.13	2.19	...	...	...	...
6	18°	...	...	...	...	32.6	32.7	2.38	2.45	...	...	...	...
7	21°	...	...	...	...	36.0	36.1	2.66	2.70	...	...	...	...
		(*c*) Run B; $\mathbf{F}_1 = 3.05$				(*f*) Run J; $\mathbf{F}_1 = 4.18$				(*i*) Run E; $\mathbf{F}_1 = 7.00$			
1	3°	20.9	21.8	1.15	1.17	15.0	16.3	1.24	1.24	10.3	10.6	1.44	1.41
2	6°	24.0	24.6	1.31	1.36	18.5	18.9	1.48	1.49	12.9	13.4	1.87	1.83
3	9°	27.0	27.6	1.52	1.56	21.4	21.8	1.76	1.76	15.7	16.2	2.26	2.30
4	12°	29.4	30.6	1.70	1.76	24.2	24.8	2.06	2.03	18.4	19.1	2.67	2.78
5	15°	33.2	34.0	1.93	1.96	27.6	27.8	2.36	2.32	20.3	22.1	3.32	3.26
6	18°	36.6	37.4	2.11	2.17	30.8	31.1	2.62	2.59	23.6	25.2	4.00	3.72

[a] Run I-1, I-2, I-3, etc.

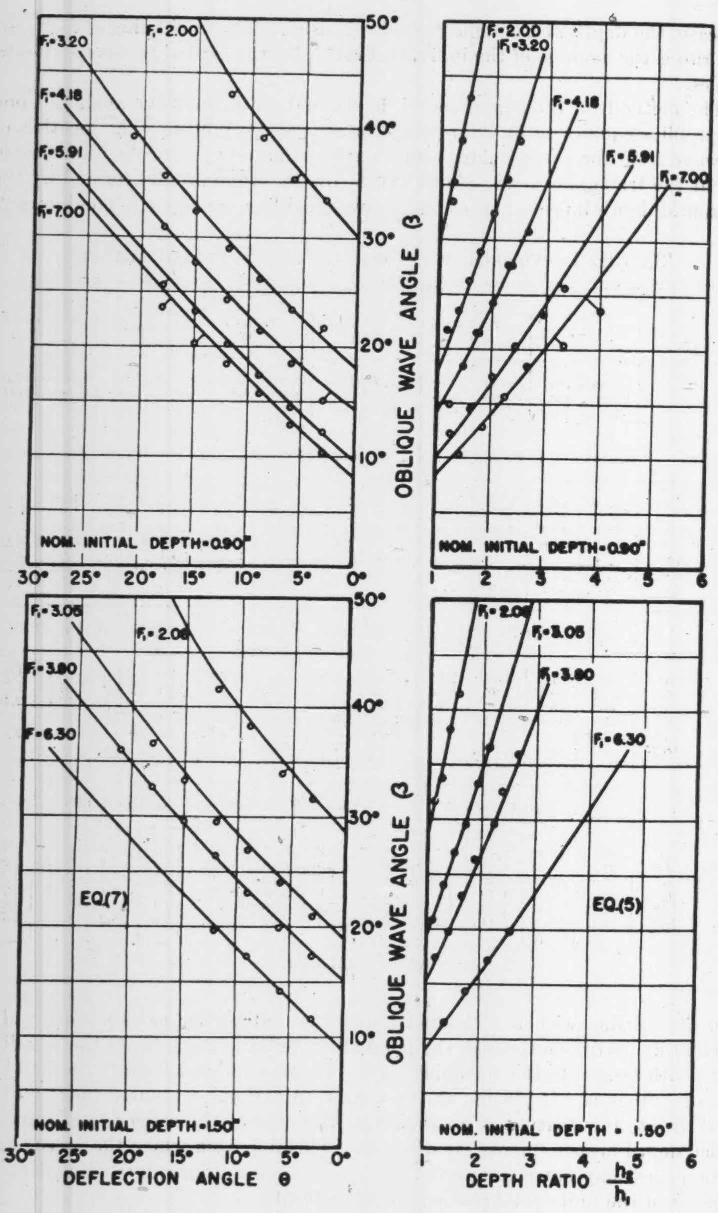

FIG. 7.—COMPARISON OF EXPERIMENTAL AND THEORETICAL DEFLECTION ANGLES AND DEPTH RATIOS OF AN OBLIQUE HYDRAULIC JUMP

The experimental results and a comparison with theory are summarized in Table 1. Fig. 7 shows the comparisons in graphical form. The wave angle β is plotted against the deflection angle and the depth ratio for the various initial Froude numbers. For purposes of clarity, the curves are separated according to their nominal initial depths of 0.90 in. and 1.50 in. The average agreement between theory and experiment for both the wave angle and the depth ratio is of the order of 2%. Larger differences appear for the minimum and maximum

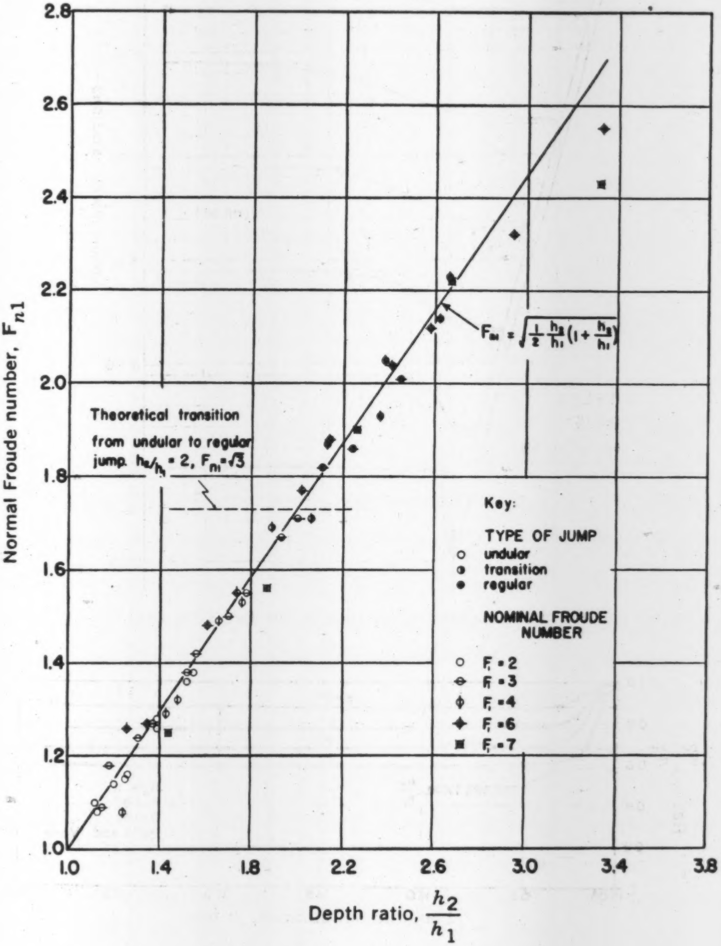

FIG. 8.—CLASSIFICATION OF JUMP FORM BY USE OF THE FROUDE NUMBER NORMAL TO THE WAVE FRONT

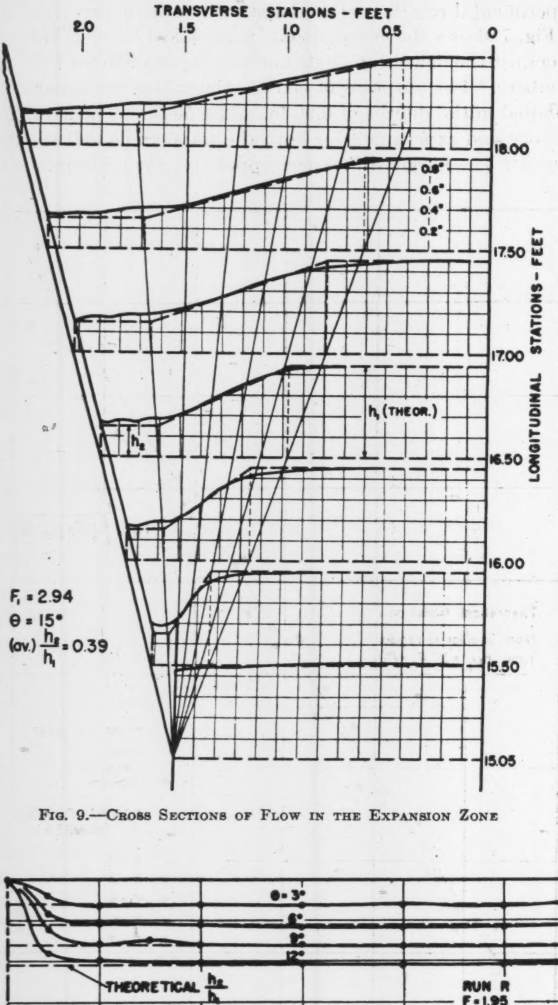

FIG. 9.—CROSS SECTIONS OF FLOW IN THE EXPANSION ZONE

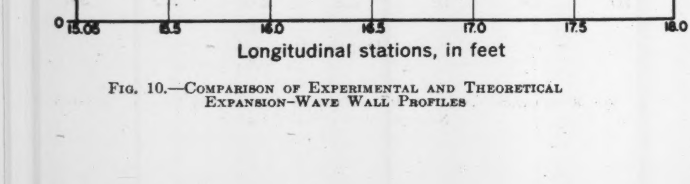

FIG. 10.—COMPARISON OF EXPERIMENTAL AND THEORETICAL EXPANSION-WAVE WALL PROFILES

deflection angles because of the small depth changes involved for the wave angle and the eddying of the roller and large vertical accelerations for the depth ratio.

The depth ratio may also be presented in a much simpler manner in terms of the Froude number normal to the wave front F_{n1} which can be computed from the experimental values of F_1 and β because $\mathsf{F}_{n1} = \mathsf{F}_1 \sin \beta$. The right-hand curves of Fig. 7 are then reduced to a single curve that represents the momentum equation of the normal hydraulic jump (Eq. 4*b*). For each experimental run, the value of F_{n1} was computed and plotted for the corresponding experimental depth ratio as shown in Fig. 8. In addition, a classification of "undular" or "roller" was assigned to each run by observing the form of the wave profile. In a few runs the classification was not clear and these runs were labeled "transition." Fig. 8 shows that the regions of the two wave types are clearly defined and confirm the analysis that indicated the limit of undular jumps at a depth ratio of two.

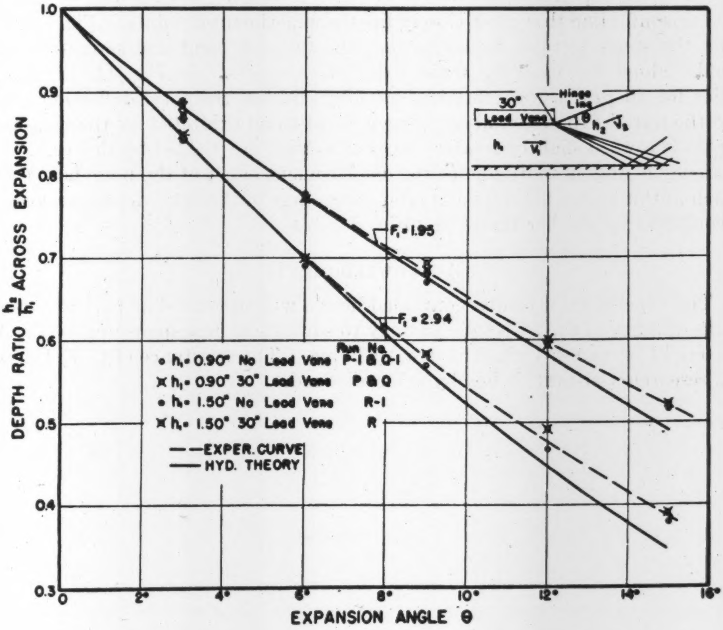

FIG. 11.—COMPARISON OF EXPERIMENTAL AND THEORETICAL DEPTH RATIOS ACROSS EXPANSION WAVES

Expansion Waves.—The experimentally determined depth profiles of the expansion wave were plotted in the same manner as in Figs. 5 and 6. A representative plot is shown in Fig. 9 for the conditions $\mathsf{F}_1 = 2.94$, $\theta_t = 15°$, and $h_1 = 0.90$ in. Superimposed upon the experimental depths are the theoretical water-depth profiles shown as dashed lines. The characteristic-depth or constant-depth lines are also shown in increments of three degrees of expansion; thus, the beginning and end of the theoretical expansion zone are determined by the initial and final line of this series that radiates from the leading edge of the deflector vane. In general, both the slope and position of the experimental profile agree reasonably closely with the theoretical profile except for the region close to the leading edge. In this area, the nonhydrostatic pressure distribution due to large vertical accelerations accounts for this disagreement. In the region of constant depth h_2 between the deflector vane and the last disturbance line, the experimental value of h_2 is determined for each profile by finding the horizontal line that most closely fits the experimental points. Fig. 10 indicates the steep decrease in depth near the turn-off point and shows the wall profiles along the vane for various deflection angles. In Fig. 11, the depth ratios for all runs are summarized as a function of the total deflection angle and the initial Froude number. The general trend exhibited by the measured depths is toward slightly greater values of h_2 than are yielded by theory. This tendency is undoubtedly due to the displacement effect of the boundary layer, which in this region assumes a greater percentage of the total depth, because h_2 is considerably smaller than the initial depth h_1.

Acknowledgments

The experimental results contained herein were obtained as part of a study of the validity of the hydraulic analogy to supersonic flow sponsored by the Air Materiel Command, United States Air Force. The assistance of C. E. Carver, Jr., research assistant, is hereby acknowledged.

AMERICAN SOCIETY OF CIVIL ENGINEERS
Founded November 5, 1852
TRANSACTIONS

Paper No. 2816

SAFE LOADS ON DOG-LEG PILES

By James D. Parsons,[1] M. ASCE, and Stanley D. Wilson,[2] A. M. ASCE

With Discussion by Messrs. A. E. Cummings; and James D. Parsons and Stanley D. Wilson

Synopsis

One of the essential requirements for the acceptability of steel-encased or pipe piles is often based on whether or not some portion of the bottom of such piles can be seen after they have been driven. As this requirement involves the loss of considerable numbers of piles on most pile installations, it is desirable to salvage those having structural value. For this purpose, the equipment described in this paper, which can be lowered into piles to measure their curvature, was devised. In the paper are described several projects where the equipment was used, and a logical analytical method is presented for evaluating the load-carrying capacity of such piles—the method having been verified by load tests.

Introduction

It has long been general practice in the driving of steel-encased concrete or pipe piles to base their acceptance on (among other things) whether or not any portion of the bottom of the piles can be seen after they have been driven. If the alinement of a pile, after it has been driven, is such that it is not possible to see any portion of the bottom of the pile with the aid of a light lowered into the pile, it is abandoned and presumed to have no bearing value irrespective of its driving characteristics. This is accepted practice even if the piles meet refusal on rock at depths that are consistent with known depths to rock established by borings. This requirement is unquestionably extremely rigid, particularly if the lengths and cost of the piles are great, and it places piles of

---

Note.—Published, essentially as printed here, in August, 1954, as *Proceedings-Separate No. 475.* Positions and titles given are those in effect when the paper or discussion was approved for publication in *Transactions.*

[1] Associate Partner, Moran, Proctor, Mueser & Rutledge, New York, N. Y.

[2] Partner, Shannon & Wilson, Seattle, Wash.

this type at a distinct disadvantage compared to piles of a type that cannot be inspected after driving. In fact, in the instances of wood or H-piles little or no thought is given to alinement of the pile below ground in spite of the fact that large loads must be carried by the latter to justify their use. Although engineers have no way of knowing the condition of such piles below grade, they often place complete confidence in them to carry large loads.

In the interest of economy, no doubt, many engineers have wondered about the validity of existing rules governing the acceptance of open piles, but unfortunately they have been unable to demonstrate the degree of curvature existing in piles, the bottoms of which could not be seen and therefore have not been able to assign realistic bearing values to the piles. To permit the salvaging of such piles required first the development of suitable equipment that could be lowered into the piles to determine the curvature of the piles at various points along their lengths and then the development of an analytical approach that could be utilized to evaluate the influence of such curvature on the load-carrying capacity of the piles. Experience has proved that large loads can be supported by piles having some curvature; it is the

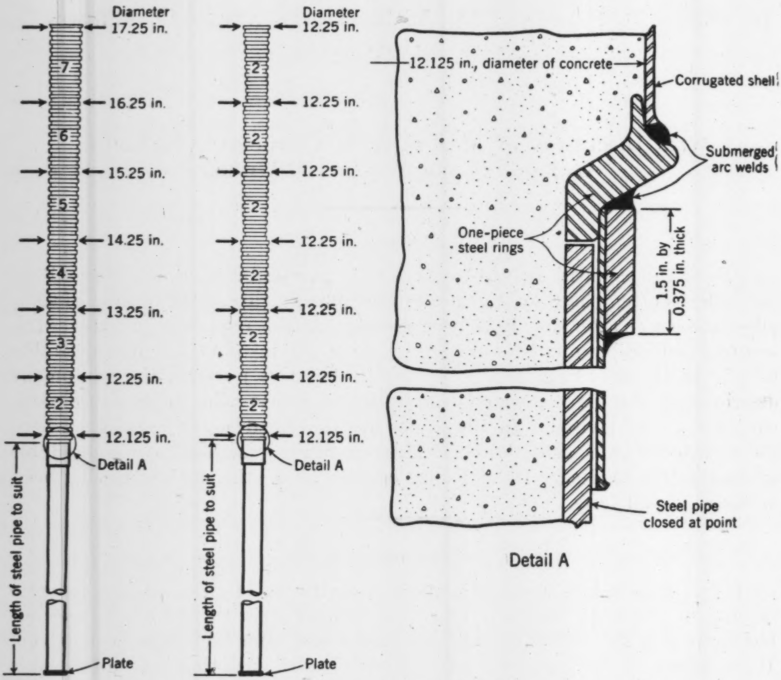
Diameter
17.25 in.
7
16.25 in.
6
15.25 in.
5
14.25 in.
4
13.25 in.
3
12.25 in.
2
12.125 in.
Detail A
Length of steel pipe to suit
Plate
Diameter
12.25 in.
2
12.25 in.
2
12.25 in.
2
12.25 in.
2
12.25 in.
2
12.25 in.
2
12.125 in.
Detail A
Length of steel pipe to suit
Plate
12.125 in., diameter of concrete
Corrugated shell
Submerged arc welds
One-piece steel rings
1.5 in. by 0.375 in. thick
Steel pipe closed at point
Detail A

FIG. 1.—DETAILS OF CASE A PILES

purpose of this paper to present a logical method of evaluating their capacity and thus provide a means of justifying their use—the approach having been verified by load tests.

The need for the development of both a means of measuring the inclination of piles exhibiting curvature and a method of analyzing their load-carrying capacity recently arose on two large New York City projects. These will be referred to as cases A and B. In the first of these instances composite piles ranging from 80 ft to 140 ft in length were being driven. Of the first 93 piles driven for this project 13 were found to exhibit curvature, and their bottoms could not be seen. Because the contract drawings called for the driving of approximately 800 composite piles it became evident, at the outset, that much money and time might be saved if the dog-leg piles could be salvaged—particularly if the early indications of the ratio of dog-leg piles to straight piles continued—because the cost of one of these piles was in excess of $500.

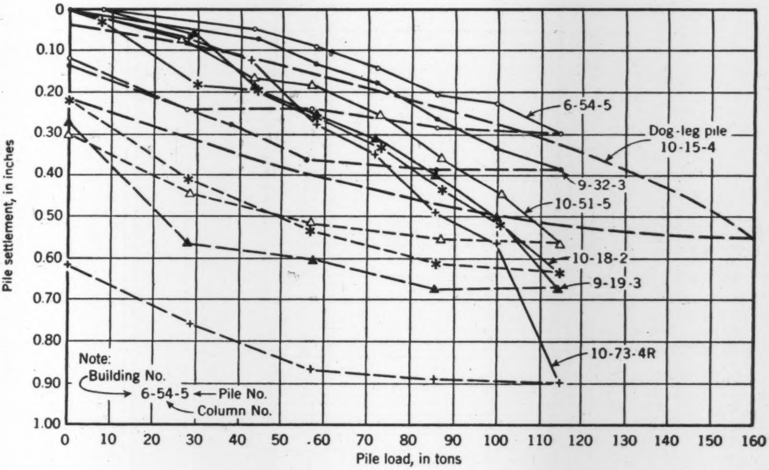

FIG. 2.—LOAD TESTS ON CASE A PILES

DESCRIPTION OF COMPOSITE PILES—CASE A

The lower portion of the composite piles analyzed consisted of closed-end steel pipe of $10\frac{3}{4}$-in. outside diameter ($\frac{3}{8}$-in. wall thickness) and the upper portion, of corrugated shell. Four-thousand-pound concrete was used in each, and the piles were driven closed-ended as point-bearing piles to carry a design load of $57\frac{1}{2}$ tons each. Details of the piles, including the connection between the corrugated section and pipe section, are shown in Fig. 1. The original design for the piles called for a tapered shell in the upper portion, but because of the extremely hard driving evidenced by the first piles driven this was later changed to a straight $12\frac{1}{2}$-in.-diameter shell. Even after this change was

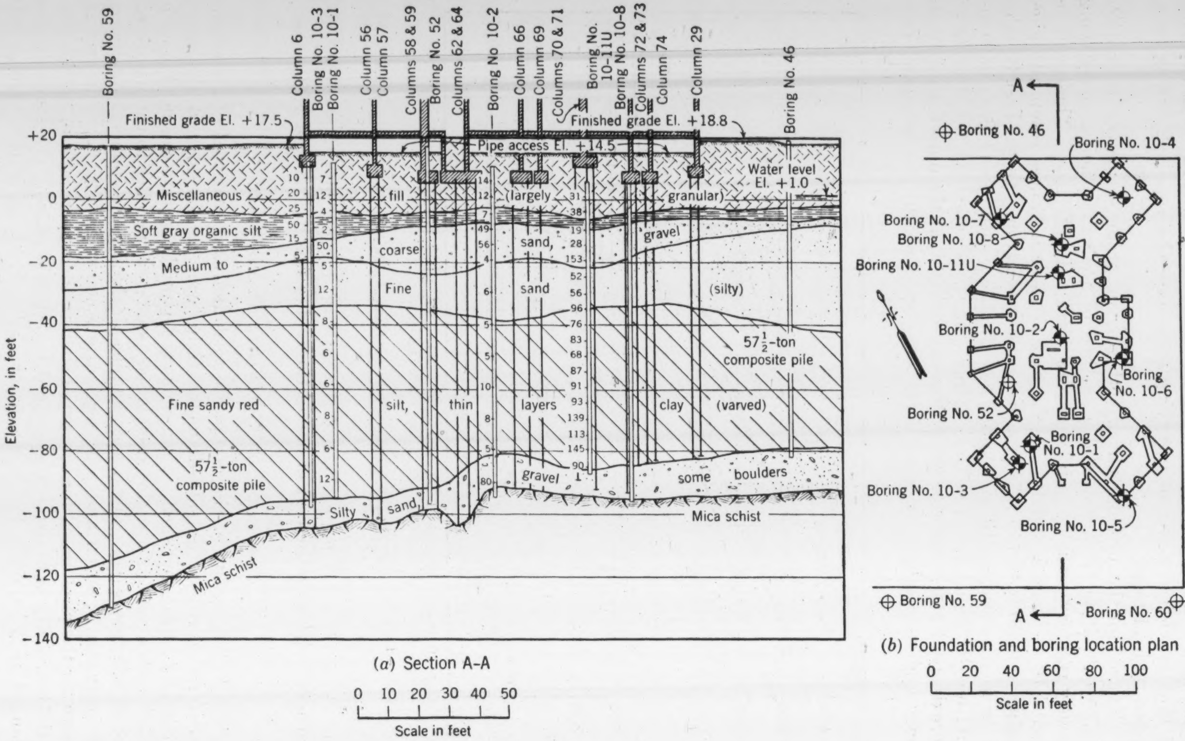
Boring No. 59
Column 6
Boring No. 10-3
Boring No. 10-1
Column 56
Column 57
Columns 58 & 59
Boring No. 52
Columns 62 & 64
Boring No 10-2
Column 66
Column 69
Columns 70 & 71
Boring No. 10-11U
Boring No. 10-8
Columns 72 & 73
Column 74
Column 29
Boring No. 46
Finished grade El. +17.5
Finished grade El. +18.8
Pipe access El. +14.5
Water level El. +1.0
Elevation, in feet
+20
0
-20
-40
-60
-80
-100
-120
-140
Miscellaneous fill (largely granular)
Soft gray organic silt
Medium to coarse sand, gravel
Fine sand (silty)
Fine sandy red silt, thin layers clay (varved)
57½-ton composite pile
57½-ton composite pile
Silty sand, gravel, some boulders
Mica schist
Mica schist
(a) Section A-A
0 10 20 30 40 50
Scale in feet
A
A
Boring No. 46
Boring No. 10-4
Boring No. 47
Boring No. 10-7
Boring No. 10-8
Boring No. 10-11U
Avenue
Boring No. 10-2
Boring No. 10-6
Boring No. 52
Boring No. 10-1
Boring No. 53
Boring No. 10-3
Boring No. 10-5
Fifth
Boring No. 59
Boring No. 60
(b) Foundation and boring location plan
0 20 40 60 80 100
Scale in feet

FIG. 3.—CASE A—BORING LOCATION PLAN AND GEOLOGICAL SECTION

made it was found necessary first to drive an outer 14-in.-diameter shell to a limited depth to eliminate friction along the upper portion of the pile, this shell being pulled in each case immediately after completing the driving of the pile. This action permits the granular soil surrounding the shell to fill the annular space between the shell and the pile. Six load tests, three on each of the two types of piles, were performed in accordance with the requirements stipulated in the New York City Building Code. The maximum design load permitted for these piles was governed by the maximum allowable unit stress permitted by the code for 4,000-lb concrete of f_c = 1,000 lb per sq in., the controlling cross-sectional area being that of the lower $12\frac{1}{8}$-in.-diameter shell of the upper section.

The load-settlement diagrams for the six load tests performed on straight piles are included in Fig. 2. The loads were in each case applied in the increments stipulated by the building code to a maximum test load of twice the design load or 115 tons; as may be seen in Fig. 2, the piles satisfactorily carried this load because the maximum deflection in each case was less than the maximum gross settlement of 1 in. permitted by the code.

SOIL FORMATION—CASE A

The specifications governing the driving of the composite piles stipulated that the piles were to be driven through the fill and underlying sand and silt formation to rock or to the gravel boulder formation directly overlying rock to a minimum penetration resistance of 8 blows per in. with a 15,000-ft-lb hammer. A typical foundation plan and geological section through one of the buildings involved in Case A is shown in Fig. 3. Beneath the thirteen-story and fourteen-story buildings of Case A, the prevailing formation in sequence of depth consists of a surface fill averaging approximately 20 ft in thickness, a thin bed of organic silt from 3 ft to 8 ft thick, a bed of medium to coarse sand and gravel approximately 10 ft thick, a layer of silty fine sand averaging approximately 15 ft thick, and a deep bed of sandy red silt containing thin layers of gray clay ranging in thickness from a minimum of 40 ft to a maximum of 53 ft. The latter formation is a glacial lake formation that extends over a rather large area along the northern and easterly parts of Manhattan Island. It is quite often referred to as "bull's liver" by the construction industry and is extremely difficult to sample because of its sensitivity to vibration. Below the varved-silt formation and overlying bedrock was encountered a bed of silty sand and gravel containing some boulders, the formation averaging about 8 ft in thickness. Bedrock of mica schist along this section is at a depth of from 110 ft to 115 ft below existing grade.

Because the 40-ft to 60-ft upper sections of the piles at this site were driven with a heavy mandrel, the alinement of which could be carefully controlled, this section (in the instance of each of the piles analyzed) was found to be straight and in most instances vertical. The curved or dog-leg section was found to be in the lower $10\frac{3}{4}$-in.-outside-diameter pipe section, and in most cases this curvature was very gradual and limited to the lower portion of the pipe. Considering the very high length-diameter ratio of these piles, it is not surprising that so many were found to have some curvature, particularly in those instances in which hard driving was required. The tips of some of the piles were found to be as much as 6 ft out of line with a vertical through the tops of the piles. In a few cases the pipe section was not found to be tangent with the upper shell section and such sections were considered the most critical as a substantial reduction in the allowable load to be carried by them had to be made.

Of the 63 piles at the site requiring curvature measurements because the tips could not be seen with a light, approximately 45% were found to be less than 2% out of plumb, which is the limiting value permitted by the building code before compensating measures must be taken. Even so, these piles would have been replaced had not the measurements been made as no portion of their bottoms could be seen.

Soil Formation and Description of Piles—Case B

In the second group of piles analyzed by the writers, the piles were closed-end pipe piles of 10¾-in. outside diameter driven to rock or the sand and gravel formation immediately overlying rock. A limited number of these piles were driven as replacement piles for 25-ton (design load) creosoted wood piles that had been damaged in driving through fill containing boulders and broken rock for the support of a seven-story, reinforced concrete building. Cost estimates indicated that if such replacement piles could be successfully driven through the areas of rock and boulders, a considerable saving could be accomplished over the removal of the rock and boulders by excavation, as parts of the adjacent foundation had already been installed and backfilled. The replacement piles were driven to support a design load of 30 tons each.

The foundation plan for the building is shown in Fig. 4. Also shown in this illustration are the locations of the exploratory borings in the building area and a longitudinal section through the building. As may be seen on the section, the prevailing formation in sequence of depth consists of a surface fill 20 ft thick placed to replace the objectionable fill containing boulders that had been removed to permit the driving of wooden piles. Below the new fill was encountered old fill containing rock and boulders. This bed is approximately 8 ft thick and, as previously explained, the failure to remove all this bed in the central part of the building where concentrations of rock were found was responsible for the timber-pile breakage. Below the old fill is a bed of soft gray organic silt averaging from 4 ft to 8 ft in thickness. Some of the rock from the overlying fill was found to have penetrated into this formation. Under the organic silt bed was encountered a 15-ft bed of reasonably compact medium-to-fine silty gray sand and between this and bedrock, a 2-ft to 8-ft layer of medium-to-coarse sand and gravel. Bedrock of mica schist ranged between 45 ft and 55 ft below cutoff level. Most of the successfully driven wooden piles penetrated to the bed of medium-to-coarse sand and gravel overlying bedrock.

The 10¾-in.-diameter pipe replacement piles included in this group were driven with points, and even though a spud was used to facilitate driving through the rock-boulder formation, considerable difficulty was experienced and a large percentage of the replacements were bent in penetrating this

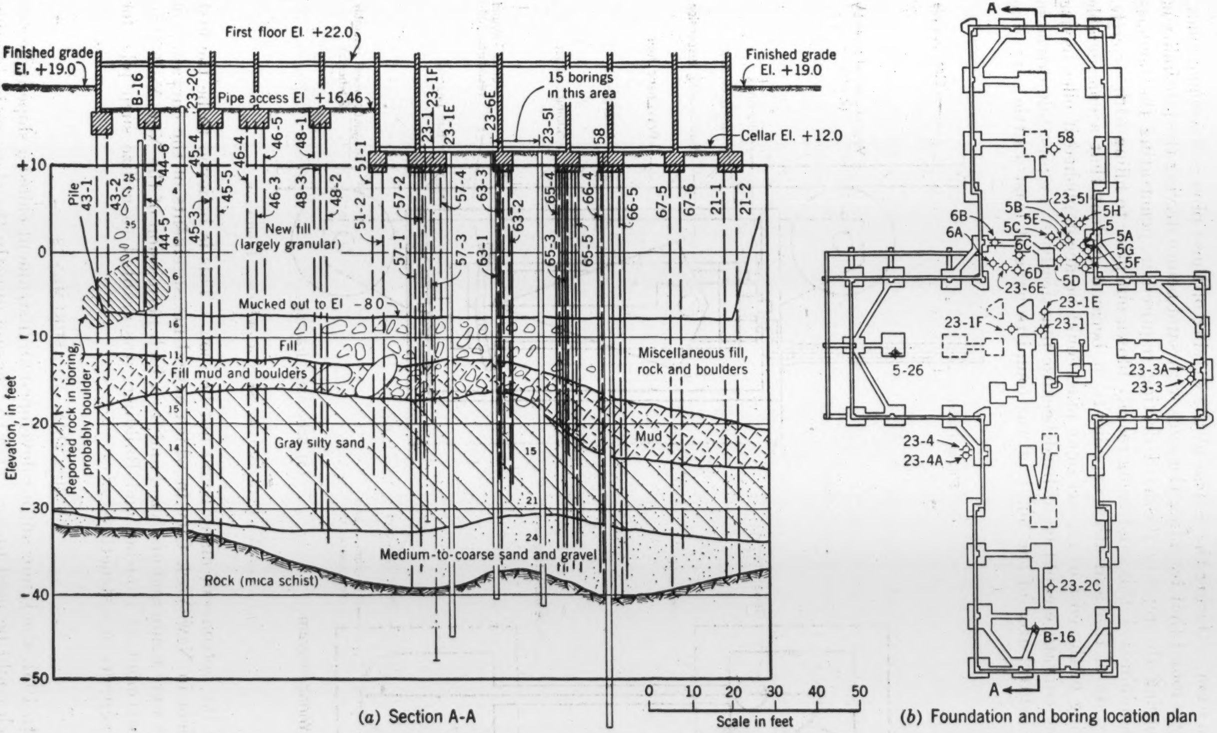
First floor El. +22.0
Finished grade El. +19.0
Finished grade El. +19.0
Pipe access El +16.46
15 borings in this area
Cellar El. +12.0
B-16
23-2C
23-1
23-1F
23-1E
23-6E
23-5I
58
Pile 43-1
43-2
44-6
44-5
45-4
45-3
45-5
46-4
46-3
46-5
48-1
48-3
48-2
51-1
51-2
57-2
57-1
57-4
57-3
63-3
63-2
63-1
65-4
65-3
65-5
66-4
66-5
67-5
67-6
21-1
21-2
New fill (largely granular)
Mucked out to El -8.0
Fill
Fill mud and boulders
Miscellaneous fill, rock and boulders
Reported rock in boring, probably boulder
Gray silty sand
Mud
Medium-to-coarse sand and gravel
Rock (mica schist)
Elevation, in feet
+10
0
-10
-20
-30
-40
-50
0
10
20
30
40
50
Scale in feet
A
A
58
6B
6A
6C
6D
23-6E
5B
5C
5E
23-5I
5H
5
5A
5G
5F
5D
23-1E
23-1F
23-1
5-26
23-3A
23-3
23-4
23-4A
23-2C
B-16

(*a*) Section A-A

(*b*) Foundation and boring location plan

FIG. 4.—CASE B—BORING LOCATION PLAN AND GEOLOGICAL SECTION

formation. During the course of the driving of these pipe replacement piles, it was found that by filling the piles with sand before driving the possibility of crimping the pipe in the hard driving required in penetrating the boulders was minimized, this sand being readily blown out prior to filling with concrete. In spite of this and other expedients, it became evident that a considerable saving in the cost of replacement piles could be accomplished if piles having some curvature could be utilized because practically every pipe pile driven in the central area of the building was found to have at least a little curvature and the bottoms of many could not be seen. This is believed to be the first project in New York City in which actual measurements of the curvature in piles were made and analyzed and for which permission of the New York City Department of Housing and Buildings was granted to utilize such piles for the support of a structure.

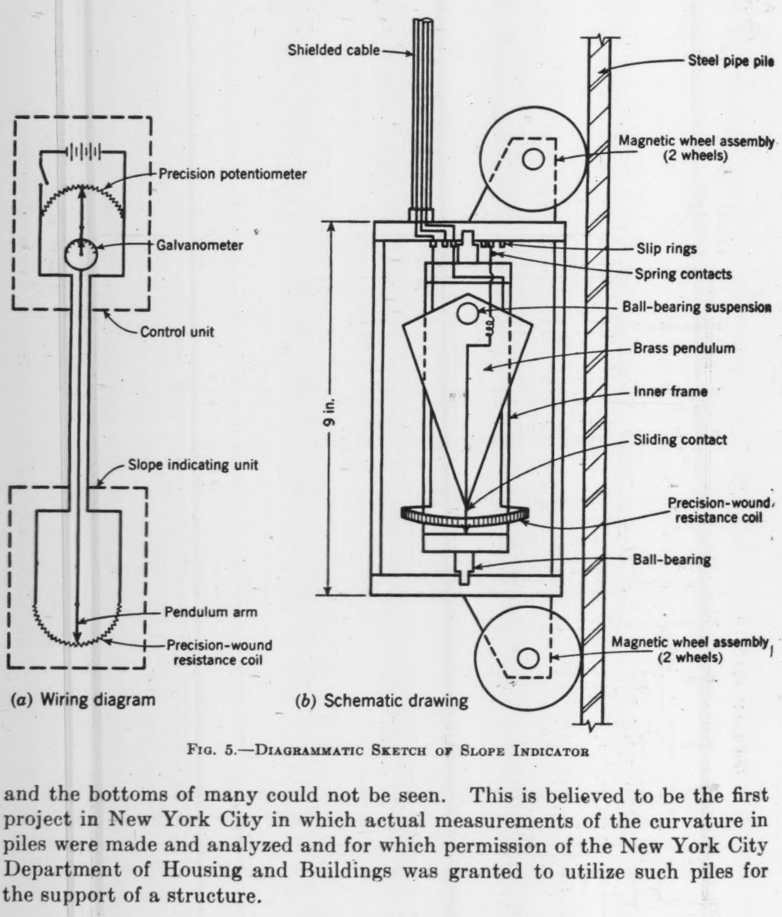
Precision potentiometer
Galvanometer
Control unit
Slope indicating unit
Pendulum arm
Precision-wound resistance coil
Shielded cable
Steel pipe pile
Magnetic wheel assembly (2 wheels)
Slip rings
Spring contacts
Ball-bearing suspension
Brass pendulum
Inner frame
Sliding contact
9 in.
Precision-wound resistance coil
Ball-bearing
Magnetic wheel assembly (2 wheels)

(*a*) Wiring diagram (*b*) Schematic drawing

FIG. 5.—DIAGRAMMATIC SKETCH OF SLOPE INDICATOR

DEFLECTION MEASUREMENTS

In 1951, the junior author developed an instrument called a slope indicator which could be used under water to measure directly the slope or inclination of steel sheet-piling at various depths. This was described in a paper presented before the Boston Society of Civil Engineers in 1953. The inclination, however, could be measured only in a plane normal to the surface against which the instrument was in contact, and the range of tilt was limited to approximately 8° from the vertical. The tips of some of the piles described in this paper were found to be inclined at angles in excess of 15°. It was therefore necessary to design and construct a new instrument that could be used to measure the maximum inclination at any depth regardless of the orientation of the instrument with respect to the pipe. Fortunately, it was necessary to ascertain the magnitude only—not the direction of the inclination.

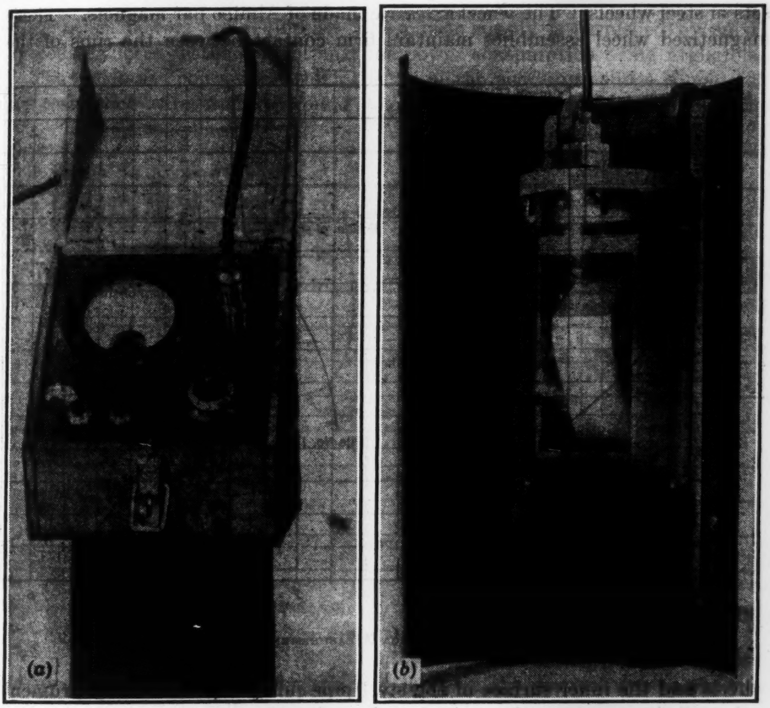

FIG. 6.—SLOPE INDICATOR SHOWING (a) THE CONTROL BOX CONTAINING A PRECISION POTENTIOMETER AND BATTERIES AND (b) THE INSTRUMENT CONTAINING A NONMAGNETIC PENDULUM

The slope-indicating system used in the revised instrument is basically the same as that devised for the earlier model and is based on the well-known Wheatstone Bridge circuit as illustrated in Fig. 5. For any given position of the pendulum arm in the slope-indicating unit, there is only one position of the potentiometer arm at which no current flows through the neutral wire connecting the two arms. A sensitive galvanometer indicates when a balance point is attained.

The slope indicator itself, shown in Figs. 5 and 6, is contained inside a 5-in.-diameter plastic tube, 9 in. long. A heavy brass pendulum with ball-bearing suspension is mounted on an inner frame that is free to rotate on ball bearings about its longitudinal or vertical axis. The tip of the pendulum slides along a precision-wound resistance coil that is also attached to the inner frame. The electrical leads from the ends of the coil and from the tip of the pendulum are brought to the case through slip rings to the surface of the ground in a 3-conductor shielded cable.

The watertight plastic case enclosing the inner frame is mounted on two sets of steel wheels. The wheel axles are made of Almico bar magnets. These magnetized wheel assemblies maintain firm contact between the rims of the wheels and the inner surface of the steel pipe pile yet permit the instrument to be rolled up or down the entire length of the pile.

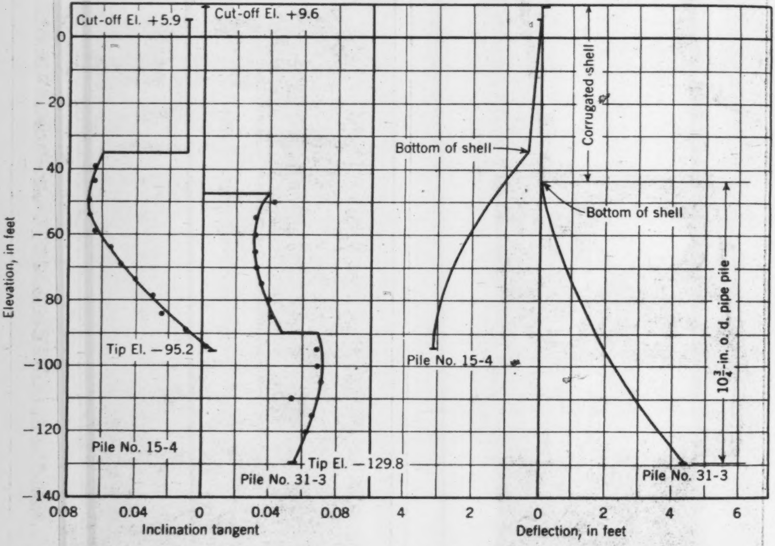

FIG. 7.—CASE A—TYPICAL DEFLECTION MEASUREMENTS FOR COMPOSITE PILES

In operation, the instrument is placed in a vertical position with the wheels in contact with the inside wall of the pipe. The nonmagnetic pendulum assumes a vertical position under the influence of gravity, whereas the longitudinal axis of the inner frame remains parallel to the axis of the pipe. If the plane of maximum inclination is perpendicular to the surface with which the wheels are in contact, the horizontal axis of the pendulum will remain parallel to the wheel axles and there will be no rotation of the inner frame. If the plane of maximum inclination shifts (as in a corkscrew pile) or if the instrument tends to rotate as it is being lowered, the inner frame rotates under the force of gravity until the pendulum swings in the plane of maximum inclination. Check observations were made by lowering the instrument down on several sides of some piles with no significant change in slopes indicated.

The downward descent of the instrument is stopped at desired intervals of depth and held stationary until the motion of the pendulum has ceased. The precision potentiometer in the control box, which remains above ground at all times, is adjusted until the bridge circuit is in balance, and the corresponding dial reading is recorded. The true inclination of the pile is then determined from the calibration curve of the instrument. No corrections for temperature or for other factors are required. The power supply is furnished by small dry cells enclosed in the control box, the power consumption being negligible.

The resistance coil across which the tip of the pendulum slides is made of fine resistance wire wound around a plastic core. The sensitivity of the instrument is such that a deflection of 1 in. from the vertical axis at the tip of a 40-ft-long pile will produce a measurable reading. Because surface imperfections on the inner surface of the piles sometimes produce changes in the instrument reading of this order of magnitude, greater sensitivity is not desired.

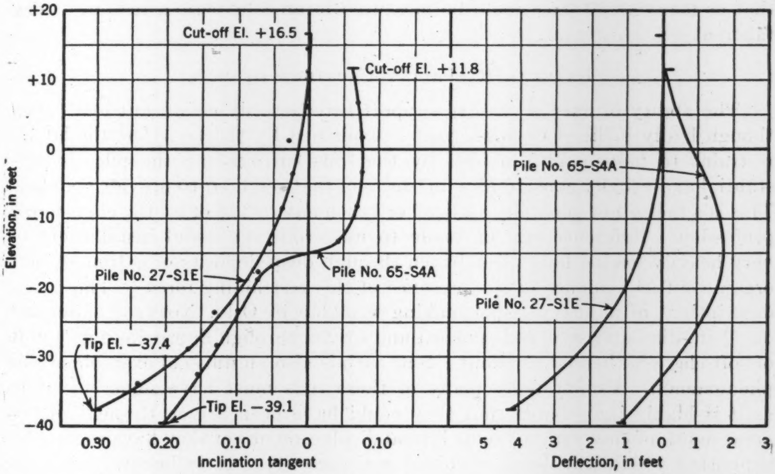

FIG. 8.—CASE B—TYPICAL DEFLECTION MEASUREMENTS FOR THE PIPE PILES

After the dial readings have been converted to inclination tangents (the tangent of the angle between the vertical axis and the axis of the pile), a plot relating the inclination tangent and the depth is prepared as shown on the left-hand plots of Figs. 7 and 8. Smooth curves are drawn through these points to iron out the effects of surface irregularities after which the deflections are determined by simple algebraic computations and plotted as shown on the right-hand plots of Figs. 7 and 8.

The direction of the bending in the pipe piles cannot be ascertained except by visual observation when the piles are dewatered. Most of the measurements were made with the piles full of water. The deflection diagrams have been drawn as though the piles were deflected in one plane only. It is possible that some were deflected in a cork-screw pattern. However, the assumption of deflection in a single plane represents the most critical condition, and all design computations were made on the basis of this assumption.

In a few instances piles were measured with the slope indicator prior to dewatering and were found to be both straight and plumb. Some of these piles were later dewatered, thus affording a positive check on the reliability of the instrument.

The slope indicator is light and even in the case of a 150-ft-long pile can be easily handled by one man. Another man, of course, is required to record the readings. It was found in the case of the piles described earlier in Case A that as many as 30 piles could be measured in an 8-hr period, readings being taken at depth intervals of 5 ft.

LATERAL RESTRAINT PROVIDED BY SOIL

The ability of curved piles to support satisfactorily significant loads even though badly inclined or dog-legged is explained by the fact that the lateral restraint to movement provided by the soils surrounding the piles is substantial and usually considerably in excess of that required to provide stability. This is a factor not generally realized or taken advantage of by the engineering profession. Reference can be made to numerous successful installations of very heavily loaded long piles driven through deep deposits of extremely soft organic silt as evidence of the presence of this restraining force.[3] The recent description[4] of a heavy paper-making machine in Oslo, Norway, supported on $1\frac{1}{4}$-in.-diameter steel rods pushed and driven through approximately 150 ft of soft clay and loaded to about 8 tons each is also an unusual example of this phenomenon. Undoubtedly many of these rods must have some curvature as it is highly improbable that they could have been driven through such a great depth of clay without some lateral displacement yet they have reportedly supported the heavy loads involved satisfactorily. It is believed that, as more cases of this type are revealed, the profession as a whole will be less hesitant to accept the fact that even the softest soils provide substantial restraint to lateral movement.

ANALYSES OF CASE A COMPOSITE PILES

In the determination of the allowable loads to be carried by the dog-leg piles considered in cases A and B, it was necessary (to fulfill the requirements of the New York City Building Code) to demonstrate that the unit stresses in the piles were within the limits permitted by the code. The allowable unit stresses controlling the design are (*a*) f_c = 1,000 lb per sq in. for 4,000-lb concrete and (*b*) f_s = 9,000 lb per sq in. for steel. An acceptable analysis therefore had to be developed to demonstrate that the stresses in the piles, irrespective of the results of load tests, were within these limits and the results had to be transmitted to the city's Department of Housing and Buildings for approval.

---

[3] "Influence of Soft Ground on the Design of Long Piles," by George W. Glick, *Proceedings*, Second International Conference on Soil Mechanics and Foundations, Vol. IV, June, 1948, p. 84.

[4] "Machine Foundation Supported by Steel Rods Driven Through Clay," by Ernest E. Howard, *Civil Engineering*, April, 1953, p. 60.

The soil formations prevailing at the location of each site had to be defined by an adequate number of borings. The upper portions of the piles included in Case A were surrounded by sand, and their lower or pipe sections were embedded principally in varved red silt—the physical properties of the latter formation being required in the analyses. Accordingly, a 3½-in.-diameter undisturbed sample boring located in the central area of one of the buildings was made for the purpose of obtaining continuous undisturbed samples for laboratory analysis. Although the principal properties involved in the analyses were the strength and elastic properties of the silt, the laboratory analyses included natural water content, liquid and plastic-limit determinations, consolidation tests, and triaxial compression tests of the quick and consolidated-quick types.

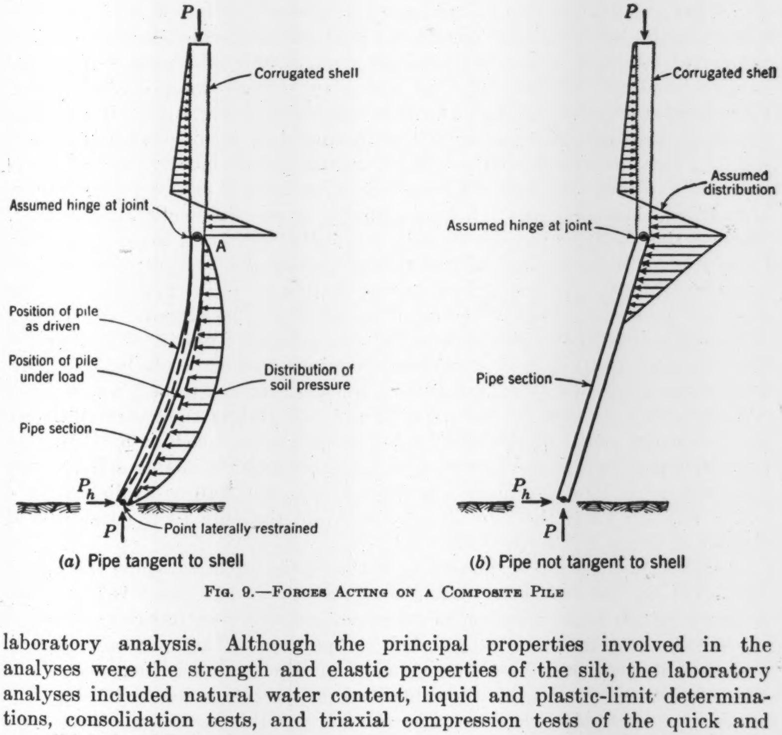
P
Corrugated shell
Assumed hinge at joint
A
Position of pile as driven
Position of pile under load
Distribution of soil pressure
Pipe section
P_h
P
Point laterally restrained
P
Corrugated shell
Assumed distribution
Assumed hinge at joint
Pipe section
P_h
P

(a) Pipe tangent to shell (b) Pipe not tangent to shell

FIG. 9.—FORCES ACTING ON A COMPOSITE PILE

The curvature in the pipe section of the composite piles—although gradual and usually limited to the lower end of this section—was sometimes found to extend to the joint between the shell and pipe section so that the pipe section was found not to be tangent with the shell section in some cases. The piles requiring analyses were therefore divided into two groups—(1) those in which the upper part of the pipe section was found to be tangent to or on the axis of the shell section and (2) those exhibiting a definite break in the alinement between the pipe section and shell section, in which case the upper portion of the pipe section was found not to be tangent to the axis of the shell section. The latter group was substantially in the minority, which was fortunate because an appreciable reduction in the allowable load to be carried by these piles had to be made. A description of the analysis for each of the foregoing two cases is included subsequently.

Basic Assumptions.—In Fig. 9(*a*) are shown the forces acting on the upper and lower sections of a typical Case A dog-leg pile of the type previously described as group 1. The pile in its original position before loading is indicated by the solid lines. Under the influence of an applied vertical load at the top the shell section, being vertical, deflects axially. However, as the bottom of the lower inclined section is sufficiently embedded in firm material to prevent lateral movement at this point and as the deformation of the top is almost entirely vertical, the section will experience its maximum lateral movement at its center as shown by the dashed line in Fig. 9(*a*). In so doing, it will develop pressures in the soil proportional to its displacement, which will be a maximum at its center, zero at its tip, and essentially vertical at the top, and the resulting pressure distribution in the soil can thus be approximated by a sinusoidal curve such as is shown on the pipe section in Fig. 9(*a*). Because the shell section moves only vertically additional assumptions had to be made in determining the soil pressure along this section; these as well as others which were required to permit a solution were: (*a*) The joint between the pipe and shell sections of the pile is considered to be hinged. (*b*) Because of the curvature in the pipe section, lateral restraint from the soil along the lower part of the straight shell section is required in order to produce stability. The pressure providing this lateral restraint was assumed to be $\frac{1}{2}\,\gamma\,h$ in which γ is the unit weight of the soil. (*c*) The distribution of the restraining force at the bottom of the shell section was assumed to approach as nearly a concentrated reaction as is permitted by the maximum available soil pressure assumed in (*b*). (*d*) No horizontal force was assumed to be available at the top of the pile from the pile cap or strut, and the only force considered at this location was the vertical pile load.

In assuming that the connection between the shell and pipe sections is hinged, recognition of some weakness of the pile at this point is taken into account. Such an assumption in effect renders necessary greater stresses in the soil along the lower part of the shell section than will actually be mobilized, and thus the computed bending moment in this section is increased above the actual moment and the allowable load on the pile is reduced. The true stresses at this point were not known, and for this reason a conservative assumption had to be made. In making this assumption the problem was reduced to one statically indeterminate to the first degree.

In connection with distribution of soil pressure on the pipe, the influence of assuming a uniform, triangular, or trapezoidal distribution was also investigated and found to have a negligible effect on the results.

In the foregoing assumptions (*b*) and (*c*), it should be pointed out that the maximum available restraining force from the soil on the upper or shell section is the difference between the full passive and active pressures, or approximately 3 γh, because the soil surrounding this section is sand. A value of $\frac{1}{2} \gamma h$ was used in the analyses. This was done because of uncertainties regarding the true stress conditions prevailing at the joint and the fact that the lateral deformation in the lower part of the shell is small. The value of $\frac{1}{2} \gamma h$ was considered sufficiently conservative to compensate for these factors. In regard to the distribution of this force it must be recognized that, as a result of the curvature in the lower section, a concentrated horizontal force P_r at the top of the section is required in order to produce stability in this section. An equal and opposite force at the lower end of the shell is therefore required, and this is provided by the soil pressure acting against the shell. As the maximum restraining soil pressure available was assumed to be $\frac{1}{2} \gamma h$, the pressure must act over a finite length of the pile. The triangular distribution shown on the right-hand side of the shell results. This pressure produces a moment in the shell which must be resisted by soil pressure acting on the other side of the shell, the moment of which about the bottom of the pile must be equal to the moment of the former—hence, the distribution on the opposite side.

Because the shell of the piles was found to be vertical in almost every case it is unlikely that the top of the shell exerts a horizontal force on the pile cap or tends to move horizontally under a vertical load. These possibilities, however, were further investigated by assuming that the soil pressure on the entire length of the pile was sinusoidal, and the required horizontal force at the top was found to be sufficiently small to neglect.

The pipe section in each case was the first to be analyzed. Because it is statically indeterminate to the first degree the horizontal force P_r required at the top in order to produce stability was taken as the redundant. The vertical force at the top of this section was first taken as the full design load of 115 kips and was later reduced if the resulting stresses in the section were found to be in excess of those allowable. The method of analysis consists of determining the deflection of point A at the top of the pipe when force P_r equals zero and then computing the value of P_r required for elimination of this deflection. In the analysis for P_r the effects of axial stresses and shearing stresses, in addition to bending stresses, were considered. It was observed, however, that by omitting these the computed value of P_r was changed only by about 5%. Consequently, in the analyses of the other piles these stresses were omitted.

Pipe Section Tangent to Shell Section.—In Fig. 10(*a*) is shown a sketch of inclined composite pile No. 59–2, which falls into group 1, because as may be seen the pipe section is tangent to the shell section. In Fig. 10(*b*) are shown the force diagrams for the shell and pipe sections of this pile. In the treatment of the pipe section, when first considering the influence of the full design load of 115 kips, the value of the redundant P_r was found to be 3.10 kips. The soil pressure exerted on the pipe under this load is 251 lb per sq ft which produces a combined stress from bending and axial load of 1,200 lb per sq in. in the concrete. Because this stress exceeds that allowable, the load was reduced from 115 kips to 96 kips to satisfy the stress limitations of the section.

It was later found necessary to reduce this load further as it was determined that the controlling stresses were those in the shell section.

The foregoing analysis is strictly correct only if the top of the pipe is prevented from moving laterally. Actually, there is a small movement at this point which decreases the computed value of P_r and increases the maximum soil pressure. The maximum soil pressure, however, can never exceed the pressure computed for $P_r = 0$ and in all the piles analyzed it was found to be less than 10% of the available restraining pressure from the soil. The average overburden pressure, alone, at the center of this section is of the order of 3,000 lb per sq ft. It will be shown subsequently that the magnitude of P_r controls the stress in the concrete in the corrugated shell section and, consequently, the allowable load on the pile. Therefore, any reduction in the value of P_r will reduce stresses in the pile and permit the allowable load on the pile to be increased.

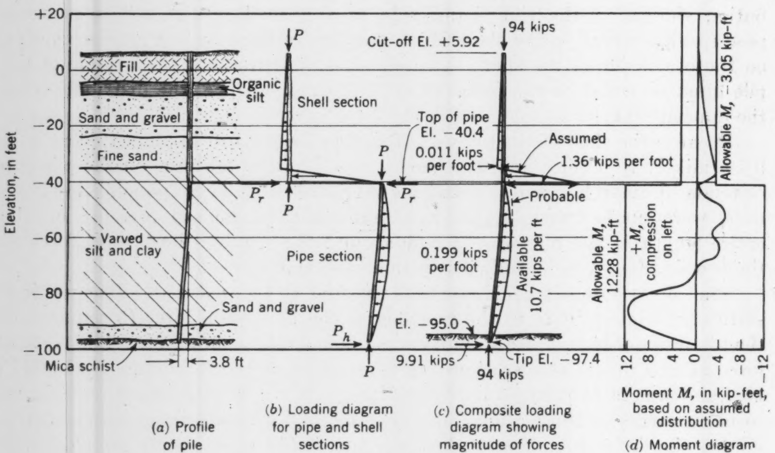
+20
0
−20
−40
−60
−80
−100
Elevation, in feet
Fill
Organic silt
Sand and gravel
Fine sand
Varved silt and clay
Sand and gravel
Mica schist
3.8 ft
P
Shell section
P
P
P_r
P_r
P
Pipe section
P_h
P
Cut-off El. +5.92
94 kips
Top of pipe El. −40.4
0.011 kips per foot
Assumed
1.36 kips per foot
Probable
0.199 kips per foot
Available 10.7 kips per ft
El. −95.0
9.91 kips
Tip El. −97.4
94 kips
Allowable M, 12.28 kip-ft
+M, compression on left
Allowable M, −3.05 kip-ft
12
8
4
0
−4
−8
−12
Moment M, in kip-feet, based on assumed distribution

(a) Profile of pile

(b) Loading diagram for pipe and shell sections

(c) Composite loading diagram showing magnitude of forces

(d) Moment diagram

FIG. 10.—CASE A—PIPE TANGENT TO SHELL

The loads acting on the corrugated shell of pile No. 59–2 are shown in Fig. 10(*b*). The distribution of loading has been explained earlier in this paper, and the determination of magnitudes is straightforward as the shell section is statically determinate. The stress resulting from the axial load and bending is 1,015 lb per sq in. if the allowable load of 96 tons based on the results of the pipe section is used. Consequently, to limit the stress in the concrete to 1,000 lb per sq in. the permissible load on the pile had to be reduced from 96 kips to 94 kips. This was the design load recommended and approved by the city, and in Figs. 10(*c*) and 10(*d*) are shown the final results of the analyses. The allowable load of 94 kips requires a soil pressure along the pipe section of 0.199 kips per ft which is equivalent to a unit stress of 222 lb per sq ft in the soil. This is obviously only a small fraction of the restraining pressure available. In Fig. 10(*c*) the estimated probable distribution has been indicated by a dashed line and the assumed distribution by a solid line. The principal difference is in the distribution of loading around the joint. Although this difference was fully realized in developing the analysis, the assumed distribution was required in order to permit development of a practical approach, and the results so obtained are recognized to be on the conservative side. The moment diagram in Fig. 10(*d*) is based on the assumed loading distribution, and the stress in the concrete was determined on the basis of the combined bending stress and axial load.

Pipe Section Not Tangent to the Axis of the Shell Section.—In Fig. 9(*b*) are shown the forces acting on a typical Case A dog-leg pile exhibiting at the joint a definite break in the alinement of the pipe and shell sections. With a vertical load at the top, the shell section, being vertical, is deflected axially.

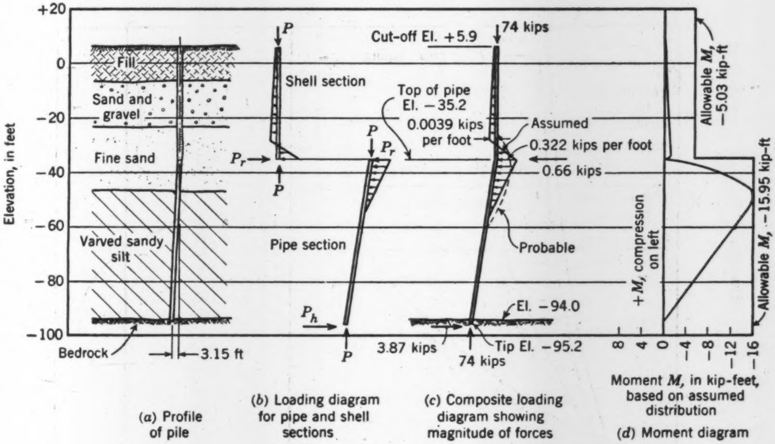
+20
0
-20
-40
-60
-80
-100
Elevation, in feet
Fill
Sand and gravel
Fine sand
Varved sandy silt
Bedrock
3.15 ft
P
Shell section
P_r
P
Pipe section
P_h
P
Cut-off El. +5.9
74 kips
Top of pipe El. −35.2
0.0039 kips per foot
Assumed
0.322 kips per foot
0.66 kips
Probable
El. −94.0
3.87 kips
Tip El. −95.2
74 kips
Allowable M, −5.03 kip-ft
Allowable M, −15.95 kip-ft
$+M$, compression on left
8
4
0
−4
−8
−12
−16
Moment M, in kip-feet, based on assumed distribution

(*a*) Profile of pile

(*b*) Loading diagram for pipe and shell sections

(*c*) Composite loading diagram showing magnitude of forces

(*d*) Moment diagram

FIG. 11.—CASE A—PIPE NOT TANGENT TO SHELL

The straight lower inclined section, however, with a vertical load at its top will be deflected laterally. The pipe section was analyzed alone under the forces shown in Fig. 9(*b*) and was found to have relatively large bending deflections under this distribution of forces. It was therefore evident that the pipe was less rigid than the surrounding soil and that the soil reaction on the pipe would be concentrated near the upper end. Hence, the distribution was assumed to be triangular and limited to the upper third of the section, as shown in Fig. 9(*b*).

The distribution of soil pressure along the shell section is the same as that previously used for pile No. 59–2. On the basis of this distribution and that previously described for the pipe section and of the assumption that the joint between the two sections is hinged, the problem of determining the magnitude of the soil pressures required to produce stability reduces itself to one that is statically determinate. For the allowable loads considered for these piles, the order of magnitude of the deformations at the joint were computed on the basis of the resulting moment diagram and were found to be sufficient to develop the necessary soil pressure without exceeding the allowable stress of 1,000 lb per sq in. in the concrete in the shell.

In Fig. 11 is a sketch of pile No. 15–4, which is a specific case of a definite break in the alinement of the pile at the joint. In Fig. 11(*b*) are shown the force diagrams for both the shell and pipe sections. It was found that the soil pressure required for the full design load of 115 kips on this pile was 500 lb per lin ft. This produced a P_h-force of 6.02 kips at the tip resulting in a moment that produced excessive stress in the pipe. Accordingly, the loads had to be reduced to those shown in Fig. 11(*c*) in order to keep the stresses within allowable limits. The allowable load on the pile therefore had to be reduced from 115 kips to 74 kips. This represents an increase of approximately 25% over the allowable load of 60 kips approved for this pile by the city authorities, which was based on the original premise that the pipe section acted as a batter pile and therefore could be subjected to axial loading only. The results of the load test subsequently considered completely justified the latter approach.

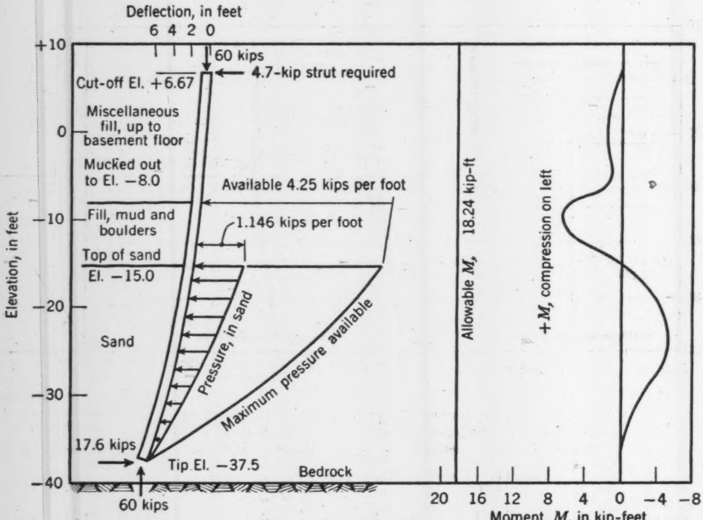
Deflection, in feet
6 4 2 0
+10
0
−10
−20
−30
−40
Elevation, in feet
60 kips
4.7-kip strut required
Cut-off El. +6.67
Miscellaneous fill, up to basement floor
Mucked out to El. −8.0
Available 4.25 kips per foot
Fill, mud and boulders
1.146 kips per foot
Top of sand El. −15.0
Sand
Pressure, in sand
Maximum pressure available
17.6 kips
Tip El. −37.5
Bedrock
60 kips
Allowable M, 18.24 kip-ft
+M, compression on left
20 16 12 8 4 0 −4 −8
Moment, M, in kip-feet

FIG. 12.—CASE B—STEEL PIPE PILE

Case A Piles Analyzed.—Of the Case A piles measured, 29 were found to be less than 2% out of plumb and thus were approved without analyses for a full design load of 57½ tons, 16 were assigned loads between 75% and 100% of the full design load, and 16 were approved for 50% to 75% of the design load. Only two of the piles measured had to be rejected.

Analysis of Case B Piles

As described under the heading, "Soil Formation and Description of Piles—Case B," the second group of piles analyzed by the writers were $10\frac{3}{4}$-in.-diameter steel pipe piles that were required to be driven through fill and organic silt containing a sufficient quantity of boulders to produce at least some curvature in almost every one of the piles driven. Because they were driven as replacements for wood piles that had been broken in penetrating the formations they were each required to carry a design load of only 30 tons. A typical example of the curvature resulting from the necessary hard driving is exhibited in pile No. 15–S2, shown in Fig. 12. Also shown in this illustration are the forces acting on the pile.

Although the curvatures in the piles analyzed at this site in some cases were excessive, they were generally found to be uniform and to extend throughout the entire length of the pile. The maximum lateral deflection in the piles under the influence of load could, therefore, be expected to occur at approximately the center of the piles which—as may be judged from the soil section shown in Fig. 12—is at about the level of the bottom of the organic silt formation.

Although it is recognized that some lateral support to the pile is provided by the organic silt and overlying fill, it was neglected in analyzing the Case B piles because of the large restraining forces available in the sand formation immediately underlying the silt and the fact that considerably smaller deformations are required for producing large restraining pressures in the sand than in the overlying silt and fill. Also, and perhaps of even greater significance is the fact that the relative flexibility of the pile and the soil surrounding it at the point of maximum curvature will dictate this to be the case. In the light of these considerations, the triangular distribution of soil pressure along the pile shown in Fig. 12 as an approximation for part of the sinusoidal distribution previously used is considered reasonable but is recognized to be conservative.

In the analysis of Case B piles a procedure similar to that adopted for the pipe section of the composite piles was used, the only difference between the two being in the treatment of the force P_r and the distribution of the soil pressure along the pile. In the instance of these piles the force P_r was replaced at the top of the pile with a force P_s from a strut, and the soil pressure instead of being sinusoidal over the entire length of the pipe was assumed as triangular over the lower half of the pile, which was embedded in sand. In this connection it may again be pointed out that the choice between the uniform distribution, the trapezoidal distribution, or the sinusoidal distribution will have but a minor influence on the final results.

The stresses in the concrete and the steel shell were computed on the basis of the combined effects of the axial force and the bending moment. The limiting values for the stresses were the same as those mentioned for the composite piles. Where necessary, the pipe was permitted to take some tension; this was considered safe in view of its $\frac{3}{8}$-in. wall thickness. The maximum soil pressure at the top of the sand stratum was assumed to be one half of the difference between the passive pressure and the active pressure in the sand. In only one case did this limiting value govern the load that could be carried by the pile, and in most cases only a small fraction of the available restraining force was developed.

In the instance of pile No. 15–S2 shown in Fig. 12, by installing a strut at the top of the pile capable of providing a horizontal force of 4.7 kips, it was found that the full design load of 60 kips could be applied. Under the influence of this load, a restraining force of only 1.15 kips was required, 4.25 kips per ft being available at the top of the sand bed.

Case B Piles Analyzed.—Of the 24 Case B piles measured in the field and analyzed, 4 were found to be less than 2% out of plumb and thus could be immediately assigned a design load of 30 tons without analysis, 11 when analyzed were found to be able to support safely 30 tons, 8 were assigned loads varying from 75% to 100% of the design load, and one had to be assigned a design load of 17 tons.

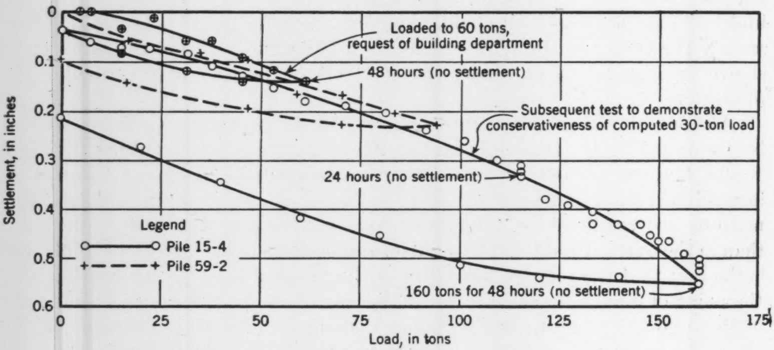

Fig. 13.—Case A—Load Tests on Dog-Leg Piles

Pile Load Tests

In order to demonstrate the performance of the Case A dog-leg composite piles analyzed, the New York City Department of Housing and Buildings required that a minimum of two of these piles be load tested. The tests were to be performed in accordance with the stipulations of the building code, and thus the piles had to be subjected to twice the allowable design load computed on the basis of the analyses. Accordingly, representative piles of each of the two foregoing types under Case A were selected. Each, however, had exhibited more than average inclination and had been assigned a design load, based on the results of analysis, somewhat less than the allowable load of $57\frac{1}{2}$ tons for a straight pile. Pile No. 59–2, representative of piles the pipe sections of which were found to be tangent to the shell sections, was assigned a design load of 47 tons, and pile No. 15–4 the pipe section of which was not tangent to the shell section was permitted a load of only 30 tons. The load-settlement diagram for each of these piles is included in Fig. 13.

As may be seen in Fig. 13, the total settlement in pile No. 59–2 under a load of 94 tons was 0.227 in. and on removal of the load it rebounded to 0.1 in.

Pile No. 15–4 showed a total settlement of only 0.142 in. under a 60-ton load and rebounded to 0.0034 in. on removal of the load. As required by the building code, in each of these tests twice the design load was to be maintained on the pile for not less than 48 hr without any observable settlement. As may be judged from the magnitude of the settlements observed, they were considerably less than the maximum permitted by the building code and thus satisfied the requirements of the New York City Department of Housing and Buildings in this respect. Actually, the maximum settlements of these piles were less than the average settlement observed for comparable loads on the straight piles. This, the writers believe, may be attributable to the fact that the time interval between driving and load testing was somewhat greater in the instance of the dog-leg piles.

For the purpose of demonstrating the conservativeness of the assumptions made in connection with the analyses for the determination of the design loads for the dog-leg piles, one of the two piles described—namely, pile No. 15–4—was subjected to a second load test and was loaded to 160 tons, approximately 5.3 times its design load. The results are included in Fig. 13, and as may be seen the gross settlement under the 160-ton load was only 0.55 in. The maximum load in this instance was maintained on the pile for 48 hr without settlement before being removed. This test has also been plotted in Fig. 2 for comparison with the results of those on straight piles. The writers believe that the results of the load test demonstrate conclusively that the method of analysis adopted renders design loads that are without question safe and on the conservative side. The extent of conservativeness, however, cannot be evaluated on the basis of the load test results alone as the stresses in the pile even under the maximum applied load cannot be determined by this means for comparison with the limiting stresses permitted by the building code.

The New York City Department of Housing and Buildings accepted the computed design loads for the Case B dog-leg piles on the bases of the analyses made, without requiring load tests. The performance of those piles, however, has been thoroughly demonstrated by semimonthly continuous settlement observations which have been made for each of the columns supported on dog-leg piles. The observations cover the entire period of building construction, and as of this date which is about a year after their installation the settlements range between 0.1 in. and 0.5 in., the average being 0.25 in., which is approximately their elastic shortening. This evidence is believed to be even more conclusive than that provided by the load tests as it demonstrates the favorable performance of such piles under load over a much longer time period.

CONCLUSIONS

The development of the facilities described herein for analyzing dog-leg piles affords an inexpensive, rapid, and safe means of evaluating their load-carrying capacity. Although the load test indicated that the assumptions made in the analyses yielded allowable loads on the piles which were on the conservative side, of considerably greater importance is the fact that the dog-leg piles analyzed were used and not abandoned as has long been the accepted practice. In the instance of the Case A piles the cost of the dog-leg piles salvaged was in excess of $30,000. Of perhaps greater significance is the fact that the salvaging of the Case B piles eliminated the necessity of removing the entire existing building foundation and mucking out the obstructions encountered.

The procedure described for determining the safe loads on dog-leg piles, the writers believe, may prove to be of value to other engineers in effecting considerable savings in foundation costs where steel-encased piles or pipe piles are used because on almost every job involving long piles, some of the piles are found to be dog-legged.

ACKNOWLEDGMENTS

Suggestions for this study were made by Philip C. Rutledge, M. ASCE, who has reviewed this paper and has made valuable suggestions which were incorporated in it. Louis J. Capozzoli, Jr., J. M. ASCE, conducted the analyses of the piles discussed herein.

DISCUSSION

A. E. Cummings,[5] M. ASCE.—This paper is concerned with a subject in which the writer has been interested for many years. As the authors have remarked, many engineers give little or no thought to the probable alinement of long wood piles or H-beam piles after they are driven into the ground. Regardless of the fact that no inspection of such piles can be made, they are often allowed to support substantial loads. With the increase in use of long pipe piles and especially the combination pipe-and-shell piles it has been generally observed that the driven piles are not always perfectly plumb and perfectly straight. During driving, piles are sometimes distorted into long-pitch helical curves, sometimes into long sweeping bends, and occasionally into sharper bends which the authors describe as dog-leg.

As soon as it became known that such misalinements were occurring, field investigations of all kinds were undertaken to determine whether or not the misalinement affected the carrying capacity of the pile and, if so, to what extent. Slope indicators similar to that described by the authors have been in use in the oil-well drilling industry for years. Some of these tools can determine not only the slope but also its direction with respect to the compass. Equipment of this kind has also been used to determine the alinement of driven piles. Furthermore, many field-loading tests have been made on piles with various amounts of misalinement and various soil conditions. The results are always similar to those shown in Fig. 2. The piles which were out of alinement supported the test loads and rebounded when unloaded just as satisfactorily as did piles that were straight and vertical.

In the writer's opinion, the satisfactory behavior of piles that are not in perfect alinement is due largely to a factor which the authors have neither mentioned nor taken into account in their theoretical analysis. They have considered the ability of the surrounding soil to stabilize the pile against horizontal displacement but have written nothing about the interaction between the pile and the soil in the vertical direction. When an external vertical load is applied to the head of a pile, this load is distributed in various ways to the soil in which the pile is imbedded. It is customary to refer to piles as friction piles or point-bearing piles. Actually all piles are combinations of the two types as some of the load goes into the soil by friction along the pile shaft and the remainder is delivered to the soil at the point of the pile.

Numerous full-scale field tests have been made to investigate the manner in which piles distribute their loads to the soil in which they are embedded.[6, 7] Recent tests of this type are those made by the Nebraska Department of Roads and Irrigation at Omaha[8] and those made by the Corps of Engineers,

---

[5] Director of Research, Raymond Concrete Pile Co., New York, N. Y. (Mr. Cummings died on July 20, 1955).

[6] "Electrical Resistance Strain Gages for Determining the Transfer of Load from Driven Piling to Soil," by L. Leroy Crandall, *Proceedings*, Second International Conference on Soil Mechanics and Foundation Eng., Vol. IV, 1948, p. 122.

[7] "Static Load Tests for Bearing Piles," by V. Hansen and F. N. Kneas, *Civil Engineering*, Vol. 12, 1942, p. 545.

[8] "Group Pile Loads in Plastic Soils," by Henry G. Schlitt, *Proceedings*, Highway Research Board, National Research Council, Washington, D. C., Vol. 31, 1952, p. 62.

United States Department of the Army, at the West Atchafalaya Floodway in Louisiana.[9] The tests described in these publications were made on several types of piles under various soil conditions. In the case of piles that were not driven to point bearing on hard ground, almost all the load was delivered to the soil along the pile shaft and almost none of it reached the point of the pile. Even when a long pile was driven through a deep bed of soft soil to high point resistance in hard ground, only a small percentage of the test load reached the pile point. The results of such a test made by the Corps of Engineers in Louisiana are shown in Fig. 14.

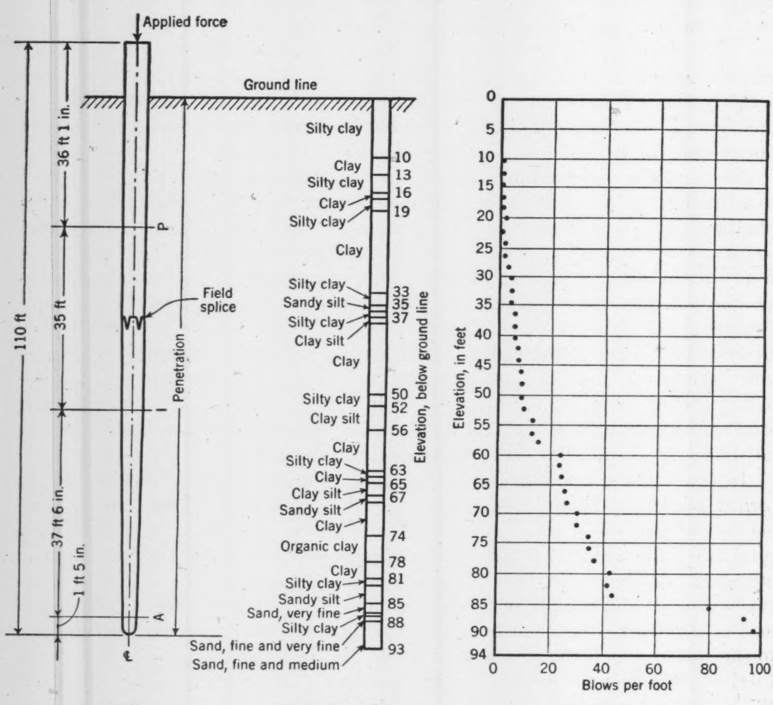

(*a*) Pile (*b*) Log of borings (*c*) Driving record

FIG. 14.—FIELD TEST RESULTS

The pile was a hollow tapered pile made of No. 3 gage steel plate. It had a point diameter of 8 in. and a butt diameter of 16 in. It was driven with a single-acting steam hammer having a 5,000-lb ram and a 3-ft stroke. The soil consisted of clays and silts to a depth of approximately 85 ft below the ground surface where a bed of compact sand was encountered. As can be seen from the driving record, the resistance increased gradually to approximately 45 blows per ft when the pile point was about to reach the sand stratum. Within a few feet thereafter the resistance increased rapidly to approximately 100 blows per ft and then to 435 blows per ft; driving was stopped at a final resistance of 100 blows for the last ½ in. with the pile point about 90 ft below the ground surface.

---

[9] "Steel and Timber Piles Tests, West Atchafalaya Floodway," New Orleans, Texas and Mexico Railway, "Advance Report of Committee 8, Masonry," *Bulletin No. 489*, A.R.E.A., Vol. 52, September-October, 1950, p. 149.

Before the pile was driven SR-4 strain gages were attached to the inner surface of the tube at vertical intervals of approximately 5 ft. The strain gages were installed and operated by the Office of the Research Engineer of the Association of American Railroads. When the static test load was applied, strain-gage readings were made at each load increment in order to determine how much of the load was in the pile shaft at various levels. The results of some of these readings are shown in Fig. 15. When the test load amounted to 140 kips, most of the load was transmitted to the soil along the upper half of the pile shaft and only approximately 20 kips reached the point. Even at the maximum load of 300 kips, only approximately 50 kips reached the point of the pile. The testing of this pile took 5 days, and the pile supported the maximum test load for 24 hr without settlement. Similar results have been obtained in all tests that have been made to investigate the transmission of load from pile to soil.

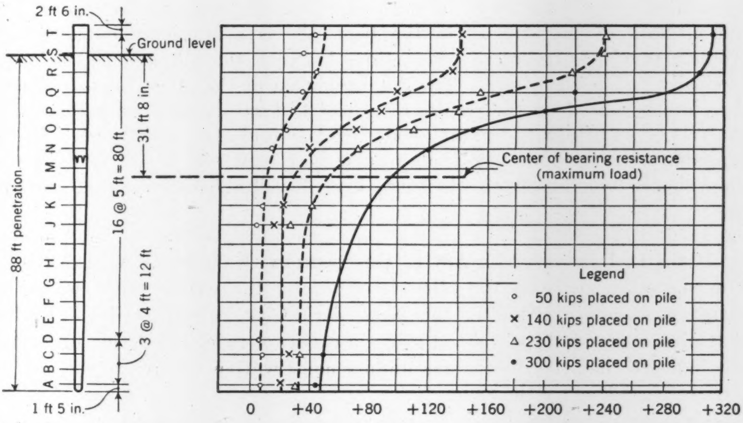

FIG. 15.—PILE REACTIONS AT EACH SECTION, IN KIPS

In the force diagrams of Figs. 10 and 11, it has been assumed that all the load at the top of the pile is transmitted undiminished to the pile point. Stresses in the pile were computed on the basis of this assumption. In both cases, the embedded surface of the pile below the level of the filled ground amounted to approximately 250 sq ft. An average frictional resistance of

375 lb per sq ft would support the entire 94 kips of Fig. 10, and only 295 lb per sq ft would be required to support the 74 kips of Fig. 11. From such considerations and from the results of the field test previously referred to, it is evident that only a fraction of the load applied to the pile head could have reached the pile point. Computations of bending moments and stresses in the pile based on the assumption of full point-bearing are therefore extremely conservative. Even when the pile has been driven to hard ground through saturated plastic soils subject to consolidation, it need not be expected that a pile that is not in perfect alinement will behave much differently from a pile that is perfectly straight and plumb.

The authors have made a valuable contribution to this subject by showing that piles should not be abandoned simply because the bottom of the pile cannot be seen from the top. However, it is the writer's opinion that it is not necessary to reduce the allowable load on the pile whenever the results of a load test are as satisfactory as those observed on piles 15–4 and 59–2. The computation of the stresses in the bent pile is a statically indeterminate problem involving unknown interactions between the pile and the soil both vertically and horizontally. The determination of the allowable load should therefore be based on the results of a load test rather than on a theoretical analysis or an arbitrary building-code regulation about straightness. All the available evidence indicates that a curved or bent pile is not in danger of collapsing or buckling even when it is loaded well above the normal working load.

James D. Parsons,[10] M. ASCE, and Stanley D. Wilson,[11] A. M. ASCE.–The allowable loads on the piles described by the writers were limited by design stresses stipulated in the New York City building code. The fact that piles successfully withstood loads in excess of twice the design loads does not indicate that the design was unduly conservative relative to the limiting stresses permitted by the code.

Mr. Cummings has made a strong plea for the acceptance of load tests on dog-leg piles in lieu of the analysis presented in the paper. Although the writers also urge the performance of load tests, they disagree with Mr. Cummings' conclusion that load tests alone should be used in the final analysis. If the tip of the pile cannot be seen with a lowered light or if the pile cannot be dewatered, the field engineer has no way of knowing how much the pile is bent unless measurements are taken. Pile-load tests, if performed on every pile suspected of being bent, would cost more than the replacement value of the piles.

The results of full-scale field tests such as those referred to by Mr. Cummings are quite interesting but unfortunately do not provide all the necessary information. All the tests conducted to date (1955) with which the writers are familiar have been short-time tests, and there is no question but that in such tests most of the load is transferred to the soil from the upper part of the pile and only a small percentage reaches the tip. If this condition remained unchanged with time, it would mean that a lot of money has been wasted on overlength piles. In reality, of course, the compressible soils in the upper region become consolidated and settle slowly with time, transferring an increasing percentage of the load to the tip of the pile. This is particularly true of piles penetrating through sands overlying a compressible stratum for which load tests would not reflect the true performance of the piles over an extended period. It is, therefore, important that the measurement of the curvature of the piles and an analysis of the stresses be conducted when the piles are known to be badly bent, regardless of the results of load tests.

---

[10] Associate Partner, Moran, Proctor, Mueser & Rutledge, New York, N. Y.

[11] Partner, Shannon and Wilson, Seattle, Wash.

AMERICAN SOCIETY OF CIVIL ENGINEERS
Founded November 5, 1852
TRANSACTIONS

Paper No. 2817

AIRPORT STANDARDS

By JOHN M. KYLE,[1] M. ASCE

SYNOPSIS

Only by continuous cooperation between the airplane manufacturer and the airport operator can the airplanes that are being built be able to use the facilities at the various airports. Similarly, satisfactory liaison can enable the airport owner to anticipate the needs of the air-transport industry. Prominent among the mutual problems are the lengths of runways and the strengths of pavements; the runways cannot be excessively long nor can the pavements be too weak. Another problem, although not one of airport design, is the suppression of noise. The noise level at airports must be lowered if the public is to accept the industry as a commonplace activity.

INTRODUCTION

From a study of the volume of traffic, it is apparent that the air-transport industry has "come of age." For example, in the twelve-month period ending April, 1952, 10,567,214,000 passenger-miles were flown in domestic air travel as compared with 9,859,000,000 for rail travel in Pullman accommodations. In the same period, 698,028 passengers were carried across the Atlantic Ocean by airplanes whereas only slightly more—783,614—were transported by ships. In 1952, with tourist air travel rates in effect, the volume of overseas air travel increased 25%. Therefore, if service to the public is considered as a measure of maturity, air transportation is no longer an infant industry. Why then, with regard to technology, is this transport medium coddled?

The industry's leaders (as of 1952) talk in terms which lead one to suspect that they are not cognizant of the economics of furnishing ground facilities to land and take-off transport ships used in air commerce.

To illustrate the foregoing, there are presented subsequently examples of two aspects of airfield design which are being handled in a manner that does not always bring credit to the engineering profession.

NOTE.—Presented at the Centennial Convocation, Chicago, Ill., September, 1952. Published, essentially as printed here, in August, 1953, as *Proceedings-Separate No. 237*. Positions and titles given are those in effect when the paper was approved for publication in *Transactions*.

[1] Chf. Engr., Port of New York Authority, New York, N. Y.

Airfields throughout the United States have evolved from small landing areas to major air terminals. In each community, the engineers, with the help of such agencies as the Civil Aeronautics Administration, United States Department of Commerce (CAA), have tried to anticipate future runway requirements. Most large cities have an airport capable of receiving (as of 1952) ship sizes up to the DC-6 with a fair margin of safety. This means, for continental airports, a minimum 6,000-ft runway with a load capacity of 50,000 lb per dual-wheel assembly. Some of the newer fields have expansion possibilities up to 8,000 ft, the only penalty for such expansion being a greatly increased financial burden on the owner or operator of the airport.

In Los Angeles, Calif., in 1951, a conference was held to discuss the need for lengthening the runways for future use. An immediate decision was needed because it was necessary to make provision for a highway underpass at the end of one of the major runways. Engineers working in the field of airport design were astonished to hear representatives of four manufacturers, supposedly speaking for the aircraft industry, state that in their opinion provisions would have to be made for runways from 12,000 ft to 15,000 ft long. They further stated that such runways would be required for airplanes then on the drawing boards. This airplane development had evidently been proceeding without any advice or concurrence from airport operators, who, in the last analysis, would be the ones "saddled" with the burden of supporting such runways. There was only the remotest possibility that airport owners or operators could possibly afford the construction and maintenance of such runways and, in any event, because of terrain conditions or available real estate such runways could not be constructed at 90% of the existing airfields in the United States.

In contrast to this attitude is the cooperative effort which went into the development of a jet airliner which was developed to land and take off successfully from existing fields without damage to their pavements either from imposed load or the angle of incidence of the jet to the runway surface.

It must be remembered that the length of a runway needed for airplane take off or landing is merely a function in the design of the plane and can be corrected within a fairly wide range by adequate design of the airplane motive-power characteristics, braking devices, and landing gear.

This is not an isolated problem in Los Angeles, but rather a problem common to all major air centers in the United States and throughout the world.

Many of the air fields in the United States have been expanded to meet the requirements of CAA Technical Standard Order (TSO) N-6a. This technical order has been the criterion in the design of landing areas. It specified 5,900-ft runways for continental fields and up to 8,400-ft runways for intercontinental fields.

It is suggested that that segment of the civil engineering profession which is involved in airport design take a firm stand so that the requirements laid down by TSO N-6a shall be considered as the ultimate limits to which airports will be constructed and that the plane designers be advised that this is the maximum they can anticipate in runway construction. With this restriction in mind, the designers can propose aircraft that can be operated safely at the airports of the world; therefore, modifications would have to be built into the airplanes rather than into the runways. When one considers that more than

$2,300,000 (as of 1952) have been invested in landing fields, the magnitude of any change in this category can be readily appreciated.

Another aspect of the problem seems to have been completely overlooked. One accepts as a matter of course the great changes in landing techniques that have occurred because of the use of landing flaps and reversible propellers; both of these have changed landing distances. With rotary wing aircraft and converter planes beyond the blueprint stage (as of 1952), is it not conceivable that still more startling changes in runway lengths and requirements will occur? Should this happen, huge investments in inordinately long runways would be rendered useless and, in fact, would become a liability, requiring as they do constant maintenance, policing, and rehabilitation.

The second engineering problem requiring the coordinated efforts of the engineering profession is pavement strength. The railroad industry has solved similar problems in their development and have evolved a valid formula for the relation of motive power to design and construction of the right of way.

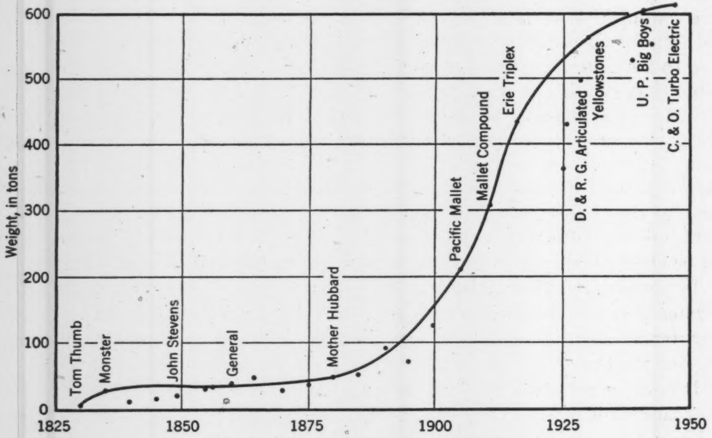

Fig. 1.—Increases of Locomotive Weights

In Fig. 1 the development of the locomotive in the United States from 1829 to 1950 is traced. Obviously, no stagnation of development is shown, yet even the newest engines fall within the allowable stresses on existing bridges, trestles, and embankments. This was accomplished by cooperative efforts within the industry by which the civil engineer and the mechanical engineer, working side by side adopted standards and held to these standards for clearances and axle loading. The latter standard is, of course, well known to all designers and is reflected in the Cooper loadings. Because both the purchase of engines and the construction of the railroads were the concern of the same organization it was a simple matter to assure thorough cooperation between the two groups of engineers. This is not the case in aircraft operation; usually the owner of an airport is not an aircraft operator and, in any event, all major airports are used by a multiplicity of operators.

The economic necessity of cooperation by the airport designers and the aircraft designers is not as easily shown as it is in the railroad industry. However, the same economic problems must be explained to the aircraft industry as were demonstrated to the railroad industry.

In paralleling the locomotive-design problem, Fig. 2 shows the weights of the largest of the new commercial aircraft developed from 1920 to 1950. The pattern in Fig. 2 is similar to that in Fig. 1. However, the pattern of a standard design criterion has been lacking. In the development of a long-term lease between the Port of New York (N.Y.) Authority and the various airlines, it has been necessary to investigate the various runway-design formulas to determine which formula would be applicable over a long period of time in order to decide which of the new airplanes would be able to land on the airfields without damage to the pavements. Investigations have led engineers of the Port of New York Authority to conclude that the best formulas evolved for the determination of pavement strength were presented[2] by Guthlac Wilson and G.M.J. Williams, A.M. ASCE. It is therefore proposed that the air-transport industry accept the use of influence charts (Fig. 3) and the following design formula[3] as its counterpart of the Cooper loading—

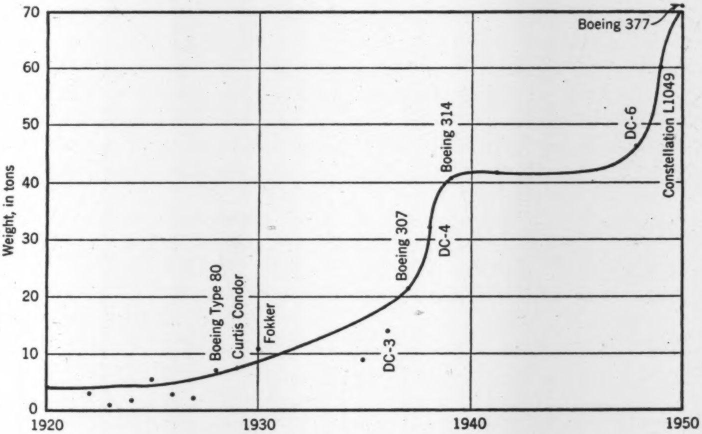

Fig. 2.—Increase of Aircraft Weights

$$M_n = \frac{Q\,L^2\,N}{10{,}000} \qquad (1)$$

in which Q is the intensity of the loading, N denotes the number of positive blocks in Fig. 3 minus the number of negative blocks (shaded blocks in Fig. 3

---

[2] "Pavement Bearing Capacity Computed by Theory of Layered Systems," by Guthlac Wilson and G. M. J. Williams, *Transactions*, ASCE, Vol, 116, 1951, p. 750.

[3] "Influence Charts for Concrete Pavements," by Gerald Pickett and G. K. Ray, *ibid.*, p. 64, Fig. 3(a).

are fractional), and

$$L = \left(\frac{D}{K}\right)^{1/4} \dots\dots\dots\dots (2)$$

in which D is the flexural rigidity of the pavement and K is the rigidity of the subgrade or the density of the liquid.

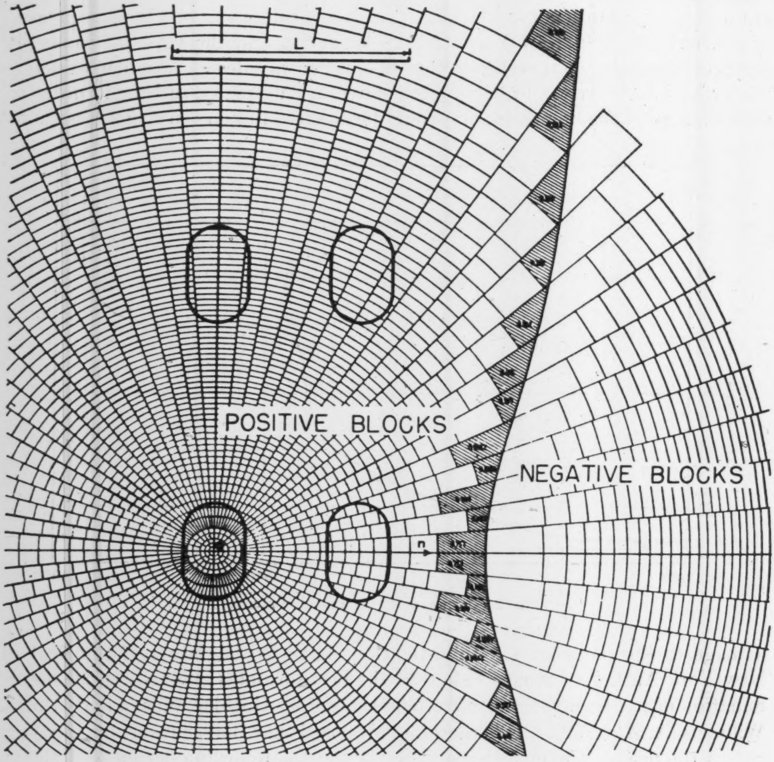

Fig. 3.—Influence Chart for the Moment M_n in a Concrete Pavement Due to a Load in the Interior of the Slab (Subgrade Assumed to Be a Dense Liquid; Poisson's Ratio for Pavement Assumed to be 0.15)

Eq. 1 is predicated on the use of an influence chart (Fig. 3) on which are plotted the loadings of the various supporting gears of an aircraft. At each airport there is a certain pavement thickness and subgrade modulus which can be matched with a standard aircraft design; it then becomes a simple arithmetic computation to determine if any given plane, when it is still in its design stages, will be acceptable at a given airport. In the event that the plans appear unacceptable, modifications can be made in the airplane without excessive hardship on either the manufacturer or the potential user of the plane. If, despite the knowledge that a plane will be destructive to the airports, the manufacturer still persists in a poorly engineered design, airport operators should refuse to allow planes of this design to use the fields.

Fortunately, an organization for the coordination of the work of airport operators has been established. This organization numbers among its members operators of all the major air terminals in the United States. The technical staffs of the member organizations might well serve as a nucleus for implementing this procedure.

One other factor of aircraft design, although it does not impinge directly on the design of the airport, should receive prompt comprehensive engineering study. This is the factor of noise which has received much attention because of its close association in the public's mind with aircraft accidents. Prominent engineers have stated (as of 1952) that it is not possible to disassociate airplane noise from more efficient aircraft operation, particularly in the field of jet planes. Although this conclusion may be correct from an aeronautical point of view, it is doubtful whether people living near airports will be satisfied with so academic an approach to the problem. As an example, despite the fine mechanical performance of the steam automobile, it diminished in use not because of the technological superiority of the gasoline automobile but because it had certain inherent characteristics which were unacceptable to the public. Therefore, should the airplane designers persist in making their products in such a manner that the noise levels produced seriously affect those living in the vicinity of airports and air routes, there would undoubtedly be a public insistence that such aircraft be banished from the skies or at least from all areas adjacent to large cities.

The Port of New York Authority is (as of 1952) sponsoring a study to determine the characteristics and noise levels caused by ground run-up of aircraft in areas adjacent to its airports. Upon completion of this study, an attempt will be made to develop noise-baffling devices for use in the vicinity of warm-up hangar and test areas.

CONCLUSIONS

It is suggested that the interrelationship of aircraft design with design of airport facilities be examined, particularly with regard to the runways needed for the ground movement and take-off of such aircraft. The goals to be achieved would be the following:

a. Runway lengths should be limited by fixed criteria, the suggested criteria to be in accordance with TSO N-6a.

b. The weight of aircraft and configuration of aircraft landing gear should impose no greater unit tensile stress, in accordance with Eq. 1, than 485 lb per sq in.

c. Noise-baffling devices should be used at airports and on airplanes.

AMERICAN SOCIETY OF CIVIL ENGINEERS
Founded November 5, 1852
TRANSACTIONS

Paper No. 2818

ANALOG COMPUTERS APPLIED TO ELASTO-PLASTIC SYSTEMS

By Leo Schenker,[1] A. M. ASCE, and Gunther Martin[2]

With Discussion by Messrs. John S. Archer and Allen Lange

Synopsis

There is described herein a circuit which can adapt differential analog computers to solve the equations of motion of systems incorporating springs with elasto-plastic resistance characteristics. The application of this method to a single-story structure is described and illustrated. The circuit can be used in conjunction with multi-degree-of-freedom systems with or without viscous damping. Interesting possibilities for further research are briefly described.

Introduction

The use of differential analog computers for the analysis of the dynamic behavior of elastic systems has become a standard procedure and is fully described in the literature.[3] Briefly, the fundamental units of the computer are operational amplifiers that can perform the processes of (1) multiplication by a constant and (2) integration. It is also a characteristic of these units that they will change the sign of the input in addition to carrying out operation (1) or (2). For example, a steady voltage of +10 volts fed into a unit set up to multiply by 2 will be transformed into a steady voltage of −20 volts. A steady positive voltage fed into an integrator will emerge as a voltage increasing at a constant rate with a negative sign. Thus, a combination of operational amplifiers can be so connected as to carry out operations prescribed by a mathematical equation.

As an illustration, the equation of motion of an undamped single-degree-of-freedom system acted on by a force $F(t)$ is considered:

Note.—Published, essentially as printed here, in October, 1954, as *Proceedings-Separate No. 528.* Positions and titles given are those in effect when the paper or discussion was approved for publication in *Transactions.*

[1] Member of the Technical Staff, Bell Telephone Labs., Inc., Murray Hill, N. J.

[2] Research Engr., Ford Motor Co., Dearborn, Mich.

[3] "Electronic Analog Computers," by G. A. Korn and T. M. Korn, McGraw-Hill Book Co., Inc., New York, N. Y., 1952.

$$m\,\ddot{x} + k\,x = F(t) \ldots\ldots\ldots\ldots\ldots\ldots\ldots (1a)$$

in which m represents mass and x denotes deflection. The circuit is shown in Fig. 1(a). To examine this, let it be assumed that the output of the second operational amplifier is $-x$, as shown in the illustration. Feeding this into a potentiometer set at a value equal to the coefficient k and then into an operational unit to multiply by -1 results in a value $k\,x$. Force $F(t)$ can be represented by a voltage signal similar to the actual force. However, Eq. 1a is a statement that $k\,x - F(t) = -\,m\,\ddot{x}$. Therefore, passing $k\,x - F(t)$ through an integrator set to multiply by $1/m$ at the same time should produce $\dot{x}$, and sending $\dot{x}$ through another integrator should result in the output $-x$. Hence, the original assumption that the output of the second unit in Fig. 1(a) is $-x$ is justified. The variation of x with time can be recorded and represents the solution of Eq. 1a to a scale that can be determined.

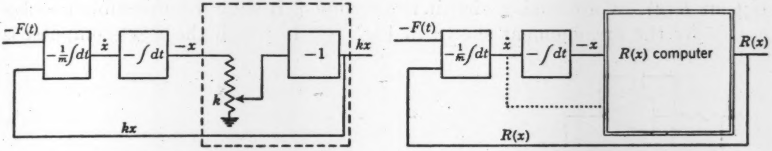

(a) Elastic system (b) Elasto-plastic system

FIG. 1.—ANALOG COMPUTER CIRCUIT FOR AN UNDAMPED, SINGLE-DEGREE-OF-FREEDOM SYSTEM

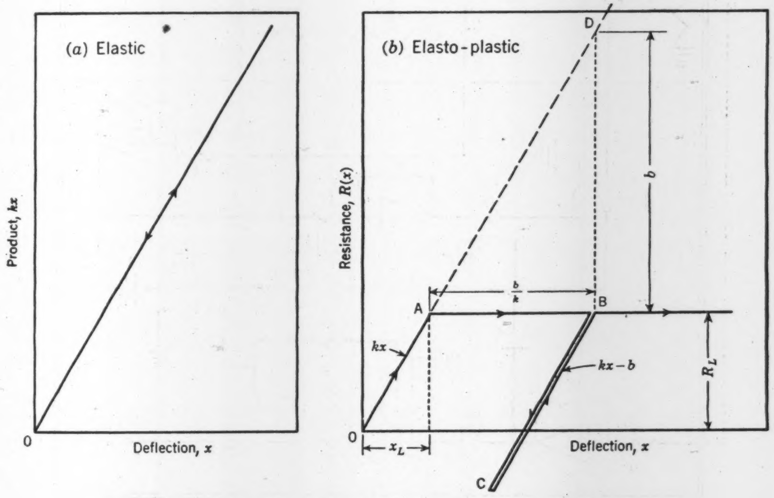

FIG. 2.—ELASTIC AND ELASTO-PLASTIC RESISTANCE FUNCTIONS

The purpose of the study described herein is to develop a procedure suitable for the analysis of systems in which the resistance $R(x)$ to a displacement x is not at all times proportional to x. Specifically, it is desired to solve the equation,

$$m\,\ddot{x} + R(x) = F(t) \quad\ldots\ldots\ldots\ldots\ldots\ldots\ldots\ldots\ldots\ldots (1b)$$

in which $R(x)$ is the elasto-plastic resistance curve shown in Fig. 2(*b*). For the computer circuit, this requires the replacement of the components shown in the dashed box in Fig. 1(*a*) by a circuit in which the input $-x(t)$ will produce an output $R(x)$. Once such a circuit is developed, it should be possible to solve Eq. 1*b* by the arrangement shown in Fig. 1(*b*) in which the $R(x)$-computer is

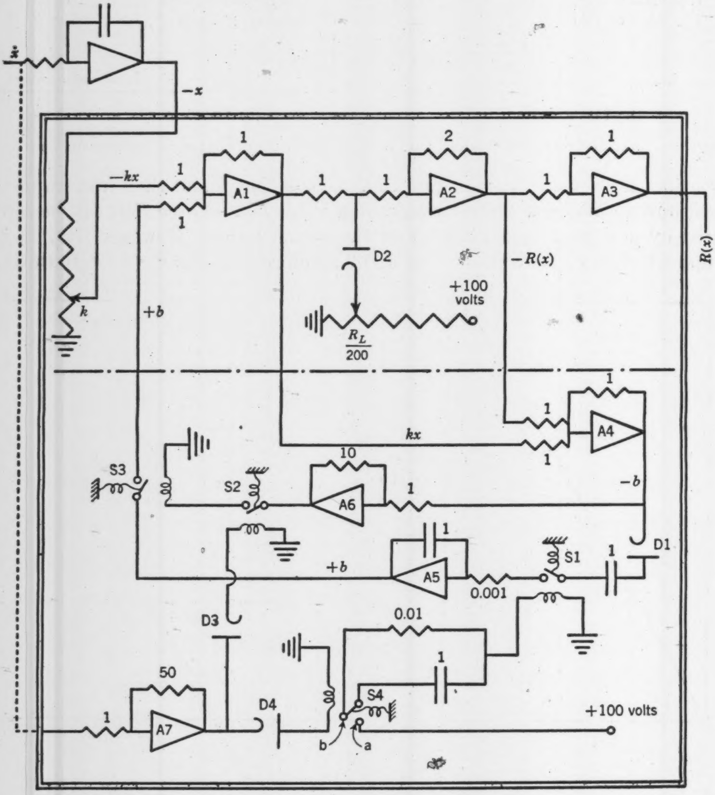
$\dot{x}$
$-x$
1
2
1
$-kx$
1
A1
1
1
1
A2
1
A3
1
D2
$-R(x)$
$R(x)$
+100 volts
k
$+b$
$\frac{R_L}{200}$
1
1
A4
kx
1
10
S3
S2
A6
1
$-b$
1
D1
S1
1
A5
$+b$
0.001
0.01
D3
1
50
S4
D4
A7
1
+100 volts
b
a

FIG. 3.—ELASTO-PLASTIC RESISTANCE FUNCTION CIRCUIT (RESISTANCE VALUES IN MEGOHMS, CAPACITANCE VALUES IN MICROFARADS)

shown as a solid box. Because information about the sign of $\dot{x}$ will clearly be required, a dotted line supplying this information is also shown. The chief obstacle is that one cannot foretell when x will reach a peak value.

CIRCUIT FOR THE ELASTO-PLASTIC RESISTANCE FUNCTION

First, it is necessary to define $R(x)$ for any value of x. The function $R(x)$ is not single-valued; it depends on the history of x as well as on its instantaneous value. By reference to Fig. 2(*b*), three states of $R(x)$ can be defined, as shown in Table 1. In the table, the subscript L denotes the elastic limit.

A circuit that will follow the "instructions" in Table 1 and will therefore compute $R(x)$ in accordance with Fig. 2(*b*) is shown in Fig. 3. Fig. 4 is a photograph of an oscillograph record showing the relation between $R(x)$ and x in parametric form because they are both necessarily plotted against time. Before describing the salient features of the circuit, it should be explained that, if it were desired to reproduce the relation between $R(x)$ and x for increasing x-values only ($\dot{x}$ never negative), only that part of the circuit in Fig. 3 above the dash-dot line would be required. If only this upper portion of the circuit were used, then for decreasing values of x (when $x > x_L$) $R(x)$ would retrace B A (Fig. 2(*b*)) rather than the line BC expressed by the equation $R(x) = k\,x - b$. It will be observed from Fig. 4 that, as soon as x is decreased ($x > x_L$), $R(x)$ is decreased also—that is, $R(x)$ is generated in accordance with Table 1.

TABLE 1.—THREE STATES OF $R(x)$

State	Magnitude of x	History of x	$R(x)$
1	$x < x_L$	x has never before been as great as x_L	$R(x) = k\,x$
2	$x < x_L + \frac{b}{k}$	x has been equal to $x_L + \frac{b}{k}$	$R(x) = k\,x - b$
3	$x > x_L$	x has never exceeded its present value	$R(x) = R_L = k\,x_L$

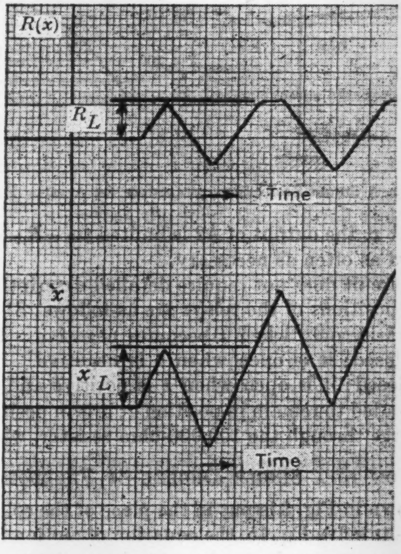

FIG. 4.—OSCILLOGRAPH RECORD OF $R(x)$ AND x

In the circuit shown in Fig. 3, the output of amplifier A1 is $k\,x$, corresponding to OAD in Fig. 2(*b*). Because diode D2 is biased to pass any positive voltage in excess of R_L, the output of amplifier A2 follows lines OAB in Fig. 2(*b*) with a negative sign (states 1 and 3). The difference between the output of A1 and A2 is b (Fig. 2(*b*)). Amplifier A4 may therefore be called the *b*-computer.

Amplifier A5 acts as a sign changer, except that condensers are used instead of the usual resistors. (The 1,000-ohm resistor between relay S1 and A5 is included for circuit stability.) Relay S1 is normally open and is closed momentarily at the instant that $\dot{x}$ becomes negative. Thus, A5 is used as a "memory" for the last value of b, and it is made to store this value during state 2 when $R(x) = k\,x - b$—that is, BCB in Fig. 2(*b*). The manner in which $R(x)$ is made to follow BCB is this: As soon as $\dot{x}$ becomes negative, relay S1 closes and b is stored on A5. A fraction of a second later, S3 closes, allowing b to be an additional input into A1. The total input into A1 is now $-k\,x + b$. Its output is $k\,x - b$.

As $R(x)$ comes up curve CB (Fig. 2(*b*)) and reaches the value of R_L, relay S3 is opened and the input of b into A1 is interrupted. Thus, the output of A1 reverts suddenly to $k\,x$; the output of A2 is limited to $-R_L$ as before (state 3). This can be repeated as often as necessary.

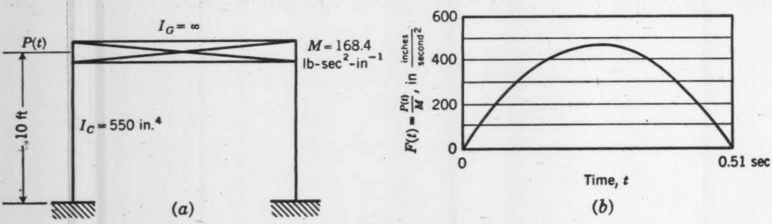
$I_G = \infty$
$P(t)$
$M = 168.4$ lb-sec^2-in^{-1}
10 ft
$I_C = 550$ in.^{4}
(*a*)
600
400
200
0
$F(t) = \frac{P(t)}{M}$, in $\frac{\text{inches}}{\text{second}^2}$
0
0.51 sec
Time, t
(*b*)

FIG. 5.—A SINGLE-STORY STRUCTURE WITH AN APPLIED FORCE

The rest of the circuit does not require detailed description. Examination will reveal that the positions of the relays are as follows: S1 is normally open; it is closed momentarily only when $\dot{x}$ becomes negative. Relay S2 is spring loaded to remain closed; it is open when $\dot{x}$ is negative. Relay S3 is spring loaded to remain closed; it is open when $\dot{x}$ is positive and when $R(x) = R_L$. Relay S4 is spring loaded to remain in position a; it is in position b, allowing the condenser to discharge through the 100,000-ohm resistor, when $\dot{x}$ is positive.

APPLICATION TO A SINGLE-DEGREE-OF-FREEDOM SYSTEM

If the circuit shown in Fig. 3 is put in the place of the solid box in Fig. 1(*b*), it should be possible to solve Eq. 1*b*, the equation of motion for a single-degree-of-freedom system having an elasto-plastic spring. To confirm whether this can in fact be done, a numerical example was solved which has been used by Nathan M. Newmark,[4] M. ASCE. This example might represent a single-story structure acted on by a variable force, as shown in Fig. 5. After dividing by the numerical value of the mass, the equation of motion in inch-kip-second units is

---

[4] "Methods of Analysis for Structures Subjected to Dynamic Loading," by N. M. Newmark, Report to Physical Vulnerability Branch, Air Targets Div., Directorate of Intelligence, U. S. Air Force, December, 1950 (Revised).

$$\ddot{x} + R(x) = 3{,}720\,t - 7{,}300\,t^2, \quad 0 < t < 0.51 \ldots\ldots\ldots\ldots (2)$$

in which $R(x)$ is an elasto-plastic resistance function, such as in Fig. 2(*b*), with the value of $k = 1{,}362\ \text{sec}^{-2}$ and $R_L = 439.6\ \text{in. sec}^{-2}$. The solid curve in Fig. 6 represents the analytical solution of Eq. 2, and the dashed curve is the solution by the Newmark numerical method with time intervals of 0.04 sec. Values scaled off the analog computer solution are also shown in Fig. 6. The oscillograph records (Fig. 7) represent the solutions of Eq. 2 and three similar equations in which the input function has different intensities, as follows:

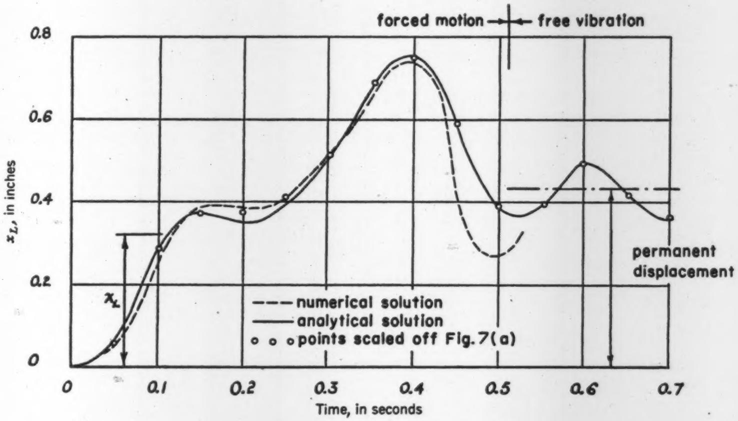

FIG. 6.—SOLUTION OF EQ. 2 BY VARIOUS METHODS

Part of Fig. 7	Input function
(*a*)	$F(t) = 3{,}720\,t - 7{,}300\,t^2$
(*b*)	$F(t) = 2{,}065\,t - 4{,}060\,t^2$
(*c*)	$F(t) = 2{,}810\,t - 5{,}520\,t^2$
(*d*)	$F(t) = 3{,}780\,t - 7{,}420\,t^2$
(*e*)	$F(t) = 3{,}720\,t - 7{,}300\,t^2$

In Fig. 7(*e*), the response of the system is shown when subjected to about 10% of the critical viscous damping.

The accuracy of the method is considered to be of approximately the same order as that of normal analog-computer operations. This statement is made despite the fact that it was found that the maximum deflection was extremely sensitive to variations in the settings for R_L. However, such sensitivity is a true characteristic of an elasto-plastic system and is emphasized by the analog computer. This characteristic might be missed when other methods are used to compute the deflections, with the result that false confidence may be placed in the accuracy of the computations.

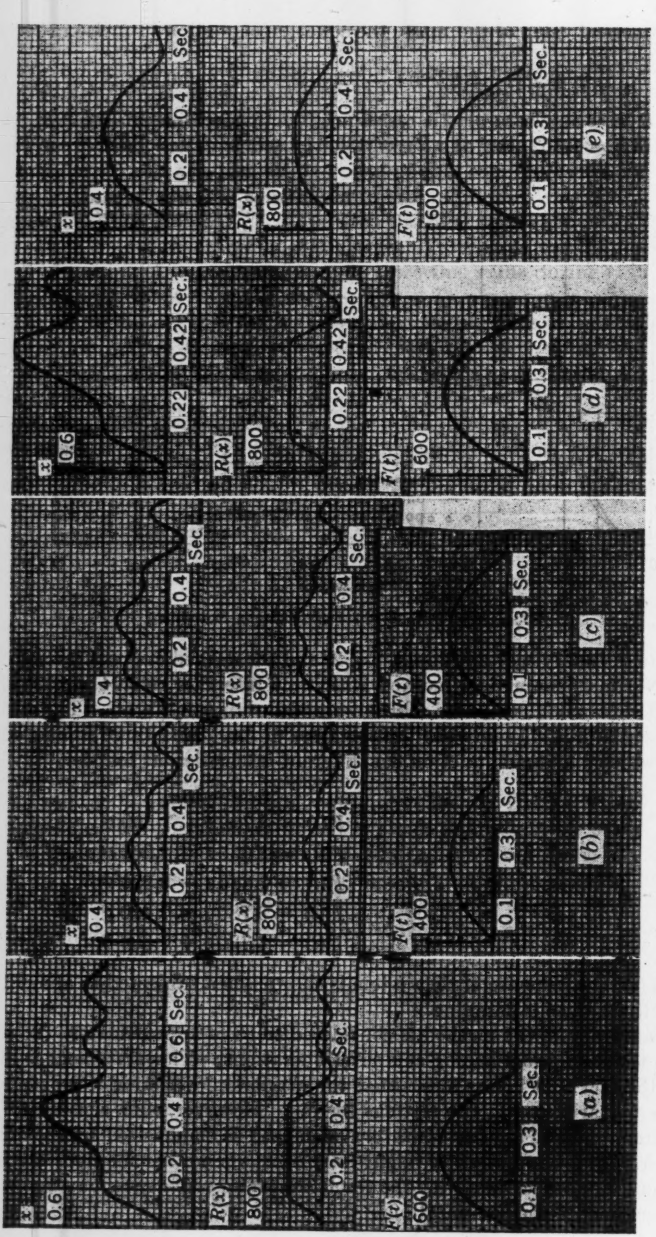

Fig. 7.—Oscillograph Records of the Response of the Elasto-Plastic System to Various Forcing Functions (Time Scale Nominal; Approximate Correction Factor, 36/27)

EVALUATION OF METHOD

Using standard components, an analog-computer circuit has been developed that will produce an elasto-plastic resistance relationship. Although this circuit may appear complex, an experienced operator will be able to make the necessary connections in less than half a day. Almost every dynamic problem involving an elasto-plastic system will take longer to solve by analytical methods. Numerical methods may yield answers more quickly, but they are not as flexible as the computer method and therefore not as suitable for design purposes. For example, it may be desirable to study the effects of changing the stiffness, of introducing damping (Fig. 7 (*e*)), or of varying the intensity of the applied force. This can be done by means of the analog computer in only a few minutes, after the first solution has been obtained.

If the force $F(t)$ causing the disturbance is completely irregular, as in the case of seismic disturbances, special arrangements are usually required to reproduce such an irregular function faithfully. In the simpler cases, it may be possible to make a harmonic analysis of the function and then to represent it as the sum of several sine curves. In other cases, the use of servo-mechanisms and representation by power series may be necessary. Several methods permit the exact generation of irregular functions. Some of these are discussed by G. A. Korn and T. M. Korn.[3]

Although the use of the method has been demonstrated for a single-degree-of-freedom system, it has a more general use. If the circuit shown in Fig. 3 is thought of simply as an operational unit which will generate $R(x)$, its application to multi-degree-of-freedom systems becomes immediately evident. Because the $R(x)$-generating circuit requires seven extra amplifiers, the use of two or more such circuits will normally be governed by the availability of equipment. In most cases, it will not be necessary to use more than one elasto-plastic circuit in the analysis of a system. A completely elastic circuit can be used initially to investigate which spring of the multi-degree-system will enter the plastic range first. Thereafter, only the circuit representing this particular spring need be of the elasto-plastic type, unless the subsequent yielding of other springs is of interest also. On this basis, the method has in fact been successfully applied to a multi-degree-of-freedom system.

The circuit of Fig. 3 functions only so long as x does not reach the plastic range in the negative direction, but it would be a simple matter to modify the circuit so that it will generate the elasto-plastic resistance function in both directions. One immediate application of such an improved circuit would be the investigation of the effect of yielding on the phenomenon of resonance. This would be of particular interest in the study of the effect of earthquakes on structures.

ACKNOWLEDGMENTS

This unsponsored study was conducted at the University of Michigan (Ann Arbor) by the department of civil engineering of which Earnest Boyce, M. ASCE, is chairman. The writers wish to express their gratitude to Leo M. Legatski, A.M. ASCE, whose efforts are responsible for the availability of an analog computer in the department.

DISCUSSION

JOHN S. ARCHER,[5] J. M. ASCE, AND ALLEN LANGE.[6]—It is indeed a pleasure to see in this paper a further application of the analog computer to complicated nonlinear problems. The analog computer has apparently unlimited fields of usefulness, one of which Messrs. Schenker and Martin have clearly delineated here.

The civil engineering department of the Massachusetts Institute of Technology is engaged in the study of elasto-plastic problems like the one described in the paper. The circuit described in this discussion has been devised to simulate the elasto-plastic phenomenon on a high-speed electronic computer, such as the general purpose simulator at the school's instrumentation laboratory.

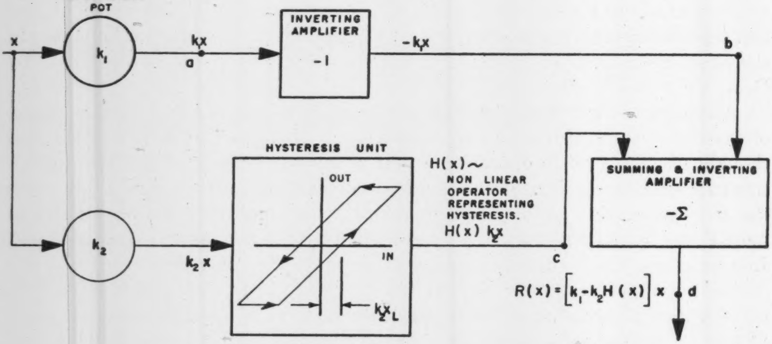

FIG. 8.—CIRCUIT SIMULATING THE ELASTO-PLASTIC PHENOMENON

It should be noted that this circuit functions properly for both positive and negative values of x. Also, because this circuit is intended for use with high-speed computers it does not use relays as circuit elements. Elimination of the relays permits a more accurate representation of the elasto-plastic phenomenon because the finite delays involved in the opening and closing of the relays are eliminated.

This circuit makes use of three standard analog-computer devices—summing and inverting amplifiers, coefficient pots, and hysteresis units.

The algebraic expression describing the nonlinear operation is quite cumbersome in this case; consequently, the operation of the circuit is analyzed by considering wave forms at various points in the circuit. Fig. 8 shows the circuit used. Fig. 9 illustrates the wave forms that appear in various parts of this circuit. In the case shown, $k_1 = k_2 = k$. In all these diagrams, x and

---

[5] Asst. Prof., Civ. Eng. Dept., Massachusetts Inst. of Technology, Cambridge, Mass.

[6] Research Engr., Instrumentation Lab., Massachusetts Inst. of Technology, Cambridge, Mass.

$R(x)$ are shown plotted against time t. Fig. 10 shows $R(x)$ plotted against x, with the numbers 1, 2, 3, . . . corresponding to $t = t_1$, $t = t_2$, ...

The adjustment of the hysteresis unit determines the hysteresis dead zone in terms of the percentage of the full-scale signal. Physically, this dead zone is analogous to the elastic-limit deflection, or elastic-limit resistance, and the full-scale signal is analogous to the maximum expected value of deflection, in accordance with the usual analog-computer scaling techniques.

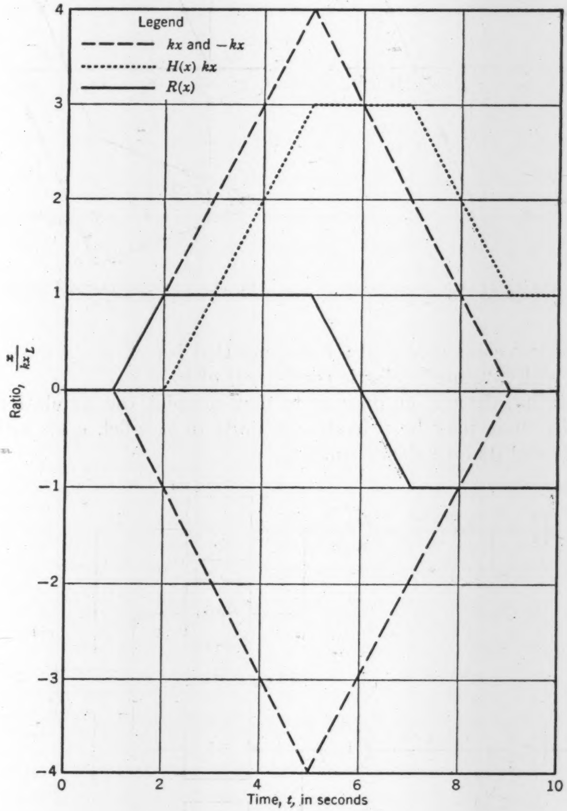

FIG. 9.—WAVE FORMS ($k_1 = k_2 = k$)

The relative values of k_1 and k_2 determine the characteristics of the elastoplastic resistance function. For example, when $k_1 = k_2$, the $R(x)$-function is the same as that used by Messrs. Schenker and Martin. The two cases for $k_1 > k_2$ and $k_1 < k_2$ are shown in Fig. 11, labeled a and b, respectively. Phy-

UNIVERSITY OF MICHIGAN LIBRARIES

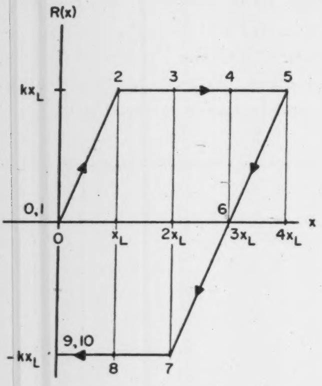

FIG. 10.—ELASTO-PLASTIC RESISTANCE FUNCTION ($k_1 = k_2 = k$)

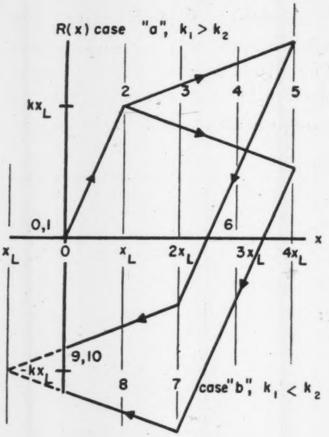

FIG. 11.—ELASTO-ELASTIC RESISTANCE FUNCTION

sically, these two cases represent a resistance that is at first elastic, then elastic and plastic with a "slope" (elastic coefficient) of $k_1 - k_2$.

Theoretically, there is no limit as to how complex the simulation may be. For example, there may be n hysteresis units in parallel, each with its own coefficient k_i and its own elastic limit x_{Li}.

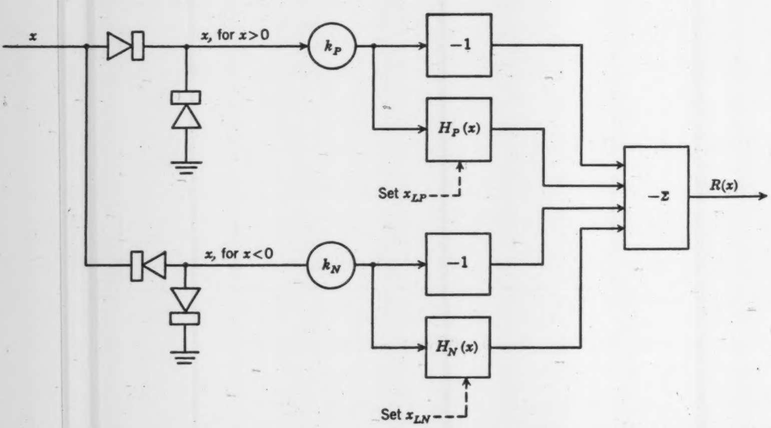

FIG. 12.—ASYMMETRIC CIRCUIT (SUBSCRIPT P APPLIES WHEN $x > 0$, SUBSCRIPT N WHEN $x < 0$)

Another physically important factor is that of asymmetry. Either k or x_L may be different for $x > 0$ or $x < 0$. The simulation of this case is shown in Fig. 12, using simple germanium diodes in shunt arrangement for rectifying.

AMERICAN SOCIETY OF CIVIL ENGINEERS
Founded November 5, 1852
TRANSACTIONS

Paper No. 2819

RIVER SURVEYS IN UNMAPPED TERRITORY

By Gerard H. Matthes,[1] Hon. M. ASCE

With Discussion by Messrs. Frederic T. Mavis, T. H. F. Nevins, Chesley J. Posey, Edward Kuiper, and Gerard H. Matthes

Synopsis

There are presented herein methods designed to assist engineers concerned with river-utilization problems in unmapped areas and in areas where streamflow data generally are lacking. The subject is treated under two headings: (*a*) Short-cut methods adapted to exploratory or reconnaissance surveys which limit engineers to the use of hand instruments, the slide rule, and expedients for estimating river discharge and river gradients; (*b*) methods of providing reliable surveys of specific local areas and also of providing more extensive maps which include the use of aerial photogrammetric methods. Convenient tables and diagrams are submitted. The hope is expressed that additional methods of this nature may be submitted by other engineers as the fruits of their experience.

Introduction

The growing demand for expert advice in matters pertaining to water-resources utilization in regions as yet unmapped, or only partly mapped, has prompted the outlining herein of field methods that experience has shown to be of considerable assistance whenever conditions require that instrumental equipment and personnel be reduced to a minimum. In addition to surveying and mapping methods, some of which rate no better than expedients, short-cuts for estimating river gradients and discharge are presented.

Exploratory or Reconnaissance Surveys

Exploratory work, usually of a tentative character, differs basically from the accurate final surveys required after a river project has reached the status

---

Note.—Published, essentially as printed here, in February, 1955, as *Proceedings-Separate No. 612.* Positions and titles given are those in effect when the paper or discussion was approved for publication in *Transactions.*

[1] Cons. Hydr. Engr., New York, N. Y.

UNIVERSITY OF MICHIGAN LIBRARIES

at which its development becomes assured. The exploratory phase recalls the situation that confronted engineers some fifty-five years ago in the arid western section of the United States which was then largely unsurveyed and devoid of stream-flow records. Prospective irrigation development then was the keynote and every ranchman and villager could direct one to what he considered to be a good dam site. Today the limitations confronting the engineer required to report on foreign project possibilities are more severe owing to differences in languages, local customs, and modes of travel. In exploratory work the mode of travel usually determines the type of instrumental equipment to be used. In most cases this equipment must be confined to articles that can be carried in coat pockets or a traveling bag, such as a compass, hand level or clinometer, aneroid, stopwatch, tape, slide rule, and magnifying glass. For the purposes of this paper it is assumed that even a current meter must be ruled out. Certain items can be added, however, to the foregoing list depending upon the facilities for travel that the country affords. Among them is the rolled, graduated cloth strip that can be nailed to a pole to serve as a leveling or stadia rod, a camera with tripod, and a barometer of the Paulin type. This latter instrument, however, is too delicate for rough travel, as on horseback or camel-back. A first reconnaissance by airplane or hydroplane is always helpful toward gaining a comprehensive view of the river, its valley and tributary characteristics, and the extent of settlements, roads, or trails. When a river is at all navigable it is wiser to travel by water than on land, in whatever type of craft is in local use, employing native boatmen thoroughly familiar with the river. The need for an interpreter in the party is essential. Traveling upstream has the advantage of providing ample time for detailed study of the river, its banks, bars, shoals, islands, and split channels. Because no two rivers are alike nothing should be taken for granted, and frequent inquiries are necessary. Native boatmen have a fund of information relating to low-water depths on shoals, the type of craft most used for transporting freight, the height and frequency of floods, their seasonal occurrence, and the extent of flood-plain lands overflowed.

Alluvial river characteristics are not limited to the lower courses of rivers. The 1,800-mile-long Rio Grande in North America, for instance, traverses a succession of canyons alternating with alluvial plains. The Colorado River meanders in an alluvial valley at an altitude of 7,200 ft. Streams of this type are worthy of detailed study because they afford potential sites for high dams and large reservoirs. On the other hand, such streams pose difficult problems as regards reconnaissance procedure because travel through mountain gorges and box canyons can be done, as a rule, only on foot rather than by boat or on horseback. In open valleys horseback travel is to be recommended. In this connection, it has been the writer's experience that, for determining distances by pacing, a horse does a better job than a man. That is, over rough ground a horse's steps vary less in length than those of a man. The writer has also found that hand-level surveying in the saddle has advantages over similar work on foot if a steady horse is procurable. All of the smaller hand instruments are readily transported in coat pockets and saddlebags; bedding, tents, and food are carried in boats or on pack animals.

In steep mountainous terrain and in canyons where a horse is more often a hindrance than a help, reconnaissance is done on foot with much physical exertion. In the absence of any trail it may be necessary to carry packs and stop to make camp when a promising site demands careful investigation. Because many river gorges and narrow valleys owe their origin to geological faults or crushing zones that were easily eroded by stream flow, search for evidences of such planes of weakness is of major importance in dam-site reconnaissance. However, not all gorges or canyons follow fault lines. For many miles the Grand Canyon of the Colorado River does not follow any of the many faults that intersect its high plateau region.

When a desirable site, or alternative sites, for a dam have been found in a gorge or narrow valley, rough cross sections can be sketched in a notebook by determining elevations above the river bed using the hand level or Paulin-type barometer and by estimating distances across the river by means of rough paper triangulation, using the camera tripod head equipped for use as a miniature plane table. If aerial photographs happen to be available, distances may be scaled between identifiable points, but no great accuracy is thus afforded because the scale of aerial photographic detail varies with height.

Individual photographs, overlapping each other about 50% or more, are invaluable for viewing terrain that stereoscopically appears suitable for dams. On reconnaissance surveys, the art of stereoscopic viewing with the naked eyes (thus dispensing with cumbersome stereoscopes) is worth cultivating. In fact, once the eyes have been trained to combine the overlapping portions of two photographs, the stereoscopic view so obtained has the added benefit of undiminished clarity whereas there is always a loss of light in a stereoscope. Eyestrain which is experienced at first affects only the eyeball muscles and not the optic nerves.

Whenever travel by water is possible a chartered boat has greater advantages than a regular passenger boat or tow boat of a barge line because it permits stops to be made to facilitate observations. For trips of undeterminate length a steamboat is preferable to a motor boat as it may not be possible to procure gasoline in the area to be explored. It is always possible to gather driftwood for firing a boiler if the necessity should arise. A stern-wheeler is safer for negotiating shallow water than a screw-propelled craft. On one reconnaissance for canalizing a 200-mile stretch of rock-bottomed river, the writer used a steamboat drawing only 23 in. By keeping all fuel on a small barge this draft was uniformly maintained. It was thus possible to paint a scale of elevations above water level on the sides of the cabin and up to the top of the pilot house to use in determining the height of bank while traveling by sighting with a hand level. Elevations up to approximately 30 ft above water level could so be estimated. All sites of merit were inspected in less than three days. The trip was expedited by having sleeping quarters and a small galley for cooking on board. Approximate river distances were scaled from aerial photographs.

DISCHARGE MEASUREMENTS

In the absence of a current meter, much can be accomplished toward determining the momentary discharge of a river regardless of its size or stage by timing floats or driftwood—preferably logs—in the swiftest part of the current. The relation between the maximum central surface velocity and the mean velocity in the entire cross section has become a serviceable tool for engineers because of extensive research by observers in several countries. In the case of small rivers subject to rapid changes in stage, especially when in flood, complete flood hydrographs of discharge are obtainable with this method by timing floats at, say, half-hour intervals. The results so obtained have repeatedly been found superior to those from current-meter measurements. The (V/V_{cs})-method, as it is called—in which V is the mean velocity in the entire cross section and V_{cs} is the maximum central surface velocity—is peculiarly suited to reconnaissance surveys, requiring only a stopwatch and a tape. The difficult part of the procedure is the determination of the wetted cross-sectional area. Soundings are indispensable and horizontal distances may have to be estimated from aerial photographs or by rough triangulation from a measured base. These difficulties are identical with those of current-meter measurements made under the same circumstances. The (V/V_{cs})-method is applicable only to straight reaches between well-defined parallel banks, where all flow is confined to a single channel. The locus of swiftest flow may not always be exactly in the center of the channel, but in a straight reach of river the axis of the current is usually found there. In doubtful cases it is advisable to time floats at several points. Because the thread of maximum velocity is not at the surface but approximately a foot below it, drifting logs that are well immersed and have no projecting limbs are suitable for float observations. In no event should chips or surface trash be used for V_{cs}-observations.

TABLE 1.—RATIOS OF $V/V_{cs} = \dfrac{\text{Mean Velocity in Cross Section}}{\text{Maximum Central Surface Velocity}}$

Hydraulic radius, in feet	VALUES OF MANNING'S *n*				
	0.021	0.024	0.028	0.037	0.045
2	0.75	0.70	0.66	0.62	0.53
3	0.77	0.72	0.69	0.64	0.57
4	0.78	0.74	0.71	0.66	0.60
5	0.79	0.75	0.72	0.68	0.62
6	0.79	0.76	0.73	0.69	0.64
8	0.80	0.77	0.74	0.71	0.66
10	0.81	0.78	0.75	0.72	0.68
12	0.81	0.79	0.76	0.73	0.69
15	0.82	0.79	0.77	0.74	0.70
20	0.82	0.80	0.78	0.76	0.72
30	0.83	0.81	0.80	0.78	0.74
50	0.84	0.82	0.81	0.79	0.77

Table 1 presents a composite of (V/V_{cs})-ratios compiled from different sources. Where accuracy is desired the effect of Manning's n and the length of hydraulic radius should be taken into account, but for quick estimates 0.8 is an average value for smooth, approximately rectangular, cross sections. Ratios for trapezoidal cross sections run nearer 0.7. Triangular cross sections in bends should be avoided as their (V/V_{cs})-ratio is low and variable. For rough rock beds or weedy channels the ratio drops to 0.5 or 0.4. The (V/V_{cs})-

ratio method has become increasingly popular in Europe and India for regular stream-gaging practice with either current meters or floats, notably for use on small streams whose flows vary half-hourly and also on large rivers in which any detailed procedure is not only time-consuming but involves the risk of losing current-meter equipment through entanglement with driftwood.

In the case of torrential-type streams it becomes important to estimate the superelevation of the midstream water surface when computing the wetted cross-sectional area. This superelevation is frequently several feet along the axis of swiftest flow thus causing a marked increase in cross-sectional area. In large rivers this superelevation is negligible.

BANK-FULL DISCHARGE CAPACITY

A formula devised by Gerald Lacey[2] yields a close approximation to the bank-full discharge capacity, in cubic feet per second, of any river whose bed and banks are composed of erodible materials of the same kind as that which the river transports. The formula is applicable only to river channels with high, well-defined banks, devoid of back channels, sloughs, and islands, and is written as

$$Q = \frac{b^2}{2.67} \qquad (1)$$

in which b is the width in feet between high banks and Q is in cubic feet per second. Because b is the only parameter that needs determination and may have to be estimated from aerial photographs or by eye, it is advisable to take the mean of several estimates made at different crossings. Eq. 1 is empirical, having been derived from numerous alluvial rivers in all parts of the world. It is important to remember the fact that b represents that width which, multiplied by the average bank-full depth, should give the area of the river's cross section for use in discharge computations. No limit is placed on the grain size of the alluvial bank materials, which may range from fine silt to coarse gravel. For example, a river 3,600 ft wide, in a straight reach where fairly steep parallel banks prevail for some distance on both sides, would have an approximate bank-full discharge capacity of 1,800,000 cu ft per sec. Eq. 1 is not applicable to rivers flowing in rock beds or between erosion-resistant materials such as riprap or quay walls, nor is it applicable to tidal estuaries.

RIVER GRADIENTS

When traveling by boat or launch, few things about a river are more difficult to estimate than its gradient. The following approximate method of estimating the slope of a river by reference to the coarsest particles in its bed load yields answers closer than can be obtained from aneroid observations of altitude plus guessing at river lengths. Because a river profile, when plotted, is not a straight line, observations should be made at frequent intervals. The slopes so determined pertain to bank-full or flood flow only. The concept used is known as the stream's "competence" for moving coarse rock debris. Competence, often stated as being indicated by the largest gravel or boulder that a stream is capable of moving when in flood, is more accurately defined by the largest "rolling diameter" of such gravel or boulder. This amounts to considering their rolling propensity as akin to that of a barrel. The length of a stone and its weight then become immaterial because the pushing force of the flowing water is the same on each unit of length along its upstream face. The well-known DuBoys formula for tractive force—$T = w\,D\,S$—is used, which, by transposition, yields $S = T/w\,D$, in which S is the water-surface slope for the bank-full stage or for a higher stage; T is the tractive force exerted at the bed, usually expressed in pounds per square foot or in kilograms per square meter; D is the depth at the bank-full stage or for a higher stage at points where the largest stones come to rest; and w is the weight of a cubic foot of water plus its sediment content, taken as from 62.5 lb to 63.0 lb. Fig. 1 was compiled by plotting, against bank-full depth and slope, the values of the tractive forces that moved the largest stones that could be found in streams in all parts of the United States. A few data were also obtained from rivers in other countries. The tractive-force values were then converted into terms of "rolling diameter," as previously defined. The consistency of the plotted values proved to be truly remarkable. On the other hand, the plot revealed a wide difference in the tractive effort exerted by torrential flow in headwater streams and that exerted by tranquil flow in deep rivers. The reason is that steep headwater streams (omitting those of the cascading type) have extremely rough beds, develop much ineffective turbulence and, in addition, entrain considerable free air which reduces the weight per cubic foot of water. Consequently, the data for these streams showed many inconsistencies and were not used in the main diagram (Fig. 1(*a*)) which applies to tranquil-flow rivers having flood depths exceeding 10 ft. In Fig. 1(*b*) are shown values applying to torrential headwater streams having flood depths of 20 ft and less. Slopes are shown as abscissas in feet per mile and in meters per kilometer. Slopes in terms of feet per foot, if desired for use in flow formulas, are conveniently determined by adding three decimal ciphers to the meter-per-kilometer values. All slope values represent water-surface slopes for ordinary and higher stages but are not applicable to low-water stages because river profiles at these stages consist of nearly level pools separated by riffles or crossing bars, and the transport of coarse debris does not occur.

---

[2] "Stable Channels in Alluvium," by Gerald Lacey, *Minutes of Proceedings*, Inst. of C. E., London, Vol. 229, 1929–1930, p. 270.

Loss of weight of stones by submergence in water, which is always allowed for in hydraulic laboratory studies of tractive force, is eliminated in this procedure by assuming a uniform specific gravity for all rock matter between 2.6 and 2.8, a range which includes the majority of rock species found in streams, as, for example, granite, gneiss, limestone, dolomite, quartzite, flint, and the heavier sandstones. Not included are trap rock and basalt (specific gravity exceeding 3.0) nor the lightweight shales and shaly sandstones. Because the latter are worn down rapidly by streams and the former are relatively scarce it is believed that the diagram will prove useful in the majority of cases.

Field application of this method calls for accurate observations of gravel and boulder sizes. Any one not familiar with the path followed by coarse bed-load travel in streams, which in general coincides with the path of strongest

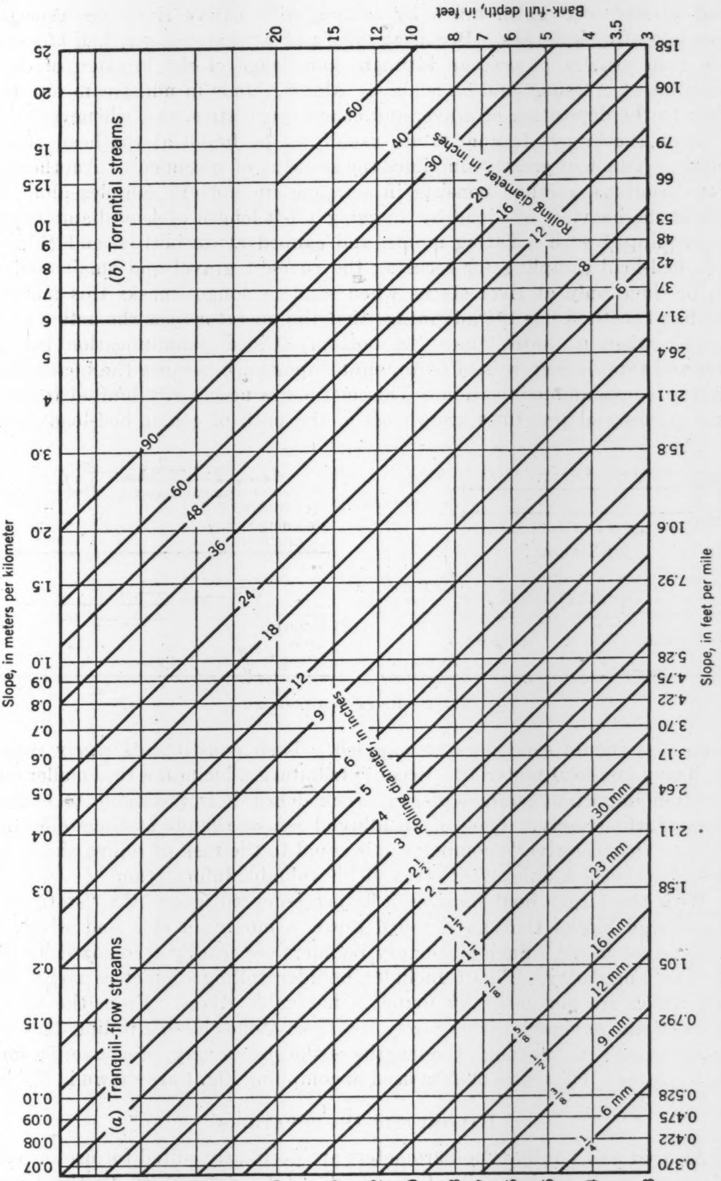

FIG. 1.—TRACTIVE-FORCE DIAGRAM FOR ESTIMATING SLOPE IN TERMS OF BANK-FULL DEPTH AND ROLLING DIAMETER OF LARGEST STONE

flood current, can glean much by talking with native rivermen, especially those operating launches. Because gravel and large stones are their *bête noire,* such men usually possess an intimate knowledge of the location of coarse debris, as at crossings and on islands. Many islands in midstream owe their origin to the deposition of gravel and coarser rock sizes, and whenever this is the case, the largest fragments are usually to be found at the head of such islands. This fact greatly simplifies the securing of specimens. Another, but more laborious, method consists in scraping up bottom samples along the path of the heaviest bed load by dragging a 4-ft length of 4-in.-diameter steel pipe equipped with a flaring mouth and capped at its bottom end (Fig. 2). Such bed-load sampling for securing the coarsest gravel and small boulders can be done only at river stages when sand no longer masks this material. The hand method has the advantage that the operator feels the action of the sampler when it "bites" into the bottom. Close communication between pilot and sampling crew is of paramount importance because the boat's speed requires constant modification. This method is necessarily limited to small-sized stones and presumes knowledge of the path of coarse bed-load debris.

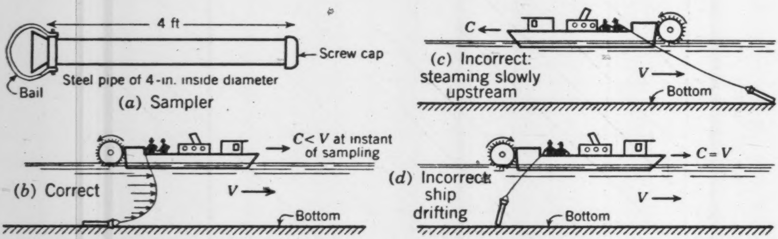
4 ft
Screw cap
Steel pipe of 4-in. inside diameter
Bail
(a) Sampler
C
(c) Incorrect: steaming slowly upstream
V
Bottom
C< V at instant of sampling
(b) Correct
V
Bottom
(d) Incorrect: ship drifting
C = V
V
Bottom

FIG. 2.—RIVER-BED SAMPLING

In no case should sand bars be sampled. Their constituents rarely contain any heavy bed-load material. Because tributaries, including the smaller ones, are often important sources of large rock debris it is profitable to examine their mouths closely. Lack of an alluvial fan or islands at their mouths is evidence that the river's competence is equal to the task of rolling the largest sizes of debris. A quick visit often yields valuable information.

With the larger boulder sizes it is necessary to ignore the "stationary" type—large blocks that have rolled down a mountain side and which the river cannot move. Such stationary boulders are readily recognized by their size and angularity. Fig. 1 includes boulder rolling diameters larger than 4 ft, which are not generally found in navigable rivers. From the writer's observations, navigable rivers rarely transport stones having rolling diameters greater than 8 in., although the lengths of the stones may, of course, be somewhat greater. Examples of data used in compiling Fig. 1 are shown in Table 2.

BAROMETRIC OBSERVATIONS

Aneroid and Paulin-type barometers are peculiarly suited for use in reconnaissance surveys where elevations need not be determined to the nearest foot. By correcting their readings for temperature changes of the air with the aid of conversion tables prepared for that purpose, errors can be reduced to within a few feet provided the readings are taken in closed circuits. Dependable results can be obtained only during steady weather conditions and by closing circuits every two hours or more often. Because diurnal variation within such periods is almost wholly caused by changes in the temperature of the air and only slightly by weather conditions, good working data are obtainable by taking temperature readings at frequent intervals. A blue sky with "fair-weather" clouds blown by strong winds is one of the worst conditions for barometric work. A completely overcast sky with gentle or no wind is best. On windy days, barometer readings taken on the lee side of a vehicle, building, ship's cabin, or pilot house, invite serious errors owing to unstable low-pressure areas at such points. Whenever practicable, a second instrument should be read at frequent intervals at a base station for the purpose of providing a correction curve. It will be readily seen that barometric observations are not satisfactory for reconnaissance work when travel is by boat on a river because of the impracticability of making closed circuits or for providing for observations at a base station. In no case are barometric elevations of any value for determining river gradients.

TABLE 2.—TRACTIVE-FORCE (*T*) DATA

River	Location	Diameter of gravel or boulder rolled, in inches	Slope		Depth, in feet	*T*, in lb per sq ft
			Feet per mile	Feet per foot		
Sacramento (California)	Mile 159 above Moulton Weir	3½[a]-4	1.1	0.00021	28	0.37
Sacramento (California)	Mile 120 above Tisdale Weir	2½-3[b]	0.69	0.00014	29	0.25
Mississippi (Illinois)	Above Confluence with Ohio River	3	0.55 -0.60	0.000104 -0.00011	34	0.19 -0.24
Missouri (Missouri)	Below St. Charles	1¼	0.71	0.000134	12.9	0.108
Kootenay (Montana)	20 miles below Yarnell	13-15	4.5	0.00085	25	1.33
Wenatchee (Montana)	Between Cashmere and Peshastin	24[c]	30	0.00057	6	2.15
Bear River (California)		8[d]	7	0.001325	8	0.66
Devil's River (Texas)	Above Gaging Station	48[e]	8.45	0.0016	40	4.05
Rio Grande (Texas)	Above El Paso (1932)	1¼-1½[f]		0.00052	5-6	0.17 -0.20

[a] A specimen 6 in. by 3½ in. by 3 in., partly rounded weighed 3 lb. [b] Sub-angular gravel; one specimen weighed 1.25 lb. [c] Rounded. [d] Mining debris; maximum diameter moved. [e] A boulder 9 ft long. [f] Some of the specimens weighed 0.25 lb; the writer was told coarser gravel had been found.

PROJECT SURVEYS

Surveys and stream-flow measurements needed in the design, construction, and operation of river development projects in unmapped regions must be made with the same care and accuracy that are required for similar purposes in highly developed, well-mapped countries. This statement applies with equal force to projects in which are contemplated water diversions for irrigation or for flood relief. Good topographic detail and an accurate net of level lines and transit traverses or triangulation control are of basic importance in all such cases. However, in the absence of sea-level elevations an assumed datum for elevations is sufficient, except in the case of harbor or navigable lower-river projects where elevations above mean sea level are of basic importance.

Accurate topographic and hydrographic survey operations in foreign lands are hampered by language differences, personnel problems, and by time lost waiting for supplies or repair parts. Mechanical equipment of all kinds, from surveying instruments to motors, propellers, and shafts for boats, entails the need for many spare parts and replacement parts. Climatic conditions impose barriers to progress by limiting the time for field operations to specific times of the year. Monsoon rainfall during certain months, alternating with periods of extreme heat, necessitate careful planning of survey operations. In some South American countries cutting down trees and clearing brush along river banks is prohibited except by special permit. In jungle areas clearing is costly and often a waste of time.

Floating equipment must be adapted to fit the job. Survey boats for field parties should be of the motorized shallow draft, scow-bow type which can push barges and make landings anywhere; native craft, when motor driven, usually is adapted only for reconnaissance work, the transferring of survey men to points within the survey area, and for moving light supplies. Jungles and swamps bordering rivers render transit-traverse surveys impracticable. In such cases permanent triangulation stations must be established. Three-legged steel pipe markers are recommended for this purpose. For their erection a work boat equipped with a drop hammer and powered by a diesel engine is required. Quarter-boats are superior to tents by providing better living conditions and better control of personnel; they also serve as bases of supply. During floods, when large areas of valley lands are overflowed, quarter-boats are invaluable. Important in the matter of keeping native personnel contented is the procurement of foodstuffs that they are accustomed to eating. On any job that is likely to take them long distances away from home, a thorough understanding with them must be had beforehand. Capable surveymen are sometimes found among foreigners, but they need careful screening; they must also be agreeable to working with American-made, four-leveling-screw instruments, which they regard as inferior to the European three-leveling-screw type.

INSTRUMENTAL EQUIPMENT

In tropical or desert regions where solar heat is intense the metal parts of surveying instruments become too hot to handle with bare hands unless wound with muslin. Spirit levels need a lid-shaped cloth that permits raising for noting the position of the bubble. If this precaution is not taken, the bubble will shrink to the size of a small pea, making it too sluggish for accuracy. Umbrellas are helpful to plane-table surveyors but not to transitmen or levelmen, who normally spend more time walking than standing at a station.

In planning the establishment of permanent gaging stations it is advisable to pattern one's methods after those adopted by the federal engineers of the country visited, in order that velocity and discharge figures may be on a comparable basis. The reason is, even with the best of instruments and care, measurements of discharge made with current meters are subject to systemic errors peculiar to the methods adopted for making the observations. These errors are in addition to the usual errors affecting stream gaging, which are of the order of 5%± from actual values. A gaging station, after it is well established in connection with a project, is also likely to prove valuable as a permanent station for local federal engineers. In such a case, the record continued by them will possess consistency.

If a current meter in one's outfit is of the revolving-cup type, it is not good practice to try to check its rating by some improvised method. So long as the cups rotate freely when blown into and the pivot point is in fair condition, it is best to use the instrument as is. A reasonable amount of wear does not usually affect the meter's performance at velocities of 1.0 ft per sec or greater. If a current meter needs overhauling or rerating it is best to complete such measurements with it as are of immediate importance before shipping it to the National Bureau of Standards, United States Department of Commerce, Washington, D. C., or to an Agricultural Experiment Station, that has special facilities for meter rating. A request should accompany the meter in such cases, to have it rated first in its existing condition and again after overhauling. This enables corrections to be applied to the measurements which were made last.

ECHO SOUNDINGS

The market affords a choice of echo-sounding apparatus suited for use under a variety of conditions. The more sensitive electronic instruments record not only the depth of water but, in the case of harbors and estuaries, the "interface" layer of brackish water that separates fresh and salt waters and also the top of flocculated clay deposits. Depth finders of this type are now available; they record the depth of bedrock through sedimentary deposits overlying it and thus provide better information than is obtainable by making borings. This is of great assistance in planning seawalls and harbor installations. As sound travels in water with velocities of from 4,740 ft per sec to 5,220 ft per sec, owing to differences in density due to temperature, salinity, and suspended sediment concentrations, calibration of any electronic depth finder is necessary at intervals during each day's work. In water and in liquid mud, calibration is quickly effected by lowering a flat piece of steel, usually a 4-ft or 5-ft length of T-bar or steel channel, suspended horizontally with the flat side up, at several known depths directly below the oscillator, thus checking the depths that it records. The rate of sound-travel through soil down to bedrock must be obtained from the instrument maker or by trial at locations where depth of bedrock is definitely known. For use on river trips small portable outfits weighing approximately 200 lb are available, composed of an outboard oscillator that can be hung from the side of the vessel, a battery, and a graphical recorder, suitable for transporting in an automobile or truck. Because spare parts are difficult to obtain in foreign lands it is important to lay in a liberal supply at the outset together with necessary tools. On important dredging jobs it is advisable to have three sets—one in service, one in reserve, and one undergoing repair by the manufacturer. Electronic instruments are delicate, hence require care in handling and in transportation. However, such instruments are capable of supplying a vast amount of information in a fraction of the time required for sounding with a lead line and they thus soon repay their cost. Special care must be exercised in suspending the oscillator alongside the boat to avoid its being in the path of air bubbles or foam from the bow. These interfere with sound transmission in water. To secure preliminary data, one engineer, thoroughly familiar with the instrumental equipment, can, with the aid of a launch runner and one deckhand, obtain in one hour enough data in a harbor to keep a draftsman busy plotting soundings the rest of the day, assuming that sufficient shore markers or range lines have previously been provided. On long river reaches prominent features along the shores can be used as fixes. In some cases aerial photographs can be used to advantage for locating the approximate position of the boat and for plotting the soundings. However, in accurate hydrographic surveys it is necessary to establish ground-survey control lines with suitable markers and range lines. The position of the boat is then established either by transit or by two surveyors on board using sextants to read angles on shore markers. By varying the rate of travel of the recording strip of paper and the speed of the boat, a wide choice of horizontal scales of the recorded soundings is obtainable. It is therefore desirable to select a depth finder that permits changing the rate of travel of the recording paper strip. In most makes, the vertical scale admits of no change. The limit of accuracy of the recorded depths is usually of the order of half a foot, which is sufficient for most purposes.

Night Photography

In estuaries, ebb and tide currents usually take different paths. Permanent records of their locations can sometimes be obtained by setting up a camera on a high point overlooking a sinuous stretch of river reputed to be troublesome for navigation and exposing a photographic plate during a dark night on which illuminated floats register tracks. In the absence of any high ground from which to obtain suitable views it is necessary to erect temporary wooden towers. The method consists in making a first exposure in early evening while the light is still strong enough to produce a faint image of the shore lines. When this is accomplished, the shutter is closed and not opened again until complete darkness prevails. It is then opened and left undisturbed throughout the period covered by the passage of the illuminated floats. Each float consists of a piece of lumber on which a small torch or an electric bulb, fed by dry battery, is mounted. Assuming that, initially, the ebb current has thus registered its track, the camera is left open and undisturbed until flood tide, when another series of illuminated floats is released. In this manner, the positions of both currents are photographed on the same plate. This method can also be used for registering the main path of the entering salt-water wedge, the floats in such a case being motivated by subsurface vanes of the type used in tidewater hydrographic work. Night photography of the kind described originated in hydraulic laboratories where the camera is suspended from a high support with the optical axis vertical. The field method is necessarily confined to oblique exposures, but some excellent results have thus been obtained.

AERIAL PHOTOGRAPHIC MAPS

Aerial photography is a valuable aid in exploratory surveys as well as in the final planning of river projects. The methods used for each of these purposes require separate consideration. For exploration and reconnaissance purposes small-scale mosaics covering large areas are preferable because they provide good orientation for travel and also general information. Shoran, the radar method of triangulation control between ground points and aircraft, provides a satisfactory control for small-scale mosaics of lengths as great as 100 miles or 200 miles. A single flight made on a clear day, at a scale of 1:50,000, will survey a strip from 7 miles to 8 miles wide, on one series of overlapping photographs. These will generally cover the windings of the average river including the entire width of its valley. Enlarged to a scale of 1:10,000 the prints permit detailed study, and from them a map may be drawn by photogrammetry at a scale as large as 1:6,000 (1 in. equals 500 ft) with 25-ft contours in selected areas. A continuous mosaic map compiled in the form of atlas sheets can be made on the original 1:50,000 scale or, if desired, to a scale of 1:20,000 by enlargement. However, a mosaic on the larger scale would require good ground control if it is to serve for the planning of project structures.

A single flight, and the successive uses that can be made of the pictures taken, as outlined here, can be accomplished only by an aerial mapping concern having suitable photographic equipment and a specially built airplane because the required altitude is 25,000 ft or more, depending on the focal length of the camera. At lower altitudes, more than one strip of exposures would be needed, requiring additional flights, and the steps involving enlargement and mosaic building would correspondingly be more complex and costly.

In heavily timbered or jungle areas ground control often has to be limited to occasional astronomically determined points. In regions of moderate relief this method yields fair results but it is less satisfactory in high mountainous areas owing to deflection of the plumb line. The results obtained with the conventional use of shoran show promise that this method may supersede astronomic observations. This statement applies only to rivers whose water surface can be used as a reference plane for altitude and scale.

Photogrammetry has been used successfully for contouring proposed reservoir sites, thus permitting their approximate capacity to be estimated without ground survey. As an example, the capacity of a reservoir site on a river in Mexico, determined from an aerial photographic survey of a 60-mile stretch of river flown without any ground control whatever, was later found by actual survey to be correct within 7%. Improvements in the art of photogrammetry now render closer determinations of this kind practicable except in cases where a proposed reservoir site is largely covered with a dense growth of jungle or timber that effectually conceals the ground surface. The method of drawing contour lines on the tops of the trees and correcting these later for average height of trees is not recommended except when only a rough approximation is desired.

Aerial photographic maps for use in planning and for design purposes are best made to scales of 1:1,000 or 1:2,400 with 5-ft contours. If the photographs taken at the 1:50,000 scale are sharp, they may permit enlargement to scales as great as 1:10,000. However, for the larger scales mentioned here special flights will usually be required covering the specific areas selected for detailed study. If the vegetation is not dense photogrammetry can provide contours at 5-ft intervals but not in stretches where the terrain has very flat slopes. Only a plane-table survey can supply contour lines in such places, and the interval may have to be as small as 2 ft. As previously stated, photogrammetric delineation of contours becomes impracticable whenever the ground surface is obscured by dense vegetation. On the other hand, in steep mountainous terrain photogrammetry is preferable to plane-table surveying as regards time, cost, and accuracy.

In deciding on a suitable horizontal scale for any map, two factors need consideration. If the scale chosen is to enable distances to be scaled accurately, the scale of the negatives must be commensurate with the final accuracy required. If, however, the scale is chosen to cover a wide expanse of working paper for over-all project layouts, a lower order of accuracy will suffice and the desired scale can be achieved through enlargement. By this method one, of course, also enlarges the errors.

A single photograph enlarged to a 1:10,000 scale would be large enough to serve as a plane-table sheet on which to plot accurate contour lines for project study. The topographer in such an event would have to determine the precise scale by reference to distances measured between objects readily identified on the ground. The use of aerial photographs on the plane table has many advantages over the orthodox way of making a map by starting with a sheet of paper having only the control points marked on it. It provides greater accuracy of detail and saves time. Furthermore, plane-table triangulation on aerial photographs is suitable for control for local surveys, as for barge terminals, small harbors, and the location of soundings.

DISCUSSION

Frederic T. Mavis,[3] M. ASCE.—The author has combined in this paper the romance of exploring geographical frontiers with the reality of present-day reconnaissance by engineers who must travel "light." In a literature that is mounting with refinements in methods, instruments, and techniques, it is stimulating to read a paper that encourages the civil engineer to train his eyes to see, his mind to reason and consider, and his whole being to be resourceful and alert.

The writer would emphasize the following excerpts in a different order and possibly with a different meaning from that which may have been intended:

> "* * * Today the limitations confronting the engineer required to report on foreign project possibilities are more severe owing to differences in languages, local customs, and modes of travel. In exploratory work the mode of travel usually determines the type of instrumental equipment to be used. * * * [Some instruments are] too delicate for rough travel, as on horseback or camel-back. A first reconnaissance by airplane or hydroplane is always helpful toward gaining a comprehensive view of the river, its valley and tributary characteristics, and the extent of settlements, roads, or trails. * * * The need for an interpreter in the party is essential. * * * Because no two rivers are alike nothing should be taken for granted, and frequent inquiries are necessary. Native boatmen have a fund of information relating to low-water depths on shoals, the type of craft most used for transporting freight [among other things] * * *."

The foregoing quotation would hardly be out of context either in exploring an uncharted reach of river (as in the paper) or in exploring mathematical "wildernesses" or the applications of nuclear science to engineering practice. However, in scientific exploration it is not always easy to distinguish between "native boatmen" and opportunists who have yet to make their first trip.

The progressive civil engineer must use many devices to acquire information he needs to solve his problem. He may make "a first reconnaissance by airplane" or a flight of fancy, he may follow a hunch, he may experience "rough travel as on horseback or camel-back" through fields of mathematics or science that are unexplored by him.

The reader would do well to look behind the printed word (which in itself is good) and to build his own allegory. He can find stimulation in the paper whether his aim is to make river surveys in unmapped territory or to explore the unknown in the unmapped territory of science and the art of civil engineering.

The author has modestly woven experience, fact, and folklore into a paper whose impact on his readers may be far greater than he had expected. He might have prefaced it with the quotation from Thomas Campbell:

" 'Tis the sunset of life gives me mystical lore
And coming events cast their shadows before."

---

[3] Prof. and Head, Dept. of Civ. Eng., Carnegie Inst. of Technology, Pittsburgh, Pa.

T. H. F. NEVINS.[4]—All engineers who have worked on projects in recently developed countries will appreciate the author's knowledge of the practical difficulties to be overcome. Not the least of these is language, even if one speaks the local tongue. In collecting data from the riverside population one must guard against misinterpretation and frame one's questions in accordance with the local mode of living. The writer, speaking the vernacular, once asked a village headman in Bengal if the Ganges River floodwaters rose to where he and the writer were standing. The headman thought this an adsurdity because the river was two miles away. By asking how high the women tucked up their skirts when planting rice, however, it was deduced that there was one and one half feet of floodwater there.

Although New Zealand has been settled for more than a century, it is only since the passing of the Soil Conservation and Rivers Control Act in 1941 that there has been general widespread activity on river-control schemes. Early hydrological records are meager and much of the investigation work has had to be done as for "unmapped territory." First-class aerial photographs are available and much use is made of the work of Mr. Lacey.[2, 5, 6] Several of Mr. Lacey's relationships have been checked against observed values in New Zealand and found to be in reasonable agreement.

In using Eq. 1 it is sometimes difficult to establish the regime width of channel, and when aerial photographs are available a more convenient approach is by means of the minimum radii of stable bends in alluvium. A. P. Grant[7] expresses this radius r, in feet, as

$$r = 11\sqrt{Q} \qquad (2)$$

When marks enable a reasonable estimate to be made of a bank-full flood gradient in incohesive alluvium, the Lacey formula—$V = 16\, R^{2/3} S^{1/2}$—is a valuable reconnaissance aid.

For velocity observations bamboo poles make useful floats and are often readily obtainable in tropical countries. They can be weighted at one end to submerge them through much of the depth of the water. Their speed then approaches the mean velocity for the vertical filament in which they travel.

The author's slope-competence-depth relationship is a notable contribution and will receive further attention in New Zealand, where rivers are short and many carry shingle all the way to the sea. It is immediately apparent that no New Zealand river carrying shingle in any quantity is tranquil as few rivers transport stones at slopes of less than from 5 ft to 6 ft per mile. Unfortunately, the writer has few data on the largest rolling diameter, local observations being concentrated on the mean diameter. In the few checks it has been possible to make there is a reasonable agreement with the torrential curves (Fig. 1(*b*)).

---

[4] Soil Conservation and Rivers Control Council, Wellington, New Zealand.

[5] "Regime Flow in Incoherent Alluvium," by Gerald Lacey, *Publications No. 20*, Central Board of Irrig., India, July 18, 1930.

[6] "A General Theory of Flow in Alluvium," by Gerald Lacey, *Journal*, Inst. of C. E., London, No. 1, November, 1946, pp. 16–47.

[7] "Channel Improvements in Alluvial Streams," by A. P. Grant, *Proceedings*, New Zealand Inst. of Engrs., Vol. XXXIV, 1948, pp. 231–304.

Chesley J. Posey,[8] M. ASCE.—The profession is indebted to Mr. Matthes for presenting in this paper a host of valuable items of information that only an engineer of his experience and scientific ability could have accumulated. At one point the author's logic eludes the writer who has supposed that there is no reason to expect appreciable superelevation of the midstream water surface of even the swiftest stream unless the cross-sectional shape is changing. This case seems to be ruled out by the stipulation that "the (V/V_{cs})-method is applicable only to straight reaches between well-defined parallel banks * * *."

In measuring currents in models with the aid of photography it is sometimes impossible to tell in which direction a float moved along the streak recorded on the photograph. The writer has described a method for circumventing this difficulty by means of a flash at or near the end of the time interval of the exposure.[9] Possibly some variant of this technique could be used with actual estuaries.

Edward Kuiper[10].—The interesting treatment of short-cut river survey methods by Mr. Matthes was greatly appreciated. During hydrometric surveys on the Assiniboine River and the Saskatchewan River in Canada, the writer had the opportunity to test similar methods and came to conclusions which strongly confirmed the findings of Mr. Matthes. By analyzing numerous current-meter measurements, it was also found that the ratio between the average velocity and the maximum surface velocity was roughly 0.8.

When timing the velocity of driftwood through a particular length of river channel became difficult because of the inaccessibility of the river banks in which the distance had to be laid out, the following method was used. The boat was kept floating on the river in the middle of the current. The velocity was determined by timing the progress of the boat on aerial photographs for several miles. At the same time, the maximum depth was determined by continuous sounding. Because the scale of the aerial photographs was known the width of the river and the length of the timed section could be determined. By multiplying the velocity of the boat by a factor of 0.8 the mean velocity was estimated. By multiplying the average sounded depth by a factor of 0.66 the mean depth was estimated. By multiplying the mean velocity by the mean depth and the mean width from the photographs the estimated discharge was determined. It was recognized that the result could be as much as 30% in error, but failing more accurate measurements such a rough estimate was often valuable.

A short method of determining the approximate sediment concentration in a river was devised, based on a method that is reported to be used in Russia. A disk, painted white, is attached to a stick or pole and submerged in the river. The maximum depth at which the disk is visible is measured on the pole with a tape. When a few suspended-sediment samples taken during medium, extreme low, and high measurements of visibility are analyzed in the laboratory, a rating curve relating visibility to sediment concentration can be composed.

---

[8] Head, Dept. of Civ. Eng., State Univ. of Iowa, Iowa City, Iowa, and Director, Rocky Mountain Hydr. Lab., Allenspark, Colo.

[9] "Photographic Technique for Recording Direction of Surface Currents in Models," by C. J. Posey, *Civil Engineering*, Vol. 9, 1939, p. 619.

[10] Senior Hydr. Engr., P. F. R. A., Dept. of Agriculture, Canada.

The writer cannot quite agree with the method that Mr. Matthes proposed for determining the river gradient by measuring the largest diameter of the river bed material. First, the slope of a river depends not only on the size of the largest bed-material particles but also on the gradation of the bed material and on the quantity of sediment that is transported. It would seem, therefore, that a unique relationship between the largest rolling diameter and the slope of the river cannot exist. On the Saskatchewan River, for instance, it was found at the head of the delta area that the largest rolling diameter was approximately 10 mm, the depth of flow 20 ft, and the slope 1 ft per mile. In the middle of the delta area, the largest rolling diameter was approximately 2 mm, the depth of flow 40 ft, and the slope 0.25 ft per mile. These data do not fit Fig. 1.

Instead of using the bed-material diameter as an index, it may be possible to estimate the slope of the river by using velocity measurements and the Manning formula. If the maximum surface velocity and the maximum depth are measured as discussed before, the average velocity and hydraulic radius can be determined by multiplying the results by 0.8 and by 0.66, respectively. If the observer is trained in estimating the hydraulic roughness of the channel on the basis of the appearance of the river and the composition of the bed material, the slope of the river can be simply computed.

If a current meter is available, a more refined method can be followed. This method is based on the logarithmic velocity formula:

$$V_y = 33 \log 30 \frac{y\,x}{K_s} \sqrt{R\,S} \dots\dots\dots\dots\dots\dots\dots (3)$$

in which V_y equals the velocity at distance y from the bed; y equals the distance from the bed; x equals a parameter; K_s equals the roughness of the bed; R equals the hydraulic radius; and S equals the slope of the river.

When this equation is solved for two values of y that differ by a factor of 10 in magnitude and the two equations are subtracted, the following equation remains:

$$V_{y10} - V_{y1} = 33 \sqrt{R\,S} \dots\dots\dots\dots\dots\dots\dots (4)$$

This equation can be solved for S simply by measuring the velocity near the surface of the river and at one tenth of the depth measured from the bottom. By subtracting these two values and after substituting for R the measured depth times 0.66, the value for S can be quickly computed.

Both methods have been applied to several observations on the Saskatchewan River. Errors of 100% in the slope estimate were possible, especially if it was assumed that only the velocity and depth at one vertical were known. Because it seems that Fig. 1 also contains some degree of error it may be of advantage to apply all three methods in a particular case. Agreement of the three answers would be a strong indication that the slope estimate was nearly correct.

GERARD H. MATTHES,[11] HON. M. ASCE.—The discussions have contributed valuable information derived from actual experience. They have been greatly appreciated by the writer and they have impressed upon him the need for clarifying the limitations besetting the relationships between slope, depth, and the rolling diameter (Fig. 1). These relationships are strictly applicable only to rivers whose bed load has suffered no loss by interception when passing through lakes or by flow diversions of any kind. Furthermore, they are applicable only to rivers whose bank-full flow is carried within a channel free from dams, islands, split-channel conditions, and flow diversions, whether into floodways, head races of power developments, or irrigation canals. These all rob the main channel of bed load. The rather severe limitations cited here were kept in mind by the writer whenever he made searches for bed-load specimens. In the course of his endeavors he discovered, first in the Mississippi River, and later in the Sacramento River (before any high dams were built on the latter) that a low swale across the narrow neck of a bend afforded unusual opportunities for finding coarse bed-load material. The reason is that water diverted through such a swale during a high flood stage consists mainly of bottom water plus bed load. The significance of bed-load diversions of this kind was first made clear by laboratory studies conducted by H. Thoma at Munich in 1919, confirmed by Th. Rehbock[12] in 1922 in the hydraulic laboratory at Karlsruhe, and conducted in considerable detail in 1932 at the U. S. Waterways Experiment Station at Vicksburg, Miss., at the writer's request. These experiments demonstrated that a 50% flow diversion may carry with it as much as 80% of the river's bed load. These experiments revealed further that, at a sharp river bend, a 10% flow diversion made along the convex bank entrained as much as 90% of the bed load. In all these cases it was found that the swift top water, owing to its momentum, suffered no appreciable diversion, the water diverted being chiefly bottom water carrying the bulk of the bed load. The point raised by Mr. Kuiper to the effect that the largest rolling diameter of gravel found by him in the lower reaches of the Saskatchewan River did not agree with the relationships shown in Fig. 1 is quite understandable when account is taken of the fact that many of the Saskatchewan River's tributaries are noted for the large lakes that they traverse. These tributaries are thus prevented from supplying coarse bed-load material to the parent stream. This consideration particularly affects the lower reaches of the river. Mr. Kuiper's methods of estimating mean velocity, mean depth, and discharge from a boat floating down the axis of the current are ingenious and thoroughly practical and emphasize the usefulness of aerial photographs in exploratory river surveys.

Mr. Posey's method of establishing by means of a flash the time intervals during photographic recording of floats in model experiments is simple and worthy of adoption elsewhere. Mr. Posey questions the occurrence of superelevation of a stream's water surface along the axis of flood flow, except where the channel's cross section changes, as at bends. The writer has observed noticeable superelevation in straight reaches of many streams. During a sudden rise in a mountain stream in California, witnessed by him, the upward thrust along the axis of swiftest flow not only raised the central water surface appreciably, but lifted small boulders to its surface at intervals. A flood in Cherry Creek in Denver, where its channel is straight and confined between concrete walls, afforded the writer an opportunity to note the central rise of the water surface, which was sufficient to hide from view the top of the concrete wall along the opposite side. Some conception of what occurs within the cross section of a torrential stream in flood is made apparent by watching a mud flow descend from a steep ravine into the plain—a common occurrence down the front of the Wahsatch Mountains in Utah. Not only is the center of a mud flow appreciably higher than its edges, but large rock fragments are forced upward within it and ride on its bulging surface for some distance before sinking out of sight. The nature of this phenomenon needs study, but it presents many practical difficulties for reproduction in a laboratory.

---

[11] Cons. Hydr. Engr., New York, N. Y.

[12] "Hydraulic Laboratory Practice," edited by John R. Freeman, ASME, 1929, pp 179-180.

The contribution made by Mr. Nevins is particularly welcome as it sums up in a measure the concensus of 15 years of experience of the highly trained staff of river engineers of New Zealand's Soil Conservation and Rivers Control Council, whose exclusive task concerns the control of some of the world's most unusual rivers. Their bed loads consist preponderantly of shingle (slab rock); hence they lack, unfortunately, the rolling-diameter factor needed for plotting in Fig. 1. Strangely, these rivers, upon debouching into the coastal plains, build equally well-shaped meanders as do rivers transporting sand and gravel. Mr. Nevins' reference to the formula for minimum radii of stable bends in alluvium (Eq. 2), recommended by A. P. Grant, is worthy of note by American river engineers. Mr. Grant's works establish him as one of the ablest river engineers of his time. Eq. 2 has its practical applications in connection with river surveys in unmapped territory, as pointed out by Mr. Nevins.

AMERICAN SOCIETY OF CIVIL ENGINEERS
Founded November 5, 1852
TRANSACTIONS

Paper No. 2820

NONUNIFORM TORSION OF PLATE GIRDERS

By Gerald G. Kubo,[1] A. M. ASCE, and Bruce G. Johnston[2] and William J. Eney,[3] Members, ASCE

With Discussion by Messrs. DeForest A. Matteson, Jr.; and Gerald G. Kubo, Bruce G. Johnston, and William J. Eney

Synopsis

As one part of a comprehensive investigation of the torsional behavior of built-up structural members, a group of full-size plate-girder specimens were tested under nonuniform torsion conditions. The measured stresses and angular distortions were compared with computed values based on available theories. It was found that the theory of S. Timoshenko agreed closely with experimental results for the rolled beam and for the plate girders with relatively high ratios of web thickness to flange thickness. However, the theory was inadequate when applied to specimens with a low ratio of web thickness to flange thickness, for which the web deformation effect is significant.

A procedure based on the compatibility of test data, by which measured web distortions and flange distortions were used as a basis for computing the flange bending stresses, established the validity of a suggested grouping of section properties for plate girders. Subsequent application of the theory of J. N. Goodier and M. V. Barton, in which is considered the web-deformation effect, indicated that the method can be successfully adapted to plate girders. The effect of a reduction in the torsion constant under nonuniform-torsion loading was also investigated.

Introduction

The behavior of members of solid section under uniform torsion and nonuniform torsion has been studied by many investigators. Most of the theories

---

Note.—Published, essentially as printed here, in June, 1954, as *Proceedings-Separate No. 449*. Positions and titles given are those in effect when the paper or discussion was approved for publication in *Transactions*.

[1] Associate Prof. of Civ. Eng., New York Univ., New York, N. Y.; formerly Research Associate, Fritz Eng. Lab., Lehigh Univ., Bethlehem, Pa.

[2] Prof. of Structural Eng., Univ. of Michigan, Ann Arbor, Mich.; formerly Director, Fritz Eng. Lab., Lehigh Univ., Bethlehem, Pa.

[3] Prof. and Head, Dept. of Civ. Eng. and Mechanics, and Director, Fritz Eng. Lab., Lehigh Univ., Bethlehem, Pa.

developed for rolled beams have been checked experimentally—a notable exception being the effect of web deformation on beams subjected to nonuniform torsion. The entire field of built-up members under torsion has only recently been systematically investigated.

A comprehensive study of full-size plate girders under torsion loading was undertaken at the Fritz Engineering Laboratory of Lehigh University (Bethlehem, Pa.). A special torsional testing machine had been designed and built for this purpose.

The first phase of the program, covering the uniform torsion of built-up structural members, was completed by F. K. Chang, A. M. ASCE, and one of the writers.[4] The third phase was based on the tests[5] involving combined bending and torsion, performed at Swarthmore College (Swarthmore, Pa.) with the cooperation of Samuel T. Carpenter, M. ASCE.

This report, which deals with the nonuniform-torsion problem of plate girders, completes the second phase. The main objectives of the writers were to compare the theoretically predicted behavior with observed behavior and to determine the modifications which were indicated by the characteristics of the built-up section.

SUMMARY OF TORSION THEORY

Classification of Torsion.—The development of the torsion theory for structural members is thoroughly documented. Following the pioneer work of St. Venant,[6] major contributions have been made by L. Prandtl,[7] S. Timoshenko,[8,9] and many others. The following review of pertinent highlights of the available background material forms a basis for the present investigation.

A twisted structural member is considered to be in a state of uniform torsion when the angle of twist per unit length is constant over portions subjected to constant torque. Because longitudinal warping of circular sections is insignificant these sections will be in uniform torsion regardless of the condition of end restraint. The terms "pure torsion," "simple torsion," and "St. Venant torsion" have also been used to designate this condition in which only transverse torsional shear stresses exist over the cross section.

Noncircular sections when twisted undergo longitudinal warping as well as angular distortions. Plane sections before twisting do not remain plane after twisting. If this warping tendency is not restrained, the member will exhibit a constant unit angle of twist and will therefore be subjected to uniform torsion. If, however, the warping distortion is arrested in any way, longitudinal normal stresses are produced in addition to the torsional shear stresses. The angle of twist per unit of length will no longer be constant. Therefore, nonuniform torsion is considered to exist in a member of noncircular section with restraint against warping.

---

[4] "Torsion of Plate Girders," by F. K. Chang and Bruce G. Johnston, *Transactions*, ASCE, Vol. 118, 1953, p. 337.

[5] "Combined Bending and Torsion of Plate Girders," by G. G. Kubo, S. T. Carpenter, W. J. Eney, and B. G. Johnston, *Report*, Inst. of Research, Lehigh Univ., Bethlehem, Pa., 1954.

[6] "De la torsion des prismes," by St. Venant, *Memoires*, l'Académie des Sciences, Paris, Vol. XIV, 1855.

[7] "Zur Torsion von prismatischen Staben," by L. Prandtl, *Physikalische Zeitschrift*, Vol. IV, 1903, p. 758.

[8] "Theory of Bending, Torsion and Buckling of Thin-Walled Members of Open Cross Section," by S. Timoshenko, *Journal*, Franklin Inst., April, 1945.

[9] "Strength of Materials," by S. Timoshenko, Pt. II, D. Van Nostrand Co., Inc., New York, N. Y., 2d Ed., 1941.

The behavior under torsion of open sections such as I-beams and plate girders is significantly altered by certain conditions of support and loading which introduce longitudinal restraint. Some common cases of nonuniform torsional loading with and without vertical bending are as follows: (1) A cantilevered beam under shaft torque loading, (2) a cantilevered beam with eccentrically applied transverse loading, (3) a simply supported beam subjected to a twisting couple at some intermediate point, and (4) a simply supported beam with an eccentrically applied transverse load.

Uniform-Torsion Theory.—The relationship between the applied torque, M, and the angular distortion for membets under uniform torsion is expressed by

$$M = K\,G\,\frac{d\psi}{dz} = K\,G\,\theta \ldots\ldots\ldots\ldots\ldots\ldots \quad (1)$$

in which K is the torsion constant, in inches^4; G, the modulus of elasticity in shear, in pounds per square inch; ψ, the angle of twist, in radians; z, the variable distance along the longitudinal axis, in inches; and θ, the angle of twist per unit length, in radians per inch.

The torsion constant is a function of the geometry of the cross section and can be computed or evaluated experimentally. The value for a narrow rectangle as developed by St. Venant is

$$K = \tfrac{1}{3}\,w\,t^3 - 0.21\,t^4 \ldots\ldots\ldots\ldots\ldots\ldots \quad (2)$$

in which w is the width and t is the thickness.

A wide-flange beam with parallel-sided flanges can be considered as an aggregation of three component rectangles. The end loss effect, represented by the last term of Eq. 2, can be neglected in design computations because it is small and offset by other compensating factors.

The torsion constant can be evaluated experimentally for solid sections by use of the membrane analogy proposed by Mr. Prandtl.[7] This technique has been used by G. I. Taylor and A. A. Griffith,[10] G. W. Trayer and H. W. March,[11] and by Inge Lyse, A. M. ASCE, and one of the writers[12] to check the torsion constant for a wide range of structural sections.

Another laboratory procedure for evaluating K is to subject the member to uniform torsion. The torque is plotted against the unit angle of twist. From Eq. 1 the torsional rigidity $K\,G$ will equal the slope of the straight-line part of the curve.

The uniform-torsion problem for built-up structural members held together by bolts, rivets, or welds has been investigated by I. Madsen,[13] M. ASCE, and others.[4] A typical member of a plate-girder section would have a torsional rigidity intermediate between the extreme limits of separate-action and solid-section behavior—a considerable difference in most cases.

---

[10] "The Use of Soap Films in Solving Torsion Problems," by G. I. Taylor and A. A. Griffith, *Reports and Memoranda No. 333*, Great Britain Rep. and Mem., Aeronautical Research Comm., London, Vol. 3, 1917–1918.

[11] "The Torsion of Members Having Sections Common in Aircraft Construction," by G. W. Trayer and H. W. March, *Report No. 334*, National Advisory Committee for Aeronautics, Washington, D. C., 1939.

[12] "Structural Beams in Torsion," by Inge Lyse and Bruce G. Johnston, *Transactions*, ASCE, Vol. 101, 1936, p. 857.

[13] "Report of Crane Girder Tests," by I. Madsen, *Iron and Steel Engineer*, Vol. 18, November, 1941, pp. 47–95.

At the upper limit of torsional rigidity, the cross section would be equivalent to that of a rolled beam of the same external dimensions. At the lower limit, the separate-action K_S-value is computed on the premise that all elements of the cross section are twisted through the same angle, but independently. Relative warping distortions are not restrained by the connectors. For a plate girder dimensioned as shown in Fig. 1(*a*) with *n* cover plates of equal thickness per flange, the torsion constant K_S is expressed by

$$K_S = \frac{1}{3}\left[2\,n\,w\,t^3_F + h\,t^3_W + 4\left(e + f + m + \frac{b - t_W}{2}\right) t^3_A\right] \ldots \quad (3)$$

Because the elements of a bolted or riveted plate girder are actually connected along well-defined gage lines and interplane friction exists, the value of the so-called integral-action constant, K_I, must be between the two extreme values. Based on the concept proposed by Karl de Vries,[14] M. ASCE, it is assumed that the core portion in each flange acts as a solid section whereas the remainder of the section acts as separate rectangles when the section is twisted. The core is assumed to be the T-section formed between the outside pair of gage lines in the flange and the outside gage line in the downstanding leg of the flange angle as shown in Fig. 1(*b*).

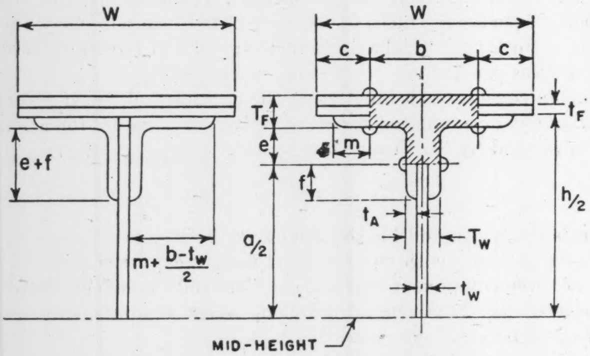

(*a*) SEPARATE ACTION K_S (*b*) INTEGRAL ACTION K_I

FIG. 1.—THE TORSION CONSTANT, *K*

As the integral-action constant for use in design, the following formula was proposed:[4]

$$K_I = \frac{2}{3} b\,T^3_F + \frac{2}{3} e\,T^3_W + \frac{4}{3} n\,c\,t^3_F + \frac{4}{3} m\,t^3_A + \frac{4}{3} f\,t^3_A + \frac{1}{3} a\,t^3_W \ldots \quad (4)$$

---

[14] "Strength of Beams as Determined by Lateral Buckling," by Karl de Vries, *Transactions*, ASCE, Vol. 112, 1947, p. 1245.

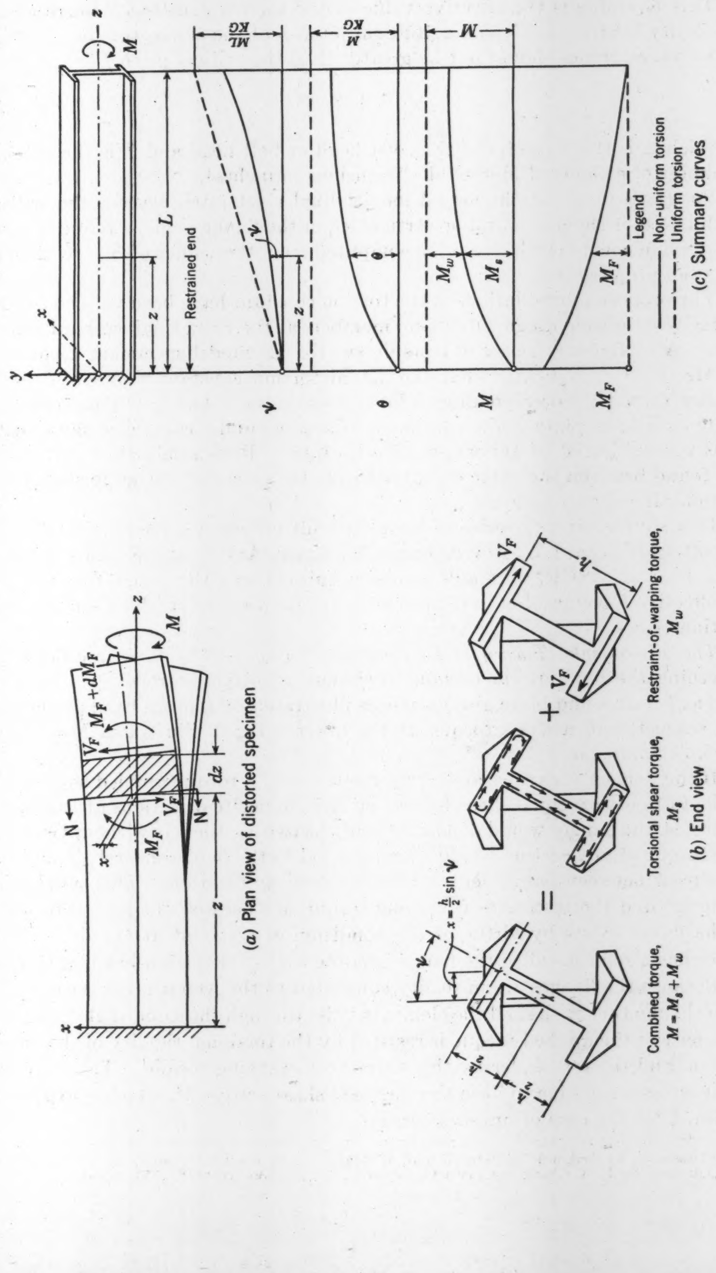
x
z
N
N
x
M_F
V_F
V_F
$M_F + dM_F$
dz
z
M
(a) Plan view of distorted specimen
$x = \frac{h}{2} \sin \psi$
ψ
$\frac{h}{2}$
$\frac{h}{2}$
=
+
V_F
V_F
h
Combined torque, $M = M_s + M_w$
Torsional shear torque, M_s
Restraint-of-warping torque, M_w
(b) End view
y
x
z
L
Restrained end
M
z
ψ
z
$\frac{ML}{KG}$
ψ
θ
θ
$\frac{M}{KG}$
M
M_w
M_s
M
M_F
M_F
Legend
Non-uniform torsion
Uniform torsion
(c) Summary curves

FIG. 2.—THE TIMOSHENKO THEORY—WF BEAM UNDER NONUNIFORM TORSION

This K_I-value is the effective value of the torsion constant if longitudinal continuity is insured. The longitudinal pitch p of the connectors in both legs of the flange angles should not be greater than the critical pitch p'—

$$p' = A + T \quad \text{(5)}$$

in which A is the diameter of the rivet head or bolt head and T is the over-all thickness of connected plates (all dimensions in inches).

For cases in which the actual longitudinal rivet pitch exceeds the critical pitch in either the horizontal or vertical leg of the flange angle, a reduced effective torsion constant which can be computed from the values of K_S, K_I, and p' has been proposed.[4]

The proposed formulations of the torsion constant have been verified experimentally for a wide range of built-up members at the Fritz Engineering Laboratory. A preliminary series of tests on small-scale model specimens performed by Mr. Madsen indicated that the actual torsion constant was considerably smaller than the corresponding solid-section value. Later, a representative group of full-size plate-girder specimens fabricated under controlled shop conditions was subjected to uniform-torsion loading.[4] Reasonably close agreement was found between the value computed from the proposed design formulas and that obtained experimentally.

In a supplementary series of tests on built-up column sections, Arthur P. Jentoft and Richard W. Mayo, Junior Members, ASCE, and E. Russell Johnston, Jr.,[15] M. ASCE, were able to check quite closely the design formulas for the effective K-values that have been proposed for members without longitudinal continuity.

The Timoshenko Theory of Nonuniform Torsion.—The basic relationships governing the nonuniform torsional behavior of bisymmetrical open sections such as I-beams and plate girders can be illustrated by a beam fixed at one end and subjected to a shaft torque at the other. Fig. 2 illustrates Mr. Timoshenko's approach.

If the flanges were separated from the web and a torque applied as a couple in the form of two equal shear forces acting in opposite directions at the flange centroids, the flanges would deflect laterally as two cantilevers without twisting. The torque at any section would then be equal to the flange shear V_F times the distance h between flange centroids before load application. This couple will be designated the restraint-of-warping torque M_w because the lateral bending of the flange exists by virtue of the condition of restraint at one end. This factor has also been called the flange-bending torque or torsion-bending torque.

Because the flanges are in reality connected to the web it is assumed in the Timoshenko theory that all the elements twist through the same angle. Therefore, part of the applied torque is resisted by the torsional rigidity of the whole section, and the remainder by the restraint-of-warping torque. The torsional shear stresses combine to form the torsional shear torque M_s which is expressed by Eq. 1 for the case of uniform torsion.

---

[15] Discussion by Arthur P. Jentoft, Richard W. Mayo, and E. Russell Johnston, Jr., of "Torsion of Plate Girders," by F. K. Chang and Bruce G. Johnston, *Transactions*, Vol. 118, 1953, p. 383.

The relationship between the angle of twist and the lateral bending of the flange is based on the geometry of the twisted section. Using the notation shown in Fig. 2, the lateral displacement of the flange centroid can be written for small angles of twist ψ as

$$x = \frac{h}{2} \sin \psi \approx \frac{h}{2} \psi \quad \text{(6)}$$

By introducing the elementary beam theory and certain substitutions, the equilibrium equation of torsion can be written as

$$M = M_s + M_w = K\,G \frac{d\psi}{dz} - \frac{E\,I_y\,h^2}{4} \frac{d^3\psi}{dz^3} \quad \text{(7)}$$

in which $K\,G$ is the torsional rigidity and $E\,I_y$ is the flexural rigidity about the vertical axis.

The general solution together with the assumed boundary conditions leads to the following expressions for the angular distortions:

$$\psi = \frac{M}{K\,G\,r} [r\,z - \sinh r\,z + \tanh r\,L\,(\cosh r\,z - 1)] \quad \text{(8)}$$

and

$$\theta = \frac{d\psi}{dz} = \frac{M}{K\,G} \left[1 - \frac{\cosh r\,(L - z)}{\cosh r\,L} \right] \quad \text{(9)}$$

in which r equals $\frac{2}{h}\sqrt{\frac{K\,G}{E\,I_y}}$.

The flange bending moment from which the bending stresses can be computed is expressed by

$$M_F = \frac{M}{r\,h} \left[\frac{\sinh r\,(L - z)}{\cosh r\,L} \right] \quad \text{(10)}$$

The web shear stress at a point is the torsional shear stress at that point. The flange shear stress at any point is determined by superimposing the corresponding transverse shear and torsional shear stresses. The variation of representative functions along the span for the cantilevered I-beam under nonuniform-torsion loading is summarized in Fig. 2(*c*).

The uniform-torsion solution is also presented for comparison. The net effect of the restraint of warping is to reduce the angular distortions and to increase the longitudinal stresses in the flange.

The Goodier-Barton Theory of Nonuniform Torsion.—It has been explained by J. N. Goodier and M. V. Barton[16] that the Timoshenko solution has certain limitations inherent in its derivation. For example, the division of torque at the free end cannot be modified to fit different boundary conditions. Certain of these limitations are removed by the Goodier-Barton theory in which the effect of web deformation on the torsional behavior of I-beams is considered.

---

[16] "The Effects of Web Deformation on the Torsion of I-Beams," by J. N. Goodier and M. V. Barton, *Journal of Applied Mechanics*, March, 1944, p. A-35.

The twisting of an I-beam under nonuniform-torsion loading is geometrically related to the lateral deflection of the flange. Such deflection implies a nonzero fourth derivative corresponding to some distributed load applied to the flange by the web. The interacting forces between web and flange—the lateral load q per unit of length and the twisting moment m per unit of length—cause the web to deform as a plate into an S-curve. This web deformation, shown highly magnified in Fig. 3, is accompanied by a reduction in the flange angle of twist by an angle α equal to the web-chord rotation.

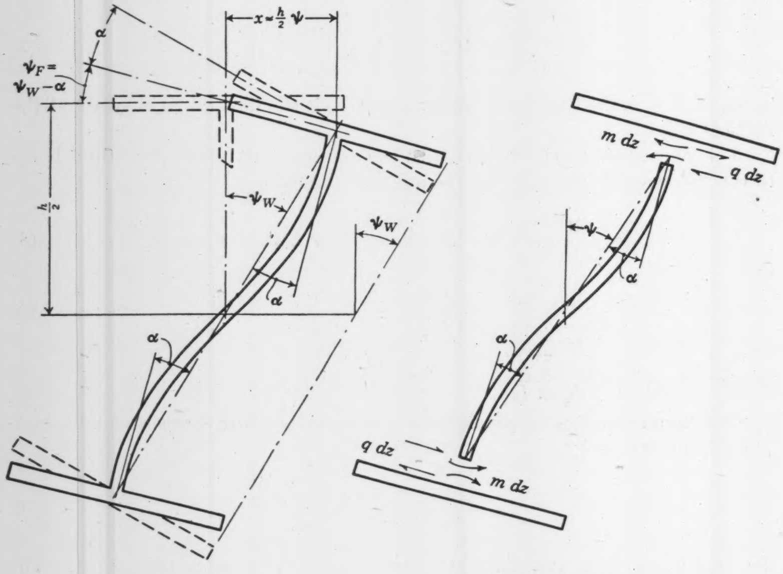

(*a*) Angle of twist with web deformation

(*b*) Interaction forces per unit of length

Fig. 3.—The Goodier-Barton Theory—WF Beam Under Nonuniform Torsion

It is demonstrated that the relative dimensions of the web and flange influence the quantitative division of applied torque between restraint-of-warping shear and torsional shear.

By careful consideration of the lateral bending and twisting of the flange and of the bending and twisting of the web as a plate, Messrs. Goodier and Barton have deduced a set of simultaneous differential equations in terms of the angular distortions ψ and α:

$$k_3 h^2 (\psi'' - \alpha'') + k_4 \alpha = 0 \ldots\ldots\ldots\ldots\ldots\ldots (11)$$

and

$$k_1 h^4 \psi^{IV} - k_2 h^2 \psi'' + 2 k_4 \alpha = 0 \ldots\ldots\ldots\ldots\ldots\ldots (12)$$

in which

$$k_1 = \frac{E\,I_y}{4\,K\,G}, \quad k_2 = \frac{K_W}{K}$$

$$k_3 = \frac{K_F}{K}, \quad k_4 = \frac{6\,D_W\,h}{K\,G}$$

and

$$D_W = \frac{E\,t^3_W}{12\,(1 - \mu^2)}$$

in which μ is the Poisson ratio, K_W is the torsion constant for the web, and K_F is the torsion constant for the flange.

By substituting the exponential forms:

$$\left.\begin{aligned} \psi &= C_1\,e^{\lambda z} \\ \alpha &= C_2\,e^{\lambda z} \end{aligned}\right\} \qquad (13)$$

and

in the system of simultaneous differential equations and setting the determinant of the coefficients of C_1 and C_2 equal to zero, a quadratic equation in $(\lambda h)^2$ is obtained whose roots are given by

$$(\lambda\,h)^2 = \frac{\mathcal{K}_1}{2}\,(1 \pm \sqrt{1 - \mathcal{K}_2}) \qquad (14)$$

in which

$$\mathcal{K}_1 = \frac{k_2}{k_1} + \frac{k_4}{k_3}$$

and

$$\mathcal{K}_2 = \frac{\dfrac{4\,k_4}{k_1}\left(2 + \dfrac{k_2}{k_3}\right)}{\mathcal{K}^2{}_1}.$$

For any particular specimen the combined dimensionless constants $\mathcal{K}_1$ and $\mathcal{K}_2$ and the two roots $(\lambda\,h)^2$ can be computed from the dimensions and properties of the section. The roots are real or complex depending on whether $\mathcal{K}_2$ is less than unity or greater than unity; I-beam sections with relatively thick webs have been found to yield real roots. When the roots of the quadratic are real, there will be four possible values of λ, designated $\pm\chi$ and $\pm\xi$.

The complete solution for the angle of twist and the flange reduction is

$$\psi = A_1 + A_2\,z + A_3\,e^{\chi z} + A_4\,e^{-\chi z} + A_5\,e^{\xi z} + A_6\,e^{-\xi z} \qquad (15)$$

and

$$\alpha = [k_5\,(\chi\,h)^2 = k_6\,(\chi\,h)^4][A_3\,e^{\chi z} + A_4\,e^{-\chi z}] + [k_5\,(\xi\,h)^2 - k_6\,(\xi\,h)^4][A_5\,e^{\xi z} + A_6\,e^{-\xi z}] \qquad (16)$$

in which $k_5 = k_2/2\,k_4$ and $k_6 = k_1/2\,k_4$.

The arbitrary constants are evaluated by introducing a system of compatible boundary conditions. The "long-beam" solution is based on an assumed condition at the free end which is not attained by the relatively short specimens used in the present investigation.

In the "finite-beam" solution, the specimen is assumed to be rigidly attached at both ends to heavy plates which remain parallel to each other and normal to the longitudinal axis while being twisted through equal angles in opposite directions (Fig. 4).

With the origin at the center of the span, the angular distortions for this special case are expressed by

$$\psi = A_2 z_2 + B_3 \sinh \chi z_2 + B_5 \sinh \xi z_2 \quad \text{(17a)}$$

and

$$\alpha = [k_5 (\chi h)^2 - k_6 (\chi h)^4] B_3 \sinh \chi z_2 + [k_5 (\xi h)^2 - k_6 (\xi h)^4] B_5 \sinh \xi z_2 \quad \text{(17b)}$$

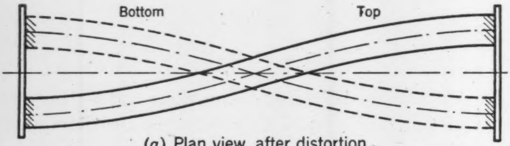

(a) Plan view, after distortion

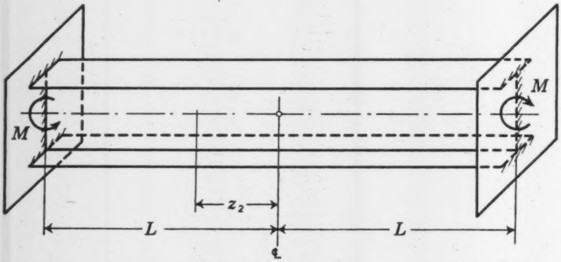

(b) Fixed-ended beam

FIG. 4.—THE FINITE BEAM OF THE GOODIER-BARTON THEORY

From the boundary conditions at the fixed end ($z_2 = L$, $\alpha = \psi' = 0$, and $\psi = \psi_m$), the arbitrary constants A_2, B_3, and B_5 can be evaluated in terms of the maximum angle of twist, ψ_m.

The equilibrium equation of torsion considering web deformation is

$$M = K G \psi' - \tfrac{1}{4} E I_y h^2 \psi''' - 2 K_F G \alpha' \quad \text{(18)}$$

Eq. 18 is used to find ψ_m in terms of the applied torque. When this value is substituted into Eq. 17*a*, the desired angular distortions and stress functions can be evaluated.

EXPERIMENTAL PROGRAM

Test Specimens.—An extensive investigation of the behavior of full-size built-up structural members under uniform-torsion loading was in progress at the Fritz Engineering Laboratory in the summer of 1949. Because the initial tests were kept in the elastic range it was felt that the same specimens could be used in a second series of tests designed to study the behavior of plate girders under nonuniform torsion. Seven specimens were made available for this purpose.

The important features and section properties of the specimens tested are summarized in Table 1. Design and fabrication details are to be found in the uniform-torsion report.[4] All specimens were 14 ft 9 in. long.

The high-strength bolts used in the bolted specimen were all tightened to a value of 300 ft-lb by a calibrated torque wrench to insure integral action in the low-load range. All rivets were machine-driven under controlled shop conditions. Welds were continuous except for those welds used to connect the cover plates to flanges.

The experimental value of the torsion constant K_A, later used in computation T, was obtained from the results of the uniform-torsion tests. The torsion constant $(K_S)_D$ was computed on the assumption of separate-action behavior.

TABLE 1.—SUMMARY OF TEST SPECIMENS

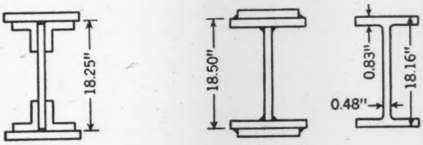

Web plate 18 by ⅜
Flange angles 4 by 3½ by ½
Cover plate 9½ by ⅜

Web plate 17¼ by ⅜
Flange plate 9½ by ⅝
Cover plate 8½ by ½

18 WF 77

Fabrication	Riveted			Bolted	Welded		Rolled
Mark	T1-R	T2-R	T5-R	T3-B	T7a-W	T7b-W	T9-WF
Cover plates per flange	None	1	3	1	None	1	
Test K_A, (in.^{4})	1.86	6.61	17.40	7.42	2.35	6.35	3.83
Computed $(K_S)_D$ (in.^{4}), separate action	1.56	1.87	2.43	1.87		2.35	

Test Apparatus.—The analytical solutions are predicated on the assumption that one end of the beam is completely restrained. This fixed-end condition is extremely difficult to produce externally. The logical arrangement was to attain fixity internally by loading the specimen symmetrically about the center line of the span.

The specimen was simply supported at both ends by web framing angles attached to the end-support plates of the special torsion testing machine. The ends of the specimen were held against twisting by a pair of flange lugs at diametrically opposite corners.

The torsional moment was introduced at the center of the span by a specially designed yoke with cantilevered loading arms. The yoke, when placed around the specimen, was held in position by a series of special fillers, each backed by a matching pair of machined wedges. A schematic sketch of the test setup is shown in Fig. 5(*a*).

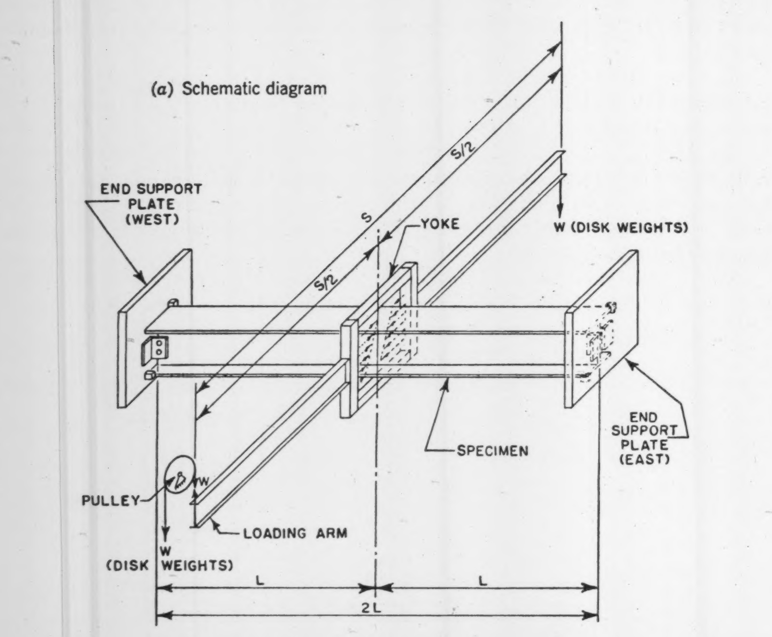

(a) Schematic diagram

(b) General view

S/2
S
S/2
END SUPPORT PLATE (WEST)
YOKE
W (DISK WEIGHTS)
END SUPPORT PLATE (EAST)
SPECIMEN
B
W
PULLEY
LOADING ARM
W
(DISK WEIGHTS)
L
L
2L

FIG. 5.—TEST APPARATUS

Disk weights were suspended directly from the end of one loading arm. An equal force was applied in the opposite direction at the other end by suspended weights attached to the loading arm by a cable passing over a ball-bearing pulley.

Under this arrangement, a specimen was divided into two symmetrical half-spans each subjected to the same shaft torque. No vertical bending loads were introduced. Complete restraint against longitudinal warping was automatically provided at the plane of symmetry for each half. Except for some unavoidable contact friction at the flange lugs, the outer ends were free to warp.

Instrumentation.—Because each specimen was divided into equal halves, strains were measured in one half and angular distortions in the other half (Fig. 5(*b*)).

In order to check the distributions of bending and shear stress, which vary along the span as well as around the section, an extensive network of strain gages was required. Approximately seventy SR-4 strain gages were cemented to each specimen at selected stations.

A 3-in. level bar equipped with a spirit level and an adjustable micrometer screw was used to measure the angle of twist. The portable level bar could be seated in prepared holes provided at the top of the level-bar supports.

Because the angular distortions are not constant along the span, it was necessary to have an integrated system of angle measuring stations. The level-bar supports for both the flange and web were uniformly spaced 11 in. apart along the longitudinal axis of each specimen. For the flange, these supports were tack-welded to the top along the longitudinal center line.

Level-bar supports, if attached directly to the web, would have led to erroneous readings because of web deformation. A more representative value of web twist was determined by basing the angular measurement on the movement of the flange sides. An auxiliary vertical bar, equipped with a hook at the top end, was held tightly against the sides of the flanges by elastic bands. The level-bar support was tack-welded to this vertical bar.

Laboratory Tests.—Most of the preliminary tests, such as tension tests of coupons, had already been performed as part of the uniform-torsion program. For use in computations, the following average values were adopted: $E =$ 29,500 kips per sq in. and $G = 11{,}450$ kips per sq in.

One plate-girder specimen was subjected to a lateral bending test in order to check the computed value of I_y. Because the comparison was favorable, the computed value of I_y was assigned to all specimens.

After a series of "shake-down" runs, the shaft-torque loading was applied to the specimen and removed in increments. Observations were recorded at each stage.

The magnitude of the torque applied to each specimen was limited to a value that would insure elastic behavior. In order to have a basis for comparison among the various specimens, an arbitrary end torque of 40,000 in-lb was established as a standard value and used in the subsequent computations.

The test data were first examined by plotting the increment of strain reading against the corresponding increment of end torque. With the exception of an explainable shift of some readings in the built-up specimens and some irregularity in lightly stressed gages, the test data showed good linearity.

Wherever possible, strain gages were paired so that the average test value could be used. The conversion of SR-4 strain readings to stresses included consideration of the transverse correction.

The level-bar readings were converted to angles of twist by use of the tangent relationship between the micrometer movement and the gage length. The unit angle of twist for a point midway between two adjacent stations was determined by dividing the relative change in the twist angle by the distance between the stations.

ANALYTICAL STUDY OF RESULTS

Comparison of Theories for Rolled Sections.—Because the available theories are based on an ideal solid section, they were first applied to specimen T9, a wide-flange steel beam incorporated in the test program as a control. The solution for the angle of twist was extended to obtain the unit angle of twist in addition to the normal stresses and shear stresses in the web and flange. However, for comparative purposes only the angle of twist and the flange bending-stress variation will be discussed.

The solution based on the Timoshenko theory and on the test value of the torsion constant K_A was designated computation T. The actual distance from the vertical axis to the line of strain gages in the flange was used in the computation of the flange normal stress.

The finite-beam solution of the Goodier-Barton theory was used in this comparative study and is designated computation G-B. The transposition of the computed values from the origin of coordinates at the torsion-free end to the restrained end was required in order to make the results comparable. It was also necessary to divide the test value of the torsion constant for the section into separate portions for the web and flange. The computed and measured values of the flange bending stress are compared graphically in Fig. 6(*a*).

For this specimen, solutions based on the Timoshenko and Goodier-Barton theories yield almost identical σ-values, as predicted by the latter. The web-deformation effect is small in this 18WF77 beam having a relatively thick web. Both computed curves agree closely with the measured values.

The angle-of-twist curves are compared in Fig. 6(*b*). The Timoshenko theory yields one value of angular distortion for the section as a whole whereas the Goodier-Barton theory yields separate values for the web and flange. The boundary conditions assumed in the finite-beam solution are such that the flange reduction angle α is equal to zero at both ends, as is evident from the converging computed curves for twist of the web and flange. The angle α, being the angle by which the flange lags behind the web, is represented by the difference between the twist angles of the web and the flange. The measured values tend to diverge at the free end. This reflects in part the unavoidable local effect of the flange lugs which are used to prevent the section from twisting at the ends. However, at other sections the magnitude of the measured flange reduction angle checks quite closely with the anticipated values. In general, the solid sections represented by the rolled beam and the welded girder without cover plates performed as predicted by the Timoshenko and Goodier-Barton theories.

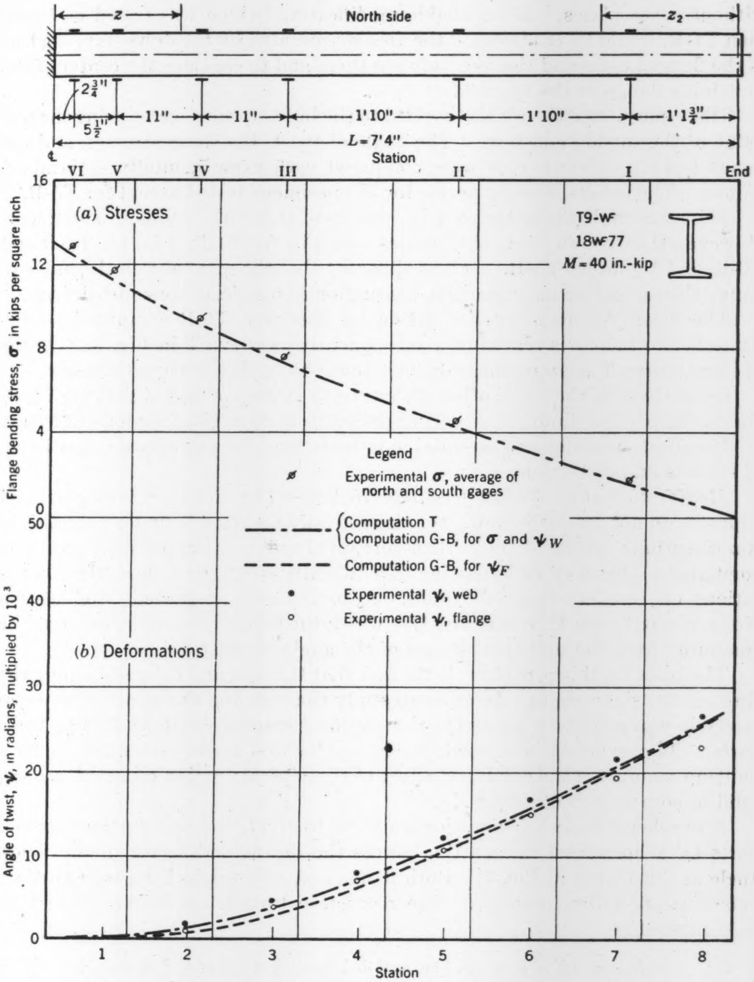

FIG. 6.—COMPARISON AMONG EXPERIMENTAL AND COMPUTED VALUES OF σ AND ψ

Application of Theories to Plate Girders.—For a plate girder, some questions exist as to the proper assumptions regarding section properties because the material is not as compactly arranged as in a rolled beam. The effective height h_e, the distance between flange centroids, is one of the dimensions required. It was found by comparing computed values that h_e may be varied over a limited range without any significant effect on the results. The usual procedure for locating the centroid therefore may be used, except in the case of a plate girder without cover plates. A reasonable modification, which was tested on specimen T1-R, would be to disregard the area represented by the downstanding legs of the flange angles and the web between them and to consider the center of the remaining flange as the centroid.

The Timoshenko theory was applied to the built-up specimens, using the test value of the torsion constant. The angle of twist, the shear stresses, and the flange bending-stress curves were compared with experimentally determined values. The results were favorable for all specimens tested except for T5-R.

The same web thickness of $\frac{3}{8}$ in. was used in all the built-up specimens. However, the over-all flange thicknesses were $\frac{1}{2}$ in. for T1-R, $\frac{7}{8}$ in. for T2-R and T3-B, and 1 $\frac{5}{8}$ in. for T5-R. It was apparent that the ratio of web thickness to flange thickness had an important bearing on nonuniform-torsion behavior.

The flange bending-stress variation for specimen T5-R computed by the Timoshenko theory is reproduced subsequently as curve T in Fig. 9. On the average, curve T is approximately 20% lower than the measured stresses.

On the basis of these and other observations, it was concluded that the Timoshenko theory has limitations when applied to certain plate girders. Certain modifications were deemed essential in order to provide an improved prediction of stresses and distortions.

Modification of the Theory for Plate Girders.—The fact that the actual end supports do not precisely match the theoretically assumed boundary conditions is a disturbing source of error when computed and measured values are to be compared. One way of bypassing this difficulty would be to base the computations on certain observed values. A procedure, designated Modification No. 1, computation H, was devised by which the flange bending stress could be computed from the measured values of the angle of twist.[17]

The basis for this procedure is the fact that the web and flanges do not twist through the same angle. In order to study the web and the two flanges separately it was necessary to divide the section torsional constant K into three parts. As previously developed, the integral-action torsion constant K_I for a built-up member is the combined effect of the separate action constant K_S and solid or core section constant K_C.

A simple yet logical assumption would be to divide the core portion into two parts by a horizontal line cutting across the downstanding leg of the flange angle as illustrated in Fig. 7. Both flange and web would have core portions and separate-action portions. The respective torsion constants would then be expressed as

$$K_F = (K_C)_F + (K_S)_F = \tfrac{1}{3}\, b\, T^3{}_F + \tfrac{2}{3}\, n\, c\, t^3{}_F + \tfrac{2}{3}\, m\, t^3{}_A \ldots\ldots (19a)$$

and

$$K_W = (K_C)_W + (K_S)_W = \frac{1}{3}\, e\, T^3{}_W + \frac{4}{3} f\, t^3{}_A + \frac{1}{3}\, a\, t^3{}_W \ldots\ldots (19b)$$

The torsional shear torque M_s was then expressed in terms of its component parts, $(M_s)_W$ for the web and $(M_s)_F$ for each flange as follows:

$$M_s = (M_s)_W + 2\,(M_s)_F = K_W\, G\, \theta_W + 2\, K_F\, G\, \theta_F \ldots\ldots\ldots (20)$$

---

[17] "Non-uniform Torsion of Plate Girders," by Gerald G. Kubo, thesis presented in 1952 to Lehigh University at Bethlehem, Pa., in partial fulfilment of the requirements for the degree of Doctor of Philosophy.

When the measured values of the unit angle of twist θ are introduced, the torsional shear torque can be evaluated at corresponding points. The restraint of warping torque M_w can then be computed by taking the difference between the applied torque M and M_s. The flange shear V_F is determined by dividing M_w by the effective height h_e. The flange bending-moment curve M_F is based on the fact that the change in bending moment between any two points is equal to the area under the shear curve between the same two points. The flange bending stress is determined from the flexure formula. The sequence of steps taken is shown diagramatically in Fig. 8.

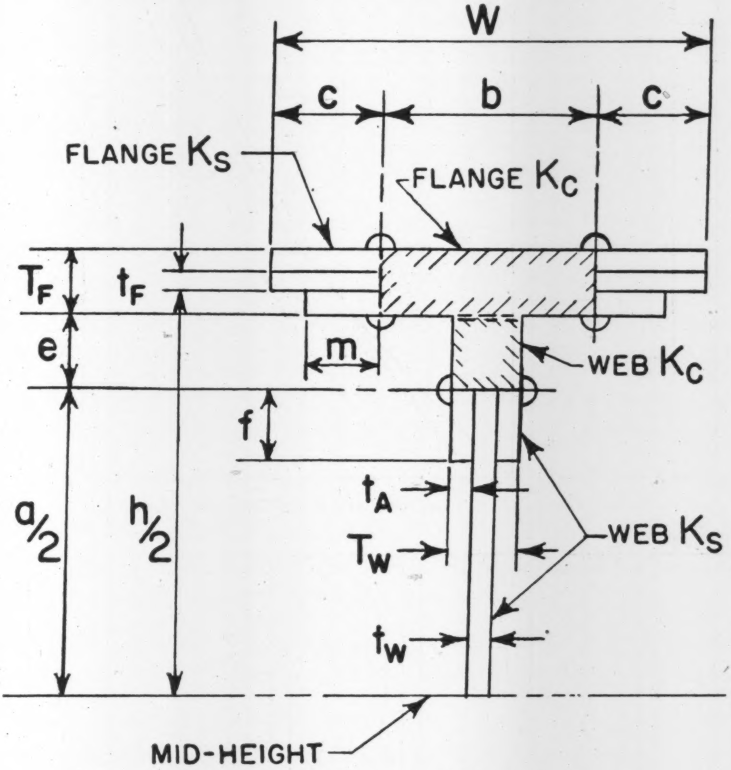

FIG. 7.—DIVISION OF THE TORSION CONSTANT, K

When plotted, the measured values of the unit angle of twist for both flange and web revealed a gradual but decided decrease near the free end. Considering the end supports used in the actual tests, it was assumed that the θ-curves and consequently the M_s-curves both converge to zero as shown by the dotted lines.

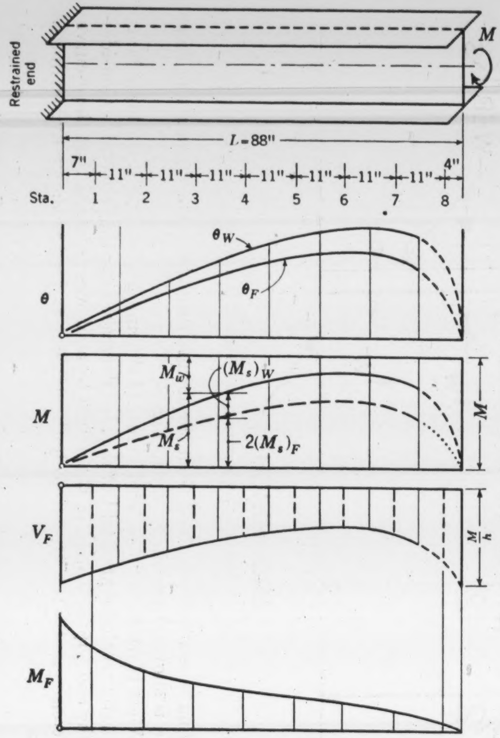
Restrained end
M
L=88"
7"
11"
11"
11"
11"
11"
11"
11"
11"
4"
Sta.
1
2
3
4
5
6
7
8
θ
θ_W
θ_F
M
M_w
$(M_s)_W$
M_s
$2(M_s)_F$
M
V_F
$\frac{M}{h}$
M_F

FIG. 8.—COMPUTATION H, MODIFICATION NO. 1

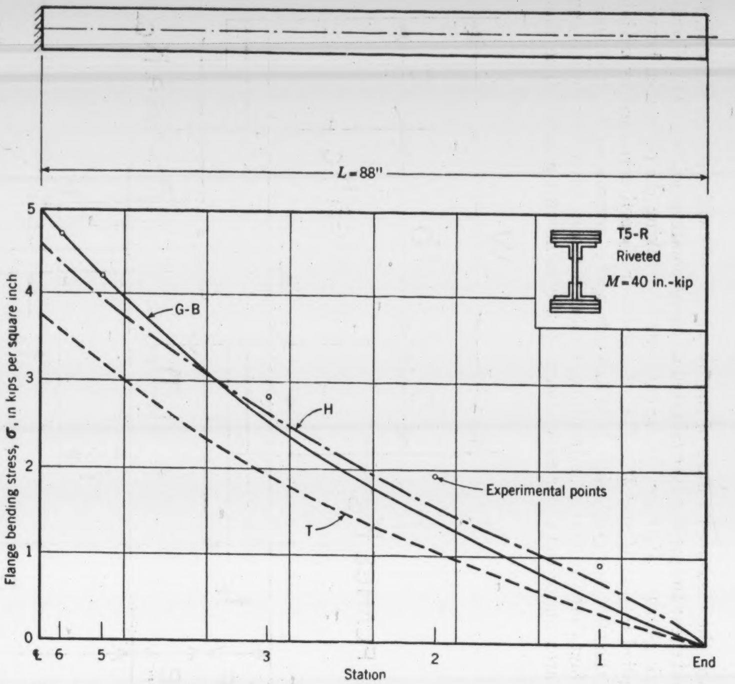

FIG. 9.—COMPARISON AMONG EXPERIMENTAL AND COMPUTED σ-VALUES

The area under the V_F-curve between substations was computed assuming straight-line segments. Beginning at the free end where the bending moment was assumed to be zero, the flange bending moment at the successive stations was computed as the cumulative sum of the shear-curve areas.

This procedure was applied to each of the built-up plate girders tested. The resulting flange bending stress variation was plotted as computation H. An inspection of Fig. 9 for T5-R emphasizes the decided improvement in the check against measured stresses as compared to the solution by means of the Timoshenko theory, even to the unexpected hump near the free end. Similar results were obtained for the other built-up specimens.

This study brought out the fact that the readjustment in the division of torque near the free end and the differential angular distortions of web and flange affect the stress distribution throughout the span. The division of the torsion constant between flange and web previously assumed was found to lead to reasonable results and hence was adopted for use in the subsequent computations.

Application of the Goodier-Barton Theory to Plate Girders.—The finite-beam analysis was applied to the built-up sections under shaft torque with restraint of warping. After the section properties were converted into the specified dimensionless constants, the roots of the characteristic equation were determined. The arbitrary constants were computed from the boundary conditions. The resulting solution for the angular distortions were used to compute the stresses. For all specimens with relatively high ratios of web thickness to flange thickness, the roots were real. Very little difference could be found between solutions based on the Goodier-Barton theory and the Timoshenko theory.

However, for the flange-heavy specimen T5-R, the roots were complex. The finite-beam solution was carried out as outlined by Messrs. Goodier and Barton, but with the following modifications:

1. In Eq. 17*a* for the angle of twist the first arbitrary constant A_2 was considered a complex number rather than a real number.
2. The three equations based on boundary conditions required to evaluate the arbitrary constants were set up in terms of all the real and imaginary parts. Only after the three sets of arbitrary constants had been determined were the imaginary parts discarded on the basis of physical considerations.

The finite-beam solution for the flange bending stress in specimen T5-R is shown in Fig. 9 as curve G-B. The improvement over curve T in the check against measured values is quite marked.

On the basis of this limited investigation it appears that the Goodier-Barton theory should be used in those cases in which the nonuniform-torsion stresses are important or the cross section is of such proportions that the web-deformation effect is accentuated.

Variable Torsion Constant.—For purposes of checking the theory of nonuniform torsion, it was desirable to keep the specimens as simple as possible. Consequently, the cross section and the spacing of connectors were kept constant. However, a plate girder with cover plates of variable lengths will be a case of a

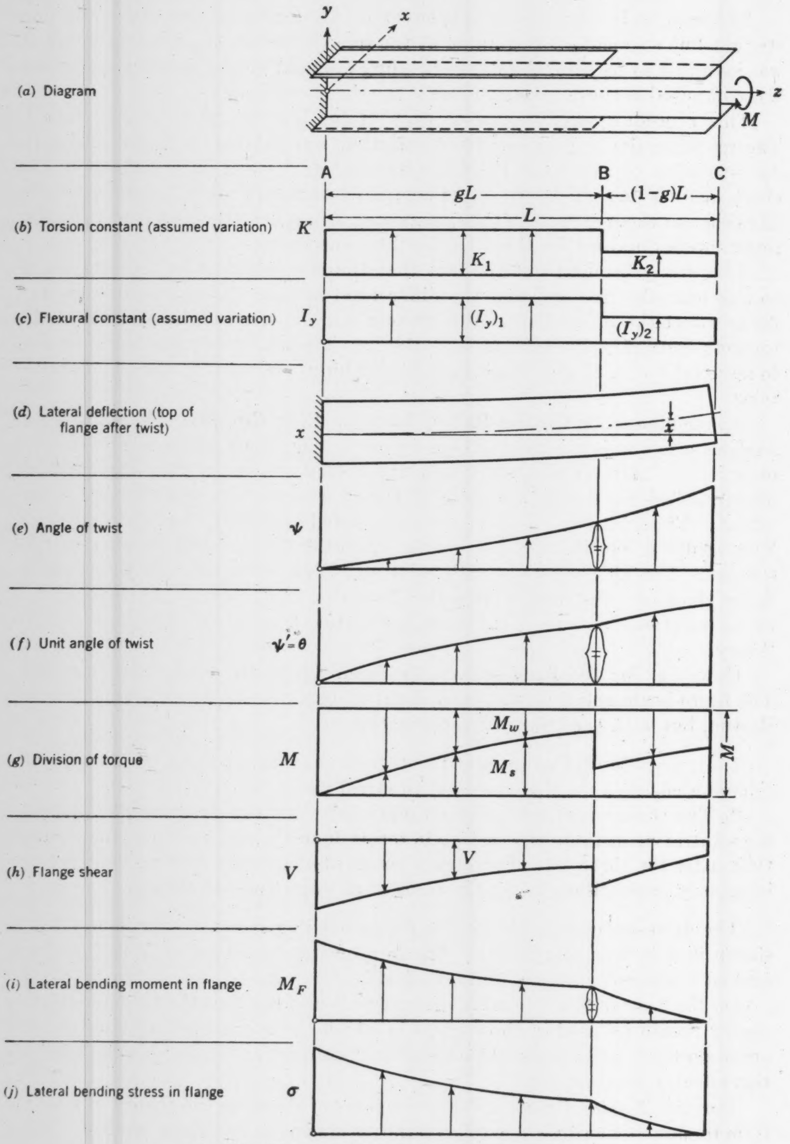
(a) Diagram
y
x
z
M
A
B
C
gL
(1-g)L
L
(b) Torsion constant (assumed variation)
K
K_1
K_2
(c) Flexural constant (assumed variation)
I_y
$(I_y)_1$
$(I_y)_2$
(d) Lateral deflection (top of flange after twist)
x
(e) Angle of twist
ψ
(f) Unit angle of twist
$\psi' = \theta$
(g) Division of torque
M
M_w
M_s
(h) Flange shear
V
(i) Lateral bending moment in flange
M_F
(j) Lateral bending stress in flange
σ

FIG. 10.—VARIABLE *K*-VALUE, MODIFICATION NO. 2

specimen with different values of torsional and lateral bending rigidities in each segment.

A plate girder with a variable torsion constant K, with or without a corresponding change in I_y, can be solved by an extension of the Timoshenko theory. In Modification No. 2 a cantilevered girder with K_1 and $(I_y)_1$ effective over a given portion and K_2 and $(I_y)_2$ effective over the balance of the span was subjected to a shaft torque M at the free end as shown in Fig. 10.

The equations for the angle of twist ψ, the unit angle of twist θ, and the flange bending moment M_F are written for each segment in terms of six arbitrary constants. These are evaluated by utilizing the following six consistent boundary conditions: At the fixed end, both ψ and θ are equal to zero; M_F is zero at the free end; and, at the junction point where the section properties change, the values of ψ, θ, and M_F from the left and right segments must be equal because of physical considerations. Substitution of the arbitrary constants leads to the expressions that will give the desired angular function and stress function. A characteristic cusp is developed in both the θ-curve and the M_F-curve.

The foregoing procedure was applied to several specimens to establish the effect of a reduction in K at the ends. It was found that if, for any reason, the effective K-value is reduced in any portion, the result will be an increase in the angular distortion and the flange bending stress throughout the span. This effect was noticeable in the built-up specimens in which the connectors were not continued clear to the free end.

CONCLUSIONS

In general, the experimental phase of this investigation progressed according to plan. The loading and support arrangements used in the laboratory tests were satisfactory. The instrumentation proved to be adequate. The use of a vertical bar braced against the flange sides to measure the angular twist of the web "bypassed" the possible complications due to web deformation.

On the basis of the observed behavior and the analytical study of results, the following conclusions were reached:

1. The test of the rolled beam was a further confirmation of the contention that the Timoshenko theory is an adequate basis for predicting the magnitude of stresses developed in solid sections of the usual dimensions under nonuniform torsion.
2. The Timoshenko theory was also found to be applicable to plate girders with a relatively high ratio of web thickness to flange thickness.
3. The Timoshenko theory, however, was found to err appreciably on the low side when used to compute the flange bending stresses in a plate girder with relatively heavy flanges.
4. A procedure was developed to check the validity of a suggested grouping of section properties for plate girders. Based on the compatibility of test data, the measured values of web and flange distortions were used to compute the flange bending stresses which compared closely with measured values.

5. By means of the finite-beam solution of the Goodier-Barton theory, it was possible to predict with reasonable accuracy the effect of web deformation on the angle of twist of cantilevered girder specimens subjected to shaft torque.

6. The finite-beam solution gave flange bending stresses which checked closely with measured values in all the plate-girder specimens tested.

7. Any reduction in the effective torsion constant along the span will result in an increase in stresses and angular distortions.

8. In those cases in which the stresses and distortions must be determined with precision, the Goodier-Barton theory is indicated. For design purposes the much simpler Timoshenko theory may be preferred.

ACKNOWLEDGMENT

This investigation was sponsored by the Pennsylvania State Department of Highways in cooperation with the Bureau of Public Roads, United States Department of Commerce. The experimental work was conducted in the Fritz Engineering Laboratory of Lehigh University with the assistance of Kenneth Harpel and others. The technical counsel contributed at various fimes by Messrs. de Vries and Chang and especially by C. H. Yang is greattully acknowledged.

DISCUSSION

DeForest A. Matteson, Jr.,[18] A. M. ASCE.—Vertical web stiffeners on a thin-webbed plate girder subject to nonuniform torsion would probably cause the girder to conform more closely to Mr. Timoshenko's analysis than does an unstiffened girder. Torsional bending stresses in the flanges may be great relative to the primary flexural stresses, and Fig. 9 suggests that the possible 20% + maximum stress reduction to be realized by making the girder conform to the Timoshenko analysis might justify the addition of vertical web stiffeners for this purpose in actual practice. This aspect of the authors' general problem suggests further study. The writer is under the impression that the specimens tested were unstiffened.

Because torsional forces at midspan were applied by the authors not only to the web but also to the flanges, it would have been realistic to connect the flanges to the end-support plates in some semirigid manner. However, of considerable difficulty in an experimental study of this type is the problem of devising end connections to conform with the assumed boundary conditions of the theory.

In the member of Fig. 4(*a*), the S-shape of the web cross section in the right-hand half of the beam would be the reverse of the S-shape of the web of the left-hand half. As explained under the heading, "Analytical Study of Results: Comparison of Theories for Rolled Sections," and as illustrated by Fig. 6(*b*), continuity at midspan (plus the boundary conditions of the finite-beam analysis) causes α to equal zero at the midspan section of the beam of Fig. 4, at which section $\sigma = 0$.

By contrast, the four cases of nonuniform torsional loading listed under the heading, "Summary of Torsion Theory: Classification of Torsion," are all of the type in which α does not equal zero at the section at which σ (due to torsion) vanishes. According to the "long-beam" analysis of Messrs. Goodier and Barton, if the cantilevered beam is very long, α remains slight but finite as σ vanishes. If the cantilevered beam is short—that is, if the free end is close to the restrained section—it seems probable that α at the free end will be larger than at the free end of a long beam because it is closer to the boundary condition of restraint which indirectly causes web deformation.

In the beam of Fig. 4, α is forced to vanish where the two opposite shapes of web deformation merge, but this situation is not true of the cantilevered beam. A distinct S-shape due to relative flange displacements might exist at the free end of the short cantilevered member.

Two items of evidence are pertinent: (1) The tests of specimen T9–WF (Fig. 6(*b*)) show clearly that, whatever the cause may have been, α was distinctly nonzero at the free end; and (2) the distance from midspan to the end of each girder used by the authors was less than five times its depth so that the girders could be termed "short" when considering torsion bending. Therefore, the writer suggests that, by providing internal fixity in place of external fixity, the authors created specimens to which the finite-beam analysis is not truly applicable in that, for computation G-B, α is assumed to become zero at the right-hand end of the beam of Fig. 6(*b*). Because this condition probably could not be true of a short cantilevered beam subject to shaft torque and because the experimental values plotted in Fig. 6(*b*) demonstrate that it was not true of the test specimens, analysis based on the Goodier-Barton theory seems to have been inadequate for computing ψ-values for the specimens of this experiment. This analysis did, however, provide an accurate prediction of the σ-values.

---

[18] Editor, Technical Publications, ASCE, New York, N. Y.

Conclusion No. 5 is thus misleading and of questionable justification. Conclusion No. 6 cannot be questioned, but a possible need for a theory of torsion bending in short beams is seen.

The foregoing discussion indicates that the authors may be unjustified in suggesting that what is probably a natural divergence of the experimental values in Fig. 6(*b*) "*** reflects in part the unavoidable local effect of the flange lugs" (under the heading, "Analytical Study of Results: Comparison of Theories for Rolled Sections"). This statement seems particularly unjustified because it is apparently opposed to the authors' later assertion (under "Analytical Study of Results: Modification of the Theory for Plate Girders") that consideration of the actual end supports led them to assume that, for plate girders, θ_W and θ_F of their specimens converged to zero at the free end. This assumption credits the use of the end supports with causing the values of ψ to become constant which means that the ψ-values for the web and flange were assumed to have been prevented from diverging. The writer will explain his reasons for suggesting that the θ-values in the experiment (Fig. 8) were decreased to a small nonzero value at the free end as the result of interference by the flange lugs.

Under the heading, "Experimental Program: Test Apparatus," the authors have explained that "Except for some unavoidable contact friction at the flange lugs, the outer ends were free to warp." If the free end of a cantilevered beam subject to nonuniform torsional loading is entirely free to warp, the longitudinal stresses will vanish at the free end, at which idealized section the conditions will approximate those of St. Venant torsion. Where this type of torsion prevails, θ is a nonzero constant value. This constant value will be the maximum θ-value for the beam, somewhat as in Fig. 10(*f*).

The two flange lugs were both at the particular edges of the flanges that would move toward the end-support plates as torsional warping occurred. The lugs, in resisting the movement of the extreme fibers toward the end plates, must have produced small longitudinal friction forces acting toward the fixed section.

Contact friction at the flange lugs could be responsible for the decrease in θ_W and θ_F (depicted at the right end of the beam of Fig. 8) if the frictional forces produced exterior moments in the horizontal flange planes of the same sense as that of the exterior reaction moments at the fixed (left) ends of the flanges. These moments would produce a decrease in dx/dz (Fig. 10(*d*)). If the opinion that the lugs resisted torsional warping is accepted, the longitudinal frictional forces at the flange lugs are each replaceable by a parallel force and the previously described moment (couple) of the proper sense for reducing θ. This resistance to torsional warping may, for this type beam, be thought of validly as a torsion bending moment. If the moment had produced complete fixity against angle change, θ would have been reduced to zero, just as complete fixity at the left-hand end of the cantilevered beam of Fig. 8 caused θ to be zero at that end. Considerable, if incomplete, elongation of the extreme tension fiber doubtlessly occurred, and θ at the right-hand end was probably reduced to some finite value between zero and the maximum θ-value.

Thus, because the measured values of θ as published by the authors showed a distinct decrease near the free end, the writer suggests that a negative moment may have been introduced in the flanges at each support. Because M/h is a specified value unaffected by the distribution of stresses, the introduction of additional restraining forces into the system must be accompanied by a decrease in the over-all ψ-value (the area under the θ-curve). The measured θ-values show that this decrease in area was an actuality, supporting the idea that unintentional restraining forces were present. The writer's suggestion of finite θ-values at the "free" end implies a smaller area under the V_F-curve than that computed by the authors and an accompanying small decrease in M_F.

It seems to the writer that the foregoing hypothesis concerning the effect of the flange lugs may be invalid for extremely large values of ψ.

Theoretically, the total area under each of the θ-curves is equal to the corresponding value of ψ at the rotating end of the beam. Possibly the test apparatus included instruments for measuring ψ close enough to the midspan yoke to yield an approximation of the maximum value of ψ for the span. By sketching to a large scale the θ-curves in the last segment (station 8, Fig. 8) in such a manner as to make the area under the entire θ-curve equal the maximum ψ-value, the nonzero value of θ, suggested by the writer as existing at the extreme free end, might be determined approximately. Different θ-values at the free end might be tried until the proper area is obtained.

The writer has opined that a small negative value of M_F existed at the free end, in which case moment computations should not begin from zero. A rough approximation to the moment at the free end may be obtained by assuming the effect of the flange lugs to be negligible on that portion of the beam (Fig. 8) to the left of the minimum value of V_F. The tangent to the V_F-curve may be drawn at its minimum ordinate, and the shear area to the right of this point and beneath the tangent may be assumed, as an approximation, to be entirely attributable to the negative moment. The area above the V_F-curve not attributable to the flange-lug interference will be similar in shape to that of length AB of Fig. 10(*h*) or to the *M*-curve of Fig. 3. Beginning at the right-hand end (Fig. 8) with a negative moment equal to the shear area attributable to this moment, the values of M_F may then be plotted by the authors' original procedure, using the entire original area above the shear curve. The curve of Fig. 8 would begin below the zero-line at the right-hand end and would change sign in the vicinity of station 8.

If a solid rectangular shaft is fixed at one end and free at the other, and if it resists an applied torque, torsional bending stresses will develop as a result of fixity. Hence, it seems possible for each flange of a girder to resist torsion independently as a shaft, developing a secondary system of longitudinal stresses within the system of torsion bending stresses studied by the authors. Apparently the authors considered such stresses either impossible or too small to distort the experimental values of M_F, even in short, heavy girders.

The primary objectives of this experimental program were admirably attained. The writer's comments are concerned with details that had insignificant effects on the results of this particular study. He believes that such detailed scrutiny, even though based on limited qualitative information and consisting of opinion rather than fact, can be valuable in clarifying certain concepts that may be of greater significance in future research.

GERALD G. KUBO,[19] A. M. ASCE, AND BRUCE G. JOHNSTON[20] AND WILLIAM J. ENEY,[21] MEMBERS, ASCE.—Mr. Matteson is to be commended for his searching analysis of the paper. Several of his comments appear at first to be at variance with the writers' statements. However, much of the seeming difference can be attributed either to the vagaries of interpretation or abridgment. In summarizing the material in the original report for publication, some of the background material had to be omitted.

The specimens tested and analyzed in this phase of the torsion program were shallow, relatively short plate girders without web stiffeners. In plate girders subjected to torsion the presence of properly designed and fabricated vertical web stiffeners would insure the maintenance of the original cross section, thereby eliminating the possibility of web deformation. As Mr. Matteson points out, this aspect of the torsion problem requires further study.

Each specimen was divided into two symmetrical half-spans with complete restraint against longitudinal warping at the plane of symmetry. In order to conform to the applicable theories as developed by Mr. Timoshenko and by Messrs. Goodier and Barton, it was necessary to have at the outer ends means whereby torsional moment could be resisted without restraint of longitudinal warping. The flange-lug arrangement at diametrically opposite corners was a practical compromise, as noted. On the other hand, to follow the discusser's suggestion that the flanges be connected to the end-support plates in some semirigid manner would be a step in the wrong direction.

The writers agree with the comments of Mr. Matteson relative to the finite beam, the long beam, and the actual loading conditions. Certain basic differences in boundary conditions preclude the use of either solution as a direct comparison with test results. It was necessary, therefore, to utilize selected portions of the available theories. Apparently the intent of the writers in using the finite-beam solution in the analysis of the angular twist in Fig. 6(*b*) was misinterpreted. As explained, the finite-beam solution was used to indicate that the flange reduction angle α, as measured, was of the same order of magnitude as that calculated for intermediate sections other than at the ends. It is agreed that Conclusion No. 5 should have been so qualified.

---

[19] Associate Prof. of Civ. Eng., New York Univ., New York, N. Y.; formerly Research Associate, Fritz Eng. Lab., Lehigh Univ., Bethlehem, Pa.

[20] Prof. of Structural Eng., Univ. of Michigan, Ann Arbor, Mich.; formerly Director, Fritz Eng. Lab., Lehigh Univ., Bethlehem, Pa.

[21] Prof. and Head, Dept. of Civ. Eng. and Mechanics, and Director, Fritz Eng. Lab., Lehigh Univ Bethlehem, Pa.

Mr. Matteson advances a logical explanation for the observed divergence from the expected pattern of the flange angle of twist at the free end. However, the essential difference between the discusser's suggested procedure and that used by the writers in computation H appears to be one of degree. In the absence of a definite value for the unit angle of twist ψ' at the end, the writers took the simple and conservative value of zero.

The secondary system of longitudinal normal stresses that are developed in wide plates under torsion has also been mentioned by the discusser. This effect, explained by Mr. Timoshenko,[8] has been extended to plate girders under uniform torsion by others.[4] The same specimens used in these tests had previously been subjected to uniform-torsion loading. Mr. Chang and one of the writers[22] had concluded that

> "* * * these longitudinal normal stresses are only important in estimating the ultimate torsion-carrying capacity. In the useful load range (lower elastic range) their effect can be ignored."

The end-support detail at one end was arranged so that there was no restraint of the tendency of the twisted specimen to be shortened. Although the pattern of these longitudinal stresses will be different in the nonuniform-torsion case, the relatively low torque range used indicated that this effect would be negligibly small.

The discusser's thoughtful suggestions have contributed to the value of the paper.

---

[22] "Torsion of Built-Up Structural Members," by F. K. Chang, thesis presented in 1950 to Lehigh University at Bethlehem, Pa., in partial fulfilment of the requirements for the degree of Doctor of Philosophy, p. 60.

AMERICAN SOCIETY OF CIVIL ENGINEERS
Founded November 5, 1852
TRANSACTIONS

Paper No. 2821

LATERAL BUCKLING OF CANTILEVERED I-BEAMS UNDER UNIFORM LOAD

By Stanley Poley,[1] J. M. ASCE

Synopsis

The differential equation and boundary conditions are derived which describe the lateral buckling of a cantilevered I-beam subjected to a uniform load. The resulting boundary-value problem, intractable by purely analytical methods, is solved numerically with the aid of a card-programmed calculator and the results are presented.

Introduction

The engineer has become more conscious of the weight-to-rigidity ratio of structures. This has led to a re-examination of the design of structural units from a more exact standpoint. As a result, there have been encountered boundary-value problems in elastic stability which are intractable by analytical methods. Before the development of high-speed computing machines, the labor involved in obtaining numerical solutions made numerical methods impractical in many important cases. An example of one of these is the problem of the lateral buckling of a cantilevered I-beam subjected to a uniform load. A numerical solution of this problem, obtained with the aid of a card-programmed calculator, is presented subsequently.

Differential Equations and Boundary Conditions

With coordinate axes as shown in Fig. 1, the total energy, V, of an I-beam that has buckled laterally under the action of a uniform normal load acting along the centroidal axis of the cross section is given[2] by

$$V = \frac{1}{2}\int_0^L \left[B(u'')^2 + C(\beta')^2 + \frac{D\,h^2}{2}(\beta'')^2 + 2\,M\,\beta\,u''\right] dz \ldots\ldots (1)$$

in which L is the length of the beam, B denotes the minimum flexural rigidity of the beam, u is the lateral deflection of the beam in the plane of minimum

---

Note.—Published, essentially as printed here, in October, 1954, as *Proceedings-Separate No. 527*. Positions and titles given are those in effect when the paper was approved for publication in *Transactions*

[1] Graduate Student, Dept. of Civ. Eng., Columbia Univ., New York, N. Y.

[2] "Lateral Buckling of Beams in Bending and Compression," by F. DiMaggio, A. Gomza, W. E. Thomas, and M. G. Salvadori, *Journal of the Aeronautical Sciences*, August, 1952, pp. 574–575.

rigidity, C represents the torsional rigidity of the cross section, β is the angular rotation of the section at an abscissa equal to z, D denotes the flexural rigidity of one flange in its own plane, h is the depth of the beam, and M represents the bending moment in the plane of maximum flexural rigidity of the section having an abscissa equal to z. The value of M is determined from

$$M = \frac{q}{2}(L - z)^2 \qquad (2)$$

in which q is the intensity of the uniform normal load. In Eq. 1, primes indicate differentiation with respect to z.

Eq. 1 is derived under the same assumptions used[3] by S. Timoshenko; it is applicable, therefore, to doubly symmetrical I-sections with the principal moment of inertia I_y much smaller than I_x.

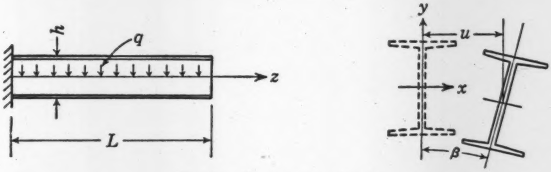

Fig. 1.—Coordinate Axes

Applying the usual methods of the calculus of variations to Eq. 1, the differential equation governing β is found to be

$$\beta^{IV} - \frac{2\,C}{D\,h^2}\beta'' - \frac{2\,M^2}{B\,D\,h^2}\beta = 0 \qquad (3)$$

and the boundary conditions are

$$\beta(0) = \beta'(0) = \beta''(L) = \left(\beta''' - \frac{2\,C}{D\,h^2}\beta'\right)_{z=L} = 0 \qquad (4)$$

Letting

$$x = \frac{z}{L} \qquad (5a)$$

$$\frac{1}{a^2} = \frac{2\,C}{D\,h^2} \qquad (5b)$$

and

$$\frac{1}{d^4} = \frac{q^2\,L^4}{2\,B\,D\,h^2} \qquad (5c)$$

Eq. 3, the buckling equation, becomes

$$\beta^{IV} - \frac{L^2}{a^2}\beta'' - \frac{L^4}{d^4}(1 - x)^4\,\beta = 0 \qquad (6)$$

---

[3] "Theory of Elastic Stability," by S. Timoshenko, McGraw-Hill Book Co., Inc., New York, N. Y., 1936.

in which, and subsequently, primes indicate differentiation with respect to x. The boundary conditions, Eq. 4, then become

$$\beta(0) = \beta'(0) = \beta''(1) = \left(\beta''' - \frac{L^2}{a^2}\beta'\right)_{x=1} = 0 \qquad (7)$$

SOLUTION BY FINITE DIFFERENCES

Subdividing the interval from 0 to 1 into n equal parts of length $\bar{h}$ and taking the first terms in the expansions of the derivatives in terms of central differences,[4] Eq. 6 becomes

$$\delta^4 \beta_i - \frac{L^2}{a^2} \bar{h}^2 \delta^2 \beta_i - \frac{L^4}{d^4} \bar{h}^4 (1 - x_i)^4 \beta_i = 0 \qquad (8)$$

in which δ is the central difference operator and

$$\beta_i \equiv \beta(x_i) \qquad (9)$$

In Eq. 9, x_i is the pivotal abscissa of the interval from 0 to 1. Substituting into Eq. 8 the values of the central differences in terms of pivotal values, there results

$$\beta_{i-2} - S\,\beta_{i-1} + [2(S - 1) - K^2(1 - x_i)^4]\,\beta_i - S\,\beta_{i+1} + \beta_{i+2} = 0 \qquad (10)$$

in which

$$S = 4 + \left(\frac{L}{a}\bar{h}\right)^2 \qquad (11a)$$

and

$$K^2 = \left(\frac{L}{d}\bar{h}\right)^4 \qquad (11b)$$

Similarly, the boundary conditions, Eq. 10, become

$$\beta_0 = 0 \qquad (12a)$$

$$\beta_{-1} = \beta_1 \qquad (12b)$$

$$\beta_{n+1} = 2\,\beta_n - \beta_{n-1} \qquad (12c)$$

and

$$\beta_{n+2} = 2(S - 2)(\beta_n - \beta_{n-1}) + \beta_{n-2} \qquad (12d)$$

From Eqs. 5*b*, 5*c*, and 11*b*, the critical load takes the form:

$$(q\,L)_{cr} = m\,\frac{\sqrt{B\,C}}{L^2} \qquad (13)$$

in which

$$m = \frac{2\,K\,n^2}{(L/a)} \qquad (14)$$

---

[4] "Numerical Computation of Buckling Loads by Finite Differences," by Mario G. Salvadori, *Transactions*, ASCE, Vol. 116, 1951, p. 590.

To solve the boundary-value problem defined by Eqs. 10 and 12, a value is fixed for both L^2/a^2 and n. Eq. 10 is then applied at the pivotal x_i ($i = 1, 2, \cdots, n$) using Eqs. 12 to eliminate β_0, β_{-1}, β_{n+1}, and β_{n+2}. This yields a set of n linear, algebraic, homogeneous equations in the n unknowns $\beta_1, \cdots, \beta_n$ and this system has solutions β_i not identically zero, if and only if its determinant Δ (which is a function of K^2) is equal to zero. In problems of elastic stability, the designer will be primarily interested in the lowest buckling load, and hence the determinantal equation,

$$\Delta(K^2) = 0 \qquad (15)$$

is solved for the smallest root. Having done this for one value of n, the operation is repeated with a larger n to obtain a better approximation of the true value of K^2. By increasing the number of pivotal points, K^2 can be evaluated, theoretically, to any degree of accuracy.

For large values of n, the evaluation of the roots of Eq. 15 is impractical without the use of special computing devices. The actual computations for this problem were performed on a card-programmed calculator. A detailed account of the method used for the computations is available.[5]

RESULTS

For a given I-beam, L^2/a^2 is computed from

$$\frac{L^2}{a^2} = \frac{2\,C\,L^2}{D\,h^2} \qquad (16)$$

The corresponding value of m is obtained from the following tabulation, and the critical load is computed from Eq. 13:

Value of L^2/a^2	Value of m	Value of L^2/a^2	Value of m
1	66.9	12	28.3
2	50.9	14	27.1
3	44.0	16	26.0
4	39.8	24	23.5
6	34.9	32	21.9
8	31.9	40	20.9
10	29.8	100	17.6

It should be noted that as the ratio L^2/a^2 increases, the factor m decreases and approaches as a limit the value 12.85; this same value was obtained for lateral buckling of a cantilevered rectangular beam under similar loading conditions.[6]

EXAMPLE

For a 24 I 79.9 section with L equal to 20 ft, the flexural rigidity, D, of a flange can be assumed to be one half the flexural rigidity of the I-beam in the lateral direction and the torsional rigidity, C, can be computed from the approximate formula:[7]

---

[5] "Lateral Buckling of Cantilevered I-Beams Under Uniform Loads," by S. Poley, thesis presented to Columbia University, in New York, N. Y., in 1953, in partial fulfilment of the requirements for the degree of Master of Science in Civil Engineering.

[6] "Theory of Elastic Stability," by S. Timoshenko, McGraw-Hill Book Co., Inc., New York, N. Y. 1936, p. 259.

$$C = \frac{G}{3}\,(2\,b\,t^3 + h\,t^3_1) \ldots\ldots\ldots\ldots\ldots\ldots\ldots (17)$$

in which b is the flange width, t denotes the average flange thickness, t_1 is the web thickness, and G is the shear modulus. For this section, b is equal to 7 in., t is equal to 0.87 in., t_1 is equal to 0.5 in., h is equal to 24 in., B is equal to 42.9 E in.^{4}, and D is equal to 21.5 E in.^{4}, in which E is the elastic modulus. Assuming E equal to 2.6 G, there results for C a value of 1.57 in.^{4}. Thus,

$$\frac{L^2}{a^2} = \frac{2\,C\,L^2}{D\,h^2} = \frac{2 \times 1.57 \times 20^2}{21.5 \times 2^2} = 14.6.$$

From the foregoing tabulation, m is equal to 26.8. With E equal to 30×10^6 lb per sq in.,

$$\begin{aligned}(q\,L)_{cr} &= m\,\frac{\sqrt{B\,C}}{L^2} = 26.8 \times 30 \times 10^6 \times \frac{\sqrt{42.9 \times 1.57}}{(20 \times 12)^2} \\ &= 115{,}000 \text{ lb.}\end{aligned}$$

CONCLUSIONS

The present theory is applicable to a variety of practical problems and was suggested by the actual buckling of long I-beams when lifted during construction. The results here obtained may increase the safety of this type of beam which is so often encountered in structures under loading conditions very similar to those considered.

---

[7] "Buckling Strength of Metal Structures," by F. Bleich, McGraw-Hill Book Co., Inc., New York N. Y., 1951.

AMERICAN SOCIETY OF CIVIL ENGINEERS
Founded November 5, 1852
TRANSACTIONS

Paper No. 2822

CORROSION AND CORROSION RESEARCH

BY THOMAS R. CAMP,[1] M. ASCE

WITH DISCUSSION BY MESSRS. EDWARD W. MOORE, AND THOMAS R. CAMP

SYNOPSIS

The elements of the corrosion cell are described and it is demonstrated that a great variety of half-cell reactions are possible whose single electrode potentials can be computed from thermodynamic constants and the composition of water. It is shown that only those half-cell reactions which produce the greatest electromotive force can occur. The method of identification of the half-cell reactions for a particular case is illustrated. It is shown that the theory can be used to great advantage in selecting water-treatment processes for corrosion control. The theory underlying the correct procedure for polarization tests is developed, and it becomes evident that all unknowns can be evaluated if the single electrode potentials are computed first.

INTRODUCTION

The corrosion of a metal consists of the solution of the metal in water (or in an aqueous solution with which it is in contact) or of the reaction of the solid metal with ions and other dissolved constituents of the solution. Either reaction is an oxidizing reaction accompanied by the release of electrons which flow back through the metal as a negative electric current. Because the water or aqueous solution is a part of the electric circuit, the complete circuit is an electric cell including (1) the anode at which the corrosion is taking place, (2) a cathode which is connected to the anode by the metal as a conductor and at which a reducing reaction takes place, and (3) the electrolyte between the anode and cathode.

The basic theory underlying the electrochemical process of corrosion of metals in contact with water was first developed by Josiah Willard Gibbs.[2]

NOTE.—Published, essentially as printed here, in May, 1955, as *Proceedings-Separate No. 685*. Positions and titles given are those in effect when the paper or discussion was approved for publication in *Transactions*.

[1] Partner, Camp, Dresser & McKee, Cons. Engrs., Boston, Mass.

[2] "On the Equilibrium of Heterogeneous Substances," *Transactions of the Connecticut Academy*, III, October, 1875–May 1876, pp. 108–248, and May 1877–July, 1878, pp. 343–524.

Mr. Gibbs' great contributions to electrochemistry were not used to any considerable extent in the United States until after the publication[3] of the work of G. M. Lewis and M. Randall in 1923. Since 1923 a great mass of experimental data has been collected relating to free energies of chemical substances and single electrode potentials, much of which has been used in the evaluation of equilibrium constants. Unfortunately, little of this very useful information has been applied to the development of the electrochemical theory of corrosion. Because of the economic importance of corrosion, there has been considerable research activity but most of it has been directed toward tests of the relative merits of various metals and their alloys, of various protective coatings, and of cathodic protection. Little attention has been given the half-cell reactions which take place during the corrosion process and the complete electric circuit.

As a step toward filling this vacuum in the knowledge of corrosion, two papers[4,5] have been published. In these papers much of the basic theory relating to the equilibria of corrosion reactions was presented, and it was shown that the half-cell reactions which actually take place in a corrosion process can be identified from the analysis of the water and the comparison of the single electrode potentials of the possible reactions.

The principles presented therein have been extremely useful in explaining what occurs during various corrosion phenomena and in evaluating protective coatings and corrective water-treatment processes. The application of these principles indicates that some of the reactions said to take place in the conventional literature[6,7] on corrosion do not take place under normal conditions and that many other half-cell reactions which are uniformly neglected actually can and do occur. Because the rate of corrosion depends on the potentials of the half-cell reactions and the resistances in the electric circuit, it should be obvious that any worthwhile fundamental research on rate of corrosion should begin with the identification of the electrochemical reactions which are taking place and the evaluation of the resistances in the circuit.

Since 1946 the principles[4,5] that were promulgated at that time have been seldom used. The purpose of this work is to present again in brief and simplified form the essentials of these papers[4,5] together with proof of their validity and a development of the theory of the electric circuit in the corrosion process. It is hoped that the principles involved will thus be better understood and more widely used in corrosion laboratories and by consultants on corrosion. Examples of the application of the principles are also presented to illustrate the procedures and the results which can be obtained.

ELEMENTS OF THE CORROSION CELL

In order for corrosion to take place there must be moisture in contact with the metal and the moisture must contain ions to form the electrolyte.

---

[3] "Thermodynamics and the Free Energy of Chemical Substances," by G. M. Lewis and M. Randall, McGraw-Hill Book Co., Inc., New York, N. Y., 1923.

[4] "Corrosiveness of Water to Metals," *Journal*, New England Water Works Assn., Vol. LX, No. 2, 1946, p. 188.

[5] *Ibid.*, No. 3, p. 282.

[6] "Corrosion," by F. N. Speller, McGraw-Hill Book Co., Inc., New York, N. Y., 1951, pp. 13-14.

[7] "Corrosion Handbook," by H. H. Uhlig, John Wiley and Sons, Inc., New York, N. Y., 1948, p. 125.

There must be anodic areas at which the anodic half-cell reactions or oxidations occur and cathodic areas at which the cathodic half-cell reactions or reductions take place. The anode and the cathode of an elementary corrosion cell must be connected by an electrical conductor, usually the metal undergoing corrosion, but also—in many cases—including the films or coatings on the metal surface. In the initial stages of the common form of corrosion the anode and cathode are close together because the principle of least action requires that the path of current flow and the resistance be the least. Therefore, in normal corrosion the anode may be only a few molecules removed from the cathode—so close, in fact, that the casual observer will overlook the fact that two separate electrochemical reactions are occurring.

In Fig. 1 are shown metals in contact with water where several different types of half-cell corrosion reactions are taking place. Fig. 1 indicates that the anode and cathode are completely separated in space as they are in fact. At the anodic reaction, electrons are released by the corroding metal, which flow back through the metal and the films to the cathode where they are captured in the cathodic reaction. The so-called positive electric current flows through the electrolyte from the anode to the cathode.

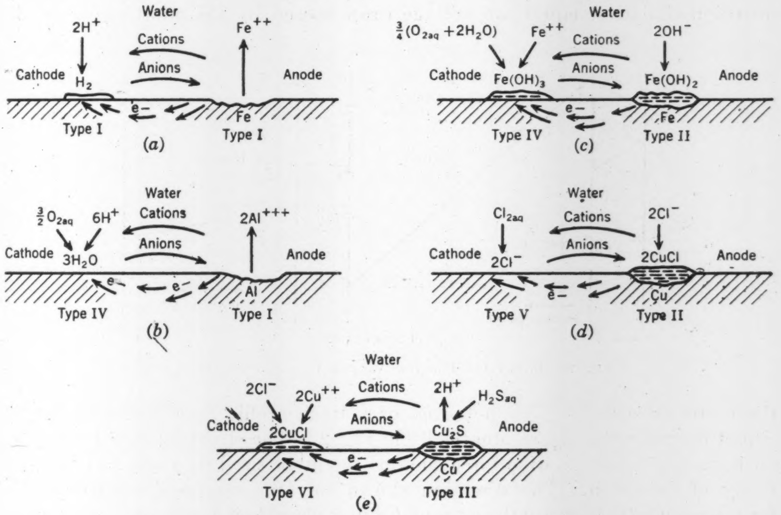
Water
2H⁺
Cations
Fe⁺⁺
Anions
Cathode
H₂
Anode
e⁻
Fe
Type I
Type I
(a)
Water
¾(O₂aq + 2H₂O)
Fe⁺⁺
Cations
2OH⁻
Anions
Cathode
Fe(OH)₃
Fe(OH)₂
Anode
e⁻
Fe
Type IV
Type II
(c)
Water
³⁄₂ O₂aq
6H⁺
Cations
2Al⁺⁺⁺
Anions
Cathode
3H₂O
Anode
e⁻
Al
Type IV
Type I
(b)
Water
Cl₂aq
Cations
2Cl⁻
Anions
Cathode
2Cl⁻
2CuCl
Anode
e⁻
Cu
Type V
Type II
(d)
Water
2Cl⁻
2Cu⁺⁺
Cations
2H⁺
H₂Saq
Anions
Cathode
2CuCl
Cu₂S
Anode
e⁻
Cu
Type VI
Type III
(e)

FIG. 1.—TYPES OF REACTIONS OCCURRING IN CORROSION OF METALS IN CONTACT WITH WATER

It will be noted in Fig. 1 that several different types of anodic reactions other than the solution of the metal may take place. The reactions shown in Fig. 1(*a*) are those which are said to occur by conventional theory in the corrosion of iron. A study of the principles indicates that at high pH-values the anodic reaction shown in Fig. 1(*c*) may take place, or carbonate and bicarbonate ions may "plate out" at the anode to form ferrous carbonate.

A study of the principles also indicates that plating out of hydrogen ions at the cathode as shown in Fig. 1(*a*) does not occur except at very low pH-values. A study of the principles also shows that the formation of water at the cathode takes place as shown in Fig. 1(*b*) rather than by the plating out of atomic hydrogen and its subsequent reaction with dissolved oxygen as has been claimed.[8] The chemical combination of hydrogen and oxygen to form water in the absence of an electric cell occurs only at high temperatures. A study of the principles also shows that ferric-iron rust is formed as shown in (Fig. 1(*c*)). This reaction will prevail instead of the cathodic reaction involving the formation of water if there is a measurable amount of ferrous iron in solution. The claim[8] that ferric-iron rust is formed by a chemical reaction not a part of the electrochemical cell does not explain why the rust is nearly always attached to the corroding metal.

In accordance with Kirchhoff's second law, the electromotive force of the corrosion cell must equal the voltage drop caused by the resistance around the corrosion circuit. The potential or voltage profile around the corrosion circuit is illustrated diagrammatically in Fig. 2. The circuit in Fig. 2 includes an impressed electromotive force such as might be used in a test cell for the study of corrosion. The direction shown for the impressed electromotive force is such as to increase the current I, but it should be noted that the current might be reduced to zero or reversed by an electromotive force of sufficient magnitude in the opposite direction. In the interest of completeness the circuit also includes an anodic film or coating and a cathodic film or coating. In accordance with Kirchhoff's second law,

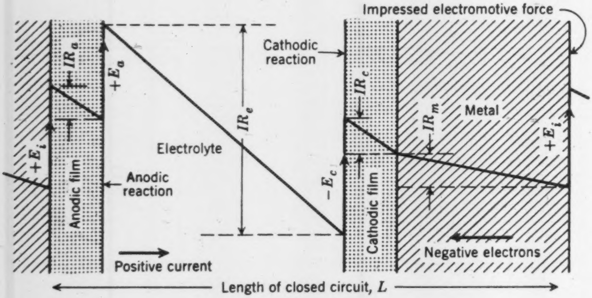

FIG. 2.—POTENTIAL PROFILE AROUND CORROSION CIRCUIT

$$E_i + E_a - E_c = I\,(R_a + R_e + R_c + R_m) \ldots\ldots\ldots\ldots (1)$$

in which E_i is the impressed electromotive force, E_a denotes the single-electrode potential at the anode, E_c is the single-electrode potential at the cathode, I represents the corrosion current, R_a is the resistance of the anodic film or coating, R_e is the resistance of the electrolyte, R_c is the resistance of the cathodic film or coating, and R_m denotes the resistance of the metal.

---

[8] "Corrosion," by F. N. Speller, McGraw-Hill Book Co., Inc., New York, N. Y., 1951, p. 14.

For a clear understanding of the corrosion process, one must realize that there are two separate regions in a corrosion cell where electrochemical half-cell reactions take place and that the reactions at the anode are completely independent of the reactions at the cathode, except that no current can flow without two half-cell reactions. Moreover, the electromotive force at the anode and the electromotive force at the cathode are completely independent of the rate of current flow despite opinions expressed to the contrary.[9,10,11] The potentials of the half-cell reactions depend only on the temperature, the participating substances, and the activities of the participating substances as shown subsequently.

The circuit shown in Fig. 2 is idealized to indicate complete separation of anode and cathode and a single length for the path of flow of the electric current. The actual corrosion cell is, of course, much more complicated. There are numerous stream paths of different length for current flow and variable thicknesses of films. In order to study the process, however, it is essential to separate the variables, and this can only be done in the laboratory by use of an experimental corrosion cell in which all factors are measurable and controllable. Fig. 2 represents such an idealized circuit.

The rate of corrosion is the time rate at which the reactions at the anode occur. The rate is the same at the cathode and throughout the corrosion circuit and is measured by the corrosion current. In accordance with Faraday's law, the corrosion current—in amperes—is equal to 96,500 times the number of equivalents per second taking part in the anodic reactions or in the cathodic reactions. For example, for a corrosion rate of 0.01 in. per yr for iron, the corrosion current is approximately 2.16×10^{-5} amperes per sq cm of iron surface provided, however, that ferrous iron is participating in all the reactions at the anode.

An examination of Eq. 1 or Fig. 2 will indicate that for a given total electromotive force the corrosion current, and hence the rate of corrosion, depends on the resistance of the corrosion circuit. In fundamental corrosion research, therefore, it is important to know the resistances of the elements of the corrosion circuit. The resistance of the electrolyte can be computed from its equivalent conductance, and the resistance of the metals and films can be computed from the specific resistance of the substances—if the lengths are known. Unfortunately, there is little information available relative to the specific resistance of the films encountered in the corrosion process. This is one of the fertile fields for future research.

PRINCIPLES FOR THE IDENTIFICATION OF HALF-CELL REACTIONS

The reactions at the electrodes of a corrosion cell will depend on the metals and on the kind and concentration of ions and other solutes adjacent to the electrodes. Of all possible anodic reactions, the reaction or reactions with the highest potential will prevail, and of all possible cathodic reactions those

---

[9] "Null Methods Applied to Corrosion Measurements," by J. M. Pearson, *Transactions*, Electrochemical Soc., Inc., Vol. 81, 1942, p. 489.

[10] "Corrosion Handbook," by H. H. Uhlig, John Wiley & Sons, Inc., New York, N. Y., 1948, p. 483.

[11] "Mechanism of Internal Corrosion of Water Pipe," by Rolf Eliassen and J. C. Lamb, *Journal* A.W.W.A., Vol. 45, 1953, p. 1290.

with the lowest potential will prevail. Thus, at any instant, the reactions will be those which produce the greatest electromotive force for the cell. At any instant there is a single electromotive force corresponding to the half-cell reactions at each electrode. If two or more half-cell reactions are occurring simultaneously at a point in an electrode, therefore, the concentrations of the reactants must be such as to produce the same electromotive force. This principle is the basis for the identification of the corrosion reactions. Arguments in support of the validity of the principle are presented herewith.

As is well known, the electromotive series of metals is a table of standard single electrode potentials arranged in order of magnitude of the electromotive forces with those of greatest magnitude at the top. If any two of the metals are immersed as electrodes in an aqueous solution containing molal concentrations of the metals, the metal highest in the series will enter solution and the other will plate out. The electromotive force of the cell will be the difference of the standard single-electrode potentials. If the concentrations of the ions of the two metals are different from the molal concentrations, the single-electrode potentials will differ from the standard potentials; but the metal with the highest potential will be the anode, and the electromotive force of the cell will be the difference of the actual potentials.

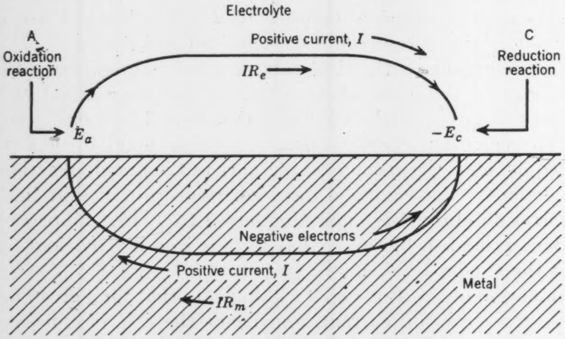

FIG. 3.—CURRENT STREAMLINE IN CORROSION CELL

The single-electrode reactions of the metals are only special cases of the more general type of half-cell reaction which must be considered in corrosion phenomena. The same laws govern in all cases and, if only two half-cell reactions are possible in a corrosion cell, the one with the highest potential will be the anodic reaction. If more than two half-cell reactions are possible, it is easy to realize that the direction of flow of positive current will be from the reactions of higher potential to those of lower potential. It is not so obvious, however, which of the reactions will prevail at anode and cathode.

In Fig. 3 there is shown a single current streamline in a corrosion cell, with the anodic reactions occurring at point A and the cathodic reactions at point C. For the corrosion current, I, at any instant, it is obvious that there can be only one value of the IR-drop through the electrolyte, metal, and films because there is only one value of the total resistance along the current streamline. Because the total *IR*-drop is equal to the difference in electromotive force of the half-cell reactions, this difference also has only one value, and each of the half cells has only one value for its potential. Two or more half-cell reactions may occur simultaneously at either electrode, but only if their potentials are equal.

Now, which of the possible half-cell reactions do occur at the anode—those with the highest, those with the lowest, or those with intermediate potentials? Applying what is already known, the reactions with the highest potential will be anodic to those with the lower potentials and will prevail at the anode. The possible reactions at the anode with the lower potentials tend to be cathodic to the anodic reactions which prevail, but they are anodic to the prevailing reactions at the cathode. These reactions cannot take place, therefore, because they would proceed in both directions at the same time and would result in a flow of current in both directions through the same point in the metal interface at the same time. Moreover, they would result in more than one value for the total *IR*-drop. Similar reasoning will show that of all possible cathodic reactions, those with the lowest potential will prevail and all others will be inactive.

It is evident from Fig. 3 that all parallel current streamlines in the corrosion circuit must follow the same laws. Therefore, at all points in the anodic area. the half-cell reactions with the highest potential will prevail; and at all points in the cathodic area, the reactions with the lowest potential will prevail. All other possible reactions will be inactive.

From the foregoing it follows that the half-cell reactions which actually occur in a corrosion cell may be identified by comparing all possible reactions until those are found which produce the highest electromotive force for the cell, The conclusions previously drawn relative to the half-cell reactions illustrated in Fig. 1 were arrived at by this procedure.

In order to determine the electromotive force of a half-cell reaction, it is necessary to have available or to determine the so-called standard electrode potential of the reaction—which is based on an activity of unity for each of the reacting substances—and to modify this potential to conform with the actual concentrations of the reacting substances. The standard electrode potentials may be computed from the free energies of formation of the reacting substances. The free energies of a large number of substances are available[12] for the standard temperature of 25° C.

In formulating half-cell reactions it is conventional to write them in the oxidation direction proceeding from left to right, and the potentials are computed in the same direction. When a reaction becomes cathodic, the direction is reversed and the potential changes sign. The standard oxidation potential of any half-cell reaction at any temperature *T* may be computed from the standard free-energy change at the same temperature as follows:

$$E°_T = -\frac{4.183}{96{,}500\,n}\Delta F°_T \ldots\ldots\ldots\ldots\ldots\ldots\ldots (2)$$

---

[12] "Oxidation Potentials," by W. M. Latimer, Prentice-Hall, New York, N. Y., 1938 and 1952.

in which $E°_T$ is the standard oxidation potential referred to the hydrogen electrode, n denotes the number of electrons transferred per mole, 4.183 is the number of joules per calorie, 96,500 is the number of coulombs per Faraday, and $-\Delta F°_T$ represents the decrease in free energy of the half-cell reaction in calories per mole..

The actual oxidation potential of a half-cell reaction at temperature T can be computed from the standard oxidation potential and the activities of the participating substances as follows:

$$E_T = E°_T - \frac{4.183 \times 2.302\,RT}{96{,}500\,n} \log Q \quad \text{(3a)}$$

or

$$E_T = E°_T - \frac{1.978 \times 10^{-4}\,T}{n} \log Q \quad \text{(3b)}$$

in which E_T is the oxidation potential at absolute temperature T ($T = 298°$ K for 25° C), R is the gas constant (1.985 calories per mole per ° K), and Q represents the ratio of the product of the activities of the products of the reaction to the product of the activities of the reactants.

At the temperature of 25° C, Eq. 3*b* reduces to

$$E_{25} = E°_{25} - \frac{0.05914}{n} \log Q \quad \text{(4)}$$

in which E_{25} is the oxidation potential at 25° C and $E°_{25}$ is the standard oxidation potential at 25° C.

Because most of the thermodynamic constants on free energy, standard potentials, entropies, and heats of reactions have been referred to a temperature of 25° C and are available in tables,[13] it is convenient to begin all computations for this temperature and then adjust to the actual temperature T. For the temperature adjustment, the Gibbs-Helmholtz equation[14] may be used. This equation, in a convenient form is

$$E°_T = E°_{25} + \frac{T - 298}{T_{avg}} \left(E°_{25} + \frac{\Delta H°_{25}}{23{,}066\,n} \right) \quad \text{(5)}$$

in which

$$T_{avg} = \frac{298°\text{ K} + T}{2} \quad \text{(6)}$$

and $\Delta H°_{25}$ is the heat of the reaction at 25° C. If the heat of the reaction is not available, it may be computed from the free energy and entropy by

$$\Delta H°_{25} = \Delta F°_{25} + 298\,\Delta S°_{25} \quad \text{(7)}$$

in which $\Delta S°_{25}$ is the change in entropy of the reaction at 25° C.

---

[13] "International Critical Tables of Numerical Data, Physics, Chemistry and Technology," by the National Research Council, McGraw-Hill Book Co., Inc., New York, N. Y., 1933.

[14] "The Principles of Electrochemistry," by D. A. MacInnes, Reinhold Publishing Corp., New York, N. Y., 1939, p. 110.

APPLICATION OF THEORY TO IDENTIFY HALF-CELL REACTIONS

Example 1.—Compute the oxidation potential of the reaction

$$CO_3^{--} + \underline{Fe} \rightarrow \underline{FeCO_3} + 2\,e^-$$

at 10° C, if the carbonate-ion concentration is 2.5 ppm.

The free energies of formation at 25° C are − 126,390 for the carbonate ion, zero for the metallic iron, and − 161,260 for the solid ferrous carbonate; and the corresponding entropies at 25° C are − 13, + 6.5 and + 22.2. Therefore,

$$\Delta F^\circ_{25} = -\,161{,}260 + 126{,}390 = -\,34{,}870 \text{ calories}$$

$$E^\circ_{25} = -\,\frac{4.183}{96{,}500 \times 2}\,(-\,34{,}870) = +\,0.755 \text{ volts}$$

$$\Delta S^\circ_{25} = +\,22.2 + 13 - 6.5 = +\,28.7$$

$$\Delta H^\circ_{25} = -\,34{,}870 + 298 \times 28.7 = -\,26{,}310 \text{ calories}$$

$$E^\circ_{10} = +\,0.755 + \frac{-\,15}{290.5}\left(+\,0.755 + \frac{-\,26{,}310}{23{,}066 \times 2}\right)$$

$$= +\,0.745 \text{ volts}$$

For 2.5 ppm of CO_3^{--}, the molal concentration is

$$[CO_3^{--}] = \frac{2.5}{60} \times 10^{-3} = 4.167 \times 10^{-5}$$

For the dilute concentrations usually encountered in waterworks practice, the activity of an ion may be taken as equal to its concentration without appreciable error. Then for 10° C or $T = 283°$ K,

$$E_{10} = +\,0.745 - \frac{1.978 \times 10^{-4} \times 283}{2} \log\left(\frac{1}{4.167 \times 10^{-5}}\right)$$

$$= +\,0.684 \text{ volts.}$$

The standard oxidation potentials at 25° C, E°_{25}, are available[12,13,4,5] for numerous half-cell reactions and do not need to be computed as was done in the foregoing.

Example 2.—The procedure to be used in identifying the half-cell reactions for a particular case will be illustrated herewith for a soft water at high pH in contact with iron. This water is typical of soft New England waters following pH adjustment with sodium hydroxide. The analysis of the water has been assumed so that $Fe(OH)_2$, $CaCO_3$, $Ca(OH)_2$, and $Mg(OH)_2$ are below saturation. There is a slight supersaturation of $FeCO_3$ and $MgCO_3$ so that some precipitation of these compounds might occur by ordinary chemical reactions. For simplicity the temperature has been taken at 25° C.

Determine the anodic and cathodic reactions for the corrosion of an iron pipe in contact with water at 25° C, the water having a pH of 9.5 and containing 4 ppm of calcium, 1.0 ppm of magnesium, 0.06 ppm of ferrous iron, 2.5 ppm of carbonate, 17.1 ppm of bicarbonate, and 6.4 ppm of dissolved oxygen.

The concentrations of the reacting substances are as follows:

$$[\mathrm{H^+}] = 10^{-9.5} = 3.16 \times 10^{-10}$$

$$[\mathrm{OH^-}] = 10^{-4.5} = 3.16 \times 10^{-5}$$

$$[\mathrm{Ca^{++}}] = \frac{4}{40} \times 10^{-3} = 10^{-4}$$

$$[\mathrm{Mg^{++}}] = \frac{1}{24.3} \times 10^{-3} = 4.12 \times 10^{-5}$$

$$[\mathrm{Fe^{++}}] = \frac{0.06}{55.8} \times 10^{-3} = 1.074 \times 10^{-6}$$

$$[\mathrm{CO_3^{--}}] = \frac{2.5}{60} \times 10^{-3} = 4.167 \times 10^{-5}$$

$$[\mathrm{HCO_3^-}] = \frac{17.1}{61} \times 10^{-3} = 2.81 \times 10^{-4}$$

$$[\mathrm{O_{2\mathit{aq}}}] = \frac{6.4}{32} \times 10^{-3} = 2 \times 10^{-4}$$

The following possible reactions have been arranged in order of decreasing potential:

1. $\mathrm{CO_3^{--}} + \underline{\mathrm{Fe}} \rightarrow \underline{\mathrm{FeCO_3}} + 2\,e^-$ $\qquad E^\circ_{25} = +\ 0.755$ volts

$$E_{25} = +\ 0.755 - \frac{0.05914}{2} \log \left(\frac{1}{4.167 \times 10^{-5}} \right) = +\ 0.625 \text{ volts}$$

2. $\underline{\mathrm{Fe}} \rightarrow \mathrm{Fe^{++}} + 2\,e^-$ $\qquad E^\circ_{25} = +\ 0.44$ volts

$$E_{25} = +\ 0.44 - \frac{0.05914}{2} \log\, (1.074 \times 10^{-6}) = +\ 0.616 \text{ volts}$$

3. $2\mathrm{OH^-} + \underline{\mathrm{Fe}} \rightarrow \underline{\mathrm{Fe(OH)_2}} + 2\,e^-$ $\qquad E^\circ_{25} = +\ 0.877$ volts

$$E_{25} = +\ 0.877 - \frac{0.05914}{2} \log \left[\frac{1}{(10^{-4.5})^2} \right] = +\ 0.611 \text{ volts}$$

4. $\mathrm{H_2} \rightarrow 2\mathrm{H^+} + 2\,e^-$ $\qquad E^\circ_{25} = 0.0$ volts

$$E_{25} = 0.0 - \frac{0.05914}{2} \log\, [(10^{-9.5})^2] = +\ 0.561 \text{ volts}$$

5. $\underline{\mathrm{CaCO_3}} + \mathrm{OH^-} \rightarrow \tfrac{1}{2}\mathrm{O_{2\mathit{aq}}} + \mathrm{Ca^{++}} + \mathrm{HCO_3^-} + 2\,e^-$

$E^\circ_{25} = -\ 0.798$ volts

$$E_{25} = -\ 0.798 - \frac{0.05914}{2} \log \left[\frac{(2 \times 10^{-4})^{\frac{1}{2}}\, (10^{-4})\, (2.81 \times 10^{-4})}{3.16 \times 10^{-5}} \right]$$
$$= -\ 0.653 \text{ volts}$$

6. $2\mathrm{OH^-} \rightarrow \tfrac{1}{2}\mathrm{O_{2\mathit{aq}}} + \mathrm{H_2O} + 2\,e^-$ $\qquad E^\circ_{25} = -\ 0.444$ volts

$$E_{25} = -\ 0.444 - \frac{0.05914}{2} \log \left[\frac{(2 \times 10^{-4})^{\frac{1}{2}}}{(10^{-4.5})^2} \right] = -\ 0.655 \text{ volts}$$

7. $2CO_3^{--} + H_2O \rightarrow \frac{1}{2}O_{2aq} + 2HCO_3^- + 2\,e^- \qquad E^\circ_{25} = -\,0.661$ volts

$$E_{25} = -\,0.661 - \frac{0.05914}{2}\log\left[\frac{(2 \times 10^{-4})^{\frac{1}{2}}\,(2.81 \times 10^{-4})^2}{(4.167 \times 10^{-5})^2}\right] = -\,0.655 \text{ volts}$$

8. $H_2O \rightarrow \frac{1}{2}O_{2aq} + 2H^+ + 2\,e^-, \qquad E^\circ_{25} = -\,1.272$ volts

$$E_{25} = -\,1.272 - \frac{0.05914}{2}\log\left[(10^{-9.5})^2\,(2 \times 10^{-4})^{\frac{1}{2}}\right] = -\,0.655 \text{ volts}$$

9. $\underline{MgCO_3} + OH^- \rightarrow \frac{1}{2}O_{2aq} + Mg^{++} + HCO_3^- + 2\,e^-$

$E^\circ_{25} = -\,0.822$ volts

$$E_{25} = -\,0.822 - \frac{0.05914}{2}\log\left[\frac{(2 \times 10^{-4})^{\frac{1}{2}}\,(4.12 \times 10^{-5})\,(2.81 \times 10^{-4})}{3.16 \times 10^{-5}}\right] = -\,0.665 \text{ volts}$$

10. $\underline{Fe(OH)_3} \rightarrow \frac{3}{4}O_{2aq} + Fe^{++} + \frac{3}{2}H_2O + 2\,e^- \qquad E^\circ_{25} = -\,1.386$ volts

$$E_{25} = -\,1.386 - \frac{0.05914}{2}\log\left[(1.074 \times 10^{-6})\,(2 \times 10^{-4})^{\frac{3}{4}}\right] = -\,1.126 \text{ volts}$$

These reactions are not all the possible reactions that can take place, but others examined appear not to be important. Now if there is no film on the iron, it is evident that reaction 1—the plating out of carbonate at the anode—will prevail at the beginning of the process and reaction 10—the formation of ferric iron oxide—will prevail at the cathode.

A study of the reactions and potentials of Example 2 leads to many interesting conclusions. In the first place, the plating out of carbonate at the anode can continue only until all the exposed metallic iron has reacted with the carbonate to produce a ferrous carbonate film one molecule deep; unless, however, some of the ferrous carbonate molecules are torn loose from the metal by the violence of the reaction. Thereafter the metal is no longer exposed to the reaction or to reaction 2 or reaction 3. Corrosion, as defined, must therefore cease. Current may continue to flow in the corrosion cell, however, with other reactions having lower potential becoming anodic. Next in order is reaction 4—the formation of hydrogen ions from molecular hydrogen. Because no molecular hydrogen is available, reaction 4 can proceed only in the reverse direction and is inactive at the anode. Next in order as an anodic reaction is 5, but because no solid calcium carbonate is available this reaction is inoperative. Reactions 6, 7, and 8 will prevail concurrently at the anode and if allowed to continue, so as to change the composition of the water, will lower the pH in the anodic areas.

Because no iron is derived from the wall of the pipe the iron must be a constituent of the water in the pipe. If the dissolved iron and oxygen are continuously replenished from the supply, ferric-iron rust will continue to plate out at the cathode as indicated by reaction 10. If the iron is not replenished from the supply, as could be the case with a dead-end pipe, the ferrous iron will be reduced in concentration by reaction 10 until the potential is increased to that of reaction 9. Thereafter magnesium carbonate will plate out along with iron rust until the electromotive force of the cell is reduced to zero and the current flow ceases.

It is of interest to note that in the absence of soluble ferrous iron, magnesium carbonate will plate out at the cathode in Example 2 by means of a half-cell electrochemical reaction involving dissolved oxygen. This reaction has been encountered in a case in the writer's practice where magnesium carbonate crystals were found at cathodic areas on the exterior of a steel pipe which had been subjected to stray-current electrolysis. It may be shown that $MgCO_3$ plates out in preference to $CaCO_3$ at 25° C unless the concentration of calcium is more than 6.5 times the magnesium concentration.

Most of the reactions in Example 2 are not to be found in the literature and experimental proof of their occurrence is desirable. Some experiments[15] by T. E. Larson and R. M. King furnish confirmatory evidence to this end on some of the reactions. In this work an experimental corrosion cell was devised with iron electrodes and nine compartments between the electrodes separated by porous Alundum plates. Tap water with a pH of 7.4, a hardness of 250 ppm, and an alkalinity of 330 ppm was used for the electrolyte and was allowed to flow continuously through the middle compartment. The water had a trace of iron and manganese, 60 ppm of calcium, 24 ppm of magnesium, and 6.0 ppm of dissolved oxygen. Current was allowed to flow through the cell in one direction with an impressed electromotive force. The objective was to study ion migration.

Progressive quality changes occurred in each compartment with continuation of current flow. In the cathode compartment, the pH rose to 11, the calcium and magnesium decreased almost to the vanishing point, and the alkalinity remained almost constant. These phenomena are fully explained by reactions 5 to 9 of Example 2. In the anode compartment, the pH decreased slightly and the alkalinity decreased to approximately one sixth its original value. These changes may be explained by the plating out of bicarbonate on some anodic areas in a reaction similar to 1 of Example 2 concurrently with the solution of ferrous iron (reaction 2 of Example 2) at other spots. Unfortunately, the changes in dissolved oxygen and ferrous-iron concentration were not reported.

Some speculation is now in order about what occurs in the corrective treatment of water by use of the calcium-carbonate equilibrium. The conventional treatment is to use alkali to supersaturate slightly the water with calcium carbonate. It is thought that the precipitation of calcium carbonate forms a protective coating on the pipe wall. Why the precipitation of calcium carbonate by an ordinary chemical reaction instead of by a half-cell reaction should form a wall coating instead of a slurry has not been explained.

It is now evident from Example 2 that calcium carbonate films are formed by an electrochemical reaction involving dissolved oxygen. It is apparent, however, that the protection against corrosion is afforded by the anodic reaction and not the calcium-carbonate film. The important feature is the high pH which prevents the solution of ferrous iron and results in the plating out of carbonate or hydroxide at the anode. As further evidence of this point, iron or steel in contact with strong solutions of sodium carbonate or sodium hydroxide do not corrode. The effectiveness of cement lining in protecting iron pipe from corrosion may be explained by the fact that the pH in the pore water adjacent to the metal is about 12.4 in newly-lined pipe.

---

[15] "Corrosion by Water at Low Flow Velocity," by T. E. Larson and R. M. King, *Journal*, A.W.W.A., Vol. 46, 1954, p. 1.

POLARIZATION TESTS

A piece of corroding metal may be described as an aggregation of numerous small corrosion cells, each with an anodic and cathodic area. If a separate electrode, electrically connected to the piece of metal, is immersed in the electrolyte and a current is made to flow between the separate electrode and the piece of metal by means of an impressed electromotive force, the so-called local or corrosion current on the piece of metal may be modified. This change in the magnitude of the corrosion current is termed "polarization." Many investigations have been made in an effort to determine the relation between the polarizing current and the local corrosion current. If the separate electrode is made an anode, the polarizing current may be increased to a point where there is no flow of local corrosion current and the entire piece of metal is cathodic. Such a current is herein designated an "anode-polarizing current" because it polarizes the anodic areas of the specimen. It is also referred to in the literature as a "cathodic-protection current" because it is the type of current used in cathodic protection of submerged metals. Similarly, if the external electrode is made a cathode, the current may be increased in the reverse direction to a point where there is no flow of local corrosion current and the entire piece of metal is anodic. Such a current is herein designated a "cathode-polarizing current." The polarizing current required to produce these results is of particular importance in indicating the current density required for cathodic protection of submerged metals.

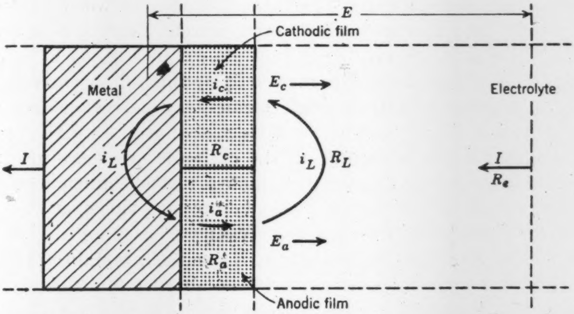

FIG. 4.—POLARIZING OF ELEMENTARY CORROSION CELL WITH ANODE-POLARIZING CURRENT.

Ingenious "null" methods have been devised for measuring the potential between the electrolyte and the corroding metal which automatically eliminate the IR-drop of the polarizing current through the electrolyte.[16] The potential thus measured reflects the increased IR-drop through the cathodic films of the test specimen for an anode-polarizing current and the increased IR-drop through the anodic films of the specimen for a cathode-polarizing current. Plots of these potential measurements against corresponding polarizing currents are known as polarization curves.

---

[16] "Null Methods Applied to Corrosion Measurements," by J. M. Pearson, *Transactions*, Electrochemical Soc., Inc., Vol. 81, 1942, p. 485.

Fig. 4 shows diagrammatically the direction of the current flow in the polarization of an elementary corrosion cell with an anode-polarizing current. Fig. 4 shows (1) the local current, i_L, as modified by the polarizing current, I, with the corresponding resistance, R_L, through the electrolyte, (2) the total current, i_c, through the cathodic film with the corresponding resistance, R_c, of the cathodic film, (3) the total current, i_a, through the anodic film with the corresponding resistance, R_a, through the anodic film, (4) the resistance of the electrolyte, R_e, to the polarizing current, I, and (5) the electromotive forces of the anodic area, E_a, and the cathodic area, E_c. The resistance through the metal itself to both the local current and the polarizing current is infinitesimally small as compared to the resistance through the films and the electrolyte and has therefore been assumed equal to zero in order to simplify the mathematical development. The total potential between a selected point in the electrolyte and the test metal for a current flowing between the test specimen and the separate electrode (not shown in Fig. 4) is designated in Fig. 4 as E. The potential which is measured by the null methods is $E - I R_e$. Although Fig. 4 pictures only a single elementary corrosion cell, it may be considered as representing an entire test specimen where all the anodic areas are grouped into a single area and all the cathodic areas are grouped into a single area. Measurements made with such a test specimen would result in average values for all the elementary cells comprising this specimen.

In order to develop the theory, it is necessary to assume that all the resistances and the single-electrode potentials, E_a and E_c, remain constant during testing. The local corrosion current, i, in the absence of a polarizing current, which is one of the unknowns to be determined, is also assumed to remain constant. As will be shown subsequently, K_a and K_c are also constant, K_a being the fraction of an anode-polarizing current I by which the local corrosion current i is reduced at the anodic areas and K_c being the fraction of a cathode-polarizing current I by which the local corrosion current i is increased at the anodic areas. The conditions during testing must therefore be such that the thickness of the films and the temperature and composition of the electrolyte in the anodic and cathodic areas are not substantially changed during the current flow. The initial thicknesses of the films should be substantial, the electrolyte should be replaced or mixed continuously, and the duration of the test should be short. It is obvious that experiments beginning with clean metal specimens will not conform to these requirements and will yield results which are difficult to interpret.

Fig. 5(a) shows an analysis of a local corrosion cell with no polarizing current. The potential drops around the circuit are shown diagrammatically with

$$I = 0 \qquad (8)$$

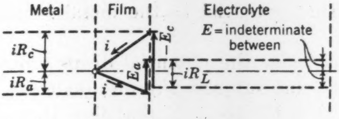
Metal
Film
Electrolyte
E = indeterminate between
iR_c
iR_a
i
i
E_a
$-E_c$
iR_L

(*a*) Zero polarizing current

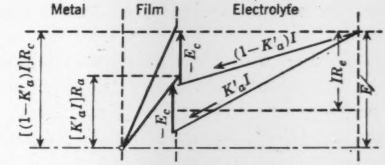
Metal
Film
Electrolyte
$[(1-K'_a)I]R_c$
$[K'_aI]R_a$
$-E_c$
$-E_c$
$(1-K'_a)I$
K'_aI
IR_e
E

(*d*) Anode polarizing current greater than I_a

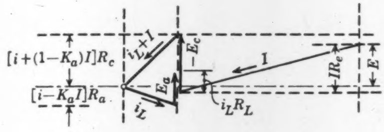
$[i+(1-K_a)I]R_c$
$[i-K_aI]R_a$
i_L+I
i_L
E_a
$-E_c$
I
IR_e
E
i_LR_L

(*b*) Anode polarizing current less than I_a

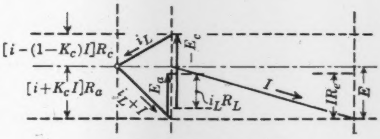
$[i-(1-K_c)I]R_c$
$[i+K_cI]R_a$
i_L
i_L+I
$-E_c$
E_a
i_LR_L
I
IR_e
E

(*e*) Cathode polarizing current less than I_c

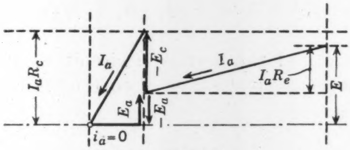
I_aR_c
I_a
$-E_c$
I_a
I_aR_e
E
E_a
$-E_a$
$i_a=0$

(*c*) Anode polarizing current equal to I_a

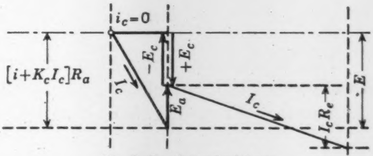
$i_c=0$
$[i+K_cI_c]R_a$
I_c
$-E_c$
$+E_c$
E_a
I_c
I_cR_e
E

(*f*) Cathode polarizing current equal to I_c

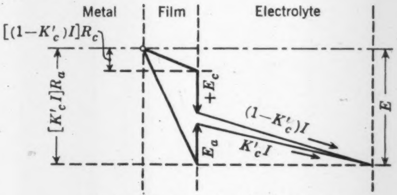
Metal
Film
Electrolyte
$[(1-K'_c)I]R_c$
$[K'_cI]R_a$
$+E_c$
$(1-K'_c)I$
K'_cI
E_a
E

(*g*) Cathode polarizing current greater than I_c

FIG. 5.—ANALYSIS OF LOCAL CORROSION CELLS

and

$$i_a = i_c = i_L = i \qquad (9)$$

By application of Kirchhoff's second law,

$$E_a - E_c = i\,(R_a + R_L + R_e) \qquad (10)$$

from which

$$i = \frac{E_a - E_c}{R_a + R_L + R_e} \qquad (11)$$

From Eq. 11 the local corrosion current can be evaluated in terms of the electromotive force of the corrosion cell and the resistances of the circuit. It can be seen from Fig. 5(*a*) that the external potential to the metal is indeterminate.

In Fig. 5(*b*) there is shown diagrammatically the potential drops around the corrosion circuit when the specimen is being subjected to an anode-polarizing current of insufficient magnitude to stop the local current flow through the anode—I_a being the anode-polarizing current just sufficient to reduce the current through the anodic areas, i_a, to zero. From Fig. 5(*b*) it can be seen that

$$I > 0 < I_a \tag{12}$$

$$i_a = i_L = i - K_a I \tag{13}$$

$$i_c = i_L + I = i + (1 - K_a) I \tag{14}$$

and

$$E_a - E_c = (i - K_a I)(R_a + R_L + R_c) + I R_c \tag{15}$$

which results from the application of Kirchhoff's second law. From Fig. 5(*b*) the external potential to the metal is

$$E - I R_e = E_c + [i + (1 - K_a) I] R_c = E_a - (i - K_a I)(R_a + R_L) \tag{16}$$

Fig. 5(*c*) shows the potential drops around the corrosion circuit with an anode-polarizing current, I_a, just sufficient to stop the flow of current through the anode. From Fig. 5(*c*) it can be seen that

$$I > 0 = I_a \tag{17}$$

$$i_a = i_L = 0 \tag{18}$$

$$i_c = I_a \tag{19}$$

and

$$i = K_a I_a \tag{20}$$

By application of Kirchhoff's second law,

$$E_a - E_c = I_a R_c \tag{21}$$

The external potential to the metal is

$$E - I_a R_e = E_c + I_a R_c = E_a \tag{22}$$

It will be noted in Fig. 5(*c*) that the anode potential is just on the point of reversing in direction for this case.

Fig. 5(*d*) represents the potential drop through the specimen with an anode-polarizing current in excess of that required to stop the flow of current through the anode. In this case, the entire specimen is cathodic. It is probable that the half-cell reaction which occurred at the anode while it was still anodic will ~~not~~ now take place with the reversal of direction because other reactions are more cathodic. Hence, in Fig. 5(*d*) a different potential has been shown for the cathodic reaction on the areas which previously were anodic. In Fig. 5(*d*),

$$I > 0 > I_a \tag{23}$$

$$i_L = 0 \tag{24}$$

$$-i_a = K'_a I \tag{25}$$

and

$$i_c = (1 - K'_a I) \tag{26}$$

Because the entire specimen becomes cathodic (*a*) E_a is replaced by $-E_c$ on previously anodic areas, (*b*) the current I is divided with different IR-drops through R_a and R_c, and (*c*) discontinuity in the polarization curve is to be expected as I exceeds I_a with the value of K_a being replaced with a variable factor K'_a.

Fig. 5(*e*) shows diagrammatically the potential drops for the corrosion circuit subjected to a cathode-polarizing current of a magnitude insufficient to stop the flow of current through the cathodic areas of the specimen—I_c being the cathode-polarizing current just sufficient to reduce the current through the cathodic areas, i_c, to zero. In Fig. 5(*e*),

$$I < 0 > I_c \tag{27}$$

$$i_c = i_L = i - (1 - K_c)\, I \tag{28}$$

$$i_a = i_L + I = i + K_c I \tag{29}$$

and from Kirchhoff's second law,

$$E_a - E_c = (i + K_c I)\,(R_a + R_L + R_c) - I\,(R_L + R_c) \tag{30}$$

The external potential to the metal is

$$E - I R_e = E_c + [i - (1 - K_c)\, I]\,(R_L + R_c) = E_a - (i + K_c I)\, R_a \tag{31}$$

In Fig. 5(*f*) are shown the potential drops around the corrosion circuit for a specimen subjected to a cathode-polarizing current, I_c, just sufficient to stop the flow of current through the cathodic areas. In Fig. 5(*f*),

$$I < 0 = I_c \tag{32}$$

$$i_c = i_L = 0 \tag{33}$$

$$i_a = I_c \tag{34}$$

and

$$i = (1 - K_c)\, I_c \tag{35}$$

By applying Kirchhoff's second law to the corrosion circuit there results

$$E_a - E_c = I_c R_a \tag{36}$$

and the external potential to the metal is

$$E - I_c R_e = E_c = E_a - I_c R_a \tag{37}$$

In Fig. 5(g) there are shown the potential drops corresponding to a cathode-polarizing current sufficient to reverse the direction of current flow through the cathodic areas of the specimen. In Fig. 5(g) the same cathode reaction is shown in reverse, indicating the dissolving of the film previously formed on the cathodic areas. If other reactions would produce a greater potential on the cathodic areas, they would supersede the ones which previously took place. In Fig. 5(g),

$$I < 0 < I_c \qquad (38)$$

$$i_a = K'_c I \qquad (39)$$

and

$$-i_c = (1 - K'_c)\, I \qquad (40)$$

Because the entire specimen becomes anodic (a) $- E_c$ is changed to an anodic potential corresponding to the possible reactions with highest potential over the cathodic film previously formed, (b) the potential may be $+ E_c$ if no other reaction is possible until the film is dissolved, (c) the current I is divided with different IR-drops through R_a and R_c, and (d) discontinuity in the polarization curve is to be expected as I exceeds I_c—the value of K_c being replaced with a variable factor K'_c.

The values of E_a and E_c should be computed before the start of the polarization tests by the methods previously illustrated. During the tests I_a may be evaluated by noting the anode-polarizing current when the external potential to the metal equals E_a (Eq. 22). Similarly, I_c may be evaluated by noting the cathode-polarizing current when the external potential to the metal equals E_c (Eq. 37). If, however, R_a is zero—as will probably be the case at low pH-values—the external potential to the metal is constant and equal to E_a with cathode-polarizing currents up to the magnitude of I_c (Eq. 31). The resistances R_c and R_a may be evaluated by Eqs. 21 and 36. When the tests are completed and the polarization curves are plotted, other unknowns may be evaluated from the curves.

If Eq. 10 is subtracted from Eq. 15, K_a may be expressed in terms of the resistances as

$$K_a = \frac{R_c}{R_a + R_L + R_c} \qquad (41)$$

It follows therefore that, if the resistances remain constant during the tests, K_a is constant for values of the anode-polarizing current up to I_a.

The value of K_a may not be computed directly from Eq. 41 because the value of R_L is not yet known. It may, however, be evaluated from the experimental data for any two points on the anode-polarization curve for values of I less than I_a. If Eq. 16 is solved for i in terms of R_c for the data from any two points and the two values of i are equated—

$$K_a = 1 - \frac{(E - I\,R_c)_2 - (E - I\,R_c)_1}{(I_2 - I_1)\,R_c} \qquad (42)$$

in which $(E - I R_e)_2$ and $(E - I R_e)_1$ are the external potentials to the metal for points 2 and 1, respectively, on the anode-polarization curve, and I_2 and I_1 are the corresponding anode-polarizing currents, both being less than I_a.

If the value of K_a computed from Eq. 42 is inserted into Eq. 41 with the already known values of R_a and R_c, R_L may be evaluated. The current i may then be evaluated from Eq. 10 or from any point on the anode-polarization curve by Eq. 16.

If Eq. 10 is subtracted from Eq. 30, K_c may be expressed in terms of the resistances—

$$K_c = \frac{R_c + R_L}{R_a + R_L + R_c} \quad \text{(43)}$$

A comparison of Eq. 43 with Eq. 41 will show that K_a and K_c are not equal. The assumption that K_a equals K_c which has been made in many previous investigations[17,16,18] involves the complete neglect of R_L. The equation,

$$i = \frac{I_a I_c}{I_a + I_c} \quad \text{(44)}$$

used by these investigators follows directly from the erroneous assumption that K_a equals K_c.

The value of K_c may be computed directly from Eq. 43 when all resistances are known. However, as a check, K_c may also be evaluated from the experimental data for any two points on the cathode-polarization curve for values of I less than I_c. If Eq. 31 is solved for i in terms of R_c for the data from any two points and the two values of i are equated,

$$K_c = 1 - \frac{(E - I R_e)_1 - (E - I R_e)_2}{(I_2 - I_1)(R_L + R_e)} \quad \text{(45)}$$

Now, if R_a is zero and the external potential to the metal is constant, as has been demonstrated previously, $K_c = 1$ from Eq. 43 or Eq. 45.

A critical examination of Eq. 16, which is the equation for the anode-polarization curve, will reveal that if the conditions for testing are properly maintained only the polarizing current and external potential to the metal are variables. Eq. 16 represents a straight line, and all anode-polarization curves also should be straight lines. Curvature indicates changes in resistance or composition of the electrolyte during testing. Similarly, Eq. 31 indicates that all cathode-polarizing curves should be straight lines as curvature indicates failure to control the conditions of the test as required. The terms K_a and K_c are functions of the slope of the straight-line polarization curves.

In order to study the rate of growth and the rate of increase in resistance of films, it is desirable to begin with clean metal specimens and a constant polarizing current I which is greater in magnitude than I_a for anode-polarizing currents and I_c for cathode-polarizing currents. The specimen will be all

---

[17] "The Effect of Cathodic Reactions on the Corrosion of Metals from the Viewpoint of the Local Cell Theory," by W. J. Muller, *Transactions*, Electrochemical Soc., Inc., Vol. 76, 1939, p. 167.

[18] "Thermodynamics of Irreversible Processes Applied to Corrosion," by P. A. Johnson and A. L. Babb, *Industrial and Engineering Chemistry*, March, 1954, p. 518.

anode for the one case and all cathode for the other case. With the anode-polarizing current,

$$E - I\,R_e = E_c + I\,R_c \tag{46}$$

and with the cathode-polarizing current,

$$E - I\,R_e = E_a - I\,R_a \tag{47}$$

If I is kept constant, the change with time in the external potential to the metal is a direct measure of the rate of increase in the resistance of the film.

Moreover, I is a measure of the rate of deposit of film. If the composition of the film is previously identified, as it must be to compute the single-electrode potential, the rate of deposit by weight may be computed directly from I.

CONCLUSIONS

It is hoped that this work will be studied carefully by all investigators in the corrosion field so that corrosion research may be placed on a more scientific basis. The principles presented should be examined critically—both by theoretical analysis and experimentation—for the elimination of errors.

DISCUSSION

EDWARD W. MOORE.[19]—A comprehensive, highly condensed presentation of the electrochemical theory of corrosion as it applies to conditions encountered in water supplies has been made by Mr. Camp. Although the material presented is already in existence in the more advanced textbooks on electrochemistry and in the literature of corrosion, the author's contribution is to assemble the material in such a way that it can be assimilated and applied by engineers sufficiently interested to devote the study necessary to follow the rigorous mode of presentation.

To one interested in corrosion theory for itself and in research that will lead to better understanding of the nature of the corrosion process, the value of the paper is obvious. It may be less obvious to the engineer interested primarily in using corrosion theory to evaluate protective coatings and corrective water-treatment processes. Mr. Camp states that the principles have been useful for these purposes; this aspect of the matter is not, and probably should not be, emphasized in this work. However, it is hoped that more work emphasizing the application of the theory to particular instances will be forthcoming. Such papers may convince a larger number of engineers that the rigorous study called for is worth the effort.

Mr. Camp is correct in deploring the little attention given to the development of corrosion theory in contradistinction to the vast effort expended on evaluation tests. It is not improbable that a little more attention devoted to basic theory would have eliminated the need for many an expensive testing program.

No important exception can be taken to the theory as presented in the main body of the paper. The facts, and the pertinent equations—chemical and thermodynamic—are set forth with clarity and precision. The selection, from the large mass of data available, has been judiciously made to include those elements most significant to waterworks practice. A careful study will result in a sound knowledge of the electrochemical theory of corrosion and its potential applications.

Certain minor criticisms might be offered. One wishes, for example, that the significance and potential utility of the equations relating to the polarization tests had been more completely explained. Most engineers will certainly not be clear as to where this material leads.

Under the heading, "Application of Theory to Identify Half-Cell Reactions: Example 2," it appears to be implied that chemical reactions always give slurry precipitates, and only electrochemical reactions give wall coatings. Although it is a well-known fact that rapid precipitations in the presence of large quantities of chemical reagents give slurries, many slow-precipitation reactions result in coatings on solid surfaces. Supersaturated solutions of many calcium and magnesium salts produce suspended precipitates only with difficulty but readily deposit on the glass walls of their containers; crystallization from solutions often begins at the walls; boiler scales not only form at walls but adhere tightly to them. Therefore, there is the whole range of adsorption phenomena to be considered.

---

[19] Associate Prof. of San. Chemistry, Div. of Eng. and Applied Physics, Harvard Univ., Cambridge, Mass.

The foregoing does not, however, imply rejection of the conclusion that calcium-carbonate precipitation on the walls is associated with the electrochemical reactions. Some recent research[20] using radioactive calcium to form the calcium-carbonate supports Mr. Camp's thesis as the quantity of calcium carbonate precipitated is directly related to the amount of iron corroded for the first few days of immersion of the specimen.

The writer has a semantic objection to the term "plate out" when applied to the electrochemical decomposition of materials like hydrogen ion, bicarbonate ion, normal carbonate ion, and the like. The term is derived from the electroplating of metals which is a special application of electrochemical decomposition resulting in a true surface plating. It has no useful function when applied to nonmetallic materials and merely tends to confuse.

There is available a most complete tabulation of chemical thermodynamic values from which, as shown by the author, oxidation potentials may be derived.[21] Therein, the thermochemical calorie is defined as 4.1840 absolute joules, and Faraday's constant is 96,485.3 coulombs. However, such minor revisions in values are of little significance in this field.

THOMAS R. CAMP,[22] M. ASCE.—The writer greatly appreciates the discussion contributed by Mr. Moore and he regrets that the many others who evidenced an interest in the subject matter by letters were unable to find the time to prepare written discussions for publication.

Mr. Moore has questioned the significance and utility of the equations developed in the section on polarization tests. Polarization tests are commonly used for estimating the currents and potentials necessary for cathodic protection. The writer believes that laboratory tests of this type must be used to verify the theory presented, to measure the resistance through the films, and to measure the rates of corrosion. The purpose of the equations is to regulate the laboratory tests so that they may not be misinterpreted.

The equations developed in the section on polarization tests are all based on the assumption that the electromotive force at the anode and the electromotive force at the cathode are completely independent of the rate of current flow. The writer has stated that this is so, despite opinions expressed to the contrary in current literature. No experimental confirmation of this statement has been presented by the writer, but such confirmation may be obtained by carefully conducted laboratory tests such as are described in the section on polarization tests.

The writer's statement that the electromotive force at the anode and the electromotive force at the cathode are completely independent of the rate of current flow was based on the form of Eqs. 2, 3, and 4 which are derived from thermodynamic principles and which include no term for rate of current flow. It was further based on the fact that the physical nature of the interfacial reactions which determine the electromotive forces is not affected by the rate of current flow.

---

[20] "Calcium Carbonate Deposition at Iron Surfaces," by Werner Stumm, *Journal*, A.W.W.A., March, 1956.

[21] "Selected Values of Chemical Thermodynamic Properties," *Circular No. 500*, National Bureau of Standards, Washington, D. C., February, 1952.

[22] Partner, Camp, Dresser & McKee, Cons. Engrs., Boston, Mass.

Consider, for example, an iron anode in contact with an electrolyte of constant composition. Metallic iron enters solution as ferrous ions, but ferrous ions likewise condense on the metal. At equilibrium—that is, no current flow—the rate of solution is equal to the rate of condensation. In order to induce current flow, it is necessary that the electromotive force at the cathode be such that there is a total electromotive force for the cell which will produce a greater rate of solution of the metallic iron than the rate of condensation of ferrous ions. If the electromotive force at the cathode exactly counteracts the electromotive force at the anode, the rate of solution of metallic iron will be exactly equal to the rate of condensation of ferrous ions. Now, from Eq. 3 the electromotive force at the anode depends on the concentration of the ferrous ions at the anode. If they are being produced faster than they condense on the metal, which is the case with the current flowing, it will be necessary to replace the electrolyte continuously in order to keep the concentration of ferrous ions constant, a condition for a constant electromotive force. This condition is easily met in most water lines with flowing water because the rate of corrosion is extremely slow as compared to the rate of movement of the water.

It will be noted from the foregoing examination that, if the concentration of ferrous ions is maintained constant at the anode during current flow, there is no physical change at the anode because of the flow of electric current. There is no reason, therefore, to suppose that the electromotive force should change because of current flow.

Actually, in most polarization tests there is a change in the measured potentials with increase in current flow, even after compensating for the potential drop through the electrolyte. It is the writer's contention that this change in potential includes the resistance through the films on the electrodes.

Mr. Moore rightly objects to the writer's terms "plate out" when applied to electrochemical decomposition of materials like hydrogen ion, bicarbonate ion, normal carbonate ion, and the like. The term was used in order to distinguish clearly between interfacial reactions requiring the transfer of electrons at a solid boundary and ordinary chemical reactions taking place within the body of the electrolyte and having nothing to do with the corrosion cell. For example, in the writer's reaction 1, normal carbonate is said to be "plated out" at the anode. The reaction involves the combination of ionic carbonate with metallic iron at the interface. This is not plating out in the sense that a metal plate is formed, but a more descriptive term than plating out is difficult to find.

AMERICAN SOCIETY OF CIVIL ENGINEERS
Founded November 5, 1852
TRANSACTIONS

Paper No. 2823

CONTINUOUS PRESTRESSING

By Robert B. B. Moorman,[1] M. ASCE

With Discussion by Messrs. Abdel F. Diwan, Leopold J. Mensch, and Robert B. B. Moorman

Synopsis

The nature and treatment of prestress loads for continuous prestressed concrete beams are considered, and two examples are presented. There is examined an approximate method of determining friction losses; a procedure for analysis and design is included.

Introduction

Continuous beams whether prestressed or not, are subjected to moments as a result of continuity. For nonprestressed beams the moments are caused by dead load and applied loads. For prestressed beams the same moments occur; however, there are also moments resulting from the effects of prestressing.

The effects of prestressing can be expressed as lateral loads[2,3,4,5,6,7,8] and longitudinal loads, either axial or eccentric. Any of the usual methods of structural analysis can be used to analyze a concrete structure to determine the effects of the prestressing loads. If the principle of superposition is accepted as valid in the case of prestressed statically indeterminate structures, the dead

---

Note.—Published, essentially as printed here, in January, 1955, as *Proceedings-Separate No. 588*. Positions and titles given are those in effect when the paper or discussion was approved for publication in *Transactions*.

[1] Chairman, Dept. of Civ. Eng., Syracuse Univ., Syracuse, N. Y.

[2] "A Study of Continuous Beams and of Some Statically Redundant Systems in Prestressed Concrete," by M. Y. Guyon, *Translation No. 33*, Cement and Concrete Assn., London, 1951.

[3] "Analysis of Continuous Prestressed Concrete Structures," by A. L. Parme and G. H. Paris, *Proceedings*, First U. S. Conference on Prestressed Concrete, Cambridge, Mass., 1951, p. 195.

[4] "Designing for Continuity in Prestressed Concrete Structures," by A. L. Parme and G. H. Paris, *Journal*, A. C. I., Vol. 23, No. 1, September, 1951, p. 45.

[5] "Equivalent Load Method for Analyzing Prestressed Concrete Structures," by Robert B. B. Moorman, *ibid.*, No. 5, January, 1952, p. 405.

[6] "A Symposium on Prestressed Concrete Statically Indeterminate Structures: Determination of Continuity Bending Moments in Prestressed Continuous Beams," by E. G. Trimble, Cement and Concrete Assn., London, 1953, p. 95.

[7] "A Symposium on Prestressed Concrete Statically Indeterminate Structures: A Theoretical Treatment of Continuity in Prestressed Concrete," by Y. Guyon, Cement and Concrete Assn., London, 1953, p. 131.

[8] "Continuous Prestressed Concrete Beams," by Fritz Leonhardt, *Journal*, A. C. I., Vol. 24, No. 7, March, 1953, p. 617.

load, applied loads, and prestressing forces can be examined separately. The resulting moments can then be added algebraically to obtain the actual maximum and minimum values for the loaded structure.

Assumptions.—It is assumed herein that (1) Hooke's law is valid, (2) the principle of superposition holds, (3) the horizontal component of the tension in the cable is equal to the tension in the cable, (4) the friction force is negligible, (5) the lateral force from the cable is either vertical or normal to the axis of the member, (6) the loss of cable tension caused by creep is negligible, and (7) the reduction in cross-sectional area because of the cable ducts is negligible.

NATURE OF PRESTRESSED LOADS

The prestressing unit produces loads on the concrete in the form of reactions at the end anchorages, lateral reactions between the cable and the sheath (for curved cables), tangential frictional reaction along the cable, and external reactions caused by bending deformation of the beam when the beam is statically indeterminate. Fig. 1 shows the horizontal and vertical end-anchorage forces, the lateral force, and the frictional force acting on part of the beam.

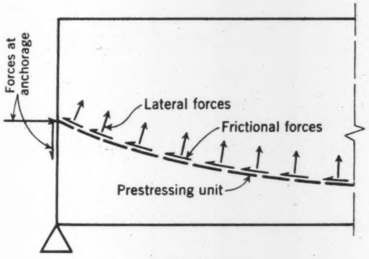

FIG. 1

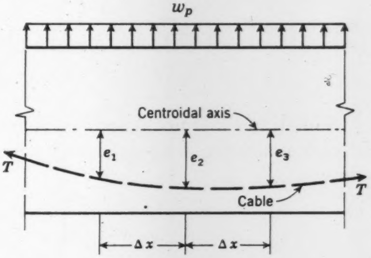

FIG. 2

For purposes of analysis, prestressed concrete can be considered to be a homogeneous material; then it remains only to consider the forces applied to the concrete structure. These forces may consist of end-anchorage reactions, normal reaction along the cable, frictional reaction along the cable, dead load, various types of live loads, and the reactions produced by the foregoing loads.

It cannot be overemphasized that, in the initial stages of analysis of a prestressed concrete beam, the beam should be treated as a member consisting of homogeneous material. The beam should be analyzed for the usual live loads and dead loads and then it should be analyzed for the prestress loads. The principle of superposition may be used to find the net results of the analyses.

In the computation of the ultimate or failure loads, the beam is considered to act as a reinforced concrete beam. In such a case, an ultimate theory should be used in the analysis of stress and moment.

EQUIVALENT LOAD

If M is the bending moment caused by an eccentric cable, T the resultant (horizontal) tension in the cable, and e the eccentricity of the resultant tension,

$$M = -T\,e \qquad (1)$$

If T is assumed constant and if the expression,

$$\frac{d^2M}{dx^2} = -w \quad \text{(2a)}$$

is used,

$$\frac{dM}{dx} = -T\frac{de}{dx} \quad \text{(2b)}$$

and

$$\frac{d^2M}{dx^2} = -T\frac{d^2e}{dx^2} = -w_p \quad \text{(2c)}$$

in which x is a horizontal distance, w denotes a distributed load, and w_p is an equivalent load resulting from an eccentric prestressing cable.

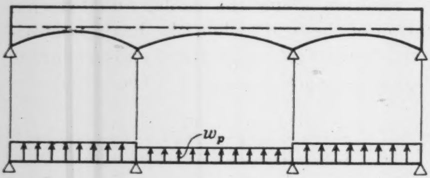

FIG. 3

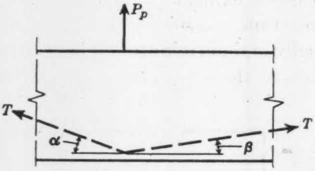

FIG. 4

Sometimes it is not possible to express e in a convenient mathematical form. In such instances it is sufficiently accurate for all practical purposes to use the expression,

$$\frac{d^2e}{dx^2} \approx \frac{e_1 - 2\,e_2 + e_3}{(\Delta x)^2} \quad \text{(3)}$$

in which e_1, e_2, and e_3 are the eccentricities at any three consecutive points along the beam axis and Δx is the distance between the points (measured along the beam). The equivalent load may then be expressed as

$$w_p = T\left(\frac{e_1 - 2\,e_2 + e_3}{(\Delta x)^2}\right) \quad \text{(4)}$$

Eq. 4 can be used for members of variable section as well as for those of constant section; e is positive when the distance is below the centroidal axis, w_p is negative if the load acts upward, and the beam is divided into equal segments Δx (Fig. 2). If the post-tensioning cable is straight between supports, the equivalent load w_p is used only for determining the bending moments; to compute the shears and reactions the load is set equal to zero (Fig. 3). If the member is straight and the post-tensioned cable is curved, the equivalent load w_p should be used for determining bending moments, shears, and reactions.

If the equivalent load w_p is based on an e-value that results from curvature of the post-tensioned cable as well as from curvature of the axis of the beam, there are two loads to be considered in the analysis. The total load w_p is used to compute the bending moments. Then, to find the part of w_p to be used in the computations for reactions and shears, any convenient horizontal straight line is selected (above the cable) as a datum to determine the *e*-value to be used in the equivalent-load expression.

When the cable is placed as shown in Fig. 4, the equivalent load P_p is concentrated. The expression for this load is

$$P_p = -T(\tan\alpha + \tan\beta) \qquad (5)$$

When a parabolic cable has a span *L* and a sag *e*, the equivalent load is

$$w_p = -\frac{8\,T\,e}{L^2} \qquad (6)$$

When the end anchorage is eccentric, as in Fig. 5, the equivalent loading consists of moments at the ends.

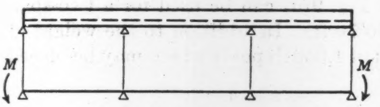

FIG. 5

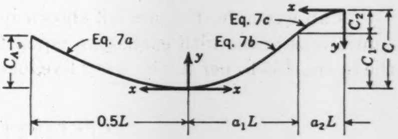

FIG. 6

PARABOLIC CURVES

Probably the most suitable cable form is parabolic; at least it is the simplest form with which to work. Fig. 6 shows a continuous curve consisting of three parabolas. The equations for the curves are

$$y = \frac{4\,x^2\,C_A}{L^2} \qquad (7a)$$

$$y = \frac{x^2\,C_1}{(a_1\,L)^2} \qquad (7b)$$

and

$$y = \frac{x^2\,C_2}{(a_2\,L)^2} \qquad (7c)$$

for the respective parts of the curve. In order for Eqs. 7*b* and 7*c* to be tangent at their common point,

$$C_1 = 2\,a_1\,C \qquad (8a)$$

and

$$C_2 = 2\,a_2\,C \qquad (8b)$$

From left to right, the equations for the equivalent loads caused by curvature are

$$w_p = -\frac{8\,T\,C_A}{L^2} \qquad (9a)$$

$$w_p = -\frac{4\,T\,C}{a_1\,L^2} \qquad (9b)$$

and

$$w_p = +\frac{4\,T\,C}{a_2\,L^2} \qquad (9c)$$

respectively.

For preliminary design purposes, the shape in Fig. 7 may be used for end spans and the shape in Fig. 8 for intermediate spans. The initial values of a may be taken as $a_1 = 0.35$ and $a_2 = 0.15$. After an analysis, these values can be adjusted in any manner deemed desirable.

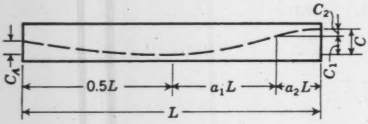
C_2
C
C_A
C_1
0.5L
a_1L
a_2L
L

FIG. 7

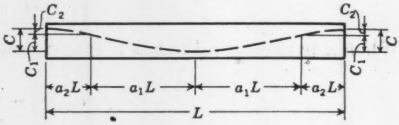
C_2
C
C_1
C_2
C
C_1
a_2L
a_1L
a_1L
a_2L
L

FIG. 8

EXAMPLES

As an example, the section shown in Fig. 9(*a*) can be used for a two-span continuous beam with each span equal to 70 ft. In addition to the weight of the beam, 653 lb per ft, there is a live load of 1,066 lb per ft which may be placed in either or both spans. A concrete working stress of 2,000 lb per sq in. is used.

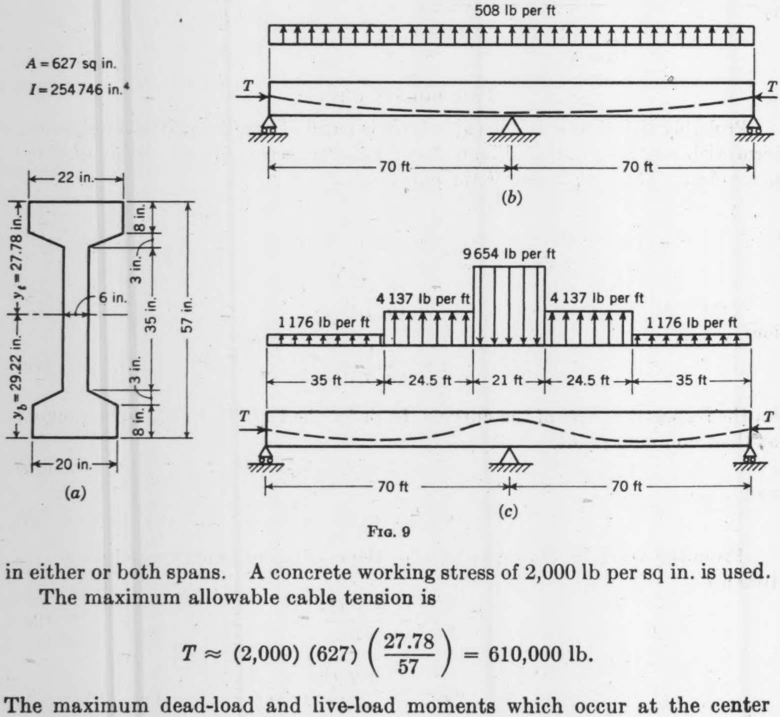
A = 627 sq in.
I = 254 746 in.^{4}
22 in.
8 in.
3 in.
6 in.
35 in.
57 in.
y_t = 27.78 in.
y_b = 29.22 in.
3 in.
8 in.
20 in.
(a)
508 lb per ft
T
T
70 ft
70 ft
(b)
9654 lb per ft
4137 lb per ft
4137 lb per ft
1176 lb per ft
1176 lb per ft
35 ft
24.5 ft
21 ft
24.5 ft
35 ft
T
T
70 ft
70 ft
(c)

FIG. 9

The maximum allowable cable tension is

$$T \approx (2{,}000)\ (627)\left(\frac{27.78}{57}\right) = 610{,}000 \text{ lb.}$$

The maximum dead-load and live-load moments which occur at the center support are

$$M_{dl} = -\ (\tfrac{1}{8})\ (653)\ (70)^2 = -\ 400{,}000 \text{ ft-lb} = -\ 4{,}800 \text{ in.-kips}$$

and

$$M_{ll} = -\left(\tfrac{1}{8}\right)(1{,}066)(70)^2 = -652{,}900 \text{ ft-lb} = -7{,}834.8 \text{ in.-kips.}$$

In the subsequent solutions the shapes of the cables are (1) the single parabolic shape shown in Fig. 9(*b*) and (2) the shape consisting of five parabolas shown in Fig. 9(*c*).

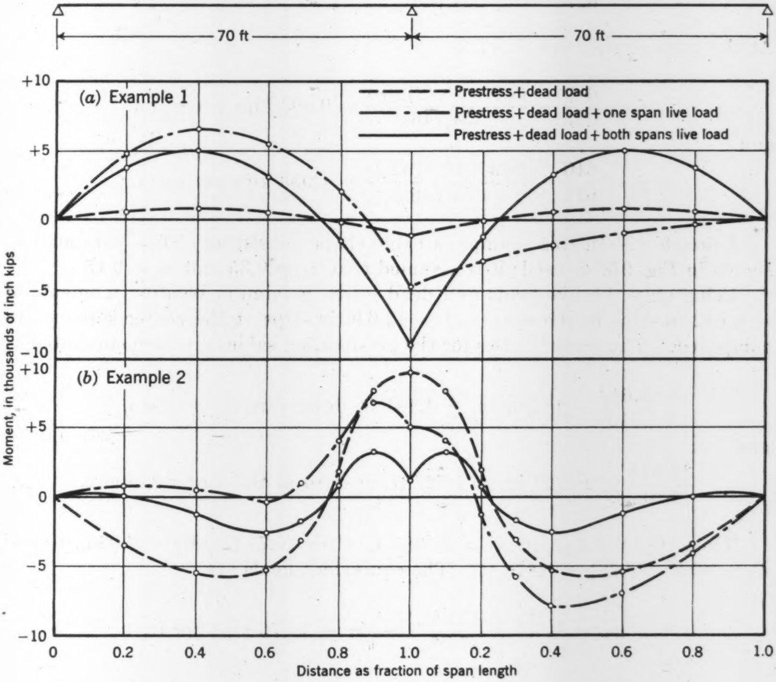

FIG. 10

Example 1.—In this example a single parabola is used for the shape of the cable. If at the center support the eccentricity of the cable is taken as 24.5 in. downward, the equivalent load is

$$w_p \approx -\frac{2\,T\,e}{L^2} = -\frac{(2)\ (610)\ (24.5)}{(12)\ (70)^2} = -\ 0.508 \text{ kips per ft}$$

as shown in Fig. 9(*b*).

The bending moment at the support caused by prestressing is

$$M_p = \left(\tfrac{1}{8}\right)(508)(70)^2 = 311{,}000 \text{ ft-lb} = 3{,}733.8 \text{ in.-kips.}$$

The curves of maximum moments are shown in Fig. 10(*a*). The unit stresses at the top and bottom of the beam in the span are

$$f_t = \frac{610}{627} + \frac{(6{,}551.6)\ (27.78)}{254{,}746} = 1.687 \text{ kips per sq in.}$$

and

$$f_b = \frac{610}{627} - \frac{(6{,}551.6)\ (29.22)}{254{,}746} = 0.221 \text{ kips per sq in.}$$

At the support they are

$$f_t = \frac{610}{627} - \frac{(8{,}901.0)\ (27.78)}{254{,}746} = 0.003 \text{ kips per sq in.}$$

and

$$f_b = \frac{610}{627} + \frac{(8.901.0)\ (29.22)}{254{,}746} = 1.993 \text{ kips per sq in.}$$

Example 2.—In this example a cable shape consisting of five parabolas as shown in Fig. 9(*c*) is used; it is assumed that $a_1 = 0.35$ and $a_2 = 0.15$.

Using only the live loads and dead loads, maximum bending moments of + 8,642 in.-kips in the span and − 12,640 in.-kips at the center support are computed. The eccentricities for the prestressing cables are then computed as

$$\frac{8{,}642}{610} = 14.167 \text{ in.} = 1.181 \text{ ft, downward at midspan,}$$

and

$$\frac{12{,}640}{610} = 20.721 \text{ in.} = 1.727 \text{ ft, upward at the center support.}$$

Thus, $C_A = 1.181$ ft, $C = 2.908$ ft, $C_1 = (0.7)\ (2.908) = 2.036$ ft, and $C_2 = (0.3)\ (2.908) = 0.872$ ft. The equivalent loads are

$$w_p = -\frac{(8)\ (610)\ (1.181)}{(70)^2} = -1.176 \text{ kips per ft,}$$

$$w_p = -\frac{(4)\ (610)\ (2.908)}{(0.35)\ (70)^2} = -4.137 \text{ kips per ft,}$$

and

$$w_p = +\frac{(4)\ (610)\ (2.908)}{(0.15)\ (70)^2} = +9.654 \text{ kips per ft.}$$

These loads are shown in Fig. 9(*c*). Using the coefficients shown in Fig. 11, the fixed end moments caused by the prestressing loads are computed at the exterior support as

$$\begin{aligned} 1.176\ (70)^2\ (0.05729) &= 330.13 \text{ ft-kips} \\ 4.137\ (70)^2\ (0.02504) &= 507.59 \text{ ft-kips} \\ -9.654\ (70)^2\ (0.000998) &= \underline{-47.21 \text{ ft-kips}} \\ & \quad +790.51 \text{ ft-kips} \end{aligned}$$

and at the interior support as

$$\begin{aligned} 1.176\,(70)^2\,(0.02604) &= \;150.05 \text{ ft-kips}\\ 4.137\,(70)^2\,(0.04817) &= \;976.47 \text{ ft-kips}\\ -\,9.654\,(70)^2\,(0.00913) &= -\;\underline{431.89 \text{ ft-kips}}\\ &\; +\;694.63 \text{ ft-kips} \end{aligned}$$

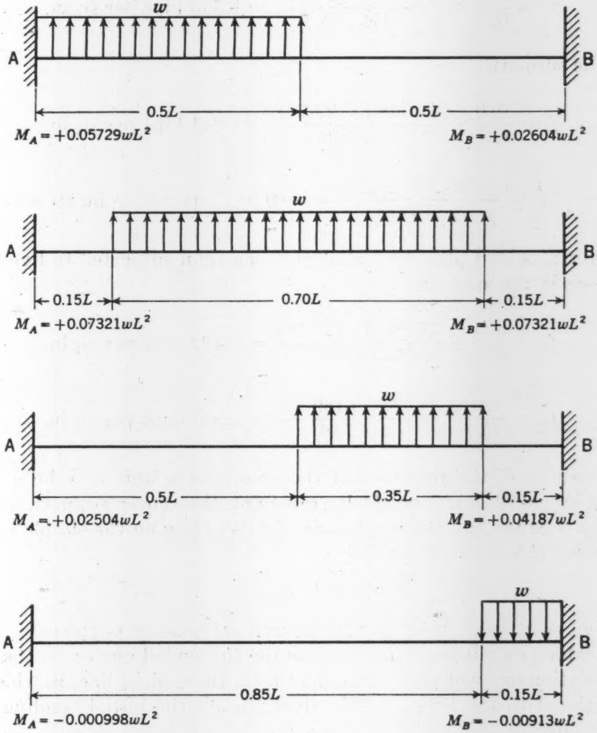
w
A
B
0.5L
0.5L
$M_A = +0.05729wL^2$
$M_B = +0.02604wL^2$
w
A
B
0.15L
0.70L
0.15L
$M_A = +0.07321wL^2$
$M_B = +0.07321wL^2$
w
A
B
0.5L
0.35L
0.15L
$M_A = +0.02504wL^2$
$M_B = +0.04187wL^2$
w
A
B
0.85L
0.15L
$M_A = -0.000998wL^2$
$M_B = -0.00913wL^2$

FIG. 11

The bending moment at the interior support caused by the prestressing loads is found by balancing the moment at the exterior support and carrying over $-\,0.5$ to the interior support. Thus,

$$-\,0.5\,(-790.51) + 694.63 = 1{,}089.89 \text{ ft-kips} = 13{,}078.7 \text{ in-kips}$$

is the bending moment at the interior support.

The curves of maximum moments are shown in Fig. 10(*b*). The computed points through which the curves are drawn are shown as circles. It should be noted that the most favorable condition occurs when the beam is subjected to prestress load, dead load, and live load on both spans.

The unit stresses at the top and bottom of the beam for prestress load plus dead load are (in the span)

$$f_t = \frac{610}{627} - \frac{(5{,}436.3)\ (27.78)}{254{,}746} = 0.382 \text{ kips per sq in.}$$

and

$$f_b = \frac{610}{627} + \frac{(5{,}436.3)\ (29.22)}{254{,}746} = 1.596 \text{ kips per sq in.}$$

and (at the support)

$$f_t = \frac{610}{627} + \frac{(8{,}908.7)\ (27.78)}{254{,}746} = 1.944 \text{ kips per sq in.}$$

and

$$f_b = \frac{610}{627} - \frac{(8{,}908.7)\ (29.22)}{254{,}746} = -\ 0.048 \text{ kips per sq in. (tension).}$$

For prestress load plus dead load plus one span subjected to live load, the unit stresses in the span are

$$f_t = \frac{610}{627} - \frac{(7{,}786.7)\ (27.78)}{254{,}746} = 0.124 \text{ kips per sq in.}$$

and

$$f_b = \frac{610}{627} + \frac{(7{,}786.7)\ (29.22)}{254{,}746} = 1.865 \text{ kips per sq in.}$$

The position of the resultant of the prestressing unit may be determined either (*a*) by use of Eq. 7 or (*b*) by removing the center support, computing the moments caused by the prestressing loads acting on the simple beam, and then dividing this moment by T.

FRICTION

Friction may result from (*a*) the intentional passage of the cable around a curve, in which case it is proportional to the subtended angle; (*b*) the unintentional deviation or "wobble" of the duct from the desired line, in which case it is proportional to the length of the duct; or (*c*) the initial bonding between cable and duct.

An approximate method of ascertaining the effects of friction in post-tensioned prestressing systems has been presented by E. H. Cooley.[9] This method is presented in Table 1 for the two examples included herein.

The method consists of dividing the tensioning unit into several sections the lengths of which are not to exceed 30 ft. The ratio, T_R, of the tensions at the two ends of each section is then computed from

$$T_R \approx 1 - \frac{\mu L}{r} \qquad \text{(10)}$$

---

[9] "Friction in Post-Tensioned Prestressing Systems," by E. H. Cooley, *Research Report No. 1*, Cement and Concrete Assn., London, October, 1953.

in which r is the radius of the section, μ is the friction constant for the prestressing unit used, and L is the length of the section. A "wobble" factor is included in the work of Mr. Cooley[9] but it is omitted herein.

From Fig. 6, Eq. 7*a* leads to

$$\frac{d^2y}{dx^2} = \frac{8\,C_A}{L^2} \tag{11}$$

TABLE 1.—COMPUTATIONS FOR CONTINUOUS PRESTRESSED BEAMS

Section	Length, in feet	Radius, in feet	Value of μ	$\mu L/r$	$1-(\mu L/r)$	Tension factor	Tension, in kips	Cable Extension: Jack end	Cable Extension: Far end	Average tension factor	Effective length, in feet
(*a*) Tensioning from One End (Example 1)											
A						1.000	610.00				
	17.5	1,200	0.07	0.001	0.999			1.000	0.999	0.9995	17.49
B						0.999	609.39				
	17.5	1,200	0.07	0.001	0.999			0.999	0.998	0.9985	17.47
C						0.998	608.78				
	17.5	1,200	0.07	0.001	0.999			0.998	0.997	0.9975	17.46
D						0.997	608.17				
	17.5	1,200	0.07	0.001	0.999			0.997	0.996	0.9965	17.44
E						0.996	607.56				
	17.5	1,200	0.07	0.001	0.999			0.996	0.995	0.9955	17.42
F						0.995	606.95				
	17.5	1,200	0.07	0.001	0.999			0.995	0.994	0.9945	17.40
G						0.994	606.34				
	17.5	1,200	0.07	0.001	0.999			0.994	0.993	0.9935	17.39
H						0.993	605.73				
	17.5	1,200	0.07	0.001	0.999			0.993	0.992	0.9925	17.37
I						0.992	605.12				
(*b*) Tensioning from Two Ends (Example 2)											
A						1.000	610.00				
	17.5	519	0.07	0.002	0.998			1.000	0.998	0.999	17.48
B						0.998	608.78				
	17.5	519	0.07	0.002	0.998			0.998	0.996	0.997	17.45
C						0.996	607.56				
	24.5	147	0.07	0.012	0.988			0.996	0.984	0.990	24.26
D						0.984	600.24				
	10.5	63	0.07	0.012	0.988			0.984	0.972	0.978	10.27
E						0.972	592.92				
(*c*) Tensioning from One End (Example 2)											
A						1.000	610.00				
	17.5	519	0.07	0.002	0.998			1.000	0.998	0.999	17.48
B						0.998	608.78				
	17.5	519	0.07	0.002	0.998			0.998	0.996	0.997	17.45
C						0.996	607.56				
	24.5	147	0.07	0.012	0.988			0.996	0.984	0.990	24.26
D						0.984	600.24				
	10.5	63	0.07	0.012	0.988			0.984	0.972	0.978	10.27
E						0.972	592.92				
	10.5	63	0.07	0.012	0.988			0.972	0.960	0.966	10.14
F						0.960	585.60				
	24.5	147	0.07	0.012	0.988			0.960	0.948	0.954	23.37
G						0.948	578.28				
	17.5	519	0.07	0.002	0.998			0.948	0.946	0.947	16.57
H						0.946	577.06				
	17.5	519	0.07	0.002	0.998			0.946	0.944	0.945	16.54
I						0.944	575.84				

Then

$$r \approx \frac{1}{\dfrac{d^2y}{dx^2}} = \frac{(0.5\,L)^2}{2\,C_A} \tag{12a}$$

and Eqs. 7*b* and 7*c* lead to

$$r = \frac{(a_1\,L)^2}{2\,C_1} \tag{12b}$$

and

$$r = \frac{(a_2\,L)^2}{2\,C_2} \tag{12c}$$

For Example 1,

$$r = \frac{(70)^2}{2(2.044)} = 1{,}200 \text{ ft}$$

and for Example 2,

$$r = \frac{(35)^2}{2\ (1.181)} = 519 \text{ ft}$$

$$r = \frac{(24.5)^2}{2\ (2.036)} = 147 \text{ ft}$$

and

$$r = \frac{(10.5)^2}{2\ (0.872)} = 63 \text{ ft}$$

A value of $\mu = 0.07$ has been selected to illustrate the method suggested by Mr. Cooley.[9] The method applied to Examples 1 and 2 is given in Table 1.

Recommended Procedure

1. Using the live loads and dead loads, compute the maximum negative bending moment at the support and the maximum positive bending moment in the span for the continuous structure as if it were composed of homogeneous material.

2. Select a section and estimate the prestressing force. This estimate can be made by multiplying the area of the section by the product of the allowable compressive unit stress and the smaller distance from the centroidal axis to the extreme fiber and dividing by the depth of the section.

3. To obtain e below the centroidal axis at the center of the span, divide the maximum live-load and dead-load positive bending moment in the span by the prestressing force.

4. To obtain e above the centroidal axis at the support, divide the maximum live-load and dead-load bending moment at the support by the prestressing force.

5. These e-values must lie within the beam. Otherwise it is necessary to select a new beam section for trial.

6. Compute the equivalent prestress loads, if the beam is straight, by use of

$$w_p = -\frac{4\ T\ C_n}{(a_n\ L)^2} \qquad (13)$$

or, if the beam is haunched, by use of Eq. 4.

7. If the friction is to be considered, use the average tension over the sectional length for T.

8. Using the prestress load w_p, analyze the continuous structure.

9. Using the principle of superposition, add the moments caused by the prestress loads to the moments caused by dead load and live load in order to obtain values for the curves of maximum moments.

10. Keeping in mind that there is a normal force caused by prestressing, compute the unit stresses at the critical points.

11. Check the ultimate load for the beam as if it were a reinforced concrete beam.

12. Revise design if necessary.

CONCLUSIONS

Continuous prestressed concrete structures may be analyzed by use of any of the usual methods such as moment distribution, slope deflection, three-moment theorem, and moment areas. Consideration of frictional forces along the cable complicates the analysis but may be included with a reasonable amount of extra work.

The effect of prestressing may be expressed in terms of equivalent forces or loads and moments which are to be applied to the structure as external effects. The equivalent distributed load may or may not be uniform. However, if the eccentricity has a parabolic variation, the equivalent load is uniform and this type of load is the easiest to treat in an analysis.

DISCUSSION

Abdel F. Diwan,[10] A.M. ASCE.—Representation of the effects of prestressing by an equivalent load in the case of continuous prestressed beams appears to be of rather limited value. It is useful only when the prestressing cable is arranged so that the function of the eccentricity e is a second-degree parabola, in which case the equivalent load will have a constant value. Even so, it is also necessary that the coefficients for fixed end moments for partly loaded beams be determined. It cannot be stated that this cable arrangement will be the most suitable, although it may be the most convenient one to justify the application of the equivalent-load concept. Gustave Magnel, for example, suggests[11] a parabola of the fourth degree for the shape of the prestressing cable. In this and similar cases, the equivalent load will have a variable intensity for which the coefficients for the fixed end moments are not readily available. To determine these moments one must consider the bending-moment diagram for any statically determinate system, the most convenient of which is a system of simple spans. For a simple span the bending-moment diagram resulting from prestressing is given by the curve enclosed by the cable and the axis of the beam, multiplied by the resultant (horizontal) tension in the cable. With this curve representing the bending-moment diagram for the statically determinate system, the final diagram for the continuous beam can be computed readily by any of the classical methods. Of these the most suitable appears to be the three-moment equation.

Fig. 12(*a*) shows Example 1 as presented by Mr. Moorman; the prestressing cable is in the shape of a single second-degree parabola. The total elastic load on each span is

$$E\,I\,P_e = -\frac{2}{3} L\,e\,T \quad\text{(14)}$$

in which E is the modulus of elasticity. The elastic reaction at support B with both spans loaded is

$$R_B = \frac{5}{4} P_e = -\frac{5}{6}\left(\frac{T\,e\,L}{E\,I}\right) \quad\text{(15)}$$

From the equation of three moments,

$$4\,M\,L = -6\,R_B \quad\text{(16a)}$$

or

$$M = 1.25\,T\,e \quad\text{(16b)}$$

The net moment at B is

$$M_B = T\,e\,(1.25 - 1.0) = 0.25\,T\,e \quad\text{(17)}$$

---

[10] Asst. Prof., Structural Dept., Faculty of Eng., Alexandria Univ., Alexandria, Egypt.

[11] "Prestressed Concrete," by Gustave Magnel, Concrete Publications, Ltd., London, 1948, p. 84.

which leads to

$$M_B = 0.25 \times 610 \times \frac{24.5}{12} = 311 \text{ kip-ft.}$$

The bending-moment diagram is shown in Fig. 12(*b*).

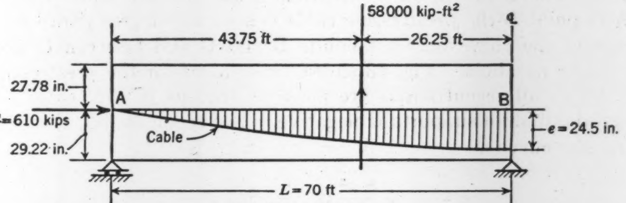
58000 kip-ft²
℄
43.75 ft
26.25 ft
27.78 in.
A
B
T=610 kips
Cable
e=24.5 in.
29.22 in.
L=70 ft

(*a*) Example 1, loads

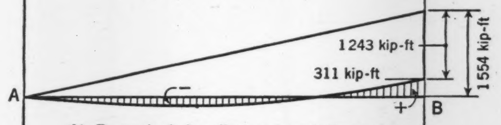
1243 kip-ft
311 kip-ft
1554 kip-ft
A
−
+
B

(*b*) Example 1, bending-moment diagram

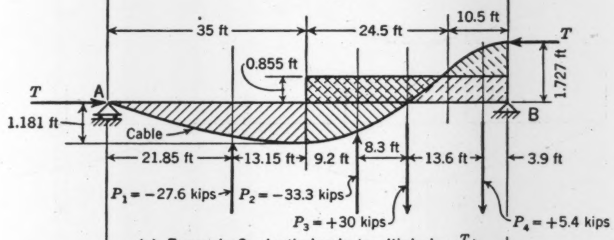
35 ft
24.5 ft
10.5 ft
T
0.855 ft
1.727 ft
T
A
B
1.181 ft
Cable
21.85 ft
13.15 ft
9.2 ft
8.3 ft
13.6 ft
3.9 ft
P₁ = −27.6 kips
P₂ = −33.3 kips
P₃ = +30 kips
P₄ = +5.4 kips

(*c*) Example 2, elastic loads (multiply by $\frac{T}{EI}$)

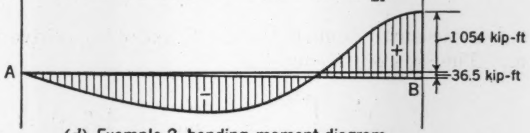
1054 kip-ft
+
36.5 kip-ft
A
−
B

(*d*) Example 2, bending-moment diagram

FIG. 12

For Example 2, the elastic loads are shown in Fig. 12(*c*). The elastic reaction at B is

$$E\,I\,R_B = -\,2.8\,T \ldots\ldots\ldots\ldots\ldots\ldots\ldots (18)$$

The continuity moment necessary at B is

$$M = \frac{6(2.8)}{4(70)}\,T = 0.06\,T \ldots\ldots\ldots\ldots\ldots\ldots (19)$$

The resultant moment at B is

$$M_B = (1.727 + 0.060)\ T = 1.787\ T \dots\dots\dots\dots (20)$$

For $T = 610$ kips, $M = 1{,}090.5$ kip-ft.

A more complicated shape for the curve of the prestressing cable is shown in Fig. 13 which represents a continuous beam of three equal spans. From point A to point B the prestressing cable is a second-degree parabola, whereas the shape of the curve between points B and C and between C and D is a fourth-degree parabola. Fig. 13 shows two shapes for the prestressing cable. In Fig. 13(*a*), all eccentricities are positive whereas in Fig. 13(*b*) the eccentricity at the middle supports is negative. For segment BC, the equation of the parabolic curve is

$$e = e_1 + \frac{8\,x^2}{L^4}\,(e_1 - e_2)(2\,x^2 - L^2) \dots\dots\dots\dots (21)$$

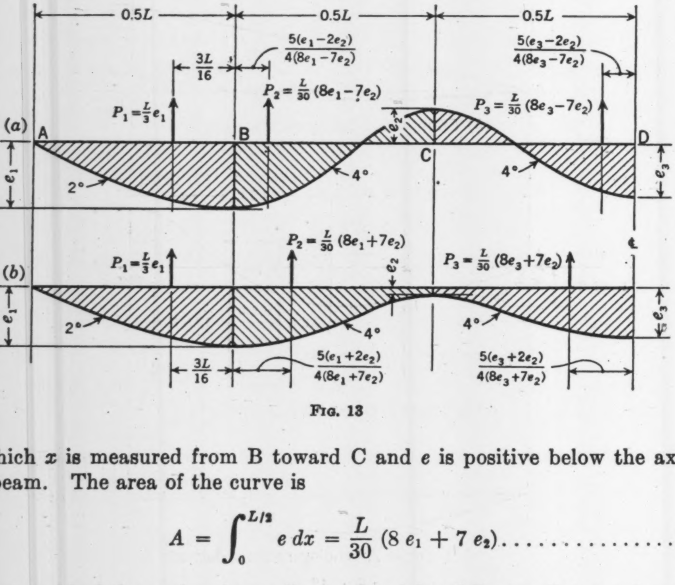
0.5L
0.5L
0.5L
$\frac{5(e_1-2e_2)}{4(8e_1-7e_2)}$
$\frac{5(e_3-2e_2)}{4(8e_3-7e_2)}$
$\frac{3L}{16}$
$P_2 = \frac{L}{30}(8e_1-7e_2)$
$P_3 = \frac{L}{30}(8e_3-7e_2)$
$P_1 = \frac{L}{3}e_1$
(a)
A
B
C
D
e_2
e_1
e_3
2°
4°
4°
$P_2 = \frac{L}{30}(8e_1+7e_2)$
$P_1 = \frac{L}{3}e_1$
$P_3 = \frac{L}{30}(8e_3+7e_2)$
℄
(b)
e_2
e_1
e_3
2°
4°
4°
$\frac{3L}{16}$
$\frac{5(e_1+2e_2)}{4(8e_1+7e_2)}$
$\frac{5(e_3+2e_2)}{4(8e_3+7e_2)}$

FIG. 13

in which x is measured from B toward C and e is positive below the axis of the beam. The area of the curve is

$$A = \int_0^{L/2} e\,dx = \frac{L}{30}\,(8\,e_1 + 7\,e_2) \dots\dots\dots\dots (22)$$

The centroid of the enclosed area lies to the right of B at a distance $\bar{x}$ so that

$$\bar{x} = \frac{\int_0^{L/2} e\,x\,dx}{A} = \frac{5\,(e_1 + 2\,e_2)}{4\,(8\,e_1 + 7\,e_2)} \dots\dots\dots\dots (23)$$

The total elastic reaction at C caused by the elastic loading on both spans is

$$E\,I\,R_C = -\,\frac{L\,T}{240}\,(67\,e_1 + 104\,e_2 + 64\,e_3) \dots\dots\dots\dots (24)$$

Thus, the continuity moment at C is

$$5\,L\,M_C = -\,6\,R_C \qquad (25)$$

from which

$$M_C = T\,(0.335\,e_1 + 0.52\,e_2 + 0.32\,e_3) \qquad (26)$$

These equations apply to both types of prestressing cables provided that the appropriate sign is taken for e.

It is also of interest to study the effect of external loading on the tension in the prestressing cable although for most practical cases this effect is negligible.

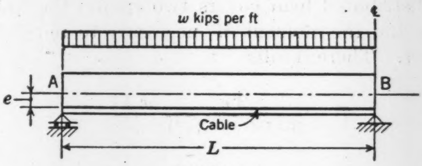

(a) Beam

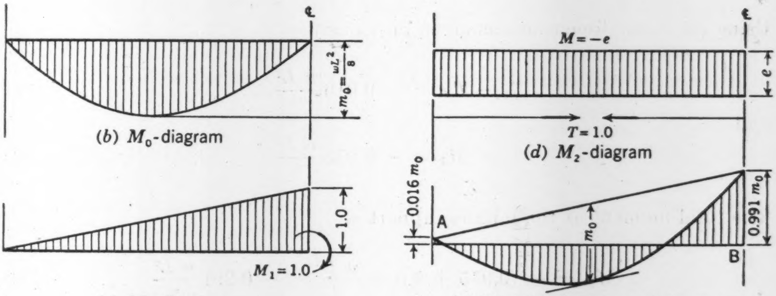

(b) M_0-diagram

(c) M_1-diagram

(d) M_2-diagram

(e) Final bending-moment diagram

FIG. 14

A prestressed, simply supported, one-span beam is, in fact, internally statically indeterminate to the first degree. For the case of a straight prestressing cable, by the method of "virtual work," the force produced in the cable as a result of a uniformly distributed load covering the full span L of the beam is

$$T = \frac{2\,e}{3\,C}\,\frac{w\,L^2}{8} \qquad (27a)$$

in which

$$C = \left(e^2 + \frac{I}{n\,A_s} + \frac{I}{A}\right) \qquad (27b)$$

A_s is the area of the prestressing cable, and $n = E_s/E_c$. Using the same cross section as does Mr. Moorman and assuming $e = 25$ in., $A_s = 6$ sq in., and $n = 7$, then $C = 7{,}080$ in.^{2}

The moment produced by the tension is

$$M = -\frac{2\,e^2}{3\,C}\,\frac{w\,L^2}{8} = -\,0.06\left(\frac{w\,L^2}{8}\right) \qquad (28)$$

Thus, the maximum moment is reduced by 6% as a result of additional force produced in the prestressing cable.

The case of a two-span continuous beam with a straight prestressing cable is shown in Fig. 14; this problem is statically indeterminate to the second degree.

The uniformly distributed load covers two spans; the unknowns are the force T in the cable and the moment M_1 necessary to re-establish continuity at the middle support. There results

$$T = \frac{2\,e}{3\,(4\,C - 3\,e^2)}\,\frac{w\,L^2}{8} \qquad (29)$$

and

$$M_1 = \frac{4\,(C - e^2)}{4\,C - 3\,e^2}\,\frac{w\,L^2}{8}\ \text{(negative)} \qquad (30)$$

Using the same dimensions as given previously—

$$-\,T\,e = -\,0.016\,\frac{w\,L^2}{8} \qquad (31)$$

and

$$+\,M_1 = -\,0.975\,\frac{w\,L^2}{8} \qquad (32)$$

The total moment at the middle support is

$$M_B = -\,(0.975 + 0.016)\,\frac{w\,L^2}{8} = -\,0.991\,\frac{w\,L^2}{8} \qquad (33)$$

The total effect of the additional tension in the cable is much less than that previously obtained for the single-span beam. This is obviously caused by the fact that the prestressing cable is in regions of both compressive and tensile stresses in the continuous beam, which greatly reduces the final elongation necessary in the cable. However, this will not be the case for the cable used in Figs. 12(*c*) and 13(*a*) where the full length of the cable lies in the region of tensile stresses. In these cases the necessary integrations may be obtained by a summation process.

LEOPOLD J. MENSCH,[12] M. ASCE.—The use of prestressed concrete has caused a wealth of papers on the strength of prestressed beams and slabs, based primarily on the laws of elasticity of isotropic materials following Hooke's law. However, concrete is neither isotropic nor does it follow Hooke's law. Therefore, the designer of prestressed concrete members should hesitate before using rules and formulas obtained by this theory. Factors which are to be used in modifying the theoretical formulas must be found from tests made by experienced investigators.

---

[12] Civ. Engr. and Contr., Evanston, Ill.

A number of these factors has been determined. In the case of a prismatic plain concrete beam of rectangular section, the theoretical bending moment at the ultimate load is given by

$$M_{ult} = \frac{f_t\, b\, d^2}{6} \quad \text{.........................} \quad (34)$$

in which f_t is the unit strength in tension. However, many tests have shown that the ultimate bending moment is much greater than that given by Eq. 34, and it has been customary to assume that there is good agreement with the tests if one uses a tensile strength of twice the value of the actual tensile strength of the concrete in the theoretical formula. What the compressive stresses are at the ultimate load or at a fraction of this load has not yet been determined (as of 1955). In the writer's opinion there cannot exist a higher tensile strength than that obtained by careful tensile tests; therefore, the assumed value for the resisting moment is in error. The resisting moment for tension becomes larger if the neutral axis approaches the compression face. This movement will make the resisting moment for compression smaller, and therefore the maximum compression will be much larger.

The correction factor was found[13] in the case of eccentrically loaded plain and reinforced columns by Armand Considère in 1903. These tests showed that the columns fail at a load from 30% to 50% greater than that derived from elastic theory.

For the continuous beam on three supports with two equal spans, tests[14] by Hermann Scheit and Emil H. Probst in 1912 showed that the ultimate moment at the center support is given by $w\,L^2/10$ rather than the theoretical moment $w\,L^2/8$.

The engineer who uses Mr. Moorman's method of designing a continuous prestressed structure will produce a safe design but will not be able to ascertain its actual strength accurately.

ROBERT B. B. MOORMAN,[15] M. ASCE.—Many thanks are offered to Messrs. Diwan and Mensch for their contributions to the paper.

Contrary to Mr. Diwan's statements, the equivalent load is not of limited value and the eccentricity does not have to be a second-degree parabola. However, if the eccentricity is a second-degree parabola, the equivalent load is uniform.

For any variation of the eccentricity the equivalent load can be computed from Eq. 4 which gives the intensity of w_p along the member, whether it is variable or uniform. Furthermore, coefficients are not necessary for fixed end moments for partly loaded beams. The fixed-end moments for beams of constant section (as shown in Fig. 15) may be computed from

---

[13] "Experimental Researches on Reinforced Concrete," by Armand Considère, McGraw-Hill Book Co., Inc., New York, N. Y., 1903, pp. 119–188.

[14] "Untersuchungen an durchlaufenden Eisenbetonkonstruktionen," by Hermann Scheit and Emil Probst, Julius Springer, Berlin, 1912, p. 63.

[15] Prof. and Chairman, Dept. of Civ. Eng., Syracuse Univ., Syracuse, N. Y.

$$M_{FA} = -\sum \frac{P\,a\,b^2}{L^2} = -\sum \frac{(w_p\,\Delta x)\,a\,b^2}{L^2} \qquad (35a)$$

and

$$M_{FB} = -\sum \frac{P\,a^2\,b}{L^2} = -\sum \frac{(w_p\,\Delta x)\,a^2\,b}{L^2} \qquad (35b)$$

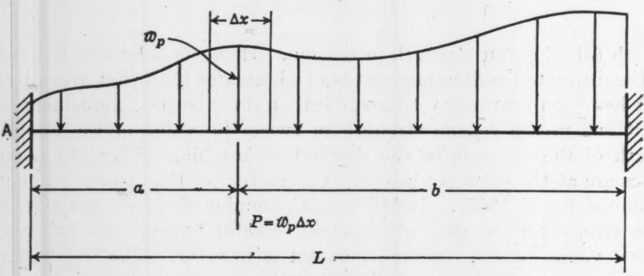

Fig. 15

It should be realized that the final bending-moment diagram (Fig. 14) represents only the effects of the load p and the change in tension in the tendon. Substitution into Eq. 29 gives $T' = 8$ kips, approximately. It should also be noted that the equivalent-load method aids in the analysis for shearing forces as well as for bending moments and that any method of analysis, classical or modern, may be used when equivalent loads are determined.

Mr. Mensch presents an interesting, although brief, discussion of ultimate moment. However, it is believed that safety, unless carried to an extreme, is not a deficiency in a design.

AMERICAN SOCIETY OF CIVIL ENGINEERS
Founded November 5, 1852
TRANSACTIONS

Paper No. 2824

THE PRESENT STATUS OF RESEARCH ON SEDIMENT TRANSPORT

BY NING CHIEN,[1] A. M. ASCE

WITH DISCUSSION BY MESSRS. THOMAS BLENCH; JAN M. JORDAAN, JR.; JOE M. LARA; NAVINCHANDRA L. RUPANI AND JOHN B. STALL; HSIN-KUAN LIU; AND NING CHIEN AND HANS A. EINSTEIN

SYNOPSIS

The problem of sediment transport, as it is known today, has been examined briefly in this paper. The significance and implications of the various phases of the problem have been emphasized; controversial issues have been discussed; and efforts have been made to unify some of the highly diversified results.

INTRODUCTION

Research on the movement of sediment along the beds of alluvial rivers was first undertaken by P. DuBoys (1)[2] who, in 1879, published a formula for bed-load transport rate in which he first introduced the idea of tractive force. It was G. K. Gilbert (2) who pioneered in conducting sediment-transportation experiments in flumes in 1909–1914. His techniques in making systematic observations and measurements on sediment movement under controlled conditions greatly advanced research in this field, and they are still being used. Because of the rapid expansion of activity in both engineering and geology in the past few decades, the importance of this problem has been felt increasingly and the subjects of interest have been rapidly widened. In consequence, a great number of papers have been written but many of them are not readily accessible. Facing such a huge number of papers—many of which contradict each other—the ordinary reader, who is interested in but has not been able to devote much time to this subject, loses perspective on the development, present status, and possible future directions of sediment research. It is for these readers that this paper was prepared. New information and interpretations are included which may also interest engineers in this field.

NOTE.—Published, essentially as printed here, in December, 1954, as *Proceedings-Separate No. 565.* Positions and titles given are those in effect when the paper or discussion was approved for publication in *Transactions.*

[1] Associate Prof. of Hydraulics, Tsing Hwa Univ., Peiping, China.

[2] Numerals in parenthesis—thus, (1)—refer to corresponding items in the Bibliography (see Appendix).

In spite of the broadening of the horizons, the basic question in the field of sedimentation remains the same: How much sediment will be carried through a channel by a certain flow in a certain reach of the stream? To answer this question, one must first know how to describe the flow of an alluvial channel and then proceed to determine how the flow affects the sediment which composes the bed. In this paper the writer has attempted to outline briefly what is now known or, more correctly, what engineers think they know about these and other related phases of the sediment problem.

HYDRAULICS OF ALLUVIAL-CHANNEL FLOW

In any open-channel flow there is a definite relationship between slope, depth, velocity, and the roughness of the boundary. This relationship cannot be established easily when the channel is alluvial. An alluvial channel contains a bed of loose sediment of the same type that is moved along the bed. Such a channel seldom remains flat and even. Bars and ripples are developed at the bed surface at low stages. They become longer when the discharge increases and eventually may disappear at high flows. At unusually high flows, large and nearly symmetrical sand bars may appear again, accompanied by surface waves in phase with the bottom undulations. These surface waves are commonly termed sand waves and their existence is a highly unstable situation. They may appear for a short duration and disappear again. The sand bars and ripples represent another type of roughness, in addition to the roughness of the grains which compose the channel bed. The problem is complicated because the roughness not only defines the flow, but the flow itself also molds the roughness.

To understand the mechanism of these two different systems of roughness, one must first attempt to identify their respective effects on the flow from the over-all flow conditions. This is necessary because one system of roughness depends largely on the flow and the other does not, at least for the case when the grain resistance behaves hydraulically rough. It becomes even more important when one considers the different roles the two types of roughness play in the sediment motion.

The frictional resistances of these two different systems of roughness are developed in two distinctly different ways. The resistance caused by the grain roughness is the same as the skin friction imposed on the flow by a wall. One recalls that J. Nikuradse proposed to measure the roughness of a pipe by an equivalent sand size. In an alluvial channel, this equivalent sand size of the boundary becomes the grain size of the bed material itself when the material is uniform; it is equal to a representative size, K_s, when the bed material is a mixture. The transmission of shear to the boundary through skin friction is accompanied by a transformation of flow energy into energy of turbulence. This turbulence is generated in the immediate vicinity of the grains and has a great effect on the bed-load motion. On the other hand, if sand bars develop at the bed surface, the streamlines of the flow do not follow the bottom contours but separate from the bed surface at the crests of the sand bars. This separation results in a pressure difference between the front and rear sides of each bar so that part of the flow resistance is transmitted to the boundary by the shape resistance. This part of the flow energy is transformed into turbulence at the interface between the wake and the free stream flow. This turbulence is generated at a considerable distance from the grains and may not contribute to the bed-load motion of the particle (3).

Most natural alluvial streams are shallow and wide without any appreciable bank friction. In small streams and especially in the distorted stream models, bank friction is quite important. Naturally, the turbulence generated at the banks by the bank friction has nothing to do with the motion of sediment along the bed, and its effect must also be separated and excluded.

Knowing the necessity of separating the individual effects of different friction devices from their over-all effect on the flow, one turns to the problems of how this can be accomplished and of how the effect of each individual roughness system can be described.

Linearity of Friction in Open Channels (*4*) (*5*).—It has been found that in flow systems in which a rough surface is arranged in an irregular manner so that the irregularities are at least five to ten times larger than the roughness—that is, where two or more systems of roughness of different orders of magnitude are superimposed—the contributions of the individual systems can be computed independently and added to determine the resulting total frictional force. The total shear stress along the boundary, T, thus can be expressed as

$$\frac{T}{\rho_f} = \sum \frac{T_m}{\rho_f} = \sum S_m R_m g \ldots\ldots\ldots\ldots\ldots\ldots \tag{1}$$

in which ρ_f is the density of the fluid, S the energy slope, R the hydraulic radius, g the gravitational acceleration, and the subscript m refers to the "roughness system m." Both R and S may vary with m, and the physical understanding of the process of superposition can be simplified considerably if one of these two variables is assumed to be common to the different systems of roughness. If R is interpreted as a purely geometric description of the cross section, S must be divided between the different systems of roughness. Thus, H. L. Cook (6) divided the energy slope of an alluvial channel flow into six component parts. The same scheme was also adopted by E. Meyer-Peter and R. Muller (7). On the other hand, the energy slope is the number of foot-pounds that each pound of fluid loses per foot of travel. If S is different for different systems, it is difficult to visualize how every pound of fluid contributes energy to all these different systems. A better interpretation is to hold S constant and to assume that the total energy used at any point in the flow contributes at its full rate to one friction system only. The cross section may be divided into parts contributing to the different systems. If A_m designates the part of the cross-sectional area A contributing energy to the mth system, then $R_m = A_m/p$ is the corresponding hydraulic radius in which p is the common perimeter. Accordingly, one may make the following divisions for an alluvial channel flow:

$$\text{Total hydraulic radius, } R \begin{cases} \text{Hydraulic radius of the banks, } R_w \\ \text{Hydraulic radius of the bed, } R_b \begin{cases} \text{Hydraulic radius of the grain resistance, } R'_b \\ \text{Hydraulic radius of the bar resistance, } R''_b \end{cases} \end{cases}$$

This system will be used throughout this section.

The Grain Resistance.—The frictional resistance of sediment grains at the bed surface can best be described by the logarithmic formula based on the similarity theorem of Theodor von Kármán, Hon. M. ASCE. The average velocity, V, of the flow in the vertical direction may be given by the equation:

$$\frac{V}{(R'_b\, S\, g)^{\frac{1}{2}}} = \frac{2.3}{k} \log_{10}\left(12.27\, x\, \frac{R'_b}{K_s}\right) \qquad (2)$$

in which x is a corrective parameter for the transition from smooth to rough and is itself a function of K_s/δ (δ being the thickness of the laminar sublayer); x is unity for a hydraulically rough bed; k denotes the von Kármán universal constant of turbulent exchange; and K_s is the representative grain size of the bed material. Hans A. Einstein, M. ASCE, and E. S. A. El-Samni, A. M. ASCE (8), found that the representative grain size of a mixture is equal to D_{65}, the size of which 65% by weight is finer. Messrs. Meyer-Peter and Muller suggested the value D_{90} instead. There is not enough experimental evidence to indicate which proposal is more reliable. Determination of the grain size also involves the question of which part of the bed is taken as the representative bed mixture. Both Messrs. Meyer-Peter and Muller emphasize the coarser part of the mixture, which is more important in influencing the roughness.

It has been found from both flume studies and river measurements that the k-value for a sediment-laden flow is, in general, less than 0.4, the value first determined by Mr. Nikuradse from pipe flow with clear water. Vito A. Vanoni, M. ASCE (9) (10), and Hassan M. Ismail, A. M. ASCE (11), have suggested that sediment damps the turbulence and reduces the momentum transfer. In effect, this results in a reduction of k, and it has been shown that there is a definite tendency for k to decrease with increased sediment load. On the other hand, Emmett M. Laursen, A. M. ASCE, and Pin-Nam Lin (11*a*) challenged this view and attributed the change in k to the change in bed roughness.

A change in k means a change in velocity distribution. It will be shown subsequently that the theory of suspension yields only the concentration distribution of the suspended sediment, and the rate of suspended-load transport is determined by integrating the product of local velocity and concentration from the surface of the bed layer up to the water surface. If velocity distribution changes, one should determine what causes the change and how the change can be predicted. The controversy over the possible reason for the change of k must be settled if further progress toward a general solution of the sediment transportation problem is to be made.

The k-value was first introduced by Mr. von Kármán (12) in his similarity theorem of turbulent flow pattern, from which he established the velocity deficiency law. In circular pipes with radius, r, the equation of velocity deficiency assumes the form:

$$\frac{V_{max} - V_y}{V_*} = -\frac{1}{k}\left[\log_e\left(1 - \sqrt{1 - \frac{y}{r}}\right) + \sqrt{1 - \frac{y}{r}}\right] \qquad (3)$$

in which V_{max} is the maximum velocity; V_y, the velocity at a distance y from the wall; and V_*, the shear velocity at the wall. The law states that at high Reynolds numbers the ratio (velocity deficiency/shear velocity) is a universal function of the relative distance from the center and is independent of the Reynolds number, the roughness of the wall, and the shape of the section. From Eq. 3 one may conclude that k is independent of the roughness, and the effect of roughness seems to be confined exclusively to the region immediately adjacent to the wall. This has been verified in the laboratory (13) (14) by measurements of open-channel flows with various cross sections and roughnesses and in the field (15) by analyzing the velocity distribution in nonalluvial stream channels which involve no sediment motion. The von Kármán theory may possibly break down only when the height of the roughness element becomes comparable with the depth of flow. This seems to be true according to the findings of the Iowa Institute of Hydraulic Research at Iowa City.

The Iowa results, which indicate that k changes with roughness, have not been published as yet. From the statement of Walter Rand, A. M. ASCE (16), the factor k appears to vary with the size and geometry of the roughness and the relative roughness h/d—in which h is the height of the roughness element and d is the average depth of flow. For instance, values of k for $\frac{1}{4}$-in., square-strip roughnesses spaced at 1-in. intervals on the bottom of the channel were 0.3 for $h/d = 0.3$ and 0.37 for $h/d = 0.003$. However, for the roughness formed by ordinary fly-screen, k proved to be from 0.37 to 0.40, even for (h/d)-values as great as 0.06.

Other measurements have been made in which the types of roughness element used were similar to those used in the Iowa experiments. H. Bazin, as reported by G. H. Keulegan (13), used wooden strips 1 cm high and 2.7 cm wide, placed 1 cm or 5 cm apart across the rectangular channel and perpendicular to the flow. The ratio of the height of the strips to the hydraulic radius varied from 0.03 to 0.18 for closely spaced strips and from 0.025 to 0.14 for widely spaced strips. H. Schlichting (14) studied the effect of roughness on the velocity distribution in a closed rectangular channel, with three sides smooth and the top plate rough. His roughness elements consisted of spheres, spherical segments, cones, short angles, and long angles. The form and arrangement of the short angles were closely similar to those of the strips used in Iowa. The ratio of the height of the short angles to the distance from the rough wall to the point near the center of the section, beyond which the flow is affected by the opposite smooth wall, varied from 0.10 to 0.12. The results of these two studies all show that k is 0.4. These two measurements were conducted with considerable care, and the Bazin results are especially reliable because he used a flume $6\frac{1}{2}$ ft wide and more than 1,000 ft long. During 1951–1953, the Corps of Engineers (United States Department of the Army) made a series of measurements on velocity and sediment-concentration distribution in the Missouri River near Omaha, Nebr. A topographic survey of the bottom configuration was made with sufficient accuracy to detect the existence of any sand bars with heights exceeding 0.15 of the depth of flow. At the center flat area of the stream, where the topographic survey revealed no such appreciable bottom undulations, the results of velocity distribution measurements indicated that k, as an average, had a value of approximately 0.25.

The question of whether the sediment motion has any effect on the change of k can be settled in a more direct manner. The writer has conducted three sets of experiments with three different sands (1.55 mm, 0.94 mm, and 0.27 mm). For each experiment, the bottom of the flume was coated with a layer of sand. Velocity distribution with clear water indicated that k is close to 0.4. Enough sand of the same diameter as that glued on the bed was then added to the flow to keep the rate of transport as rapid as possible and still avoid any significant deposition on the bed. The particles moving along the lower part of the flume occasionally settled to the bed, but the duration of rest was small because of the rapid transport rate. Because the bottom was coated with the same sand as that in motion, the widely-scattered, temporary deposition of individual particles at the bed surface in no way affected the bed roughness. However, the experimental results showed that the value of k was approximately 0.30 for all three experiments.

From the foregoing evidence one may safely conclude that (*a*) the sediment motion affects the velocity distribution and (*b*) if roughness changes k, the roughness element must be so pronounced that its height becomes comparable with the depth of flow.

Indeed, there are reasons to believe that the sediment motion must affect the velocity distribution. In a sediment-laden flow, the vertical distribution of the large sediment grains is highly skewed. Near the bed there is a zone where the sediment is heavily concentrated, and the concentration of sediment is reduced progressively toward the water surface. For simplicity of argument, the sediment-laden flow may be considered as consisting of two parts: A relatively shallow zone near the bed where the sediment is highly concentrated (heavy-fluid zone), and the remaining area where the concentration is so small that the density of the fluid remains materially unchanged (light-fluid zone). The presence of the heavy-fluid zone near the bed is very important in the following respects—when the turbulence generated at the bed in the heavy-fluid zone enters the light-fluid zone, the momentum exchange may become less effective due to the reduction of mass of the exchange flow. In the heavy-fluid zone part of the shear may also be transmitted to the boundary through the sediment particle in motion. These two effects, in combination with the decrease in turbulence level because of the energy spent in keeping sediment in suspension, are all accounted for by a reduced value of k.

The effect on the velocity distribution of a heavy sediment concentration close to the bed is demonstrated by the writer's experiment on coarse sediment. The material in motion was confined to a zone close to the bed, approximately one tenth of the depth of flow in thickness. Outside this zone, the water was practically clear; the result shows a significant reduction in the value of k. There are some indications that the mechanism which causes a change of velocity distribution probably occurs in a zone close to the bed, although the end product of this effect manifests itself in the main part of the flow where measurements usually are made. The sediment particles suspended in the main part of the flow are of smaller sizes, and it does not take much energy to keep them in suspension. This may account for the apparent constancy in the value of k with depth.

Mr. Einstein and the writer (17) proposed to measure the reduction in the value of k by the amount of turbulent energy spent in supporting the sediment in suspension. The rate at which frictional energy is spent per unit weight of fluid and per unit time in supporting the sediment in suspension, $\sum \frac{C_s V_s}{V S} \frac{\rho_s - \rho_f}{\rho_s}$, is correlated with k in Fig. 1. Here C_s is the average con-

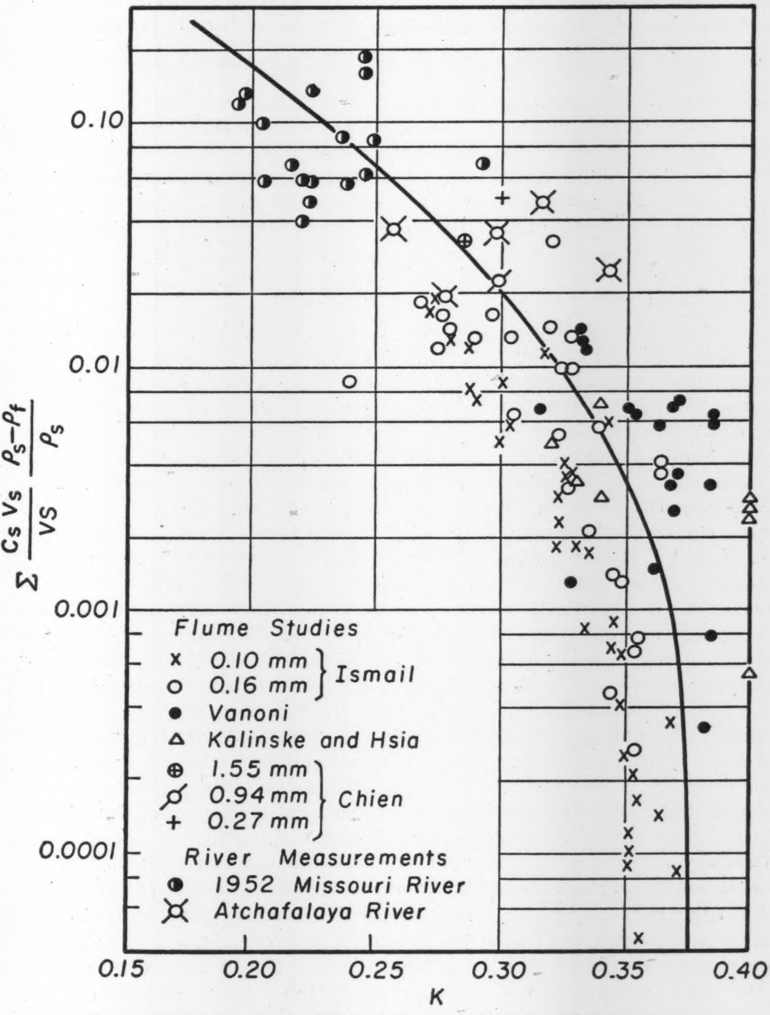

FIG. 1.—THE EFFECT OF SUSPENDED SEDIMENT ON VELOCITY DISTRIBUTION

centration by weight of a given grain size with settling velocity V_s in the vertical, ρ_s is the density of the solid, and the summation sign designates a summation over all the particles in suspension. The data plotted in Fig. 1 include (*a*) flume studies by Messrs. Vanoni (9) and Ismail (11), A. A. Kalinske, M. ASCE, and C. H. Hsia (18), and the writer, and (*b*) field measurements on the Missouri River at Omaha and on the Atchafalaya River at Simmsport, La. The scatter of the points is wide because the effect of heavy sediment concentration near the bed may be different under different conditions; yet the over-all trend that *k* decreases with an increase in the parameter $\sum \frac{C_s V_s}{V S} \frac{\rho_s - \rho_f}{\rho_s}$ is beyond doubt.

A reduction of *k* from 0.4 to, say, 0.2 does not mean that the average velocity of the sediment-laden flow will be twice that of the corresponding sediment-free flow. Evidently Eq. 2 is no longer adequate in describing a sediment-laden flow. The development of a new equation on velocity distribution must wait until the effect of heavy sediment concentration near the bed becomes better understood. It is believed, however, that the difference in average velocity between the sediment-laden flow and the sediment-free flow will not be appreciable.

Bar Resistance.—The mechanism of ripple formation remains a puzzling problem. R. A. Bagnold (19) was able to show that the ripple formation on desert sand is closely associated with the motion of saltation of the bed-load particles. Although saltation is the dominating mode of transportation of aeolian sediment, Mr. Kalinske (20) has shown that it is insignificant for sediment motion in water. F. M. Exner (21) has published a formula indicating that the rate of change of bed elevation is proportional to the longitudinal variation of the bottom velocity. If the channel has a smooth bed initially, what causes the longitudinal variation of bottom velocity? A. G. Anderson, A. M. ASCE (22), suggested that this variation is associated with the surface waves. Observations made at the University of California at Berkeley on the movement of lightweight materials revealed that the bottom undulations can be as high as from $\frac{1}{4}$ to $\frac{1}{3}$ of the water depth, yet the water surface remains almost mirror smooth. Perhaps Mr. Anderson's description applies only to the case of sand waves, the last developmental stage of the bottom undulations.

The initiation of ripples has been shown by H. K. Liu (23) to be as in Fig. 2, using V_*/V_s and $V_* D/\nu$ as the characteristic parameters (D denotes the grain size and ν the kinematic viscosity of the fluid). In the same graph the results obtained by A. Shields (24) on the beginning of bed-load movement and the data of M. S. Quraishy (25) on the commencement of general movement of the bed load are included. The general movement of bed load is defined by Mr. Quraishy as the stage of movement when all sediment sizes of the bed material are in motion and the movement is strong enough to develop bed configurations. According to Fig. 2, ripples usually appear and develop right after the bed-load movement begins, but before the movement is strong enough that there may develop a layer close to the bed in which the sediment is heavily concentrated. The same phenomenon was also observed in India (26). This seems to rule out the possibility that ripple formation is a phenomenon associated with the instability at the interface of two flows with different densities.

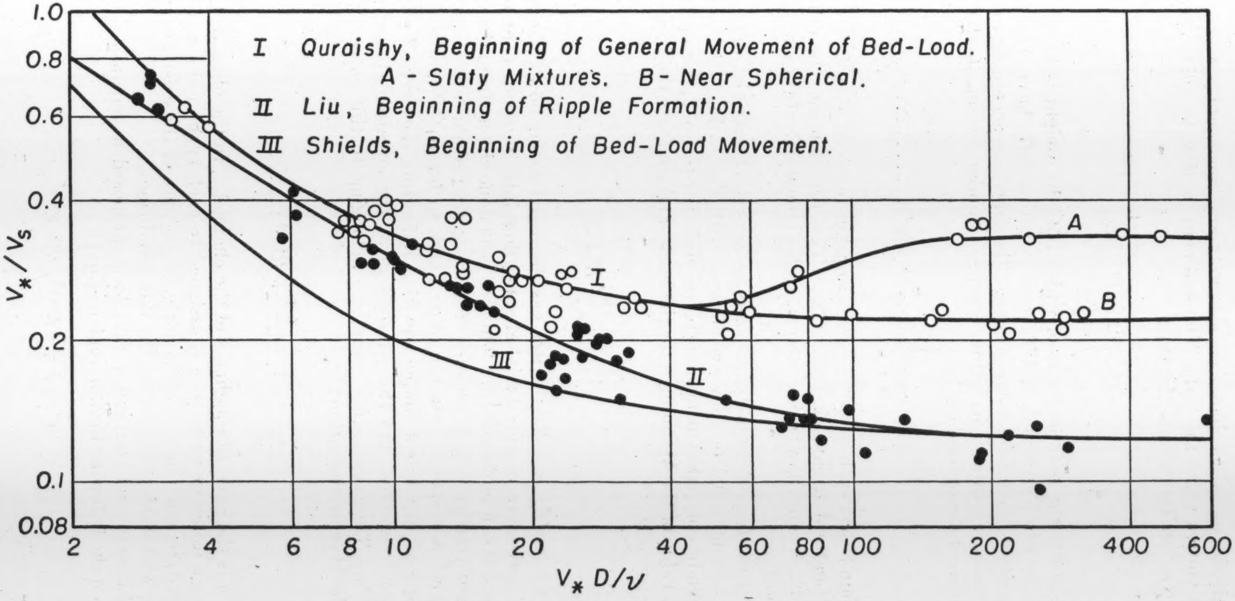

FIG. 2.—THE BEGINNING OF BED-LOAD MOVEMENT AND RIPPLE FORMATION

The ripples and bars change considerably and consistently with the rate of sediment motion along the bed. The sediment motion, as will be seen later, is related to a flow function of the type—

$$\psi' = \frac{\rho_s - \rho_f}{\rho_f} \frac{D_{35}}{R'_b\, S} \quad \text{(4)}$$

in which D_{35} is the sediment size of which 35% by weight is finer. Toichro Tsubaki, Tsuruo Kawasumi, and Takeshi Yasutomi (27) have shown that the flow intensity ψ' governs the dimensions of the sand bars according to the result of field measurements in irrigation flumes. Similar to Eq. 2, the sand-bar resistance can be expressed as

$$\frac{V}{\sqrt{R''_b\, S\, g}} = f_1(\psi') \quad \text{(5)}$$

It was found that such a universal relationship between $V/\sqrt{R''_b\, S\, g}$ and ψ' exists for natural stream channels (28). This function may be different for more confined canal flow; other factors, such as the width of the channel, might be of importance.

Bank Friction.—Stream banks usually consist of material different from movable bed material or they are covered with vegetation. Although bank friction can be computed using an expression similar to Eq. 2, it is customary to assume a value of the Manning n for the banks and compute the friction by the Manning formula:

$$V = \frac{1.486}{n_w} R^{\frac{2}{3}}_w\, S^{\frac{1}{2}} \quad \text{(6)}$$

Over-All Resistance.—The writer has discussed so far how to separate the frictional resistance of an alluvial-channel flow into its component parts and how each part can be described. This has been done chiefly from the viewpoint of sediment transportation because only the grain resistance is responsible for the bed-load movement. On the other hand, so far as the flow itself is concerned, one often needs a simple equation indicating the over-all effect of all systems of roughness, and the parameters of the equation should be easily identifiable. There are a few equations belonging to this category—for instance, the Manning equation:

$$V = \frac{1.486}{n} R^{\frac{2}{3}}\, S^{\frac{1}{2}} \quad \text{(7)}$$

in which n is the over-all roughness of the channel. In the older textbooks on hydraulics a different value of n is assigned to each type of channel material. This procedure, one now knows, is not valid because of the existence of the bar resistance and its dependence on the flow conditions.

Mr. Einstein and the writer (29) have proposed a generalized Manning equation of the following form to replace Eq. 7:

$$V = c\,\sqrt{g}\, R^{m+\frac{1}{2}}_T\, S^{\frac{1}{2}}\, K^{-m}_s \quad \text{(8)}$$

in which

$$R_T = \frac{A_T}{p_b} \qquad (9)$$

A_T being the cross-sectional area and p_b the channel width. The constant c and the exponent m can be determined graphically with due consideration of the effects of different components of the frictional resistance. Eq. 8 becomes identical with Eq. 7 if m is taken equal to $\frac{1}{6}$ and if one uses the relation (30) of A. Strickler:

$$n = \frac{K^{\frac{1}{6}}_s}{A} \qquad (10)$$

in which

$$c = \frac{1.486\ A}{\sqrt{g}} \qquad (11)$$

The constant A is usually taken as 29.3 in foot-pound-second units. The constants c and m in Eq. 8 presumably change with a change in the range of R_T/K_s under consideration. A closer approximation may be obtained by introducing two sets of values of c and m, one set for the low stages and the other for the high stages. The constants c and m for high stages should not differ much from Eq. 11 and $\frac{1}{6}$, respectively, provided that the bank friction is not appreciable.

Another method of describing the over-all resistance of alluvial-channel flow has been outlined by James J. Doland, M. ASCE, and Ven T. Chow, A. M. ASCE (28*a*). They retained the use of the Manning equation by modifying Eq. 10 to the following:

$$n = \frac{\dfrac{K^{\frac{1}{6}}_s}{A}}{\left(\dfrac{R'_b}{R}\right)^{\frac{2}{3}}} \qquad (12)$$

in which the ratio R'_b/R indicates the effect of sand bars. A graphical solution of R'_b/R has been given in terms of R/K_s and $D_{35}/R\ S$, which is valid if the bank friction can be ignored.

SEDIMENT–TRANSPORT RATE

Sediment has been divided into bed load and suspended load according to the difference in the mode of movement and in the laws that govern its motion and into bed-material load and wash load according to the difference in the source of material.

Suspended Load.—Suspended load is the material moving in suspension in a fluid, being held up by the upward component of the turbulent current.

Based on the mechanics of turbulent flow of fluids, it has been established that the distribution of the relative concentration of the suspended load is of the following form (9) (31):

$$\frac{C_y}{C_a} = \left(\frac{d - y}{y}\,\frac{a}{d - a}\right)^z \qquad (13)$$

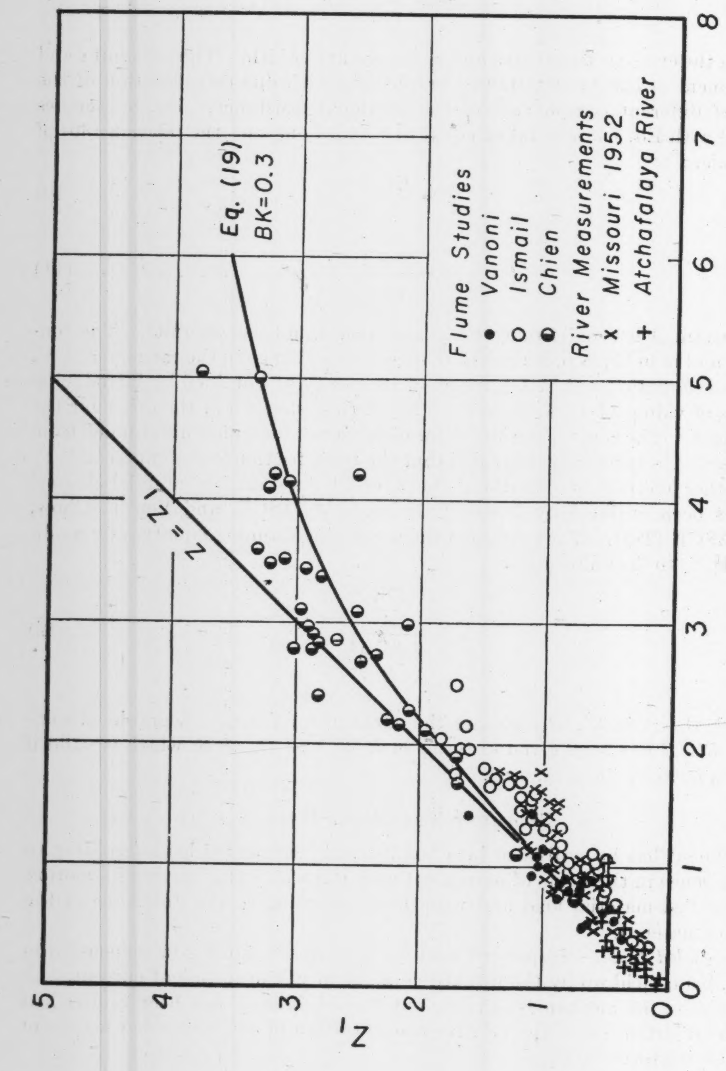

FIG. 3.—THE RELATIONSHIP BETWEEN z AND z_1

with

$$z = \frac{V_s}{k\,V_*} \ldots\ldots\ldots\ldots\ldots\ldots\ldots\ldots (14)$$

in which C_y and C_a are the concentrations of a grain size with settling velocity V_s at distances y and a from the bed, respectively; k is the von Kármán universal constant; and d is the depth of the flow. J. N. Hunt (32), taking into consideration the space occupied by the sediment particles, introduced a more exact distribution function as follows:

$$\frac{C_y}{1 - C_y}\,\frac{1 - C_a}{C_a} = \left\{\left(\frac{1 - \frac{y}{d}}{1 - \frac{a}{d}}\right)^{\frac{1}{2}} \left[\frac{B_s - \left(1 - \frac{a}{d}\right)^{\frac{1}{2}}}{B_s - \left(1 - \frac{y}{d}\right)^{\frac{1}{2}}}\right]\right\}^{z} \ldots\ldots (15)$$

in which B_s is a constant that was found to be slightly smaller than unity.

Eqs. 13 and 15 have been shown to describe the suspended-sediment distribution sufficiently well, except that the value of the exponent z yielded by Eq. 14 does not agree with z_1, the exponent that fits the measured data (9) (11) (33) (34). For small z-values, the measured exponent z_1 is the same as z. For large z-values, the measured values of z_1 are smaller than z, indicating that the distribution of the suspended load is more uniform than that indicated by the theory. Fig. 3 shows the relationship between z and z_1 according to the results of measurements in both rivers and flumes. Messrs. Vanoni (9) and Ismail (11) proposed that the sediment-transfer coefficient, ϵ_s, is not the same as the momentum-transfer coefficient, ϵ_m, but that they are related by the following formula:

$$\epsilon_s = \beta\,\epsilon_m \ldots\ldots\ldots\ldots\ldots\ldots\ldots\ldots (16)$$

in which β seems to be a function of the particle size. Also,

$$z_1 = \frac{V_s}{\beta\,k\,V_*} = \frac{z}{\beta} \ldots\ldots\ldots\ldots\ldots\ldots (17)$$

which indicates the deviation of z_1 from z. Mr. Hunt (32) introduced a different universal constant k_s for suspended-sediment distribution such that

$$z_1 = \frac{V_s}{B_s\,k_s\,V_*} = \frac{z\,k}{B_s\,k_s} \ldots\ldots\ldots\ldots\ldots\ldots (18)$$

No detailed explanations have been given as to what basically causes the difference between z and z_1 and what determines the value β or $B_s\,k_s/k$. On the other hand, Mr. Einstein and the writer (17) revised the suspended-load theory in the following aspects:

a. The difference in sediment concentration at a vertical distance l apart—l symbolizing the mixing length of the turbulent flow—is expressed by $l\;dC_y/dy$ only for fine particles. For coarse particles, the sediment distribution is highly skewed, and the higher-derivative terms of the concentration C_y with respect to the vertical distance y have to be included.

b. It is unrealistic to assume that the turbulence eddy maintains its identity until it travels a certain distance, l, and only then begins mixing. The model of the turbulence eddy is rather to be visualized as if the fluid carried by the eddy continuously mixes with the surrounding fluid on the course of the traverse of the eddy. However, the process of mixing is much more active near the origin of the eddy than at points farther away. In other words, the mixing length is assumed to follow a certain probability distribution instead of possessing a finite value.

c. Because the turbulence is generated at the bed and dissipated toward the water surface the characteristics of turbulence are not necessarily symmetric. In other words, for an upward flow and a downward flow originating from the same point, the mixing length and fluctuating velocity of the upward flow might not be the same as those of the downward flow.

The detailed description of the second approximation to the solution of the suspended-load theory cannot be given here. In one case where the fluctuating velocity and mixing length of the turbulent flow were assumed to follow the normal error law and a certain probability-distribution function, respectively, and where the higher derivative terms of the concentration gradient were included, z and z_1 were shown to be related by the following expression:

$$z_1 = \frac{z}{e^{-\alpha} + 2\sqrt{\frac{\alpha}{2}}\int_0^{\sqrt{2\alpha}} e^{-x^2/2}\,dx} \qquad (19)$$

in which

$$L = \log_e (1 + B\,k) \qquad (20a)$$

and

$$\alpha = \frac{L^2\,z^2}{\pi} \qquad (20b)$$

and B is a constant. Eq. 19 has been plotted in Fig. 3, and the results can be compared with those determined by actual measurements. For practical purposes, the difference between z and z_1 perhaps can be ignored because it affects only the coarse particles, and the number of coarse particles in suspension is usually of secondary importance.

In addition to the flow conditions, the settling velocity of the sediment grains is the determining factor in the suspension of material. The general expression for the settling velocity of a sediment particle is as follows:

$$V^2_s = A\,\frac{1}{C_D}\,\frac{\rho_s - \rho_f}{\rho_f}\,g\,D \qquad (21)$$

in which C_D is the coefficient of drag. For large grains which settle with a turbulent wake, C_D is constant. If the fall velocity is in the viscous range,

$$C_D = \frac{24}{\mathsf{R}} = \frac{24\,\nu}{V_s\,D} \qquad (22)$$

and

$$V_s = \frac{A}{24} \frac{\rho_s - \rho_f}{\rho_f} \frac{1}{\nu} g D^2 \qquad (23)$$

Eq. 23 has been used quite extensively in the size analysis of fine materials by the sedimentation method.

The constant A in Eqs. 21 and 23 depends on a number of factors—for instance, the particle shape, the boundary proximity, the sediment concentration, and the turbulence of the flow. Extensive research to relate A to these factors has been conducted not only by engineers but by geologists, soil scientists, and chemists as well. To measure the shape factor, geologists used "sphericity" (35) which is defined as the ratio of the surface area of that sphere having the same volume as the particle to the actual surface area of the particle. For practical purposes, the sphericity of a particle can be approximated by combinations in various forms of the maximum, intermediate, and minimum mutually perpendicular axes. Some of the recent works in this phase of the problem include those by W. C. Krumbein (36), J. S. McNown, M. ASCE, J. Malaika, A. M. ASCE, and H. R. Pramanik, A. M. ASCE (37), and M. L. Albertson, M. ASCE (38). The effect of the boundary proximity on the settling velocity has been summarized, together with other effects, by Mr. McNown (39). Messrs. McNown and Lin (40) also showed that, for 0.1-mm sand at a concentration of 30 g per liter, the decrease in fall velocity is as much as 20%. The effect of very high sediment concentration has been studied by H. H. Steinour (41) and B. W. Wilson, A. M. ASCE (42). Sediment mixtures settle collectively as a unit at high concentrations despite the spread in particle sizes. P. G. W. Hawksley (43) showed that there is a continuity from the effect of sediment concentration on the settling of suspensions to the flow through porous media, the latter being the upper limit of the former. When sediment settles in a turbulent flow, not only the particle itself but also the turbulent wake behind the particle is subjected to the acceleration and deceleration of the flow. This phenomenon introduces the virtual-mass problem which has been studied by H. W. Iversen and R. Balent (44). A recent investigation by the Missouri River Division, Corps of Engineers, indicated that for the turbulence generally existing in natural streams its effect on the settling velocity is of minor importance.

In spite of the fact that the problem of relating the properties of the sediment and fluid to the fall velocity of the particles has received more attention than any other phase of sedimentation, much still remains to be done. Most investigations, of which only a few are cited here, are begun from the viewpoint of sediment-size analysis and are, therefore, confined to fine particles in the Stokes range. Much more important to river engineers is the behavior of coarse particles, the transport rate of which is a governing factor on channel stability. How the various factors affect the settling velocity of these coarse particles deserves special consideration.

The suspended-load theory breaks down for flow near the bed where the particle size is of the same order of magnitude as the size of the eddies around the particle. The particle merely settles down between eddies without being

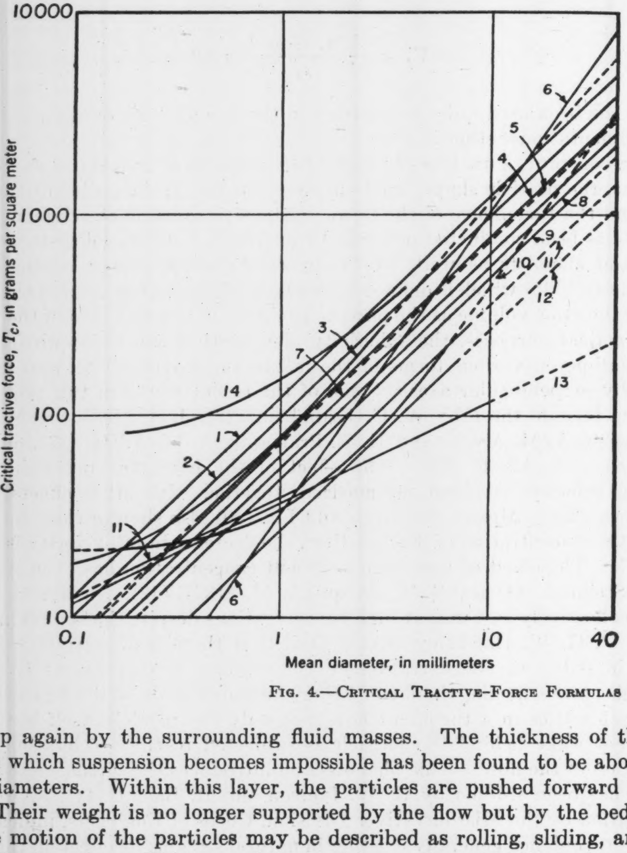

Fig. 4.—Critical Tractive-Force Formulas Showing

lifted up again by the surrounding fluid masses. The thickness of the bed layer in which suspension becomes impossible has been found to be about two grain diameters. Within this layer, the particles are pushed forward by the flow. Their weight is no longer supported by the flow but by the bed itself, and the motion of the particles may be described as rolling, sliding, and, occasionally, jumping. This part of the load is usually called the bed load.

Bed Load.—Bed-load movement has received much attention by many investigators, and almost every investigator has proposed a formula of his own, relating the bed-load transport rate to the flow conditions. A historical development of these bed-load equations has been outlined by Mr. Vanoni (45) (46); only the most important ones will be presented herein in their final forms. Attempts will be made to explain how one can achieve a certain degree of unification among the various formulas.

1. Tractive-Force Theory.—The most common concept of the mechanics of bed-load movement is that of a dragging force existing on the stream bed due to the flowing water. This force, termed the "tractive force," is the entraining force exerted at the base of a prism of water of unit area of the bed and of height equal to the water depth, sliding (under the influence of gravity) down an inclined plane having a specified slope. When the tractive force is

Curve No.	Sources	Value of ψ_c
1	Prussian Experiment Institute[a]	13.2
2	H. Krey[a] and A. Shields[b,c]	16.7
3	Hugh J. Casey[d]	...
4	E. Meyer-Peter[e,f]	21.4
5	C. M. White[g]	22.2
6	Armin Schoklitsch[h]	...
7	A. A. Kalinske[i]	25.7
8	M. P. O'Brien and B. D. Rindlaub[j]	29.5
9	E. Meyer-Peter[b,f] and A. Shields[e,c]	33.3
10	H. K. Liu[k]	...
11	Y. L. Chang[l]	45.2
12	Hans Kramer[m]	60.2
13	United States Waterways Experiment Station[n]	...
14	L. G. Straub[o]	...

[a] "Elbe Experiments," Report of the Preussische Versuchsanstalt für Wasserbau und Schiffbau, Berlin, under H. Krey (unpublished).

[b] Second plot.

[c] "Anwendung der Aechlichkeitsmechanik und der Turbulenzforschung auf die Geschiebebewegung," by A. Shields, *Mitteilungen*, Preussische Versuchsanstalt für Wasserbau und Schiffbau, Berlin, 1936.

[d] "Ueber Geschiebebewegung," by Hugh J. Casey, *ibid.*, 1935.

[e] First plot.

[f] "Formulas for Bed-Load Transport," by E. Meyer-Peter and R. Muller, *Proceedings*, Third Meeting, International Assn. for Hydr. Research, Stockholm, 1948.

[g] "The Equilibrium of Grains on the Bed of a Stream," by C. M. White, *Proceedings*, Royal Soc. of London, Series A, No. 958, Vol. 174, February, 1940, pp. 322–338.

[h] "Ueber Schleppkraft und Geschiebebewegung," by Armin Schoklitsch, Wilhelm Engelmann, Berlin, 1914, pp. 20–26.

[i] "Movement of Sediment as Bed Load in Rivers," by A. A. Kalinske, *Transactions*, Am. Geophysical Union, Vol. 28, 1947, pp. 615–620.

[j] "The Transportation of Bed-Load by Streams," by M. P. O'Brien and B. D. Rindlaub, *ibid.*, Vol. 15, 1934, pp. 593–603.

[k] "Ripple Formation and Its Relation to Bed-Load Movement," by H. K. Liu, thesis presented to the University of Minnesota, at Minneapolis, in 1953, in partial fulfilment of the requirements for the degree of Doctor of Philosophy.

[l] "Laboratory Investigation of Flume Traction and Transportation," by Y. L. Chang, *Transactions*, ASCE, Vol. 104, 1939, pp. 1246–1313.

[m] "Sand Mixtures and Sand Movement in Fluvial Models," by Hans Kramer, *ibid.*, Vol. 100, 1935, pp. 798–838.

[n] "Studies of River Bed Materials and Their Movement with Special Reference to the Lower Mississippi River," *Professional Paper 17*, U. S. Waterways Experiment Station, Vicksburg, Miss., 1935.

[o] *House Document No. 238*, 73d Cong., 2d Session, 1935, U. S. Govt. Printing Office, Washington, D. C., pp. 1125–1139.

ψ_c-VALUES FOR RESULTS FROM THE SOURCES LISTED

sufficient to overcome the resistance of the particles, sediment begins to move as bed load. The force which creates the commencement of movement of the bed material is called the critical tractive force.

The idea of tractive force was first introduced by DuBoys (1) in the nineteenth century. Since then, numerous flume studies have been conducted in order to ascertain a relationship between the various factors influencing the beginning of bed-load movement. Some of the results were summarized by Y. L. Chang (47). A recent analysis by A. C. Carter (48) indicated that most of the dimensionally correct critical-tractive-force equations can be reduced to the form:

$$\frac{T_o}{(\gamma_s - \gamma_f)\,D} = A \qquad (24)$$

in which T_o is the critical tractive force; γ_s and γ_f, the specific weight of the sediment and the fluid, respectively; D, the grain size; and A, a constant. Mr. Shields (24) showed that A is actually a function of D/δ. The term A becomes a constant only when there is fully developed turbulent flow at the bed.

It has been shown (49) that the "critical" conditions for the commencement of sediment movement actually correspond to a particular value of flow intensity ψ, the parameter introduced by Mr. Einstein (3) in his bed-load function. Fig. 4, after E. W. Lane, M. ASCE (50), and Mr. Carter (48), shows a plot of the various critical tractive-force equations. Eq. 24 is a straight line of 1 to 1 slope when represented as in Fig. 4. The value of ψ corresponding to the "critical" conditions varies considerably for results of different investigators and is given in Fig. 4. A closer survey of these equations reveals that the so-called "critical" value in some cases is a practical value, indicating zero transportation. In some other cases, it is a constant of the transportation law. These two are so different in nature that one should not be astonished by the apparent spread of the critical value.

Based on the idea of critical tractive force, the sediment transportation should be a function of the difference between the tractive force and the critical tractive force of the material in the bed. Thus, DuBoys proposed his classical bed-load formula as follows:

$$q_B = C_B\, T\, (T - T_o) \qquad (25)$$

in which q_B is the transport rate measured in weight per unit width and time; T, the tractive force; and C_B, a sediment parameter. He based his analysis on the oversimplified picture of sliding layers of bed material kept in motion by the tractive force of the moving fluid. His reasoning was improved by M. P. O'Brien, M. ASCE, and B. D. Rindlaub (51) to yield a bed-load formula of the type—

$$q_B = K\, (T - T_o)^m \qquad (26)$$

in which K and m are constants. Eq. 26 has been used by the United States Waterways Experiment Station (52) at Vicksburg, Miss. The exponent m varies from 1.4 to 1.8 depending on the material tested.

There are numerous other equations derived directly or indirectly from the DuBoys tractive-force theory which are different in form from Eqs. 25 and 26. Some of the expressions have been tabulated by Mr. Vanoni (45) and Carl B. Brown, M. ASCE (53). Joe W. Johnson, M. ASCE (47*a*) has shown that they all fit the date of flume experiments equally well.

Mr. Kalinske (54), using the idea of critical tractive force and applying some of the results of modern turbulence research, developed a theory for bed-load transport as follows:

$$\frac{Q_B}{V_* \gamma_s D} = f_2\left(\frac{T_o}{T}\right) \qquad (27)$$

in which the function f_2, which involves the characteristics of the fluid turbulence, is analytically described. M. G. Mostafa, A. M. ASCE (55), has shown that Eq. 27 is similar to the Einstein bed-load function, with the difference lying in the definition of a velocity scale.

2. The Einstein Bed-Load Function.—It was first concluded on the basis of special experiments that a given particle size moves in a series of steps of a constant average length and that the particles are periodically deposited in the bed after performing such a step. The number of particles deposited per unit of

time in the unit of bed area may be expressed in terms of the rate of transport and the size and weight of the particles. The rate at which these sediment particles will be eroded from the bed is proportional to the number of particles in the surface of the bed area and to the probability that such a particle will be eroded during the unit time. This probability is then expressed as a function of the ratio of dynamic lift on the particle to the weight of the particle under water. The equilibrium rate of bed-load transportation is then determined by equating the number of particles deposited on the unit bed area and on the number eroded from it, per unit time. This leads to a functional relationship between the flow intensity, ψ, and the intensity of bed-load transport, ϕ:

$$\phi = f_3(\psi) \qquad (28)$$

Eq. 28 was defined empirically in 1942 (56) and was replaced in 1950 (3) by an analytical function as follows:

$$1 - \frac{1}{\sqrt{\pi}} \int_{-B_* \psi - (1/\eta_o)}^{B_* \psi - (1/\eta_o)} e^{-t^2}\, dt = \frac{A_* \phi}{1 + A_* \phi} \qquad (29)$$

in which

$$\phi = \frac{q_B}{\rho_s\, g} \left(\frac{\rho_f}{\rho_s - \rho_f} \right)^{\frac{1}{2}} \left(\frac{1}{g\, D^3} \right)^{\frac{1}{2}} \qquad (30)$$

$$\psi = \frac{\rho_s - \rho_f}{\rho_f} \frac{D}{R'_b\, S} \qquad (31)$$

and A_*, B_*, and η_o are universal constants, with $A_* = 1/0.023 = 43.5$, $B_* = 1/7 = 0.143$, and $1/\eta_o = 2$. (Eq. 29 and the numerical values of the universal constants as published in Mr. Einstein's paper (3) involve certain typographical errors.)

3. Meyer-Peter Formula.—The Meyer-Peter formula was developed at the Zurich Hydraulic Laboratory in Zurich, Switzerland, and has been used quite extensively in Europe. It was first published in 1934 (57) as follows:

$$\frac{q^{\frac{2}{3}}_b\, S}{D} = a + b\, \frac{q^{\frac{2}{3}}_b}{D} \qquad (32)$$

in which $q_b = V\, R_b$—V being the average velocity of the flow, R_b the hydraulic radius of the bed, and a and b, constants.

Eq. 32 was derived empirically, using the Froude law of similarity as the guide, because it can be seen that the quotient $q^{\frac{2}{3}}_b\, S/D$ is independent of the scale, both the numerator and denominator varying with the scale in a linear manner. In 1948, Messrs. Meyer-Peter and Muller (7) modified Eq. 32 in two respects—namely, the inclusion of the effect of sediment density and the separation of the bar resistance from the total bed resistance—to provide a new equation of the form:

$$\gamma_f \frac{q_b}{q} \left(\frac{K_b}{K'_b} \right)^{\frac{3}{2}} dS = a(\gamma_s - \gamma_f) D + B \left(\frac{\gamma_f}{g} \right)^{\frac{1}{3}} \left(\frac{\rho_s - \rho_f}{\rho_s} \right)^{\frac{2}{3}} q^{\frac{2}{3}}_b \qquad (33)$$

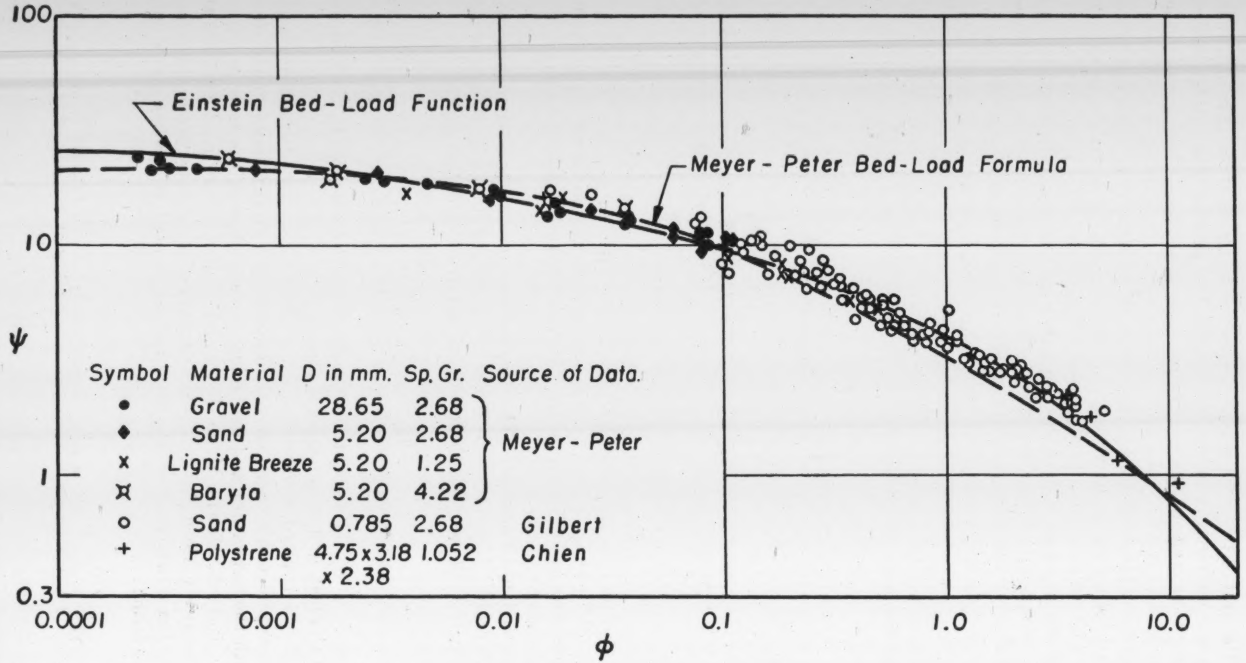

FIG. 5.—TRANSPORT OF UNIFORM MATERIALS

in which $q = V\,d$, d is the average depth of flow, $K_b = V/(R^{2/3}_b\, S^{1/2})$, $K'_b = V/[R^{2/3}_b(S'_b)^{1/2}]$, A and B are constants, and q_b is the sediment-transport rate measured as dry weight per unit of width per unit of time.

The division of the bed resistance into its component parts is accomplished by holding R_b constant and dividing the energy slope, S, into two parts—the energy slope with respect to the grain resistance, S'_b, and the energy slope with respect to the bar resistance, S''_b.

The writer (49) has shown that Eq. 33 can be modified to express the following relationship between ϕ and ψ—the same parameters introduced by Mr. Einstein in his bed-load function:

$$\phi = \left(\frac{4}{\psi} - 0.188\right)^{3/2} \qquad (34)$$

Eq. 34, together with Eq. 29, is plotted in Fig. 5. It shows excellent agreement between the Einstein bed-load function and the Meyer-Peter equation up to a ϕ-value of 10. With larger ϕ-values, the Meyer-Peter equation yields a larger transport rate than that indicated by the Einstein bed-load function.

The experimental results plotted in Fig. 5 were obtained under the following ranges of conditions for particle shapes ranging from nearly spherical to rectangular:

Condition	Range
Slope, in percentage	0.15–20
Particle size, in millimeters	0.8–30
Water depth, in feet	0.03–4
Discharge, in cubic feet per second per foot	0.0215–21.5
Specific gravity of sediment	1.05–4.2

The fact that the experimental points which are derived from such a wide range of variables fall exactly on the curves clearly demonstrates the merit of both methods.

Eq. 33 also can be reduced to the form (49):

$$q_b = K_1(T - T_o)^{3/2} \qquad (35)$$

which is identical with Eq. 26, one of the equations derived from the DuBoys tractive force theory with m equal to $\frac{3}{2}$.

The Meyer-Peter equation also has been shown (49) to be similar to the Bagnold equation (19) for sediment transport in air, taking into consideration the large difference in density between air and water.

One now sees that the various bed-load transport formulas as proposed by different investigators are actually of compatible form and consist of the same parameters.

4. Sediment Mixtures.—All the theories examined thus far were derived originally from experiments with uniform sediment. For any given sediment mixture there is some grain size which, using these theories, will give the same rate of movement as the mixture does. Whereas Mr. Einstein (58) proposed to use D_{35} as the effective diameter, Messrs. Meyer-Peter and Muller (7) suggested

the use of a sediment size of the following value:

$$D_m = \sum D \frac{\Delta p}{100} \qquad (36)$$

in which Δp is the percentage by weight of the bed material having grain size D. Mr. Kalinske (54) recommended that the medium diameter be used. At large transport rates it becomes immaterial which one of these is regarded as the effective size (49).

The nature of the sediment problem is often such that one needs to know the composition of the bed load as well as the total transport rate. Basically one may still apply the normal bed-load equations to the different components of a bed with due regard to the mutual interference effects between bed particles of different sizes. For instance, fine particles may be hidden behind large protruding particles at the bed surface and, in consequence, are not subject to the same velocity as in the case where the whole bed is composed of material of only that size. This effect differs considerably, depending on whether the bed material is homogeneous or is locally sorted (59). Mr. Einstein and the writer took into consideration the "interference effect" of sediment mixtures by introducing a set of correction factors. In applying the Einstein bed-load function to the components of a mixture, the flow intensity and the intensity of bed-load transport should be modified to assume the following form:

$$\phi_* = \phi \frac{i_B}{i_b} \qquad (37)$$

and

$$\psi_* = \frac{\xi \; Y \; (\beta/\beta_x)^2}{\theta} \psi \qquad (38)$$

in which i_B equals the fraction of the bed load in a particular grain-size range; i_b equals the fraction of bed material in a particular grain-size range; and ξ, Y, $(\beta/\beta_x)^2$, and θ are correction factors introduced for nonuniform materials (3) (59). These correction factors, although constituting the only working tool available at the present, should by no means be considered as the final solution. In fact, it is anticipated that they may be considerably simplified if some phases of the sediment-transport problem—for instance, the effect that the heavy sediment concentration near the bed exerts on the flow and the sediment motion—becomes known.

Evaluation of Total Load.—So far sediment motion has been described separately as it relates to suspended load and bed load because of the difference in laws which govern their motion. This fact does not imply that the two modes of transportation are completely unrelated. Indeed, sediment motion must be continuous from the bed up to the water surface. Not only the bed load but also the suspension must relate to the composition of the stream bed.

Currently there exist two methods in linking a point in the flow to a point on the bed. Messrs. Lane and Kalinske (60) argued that sediment can only be kept in suspension when it is available on the bed and when the vertical fluctuating velocity of the turbulent flow is larger than the settling velocity of the particle. The rate at which particles of a given size are picked up and placed in suspension is, therefore, proportional to (*a*) the relative number of these particles in the bed, (*b*) the magnitude of the vertical turbulent velocity components which are present and capable of picking them up, and (*c*) the percentage of time during which velocities exist that are capable of causing the fluid to pick up particles of that size. This approach thus links a point in the flow directly to a point on the bed and implies that the suspended-load theory can be extended to apply to the bed. On the other hand, Mr. Einstein (3) has argued that sediment cannot be kept in suspension close to the bed where the size of the eddies becomes comparable to the size of the particles. The layer close to the bed within which suspension becomes impossible has been termed "bed layer," and it has been shown how the flow together with the sediment composition of the bed determines the transport of sediment as bed load in the bed layer. The relationship was found to be governed by the exchange of sediment particles between the bed layer and the bed. In a similar manner, one can also establish the relationship governing the concentration at the lower edge of the suspension (that is, at the upper boundary of the bed layer) by writing an expression for the exchange of sediment particles between the suspension and the bed layer. Taking this concentration as the reference concentration C_a—in which a is the thickness of the bed layer—one can use Eq. 13 to determine the distribution of suspended load along the vertical. In this way a point in the flow is linked directly to a point in the bed layer, and thereby is indirectly connected to a point on the bed. The transport rate of suspended load is determined by integrating the product of local velocity and sediment concentration from the bed layer up to the water surface. Knowing the rates of transport of suspended load and bed load, the total sediment discharge moving across the section is merely the sum of the two.

Wash Load (61).—Basically, the sediment supply is the primary factor determining the behavior of the stream. The channel will be aggraded or degraded depending on whether the sediment inflow into the reach is larger or smaller than the capacity of the channel to transport the material. In the past, sediment has been furnished, and in most streams it still is being furnished, by the watershed at a rate that is higher than the capacity load. Most streams are continuously subjected to a very slow process of aggradation.

Recent studies on the behavior of aggrading channels (59) seem to indicate that (*a*) coarse particles tend to accumulate in the entire bed, and a very large percentage of this material in the bed maintains a small percentage of the same material in motion; and (*b*) fine particles tend to remain at the bed surface, and their presence in the bulk of bed deposits is insignificant. Although fine particles constitute only a small part of the bed material, they represent most of the sediment in motion.

In the course of centuries the stream channel has been continuously built up by sediment deposits of which the coarse particles contribute the most. If for any reason the sediment inflow temporarily changes, the local deposition or scour will not materially affect the quantity of coarse particles available at the bed surface. Any additional particles deposited on the bed surface will be stored in the bed, and any particles removed from the bed surface will be quickly replaced from the bed beneath. Because the bed composition essentially remains constant and if the change in sediment supply is only of short duration, the sediment-transport rate is determined solely by the flow conditions. By the same reasoning—although the coarse material must have been eroded or otherwise have been made available in the watershed—its immediate source is the upstream reach of the channel. This type of material is termed the "bed-material load."

On the other hand, the fine particles accumulate only in the surface layer of the bed in any significant amount. Even if this small percentage of fine particles in the bed permits the prediction of the large rate of such particles moving with the flow at that instant (62), it is not sufficient to make up for a lack of supply of such particles from upstream, nor does the bed provide room for the deposit of a surplus in the upstream supply. The bed composition will thus change with the supply; the transport, representing the major part of the supply, will not be affected by temporary bed storage but will fluctuate with the supply. This type of material originates in the upstream watershed. On its route to a given reach, a very small part of it may settle out, or some may be picked up from the channel bed in accordance with the local conditions. Essentially, however, it maintains its identity, and its transport rate depends primarily on how much of it is produced at its points of origin in the upstream watershed. In contrast with the bed-material load, this type of material is called "wash load."

The differentiation between the "bed-material load" and the "wash load" has its practical significance. Consider, for instance, that the regime of the channel is upset by a permanent change in sediment supply. This will lead to certain changes in channel characteristics until the capacity of the channel to transport the sediment equals the sediment supply, and only then will the channel attain a new equilibrium state. If the change in supply involves only the wash-load material, the composition of the channel is only slightly modified at the bed surface. If, however, the change in sediment supply involves the bed-material load, the channel must undergo a significant modification of its characteristics, involving substantial deposition or scour of the channel bed. The transport rate of the bed-material load, therefore, is the governing factor on channel stability. On the other hand, wash load, which has a minor effect on the channel stability, contributes the bulk of the deposition in lakes and reservoirs.

The rate of transport of wash load depends essentially on the different factors determining the availability of the material from the watershed. H. W. Anderson (63), in analyzing twenty-nine watersheds of western Oregon, has associated quantitatively the variation in the suspended-sediment discharge (of which presumably the wash load constitutes the major part) with differences in stream flow, topography, soils, land use, and bank conditions of the watershed. This type of analysis should definitely be extended to take advantage of the great volume of reservoir and basin survey data accumulated in the last two decades by various federal agencies (64) so that a general relationship between the quantity of wash load and the characteristics of the watershed may finally be established.

OTHER PHASES OF SEDIMENT RESEARCH

Owing to the diversity of interests of research workers and to the complexity of the sediment problem itself, the horizon of sediment research has broadened greatly in recent years. Because of the limitation of space, only those problems which are related to sediment transportation in open channels will be examined here briefly.

Field Sampling.—All the sediment-transportation equations were developed from flume experiments in the laboratory, and it is very important to determine their applicability to natural streams by making field measurements. Field sampling at present consists mostly of suspended-sediment measurement by either depth-integrating samplers or point-integrating samplers. The depth-integrating samplers cannot be used to sample down to the bed and, therefore, trap only a part of the total sediment load moving across the vertical. Methods (65) (66) have been developed to correct this inherent error of sampling. For small streams, there is also a method (67) of causing, by natural or artificial means, all the material to go into suspension so that the suspended-load measurement will yield the total transport rate. Comparisons of field data with existing theories (68) seem to favor the Einstein bed-load function and the Meyer-Peter equation. It has been pointed out (69) that almost all the flume studies are confined to relatively small depths and steep slopes. The ratio of flow depth to the bed-material grain size is comparatively small. These conditions correspond to a stream with a steep slope, a shallow water depth, and a large sediment size. The constants and functions of the sediment-transport formulas as determined from the flume studies may have to be modified in applying the formulas to deep rivers with a small bed-material grain size and flat slopes. It is in this range of conditions that the field measurements are most urgently needed.

The current trend in determining the total sediment-transport rate of a river reach, in connection with the basin planning, is to combine the analytical method with the suspended-sediment sampling program. The transport rate of coarse particles is computed according to the existing theories, and the measured results are used to determine the transport rate of fine particles. This is a logical step because (*a*) coarse particles move essentially close to the bed and cannot be sampled by suspended-load samplers and (*b*) fine particles behave like wash load and their transport rate cannot be predicted by analytical methods.

Channel Cross Section.—One of the most basic questions confronting a river engineer is the following: Given the bed material, what should be the width, depth, and slope of the channel in order that a given discharge and a given sediment inflow will be accommodated? In designing canal systems with rigid boundaries and without sediment motion, two of these three variables must be known. For alluvial channels, the condition necessary for sediment to be transported at a certain rate fixes another variable, according to the theories as depicted in the preceding two sections. Fig. 6, for example, shows how the depth and slope can be determined from the given unit discharge and total sediment-transport rate, assuming a representative bed-material size of 0.25 mm (70). In most cases a change of sediment load, say, by 50%, does not

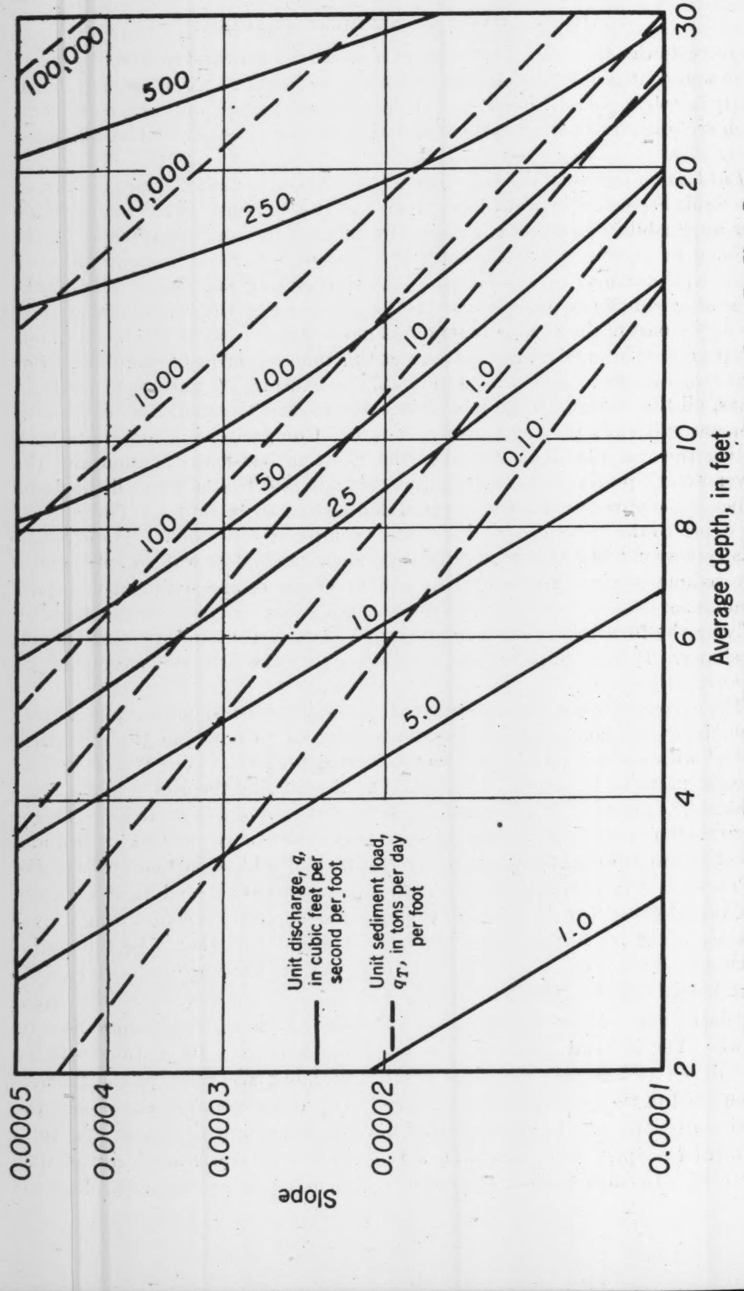

FIG. 6.—DESIGN OF ALLUVIAL CHANNELS TO CARRY A SPECIFIED DISCHARGE AND SEDIMENT LOAD; FINE SAND BED ($D = 0.25$ MM); BANK FRICTION NEGLECTED

materially affect the slope and the depth. So far as the design of alluvial channels is concerned, considerable tolerance can be allowed in determining the sediment-transport rate. This fact clearly demonstrates that, although efforts should be made to improve the existing sediment-transport formulas, any hasty rejection of these formulas because in some cases they fail to agree closely with the measured data is highly unwarranted. Graphs such as Fig. 6 are valuable aids in gaining insight into the change of river morphology by engineering measures.

On the other hand, one variable remains undetermined. What, for instance, should be the width of a natural stream channel? As early as 1919, E. S. Lindley, A. M. ASCE (71), stated that the "***dimensions, width, depth, and gradient of a [regime] channel to carry a given supply loaded with a given silt charge were all fixed by nature." By channel in regime is meant a channel at equilibrium. Since then, based on observations on the behavior of irrigation canals, engineers in India have succeeded in developing a set of rules that control the cross section and gradient of regime channels. For instance, G. Lacey claimed that the wetted perimeter, p, is related to the discharge, Q, as follows:

$$p = 2.67\, Q^{\frac{1}{2}} \qquad \text{(39)}$$

Investigations by L. P. Leopold and Thomas Maddock, Jr., M. ASCE (72), indicated that for natural streams the constant in Eq. 39 among others, should be, a function of the bed material.

The mass of data and experience gathered by engineers in India is so large that even a brief outline would overburden a paper of this nature. Reference is made to Mr. Lacey's original works (73) (74) and a summary of the regime theory by T. Blench, M. ASCE (75). A comparison between the Indian regime theory and the Einstein bed-load function is currently being undertaken by the writer (76). The results of preliminary analysis seem to indicate that, within the range of conditions prevailing in India, the Indian regime theory, through proper selection of the various "silt factors," yields nearly the same results as those given by the Einstein bed-load function. Outside the range of conditions in India, the use of regime theory is difficult because the "silt factors" then depend not only on the characteristics of sediment but also on the hydraulic characteristics of the channel.

Messrs. Leopold and Maddock have developed an empirical quantitative relation among width, depth, velocity, discharge, and suspended-sediment load from data on natural streams in the United States. The inclusion of sediment load in this type of empirical formula is significant and interesting. Application has been made of the Leopold-Maddock relationship in the actual design of stream channels (77).

In connection with the foregoing problem is the design of stable channels. The regime channel, by definition, is stable. Progress also has been made by the Bureau of Reclamation, United States Department of the Interior, under the direction of Mr. Lane (50) (78) in clarifying the general principles of stable-channel design and in developing methods of designing unlined earth canals to insure freedom from scour.

Density Current.—A density current is a gravity flow of a liquid or gas through, under, or over a fluid of approximately equal density (79). The density difference is due to dissolved solids, to temperature differences, and to suspended sediment. Geologists and oceanographers have used the term, "turbidity current," to identify a particular type of density current which contains suspended sediment and flows along the floor of a still body of clear water.

The most intricate feature of a turbidity current is its ability to maintain its identity. The stability of a turbidity current involves two aspects—that is, (*a*) the stability at the interface of the turbidity current and the flow above it and (*b*) the stability of the current itself. The first phase of the stability problem has been studied by several research workers, including Mr. Keulegan (80) (81) (82), A. T. Ippen, M. ASCE, and D. R. F. Harleman, J. M. ASCE (83), and R. R. Long (84), among many others. On the other hand, it still remains a mystery today how underflows of fluids with Reynolds numbers as great as 100,000 or more are not mixed with the flow above. Certain mechanisms must exist which prevent the turbulence created along the bed from penetrating the interface. Mr. Einstein (85) suggested that at high sediment concentrations and especially when sediment is flocculated, the underflow is no longer viscous but becomes plastic; the plasticity of the flow appears to be highly responsible for the existence of nonmixing underflows at large Reynolds numbers. Recent analysis of the structure of the sediment suspended in Lake Mead in Colorado and Arizona (86) indicated that the sediment does travel in a flocculated state.

Since the passage of turbid water through the tunnel outlets of Hoover Dam was first reported in 1938 by Nathan C. Grover, M. ASCE, and Charles S. Howard (87), considerable interest has been stimulated on the density current as a possible means of relieving the rate of reservoir silting. A follow-up survey of sedimentation in Lake Mead revealed that occasionally substantial portions of the inflow into Lake Mead traveled along the bottom of the reservoir, following the old river bed, and resulted in a deposit more than 100 ft thick (88) (89). However, to rely on the density current as an effective means of releasing sediment from reservoirs requires practical consideration. A density current is possible only when there is high sediment concentration in the inflow. In order to release the sediment carried by a density current, one must open the outlet by the time the density current reaches the dam. After the sediment in the density current has settled out of suspension, it has such a high resistance against scour that further flushing will only cut a deep gorge near the outlet and will have little effect on the deposits elsewhere. The design and maintenance of large outlets placed at low levels in a dam are not simple matters, and the high erosive action resulting from flow with large sediment concentration moving at relatively high velocity must be considered. Considerable water will be lost from the impounding reservoir in passing a density current through the reservoir.

Perhaps some thought should be given to another phase of the turbidity current—namely, the low unit weight of the reservoir deposits brought in either by density currents or by other means. In Lake Mead, for instance, the over-all unit weight of the deposits is 64.8 lb per cu ft. However, the deposits of fine-textured sediment have extremely high porosities and low specific weights (86). One of the cores showed that in the first 15 ft of deposits the specific weight varied from only 20 lb per cu ft to 40 lb per cu ft. If some means can be devised to release the water trapped in the deposits and thereby increase the unit weight, the space of the reservoir lost to the sediment deposits will be greatly reduced. Means have been devised to compact soil (90) for better foundations. These methods, as they stand now, cannot be applied to compacting the reservoir deposits because of the high costs involved and the relatively low efficiency. However, with the problem of reservoir silting becoming increasingly serious and with proper dam sites becoming more and more scarce, these methods, or others, should be studied and improved. Eventually they may prove feasible in attempting to increase reservoir life.

ACKNOWLEDGMENT

In preparing the paper, material has been drawn freely from the works of Mr. Einstein. The writer is the joint author of some of these works.

APPENDIX. BIBLIOGRAPHY ON SEDIMENT TRANSPORT

(1) **"Études du Régime du Rhone et l'action exercée par les eaux sur un lit a fond de graviers undefiniment affouillable,"** by P. DuBoys, *Annales des Pont et Chaussees*, Series 5, Vol. 18, 1879, pp. 141–195.

(2) **"The Transportation of Debris by Running Water,"** by G. K. Gilbert, *Professional Paper No. 86*, Geological Survey, U. S. Dept. of the Interior, Washington, D. C., 1914.

(3) **"The Bed-Load Function for Sediment Transportation in Open Channel Flows,"** by H. A. Einstein, *Technical Bulletin No. 1026*, U. S. Dept. of Agriculture, Washington, D. C., 1950. (*a*) p. 10.

(4) **"Fluid Resistance of Composite Roughness,"** by H. A. Einstein and R. B. Banks, *Transactions*, Am. Geophysical Union, Vol. 31, 1950, pp. 603–610.

(5) **"Linearity of Friction in Open Channels,"** by H. A. Einstein and R. B. Banks, Assn. Internationale d'Hydrologie Scientifique, Assemblée Générale de Bruxelles, 1951, pp. 488–498.

(6) **"Outline of the Energetics of Stream-Transportation of Solids,"** by H. L. Cook, *Transactions*, Am. Geophysical Union, 1935, pp. 456–463.

(7) **"Formulas for Bed-Load Transport,"** by E. Meyer-Peter and R. Muller, *Proceedings*, Third Meeting, International Assn. for Hydr. Research, Stockholm, 1948.

(8) **"Hydrodynamic Forces on a Rough Wall,"** by H. A. Einstein and E. S. A. El-Samni, *Reviews of Modern Physics*, Vol. 21, 1949, pp. 520–524.

(9) **"Transportation of Suspended Sediment by Water,"** by Vito A. Vanoni, *Transactions*, ASCE, Vol. 111 1946, pp. 67–133.

(10) **"Some Effects of Suspended Sediment on Fluid Characteristics,"** by Vito A. Vanoni, *Proceedings*, Fifth Iowa Hydr. Conference, 1952, pp. 137–158.

(11) **"Turbulent Transfer Mechanism and Suspended Sediment in Closed Channels,"** by Hassan M. Ismail, *Transactions*, ASCE, Vol. 117, 1952, pp. 409–446. (*a*) p. 435.

(12) **"Turbulence and Skin Friction,"** by Theodor von Kármán, *Journal of the Aeronautical Sciences*, Vol. 1, No. 1, 1934, pp. 1–20.

(13) **"Laws of Turbulent Flow in Open Channels,"** by G. H. Keulegan, *Research Publication No. 1151*, National Bureau of Standards, Washington, D. C., 1938.

(14) **"Experimental Investigation of the Problem of Surface Roughness,"** by H. Schlichting, *Technical Memorandum No. 823*, National Advisory Committee for Aeronautics, Washington, D. C., 1937.

(15) **"Notes on the Turbulence Function *k*,"** Missouri River Div., Corps of Engrs., U. S. Dept. of the Army, Omaha, Nebr., 1953 (unpublished).

(16) Discussion by Walter Rand of **"Wind Tunnel Studies of the Movement of Sedimentary Material,"** by A. W. Zingg, *Proceedings*, Fifth Iowa Hydr. Conference, 1952, pp. 132–133.

(17) **"Second Approximation to the Solution of the Suspended-Load Theory,"** by H. A. Einstein and Ning Chien, *Sediment Series No. 3*, Corps of Engrs., Missouri River Div., U. S. Dept. of the Army, Omaha, Nebr., January, 1954.

(18) **"Study of Transportation of Fine Sediments by Flowing Water,"** by A. A. Kalinske and C. H. Hsia, Studies in Engineering, *Bulletin No. 29*, Univ. of Iowa, Iowa City, Iowa, 1945.

(19) **"The Physics of Blown Sand and Desert Dunes,"** by R. A. Bagnold, William Morrow & Co., New York, N. Y.

(20) **"Criteria for Determining Sand-Transport by Surface Creep and Saltation,"** by A. A. Kalinske, *Transactions*, Am. Geophysical Union, Vol. 23, 1942, pp. 639–643.

(21) **"Über die Wechselwirkung Zwischen Wasser und Geschiebe in Flussen,"** by F. M. Exner, *Sitzenberichte*, Academie der Wissenshaften, Vienna, Vols. 3–4, 1925.

(22) **"The Characteristics of Sediment Waves Formed by Flow in Open Channels,"** by A. G. Anderson, *Proceedings*, Third Midwestern Conference on Fluid Mechanics, Univ. of Minnesota, Minneapolis, Minn., 1953, pp. 379–395.

(23) **"Ripple Formation and Its Relation to Bed-Load Movement,"** by H. K. Liu, thesis presented to the University of Minnesota, at Minneapolis, in 1953, in partial fulfilment of the requirements for the degree of Doctor of Philosophy.

(24) **"Anwendung der Aechlichkeitsmechanik und der Turbulenzforschung auf die Geschiebebewegung,"** by A. Shields, *Mitteilungen*, Preussische Versuchsanstalt für Wasserbau und Schiffbau, Berlin, 1936.

(25) **"The Critical Shear Stress,"** by M. S. Quraishy, *Journal*, Univ. of Bombay, India, Vol. 12, Pt. 3, 1943, pp. 37–46.

(26) **"Bed Ripples and Bed Dunes,"** by C. C. Inglis, Appendix 2 in "The Behavior and Control of Rivers and Canals," *Research Publication No. 13*, Central Waterpower Irrig. and Navig. Research Station, Poona, India, 1949, pp. 459–467.

(27) **"On the Influences of Sand Ripples upon the Sediment Transport in Open Channels,"** by Toichro Tsubaki, Tsuruo Kawasumi, and Takeshi Yasutomi, Reports of Research Inst. for Applied Mechanics, Kyushu Univ., Japan, Vol. 2, No. 8, 1953, pp. 241–256.

(28) **"River Channel Roughness,"** by H. A. Einstein and Nicholas L. Barbarossa, *Transactions*, ASCE, Vol. 117, 1952, pp. 1121–1146. (*a*) pp. 1134–1139.

(29) **"Similarity of Distorted River Models with Movable Bed,"** by H. A. Einstein and Ning Chien, *Proceedings-Separate No. 566*, December, 1954.

(30) **"Beitrag zur Frage der Geschwinddigkeitsformal und der Rauhigkeitszahlen für Strom Kanale und Geschlossene Leitungen,"** by A. Strickler *Mitteilungen*, Eidg. Amtes für Wasserwirtschaft, No. 16, Bern, 1923.

(31) **"Modern Conceptions of the Mechanics of Fluid Turbulence,"** by Hunter Rouse, *Transactions*, ASCE, Vol. 102, 1937, p. 534.

(32) **"The Turbulent Transport of Suspended Sediment in Open Channels,"** by J. N. Hunt, *Proceedings*, Royal Soc. of London, Series A, Vol. 224, No. 1158, 1954, pp. 322–335.

(33) **"Distribution of Suspended Sediment in a Natural Stream,"** by A. G. Anderson, *Transactions*, Am. Geophysical Union, Vol. 33, Pt. 2, 1942, pp. 678–683.

(34) **"Sediment Transportation Characteristics Study of Missouri River at Omaha, Nebraska,"** Corps of Engrs., Missouri River Div., U. S. Dept. of the Army, Omaha, Nebr., 1953 (unpublished).

(35) **"Manual of Sedimentary Petrography,"** by W. C. Krumbein and E. J. Pettijohn, Appleton-Century-Crofts, Inc., New York, N. Y., 1938.

(36) **"Settling Velocities and Behavior of Non-Spherical Particles,"** by W. C. Krumbein, *Transactions*, Am. Geophysical Union, Vol. 23, 1942, pp. 621–633.

(37) **"Particle Shape and Settling Velocity,"** by J. S. McNown, J. Malaika, and H. R. Pramanik, Report on the Fourth Meeting, International Assn. for Hydr. Research, Bombay, India, 1953, pp. 511–522.

(38) **"Effect of Shape on the Fall Velocity of Gravel Particles,"** by M. L. Albertson, *Proceedings*, Fifth Iowa Hydr. Conference, 1952, pp. 243–261.

(39) **"Particles in Slow Motion,"** by J. S. McNown, *La Houille Blanche,* Vol. 6, 1951, pp. 701–722.

(40) **"Sediment Concentration and Fall Velocity,"** by J. S. McNown and Pin-Nam Lin, *Proceedings*, Second Midwestern Conference on Fluid Mechanics, 1952, pp. 401–411.

(41) **"Rate of Sedimentation,"** by H. H. Steinour, *Industrial and Engineering Chemistry*, 1944, pp. 618–624, 840–847, and 901–907.

(42) **"The Sedimentation of Dense Suspensions of Microscopic Spheres,"** by B. W. Wilson, *Australian Journal of Applied Science*, Vol. 4, 1953, pp. 274–299.

(43) **"The Effect of Concentration on the Settling of Suspensions and Flow Through Porous Media,"** by P. G. W. Hawksley, in "Some Aspects of Fluid Flow," Edward Arnold & Co., London, 1951.

(44) **"A Correlating Modulus for Fluid Resistance in Accelerated Motion,"** by H. W. Iversen and R. Balent, *Journal of Applied Physics*, March, 1951.

(45) **"Development of the Mechanics of Sediment Transportation,"** by V. A. Vanoni, *Proceedings*, Federal Inter-Agency Sedimentation Conference, Bureau of Reclamation, U. S. Dept. of the Interior, Washington, D. C., 1947, pp. 209–224.

(46) **"A Summary of Sediment Transportation Mechanics,"** by V. A. Vanoni, *Proceedings*, Third Midwestern Conference on Fluid Mechanics, 1953, pp. 129–160.

(47) **"Laboratory Investigation of Flume Traction and Transportation,"** by Y. L. Chang, *Transactions*, ASCE, Vol. 104, 1939, pp. 1246–1313. (*a*) pp. 1287–1293.

(48) **"Critical Tractive Forces Which Start Movement of Sediment in a Channel,"** by A. C. Carter, *Report HYD–296*, Hydraulics Lab., Bureau of Reclamation, U. S. Dept. of the Interior, Washington, D. C., 1950.

(49) **"The Meyer-Peter Formula for Bed-Load Transport and Einstein Bed-Load Function,"** by Ning Chien, *Sediment Series*, Corps of Engrs., Missouri River Div., U. S. Dept. of the Army, Omaha, Nebr., (unpublished).

(50) **"Progress Report on Results of Studies on Design of Stable Channels,"** by E. W. Lane, *Report HYD–352*, Hydraulics Lab., Bureau of Reclamation, U. S. Dept. of the Interior, Washington, D. C., 1952.

(51) **"The Transportation of Bed-Load by Streams,"** by M. P. O'Brien and B. D. Rindlaub, *Transactions*, Am. Geophysical Union, Vol. 15, 1934, pp. 593–603.

(52) **"Studies of River Bed Materials and Their Movement with Special Reference to the Lower Mississippi River,"** *Professional Paper 17*, U. S. Waterways Experiment Station, Vicksburg, Miss., 1935.

(53) **"Sediment Transportation,"** by Carl B. Brown, in "Engineering Hydraulics," edited by H. Rouse, John Wiley & Sons, Inc., New York, N. Y., 1950, Chapter 7, p. 795.

(54) **"Movement of Sediment as Bed Load in Rivers,"** by A. A. Kalinske, *Transactions*, Am. Geophysical Union, Vol. 28, 1947, pp. 615–620.

(55) **"Analytical and Experimental Study of the Effects of Flow Characteristics and Fluid Viscosity Upon the Movement of Bed-Load in the Open Channel,"** by M. G. Mostafa, thesis presented to the University of Minnesota at Minneapolis, in 1949, in partial fulfilment of the requirements for the degree of Doctor of Philosophy.

(56) **"Formulas for the Transportation of Bed Load,"** by H. A. Einstein, *Transactions*, ASCE, Vol. 107, 1942, pp. 561–573.

(57) **"Neuere Versuchsresultate uber den Geschiebetrieb,"** by E. Meyer-Peter, H. Favre, and Hans A. Einstein, *Schweizer Bauzeitung*, Vol. 103, No. 13, 1934, pp. 147–150.

(58) **"Bed-Load Transportation in Mountain Creek,"** by H. A. Einstein, *Technical Publication No. 55*, SCS, U. S. Dept. of Agriculture, Washington, D. C., 1944.

(59) **"Transport of Sediment Mixtures with Large Ranges of Grain Sizes,"** by H. A. Einstein and Ning Chien, *Sediment Series No. 2*, Corps of

Engrs., Missouri River Div., U. S. Dept. of the Army, Omaha, Nebr., 1953.

(60) **"The Relation of Suspended to Bed Material in Rivers,"** by E. W. Lane and A. A. Kalinske, *Transactions*, Am. Geophysical Union, Vol. 20, 1939, pp. 637–641.

(61) **"A Distinction Between Bed-Load and Suspended-Load in Natural Streams,"** by H. A. Einstein, A. G. Anderson, and J. W. Johnson, *ibid.*, Vol. 21, 1940, pp. 628–630.

(62) **"Can the Rate of Wash Load be Predicted from the Bed-Load Function?"** by H. A. Einstein and Ning Chien, *ibid.*, Vol. 34, 1953, pp. 876–882.

(63) **"Suspended Sediment Discharge as Related to Streamflow, Topography, Soil, and Land Use,"** by H. W. Anderson, *ibid.*, Vol. 35, No. 2, April, 1954, pp. 268–281.

(64) **"Summary of Reservoir Sedimentation Surveys in the United States Through 1950,"** by Federal Inter-Agency Subcommittee on Sedimentation, *Sedimentation Bulletin No. 5*, Bureau of Reclamation, U. S. Dept. of the Interior, Washington, D. C., 1953.

(65) **"The Efficiency of Depth-Integrating Suspended Sediment Sampling,"** by Ning Chien, *Transactions*, Am. Geophysical Union, Vol. 33, 1952, pp. 693–698.

(66) **"Total Suspended Sediment Load from Vertical Transport Distribution,"** by K. B. Schroeder and D. B. Raitt, Bureau of Reclamation, U. S. Dept. of the Interior, Washington, D. C., 1952.

(67) **"Total Sediment Load Measured in Turbulence Flume,"** by Paul C. Benedict, Maurice L. Albertson, and Donald Q. Matejka, *Transactions*, ASCE, Vol. 120, 1955, p. 457.

(68) **"Application of Bed-Load Formulas to the Bed-Load Transport on the Middle Loup River, Dunning, Nebraska,"** by E. L. Pemberton, Bureau of Reclamation, U. S. Dept. of the Interior, Washington, D. C., 1950.

(69) **"Sediment Movement in Bear River, Utah,"** by C. G. Clyde, thesis presented to the University of California, at Berkeley, in 1953, in partial fulfilment of the requirements of the degree of Civil Engineer.

(70) **"Graphic Design of Alluvial Channels,"** by Ning Chien, *Transactions*, ASCE, Vol. 121, 1956.

(71) **"Regime Channels,"** by E. S. Lindley, *Proceedings*, Punjab Eng. Cong., Vol. 7, 1919, pp. 63–74.

(72) **"The Hydraulic Geometry of Stream Channels and Some Physiographic Implications,"** by L. B. Leopold and Thomas Maddock, Jr., *Professional Paper No. 252*, Geological Survey, U. S. Dept. of the Interior, Washington, D. C., 1953.

(73) **"Stable Channels in Alluvium,"** by G. Lacey, *Proceedings*, Inst. of C. E., London, Vol. 229, 1930, pp. 259–292.

(74) **"Regime Flow in Incoherent Alluvium,"** by G. Lacey, *Publication No. 20*, Central Board of Irrig., India, 1939.

(75) **"Hydraulics of Sediment-Bearing Canals and Rivers,"** by T. Blench, Evans Industries, Ltd., Vancouver, B. C., Canada, 1951.

(76) **"A Concept of Lacey's Regime Theory,"** by Ning Chien, *Proceedings-Separate No. 620*, February, 1955.

(77) **"A Plan of Channel Erosion Control, Five Mile Creek, Riverton Project, Wyoming,"** by Sedimentation Section, Bureau of Reclamation, U. S. Dept., of the Interior, Washington, D. C., 1953.

(78) **"Some Factors Affecting the Stability of Canals Constructed in Coarse Granular Materials,"** by E. W. Lane and E. J. Carlson, *Proceedings*, Minnesota International Hydr. Conference, Minneapolis, Minn., 1953, pp. 37–48.

(79) **"Density Currents as Agents for Transporting Fine Sediments,"** by H. S. Bell, *Journal of Geology*, Vol. L, No. 5, 1942, pp. 512–547.

(80) **"Laminar Flow at the Interface of Two Liquids,"** by G. H. Keulegan, *Research Publication No. 1591*, National Bureau of Standards, Washington, D. C., 1944.

(81) **"Interfacial Instability and Mixing in Stratified Flows,"** by G. H. Keulegan, *Research Publication No. 2040*, National Bureau of Standards, Washington, D. C., 1949.

(82) **"Characteristics of Internal Solitary Waves,"** by G. H. Keulegan, *Research Publication No. 2442*, National Bureau of Standards, Washington, D. C., 1953.

(83) **"Steady-State Characteristics of Subsurface Flow,"** by A. T. Ippen and D. R. F. Harleman, in "Symposium of Gravity Waves," *Circular No. 521*, National Bureau of Standards, Washington, D. C., 1952, pp. 79–93.

(84) **"Some Aspects of the Flow of Stratified Fluids, Part I,"** by R. R. Long, *Tellus*, Vol. 5, No. 1, 1953, pp. 42–58.

(85) **"The Viscosity of Highly Concentrated Underflows and Its Influence on Mixing,"** by H. A. Einstein, *Transactions*, Am. Geophysical Union, Vol. 22, 1941, pp. 597–603.

(86) **"Flocculent Structure of Sediment Suspended in Lake Mead,"** by I. Sherman, *ibid.*, Vol. 34, 1953, pp. 394–406.

(87) **"The Passage of Turbid Water Through Lake Mead,"** by Nathan C. Grover and Charles S. Howard, *Transactions*, ASCE, Vol. 103, 1938, pp. 720–790.

(88) **"Sediment Problems in Lake Mead and Downstream on the Colorado River,"** by C. P. Vetter, *Transactions*, Am. Geophysical Union, Vol. 34, 1953, pp. 249–256.

(89) **"Some Quantitative Aspects of Lake Mead Turbidity Currents,"** by H. R. Gould, *Special Publication No. 2*, Soc. of Economic Paleontologists and Mineralogists, 1951, pp. 34 and 52.

(90) **"Electro-Osmotic Stabilization of Solids,"** by L. Casagrande, *Journal*, Boston Soc. of Civ. Engrs., Vol. 39, No. 1, 1952.

(91) **"Regime Theory for Self-Formed Sediment-Bearing Channels,"** by Thomas Blench, *Transactions*, ASCE, Vol. 117, 1952, p. 383.

(92) **"Effect of Dynamic Shape on Lacey Relations,"** by T. Blench, *Papers 75–84, Publication No. 27*, Central Board of Irrig., Annual Report (Technical) 1941, Govt. of India Press, Simla, 1942.

(93) **"Practical Regime Theory Design of Artificial Channels with Self-Adjustable Boundaries,"** by T. Blench, presented at the ASCE Convention, St. Louis, Mo., June, 1955.

(94) **"Regime Formulas for Bed-Load Transport,"** by T. Blench, *Proceedings*, International Assn. for Hydr. Research, 1955.

(95) **"Analysis of Bed-Load Data,"** by R. B. Erb, thesis presented to the University of Alberta, at Edmonton, Alta., Canada, in 1955, in partial fulfilment of the requirements for the degree of Master of Science.

(96) **"Notes on Bedload Formula Curves,"** by Odin Hanson, Bureau of Reclamation, U. S. Dept. of the Interior, Denver, Colo. (unpublished report of the Hydraulic Lab.)

(97) **House Document No. 238,** 73d Cong., 2d Session, U. S. Govt. Printing Office, Washington, D. C., 1935.

(98) **"The Schoklitsch Bed-Load Formula,"** by Samuel Shulits, *Engineering*, London, June 21, 1935.

(99) **"Computations of Total Sediment Discharge—Niobrara River near Cody, Nebraska,"** by B. R. Colby and C. H. Hembree, *Water Supply Paper No. 1357*, Geological Survey, U. S. Dept. of the Interior, Washington, D. C.

(100) **"Observations on Channel Changes, Degradation, and Scour below Dams,"** by G. A. Hathaway, Corps of Engrs., U. S. Dept. of the Army, International Assn. for Hydr. Structures, Research Report 2, December 31, 1948, Appendix 16, pp. 287–307.

(101) **"Degradation Below Proposed Red Bluff Diversion Dam on Sacramento River,"** by C. R. Miller, Bureau of Reclamation, U. S. Dept. of the Interior, Denver, Colo., 1953 (unpublished report).

(102) **"A Reappraisal of the Beginnings of Bed-Movement-Competent Velocity,"** by F. T. Mavis and L. M. Laushey, International Assn. for Hydr. Research, Second Meeting, Stockholm, June 7–9, 1948.

(103) **"Studies of the Morphological Activity of Rivers As Illustrated by the River Fryis,"** by F. Hjulstrom, *Bulletin*, Geological Inst., Uppsala, Univ., Vol. 25, 1935, pp. 221–528.

(104) **"Stable Channels in Erodible Material,"** by E. W. Lane, *Transactions* ASCE, Vol. 102, 1937, p. 138.

(105) **"A Theory of Silt and Scour,"** by W. M. Griffith, *Proceedings*, Inst. of C. E., London, Vol. 223, 1937.

(106) **"Studies of Sediment Yields from Watersheds,"** by L. M. Glymph, Jr., *Publication No. 36*, l'Association Internationale d'Hydrologie (Assemblée générale de Rome, tome I), September, 1954, Extrait, pp. 178–191.

(107) **"Erosional Development of Streams and Their Drainage Basins: Hydrophysical Approach to Quantitative Morphology,"** by R. E. Horton, *Bulletin*, Geological Soc. of America, Vol. 56, 1945, pp. 275–370.

(108) **"Soil Erosion Studies,"** by W. D. Ellison, Pts. I–VI, *Agricultural Engineering*, Vol. 28, 1947, pp. 197–201, 245–248, 297–300, 349–351, 402–408, 442–450.

(109) **"Silt Transportation and Its Relation to Regime Channel Sections,"** by W. M. Griffith, *Journal*, Inst. of C. E. London, Vol. 22, 1944, pp. 107–120.

(110) **"Die Massenaustauch in freien Luft und verwandte Erscheinungen,"** by W. Schmidt, H. Grand, Hamburg, 1925.

(111) **"Review of the Theory of Turbulent Flow and Its Relation to Sediment Transportation,"** by M. P. O'Brien, *Transactions*, Am. Geophysical Union, Vol. 14, Part 2, 1933, p. 487.

(112) **"Elementary Mechanics of Fluids,"** by Hunter Rouse, John Wiley & Sons, Inc., New York, N. Y., 1947, p. 171.

(113) **"Bed Sediment Segregation in a Degrading Bed,"** by A. S. Harrison *Technical Report 33-1*, Inst. of Eng. Research, Univ. of California Berkeley, Calif., 1950.

(114) **"Observations on the Nature of Scour,"** by E. M. Laursen, *Proceedings*, Fifth Hydraulics Conference, Iowa Inst. of Hydr. Research, Iowa City, Iowa, June, 1952.

DISCUSSION

Thomas Blench,[3] M. ASCE.—The knowledge outlined by Mr. Chien has been obtained almost entirely from work with laboratory flumes. The various formulas cited, with the mixture of assumptions, approximations, and ingenious ideas behind them, are ably presented; the great complexity of the more exhaustive methods is manifest. The vast amount of observations on canals in the field, the dynamical aspect of the formulas evolved therefrom, and the fact that these formulas provide a simple and adequate means of practical design that has been used widely for many years receive no comment—although from the Bibliography (see Appendix at the end of the paper) (71) (73) (74) it is seen that the information was available for study. Instead, Fig. 6 is proffered, apparently based on laboratory flume experiments with trifling discharges, uniform sediments, and very poorly measurable slopes to replace the unmentioned formulas that represent the observed self-adjustment of field channels with discharges up to 10,000 cu ft per sec, naturally graded bed material, and excellently observable slopes. As Fig. 6 deals with channels with "bank friction neglected" it cannot be tested as rigorously as a chart for real channels and, of course, as bed load cannot be measured in the field its prophesies about transport cannot be checked at all, except on a laboratory scale. However, it seems reasonable to assume that the results are intended to approximate those for channels having hydraulically smooth sides. Making that assumption, loci of equal charge ("charge" being measured by the ratio of sediment-load weight per second to water weight per second) being also loci of equal bed factor (75) (91) would have the following two properties: The channel slope and the depth along any one locus would vary as the inverse cube root and the cube root of the square of the discharge intensity, respectively. (Discharge intensity is measured in cubic feet per second per foot.) One point on such a locus is where the lines representing 5.0 cu ft per sec per ft and the 0.10 ton per day per ft intersect; another on the same locus is where the lines representing 50 cu ft per sec per ft and 1.0 ton per day per ft intersect. The former point is at a slope of 0.0003 and at a depth of about 3.5 ft. Using the foregoing law of variation, the latter point should indicate a slope of 0.00014 and a depth of 16.4 ft, but it shows 0.0001 and 20 ft instead. This is misleading enough, practically; but even more confusing is the fact that regime equations (which represent what real channels actually do) indicate 13.6 ft of depth corresponding to 0.25 mm of sand, negligible charge, and 50 cu ft per sec per ft and indicate less depth as charge increases. The writer has had sufficient experience with that set of conditions to know that 13.6 ft is exceedingly close to the condition found in nature, and 20 ft has no prospect of realization as an equilibrium condition.

Incidentally, the one formula quoted from original regime theory—namely, Eq. 39—was investigated in the field by several Indian provincial irrigation research organizations which found that the "constant" depended on the nature of the bed material. (However, the functional form of the original Lacey relationships has never had to suffer amendment.) The writer used this information to replace the constant by a simple function of bed and side factors and published his method in 1941 (92); the results are in several subsequent references (75) (91). This matter is recorded because the author might be thought to have attributed the discovery to Messrs. Leopold and Maddock in 1953 (72).

---

[3] Cons. Engr. and Prof. of Civ. Eng., Univ. of Alberta, Edmonton, Alta., Canada.

The writer regards the laboratory and field approaches to sediment-transport problems as equally valid, complementary to each other, but from opposite directions. His comments are not intended to detract from the former but to warn against injudicious extrapolation from its results; they are also intended to draw attention to the existence and status of the complementary approach. As there is a readily available summary of regime theory (91) and a paper in preparation by the writer on its practical use (93) no details will be given here. Methods of applying regime theory to laboratory data are under study (94) (95) and are showing the inadequacy of the data for extrapolation.

Jan M. Jordaan, Jr.[4]—In the section entitled "Other Phases of Sediment Research: Density Current," the author has emphasized the need for a practical approach to determine the usefulness of density currents for conducting silt through reservoirs.

The writer concurs in the opinion that practical considerations are as important as the theoretical in an analysis of this nature. Irregularity of frequency and magnitude of inflows, variation in reservoir levels, temperature and density distributions, slopes, and cross sections may cause the most painstaking analytical treatment to be misleading and of little value where the practical approach is incorrect. Sedimentation in reservoirs is an irregular process in which the greatest damage is done at rare intervals during abnormal floods.

The application of the regime theory to channels may be extended to regime establishment under backwater conditions. In a reservoir the cross sections in the headwaters progressively become shallower as the sedimentation continues. Stored water, distributed over a large area, becomes subject to increased evaporation losses. The reduction of storage capacity, which may be regained by raising the dam, is not as important a factor in limiting the useful life of a reservoir as the increased evaporation losses resulting from the flattening of the cross sections.

In the writer's opinion, suitable outlet works may be designed for a particular site to release sediment-carrying density currents by the following method of operation:

1. During floods the clear water in the reservoir may be retained long enough for the peak of the turbulent inflow carrying the most sediment to be passed as a density current.

2. Release of the suspended silt at the dam under flood conditions could be effected by a curtain-wall structure built in front of the spillway crest and extending downward to restrict the region of drawoff to the denser bottom

---

[4] Research Assistant, Dept. of Civ. Eng., Massachusetts Inst. of Technology, Cambridge, Mass.; formerly Asst. Engr., Irrig. Dept., Pretoria, South Africa.

layers, progressing as a density underflow. Silt-bearing water would then be conducted vertically upward against the dam face in the draft-conduit thus created and would spill freely under normal crest head.

It should be borne in mind that such outlet works in the prototype are only useful during rare intervals of flood. Effective operation, however, would increase the useful life of the reservoir but would have to be verified by model analysis—due consideration being given to an accurate representation of the hydrologic features of the site.

Joe M. Lara,[5] J.M. ASCE.—This excellent paper meets its objective of acquainting the "nonsediment" technologist with the progress that has been made in sediment research. For such a broad subject it would be difficult to expand on the many phases. Mr. Chien, however, has examined briefly some of the current methods for computing sediment transport. Needless to say, there are other research studies being conducted at present to modify or improve the methods. The paper also contains a convenient set of references for those desiring more details of the technical background.

Odin Hanson of the Bureau of Reclamation has prepared a set of curves (96) which show a multiplotting of the (*S R*)-values against the unit sediment load as computed by the equations of Messrs. Einstein, Meyer-Peter, and Kalinske, L. G. Straub, M. ASCE (97), and A. Schoklitsch (98). Fig. 7 shows a graph excerpted from a set of these curves for a 0.125-mm grain size. From this plotting, it is indicated that further research is needed to reconcile the highly divergent results of the bed-load formulas to within a comparable range of practical limits. This objective might be attained by the further definition of the existing parameters, empirical coefficients, and other variables and constants contained in the different bed-load expressions. Progress toward this end is being made by the experiments and studies of Messrs. Chien and Einstein and other sedimentologists.

For current sediment studies it is necessary for the practical engineer to rely greatly on his judgment and experience in selecting the proper bed-load equation for the problem under consideration. This can be accomplished by making a few preliminary analyses of the various formulas he thinks will be applicable. Mr. Hanson's curves can be used as a guide in making the initial selection, provided that the engineer is sufficiently acquainted with the underlying theory of each formula and understands its limits of practical application.

It seems that one of the major pitfalls associated with the formulas developed by flume experiments is that, when they are applied to river channels, they fail to yield comparable results for the same variables that are empirically related by theory or experiment. These formulas may provide a reliable answer on one river system but for practical purposes fail when applied to another system. The current trend is to bring about better correlative agreement between the results of model studies and prototype data. The studies of E. L. Pemberton (68), B. R. Colby and C. H. Hembree (99), and the author and Mr. Einstein (17) are a step in this direction. Many of the practical aspects are being considered, and a more thorough analysis is being made of each of the natural, influential, or dominating factors. Mr. Chien cited examples of these in the studies being made of the von Kármán k-constant and the z-exponent of the suspended-load theory. These are some of the important steps which will bring the classical theories of experimental verification in closer agreement with the practical results. Research studies should be continued to keep these two conditions abreast of each other.

---

[5] Junior Member, Sedimentation Section, Hydrology Branch, Div. of Project Investigations, Bureau of Reclamation, U. S. Dept. of the Interior, Denver, Colo.

The study of Messrs. Colby and Hembree (99) illustrates a realistic approach to research work. The objective of the study was to check the various bed-load formulas by using the data collected at a test reach on the Niobrara River near Cody, Nebr. Of all the formulas tried, it was found that the computed values using the Einstein method yielded the best results when compared to the observed sediment discharge. In a further analysis, however, another method was developed for computing the sediment load. The method called the modified Einstein procedure is based on Mr. Einstein's theory except that different methods of computation are used to determine (a) the exponential measure of z, (b) the shear velocity with respect to the sediment particles, u_*, and (c) the intensity of bed-load transport ϕ_*. The z-values are determined by a trial-and-error solution of the equation:

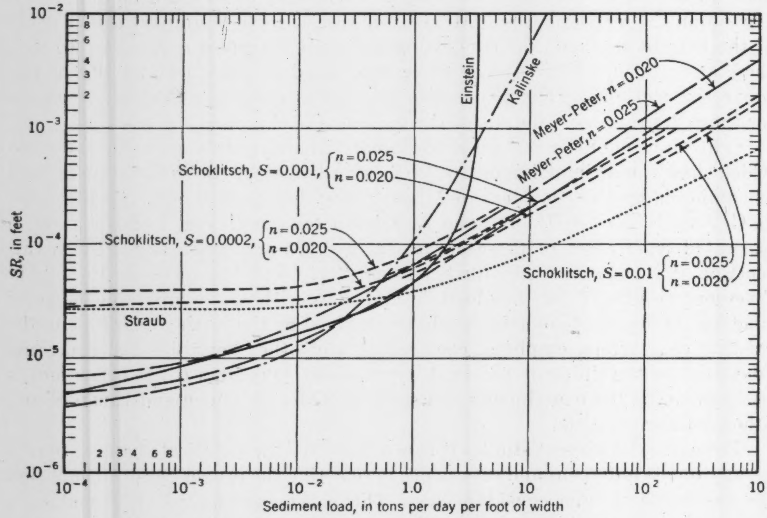

FIG. 7.—BED-LOAD EQUATIONS (GRAIN SIZE, 0.125 MM)

$$(P\,I''_1 + I''_2)\left(\frac{P\,J'_1 + J'_2}{P\,J''_1 + J''_2}\right) \ldots\ldots\ldots\ldots\ldots (40)$$

and by using the ratio of fall velocities. The shear velocity with respect to the sediment particles is also determined by a trial-and-error procedure to solve the modified equation (3*a*):

$$\bar{u} = 5.75 \left[g \, (S\,R)_m \right]^{\frac{1}{2}} \log_{10} \frac{12.27\, d x}{k_s} \ldots\ldots\ldots\ldots\ldots (41)$$

in which $\bar{u}$ is the average velocity for the cross section taken from a stream-flow measurement. The quantity $(S\,R)_m$ is determined by solving Eq. 41 knowing the $\bar{u}$-value and assuming the x-value; d is the average depth of the cross section, rather than R' as given by Mr. Einstein; x is the parameter for transition of smooth-rough boundaries and is an indirect function of the shear velocity u_*; u_* results from the evaluation of the terms under the radical sign $\sqrt{g\,(S\,R)_m}$. The intensity of the bed-load transport, ϕ_* is read from Mr. Einstein's graph relating ϕ_* and ψ_*. The appropriate value for ψ_*, however, is selected by solving the two equations:

$$\left.\begin{aligned} \psi_m &= \frac{1.65\, D_{35}}{(S\,R)_m} \\ \text{and} \qquad \psi_m &= \frac{0.66\, D}{(S\,R)_m} \end{aligned}\right\} \ldots\ldots\ldots\ldots\ldots\ldots\ldots\ldots (42)$$

The equation yielding the larger value of ψ_m is used.

The major advantage of the procedure is that it greatly reduces the necessary field work required for use in the original Einstein equation. Information is collected at only one cross section, and neither point-integrated samples nor water-surface slopes are required. The procedure is also closely tied to more of the measured field data.

A need exists for two more types of research work: (*a*) The determination of loads carried in cobble-bottom channels and (*b*) a method for computing the degradation below dams. These two problems are commonly encountered and are highly important to the practical engineer. To the writer's knowledge, no other studies have been made or methods developed for including sediments coarser than the 30-mm size, the upper limit of the Meyer-Peter formula mentioned by Mr. Chien. Computations based on any of the prevailing methods have not always yielded favorable results when applied to cobble-bed streams. Further experimentation with or modification of present or newer methods is definitely needed. On checking the available literature on sediment research, the writer could find no methods for computing degradation below proposed dams. There are studies (100) in which the degradation was measured or observed subsequent to the construction of the dam. C. R. Miller, J.M. ASCE, has investigated (101) some of the practical methods of approach for computing the probable degradation which bear mentioning. His analyses involve the use of (*a*) the tractive-force principle, (*b*) the competent bottom velocity using the curve developed by F. T. Mavis, M. ASCE, and L. M. Laushey, A.M. ASCE (102), (*c*) the bed-load transport equations utilizing Mr. Hanson's curves (96), and (*d*) canal stability, which involves the chart of F. Hjulstrom (103). The procedure essentially consists of plotting the discharge against the movable-size material and checking the size analysis curve for the degradation limit of the channel being considered. On establishing a reasonable estimate of the degradation, it is combined with the tailwater rating curve for use in designing the stilling pool.

It is hoped that this discussion will serve to stimulate further research work in the two problems just mentioned and the continuance of present research studies along the other practical lines suggested earlier in this report.

Navinchandra L. Rupani,[6] J. M. ASCE, and John B. Stall.[7]—This stimulating paper will be welcomed in the sediment-transport field.

Grain Resistance.—The suspended-sediment transportation theory requires essentially the understanding and application of laws governing the velocity distribution in a vertical. Mr. Von Kármán's velocity deficiency law applied to circular pipes is given by Eq. 3. The numerical value of Mr. Von Kármán's universal constant as evaluated from the Nikuradse experiments is found to be 0.4 for clear-water flow in circular pipes. That the velocity distribution in a vertical for a sediment-laden flow is different from that of a clear-water flow is demonstrated by the variation in the universal constant k from 0.2 to 0.4. There appear to be two schools of thought as to the probable cause of change in the k-value. One school subscribes to the belief that the sediment in suspension causes damping of the turbulent eddies, and the other attributes the change in the k-value to the bed roughness. With due respect to the latter, the writers favor the former school. Undoubtedly, when the bed protrusions caused by the sediment become comparable to the depth of flow, the velocity distribution may be expected to change; however, it is not clear how the problem of suspended sediment is affected by such bed roughness. First, there must be sufficient sediment grains in the bed for some grains to go into suspension. The space between the protrusions may then be expected to be filled in by these relatively fine particles, thus reducing the ultimate effect of the protrusion height as a rough surface. However, if relatively fine sediment grains do not exist in the bed, the problem of suspension does not arise.

The author's arbitrary division of sediment-laden flow into a heavy-fluid zone and a light-fluid zone indicates the damping effect of the highly concentrated zone on the turbulence generated at the bed. Messrs. Kalinske and Hsia (18), using particles having a median diameter of 0.011 mm, found the suspended-sediment distribution uniform throughout the vertical with concentrations as high as 11%. Whether the reduction in the k-value can be similarly explained by the damping effect is not understood.

Remembering that the scatter is wide even when plotted on semi-log paper, the relationships between the parameter $\sum \frac{C_s\, V_s}{VS} \frac{\rho_s - \rho_f}{\rho_s}$ and k are of considerable interest. If the wash load with extremely high concentrations exerts any significant influence on the damping of turbulent eddies, the relationships shown in Fig. 1 may be expected to change.

---

[6] Asst. Engr., State Water Survey, Urbana, Ill.

[7] Asst. Engr., State Water Survey, Urbana, Ill.

Bar Resistance.—When evaluating the frictional component due to channel irregularities, one must resort to such functional relationships as

$$\psi' = \frac{\rho_s - \rho_f}{\rho_f} \frac{D_{35}}{R'_b S} \text{ versus } \frac{U}{U''_*}$$

developed by Mr. Einstein (3) from field measurements. Mr. Lane (104) observes that

> "* * * If a channel is supplied with a heavy bed load, in order to be stable it must move this load along; * * * To be stable, the channel carrying bed loads, therefore, should have a higher velocity along the bed, but the same velocity along the banks, and this could only occur with a wider, shallower section."

W. M. Griffith (105) has also observed similar phenomena in India. In these channels evaluation of bar resistance becomes important. Preliminary computations, representing Illinois streams and sediment characteristics, indicate a ψ'-value as low as 0.05 for an average depth of 7 ft. Mr. Einstein (3) gives the lowest ψ'-value as 0.48 based on river measurements. Field measurements for rivers with fine sediment loads, relatively flat slopes, and shallow depths could be of great value to field engineers in evaluating bar resistance. Laboratory flume studies do not yield satisfactory results because of the side-wall influence on the flow, which tends to straighten out the channel irregularities (3).

Wash Load.—Average grain-size distributions of sediment from eight reservoirs in central and southern Illinois show that 90% of the sediment by weight is finer than 40 microns (0.04 mm). Thus, sedimentation of reservoirs in Illinois is a problem of suspended-sediment transportation. This confirms the statement by Mr. Chien that "* * * wash load * * * contributes the bulk of the deposition in lakes and reservoirs."

In an earlier article Messrs. Einstein and Chien showed (62) quite conclusively the impracticability of predicting the wash load from the hydraulic characteristics of the river channels. In the present article the author suggests further work in establishing quantitative relationships between the wash load and watershed factors. Mr. Anderson (63) has pioneered in this field. L. M. Glymph, Jr. (106), has reported and compared a number of other fundamental works in an attempt to establish such relationships. Attempts are underway in Illinois to improve this quantitative relationship.

As a stream channel develops over a geologic era the composition of the bed material is a result of the discriminatory transport of the parent materials by the flowing stream. The parent materials within the drainage area above the channel may be heterogeneous and thus confound efforts to understand sediment transport by studies of the bed composition and the hydraulic characteristics of the channel.

The wash load might be traced back upstream to the micro-channel into which runoff first collects. R. E. Horton (107) has contributed fundamental thinking regarding these soil channels. The recent work of W. D. Ellison (108) is also of basic importance. The bed composition of this small rill of micro-channel could consist of soil particles having a known size distribution, and the characteristics of this channel could be determined.

In this rill the water flow will be found to have discriminated much less among the soil particles in motion than it would have in a downstream river channel. The material moved in this rill will have a composition much more nearly identical to the bed material than would be the case downstream where the river has collected flow from widely heterogeneous soils and channels. The close identity of the sediment load and the bed material in the rill or micro-channel offers the possibility of a better understanding of the true sediment-transport function which relates the former to the latter.

The sediment load moved in this micro-channel later constitutes a fraction of the total sediment load of a downstream channel although the mode of transport of the different components of the load at the downstream location may not yet be readily classified as bed-material load or wash load. Research into the movement of the load in this micro-channel might reveal the laws which it follows. This research can be done in the laboratory; the model, however, may be larger than the prototype. If some new functions could explain sediment movement in this micro-channel, this load could be traced downstream to the point where it becomes wash load. It appears that research to understand better the upper networks of the stream systems is requisite to the control of the damaging wash load.

Channel Stability.—The problem of stability of river channels and earthen canals deserves a more rigorous approach based on the modern theory of fluid mechanics. It is probably an oversimplification to postulate that such a simple relationship as Eq. 39, developed by Mr. Lacey, governs the hydraulics of a stable channel. This empirical equation, although applicable to local conditions in India, has shown a variation of the value of the constant from 2.32 to 3.1 (109).

No satisfactory explanation as to what factors govern this variation is available. The writers believe that the following factors, among others, affect the value of the constant: (*a*) The shape of the channel section; (*b*) the hydraulics of the channel (roughness, energy slope, and similar factors); and (*c*) sediment characteristics.

Mr. Lacey has also stated that the exponent is invariably 0.5. Messrs. Leopold and Maddock (72) investigated a large variety of rivers in the Great Plains and the southwest regions of the United States. They found an average value of 0.26 for natural streams instead of the value of 0.5 which was obtained strictly from data on stable (regime) irrigation canals in India.

The modern concept of sediment transportation based on the theory of fluid mechanics developed by W. Schmidt (110), Mr. O'Brien (111), and Mr. Einstein (3) provides a valid approach to the solution of this difficult problem of sediment transportation. It is gratifying to learn from the paper that Mr. Einstein's bed-load function gives results that agree with those obtained when proper "silt factors" are used in Mr. Lacey's regime theory. It is hoped, as more field experience is gathered covering wide ranges, that the Einstein bed-load function will replace existing empirical relationships, thus providing a universal solution to the difficult problem of sediment transportation in open-channel flows.

Hsin-Kuan Liu[8].—To make a brief summary of what has been studied and found in the field of sediment transport is not an easy task because numerous papers dealing with the mechanics of this subject have been published. It is even more difficult to draw conclusions from various studies because of the widely spread opinions among them. The author certainly has prepared an excellent, timely summary which helps the advancement of research in the field of sediment transport.

In discussing the initiation of ripples, the author introduced the writer's results as shown in Fig. 2, Curve II. In order to distinguish among the sources of data and to understand the significance of Curve II more clearly, the original graph (23) is presented as shown by Fig. 8 in this discussion. The result is based on the reasoning that ripples are due to instability of the interface (or boundary) between the flow and the movable bed. The author argued that, because the sediment rate is not large enough to create any difference in density between the clear water and the sediment-laden water, ripples cannot be associated with the instability at the interface of two flows of different densities. Apparently the author misunderstood the term "interface" as used by the writer. The writer's concept of interfacial instability between the movable bed and the superposed fluid which leads to a possible explanation of the mechanics of ripple formation is briefly summarized as follows:

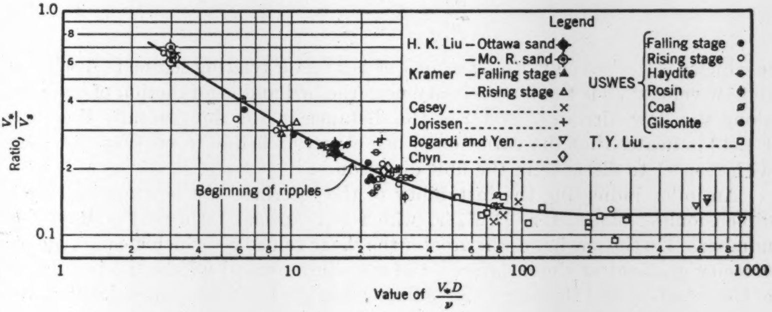

Fig. 8.—Criterion of Ripple Formation As a Function of V_*/V_s and $V_* D/\nu$

Owing to the difference in velocity between the flow and the movable bed, there exists close to the bed a zone which has a high velocity gradient. Such a zone, very thin in nature, is defined here as an "interface." Furthermore, such an interface is particularly unstable because of this high-velocity gradient. In the case of flow over a rigid boundary, turbulence from the boundary is caused by the instability of this interface, which rolls up into small eddies. In the case of an alluvial bed, the roll-up effect of the interface can produce turbulence as well as change the bed configuration. In order to analyze the mechanics of ripple formation it is necessary to examine the nature of the interface and its effect on the bed configuration. Because the bed is movable, the

---

Asst. Prof., Dept. of Civ. Eng., Colorado Agri. & Mech. College, Fort Collins, Colo.

bed configuration is readily affected by temporal variations of the flow pattern, if the local flow velocity is large enough to transport the bed material. The next question is: What causes this temporal variation of flow pattern which results in the instability of the interface? This question can be answered, at least in part, by the analysis which Hunter Rouse, M. ASCE, used in explaining the instability of flow at a hypothetical surface of discontinuity (112). At any instant the streamline at the interface may deviate from a straight line due to a sufficient disturbance which probably exists in the flow. The effect of the disturbance on the flow pattern depends on the instability of the interface (or boundary). According to the principle of the flow net, the local velocity will decrease as the neighboring streamlines diverge and will increase as they converge. If the local velocity of the flow is large enough to transport the sediment, the periodic change in velocity along the interface will result in a change of bed configuration. Mr. Exner (21) has established a differential equation for sediment transport in two-dimensional flow. That is,

$$\frac{\partial \eta}{\partial t} + K \frac{\partial v}{\partial x} = 0 \quad \ldots\ldots (43)$$

in which η is the bed elevation, t is time, K is a factor relating sediment discharge to flow velocity, v is the flow velocity near the bed and is a function of distance along the flow direction, and x is the distance in the downstream direction. Eq. 43 indicates that the variation of bed elevation is due to velocity variation with respect to distance in the flow direction.

An index indicating the instability of the interface can be expressed by a dimensionless parameter, $D\ V_*/\nu$, which is a special form of the Reynolds number. On the one hand, the greater the shear velocity—which means a higher velocity gradient at the interface—the more pronounced will be the instability of the interface and the larger the sediment size the more pronounced will be the tendency to produce eddies. On the other hand, the higher the kinematic viscosity the more the internal shear will tend to oppose further differences in velocity.

The capability of the flow to transport the sediment and change the bed configuration depends on the scouring force of the flow and the resistance force of the sediment. The scouring force can be expressed as (23)

$$F_1 = C_1 \tfrac{1}{4} \pi D^2 \left(\tfrac{1}{2} \rho_f V^2{}_*\right) \quad \ldots\ldots (44)$$

and the resistance force of the sediment to the flow is (23)

$$F_2 = C_2 \tfrac{1}{4} \pi D^2 \tfrac{1}{2} \left(\rho_f V^2{}_s\right) \quad \ldots\ldots (45)$$

in which F_1 is the erosive force of the flow and F_2 is the resistance force of the sediment.

Laboratory experiments indicate that ripples occur shortly after the beginning of bed-load movement. Therefore, it can be assumed without serious error that, at the moment ripples occur, the scouring force is equal to the critical scouring force.

$$F_1 = F_2 \quad \ldots\ldots (46)$$

so that

$$\frac{V_*}{V_s} = \text{function}\left(\frac{D\,V_*}{\nu}, \text{shape factor}\right) \qquad (47)$$

If the shape factor is considered to be of secondary importance, Eq. 47 can be written as

$$\frac{V_*}{V_s} = \text{function}\left(\frac{D\,V_*}{\nu}\right) \qquad (48)$$

At the moment at which ripples occur, two conditions must be satisfied: (*a*) The flow must be strong enough to transport the sediment and (*b*) the interface between the flow and the movable bed must become unstable; consequently, it causes velocity variation along the flow direction. It should be noted that $D\,V_*/\nu$ is a parameter that serves two functions: (*A*) It indicates the instability of the interface and (*B*) it correlates the flow velocity at the grain level with the shear velocity in accordance with the von Kármán-Prandtl theory, thereby defining the scouring force. By plotting data which are the average between those for a smooth bed and those for the first appearance of ripples in terms of V_*/V_s against $D\,V_*/\nu$, Fig. 8 was obtained. Conditions (*a*) and (*b*) are both satisfied when data pertaining to the flow and the sediment fall above the curve. The scatter of the data is due to such causes as error in measurements, difficulties of defining the first appearance of ripples, shape factor, and effect of mixture.

The author pointed out that there are many bed-load equations in existence. However, their application to engineering problems is limited for various reasons. Those of Messrs. Einstein, Kalinske, and Meyer-Peter are sound in theory, yet too complicated for many hydraulic engineers to use in practice. Furthermore, because there is no way of measuring the actual bed load in a large river, their applicability to a large river is uncertain. Many investigators are still searching for a better bed-load equation and also a better method of measuring bed load

The writer's experiment on sand-wave movement, as will be explained, seems to indicate the possibility of obtaining a type of bed-load equation in terms of sand-wave motion and of measuring the bed load transported by investigating the sand-wave motion.

In performing the experiments the writer used a recirculating, open-channel, laboratory flume 40 ft long, 1 ft wide, and 2 ft deep. There were two 5-ft-long glass sections on one side and one 5-ft-long section on the other to facilitate observation. Water was supplied from a floor-level sump 8 ft long by 2.5 ft by 2.5 ft through a centrifugal pump to a 4-in.-diameter feed pipe. Flow was measured through an orifice meter and returned to the supply sump over an adjustable tailgate at the downstream end of the flume. Sand was supplied at the upstream end of the flume by an elevator. The elevator was operated by a variable-speed motor, chain, and sprocket-wheel connected to a screw-lift mechanism. Ottawa sand, passing a No. 20 sieve and retained on a No. 30 sieve, was used as sediment. Sand transported to the downstream end of the flume was trapped in a bucket and weighed to verify the rate of sediment feed. The experiments were conducted at the St. Anthony Falls Hydraulic Laboratory of the University of Minnesota at Minneapolis. The entire work was part of the writer's doctoral dissertation under the guidance of Mr. Straub.

The purpose of the experiments was to determine the quantitative relationship between sand-wave motion and bed-load transport. It was found that approximately 100% of the bed load is transported in the form of sand waves, except when there is appreciable saltation load in the stream. In these experiments, the discharge was kept constant at 0.4 cu ft per sec. The rate of sediment feed, in pounds per hour, ranged from 600, 300, 150, and 75, to 38.3. The bed slope was varied from 0.0115 to 0.002. The mean velocity of the flow varied from 2.3 ft per sec to 1.5 ft per sec. The depth of flow varied from 0.174 ft to 0.267 ft. The Froude number ranged from 0.97 to 0.512.

The velocity of the sand waves was measured by two methods: (*a*) Counting the number of waves passing a certain station per unit of time and multiplying this by the wave length and (*b*) measuring the time required for a certain wave to travel a certain distance. The wave length was obtained by averaging the total length of several waves. It was found, as shown in Fig. 9, that the velocity of the sand waves for the case in which $q = 0.40$ cu ft per sec with the size of Ottawa sand used ($d = 0.690$ mm) was

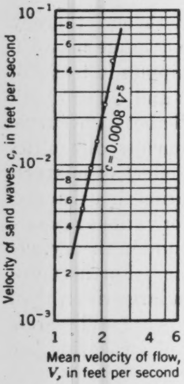

FIG. 9.—RELATIONSHIP BETWEEN THE VELOCITY OF THE SAND WAVE AND THE VELOCITY OF FLOW

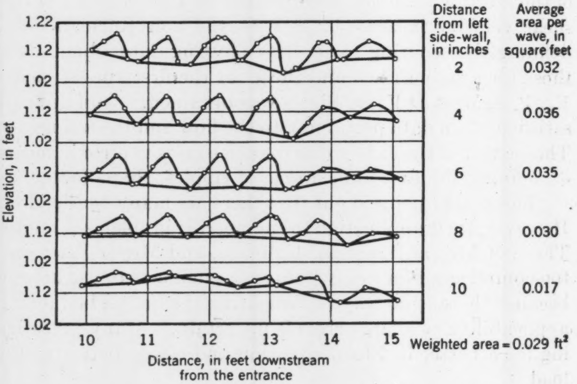

FIG. 10.—EXAMPLE OF PLOT OF SAND-WAVE PROFILES (RUN 2-2, $q = 0.4$ CU FT PER SEC, $q_B = 300$ LB PER HR)

$$c = 0.0008\ V^5 \ldots\ldots\ldots\ldots\ldots\ldots\ldots\ldots (49)$$

in which c is the sand-wave velocity and V is the mean velocity of flow. Inasmuch as the wave velocity varies with a large exponential power of the mean velocity of the flow, the wave velocity is highly sensitive to change in the flow velocity.

In studying the relationship between sand-wave motion and rate of bed-load transport, the bed profile was measured using a point gage with an electric device attached. As the point touched the wetted bed surface, a red light appeared on the gage. The depth of the flow was the vertical distance between the water surface and the mean bed elevation. In order to compute the bulk volume of the sand wave during each run, five bed profiles were taken along the flume. The lower boundary of the sand waves was considered to be the line joining the lowest point of the troughs. The average volume per sand wave was that of the total volume of sand waves above the lower boundary divided by the number of waves. The volume of sand waves per unit of width was measured from the bed profiles by means of a planimeter. Profiles of Run 2-2 are shown in Fig. 10. Results of the experiments are listed in Table 1. The last two lines in Table 1 show both the actual and the computed quantity of sediment transported. It indicates that bed load is entirely in wave forms. Translation of sediment along the bed is negligible. The computed quantity of sediment in Run 2-1 is considerably less than the actual amount of sediment introduced. This can be explained by the fact that the sediment feed was heavy and a considerable amount of it was moving as saltation load.

TABLE 1.—SUMMARY OF EXPERIMENTAL RESULTS OF PROPERTIES OF SAND WAVES

Description	Run No.				
	2-1	2-2	2-3	2-4	2-5
Discharge, in cubic feet per second	0.4	0.4	0.4	0.4	0.4
Depth, in feet	0.174	0.190	0.215	0.236	0.267
Velocity, in feet per second	2.3	2.1	1.86	1.70	1.50
Slope	0.0115	0.0086	0.0054	0.0032	0.002
R_w, in feet	0.035	0.051	0.06	0.077	0.092
R_b, in feet	0.162	0.171	0.189	0.189	0.218
Froude Number, **F**	0.972	0.848	0.707	0.615	0.512
Amplitude, in feet	0.089	0.078	0.059	0.037	0.053
Wave length, in feet	0.92	0.835	0.834	0.715	1.58
Wave velocity, in feet per second	0.0455	0.0236	0.014	0.0093	0.0051
Temperature, in degrees Fahrenheit	72	77	73	76	75
T_b, in pounds per foot, $= \gamma_f R_b S$	0.116	0.092	0.064	0.038	0.027
Shear velocity V_*, in feet per second	0.245	0.22	0.18	0.14	0.12
Sediment supply, in pounds per hour	600	300	150	75	38.3
Computed sediment, in pounds per hour	440	297	157	72.5	39.6

Results previously shown suggest that a formula for bed-load transport in terms of sand-wave motion, sediment properties, and flow properties might possibly be obtained by extensive experiments. The formula, if obtained in the future, could be used to verify existing bed-load equations. Field measurements of rate of bed-load transport could be made by observing the sand-wave velocity during flood stage, and the bed profile could be taken by echo sound devices.

NING CHIEN,[9] A. M. ASCE.—Owing to the large number of papers published in the field of sediment engineering, it is almost impossible to cover every phase of the research that has been conducted by various persons and agencies. It was the writer's hope that some of the important research programs which did not receive enough attention in the summary of the paper would be reported on in more detail by those familiar with these programs.

---

[9] Formerly Asst. Research Engr., Inst. of Eng. Research, Univ. of California, Berkeley, Calif.

In this respect, the discussions contributed by Messrs. Lara, Rupani and Stall, and Liu are especially constructive and valuable. Also, Mr. Blench's suggestions of using field observations are highly supported. Empirical laws, however, which are derived from field observations in certain types of channels should not be applied to different types of channels without previously checking such channels.

At low or moderate flows when the bed is covered by sand bars, the motion of the bed load can be determined by either measuring the transport rate of individual particles in the bed layer or by measuring the collective motion of sand bars. However, as suggested by Mr. Liu, a bed-load formula in terms of the collective motion of sand bars is not necessarily certain to be more accurate than the existing ones that are derived on the basis of the motion of individual particles. Not only are the basic mechanics that initiate the sand-bar formation not well understood as yet, but the link between the motion of bed load and the distribution of suspended sediment will be lost if the former is expressed in terms of the collective motion of bed particles. It is the writer's opinion that enough bed-load formulas have already been proposed, and any new formulas developed on the basis of the same data probably will not differ materially from the existing ones—even if they may assume different mathematical forms. It is much more important to extend the range of application of the existing theories and to determine their limitations. Mr. Lara has mentioned the difficulties in applying the prevailing methods to determine the loads carried by cobble-bottom channels. An even more important step is the extension of present theories to streams that drain watersheds supplying silty sediment at high rates. This is especially true in arid areas with only rare but heavy precipitation and with large deposits of unconsolidated silt ready for erosion. The extremely high concentration of silty sediment at all significant flows makes the division of flow into a liquid and into a solid phase illogical, as explained by Messrs. Rupani and Stall. The liquid and solid actually blend into a liquid of entirely different characteristics, such as density and viscosity, of all possible stages of transition from water to a mud flow. Mr. Lara also called for research on developing a method for computing the degradation below dams. Attention is directed to an excellent work by A. S. Harrison, J. M. ASCE (113), which has not been reported by the writer because it falls into the field of sediment erosion. In the same general field the work by Mr. Laursen (114) also warrants recommendation. Information is equally meager in the last phase of the sedimentation process—sediment deposition—with the exception of deposition in reservoirs.

Mr. Lara has reported the work of field engineers in modifying the Einstein method to reduce the necessary field work. In spite of the fact that such attempts have been proved beneficial to field workers and should definitely be encouraged, the writer wishes to express a few words of caution. The Einstein method covered a wide range of conditions, as reported in the writer's paper. Changes in any one phase of the whole description must be thoroughly checked against all these conditions. If this is not done, such modifications may yield accurate results in a certain range of conditions but may lead to gross error in other ranges. Furthermore, every step of development that leads to the Einstein bed-load function of its present form has its physical significance. For instance, the use of Eq. 2 is based on the linearity of friction in open channels, which allows the linking together of grain roughness K_s with its corresponding hydraulic radius R'_b. The replacement of R'_b in the logarithmic term in Eq. 2 by the total depth d may simplify the computation procedures but, in the meantime, also divorces the equation from its physical background. However, such a step has little practical consequence as any moderate change in a variable affects the logarithm of the variable even to a lesser extent.

Some of the results as quoted by the discussers appear to be in error. The one-half power in Eq. 39 has been verified according to the investigations of Messrs. Leopold and Maddock (72). The power 0.26 as reported by Messrs. Leopold and Maddock and as quoted by Messrs. Rupani and Stall applies only to the variation in a particular cross section of a river. The Einstein curve prepared by Mr. Hanson and cited by Mr. Lara was based on the old $(\phi - \psi)$-relationship (56) and should be reconstructed according to the new Einstein bed-load function (3). This will eliminate the part that gives almost constant sediment load over a range of $(S\,R)$-values. In reality this part of the curve has not much physical significance because rivers with a bed-material size of 0.125 mm seldom, if ever, flow at a product of $S\,R$ greater than 0.005.

HANS A. EINSTEIN,[10] M. ASCE.—Before leaving the United States, the author authorized the writer to answer additional comments referring to his paper.

Mr. Blench makes it an important point of his discussion that the superiority of the "simple and adequate" formulas preferred by him follow logically from the fact that they are derived from field measurements in full-sized canals rather than from flume experiments with "trifling" discharges. The writer would like to take issue with this statement. Every empirical equation is adequate, at least in the eyes of the engineer, if the constants of that equation are known and can be predicted for every case which needs to be calculated. In following the recent papers and publications on the development of the "simple and adequate" regime-theory equations, the writer noticed that even the proponents of that general approach do not agree on the choice of these constants and that not even general agreement exists on the parameters upon which they depend. The American engineer who lacks the necessary years of experience with these formulas thus stands a grave chance of choosing wrong constants and of emerging with a wrong result, despite the correct use of the formulas. Naturally, this is exactly the same with any other equation such as the Manning formula, and the best results will always be obtained if the engineer uses that formula for which he best knows the constants and with which he has had the most experience.

If Mr. Blench maintains that bed-load rates cannot be measured in natural streams, he must not be familiar with the rather large list of such measurements that have been made in Austria, Switzerland, Holland, and the United

---

[10] Prof. of Mech. Eng., Univ. of California, Berkeley, Calif.

States. What he should state is that the measurements in the natural canals with the greater-than-trifling discharges on which his formulas are based did not include the determination of bed-load rates. However, even a quick check into the Indian canal data reveals that all data were taken within a very narrow range of bed-load conditions. Even if the bed-load rates had been measured, no interesting results could have been revealed. The writer is rather doubtful as to whether the derived formulas can be assumed valid for changed bed-load conditions existing in many American rivers.

The previously mentioned river measurements of bed-load transport also provide a complete hydraulic measurement of the flows and have permitted the proof of applicability to a wide variety of rivers of the formulas which the writer and others have derived from flume experiments with small discharges.

With respect to the introduction of the bed-load rates as a weight concentration only, the writer is not able to follow Mr. Blench's arguments. The writer has seen rivers carrying 1% of gravel and others carrying 1% of silt or fine sand. The effect of the two loads on the streams was distinctly different and thus cannot be expressed by the concentration only.

As a last and concluding remark, the writer agrees heartily with Mr. Blench's idea that the sediment problem can only be solved by a combined attack in the laboratory and in the field. It is a fallacy, however, to think that field measurement is identical with regime theory. The writer is actually glad to have spent a number of years in the field studying natural stream behavior, and it is this prototype study which has guided him in the organization of the laboratory work and its analysis and which has forced him to view the general applicability of the regime theory with suspicion.

AMERICAN SOCIETY OF CIVIL ENGINEERS
Founded November 5, 1852
TRANSACTIONS

Paper No. 2825

PITTSBURGH'S COMPREHENSIVE IMPROVEMENT PROGRAM

By Park H. Martin,[1] M. ASCE

Synopsis

Recent redevelopment activities in Pittsburgh, Pa., have been unusually extensive, and the author describes the planning, execution, and financing of this work. The various organizations that have been established, the legislation that has been enacted, and the negotiations that have been necessary for the accomplishment of the plan are described. The over-all project involves smoke and flood control, highways, parking, airports, mass transit, sanitation and public health, recreation and conservation, zoning and urban redevelopment, libraries and other cultural institutions, and economic development.

Introduction

This is the second paper that the writer has had published under the auspices of the Society on the so-called "Pittsburgh (Pa.) Story." The first paper[2] described the Allegheny Conference, the Pittsburgh Program, what had then been accomplished, and what was either in process or planned.

The present paper describes the accomplishments as of October, 1954. Many articles have appeared in magazines of national circulation setting forth the "Pittsburgh Story." Mostly written in a dramatic vein, they have been devoted largely to personalities. Although the writer recognizes the value of individuals in planning and carrying out the program, this paper is more concerned with the way the program was developed, what has been accomplished, and how the program has been financed.

Pittsburgh Background

The City of Pittsburgh is not only the center of Allegheny County but also the hub of the Pittsburgh industrial area (Fig. 1). Within the corporate

---

Note.—Published, essentially as printed here, in January, 1955, as *Proceedings-Separate No. 601*. Positions and titles given are those in effect when the paper was approved for publication in *Transactions*.

[1] Executive Director, Allegheny Conference on Community Development & Pittsburgh Regional Planning Assn., Pittsburgh, Pa.

[2] "The Allegheny Conference—Planning in Action," by Park H. Martin, *Transactions*, ASCE, Vo 1953, p. 235.

limits of the city are 54 sq miles and 676,000 persons. The County of Allegheny, including Pittsburgh, contains 745 sq miles and a population of 1,515,000 according to the 1950 census.

Within the limits of the county are 129 separate municipal subdivisions. There is a County Planning Commission which has limited operations and also an effective Pittsburgh City Planning Commission which operates inside the city limits; some other municipalities have local planning commissions.

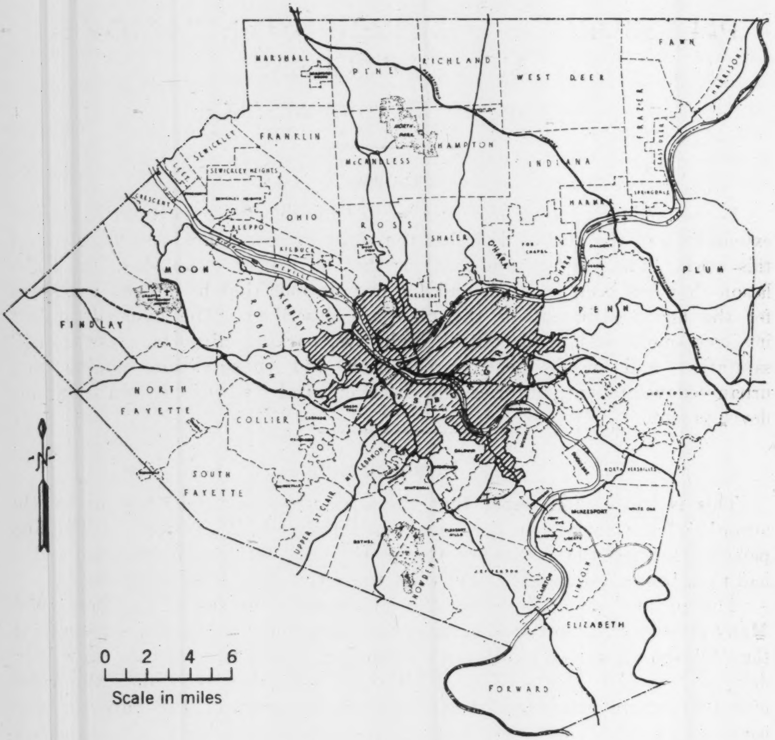
MARSHALL
PINE
RICHLAND
WEST DEER
FAWN
HARRISON
FRAZER
EAST DEER
FRANKLIN
McCANDLESS
HAMPTON
INDIANA
SEWICKLEY
LEET
SEWICKLEY HEIGHTS
CRESCENT
ALEPPO
OHIO
ROSS
SHALER
O'HARA
FOX CHAPEL
HARMAR
SPRINGDALE
PLUM
MOON
KILBUCK
NEVILLE
STOWE
KENNEDY
ROBINSON
PENN
FINDLAY
NORTH FAYETTE
COLLIER
SOUTH FAYETTE
MT LEBANON
UPPER ST CLAIR
BALDWIN
BETHEL
SNOWDEN
JEFFERSON
MONROEVILLE
WILKINS
NORTH VERSAILLES
McKEESPORT
WHITE OAK
CLAIRTON
LINCOLN
ELIZABETH
FORWARD
N
0 2 4 6
Scale in miles

FIG. 1.—ALLEGHENY COUNTY

The State Department of Highways and the County of Allegheny are responsible for the major highway routes and most secondary highways.

The Pittsburgh industrial area has long been known as an area of heavy industry. Because of this and because it was founded in part on the great bituminous coal fields in the region, Pittsburgh over the years had acquired a rather unsavory reputation for smoke and dirt. Its traffic problems were mounting, the parking problem had not been attacked, a new airport was greatly needed, assessed valuations in the city declined from a high of $1,211,867,000 in 1936 to a low of $961,000,000 in 1947, with the "Golden Triangle" showing a higher rate of decline. All this had become a matter of grave concern to its business and political leaders and, near the end of World War II, it was decided to do something constructive about the situation.

The Allegheny Conference on Community Development

It was agreed first to form a citizens' organization concerning itself with the future of the region. Known as the Allegheny Conference on Community Development and now commonly called "The Allegheny Conference," its purpose was to stimulate and coordinate research and planning, having as its goal a unified community plan for the entire region. The Allegheny Conference was to secure, by educational means, public support of projects that were approved by the conference as parts of the over-all unified plan and to expedite the fulfilment of the plans. Where qualified agencies existed, the Allegheny Conference obtained from them research and planning assistance. In certain fields where no such qualified agency existed, the conference created its own staff to do the research and planning. Committees were formed to study various phases of the community's needs and to make recommendations in relation thereto.

Strong emphasis has been placed on the Golden Triangle. It is the business and commercial heart of the city and county, and its assessed valuation represents approximately one quarter of the assessed valuation of the entire city. The need for preserving and protecting the stability of the Golden Triangle was recognized and accepted, and the program deliberately placed great emphasis on this area. Although the county's suburban areas are growing both residentially and commercially it is believed that the central core must be preserved.

The emphasis on preserving the values in the Golden Triangle is further recognized in the highway program and mass-transit studies.

A Comprehensive Program

It is the feeling of the Allegheny Conference that a community improvement program must be broad and balanced. With that in mind, the conference has been concerned with smoke and flood control, highways, parking, airports, mass transit, sanitation and public health, recreation and conservation, zoning and urban redevelopment, libraries and other cultural institutions, and economic development.

The order in which these subjects are herein mentioned does not necessarily reflect their relative importance, except in the case of smoke and flood control. It is believed that had these two projects not been successful the entire program might have failed.

Smoke Abatement.—Since the early 1900's, the people of Pittsburgh have been concerned about smoke control. In 1911 the Pennsylvania Legislature passed laws permitting the City of Pittsburgh to control smoke from all sources, but powerful opposition and civic lethargy blocked all efforts to pass a city ordinance. However, in 1941 the City Council passed an effective smoke-control ordinance. Because of World War II the effective date of the ordinance was not set. In 1946, with urging and support from the Allegheny Conference, the City Council fixed the effective date as October 1, 1946, requiring industries and railroads to burn solid fuels smokelessly or use other types of fuels. On October 1 of the following year, households within the city limits came under the provisions of the ordinance.

During the eight years that the ordinance has been in full effect (as of 1954) amazing results have been produced in this heart of the bituminous coal industry. Official figures of the Weather Bureau of the United States Department of Commerce show that Pittsburgh is now receiving 89% more sunshine than prior to smoke control. Soot and dustfall records reflect an average reduction of 20% for the period of 1938–1953, years of high industrial activity. In eight years—1946–1953—the hours of heavy smoke, as compiled by the Weather Bureau, have been reduced by 94.4%.

As a result of smoke control, building owners and managers in the Golden Triangle alone have spent more than $1,500,000 on exterior building cleaning, and other office building cleaning projects are planned.

The benefits of this smoke-abatement program have now been extended to all of Allegheny County. In 1949, the Board of County Commissioners enacted a county-wide ordinance which embodies the principal features of the Pittsburgh ordinance. To date, industry in Allegheny County has spent more than $200,000,000 in advancing smoke control. The installation of modern conbustion equipment, dust collectors, new boiler plants, precipitators, and other modern devices are contributing greatly to the elimination, reduction, and control of smoke and other industrial pollutants.

Dieselization of the railroads has practically solved the problem of railroad smoke. Railroad operations throughout Allegheny County are now 81% dieselized and yard operations, 91%. Even the colorful, smoking, sternwheel river boats have largely been discarded for diesel power, and now these operations are 78% dieselized.

The result of the smoke-control program in Pittsburgh and Allegheny County is all the more remarkable because of the fact that this center of heavy industry consumes about 50,000,000 tons of coal annually.

Flood Control.—In 1936 a disastrous flood occurred at Pittsburgh and in the upper Ohio River valley. Flood crests from the Monongahela River and the Allegheny River converged at the "point," flooding the lower part of the Golden Triangle to a depth of about 10 ft. Property damage in the Pittsburgh district reached $94,000,000 and in the upper Ohio River valley, approximately $200,000,000.

Since 1936 the federal government, through the Corps of Engineers (United States Department of the Army), has constructed a $100,000,000 flood control system in this region. Eight major dams have been erected in the watersheds of the Allegheny River and the Monongahela River and are all now in operation. If the dams had been in operation at the time of the 1936 flood, the Corps of Engineers estimates the flood level at the "point" would have been reduced 10.5 ft.

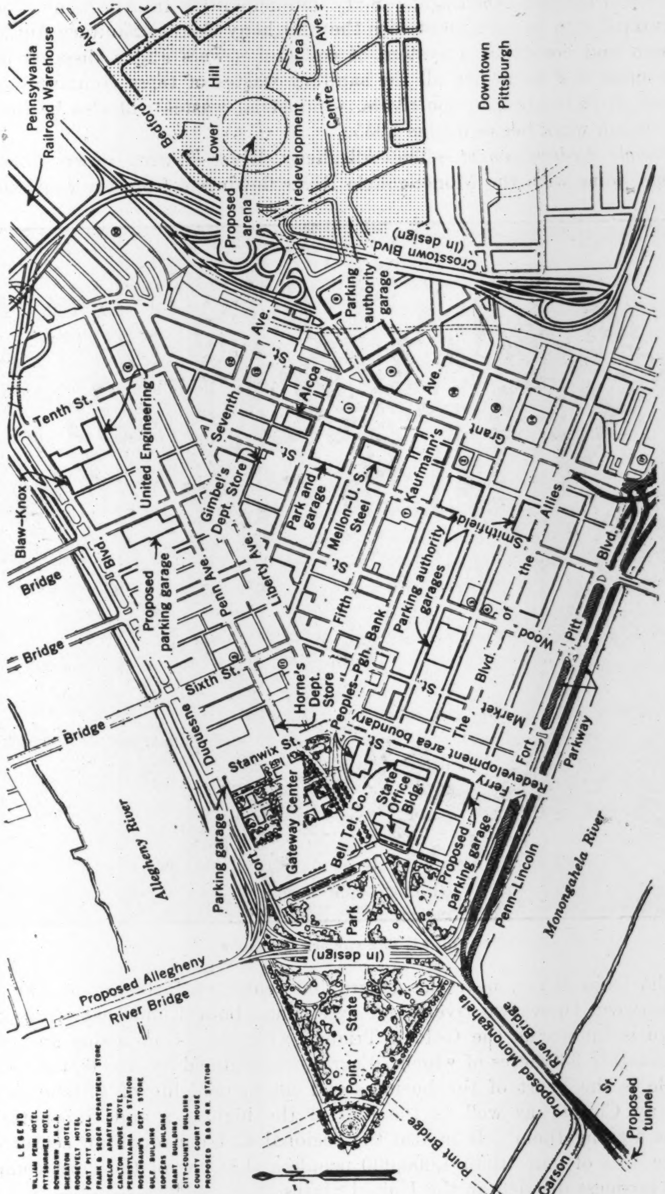
LEGEND
1 WILLIAM PENN HOTEL
2 PITTSBURGHER HOTEL
3 DOWNTOWN Y.M.C.A.
4 SHERATON HOTEL
5 ROOSEVELT HOTEL
6 FORT PITT HOTEL
7 FRANK & SEDER DEPARTMENT STORE
8 BIGELOW APARTMENTS
9 CARLTON HOUSE HOTEL
10 PENNSYLVANIA RR. STATION
11 ROSENBAUM'S DEPT. STORE
12 GULF BUILDING
13 KOPPERS BUILDING
14 GRANT BUILDING
15 CITY-COUNTY BUILDING
16 COUNTY COURT HOUSE
17 PROPOSED B&O RR STATION
Pennsylvania Railroad Warehouse
Bedford Ave.
Lower Hill
Proposed arena
redevelopment area
Centre Ave.
Downtown Pittsburgh
Crosstown Blvd. (In design)
Parking authority garage
Tenth St.
Blaw-Knox
United Engineering
Seventh Ave.
St.
Alcoa
Gimbel's Dept. Store
Park and garage
Mellon-U. S. Steel
Kaufmann's
Grant
Ave.
Smithfield
Allies
Blvd.
Bridge
Blvd.
Proposed parking garage
Penn Ave.
Liberty Ave.
Fifth
St.
Parking authority garages
of the
Wood
Pitt
Bridge
Sixth St.
Horne's Dept. Store
Peoples-Pgh. Bank
St.
The Blvd.
Market
Fort
Parkway
Bridge
Duquesne
Stanwix St.
Redevelopment area boundary
Ferry
Parking garage
Fort
Gateway Center
Bell Tel. Co.
State Office Bldg.
Proposed parking garage
Penn-Lincoln
Allegheny River
Monongahela River
Park
(In design)
Proposed Allegheny River Bridge
State
Point
Proposed Monongahela River Bridge
Point Bridge
Carson
St.
Proposed tunnel
N

FIG. 2.—PUBLIC IMPROVEMENT PROJECTS COMPLETED, UNDER CONSTRUCTION, OR PLANNED

Stream Pollution Abatement.—Sixty municipalities in Allegheny County have entered into an agreement with the Allegheny County Sanitary Authority to design and construct a system of collector sewers and a disposal plant. At the present time nearly all the sanitary wastes of these communities are disposed of, untreated, in the rivers. Industrial wastes will also be treated. Construction work began during 1955.

Triangle Redevelopment.—The Allegheny River flowing down from the northeast joins with the Monongahela River flowing in from the southeast to form the Ohio River, near the geographic center of Pittsburgh. The area lying between these two rivers and extending about 1 mile east from their juncture is known as the Golden Triangle (Fig. 2). Comprising an area of approximately 330 acres of which 70 acres are occupied by streets, the Golden Triangle is the heart of the business and commercial life of Pittsburgh and Allegheny County as well as the hub of the highways and transportation systems serving them. It is also the regional and metropolitan center of a tri-state area of more than 4,000,000 people and is one of the most compact central business districts in the United States.

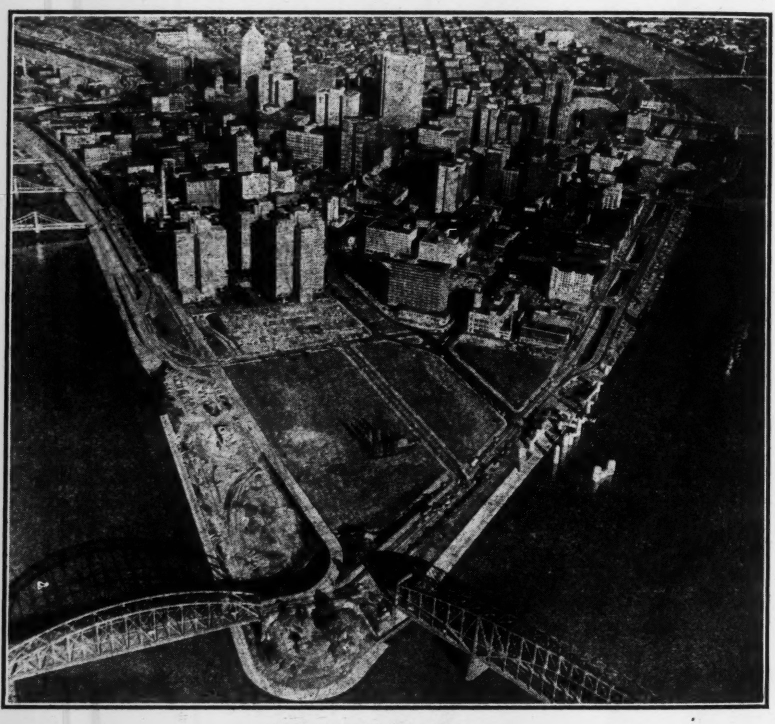

Fig. 3.—The Golden Triangle

Point Park and Gateway Center Development.—The area at the juncture of the Allegheny and Monongahela rivers is known as "the point" (Fig. 3). This was the site of Fort Duquesne and Fort Pitt and it was here that the city was originally founded. To preserve the site of the two forts, the Commonwealth of Pennsylvania is constructing a historical park comprising 36 acres. Begun in 1945, this project is being financed entirely by the commonwealth and to date it has cost more than $7,500,000 in land acquisition alone. All the buildings in the area have been razed, and grading and landscaping is partly completed. A river wall around the park has been built together with riverbank slope paving.

In the park area an elaborate traffic interchange will be built which will connect Fort Pitt Boulevard along the Monongahela River and Fort Duquesne Boulevard along the Allegheny River with the street system in the lower triangle. Two double-deck bridges across the rivers will also be constructed by the commonwealth. Construction has begun on the bridge across the Monongahela River.

Early in this project the state requested the Allegheny Conference to represent it in the development of plans for the park and to coordinate local interest. This responsibility was accepted by the conference.

In addition to initiating studies on the park project, the conference studied the adjacent area as well. This area covering 23 acres was largely deteriorated as a result of floods, railroad yards, and old loft buildings. The Allegheny Conference evolved a plan for the redevelopment of the entire area. In July, 1946, conference representatives presented the plan to the Equitable Life Assurance Society of the United States with the request that that organization become the redeveloper.

It was apparent from the beginning of negotiations that, to acquire the land where so many different owners and relatively small parcels of land were involved, the power of eminent domain would be essential if the project were to succeed. At this time the City of Pittsburgh did not have an Urban Redevelopment Authority. The conference recommended to the City Council that such an agency of government with the power of eminent domain be created, and on November 18, 1946, the Urban Redevelopment Authority of Pittsburgh was established by action of the mayor and the City Council.

An essential step in the urban redevelopment process is the certification of an area as being subject to redevelopment by the City Planning Commission. After thorough studies the City Planning Commission certified the entire area of both the proposed 36-acre park and the 23-acre adjoining property as a redevelopment area. The Urban Redevelopment Authority acted as the land-assembler of the 23-acre tract and entered into an agreement with the Equitable Life Assurance Society to be the redeveloper. Called "Gateway Center," the plan provided for complete readjustment of the street pattern and the initial construction of three large office buildings with only 25% land coverage. Off-street loading and parking were required as part of the redevelopment plan.

Leading Pittsburgh corporations signed long-term leases with the Equitable Life Assurance Society to occupy space in the new buildings. These agreements were executed in February, 1950, by the Jones & Laughlin Steel Corporation, Mellon National Bank and Trust Company, National Supply Company, Peoples Natural Gas Company, Pittsburgh Plate Glass Company, Union Switch and Signal Company, Westinghouse Air Brake Company, and Westinghouse Electric Corporation. It is interesting to note that the agreements were negotiated before all the land had been acquired in Gateway Center and before the buildings were completely designed. At the present time (1954) two 20-story buildings and one 24-story building have been completed and are occupied. The Equitable Life Assurance Society's investment in Gateway Center to date is approximately $43,000,000. Occupancy began in the spring of 1952.

Construction of a fourth building (15 stories high) in Gateway Center will begin this fall (1954). It is being built, at an estimated cost of $6,000,000, by the commonwealth to house all of its departments now renting space in numerous buildings in the city. The Peoples First National Bank and Trust Company, in September, 1953, announced its intention of constructing a bank and office building in the area.

Gateway Center provides for open space around the buildings, creating, in effect, an extension of Point Park. The city has widened and relocated Liberty Avenue as part of the project, and certain other thoroughfares in the area will also be widened and relocated; others have been vacated.

The ultimate plan for Gateway Center provides for additional structures, including an open-deck parking garage. The existing Stanwix Garage in the area has already been enlarged by the addition of one story, providing a total capacity for 600 cars.

Jones & Laughlin Steel Corporation Expansion.—Another major project accomplished through the services of the Urban Redevelopment Authority has been the expansion of the mills of the Jones & Laughlin Steel Corporation on the south side of Pittsburgh (Fig. 4). As in the case of Gateway Center the Urban Redevelopment Authority acted as the land-assembling agency after the City Planning Commission had studied and certified the area as being subject to redevelopment under the terms of the Redevelopment Law of the Commonwealth of Pennsylvania. Because it represented an expenditure of more than $50,000,000, it is unlikely that this expansion would have occurred within the city had there not been a Redevelopment Authority to acquire the land. The Jones & Laughlin Steel Corporation has also agreed to be the redeveloper of a blighted area in what is known as the Hazelwood section of the city (Fig. 4). This area has been certified by the City Planning Commission. The project contemplates the removal of a blighted residential area and the construction of a new mill.

University of Pittsburgh Expansion.—Another instance of the effectiveness of the Urban Redevelopment Authority is the expansion of the University of Pittsburgh's facilities for its Graduate School of Public Health. In this case also, after certification of the City Planning Commission, the Urban Redevelopment Authority entered into an agreement with the university to act as redeveloper of the certified area. Demolitions are in progress (1954), and construction for the new buildings will follow.

Parking.—During the years of 1945 through 1946 the Allegheny Conference and the Pittsburgh Regional Planning Association conducted an exhaustive study of the parking problem in the Golden Triangle. This study revealed the existing situation, with an analysis of future needs and recommendations as to how the needs should be met. As a result, the 1947 session of the Pennsylvania Legislature enacted enabling legislation permitting the city to create a Public Parking Authority. The authority was created by the city during the same year. Since that time the authority has completed and has in

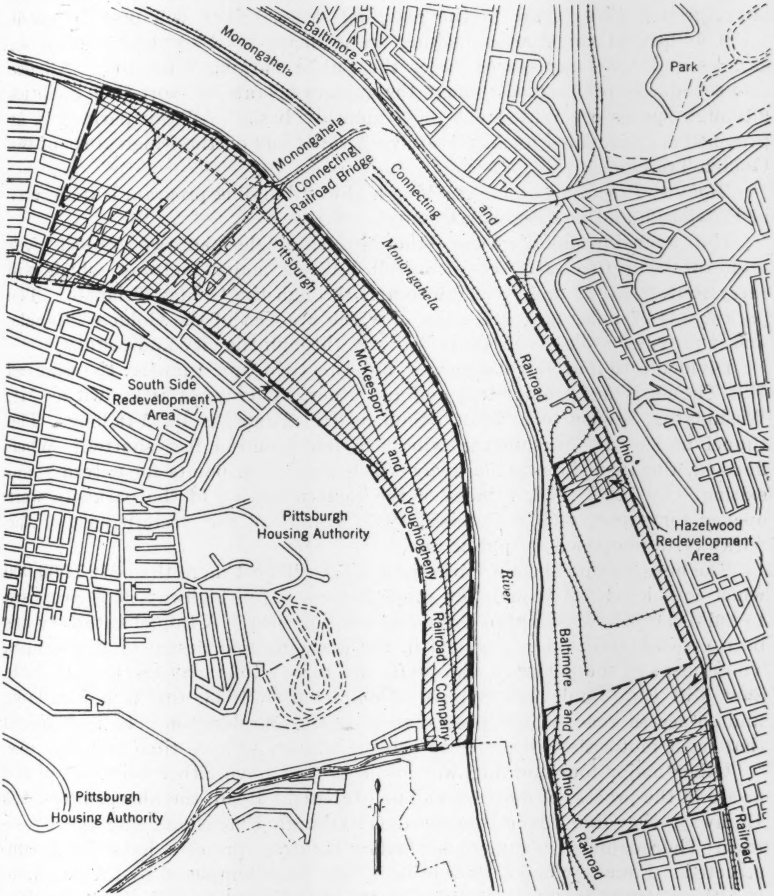
Monongahela
Baltimore
Park
Monongahela
Connecting
Railroad Bridge
Connecting
and
Pittsburgh
Monongahela
Railroad
McKeesport
South Side
Redevelopment
Area
Ohio
and
Youghiogheny
Pittsburgh
Housing Authority
Hazelwood
Redevelopment
Area
River
Railroad
Company
Baltimore
and
Ohio
Railroad
Railroad
N
Pittsburgh
Housing Authority

FIG. 4.—URBAN REDEVELOPMENT AUTHORITY PROJECTS FOR JONES & LAUGHLIN STEEL CORPORATION, PITTSBURGH

operation two above-ground, open-deck garages, providing approximately 1,550 car spaces. It has in construction a 6-story underground garage under Mellon Square which will provide approximately 900 car spaces. Bids were received for the construction of two additional above-ground, open-deck garages which will provide a total of 1,392 car spaces. Two more open-deck, above-ground garages are in the planning stage. They will provide about 1,450 additional car spaces, making an ultimate total ownership of seven garages and 5,300 car spaces under the Public Parking Authority. All the rate schedules are designed to have the garages operate as short-time facilities although spaces are rented out on a monthly basis. All-day parking is at present being provided for in privately operated lots on the fringe areas of the Golden Triangle.

Highway Program.—A far-reaching highway building program is underway in Pittsburgh and in Allegheny County.

The Penn-Lincoln Parkway—the biggest single highway project ever undertaken in this area—is a controlled-access major highway which will carry routes No. 22 and No. 30 into and through the Golden Triangle. The parkway is 27 miles long, 9.5 miles of which are east of the Golden Triangle, and it provides a direct east-west highway through the city and county.

Divided into four and six lanes, it has two twin-tube tunnels; the Squirrel Hill Tunnel is now completed, and the other, under what is known as Mt. Washington, is soon to be built. Squirrel Hill Tunnel is 4,225 ft long. The tunnel under Mt. Washington will be a few hundred feet shorter. When finished, the Penn-Lincoln Parkway will have sixteen points for entering and exiting. In June, 1953, 7 miles of the eastern section of the parkway were opened for travel, and in October, 1953, 9 miles of the western part of the parkway were opened for public use.

The entire Penn-Lincoln Parkway project will cost more than $125,000,000 when completed. Although the project is not a toll highway, it is proposed to build the Mt. Washington Tunnel as a toll project. A tunnel authority has been created and is now engaged in the planning and design of this tunnel. Those users of the parkway who prefer not to pay tolls may use the alternate Saw Mill Run Boulevard Bypass. Completed in 1953, this is a four-lane, limited-access road which passes around Mt. Washington. It is believed that most motorists will prefer to use the tunnels to save time and distance.

Other major four-lane highway projects that have either been completed or are in the process of design are: The McKnight Road, the Sharpsburg-Etna Highway, the Ohio River Boulevard (Pittsburgh Extension), and the Crosstown Thoroughfare. Numerous smaller highway projects have been constructed. Four new major river bridges have been completed by the commonwealth or county in the past several years—the Tarentum, Elizabeth, Rankin, and Dravosburg bridges—representing more than $27,000,000 of expenditure of public funds.

The western extension of the Pennsylvania Turnpike was opened for traffic in December, 1951. It passes north of Pittsburgh and about 15 miles from the Golden Triangle, and ready access to it is provided by means of the Penn-Lincoln Parkway East and State Routes No. 8 and No. 19 to the west.

Lower Hill Redevelopment Project.—Adjoining the Golden Triangle on the east is a section known as the "hill district." One of the older sections of the city, a large part of it has many characteristics of a slum area with an extremely wasteful street pattern of land use. After careful study the City Planning Commission has certified 105 acres immediately adjoining the Golden Triangle as being subject to redevelopment. The Urban Redevelopment Authority of the city is now in the process of working out an agreement with the federal Housing and Home Finance Agency for federal aid in the redevelopment of the area.

The plan provides for use of one half the area for a combined public auditorium and sports arena, a symphony and grand opera building, and a building for the Pittsburgh Playhouse. The remainder of the area is planned for modern tower apartments. To act as redeveloper for the area being set aside for the auditorium, a Public Auditorium Authority has been created. The plan for the auditorium-sports arena is unique. It provides for a retractable roof when the auditorium is in use during the summer by the Civic Light Opera Association. For light opera purposes, 9,000 seats are to be provided. During the fall and winter season when the auditorium is being used for sports events, such as basketball, boxing, and ice hockey, as many as 11,000 seats will be provided. Conventions may also be held in the auditorium with provision made for exhibition space. This project has progressed to the extent (1954) that the city and county governments have each agreed to contribute $1,500,000; a local foundation has agreed to contribute $1,000,000; and $2,000,000 is to be raised from corporations and the public. The balance of the funds, estimated at $3,000,000, is to be raised by the sale of revenue bonds by the Urban Redevelopment Authority. It was expected that demolitions would be begun in the area during 1955. Approximately 80% of the 3,000 families in this area are eligible for public housing. The Public Housing Authority has recently completed 1,550 housing units, making a total of 7,011 permanent public housing units. These will form the major reservoir to house displaced persons eligible for public housing.

Reference has been made previously to the Crosstown Thoroughfare. Planned to connect with the Penn-Lincoln Parkway, it lies along the base of the Golden Triangle through the 105-acre redevelopment area. With two free-moving lanes in each direction, it also provides for an additional acceleration or deceleration lane on each side with elaborate connections to the auditorium area. Circular in shape and 400 ft in diameter, the auditorium is completely and immediately surrounded with surface parking areas for about 1,700 automobiles. Additional parking near the auditorium will provide at least 300 more spaces. Two blocks from the auditorium is Garage No. 1 of the Public Parking Authority with 786 car spaces.

The first-stage plans for the Crosstown Thoroughfare are in design (1954) so that construction may keep abreast of the Lower Hill Redevelopment Project.

Mass Transportation.—The Allegheny Conference has not been unmindful of the important role of mass transportation in the movement of people. The conference conducted two studies of the mass-transit problem in the

Pittsburgh area. In Allegheny County there are fifty-one different operating mass-transit companies. Seventeen of these are long-line carriers, seventeen operate outside the city in the county, and seventeen enter the Golden Triangle. As a result of its studies, the conference recommended unification of all the carriers into one company excluding the long-line carriers. The Board of County Commissioners, subsequent to the conference reports, conducted a study through a committee called the Allegheny County Mass Transportation Study Committee. This committee filed its report in June, 1953; it recommended not only unification but also the creation of a mass-transit authority to accomplish the unification. Because it is believed desirable that special legislation be passed to authorize the creation of the authority, a committee appointed by the Board of County Commissioners is now (1954) drafting the legislation to be submitted to the 1955 session of the State Legislature.

Greater Pittsburgh Airport.—The great expansion in the aviation industry had made the old County Municipal Airport obsolete for modern commercial planes and jet planes. The field and the terminal facilities were both inadequate.

In May, 1952, the County of Allegheny completed and opened an airport terminal building at a new landing field which had been constructed during the early years of World War II, about 14 miles west of the city (Fig. 1). With runways of adequate length for modern aviation and protected approach zones, the new field and terminal building should adequately serve the district for many years to come. A new four-lane divided access highway from the airfield connects the airport directly with the Penn-Lincoln Parkway West. Over these modern highways the present driving time to the field from the Golden Triangle is twenty-five minutes. When the new tunnels are completed under Mt. Washington, this time will probably be reduced to twenty minutes.

Recreation.—Recreational facilities in the Pittsburgh area have been expanded during recent years. In 1947 the voters approved a bond issue of $4,000,000 for new swimming pools and playgrounds. There have been constructed in Pittsburgh what are called "parklets"; twelve of these parklets have been built. Initially begun and financed by a private citizen, the city has continued the program with city funds. Parklets are small play areas in congested parts of the city. They are approximately ½ acre to 1 acre in area and they are fenced for the children's safety. They have slides, swings, sandboxes, and shower pools for younger children.

Through the combination of private funds and city funds, a children's zoo has been built, as well as a new aviary-conservatory paid for by city funds. Beyond the city and county limits and yet within reasonable driving distance, the commonwealth has built Raccoon Creek Park and Shawnee Park. The Western Pennsylvania Conservancy, a privately-financed group interested in conservation and recreation, has also acquired two sites—one known as Ferncliff Park at Ohiopyle is south of the city and the other, planned to embrace 6,000 acres, is north of the city at historic McConnell's Mill.

Cultural and Educational Facilities.—It was previously stated that members of the Allegheny Conference felt that a community improvement program must be broad and well-balanced. Therefore, an expansion of educational and cultural facilities has been conducted. Although the conference as an organization cannot claim credit for much of this expansion, many of the conference sponsors are on the boards of direction of the institutions of higher learning and other cultural agencies.

The University of Pittsburgh has a building program in progress requiring expenditures of more than $19,500,000. Its Medical Center is engaged in a large expansion program. Carnegie Institute of Technology, Pennsylvania College for Women, Mt. Mercy College, and Duquesne University are all either engaged in or have completed large physical expansion programs.

In the fall of 1953 the Federal Communications Commission granted a construction permit to Pittsburgh's Educational Television Station WQED. With construction funds provided by private grants, this station began broadcasting in April, 1954.

Finance.—Where has the money for these projects come from? It has come from several sources—public funds, private funds, and, at times, from a combination of public and private money. State highway projects such as the Penn-Lincoln Parkway have been financed largely from state highway funds and normal federal aid. The County of Allegheny contributed $5,000,000 and the City of Pittsburgh gave $1,000,000 toward the cost of the Penn-Lincoln Parkway East. County highway and bridge projects have been financed by the sale of general obligation bonds of the county. Point Park has been constructed with funds provided by the Commonwealth of Pennsylvania. Gateway Center has been financed by funds from the Equitable Life Assurance Society. Readjustment of street facilities have been supported by the City of Pittsburgh through the sale of general obligation bonds. The Crosstown Thoroughfare is being financed by a grant of $2,500,000 by the County of Allegheny and $2,750,000 of city bond funds. Mention has previously been made of the financing of the auditorium on the Lower Hill Redevelopment. The remainder of the project will be supported by private funds. Federal funds to help cover the writedown cost of the buildings to be razed will also be made available. The parking authority program has been financed largely by the sale of revenue bonds. No credit or funds of the City of Pittsburgh have been involved, except that the city made available parking-meter receipts to support the sale of the revenue bonds for the first two garages built by the parking authority. Buildings such as the Mellon-Steel, Alcoa, Kaufmann Department Store expansion, and similar private projects, have been financed entirely by private funds. The Jones & Laughlin Steel Company's expansion has been financed by the company's private funds, and the new Greater Pittsburgh Airport has been largely financed by funds provided by Allegheny County with minor assistance from the Civil Aeronautics Authority and the Commonwealth of Pennsylvania. The flood control program has been financed by federal funds. This indicates, in general, the pattern of financing the major projects in the program. The Allegheny Conference itself is financed by private funds provided by business and industry.

Corollary Benefits.—It would be safe to say that no one initially interested in the Allegheny Conference could foresee the broad benefits to the community that have resulted from the program as planned. The total of assessed valuations in the city has risen almost $200,000,000; in the Golden Triangle alone assessed valuations have risen more than $51,000,000. However, who then could foresee the $1,500,000,000 investments in plant expansion and new plants that have occurred in the four-county area around Pittsburgh during the period from 1946 to 1954? No one could foresee the construction of the 41-story Mellon-Steel Building or the new Alcoa Building, the great expansion in the Golden Triangle or the expansion of Kaufmann's Department Store, or that great national corporations would definitely establish their home offices in Pittsburgh and that great company research centers would be established there. However, the greatest change that has taken place has been the change in attitudes. At all levels of society the people of Pittsburgh now believe in their city; top level business leaders have accepted civic responsibility along with their business responsibility. Pittsburgh has been and still is experiencing a civic renaissance which may serve as an inspiration to other cities.

AMERICAN SOCIETY OF CIVIL ENGINEERS
Founded November 5, 1852
TRANSACTIONS

Paper No. 2826

ECONOMY AND SAFETY OF CONCRETE DAMS

BY AUGUST E. KOMENDANT,[1] M. ASCE

WITH DISCUSSION BY MESSRS. JARO J. POLIVKA, AND AUGUST E. KOMENDANT

SYNOPSIS

The design and construction methods in use for dams fall far short of the obtainable economy and safety because of the complexity of the problems involved in space structures. To avoid these complexities the thickness of dams is generally increased, thus sacrificing economy to attain illusory safety. The possible extreme stresses in dams computed by the shell theory are presented as is a comparison of the economy and safety of various dams. It is shown that the laminated arch dam with forked abutments can be most practically realized in a leaf-spring type shell dam that has prestressed abutments and is constructed by the use of sliding forms.

NOTATION

The letter symbols adopted for use in this paper are defined where they first appear, in the illustrations or in the text, and are arranged alphabetically, for convenience of reference, in the Appendix.

INTRODUCTION

Of the various types of dams, gravity dams, arched gravity dams, arch dams, and buttressed dams combined with multiple arches, slabs, or domes are currently (1956) in use. In the United States, for narrow and deep valleys, mostly gravity dams or arched gravity dams are used, and for relatively flat valleys earth-fill dams or gravity dams are built. In other countries, especially in Europe, for damming off narrow and deep valleys arch dams are utilized, and for flat valleys buttressed dams are preferred; recently, prestressing has been used in the buttresses.

NOTE.—Published, essentially as printed here, in May, 1955, as *Proceedings-Separate No. 684*. Positions and titles given are those in effect when the paper or discussion was approved for publication in *Transactions*.

[1] Cons. Engr., New York, N. Y.

Which dam design should be advocated with respect to its economy and safety for a certain location has been the subject of many scientific works and comparative studies. It is apparent that the geology and topography at the dam site determine, to a certain degree, the general features of the design, but for typical conditions the economy of a design is primarily controlled by (*a*) the quantities of material and labor required for construction, their price, and their relationship; (*b*) the time necessary for erection of the dam; and (*c*) maintenance costs. However, the quantities required are dependent on how efficiently the materials are used and on the safety required. The labor and time required for erection are, to a great extent, controlled by the quantities, dimensions, and methods of placement of the concrete. The maintenance costs are dependent on the type of the dam and the quality of the concrete.

GRAVITY DAMS

The controlling principle for the design of a gravity dam is that no tensile stresses should develop either in the base or in any other section of the dam. For assumed linear pressure distribution, this condition can be satisfied only if the resultant of all the forces which act above the base or sections being considered comes within the middle third of the base or section of the dam. Disregarding uplift, earthquake, and ice or wave pressure, the required width b of the base is given by

$$W \frac{b}{3} = P \frac{h}{3} \qquad (1)$$

in which W is the total weight of a unit length of the dam having a height h and P denotes the total water pressure acting on the unit length. Assuming a triangularly shaped cross section, the weight of the dam is

$$W = \frac{h\,b}{2} \gamma_c \qquad (2)$$

in which γ_c is the unit weight of the concrete.

The total water pressure is

$$P = \frac{h^2}{2} \gamma_w \qquad (3)$$

in which γ_w is the unit weight of water. Substituting the values from Eqs. 2 and 3 into Eq. 1 there results, for the minimum width b_{min},

$$b_{min} = h \sqrt{\frac{\gamma_w}{\gamma_c}} \qquad (4)$$

As the unit weight of water is 64 lb per cu ft and the unit weight of concrete is 150 lb per cu ft, the minimum width of the base is approximately 0.65 h. However, considering uplift, ice or wave pressure, and earthquake forces, the base width commonly required is as great as 0.85 h. Despite the considerable width of the base and the volume of concrete in the dam, the safety of gravity dams is relatively low because a linear stress distribution does not exist, and extremely high stresses are developed by shrinkage and temperature stresses in such a massive concrete dam.

The variations in the elasticity of the foundation result in relatively high tensile stresses at the heel when the basin is filled and at the toe when the basin is empty. Such high tensile stresses have been measured on large-scale models and can be easily determined by use of Airy's stress function. Because of the high tensile stresses at the heel the full uplift pressure is developed, thus resulting in reduced safety and causing leakage of the gravity dam. Furthermore, in ordinary concrete works, especially when large volumes are involved, complete hydration of the cement will never take place inside the concrete. Thus, the variations in the elasticity and strength of the concrete can be considerable throughout the dam.

Incomplete Hydration.—Cement consists of clinker fragments formed principally of

dicalcium silicate	$2\,\mathrm{Ca\,O\,Si\,O_2}$
tricalcium silicate	$3\,\mathrm{Ca\,O\,Si\,O_2}$
tricalcium aluminate	$3\,\mathrm{Ca\,O\,Al_2\,O_3}$
tetracalcium alumino-ferrite	$4\,\mathrm{Ca\,O\,Al_2\,O_3\,Fe_2\,O_3}$

The size of these fragments ranges approximately from 75 microns to less than 1 micron. When water is added to these fragments it is attracted by the grains, thus resulting in a softening of the surface and the forming of calcium hydroaluminate and calcium hydrosilicate colloids. The speed of the water attraction and the softening of the fragments is very different—it is especially slow for dicalcium silicate and fastest for tricalcium aluminate. The chemical reaction causes heat to be generated, creating vapor pressure which hinders the rapid penetration of the large-diameter grains by the water. Furthermore, swelling of the colloids occurs and the colloids are pressed together if the amount of water or space present is insufficient to allow spreading. As a result, clusters of slow-softening fragments are formed which further hinder the complete hydration of the cement grains and render these into colloidal solution; in this state crystallization takes place. The cluster formation is reduced if some admixture or air-entrainment agents are added to the cement. Crystallization begins at the outmost surface of the grains or clusters where the hydration is more complete. In this state the capillary and crystallization pressure in concrete is quite high. These pressures resist the swelling connected with hydration, thereby hindering and delaying further hydration of the nucleus of the fragments or clusters. It is possible that, after several years, the hydration of cement grains inside massive concrete is complete in no more than 1 to 2 microns from the surface of particles. The inside part of particles larger than 4 microns in diameter is believed to be entirely in an amorphous state. The amorphous substance offers relatively small resistance to the high capillary pressure and thus large-scale shrinkage takes place in such concrete. The magnitude of the capillary pressure present at the equilibrium of evaporation can be estimated by use of the theory developed by E. Freyssinet.[2] In accordance with this theory, the normal pressure, p_{nc}, in milligrams per square millimeter, in the capillary tubes is

$$p_{nc} = \frac{2\,\Gamma}{D_f} \qquad (5)$$

---

[2] "Une révolution dans les Techniques des Bétons," Librarie de l'enseignement Technique, Editeur Léon Eyrolles, Paris, 1936.

in which Γ is the capillary constant (approximately 8 mg per mm) and D_f is the smallest diameter of capillary tubes at which water completely evaporates under a given air humidity (f). The value of D_f, in millimeters, is

$$D_f = \frac{2\,\Gamma}{1.3 \times 10^7 \ln\left(\frac{1}{f}\right)} \qquad (6)$$

Assuming a moderate climate with a relative humidity of 40%, p_{nc} is computed to be 17,000 lb per sq in. Estimating that the proportion of tubes up to the limiting size is 4%, the pressure will be approximately 700 lb per sq in. It is obvious that such a high pressure, unequally distributed over the cross section, results in high tensile and shearing stresses in concrete. As the capillary stresses develop, the plastic flow of concrete occurs simultaneously at a much lower rate than the stresses, especially in the later state of the hardening of the concrete. Thus, crack formation can be avoided or at least curtailed if the development of capillary forces is delayed so that there is time for plastic flow to take place and for concrete to gain strength. To delay shrinkage and also to allow water to penetrate the cement particles, hydration heat must be reduced, especially if concrete is being placed in large quantities (up to 20,000 cu yd per day). This cooling is done by artificial methods—water cooling or ice lenses—reducing the cement amount in concrete and using low-heat cements. Regardless of these procedures, high initial stresses cannot be avoided because artificial cooling creates disuniformity of temperature distribution and variation in elastic properties of concrete which leads again to increased high internal stresses resulting in increased crack formation; this is especially true if water cooling is used.

As test specimens cut out of massive concrete illustrate, the compressive strength of such concrete can be relatively high. This high strength indicates, however, only that the hydrated part of the cement is strong enough to prevent lateral flow of particles; it does not indicate that it can resist weathering and assure watertightness. These latter two requirements are, in dam construction, far more important than the compressive strength. To control leakage through the dam and corrosion of the concrete, drainage and control gangs must be provided inside the dam.

The almost continuous change of pressure in the bedrock beneath the foundation also favors the development of leakage. This leakage decreases the already low safety of gravity dams regardless of the large masses involved and the very safe appearance of the dam. This fact is proved by the much easier destruction of gravity dams than arch dams during wartime.

The large masses, chemical heat, and shrinkage problems are the controlling factors in the choice of construction methods, in efficiency, and in construction time of the dam. Satisfying even the minimum requirements for quality of the concrete in a dam can only be accomplished (as of 1956) by lengthening the construction time by several years, utilizing special methods for cooling, placing of concrete in small sections, and providing joints. To avoid leakage, the foundation for gravity dams must be carefully constructed and even the bedrock density must be improved by forcing in large quantities of cement under high pressure. All of the foregoing reduce the economy of gravity dams.

The labor required for the construction of gravity dams is very often less than that needed for arch dams regardless of the large volumes involved. This is obvious because standard forms are used which do not require much labor. Furthermore, the simplicity of construction and large quantities justify almost entirely mechanized construction. Because labor in the United States is relatively more expensive than material, resulting in high mechanization at large construction sites, gravity dams are favored regardless of the many deficiencies inherent in them.

ARCHED GRAVITY DAMS

The safety of an arched gravity dam is relatively higher than that of a gravity dam. In the case of the arched gravity dam the water pressure is partly transmitted by arch action into the flanks of the valley (as for arch dams). The tensile stresses developed at the heel, resulting in increased uplift, do not reduce the safety of this type of dam because the decreased cantilever action caused by uplift will be automatically balanced by increased arch action. The other features of an arched gravity dam are the same as for gravity dams described previously.

ARCH DAMS

The most economical arch dam would be a cylindrical arch in which the stresses are approximately equal across any section. This condition would be satisfied only in a dam with triangular cross section having a zero wall thickness, t, at the water-surface elevation, a constant radius, r, and constant radial deflection throughout the dam. The arch thrust in such an arch is proportional to the depth, z, from the water-surface elevation to the radius r of the arch. Thus, the normal force and corresponding normal stress are, respectively,

$$N_{\beta o} = z \gamma_w r_e \quad \text{(7a)}$$

and

$$\sigma_{\beta o} = \frac{N_{\beta o}}{t_z} = \text{constant} \quad \text{(7b)}$$

in which the subscript o indicates the use of the cylinder formula, r_e denotes the radius of the extrados, and t_z is the thickness of the wall at a distance, z, below the water-surface elevation. The radial deflection for constant modulus of elasticity, E, is given by

$$\omega_o = \frac{\sigma_{\beta o} r}{E} = \text{constant} \quad \text{(8)}$$

It is apparent that such an arch dam cannot exist because the radial deflection, ω, of the wall at its boundaries is approximately zero and the edge of the wall cannot be made movable. Furthermore, for the case of a large base width the wall is restrained in the foundation. As a consequence, the water pressure at the bottom part of the dam is vertically transmitted by cantilever action into the bedrock. This cantilever action is assumed to be limited to the lower third of the dam. However, this is not true, and the cantilever action affects the stress distribution in the wall almost throughout the entire height of the dam. As the result of boundary disturbances, large flexural stresses are developed in arch dams which lead to extensive cracks. To estimate the flexural stresses even to a reasonable degree makes the analysis of an arch dam rather complicated. Furthermore, the most advanced theories involve numerous assumptions and introduce uncertainties.[3]

To examine the safety and economy of arch dams, their stress condition should be considered. However, because the complete stress analysis of dams is beyond the scope of the present undertaking, the stresses will be cited only to the extent necessary in the development of the subject.

Each section of the wall under consideration is subjected to normal water pressure, p. A part, p_β, of this pressure is transmitted by arch action whereas the remaining part, p_z, is transmitted by cantilever action (Fig. 1). The part, p_β, develops the thrust H. The strain e caused by the thrust, the shrinkage s, the change of temperature ΔT, and the displacement of abutments Δ, result in a reduction, ΔH, of the statically determinate thrust, H. If the water pressure transmitted by arch action is known, the magnitude of H can be computed for any restraint ratio ρ at the abutment by applying the theory of elasticity—

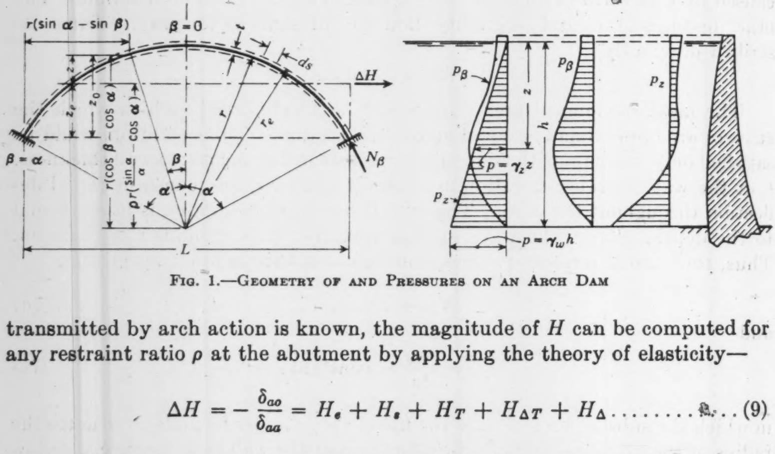

FIG. 1.—GEOMETRY OF AND PRESSURES ON AN ARCH DAM

$$\Delta H = -\frac{\delta_{ao}}{\delta_{aa}} = H_e + H_s + H_T + H_{\Delta T} + H_\Delta \qquad (9)$$

in which δ_{ao} is the change of span of the statically determinate circular arch because of the thrust p_β caused by water pressure, shrinkage, uniform and unequal temperature change, and displacement of abutments, and δ_{aa} is the change of the span due to $H' = 1$. From the foregoing:

$$\begin{aligned} \delta_{ao} &= \delta_{ae} + \delta_{as} + \delta_{aT} + \delta_{a\Delta T} + \delta_{a\Delta} \\ &= 2 \int_{\beta=0}^{\alpha} N_\beta \cos\beta \frac{r\,d\beta}{E\,A} + \epsilon_s\, 2\, r \sin\alpha \mp \epsilon_T\, 2\, r \sin\alpha \\ &\quad - 2\frac{\epsilon \Delta T}{t} \int_{\beta=0}^{\alpha} \left[(\cos\beta - \cos\alpha) - \rho \left(\frac{\sin\alpha}{\alpha} - \cos\alpha \right) \right] r\,d\beta + 2\,\Delta \qquad (10) \end{aligned}$$

---

[3] "Wasserkraftanlagen," by F. Toelke, edited by A. Ludin, J. Springer, Berlin, 1938.

and

$$\delta_{aa} = 2 \int_{\beta=o}^{\alpha} (z^2_o - z_o\, z_e)\, \frac{ds}{E\, I} + 2 \int_{\beta=o}^{\alpha} \cos^2 \beta\, \frac{ds}{E\, A} \qquad (11)$$

in which ϵ_s is the change in length caused by shrinkage, ϵ_T denotes the change in length due to temperature change, T, and $\epsilon\, \Delta T$ is the lengthening of the fiber with respect to the center line due to unequal temperature change and is considered to be positive if the fiber on the air side is lengthened.

The ordinates in Fig. 1 are

$$z_e = r\, (\cos \beta - \cos \alpha) \qquad (12a)$$

$$z_o = \rho\, r \left(\frac{\sin \alpha}{\alpha} - \cos \alpha \right) \qquad (12b)$$

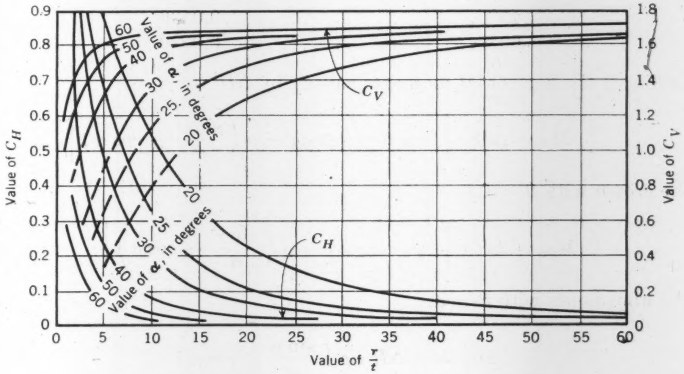

FIG. 2.—ESTIMATING HORIZONTAL AND VERTICAL STRESSES

and

$$z = z_o - z_e \qquad (12c)$$

After integrating, rearranging the expressions, and considering the influence of plastic flow on H_s and H_Δ, there results

$$H_e = - N_\beta\, C_H \qquad (13a)$$

$$H_s = - \epsilon_s\, E\, t\, C_H\, \frac{1 - e^{-\phi}}{\phi} \qquad (13b)$$

$$H_T = \mp\, \epsilon_T\, E\, t\, C_H \qquad (13c)$$

$$H_{\Delta T} = \epsilon\, \Delta T\, E\, r\, C_H\, F_{\Delta H} \qquad (13d)$$

and

$$H_\Delta = - \frac{\Delta E\, t}{r \sin \alpha}\, C_H\, e^{-\phi} \qquad (13e)$$

in which

$$\phi = \frac{\text{plastic flow}}{\text{elastic strain}} \sim 2.0 \qquad (14a)$$

$$F_{\Delta H} = (1 - \alpha \cot \alpha)(1 - \rho) \qquad (14b)$$

and

$$C_H = \sin\alpha \div \left\{ \tfrac{1}{4}(\sin 2\alpha + 2\alpha) + 12\frac{r^2}{t^2}\left[\alpha(\cos^2\alpha + \tfrac{1}{2}) - \tfrac{3}{4}\sin 2\alpha - \rho\alpha\left(\frac{\sin\alpha}{\alpha} - \cos\alpha\right)^2\right]\right\} \quad \text{(14c)}$$

The C_H-values—dependent on center angles and radius-to-depth ratios for an assumed $\rho = 0.75$—are represented in Fig. 2. The $F_{\Delta H}$-values for common center angles and for an assumed $\rho = 0.75$ are

Value of α	Value of $F_{\Delta H}$
20°	0.0102
25°	0.0161
30°	0.0233
45°	0.0536
60°	0.0989

In Fig. 2 the horizontal moments caused by ΔH are

$$M_\beta = \Delta H\, r\left[(\cos\beta - \cos\alpha) - \rho\left(\frac{\sin\alpha}{\alpha} - \cos\alpha\right)\right] \quad \text{(15a)}$$

At the crown with $\beta = 0$,

$$M_{\beta c} = \Delta H\, r\left[(1 - \cos\alpha) - \rho\left(\frac{\sin\alpha}{\alpha} - \cos\alpha\right)\right] \quad \text{(15b)}$$

At the abutments with $\beta = \alpha$,

$$M_{\beta a} = -\,\Delta H\, r\,\rho\left(\frac{\sin\alpha}{\alpha} - \cos\alpha\right) \quad \text{(15c)}$$

The corresponding stresses at the crown are

$$\sigma_{\beta c} = -\,\frac{H - \Delta H}{t} \pm \frac{6\,\Delta H}{t}\,\frac{r}{t}\left[(1 - \cos\alpha) - \rho\left(\frac{\sin\alpha}{\alpha} - \cos\alpha\right)\right] \quad \text{(16a)}$$

At the abutments,

$$\sigma_{\beta a} = -\,\frac{H - \Delta H}{t} \pm \frac{6\,\Delta H}{t}\,\frac{r}{t}\,\rho\left(\frac{\sin\alpha}{\alpha} - \cos\alpha\right) \quad \text{(16b)}$$

In terms of the normal stresses,

$$\sigma_\beta = \frac{H - \Delta H}{t} \quad \text{(17a)}$$

$$\Delta\sigma_\beta = \frac{\Delta H}{t} \quad \text{(17b)}$$

$$\sigma_{\beta c} = -\,\sigma_\beta \pm 6\,\Delta\sigma_\beta\,\frac{r}{t}\left[(1 - \cos\alpha) - \rho\left(\frac{\sin\alpha}{\alpha} - \cos\alpha\right)\right] = -\,\sigma_\beta \pm \Delta\sigma_{\beta c} \quad \text{(17c)}$$

and

$$\sigma_{\beta a} = -\,\sigma_\beta \pm 6\,\Delta\sigma_\beta \frac{r}{t}\rho\left(\frac{\sin\alpha}{\alpha} - \cos\alpha\right) = -\,\sigma_\beta \pm \Delta\sigma_{\beta a} \ldots\ldots (17d)$$

The values of the multiplier of $6\,\Delta\sigma_\beta\,(r/t)$ in Eq. 17*c* and of $6\,\Delta\sigma_\beta\,(r/t)\,\rho$ in Eq. 17*d* are approximately equal for $\rho = 0.75$ and, as an average, for $\alpha = 30°$ they are 0.067 and 0.25 for $\alpha = 60°$. Assuming the normal stress $\sigma_\beta = 1{,}000$ lb per sq in., shrinkage $= 35 \times 10^{-5}$, plastic flow $\phi = 2.0$, change of temperature in concrete $\epsilon_T = -\,20°\ \mathrm{F} \times 6.0 \times 10^{-6}$, and modulus of elasticity $E = 3.0 \times 10^6$ lb per sq in., there results

Value of α	Value of r/t	Value of $\sigma_\beta \pm \Delta\sigma_\beta$, in pounds per square inch
30°	4	$0 \pm 1{,}685$
30°	35	-962 ± 440
60°	4	-857 ± 856
60°	35	-998 ± 105

The foregoing indicates clearly that the flexural stresses increase as the ratio r/t and α decrease. As a consequence, the deeper the arch ring under investigation is located, the more the flexural stresses increase. For small (r/t)-ratios and center angle α, the direct compressive stress (arch action) is negligible in comparison with flexural stresses (beam action) and thus, in such cases, the water pressure p_β is transmitted to the flanks of the valley almost entirely by beam action. In the case of constant-angle dams the decrease of the ratio r/t at the lower part of the dam is counteracted by a large center angle, α. This fact makes the constant-angle dam far superior to the conventional type of arch dam. However, even for a moderately large center angle and fairly large (r/t)-ratios, the combined flexural stresses (Eqs. 13) become critical and exceed the tensile strength of the concrete. As a result, extensive crack formation appears in the tension zones of the arch dams, especially in those designs having a relatively large base width and small center angles.

There is no simple method for the determination of the water-pressure distribution between the arch (p_β) action and the cantilever (p_s) action. The determination can be made by considering the dam as being divided into vertical and horizontal strips. Each such strip is loaded with water pressure p_s and p_β, respectively; for the points of intersection the deflection of strips must be equal. This method involves a great number of simultaneous linear equations which have to be solved for p_s or p_β. To obtain the desired accuracy, the number of equations required becomes considerable and their solution complicated and time consuming. Furthermore, this method does not take into account the influence of the twisting moments and thus is, at best, a rough approximation; the foregoing also applies to the trial-load method.

The best known and simplest solution to the problem is the method of successive approximation. In accordance with this method the dam is considered as a cylindrical shell with varying thickness and the stresses in such a shell are determined.[4] The dam wall is divided into sections with each section consid-

---

[4] "Ueber die Festigkeit achsensymmetrischer Schalen," by J. W. Geckeler. *Forschungsarbeiten*, Ingenieurwesen, Berlin, 1926.

ered to be a cylindrical shell with assumed constant depth. Starting from the bottom edge, the boundary forces acting at the top edge of the first shell serve as the boundary forces for the bottom edge of the following section. In this way the internal forces N_β, Q_z, and M_z, or respective stresses and displacements in horizontal and vertical directions can be determined; the water pressure in both directions can be obtained by differentiation. However, these stresses and the water-pressure distribution are not the true ones because the dam does not act as a closed cylinder but as a segment of the cylinder; that is, the points at the abutments are not free to move in a radial direction as is the case with a closed cylinder. The effect is similar to the displacement of the abutments and results in increased deflection and corresponding higher vertical stresses in the dam. The actual stresses and water-pressure distribution can be obtained by successive approximations from the results of the arch action (Eqs. 9 through 17) and values from the theory of the closed cylindrical shell. The water-pressure distribution for a trapezoidal cross section is illustrated in Fig. 1.

Results obtained by the application of the method of successive approximations reveal that the cantilever influence at the bottom edge of the variable cross section is slightly higher than for a cylindrical shell having a constant thickness. However, the upward damping of the moments is greater because the characteristic length L_e becomes smaller with decreasing thickness of the wall. The vertical stress for a constant-thickness cylindrical shell is

$$\sigma_z = 1.74 \left(\sigma_{\beta o} + L_e \frac{d\sigma_{\beta o}}{dz} \right) \dots\dots\dots\dots\dots\dots (18)$$

Disregarding the relatively small value of $d\sigma_{\beta o}/dz$ for the bottom edge of the wall, the maximum vertical stress caused by the water pressure becomes

$$\sigma_z = 1.74\, \sigma_{\beta o} \dots\dots\dots\dots\dots\dots\dots\dots (19)$$

in which

$$\sigma_{\beta o} = \frac{N_{\beta o}}{t} = \frac{r_e\, p}{t} \dots\dots\dots\dots\dots\dots\dots\dots (20)$$

is the cylindrical stress at the bottom edge of the wall.

The stresses given by Eqs. 18 and 19 are required to balance the radial deflection of the wall, ω_o, caused only by the water pressure. Considering the influence of the horizontal moments, temperature changes, shrinkage, and change in the span length of the wall, the maximum vertical stress, σ_z, developed at the edge becomes C_V times higher than the stress given by Eq. 19 (Fig. 2).

From the foregoing, it can be seen that the flexural stresses in arch dams are considerable. As a result, numerous cracks are formed in the tension zones both in vertical and horizontal directions of the arch. However, regardless of the extensive cracks found, not a single arch dam has failed (as of 1956) because of structural weakness.

No failures have occurred because crack development in an arch dam results in a formation of a relatively thin secondary arch in which water pressure is no longer transmitted by flexural stresses (beam action) but primarily by normal stresses (σ_β) to the flanks and bottom of the valley. Thus, the loss in cross section because of cracks is balanced by more efficient water-pressure transmission to the foundations. The structural safety of arch dams seems not to be reduced by crack formation but rather to be increased. However, the safety may be considerably decreased if corrosion as a result of the crack formation is allowed to develop.

The foregoing illustrates that the efficiency and safety of an arch dam increases with the decrease of the thickness and radius of the wall. Making use of this fact, and to increase the economy of the arch dams, the recently designed (1955) dams in France have been relatively thin. The base width has been reduced to as low as $b = 0.17\ h$ or approximately one quarter of the minimum base width required for gravity dams. In this manner, the volume of concrete could be reduced to 25% of that of gravity dams.

In the constant-angle dam the radius decreases constantly downward; thus, the flexural stresses are reduced because of the small radius and large constant center angle. Therefore, the material in this design is more efficiently used than in the other types of arch dams. However, even this design is far from the ideal in which the entire water pressure is transmitted by normal stresses.

As the mass of arch dams ranges from 25% to 40% that of gravity dams, the use of material in arch dams is far more economical. However, this economy is greatly reduced because the extrados and intrados of slender arch dams are doubly curved, making the form work complicated and expensive, especially in countries with high labor costs. This is one of the reasons why gravity dams, which are simply constructed and which use standard forms, are favored in the United States.

LEAF-SPRING TYPE SHELL DAM

By use of the leaf-spring type shell dam, simplicity in design and construction, safety, and economy are realized. The water pressure is almost entirely transmitted by arch action into the flanks of the valley and higher compressive stresses always occur in the bedrock on the water side rather than at the air side of the dam, regardless of whether the basin is empty or filled. This is not possible in any other type of dam and it results in higher safety for this type. Erection of the cylindrical shells can be accomplished by the use of slip forms. In principle, the design[5] is illustrated in Fig. 3. The shell arches with decreasing heights are numbered 1 to n ($n = 3$ in Fig. 3). Every shell—each with varied height—sustains approximately the same hydrostatic pressure. The shells are separated with thin layers of asphalt or similar material of an adequate consistency. By the use of this material it is possible to eliminate the sliding friction of the separating layer entirely; this is of special importance because the pressure on the separation layer is continuous and of long endurance. The advantage of the asphalt layer is an increased watertightness of the dam.

The basic idea of this dam type is not new. In 1927, A. Mesnager proposed[6] the use of five entirely separated, very slender reinforced concrete arched dams, arranged behind each other—with decreasing height—and separated with water space, rather than one thick arch dam for the Marège Dam on the Dordogne River, in France. A similar stepped-off dam type has also been proposed[7] by R. Maillart. However, the most complete study of such a dam has been made[8] by Fred A. Noetzli. This dam is characterized by (*a*) the use of a special type of buttress to take the thrust of the upper arch elements, thereby reducing the required maximum arch span and hence the maximum radius; (*b*) the pronounced upstream sloping from the crest of the crown of the dam, thereby securing the minimum radii for the lower arch elements; (*c*) the subdivision, where necessary, of the total arch thickness into two or more separate arches, thereby keeping the arches thin, or relatively so, and maintaining throughout the dam the corresponding advantages.

---

[5] "Prestressed Concrete Structures," by A. E. Komendant, McGraw-Hill Book Co., Inc., New York, N. Y., 1952.

[6] "Sur les barrage-réservoirs à voûtes et à charge fractionnée," by A. Mesnager, *Revue Générale de l'Électricité*, October 29, 1927.

Regardless of the technical superiority of these proposals above gravity and conventional arch dams, they have failed to draw sufficient attention and to prove their superiority for utilization. The following reasons are believed to be responsible for this.

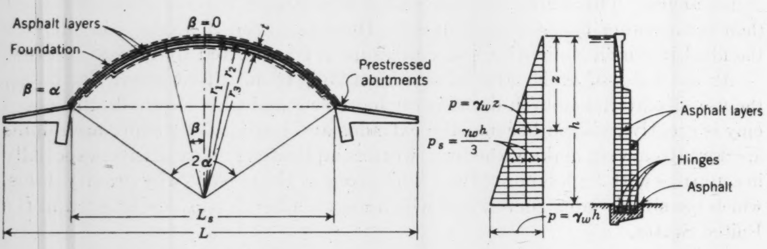

FIG. 3.—LEAF-SPRING TYPE SHELL DAM PLAN AND SECTIONS

The separated structures require more form work, and their foundations are more expensive than for a single structure. Furthermore, if any one of the separated structures fails, the entire dam will collapse by chain reaction. In the case of the laminated arch dam with forked abutments, the strongly pronounced crest and doubly curved extrados and intrados of each lamina make the form work complicated and require much labor. The chemical-heat problems are the same as in any other massive dam and because of the overhang it is difficult to avoid tensile stresses at the heel of the dam. The use of forked abutments introduces a point for differential displacements resulting in increased danger of crack formation. In the leaf-spring shell dam all these objections are eliminated.

The safety of the leaf-spring shell dam is primarily controlled by the stability against buckling. In accordance with Euler's formula, the buckling strength, P_B, of a straight column of length L and section modulus I is

---

[7] "Gewoelbe-Staumauern mit abgestuften Druckhoehen," by R. Maillart, *Schweizerische Bauzeitung*, April 14, 1928.

[8] "Laminated Arch Dam with Forked Abutments," by Fred A. Noetzli, *Transactions*, ASCE, Vol. 95, 1931, p. 533.

$$P_B = \frac{\pi^2 E I}{L^2} \qquad (21)$$

By the use of

$$I = A\, i^2 \qquad (22a)$$

and taking

$$i^2 = \frac{t^2}{12} \qquad (22b)$$

the buckling stress σ_B will be

$$\sigma_B = \frac{\pi^2 E t^2}{12 L^2} \qquad (22c)$$

in which A is the cross-sectional area. For a restrained cylindrical shell having a center angle $2\,\alpha$, the buckling length is

$$L_B = \tfrac{1}{3}\, 2\,\alpha\, r \qquad (23)$$

Substituting this value into Eq. 22*c* and assuming

$$\sigma_B = n\,\sigma_d \qquad (24)$$

in which n is the factor of safety against buckling and σ_d is the allowable design stress, there result the limiting ratios r/t for individual shells—

$$\frac{r}{t} = \frac{1.364}{\alpha}\sqrt{\frac{E}{n\,\sigma_d}} \qquad (25a)$$

or taking $n = 4$

$$\frac{r}{t} = \frac{0.68}{\alpha}\sqrt{\frac{E}{\sigma_d}} \qquad (25b)$$

For commonly encountered center angles (50° to 60° for the upper part of the shells) and lowest value (4,000) of E/σ_d, the ratio r/t must lie approximately between 40 and 50 to avoid buckling. The minimum thickness, t_{min}, for the individual shells, as controlled by buckling, is

$$t_{min} = \frac{r\,\alpha}{0.68\sqrt{\dfrac{E}{\sigma_d}}} \sim \frac{r}{40 \text{ to } 50} \qquad (26)$$

The horizontal stresses in the shells can be estimated by Eqs. 13, 15, 16, and 17. As shown previously, for large center angles and large ratios of r/t the horizontal flexural stresses are negligible in comparison with the normal stresses. For small center angles (such as those at the lower part of the dam), the values of N_β or σ_β are superposed by boundary forces resulting, respectively, in reduced horizontal flexural stresses. As a consequence, the horizontal flexural stresses are of secondary order. Considering that they are superposed by high normal stresses, no crack formation occurs in the horizontal direction in the shell dam.

The radial deflection of the determinate shells as a result of the horizontal forces $N_{\beta o}$ and ΔH and the moment M_β is

$$\omega_o = \frac{1}{E\,A}\int_{\beta=o}^{\alpha}(N_{\beta o} + \Delta H \cos\beta)\sin\beta\, r\, d\beta + \frac{\Delta H\, r^3}{E\,I}\int_{\beta=o}^{\alpha}\left[(\cos\beta - \cos\alpha) - \rho\left(\frac{\sin\alpha}{\alpha} - \cos\alpha\right)\right](\sin\alpha - \sin\beta)\, d\beta \quad (27)$$

Substituting $I = t^3/12$ and $A = t$ after integration there results

$$E\,\omega_o = N_{\beta o}\frac{r}{t}\left[(1 - \cos\alpha) - \frac{\Delta H}{4\,N_{\beta o}}(1 - \cos 2\,\alpha)\right] + 12\,\Delta H\left(\frac{r}{t}\right)^2 r\, f_\omega \quad (28)$$

and

$$\omega_o = \frac{N_{\beta o}}{E}\frac{r}{t}\left\{(1 - \cos\alpha) + \frac{\Delta H}{N_{\beta o}}\left[12\left(\frac{r}{t}\right)^2 f_\omega - \tfrac{1}{4}(1 - \cos 2\,\alpha)\right]\right\} = \frac{N_{\beta o}}{E}\frac{r}{t}\,C_V \quad (29)$$

The radial deflection in terms of normal stresses, $\sigma_{\beta o} = N_{\beta o}/t$ and $\Delta\sigma_\beta = \Delta H/t$, is

$$\omega_o = \frac{\sigma_{\beta o}}{E}\, r\left\{(1 - \cos\alpha) + \frac{\Delta\sigma_\beta}{\sigma_{\beta o}}\left[12\left(\frac{r}{t}\right)^2 f_\omega - \tfrac{1}{4}(1 - \cos 2\,\alpha)\right]\right\} = \frac{\sigma_{\beta o}}{E}\, r\, C_V \quad (30)$$

in which $\Delta\sigma_\beta$ is the change of the normal stress $(\sigma_{\beta o})$ due to the rib shortening, shrinkage, and temperature change, and

$$f_\omega = \sin^2\alpha - \frac{\alpha}{2}\sin 2\,\alpha - \tfrac{1}{4}(1 - \cos 2\,\alpha) + (1 - \cos\alpha)\cos\alpha - \rho\left(\frac{\sin\alpha}{\alpha} - \cos\alpha\right)(\alpha\sin\alpha + \cos\alpha - 1) \quad (31)$$

The f_ω-values for common center angles with $\rho = 1.00$ are

Value of α	Value of f_ω
25°	0.00145
30°	0.00293
35°	0.00532
40°	0.01141
45°	0.0137
50°	0.01757
60°	0.0384

The terms $\frac{N_{\beta o}}{E}\frac{r}{t}(1 - \cos\alpha)$ or $\frac{\sigma_{\beta o}}{E}r(1 - \cos\alpha)$ in Eqs. 28 and 30 indicate the deflection caused by the determinate cylindrical stress $(\sigma_{\beta o})$ and the terms

$$\frac{\Delta H}{E}\frac{r}{t}\left[12\left(\frac{r}{t}\right)^2 f_\omega - \tfrac{1}{4}(1 - \cos 2\,\alpha)\right] \text{ or } \frac{\Delta\sigma_\beta}{E}\, r\left[12\left(\frac{r}{t}\right)^2 f_\omega - \tfrac{1}{4}(1 - \cos 2\,\alpha)\right]$$

indicate the influence of horizontal bending and the rib shortening caused by the indeterminate stress resulting from the arch thrust, ΔH. The value of C_V is almost constant for large values of the center angle α and is not significantly affected by the ratio r/t—it can usually be as great as 1.7 (Fig. 2). However, for smaller center angles, C_V is considerably affected by r/t and can become even less than unity.

The radial deflection ω_o from Eq. 30 and angular rotation $d\omega_o/dz$ must be zero at the bottom edge of the shell. These conditions can be satisfied by introducing a horizontal boundary force X_1 and a boundary moment X_2 at the bottom edge of the shell to balance ω_o and $d\omega_o/dz$. In accordance with the theory of cylindrical shells,[9,5] the values of X_1 and X_2 are

$$X_1 = \frac{L_c\, E}{2\,\frac{r}{t}\,r}\left(2\,\omega_o + \frac{d\omega_o}{d\xi}\right) = \frac{0.38\,E}{\sqrt{\left(\frac{r}{t}\right)^3}}\left(2\,\omega_o + \frac{d\omega_o}{d\xi}\right)\ldots\ldots\ldots(32a)$$

and

$$X_2 = \frac{L^2_c\, E}{2\,\frac{r}{t}\,r}\left(\omega_o + \frac{d\omega_o}{d\xi}\right) = \frac{0.29\,E\,t}{\frac{r}{t}}\left(\omega_o + \frac{d\omega_o}{d\xi}\right)\ldots\ldots\ldots(32b)$$

in which

$$\xi = \frac{z}{L_c}\ldots\ldots\ldots(33a)$$

and

$$L_c = \frac{0.76\,r}{\sqrt{\frac{r}{t}}}\ldots\ldots\ldots(33b)$$

and is termed the characteristic length of cylindrical shell. The values of normal force N_β and moment M_z are obtained by superposition—

$$N_\beta = N_{\beta o} + X_1\,N_{\beta 1} + X_2\,N_{\beta 2}\ldots\ldots\ldots(34a)$$

and

$$M_z = M_{zo} + X_1\,M_{z1} + X_2\,M_{z2}\ldots\ldots\ldots(34b)$$

in which $N_{\beta 1}$, $N_{\beta 2}$, M_{z1}, and M_{z2} are the normal forces and moments in the statically determinate shell caused by the boundary forces $X'_1 = 1$ and $X'_2 = 1$, respectively. They are

$$N_{\beta 1} = -\frac{2\,r}{L_c}\,e^{-\xi}\cos\xi\ldots\ldots\ldots(35a)$$

$$N_{\beta 2} = \frac{2\,r}{L^2_c}\,e^{-\xi}\,(\cos\xi - \sin\xi)\ldots\ldots\ldots(35b)$$

$$M_{z1} = -\,L_c\,e^{-\xi}\sin\xi\ldots\ldots\ldots(35c)$$

and

$$M_{z2} = e^{-\xi}\,(\sin\xi + \cos\xi)\ldots\ldots\ldots(35d)$$

---

[9] "Die Statik in Eisenbetonbau," by K. Beyer, J. Springer, Berlin, Vol. 2, 1934.

Introducing the values from Eqs. 32 and 35 into Eqs. 34, there results

$$N_\beta = N_{\beta o} - \frac{E}{\frac{r}{t}} e^{-\xi} \left[\left(2\,\omega_o + \frac{d\omega_o}{d\xi}\right) \times \cos\xi + \left(\omega_o + \frac{d\omega_o}{d\xi}\right) (\cos\xi - \sin\xi) \right] \quad (36a)$$

and

$$M_z = - \frac{0.29\,E\,t}{\frac{r}{t}} e^{-\xi} \left[\left(2\,\omega_o + \frac{d\omega_o}{d\xi}\right) \times \sin\xi + \left(\omega_o + \frac{d\omega_o}{d\xi}\right) (\sin\xi + \cos\xi) \right] \quad (36b)$$

The water pressure carried by cantilever and arch action can be obtained by differentiation of M_z:

$$p_z = \frac{d^2 M_z}{dz^2} = \frac{d^2 M_z}{L^2_c\, d\xi^2} \quad (37a)$$

and

$$p_\beta = p_s - p_z \quad (37b)$$

The actual deflection of the wall is obtained by applying the principle of superposition—

$$\omega = \omega_o + X_1\,\omega_1 + X_2\,\omega_2 \quad (38)$$

wherein ω_o is the deflection from Eq. 30 and ω_1 and ω_2 are the deflections due to $X'_1 = 1$ and $X'_2 = 1$, respectively—

$$\omega_1 = \frac{2\,r}{L_c\,E}\frac{r}{t} e^{-\xi} \cos\xi \quad (39a)$$

and

$$\omega_2 = - \frac{2\,r}{L^2_c\,E}\frac{r}{t} e^{-\xi} (\cos\xi - \sin\xi) \quad (39b)$$

Introducing the ω_o-value from Eq. 30 into Eq. 32 and disregarding the value $d\omega_o/d\xi$ because it is relatively small for thin shells subjected to a constant pressure, there results the cantilever moment at the edge of the shell—

$$M_z = X_2 = 0.29\,t^2\,\sigma_{\beta o} \left\{ (1 - \cos\alpha) + \frac{\Delta\sigma_\beta}{\sigma_{\beta o}} \left[12\left(\frac{r}{t}\right)^2 f_\omega - \tfrac{1}{4}\,(1 - \cos 2\,\alpha) \right] \right\} = 0.29\,t^2\,\sigma_{\beta o}\,C_V \quad (40)$$

The corresponding vertical stress is

$$\sigma_z = \frac{M_z}{S} = \frac{6\,M_z}{t^2} = 1.74\,\sigma_{\beta o} \left\{ (1 - \cos\alpha) + \frac{\Delta\sigma_\beta}{\sigma_{\beta o}} \left[12\left(\frac{r}{t}\right)^2 f_\omega - \tfrac{1}{4}\,(1 - \cos 2\,\alpha) \right] \right\} = 1.74\,\sigma_{\beta o}\,C_V \quad (41)$$

Using the same values for computing $\Delta\sigma_\beta$ as used previously, the σ_z-stresses for $\rho = 1.0$ are, by Eq. 41,

Value of α	Value of $\frac{r}{t}$	Value of σ_z
30°	4	$1.74 \times 0.57\ \sigma_{\beta o}$
30°	35	$1.74 \times 1.48\ \sigma_{\beta o}$
60°	4	$1.74 \times 1.50\ \sigma_{\beta o}$
60°	35	$1.74 \times 1.60\ \sigma_{\beta o}$

The foregoing shows that the cantilever stresses cannot be reduced by lamination of the dam wall as was believed by Mr. Noetzli. It is apparent that stresses too high for concrete are developed in the vertical direction of the wall and, as a result, large cracks occur at the bottom margin of the dam. The fact that $C_V < 1$, which occurs with small (r/t)-values, indicates that arch action is negligible and the water pressure is primarily transmitted horizontally by beam action—that is, very high flexural stresses are developed at the lower part of the dam. In the leaf-spring shell dam the intolerable vertical stresses, σ_z, have been eliminated by providing a hinge at the base; this is easily done because of the thinness of the shells. Furthermore, such high stresses can also be greatly reduced by lowering the base somewhat below the elevation of the impermeable stratum, thus decreasing the $N_{\beta o}$-value to such an extent that the values of σ_z become negligible.

The maximum vertical tensile stresses on the air side of the dam are approximately 40% higher for hinged bases than for fixed bases. However, these stresses can be reduced by arranging the hinge eccentrically with respect to the center line of the wall.

The magnitude of σ_β and σ_z with the hinged support can be easily computed in accordance with Eqs. 30 and 32. Considering that $X_2 = 0$, there results

$$N_\beta = N_{\beta o} - \frac{E}{\frac{r}{t}}\, e^{-\xi} \left(2\, \omega_o + \frac{d\omega_o}{d\xi}\right) \cos \xi \ldots\ldots\ldots\ldots (42a)$$

$$M_z = - \frac{0.29\, E\, t}{\frac{r}{t}}\, e^{-\xi} \left(2\, \omega_o + \frac{d\omega_o}{d\xi}\right) \sin \xi \ldots\ldots\ldots\ldots (42b)$$

and

$$\sigma_z = \pm\, 1.74\, \sigma_{\beta o}\, e^{-\xi} \sin \xi \left\{ (1 - \cos \alpha) + \frac{\Delta\sigma_\beta}{\sigma_{\beta o}} \left[12 \left(\frac{r}{t}\right)^2 f_\omega - \frac{1}{4}\,(1 - \cos 2\,\alpha) \right] \right\} = \pm\, 1.74\, \sigma_{\beta o}\, C_V\, e^{-\xi} \sin \xi \,.\,.\, (42c)$$

Because the maximum value of $e^{-\xi} \sin \xi$ is approximately 0.32 and the value of C_V is up to 1.7, the maximum vertical stress will be approximately of the same order as the cylindrical stress. As already shown, this stress can be reduced by an eccentric hinge. Thus, the moment caused by eccentricity is

$$M'_z = W\,a \tag{43a}$$

and the stresses, in accordance with Eq. 42*c*, are

$$\sigma_z = \mp \frac{6\,W\,a}{t^2} \pm 1.74\,\sigma_{\beta o}\,C_V\,e^{-\xi}\sin\xi \tag{43b}$$

in which *a* is the eccentricity of the hinge. In this manner, the σ_z-stress condition in the wall can be improved considerably.

Considering that the vertical stress is superposed by the normal stresses because of the weight of the wall and the tensile stresses appear on the air side, no harmful crack formation is expected. However, if any doubt exists, the tensile stresses can be easily avoided by application of prestressing.

The stress analysis of the design of a leaf-spring shell dam is relatively simple in comparison with that for a conventional arch dam. Furthermore, no uncertain assumptions are required in the theory—the stresses determined are of sufficient accuracy. Taking these facts into consideration, much higher allowable stresses can be used for the design without sacrificing safety.

The safety of the leaf-spring shell dam against earthquake or other dynamic effects is considerably higher than for other types of dams because of the reduced masses and, consequently, small acceleration forces acting on the dam. Furthermore, the acceleration forces are greatly damped by the flexibility of the wall and the asphalt layer between the individual shells. Thus, resonance possibilities are unlikely with shell dams.

The fact that the pressure on the soil foundation is independent of the filling height of the basin and is always higher at the water side contributes considerably to the safety against leakage through the base. Furthermore, the safety of the leaf-spring shell dam is not affected by the uplift.

It is apparent that the allowable stresses are most efficiently used in a leaf-spring shell dam in comparison with other dams. The base thickness of gravity dams is approximately 0.85 *h* and, as an average, 0.25 *h* for arch dams, but the base thickness of the shell dam can be less than 0.1 *h*. Thus, the volume of concrete required would be approximately 15% that of gravity dams and 40% that of conventional arch dams. Making use of forked abutments[8] for supporting the upper part of the water-side shell, the radius and the span of the shells can be considerably reduced, allowing for the further reduction of the thickness of the shells and resulting in increased economy of the dam. By applying prestressing to the abutments the displacements at the junction of the shell and abutment can be closely controlled, and differential displacements can be eliminated entirely. The application of prestressing to the forked abutments not only reduces the possibility of crack formation but increases the economy and safety of the abutments and the dam itself. In view of the construction time, forked abutments, which are to be considered as separated structures, can be completed simultaneously with the foundation of the dam. This simplifies the construction and reduces the construction time considerably.

In locations where the bedrock upon which the dam is to be built lies at a great depth beneath the grade and the overlying strata carry a ground-water stream, the relative thinness of the leaf-spring shell dam makes it possible to erect the dam upon one single caisson or upon a row of caissons. Such a caisson can be easily constructed by the use of slip forms. In this process the caisson is constantly increased in height above the ground-water level. In this manner, the feasibility of such locations is made economically possible.

The constant and relatively small thickness of all shells allows for the use of slip forms for pouring concrete. As an average, it can be assumed that the wall is raised 8 in. per hr or approximately 16 ft per 24 hr; thus, the placing of concrete of an individual shell having a height of 600 ft requires approximately 40 days (24-hr pour). The shell on the water side of the dam will be erected first and then, using the same forms, the third shell is constructed, and then the fifth. The second and fourth shells require only a limited number of forms because the adjoining shells provide the form for them. Because of the small thickness of the shells and the possibility of making the shells at separate times, the influence of chemical heat during hardening of the concrete is considerably reduced. Such a dam can therefore be constructed in a relatively short time.

The depth of the slip form is about 4 ft and it can be used several times; approximately forty hydraulic jacks can be lifted and controlled by only one man, and the quantity of concrete required is small. It is therefore obvious that the labor involved for the construction of the leaf-spring shell dam is less that that for any other dam type.

As to the quality of concrete poured by the use of slip forms, there has been and still exists the concept that concrete should not be disturbed in any way after the initial setting has started—that is, after 1 hr. Therefore, many engineers are skeptical about the quality of concrete poured into slip forms. However, experience and tests show that the quality of concrete can be considerably increased when it is vibrated during the early stage of the initial setting. This is because during the initial-set period the cement grains become engaged with water and hydration of the cement begins; great temperature differences and high capillary forces exist in the concrete. Because of the use of the slip form and the continuous placing of the concrete the temperature differences and capillary forces are more equally distributed by the vibration, resulting in decreased initial stress and increased hydration of the cement grains. The formation of crystals in concrete is also increased by vibration. In accordance with the results of tests made by the author, the best results have been obtained when vibration was applied approximately from 3 hr to 4 hr after placing of the concrete. However, the time is largely controlled by the type of cement used, the quantity of water present, the atmospheric temperature, and the humidity. Furthermore, the pour is continuous with slip forms and therefore all construction joints and discontinuity places are eliminated, which results in a very uniform concrete throughout the structure. The surfaces leaving the slip form (after approximately 5 hr) are rubbed, causing a very dense concrete at the surface and increased resistance against corrosion.

This method of placing the concrete makes it possible to start the filling of the basin much earlier than for other dams. After the first shell is constructed the filling can be started. Therefore, to the great economy of the construction cost a considerable saving of capital interest for the total project has to be added. The savings in cost as compared with the conventional arch dam is up to from 50% to 70% in locations favorable for this design. Without sacrificing safety, the construction time is reduced to one third that required for the other dam types.

Buttressed Dams

Buttressed dams are used for damming off flat valleys. In such locations, neither the conventional arch nor the leaf-spring shell dam is suitable because of the large radius and other factors. The dead load of the dam that is used to counteract the water pressure in this case must be balanced by water weight—that is, the dam wall must be inclined in the direction of the air side. In this way, the resultant of the forces acting on the dam can be kept within the middle third of the base. As the base for such a dam is primarily concentrated under the buttresses and is rather small, uplift is not a serious problem. The safety of buttressed dams against overturning is relatively large in comparison with gravity dams. However, rather small dimensions can lead to serious leakage and corrosion, especially if reinforcing is used.

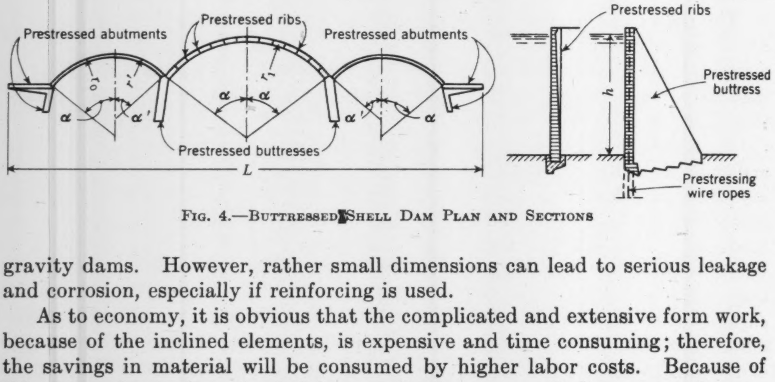

Fig. 4.—Buttressed Shell Dam Plan and Sections

As to economy, it is obvious that the complicated and extensive form work, because of the inclined elements, is expensive and time consuming; therefore, the savings in material will be consumed by higher labor costs. Because of this, for moderate damming heights gravity dams or earth dams are to be considered more economical than buttressed dams, especially in countries with high labor costs. However, using prestressed buttresses, the wall can be constructed vertical. Furthermore, if one utilizes leaf-spring shells or single shells between the buttresses the number of intermediate buttresses can be reduced to two and, in this way, even a relatively flat valley can be economically dammed. The principle of such design is illustrated in Fig. 4.

The tensile stresses on the air side can be easily avoided in this case by providing ribs on the air side and prestressing the ribs. Thus, the shell acts in a vertical direction as a T-beam. The cross section of the wall can be trapezoidal or of constant thickness. The buttresses will be prestressed by high-strength wire ropes arranged as required in the ducts left for them by the slip forms. After the prestressing, the wire ropes are grouted in. The wall, as well as the buttresses, are poured by use of slip forms.

This type of design is especially economical in locations where the stratum lying above the bedrock is relatively thick and impermeable or can easily be made impermeable, because only the buttresses have to be founded on bedrock. Furthermore, this design can be used in similar locations where the stratum above the bedrock carries flowing ground water and has to be cut off by a caisson. The very narrow width of the shell permits the easier and more economical construction of the foundation than for a thick wall. The general advantages and economy of such a dam are the same as for leaf-spring shell dams.

Conclusions

The gravity dams, arched gravity dams, arch dams, leaf-spring type shell dams, and buttressed dams have been critically considered and compared with respect to their safety and economy.

The criterion for safety of a dam has been based on the stress condition and corrosion. It has been shown by stress analysis that the stress condition of arch dams in vertical and horizontal directions is more severe than is commonly realized. At the lower part, even up to moderately large center angles and (radius/depth)-ratios, the water pressure is carried to the bottom and flanks of the valley by beam action. The arch action in this part of the wall develops after the crack formation has occurred. The safest dams are the leaf-spring shell dam and the multiple single-shell dam with prestressed buttresses. This conclusion is proved by the shell theory; it is shown that no tensile stresses occur in the shells and the stresses in the soil beneath the foundation are always higher at the water side regardless of whether the basin is empty or filled. This is not possible in any other known type of dam.

The criterion for safety against corrosion is based on the degree of hydration of the cement in massive concrete. The process and initial stresses during hydration, conditions favoring the hydration, and reduction of the initial stresses have been described.

The criteria for economy have been based on the simplicity and exactness of the stress analysis, the efficiency of the use of materials, the simplest and most rapid construction possible, and the lowest maintenance costs. It has been shown that the leaf-spring type shell and buttressed-shell dams are also the dam types nearest to the ideal conditions. This is because (*a*) the design is simple and the stress conditions in the shell can be described in desired limits without making uncertain assumptions; (*b*) the water pressure is transmitted to the flanks of the valley almost entirely by arch action, thus resulting in the least possible volume of the dam without sacrificing safety; (*c*) the shells are erected rapidly by slip forms lifted by hydraulic jacks in a continuous pour. One set of forms can be used for erection of all the individual shells. Chemical heat is not a serious problem because of the small thickness of the shells and the possibility of constructing the individual shells at separate times; and (*d*) the maintenance costs are low because of the high quality of the concrete and dense surfaces obtained by slip forms. Also, there are no cracks and hence no leakage.

APPENDIX. NOTATION

The following symbols, adopted for use in the paper and for the guidance of discussers, conform essentially with "American Standard Letter Symbols for Structural Analysis" (ASA Z10.8-1949), prepared by a committee of the American Standards Association with Society representation, and approved by the Association in 1949:

A = cross-sectional area;
a = eccentricity of the hinge;
b = width of the base;
b_{min} = minimum width;
C_H = term used for estimating horizontal shear;
C_V = term used for estimating vertical stress;
D_f = diameter of the capillary tubes;
E = modulus of elasticity;
e = strain caused by thrust;
$F_{\Delta H}$ = term defined by Eq. 14*b*;
f = air humidity;
f_ω = term defined by Eq. 31:
H = arch thrust;
h = height of the dam;
I = moment of inertia;
L = span:
    L_B = buckling length;
    L_c = characteristic length of the cylindrical shell;
M = moment:
    M_β = horizontal moment caused by H;
    $M_{\beta a}$ = moment at the abutments;
    $M_{\beta c}$ = horizontal moment at the crown;
$N_{\beta o}$ = normal force;
n = factor of safety against buckling;
P = total water pressure acting on the unit length;
P_B = buckling strength;
p = normal water pressure:
    p_{nc} = normal pressure in the capillary tubes;
    p_z = part of the water pressure transmitted by cantilever action;
    p_β = part of the water pressure transmitted by arch action;
r = radius of arch dam;
r_e = radius of the extrados;
s = shrinkage;
T = temperature;
t = wall thickness:
    t_{min} = minimum wall thickness;
    t_z = thickness at depth z;

W = total weight of a unit length of the dam having a height h;
X_1 = horizontal boundary force;
X_2 = boundary moment;
z = depth from water-surface elevation;
α = center angle;
Γ = capillary constant;
γ = unit weight:
  γ_c = unit weight of concrete;
  γ_w = unit weight of water;
Δ = displacement of abutments;
δ_{aa} = change of span due to $H' = 1$;
δ_{ao} = change of span because of thrust;
ϵ = change in length:
  ϵ_s = change in length due to shrinkage;
  ϵ_T = change in length as a result of temperature change;
  $\epsilon_{\Delta T}$ = change in length because of unequal temperature change;
ξ = term defined by Eq. 33a;
ρ = restraint ratio;
σ = stress:
  σ_B = buckling stress;
  σ_d = allowable design stress;
  σ_β = change of normal stress due to rib shortening;
  $\sigma_{\beta c}$ = stress at crown;
  $\sigma_{\beta o}$ = normal stress;
ϕ = plastic-flow factor; and
ω = radial deflection.

DISCUSSION

Jaro J. Polivka,[10] M. ASCE.—This paper should be of special interest not only to designers of larger dams but also to authorities responsible for water power, irrigation, and water supply for both agricultural and domestic needs. These projects are constructed in the public interest so that everyone must be concerned with their economy and safety. Mr. Komendant has reminded both engineers and authorities that they must, in each case, investigate these important factors. Additional fees and expenses may be involved as a result of a study of the possible alternate designs, but in most cases much money can be saved. The author has cited the considerable economy of constant-angle arch dams developed by Lars R. Jorgensen, M. ASCE. It has been shown[11,12] that approximately $36,000,000 was saved in the construction of sixty-one dams of this type built in the period from 1912 to 1950.

It is clear that the leaf-spring type shell dam originated by Mr. Komendant and F. Dischinger is very economical. As the author has stated, the basic idea of such a dam was conceived by R. Maillart,[13] A. Mesnager,[14] Mr. Noetzli,[8] and others.[15]

Mr. Komendant has stated that straight gravity dams—regardless of their tremendously large volumes of concrete—have relatively low safety because of stress concentrations; linear stress distributions under the water pressure combined with the proper weight do not exist. The stress analysis is, both theoretically and experimentally, very intricate. It should be remembered that H. M. Westergaard was able to determine,[16] by the slab-analogy method, only the stresses inside Hoover Dam (Arizona-Nevada). However, it was then found—by photoelastic stress analysis—in certain horizontal sections of the dam the boundary stresses increased dangerously, especially as a result of stress concentrations at the re-entrant corners between the body of the dam and the foundation block.[17] The tests were concerned with gravity forces and the experimental stresses were incorporated ("frozen") into a bakelite model in a centrifuge oven by slow annealing during a rotation of about 1,000 rpm; they prove that the gravity stresses in critical sections considerably exceed the average values. Usually, gravity dams are built in an arched shape which increases structural resistance; if this were not done some gravity dams would be still less economical.

---

[10] Cons. Engr., Berkeley, Calif., and Lecturer, Stanford Univ., Stanford, Calif.

[11] "Large Savings Estimated from Constant-Angle Dam Design," by J. J. Polivka, *Civil Engineering*, November, 1950, No. 11, Vol. 20, p. 45.

[12] "Constant Angle Arch Dams Compared with Other Types," by J. J. Polivka, *ibid.*, April, 1951, p. 47.

[13] "Gewoelbe-Staumauern mit abgestuften Druckhoehen," by R. Maillart, *Schweizerische Bauzeitung* April 14, 1928, p. 183.

[14] "Sur les barrage-réservoirs à voûtes et à charge fractionnée," by A. Mesnager, *Revue Générale de l'Électricité*, October 29, 1927, p. 681.

[15] "Dams with Stepped Water Levels," by A. Floris, *Western Construction News*, October 25, 1928, p. 666.

[16] "Boulder Canyon Projects—Final Reports," Part V, Technical Investigations, *Bulletin No. 2*, Bureau of Reclamation, U. S. Dept. of the Interior, Denver, Colo., 1938, p. 184.

[17] "Analysis of Gravity Load Stresses by Photoelastic Methods," by J. J. Polivka, *Proceedings*, 16th, Semi-Annual Photoelasticity Conference, Illinois Inst. of Technology, Chicago, Ill., 1942.

It may also be of interest to investigate and to compare the economy and the safety of steel dams built in the United States and elsewhere at the beginning of the twentieth century.[18, 19, 20, 21, 22, 23] These dams were from 30% to 50% less expensive than concrete dams. The construction of steel dams was abandoned because of corrosion—a disadvantage which (as of 1956) can be successfully prevented by protective coatings and new metal alloys. Also, new, more economical structural schemes have been proposed as, for example, the shell-type dam invented by G. Krivochéine, J. Fultner, and J. Sekla.[24]

August E. Komendant,[25] M. ASCE—The reminder by Mr. Polivka that engineers and responsible public officials should investigate economy and safety even though additional expense may be involved is a fact which is not always recognized—especially if a new design is involved. To use a "proven" design is not justifiable; such a principle would have stagnated engineering science.

Engineers are always seeking new ways to extend the boundaries of knowledge. Therefore, from day to day, that which one "knows" changes, disappears, and gives way to new principles and achievements. The progress in science is so extensive and rapid that it appears to be limitless. It is an obligation of engineers to investigate every new idea which is sound from the theoretical point of view. The design of leaf-spring type shell dam is theoretically clear. This dam widens the range of application of concrete dams and even makes possible damming at locations where other types of dams are eliminated because of foundation difficulties or economy. The leaf-spring type shell dam, therefore, has a wide range of application. It can be combined with an earth-fill dam wherein use can be made of the passive-earth pressure, and with this combination the economy of the dam is considerably increased. Even an earth dam of one third the height of the total dam requires only a fraction of the volume of a complete earth-fill dam but also results in a reduction of the number of shells and flexural stresses; it also allows for the control, to a great extent, of the boundary disturbances in the shells. Additionally, the earth dam improves the architectural appearance of a concrete dam. Furthermore, the leaf-spring type shell dam can also be designed as a buttressed dam for damming relatively wide and flat valleys. In this case, however, the buttress and abutments should be prestressed.

---

[18] "Steel Dams," by O. L. Hovey, A.I.S.C., New York, N. Y., 1935.

[19] "Design and Construction of Dams," by E. Wegman, John Wiley and Sons, Inc., New York, N. Y., 8th Ed., 1927.

[20] "Structural Steel Dams," by F. H. Bainbridge, *Journal*, Western Soc. of Engrs., Vol. 8, 1903, p. I and Vol. 10, p. 615.

[21] "Four Steel Dams—Their Design and History," by J. F. Jackson, *Engineering News-Record*, 1930, p. 281.

[22] "Why Not Steel Dams?," by C. M. Stanley, *ibid.*, 1932, p. 652.

[23] "Force of Habit," editorial, *ibid.*, 1932, p. 658.

[24] "Steel Dams," by G. Krivochéine, *Proceedings*, Second Cong., International Assn. for Bridge and Structural Eng., Zurich, 1938.

[25] Cons. Engr., New York, N. Y.

Considering that (*a*) the shells can be poured rapidly by the use of slip forms, (*b*) relatively small quantities of concrete are required, (*c*) the shells can be built separately, and (*d*) the influence of chemical heat during the hydration of cement can be eliminated, the economy of the leaf-spring type shell dam is obvious and therefore this type of dam should be adopted. Model tests should be made to prove the soundness of the theory and to obtain information about the actual behavior of this dam type under water pressure and dynamic effects.

AMERICAN SOCIETY OF CIVIL ENGINEERS
Founded November 5, 1852
TRANSACTIONS

Paper No. 2827

EFFECT OF SAMPLE DISTURBANCE ON THE STRENGTH OF A CLAY

BY MAX L. CALHOON,[1] J. M. ASCE

WITH DISCUSSION BY MESSRS. JOHN H. SCHMERTMANN, AND MAX L. CALHOON

SYNOPSIS

Of the many variables that influence the laboratory-test shearing strength of saturated homogeneous clays, the effect of sample disturbance (partial remolding) has received little constructive analysis. It has generally been assumed that sample disturbance reduces the laboratory shearing strength and thereby results in an added factor of safety when the test results are applied to field design. It will be demonstrated herein for certain clay soils of the type tested that, due to sample disturbance, the actual field shear strength may be less than the laboratory-test shear strength. A method of analyzing strength data is described, in which is considered the effect of sample disturbance.

INTRODUCTION

Disturbances to the soil during sampling operations, removal of the soil sample from the sampling tube, and the process of trimming the specimen to size for a strength test cause a partial remolding of undisturbed soil specimens. In saturated clays that are sensitive to remolding, these disturbances cause a major deviation between observed laboratory strength and actual field strength. The effect of this variable frequently is not directly considered in analyzing laboratory strength results or in applying these results to the design of earth structures and foundations. Its effect is usually included in a factor of safety that is applied to the design, and the designer hopes he has thereby adequately compensated for the sample disturbance. The fact that disturbances exist in all test specimens can lead to erroneous interpretations of triaxial shear test results which may be on the unsafe side in many saturated clays. A method of evaluating triaxial shear test results in which the effect of sample disturbance is

---

NOTE.—Published, essentially as printed here, in December, 1954, as *Proceedings-Separate No. 570.* Positions and titles given are those in effect when the paper or discussion was approved for publication in *Transactions.*

[1] Soils Engr., Howard, Needles, Tammen and Bergendoff, New York, N. Y.

considered is presented herein. This method is based on the results of studies made by the writer at Northwestern University, at Evanston, Ill.[2]

GENERAL TEST INFORMATION

The following three definitions are significant as used in this paper: The term "clay" will refer to an extremely fine-grained, highly plastic, highly impervious, homogeneous, cohesive, saturated soil. A sensitive clay is one that loses part of its shearing strength when in a partly or completely remolded condition. The "sensitivity" of a clay is defined as the ratio of its unconfined compressive strength at the natural water content in the undisturbed condition to its unconfined compressive strength at the natural water content in a completely remolded condition. The value of the sensitivity ratio for most clays is between 2 and 4. For "sensitive" clays this ratio will be between 4 and 8. If the ratio is greater than 8, the clay is "extra-sensitive." The compressive strength of a clay (the difference between the major and minor principal stresses) is used to define the maximum applied axial stress which a triaxial compression test specimen will sustain before failing. Because a saturated clay has an effective internal friction angle equal to zero under conditions of no water-content change during failure, the shearing strength of the clay is equal to one half of the compressive strength.

The soil sample used in this study was obtained in conjunction with an extensive foundation investigation at the Milwaukee (Wis.) sewage disposal plant. This investigation was reported on by Philip C. Rutledge, M. ASCE, and C. R. Holdampf, in a paper presented at a meeting of the Society in 1952. It was taken in a 5-in.-diameter, thin-walled tube in a sampler developed by Jorg O. Osterberg,[3] A. M. ASCE, of Northwestern University. The sample came from a depth of from 38.5 ft to 42.3 ft below the ground surface and from 29.5 ft to 33.3 ft below the Milwaukee datum (mean level of Lake Michigan).

The sample was part of an unusually uniform deposit of saturated clay with some organic matter and was highly sensitive to remolding and to sample disturbance. Its sensitivity ratio was in the vicinity of 8. The remolded unconfined compressive strength at the natural water content was difficult to determine accurately because a remolded specimen would scarcely stand under its own weight. The soil appeared to be normally consolidated (never consolidated to any pressure greater than the existing effective overburden pressure) to a pressure of 1.1 tons per sq ft as determined from the results of a one-dimensional consolidation test. This clay was a sedimentary deposit and was probably formed in a paludal environment of one of the ancient glacial great lakes. Its liquid limit was 71%, its plasticity index was 30, and its specific gravity was 2.67. Its average natural dry density was 59.2 lb per cu ft and its average natural water content was 67.7%. Its relative water content was 89% (also known as liquidity index or water-plasticity ratio). The uniform compressible stratum from which this soil came is approximately 35 ft in thickness. Tests for natural moisture content and unconfined compressive strength on undisturbed specimens throughout the depth of the stratum revealed no consistent trends toward lower moisture content or increased compressive strength as depth increased. These two facts may indicate that this clay is of the type described by Karl Terzaghi,[4] Hon. M. ASCE, as having a quicksand type of structure.

---

[2] "The Effect of Remolding on the Strength of a Saturated Clay," by Max L. Calhoon, thesis presented to Northwestern Univ., at Evanston, Ill., in 1952, in partial fulfilment of the requirements for the degree of Master of Science.

[3] "New Piston-Type Soil Sampler," by Jorg O. Osterberg, *Engineering News-Record*, April 24, 1952, p. 77.

Method of Presenting Test Data.—The commonly used method of evaluating test shear-strength data is through the use of a Mohr diagram. Anyone familiar with such diagrams for clays knows that the simplified straight-line concept proposed by Coulomb is usually not observed in these soils. There are frequently erratic test results due to minor sample variations that are almost impossible to smooth intelligently on such diagrams. Therefore, a hypothesis proposed by Mr. Rutledge[5] for interpretation of results has been used.

Before describing this method, several types of shear tests for saturated clays should be reviewed. The first type is the quick triaxial test (Q test). In this test the specimen is placed in the shear device at its natural water content. A lateral pressure is applied, but no water is allowed to drain from the specimen. An axial load is then rapidly applied until the specimen fails. It has been confirmed through many years of research that a given clay at constant water content will exhibit the same value of compressive strength regardless of the magnitude of the lateral pressure. If the lateral pressure is zero, the test is an unconfined compression test.

In a consolidated-quick triaxial test (Qc test) water is allowed to drain from the specimen under the influence of the lateral pressure. After drainage is essentially complete, the specimen is sealed against further drainage and the axial load is rapidly applied. After the specimen is sealed against drainage, the lateral pressure can be changed to any magnitude and the specimen will still show the same compressive strength in a manner similar to a quick test. Because the water content at failure is reduced from the natural water content the void ratio is also proportionately decreased. Therefore, the compressive strength is increased over that of the quick test. It should be explained that this increase in strength is not due to frictional properties and that the effective Qc friction angle is equal to zero.

In a slow triaxial test (S test) the specimen is allowed to drain under the lateral pressure similar to the Qc test. When this drainage is essentially complete, the axial load is applied without sealing the specimen against drainage. In this test the axial load is applied slowly so that essentially complete drainage is achieved under each increment of axial load. Tests of this type generally yield higher shear-strength values than does the Qc test.

Mr. Rutledges's hypothesis for evaluating shear data will now be explained. There are two curves involved (Fig. 1). Curve A represents water content (or void ratio) plotted against logarithm of pressure, and it is unique in that it can be defined by either one-dimensional or triaxial consolidation. This implies that consolidation is independent of the minor principal stress. Curve B is a curve of water content (or void ratio) plotted against logarithm of compressive strength, which is unique in that it can be defined by unconfined compression tests, consolidated-quick tests, or slow triaxial tests. Curve B is independent of pore-water pressure. Curves A and B are essentially parallel when both are plotted on semilogarithmic paper.

---

[4] "Shear Characteristics of Quicksand and Soft Clay," by Karl Terzaghi, *Proceedings*, Seventh Texas Conference on Soil Mechanics and Foundation Eng., Bureau of Eng. Research, Univ. of Texas, Austin, Tex., January, 1947.

[5] "Review of the Cooperative Triaxial Research Program of the War Department, Corps of Engineers," by Philip C. Rutledge, in "Soil Mechanics Fact Finding Survey, Progress Report: Triaxial Shear Research and Pressure Distribution Studies on Soils," U. S. Waterways Experiment Station, Vicksburg, Miss., April, 1947.

The unconfined compression or the quick triaxial compressive strength is the strength shown by curve B at the natural water content, W_n (Fig. 2).

The consolidated-quick test strength is the compressive strength shown by curve B at the water content at which the specimen failed. This water content is determined from curve A and corresponds to the lateral pressure used in the test (Fig. 2).

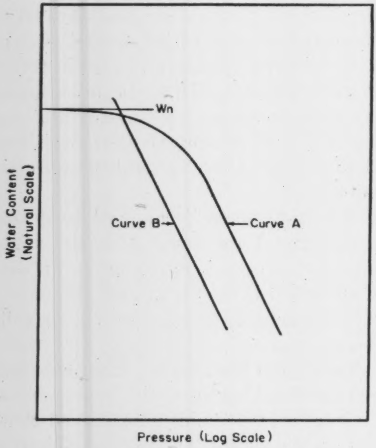

FIG. 1.—CONSOLIDATION AND COMPRESSIVE-STRENGTH CURVES

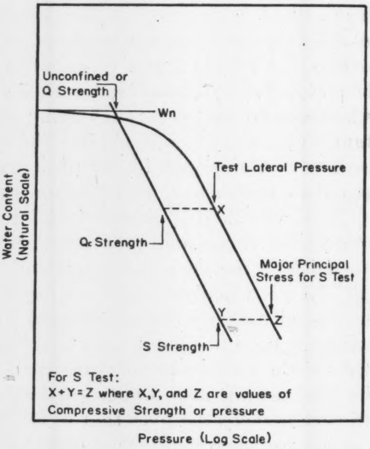

FIG. 2.—DETERMINATION OF UNCONFINED, Q, QC, AND S COMPRESSIVE STRENGTHS

The slow triaxial test strength is the compressive strength which, when added to the test lateral pressure, is equal to the pressure on curve A at the same water content as the compressive strength. There is only one such combination of values for each lateral-pressure value selected. (Fig. 2 provides a graphical illustration of the determination of the slow-test strength.)

It can therefore be seen that, although curve B is defined entirely by unconfined compression tests (moisture content lowered by slow drying in a humid room), the Q, Qc, and S triaxial strengths can be determined without performing these tests.

The use of this method of analyzing test data allows the designer to smooth intelligently erratic data and also provides valuable information as to possible causes of erratic data.

Tests Used.—The tests used in this investigation were as follows: Nineteen Qc triaxial tests of undisturbed soil, eight Qc triaxial tests of remolded soil,

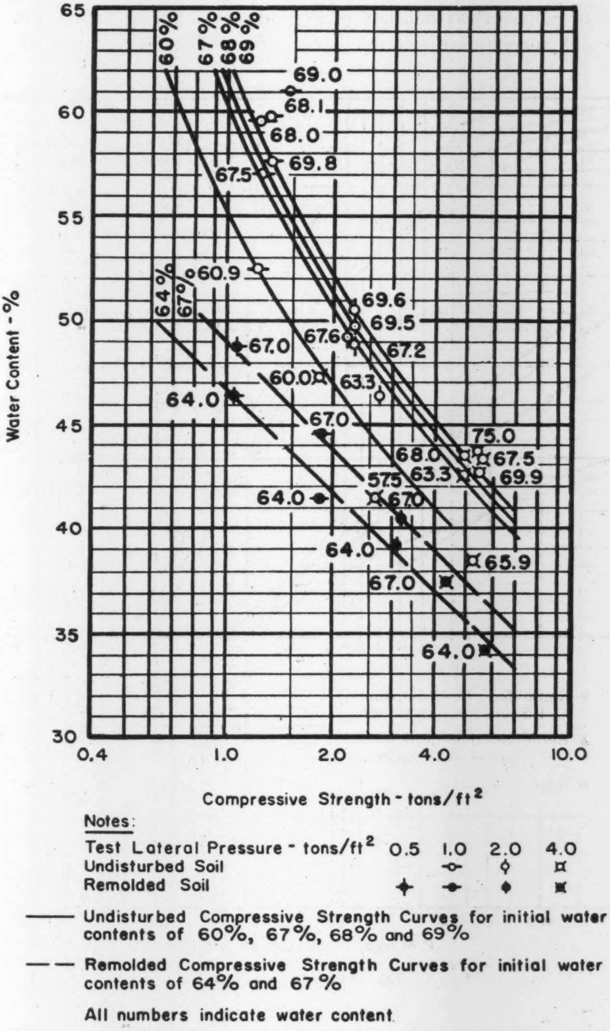

FIG. 3.—RESULTS OF TRIAXIAL SHEAR TESTS

one one-dimensional consolidation test using a 1.5-in.-thick specimen of undisturbed soil, two one-dimensional consolidation tests with 0.75-in.-thick specimens of undisturbed soil, and one one-dimensional consolidation test with a 1.5-in.-thick specimen of remolded soil. The 0.75-in.-thick, one-dimensional consolidation specimens were remolded at the completion of consolidation, brought back to their natural moisture contents, and then reconsolidated. All one-dimensional consolidation-test specimens had an area of 100 sq cm. The average size of the triaxial test specimens was 3.6 cm in diameter and 6.0 cm in height. The results of all these tests are shown in Figs. 3 and 4.

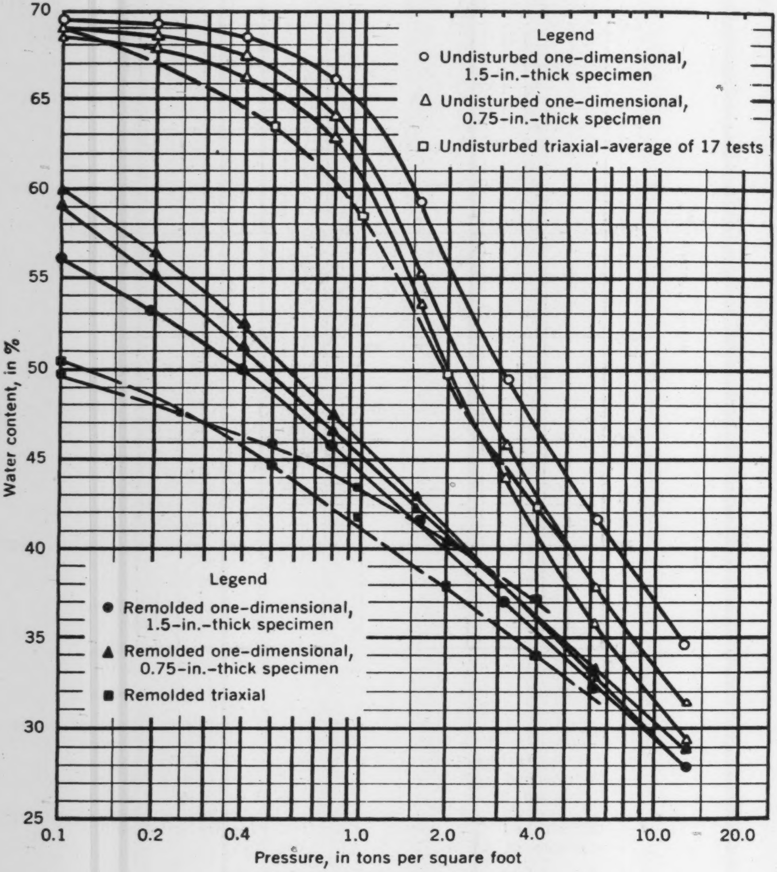

FIG. 4.—RESULTS OF CONSOLIDATION TESTS

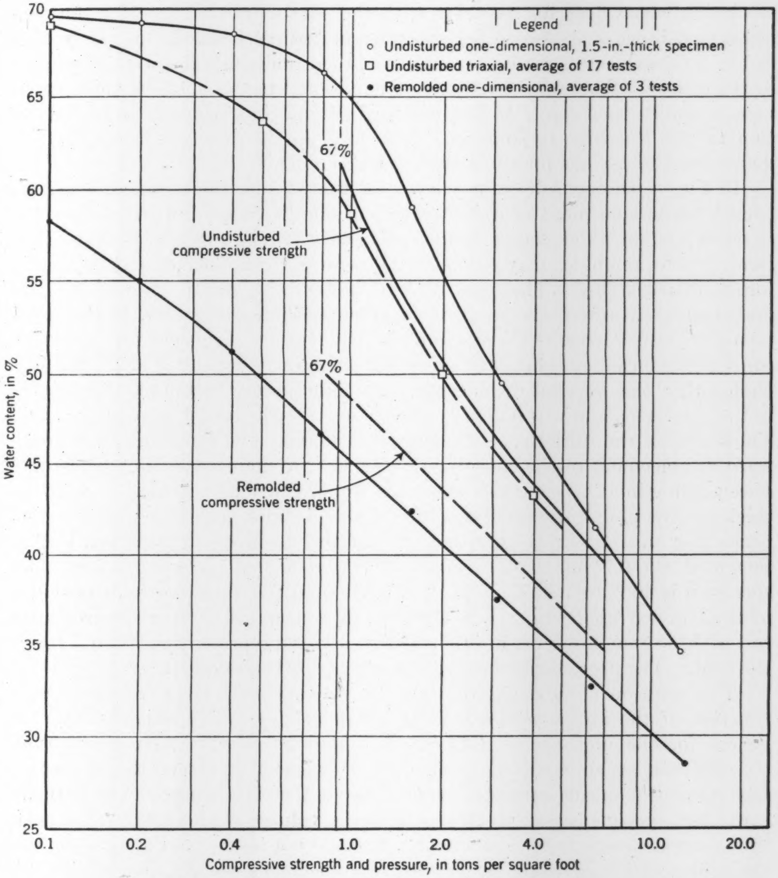

FIG. 5.—RELATIVE POSITIONS OF VARIOUS CONSOLIDATION CURVES AND STRENGTH CURVES FOR UNDISTURBED AND REMOLDED SOIL

It can be seen that the undisturbed compressive-strength results are not as uniform as might be desired, but curves representing various initial water contents could be drawn with moderate accuracy.[6] The nonuniform behavior was probably due to slight variations among specimens in the initial condition of the soil.

ANALYSIS OF TEST RESULTS

Validity of the Rutledge Hypothesis.—The undisturbed and remolded compressive-strength curves representing an initial water content of 67% have been selected for analysis. Fig. 4 shows that the average undisturbed triaxial consolidation curve does not coincide with the consolidation curve for the one-dimensional test of a 1.5-in.-thick specimen of undisturbed soil. It can be seen in Fig. 5 that the compressive-strength curve for undisturbed soil is not parallel to the consolidation curve for the one-dimensional test of a 1.5-in.-thick specimen of undisturbed soil. At first one might think that this is in direct opposition to the Rutledge hypothesis. Therefore, further analysis is required to determine the reasons for these apparent discrepancies.

---

[6] "Sampling, Testing, and Averaging," by Karl Terzaghi, *Proceedings*, Purdue Conference on Soil Mechanics and Its Applications, Purdue Univ., Lafayette, Ind., 1940.

In Fig. 4, the consolidation curves for the 0.75-in.-thick, one-dimensional consolidation specimens of undisturbed soil are displaced downward from the curve of a 1.5-in.-thick consolidation specimen. It is known that the consolidation curve for remolded clay is displaced downward from the consolidation curve for undisturbed clay. Theodore W. Van Zelst,[7] J. M. ASCE, showed that, for undisturbed saturated clays and for a given specimen diameter, as the specimen thickness decreases the consolidation curves are displaced further downward toward the consolidation curve for completely remolded soil. He concluded that this vertical displacement was due mainly to sample disturbance in the specimens and was inversely proportional to the initial specimen volume. Therefore, as the initial specimen size is decreased, the remolding and downward displacement of the consolidation curves are increased. The percentage of remolding in a 0.75-in.-thick specimen would thus be twice that in a 1.5-in.-thick specimen, and the remolding in a 0.375-in.-thick specimen would be four times that in a 1.5-in.-thick specimen. If the 1.5-in.-thick specimen is 10% remolded, the 0.75-in.-thick specimen is 20% remolded and the 0.375-in.-thick specimen is 40% remolded. Mr. Van Zelst used this phenomenon to devise a method of extrapolating the position of a consolidation curve representing soil with no remolding or, in other words, a curve representing natural soil in the field. The procedure for doing this is described subsequently.

The position of consolidation curves for saturated clays is, therefore, a function of the initial volume of the test specimen. This explains why the curves for the undisturbed 0.75-in.-thick and 1.5-in.-thick, one-dimensional consolidation specimens do not coincide. It is logical to extend this idea to the triaxial consolidation curve for undisturbed soil. The volume of the triaxial shear test specimens was much less than the volume of the 1.5-in.-thick, one-dimensional consolidation specimens. It could not be expected, therefore, that the consolidation curve for the triaxial test specimens would coincide with that of the 1.5-in.-thick, one-dimensional consolidation-test specimen.

Fig. 5 shows that the compressive-strength curve for undisturbed soil is parallel to the average triaxial consolidation curve for undisturbed soil. The compressive-strength curve is therefore parallel to the consolidation curve that represents the same degree of remolding as the strength curve represents.

The foregoing facts suggest that the Rutledge hypothesis should be modified for soils that are sensitive to remolding as follows:

1. Curve A (Fig. 1) is unique in that it can be defined by either triaxial or one-dimensional consolidation if the triaxial and one-dimensional consolidation specimens are disturbed to the same degree.

---

[7] "An Investigation of the Factors Affecting Laboratory Consolidation of Clay," by Theodore W. Van Zelst, *Proceedings*, Second International Conference on Soil Mechanics and Foundation Eng., Rotterdam, Vol. VII, 1948, pp. 52–61.

2. Curve B is unique if all test specimens are disturbed to the same degree.
3. Curves A and B are parallel only if they both represent soil specimens which were disturbed to the same degree.

Method of Determining Field Strength.—Because it has been rather definitely shown that the degree of remolding affects the position of the consolidation curves, it is logical to surmise that the degree of remolding would also affect the position of the compressive-strength curves. Fig. 5 shows the compressive-strength curve for the remolded specimen which is displaced downward from that for the undisturbed specimen. If the amount of disturbance in the undisturbed triaxial-shear-test specimens were known, it would be possible to compute the position of a compressive-strength curve representing soil with no disturbance. Assuming that the percentage of disturbance in the undisturbed triaxial specimens is known—for example, 20%—the computation would be as follows: The vertical distance (at any value of compressive strength) between the undisturbed-strength curve and the 100% remolded-strength curve is equal to 80% or 8 units. The curve representing 0 remolding is therefore 2 units above the undisturbed curve. The position of the strength curve representing no remolding may be determined either mathematically, by reference to the vertical scale on the graph, or graphically, through the use of a scale and dividers. Several points on the strength curve for 0 disturbance should be located and then connected with a smooth curve.

The percentage of remolding in the undisturbed triaxial specimens could be computed if the position of a consolidation curve representing 0 remolding were known by noting the position in the vertical direction of the average triaxial consolidation curve for undisturbed soil with respect to the 100% remolded consolidation curve and the consolidation curve for 0 remolding. This computation would be similar to the foregoing one. The vertical distance between the curves for 0% and 100% remolding represents 10 units (at any value of pressure). If the average triaxial consolidation curve for undisturbed soil is 2 units below the consolidation curve for 0 remolding, the triaxial test specimens would be 20% remolded, and so on.

The first problem, then, was to obtain a consolidation curve representing natural soil in the field which is not disturbed in any way (0% remolded). To do this, the method proposed by Mr. Van Zelst[7] was utilized.

This method assumes that the operation of trimming undisturbed one-dimensional consolidation specimens disturbs the specimens to the same depth, no matter what the thickness of the consolidation specimen may be. This assumption is merely an analogy to express the idea that, for example, a 0.75-in.-thick specimen is remolded twice as much as a 1.5-in.-thick specimen of the same diameter. This is a reasonable assumption because the trimming operation for all specimen sizes is the same.

The tests that are required are one undisturbed, one-dimensional consolidation test using a thick specimen (say, 1.5 in.) and one test using a thin specimen (say, 0.75 in.). Also, a one-dimensional consolidation test of a completely remolded specimen is needed, using either of the previously mentioned specimen sizes.

The diagrams relating moisture content and log pressure are plotted for each of the foregoing three tests. A percentage of remolding (P_1) is assumed for the thick specimen (thickness = T_1). The percentage of remolding (P_2) for the thin specimen (thickness = T_2) is equal to (T_1/T_2) P_1. (This is true only if the areas of both specimens are equal.) The percentage of remolding for the remolded specimen is 100%. The three consolidation curves are then examined to determine whether the assumed percentages of remolding (P_1 and P_2) place the three consolidation curves correctly in the vertical direction with respect to each other. For example, if P_1 is assumed to be 10% for a 1.5-in.-thick undisturbed specimen, P_2 is 20% for a 0.75-in.-thick undisturbed speci-

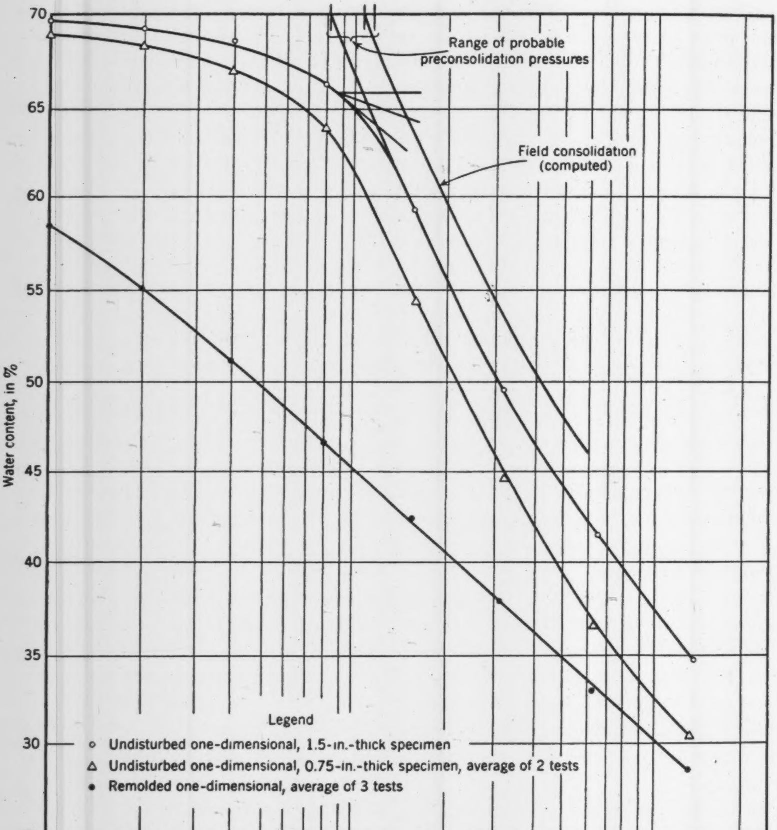

FIG. 6.—FIELD CONSOLIDATION CURVE AND CONSOLIDATION CURVES USED TO COMPUTE IT

men. The vertical distance between the curve for the 100% remolded specimen and the curve for the 1.5-in.-thick specimen is 90% or 9 units (at any value of pressure). The vertical distance between curves for the 1.5-in.-thick and 0.75-in.-thick specimens should be 1 unit and the vertical distance between the 0.75-in.-thick and the 100% remolded curve should be 8 units. The distance is then measured on the graph of the three curves and, if they are actually spaced vertically with respect to each other so that the foregoing percentages hold true, the assumed values of P_1 and P_2 are correct. Values of P_1 and P_2 are determined by trial and error. After the correct values for P_1 and P_2 are

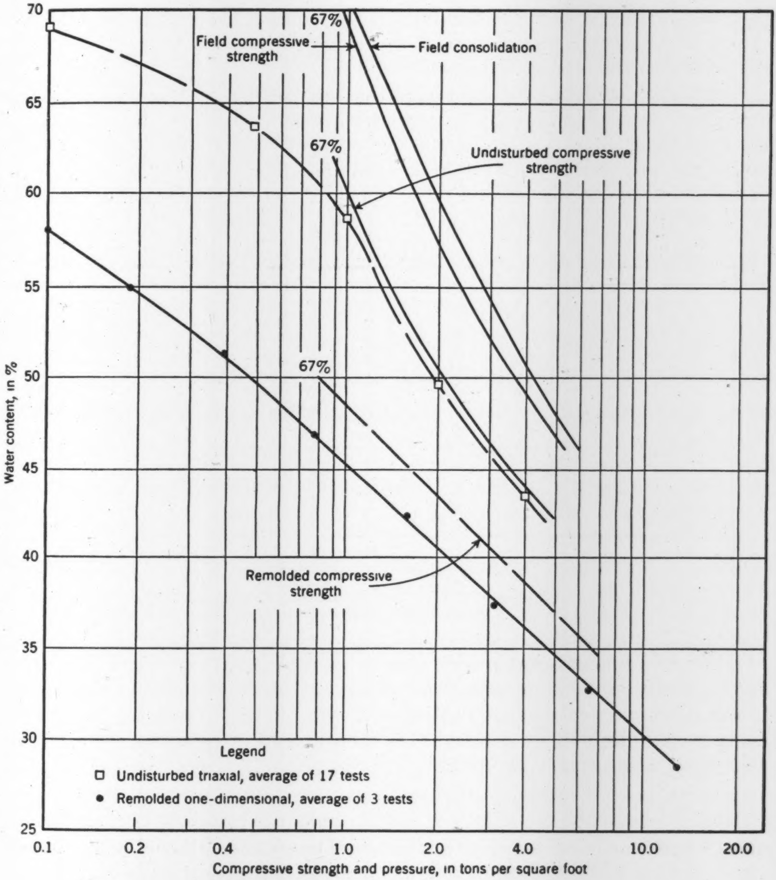

FIG. 7.—FIELD STRENGTH CURVE AND THE COMPRESSIVE-STRENGTH CURVES AND CONSOLIDATION CURVES USED TO COMPUTE IT

determined, a consolidation curve representing 0 remolding can be easily extrapolated. If P_1 and P_2 are found actually to be equal to 10% and 20%, respectively, the curve representing 0 remolding would be 1 unit above the curve for the 1.5-in.-thick specimen.

Fig. 6 shows the previously mentioned average test curves plus the computed consolidation curve for a natural soil in the field. It is interesting to note that this computed curve at the initial water content lies within the probable range of preconsolidation pressures for the undisturbed 1.5-in.-thick consolidation specimen and is therefore considered valid.

After the positions of the consolidation curves representing 0% remolding and 100% remolding have been determined, it is a simple matter to compute the percentage of remolding in the undisturbed triaxial shear specimens by noting the position of the average triaxial consolidation curve in the vertical direction relative to the 0% and 100% remolded consolidation curves, as shown previously.

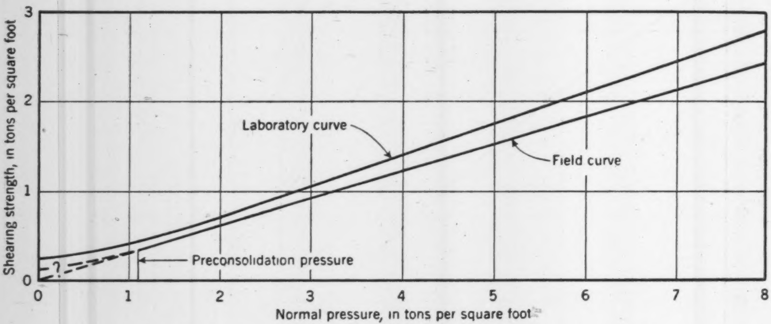

FIG. 8.—QC SHEAR-STRENGTH ENVELOPES, LABORATORY AND FIELD (67% INITIAL WATER CONTENT)

It is thus known what percentages of remolding the remolded and undisturbed compressive-strength curves represent. A simple extrapolation of distances in the vertical direction will give the position of a compressive-strength curve representing 0% remolding or, in other words, representing the compressive strength of natural soil in the field. An example of this extrapolation has been presented previously.

Fig. 7. shows the laboratory (triaxial) and field (computed) consolidation curves and compressive-strength curves. The average triaxial consolidation curve is used for the laboratory curve A because it and the laboratory compressive-strength curve both represent the same degree of disturbance.

Fig. 8 shows consolidated-quick shearing-strength envelopes which are drawn from Fig. 7. The magnitude of the ordinate to the field curve at 0 normal pressure is unknown because it is not known whether the field consolidation curve progresses upward above the natural water content as a straight line to 0 pressure or whether it bends to the left somewhat above the liquid limit as suggested by Mr. Terzaghi.[8] If the field consolidation curve is a straight line to 0 pressure and the compressive-strength curve is parallel to it, the shearing strength of the soil is 0 at 0 normal pressure. This implies that "cohesion" is a function of the pressure history of the soil. An important fact is readily seen: The field shearing-strength curve is below the laboratory shearing-strength curve at all values of normal pressure. This phenomenon may not necessarily be confined to highly sensitive clays. It is entirely possible that clays of low and medium sensitivity may exhibit lower shearing strength in the field than in the laboratory.

Discussion of Results

An analogy can be made wherein the undisturbed triaxial specimens are considered to consist of a core of soil which is completely undisturbed and is surrounded by an annulus of completely remolded soil. The average consolidation curve of this specimen would necessarily lie somewhere between a curve representing no disturbance and a curve representing 100% remolding. The undisturbed core would follow the same consolidation curve as completely undisturbed soil and the remolded annulus would follow the same consolidation curve as completely remolded soil. Because the remolded soil exhibits a higher compressive strength than the undisturbed soil for any specified value of test lateral pressure, it would be expected that the average compressive strength of this specimen would be greater than the compressive strength of a specimen of completely undisturbed soil.

It should be noted in Fig. 8 that the natural shearing strength in the field is the ordinate to the field curve at the preconsolidation pressure which was determined from the calculated field consolidation curve. This shearing strength is greater than the laboratory unconfined-test shearing strength (ordinate to the laboratory shearing-strength curve at 0 normal pressure).

One might logically wonder, then, since the natural field shearing strength is greater than the laboratory unconfined-test shearing strength, why failures occur in the field when the design was based on the laboratory unconfined-test shearing strength. The shearing strength of clays is a highly complex phenomenon and is a function of many variables. One of these variables which appears to be important is the rate of application of the axial load to the specimens in the laboratory as compared to the rate of loading in the field during construction. A fairly complete discussion of this subject has been presented by Arthur Casagrande, M. ASCE, and Stanley D. Wilson,[9] A. M. ASCE. Some other factors that affect the strength and stability of clays which the designer may not consider are planes of weakness in the clay; progressive failure in the field; short-term fluctuations in ground-water pressures, possibly for as briefly as an hour; test specimens that are too small to be representative of the average condition of the soil; and an incorrect assumption as to the stress conditions in the field prior to failure. It is evident that failure can be the result of a multitude of causes other than the use of an incorrect value for the shearing resistance of the soil.

---

[8] "Undisturbed Clay Samples and Undisturbed Clays," by Karl Terzaghi, *Journal*, Boston Soc. of Civ. Engrs., July, 1941, pp. 45–65.

[9] "Effect of Rate of Loading on the Strength of Clays and Shales at Constant Water Content," by Arthur Casagrande and Stanley D. Wilson, *Geotechnique*, Vol. 2, No. 3, June, 1951, pp. 251–263. (Reprinted in the *Soil Mechanics Series, No. 39*, Harvard Univ., Cambridge, Mass.)

The shearing resistance shown on the laboratory curve of Fig. 8 at the preconsolidation pressure is somewhat unsafe and should not be used. Many designs have been based on this value of shearing resistance. In some cases it may be overconservative also to use the unconfined compression test results. Therefore, a careful study should be made of the shearing resistance, considering all factors before selecting a value to be used for design.

Conclusions and Recommendations

On the basis of the studies made it has been found that, for a sensitive saturated clay, the actual shearing strength of this soil in the field would be less than the laboratory-test shearing strength at any specified value of normal pressure.

A recommended testing program and method of analysis to determine shearing resistance for clays of the general type used in this investigation are as follows:

1. Samples should be carefully obtained by means of handcutting or by the use of large-diameter sampling tubes (at least 3.5 in. in diameter).
2. Laboratory testing should include the following:

a. One undisturbed, one-dimensional consolidation test using a thick specimen—say, 1.5 in.;

b. One undisturbed, one-dimensional consolidation test using a thin specimen—say, 0.75 in.;

c. One remolded, one-dimensional consolidation test using either of the specimen sizes of item *a* or item *b*;

d. Two or three unconfined compression tests on undisturbed soil at the natural water content;

e. Two or three unconfined compression tests on remolded soil at the natural water content to determine the sensitivity ratio;

f. At least four consolidated-quick triaxial shear tests on undisturbed soil, each at different lateral pressures (if the natural water content of the specimens varies by more than 1% and if the soil tends to show different strength curves for different initial water contents, enough specimens should be used to establish compressive-strength curves for a range of initial water contents; the triaxial consolidation characteristics should be carefully observed so that the triaxial consolidation curve can be constructed); and

g. At least four consolidated-quick triaxial shear tests on remolded soil, each at different lateral pressures.

The procedure for analyzing the data based on the methods described in this paper would be as follows:

A. The field virgin consolidation curve is extrapolated from the foregoing tests in *a*, *b*, and *c*.

B. Undisturbed triaxial consolidation curve and undisturbed compressive strength curve are plotted.

C. The remolded consolidation curve (this may be either one-dimensional, triaxial, or an average of both, depending on the validity of the data) and the remolded compressive strength curve are plotted.

D. The percentage of remolding in undisturbed triaxial specimens is determined.

E. The field compressive-strength curve for the average natural water content expected in the field is determined.

F. Shear-strength envelopes for the laboratory and field similar to Fig. 8 are plotted, using the triaxial consolidation curve as the laboratory curve A (both shear envelopes should represent the same initial water content).

G. The shearing strength to use in the design is determined from an analysis of the foregoing curves.

ACKNOWLEDGMENTS

The writer wishes to express appreciation to Mr. Rutledge for the conception of the initial idea for this investigation, for his many helpful suggestions during the early part of the testing, and for his critical review of the manuscript; to Mr. Osterberg for his suggestions and criticisms throughout the entire investigation; and to John W. N. Fead, A. M. ASCE, and Elmer A. Richards, J. M. ASCE, for their constructive criticisms and assistance in performing many of the laboratory tests.

DISCUSSION

JOHN H. SCHMERTMANN,[10] J. M. ASCE.—Mr. Calhoon has presented a thoughtful analysis of his fine laboratory investigation. He has brought the attention of his colleagues to the important practical problem of the proper evaluation of the effect of sample disturbance on laboratory shear-strength results. The paper will serve as an aid to engineers faced with the problems of evaluating and using laboratory strength data.

Before beginning a more direct discussion of Mr. Calhoon's paper, a few statements regarding the probable significance of void ratio in relation to the strength of a clay may seem appropriate.

Strength and Void Ratio.—Soil mechanics was developed through a mechanical approach to mass soil behavior. The initial success of the use of the Coulomb equation, later combined with pore-pressure corrections, as an expression for the strength of a clay has resulted in a tendency to continue to think of this strength in mechanical terms. However, recent problems, particularly in the field of soil stabilization, have shown the superiority of the more fundamental electrochemical explanation of the behavior of clay.[11,12,13,14]

Striking laboratory and field tests have been performed in which the strengths of clays have been significantly altered without any external stress changes by changing the interparticle energy-potential relationships with trace chemicals[14] and with external electrical potentials.[15,16] Strength alterations can be accomplished in two general ways: (*a*) Changing the nature of the soil ions or their concentrations and (*b*) changing the structural arrangement or the distance between particles, or both. The latter method is of particular interest here.

Clay can be considered as a colloid with small interparticle distances.[14] The summation of the various attractive forces between such particles probably varies as some function of $(1/r)^n$, in which r is the distance between particles and n may vary[14] from 2 to 7. The soils engineer can change this distance by the application of an external stress which causes consolidation and, in turn, results in a closer spacing of the colloidal clay particles. For a given initial structural arrangement of a clay soil, change of void ratio is a convenient parameter for measuring the more fundamental change of particle spacing.

Mr. Rutledge has repeatedly shown in laboratory work with saturated natural clays that compressive strength increased exponentially as failure void ratio decreased arithmetically (Fig. 14).[5] This relationship was found to be

---

[10] Graduate Student, Northwestern Technological Inst., Northwestern Univ., Evanston, Ill.

[11] "Altering Soil Water Relationships by Chemical Means," by Alan S. Michaels, *Proceedings*, Conference on Soil Stabilization, Massachusetts Inst. of Technology, Cambridge, Mass., June, 1952.

[12] "Electrical Stabilization in Earthwork and Foundation Engineering," by Leo Casagrande, *ibid.*, p. 84.

[13] "Soil Stabilization by Chemical Means," by George E. Murray, *ibid.* p. 107.

[14] "The Structure of Inorganic Soil," by T. W. Lambe, *Proceedings-Separate No. 315*, ASCE, October, 1953.

[15] "The Influence of Direct Current Potential on the Adhesion between Clay and Metal Objects. Laboratory and Full Scale Tests," by Ir H. K. S. Ph. Begemann, *Proceedings*, Third International Conference on Soil Mechanics and Foundation Eng., Zurich, Vol. 1, 1953, p. 89.

[16] "Electro-Osmotic Stabilization of Soils," by A. Casagrande, *Soil Mechanics Series No. 38*, Harvard Univ., Cambridge, Mass., 1952.

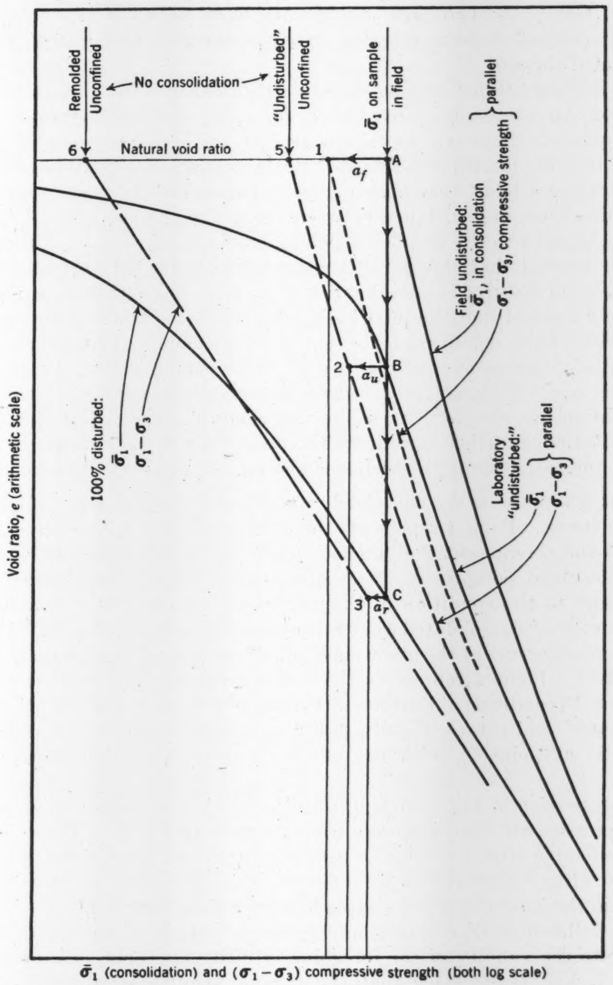

Fig. 9.—Effect of Disturbance on Consolidated Strength (If $a_f > a_u > a_r$, Consolidated Strength Increases with Sample Disturbance)

unique in that it was almost independent of the pore-water pressure at failure and the manner in which the final void ratio was reached (minor principal stress). Milton Vargas, A. M. ASCE, found that the same relationships existed for two natural, partly saturated, Brazilian residual clays.[17] More recently, Gerald A. Leonards, A. M. ASCE, obtained similar results with carefully controlled tests on two partly saturated, compacted, and then consolidated clays.[18]

---

[17] "Correlation between Angle of Internal Friction and Angle of Shearing Resistance in Consolidated Quick Triaxial Compression Tests on Residual Clays," by Milton Vargas, *Proceedings*, Third International Conference on Soil Mechanics and Foundation Eng., Zurich, Vol. 1, 1953, p. 72.

The Rutledge Hypothesis on Sample Disturbance.—By laboratory experimentation Mr. Rutledge proved that for many natural saturated clays a semilog plot of void ratio at failure against compressive strength $(\sigma_1 - \sigma_3)$ resulted in a unique curve—almost a straight line and closely parallel to the virgin slope of a laboratory one-dimensional consolidation test. Referring to Fig. 9, the horizontal distance between these two curves, measured positive from the lettered to the numbered points, has been labeled a. Although Mr. Rutledge showed that this parallel relationship exists only between the best obtainable undisturbed consolidation-test and strength-test samples, he intuitively guessed that the relationship might also be true for the completely undisturbed field conditions, the completely remolded condition, and all intermediate degrees of disturbance—of which the laboratory "undisturbed" sample is one. Following the known effects of sample disturbance on the consolidation test results[19,20] these limiting conditions are also shown in Fig. 9.

Mr. Rutledge further considered the possibility of the a-distances decreasing with increased sample disturbance and reasoned the effect as follows:

> Point A represents the completely undisturbed natural field void ratio and effective stress. Point 1 represents the field unconfined compressive strength. Points 5 and 6 represent the "undisturbed" and completely remolded laboratory unconfined compressive strengths at the natural void ratio. Partial disturbance to the condition of the laboratory "undisturbed" sample results in a decrease of consolidated void ratio from point A to point B. The void-ratio decrease occurs at the given constant stress here taken as $\bar{\sigma}$ on the sample in the field. Point 2 represents the compressive strength for the sample at the point B condition. Further disturbance results in further decreases of consolidated void ratio. Finally, 100% disturbance results in a consolidated void ratio at point C, with the new compressive strength represented by point 3.

It can be seen in Fig, 9 that, if a_f is greater than a_u and a_u is greater than a_r, compressive strength increases from points 1 to 2 to 3. Thus, for a particular effective stress, it may be possible for consolidated shear strengths to increase with increased sample disturbance. However, at any particular void ratio the least disturbed sample has the greater strength.

Mr. Calhoon made a careful and systematic study of one uniform clay to investigate the validity of the foregoing intuitive concepts. As may be seen in Fig. 7, his results show that the parallel semilog strength-consolidation relationship actually did exist for various degrees of sample disturbance and that the a-distances actually did decrease, and in fact became negative with increased disturbance. His results therefore check the prediction of increased consolidated strength with increased disturbance.

---

[18] "Strength Characteristics of Compacted Clays," by Gerald A. Leonards, *Transactions*, ASCE, Vol. 120, 1955, p. 1420.

[19] "Relation of Undisturbed Sampling to Laboratory Testing," by P. C. Rutledge, *ibid.*, Vol. 109, 1944, p. 1155.

[20] "The Undisturbed Consolidation Behavior of Clay," by John H. Schmertmann, *ibid.*, Vol. 120, 1955, p. 1201.

Nature of Clay Investigated.—Mr. Calhoon has stated that the apparent constant water content of the uniform clay bed, of which his samples were a part, may indicate that the clay he studied had a quicksand[8] type of structure. Because the nature of the clay studied is of importance when applying the results of Mr. Calhoon's work, the writer reinvestigated the consolidation and water content data utilizing additional data not available at the time of the original work. These data are presented in Fig. 10.

Inspection of the available data indicates that only the 20-ft depth shown can be considered sufficiently uniform to permit evaluation of the significance

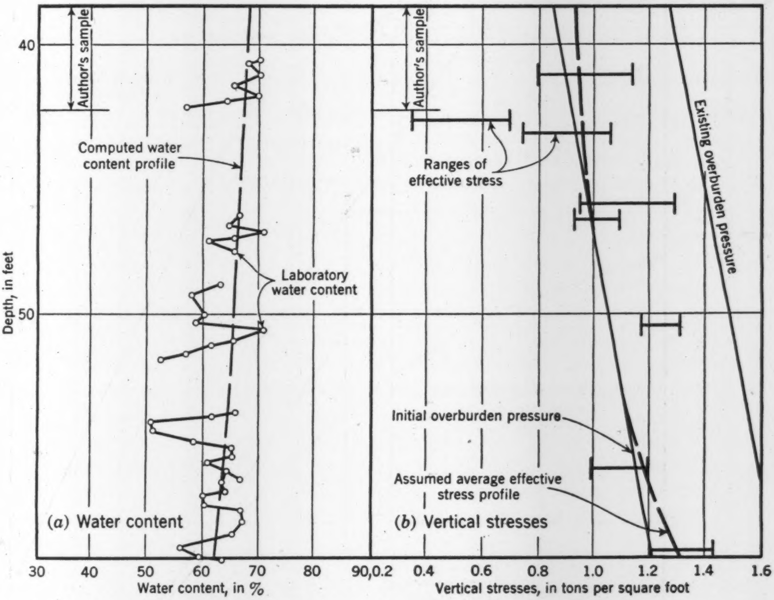

FIG. 10.—CONSOLIDATION AND WATER CONTENT OF MILWAUKEE CLAY

of the water-content profile. The location of Mr. Calhoon's sample is shown in the illustration.

In Fig. 10(*a*) are presented the detailed water-content data for the bed. Mr. Calhoon's detailed data from his sample are not shown. His average water content value of 67.7% is consistent with the data presented. In Fig. 10(*b*) are presented the effective stress ranges interpreted from the individual consolidation tests and the effective stress profile assumed from these results. The total initial overburden pressure (before fill) and the existing overburden pressure are also shown for comparison. It may be seen that the clay is partly consolidated under the added fill stress.

Assuming that field consolidation occurred along a virgin effective-stress slope parallel to the laboratory virgin slope of Mr. Calhoon's 1.5-in. consolidation test, it was possible to compute the expected distribution of water content for the depth of the clay layer. This computed distribution is indicated in Fig. 10(*a*) for direct comparison with the actual water-content data. If one makes allowances for the probable local variations in the soil, it may be seen that there is reasonable agreement between the computed distribution and the actual data.

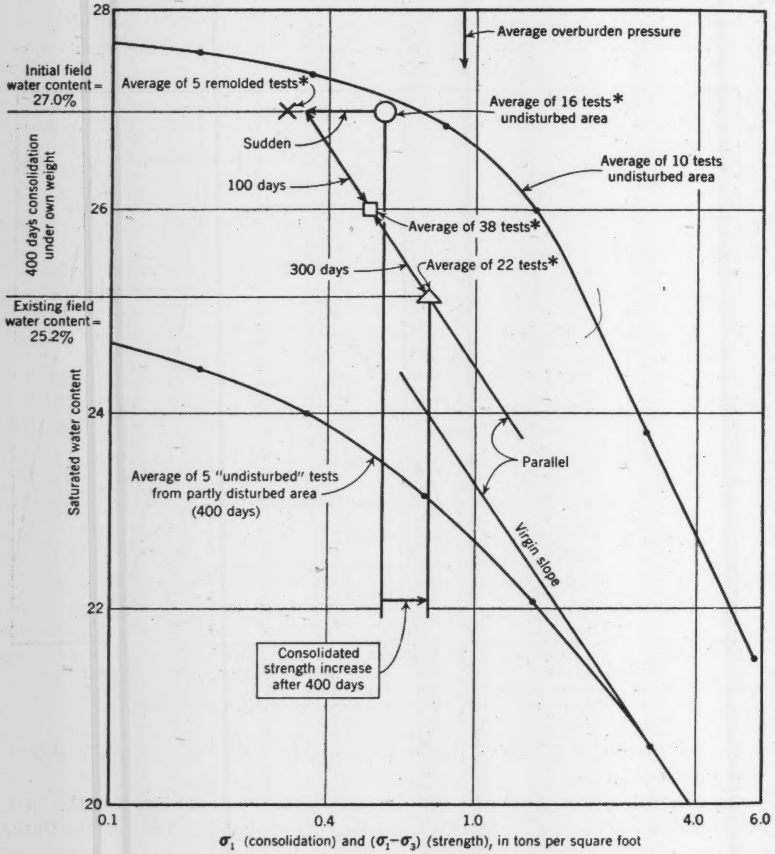

FIG. 11.—CONSOLIDATED STRENGTH INCREASE RESULTING FROM FIELD DISTURBANCE (*ALL TESTS UNCONFINED COMPRESSION)

It appears that the clay tested may have no unusual structural features but behaves in consolidation as would be predicted from laboratory consolidation tests. Because of the small variation in water content with depth, it appears probable that other variables, such as soil variation, degree of disturbance, and test technique, may predominate and completely account for the reported lack of trend in the unconfined-compression-test strengths.

Data from Another Saturated Clay.—Extensive data were obtained on the effect of partial disturbance on the compressive strength of another saturated clay. This clay is a glacial till. Its sensitivity was approximately 2.5. It had average liquid and plastic limits of 34% and 18%. A water content-consolidation data correlation, similar to that shown in Fig. 10, indicated that the water-content profile in the field was in close agreement with laboratory consolidation-test data.

Construction activities were such that the clay layer was significantly disturbed over a portion of the construction site. Three sets of "undisturbed" samples were obtained to help evaluate the cause and effect of this disturbance. Two sets were obtained within the disturbed portion of the site. One was taken about 100 days after the date of the disturbance and the other about 400 days after. The third set of samples was obtained from a portion of the same site known to be undisturbed. Lateral uniformity of the clay deposit permitted comparison of the results obtained from the three sets of samples. A summary of the results of the consolidation and unconfined compression strength tests from these samples is presented in Fig. 11.

As may be seen in Fig. 11, the clay disturbed in the field has become consolidated under its own weight thereby losing an average of 1.8% of its water content in 400 days. This is about one half the ultimate expected decrease in water content resulting from this consolidation.

It may also be seen that immediately after the disturbance the clay lost strength. As it was consolidated it regained this strength so that after 400 days its strength was approximately 33% greater than the average laboratory strength value obtained from samples from the undisturbed part of the site. Although it is possible that the 400-day strength is still less than the completely undisturbed field strength, it is expected that the 50% consolidation still to be achieved will increase the disturbed sample strength to about 1.9 tons per sq ft. This value should be much greater than the undisturbed field strength.

This, then, is another instance in which the consolidated strength of partly disturbed samples is significantly greater than the true strength in the field. This situation could have occurred in the laboratory as it did in the field.

As shown by the example in Fig. 11, a certain amount of consolidation is necessary before the disturbed-sample strength can "catch up" to the completely undisturbed strength. Thus, it is believed that Fig. 8 is in error in the range of low normal stresses. At 0 normal stress (unconfined compression test) the unconsolidated natural void ratio condition exists. As discussed previously, under the heading, "The Rutledge Hypothesis on Sample Disturbance," at constant void ratio, the least disturbed sample has the greatest strength. Therefore, the undisturbed Mohr stress envelope must be above that for the partly remolded samples at low consolidating stresses and must cross it and become lower at higher stresses.

Silts.—It is sometimes desirable to make a laboratory determination of the angle of internal friction of cohesionless, or near-cohesionless, silts. Saturated natural silt soils are often highly sensitive to sample disturbance and may easily become quick when handled. It is often almost impossible to obtain samples and trim specimens without significant and noticeable sample disturbance. Therefore, this is a situation in which great additional consolidation due to sample disturbance may be expected, with the possibility that consolidated-strength tests may yield friction angles that are entirely too large for the soil in its natural state.

As examples of this difficulty, results of triaxial consolidated-quick tests for two sensitive natural silt soils are presented in Fig. 12. Fig. 12(*a*) shows results from a slightly clayey silt with approximately 80% of the grains in the silt size range (MIT (Massachusetts Institute of Technology) classification). Fig. 12(*b*) shows results from a cohesionless fine sandy silt.

The writer believes that the friction angles of 29° and 47° determined from these tests are considerably in excess of the true strengths. Perhaps the most plausible explanation is that additional consolidation took place because of sample disturbance and, therefore, the natural soil was not tested each time but instead an appreciably denser sample with each increased lateral pressure. Inspection of the decrease in water contents at failure of the saturated samples supports the foregoing explanation.

Simplified Test and Analysis Procedure.—Mr. Calhoon has recommended a test series and analysis procedure in order to determine by extrapolation the variation of the completely undisturbed field strength with the void ratio. His recommendation probably represents the most thorough approach to the problem. However, the writer questions the general practicability of so extensive a laboratory test series. An alternate method is herein suggested which requires a simpler procedure and fewer laboratory tests.

Instead of consolidated-quick triaxial strength tests on series of "undisturbed" and remolded samples, the writer recommends that these samples be cut and slowly dried until the approximate desired void ratio is reached and that they then be tested for strength using the unconfined compression test. As may readily be seen in Fig. 14—in which the crosses represent results of unconfined compression tests of slowly dried samples (except within the natural density area)—void-ratio reduction by slow drying can be substituted for triaxial consolidation. In Fig. 14, L_w indicates liquid limit, P_w indicates plastic limit, and G is the specific gravity of solids.

When preparing slowly dried test samples, it is important that the drying be slow enough to permit water migration to the surface and thereby eliminate possible formation of a "crust" of drier clay at the sample surface. Clays containing sand or very silty layers may prove difficult to slow-dry uniformly without developing partings or warping. Triaxial testing would be the best procedure for such clays.

The foregoing suggested substitution would offer a number of important advantages. The unconfined test equipment is less expensive, more generally available, and requires far less preparation and testing time. Unconfined samples can conveniently be cut to any size or shape, up to the maximum diameter of the undisturbed sample. Triaxial specimens, on the other hand, may be limited by the triaxial equipment. As Mr. Calhoon explained, the

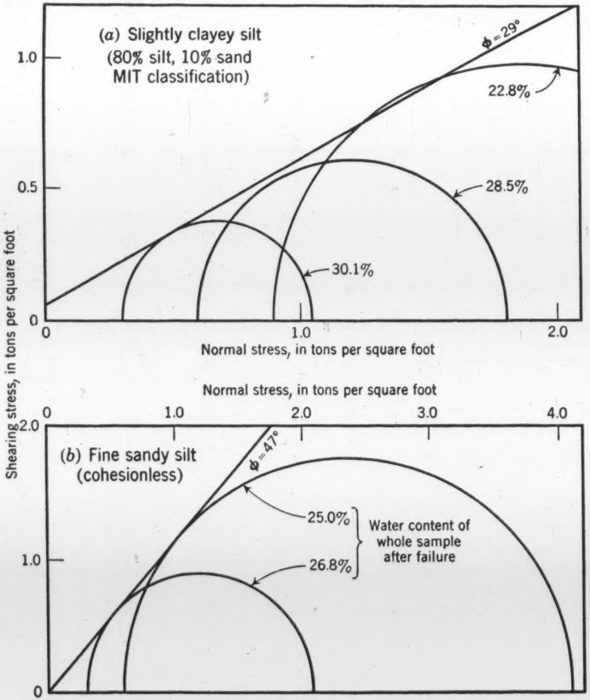

FIG. 12.—CONSOLIDATED-QUICK SHEAR TESTS ON NATURAL SILTS

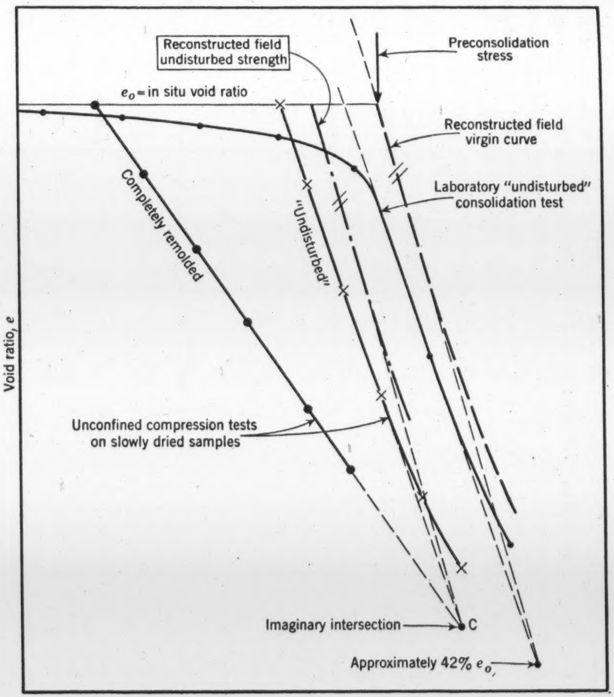

FIG. 13.—ALTERNATE METHOD OF RECONSTRUCTING THE FIELD UNDISTURBED STRENGTH

trimming disturbance of his 1.4-in.-diameter triaxial samples was proportionally larger than the disturbance of the 1.5-in.-thick consolidation sample, thus necessitating a triaxial consolidation curve for comparison purposes. Unconfined samples can be cut large enough so that trimming disturbance will be approximately the same (equal surface areas per unit volume) as that of the least disturbed (largest) "undisturbed" consolidation-test sample.

Referring to Fig. 13, let it be assumed that the "undisturbed" and remolded series of slowly dried unconfined compression strength tests and the "undisturbed" consolidation test are completed. These are the only tests required.

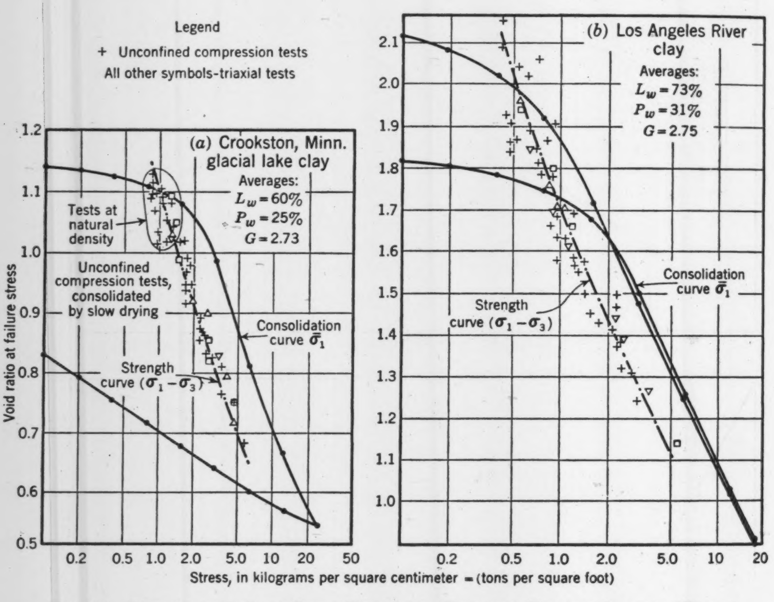

FIG. 14.—COMPARISON OF SLOW-DRIED UNCONFINED TESTS AND TRIAXIAL STRENGTH TESTS

The following procedure is recommended for extrapolating the field compressive strength curve:

1. The first step is to reconstruct the undisturbed field consolidation curve. It is recommended that this be done according to the procedures described elsewhere by the writer.[20] In this case one is interested in the slope of the virgin curve in the vicinity of the natural void ratio, which is generally the void ratio range of practical interest. The recommended procedure is sufficiently accurate for this purpose and requires no completely remolded or reduced thickness consolidation tests.

2. Next, point C must be determined. As shown in Fig. 13, this point is determined from the "undisturbed" and remolded e against $(\sigma_1 - \sigma_3)$-curves by

extending them as straight lines until they intersect at C. These lines are drawn so as to continue the slope of the strength curves at the void ratio at which the clay was disturbed. The strength-curve slopes are essentially constant for moderate decreases from this void ratio, and the proper extension slope is easily determined.

3. The last step is to make use of the Rutledge parallel relationship and construct a line through point C and parallel to the reconstructed field virgin curve. As shown in Fig. 13, the upper part of this constructed line forms the basis for the curve of the reconstructed field undisturbed strength.

The significance of point C will next be explained. One knows from the nature of the sample disturbance effect on the curves of consolidation e against the logarithm of the pressure[19,20] that the virgin slope decreases in magnitude and is displaced to the left with increasing sample disturbance. All data indicate that disturbance has this effect on the curve of the void ratio against compressive strength $(\sigma_1 - \sigma_3)$. As with the consolidation test, the process is continuous—increments of increased disturbance result in increments of slope flattening and displacement to the left.[7,19,20] It is assumed here that all the strength slopes, from the completely undisturbed to the completely remolded, are radial with a common center, point C.

One may note that, in Fig. 7, a C-point at 33% and 9 tons per sq ft would be a reasonable common intersection point for the three strength curves presented. It should be stated that, although the C-point assumption is believed by the writer to be approximately correct, it is conceivable that its use may yield undisturbed-strength extrapolations that are too high. Research to determine the manner in which these slopes intersect would be valuable.

The strength slopes should be determined over a moderate void-ratio range below the void ratio at which the disturbance occurred—at greater ranges the clay structure is significantly changed by the consolidation with the often observed result that, on the semilogarithmic plot, the strength-curve slope gradually flattens, thereby increasing the rate of strength gain with further void-ratio reduction.

The strength correction procedures suggested by Mr. Calhoon and the writer have yet to stand the hard test of practical utilization. Such experience with the latter is limited to two jobs, both dealing with sensitive marine organic clays.

On one job a strength correction analysis indicated that the laboratory-tested samples had greatly reduced strengths as a result of sample disturbance. New samples were obtained with a better sampler. The new strengths proved significantly higher than the original values but were still below the analysis-predicted, completely undisturbed values. The new strength values were successfully, and perhaps conservatively, used for design. On the other job, a two-dimensional stability analysis indicated a factor of safety of 0.85 when laboratory "undisturbed" strengths were used. The use of disturbance-corrected strength values yielded a factor of safety of 1.1. It was decided to use the latter. The fully loaded structure has proved stable.

It would be valuable if Mr. Calhoon would present any experiences he or others have had using the correction procedure he presented.

Acknowledgments.—The concepts presented in Fig. 9 were obtained from the class notes of a soil mechanics course taught by Mr. Rutledge in 1951 at Northwestern University.

The data in Figs. 10 and 14 were obtained from Mr. Osterberg, professor of civil engineering at Northwestern University. The tests were performed at Northwestern University.

The data in Figs. 11 and 12 were obtained from the files of Moran, Proctor, Mueser & Rutledge, consulting engineers, New York, N. Y. James D. Parsons, M. ASCE, supervised the analysis presented in Fig. 11.

MAX L. CALHOON,[21] J.M. ASCE.—The writer appreciates Mr. Schmertmann's thoughtful discussion and particularly his excellent explanation of the Rutledge hypothesis concerning the effects of sample disturbance on test results of undisturbed soil samples.

It may be of interest, in connection with the phenomenon of the compressive strength increasing exponentially as the failure void ratio (or water content) decreases arithmetically, that, in addition to saturated clays, it has been found that saturated peat soils behave in the same manner. Fig. 15 shows a typical example. It can also be seen that the compressive-strength curve is essentially parallel to the triaxial-consolidation curve.

Mr. Schmertmann has presented some very interesting data on the strength of a remolded saturated clay that was remolded during construction operations. As shown in Fig. 11, the a_r-value is negative. It may be seen in Fig. 7 that the a-values for both the completely remolded and undisturbed specimens (approximately 50% remolded) are negative. It is the opinion of the writer that a negative a-value indicates serious disturbance and that when this is found in presumably undisturbed samples, serious disturbance has actually occurred and the test results should be corrected before the data are used in design.

Mr. Schmertmann states that he believes that Fig. 8 of the paper is in error in that the undisturbed Mohr stress envelope must be above that for the partly remolded samples at low consolidating stresses and must cross it and become lower at higher stresses. An explanation as to how Fig. 8 was plotted is therefore warranted. The ordinates are equal to $(\sigma_1 - \sigma_3)/2$ and the abscissas are equal to $\sigma_3 + (\sigma_1 - \sigma_3)/2$. To plot a graph similar to Fig. 8 from Fig. 9, the shear strength for point 5 (equal to one half the compressive strength at point 5) would be plotted at a normal pressure of zero plus one half point 5, for point 6 at zero plus one half point 6, and for point 1 at A plus one half point 1. It is believed that Mr. Schmertmann was plotting point 1 at zero plus one half the compressive strength at point 1 which is incorrect. Therefore, Fig. 8 is correct as shown.

The writer agrees completely with Mr. Schmertmann on the impracticability of the laboratory test series for the evaluation of strength data presented in the original paper. A simpler approach must be found. Mr. Schmertmann has proposed a tentative procedure, but the writer does not favor it for several reasons. Mr. Schmertmann has gone to great length to extrapolate a field virgin consolidation curve that depends on reliable knowledge of the natural void ratio and preconsolidation pressure in the field. It has long been known that, for normally loaded clays, if the natural void ratio and preconsolidation pressure in the field are known, a virgin consolidation curve passing through this point on a graph and either parallel to or slightly steeper than the best laboratory virgin consolidation curve represents an acceptable field consolidation curve. It is not believed that Mr. Schmertmann's concept of the initial virgin slopes of all consolidation curves passing through a common point at 42% of the initial void ratio is any more accurate or more acceptable than the foregoing method. He has then further assumed that all curves relating the void ratio to the logarithm of the compressive strength pass through a common point and he gives such a point for the data in the paper as 33% water content and 9 tons per sq ft compressive strength (Fig. 7). If the field-strength curve were not

---

[21] Soils Engr., Howard, Needles, Tammen and Bergendoff, New York, N. Y.

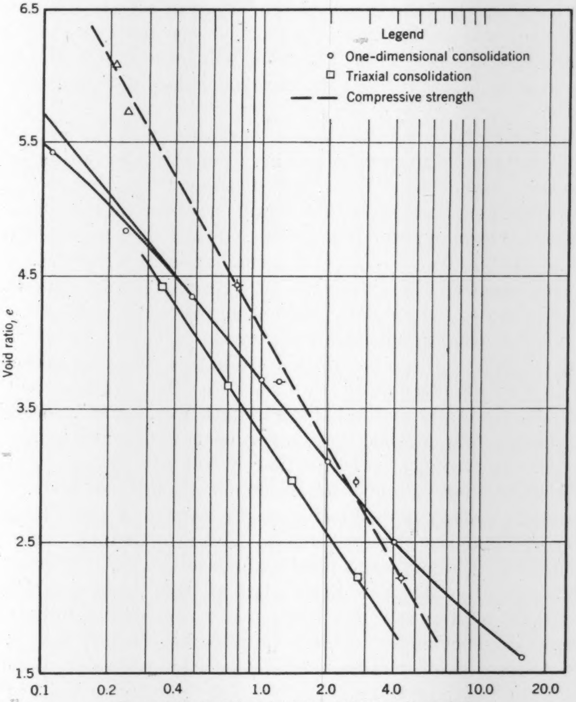

FIG. 15.—CONSOLIDATION AND STRENGTH CURVES FOR A PEAT SOIL

already plotted in Fig. 7 for reference, it is believed that a different point, say, 34% and 4 tons per sq ft would logically have been chosen by Mr. Schmertmann and would result in a field-strength curve that would be quite different from that shown in Fig. 7.

Mr. Schmertmann has also stated in his method that unconfined compression samples could be cut large enough so that trimming disturbance would be approximately the same (equal surface areas per unit volume) as that of the least disturbed consolidation test sample. By this statement Mr. Schmertmann apparently assumes that the depth of remolding in a triaxial specimen is approximately the same as that in a consolidation specimen due to the sampling and trimming operations. From Fig. 15 it will be seen that the triaxial consolidation curve is below the one-dimensional consolidation curve. The triaxial specimen was 1.4 in. in diameter by 2.8 in. in length, and the one-dimensional consolidation specimen was 2.5 in. in diameter by 0.75 in. in thickness. Therefore, if the remolding was to be the same depth in both specimens, the triaxial specimen should have been remolded to a lesser degree than the one-dimensional specimen, and the triaxial virgin curve should have been above the one-dimensional virgin curve. It is concluded that the two different trimming operations do not produce comparable disturbance, and therefore a consolidation curve representing the same amount of remolding as does the strength curve is a necessity to the strength evaluation procedure, so that the remolding can be included in the strength computations.

The writer here proposes an untried strength evaluation procedure in the interest of sharing his ideas on the subject with other engineers with the hope that eventually a simple and reliable strength evaluation procedure will be found. Although this method has never been tried in the laboratory, all available evidence strongly indicates that it will prove workable. This proposed method requires two one-dimensional consolidation tests, two triaxial shear tests, and as many unconfined strength tests (or triaxial tests if desired) as necessary to define two strength curves. Four unconfined compression tests would probably be the minimum possible for use.

It was shown by Mr. Van Zelst[7] that all significant remolding to one-dimensional consolidation samples occurs in trimming and planning the horizontal surfaces of the specimens. This is revealed by the fact that specimens of various thicknesses show virgin consolidation curves that are displaced vertically so that the two equations presented subsequently as Eq. 1 and Eq. 2 are satisfied. Therefore, peripheral disturbance is apparently negligible. On the basis of the foregoing, a simpler method of extrapolating the field virgin consolidation curve than that proposed by Mr. Van Zelst and used in the writer's paper has been found.

If it is assumed that the depth of remolding in one-dimensional consolidation specimens of the same area is equal in specimens of all thicknesses, it can be shown that the ratio of percentage of disturbance in a thin specimen to that in a thick specimen is proportional to the ratio of the thickness of the thick specimen to that of the thin specimen (neglecting peripheral disturbance). In equation form:

$$R = \frac{T_1}{T_2} \qquad \text{(1)}$$

in which R is the ratio of disturbance of the thin specimen to that of the thick specimen, T_1 is the thickness of the thick specimen, and T_2 is the thickness of the thin specimen. From Fig. 16 it may be seen that the vertical distance from curve 1 to curve 3 must be R times the vertical distance from curve 1 to curve 2 because distances in the vertical direction are proportional to the percentages of

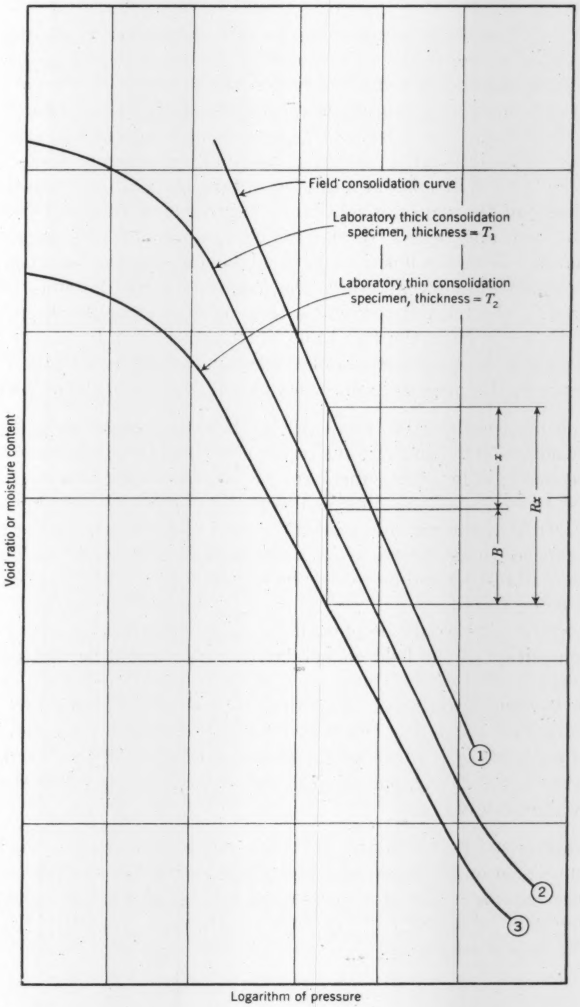
Field consolidation curve
Laboratory thick consolidation specimen, thickness = T_1
Laboratory thin consolidation specimen, thickness = T_2
x
Rx
B
①
②
③
Void ratio or moisture content
Logarithm of pressure

FIG. 16.—METHOD OF EXTRAPOLATING THE FIELD CONSOLIDATION CURVE

disturbance as shown by Mr. Van Zelst.[7] In equation form:

$$\left.\begin{aligned} R &= \frac{B + x}{x} \\ \text{or} \qquad x &= \frac{B}{R - 1} \end{aligned}\right\} \qquad (2)$$

Because R and B are known quantities, x can be computed at various pressures and the location of the field virgin consolidation curve can be plotted.

To evaluate the strength characteristics, two strength curves are required—one obtained from small compression specimens—say, 1.4 in. in diameter by 2.8 in. in length and the other from large compression specimens, say, 2.8 in. in diameter by 5.6 in. in length. At least one small specimen and one large specimen must be tested in triaxial shear to obtain triaxial consolidation curves. The remainder of the strength specimens may be consolidated by slow-drying in a humid room and tested by unconfined compression as suggested by Mr. Schmertmann. With the positions of the field consolidation curve and the two triaxial consolidation curves known, the R-value for triaxial consolidation can be computed. The triaxial R-value is then used to compute the position of a field-strength curve from the two known strength curves by use of Eq. 2 in a manner similar to the computation of the position of the field consolidation curve.

In summary, the procedure proposed herein consists of the following points.

1. Using undisturbed soil, one consolidation test would be performed in a thick ring and one in a thin ring; one triaxial test on a large specimen and one on a small specimen; at least two unconfined compression tests on large specimens and at least two on small specimens all consolidated by slow-drying. (It must be emphasized that the unconfined compression specimens must be trimmed by the same procedure as the triaxial specimens were trimmed.) The foregoing is a minimum of testing and more may be required, depending on the uniformity of the soil being tested.
2. All test results would be plotted on the same graph.
3. The position of the field consolidation curve would be plotted by use of Eqs. 1 and 2.
4. The R-value for triaxial consolidation would be computed by use of the field consolidation curve, the two triaxial consolidation curves, and Eq. 2.
5. The field-strength curve would be plotted by use of the triaxial R-value found in step 4 and Eq. 2, the x-value and B-value being referred to the two laboratory strength curves.

It is emphasized that this procedure has never been tried in the laboratory but is proposed in order to provoke more thought on the subject.

Acknowledgments.—The data presented in Fig. 15 were obtained from the files of the soils laboratory of the firm of Howard, Needles, Tammen and Bergendoff, New York, N. Y.

AMERICAN SOCIETY OF CIVIL ENGINEERS
Founded November 5, 1852
TRANSACTIONS

Paper No. 2828

THE BOX INLET DROP SPILLWAY AND ITS OUTLET

By Fred W. Blaisdell,[1] M. ASCE, and
Charles A. Donnelly[2]

With Discussion by Messrs. Neal E. Minshall; and Fred W. Blaisdell and Charles A. Donnelly

Synopsis

Model experiments were performed to determine the free-flow capacity and the effect of submergence on flow over box inlet drop spillways; the development of a spillway outlet is described. Data are presented for the determination of both the free-flow capacity and the hydraulic proportions of the outlet structure; design data for the effect of submergence are omitted as they are quite voluminous.

Two control sections—the crest of the box inlet and the headwall opening—are shown to govern the head-discharge relationship; the control section changes from the former to the latter as the flow increases. Flow over the box-inlet crest is affected by the head on the box inlet, the shape of the box inlet, the width of the approach channel, and the location of the dikes. These effects are described, and the corrections which must be applied to the discharge coefficient are evaluated for a wide range of conditions. When the control section is at the headwall opening the discharge coefficient varies with the depth of the box inlet. In addition, the head, which is measured from the crest of the box inlet, must be corrected by adding a quantity which is a function of the relative depth of the box inlet.

Submergence greatly affects the flow through box inlet drop spillways. The effect decreases as the flared outlet is widened and varies with the discharge—the greatest effect occurring at the discharge at which the free-flow control changes from the box-inlet crest to the headwall opening.

Note.—Published, essentially as printed here, in November, 1954, as *Proceedings-Separate No. 534*. Positions and titles given are those in effect when the paper or discussion was approved for publication in *Transactions*.

[1] Project Supervisor, Agri. Research Service, U. S. Dept. of Agriculture, St. Anthony Falls Hydr. Lab., Minneapolis, Minn.

[2] Hydr. Engr., Agri. Research Service, U. S. Dept. of Agriculture, St. Anthony Falls Hydr. Lab., Minneapolis, Minn.

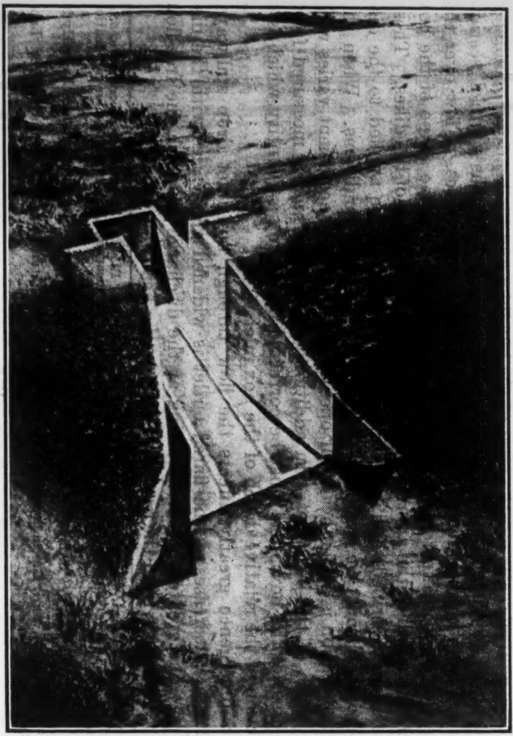

Fig. 1.—A Spillway and Its Outlet

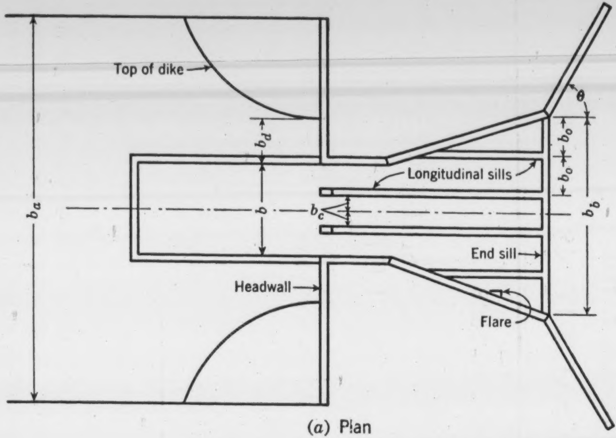
Top of dike
b_d
b_a
b
b_c
Headwall
Longitudinal sills
End sill
Flare
θ
b_o
b_o
b_b

(a) Plan

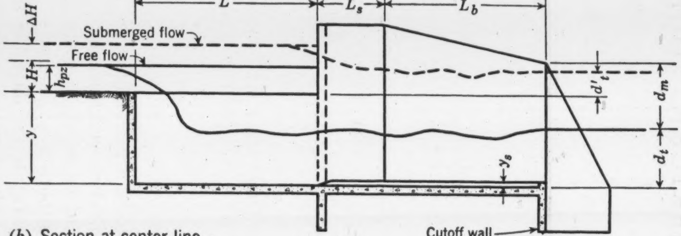
L
L_s
L_b
ΔH
Submerged flow
Free flow
H
h_{pz}
y
y_s
d'_t
d_m
d_t
Cutoff wall

(b) Section at center line

Fig. 2.—Proportions and Dimensions of a Spillway

The outlet structure can be adjusted to fit a wide variety of field conditions. It is possible to lengthen the straight section and to cover it to form a highway culvert. The stilling-basin sidewalls can be flared, if desired, thus permitting discharges into a narrow channel or onto a wide flood plain. Flaring the sidewalls also makes it possible to adjust the tailwater depth to the depth naturally available.

Introduction

The box inlet drop spillway can be described as a rectangular box open both at the top and at the downstream end; an outlet structure is attached to the open end of the box inlet. A spillway and its outlet are shown in Fig. 1, and their general proportions and dimensions are defined in Fig. 2. Runoff water is directed to the crest of the box inlet by earth dikes and headwalls, enters over the upstream end and two sides, and leaves the spillway and enters the outlet through the open downstream end. The long crest of the box inlet permits large flows to pass with relatively low heads and correspondingly low dikes, yet the width of the spillway need be no greater than that of the downstream channel.

There are uses for the box inlet drop spillway in the fields—among others—of irrigation, drainage, gully control, water conservation, and highways. In the field of soil and water conservation, it is used as a gully control structure and as an outlet for artificial ponds to control vertical drops of from 2 ft to 12 ft. As a drainage structure it is used to permit excess surface water to enter the drainage ditch without causing erosion of the ditch head or banks and at the same time it provides an outlet structure for drainage tile. In highway use the so-called straight section of the outlet can be lengthened and covered to form a culvert. The cases in which the special characteristics of this type of spillway can be utilized are numerous.

Previous Work

The earliest investigation of box inlet drop spillways is that reported[3] by Lewis H. Kessler, M. ASCE, in 1934. Some use of these results was made during the 1930's but they are now (1955) considered to be obsolete.

A more complete series of experiments was reported[4] by A. N. Huff in 1944. The results of these experiments apply particularly to entrances to chute spillways. Messrs. Huff and Kessler both found that a level approach (as compared to a deeper approach) serves to lower capacity. Mr. Huff presented some data indicating the great effect of the width of the approach channel on flow capacity and also briefly cited the effect of submergence; the latter points are investigated fully herein.

Studies of outlets for box inlet drop spillways were initiated late in 1942 and were reported on[5] by Mr. Huff in 1944. Because the outlet reported by

---

[3] "Experimental Investigation of the Hydraulics of Drop Inlets and Spillways for Erosion Control Structures," by L. H. Kessler, *Series No. 80*, Bulletin, Univ. of Wisconsin Eng. Experiment Station, Madison, Wis., 1934, pp. 56–66.

[4] "The Hydraulic Design of Rectangular Spillways," by A. N. Huff, *SCS-TP-71*. Soil Conservation Service, U. S. Dept. of Agriculture, Washington, D. C., February, 1944.

[5] "Progress Report on Design of an Outlet Structure for Head Spillways," by A. N. Huff, Soil Conservation Service, U. S. Dept. of Agriculture, Washington, D. C., December, 1944.

Mr. Huff is limited in its application, a new outlet for box inlet drop spillways was developed by the junior writer.[6] This design results in a backwater effect on the flow over the crest of the box inlet if the drop in the box inlet is low or if the flows are high enough to submerge the box-inlet crest. Therefore, the discharge tables presented by Mr. Huff[4] are invalid for many flows through box inlet drop spillways. The submergence data presented by Mr. Huff[4] also are invalid as a result of the change in outlet design. The necessity for additional studies thus becomes apparent.

NOTATION

The letter symbols adopted for use in this paper are defined where they first appear and are arranged alphabetically, for convenience of reference, in the Appendix.

EXPERIMENTAL PROGRAM

The information presented herein is based on extensive programs of experimental investigation. The free-flow and submerged-flow studies comprise 361 tests, each test differing in some respect from the others and each requiring approximately 35 runs made with differing flow conditions. The design procedure related to discharge is based on more than 12,000 runs. Similarly, the outlet design is based on 386 tests representing (*a*) the exploratory tests determining the general form of the outlet, (*b*) the tests determining the general design rules for each element of the outlet, and (*c*) the tests verifying the design rules. Subsequently, the outlet design was modified slightly as a result of special wingwall studies. Details of the test programs are cited subsequently under the three subdivisions into which it is convenient to divide the studies—that is, free-flow tests, submerged-flow tests, and outlet tests.

Free-Flow Tests.—An analysis of the dimensions of several box inlets constructed by the Soil Conservation Service of the United States Department of Agriculture (SCS) indicated that relative box-inlet depths, y/b, ranging from 1/8 to 1 and relative box-inlet lengths, L/b, ranging from 0.25 to 2 would cover the anticipated range of field conditions although the range of tests for L/b was from 0 to 4; b is the width, y is the depth, and L is the length, respectively, of the box inlet drop spillway.

Because Mr. Huff's investigation[4] indicated little effect of approach-channel width when $b_a/L_c \geq 3$, this width was adopted as standard for the tests. However, in order to determine independently the effect of approach-channel width, tests were made with relative approach-channel widths, b_a/L_c, as narrow as 0.4 and as wide as 10; b_a is the approach-channel width, and L_c is the crest length, equivalent to $2L + b$.

The magnitudes of the several variables for which free-flow tests were run are presented in Table 1(*a*). However, not all combinations of these variables were tested.

Submerged-Flow Tests.—Approximately 50 exploratory tests were made before the program of submergence tests was planned. Indications were that a considerable number of tests would be required to define the submergence effect properly. Considerable thought was given to this phase of the test program in order to reduce the number of tests to a minimum but still to cover the range of conditions anticipated in the field. The values of the variables utilized during the test program are given in Table 1(*b*); in Table 1(*b*), b_b is the width of the exit from the stilling basin and Q is the discharge.

---

[6] "Design of an Outlet for Box Inlet Drop Spillway," by C. A. Donnelly, *SCS-TP-63*, Soil Conservation Service, U. S. Dept. of Agriculture, Washington, D. C., November, 1947.

Outlet Tests.—It was not possible to design in advance any clear-cut program for the outlet tests. Nevertheless, the program can be divided into three phases—the exploratory tests, the evaluation tests, and the check tests. The initial tests were exploratory and served to determine the important features of the outlet in a general way. During the next phase of the study, the proportions of the various features were varied one by one to discover how the performance of the outlet was affected. The final phase of the study was begun after the design rules had been developed. These rules were checked by designing a series of outlets and testing them under the range of conditions that each was supposed to accommodate.

APPARATUS AND PROCEDURE

Two different test arrangements were used for these tests; both are described herein.

Free-Flow and Submerged-Flow Tests.—The experimental arrangement used for the study of the box inlet drop spillway was especially designed for the submergence tests. The special features incorporated in it also facilitated the rating tests. A general view of the setup is shown in Fig. 3(*a*).

TABLE 1.—VALUES OF VARIABLES

Variable	(*a*) Free-flow tests	(*b*) Submerged-flow tests
L/b	0, 0.25, 0.5, 1, 2, 3, 4	0.5, 1, 2
y/b	1/8, 1/4, 1/2, 1	1/4, 1/2, 1
b_a/L_e	0.4, 0.6, 0.8, 1.0, 1.15, 1.3, 1.5, 2.0, 3.0, 5.0, 10.0	
b_b/b		1.0, 1.25, 1.5, 2.0
$Q/b^{5/2}$		0.6, 1.0, 1.5, 2.0, 3.0, 4.0, 6.0

The approach-channel floor was made of cement mortar and was level with the crest of the box inlet. The headwater piezometer opening was located at the center of the channel, 3.5 ft upstream from the headwall. The tailwater piezometer opening was located 5 ft downstream from the headwall. Point gages were used to determine the water levels, and water-level recorders were used for control purposes. The recorders served to increase the reliability of the reading as well as to save time.

Outlet Tests.—The arrangement of the test apparatus for the outlet tests is shown in Fig. 3(*b*). All models were halved (split along their longitudinal center lines) and set against a glass panel in the channel as previous experiments had shown that identical results could be obtained from full and half models.

Near the conclusion of the tests, this half-model method of conducting tests was checked on a full model half the size of the half models. This model is shown in Fig. 4(*c*). After the full model had been tested, a lucite plate was placed at the center line of the structure to give, in effect, two half models as

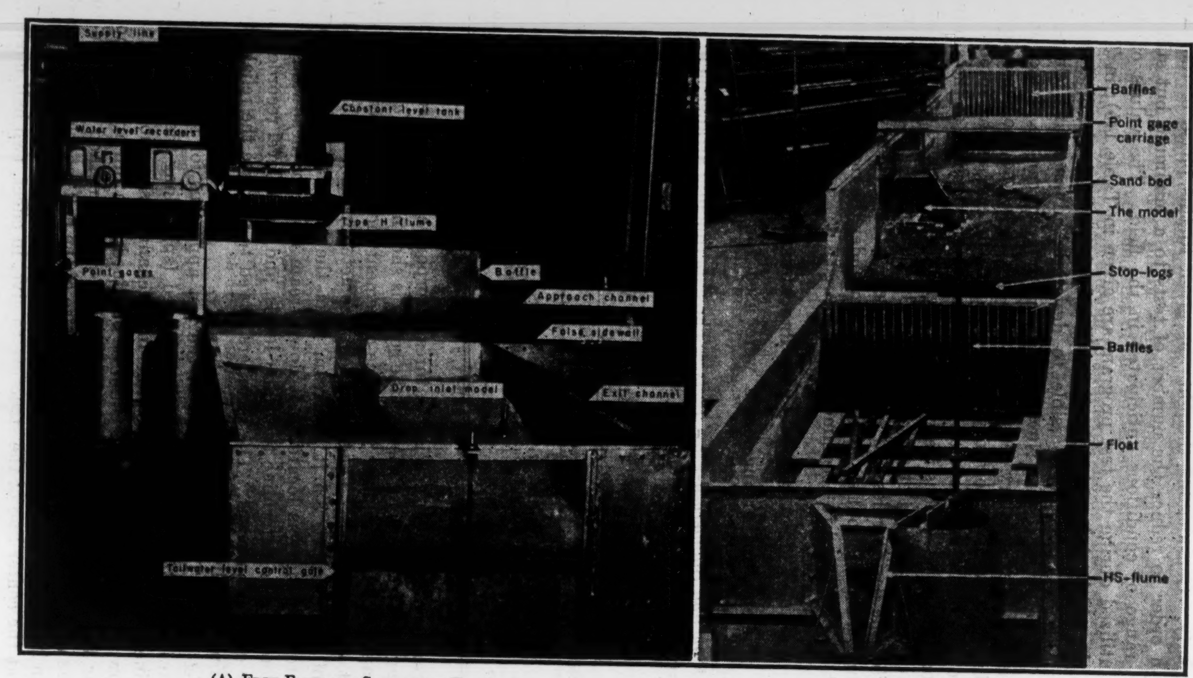
Supply line
Constant level tank
Water level recorders
Type H flume
Point gages
Baffle
Approach channel
False sidewall
Drop inlet model
Exit channel
Tailwater level control gate
Baffles
Point gage carriage
Sand bed
The model
Stop-logs
Baffles
Float
HS-flume

(A) Free Flow and Submerged Tests

(B) Outlet Tests

Fig. 3.—Test Arrangement

shown in Fig. 4(*d*), and the test was repeated. The results of the tests are shown in Fig. 4. Confetti was sprinkled on the water surface for the flow photographs (Figs. 4(*a*) and 4(*b*)) to show the stream lines. A careful comparison of the two photographs shows that the flow patterns are identical within the limits of precision of the experiment. The scour patterns are compared in Figs. 4(*c*) and 4(*d*). A small disagreement in scour patterns will be noted between the two halves of Fig. 4(*d*). However, the bed slopes are small, and a considerable displacement in plan position of the contours represents only small differences between the depths on either side of the center line.

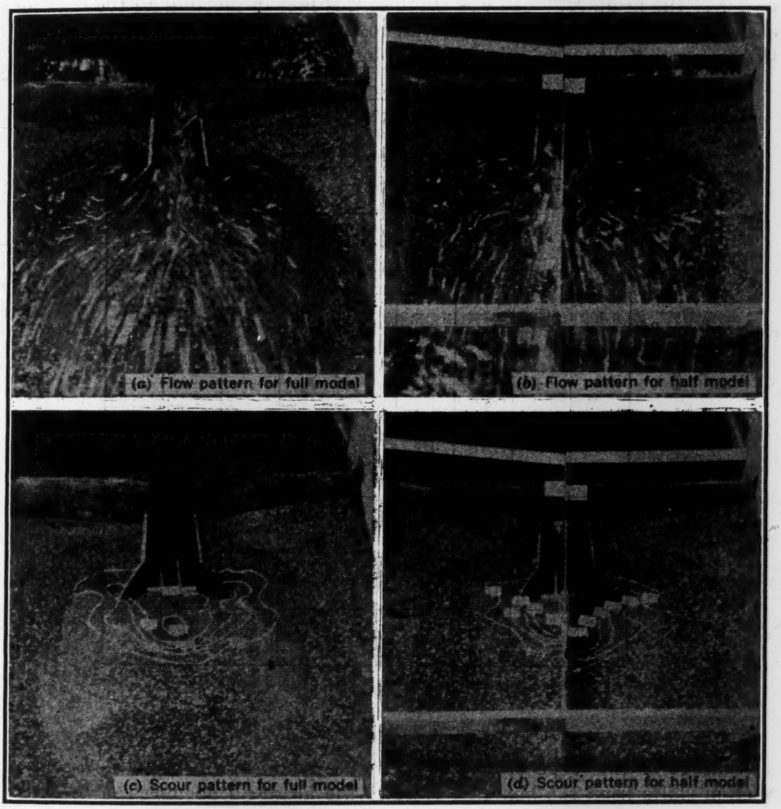
(a) Flow pattern for full model
(b) Flow pattern for half model
(c) Scour pattern for full model
(d) Scour pattern for half model

FIG. 4.—COMPARISON OF RESULTS USING FULL AND HALF MODELS

Ordinary concrete sand passing an 8-mesh screen was used for the stream bed downstream from the outlet. The erosion of the sand bed below the level of the outlet floor was used as a measure of the efficiency of the outlet.

RESULTS OF FREE-FLOW TESTS

Considerable study was necessary to find the best method for analyzing the data. The adopted method is described subsequently and is followed by separate presentations of the results obtained when the control was at the box-inlet crest and when it was at the headwall opening.

Analysis of Data.—Both the flow, Q, over the crest of the box inlet and that through the headwall opening are theoretically proportional to the three-halves power of the head, H. Use was made of this fact in plotting all the data for each test on a single sheet. However, to simplify the analysis, both terms in this proportionality were raised before plotting to the two-thirds power. The advantage of this type of plot is that the point at which the flow-control section shifts from the box-inlet crest to the headwall opening can be determined readily. Furthermore, if the data points fall on a straight line, it is an indication that the theoretical exponent is correct.

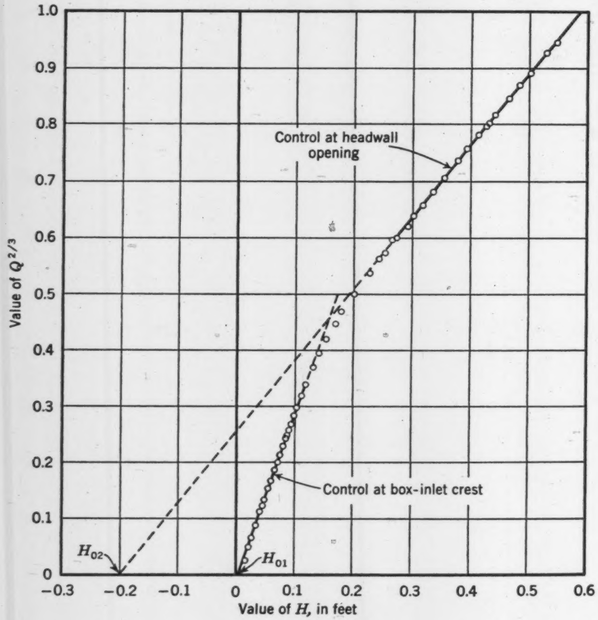

FIG. 5.—TYPICAL PLOT OF DATA

A typical plot of data is shown in Fig. 5. It will be noted that a number of points fall on neither the box-inlet crest nor the headwall-opening curves in the vicinity of their intersection; therefore, these points were not used in computing the rating curves. In addition, a few of the lowest points were discarded when they deviated from the curve, probably as a result of surface-tension effects. With minor exceptions, this deviation was characteristic of

TABLE 2.—SUMMARY OF DATA FOR FREE-FLOW TESTS WITH $b_b/b = 2.0$

Run	L/b	L/y	y/b	b_a/L_c	Eq. 1a			Eq. 1b			
					C_1	H_{01}	N	C_2	H_{02}	H_{02}/y	N
49	2.0	2.0	1.0	3.0	0.416	0.006	9	0.414	−0.370	−0.740	8
77				2.0	0.399	0.007	23	0.449	−0.335	−0.670	10
78				1.5	0.390	0.008	24	0.439	−0.340	−0.680	11
79				1.3	0.378	0.008	29	0.461	−0.318	−0.636	10
80				1.15	0.366	0.008	16	0.445	−0.332	−0.664	12
81				1.0	0.346	0.010	22	0.414	−0.364	−0.728	9
82a				0.8	0.307	0.007	20	0.560	−0.236	−0.472	5
83				0.6	0.234	0.005	13	[d]	[d]	[d]	[d]
83a				0.6	0.235	0.007	9	[d]	[d]	[d]	[d]
84				0.4	0.157	0.006	24	[d]	[d]	[d]	[d]
85	1.0	1.0	1.0	3.0	0.429	0.004	14	0.432	−0.253	−0.506	9
114				2.0	0.416	0.004	16	0.423	−0.263	−0.526	10
115 & 115*a*				1.5	0.407	0.005	13	0.433	−0.252	−0.504	21
116				1.3	0.400	0.006	11	0.446	−0.239	−0.478	7
117				1.0	0.364	0.006	13	0.468	−0.213	−0.426	8
118				0.8	0.304	0.005	16	[e]	[e]	[e]	[e]
119				0.6	0.228	0.007	23	[d]	[d]	[d]	[d]
120				0.4	0.153	0.006	13	[d]	[d]	[d]	[d]
121				1.15	0.385	0.006	12	0.434	−0.249	−0.498	8
122				5.0	0.431	0.005	11	0.410	−0.280	−0.560	6
123	0.5	0.5	1.0	10.0	0.436	0.005	9	0.402	−0.152	−0.304	6
124				0.6	0.234	0.008	23	[d]	[d]	[d]	[d]
125				0.8	0.302	0.004	25	[d]	[d]	[d]	[d]
126				1.0	0.364	0.006	10	0.457	−0.119	−0.238	11
127				1.15	0.396	0.006	8	0.430	−0.142	−0.284	11
128				1.3	0.410	0.006	6	0.377	−0.197	−0.394	7
129				1.5	0.421	0.006	11	0.384	−0.183	−0.366	13
130				2.0	0.439	0.007	7	0.393	−0.169	−0.338	11
131				5.0	0.433	0.004	6	0.394	−0.160	−0.320	11
132				3.0	0.445	0.006	13	0.398	−0.158	−0.316	13
165	0.25	0.25	1.0	3.0	0.405	0.000	7	0.424	−0.059	−0.118	15
166				2.0	0.397	−0.003	8	0.434	−0.060	−0.120	17
167	0.0	0.0	1.0	3.0	0.423	0.002	24	0.423	0.002	0.004	25
168				2.0	0.446	0.007	25	0.446	0.007	0.014	25
169 & 169*a*	2.0	4.0	0.5	3.0	0.392	0.004	18	0.351	−0.227	−0.908	17
226	1.0	2.0			0.419	0.004	17	0.356	−0.199	−0.796	19
227	0.5	1.0			0.447	0.005	15	0.351	−0.136	−0.544	28
252	0.25	0.5			0.429	0.001	11	0.361	−0.079	−0.316	33
253	0.0	0.0			0.420	0.002	36	0.420[a] 0.386[b]	0.002[a] −0.014[b]	0.008[a] −0.056[b]	36[a] 34[b]
254	2.0	8.0	0.25		0.411	0.005	11	0.334	−0.116	−0.928	37
285	1.0	4.0			0.388	0.002	10	0.340	−0.113	−0.904	30
324	0.5	2.0			0.467	0.007	12	0.352	−0.085	−0.680	26
330	0.25	1.0			0.476	0.005	6	0.354	−0.060	−0.480	22
331	0.0	0.0			0.456	0.006	13	0.368	−0.014	−0.112	27
332			0.125		0.417[c] 0.406	0.003[c] 0.007	4 7	0.349	−0.007	−0.112	31
333	0.25	2.0		3.0	0.459	0.010	10	0.341	−0.032	−0.512	29
334	0.5	4.0		0.6	0.208	0.011	56	0.415	0.011	0.176	56
335				1.0	0.337	0.011	10	0.356	−0.036	−0.576	28
336				1.5	0.334	0.012	7	0.346	−0.038	−0.608	30
337				3.0	0.347	0.012	6	0.341	−0.039	−0.624	32
338	1.0	8.0		0.6	0.235	0.013	12	0.349	−0.042	−0.672	25
339				1.0	0.239	0.011	10	0.340	−0.046	−0.736	28
340				1.5	0.252	0.012	8	0.345	−0.042	−0.672	31
341				3.0	0.235	0.010	12	0.343	−0.042	−0.672	33
342				0.4	0.167	0.011	10	[d]	[d]	[d]	[d]
343	2.0	16.0		0.4	0.158	0.014	7	0.346	−0.045	−0.720	29
344				0.6	0.143	0.011	11	0.346	−0.044	−0.704	33
345				1.0	0.139	0.009	11	0.343	−0.044	−0.704	29
346				1.5	0.140	0.011	10	0.343	−0.043	−0.688	38
347				3.0	0.142	0.011	9	0.338	−0.047	−0.752	30
348	4.0	4.0	1.0	2.0	0.389	0.002	24	0.361	−0.459	−0.918	23
349	3.0	3.0	1.0	2.0	0.396	0.004	18	0.399	−0.463	−0.806	21

[a] Free nappe. [b] No air under nappe. [c] No end sill. [d] No data obtainable. [e] Insufficient data.

all the data obtained during the tests. The deduction from this observation is that the theoretical exponent is correct.

The constants in the discharge equations are presented in Table 2; they were determined by the method of least squares after it was found that fitting the curves by eye resulted in intolerable personal errors. The equations used had the form,

$$Q = C_1 L_c \sqrt{2g} (H - H_{01})^{3/2} \qquad (1a)$$

for the box-inlet-crest part of the rating curve, and

$$Q = C_2 b \sqrt{2g} (H - H_{02})^{3/2} \qquad (1b)$$

for the headwall-opening part of the rating curve. In Eqs. 1, C_1 and C_2 are coefficients of discharge, g denotes gravitational acceleration, H_{01} is the apparent specific head at zero flow with control at the box-inlet crest, and H_{02} denotes the apparent specific head at zero flow with control at the headwall opening.

It will be noted that neither of the curves shown in Fig. 5 pass through the origin. This had been anticipated for the headwall-opening part of the rating curve because the assumption of the origin of heads at the crest of the box inlet is obviously incorrect. The form of Eq. 1*b* was adopted, for one reason, so that the correction H_{02} could be obtained. However, there was no reason to believe that the value of H_{01} in Eq. 1*a* would be other than zero. The fact remains that H_{01} was consistently found to be so much greater than zero that there was no doubt as to its statistical significance.

TABLE 3.—CORRECTION FOR DIKE EFFECT WITH CONTROL AT BOX-INLET CREST

Value of $\frac{L}{b}$	Value of b_d/H					
	0.0	0.7	1.4	2.9	5.7	∞
2.0 (actual)	0.84	0.85	0.93	0.97	0.99	1.00
1.0 (estimated)	0.73	0.75	0.88	0.95	0.98	1.00
0.5 (estimated)	0.60	0.62	0.82	0.92	0.98	1.00

At first it was thought that the determination of the zero reading of the head gage was in error, but repeated checks eliminated this possibility. The possibility of surface-tension effects is also eliminated by the manner in which the curve is drawn. The only conclusion that can be reached is that the significance of H_{01} has eluded detection.

Control at Crest of Box Inlet.—Four factors which affect the flow through box inlet drop spillways when the control section is at the crest of the box inlet are considered subsequently, as is the precision of the results.

Although it was shown by Messrs. Kessler[3] and Huff[4] that the level of the approach channel affects the discharge, no tests were made to evaluate this effect; the approach-channel surface was level with the box-inlet crest simulating a natural approach channel silted full.

Effect of Position of Dike.—Free access to part of the box-inlet crest is cut off as the dike is moved closer to the crest of the box inlet. Although few data were obtained, information which can be utilized to evaluate the dike effect is presented herewith for its qualitative value.

Tests were made with $b_d/H = 0, 0.7, 1.4, 2.9, 5.7$, and ∞ (no dike). The distance from the box-inlet crest to the toe of the dike b_d is zero at the point where the toe of the dike just touches the crest. The relative head H/b at which the tests were made was 0.35. Because the dike slope was 1 on 3, the toe of the dike projected upstream $3\,H$ from the headwall. The tests were conducted for only a single box inlet having a relative length $L/b = 2$. The ratio of the discharge in a spillway with a dike to the discharge in the same spillway without a dike was computed for each of the dike positions with the results shown in Table 3 for $L/b = 2$. Apparently the toe of the dike should be located from $3\,H$ to $5\,H$ from the box-inlet crest in order to minimize the dike effect.

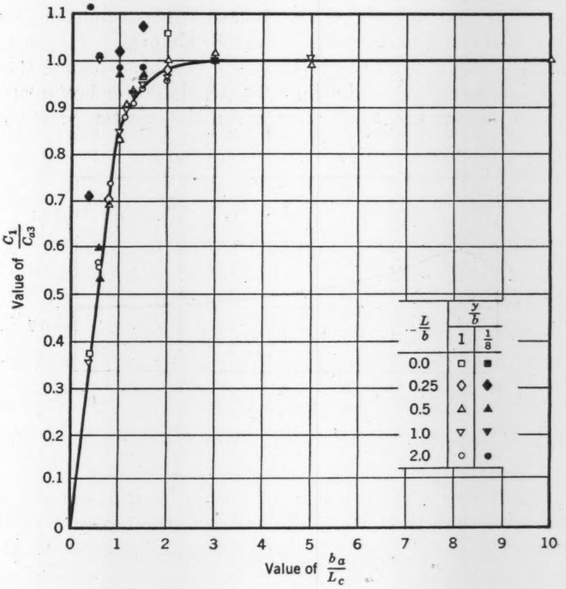

Fig. 6.—Relative Effect of Approach-Channel Width with Control at Box-Inlet Crest

If the effect of the dike on the discharge over other box inlets can be assumed to be inversely proportional to the length of the crest, then for a box-inlet shape of $L/b = 1$, in which the crest length is $3\,b$ as compared to $5\,b$ when $L/b = 2$, the decrease in the relative discharge will be $5\,b/3\,b$ or 1.7 times as great. The corresponding value for $L/b = 0.5$ is $5\,b/2\,b$ or 2.5. Based on these assumptions, Table 3 has been prepared to facilitate correcting for the dike effect. The importance of keeping the toe of the dike well away from the crest of the box inlet is quite apparent from the values shown therein.

In using the values shown in Table 3 to determine the dike effect, it should be realized that the data are too few to permit the determination of completely reliable figures. The data are presented in the absence of any better information, primarily for their qualitative value.

Effect of Approach-Channel Width.—One phase of the test program was designed to determine the effect, both quantitatively and accurately, of the width of the approach channel. The results are presented in Fig. 6 in dimensionless form. The discharge coefficient C_1 was divided by the average discharge coefficient for channel widths equal to or greater than three crest lengths, C_{a3}, before plotting so that the plotted values would indicate directly the throttling effect of the narrower approach channel. The tests with the deeper box inlets (larger y/b) are the more reliable because they cover a wider range of discharges than do those for the shallower box inlets; the data obtained for the deeper box inlets were given the greater weight in drawing the curves.

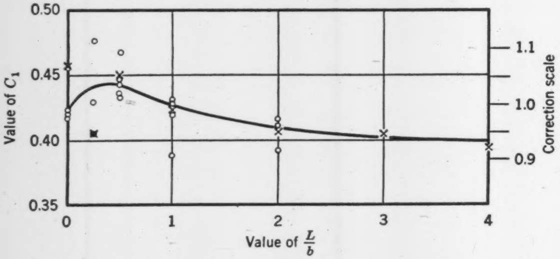

Fig. 7.—Effect of Box-Inlet Shape on Discharge Coefficient with Control at Box-Inlet Crest

The relative discharge coefficient is unaffected by approach-channel widths equal to or greater than three times the length of the box-inlet crest. Therefore, all design criteria are based on wide approach channels, and the curve in Fig. 6 is suggested for use in correcting for the effect of narrow channels.

Effect of Shape of Box Inlet.—In analyzing the results, it was observed that the coefficient of discharge C_1 in Eq. 1*a* was a function of L/b. The discharge coefficients are plotted in Fig. 7. In preparing Fig. 7, open circles were used when the relative channel width was equal to or greater than 3. The coefficients obtained from tests made with a relative approach-channel width of 2 were corrected for the effect of approach-channel width by using the curve in Fig. 6; they were used to locate the curve for the longer boxes. The corrected coefficients are plotted as crosses in Fig. 7. The data obtained for the shallowest box inlets ($y/b = 1/8$) were not plotted because the end sill caused submergence of the weir crest at all flows.

It is intended that the curve in Fig. 7 be used for design purposes. Despite the scatter in the data, particularly for the shorter box inlets (low L/b), it is felt that values taken from the curve are valid to within ±10%.

A correction scale is shown on the right side of Fig. 7. This scale is based on the assumption that no correction is required for a discharge coefficient of 0.4275 when $L/b = 1$, but that a correction is required for other box-inlet shapes.

Variation of Discharge Coefficient with Head.—Although the coefficient C_1 in Eq. 1*a* is a constant, the use of Eq. 1*a* with its zero-flow-head correction, which assures the constancy of C_1, is open to some objection. Accordingly, a method was sought to eliminate the zero-flow-head correction altogether even though this necessitated the use of a variable discharge coefficient. The resulting equation for discharge over a box-inlet crest has the form,

$$Q = C_3 L_c \sqrt{2\,g}\, H^{3/2} \qquad (2)$$

in which C_3 varies with the head.

To determine the coefficient of discharge in Eq. 2, C_3 was computed for each run of all pertinent tests. The coefficient C_3 was then corrected for the effect of approach-channel width and box-inlet shape. The corrected discharge coefficients are plotted in Fig. 8 against the relative head H/b. The only data not appearing in Fig. 8 are those obtained for shallow boxes where submergence caused by the sill at the outlet exit affects the discharge even at very low flows. Some shallow-box data have been included for runs in which the end sill was removed. Data from fifty-one of the sixty-two tests listed in Table 2 appear in Fig. 8.

A mean curve has been drawn as a solid line in Fig. 8. The coefficient of discharge for a given relative head may be taken from this curve, multiplied by the approach-channel-width correction and the box-inlet-shape correction, and substituted into Eq. 2 to determine the capacity of the box inlet drop spillway when the box-inlet crest controls the discharge. A second method for determining the discharge is outlined herewith using the correction scale to the right of Fig. 8.

It will be noted that the discharge coefficient is constant in Fig. 8 when H/b is greater than 0.6. Therefore, Eq. 2 can be written

$$Q = 0.4275\, L_c \sqrt{2\,g}\, H^{3/2} \qquad (3a)$$

or, in English units,

$$Q = 3.43\, L_c\, H^{3/2} \qquad (3b)$$

Eqs. 3 are valid when $L/b = 1$, $b_a/L_c \geq 3$, and $H/b \geq 0.6$. For other box-inlet lengths, narrower approach channels, and lower heads, the corrections given by the curves in Figs. 6, 7, and 8 or the tables of the design report[7] must be applied.

Precision of Results.—Fig. 8 has been prepared to a large scale in order to facilitate plotting the data. Therefore, the scatter is not as great as might be assumed at first glance. It can be seen that most of the observed data fall within ±5% of the mean line. Fig. 8 can therefore be considered as verifying Eq. 2 when C_3 is taken from Fig. 8 and corrected by the use of Figs. 6 and 7. Similar comments apply to Eqs. 3 when corrected by the use of Figs. 6, 7, and 8.

---

[7] "Hydraulic Design of the Box Inlet Drop Spillway," by Fred W. Blaisdell and Charles A. Donnelly, *SCS-TP-106*, Soil Conservation Service, U. S. Dept. of Agriculture, Washington, D. C., July, 1951.

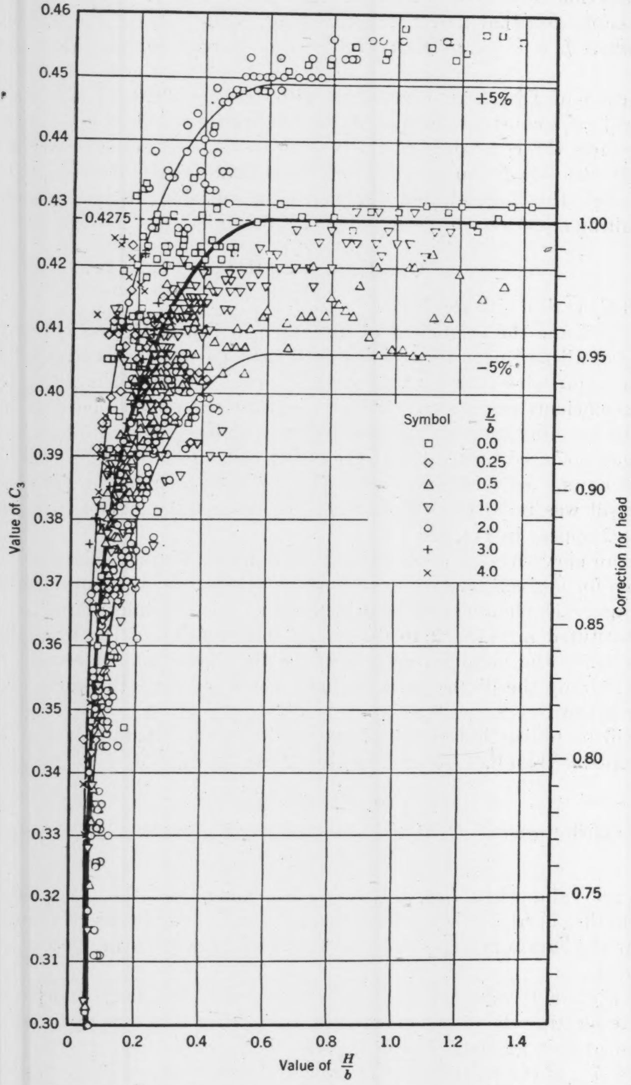

FIG. 8.—RELATIONSHIP BETWEEN C_3 AND H/b WITH CONTROL AT BOX-INLET CREST

Control at Headwall Opening.—At the higher flows the box inlet becomes flooded out, and the section controlling the flow shifts from the box-inlet crest to the opening in the headwall, as can be seen by referring to the typical plot presented in Fig. 5. This part of the rating curve is defined by Eq. 1*b*.

A detailed analytical study was made to determine the factors that affect the discharge coefficient and the zero-flow-head correction in Eq. 1*b*. It was discovered that the dike position, the box-inlet shape, and the approach-channel width had no effect on the discharge coefficient C_2, but that the coefficient was a function of the depth of the box inlet. With regard to the zero-flow-head correction H_{02}, it was discovered that H_{02} was independent of the approach-channel width and the dike position was but a function of both the relative length L/b and the relative depth y/b of the box inlet. The effect of the relative depth of the box inlet on the discharge coefficient and the head correction are herein separately considered.

Effect of Depth of Box Inlet on Discharge Coefficient.—When the discharge coefficient C_2 in Eq. 1*b* is plotted against the relative depth of the box inlet y/b, it is found that C_2 increases with y/b. This is shown in Fig. 9. Even though there is considerable spread to the data, other plots not presented show that C_2 is independent of both L/b and b_a/L_c, and it seems unlikely that the spread can be decreased.

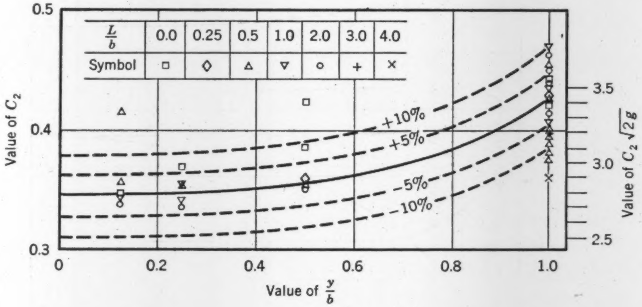

FIG. 9.—COEFFICIENT OF DISCHARGE WITH CONTROL AT HEADWALL OPENING

For design purposes the solid curve in Fig. 9 is suggested for use in determining the coefficient of discharge in Eq. 1*b*.

Head Correction.—The tests showed that the head correction is independent of both the approach-channel width and the width of the box inlet, but that it is a function of the ratio of the box-inlet length to its depth, L/y. In Fig. 10(*a*) the ratio H_{02}/y has been plotted against L/y. It will be noted that the data for box inlets having relative depths y/b of 1, $\frac{1}{2}$, and $\frac{1}{4}$ fall on a single curve, but that for a relative box-inlet depth of $\frac{1}{8}$ the data fall on a separate well-defined curve. The reason for this has not been determined.

Because shallow boxes are uneconomical in most cases for the higher flows (when the headwall opening controls the discharge) the solid curve in Fig. 10(*a*) is presented for design purposes for box inlets equal to or greater in depth than $b/4$. In order to cover relative box-inlet depths between $\frac{1}{4}$ and $\frac{1}{8}$ as well as the deeper box inlets, the data have been plotted in a different form in Fig. 10(*b*). Although Fig. 10(*a*) is simpler to use than Fig. 10(*b*), Fig. 10(*b*) may be used in place of Fig. 10(*a*) and must be used for the shallower boxes.

Precision of Results.—Dashed curves have been added to Fig. 9 parallel to the solid curve and 5% and 10% above and below it to indicate the spread of the data. Although occasional data points fall outside the ±10% limits, sufficient data fall inside this range to indicate that the coefficient of discharge can reasonably be expected to be within 10% of the value given by the solid curve.

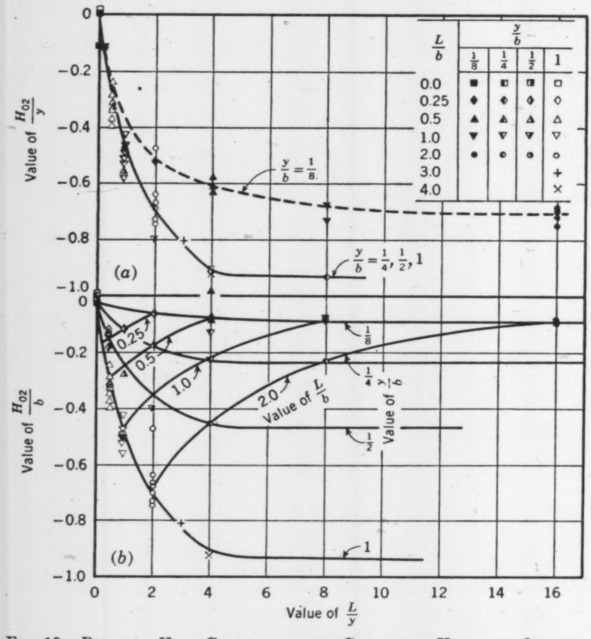

FIG. 10.—RELATIVE HEAD CORRECTION WITH CONTROL AT HEADWALL OPENING

With regard to the head correction, it appears that the curve of Fig. 10(*a*) can generally be expected to give this correction to within approximately 10%. At low values of L/y the curve is steep, and it seems likely that the head correction may vary by as much as 20% from the curve. Little can be said regarding the accuracies obtainable through the use of Fig. 10(*b*), but it seems likely that the comments made regarding Fig. 10(*a*) also apply to Fig. 10(*b*).

It was noted when analyzing the data that the coefficient of discharge and the head correction varied in such a manner that a deviation of one from the curve was at least partly corrected by a compensating deviation of the other.

To some degree, at least, the variations from the design curves of Figs. 9 and 10(*a*) are therefore probably compensating.

RESULTS OF SUBMERGED FLOW TESTS

A determination of the effect of submergence on the flow through box inlet drop spillways was necessary because there are many field locations where high tailwater elevations are likely. As the relative importance of the various factors which affect submergence were unknown, preliminary tests were conducted to determine the effect of each factor. The subsequent material is devoted to the preliminary tests and the submergence calibration tests, which were voluminous because no simple method had been discovered by which the results could be systematized.

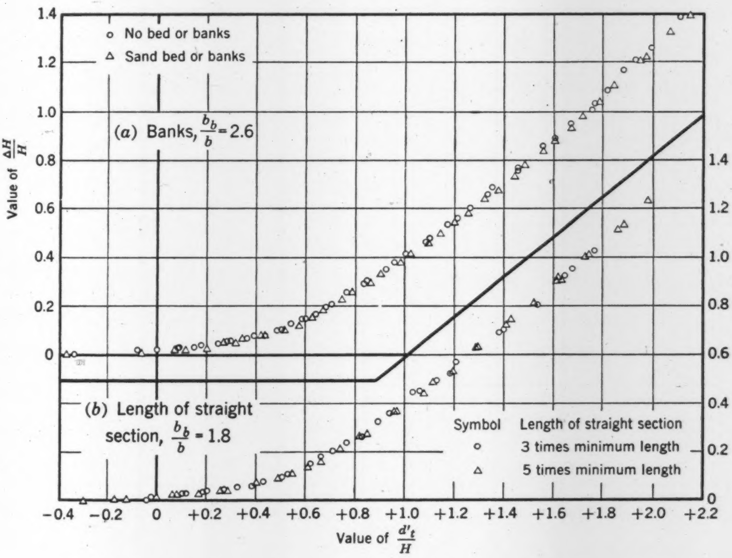

Fig. 11.—Effect of Banks in Exit Channel and Length of Straight Section with $L/b = 2$, $y/b = 1$, $b_0/L_e = 3$, and $Q/b^{5/2} = 3$

Preliminary Tests.—The preliminary tests and analyses relate to the effect of the banks in the exit channel, the effect of varying the length of the straight section in the outlet, the effect of the width of the outlet, and the effect of varying the rate of flow.

Effect of the Banks in the Exit Channel.—Because it was more convenient not to simulate the exit channel, a test was made to determine whether the submergence curve was affected by the presence or absence of the downstream channel.

In Fig. 11(*a*) the points shown as triangles were obtained when a downstream channel was filled with sand, the shape being formed by water running over it with the tailwater at about its normal level. The points shown as circles were obtained with no sand in the downstream channel. From Fig. 11 (*a*) it can be seen that the presence or absence of the bed and banks in the downstream channel had no effect on the submergence curve. As a result, all subsequent submergence curves were obtained without stream banks in the downstream channel. This greatly facilitated the study without detracting from its value.

Effect of Length of Straight Section.—The outlet for the box inlet drop spillway has a straight or parallel-sided section between the box inlet and the stilling basin the length of which may be varied according to the site conditions. Data obtained with straight sections having lengths equal to three and five times the minimum lengths given by the design equations are plotted in

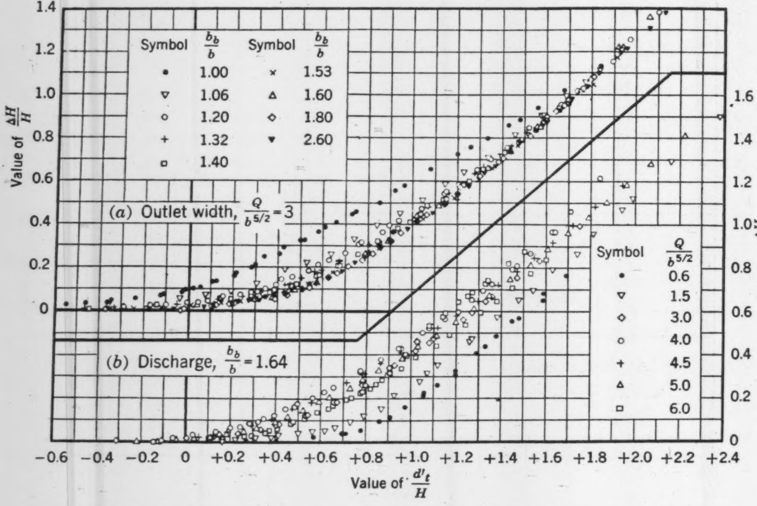

FIG. 12.—EFFECT OF OUTLET WIDTH AND DISCHARGE WITH $L/b = 2$, $y/b = 1$, AND $b_o/L_c = 3$

Fig. 11 (*b*). In Fig. 11 (*b*) it may be seen that the points fall on a single curve within the limits of experimental precision. There are no comparable data for the minimum length of the straight section. It is concluded that the length of the straight section does not affect the submergence curve.

Effect of Width of Outlet.—The stilling basin can be constructed either with parallel sidewalls that are extensions of the straight-section walls or with flaring sidewalls. If flaring sidewalls are used, it is likely that there will be a recovery of velocity head in the outlet that may mitigate the submergence effect. Therefore, the influence of flaring the outlet sidewalls was investigated.

A study of the data indicates that, within reasonable limits, the rate of flare of the outlet sidewalls does not affect the submergence curves. Flares tested varied from 1 in ∞ (no flare) to 1 in 2, the maximum permitted by the outlet design.

The width b_b at the outlet exit determines the energy recovered in the outlet; this is shown in Fig. 12(*a*). As would be anticipated, the effect of the width decreases as the width increases until, in the case cited in Fig. 12(*a*), there is no benefit in using outlets wider than approximately 1.5 *b*.

The results of this investigation show the significant effect of the width of the outlet and indicate the necessity of considering the outlet width as one of the variables in a study of the effects of submergence on flow through box inlet drop spillways.

Effect of Varying Discharge.—The results of a study of the variation in the effects of submergence on discharge are shown in Fig. 12(*b*) in which it can be seen that the submergence effect increases with the discharge up to the point where $Q/b^{5/2} = 4$; at still higher discharges the submergence effect decreases. An excellent correlation was obtained showing that the discharge which produces the greatest submergence effect corresponds to the discharge on the free-flow rating curve at which the control changes from the box-inlet crest to the headwall opening.

As a result of this phase of the study, it was seen that the submergence effect is a function of the discharge.

Submergence Calibration Tests.—The preliminary tests cited in the foregoing bear out comments made by Horace W. King on the submerged-weir experiments conducted by H. Bazin. Mr. King states,[8]

> "Each type of weir is a problem in itself and if the laws governing [submerged] flow over it are to be determined, each requires an extensive experimental investigation, covering a wide range of conditions."

The test program was designed to provide the "extensive experimental investigation" which Mr. King requires. The range of variables involved is given in Table 1(*b*). The data for each of the 36 models or variations were plotted on separate sheets, each of the six constant discharges recorded on each sheet being represented by a different curve. Fig. 12(*b*) is representative of these plots. For use in determining the flow over box inlet drop spillways under submerged flow conditions, 216 submergence curves (less the data points) have been prepared.[7]

RESULTS OF OUTLET TESTS

The test program for the study of outlets for box inlet drop spillways may be conveniently divided into (1) the initial tests, (2) the definition tests, and (3) the check tests. The initial tests were exploratory in nature—that is, several different forms of the outlet were devised and tested to determine the important features of the outlet; the general form of the outlet was evolved from these exploratory tests. The definition tests were made to define the design rules, to evaluate the design equations, and to determine the ranges of their application. The check tests covered the anticipated range of each of the variables and served to verify the design rules. Subsequently, each element entering into the design will be noted in a manner that will permit one to verify the adequacy of the design data independently.

---

[8] "Handbook of Hydraulics," by Horace W. King, McGraw-Hill Book Co., Inc., New York, N. Y., 2d Ed., 1929, p. 162.

Because the form of the outlet is determined primarily by the manner in which the flow leaves the box inlet, it is pertinent to describe the outflow briefly. The water passing over the sides of the box inlet springs clear of the sidewalls and creates a space between and under the nappes and the sidewalls. These spaces are filled with water moving helically about a horizontal axis. At the exit of the box inlet, the helices from the opposite sides of the spillway enter the outlet along the sidewalls and create a considerable disturbance and uneven distribution of flow across the outlet. It is this poor velocity distribution and attempts to improve it that cause the major problems in the development of the outlet.

Critical Depth.—In order to determine the proportions of the outlet it is necessary to determine the critical depth at two points in the outlet—in the straight section (L_s in Fig. 2) and at the exit.

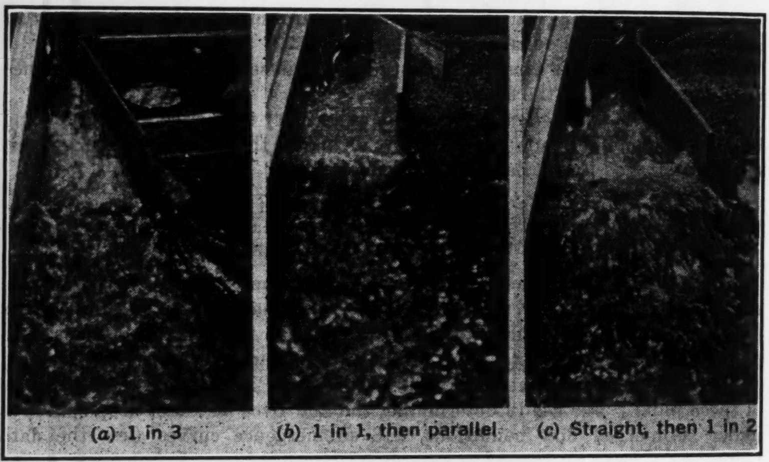

FIG. 13.—EFFECT OF VARIOUS SIDEWALL FLARES

The equation for the critical depth in the straight section of the outlet d_c is

$$d_c = \sqrt[3]{\frac{(Q/b)^2}{g}} \qquad (4)$$

At the end of the stilling basin Eq. 4 becomes

$$d'_c = \sqrt[3]{\frac{(Q/b_b)^2}{g}} \qquad (5)$$

in which d'_c is the critical depth at the stilling-basin exit.

Straight Section.—A straight section is used between the box inlet and the stilling basin to assist in breaking up the helical rollers described previously, to improve the flow distribution, to make better use of the available tailwater, and to improve the scour pattern. The necessity for the straight section is shown in Fig. 13. The outlet sidewall in Fig. 13(*a*) has a flare of 1 (transverse) in 3 (longitudinal) for its entire length. The roller clings to the sidewall, and at the stilling-basin exit the high velocity is at the sidewall. Therefore, there are high velocities along the sides of the downstream channel, resulting in scour of the banks and the bed along the sides of the channel. In Fig. 13(*b*) the outlet sidewall first flares 1 in 1 in an attempt to give the roller a chance to spread out and then is made parallel to the outlet center line. Although the rollers fall to the floor of the outlet and spread out, the transverse component of the velocity creates an impact wave against the sidewalls and high velocities along the walls. The uneven velocity distribution at the end of the outlet causes eddies in the downstream channel and results in poor scour patterns. In both models various combinations of baffles, angular sills, cross sills, longitudinal sills, and end sills were tried in an effort to obtain a satisfactory flow pattern, but no combination was successful.

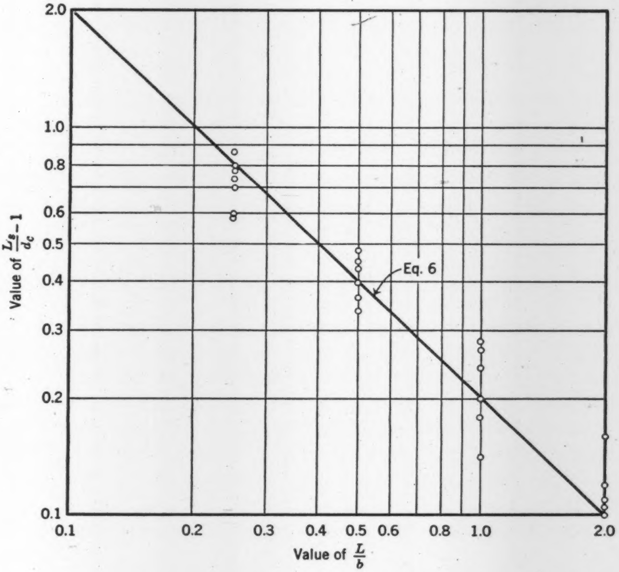

FIG. 14.—DETERMINATION OF THE LENGTH OF THE STRAIGHT SECTION WITH $d_t = 1.5\, d'_c$, $y_s = b/8$, AND $0.25 < L/b < 2.0$

After conducting tests with several types of sidewalls, it was found that, when a straight section (one having parallel sidewalls) equal to the box inlet in width was used between the box inlet and the outlet proper, the roller was broken up, the flow distribution was improved, better use was made of the tailwater, and the resulting scour pattern was improved. Fig. 13(*c*) shows the flow conditions when this straight section was used.

The data obtained from the tests determining the length of the straight section are plotted in Fig. 14 using as coordinates $(L_s/d_c) - 1$ and L/b; the selection of the coordinates was by trial and error. The curve drawn through the plotted data has the equation,

$$L_s = d_c \left(\frac{0.2}{L/b} + 1 \right) \ldots\ldots\ldots\ldots\ldots\ldots\ldots (6)$$

The points are scattered in Fig. 14 because of the manner in which the data were obtained. The rate of flow which gave good flow distribution over the end sill was determined only by visual observation. For the same length of straight section, it is possible that two or more flows could be equally acceptable. Check tests on this part of the outlet and tests on the other parts show that, ordinarily, Eq. 6 results in a straight section that is too short for practical use. When this is so, the straight section may be lengthened to suit the site with assurance that it will function properly.

It will be noted that L/b appears in the denominator of Eq. 6. As L/b approaches zero, the minimum length of the straight section therefore becomes infinite; this seems unreasonable. Eq. 6 is valid and should be used only for values of $L/b \geq 0.25$—the minimum covered by the tests. It is not intended that the outlet described herein be used for straight overfalls such as would be the case if $L/b = 0$.

Stilling-Basin Section.—The stilling-basin section of the outlet is used to remove destructive energy from the flow and to discharge water into the downstream channel in a manner that will not damage the bed, the banks, or the structure itself. There are a number of elements that comprise the stilling basin; the tests made on each of these elements will be cited.

Tests showed that the sidewalls either could be parallel extensions of the straight-section sidewalls or could flare as much as 1 in 2. If the sidewall flare is greater than 1 in 2, the flow does not spread out rapidly enough to follow the sidewalls, the main stream is concentrated at the center of the stilling basin, and whirls develop between the stream and the walls. The choice between the limits 1 in ∞ (no flare) and 1 in 2 depends on site conditions; these broad limits permit the adaptation of the outlet to almost any field situation.

Length.—Tests were conducted to determine the minimum length of the stilling basin for box inlets having shape ratios, L/b, of 2.0, 1.5, 1.0, and 0.5; a depth ratio b/y of 1; the previously determined straight section length; a tailwater depth of 1.6 d'_c; end and longitudinal sills $b/8$ high; and wingwalls set at a 45° angle and cut on a 45° top slope.

Observation showed that, for the short box inlets, the jet shoots out at a high level and takes a relatively greater distance to level out than for the longer boxes and that the basin length must be proportionately greater for the same discharge. When the box inlet is long, water shoots out from the bottom of the box and levels out in a relatively short distance, thereby requiring less basin length.

The data obtained during these tests may be found in Table 4. A comparison of the values listed in the column showing (L_b/L_c) (L/b) with the

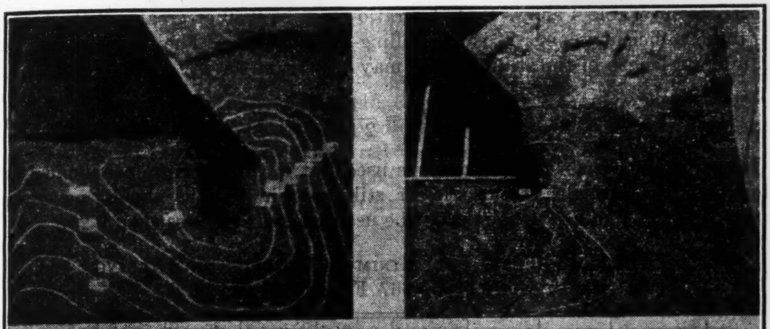

(*a*) No sills (*d*) No wingwall

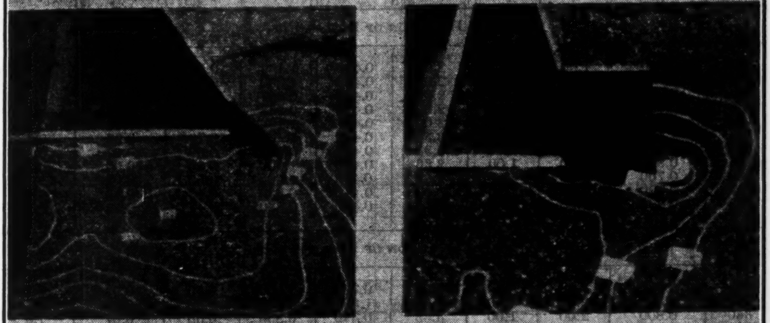

(*b*) End sill only (*e*) Rectangular wingwall

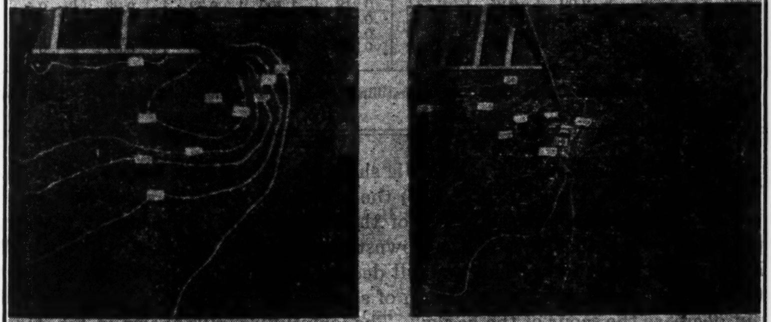

(*c*) End and longitudinal sills (*f*) Sidewall extended and cut

FIG. 15.—SCOUR PATTERNS AS A RESULT OF SILLS AND WINGWALLS

footnotes in Table 4 shows that this ratio must be 0.50 or greater if the basin is to be sufficiently long; L_b is the stilling-basin length. The equation for the minimum length of the stilling basin may be written as

$$L_b = \frac{L_c}{2\,L/b} \qquad (7)$$

Greater stilling-basin lengths may be used but it will be more economical to lengthen the straight section; lesser stilling-basin lengths should never be used. Eq. 7, like Eq. 6, should not be used when L/b is less than 0.25.

TABLE 4.—TESTS FOR MINIMUM LENGTHS OF STILLING BASIN WITH $b = 0.667$ FT AND $d_t = 1.60\ d'_c$

Run	Q in, cubic feet per second	L/b	y/b	L_c, in feet	L_s, in feet	L_b, in feet	$\frac{L_b}{L_c} \times \frac{L}{b}$	SCOUR, IN FEET	
								Maximum[a]	Distance[b]
				(a) DURATION OF RUN = ½ hr					
163[c]	0.700	1.00	1.00	2.00	0.410	1.160	0.58	0.07	0.7
164[c]	0.700	1.00	1.00	2.00	0.410	1.000	0.50	0.07	0.7
165[d]	0.700	1.00	1.00	2.00	0.410	0.667	0.34	0.07	0.7
166[d]	0.700	1.00	1.00	2.00	0.410	0.583	0.29	0.07	0.5
182[c]	0.700	1.00	1.00	2.00	0.410	1.160	0.58	0.12	0.7
183[c]	1.130	2.00	1.00	3.33	0.410	1.160	0.70	0.07	0.6
184[c]	1.130	2.00	1.00	3.33	0.410	1.000	0.60	0.07	0.7
185[c]	0.824	1.50	1.00	2.66	0.410	1.000	0.56	0.05	0.5
186[c]	0.700	1.00	1.00	2.00	0.410	1.000	0.50	0.02	0.4
187[d]	0.700	1.00	1.00	2.00	0.410	0.830	0.42	0.15	0.6
188[d]	0.824	1.50	1.00	2.66	0.410	0.830	0.47	0.15	0.7
				(b) DURATION OF RUN = 4 hr					
358[c]	0.530	1.00	0.50	2.00	0.324	1.000	0.50	0.07	0.8
359[c]	0.810	2.00	0.50	3.33	1.330	0.830	0.50	0.06	0.6
360[c]	0.800	2.00	1.00	3.33	0.390	0.830	0.50	0.07	1.0
361[c]	0.305	1.00	0.25	2.00	0.224	1.000	0.50	0.03	0.5
363[c]	0.530	1.00	0.50	2.00	0.324	1.200	0.60	0.08	0.7
365[c]	0.810	2.00	0.50	3.33	0.396	0.830	0.50	0.05	0.6
369[c]	0.345	0.50	0.25	1.33	0.288	1.330	0.50	0.03	0.5
371[c]	0.305	1.00	0.25	2.00	0.224	1.200	0.60	0.06	0.7
373[c]	0.328	2.00	0.25	3.33	0.218	1.200	0.72	0.03	0.5
374[c]	0.400	1.00	0.25	2.00	0.268	1.200	0.60	0.05	0.2
375[c]	0.405	2.00	0.25	3.33	0.247	0.830	0.50	0.02	0.4
386[c]	0.750	1.50	1.00	2.66	0.390	0.880	0.55	0.07	0.7

[a] Below floor of stilling basin. [b] From end of stilling basin. [c] Basin length satisfactory. [d] Basin too short.

Sills.—The necessity for the sills is shown in Figs. 15(*a*), 15(*b*), and 15(*c*). When no sills were used (Fig. 15(*a*)) the maximum depth of scour was below −0.20 ft relative to the elevation of the model basin floor, and it was not possible to hold the bank of the downstream channel in place. An end sill is shown in Fig. 15(*b*). This end sill decreased the maximum depth of scour to −0.12 ft and decreased the depth of scour at the end of the basin but did not decrease the scour of the banks. The longitudinal sills shown in Fig. (15*c*) straightened out the flow and prevented the direct action on the stream banks. They also served to decrease the maximum depth of scour to −0.08 ft and improved the form of the scour pattern.

The results of the tests determining the best height of the end sill are presented in Fig. 16(*a*). During the tests it was noted that, when the end sill was too high, the jet leaving the basin jumped over the sill and landed some distance from the end of the basin, causing severe erosion at that location. However, when the end sill was too low the water leaving the basin caused the same severe erosion, but it occurred very near the end of the basin. This explains the solid points indicating poor performance both above and below the curve drawn in Fig. 16(*a*) which designates the proper height of the end sill. This curve has the equation,

$$y_s = \frac{d_t}{6} \qquad (8)$$

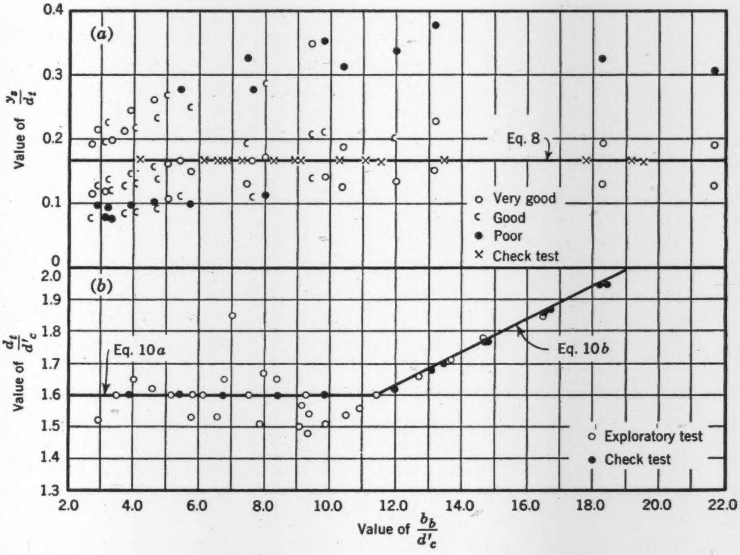

FIG. 16.—DETERMINATION OF END SILL HEIGHT AND TAILWATER DEPTH

in which y_s is the height of the end sill and d_t is the tailwater depth over the basin floor. The determination of the required tailwater depth is given subsequently.

Although several different heights of longitudinal sills were tested, it was found that the apparently most satisfactory height was equal to that used for the end sill.

Longitudinal sills may be omitted if the stilling-basin sidewalls are parallel extensions of the straight-section sidewalls. They should be used whenever the stilling-basin sidewalls flare. The longitudinal sills extend from the exit of the box inlet to the end sill. Tests showed that only a single pair of sills need be used if b_b is less than 2.5 b. Their distance either side of the outlet center line should be between $b/6$ and $b/4$. When b_b is greater than 2.5 b

an additional pair of sills is required; they should be located midway between the center pair of sills and the sidewalls at the stilling-basin exit.

Sidewall Height.—The minimum height, d_m, of the stilling-basin sidewalls at the exit of the stilling basin above tailwater level should be

$$d_m = \frac{d_t}{3} \qquad (9)$$

In order to prevent overtopping and the resulting erosion of the dam fill, the outlet sidewalls should always extend above the tailwater level. Therefore, under submerged-flow conditions, much higher sidewalls may be required; however, the freeboard above the tailwater level may be safely reduced somewhat because the water surface will be smoother.

Wingwalls.—The shape and the position of the wingwalls have more effect on the scour of the bed and the dam fill near the end of the stilling basin than has been commonly supposed. Considerable study was given to the shape and location of wingwalls that would best protect the dam fill.

The effect of the wingwalls on the scour pattern is shown in Figs. 15(*d*), 15(*e*), and 15(*f*). If no wingwall is used, as in Fig. 15(*d*), a deep hole is scoured at the end of the sidewall. The possibility of undermining the outlet is apparent, and severe erosion of the dam fill takes place. A common type of wingwall is the rectangularly shaped wall placed perpendicular to the outlet center line. The results of the test on this wall are shown in Fig. 15(*e*). The scour is severe at the end of the wingwall, and the dam fill has been badly eroded. The scour is caused by a whirl on the side of the main stream. The streamlines of the whirl are forced close together as they pass around the end of the wingwall, and the resulting high velocities cause the scour. This is not an isolated circumstance observed only in the laboratory; several field structures have been badly damaged by the same phenomenon. In Fig. 15(*f*), the wingwall has been formed by extending the sidewall and cutting it to fit the slope of the dam fill. No scour took place outside the wingwall, but a rather deep hole was scoured at its end. When the wingwall, shown in Fig. 15(*c*) was installed, the dam-fill material rested at its angle of repose, indicating that there was no scour in back of the wingwall.

Of the many different types of arrangements of wingwalls studied, none gave scour patterns which were an improvement over that of the wingwall that was triangular in elevation. Tests were therefore conducted to determine the optimum position of the wingwall with the results shown in Table 5. It was noted that slight scour may occur near the wingwalls as a result of the eddies along the side of the channel or that the scour may be at the center line of the channel. The magnitude and location of the maximum scour depth are given in Table 5. In no case was the scour sufficient to endanger the outlet or cause concern.

From a study of the data shown in Table 5, it appears that wingwalls having top slopes of 45° and set at angles, θ, of 45° and 60° with the outlet center line are slightly superior to the others. With this type of wingwall, there was little bank erosion and none at all in back of the wingwall where the fill material rested at its angle of repose, as can be observed in Fig. 15(*c*).

TABLE 5.—TESTS DETERMINING WINGWALL POSITION AND TOP SLOPE[a]

Run	Q, in cubic feet per second	L, in feet	L_s, in feet	L_b, in feet	b_b, in feet	WINGWALL		DEPTH OF SCOUR, IN FEET[b]	
						Angle from center line, in degrees	Angle of top slope from horizontal, in degrees	Near wingwall	Near center line
240	1.28	1.000	0.550	1.2	1.86	60	30	0.09	
241						45	30	0.13	
242						30	30	0.10	
243						60	37.5	0.06	
244						45	37.5	0.06	
245						30	37.5		0.03
246						30	45		0.07
247						45	45	0.03	
248						60	45		0.05
249						30	33.5	0.05	
250						45	33.5	0.10	
251						60	33.5	0.04	
252	1.28	1.000	0.550	1.2	1.06	30	30	0.07	
253						45	30	0.05	
254						60	30	0.02	
255						30	37.5	0.07	
256						45	37.5	0.03	
257						60	37.5	0.00	
258						30	45	0.02	
259						45	45	+0.01	
260						60	45	+0.02	
261	1.04	0.667	0.508	1.2	1.46	60	45		0.03
262						45	45		0.12
263						30	45		0.07
264						60	37.5		0.05
265						45	37.5		0.07
266						30	37.5		0.12
267						45	0[c]		0.13
268						45	30		0.07
269	1.13	1.333	0.493	1.2	1.46	45	45	0.12	
270						45	37.5	0.07	
271						30	37.5		0.07
272						30	37.5		0.08
273						60	37.5	0.04	
274						60	30	0.03	
275						60	45	+0.02	
276						45	45	0.02	
277	0.80	1.333	0.391	1.1	1.03	60	37.5	0.05	
278						45	37.5		0.05
279						30	37.5		0.07
280						60	45		0.05
281						45	45		0.07
282						30	45	0.07	0.07
283						60	30		0.07
284						45	30	0.07	0.07
285	0.69	1.000	0.360	1.1	1.03	60	37.5		0.04
286						45	37.5		0.03
287						30	37.5		0.02
288						60	45		0.02
289						45	45		0.02
290						30	45		0.02
291						60	30	0.02	
292						45	30		0.02
293						30	30		0.02
294	0.56	0.667	0.336	1.1	1.03	30	30		0.07
295						45	30		0.04
296						60	30	0.04	
297						60	45		0.02
298						45	45		0.04
299						30	45	0.03	0.03
300						60	37.5		0.03
301						45	37.5		0.03
302						30	37.5	0.03	0.03

[a] Duration of run = 4 hr; $b = 0.667$ ft, $y = 0.667$ ft, $d_t = 1.60\ d'_c$. [b] Below floor of stilling basin.
[c] Rectangular wingwall; top horizontal.

After these outlet tests had been completed, a special study of wingwalls for another type of outlet was made. These tests confirmed the poor performance of the wingwall that is rectangular in elevation and located perpendicular to the outlet center line. They also confirmed the satisfactory performance of the wingwall that is triangular in elevation located at an angle of from 45° to 60° with the outlet center line. The later tests indicated, however, that the top of the wingwall could be sloped to fit the dam fill, if desired.

Tailwater Depth.—Tests defining the required tailwater depth were conducted before the sill heights had been determined; the height of the longitudinal sills was taken as $b/8$ for this group of tests. The box inlets had relative lengths L/b of 0.5, 1.0, 1.5, and 2.0 and a relative depth y/b of 1. The length of the straight section was based on Eq. 6, and the wingwalls were set at an angle of 45° from the outlet center line and cut on a 45° top slope.

The minimum depth of tailwater that would keep the hydraulic jump in the outlet was determined for each test. These minimum relative depths measured above the basin floor, d_t/d'_c, have been plotted in Fig. 16(*b*) as open circles against the relative widths of the exit of the stilling basin, b_b/d'_c. Curves were drawn through these data and used for the subsequent tests. Up to b_b/d'_c equal to 11.5, the equation of the curve takes the form,

$$d_t = 1.6\,d'_c \qquad \text{(10a)}$$

For values of b_b/d'_c in excess of 11.5, the equation of the curve is

$$d_t = d'_c + 0.052\,b_b \qquad \text{(10b)}$$

Eq. 10*b* is used at the higher ratios of b_b/d'_c because the tests showed that dead or nearly dead water exists along the wingwalls near the end of the basin when this ratio is greater than 11.5. That part of the outlet occupied by dead water is obviously not used to dissipate energy, and the outlet would operate just as well if it were eliminated. Satisfactory results can be obtained with outlets wider than 11.5 d'_c if the tailwater depth is computed from Eq. 10*b*, but the wider basins result in inefficient use of the outlet and are probably more expensive than basins with narrower outlet widths.

The check tests, which were conducted using the recommended sill heights and tailwater depths computed from Eqs. 10, showed that these equations give satisfactory tailwater depths. The check tests are plotted in Fig. 16(*b*) as solid circles. Another group of tests conducted with tailwater depths greater than those given in Eqs. 10 produced scour patterns as good as or better than those produced when the design tailwater depth was used.

Depth of Box Inlet.—The depth of the box inlet was not ignored; it was considered in each step of the test program. However, it will be noted that the box-inlet depth does not appear in any of the design equations because of the manner in which the water flows through the box inlet. The flow in the box is quite turbulent, and much of the energy at the drop is dissipated so that it is the depth of flow in the box inlet (which is related to the critical depth used in the outlet equations) rather than the box-inlet depth itself that determines the proportions of the outlet

Check Tests.—Each of the various elements comprising an outlet has an individual effect on the performance of the structure. These effects are, of course, interrelated so that a variation in one element can cause a change in the performance of some other element. However, the only logical way to conduct the experiments was to vary only one element at a time and disregard, temporarily, its effect on the other elements. In order to be sure that all interrelated elements would lead to the desired final result, a comprehensive series of check tests was required. These check tests were made after the design equations had been tentatively adopted and before they were considered final.

TABLE 6.—RESULTS OF CHECK TESTS[a]

Run	Q, in cubic feet per second	L, in feet	y, in feet	d_c, in feet	L_s, in feet	L_b, in feet	SIDEWALL		y_s, in feet	b_b, in feet	d'_e, in feet	d_t, in feet	SCOUR, IN FEET	
							Flare	Height, in feet					Maximum[b]	Distance[c]
358	0.530	0.667	0.333	0.270	0.324	1.00	4:1	0.400	0.050	1.16	0.187	0.299	0.07	0.8^d
359	0.810	1.333	0.333	0.358	1.330	0.83	3:1	0.516	0.065	1.20	0.242	0.387	0.06	0.6^e
360	0.800	1.333	0.667	0.355	0.390	0.83	4:1	0.548	0.070	1.08	0.257	0.413	0.07	1.0^d
361	0.305	0.667	0.166	0.186	0.224	1.00	4:1	0.260	0.033	1.16	0.129	0.196	0.03	0.5^d
362	0.395	0.333	0.333	0.221	0.311	1.60	4:1	0.280	0.035	1.46	0.131	0.210	0.03	0.6^d
363	0.530	0.667	0.333	0.270	0.324	1.20	3:1	0.344	0.043	1.46	0.160	0.257	0.08	0.7^d
364	0.960	1.333	0.667	0.401	0.600	1.87	4:1	0.452	0.056	1.62	0.222	0.340	0.10	0.4^e
365	0.810	1.333	0.333	0.358	0.396	0.83	3:1	0.516	0.065	1.20	0.242	0.387	0.05	0.6^d
366	0.240	0.333	0.166	0.159	0.224	1.60	2:1	0.248	0.031	2.26	0.070	0.187	0.06	0.6^d
367	0.345	0.333	0.166	0.202	0.288	1.50	6:1	0.300	0.037	1.16	0.140	0.224	0.02	0.6^d
368	0.240	0.333	0.166	0.159	0.224	1.50	3:1	0.228	0.028	1.66	0.087	0.172	0.06	0.7^d
369	0.345	0.333	0.166	0.202	0.288	1.33	4:1	0.272	0.034	1.32	0.128	0.204	0.03	0.5^d
370	0.405	1.333	0.166	0.225	0.247	1.50	3:1	0.264	0.033	1.66	0.123	0.197	0.07	0.2^e
371	0.305	0.667	0.166	0.186	0.224	1.20	6:1	0.292	0.037	1.06	0.138	0.220	0.06	0.7^d
372	0.400	0.667	0.166	0.223	0.268	1.40	2:1	0.284	0.035	2.06	0.105	0.212	0.06	0.5^d
373	0.328	1.333	0.166	0.196	0.218	1.20	6:1	0.300	0.038	1.06	0.144	0.226	0.03	0.5^d
374	0.400	0.667	0.166	0.223	0.268	1.20	3:1	0.284	0.035	1.46	0.132	0.212	0.05	0.2^e
375	0.405	1.333	0.166	0.225	0.247	0.83	4:1	0.348	0.044	1.08	0.164	0.262	0.02	0.4^d
376	0.810	1.333	0.333	0.358	0.396	1.60	4:1	0.452	0.057	1.46	0.212	0.340	0.03	0.9^d
377	0.690	0.667	0.333	0.321	0.387	1.60	6:1	0.484	0.060	1.13	0.226	0.362	0.07	0.8^d
378	0.675	1.333	0.333	0.317	0.348	1.60	6:1	0.476	0.059	1.13	0.223	0.356	0.07	0.7^d
379	0.690	0.667	0.333	0.321	0.387	1.40	4:1	0.428	0.053	1.36	0.200	0.322	0.03	0.4^e
380	0.675	1.333	0.333	0.317	0.348	1.20	2:1	0.344	0.043	1.86	0.160	0.257	0.07	0.4^e
381	0.395	0.333	0.333	0.221	0.311	1.70	6:1	0.316	0.039	1.23	0.147	0.237	0.07	0.6^d
382	0.960	1.333	0.667	0.401	0.600	1.87	6:1	0.552	0.070	1.28	0.259	0.415	0.07	0.8^d
383	0.860	1.000	0.667	0.373	0.422	2.47	∞:1	0.802	0.100	0.67	0.373	0.595	0.07	0.8^d
384	0.556	0.333	0.667	0.279	0.390	1.60	4:1	0.356	0.045	1.46	0.165	0.268	0.07	0.3^e
385	0.800	1.333	0.667	0.355	0.390	1.60	4:1	0.448	0.056	1.46	0.210	0.337	0.07	0.4^e
386	0.750	1.000	0.667	0.340	0.390	0.88	4:1	0.520	0.065	1.10	0.244	0.390	0.07	0.7^d

[a] b = 0.667 ft., wingwall at 60° from center line, wingwall top slope is 45° from horizontal, and duration of run = 4 hr. [b] Below floor of stilling basin. [c] From end of stilling basin. [d] Scour near center line. [e] Scour near wingwall.

The check tests are summarized in Table 6. The tests showed that no changes were required in the design equations and rules and that the operation of the outlet was satisfactory.

SUMMARY OF RESULTS

The results of the tests made to evaluate the discharge over box inlet drop spillways and to determine the design of the outlet may be summarized as follows:

A. When the discharge over the box inlet drop spillway is controlled by the crest of the box inlet—

1. The general formula for the discharge is given by Eqs. 3.

2. The discharge coefficients in Eqs. 3 must be multiplied by (*a*) the correction for head given in Fig. 8; (*b*) the correction for box-inlet shape given in Fig. 7; (*c*) the correction for approach-channel width given in Fig. 6; and (*d*) the correction for dike proximity to the box-inlet crest given in Table 4, these values being of low precision.

3. The approach channel is silted level with the crest of the box inlet.

4. The precision of the design curves is within ±7%.

B. When the discharge over the box inlet drop spillway is controlled by the headwall opening—

1. The general formula for the discharge is given by Eq. 1*b*.

2. The discharge coefficient C_2 may be obtained from Fig. 9.

3. The head correction H_{02} may be obtained from Fig. 10(*b*). If y/b is between $\frac{1}{4}$ and 1, H_{02} may be more readily determined from Fig. 10(*a*).

4. The precision of the design curves is probably within ±10%.

C. When the box inlet drop spillway operates under submerged conditions, both the width of the outlet and the discharge influence the effect of submergence.[7]

D. The rules for the design of the outlet for a box inlet drop spillway are—

1. The critical depth in the straight section is given by Eq. 4.

2. The critical depth at the exit of the stilling basin is given by Eq. 5.

3. The minimum length of the straight section is given by Eq. 6 for values of $L/b \geq 0.25$. Greater lengths of straight section may be used.

4. The sidewalls of the stilling basin may flare from 1 in ∞ (parallel extensions of the straight section walls) to 1 in 2.

5. The minimum length of the stilling basin is given by Eq. 7 for values of $L/b \geq 0.25$. Longer lengths of stilling basin may be used, but less material will be required if the straight section is lengthened to secure the same over-all outlet length.

6*a*. When the stilling basin is less than $11.5\,d'_c$ wide at its exit, the minimum tailwater depth over the basin floor is given by Eq. 10*a*.

6*b*. When the stilling basin is more than $11.5\,d'_c$ wide at its exit, the minimum tailwater depth over the basin floor is given by Eq. 10*b*. However, stilling basins wider than $11.5\,d'_c$ may result in inefficient use of the outlet.

6*c*. Greater tailwater depths may be used; lesser depths will cause more scour in the downstream channel.

7. The height of the end sill is given by Eq. 8.

8. Longitudinal sills improve the flow distribution in the outlet. They should be located as follows: (*a*) When the stilling-basin sidewalls are parallel, longitudinal sills may be omitted. (*b*) The center pair of longitudinal sills

should extend from the exit of the box inlet through the straight section and stilling basin to the end sill. (*c*) When b_b is less than 2.5 b, only two sills are needed. These sills should be located at a distance b_c of from $b/6$ to $b/4$ each side of the center line. (*d*) When b_b exceeds 2.5 b, two additional sills are required. These sills should be located parallel to the outlet center line and midway between the center sills and the sidewalls at the exit of the stilling basin. (*e*) The height of the longitudinal sills should be the same as the height of the end sill.

9. The minimum height of the sidewalls above the water surface at the exit of the stilling basin should be as given in Eq. 9, or greater. The sidewalls should extend above the tailwater surface under all conditions.

10*a*. The wingwalls should be triangular in elevation and have top slopes of 45° with the horizontal. Top slopes as flat as 30° are permissible.

10*b*. The wingwalls should flare in plan at an angle of 60° with the outlet center line. Flare angles of 45° are permissible. Wingwalls parallel to the outlet center line are not recommended.

ACKNOWLEDGMENTS

The work reported on herein was performed by the staff of the SCS, assigned to the St. Anthony Falls Hydraulic Laboratory in Minneapolis, Minn. On January 1, 1954, the SCS research project at the St. Anthony Falls Hydraulic Laboratory was transferred to the Agricultural Research Service, United States Department of Agriculture. The SCS, the Minnesota Agricultural Experiment Station, and the St. Anthony Falls Hydraulic Laboratory of the University of Minnesota are cooperating in the solution of problems concerning the hydraulics of conservation structures. The study was performed under the administrative direction of M. L. Nichols, chief of research (SCS), and Lewis A. Jones, M. ASCE, chief of the Division of Drainage and Water Control (SCS).

The experimental work and much of the analysis of the data were performed by the junior writer. The remainder of the analysis was performed by the senior writer with the assistance of other members of the staff. Many persons contributed their talents to achieve the results summarized herein; it is not possible to acknowledge specifically the contribution which each individual has made. However, these contributions are gratefully appreciated even though they are not specifically cited.

APPENDIX. NOTATION

The following symbols, adopted for use in the paper and for the guidance of discussers, conform essentially with "American Standard Letter Symbols for Hydraulics" (ASA Z10.2—1942), prepared by a committee of the American Standards Association, with Society representation, and approved by the Association in 1942:

b = width of the box inlet drop spillway:

b_a = width of the approach channel;
b_b = width of the stilling-basin exit;
b_c = spacing of center pair of longitudinal sills from the outlet center line;
b_d = distance from the box-inlet crest to the toe of the dike;
b_o = spacing of the outer pair of longitudinal sills;

C_1, C_2, C_3 = coefficients of discharge;
C_{a3} = the average discharge coefficient for channel widths equal to or greater than three crest lengths;

d = depth:

d_c = critical depth in the straight section;
d'_c = critical depth at the stilling-basin exit;
d_m = minimum height of the stilling-basin sidewalls above tailwater;
d_t = tailwater depth referred to the stilling-basin floor;
d'_t = tailwater level referred to the box-inlet crest;

g = acceleration due to gravity;
H = head:

H_{01} = apparent specific head at zero flow with control at the box-inlet crest;
H_{02} = apparent specific head at zero flow with control at the headwall opening;
ΔH = increase over free-flow head caused by high tailwater level;

h_{pz} = piezometic head;

L = length of the box inlet drop spillway:

L_b = length of the stilling basin;
L_c = crest length $= 2L + b$;
L_s = length of the straight section;

N = number of observations;
Q = discharge;
y = depth of the box inlet drop spillway;
y_s = height of the end and longitudinal sills; and
θ = angle of the wingwalls with the center line.

DISCUSSION

Neal E. Minshall,[9] A.M. ASCE.—Several variations of the general type of structure reported on by the authors were built in southwestern Wisconsin during the period from 1933 to 1938. As stated by Messrs. Blaisdell and Donnelly, the type tested by them has replaced those formerly used, and the inlet has been further modified to overcome design and construction difficulties and effect a substantial saving.

The writer examined fifty two of the original type during a four-county survey of structures in Wisconsin in 1949.[10] Although the authors' tests were limited to a maximum (y/b)-ratio of 1.0, field examination showed that one third of the structures in this area had (y/b)-ratios of approximately 1.5. Because many of the existing structures might well be used as sites for estimating peak discharges from unusual floods, it is unfortunate that complete data are not available for this higher ratio. If the structure is to be used for vertical drops of up to 12 ft and if the (y/b)-ratio is limited to 1.0, the structure will probably be wider than necessary. In general, the minimum concrete quantity for the box inlet drop spillway will be obtained with a structure which is no wider at the headwall than necessary to discharge the required Q for the design values of H and y. A wider structure will not permit a significant reduction in total weir length, and for a specific y-value the base area of the inlet will increase as the (y/b)-ratio decreases.

Still another modification of this type of inlet eliminates the long headwall and continues the sidewalls up along fill slopes of 3 to 1, using only a moderate length of cutoff under the center of the fill. Tests determining the hydraulic capacity of this type structure were made at the writer's suggestion in 1953.[11] This inlet has been designated as a trapezoidal weir box inlet. Some of the results obtained for the trapezoidal weir box inlet are available.[12] Advantages of this type of inlet are a saving of material and a reduction of scour around the inlet and at the toe of the fill.

For a comparison of inlet types the same model (previously used on the trapezoidal weir box inlet) was used for tests on the standard inlet (Fig. 2) to determine the effect of dike location on discharge for various ratios of L/b. The tests were made for a range of designs, as shown in Table 7. Each of these listings represents a series of about 15 individual test runs. The total number of runs was approximately 1,000.

The effects of the dike position on the discharge coefficients for (L/b)-values of 1.0 and 0.5 are not the same as those assumed by the authors. Comparison of the results in Table 3 with the values obtained in tests at the University of

---

[9] Hydr. Engr., Soil and Water Conservation Branch, Agri. Research Service, Madison, Wis.

[10] "Evaluation of Gully Control Structures in Southwestern Wisconsin," by Neal E. Minshall, *Technical Publication No. 116*, Soil Conservation Service, U. S. Dept. of Agriculture, Washington, D. C., September, 1953.

[11] "Model Test of Head Spillway," by R. K. Bastain, E. G. Olson, and F. L. Plautz, thesis presented to the University of Wisconsin at Madison in June, 1953, in partial fulfilment of the requirements for the degree of Bachelor of Science.

[12] "Evaluation of Wisconsin Gully Control Structures," by Neal E. Minshall, *Agricultural Engineering*, January, 1955, p. 35.

Wisconsin at Madison are shown in Table 8. The slight disagreement in the correction values for L/b equal to 2.0 results from the fact that in the Wisconsin tests the height of dike was approximately equal to 1.33 H to allow for freeboard. Thus the toe of the dike extended upstream a distance of 4 H from the headwall rather than 3 H. The Wisconsin tests shown in Table 8 were made for a design value of H/b of 0.42 whereas those reported in Table 3 were for $H/b =$ 0.35. Thus, for b_d/H equal to 1.0, the toe of the slope in the Wisconsin tests was 0.07 b farther from the spillway crest. Values of the discharge coefficient for b_d/H equal to 1.0, 0.5, and 0 only were determined in the Wisconsin tests as nearly all field installations have been designed with the toe of the fill back a distance H from the weir crest. These results show that for L/b equal to zero—that is, in a straight drop spillway—the effect of the dike is to increase the discharge, the greatest capacity resulting when $b_d/H = 0.5$.

TABLE 7.—DESIGN VALUES OF H/b TESTED TO DETERMINE EFFECT OF DIKE LOCATION

Value of y/b	Value of b_d/H	VALUE OF L/b: 0.0	0.5	1.0	1.6	2.0
0.5	0	0.22, 0.42	0.22	0.22	0.22	0.22
	1.0	0.22, 0.42	0.22	0.22	0.22	0.22
1.0	0	0.42, 0.60	0.42, 0.60	0.42, 0.60	0.42, 0.60	0.42, 0.60
	0.5	0.42	0.42, 0.60	0.42	0.42	0.42, 0.60
	1.0	0.42	0.42, 0.60	0.42, 0.60	0.42	0.42, 0.60
1.5	0.5	0.50	0.50	0.50	0.50	0.50
	1.0	0.50	0.50	0.50	0.50	0.50

TABLE 8.—CORRECTION FOR DIKE EFFECT WITH CONTROL AT THE BOX-INLET CREST

Value of L/b	VALUE OF b_d/H: 0.0		0.5	0.7		1.0
	Table 3[a]	Wis.[b]	Wis.[b]	Table 3[a]	Wis.[c]	Wis.[b]
2.0	0.84	0.72	0.82	0.85	0.84	0.86
1.5	...	0.73	0.85	...	0.87	0.89
1.0	0.73	0.78	0.92	0.75	0.94	0.96
0.5	0.60	0.93	1.01	0.62	1.01	1.01
0.0	...	1.04	1.08	...	1.06	1.04

[a] $H/b = 0.35$, toe of slope extends upstream 3 H or 1.05 b. [b] $H/b = 0.42$, toe of slope extends upstream 4 H or 1.68 b. [c] Interpolation.

The corrections shown in Table 8 apply only at the specific design head $H = 0.42\ b$. For heads less than the design head there will be a slight additional reduction in the discharge coefficient as shown in Fig. 17.

The effect of box-inlet shape L/b on the discharge coefficient, as determined from the Wisconsin tests, shows good agreement with the curve in Fig. 7. These tests also indicate that the value of $C_2\sqrt{2\,g}$ in Eq. 1*b* may be a constant for all ratios of y/b greater than 1.0.

Messrs. Blaisdell and Donnelly state (under the heading, "Results of Free-Flow Tests: Control at the Crest of The Box Inlet: Variation of Discharge Coefficient with Head"), "It will be noted that the discharge coefficient is constant in Fig. 8 when H/b is greater than 0.6." Fig. 5 does not bear out this statement but indicates, for that particular test, a reasonably constant coefficient between the limits of $H = 0.05$ and $H = 0.15$ and a gradual decrease in C_3 for higher heads. In Eq. 3*b*, which applies to the lower part of the curve in Fig. 5, control is at the spillway crest. For convenience of plotting, the authors have shown $Q^{2/3}$ versus H which is the same as raising both sides of Eq. 5 to the two-thirds power. Thus,

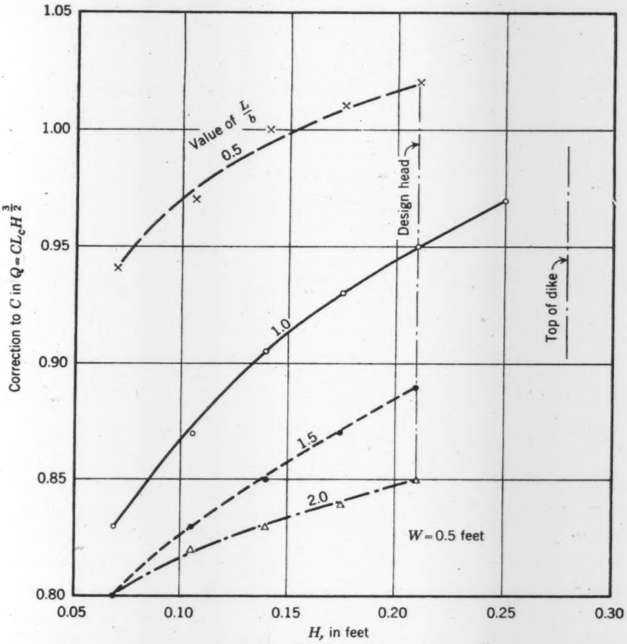

FIG. 17.—CORRECTION FOR DIKE EFFECT FOR HEADS LESS THAN THE DESIGN HEAD

$$Q^{2/3} = 3.43^{2/3}\, L^{2/3}\, H \qquad \text{(11a)}$$

or

$$Q^{2/3} = K\, H \qquad \text{(11b)}$$

in which

$$K = (3.43\ L)^{2/3} \qquad \text{(11c)}$$

Eq. 11*b* can also be written as

$$Y = K\ X \qquad \text{(12)}$$

in which $Y = Q^{2/3}$, $X = H$, and K is a constant. Eq. 12 is the equation of a straight line of slope K passing through the origin. For heads higher than 0.15 the line does not pass through the origin and the coefficient therefore cannot be a constant.

In the Wisconsin tests, for the deepest box ($y/b = 1.5$) the spillway crest appeared to be submerged at a (H/b)-value of approximately 0.5. During the tests on the trapezoidal weir box inlet, water-surface profiles were taken at the toe of the slope of the 3 to 1 dike. One series of these profiles for H/b equal to about 0.5 and for various ratios of L/b is shown in Fig. 18. From Fig. 18 it appears that the flow over the sides probably becomes a submerged weir at some point below $H/b = 0.5$ with a resultant decrease in discharge coefficient for higher heads. Discharge coefficients for the Wisconsin series of tests with headwalls similar to Fig. 2, without dikes, and for $y/b = 1.5$ are shown in Fig. 19. The significance of these coefficients is that they are reasonably constant for heads between 0.05 and 0.20 while the control remains at the crest. With control at the headwall, which condition begins below $H/b = 0.5$ for most boxes, the coefficients based on Eq. 3*b* or Fig. 8 for (H/b)-ratios above 0.5 have little practical significance. The only exceptions to the results shown in Fig. 19 would be at $L/b = 0$ or for a straight drop spillway in which the coefficient might remain reasonably constant through a wide range in heads until the spillway is submerged by high tailwater.

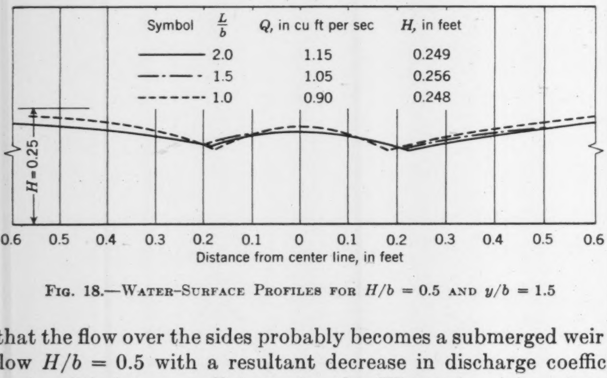

FIG. 18.—WATER-SURFACE PROFILES FOR $H/b = 0.5$ AND $y/b = 1.5$

The discharge over the sloping section of the trapezoidal weir box inlet was determined by plotting, on the same set of axes, discharge against head for this type and for the spillway shown in Fig. 2 without dikes. The difference in discharge at any head was credited directly to the sloping section. The differences in discharge plotted against head were fairly constant for all (L/b)-ratios. This method of direct comparison eliminated the necessity of applying corrections for (L/b)- and (H/b)-ratios to Eq. 3b. The flow over the sloping section can be considered as that over a triangular weir in which the discharge is proportional to the five-halves power of the head or

$$Q_s = C_s H^{5/2} \qquad (13)$$

Computations for a range of (H/b)-ratios between 0.20 and 0.40 gave an average value of $C_s = 9$. The equation for the trapezoidal weir box inlet without headwalls can therefore be written as

$$Q = 3.5\, L_c H^{3/2} + 9\, H^{5/2} \qquad (14)$$

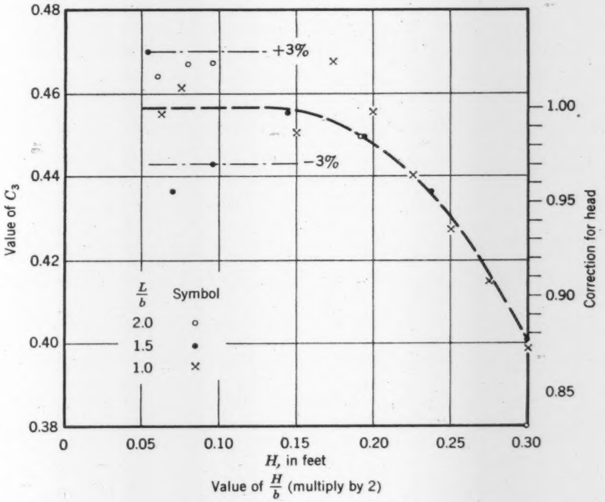

FIG. 19.—EFFECT OF H/b ON C_3-VALUES

In Eq. 14 the only correction which need be made is for the effect of the (L/b)-ratio. Comparison of discharges for the spillway shown in Fig. 2 where the toe of the dike was a distance H from the spillway crest and the trapezoidal weir inlet with sidewalls sloping up along 3 to 1 fill slopes gave an increase of approximately one third for most (L/b)-ratios.

The authors state (under the heading, "Results of Free-Flow Tests: Control at Crest of Box Inlet: Effect of Position of Dike") that "Apparently the toe of the dike should be located from 3 H to 5 H from the box-inlet crest in order to minimize the dike effect" and "The importance of keeping the toe of the dike well away from the crest of the box inlet is quite apparent from the values shown therein." These statements would perhaps be true if the main criterion of good design were to keep the crest length at a minimum. There are many situations in which keeping the dike back the recommended distances would require extensive and costly excavation as the headwall is usually carried 3 ft or more below the spillway floor to act as a cutoff. The differential loading on the long headwalls require that they be designed as cantilever retaining walls with footings.

In comparing the two types of inlets to determine the difference in concrete volume for structures of equal capacity, two designs were made for Fig. 2, and a third was made using the trapezoidal weir inlet. For all three designs $Q =$ 500 cu ft per sec, $y = 6$ ft, $b = 7.5$ ft, and $H = 3$ ft. Only the length of the level part of the inlet (L) and the length of the headwall were variable. For design 1, $b_d = 3\ H$, $L = 11.5$ ft, and the length of headwall was 21 ft on each side. For design 2, $b_d = H$, L was increased to 12.5 ft, and the headwall lengths were reduced to 15 ft, with a resultant saving in concrete of about 8%. Moving the toe of the dike closer than a distance H from the spillway crest does not result in additional savings in concrete quantities. For design 3 (the trapezoidal weir box inlet), $L = 6.5$ ft; with the length of cutoff equal to 5.0 ft, there is a further saving in concrete volume of 10% more than for design 2.

On the basis of this limited analysis, it appears that the most logical design for the inlet shown in Fig. 2 is with $b_d = H$, which places the toe of the fill as far from the spillway as possible without increasing the concrete required. Of course, as the toe of the dike is moved nearer the spillway crest, it may become necessary to place riprap at the end of the fill to prevent excessive scour.

For large structures further savings might be effected by flaring the sides uniformly from a minimum b of $2\ H$ at the upstream end of the inlet to b_b at the outlet cutoff. This change might require re-evaluation of both the inlet and outlet characteristics.

In all the tests discussed herein, the approach channel was level with the box-inlet crest. Many of the structures examined in the field have built up silting gradients of about 1% above the spillway crest. Therefore, during future tests it would be advisable to determine the effect of silting gradients on the discharge capacity.

FRED W. BLAISDELL,[13] M. ASCE, AND CHARLES A. DONNELLY.[14]—The writers greatly appreciate Mr. Minshall's discussion. He neglected to note that his association with this type of structure began in 1933 when he worked with Mr. Kessler in making some early tests.[3] Mr. Minshall also worked on the design and construction of many of the box inlet drop spillways built in western Wisconsin in the 1930's. He did cite the evaluation of their performance which he made in 1949. Mr. Minshall is, therefore, well qualified to discuss the writers' paper.

The studies reported by the writers were made to obtain design information for use by the SCS, and the limits of the test variables, including the limitation of y/b to a maximum of 1.0, were largely set by the SCS design engineers. It is unfortunate, as Mr. Minshall notes, that information was not obtained that could be used for estimating peak discharges through the older structures having higher values of y/b.

---

[13] Project Supervisor, Agri. Research Service, U. S. Dept. of Agriculture, St. Anthony Falls Hydr. Lab., Minneapolis, Minn.

[14] Hydr. Engr., Agri. Research Service, U. S. Dept. of Agriculture, St. Anthony Falls Hydr. Lab., Minneapolis, Minn.

The data on the effect of the position of the dike, on which Table 3 was based, were scanty, as was carefully emphasized. Time limitations and a need for concentration of efforts on other studies made it impossible to give the effect of dike position the study it deserved. It appears that the assumptions used to extrapolate Table 3 beyond the range of the tests were not completely correct. For these reasons, the additional data presented by Mr. Minshall are most welcome.

Mr. Minshall states that for $L/b = 0$ (straight drop spillway) the greatest capacity of the spillway is reached when $b_d/H = 0.5$. This statement is at least qualitatively verified by unreported tests made by the junior writer at the St. Anthony Falls Hydraulic Laboratory. These tests, made with vertical parallel approach-channel walls, show that the maximum capacity of the straight drop spillway is reached when the width of the approach channel is 1.25 times the length of the straight drop spillway crest.

It is unfortunate that several of Mr. Minshall's comments indicate that he has assumed that Fig. 8 and Eq. 3*b* apply to the entire curve of Fig. 5. Fig. 8 and Eq. 3*b* apply only to that part of the curve of Fig. 5 which represents the control at the box-inlet crest. Eq. 1*b* applies when the control is at the headwall opening. The latter equation includes a correction for the fact that the straight line representing the high head data of Fig. 5 does not pass through the origin. A constant coefficient C_2 is obtained when this H_{02}-correction is applied, as is indicated by the straight line in Fig. 5 when the control is at the headwall opening. Mr. Minshall's use of Eq. 2 for both crest control and submerged-crest control undoubtedly accounts for the reduction in C_3 at the higher heads shown in Fig. 19.

The writers' experiments show that the shift from crest control to headwall control takes place when the crest becomes affected by submergence, as Mr. Minshall has shown in Fig. 18, and that at higher heads a constant coefficient is obtained if Eq. 1*b* is used. The data show that this shift may occur at (H/b)-values ranging from 0.1 to 1.4—the maximum value of H/b included in the test—indicating that the shift from crest control to headwall control does not occur at a definite value of H/b. The writers' data also show that headwall control sometimes begins at (H/b)-values considerably greater than 0.5, contrary to Mr. Minshall's statement. Values of H/b in excess of 0.5 were obtained for tests 82*a* to 84, 114 to 122, and 124 to 129. It will be noted from Table 2 that these tests include those conducted on the narrower approach channels and the deepest box inlets.

The writers have observed that the toe of the dike is frequently pushed closer to the crest during construction than is specified by the plans; this reduces the capacity of the spillway below the design value. When a trapezoidal weir box inlet is used, the sloping sidewall part of the crest provides a definite line to which the fill can be graded. This helps to assure that construction is performed according to the design. Eq. 14, which gives the discharge for this type of weir crest when the fill slope is 1 on 3, is therefore a welcome contribution.

Some of the thoughts expressed in the foregoing regarding the proximity of the dike toe to the box-inlet crest were in the minds of the writers when they stated that it is important to keep the toe of the dike well away from the crest. Mr. Minshall has correctly noted that the designer must provide the most economical structure. The hydraulic criteria presented in the paper should provide sufficient latitude to permit choice among several possible combinations of dimensions to fit the site and achieve this end.

The writers are in full agreement that the effect of silting gradients on the discharge capacity should be determined. Other items which might be considered are the effects of channeling through the silt deposits and the effects of lack of maintenance on the capacity.

AMERICAN SOCIETY OF CIVIL ENGINEERS
Founded November 5, 1852
TRANSACTIONS

Paper No. 2829

THE OCTAGONAL-GIRDER FOUR-COLUMN SPACE FRAME

BY PAUL C. DISARIO, JR.,[1] A. M. ASCE, JOHN S. PODOLAN,[2]
AND NICHOLAS A. WEIL,[3] J. M. ASCE

WITH DISCUSSION BY MESSRS. ABDEL F. DIWAN; SIDNEY SHORE AND HUMBERTO RINCON; AND PAUL C. DISARIO, JR., JOHN S. PODOLAN, AND NICHOLAS A. WEIL

SYNOPSIS

This paper presents the analysis of a space frame consisting of a closed octagonal ring supported rigidly on four columns. A solution was obtained in closed form for three types of loading: (*a*) Uniformly distributed vertical loading, (*b*) concentrated horizontal (or shear) loading, and (*c*) linearly varying antisymmetrical (moment) loading. In the derivation it has been assumed that the girder is infinitely rigid in its plane; this stipulation is physically very nearly correct.

The computations have been extended to include the fixed and hinged conditions at the bottom of the supporting columns. The moments at the segmental points and at the column-ring junctions as well as the end reactions are expressed explicitly and are presented in tabular form; these expressions appear as functions of the load, the ratio of bending to torsional stiffness of the ring (k), and the ratio of relative bending stiffness of the ring and the columns (n).

In addition to an extended analysis of horizontal and moment loading for fixed columns, a modified analysis is presented from which considerable simplification of the functions involved in the moment expressions results. Both types of analyses are accompanied by numerical examples.

The general method of analysis is adaptable to ring girders of different shapes or having a greater number of supporting columns.

NOTE.—Published, essentially as printed here, in November, 1954, as *Proceedings-Separate No. 542*. Positions and titles given are those in effect when the paper or discussion was approved for publication in *Transactions*.

[1] Section Head, Foundations and Concrete Section, M. W. Kellogg Co., New York, N. Y.

[2] Structural Engr., M. W. Kellogg Co., New York, N. Y.

[3] Development Engr., M. W. Kellogg Co., New York, N. Y.

NOTATION

The letter symbols in this paper are defined where they first appear, in the text or in the illustrations, and are assembled alphabetically in Appendix III.

INTRODUCTION

The majority of structures in existence are space structures subjected to loads in three dimensions. Curved or segmental frames are frequently used in the form of supporting structures for chemical equipment, in ship construction, for bins or water towers, curved balcony frames, arches, horizontally curved bridges, or components of piping systems.

For convenience and simplicity, most of these structures are reduced in design to planar considerations. This simplification, however, leaves unanswered several questions pertaining to the load-carrying capacity of these structures. It becomes necessary, therefore, to use a higher factor of safety, and thus the inherent strength of spatial frames is not fully utilized.

As an example, present refinery tower supports normally consist of a square slab with a central octagonal cutout, supported at the corners on four columns. Obviously, this type of structure, square in plan and supporting a circular vertical vessel, is not the ideal solution from the esthetic and engineering viewpoints. Because vertical loading alone induces moments in the columns in two directions—thus considerably affecting column sizes—the objective of economical design is far from being truly attained. In comparison, by placing columns in the center of four sides of the octagonal ring girder (Fig. 1), column moments in the directions of the sides are eliminated and the magnitude of column moments normal to the sides is considerably reduced. This situation is true for symmetrical vertical loading only. Comparative studies indicate that much material can be saved if an octagonal-ring girder structure is used instead of the usual square structure.

The analysis of these structures is by necessity quite involved. A systematic, although somewhat brief, study of horizontally curved beams is given by S. Timoshenko and D. H. Young (1).[4] In addition, many investigators (2) (3) (4) (5) (6) (7) (8) (9) (10) (11) (12) (13) (14) (15) (16) have studied various aspects of the problem of curved beams having different modes of end fixity and being loaded normal to their plane of curvature. Spatially curved piping systems, a special group of the spatial frame problems, have also been subjected to numerous analytical studies (17) (18) (19) (20) (21) (22).

To the writers' knowledge, however, no study exists in which the stresses in space frames with horizontally curved members, subject to loading in, or normal to, their plane of curvature are analyzed. This study was conducted to initiate an analysis of structures of this nature and to foster interest for further development in this field.

The structures analyzed herein are space frames consisting of a closed octagonal ring, supported rigidly on four evenly spaced columns, which are either hinged or fixed to their foundations. The method of solution presented is easily extendable to ring structures of a different shape, or to an arbitrary number of supporting columns.

---

[4] Numerals in parentheses—thus, (1)—refer to corresponding items in the Bibliography (see Appendix II).

EXTENDED ANALYSIS

Designation of Forces and Method of Attack.—The general shape of this structure is shown in Fig. 1. The octagonal ring has a rectangular cross section, the width of which is denoted by b and the depth by d. The columns are assumed to have a square cross section (length of sides equal to c) although this is not a mandatory assumption from the viewpoint of analysis.

The solution in most cases is based on the Castigliano theorem or the principle of least work (23). A curvilinear orthogonal coordinate system is used whose positive x-axis is directed in the forward sense of travel from A to B to C to D (Fig. 1). The positive y-axis is obtained by a 90° clockwise rotation of the x-axis (that is, the y-axis always points toward the outside of the ring). This coordinate system suffers abrupt directional changes at the corner-points of the octagonal ring.

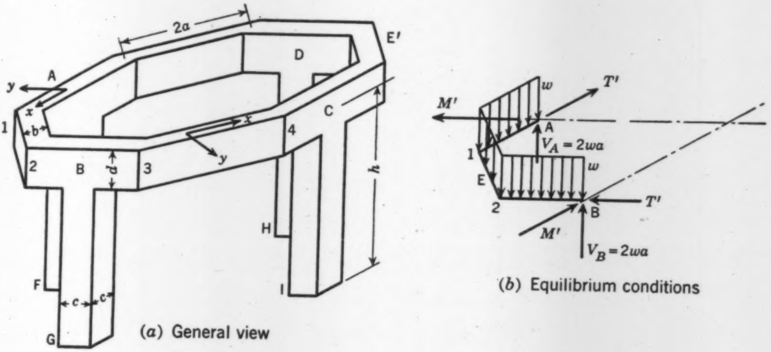

(*a*) General view

(*b*) Equilibrium conditions

FIG. 1.—OCTAGONAL FRAME, SHOWING FORCES ON A QUADRANT SUPPORTING A UNIFORMLY DISTRIBUTED VERTICAL LOAD

A vector notation, using the right-hand-screw rule, is used to designate the moments. Bending and twisting moments in the girder are denoted by M and T, and are considered positive if their vectors point in the direction of the positive y-axis and x-axis, respectively. Vertical forces are positive if their vectors point downward. A double subscript on moments depicts a generalized moment over a member of the closed ring; a concurrent subscript and superscript indicate a specific moment, whose location is denoted by the subscript and orientation by the superscript. Moments at any particular location in the ring will be understood to act on the right side (far side in the sense of travel) of the section.

Bending moments in the supporting columns will be considered positive if their vectors are oriented parallel to the positive sense of the x-axis or the

y-axis. These moments will also bear a subscript indicating their location and a superscript indicating their orientation in the columns.

Uniformly Distributed Vertical Load.—Under a uniformly distributed vertical loading the distribution of applied and reacting forces and moments is symmetrical about both the AC-axis and the BD-axis; consequently it suffices to scrutinize only one quadrant of the structure as shown in Fig. 1 (b) in which M' and T' denote the redundant bending moment and torque, respectively. Static equilibrium contributes the following equation,

$$M' = \frac{3}{2} w\, a^2 - T' \quad \dots\dots\dots\dots\dots\dots (1)$$

The ensuing analysis is presented in full for the sake of clarity and to eliminate the tedium of repetitive details throughout the paper.

The moment expressions for the members of the quadrant take the following form:

$$M_{A-1} = -2\, w\, a\, x + \frac{w\, x^2}{2} + M'$$

$$T_{A-1} = -T'$$

$$M_{1-2} = \frac{-3}{2\sqrt{2}} w\, a^2 - w\, a\, x + \frac{w\, x^2}{2} + \frac{M'}{\sqrt{2}} - \frac{T'}{\sqrt{2}}$$

$$T_{1-2} = \frac{3}{2\sqrt{2}} w\, a^2 - \frac{M'}{\sqrt{2}} - \frac{T'}{\sqrt{2}}$$

$$M_{2-B} = w\, a\, x + \frac{w\, x^2}{2} - T'$$

$$T_{2-B} = \frac{3}{2} w\, a^2 - M'.$$

By the Castigliano theorem, the torsional rotation at point A or point B under the external forces shown in Fig. 1 (b) is determined from the equation:

$$\theta^T{}_A = \frac{\partial U}{\partial T'} = -\frac{\partial}{\partial T'}\left[\sum_{\text{Member A-1}}^{\text{Member 2-B}} \int_0^l \left(\frac{M^2}{2\,E\,I} + \frac{T^2}{2\,G\,J}\right) dx\right]$$

$$= -\sum_{\text{Member A-1}}^{\text{Member 2-B}} \left[\frac{1}{E\,I} \int_0^l \left(M \frac{\partial M}{\partial T'} + k\, T \frac{\partial T}{\partial T'}\right) dx\right]$$

$$= \left[\frac{2-\sqrt{2}}{3} w\, a^2 - (3 + k)\, T'\right] \frac{a}{E\,I} \quad \dots\dots\dots\dots\dots\dots (2)$$

in which $k = E\,I/G\,J$ and l is the length of the member in question.

Further analysis must take into account the degree of fixity of the columns.

1. Columns Hinged at the Base.—By symmetry, the bending moments in the ring on two sides of any support are equal and opposite so that the columns

are subject to bending only in the diametral normal planes of the ring (planes AFIC and BGHD in Fig. 1) under a moment equal to 2 T' applied at their tops. Hence, for hinged-base columns, the top rotation is

$$\theta^{xx}{}_{cA} = \frac{2\,T'\,h}{3\,E_c\,I_c} \qquad (3)$$

in which the subscripts c refer to the columns.

Because the torsional rotation of the ring at the supports must equal the bending rotation of the top of the columns, one has to satisfy the condition,

$$\theta^{T}{}_{A} = \theta^{xx}{}_{cA} \qquad (4)$$

Assuming that $E_c = E$ (this assumption is tacitly understood throughout this paper) and denoting the relative stiffness of the ring and column by

$$n = \frac{h}{a}\,\frac{I}{I_c}$$

one obtains by substitution of Eqs. 2 and 3 into Eq. 4

$$T' = \beta_1\,w\,a^2 \qquad (5)$$

in which

$$\beta_1 = \frac{0.5858}{2\,n + 3\,k + 9} \qquad [a]$$

Substituting Eq. 5 into Eq. 1,

$$M' = (1.5 - \beta_1)\,w\,a^2 \qquad (6)$$

Knowing values of M' and T', it is possible to derive explicit expressions for the moments at any point in the ring and in the columns from the moment equations given at the outset. These moments are determined by substituting β_1 for β in Table 1. The twisting moments over member 1–2 are equal to zero because symmetry about the axis EE′ excludes the presence of a torque at E.

When either $n \longrightarrow \infty$ or $k \longrightarrow \infty$, β_1 vanishes; in these cases both twisting moments in the ring and bending moments in the columns also tend toward zero, and the solution reverts to a statically determinate one.

A simplification from the standpoint of design can be achieved in the following way:

For a rectangular cross section (width b, depth d), $I = 0.08333\,b\,d^3$. Theoretically (23*a*), $G = E/2\,(1 + \nu)$ and assuming $\nu = 0.15$ for reinforced concrete, $G = 0.4348\,E$.

Furthermore, for a cross section with a depth-to-width ratio varying from 0.33 to 3.0, an excellent approximation is obtained if one assumes (23*b*)

$$J = \frac{0.286}{b^2 + d^2}\,b^3\,d^3.$$

With these expressions the equation for k can be rearranged into the following form,

$$k = \frac{E\,I}{G\,J} = 0.6702\left(1 + \frac{d^2}{b^2}\right) \qquad (7)$$

this formula being valid over the range $(1/3) < (d/b) < 3$.

TABLE 1.—PEDESTAL UNDER UNIFORMLY DISTRIBUTED VERTICAL LOAD,[a] w

(a) OCTAGONAL RING

Location and Direction	Bending Moments	Twisting Moments
At A in direction of 1	$M^{1}{}_{A} = (1.5 - \beta)\,w\,a^2$	$T^{1}{}_{A} = -\beta\,w\,a^2$
At 1 in direction of A	$M^{A}{}_{1} = -\beta\,w\,a^2$	$T^{A}{}_{1} = -\beta\,w\,a^2$
At 1 in direction of E	$M^{E}{}_{1} = -\sqrt{2}\,\beta\,w\,a^2$	$T^{E}{}_{1} = 0$
At E	$M_E = -(0.5 + \sqrt{2}\,\beta)\,w\,a^2$	$T_E = 0$
At 2 in direction of E	$M^{E}{}_{2} = -\sqrt{2}\,\beta\,w\,a^2$	$T^{E}{}_{2} = 0$
At 2 in direction of B	$M^{B}{}_{2} = -\beta\,w\,a^2$	$T^{B}{}_{2} = \beta\,w\,a^2$
At B in direction of 2	$M^{2}{}_{B} = (1.5 - \beta)\,w\,a^2$	$T^{2}{}_{B} = \beta\,w\,a^2$

(b) COLUMNS

Bending Moments at Column Tops	Hinged Bases	Fixed Bases
	Bending Moments at Column Bases	
$M^{xx}{}_{cA} = -2\,\beta\,w\,a^2$	$M^{xx}{}_{cF} = 0$	$M^{xx}{}_{cF} = \beta_2\,w\,a^2$
$M^{yy}{}_{cA} = 0$	$M^{yy}{}_{cF} = 0$	$M^{yy}{}_{cF} = 0$
$M^{xx}{}_{cB} = -2\,\beta\,w\,a^2$	$M^{xx}{}_{cG} = 0$	$M^{xx}{}_{cG} = \beta_2\,w\,a^2$
$M^{yy}{}_{cB} = 0$	$M^{yy}{}_{cG} = 0$	$M^{yy}{}_{cG} = 0$
Vertical Loads	**Horizontal Reactions at Bases**	
$V_{cA} = 4\,a\,w$	$H^{xx}{}_{cF} = 0$	$H^{xx}{}_{cF} = 0$
$V_{cB} = 4\,a\,w$	$H^{yy}{}_{cF} = (2\,\beta_1/h)\,w\,a^2$	$H^{yy}{}_{cF} = (3\,\beta_2/h)\,w\,a^2$
	$H^{xx}{}_{cG} = 0$	$H^{xx}{}_{cG} = 0$
	$H^{yy}{}_{cG} = (2\,\beta_1/h)\,w\,a^2$	$H^{yy}{}_{cG} = (3\,\beta_2/h)\,w\,a^2$

[a] In place of β, substitute β_1 (Eq. [a]) when hinged columns are used and β_2 (Eq. [b]) when fixed columns are used, except where these already appear.

The values of d/b represent tangible design dimensions. It has to be borne in mind, however, that for extremely flat or deep cross sections the expression for J will not hold; in these cases recourse has to be made to Mr. Timoshenko's study (23b). Furthermore, for steel structures ν is equal to 0.30 which will also alter the character of Eq. 7.

2. Columns Fixed at the Base.—The approach in this case is similar to that of the previous case, except that Eq. 3 is modified to

$$\theta^{xx}{}_{cA} = \frac{T' h}{2 E_c I_c} \qquad (8)$$

Thus, combining Eqs. 2, 8, and 4, there results

$$T' = \beta_2 \, w \, a^2 \qquad (9)$$

in which

$$\beta_2 = \frac{0.3905}{n + 2k + 6} \qquad [b]$$

Substitution of Eq. 9 into Eq. 1 yields

$$M' = (1.5 - \beta_2) \, w \, a^2 \qquad (10)$$

The bending and twisting moments for a uniformly loaded octagonal pedestal on four fixed-ended columns are determined by substituting β_2 for β in Table 1. For both cases (hinged or fixed-ended columns) maximum bending moments and torques are to be found at point A in the octagonal ring.

Comparing the solutions for the hinged columns and fixed-ended columns, it appears that $\beta_1 = \beta_2$ when $n = 0$ or $n = \infty$; for these cases, therefore, the solutions coincide. When $0 < n < \infty$, $\beta_1 < \beta_2$, so that greater maximum bending moments but smaller maximum torques are developed in the ring of the hinged-column pedestal. The bending moments in the columns are also smaller in this case as compared to the pedestal with fixed columns.

Horizontal Shear Loading.—Wind pressures on the supported tower or equipment are transmitted to the frame as a concurrent horizontal shear and overturning moment. Although the exact distribution of these shear forces is not known, it is a plausible approach to unify them into a single resultant and then study the action of the frame under the attack of a concentrated horizontal force in the plane of the ring.

In the following analysis the ring is assumed to be infinitely rigid in its plane; hence, no bending moments can develop in this plane. This assumption is physically very nearly correct and permits great simplifications in solving the problem.

The structure may be exposed to a wind attack from any arbitrary direction. Greatest bending moments and vertical shears occur, however, when the wind load is parallel to the planes defined by a set of diametrically opposite columns (such as plane AFIC in Fig. 1); greatest twisting moments occur when the wind load attacks on vertical planes oriented at 45° to the previous direction. The analysis scrutinized in detail herein refers to the lateral loading directed in the plane AFIC. The functions for wind loading P at 45° to this direction can be obtained by superimposing the component effects of two loads of 0.7071 P magnitude, attacking on the perpendicular planes AFIC and BGHD, respectively.

As an auxiliary part of the solution, a study of the octagonal ring subjected to two equal moments $\bar{T}$ applied at A and C and two equal moments $\bar{M}$ applied at B and D has to be made, these four moments being undirectional, as shown in Fig. 2(*a*). The geometry of structure and loading produce the following limitations:

From antisymmetry about axis BD,

$$V_B = V_D = M_B = M_D = \theta^T{}_B = \theta^T{}_D = 0$$
$$V_A = -V_C.$$

From symmetry about axis AC,

$$T_A = T_C = \theta^M{}_A = \theta^M{}_C = 0.$$

Symmetry also permits limiting the study to the semi-octagonal ring extending from A to C (Fig. 2(*b*)). This illustration shows, in addition to the external moments $\bar{T}$ and $\bar{M}$, a moment M'' which represents the redundant bending moment existing at supports A and C.

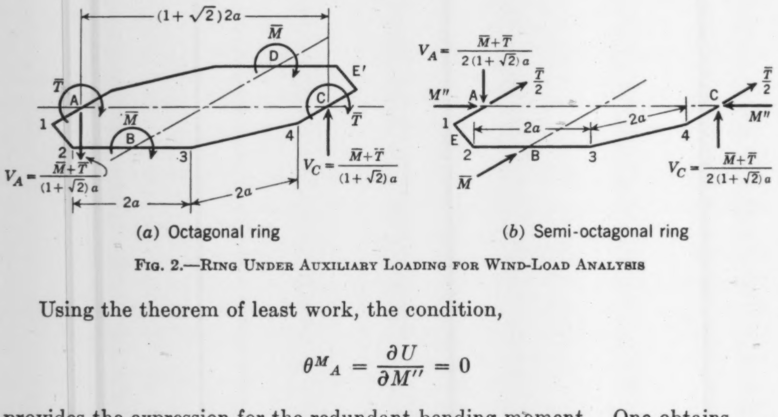

(*a*) Octagonal ring (*b*) Semi-octagonal ring

FIG. 2.—RING UNDER AUXILIARY LOADING FOR WIND-LOAD ANALYSIS

Using the theorem of least work, the condition,

$$\theta^M{}_A = \frac{\partial U}{\partial M''} = 0$$

provides the expression for the redundant bending moment. One obtains

$$M'' = \frac{0.3536\,k + 0.3018}{k+1}\,\bar{M} + \frac{0.6036\,k + 0.05178}{k+1}\,\bar{T}.$$

This expression enables one to determine the torsional rotation over support A and the bending rotation of the ring over support B solely in terms of the applied external moments $\bar{M}$ and $\bar{T}$:

$$\left.\begin{aligned}\theta^T{}_A &= \frac{\partial U}{\partial \bar{T}} = \frac{a}{E\,I}\,(\zeta_1\,\bar{M} + \zeta_2\,\bar{T}) \\ \theta^M{}_B &= \frac{\partial U}{\partial \bar{M}} = \frac{a}{E\,I}\,(\zeta_3\,\bar{M} + \zeta_1\,\bar{T})\end{aligned}\right\}\ldots\ldots\ldots\ldots\ldots(11)$$

in which ζ_1, ζ_2, and ζ_3 can be represented to four-digit accuracy by the following functions:

$$\zeta_1 = \frac{-\,0.06066\,k^2 + 0.001944\,k - 0.05167}{k+1}$$

$$\zeta_2 = \frac{0.5430\,k^2 + 1.8644\,k + 0.10366}{k+1}$$

and

$$\zeta_3 = \frac{0.08579\,k^2 + 0.6395\,k + 0.5430}{k+1}.$$

Eqs. 11 satisfy the conditions of the Maxwell law of reciprocal relations. Further treatment of this problem must again be subdivided according to the mode of fixity of the columns.

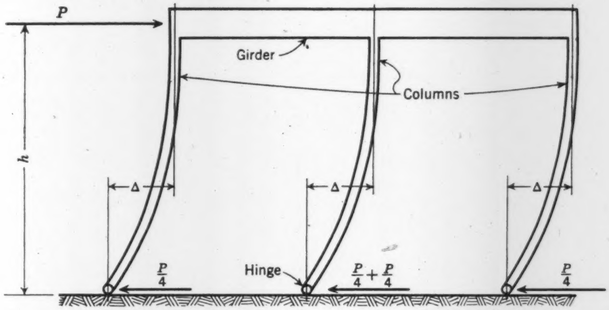

FIG. 3.—DISTORTION OF A FRAME HAVING A VERY STIFF GIRDER, UNDER A HORIZONTAL LOAD

1. Columns Hinged at the Base.—Fixing the columns momentarily at the top and treating the octagonal ring as a rigid beam, every column is deflected through a distance Δ under the horizontal load (Fig. 3). The resulting moment at the top of each column is

$$M_c\ (\text{top}) = \frac{3\,E\,I_c}{h^2}\,\Delta = \frac{P\,h}{4}.$$

If the column-ring joints are released, the displacements are increased to Δ_1, while the column-ring junctions are rotated through an angle of $\theta^T{}_A$ at A and $\theta^M{}_B$ at B. Hence, the moments in the columns become

$$M^{xx}{}_{cA} = \frac{3\,E\,I_c}{h}\left(\frac{\Delta_1}{h} - \theta^T{}_A\right)$$

$$M^{yy}{}_{cB} = \frac{3\,E\,I_c}{h}\left(\frac{\Delta_1}{h} - \theta^M{}_B\right).$$

Eliminating Δ_1 from these equations,

$$\frac{h}{3\,E\,I_c}\,M^{xx}{}_{cA} + \theta^T{}_A = \frac{h}{3\,E\,I_c}\,M^{yy}{}_{cB} + \theta^M{}_B.$$

Combining this expression with the condition,

$$M^{xx}{}_{cA} + M^{vv}{}_{cB} = \frac{P\,h}{2}$$

one arrives at the following relations for the column-top moments:

$$\left.\begin{aligned} M^{xx}{}_{cA} &= \frac{P\,h}{4} + \frac{3\,E\,I_c}{2\,h}\,(\theta^M{}_B - \theta^T{}_A) \\ M^{vv}{}_{cB} &= \frac{P\,h}{4} + \frac{3\,E\,I_c}{2\,h}\,(\theta^T{}_A - \theta^M{}_B) \end{aligned}\right\}\ldots\ldots\ldots\ldots\ldots (12)$$

The condition that moments in the ring and columns be equal at their junction demands that

$$M^{xx}{}_{cA} = \bar{T}$$
$$M^{vv}{}_{cB} = \bar{M}$$

in which $\bar{T}$ and $\bar{M}$ are the moments under whose action the ring was analyzed previously. Using this condition, substituting Eqs. 11 into Eqs. 12, and solving the resulting simultaneous equations for the column-top moments yields the expressions:

$$M^{xx}{}_{cA} = \frac{n + 3\,(\zeta_3 - \zeta_1)}{2\,[2\,n + 3\,(\zeta_2 + \zeta_3 - 2\,\zeta_1)]}\,P\,h$$

$$M^{vv}{}_{cB} = \frac{n + 3\,(\zeta_2 - \zeta_1)}{2\,[2\,n + 3\,(\zeta_2 + \zeta_3 - 2\,\zeta_1)]}\,P\,h.$$

Finally, substituting the ζ-functions into these expressions and observing that $T^1{}_A = -\,\frac{1}{2}\,M^{xx}{}_{cA}$ and $M^2{}_B = \frac{1}{2}\,M^{vv}{}_{cB}$ leads to the results:

and

$$\left.\begin{aligned} T^1{}_A &= (\gamma_1 - 0.25)\,P\,h \\ M^2{}_B &= \gamma_1\,P\,h \end{aligned}\right\}\ldots\ldots\ldots\ldots\ldots\ldots (13)$$

The moments and forces at any point in the structure can thus be expressed in terms of the following two functions:

$$\left.\begin{aligned} \gamma_1 &= \frac{1}{A}\,[0.125\,n\,(k + 1) + 0.2263\,k^2 + 0.6984\,k + 0.05825] \\ \gamma_2 &= \frac{1}{A}\,[n\,(0.2393\,k + 0.08839) + 0.2263\,k^2 + 0.6984\,k + 0.05825] \end{aligned}\right\}\ldots .[\mathrm{c}]$$

in which

$$A = n\,(k + 1) + 1.125\,\left(k^2 + \frac{10}{3}\,k + 1\right).$$

The design quantities at the significant points in quadrant AB of the pedestal are listed in Table 2. Over quadrant BC the torques are equal whereas bending moments are equal in magnitude but opposite in sign, as compared to those acting in quadrant AB.

TABLE 2.—PEDESTAL UNDER CONCENTRATED HORIZONTAL LOAD, P

(a) OCTAGONAL RING

Bending Moments	Twisting Moments
Hinged Column Bases	
$M^1{}_A = -\gamma_2 P h$	$T^1{}_A = (\gamma_1 - 0.25) P h$
$M^A{}_1 = -(\gamma_2 - 0.10355) P h$	$T^A{}_1 = (\gamma_1 - 0.25) P h$
$M^E{}_1 = 0.7071 (\gamma_1 - \gamma_2 - 0.14645) P h$	$T^E{}_1 = 0.7071 (\gamma_1 + \gamma_2 - 0.3536) P h$
$M_E = 0.7071 (\gamma_1 - \gamma_2) P h$	$T_E = 0.7071 (\gamma_1 + \gamma_2 - 0.3536) P h$
$M^E{}_2 = 0.7071 (\gamma_1 - \gamma_2 + 0.14645) P h$	$T^E{}_2 = 0.7071 (\gamma_1 + \gamma_2 - 0.3536) P h$
$M^B{}_2 = (\gamma_1 - 0.10355) P h$	$T^B{}_2 = (\gamma_2 - 0.25) P h$
$M^2{}_B = \gamma_1 P h$	$T^2{}_B = (\gamma_2 - 0.25) P h$
Fixed Column Bases	
$M^1{}_A = -\gamma_4 P h$	$T^1{}_A = (\gamma_3 - \gamma_5) P h$
$M^A{}_1 = -(\gamma_4 - 0.4142 \gamma_5) P h$	$T^A{}_1 = (\gamma_3 - \gamma_5) P h$
$M^E{}_1 = 0.7071 (\gamma_3 - \gamma_4 - 0.5858 \gamma_5) P h$	$T^E{}_1 = 0.7071 (\gamma_3 + \gamma_4 - 1.4142 \gamma_5) P h$
$M_E = 0.7071 (\gamma_3 - \gamma_4) P h$	$T_E = 0.7071 (\gamma_3 + \gamma_4 - 1.4142 \gamma_5) P h$
$M^E{}_2 = 0.7071 (\gamma_3 - \gamma_4 + 0.5858 \gamma_5) P h$	$T^E{}_2 = 0.7071 (\gamma_3 + \gamma_4 - 1.4142 \gamma_5) P h$
$M^B{}_2 = (\gamma_3 - 0.4142 \gamma_5) P h$	$T^B{}_2 = (\gamma_4 - \gamma_5) P h$
$M^2{}_B = \gamma_3 P h$	$T^2{}_B = (\gamma_4 - \gamma_5) P h$

(b) COLUMNS

Hinged Base	Fixed Base	Hinged Base	Fixed Base
Bending Moments at Column Tops		**Bending Moments at Column Bases**	
$M^{xx}{}_{cA} = -(0.5 - 2\gamma_1) P h$	$M^{xx}{}_{cA} = -2 (\gamma_5 - \gamma_3) P h$	$M^{xx}{}_{cF} = 0$	$M^{xx}{}_{cF} = (-\gamma_3 - 0.5\gamma_5 + 0.25) P h$
$M^{yy}{}_{cA} = 0$	$M^{yy}{}_{cA} = 0$	$M^{yy}{}_{cF} = 0$	$M^{yy}{}_{cF} = 0$
$M^{xx}{}_{cB} = 0$	$M^{xx}{}_{cB} = 0$	$M^{xx}{}_{cG} = 0$	$M^{xx}{}_{cG} = 0$
$M^{yy}{}_{cB} = -2\gamma_1 P h$	$M^{yy}{}_{cB} = -2\gamma_3 P h$	$M^{yy}{}_{cG} = 0$	$M^{yy}{}_{cG} = (+\gamma_3 - 1.5\gamma_5 + 0.25) P h$
Vertical Loads		**Horizontal Reactions at Bases**	
$V_{cA} = -\frac{0.2071}{a} P h$	$V_{cA} = -\frac{0.8284}{a} \gamma_5 P h$	$H^{xx}{}_{cF} = 0$	$H^{xx}{}_{cF} = 0$
$V_{cB} = 0$	$V_{cB} = 0$	$H^{yy}{}_{cF} = (0.5 - 2\gamma_1) P$	$H^{yy}{}_{cF} = -(3\gamma_3 - 1.5\gamma_5 - 0.25) P$
		$H^{xx}{}_{cG} = -2\gamma_1 P$	$H^{xx}{}_{cG} = -(3\gamma_3 - 1.5\gamma_5 + 0.25) P$
		$H^{yy}{}_{cG} = 0$	$H^{yy}{}_{cG} = 0$

For the horizontal shear-loading, the location of maximum and minimum moments depends on the values of k and n. However, within the range of variables normally encountered, the greatest negative bending moment and greatest absolute torque occur at point A, whereas the maximum positive bending moment in the ring exists at junction B.

2. Columns Fixed at the Base.—A rigid horizontal translation Δ of the ring induces the following moments at the column junctions:

$$M_c \text{ (top)} = \frac{6\,E\,I_c}{h^2}\,\Delta.$$

If the junctions are released, the ensuing deflections and rotations will modify these moments as follows:

$$M^{xx}{}_{cA} = \frac{4\,E\,I_c}{h}\left(\frac{3\,\Delta_1}{2\,h} - \theta^T{}_A\right)$$

$$M^{vv}{}_{cB} = \frac{4\,E\,I_c}{h}\left(\frac{3\,\Delta_1}{2\,h} - \theta^M{}_B\right).$$

Elimination of Δ_1 yields the identity:

$$M^{xx}{}_{cA} - M^{vv}{}_{cB} = \frac{4\,E\,I_c}{h}\,(\theta^M{}_B - \theta^T{}_A).$$

The governing condition for a concentrated horizontal force is thus expressed as

$$M^{xx}{}_{cA} + M^{vv}{}_{cB} = \frac{P\,h}{4} - \frac{E\,I_c}{h}\,(\theta^M{}_B + \theta^T{}_A).$$

The latter two equations can be solved for the column-top moments. Further substitution of Eqs. 11 and the continuity condition into the solutions yields

$$M^{xx}{}_{cA} = \frac{n\,[n + 4\,(\zeta_3 - \zeta_1)]}{4\,[2\,n^2 + n\,(5\,\zeta_2 + 5\,\zeta_3 - 6\,\zeta_1) + 8\,(\zeta_2\,\zeta_3 - \zeta^2{}_1)]}\,P\,h$$

and

$$M^{vv}{}_{cB} = \frac{n\,[n + 4\,(\zeta_2 - \zeta_1)]}{4\,[2\,n^2 + n\,(5\,\zeta_2 + 5\,\zeta_3 - 6\,\zeta_1) + 8\,(\zeta_2\,\zeta_3 - \zeta^2{}_1)]}\,P\,h.$$

Insertion of the ζ-functions in turn changes these expressions to

$$\left.\begin{aligned} T^1{}_A &= -\frac{1}{2}\,M^{xx}{}_{cA} = (\gamma_3 - \gamma_5)\,P\,h \\ \text{and}\qquad M^2{}_B &= \frac{1}{2}\,M^{vv}{}_{cB} = \gamma_3\,P\,h \end{aligned}\right\}\ldots\ldots\ldots\ldots\ldots(14)$$

so that all quantities of interest can be expressed with the aid of three auxiliary functions:

$$\left.\begin{aligned}
\gamma_3 &= \frac{n}{B}[0.0625\,n\,(k+1) + 0.15089\,k^2 + 0.4656\,k + 0.03883] \\
\gamma_4 &= \frac{n}{B}[n\,(0.11964\,k + 0.04419) + 0.15089\,k^2 + 0.4656\,k + 0.03883] \\
&\text{and} \\
\gamma_5 &= \frac{n}{B}[0.125\,n\,(k+1) + 0.1875\,k^2 + 0.625\,k + 0.1875]
\end{aligned}\right\}\ldots\ldots[\mathrm{d}]$$

in which

$$B = n^2\,(k+1) + n\,(1.7537\,k^2 + 6.254\,k + 1.7717) + 0.17157\,k^3 + 1.8579\,k^2 + 4.101\,k + 0.2145.$$

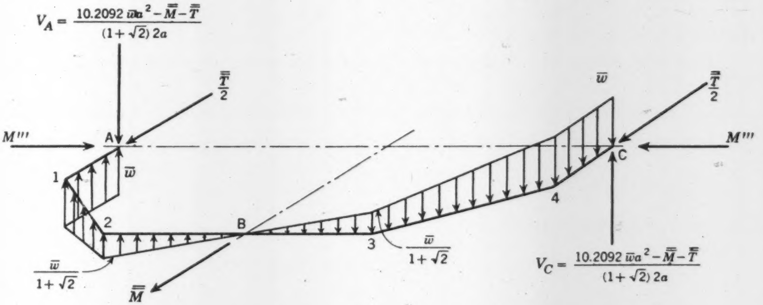
$V_A = \frac{10.2092\,\bar{w}a^2 - \bar{\bar{M}} - \bar{\bar{T}}}{(1+\sqrt{2})\,2a}$
$\frac{\bar{\bar{T}}}{2}$
$\bar{w}$
$\frac{\bar{\bar{T}}}{2}$
M'''
A
M'''
C
1
$\bar{w}$
4
2
B
3
$\frac{\bar{w}}{1+\sqrt{2}}$
$V_C = \frac{10.2092\,\bar{w}a^2 - \bar{\bar{M}} - \bar{\bar{T}}}{(1+\sqrt{2})\,2a}$
$\frac{\bar{w}}{1+\sqrt{2}}$
$\bar{\bar{M}}$

FIG. 4.—EXTERNAL AND INTERNAL FORCES, OVERTURNING-MOMENT ANALYSIS OF THE OCTAGONAL FRAME

The moments and forces at the significant points in the fixed-based pedestal under a horizontal force are given in Table 2. The location of moment maxima and minima are similar to those found for the hinged pedestal. The absolute maximum bending moment in the structure occurs at the base of column BG. The condition $k = \infty$ produces equal moments in the four columns.

Although the foregoing analysis is concerned with moments due to the action of wind, it is equally adaptable to any extraneous loading resulting in horizontal forces on the structure, as for instance earthquake effects or bomb blasts. It provides, furthermore, a procedure for sidesway analysis.

Moment Loading.—The last part of the analysis is the study of the effect of an overturning moment arising from wind pressure exerted on the tower or equipment. This type of loading is equivalent to a linearly varying distributed load on the ring, asymmetrical about the BD-axis, as shown in Fig. 4. The greatest intensity of this load is $\bar{w}$, and it can be related to the overturning moment through the equation,

$$M_o = 20.418\,\bar{w}\,a^2 \ldots\ldots\ldots\ldots\ldots\ldots\ldots (15)$$

The vertical plane of the overturning moment is selected to coincide with the horizontal force described under the heading, "Horizontal Shear Loading." Symmetry about the AC-axis facilitates a restriction of the analysis to one half of the structure. Some further conditions simplifying the analysis can be formulated in a manner identical to those described previously under the same heading. Owing to antisymmetry,

$$V_B = V_D = M_B = M_D = \theta^T{}_B = \theta^T{}_D = 0$$

and

$$V_A = - V_C.$$

Owing to symmetry,

$$T_A = T_C = \theta^M{}_A = \theta^M{}_C = 0.$$

In addition to the external loads, there appears in Fig. 4 a torque $\bar{\bar{T}}$ and a bending moment $\bar{\bar{M}}$, acting at the end points of the diameters AC and BD, respectively. These represent virtual couples needed for obtaining the rotation of the ring at these points.

Only the important features of the analysis are presented herein, without elaboration of the moment equations and derivatives.

The redundant bending moment may be determined from the condition that

$$\theta^M{}_A = \left.\frac{\partial U}{\partial M'''}\right]_{\bar{\bar{M}}=\bar{\bar{T}}=0} = 0.$$

This condition leads to

$$M''' = \frac{1.8333\,k + 1.6381}{k + 1}\,\varpi\,a^2 \dots\dots\dots\dots \tag{16}$$

The torsional rotation of the ring at supports A or C, under the loading shown, is determined from

$$\theta^T{}_A = \left.\frac{\partial U}{\partial \bar{\bar{T}}}\right]_{\bar{\bar{M}}=\bar{\bar{T}}=0} = k_1\,\frac{\varpi\,a^3}{E\,I} \dots\dots\dots\dots \tag{17}$$

in which

$$k_1 = \frac{-\,0.09069\,k^2 + 0.2570\,k - 0.08326}{k + 1}.$$

Similarly, the external loads initiate a bending rotation at support B or support D equal to

$$\theta^M{}_B = \left.\frac{\partial U}{\partial \bar{\bar{M}}}\right]_{\bar{\bar{M}}=\bar{\bar{T}}=0} = k_2\,\frac{\varpi\,a^3}{E\,I} \dots\dots\dots\dots \tag{18}$$

in which

$$k_2 = \frac{0.12826\,k^2 + 1.0692\,k + 0.9005}{k + 1}.$$

It can easily be demonstrated that the torsional rotation at supports B and D is zero; this result could also be deduced from asymmetry considerations.

The moments actually present in the structure under the type of loading shown in Fig. 4 depend on the conditions of fixity at the base of the columns.

1. Columns Hinged at the Base.—Every point of the octagonal ring is subject to bending and torsional rotations from two sources: The external load and the moments transmitted by the columns. The rotations at the points of support were obtained in Eqs. 17, 18, and 11, respectively. Continuity requires that the rotation of the ring and column at their junction be equal; this condition stipulates that at support A,

$$k_1\,\varpi\,a^2 - (\zeta_2\,\overline{\overline{T}} + \zeta_1\,\overline{\overline{M}}) = \frac{n}{3}\,\overline{\overline{T}}$$

at support B,

$$k_2\,\varpi\,a^2 - (\zeta_1\,\overline{\overline{T}} + \zeta_3\,\overline{\overline{M}}) = \frac{n}{3}\,\overline{\overline{M}}$$

in which $\overline{\overline{T}}$ and $\overline{\overline{M}}$ represent the moments being developed at the column-to-ring junctions. Solving for $\overline{\overline{T}}$ and $\overline{\overline{M}}$ produces

$$\left.\begin{aligned}\overline{\overline{T}} &= \frac{n\,k_1 + 3\,(k_1\,\zeta_3 - k_2\,\zeta_1)}{\frac{n^2}{3} + n\,(\zeta_2 + \zeta_3) + 3\,(\zeta_2\,\zeta_3 - {\zeta^2}_1)}\,\varpi\,a^2\\ \overline{\overline{M}} &= \frac{n\,k_2 + 3\,(k_2\,\zeta_2 - k_1\,\zeta_1)}{\frac{n^2}{3} + n\,(\zeta_2 + \zeta_3) + 3\,(\zeta_2\,\zeta_3 - {\zeta^2}_1)}\,\varpi\,a^2\end{aligned}\right\}\ldots\ldots\ldots(19)$$

The continuity moments expressed by Eqs. 19 represent concurrently the moments applied to the top of the supporting columns. These moments produce a total horizontal reaction of

$$P_o = \frac{2}{h}\,(\overline{\overline{T}} + \overline{\overline{M}})\ldots\ldots\ldots\ldots\ldots\ldots\ldots(20)$$

Equilibrium demands that the sum of the horizontal reactions vanish; hence, for the moment loading shown, one must introduce a sidesway force acting in the sense of the force described under the heading, "Horizontal Shear Loading," and equal in magnitude to Eq. 20. The moment corrections due to a sidesway can then be determined from Table 2.

The use of Eqs. 16 and 19, substitution of the k-function and the ζ-function, and the sidesway considerations permit a final formulation of the moments developed in the frame, with the aid of two functions:

$$\left.\begin{aligned}\eta_1 &= \frac{1}{A}\,(0.008025\,k^2 + 0.02979\,k + 0.03613)\\ &\text{and}\\ \eta_2 &= \frac{1}{A}\,[n\,(0.08979\,k + 0.08023) + 0.1050\,k^2 + 0.3328\,k + 0.07217]\end{aligned}\right\}\ldots[\text{e}]$$

TABLE 3.—PEDESTAL LOADING WITH AN OVERTURNING MOMENT, M_o

(a) OCTAGONAL RING

Bending Moments	Twisting Moments
Hinged Column Bases	
$M^1{}_A = -\eta_2 M_o$ $M^A{}_1 = -(\eta_2 - 0.07907) M_o$ $M^E{}_1 = -0.7071 (\eta_1 + \eta_2 - 0.07907) M_o$ $M_E = -0.7071 (\eta_1 + \eta_2 - 0.125) M_o$ $M^E{}_2 = -0.7071 (\eta_1 + \eta_2 - 0.12196) M_o$ $M^B{}_2 = -(\eta_1 - 0.02145) M_o$ $M^2{}_B = -\eta_1 M_o$	$T^1{}_A = -\eta_1 M_o$ $T^A{}_1 = -\eta_1 M_o$ $T^E{}_1 = -0.7071 (\eta_1 - \eta_2 + 0.07907) M_o$ $T_E = -0.7071 (\eta_1 - \eta_2 + 0.07907) M_o$ $T^E{}_2 = -0.7071 (\eta_1 - \eta_2 + 0.07907) M_o$ $T^B{}_2 = (\eta_2 - 0.10051) M_o$ $T^2{}_B = (\eta_2 - 0.10051) M_o$
Fixed Column Bases	
$M^1{}_A = -\eta_4 M_o$ $M^A{}_1 = -(\eta_4 + 0.4142 \eta_5 - 0.07907) M_o$ $M^E{}_1 = -0.7071 (\eta_3 + \eta_4 - 0.5858 \eta_5 - 0.07907) M_o$ $M_E = -0.7071 (\eta_3 + \eta_4 - 0.125) M_o$ $M^E{}_2 = -0.7071 (\eta_3 + \eta_4 + 0.5858 \eta_5 - 0.12196) M_o$ $M^B{}_2 = -(\eta_3 - 0.4142 \eta_5 - 0.02145) M_o$ $M^2{}_B = -\eta_3 M_o$	$T^1{}_A = -(\eta_3 - \eta_5) M_o$ $T^A{}_1 = -(\eta_3 - \eta_5) M_o$ $T^E{}_1 = -0.7071 (\eta_3 - \eta_4 - 1.4142 \eta_5 + 0.07907) M_o$ $T_E = -0.7071 (\eta_3 - \eta_4 - 1.4142 \eta_5 + 0.07907) M_o$ $T^E{}_2 = -0.7071 (\eta_3 - \eta_4 - 1.4142 \eta_5 + 0.07907) M_o$ $T^B{}_2 = (\eta_4 + \eta_5 - 0.10051) M_o$ $T^2{}_B = (\eta_4 + \eta_5 - 0.10051) M_o$

(b) COLUMNS

Hinged Base	Fixed Base	Hinged Base	Fixed Base
Bending Moments at Column Tops		Bending Moments at Column Bases	
$M^{xx}{}_{cA} = -2 \eta_1 M_o$ $M^{yy}{}_{cA} = 0$ $M^{xx}{}_{cB} = 0$ $M^{yy}{}_{cB} = 2 \eta_1 M_o$	$M^{xx}{}_{cA} = -2 (\eta_3 - \eta_5) M_o$ $M^{yy}{}_{cA} = 0$ $M^{xx}{}_{cB} = 0$ $M^{yy}{}_{cB} = 2 \eta_3 M_o$	$M^{xx}{}_{cF} = 0$ $M^{yy}{}_{cF} = 0$ $M^{xx}{}_{cG} = 0$ $M^{yy}{}_{cG} = 0$	$M^{xx}{}_{cF} = (\eta_3 + 0.5 \eta_5) M_o$ $M^{yy}{}_{cF} = 0$ $M^{xx}{}_{cG} = 0$ $M^{yy}{}_{cG} = -(\eta_3 - 1.5 \eta_5) M_o$
Vertical Loads		Horizontal Reactions at Base	
$V_{cA} = -\frac{0.2071}{a} M_o$ $V_{cB} = 0$	$V_{cA} = \frac{0.2071}{a} (4 \eta_5 - 1) M_o$ $V_{cB} = 0$	$H^{xx}{}_{cF} = 0$ $H^{yy}{}_{cF} = \frac{2 \eta_1}{h} M_o$ $H^{xx}{}_{cG} = \frac{2 \eta_1}{h} M_o$ $H^{yy}{}_{cG} = 0$	$H^{xx}{}_{cF} = 0$ $H^{yy}{}_{cF} = (3 \eta_3 - 1.5 \eta_5) \frac{M_o}{h}$ $H^{xx}{}_{cG} = (3 \eta_3 - 1.5 \eta_5) \frac{M_o}{h}$ $H^{yy}{}_{cG} = 0$

The forces and moments developed at various points in the frame subject to a moment loading are expressed in terms of η_1 and η_2 in Table 3 in which recourse was made to the external moment by means of Eq. 15. Table 3 contains the critical points of only quadrant AB because the bending moments simply reverse their sense of action whereas torques retain their signs over the quadrant BC.

2. Columns Fixed at the Base.—The continuity equations for the fixed-base pedestal assume the following form: At support A,

$$k_1\, \varpi\, a^2 - (\zeta_2\, \overline{\overline{T}} + \zeta_1\, \overline{\overline{M}}) = \frac{n}{4}\, \overline{\overline{T}}$$

and at support B,

$$k_2\, \varpi\, a^2 - (\zeta_1\, \overline{\overline{T}} + \zeta_3\, \overline{\overline{M}}) = \frac{n}{4}\, \overline{\overline{M}}.$$

The continuity moments can now be expressed as

$$\left.\begin{aligned} \overline{\overline{T}} &= \frac{n\, k_1 + 4\, (k_1\, \zeta_3 - k_2\, \zeta_1)}{\dfrac{n^2}{4} + n\, (\zeta_2 + \zeta_3) + 4\, (\zeta_2\, \zeta_3 - \zeta^2{}_1)}\, \varpi\, a^2 \\ \overline{\overline{M}} &= \frac{n\, k_2 + 4\, (k_2\, \zeta_2 - k_1\, \zeta_1)}{\dfrac{n^2}{4} + n\, (\zeta_2 + \zeta_3) + 4\, (\zeta_2\, \zeta_3 - \zeta^2{}_1)}\, \varpi\, a^2 \end{aligned}\right\} \dots\dots\dots\dots (21)$$

The analysis has to be augmented in this case by considering a sidesway force,

$$P_o = \frac{3}{h}\, (\overline{\overline{T}} + \overline{\overline{M}}) \dots\dots\dots\dots\dots\dots (22)$$

The resulting final moments for the fixed-base condition are tabulated in Table 3; the functions η_3, η_4, and η_5 incorporated in these moment expressions can be given as

$$\left.\begin{aligned} \eta_3 &= \frac{1}{B}\, [n\, (0.01118\, k^2 + 0.05602\, k + 0.05819) + 0.00628\, k^3 \\ &\qquad + 0.07582\, k^2 + 0.1670\, k + 0.0095] \\ \eta_4 &= \frac{1}{B}\, [n^2\, (0.08979\, k + 0.08023) + n\, (0.162\, k^2 + 0.5235\, k \\ &\qquad + 0.111) + 0.0108\, k^3 + 0.1078\, k^2 + 0.2271\, k + 0.0115] \\ \eta_5 &= \frac{1}{B}\, [n\, (0.00092\, k^2 + 0.03248\, k + 0.02001) + 0.006282\, k^3 \\ &\qquad + 0.07836\, k^2 + 0.1814\, k + 0.008958] \end{aligned}\right\} \dots [f]$$

As before, over the quadrant BC bending moments are opposite and torques are equal to those listed in Table 3 for the case of fixed bases.

MODIFIED ANALYSIS

The moment expressions, and especially the evaluation of the functions in the analysis of horizontal shear and overturning-moment loading for fixed columns involve lengthy and time-consuming computations. These expressions can be simplified considerably by adopting the modifying assumption that, under the horizontal shear loading P, identical horizontal reactions $(P/4)$ are developed at the base of each column. Similarly, under the moment loading M_o for fixed columns, the induced moments at the base of each column are assumed to be equal. Although these assumptions will not strictly satisfy the elastic equations, they lead rapidly to results which are, as shown subsequently, in close agreement with the extended analysis. In addition, the significant curtailment of arithmetic computations and the degree of accuracy with which wind loads can be predicted justify use of the modified analysis in most cases.

Assuming H (col.) $= P/4$ for every column, the functions involved in Table 2 for the hinged-base columns are simplified to

$$\left.\begin{aligned} \gamma_1 &= 0.125 \\ \gamma_2 &= \frac{0.2393\,k + 0.08839}{k + 1} \end{aligned}\right\} \cdots\cdots\cdots\cdots\cdots [c']$$

(These equations will satisfy the extended analysis only when $k = 0.32$ or $k = -3$, which is a physically meaningless condition; Eq. 7 shows that in actual cases $k > 0.6702$.) Denoting the second of Eqs. [c′] by $\bar{\gamma}_2$, the simplifying assumption will transform the expressions in Table 2 for the hinged-base condition into those shown in Table 4 for the same condition.

For the frame with the fixed-base columns, the assumption of equal horizontal reactions reduces the auxiliary functions involved in the extended analysis to the following expressions:

$$\left.\begin{aligned} \bar{\gamma}_3 &= \frac{[0.06961\,n\,(k + 1) + 0.014128\,(0.2538\,k^2 + 1.2473\,k + 0.2718)]}{[n\,(k + 1) + 0.2538\,k^2 + 1.2473\,k + 0.2718]} \\ \bar{\gamma}_4 &= \frac{n\,(0.11973\,k + 0.04423)}{n\,(k + 1) + 0.2538\,k^2 + 1.2473\,k + 0.2718} \end{aligned}\right\} \cdots [d']$$

Eqs. [d′] again involve the physically impossible condition that $k = 0.32$ or $k = -3$. The moment and force expressions for a fixed-based condition of the pedestal resisting horizontal thrust, using the modified analysis, are reproduced in Table 4.

In like manner the simplifying assumption of equal column-base moments for the overturning-moment loading on fixed columns leads to greatly abbreviated expressions. Consequently, the moments and forces can be expressed in

TABLE 4.—MODIFIED ANALYSIS OF A PEDESTAL WITH A CONCENTRATED HORIZONTAL LOAD, P

(a) OCTAGONAL RING

Bending Moments	Twisting Moments
Hinged Column Bases	
$M^1{}_A = -\bar{\gamma}_2 P\,h$	$T^1{}_A = -0.125\,P\,h$
$M^A{}_1 = -(\bar{\gamma}_2 - 0.10355)\,P\,h$	$T^A{}_1 = -0.125\,P\,h$
$M^E{}_1 = -0.7071\,(\bar{\gamma}_2 + 0.02145)\,P\,h$	$T^E{}_1 = 0.7071\,(\bar{\gamma}_2 - 0.2286)\,P\,h$
$M_E = -0.7071\,(\bar{\gamma}_2 - 0.125)\,P\,h$	$T_E = 0.7071\,(\bar{\gamma}_2 - 0.2286)\,P\,h$
$M^E{}_2 = -0.7071\,(\bar{\gamma}_2 - 0.2714)\,P\,h$	$T^E{}_2 = 0.7071\,(\bar{\gamma}_2 - 0.2286)\,P\,h$
$M^B{}_2 = 0.02145\,P\,h$	$T^B{}_2 = (\bar{\gamma}_2 - 0.25)\,P\,h$
$M^2{}_B = 0.125\,P\,h$	$T^2{}_B = (\bar{\gamma}_2 - 0.25)\,P\,h$
Fixed Column Bases	
$M^1{}_A = -\bar{\gamma}_4 P\,h$	$T^1{}_A = -\bar{\gamma}_3 P\,h$
$M^A{}_1 = (0.8284\bar{\gamma}_3 - \bar{\gamma}_4)\,P\,h$	$T^A{}_1 = -\bar{\gamma}_3 P\,h$
$M^E{}_1 = -0.7071\,(0.17157\bar{\gamma}_3 + \bar{\gamma}_4)\,P\,h$	$T^E{}_1 = -0.7071\,(1.8284\bar{\gamma}_3 - \bar{\gamma}_4)\,P\,h$
$M_E = 0.7071\,(\bar{\gamma}_3 - \bar{\gamma}_4)\,P\,h$	$T_E = -0.7071\,(1.8284\bar{\gamma}_3 - \bar{\gamma}_4)\,P\,h$
$M^E{}_2 = 0.7071\,(2.172\bar{\gamma}_3 - \bar{\gamma}_4)\,P\,h$	$T^E{}_2 = -0.7071\,(1.8284\bar{\gamma}_3 - \bar{\gamma}_4)\,P\,h$
$M^B{}_2 = 0.17157\bar{\gamma}_3 P\,h$	$T^B{}_2 = -(2\bar{\gamma}_3 - \bar{\gamma}_4)\,P\,h$
$M^2{}_B = \bar{\gamma}_3 P\,h$	$T^2{}_B = -(2\bar{\gamma}_3 - \bar{\gamma}_4)\,P\,h$

(b) COLUMNS

Hinged Base	Fixed Base	Hinged Base	Fixed Base
Bending Moments at Column Tops		Bending Moments at Column Bases	
$M^{xx}{}_{cA} = -0.25\,P\,h$	$M^{xx}{}_{cA} = -2\bar{\gamma}_3 P\,h$	$M^{xx}{}_{cF} = 0$	$M^{xx}{}_{cF} = (-2\bar{\gamma}_3 + 0.25)\,P\,h$
$M^{yy}{}_{cA} = 0$	$M^{yy}{}_{cA} = 0$	$M^{yy}{}_{cF} = 0$	$M^{yy}{}_{cF} = 0$
$M^{xx}{}_{cB} = 0$	$M^{xx}{}_{cB} = 0$	$M^{xx}{}_{cG} = 0$	$M^{xx}{}_{cG} = 0$
$M^{yy}{}_{cB} = -0.25\,P\,h$	$M^{yy}{}_{cB} = -2\bar{\gamma}_3 P\,h$	$M^{yy}{}_{cG} = 0$	$M^{yy}{}_{cG} = (-2\bar{\gamma}_3 + 0.25)\,P\,h$
Vertical Loads		Horizontal Reactions at Base	
$V_{cA} = -\dfrac{0.2071}{a}\,P\,h$	$V_{cA} = -\dfrac{1.6569}{a}\bar{\gamma}_3 P\,h$	$H^{xx}{}_{cF} = 0$	$H^{xx}{}_{cF} = 0$
$V_{cB} = 0$	$V_{cB} = 0$	$H^{yy}{}_{cF} = 0.25\,P$	$H^{yy}{}_{cF} = 0.25\,P$
		$H^{xx}{}_{cG} = -0.25\,P$	$H^{xx}{}_{cG} = -0.25\,P$
		$H^{yy}{}_{cG} = 0$	$H^{yy}{}_{cG} = 0$

terms of two reduced auxiliary functions:

$$\left.\begin{aligned}\bar{\eta}_3 &= \frac{0.01070\,k^2 + 0.0397\,k + 0.04815}{n\,(k+1) + 1.5\left(k^2 + \frac{10}{3}\,k + 1\right)}\\ \bar{\eta}_4 &= \frac{n\,(0.08979\,k + 0.08022) + 0.1400\,k^2 + 0.4434\,k + 0.0965}{n\,(k+1) + 1.5\left(k^2 + \frac{10}{3}\,k + 1\right)}\end{aligned}\right\}\ldots[\mathrm{f}']$$

TABLE 5.—MODIFIED ANALYSIS OF A PEDESTAL HAVING FIXED COLUMN BASES WITH AN OVERTURNING MOMENT, M_o

(a) OCTAGONAL RING

Bending Moments	Twisting Moments
$M^{1}_{A} = -\bar{\eta}_4\,M_o$	$T^{1}_{A} = -\bar{\eta}_3\,M_o$
$M^{A}_{1} = -(\bar{\eta}_4 - 0.07907)\,M_o$	$T^{A}_{1} = -\bar{\eta}_3\,M_o$
$M^{E}_{1} = -0.7071\,(\bar{\eta}_3 + \bar{\eta}_4 - 0.07907)\,M_o$	$T^{E}_{1} = -0.7071\,(\bar{\eta}_3 - \bar{\eta}_4 + 0.07907)\,M_o$
$M_E = -0.7071\,(\bar{\eta}_3 + \bar{\eta}_4 - 0.125)\,M_o$	$T_E = -0.7071\,(\bar{\eta}_3 - \bar{\eta}_4 + 0.07907)\,M_o$
$M^{E}_{2} = -0.7071\,(\bar{\eta}_3 + \bar{\eta}_4 - 0.12196)\,M_o$	$T^{E}_{2} = -0.7071\,(\bar{\eta}_3 - \bar{\eta}_4 + 0.07907)\,M_o$
$M^{B}_{2} = -(\bar{\eta}_3 - 0.02145)\,M_o$	$T^{B}_{2} = (\bar{\eta}_4 - 0.10051)\,M_o$
$M^{2}_{B} = -\bar{\eta}_3\,M_o$	$T^{2}_{B} = (\bar{\eta}_4 - 0.10051)\,M_o$

(b) COLUMNS

Bending Moments at Column Tops	Bending Moments at Column Bases
$M^{xx}_{cA} = -2\,\bar{\eta}_3\,M_o$	$M^{xx}_{cF} = \bar{\eta}_3\,M_o$
$M^{yy}_{cA} = 0$	$M^{yy}_{cF} = 0$
$M^{xx}_{cB} = 0$	$M^{xx}_{cG} = 0$
$M^{yy}_{cB} = 2\,\bar{\eta}_3\,M_o$	$M^{yy}_{cG} = -\bar{\eta}_3\,M_o$

Vertical Loads	Horizontal Reactions at Base
$V_{cA} = -\frac{0.2071}{a}\,M_o$	$H^{xx}_{cA} = 0$
$V_{cB} = 0$	$H^{yy}_{cA} = \frac{3\,\bar{\eta}_3}{h}\,M_o$
	$H^{xx}_{cB} = \frac{3\,\bar{\eta}_3}{h}\,M_o$
	$H^{yy}_{cB} = 0$

The expressions for forces and moments based on the modified approach for the frame with fixed columns under overturning-moment loading are presented in Table 5. This table is similar to Table 3 if allowance is made for the different functions encountered.

To compare orders of magnitude, the octagonal frame solved in the numerical example was reanalyzed by means of the modified method. These values are listed in Tables 6 and 7 for the hinged-base and fixed-base frames, respectively, and the appropriate values derived from the extended analysis (Table 7 and Appendix I) are also shown for comparative purposes. Moments and forces due to uniform vertical loading for hinged or fixed columns were not tabulated. Likewise moments and forces under overturning-moment loading for hinged columns were omitted because no modifying assumptions were made in the analyses of these three conditions.

TABLE 6.—COMPARISON BETWEEN THE EXTENDED ANALYSIS AND THE MODIFIED ANALYSIS—PEDESTAL ON HINGED COLUMNS

(a) OCTAGONAL RING

Direction and Location	HORIZONTAL FORCE, *P*		Direction and Location	HORIZONTAL FORCE, *P*	
	Extended	Modified		Extended	Modified
Bending Moment, in Foot-Kips			Twisting Moment, in Foot-Kips		
$M^1{}_A$	−98.3	−99.2	$T^1{}_A$	−60.2	−70.9
$M^A{}_1$	−39.6	−40.4	$T^A{}_1$	−60.2	−70.9
$M^E{}_1$	−70.6	−78.7	$T^E{}_1$	−14.6	−21.5
M_E	−11.9	−20.0	T_E	−14.6	−21.5
$M^E{}_2$	+46.8	+38.7	$T^E{}_2$	−14.6	−21.5
$M^B{}_2$	+22.8	+12.2	$T^B{}_2$	−43.4	−42.6
$M^2{}_B$	+81.5	+70.9	$T^2{}_B$	−43.4	−42.6

(b) COLUMNS

Bending Moments at Column Tops, in Foot-Kips			Bending Moments at Column Bases, in Foot-Kips		
$M^{xx}{}_{cA}$	−120.5	−141.8	$M^{xx}{}_{cF}$	0	0
$M^{yy}{}_{cA}$	0	0	$M^{yy}{}_{cF}$	0	0
$M^{xx}{}_{cB}$	0	0	$M^{xx}{}_{cG}$	0	0
$M^{yy}{}_{cB}$	−163.0	−141.8	$M^{yy}{}_{cG}$	0	0
Vertical Loads, in Kips			Horizontal Reactions at Bases, in Kips		
V_{cA}	−26.9	−26.9	$H^{xx}{}_{cF}$	0	0
V_{cB}	0	0	$H^{yy}{}_{cG}$	5.4	6.3
			$H^{xx}{}_{cF}$	−7.2	−6.3
			$H^{yy}{}_{cG}$	0	0

TABLE 7.—COMPARISON BETWEEN THE EXTENDED ANALYSIS AND THE MODIFIED ANALYSIS—PEDESTAL ON FIXED COLUMNS

(a) OCTAGONAL RING

Direction and Location	TYPE OF LOADING				Direction and Location	TYPE OF LOADING			
	Horizontal Force, P		Moment, M_o			Horizontal Force, P		Moment, M_o	
	Extended	Modified	Extended	Modified		Extended	Modified	Extended	Modified
	Bending Moment, in Foot-Kips					Twisting Moment, in Foot-Kips			
M^1_A	−41.5	−41.4	−77.9	−81.3	T^1_A	−24.6	−29.6	− 2.9	− 5.0
M^A_1	−16.7	−16.9	− 5.2	− 6.6	T^A_1	−24.6	−29.6	− 2.9	− 5.0
M^E_1	−29.2	−32.8	− 5.7	− 8.2	T^E_1	− 5.6	− 9.0	+ 1.6	+ 1.2
M_E	− 4.4	− 8.3	+22.9	+22.5	T_E	− 5.6	− 9.0	+ 1.6	+ 1.2
M^E_2	+20.4	+16.2	+18.8	+20.5	T^E_2	− 5.6	− 9.0	+ 1.6	+ 1.2
M^B_2	+10.4	+ 5.1	+14.4	+15.3	T^B_2	−18.4	−17.8	−12.1	−13.6
M^2_B	+35.2	+29.6	− 7.9	− 5.0	T^2_B	−18.4	−17.8	−12.1	−13.6
(b) COLUMNS									
M^{xx}_{cA}	−49.3	−59.2	− 5.8	− 9.9	M^{xx}_{cF}	+76.7	+82.6	+10.4	+ 5.0
M^{yy}_{cA}	0	0	0	0	M^{yy}_{cF}	0	0	0	0
M^{xx}_{cB}	0	0	0	0	M^{xx}_{cG}	0	0	0	0
M^{yy}_{cB}	−70.4	−59.2	+15.8	+ 9.9	M^{yy}_{cG}	+87.2	+82.6	− 0.4	− 5.0
	Vertical Loads, in Kips					Horizontal Reactions at Bases, in Kips			
V_{cA}	−11.4	−11.2	−43.9	−44.8	H^{xx}_{cF}	0	0	0	0
V_{cB}	0	0	0	0	H^{yy}_{cF}	+5.6	+6.3	+0.7	+0.7
					H^{xx}_{cF}	+7.0	−6.3	+0.7	+0.7
					H^{yy}_{cG}	0	0	0	0

Tables 6 and 7 show that the modified method is in close over-all agreement with the extended approach. With the exception of the evident differences in column moments under the moment loading for fixed columns, all other deviations occur at points of low moment values which, from an engineering standpoint, are insignificant because they do not govern design.

ACKNOWLEDGMENTS

The writers wish to acknowledge the encouragement and interest provided by D. B. Rossheim, M. ASCE, and J. J. Rush during the preparation of this paper.

APPENDIX I. NUMERICAL EXAMPLE

An octagonal frame is to carry a refinery tower having a diameter of 21.6 ft and an operating weight of 391.0 kips. In order to eliminate local torsion the diameter of the inscribed circle of the octagon is assumed to be 0.975 of that of the loading circle. The base of the vessel has to be supported at an elevation of 23.5 ft; the maximum wind force acting on the superstructure is 25.2

TABLE 8.—NUMERICAL EXAMPLE: PEDESTAL ON HINGED COLUMNS

(a) OCTAGONAL RING

Location and Direction	TYPE OF LOADING			Total	Location and Direction	TYPE OF LOADING			Total
	Vertical Load, w	Horizontal Force, P	Moment, M_o			Vertical Load, w	Horizontal Force, P	Moment, M_o	
Bending Moments, in Foot-Kips					Twisting Moments, in Foot-Kips				
$M^1{}_A$	+174.3	∓98.3	∓81.3	+353.9 − 5.3	$T^1{}_A$	−3.0	∓60.2	∓ 4.2	−67.4
$M^{A}{}_1$	− 3.0	∓39.6	∓ 6.5	+ 43.2 − 49.2	$T^{A}{}_1$	−3.0	∓60.2	∓ 4.2	−67.4
$M^{E}{}_1$	− 4.2	∓70.6	∓ 7.6	+ 74.0 − 82.4	$T^{E}{}_1$	0	∓14.6	± 1.7	±12.9
M_E	− 63.3	∓11.9	±23.1	− 74.5	T_E	0	∓14.6	± 1.7	±12.9
$M^{E}{}_2$	− 4.2	±46.8	±21.0	+ 63.6 − 72.0	$T^{E}{}_2$	0	∓14.6	± 1.7	±12.9
$M^{B}{}_2$	− 3.0	±22.8	±16.1	+ 35.9 − 41.9	$T^{B}{}_2$	+3.0	∓43.4	∓13.7	+60.1
$M^2{}_B$	+174.3	±81.5	∓ 4.2	+251.6	$T^2{}_B$	+3.0	∓43.4	∓13.7	+60.1

(b) COLUMNS

Bending Moments at Column Tops, in Foot-Kips					Bending Moments at Column Bases, in Foot-Kips				
$M^{zz}{}_{cA}$	−5.9	∓120.5	∓8.4	+123.0 −134.8	$M^{zz}{}_{cF}$	0	0	0	0
$M^{yy}{}_{cA}$	0	0	0	0	$M^{yy}{}_{cF}$	0	0	0	0
$M^{zz}{}_{cB}$	−5.9	0	0	− 5.9	$M^{zz}{}_{cG}$	0	0	0	0
$M^{yy}{}_{cB}$	0	∓163.0	±8.4	±154.6	$M^{yy}{}_{cG}$	0	0	0	0
Vertical Loads, in Kips					Horizontal Reactions at Base, in Kips				
V_{cA}	+108.2	∓26.9	∓44.8	+179.9	$H^{zz}{}_{cF}$	0	0	0	0
V_{cB}	+108.2	0	0	+108.2	$H^{yy}{}_{cF}$	+0.3	±5.4	±0.4	+6.1 −5.5
					$H^{zz}{}_{cG}$	0	∓7.2	±0.4	±6.8
					$H^{yy}{}_{cG}$	+0.3	0	0	+0.3

TABLE 9.—NUMERICAL EXAMPLE: PEDESTAL ON FIXED COLUMNS

(a) OCTAGONAL RING

Location and Direction	Type of Loading			Total	Location and Direction	Type of Loading			Total
	Vertical Load, w	Horizontal Force, P	Moment, M_o			Vertical Load, w	Horizontal Force, P	Moment, M_o	
Bending Moments, in Foot-Kips					Twisting Moments, in Foot-Kips				
M^{1}_{A}	+173.9	∓41.5	∓77.9	+293.3	T^{1}_{A}	−3.3	∓24.6	∓ 2.9	−30.8
M^{A}_{1}	− 3.3	∓16.7	∓ 5.2	+18.6 −25.2	T^{A}_{1}	−3.3	∓24.6	∓ 2.9	−30.8
M^{E}_{1}	− 4.7	∓29.2	∓ 5.7	+30.2 −39.6	T^{E}_{1}	0	∓ 5.6	± 1.6	± 4.0
M_{E}	− 63.8	∓ 4.4	±22.9	−82.3	T_{E}	0	∓ 5.6	± 1.6	± 4.0
M^{E}_{2}	− 4.7	±20.4	±18.8	+34.5 −43.9	T^{E}_{2}	0	∓ 5.6	± 1.6	± 4.0
M^{B}_{2}	− 3.3	±10.4	±14.4	+21.5 −28.1	T^{B}_{2}	+3.3	∓18.4	∓12.1	+33.8
M^{2}_{B}	+173.9	±35.2	∓ 7.9	+201.2	T^{2}_{B}	+3.3	∓18.4	∓12.1	+33.8

(b) COLUMNS

Bending Moments at Column Tops, in Foot-Kips					Bending Moments at Column Bases, in Foot-Kips				
M^{xx}_{cA}	−6.7	∓49.3	∓ 5.8	+48.4 −61.8	M^{xx}_{cF}	+3.3	±76.7	±10.4	+90.4 −83.8
M^{yy}_{cA}	0	0	0	0	M^{yy}_{cF}	0	0	0	0
M^{xx}_{cB}	−6.7	0	0	− 6.7	M^{xx}_{cG}	+3.3	0	0	+ 3.3
M^{yy}_{cB}	0	∓70.4	±15.8	±54.6	M^{yy}_{cG}	0	±87.2	∓ 0.4	±86.8
Vertical Loads, in Kips					Horizontal Reactions at Base, in Foot-Kips				
V_{cA}	+108.2	∓11.4	∓43.9	+163.9	H^{xx}_{cF}	0	0	0	0
V_{cB}	+108.2	0	0	+108.2	H^{yy}_{cF}	+0.4	± 5.6	± 0.7	+6.7 −5.9
					H^{xx}_{cG}	0	∓ 7.0	± 0.7	±6.3
					H^{yy}_{cG}	+0.4	0	0	+0.4

kips and attacks horizontally at an elevation of 36.5 ft above the base. Assuming that the columns as well as the octagonal ring would have a cross section of 2 ft by 2 ft, the question is whether it would be more economical to design the pedestal with a hinged or a fixed base.

With these data, the design dimensions and forces can be listed as follows: $a = 4.367$ ft, $b = c = d = 2.0$ ft, $h = 22.5$ ft, $w = 6.196$ kips per ft (distributed weight of supported equipment plus dead load), $P = 25.2$ kips, $M_o = 945$ ft-kips, $k = 1.3404$, and $n = 5.153$.

The auxiliary functions will, in turn, have the following values:

For the hinged-base condition, from Eqs. [a], [c], and [e], $\beta_1 = 0.02511$, $\gamma_1 = 0.14375$, $\gamma_2 = 0.17344$, $\eta_1 = 0.004468$, and $\eta_2 = 0.08602$.

For the fixed-base condition, from Eqs. [b], [d], and [f], $\beta_2 = 0.02822$, $\gamma_3 = 0.06205$, $\gamma_4 = 0.07310$, $\gamma_5 = 0.10550$, $\eta_3 = 0.008384$, $\eta_4 = 0.08239$, and $\eta_5 = 0.005309$.

The moments and forces determined with the aid of these auxiliary functions are listed for the hinged-base and fixed-base condition in Tables 8 and 9, respectively. Based on these tables, the comparison in Table 10 can be drawn between the design conditions for the different modes of base fixity.

TABLE 10.—COMPARISON BETWEEN THE EFFECTS OF HINGED-BASE COLUMNS AND THOSE OF FIXED-BASE COLUMNS

Description	Hinged-Base Condition	Fixed-Base Condition
MOMENTS, IN FOOT-KIPS		
${M^1}_A$	353.9	293.3
${M^A}_1$	43.2 −49.2	18.6 −25.2
${M^E}_1$	74.0 −82.4	30.2 −39.6
M_E	−74.5	−82.3
${T^1}_A = {T^A}_1$	67.4	30.8
${T^E}_1 = T_E$	12.9	4.0
M_c (Top)	−160.5 +148.6	61.3 −47.9
M_c (Base)	0	90.4 −83.8
FORCES, IN KIPS		
V_c	179.9	163.9
H_c	7.1	6.7

This comparison shows that most of the bending moments and all the torques (which often govern design in reinforced concrete structures) are materially smaller for the fixed-base condition.

APPENDIX II. LIST OF REFERENCES

(1) **"Theory of Structures,"** by S. Timoshenko and D. H. Young, McGraw-Hill Book Co., Inc., New York, N. Y., 1945.

(2) **"Berechnung des senkrecht zu seiner Ebene belasteten Bogenträgers,"** by K. Federhofer, *Zeitschrift für Mathematics und Physik*, Vol. 62, 1914, pp. 40–63.

(3) **"Zur Berechnung gekrümmter Träger,"** by W. L. Andree, *Der Eisenbau*, Vol. 9, 1918, pp. 184–190.

(4) **"The Design of Walls, Bins and Grain Elevators,"** by M. S. Ketchum, McGraw-Hill Book Co., Inc., New York, N. Y., 3rd Ed., 1929, pp. 206–212.

(5) **"Der kontinuierliche, halbkreisförmig gebogene und gleichmässig belastete Eisenbetonträger mit rechteckigem Querschnitt auf drei und vier gleich weit entfernten Stützen,"** by S. Hessler, *Beton und Eisen*, Vol. 29, 1930, pp. 149–154.

(6) **"Beitrag zur Berechnung gekrümmter Träger,"** by J. Hailer, *Die Bautechnik*, Vol. 10, 1932, p. 372.

(7) **"Bending and Torsion in Horizontally Curved Beams,"** by I. Oesterblom, *Proceedings*, A.C.I., Vol. 28, 1932, pp. 597–606.

(8) **"Circular Beams Loaded Normal to the Plane of Curvature,"** by M. B. Hogan, *Transactions*, ASME, Vol. 60, 1938, p. A-81.

(9) **"Stresses in a Curved Beam Under Loads Normal to the Plane of its Axis,"** by R. B. B. Moorman, *Bulletin No. 145*, Eng. Experiment Station, Iowa State College, Ames, Iowa, 1940.

(10) **"Strength of Materials,"** by S. Timoshenko, D. Van Nostrand Co., New York, N. Y., 2d Ed., 1941, Pt. II, pp. 112–117.

(11) **"Circular Beams Loaded Normal to the Plane of Curvature—2,"** by M. B. Hogan, *Journal of Applied Mechanics*, Vol. 11, 1944, p. 51.

(12) **"Theory of Indeterminate Structures,"** by L. C. Maugh, John Wiley & Sons, Inc., New York, N. Y., 1946.

(13) **"Influence Lines for Horizontally Curved Fixed-End Beams of Circular Arc Plan,"** by R. B. B. Moorman, *Bulletin No. 35*, Univ. of Missouri Eng. Experiment Station, Columbia, Mo., 1947.

(14) **"Stresses in a Uniformly Loaded Circular Arc I-Beam,"** by R. B. B. Moorman, *Bulletin No. 36*, Univ. of Missouri, Eng. Experiment Station, Columbia, Mo., 1947.

(15) **"Laterally Loaded Plane Structures and Structures Curved in Space,"** by Frank Baron and James P. Michalos, *Transactions*, ASCE, Vol. 117, 1952, p. 279.

(16) **"Horizontally Curved Box Beams,"** by Charles E. Cutts, *ibid.*, Vol. 118, 1953, p. 517.

(17) **"Application of the Elastic-Point Theory to Piping Stress Calculations,"** by S. W. Spielvogel and S. Kameros, *Transactions*, ASME, Vol. 57, 1935, p. 165.

(18) **"Stresses in Three-Dimensional Pipe Bends,"** by W. Hovgaard, *ibid.*, pp. 401–415.

(19) **"Further Studies of Three-Dimensional Pipe Bends,"** by W. Hovgaard, *ibid.*, Vol. 59, 1937, p. 647.

(20) **"Piping Stress Calculations Simplified,"** by S. W. Spielvogel, McGraw-Hill Book Co., Inc., New York, N. Y., 1943.

(21) **"Design of Piping Systems,"** The M. W. Kellogg Co., John Wiley & Sons, Inc., New York, N. Y., 1956.

(22) **"A Matrix Method for Flexibility Analysis of Piping Systems,"** by J. E. Brock, *Journal of Applied Mechanics*, Vol. 19, 1952, pp. 501–516.

(23) **"Theory of Elasticity,"** by S. Timoshenko, McGraw-Hill Book Co., Inc., New York, N. Y., 1st Ed., 1934, pp. 145–151. (*a*) p. 10; (*b*) pp. 245–249.

(24) **"Numerical Analysis of Continuous Frames in Space,"** by James Michalos, *Transactions*, ASCE, Vol. 119, 1954, p. 565.

(25) **"Numerical Analysis of Frames with Curved Girders,"** by James Michalos, *ibid.*, Vol. 121, 1956.

APPENDIX III. NOMENCLATURE

The following symbols, adopted for use in the paper, and for the guidance of discussers, conform essentially with "American Standard Letter Symbols for Structural Analysis" (ASA Z10.8—1942), prepared by a Committee of the American Standards Association, with Society representation, and approved by the Association in 1942:

a = one half of segmental length of horizontal girder;
b = width of horizontal girder;
c = side length of cross section of supporting square columns;
d = depth of horizontal girder;
E = modulus of elasticity of horizontal girder;
E_c = modulus of elasticity of supporting square columns;
G = shear modulus of horizontal girder;
h = height of supporting square columns;
I = moment of inertia of horizontal girder;
I_c = moment of inertia of supporting square columns;
J = torsional moment of inertia of horizontal girder;
$k = \frac{E\,I}{G\,J}$, ratio of bending to torsional stiffness of ring;
M = bending moment;
M_o = extraneous moment acting perpendicular to the plane of the girder;
$n = \frac{h\,I}{a\,I_c}$, ratio of relative bending stiffnesses of ring and columns;
P = extraneous horizontal load acting in the plane of the girder;
T = torsional moment;
U = total strain-energy in loaded structure;
V = shear or vertical force;
w = vertical loading per unit of length;
Δ = translation or deflection of structural element; and
θ = rotation of structural element.

Note: Double subscripts denote generalized moments in, or rotation of, a member indicated by the subscript. In case of a concurrent subscript and superscript, the subscript denotes the location and the superscript the direction of the moment or the sense of rotation in question.

DISCUSSION

Abdel F. Diwan,[5] **A. M. ASCE.**—The paper is concerned with a special type of space frame—namely, the octagonal girder rigidly supported on four columns. The work involved is indeed remarkable, although its value is limited to the narrow scope of the octagonal girder under two particular cases of loading. The coefficients obtained for the bending and twisting moments are very useful to all concerned with the design of frames of this type.

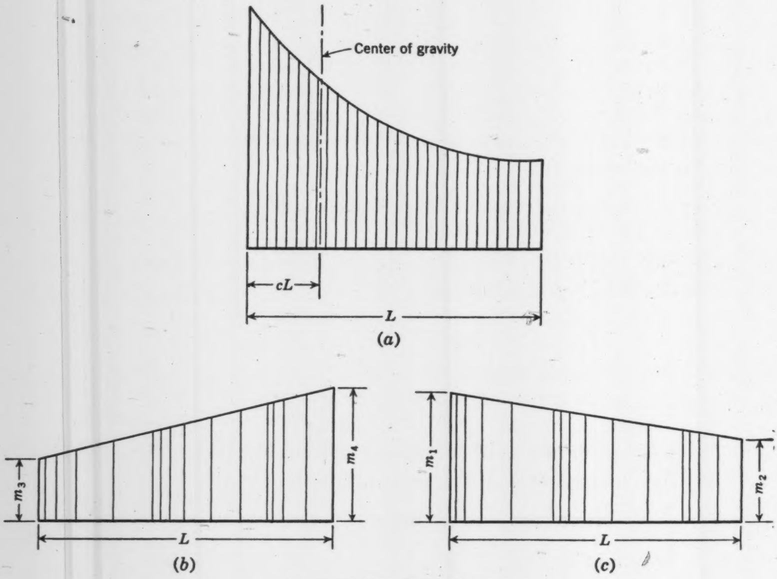

Fig. 5.—Moment Diagrams

The authors have used the Castigliano theorem in computing the angles of rotation θ as expressed by

$$\theta^T{}_A = \frac{\partial U}{\partial T'}\left[\Sigma \int \left(\frac{M^2}{2\,E\,I} + \frac{T^2}{2\,G\,J}\right) dx\right]$$

$$= \frac{1}{E\,I}\left[\Sigma \int \left(M\,\frac{\partial M}{\partial T'} + k\,T\,\frac{\partial T}{\partial T'}\right) dx\right] \ldots\ldots\ldots\ldots (23)$$

However, the writer finds it much easier to use the method of "virtual work" which he regards as a refined form of the Castigliano equations. Referring to Eq. 23, it can be seen that the terms $\partial M/\partial T'$ and $\partial T/\partial T'$ are in fact the bending moments and twisting moments, respectively, produced by unit torques $T' = 1.0$ acting at points A and C.

---

[5] Structural Dept., Faculty of Eng., Alexandria Univ., Alexandria, Egypt.

Using the following notation—

M_m, T_m = bending moments and twisting moments, respectively, due to unit moments $M = 1$ at B and D;
M_t, T_t = bending moments and twisting moments, respectively, due to unit torques $T = 1$ at A and C; and
M_o, T_o = bending moments and twisting moments, respectively, due to any specified case of loading

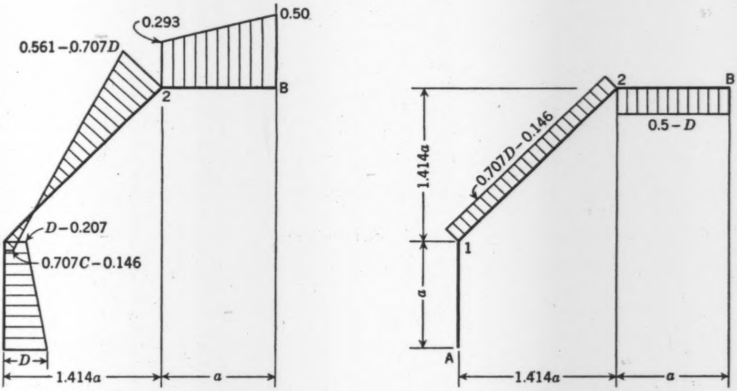

(a) M_m-diagram (b) T_m-diagram

FIG. 6.—MOMENT DIAGRAMS FOR ONE QUADRANT $C = (0.3536\,k + 0.3018)/(k + 1)$

—the angles of rotation θ for this given case of loading as determined from Eq. 23 will be

$$\theta^T{}_A = \frac{1}{E\,I}\left[\Sigma \int (M_o\,M_t + k\,T_o\,T_t)\,dx\right] \ldots\ldots\ldots\ldots (24a)$$

and

$$\theta^M{}_B = \frac{1}{E\,I}\left[\Sigma \int (M_o\,M_m + k\,T_o\,T_m)\,dx\right] \ldots\ldots\ldots\ldots (24b)$$

These are the equations of virtual work. The problem is thus reduced to integrating two moment diagrams for each member. The first of these diagrams corresponds to the particular load system producing the rotation θ and the second to the case of loading $M = 1.0$ or $T = 1.0$. The second of these diagrams being linear, the integration for a prismatic member is simply determined as $A_o\,M^*$ or $A_o\,T^*$ in which A_o is the elastic area under the first diagram (M_o or T_o); and M^* and T^* are the ordinates of the second diagram (M_t, M_m, T_t, and T_m) measured at the center of gravity of the first diagram. Fig. 5 shows three moment diagrams, the first two of which may correspond to the

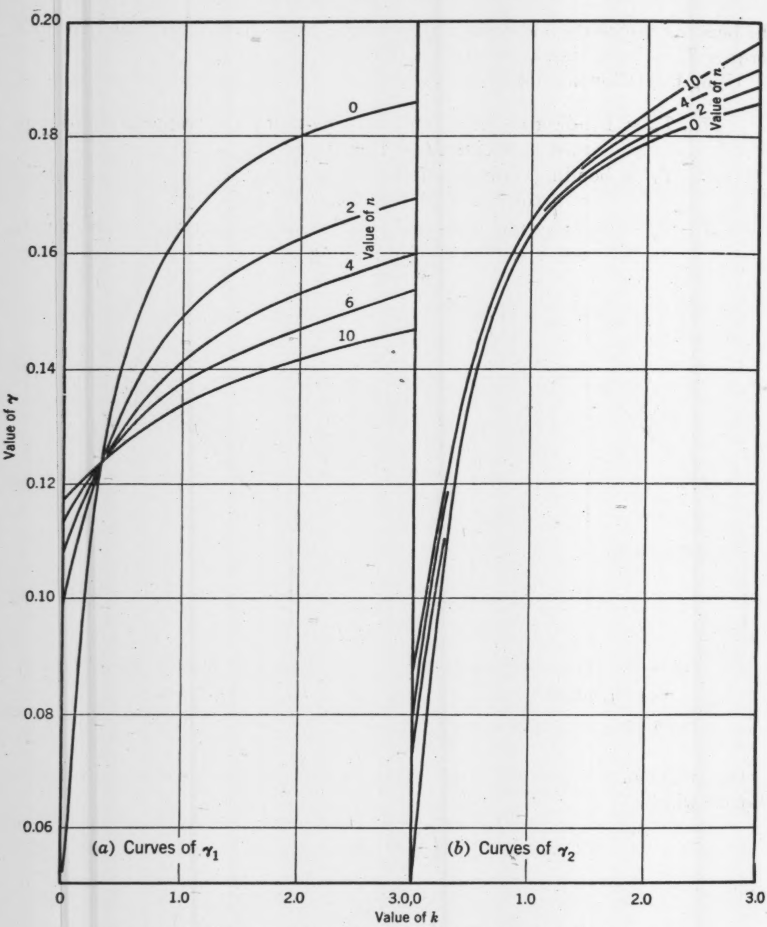

FIG. 7.—CURVES OF $\gamma_1 = M_B/P\,h$ AND $\gamma_2 = -M_A/P\,h$ (FROM TABLE 3)

case M_o and the third, say, to the case M_m. If both diagrams M_o and M_m (or T_o and T_m, or any other pair) are linear as those in Fig. 5(*b*) and Fig. 5(*c*), say, the integration will become

$$I = \frac{\bar{L}}{3}\left[2\ (m_1\, m_3 + m_2\, m_4) + (m_1\, m_4 + m_2\, m_3)\right] \dots\dots\dots (25)$$

In the special case when Figs. 5(*b*) and 5(*c*) are similar—that is, when integrating diagram *c* by itself—the result will be

$$I = \frac{\bar{L}}{3}\ (m_1^2 + m_2^2 + m_1\, m_2) \dots\dots\dots\dots\dots\dots (26)$$

in which $\bar{L}$ equals $L/E\,I$ for bending-moment diagrams, and $L/G\,J$ for twisting-moment diagrams.

Eq. 11 is considered next—$\theta^{M}_{B} = \frac{a}{E\,I}\,(\zeta_3 \bar{M} + \zeta_1 \bar{T})$. In this equation it can be seen that ζ_3 will be the rotation $E\,I/\alpha(\theta^{M}_{B})$ due to unit bending moments $M = 1.0$ acting at B and D so that

$$\zeta_3 = \left[\Sigma \int (M^2_m + k\,T^2_m)\,dx\right]\frac{1}{a} \ldots\ldots\ldots\ldots\ldots (27)$$

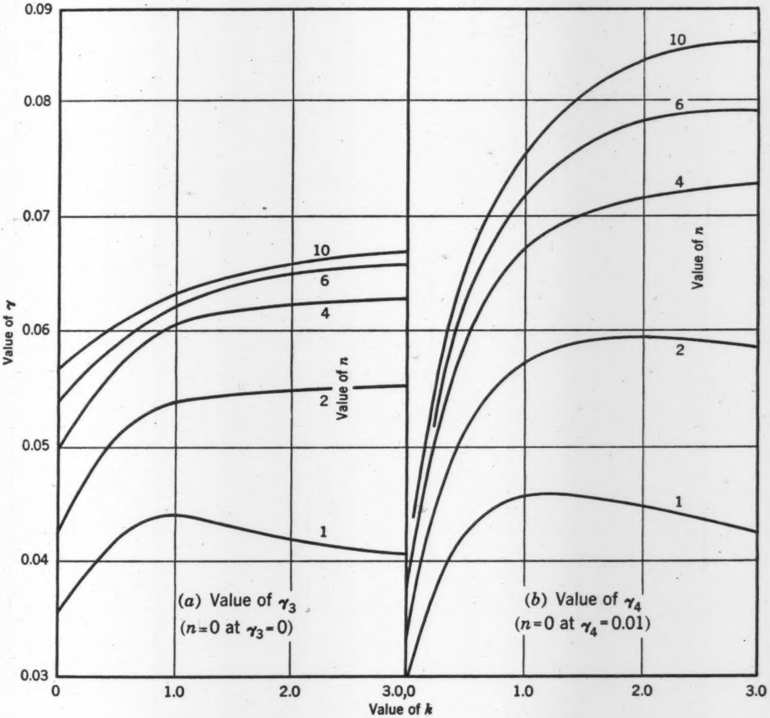

FIG. 8.—CURVES OF $\gamma_3 = M_B/P\,h$ AND $\gamma_4 = -M_A/P\,h$ (FROM TABLE 4)

The integration is being carried over two quadrants of the girder. Fig. 6 shows the bending-moment and twisting-moment diagrams M_m and T_m for one quadrant. The redundant bending moment in this case is $M'' = D = (0.3536\,k + 0.3018)/(k + 1)$, as given in the text.

Using Eq. 26, the integration of Eq. 27 over two quadrants will yield

$$\zeta_3 = \frac{0.0858\,k^2 + 0.0638\,k + 0.541}{k + 1} \ldots\ldots\ldots\ldots\ldots (28)$$

The solution of the problem using the classical methods of Castigliano or virtual work as presented by the authors is too complex, although the derivation of the authors' formulas is indeed excellent. The writer has, however, developed a simple method for the analysis of statically indeterminate frames loaded normal to their plane using the concept of "elastic poles." The method is easily applied in the analysis of space frames, such as that dealt with by the authors. This is the subject of a paper which the writer hopes will be ready for presentation soon. Applying his method to the problem of the octagonal girder, the writer arrived at the following functions for the moment coefficients:

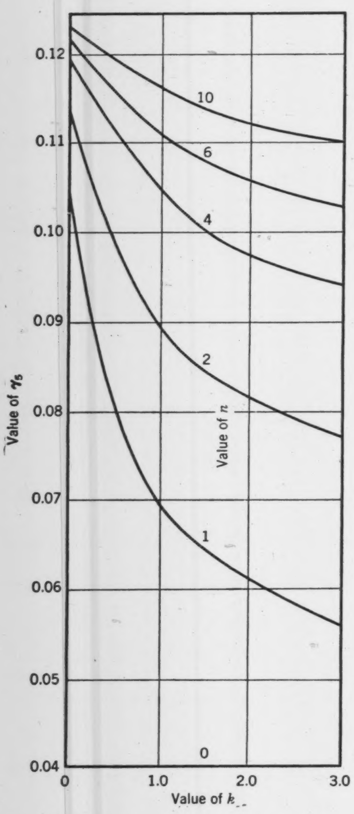

FIG. 9.—CURVES OF γ_5 IN THE EXPRESSION $T_A = (\gamma_3 - \gamma_5) P h$ (FROM TABLE 4)

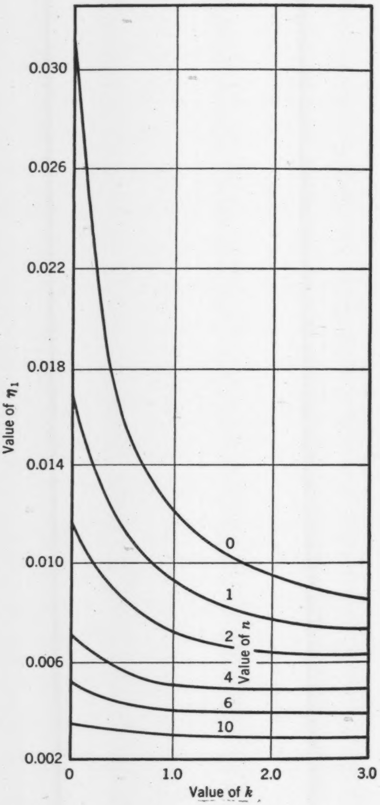

FIG. 10.—CURVES OF $\eta_1 = -M_B/M_o$ (FROM TABLE 5)

$$\left.\begin{aligned}
\gamma_1 &= \frac{n\,(k+1) + 1.81\,k^2 + 5.587\,k + 0.466}{3\,H} \\
\gamma_2 &= \frac{n\,(1.914\,k + 0.707) + 1.81\,k^2 + 5.56\,k + 0.466}{3\,H} \\
\gamma_3 &= \frac{n\,A}{4\,B} \\
\gamma_4 &= \frac{n\,F}{4\,B} \\
\gamma_5 &= \frac{2.9\,n\,H^2}{4\,B}
\end{aligned}\right\}\ldots\ldots(29)$$

and

$$\left.\begin{aligned}
\eta_1 &= -\,\frac{0.096 + 0.079\,k + 0.021\,k^2}{H} \\
\eta_2 &= \frac{0.19 + 0.883\,k + 0.279\,k^2 + n\,(0.212 + 0.238\,k)}{H}
\end{aligned}\right\}\ldots\ldots(30)$$

in which

$$\left.\begin{aligned}
A &= 5.8\,n^2\,(k+1)^2 + n\,(22.7\,k^3 + 95\,k^2 + 85\,k + 12) \\
&\quad + (21\,k^4 + 135\,k^3 + 244\,k^2 + 83\,k + 5.5) \\
B &= 23\,n^3\,(k+1) + n^2\,(80\,k^3 + 324\,k^2 + 340\,k + 76) \\
&\quad + n\,(65\,k^4 + 466\,k^3 + 985\,k^2 + 522\,k + 66) \\
&\quad + (6\,k^5 + 85\,k^4 + 366\,k^3 + 551\,k^2 + 167\,k + 7) \\
F &= n^2\,(k+1)\,(11\,k + 4.1) + n\,(30.7\,k^3 + 117\,k^2 + 85\,k + 10) \\
&\quad + (21\,k^4 + 135\,k^3 + 244\,k^2 + 83\,k + 5.5) \\
H &= 3 + 10\,k + 3\,k^2 + 2.667\,n\,(k+1)
\end{aligned}\right\}\ldots\ldots(31)$$

For the given dimensions of girder and columns, the writer obtained the numerical values of Table 11 for the moment coefficients.

Throughout the computations, the writer has used an ordinary 10-in. slide rule, and no simultaneous equations were necessary in the solution.

The great value of the authors' paper is in the closed-form coefficients obtained for the moments. However, as the authors themselves admit, the expressions presented for these moment coefficients are extremely complex, and require extensive computations to determine numerical values corresponding to any particular n and k. This overshadowed the real importance of the paper, and it became necessary for the authors to seek a modified simple

TABLE 11.—MOMENT COEFFICIENTS

Coefficient	Writer's value	Authors' value	Coefficient	Writer's value	Authors' value
γ_1	0.144	0.14375	η_1	0.00445	0.004468
γ_2	0.173	0.17344	η_2	0.0855	0.08602
γ_3	0.062	0.067205	η_3	0.0085	0.008384
γ_4	0.073	0.07310	η_4	0.083	0.08239
γ_5	0.1075	0.10550	η_5	0.0056	0.005309

analysis. To make these moment coefficients easily applicable, they should be given in a curve form—a form which appeals to all engineers. The writer has put the coefficients of Eqs. 29 and 30 in the curve form shown in Figs. 7 to 11.

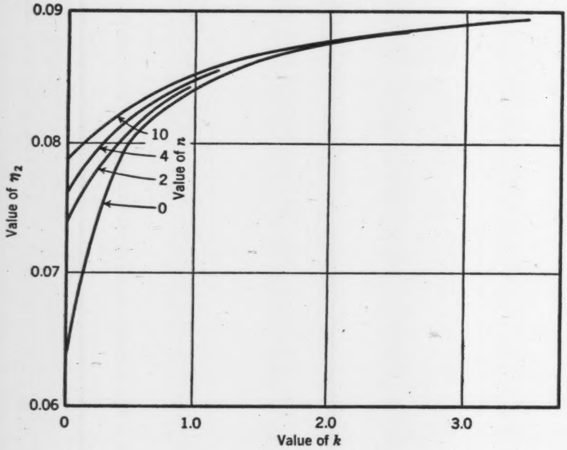

FIG. 11.—CURVES OF $\eta_2 = -M_A/M_o$ (FROM TABLE 5)

These curves cover the ranges from $k = 0$ to $k = 3$ and from $n = 0$ to $n = 10$. The authors may extend these curves more accurately to a wider range.

SIDNEY SHORE,[6] J. M. ASCE, AND HUMBERTO RINCON.[7]—In the "Introduction" of the paper it is stated that

> "To the writers' knowledge, however, no study exists in which the stresses in space frames with horizontally curved members, subject to loading in, or normal to, their plane of curvature are analyzed."

To the contrary, there appear in the literature methods that can be adapted quite easily to analyze the type of space frame being discussed. For example, if the members of the space frame are either segmental (24) in the horizontal plane or of circular arc plan (25) the moment-distribution techniques offer avenues for solutions. Although the moment-distribution solution is not usually of the "closed form," its versatility justifies its use. This appears to be particularly true in the case of supporting structures for chemical equipment and bins because each type of structure requires its own geometrical configuration. The closed form is most advantageous when a series of structures of the same general configuration are designed.

---

[6] Associate Prof. of Civ. Eng., Univ. of Pennsylvania, Philadelphia, Pa.

[7] Graduate Student, The School of Civ. Eng., University of Pennsylvania, Philadelphia, Pa.

TABLE 12.—DISTRIBUTION OF MOMENTS, IN FOOT-KIPS, ABOUT THE x-AXIS; w = 6.196 KIPS PER FT (NO JOINT TRANSLATION PERMITTED)

Joint	A			1		2		B
Member	A8	AF	A1	1A	12	21	2B	B2
$K/\Sigma K$	0.361	0.278	0.361	0.387	0.613	0.230	0.770	
C	$C'_{zz} = -1.0$	$C'_{zz} = 0$	$C'_{zz} = -1.0$	$C'_{zz} = -1.0$	$C'_{zz} = 0.263$ $C'_{zz} = 0.579$ $C_{zz} = 0.686$	$C'_{zz} = 0.263$ $C'_{zz} = 0.579$ $C_{zz} = 0.686$	$C'_{zz} = 0.50$	
F.E.M.					−27.85	+27.85	−9.90	+9.90
Dist.				+10.80	+17.05	−4.15	−13.80	
COM (x)	−10.80		−10.80		−1.09	+4.50		−6.90
COM (z)					−9.85 +2.84	−11.70 +2.40		
Subtotal	−10.80		−10.80	+10.80	−18.90	+18.90	−23.70	+3.00
Dist.	+7.80	+6.00	+7.80	+3.14	+4.96	+1.10	+3.70	
COM (x)	−3.14		−3.14	−7.80	+0.29	+1.30		+1.85
COM (z)					−2.87 −0.75	−3.40 −0.64		
Subtotal	−6.14	+6.00	−6.14	+6.14	−17.27	+17.26	−20.00	+4.85
Dist.	+2.26	+1.76	+2.26	+4.30	+6.83	+0.63	+2.11	
COM (x)	−4.30		−4.30	−2.26	+0.17	+1.80		+1.05
COM (z)					−3.95 −0.43	−4.70 −0.36		
Subtotal	−8.18	+7.76	−8.18	+8.18	−14.65	+14.63	−17.89	+5.90
Dist.	+3.10	+2.40	+3.10	+2.50	+3.97	+0.75	+2.51	
COM (x)	−2.50		−2.50	−3.10	+0.20	+1.05		+1.25
COM (z)					−2.30 −0.51	−2.72 −0.43		
Subtotal	−7.58	+10.16	−7.58	+7.58	−13.29	+13.28	−15.38	+7.15
Dist.	+1.80	+1.40	+1.80	+2.21	+3.50	+0.48	+1.62	
COM (x)	−2.21		−2.21	−1.80	+0.13	+0.92		+0.81
COM (z)					−2.02 −0.33	−2.40 −0.28		
Subtotal	−7.99	+11.56	−7.99	+7.99	−12.01	+12.00	−13.76	+7.96
Dist.	+1.59	+1.24	+1.59	+1.55	+2.47	+0.40	+1.36	
COM (x)	−1.55		−1.55	−1.59	+0.10	+0.65		+0.68
COM (z)					−1.43 −0.27	−1.70 −0.23		
Subtotal	−7.95	+12.80	−7.95	+7.95	−11.14	+11.12	−12.40	+8.64
Dist.	+1.12	+0.86	+1.12	+1.23	+1.96	+0.29	+0.99	
COM (x)	−1.23		−1.23	−1.12	+0.07	+0.52		+0.48
COM (z)					−1.13 −0.20	−1.34 −0.17		
Subtotal	−8.06	+13.66	−8.06	+8.06	−10.44	+10.42	−11.41	+9.12
Dist.	+0.96	+0.74	+0.96	+0.92	+1.46	+0.22	+0.77	
COM (x)	−0.92		−0.92	−0.96	+0.06	+0.38		+0.38
COM (z)					−0.85 −0.15	−1.00 −0.13		
Subtotal	−8.02	+14.40	−8.02	+8.02	−9.92	+9.92	−10.64	+9.50
Dist.	+0.59	+0.46	+0.59	+0.74	+1.16	+0.17	+0.55	
Final	−7.43	+14.86	−7.43	+8.76	−8.76	+10.09	−10.09	+9.50

To demonstrate a typical moment-distribution solution, the same octagonal frame solved numerically in Appendix I will be analyzed for the case of distributed loading and columns hinged at the base. It is not feasible to use the same nomenclature and sign convention regarding moments as the authors used. In this discussion the sign convention for moments acting on the ends of a member is shown in Fig. 12, and the nomenclature is that used by James Michalos, M. ASCE (24). The right-hand-screw rule will determine the sense of the moment vector which is denoted by a double-headed arrow. Following are the values of the stiffness (K) and carry-over factors (C) for member 1–2, the only member skewed with respect to the reference axes, x, y, and z.

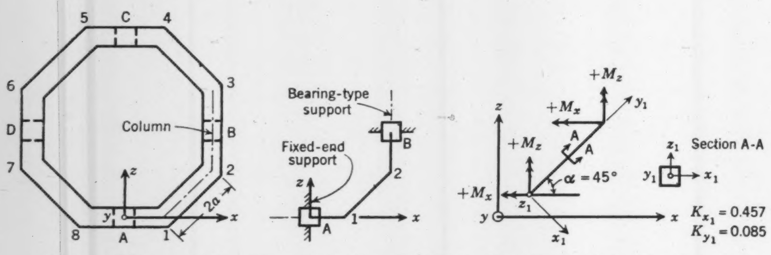

FIG. 12.—DIAGRAM OF OCTAGONAL RING SHOWING MOMENT-DISTRIBUTION SIGN CONVENTION

$$K_z = K_{y_1} \sin^2 \alpha + K_{x_1} \cos^2 \alpha = 0.271$$
$$K_x = K_{y_1} \cos^2 \alpha + K_{x_1} \sin^2 \alpha = 0.271$$
$$K_y = K_{z_1}$$
$$C_{xz} = \frac{(K_{x_1} - K_{y_1}) \sin \alpha \cos \alpha}{K_z} = 0.686$$
$$C_{zx} = \frac{(K_{x_1} - K_{y_1}) \sin \alpha \cos \alpha}{K_x} = 0.686$$
$$C_{yz} = C_{yx} = C_{zy} = C_{xy} = 0$$
$$C'_{xz} = (C^{x_1}{}_{12} + 1) \sin \alpha \cos \alpha + C_{xz}(C^{x_1}{}_{12} \sin^2 \alpha - \cos^2 \alpha) = 0.579$$
$$C'_{zz} = C^{x_1}{}_{12} \cos^2 \alpha - \sin^2 \alpha + C_{xz} \sin \alpha \cos \alpha (C^{x_1}{}_{12} + 1) = 0.263$$
$$C'_{xx} = C^{x_1}{}_{12} \sin^2 \alpha - \cos^2 \alpha + C_{zx} \sin \alpha \cos \alpha (C^{x_1}{}_{12} + 1) = 0.263$$
$$C'_{zx} = (C^{x_1}{}_{12} + 1) \sin \alpha \cos \alpha + C_{zx}(C^{x_1}{}_{12} \cos^2 \alpha - \sin^2 \alpha) = 0.579$$
$$C^{x_1}{}_{12} = C^{z_1}{}_{12} = 0.5$$
$$C'_{yz} = 0, \quad C'_{zy} = 0, \quad C'_{yx} = 0, \quad \text{and} \quad C'_{xy} = 0$$
$$C'_{yy} = C^{z_1}{}_{12} = 0.5$$

Owing to the symmetry of the octagonal girder and the uniformly distributed loading, only one quarter of the structure (A12B) has to be considered; furthermore, the distribution about only one of the two coordinate axes, x and z (Fig. 12), is necessary. In Tables 12 and 13 the distribution about the x-axis

TABLE 13.—Distribution of Moments, in Foot-Kips, About the x-Axis (Joint Translation Only)

Joint	A			1		2		B
Member	A8	AF	A1	1A	12	21	2B	B2
$K/\Sigma K$	0.361	0.278	0.361	0.387	0.613	0.230	0.770	
C	$C'_{zz} = -1.0$	$C'_{zz} = 0$	$C'_{zz} = -1.0$	$C'_{zz} = -1.0$	$C'_{zz} = 0.263$ $C'_{zz} = 0.579$ $C_{zz} = 0.686$	$C'_{zz} = 0.263$ $C'_{zz} = 0.579$ $C_{zz} = 0.686$	$C'_{zz} = 0.50$	
F.E.M.							+100	+100
Dist.						−23.00	−77.00	
COM (x)					−6.05			−38.50
COM (z)					+15.80	+13.30		
Subtotal					+9.75	−9.70	+23.00	+61.50
Dist.				−3.77	−5.98	−3.10	−10.20	
COM (x)	+3.77		+3.77		−0.82	−1.57		−5.10
COM (z)					+3.45 +2.12	+4.10 +1.79		
Subtotal	+3.77		+3.77	−3.77	+8.52	−8.48	+12.80	+56.40
Dist.	−2.71	−2.12	−2.71	−1.84	−2.91	−1.00	−3.32	
COM (x)	+1.84		+1.84	+2.71	−0.26	−0.77		−1.66
COM (z)					+1.68 +0.69	+2.00 +0.58		
Subtotal	+2.90	−2.12	+2.90	−2.90	+7.72	−7.67	+9.48	+54.74
Dist.	−1.33	−1.02	−1.33	−1.86	−2.96	−0.42	−1.39	
COM (x)	+1.86		+1.86	+1.33	−0.11	−0.78		−0.69
COM (z)					+1.71 +0.29	+2.03 +0.24		
Subtotal	+3.43	−3.14	+3.43	−3.43	+6.65	−6.60	+8.09	+54.05
Dist.	−1.34	−1.04	−1.34	−1.24	−1.98	−0.34	−1.15	
COM (x)	+1.24		+1.24	+1.34	−0.09	−0.52		−0.57
COM (z)					+1.14 +0.23	+1.36 +0.20		
Subtotal	+3.33	−4.18	+3.33	−3.33	+5.90	−5.90	+6.94	+53.48
Dist.	−0.90	−0.68	−0.90	−1.00	−1.57	−0.24	−0.80	
COM (x)	+1.00		+1.00	−0.06	−0.41			−0.40
COM (z)				+0.91 +0.16	+1.08 +0.14			
Subtotal	+3.43	−4.86	+3.43	−3.43	+5.34	−5.33	+6.14	+53.08
Dist.	−0.72	−0.56	−0.72	−0.74	−1.17	−0.19	−0.62	
COM (x)	+0.74		+0.74	−0.05	−0.31			−0.31
COM (z)				+0.68 +0.13	+0.80 +0.11			
Subtotal	+3.45	−5.42	+3.45	−3.45	+4.93	−4.92	+5.52	+52.77
Dist.	−0.53	−0.42	−0.53	−0.57	−0.91	−0.14	−0.46	
COM (x)	+0.57		+0.57	+0.53	−0.04	−0.24		−0.23
COM (z)					+0.53 +0.10	+0.62 +0.08		
Subtotal	+3.49	−5.84	+3.49	−3.49	+4.61	−4.60	+5.06	+52.54
Dist.	−0.42	−0.30	−0.42	−0.43	−0.69	−0.11	−0.35	
Final	+3.07	−6.14	+3.07	−3.92	+3.92	−4.71	+4.71	+52.54
$\frac{Y_1}{Y'_1} x$ (Final)	+9.58	−19.17	+9.58	−12.22	+12.22	−14.70	+14.70	+164.10

only is shown because the carry-over moments from the z-axis to the x-axis are determined by the following relationships,

$$\text{COM}(z) = (+\,C_{zz})(\text{distributed moment})_z = (-\,C'_{zz})(\text{distributed moment})_x$$

and

$$\text{COM}(z) = (+\,C'_{zz})(\text{distributed moment})_z = (-\,C_{zz})(\text{distributed moment})_x.$$

Essentially, the number of degrees of freedom that the segment A12B has is two. However, owing to symmetry of loading and structure, the translation of both joints 1 and 2, perpendicular to plane xz, will be identical. Therefore, in Table 12 are listed the end moments due to the uniformly distributed loading of 6.196 kips per ft, with joints 1 and 2 restrained against translation. In Table 13 is presented the distribution of moments produced by giving joints 1 and 2 any arbitrary, but equal, displacements perpendicular to the xz-plane. In fact, these arbitrary displacements are of such a magnitude to produce fixed-end moments of 100 ft-kips at the ends of members A1 and 2B. From the results of Tables 12 and 13, the final end moments were computed from the conditions that in the actual structure there were no supports at joints 1 and 2.

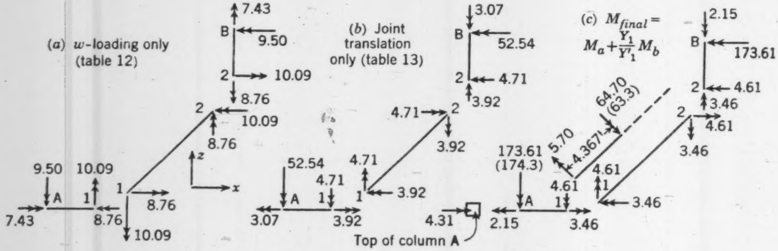
(a) w-loading only (table 12)
7.43
B
9.50
2
10.09
8.76
2
10.09
8.76
z
x
9.50
10.09
A
1
1
7.43
8.76
8.76
10.09
(b) Joint translation only (table 13)
3.07
B
52.54
2
4.71
3.92
4.71
2
3.92
52.54
4.71
4.71
A
1
1
3.92
3.07
3.92
4.31
Top of column A
(c) $M_{final} = M_a + \frac{Y_1}{Y'_1} M_b$
2.15
B
173.61
2
4.61
3.46
64.70
(63.3)
4.367'
5.70
173.61
(174.3)
2
4.61
3.46
4.61
4.61
1
A
1
3.46
2.15
3.46

FIG. 13.—COMPUTATION OF END MOMENTS, IN FOOT-KIPS (MOMENTS IN PARENTHESES ARE FROM TABLE 8)

The procedure for computing the final end moments are shown in Fig. 13, in which $Y_1 = \left[\frac{(6.196)(4.367)}{2} + \frac{10.09 - 9.50}{4.367}\right] + \left[\frac{(6.196)(8.734)}{2}\right] = 40.85$ kips upward due to the w-loading, and $Y'_1 = \frac{52.54 + 4.71}{4.367} = 13.10$ kips downward due to joint translation.

It can be seen that the moment-distribution results agree closely with those of Table 8 at the locations of maximum moments. At those locations where the moments are rather small, the discrepancies, percentagewise, appear large, but this is of little consequence because the design of the member will not be based on these small values. Of course, closer correlation could have been obtained if several more cycles of distribution had been performed. However, it is felt that the technique has been adequately demonstrated by the nine distribution cycles shown in Tables 12 and 13.

The solution of the other two conditions of loading—that is, horizontal shear loading and moment loading—will not present any difficulties, the only variation being that the two degrees of freedom of the segment A12B will manifest themselves under these loadings.

Paul C. Disario, Jr.,[8] A. M. ASCE, John S. Podolan,[9] and Nicholas A. Weil,[10] J. M. ASCE.—The writers wish to thank the discussers for their interest. Each has contributed to the analysis by his comments.

The writers agree with Mr. Diwan that the solution given is complex; however, included in the paper is a "modified analysis," which produces substantially the same results with considerably less effort. This solution is used in the actual design of these frames and with the aid of curves makes the design reasonably simple. The writers have not attempted to publish such curves here but agree wholeheartedly with Mr. Diwan that such a presentation is ideal for office use. A preference on the part of the writers for the Castigliano theorem does not mean that the method of virtual work is not equally adaptable to this problem. The amount of work involved using either method is substantially the same.

Messrs. Shore and Rincon have in their discussion questioned the writers' statement that no previous study of the subject exists. The writers believe this statement continues to be essentially correct for the scope of the paper presented. They have attempted to produce coefficients of closed form which can be adopted to the curve type of presentation for the rapid solution of design problems.

Messrs. Shore and Rincon have used the obvious method of moment distribution to arrive at moments for uniformly distributed vertical load; based on this method they have stated that "horizontal shear loading and moment loading will not present any difficulties," but they have not attempted to prove this point more thoroughly. It is the writers' belief that the method of moment distribution when applied to the octagonal-girder space frame under horizontal loading and moment loading will present difficulties not normally encountered in usual design problems.

---

[8] Section Head, Foundations and Concrete Section, M. W. Kellogg Co., New York, N. Y.

[9] Structural Engr., M. W. Kellogg., New York, N. Y.

[10] Development Engr., M. W. Kellogg Co., New York, N. Y.

AMERICAN SOCIETY OF CIVIL ENGINEERS
Founded November 5, 1852
TRANSACTIONS

Paper No. 2830

BEAM RESTRAINTS PROVIDED BY WALLS WITH OPENINGS

By Ibrahim A. Mohammed,[1] J. M. ASCE, and
Egor P. Popov,[2] A. M. ASCE

Synopsis

No generally accepted design criteria are available for determining the restraint that a reinforced concrete wall exerts on a beam framing into it. By means of graphs the authors of this paper attempt to provide this information in a convenient form. The report includes the results of an analytical solution for a plate, considered to be equivalent to a wall, to which a local edge moment is applied. The effective stiffness of the plate is converted into an equivalent beam stiffness. Then, based on experimental evidence, the reduction in restraint caused by certain types of rectangular openings is indicated. These results are shown on graphs, which enable one to determine easily the effective stiffness of a plate or a wall without openings—or with openings of different heights but of width equal to the height of the wall—in terms of the restraint of an equivalent beam. The proposed method of analysis is based on the assumption of the elastic behavior of material.

Introduction

A common element of construction—the reinforced concrete bearing wall—has received relatively little attention by analysts. No generally accepted design criteria are available for determining the restraint provided by a wall to a beam framing into it. However, such information is necessary for the proper design of the reinforcement of a beam and a wall.

The problem is solved by idealizing the actual situation. First it is assumed that the wall behaves elastically and that the material of which it is made is isotropic. This assumption, although somewhat at variance with the actual facts, is nevertheless commonly used in the analysis and design of reinforced concrete flexural members. Second, the axial stresses in a bearing wall are so small that their effect may be neglected in determining the flexural stiffness of

---

Note.—Published, essentially as printed here, in October, 1954, as *Proceedings-Separate No. 529.* Positions and titles given are those in effect when the paper was approved for publication in *Transactions.*

[1] Graduate student in Civ. Eng., Univ. of California, Berkeley, Calif.

[2] Prof. of Civ. Eng., Univ. of California, Berkeley, Calif.

the wall. Under these assumptions, the determination of the effective stiffness of a wall is reduced to the problem of an elastic plate subjected to a locally applied moment. The writers present an analytical solution of this problem. The solution is applicable to a solid, rectangular, simply supported plate with a local moment applied parallel to one pair of the edges. The solution shows that in determining the effective stiffness of a solid plate to a locally applied moment it is possible to replace the wall with an equivalent beam.

When the plate is weakened by openings, such as window and door openings in the case of a bearing wall, the determination of the stiffness of the perforated plate is very involved mathematically. An analytical solution of this problem was not attempted. Instead, experimental investigations were made on a steel plate with rectangular openings of various sizes. Although the height of these openings was varied, their width in all cases was equal to the height of the plate. The results of this investigation provide experimentally determined factors which, in percentages, represent the restraint provided by the perforated plate relative to the restraint provided by the solid plate. An example of the application of this theory to a practical problem is also presented.

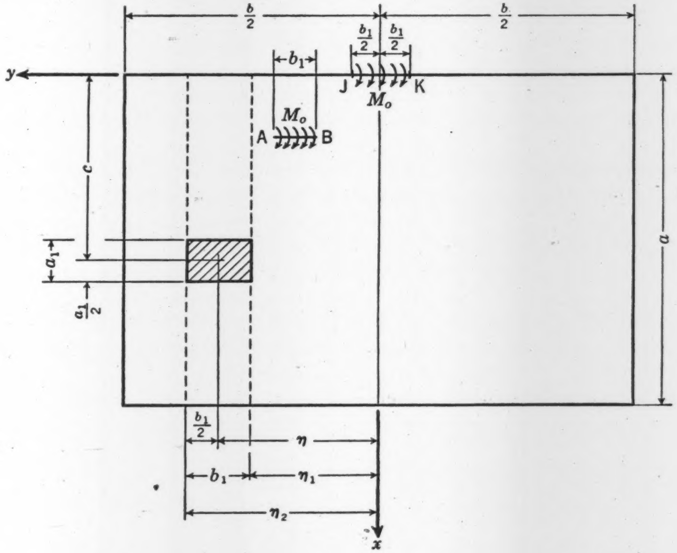

Fig. 1.—General Case of the Simply Supported Rectangular Plate

Theoretical Investigation

If consideration is limited to simply supported rectangular plates, the general problem requires the determination of the deflection of the plate subjected to a local moment. In a general case (Fig. 1) it is necessary to know the deflection of the plate caused by a local moment M_o acting along a line such as AB. This solution has been previously reported[3] and is briefly reviewed herein.

The deflection w of a plate is expressed by the well-known differential equation

$$\frac{\partial^4 w}{\partial x^4} + 2\,\frac{\partial^4 w}{\partial x^2\,\partial y^2} + \frac{\partial^4 w}{\partial y^4} = \frac{q}{D} \qquad (1)$$

in which q is the intensity of the load and D, the flexural rigidity of the plate, is $E\,t^3/12(1-\mu^2)$. In the latter expression, E is the elastic modulus, t is the thickness of the plate, and μ is the Poisson ratio.

The deflection w produced by a uniformly distributed load q on the shaded portion in Fig. 1, for example, may be expressed in a series form.[4] One of these series applies in the region $y < \eta_1$, another in the region $y > \eta_2$, and a third series applies to that portion in the interval $\eta_1 < y < \eta_2$. By expanding the applied load q into a Fourier series and making use of the boundary conditions and continuity conditions, all the necessary constants for the foregoing series may be determined.[3,4] This procedure yields a solution for the deflection of a plate caused by a uniformly distributed load on the area $a_1\,b_1$, shown shaded in Fig. 1. By letting a_1 approach zero as $a_1\,b_1\,q = P$ is maintained constant, one obtains an expression for w caused by a line load P acting over a distance b_1.

On introducing in the interval $\eta_1 < y < \eta_2$ two adjacent equal line loads of magnitude P acting in opposite directions, the deflection of the plate may be determined by superposition. By letting the distance λ between the two line loads approach zero as $P\,\lambda = M_o$ is maintained constant, one obtains an expression[3] for w caused by a moment M_o uniformly distributed along the distance b_1. The resulting expression is highly involved (Eqs. 8*a* and 9*a*). However, it is greatly simplified if b approaches ∞, $c = 0$, and $\eta = 0$. For this special case the expression is reduced to[3]

$$w = \frac{M_o\,a^2}{b_1\,D\,\pi^3} \sum_{m=1}^{\infty} \frac{1}{m^3} \sin\frac{m\,\pi\,x}{a} \left\{ 2 + \left[\frac{m\,\pi\,y}{a} \sinh\frac{m\,\pi\,y}{a} - \left(2 + \frac{m\,\pi\,b_1}{2\,a}\right) \cosh\frac{m\,\pi\,y}{a} \right] e^{-m\pi b_1/2a} \right\} \qquad (2)$$

in which m is an integer.

For practical applications Eq. 2 is particularly significant. It expresses the deflection w for a simply supported long plate loaded with a local moment M_o along the line JK in Fig. 1. This case closely corresponds to a bearing wall into which a horizontal beam of width b_1 is framed.

A study of Eq. 2 and analogous expressions given in the Appendix shows that significant deflections of the plate occur in close proximity to the loaded strip $y = \pm b_1/2$. At y-distances comparable to the width a of the plate, the deflections become small. This fact may be seen by examining Fig. 2, in which

---

[3] "Effective Stiffness of a Plate Subjected to a Local Edge Moment," by Ibrahim A. Mohammed and Egor P. Popov, *Proceedings*, Second U. S. National Cong. of Applied Mechanics, Ann Arbor, Mich., June 14–18, 1954, pp. 423–426.

[4] "Theory of Plates and Shells," by S. Timoshenko, McGraw-Hill Book Co., Inc., New York, N. Y., 1940, pp. 147 and 150–152.

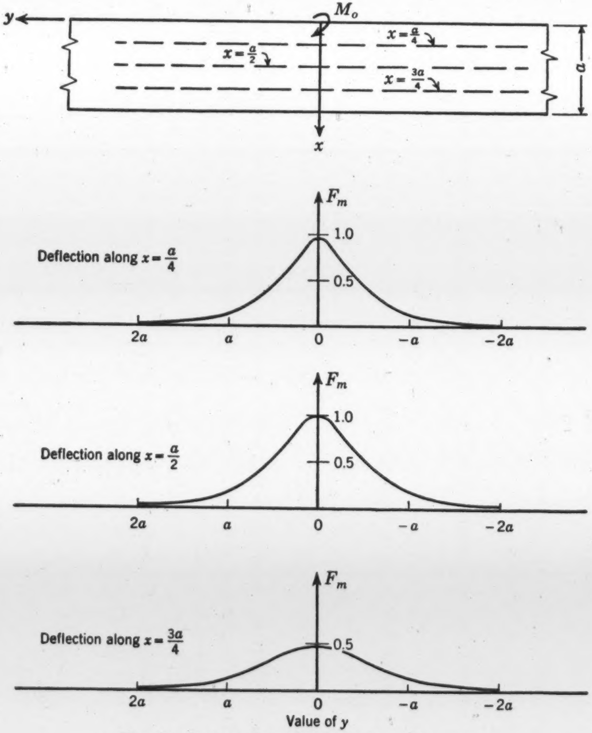

FIG. 2.—DEFLECTIONS COMPUTED USING EQS. 3

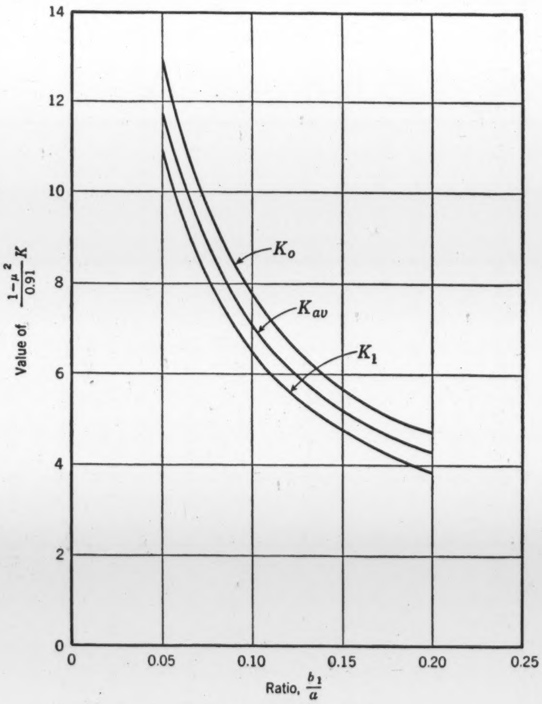

FIG. 3.—CONSTANT, K

is shown the deflection variation caused by a concentrated moment M_o applied at $x = y = 0$ along several lines of constant x-values. The computations were based on the equations for concentrated moment, Eqs. 6*b* and 7*b*, in the form,

$$w = \frac{M_o\, a}{2\, D\, \pi^2} F_m \qquad \text{(3a)}$$

in which

$$F_m = \sum_{m=1}^{\infty} \frac{\sin \dfrac{m\, \pi\, x}{a}}{m^2} \left(1 + \frac{m\, \pi\, y}{a}\right) e^{-m\pi y/a} \qquad \text{(3b)}$$

The first partial derivative of Eq. 2 with respect to x shows that for a moment M_o distributed along a distance b_1 the rotation of the edge of the plate varies within this distance. This rotation of the plate within the width b_1 at $x = 0$ is particularly significant. It is this rotation, a function of the applied moment M_o, that is directly related to the restraint that a plate provides to a beam. However, the moment is usually applied to the plate by means of a beam of enormous rigidity. Such a beam, of width b_1, tends to force a uniform rotation of the plate within this width. Thus, the condition of uniform distribution of the moment is not satisfied. Also, there is a question as to which rotation of the plate should be used in establishing an equivalent beam having a stiffness equal to the stiffness of the plate. This problem may be resolved by investigating the two extreme values of the rotation of the plate within the distance b_1—that is, at $y = 0$ and at $y = \pm b_1/2$. It was found that the difference between these two solutions is not large, and the correct answer, lying between the two extremes, may be estimated with reasonable accuracy (Fig. 3).

From Eq. 2 the maximum slope of the loaded plate occurs at $x = y = 0$. It may be determined by differentiating Eq. 2 with respect to x and then setting $x = y = 0$. On the other hand, the maximum slope of the elastic curve for a simply supported beam loaded with an end moment M_o is given by the expression,

$$\left(\frac{dw}{dx}\right)_{x=0} = \frac{M_o\, a}{3\, E\, I} = \frac{4\, M_o\, a}{E\, B\, t^3} \qquad \text{(4)}$$

in which a is the span, B is the width of the beam, and t is its depth.

If the maximum slope or rotation of the plate is regarded as a measure of the stiffness of the plate in resisting an applied moment, then the corresponding expression for the rotation of an equivalent simple beam must equal this maximum rotation. By formulating this equality, it is possible to relate the width B of the equivalent beam to the width b_1:

$$B = K_o\, b_1 \qquad \text{(5a)}$$

in which

$$\frac{1}{K_o} = \frac{3(1 - \mu^2)}{\pi^2} \sum_{m=1}^{\infty} \frac{1}{m^2} \left[2 - \left(2 + \frac{m\, \pi\, b_1}{2\, a}\right) e^{-m\pi b_1/2a}\right] \qquad \text{(5b)}$$

Analogously, if the rotation of the plate at $y = \pm b_1/2$ is regarded as a measure of the plate's stiffness, the constant K_o in Eq. 5*a* must be replaced by K evaluated at $y = \pm b_1/2$, designated K_1 and defined as

$$\frac{1}{K_1} = \frac{3(1 - \mu^2)}{\pi^2} \sum_{m=1}^{\infty} \frac{1}{2\,m^2}\left[2 - \left(2 + \frac{m\,\pi\,b_1}{a}\right) e^{-m\pi b_1/a}\right] \ldots\ldots (5c)$$

The series defined by Eqs. 5*b* and 5*c* converge very slowly. Direct evaluation of the constants K_o and K_1 is rather lengthy. To minimize the work in applications, Fig. 3 may be used for a considerable range of values of the parameter b_1/a. However, as stated previously, a beam framing into a wall has enormous rigidity and tends to force a uniform rotation at the edge of the wall within the distance b_1. Thus, neither K_o nor K_1 is the exact constant for the solution of the actual problem. However, for a practical problem it is sufficiently accurate to use the constant $K_{av} = (K_o + K_1)/2$. This follows from the assumption of a linear variation of the rotation of the edge of the plate from $y = 0$ to $y = \pm b_1/2$. This approximation is not accurate for large values of b_1.

For practical applications one may compute the value of the width B from the relationship,

$$B = K_{av}\,b_1 \ldots\ldots\ldots\ldots\ldots\ldots\ldots\ldots (5d)$$

The curve for K_{av} is shown in Fig. 3.

EXPERIMENTAL INVESTIGATION

Because there are almost invariably door openings and window openings in bearing walls, the restraint of beams caused by such walls is an important problem related to the foregoing one. As mathematical difficulties precluded the analytical solution of this problem a limited aspect was studied experimentally. The experiments performed are described subsequently. The analysis of the experimental data permitted the construction of curves which enable one to determine that restraint provided to a beam by a wall weakened by various openings as a fraction of the restraint given by a similar solid wall. In all cases the horizontal width of the openings investigated was equal to the height of the wall.

A general view of the test arrangement is shown in Fig. 4(*a*). A wall was simulated by a steel plate 24 in. by ¼ in. by 8 ft, which was hung vertically from four cables. At the top and bottom, "simple supports" for the plate were provided by aluminum strips ½ in. by 1/16 in. by 1 ft 1 in., spaced approximately 1.5 in. on centers and attached to the plate with machine screws. Because the plate was long in relation to its width, the two short edges of the plate were left free. The moment at the middle of the top edge could be applied by means of six levers (Fig. 4(*a*)). By applying known upward forces on one end of the levers and equal downward forces on the other end, it was possible to apply external edge moments of the desired magnitudes. The magnitudes of the forces were controlled by placing weights on pans attached to the ends of the levers by means of a pulley arrangement (Fig. 4(*a*)). The levers were so con-

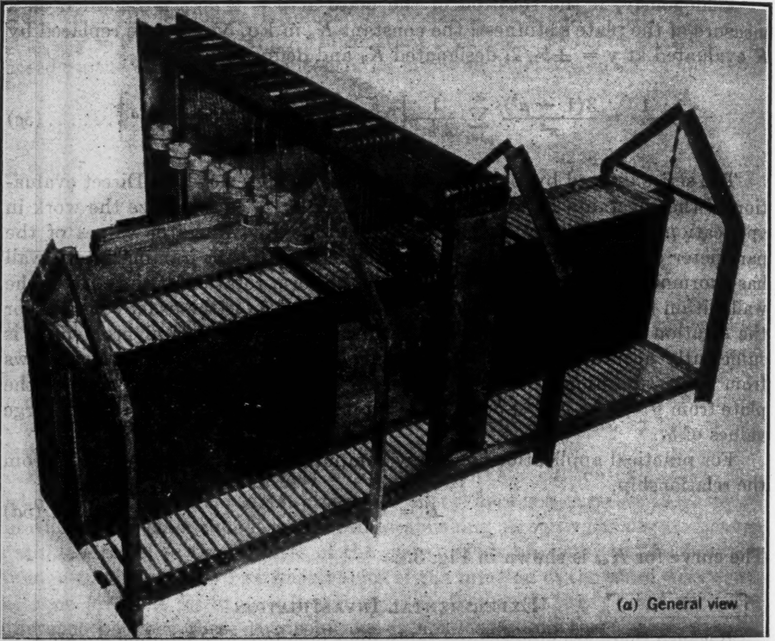

(a) General view

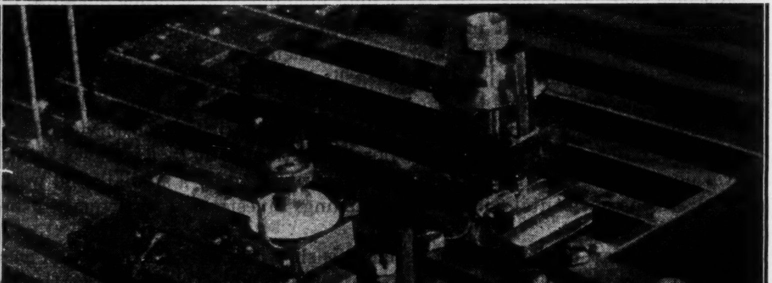

(b) Detail

FIG. 4.—TEST APPARATUS

structed that the moment was applied within $\frac{7}{16}$ in. of the top of the plate. The rotation of the plate caused by the applied moments was measured using highly sensitive clinometers which were mounted on short rods (Fig. 4(*b*)).

In several tests, the outer two or the outer four levers were left unloaded in order to study the effect of various widths of beams framing into the plate. In some tests the loaded levers were rigidly clamped together in order to enforce a uniform rotation of the edge of the plate within the loaded edge; these cases more nearly correspond to actual beams framing into a wall.

The initial tests were performed on a solid plate. Then a saw cut 24 in. long was made in the plate 10 in. above the bottom and parallel thereto. Subsequently, analogous tests were made by increasing the height of the opening in 3-in. steps. In this manner data were obtained for rectangular openings 3 in., 6 in., 9 in., 12 in., 15 in., and 18 in. high. In all cases, the width of the opening was maintained at 24 in. The location of these openings is shown diagrammatically in Fig. 5.

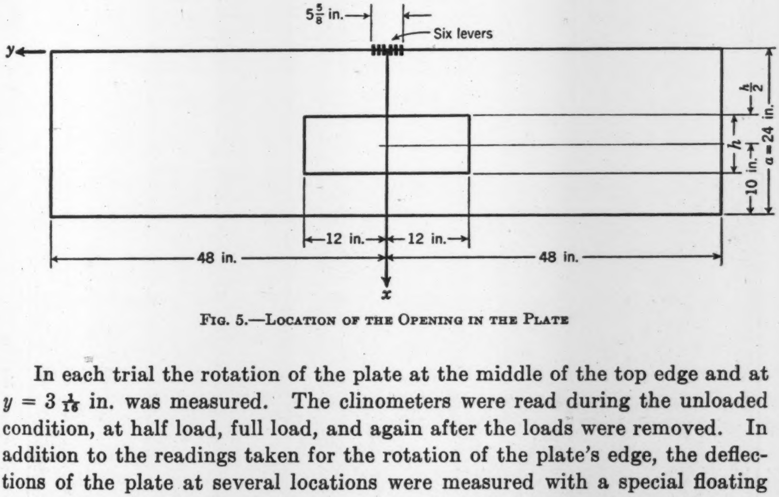

FIG. 5.—LOCATION OF THE OPENING IN THE PLATE

In each trial the rotation of the plate at the middle of the top edge and at $y = 3\frac{1}{16}$ in. was measured. The clinometers were read during the unloaded condition, at half load, full load, and again after the loads were removed. In addition to the readings taken for the rotation of the plate's edge, the deflections of the plate at several locations were measured with a special floating meter (Fig. 6). In Fig. 6 the meter is located at a distance 24 in. from the center of the plate. The opening in the plate in Fig. 4(*a*) is the largest one investigated.

The deflections of the solid plate used in these experiments caused by an effective moment $M_o = 930$ in.-lb applied by means of six levers are shown in Fig. 7. Three curves, giving the deflection at $y = a = 24$ in., $y = a/2 = 12$ in., and $y = 0$, show the results when all six levers acted independently; one curve for $y = 0$ is shown for the case when all levers were rigidly clamped together. Although the loaded region was relatively wide, the difference between the deflections at $y = 0$ when the levers were separate and when they were clamped together is rather small.

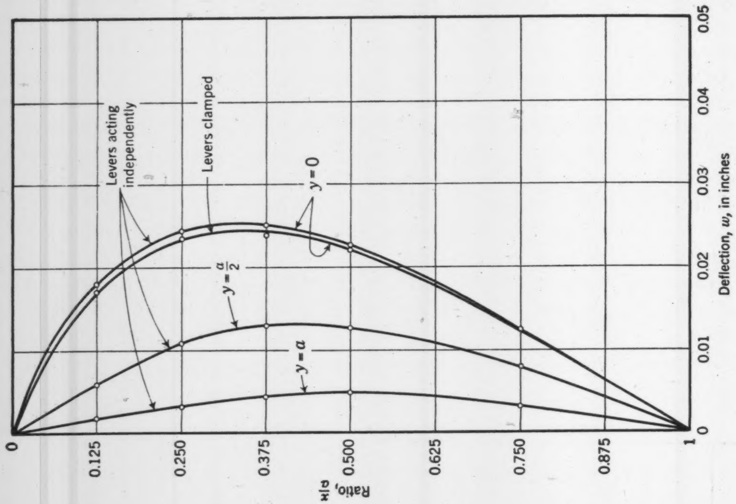

Fig. 7.—Deflections Produced by Six Levers Fully Loaded

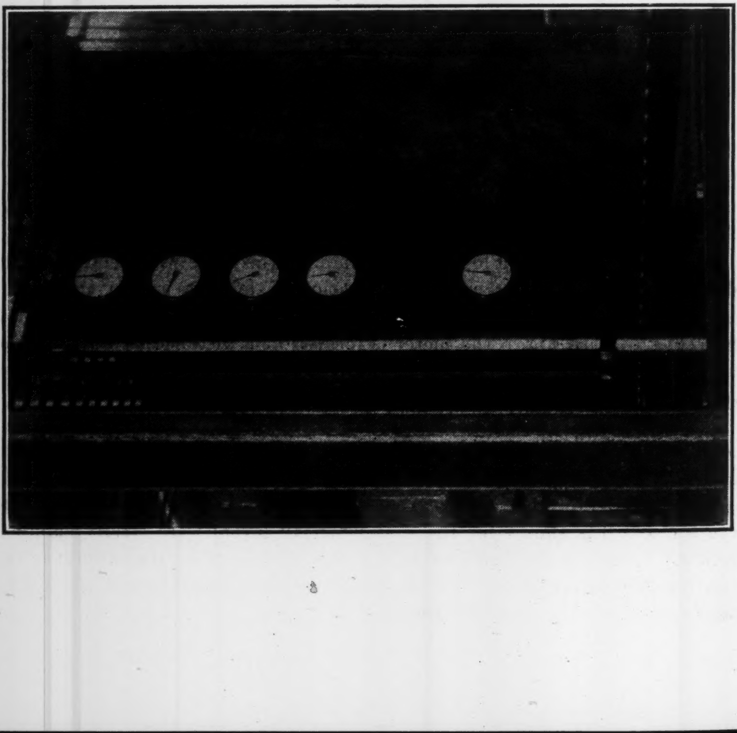

Fig. 6.—Floating Meter

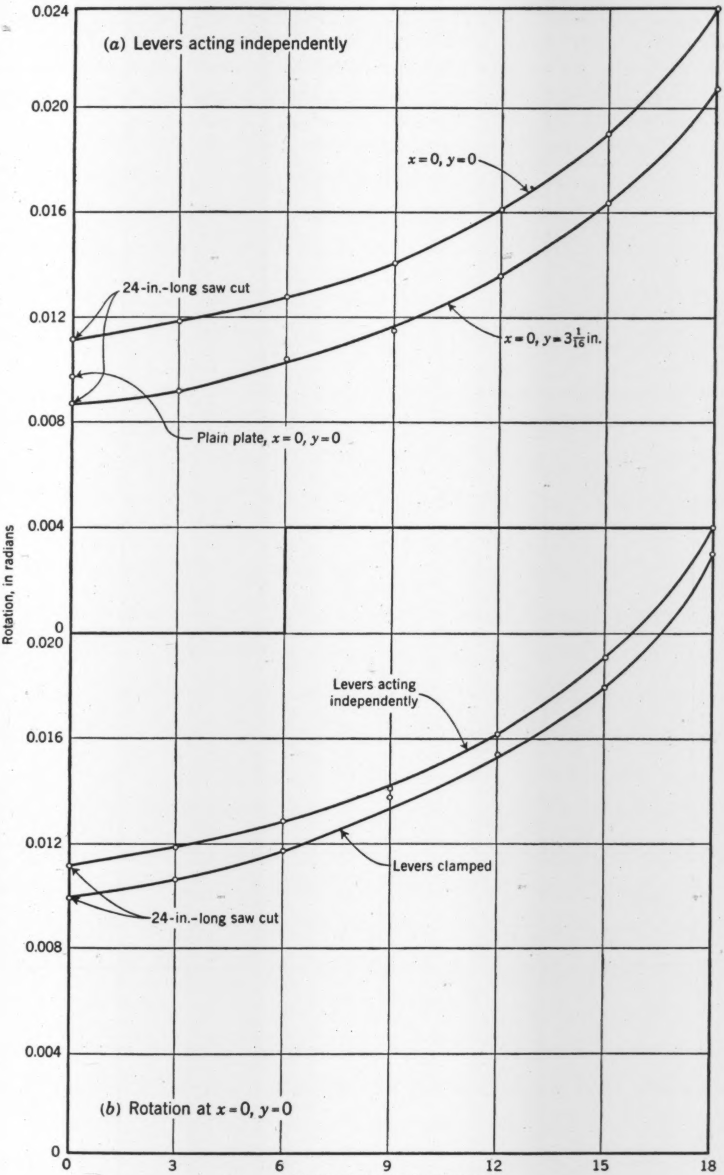

FIG. 8.—ROTATION MEASUREMENTS, ALL LEVERS FULLY LOADED

The variation in the rotations of the plate's edge at the middle and near the edge of the loaded region may be seen from Fig. 8(*a*). The curves show the effect of the six levers acting independently with a total effective moment of 930 in.-lb. The readings were made using the two clinometers shown in Fig. 4(*b*). The outer clinometer was mounted at $y = 3\,\frac{1}{16}$ in., whereas the edge of the exterior lever was at $y = 2\,\frac{13}{16}$ in. Therefore, the difference between the two curves exaggerates the actual difference in the rotations at the middle and at the edge of the exterior lever.

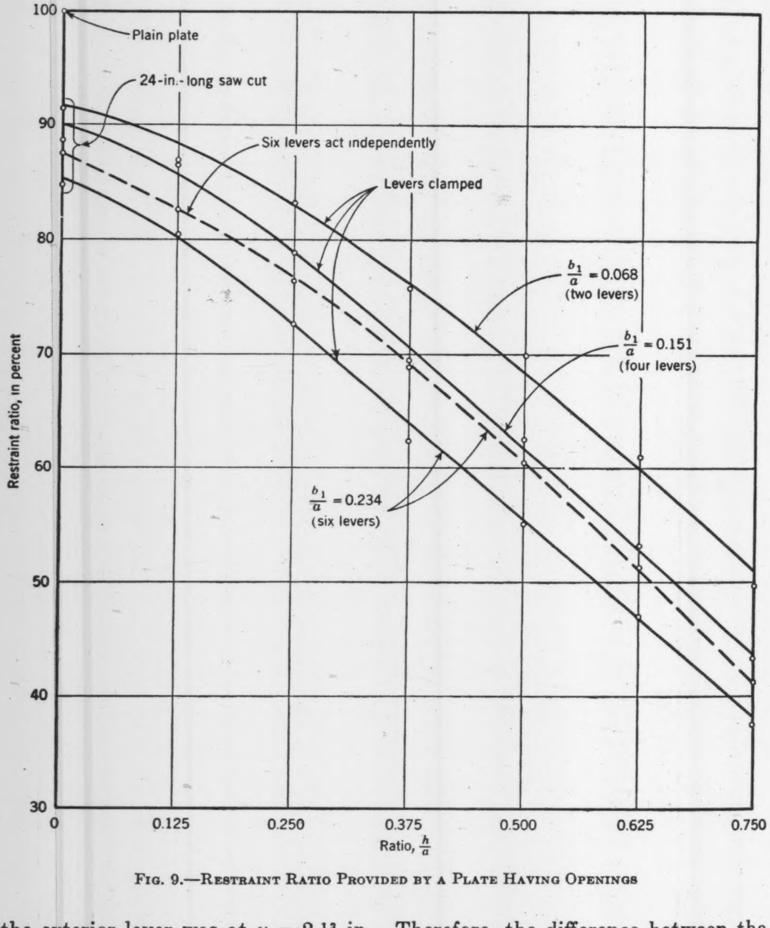

FIG. 9.—RESTRAINT RATIO PROVIDED BY A PLATE HAVING OPENINGS

The rotations at the middle of the top plate produced by the six levers acting independently and by the six levers clamped together are plotted in

Fig. 8(*b*). In both cases the effective applied moment was 930 in.-lb. For narrower beams—that is, for four-lever or two-lever loading—the difference (not shown) between the corresponding curves is smaller.

The various observed maximum rotations of the perforated plate were compared with the corresponding maximum rotation, caused by the same loading, of the solid plate. This permitted the computation of the restraint provided by the plate with openings of different sizes as a percentage of the restraint given by the solid plate. The height h of the opening was expressed as a fraction of the height a of the wall. Using these dimensionless parameters, the curves shown in Fig. 9 were established. Each curve corresponds to a particular ratio of the width b_1 of the beam to a, the height of the wall into which the beam frames. By interpolating between these curves a considerable range of possible beam widths and opening sizes may be analyzed. The curve shown in Fig. 9 for the six levers acting independently is of some theoretical interest.

COMPARISON OF EXPERIMENTAL AND THEORETICAL RESULTS

The results of the experiments on a solid plate loaded with levers acting independently may be compared with the established analytical expressions. For this purpose the mechanical properties of the steel plate were determined, and the sources of the experimental errors were analyzed and compensated for in the comparison.

A sample of the steel plate 1.00 in. by 0.251 in. by 2 ft 0 in. was tested in pure bending, and from the data the modulus of elasticity E was found to be 31.2×10^6 lb per sq in. The Poisson ratio μ was assumed to be 0.30. These values of E and μ were used in all computations.

It was believed that the readings obtained with the clinometers and dial gages were reliable. However, the cables used in the loading arrangement were not sufficiently flexible, and there was considerable friction in the pulleys. Therefore, it was necessary to calibrate the loading system and to determine accurately the magnitude of the actual forces delivered to the ends of the levers. This calibration showed that approximately 26.3% of the force originating from the loads in the pans was lost in pulley friction and bending of the cables. All other sources of experimental error were rather small. Nevertheless, an attempt to compensate for them was also made as follows:

1. The aluminum strips at the top and bottom of the plate provided some restraint—that is, the support was not truly "simple." Based on certain assumptions, the computations show that the restraint given to the plate by these strips was about 1.0% of the applied moment.
2. Because the plate was actually hung vertically from four cables the weight of the plate tended to straighten out the plate and therefore the observed deflections and rotations were reduced. It is estimated that this effect also amounted to about 1.0%.
3. The fact that the moment could not be applied precisely at the edge of the plate also reduced the applied moment by 0.2%.

It was felt that other sources of experimental error could be ignored.

Based on the foregoing analysis of the possible experimental errors, it was concluded that the moment applied to the plate was reduced by approximately 29%. Therefore, when each of the twelve pans was loaded with a weight of 10 lb. and the moment arm for each force in the lever arrangement was 10 in., the moment, in inch-pounds, applied to the top of the plate, would not be 1,200 but 1,200/1.29 = 930. This is the magnitude previously cited.

TABLE 1.—DEFLECTION OF THE PLATE, IN THOUSANDTHS OF AN INCH, ALL LEVERS ACTING INDEPENDENTLY

$\frac{x}{a}$	6 LEVERS LOADED						INNER 4 LEVERS LOADED						INNER 2 LEVERS LOADED					
	$y=0$		$y=a/2$		$y=a$		$y=0$		$y=a/2$		$y=a$		$y=0$		$y=a/2$		$y=a$	
	A[a]	B[a]	A	B	A	B	A	B	A	B	A	B	A	B	A	B	A	B
0	0	0	0	0	0	0	0	0	0	0	0	0	0	0	0	0	0	0
⅛	23.3	23.2	8.0	7.7	2.3	2.2	16.1	16.0	5.2	4.9	1.5	1.5	8.3	8.9	2.6	2.5	0.8	0.9
¼	30.9	31.6	13.9	13.9	4.2	4.0	21.4	21.3	9.2	8.8	2.8	2.6	10.6	11.4	4.6	4.0	1.4	1.3
⅜	31.9	32.2	17.0	16.6	5.5	5.3	21.5	21.4	11.3	10.6	3.6	3.6	10.8	11.5	5.6	5.2	1.8	1.7
½	29.3	29.0	17.2	16.6	5.8	6.2	19.7	19.5	11.4	10.7	3.8	3.9	9.9	10.3	5.7	5.4	1.9	1.9
⅝	23.9	...	14.9	...	5.3	...	16.0	...	9.9	...	3.5	...	8.0	...	5.0	...	1.8	...
¾	16.7	16.0	10.9	10.5	4.0	3.9	11.2	10.5	7.3	7.1	2.6	2.3	5.6	5.4	3.6	3.9	1.3	1.0
⅞	8.7	...	5.8	...	2.1	...	5.8	...	3.8	...	1.4	...	3.0	...	1.9	...	0.7	...
1	0	0	0	0	0	0	0	0	0	0	0	0	0	0	0	0	0	0

[a] Columns marked A contain the computed values of deflection; columns marked B contain the observed values of deflection, multiplied by 1.29.

Because the derived analytical expressions are based on the assumption of a uniformly distributed moment, a comparison must be made between them and the experiments in which the levers acted independently (not clamped together). The nature of the agreement found between the computed and the adjusted observed values may be seen in Table 1.

TABLE 2.—ROTATION, IN RADIANS, OF THE PLATE AT $x = 0$, $y = 0$, ALL LEVERS ACTING INDEPENDENTLY

6 LEVERS LOADED		INNER 4 LEVERS LOADED		INNER 2 LEVERS LOADED	
Computed	Observed ×1.29	Computed	Observed ×1.29	Computed	Observed ×1.29
0.0125	0.0126	0.00946	0.00967	0.00570	0.00603

An examination of the data in Table 1 shows an excellent agreement between the computed values and the adjusted observed values for the deflection of the plate. Equally close agreement between the computed and the experimental values was found for the maximum rotation of the plate, as may be seen in Table 2.

ILLUSTRATIVE EXAMPLE

The restraint exerted by the vertical member on the beam is compared for the two cases shown in Fig. 10. In the first case, a 12-in.-wide beam is framed into a 12-in. by 10-in. column, simply supported at its bottom (Fig. 10(*a*)); in the second case, an identical beam is framed into a 10-in.-thick wall with an opening 10 ft by 3 ft 9 in. (Fig. 10(*b*)). The wall is supposed to be long and simply supported along the top and bottom edges. Both the wall and the column are made of concrete for which $\mu = 1/6$.

It is required to find the ratio of the restraint encountered by the beams in the two cases.

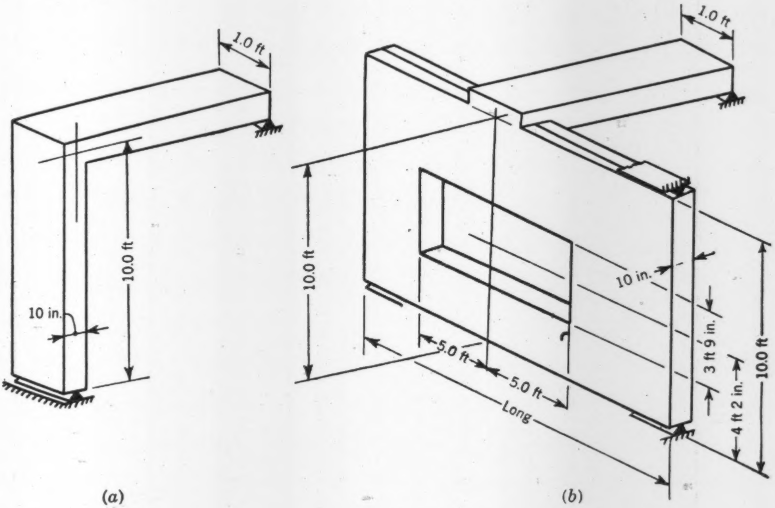

FIG. 10

Solution.—For the second case, the width and the location of the opening are of the same ratio as those shown in Fig. 5. Thus, the problem can be solved by means of the curves shown in Figs. 3 and 9.

The ratio of the width of the beam b_1 to the height of the wall a is $b_1/a = 1.00\text{ ft}/10.00\text{ ft} = 0.10$. For this ratio and using Fig. 3, the coefficient K_{av} equals 7.10. Because $\mu = 1/6$, the coefficient K_{av} must be multiplied by the factor, $0.91/[1 - (1/6)^2] = 0.936$; hence,

$$K_{av} = 6.64.$$

Because of the opening in this wall, the restraint is reduced to a percentage that may be determined from Fig. 9. Thus, using the ratio of the height of the opening h to the height of the wall a—that is, $h/a = 3.75\text{ ft}/10.00\text{ ft} =$

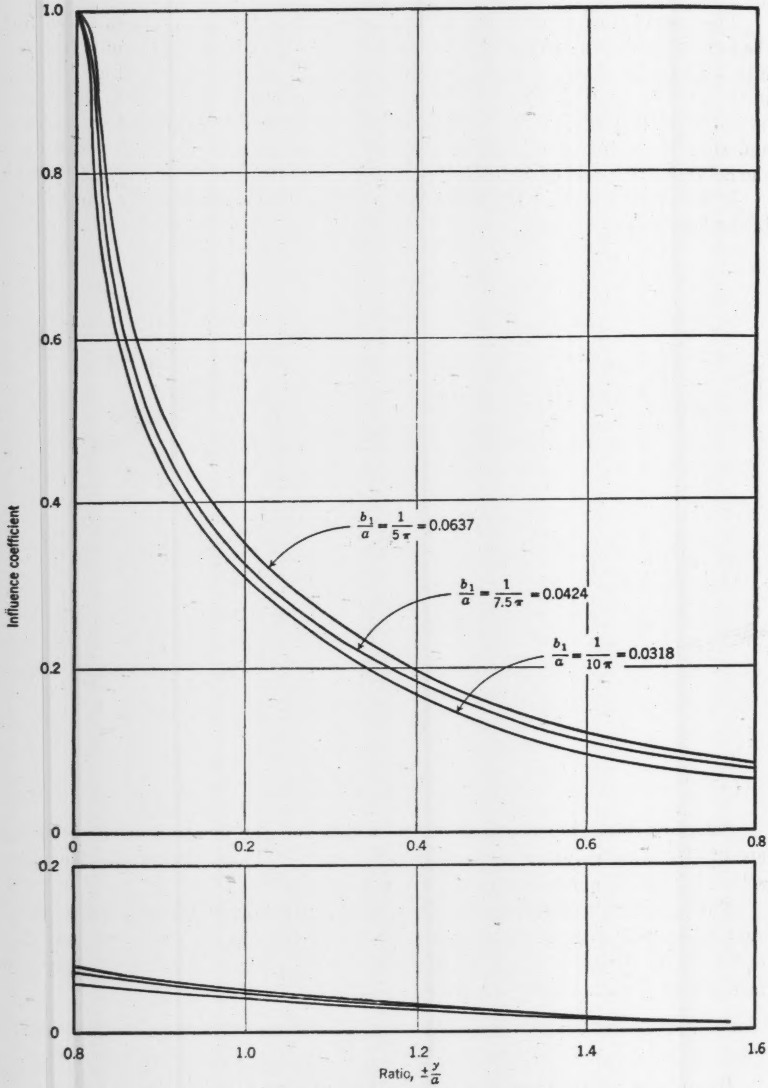

FIG. 11.—INFLUENCE LINES FOR ROTATION AT $x = 0$

0.375—one obtains from Fig. 9 the restraint ratio, 73%. Therefore, the reduced $K_{av} = 6.64 \times 0.73 = 4.85$.

Accordingly, the equivalent width of the column providing the same restraint exhibited by the perforated wall would be, using Eq. 5*d*, equal to

$$B = K_{av} \times b_1 = 4.85 \text{ ft.}$$

A wall with an opening such as the one shown in Fig. 10(*b*) therefore provides 4.85 times as much restraint to the horizontal beam as does the column shown in Fig. 10(*a*).

CONCLUDING REMARKS

The stiffness of a simply supported solid plate subjected to a local edge moment was studied by the writers. Fig. 3 was established for determining the width of a simply supported beam which has the same effective stiffness as a solid plate. However, in practice, more than one beam frames into the wall at various spacings. In such circumstances, when the edge moments are simultaneously applied to the wall by several beams, the rotation of the wall at the location of any one beam is influenced by the other beams. This may be accounted for by using the influence lines shown in Fig. 11. These curves represent the relative rotation of the top edge of a simply supported long plate subjected to a moment uniformly distributed along a distance b_1 located at the middle of this edge. These curves are for three different ratios of b_1/a; for other values of b_1/a interpolation and extrapolation may be used. To establish these curves, values of $\partial w/\partial x$ at $x = 0$ for several values of y were computed. The expression for w is given by Eqs. 8*b*, 8*c*, and 9*b*. The series for $\partial w/\partial x$ converge slowly and a large number of terms was used.

For a particular ratio of b_1/a the corresponding influence line shown in Fig. 11 may be used as follows: First, the positions of the adjoining beams are marked off along the abscissa. Then, the ordinates to the curve are scaled at each of the beam positions. The sum of all the ordinates so found is the magnification factor by which the maximum rotation of the plate at the selected beam is increased. By dividing the width B (Eq. 5*d*) by this magnification factor, one determines the width of a simply supported beam having a stiffness equivalent to the stiffness of the plate loaded with several discrete moments.

The curves of Fig. 9, based on experiments, make it possible to determine the percentage of restraint provided by a plate with an opening relative to the restraint of a solid plate. The width of the opening to which these curves apply must be equal to the height of the wall. Additional experiments must be performed to enable engineers to analyze walls with different widths of openings.

ACKNOWLEDGMENTS

The experimental work described in this paper was financed by the University of California at Berkeley. The funds were administered by H. A. Schade, Director of the Institute of Engineering Research. The work de-

scribed herein was done in the Engineering Materials Laboratory, the director of which was R. E. Davis, M. ASCE. H. D Eberhart and R. W. Clough, Associate Members, ASCE, of the Division of Civil Engineering and Irrigation, offered helpful suggestions regarding the design of the apparatus for which the authors are very grateful.

APPENDIX. MATHEMATICAL EXPRESSIONS

Concentrated Moment.—The following equations apply to a simply supported plate subjected to a concentrated moment M_o (Fig. 12(a)).

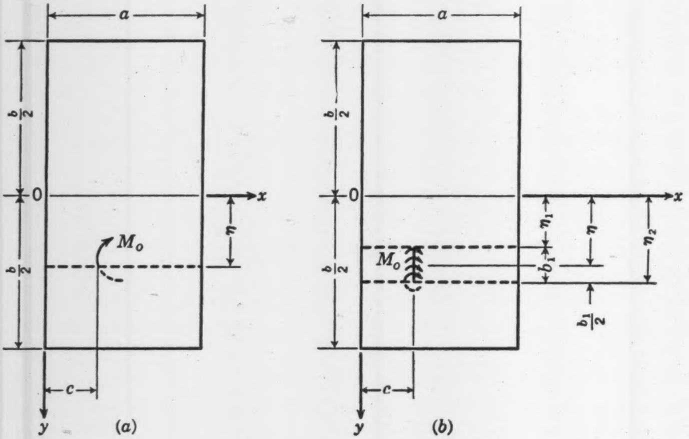

FIG. 12.—PLATE HAVING ALL EDGES SIMPLY SUPPORTED

The deflection w along $y = \eta$ is

$$w = \frac{M_o\, a}{2\, D\, \pi^2} \sum_{m=1}^{\infty} \frac{\cos\frac{m\,\pi\,c}{a}\sin\frac{m\,\pi\,x}{a}}{m^2}\left[\cosh^2\frac{m\,\pi\,\eta}{a}\left(\tanh\alpha_m - \frac{\alpha_m}{\cosh^2\alpha_m}\right)\right.$$
$$- \sinh^2\frac{m\,\pi\,\eta}{a}\left(\coth\alpha_m + \frac{\alpha_m}{\sinh^2\alpha_m}\right)$$
$$\left. - 2\,\frac{m\,\pi\,\eta}{a}\sinh\frac{m\,\pi\,\eta}{a}\cosh\frac{m\,\pi\,\eta}{a}\left(\tanh\alpha_m - \coth\alpha_m\right)\right] \quad (6a)$$

in which $\alpha_m = \frac{m\,\pi\,b}{2\,a}$.

If $c = 0$, $\eta = 0$, and $b \to \infty$, Eq. 6a reduces to

$$w = \frac{M_o\, a}{2\, D\, \pi^2} \sum_{m=1}^{\infty} \frac{\sin \dfrac{m\, \pi\, x}{a}}{m^2} \qquad (6b)$$

The deflection w' for the region $y > \eta$, or the deflection w'' for the region $y < \eta$, is

$$\begin{aligned}
\begin{matrix} w' \\ w'' \end{matrix}\Big\rangle &= \frac{M_o\, a}{2\, D\, \pi^2} \sum_{m=1}^{\infty} \frac{\cos \dfrac{m\, \pi\, c}{a} \sin \dfrac{m\, \pi\, x}{a}}{m^2} \\
&\times \Bigg\{ + \Bigg[\left(\tanh \alpha_m \cosh \frac{m\, \pi\, \eta}{a} \pm \sinh \frac{m\, \pi\, \eta}{a} \right) \\
&\mp \frac{m\, \pi\, \eta}{a} \left(\cosh \frac{m\, \pi\, \eta}{a} \pm \tanh \alpha_m \sinh \frac{m\, \pi\, \eta}{a} \right) - \alpha_m \frac{\cosh \dfrac{m\, \pi\, \eta}{a}}{\cosh^2 \alpha_m} \Bigg] \cosh \frac{m\, \pi\, y}{a} \\
&+ \Bigg[\mp \left(\cosh \frac{m\, \pi\, \eta}{a} \pm \coth \alpha_m \sinh \frac{m\, \pi\, \eta}{a} \right) \\
&+ \frac{m\, \pi\, \eta}{a} \left(\coth \alpha_m \cosh \frac{m\, \pi\, \eta}{a} \pm \sinh \frac{m\, \pi\, \eta}{a} \right) - \alpha_m \frac{\sinh \dfrac{m\, \pi\, \eta}{a}}{\sinh^2 \alpha_m} \Bigg] \sinh \frac{m\, \pi\, y}{a} \\
&- \left(\tanh \alpha_m \cosh \frac{m\, \pi\, \eta}{a} \pm \sinh \frac{m\, \pi\, \eta}{a} \right) \frac{m\, \pi\, y}{a} \sinh \frac{m\, \pi\, y}{a} \\
&\pm \left(\cosh \frac{m\, \pi\, \eta}{a} \pm \coth \alpha_m \sinh \frac{m\, \pi\, \eta}{a} \right) \frac{m\, \pi\, y}{a} \cosh \frac{m\, \pi\, y}{a} \Bigg\} \qquad (7a)
\end{aligned}$$

When $c = 0$, $\eta = 0$, and $b \to \infty$, Eq. 7a reduces to

$$\begin{matrix} w' \\ w'' \end{matrix}\Big\rangle = \frac{M_o\, a}{2\, D\, \pi^2} \sum_{m=1}^{\infty} \frac{\sin \dfrac{m\, \pi\, x}{a}}{m^2} \left(1 \pm \frac{m\, \pi\, y}{a} \right) e^{\pm m \pi y / a} \qquad (7b)$$

Uniformly Distributed Moment.—The following formulas apply for a simply supported plate subjected to a moment M_o uniformly distributed along a distance b_1 (Fig. 12(b)).

The deflection w for $\eta_1 \leqslant y \leqslant \eta_2$ is

$$
\begin{aligned}
w = \frac{2\,M_o\,a^2}{b_1\,D\,\pi^3} \sum_{m=1}^{\infty} \frac{\cos\dfrac{m\,\pi\,c}{a}\sin\dfrac{m\,\pi\,x}{a}}{m^3} \Bigg\{ &+ 1 \\
&- \left[\left(\cosh\frac{m\,\pi\,b_1}{2\,a} - \tanh\alpha_m \sinh\frac{m\,\pi\,b_1}{2\,a}\right) + \frac{m\,\pi\,b_1}{4\,a}\left(\tanh\alpha_m\cosh\frac{m\,\pi\,b_1}{2\,a} - \sinh\frac{m\,\pi\,b_1}{2\,a}\right) + \alpha_m \frac{\sinh\dfrac{m\,\pi\,b_1}{2\,a}}{2\cosh^2\alpha_m}\right]\cosh\frac{m\,\pi\,\eta}{a}\cosh\frac{m\,\pi\,y}{a} \\
&+ \left[\left(\cosh\frac{m\,\pi\,b_1}{2\,a} - \coth\alpha_m \sinh\frac{m\,\pi\,b_1}{2\,a}\right) + \frac{m\,\pi\,b_1}{4\,a}\left(\coth\alpha_m\cosh\frac{m\,\pi\,b_1}{2\,a} - \sinh\frac{m\,\pi\,b_1}{2\,a}\right) - \alpha_m \frac{\sinh\dfrac{m\,\pi\,b_1}{2\,a}}{2\sinh^2\alpha_m}\right]\sinh\frac{m\,\pi\,\eta}{a}\sinh\frac{m\,\pi\,y}{a} \\
&+ \left[\left(\cosh\frac{m\,\pi\,b_1}{2\,a} - \tanh\alpha_m\sinh\frac{m\,\pi\,b_1}{2\,a}\right)\frac{m\,\pi\,\eta}{2\,a} - \left(\cosh\frac{m\,\pi\,b_1}{2\,a} - \coth\alpha_m\sinh\frac{m\,\pi\,b_1}{2\,a}\right)\frac{m\,\pi\,y}{2\,a}\right]\sinh\frac{m\,\pi\,\eta}{a}\cosh\frac{m\,\pi\,y}{a} \\
&- \left[\left(\cosh\frac{m\,\pi\,b_1}{2\,a} - \coth\alpha_m\sinh\frac{m\,\pi\,b_1}{2\,a}\right)\frac{m\,\pi\,\eta}{2\,a} - \left(\cosh\frac{m\,\pi\,b_1}{2\,a} - \tanh\alpha_m\sinh\frac{m\,\pi\,b_1}{2\,a}\right)\frac{m\,\pi\,y}{2\,a}\right]\cosh\frac{m\,\pi\,\eta}{a}\sinh\frac{m\,\pi\,y}{a}\Bigg\} \ldots (8a)
\end{aligned}
$$

If $c = 0$, $\eta = 0$, and $b \rightarrow \infty$, Eq. 8*a* is reduced to

$$
w = \frac{M_o\,a^2}{b_1\,D\,\pi^3} \sum_{m=1}^{\infty} \frac{\sin\dfrac{m\,\pi\,x}{a}}{m^3} \left\{2 + \left[\frac{m\,\pi\,y}{a}\sinh\frac{m\,\pi\,y}{a} - \left(2 + \frac{m\,\pi\,b_1}{2\,a}\right)\cosh\frac{m\,\pi\,y}{a}\right] e^{-m\,\pi\,b_1/2\,a}\right\} \ldots\ldots\ldots\ldots (8b)
$$

If $y = 0$, Eq. 8*b* is reduced to

$$w = \frac{M_o\, a^2}{b_1\, D\, \pi^3} \sum_{m=1}^{\infty} \frac{\sin \frac{m\,\pi\, x}{a}}{m^3} \left[2 - \left(2 + \frac{m\,\pi\, b_1}{2\,a}\right) e^{-m\,\pi\, b_1/2\,a}\right] \ldots\ldots (8c)$$

The deflection w' for the region $y \geqslant \eta_2$, or the deflection w'' for the region $y \leqslant \eta_1$, is

$$\begin{aligned}
\left.\begin{matrix} w' \\ w'' \end{matrix}\right\rangle &= \frac{M_o\, a^2}{b_1\, D\, \pi^3} \sum_{m=1}^{\infty} \frac{\cos \frac{m\,\pi\, c}{a} \sin \frac{m\,\pi\, x}{a} \sinh \frac{m\,\pi\, b_1}{2\,a}}{m^3} \\
&\times \left\{ + \left[\left(2 - \frac{m\,\pi\, b_1}{2\,a} \coth \frac{m\,\pi\, b_1}{2\,a}\right)\left(\tanh \alpha_m \cosh \frac{m\,\pi\, \eta}{a} \pm \sinh \frac{m\,\pi\, \eta}{a}\right) \right.\right. \\
&\left. \mp \frac{m\,\pi\, \eta}{a}\left(\cosh \frac{m\,\pi\, \eta}{a} \pm \tanh \alpha_m \sinh \frac{m\,\pi\, \eta}{a}\right) - \alpha_m \frac{\cosh \frac{m\,\pi\, \eta}{a}}{\cosh^2 \alpha_m} \right] \cosh \frac{m\,\pi\, y}{a} \\
&+ \left[\left(\mp 2 \pm \frac{m\,\pi\, b_1}{2\,a} \coth \frac{m\,\pi\, b_1}{2\,a}\right)\left(\cosh \frac{m\,\pi\, \eta}{a} \pm \coth \alpha_m \sinh \frac{m\,\pi\, \eta}{a}\right) \right. \\
&\left. + \frac{m\,\pi\, \eta}{a}\left(\coth \alpha_m \cosh \frac{m\,\pi\, \eta}{a} \pm \sinh \frac{m\,\pi\, \eta}{a}\right) - \alpha_m \frac{\sinh \frac{m\,\pi\, \eta}{a}}{\sinh^2 \alpha_m} \right] \sinh \frac{m\,\pi\, y}{a} \\
&- \frac{m\,\pi\, y}{a}\left(\tanh \alpha_m \cosh \frac{m\,\pi\, \eta}{a} \pm \sinh \frac{m\,\pi\, \eta}{a}\right) \sinh \frac{m\,\pi\, y}{a} \\
&\left. \pm \frac{m\,\pi\, y}{a}\left(\cosh \frac{m\,\pi\, \eta}{a} \pm \coth \alpha_m \sinh \frac{m\,\pi\, \eta}{a}\right) \cosh \frac{m\,\pi\, y}{a} \right\} \ldots\ldots\ldots\ldots (9a)
\end{aligned}$$

If $c = 0$, $\eta = 0$, and $b \rightarrow \infty$, Eq. 9*a* is reduced to

$$\begin{aligned}
\left.\begin{matrix} w' \\ w'' \end{matrix}\right\rangle &= \frac{M_o\, a^2}{b_1\, D\, \pi^3} \sum_{m=1}^{\infty} \frac{\sin \frac{m\,\pi\, x}{a} \sinh \frac{m\,\pi\, b_1}{2\,a}}{m^3} \left(2 \pm \frac{m\,\pi\, y}{a}\right. \\
&\qquad \left. - \frac{m\,\pi\, b_1}{2\,a} \coth \frac{m\,\pi\, b_1}{2\,a}\right) e^{\mp m\,\pi\, y/a} \ldots (9b)
\end{aligned}$$

AMERICAN SOCIETY OF CIVIL ENGINEERS
Founded November 5, 1852
TRANSACTIONS

Paper No. 2831

THE VIBRATIONS OF STEEL STACKS

By Walter L. Dickey[1] and Glenn B. Woodruff,[2]
Members, ASCE

With Discussion by Messrs. Richard Jenney; George S. Vincent; John N. Pirok; Frederick B. Farquharson; W. Watters Pagon; Robert H. Sherlock; and Walter L. Dickey and Glenn B. Woodruff

Synopsis

Few of the many instances of excessive vibrations of self-supported steel stacks have been reported in technical literature. There is little information concerning the magnitude of the forces produced by periodic vortex discharge or the damping properties of the stacks in absorbing the energy resulting from these periodic forces. In this paper the authors analyze various data and give tentative values for several unknowns; these values appear to be of the correct magnitude.

Notation

The letter symbols adopted for use in this paper are defined where they first appear and are arranged alphabetically, for convenience of reference, in the Appendix.

Introduction

During the construction of the Moss Landing Steam Plant on Monterey Bay in California comparatively severe vibrations occurred.[3] Similar difficulties were encountered at the Oleum Steam Plant in Oleum, Calif. To investigate the matter, the owner of these plants initiated the research described herein.

Source of Vibrations

When a fluid such as air flows past an obstacle such as a cylindrical stack, certain forces develop as a result of changes in the velocity or direction of the

---

Note.—Published, essentially as printed here, in November, 1954, as *Proceedings-Separate No. 540*. Positions and titles given are those in effect when the paper or discussion was approved for publication in *Transactions*.

[1] Chf. Structural Engr., Power Div., Bechtel Corp., San Francisco, Calif.

[2] Cons. Engr., San Francisco, Calif.

[3] "Resonant Vibration of Steel Stacks," by Ernest A. Dockstader, William F. Swiger, and Emory Ireland, *Transactions*, ASCE, Vol. 121, 1956, p. 1088.

stream. The unit force or drag P (in pounds per square foot) on the obstruction can be expressed as

$$P = \frac{C_D\, \rho\, v^2}{2} = 0.00119\, C_D\, v^2 \ldots\ldots\ldots\ldots (1)$$

in which C_D is the drag coefficient which varies with the shape of the obstruction and is also dependent on the Reynolds number $\mathbf{R}$, ρ denotes the mass density of air, and v is the velocity of the wind in feet per second. For air,

$$\mathbf{R} = \frac{v\, D}{\nu} = 6{,}380\, v\, D \ldots\ldots\ldots\ldots (2)$$

in which D is the diameter of the stack in feet and ν is the kinematic viscosity.

The range of Reynolds numbers between 120,000 and 250,000 is termed "critical." Within this range the air flow changes from "laminar" to "turbulent." Within the range of Reynolds numbers from 10,000 to 120,000, C_D has a value of approximately 1.2. Through the critical range this value decreases to approximately 0.30. Some experiments show this value to be constant for values of $\mathbf{R}$ up to 500,000. R. H. Sherlock, M. ASCE, and E. A. Stalker found[4] values of 0.30 for $\mathbf{R} = 270{,}000$ and 0.40 for $\mathbf{R} = 450{,}000$. No data have been found for the values ($\mathbf{R} = 3{,}000{,}000$ to $10{,}000{,}000$) connected with stack vibrations; therefore, it has been assumed that $C_D = 0.35$.

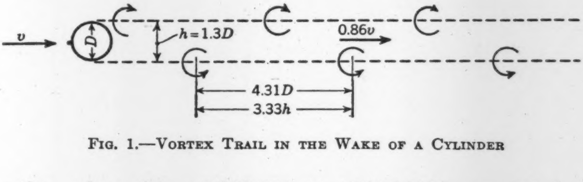

FIG. 1.—VORTEX TRAIL IN THE WAKE OF A CYLINDER

When a wind stream passes a cylindrical obstruction alternating vortices are shed periodically, forming the vortex trail described by Theodor von Kármán, Hon. M. ASCE. The pattern of the trail and the spacing of the vortices are shown in Fig. 1. The frequency of these vortices is determined by the Strouhal number, S—

$$S = \frac{f\, D}{v} \approx 0.19 \ldots\ldots\ldots\ldots (3)$$

in which f is the frequency of vortex shedding or vibration in cycles per second.

Most experimentation as to the value of the Strouhal number has been in the subcritical range ($\mathbf{R} < 120{,}000$). E. F. Relf and L. G. F. Simmons found[5] that this number increased with larger Reynolds numbers; other experimenters have reached the conclusion that with turbulent flow the shedding of the vortices becomes aperiodic.

---

[4] "A Study of Flow Phenomena in the Wake of Smoke-stacks," by R. H. Sherlock and E. A. Stalker, *Engineering Research Bulletin No. 29*, Univ. of Michigan, Ann Arbor, Mich., 1940.

[5] "The Frequency of the Eddies Generated by the Motion of Circular Cylinders Through a Fluid," by E. F. Relf and L. G. F. Simmons, *Reports and Memoranda No. 917*, Aeronautical Research Committee London, 1924–1925.

As in the case of suspension bridges,[6] the vibrations of stacks may be considered to be self-excited vibrations (negative air damping) rather than forced vibrations at resonance. The frequency of vortex shedding is determined by the natural frequency of the stack rather than by the velocity of the approaching air. The only significance of the Strouhal number seems to be that it indicates the velocity at which the vortex shedding, and therefore the response of the stack, will be most vigorous.

In the experimental work on suspension bridges[6] two types of self-excited vibrations were observed. In the first, the "restricted" type, vibrations in a given mode occurred over a considerable range of velocities—reaching a maximum amplitude at a certain wind velocity. As the velocity was increased above this point, the amplitudes decreased. When the velocities were still further increased, vibrations in the same mode reoccurred at twice the velocity of the first appearance. In the second, the "catastrophic" type, vibrations began at a critical wind velocity, and as the velocity increased the amplitudes built up rapidly—resulting in failure of the structure.

It has been assumed, possibly without sufficient evidence, that the vibrations of stacks are of the restricted type and that, if the stacks are so designed that no damaging stresses occur at the lower critical velocity, such stacks will be safe for all wind velocities below twice the lower critical velocity.

LATERAL FORCES

As von Kármán vortices are alternately discharged, the velocities and the pressures on opposite sides of the cylinder vary, producing an alternating force—

$$P_a = \frac{C_L \rho v^2}{2} \qquad (4)$$

in which C_L is a coefficient of lateral forces resulting from vortex shedding. No data have been found as to the values of C_L within the range of Reynolds numbers herein considered. For lower Reynolds numbers, D. B. Steinman, M. ASCE, gives[7] values of 1.9 C_D. In the absence of more complete information for high Reynolds numbers, it is assumed that $C_L = 0.66$.

The amplitudes of vibration which will result from these alternating periodic forces depend on (*a*) the magnitude of the alternating forces or the energy input per cycle, (*b*) the number of cycles applied, and (*c*) the damping characteristics. Assumptions as to the alternating forces have been cited previously. At critical velocities the maximum amplitudes build up rapidly until the "steady state" at which the input and dissipation of energy per cycle are equal.

DAMPING

Damping forces are those which absorb energy from any vibrating body. In the case of stacks, these forces are the sum of (*a*) the structural damping resulting from the hysteresis effect in stress reversal, (*b*) the energy dissipated at the foundations, (*c*) the aerodynamic damping or friction between the air and the vibrating stacks, and (*d*) the energy dissipated by any external energy absorbers that may be used.

---

[6] "Aerodynamic Stability of Suspension Bridges with Special Reference to the Tacoma Narrows Bridge," *Report No. 116*, Univ. of Washington Eng. Experiment Station, Seattle, Wash., 1949–1954.

[7] "Problems of Aerodynamic and Hydrodynamic Stability," by D. B. Steinman, *Bulletin No. 31*, Univ. of Iowa Studies in Eng., Iowa City, Iowa, 1947.

In an unlined welded stack, the only structural damping within the stack arises from the hysteresis effect. In the stress-strain diagram most of the elongation is elastic; this is accompanied by some plastic deformation. During each vibration cycle the energy, ΔW, within the hysteresis loop is dissipated by heat; the damping ratio,

$$\psi = \frac{\Delta W}{W} \qquad (5)$$

in which W is the work of deformation stored in the extreme position. The damping ratio may also be expressed by the logarithmic decrement, δ. The successive amplitudes can be observed after the disturbing force has been removed and, if the envelopes of the successive amplitudes are plotted, δ can be computed;[8] for small damping, $\delta = \psi/2$. There is little information as to the damping ratios of various structural materials. Most excessive stack vibrations have occurred in welded stacks; this fact confirms the experimental finding that damping is greatly increased by the friction on faying surfaces of riveted construction. Because the ratio of plastic elongation to total elongation increases with the unit stress, δ is not constant but increases with the stress. L. W. Teller, M. ASCE, and E. G. Wiles tested bolted trusses and solid sections.[9] At unit stresses of 2 kips per sq in. the respective decrements were 0.009 and 0.003 and at 10 kips per sq in. they were 0.048 and 0.007.

Because the stress-strain curve for concrete does not follow Hooke's law as closely as does that for steel, it may be inferred that the damping characteristics of the former will be considerably greater. Carl F. Muckenhoupt found values of 0.10 for δ at stresses of 200 lb per sq in. with rapid increases as the ultimate tensile strength was approached. In many investigations of vibrations it has been found that the greatest source of damping is in the energy absorbed by the foundations. Again, few specific data applicable to stacks are available. With the comparatively small velocities that are involved, it is probable that positive aerodynamic damping in still air or with a wind of constant velocity is negligible.

VIBRATION FREQUENCIES

The natural frequency of a vibrating system is given by

$$f = \frac{1}{2\,\pi} \sqrt{\frac{k}{m}} \qquad (6)$$

in which k is the spring constant and m is the mass. With damping (assumed to be viscous and small) the amplitude A can be determined from

$$A = y\,N = \frac{\pi\,y}{\delta} \qquad (7)$$

---

[8] "Vibration Problems in Engineering," by S. Timoshenko, D. Van Nostrand Co., New York, N. Y., 1955.

[9] "Tests of Structural Damping," by L. W. Teller and E. G. Wiles, *Public Roads*, October, 1953, p. 203.

in which y is the deflection which would be produced by the disturbing force acting statically and N is the magnification factor. The significance of N becomes apparent when δ for steel is only about 0.007 and N is approximately equal to 400.

In investigating the probabilities of resonance with the alternating forces, a determination of the frequency of the stack being designed is necessary. For a cantilever of uniform section, fixed at its base, Eq. 6 reduces to

$$f = \frac{C}{2\,\pi\,L^2}\sqrt{\frac{E\,I\,g}{w}} \quad \text{.....................} (8)$$

in which C is a constant depending on the mode of vibration, L denotes the length of the cantilever in feet, E is the modulus of elasticity, I is the moment of inertia, and w represents the weight in pounds per foot. The fundamental value of C is denoted as C_1 and is equal to 3.515; also $C_2 = 22.0$ and $C_3 = 61.7$.

Generally the sections of stacks are not uniform; the plate thickness, weight, and often the diameter decrease from bottom to top. In such cases, the frequency may be found by the Rayleigh-Ritz method of summation—

$$f = \frac{1}{2\,\pi}\sqrt{\frac{g\,\Sigma\,F\,x}{\Sigma\,F\,x^2}} \quad \text{.......................} (9)$$

In the solution of Eq. 9, it is necessary to divide the height of the stack into several sections. In Eq. 9, F is the weight of each section and x is the resulting dead-load deflection at the center of each section when the stack acts as a horizontal cantilever beam.

Preliminary estimates of the frequency of an unlined stack can be made from

$$f = \frac{D\,(3{,}040\,t + 2{,}520)}{h^2} \quad \text{...................} (10)$$

in which t is the thickness of the shell, in inches, at the bottom of the vertical section of the stack and h is the equivalent height for the vibration computation. The value of h is determined from

$$h = h_s + \frac{h_f}{3} + \frac{D}{2} \quad \text{.....................} (11)$$

in which h_s is the height of the straight shaft and h_f is the height of the flare. A comparison of computed and observed frequencies for the examples herein reported is given in Table 1. From Table 1 it can be seen that the observed frequency is less than that computed. It is probable that the stacks are not completely fixed at their bases and that there is some movement of the foundations. It appears reasonable to divide the computed frequency by 1.15 for unlined stacks. For gunite-lined stacks, using $n = 20$ (in which n is the ratio of the moduli of elasticity of steel and gunite), the corresponding factor becomes about 1.05. No data have been found as to the interaction between steel and a brick lining.

In some cases, the variations are such that they can be approximated by sections with such variables that Eq. 9 can be integrated; some of these cases have been presented elsewhere.[10]

---

[10] "Mechanical Vibrations," by J. P. Den Hartog, McGraw-Hill Book Co., Inc., New York, N. Y., 1940.

The frequency of ovalling, or breathing, of an unlined stack[11] in the first mode is given by

$$f = 24{,}500 \frac{t}{r^2} \quad \text{(12)}$$

in which r is the radius of the stack, in inches.

Experiments and Observations

Because of its importance in the design of stacks, an investigation was made as to the best method of restricting stack vibrations to amplitudes that would not involve serious stresses. This investigation primarily covered the damping effects of a gunite lining.

Model Tests.—Preliminary tests were made on a model consisting of a 6-in.-diameter steel pipe cantilevered from a concrete base. Vibrations were initiated by abruptly releasing a horizontal pull applied at the free end. The essential results are given in Table 2. The following comments are pertinent:

TABLE 1.—Comparison of Computed and Observed Frequencies

Stack	Frequency, in Cycles per Second			Ratio, computed frequency to observed frequency
	Computed from		Observed	
	Eq. 9	Eq. 10		
Steel tube, plain	3.94[a]	3.68	3.75	1.05
Steel tube, gunite encasement	2.72[b]	...	2.20	1.24
Moss Landing, unlined	1.23	0.63	1.12	1.10
Moss Landing, lined	0.85	...	0.82	1.04
Contra Costa, unlined	1.12	1.06	0.97	1.16
Contra Costa, lined	0.75	...	0.71	1.05
Detroit, unlined	1.24	1.24	1.00	1.24

[a] Eq. 8. [b] $n = 20$.

1. The logarithmic decrement of 0.007 for the unlined stack is in agreement with those given previously. As the amplitudes decreased, smaller stresses resulted and there was some decrease in the decrement.

2. For the gunite-encased specimen, the decrement was increased approximately thirty times. In this case, however, the decrement increased with decreasing amplitudes (characteristic of Coulomb friction damping[12]).

3. At maximum amplitudes the stress in the concrete at the base would be approximately 320 lb per sq in., probably approaching its ultimate strength. The frequency computations based on the value of $E\,I$ determined by the dynamometer test agree with the observations. Evidently for these conditions the analysis should be made on the basis of a "cracked" section, or the value of n should be increased. For gunite with lightweight aggregate, a value of $n = 20$ appears reasonable.

---

[11] "Vibration Problems in Engineering," by S. Timoshenko, D. Van Nostrand Co., New York, N. Y., 2d Ed., 1937.

[12] "Aerodynamic Stability of Suspension Bridges: 1952 Report of the Advisory Board on the Investigation of Suspension Bridges," *Transactions*, ASCE, Vol. 120, 1955, p. 721.

4. The values of both the frequency and the decrement indicate a truly fixed condition at the base.

Moss Landing Stacks.—The vibration observed at the Moss Landing stacks prior to their lining, the test made on the stacks, and the measures used to inhibit troubles in the completed stacks have been described.[3] Conclusions can be drawn as follows:

1. Breathing.—Substituting the value of 68 in. for r in Eq. 12, the theoretical frequency for the $\frac{5}{16}$-in. plates would be 1.67 cycles per sec or 100 cycles per min, a somewhat higher value than the 88 cycles per min that was observed. Assuming the latter value and also the estimated wind velocity of 25 miles per hr (37 ft per sec) to be correct, the Strouhal number would become 0.45 and R would be 2,650,000. The reasons for the discrepancy in frequency may be—

TABLE 2.—TESTS ON STEEL TUBE

PLAIN TUBE		TUBE ENCASED WITH 1.92 IN. OF GUNITE	
Basic Data			
Outside diameter	6.000 in.	Outside diameter	9.84 in
Inside diameter	5.624 in.	I_g	396 in.^{4}
Wall thickness	0.188 in.	n	20
Length	20.15 ft	E_g	1.45 × 10^6 lb/in.^{2}
I	14.42 in.^{4}	I_g/n	19.8 in.^{4}
E (assumed)	2.90 × 10^7 lb/in.^{2}	$I_s + I_g/n$	34.22 in.^{4}
$E\,I$	2.90 × 10^6 lb-ft^2	$E\,I$ (computed)	6.90 × 10^6 lb-ft^2
Weight	11.67 lb/ft	$E\,I$ (dynamometer test)	4.36 × 10^6 lb-ft^2
		Weight	57.5 lb/ft
Frequency, f, in Cycles per Second			
Computed from Eq. 8	3.94	Computed from Eq. 8:	
Observed	3.75	with $E\,I$ = 6.90 × 10^6	2.72
		with $E\,I$ = 4.36 × 10^6	2.15
		Observed	2.20
Amplitude, A, in Inches			
At t = 0	1.25	At t = 0	1.13
t = 15 sec	0.83	t = 3.4 sec (7.5 cycles)	0.33
t = 30 sec	0.57	t = 6.8 sec (15.0 cycles)	0.06
Logarithmic Decrement δ			
t_0 to t_{15}	0.0073	t_0 to $t_{3.4}$	0.164
t_{15} to t_{30}	0.0068	$t_{3.4}$ to $t_{6.8}$	0.227
t_0 to t_{30}	0.0070	t_0 to $t_{6.8}$	0.196

a. The velocity of 25 miles per hr was estimated. Again assuming the estimate to be correct near the ground, the velocity[13] at a height of 200 ft would be approximately 48 ft per sec. With a frequency of 1.47 cycles per sec, the Strouhal number would become 0.35.

---

[13] "Variation of Wind Velocity and Gusts with Height," by R. H. Sherlock, *Transactions*, ASCE, Vol. 118, 1953, p. 463.

b. Assuming a Strouhal number of 0.19, the critical velocity (Eq. 3) would become 88 ft per sec or about double that assumed. It is possible that the frequency of vibration was twice that of the vortex shedding.

c. When the breathing was observed there were only inappreciable movements of the stacks as cantilevers so that the stacks can be considered to be fixed in space. The evidence is conclusive that with cantilever vibrations the value of S is constant within the range of Reynolds numbers herein considered. The higher values[5] of S may apply for fixed cylinders.

2. Cantilever Vibrations.—In the cantilever vibrations of October 18, 1949, the wind velocity was estimated at between 30 miles per hr and 40 miles per hr and the frequency was observed to be 73 cycles per min. In the tests determining the damping properties of the stack, the frequency was 67 cycles per min. Assuming a frequency of 1.20 cycles per sec and a Strouhal number of 0.19, the wind velocity would be 72 ft per sec or 49 miles per hr. Perhaps the velocity at the top of the stack was of this general order. Assuming a wind velocity of 72 ft per sec and C_L at 0.66, P_a from Eq. 4 would be 4.1 lb per sq ft of stack. For such a load applied over the cylindrical section of the stack only, the static deflection at the top of the stack has been computed to be 0.88 in. The maximum observed amplitude was 16 in. resulting in a magnification factor of about 18.

Contra Costa Stacks.—The Contra Costa Steam Plant at Antioch, Calif. (completed in 1953) has a total capacity of 570,000 kw. There are two sets of three stacks, one for each boiler, the axis of each set being due north. Each stack has an inside diameter of 11 ft. Beginning at the top, there are 105 ft of $\frac{5}{16}$-in. plate, 40 ft of $\frac{3}{8}$-in. plate, and 55 ft of $\frac{1}{2}$-in. plate. All the stacks were lined with 3 in. of lightweight gunite, except that in the lower 51 ft of the stack the thickness tapered from 3 in. to 8 in. The stacks were designed for a static wind pressure of 20 lb per sq ft of projected area.

The properties of the gunite as determined by nine test cylinders at 28 days were—

	Range	Average
Compressive strength, in pounds per square inch	2,820–4,300	3,520
Unit weight, in pounds per cubic foot	107.3–113.5	110.2
E, in pounds per square inch	2.01×10^6–3.27×10^6	2.37×10^6

Vibration was initiated by releasing a horizontal force at the top of the stacks. Tables 3 and 4 give the ordinates of the decay curves for the unlined and the lined stacks, respectively, and also the computations for the logarithmic decrement. The observed frequencies and the computed frequencies have been presented in Table 1. A plotting of decrements versus amplitudes indicates a considerable increase of decrement with the larger amplitudes or stresses.

Because of the experience at Moss Landing, the Contra Costa stacks were guyed immediately upon their erection, the guys being removed on the completion of the lining. With a Strouhal number of 0.19 and a frequency of 42.5 cycles per min (0.71 cycle per sec), the critical velocity of the lined stacks would be 42.6 ft per sec, or 29 miles per hr. With this velocity, the stagnation pressure would be 2.14 lb per sq ft. Using the value of C_L of 0.66, the lateral force would be 16.0 lb per lin ft of stack. The static deflection at the top of the stack under this force would be 0.30 in.

Following the completion of the lining, several wind velocities of 30 miles per hr have occurred. The maximum observed amplitude is 3 in., corresponding to a magnification factor of 10. With this magnification factor, the equivalent wind pressure would be 21.4 lb per sq ft, and the unit stress at the base of the stack, based on composite action would be 3,500 lb per sq in.

The question arises as to what would happen in the case (not anticipated in this particular location) of a wind twice the critical wind. If the vortices of four times the intensity were shed, the deflections at the top of the stack would be about 12 in. and the unit stress in the shell would be 14,000 lb per sq in.

Oleum Steam Plant.—At the Oleum Steam Plant there are three stacks on 31-ft centers; the stacks are 200 ft high. The upper 110 ft have an outside diameter of 6.5 ft, the lower part tapering to a diameter of 9 ft at the base. In the original design, there was a heavy truss 10 ft deep and 100 ft above the base tying the stacks together; the design also provided for gunite lining.

TABLE 3.—ORDINATES OF DECAY CURVES FOR UNLINED CONTRA COSTA STACKS

NUMBER OF		AMPLITUDE, IN INCHES					Ratio, $\frac{A_{n-1}}{A_n}$	Log $_e$ $\frac{A_{n-1}}{A_n}$	Value of δ
Seconds	Cycles	Run 1	Run 2	Run 3	Run 4	Average			
0.0	0.0	5.00	5.00	5.00	5.00	5.00	1.07	0.068	0.028
2.5	2.43	4.56	4.58	4.68	4.81	4.66	1.09	0.086	0.036
5.0	4.85	4.13	4.16	4.25	4.56	4.28	1.10	0.095	0.039
7.5	7.28	3.76	3.75	3.77	4.22	3.88	1.13	0.122	0.050
10.0	9.71	3.38	3.33	3.26	3.77	3.43	1.13	0.122	0.050
12.5	12.14	3.00	2.94	2.84	3.37	3.04	1.12	0.113	0.047
15.0	14.56	2.68	2.65	2.51	3.00	2.71	1.25	0.223	0.046
20.0	19.42	2.14	2.12	1.99	2.42	2.17	1.20	0.182	0.038
25.0	24.27	1.84	1.74	1.66	2.00	1.81	1.17	0.157	0.032
30.0	29.13	1.61	1.48	1.40	1.68	1.54	1.18	0.165	0.034
35.0	33.98	1.35	1.29	1.14	1.40	1.30	1.18	0.165	0.034
40.0	38.83	1.13	1.08	0.99	1.18	1.10	1.22	0.199	0.041
45.0	43.69	0.88	0.83	...	0.99	0.90	...	...	...
Average									0.039

On August 11, 1941, before the gunite lining had been applied, two or more of the stacks vibrated violently in the wind. The shell of the center stack cracked at a point just above the truss. The wind velocity was estimated at 45 miles per hr in a direction nearly parallel to the axis of the group. An eye witness states that the tops of the stacks were moving in opposite directions and normal to the direction of the wind; no estimate of the frequency is available. It may or may not be pertinent to note that the spacing of the stacks is close to the spacing, 4.31 D, of the von Kármán vortices. Without the heavy truss, the frequency of the stacks would have been about 1.0 cycle per sec, and the critical velocity (assuming $S = 0.19$) would have been approximately 20 miles per hr. Without definite knowledge as to the direction of the wind, it is impossible to compute the effect of the truss on the period. It is possible that the vibrations resulted from a wind twice the critical. As a corrective measure,

TABLE 4.—ORDINATES OF DECAY CURVES FOR LINED CONTRA COSTA STACKS

NUMBER OF		RUN 2				RUN 3				RUN 4				RUN 5				Average value of δ
Seconds	Cycles	Amplitude, in inches	$\frac{A_{n-1}}{A_n}$	Log$_e$ $\frac{A_{n-1}}{A_n}$	Value of δ	Amplitude, in inches	$\frac{A_{n-1}}{A_n}$	Log$_e$ $\frac{A_{n-1}}{A_n}$	Value of δ	Amplitude, in inches	$\frac{A_{n-1}}{A_n}$	Log$_e$ $\frac{A_{n-1}}{A_n}$	Value of δ	Amplitude, in inches	$\frac{A_{n-1}}{A_n}$	Log$_e$ $\frac{A_{n-1}}{A_n}$	Value of δ	
0.0	0.0	5.00	1.22	0.199	0.112	5.00	1.20	0.182	0.103	5.00	1.22	0.199	0.112	7.33	1.43	0.358	0.202	0.132
2.5	1.77	4.11	1.23	0.207	0.116	4.17	1.22	0.199	0.112	4.11	1.19	0.174	0.098	5.11	1.17	0.157	0.088	0.103
5.0	3.55	3.35	1.22	0.199	0.112	3.42	1.23	0.207	0.116	3.45	1.16	0.148	0.084	4.37	1.13	0.122	0.069	0.095
7.5	5.32	2.74	1.22	0.199	0.112	2.79	1.18	0.165	0.093	2.97	1.13	0.122	0.069	3.86	1.12	0.113	0.064	0.084
10.0	7.09	2.24	1.18	0.165	0.093	2.37	1.18	0.165	0.093	2.63	1.12	0.113	0.064	3.43	1.10	0.095	0.054	0.076
12.5	8.87	1.89	1.19	0.174	0.098	2.01	1.10	0.095	0.054	2.34	1.08	0.077	0.043	3.10	1.13	0.122	0.064	0.065
15.0	10.64	1.59	1.36	0.307	0.087	1.82	1.27	0.239	0.068	2.16	1.17	0.157	0.044	2.75	1.19	0.174	0.049	0.062
20.0	14.18	1.17	1.39	0.329	0.093	1.43	1.22	0.199	0.056	1.84	1.16	0.148	0.042	2.31	1.20	0.182	0.051	0.060
25.0	17.73	0.84	1.22	0.199	0.056	1.17	1.32	0.278	0.078	1.58	1.19	0.174	0.049	1.93	1.18	0.165	0.046	0.057
30.0	21.28	0.69				0.89	1.25	0.223	0.063	1.33	1.19	0.174	0.049	1.64	1.22	0.199	0.056	0.056
35.0	24.82					0.71				1.12	1.08	0.077	0.022	1.34	1.21	0.191	0.054	0.038
40.0	28.37									1.04				1.11				
Average				1.981	0.093			1.952	0.079			1.570	0.055			1.887	0.067	0.074

a horizontally rigid truss was installed near the top of the stacks and the stacks were lined with gunite. No further vibrations of material amplitudes have been observed since (as of 1955).

Baltimore Stacks.—The vibrations of two stacks in Baltimore, Md., have been described[14] by W. Watters Pagon, M. ASCE. Observations pertinent to this investigation are:

1. The critical velocity was 53 miles per hr or 78 ft per sec with a frequency of 1.33 cycles per sec. For a stack diameter of 11 ft, the Strouhal number was 0.187 at a Reynolds number of 5,500,000.
2. Vibrations were observed in the leeward stack only. The stacks are spaced 48 ft on centers or 4.36 D as compared to 4.31 D for the spacing of the von Kármán vortices.
3. Very severe ovalling occurred with a frequency of 2.20 cycles per sec. From Eq. 12 the frequency would be 1.75 cycles per sec and 1.40 cycles per sec for the $\frac{5}{16}$-in. and $\frac{1}{4}$-in. plates, respectively. Mr. Pagon has given[14] corresponding frequences of 2.30 cycles per sec and 1.90 cycles per sec, respectively.

Guam Stacks.—On August 3, 1941, a typhoon struck the Island of Guam with maximum winds of 125 miles per hr. The power plant stacks, 9 ft in diameter and 150 ft high, reacted in a manner which observers have characterized as a "typhoon shimmy." This movement is described as being fully as spectacular as the movements of the Tacoma Narrows Bridge, near Tacoma, Wash., before its failure in 1940.[15] The stack movement consisted of a rhythmic panting, with the cross section becoming oval first in one direction and then in the other; this movement caused the upper section to appear to have a diameter of 11 ft at one instant and the next instant the diameter appeared to be 7 ft. The motion was quite rapid—being timed at 105 vibrations per min—and was accompanied by a "hula twist" whose amplitude was not of sufficient magnitude to be considered dangerous. Although the winds during the typhoon were excessive, there was no fear that the stack would collapse because the stack was examined for damage, repaired, and shortened following a typhoon which occurred in November, 1940.

No details are available concerning this stack. Assuming a shell thickness of $\frac{1}{4}$ in. at the top and $\frac{1}{2}$ in. at the bottom, the frequency as a cantilever from Eq. 10 would be 1.86 cycles per sec or 112 cycles per min, and the frequency of the $\frac{1}{4}$-in. plate in breathing would be 2.1 cycles per sec or 125 cycles per min, both being fairly close to the observed 105 cycles per min; the Strouhal number would be 0.105.

The observations indicate and the computations confirm the simultaneous occurrence of breathing and cantilever vibrations. There is no record of a Strouhal number as low as that given previously. The most probable explanation seems to be that the critical velocity of the stacks as a cantilever is 60 miles per hr, and the stack responds either to vortices shed at twice the frequency of the stack or controls the vortex shedding so that the vortices are shed at half the usual rate. At a velocity of 120 miles per hr the stagnation pressure would be 37 lb per sq ft. When C_L equals 0.66 the lateral pressure will be about 25 lb per sq ft. Without details of the design, it would appear that in this case the magnification factor was comparatively low.

---

[14] "Wind Design by Aerodynamic Principles," by W. Watters Pagon, *Engineering News-Record*, March 15, 1934–October 31, 1935.

[15] "The Failure of the Tacoma Narrows Bridge; A Report to the Federal Works Agency," by O. H. Ammann, Theodor von Kármán, and Glenn B. Woodruff, March 28, 1941.

Pittsburgh Stacks.—On June 12, 1951, observations were recorded of the vibrations of stacks near Pittsburgh, Pa.; the stacks were 250 ft high with a diameter at the top of 8 ft 7 in. Shell thicknesses were 95 ft of $\frac{5}{16}$-in. plate, 40 ft of $\frac{3}{8}$-in. plate, 40 ft of $\frac{7}{16}$-in. plate, and 75 ft of $\frac{1}{2}$-in. plate. The vertical section was 200 ft, flaring to a diameter of 11 ft 8 in. at the base. Deflections of from 24 in. to 30 in. on either side of the center line were noted when the wind was blowing at 17 miles per hr. These deflections were transverse to the direction of the wind indicating that they were the result of aerodynamic forces synchronized with the natural mode of vibration of the stacks.

From Eq. 9, the frequency of these stacks is 0.635 cycle per sec. Using a factor of 1.15 to allow for action at the base, the frequency is 0.55 cycle per sec. At a Strouhal number of 0.19, the critical velocity is 24.8 ft per sec or 17 miles per hr. With this velocity and a C_L-value of 0.66 the lateral force would be 0.48 lb per sq ft. The static deflection for such a load would be 0.45 in. For an observed amplitude of 30 in., the magnification factor becomes 67.

The manager of contract engineering for the fabricator of the stacks has furnished the following information:

> "We have had several experiences with stacks vibrating at their natural period, such vibration being excited by resonant vortex shedding. We had serious trouble with a stack 6 ft. diameter × 179 ft. in height. The height above the bell in this case was 126 ft. 11½ in., H/D ratio 21.2.
>
> "We had moderate trouble with a stack 6 ft. 9 in. diameter × 150 ft. high in which the height above the bell was 100 ft., H/D 14.8.
>
> "We had very serious trouble with several stacks which were 8 ft. 7 in. diameter × 250 ft. in height in which the height above the bell was 200 ft., the H/D 23.3.
>
> "We have not found any way to effectively damp the vibrations where resonance occurs. Our present policy is to avoid stacks with a diameter to height ratio greater than 20."

Detroit Stacks.—In 1952 three stacks, 300 ft high, were being erected near Detroit, Mich. The stacks had a diameter of 16 ft at the top, flaring to 18 ft at 96 ft above the base and 27 ft at the base. From the top, shell thicknesses were 100 ft of $\frac{1}{4}$ in., 22 ft of $\frac{5}{16}$ in., 30 ft of $\frac{3}{8}$ in., 22 ft of $\frac{7}{16}$ in., 30 ft of $\frac{1}{2}$ in., 28 ft of $\frac{9}{16}$ in., and 68 ft of $\frac{5}{8}$ in.

On November 26, 1952, when two of the stacks were completed except for the proposed gunite lining and the third stack was completed to within 40 ft of the top, a severe storm occurred. At a nearby airport steady winds of 65 miles per hr were reported with somewhat higher gust velocities. The two completed stacks swayed violently; the movements of the incompleted stack were negligible. The motion at the top of the completed stacks is reported to have been circular.

The two completed stacks failed at a point about 90 ft from the top. Initial failure was by buckling followed by a tearing of the plate. After failure, the movement of the stacks decreased and the upper sections remained in place. There were also considerable movements at the base of the stacks. The concrete surrounding the base plate was cracked loose, and some elongation of the anchor bolts occurred.

The hypotheses previously presented may be applied to the information concerning the Detroit stacks—

Computed frequency of stacks, Eq. 9, in cycles per second	1.24
Correction factor	1.15
Corrected frequency of stacks, in cycles per second	1.08
Observed frequency of stacks, in cycles per second	1.00

Assuming $f = 1.08$, $S = 0.19$, and $D = 16.5$ (average for the top 102 ft of stack)—

Critical velocity, in feet per second	94
Stagnation pressure, in pounds per square foot	10.5
C_L	0.66
Lateral pressure, static, in pounds per square foot	6.94
Magnification factor (assumed)	14.5
Equivalent static pressure, in pounds per square foot	100.0
Stress in anchor bolts, in kips per square inch	54.5

and

Shell thickness, in inches	Maximum compression, in kips per square inch	Critical buckling, in kips per square inch
$\frac{1}{4}$	12.0	12.4
$\frac{5}{16}$	14.0	15.2
$\frac{3}{8}$	17.4	17.9
$\frac{7}{16}$	19.4	20.5
$\frac{1}{2}$	22.6	23.1
$\frac{9}{16}$	19.6	22.5
$\frac{5}{8}$	16.8	19.3

On the basis of the foregoing, the following observations were made:

1. The magnification factor of 14.5 was assumed arbitrarily to produce results comparable with the buckling strength of the shell. It is somewhat lower than would have been assumed from other data. Quite likely the taper of the stack had a beneficial effect in that the critical velocities, and therefore the maximum forces would vary over the length of the stack.
2. The absence of appreciable vibrations in the incompleted stack is readily explained by the fact that the natural frequency of the shorter stacks was great enough so that the critical wind velocity was not reached.

Concrete Stacks.—Although this investigation was primarily directed to steel stacks, vibration of concrete stacks has been reported[16] by Walther Frank. Results from Mr. Frank's report are given in Table 5.

---

[16] "Vibrations of Smokestacks Induced by Flow," by Walther Frank, *Journal*, Archiv für Warmewirtschaft und Dampfkesselwesen, Prague, Vol. 22, No. 2, 1941, Fig. 3.

The observed amplitude of Stack 1 was 1.29 ft. This may indicate that at least considerable taper is necessary to avoid vibration from periodic wind forces.

Mr. Frank attributes the apparently circular orbit observed at the top of stacks to a combination of lateral forces produced by the von Kármán vortices and longitudinal forces produced by gusts. He further advises that the frequency of the stack be kept as low as possible.

Evaluation of Data

Although the foregoing data are incomplete, it is believed certain tentative conclusions can be drawn therefrom:

1. The damping of the unlined stacks at low amplitudes at the Contra Costa and Moss Landing plants was approximately eight times that which might have been anticipated from the damping characteristics of the welded steel; at higher amplitudes the damping increased. The most apparent conclusion is that the major source of energy dissipation was at the foundation. In both cases the stack foundations consisted of a concrete mat supported by piles. Further observations are desirable to determine what decrements can safely by assumed for an unlined stack.

TABLE 5.—Concrete Stacks

Smoke stack	Height, in feet	Diameter, in Feet			Frequency, in cycles per second	Critical Velocity	
		Top	Bottom	Average		In feet per second	In miles per hour
1	549.60	27.55	42.65	35.10	0.39	91.7	62.7
2	360.89	17.58	26.74	22.18	0.40	59.0	40.3
3	328.83	18.04	27.00	22.54	0.435	65.9	45.0
4	328.08	18.44	38.71	28.57	0.585	111.9	76.2

2. Greater additional damping was expected from the gunite linings. However, the additional damping was considerable in view of the fact that the damping of the foundation was probably about the same in both cases so that there was a material increase in the damping of the stack itself. Other instances of stacks exhibiting excessive vibrations before lining and no appreciable vibrations thereafter are known; in one case, a brick lining was used. Possibly more friction would develop in this case than when a gunite lining is used.

3. A lining has the advantage of lowering the critical velocity provided that it is not lowered to the point where the stack would be subject to subharmonic vibrations from winds of higher velocity.

4. From many cases of reported vibrations in groups of two or more stacks, it appears usual that large amplitudes occur on only one of the stacks. This is a matter for which no satisfactory answer has been found.

5. The importance of lining may be emphasized by stating that no instance of excessive vibrations of lined stacks is known.

DESIGN OF STACKS

The foregoing appears to permit some tentative suggestions for the design of stacks in so far as vibrations are concerned:

1. The highest probable wind velocity should be assumed. Eliminating the tornado from consideration, velocities of 120 miles per hr may occur in Florida hurricanes and slightly lower velocities along the Atlantic Coast and Gulf Coast of the United States. Velocities of the same order may be anticipated on the summits of high hills. With these exceptions, a velocity of 80 miles per hr may be considered a safe assumption for other locations within the continental United States.
2. It is possible to make the diameter of the stack sufficiently great so that its natural frequency would be greater than that of the vortices. For stacks taller than 150 ft this would usually result in a greater diameter of stack than is economical.
3. The stack might be designed as a frustum of a cone for its entire height with the result that the critical velocity would differ throughout its height. The moment of inertia of this type of section would be large in comparison with a similar stack of uniform section with a resultant large increase in the natural frequency of the stack vibration.
4. When it is possible to introduce rigid bracing between the stack and adjoining structures, the frequency of the stacks may be increased by such bracing. The optimum location is at a point about two thirds the height of the stacks.
5. When there are two or more adjoining stacks, the vibrations may be inhibited by introducing a system of bracing near their tops. The probability of two or more stacks vibrating together as a result of vortex shedding appears to be remote.
6. Energy-absorbing devices may be installed, or the design may take advantage of the greater damping properties of masonry and concrete in comparison to those of steel.
7. The most economical procedure is to design the stacks so that their natural frequency is that of the vortex shedding at a wind velocity of 45 miles per hr. With proper design, the energy of the vortices at this velocity will not be sufficient to produce excessive stresses; the stack would be safe against excessive vibrations up to a velocity of 80 miles per hr. It should be noted that this conclusion is based on the unconfirmed assumption of the restricted type of self-induced vibrations.

FURTHER INVESTIGATIONS

The design of stacks is a matter of considerable economic importance to power and other industrial companies. Further information is desirable to eliminate the uncertainties in many of the assumptions made herein. Among these uncertainties are: (1) The drag coefficient for cylinders with Reynolds numbers in the range of from 3×10^6 to 10×10^6; (2) the drag coefficient for vibrating cylinders; (3) the corresponding lateral coefficients of force; (4) confirmation or negation of the assumption as to the type of self-excited vibrations;

(5) damping characteristics for welded stacks, both lined and unlined and with varying types of foundation restraint—considerable statistical data could be obtained from observations on existing stacks; and (6) design of any practical devices by which the shedding of periodic vortices may be eliminated.

ACKNOWLEDGMENTS

The investigation herein described was sponsored by the Pacific Gas and Electric Company of San Francisco, Calif. At the beginning of the investigation, I. C. Steele, M. ASCE, was vice president in charge of engineering. Mr. Steele was succeeded by Walter Dreyer, M. ASCE. Carl Appleford, M. ASCE, supervising civil engineer, represented the company for the structural design of the Moss Landing and Contra Costa plants. The Moss Landing plant was designed by the Stone & Webster Engineering Corporation of Boston, Mass., with E. A. Dockstader, M. ASCE, as chief engineer. The data given herein in regard to the Moss Landing stacks have been taken from a report by the Stone & Webster Engineering Corporation to the Pacific Gas and Electric Company. The Contra Costa plant was designed and constructed by the power division of the Bechtel Corporation of San Francisco, with J. N. Landis as chief power engineer, the senior author as chief structural engineer, and the junior author as consultant. I. E. Boberg, M. ASCE, chief engineer of the Chicago Bridge and Iron Company, furnished the data for the Detroit stacks.

APPENDIX. NOTATION

The following symbols, adopted for use in the paper and for the guidance of discussers, conform essentially with "American Standard Letter Symbols for Structural Analysis" (ASA Z10.8—1949), prepared by a committee of the American Standards Association with Society representation, and approved by the Association in 1949:

A = amplitude;
C = constant depending on the mode of vibration;
C_D = coefficient of drag varying with the shape of the body and with the Reynolds number;
C_L = coefficient of lateral forces resulting from vortex shedding;
D = diameter of stack or cylinder;
E = modulus of elasticity;
F = weight of section into which the stack is divided for analysis;
f = frequency of vortex shedding or vibration;
g = acceleration of gravity;
h = equivalent height of the stack:
    h_f = height of the flare;
    h_s = height of the straight shaft;
I = moment of inertia;
k = spring constant of a vibrating body;
L = length of cantilever;
m = mass of a vibrating body;

N = magnification factor;
n = ratio of the moduli of elasticity for steel and concrete;
P = unit force or drag;
P_a = alternating force;
R = Reynolds number;
r = radius of stack;
S = Strouhal number;
t = thickness of stack shell;
v = velocity of wind;
W = work of deformation;
w = weight per unit length;
x = dead-load deflection at the center of each section when the stack acts as a horizontal cantilever;
y = deflection which would be produced by the disturbing force acting statically;
δ = logarithmic decrement;
ν = kinematic viscosity;
ρ = mass density of air; and
ψ = damping ratio.

DISCUSSION

Richard Jenney,[17] M. ASCE.—An assemblage in usable form of all that is known regarding the behavior of tall stacks in the wind has been made by Messrs. Dickey and Woodruff. The constructive suggestions for design and further investigation should be of considerable interest to the engineering profession.

The incidence of serious vibrations is still, however, not entirely predictable. The freedom of some stacks from such troubles is somewhat puzzling. In the belief that negative experience may also be of some interest, the writer refers to a stack built near New London, Conn., in 1953. This stack was very similar to the Moss Landing stacks, having a top diameter of 11 ft 5 in. and a height of 244 ft. The flared base was 80 ft high and had a diameter of 17 ft at the bottom; there was a parabolic transition at the top of the flare. Plate thicknesses, from the top, were 74 ft of $\frac{3}{8}$ in., 20 ft of $\frac{7}{16}$ in., 20 ft of $\frac{1}{2}$ in., 20 ft of $\frac{9}{16}$ in., and 110 ft of $\frac{5}{8}$ in., all laid up in 5-ft lifts. Ring stiffeners were applied internally at 10-ft intervals, and butt-welded construction was used throughout. During construction and until gunite was applied, the stack was guyed by three $\frac{3}{4}$-in. steel wire ropes sloping about 40° and spaced at 120° on a guy ring 190 ft from the ground. After applying gunite to a thickness of $2\frac{1}{2}$ in., the guy ropes were slacked off to a 12-ft sag and left in place for security until the behavior of the stack could be observed under a variety of conditions for at least one winter season. The foundation was an octagonal pad on 14 BP 73 piles 100 ft long acting as friction units in nearly uniform, very fine, gray sand.

Although the design is obviously on the conservative side by conventional standards (wind load of 25 lb per sq ft on the projected area), the stack is quite slender and the computed dynamic properties are such as might lead one to expect difficulties—

	Unlined	Lined
Natural frequency, in cycles per second	0.96	0.71
Period, in seconds	1.04	1.41
Static deflection, in inches	8	6
Critical wind velocity, in miles per hour	39.4	29.1

Judging by these data, noticeable vibrations might have been expected from a wind velocity of 60 miles per hr on the completed stack, and preparations were made to take up slack in the guys if necessary to moderate the sway. However, a hurricane that struck on August 31, 1954, resulted in no serious amplitudes, at least so far as could be seen with the naked eye, and it was at no time deemed necessary to take up the guys.

The only features of this stack which might be considered at all unusual are the rigid stiffening against ovalling and the excess plate thickness of between $\frac{1}{16}$ in. and $\frac{1}{8}$ in. Of course, the platform at the top may, to some extent, have prevented the regular formation of vortices at the point where they exert the greatest influence. There may also have been appreciable energy absorption through the whipping of the guys by the elastic working of the piles in the sand and by the damping effect of the lining.

---

[17] Structural Engr., United Engineers & Constructors, Inc., Philadelphia, Pa.

It is unfortunate that the proportions of stacks dictated by functional requirements together with the trend toward all-welded construction tend to produce undesirable elastic behavior within the critical range of response to winds of reasonably frequent occurrence.

Considering the extremely high cost of serious stack damage, a substantially increased first cost may be justified to assure reliable and predictable behavior in a utility power stack. Except in earthquake zones, however, such an increased cost may easily result in steel stacks which compare quite unfavorably with corresponding concrete stacks, particularly for heights greater than 200 ft.

It is agreed that much further study is necessary. It is suggested that, until firm design criteria have been developed by further investigation, it may be wise not to use exclusively all-welded construction for slender steel stacks except when special requirements dictate their use and the designer is made fully aware of the physical and economic hazards involved.

That this conclusion should follow so closely on the completion of an apparently satisfactory stack may seem inconsistent, but it is to be considered whether any structure which can cause its designer continuing concern and demand of its owner continuing vigilance can be counted wholly successful. There persists a suspicion of unsoundness as to the choice of materials, proportions, and design assumptions to the detriment of the over-all reliability of the plant.

GEORGE S. VINCENT,[18] M. ASCE.—A worthwhile advance in the knowledge of the action of wind on engineering structures has been made by the authors. The specific data concerning the behavior of several steel stacks in winds of various velocities suggest certain design criteria which are noted by Messrs. Dickey and Woodruff. Furthermore, the data represent large-scale experiments that extend the knowledge of wind action around a cylinder and shed further light on the oscillation of transmission lines and even on some forms of the more complex excitation of suspension-bridge sections.

As shown by the authors, the Strouhal number is the most significant parameter concerning the behavior of a stack in the wind. Some of the variation in the computed values of S arises from uncertainty as to the actual wind velocity at a given time and at the elevation at which the dominant wind effect occurs as well as to the variability of the wind. In some cases the computed value differs so much from the standard range that an explanation is sought. A closer study of the wind pattern and its resulting forces on a cylinder may be helpful to this end.

Fig. 2(*a*) is taken from a more comprehensive diagram.[19] Figs. 2(*b*), 2(*c*), 2(*d*), and 2(*e*) show the stream flow around a cylinder at various stages. Fig.

---

[18] Bridge Engr., Physical Research Branch, Bureau of Public Roads, U. S. Dept. of Commerce, Washington, D. C.

[19] "What Aerodynamics Can Teach the Civil Engineer," by W. Watters Pagon, *Engineering News-Record*, March 15, 1934, p. 351, Fig. 3.

2(*b*) shows the "potential flow" which exists briefly after the beginning of motion. This flow pattern corresponds to the pressure diagram for ideal flow (labeled I in Fig. 2(*a*)). The forces required to deflect the wind act toward the centers of curvature of the streamlines, and the forces on the cylinder act in the opposite direction. At the center of the windward side the wind comes to rest at a "stagnation point," and the pressure therefore reaches its maximum positive value,

$$q = \frac{\rho\, v^2}{2} \quad \text{.........................} \quad (13)$$

The same pressure pattern, occurring on the leeward side of the cylinder, accelerates the air at the leeward stagnation point from no velocity to the

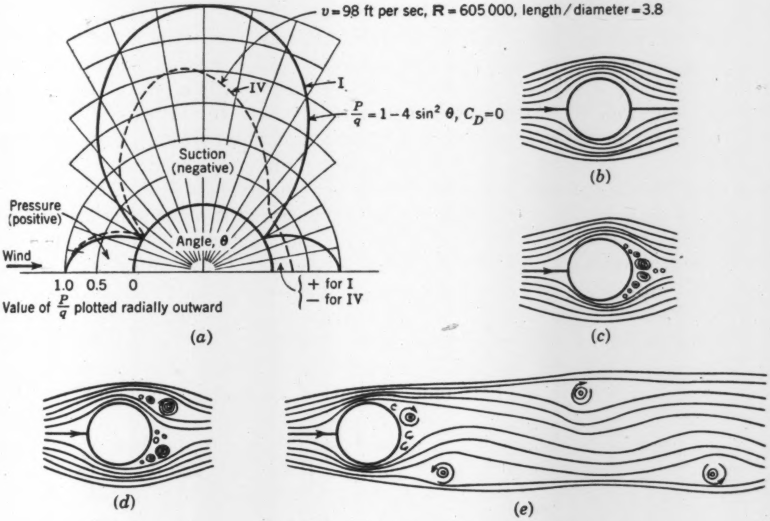
v = 98 ft per sec, R = 605 000, length/diameter = 3.8
IV
I
$\frac{P}{q} = 1 - 4 \sin^2 \theta,\ C_D = 0$
Suction (negative)
Pressure (positive)
Angle, θ
Wind
1.0
0.5
0
Value of $\frac{P}{q}$ plotted radially outward
+ for I
− for IV
(a)
(b)
(c)
(d)
(e)

FIG. 2.—WIND PATTERNS

stream velocity, *v*. It is in the negative pressure region at the sides that large pressures occur, up to three times the dynamic pressure. For the ideal or potential flow there is no net force tending to move the cylinder.

Because of viscosity, the air flow near the cylinder is slowed down, and air from the leeward stagnation area moves upstream (Fig. 2(*c*)). The accumulating air in the leeward stagnation zone crowds the streamlines, reducing their curvature and modifying the pressure pattern as is typified by IV in Fig. 2(*a*). This accumulation must be released at intervals which naturally depend on the wind velocity and dimensions of the area involved, giving rise to the periodic discharge of vortices as idealized in Figs. 2(*d*) and 2(*e*); photographs taken with the fluid and camera stationary and the cylinder moving show a strong circular pattern affecting all the streamlines, but the pattern is elongated when considered with the fluid in motion and the cylinder stationary. The chance discharge of the first vortex from one side sets up an oscillation in the leeward stagnation zone which results in the subsequent alternation of discharges, one from each side per cycle of the Strouhal frequency. The pressure diagram labeled IV in Fig. 2(*a*) represents the average condition. Associated with the alternating vortex discharge is a variation in the pressure pattern alternating from side to side with respect to the longitudinal axis (parallel to the stream flow). The maximum value of this periodic pressure variation is expressed as an average transverse pressure in Eq. 4.

Eq. 7, involving the magnification factor as π/δ, is applicable only at, or reasonably near, resonance. The velocity range in which excitation occurs is broadened if the bending oscillation is large as the effect of the motion is to add the double amplitude to D in Eq. 3. For a uniform diameter, $D + 2\ A$ increases with height as does the wind velocity.

The reoccurrence of a mode at approximately twice the wind velocity indicated by the Strouhal number involves "sub-harmonic excitation" in which the force is applied at twice (or some other multiple of) the frequency of the oscillation.[10] Such excitation is possible only to the extent that the exciting force or the oscillation or both are nonlinear. Thus, although the wind forces would be increased fourfold as noted under the heading, "Vibration Frequencies: Contra Costa Stacks," their net effectiveness in exciting motion might be quite small. The relative ineffectiveness of subharmonic excitation undoubtedly is the reason for the low magnification factor noted in the behavior of the 9-ft-diameter stack on Guam at a velocity of 120 miles per hr. It would be interesting to know the subsequent history of this stack. If it has survived several typhoons, fatigue may become an important factor.

Mr. Frank's advice[16] that the frequency of the stack be kept as low as possible seems intended to permit resonant excitation at low velocities with the expectation that subharmonic excitation at higher velocities will be inefficient.

The pressure pulsations which cause breathing or ovalling occur twice per vortex cycle—that is, once for each vortex. If this is taken into account, the data for the breathing of the Moss Landing stacks indicate Strouhal numbers of 0.225 and 0.175 for velocities of 37 ft per sec and 48 ft per sec, respectively. The breathing of the Guam stack was evidently subharmonically excited. If, for example, the effective velocity is 108 miles per hr and S is assumed to be 0.2, the vortex cycle frequency is found to be 210 cycles per min. If the maximum estimated diameter of the oval, 11 ft, is assumed to be the effective diameter, a frequency of 210 cycles per min would result for velocities up to $\frac{11}{9} \times 108 = 132$ miles per hr. It is evident that two complete vortex cycles (four individual vortex discharges) occurred per cycle of breathing.

The behavior of the stacks in groups recalls the oscillation of individual strands of the open-stranded cables of the Peace River and Liard River suspension bridges on the Alaska Highway.[20] The cable of the former consists of twenty-four $1\frac{7}{8}$-in. strands arranged in six horizontal layers of four strands each spaced at $3\frac{1}{2}$ in. on centers both ways. The Liard Bridge cable has twelve $2\frac{1}{16}$-in. strands arranged in four horizontal layers at the same spacing. Before spacer blocks were placed at the middle of each panel (approximately 40 ft long), the individual strands vibrated frequently in the wind. Strands in the windward tier of the cable were never seen to vibrate but those in the adjacent tiers did, evidently under the influence of the vortex trail of the windward strands. At the Peace River bridge practically all the individual wire breaks were nearly equally divided between the two interior tiers whereas at the Liard River bridge over half were in the middle tier. Apparently the tier next to the windward one was most affected. Action was greater and more frequent in the windward cable; evidently the turbulence shed by this cable as a whole weakened or destroyed excitation on the leeward cable.

---

[20] "Cable Vibrations on Alaska Highway Suspension Bridges," by Raymond Archibald, *Engineering News-Record*, September 2, 1948, p. 79.

As both the clear length between hangers and the tension in the strand increased toward the tower, the frequency was fairly constant (588 cycles per min measured at Peace River and 420 cycles per min at Liard River), and motion was observed in practically all panels, depending on the direction of the wind. Usually only half a dozen panels were involved at a time. Because the vibration was noticed in winds of from a few miles per hour up to 40 miles per hr it is evident that the excitation must have been subharmonic.

Tests on bridges have shown distinctly greater damping when on pile foundations rather than on piers founded on rock, and greater effects of foundation conditions are to be expected when the foundation directly supports a vibrating cantilever.

The increase in damping obtained by adding a 1.92-in. gunite encasement to a 6-in. steel pipe (Table 2) must be much greater than that which would result from guniting a steel stack as the thickness of gunite used on the model was 32% of the outside diameter of the steel pipe, although the relative thickness of steel and gunite was reasonably consistent with an actual design.

John N. Pirok,[21] M. ASCE.—Gas volume and draft requirements are the criteria that usually determine the proportions of stacks. Various rules of thumb are used in adjusting proportions to guard against aerodynamic difficulties. Designers cognizant of the vibration induced by wind often find it difficult to obtain acceptance of needed changes in proportions to meet aerodynamic requirements. However, the theory presented by the authors gives a basis to the aerodynamic design of stacks. Dynamic stability sometimes requires stack diameters larger than those actually needed to accommodate gas volumes.

The wind-pressure formula with which engineers are most familiar is

$$P = K\,v^2 \quad \text{.........................} \quad (14)$$

in which K is a coeffcient varying from 0.002 to 0.005. Eq. 14 is similar in form to Eq. 1. The value of K is determined from

$$K = \tfrac{1}{2}\,\rho\, C_D \left(\frac{88}{60}\right)^2 \quad \text{....................} \quad (15)$$

---

[21] Structural Engr., Chicago Bridge & Iron Co., Chicago, Ill.

If one uses $C_D = 0.35$ and $\rho = 0.00238$ as suggested by Messrs. Dickey and Woodruff, K becomes 0.00086. The value suggested for C_D is obviously too low; it should be at least 0.60 when Eq. 1 is used to compute the wind pressure to be used for stack design.

The frequency of the alternating vortices as expressed by Eq. 3 must not be assumed to be precisely determined by this formula for any given stack. The wind velocity is not uniform over the full height of the stack.[22] The variation is given as

$$v_z = v_{30} \sqrt[7]{\frac{z}{30}} \quad \text{.......................} (16)$$

in which v_{30} is the wind velocity 30 ft above the ground and v_z is the wind velocity z feet above the ground. For stacks 100 ft or less in height, the variation is not significant. For stacks 200 ft high, the velocity at the top may be 30% greater than at ground elevation. The velocity at the top of 500-ft-high stacks may be 50% greater than at ground elevation.

The Strouhal number S has not been established for all velocity ranges influencing stack design. Mr. Frank[16] has given a value for S of 0.15 for stacks; the authors used $S = 0.19$ in Eq. 3. Stacks are not always cylinders throughout their full height; the diameter varies from top to bottom in conical stacks. If resonance is to be avoided, stacks should be designed for wind velocities at least 25% greater than those recorded for the area. A stack may be designed for a resonant velocity of 80 miles per hr, yet actual resonance may occur at 65 miles per hr because vortex frequency cannot be precisely determined. If velocities of 65 miles per hr frequently occur, the stack is certain to experience difficulty. Wind-velocity records must be studied for each location, and natural permanent obstructions must be taken into account. Experience and judgment must still be reflected in the design.

The authors state, under the heading, "Damping," that "most excessive stack vibrations have occurred in welded stacks * * *." Is this all-inclusive statement justified? Did excessive vibrations occur because of the welded construction? There are few published data on the vibration of riveted stacks, and not many on the vibration of welded stacks. With the use of welding there occur changes that affect vibration characteristics of stacks—(*a*) the linings are made thinner and of lighter materials, (*b*) the steel plates are thinner, and (*c*) because the linings are thinner, the stack diameters are smaller. Also more unlined stacks are built than in the era of riveted construction and better dispersion of ash and other products of combustion demands taller stacks. With an increased demand for taller stacks, vibration difficulties increase. The greatest change is caused by the reduction in lining because the weight is reduced more than 50%. This weight reduction increases the natural frequency of stacks with resonance occurring at higher wind velocities.

The Rayleigh-Ritz method is a rapid procedure for determining the natural frequency of lined or unlined stacks. The computed frequency of stacks lined with 2 in. of gunite is approximately 70% of the natural frequency of unlined stacks. The usefulness of Eq. 10 can be extended to lined stacks by determining the factor for materials other than gunite.

---

[22] "Frequency of Maximum Wind Speeds," by H. C. S. Thom, *Proceedings-Separate No. 539*, ASCE, November, 1954.

Eq. 12 does not make allowance for stiffeners on stacks. Ovalling or breathing can be prevented with stiffeners as is borne out by experience. A stack built in 1945 in Hammond, Ind., was 100 ft tall and 4 ft in diameter. This stack vibrated severely as a cantilever and measurements showed dilation or ovalling. Addition of stiffeners (6-in. by 4-in. by $\frac{3}{8}$-in. angles spaced at 25 ft on centers measured from the top) stopped both the ovalling and the cantilever vibrations, indicating that there is a relationship between ovalling and cantilever vibrations.

The lining of stacks does more than provide corrosion resistance. It backs up the plate, thus increasing its ultimate strength from tubular buckling to the yield strength of steel plate. This may account for the fact that there is no record of lined-stack failures. Lined stacks should be designed for lined conditions. They should be temporarily guyed during construction if the critical velocity could occur before the lining is installed. External damping devices are not good solutions; these gadgets require maintenance and can be inoperative when they are most needed.

Frederick B. Farquharson,[23] M. ASCE.—Essential information has been provided regarding the wind-excited oscillation of several large steel stacks. Under the heading, "Source of Vibrations," Messrs. Dickey and Woodruff have made reference to experimental work on suspension bridges. The statement regarding a velocity ratio of two between the first and second appearances of the same mode applies only to a limited category of suspension-bridge sections. This ratio was found only on plate-girder-stiffened sections for which the ratio of depth of the girder to width of the section was approximately 0.2. The same ratio was found to exist in the cases of torsional and vertical (or bending) modes and was observed on dynamic section models as well as models on the complete bridge.[6] Two appearances of each vibration mode have been observed on other types of suspension-bridge sections but never with a ratio of two between their critical velocities.

It is also important to note that this multiple appearance of the same mode (under some circumstances there are more than two appearances) is assumed to indicate a condition of subharmonic resonance. It does not necessarily follow that the later manifestations of a given mode must be catastrophic. Theoretical considerations have revealed the probable existence of other manifestations of both torsional and vertical vibration modes at still lower wind velocities. However, their development in the wind tunnel has been prevented because of the inability to reduce sufficiently the structural damping inherent in the model suspension.

It appears that the exciting mechanism involved in suspension bridges of the girder-stiffened type with depth-to-width ratios of less than 0.22 has its origin in the discharge of vortices. For sections with ratios greater than 0.225 another type of excitation is superimposed on the vortex action.

---

[23] Prof. of Civ. Eng. and Director, Eng. Experiment Station, Univ. of Washington, Seattle, Wash.

The only similarity between the vibrations of cylindrical stacks and of suspension bridges like the original Tacoma Narrows Bridge[6] is that they are both vortex-excited. It would appear that the steel stack is harmonically excited by the vortex discharge and that a single appearance of the vibration mode will develop.

An excellent parallel exists between the cylindrical stack and the vibrating transmission line. In the course of an investigation of the high-frequency vibration of power-transmission lines (not to be confused with the galloping of such lines when coated with ice), a series of tests was performed on smooth cylinders of several diameters. In these tests, which were run on rigid-section models, only one vertical mode was isolated, and it was quite evident that the excitation was harmonic—the exciting wind velocity being determined by the natural frequency of the model in its spring mounting. It was observed that vibrations were initiated on these models when the rate of vortex discharge corresponded approximately to a natural frequency of the model in its spring suspension. The wind velocity at which vibration started corresponded closely to the velocity appropriate to $S \approx 0.2$.

As the wind velocity was increased above the point where motion was first evident, the structure constrained the vortex shedding to correspond with the frequency of the model. The structure was capable of controlling the vortex frequency over a limited range of wind velocity, depending principally on the magnitude of the structural damping present in the model suspension, and eventually the model came to rest. Further increase in wind velocity caused a discharge of vortices at a rate appropriate to the Strouhal number and the wind velocity, with the vibration phenomenon repeating itself when the vortex frequency again corresponded with a natural frequency of the structure.

In considering aerodynamic forces acting on the stack, the authors have assumed that C_D is equal to 0.35, a value which corresponds closely to the minimum shown in Fig. 3. Experiments by N. K. Delany and N. E. Sorensen[24] on cylinders of various shapes have revealed values of $S = 0.4$ corresponding to $C_D \approx 0.4$ for circular cylinders at $\mathsf{R} = 2{,}300{,}000$—well above the conventional critical value. This high value of S suggests that the steep characteristic of the S-curve in Fig. 3 may be maintained as R is increased above the critical region. However, the value of C_L, the alternating lift coefficient, which is given as $C_L = 0.66$ (for $\mathsf{R} \approx 700{,}000$) is just one half the value computed by L. Landweber[25] for similar conditions. Computations by R. Ruedy[26] from observation of pressure distribution over circular cylinders at $\mathsf{R} = 962{,}000$ indicate $C_L = 1.13$.

J. P. Den Hartog[27] has remarked that the meager information on the value of the Strouhal number and the alternating lift coefficient has been obtained at relatively low values of the Reynolds number and only on fixed cylinders. He comments further that the alternating force will be greater for the vibrating cylinder than for the cylinder at rest.

---

[24] "Low Speed Drag of Cylinders of Various Shapes," by N. K. Delany and N. E. Sorensen, *Technical Note, No. 3038*, National Advisory Committee for Aeronautics, Washington, D. C., November, 1953.

[25] "Flow About a Pair of Adjacent Parallel Cylinders Normal to a Stream," by L. Landweber, *Report No. 485*, David W. Taylor Model Basin, Washington, D. C., July, 1942.

[26] "Vibrations of Power Lines in a Steady Wind," by R. Ruedy, *Canadian Journal of Research*, No. 13, Sect. A, November, 1935, pp. 99–110.

[27] "Recent Technical Manifestations of Von Karman's Vortex Wake," by J. P. Den Hartog, *Proceedings*, National Academy of Sciences, Vol. 40, 1954.

It is a matter of great interest that field observations of the vibration of a number of steel stacks have shown resonant vibration at values of the Reynolds number well beyond the range in which many careful laboratory investigations have established a transition to turbulent flow. Fig. 3 shows the variation of the drag coefficient C_D and the Strouhal number S with the Reynolds number **R** obtained on circular cylinders in two laboratories. Evidently regular vortex shedding did not occur beyond **R** $\approx$ 200,000 to 550,000. The subsequent discussion may shed some light on this discrepancy.

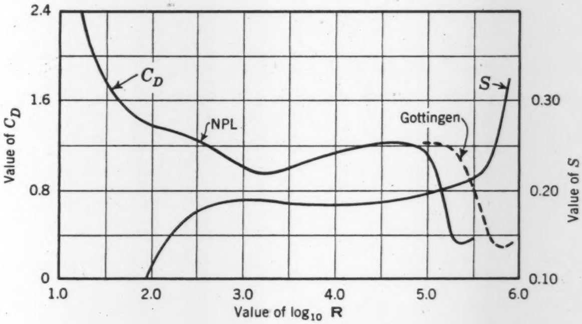

FIG. 3.—VARIATION OF C_D AND S WITH **R**

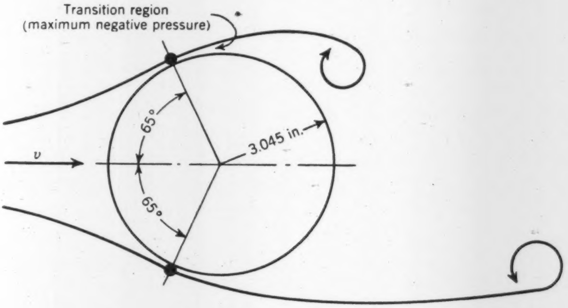

FIG. 4.—TEST ARRANGEMENT

A. Fage and J. H. Warsap[28] measured the drag of a 6.09 in.-diameter cylinder when wires of various diameters were placed along generators at $\theta = \pm 65°$ (Fig. 4). The results of these tests are summarized in Fig. 5(*a*) in which it will be noted that the shape of the drag curve suffered a regular change as the diameter of the wires was increased, the largest wire producing the most marked change. When the angle θ was changed to ±25° the same wires had no appreciable effect.

---

[28] "The Effects of Turbulence and Surface Roughness on the Drag of a Circular Cylinder," by A. Fage and J. H. Warsap, *Reports and Memoranda No. 1283*, Aeronautical Research Committee, Great Britain, 1930.

In similar tests from the same source, the effect of uniform roughening developed on the surface of the cylinders by covering them with fine sandpaper of varying coarseness was investigated. In Fig. 5(*b*) it will be seen that the drop in C_D occurs at a lower value of **R** and becomes smaller as the surface roughness is progressively increased. The range of velocities covered in these tests corresponds to Reynolds numbers between 45,000 and 210,000, the higher value approximating the critical value ($\mathbf{R} = 6{,}380\, v\, L$).

Many laboratory tests have also demonstrated that the critical range of the Reynolds number is also markedly reduced by increased turbulence in the wind stream. Observations in the field on several stacks have revealed oscillations at values of **R** as high as 5,500,000, which is well above the critical values shown in Fig. 3 which are commonly accepted in the classical literature.[29] In Fig. 3 it will be seen that two sources place the critical value of **R** between 250,000 and 600,000—the higher value developing in the wind tunnel with the lowest turbulence. These values were all determined for highly polished cylinders.

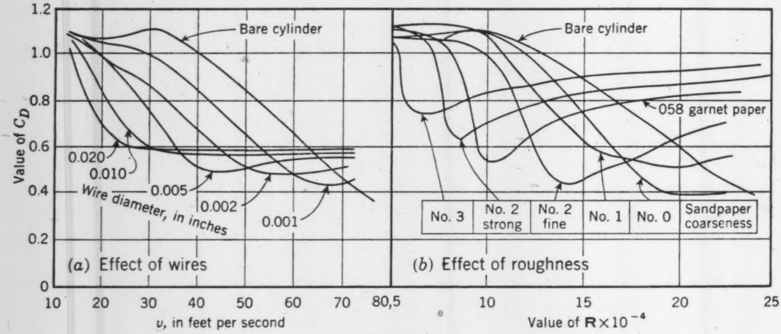

FIG. 5

The results of tests by Messrs. Fage and Warsap suggest (Fig. 5) that the coarse texture of the surface of the typical stack, plus the presence on many of them of either a series of lapped and riveted joints or butt-welded seams, has provided a partial explanation of oscillations of the high Reynolds numbers observed in the field. In Fig. 5(*a*) it is evident that the largest wire used reduced C_D to 0.59 at $v = 30$ ft per sec ($\mathbf{R} = 97{,}000$) whereas the bare cylinder showed the same value of C_D at $v = 63$ ft per sec ($\mathbf{R} = 204{,}000$). This effect alone has resulted in a 47.5% reduction in critical **R**.

Fig. 5(*b*) indicates that the effect of surface roughness was most pronounced for the garnet paper at $C_D = 0.52$ with a reduction of 47% in **R**.

---

[29] "Modern Developments in Fluid Mechanics," by S. Goldstein, Clarendon Press, London, 1st Ed., 1938, Vol. II, p. 419.

A measure of the effect of turbulence is found in Fig. 3 where the Göttingen tunnel is known to have the least turbulent flow and the critical value of **R** is found to be markedly lower for the more highly turbulent NPL tunnel. The turbulence in both these wind tunnels is of a much lower order than that in natural wind; thus, the effect of field turbulence could be expected to be somewhat greater. S. Goldstein has summarized[29] this situation as follows:

> "* * * the critical range of **R**, in which the drag coefficient experiences a large drop, can be changed progressively by ordered changes in the turbulence of the general stream, in the general roughness of the surface and by small excrescences * * * on the surface near the position of maximum negative pressure."

An examination of the data assembled from the six steel stacks which have oscillated under wind confirms the conclusion toward which this discussion has been directed. In the case of all but the Guam stack the evidence seems to point conclusively to a condition of resonance between the vortex frequency and the natural frequency of the fundamental mode of the stack.

The Guam report presents somewhat conflicting evidence. It seems possible that ovalling at 1.75 cycles per sec could have been of a subharmonic origin and might have been coupled with a subharmonically excited bending mode. The frequency of the vortex shed by the undistorted stack would have been $f \approx 3.88$ cycles per sec for a Strouhal number of 0.19.

Under the heading, "Evaluation of Data," a warning is sounded regarding the danger of reducing the critical velocity through added damping, the fear being expressed that a subharmonic excitation might occur at a higher wind velocity. The laboratory tests on circular cylinders mentioned previously have indicated that only one appearance of the fundamental mode is possible. Of course there is always the possibility that the stack might vibrate in a higher mode—that is, with a different wave form. As Messrs. Dickey and Woodruff have mentioned, for a stack of constant cross section the frequency in the second mode is 6.25 times that in the first mode. Realizing that the critical wind velocity varies directly with the natural frequency, it seems clear that for any but the most limber stacks only the fundamental mode need be considered.

It was further suggested as a design procedure that stacks be designed for a natural frequency equivalent to the vortex frequency at 45 miles per hr—that the stack would be safe until a velocity of 80 miles per hr was reached. This procedure simply involves a harmonic resonant condition in the vicinity of 45 miles per hr which could be disastrous under low damping conditions. At 80 miles per hr the Moss Landing stack would operate at

$$\mathsf{R} = (6{,}380)(117)(11.3) = 8{,}450{,}000$$

which, even allowing for turbulence and roughness corrections, should place the stack above the critical value of **R** where vortices are not regularly shed.

In line with the material under the heading, "Further Investigations," it is felt that items 1 to 3 need no further study as the wind force on a fixed member controls if methods can be found for eliminating vibration. The present discussion is submitted as a partial answer to item 4. The damping characteristics mentioned in item 5 are important as this feature represents an element in the control of the critical velocity. The elimination of vortex shedding (item 6) is probably a practical impossibility because of the fact that the wind may blow from all points of the compass.

One might suggest the following investigations:

1. The design of a practical stiffening ring to eliminate ovalling.
2. The mounting of vertical vanes in the manner of the wires in Fig. 4, placed 45°, 51.5°, or 60° apart, completely around the stack and within the boundary layer. It may be assumed that such a device might serve to reduce the drag much as shown in Fig. 5(*a*) and thus the strength of the vorticity. Wind-tunnel experimentation would develop an optimum depth and spacing of these vanes.
3. Wind-tunnel studies on a special type of flexible model to determine the taper which might effectively eliminate oscillation.

W. WATTERS PAGON,[30] M. ASCE.—A welcome addition has been made to the recorded data concerning stack swaying and ovalling. These facts have been integrated with a theory and thus are brought within the purview of the designing engineer.

The problem is one of many variables which differ between power plants. These variables are (*a*) the probable velocity of the wind and its turbulent nature; (*b*) the orientation of the stack group to probable winds of suitable velocity; (*c*) the height-to-diameter ratio of the stacks; (*d*) the ratio of bell length to cylindrical length; (*e*) the soil characteristics (for ground-level foundations); (*f*) the vibration frequency of the roof supports if any;[15] (*g*) the shell thickness; (*h*) the presence or absence of ring stiffening; (*i*) the effect of lining on the period, damping, and rigidity; and (*j*) the effect of welding as opposed to riveting.

It is of value to add to the information that was presented by Messrs. Dickey and Woodruff and to call attention to a wealth of theoretical material that is unused by the designer. For example, it is of importance to note that the Baltimore stacks were lap riveted and that the swaying was apparently caused by the flexibility of the roof structure. The swaying was corrected by stiffening this structure; and ring reinforcing was added to eliminate ovalling. As these stacks approached the end of their useful life (approximately fourteen years) and when rusting in the vicinity of the lap joints became increasingly serious, more rings were added, which increased the moment of the weight but had no effect on swaying.

The most serious deficiency in stack-designing theory is the lack of data on the influence of one stack on adjacent stacks. Does the 4-diameter spacing for the Moss Landing stacks or the 4.45-diameter spacing for the Baltimore stacks have significance? The swaying of the latter resulted when the eddies on one side of the windward stack during a quartering wind enveloped the leeward stack; ovalling was primarily confined to the leeward one (being reversed for wind in the reverse direction). The smoke trails which were visible indicated that the stack spacing was approximately equal to the eddy spacing.

---

[30] Cons. Engr., Baltimore, Md.

There is a considerable lack of knowledge as to what happens when there are two, three, or more stacks in a row. No satisfactory data exist (as of 1955) concerning the eddy frequency and drag coefficient for multiple cylinders, either in a row in line with the wind or in echelon for a quartering wind. Anatol Roshko has amplified[31] the previous data[32, 33, 34] on this subject. These studies are based on the same method as was used[35] by the writer. Briefly, Mr. Roshko has reverted to the earlier studies of Herman Ludwig Ferdinand von Helmholtz,[36] as extended by Gustav Robert Kirchhoff[37] and by John William Strutt Rayleigh[38] on the drag of a flat plate. In these earlier studies it was assumed that the base pressure on the leeward face of the plate is the same as the pressure "at infinity" in the free stream. However, Mr. Roshko has changed this assumption to one wherein this base pressure is a function of the velocity within the wake in the vicinity of the body—before the vortex street has degenerated into mixed turbulence from the interaction of the two sheets of alternating eddies. The results obtained by Mr. Roshko apply only in the vicinity of the body; however, it is at this point that the base pressure is developed, and there results in Mr. Roshko's work[39] the same agreement that the writer found.[40, 41]

In Mr. Roshko's work there are found (*a*) the relationship between the coefficient of drag and the width of the wake for a normal plate, for a 90° wedge, and for a circular cylinder;[42] (*b*) the effect of a "splitter plate" on the coefficient of drag of a circular cylinder;[43] (*c*) the effect of varying the distance from splitter plate to cylinder;[44] (*d*) the variation of the wake-pressure coefficient;[44] (*e*) the variation of the Strouhal number;[44, 45, 46] and (*f*) the conclusion that the processes in the wake are essentially unchanged for Reynolds numbers above the critical.[47] Also of interest in this matter is the information obtained by Herman M. Spivak from tests[48] on two parallel cylinders exposed to a wind normal to the line joining them.

---

[31] "On the Wake and Drag of Bluff Bodies," by Anatol Roshko, *Journal of the Aeronautical Sciences*, February, 1955, pp. 124–132.

[32] "A New Hodograph for Free Streamline Theory," by Anatol Roshko, *Technical Note No. 3168*, National Advisory Committee for Aeronautics, Washington, D. C., July, 1954.

[33] "On the Drag and Shedding Frequency of Bluff Cylinders," by Anatol Roshko, *Technical Note No. 3169*, National Advisory Committee for Aeronautics, Washington, D. C., July, 1954.

[34] "On the Development of Turbulent Wakes from Vortex Streets," by Anatol Roshko, *Technical Note No. 2913*, National Advisory Committee for Aeronautics, Washington, D. C., 1953.

[35] "Wind Tunnel Studies Reveal Pressure Distribution in Buildings," by W. Watters Pagon, *Engineering News-Record*, December 27, 1934, p. 352, Fig. 4.

[36] "On the Discontinuous Motions of a Fluid," by Herman Ludwig Ferdinand von Helmholtz, *Monatsberichte der Königlich*, Preussischen Akademie der Wissenschaften zu Berlin, 1868, pp. 215–228.

[37] "Zur Theorie freie Flussigkeitsstrahlen," by Gustav Robert Kirchhoff, *Crelles Journal für die reine und angewandte Mathematik*, Vol. 70, 1869, p. 269.

[38] "On the Resistance of Fluids," by John William Strutt Rayleigh, *Philosophical Magazine*, Series V, Vol. II, 1878, pp. 430–441.

[39] "A New Hodograph for Free Streamline Theory," by Anatol Roshko, *Technical Note No. 3168*, National Advisory Committee for Aeronautics, Washington, D. C., July, 1954, p. 34, Fig. 1.

[40] "The Structure of Vortex Streets," by A. Fage and F. C. Johansen, *Reports and Memoranda No. 1143*, Aeronautical Research Committee, Great Britain, 1927.

[41] *Philosphical Magazine*, Series 7, Vol. 5, No. 13, February, 1928, pp. 417–441.

[42] "On the Wake and Drag of Bluff Bodies," by Anatol Roshko, *Journal of the Aeronautical Sciences*, February, 1955, p. 127, Figs. 2 and 3.

[43] *Ibid.*, p. 127, Fig. 4.

[44] *Ibid.*, p. 127, Fig. 5.

[45] *Ibid.*, p. 128, Table 1.

[46] *Ibid.*, p. 131, Fig. 7.

[47] *Ibid.*, p. 132.

One other element that is uncertain is the shape of the wake and the shedding frequency behind the central cylinder in comparison with that of the two outer cylinders. Because the size of boiler installations generally necessitates a spacing between the stacks of more than one diameter, it would appear that each stack would be independent of adjacent stacks as far as wake and frequency are concerned. However, if the several stacks are found to be subject to wakes that vary markedly so that swaying is not in phase for all the group, then longitudinal bracing could be provided to secure a horizontal beam of width equal to the stack diameter designed for the condition when adjacent stacks are in reverse phase, for wind from any direction.

Robert H. Sherlock,[49] M. ASCE.—The subject matter of this paper is still in the pioneer stage (as of 1955); it will probably continue to be so for some years to come. Nevertheless, engineers must design and construct high stacks as height is one of the considerations involved in the proper dispersion of gases. Under this condition it is especially important that engineers in this field make available to the profession the results of their experience and thinking. The authors have provided a welcome addition to the meager literature on this subject.

Of particular interest to the writer is item 4 under the heading, "Further Investigations." It is general practice to accept the von Kármán vortex trail in explanation of the exciting forces necessary to produce vibration across the wind stream. The theory has been validated for values of the Reynolds number below the critical value. Even above this critical value, cylindrical smoke stacks vibrate as would be expected if the flow around and behind the stacks followed the von Kármán theory. In the present (1955) state of the art and its underlying sciences, the von Kármán theory serves as a useful framework on which to base coefficients determined by experience. It cannot be said, however, that at high values of the Reynolds number the reality of the theory has been established.

A cylindrical stack is an obstruction in the air stream. The air is forced to flow around it and resumes the undisturbed conditions of flow as soon as possible downstream from the obstruction. If air were a perfect gas, there would be no loss as a result of viscosity and friction in the boundary layer, and the air would resume its undisturbed condition of flow without separation of the boundary layer from the surface of the stack. In such a case there would be an increase in the velocity and kinetic energy of the layers adjacant to the sides of the cylinder on the upstream side with a corresponding decrease in static pressure so that at the cross-wind axis of the cylinder these layers would have gained the exact amount of kinetic energy necessary to permit them to return to their original line of flow against the increasing static pressure at the downstream surface.

---

[48] "Vortex Frequency and Flow Pattern in the Wake of Two Parallel Cylinders at Varied Spacing Normal to an Air Stream," by Herman M. Spivak, *Journal of the Aeronautical Sciences*, June, 1946, No. 6, pp. 289–301.

[49] Prof. of Civ. Eng., Univ. of Michigan, Ann Arbor, Mich.

Actually, however, air is not a perfect gas but is viscous, and the conditions of flow are different from those of a perfect gas. The boundary layers lose energy through friction and viscosity on the upstream sides and are eventually forced to separate from the surface of the cylinder, thus enclosing a region in which the static pressure is lower than that of the freely flowing air but higher than that of the fast-moving enclosing layers.

Because of its momentum, each layer is able to support a difference in pressure between the air spaces inside and outside the layer. However, this difference in pressure cannot be supported indefinitely, and, in those cases to which the von Kármán theory is applicable, the layers turn inward and roll up into vortices with their axes of rotation parallel to the axis of the cylinder. The vortices flow downstream and eventually disintegrate as the velocities in the component parts of the wake approach the velocities in the undisturbed air stream. This formation is termed the "von Kármán trail," and the reality of its existence at Reynolds numbers below the critical value has been established in the laboratory.

At the Reynolds numbers which exist around smoke stacks during high winds, trailing vortices are occasionally outlined by entrapped smoke. They appear as vertical tails spinning their way downwind. The vortices rarely show even a quasi-periodicity even in the case of rough stacks. At one plant where there are eight vertical angles on the outside of the stack which give the effect of great roughness, these trailing vortices can be seen frequently. However, even if the reality of the vortex trail were established at high Reynolds numbers in a wind tunnel, there might still be considerable doubt as to its existence in the free atmosphere during high winds.

There are a number of differences between the conditions of a stack in the free atmosphere and those of a cylinder in a wind tunnel:

1. The stacks are not stationary but are vibrating, often through a considerable amplitude.
2. The stacks are not always cylindrical but sometimes have the shape of truncated cones so that vortices would be generated at different frequencies along the height of the stacks, according to the von Kármán theory.
3. During wind storms there is usually a considerable temperature-lapse rate in the atmosphere, with consequent turbulence which varies throughout the height of the stack.
4. The wind is gusty so that the velocity is constantly changing.

It does not follow that there are no lateral exciting forces even though the von Kármán vortices do not have an opportunity to form in the immediate wake of the stack; other hypotheses are possible. For example, if it is assumed that the von Kármán vortices do not form downwind from the stack, the boundary layer would still form on the upstream and lateral sides of the stack and these layers would be forced to separate from the downwind surfaces of the stack. They would flow downwind as layers of high momentum capable of enclosing a low pressure zone for some distance. The presence of this low pressure zone is frequently marked by a bulbous protrusion on the bottom of a horizontal smoke plume close to the stack. As the stack vibrates across the wind, the angle of incidence of the wind will change periodically, and the period will be controlled by that of the stack. Likewise, the points of separation of the boundary layers will move back and forth with the period of the stack. This should cause a difference in the simultaneous velocities of the boundary layers on the two sides, with a consequent periodic difference in pressures. In this concept of the exciting mechanism the period of the alternating pressures is always controlled by the period of the stack. The incidence of catastrophic vibration would not depend on resonance between the period of the vortices and that of the stack but on the frequency of occurrence of atmospheric conditions favorable to this orderly behavior of the boundary layer. The role of damping is the same under both hypotheses.

Under the heading, "Further Investigations," there might be added:

1. To what extent does the turbulence usually associated with high wind velocities inhibit the development of large periodic lateral forces?
2. What is the probable frequency of occurrence of those types of high winds that are favorable to the development of large periodic lateral forces?

Item 1 deals primarily with aerodynamics, item 2 with meteorology.

Walter L. Dickey[50] and Glenn B. Woodruff,[51] Members, ASCE.—Much has been done by the several discussers toward formulating the questions which must be answered before any sound specification for the design of steel stacks can be prepared.

Mr. Sherlock has noted the failure to consider the effects of turbulence at high wind velocities and the probable frequencies of comparatively nonturbulent winds of high velocity. Turbulence will interfere with the uniformity of vortex discharge and generally exists with high velocities. The effect of this turbulence can be termed wind efficiency, the numerical value of which decreases with increasing velocity and is also affected by the terrain. A low wind efficiency is the most plausible reason why the amplitudes in the case described by Mr. Jenney were not serious.

A considerable part of the discussion was based on the Strouhal number. An investigation at Stanford University at Stanford, Calif., under the direction of E. G. Reid indicates that above the critical Reynolds number the amplitudes increase as the square of the velocity except as affected by changes in damping and wind efficiency. These tests gave equal amplitudes at stagnation pressures of 5.25 lb per sq ft and 13.65 lb per sq ft ($\mathbf{R} = 465{,}000$ and $685{,}000$, respectively), indicating that the ratio of 1.71 and 0.66 assumed by the writers for C_L below and above the critical Reynolds number is approximately correct. Mr. Farquharson quotes Mr. Landweber as giving a value for C_L of 3.8 (below the critical Reynolds number) or more than twice the value given by Mr. Steinman.[7]

Mr. Jenney suggests that until firm design criteria become available the use of welded steel stacks should be avoided in favor of reinforced concrete stacks. Especially when area requirements are such that the stacks must be placed on top of building steel, the latter are considerably more expensive. No cases of vibrations of lined stacks with amplitudes sufficient to produce excessive stresses were mentioned by the discussers.

---

[50] Chf. Structural Engr., Power Div., Bechtel Corp., San Francisco, Calif.

[51] Cons. Engr., San Francisco, Calif.

Mr. Pirok questions the values for C_D and the assumption that welded stacks are more subject to vibration than riveted ones. The value of 0.35 for C_D was not intended as a design recommendation; for this purpose, the writers use recommendations for ordinary exposures and increase the specified pressures in locations subject to hurricanes. Mr. Pirok offers additional explanations of excessive vibrations in unlined welded steel stacks.

Mr. Pirok's statement of the relationship between ovalling and cantilever vibrations deserves further investigation. The writers have no comments other than that they believe ovalling is generally a forced vibration, the disturbing force being the vortices discharged at a frequency controlled by the natural frequency of the stack. The writers agree with Mr. Pirok's opinion of external damping devices. Such devices may be economical in the case of completed stacks which are subject to excessive vibrations.

Mr. Vincent furnished considerable detail as to the nature of the disturbing force; he also adds twice the amplitude to the effective diameter of the stack. In the usual case the relationship of the amplitude to the diameter is so small that the correction therefor is minor compared to the other unknowns. Mr. Vincent questions the value of π/δ for the magnification factor. The writers believe this value to be high; a factor of $1/\delta$ corresponds more closely to observations.

Messrs. Vincent and Pagon furnish additional observations as to the forces on leeward stacks. Wind-tunnel tests at values of R above the critical are needed.

Mr. Farquharson adds considerable information as to critical values of R and suggests the addition of "spoilers" which would reduce the intensity of the lateral forces. Both these matters were investigated in the previously cited Stanford tests. These tests indicated an effective system of spoilers but none that appeared more economical than designing the stacks to allow for the dynamic forces.

In the Stanford tests, C_D decreased from 0.9 at $\mathsf{R} = 250{,}000$ to 0.3 at $\mathsf{R} = 600{,}000$. The maximum response at a subcritical Reynolds number occurred at $\mathsf{R} = 425{,}000$ with a Strouhal number of 0.34.

The economical design of steel stacks and circular pressure vessels is important to industry. The writers trust that methods will be found to explore the many unknowns that exist.

AMERICAN SOCIETY OF CIVIL ENGINEERS
Founded November 5, 1852
TRANSACTIONS

Paper No. 2832

RESONANT VIBRATION OF STEEL STACKS

BY ERNEST A. DOCKSTADER,[1] WILLIAM F. SWIGER,[2] AND
EMORY IRELAND,[3] MEMBERS, ASCE

WITH DISCUSSION BY MESSRS. CEDRIC MARSH; AND ERNEST A. DOCKSTADER,
WILLIAM F. SWIGER, AND EMORY IRELAND

SYNOPSIS

Soon after their completion, the steel stacks of the Moss Landing steam plant (south of San Francisco, Calif.,) were excited to violent vibrational movement by a steady wind of moderate velocity. These stacks were conservatively designed in accordance with commonly accepted practice and were capable of withstanding, as a static force, the drag from a wind of several times the velocity which occurred. Investigation indicated that vibration was caused by periodic forces which developed during the formation of von Kármán vortices in the air stream around the stacks. There are cited herein the character and magnitude of the disturbing aerodynamic forces, the investigation and studies made, and the design of corrective measures taken to protect the stacks from similar disturbances in the future.

NOTATION

The letter symbols adopted for use in this paper are defined where they first appear and are arranged alphabetically, for convenience of reference, in the Appendix.

INTRODUCTION

From the early days of civil engineering, the generally accepted practice has been to design bridges, buildings, and other structures to resist wind, on the premise that wind forces could be replaced, for design purposes, by some equivalent system of static loads. Since the beginning of the twentieth century, the rapid growth of airplane design has led to widespread research—both the-

---

NOTE.—Published, essentially as printed here, in November, 1954, as *Proceedings-Separate No. 541*. Positions and titles given are those in effect when the paper or discussion was approved for publication in *Transactions*.

[1] Chf. Structural Engr., Stone & Webster Eng. Corp., Boston, Mass.

[2] Structural Engr., Stone & Webster Eng. Corp., Boston, Mass.

[3] Structural Engr., Stone & Webster Eng. Corp., Boston, Mass.

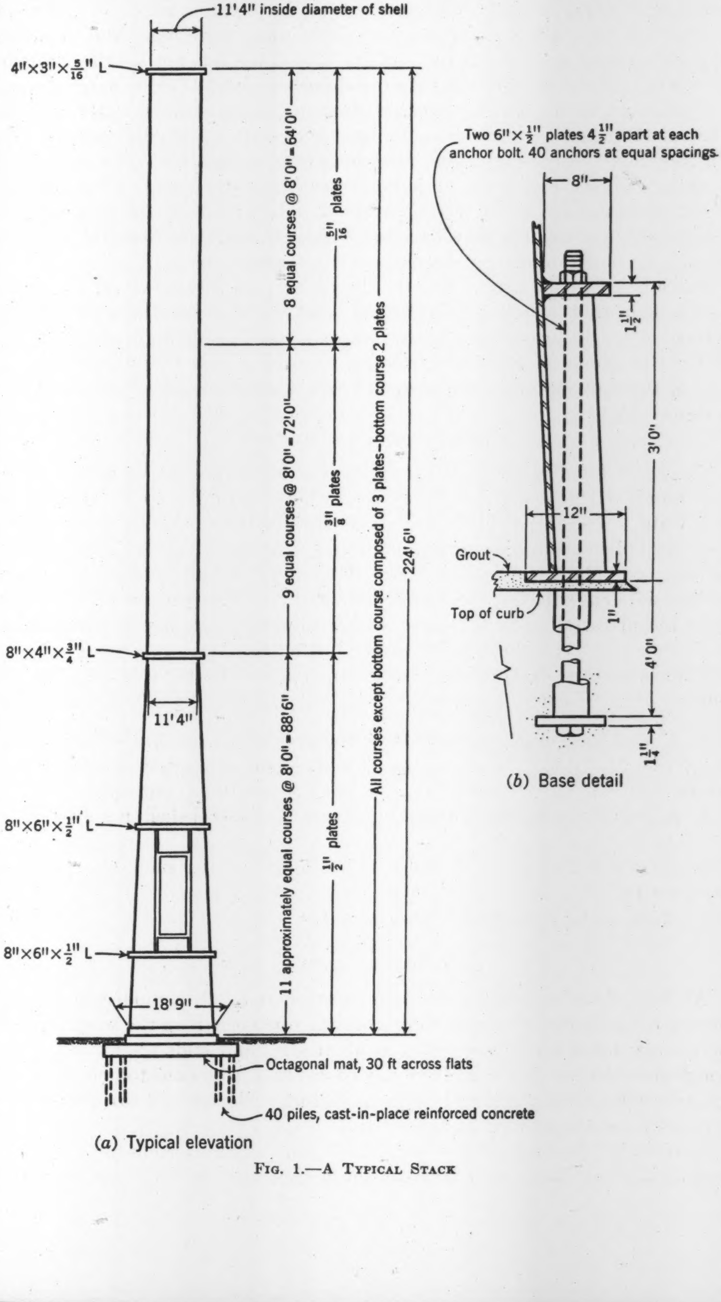
11'4" inside diameter of shell
4"×3"×5/16" L
8 equal courses @ 8'0" = 64'0"
5/16" plates
9 equal courses @ 8'0" = 72'0"
3/8" plates
All courses except bottom course composed of 3 plates–bottom course 2 plates
224'6"
8"×4"×3/4" L
11'4"
11 approximately equal courses @ 8'0" = 88'6"
1/2" plates
8"×6"×1/2" L
8"×6"×1/2" L
18'9"
Octagonal mat, 30 ft across flats
40 piles, cast-in-place reinforced concrete
Two 6"×1/2" plates 4 1/2" apart at each anchor bolt. 40 anchors at equal spacings.
8"
1 1/2"
3'0"
12"
Grout
Top of curb
1"
4'0"
1 1/4"

(*a*) Typical elevation

(*b*) Base detail

FIG. 1.—A TYPICAL STACK

oretical and experimental—with respect to aerodynamic forces. However, the generally satisfactory performance of bridges, buildings, and structures designed to resist wind on the basis of static loadings has not led the structural designer to make extensive use of the developments in the field of aerodynamics.

The dangerous effects to machine elements or structures, if their natural period of vibration happens to be in resonance with a periodic exciting force, even though small in magnitude, have long been recognized. That a wind of moderate velocity can exert periodic forces upon structures or bridges with disastrous results has not been fully appreciated; it required the collapse of the Tacoma Narrows Bridge, near Tacoma, Wash., to focus the attention of bridge designers on the importance of aerodynamic forces.

There are described subsequently the unforeseen serious vibrations experienced at low wind velocities by tall steel stacks. These stacks were conservatively designed in accordance with accepted practice for high wind velocities and for the effects of possible earthquake action. The investigations of the cause of these phenomena, the corrective measures taken, and the conclusions are described.

General Description

The Moss Landing steam plant is situated on the eastern or inshore side of Moss Landing Harbor on Monterey Bay, about 100 miles south of San Francisco, Calif. The initial plant, which consists of three 100,000-kw steam turbines, six boilers, and associated auxiliaries, was completed in 1950. An extension to the plant, consisting of two 100,000-kw steam turbines, two boilers, and associated auxiliaries, was completed in 1953. The primary concern herein is the initial installation stacks of which there are six, one for each boiler. The details of a typical stack are shown in Fig. 1.

The stacks were designed to be self-supporting under the following specifications:

1. A wind load of 25 lb per sq ft on the projected area or a seismic force of 0.2 g; the wind load governed the design. The computed maximum compressive stress in the steel shell on this basis was 6,700 lb per sq in.
2. A ratio of the diameter to the thickness of the steel shell, not greater than 500 to 1.
3. A ratio of any given diameter to the height of the stack above, not less than 1 to 12.
4. Stack plates butt-welded throughout.

Observations

At Moss Landing during the late summer and fall, a moderate wind frequently begins about noon, blowing from the open ocean on the west across the flat unobstructed shore line and the plant site, and ends about 5 p.m. Although the velocity may vary from day to day and from hour to hour on a given day, this wind is characterized by (*a*) a uniform velocity and (*b*) freedom from turbulence for appreciable periods of time.

Late in the afternoon of October 5, 1949, with the steel shells for stacks 2 and 3 completed but unlined and under the action of a moderate wind, a slight breathing or ovalling of short duration was noticed about halfway up the straight section of stack 3.

On the following afternoon with a wind from slightly north of west at an estimated velocity of 25 miles per hr, stack 3 again ovalled or breathed in and out for an appreciable distance above and below the middle of its straight section. No definite measurements were taken, but the movement was noticeable and probably was several inches; it had a definite cadence estimated at 88 times per min. The base of the stack appeared perfectly rigid, and there was no noticeable movement of the top of the stack. A spreader spider was immediately installed inside stack 3 near the midpoint of its straight section.

On the next afternoon, October 7, 1949, a similar wind from slightly south of west at a somewhat higher velocity, possibly from 30 miles per hr to 35 miles per hr, caused no breathing or vibration of stack 3. However, the top of stack 2, which had neither breathed nor moved noticeably previously, swayed back and forth from about 4 in. to 6 in. in regular cadence. This swaying affected stack 2 throughout its entire height and there was evidence that the grout under the base ring had spalled and that a few anchor bolts could be tightened about $\frac{1}{8}$ turn. In no case was it possible to tighten two adjacent anchor bolts. The next day, two $\frac{3}{4}$-in. steel cable guys were installed on opposite sides of stack 2, about 64 ft down from the top, leading to two dead-men ground anchors, one northwest and the other southwest of this stack.

Preparations were made to take instrument readings of stack movements, and an anemometer was installed at the top of stack 2 to record wind velocity. The next observable movement occurred on the afternoon of October 18, 1949, when the most violent movements were experienced. A summary of conditions at this time follows: An internal spreader spider was in place at about the midheight of the straight section of stack 3, and a $\frac{1}{4}$-in. painter's trolley line was attached at the top of this stack on the southwest side but was hanging loose. Stack 2 had no internal spider but had two $\frac{3}{4}$-in. steel guy cables to the dead-men anchors. The steel shell of stack 1, which was completed except for the top 8-ft-high ring, contained no internal spiders and was not guyed. Gunite linings had not been started in any of the stacks.

The wind and attendant swaying of the stacks commenced at about 12:45 p.m. and continued until shortly after 4:00 p.m. The anemometer on the top of stack 2 failed to register. The wind velocity was estimated to be between 30 miles per hr and 40 miles per hr at the ground level and was from slightly north of west. Stack 3 began moving first; the erector crew immediately attached the $\frac{1}{4}$-in. line to a box car which was located near the base of the stack. This was done before instruments were set up to measure the movement. Visual observation indicated that fastening this line to the box car restricted the movement, although it is impossible to estimate to what extent. Stack 2 began moving a few minutes after stack 3. The paths described by the top of both stacks were elongated ellipses, the major axis being north and south or generally at right angles to the direction of the wind. The amplitudes of movement were erratic during the afternoon. Movement would at first be slight, then increase to a maximum which would continue for various lengths of time and then die down. Movements of the stacks were independent of each other.

First one stack would move and then the other; frequently both were swaying. At times movement was in phase, and at other times out of phase. The length of time of any period of movement was varied and did not follow any specific pattern. However, the frequency was constant throughout at from 72 cycles per min to 74 cycles per min. Movements of the top of the stacks at various times during the afternoon were measured with transits and are recorded in Table 1. The maximum observed total sway was more than 32 in.

The guy wires on stack 2 and the painter's trolley on stack 3 absorbed, by stretching, whipping, and movement of their anchorages, appreciable vibrational energy of the stacks, thus limiting amplitudes of vibration. These lines had to be pulled up several times during the afternoon because they elongated. The force transmitted through the painter's trolley rocked the box car to which it was attached so violently that this line was transferred to a heavy caterpillar crane.

TABLE 1.—MOVEMENT OF STACKS[a]

Time of Day	Stack 3[b]			Stack 2[c]		
	Movement at Top from Normal		Total movement, in inches	Movement at Top from Normal		Total movement, in inches
	North, in inches	South, in inches		North, in inches	South, in inches	
1:00 p.m.	14	16	30	15¾	14¼	30
2:00 p.m.	16¾	14¼	31	12	13½	25½
3:00 p.m.	17½	15	32½	13½	15	28½
4:00 p.m.	10¾	9	19¾	8	9½	17½

[a] Wind velocity of 30 miles per hr to 40 miles per hr. Wind direction was north of west. [b] Throughout the observations, stack 3 underwent practically uniform movement to the east and west of approximately 2½ in. in each direction for a total movement of 5 in. [c] Throughout the observations stack 2 underwent practically uniform movement to the east and west of approximately 2 in. in each direction for a total movement of 4 in.

There was appreciable vibration of the base of the stacks and of the concrete foundation. The stack mat at the anchor bolt ring moved vertically by as much as 0.01 ft. On the north side of the foundations of both stacks 2 and 3, the earth cracked over the edge of the foundation mat. Several bolts on the north and south sides of both stacks were sufficiently loosened so that, in a few cases, the nuts could be turned by hand. During periods of maximum stack movement, there was a noticeable squeaking noise at the tops of the bolts. Pieces of grout up to 3 in. long by 1½ in. wide by ⅝ in. deep flaked out from between the stack base and the top of the concrete foundation at the north and south sides of both stacks 2 and 3.

Stack 1, at this time only 8 ft less in height, showed no appreciable vibration or movement. Movements ceased when the wind dropped shortly after 4 p.m. About 4:30 p.m., a squall with heavy rain came up, during which time it was estimated that the wind blew even harder than at any time earlier that afternoon. This wind lasted only a short time, but during this time there was no observable movement of any of the stacks.

Following these violent movements, both stacks 2 and 3 were thoroughly examined. A visual check did not indicate any cracked or broken welds. Welds located at critical points were magnafluxed both inside and outside. This check indicated that none of the welds had been cracked. Two coupons taken at random indicated that full penetration was obtained in the welding. Diameters of the stacks were measured at a number of locations. Maximum variations from specified diameters were $+1\frac{1}{4}$ in. and $-1\frac{1}{2}$ in. Stacks were checked for plumbness at a time when there was no wind or sun, and the maximum deviation was only 0.46 ft. These examinations indicated that the stacks had suffered no permanent distortion or damage.

As a temporary protective measure during the remainder of the construction program and until permanent corrective measures could be taken, all stacks were guyed three ways and at two levels immediately following erection of the stack shell. Also, additional steel stiffener rings were welded to the stacks at intervals of 16 ft throughout the cylindrical part to prevent ovalling. These consisted of 6-in. by 4-in. by $\frac{1}{2}$-in. circumferential angles welded to the stack shell with the 4-in. leg out and turned down.

AERODYNAMIC FORCES

Analysis indicated that the Moss Landing stacks compared favorably in strength and stiffness with numerous stacks throughout the United States which had performed satisfactorily. The rhythmic character of the movement and its dependence on a particular wind condition directed the study to their aerodynamic characteristics.

The drag of a cylinder moving at uniform velocity through a fluid is the sum of frictional forces and of energy losses resulting from eddies set up in the fluid. Between Reynolds numbers, R, of approximately 1,000 and some larger number termed the critical value of the Reynolds number, eddies are shed in a regular pattern from alternate sides of the cylinder. For a nonoscillating cylinder or for a cylinder which vibrates through a small amplitude relative to the diameter of the cylinder, the approximate relations among the distance between eddy paths, d; the distance between eddies in a single path, l; the diameter of the cylinder, D; the velocity of the cylinder, v; the and frequency of eddy formation, f_e are

$$\frac{d}{l} \approx 0.3 \qquad \text{(1a)}$$

$$\frac{d}{D} \approx 1.3 \qquad \text{(1b)}$$

$$\frac{l}{D} \approx 4.3 \qquad \text{(1c)}$$

and

$$f_e \approx 0.2\,\frac{v}{D} \qquad \text{(1d)}$$

The dimensionless ratio,

$$S = \frac{f_e\,D}{v} \qquad \text{(2)}$$

is termed the Strouhal number.

While an eddy is forming, the fluid on the side opposite the eddy has a higher velocity as it passes the cylinder. In accordance with Bernoulli's theorem, this increased velocity must be accompanied by a decrease in pressure. There is consequently a lift or force exerted on the cylinder acting in a direction away from the side on which the eddy is forming. Because the eddies form alternately on opposite sides of the cylinder, the cylinder is subjected to an alternating force of a frequency equal to the frequency of formation of the eddies.

The lift or lateral force P exerted during the formation of vortices may be expressed by the term,

$$P = C_L \rho \frac{v^2}{2} D \ldots\ldots\ldots\ldots\ldots\ldots\ldots\ldots \quad (3)$$

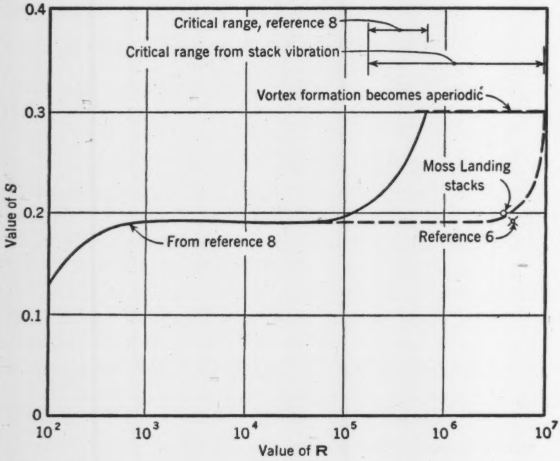

FIG. 2.—RELATIONSHIP BETWEEN THE STROUHAL NUMBER AND THE REYNOLDS NUMBER

in which C_L is the coefficient of lift and ρ is the density of air. It is common in investigations involving periodic vortices to assume that C_L varies as a simple harmonic function. Experimental or analytical determinations of C_L are rather limited.

David B. Steinman, M. ASCE, showed[4] analytically that for an infinitely long, nonoscillating cylinder the maximum value of C_L was 1.71. R. Ruedy derived[5] analytically a maximum value of C_L of 0.93 and has given experimental values of C_L varying from 0.61 to 1.05. Computation of C_L from experimentally determined values of pressure reduction along the sides of cylinders indicates[6,7] C_L equal to 1.13 at **R** = 962,000. These values are the maximum values of C_L in a single cycle.

---

[4] "Problems of Aerodynamic and Hydrodynamic Stability," by David B. Steinman, *Proceedings*, Third Hydr. Conference, Univ. of Iowa, Iowa City, Iowa, 1946, p. 136.

[5] "Vibrations of Power Lines in a Steady Wind," by R. Ruedy, *Canadian Journal of Research*, October, 1935, Vol. 13, No. 4, p. 82.

[6] "What Aerodynamics Can Teach the Civil Engineer," by W. Watters Pagon, *Engineering News-Record*, March 15, 1934, p. 348.

[7] *Ibid.*, July 12, 1934, p. 41.

Above the critical value of **R**, the boundary layer ceases to be laminar and becomes turbulent. This causes the breaking-away point of the eddies to move backward along the body, thus reducing the size of the eddies and the width between eddy trails. Because the vortex trail is stable only for the constant ratio given in Eq. 1*a* reduction in the width between eddy trails d also reduces l and causes a corresponding sharp increase in the frequency and the Strouhal number as shown in Fig. 2.

The actual range of the Strouhal number is not large. J. P. Den Hartog[8] gives the range of S as being between 0.18 and 0.27 for cylinders. A mean value of $S = 0.22$ was used generally in the subsequent analysis. E. F. Relf, and others,[9,10,11,12,13] show that above this critical range the flow becomes turbulent and formation of vortices ceases to be periodic.

The critical Reynolds number is not a sharply defined value but extends over a considerable range, depending on the turbulence in the air stream and on the relative smoothness of the cylinder. Wind-tunnel experiments have indicated[13] that the critical range for **R** lies between 200,000 and 500,000. However, as illustrated in Fig. 2, observations of large diameter stacks by W. Watters Pagon,[6,7] M. ASCE, and at Moss Landing, have shown formation of periodic vortices at $S \approx 0.2$ for Reynolds numbers of approximately 5,000,000.

Resonance of Stacks

The alternating forces exerted upon an elastic cylinder attendant to the forming of periodic vortices in the air stream may cause the cylinder to vibrate either by ovalling—that is, vibration as an elastic ring—or by swaying—that is, vibration as an elastic cantilever. Both types of vibration were noted at Moss Landing, the first movement being ovalling.

The lowest or fundamental frequency of vibration, f, of an elastic ring may be reduced for a steel cylinder to

$$f = 41{,}000 \frac{t}{D^2} \qquad (4)$$

in which t is the thickness of the shell, in inches, and D is the diameter, in feet. Solution of Eq. 4 for the Moss Landing stacks shows a natural frequency of 120 cycles per min for the $\frac{3}{8}$-in. plate and 100 cycles per min for the $\frac{5}{16}$-in. plate sections of the stack.

Because the pressure reductions during the formation of vortices occur alternately on opposite sides of the stack, periodic vortices will excite ovalling at double their own frequency, as illustrated in Fig. 3.

---

[8] "Mechanical Vibrations," by J. P. Den Hartog, McGraw-Hill Book Co., Inc., New York, N. Y., 1934 (revised 1947).

[9] "Singing of Circular and Streamlined Wires," by E. F. Relf and E. Ower, *Reports and Memoranda, No. 825*, Aeronautical Research Committee, London, 1921.

[10] "Frequency of the Eddies Generated by the Motion of Circular Cylinders Through a Fluid," by E. F. Relf and L. F. G. Simmons, *Reports and Memoranda, No. 917*, Aeronautical Research Committee, London, 1924.

[11] "On the System of Vortices Generated by a Circular Cylinder in Steady Motion Through a Fluid," by C. N. H. Lock, *Reports and Memoranda, No. 986*, Aeronautical Research Committee, London, 1925.

[12] "The Strength and Position of the Eddies Behind a Circular Cylinder," by A. Thorn, *Reports and Memoranda, No. 1373*, Aeronautical Research Committee, London, 1931.

[13] "Modern Developments in Fluid Dynamics," by S. Goldstein, Clarendon Press, London, 1938, Vols. I and II.

The vortex frequency of Theodor von Kármán, Hon. M. ASCE, for a wind velocity of 25 miles per hr and an 11.4-ft-diameter cylinder would be 42 cycles per min at a Strouhal number of 0.22. Twice this would be 84 cycles per min which is reasonably close to the frequency of 88 cycles per min observed on October 6. It is believed that pressure variations from vortices forming at a Strouhal number of $S \approx 0.22$ excited near-resonant ring vibrations of these stacks, thus causing the ovalling.

Swaying occurred on October 7 and again on October 18, the amplitude on the latter date being much greater and the record more complete. The wind velocity on October 18 near ground level was estimated to be from 30 miles per hr to 40 miles per hr. The frequency of the vortices computed from Eq. 1*c* for a wind velocity of 40 miles per hr and a stack diameter of 11.4 ft is 68 cycles per min at a Strouhal number of 0.22. The observed frequency of vibration for stacks 2 and 3 was from 72 cycles per min to 74 cycles per min which is in reasonably close agreement with the value derived previously.

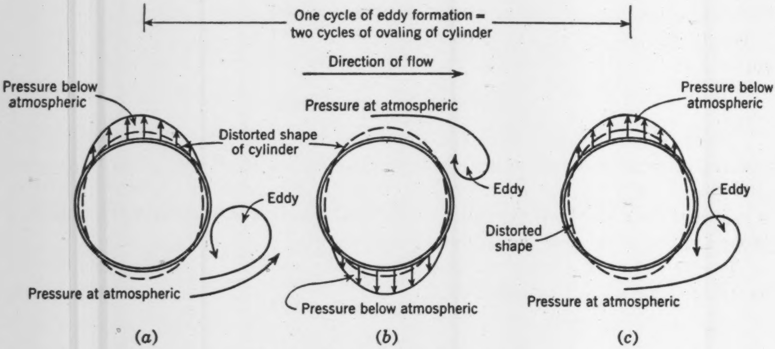
One cycle of eddy formation = two cycles of ovaling of cylinder
Direction of flow
Pressure below atmospheric
Distorted shape of cylinder
Pressure at atmospheric
Eddy
Pressure at atmospheric
Eddy
Pressure below atmospheric
Pressure below atmospheric
Eddy
Distorted shape
Pressure at atmospheric
(a)
(b)
(c)

FIG. 3.—OVALLING OF A CYLINDER

Rigorous computation of the frequency of vibration of these stacks as cantilevers would be extremely complicated because of the variable moment of inertia and the variable mass. However, reasonably close approximations can be made by several methods such as the Rayleigh-Ritz method. An easier method of approximation results from the fact that it can be shown, for inch-pound units, that the fundamental frequency f of a uniform cantilever is approximately

$$f = 11.8 \sqrt{\frac{K}{m}} \quad \ldots\ldots\ldots\ldots\ldots\ldots (5)$$

in which K is the stiffness in terms of the total force uniformly distributed over the length that is required to deflect the cantilever 1 in. at the top, and m is the total mass, F/g, when F equals the weight in pounds and g is acceleration due to gravity (386 in. per sec²). For the unlined stacks, K was computed to be 12,400 lb per in., F was approximately 150,000 lb, and f equaled 67 cycles per min.

This frequency includes the effect of the variable stiffness but does not include the effect of the distribution of mass because of the variable plate thickness and flared base. The actual distribution of mass would cause a slightly higher natural frequency, and the rotation of the concrete foundation would cause a lower natural frequency.

The computed frequency of the vortices and the computed natural frequency of the stacks were in reasonable agreement with the observed type of motion and observed frequency of stack swaying. It was concluded that swaying of these unlined stacks was caused by resonant vibrations actuated by the forces attending the formation of periodic vortices in a steady air stream.

Computations using available data with respect to the elastic properties of the lining indicated that the natural frequency of the stacks after lining would be somewhat lower than that of the unlined stacks. Consequently, after lining, the stacks would be resonant with winds of somewhat lower velocities—which might occur more frequently.

Because the internal friction or damping of concrete is many times that of steel, it was anticipated that the lined stacks would have appreciably more damping than the unlined stacks. The logarithmic damping decrement[8] of the lined stack was computed[14] to be 0.08 according to available data on the damping characteristics of concrete and ignoring foundation damping. Although this damping would limit vibration, computations indicated that the amplitude would be excessive. Further analysis showed that variations in thickness of the lining within the limits indicated by stresses in the shell and foundation under earthquake loads would not change the damping decrement sufficiently to bring the computed amplitudes of vibration within acceptable limits.

Because of the location and climatic conditions, the Moss Landing site is subject to steady, nonturbulent winds of near-resonant velocity a number of times during a year. It was considered probable, therefore, that unless corrective measures were undertaken resonant vibration would again occur with probable damage to one or more stacks. Consequently, complete protection against the effects of periodic vortices was considered essential.

CORRECTIVE MEASURES

Resonant vibration of elastic structures may be limited or prevented by (*a*) removing the source of vibration, (*b*) changing the resonant frequency of the elastic structure so that it is no longer resonant with the driving forces, or (*c*) providing damping to absorb and dissipate the energy of vibration.

A system of fins or spoilers on the stack to prevent the formation of vortices was considered. Some experimental work had been done on submarine periscopes at $\mathsf{R} \approx 4{,}000$ which indicated that spoilers in order to be effective would have to extend about one diameter from the cylinder. Such spoilers attached to the upper part of the stacks would have increased the maximum wind resistance sufficiently to overstress the stack shells and foundations. Other information indicated that smaller spoilers might be effective but this hypothesis was unsupported by experimental data and, until proved, could not be depended on; this procedure was therefore eliminated.

---

[14] "Structural Damping in Suspension Bridges," by Friedrich Bleich and L. W. Teller, *Transactions*, ASCE, Vol. 117, 1952, p. 165.

The maximum wind velocity, in the records studied, at which periodic vortex-induced vibration of stacks has occurred, is approximately 60 miles per hr. Close to the earth's surface, winds having a velocity in excess of approximately 60 miles per hr to 65 miles per hr probably are sufficiently turbulent to prevent the formation of periodic vortices for cylinders having diameters causing Reynolds numbers of more than 1,000,000. From this, it has been concluded that stacks should be free of vortex-induced vibration if they are made so stiff that their fundamental frequency as a cantilever or twice their fundamental frequency as a ring were equal to or greater than the frequency of eddy formation for a wind velocity of 70 miles per hr computed for a Strouhal number of 0.22 (80 miles per hr if S is selected equal to 0.19).

The arrangement of the Moss Landing stacks is such that a conventional guying system for each stack, using normal size guy wires, would seriously interfere with normal plant operations at ground level. Furthermore, such guys would not theoretically increase the natural frequency of the stacks sufficiently to eliminate the start of resonant stack movement. Because the guyed stacks would be an elastic system, under resonant periodic forces resulting from the wind, they could be set into a vibration which would theoretically increase until sufficient damping developed from stretching of the guys to limit the vibration at some value. Thus, during each period of vibration the guys would have to be tightened to remove the stretch caused by the vibration in order to prevent excessive amplitude of movement. This method would suffice for temporary protection, but it was not considered satisfactory as a permanent measure.

Methods of increasing the stiffness of the stacks sufficiently by portal bracing and by rigid bracing to the powerhouse to make them nonresonant with winds below 70 miles per hr did not appear practical or economical because of the difficulty of accommodating thermal movements of the individual stacks. Because increasing the stiffness of these stacks sufficiently to eliminate resonance did not appear practical or economical, attention was turned to damping systems in which the energy input of the periodic forces would be absorbed.

Swaying would not be entirely eliminated by the damping system because energy can be dissipated by the dampers only when there is movement. However, by providing the proper degree and type of damping, the amplitudes of vibration would be limited to values well below normal deflections in high winds. Limitation of the double amplitudes of vibration to approximately 2 in. at the top was found entirely practicable and was considered desirable from the psychological effect and for the protection of the gunite lining.

It can be shown that, for an elastic cantilever W, the energy input per cycle —caused by a simple harmonic force applied uniformly along the length of the cantilever and having a maximum value of w per unit length acting in resonance with the vibration of the cantilever—is

$$W = \frac{2\pi}{5} y\, w\, L \qquad (6)$$

in which y is the elastic deflection of the end of the cantilever under a uniform static load of w per unit length and L is the length of the cantilever. For stacks, w is equal to the lift, P, developed during formation of the vortices (Eq. 3). As previously outlined, the value of C_L is only imperfectly established. On the basis of available data and considering circulation over the top of the stacks, a value of $C_L = 1.0$ was assumed herein. Computation of the fundamental frequency after lining gave a value of 55 cycles per min for an assumed modulus of elasticity of 2,000,000 lb per sq in. for the 2-in. gunite lining. This would correspond to a wind velocity of 32 miles per hr for $S = 0.22$ or of 37 miles per hr for $S = 0.19$.

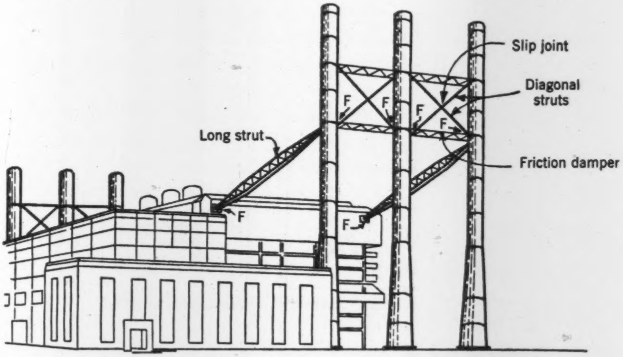
Slip joint
Diagonal struts
Long strut
Friction damper
F
F
F
F
F
F

(a) Arrangement of damping system

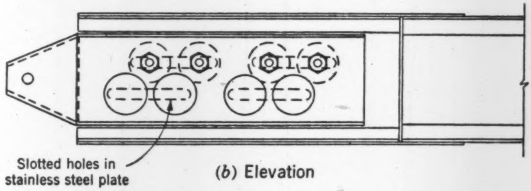
Slotted holes in stainless steel plate

(b) Elevation

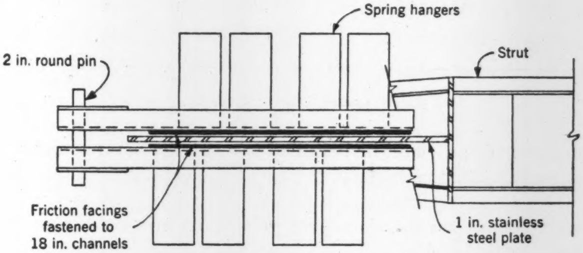
Spring hangers
2 in. round pin
Strut
Friction facings fastened to 18 in. channels
1 in. stainless steel plate

(c) Plan

Fig. 4.—Details of Friction Damper

A wind velocity of 40 miles per hr was selected for design of the damping system, for which $w = 45.6$ lb per ft of height of the cylindrical part of the stack. From Eqs. 3 and 6, $W = 1{,}070\ y$ ft-lb per cycle.

A damping system using viscous dampers, such as are found in hydraulic shock absorbers, could have been used. Although viscous damping is smoother, dry-friction damping is more effective in limiting small amplitudes of motion at low velocities. Also, it was believed that a friction-type damper system would require less maintenance and could be installed in a simpler arrangement. The final design was prepared using friction dampers; the arrangement is shown in Fig. 4.

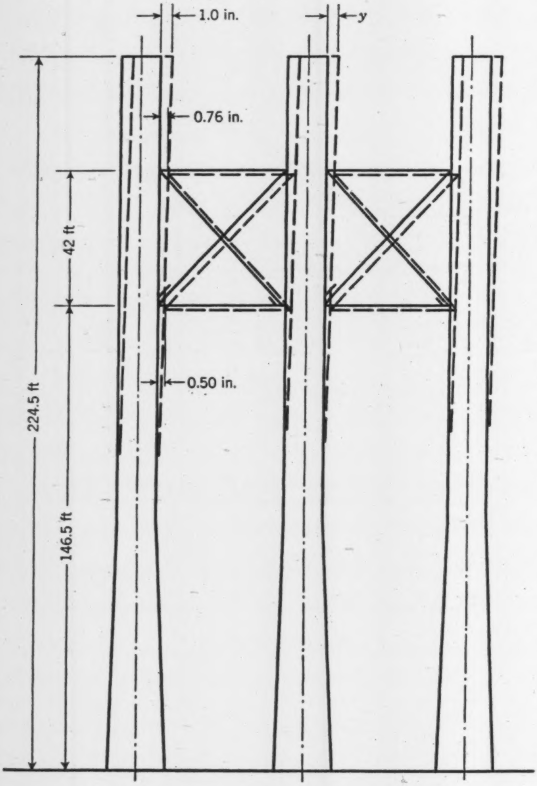

Fig. 5.—Relative Deflections

For each group of three stacks, there are two sets of horizontal trusses which are pin-connected to the stacks. These trusses permit vertical movement of any individual stack but force the three stacks to move in unison in the north-south direction. Crossed diagonals are provided with friction connections at their lower ends to form the damping system in the north-south direction. The diagonals are not connected to each other where they cross. The friction forces in the connections are not large enough to restrict thermal expansion of any stack.

Long struts with friction connections are provided, extending from the two end stacks to the boiler-supporting structure. The struts with the horizontal trusses form the damping system in the east-west direction.

For movements in a north-south direction in the plane of the stacks, the lengths of the diagonals change by some amount x which is proportional to the deflection y of the tops of the stacks. These values for the limiting deflections selected for the Moss Landing stacks are shown in Fig. 5. This change in length of the diagonals causes slippage of the friction connections at their lower ends. The total energy, W_{td}, dissipated in $\frac{1}{4}$ cycle by four dampers for three stacks is determined from

$$W_{td} = 4\,(x - \Delta x)\,P_f \qquad \text{(7)}$$

in which P_f is the frictional force of each damper and Δx is the elastic shortening of the struts for the frictional force developed at each connection. By selecting P_f properly, the energy dissipated in each cycle could be made equal to or larger than the energy put into the system by the wind. Similarly, in the direction perpendicular to the plane of the stacks, energy is dissipated in the dampers at the boiler house. It was convenient to use commercially available springs and friction materials to dissipate about 10% more energy per cycle than would be put into the stacks by a wind of 40 miles per hr. There also is some additional damping provided by the stack lining and by the structural connections.

An available industrial friction material with a nominal coefficient of friction of approximately 0.45 was chosen for the friction dampers. It was found that the nominal coefficient of 0.45 was based on dynamometer tests of kinetic friction set up in the manner of common industrial usage with braking at high speed and, consequently, at high temperatures. Tests indicated that at low speeds the coefficients of both static and kinetic friction would be about half this value. A coefficient of friction of 0.2 was used in the design.

All structural members and connections were designed for more than three times the design friction forces without exceeding allowable working stresses. This was done to provide a factor of safety should the coefficient of friction in the friction material increase from the value of 0.2 at low loading velocities to the value of 0.45 or higher.

VIBRATION TESTS

In the foregoing analysis, it was shown that on a theoretical basis the installation of 2-in. gunite linings could not be depended on to reduce stack vibrations to acceptable safe limits under the conditions which exist at Moss Landing. However, there was practically no experimental data to substantiate this conclusion.

It was suggested that full-scale tests be made on the Moss Landing stacks to determine the actual natural periods of the stacks in both unlined and lined conditions, together with the damping characteristics present in both conditions. Although stacks 2 and 3 were the ones that had shown excessive movement under wind forces, these stacks were placed in service almost immediately after their linings had been completed and it was decided to make the tests on stack 6. For each test the stack was deflected a predetermined distance and was suddenly released. The stack was tested in a north-south direction and in an east-west direction. For each test the frequency of vibration and the decay curve were established.

TABLE 2.—TRANSIT OBSERVATIONS OF VIBRATION DAMPING OF UNLINED STACK 6

Run	OBSERVATIONS					COMPUTATIONS		
	Frequency, in cycles per second	Zero on rod, in feet	Reading on rod, in feet	Single amplitude, in feet	Cycles from release	Amplitude ratio, Y_2/Y_1	Increment of cycles	Damping decrement, $1-(Y_2/Y_1)^{1/n}$
				NORTH-SOUTH VIBRATION				
		10.85	10.70	0.15	17			
1	68	10.87	10.80	0.07	59	0.467	42	0.018
		10.88	10.90	0.02	96	0.286	37	0.033
Mean						0.133	79	0.025
		10.85	10.70	0.15	16			
2	68	10.87	10.80	0.07	55	0.467	39	0.019
		10.87	10.90	0.03	89	0.428	34	0.025
Mean						0.200	73	0.022
		10.86	10.70	0.16	13			
3	68	10.87	10.80	0.07	49	0.438	36	0.023
		10.88	10.90	0.02	76	0.286	27	0.045
Mean						0.125	63	0.032
				EAST-WEST VIBRATION				
		8.01	7.70	0.31	7			
4	66	8.01	7.80	0.21	12	0.677	5	0.075
		8.01	7.90	0.11	51	0.524	39	0.016
Mean						0.355	44	0.023
		8.02	7.70	0.32	6			
5	66	8.02	7.80	0.22	12	0.687	6	0.061
		8.02	7.90	0.12	41	0.545	29	0.021
Mean						0.375	35	0.028
		8.00	7.70	0.30	7			
6	66	8.00	7.80	0.20	16	0.667	9	0.044
		8.00	7.90	0.10	43	0.500	27	0.025
Mean						0.333	36	0.030
		8.02	7.70	0.32	7			
7	66	8.02	7.80	0.22	15	0.687	8	0.046
		8.02	7.90	0.12	42	0.545	27	0.022
Mean						0.375	35	0.028
Average								0.027

To measure the vibration, SR-4 strain gages were placed just above the bell as this was the point of maximum stress. A gage located on the axis parallel to the movement of the stack was attached to a strain indicator, and a motion picture was taken of the movement of the needle. In a supplementary method engineers' transits were used. Two sections of a level rod were attached in a horizontal position to the top of the stack, one extending north and south for the tests in the north-south direction and one extending east and west for the tests in the east-west direction. Several transits were set on a rod reading approximately on the center line of the stack. When the stack was deflected and released, each transitman counted the number of cycles from the time of release until a predetermined amplitude was coincident with his line of sight. These data established a number of points along the decay curve, and from them the decay curves of each test were plotted.

TABLE 3.—TRANSIT OBSERVATIONS OF VIBRATION DAMPING OF LINED STACK 6

Run	Observations					Computations		
	Frequency, in cycles per minute	Zero on rod, in feet	Reading on rod, in feet	Single amplitude, in feet	Cycles from release	Amplitude ratio, Y_2/Y_1	Increment of cycles	Damping decrement, $1-(Y_2/Y_1)^{1/n}$
NORTH-SOUTH VIBRATION								
1	50	11.00	10.75	0.25	3			
			10.80	0.20	8	0.800	5	0.044
			10.85	0.15	15	0.750	7	0.040
			10.90	0.10	26	0.667	11	0.036
			10.95	0.05	48	0.500	22	0.031
Mean						0.200	45	0.035
2	50	11.00	10.75	0.25	4			
			10.80	0.20	9	0.800	5	0.044
			10.85	0.15	14	0.750	5	0.056
			10.90	0.10	26	0.667	12	0.033
			10.95	0.05	47	0.500	21	0.033
Mean						0.200	43	0.037
3	50	11.00	10.75	0.25	3			
			10.80	0.20	9	0.800	6	0.036
			10.85	0.15	15	0.750	6	0.047
			10.90	0.10	27	0.667	12	0.033
			10.95	0.05	45	0.500	18	0.038
Mean						0.200	42	0.038
EAST-WEST VIBRATION								
4	48	8.00	7.75	0.25	2			
			7.80	0.20	5	0.800	3	0.072
			7.85	0.15	9	0.750	4	0.069
			7.90	0.10	19	0.667	10	0.040
			7.95	0.05	34	0.500	15	0.045
Mean						0.200	32	0.049
5	48	8.00	7.75	0.25	3			
			7.80	0.20	7	0.800	4	0.054
			7.85	0.15	11	0.750	4	0.069
			7.90	0.10	22	0.667	11	0.036
			7.95	0.05	38	0.500	16	0.042
Mean						0.200	35	0.045
6	48	8.00	7.75	0.25	3			
			7.80	0.20	7	0.800	4	0.054
			7.85	0.15	12	0.750	5	0.056
			7.90	0.10	22	0.667	10	0.040
			7.95	0.05	42	0.500	20	0.033
Mean						0.200	39	0.040
Average								0.041

To deflect the stack in the north-south direction, a wire line was connected horizontally between the tops of stacks 5 and 6. A downhaul line was attached near the midpoint of the horizontal line which, when loaded, pulled the stacks together. A strain link was provided in the line near stack 6 to measure the load required to deflect the stack. A quick-release hook tripped from the ground released the stack sharply, permitting it to vibrate freely and with a minimum of interference. Stack 6 was deflected in an east-west direction by pulling it with a line attached to the boiler house.

TABLE 4.—STRAIN-GAGE RECORDS OF VIBRATION DAMPING OF STACK 6

Run	Frequency, in cycles per second	Amplitude, in micro-inches	Time from release, in seconds	Amplitude ratio, Y_2/Y_1	Increment of time, in seconds	Increment of cycles	Damping decrement, $1-(Y_2/Y_1)^{1/n}$
UNLINED, EAST-WEST VIBRATION							
7	66	120	2				
		100	5	0.833	3	3.3	0.054
		40	26				
		20	46	0.500	20	22	0.031
Mean				0.167	44	48.4	0.036
LINED, NORTH-SOUTH VIBRATION							
2	50	120	2				
		100	9	0.833	7	5.83	0.031
		40	36.5				
		20	52	0.500	15.5	12.9	0.052
Mean				0.167	50	41.7	0.042
3	50	120	6				
		100	10.5	0.833	4.5	3.8	0.047
		40	32				
		20	43.5	0.500	11.5	9.58	0.070
Mean				0.167	37.5	31.3	0.056
LINED, EAST-WEST VIBRATION							
4	48	120	8.5				
		100	13.5	0.833	5	4	0.045
		40	41				
		20	57.5	0.500	16.5	13.2	0.060
Mean				0.167	49	39.2	0.045
5	48	120	1				
		100	7	0.833	6	4.8	0.037
		40	29				
		20	41	0.500	12	9.6	0.070
Mean				0.167	40	32	0.054
6	48	120	5.5				
		100	11	0.833	5.5	4.4	0.042
		40	37.5				
		20	54.5	0.500	17	13.6	0.050
Mean				0.167	49	39.2	0.045
Average							0.048

The first series of tests was made on the unlined shell of stack 6 on January 6 and 7, 1950. The lining of stack 6 was completed on March 17, 1950, and the second series of tests was made on April 17, 1950. The weather for both series was satisfactory, with little or no wind. The observations of the decay of vibration by transit and the computed damping decrements are given in Tables 2 and 3.

The motion picture observations of the decay of vibration of a strain indicator attached to a SR-4 gage and damping decrements computed from these observations are given in Table 4. Only one successful observation was made by this method on the unlined stack, and five successful observations were made on the lined stack.

It is mathematically convenient to investigate damping by assuming that, for short intervals at least, the damping approximates viscous damping. For true viscous damping, the amplitude of each cycle has a constant ratio to the amplitude of the preceding cycle. The ratio of the reduction in amplitude to the amplitude, which is termed the damping decrement, can be expressed as

$$\delta = 1 - \frac{y_{n+1}}{y_n} \qquad (8a)$$

and for n number of cycles

$$\delta = 1 - \left(\frac{y_n}{y}\right)^{1/n} \qquad (8b)$$

The average damping decrement for the steel shell was found to be 0.027, and the average damping decrement of the stack with lining was found to be 0.045—less than the estimated value of 0.08.

Values of the damping decrement were quite erratic in the various tests. There was an indication that it was not constant, which would be the case for true viscous damping, but that it increased with amplitude. Averaging all test results for the lined stacks indicates an average damping decrement in the lined condition varying from $\delta = 0.02$ at zero amplitude to $\delta = 0.068$ at an amplitude of 4 in. This trend, if extrapolated, gives a value of $\delta = 0.15$ at an amplitude of 10 in.

The fundamental frequency of the completed stack had been computed at 55 cycles per min, assuming $E = 2{,}000{,}000$ lb per sq in. for the gunite lining. The actual frequency was 49 cycles per min. which corresponds with the frequency of eddy formation for a wind velocity of 29 miles per hr at a Strouhal number of 0.22. The input energy W per cycle for this wind velocity would be 556 y ft-lb per cycle.

Computation of the stiffness of the stack after lining from the observed frequency indicated that the lining increased the stiffness by only 5%. The energy dissipated by viscous damping per cycle, ΔW, is given by

$$\Delta W = 2\,\delta\,W_{ta} \qquad (9)$$

in which W_{ta} is the total accumulated energy at the end of any cycle which is equal to the potential energy at the point of maximum deflection. For the lined stack, based on the stiffness obtained in the tests, W_{ta} is equal to 216 y^2 ft-lb for any amplitude of vibration. Then the energy dissipated per cycle is

$$W = 2\,\delta\,216\,y^2 \qquad (10)$$

Under steady-state excitation, vibration of these stacks as individual structures would build up until the energy dissipated in each cycle of vibration just equaled the input energy of the wind forces. The energy input per cycle at various wind velocities and that dissipated per cycle for various degrees of damping are shown graphically in Fig. 6.

The energy dissipated by damping at $\delta = 0.045$, the average value found in tests on the lined stack, is so small that (Fig. 6) the resulting amplitude of vibration would be so large as to destroy the protective gunite lining and probably result in failure of the stack shell. As noted, there was some indication that the damping increased with amplitude, possibly reaching $\delta = 0.15$ at an amplitude of about 10 in. Assuming this damping did develop, it would limit vibration of the stacks to an amplitude of about 9 in. for a wind of 29 miles per hr. Continued vibration of this amplitude would undoubtedly cause severe cracking of the lining.

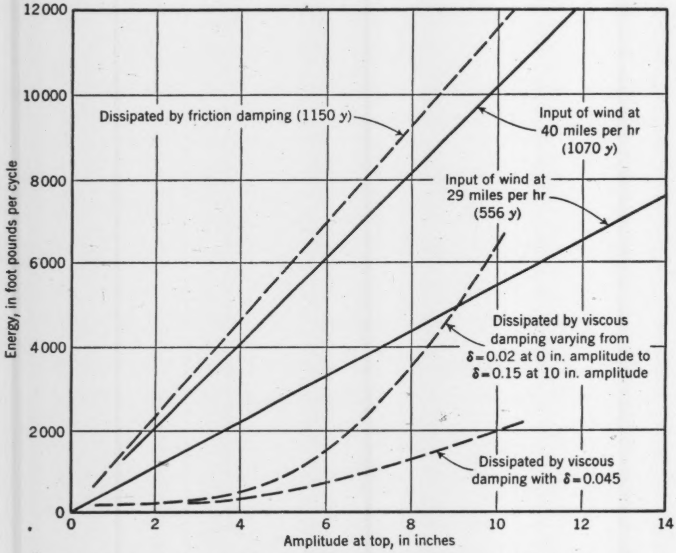

FIG. 6.—ENERGY INPUT OF WIND AND ENERGY DISSIPATED BY VISCOUS DAMPING

The foregoing analyses have been based on steady-state conditions. The wind, even under the very uniform conditions at Moss Landing, is never perfectly constant. The time required to build up to excessive vibrational amplitudes was also investigated. The energy stored in the stack at its point of maximum deflection at any cycle of vibration is equal to the potential energy at the same point of the previous cycle, plus input energy during the cycle, less the energy dissipated by damping during the cycle.

Computations indicated that, for a damping decrement increasing uniformly from $\delta = 0.02$ at zero amplitude to $\delta = 0.15$ at 10-in. amplitude, vibration of these stacks without an external damping system would build up very quickly, reaching almost maximum amplitude within 20 sec. Steady-state winds of several times this duration and of critical velocity may be expected many times in the life of these stacks. Also, investigations as reported[4] by Steinman have shown that once movement has begun eddy formation tends to be self-exciting and will continue at constant frequency, even though the stream velocity changes appreciably.

This analysis has assumed that the force developed by the formation of the vortices was uniform from top to bottom of the stack. This is conservative because vortices possibly are not formed near ground level. However, it can be shown from the deflection curve of the stack that the energy input from the bottom third, assuming uniform load, is only 4% of the total energy input in any one cycle.

This test program showed that damping in the gunite-lined stacks was actually less than that computed from available data on the damping effect of concrete. This verified the conclusions that the lining alone, either as designed or for a reasonable increase in thickness, would not provide sufficient damping to limit the vibration acceptably and that a suitable external damping system was necessary. The additional stiffness under dynamic loading contributed by the lining was surprisingly small.

Design of an Independent Self-Supporting Stack

For the extension to this station, it was necessary to erect two additional stacks of larger diameter so arranged that a damping system would have been expensive and difficult to install. These new stacks were designed to be nonresonant with the eddy frequency for all wind velocities below 70 miles per hr. For maximum economy these stacks were tapered from top to bottom. The average diameter of the top 25% was used in computing the eddy frequency as this contributes the greatest part of the driving energy. These stacks are 224.5 ft high with a base diameter of 27 ft 8 in. and a top diameter of 12 ft 8 in. inside the 2-in. gunite lining.

It might appear from the foregoing analyses that the use of a tapering section would automatically prevent formation of eddies because their frequency would be changing continuously with the stack diameter. Actually, test data indicate that the width of the eddy trail and the Strouhal number are not rigidly fixed but can vary moderately. Consequently, an appreciable length of a tapered stack could be acted upon by vortices of uniform frequency. Thus, even a tapered stack, if it had a natural frequency resonant with the frequency of eddy formation for its upper quarter, could be excited to excessive amplitudes of vibration.

Conclusions

Steel stacks of many diameters and heights have been used for many years throughout the United States. However, reports of serious stack vibration at moderate wind velocities were rare until recently (1955) when increasing instances of this phenomenon were being experienced. It also appears significant that until recent years most steel stacks were of riveted construction.

Review of published experimental data and theory concerning vortices indicates that formation of the vortices is primarily a shape function below

Reynolds numbers of approximately 200,000. However, for Reynolds numbers in excess of approximately 1,000,000, formation of the vortices is in a condition of critical instability. This suggests that relatively small spoilers tripping only the boundary layer would protect stacks of conventional size and design against formation of periodic vortices. This may explain why riveted stacks, which are much rougher than butt-welded stacks because of lap joints and rivet heads, have apparently been almost free from vortex-induced vibration. Unfortunately, very little if any experimental work has been done at these very large Reynolds numbers, and consequently this hypothesis is not supported by experimental data. The possibility that small spoilers would be effective should be investigated fully.

However, until the effect of surface roughness on eddy formation is demonstrated, it is believed that increasing instances of phenomena similar to those described and analyzed herein should lead designers of steel stacks, whether riveted or butt-welded, to consider carefully the possibility that the forces caused by eddy formation may be present. Available information indicates that eddies form only in steady, nonturbulent air streams. Consequently, sites located on flat terrain or adjacent to large bodies of water offer favorable conditions for eddy formation, with the attendant hazard of resonant vibration, unless the stack is designed to be nonresonant for wind velocities below the critical range of eddy formation. Conversely, sites in rugged terrain or where there are other adjacent structures provide less favorable conditions for eddy formation, although the possibility should not be overlooked that an appreciable part of the upper portion of a tall stack may be above the turbulent air flow.

Available data indicate that stacks designed to be nonresonant with the frequency of eddies for wind velocities below 70 miles per hr should not experience difficulty. Consideration must be given to both vibration as an elastic cantilever and vibration as an elastic ring. In the latter case, the eddies will induce vibration at twice their own frequency.

The magnitude of lateral forces induced by eddy formation is uncertain. Reported experimental and theoretical values of C_L range from 0.65 to 1.71. Rigorous experimental determination of C_L at high Reynolds numbers and laminar-flow conditions for nonoscillating cylinders would be of considerable value in resolving this uncertainty.

Damping and additional stiffness from the gunite lining which was about 2 in. thick were surprisingly small. For the stacks described, this damping was insufficient to limit acceptably the vibration. The basic principles and criteria of design of a damping system which has proved satisfactory have been outlined.

ACKNOWLEDGMENTS

The Moss Landing plant was designed and constructed by the Stone & Webster Engineering Corporation of Boston, Mass., in collaboration with the Pacific Gas and Electric Company of San Francisco.

The test program described was suggested by and performed in collaboration with and at the expense of the Pacific Gas and Electric Company. Ferdinand F. Mautz, A. M. ASCE, and Mr. Swiger supervised the tests. At the time of the test program, I. Cleveland Steele, M. ASCE, was vice president in charge of

engineering. Mr. Steele has been succeeded by Walter Dreyer, M. ASCE. Carl Appleford, M. ASCE, supervising civil engineer, represented the company in matters relating to these stacks. Mr. Den Hartog served as consultant on the design of the vibration damping system.

APPENDIX. NOTATION

The following symbols, adopted for use in the paper and for the guidance of discussers, conform essentially with "American Standard Letter Symbols for Structural Analysis" (ASA Z10.8-1949), prepared by a committee of the American Standards Association with Society representation, and approved by the Association in 1949:

C_L = coefficient of lift;
D = diameter of the cylinder;
E = modulus of elasticity;
F = weight;
f = fundamental frequency;
f_e = frequency of eddy formation;
g = acceleration of gravity;
K = stiffness;
L = length of the cantilever;
l = distance between eddies in a single path,
m = mass;
P = lift or lateral force;
P_f = frictional force;
R = Reynolds number;
S = Strouhal number;
t = thickness of shell;
v = velocity of cylinder or of wind;
W = input energy:
  W_{ta} = total accumulated energy at the end of any cycle;
  W_{td} = total energy dissipated in $\frac{1}{4}$ cycle by four dampers;
w = force per unit length;
x = change in length of diagonals;
y = elastic deflection of end of cantilever;
δ = logarithmic decrement; and
ρ = density of air.

DISCUSSION

Cedric Marsh[15].—The problem of wind-induced vibration is far from being a new one but it is equally far from being satisfactorily resolved.

The writer encountered a case identical to that described by the authors in the design of a welded 100-ft-high tubular aluminum tower with a base diameter of 4.5 ft. During the design stages, a thorough study of the possibility of forced vibration was made, but—although the natural frequency of towers, the period of wind impulses, and the energy input by the wind can all be computed more or less accurately—there is little or no information available on the actual energy absorbed by a tower itself, thus making it impossible to establish what would be the maximum steady amplitude of the tower when subjected to reasonant impulses. In the writer's own case, one of the design considerations was that, when vibrating in the steady state, the maximum stress would not exceed the fatigue strength of the welded joints, but only after the tower was erected and field tests performed was it possible to establish that the energy absorbed by the tower was sufficient to restrict the amplitude to the necessary limits.

Information on the damping characteristics of towers being so scarce, it is worth recording that the damping decrement for this aluminum tower varied from 0.05 at a 6-in. amplitude to 0.1 at a 12-in. amplitude, the natural frequency being 46 cycles per min. This range is surprisingly similar to that for the steel stack despite the different proportions of the structures, and it would appear that for design purposes a value of 0.1 for the damping decrement may be assumed in establishing the magnitude of the steady amplitude.

Another feature of interest concerning the aluminum tower is that, although vibrations occur usually at wind speeds of between 6 miles per hr and 10 miles per hr, they also arise in a range of wind speeds between 40 miles per hr and 45 miles per hr—that is, when the impulses from eddies are some five times that of the tower although at this wind speed the impulses should not be periodic. The steady amplitude is only slightly greater than for the oscillations at the lower resonant wind speeds as the energy input is of the same order.

Ernest A. Dockstader,[16] William F. Swiger,[17] and Emory Ireland,[18] Members, ASCE.—The general mechanism of vortex-excited resonant vibration of individual tall stacks and similar structures seems well established. The assembly of data which may be used in the design of such structures, however, has just been begun (as of 1955). It is important to obtain additional information concerning (*a*) the damping characteristics of various types of structures and their foundations, (*b*) the coefficients of lift for the computation of exciting forces, (*c*) the mutual interference or effects of several stacks, and (*d*) the effects of boundary-layer tripping devices on vortex formation.

---

[15] Chief of Design, Aluminum Laboratories, Ltd., Geneva, Switzerland.

[16] Chf. Structural Engr., Stone & Webster Eng. Corp., Boston, Mass.

[17] Structural Engr., Stone & Webster Eng. Corp., Boston, Mass.

[18] Structural Engr., Stone & Webster Eng. Corp., Boston, Mass.

The data supplied by Mr. Marsh concerning the damping of an aluminum tower in Switzerland are most welcome as they furnish damping characteristics of a structure of markedly different proportions and of different material than the stacks which have been reported on previously. Internal damping in a welded aluminum structure should account for only a small part of the total values reported by Mr. Marsh. External damping for such a structure could originate in the foundation or from air drag. Air drag would be viscous in character and the damping decrement would be constant. However, the marked increase in the damping decrement with increasing amplitude strongly indicates the damping in this structure probably originated in the foundation. If this is true, variation in the damping decrement could be expected for different foundation conditions and more data covering a variety of foundations would be desirable before acceptance of a general value of 0.1 for the damping decrement.

Such data as are available on damping characteristics are limited to stacks supported on their own foundations. Additional data covering stacks supported on the roofs of boiler houses or other structures would be of value in further analysis of this phenomenon.

The need for data on the coefficient of lift at these large Reynolds numbers is self-evident. Theoretical values of this coefficient range from 0.9 to 1.71. Experimentally determined values at Reynolds numbers below 1×10^6 range from 0.61 to 1.13. Experimental data or reliable observations from which this coefficient can be computed at Reynolds numbers of interest in stack design are totally lacking. Therefore, the observations of Mr. Marsh that the amplitudes of vibration of the aluminum tower at winds of from 40 miles per hr to 45 miles per hr were only slightly greater than at winds of from 6 miles per hr to 10 miles per hr and that the energy input at this higher velocity is of the same order are most interesting. It is hoped that the data and reasoning leading to this conclusion will be made available in some other publication.

Information advanced[19] by Mr. Pagon, together with his observations[6, 7] in Baltimore, Md., indicate that in a quartering wind or for wind along the line of a group of stacks the mechanism of excitation may be markedly different than for a single stack. Additional data showing marked excitation of the second of two stacks in line, together with marked directional effects, have become available.[20]

Exciting winds at Moss Landing were in a direction almost normal to the line of stacks. The observations indicated there was no coupling of the stacks under these conditions. Stacks 2 and 3 vibrated at the same frequency, but their motion was completely independent. At times, only one of the two stacks would be moving and at other times, both. When they were both in motion, movement was sometimes in phase and sometimes out of phase. It is perhaps significant that stack 1, which was completed except for the top 8-ft high ring, did not move. This would indicate that, for a line of stacks spaced about 4.5 diameters apart and a wind normal to the line, there is no mutual interference.

---

[19] Discussion by W. Watters Pagon of "The Vibrations of Steel Stacks," by Walter L. Dickey and Glenn B. Woodruff, *Transactions*, ASCE, Vol. 121, 1956, p. 1082.

[20] "Factors Influencing the Dynamic Behavior of Tall Stacks Under the Action of Wind," by M. S. Ozker and J. O. Smith, *Paper No. 55-A-69*, ASME, 1955.

Connecting the stacks at Moss Landing with a horizontal beam was considered. Because experience indicated that they could vibrate in phase as readily as out of phase and considering the definite self-excitation characteristics described[4] by Mr. Steinman, it was believed that a simple horizontal beam system would not be effective in preventing vibration.

Additional observations on multiple-stack installations would be most welcome as installations with two, three, four, or more stacks in line are quite common. If the mechanism of excitation for quartering winds or for wind along the line of stacks is different from that of a single stack or for winds nearly normal to the line of stacks, the methods of analysis and data developed for single stacks could give misleading results when applied to multiple-stack installations.

The possibility of devices for tripping the boundary layer which might prove effective in preventing vortex-induced motion is again cited because of the probable economy such a device would offer, as compared with designs based on nonresonance to extremely high wind velocities or on damper systems. There are theoretical reasons for believing that such boundary-layer trippers might be effective, but, until supported by experimental data, dependence certainly could not be placed on them for structures as important and expensive as the stacks for major power or industrial plants.

AMERICAN SOCIETY OF CIVIL ENGINEERS
Founded November 5, 1852
TRANSACTIONS

Paper No. 2833

PIPELINE TRANSPORTATION IN THE UNITED STATES

By Eldon V. Hunt,[1] M. ASCE

Synopsis

The pipeline industry is described from an over-all viewpoint, beginning with its early history in the United States and including technological developments leading to the present complex network of oil and gas pipelines. The economics and management of the lines are discussed and statistics are presented to indicate the magnitude of the development of this industry.

Introduction

Across all or part of every state in the United States there is a pipeline, either for crude oil, petroleum products, or natural gas. This transportation network measures more than 594,000 miles and includes the mileage of pipes in the distribution systems of towns and cities, but it does not include service lines or pipes that conduct water, drainage, or sewage. Of the three types of pipelines the crude-oil lines have the longest history in the United States; however, it is of historical interest to note that the ancient Chinese transported natural gas through bamboo pipes considerable distances for evaporating water from brine to obtain salt.

These pipelines are a vital factor in the economic life of the United States and influence the planning for national defense. They affect the land from which the oil or gas comes, the lands they traverse, the industries they serve, and the industries that mine, produce, and fabricate the steel with which they are made and maintained. They are a part of the investments supporting millions of life insurance policies and they exert a personal influence on the individual lives of nearly every citizen.

The development and expansion of the nation's pipeline systems are of recent years and the trend is toward their continued growth and importance. Fig. 1 shows the breakdown of pipeline mileage among the various states as of 1953.

Note.—Published, essentially as printed here, in February, 1955, as *Proceedings-Separate No. 633*. Positions and titles given are those in effect when the paper was approved for publication in *Transactions*.

[1] Asst. Constr. Mgr., Ebasco Services, Inc., New York, N. Y.

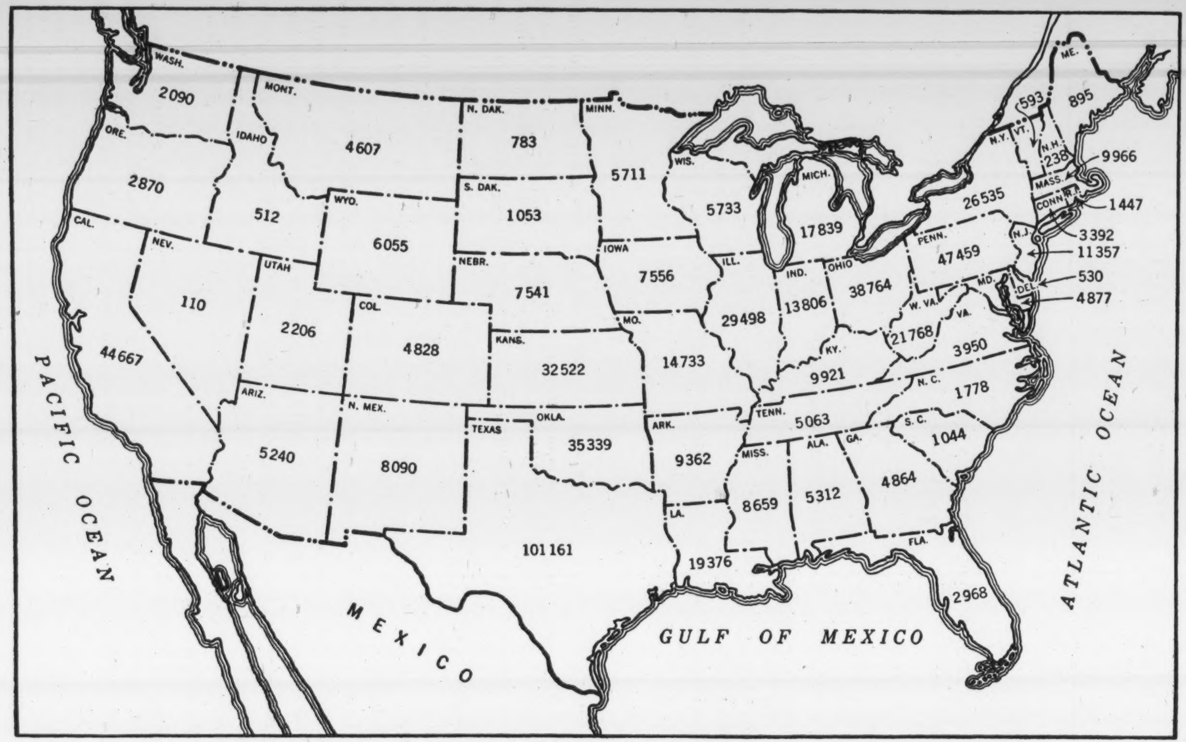
WASH.
2090
MONT.
4607
N. DAK.
783
MINN.
5711
WIS.
5733
MICH.
17839
N.Y.
26535
VT.
593
ME.
895
N.H.
238
9966
MASS.
CONN.
R.I.
1447
3392
N.J.
11357
530
4877
DEL.
MD.
PENN.
47459
OHIO
38764
IND.
13806
ILL.
29498
IOWA
7556
S. DAK.
1053
NEBR.
7541
WYO.
6055
IDAHO
512
ORE.
2870
CAL.
44667
NEV.
110
UTAH
2206
COL.
4828
KANS.
32522
MO.
14733
KY.
9921
W. VA.
21768
VA.
3950
N. C.
1778
S. C.
1044
GA.
4864
ALA.
5312
TENN.
5063
MISS.
8659
ARK.
9362
LA.
19376
OKLA.
35339
TEXAS
101161
N. MEX.
8090
ARIZ.
5240
FLA.
2968
PACIFIC OCEAN
ATLANTIC OCEAN
GULF OF MEXICO
MEXICO

FIG. 1.—TOTAL PIPELINE MILEAGES FOR TRANSMISSION AND DISTRIBUTION OF OIL AND GAS AND THEIR PRODUCTS, 1953

DEVELOPMENT OF LINES FOR PETROLEUM AND ITS PRODUCTS

The first impetus for pipeline construction had its origin in the discovery of oil by Colonel Drake at Oil City, Pa., in 1859. The boom thus initiated occurred along Oil Creek in very rough terrain several miles from a railroad. The oil was hauled in barrels by wagons and teams to the railroads at a cost of from $3 to $5 per barrel for a distance of 25 miles. Within a year, oil cartage grew into a huge, fiercely competitive business employing several thousand teamsters.

In 1861, an attempt was made to build a pipeline of wooden pipe to carry this oil. The venture was abandoned when the irate teamsters dug up the pipe at night which had been laid during the day, causing fighting and bloodshed to occur. Four years later, however, Samuel Van Sychel built the first crude-oil line from Pithole City to Millers Farm in western Pennsylvania. It was of wrought iron, 2 in. in diameter and 5 miles long. It had a capacity of approximately 800 bbl per day and operated at a pressure of approximately 200 lb per sq in., the motive power being furnished by three steam-driven pumps in two stations. This capacity was equal to approximately 300 teams of horses working ten hours per day. During the construction of this line two crews were used—one to stand guard at night over the finished work to prevent its destruction by the angry teamsters, and the other crew to do the work by day.

At first the railroad companies were pleased with this new industry because it gave them revenue from hauling pipe but soon they recognized pipelines as competition that they were not inclined to accept. They fought the building of other pipelines by every means available and, together with the teamsters and barge companies, formed powerful lobbies. They refused to allow pipelines to go under their tracks and, on one occasion, a locomotive was used to pull out a pipeline that had been laid parallel to the tracks. However, the economics of pipeline transportation for oil proved to be too strongly supported to enable them to prevent its development by either violent or legal means.

In 1874, a 60-mile, 9-in.-diameter line terminating in Pittsburgh (Pa.) was built by Dr. Hostetter, who was a patent-medicine manufacturer. (Crude oil was sold in bottles at prices of from 50¢ to $1 for a half pint and was purported to be a cure for almost any ailment.) In 1879, a 6-in.-diameter crude-oil line of wrought-iron pipe, using thread-connected couplings, was built from Coryville, Pa., to Williamsport, Pa., and was later extended to Bayonne, N. J. By 1900 there were 18,000 miles of crude-oil pipelines of different sizes and lengths fanning outward in all directions from the Pennsylvania fields.

In 1901 the famous Lucas gusher in the Spindletop Field of Texas was "brought in" and with it there was created another pipeline situation—one of a vastly different magnitude. Until this time, the crude-oil lines had been confined mostly to the Pennsylvania fields and adjacent refineries. However, this new oil field and the fields subsequently "brought in" were 1,500 miles from the consuming markets of the Chicago (Ill.) area and the eastern seaboard. It was only natural, therefore, that the first trunk lines were to spread out from the Texas fields to the tidewater where the oil could be moved by tanker to the eastern markets.

The Kern River fields of California were also brought into production at approximately this same time and the Standard Oil Company built an 8-in.-

diameter line 300 miles long to San Francisco, Calif.; in 1904, a 100-mile, 6-in.-diameter line was built into Monterey, Calif., to carry crude oil. Because of the high viscosity of this California crude oil much difficulty was encountered in pumping it through these lines. Finally, in 1906, the Southern Pacific Company developed a "rifled pipeline" that helped to solve this problem. Their method was to rifle the pipe, thus making its interior appearance similar to that of a rifle barrel. A small percentage of water was pumped into the line with the oil. The rifling of the pipe caused the entire mass to whirl and because the water was heavier than the oil it was thrown to the exterior of the mass, thus causing the envelopment of the oil by a thin film of water which acted as a lubricant.

Oil-products lines had their beginning in 1901 when two 4-in.-diameter lines, originally built to carry crude oil from Titusville, Pa., to Wilkes-Barre, Pa., were converted to the transportation of kerosene. By 1930 the total mileage of pipelines devoted to the movement of products was only 1,300 miles but since then their growth has been very rapid, until now there are 24,000 miles of lines carrying petroleum products.

In 1910 there were 40,000 miles of lines for crude oil and its products. At the start of World War II the total had increased to 125,000 miles. Because of the vulnerability of tankers to Nazi submarine attacks, the Big Inch and Little Inch lines were rushed to completion as a wartime measure. These, together with recent additions, have brought the present total mileage to approximately 170,000 miles of crude-oil and oil-products pipelines in service.

It is interesting to note how the oil-products lines maintain the identity of the individual consignments that are being moved through the line. Frequently a line will contain many batches along its length which differ as to type, grade, and ownership. One long line has had as many as 65 different batches moving along it simultaneously. These products are simply introduced into the line one behind the other and each pushes the batch ahead. The mixing is negligible, and the small amounts of mixed products are blended into other shipments in such quantities as not to affect them. It is essential to know the location of the "faces" of these batches at all times because these products move at approximately 4 miles per hour, which means that the quantity or "face" that has intermixed would pass the valves at a station within a few minutes. Valve operations must be timed to a few seconds to keep the products separated and "switched" into their proper tanks. It has been found that the introduction of minute quantities of radioactive isotopes at the beginning of a shipment gives the pipeline operating personnel an accurate indication of the location of that shipment through the use of radiation counters at appropriate points along the line.

ECONOMICS OF OIL AND PRODUCTS PIPELINES

The advantage that pipelines have over any other means of transportation for the movement of fluid products is that there are no empty vehicles to return and no cars to build or to service. Fluids present no problem as to size or shape and require no packaging or crating. There is no waste power. Delivery is continuous, and the quantities to be delivered can be accurately predicted.

The system is out of the way, below ground, and is free from most of the maintenance problems of surface transportation. Theft is almost impossible, and there are no traffic accidents. The labor required for operations is small. When one compares the cost of from $3 to $5 per barrel for moving barrels of oil by team and wagon in the early days with the cost of approximately 5¢ per barrel for electric power to pump oil a distance of more than 1,000 miles, the economics of pipelines for oil and oil-products transportation is apparent and shows the great advances the industry has made.

The industry is characterized by high capital costs and low operating expenses. The average per-mile investment in pipelines for oil and oil products is approximately $97,000, whereas the railroads have a per-mile investment of approximately $135,000. These figures are presented for the purpose of comparison only; they have no other relationship. There are approximately 27,000 persons employed by the pipeline companies. The average annual salary per person is in excess of $4,300 per year.

Every year approximately 2,500,000,000 bbl of oil in the United States are moved from 500,000 producing wells to approximately 350 refineries and the resultant refined products distributed throughout the nation. A large portion of these products are transported through pipelines; this amounted to considerably more than 100,000,000,000 ton-miles in 1954. Nearly 2,500 pumping stations furnished the motive power for this movement. Of the ton-miles of all freight traffic transported in the United States in 1953, the railways hauled 58.5%, trucks hauled 12.5%, Great Lakes shipping hauled 11.1%, and oil pipelines conveyed 12.8%. These oil and oil-products pipelines constitute only one quarter of the total pipeline mileage of the country. To illustrate further the economic advantages of pipelines for the transportation of fluid products, there are approximately 103,000 tank cars in the country devoted to the movement of petroleum products. These cars travel more than 2,225,000,000 miles annually—the return of the empty cars constitutes half this distance.

Pumping Stations on Pipelines for Oil and Oil Products

The early pumping stations on crude-oil lines and oil-products lines obtained power from steam. The horizontal air-injection oil engine was next, only to be followed by the vertical diesels of larger horsepower and greater efficiencies. Among the early pumps was the Dow duplex pump with outside-packed plunger, having a capacity of about 6,000 bbl per day when working against a pressure of 1,000 lb. Some of the largest modern pumps in oil-line service are two 6,000-hp, steam-turbine-driven centrifugal units on the Arabian-American Oil Company line. Either pump can deliver full line throughput—as much as 400,000 bbl daily at a discharge pressure of 800 lb per sq in.

The trend on these lines is toward electric drive in pumping stations, using power supplied by the electric utility companies. This development is caused by the broad extension of electric power during the past ten years which has made electricity available even in remote areas. The electric-motor drive has one distinct advantage—its adaptability to automatic and remote controls. The electric-powered stations have the additional advantage of requiring much less manpower for operation and maintenance.

Development of Natural-Gas Pipelines

In 1821, at Fredonia, N. Y., natural gas was first piped from shallow wells to several homes in the vicinity where it was used for illumination. In 1825, while on a visit to the United States, General Lafayette arrived by stage coach at the old Taylor House in Fredonia at night and found the place brilliantly illuminated in his honor by this natural gas. The Fredonia Gas Light and Water Works Company was formed in 1865 to become the first company organized to engage in the natural-gas business in the United States.

It is of interest to note that George Washington became a partial owner of a natural-gas field in 1776. He wrote of a

> "tract of which 123 acres is a moiety [half-interest] and which was taken by General Andrew Lewis and myself for and on account of, a bituminous spring which it contains, of so inflammable a nature as to burst forth as freely as spirits and is nearly as difficult to extinguish."

This "burning spring" was on the banks of the Kanawha River near Charleston, W. Va., in what was later to become the first great natural-gas-producing region.

It has been only in the past few decades that natural gas has had more than local significance as a source of energy. The principal explanation for this is that there was no feasible way to transport the gas before the advent of a suitable pipe—particularly steel pipe. This fact restricted the use of natural gas to domestic and local uses and to such manufacturing processes as were oriented to the fuel source rather than to the market.

However, the use of gas for illuminating purposes had been known as early as 1691, when coal gas was used for this purpose in Ireland. The invention of the "gas chimney" by Armond in 1784 improved the lighting qualities of this gas, and in 1803 Baltimore (Md.) had gas lights. By 1812 there were approximately 120 miles of mains in London, England; Westminster Abbey was gas-lighted in 1814.

Pipe manufacture has been the dominant factor in the development of gas pipelines. The cast-iron pipe which was first used left much to be desired although it is still used in low-pressure lines today. Wrought-iron pipe came into use about 1830 and was much lighter and tougher than cast-iron pipe; it made possible the screw joint and thereby reduced the leakage in gas transmission. About 1871, an attempt was made to construct a gas line from West Bloomfield, N. Y., to Rochester, N. Y., using pipe made of pine logs which had been bored with 8-in. holes. This line was a failure. In 1872, about 6 miles of 2-in. iron pipe was laid between Newton Wells (Pa.) and Titusville, but the high pressures and greater capacities of gas lines did not develop until about 1891 when Solomon R. Dresser, a manufacturer of oil-well equipment, developed a flexible and leak-proof joint which bears his name.

To prove the worth and advantage of his coupling, Mr. Dresser built, at his own expense, a 5-in. line several miles long from a gas field into the town of Malta, Ohio. This line became the first successful gas-tight or leak-proof gas line in the country. A second line using Dresser couplings was laid in 1896 by the United Natural Gas Company to bring gas to Buffalo, N. Y., through a 12-in. line, and the third Dresser line was built into Pittsburgh in 1898. The East Ohio Gas Company built a line from the West Virginia fields to the industrial area of north central Ohio in 1899. In the same year, a 10-in. line 100 miles long and using Dresser couplings brought gas from Sugar Grove in central Ohio to Toledo, Ohio, for the purpose of serving the glass industry there. Until the late 1920's the transmission of natural gas had been developed in a limited way in the southwestern and Appalachian areas of the United States to supply gas to nearby cities and industries. In the late 1920's and early 1930's, rapid expansion began with pipelines being built to New Orleans (La.), Memphis (Tenn.), Chicago, St. Louis (Mo.), Denver (Colo.), Atlanta (Ga.), Los Angeles (Calif.), and San Francisco. The manufactured gas facilities were converted to distribute natural gas. There was a lull in building during the depression, but thereafter, natural gas has been supplied to practically all of the United States with the exception of the northwestern states. In addition, large pipelines have been built from Texas to California to supplement their local production. Natural-gas lines have spread out from producing fields until, at the end of 1952, the combined network of field and gathering, transmission, and distribution lines operated by the gas utility and gas pipeline industry aggregates more than 424,000 miles of pipe of all sizes. By way of comparison, on December 31, 1952, there were 375,296 miles of railroad trackage owned and operated by the railroads of the United States.

Throughout the years, the sizes of pipe have gradually increased until now the 30-in. line is considered commonplace, and considerable work is being done by pipe manufacturers and equipment companies to develop a 36-in. steel pipe and the means of handling it on cross-country lines.

The aggregate consumption of energy in the United States during 1952 was $38{,}773 \times 10^9$ Btu. The annual energy consumption has gained 391% during the course of the century and 42% since 1941. In the prewar decade coal contributed 54.9% of this total; petroleum, 30.7%; and natural gas, 10.6%. During 1952, the distribution was 34.0% for coal, 39.4% for petroleum, and 22.5% for natural gas. Natural gas now heats almost as many homes as are heated by coal and furnishes approximately 20% of the fuel consumed by the electric-utility industry. To move this natural gas, a volume of approximately 7.5×10^9 cu ft with a heating potential equivalent to 31,250,000 tons of bituminous coal, the gas pipelines have 6,500,000 hp installed in their compressor stations. This total horsepower is equivalent to the horsepower that could be developed by approximately 4,700 diesel-electric railroad locomotives.

During the four years from 1953 through 1956, the plan of the gas utilities and pipeline industry is to spend almost $4,000,000,000 for the construction of new facilities and the expansion of the present plants. About $1,900,000,000 will be spent on transmission facilities, $1,400,000,000 on distribution, and about $637,000,000 on production, underground storage, and general facilities. Since 1945, the natural-gas pipelines have used nearly 12,000,000 tons of steel in their line pipe.

COMPRESSOR STATIONS

Gas compressor stations have undergone a distinct change. The very early stations used steam because it was the only type of power then available. Steam is being used again in turbines to furnish power for the centrifugal compressors that owners of several gas pipelines have recently installed. However, most of this work is done by reciprocating gas-engine units which range in size from 500 hp to 2,400 hp. Compressor stations are spaced at approximately 80-mile intervals and it has been found that additional stations giving frequent but smaller pressure boosts are the most economical.

One of the new developments is the gas turbine which has already shown great promise in the transmission of gas. The first installation of this type was made in 1949 when a 1,800-hp unit was placed in operation at a compressor station in Arkansas. This was the first commercial gas turbine in the United States to burn natural gas and the first installation in the world of a gas-turbine power plant driving a centrifugal compressor for natural-gas transmission.

The Texas Eastern line has 20 compressor stations equipped with single-stage centrifugal compressors, each directly connected to an electric motor. These stations range in size from 3,750 hp to 19,000 hp and constitute 221,250 hp of the total installed compressor-station power of 357,410 hp now on this pipeline.

PIPELINE COMMUNICATIONS

An efficient communication system is essential to the successful operation of any pipeline. In the earlier days, parallel telegraph and telephone lines were built for dispatching purposes and general communication uses. Telephone booths, which the linewalkers used to report any leaks or other troubles, were placed at regular intervals along a line. Hourly gage or pressure reports were sent by the field locations to the central dispatching offices, and the lines were regulated from these reports.

Because communications are so essential to pipelines, it was only natural that the pipeline industry would be among the first to adopt radio and microwave facilities for their dispatching, message transmission, and remote control of station operations. By the use of remote controls and electric pumps and compressors, a pipeline becomes almost automatic in its operation and an oil line in Ohio is now being remotely controlled by the dispatcher in New York, N. Y.

STORAGE FACILITIES

The storage of pipeline deliveries at the terminal end of a line is a problem that both liquid-pipeline and gas-pipeline operators have in common. Liquid products are stored in large tanks in the familiar oil company "tank farms" and the only limit is that of tank capacity. However, gas volumes are too great to store in tanks in sufficient quantity to take up the slack between the necessary economical uniform flow and the seasonal and industrial demand. This problem has been solved in several cases through the use of exhausted gas and oil fields and salt domes near areas of consumption. Abandoned quarries have also been studied for this purpose.

At the beginning of the 1952–1953 heating season, about 700,000,000,000 cu ft of natural gas were in underground storage. It would require 40,000 of the largest-size gas holders to store this volume.

The crude-oil trunk and gathering lines have a pipeline "fill" of 50,000,000 bbl, which represented about 18% of the crude petroleum in storage as of December 31, 1952. The corresponding "fill" of the products lines is nearly 10,000,000 bbl, which is equal to about 4% of the stock total of all light products. There are no accurate figures available to show the volume of gas in the "fill" of gas lines but it constitutes billions of cubic feet.

INFLUENCE OF PIPELINES ON PROPERTY AND BUSINESS

That pipelines exert an influence on the lands over which they have a right of way is illustrated by the rights-of-way problems encountered on the recently completed 154-mile gas pipeline which the writer supervised as the construction superintendent and which was built for the South Carolina Natural Gas Company by Ebasco Services, Inc., of New York. This line began at Aiken, S. C., and ended in Columbia, S. C., and Charleston, S. C. It crossed 750 different tracts of land. An abstract of ownerships extending back more than 25 years was made on each tract. Local attorneys were employed to make title searches. Defective titles were cleared before easements could be executed. Estates which had been divided years before but not legally settled were settled, guardians were appointed by the courts for minor heirs and for those who were mentally or otherwise incompetent. Nonresident owners were contacted either by right-of-way agents or by attorneys living in their towns, and signatures were obtained on the necessary documents. Consent to construct the line and to enter upon the properties was obtained from all tenants. Disputed land lines were surveyed by licensed surveyors and re-established to the satisfaction of the adjoining owners and the owner. Subordination of all liens was obtained from those who held the mortgages or rights. All executed easements and damage releases were recorded at the respective county court houses.

Upon completion of the construction, each owner and tenant was again contacted and a settlement made to cover any construction damage he might have sustained. When the work was complete, more than 3,000 documents had been recorded to cover the land grants for this 150 miles of pipeline. For this purpose, the field agents drove nearly 250,000 miles calling on landowners during a period of seven months. These landowners were paid the standard rate of $1 per rod for the easement rights. If one adds to these payments the money paid for the settlement of construction damages, the total is in excess of $250,000 for the land rights for this line. The various communities along the line were benefitted by this money.

In 1953, pipelines for oil and gas used more than 3,500,000 tons of line pipe, most of which was for new construction. This new construction increased the property values on which taxes are collected for schools, roads, and other public improvements. The life insurance companies of the country have invested more than $1,500,000,000 in pipeline securities compared to approximately $14,000,000,000 that they have invested in other public utilities.

Pipeline Construction Materials and Methods

As stated previously, pipe has been perhaps the primary factor in the development and expansion of pipeline systems in the United States. Cast-iron and wrought-iron pipes were not as adaptable as steel pipe for cross-country lines, although both of these types of pipe have special favorable qualities and are used for certain purposes in the industry.

The progress made in steel-pipe manufacture was prompted by the economics of bigger size and higher working pressures. For example, the per-barrel-mile costs on a 20-in. or 24-in. oil line running at full load are about 40% and 36%, respectively, of the equivalent full-load costs on a 10-in. line in the same territory.

The advent of the Dresser coupling helped to make the use of larger size pipe possible because it provided a gas-tight joint that was also somewhat flexible. This coupling, which consists of a center ring or sleeve into which the two joints of pipe fit and two follower rings containing equally-spaced bolt holes, has a special rubber gasket which is expanded against the sides of the pipe and center ring when the bolts are tightened, thus making a gas-tight joint or coupling. This coupling or center ring has a tolerance which allows a deflection angle of a degree or more per joint, thus reducing the necessity for bending the pipe itself.

Oxyacetylene welding was introduced in about 1920 and, to some extent, displaced the Dresser coupling for cross-country pipelines, although this coupling is still widely used in distribution systems and other installations. By 1928 the electric arc-welding process displaced oxyacetylene welding and is now the universal process in pipeline construction. During this period, the sizes and strengths of pipe steadily increased. In 1936 only one fourth of the crude-oil lines were larger than 8 in. but now most of the crude-oil lines are in excess of 10 in. in diameter; more than 5,000 miles are greater than 12 in. The recently completed Lakehead pipeline (crossing the Mackinac Straits) is 30-in. pipe, and the largest gas lines are 34 in.

The development of x-ray and radioactive methods of inspecting metal has greatly improved the quality of welding and has, of course, had an influence on the development of these pipelines.

Pipe lengths have increased from the early 10-ft joints of cast pipe to the 40-ft joints of 30-in. and larger steel pipe of today. Some of the smaller sized pipes come in joints as long as 60 ft. This increase in the length of joints has accelerated construction and lowered construction costs correspondingly. One of the systems widely used is "double jointing," or the welding together of two joints of pipe at yards or storage areas, and moving these double-length pieces of pipe to the line as a unit instead of as single joints.

Construction machinery and equipment has kept pace with other developments or has perhaps made possible the development of the long joints of pipe. A 40-ft joint of 30-in. pipe may weigh as much as 2.5 tons. This weight could not be man-handled into ditch as the pipe was handled during the pioneer days of pipelining. The most spectacular of any of the machines devoted to pipeline construction is the famous "side-boom" tractor which was developed by pipeliners and is almost the universal symbol of the industry. Legend has it that the first side boom was an improvised gadget made on the job by a "lazy foreman" of a pipe gang.

The modern ditching or trenching machine can excavate a trench 4 ft wide and from 5 ft to 7 ft deep and can do this at the rate of $1\frac{1}{2}$ miles per day, depending on the type of soil and the volume of rock encountered in the ditch line. Customary pipeline specifications require a minimum cover of 30 in. over the top of a pipe so that a 30-in. line will require a ditch of a 5-ft-deep minimum. For every mile of such line approximately 3,900 cu yd of excavation is piled up on the bank and then moved back into the ditch after the pipe has been lowered into it.

In the early days, bending was done by snubbing the pipe to a large tree or post and bending it with whatever power was available—mostly manpower and mule-power. Large-diameter pipe was placed on a pair of supports, and a fire was built under the middle of the joint to make the bend. Specifications in some of the contracts prescribed a cherry-red color before bending and certain conditions for cooling it after the bend had been made. Currently, a specially designed bending machine can make smooth bends in pipe as large as 36 in. in diameter without heating the pipe or disturbing the wall thickness. These machines are hydraulically operated with the power furnished by a small gasoline engine.

The machines that clean, coat, and wrap pipe with protective asbestos and fiber-glass wrapper are a specialty of the industry. In the olden days of pipelines this work was done by hand, and many miles of line have been flood-coated and "granny ragged."

Each river crossing, regardless of the size of the pipe, constitutes a separate and special engineering problem, and it is not within the scope of this paper to discuss this challenging phase of pipelining. However, it is appropriate to mention the latest and perhaps most heroic crossing—that of the Lakehead line laid across the Mackinac Straits.

CONCLUSION

Pipelines are an important segment of the economic life of the United States. Gas and oil have become a necessity to modern culture. They are relied on for heating houses, cooking meals, running automobiles, and as a raw material for a vast number of petrochemicals. Much thought is now being given to ways of assuring their supply in the event of war.

Those engaged in the industry will continue their study and work on corrosion control, the development of new and better pipe and welding processes, methods to increase the efficiency of lines and motive power, better maintenance and operating practices, and further economies in construction.

APPENDIX. LIST OF REFERENCES

(1) **"Chronology of the Natural Gas Industry,"** by Louis Hilt, *American Gas Journal*, May, 1950, pp. 29–36.

(2) **"Rifled Pipes for Conducting Heavy Crude Oil,"** by J. O. Isaacs, *Engineering News*, June 7, 1906, pp. 640–641.

(3) **"100 Mile Oil Pumping Line,"** by A. M. Hunt, *Journal of Electricity*, January, 1905, pp. 4–8.

(4) **"Lake Head Pipe Line Now in Operation,"** *Pipe Line News*, February, 1954.

(5) **"Excavating Machinery for Ditching and Trenching,"** by E. E. R. Tratman, *Engineering News*, February 23, 1911, pp. 215–217.

(6) **"Oil Pipe Lines in California,"** by B. K. Stroud, *ibid.*, March 13, 1913, pp. 500–501.

(7) **"Building a 375 Mile Pipeline in 193 Calendar Days,"** by Wm. Thompson Smith, *Engineering News-Record*, October 4, 1928, pp. 509–514.

(8) **"Pipelines Laid in English Channel Carried Gas and Oil to France,"** *ibid.*, June 7, 1945, p. 3.

(9) **"Oil Pipeline,"** *Mechanical Engineering*, March, 1952, p. 230.

(10) **"Coal Pipeline,"** *ibid.*, March, 1952, p. 230.

(11) **"Paper Pulp Transported Through Pipeline,"** *Engineering News-Record*, November 1, 1928, p. 667.

(12) **"Resistance to Flow of Molasses Found to Agree with Basic Laws,"** by Glen N. Cox, *ibid.* October 12, 1933, p. 441.

(13) **"Motor Driven Centrifugal Pumps in Oil Pipeline Service,"** *ibid.*, March 1, 1928, p. 377.

(14) **"Cast Iron Pipe Prices in Boston from 1868 to 1917,"** by Dexter Brackett, *ibid.*, May 9, 1918, p. 923.

(15) **"Reducing Cost of Bending Pipe,"** *ibid.*, October 31, 1918, p. 828.

(16) **"Concrete Oil Reservoir Fails,"** *ibid.*, March 16, 1911, p. 310.

(17) **"Gas Facts—1952,"** Am. Gas Assn., New York, N. Y., 1953.

(18) **"Petroleum Facts and Figures,"** Am. Petroleum Inst., New York, N. Y., 10th Ed., 1952.

(19) **"Natural Gas Construction Data, July 1, 1945–January 1, 1953,"** Gas Appliance Manufacturers Assn. Inc., New York, N. Y., 1953.

(20) **"Railroad Transportation, 1911–1951,"** Assn. of Am. Railroads, Washington, D. C., March, 1953.

(21) **"Insurance Fact Book, 1952,"** Inst. of Life Insurance, New York, N. Y., 1953.

(22) **"Crude Oil and Refined-Products Pipeline Mileage in the United States January 1, 1953,"** *Information Circular 7671*, Bureau of Mines, U. S. Dept. of the Interior, Washington, D. C., November, 1953.

(23) **"Sixty Fourth Annual Report on the Statistics of Railways in the United States for the Year Ended December 31, 1950,"** U. S. Bureau of Transport Economics and Statistics, Interstate Commerce Comm., Washington, D. C., 1952.

(24) **"1952 Bituminous Coal Annual,"** Bituminous Coal Inst., Pittsburgh, Pa., 1953.

AMERICAN SOCIETY OF CIVIL ENGINEERS
Founded November 5, 1852
TRANSACTIONS

Paper No. 2834

THICKNESSES OF CONCRETE PAVEMENTS FOR HIGHWAYS

By JOSEPH HERBERT MOORE,[1] A. M. ASCE

WITH DISCUSSION BY MESSRS. LAWRENCE A. PALMER, EARL C. SUTHERLAND, WARNER HARWOOD, ALBERT DE NEUFVILLE, AND JOSEPH HERBERT MOORE

SYNOPSIS

The most widely used method of determining the thickness of portland cement concrete pavements for highways is based on wheel loads placed at the corners of the slabs. This paper presents data which indicate that the longitudinal-edge loading position is really the critical loading position when the restrained-warping stresses and lateral distribution of vehicles across the traffic lanes are considered.

A table of "load percent factors" is given to simplify the recommended design method and make its application practical. For numerous traffic patterns the new design method indicates that pavements 8 in. or 9 in. thick have longest life and that pavement life can be remarkably increased by providing very strong subgrade support.

NOTATION

The letter symbols adopted for use in this paper are defined where they first appear, in the illustrations or in the text, and are arranged alphabetically, for convenience of reference, in the Appendix.

INTRODUCTION

The determination of the proper thickness of a concrete pavement slab for a highway has apparently remained so complex that highway engineers often base their choice of thickness entirely on their own previous experiences. The Portland Cement Association (PCA) method[2] of determining the thickness has

---

NOTE.—Published, essentially as printed here, in January, 1955, as *Proceedings-Separate No. 596*. Positions and titles given are those in effect when the paper or discussion was approved for publication in *Transactions*.

[1] Project Bridge Engr., Joseph K. Knoerle and Associates, Inc., Cons. Engrs., Chicago, Ill.

[2] "Concrete Pavement Design," Portland Cement Assn., Chicago, Ill., 1951.

been used by several states, but the semi-empirical equation of Gerald Pickett[3] which underlies the PCA design method is based on placing a wheel load only at the corner of the pavement slab. This type of loading would produce cracks diagonally across the corner; yet in a study of this problem made by a private company for the Joint State Government Commission of Pennsylvania in 1952, the corner crack was found to be rare whereas the large majority of cracks were transverse cracks almost at right angles to the longitudinal axis of the pavement slab.

For several years the Pennsylvania Department of Highways has collected detailed traffic data at loadometer stations throughout the state and has kept rather complete records of pavement performance for designated parts of the highways at these loadometer stations. Many of these strips were portland cement concrete pavements and presented an excellent yardstick for measuring any empirical or theoretical design method. In addition to these strips along which the traffic data were well known, one-mile strips of concrete pavement were chosen at random throughout the state, and estimates were made of the traffic on each strip and of the life of the existing pavement. The design method developed in the study was then applied to these pavements; a close correlation was noted between the computed pavement life and the field estimate thereof.

The design procedure developed was measured against highways in Pennsylvania and is therefore for pavements with a reasonable amount of distributed steel, tie bars, and dowels. The size of distributed steel mats in Pennsylvania highways has grown from 42 lb per sq yd to 72 lb per sq yd at the present time (1955). The size and spacing of dowels has varied, but the spacing of tie bars of $\frac{9}{16}$-in. diameter at 5-ft intervals across longitudinal joints has been almost uniform practice.

Assumptions or major premises used in the design method will be considered with the particular factor involved.

MAJOR FACTORS AFFECTING THE REQUIRED PAVEMENT THICKNESS

Subgrade and Drainage.—The year-round bearing capacity of the subgrade is of primary importance and is probably the most significant factor in determining how long a pavement will support heavy loads before cracking. Permanent settlement or deflection of the subgrade beneath a slab will leave the slab unsupported, and, if the soil is susceptible to pumping, a combination of heavy loads and free water beneath the slab will lead to the forming of transverse cracks approximately 4 ft or 5 ft from the end of the slab.

A major premise in this paper is that the subgrade must be so constructed as to prevent pumping. This in itself presents a major problem, in the solution of which the soils engineer, field inspector, and contractor all make important contributions.

The dependable bearing capacity of the subgrade must be known in order to determine the thickness of the pavement slab. Plate bearing tests using 30-in.-diameter plates are suggested as the most satisfactory means of determining bearing capacity.

---

[3] "A Study of Stresses in the Corner Region of Concrete Pavement Slabs Under Large Corner Loads," by Gerald Pickett, in "Concrete Pavement Design," Portland Cement Assn., Chicago, Ill., 1951, pp. 77–86.

Traffic.—To determine the thickness of a pavement slab for a particular road the engineer must obtain the following traffic data: (*a*) Total traffic per lane, (*b*) percentage of trucks or commercial traffic, (*c*) average number of axles per truck, and (*d*) number of axles in each thousand-pound weight category.

If a highway is to be designed for future traffic, someone must estimate the foregoing items; however, too often no estimate is made of the number of axles per truck and no measurements are made on comparable roads to determine the weight category of the axles. Therefore, no real consideration is given to the number of applications of the various axle loads.

Lateral Distribution of Traffic.—It is as apparent to the layman as it is to the engineer that vehicles do not "track" each other on a highway. However, a comprehensive search of the literature failed to reveal a design method for concrete pavements in which this lateral distribution of wheel loads was considered. A. Taragin[4] reported some values for the lateral distribution of traffic; Table 1 presents an interpretation of his data. As would be expected, Table 1 reveals that use of narrow pavement lanes results in more numerous truck loads near the longitudinal edge than does the use of wider pavement lanes.

Points of Largest Unit Tensile Stress.—Concrete pavements crack when they are subjected to excessive tensile stresses. The major types and sources of these stresses are (*a*) direct tensile stresses produced by contraction of the slab, (*b*) flexural tensile stresses caused by wheel loads on the slab, and (*c*) flexural tensile stresses caused by restrained warping of the slab.

TABLE 1.—LATERAL DISTRIBUTION OF COMMERCIAL TRAFFIC, IN PERCENTAGES

Placement of right wheels to the left of the right edge, in feet	LANE WIDTHS, IN FEET			
	9	10	11	12
0.5	15.7	5.8	1.6	0.7
1	17.7	11.7	3.8	1.8
1.5	23.6	17.5	8.4	3.7
2	18.6	18.7	16.6	6.6
2.5	12.5	18.6	22.9	10.6
3	6.7	14.2	17.9	15.4

Longitudinal steel is customarily placed in all concrete pavements in Pennsylvania, and the widespread practice has been to use enough steel to resist computed contraction stresses. Average values for these stresses are not difficult to compute for any length of slab if reliable values are available for the thermal coefficient of the concrete and the coefficient of friction between slab and subgrade. The proper coefficient of friction is still an open question and this paper will not include an investigation of this problem; a value of 1.5 has often been used and is apparently very conservative. Because sufficient longitudinal steel is provided in Pennsylvania highways to resist the tensile stresses introduced by contraction of the concrete slab in cold weather, this item was eliminated from further consideration in the study.

On a concrete pavement slab the wheel load may be at any of four general positions: At the interior, along a longitudinal edge, at a transverse edge, or at

---

[4] "Effect of Roadway Width on Vehicle Operation," by A. Taragin, *Public Roads*, Vol. 24, No. 6, 1945.

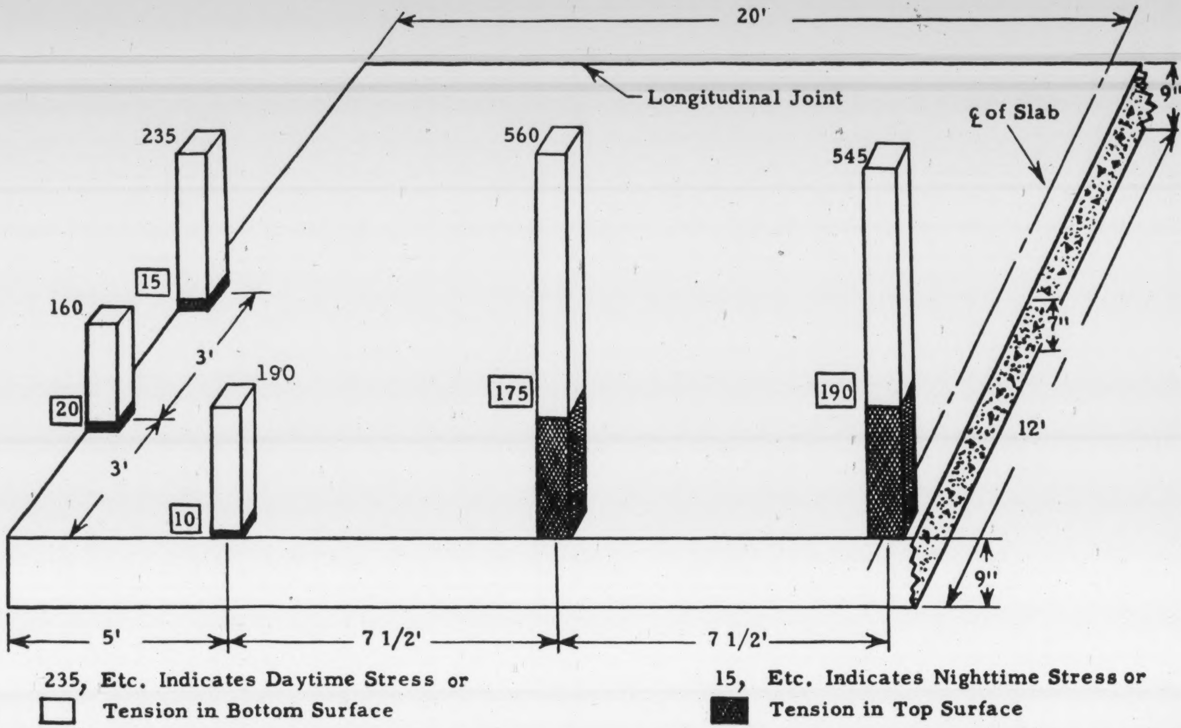
20'
Longitudinal Joint
℄ of Slab
9"
235
560
545
15
160
3'
190
175
190
7"
12'
20
3'
10
9"
5'
7 1/2'
7 1/2'
235, Etc. Indicates Daytime Stress or
☐ Tension in Bottom Surface
15, Etc. Indicates Nighttime Stress or
▨ Tension in Top Surface

Fig. 1.—Measured Stresses Caused by Restrained Temperature Warping Along Transverse Joint and Free Edge, 12-Ft by 40-Ft Slab (Road Test One-MD)

the corner of the slab. If the only stresses in the slab were those resulting from wheel loads, use of the corner loading position would probably introduce the largest unit stress in the concrete. However, the Arlington road tests[5] and Road Test One-MD[6] (Fig. 1 shows data from the latter) indicated that restrained-warping stresses along the longitudinal edge of a slab may be large, whereas near the corner or along the transverse edge they are usually insignificant. These restrained-warping stresses result from the resistance of the weight of the slab and the friction between pavement and subgrade to the free warping of the pavement which is caused by temperature and moisture differentials at the top and bottom of the slab. The designer's problem is therefore to determine whether a particular pavement slab will develop transverse cracks because of the combination of load and restrained-warping stresses at the interior or along the longitudinal edge of the slab before it fails diagonally across the corner.

A comprehensive search of the literature revealed that the analysis by H. M. Westergaard[7] and the extensive Arlington road tests[8] provide the most exact coverage of the subject. The Arlington tests were planned to check the validity of the Westergaard theoretical equations, and, in general, remarkable agreement was obtained between computed and measured load and restrained-warping stresses at various points in the slab. The chief exception to this agreement was the maximum load stress produced by loads at the interior loading position.

For this position of loading Mr. Westergaard noted that for a body continuous in two directions the reactions of the subgrade might be more closely concentrated around the load than would be the deflections. He therefore modified[9] his earlier equation for this load stress to include two additional unknowns. Unfortunately, these unknowns, L and Z, can only be evaluated by field tests on pavements at each particular site. However, both Mr. Westergaard and R. D. Bradbury[10] suggested limits for L and Z; these values were used in preliminary computations for this paper in order to ascertain whether or not the unit load and restrained-warping stresses at the bottom of the slab for interior wheel loading would be as detrimental as those for the longitudinal-edge loading position. Because values of L and Z vary widely among sites, the calculations were of little help; the longitudinal loading position appeared to present larger total unit stresses so the interior loading position was not considered further.

As the transverse-edge loading stresses and restrained-warping stresses did not prove to be of appreciable magnitude in this study, this general loading position was also eliminated—confining the study to the largest unit tensile stresses produced at the critical sections for corner loading and longitudinal-edge loading. The longitudinal edge considered was the free edge.

---

[5] "The Structural Design of Concrete Pavements, Part II—Observed Effects of Variations in Temperature and Moisture on the Size, Shape, and Stress Resistance of Concrete Pavement Slabs," by L. W. Teller and E. C. Sutherland, *Public Roads*, Vol. 16, No. 9, 1935.

[6] "Final Report on Road Test One-Md," *Special Report No. 4*, Highway Research Board, National Research Council, Washington, D. C., 1952.

[7] "Stresses in Concrete Pavements Computed by Theoretical Analysis," by H. M. Westergaard, *Public Roads*, Vol. 7, No. 2, 1926, pp. 25–35.

[8] "The Structural Design of Concrete Pavements" (Five Parts), by L. W. Teller and E. C. Sutherland, *ibid.*, October, November, December, 1935, September, October, 1936, April, May, June, 1943.

[9] "Analytical Tools for Judging Results of Structural Tests of Concrete Pavements," by H. M. Westergaard, *ibid.*, Vol. 14, No. 10, 1933.

[10] "Reinforced Concrete Pavements," by R. D. Bradbury, The Wire Reinforcement Inst., Washington, D. C., 1938, p. 31.

Mr. Westergaard's equation for the maximum unit stress in a longitudinal direction beneath a load applied during the day at the longitudinal edge of the slab is reduced to the following for a Poisson ration of 0.15:

$$\sigma_{ex} = 0.57185 \frac{P}{h^2} \left(4 \log_{10} \frac{l}{b} + 0.3593 \right) \dots\dots\dots\dots\dots (1)$$

in which σ_{ex} is the maximum unit stress as defined in the Appendix, P is the load, h is the pavement thickness, b is the radius of the circle of equivalent pressure distribution, $l = \{E\, h^3/[12\,(1 - \mu^2)\,k]\}^{\frac{1}{4}}$, E is the Young modulus, μ the Poisson ratio, and k the subgrade modulus. For the load stress at the same point at night when temperature tends to curl the slab upward at the edges, E. F. Kelley[11] presented the following modification of another Westergaard equation:

$$\sigma_{ex} = 0.57185 \frac{P}{h^2} \left(4 \log_{10} \frac{l}{b} + \log_{10} b \right) \dots\dots\dots\dots\dots (2)$$

The Westergaard equations for restrained-warping stresses[12] near the longitudinal edge were lengthy and involved hyperbolic functions. Mr. Bradbury[13] and Mr. Kelley[14] each presented simplified equations for this stress. Mr. Bradbury's equation that was used in this study is as follows:

$$s_{ex} = \frac{C\, E\, \alpha\, \Delta t}{2} \dots\dots\dots\dots\dots\dots\dots\dots (3)$$

in which s_{ex} is the maximum restrained-warping stress as defined in the Appendix, C equals the slab length divided by l, α equals the thermal coefficient, and Δt is the temperature change in degrees Fahrenheit.

For the corner loading position, Mr. Westergaard suggested the following equation:

$$\sigma_c = \frac{3\,P}{h^2} \left[1 - \left(\frac{a_1}{l} \right)^{0.6} \right] \dots\dots\dots\dots\dots\dots\dots (4)$$

in which a_1 equals the distance from the slab corner along the bisector of the corner angle to the center of the area over which the load is applied for the critical corner loading condition. Messrs. Kelley, Bradbury, and M. G. Spangler,[15] M. ASCE, have suggested modifications of this theoretical equation for various reasons, including loss of subgrade support. Mr. Pickett compared these equations and others and suggested the following equation which has the form of the Westergaard theoretical equation but which more closely follows the larger stress values determined in the Arlington tests:

---

[11] "Application of the Results of Research to the Structural Design of Concrete Pavements," by E. F. Kelley, *Public Roads*, Vol. 20, No. 5, July, 1939, p. 90.

[12] "Analysis of Stresses in Concrete Roads Caused by Variations of Temperature," by H. M. Westergaard, *ibid.*, Vol. 8, No. 3, May, 1927.

[13] "Reinforced Concrete Pavements," by R. D. Bradbury, The Wire Reinforcement Inst., Washington, D. C., 1938, p. 39.

[14] "Application of the Results of Research to the Structural Design of Concrete Pavements," by E. F, Kelley, *Public Roads*, Vol. 20, No. 5, July, 1939, p. 96.

[15] "Stresses in the Corner Region of Concrete Pavements," by M. G. Spangler, ***Bulletin No. 157***, Iowa Eng. Experiment Station, Ames, Iowa, September, 1942.

$$\sigma_c = \frac{4.2\,P}{h^2}\left(1 - \frac{\sqrt{a_1/l}}{1.1 + 0.185\,a_1/l}\right) \ldots\ldots\ldots\ldots\ldots (5)$$

Mr. Pickett's equation for the corner loading position has been widely accepted and was used in this study.

The equations for the longitudinal-edge loading stress chosen by the writer were those that showed the closest agreement with values measured in the Arlington tests.

Frequency with Which Load Stresses and Warping Stresses Are Additive.—During the day the top of a pavement is warmer than the bottom, causing the edges to curl downward. The weight of the slab and subgrade friction tend to prevent this action, and tensile stresses are thereby produced in the bottom of the slab. At night the effect is the opposite.

Wheel loads always produce tensile stresses in the bottom of the slab directly under the load for the longitudinal-edge loading position. Therefore it is only in the daytime that load stresses and warping stresses at such a point could be additive. In this study such stresses were considered to be additive for only approximately 6 hr each day.

The magnitude of the restrained-warping stresses depends on temperature and moisture differentials between the top and the bottom of the slab. The former differential has the major effect and in spring and summer it may be approximated as 3° F per in. of slab thickness; in fall and winter it may be reduced to $\frac{2}{3}$ this amount. On this basis $\frac{1}{8}$ of the annual traffic may be assumed to be passing over the slab when the largest restrained-warping stresses are additive to load stresses, and another $\frac{1}{8}$ of this annual traffic may be assumed to be passing over it when $\frac{2}{3}$ of the maximum restrained-warping stresses are additive to load stresses.

To the casual reader this condition may suggest the erroneous conclusion that the reduced volume of effective traffic would lead to earlier failure due to the corner loading. Fig. 2 shows the magnitude of the stresses that can exist for the corner or the longitudinal-edge loading positions, but it should be noted that only those stresses above 50% of the flexural modulus of rupture of the concrete (350 lb per sq in. in Fig. 2) will have any appreciable effect in producing cracking.

Influence of Lateral Position of Load on Load Stress.—Reports of both the Arlington road tests and Road Test One-MD contain data on the relation of position to stress. The latter report reveals that the stress in a longitudinal direction at a point 6 in. from the free longitudinal edge of the pavement would be reduced from 100% to 40% if the wheel were moved transversely from this point to a position 30 in. from the free edge. The stress-reduction curve is almost a straight line between these two positions. With corner loading the reduction in stress at the critical section is from 100% to 60% for a similar lateral shift of the load.

These reductions are of interest because a complete analysis of load stresses at any point must include the effect at that point of loads 1 ft, 2 ft, or possibly 3 ft away in a lateral direction.

Length of Pavement Slab.—In determining the thickness of a slab, the length of the slab is involved only in the computation of the restrained-warping stress.

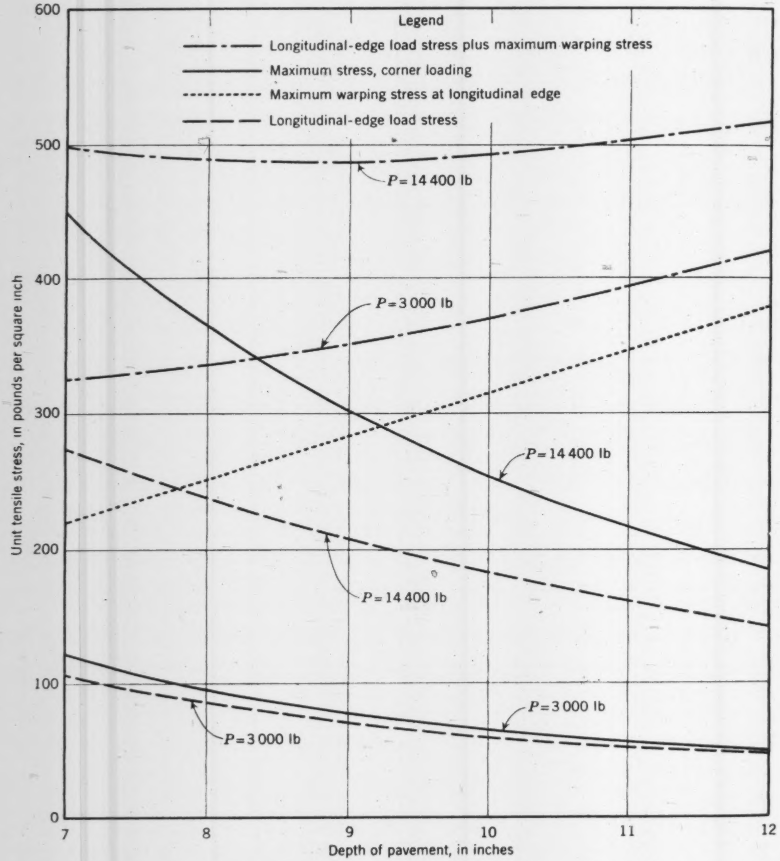

FIG. 2.—TENSILE STRESS RELATED TO THICKNESS, $k = 300$ LB PER SQ IN. PER IN., SLAB LENGTH = 30 FT, $E = 4 \times 10^6$ LB PER SQ IN., $\mu = 0.15$, AND $\alpha = 5 \times 10^{-6}$ IN. PER IN. PER DEGREE F

The Bradbury curve[16] for the coefficient C clearly indictes that beyond a length of 15 ft there is no appreciable increase in restrained-warping stress with increase in slab length. It also indicates that slabs less than 15 ft long must be used if appreciable restrained-warping stresses are to be avoided. On Pennsylvania highways, a slab length of 61.5 ft is used, and because highway slab lengths of less than 15 ft do not seem practical or economical the design values suggested in this study are based on slab lengths greater than 30 ft.

---

[16] "Reinforced Concrete Pavements," by R. D. Bradbury, The Wire Reinforcement Inst., Washington, D. C., 1938, p. 40.

Properties of the Concrete.—The flexural modulus of elasticity, the Poisson ratio, and the coefficient of thermal expansion or contraction of concrete directly affect the stresses in the slabs. Although these properties undoubtedly vary somewhat in any length of pavement, the following values were selected as representative and were used in this study: $E = 4 \times 10^6$ lb per sq in., $\mu = 0.15$, and $\alpha = 0.000005$ per degree F.

TABLE 2.—COMPUTATION OF EQUIVALENT NUMBER OF 5,000-LB LOAD REPETITIONS [a]

Wheel load, in pounds	Wheel position[b]	Longitudinal edge stress[c] (load plus warping)	Percentage of modulus of rupture	Repetitions to cause cracking	Actual repetitions per year	Equivalent 5,000-lb load repetitions per year[d]
Δt = 3° F PER IN. OF SLAB LENGTH						
3,000	a	<350	....	∞	....	0
4,000	a	363	51.8	550,000	127	39
5,000	a	384	54.8	170,000	61	61
	b	357	51.0	850,000	156	31
6,000	a	402	57.4	65,000	78	204
	b	372	53.1	340,000	200	100
7,000	a	418	59.8	30,000	78	442
	b	384	54.8	170,000	199	199
	c	351	50.1	∞	....	0
8,000	a	433	61.9	17,000	74	740
	b	396	56.6	90,000	191	361
	c	360	51.4	700,000	393	95
9,000	a	448	64.1	8,000	74	1,575
	b	408	58.3	48,000	190	673
	c	369	52.7	400,000	390	166
10,000	a	463	66.2	3,900	36	1,570
	b	421	60.1	28,000	92	553
	c	378	54.0	234,000	189	137
11,000	a	473	67.6	2,600	9.1	595
	b	428	61.2	20,000	23.4	199
	c	384	54.8	170,000	48.2	48.2
12,000	a	487	69.5	1,500	1.4	159
	b	440	62.8	12,000	3.7	52.4
	c	392	56.0	110,000	7.6	11.7
13,000	a	496	70.9	1,040	0.6	102
	b	447	63.9	8,500	1.5	30
	c	398	56.9	80,000	3.1	6.6
15,000	a	521	74.4	320	0.3	154
	b	468	66.9	3,150	0.7	37.8
	c	413	59.1	35,000	1.5	7.3
	d	358	51.2	750,000	2.7	0.6
Δt = 2° F PER IN. OF SLAB LENGTH						
9,000	a	365	52.1	500,000	74	25.2
10,000	a	380	54.3	210,000	36	29.2
11,000	a	390	55.7	120,000	9.1	12.9
12,000	a	404	57.7	60,000	1.4	4.0
13,000	a	413	59.0	37,000	0.6	2.8
	b	365	52.0	450,000	1.5	0.6
15,000	a	438	62.6	13,000	0.3	3.9
	b	383	54.7	180,000	0.7	0.6

[a] Slab depth = 8 in.; k = 200 lb per sq in. per in.; slab length = 30 ft; slab width = 12 ft. [b] Wheel positions are: Letter a—center of wheel 6 in. from longitudinal edge; letter b—center of wheel 12 in. from longitudinal edge; letter c—center of wheel 18 in. from longitudinal edge; letter d—center of wheel 24 in. from longitudinal edge. [c] In pounds per square inch. [d] Repetitions of 5,000-lb wheel loads placed at position "a" on the slab.

Resistance to failure resulting from numerous applications of unit stresses less than the yield-point unit stress is also of interest in such a study as this. Although data on fatigue in concrete beams in bending are available, there appear to be no such data on large slabs subjected to localized bending stresses. In this study the fatigue curve of Mr. Bradbury[17] was used to determine the relative detrimental effects of various unit stresses.

The Design Method

After limiting the possibilities of failure to diagonal cracking across the corner due to loads on or near the corner or to transverse cracking due to tensile stresses in the bottom of the slab at points near the longitudinal free edge of the pavement, the two loading positions were examined in detail, and curves for load stress and restrained-warping stress were constructed.

TABLE 3.—Computation of Load Percent Factors [a]

Wheel load, in pounds	Actual repetitions per year per lane	12-Ft Lane Width			11-Ft Lane Width		10-Ft Lane Width		9-Ft Lane Width	
		Equivalent 5,000-lb loads per year	Percent factors	Revised percent factors	Equivalent 5,000-lb loads per year	Percent factors	Equivalent 5,000-lb loads per year	Percent factors	Equivalent 5,000-lb loads per year	Percent factors
4,000	145,000	39	0.03	0.05	89	0.06	323	0.22	875	0.60
5,000	69,200	92	0.13	0.13	204	0.30	706	1.02	1,675	2.42
6,000	89,000	304	0.34	0.39	677	0.76	2,340	2.6	5,553	6.2
7,000	88,600	641	0.73	0.77	1,430	1.6	4,950	5.6	11,860	13.4
8,000	85,000	1,196	1.4	1.5	2,667	3.1	8,929	10.5	20,756	24.4
9,000	84,200	2,439	2.9	2.9	5,455	6.5	18,464	21.9	43,545	51.7
10,000	40,750	2,289	5.6	5.2	5,138	12.6	17,490	42.9	42,169	105.0
11,000	10,400	855	8.2	8.2	1,919	18.4	6,555	63.0	15,907	153.0
12,000	1,642	227	13.8	13.6	510	31.0	1,748	107.0	4,250	258.0
13,000	660	142	21.5	23.6	319	48.4	1,099	165.0	2,696	407.0
15,000	330	204	61.8	63.3	460	139.0	1,599	484.0	3,984	1,210.0
Totals		8,428			18,868		64,203		153,270	
Crack-resistance factor, in years		$\frac{170,000}{8,428} = 20.4$			$\frac{170,000}{18,868} = 9.1$		$\frac{170,000}{64,203} = 2.7$		$\frac{170,000}{153,270} = 1.1$	
Ratio of crack-resistance factors		$\frac{20.4}{20.4} = 1.0$			$\frac{20.4}{9.1} = 2.24$		$\frac{20.4}{2.7} = 7.55$		$\frac{20.4}{1.1} = 18.5$	

[a] Pavement depth = 8 in. and k = 200 lb per sq in. per in.

The commercial traffic on the highway lane was considered to be distributed laterally as indicated by Table 1 so that the number of wheel loads of each magnitude traveling 1 ft or 2 ft from the point under study could be known. A wheel load 1.5 ft from the edge was then known to be only 70% effective in producing longitudinal stress at a point 0.5 ft from the edge, as shown in Road Test One-MD. Such load stresses due to wheels within 2 ft or 3 ft of the point were then added algebraically to the restrained-warping stresses at this point. Of course, the worst combinations of load and restrained-warping stress for longitudinal-edge loading will only occur under approximately $\frac{1}{8}$ of the yearly traffic. Another $\frac{1}{8}$ of the yearly traffic must also be considered when studying the combined effect of load and the smaller restrained-warping stresses caused by the temperature differential of 2° F per in. of the slab depth which may be expected in fall and winter. The actual number of effective repetitions per year of various wheel loads and the combined stress at a point 0.5 ft from the longitudinal edge for a sample case is shown in Table 2.

---

[17] "Reinforced Concrete Pavements," by R. D. Bradbury, The Wire Reinforcement Inst., Washington, D. C., 1938, p. 55.

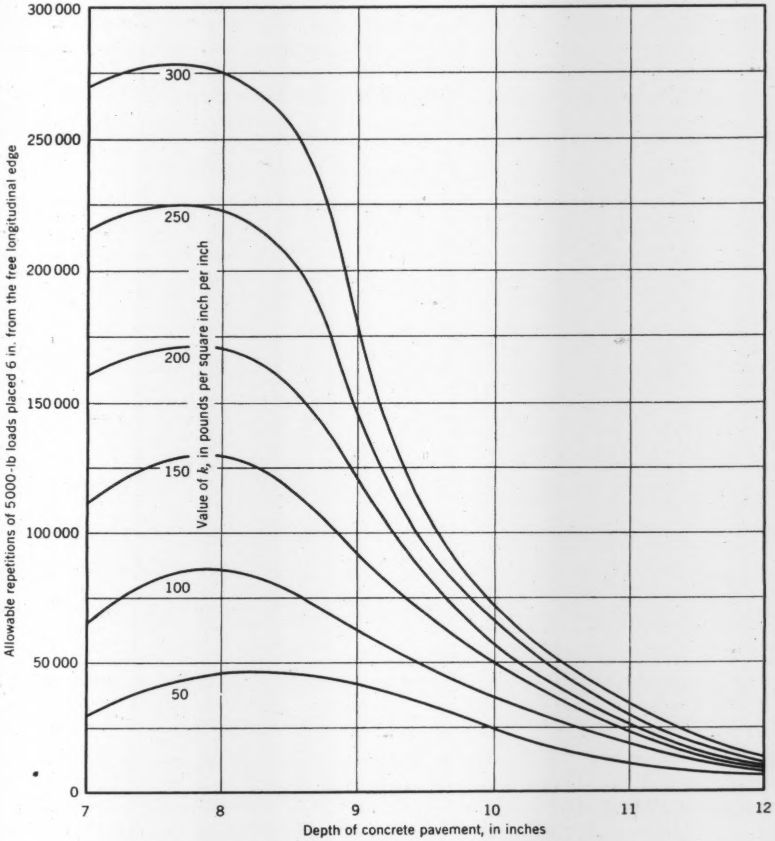

FIG. 3.—CONCRETE-PAVEMENT DESIGN CURVES FOR MODULUS OF RUPTURE OF 700 LB PER SQ IN.

To total the effects of various tensile stresses a common denominator was needed. The Bradbury fatigue curve for concrete in bending was used to determine the number of repetitions of each stress which would cause failure. From this value the actual number of repetitions of a single stress could be converted by proportion to the equivalent number of repetitions of any other stress. In this study all wheel-load effects were converted to an equivalent number of

5,000-lb wheel loads applied 0.5 ft from the edge when the maximum restrained-warping stress was effective.

For longitudinal-edge loading the number of these 5,000-lb wheel loads equivalent to the actual number of wheel loads of a particular weight traveling on a pavement slab was expressed as a "load percent factor" as shown in Table 3. The column headed "Revised percent factors" for a 12-ft lane width has been included to show that the computed percent factors produce a nearly smooth plot. In Table 4 similar percent factors for 12-ft lanes are presented for various values of pavement thickness and subgrade bearing capacity.

The "crack-resistance factor" in Table 3 was determined by dividing the number of 5,000-lb loads 0.5 ft from the edge that cause failure by the total equivalent 5,000-lb wheel loads produced by the particular traffic pattern in the problem. The numerator in this computation appears as the ordinate in Fig. 3, which was constructed using computed stress values and the Bradbury fatigue curve.

TABLE 4.—PERCENT FACTORS TO CONVERT VARIOUS WHEEL-LOAD

Wheel loads, in pounds	Value of k, in Pounds Per Square Inch Per Inch,									
	$k < 100$				$100 < k < 175$				$175 < k$	
	Concrete thickness,									
	7	8	9	10	7	8	9	10	7	8
3,000	0	0.01	0.01	0.03	0.02	0.01	0.01	0.05	0	0
4,000	0.06	0.07	0.09	0.11	0.04	0.04	0.06	0.09	0.03	0.05
5,000	0.12	0.13	0.18	0.22	0.11	0.12	0.17	0.27	0.09	0.13
6,000	0.50	0.39	0.43	0.42	0.31	0.33	0.35	0.49	0.39	0.39
7,000	1.30	0.98	0.90	0.84	0.86	0.77	0.70	0.85	0.95	0.77
8,000	3.2	2.1	2.0	1.5	2.4	1.8	1.4	1.4	2.4	1.5
9,000	8.7	5.5	3.9	2.9	5.1	3.6	2.6	2.3	5.1	2.9
10,000	22.4	12.3	7.4	5.0	10.2	6.9	4.6	3.9	9.2	5.2
11,000	40.6	25.9	13.2	7.8	18.4	11.3	7.5	5.8	15.2	8.2
12,000	50.4	34.7	23.4	13.0	31.8	19.2	11.8	8.1	25.6	13.6
13,000	78.6	47.7	38.6	20.8	54.1	31.1	19.2	12.9	48.6	23.6
15,000	199	111	80.0	42.1	148	71.5	41.2	28.1	138	63.3
17,500	468	240	149	71.7	220	142	88.0	48.0	220	117
20,000	2,880	402	281	136	370	268	162	75.0	322	252

The ratios between the crack-resistance factors illustrated in Table 3 are most interesting. Computations similar to those of Table 3 were made for lane widths of 12 ft, 11 ft, 10 ft, and 9 ft for all the combinations of depth and subgrade support indicated in Table 4. The ratios of crack-resistance factors for 11-ft, 10-ft, and 9-ft slab widths to those for the 12-ft slab width were always close to 2.25, 8.1, and 18.0, respectively. Therefore, percent factors were not presented in Table 4 for other than 12-ft slab widths.

The percent factors in Table 4 can be used to convert any traffic pattern on a pavement lane to equivalent 5,000-lb loads applied 6 in. from the longitudinal free edge of the slab. The crack-resistance factor can then be computed, and, if the pavement lane is not 12 ft wide, the ratios of 2.25, 8.1, or 18.0 can be used to convert the crack-resistance factor to its proper value. A sample design problem is presented in Table 5 to illustrate how the pavement depth providing longest pavement life can be chosen for any highway.

The life of a pavement, of course, does not become zero the day the first crack occurs; therefore, an empirical value was needed to relate the crack-resistance factor to pavement life. To determine this value and to check the design method in every possible way, detailed inspections were made of pavements at the loadometer stations throughout Pennsylvania. Superintendents from the Pennsylvania Department of Highways made estimates of the remaining life of each pavement, and separate estimates were made by the personnel conducting the study to assure uniformity in reporting the data. Soil and drainage conditions at these sites were closely observed, and possible seasonal fluctuations of traffic were considered. A traffic prediction curve was constructed, based on the collection of gasoline taxes in the past and the most reliable estimates available for the future.

EFFECTS TO EQUIVALENT 5,000-LB WHEEL LOADS (12-FT LANES)

as Determined Through Plate Bearing Tests										Wheel loads, in pounds
< 225		225 < k < 275				275 < k				
h, in inches										
9	10	7	8	9	10	7	8	9	10	
0.01	0.04	0.02	0.01	0.01	0.05	0	0	0	0.04	3,000
0.05	0.09	0.04	0.03	0.05	0.09	0.04	0.04	0.06	0.10	4,000
0.16	0.24	0.07	0.09	0.15	0.25	0.09	0.09	0.15	0.26	5,000
0.40	0.51	0.27	0.29	0.37	0.48	0.26	0.24	0.36	0.52	6,000
0.79	0.97	0.72	0.66	0.73	0.83	0.62	0.58	0.74	0.78	7,000
1.1	1.3	1.8	1.3	1.4	1.3	1.3	1.1	1.3	1.2	8,000
2.3	1.9	3.8	2.6	2.3	2.0	2.5	2.1	2.3	1.9	9,000
3.8	3.0	6.8	4.5	3.8	3.0	4.5	3.7	3.8	2.9	10,000
5.9	4.6	11.4	7.3	5.8	4.3	7.9	6.4	5.7	3.9	11,000
9.3	5.8	19.1	11.7	9.0	5.8	12.8	10.0	8.3	5.4	12,000
17.2	9.7	34.3	19.4	14.7	9.4	19.6	14.8	11.9	7.7	13,000
39.8	23.1	91.9	48.1	32.9	18.4	45.5	32.9	25.8	13.7	15,000
61.6	31.6	140	88.0	52.0	26.0	77.5	60.7	41.5	21.2	17,500
101	54.5	230	160	87.0	44.0	140	105	68.1	33.0	20,000

The conclusions of this part of the study indicated that, for pavements resting on subgrades with k-values of 250 lb per sq in. per in. or more, the pavement life would be approximately twice the crack-resistance factor. For pavements resting on poorer subgrades, the ratio of pavement life to the crack-resistance factor chosen was about 1.3.

As an example, an average daily traffic of 7,700 vehicles is assumed, of which 28% is commercial. If two 12-ft-wide lanes are to be used, and if the average number of axles per commercial vehicle is 2.60 (letting a tandem axle equal 2 axles), the current traffic rate will be $\frac{1}{2} \times 7{,}700 \times 365 \times 0.28 \times 2.60 = 1{,}022{,}000$ commercial axles per lane per year. The transverse-crack expectancy, based on the 8-in. depth determined in Table 5, is $100{,}000 \times 170{,}000/957$, or 17,750,000 axles; requiring $17{,}750{,}000/1{,}022{,}000 = 17.3$ yr. Therefore, the anticipated pavement life is $1.3 \times 17.3 = 22.5$ yr.

Using the empirical factors, the pavement life based on applications of 10,000 commercial axles per day per lane was computed for pavements of depths ranging from 7 in. to 10 in. and for soils having a wide range of bearing capacities for each of the sixteen different traffic weight patterns measured at loadometer stations. For each set of conditions, the depth of pavement that would provide the longest life and the pavement life in years are given in Table 7. The traffic weight patterns for the sixteen stations are presented in Table 6. For clarity it should be noted that 10,000 commercial axles per lane per day would be a particularly heavy traffic load and that the life values in Table 6 can be converted for any other number of commercial axles per lane per day by proportion.

TABLE 5.—Sample Design Problem: To Determine Pavement for Longest Life, If $k = 200$ Lb per Sq In., and the Traffic Pattern Is As in Col. 2

Wheel load, in pounds (1)	Commercial traffic pattern, in % (2)	Commercial traffic distribution[a] (3)	Thickness in Inches							
			7		8		9		10	
			5,000-lb percent factor (4)	Equivalent 5,000-lb load[b] (5)	5,000-lb percent factor (6)	Equivalent 5,000-lb load[c] (7)	5,000-lb percent factor (8)	Equivalent 5,000-lb load[d] (9)	5,000-lb percent factor (10)	Equivalent 5,000-lb load[e] (11)
3,000	30.3	30,000	0		0		0.01	3	0.04	12
4,000	16.4	16,400	0.03	5	0.05	8	0.05	8	0.09	15
5,000	7.9	7,900	0.09	7	0.13	10	0.16	13	0.24	19
6,000	10.1	10,100	0.39	39	0.39	39	0.40	40	0.51	52
7,000	10.0	10,000	0.95	95	0.77	77	0.79	79	0.97	97
8,000	9.6	9,600	2.4	230	1.5	144	1.1	106	1.3	125
9,000	9.6	9,600	5.1	489	2.9	278	2.3	222	1.9	181
10,000	4.6	4,600	9.2	423	5.2	240	3.8	175	3.0	138
11,000	1.2	1,200	15.2	183	8.2	98	5.9	71	4.6	55
12,000	0.2	200	25.6	51	13.6	27	9.3	19	5.8	12
13,000	0.07	70	48.6	34	23.6	17	17.2	12	9.7	7
15,000	0.03	30	138	41	63.3	19	39.8	12	23.1	7
Totals	100.00	100,000		1,597		957		760		720
Allowable loads 6 in. from edge[f]				158,000		170,000		120,000		59,000
Crack-resistance factor[g]				99		177[h]		158		82

[a] Number of axles per 100,000 axles. [b] Col. 5 = Col. 3 × Col. 4. [c] Col. 7 = Col. 3 × Col. 6. [d] Col. 9 = Col. 3 × Col. 8. [e] Col. 11 = Col. 3 × Col. 10. [f] From Fig. 3. [g] The ratio of the allowable load to the total equivalent load, in years. [h] For longest pavement life, 8-in. depth should be used.

Table 8 contains a comparison between pavement-life values estimated by careful inspection and those determined by using the foregoing design method. The pavements included in this table were chosen to illustrate problems introduced by such items as multilane highways and slabs of nonuniform depth. For values in Table 8 the average pavement depths were used in the design method; outer lanes of three-lane or four-lane highways were analyzed as 12-ft lanes regardless of their width and were assumed to carry one half the two-way commercial traffic on the road. Such assumptions for traffic on multilane highways may be questioned but they were made after considering that trucks tend to stay away from the edge of the pavement on such highways. Errors in this assumption are reflected only in Table 8 and do not affect the basic design method.

In order to ascertain whether or not the corner loading condition would have caused failure before longitudinal-edge loading, a parallel investigation was made of crack-resistance factors with corner loading. The only major difference in the method of attack was that the full commercial traffic count was considered to be effective for this loading. However, the lateral distribution of traffic on the lane and the reduction in stress at the critical section when a load was not within 6 in. of the corner, combined with the low unit stress values resulting from moderate loads (Fig. 2), materially reduced the total equivalent 5,000-lb wheel loads to only a fraction of those found for the longitudinal-edge loading condition.

TABLE 6.—COMMERCIAL TRAFFIC PATTERNS AT LOADOMETER STATIONS

Wheel loads, in pounds	STATION														
	L-53	L-182	L-123	L-502	L-136	L-169	L-88	L-32	L-132	L-110	L-104	L-159	L-12	L-192	L-59
	TRAFFIC LOAD DESCRIPTION														
	Heavy					Medium							Light		
	PERCENTAGE DISTRIBUTION OF COMMERCIAL WHEEL LOADS														
<3,000	36.4	21.8	28.2	20.2	21.1	44.6	43.3	51.7	32.8	30.3	41.0	50.0	49.2	47.5	55.7
4,000	12.8	10.4	15.2	6.5	9.4	10.3	14.5	12.3	11.8	16.4	17.2	12.1	12.6	14.7	9.8
5,000	7.3	11.2	8.6	10.5	9.5	9.1	10.8	6.4	9.8	7.9	8.0	5.0	8.3	9.1	9.5
6,000	9.9	12.8	7.7	13.7	13.8	9.1	8.7	9.3	8.3	10.1	8.2	6.1	6.2	8.1	6.7
7,000	7.3	11.4	9.4	16.1	14.3	7.9	4.3	3.5	9.7	10.0	6.3	6.6	7.9	7.4	5.5
8,000	10.3	13.3	11.2	15.6	15.2	8.2	3.9	2.5	11.0	9.6	6.5	8.8	7.0	5.7	5.5
9,000	6.8	11.2	12.1	11.5	10.5	4.5	5.8	4.4	9.4	9.6	6.8	7.5	6.2	4.7	4.0
10,000	4.3	6.0	5.7	3.9	4.2	3.0	4.3	5.9	5.6	4.6	3.5	1.9	1.5	1.9	2.7
11,000	3.6	1.3	1.1	1.3	1.6	0.6	2.3	2.0	1.1	1.2	1.6	1.7	0.9	0.4	0.3
12,000	0.8	0.4	0.5	0.5	0.1	1.5	1.7	1.5	0.5	0.2	0.6	0	0.2	0.4	0.3
13,000	0.4	0.1	0.1	0.1	0.1	0.9	0.2	0.5	0	0.06	0.2	0	0	0.1	0
15,000	0.1	0.1	0.2	0.1	0.2	0.3	0.2	0	0	0.04	0.1	0.3	0	0	0
Totals	100.0	100.0	100.0	100.0	100.0	100.0	100.0	100.0	100.0	100.0	100.0	100.0	100.0	100.0	100.0

A comparison of pavement-life values based on 10,000 commercial axles per lane per day is made in Table 9. Because 9-ft pavement lanes would suffer the most detrimental corner loading effects, most of the comparisons shown in Table 9 are for this slab width. No traffic lane would ever be subjected to as many as 10,000 commercial axle loads per day, but Table 9 clearly shows that longitudinal-edge loading is the critical loading position when lateral distribution of traffic and restrained-warping stresses are considered. The pavement-life values given for corner loading are, of course, absurd and are listed only to illustrate the importance of the longitudinal-edge loading. Occasionally, diagonal cracks will be found on pavement slabs, but these can be traced directly

TABLE 7.—PAVEMENT THICKNESS AND PAVEMENT LIFE FOR VARIOUS TRAFFIC PATTERNS AND k-VALUES [a]

Traffic load description	Station	Subgrade Modulus Classification and Value, in Lb per Sq In. per In.									
		Very Good $k > 275$		Good $275 > k > 225$		Fair $225 > k > 175$		Poor $175 > k > 100$		Very Poor $100 > k$	
		Pavement thickness[b]	Pavement life[c]	Pavement thickness[b]	Pavement life[c]	Pavement thickness[b]	Pavement life[c]	Pavement thickness[b]	Pavement life[c]	Pavement thickness[b]	Pavement life[c]
Heavy	L-53	8	16.8	8	11.3	8	4.9	9	3.0	9	0.8
	L-182	8	17.1	8	11.4	8	4.9	8	3.1	9	0.9
	L-123	8	17.2	8	11.4	8	5.0	9	3.1	9	0.9
	L-502	8	17.2	8	11.5	8	5.1	8	3.1	9	0.9
	L-136	8	17.4	8	11.6	8	5.1	8	3.2	9	1.0
Medium	L-169	8	18.9	8	12.3	8	5.2	9	3.3	10	0.9
	L-88	8	18.9	8	12.6	8	5.5	9	3.7	9	0.9
	L-32	8	20.3	8	12.2	8	5.0	9	3.6	9	1.0
	L-132	8	20.6	8	13.9	8	6.1	8	3.7	9	1.1
	L-110	8	22.1	8	14.6	8	6.4	8	4.0	9	1.1
	L-104	8	23.6	8	15.8	8	6.9	8 or 9	4.1	9	1.2
	L-159	8	25.4	8	16.6	8	7.1	9	4.5	9	1.3
Light	L-12	8	36.5	8	24.7	8	11.0	8	6.8	9	2.0
	L-192	8	38.8	8	26.1	8	11.6	8	7.1	9	2.0
	L-59	8	42.6	8	28.6	8	12.5	8	7.7	9	2.2

[a] Based on 10,000 commercial axle loads per day for the loadometer stations indicated. [b] Best choice, in inches. [c] Corresponding to the pavement thickness chosen, in years.

TABLE 8.—COMPARISON OF REMAINING PAVEMENT LIFE AS COMPUTED BY THE LONGITUDINAL-EDGE-LOADING DESIGN METHOD AND REPORTED BY FIELD INSPECTION

Station	Average daily traffic (1951)	Commercial traffic % of Col. 2	Average number axles per truck	Subgrade modulus,[a] k	Pavement Data				Remaining Pavement Life[c]	
					Thickness, in inches	No. of lanes	Lane width, in feet	Year constructed[b]	Field estimate (years)	By design method (years)
(1)	(2)	(3)	(4)	(5)	(6)	(7)	(8)	(9)	(10)	(11)
L-1	12,400	31	2.16	200	9-8-9	4	12	1929	−1	−1
L-2	2,200	29	2.20	250	9-7-9	2	9	1924	1	3
L-4	4,100	23	2.40	300	9-7-9	2	9	1928	1	−2
L-32	3,100	28	2.33	150	6-8-6	2	11	1921	−14[d]	−12
L-53	3,800	19	2.34	250	9-7-9	2	10	1936	5	5
L-59	2,750	17	2.20	200	9-7-9	2	9	1928	1	0
L-88	3,200	18	2.20	200	6-8-6	2	11	1922	−4[e]	−5
L-104	7,150	18	2.40	150	10-8-10	3	10	1933	8	11
L-110	7,700	28	2.65	200	9	4	12	1944	8	9
L-136	15,900	23	2.50	150	10-8-10	3	10	1934	−3[f]	−5
L-192	8,500	17	2.12	200	9	2	10	1935	8	8
L-202	5,500	28	2.65	250	9-7-9	2	10	1930	0	−2
L-301	9,900	18	2.40	150	10-8-10	3	10	1938	13	7
L-302	13,200	18	2.40	250	10-8-10	2 1	17.5 20	1925	10	12
L-461	8,000	20	2.65	200	10-8-10	3	10	1930	8	11
L-503	5,200	16	2.65	200	9	3	11	1948	18	24

[a] Estimated. [b] Original Construction. [c] The survey and study was made in 1952; a reported life of −1 means the pavement should have been replaced in 1951. [d] Resurfaced in 1938. [e] Replaced in 1948. Resurfaced in 1949.

to loss of subgrade support beneath the corner of the slab. Of course, with extremely heavy loads such as those of airplane wheels a pavement may crack across the corner from a single application of load. However, this paper presents a design method applicable only to slabs carrying loads of magnitudes that can be expected on highways.

CONCLUSIONS

1. Restrained-warping stresses must be considered when portland cement concrete pavement slabs are to be designed for highways.

2. For highway traffic, the critical loading position of the wheel is along the longitudinal free edge of the pavement slab—not at the corner.

TABLE 9.—COMPARISON OF PAVEMENT LIFE AS COMPUTED FOR LONGITUDINAL-EDGE LOADING AND CORNER LOADING

Station	Pavement thickness (in inches)	Subgrade modulus,[a] k	Lane width (in feet)	PAVEMENT LIFE, IN YEARS, BASED ON 10,000 COMMERCIAL AXLES PER LANE PER DAY[b]	
				Longitudinal-edge loading	Corner loading
L-53	9	50	9	0.04	767
	8	200	9	0.27	104
	8	300	9	0.93	505
L-182	9	50	9	0.05	767
	8	100	9	0.17	48
L-123	9	50	9	0.05	383
	8	200	9	0.28	73
	8	200	12	5.0	1,530
L-502	9	50	9	0.05	767
	8	100	9	0.17	48
L-136	9	50	9	0.06	383
	8	100	9	0.18	26
	8	100	12	3.2	536
L-169	10	50	9	0.05	∞
	9	100	9	0.18	∞
	8	200	9	0.29	38
L-88	9	50	9	0.05	383
	8	200	9	0.30	69

[a] In pounds per square inch per inch. [b] This number was chosen only for purposes of comparison and for simplicity of computation.

3. Highway pavement thicknesses should be chosen only after consideration is given to the number of repetitions of various wheel loads and should not be chosen on the basis of a single application of a particularly heavy wheel load.

4. The semi-empirical design method illustrated in this paper can be easily and quickly applied by using the key percent factors in Table 4.

5. Table 7 clearly indicates that pavement thicknesses need not exceed 8 in. or 9 in. for the traffic now encountered on highways. This table may also be interpreted as showing that a pavement life of thirty years may not be attained for some traffic conditions regardless of the condition of the subgrade.

6. Table 7 indicates that funds should be spent on improvement of the bearing capacity of the subgrade rather than on increased thicknesses of pavement.

APPENDIX. NOTATION

The following symbols, adopted for use in the paper and for the guidance of discussers, conform essentially with "American Standard Letter Symbols for Mechanics of Solid Bodies" (ASA Z10.3-1948), prepared by a committee of the American Standards Association with Society representation, and approved by the Association in 1948:

a = radius, in inches, of a circle of area equivalent to the area of contact of the wheel with the pavement;

$a_1 = a\sqrt{2}$ = distance, in inches, from the slab corner along the bisector of the corner angle to the center of the area over which the load is applied for the critical corner-loading condition;

b = radius, in inches, of the circle having a pressure distribution equivalent to the area of contact of the wheel with the pavement;

$C = L_x/l$ = a coefficient;

h = thickness of pavement, in inches;

E = modulus of elasticity of concrete, in pounds per square inch;

k = modulus of subgrade reaction, in pounds per square inch per inch;

L = maximum value, in inches, of the radius of the circular area within which a redistribution of subgrade reactions is made (the center of the circle is at the point of load application);

L_x = length of the pavement slab in the longitudinal direction of the highway, in inches;

$l = \sqrt[4]{\dfrac{E\,h^3}{12\,(1 - \mu^2)\,k}}$ = radius of relative stiffness, in inches;

P = vertical wheel load, in pounds;

s_{ex} = maximum longitudinal unit stress 6 in. from the free longitudinal edge of the slab produced by a temperature differential Δt between the top and bottom of the pavement slab, in pounds per square inch;

Z = reduction ratio of the maximum deflection;

α = coefficient of thermal expansion of concrete, per degree Fahrenheit;

Δt = temperature differential between the top and bottom of the pavement slab, in degrees Fahrenheit;

μ = Poisson ratio;

σ_c = maximum unit stress in the pavement slab produced by a vertical load on the pavement at a distance a_1 from the corner, in pounds per square inch; and

σ_{ex} = maximum longitudinal unit stress in the slab at a point 6 in. from the free longitudinal edge and at least 5 ft from the transverse edge produced by a vertical load P at this point on the pavement slab, in pounds per square inch.

DISCUSSION

LAWRENCE A. PALMER.[18]—Mr. Moore's paper indicates the best approach to the improved design of concrete pavement for highways. Two outstanding conclusions are that nothing is gained, economically or otherwise, by increasing the slab thickness beyond 8 in. or 9 in. and that more effort and funds should be spent on improving the subgrade support.

Highway engineers usually compute the slab thickness by using the Pickett semi-empirical expressions for exterior corner loading, assuming that only approximately 20% of the load can be transferred from one slab corner to the next. Mr. Pickett, of course, assumed in developing his expressions that for some distance from the corner there is no subgrade support. His expressions are thoroughly reliable for the assumed conditions.

It is both easy and economical to maintain adequate subgrade support at slab corners and elsewhere. A well-compacted subbase of stable earth material and of adequate thickness under a concrete pavement is not a luxury. When there is irregular, "mushroom" support of the slabs, none of the rational methods of Messrs. Westergaard, Pickett, and others is at all applicable. These methods are closely applicable, however, if there is continuous and permanent subgrade support. The application of sound engineering principles is thereby made possible.

Present specifications and design criteria of the Bureau of Yards and Docks (United States Department of the Navy) require that the subbase material under concrete have a minimum soaked California Bearing Ratio of 30 and that it be compacted to not less than 95% of the maximum density corresponding to optimum moisture as determined by the modified laboratory compaction procedure of the American Association of State Highway Officials. It is further required that the compacted subbase have a minimum Westergaard k-modulus of 200. When these requirements have been met, there has been no instance of pumping at joints known to the writer. Neither have there been instances reported of corner cracking.

When these conditions are realized on highways, thickness design should be based on anticipated maximum bending stresses at points close to the free longitudinal edges, as Mr. Moore concludes. At airfields, loads near the free edges are quite infrequent, and, if there is effective load transfer at transverse contraction joints and longitudinal keyed joints, design should be based only on loading at the slab interiors.

If plain concrete is used, the slab length must depend not only on restrained-warping stresses but also on necessary limitations to the opening of contraction joints. These joints must not open so wide as to preclude proper aggregate interlocking. The quality and maximum size of coarse aggregate are thus also factors to be considered in determining slab length.

Fig. 3 shows the advantages of designing relatively thin, heavily reinforced slabs. It shows further that the real benefit of proper subgrade support tends to be lost when the thickness of a concrete highway pavement exceeds 8 in. or

---

[18] Eng. Consultant, Soil Mechanics and Paving, U. S. Dept. of the Navy, Washington, D. C.

9 in. Obviously, flexural strength combined with flexability and also with reduction in restrained-warping stresses are in the direction of optimum conditions for longevity of concrete pavement subjected to highway traffic; it is only a small step from this conclusion to a full appreciation of the remarkable benefits that can be realized by prestressing concrete pavements for highways and airfields. The Department of the Navy has already made an excellent preliminary study of the possible advantages of such prestressing.

An additional consideration with respect to fatigue effects is that of the time between successive load repetitions. It is obvious, for example, that 50,000 load repetitions at a point with 1-min intervals between successive loads are far more damaging than the same number of loads at hourly intervals. Points near longitudinal edges are subjected to fewer load repetitions and have greater time intervals between successive loads than other points. The greater this time interval, the more "recovery" there is between shocks.

Earl C. Sutherland,[19] M. ASCE.—The subject considered by the author regarding the proper theoretical formula for designing the thickness of concrete pavements is one on which there is disagreement.

When Mr. Westergaard made his notable theoretical analysis of the stresses in concrete pavements caused by loads, two particular types of structural failure were of concern. These were (1) corner breaks at outside corners and (2) open transverse cracks that usually spalled badly.

Fig. 4(*a*) shows an outside corner break of the type analyzed by Mr. Westergaard.[7] The crack developed at distances of approximately 36 in. to 50 in. from the corner. As the author indicates, there are few breaks of this type currently to be found in pavements. This is true not only of modern pavements but also of older pavements that are still in use. The disappearance of this type of failure is probably largely due to two factors—(1) the substitution of pneumatic tires for hard rubber tires with a resulting increase in the tire contact area and (2) the increased width of pavements which results in traffic traveling at greater distances from the outside edges of the pavement.

Pavements of modern design are constructed in a manner that makes transverse cracks less objectionable than they formerly were. For example, plain concrete pavements are constructed with contraction joints at sufficiently close intervals to control transverse cracking, and expansion joints have been mostly eliminated so that the contraction joints as well as any cracks that may develop are held closed. Reinforced pavements are constructed with sufficient longitudinal reinforcement to hold transverse cracks closed, which greatly reduces the tendency for spalling or raveling. Furthermore, cracks in reinforced pavements have little if any tendency to pump except where the steel has broken.

The slab end failure which has become more common in recent years is perhaps the most troublesome type of failure in concrete pavements at the present time. A typical example is shown in Fig. 4(*b*). The actual cracking of the slab is usually preceded by severe faulting at the joint. The crack which follows is generally at distances of from 5 ft to 8 ft from the joint. This type of failure is found only in pavements carrying a considerable number of heavy trucks and is primarily the result of a loss of subgrade support under the slab end. The most common cause of this loss of subgrade support is pumping, although consolidation and softening of the subgrade by moisture are also factors.

---

[19] Senior Highway Engr., U. S. Bureau of Public Roads, Washington, D. C.

Unfortunately, none of the theoretical formulas for computing stresses in concrete pavements is applicable to the slab end load condition, nor does it seem likely that valid formulas for this load condition can be developed until more experimental data are available concerning the influence of granular subbases on the supporting properties of subgrades of a pumping nature and on the effectiveness of load transfer in reducing the magnitude of the stresses.

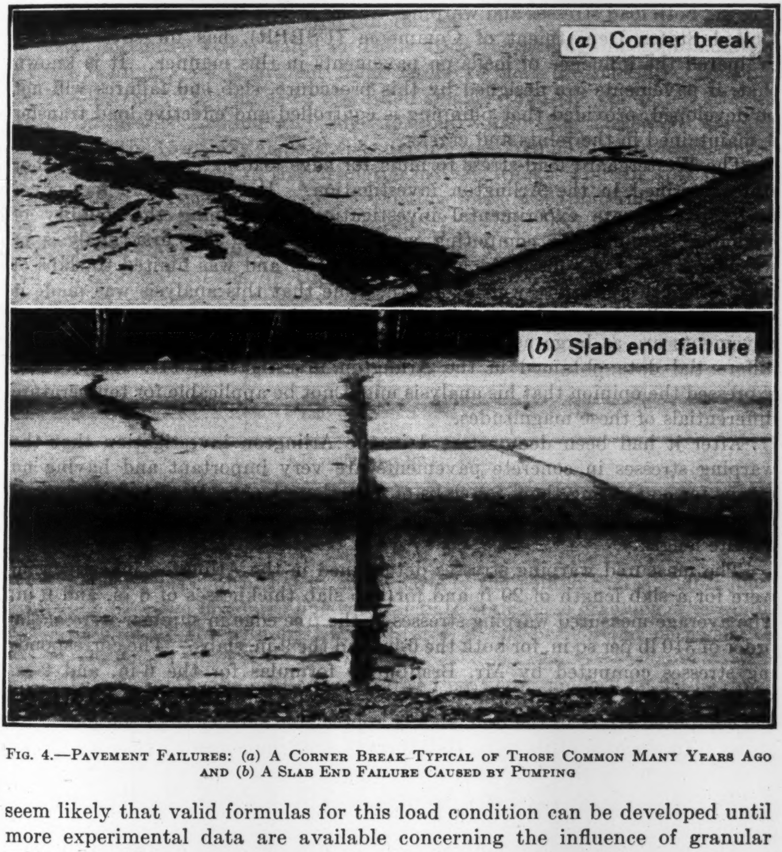

Fig. 4.—Pavement Failures: (a) A Corner Break Typical of Those Common Many Years Ago and (b) A Slab End Failure Caused by Pumping

It was stated previously that transverse cracks in modern concrete pavements do not appear to be as destructive as they were in pavements constructed many years ago. It is important, however, that pavements be designed with sufficient thickness to prevent the formation of transverse cracks at close intervals. The slabs of plain concrete pavements should be designed of the proper thickness and length to eliminate intermediate cracks in so far as possible. Reinforced pavements of the conventional type containing the usual weights of longitudinal reinforcement should be designed with sufficient thickness to avoid transverse cracking at intervals of less than approximately 15 ft or 20 ft.

There appears to be justification for the author's recommendation that concrete pavements be designed on the basis of the edge case of loading considering both load stresses and warping stresses. The Bureau of Public Roads, United States Department of Commerce (USBPR), has for several years evaluated the influence of loads on pavements in this manner. It is known that, if pavements are designed by this procedure, slab end failures will not be developed, provided that pumping is controlled and effective load transfer is maintained in the joints and cracks.

The Westergaard load-stress formula for edge loading[7] was, as the author states, verified in the Arlington investigation.[8] However, there has never been an adequate experimental investigation determining the validity of available formulas for computing warping stresses. The first analysis of warping stresses was made by Mr. Westergaard[12] and was limited to slabs of infinite length and finite width. At the time that this analysis was made it was not realized that the temperature differentials that develop in concrete pavements are as large as they are. After seeing some of the temperature differential data obtained in the Arlington investigation, Mr. Westergaard expressed the opinion that his analysis might not be applicable for temperature differentials of these magnitudes.

After it had been demonstrated in the Arlington investigation that the warping stresses in concrete pavements are very important and having no means for computing them for slabs of finite length, Mr. Bradbury developed formulas[20] for this purpose based on the Westergaard formulas for slabs of infinite length.

The measured warping stresses determined in the Arlington investigation[9] were for a slab length of 20 ft and for two slab thicknesses of 6 in. and 9 in. The average measured warping stresses at the free edge in summer were of the order of 310 lb per sq in. for both the 6-in. and the 9-in. slabs. The corresponding stresses computed by Mr. Bradbury's formulas for the 6-in. and 9-in. slabs are 245 lb per sq in. and 315 lb per sq in., respectively. For this case the computed stress in the 6-in. slab is appreciable smaller than the measured stress. In the case of the 9-in. slab there is close agreement.

Subsequent to the Arlington investigation, many warping-stress measurements were made on a pavement having a 15-ft slab length.[21] The results of this study have not been published.

The pavement on which these tests were made was constructed on the same subgrade as the Arlington pavement after the removal of the earlier pavement. The top 6 in. of the subgrade were stabilized, but this did not make an appreciable change in the modulus of subgrade resistance. The pavement was of uniform 8-in. thickness and the concrete was of two types—one containing gravel as a coarse aggregate and the other, crushed limestone. The physical properties of the two concretes were approximately the same and differed little from those of the concrete in the older Arlington test pavement. The average summertime warping stresses measured on this pavement together with the corresponding computed stresses are presented in Table 10. The temperature differential used for the computed stresses was essentially the same as the average measured differential.

---

[20] "Reinforced Concrete Pavements," by R. D. Bradbury, The Wire Reinforcement Inst., Washington, D. C., 1938.

[21] "The Investigational Concrete Pavements Progress Reports," *Research Reports No. 3B*, Highway Research Board, National Research Council, Washington, D. C., 1945, p. 89.

Each measured stress value in Table 10 is the average of approximately sixteen readings. It is evident from Table 10 that the measured warping stresses on the 15-ft-long slabs are much smaller than the computed stresses for both interior loading and edge loading. Also, the measured warping stresses for the 15-ft-long slabs at the edge are less than 50% of those measured for the 20-ft-long slabs in the Arlington investigation. Thus, it appears that the warping stresses computed by existing formulas applicable to slabs of finite length are much larger than the actual stresses if the slab length is approximately 15 ft.

TABLE 10.—AVERAGE MEASURED AND COMPUTED WARPING STRESSES ON PAVEMENT SLABS OF UNIFORM 8-IN. THICKNESS, 15 FT LONG

Coarse aggregate	INTERIOR LOADING		FREE-EDGE LOADING	
	Measured stress[a]	Computed stress[a]	Measured stress[a]	Computed stress[a]
Gravel	130	240	120	230
Crushed stone	150	265	115	250

[a] In pounds per square inch.

Experience has shown that in many parts of the United States a 20-ft joint spacing is effective in controlling intermediate transverse cracking whereas in others, expecially the western United States, it has been found necessary to reduce the length to 15 ft.

In Conclusion 5, the author has stated that under modern traffic loadings it is not necessary to use slab thicknesses greater than 8 in. or 9 in. This, of course, is true only if subgrade support is maintained. The conclusion is supported by data obtained in experimental investigations as well as by the theoretical studies considered by the author. For example, on Road Test One-MD the maximum stresses measured for the 22,400-lb single axle and the 44,800-lb tandem axle were of the order of 200 lb per sq in. or less on the natural granular subgrade on which no pumping developed.

In Conclusion 6, it is stated that funds should be spent on improving the bearing capacity of the subgrade rather than for increased thickness of pavement. This is true when the subgrade is fine-grained material and when there is danger that pumping may develop. When there is no danger of pumping, however, it is likely to prove more economical to increase the thickness of the pavement slab rather than to attempt to increase the bearing power of the subgrade because there is considerable evidence that granular subbases of usual thicknesses do little to increase the supporting power of the subgrade.

WARNER HARWOOD,[22] A. M. ASCE.—The paper focuses attention on the effect of increased width of pavement lanes in decreasing the proportion of applications of load which occur at critical locations close to the edge of the slab. However, by certain assumptions used in the determination of the load stresses and warping stresses, the author arrives at values for these stresses that are subject to question.

The paper is largely a summary of the material on rigid pavements originally presented in a report to the Pennsylvania General Assembly entitled "Technical Supplement to Highway Use and Highway Costs" in 1953. Table 2 is a copy of Table A–6 of that report, which is based on the computations of load and warping stresses shown in detail in Table A–5, of the same report.

A study of these tables indicates that, for all loadings, the edge warping stress in the 8-in.-thick slab is computed as 251 lb per sq in. for a temperature differential of 3°F per in. of depth and 167 lb per sq in. for a 2°F differential. These were computed by the formula proposed by Mr. Bradbury. The stresses computed by these formulas seem to be unreasonably high. When they were published in 1939 in a paper[23] by Mr. Kelley, a discussion was submitted by A. T. Goldbeck, M. ASCE, Mr. Kelley's predecessor as chief of the Division of Tests, USBPR. In this discussion Mr. Goldbeck states:[24]

> "I think that perhaps one of the phases of Mr. Kelley's paper which will be surprising to many, deals with the question of warping stresses. Warping stresses are really bending stresses and are shown to be very high, particularly when the slabs have lengths to which we are accustomed, for instance, 30 feet. * * * I am not convinced that the results obtained from the formulas used for calculating warping stresses are entirely correct. In this connection, let me refer to Table 9 in which are shown transverse temperature warping stresses. The effect of transverse warping is to produce bending of the slab transversely. It would seem that the greatest transverse stress which could possibly exist would be that in which the slab is so warped that it rests upon a line of support at the center of the slab. The dead load stress for a ten-foot width of a 6-in. slab thus supported is 156 psi., whereas the warping stress for a modulus of subgrade reaction of 300, is given at 210 psi. For an 8-in. slab the maximum possible dead load stress at the center, assuming the slab supported at the center and overhanging at the end, is only 117 psi. as against a calculated warping stress of 190 psi. This does not seem logical to me and I am wondering if the warping stresses in a longitudinal direction are really as high as the calculations show. * * * I note that warping stresses were observed on a test slab at Arlington. It would be very interesting to me to know how such stresses were observed. It is obvious that if deformations are taken with a strain gage, such deformations might give misleading results. It is perfectly possible, for illustration, to have high stress where no deformation is ob-

---

[22] Highways & Municipal Bureau, Portland Cement Assn., Chicago, Ill.

[23] "Application of the Results of Research to the Structural Design of Concrete Pavements," by E. F. Kelley, *Proceedings*, A.C.I., Vol. 35, 1939, p. 437.

[24] Discussion by A. T. Goldbeck of "Application of the Results of Research to the Structural Design on Concrete Pavements," by E. F. Kelley, *ibid.*, p. 464-11 and -12.

servable whatever; and, correspondingly have zero stress in spite of what seems to be a deformation."

Few additional data were published on warping stresses before the final report on Road Test One-MD which included the illustration[25] that Mr. Moore has used as Fig. 1. In this figure the stresses are of considerably greater magnitude than those which would be found by the Bradbury formula. This discrepancy casts further doubt on the accuracy of both the method of computing the stresses and the determination of these stresses in the field by the use of strain gages. The figure is referred to in the report as follows:[26]

> "The data of Fig. 151 indicate that the daytime warping stresses are quite high at some distance from the ends of the pavement slabs. Stresses of such magnitude when combined with the daytime stresses of the interior and free-edge loadings approach the modulus of rupture of the concrete, and as a result, transverse cracking might be expected. No significant cracking of the type attributable to the combined stress condition of these cases of loading was observed in this investigation."

The pavement used in the Maryland Test Road had been in service for nine years before the test was begun. At the time the test was begun there was little transverse cracking on the project and none in any of the slabs that were on a granular subgrade. The only transverse cracks that were formed during the test loading were in slabs on fine-grained soils where subgrade failure occurred during the test. The computed warping stresses added to the observed load stresses certainly exceeded the modulus of rupture of the concrete. Because no cracks formed it is evident that the actual stress was less than the sum of the computed and observed stresses. Probably both the computed and observed stresses (so-called) were greater than the actual stress.

In Mr. Moore's computation of load stresses there is also an assumption that results in higher values than exist in the field. For a wheel load placed so that the center of the wheel (or outside tire of dual-tired wheels) is 6 in. from the edge of the slab, he has computed the stresses using the Westergaard formula for edge stress. In this formula the contact area is considered to be a semicircle the diameter of which is along the pavement edge, and its use results in higher edge stresses than are present under the loading in question.

For example, for a 9,000-lb wheel load the center of gravity of the semicircular contact area as used in the Westergaard formula is 4.1 in. from the edge of the slab. By contrast, the center of gravity of a dual-tired wheel would be 12.5 in. from the edge if the center of the outside tire is 6 in. from the edge. This increase of more than 8 in. decreases the stress approximately 30% according to data from Road Test One-MD and approximately 25% when computed by the use of influence charts as outlined[27] by Mr. Pickett and G. K. Ray, A. M. ASCE. A proportionate reduction should be applied to the load stresses for other locations as they are all based on the stress computed for the case in which the load is 6 in. from the edge.

---

[25] "Final Report on Road Test One-Md," *Special Report No. 4*, Highway Research Board, National Research Council, Washington, D. C., 1952, p. 138, Fig. 151.

[26] *Ibid.*, p. 138.

[27] "Influence Charts for Concrete Pavements," by Gerald Pickett and G. K. Ray, *Transactions*, ASCE, Vol. 116, 1951, p. 49.

The result of these improper assumptions is most forcibly emphasized in Fig. 3, which indicates that a pavement 7 in. thick on a subgrade having a k-value of 300 lb per sq in. per in. would have twenty times the load-carrying capacity of a 12-in.-thick pavement on the same subgrade. Mr. Moore has indicated the absurdity of the long lives shown for corner loading in Table 9; however, the extremely short lives shown in the same table based on longitudinal-edge loading are equally absurd. One reason for this is that both the warping stresses and the load stresses that are assumed to be combined to produce longitudinal-edge failure are too high, as explained previously in this discussion. The other reason is that these lives are arbitrarily taken as twice the age at which a transverse crack would form. Experience gives no justification for this assumption. Plain pavements are jointed to prevent transverse cracking. Reinforced pavements contain steel to prevent intermediate transverse cracks from becoming points of weakness. In neither case is there any reason to establish pavement life on the basis of age at which the first crack forms.

ALBERT DE NEUFVILLE.[28]—Under the heading, "Conclusions," the author's opinion that concrete pavements 8 in. or 9 in. thick have longest life seems questionable. This conclusion is apparently based on the computation of combined load and restrained-warping stresses along the longitudinal edge, as shown in Fig. 2. The computation of restrained-warping stresses, however, is based on the Westergaard assumption of a constant temperature gradient in the pavement, an assumption that is inconsistent with the laws of heat flow.

Unfortunately, the author seems not to have read a paper by J. Thomlinson[29] in which the necessary formulas have been developed for temperature stresses in a concrete pavement having a temperature distribution consistent with the laws of heat flow. The variations of temperature in a pavement during a daily cycle as illustrated[30] in Mr. Thomlinson's paper correspond fairly closely with the temperature measurements in the Arlington road tests.[31] Mr. Thomlinson has shown[32] that the internal stress plus the restrained-warping stress is always smaller at the bottom of the slab than at the top. In a 6-in.-thick pavement, the bottom stresses are only approximately 70% of the top stresses, whereas for a 12-in.-thick pavement this percentage decreases to approximately 50%. The numerical values of the stresses computed according to the Thomlinson method cannot be directly compared to the stresses found with the Bradbury formula. In the latter the difference in temperature between the top and the bottom of the slab has to be assumed, whereas the Thomlinson analysis is based on the temperature variations at the top of the slab which are independent of the thickness of the pavement, being determined by climatic conditions instead. Under Mr. Thomlinson's assumptions the highest restrained-warping stress of approximately 280 lb per sq in. at the bottom of the slab occurs in pavements from 8 in. to 9 in. thick, thinner or thicker pavements being subjected to lower stresses at this point under these conditions.

---

[28] Asst. Prof. of Mechanics, Lehigh Univ., Bethlehem, Pa.

[29] "Temperature Variations and Consequent Stresses Produced by Daily and Seasonal Temperature Cycles in Concrete Slabs," by J. Thomlinson, *Concrete and Construction Engineering*, Vol. 35, June and July, 1940, pp. 298 and 352.

[30] *Ibid.*, p. 300, Fig. 2.

[31] "The Structural Design of Concrete Pavements," by L. W. Teller and E. C. Sutherland, *Public Roads*, November, 1935, p. 177, Fig. 9.

[32] "Temperature Variations and Consequent Stresses Produced by Daily and Seasonal Temperature Cycles in Concrete Slabs," by J. Thomlinson, *Concrete and Construction Engineering*, Vol. 35 July, 1940, p. 358, Table I.

The author's reference to the results of Road Test One-MD concerning restrained-warping stresses (Fig. 1) is not convincing because they apparently were evaluated with the probably outdated assumptions of Mr. Westergaard.

It is not appropriate for the writer to present the entire case for thicker concrete pavements in this discussion. He would like to express the opinion, in brief, that a correct evaluation of warping stresses may, for both structural reasons and economic reasons, justify the use of concrete pavements thicker than 8 in. or 9 in. in the road system.

Joseph Herbert Moore,[33] A. M. ASCE.—The writer wishes to thank the discussers of his paper for their contributions. The choice of the thickness of pavement has been treated much too lightly by those who have been designing highways, yet to the layman an early failure of the pavement represents poor engineering practice. As all the discussions have indicated, there are many variables entering into a realistic approach to the solution of this problem, and this could account for the practice of many states of simply using a standard thickness at all sites. Obviously, this is poor practice and provides no real cost comparison between the use of rigid pavements and flexible pavements.

One of the variables on which little research has been done is the fatigue property of pavement slabs. The only available data with which the writer is acquainted are those used by Mr. Bradbury and also by the PCA; these data are based on tests of beams. A slab undoubtedly deflects and rebounds very differently than does a beam, and, as Mr. Palmer has indicated, the recovery period is relatively long in the case of an actual pavement slab.

The previously unpublished data that Mr. Sutherland has furnished on measured warping stresses in 15-ft-long slabs are greatly appreciated and certainly provide an additional basis for constructive thinking. The comparison of measured and computed warping stresses in 15-ft-long slabs is not as disturbing as it may at first appear because these computed stresses increase at a rapid rate and are difficult to compute for slabs from 10 ft to 25 ft long; beyond this length the computed values are almost constant. Reports on the Arlington tests[9] did include comparisons of edge warping stresses along the sides of slabs 10 ft and 20 ft long, and the stresses along the 10-ft sides were almost 90% less than those along the 20-ft sides. Because the cost of the complex dowel arrangements needed at transverse joints cannot be and is not ignored, there is a current tendency to use fewer joints and slabs of greater length. Therefore, the irregularities in warping computations for short slabs are not of practical importance.

As Mr. Harwood has indicated, some of the material in the writer's paper was published in a report issued by the Joint State Government Commission of the Commonwealth of Pennsylvania. The writer prepared the material for that report while employed by the private research firm of Haller, Raymond, and Brown. The comparison between rigid pavements and flexible pavements was not an issue in the report or this paper; in the latter, an attempt was simply made to explain the cause of the numerous transverse cracks that tend to make concrete pavements rough and lead to high maintenance costs.

---

[33] Project Bridge Engr., Joseph K. Knoerle & Associates, Inc., Cons. Engrs., Chicago, Ill.

Obviously, the complexity of any realistic treatment of pavement design necessitates an engineering analysis of numerous variables, and an engineer's judgment and decision in simplifying any one of these variables is justly open to criticism. The design methods proposed by the writer are not purely theoretical but include a factor that represents the observed condition of many pavements in use throughout Pennsylvania. One purpose in presenting Table 9 was to show the absurd values at which one could occasionally arrive if he used either the proposed longitudinal-edge loading method or the more publicized and simpler corner loading method. However, for normal cases Table 9 clearly reveals that, if the repetitions of corner loadings are realistically computed—that is, if the effect of lane width is considered,—highway pavements will develop numerous transverse cracks long before any corner cracks appear. As cracks appear, the seepage of water into the subgrade reduces the supporting value thereof, and this soon produces pavement roughness, which is a more proper measurement of pavement life. Thus, it appears to the writer that there is a definite relationship between early pavement cracks and pavement life; at least the field studies in Pennsylvania support this statement.

AMERICAN SOCIETY OF CIVIL ENGINEERS
Founded November 5, 1852
TRANSACTIONS

Paper No. 2835

VIBRATION IN HYDROELECTRIC POWER PLANTS

By Samuel Judd,[1] M. ASCE

Synopsis

Vibrations that occur because of the forces of nature and those induced by moving or rotating equipment may cause a reduction in efficiency, objectionable noise, excessive wear, and fatigue failures, and may result in a loss of property or revenue. The vibration sources and design criteria used by the Bureau of Reclamation, United States Department of the Interior, in the structural design of hydroelectric power plants are cited.

Introduction

The many sources of vibration in a hydroelectric plant present a vexatious and controversial problem in every plant design. Those vibrations that occur because of the forces of nature, such as wind or earthquake, play an important part in the proportions and economy of structures. Others that are induced by moving or rotating equipment may cause objectionable noise, loss of efficiency, excessive wear, and fatigue failures. When vibrations exist, whether natural or man made, they may result in a loss of property or revenue.

Every object in motion produces vibrations that are exhibited in two forms—movement or noise. The form of vibration is dependent primarily on the frequency or the number of times the vibration repeats itself during a unit of time, usually a second. Stephen E. Slocum[2] stated that when this frequency is below 30 cycles per sec it is a tremor that is apparent to the sense of touch. When it is higher, between 30 cycles per sec and 50 cycles per sec, intermittent noise can be perceived; when it is between 50 cycles per sec and 10,000 cycles per sec it becomes a continuous sound.

Natural Sources of Vibration

The major sources of vibration resulting from the forces of nature arise from wind and earthquakes. Normally, structures must be designed to

---

NOTE.—Published, essentially as printed here, in March, 1955, as *Proceedings-Separate No. 637*. Positions and titles given are those in effect when the paper was approved for publication in *Transactions*.

[1] Chief, Structural and Architectural Branch, Bureau of Reclamation, U. S. Dept. of the Interior, Denver, Colo.

[2] "Noise and Vibration Engineering," by Stephen E. Slocum, D. Van Nostrand Co., Inc., New York, N. Y., 1931.

resist these forces; they cannot be controlled as can some of the destructive, man-made vibrations.

The method of designing a hydroelectric plant for wind forces is well established and is usually of secondary importance when the plant is in an area subject to earthquakes. All major earthquakes have resulted from the slippage of the earth's crust along a seam or fault. These tremors are termed "tectonic earthquakes" and cause several types of elastic surface and depth waves. The locations of these geologic faults or seams of weakness have been obtained by the Geological Survey, United States Department of the Interior. These waves are readily transmitted through saturated soils or rock as they propagate themselves in a manner similar to sound waves. In this respect it should be noted that the mere installation of a sand cushion beneath a structure is no cure-all for the waves are readily transmitted through sand. The possibility of resonance between the shock from a surface wave and a power plant is remote because of the complexity of the earthquake motion; moreover, the inherent stiffness and shape of the plant result in a natural frequency considerably greater than that of the earthquake. Although the ground vibrations are not harmonic vibrations, certain paramount periods often appear, and this effect is usually included in the designs of the structure by the application of a force equivalent to a given fraction of the dead loads and fixed-equipment loads. The fraction to be used for a given locality may be determined from the seismic-probability maps prepared from historical records by the Geological Survey. For a stiff structure such as a powerhouse, with a ratio of height to base width less than 3, this method of design is satisfactory.

MAN-MADE SOURCES OF VIBRATION

Man-made vibrations are usually controlled through isolation, elimination, damping, or absorbtion. It is generally not considered feasible to isolate the source of the vibration that arises in a hydroelectric unit because of the weight and size of the component parts. The rotor of the generator for one unit at Grand Coulee Dam (Washington), for example, weighs 500 tons and the turbine spiral cases are 50 ft in diameter. The elimination of the vibration by the most desirable method—dynamic balancing or similar corrective measures—is never completely effective because of physical and theoretical difficulties. The third method, damping, is one often used to reduce the effects of vibration, but its effectiveness is limited to a certain range of frequencies as will be illustrated subsequently. The fourth method, absorbing or minimizing the displacements resulting from vibration, is most generally used because of the many sources and frequencies, some known and some unforseen, that arise from the periodic man-made impulses.

Before investigating these causes it is well to review a basic equation portraying the effects of a forced-vibration system with damping.[3] In such a system the equation for the actual periodic displacement is

$$X_p = \frac{X_{st}}{\sqrt{(1 - r^2)^2 + \left(2 \frac{C}{C_c} r\right)^2}} \quad \ldots\ldots\ldots\ldots\ldots\ldots (1)$$

---

[3] "Elementary Mechanical Vibrations," by A. H. Church, Pitman Publishing Corp., New York and London, 1948, p. 82.

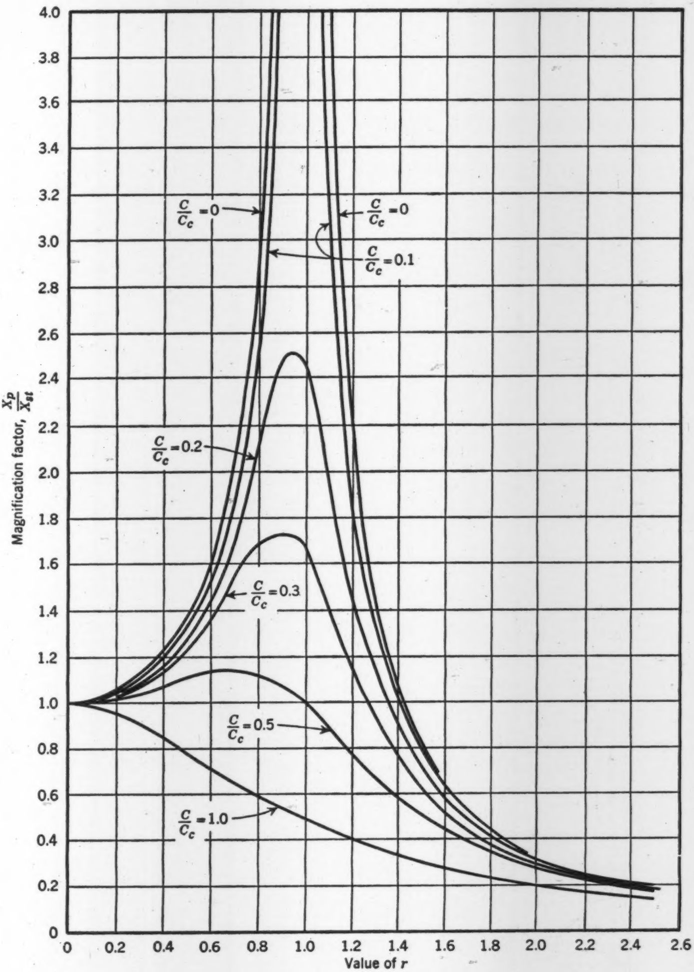

FIG. 1.—RELATIONSHIP BETWEEN THE MAGNIFICATION FACTOR AND THE RATIO OF THE IMPRESSED FREQUENCY AND THE NATURAL FREQUENCY

in which X_p is the periodic displacement, X_{st} denotes the static displacement caused by a static load equal to the maximum value of the periodically varying load, r is the ratio of the impressed frequency to the natural frequency of the structure, C represents the actual damping factor of the system, and C_c is the critical damping factor of the system. The actual periodic displacement of the structure can be made negligible by adding mass or stiffening the structure so that the static displacement is small.

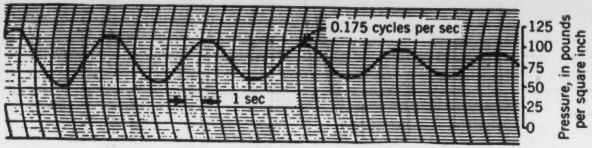

FIG. 2.—PRESSURE SURGES CAUSED BY WATER HAMMER AT TRACY PUMPING PLANT WITH L = 5,130 FT AND a = 3,600 FT PER SEC

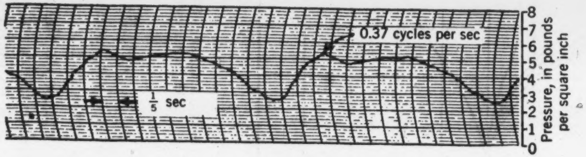

FIG. 3.—DRAFT-TUBE SURGES AT PARKER POWER PLANT WITH N = 94.7 RPM AT 0.5 GATE POSITION

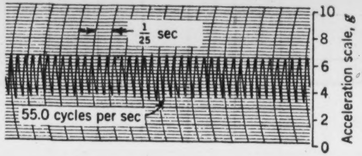

FIG. 4.—TRANSVERSE ACCELERATIONS OF TURBINE RUNNER AT PARKER POWER PLANT AT 0.8 GATE POSITION

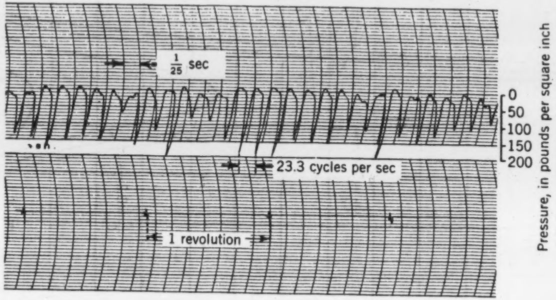

FIG. 5.—PRESSURE CHANGES AT TONGUE OF PUMP AT GRAND COULEE PUMPING PLANT WITH N = 200 RPM AND 7 IMPELLER BLADES

The magnitude of this periodic vibration of the structure also depends on the relationship between the impressed frequency of the disturbing force and the natural frequency of the building and the damping; Fig. 1 shows these relationships graphically. The periodic displacement is represented in the ratio of the periodic to static displacement, usually termed the "magnification factor." As will be observed from Fig. 1, if the impressed frequency and the natural frequency of the structure were nearly equal and very little damping were present, the resulting periodic movement would be very large. However, if the ratio of these frequencies is greater or less than unity, the resulting movement varies as shown in Fig. 1. The beneficial results of damping when the frequency of the disturbing force is $\pm$ 40% of the natural frequency are self-evident. For the remainder of the frequency ratios, however, it is seen in Fig. 1 that damping will have little effect, and the periodic displacement must be absorbed or made negligible by reducing the static displacement.

Periodic Pressure Surges Caused by Water Hammer.—A possible source of vibration in hydraulic-turbine installations is the pressure surges which occur in turbine penstocks as a result of the operaton of the turbine wicket gates. Under normal governor action during normal load changes the wicket-gate movements produce rapid changes in the flow. These changes produce water-hammer waves and rhythmic pressure surges in the turbine penstock. An example of these measured surges at the Tracy Pumping Plant near Tracy, Calif., is shown in Fig. 2. The frequency of these pressure surges is defined by

$$F = \frac{V}{4\,L} \quad \ldots\ldots\ldots\ldots\ldots\ldots\ldots\ldots\ldots\ldots\ldots (2)$$

in which F is the frequency of the pressure surges in the penstock, in cycles per second; L denotes the length of the penstock, in feet; and V is the velocity of the water-hammer waves in the penstock, in feet per second. For this type of operation, hydraulic resonance[4] will rarely occur because the pressure surges are damped out rapidly by the partial wave reflections which occur at the partly open gates as well as by the effects of the pipeline friction.

Draft-Tube Surges and Power Swings.—A significant source of low-frequency vibration in hydraulic-turbine installations results from surges in the draft tube. Draft-tube surges are the periodic surges that occur in the water column in the draft tube of hydraulic turbines when operating at partial gate openings. The hydraulic phenomenon causing this surging is not completely understood[5] (as of 1956) and does not occur at all turbine installations. However, it is believed to result from the presence of air or vapor which accumulates around the vertical axis of the draft tube just below the runner. The effect of these surges is described briefly as follows:

The fluctuation in the vacuum or pressure in the draft tube causes a fluctuation in the effective head on the turbine and thereby causes a variation in the turbine discharge. This produces a further fluctuation in the penstock pressure as a result of the effects of the water hammer. These, in turn, combine with the draft-tube surges to create a change in the head on the turbine and a variation in torque on the runner. Because the turbine is connected to a generator the electrical output of the machine also varies, and power swings occur. The magnitude of these power swings will then depend on the relation between the frequency of the draft-tube surges and the natural frequency of oscillation of the generator connected to the power-transmission system. An example of these surges measured at the Parker Power Plant near Needles, Calif., is shown in Fig. 3. The draft-tube-surge frequencies and power swings are approximately proportional to the speed of the unit for various types and sizes of units. This relationship is

---

[4] "Theory of Resonance in Pressure Conduits," by Charles Jaeger, *Transactions*, ASME, Vol. 61, 1939, pp. 109–115.

[5] "Power Swings in Hydroelectric Power Plants," by W. H. Rheingans, *ibid.*, Vol. 62, 1940, pp. 171–177.

$$F = \frac{N}{216} \qquad (3)$$

in which F is the approximate frequency of draft-tube surges, in cycles per second, and N is the speed of the turbine, in revolutions per minute.

Guide Vane-Runner Bucket Relation.—Objectionable vibrations in a hydraulic-turbine installation may be caused by having an improper relation among (*a*) speed of rotation, (*b*) number of guide vanes, (*c*) number of runner buckets, (*d*) length of the spiral case, and (*e*) velocity of propagation of water-hammer waves. J. P. Den Hartog has described[6] a power plant in which serious vibration was apparently caused by an unfortunate combination of these variables. The turbine was so proportioned that the pressure impulses caused by each runner bucket passing each guide vane were in phase, and as the various pressure waves reached the penstock, they added arithmetically to produce severe forced vibrations in the penstock.

Unbalanced Rotating Parts.—Hydraulic-turbine runners are usually balanced statically in the shop by mounting the turbine runner on a pivot and balancing the runner by the addition or removal of metal from the outer shroud band. On small generators the rotor is also balanced statically in the shop by the addition of weights in the rotor. Although the turbine runner and generator may each be in perfect static balance, the combination is seldom in dynamic balance because during rotation additional disturbing forces caused by centrifugal effects are imposed on the rotating unit. Dynamic balancing of the unit is usually obtained after rotating the unit at normal speed by attaching weights to the generator rotor. When dynamic unbalance is present, the vibration is usually quite pronounced and its frequency is[7]

$$F = \frac{N}{60} \qquad (4)$$

Turbine-Runner Vibration.—Periodic vibration of turbine runner blades on large-diameter runners (14 ft) has been observed at several turbine installations. This type of vibration has caused extensive cracking of the runner blades.[8]

---

[6] "Mechanical Vibrations," by J. P. Den Hartog, McGraw-Hill Book Co., Inc., New York and London, 3rd Ed., 1947, p. 10.

[7] "Vibration Problems in Engineering," by S. Timoshenko, D. Van Nostrand Co., Inc., New York, N. Y., 1955, p. 296.

[8] "Measurement of Hydraulic Turbine Vibration," by John Parmakian and R. S. Jacobson, *Transactions*, ASME, Vol. 74, 1952 p. 733.

The cause of the runner vibration appears to be associated with the shock-type pressure changes at the trailing edges of the runner blades as a result of the presence of vortex trails. The action of these vortices imposes periodic transverse forces on the runner blades and causes them to vibrate across the streamlines. When this vibrating tendency is close to the natural frequency of the runner blades, a condition of resonance occurs, and the vibration of the blades is magnified considerably. At Parker Power Plant, thinning of the trailing edge of the runner blades by chipping and grinding completely eliminated this type of vibration which could be heard and felt over the entire plant.

This type of vibration is also affected by the tailwater elevation. At Keswick Power Plant near Redding, Calif., the objectionable vibration disappeared when the tailwater elevation was lowered 10 ft below the center line of the unit. Air admission at the lower seal chamber reduces the noise but has little effect on the vibration within the unit. The range of frequencies measured at Parker Power Plant was from 55 cycles per sec to 65 cycles per sec as shown in Fig. 4, and that measured at Keswick Power Plant was from 150 cycles per sec to 170 cycles per sec.

Pumps.—Occasionally, a strong vibration in pump installations results from the periodic pressure surges of high intensity which form inside the pump. Although pump manufacturers do not seem to agree as to the exact cause of the phenomena, these pressure shocks appear to be the result of sudden velocity changes in the pump casing at the tongue of the pump. This seems to be borne out by the fact that insufficient clearance between the impeller and the tongue of the pump aggravates the pressure surges. These surges create shock waves which are transmitted through the water to the discharge line and pump casing. The measured pressure changes at the tongue of the pump at Grand Coulee Pumping Plant are shown in Fig. 5. The frequency of this type of vibration is determined from

$$F = \frac{N\,n}{60} \qquad (5)$$

in which n is the number of impeller vanes.

DESIGN CRITERIA

Several design criteria are used for controlling man-made vibrations resulting from the aforementioned forces—whether it is vibration resulting from objectionable movement or noise. Briefly, they are:

a. An "experience constant" for the relationship between mass and kilowatt capacity.

b. An experience constant for the ratio of the weights of the rotating parts to their concrete foundation.

c. Structural analysis for the impressed forces.

d. Mallock's nuisance vibration curve.[9]

---

[9] "Noise and Vibration Engineering," by S. E. Slocum, D. Van Nostrand, Co., Inc., New York, N. Y., 1931, p. 3.

Since the early 1930's, a minimum ratio of concrete mass to kilowatt capacity has been relied on as a guide in proportioning structures. This is admittedly a very rough guide; however, it may be rationalized because certain losses are inherent in transforming the flow of water into electrical energy through mechanical methods. Some of these losses are in the form of heat, some in friction, and some are vibration. As seen from the aforementioned examples, the known sources of vibration are several and their frequencies may vary from 1.5 cycles per sec to 150 cycles per sec (an unbalanced rotor and the turbine-runner vibration, respectively, at the Keswick Power Plant). From Fig. 1 it is obvious that one cannot rely on damping, even if its measurement were well defined, to control all vibrations because of its limited effective range. The energy lost in this transfer of kinetic energy to electrical energy is approximately 15% of the capacity of the hydroelectric unit. What part of this may be attributed to vibration is questionable, but it is undoubtedly small, probably less than $\frac{1}{4}\%$ of the capacity of the machine. However, the energy lost because of vibration must be absorbed to minimize the displacement so that it will not be objectionable. To do this and to cover the wide range of impressed forces and frequencies possible, a minimum value of 2 has been used for the ratio of the cubic feet of the concrete mass surrounding the scroll case and supporting the generator to the capacity of the machine in kilowatts; many plants, both public and private, have a higher ratio than this. This ratio has been known[10] to vary from less than 1 to more than 30. Other extenuating conditions, such as high tailwater or unusual foundation conditions, undoubtedly have contributed to the wide variations.

A reliable experience constant of this nature has been sought without success. Studies in which the mass has been varied with the rotational speed, head, discharge, specific speed, and horsepower have been attempted without reliable results. Unquestionably, one reason for such poor correlation is the lack of definite data on the proper mass to be used. The time and money required to assemble these basic data in the correct form have been prohibitive. Therefore, it is felt that a more reasonable approach to an experience constant of this nature lies in limiting the acceleration due to a periodic force to a value between 0.005 g and 0.01 g (in which g is the gravitational acceleration).

A second criterion, the ratio of the weight of the rotating parts to their support, is based on experience and is similar to that used in steam-plant design. The generator supports and scroll-case encasement concrete are proportioned to minimize eccentricity and provide a minimum of 2 to $2\frac{1}{2}$ times the weight of the rotating parts.

The third criterion, structural analysis for the impressed forces, presents varying degrees of complexity. For periodic natural forces, the analysis is made along conventional lines with the impressed movement from an earthquake applied as a horizontal or vertical force whose magnitude is determined as equal to the mass times the acceleration. For other impressed forces arising from the sources previously cited, the design requires a determination of whether the entire structure or its components will be near resonance with any of these large periodic forces.

---

[10] "Hydroelectric Handbook," by W. P. Creager and J. D. Justin, John Wiley & Sons, Inc., New York, N. Y., 2d Ed., 1950, p. 778.

It is difficult to predict accurately the natural frequencies of vibration of the complex, massive structures needed to house a hydroelectric unit. The method used in the vibration analyses of power plants is to make simplified assumptions and idealizations such that the lowest possible natural frequencies are computed. If it can be shown that the computed frequencies are considerably higher than the highest of the impressed frequencies, the powerhouse will probably be free of major vibration trouble. If the computed natural frequency is less than one of the important impressed frequencies, a redesign of part of the structure may be necessary. If this redesign proves uneconomical, it is sometimes possible to make provision for changing the natural frequencies in the initial installation by such measures as changing from simple spans to continuous spans or leaving space for the future placement of concrete to assist in damping the vibration.

It may develop that part of the powerhouse structure is in resonance with the disturbance caused by a small unit such as a compressor, sump pump, or blower. This condition is usually not considered during the design of the powerhouse; however, if the resonant condition develops, it is taken care of by changing the natural frequency of the vibrating member or by mounting the disturbing unit in a vibration-isolating suspension.

The fourth criterion to the limiting amount of acceleration permissible from one of the periodic forces has been developed by Mr. Mallock.[9] Mr. Mallock found, by experiment, that a periodic vibration which produces an acceleration of 0.01 g is perceptible and that, when the acceleration reaches 0.04 g to 0.05 g, the vibration becomes distinctly unpleasant. This criterion for a nuisance vibration is stated as

$$4\,\pi^2\,x_o\,F^2 = 0.05\,g \ldots\ldots\ldots\ldots\ldots\ldots\ldots\ldots (6)$$

in which x_o is the displacement. It should be remembered that power-plant design is never predicated on any of these criteria; that is, the layout is made with the arrangement of the equipment, the dead and live loads, and the foundation conditions in mind. Then the aforementioned criteria are used as a check or guide to a more preferable arrangement.

CONCLUSIONS

It is believed that there is a definite ratio between the mass and properties of a unit. This ratio may be used as a guide for controlling man-made vibrations; however, it has not been determined (as of 1956). Such a guide, of course, would be most beneficial during the preliminary planning stages of a plant.

It is recommended that a systematic program of vibration measurement be undertaken. Although much work has been done in this field on structures in general, little has been specifically concerned with power and pumping plants. Actual vibration records during normal operation of the units as well as during starting and emergency shut-down periods should be obtained.

Suitable locations would be on the concrete surrounding the draft tube, encasement of the scroll case, main-support structure of the generator stator, and points on all floor levels as well as main columns in the superstructure; these measurements need not be made on all plants. On the contrary, they should be performed on a selected few—in particular, the ones where vibration troubles are known to exist.

The vibration equipment which the Bureau of Reclamation has available (1956) for such measurements are a vibration meter and vibration analyzer. The "pick up" for the vibration meter is of the inertia-operated crystal type which responds to acceleration. Two stages of electrical integration are built into the vibration meter so that the velocity and displacement of the vibration can also be measured. The vibration meter gives little information about the frequencies involved. The vibration analyzer is therefore used with the vibration meter, and through tuned circuits it determines the amplitude of the various components of the periodic vibration which are included in the total vibration. This equipment has a frequency range of from 2.5 cycles per sec to 750 cycles per sec.

In addition to the foregoing measurements which would give information on actual vibration frequencies and magnitudes, another series should be made to determine the natural frequencies of the structures in as many of these locations as possible. This could be done by the use of variable-speed vibrating machines using eccentric rotating weights.

Information of this type taken at similar points in selected plants, coupled with a program of harmonic and structural analyses, could remove the uncertainties connected with present concepts and form the basis for an intelligent, analytical approach to the problem.

ACKNOWLEDGMENTS

Thanks are due to John Parmakian and William H. Wolf, Members, ASCE, and other engineers of the Bureau of Reclamation for their valuable assistance in preparing and reviewing this work.

AMERICAN SOCIETY OF CIVIL ENGINEERS
Founded November 5, 1852
TRANSACTIONS

Paper No. 2836

LATERAL BUCKLING OF ECCENTRICALLY LOADED I-COLUMNS

BY MARIO G. SALVADORI,[1] M. ASCE

SYNOPSIS

The critical combination of thrust and unequal end moments, or eccentricities, for the lateral buckling of columns that are elastically restrained against rotation about the principal axes at the end sections, and that are prevented from twisting about the column axis at the end sections, are derived for various values of the parameter L^2/a^2 and of the end-moments ratio.

It is shown that for most practical cases these critical combinations are easily obtainable from the critical value of equal end moments without thrust for columns that are free to rotate at their ends.

INTRODUCTION

The solution of the lateral-stability problem for I-columns under eccentric thrust—that is, under a combination of axial thrust and end moments—consists in the determination of "interaction curves." From these curves the critical value of the thrust can be derived for given end moments, or the critical value of the end moments can be determined for a given thrust.

The shape of the interaction curves depends essentially on (*a*) the geometric and strength characteristics of the I-column and, in particular, on the value of the parameter L^2/a^2—in which L is the column length,

$$a^2 = \frac{h^2 D}{2 C} \quad \text{(1)}$$

h is the column depth, D denotes the flexural rigidity of one flange in its own plane, and C is the torsional rigidity of the column without thrust; (*b*) the ratio r of the end moments, or eccentricities; and (*c*) the boundary conditions at the column ends.

Interaction curves for I-columns with equal end moments were obtained by B. G. Johnston,[2] M. ASCE, for columns of rectangular cross section with un-

---

NOTE.—Published, essentially as printed here, in January, 1955, as *Proceedings-Separate No. 607*. Positions and titles given are those in effect when the paper was approved for publication in *Transactions*.

[1] Prof. of Civ. Eng., Columbia Univ., New York, N. Y.

[2] "Lateral Buckling of I-Section Columns with Eccentric End Loads in the Plane of the Web," by B. G. Johnston, *Transactions*, ASME, Vol. 62, 1941, p. A-176.

equal end moments by F. DiMaggio,[3] and for I-columns with unequal end moments by the writer.[4] All these solutions considered "simply supported" columns whose ends were free to rotate around their principal axes at the ends and were prevented from twisting around the column axis there.

Interaction curves are obtained herein for I-columns whose ends are free to rotate in the plane of the web (strong plane) but are either elastically restrained or totally fixed in the plane of the flanges (weak plane) at the ends, while they are prevented from twisting around the column axis there. The consideration of unequal end moments in the plane of the web, which may be caused by continuity, allows the use of these interaction curves for columns that are elastically restrained in both the weak and the strong planes. It should be noted that the treatment is limited to stresses within the elastic limit.

LATERAL BUCKLING UNDER EQUAL END MOMENTS

A simply supported column of length L, depth h, minimum flexural rigidity B (in the plane of the flanges), torsional rigidity C, and flange rigidity D buckles laterally under the action of two equal end moments M_s in the strong plane when[5]

$$M_s = \frac{\pi \sqrt{B\,C}}{L} \sqrt{1 + \left(\frac{\pi}{L/a}\right)^2} \quad \text{(2)}$$

The moment coefficient is defined as

$$K_{0,1} = \frac{M\,L}{\sqrt{B\,C}} \quad \text{(3)}$$

in which the first subscript, 0, indicates the absence of thrust; the second, 1, indicates the equality of end moments for which the ratio r equals unity. The critical value of $K_{0,1}$ is given by

$$K_{0,1}|_s = \pi \sqrt{1 + \left(\frac{\pi}{L/a}\right)^2} \quad \text{(4)}$$

When the I-column is completely fixed in the weak plane at the ends, the critical value of the end moments is given[5] by

$$M_f = \frac{2\,\pi \sqrt{B\,C}}{L} \sqrt{1 + \left(\frac{2\,\pi}{L/a}\right)^2} \quad \text{(5)}$$

from which

$$K_{0,1}|_f = 2\,\pi \sqrt{1 + \left(\frac{2\,\pi}{L/a}\right)^2} \quad \text{(6)}$$

The critical value of $K_{0,1}$ may be expressed by a single formula if the concept of reduced length l is introduced—that is, of the length between inflection points when the same column buckles under thrust (Euler buckling). Letting

---

[3] "Laterial Buckling of Beams in Bending and Compression," by F. DiMaggio, A. Gomza, W. E. Thomas, and M. G. Salvadori, *Journal of the Aeronautical Sciences*, Vol. 19, 1952, No. 8, p. 574.

[4] "Lateral Buckling of I-Beams," by Mario G. Salvadori, *Transactions*, ASCE, Vol. 120, 1955, p. 1165.

[5] "Theory of Elastic Stability," by S. Timoshenko, McGraw-Hill Book Co., Inc., New York, N. Y., 1936.

$$l = \alpha\, L\, \tfrac{1}{2}\ (\tfrac{1}{2} \leq \alpha \leq 1) \quad \text{(7)}$$

the reduction coefficient α equals unity for columns that are simply supported in the weak plane and $\frac{1}{2}$ for columns fixed in the weak plane; it has values between $\frac{1}{2}$ and 1 for columns that are elastically restrained in the weak plane. By use of l, the expression for $K_{0,1}$ becomes, whatever the conditions of restraint in the weak plane,

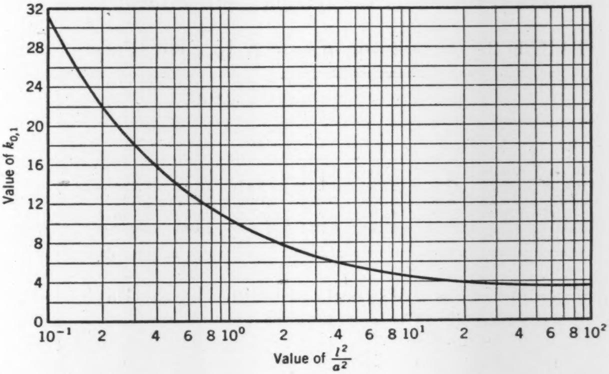

Fig. 1

$$k_{0,1} = \frac{M\, l}{\sqrt{B\, C}} = \pi \sqrt{1 + \left(\frac{\pi}{l/a}\right)^2} \quad \text{(8)}$$

TABLE 1.—Values of $K_{0,r} = K_r|_{p=0}$ for Simple Support

Value of r	Value of L^2/a^2										
	0.1	1	2	6	10	16	24	32	40	100	∞
1.0	31.40	10.36	7.66	5.11	4.43	4.00	3.73	3.59	3.51	3.29	3.14
0.5	41.40	13.68	10.11	6.75	5.84	5.27	4.92	4.73	4.62	4.33	4.12
0	58.30	19.22	14.19	9.44	8.16	7.33	6.83	6.55	6.38	5.94	5.56
−0.5	82.39	27.14	20.00	13.24	11.40	10.18	9.42	9.00	8.74	8.00	7.32
−1.0	86.07	28.40	20.98	13.95	12.07	10.85	10.09	9.69	9.43	8.72	8.03

in which $k_{0,1}$ is the reduced length bending moment coefficient for equal end moments, and the critical value of the moments is given by

$$M_{cr} = k_{0,1} \frac{\sqrt{B\, C}}{\alpha\, L} \quad \text{(9)}$$

An analogous result was obtained by George Winter,[6] M. ASCE, for beams of rectangular cross section.

---

[6] "Strength of Slender Beams," by George Winter, *Transactions*, ASCE, Vol. 109, 1944, p. 1321.

Fig. 1 gives the values of $k_{0,1}$ versus l^2/a^2, which also appear in the row $r = 1$ of Table 1, in which $l = L$ and hence $k_{0,1} = K_{0,1}$.

Lateral Buckling Under Unequal End Moments

Indicating by r the ratio of the moment $M_{0,1}$ at the bottom of the column to the moment $M_{0,2}$ at the top of the column (both without thrust), the critical values of $M_{0,2}$ and $M_{0,1} = r\, M_{0,2}$ can be obtained by the Rayleigh-Ritz method as shown in Appendix I. Tables 1 and 2 give

TABLE 2.—Values of $K_{0,r} = K_r|_{p=0}$ for Fixed Ends

Value of r	Value of L^2/a^2										
	0.1	1	2	6	10	16	24	32	40	100	∞
1.0	125.00	39.98	28.61	17.30	13.98	11.70	10.22	9.39	8.86	7.42	6.28
0.5	164.98	52.76	37.76	22.82	18.44	15.43	13.47	12.38	11.67	9.76	8.19
0	230.79	73.79	52.80	31.89	25.74	21.52	18.77	17.22	16.22	13.50	11.20
−0.5	318.97	101.93	72.91	43.94	35.40	29.52	25.66	23.48	22.06	18.10	14.40
−1.0	322.02	102.90	73.59	44.34	35.71	29.76	25.85	23.63	22.18	18.11	14.00

$$K_{0,r} = \frac{M_{0,2}\, L}{\sqrt{B\, C}} \quad\text{(10)}$$

for columns simply supported in the weak plane[4] and for columns fixed in the weak plane, respectively, in terms of L^2/a^2 and r. From the coefficients $K_{0,r}$ of Tables 1 and 2 it is easy to compute, in terms of L^2/a^2, the ratios:

$$\mu_r = \frac{K_{0,r}}{K_{0,1}} = \frac{M_{0,2}}{M_{0,2}|_{r=1}} \quad\text{(11)}$$

TABLE 3.—Values of $\mu_r = K_{0,r}/K_{0,1}$

Value of r	Condition of support	Value of L^2/a^2										
		0.1	1	2	6	10	16	24	32	40	100	∞
1	Simple	1.00	1.00	1.00	1.00	1.00	1.00	1.00	1.00	1.00	1.00	1.00
	Fixed	1.00	1.00	1.00	1.00	1.00	1.00	1.00	1.00	1.00	1.00	1.00
0.5	Simple	1.32	1.32	1.32	1.32	1.32	1.32	1.32	1.32	1.32	1.32	1.31
	Fixed	1.32	1.32	1.32	1.32	1.32	1.32	1.32	1.32	1.32	1.32	1.30
0	Simple	1.86	1.86	1.85	1.85	1.84	1.83	1.83	1.82	1.82	1.81	1.77
	Fixed	1.85	1.85	1.85	1.84	1.84	1.84	1.84	1.83	1.83	1.82	1.78
−0.5	Simple	2.62	2.62	2.61	2.59	2.57	2.55	2.53	2.51	2.49	2.43	2.33
	Fixed	2.55	2.55	2.55	2.54	2.53	2.52	2.51	2.50	2.49	2.44	2.29
−1.0	Simple	2.74	2.74	2.74	2.73	2.72	2.71	2.71	2.70	2.69	2.65	2.56
	Fixed	2.58	2.57	2.57	2.56	2.55	2.54	2.53	2.52	2.50	2.44	2.23

of the critical moment $M_{0,2}$ at the top of the column to the critical value $M_{0,2}|_{r=1}$ of the same moment when $M_{0,2} = M_{0,1}$ for the two extreme conditions of simple support and fixity in the weak plane. The term μ_r in Eq. 11 is the magnification factor for unequal end moments. Table 3 shows that for all practical purposes this ratio is independent of L^2/a^2 for $L^2/a^2 \leq 40$, and has the same value for both extreme conditions of support for $r = \frac{1}{2}$ and $r = 0$. For $r = -\frac{1}{2}$ and

$r = -1$, this ratio is slightly sensitive to the values of L^2/a^2 and to the conditions of support. Hence, it may be conjectured that, for all values of r and for $L^2/a^2 \leq 40$, the ratio μ_r will be between the extreme values corresponding to the conditions of simple support and of fixity (Fig. 2).

Noticing that in most practical cases $L^2/a^2 \leq 40$ and that errors of up to 10% are easily permissible, if on the safe side, a simplified approximate evaluation of the critical moments may be obtained by use of the following minimum, safe values $\bar{\mu}_r$ of μ_r from Table 3:

Value of r	Value of $\bar{\mu}_r$
1	1.00
0.5	1.32
0	1.82
−0.5	2.49
−1	2.50

By Eqs. 8 and 10 the critical value of $M_{0,2}$ may be obtained, whatever the degree of restraint in the weak plane, by

$$M_{0,2} = \bar{\mu}_r \, M_{0,2}|_{r=1} = \bar{\mu}_r \, k_{0,1} \frac{\sqrt{B\,C}}{\alpha\,L} \qquad (12)$$

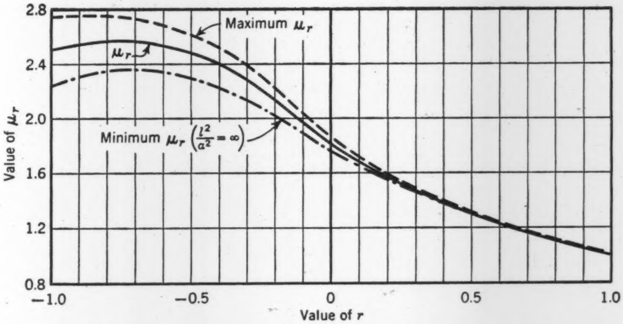

FIG. 2

in which $k_{0,1}$ is obtained from Fig. 1. It is seen by comparison of Eq. 12 with Eq. 10 that

$$K_{0,r} = \frac{\bar{\mu}_r}{\alpha} k_{0,1} \qquad (13)$$

As clearly shown by Eq. 13, the introduction of the (safe) ratios $\bar{\mu}_r$ and of the reduced length l reduces the solution of the lateral-buckling problem under unequal end moments, whatever the end restraints and the value of L^2/a^2, to the known solution of the buckling problem of a simply supported column in pure bending.

For example, an elastically restrained column of reduced length $l = 0.7\,L$ ($\alpha = 0.7$) with a moment $M_{0,2}$ at the top and no moment at the bottom ($M_{0,1}$

$= r\,M_{0,2} = 0$—that is, $r = 0$), for which $L^2/a^2 = 32$, has $l^2/a^2 = (0.7\,L)^2/a^2 = 16$. Hence, from Fig. 1 or Table 1, $k_{0,1} = 4.00$; from Fig. 2 or the foregoing tabulation, $\bar{\mu}_0 = 1.82$; and by Eq. 12

$$M_{0,2} = 1.82 \times 4.00\,\frac{\sqrt{B\,C}}{0.7\,L} = 10.4\,\frac{\sqrt{B\,C}}{L} \qquad (14)$$

A more accurate evaluation of $M_{0,2}$ may always be obtained by the values of μ_r in Table 3 but is seldom warranted in practice.

LATERAL BUCKLING UNDER EQUAL END MOMENTS AND THRUST

Indicating by

$$P_{cr} = \frac{\pi^2\,B}{(\alpha\,L)^2} \qquad (15)$$

the minimum critical value of the thrust in the absence of end moments, and by

$$M_{cr} = \pi\,\sqrt{1 + \left[\frac{\pi}{\frac{\alpha\,L}{a}}\right]^2}\,\frac{\sqrt{B\,C}}{\alpha\,L} \qquad (16)$$

the critical value of equal end moments in the absence of thrust, the critical combination of thrust P and equal end moments M (that is, the expression for the interaction curve P versus M) is given[2] by

$$\frac{P}{P_{cr}} + \left(\frac{M}{M_{cr}}\right)^2 = 1 \qquad (17)$$

Letting the thrust coefficient

$$p = \frac{P}{P_{cr}} = \frac{\alpha^2}{\pi^2}\,\frac{P\,L^2}{B} \qquad (18)$$

and

$$k_1 = \frac{M\,l}{\sqrt{B\,C}} \qquad (19)$$

there is obtained from Eq. 17

$$k_1 = \pi\sqrt{1 + \left(\frac{\pi}{l/a}\right)^2}\,\sqrt{1 - p} \qquad (20)$$

For $p = 0$—that is, no thrust—$k_1 = k_{0,1}$ and the ratio:

$$\frac{k_1}{k_{0,1}} = \sqrt{1 - p} \qquad (21)$$

is independent of L^2/a^2 and α. The curve $k_1/k_{0,1}$ versus p is identical with the curve $K_0/K_{0,1}$ versus p for $\alpha = 1$ and labeled $r = 1$ in Fig. 3 (thin line).

By use of the values $k_{0,1} = K_{0,1}$ of Fig. 1, the critical value of equal end moments with thrust is given by

$$M = k_{0,1}\,\sqrt{1 - p}\,\frac{\sqrt{B\,C}}{\alpha\,L} \qquad (22)$$

When the moments M are caused by the eccentricity e of the thrust P, the critical value of e may be computed from

$$e = \frac{M}{P} \qquad (23)$$

Similarly, Eq. 17 may be solved for P in terms of e, giving

$$P = \frac{C}{2\,e^2}\left(\frac{k_{0,1}}{\pi}\right)^2\left[-1 + \sqrt{1 + \frac{4\,\pi^2}{\alpha^2}\,\frac{B\,e^2}{C\,L^2}\left(\frac{\pi}{k_{0,1}}\right)^2}\,\right] \qquad (24)$$

Lateral Buckling Under Unequal End Moments and Thrust

The critical combinations of thrust P and of top moment M_2 for various values of the ratio r and of L^2/a^2 may be computed by the methods explained in Appendix I for conditions of simple support[4] and for conditions of fixity.

TABLE 4.—Values of $\Delta\kappa_r$

Value of r	Value of p					
	0	0.2	0.4	0.6	0.8	1.0
1.0	0	0.00	0.13	0.16	0.00	0
0.5	0	0.22	0.26	0.31	0.66	0
0	0	0.55	0.50	0.30	0.42	0
−0.5	0	1.40	2.00	1.63	0.50	0
−1.0	0	2.73	6.13	9.62	14.45	0

The critical combinations may be expressed in terms of the nondimensional ratios p (Eq. 18) and

$$\kappa_r = \frac{K_r}{K_{0,r}} \qquad (25)$$

in which

$$K_r = \frac{M_2\,L}{\sqrt{B\,C}} \qquad (26)$$

and $K_{0,r}$ is the moment coefficient without thrust. From Eq. 11 it is also seen that

$$\kappa_r = \frac{K_r}{K_{0,r}} = \frac{M_2}{M_{0,2}} \qquad (27)$$

Table 4 gives the largest percentage difference, in absolute value, between the ratios κ_r for simply supported and fixed ends—that is, the values

$$\Delta\kappa_r = \left|\frac{\kappa_r|_s - \kappa_r|_f}{\kappa_r|_f}\right|_{max} \times 100 \qquad (28)$$

It is seen that $\Delta\kappa_r$ is less than 3% for all values of L^2/a^2 and of r, except for $r = -1$. Hence, for practical purposes, the interaction curves κ_r versus p are independent of L^2/a^2 and of the conditions of restraint in the weak plane, except for $r = -1$.

Fig. 3 gives the graphs (thin curves) of the average value of κ_r versus p for $r = 1, \frac{1}{2}, 0$, and $-\frac{1}{2}$. These graphs can be used whatever the value of L^2/a^2 and the end restraints. For $r = -1$, Fig. 3 gives three separate graphs for simply supported ends (r_s) and two separate graphs for fixed ends (r_f) in terms of L^2/a^2.

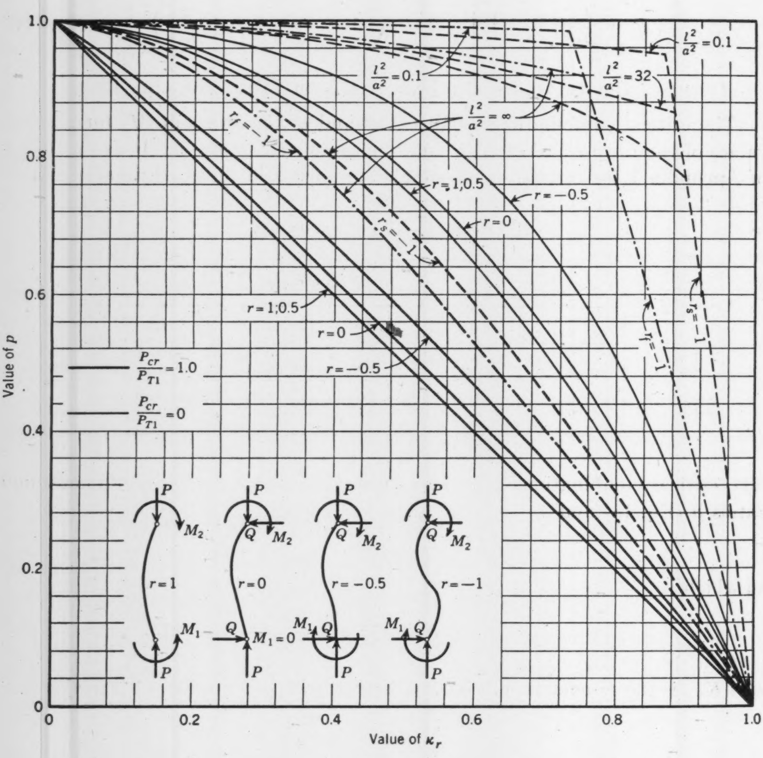

FIG. 3

The discontinuity in the slope of the curves $r = -1$ in Fig. 3 corresponds to the meeting point of two separate branches of the interaction curves. The branch valid for lower values of κ_r represents a buckling deformation in which the flanges are displaced in the same direction; the branch valid for κ_r greater than 0.8 corresponds to flange displacements in opposite directions. This last branch, if prolonged to meet the p-axis, would cross it at a value corresponding to the second Euler load—that is, at $p = 4$.

By use of the ratios κ_r of Eq. 27, the top moment M_2 may be written

$$M_2 = \kappa_r M_{0,2} \qquad (29)$$

or by Eq. 12

$$M_2 = \kappa_r \bar{\mu}_r k_{0,1} \frac{\sqrt{B C}}{\alpha L} \qquad (30)$$

To illustrate the use of Fig. 3, one might consider a column restrained in the weak plane so as to have a reduced length $l = 0.7 L$ ($\alpha = 0.7$), with $L^2/a^2 = 32$, and loaded by a thrust $P = 0.6 P_{cr}$. The restraint conditions in the strong plane are assumed to be such that $r = 0$. With $p = 0.6$ and $r = 0$, from Fig. 3, $\kappa_r = 0.66$. For $r = 0$, Fig. 2 gives $\bar{\mu}_0 = 1.82$; for $l^2/a^2 = (0.7)^2 \times 32 = 16$, Table 1 (or Fig. 1) gives $k_{0,1} = 4.00$. Hence, by Eq. 30

$$M_2 = \frac{0.66 \times 1.82 \times 4.00}{0.7} \frac{\sqrt{B C}}{L} = 6.87 \frac{\sqrt{B C}}{L} \qquad (31)$$

The corresponding eccentricity e_2 of the thrust at the top of the column is given by

$$e_2 = \frac{M_2}{P} = \frac{M_2}{0.6 P_{cr}} = \frac{6.87 \frac{\sqrt{B C}}{L}}{\frac{0.6 \pi^2 B}{(0.7 L)^2}} = 0.57 \sqrt{\frac{C L^2}{B}} \qquad (32)$$

To solve the instability problem for a given eccentricity,

$$e_2 = \epsilon_2 \sqrt{\frac{C L^2}{B}} \qquad (33)$$

in which ϵ_2 is the top-eccentricity coefficient. One should notice that

$$M_2 = P e_2 = p P_{cr} e_2 \qquad (34)$$

and that by Eq. 26

$$M_2 = K_r \frac{\sqrt{B C}}{L} \qquad (35)$$

Hence,

$$p P_{cr} e_2 = p \frac{\pi^2 B}{(\alpha L)^2} \epsilon_2 \sqrt{\frac{C L^2}{B}} = K_r \frac{\sqrt{B C}}{L} \qquad (36)$$

from which

$$K_r = \left(\frac{\pi}{\alpha}\right)^2 \epsilon_2 p \qquad (37)$$

or, dividing both sides of Eq. 37 by $K_{0,r}$,

$$p = \frac{\alpha^2 K_{0,r}}{\pi^2 \epsilon_2} \kappa_r \qquad (38)$$

The intersection of the straight line p versus κ_r of Eq. 38 with the graph of p versus κ_r of Fig. 3 gives the critical value of p and hence of P.

For example, for $e_2 = 0.4\sqrt{C\,L^2/B}$ — that is, $\epsilon_2 = 0.4$ — $\alpha = 0.7$, $L^2/a^2 = 32$, and $r = 0$, there results $l^2/a^2 = 16$, and by Eq. 13, Fig. 2, and Fig. 1

$$K_{0,r} = \frac{\mu_r}{\alpha}\,k_{0,1} = 1.82 \times \frac{4.00}{0.7} = 14.8.$$

Hence,

$$\frac{\alpha^2\,K_{0,r}}{\pi^2\,\epsilon_2} = \frac{(0.7)^2 \times 14.8}{9.87 \times 0.4} = 1.83.$$

The line through the origin of slope equal to 1.83 intersects the thin curve $r = 0$ of Fig. 3 at $p = 0.84$; therefore, the critical value of the thrust is

$$P = 0.84\,\frac{\pi^2\,B}{0.7\,L} = 1.20\,\frac{\pi^2\,B}{L} \qquad (39)$$

REDUCTION OF TORSIONAL RIGIDITY DUE TO THRUST

A column buckles in pure torsion under a thrust P_T uniformly distributed over its cross section when[7]

$$P_T = \frac{C\,A}{I_p} \qquad (40)$$

in which A is the area of the cross section and I_p its polar moment of inertia. The equivalent or reduced torsional rigidity H of the column under a thrust P is given by[7,8]

$$H = C\left(1 - \frac{P}{P_T}\right) = C\left(1 - p\,\frac{P_{cr}}{P_T}\right) \qquad (41)$$

In order to account for the reduction of torsional rigidity in the evaluation of the interaction curves, H must be substituted for C in Eq. 30 both in $\sqrt{B\,C}$ and in $k_{0,1}$.

Indicating by $k'_{0,1}$ the value of $k_{0,1}$ when H is substituted for C in l^2/a^2, the relationship between $k'_{0,1}$ and $k_{0,1}$ is found to be [7,9]

$$k'_{0,1} = k_{0,1}\,\frac{\sqrt{1 - \dfrac{P}{P_{T1}}}}{\sqrt{1 - \dfrac{P}{P_T}}} \qquad (42)$$

in which

$$P_{T1} = P_T\left[1 + \left(\frac{\pi}{l/a}\right)^2\right] \qquad (43)$$

---

[7] "Flexural-Torsional Buckling of Bars of Open Sections," by J. N. Goodier, *Bulletin No. 28*, Cornell Univ. Eng. Experiment Station, Ithaca, N. Y., January, 1942.

[8] "Refinement of the Theory of Torsional Buckling of Thin-walled Columns," by H. H. Bleich, *Proceedings*, First Midwestern Conference on Solid Mechanics, June, 1953.

[9] "Lateral Buckling of Eccentrically Loaded I-Section Columns," by H. N. Hill and J. W. Clark, *Transactions*, ASCE, Vol. 116, 1951, p. 1179.

Similarly, indicating by M'_2 the value of M_2 in Eq. 30 in which H is substituted for C, and noticing that, by Eq. 41,

$$\sqrt{\frac{H}{C}} = 1 - \frac{P}{P_T} \quad \ldots\ldots (44)$$

it is found that

$$M'_2 = \kappa_r \, \bar{\mu}_r \, k'_{0,1} \frac{\sqrt{B\,H}}{\alpha\,L} = \kappa_r \, \bar{\mu}_r \, k_{0,1} \frac{\sqrt{B\,C}}{\alpha\,L} 1 - \frac{P}{P_T} \quad \ldots\ldots (45)$$

or, by Eq. 12, that

$$\kappa'_r = \frac{M'_2}{M_{0,2}} = \kappa_r \, 1 - \frac{P}{P_T} \quad \ldots\ldots (46)$$

By the parameter,

$$\gamma = \frac{P_{cr}}{P_{T1}} = \frac{\pi^2 \, B \, I_p}{\alpha^2 \, L^2 \, C \, A \left(1 + \frac{\pi^2 \, a^2}{\alpha^2 \, L^2}\right)} \quad \ldots\ldots (47)$$

the coefficient κ'_r may be written as

$$\kappa'_r = \kappa_r \sqrt{1 - \gamma\,p} \quad \ldots\ldots (48)$$

The parameter γ varies, practically, between zero and one. When the reduction of torsional rigidity is negligible, $\gamma = 0$ and the thin curves of Fig. 3 remain unchanged. When the torsional rigidity is greatly reduced by the thrust, $\gamma = 1$ and the ordinates κ_r of these curves must be multiplied by $\sqrt{1 - p}$. The heavy curves of Fig. 3 give κ_r versus p for $\gamma = 1$ and are on the safe side for all practical cases. For intermediate values of γ, new curves may be easily computed.

To illustrate the influence of the reduction of torsional rigidity on the value of the critical moments one might consider the column of the example under the heading, "Lateral Buckling Under Unequal End Moments and Thrust." assuming the highest possible value of γ (unity) and $p = 0.6$, the moment M_2 of Eq. 31 becomes

$$M_2 = \sqrt{1 - 0.6} \times 6.87 \frac{\sqrt{B\,C}}{L} = 4.36 \frac{\sqrt{B\,C}}{L} \quad \ldots\ldots (49)$$

INFLUENCE OF DEFLECTIONS IN THE PLANE OF THE WEB

The interaction curves given previously are obtained under the assumption that the flexural rigidity of the column in the plane of the web is much greater than the rigidity in the plane of the flanges so that bending deflections in the plane of the web may be neglected.

For the case of equal end moments the influence of the deflections in the plane of the web may be taken into account by multiplying the critical bending moments M by the factor $1 - P/P_E$, in which P_E is the Euler thrust in the plane of the web. Thus, the curves $r = 1$ of Fig. 3 may be used provided $\kappa_r/(1 - p\,P_{cr}/P_E)$ be substituted for κ_r.

The influence of the deflections in the plane of the web decreases as r approaches -1. Hence, this influence may be taken empirically into account, with sufficient accuracy, by substituting for κ_r the ordinates,

$$\kappa'_r = \frac{\kappa_r}{1 - \frac{1}{2}\, p\, (r + 1)\, \dfrac{P_{cr}}{P_E}} \qquad (50)$$

In the foregoing examples, assuming a ratio $P_{cr}/P_E = I_{min}/I_{max} = 0.2$, with $r = 0$ and $p = 0.6$, the critical moment becomes

$$M_2 = 4.36\,(1 - 0.5 \times 0.6 \times 0.2)\,\frac{\sqrt{B\,C}}{L} = 4.10\,\frac{\sqrt{B\,C}}{L} \qquad (51)$$

CONCLUSIONS

The foregoing results prove that for all practical purposes the critical combinations of thrust and end moments of I-columns elastically restrained in bending about the principal axes of their end sections and fixed against twisting there may be easily obtained once the critical value of equal end moments for a simply supported column is known. By the use of the illustrations and tables the designer may evaluate critical thrusts and moments (or eccentricities) with a minimum of computations.

The most significant result achieved by this numerical research is perhaps the discovery of the practically linear relation between p and κ_r, valid for most practical cases when the reduction of torsional rigidity is taken into account.

Although it must be remembered that an extension of the present results to the inelastic range is essential to all engineering applications, it is hoped that their simplicity will encourage specification writers to adopt more accurate column formulas in order to achieve greater economy and safety in steel structures.

APPENDIX I

The values of the moment coefficients:

$$K_r = \frac{M_2\,L}{\sqrt{B\,C}} \qquad (52)$$

and of the ratios κ_r were obtained by the Rayleigh-Ritz method starting from the expression for the total energy V of an I-column buckled laterally under the action of thrusts P and end moments:[4]

$$V = \frac{B}{2}\int_0^L (u'')^2\,dz + \frac{D\,h^2}{4}\int_0^L (\beta'')^2\,dz + \frac{H}{2}\int_0^L (\beta')^2\,dz + \int_0^L M\,\beta\,u''\,dz - \frac{P}{2}\int_0^L (u')^2\,dz \qquad (53)$$

in which u is the lateral displacement of the buckled column in the plane of minimum rigidity, β denotes the angular rotation of the buckled column, and z is the abscissa along the column axis with origin at the bottom of the column. The boundary conditions for columns simply supported in the weak plane are

$$u(0) = u''(0) = u(L) = u''(L) = 0 \qquad (54a)$$

and

$$\beta(0) = \beta''(0) = \beta(L) = \beta''(L) = 0 \qquad (54b)$$

in which the primes indicate derivatives with respect to z.

For columns fixed at the ends in the weak plane the boundary conditions are

$$u(0) = u'(0) = u(L) = u'(L) = 0 \qquad (55a)$$

and

$$\beta(0) = \beta'(0) = \beta(L) = \beta'(L) = 0 \qquad (55b)$$

The conditions of Eqs. 54 are satisfied by taking

$$u(z) = \sum_{n=1}^{\infty} a_n \sin \frac{n \pi z}{L} \qquad (56a)$$

and

$$\beta(z) = \sum_{n=1}^{\infty} b_n \sin \frac{n \pi z}{L} \qquad (56b)$$

in which a_n and b_n are undetermined constants evaluated by the Rayleigh-Ritz method.[4]

To satisfy the conditions of Eqs. 55, let

$$u(z) = h \sqrt{\frac{D}{2 B}}\, \eta(z) \qquad (57)$$

in which η is the nondimensional lateral displacement and expand η and β in the series:

$$\eta(z) = \sum_{n=1}^{\infty} a_n \, \phi_n(z) + \sum_{n=1}^{\infty} c_n \, \psi_n(z) \qquad (58a)$$

and

$$\beta(z) = \sum_{n=1}^{\infty} b_n \, \phi_n(z) + \sum_{n=1}^{\infty} d_n \, \psi_n(z) \qquad (58b)$$

in which

$$\phi_n(z) = \frac{1}{4 n^2 \pi^2} \left(1 - \cos \frac{2 n \pi z}{L}\right) \qquad (59a)$$

$$\psi_n(z) = \frac{1}{4 \nu^2} \left[\frac{2 z}{L} - 1 - \frac{\sin \nu_n \ (2 z/L - 1)}{\sin \nu_n} \right] \qquad (59b)$$

and ν_n are roots of the transcendental equation:

$$\tan \nu = \nu \qquad (60)$$

The choice of these functions greatly simplifies the Rayleigh-Ritz computations as they are orthogonal together with their first and second derivatives in almost all the combinations appearing in the integrals to be evaluated in minimizing the total energy V.

In order to obtain an accuracy of 1% or better, the cases $r = \frac{1}{2}, 0, -\frac{1}{2}$, and -1 were solved taking into account one term of each series, and from the corresponding values of K_r the ratios κ_r were computed. The corresponding determinantal equations are of the fourth order. The case $r = -1$ was then solved with two terms of each series, leading to determinantal equations of the eighth order. The new K_r differed substantially from those of the first approximation, but the new ratios κ_r were practically identical with those obtained by the first approximation. Hence, the ratios κ_r of the first approximation were considered correct within the required accuracy and only the coefficients $K_{0,r}$ were computed again by means of two terms of each series for $r = \frac{1}{2}$, $r = 0$, and $r = -\frac{1}{2}$, and with two and three terms of each series for $r = -1$. In this last case the determinantal equations of order eight and twelve split, for $p = 0$, into two separate equations of order four and six, whose roots correspond to the two branches of the curves $r = -1$ of Fig. 3. The intersection of the two branches was also determined in order to draw the graphs with greater accuracy.

Acknowledgments

The extremely complicated calculations were performed by the staff of the Istituto Nazionale per le Applicazioni del Calcolo, in Rome, Italy (the mathematical laboratory of the Italian National Research Council) directed by Mauro Picone. Aldo Ghizzetti, vice-director of the institute, and Wolf Gross supervised the calculations. E. D. Broadbent, Clelia Mengotti Marzolla, and Antonio Perugini were in charge of the computations, and Virgilio Ceccarini participated in the calculations and drew the original graphs.

The writer is greatly indebted to the Istituto Nazionale per le Applicazioni del Calcolo for this accurate and laborious numerical research, which was partially supported by a grant of the Column Research Council of the Engineering Foundation, under the chairmanship of Shortridge Hardesty, Hon. M. ASCE, and which was sponsored by its Committee E, headed by H. N. Hill, M. ASCE.

APPENDIX II

The following symbols, adopted for use in the paper and for the guidance of discussers, conform essentially with "American Standard Letter Symbols for Structural Analysis" (ASA Z-10.8-1949), prepared by a committee of the American Standards Association with Society representation, and approved by the Association in 1949:

A = area;
a = term defined in Eq. 1;

B = minumum flexural rigidity of the column in the plane of the flanges;
C = torsional rigidity of the column without thrust;
D = flexural rigidity of one flange in its own plane;
e = eccentricity;
e_2 = eccentricity at the top of the column;
H = reduced torsional rigidity;
h = column depth;
I_p = polar moment of inertia;
K = bending-moment coefficient:
  K_r = moment coefficient defined in Eq. 26;
  $K_{0,r}$ = moment coefficient without thrust;
  $K_{0,1}$ = moment coefficient for absence of thrust and equal end moments;
  $K_{0,1|f}$ = critical value of $K_{0,1}$ for column that is fixed in the weak plane at the ends;
  $K_{0,1|s}$ = critical value of $K_{0,1}$ for simply supported column;
k = bending-moment coefficient:
  $k_{0,1}$ = reduced-length bending-moment coefficient for equal end moments and no thrust;
  k_1 = coefficient defined in Eq. 19;
  $k'_{0,1}$ = value of $k_{0,1}$ when H is substituted for C in expression for l^2/a^2;
L = column length;
l = reduced column length;
M = bending moment:
  M_{cr} = critical value of equal end moments without thrust;
  M_f = end moment on column that is fixed in the weak plane;
  M_s = end moment on simply supported column;
  $M_{0,1}$ = moment at bottom of column without thrust;
  $M_{0,2}$ = moment at top of column without thrust;
  M_1 = moment at bottom of column;
  M_2 = moment at top of column;
  M'_2 = value of M_2 when H is substituted for C in the expression for l^2/a^2;
P = axial thrust:
  P_{cr} = minimum critical thrust in the absence of end moments;
  P_E = Euler thrust in the plane of the web;
  P_T = torsional thrust;
  P_{T_1} = thrust term defined in Eq. 43;
p = thrust coefficient;
r = ratio of the end moments;
u = lateral displacement of buckled column in the weak plane;
V = total energy;
z = abscissa along column axis with origin at bottom;
α = column-length reduction coefficient;
β = angular rotation of buckled column;

γ = ratio of minimum Euler thrust to torsional critical thrust;
ϵ_2 = top-eccentricity coefficient;
η = nondimensional lateral displacement;
κ_r = ratio of top moments with and without thrust;
κ'_r = value of κ_r when H is substituted for C in expression for l^2/a^2;
μ_r = magnification coefficient for unequal end moments;
$\bar{\mu}_r$ = minimum safe value of μ_r;
ν_n = roots of Eq. 60;
ϕ_n = function of z for the expansion of η and β; and
ψ_n = function of z for the expansion of η and β.

AMERICAN SOCIETY OF CIVIL ENGINEERS
Founded November 5, 1852
TRANSACTIONS

Paper No. 2837

FUNDAMENTAL CONCEPTS OF RECTANGULAR SETTLING TANKS

BY ALFRED C. INGERSOLL,[1] A. M. ASCE, JACK E. MCKEE,[2] M. ASCE, AND NORMAN H. BROOKS,[3] J. M. ASCE

WITH DISCUSSION BY MESSRS. THOMAS R. CAMP; HENRY L. THACKWELL; AND ALFRED C. INGERSOLL, JACK E. MCKEE, AND NORMAN H. BROOKS

SYNOPSIS

This investigation of fundamental theories of sedimentation, scour by turbulent eddies, inlet and outlet disturbances, and sludge-thickening phenomena indicates that settling tanks should be designed on the basis of surface area and that rectangular settling tanks should be long and narrow. The authors suggest that the minimum depth of such tanks is limited not by bed-load movement resulting from direct shear, as previously supposed, but by scour resulting from turbulent eddies in accordance with the suspended-load equation. There is evidence that tanks can be made relatively shallow if the deposited sludge is protected from resuspension by means of multiple inclined baffles. These baffles also serve to produce thicker sludge.

The conventional measure of efficiency of settling tanks is highly inadequate. In its place a new rational measure, called the overflow residual efficiency, has been developed theoretically.

INTRODUCTION

The primary function of a settling tank is to separate settleable and floatable solids from the liquid in which they have become suspended. In addition, settling tanks are frequently expected to perform another major role, namely, to separate liquid from the settled solids—a process known as "sludge thickening." In a well-designed settling tank it should be possible to accomplish both

---

NOTE.—Published, essentially as printed here, in January, 1955, as *Proceedings-Separate No. 590*. Positions and titles given are those in effect when the paper or discussion was approved for publication in *Transactions*.

[1] Asst. Prof. of Civ. Eng., California Inst. of Technology, Pasadena, Calif.

[2] Associate Prof. of San. Eng., California Inst. of Technology, Pasadena, Calif.

[3] Asst. Prof. of Civ. Eng., California Inst. of Technology, Pasadena, Calif.

these functions simultaneously at optimum efficiency with maximum economy of construction and minimum costs for operation and maintenance.

Like many other phases of engineering, however, the design of settling tanks has been governed largely by empirical rules rather than by fundamental considerations. Despite the excellent theoretical treatises by Allen Hazen[4] and Thomas R. Camp,[5] M. ASCE, showing that sedimentation is primarily a function of the settling velocity of discrete particles and largely independent of depth, the design of many settling tanks for waterworks and sewage works is still being based on the detention period and on rules of thumb.

It is one of the purposes of this paper, therefore, to reiterate briefly the fundamental concepts of sedimentation, especially as they relate to the shape of rectangular settling tanks and the length-width-depth proportions. Measures of efficiency are analyzed critically, and a new method is proposed for comparing the operating efficiencies of settling tanks. In addition, the paper presents recently acquired empirical data that extend the basic knowledge and in it the writers propound some theoretical aspects of the problem that have received little emphasis in civil engineering literature. Sludge thickening is discussed in relation to the area and depth of settling tanks, and a method is proposed to hasten thickening while simultaneously improving settling efficiency. Finally, it is the intent of the writers to suggest areas in which research may be conducted in order to further the understanding of this important phase of hydraulic design. Because of limitations of space all aspects of sedimentation and the design of rectangular settling tanks cannot be included in this paper, and in many instances such aspects are treated merely by reference to other detailed and authoritative papers.

RESUME OF FUNDAMENTAL CONCEPTS

The settling of discrete nonflocculent particles in a quiescent liquid, as reported by many investigators, is described in recent textbooks on fluid mechanics. In extremely weak concentrations the particles settle individually, but in thicker suspensions the settling velocities are reduced materially by collisions and by interference of the velocity fields of particles, combined with the upward movement of displaced liquid. John S. McNown, M. ASCE, and Pin-Nam Lin[6,7] have shown that settling velocities in a suspension of 1,000 ppm by volume are decreased by as much as 13% whereas at a volumetric concentration of 10,000 ppm the settling velocity is decreased by as much as 25%. In a quiescent suspension, the concentration may be weak in the top layers but it will become progressively more concentrated with increasing depth measured from the surface. When the concentration becomes so thick that numerous particles adhere to form a continuous honeycombed structure, the resulting sludge blanket will subside initially in accordance with the laws of consolidation described subsequently under the heading, "Thickening." In flocculent suspensions, two or more particles may coalesce to form a larger agglomerate which will probably settle at an increased rate.

---

[4] "On Sedimentation," by Allen Hazen, *Transactions*, ASCE, Vol. 53, 1904, p. 45.

[5] "Sedimentation and the Design of Settling Tanks," by Thomas R. Camp, *ibid.*, Vol. 111, 1946, p. 895.

[6] "Sediment Concentration and Fall Velocity," by John S. McNown and Pin-Nam Lin, *Proceedings*, Second Midwestern Conference on Fluid Mechanics, Ohio State Univ., Columbus, Ohio, 1952, p. 401.

[7] Discussion by Emmett M. Laursen and Pin-Nam Lin of "Turbulent Transfer Mechanism and Suspended Sediment in Closed Channels," by Hassan M. Ismail, *Transactions*, ASCE, Vol. 117, 1952, p. 440.

Messrs. Hazen[4] and Camp[5] analyzed the settling of discrete particles in a so-called ideal basin, for which the following assumptions are applicable: (*a*) The direction of flow is horizontal, and the velocity is uniform in all parts of the settling zone; (*b*) the concentration of suspended particles of each size is uniform over the depth at the inlet end of the settling zone; and (*c*) particles reaching the bottom remain fixed. For these conditions it is readily demonstrated that the settling velocity of a particle that falls through a distance exactly equaling the depth of the tank during its theoretical period of detention is equal to the discharge per unit of surface area, known as the "overflow rate." All particles with settling velocities, v, greater than the overflow rate, v_o, will be separated from the suspension, whereas particles with $v < v_o$ will be removed in the ratio v/v_o. Because Mr. Hazen was the first to utilize this ratio in the sedimentation field to which he contributed so greatly, the writers propose that the ratio be named the "Hazen number"—thus, $\mathsf{H} = v/v_o$. The use and significance of the Hazen number are explained subsequently, under the heading, "Measures of Efficiency."

Sedimentation in an "ideal" tank is independent of depth, being a function merely of the discharge and surface area. Were it not for factors that militate against the assumptions of an ideal basin and interfere with the theoretical conclusions, settling tanks could be made infinitely shallow. In real basins, however, the theory is modified by the effects of flocculation, turbulence, scour, density currents, inlet and outlet disturbances giving rise to mixing and short-circuiting, and the movement of cleaning mechanisms. In describing and evaluating these effects and in prescribing for their amelioration, Mr. Camp[5] has indicated that:

1. Settling tanks should be designed on the basis of the overflow rate—that is, the settling velocity of a particle of sediment of the smallest size theoretically to be 100% removed.
2. Detention periods are of themselves immaterial; in fact, for sewage treatment long detention periods may be deleterious.
3. Tanks should be no deeper than will be required to prevent scour and to accommodate cleaning mechanisms.
4. Tanks should be long and narrow in order to minimize the effects of inlet and outlet disturbances, cross winds, density currents, and longitudinal mixing.

Despite the apparent simplicity of the theories of sedimentation and the clear relation of overflow rates to removal ratios, attempts to compare the performances of settling tanks in waterworks or sewage works have been disappointing. There appears to be little or no correlation in actual operating records between removal efficiencies and overflow rates or detention periods. Basins that are poorly designed on a theoretical basis sometimes appear to perform more satisfactorily than well-designed tanks. In an attempt to evaluate the performance of settling tanks and to find parameters by which tanks may be compared logically, the following analysis of measures of efficiency is advanced.

MEASURES OF EFFICIENCY

A true measure of the efficiency of a settling tank should satisfy two requirements: (1) It should be independent of the characteristics of the suspension and should thus reflect directly the adequacy of the hydraulic design and operation of the tank, and (2) for an ideal tank the efficiency should be 100%.

The conventional measure of efficiency—the total percentage reduction of suspended solids—does not satisfy these requirements. It is obvious that any particular tank with a particular overflow rate will remove a far larger proportion of the solids from a suspension of coarse particles than from a suspension of very fine particles. For an ideal tank, furthermore, the total reduction of suspended solids is not 100% but a variable quantity depending on the size distribution of the material in suspension. Hence, if a chosen measure of efficiency is a function largely of the size distribution and is not 100% even for an ideal tank, it is a hopeless basis for comparison of different tanks unless the overflow rates and the suspensions to be settled are identical.

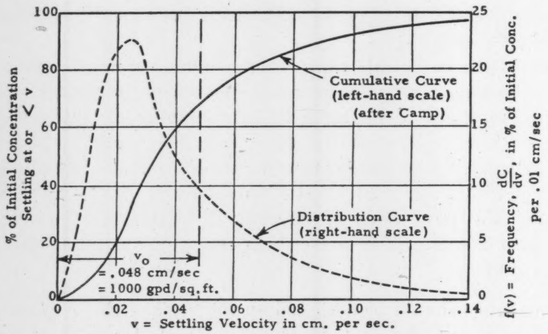

FIG. 1.—CONCENTRATION AS A FUNCTION OF SETTLING VELOCITY

The effects of various size distributions on total removal can best be visualized by considering the frequency distribution curve for the settling velocities of the particles. Such a distribution curve may be derived from a cumulative curve as illustrated by Fig. 1. A hypothetical raw (influent) distribution curve, $f_r = f_r(v)$, and the corresponding distribution curve for the effluent from an ideal tank, $f_i = f_i(v)$, are shown in Fig. 2. By definition, $f_r \, \Delta v$ is the fraction of the total material (by weight) that has a settling velocity between $v - (\Delta v/2)$ and $v + (\Delta v/2)$. The total area under the f_r-curve is unity and corresponds to the total concentration of solids.

If r_i denotes the removal ratio in an ideal tank (or simply the "ideal removal ratio") for a particular size of particle,

$$r_i = \mathsf{H} \quad \text{if} \quad \mathsf{H} < 1$$

and

$$r_i = 1 \quad \text{if} \quad \mathsf{H} \geqslant 1$$

in which H, the Hazen number, is defined as v/v_o under the heading, "Resume of Fundamental Concepts." The ideal removal ratio is shown graphically as a function of H in Fig. 3. The distribution curve f_i for the ideal effluent may then be expressed as

$$f_i = f_r \, (1 - r_i) \quad \text{(1)}$$

Referring again to Fig 2, it is noted that for $v > v_o$, f_i is always 0, indicating complete removal, whereas for $v < v_o$ the removal is proportional to v/v_o.

The total ideal removal, $\mathcal{R}_i$, is defined as the weighted average of the individual removals, r_i:

$$\mathcal{R}_i = \int_0^\infty r_i \, f_r \, dv \quad \text{(2)}$$

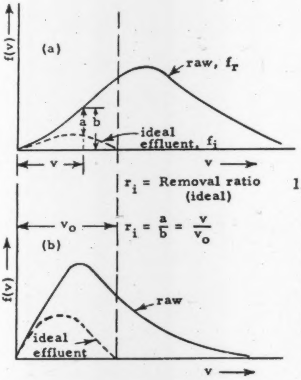

FIG. 2.—INFLUENT AND EFFLUENT RELATIONSHIPS FOR TWO SUSPENSIONS IN AN IDEAL TANK

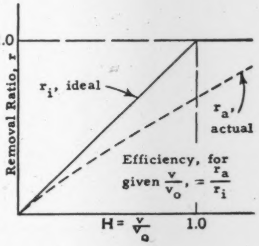

FIG. 3.—REMOVAL RATIO AS A FUNCTION OF THE HAZEN NUMBER

Because the total ideal removal ratio is also the area between the curves of f_r and f_i, divided by the area under the f_r-curve, $\mathcal{R}_i$ can also be written as

$$\mathcal{R}_i = \frac{\int_0^\infty f_r \, dv - \int_0^\infty f_i \, dv}{\int_0^\infty f_r \, dv}$$

because

$$\int_0^\infty f_r \, dv = 1, \quad \mathcal{R}_i = 1 - \int_0^\infty f_i \, dv \quad \text{(3)}$$

Comparing Fig. 2(*a*) with Fig. 2(*b*) it is quite apparent that the total ideal removal, $\mathcal{R}_i$, in case (*a*) is much larger than in case (*b*). Although the individual ideal removal ratios, r_i, are identical in cases (*a*) and (*b*) for each value of *v*, case (*b*) involves a finer suspension, and hence the sizes for which the removal is incomplete carry more weight in the integration.

Because any real tank has some turbulence, short-circuiting, and possible scouring, the actual removal ratio, r_a, will probably be less than the ideal removal ratio, r_i, as illustrated in Fig. 3. If the suspended material flocculates as it settles, it is even possible for r_a to exceed r_i. The actual effluent distribution curve, f_a, may be written in the same manner as the ideal case:

$$f_a = f_r\,(1 - r_a) \qquad (4)$$

A hypothetical actual effluent curve, f_a, is shown in Fig. 4. In contrast to f_i for the ideal effluent, f_a does not equal 0 for all values of $v > v_o$.

The total actual removal ratio, $\mathcal{R}_a$ is similar to $\mathcal{R}_i$ and is defined as

$$\left.\begin{aligned} \mathcal{R}_a &= \int_0^\infty r_a\,f_r\,dv \\ \text{or}\quad \mathcal{R}_a &= 1 - \int_0^\infty f_a\,dv \end{aligned}\right\} \qquad (5)$$

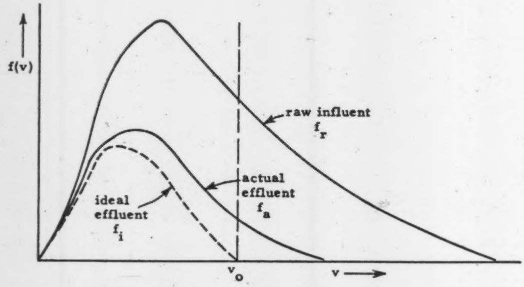

FIG. 4.—ACTUAL PERFORMANCE COMPARED WITH THAT OF THE IDEAL BASIN

This is the conventional measure of performance. Like $\mathcal{R}_i$, unfortunately, its magnitude is affected by the raw distribution. Thus, without knowing the settling-velocity distribution of the suspended matter in the influent and therefore not knowing $\mathcal{R}_i$ either, it is impossible to compare quantitatively the performances of different settling tanks merely on the basis of the total removal, $\mathcal{R}_a$, and the overflow rate, v_o.

Efficiencies.—For any particle size, the efficiency, η, may be defined as the ratio of actual to ideal removal ratios.

$$\eta = \frac{r_a}{r_i} \qquad (6)$$

This is an efficiency in the true sense because it is a measure of what the tank accomplishes relative to what the same tank should ideally accomplish, whether r_i be large or small. The amount by which η falls short of unity is entirely the net result of turbulence, short-circuiting, and flocculation. If flocculation is significant in increasing the removal of particles for which $\mathsf{H} < 1$, then it is possible for the efficiency at a particular particle size to exceed unity. It is probable that the efficiency will vary somewhat with the Hazen number. As

H becomes very large, thorough removal is assured despite short-circuiting and turbulence, and the efficiency, η, is bound to approach unity.

It is logical now to define a total or integrated efficiency, $\mathcal{E}$, as

$$\mathcal{E} = \frac{\mathcal{R}_a}{\mathcal{R}_i} = \frac{\int_0^\infty r_a f_r \, dv}{\int_0^\infty r_i f_r \, dv} \qquad (7)$$

In a sense this is a weighted average efficiency because it can also be written as

$$\mathcal{E} = \frac{\int_0^\infty \eta \, r_i f_r \, dv}{\int_0^\infty r_i f_r \, dv} \qquad (8)$$

If the efficiency, η, is constant for all values of v, then $\mathcal{E}$ is equal to η and is independent of the distribution f_r. However, because η probably varies somewhat, $\mathcal{E}$ will depend on the distribution f_r.

The main drawback of both η and $\mathcal{E}$ is that their determination is laborious. To compute η it is necessary to measure both the influent and effluent distributions, f_r and f_a, by pipette analysis or some equivalent method. For the total efficiency $\mathcal{E}$, it is easy to determine the total actual removal, $\mathcal{R}_a$, using conventional tests for suspended solids in the raw suspension and the effluent suspension, but the total ideal removal, $\mathcal{R}_i$, can only be determined from the raw distribution, f_r. Hence, a simpler measure of effciency is needed if it is to be used extensively.

Considering only the particles having a settling velocity, v, greater than the overflow rate, v_o, a partly integrated efficiency may be conveniently defined as

$$\mathcal{E}_o = \frac{\int_{v_o}^\infty r_a f_r \, dv}{\int_{v_o}^\infty r_i f_r \, dv} \qquad (9)$$

Thus, $\mathcal{E}_o$ is the area between the f_r-curve and the f_a-curve for $v > v_o$, divided by the area under the f_r-curve for $v > v_o$. If $v > v_o$, however, $r_i \equiv 1$ and $r_a = \eta$. Hence,

$$\mathcal{E}_o = \frac{\int_{v_o}^\infty \eta f_r \, dv}{\int_{v_o}^\infty f_r \, dv} \qquad (10)$$

The term $\mathcal{E}_o$ may be called the "overflow residual efficiency." It is simply the percentage removal of all material with settling velocity v greater than v_o (Fig. 5). Because an ideal tank should remove 100% of all particles for which

$v > v_o$, it is not necessary to find the size distribution of the raw suspension in order to determine $\mathcal{E}_o$.

To compute $\mathcal{E}_o$, all the information that is required is the total concentration of suspended material for which $v > v_o$, in both influent and effluent. This may be obtained for a sample of influent or effluent by separating the large particles from the small particles in an upward-flow device in which the backflow velocity is equal to the overflow rate, v_o, for the tank. The concentration of suspended matter in the measured volume of liquid remaining in the apparatus may then be determined for each sample. Such an apparatus might be developed, standardized, and made a part of sanitary engineering laboratories.

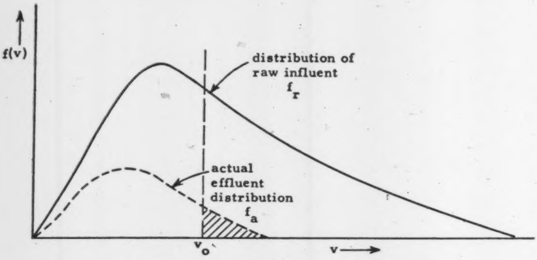

FIG. 5.—HYPOTHETICAL ACTUAL EFFLUENT DISTRIBUTION

The overflow residual efficiency, $\mathcal{E}_o$, is a relatively simple measure of efficiency to determine, but it is unfortunately still somewhat dependent on the size distribution of the material because the efficiency, η, depends on v. Nevertheless, because $\mathcal{E}_o$ is 100% for any ideal tank it should provide a reasonably valid basis for comparison between tanks of different design, whereas the total actual removal ratio $\mathcal{R}_a$, as conventionally used, is an inadequate basis for such a comparison.

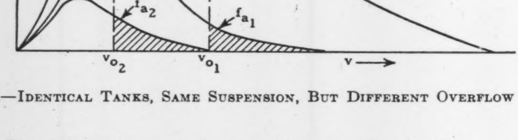

FIG. 6.—IDENTICAL TANKS, SAME SUSPENSION, BUT DIFFERENT OVERFLOW RATES

To illustrate the application of $\mathcal{E}_o$ as a measure of performance, the following combinations are examined:

(1) Identical tanks in which the v_o-values are equal, but the suspensions are different. This case is shown for an ideal tank in Fig. 2. The results for an actual tank would be similar except that part of each effluent curve would extend beyond v_o. Although the total removal, $\mathcal{R}_a$, would be quite different in the two cases, it is expected that the overflow residual efficiency, $\mathcal{E}_o$, would be almost the same.

(2) Identical tanks containing the same suspension but having different overflow rates. As shown in Fig. 6, decreasing the overflow rate will appreciably increase $\mathcal{R}_a$, whereas $\mathcal{E}_o$ will probably remain nearly constant.

(3) Two tanks of different design, containing the same suspension at the same overflow rate. This is the case of greatest interest and controversy among engineers. In Fig. 7, the area to the right of $v = v_o$ and under the actual effluent curve f_{a1} for tank No. 1 is much larger than the corresponding area for f_{a2}, for tank No. 2. Hence, the overflow residual efficiency, $\mathcal{E}_o$, for tank No. 2 is much higher than for tank No. 1. Therefore, tank No. 2 performs better than tank No. 1, at least for particles with $v > v_o$, and most probably for all values of $v < v_o$ also.

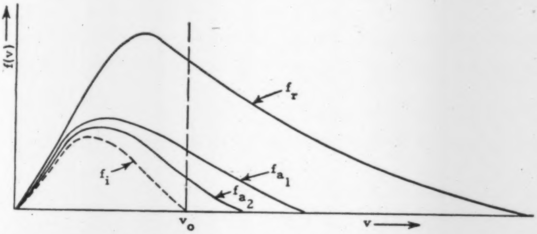

FIG. 7.—DIFFERENTLY DESIGNED TANKS, HAVING THE SAME SUSPENSION AND OVERFLOW RATE

One may next consider how some of the factors of design can be used to improve the efficiency and performance of settling tanks.

THE SHAPE OF RECTANGULAR TANKS

On the basis of the theory of ideal settling tanks, one cannot define the optimum ratios of length to width, length to depth, and depth to width in the design of a rectangular settling tank. The fundamental factors in any such determination are the kinematic quantities, such as horizontal velocity, turbulence, short-circuiting, and mixing. To the extent that the tank dimensions govern these factors they may be analyzed theoretically.

For a particular overflow rate and plan dimensions the mean horizontal velocity will vary inversely as the depth of the tank. If the horizontal velocity is limited by the scouring velocity of the particles being settled, the minimum depth allowable for the specified length and width is determined. From this reasoning alone, however, one cannot determine whether the best shape of tank is long, narrow, and deep or, for the same surface area and velocity, short, wide, and shallow. It is here that the theory must be supplemented with observations from practice.

On the subject of tank length, Mr. Camp[5] has explained that the inlet and outlet disturbance zones, even in the most well-designed structures, extend into the tank for a distance from each end that is at least equal to the depth. Therefore, a long, narrow tank will lose a minimum of its surface area to the unproductive inlet and outlet disturbance zones. Mr. Camp has indicated that the scouring velocity establishes a minimum value for the depth of a tank of fixed width, but that this dimension is rather more frequently controlled by the minimum requirement for the installation of a sludge-scraping mechanism. Commonly accepted minimum depths for mechanically cleaned tanks are between 5 ft and 8 ft.

For the settling of flocculent suspensions, Mr. Camp has presented a detailed method for determining the exact dimensions of tanks of different types. In lieu of a similar theoretical approach in this paper, the writers have found it instructive to make some observations on the results of two sets of laboratory model investigations.

Experimental Results.—At the University of Wisconsin, at Madison,[8] a model basin, 10 ft long by 5 ft wide by 2 ft deep, was tested with a 200-ppm suspension of microcrystalline wax spheres of specific gravity 0.92 and approximate diameter 0.02 cm. The basin was supplied with a vertical slotted inlet baffle obstructing 96% of the free area and a simple surface retention baffle followed by an overflow weir at the outlet. The tank was so constructed that the length could be made 5 ft or 10 ft, the width 2 ft or 5 ft, and the depth 0.2 ft, 0.4 ft, 0.6 ft, 0.8 ft, 1.0 ft, 1.5 ft, or 2.0 ft.

A similar tank was constructed at Purdue University (Lafayette, Ind.)[9] of fixed length 11.5 ft, adjustable widths of 2.0 ft, 4.0 ft, and 6.0 ft, and adjustable depths of 1.1 ft and 2.1 ft. The influent passed through two horizontal slotted baffles, obstructing 92% of the free area, while the effluent passed over a simple weir. The tank was tested with a suspension of approximately 200 ppm of diatomaceous silica. Separate tests, conducted in quiescent cylinders concurrently with the tank tests, afforded some information on the settling analysis of the suspension.

The most important difference between the two sets of tests was that the silica settled downward and was therefore subject to scour along the bed, whereas the wax moved upward to the free surface, where there was presumably no shear or scour. Actually, however, the surface of the tank containing wax soon became covered with a stagnant film of wax, held by the retention baffle, and the wax rising to the under side of this layer must have been subject to much the same shear forces as the downward-settling silica. It is not surprising, therefore, to see that both sets of tests yielded results that are closely comparable.

The data from the 37 wax tests and the 35 silica tests have been plotted together in Fig. 8 to show the total actual removal in percentages as a function of the Hazen number. (In Fig. 8, L denotes length, W width, and H depth.) It is evident that the disparity in the results of either the wax tests or the silica tests attributable to changes in shape of the tanks is far greater than the difference between the results of the two sets of tests. Although a consistent difference produced by the aforementioned condition of reduced surface shear for the wax might logically be expected, it is not apparent.

---

[8] "Hydraulic Characteristics of Gravity Type Oil-Water Separators," by Gerard A. Rohlich, *Proceedings*, Am. Petroleum Inst., Vol. 31M (III), 1951, p. 63.

[9] "An Investigation of the Effect of Varying the Width and Depth of a Sedimentation Tank," *Purdue University Progress Report No. 3*, Project No. RG1785C, Div. of Research Grants, National Inst. of Health, Bethesda, Md., 1953.

The Hazen number was computed for the median particle of the suspension in both cases. The distribution of rising velocities for wax spheres was determined by means of a sieve analysis of the wax, and values of rising velocity were computed by the laws of Stokes and Newton. The distribution of the settling velocities of silica was determined by means of quiescent settling tube tests.

Although it is difficult to draw any firm conclusions from an examination of Fig. 8, a few salient features may be noted. At a value of **H** = 0.38, the wax tests in a tank of dimensions 8.9 ft long by 2.0 ft wide by 1.5 ft deep produced a removal of 36% which is very close to that which might be expected of an ideal tank receiving a suspension of uniform particles, all the same size as the median particle of the true suspension. Varying the depth from a maximum of 1.5 ft or 2.0 ft to minimum depths of 1.0 ft, 0.8 ft, and 0.6 ft produced only negligible changes in removal, well within the range of experimental errors. When the depth was reduced to 0.4 ft, however, the removal was decreased markedly to 16%. This identical trend was observed at the other two values of the Hazen number tested with wax. Even poorer than the long shallow tank was the "square" tank, 4.5 ft by 5.1 ft by 1.0 ft. With this shape the removal was significantly improved as the depth was increased to 1.5 ft and 2.0 ft, at all values of **H**. The long, narrow tanks appear to be the most consistently satisfactory, both in the wax tests and the silica tests. The silica data from the shallow tank indicate a decreased removal at high values of the Hazen number,

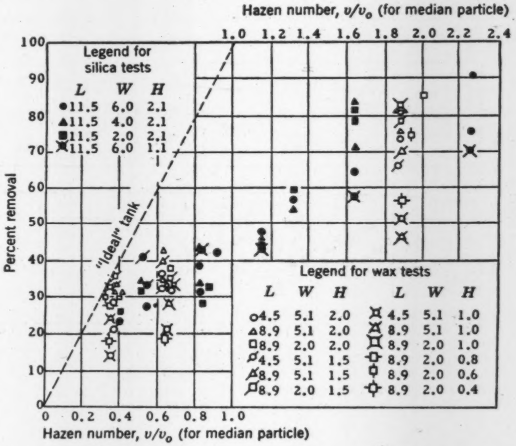

FIG. 8.—THE EFFECT OF LENGTH, WIDTH, AND DEPTH ON THE REMOVAL OF SILICA AND WAX IN MODEL BASINS (ALL DIMENSIONS IN FEET)

but this tank shows a comparatively high percentage of removal for values of H less than 1.0.

It is evident from the results of both sets of tests that the removal percentages achieved were generally far less than values on the line representing removal in the ideal tank. It is natural to inquire whether this fact may be explained on the basis of the turbulent-diffusion theory forwarded by William E. Dobbins,[10] A.M. ASCE, and discussed by Mr. Camp. Data from the wax and silica tests have been replotted in Fig. 9 utilizing exactly the same coordinates as those used by Mr. Camp in Fig. 14 of his paper.[5] In Fig. 9, V represents the flow velocity in the tank, ϵ is the mixing coefficient, and H is the total water depth. Beside each plotted point appears the value of $\mathsf{H} = v/v_o$. The two lines for Hazen numbers of 1.0 and 0.5 have been traced from Mr. Camp's curve. Both wax and silica tests—but especially the former—show a decrease in removal with an increase in horizontal velocity. For example, in the tank 8.9 ft long by 2.0 ft wide containing wax, doubling the horizontal velocity (or halving the abscissa of Fig. 9, as from 20 to 10) reduces the removal from approximately 80% to approximately 60%, for a constant Hazen number of 1.9. In the tank 11.5 ft by 6 ft containing silica, the reduction in abscissa from 51 to 27 results in a decrease in removal of from 90% to 70% for constant $\mathsf{H} = 2.28$. For wax tests in the shorter tank, a reduction in abscissa of from 102 to 51 reduces the removal from 74% to 51% for $\mathsf{H} = 1.92$.

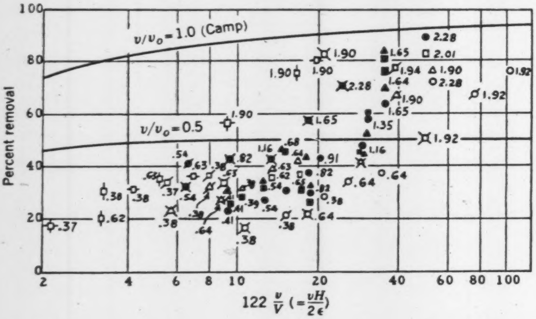

FIG. 9.—EFFECT OF TURBULENCE ON SUSPENSIONS OF WAX AND SILICA (NUMBERS INDICATE H-VALUES)

When these high rates of decreasing removal with increasing velocity are compared with the gentle slopes of the theoretical lines, it becomes clear that the effect of turbulent diffusion may be greater than is predicted from theory or that other effects such as short-circuiting or scour are operating.

In the case of the tank at Wisconsin, separate studies of short-circuiting were conducted by means of the dispersion technique, further described under the heading, "Inlets and Outlets." These tests, reported by Gerard A. Rohlich,[8] A.M. ASCE, and by the senior writer,[11] indicate that the effective overflow rate varied from about 1.10 to 1.05 times the observed overflow rate over the same range of horizontal velocities previously mentioned. This difference, of course, is not great enough to indict short-circuiting for the discrepancy between the results of theory and experiment. A more plausible explanation exists in a consideration of scour.

---

[10] "Effect of Turbulence on Sedimentation," by William E. Dobbins, *Transactions*, ASCE, Vol. 109, 1944, p. 629.

Scour by Turbulent Eddies.—Based on experiments by A. Shields and others relating to bed-load movement, Mr. Camp[5] derived a formula for the mean channel velocity, V_c, required to start motion of particles on the bottom of a settling tank. When applied to the foregoing experimental data from the University of Wisconsin and Purdue University, this formula yields values of critical channel velocities, V_c, much greater than actual tank displacement velocities, V, which might lead one to conclude that scour was not a factor in those tests.

Mr. Camp's formula can be used successfully for determining the maximum permissible velocity for sand particles in a grit chamber but, unfortunately, it is not applicable to the fine, light, flocculent material that forms the upper layer of the sludge blanket in a water tank or sewage tank. From Fig. 11 of Mr. Camp's paper,[5] it may be seen that the experimental points plotted by Mr. Shields for the critical shear for initiation of bed movement have values in the range of $0.15 < D/\delta < 40$, in which D is the particle diameter and δ is the thickness of the laminar film or sublayer at the bed, or in terms of the bed Reynolds number, $\frac{D\sqrt{\tau_o/\rho}}{\nu} = 11.6\,\frac{D}{\delta}$, in the range $1.7 < \frac{D\sqrt{\tau_o/\rho}}{\nu} < 450$, in which τ_o is the shear stress at the bed and ρ and ν are the density and kinematic viscosity, respectively, of the liquid. For typical sewage solids in a settling tank the values of $\frac{D\sqrt{\tau_o/\rho}}{\nu}$ are much smaller than 1.7, so that Mr. Shields' results cannot be applied. For example, if it is assumed that $V = 3$ ft per min and the Darcy friction factor $f = 0.025$, then $\sqrt{\tau_o/\rho} = V\sqrt{f/8} = 0.0028$ ft per sec; taking D equal to 0.1 mm and $\nu = 10^{-5}$ ft^2 per sec, the value of the bed Reynolds number is $\frac{D\sqrt{\tau_o/\rho}}{\nu} = 0.1$. For smaller horizontal velocities the value of the bed Reynolds number will be even less. In fact, the mechanism of scour in a case like this is probably completely different from the usual concept of bed-load movement.

Before the shear becomes sufficient to cause the material to slide or roll along the bed, the turbulent eddies in the stream will be strong enough to lift the material off the bed in gusts or "puffs." In a wind tunnel with two-dimensional flow, John Laufer[12] has shown that the root-mean-square value of the vertical turbulent velocity fluctuations near the wall is approximately $\sqrt{\tau_o/\rho}$ for channel Reynolds numbers of 12,300, 30,800, or 61,600. Because the Reynolds number for the flow in settling tanks is usually of this same order of magnitude,

---

[11] "Determination of Hydraulic Characteristics of Separating Chambers," by Alfred C. Ingersoll, *Proceedings*, Midwest Conference on Fluid Dynamics, Univ. of Illinois, Urbana, Ill., Vol. 1, 1950, p. 389.

[12] "Some Recent Measurements in a Two-Dimensional Turbulent Channel," by John Laufer, *Journal of the Aeronautical Sciences*, Vol. 17, 1950, p. 277.

Mr. Laufer's results can be applied generally to the present problem. In the example cited, the settling velocity, v, of a particle 0.1 mm in diameter with a specific gravity of 1.2 is 0.0019 ft per sec by the Stokes law at about 20° C. Because $\sqrt{\tau_o/\rho} = 0.0028$ ft per sec and $v = 0.0019$ ft per sec, the eddy currents will certainly be strong enough to lift material off the bed directly. It is suggested that the velocity should be kept low enough so that $\frac{v}{\sqrt{\tau_o/\rho}}$ is at least greater than 1 or 2.

Another approach to the problem of predicting when scour by turbulent eddies will occur is through the suspended-load equation described by Vito A. Vanoni,[13] M. ASCE, and others. Neglecting the turbulence caused by obstacles on the bed (such as scraper blades), the relative distribution of suspended material in the steady state in a two-dimensional channel is expressed by the suspended-load equation:

$$\frac{c_y}{c_a} = \left(\frac{H - y}{y}\right)^z \left(\frac{a}{H - a}\right)^z \dots\dots\dots\dots\dots\dots (11)$$

in which H is the total water depth; c_y is the concentration of particles of a particular size at any height, y, from the bottom; c_a is the concentration at a reference height a; and z is defined as

$$z = \frac{v}{\kappa \sqrt{\tau_o/\rho}} \approx \frac{2.5\, v}{\sqrt{\tau_o/\rho}} \dots\dots\dots\dots\dots\dots (12)$$

In Eq. 12, κ is the constant of approximately 0.4, as determined by Theodor von Kármán, Hon. M. ASCE, v is the settling velocity of the specific particle, and $\sqrt{\tau_o/\rho}$ is the conventional shear velocity. Although, strictly speaking, Eq. 11 is applicable only to two-dimensional flow (as with Mr. Camp's turbulence analysis), it nevertheless indicates that in any continuous-flow settling tank a quantity of light, fine material equivalent to the steady-state load of the basin will tend to be carried in suspension indefinitely, or, more precisely, that sludge may be continuously resuspended by turbulent eddies to maintain this steady-state load.

Although Eq. 11 is only relative, inasmuch as c_a or $c_a \left(\frac{a}{H - a}\right)^z$ cannot be determined as yet for various conditions, it is possible to set maximum or safe values for c_a. If the reference height a is taken as 0.01 H and if z equals 5, the concentration is decreased by a factor of 10^{-5} as y is increased from 0.01 H to 0.09 H (that is, from 10,000 ppm to 0.1 ppm). If z equals 2, however, the concentration is decreased by a factor of only 10^{-2} in the same height (that is, from 10,000 ppm to 100 ppm). In natural streams, material for which z is greater than 2 is usually not found in suspension in any measurable quantities.

As a safe design criterion, therefore, it is suggested that z be greater than from 3 to 5 or, by Eq. 12, $\frac{v}{\sqrt{\tau_o/\rho}}$ should be greater than from 1.2 to 2. This value agrees roughly with the value of $\frac{v}{\sqrt{\tau_o/\rho}}$ previously suggested by consideration of the magnitude of the turbulent velocity fluctuations near the bed. The shear velocity in artificial settling tanks is expressed approximately in relation to the mean horizontal velocity, V, as

---

[13] "Transportation of Suspended Sediment by Water," by Vito A. Vanoni, *Transactions*, ASCE, Vol. 111, 1946, p. 67.

$$\sqrt{\frac{\tau_o}{\rho}} = \frac{V}{18}$$

assuming a Darcy friction factor of 0.025 and, hence, V/v should be less than 9 to 15.

The application of this approach can be made clearer by considering an example. A settling tank is to be designed to pass 3.0 mgd and to remove all particles with settling velocities of 0.04 cm per sec or greater. This capacity corresponds to an overflow rate of 850 gals per day per sq ft, and hence the effective tank surface area should be 3,530 sq ft. To minimize the effect of inlet and outlet disturbances one should make the tank long and narrow—that is, 18 ft wide and 196 ft long, and perhaps 14 ft should be added to the length to allow for such disturbances.

How deep should the tank be? By Mr. Camp's formula for scour, assuming organic particles of specific gravity equal to 1.2 and diameter of 0.06 mm corresponding to the settling velocity, with conventional values for the constants, it is computed that V_c is at least 7 ft per min. On this basis, the tank need be only 2.2 ft deep to prevent scour. By analysis with the suspended-load equation, however, V should be not more than, say, 12 v_o, or 0.48 cm per sec, equivalent to about 1.0 ft per min. On this basis, the tank should be 15.5 ft deep; otherwise, a shallower and wider tank could be used.

Referring back to Fig. 9, it may be noted from Mr. Camp's discussion of Mr. Dobbin's paper,[10] that since

$$\epsilon = \frac{\kappa}{6} H \sqrt{\frac{\tau_o}{\rho}}$$

the abscissa may be rewritten as

$$\frac{v\,H}{2\,\epsilon} = 3\,\frac{v}{\kappa\,\sqrt{\tau_o/\rho}} = 3\,z.$$

On the basis of the foregoing analysis, it might be presumed that, when $\frac{v\,H}{2\,\epsilon} = 3\,z > 15$, the tanks should perform more nearly in accordance with Mr. Camp's theory because scour should be minor. However, from an inspection of Fig. 9, it appears that, although there is some relative improvement at larger abscissas, the removal is still too low. This may be due to turbulence in the tank generated by the inlets in addition to turbulence resulting from ordinary shear because the model tanks are relatively short. Indeed, the criterion given —that is, $z > 5$—may be considered necessary in preventing scour by eddies, but it may not be sufficient because of the additional sources of turbulence.

Tanks deep enough or wide enough to provide low displacement velocities are undesirable because they are costly and they may produce density currents that cause short-circuiting. In sewage works, moreover, their increased detention period favors septicity that may affect subsequent treatment adversely. It is desirable, therefore, to develop means whereby tanks can be made shallow and yet the sediment in such shallow high-velocity tanks can be protected from resuspension by turbulent eddies. A suggested design to accomplish this purpose and simultaneously to thicken the sludge is presented subsequently under the heading, "Suggested Design."

Multiple Inclined Baffles

A striking illustration of the theories of sedimentation and the ineffectiveness of depth lies in the experiments of Ralph Hayden[14] with ore "slimes," containing 2% by weight of granular sand, silt, and colloids in mechanical suspension in water. Mr. Hayden fed these slimes over an influent apron into a rectangular tank, 3 ft wide, 9 ft long, and 3 ft deep, with 3 hoppers and a conventional effluent weir. Baffles spaced 3 in. apart and inclined at 45° were inserted in various manners as follows: (*a*) As longitudinal baffles with the tops at either 4 in. or 0.5 in. below the water surface, (*b*) as transverse baffles with the tops sloping away from the feed end and either 4.5 in. or 0.5 in. below the water surface, and (*c*) as transverse baffles with tops sloping toward the feed end and only 0.5 in. below the water surface. The results of Mr. Hayden's experiments are presented in Table 1 and are illustrated in Fig. 10.

TABLE 1.—Settling of Ore Slimes in Open and Baffled Tanks[a]

Arrangement of baffles[b]	Overflow rate (gal per day per sq ft)	Removal (%)	Solids in the sludge (%)	Displacement[c] velocity (ft per min)
No baffles	347	65.9	10.9	0.097
	373	57.4	10.4	0.104
	445	63.1	12.6	0.124
	552	39.7	12.2	0.154
	721	35.3	13.8	0.201
Longitudinal baffles, 4 in. deep[b]	377	92.3	11.9	0.945
	730	76.9	15.7	1.83
	1,058	61.1	20.5	2.65
Longitudinal baffles, 0.5 in. deep[b]	589	87.6	17.0	11.8
	729	74.9	24.3	14.6
	960	76.6	25.4	19.2
Lateral baffles, 4.5 in. deep[b] with tops sloping away from the feed end	380	97.4	14.2	0.82
	522	93.6	18.7	1.16
	704	89.4	18.8	1.57
	960	70.6	25.5	2.14
Lateral baffles, 0.5 in. deep[b], with tops sloping away from the feed end	359	98.5	16.2	7.29
	533	98.3	17.7	10.68
	530	96.0	20.0	10.60
	706	86.8	24.2	14.15
	962	82.3	26.9	19.25
Lateral baffles, 0.5 in. deep[b], with tops sloping toward the feed end	533	93.4	28.6	10.68
	704	84.8	21.7	14.1
	925	68.3	27.7	18.5

[a] Influent suspension contained 2% solids, by weight. [b] Depth in this case means depth of the top edges of baffles below the effluent weir level. [c] In the area above the tops of baffles.

The transverse baffles in these tests rendered most of the tank volume ineffective except as a quiescent zone in which particles trapped from the thin surface layer could settle thereafter without serious disturbance from scour, density currents, or turbulence. Despite the intense short-circuiting (based on the entire volume), the tanks with transverse baffling produced exceptionally satisfactory results. In effect, they operated as very shallow tanks with horizontal velocities varying from 1 ft per min to 20 ft per min. Such high velocities are associated with increased turbulence, but particles that settled the short vertical distance to the top of the baffles were thereafter protected from scour or bed-load movement. As Fig. 10 indicates, tanks with transverse baffles and tops sloping away from the influent end yielded superior results, with 0.5-in. depths being as effective or more so than 4-in. depths.

---

[14] "Concentration of Slimes at Anaconda, Montana," by Ralph Hayden, *Transactions*, Am. Inst. of Mining Engrs., Montana, Vol. XLVI, 1913, p. 239.

The longitudinal baffles, extending from inlet wall to outlet wall, did not prove quite so satisfactory as the lateral baffles but they were a decided improvement over the unbaffled tank. This improvement may be attributable, in part, to the increased surface areas over which part of the suspension flowed.

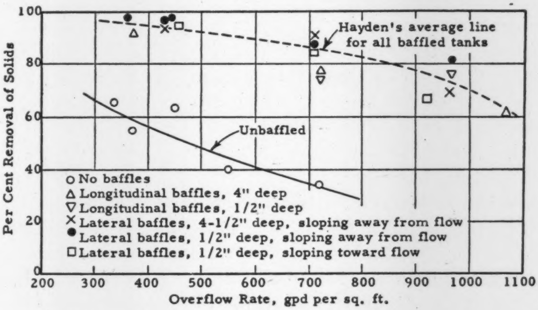

FIG. 10.—EFFECT OF MULTIPLE INCLINED BAFFLES ON THE SETTLING OF ORE SLIMES, BASED ON MR. HAYDEN'S WORK

In effect, then, the longitudinal baffles acted like trays, as advocated by Mr. Camp,[5] but with sloping surfaces.

Attention is invited particularly to the fact that the baffled tanks of all types produced much denser sludge than the unbaffled tanks. This effect of thickening by inclined baffles is examined subsequently, under the heading, "Thickening."

INLETS AND OUTLETS

Equally as important to the performance of a settling tank as the over-all shape is the matter of inlet and outlet structures. The updraft effect of the outlet weir, which is the simplest to understand, may be ascertained accurately by conformal mapping or by constructing a flow net. Ideal flow theory (required for drawing a flow net) is quite applicable to the outlet because the streamlines are converging and shear values are small. When the updraft velocity approaching the effluent weir exceeds the subsiding velocity of the particle to be settled, the particle will be entrained in the effluent.

Flow at the inlet, on the other hand, is distinctly not ideal. Invariably, the flow comes to the settling tank from a pipe or channel with a much smaller cross section than that of the tank. This means that the streamlines must in some fashion diverge upon entering the tank, with the usual result of separation and turbulence. Because the effects of turbulence caused by the inlet can extend for a considerable distance downstream, whereas the outlet weir updraft affects the flow only a very short distance upstream, the design of the inlet is generally conceded to be of much greater importance than that of the outlet.

Inlet Structure—The purposes of the inlet structure may be enumerated as follows: (1) To distribute the influent as uniformly as possible over the cross section of the settling zone, (2) to start all the flow through the settling zone in parallel horizontal paths, (3) to introduce the flow into the tank with a minimum of large-scale turbulence, and (4) to prevent a high velocity at the bottom of the tank, where sediment is gathering and being removed.

From the foregoing statement of purposes it is evident that the ideal inlet would be a diffusion wall with openings large enough to pass all of the suspension, across which there would be a head loss great enough to insure uniform velocity distribution over the cross section of the settling zone. The ideal inlet, moreover, would have expanding passageways on the downstream side so that, as nearly as possible, the kinetic energy of the influent would either be converted to potential energy or dissipated within or near the inlet wall, without becoming a disturbing influence in the main body of the tank.

In contrast to the ideal diffusion-wall inlet there is considered a simple free-fall weir, a poor type of inlet structure. The inlet weir achieves a good transverse flow distribution, but beyond this its virtues cease. The vertical velocity distribution just downstream from the weir is likely to show a strong flow along the bottom with reverse flow at the top, indicating a large eddy. The weir introduces kinetic energy equal to the free fall, but it absorbs almost none.

Between these two extremes lie the practical possibilities of inlets for settling tanks. The new design of oil-refinery waste-water separators utilizes a vertical slotted baffle with slots diverging at a 15° angle to approximate the ideal diffusion wall. The free area at the $\frac{5}{16}$-in. throat of the slots is only 4% of the cross-sectional area of the tank. The kinetic energy at the throat is therefore 625 times that in the tank. Before the flow leaves the diverging slots, however, its velocity is reduced to approximately 3 times the displacement velocity in the tank. Tests of the head loss across such a baffle have shown that there is almost no recovery of energy in the diverging slots. Therefore, the baffle converts approximately 98% of the kinetic energy existing at the throat into small-scale turbulence, which is quickly dissipated.

In sewage settling tanks this slotted baffle is not practical because it is difficult to keep clean. Workable inlets to sewage tanks generally utilize entrance ports or pipes which at least distribute the influent across the width of the tank. Various schemes, ranging from a simple tee on the end of each inlet pipe to the sloping target baffle used at Detroit (Mich.), are employed to deflect the jets from the inlet ports. All such inlets involve considerable large-scale turbulence; however, if the tank is made long and narrow, the inlet disturbance is confined to a relatively small part of the tank.

Outlet Structure.—The entraining effect of the outlet weir has been analyzed approximately in a report of the National Research Council.[15] It is shown that a certain portion of the tank volume, in the shape of a cylindrical sector with its axis at the outlet weir, is ineffective for settling because a particle entering this zone will be entrained in the effluent. The equation given for this volume is

---

[15] "Sewage Treatment at Military Installations," Report of the Subcommittee on Sewage Treatment, National Research Council, *Sewage Works Journal*, Vol. 18, 1946, p. 791.

$$\text{Ineffective volume} = \kappa \frac{q^2}{v^2} \quad \ldots\ldots\ldots\ldots\ldots\ldots (13)$$

in which q is the weir loading or flow per unit length of weir, v is the settling velocity of the particle considered, and κ is a constant ranging from 0.35 to 0.55 depending on the shape and geometry of the tank.

This analysis, based on ineffective volume, does not provide a clear comparison with ideal tank theory, which assumes a uniform vertical distribution of velocity at the outlet of the settling zone. Particles that have not actually reached the bottom are entrained in the effluent from the ideal tank and thus, according to this reasoning, even a part of the volume of an ideal tank is ineffective in settling.

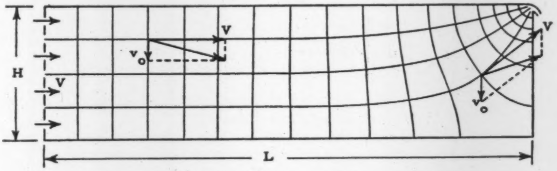

Flow Net for Two-Dimensional Rectangular Tank

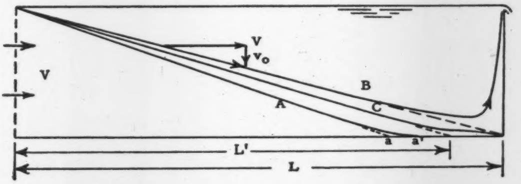

FIG. 11.—THE EFFECT OF THE EFFLUENT WEIR ON PATH LINES OF SETTLING PARTICLES

A more proper examination of the effect of the outlet weir can be made by sketching the flow net for the tank to be studied. This approach indicates the effect of the weir on the velocities through the tank and not only in the vicinity of the weir. There are considered three particles, A, B, and C, all starting at the top of the tank at the inlet. The velocity of each particle at any point is given by the vector sum of its settling velocity and the local water velocity. From such velocity vectors, the paths of the three particles have been traced in Fig. 11.

Particle A, with settling velocity, v_A, would reach the bottom at a distance, a, from the inlet in an ideal tank. By means of the flow net it may be determined that, with the effect of the outlet weir, particle A will not reach the bottom until the distance a'. Particle B, which would have just settled to the bottom in the length, L, of the ideal tank, will be entrained if the updraft velocity is greater than its settling velocity. Particle C, which may be called the critical particle, would settle in an ideal tank at a length, *c*, from the inlet. With the weir updraft, however, particle C is carried along toward the weir and finally barely escapes the strong updraft and settles to the bottom at the end of the tank. All particles with v-values greater than v_C are settled completely, and those with v-values less than v_C will be entrained in the effluent if they begin at the top of the tank. The effect of the weir, then, is to decrease the length of the equivalent tank from L to L'. To compute this accurately, a different flow net must be drawn for each value of L/H desired. It will soon be found, however, that for long tanks the distortion of the flow is negligible at a distance of a few multiples of the depth. Hence, to minimize outlet effect a long tank is again desired. It is common practice, moreover, to introduce additional launders or take-off weirs to keep the weir rate down.

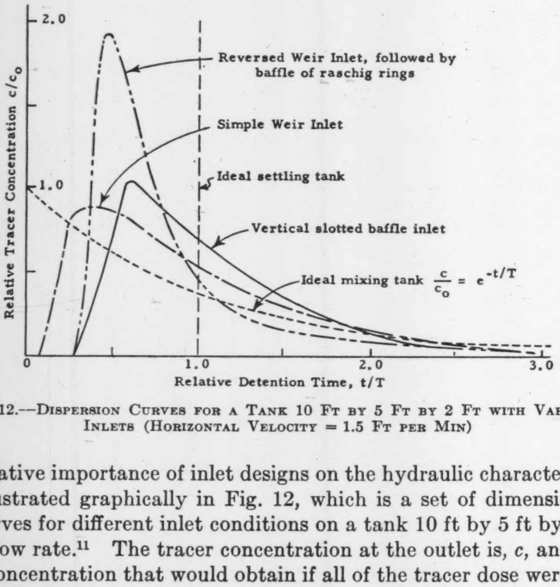

FIG. 12.—DISPERSION CURVES FOR A TANK 10 FT BY 5 FT BY 2 FT WITH VARIOUS INLETS (HORIZONTAL VELOCITY = 1.5 FT PER MIN)

The relative importance of inlet designs on the hydraulic characteristics of a tank is illustrated graphically in Fig. 12, which is a set of dimensionless dispersion curves for different inlet conditions on a tank 10 ft by 5 ft by 2 ft all at the same flow rate.[11] The tracer concentration at the outlet is, c, and c_o represents the concentration that would obtain if all of the tracer dose were distributed uniformly throughout the tank, and T is the nominal detention time. The simple weir inlet is seen to produce a dispersion curve not greatly different from that of an ideal mixing tank, indicating the ineffectiveness of this inlet arrangement. Passing the influent over a reversed-flow weir inlet followed by a tray of raschig rings produces a dispersion curve with a much higher peak, thereby indicating less mixing, but the short-circuiting is nevertheless severe. The aforementioned diverging-slot baffle inlet produces the most desirable curve of the three inlets with the greatest median and modal detention times.

With the slotted baffle for an inlet, the outlet structure was varied in at least three different ways, but no significant difference could be observed from the results (not shown in Fig. 12). In so far as dispersion characteristics are concerned, differences in outlet types are of small importance compared to differences in inlet types.

THICKENING

Particles that settle through zones of free settling or hindered settling, or of both, form a carpet of sludge when they reach a flat or inclined surface in a tank. This carpet, in its upper portion and in early stages of formation, consists of particles resting upon each other in a haphazard fashion with a high proportion of interstitial space—that is, a high porosity and a high void ratio. Flocculent particles, such as activated sludge, form carpets or blankets with extremely high porosity.

Subsequent to its formation, the sludge blanket is subjected to excess hydrostatic pressure from its own weight. The blanket tends to be compacted as water is squeezed from the interstices by increased weight or by mechanical modification of the honeycombed structure. In effect, then, thickening is the process of removing liquid from the solids, or the opposite of sedimentation, which is the removal of suspended solids from the liquid.

Thickening is generally a desirable phenomenon in settling tanks from which the sludge must be pumped and otherwise processed. A sludge with 98% moisture has approximately twice the volume per unit weight of dry solids as a sludge of 96% moisture. Denser sludges yield savings in pumping costs, pipelines, and digestion tanks, but a sludge that is too dense may become troublesome to handle.

Factors that influence the initial structure and the thickening of sludge blankets include: (1) The nature of the settleable solids—their density, shape, flocculent structure, thixotropy, content of living organisms, electrostatic charges, and other surface characteristics; (2) the concentration of settleable solids in the original suspension; (3) the dissolved substances in the interstitial water; (4) temperature; (5) the depth of the blanket; (6) the surface area of the blanket; (7) the time allowed for compaction; and (8) structural modification by mechanical action, vibrations, or pressure. Of these factors, the first three are independent of the design of the settling tank and the fourth is relatively so, although shallow tanks may become warm or cool more rapidly than deep ones. The other factors, closely related to the shape and design of settling tanks, are discussed subsequently.

Effect of Depth, Surface Area, and Time.—The initial compaction of a sludge blanket is analogous to the consolidation of a clay soil and to the cooling of a hot solid body; all of these phenomena can be formulated by the same partial differential equation. For one-dimensional consolidation of a clay soil, water in the inner regions cannot be squeezed out rapidly because it must pass upward successively through countless other interstices and capillaries as hydraulic and physical considerations permit. When the amount of compaction is small, the partial differential equation governing this phenomenon is

$$\frac{\partial u}{\partial t} = C_v \frac{\partial^2 u}{\partial z^2} \qquad (14)$$

in which u is the excess pore pressure—that is, any pressure in excess of the hydrostatic pressure; z is the longitudinal distance; and C_v is the coefficient of consolidation. When an external pressure is applied to a clay soil, the pressure is initially transmitted principally by the interstitial water, creating an excess hydrostatic pressure, u. Gradually, as water is squeezed from the upper layers of clay, the excess pressure is transferred to the grain structure. The reduction of pore pressure near the surface creates a pressure gradient which causes the pore water to flow upward. The time required for any particular degree of average consolidation to be reached in a clay layer is proportional to the square of the thickness of the layer. Hence, a shallow bed of clay will be consolidated much more quickly than a deep bed or, to express it otherwise, after a specified interval of time a shallow bed will have achieved, percentagewise, more consolidation than a deep bed.

The early stages of compaction of a sludge blanket in a settling tank are roughly analogous to the consolidation of clay under an external pressure, and hence a shallow blanket of sludge thickens more rapidly than does a deep blanket. The analogy is approximate, however, inasmuch as (*a*) the subsidence is large compared with the initial thickness and (*b*) the excess hydrostatic pressure in the case of a sludge blanket arises from the weight of the sludge itself rather than from an applied force. As more sludge accumulates, the weight increases. Moreover, as compaction of a blanket progresses, the excess force on lower layers increases as more load is transferred to the grain structure.

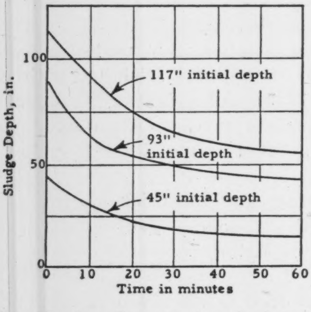

FIG. 13.—THE COMPACTING OF ACTIVATED SLUDGE, BASED ON DATA OF MESSRS. RUDOLFS AND LACY (TABLE 2)

TABLE 2.—DATA FOR FIG. 13

Initial depth, in inches	Depth of Sludge, in Percentage of Initial Depth		
	After 1 hour	After 3 hours	After 19 hours
117	46	37	12
93	40	31	14
45	32	22	16

The coefficient of consolidation in Eq. 14 is defined as

$$C_v = \frac{K\,(1 + e)}{a_v\,\gamma} \qquad (15)$$

in which K is the coefficient of permeability, e is the void ratio, a_v is the negative slope of the pressure-void ratio curve, and γ is the specific weight of water. In the consolidation of clay, the components of C_v do not change markedly, and hence C_v remains approximately constant. In the compaction of sludge, however, both k and e in the numerator are decreased rapidly as thickening progresses but a_v is also decreased as the pressure is increased.

The effect of depth on the compacting of activated sludge is illustrated by Fig. 13, from data (Table 2) presented originally by Willem Rudolfs and I. O. Lacy.[16] Identical sludges were placed in cylinders of three different depths, and the rates at which the sludge surfaces dropped were noted. The three curves are roughly parallel for the first hour; by that time the shallowest sample had thickened to 32% of its original volume and the deepest sample to only 46%. During the very early stages of compaction the bottom of the blanket has almost no effect inasmuch as compaction is occurring primarily at the surface. Hence, in absolute distance, the top of a thin layer subsides almost as rapidly as the top of a thick layer and, consequently, for a thin layer the relative compaction will be greater. The advantage of the shallowest sample was still maintained after 3 hours, but by 19 hours the deep sample had formed the densest sludge. For nonputrescible sludges long periods of compaction are beneficial, but in sewage works biological considerations require that sludge be removed from settling tanks in 1 hour or 2 hours at the most.

It is apparent, therefore, that the shallowest sludges thicken most rapidly and, consequently, for a given volume of sludge the greatest possible area should be provided. Thus, the simple initial compaction of sludge, like the settling of discrete particles, is a function of the surface area of the tank. After the first hour of such compaction, the depth of the sludge blanket becomes an important consideration. In waterworks, where alum or calcium-carbonate sludge may be allowed to accumulate for several days or weeks, additional depth for sludge should logically be provided.

Effect of Mechanical Action and Vibrations.—The honeycombed structure of sludge formed by discrete particles as well as flocculent particles is extremely unstable when subjected to lateral forces or vibrations. The grains tend to slide, roll, or slough over each other, and to realine themselves in a denser structure. Moreover, the capillaries are modified, allowing water to escape more rapidly from the pores.

This mechanical action is the basis of commercial thickening apparatus of the picket-fence type and other stirring types. It is also effective in the sludge-scraping mechanisms of rectangular tanks or circular tanks, the primary purpose of which, however, is to move the sludge to a hopper. The raking action and horizontal thrusts of such mechanisms serve to disrupt, modify, and thicken the sludge structure.

Effect of Inclined Surfaces.—Particles that settle onto an inclined surface will usually adhere and form a sludge blanket of limited depth. In this case the theory of compaction is more complicated than for simple one-dimensional consolidation. For a given water-surface area more settling surface is provided by an inclined bottom than by a level one; consequently, sludge compaction should be more rapid. The steeper the slope of the bottom surface in relation to a particular water-surface area, the greater will be the exposed area for compaction and the more rapid will be the thickening.

---

[16] "Settling and Compacting of Activated Sludge," by Willem Rudolfs and I. O. Lacy, *Sewage Works Journal*, Vol. VI, 1934, p. 647.

On steep slopes, moreover, sludge will slough or flow downward rather than accumulate as a deep blanket. This sloughing or tumbling action is similar to mechanical action or vibrations in its effect of breaking apart the flocculent honeycombed structure of the sludge and causing the individual grains to realine themselves in a denser structure.

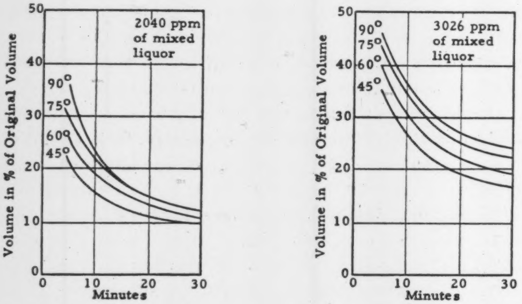

FIG. 14.—EFFECT OF INCLINATION ON THE COMPACTION OF ACTIVATED SLUDGE

The effect of various slopes on the compaction of activated sludge was also demonstrated by Messrs. Rudolfs and Lacy[16] who observed the sludge in cylinders inclined at angles of 90°, 75°, 60°, and 45° from the horizontal. A portion of their results, shown in Fig. 14, demonstrates that the greater the inclination from vertical—and hence the greater the horizontal area—the more rapid is the compaction.

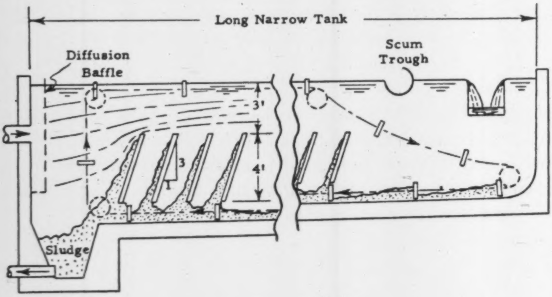

FIG. 15.—TENTATIVE SUGGESTED DESIGN OF A BAFFLED TANK FOR WATER OR SEWAGE WORKS

Mr. Hayden's work with ore slimes, described previously in this paper, corroborates the theory of thickening by inclined baffles. As shown in Table 1, the baffled tanks produced denser sludge than did the unbaffled tanks, probably because of the mechanical thickening that occurred as sludge tumbled down the baffles. It is also interesting to note that use of the higher overflow rates produced denser sludges. At higher discharges many of the finer and more flocculent particles were not removed from the suspension; consequently the larger, heavier particles formed a denser sludge.

The theories and experiments described in this section lead to the conclusion that sludge thickening in settling tanks can be hastened by providing larger surfaces on which the sludge may settle and by inclining these surfaces so that successive mechanical disruptions of structure will occur by sloughing. A suggested design for such a tank is presented in the following section.

Suggested Design

A suggested design for a settling tank for a waterworks or sewage works, with a tentative arrangement of multiple inclined baffles, is shown in Fig. 15. For fluocculent putrescible wastes inclined baffles must not be spaced so closely as to produce clogging. Inclinations should be greater than 45° to prevent heavy accumulations of sludge and to assure rapid sloughing. Tentatively, therefore, it is suggested that baffles be inclined on a slope such as 3 on 1 and that they be spaced 1 ft or more apart.

The arrangement of baffles in Fig. 15 allows the sludge-scraping mechanism to operate in a conventional manner to move sludge from the bottom of the inclined baffles to the hopper. The return flight can skim the surface, if desired, but it is likely that floating scum will be moved to the trough effectively by the high horizontal velocity without mechanical assistance. The settling zone above the baffles should be greater than the 0.5 in. or 4 in. used by Mr. Hayden for ore slimes, but depths of 2 ft or 3 ft should be adequate. This combination of inclined baffles and a shallow settling zone, free from the probability of scour, should improve the efficiency of sedimentation and favor the formation of thick sludge.

Summary

The major points of this paper may be summarized as follows:

1. The theories of Messrs. Hazen, Camp, and others, indicating that sedimentation is a function of surface area and that, for optimum efficiency, settling tanks should be long, narrow, and relatively shallow, are reiterated and supported.

2. The present method of comparing the performances of settling tanks on the basis of their total percentage removal of suspended solids is inadequate. Instead, a new method is proposed for comparing the performance of an actual tank with an ideal basin by means of the "overflow residual efficiency."

3. Results of experiments with wax spheres and silica verify to a great extent the theory that sedimentation is independent of depth, but these tests indicate that turbulence or scour, or both, at very shallow depths and high displacement velocities may be more deleterious than was formerly realized.

4. Turbulent eddies will produce a resuspension of fine light sediment and lead to inefficient removal of these solids at horizontal velocities much lower than those required to start bed-load movement in accordance with Mr. Camp's formula based on Mr. Shield's data.

5. The suspended-load equation (Eq. 11) is advanced as a logical approach to the subject of limiting horizontal velocities to avoid scour by turbulent eddies. This equation indicates that displacement velocities should be much

lower than Mr. Camp advocates; however, because, for several reasons deep tanks are undersirable, the writers propose that shallow tanks be used in conjunction with a method to prevent scour. Multiple inclined baffles appear to serve this purpose.

6. Dispersion tests indicate that inlets are more critical than outlets in controlling short-circuiting. Outlets, however, modify the flow nets so that poor designs with high weir rates cause partly settled particles to be entrapped in updrafts.

7. A given volume of sludge will thicken more rapidly during early stages of compaction in a shallow blanket than in a deep one; hence, a large bottom area should be provided for sludge thickening.

8. Thickening is accelerated by inclined surfaces and by mechanical action or vibrations.

On the basis of the foregoing analysis, it is suggested that further research and experimentation be conducted with a view toward designing rectangular settling tanks for waterworks and sewage works along the following lines: (*a*) With a surface area corresponding to the overflow rate of the particle to be 100% removed, (*b*) with high ratios—that is, 10—of length to width in order to minimize inlet and outlet disturbances, (*c*) with depths of 6 ft or more which would be great enough to accommodate mechanical scraping mechanisms, and (*d*) with multiple inclined baffles to minimize scour and to improve the thickening of sludge.

DISCUSSION

Thomas R. Camp,[17] M. ASCE.—This paper is a welcome addition to the sparse literature on the theory of sedimentation. Much remains to be done in perfecting rational theories of sedimentation and in applying these theories to the economic design of settling tanks. The authors of this paper are to be congratulated on their grasp of the proper methods of approach and should be encouraged to continue their research both in the development of the theory and in the testing of the theory by experiment. The following comments by the writer are made with the hope that they will lead to a better understanding of the theories developed thus far and will therefore be helpful to future research in this field.

The authors refer to experiments by Messrs. McNown and Lin which show reductions in settling velocities due to hindered settling which are very much greater than the reductions indicated elsewhere by the writer.[18] The graph which he presented was based on experiments by (1) W. O. Kermack, A. G. McKendrick, and E. Ponder on red blood cells, (2) the writer on lucite spheres, and (3) the writer on round sand grains. The wide discrepancy between the results obtained by Messrs. McNown and Lin and those shown in the writer's graph indicates the need for a critical study of the methods of testing in each case and possibly the need for further experimental measurements.

The authors' presentation of new means for measuring the efficiency of settling tanks is of academic interest but of little practical value to sanitary engineers because the method deals entirely with suspensions of discrete particles, whereas nearly all the suspensions dealt with in practice by sanitary engineers are suspensions of flocculent particles. It is impossible to make a settling-velocity analysis of a suspension of flocculent particles because the number of particles and the settling velocity of each one are changing continuously as a result of flocculation.

The authors have analyzed the results of settling tests made at the University of Wisconsin with a suspension of small wax spheres and of settling tests made at Purdue University with a suspension of diatomaceous silica. In the former case, removal was accomplished by flotation because the wax spheres were lighter than water, and in the latter case removal was accomplished by settling. The analysis of the results of these experiments made by the authors consisted of a comparison between the removal which would be expected from an ideal tank and the removal which might be expected from an ideal tank modified by turbulent eddies. The authors found that the actual removal was very much less than indicated for the ideal tank, and that this difference could not be explained by turbulent eddies generated from the drag on the walls and floor of the tanks. The authors conclude that a more plausible explanation for the lesser removal is in the scour from the top of the deposited sludge. They reached the further conclusion that scour of the sludge must be much greater than indicated by the experiments of Mr. Shields and others which were used as a basis for the writer's equation for critical scouring velocity.[19] The writer questions the validity of the authors' conclusions and suggests that they are the result of the authors' failure to give due consideration to the overpowering effect of residual turbulence from the inlets of the basins used in the Wisconsin and Purdue tests. The authors took cognizance of turbulence generated by the inlets but they did not evaluate its great magnitude.

---

[17] Partner, Camp, Dresser & McKee, Cons. Engrs., Boston, Mass.

[18] "Sedimentation and the Design of Settling Tanks," by Thomas R. Camp, *Transactions*, ASCE, Vol. 111, 1946, p. 899, Fig. 3.

The authors argue that the writer's equation for critical scouring velocity, derived from studies and experiments by Mr. Shields and others, is not applicable to deposits of light flocculent materials because the bed Reynolds number for flocculent materials in a settling tank will be much less than the bed Reynolds numbers corresponding to the experiments of Mr. Shields and others. The writer's equation is a rational derivation involving the assumption that the critical tractive force is directly proportional to the size and net density of the particles to be scoured. The results of Mr. Shields' experiments[20] show that this assumption is approximately valid if the value of the proportionality factor β ranges from approximately 0.03 to 0.07. There is no reason to conclude that this assumption cannot also be made outside the range of the Shields experiments, provided the value of β is known approximately.

The authors have argued that the mechanism of scour in a water or sewage settling tank is completely different from the usual concept of bed-load movement. They have stated that, before the shear is sufficient to cause the material to slide or roll along the bed, the turbulent eddies in the stream will be strong enough to lift the material off the bed in gusts or puffs. The writer believes that the mechanism of scour is the same wherever it exists and that it is a combination of rolling and lifting by puffs.

The vertical velocity fluctuations at the wall are zero, even though they may be equal to the friction velocity near the wall. For this reason, the value of the vertical velocity fluctuations must be much greater than the settling velocity of a particle in order to lift the particle. For example, as reported by W. F. Langelier, in the tunnel section where alum floc was settled with no scour at a channel velocity of 12 ft per min, the friction velocity was 0.011 ft per sec, or six times the settling velocity of a 0.1-mm particle with a specific gravity of 1.2.

The writer's presentation[21] of the effect of turbulence in retarding sedimentation—used by the authors in Fig. 9—is a graphical representation of the theory derived by Mr. Dobbins to show the effect of turbulent mixing induced by the drag on the walls and floor of the tank or channel. In this theory, no account is taken of residual turbulence from the tank inlet. The theory is applicable, therefore, only to grit chambers where the velocity at the inlet end is reduced by only one half to three fourths and to very long settling tanks where the effect of velocity reduction at the inlet end is masked by the great length of the tank.

The experimental basins used at Wisconsin and Purdue were much too short to be of any use in interpreting the theory for an ideal tank as modified by drag-induced turbulence. The tanks were not long enough to produce a uniform flow velocity distribution. Moreover, the high inlet velocities, amounting to 25 times the tank velocity for the Wisconsin tank and 12.5 times the tank velocity for the Purdue tank, further interfered with the possibility of developing stable flow patterns in the tanks.

---

[19] "Sedimentation and the Design of Settling Tanks," by Thomas R. Camp, *Transactions*, ASCE, Vol. 111, 1946, p. 913, Eq. 12.

[20] *Ibid.*, p. 912, Fig. 11.

[21] *Ibid.*, p. 918, Fig. 14.

The loss of head through the Wisconsin tank because of drag on the walls and floor has been computed by the writer for the case of the 5-ft width and 2-ft depth, using the Darcy-Weisbach formula with a value of f arbitrarily taken at 0.024. The resulting head loss is 0.054 times the velocity head in the tank. The corresponding loss of head in the inlet slots is 625 times the velocity head in the tank. The resulting ratio of the loss in energy at the inlets to the loss in energy due to drag on the walls and floor is 11,600 to 1. A similar computation for the Purdue tank, using a 6-ft width and a depth of 2.1 ft, shows that the energy loss from turbulence in the inlet jets is 2,800 times the energy loss due to drag on the walls and floor.

All the energy in the inlet jets is lost in turbulent eddies within the tank itself. It should be obvious that the turbulence produced by the inlet jets is of far greater importance in retarding settling than the turbulence produced by the drag on the walls and floors.

Most of the energy in the inlet jets is doubtless dissipated in the upstream end of the tank, but extremely slight differences in energy between the top and bottom or between jets will induce short-circuiting and encourage density currents. In tanks long enough to develop a drag along the walls and floor, the drag will tend to stabilize the effects of the inlet jets. No such stabilizing effect is possible, however, for the experimental tanks at Wisconsin and Purdue.

Another method of comparing the relative effects of drag-induced turbulence and inlet-induced turbulence is through the value of the mixing coefficient. If it is assumed that the mixing is uniform throughout the tank, whether induced by drag or by the inlet jets, the mixing coefficient is proportional to the square root of the head loss. Thus, for the Wisconsin tank, the mixing coefficient for the jets is 108 times the mixing coefficient for the drag, and for the Purdue tank the mixing coefficient for the jets is 53 times the mixing coefficient for the drag on the walls and floor.

The authors have stated that the writer's formula for critical channel velocities to prevent scour may be applied successfully to sand particles in a grit chamber but, unfortunately, is not applicable to the fine, light, flocculent material that forms the upper layer of the sludge blanket in a water tank or sewage tank. The formula was derived from the results of experiments on discrete particles of sand, barite, granite, lignite, and amber. It is true that none of these materials is flocculent, but there is no reason to conclude that flocculent materials are not also scoured by means of the same drag forces. In the writer's opinion, flocculent materials are less easily scoured than granular materials of the same density and effective size because of their adhesive characteristics. The authors have suggested that flocculent materials are more easily scoured.

The authors have suggested that the problem of scour by turbulent eddies be approached through the suspended-load theory. A continuous suspension of particles heavier than the fluid is an impossible occurrence. What appears to be continuous suspension is alternate settling out and scour. The Vanoni equation for suspended load mentioned by the authors is a relation between the concentrations of suspended matter at two depths above the bottom for steady, uniform, flow conditions. The concentrations at both depths depend on the existence of and are the result of scour at the bottom. The writer's equation for impending scour is a limiting condition in which there is no suspended matter above the bottom which was placed there by scour. Obviously, the suspended-load theory is not applicable to impending scour.

In applying the suspended-load theory to problems of scour, the authors find it necessary to select an arbitrary value of the exponent Z which is not supported by any experimental observations. In the authors' example for the determination of the depth of a tank to permit the settling of organic particles having a density of 1.2 and a size of 0.06 mm, they find a minimum depth of 2.2 ft for impending scour by means of the writer's formula and a minimum depth of 15.5 ft by means of the authors' method. The writer presumes that the authors' selection of values for particle density and size was an effort to determine probable minimum depths for settling tanks in water and sewage treatment plants. The authors' example indicates a maximum tank velocity of about 1 ft per min, whereas there are numerous settling tanks in use for water plants and sewage treatment plants which are performing very satisfactorily with much higher tank velocities.

The long, narrow rectangular primary settling tanks for the Detroit sewage treatment works were designed for a velocity of 5.17 ft per min. The wide, rectangular sedimentation basins for the Springwells water filtration plant at Detroit were designed for a velocity of 3.12 ft per min. The mean velocity in the upper passes of the tray settling tanks for the Cambridge (Mass.) filtration plant is 5.8 ft per min at nominal plant capacity with both basins in operation and 11.6 ft per min with one basin in operation. Experience indicates that the sludge begins to scour when one basin is taken out of service for cleaning. Alum flocculation is used at the Cambridge plant. The authors also referred to the following statement in the writer's paper:[22]

> "Reporting on a tunnel section with a flow velocity of 12 ft per min, W. F. Langelier stated that settling had been unusually effective in removing turbidity and color from an alum-coagulated water. For this suspension it is evident that V_c was greater than 12 ft per min. Since a velocity of about 18 ft per min (0.3 ft per sec) is considered a minimum for baffled mixing chambers to avoid too much settling of floc in the chamber, it appears that 18 ft per min is greater than V_c for alum and iron floc."

The commonly-held opinion, concurred in by the authors, that the design of inlet structures is extremely important, is the direct result of the common practice of using settling tanks that are much too short. If settling tanks are made sufficiently long and are preceded by flocculation chambers at the upstream end, the entire problem of inlet design is removed. In large treatment plants with many settling tanks in parallel, it is necessary to bring the suspension into the inlet ends of the tanks at high velocity in order to accomplish acceptably uniform division of the flow between the tanks in the battery. The designer must accept these high velocities but, if he brings the flow into flocculation basins at the upstream ends of the settling tanks, the high velocity is of no importance. With this procedure, the inlet velocity to the settling tank is the exit velocity from the flocculation chamber and it may be made as low as is desired.

---

[22] "Sedimentation and the Design of Settling Tanks," by Thomas R. Camp, *Transactions*, ASCE, Vol. 111, 1946, p. 930.

If it is necessary to bring the suspension directly into the settling tank at high velocity, the best compensation therefore is a long narrow tank. Only an inlet baffle is necessary in front of the inlet pipe to deflect the flow backward against the end wall of the tank. There will, of course, be residual turbulence from this inlet velocity which will occupy a considerable portion of the upstream length of the tank. With a relatively high velocity and a small hydraulic radius, the drag on the walls and the floor will tend to stabilize the flow pattern in the tank. The improved results obtained by Mr. Hayden by means of baffles can be explained by the more stable flow patterns resulting from increased drag. The idea of inclined transverse baffles suggested by the authors is intriguing. Tanks equipped with such baffles will be relatively more costly than shallower tanks without them, but for tanks requiring storage and consolidation of the sludge the baffles might be helpful.

HENRY L. THACKWELL,[23] M. ASCE.—The title of the paper concerns rectangular settling tanks; the paper, however, deals only with rectangular tanks having horizontal flow. Upward-flow rectangular tanks are numerous enough to have been mentioned and, consequently, the inference is drawn that only horizontal-flow tanks are to be considered.

The authors have indicated that settling tanks should be designed on the basis of surface area and that rectangular settling tanks should be long and narrow. Opinion to the contrary has been expressed elsewhere:[24]

> "Data for surface settling rates versus BOD and SS removal were plotted in a form analogous to Figures 69 to 72. A great dispersion was observed, and little correlation between surface settling rate and removal efficiency could be detected. It was inferred that surface settling rate was inferior to detention period as a measure of performance in settling tanks at military plants. This might not have been the case if flows per unit volume of tank had been larger."

For any rectangular tank having vertical sides and a uniform depth, the detention time is directly proportional to the reciprocal of the surface area. In plotting a curve having the percentage of suspended-solids removal as ordinates and the reciprocal of the surface area as abscissas, the shape of the curve should take the general form of the usual curve relating percentage removal and detention time. A break in this general curve as typified in Figure 69 usually occurs[25] between 2 hours and 3 hours detention time.

---

[23] Cons. San. Engr., Walnut Creek, Calif.

[24] "Sewage Treatment at Military Installations," Report of the Subcommittee on Sewage Treatment, National Research Council, *Sewage Works Journal*, Vol. 18, 1946, p. 883.

[25] *Ibid.*, p. 879.

Reference again is made[26] to the previously quoted article:

> "It is interesting to observe that with rectangular final tanks compliance with the foregoing criteria with respect to detention period, depth, displacement velocity, and overflow rate result in a fixed design admitting of no variation. The following equation may be derived from the foregoing relationships between variables."

This equation is here presented, with notation changed to agree with that of Messrs. Ingersoll, McKee, and Brooks:

$$b = \frac{q}{V_{max}\, d}, \quad L = \frac{V_{max}\, d}{v_o}.$$

The subcommittee then presents an example: If $q = 1.0$ mgd $= 92.8$ cu ft per min, if $V_{\max} = 0.50$ ft per min, if $T = 2.5$ hours $= 150$ min, if $v_o = 800$ gal per day per sq ft $= 0.074$ ft per min, and if $d = 9$ ft, then $b = 20.7$ ft and $L = 60.5$ ft.

In the foregoing example, the length-to-width ratio is 2.93 and the length-to-depth ratio is 6.7. This tank would prove economical for use with straight-line sludge collectors.

Under the heading, "Resume of Fundamental Concepts," the authors have stated:

> "In a quiescent suspension, the concentration may be weak in the top layers but it will become progressively more concentrated with increasing depth measured from the surface."

This statement is universally true for quiescent suspensions and is also true in most cases of turbid moving water, such as in the Mississippi River below New Orleans, La. The writer made an investigation of turbidity on the river surface and 20 ft below the surface at numerous stations and found that it was always greater at the lower depths. The cleanest water is on the surface and close to shore.

The authors have said further: "In flocculent suspensions, two or more particles may coalesce to form a larger agglomerate which will probably settle at an increased rate." Actually, this is an argument for deeper tanks. A. T. Hobb, has stated[27] in agreement:

> "As explained, the different settling rates of the suspended particles entering the tank cause flocculation, and effectiveness of this would be increased by greater depth in tank. The action is similar to that of raindrops on a window pane. The particle, or drops, initially move downwards very slowly, but as they fall they join together to form larger drops which move more rapidly and collect with them as they go other smaller and slower drops."

This statement further substantiates the opinion that deeper tanks have some features of merit. Again, in this regard, Mr. Camp[28] is quoted:

---

[26] "Sewage Treatment at Military Installations," Report of the Subcommittee on Sewage Treatment, National Research Council, *Sewage Works Journal*, Vol. 18, 1946, p. 876.

[27] "Design, Maintenance and Operation, Water Treatment Plants," in "Manual of British Water Supply Practice," A. T. Hobb, editor, W. Heffer and Sons, Ltd., Cambridge, England, 1950, Chapter II, p. 360.

[28] "Handbook of Applied Hydraulics C. V. Davis, editor, McGraw-Hill Book Co., Inc., New York, N. Y., 1st Ed., 1942, p. 795.

> "Clarification Theory: Ideal Basin and Coalescing Particles.*** It may be seen, therefore, that the removal for this suspension is not independent of the depth and is influenced by both overflow rate and retention period. If the concentration is the same for all depths at the end of the period, it will be noted that the removal is independent of the overflow rate and is a function only of the retention period."

The foregoing statement indicates that both overflow rate and retention period may be valued criteria in the design of settling basins. Frequent mention of a higher density of sludge in deep tanks over that in shallow tanks has been made by observers.

The dispersion index is less in shallow tanks than in deep ones and, as stated by E. B. Phelps:[29]

> "The more important factors which appear to govern dispersion are shape of tank, location and type of inlet and outlet devices, temperature as affecting stratification, wind action, and velocity of flow through the tank. Long narrow tanks with maximum distance between inlet and outlet are favorable to low indices. Shallow rather than deep tanks favor good distribution of flow and minimize stratification."

The foregoing statement is in general agreement with that given by the authors under the heading, "Resume of Fundamental Concepts." They observe:

> "There appears to be little or no correlation in actual operating records between removal efficiencies and overflow rates or detention periods. Basins that are poorly designed on a theoretical basis sometimes appear to perform more satisfactorily than well-designed tanks."

Is the foregoing due to paradoxes in nature or is it because engineers have not found the answers to occult factors inherent in the hydromechanical workings of sedimentation? Doubtless because of this quandary engineers have used rule-of-thumb methods for too long a time in designing such works.

In the last paragraph of the "Summary," it is suggested that further research and experimentation be conducted with a view toward designing rectangular tanks. This is well taken and should be welcomed by all sanitary engineers.

The average practicing engineer would appreciate having a few safe rules or guiding parameters for designing water-treatment settling basins. The writer studied this problem with a glass model on 1:20 scale and using potassium permanganate dye tracers which could be photographed through the sides of the glass walls. The problem was to find the economic solution for the design of water-treatment tanks which necessarily had a relatively short width-to-length ratio because to make long tanks would have required the excavation of a high rocky hill at great cost. The water supply was turbid, varying from 60 ppm to 1,100 ppm. The coagulant was to be alum. The precipitated sludge had a water content of 93%. Sludge storage was to be provided for a maximum period of 6 months, thereby necessitating a deep tank. Raw water was to be well flocculated prior to entering the tank. The entrance of influent water was to be projected downward from four inlets at average velocities of 1 ft per sec. A surge baffle which was solid for the upper half of the tank depth was set 10 ft out from the influent-end wall. This baffle absorbed the energy of the rebound from the bottom and forced the water downward again so that an even horizontal flow occurred. In order to make a greater length-width ratio, a longitudinal septum was set axially as a training wall, and it provided three disconnected sections through the middle of the tank. Each end section was 12 ft long and the central section 9 ft long. These septum walls supported baffles at the influent end and midsection as well as two rows of overflow weir channels at the effluent section. The mid-baffle was designed as a venetian blind with redwood boards 2 in. by 14 in. as horizontal slats. The top half and bottom half were designed to operate separately and to be set at any angle of opening or closure with the vertical. The bisectional arrangement was required for top and bottom variation because stratification would occur with small temperature differences.

---

[29] "Public Health Engineering," by E. B. Phelps, *Public Health Engineering*, Vol. 1, 1948, p. 440.

The design as finally adopted was as follows: The overflow rate at maximum flow was 900 gal per sq ft per day, and at average flow, 600 gal per sq ft per day; the detention time with a clean tank was, at maximum flow, 3.6 hours, and at average flow, 5.4 hours; the detention time with sludge was, at maximum flow, 2 hours, and at average flow, 3.0 hours; the width-to-length ratio, considering the septum wall was 6, and not considering the septum, 3; the maximum depth-to-length ratio with a clean tank was 6.1, and with full sludge, 12; and the maximum velocity of flow with a clean tank, 0.5 ft per min, and with full sludge load, 1.0 ft per min. The maximum flow rate over the end weir was 25,000 gal per ft of weir per day, and the average flow rate over the weir, 16,700 gal per ft per day.

The results in prototype practice are gratifying. The turbidity removals are between 96% and 99%. The effluent turbidity is rarely more than 4 ppm and is sometimes 1.5 ppm.

The writer would like to see the concept of overflow residual efficiency in general use but, until some standard method is accepted and put into practice by sanitary engineers, he suggests the following method of obtaining efficiency curves which could be plotted on an average monthly basis from plant records.

Because the coagulant dosage is influenced by and proportional to low values of color and turbidity, the coagulant dosage required for a given percentage removal may be plotted approximately on a straight line with the sum of turbidity and color values. For higher values of color and turbidity, the curve is exponential and can be plotted on logarithmic paper approximately as a straight line. Then, in any settling tanks for water treatment, the percentage removal may be plotted with overflow rates as a curve for each separate ratio of (turbidity + color) to coagulant.

After plotting, there will be many such curves of hyperbolic type which should indicate the optimum and economic point at which to operate the plant. Of course, if the plant is running at full load, there is no choice but to use a higher ratio of (turbidity + color) to coagulant if the percentage removal is to be increased. If this plan were currently adopted, it would be the means of guiding the operator toward greater economy in the use of chemicals, and his efforts at compilation would be well repaid.

Alfred C. Ingersoll,[30] **A. M. ASCE, Jack E. McKee,**[31] **M. ASCE, and Norman H. Brooks,**[32] **J. M. ASCE.**—The writers are grateful to Mr. Camp for pointing out that the experimental data presented by him[5] for reduction of fall velocities attributable to hindered settling do not agree with the analyses presented by Messrs. McNown and Lin.[6,7] Inasmuch as the latters' results are based on a theory, corroborated by experiments and also by the theories of J. M. Burgers and M. S. Smoluchowski, the cause of the discrepancy is not apparent. The writers agree with Mr. Camp that further investigation is indicated.

The writers contend that it is definitely worth while to study the mechanics of sedimentation of suspensions of discrete particles, even though the sanitary engineer always deals with suspensions that are somewhat flocculent. Great progress is made in all fields of engineering by making simplifying assumptions, especially those assumptions that lead to a better understanding of the physical phenomena. Even Mr. Camp in his earlier work[5] has made free use of the simplifying assumption of a suspension of discrete particles.

Considerations of discrete particles, however, will not solve all the problems in settling-tank design. A thorough investigation is now being made of the physical characteristics of domestic sewage under the direction of two of the writers with a grant from the United States Public Health Service. In this study specific consideration is being given to effects of flocculation and various test procedures on settling-velocity analyses. It is hoped that the performance of settling tanks will be more fully understood when more is known about the nature of the suspensions being treated. When the results of this work are known, it is not unlikely that a new and rational procedure for assessing settling-tank efficiency can be developed. Under the heading, "Measures of Efficiency," the writers presented what appeared to be a logical and simple approach to the efficiency problem in the absence of a good understanding of flocculation.

Mr. Camp has misinterpreted the writers in his inference that "the authors have suggested that flocculent materials are more easily scoured" from the bed than nonflocculent materials. The writers should have stated that light, fine materials with small settling velocities are more easily scoured from the bed than Mr. Camp's scour formula would indicate, regardless of whether the particles are flocculent or not.

Research on the problem of scour of light materials is also presently being conducted at the California Institute of Technology at Pasadena, under the writers' supervision with the previously mentioned grant from the Public Health Service. The writers' analysis of scour is perhaps largely a matter of conjecture, but Mr. Camp has not justified extrapolation of Mr. Shields' scour analysis to bed Reynolds numbers much lower than those used by Mr. Shields. Mr. Camp has stated that there is no reason why one may not extrapolate Mr. Shields' results, but the writers believe that it was Mr. Camp's responsibility to adopt a positive approach and prove that such extrapolation is valid. It is hoped that the current research will clarify the scour phenomena at very low bed Reynolds numbers $\left(\frac{D}{\nu}\sqrt{\frac{\tau_0}{\rho}} < 1.7\right)$.

---

[30] Asst. Prof. of Civ. Eng., California Inst. of Technology, Pasadena, Calif.

[31] Associate Prof. of San. Eng., California Inst. of Technology, Pasadena, Calif.

[32] Asst. Prof. of Civ. Eng., California Inst. of Technology, Pasadena, Calif.

Mr. Camp has stated that in some experiments made by Mr. Langelier

> "* * * where alum floc was settled with no scour at a channel velocity of 12 ft per min, the friction velocity was 0.011 ft per sec, or six times the settling velocity of a 0.1-mm particle with a specific gravity of 1.2."

By an application of the Stokes law for settling (assuming a spherical particle), the writers find that the settling velocity, *v*, is approximately 0.0035 ft per sec at room temperature, or about one third of the friction velocity instead of one sixth as indicated by Mr. Camp. However, Mr. Camp's contention that, in order for scour to occur, the magnitude of turbulent fluctuations near the bed (or the shear velocity) must be several times the settling velocity is probably correct.

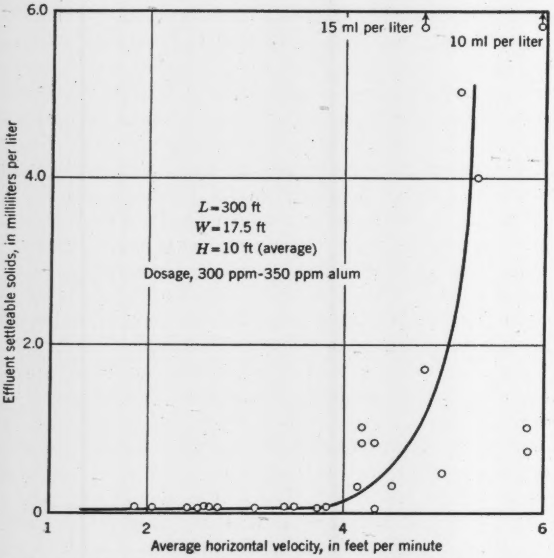

FIG. 16.—EFFECT OF VELOCITY ON EFFLUENT SETTLEABLE SOLIDS, VALLEY SETTLING BASINS, LOS ANGELES

Some recent experiments at the Valley Settling Basins of the City of Los Angeles (Calif.) have also indicated that the writers' suggested criterion for impending scour is probably too stringent. At this plant, a small quantity of raw sewage has been treated with a heavy dose of alum and settled in two rectangular tanks each 300 ft long, 17.5 ft wide, and having an average depth of 10 ft. The horizontal velocities in the basins have varied from approximately 2 ft per min to 6 ft per min. Fig. 16 shows the settleable solids in the effluent in milliliters per liter, as a function of mean tank velocity. The critical velocity for resuspension appears to be about 4 ft per min.

A rough pipette analysis of the alum floc shows that the median settling velocity of the particles is about 0.06 cm per sec, or 0.12 ft per min. The ratio of tank velocity to median settling velocity at the commencing of resuspension is thus

$$\frac{V}{v} = \frac{4}{0.12} = 33.$$

This ratio corresponds to a z-value (the exponent in the suspended-load equation) of approximately 1.5 as compared with suggested design values of from 3 to 5. However, by visual observation of the effluent it was noted that many particles larger than the median were being resuspended, indicating that the critical (V/v)-ratio is smaller than 33 (or z larger than 1.5). By comparison, the value of V/v for critical shear is 57 for the example presented by Mr. Camp from Mr. Langelier's previously mentioned data.

The writers concede that their suggested criterion for incipient scour (V/v = from 9 to 15) is probably unduly conservative; however, no reliable alternate recommendation can be made until more research has been performed. Nevertheless, the writers believe that the resuspension of fine, light material must be directly related to the fall velocities of the particles, the actual size and specific gravity of the particles being secondary.

Although the suspended-load equation cannot be applied directly to the scour problem, it indicates how readily the sediment is diffused upward after it becomes scoured from the bed. When the exponent z in Eq. 11 is large (greater than 3), the settling of the particles is so rapid that, for all practical purposes, the material is not even lifted into suspension; on the other hand, when z is small (less than 0.5), the particles settle slowly enough so that the natural turbulence is quite effective in diffusing particles upward toward the surface, resulting in a concentration profile in accordance with Eq. 11. If particles for which z is small are readily available on the bed, it is conceivable that large numbers of these would become suspended. The thin laminar sublayer that separates the bed material from the main flow could not prevent suspension.

When a stream is in equilibrium the rate of deposition just balances the rate of resuspension; in a settling tank it is desirable to deposit as many solids as possible, with a minimum of resuspension. If there is resuspension, the concentration of suspended solids will be reduced only to the point where the rate of resuspension balances the rate of deposition. It seems reasonable to suppose that if the z-value for the settling tank is too small, it will be impossible to prevent resuspension. The writers believe that Mr. Camp's statement, "Obviously the suspended-load theory is not applicable to impending scour," is not entirely justified.

Mr. Camp has directed attention to the fact that residual turbulence in a settling tank resulting from the inlet may cause considerably more diffusion and mixing than the turbulence generated by tank friction. As this is difficult to evaluate quantitatively, the writers have based the scour calculations on the turbulence caused by friction only, in the same way that Mr. Camp did in his analysis of the effects of turbulence on sedimentation.[5, 10] Also, it should be explained that Mr. Camp's scour formula gives too high a value of the critical velocity if there is appreciable residual turbulence from the inlet disturbances. In this case the bed shear stress will fluctuate more than it did in Mr. Shields' experiments (or more than is natural), and a lower mean shear will cause some scour.

With regard to the harmful effect of the inlet jets in the test tanks at the University at Wisconsin and Purdue University, Mr. Camp has stated that "Most of the energy in the inlet jets is doubtless dissipated in the upstream end of the tank * * *." This is exactly the function of the inlet baffle—to break up large-scale turbulence and, by means of a head loss, to gain an even distribution of velocity across the inlet end of the settling tank. In this design, the slotted baffle serves the same purpose as the damping screens used in the settling section of a wind tunnel upstream from the test section. The screens induce a small-scale turbulence while destroying large-scale eddies, the idea being that the small-scale disturbance is quickly damped out and converted into heat by friction. Large eddies, on the other hand, can be carried downstream for a considerable distance before they are "ground down" into smaller eddies and finally dissipated into heat. Although the turbulence induced by the inlet jets is of small scale, that arising from wall and bed friction is more likely to be of large scale—of the type that causes scour. Thus, it is not uncommon in canals to observe eddies of a size comparable to the full depth.

The extent to which the turbulence induced by the inlet jets is damped in the influent end of the tank has been indicated in the researches of A. A. Kalinske,[33] M. ASCE, and H. R. Henry,[34] J. M. ASCE. Mr. Kalinske has shown that for a three-dimensional jet in an abrupt (180°) pipe expansion the kinetic energy possessed by the turbulence is reduced to less than 1% of the expansion head loss within a distance of some 15 jet diameters downstream. The remainder of the head loss is dissipated into heat in the regions of high local shear immediately downstream from the jet. Mr. Henry's experiments on a two-dimensional sluice gate (that is, a "half-jet") show that the energy of turbulence is reduced to approximately 0.5% of the head loss within a distance of 15 full-jet widths downstream.

Translated to the University of Wisconsin tank, in what is admittedly a fairly rough analogy, Mr. Henry's experiments would mean that 99.5% of the kinetic energy of the inlet jets ($\frac{1}{8}$ in. wide) is dissipated into heat within a distance of 2 in. from the inlet. It is difficult to believe that the remaining small-scale eddies could project their influence throughout the volume of the tank, affecting the settling process as seriously as Mr. Camp has suggested. It is perfectly true that the conventional type of inlet with a single deflecting baffle will produce large-scale turbulence which will indeed exert influence throughout a short tank. The writers acknowledge the correctness of Mr. Camp's over-all head-loss computations; undeniably, the tiny fraction of the inlet head loss remaining in the form of turbulent eddies beyond the first few inches of the tank is many times the loss from the drag on the floor and walls. However, the writers disagree with Mr. Camp's computations of ratios of mixing coefficients. It is well known from the Prandtl theory that the mixing (or diffusion) coefficient is proportional to the product of the root-mean-square of the velocity fluctuations and the mixing length. Comparisons on the basis of energy alone are misleading because the mixing length (or scale) is also an important variable.

---

[33] "Conversion of Kinetic to Potential Energy in Flow Expansions," by A. A. Kalinske, *Transactions*, ASCE, Vol. 111, 1946, p. 355.

[34] Discussion by Harold R. Henry of "Diffusion of Submerged Jets," by M. L. Albertson, Y. B. Dai, R. A. Jensen, and Hunter Rouse, *ibid.*, Vol. 115, 1950, p. 687.

The writers cannot agree with Mr. Camp that the solution to inlet design problems is simply to make settling tanks so long that inlet effects are damped out by the drag on the floor and walls. It would surely seem that economics of construction might well dictate a shorter tank having a well-designed inlet achieving even distribution without large-scale turbulence, rather than a long tank having a poor inlet. Use of the flocculating basin represents progress in this direction, but not all settling tanks need flocculating basins.

The writers are indebted to Mr. Thackwell for his viewpoint on making this paper more useful to the practicing engineer. As they explained in the paper, the writers are aware that existing data from operating plants do not support overflow rate (or surface area) as the sole design criterion for settling tanks. Neither do they support detention time as the sole criterion. If all other factors can be evaluated, however, there is analytical reasoning to support overflow rate as the principal design criterion. The writers have made this assumption from the beginning of the paper and have attempted to treat some of the secondary factors—notably, inlet and outlet conditions, shape factors, and limiting horizontal velocities.

Mr. Thackwell has stated, "For any rectangular tank having vertical sides and a uniform depth, the detention time is directly proportional to the reciprocal of the surface area." For steady flow this statement is seen to be inverted because the detention time is then directly proportional to the surface area.

The writers take exception on two counts to the design example quoted by Mr. Thackwell. First, the depth, detention time, and overflow rate have been presented as though they were independent design criteria. Because they are not independent but related by the expression, $v_o = H/T$, for rectangular tanks, any two of the quantities will determine the third. In fact, the values of detention time (150 min), overflow rate (0.074 ft per min), and depth (9 ft) quoted by Mr. Thackwell are numerically inconsistent. Second, there is no reason to state arbitrarily either the depth or the detention time. Instead, it is important to determine the limiting horizontal velocity which must be established by considerations of scour. Then the length, width, and depth may be determined in accordance with the desirability of having a long narrow tank (preferably with a length-to-width ratio of 10 or more) to minimize inlet and outlet disturbances and with the need for installing mechanical cleaning devices.

With regard to Mr. Thackwell's query about paradoxes in nature as against occult factors inherent in the workings of sedimentation, the writers have been quoted out of context. Taken in its entirety, the paragraph from which Mr. Thackwell has quoted implied that the apparent disparity between the simple theories and actual performance is largely the result of the existing practice of considering percentage removal as a measure of settling-tank efficiency. In the section entitled "Measures of Efficiency" which follows that paragraph, the writers attempted to remedy this deficiency by introducing a new concept of efficiency that takes cognizance of the settling characteristics of the influent suspension in addition to the hydraulic geometry (overflow rate, detention time, and similar properties) of the tank.

The writers appreciate Mr. Thackwell's desire to have a few simple rules to guide the practicing engineer in designing settling basins. However, the writers have no reason to place further restrictions on the latitude of the designing engineer beyond the simple approach they have presented here. As more information becomes available from research and operating data on this subject, it may be that such restrictions will be warranted, but at the present time there seems to be no justification for prescribing design limits other than overflow rate and horizontal velocity (both fixed by characteristics of suspension) and length-to-width ratio (to be as great as is practicable, consistent with economics and the requirements of mechanical cleaning equipment). Additional launders at the effluent end of a long tank are also desirable.

Mr. Thackwell has proposed a scheme by which a plant operator may determine the quantity of chemical dosage he needs in order to coagulate certain raw waters for a specified overflow rate and desired quality of effluent. Two tanks of different shapes could be compared on the basis of the coagulant curves that Mr. Thackwell has proposed if it were known that the influent suspensions to both tanks had the same chemical characteristics and settling characteristics. Thus, the tank yielding the higher curve on the plot relating removal and overflow rate for a fixed coagulant ratio would be considered the more efficient tank.

Waterworks chemists and engineers know, however, that coagulation of colored or turbid waters or both, is a complex process that depends on many factors other than the concentration of color plus turbidity. The coagulant dosage is governed by the concentration of many ions, by the pH-value, by temperature, and by the type of coagulant being used. As Mr. Thackwell has explained, his plan would be a means of guiding the operator toward greater economy in the use of chemicals but it would not serve to compare sedimentation basins used for different raw waters.

The writers would like to express their appreciation for the thoughtful comments and helpful criticism offered by Mr. Camp and Mr. Thackwell in their discussions.

AMERICAN SOCIETY OF CIVIL ENGINEERS

Founded November 5, 1852

TRANSACTIONS

Paper No. 2838

A PHYSICAL APPROACH TO TURBULENT-BOUNDARY-LAYER PROBLEMS

By Donald Ross[1]

With Discussion By Messrs. William Douglas Baines, James M. Robertson, William J. Bauer, and Donald Ross

Synopsis

A new approach to the problem of incompressible, turbulent boundary layers is presented. From physical considerations involving the diffusion of turbulent stresses, the boundary layer is divided into three regions distinguished by the relative proximity of the wall. Within a distance of approximately 10% of the boundary-layer thickness from the wall, the local wall conditions have an important effect whereas the outer 75% is governed entirely by the spatial history of the boundary layer. The inner region includes the laminar sublayer, the buffer zone, and that part of the turbulent region characterized by the logarithmic velocity profile. The outer region of the turbulent boundary layer is similar to that of a wake or jet, being characterized by a sharp but irregular boundary between turbulent and nonturbulent regions. Here the velocity profile may usually be approximated by a 3/2-power deficiency relationship. The region between the inner and outer parts is a blending region more complicated than either of the other two and not easily analyzed. This new physical analysis, combined with empirical correlations, leads to a new method for computing two-dimensional turbulent boundary layers. The method usually involves only algebraic equations and is more versatile than any previously published method.

Introduction

The basic differential equations for turbulent flows were derived by Osborne Reynolds (1)[2] in 1895 by assuming that all instantaneous velocities could be

---

Note.—Published, essentially as printed here, in January, 1955, as *Proceedings-Separate No. 604*. Positions and titles given are those in effect when the paper or discussion was approved for publication in *Transactions*.

[1] Member of the Technical Staff, the Bell Telephone Labs., Whippany, N. J.; formerly Associate Prof. of Eng. Research, Ordnance Research Lab., The Pennsylvania State Univ., State College, Pa.

[2] Numerals in parentheses—thus, (1)—refer to corresponding items in the Bibliography (see Appendix).

expressed as the sums of time-average velocities and instantaneous fluctuations about the average. Reynolds inserted his expressions for instantaneous velocities and pressures in the Navier-Stokes differential equations and took a time average. The resultant equations include additional terms—known as the Reynolds stresses—which involve the correlations of the fluctuation velocities and which represent the turbulent transport of momentum. When the boundary-layer assumptions (2) of L. Prandtl are applied to these equations, some of the remaining terms still involve the Reynolds stresses. It is because of these terms that mathematical solutions of turbulent-boundary-layer problems have not been possible, as they have been for the corresponding laminar flows.

In the past thirty years, various approaches have been taken to turbulent-boundary-layer problems—all of them without real success. The present status of the problem is that the theoreticians are awaiting the results of hot-wire measurements in turbulent shear flows with the hope that these experiments will reveal the basic mechanism of turbulent stresses and thus enable the building of a rigorous theory. It is believed by most workers in the field that it will be many years before such a theory is completely developed and still more years before it can yield results of practical value to the engineer.

In the meanwhile, as engineering problems require answers and cannot wait for the ultimate theoretical solution, it is desirable that improved semi-empirical methods of computing turbulent boundary layers be developed. The present paper constitutes a report on an analytical study of turbulent boundary layers aimed at satisfying this need (3). In this study the wealth of experimental data and theoretical ideas in the literature were re-examined and re-evaluated in terms of some of the newer information and ideas concerning turbulent shear flows. One result was the development of a new method for predicting the behavior of two-dimensional boundary layers that is applicable whenever the initial spatial variation of the boundary layer is known.

DIVISION OF THE BOUNDARY LAYER INTO REGIONS

The shear stress τ in a turbulent flow of velocity u is composed of viscous and turbulent terms and it may be written as

$$\frac{\tau}{\rho} = (\nu + \epsilon)\frac{\partial u}{\partial y} \qquad (1)$$

in which ν is the molecular viscosity and ϵ the eddy viscosity associated with the turbulent fluctuations. The usual approach to the problem of the turbulent boundary layer is in terms of the relative influence of the molecular and eddy viscosities. Thus, very close to the wall there is the laminar sublayer in which the molecular viscosity predominates and in which the velocity is proportional to the distance from the wall. Farther out the molecular viscosity has a negligible effect, and the eddy viscosity governs the flow. In between, there is a buffer zone in which both viscosities must be considered. Except at the lowest Reynolds numbers, the laminar sublayer and the buffer zone are very small. One is therefore left with a single turbulent region, and solutions of the

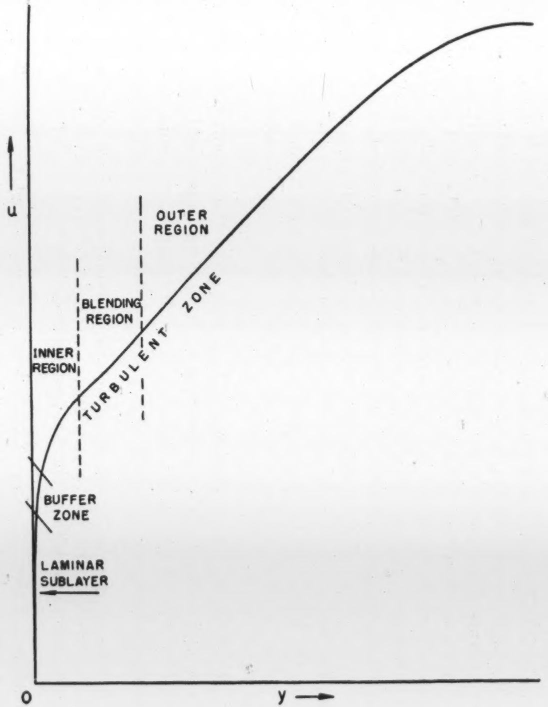
u
OUTER REGION
BLENDING REGION
INNER REGION
TURBULENT ZONE
BUFFER ZONE
LAMINAR SUBLAYER
0
y

Fig. 1.—Velocity Profile, Showing Division of the Boundary Layer into Regions

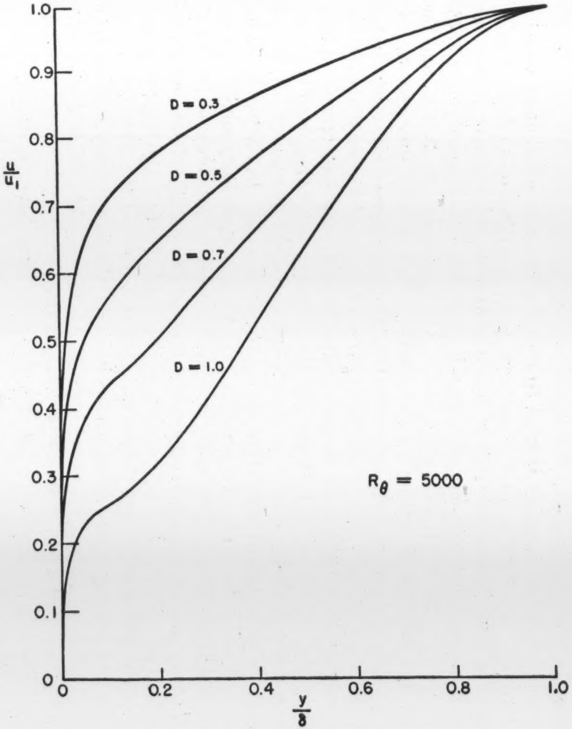

Fig. 2.—Typical Idealized Velocity Profiles

equations of motion are sought in which the molecular viscosity is practically neglected.

Usually a single function is used to describe the entire turbulent velocity distribution. The well-known power law is an example of such a formula. Sometimes it provides a reasonably close fit, but usually it is a poor approximation. Superposition formulas, developed by Busuke Hudimoto (4) in 1935, and more recently by J. Rotta (5) and J. M. Robertson, M. ASCE, and the writer (6), also fail to agree with the details of the velocity profiles. Specifically, none of these single functions admits the existence of inflections in the profiles; yet, such inflections are invariably found for profiles close to separation.

Recognizing that the usual analyses do not achieve sufficient agreement with the details of measured velocity profiles, the physical factor that would account for the experimentally observed features of turbulent boundary layers was sought. This factor is the relative proximity to the wall. In the new analysis, there is superimposed on the usual division based on viscosity considerations a division into three regions according to the relative influence of local wall conditions. These zones are approximately the inner 10% of the boundary-layer thickness, in which the proximity of the wall influences the flow; the outer 75% of the thickness, governed by the spatial history of the boundary layer; and a blending zone between the others in which the flow is influenced by both the wall proximity and the spatial history. A typical velocity profile and the superposition of the two methods of dividing the boundary layer are shown in Fig. 1 The inner region is seen to include the laminar sublayer and the buffer zone as well as an inner turbulent part.

To understand the reasoning behind this method of division it is essential to realize the fundamental distinction between laminar and turbulent shear flows. In laminar flows the property that supports the shear stress—namely, the viscosity—exists throughout the fluid in a uniform manner. The laminar boundary layer exists because the physical boundary condition of zero velocity at a solid surface differs from the potential theory solution for the main fluid flow. In the case of the turbulent boundary layer, the high-intensity turbulence that supports the shear has its origin very close to the wall and is diffused into the fluid. Because the turbulence originates very close to the wall in the region of very high velocity gradients and is diffused out into the moving fluid, it follows that the turbulence intensities and shears in the outer part of the boundary layer are governed by the spatial history of the flow whereas those near the surface are more a function of local conditions. This concept of the space history of the flow was expressed by F. Schultz-Grunow (7) in 1938 and again by H. L. Dryden (8) in 1946. Mr. Prandtl (9) was aware of this important point as early as 1935, when he stated:

> "* * * for each velocity profile develops in some regular manner from the velocity profiles situated further upstream; i.e. * * * depends on the previous history of the portion of the fluid considered."

This concept of the diffusion of turbulent stresses and of the importance of spatial history is expressed in the division of the boundary layer into the zones shown in Fig. 1.

The properties of the inner region are closely related to the presence of the wall. Here occurs the majority of the conversion of mean motion to turbulence and of turbulence to heat. Turbulence is produced faster than it is dissipated. In the outer region, both production and dissipation occur at much reduced rates, with dissipation predominating. The outer region is also characterized by an "intermittency effect" that arises from the irregular nature of the outer boundary of the turbulent region (10).

Between the inner and outer regions there is a blending region that is partly dependent on local conditions and partly on spatial history. This blending region combines the features of the other two regions and is necessarily more complex than either of the others. It is not to be confused with the "overlap" region. In analyses of equilibrium boundary layers by C. B. Millikan (11) and Richard von Mises (12) the velocity profile is considered from the wall outward and from the outside in. It is also assumed that there is an overlap region close to the wall in which both functions are equally valid. Because the overlap region is closer to the wall than the blending region the overlap condition can only be used when the outer profile is known through the blending region. Thus, the overlap concept has some apparent value when one is dealing with equilibrium boundary layers but it is of no value when dealing with the more general nonequilibrium case.

Velocity Functions.—If the methods of dimensional analysis are applied to the problem of turbulent-boundary-layer velocity profiles, using the concepts already developed, two functions result (13). The one for the inner profile:

$$\frac{u}{u_*} = f\left(\frac{y\,u_*}{\nu},\ \frac{y}{e},\ \frac{\nu}{\rho\,u^3_*}\,\frac{\partial p}{\partial x}\right) \quad (2)$$

involves the wall shear stress in the definition of the friction velocity,

$$u_* \equiv \sqrt{\frac{\tau_w}{\rho}} \quad (3)$$

the wall roughness e in the term y/e, and the local pressure gradient in the last term. The relationship for the outer profile:

$$\frac{u_1 - u}{u_1} = g\left(\frac{\delta - y}{\delta},\ \text{spatial history}\right) \quad (4)$$

expresses the velocity deficiency in terms of the relative distance from the outer edge and the spatial history (u_1 is the free-stream velocity and δ is the effective boundary-layer thickness).

The inner function consists of three parts: The laminar sublayer, the buffer zone, and the inner turbulent region. The first two of these are usually quite thin. The inner turbulent region is characterized by a logarithmic velocity profile, which can be derived directly from dimensional analysis by assuming that a most important influence on the eddy viscosity is the distance from the wall. The equation,

$$\frac{u}{u_*} = A + B \log \frac{y\,u_*}{\nu} \quad (5)$$

has been closely verified by measured velocity profiles. The "law of the wall" proposed by H. Ludwieg (14) in 1949 states that for smooth walls the coefficients A and B of the logarithmic inner profiles are practically universal constants independent of pressure gradients, of the Reynolds number, and of the past history of the flow. (The functional relationship of Eq. 2 includes a pressure-gradient term, but this may be shown to be small except for small Reynolds numbers or for extreme pressure gradients, or both.) The writer has examined approximately one dozen experiments in which both wall shear stress and velocity profiles were measured and has found no appreciable difference between the

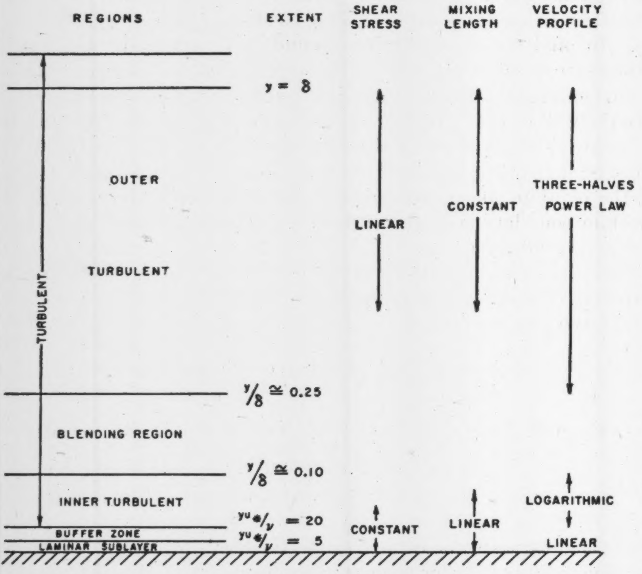
REGIONS
EXTENT
SHEAR STRESS
MIXING LENGTH
VELOCITY PROFILE
y = δ
OUTER
TURBULENT
TURBULENT
LINEAR
CONSTANT
THREE-HALVES POWER LAW
y/δ ≅ 0.25
BLENDING REGION
y/δ ≅ 0.10
INNER TURBULENT
LOGARITHMIC
yu*/ν = 20
BUFFER ZONE
CONSTANT
LINEAR
yu*/ν = 5
LAMINAR SUBLAYER
LINEAR

FIG. 3.—PROPERTIES OF THE REGIONS OF THE TURBULENT BOUNDARY LAYER

coefficients for the various types of flows. For all practical purposes, the coefficients A and B are both 5.6, and the formula for the inner turbulent region is

$$\frac{u}{u_*} = 5.6 + 5.6 \log_{10} \frac{y\, u_*}{\nu} \qquad \text{(6)}$$

This formula is valid for $(y\, u_*/\nu) > 20$ and $(y/\delta) < 0.1$.

For the outer turbulent region, a simple formula that fits most velocity profiles well is the 3/2-power deficiency law:

$$1 - \frac{u}{u_1} = D \left(1 - \frac{y}{\delta}\right)^{3/2} \qquad \text{(7)}$$

This formula, which is valid for approximately the outer 75% of the boundary layer, is similar to that proposed by Darcy nearly a century ago for the central region of pipe flow—hence, the choice of the letter *D* for the coefficient. Its local value, which depends on the spatial history of the flow, varies from approximately 0.3 for flat plates to as high as 1.3 near separation.

The various assumptions that have been used to derive the inner and outer velocity functions fail in the blending region between these two regions. The physics of this region is not such that the velocity profile can be described by any simple functional relation; neither wall conditions nor spatial history can be ignored. An infinite number of outer profiles may exist. For each outer profile a variety of inner profiles may exist, depending primarily on the local Reynolds number. The velocity profile in the blending region will depend on the combination of inner and outer profiles. For those cases in which the extrapolated inner and outer functions cross each other at an appreciable angle, the curve in the blending region will include an inflection point. Some of the possible combinations are illustrated in Fig. 2, where the inflections that occur for high *D*-profiles are clearly shown.

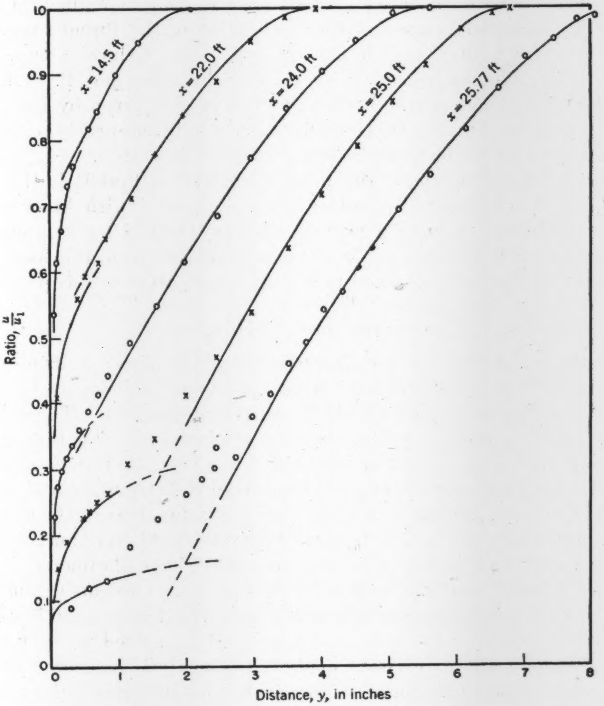

FIG. 4.—TURBULENT BOUNDARY-LAYER TRAVERSES MEASURED BY MESSRS. SCHUBAUER AND KLEBANOFF

The division of the boundary layer into inner and outer regions, superimposed on the normal division into viscous and turbulent zones, has resulted in a somewhat more complex picture of the turbulent boundary layer than that usually considered. That this additional complexity is worth while is supported by the simplifications that result in the analysis of each of the regions. In Fig. 3 the division of the boundary layer into regions is illustrated and their properties are summarized. Along with the extents of the regions and the types of velocity profiles, the general characteristics of the shear-stress profile and of the Prandtl mixing length (15) are indicated. These are based on experimental observations and are included because of the application of the Prandtl momentum-transfer theory at a later stage in the analysis. Fig. 4 shows a typical set of experimental profiles as measured by G. B. Schubauer and P. S. Klebanoff (16). The solid curves are the inner and outer profiles given by Eqs. 6 and 7. The curves progress from equilibrium, flat-plate conditions nearly to separation. The blending between the two portions is clearly illustrated.

The strongest argument for the present analysis is that it is the simplest treatment of the turbulent boundary layer consistent with known physical properties that leads to useful results. A new method for computing two-dimensional turbulent boundary layers was developed from this analysis. The remainder of this paper is devoted to a brief examination of this new method.

COMPUTATION METHOD

When the turbulent-boundary-layer problem is expressed in its most general form there are four simultaneous equations, two of which may be nonlinear differential equations and all of which are interdependent. These equations express: (1) The growth of the momentum thickness as a function of the wall shear stress, pressure gradient, and a shape parameter; (2) the shape parameter of the velocity profile as a function of the pressure distribution and the spatial history of the flow; (3) the wall shear stress as a function of the shape of the velocity profile and the momentum-thickness Reynolds number; and (4) the detailed velocity distribution as a function of the shape parameter, the boundary-layer thickness, and the local wall shear stress. Obviously, simultaneous solution of these four equations is impractical. What is required is an approximate method whereby the four equations can be solved separately and, if necessary, second approximations made. The analysis presented here makes such a solution possible for a wide variety of two-dimensional boundary layers.

The boundary layer at any station is computed as follows:

1. The momentum thickness is found as a function of the pressure distribution through a recently developed approximate integration of the momentum equation of Theodor von Kármán, Hon. M. ASCE.

2. The coefficient D of the 3/2-power, outer-velocity distribution replaces the shape parameter. A function of this coefficient is related to the spatial history by a semi-empirical equation derived from the Prandtl momentum-transfer theory. This function then leads to D itself through an empirical correlation.

3. The wall-shear-stress coefficient is related to D and the local momentum-thickness Reynolds number by the Ludwieg "law of the wall," and by a second empirical correlation.
4. Finally, the velocity distribution at the station is computed in two parts. The outer part is a 3/2-power deficiency curve having coefficient D. The inner part is logarithmic with its magnitude determined from the wall-shear-stress coefficient. A smooth curve is used to blend the two regions.

The method is applicable to redistributing flows that proceed from separation toward flat-plate equilibrium as well as to the usual boundary layer in an adverse pressure gradient that goes from equilibrium toward separation. The occurrence of separation is also correlated with the coefficient D.

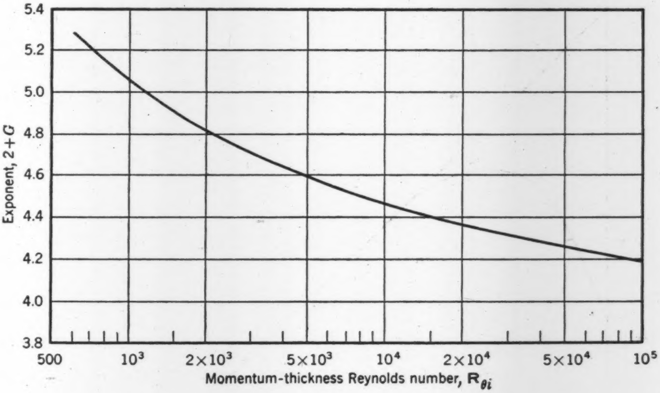

FIG. 5.—VARIATION OF THE MOMENTUM-EQUATION EXPONENT WITH THE REYNOLDS NUMBER

Growth of the Momentum Thickness.—The equation that is almost invariably used for the growth of the momentum thickness θ is the von Kármán integral momentum equation:

$$\frac{d\theta}{dx} = \frac{c_f}{2} + (2 + H)\,\frac{\theta}{\rho\, u^2{}_1}\frac{dp}{dx} \dots\dots\dots\dots\dots\dots (8)$$

in which c_f is the wall-shear-stress coefficient and H is the common shape parameter. This equation, in somewhat different form, was originally derived by Mr. von Kármán (17) in 1921 for use with laminar boundary layers. Although it is extensively applied to turbulent-boundary-layer problems in this form, actually for many turbulent flows the contributions of the turbulent normal stresses must be included as an additional term. The exact solution of the corrected equation requires the simultaneous solution of the equations for the wall-shear-stress coefficient and for the shape parameter. However, Mr. Robertson and the writer (18) have developed an approximate solution that may be used directly. They have distinguished between two cases: (a)

Small pressure gradients for which the boundary layer is close to the equilibrium condition and (*b*) large adverse pressure gradients. In the first case, step-by-step solution of Eq. 8 is utilized, with both c_f and H assumed constant for each step and each usually having the equilibrium, flat-plate value. For comparatively large pressure gradients, they have developed a simple algebraic power expression:

$$\frac{\theta}{\theta_i} = \left(\frac{u_{1i}}{u_1}\right)^{2+G} \qquad (9)$$

which agrees closely with experimental results. The exponent $2 + G$ is a function of the momentum-thickness Reynolds number at the initial station, varying from about 5.0 at transition ($\mathbf{R}_\theta \approx 10^3$) to approximately 4.2 at a high momentum-thickness Reynolds number of about 10^5 as shown in Fig. 5. Utilizing this result, the momentum thickness for any station may be readily computed without first solving the other three equations and without knowledge of the shape parameter. Usually a direct algebraic solution will be possible for θ as a function of only the potential velocity (u_1), or pressure, distribution. The momentum-thickness Reynolds number is then

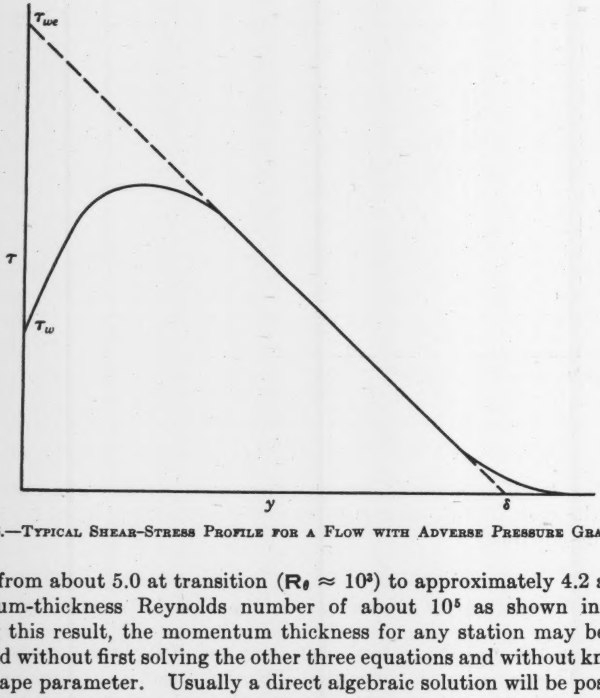

Fig. 6.—Typical Shear-Stress Profile for a Flow with Adverse Pressure Gradient

$$\mathbf{R}_\theta \equiv \theta \frac{u_1}{\nu} \approx \left(\frac{u_{1i}}{u_1}\right)^{1+G} \mathbf{R}_{\theta i} \qquad (10)$$

The wall shear stress will be shown to be partly a function of this Reynolds number.

Behavior of the Shape Parameter.—In most of the published methods of analysis a single-parameter family of velocity profiles is assumed, and a differential equation is written for the variation of the shape parameter with distance. This auxiliary equation must be solved simultaneously with the momentum equation and the equation for the wall shear stress. In the present development, the boundary layer is divided into regions, and no single parameter characterizes the entire velocity profile. However, the inner profile, like the outer one, depends on the outer shape parameter D so that solution of an equation for D is the analogous step in the computation procedure.

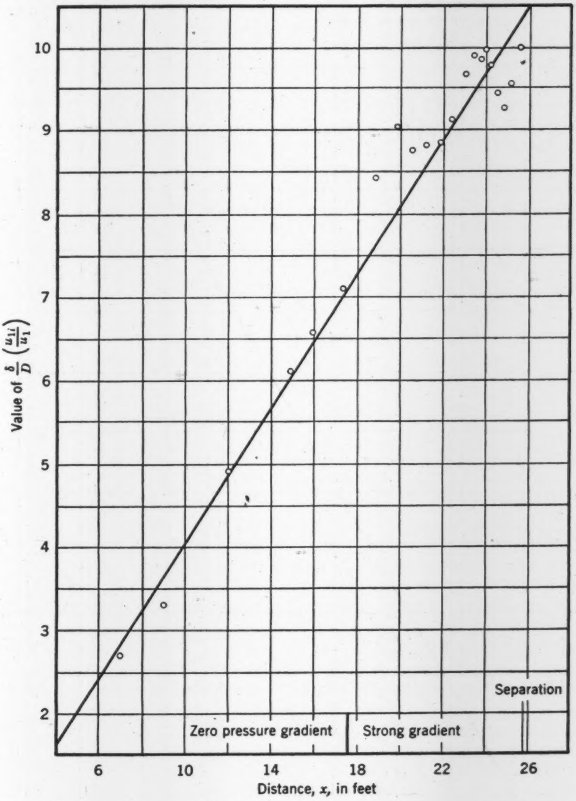

FIG. 7.—VARIATION OF THE OUTER-PROFILE PARAMETER WITH DISTANCE

The fundamental physical property governing D is the dependence of the outer velocity profile on the spatial history of the flow and its independence of local wall conditions. The problem of expressing this by an equation was

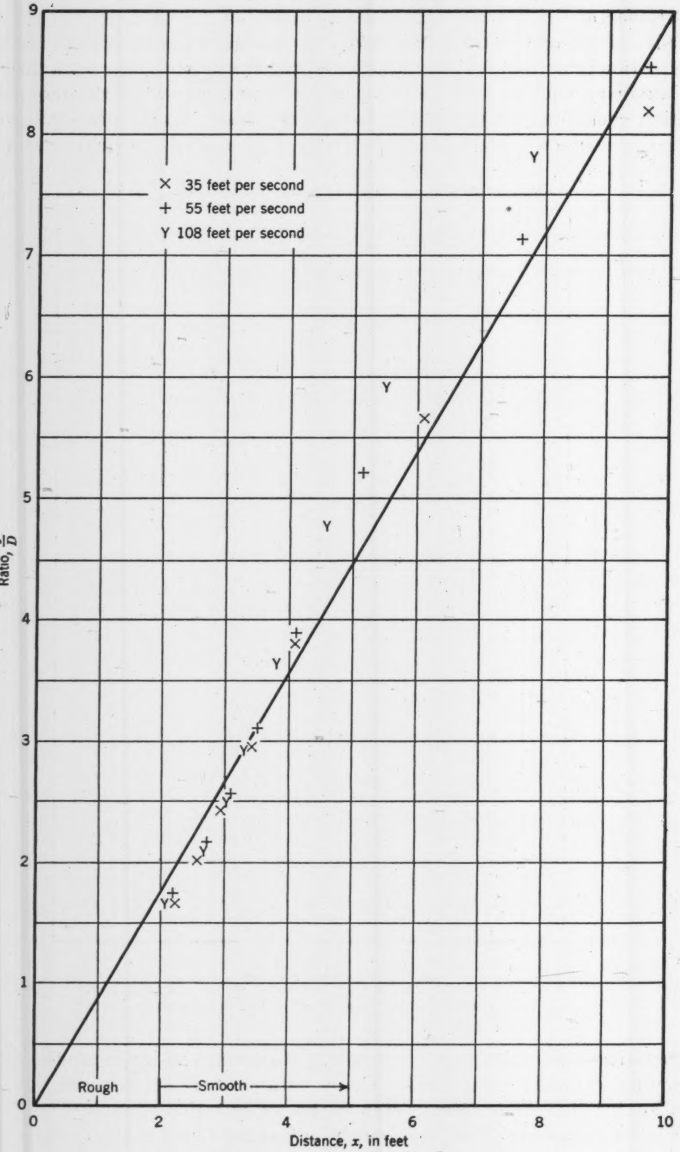

FIG. 8.—VARIATION OF THE OUTER-PROFILE PARAMETER WITH DISTANCE (SANDPAPER PLATE)

attacked through use of the Prandtl momentum-transfer theory. Although this mixing-length theory has long been held in contempt by many theoreticians, recent investigations (19)(20) based on the statistical aspects of turbulence have shown that it is a useful approximation for the computation of velocity profiles.

The Prandtl theory gives a differential equation for the velocity profile as a function of the shear-stress profile and mixing-length profile:

$$\frac{\tau}{\rho} = l^2 \frac{\partial u}{\partial y}\left|\frac{\partial u}{\partial y}\right| \qquad (11)$$

A typical shear-stress profile is shown in Fig. 6. The outer region is essentially a linear function (21) with intercepts at an effective (outer) wall shear stress, τ_{we}, and at the effective boundary-layer thickness, l. The mixing length, δ, is assumed to be constant in the region outside the influence of the wall. When the linear shear-stress profile and constant mixing length are assumed, the Prandtl theory yields the 3/2-power velocity deficiency relation with

$$D = \frac{2}{3}\frac{\delta}{L}\sqrt{\frac{\tau_{we}}{\rho\, u^2{}_1}} \qquad (12)$$

in which L is the constant mixing length; τ_{we} and δ are defined in Fig. 6. By simple algebraic manipulation one can create a parameter that should be a function of distance but not of local conditions. This combination is

$$\frac{\delta}{D}\left(\frac{u_{1i}}{u_1}\right) = \frac{3}{2} L \left(\frac{\tau_{we}}{\rho\, u^2{}_{1i}}\right)^{-\frac{1}{2}} \approx f(x) \qquad (13)$$

in which u_{1i} is measured at the initial station. It can be reasoned that, if the outer region of a turbulent boundary layer is similar to the shear flow in a wake or jet, L and τ_{we} will vary with distance in a manner independent of changes in local wall conditions and of pressure gradients.

Experimental confirmation of Eq. 13 is found in Fig. 7, which is a plot of the left-hand side of Eq. 13 for the data published in 1950 by Messrs. Schubauer and Klebanoff (16). In this experiment the flow had nearly zero pressure gradient up to the 18-ft station and a strong adverse pressure gradient beyond this point. (Separation occurred immediately preceding the 26-ft station.) The linear trend that was established in the constant-pressure region continued into the strong adverse pressure gradient. Another confirmation, in this case for a redistributing flow having constant outer velocity, is shown in Fig. 8. In this graph the 1951 data of Mr. Klebanoff and Z. W. Diehl (22) for the flow along a smooth plate preceded by 2 ft of very rough surface shows the same linear trend as in Fig. 7. This confirms a basic assumption of the present development that all turbulent flows obey the same general relationships. Most of the published analyses are particularly unsuccessful in computing the shape parameter for this type of flow. In the original study (3) several other examples of normal and of redistributing flows were presented, and it is concluded that, for a distance equal to about fifty initial-boundary-layer thicknesses, the outer velocity profile is governed by a relation of the form:

$$\frac{\delta}{D}\left(\frac{u_{1i}}{u_1}\right) = A\ (x - x_i) + \frac{\delta_i}{D_i} \qquad (14)$$

provided the flow is very closely two-dimensional. Following the linear region, the initial nature of the outer flow is considerably submerged in the turbulence generated within this distance, and a new equilibrium is established.

The coefficient A may be computed for those cases for which an equilibrium boundary layer is established in a region of zero pressure gradient ahead of a region of relatively strong pressure gradient or of change in wall conditions. As A has a constant value, it may be computed from the equilibrium, constant-pressure flow:

$$A = \frac{d}{dx}\left(\frac{\delta}{D}\frac{u_{1i}}{u_1}\right)_e \approx \left(\frac{\delta/\theta}{D}\right)_e \frac{d\theta}{dx} = \left(\frac{\delta/\theta}{D}\right)_e \left(\frac{c_f}{2}\right)_e \qquad (15)$$

For equilibrium profiles, all the quantities are related, and it is possible (3) to relate A simply to the value of the wall-shear-stress coefficient:

$$A \approx 0.025\ (1 + 12\sqrt{c_f}) \qquad (16)$$

which is in turn a function of the momentum-thickness Reynolds number, or of the relative roughness, or both.

In cases in which A is known, the value of D at any station can be computed if δ, the thickness of the boundary layer, is known. The momentum equation yields θ so that the ratio of δ to θ is sufficient. If the blending region were fully understood, it might be possible to compute this ratio; however, it was necessary to resort to empirical correlation.

In the original study (3), more than one hundred experiments were examined, and eighteen were selected for the empirical analysis. These experiments listed in Table 1 were selected as the best representatives of a wide variety of experimental conditions. It being a logical contention of the present analysis that all types of turbulent-boundary-layer flows must be governed by the same physical laws, at least one experiment for each type of two-dimensional configuration was chosen. The correlation of δ/θ with D is shown in Fig. 9(*b*). From this result, δ can be determined if D is known. Actually, referring to Eq. 14, it is D that is to be found. Eq. 14 may be written in the form:

$$\frac{\delta/\theta}{D} = \left[A\left(\frac{x - x_i}{\theta_i}\right) + \left(\frac{\delta/\theta}{D}\right)_i\right]\left(\frac{u_1}{u_{1i}}\right)\left(\frac{\theta_i}{\theta}\right) \qquad (17)$$

in which the left-hand side is the function of D presented in Fig. 9(*a*). Thus, from Eq. 17 and Fig. 9(*a*), the value of D at any station may be found provided that the value of A and the initial conditions are known. The foregoing method of computing D stresses the initial spatial variation of the outer boundary layer. It follows that boundary layers with different initial spatial histories (different

TABLE 1.—THE MAJOR EXPERIMENTS ON TWO-DIMENSIONAL TURBULENT BOUNDARY LAYERS SELECTED FOR THE PRESENT ANALYSIS

Investigators	Test object	Entrance conditions	Approximate R_θ-range	H-range	No. of stations	Symbols
Fage and Falkner (1930)	Joukowski airfoil at 0°	Transition	750– 4,000	1.4 –1.55	7	⦸,⊘
Gruschwitz (1931)	387 Airfoil at 12°	Transition	950– 5,400	1.4 –1.8	6	◬
von Doenhoff (1940)	NACA 0012 at 0°	Transition	1,200– 8,700	1.35–1.5	7	⍒,⍋
von Doenhoff and Tetervin (1942)	66, 2–216 airfoil at 10°	Transition	3,200–13,200	1.5 –2.3	6	<
von Doenhoff and Tetervin (1943)	65(216)–222 airfoil at 8°	Transition	1,000–13,000	1.5 –2.6	6	∨,∧
von Doenhoff and Tetervin (1943)	65(216)–222 airfoil at 10°	Transition	3,000–17,000	1.5 –2.8	6	>
Preston and Sweeting (1943)	Joukowski airfoil at 0°, 6°	Transition	600– 2,350	1.5 –1.8	8	⦶,⊖
Schubauer and Klebanoff (1950)	NBS simulated airfoil	Equilibrium	15,000–80,000	1.35–2.8	20	⊙
Newman (1950)	Airfoil at 9.5°	Near separation	8,400– 9,100	2.2 –2.3	3	⛛
Klebanoff and Diehl (1951)	Sand-paper plate	Fully rough	2,000–15,000	1.35–1.9	12	X,+,Y
Kehl (1943)	Channel AK III	Approximate equilibrium	9,000–29,000	1.2 –1.45	14	◫
Kehl (1943)	Channel K3	Approximate equilibrium	10,000–24,000	1.2 –1.5	18	⊟
Kehl (1943)	Channel K7	Approximate equilibrium	2,000–34,000	1.3 –1.7	16	⧅,⧄
Wieghardt and Tillmann (1944)	Channel IV	Transition at pressure dip	2,000–90,000	1.25–1.7	16	▯
Hall (1946)	10°, 2-dimensional diffuser	Transition at pressure dip	700–12,000	1.25–2.15	12	⊡
Pierpont (1947)	Plate with suction slot	Various amounts of suction	1,700–23,000	1.15–2.0	1	■
Newman (1949)	Airfoil with spoiler	Turbulent separation	18,000–52,000	1.6 –3.6	8	▲,▼
Bursnall and Loftin (1951)	66_3 airfoil at 0°	Laminar separation	1,350– 2,000	1.25–1.65	6	●

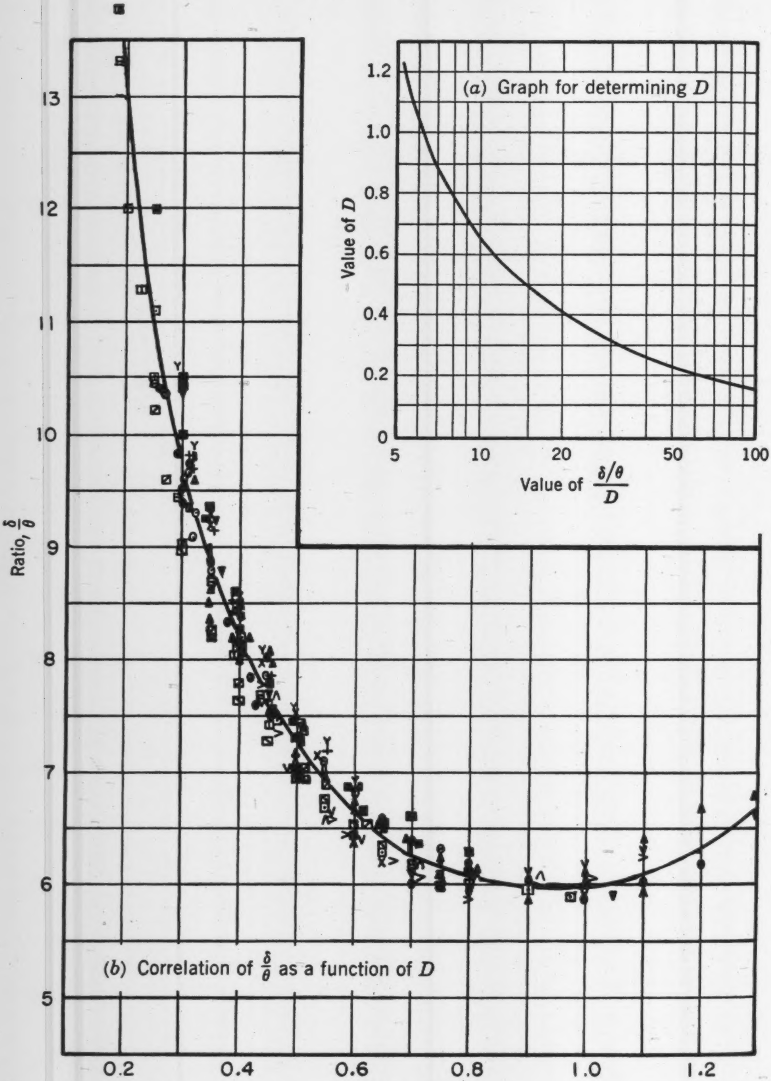

FIG. 9.—SYMBOLS IDENTIFIED IN TABLE 1

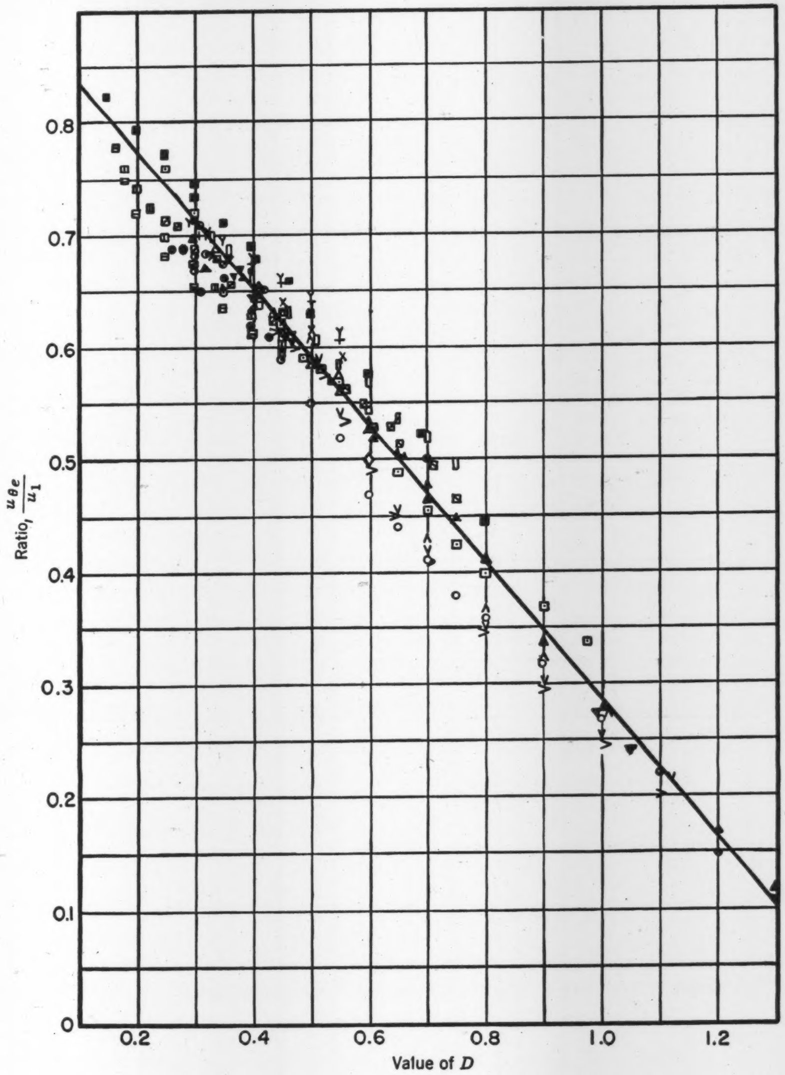

FIG. 10.—CORRELATION OF EFFECTIVE RELATIVE VELOCITY AT MOMENTUM THICKNESS AS A FUNCTION OF D (SYMBOLS IDENTIFIED IN TABLE 1)

A-values) will react quite differently when acted on by the same pressure distribution.

The Wall Shear Stress.—In Eq. 6, the inner velocity profile is given as a function of the friction velocity. A useful expression for this latter quantity results from writing the inner velocity equation for the momentum-thickness distance. The equation for this fictitious effective velocity, $u_{\theta e}$, is simply

$$\frac{u_{\theta e}}{u_*} = 5.6 + 5.6 \log \frac{\theta u_*}{\nu} \ldots\ldots\ldots\ldots\ldots\ldots (18)$$

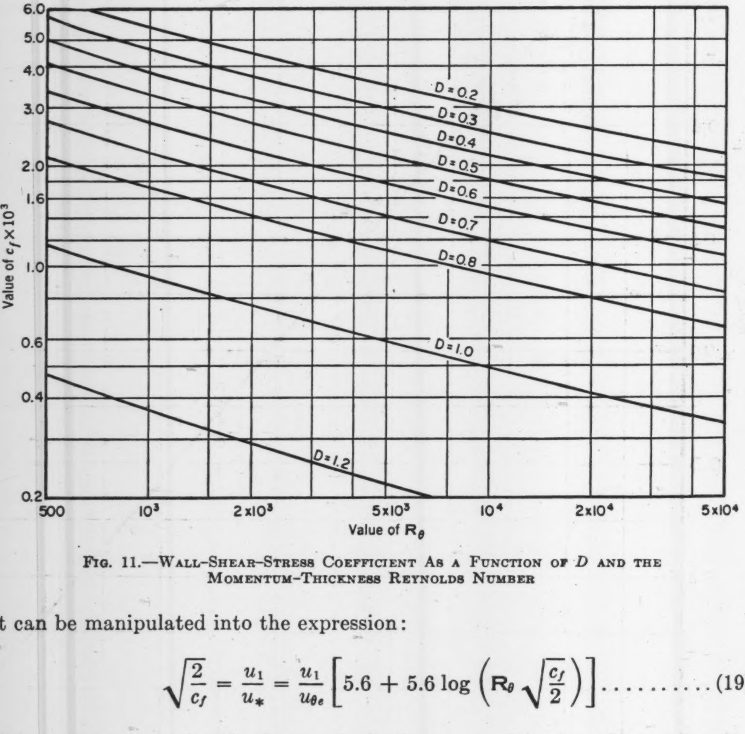

FIG. 11.—WALL-SHEAR-STRESS COEFFICIENT AS A FUNCTION OF *D* AND THE MOMENTUM-THICKNESS REYNOLDS NUMBER

It can be manipulated into the expression:

$$\sqrt{\frac{2}{c_f}} = \frac{u_1}{u_*} = \frac{u_1}{u_{\theta e}} \left[5.6 + 5.6 \log \left(\mathrm{R}_\theta \sqrt{\frac{c_f}{2}} \right) \right] \ldots\ldots\ldots\ldots (19)$$

This equation may be solved numerically for u_* as a function of R_θ and $u_{\theta e}/u_1$. The result is found to fit closely the approximate expression:

$$\frac{u_1}{u_*} \equiv \sqrt{\frac{2}{c_f}} \approx \frac{u_1}{u_{\theta e}} \left[0.7 + 5.0 \log \left(\mathrm{R}_\theta \frac{u_{\theta e}}{u_1} \right) \right] \ldots\ldots\ldots\ldots (20)$$

This formulation of the wall-friction relationship for turbulent boundary layers follows directly from the universal "law of the wall" proposed by Mr. Ludwieg (14). The friction analysis presented here parallels that of Mr. Ludwieg with the difference that the momentum-thickness velocity will be related to the new outer parameter D instead of to the usual shape parameter H. The empirical correlation of $u_{\theta e}/u_1$ with D is shown in Fig. 10. The scatter of the data is somewhat greater than that for δ/θ, but no consistent trend could be found with any other variable and the scatter is attributed less to second-order effects than to experimental error. Fig. 11 enables the rapid estimation of the wall-shear-stress coefficient as a function of the coefficient D and the momentum-thickness Reynolds number, $\mathbf{R}_\theta$.

The Velocity Distribution.—The velocity distribution is composed of the separate inner and outer profiles connected by a blending curve. Eq. 6 for the inner profile may be written

$$\frac{u}{u_1} = \frac{u_{\theta e}}{u_1}\left[1 + \frac{\log (y/\theta)}{1 + \log (\mathbf{R}_\theta \sqrt{c_f/2})}\right] \qquad (21)$$

in which all the required quantities have already been computed. Similarly, the outer profile is expressed directly by Eq. 7 in terms of known quantities. A smooth curve may be used to connect the curves in the blending region. Thus, the present analysis leads readily to the computation of the velocity distribution at a station, without requiring the simultaneous solution of a pair of differential equations.

SEPARATION

The method presented in this paper is particularly suited to the prediction of separation. The computation procedure provides a method of determining D, and the occurrence of separation may be correlated with D. Fig. 10 shows a linear variation for the velocity at the momentum thickness as a function of D. This is extrapolated to zero at D equal to about 1.45, establishing an upper limit. The actual value will depend somewhat on the Reynolds number and on the downstream flow conditions. A good criterion for separation is $D = 1.3 \pm 0.1$.

CONCLUSION

A new approach to turbulent-boundary-layer problems has been outlined. The analysis considers that a most important factor governing the velocity profile is the relative proximity of the wall. Consideration of this factor has led to the division of the boundary layer into three regions. The properties of the inner, or wall, region depend on local wall conditions and on the outer region. The latter is determined as a function of the spatial history of the flow. The resultant semi-empirical computation method is the only one developed to date that applies to redistributing flows as well as to the usual case of flow in an adverse pressure gradient. The computation procedure is also mathematically more simple because the usual simultaneous differential equations are replaced by algebraic equations. This means that analytic answers are now possible for many problems previously requiring numerical solution. The method also yields a simple criterion for predicting separation. Its most serious limitation is that, in the algebraic form, it is only applicable for a distance equal to about fifty initial-boundary-layer thicknesses.

ACKNOWLEDGMENTS

This paper includes the results of a research program conducted under the supervision of the Division of Applied Science of Harvard University (Cambridge, Mass.) while the writer was working part-time at the Ordnance Research Laboratory of The Pennsylvania State University (State College). The work was partly supported by the Office of Naval Research under Project NR 062-139.

It is with a deep sense of gratitude that the writer acknowledges the splendid cooperation of those who made this research possible. In particular, the writer wishes to acknowledge the contributions of Howard W. Emmons and George F. Carrier of Harvard University; Mr. Robertson and Earl M. Uram and J. W. Holl of the Ordnance Research Laboratory; and Natalie Nicholson and her staff in the Gordon McKay Engineering Library at Harvard.

APPENDIX. BIBLIOGRAPHY ON TURBULENT-BOUNDARY-LAYER PROBLEMS

(1) **"On the Dynamical Theory of Incompressible Viscous Fluids and the Determination of the Criterion,"** by Osborne Reynolds, *Philosophical Transactions* (London), Vol. A186, 1895, pp. 123–164.

(2) **"Motion of Fluids with Very Little Viscosity,"** by L. Prandtl, Verhandlung III, International Mathematik Kongress, Heidelberg, 1904 (Leipzig, 1905), pp. 484–491. (Translated in *Technical Memorandum No. 452*, National Advisory Committee for Aeronautics, Washington, D. C., 1928.)

(3) **"A Study of Incompressible Turbulent Boundary Layers,"** by Donald Ross, Ordnance Research Lab. Technical Memorandum, ONR Project NR 062-139-1, June 1, 1953.

(4) **"On the Turbulent Boundary Layer with Pressure Rise and Fall,"** by Busuke Hudimoto, *Memoirs*, College of Eng., Kyoto Imperial Univ., (Japan), Vol. 9, 1935, pp. 1–17.

(5) **"On the Theory of the Turbulent Boundary Layer,"** by J. Rotta, Max Planck Institut für Strömungsforschung Nr. 1, Göttingen, 1950. (Translated in *Technical Memorandum 1344*, National Advisory Committee for Aeronautics, Washington, D. C., 1953.)

(6) **"A Superposition Analysis of the Turbulent Boundary Layer in an Adverse Pressure Gradient,"** by Donald Ross and J. M. Robertson, *Journal of Applied Mechanics*, Vol. 18, 1951, pp. 95–100.

(7) **"Über das Nachwirken der Turbulenz bei örtlich und zeitlich verzögerter Grenzschichtströmung,"** by F. Schultz-Grunow, *Proceedings*, Fifth International Cong. for Applied Mechanics, Cambridge, Mass., 1938, pp. 428–435.

(8) **"Some Recent Contributions to the Study of Transition and Turbulent Boundary Layers,"** by H. L. Dryden, *Technical Note 1168*, National Advisory Committee for Aeronautics, Washington, D. C., April, 1947.

(9) **"The Mechanics of Viscous Fluids,"** by L. Prandtl, Vol. III of "Aerodynamic Theory," by W. F. Durand, Julius Springer, Berlin, 1935.

(10) **"The Turbulence Front at Free Stream Boundaries,"** by Stanley Corrsin, *Proceedings*, Third Midwestern Conference on Fluid Mechanics, March, 1953.

(11) **"A Critical Discussion of Turbulent Flow in Channels and Circular Tubes,"** by C. B. Millikan, *Proceedings*, Fifth International Cong. for Applied Mechanics, 1938, pp. 386–392.

(12) **"Some Remarks on the Laws of Turbulent Motion in Tubes,"** by Richard von Mises, in von Kármán Anniversary Volume, California Inst. of Technology, Pasadena, Calif., 1941, pp. 317–327.

(13) **"Reconsideration of the Theory of Free Turbulence,"** by H. B. Squire, *Philosophical Magazine*, Vol. 39, 1948, pp. 1–20.

(14) **"Instrument for Measuring the Wall Shearing Stress of Turbulent Boundary Layers,"** by H. Ludwieg, *Ingenieur-Archiv*, Vol. 17, 1949, pp. 207–218. (Translated in *Technical Memorandum 1284*, National Advisory Committee for Aeronautics, Washington, D. C., 1950)

(15) **"Report on Investigation of Developed Turbulence,"** by L. Prandtl, *Zeitschrift für angewandte Mathematik und Mechanik*, Vol. 5, 1925, pp. 136–139. (Translated in *Technical Memorandum 1231*, National Advisory Committee for Aeronautics, Washington, D. C., 1949)

(16) **"Investigation of Separation of the Turbulent Boundary Layer,"** by G. B. Schubauer and P. S. Klebanoff, *Technical Note 2133*, National Advisory, Committee for Aeronautics, Washington, D. C., August, 1950.

(17) **"Über laminare und turbulente Reibung,"** by Theodor von Kármán *Zeitschrift für angewandte Mathematik und Mechanik*, Vol. 1, 1921, pp. 235–252.

(18) **"An Empirical Method for Calculation of the Growth of a Turbulent Boundary Layer,"** by Donald Ross and J. M. Robertson, *Journal of the Aeronautical Sciences*, May, 1954, p. 355.

(19) **"Studies of von Kármán's Similarity Theory and Its Extension to Compressible Flows. A Critical Examination of Similarity Theory for Incompressible Flows,"** by C. C. Lin and S. F. Shen, *Technical Note 2541*, National Advisory Committee for Aeronautics, Washington, D. C., November, 1951.

(20) **"The Eddy Viscosity in Turbulent Shear Flow,"** by A. A. Townsend, *Philosophical Magazine*, Vol. 41, 1950, pp. 890–906.

(21) **"Shear Stress in a Turbulent Boundary Layer,"** by Donald Ross and J. M. Robertson, *Journal of Applied Physics*, Vol. 21, 1950, pp. 557–561.

(22) **"Some Features of Artificially Thickened Fully-Developed Turbulent Boundary Layers with Zero Pressure Gradient,"** by P. S. Klebanoff and Z. W. Diehl, *Technical Note 2475*, National Advisory Committee for Aeronautics, Washington, D. C., October, 1951.

(23) **"The Frictional Resistance of Flat Plates in Zero Pressure Gradient,"** by L. Landweber, *Transactions*, Soc. of Naval Architects and Marine Engrs., Vol. 61, 1953.

(24) **"A Literature Survey of Boundary-Layer Development on Smooth and Rough Surfaces at Zero Pressure Gradient,"** by W. D. Baines, Iowa Inst. of Hydr. Research, State Univ. of Iowa, Iowa City, Iowa, 1951.

(25) **"Zur Turbulenten Reibungsschicht bei Druckansteig,"** by K. Weighardt and W. Tillman, Zentrale für Wissenschaftliches Berichtwesen über Luftfahrtforschung, Untersuchungen und Mitteilungen 6617, November, 1944.

(26) **"Characteristics of Turbulence in a Boundary Layer with Zero Pressure Gradient,"** by P. S. Klebanoff, *Technical Note No. 3178*, National Advisory Committee for Aeronautics, Washington, D. C., 1954.

(27) **"Study of the Momentum Distribution of Turbulent Boundary Layers in Adverse Pressure Gradients,"** by V. A. Sandborn and R. J. Slogar, *Technical Memorandum No. 3264*, National Advisory Committee for Aeronautics, Washington, D. C., January, 1955.

(28) **"The Growth of an Axisymmetric Turbulent Boundary Layer in an Adverse Pressure Gradient,"** by E. M. Uram, *Proceedings*, Second U. S. National Cong. for Applied Mechanics, 1955, pp. 687–695.

(29) **"Untersuchunger über die Strömungen des Wassers in Konvergenten und Divergenten Kanälen,"** by J. Nikuradse, *Forschungsheft, No. 289*, Verein Deutscher Ingenieure, 1929.

(30) **"Water Tunnel Diffuser Flow Studies, Part III—Analytical Research,"** by D. Ross and J. M. Robertson, Pennsylvania State Univ., State College, Pa., Ordnance Research Lab. Report, NOrd 7958—230, March, 1952.

(31) **"Water Tunnel Diffuser Flow Studies, Part I—Review of Literature,"** by J. M. Robertson and D. Ross, Pennsylvania State Univ., State College, Pa., Ordnance Research Lab. Report, NOrd 7958—139, May, 1949.

(32) **"Effect of Entrance Conditions on Diffuser Flow,"** by J. M. Robertson and Donald Ross, *Transactions*, ASCE, Vol. 118, 1953, p. 1068.

(33) **"Some Contributions to the Study of the Turbulent Boundary-Layer Near Separation,"** by B. G. Newman, *Report ACA-53*, Aeronautical Research Consultative Committee, Australia, March, 1951.

(34) **"Turbulent Boundary Layer on Steep Slopes,"** by William J. Bauer, *Transactions*, ASCE, Vol. 119, 1954, p. 1212.

(35) **"The Development of the Turbulent Bounday Layer on Steep Slopes,"** by William J. Bauer, thesis presented to the State University of Iowa at Iowa City, in 1951, in partial fulfilment of the requirements for the degree of Doctor of Philosophy.

(36) **"Elementary Mechanics of Fluids,"** by Hunter Rouse, John Wiley & Sons, Inc., New York, N. Y., 1946.

(37) **"Boundary Layer Characteristics for Smooth and Rough Surfaces,"** by Francis R. Hama, *Transactions*, Soc. of Naval Architects and Marine Engrs., Vol. 62, 1954.

(38) **"Turbulent Boundary Layers in Adverse Pressure Gradients,"** by Francis H. Clauser, *Journal of the Aeronautical Sciences*, Vol. 21, 1954, p. 91.

DISCUSSION

William Douglas Baines,[3] J.M. ASCE.—There are many cases of civil engineering work in which a knowledge of the behavior of a turbulent boundary layer is important. Among these are conduit inlets in dams, entrances to tunnels, and streamlined struts immersed in water—the forces on which are primarily the result of surface friction. Open-channel flow is a form of turbulent boundary layer and it can be shown to obey the same velocity distributions used by the author. Changes in flow regime are usually analyzed by backwater computations but there are a few cases in which a detailed knowledge of the flow is required. In such a case an analysis must be made using the boundary-layer equations. The author has made an important contribution by simplifying the approach. He has eliminated the need for using differential equations and has presented useful graphs to support his analysis. However, before this method can be extensively used by civil engineers, surface roughness must be considered because this is the most common case encountered. A similar analysis and a comparable series of curves must be prepared. It is to be hoped that this phase will be investigated in the near future.

The outer law for the velocity distribution as presented by the author is compatible with the commonly accepted law for the constant pressure case. Several investigators have studied this closely (23)(24) and find that the data are best represented by the following equation:

$$\frac{u_1 - u}{u_*} = f\left(\frac{y}{\delta}\right) \qquad (22)$$

The function f has been found to be closely represented by a linear logarithmic law in the region between the edge of the laminar sublayer and the point at which y/δ becomes less than 0.15. This fact has been used (23) to derive expressions for the wall-shear-stress coefficient for the flat-plate and circular-pipe cases. In each instance no blending region has been required for joining the inner and outer velocity profiles. A question thus arises as to when a blending region is required. The author does not indicate how the blending region is defined. This is a serious omission because other investigators wishing to use his analysis will not have the benefit of his experience with the varied types of boundary-layer flow.

The right-hand side of Eq. 22 can readily be written as a function of $(1 - y/\delta)$ which is the same variable found in Eq. 7. It is significant that the function on the right-hand side can be represented by a power law. This has not been noted by other investigators and has led to a considerable simplification in the analysis. In generalized form with the power-law variation, Eq. 22 can be written as

$$1 - \frac{u}{u_1} = k_e \sqrt{\frac{c_f}{2}} \left(1 - \frac{y}{\delta}\right)^m \qquad (23)$$

in which k_e and m are constant. Comparing Eqs. 7 and 23 demonstrates that D is proportional to $\sqrt{c_f/2}$ for flat plates. The author infers that D is constant at a value of approximately 0.3. This is correct for $\mathbf{R}_\theta \approx 3{,}000$ (a typical condition in wind-tunnel investigations).

---

[3] Research Officer, National Research Council of Canada, Ottawa, Ont., Canada.

One point with which the writer does not agree is that the 3/2-power relationship provides the best fit to the experimental data. A value closer to 13/8 is better, and as evidence Fig. 12 is presented, showing some typical velocity profiles (22)(25)(26). The solid line in Fig. 12 is represented by the equation:

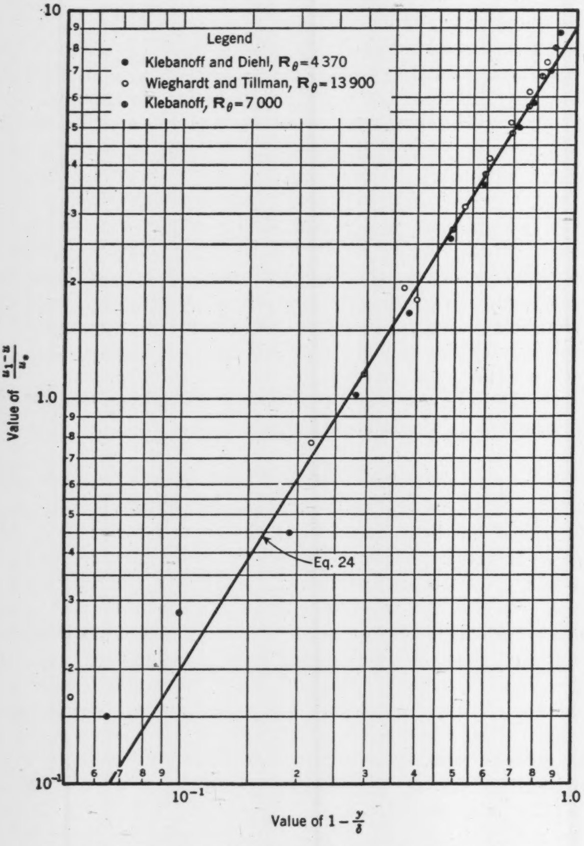

FIG. 12.—OUTER LAW VELOCITY DISTRIBUTION FOR FLAT PLATES

$$1 - \frac{u}{u_1} = 8.9\sqrt{\frac{c_f}{2}}\left(1 - \frac{y}{\delta}\right)^{1.625} \quad \ldots\ldots\ldots\ldots\ldots\ldots (24)$$

For the outer 75% of the boundary layer, the line of slope 1.625 is a close fit. Similar agreement was found by the writer for the measurements of V. A.

Sandborn and R. J. Slogar (27) in an adverse pressure gradient. It thus appears that the analysis could be refined using a larger exponent. This, however, would not change any of the author's basic assumptions. The values of D in various equations and in Figs. 7 through 11 would be changed, thus necessitating redrafting them. Use of a line of steeper slope in illustrations such as Fig. 12 results in a larger value of D for the same data.

Inasmuch as the detailed velocity distribution is not usually required in an analysis of the boundary layer, the suggested change would not produce significantly different results. The usual problem is to determine the boundary-layer thickness, the friction drag, or the point of separation. The author has based his curves on experimental evidence and as a result these quantities will be accurately predicted by his method.

The writer hopes that the author's approach to turbulent-boundary-layer problems will receive attention from engineers working in this field so that its use can be demonstrated.

James M. Robertson,[4] M. ASCE.—This paper represents an important step forward in the understanding of turbulent-boundary-layer flow. Fluid-dynamics literature is replete with studies of the turbulent boundary layer in an adverse pressure gradient in which each investigator brought forth a new theory based on his experimental data only to have the next experimenter's work discredit it. Because Mr. Ross's study is on such a firm physical basis and utilizes the widest range of test data, it is to be expected to stand for some time. As implied by Mr. Ross, a rigorous theory should appear eventually in terms of the statistical theory of turbulence—but that day appears to be far off.

Most work on the boundary-layer problem has been devoted to the two-dimensional case, and many applications fall within this category. The three-dimensional case is naturally more complex, but some applications (such as conical diffusers and flow about elongated bodies) can be treated as axisymmetric. This flow case might be termed quasi two-dimensional because the flow is symmetrical about the flow-direction axis and only two coordinates are needed to describe the geometry. Mr. Ross's approach is for two-dimensional flow cases. It is natural to hope that it can be extended to the more general case—one wonders if it should not be directly applicable to the axisymmetric flow case which for relatively thin boundary layers is effectively two-dimensional. Some studies of the axisymmetric boundary-layer flow in a conical diffuser have been conducted at the Ordnance Research Laboratory of the Pennsylvania State University by Messrs. Uram (28) and Holl and the writer. These studies indicate that, although the various relationships introduced by Mr. Ross are most useful and effective for describing the flow, the outer-profile parameter does not follow a linear type of variation with downstream distance. This might be expected from Mr. Ross's statement that Eq. 14 is applicable "provided the flow is very closely two-dimensional." Perhaps it may be possible to analyze the axisymmetric case in a manner similar to that used by Mr. Ross and obtain appropriate relationships similar to Eqs. 13 and 14. Until then empirical relationships will have to suffice and engineers will have to consider the Ross approach to be limited strictly to the prediction of two-dimensional turbulent boundary layers in adverse pressure gradients.

---

[4] Prof. of Theoretical and Applied Mechanics, Univ. of Illinois, Urbana, Ill.

It is unfortunate that this presentation of an exhaustive study had to be so greatly abbreviated. The writer hopes that Mr. Ross will rectify some of the more glaring omissions for the benefit of those students of the subject who do not have ready access to his original lengthy thesis. Not apparent in this paper is the complete physical background used by Mr. Ross in obtaining the relationships used and the pains taken in sorting out from that mass of data available relative to turbulent boundary layers the most reliable sets of experimental information for verifying the analysis and determining the empirical constants needed. For the benefit of completeness some indication of the author's criteria for sorting out the experimental data used from that rejected would be instructive and valuable. Certainly for any investigator planning further experimental research on this subject these would aid in proper design of experiments.

The division of the boundary-layer flow into two regions—an inner wall region and an outer region relatively independent of local wall conditions—with some sort of junction between them is most important. In a sense the "law-of-the-wall" concept for the inner region may be considered to have been initiated by Mr. Prandtl in stating that $u/u_* = f(y\, u_*/\nu)$ irrespective of how far away the other side of the conduit is. Mr. Ross's contribution is that of analyzing the two basic regions completely separately. Not only has he indicated a unique relationship for the inner region as others have done but he has analyzed the outer flow region as a separate entity. All previous students of the subject have included the inner or wall region in their analysis of pressure-gradient effects and history effects. The advantages of the new approach are evident in the paper.

In connection with the 3/2-power deficiency law derived for the outer boundary-layer region, it is interesting to note that Prandtl (15) in 1925 derived just such a law for the outer region in a pipe,

$$u = A - B\, r^{3/2} \ldots\ldots\ldots\ldots\ldots\ldots\ldots\ldots (25)$$

in which u is the velocity at radius r. In terms of the region in a pipe from the wall to the center line representing a boundary layer, this is equivalent to Eq. 7 with $D = B\,\delta/u_1$. The Prandtl derivation was based on his momentum-transfer theory with linear shear-stress variation and constant mixing length—in exact accord with the indications of Fig. 3.

The assumption of linear shear-stress variation in the outer region is justified as this quantity has been measured with hot-wire instrumentation (16). The constancy of the mixing length in the outer region is not subject to explicit proof because this quantity cannot be measured directly. A few investigators have determined the mixing length by working backward from velocity distributions with the aid of Eq. 11. Although this procedure is subject to accumulated errors, the results indicate that the mixing length is essentially constant in the outer region. Thus, Fig. 13 shows a universal plot of the Nikuradse (29) mixing-length data for a family of diffusers. This plot was compiled by the writer several years ago (30) but no explanation for the arbitrary constant C was found. Actually $1/C$ is an indication of the fraction of the boundary layer influenced by the wall region. Because the Nikuradse data are available for only one station in the diffuser, the manner in which the mixing length varies in the downstream direction is not clear. Evidence from other tests suggests that it may possibly increase in the flow direction directly with the boundary-layer thickness. This uncertainty has been side-stepped by Mr. Ross in combining the mixing length in the outer region with other quantities to form a parameter whose form of variation in the flow direction he then infers by reference to experiment.

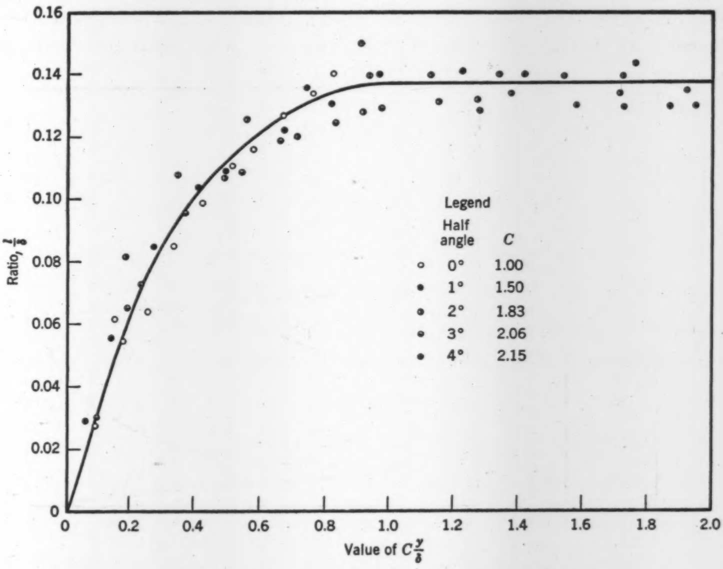

FIG. 13.—UNIVERSAL PLOT OF MIXING LENGTHS FROM J. NIKURADSE'S DIFFUSER STUDY

The writer has made a crude analysis of the longitudinal variation of the mixing length for the boundary layer of Messrs. Schubauer and Klebanoff (16) analyzed by Mr. Ross, with the results shown in Fig. 14. The effective wall-shear-stress coefficient, $c_{f_e} = \frac{\tau_{we}}{(\rho/2)\, u^2_{1i}}$, has been estimated by extrapolation to the wall of the outer part of the lateral-shear-stress variations found by Messrs. Schubauer and Klebanoff. From Eq. 13 and from the values of $\delta/D(u_{1i}/u_1)$ for this boundary layer in Fig. 7, the value of L has been computed. Both the effective wall shear stress and the mixing length in the outer region are seen to increase with distance in the flow direction at an increasing rate as separation is approached. The boundary-layer thickness varies in about the same fashion, and the ratio of L to the thickness (L/δ') is seen to be nearly constant. (The boundary-layer thickness δ' is the approximate outer limit indicated by Messrs. Schubauer and Klebanoff for the layer.)

Numerous form parameters have been used to describe the shape of the velocity profile in turbulent flow. Mr. Ross' temerity in introducing yet another can only be justified by the foregoing observation that it is not only significant but unique in being limited to the description of the outer flow region irrespective of the flow in the inner wall region. The common shape parameter H is introduced (but not defined) in Eq. 8, the von Kármán momentum-integral equation. It is the ratio of the displacement thickness δ^* to the momentum thickness θ with the boundary layer. In two-dimensional flow δ^* is a measure of the lateral displacement of the streamlines outside the boundary-layer region due to the layer; the momentum thickness is a measure of the momentum deficiency in the layer. Because this parameter is so commonly used the writer strongly urges the author to present a graph indicating the relation between H and D even though H is not germane to his new approach. As H includes a description of the inner region in addition to the outer region described by D, the Reynolds number or shear-stress coefficient will presumably occur as a secondary parameter on such a graph. The various form parameters introduced into the literature up to about 1948 have been reviewed elsewhere (31), and their unsuitability for the analysis of the case of the adverse pressure gradient was indicated (30).

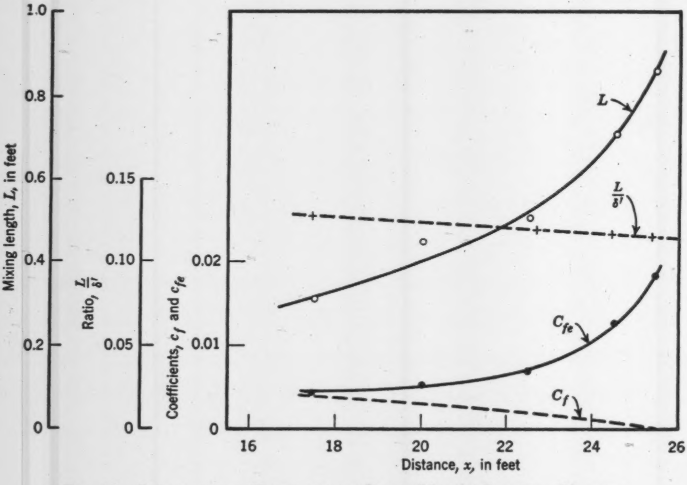

FIG. 14.—LONGITUDINAL VARIATION IN OUTER MIXING LENGTH—MESSRS. SCHUBAUER AND KLEBANOFF'S BOUNDARY LAYER

One form parameter introduced by Mr. Ludwieg and W. Tillmann (14) is $\gamma = u_{\theta e}/u_1$ which Mr. Ross uses in the wall-shear-stress relationships (Eqs. 19 and 20) and in Eq. 21. Thus, Eq. 20 can be written as

$$c_f = \frac{2\,\gamma^2}{[0.7 + 5.0\log(\gamma\,R_\theta)]^2} \qquad (26)$$

The variation in γ is small (Fig. 10) compared with that of $\mathbf{R}_\theta$ and hence its influence on the denominator is less significant than that indicated by the numerator of Eq. 26. For very large Reynolds numbers this approaches the simple expression,

$$c_f = \frac{\gamma^2}{\gamma^2_o} c_{fo} \qquad (27)$$

which was developed by Messrs. Ludwieg and Tillmann. The subscript *o* is used to indicate values that obtain without a pressure gradient. Actually, Eq. 27 differs from Eq. 26 by 30% for a flow with *D* of 1.2 at a Reynolds number of 10^5. Mr. Ross and the writer (6) on the basis of a superposition analysis developed an equivalent relationship,

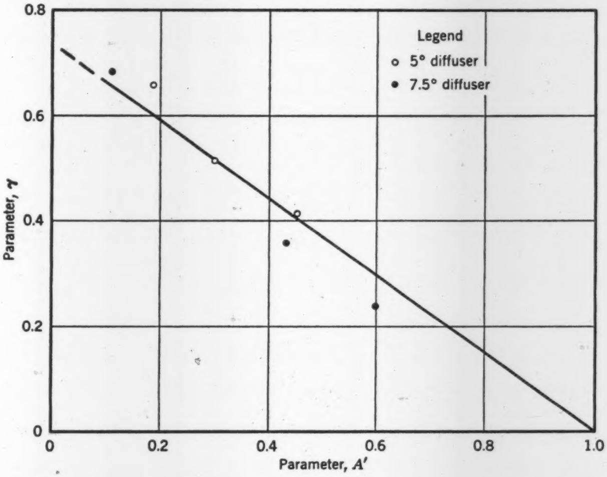

FIG. 15.—CORRELATION BETWEEN SHAPE PARAMETERS A' AND γ (BOTH DIFFUSERS HAVING A 3 + IN. DIAMETER APPROACH PIPE)

$$c_f = (1 - A')^2 c_{fo} \qquad (28)$$

in terms of A', the form parameter for the superposition analysis. The parameter A' must be related to γ by

$$\gamma = \gamma_o (1 - A') \qquad (29)$$

A rough check on this for some diffuser data (32) is indicated in Fig. 15. The parameter γ is correlated with *D* and therefore A' must also be. Besides indicating the interrelationship of several form parameters this phase of the discussion suggests that the shear-stress relationship (Eq. 20) might be more simply expressed as

$$c_f = c_{fo} f(D) \qquad (30)$$

in which the function of D could be presented on a separate plot as a factor by which the flat-plate drag is reduced due to the pressure gradient. This would permit those wishing to use a different flat-plate drag law to take advantage of the Ross analysis of the pressure-gradient effect.

In any analysis of the turbulent boundary layer in an adverse pressure gradient a very important consideration is the occurrence of separation, or how closely separation is approached. The writer is not strongly convinced that by stating $D = 1.3$ to be the criterion for separation that Mr. Ross has improved on other criteria—for example, $H = 2.5$ or $A' = 0.8$. The only improvement is that D typifies the outer flow region, and, as noted by Mr. Prandtl in 1904, "The flow separates from the surface at a point entirely determined by external conditions" (2).

TABLE 2

$R_{\theta i}$	D_i	$f_i(D)$	c_f	A	n
10^3	0.384	21.7	0.00465	0.0454	0.166
10^4	0.312	30	0.0026	0.0403	0.183
10^5	0.254	43	0.0016	0.037	0.193

As a means for analyzing boundary-layer progression in an adverse pressure gradient, the new approach can be used to predict the growth and eventual separation of the layer for a specified flow condition. Not only this, but it can be used to ascertain how much a particular boundary layer can be decelerated before it separates, without calculating the growth—that is, to ascertain deceleration in terms of the terminal conditions alone. As indicated by Mr. Ross in private communication, Eq. 17 can be used to indicate which flows will proceed toward separation and which will not. Usually one wishes the flow to proceed close to separation without its occurrence. With the aid of Eq. 9 one can write Eq. 17 as

$$f(D) = \left[A \frac{\Delta x}{\theta_i} + f_i(D)\right]\left(\frac{u_1}{u_{1i}}\right)^{3+G} \dots\dots\dots\dots\dots (31)$$

in which $f(D) = \delta\,\theta/D$ and $f_i(D)$ is its initial value. Taking $D = 1.3$ as necessary for separation, the left side of Eq. 31 is $f = 5$ (Fig. 9(*a*)). The initial value $f_i(D)$ is also determined from the initial value of D which is approximately 0.3 for a flow beginning from flat-plate conditions. The D-value in flat-plate flow varies slowly with the Reynolds number, and this variation is enough to affect significantly the present solution. The constant A is a function of the momentum-thickness Reynolds number (Eq. 16) as is also the exponent, $3 + G$ (Fig. 5). Eq. 31 has been solved for the allowable reduction in u_1 for three different values of the initial momentum-thickness Reynolds number, for which the various constants are indicated in Table 2. If $n = 1/(G + 3)$, the equation may be written as

$$\frac{u_1}{u_{1i}} = \left(\frac{5}{A \dfrac{\Delta x}{\theta_i} + f_i}\right)^n \dots\dots\dots\dots\dots\dots\dots (32)$$

Because the relationships are not applicable for $(\Delta x/\theta_i)$-values greater than 50 and because of the relative magnitudes of A and $f_i(D)$ listed in Table 2, the relationship can be written (with an error of less than 2%) as

$$\frac{u_1}{u_{1i}} = \left(\frac{5}{f_i}\right)^n \qquad (33)$$

The solution of Eq. 33 is presented in Fig. 16, which shows the permissible decrease in velocity (without separation) as a function of the initial Reynolds number. Also shown is a more conservative solution based on $D = 1.0$, for which $f(D) = 6.1$.

Three conclusions are indicated by the foregoing computation. First, the allowable velocity change is not great. Second, the rate of deceleration does not matter (the results being independent of x). Third, for greater Reynolds numbers there is less chance of separation. It must be recalled that these conclusions are subject to the limits of Eq. 9 (18) and an x-limit of 50 θ_i. As the first two conclusions were somewhat beyond the writer's expectation, a search was made for possible experimental verification. Two series of experiments were checked: The work at the National Bureau of Standards (NBS), United States Department of the Interior, by Messrs. Schubauer and Klebanoff (16) and work at Sydney University (SU) in Australia by B. G. Newman (33). These two points are plotted in Fig. 16 showing close agreement in the NBS case but an underprediction in the case of the SU work. The writer would appreciate Mr. Ross's comments on this analysis as well as an indication of other uses of Eq. 17 to predict over-all flow conditions.

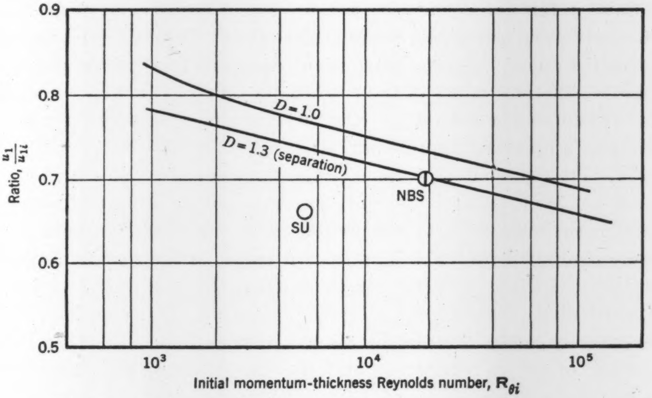

FIG. 16.—PERMISSIBLE VELOCITY DECREASE WITHOUT SEPARATION AS A FUNCTION OF THE INITIAL REYNOLDS NUMBER

WILLIAM J. BAUER,[5] J. M. ASCE.—This discussion will be limited to a comparison of the shape of the empirical velocity profile proposed by the author with measurements made by the writer in a steep laboratory flume (34). The comparison is presented graphically in Fig. 17.

In Fig. 17(*a*) u/u_* is plotted on a linear ordinate scale as a function of $y\, u_*/\nu$, the latter being plotted on a logarithmic abscissa scale. On the same field a straight line has been drawn to represent the Ludwieg "law of the wall" as presented in Eq. 6. Although the author states that this function is valid for (y/δ)-values less than 0.1, points have been plotted for (y/δ)-values up to 0.25. The seven velocity profiles presented were selected at random from a group of more than 30 profiles measured by the writer (35) above the plate glass floor of a steep laboratory flume. Except for the one profile obtained on the 40° slope at $\delta\, u_1/\nu = 2.14 \times 10^5$, the points appear to be reasonably closely bunched and in fair agreement with Eq. 6. Slight adjustment of the constant of Eq. 6 would obviously give a closer fit, however. (Eq. 6 is also known as the von Kármán-Prandtl velocity-distribution equation for flow in pipes, albeit with slightly different values of the coefficients (36)). One may conclude that the inner portion of the velocity profiles on steep slopes is adequately described by the author's proposed approximation.

In Fig. 17(*b*), the outer portions of the same seven profiles do not appear to be as closely approximated by Eq. 7, which the author proposes for describing the shape of the outer 75% of the profile. The values of *D* presented in Fig. 17(*b*) were computed from Eq. 7 for known values of the remaining variables. Even within the limits proposed by the author, the value of *D* varies rather widely, particularly for values of y/δ greater than 0.7. Nevertheless, the value of *D* is relatively constant in the middle 40% of the profile, and it can be shown that the use of an average value obtained from this region will result in a reasonably good approximation of the velocity profile outside this range because of the nature of the function. No apparent systematic variation with slope or location on the flume is evident in Fig. 17(*b*). Thus, it appears that Eq. 7 is also a useful description of the shape of the velocity profile within turbulent boundary layers on steep slopes.

As far as rough boundaries are concerned, it should be noted that the value of *D* would be considerably larger than that for smooth boundaries. This fact was evaluated by the writer by examining a corresponding series of rough-boundary velocity profiles also measured in the same steep flume. The *D*-values appear to be about 0.15 larger than those plotted in Fig. 17(*b*) for the corresponding conditions on a rough boundary of fly screen.

Finally, the values of c_f as obtained from Fig. 11 (on the basis of measured values of R_θ and *D*) are compared with values computed by the writer using the von Kármán momentum equation:

---

[5] Senior Designer, Harza Eng. Co., Chicago, Ill.

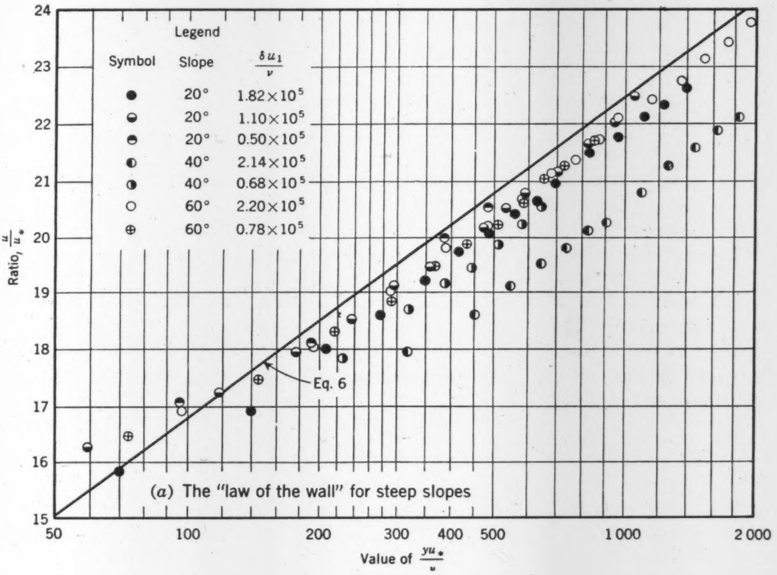

(*a*) The "law of the wall" for steep slopes

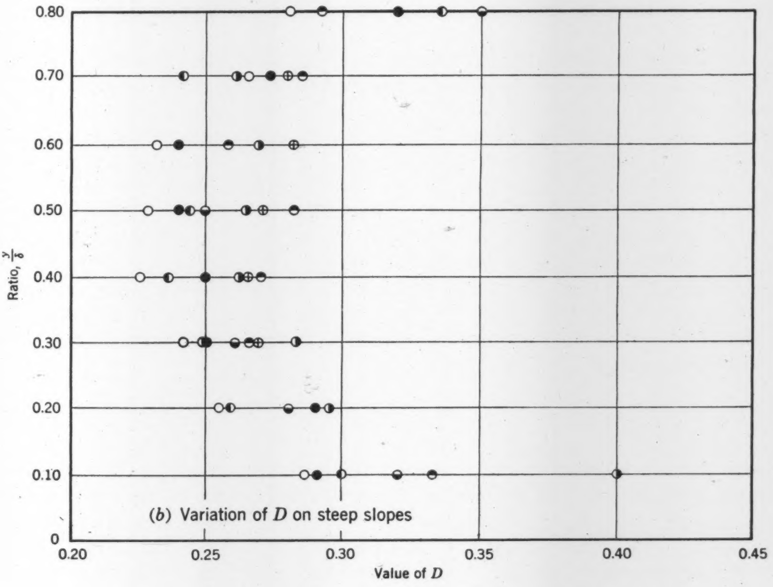

(*b*) Variation of *D* on steep slopes

FIG. 17.—COMPARISON OF VELOCITY PROFILES

R_θ	D	c_f (Fig. 11)	c_f (writer's computations)
1.63×10^4	0.24	0.0025	0.00265
1.07×10^4	0.25	0.0027	0.00275
0.46×10^4	0.27	0.00315	0.00315
2.00×10^4	0.24	0.0024	0.0028
0.64×10^4	0.28	0.00295	0.0031
2.04×10^4	0.23	0.0025	0.0025
0.72×10^4	0.27	0.00295	0.00295

The D-values are averages from the middle 40% of the profiles.

The writer congratulates the author for a straightforward presentation of a relatively simple and apparently useful approximation of the turbulent-boundary-layer velocity profile. Although his work will be most frequently applied to the calculation of boundary layers with adverse pressure gradients, the author has nevertheless presented a method that is equally valid for developments in accelerating flow.

DONALD ROSS[6].—In attacking the problem of turbulent boundary layers and in writing this paper, the writer has been primarily concerned with the case of boundary layers acted upon by adverse pressure gradients. For this reason, and also because several papers in the literature handle the subject successfully, that part of the original thesis dealing with equilibrium flows was omitted from the paper. However, Messrs. Baines and Robertson have dwelled on this case and other readers may feel that it should receive specific attention.

For equilibrium boundary layers there seems to be little question that Eq. 5 correctly represents the velocity distribution of the inner turbulent flow, although there may be some variation of the coefficients in Eq. 6. However, the velocity deficiency in the outer region may more properly be represented by the more general Eq. 23 proposed by Mr. Baines. The writer agrees with Messrs. Baines and Bauer that a higher exponent is in closer agreement with flat-plate data than the 3/2-power. The writer chose the 3/2-power because, for flows having strong adverse pressure gradients, the 3/2-power law is a closer fit than any other. Also, because the velocity deficiencies involved are so much greater near separation, the writer settled on the single formula providing the closest fit for that type of flow and accepted the error typified in Fig. 17(*b*). It is not a serious discrepancy. In Fig. 18 one may compare the writer's formula,

$$1 - \frac{u}{u_1} = 8.4\sqrt{\frac{c_f}{2}}\left(1 - \frac{y}{\delta}\right)^{3/2}$$

with those of Mr. Baines and of Francis R. Hama (37) and with the expression derived by Mr. von Kármán that the writer finds provides the best experimental fit. Fig. 18 clearly shows that the differences between the writer's formula and Mr. Baines' are not great and that both provide good average fits to experimental data. However, the true curve is not a power law—hence Mr. Bauer's result (Fig. 17(*b*)) that the value of *D* is not constant across the profile. Mr. Baines has incorporated the coefficient c_f in his formula for the outer-velocity deficiency. This is valid for the constant-pressure case, and the writer confirms that *D* is proportional to $\sqrt{c_f/2}$ for flat plates. However, in general, for nonequilibrium boundary layers—that is, boundary layers having profiles that change with distance—the local value of *D* in no way depends on the local value of c_f.

---

[6] Member of the Technical Staff, The Bell Telephone Labs., Inc., Whippany, N. J.

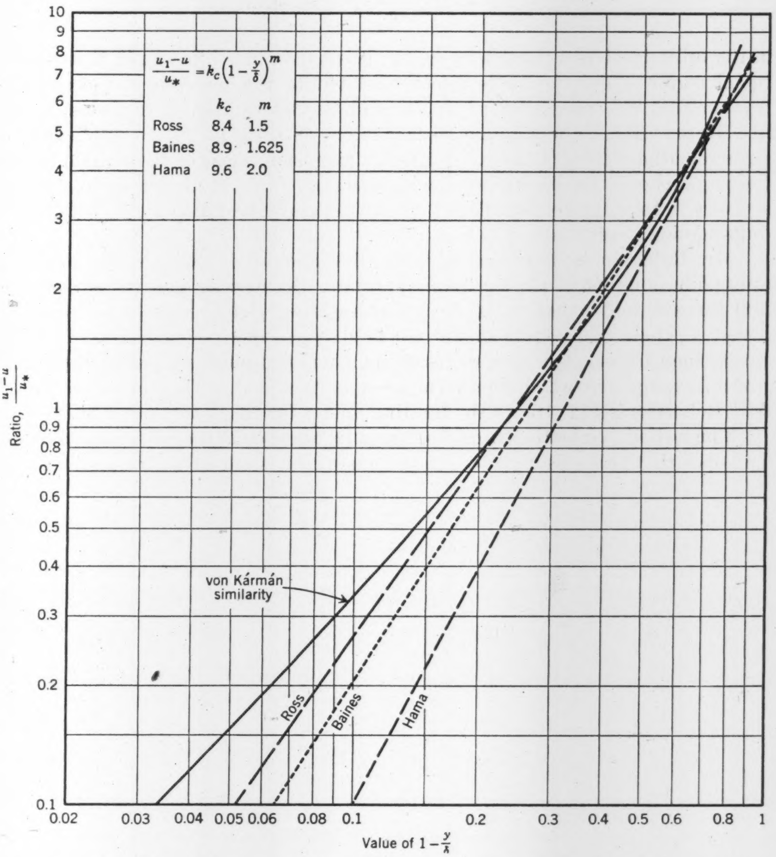

FIG. 18.—COMPARISON OF OUTER-VELOCITY FORMULAS FOR FLAT PLATES

In reply to Mr. Baines, the writer believes that the methods developed in the paper can be extended to rough surfaces in so far as these are understood. Thus, following Mr. Hama (37) and Francis H. Clauser (38), one may write for the logarithmic inner-turbulent velocity profile:

$$\frac{u}{u_*} = A + B \log \frac{y\, u_*}{\nu} - \frac{\Delta U}{u_*}$$

in which

$$\frac{\Delta U}{u_*} = B \log \frac{k\, u_*}{\nu} + \text{a constant}$$

in the fully developed roughness region; it is somewhat different in the transitional region. This factor is directly related to the increase of the surface friction that the roughness produces, and its determination is discussed by Mr. Hama (37). For a rough surface, Eqs. 18 through 20 are applicable if u_{θ_e} is replaced by $(u_{\theta_e} + \Delta U)$. With this extension, most of the remainder of the paper should be directly applicable to rough surfaces as well as to smooth surfaces. As noted by Mr. Bauer, D will generally be larger for flows in conduits having rough walls.

Mr. Robertson's discussion of separation should be valid, at least to the approximations made for his final equation. Because Δx can be as great as 500 times θ_i and A can actually be much greater than he assumes, the term involving these two factors should not be dropped relative to $f_i(D)$. In fact, the Sydney University experiments of Mr. Newman mentioned in his discussion are an example in which this term must be included. The curves shown in Mr. Robertson's Fig. 16 are the limiting values for rapid decelerations.

The writer thanks the three discussers for their constructive comments and he hopes that this closure provides the answers to some of their questions.

AMERICAN SOCIETY OF CIVIL ENGINEERS
Founded November 5, 1852
TRANSACTIONS

Paper No. 2839

RESEARCH ON BOLTED CONNECTIONS

By William H. Munse,[1] A. M. ASCE

Synopsis

The introduction of the high-strength bolt as a structural connector has made it possible to produce structural joints that are superior to and often more economical than comparable riveted joints. However, to obtain full benefit from the use of these bolts it is necessary that they be installed with a high initial tension. The reasons for and the effects of this high tension are discussed herein on the basis of (*a*) previous data and (*b*) the results of static and fatigue tests that have been conducted recently on bolts and bolted connections subjected to shear and tensile loadings.

Introduction

Seldom, if ever, has a new structural connector received such rapid and wide-spread acceptance as the high-strength bolt (bolts furnished under American Society for Testing Materials designation ASTM–A 325); within a few years, the high-strength bolt has moved from the structural research laboratory into general acceptance in the field. This acceptance is based on the economy and on the superior behavior obtained in both the field and the laboratory. In the field tests, the bolts have been used as replacements in connections in which rivets were periodically working loose. In the laboratory, much effort has been expended in studying the fundamental behavior of bolted joints and the conditions necessary for the most efficient use of the materials in such joints. The results of these studies have all been extremely promising.

The initial impetus for this work came from W. M. Wilson in 1938 when he found that high-strength bolts tightened sufficiently to eliminate slip in a structural joint did not fail in fatigue.[2] The next step in the development of the high-strength bolt as a fastener did not occur until 1945 when the late

---

Note.—Published, essentially as printed here, in March, 1955, as *Proceedings-Separate No. 650*. Positions and titles given are those in effect when the paper was approved for publication in *Transactions*.

[1] Research Prof. of Civ. Eng., Univ. of Illinois, Urbana, Ill.

[2] "Fatigue Tests of Riveted Joints," by W. M. Wilson and F. P. Thomas, *Bulletin No. 302*, Univ. of Illinois Eng. Experiment Station, Urbana, Ill., 1938.

G. A. Maney began preliminary studies on the problem.[3] In the spring of 1947, the Research Council on Riveted and Bolted Structural Joints (referred to herein as the Research Council) was formed and began a number of studies at the University of Illinois (Urbana) on joints assembled with high-strength bolts. Since then—through the sponsorship of the Research Council and the cooperation of Northwestern University (Evanston, Ill., and Chicago, Ill.), Purdue University (LaFayette, Ind.), the University of Washington (Seattle), the University of Illinois, practicing engineers, and the structural-steel fabricators—many studies have been made to determine the behavior of such joints.

By 1952 many laboratory and field studies had been completed and, very appropriately, were described to the engineering profession at the Centennial Convocation of the Society[4, 5, 6, 7, 8, 9] at Chicago. These studies included tests of the bolts themselves, plus tests of lap joints and butt joints loaded either under static conditions or repeated-load conditions and in both tension and compression.

In addition to demonstrating the economy and superior quality of the high-strength bolt, the Research Council has prepared a specification entitled, "The Assembly of Structural Joints Using High Strength Steel Bolts." This specification, adopted in January, 1951, and revised in February, 1954, has been widely accepted by the engineering profession.

GENERAL BEHAVIOR OF BOLTED JOINTS

It has long been known that the working loads on most riveted joints are resisted by means of the frictional forces in the connections rather than by shear on the rivets. Nevertheless, the design of such joints is based on the premise that the load is transferred from one portion of the member to another by means of direct shear on the rivets. In the same manner, a properly assembled joint fastened with high-strength bolts resists loads by means of the friction between the connected parts. By following the procedure recommended by the Research Council, that of substituting an equal number of bolts for rivets of the same nominal diameter and installing these bolts with an initial tension at least as great as 90% of the elastic proof load of the bolt material, connections are obtained which have properties generally superior to those of a similar riveted joint.

In order to develop the frictional resistance necessary to carry the working loads on bolted joints, a high axial tension must be maintained in high-strength bolts at all times. To maintain this tension the use of hardened washers is required under both the head and nut of the bolt. With the hardened washers and a high initial tension, it has been found, both in the laboratory and field tests, that the bolts remain tight and the joints rigid even under the most severe loading conditions. However, it is necessary that the tension in the bolts be in accordance with the recommendations of the Research Council in order for these superior results to be obtained.

---

[3] "The Effect of Various Fasteners on the Fatigue Strength of a Structural Joint," by K. H. Lenzen, *Bulletin No. 480*, A.R.E.A., June–July, 1949.

[4] "History of the Use of High-Strength Bolts," by W. C. Stewart, *Transactions*, ASCE, Vol. 120, 1955, p. 1296.

[5] "Laboratory Tests of Bolted Joints," by William H. Munse, D. T. Wright, and Nathan M. Newmark, *ibid.*, p. 1299.

[6] "Fatigue in Riveted and Bolted Single-Lap Joints," by Jack W. Carter, Kenneth H. Lenzen, and Lawrence T. Wyly, *ibid.*, p. 1353.

[7] "Comparison of Bolted and Riveted Joints," by Frank Baron and Edward W. Larson, Jr., *ibid.*, p. 1322.

[8] "Slip of Joints Under Static Loads," by R. A. Hechtman, D.R. Young, A. G. Chin, and E. R. Savikko, *ibid.*, p. 1335.

[9] "Structural Uses of High-Strength Bolts," by T. R. Higgins and E. J. Ruble, *ibid.*, p. 1389.

Some engineers have expressed concern over the possibility of slip in a high-strength bolted joint; however, those well acquainted with the behavior of such connections believe that this concern is unwarranted. Many structural members which are subjected to a stress in only one direction under both dead-load and live-load conditions are erected with the fasteners in bearing in this same direction. Consequently, there should be no question of slip in these connections. However, the frictional resistance of connections which are subjected to reversals of stress must be great enough to prevent slip. For this reason, the Research Council has concentrated a large part of its effort on the determination of the conditions necessary to inhibit slip in a bolted structural joint and in the preparation of a specification that will insure that these conditions are met.

A connection of so-called balanced design is one in which the parts are so proportioned that the allowable unit working stresses in all parts will be reached simultaneously. Thus, for present specifications the net tensile area for a balanced design would be 0.75 times as great as the shear area of the fasteners based on their nominal diameter. It can be shown that, for a bolted joint of balanced design and an apparent coefficient of friction of 0.25, the stress in the member at slip is equal to approximately one third the unit axial tension on the nominal area of the bolts. (Tests at the University of Washington[8] and at the University of Illinois[5] have shown that the apparent frictional coefficient for properly designed bolted joints will be between 0.25 and 0.35.) Thus, a tensile stress of approximately 54,000 lb per sq in. would be required in the bolts to eliminate slip in a joint stressed to 18,000 lb per sq in. on the net section of the connection. An axial tensile stress of this magnitude can be produced readily in high-strength bolts, ASTM-A 325. In fact, it corresponds to only about 84% of the elastic proof load of the bolts. In addition, any reduction of the ratio of rivet shear to plate tension, necessitating more or larger rivets, or any increase of the coefficient of friction over the minimum of 0.25 previously mentioned, will increase the frictional resistance of a joint. Therefore, bolted structural joints that are assembled properly can be expected to perform at stresses at least as great as the normal working stresses without slipping into bearing.

Bolted Joints Subjected to Repeated Loads

Because high-strength bolts provide a joint in which the load is carried by friction rather than bearing, such joints are found to be extremely effective for members that are subjected to reversals of stress. There is little or no change in axial stress in the bolts of joints which are subjected to shear-type loadings and, consequently, the fatigue life of the bolts is especially great. This statement is strongly supported by the fact that to date no bolt failures have occurred in bolted joints in which the load is transferred by friction. It is important also to note that in no case have properly assembled high-strength bolts become loose even under the most severe loading conditions.

Several recent fatigue tests have been conducted in an attempt to obtain further information concerning the behavior of bolted joints that are subjected to repeated loads and in which the bolts are loaded in either shear or tension. The results of these studies have, in part, served as a basis for the recommendations of the Research Council for the proper procedures to be followed in the assembly of high-strength bolted structural joints and will be examined briefly in this paper.

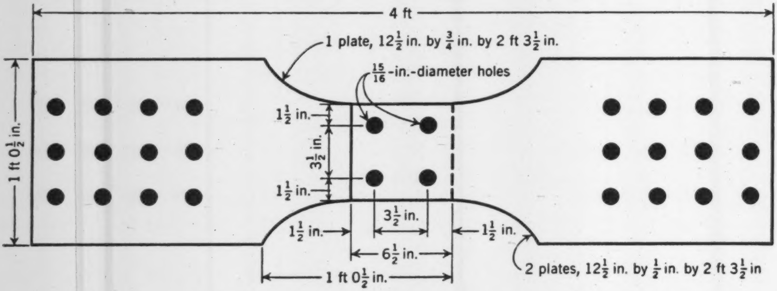

FIG. 1.—TEST SPECIMEN, BOS SERIES, FASTENED WITH ⅞-IN.-DIAMETER BOLTS AND CARBURIZED WASHERS

a. Bolts in Shear.—Because of the Research Council's recommendation that high-strength bolts be torqued to at least 90% of the elastic proof load, some engineers have been concerned with the possibility of over-torqueing the bolts. To alleviate these fears, a short series of fatigue tests was conducted on specimens of the type shown in Fig. 1, in which the bolts were tightened greatly beyond the elastic limit.

Prior to conducting these tests, it was found that, after the nut was hand tight, from two to three turns were still required in order to rupture the bolts in the specimen; one and one-half turns produced the maximum axial tension that could be developed in the bolts and also produced a reduction in the bolt area of approximately 10% as a result of plastic deformation during the torqueing.

TABLE 1.—FATIGUE TESTS OF JOINTS WITH OVERSTRESSED BOLTS

Specimen No.	Stress cycle on net section, in pounds per square inch	Number of cycles to failure of plates
BOS-1	±22,800	1,206,000
BOS-2[a]	0 to +30,000	2,130,000[b]
	±15,000	31,000[b]
	±20,000	2,168,000
BOS-3	±20,000	4,405,000
BOS-4	±20,000	2,083,000

[a] Coat of grease placed on contact surfaces before test. [b] Specimen did not fail. Cycle changed and test continued.

Four fatigue tests were conducted on specimens in which the bolts had been tensioned by rotating the nuts one and one-half turns. The results of these fatigue tests are presented in Table 1 and demonstrate that the bolts did not fail in fatigue, even under these unusually severe loading conditions.

The American Railway Engineering Association allows, in its specifications for steel railway bridges, a stress of ±12,000 lb per sq in. for members subjected to a complete reversal of stress. However, all the joints summarized in Table 1 withstood or would have withstood at least 2,000,000 cycles of loading in which the stress on the net section was ±20,000 lb per sq in. Similar riveted joints[5] when subjected to a stress of ±18,000 lb per sq in. withstood only approximately 600,000 cycles before failure. Thus, the large initial tension in the bolts is seen to be very effective in increasing the fatigue resistance of the connections.

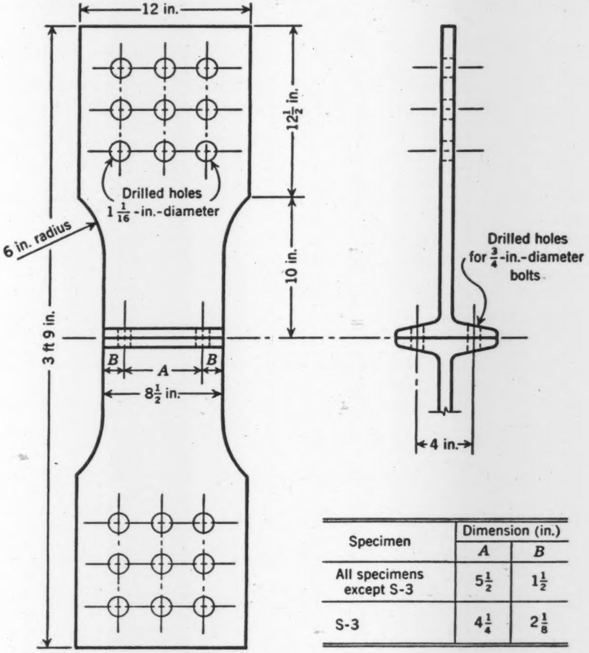

Specimen	Dimension (in.)	
	A	B
All specimens except S-3	5½	1½
S-3	4¼	2⅛

FIG. 2.—DETAILS OF TEST SPECIMENS FOR TENSION TESTS

These tests also help to demonstrate the desirability of having a high initial tension in the bolts to protect against slip. One of the members, specimen BOS–2, withstood more than 2,000,000 cycles of stressing to 30,000 lb per sq in. without slipping, in spite of the fact that this joint had been coated with a heavy grease before testing.

b. Bolts in Tension.—For many years, engineers have disagreed on the use of rivets and bolts in direct tension. Some have mistakenly reasoned that the tension in the fastener increases immediately upon application of an external load while others have stated that the tension does not change until the applied external load equals the total initial tension. Because of this difference of opinion and the extremely high initial tensions in the bolts of joints assembled with high-strength bolts, it was considered desirable to study the behavior of connections—such as the member in Fig. 2—in which the bolts are subjected to repeated direct tensile loads. In these repeated-load (fatigue) tests, studies have been made to determine the effect of initial bolt tension, in addition to other variables, on the behavior of the bolts.

The specimens for the direct-tension tests were fabricated from 24-in.-deep, I-sections. Four $\frac{3}{4}$-in.-diameter, high-strength bolts (ASTM–A 325) or four $\frac{3}{4}$-in.-diameter rivets (ASTM–A 141) were used to fasten the abutting flanges together. A beveled washer having a 1 on 6 slope (a slope equal to that of the I-beam flange) was placed under the head and nut of each bolt in all but two specimens. In these two specimens, a flat hardened washer was placed under the head of the bolt whereas a beveled washer was placed under the nut, thus causing the head of the bolt to bend through an angle of approximately 10° as it was torqued into position.

TABLE 2.—SUMMARY OF RESULTS OF FATIGUE TESTS OF BOLTS IN TENSION

Specimen No. (1)	Beveled washer under bolt head[a] (2)	Total prestress on four bolts,[b] in kips (3)	Total applied load, in kips (4)	Number of cycles prior to failure (5)	Maximum bolt stress in pounds per square inch (6)
F-1A	Yes	11.2	68.0	9,700	42,500
F-1B	Yes	11.2	53.0	13,400	39,600
F-2A1	Yes	68.0	102.4	1,040	82,300
F-2A2	Yes	68.0	102.4	5,400	94,900
F-2B	Yes	68.0	68.0	127,600	65,000
F-2C1	Yes	68.0	53.0	189,100	64,300
F-2C2	Yes	68.0	53.0	490,000	58,600
F-3A	Yes	102.4	102.4	10,800	102,600
F-3B1	Yes	102.4	68.0	389,400	88,200
F-3B2	Yes	102.4	68.0	115,600	90,400
F-3B3	Yes	102.4	68.0	188,900	89,500
F-3C	No	102.4	102.4	1,950	....
F-3D	No	102.4	68.0	13,500	....
F-3E	Yes	102.4	53.0	+2,271,600[c]	82,700
F-4A1	Yes	136.0	102.4	20,900	108,300
F-4A2	Yes	136.0	102.4	24,200	106,000
F-4B1	Yes	136.0	68.0	434,600	101,300
F-4B2	Yes	136.0	68.0	471,100	102,600
F-5A	Riveted	....	46.9	230,600	....
F-5B	Riveted	....	46.9	1,121,200	....
F-5C	Riveted	....	60.0	117,700	....

[a] Beveled washer under the nut on all bolts; no washers under rivet heads. [b] Bolt tensions were equal to 0.1, 0.6, 0.9 and 1.2 of the elastic proof load. [c] The specimen did not fail.

In the fatigue tests of the tension specimens, the behavior of the bolts was studied for various prestresses and applied loads. The prestress was varied between 0.1 and 1.2 times the elastic proof load, and the applied load was either 0.47, 0.6, or 0.9 times the elastic proof load of the bolts.

The results of the fatigue tests are presented in Table 2. In this table, the prestress is the nominal tension placed in the bolts before the fatigue tests were started. However, the actual tension in the bolts during the tests might have been somewhat less than this reported value because the bolts and washers tend to slide down the flanges. The range of applied external load was from zero to the total applied load listed in Col. 4, Table 2. Because the maximum stress in the bolts was not always proportional to this applied load, the maximum stress is also reported and is the stress on the effective bolt area (based on a diameter equal to the average of the pitch and root diameters) as determined by elongation measurements of the bolts. All the bolted specimens except specimen F-3E failed by rupture of one or more of the bolts. The straight bolts (beveled washers under the heads) failed in the threads at the face of the nut, whereas the bent bolts in the two specimens without beveled washers under the bolt head failed at the junction of the head and the shank.

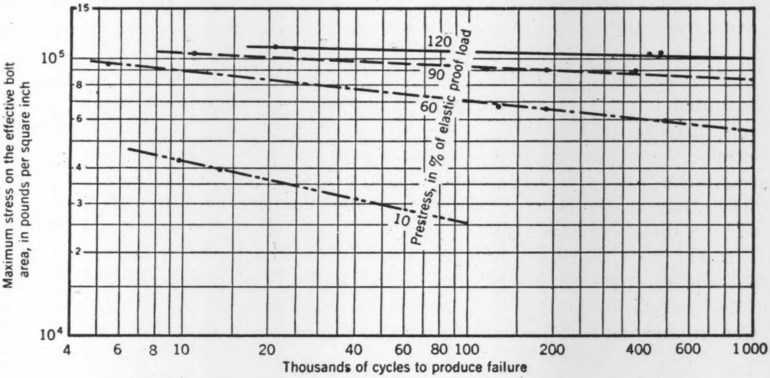

FIG. 3.—FOUR (*s*-*N*)-CURVES FOR BOLTS IN TENSION

The effect of the initial tension in the bolts is readily evident from a comparison of the results of the tests on specimens F-3E and F-1B. The maximum load applied to these specimens was the same. However, specimen F-1B failed after only 13,400 cycles of loading while specimen F-3E had not failed in more than 2,000,000 cycles of loading. Thus, the greater prestress in the F-3E specimen provided a large increase in the resistance of the bolts to repeated loads.

A more complete picture of the effect of the initial prestress may be obtained from the (*s*-*N*)-curves shown in Fig. 3. In this figure, the maximum stress on the effective bolt area has been plotted against the number of cycles required to produce failure; as the prestress is increased the bolts withstand increasingly larger maximum stresses for the same number of cycles to failure. The curves are not parallel but become successively flatter as the prestress is increased; thus, as the prestress increases the fatigue life becomes more sensitive to changes in maximum stress.

It may also be noted in the results of Table 2 that the fatigue life of the high-strength bolts was much greater than that of rivets tested under similar conditions. However, when the bolt head was caused to bend to the slope of the I-section flange, the fatigue life was greatly reduced; it is essential that the bending in bolts used in direct tension be kept to a minimum. It is also desirable that the bolts be installed in such a manner that the washers cannot slip down the sloping flanges as the members are loaded. If, for standard I-sections, the washers slip down the flanges, the bolts will lose some of their initial tension and, as a result, will be weaker under repeated loading conditions.

These tests, in addition to many others that have been reported previously, demonstrate the need for maintaining a high initial tension in the high-strength bolts. The loss of this tension permits a shear joint to slip at a much reduced level of tension, and in a joint in which the bolts carry tensile loading it provides a much lower resistance to fatigue-type loadings. In addition, the use of the high bolt tensions in no way endangers or reduces the strength of the bolts. On the contrary, those connections in which the bolts have been over-torqued have been found to be the most efficient.

BOLTED JOINTS SUBJECTED TO STATIC LOADS

Bolted joints that are designed in accordance with present recommendations provide for the substitution of a bolt for a rivet of equal diameter. Because the bolts are of high-strength material, any connection designed in accordance with the recommended practice will fail in the member itself rather than in the bolts. However, riveted connections often are found to fail by a shearing of the rivets.

In the tests that have been conducted on bolted joints, it has been found that the ultimate static strength of the connections is not affected by the initial tension in the bolts. However, as noted previously, both the fatigue strength and the resistance of the joint to slip depend greatly upon the clamping force of the bolts.

Several recent studies of connections fabricated with high-strength bolts are of interest in studying the strength and slip behavior of bolted joints. These studies have included tests of bolts both in shear and in tension.

a. Bolts in Shear.—Two groups of tests in which the bolts were subjected to shear will be described briefly. The first of these was a test of flat plates fabricated with bolts which were over-torqued, and the second group of tests constituted a study of the strength of bolted connections in large I-sections.

A specimen of the type shown in Fig. 1 and assembled with overstressed bolts was tested statically. This specimen, being of balanced design, had a net tensile area which was only three quarters as large as the shearing area of the fasteners. The bolts were torqued to one and one-half turns of the nut or approximately the maximum strength of the bolt material. With this extremely high initial tension in the bolts, the joint withstood a stress of approximately 27,000 lb per sq in. on the net section of the plates before slipping into bearing and an ultimate strength of 212,800 lb or 60,400 lb per sq in. It is apparent from these data that the bolt tension again did not affect the ultimate strength of the connection. However, the high bolt tension had a great retarding effect upon the slip of the connection and provided much frictional resistance.

The second group of static tests consisted of tensile tests of three large I-sections. One of the specimens was fabricated with hot-driven rivets whereas the other two were bolted. The general details of the specimens, designated S-1, S-2, and S-3, are shown in Fig. 4. Specimens S-1 and S-2 were fabricated with high-strength steel bolts. Specimen S-1 was assembled with hardened beveled washers between the heads of the bolts and the sloping faces of the I-beam flanges to provide parallel bearing surfaces for each bolt. However, for specimen S-2, only flat hardened washers were used. Consequently, as the bolts for specimen S-2 were torqued, the bolt shanks were bent through an angle of approximately 10° as the bolt heads were pulled into contact with the flat washers on the sloping faces of the flanges.

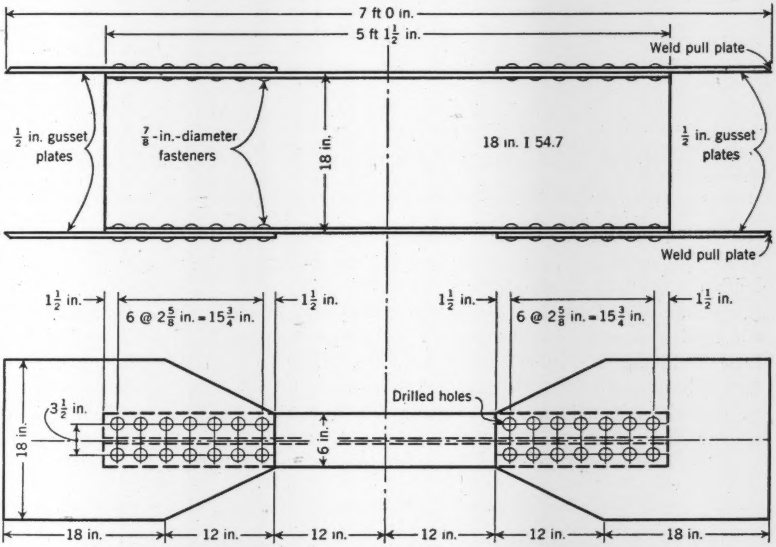
7 ft 0 in.
5 ft $1\frac{1}{2}$ in.
Weld pull plate
$\frac{1}{2}$ in. gusset plates
$\frac{7}{8}$-in.-diameter fasteners
18 in.
18 in. I 54.7
$\frac{1}{2}$ in. gusset plates
Weld pull plate
$1\frac{1}{2}$ in.
6 @ $2\frac{5}{8}$ in. = $15\frac{3}{4}$ in.
$1\frac{1}{2}$ in.
$1\frac{1}{2}$ in.
6 @ $2\frac{5}{8}$ in. = $15\frac{3}{4}$ in.
$1\frac{1}{2}$ in.
$3\frac{1}{2}$ in.
18 in.
6 in.
Drilled holes
18 in.
12 in.
12 in.
12 in.
12 in.
18 in.

Specimen	Fasteners
S-1	Bolted, beveled washers
S-2	Bolted, plain washers
S-3	Riveted

FIG. 4.—DETAILS OF TEST SPECIMENS FOR I-SECTION TESTS

The two bolted members slipped into bearing at loads of approximately 366,000 lb. This load corresponds to an average nominal shearing stress on the bolts of approximately 21,000 lb per sq in. and, based on the initial tension in the bolts, is equivalent to an apparent coefficient of friction of approximately 0.40. Apparently the frictional resistance developed in the long connections of these members was somewhat greater than has been developed in the smaller flat-plate joints reported in a number of other studies.

The results of the tests of the three large I-sections are briefly summarized in Table 3. It will be noted that the bolted members failed at loads of 798,000 lb and 808,000 lb and at a test efficiency of approximately 74%. The test efficiency is computed as the ultimate strength by test, divided by the theoretical strength of the gross section based on the coupon strength of the material. Both of these failures occurred through the net section of the I-beam. The riveted member, specimen S–3, failed by a shearing of the rivets in one connection at a load of 760,000 lb. After this initial shear failure, all the rivets in the connnection were removed and the joint was reassembled using high-strength bolts and beveled washers. The specimen was again loaded and failed by shearing of the rivets of the second connection at a maximum load of 818,000 lb. After bolting the second connection of the member, the load was again increased until the member failed in the net section at a load of 870,000 lb. This fracture load is considerably greater than that for the two bolted members. However, the material in the connection was subjected to considerable cold-working during the first two loadings when the rivets failed in shear and may have been increased in strength by these previous loadings.

TABLE 3.—STATIC TESTS OF I-SECTIONS

Specimen No.	Load at failure, in pounds	Test efficiency[a] (%)	Location of the fracture
S–1	798,000	73.9	Net section
S–2	808,000	74.9	Net section
S–3	760,000		Rivets[b]
	818,000		Rivets[c]
	870,000	80.6	Net section

[a] Theoretical efficiency equals 83.6%. [b] Failed by shearing of the rivets in one joint. All the rivets in this joint were replaced with bolts. [c] Failed by shearing of the rivets in the second joint. All rivets were replaced with bolts.

TABLE 4.—SUMMARY OF RESULTS OF STATIC TESTS ON BOLTS IN TENSION

Specimen No.	Beveled washer under the bolt head[a]	Total prestress on four bolts, in kips	Fastener spacing parallel to the web, in inches	Ultimate load, in pounds
S–1	Yes	11.2	5.5	157,300
S–2	Yes	102.4	5.5	154,200
S–3	Yes	102.4	4.25	152,700
S–4	No	102.4	5.5	163,800
S–4B	No	102.4	5.5	169,300
S–5	Riveted	....	5.5	120,100

[a] Beveled washer under the nut on all bolts; no washers under rivet heads.

The bolted joints with beveled washers did not produce greatly different results from those without washers. Some slight differences were noted in the manner in which the joints slipped into bearing; however, the ultimate strengths were almost the same.

b. Bolts in Tension.—In the discussion of the fatigue tests in which the bolts were loaded in tension, mention was made of the concern of engineers over the tensile loading of bolts which are under high initial tensions. Many of the questions that have been raised can be answered by means of the results of the static tests and fatigue tests conducted on the specimens shown in Fig. 2 and the results of other tests reported in the literature.[10]

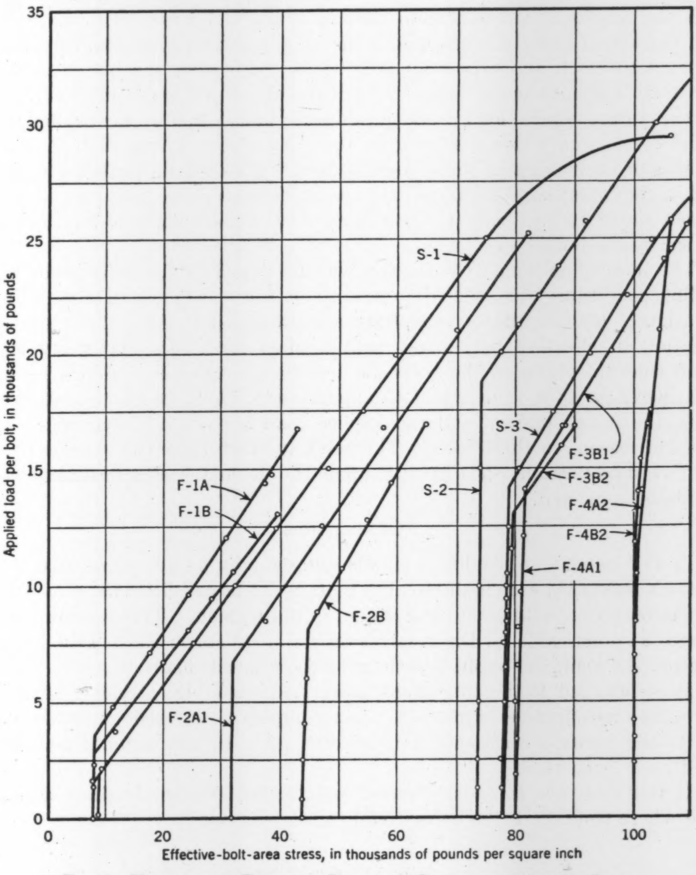

FIG. 5.—VARIATION IN EFFECTIVE BOLT-AREA STRESS WITH APPLIED LOAD

As a means of studying the behavior of bolts loaded in tension under static loading conditions, six static tests of members as shown in Fig. 2 were conducted and are summarized in Table 4. This table includes the results of tests on five bolted joints and on one riveted joint. The data show that decreasing the prestress from 0.9 to 0.1 of the elastic proof load (25.6 kips per bolt to 2.8 kips per bolt) caused little change in the ultimate strength of the bolts. Thus, the prestress in a bolt has little, if any, effect on its capacity for carrying static loads, as contrasted with its great effect upon its capacity for resisting repetitive loads.

---

[10] "Does Torque Weaken Bolts," by H. O. Hill, *Engineering News-Record*, July 24, 1947, p. 78.

One of the most significant observations was that the ultimate static tensile strength of the bolts was well below that which would have been computed from the results of direct tension tests of individual bolts. On the basis of such individual tests, the ultimate loads on these specimens could have been expected to reach approximately 187,000 lb. However, the bolted members withstood ultimate loads which were only about 85% of this load. This decrease in the applied load producing rupture was caused by the prying action in the connection which results from the compression forces that develop at the toes of the flanges as the fittings deform. This prying provides a greater load in the bolts than is applied externally. The ultimate load carried by the riveted specimen was only 120,000 lb, a value considerably lower than that carried by the bolted specimens.

The manner in which the tension was developed in the bolts under static loading conditions was studied in several of the specimens that were tested in fatigue. The results of this study are presented in Fig. 5 and show the variation in effective bolt stress with applied load. In this study it was found that the stress in the bolts did not change until the applied load had been increased to a value equal to approximately 60% of the initial tension. Thus, the initial tension and the applied load are not additive in the early stages of loading in these tests. The point at which these two stresses become additive doubtless depends greatly upon the geometry and flexibility of the members connected.

CONCLUSION

In this paper one condition stands out strongly as being essential if connections assembled with high-strength bolts are to be as efficient and economical as possible: The bolts must have a high initial tension. This tension must be as high as practicable for the greatest resistance to static and fatigue loadings, whether the loads are applied as shear loads or tensile loads.

It is believed that connections assembled with high-strength steel bolts will prove as effective or more so than comparable riveted joints, providing the bolted joints are assembled in accordance with the recommendations of the Research Council.

If the bolts are to resist direct-tension loads, beveled washers should be used where bending of the bolts would otherwise occur.

ACKNOWLEDGMENTS

The tests described herein constitute a part of the Structural Research Program in the Engineering Experiment Station at the University of Illinois under the general direction of N. M. Newmark, M. ASCE, and were sponsored by the Illinois Division of Highways, the Bureau of Public Roads (United States Department of Commerce), and the Research Council. J. R. Fuller and T. F. Leahey, research assistants in civil engineering at the University of Illinois, conducted the various laboratory tests discussed herein.

AMERICAN SOCIETY OF CIVIL ENGINEERS
Founded November 5, 1852
TRANSACTIONS

Paper No. 2840

GRAPHIC DESIGN OF ALLUVIAL CHANNELS

BY NING CHIEN,[1] A. M. ASCE

WITH DISCUSSION BY MESSRS. THOMAS BLENCH,
EMORY W. LANE, AND NING CHIEN

SYNOPSIS

The determination of channel depth and slope to conduct a specified unit discharge and sediment load is presented in graphical form on the basis of the Einstein bed-load function. Applications of these curves are made to evaluate the effects on river regimen by the diversion of flows, construction of dams, contraction of channels, elimination of river forks, and cutoff of bends. The deficiencies of knowledge in describing the canal flows and in determining the sediment supply to the canal systems still prevent the use of this method in designing irrigation canals.

INTRODUCTION

The design of alluvial channels to conduct a specified flow is one of the important problems in the field of hydraulic engineering. As early as the eighteenth century, Chezy developed a formula in which the depth and slope of the channel are related to the velocity of flow. As time passed, engineers realized that the problem is complicated by the fact that alluvial streams carry not only the water flow but also sediment of the same type as that which composes the bed. Erosion or deposition will occur if no proper provisions are made for the sediment flow and thereby changes the characteristics of the channel completely. The writer will attempt to show how one can utilize the results of sediment research to develop a more rational approach to the problem of alluvial-channel design.

The Problem.—The problem of alluvial-channel design can be stated as follows: For a specific bed material, what should be the width, depth, and slope of the channel to accommodate the specified discharge and sediment

---

NOTE.—Published, essentially as printed here, in February, 1955, as *Proceedings-Separate No. 611.* Positions and titles given are those in effect when the paper or discussion was approved for publication in *Transactions.*

[1] Associate Prof. of Hydraulics, Tsing Hwa Univ., Peiping, China.

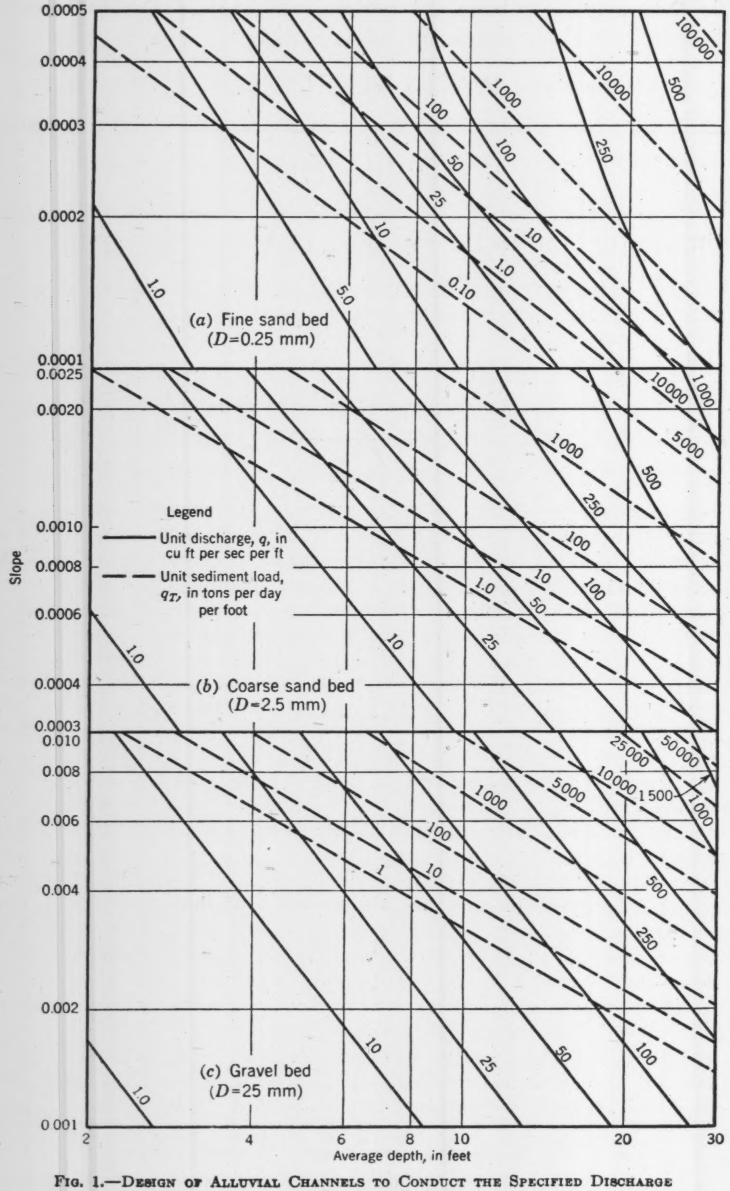

Fig. 1.—Design of Alluvial Channels to Conduct the Specified Discharge and Sediment Load

inflow? The sediment inflow and the discharge can be regarded as conditions, imposed on the channel by the watershed, which are independent of the channel itself. For a channel in equilibrium, there are two conditions to be satisfied, and three variables. This situation leaves one of the three variables undetermined according to the present state of knowledge.

It is to be noted that by the term "sediment inflow" the writer refers essentially to the bed-material load.[2] The wash load, despite the fact that it is often the major part of the sediment load and the deciding factor in the silting of reservoirs and lakes, plays only a minor role in the problem of channel stability. Indirectly, the presence of large quantities of wash load may be a determining factor in the use of permeable structures for construction works and regulating measures.

THE DESIGN CURVES

The design of alluvial channels is greatly facilitated by the use of a graphical presentation first suggested by J. P. Raynaud[3] in 1953. The theories developed by Hans A. Einstein,[4] M. ASCE, in describing the alluvial-channel flow and in relating the sediment transport rate to the flow conditions are used as the basis for the construction of the design curves. For illustrative purposes, the following simplifications are introduced so that the curves are of more general use: (*a*) Bank friction is neglected and (*b*) bed material is considered uniform in size. It is understood that, in the actual design, when there are not more than a few particular channels to be considered, one can always take all the local conditions into consideration and thereby construct more reliable curves.

Fig. 1 contains the design curves for the determination of the slope and depth with a particular discharge and sediment inflow—including both the suspended load and bed load—for channels of fine sand (grain size $D = 0.25$ mm), of coarse sand ($D = 2.5$ mm), and of gravel ($D = 25$ mm), respectively. The discharge and sediment inflow are expressed in terms of quantities per unit width of the channel, leaving unaccountable the effect of variation in width. These curves are applicable only for stages up to the bank-full stage.

The absence of width from the design curves is not as detrimental as it first appears. Plans on river improvements usually include some bank stabilization work, and the width of the channel can be chosen freely within limits. In nature, river channels may also be confined in canyons or the banks may be consolidated by the growth of vegetation. On the other hand, Gerald Lacey[5] claimed that the width, p, of a natural channel is related to the discharge, Q, by the following formula:

$$p = 2.67\, Q^{1/2} \quad \text{.......................} \quad (1)$$

---

[2] "The Laws of Sediment Transportation," by H. A. Einstein and J. W. Johnson, Chapter 3 of "Applied Sedimentation," edited by P. D. Trask, John Wiley & Sons, Inc., New York, N. Y., 1950, pp. 62–71.

[3] "Study of Saturated Rivers by Means of a Graphical Presentation," by J. P. Raynaud, *Proceedings*, Fourth Meeting of the International Assn. for Hydr. Research, Bombay, India, 1953, pp. 393–416.

[4] "The Bed-Load Function for Sediment Transportation in Open Channel Flows," by H. A. Einstein, *Technical Bulletin No. 1026*, U. S. Dept. of Agriculture, Washington, D. C. 1950.

[5] "Regime Flow in Incoherent Alluvium," by G. Lacey, *Publication No 20*, Central Board of Irrig., India, 1939.

Luna B. Leopold, A. M. ASCE, and Thomas Maddock,[6] M. ASCE, after analyzing many streams in the Great Plains and the southwestern United States, have come to the conclusion that (*a*) the relationship between channel width and discharge in Eq. 1 is valid only for the comparison of various cross sections at corresponding discharges; (*b*) the constant of proportionality in Eq. 1 is actually, among other things, a function of the bed material size; and (*c*) the channel width varies only with the 0.26 power of the discharge when considering the variation in a particular cross section of a river.

An examination of Fig. 1 indicates that, for a particular slope (or depth), the sediment transport rate increases considerably with a slight increase in depth (or slope). This implies that, in so far as the design of alluvial channels is concerned, considerable tolerance can be allowed in the determination of the sediment transport rate, a fact that should be welcomed by engineers who may have doubts concerning the reliability of existing sediment transport theories. Fig. 1 also shows that an increase in discharge results in a much larger increase in the capacity of the flow to transport sediment. This fact has considerable bearing on the planning of river works and will be made clear in the examples cited later.

Planning of River Works.—When planning river works the problem often is not the designing of new channels to carry the discharge and sediment load but rather the regulation and improvement of existing channels so that they will function properly. Any alteration of the channel naturally upsets the existing regimen of the river; it is very important to know how the channel adjusts its width, depth, and slope to achieve the new equilibrium. A comparison between the existing regimen and the future regimen will then reveal whether or not the plan serves its purposes. In this respect, design curves such as those in Fig. 1 are of great help. In the following material, hypothetical examples will be cited to illustrate how different engineering measures affect the characteristics of streams.

1. Diversion of Flow.—Flow is diverted from streams either to relieve downstream flooding or for irrigation and other domestic and industrial uses. A division of flow naturally induces certain changes downstream, and it is important to ascertain whether or not the changes will lead to adverse consequences. For instance, for several years part of the Mississippi River flow has been diverted to the sea through the Old River-Atchafalaya channel 320 miles upstream from its mouth. The latter channel is enlarging at an alarmingly rapid rate, and currently takes 23% of the Mississippi River flow. A control structure has been planned by the Corps of Engineers, United States Department of the Army, to be installed in the Old River. Unless this is done during the next 20 years, most of the flows will be diverted away from the lower Mississippi River, leaving the port of New Orleans (La.) somewhat isolated. A crisis of this kind arises essentially from an unfavorable division of the sediment load between the two channels, causing aggradation in one channel and degradation in the other. The amount of sediment drawn by the

---

[6] "The Hydraulic Geometry of Stream Channels and Some Physiographic Implications," by L. B. Leopold and Thomas Maddock, *Profession Paper No. 252*, Geological Survey, U. S. Dept. of the Interior, Washington, D. C., 1953.

branch channel depends greatly on the local conditions, the controlling factors of which have been clearly pointed out by Anthony R. Thomas,[7] M. ASCE. One must either control the division of flow according to the existing conditions or change the flow patterns at the point of diversion by engineering measures so that the resulting load division will cause neither erosion nor deposition downstream. In either case, the question to be answered is what division of the sediment supply for a specific division of flow will result in equilibrium flow at existing channel slopes. This can best be answered by plotting the sediment rating curves at constant slopes, several of which are presented in Fig. 2 for different channels. The smaller the slope of a curve, the larger the percentage of sediment load that must be diverted by the branch channel without upsetting the equilibrium of the main channel downstream.

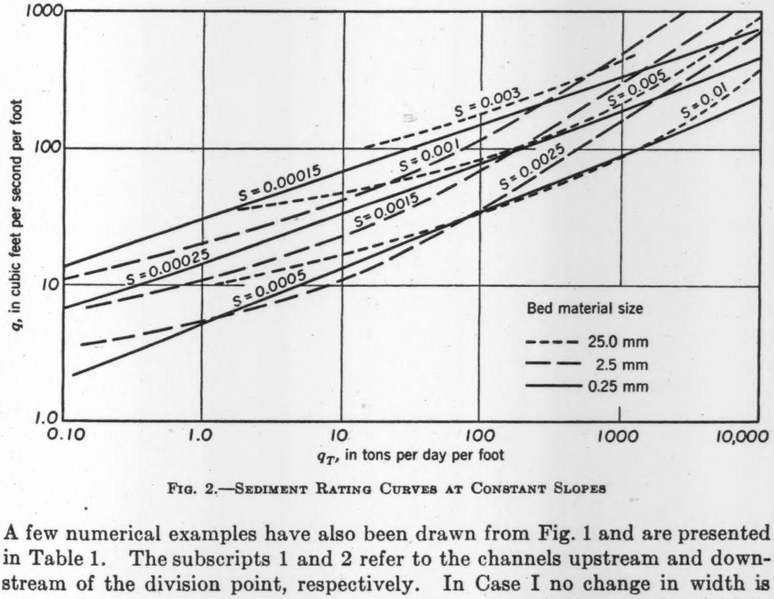

FIG. 2.—SEDIMENT RATING CURVES AT CONSTANT SLOPES

A few numerical examples have also been drawn from Fig. 1 and are presented in Table 1. The subscripts 1 and 2 refer to the channels upstream and downstream of the division point, respectively. In Case I no change in width is assumed to occur as the result of flow diversion, and in Case II the width is assumed to change in proportion to the 0.26th power of the discharge.

An examination of Fig. 2 and Table 1 reveals the following:

a. Because the slope of the sediment rating curves is smaller than 45°, the only circumstance under which the downstream channel will not aggrade is when the percentage of sediment load diverted is larger than the percentage of flow diversion.

b. For the conditions shown in Table 1, diversions of 50% and 25% of the flow require diversions of 65%–90% and 35%–75% of the sediment load,

---

[7] Discussion by A. R. Thomas of "Diversions from Alluvial Streams," by C. P. Lindner, *Transactions*, ASCE, Vol. 118, 1953, pp. 276–278.

TABLE 1.—EFFECT OF FLOW DIVERSIONS FOR THREE BED-MATERIAL SIZES

$\frac{Q_2}{Q_1}$, in %[a]	q_1, in cu ft per sec per ft	Slope, S	q_{T1}, in tons per day per ft	CASE I, B = CONSTANT			CASE II, $B \propto Q^{0.26}$		
				q_2, in cu ft per sec per ft	q_{T2}, in tons per day per ft	$\frac{Q_{T2}}{Q_{T1}}$, in %[b]	q_2, in cu ft per sec per ft	q_{T2}, in tons per day per ft	$\frac{Q_{T2}}{Q_{T1}}$, in %[b]
D = 0.25 mm									
50	100	0.00015	32	50	4	13.8	60	7	18.3
		0.00025	195		30	15.4		45	19.3
		0.00050	1,400		260	18.6		400	23.8
	250	0.00015	430	125	60	14.0	150	100	19.4
		0.00025	2,200		340	15.4		600	22.8
		0.00050	12,000		2,400	20.0		4,000	27.8
75	100	0.00015	32	75	14	42.8	80	16	46.4
		0.00025	195		88	45.1		100	47.5
		0.00050	1,400		700	50.0		800	53.0
	250	0.00015	430	187.5	190	44.2	200	250	53.9
		0.00025	2,200		1,000	45.5		1,300	54.8
		0.00050	12,000		6,200	51.8		7,000	54.2
D = 2.5 mm									
50	100	0.0010	75	50	17	22.0	60	25	27.8
		0.0015	180		54	30.0		80	37.1
		0.0025	495		168	33.9		250	42.1
	250	0.0010	340	125	110	32.3	150	150	36.8
		0.0015	740		250	33.8		350	39.5
		0.0025	2,000		690	34.5		1,000	41.8
75	100	0.0010	75	75	41	54.7	80	45	55.8
		0.0015	180		110	61.1		130	67.0
		0.0025	495		315	63.6		375	70.4
	250	0.0010	340	187.5	216	63.5	200	230	62.8
		0.0015	740		475	64.2		500	62.7
		0.0025	2,000		1,270	63.5		1,350	62.6
D = 25 mm									
50	100	0.003	13	50	...	...	60	1	5.2
		0.005	175		13	7.2		35	16.7
		0.010	1,350		285	21.1		450	27.8
	250	0.003	270	125	30	11.1	150	50	15.5
		0.005	1,350		305	22.6		475	29.4
		0.010	5,700		2,000	35.1		3,000	44.0
75	100	0.003	13	75	3	22.0	80	5	35.7
		0.005	175		70	40.0		100	53.0
		0.010	1,350		730	54.0		800	55.0
	250	0.003	270	187.5	118	43.7	200	140	48.1
		0.005	1,350		760	56.3		850	58.5
		0.010	5,700		3,800	66.7		4,500	73.2

[a] The ratio Q_2/Q_1 is the percentage of the original flow that enters the downstream channel; $(1 - Q_2/Q_1)$ is the percentage of flow that is diverted. [b] The ratio Q_{T2}/Q_{T1} is the percentage of the original bed-material load that is allowed to enter the downstream channel without changing the channel slope.

respectively, if the channel width remains constant. These percentages for the required diversion of sediment load are reduced to 60%–85% and 30%–55% if the channel width also varies with variation in $Q^{0.26}$.

c. The percentage of sediment load that must be diverted to satisfy the original equilibrium conditions of the channel (*i*) decreases with the slope and the discharge for the same bed-material size; (*ii*) increases with the bed-material size for small streams that carry little sediment load; and (*iii*) decreases as the bed-material size for large streams with heavy sediment loads.

2. Construction of Dams.—The changes in river regimen caused by the construction of dams across the river have received considerable attention in recent years. The completion of several large dams, including Hoover Dam (Arizona-Nevada) and Elephant Butte Dam (New Mexico), also offers a rare opportunity for close field observations. As a result, it has become common knowledge that damming a channel will induce aggradation upstream and degradation downstream, two of the immediate effects that can also be derived easily from Fig. 1. However, less obvious is the answer to the question of what the changes in river regimen will be below the junction of a sizable tributary downstream from the dam. The elimination of peak flows by the regulation of the reservoir greatly reduces the capacity of the channel to transport sediment. In fact, if the total annual discharge is released from the reservoir at a constant rate, the downstream channel may carry less than one tenth the sediment load that the same total annual discharge would carry if it flowed according to its natural pattern. Or, in other words, the building fo a dam upstream reduces both the sediment capacity and the sediment supply in the channel below the junction point, the net effect of which can only be determined by examining the design curves.

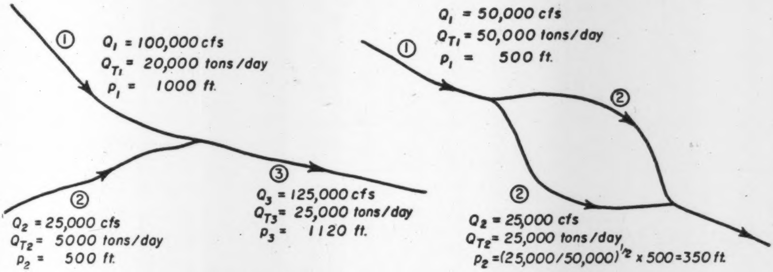
①
Q_1 = 100,000 cfs
Q_{T_1} = 20,000 tons/day
p_1 = 1000 ft.
②
Q_2 = 25,000 cfs
Q_{T_2} = 5000 tons/day
p_2 = 500 ft.
③
Q_3 = 125,000 cfs
Q_{T_3} = 25,000 tons/day
p_3 = 1120 ft.
Q_1 = 50,000 cfs
Q_{T_1} = 50,000 tons/day
p_1 = 500 ft.
①
②
②
Q_2 = 25,000 cfs
Q_{T_2} = 25,000 tons/day
$p_2 = (25{,}000/50{,}000)^{1/2} \times 500 = 350$ ft.

(*a*) Junction of Stream with Comparatively Large Tributary

(*b*) Flow at River Fork

FIG. 3.

For example, the junction of the two channels is considered, as shown in Fig. 3(*a*). Will the channel below the junction degrade or aggrade if the discharge from the main channel is reduced to 20,000 cu ft per sec by the regulation of a reservoir? Table 2(*a*) gives the characteristics of these three channels before the construction of the dam in channel 1 of Fig. 3(*a*). It can be seen that the slope of the channel below the junction is lower than that of either of the confluents, a fact substantiated by many field observations.[8] The slope of the main channel below the confluence wtih a sizable tributary is steeper than that above the junction only if (*a*) the tributary brings in sediment substantially coarser than that carried by the main stream, such as the increase in the Missouri River slope below the mouth of the Platte River; or (*b*) the tributary carries a disproportionately large sediment load with respect to its discharge, such as the steepening of the Rio Grande below the confluence of Rio Puerco. In Table 2(*b*) is indicated the change in channel characteristics after the completion of a dam in channel 1. Two cases are presented. In Case I the degradation below the dam has not yet been extended to the reach immediately above the junction so that the slope of the channel in that reach remains unchanged. In Case II the degradation below the dam has been completed, and channel 1 has become essentially nonalluvial in nature and carries almost no sediment. In both cases the channel below the junction is substantially accreted. This is also true for channels other than those cited in the foregoing example. It appears that the effect of reduction in peak discharge by the operation of the reservoir greatly outweighs the effect of a decrease in sediment supply, and one may regard the aggradation of the main channel downstream of the dam and below the junctions with tributaries as a condition common to many alluvial streams.

---

[8] "Concept of the Graded River," by J. Hoover Mackin, *Bulletin*, Geological Soc. of America, Vol. 59, 1948, pp. 463–512.

TABLE 2.—CHANNEL CHARACTERISTICS AT A JUNCTION OF A COMPAR

(*a*) BEFORE THE CONSTRUCTION OF A

Channel	Discharge, Q, in cubic feet per second	Sediment load, in tons per day	Width,[b] p, in feet	Unit discharge, in cubic feet per second per foot	Unit sediment load, in tons per day per foot
1	100,000	20,000	1,000	100	20
2	25,000	5,000[c]	500	50	10
3	125,000	25,000	1,120	112	22

(*b*) AFTER THE CONSTRUCTION OF A

Channel	Case	Discharge, Q', in cubic feet per second	Width, p', in feet	Unit discharge, in cubic feet per second per foot	$D = 0.25$ MM				
					Total sediment load[d]	Unit sediment load[e]	Slope, S'	Depth, d', in feet	$\frac{S'_3 - S_3}{S_3}$, in %[f]
1	I	20,000	658[g]	30.4	658	1.0	0.00014	12.5	...
	II				0	0	...	...	...
2	I, II	25,000	500	50.0	5,000	10.0	0.00020	10.7	...
3	I	45,000	858[g]	52.5	5,658	6.5	0.00016	13.5	23.1
	II				5,000	5.8	0.000155	14.0	19.2

[a] Change in slope of the main stream after the junction with a comparatively large tributary. [b] Width
Leopold and Maddock (1953): $d_2 \doteq (Q_2/Q_1)^{0.4} d_1$. [d] In tons per day. [e] In tons per day per foot. [f] Change
$(Q'_1/Q_1)^{0.26} p_1$ and $p'_3 = (Q'_3/Q_3)^{0.26} p_3$.

3. Contraction of the Channel.—One of the most common measures in increasing the navigable depth of a river is to confine the channel between jetties or training walls for limited or extensive reaches. A reduction in width produces a proportionate increase in the unit discharge and unit sediment supply; the effect of these factors on the channel characteristics can be derived from the design curves. Table 3 shows the changes in slope and water depth that occur if the channel is contracted by 50%. Subscripts in Table 3 denote conditions above and at the contraction. Generally speaking,

this results in an increase in depth of from 45%–80% and a decline in slope of from 15%–30%. Lorenz G. Straub,[9] M. ASCE, has developed a formula expressing the depth in the contracted section in terms of the flow conditions in the uncontracted section as follows:

$$d_2 = \frac{\dfrac{d_1}{(1-\alpha)^{3/7}}\left\{\dfrac{-T_o}{\gamma S_1} + \left[\left(\dfrac{T_o}{\gamma S_1}\right)^2 + \dfrac{4\,d_1\left(d_1 - \dfrac{T_o}{\gamma S_1}\right)}{1-\alpha}\right]^{1/2}\right\}^{3/7}}{\left[2\left(d_1 - \dfrac{T_o}{\gamma S_1}\right)\right]^{3/7}} \qquad \text{. . . (2)}$$

ATIVELY LARGE TRIBUTARY (SUBSCRIPTS DENOTE CHANNEL NUMBERS)

DAM IN THE UPSTREAM MAIN CHANNEL

D = 0.25 MM			D = 2.5 MM			D = 25 MM			Channel
Slope, S	Depth, d, in feet	$\frac{S_3 - S_1}{S_1}$, in %[b]	Slope, S	Depth, d, in feet	$\frac{S_3 - S_1}{S_1}$, in %[b]	Slope, S	Depth, d, in feet	$\frac{S_3 - S_1}{S_1}$, in %[b]	
0.00014	18.0	...	0.00068	16.8	...	0.00325	13.5	...	1
0.00020	10.7	...	0.00089	10.4	...	0.00477	7.6	...	2
0.00013	20.0	−7.15	0.00063	18.5	−7.35	0.00308	14.8	−5.23	3

DAM IN THE UPSTREAM MAIN CHANNEL

D = 2.5 MM					D = 25 MM					Channel
Total sediment load[d]	Unit sediment load[e]	Slope, S'	Depth, d', in feet	$\frac{S'_3 - S_3}{S_3}$, in %[f]	Total sediment load[d]	Unit sediment load[e]	Slope, S'	Depth, d', in feet	$\frac{S'_3 - S_3}{S_3}$, in %[f]	
526	0.8	0.00068	10.2	...	66	0.1	0.00325	7.5	...	1
0	0	...	...	...	0	0	...	...	...	
5,000	10.0	0.00089	10.4	...	5,000	10.0	0.00477	7.5	...	2
5,526	6.5	0.00079	11.6	25.4	5,066	5.9	0.00416	8.4	35.1	3
5,000	5.8	0.00078	11.7	23.8	5,000	5.8	0.00416	8.4	35.1	

$\propto Q^{1/2}$. [e] The sediment load carried by channel No. 2 is assumed to conform to the relationship of Messrs. in slope below the junction after the completion of a dam in the upstream main channel. [g] Width, p'_1 =

in which d_2 is the water depth at the contracted section; d_1 is the water depth at the uncontracted section; T_o is the critical tractive force; S_1 is the slope in the uncontracted section; γ is the unit weight of the water; and α is the amount of contraction, equal to $(p_1 - p_2)/p_1$, if p_1 and p_2 are the widths of the channel at the normal and contracted sections, respectively. For most of the streams, the critical tractive force is small and can be ignored, in which case Eq. 2 becomes

$$d_2 = \frac{d_1}{(1-\alpha)^{9/14}} \qquad \text{. . . . . (3)}$$

---

[9] "Effect of Channel Contraction Works Upon Regimen of Movable-Bed Streams," by L. G. Straub, *Transactions*, Am. Geophysics Union, Vol. 15, 1934, pp. 454–463.

and

$$\frac{d_2 - d_1}{d_1} = \frac{1}{(1 - \alpha)^{9/14} - 1} \qquad (4)$$

For 50% reduction of channel width, α equals 0.5; Eq. 4 indicates an increase in depth of 56%, a value which checks well with the results in Table 3.

TABLE 3.—EFFECT ON THE CHANNEL CHARACTERISTICS CAUSED BY CONTRACTING THE CHANNEL 50%

Slope, S_1	Value[a] of q_1	Value[b] of q_{T1}	d_1, in feet	Value[a] of q_2	Value[b] of q_{T2}	Slope, S_2	d_2, in feet	$\frac{S_2 - S_1}{S_1}$, in %	$\frac{d_2 - d_1}{d_1}$, in %
D = 0.25 mm									
0.002	12.5	0.4	6.75	25.0	0.8	0.000157	10.5	−21.5	55.6
	25.0	2.5	8.80	50.0	5.8	0.000150	13.9	−25.0	58.0
	50.0	12.5	10.75	100.0	25.0	0.000145	17.4	−27.5	61.8
	100.0	80.0	13.30	200.0	160.0	0.000140	21.0	−30.0	57.9
0.004	5.0	0.5	2.90	10.0	0.9	0.000300	4.6	−25.0	60.0
	12.5	4.0	3.90	25.0	8.0	0.000300	6.2	−25.0	59.0
	25.0	25.0	5.20	50.0	50.0	0.000310	7.7	−22.5	48.1
	50.0	125.0	6.50	100.0	250.0	0.000285	10.6	−28.7	63.1
	100.0	600.0	8.95	200.0	1,200.0	0.000230	16.5	−42.5	84.3
	200.0	4,000.0	13.30	400.0	8,000.0	0.000255	23.6	−36.2	77.5
D = 2.5 mm									
0.002	12.5	4.0	3.25	25.0	8.0	0.0014	5.7	−30.0	74.5
	25.0	25.0	4.50	50.0	50.0	0.0015	7.5	−25.0	66.7
	50.0	125.0	6.20	100.0	250.0	0.0017	9.2	−15.0	48.3
	100.0	350.0	8.45	200.0	700.0	0.00174	11.8	−13.0	41.3
	200.0	900.0	11.00	400.0	1,800.0	0.00165	17.2	−17.5	56.3
0.001	12.5	0.1	5.40	25.0	0.2	0.00073	8.6	−27.0	58.4
	25.0	2.0	7.00	50.0	4.0	0.00072	12.0	−28.0	71.5
	50.0	15.0	9.65	100.0	30.0	0.00077	15.4	−23.0	59.6
	100.0	65.0	12.80	200.0	130.0	0.00083	18.5	−17.0	44.5
	200.0	180.0	16.00	400.0	360.0	0.00075	26.0	−25.0	62.5
D = 25 mm									
0.003	50.0	0.2	9.90	100.0	0.4	0.0020	18.0	−33.3	81.8
	100.0	12.5	14.20	200.0	25.0	0.0022	23.1	−26.6	62.7
	200.0	140.0	19.30	400.0	280.0	0.0023	34.0	−23.3	76.2
0.006	25.0	1.5	4.70	50.0	3.0	0.0042	8.1	−30.0	72.3
	50.0	40.0	6.60	100.0	80.0	0.0041	11.7	−31.6	77.3
	100.0	300.0	9.30	200.0	600.0	0.0047	14.9	−21.6	60.2
	200.0	1,300.0	12.90	400.0	2,600.0	0.0047	20.8	−21.6	61.2

[a] In cubic feet per second per foot. [b] In tons per day per foot.

4. Closure of River Forks.—When a river flows in a divided channel the water depth in either of the channels is often insufficient for navigation at low water, and it is desirable to eliminate the forks. For example, it is assumed that half of the flow goes down each branch as shown in Fig. 3(*b*). Table 4 shows the channel characteristics of the river at the fork and in the undivided reach. The water depth in each branch is only 80% of the depth

in the single course if the flow is equally divided at the fork. O. Franzius[10] found the ratio of d_2/d_1 to be between 0.777 and 0.80 by making several assumptions concerning the hydraulics of the channel.

5. Cutoff.—When a stream flows in excessive meander loops, the water at high stages may take a shorter route across the narrow necks of overdeveloped bends. This natural process is often assisted by engineering measures to relieve the flood pressure upstream and, to a lesser degree, to facilitate the maneuvering of barge fleets. A cutoff of the bends means a shortening of the river course and, consequently, a local steepening of the channel. This local increase in slope will eventually be cancelled by lowering of the bed upstream and by raising of the river bottom downstream, as shown in Fig. 4(a). If the channel is subject to slow accretion, this step will be absorbed in the final adjustment of the profile, reducing the aggradation of the upstream

TABLE 4.—CHANNEL CHARACTERISTICS OF A RIVER AT THE FORK AND IN THE UNDIVIDED REACH

D (mm)	UNDIVIDED CHANNEL		CHANNELS AT THE FORK		$\frac{d_2}{d_1}$
	d_1 (ft)	S_1	d_2 (ft)	S_2	
0.25	12.7	0.000214	10.3	0.000250	0.81
2.5	11.8	0.00114	9.7	0.00126	0.82
25	11.3	0.00430	8.8	0.00500	0.78

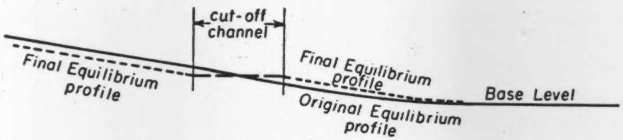
cut-off channel
Final Equilibrium profile
Final Equilibrium profile
Base Level
Original Equilibrium profile

(a) Original Channel in Regimen

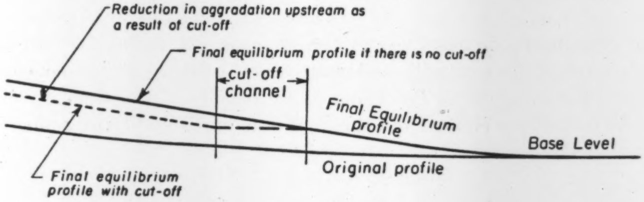
Reduction in aggradation upstream as a result of cut-off
Final equilibrium profile if there is no cut-off
cut-off channel
Final Equilibrium profile
Base Level
Original profile
Final equilibrium profile with cut-off

(b) Original Channel Subject to Slow Aggradation

FIG. 4.—EFFECTS OF CUTOFF ON RIVERS IN REGIMEN AND ON AGGRADING RIVERS

channel to a depth equal to the product of the length of the cutoff channel and the final equilibrium slope, as in Fig. 4(*b*). The reliance on cutoffs in reducing flood stages upstream, therefore, is only effective when the channel is being slowly aggraded or when the downstream aggradation causes no serious local damage.

---

[10] "Waterway Engineering," by O. Franzius, translated by L. G. Straub, Technology Press, Massachusetts Inst. of Technology, Cambridge, Mass., 1936, pp. 37–40.

The writer has demonstrated that valuable information on the interdependent effects of changes of the channel characteristics, the sediment supply, and the flow can be derived from proper use of the design curves. In addition to this, there are other complications that must be considered in order to obtain as complete a general picture as possible. Any change in conditions may lead to other changes, and thereby further complicate the final adjustment. For instance, lowering of the channel bed may increase the sediment inflow from tributaries as a result of the increase in slopes near their mouths.[11] There are also conditions peculiar to the particular stream under consideration. No two natural streams are exactly alike. Each has its own complex history and possesses certain features and irregularities not to be found in other similar drainage basins. For instance, the existence of gravel lenses or outcrops of rock in the bed may allow the bed to be scoured only to a certain extent, after which the flow is forced to widen the channel, which may not be the case without the lenses or outcrops. The slope may be adjusted as a result of the difference in channel filling or scouring between the upstream and downstream part of the reach or it may be achieved by the change in meander pattern, depending very much on the erodibility of the bank material. W. W. Rubey[12] has also explained that a change in regimen is liable to be counteracted by an adjustment in cross section in some cases and by modification of slope in others, depending on the historical background and physiographical and geological features of the watershed.

The design curves also do not aid in determining the time factor involved in planning the river works. In addition to the outcome of the regulating measures, it is equally important to know how long the river takes to reach its new equilibrium in response to the changes. A plan that will produce immediate relief but that will eventually allow a retreat to former conditions may nevertheless prove to be economically feasible if the time involved between the immediate change and the final outcome is sufficiently long.

DESIGN OF IRRIGATION CANALS

The design curves in Fig. 1 cannot be used for irrigation-canal design because of the lack of certain information. The difficulties are partly in the hydraulic description and partly in the determination of the sediment supply.

Irrigation canals are usually of a much smaller size than natural streams. The bank friction is a significant part of the total resistance. The intensity of bank friction depends greatly on the shape of the channel, thus making the construction of generalized design curves impossible. Also lacking are systematic studies on the factors that govern the additional resistance caused by the existance of sand bars and other irregularities at the bed surface of narrow channels. It has been found that the bar resistance in natural streams is a function of bed-load transport[13] and the functional relationship between the two has been incorporated in the preparation of Fig. 1. For more confined canal flows, this empirical relationship between the bed-load transport and the bar resistance appears to be somewhat different. There are also indications that other factors, such as the width of the channel, may also influence the flow. This deficiency of knowledge necessitates prototype measurements which must be analyzed on the basis of modern concepts of friction in open-channel flow.[14]

---

[11] Discussion by E. W. Lane of "Missouri River Slope and Sediment," by William Whipple, Jr., *Transactions*, ASCE, Vol. 107, 1942, pp. 1205–1211.

[12] "Geology and Mineral Resources of the Hardin and Brussels Quadrangles in Illinois," by W. W. Rubey, *Professional Paper 218*, U. S. Geological Survey, U. S. Dept. of the Interior, Washington, D. C., 1952.

The determination of sediment inflow in canals is rather complicated. In planning river works, the sediment supply to the reach under consideration can be calculated by applying the Einstein bed-load function to data obtained in the reach immediately upstream. The sediment inflow to the canal system, however, depends not only on the sediment load of the stream from which the water is diverted but also on the division of sediment load as the result of flow diversion. The latter differs considerably according to the local conditions; the data available are so meager that not even a "rule of thumb" can be made at present. This situation may be improved considerably if data on the division of sediment load under a variety of flow conditions can be collected either through direct field measurements of sediment load or by the application of the Einstein bed-load function to data from both the stream and the canal after the latter has become stable, and provided the bar resistance of canal flows has been properly described. In many irrigation systems, provisions have been made to eject the coarse material from the canal at, or close to, the canal entrance. Little is known as yet concerning the effectiveness of these ejectors. The distribution of fine sediment in a stream is generally more uniform than that of coarse sediment, and the division of these particles is probably proportional to the division of discharge at the canal entrance. In case the ejectors are proved to exclude all the coarse sediment so that the material drawn from the stream to the canal consists mainly of the fine particles, the foregoing relationship between sediment and discharge will permit the determination of sediment inflow to the canal system with ease. However, there is one further complication. The canal inflow doubtless carries with it its share of the wash-load material. Because the velocity in the canal is lower than that in the stream, part of the wash load may settle out in the canal and form a significant part of the bed. In other words, these fine particles which behave like wash load in the stream may behave like bed-material load in the canal, and their transport rate must also be included in the stability consideration. How much of this part of the load is diverted depends not only on the flow but also on the availability of the material from the upstream watershed. For a small watershed it may be possible to establish a rating curve of the wash-load material by a tedious sediment-load sampling program. This task becomes increasingly complex if the watershed is large, if the topography, soil, and vegetation vary considerably over the watershed area, and if the local rainfall patterns cover only part of the entire area. One does not need to know the sediment inflow very accurately, and perhaps complications like these can be ignored with only minor consequences; however, no experience in this matter has been recorded.

---

[13] "River Channel Roughness," by H. A. Einstein and Nicholas L. Barbarossa, *Transactions*, ASCE, Vol. 117, 1952, p. 1121.

[14] "Linearity of Friction in Open Channels," by H. A. Einstein and R. B. Banks, Assn. Internationale d'Hydrologie Scientifique, Assemblée Générale de Bruxelles, 1951, pp. 488–498.

DISCUSSION

Thomas Blench,[15] M. ASCE.—The design diagrams in Fig. 1 represent a remarkably bold extrapolation. The data on which they are based are from laboratory flume experiments with trifling discharges, unnatural uniform sediments, and poorly measurable slopes. The proposed field of application is enormous; for example, a channel whose discharge intensity is 50 cu ft per sec per ft, with average loam sides and bed material of size $D = 0.25$ mm in negligibly small quantities, would have a natural width of approximately 250 ft and a discharge of 12,500 cu ft per sec. It would also be approximately 13.6 ft deep, but Fig. 1(*a*) indicates that it would be 20 ft deep. If the data on which the diagrams are based were plotted thereon, they would lie either outside or in a small zone in the left-hand corner. Moreover, they would not be the original data, but the results of "removing the effect of the sides" by making the incorrect assumption that velocity is uniform over a section; a separation will then be performed based on the further assumption that the Manning equation applies to the rather peculiar parts into which the section is divided.[16]

Although there is no direct means of checking in the field the reliability of the load curves—bed load cannot be measured in the field—the formulas of regime theory[17,18,19] which fit the dimensions to which channels actually adjust in the field can be applied to verify whether the diagrams are functionally correct along loci of equal ratios of load to discharge. The writer includes details of such a check in his discussion of another paper by Mr. Chien[20] and is satisfied that the diagrams are functionally incorrect. Furthermore, from examples such as the foregoing in which the diagrams indicate depths of 20 ft as against nature's approximate depth of 13.6 ft, he is satisfied that Fig. 1 is factually too incorrect to be recommended for practical use.

The writer feels that the references to Mr. Lacey[5] and Messrs. Leopold and Maddock[6] are misleading and therefore attempts to put matters in a wider perspective. Mr. Lacey laid the quantitative basis of modern regime theory in the 1920's when he was placed on special duty by the government of the United Provinces of India for that purpose. Whatever views may be held about the theoretical aspect of the theory, its importance to the engineer is that the three fundamental formulas resulted from observations of the actual adjustments of canals in the field and so permit nature to be copied. Mr. Lacey's initial work is readily available.[21,22] His formulas were recommended for use in 1933 by the Central Board of Irrigation of the government of India.[23] No one has successfully assailed the functional correctness of the Lacey equations, but they have a defect that might be nontechnically stated as "averaging the relative importance of bed and sides." This defect arose from the nature of the data available and affected only the coefficients in the formulas. Practical engineers dealt with this secondary difficulty by various means, including the use of the formulas in a definite sequence. Claude C. Inglis, M. ASCE, described the situation by saying that all Lacey channels were regime channels but not all regime channels were Lacey channels. During the 1930's the Irrigation Research Institutes of India and various individual engineers made exhaustive field studies aimed at resolving the difficulty. Using the information they gathered, Cuthbert King of the Punjab Irrigation Service and the writer were able to suggest how to account for the bed and the sides separately. Their findings were published in 1941 and 1943;[24,25] they were confirmed in a later and more readily available publication.[26] These findings affected all three Lacey formulas; Eq. 1 was replaced by

---

[15] Prof. of Civ. Eng., Univ. of Alberta, Edmonton, Alta., Canada, and Cons. Engr.

[16] "The Present Status of Research on Sediment Transport," by Ning Chien, *Transactions*, ASCE, Vol. 121, 1956, p. 833.

[17] "Canals, Channels and Rivers," by T. Blench in "Civil Engineering Reference Book," Butterworths, London, 1951.

[18] "Hydraulics of Sediment-Bearing Canals and Rivers," by T. Blench, Evans Industries, Ltd., Vancouver, B. C., Canada, 1951.

[19] "Regime Theory for Self-Formed Sediment-Bearing Channels," by T. Blench, *Transactions*, ASCE, Vol. 117, 1952, p. 383.

[20] Discussion by T. Blench of "The Present Status of Research on Sediment Transport," by Ning Chien, *Transactions*, ASCE, Vol. 121, 1956, p. 869.

[21] "Stable Channels in Alluvium," by Gerald Lacey, *Proceedings*, Inst. of C. E., London, Vol. 229, 1930.

[22] "Uniform Flow in Alluvial Channels," by Gerald Lacey, *ibid.*, Vol. 239, 1933–1934.

$$b = \left(\frac{F_b Q}{F_s}\right)^{0.5} \qquad (5)$$

in which F_b and F_s depend on the nature of the bed and of the sides, respectively. World War II interrupted further work and publications. After the war, the writer attempted to apply further the valuable information obtained in Pakistan and India[17,27] and to continue to extend the results to apply to rivers.[28] The work of Messrs. Leopold and Maddock[6] was, so far as the writer knows, the first comprehensive scientific attempt to analyze actual river data and merits the closest study. These engineers have used their personal methods of analysis; however, the writer considers their work accomplishes with regard to rivers, what Mr. Lacey did in the case of canals. Their work agrees exactly with the functional correctness of Eq. 1, with discharge taken as the long-period arithmetic mean. Unfortunately, the author has cited a reference by Messrs. Leopold and Maddock to "variation in a particular cross-section of a river"[29] in a manner irrelevant to the context of their work to suggest they found an index of 0.26 for Eq. 1. Later in their book they have referred to "variation downstream" and have shown that they found the Lacey value of 0.5 instead of the erroneously quoted[30] 0.26.

---

[23] "Constitution of the Research Committee of the Central Board of Irrigation with Resolutions * * *," Central Board of Irrig., Simla, India, 1940.

[24] "Effect of Dynamic Shape on Lacey Relations," by T. Blench and C. King, *Proceedings*, Central Board of Irrig. Research Committee, India, Pbn. 27, 1941.

[25] "Practical Design Formulae for Stable Irrigation Channels," by C. King, *ibid.*, Pbn. 31, 1943.

[26] "Historical Note on Empirical Equations Developed by Engineers in India for Flow of Water and Sand in Alluvial Channels," by Claude Inglis, *Proceedings*, Second Meeting of the International Assn. for Hydr. Structures Research, Stockholm, 1948.

[27] "Practical Regime Theory Design of Artificial Channels with Self-Adjustable Boundaries," by T. Blench, presented at the ASCE Convention, St. Louis, Mo., June, 1955.

[28] "Regime Theory Equations Applied to a Tidal River Estuary," by T. Blench, *Proceedings*, International Hydraulics Convention, Minneapolis, Minn., 1953, p. 77.

[29] "The Hydraulic Geometry of Stream Channels and Some Physiographic Implications," by L. B. Leopold and Thomas Maddock, Jr., *Professional Paper No. 252*, Geological Survey, U. S. Dept. of the Interior, Washington, D. C., 1953, p. 9.

[30] *Ibid.*, p. 16.

Relative to the author's information on the Atchafalaya channel, the writer has also shown how simple regime formulas can be applied to explain occurrences.[31]

Recently, some investigations were made of small-flume data using regime-theory methods.[27,32,33] The basic data are readily amenable to this treatment. The writer's opinion is that the data require tremendous amplification by improved methods before there can be the least justification for extrapolation into the field of practice.

It is difficult to understand why the author expressed doubt concerning the application of his laboratory flume data to canals while being confident of their application to rivers that obey the same laws but are complicated by variations of discharge and by meandering; meandering can alter slope by at least 100%.

EMORY W. LANE,[34] M. ASCE.—The writer believes that the development of improved methods for solving sediment problems will involve learning to determine the flow and deposit of sediment quantitatively, just as engineers now study the flow and storage of water. Of course, the methods for handling sediment are much more difficult to devise than those for handling water, but rapid progress is being made and reasonably satisfactory quantitative solutions of many problems can be expected in the near future. Mr. Chien's paper is a valuable forward step in this advance. The author's examples show the way many problems can be solved by the application of the laws of sediment transport.

In nearly all sediment problems, at the present state of development of the science, highly exact answers cannot be secured. It is therefore probable that Mr. Chien's results are not highly accurate, but they are likely to be the most accurate that it is now possible to obtain.

In the paper as well as in his investigation of the Lacey regime theory,[35] Mr. Chien has discussed the problem of determining channel width but has not presented any method for selecting the width because he has concluded that it is not important. The writer does not share this view but rather believes that for artificial channels it is possible to compute the most favorable channel width. For natural streams it seems possible now only to list the most important factors that influence this width.

In order that an artificial channel in earth may be stable it must be free from scour and deposition. To be free from scour, the shear at all points of the bed and banks must be less than the value that will cause scour. To prevent deposition, the shear and resulting turbulence and secondary currents at all points must be great enough to prevent the deposition of sediment or, in other words, shear on the bed and banks must be of such magnitude and distribution that all the sediment entering the channel will be transported through it. The shape of the cross section and the longitudinal slope of the canal must be such that both of these requirements are met. Fulfilment of these conditions will fix the width of the channel. A method for designing channels which will satisfy these requirements has been developed by the Bureau of Reclamation, U. S. Department of the Interior. In the report on this method[36] the writer has discussed in only general terms the design of channels carrying heavy sediment loads and has not presented methods of computing the sediment load which would be carried under specific conditions; however, he gives in some detail methods of designing channels that will not scour on the banks. The author's diagrams appear to be a valuable aid in determining the conditions necessary to transport the sediment load required to prevent deposition.

---

[31] Discussion by T. Blench of "Diversions from Alluvial Streams," by C. P. Lindner, *Transactions*, ASCE, Vol. 118, 1953, pp. 270–272.

[32] "Bed-Load Transportation Formulas for Uniform Sediment in Uniform Flumes with Smooth Sides," by T. Blench, *Proceedings*, International Assn. for Hydr. Research, Delft (Netherlands), September Meeting, 1955.

[33] "Analysis of Bed-Load Data," by R. B. Erb, thesis presented to the University of Alberta, at Edmonton, Alta., Canada, in 1955, in partial fulfilment of the requirements for the degree of Master of Science.

[34] Hydr. Engr., Fort Collins, Colo.

[35] "A Concept of Lacey's Regime Theory," by Ning Chien, *Proceedings Paper No. 620*, ASCE, February, 1955.

The factors that influence natural stream width are numerous. If such a stream is in equilibrium, these factors are substantially constant, even though the stream channel may shift in places so that it occupies an entirely new position. This frequently happens in a meandering channel such as that of the lower Mississippi River. In this case the width of the channel is the result of a balance between the conditions which tend to widen the channel by cutting away the banks and those which tend to resist widening or tend to narrow it by building up the banks on the side of the stream opposite the places where bank scour is occurring. To keep the width the same, the building up of the banks must be at the same rate as the bank cutting; and the channel width of a stable stream is that width, which, under the existing conditions, will produce this balance. The conditions that tend toward a high rate of bank cutting are: (1) High discharge, great discharge variability, steep slopes, large depths, and great curvature of alinement; and (2) low resistance to widening due to the presence of noncohesive materials of small grain size and to a lack of vegetal growth. The principal conditions tending to produce resistance to widening constitute the resistivity of the bank material to scour and are the opposite of those listed under (2) as producing low resistance to widening. The principal factors promoting rapid building up of the banks are a high concentration and settling rate of the transported material and the tendency of this sediment to form cohesive material, as well as channel alinement such as to produce little shear and turbulence at those places that are favorable to the deposition of the transported material. There is considerable interdependence of the factors mentioned, and some are undoubtedly less important than others. The more accuracy required in determining the width, the larger the number of factors that must be considered. Some of the factors are difficult to express in quantitative terms. Under these conditions a formula for determining width of a natural stream with satisfactory accuracy will be particularly difficult to obtain, but a listing of the variables involved may help in reaching a solution.

The writer wishes to acknowledge the assistance of Maurice L. Albertson, M. ASCE, in preparing this discussion.

---

[36] "Design of Stable Channels," by Emory W. Lane, *Transactions*, ASCE, Vol. 120, 1955, p. 1234.

NING CHIEN,[37] A. M. ASCE.—Mr. Lane correctly stated that research on the determination of alluvial-channel width is urgently needed, and his outline of the factors involved in the problem should prove helpful in planning such a research program. The writer wishes to add another factor—the secondary current, which is believed to have an important effect on both the channel width and the meander pattern.

The writer has some difficulty in following the arguments presented by Mr. Blench. If the use of flume data to predict river conditions represents a "bold extrapolation," then, considering the differences between irrigation canals and rivers like the Missouri River or the Mississippi River, surely the "extrapolation" of the observations from canals to rivers is just as bold. The design diagrams presented by the writer were constructed according to the Einstein method which is derived from measurements covering a wide range of conditions, as follows: Slope, from 0.015% to 2.0%; particle size, from 0.8 mm to 30 mm; water depth, from 0.03 ft to 4 ft; discharge, from 0.0215 cu ft per sec per ft to 21.5 cu ft per sec per ft; specific gravity of sediment, from 1.05 to 4.2; and particle shape, from nearly spherical to flat and rectangular. The method has been checked by application to various rivers. Recent extension of the theory[38] also covered sediment mixtures with sizes varying between 4 mm and 0.005 mm and with a sorting coefficient as high as 2.5, which is higher than for most of the natural river sediment.[39] The use of lightweight material actually extends the ranges of flow conditions even more than those in the foregoing list according to any suitable model laws (including Mr. Blench's). In fact, the writer has conducted a special set of flume experiments for the Corps of Engineers by using lightweight material (specific gravity = 1.05) having the same gradation as Missouri River sand and by reproducing the Missouri River flows from low stages to floods according to the model laws. The results thus obtained follow quite closely the theories advanced by Mr. Einstein. Despite this, Mr. Blench claimed that all these data are either trifling in range, unnatural in material, or poorly measurable. On the other hand, the regime theory was developed in the Indian plains where the bed-material size varies[35] only from 0.05 mm to 0.38 mm.

The writer has assumed uniform material and has ignored the bank friction in constructing the design curves so that these curves would be sufficiently general to illustrate their various possible uses in aiding the planning of river control works. It has never been the writer's contention that Fig. 1 is the one and only set of curves to be used by every river engineer. In fact, he has specifically explained in the paper that one should take all the local conditions including the bank friction and the gradation of bed material into consideration and construct more reliable curves for the individual case using the same basic methods.

---

[37] Associate Prof. of Hydraulics, Tsing Hwa Univ., Peiping, China.

[38] "Transport of Sediment Mixtures with Large Ranges of Grain Sizes," by H. A. Einstein and Ning Chien, *Sediment Series No. 2*, Missouri River Div., Corps of Engrs., U. S. Dept. of the Army, Omaha, Nebr., 1953.

[39] Discussion by H. A. Einstein and Ning Chien of "Mechanics of Streams with Movable Beds of Fine Sand," by Norman H. Brooks, *Proceedings Paper No. 841*, ASCE, November, 1955.

A much more serious question raised by Mr. Blench's criticism is the following: Can engineers rely on flume data for predicting river conditions? The answer to this question depends on the types of information to be sought and also on the way the flume experiments are conducted. In the particular problem of sediment transportation, the basic mechanics of transport are studied on the basis of both actual observations and physical reasonings. Such a description on the basis of the forces which move the sediment actually involves studying the way it moves, the factors that control its rate of movement, and the mutual effect between the liquid and solid phase of the mixture; it is equally applicable to flumes and to rivers because most important dimensionless parameters have equal values in both scales. The transformation from theoretical considerations into practical engineering tools, however, involves the determination of certain constants or functions. This is accomplished by conducting flume studies, and the limitations imposed on the flumes naturally are also inherent in the results obtained through use of the flumes. The limitation on the range of flow conditions available in laboratories can partly be overcome by using as sediment lightweight material which moves more easily in the flow. On the other hand, it is obvious that meander patterns cannot be studied in a narrow channel. It has also been found that the bar resistance is not developed to its full effect in a narrow channel. Such deficiencies in flume data must be supplemented by using actual river measurements. Thus, Mr. Einstein and Nicholas L. Barbarossa,[13] A. M. ASCE, derived the bar-resistance effect from the river data and, for this reason, it cannot be used for narrow irrigation canals without certain modifications.

On the other hand, the flume flow, because of its confinement by two side walls, is affected more strongly by bank friction than are the natural river flows. Mr. Einstein has devised a method[40] to remove this bank effect from the over-all flow resistance. This method, incorrect as it may appear to Mr. Blench, has a physical basis.[14,41] It has also been verified repeatedly by independent measurements, such as those of A. M. Yassin[42] and the unpublished data obtained in 1953 by J. A. Kerr, and is now generally accepted as a standard procedure in analyzing flume data. Because this theory on sediment transport is not directly affected by the bank friction, its range of applicability is again greatly extended. Mr. Blench, however, preferred the use of original data which include the effect of bank friction. He has also stated[18] that in the Indian plains where the regime theory originated the banks behave hydraulically smooth. The question immediately arises as to whether the same theory which includes the effect of friction of smooth side walls can be applied to channels with rough banks. Again, Mr. Blench has never made this point clear in his writings.

Mr. Blench, from his experience with a single case, claimed that the Einstein method is wrong, both "functionally" and "factually." There are some questions to be considered before this challenge can withstand further scrutiny.

---

[40] "Formulas for the Transportation of Bed Load," by H. A. Einstein, *Transactions*, ASCE, Vol. 107, 1942, pp. 561-573.

[41] "Der Hydraulische oder Profil-Radius," by H. A. Einstein, *Schweizerische Bauzeitung*, Vol. 103, No. 8, February, 1934.

[42] "Mean Roughness Coefficient in Open Channels with Different Roughness of Bed and Side Walls," by A. M. Yassin, *Mitteilungen aus der Versuchsanstalt für Wasserbau und Erdbau*, Zurich, No. 27, 1953.

Mr. Blench admittedly has not determined the sediment transport rate in the canal which he used to test the proposed graph. It seems possible, therefore, that the sediment load in it was not as small as he assumed. If it actually was three times as large (including suspended bed material), the observed depth would have been obtained from the graph exactly. On the other hand, Mr. Blench evidently ignored many field measurements which essentially prove the reliability of the Einstein method in determining the sediment transport rate of natural river channels. In this respect the writer is in full agreement with Mr. Lane[43] that the greatest need in the sediment engineering field is extensive field measurement of the rate of sediment transport in channels under a wide range of conditions, against which the various theories may be thoroughly checked. Before this is done, the Einstein method because of its physical soundness and its coverage of a wide range of conditions is likely to be the best tool available to the field engineers.

---

[43] Discussion by E. W. Lane of "A Concept of Lacey's Regime Theory," by Ning Chien, *Proceedings, Paper No. 808*, ASCE, September, 1955.

AMERICAN SOCIETY OF CIVIL ENGINEERS
Founded November 5, 1852
TRANSACTIONS

Paper No. 2841

MULTIPLE-SPAN GABLED FRAMES

By John D. Griffiths,[1] M. ASCE

With Discussion by Messrs. Abdel F. Diwan, and John D. Griffiths

Synopsis

Methods available for the solution of multiple-span frames are characterized by extensive, excessively time-consuming operations. This paper is a presentation of a simplified procedure based on an analysis by parts, not requiring the solution of simultaneous equations. It may be extended to structures containing joints having three degrees of freedom.

Introduction

Multiple-span frames of the type shown in Fig. 1 have long been recognized as being efficient and economical and as providing a most acceptable architectural form. However, in spite of their many attributes, they have not been as widely popular as single-span frames. Their limited use has been due, in no small measure, to the complexity of their analysis and design.

In the paper the writer has outlined a procedure of analysis that has been found to be less laborious than methods commonly used. This procedure, an analysis by parts, does not require the solution of simultaneous equations, and reasonable accuracy of results may be obtained by slide-rule computation. The presentation of this material presupposes a knowledge on the part of the reader of the basic concepts and terminology of the method of moment distribution[2] of Hardy Cross, Hon. M. ASCE.

General Considerations

The great labor involved in the analysis of multiple-span gabled frames is due primarily to the difficult types of simultaneous equations that must be solved. Too often, the simultaneous equations that express joint translation

---

Note.—Published, essentially as printed here, in January, 1955, as *Proceedings-Separate No. 586*. Positions and titles given are those in effect when the paper or discussion was approved for publication in *Transactions*.

[1] Chf. Engr., Gate City Steel Inc., Boise, Idaho.

[2] "Continuous Frames of Reinforced Concrete," by Hardy Cross and N. D. Morgan, John Wiley & Sons, Inc., New York, N. Y., 1932.

(or sidesway) converge quite slowly. This lack of convergence of joint-translation equations is in contrast to the rapid convergence of equations which express only joint rotation. The latter type are readily solved by means of moment distribution or other procedures of iteration.[3]

A primary reason for the marked difference in the rates of convergence of the two types of equations can be realized from a consideration of moment and thrust carry-over factors. The moment carry-over factor is usually $\frac{1}{2}$, and, thus, each cycle of distribution reduces fixed-end moments remaining from the previous cycle by more than 50%. On the other hand, thrusts are carried over from one joint to the next at their full numerical value in order that ΣH may remain equal to zero. Therefore, the thrusts (associated with joint translations) tend to remain in the structure and will proceed toward the supports at only a slow rate under the "pressure" of a balancing procedure. This is particularly true in hinged-base gabled frames having relatively flexible columns.

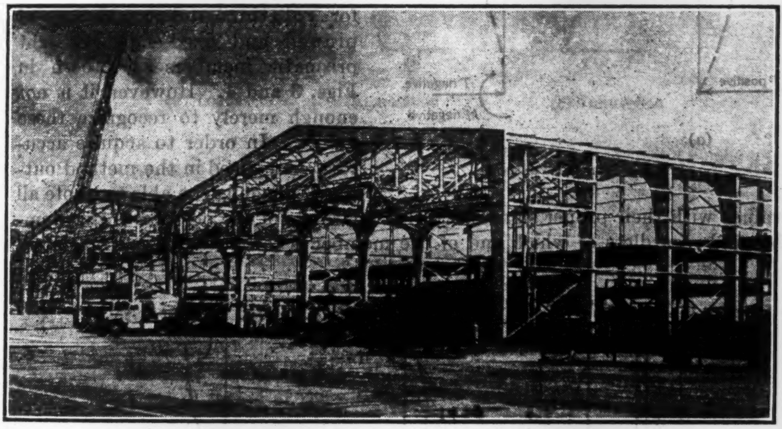

FIG. 1.—PHILADELPHIA INTERNATIONAL AIRPORT HANGARS

It is possible to "distribute" thrusts throughout a structure in a single operation by use of a spring analogy as discussed by A. J. Francis.[4] However, this operation can be used only for pure translation (without rotation). Therefore, this direct-thrust distribution produces new moments which must be distributed and which produce in turn new thrusts, and so on.

Equations that will yield a direct final solution must express combined joint-rotation and translation relationships. Unfortunately, these equations inherit much of the tendency for slow convergence from the expressions of pure translation. Such equations may result from a classical analysis such as slope deflection or from the sidesway correction operations of the method of moment distribution.

---

[3] "Analysis of Rigid Frames," by A. Amirikian, U. S. Govt. Printing Office, Washington, D. C., 1942.

[4] "The Analysis of Single-Storey Multi-Bay Gabled Rigid Frames," by A. J. Francis, *The Structura Engineer*, July, 1951, p. 189.

It is desirable to (1) eliminate the requirement for solution of complicated simultaneous equations and (2) avoid the necessity for successive cycles of moment-thrust distribution.

SIGN CONVENTION

The following sign convention (Fig. 2) will be used in this paper: Clockwise rotations are positive, clockwise moments are positive, translations to the right are positive, and thrusts to the right are positive.

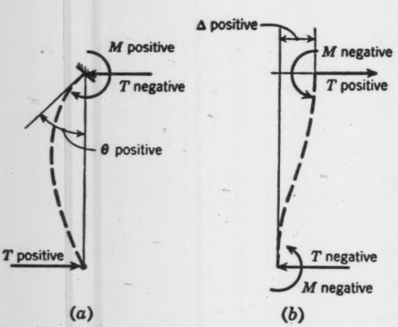
Δ positive
M positive
T negative
θ positive
T positive
M negative
T positive
T negative
M negative
(a)
(b)

FIG. 2.—SIGN CONVENTION

BASIC DATA

The reader, familiar with moment distribution, should recognize the values of moments and thrusts for rotation and translation of pinned and fixed-ended straight prismatic members as shown in Figs. 3 and 4. However, it is not enough merely to recognize these values. In order to acquire accuracy and speed in the method outlined, one must be able to quote all values with their proper signs instantly, regardless of the position of the member and regardless of which end of the member is to be rotated or translated.

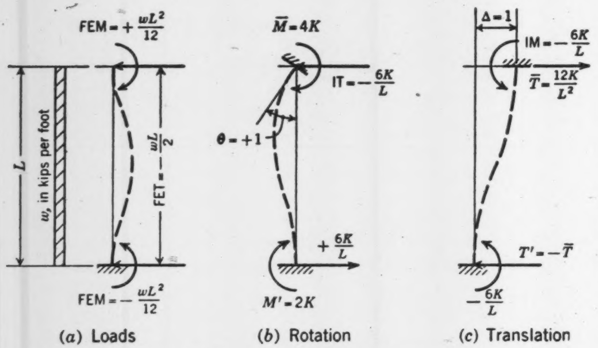
FEM = + $\frac{wL^2}{12}$
L
w, in kips per foot
FET = − $\frac{wL}{2}$
FEM = − $\frac{wL^2}{12}$
$\bar{M}$ = 4K
IT = − $\frac{6K}{L}$
θ = +1
+ $\frac{6K}{L}$
M' = 2K
Δ = 1
IM = − $\frac{6K}{L}$
$\bar{T}$ = $\frac{12K}{L^2}$
T' = −$\bar{T}$
− $\frac{6K}{L}$

(a) Loads (b) Rotation (c) Translation

FIG. 3.—FIXED-ENDED MEMBERS

If any term is not familiar to the reader, the derivation of that term should, of course, be reviewed in one of the standard textbooks on indeterminate structures.[5,6,7]

---

[5] "Statically Indeterminate Structures," by L. C. Maugh, John Wiley & Sons, Inc., New York, N. Y., 1946.

[6] "Theory of Modern Steel Structures," by Linton Grinter, The Macmillan Co., New York, N. Y., 1937.

[7] "Statically Indeterminate Structures," by Chu-Kia Wang, McGraw-Hill Book Co., New York, N. Y., 1953.

Because only relative values of rotation and translation are required, the term E has been omitted in Figs. 3 and 4. For exact values, each term associated with rotation and translation should be multiplied by E.

The following system of notation is used in Figs. 3 and 4:

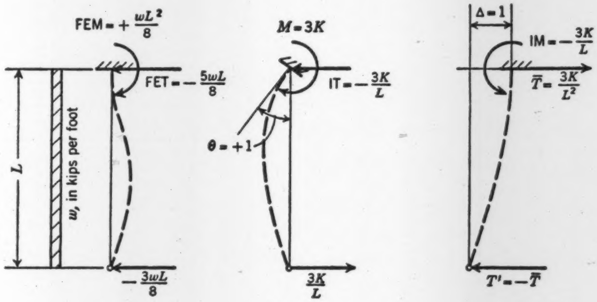

(*a*) Loads (*b*) Rotation (*c*) Translation

FIG. 4.—PINNED MEMBERS

F.E.M. = fixed-end moment;

F.E.T. = fixed-end thrust;

$\bar{M}$ = rotation stiffness;

M' = moment carried over to the far end of a member by a unit rotation of the near end;

I.T. = thrust induced by a unit rotation;

$\bar{T}$ = translation stiffness;

T' = thrust carried over to the far end of a member by a unit translation of the near end;

I.M. = moment induced by a unit translation;

I = moment of inertia;

$K = I/L$; and

w = load, in pounds per linear foot.

However, in the actual analysis of frames, all moments will be designated simply as M regardless of the cause for their existence. Likewise, all thrusts will be designated simply as T.

The values of I.T. and I.M. are statically determinate if the values for $\bar{M}$ and M' or $\bar{T}$ and T' are known. Also, for any member the values of I.M. and I.T. are numerically equal and of like sign. It has been shown by Alfred Niles, A. M. ASCE, and Joseph Newell[8] that such equality will always exist for any member or combination of members at a single joint, provided that the induced moments and induced thrusts result from unit rotations and unit translations.

---

[8] "Airplane Structures," by Alfred Niles and Joseph Newell, John Wiley & Sons, Inc., New York, N. Y., 1943, Vol. I.

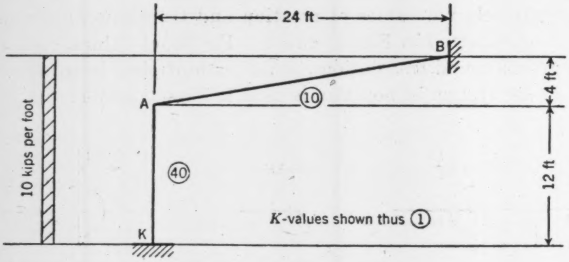

Line No.	Description	Joint A		Joint A		Joint B	
		θ	Δ	M, in kip-feet	T, in kips	M, in kip-feet	T, in kips
1	θ_{AK}			+160	−20		
2	θ_{AB}			+ 40		+20	
3	Total	+1.0		+200		+20	− 20
4	Loads, AK			+120	−60		
5	Loads, AB			− 13.3	−20	+13.3	− 20
6	Total			+107		+13.3	−100
7	Balance M	−0.535		−107		−10.7	+ 10.7
8	Loads, BK	−0.535		0		+ 2.6	− 89.3
9	θ_{BA}			+ 20		+40	
10	Balance M	−0.1		− 20		− 2	+ 2
11	θ_{BK}	−0.1		0		+38	+ 2
12	Δ_{BA}			− 20			+ 3.33
13	Balance M	+0.1		+ 20		+ 2	− 2
14	Δ_{BK}	+0.1		0		+ 2	+ 1.33

Structure BK

15	Description	M, in kip-feet	T, in kips	θ_A	Δ_A	θ_B	Δ_B
16	Loads, BK	+ 2.6	−89.3	−0.535	0		
17	+2 θ_{BK}	+76	+ 4	−0.2	0	+2[a]	
18	−3 Δ_{BK}	− 6	− 4	−0.3	−3		−3[a]
19	Total	+72.6	−89.3	−1.04	−3		

Member AK

20	Description	M, in kip-feet	T, in kips
21	Loads, AK	+120	−60
22	−1.04 θ_{AK}	−166	+20.8
23	−3 Δ_{AK}	+ 60	−10
24	Total	+ 14	−49.2

[a] Assumed movements of joint B due to forces not indicated in the sketch.

Fig. 5.—Solution of Example No. 1

Example No. 1

Fig. 5 provides an analysis, in tabular form, of a two-member frame. This frame will subsequently be considered as a part of a more complex structure. A detailed description of the analysis follows:

Step 1, Line 1.—Moments and thrusts associated with a positive unit rotation (θ_{AK}) of end A of member AK are recorded. The moment at A is

$\bar{M} = 4K = 4 \times 40 = 160$ kip-ft. The thrust at A is I.T. $= -6K/L = -6 \times 40/12 = -20$ kips.

Step 2, Line 2.—Moments associated with a positive unit rotation of end A of member AB are recorded. The moments are $\bar{M} = 4K = 4 \times 10 = 40$ ft-kips at A and $M' = 2K = 2 \times 10 = 20$ ft-kips at B. The thrusts at A and B due to this rotation of A will be equal and opposite ($\Sigma H = 0$). Therefore, their combined effect on the frame reactions and on frame deformations is zero (deformations due to direct stress are disregarded). For these reasons, the thrust values associated with this operation are not required and are therefore not recorded in the tabular solution.

Step 3, Line 3.—Lines 1 and 2 are added to determine the moments and thrusts for a unit rotation of joint A. On the basis of the same reasoning as outlined under Step 2, the thrust of −20 kips at A is transferred directly to B. The frame reactions and deformations are unaffected thereby.

Step 4, Lines 4, 5, and 6.—The F.E.M. and F.E.T. due to loads are recorded for each individual member, and these values are added to determine the total F.E.M. and F.E.T. In the addition (line 6), the thrust at A (−80 kips) is again transferred directly to B.

Step 5, Line 7.—The F.E.M. at A (107 ft-kips) is balanced by the application of an equal and opposite moment. Obviously, if +200 ft-kips (line 3) is associated with a rotation at A of +1.0 units, a moment of −107 ft-kips will be associated with a rotation of $-107/200 = -0.535$ units. All the figures on line 3 are therefore multiplied by −0.535, and the results are recorded on line 7.

Step 6, Line 8.—Lines 6 and 7 are added. If frame BAK were not to be subsequently considered as a part of a larger structure, line 8 would complete the analysis.

It has thus been determined that, under the specified loads, joint A will rotate −0.535 units (relatively), and the reactions at B will be $M = +2.6$ ft-kips and $T = -89.3$ kips. These values of moment and thrust may be considered as values of F.E.M. and F.E.T. for member BK on the basis of the assumption that the frame BAK acts as a single member with joint A eliminated, or at least temporarily disregarded.

If BK is a part of a more complex frame that extends beyond joint B, it will be desirable to determine its rotation and translation stiffness at joint B. This can be done as follows:

Step 7, Line 9.—Moments associated with a unit rotation of joint B are recorded. As indicated under Step 2, it is not necessary to record thrusts in this case.

Step 8, Lines 10 and 11.—Moments at A are balanced as outlined under Steps 5 and 6. The moment of +38 ft-kips is the moment stiffness of BK (that is, it is the moment associated with a unit rotation of BK, joint A being relaxed). The thrust of +2 kips is the induced thrust for BK.

Step 9, Lines 12 Through 14.—As joint B is translated one unit (without vertical movement of that joint and without rotation of joint A), no bending deformation occurs in member BA. Also, the entire thrust applied at B is transmitted to A. Therefore, the thrust required for unit translation of joint B is equal to the thrust required for unit translation of end A of the member AK. The moments and thrust associated with this translation are recorded and joint A is balanced in accordance with procedures previously outlined. The translation stiffness (+1.33 kips) and the induced moment (+2.0 kip-ft) for BK have thus been determined.

The total end moment for any member of a structure will always be the sum of the following three values: (1) The original fixed-end moment, (2) the moment due to joint rotations, and (3) the moment due to joint translations. Let it be assumed that joint B, because of action of the frame extending beyond that joint, is rotated +2 units and translated −3 units. The total moments in the frame will be determined on the basis of this arbitrary assumption.

Step 10, Lines 15 Through 24.—Fig. 5 provides the following values for BK: F.E.M. (or loads BK) = + 2.6 (line 8), rotation stiffness = + 38 (line 11), and I.M. = + 2 (line 14). Therefore,

$$M_{BK} = +2.6 + 2 \times 38 - 3 \times 2 = +72.6 \text{ ft-kips.}$$

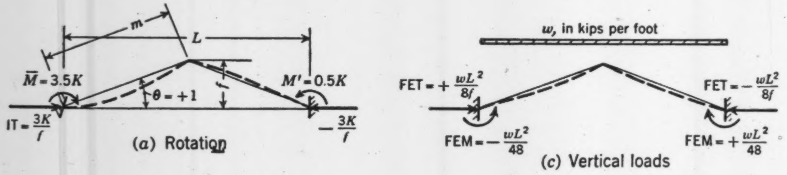
m
L
$\bar{M} = 3.5K$
$M' = 0.5K$
$\theta = +1$
$IT = \frac{3K}{f}$
$-\frac{3K}{f}$
w, in kips per foot
$FET = +\frac{wL^2}{8f}$
$FET = -\frac{wL^2}{8f}$
$FEM = -\frac{wL^2}{48}$
$FEM = +\frac{wL^2}{48}$

(*a*) Rotation (*c*) Vertical loads

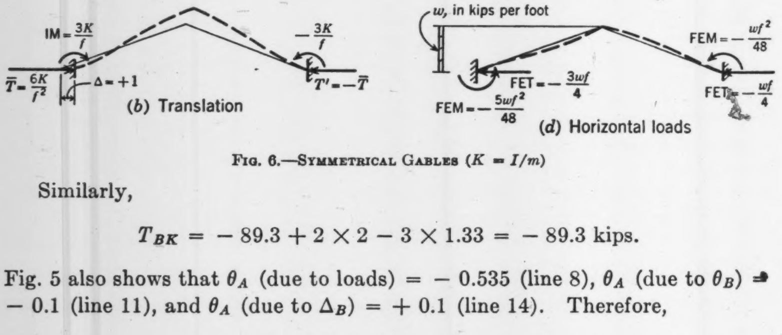
$IM = \frac{3K}{f}$
$-\frac{3K}{f}$
$\bar{T} = \frac{6K}{f^2}$
$\Delta = +1$
$T' = -\bar{T}$
w, in kips per foot
$FEM = -\frac{wf^2}{48}$
$FET = -\frac{3wf}{4}$
$FET = -\frac{wf}{4}$
$FEM = -\frac{5wf^2}{48}$

(*b*) Translation (*d*) Horizontal loads

FIG. 6.—SYMMETRICAL GABLES ($K = I/m$)

Similarly,

$$T_{BK} = -89.3 + 2 \times 2 - 3 \times 1.33 = -89.3 \text{ kips.}$$

Fig. 5 also shows that θ_A (due to loads) = − 0.535 (line 8), θ_A (due to θ_B) = − 0.1 (line 11), and θ_A (due to Δ_B) = + 0.1 (line 14). Therefore,

$$\theta_A = -0.535 - 2 \times 0.1 - 3 \times 0.1 = -1.04.$$

The translation of joint A is equal to the translation of joint B ($\Delta_A = -3$). Fig. 5 provides the following values for AK: F.E.M. = + 120 (line 4), rotation stiffness = + 160 (line 1), and I.M. = − 20 (line 12). Therefore,

$$M_{AK} = +120 - 1.04 \times 160 + 3 \times 20 = +14 \text{ ft-kips.}$$

Similarly,

$$T_{AK} = -60 + 1.04 \times 20 - 3 \times 3.33 = -49.2 \text{ kips.}$$

With the foregoing moments and thrusts determined, all other moments and reactions of the frame may be determined using statics. It would be well for the reader, at this stage, to review the foregoing description until he is able to set down the tabulation of Fig. 5 without reference to written material and without the use of scratch paper.

SYMMETRICAL GABLES

Fig. 6 provides general values of stiffness and other quantities for symmetrical gables. The derivation of these values is outlined in the Appendix.

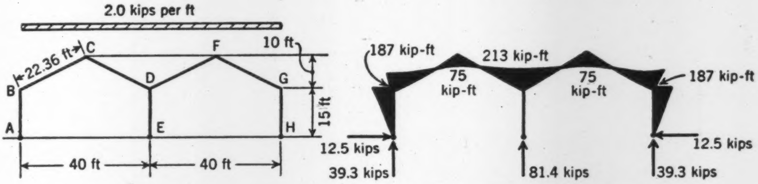

(*a*) Loaded structure

(*b*) Final moments and reactions

Description	JOINT B		JOINT B		JOINT D	
	θ	Δ	M, in kip-feet	T, in kips	M, in kip-feet	T, in kips
θ_{BA}			+200	−13.3		
θ_{BD}			+157	+13.4	− 22.4	−13.4
Total	+1.0		+357	0	− 22.4	−13.4
Δ_{BA}			− 13.3	+ 0.89		
Δ_{BD}			+ 13.4	+ 2.68	− 13.4	− 2.68
Total		+ 1.0	0	+ 3.57	− 13.4	− 2.68
Loads, DB			− 66.7	+40	+ 66.7	−40
Balance M	+0.187		+ 66.7	0	− 4.2	− 2.5
Balance T		−11.2	0	−40	+150	+30
Loads, DA	+0.187	−11.2	0	0	+213	−12.5

FIG. 7.—SOLUTION OF EXAMPLE NO. 2 (ALL *I*-VALUES EQUAL 1,000 IN.^{4})

EXAMPLE NO. 2

The frame of Fig. 7 has also been analyzed by Martin Korn,[9] M. ASCE, by the method of work. The moment and reaction values determined in Fig. 7 agree (within less than 1%) with the work solution. This frame is of such proportions that a rotation of joint B does not result in an induced thrust at that joint. Because of symmetry of frame and loading, no rotation or translation of the center joint B will occur. These conditions, of course, simplify the required solution. The computations indicated in Fig. 7 are in accordance with the principles described for Example No. 1. The reader should be able to reproduce the data of Fig. 7 without reference to any written material except Fig. 6 and without the use of scratch paper except for computations of statics required for the final moment diagram.

---

[9] "Steel Rigid Frames," by Martin Korn, J. W. Edwards, Inc., Ann Arbor, Mich., 1953.

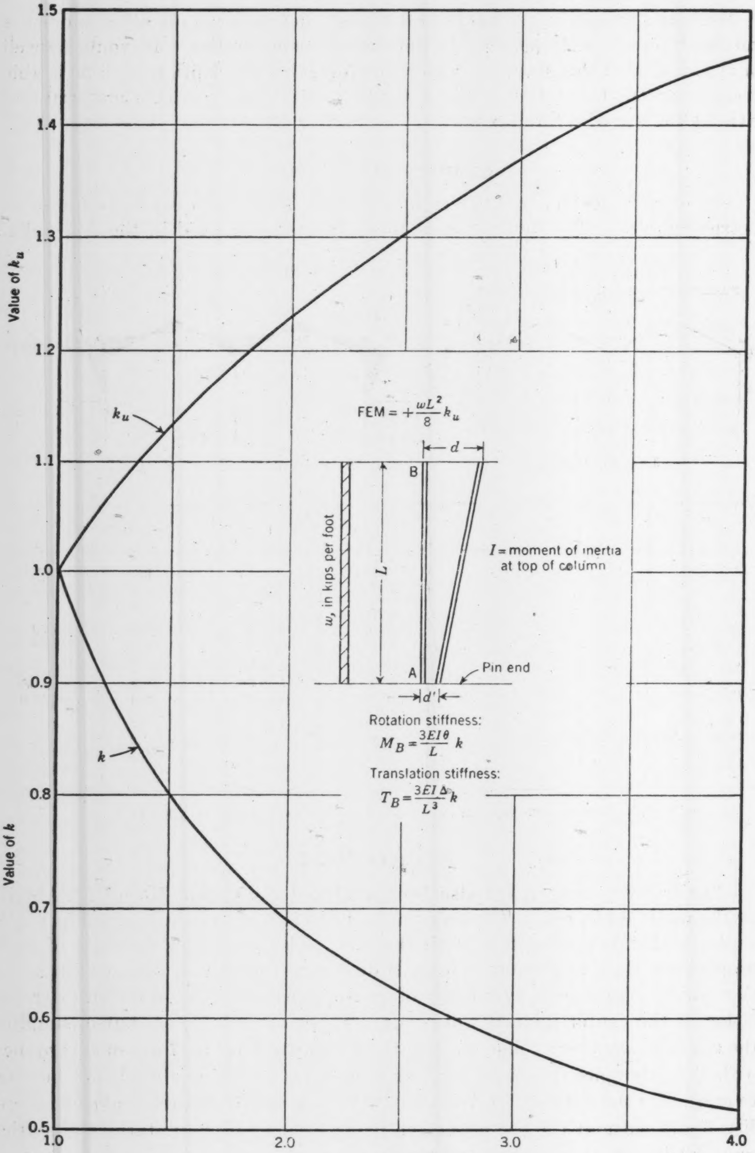

FIG. 8.—FACTORS FOR TAPERED PINNED MEMBERS

VARIABLE-DEPTH MEMBERS

It is generally economical to reinforce the frame members at the juncture of columns and gables by the use of a straight haunch or a curved haunch. The deepened section thus provided will cause increased moment at the haunch. For a haunched knee of unusual proportions, the computed value of such a moment increase will rarely exceed 5%. The actual moment increase may be even less than that computed because of the nonuniform stress distribution across the knee. An investigation of a curved knee frame at Lehigh University[10] at Bethlehem, Pa., indicated a reduction of approximately 3.5% from the calculated knee moment because of the shift of the neutral axis toward the inner flange.

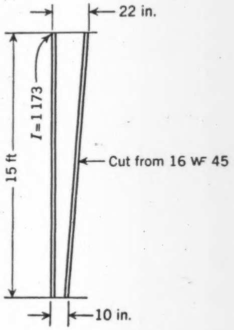

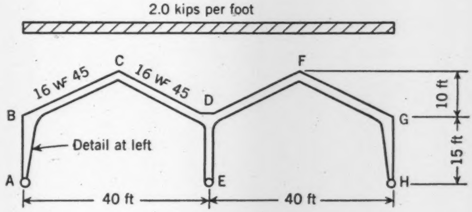

$$\frac{d}{d'} = 2.2$$

$$\theta_{BA}: M = \frac{3 \times 1\,173}{13} \times 0.67 = 157 \text{ units}$$

$$\Delta_{BA}: T = \frac{3 \times 1\,173}{15^3} \times 0.67 = 0.699$$

Line No.	Description	JOINT B		JOINT B		JOINT D	
		θ	Δ	M, in kip-feet	T, in kips	M, in kip-feet	T, in kips
1	θ_{BA}			+157	−10.5		
2	θ_{BD}			+ 91	+ 7.83	− 13.0	− 7.83
3	Total	+1.0		+248	− 2.67	− 13.0	− 7.83
4	Δ_{BA}			− 10.5	+ 0.699		
5	Δ_{BD}			+ 7.83	+ 1.57	− 7.83	− 1.57
6	Total		+ 1.0	− 2.67	+ 2.27	− 7.83	− 1.57
7	Balance M	+0.0108		+ 2.67	− 0.03	− 0.14	− 0.08
8		+0.0108	+ 1.0	0	+ 2.24	− 7.97	− 1.65
9	Loads, DB			− 66.7	+40	+ 66.7	−40
10	Balance M	+0.269		+ 66.7	− 0.72	− 3.5	− 2.1
11	Balance T	−0.189	−17.5	0	−39.3	+139	+28.9
12	Loads, DA	+0.080	−17.5	0	0	+202	+13.0

FIG. 9.—SOLUTION OF EXAMPLE NO. 3

Some engineers neglect entirely the effect of a haunch; others neglect the haunch during analysis but, for design purposes, arbitrarily increase the uniform-section knee moments[11] by from 3% to 5%. In any case, it is generally agreed that an exact analysis of the effect of a typically proportioned haunch is rarely, if ever, justified.

---

[10] "An Investigation of Steel Rigid Frames," by Inge Lyse and W. E. Black, *Transactions*, ASCE, Vol. 107, 1942, p. 127.

[11] "Single Span Rigid Frames in Steel," by John D. Griffiths, A.I.S.C., 1948.

The foregoing observation regarding haunches of usual proportion does not necessarily apply to the case of tapered members. A large variation in the moment of inertia extending over a considerable portion of the frame may materially affect the distribution of moment and thrust. Fig. 8 provides factors for the rotation and translation stiffness of pinned tapered sections. The curves shown are based on the assumption that I for a WF-section varies as $d^{2.3}$.

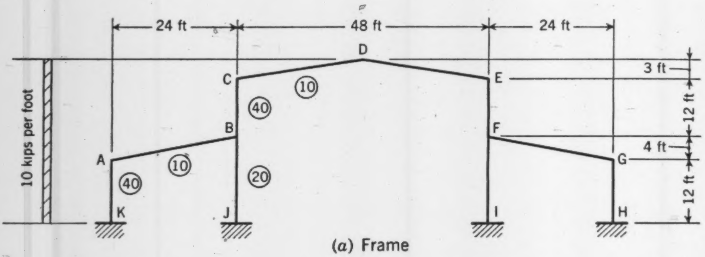

(*a*) Frame

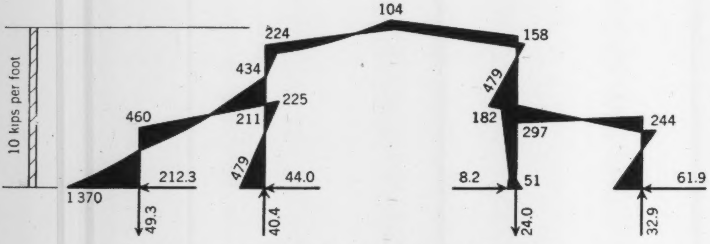

(*b*) Moments in foot-kips and thrusts in kips

FIG. 10.—EXAMPLE NO. 5

EXAMPLE NO. 3

The frame of Example No. 2 has been re-analyzed in Fig. 9 on the basis of tapered columns. It will be noted that the horizontal reactions at B and G are increased from 12.5 kips for straight columns to 13.0 kips for the tapered columns. This is an increase of only 4% for this particular condition of frame geometry and loading.

All computations for the tabular analysis of Fig. 9 are in accordance wit steps previously outlined. The values in line 8 were determined from line 6 by a typical moment balance. By use of the values on line 8, thrusts at joint B may be balanced without inducing a moment at that joint. Line 8 provides values for a combined rotation and translation operation by means of which successive cycles of moment-thrust distribution may be avoided.

EXAMPLE NO. 4

A fourth example is the analysis shown subsequently as lines 1 through 24 of Table 1(*b*). The BAK portion of the frame of Table 1(*b*) was analyzed in Example No. 1. Therefore, the values on lines 1, 15, and 19 of Table 1(*b*) are copied directly from the results of Example No. 1. Each step in Example

TABLE 1(*a*).—SOLUTION OF MEMBER BK OF FIG. 10

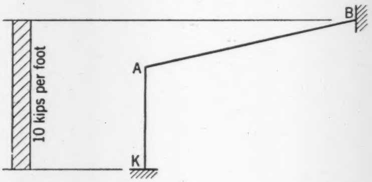

Description	JOINT A	JOINT A		JOINT B	
	θ	*M*, in kip-feet	*T*, in kips	*M*, in kip-feet	*T*, in kips
		FRAME PROPERTIES			
θ_{AK}		+160	−20		
θ_{AB}		+ 40		+20	
Total	+1.0	+200		+20	− 20
θ_{BA}		+ 20		+40	
Balance *M*	−0.1	− 20		− 2	+ 2
θ_{BK}	−0.1	0		+38	+ 2
Δ_{BA}		− 20			+ 3.33
Balance *M*	+0.1	+ 20		+ 2	− 2
Δ_{BK}	+0.1	0		+ 2	+ 1.33
		LOADS			
Loads, AK		+120	−60		
Loads, AB		− 13	−20	+13.3	− 20
Total		+107		+13.3	−100
Balance *M*	−0.535	−107		−10.7	+ 10.7
Loads, BK	−0.535	0	0	+ 2.6	− 89.3

FINAL RESULTS

Description	*M* in AK, kip-feet	θ_A	Δ_A	θ_B	Δ_B
Loads	+ 120	−0.535			
+8.53 θ_{AK}	+1,360	−0.63		+6.29	
+97.0 Δ_{AK}	−1,940	+9.70	+97.0		+97.0
Total	− 460	+8.53	+97.0		

Description	*M* in GH, kip-feet	θ_G, in radians	Δ_G, in inches	θ_F, in radians	Δ_F, in inches
+3.20 θ_{GH}	+517	−0.58		+5.82	
+37.8 Δ_{GH}	−756	+3.78	+37.8		+37.8
Totals	−244	+3.20	+37.8		

No. 4 is in accordance with previously explained procedures. The information obtained through the computations of Table 1 (*b*) will allow the frame CJK to be considered as a part of a still more complex structure.

Example No. 4 does not include the computation of moments and thrusts at the ends of the individual members. These values may be determined if desired by the procedure described for lines 15 through 24, Example No. 1.

TABLE 1 (*b*).—SOLUTION OF MEMBER CK OF FIG. 10

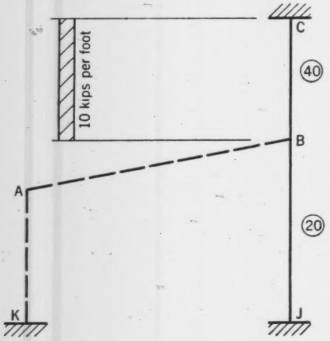

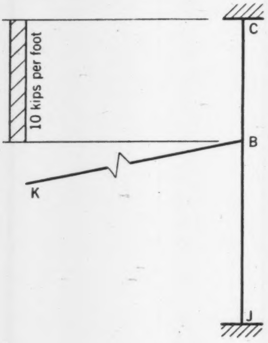

Line No.	Description	JOINT B		JOINT B		JOINT C	
		θ	Δ	M, in kip-feet	T, in kips	M, in kip-feet	T, in kips
1	θ_{BK}			+ 38	+ 2		
2	θ_{BJ}			+ 80	− 7.5		
3	θ_{BC}			+160	+ 20	+ 80	− 20
4	Total	+1.0		+278	+ 14.5	+ 80	− 20
5	Δ_{BK}			+ 2	+ 1.33		
6	Δ_{BJ}			− 7.5	+ 0.94		
7	Δ_{BC}			+ 20	+ 3.33	+ 20	− 3.33
8	Total		+1.0	+ 14.5	+ 5.60	+ 20	− 3.33
9	Balance *M*	−0.0522		− 14.5	− 0.76	− 4.2	+ 1.04
10		−0.0522	+1.0	0	+ 4.84	+ 15.8	− 2.29
11	θ_{CB}			+ 80	+ 20	+160	− 20
12	Balance *M*	−0.288		− 80	− 4.2	− 23	+ 5.76
13	Balance *T*	+0.170	−3.26	0	− 15.8	− 51.5	+ 7.47
14	θ_{CK}	−0.118	−3.26	0	0	+ 85.5	− 6.77
15	Δ_{CB}			− 20	− 3.33	− 20	+ 3.33
16	Balance *M*	+0.0719		+ 20	+ 1.04	+ 5.75	− 1.44
17	Balance *T*	−0.0247	+0.473		+ 2.29	+ 7.47	− 1.08
18	Δ_{CK}	+0.0472	+0.473	0	0	− 6.78	+ 0.81
				LOADS			
19	Loads, BK			+ 2.6	− 89.3		
20	Loads, BC			−120	− 60	+120	− 60
21	Total			−117	−149	+120	− 60
22	Balance *M*	+0.421		+117	+ 6.1	+ 33.7	− 8.42
23	Balance *T*	−1.54	+29.5		+143	+466	− 67.6
24	Loads, CK	−1.12	+29.5	0	0	+620	−136

TABLE 1(*b*).—*Continued*

Line No.	Description	JOINT B		JOINT B		JOINT C	
		M in BK, kip-feet	*T* in BK, kips	θ_B	Δ_B	θ_C	Δ_C
25	Loads	+ 2.6	− 89.3	−1.12	+29.5		
26	+6.29 θ_{BK}	+239	+ 12.6	−0.38	−10.5	3.23	
27	+97.0 Δ_{BK}	+194	+129	+7.79	+78.0		+165
28	Total	+436	+ 52.3	+6.29	+97.0		
	Description	*M* in BJ, kip-feet	*T* in BJ, kips				
29	+6.29 θ_{BJ}	+503	−47.2				
30	+97.0 Δ_{BJ}	−728	+91.2				
31	Total	−225	+44.0				
	Description	*M* in FH, kip-feet	*T* in FH, kips	θ_F	Δ_F	θ_E	Δ_E
32	+5.82 θ_{FH}	+221	+11.6	−1.17	−32.2	+9.89	
33	+37.8 Δ_{FH}	+ 76	+50.3	+6.99	+70.0		+148
34	Total	+297	+61.9	+5.82	+37.8		
	Description	*M* in FI, kip-feet	*T* in FI, kips				
35	+5.82 θ_{FI}	+466	−43.7				
36	+37.8 Δ_{FI}	−284	+35.5				
37	Total	+182	− 8.2				

EXAMPLE NO. 5

Arsham Amirikian, M. ASCE, has presented elsewhere[3] a solution for the structure of Fig. 10. The results in Table 1 agree closely with those in the referenced text. The greatest difference between the two solutions for any final moment is 8 ft-kips for M_{KA} (less than 1% error).

It will be observed that the solution shown in Table 1 is divided into four parts. In Table 1(*a*), frame BAK is that of Example No. 1. In Table 1(*b*), frame CJK (or CK) is Example No. 4. The computations for Example No. 1 reappear in Table 1 slightly rearranged. This revised arrangement is used to separate completely the computations of frame properties and of loads. If a second loading arrangement is to be investigated later, it will not be necessary to recompute the frame properties.

The steps involved in the solution of Table 1 are in accordance with procedures previously described. However, a few general comments regarding the computations are in order. By symmetry of the frame, the moments and thrusts associated with a unit rotation or a unit translation of EH are numerically equal to those associated with a unit rotation or a unit translation of CK. These equalities are used in the analysis of joint E. The determination of frame properties and loading effects proceeds from the left (joint A) to the right (joint E). The determination of final joint rotations and translations, on the other hand, proceeds from E toward A for the loaded portion of the frame and from E toward G for the unloaded portion.

Computations are to an accuracy of three significant figures. All computations for the indeterminate analysis, except direct slide-rule operations, are listed. The computations of statics for the final moment diagram are not shown. No equations are used except for the relationships indicated in Figs. 3, 4, and 6.

TABLE 1(*c*).—SOLUTION OF MEMBER EK OF FIG. 10

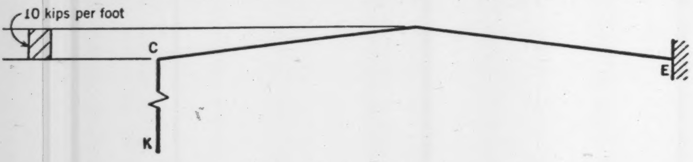

Description	JOINT C		JOINT C		JOINT E	
	θ	Δ	*M*, in kip-feet	*T*, in kips	*M*, in kip-feet	*T*, in kips
			FRAME PROPERTIES			
θ_{CK}			+ 85.5	− 6.77		
θ_{CE}			+ 35.0	+ 10	− 5	− 10
Total	+1.0		+120	+ 3.23	− 5	− 10
Δ_{CK}			− 6.78	+ 0.81		
Δ_{CE}			+ 10	+ 6.67	− 10	− 6.67
Total		+ 1.0	+ 3.22	+ 7.48	− 10	− 6.67
Balance *M*	−0.0268		− 3.22	− 0.09	+ 0.13	+ 0.27
	−0.0268	+ 1.0	0	+ 7.39	− 9.87	− 6.40
θ_{EC}			− 5	− 10	+ 35	+ 10
Balance *M*	+0.0417		+ 5	+ 0.13	− 0.21	− 0.42
Balance *T*	−0.0359	+ 1.34	0	+ 9.90	− 13.2	− 8.58
θ_{EK}	+0.0058	+ 1.34	0	0	+ 21.6	+ 1.00
Δ_{EC}			− 10	− 6.67	+ 10	+ 6.67
Balance *M*	+0.0833		+ 10	+ 0.27	− 0.42	− 0.83
Balance *T*	−0.0232	+ 0.866	0	+ 6.40	− 8.55	− 5.54
Δ_{EK}	+0.0601	+ 0.866	0	0	+ 1.03	+ 0.30
			LOADS			
Loads, CK			+620	−136		
Loads, CE			− 9	− 22	− 2	− 7.5
Total			+611	−158	− 2	− 7.5
Balance *M*	−5.09		−611	− 16.4	+ 25.5	+ 50.9
Balance *T*	−0.63	+23.5		+174	−232	−150
Loads, EK	−5.72	+23.5	0	0	−208	−107

FINAL RESULTS

Description	*M* in CK, kip-feet	*T* in CK, kips	θ_C	Δ_C	θ_E	Δ_E
Loads	+ 620	−136	−5.72	+ 23.5	+9.89	+148
3.23 θ_{CK}	+ 276	− 21.9	+0.06	+ 13.3		
+165 Δ_{CK}	−1120	+134	+8.89	+128		
Total	− 224	− 23.9	+3.23	+165		

TABLE 1(*d*).—SOLUTION OF MEMBER HK OF FIG. 10

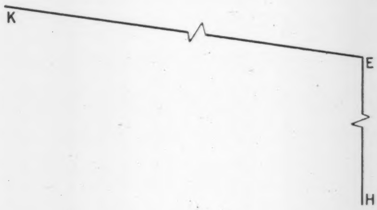

Description	Joint E			
	θ	Δ	*M*, in kip-feet	*T*, in kips
Frame Properties				
θ_{EK}			+ 21.6	+ 1.00
θ_{EH}			+ 85.5	− 6.77
Total	+1.0		+107	− 5.77
Δ_{EK}			+ 1.03	+ 0.30
Δ_{EH}			− 6.78	+ 0.81
Total		+ 1.0	− 5.75	+ 1.11
Balance *M*	+0.0537		+ 5.75	− 0.31
	+0.0537	+ 1.0	0	+ 0.80
Loads				
Loads, EK			−208	−107
Balance *M*	+1.94		+208	− 11
Balance *T*	+7.95	+148	0	+118
	+9.89	+148	0	0

Final Results

Description	*M* in EK, kip-feet	*T* in EK, kips
Loads	−208	−107
+9.89 θ_{EK}	+214	+ 9.9
+148 Δ_{EK}	+152	+ 44.4
Total	+158	− 52.7

CONCLUSION

As stated previously, the "analysis by parts" has been found to be less laborious than other methods for the design of multiple-span gabled frames. Obviously, this procedure is applicable to the case of wedge-beam framing[12] and its use may be extended to the case of more complex structures where joints have three degrees of freedom instead of only two.

---

[12] "Wedge-Beam Framing," by Arsham Amirikian, *Transactions*, ASCE, Vol. 117, 1952, p. 596.

The analysis of structures such as those described herein and the analysis of even more complex structures bring to mind the final footnote in a textbook[13] by Linton Grinter, M. ASCE. In part, Mr. Grinter stated:

> "Before permitting the second volume of this series on structural theory to go into print, the author desires to emphasize his dissatisfaction with the theories presented * * *"

With such thoughts as this, it is encouraging to note the considerable research effort being directed toward the study of plasticity. The several research programs on this subject offer hope for substantial simplifications of analysis as well as for a more rational approach to the design of continuous frames of ductile material.

APPENDIX. PROPERTIES OF GABLES

Fig. 11 (*a*) indicates a unit positive translation of end A of the unsymmetrical gable ABC. An enlargement of the deflection triangle AA_2A_1 is shown in Fig. 11 (*b*). It is convenient to consider that the deflection AA_1 occurs in two steps—first, the deflection AA_2 (or Δ_3) which causes bending in member AB only and, second, the deflection A_2A_1 (or Δ_4) which causes bending in member BC only. From the relationships between similar triangles:

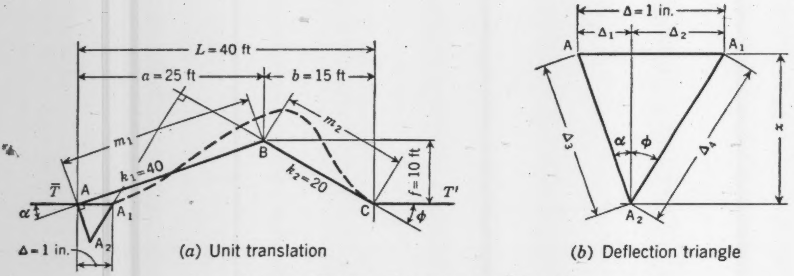

(*a*) Unit translation (*b*) Deflection triangle

FIG. 11.—POSITIVE TRANSLATION OF END A

$$x = \frac{a\,\Delta_1}{f} = \frac{b\,\Delta_2}{f}\,;\quad \frac{\Delta_1}{b} = \frac{\Delta_2}{a} = \frac{\Delta}{L} \qquad (1)$$

Therefore,

and

$$\left.\begin{aligned}\Delta_1 &= \frac{b\,\Delta}{L}\\ \Delta_2 &= \frac{a\,\Delta}{L}\end{aligned}\right\} \qquad (2)$$

---

[13] "Theory of Modern Steel Structures," by Linton Grinter, The Macmillan Co., New York, N. Y., 1937, p. 270.

Also,

$$\left.\begin{aligned}\Delta_3 &= \frac{m_1\,\Delta_1}{f} = \frac{b\,m_1\,\Delta}{f\,L}\\ \text{and}\qquad \Delta_4 &= \frac{a\,m_2\,\Delta}{f\,L}\end{aligned}\right\}\qquad\qquad (3)$$

The moment at each end of AB due to the deflection Δ_3 (with joint B restrained from rotation) is

$$\text{I.M.} = +\frac{6\,K_1\,\Delta_3}{m_1} = +\frac{6\,K_1\,\Delta}{f}\,\frac{b}{L}\qquad\qquad (4)$$

(*a*) Relaxation of Joint B

Description	θ at joint B, in radians	Moments, in Foot-Kips		
		Joint A	Joint B	Joint C
θ_{BA}		+80	+160	
θ_{BC}			+ 80	+40
θ_B	+1.0	+80	+240	+40
Δ_3		+ 9	+ 9	
Δ_4			− 7.5	− 7.5
Total		+ 9	+ 1.5	− 7.5
Balance *M*	−0.00625	− 0.5	− 1.5	− 0.25
Δ_{AC}		+ 8.5	0	− 7.75

(*b*) Thrust-Stiffness Determination

$V_2 = \frac{0.75}{40} = 0.00188$ kips $= V_1$

$M_{BA} = +9 - 0.00625 \times 160$
$= +8$ ft-kips

$\Sigma M_B = 0 = +8 + 8.5$
$-0.00188 \times 25 - 10\,\overline{T}$

$\overline{T} = +1.645$ kips

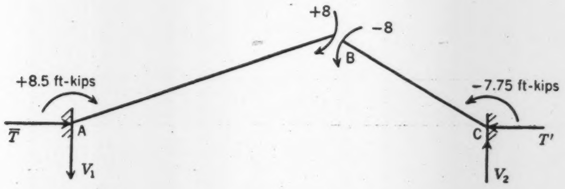

Fig. 12.—Moments and Thrust in an Unsymmetrical Gable

Likewise, the moment at each end of BC due to the deflection Δ_4 (with joint B restrained from rotation) is

$$\text{I.M.} = -\frac{6\,K_2\,\Delta}{f}\,\frac{a}{L}\qquad\qquad (5)$$

If $K_1 = K_2 = K$ and $a = b = L/2$, Eqs. 4 and 5 are both reduced to $\pm 3\,K/f$ for unit translation. In such a case, there will be no unbalanced moment at joint B and therefore no tendency of that joint to rotate. Thus, for the symmetrical case, $+3\,K/f$ and $-3\,K/f$ are the induced moments at A and C, respectively, even after joint B is relaxed. The thrust stiffness $\bar{T}$ may be determined from these moments by statics. (See also the statics calculations of Fig. 12(*b*))

$$\left.\begin{aligned} \Sigma M_B &= +\frac{3\,K}{f} + \frac{3\,K}{f} - \bar{T}\,f = 0 \\ \bar{T} &= +\frac{6\,K}{f^2} \end{aligned}\right\} \qquad (6)$$

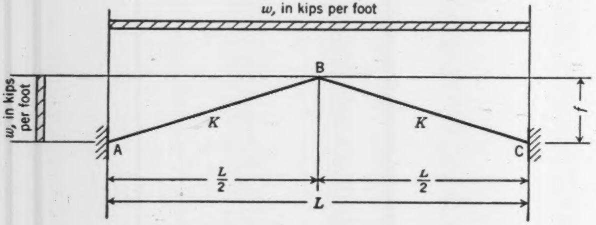

Description	θ at joint B, in radians	Moments, in Foot-Kips: Joint A	Joint B	Joint C
		Rotation		
θ_{BA}		+2 *K*	+4 *K*	
θ_{BC}			+4 *K*	+2 *K*
θ_B	+ 1.0	+2 *K*	+8 *K*	+2 *K*
θ_{AB}		+4 *K*	+2 *K*	
Balance *M*	− 0.25	−0.5 *K*	−2 *K*	−0.5 *K*
θ_{AC}	−25	+3.5 *K*	0	−0.5 *K*
		Vertical Loads		
Loads, BA		$-\frac{w\,L^2}{48}$	$+\frac{w\,L^2}{48}$	
Loads, BC			$-\frac{w\,L^2}{48}$	$+\frac{w\,L^2}{48}$
Total, AC	0	$-\frac{w\,L^2}{48}$	0	$+\frac{w\,L^2}{48}$
		Horizontal Loads		
Loads, BA		$-\frac{w\,f^2}{12}$	$+\frac{w\,f^2}{12}$	
Balance *M*	$-\frac{w\,f^2}{96\,K}$	$-\frac{w\,f^2}{48}$	$-\frac{w\,f^2}{12}$	$-\frac{w\,f^2}{48}$
Loads, AC	$-\frac{w\,f^2}{96\,K}$	$-\frac{5\,w\,f^2}{48}$	0	$-\frac{w\,f^2}{48}$

FIG. 13.—MOMENTS IN A SYMMETRICAL GABLE

For the unsymmetrical gable of Fig. 11, the induced moments at each end of AB are: $+(6\,K_1\,b)/f\,L = +\,9$ ft-kips. Likewise, the induced moments at each end of BC are -7.5. Joint B may now be relaxed by moment distribution, as indicated in the table of Fig. 12(*a*), in order to determine the final induced moments. Subsequently, the thrust stiffness may be determined by means of statics as indicated in Fig. 12(*b*).

In Fig. 13, values have been obtained for moments due to uniform loads and unit rotation of a symmetrical gable. The thrusts associated with these moments may be determined by means of statics as indicated in Fig. 12(*b*).

DISCUSSION

Abdel F. Diwan,[14] A.M. ASCE.—The main difficulty in analyzing continuous structures by the classical methods lies in the necessity of preparing and solving as many simultaneous equations as there are indeterminacies in the structure. Many attempts have therefore been made by structural engineers to develop more practical and simple methods of analysis in which such simultaneous equations are not needed. The most successful attempt is the moment-distribution method presented by Mr. Cross.[2] Later developments have been added to his original method, all of which tend to accelerate the convergence of the process, or even to produce a direct one-step relaxation. The method presented by the author, an analysis by parts, is one of the modifications to the original method of Mr. Cross. Proceeding from one end of the frame, the joints are successively relaxed until the other end is reached, when moments and thrusts at all joints will be balanced. Once any joint is unlocked, it remains unlocked, and the modified fixed-end moment, thrust, and the rotation and translation stiffnesses at the next joint are computed.

Almost all the joints have two degrees of freedom, and the necessary balancing displacement consists of a rotation θ and a horizontal translation Δ. In the suggested solution, the joint is first allowed to rotate until the moment acting there is balanced. The resulting force, together with that originally acting on the joint, is next balanced by allowing translation Δ with appropriate rotation θ so that no moments are developed at the joint. This is, of course, a modification of the original method of Mr. Cross in which pure rotation and translation are separately produced at the so-called "neutral point" for the joint.

In the author's paper, the simple unit considered is always one straight bar, except for CDE which is considered one unit. This makes the procedure rather lengthy, although it simplifies it.

It is however more convenient, in the writer's opinion, to reduce the number of the simple units as much as possible and still avoid solving any equations—thus reducing the number of the joints that are to be relaxed and at which the displacements θ and Δ are to be computed. For the frame in Example No. 5, only joints B and F need to be locked at the start, thus dividing the frame into three parts—namely, (BK + BJ), BDF, and (FH + FI).

These three units are added together in series whereas the parts in parentheses are added together in parallel to form one unit each.

The analysis of continuous frames in the paper is simplified greatly by the concepts of equivalent elastic systems[15,16] and stiffness factors[17] that have been published by the writer, together with L. Beaufoy, M. ASCE. It is interesting to show the application of these concepts to the solution of the frame in

---

[14] Asst. Prof., Structural Dept., Faculty of Eng., Alexandria Univ., Alexandria, Egypt.

[15] "Equivalent Elastic Systems in the Analysis of Continuous Structures," by L. Beaufoy and A. Diwan, *Concrete and Construction Engineering*, Vols. 11 and 12, 1950.

[16] "Analysis of Pin-Jointed Redundant Plane Frameworks Using Equivalent Elastic Systems," by L. Beaufoy and A. Diwan, *Quarterly Journal of Mechanical and Applied Mathematics*, Pt. 1, 1950.

[17] "Analysis of Continuous Structures by the Stiffness Factors Method," by L. Beaufoy and A. Diwan, *ibid.*, Pt. 3, 1949.

Fig. 14. Computations are all made by slide rule, and no equations are needed. The writer will first explain the method.

For any elastic member AB (Fig. 15(*a*)), polygonal or straight, with constant or variable cross section, the following terms are called the elastic constants:

$$\bar{s} = \int \frac{ds}{E\,I} = \int d\bar{s} \quad \text{(7)}$$

$$I_x = \int y^2\,d\bar{s} \quad \text{(8)}$$

$$I_y = \int x^2\,d\bar{s} \quad \text{(9)}$$

$$I_{xy} = \int x\,y\,d\bar{s} \quad \text{(10)}$$

and C is the centroid of the elastic lengths $d\bar{s}$.

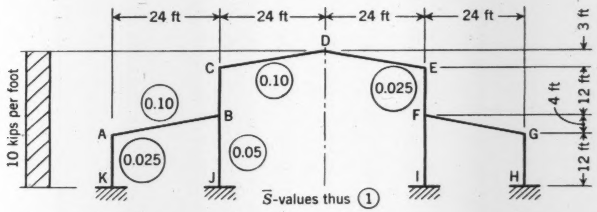
24 ft
24 ft
24 ft
24 ft
3 ft
D
C
E
0.10
0.025
0.10
4 ft
12 ft
B
F
A
G
0.025
0.05
12 ft
K
J
I
H
10 kips per foot
$\bar{S}$-values thus ①

FIG. 14.—FRAME SIMILAR TO THAT OF FIG. 10

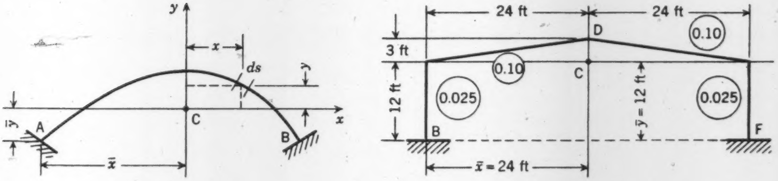
y
x
ds
y
$\bar{y}$
A
C
B
x
$\bar{x}$
24 ft
24 ft
D
0.10
3 ft
0.10
C
12 ft
0.025
$\bar{y}$ = 12 ft
0.025
B
F
$\bar{x}$ = 24 ft

(*a*) Elastic member

(*b*) Middle part of frame

FIG. 15

From these elastic constants, the rotation θ and the horizontal and vertical translations, Δ and λ, respectively, of the elastic centroid C due to a moment M, a horizontal thrust T, and a vertical force V, acting at C will be

$$\theta^C = M\,\bar{s} \quad \text{(11)}$$

$$\Delta^C = T\,I_x - V\,I_{xy} \quad \text{(12)}$$

$$\lambda^C = V\,I_y - T\,I_{xy} \quad \text{(13)}$$

Positive moments and rotations are clockwise, and positive translations and forces are upward and to the right.

The displacement of end A assumed as rigidly connected to C in terms of the displacement of C will then be

$$\theta^A = \theta^C \qquad (14)$$

$$\Delta^A = \Delta^C - \bar{y}\,\theta^C \qquad (15)$$

$$\lambda^A = \lambda^C + \bar{x}\,\theta^C \qquad (16)$$

On the other hand, the moment M and forces T and V necessary to act at C to produce a unit rotation θ and unit translations Δ and λ will be

$$M = \frac{1}{s} \qquad (17)$$

$$T = \frac{\Delta'}{I'_x} \qquad (18)$$

$$V = \frac{\lambda'}{I'_y} \qquad (19)$$

in which

$$I'_x = I_x - \frac{I^2_{xy}}{I_y} \qquad (20)$$

$$I'_y = I_y - \frac{I^2_{xy}}{I_x} \qquad (21)$$

$$\Delta' = \Delta + \lambda\,\frac{I_{xy}}{I_y} \qquad (22)$$

and

$$\lambda' = \lambda + \Delta\,\frac{I_{xy}}{I_x} \qquad (23)$$

The term "stiffness factors" denotes the moment and the horizontal and vertical forces necessary to produce unit rotation and horizontal or vertical translation at a particular joint. These factors are expressed as M_θ, T_θ, and V_θ for a unit rotation θ; M_Δ, T_Δ, and V_Δ for a unit translation Δ; and M_λ, T_λ, and V_λ for a unit translation λ.

The reciprocal relationship is valid so that these rotation and translation stiffnesses for joint A of the elastic member AB will be

$$T_\Delta = \frac{1}{I'_x} \qquad (24a)$$

$$V_\lambda = \frac{1}{I'_y} \qquad (24b)$$

$$V_\Delta = T_\lambda = \frac{I_{xy}}{I'_x\, I_y} \qquad (24c)$$

$$M_\Delta = T_\theta = \bar{y}\,T_\Delta - \bar{x}\,V_\Delta \qquad (24d)$$

$$M_\lambda = V_\theta = \bar{y}\,T_\lambda - \bar{x}\,V_\lambda \qquad (24e)$$

and

$$M_\theta = \frac{1}{\bar{s}} + \bar{y}\, T_\theta - \bar{x}\, V_\theta \qquad (24f)$$

Applying Eqs. 20 through 24 to the middle part BDF of the frame as shown in Fig. 15(*b*), the following are the values for the elastic constants of the frame and for the stiffness factors at end B, assuming joint F to be fixed.

$$\begin{aligned} s &= 2\ (0.10 + 0.025) = 0.250 \\ I_x &= 3.0 = I'_x \\ I_y &= 67.2 = I'_y \\ I_{xy} &= 0 \end{aligned}$$

Therefore, $T_\Delta = 0.333$, $T_\theta = 4.0 = M_\Delta$, $V_\theta = -0.357$, and $M_\theta = 60.57$. The carry-over moments to end F will be $M'_\Delta = -4.0$ and $M'_\theta = -43.43$.

If the stiffness factors for any joint, in which two or more elastic members intersect, are known, the elastic behavior of the joint can be represented by that of a single elastic member connected to the joint, and called the equivalent elastic system.

The elastic constants for this symbolic system in terms of the stiffness factors for the joint are presented in Table 2 for the general case of a joint having three degrees of freedom and for the special cases of only two degrees of freedom.

TABLE 2.—ELASTIC CONSTANTS IN TERMS OF STIFFNESS FACTORS

Elastic constants	General case of three degrees of freedom[a]	SPECIAL CASES OF TWO DEGREES OF FREEDOM	
		Only Δ and θ possible	Only λ and θ possible
$\bar{s}$	D_1/D	T_Δ/D_4	V_λ/D_5
$\bar{x}$	D_2/D_1	0	$-V_\theta/V_\lambda$
$\bar{y}$	D_3/D_1	T_θ/T_Δ	0
I_x	V_λ/D_1	$1/T_\Delta$	0
I_y	T_Δ/D_1	0	$1/V_\lambda$
I_{xy}	V_Δ/D_1	0	0

[a] Notation: $D_1 = T_\Delta V_\lambda - V^2_\Delta$; $D_2 = T_\theta V_\Delta - V_\theta T_\Delta$; $D_3 = T_\theta V_\lambda - V_\theta V_\Delta$; $D_4 = M_\theta T_\Delta - T^2_\theta$; $D_5 = M_\theta V_\lambda - V^2_\theta$; and $D = M_\theta T_\Delta V_\lambda - M_\theta V^2_\Delta - T_\Delta V^2_\theta - V_\lambda T^2_\theta + 2\, V_\theta T_\theta V_\Delta$.

Considering, for example, the two members FH and FI intersecting at F and added in parallel, the sum of their stiffnesses with joint G unlocked will be (Fig. 16(*a*)) $M_\theta = 38 + 80 = 118$, $T_\theta = 2 - 7.5 = -5.5$, and $T_\Delta = 1.33 + 0.94 = 2.27$.

Because only rotation and horizontal translation can occur at F, the elastic constants in the equivalent elastic symbolic system for Fig. 16(*a*) will be (Table 2). $\bar{y} = -\frac{5.5}{2.27} = -2.43$ ft, $I_x = \frac{1}{2.27} = 0.44$, $s = \frac{2.27}{118\ (2.27) - (5.5)^2} = 0.0095$, and $I_y = I_{xy} = \bar{x} = 0$. If this symbolic system is added in series to BDF as shown in Fig. 16(*b*), one obtains a new virtual elastic system for which the elastic constants will be $\hat{s} = 0.2595$, $I_x = 5.35$, $I_y = 72.5$, and $I_{xy} = -3.18$. Then, $I'_x = 5.20$ and $I'_y = 70.5$.

The stiffness factors for end B of this virtual system will be the real stiffnesses for that end with no external additional restraint applied anywhere to the right of B. The same values, of course, apply to end F of FDB because of symmetry.

These real stiffnesses will be (Eqs. 24) $T_\Delta = 0.192$, $V_\Delta = -0.0085$, $M_\Delta = 2.41 = T_\theta$, $V_\theta = -0.450$, and $M_\theta = 42.80$. The displacements induced at the far joint F by unit translation or unit rotation at B are determined from the moment and thrust acting at the centroid O of the symbolic system (Eqs. 11 through 16). Thus, for unit translation Δ at B, the moment and thrust at O are $T = 0.192$ and $M = 2.41 + 0.192 \times 2.43 - 0.0085 \times 48 = 2.47$.

The displacements at F will then be (Eqs. 11 through 16) $\theta_\Delta = 2.47 \times 0.0095 = 0.0235$ and $\Delta_\Delta = 0.0235 \times 2.43 + 0.192 \times 0.44 = 0.142$. Similarly, for a unit rotation at B, the induced motion at F will be $\theta_\theta = 0.257$ and $\Delta_\theta = 1.68$.

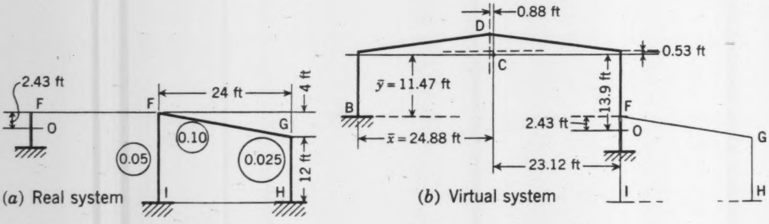

(*a*) Real system (*b*) Virtual system

FIG. 16.—FORMATION OF THE VIRTUAL SYSTEM

The actual rotation and translation stiffnesses for joint B with the three intersecting members and with no restraint applied anywhere else in the frame can be determined. They are $M_\theta = 38 + 80 + 42.8 = 160.8$, $T_\theta = 2 - 7.5 + 2.41 = -3.09$, and $T_\Delta = 1.333 + 0.94 + 0.192 = 2.465$.

The elastic constants for the symbolic system equivalent to joints B and F in the full frame will be $\hat{s} = 0.00638$, $I_x = 0.407$, and $\bar{y} = 1.25$ ft. With these values determined, a direct one-step relaxation is possible. The steps of the solution will be as follows:

1. With only joints B and F locked, the moments and thrusts at these joints are evaluated using any convenient method—for example, column analogy for BDF and ordinary moment distribution for BK. Thus, at B, $M = 581 - 2.6 = 578.4$ ft-kips and $T = 118.1 + 89.3 = 207.4$ kips; and at F, $M = 326$ ft-kips and $T = 31.9$ kips.
2. These moments and thrusts must be transferred to the elastic centroids of the joints, yielding λ at joint B, $M = 207.4 \times 1.25 + 578.4 = 837.6$ ft-kips and $T = 207.4$ kips; and at joint F, $M = 31.9 \times 1.25 + 326 = 366$ ft-kips and $T = 31.9$ kips.

3. The balancing displacements are evaluated at each joint using Eqs. 11 through 16, and those consequently induced at the opposite joint are evaluated using the coefficients: $\theta_\theta = 0.257$, $\Delta_\theta = 1.68$, $\theta_\Delta = 0.0235$, and $\Delta_\Delta = 0.142$. These displacements are listed in Table 3.

TABLE 3.—TOTAL JOINT DISPLACEMENTS

Description	Joint B		Direction of procedure	Joint F	
	θ, in radians	Δ		θ, in radians	Δ
Balancing displacement at B and induced displacement at F	5.32		→	1.36	9.00
		90.9	→	2.14	12.90
Balancing displacement at F and induced displacement at B	0.60	3.94	←	2.34	
	0.38	2.26	←		13.90
Total displacements	6.30	97.1		5.84	37.8

4. The moments M and forces R, acting on the terminals at each joint are next computed as shown in Table 4. From these values, the moments and forces at any other section in the frame are easily determined by means of simple statics.

TABLE 4.—COMPUTATION OF MOMENTS AND THRUSTS

Description	Joint B			Joint F		
	Member BK	Member BJ	Member BF	Member FB	Member FI	Member FH
MOMENTS						
Fixed-end moment	2.6	0	−581	−326	0	0
Rotation $\theta^B = 6.3$	239.4	504	382	−273		
Rotation $\theta^F = 5.84$			−253	354	469	221
Translation $\Delta^B = 97.1$	194	−728	388	−388		
Translation $\Delta^F = 37.8$			−151	151	−284	76
Final moments, ΣM	436	−224	−215	−482	185	297
THRUSTS						
Fixed-end thrust	−89.3	0	−118.1	−31.9	0	0
Rotation $\theta^B = 6.3$	12.6	−47.3	25.2	− 25.2		
Rotation $\theta^F = 5.84$			−23.4	23.4	−43.8	11.7
Translation $\Delta^B = 97.1$	129.5	91.2	32.3	−32.3		
Translation $\Delta^F = 37.8$			−12.6	12.6	35.4	50.4
Final thrusts, ΣT	52.8	43.9	−96.5	−53.4	−8.4	62.1

The results obtained for the displacements θ and Δ and for the moments M and thrusts T agree with those of the author with a maximum difference of less than 0.5%. The method is self-checking because the final moments and forces at any joint must total zero.

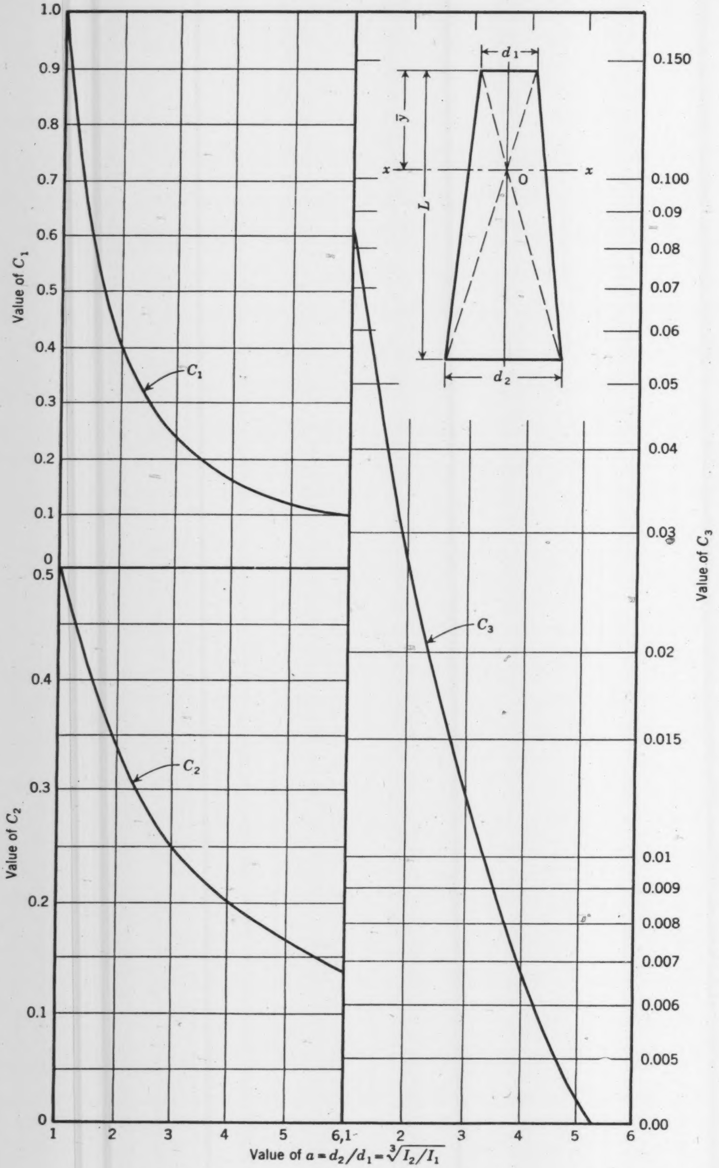

FIG. 17.—ELASTIC CONSTANTS FOR TAPERED BEAMS

Finally, Fig. 17 shows the coefficients C_1, C_2, and C_3 for tapered members in which the moment of intertia varies as d^3. These are

$$\left.\begin{aligned} C_1 &= \frac{1 + a}{2\,a^2} \\ C_2 &= \frac{1}{1 + a} \\ \text{and} \qquad C_3 &= \frac{1}{(a - 1)^3}\left[\log a - \frac{2\,(a - 1)}{a + 1}\right] \end{aligned}\right\} \ldots\ldots\ldots\ldots (25)$$

The elastic constants, in terms of these coefficients will be

$$\left.\begin{aligned} s &= C_1 \frac{L}{E\,I_1} \\ \bar{y} &= C_2\,L \\ \text{and} \qquad I_x &= C_3 \frac{L^3}{E\,I_1} \end{aligned}\right\} \ldots\ldots\ldots\ldots (26)$$

for cases of members either totally fixed or hinged at the far end. In the latter case the centroid lies at the hinge. From these elastic constants the stiffness factors can be readily evaluated. It is hoped that these concepts of equivalent elastic systems and stiffness factors will prove useful to all concerned with the design of continuous structures.

John D. Griffiths,[18] M. ASCE.—The alternate procedures recommended by Mr. Diwan will be found helpful to many who must analyze multiple-span frames on the basis of elastic theory. Basically, Mr. Diwan suggests the use of fewer frame subdivisions. By the use of fewer subdivisions, the final analysis by parts is simplified because of the reduction in the number of joints to be relaxed. On the other hand, the subdivisions become more complex as their numbers are reduced. Each designer must decide individually on the degree of subdivision that will require the minimum total effort for any particular structure.

It should be realized that basic data including stiffness and carry-over factors for any subdivision may be determined using the methods of virtual work, strain energy, column analogy, or other similar procedures as well as by means of the "concept of equivalent elastic systems."

Advice has been received that the procedure outlined in the original paper has been used in the design of several structures such as the multiple-span frames for the Kentucky State Fair buildings at Louisville (Fig. 18). Edwin R. Leonard, M. ASCE, was the structural designer of these buildings.

---

[18] Chf. Engr., Gate City Steel, Inc., Boise, Idaho.

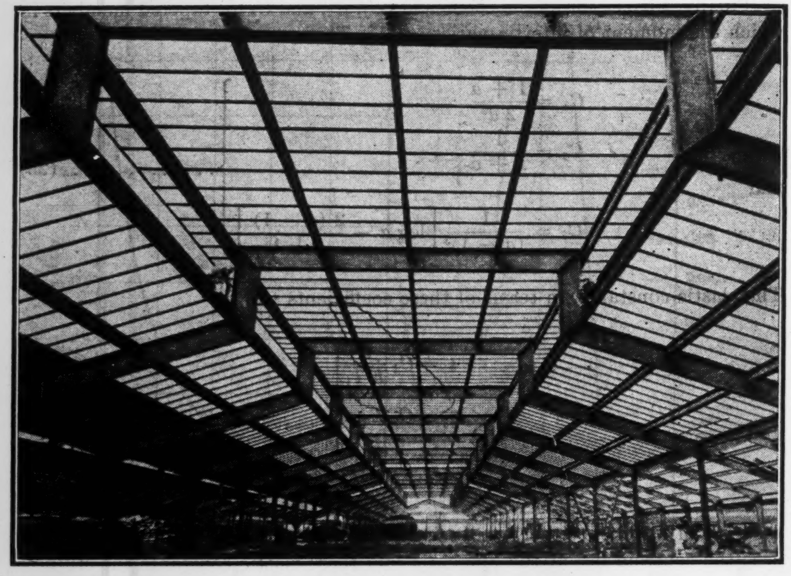

FIG. 18.—KENTUCKY STATE FAIR BUILDINGS

It is of course a source of satisfaction to the writer to know that the procedure has been used in the design of buildings actually constructed. However, it should be again emphasized that the most worthwhile simplifications of design procedure will be based on plastic analysis rather than on the elastic analysis described in this paper.

AMERICAN SOCIETY OF CIVIL ENGINEERS
Founded November 5, 1852
TRANSACTIONS

Paper No. 2842

CONSTANT-SEGMENT METHOD FOR ANALYSIS OF NONUNIFORM MEMBERS

By Walter E. Hanson,[1] M. ASCE, and Wallace F. Wiley[2]

With Discussion by Messrs. Thomas F. Hickerson; Eugene J. Vayda; Jaro J. Polivka; and Walter E. Hanson and Wallace F. Wiley

Synopsis

There are several general methods of analysis for beams having variable moments of inertia. Although precise, these methods are time-consuming and subject to numerical errors. Even the combination of column analogy and moment distribution sometimes becomes quite laborious.

A method is presented herein which requires comparatively little computation and which is simple in concept and use. The method is based on the division of a flexural member into a number of segments of equal length, each segment being assumed to have a constant cross section and modulus of elasticity. In this respect the method may be considered an approximation; however, the accuracy afforded is very high, and even with slide-rule computations it is entirely sufficient for all design purposes.

The material presented herein covers only the computation of stiffness, carry-over factors, fixed-end moments, and dead-load deflections; however, the method is applicable to similar problems.

Basic Concepts

The behavior of a flexural member acted on by any combination of transverse loads and end moments is dependent on the angle changes produced along the beam. These angle changes can be computed from the properties of the $(M/E\,I)$-diagram; M is the applied bending moment, E represents the modulus of elasticity, and I is the moment of inertia.

Note.—Published, essentially as printed here, in March, 1955, as *Proceedings-Separate No. 649*. Positions and titles given are those in effect when the paper or discussion was approved for publication in *Transactions*.

[1] Cons. Engr., Hanson, Collins & Rice, Springfield, Ill.

[2] Senior Bridge Designer, Illinois Div. of Highways, Springfield, Ill.

For any nonuniform beam the shape of the (*M*/*E I*)-diagram is irregular and may present difficulties in the computation of slopes and deflections. Such difficulties can be overcome by using the principle of superposition; the total slope or deflection at any one particular point is the summation of the slopes or deflections at that point produced by all segments of the (*M*/*E I*)-diagram, each segment acting individually. While one segment is being considered, all other segments of the beam are assumed at that time to have an infinite value of *E I*. Fig. 1 shows the behavior of a beam in which only the segment e f is assumed to be active.

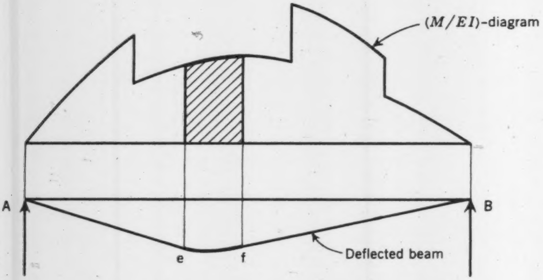

Fig. 1.—Action of One Flexural Segment

If each segment may be considered to have a constant value of *E I* throughout its length, numerical computations can be greatly simplified by the use of predetermined coefficients. These coefficients represent the effects of a segment of the moment diagram if this segment of the beam has a unit value of *E I*. In use, the coefficient for each segment is divided by the actual value of *E I* for that segment, and the results are summed across the beam to obtain the total effect.

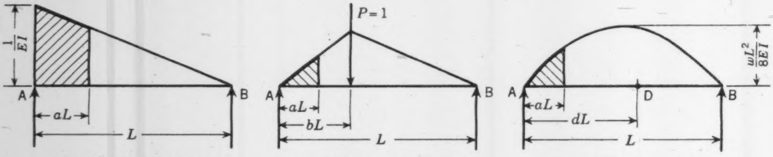

(*a*) Unit end moment (*b*) Concentrated load (*c*) Uniform load

Fig. 2.—(*M*/*E I*)-Diagrams

For purposes of computation, it is convenient to divide all beams into the same number of equal segments; the ten-segment scheme has been chosen for use herein. Each of the segments in this scheme is considered to have a constant value of *E I* throughout its length. If the value of *E I* changes within the segment, the weighted average value of 1/*E I* in the segment is used.

No sign convention is followed herein. The solution of any one of the equations will result in a positive quantity; the proper sign is applied according to the problem.

End Slopes Produced by Unit End Moments.—The slope at the end of a beam is numerically equal to the reaction of the $(M/E\,I)$-diagram at that end. If a unit moment is applied to end A of the beam AB which has a constant value of $E\,I$, the $(M/E\,I)$-diagram is as shown in Fig. 2(*a*). If only the shaded segment is then assumed to have a finite value of $E\,I$, the end slopes caused by this segment are the reaction of the segment of the $(M/E\,I)$-diagram—that is,

$$\theta^A{}_A = \frac{L}{E\,I}\left(a - a^2 + \frac{a^3}{3}\right) \quad (1)$$

and

$$\theta^A{}_B = \frac{L}{E\,I}\left(\frac{a^2}{2} - \frac{a^3}{3}\right) \quad (2)$$

Similarly, for a unit moment applied at B,

$$\theta^B{}_B = \frac{L}{E\,I}\left(\frac{a^3}{3}\right) \quad (3)$$

and

$$\theta^B{}_A = \frac{L}{E\,I}\left(\frac{a^2}{2} - \frac{a^3}{3}\right) \quad (4)$$

In Eqs. 1 through 4, $\theta^A{}_A$ is the slope at A caused by a unit moment applied at A, $\theta^A{}_B$ denotes the slope at B caused by a unit moment applied at A, $\theta^B{}_B$ is the slope at B caused by a unit moment applied at B, $\theta^B{}_A$ represents the slope at A caused by a unit moment applied at B, L is the span length, and a denotes the ratio of a distance measured from the left support A to the span length.

It should be noted that Eqs. 2 and 4 are equal and by the law of reciprocal relations this is true for any beam, no matter how the value of $E\,I$ varies; that is,

$$\theta^A{}_B = \theta^B{}_A \quad (5)$$

The quantities in parentheses in Eqs. 1 through 4 are coefficients of end slopes produced by a unit moment applied to the end of a beam having a constant value of $E\,I$. They represent, however, the slopes caused only by that segment of the $(M/E\,I)$-diagram extending a distance $a\,L$ along the beam—that is, all of the beam except this segment is considered to have an infinite value of $E\,I$.

The value of a coefficient for a segment extending from $a_1\,L$ to $a_2\,L$ is the difference between the values obtained by substituting successively for a the values of a_1 and a_2 in the factor in parentheses. Values of these coefficients for ten segments of equal length are presented in Table 1(*a*).

When the value of $E\,I$ is not constant throughout the length of the beam, the true value of an end slope is obtained by summation, thus:

$$\theta^A{}_A = L\left(\frac{C_1}{E\,I_1} + \frac{C_2}{E\,I_2} + \cdots + \frac{C_{10}}{E\,I_{10}}\right) \quad (6)$$

in which C_1 through C_{10} are segmental coefficients for end slopes or deflections given in Tables 1 through 3. Because E is generally a constant it can be placed outside the parentheses. Also, for convenience of computation, if some value, I_0 of the moment of inertia is taken as a reference value,

$$\theta^A{}_A = \frac{L}{E\,I_0}\left(C_1\frac{I_0}{I_1} + \frac{C_2\,I_0}{I_2} + \cdots + C_{10}\frac{I_0}{I_{10}}\right) \ldots\ldots\ldots\ldots (7)$$

Eq. 7 represents the general procedure used herein to evaluate the properties and behavior of beams that have nonuniform sections.

TABLE 1.—COEFFICIENTS FOR END SLOPES

Segment	(a) END MOMENTS			(b) UNIFORM LOAD	
	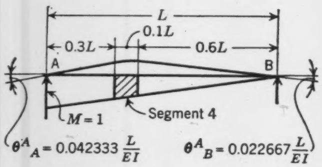 L 0.3L 0.1L 0.6L A B M=1 Segment 4 $\theta^A{}_A = 0.042333\frac{L}{EI}$ $\theta^A{}_B = 0.022667\frac{L}{EI}$			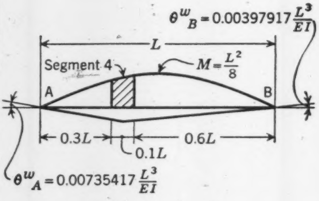 $\theta^w{}_B = 0.00397917\frac{L^3}{EI}$ L Segment 4 $M = \frac{L^2}{8}$ A B 0.3L 0.1L 0.6L $\theta^w{}_A = 0.00735417\frac{L^3}{EI}$	
	$\theta^A{}_A$	$\theta^B{}_B$	$\theta^A{}_B = \theta^B{}_A$	$\theta^w{}_A$	$\theta^w{}_B$
1	0.090333	0.000333	0.004667	0.00217917	0.00015417
2	0.072333	0.002333	0.012667	0.00535417	0.00097917
3	0.056333	0.006333	0.018667	0.00697917	0.00235417
4	0.042333	0.012333	0.022667	0.00735417	0.00397917
5	0.030333	0.020333	0.024667	0.00677917	0.00555417
6	0.020333	0.030333	0.024667	0.00555417	0.00677917
7	0.012333	0.042333	0.022667	0.00397917	0.00735417
8	0.006333	0.056333	0.018667	0.00235417	0.00697917
9	0.002333	0.072333	0.012667	0.00097917	0.00535417
10	0.000333	0.090333	0.004667	0.00015417	0.00217917

Carry-Over and Stiffness Factors.—The moment carry-over factor from end A to end B of a beam is defined as the moment produced at the fixed end B by a unit moment applied at A. It can be shown that

$$C_{AB} = \frac{\theta^A{}_B}{\theta^B{}_B} \ldots\ldots\ldots\ldots\ldots\ldots\ldots\ldots (8a)$$

and

$$C_{BA} = \frac{\theta^B{}_A}{\theta^A{}_A} \ldots\ldots\ldots\ldots\ldots\ldots\ldots\ldots (8b)$$

in which C_{AB} is the moment carry-over factor from end A to end B and C_{BA} is the moment carry-over factor from end B to end A.

Because the stiffness factor K at the end of a beam is defined as the moment required to rotate that end through a unit angle, it follows that when end B is simply supported

$$K_{AB} = \frac{1}{\theta^A{}_A} \quad \text{(9)}$$

and when end B is fixed

$$K'_{AB} = \frac{\theta^B{}_B}{\theta^A{}_A\,\theta^B{}_B - \theta^A{}_B\,\theta^B{}_A} \quad \text{(10)}$$

in which K_{AB} is the stiffness factor at end A if end B is simply supported and K'_{AB} denotes the stiffness factor at end A if end B is fixed. When end A is simply supported,

$$K_{BA} = \frac{1}{\theta^B{}_B} \quad \text{(11)}$$

and when A is fixed

$$K'_{BA} = \frac{\theta^A{}_A}{\theta^A{}_A\,\theta^B{}_B - \theta^A{}_B\,\theta^B{}_A} \quad \text{(12)}$$

in which K_{BA} is the stiffness factor at end B when end A is simply supported and K'_{BA} represents the stiffness factor at end B when end A is fixed.

Thus, it is evident that, after the values of the end slopes have been determined, the carry-over factor and stiffness factor may be found by using Eqs. 8 to 12. Also, it should be noted that the units of Eqs. 9 to 12 are such that the stiffness factors vary directly as the moment of inertia times the modulus of elasticity and inversely as the length of the beam.

Fixed-End Moments.—Fig. 2(*b*) shows the $(M/E\,I)$-diagram for a simple beam having a constant value of $E\,I$ and acted on by a unit concentrated load. For any segment extending a distance $a\,L$ along the beam from the left support A, when $a < b$,

$$\theta^P{}_A = \frac{L^2}{E\,I}\left[\left(\frac{a^2}{2} - \frac{a^3}{3}\right)(1 - b)\right] \quad \text{(13)}$$

and

$$\theta^P{}_B = \frac{L^2}{E\,I}\left[\frac{a^3}{3}(1 - b)\right] \quad \text{(14)}$$

in which b is the ratio of the distance measured from the left support to the point of application of load P to the span length, $\theta^P{}_A$ denotes the slope at end A caused by a unit concentrated load, and $\theta^P{}_B$ is the slope at end B caused by a unit concentrated load.

When $a > b$,

$$\theta^P{}_A = \frac{L^2}{E\,I}\left[b\left(a - a^2 + \frac{a^3}{3}\right) - \frac{b^2}{2} + \frac{b^3}{6}\right] \quad \text{(15)}$$

and

$$\theta^P{}_B = \frac{L^2}{E\,I}\left[b\left(\frac{a^2}{2} - \frac{a^3}{3}\right) - \frac{b^3}{6}\right] \quad \text{(16)}$$

The quantities in brackets in Eqs. 13 through 16 are coefficients for end slopes produced by a segment of the $(M/E\,I)$-diagram extending a distance $a\,L$ from end A. Coefficients for ten equal segments have been evaluated from these equations and are given in Table 2. By the use of these coefficients the total

TABLE 2.—COEFFICIENTS FOR END SLOPES PRODUCED BY A CONCENTRATED LOAD

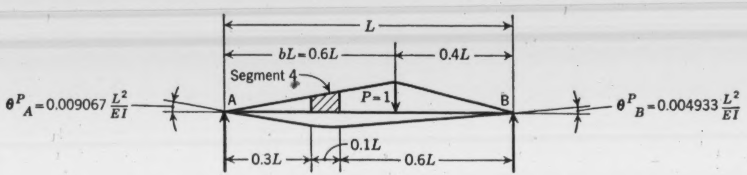
$\theta^P_A = 0.009067 \frac{L^2}{EI}$
$\theta^P_B = 0.004933 \frac{L^2}{EI}$
L
$bL = 0.6L$
$0.4L$
Segment 4
$P=1$
A
B
$0.3L$
$0.1L$
$0.6L$

Segment	For θ^P_A									
	VALUES OF b									
	0.1	0.2	0.3	0.4	0.5	0.6	0.7	0.8	0.9	
1	0.004200	0.003733	0.003267	0.002800	0.002333	0.001867	0.001400	0.000933	0.000467	10
2	0.007233	0.010133	0.008867	0.007600	0.006333	0.005067	0.003800	0.002533	0.001267	9
3	0.005633	0.011267	0.013067	0.011200	0.009333	0.007467	0.005600	0.003733	0.001867	8
4	0.004233	0.008467	0.012700	0.013600	0.011333	0.009067	0.006800	0.004533	0.002267	7
5	0.003033	0.006067	0.009100	0.012133	0.012333	0.009867	0.007400	0.004933	0.002467	6
6	0.002033	0.004067	0.006100	0.008133	0.010167	0.009867	0.007400	0.004933	0.002467	5
7	0.001233	0.002467	0.003700	0.004933	0.006167	0.007400	0.006800	0.004533	0.002267	4
8	0.000633	0.001267	0.001900	0.002533	0.003167	0.003800	0.004433	0.003733	0.001867	3
9	0.000233	0.000467	0.000700	0.000933	0.001167	0.001400	0.001633	0.001867	0.001267	2
10	0.000033	0.000067	0.000100	0.000133	0.000167	0.000200	0.000233	0.000267	0.000300	1
	0.9	0.8	0.7	0.6	0.5	0.4	0.3	0.2	0.1	
	VALUES OF b									Segment
	For θ^P_B									

values of end slopes for beams with variable moments of inertia may be found by a summation process similar to that indicated by Eq. 7.

For a unit uniform load w (Fig. 2(c)),

$$\theta^w{}_A = \frac{L^3}{E\,I}\left(\frac{a^2}{4} - \frac{a^3}{3} + \frac{a^4}{8}\right) \qquad (17)$$

and

$$\theta^w{}_B = \frac{L^3}{E\,I}\left(\frac{a^3}{6} - \frac{a^4}{8}\right) \qquad (18)$$

in which $\theta^w{}_A$ is the slope at end A caused by a unit uniformly distributed load and $\theta^w{}_B$ is the slope at end B caused by a unit uniformly distributed load. The coefficients of these slopes for ten equal segments are given in Table 1(*b*).

With the end slopes evaluated, equations can be used to determine the fixed-end moments; for a concentrated load P, when both ends of the beam are fixed,

$$M^F{}_A = P\,(\theta^P{}_A\,K'_{AB} - \theta^P{}_B\,C_{BA}\,K'_{BA}) \qquad (19)$$

and

$$M^F{}_B = P\,(\theta^P{}_B\,K'_{BA} - \theta^P{}_A\,C_{AB}\,K'_{AB}) \qquad (20)$$

in which $M^F{}_A$ is the fixed-end moment at end A of span AB and $M^F{}_B$ is the fixed-moment at end B.

For uniform loads when both ends of the beam are fixed,

$$M^F{}_A = w\,(\theta^w{}_A\,K'_{AB} - \theta^w{}_B\,C_{BA}\,K'_{BA}) \qquad (21)$$

and

$$M^F{}_B = w\,(\theta^w{}_B\,K'_{BA} - \theta^w{}_A\,C_{AB}\,K'_{AB}) \qquad (22)$$

For concentrated loads when end A is simply supported,

$$M^F{}_B = P\,(\theta^P{}_B\,K_{BA}) \qquad (23)$$

For uniform loads when end A is simply supported,

$$M^F{}_B = w\,(\theta^w{}_B\,K_{BA}) \qquad (24)$$

It should be noted that the units of the terms in parentheses in Eqs. 19, 20, and 23 are such that the moments are the product of load and length. Similarly, the moments from Eqs. 21, 22, and 24 reduce to the form of load per unit length times length squared.

Dead-Load Deflections.—The dead-load deflection at any point on a beam can also be computed by the method of constant ($E\,I$)-segments. In this case, however, the quantities used are the moments of the segments of the ($M/E\,I$)-diagram rather than the reactions.

In order to compute the dead-load deflections of both simple and continuous beams, parabolic, triangular, and rectangular moment diagrams may be considered. The parabolic diagram is used to compute the simple-beam deflections; the triangular and rectangular diagrams serve for computing the deflections caused by end moments.

Fig. 2(*c*) shows a beam having a constant value of $E\,I$ subjected to a parabolic $(M/E\,I)$-diagram resulting from a uniformly distributed load of w per unit length. The deflection Δ_D at point D (which is a distance d from A) caused by that segment of the $(M/E\,I)$-diagram extending a distance $a\,L$ along the beam from the left support A can be expressed, when $a < d$, as

$$\Delta_D = \frac{w\,L^4}{E\,I}\left[\tfrac{1}{2}\,(1 - d)\left(\frac{a^3}{3} - \frac{a^4}{4}\right)\right] \dots\dots \quad (25)$$

When $a > d$,

$$\Delta_D = \frac{w\,L^4}{E\,I}\left[\frac{d}{2}\left(\frac{a^2}{2} - \frac{2\,a^3}{3} + \frac{a^4}{4}\right) - \frac{d}{2}\left(\frac{d^2}{6} - \frac{d^3}{12}\right)\right] \dots\dots \quad (26)$$

Similarly, for a moment M_T applied at end B, when $a < d$,

$$\Delta_D = \frac{M_T\,L^2}{E\,I}\left[(1 - d)\,\frac{a^3}{3}\right] \dots\dots \quad (27)$$

When $a > d$,

$$\Delta_D = \frac{M_T\,L^2}{E\,I}\left[d\left(\frac{a^2}{2} - \frac{a^3}{3}\right) - \frac{d^3}{6}\right] \dots\dots \quad (28)$$

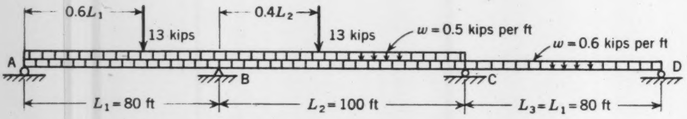

FIG. 3.—THREE-SPAN CONTINUOUS BEAM AND LOADINGS

For a rectangular moment diagram with equal moments applied at ends A and B when $a < d$,

$$\Delta_D = \frac{M_R\,L^2}{E\,I}\left[(1 - d)\,\frac{a^2}{2}\right] \dots\dots \quad (29)$$

When $a > d$,

$$\Delta_D = \frac{M_R\,L^2}{E\,I}\left[a\,d\left(1 - \frac{a}{2}\right) - \frac{d^2}{2}\right] \dots\dots \quad (30)$$

In Eqs. 25 through 30 the quantities in brackets are coefficients of the deflection of point D on a beam having a constant value of $E\,I$. These quantities are due only to the segment $a\,L$ of the $(M/E\,I)$-diagram. Coefficients are evaluated for ten equal segments in Table 3 for values of d of $\frac{1}{4}$, $\frac{1}{2}$, and $\frac{3}{4}$.

For beams of nonuniform section the deflections are computed by the same process of summation as that indicated by Eq. 7 for end slopes.

EXAMPLES OF APPLICATION

Fig. 3 shows a three-span continuous beam and loading; there will be determined the negative moments at supports B and C and the deflection at the $\frac{1}{2}$ point of span AB due to the uniform dead load of 0.6 kip per ft.

TABLE 3.—Coefficients for Deflections

(*a*) Parabolic Moment Diagram

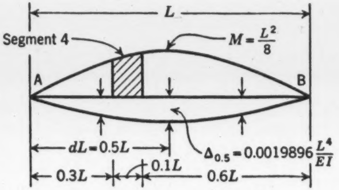
L
Segment 4
$M=\frac{L^2}{8}$
A
B
$dL=0.5L$
$\Delta_{0.5}=0.0019896\frac{L^4}{EI}$
$0.3L$
$0.1L$
$0.6L$

(*b*) Triangular Moment Diagram

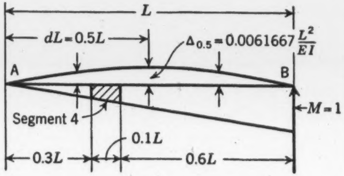
L
$dL=0.5L$
$\Delta_{0.5}=0.0061667\frac{L^2}{EI}$
A
B
$M=1$
Segment 4
$0.1L$
$0.3L$
$0.6L$

(*c*) Rectangular Moment Diagram

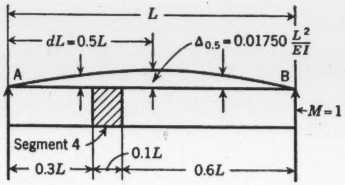
L
$dL=0.5L$
$\Delta_{0.5}=0.01750\frac{L^2}{EI}$
A
B
$M=1$
Segment 4
$0.1L$
$0.3L$
$0.6L$

Segment	Values of d								
	(*a*) Parabolic Moment Diagram			(*b*) Triangular Moment Diagram			(*c*) Rectangular Moment Diagram		
	1/4	1/2	3/4	1/4	1/2	3/4	1/4	1/2	3/4
1	0.0001156250	0.0000770833	0.0000385417	0.00025000	0.00016667	0.00008333	0.003750	0.002500	0.001250
2	0.0007343750	0.0004895833	0.0002447917	0.00175000	0.00116667	0.00058333	0.011250	0.007500	0.003750
3	0.0016388021	0.0011770833	0.0005885417	0.00439583	0.00316667	0.00158333	0.017500	0.012500	0.006250
4	0.0018385417	0.0019895833	0.0009947917	0.00566667	0.00616667	0.00308333	0.016250	0.017500	0.008750
5	0.0016947917	0.0027770833	0.0013885417	0.00616667	0.01016667	0.00508333	0.013750	0.022500	0.011250
6	0.0013885417	0.0027770833	0.0016947917	0.00616667	0.01233333	0.00758333	0.011250	0.022500	0.013750
7	0.0009947917	0.0019895833	0.0018385417	0.00566667	0.01133333	0.01058333	0.008750	0.017500	0.016250
8	0.0005885417	0.0011770833	0.0016388021	0.00466667	0.00933333	0.01310417	0.006250	0.012500	0.017500
9	0.0002447917	0.0004895833	0.0007343750	0.00316667	0.00633333	0.00950000	0.003750	0.007500	0.011250
10	0.0000385417	0.0000770833	0.0001156250	0.00116667	0.00233333	0.00350000	0.001250	0.002500	0.003750

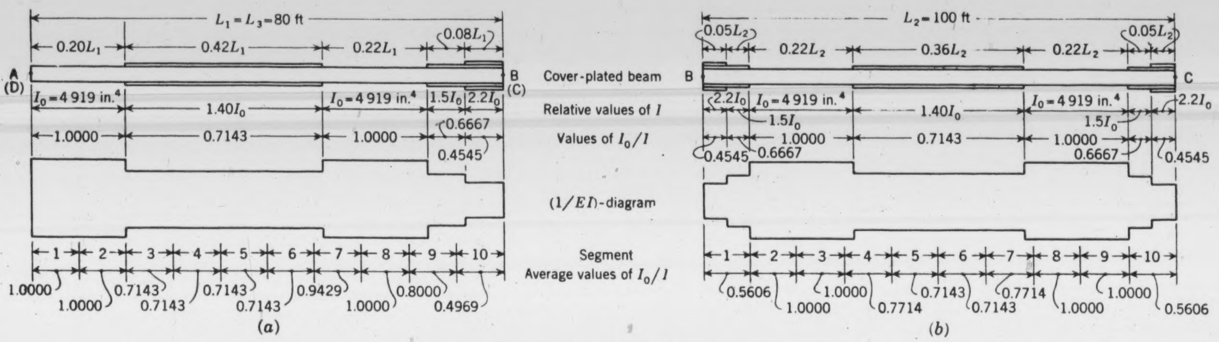
$L_1 = L_3 = 80$ ft
$0.20L_1$
$0.42L_1$
$0.22L_1$
$0.08L_1$
A
(D)
B
(C)
$I_0 = 4\,919$ in.^{4}
$1.40I_0$
$I_0 = 4\,919$ in.^{4}
$1.5I_0$
$2.2I_0$
1.0000
0.7143
1.0000
0.6667
0.4545
1
2
3
4
5
6
7
8
9
10
1.0000
1.0000
0.7143
0.7143
0.7143
0.7143
0.9429
1.0000
0.8000
0.4969
(a)
Cover-plated beam
Relative values of I
Values of I_0/I
$(1/EI)$-diagram
Segment
Average values of I_0/I
$L_2 = 100$ ft
$0.05L_2$
$0.22L_2$
$0.36L_2$
$0.22L_2$
$0.05L_2$
B
C
$2.2I_0$
$I_0 = 4\,919$ in.^{4}
$1.5I_0$
$1.40I_0$
$I_0 = 4\,919$ in.^{4}
$1.5I_0$
$2.2I_0$
0.4545
0.6667
1.0000
0.7143
1.0000
0.6667
0.4545
1
2
3
4
5
6
7
8
9
10
0.5606
1.0000
1.0000
0.7714
0.7143
0.7143
0.7714
1.0000
1.0000
0.5606
(b)

Fig. 4.—Properties of Spans

TABLE 4.—Computations for Beam in Fig. 4

Seg-ment	(a) Span AB						(b) Span BC									
	For θ^B_B		For θ^P_B		For θ^w_B		For $\theta^B_B = \theta^C_C$		For $\theta^B_C = \theta^C_B$		For θ^P_B		For θ^P_C		For $\theta^w_B = \theta^w_C$	
	Table 1(a)	θ^B_B	Table 2	θ^P_B	Table 1(b)	θ^w_B	Table 1(a)	$\theta^B_B = \theta^C_C$	Table 1(a)	$\theta^B_C = \theta^C_B$	Table 2	θ^P_B	Table 2	θ^P_C	Table 1(b)	$\theta^w_B = \theta^w_C$
1	0.00033	0.0003	0.00013	0.00013	0.00015	0.00015	0.09033	0.0506	0.00467	0.0026	0.00280	0.00157	0.00020	0.00011	0.00218	0.00122
2	0.00233	0.0023	0.00093	0.00093	0.00098	0.00098	0.07233	0.0723	0.01267	0.0127	0.00760	0.00760	0.00140	0.00140	0.00535	0.00535
3	0.00633	0.0045	0.00253	0.00181	0.00235	0.00168	0.05633	0.0563	0.01867	0.0187	0.01120	0.01120	0.00380	0.00380	0.00698	0.00698
4	0.01233	0.0088	0.00493	0.00352	0.00398	0.00284	0.04233	0.0326	0.02267	0.0175	0.01360	0.01050	0.00740	0.00571	0.00735	0.00567
5	0.02033	0.0145	0.00813	0.00581	0.00555	0.00396	0.03033	0.0217	0.02467	0.0176	0.01213	0.00867	0.00987	0.00705	0.00678	0.00484
6	0.03033	0.0217	0.01213	0.00867	0.00678	0.00484	0.02033	0.0145	0.02467	0.0176	0.00813	0.00581	0.00987	0.00705	0.00555	0.00396
7	0.04233	0.0399	0.01360	0.01283	0.00735	0.00693	0.01233	0.0095	0.02267	0.0175	0.00493	0.00380	0.00907	0.00700	0.00398	0.00307
8	0.05633	0.0563	0.01120	0.01120	0.00698	0.00698	0.00633	0.0063	0.01867	0.0187	0.00253	0.00253	0.00747	0.00747	0.00235	0.00235
9	0.07233	0.0579	0.00760	0.00608	0.00535	0.00428	0.00233	0.0023	0.01267	0.0127	0.00093	0.00093	0.00507	0.00507	0.00098	0.00098
10	0.09033	0.0449	0.00280	0.00139	0.00218	0.00108	0.00033	0.0002	0.00467	0.0026	0.00013	0.00007	0.00187	0.00105	0.00015	0.00008
Total		0.2511		0.05237		0.03372		0.2663		0.1382		0.05268		0.04571		0.03450

The variation in the moment of inertia and values of I_0/I for the end spans and center span are given in Fig. 4. The average values of I_0/I for each of the 10 equal segments in each span are also shown in this illustration.

In Table 4 there is shown a typical form of the computations for determining the end slopes at end B of span AB and at both ends B and C of span BC. The values of I_0/I are obtained from Fig. 4, and the values of the coefficients are taken from Tables 1 and 2. The value of the coefficient for each segment is multiplied by the value of I_0/I for that segment, and the product is entered in the adjoining column. The columns are then totaled; the values of these column totals, when multiplied by the ratio $L/E\,I_0$, yield the end slopes.

Carry-Over Factors and Stiffness Factors.—Span AB is simply supported at A; therefore, the stiffness is found by Eq. 11—

$$K_{BA} = \frac{1}{0.2511} = 3.98\,\frac{E\,I_0}{L_1}.$$

The beam is continuous over supports B and C; therefore, carry-over factors and stiffness factors for span BC are computed from Eqs. 8, 10, and 12:

$$C_{BC} = C_{CB} = \frac{0.1382}{0.2663} = 0.519$$

$$K'_{BC} = K'_{CB} = \frac{0.2663}{(0.2663)^2 - (0.1382)^2} = 5.14\,\frac{E\,I_0}{L_2}.$$

It should be noted that, when the coefficients in Table 1(*a*) are used for the analysis of span BC, end A becomes B and end B becomes C. Because of symmetry the computations for span BC are reduced considerably, and the stiffness determined for span AB also applies to span CD.

Fixed-End Moments.—The fixed-end moment at support B is for the concentrated load, from Eq. 23,

$$M^F{}_B = 13.0\ (80)\ (0.05237 \times 3.98) = 217\text{ ft-kips}$$

and for the uniform load, from Eq. 24,

$$M^F{}_B = 1.1\ (80)^2\ (0.03372 \times 3.98) = 944\text{ ft-kips}$$

which results in a total $M^F{}_B$ of 1,161 ft-kips.

The coefficients for the end slope at B are obtained from Tables 2 and 1(*b*). After the end slopes at B resulting from the concentrated and uniform loads have been determined, the respective fixed-end moments are computed from Eqs. 23 and 24.

In a similar manner, the fixed-end moments are obtained at supports B and C for the loads in span BC. Because the span is fixed at both ends, the moments are found from Eqs. 19, 20, 21, and 22—

For the concentrated load, from Eq. 19,

$$M^F{}_B = 13.0\ (100)\ [(0.05268 \times 5.14) - (0.04571 \times 0.519 \times 5.14)] = 194\text{ ft-kips.}$$

For the uniform load, from Eq. 21,

$$M^F{}_B = 1.1\ (100)^2\,[(0.03450 \times 5.14) - (0.03450 \times 0.519 \times 5.14)] = 939 \text{ ft-kips.}$$

These result in a total $M^F{}_B$ of 1,133 ft-kips. For the concentrated load, from Eq. 20,

$$M^F{}_C = 13.0\ (100)\,[(0.04571 \times 5.14) - (0.05268 \times 0.519 \times 5.14)] = 123 \text{ ft-kips.}$$

For the uniform load, from Eq. 22,

$$M^F{}_C = M^F{}_B = 939 \text{ ft-kips.}$$

These result in a total $M^F{}_C$ of 1,062 ft-kips.

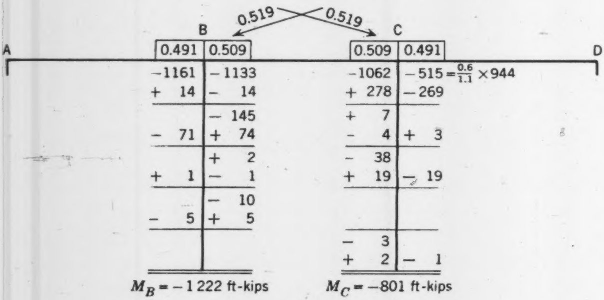
0.519
0.519
A
B
C
D
0.491
0.509
0.509
0.491
−1161
+ 14
− 71
+ 1
− 5
− 1133
− 14
− 145
+ 74
+ 2
− 1
− 10
+ 5
−1062
+ 278
+ 7
− 4
− 38
+ 19
− 3
+ 2
− 515 = 0.6/1.1 × 944
− 269
+ 3
− 19
− 1
M_B = −1 222 ft-kips
M_C = −801 ft-kips

(*a*) Moments due to dead load plus live load

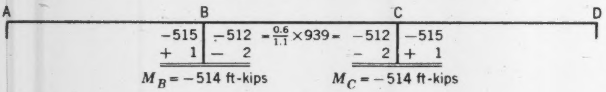
A
B
C
D
−515
+ 1
−512 = 0.6/1.1 × 939 = −512
− 2
− 2
−515
+ 1
M_B = −514 ft-kips
M_C = −514 ft-kips

(*b*) Moments due to dead load

FIG. 5.—MOMENT-DISTRIBUTION COMPUTATIONS

It should be noted that these computations are reduced because of symmetry of the uniform load and of the properties of the beam.

No computations for the fixed-end moment in span CD have been made because the moment may be determined by a ratio after the computations for the uniform load in span AB have been made.

Moment Distribution.—The actual moments at supports B and C due to the total loading on the three-span continuous unit are computed in Fig. 5(*a*); the dead-load moments are determined in Fig. 5(*b*). The stiffnesses are

$$K_{BA} = \frac{3.98}{80} = 0.0497$$

and

$$K'_{BC} = \frac{5.14}{100} = \frac{0.0514}{0.1011}.$$

The distribution factors are

$$BA = CD = \frac{0.0497}{0.1011} = 0.491$$

and

$$BC = CB = \frac{0.0514}{0.1011} = 0.509.$$

These computations are self-explanatory. It is important to note that the computations for relative stiffness and distribution factors take into account the differences in span lengths. Because the same reference value of I_0 was used in determining the values of relative I in all spans and because E is constant, these values need not be included in the computations for the relative stiffnesses.

TABLE 5.—DEAD–LOAD DEFLECTION AT MIDPOINT OF AB

Segment	I_0/I	FOR UNIFORM LOAD		FOR MOMENT AT B	
		Table 3 (*a*)	$\Delta_{\frac{1}{2}}$	Table 3 (*b*)	$\Delta_{\frac{1}{2}}$
1	1.0000	0.0000771	0.000077	0.0001667	0.000167
2	1.0000	0.0004896	0.000490	0.0011667	0.001167
3	0.7143	0.0011771	0.000840	0.0031667	0.002260
4	0.7143	0.0019896	0.001416	0.0061667	0.004400
5	0.7143	0.0027771	0.001976	0.0101667	0.007250
6	0.7143	0.0027771	0.001976	0.0123333	0.008790
7	0.9429	0.0019896	0.001873	0.0113333	0.010690
8	1.0000	0.0011771	0.001177	0.0093333	0.009333
9	0.8000	0.0004896	0.000392	0.0063333	0.005060
10	0.4969	0.0000771	0.000038	0.0023333	0.001160
Total			0.010255		0.050277

Deflection.—The dead-load deflection at the ½ point of span AB is computed in Table 5 using the coefficients from Table 3. It should be noted that this deflection is made up of two parts. The deflection resulting from the simple beam, parabolic moment diagram is downward, whereas the deflection due to the triangular variation in negative moment, Fig. 5 (*b*), is upward:

$$\Delta_{\frac{1}{2}}\downarrow = \frac{0.010255 \times 0.6 \times 80^4}{30{,}000 \times 4{,}919} = 0.001710 \times (12)^3 = 2.95 \text{ in.}\downarrow$$

$$\Delta_{\frac{1}{2}}\uparrow = \frac{0.050277 \times 514 \times 80^2}{30{,}000 \times 4{,}919} = 0.001121 \times (12)^3 = \frac{1.94 \text{ in.}\uparrow}{1.01 \text{ in.}\downarrow} = \Delta_{\frac{1}{2}}.$$

CONCLUSIONS

The example contained herein demonstrates the constant-segment method of analysis and the usefulness of predetermined constants. Tables 4 and 5 represent much less labor than that required by any other method of analysis. The method and constants presented herein have been used to obtain a direct solution for moments and deflections but they are also useful in the development of influence lines.

It should be noted that one of the distinct advantages of the use of the constants given in Tables 1, 2, and 3 is the ease with which computations such as those given in Tables 4 and 5 may be developed by single settings of the values of I_0/I on the slide-rule or computing machine.

DISCUSSION

Thomas F. Hickerson,[3] M. ASCE.—Although not specifically stated by the authors, this work is based on the conjugate-beam method. In the belief that this principle offers the best approach to structural analysis and particularly to beam slopes and deflections, it has been used exclusively in a similar work.[4]

Comparing Fig. 6(*a*) and Fig. 6(*b*), it is obvious Eq. 5 is correct without citing Maxwell's law of reciprocal relations.

At the bottoms of Tables 1 through 3, the totals could have been given to advantage. Thus, in Table 1(*a*), from left to right, the totals would be 0.33333, 0.33333, and 0.16667, indicating that, as a limiting condition, when *I* is constant throughout the member,

$$\theta^A{}_A = \frac{1}{3}\frac{L}{E\,I} \qquad (31)$$

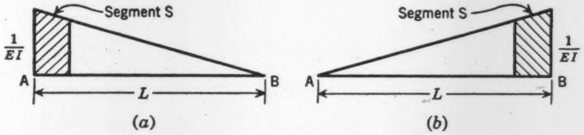

Fig. 6.—($M/E\,I$)—Diagrams for Span AB

and

$$\theta^B{}_A = \frac{1}{6}\frac{L}{E\,I} \qquad (32)$$

for a unit moment at A.

Also, in Table 2 for $b = 0.4$, the total is 0.064. Hence, if *I* is constant,

$$\theta^P{}_A = 0.064\,\frac{P\,L^2}{E\,I} \qquad (33)$$

The stiffness, carry-over, and distribution factors are based on the assumption that the other end of the member is fixed—a condition that usually does not exist. Hence, distribution and carry-over must take place through a few cycles in order to obtain the final correct result.

The inclusion of coefficients for deflections produced by a concentrated load would have added to the completeness of the paper. Perhaps Messrs. Hanson and Wiley wished to avoid dealing with absolute maximum deflections. However, the midspan-deflection coefficients are closely representative of the maximum deflections.

The neatness, clarity, and accuracy of the paper is commendable. However, one may doubt whether it presents the simplest and shortest procedure for obtaining slopes, deflections, or moments when *I* is variable.

---

[3] Formerly Prof. of Civ. Eng., Univ. of North Carolina, Chapel Hill, N. C.

[4] "Statically Indeterminate Frameworks: Beam Deflection When *I* Is Constant or Variable," by Thomas F. Hickerson, University Press, Chapel Hill, N. C., 1949.

Eugene J. Vayda,[5] M. ASCE.—The interpretation and presentation of this subject by Messrs. Hanson and Wiley are to be commended. To illustrate this method of analysis, the fixed-end moment at the top of a haunched column that is bent by an offset force and hinged at the bottom, as shown in Fig. 7 (a), shall be determined.

The elastic line of the simply supported beam AB, bent by a moment M (in which $M = P\,e$), will have a slope with the horizontal of θ_P at point B (Fig. 7 (*b*)). The moment of inertia is computed at the center of gravity of each division (Fig. 7 (*c*). After finding M_P and M_P/I at the center of gravity of each division, the reaction of the conjugate beam, loaded with the (M_P/I)-diagram, is R_P at point B (Fig. 7 (*d*)) and

$$E\,\theta_P = R_P \qquad (34)$$

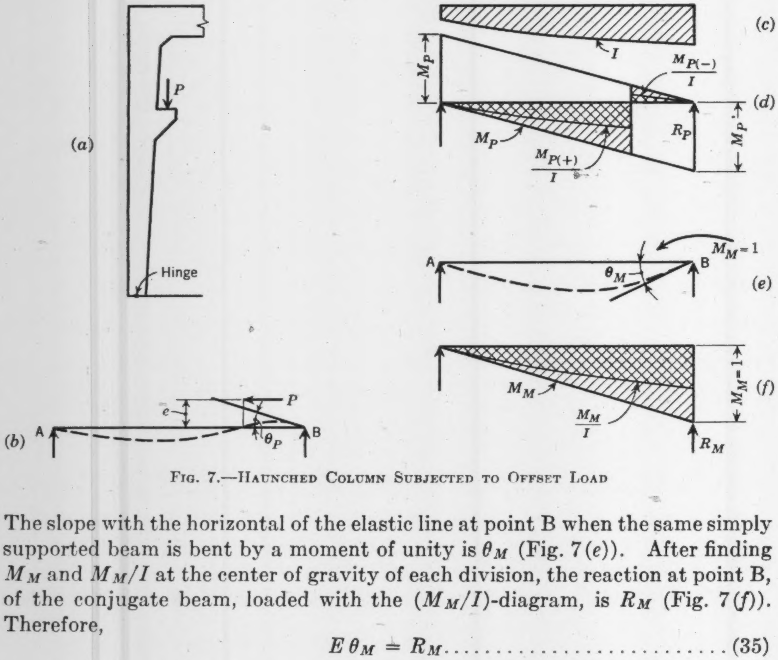

Fig. 7.—Haunched Column Subjected to Offset Load

The slope with the horizontal of the elastic line at point B when the same simply supported beam is bent by a moment of unity is θ_M (Fig. 7 (*e*)). After finding M_M and M_M/I at the center of gravity of each division, the reaction at point B, of the conjugate beam, loaded with the (M_M/I)-diagram, is R_M (Fig. 7 (*f*)). Therefore,

$$E\,\theta_M = R_M \qquad (35)$$

and if the total slope of the elastic line at the fixed end B is θ_B,

$$E\,\theta_B = E\,(\theta_P + \theta_M) = R_P + R_M\,M_M = 0 \qquad (36)$$

from which

$$M_M = -\frac{R_P}{R_M} \qquad (37)$$

---

[5] Designer, Tippetts-Abbett-McCarthy-Stratton, Engrs., New York, N. Y.

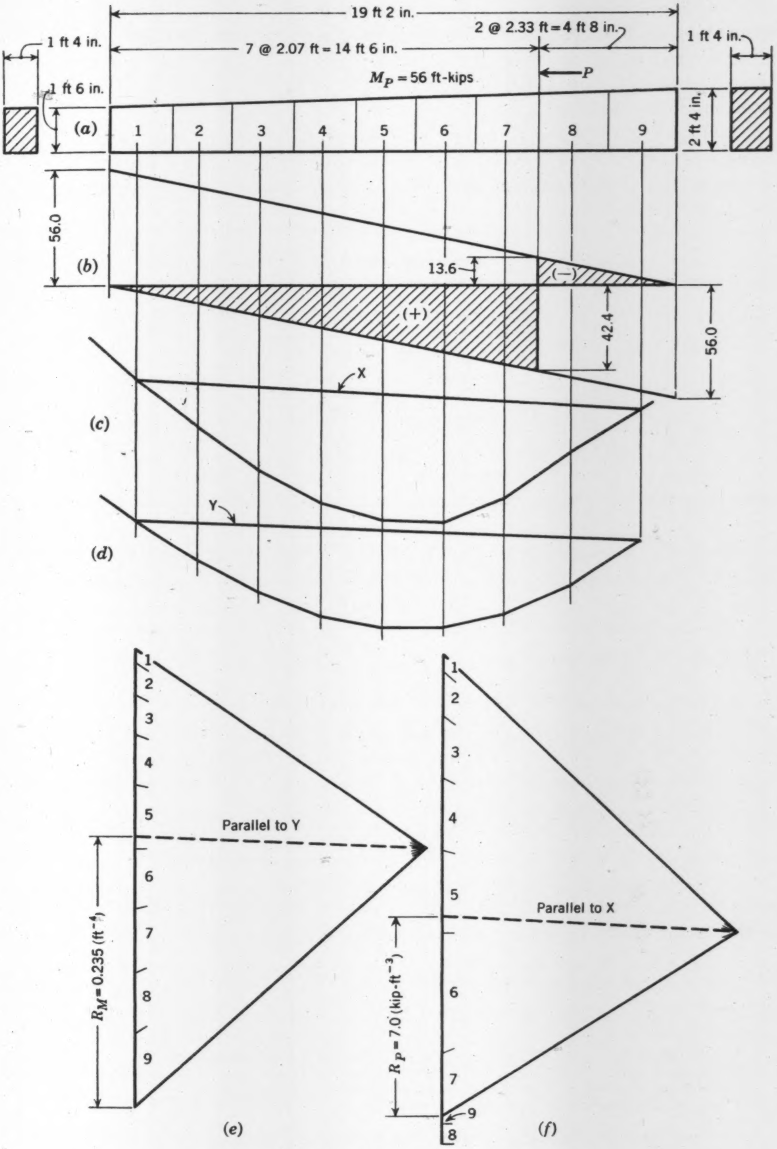
19 ft 2 in.
2 @ 2.33 ft = 4 ft 8 in.
1 ft 4 in.
7 @ 2.07 ft = 14 ft 6 in.
1 ft 4 in.
M_P = 56 ft-kips
P
1 ft 6 in.
(a)
1
2
3
4
5
6
7
8
9
2 ft 4 in.
56.0
(b)
13.6
(−)
(+)
42.4
56.0
X
(c)
Y
(d)
1
2
3
4
5
Parallel to Y
6
7
8
9
R_M = 0.235 (ft^{-4})
(e)
1
2
3
4
5
Parallel to X
6
7
9
8
R_P = 7.0 (kip-ft^{-3})
(f)

FIG. 8.—GRAPHICAL ANALYSIS

Graphical analysis offers a fast solution of the problem in which a crane runway is attached to the vertical member of a rigid frame. It is assumed that a bending moment of 56 ft-kips is created (Fig. 8(*a*)) and that the column is hinged at the 1 ft-6 in. end and fixed at the 2 ft-4 in. end; the computations have been made in Table 6.

In Fig. 8(*b*), M_P is determined for each division point. With the (M_P/I)-force polygon (Fig. 8(*f*)) the funicular polygon of Fig. 8(*c*) is drawn; the line drawn in Fig. 8(*f*) parallel to the line X of Fig. 8(*c*) cuts of the reaction of the conjugate beam, R_P.

TABLE 6.—COMPUTATIONS FOR FIG. 8

Segment	Value of I, in ft^4	Value of M_P, in foot-kips	Value of M_P/I	Value of M_M for unit moment at B	Value of M_M/I
1	5.00	3.03	0.61	0.054	0.0108
2	5.92	9.08	1.53	0.162	0.0273
3	6.94	15.13	2.18	0.270	0.0390
4	8.20	21.18	2.58	0.378	0.0460
5	9.30	27.73	2.94	0.486	0.0521
6	10.70	33.28	3.11	0.594	0.0555
7	12.10	39.33	3.25	0.702	0.0580
8	13.90	−10.20	−0.735	0.815	0.0585
9	15.90	− 3.40	−0.214	0.950	0.0600

From the force polygon (Fig. 8(*e*)) the funicular polygon of Fig. 8(*d*) is drawn. The line in the (M_M/I)-force polygon (Fig. 8(*e*)) parallel to the line Y of Fig. 8(*d*) cuts off the reaction R_M of the conjugate beam.

The fixed-end moment M_F at the large end is the quotient of the two conjugate-beam reactions.

JARO J. POLIVKA,[6] M. ASCE.—In the "Synopsis" it is noted that there are other methods of analysis for beams having variable moments of inertia but these are said to be more time-consuming and subject to numerical errors. One method which proves to be very simple and permits checking during various steps of the computations is the method of constant centers of elastic rotations or fixed points.[7, 8, 9] This method is advantageous in that a great part of the computations can be applied to any type of loading. The continuous beam analyzed as an example by Messrs. Hanson and Wiley needs only two fixed points to be determined because of symmetry, and the resulting bending moments for any type of loading can be found directly, with any accuracy required, without using a series of approximations characteristic of the method of moment distribution. The fixed points are determined by slopes $\theta^A{}_A$, $\theta^B{}_B$, and $\theta^A{}_B$ computed either by the method presented by the

---

[6] Cons. Engr., Berkeley, Calif., and Lecturer, Stanford Univ. Stanford, Calif.

[7] "Graphical Methods of Analyzing Statically Indeterminate Structures," by J. J. Polivka, *Mimeographed Lectures*, Univ. of California, Berkeley, Calif., 1940, and 2d Ed., 1942.

[8] "Frames and Bents in Reinforced Concrete," by J. J. Polivka, *Revue du Béton Armé*, Vols. 9 and 10, Brussels, 1920.

[9] "Continuous Arches on Elastic Supports," by J. J. Polivka, *Der Brueckenbau*, Vols. 4, 5, and 6, Heidelberg, 1920.

authors, or, more accurately, by the same moment-area method, but applied to actual segments having different moments of inertia; there is practically no difference in the results of both methods. For example, Table 4(*b*) indicates the values $\theta^B{}_B = 0.2663$ and $\theta^B{}_C = 0.1382$, and the writer computed the corresponding values to be $\theta^B{}_B = 0.263996$ and $\theta^B{}_C = 0.140636$, their sum being 0.404632 as compared with the authors' sum of 0.4045.

Every such analysis should be checked for final results. A simple method consists in computing the final slopes under any given loading at supports B and C for both adjacent spans, and these slopes must be numerically equal. It is suggested that one perform this checking for any of the assumed types of loading.

WALTER E. HANSON,[10] M. ASCE, AND WALLACE F. WILEY[11].—The discussions that have been presented are most interesting and have contributed to the understanding of the method and its application; the comments have been constructive in nature and clearly presented. The writers appreciate these discussions as well as the many favorable comments from engineers who have recognized the time-saving features of the method in the analysis of indeterminate highway bridge girders having variable moments of inertia.

The writers agree with Mr. Hickerson that the paper is based on the conjugate-beam method. However, many other methods could be listed as bases for the work—among these are moment area, elastic weights, and angle changes. It is preferred to group all these methods under the general classification of geometry of small angle changes.

Mr. Hickerson states that "the stiffness, carry-over, and distribution factors are based on the assumption that the other end of the member is fixed—a condition that usually does not exist." Apparently, Eqs. 9 and 11 were overlooked; these give the stiffness factors, and Eqs. 23 and 24 give the fixed-end moments when one end of the span is simply supported.

Messrs. Vayda and Polivka both discussed interesting and expeditious methods of analysis involving some graphics. It is agreed that graphical procedures often expedite the solutions of many structural problems.

During the development of the paper the writers were primarily concerned with its application to the analysis of continuous highway bridges. The example used is easily recognized as a typical three-span beam with cover plates subjected to the uniform and roving concentrated live loads given in the specifications of the American Association of State Highway Officials (AASHO). Moreover, the method was extended to computations for dead-load deflections which are commonly shown on bridge plans to facilitate the construction of forms to proper elevations and dimensions to compensate for deflections caused by dead weight.

Subsequent to the publication of the paper, the writers have used the method in the analysis of several welded, haunched, highway bridge girders.

---

[10] Cons. Engr., Hanson, Collins & Rice, Springfield, Ill.

[11] Senior Bridge Designer, Illinois Div. of Highways, Springfield, Ill.

In these designs the H-S truck loading given in the AASHO specifications[12] has governed the positive moment values at the center of the spans. Unless the span length is exactly 140 ft, the concentrated wheel loads of this specified truck do not coincide with the $\frac{1}{10}$ points of the span. The writers have concluded that for this condition of loading it is sufficiently accurate, for purposes of design, to compute equivalent simple-beam reactions at the $\frac{1}{10}$ points and to use these reactions as the loads applied to the girder. In this way, Table 2 can be readily utilized in the analysis of this type of loading.

---

[12] "Standard Specifications for Highway Bridges," A.A.S.H.O., 6th Ed., 1953, p. 162.

AMERICAN SOCIETY OF CIVIL ENGINEERS
Founded November 5, 1852
TRANSACTIONS

Paper No. 2843

SAFETY AND THE PROBABILITY OF STRUCTURAL FAILURE

BY ALFRED M. FREUDENTHAL,[1] M. ASCE

WITH DISCUSSION BY MESSRS. ANTHONY CHIBARO, LLOYD S. LAWRENCE, JOSÉ M. CORSO, OLIVER G. JULIAN, AIDEN R. GIERASCH, AND ALFRED M. FREUDENTHAL

SYNOPSIS

Applied loads are examined as are the probabilities of unserviceability and of failure. It is shown that these two items are equally as important as the stress analysis. Only from a complete structural analysis can rational estimates of the safety factors be obtained. The concepts of unserviceability and of failure are defined, and procedures are outlined for the numerical evaluation of factors of safety. These factors are based on the expected variation of loadings and of strength properties of the structural materials, together with the economic aspects involved.

INTRODUCTION

The preoccupation of engineers with carrying capacity and safety is evidence that significant advances in structural theory can be expected from a reevaluation of the basis of such theory rather than from further refinement of the methods of stress analysis. Present (1956) structural analyses result in designs in which safety is neither balanced nor clearly specified. The formulation of a rational concept of safety and of methods for measuring safety are tasks of considerable urgency. The fact that design procedures generally result in structures of excessive safety rather than in unsafe structures is an indication of the caution exercised by designers and responsible authorities rather than of the reliability and accuracy of the procedures.

Because the design of a structure embodies uncertain predictions of the performance of structural materials as well as of expected load patterns and

---

NOTE.—Published, essentially as printed here, in August, 1954, as *Proceedings-Separate No. 468.* Positions and titles given are those in effect when the paper or discussion was approved for publication in *Transactions.*

[1] Prof. of Civ. Eng., Columbia Univ., New York, N. Y.

intensities the concept of probability must form an integral part of any rational design; any conceivable condition is necessarily associated with a numerical measure of the probability of its occurrence. It is by this measure alone that the structural significance of a specified condition can be evaluated.

The foregoing does not imply that the use of the probability theory is, in itself, sufficient to make design procedures more adequate and reliable. Probability concepts and statistical methods based thereon can be used effectively only in conjunction with a thorough knowledge of the operating conditions of the structure and of its structural action. These concepts and methods provide objective guidance for sound engineering judgment whenever random phenomena and random magnitudes have to be considered; they are useless in the analysis of nonrandom phenomena and effects.

Ignorance of the cause of variation does not make such variation random. Random variability is controlled by many factors. The effect of any one of the factors is small in comparison to that of all the others; the identification of the effect of any cause on the variation becomes, therefore, either impossible or irrelevant. Once randomness is established, however, the rules governing the variation are as rigid as those in classical mechanics governing the relations between cause and effect.

Design Procedure

Conditions of Failure and of Unserviceability.—The principal aspects of the operating conditions of a load-carrying structure are the limiting conditions of service and of failure. Both conditions can be rationally specified only in terms of a characteristic load carried under defined conditions. Specification of the critical conditions in terms of stresses rather than loads presupposes proportionality between loads and stresses. The validity of this assumption is, however, limited to perfectly elastic structures, the deformations of which are small in relation to their dimensions. Because under almost all loading conditions real structures fail after extensive inelastic deformation—with substantial modifications of the initial (elastic) structural action—the specification of the failure condition in terms of a stress cannot reflect the behavior of the structure at or close to the instant of failure.

Under conditions of service, a structure should be able to sustain an infinite number or, in certain cases, a specified finite number of load applications without any noticeable effect on its usefulness or serviceability. Because, prior to failure, this usefulness can only be reduced by a change of shape (either permanent or transient) which would impair the function of the structure, the service-condition specification should contain a requirement of perfect reversibility of the deformation of the structure in conjunction with a limitation of the maximum value of such deformation. The limiting condition of serviceability is therefore defined by a characteristic (or standard) load, the repeated application of which would produce reversible deformation of the limiting magnitude.

This definition in terms of reversibility does not imply a constant, perfectly elastic condition of the structure. The most important condition for the successful elastic design of structures is that of an inelastic response of the

ductility

structural material. This response should be sufficiently pronounced to reduce to manageable levels the unavoidable stress concentrations in and close to structural connections, points of load application, and changes in cross section. In a perfectly elastic structure these concentrations would cause fracture under loads far below reasonable service loads. As a result of the localized inelastic strains that are produced in the vicinity of the stress concentration by the first few load applications, residual stresses can be created which under subsequent applications of smaller loads prevent further inelastic deformation of the structure. This load, therefore, is a "service load" despite the permanent deformation produced by its first few applications, provided that such initial permanent deformation does not impede the effective functioning of the structure.

There appears to be no valid reason for restricting the definition of limiting service load to loads which, on initial application, produce limited permanent deformation only in the connections and at points of load application. Provided that the permanent deformation resulting from initial loading is rapidly stabilized and that its magnitude is not objectionable, the specification of serviceability can be extended to such loads which, in the first few applications, cause a permanent deformation of acceptable magnitude within certain structural elements, followed by fully reversible deformations under all subsequent applications of the same or smaller loads. Such a specification of the maximum service load has, in fact, been established in the design of gun barrels (auto-frettage), steel containers under high internal pressures, heavy coil springs, crane hooks, and other machine parts with highly nonuniform elastic stress distribution; it cannot be easily translated into conventional terms of stress.

Conditions of Loading.—The load in terms of which unserviceability and failure are to be defined is a relatively simple force pattern that is, or can be made, representative of the variety of actual loads to which the structure might be subjected during its period of service. It is expedient to distinguish between (*a*) "simple" or "proportional" loads that do not vary in location, distribution, or composition but only in intensity and (*b*) "complex" loads which vary in location, distribution, and composition, as well as in intensity. Depending on the range of variation in location and distribution, certain types of complex loads can be approximately considered to be proportional loads.

Examples of proportional loads are acceleration and landing forces acting on airplanes, seismic forces, column loads, the weight of fluids in storage tanks, and forces resulting from restriction of the deformation of a structure. Complex loads that can be approximated by proportional loads are traffic loads on simple, single-span bridge members which can accommodate not more than a single traffic unit, floor loads of buildings, and wind-gust and blast forces. Complex loads that cannot be reduced to simple loads are movable forces which, because of the variation in location, may produce a change in sign of the resulting effect, as well as load combinations the components of which are independently variable. Examples of the latter are the combination of bending moments caused by wing loads (depending on acceleration) and torque (depending on speed) which act jointly on aircraft wings or axial loads and bending moments acting jointly on frame columns. The complexity of the load is as much a result of the type of the structure as of the load. In general, design procedures are much simpler for proportional loads than for complex loads.

The definition of the critical operating conditions requires the specification of (*a*) a characteristic load pattern, (*b*) the expected range of variation of the load intensity, (*c*) the expected range of variation of the rates of load application, (*d*) the duration of loading cycles, and (*e*) the characteristic pattern of the expected load sequences. The response of the designed structure may change considerably in terms of deformation and failure with the variation of any one of these characteristics.

Sequence of Design.—A rational procedure of structural design in which operating conditions and structural action are integrated with the probability of their occurrence should include the following steps:

Load Analysis.—

a. Specification of the standard load pattern and of its relationship to the actual loading conditions.

b. Evaluation of the probability of occurrence of various intensities of the standard load.

c. Analysis of the time dependence of the standard load and of its variability.

Structural Analysis.—

a. Determination of the maximum intensity of that standard load which can be applied to the idealized structure without causing structural failure during the expected period of service, either on a single application or after repeated or sustained applications. The idealization refers to the deformational response of the structural material as the structure approaches the failure load.

b. Evaluation of the probability distribution of the standard load producing failure resulting from random variations of the deformation and strength properties of the real material and from the effect of random variations of the loading rate and of the duration and sequence of load applications on those properties.

c. Determination of the limiting intensity of that standard load the repeated application of which does not impair the serviceability of the idealized structure, as defined by functionally acceptable limits of the permanent deformation under the first applications of the load and of the recoverable deformation under all subsequent load applications.

d. Evaluation of the probability distribution of the limiting intensity of the standard load of unserviceability resulting from random variation of the deformational properties of the real material and of their variation because of random variation of rate, duration, and sequence of loading.

Safety Analysis.—

a. Formulation of rules for the selection of the design conditions of the structure with respect to unserviceability and failure and choice of the optimal rule. These rules can be formulated on the basis of two fundamentally different approaches: (1) The direct probability approach specifies numerical values for the probabilities with which both failure and unserviceability are to be avoided. (2) The economic approach compares the cost of increasing the carrying capacity of the structure and the risk and eventual cost of failure. The sum of the cost of the structure and the probable cost of failure or of unserviceability shall be a minimum.

b. Determination of the intensities of the standard load associated with the acceptable probabilities of failure and of unserviceability that have resulted from the selected decision rules. The lower of these intensities, which represents the limiting standard load for which the structure is designed with the specified probability of either failure or unserviceability, is then related to the real loading conditions by inversion of step (*a*) of the "Load Analysis," thus completing the design.

The Concept of Safety.—A procedure of structural design can thus be established in which the conventional engineering concepts of safety and safety factors and load factors or permissible stresses do not appear. Considering the individual steps of the procedure it is, in fact, not immediately obvious how any of these concepts could be introduced without disturbing, by arbitrary assumptions, the sequence of design for a specified probability of failure or unserviceability.

However, because the concept of safety is deeply rooted in engineering design whereas the notion that a finite (no matter how small) probability of failure or at least of unserviceability is repulsive to a majority of engineers, it appears desirable to retain the concept of "safety" rather than to replace it by that of "probability of failure" and to reformulate the former in terms of the latter. The safety factor is thus transformed into a parameter that is a function of the random variation of all design characteristics as well as of the nonrandom variations essentially caused by the process of construction. Only the part representing the random variations can be derived from the relevant probabilities; that part represents, therefore, the objective minimum value of the safety factor. The selection of the actual engineering safety factor should be guided by this minimum value in conjunction with sound judgment concerning the possible uncertainties associated with actual construction.

An attempt has been made (1)[2] to derive this minimum safety factor from the statistical variations of the design characteristics. The assumption used concerning structural action was the invariability of such action over the entire range of operating conditions, including the limiting condition of failure. The minimum safety factor and the associated probability of failure were obtained by correlating that stress in excess of the design stress produced by a rather improbably high load fluctuation with the difference between the design strength and an improbably low value of strength of the structural material, and by multiplying the probabilities of occurrence of those extreme values of stress and strength.

Following this attempt and a subsequent one (2), the concept of safety was extensively considered, particularly in England (3), France (4), Spain (5), and Sweden (6). The subject of the safety of structures has also been discussed during the International Congresses for Bridge and Structural Engineering in 1948 (7) (8) and 1952 (9) (10). In the United States and in England, committees have been formed to deal with the subject of structural safety and to recommend such modifications of standard structural-design procedures which would embody the most adequate formulation of the concept of safety. Considerable effort has also been made in the United States (11) (11a) and in England (12) (12a) to evaluate failure loads of structures of idealized inelastic response, particularly of ideal plastic structures; part of this work, however, is duplication of earlier research (13) (14). Finally, investigations have been made in an attempt to determine the actual shape of the statistical variation of various types of loadings, such as highway loads (15), building-floor loads (6), and wind and gust forces (16), as well as of the deformational and strength properties of structural materials, such as the yield point of structural steel, the compressive strength of concrete (17) (18), the number of stress cycles to fatigue fracture (fatigue life) (19), the fatigue strength (20), and the energy absorbed in dynamic fracture under specific testing conditions (21).

---

[2] Numerals in parentheses—thus, (1)—refer to corresponding items in the Bibliography (see Appendix).

The ultimate purpose of each of these investigations was to contribute to the improvement of the procedures of structural design. Hence, their relative importance can be judged in relation to the individual steps of the design sequence. On the basis of this interrelationship it is obvious that no single line of investigation can produce a solution to the design problem; this fact illustrates the futility of the claim, not infrequently heard, that the application of plastic or "limit" design methods represents the complete rational solution of the design problem. In itself, the "plastic" concept of safety is as limited as the conventional one; only an integrated approach to the design problem as a whole, with consideration of all steps in the design procedure, can lead to such a solution.

LOAD ANALYSIS

The Standard Load.—Because the analysis of a structure cannot be better than the load analysis underlying it, refinement of structural analysis cannot make up for crudeness of load analysis. Despite its self evidence, this fact is frequently forgotten in structural design.

Whenever the operating conditions of structures are such that the loads are of different patterns and of different weights—as, for example, in highway bridges carrying different vehicle types and loads—a "standard load" has to be established. This standard load defines a loading pattern which is sufficiently characteristic of the real load patterns to make the structural action equivalent or comparable; on this basis methods can be developed for the conversion of real loads into standard loads.

For this method the criterion of equivalence can be defined in terms of failure or unserviceability or simply in terms of weight. The more elaborate procedures of conversion of real loads into standard loads—by equalizing the load intensities which produce failure or unserviceability of the structure—are applied whenever the differences between the actual load patterns and the standard pattern produce significant differences between the gross weights of the actual load and the equivalent standard load, as, for example, in short bridge spans. The standard load becomes a function of the span, type, and structural action of the designed structure; therefore, standard-load intensities only of similar structures can be related. As the length of the span increases and more traffic units are accommodated, differences in pattern become less significant, and a simple conversion of the actual loads into standard loads of the same gross weight may be sufficiently accurate.

An extensive investigation has been published (15) in which the load patterns of several thousand heavy trucks and truck combinations of fourteen different types were converted into equivalent standard H-truck loads for simple bridge girders of spans between 10 ft and 100 ft. The basis of comparison was the maximum bending moment produced by the equivalent loads; for the simple span this is identical with a comparison of conditions of either failure or unserviceability. The results of this investigation clearly show the effect of span on the standard load. For all vehicles considered the average equivalent H-truck load intensity increased from approximately 12 tons for the 10-ft span to 18 tons for the 100-ft span, whereas the span-independent, mean-gross-weight equivalent was as high as 21 tons.

For spans that are long in relation to the length of the traffic unit, the actual load pattern is relatively unimportant. A uniformly distributed standard load is usually determined from the gross weight of the applied load units and the space which they occupy on the structure under operating conditions (2).

When a load is always applied in essentially the same pattern, the standard-load pattern differs very little from that of the real load. Loads of this type are loads proportional by definition, such as wind and gust forces, or mass forces acting at the mass centers of structures (acceleration and seismic forces or centrifugal forces). The pattern of such loads is usually very simple.

Because structures are expected to be of service for future periods and because the load pattern applied in their design has necessarily been derived from load observations preceding the time of design, a certain adjustment of the standard load has to be made for anticipated changes in the loading conditions. Such adjustments are matters of engineering judgment, based on an evaluation of the trend in the operating conditions of the structure.

Random Variation of Standard-Load Intensity.—The intensities of real loads and standard loads can usually be considered to be design parameters subject to random variations. Probability concepts and statistical methods can be used, therefore, for the prediction and presentation of this variation in a form suitable for application in design. The only exception would be in the case in which a maximum load intensity of relatively high frequency of occurrence can actually be specified in a nonstatistical manner, as in the cases of floor loads in warehouses, fluid loads and pressures in storage tanks, and maximum train loads on railroad bridges. In these cases the maximum load is not the result of a random variation but of arbitrarily established limitations. An illustration is the difference in the concept of the maximum loads used in the design of a water storage tank and that of a multiple-purpose dam. For the storage tank, the maximum load caused by a completely filled tank represents the maximum design load to be considered in relation to serviceability rather than to failure. The maximum load to be carried by the dam in the course of its anticipated life, however, can only be statistically predicted from extrapolation on the basis of previous records of the random variation of flood levels. The maximum load represents a "catastrophic" load to be sustained without failure but probably not without some damage, which is acceptable because of its rare occurrence and because its complete prevention would require the consideration of the catastrophic load as the actual service load, perhaps leading to an economically unjustifiable increase in the cost of the structure.

When the variation of the load intensity is random, the form of the variation is described either by its frequency distribution—which indicates the relative frequencies of occurrence $f_i(S)$ of various load intensities S—or by its cumulative frequency functions,

$$F_i(S) = \sum_0^i f_i(S) \qquad (1a)$$

which indicates the relative frequencies of occurrence of load intensities smaller than or equal to S, or

$$F^*_i(S) = \sum_i^\infty f_i(S) = 1 - F_{i-1}(S) \qquad (1b)$$

which indicates the relative frequencies of occurrence of load intensities equal to or greater than S.

For proportional loads, such functions are obtained from systematic, extensive records of observed load intensities by the application of standard statistical methods to the collected data; extensive records of wind and gust loads on structures (16) and of flood levels in rivers (22) (23) have, in fact, been so analyzed and presented.

Information concerning the variation of observed loads is, however, of limited value unless it is possible to deduce from the information the general pattern of random variation in terms of theoretical probability distributions $p(S)$ or probability functions

$$P(S) = \int_o^S p(S)\, dS \qquad (2a)$$

and

$$P^*(S) = 1 - P(S) \qquad (2b)$$

It then appears justifiable to assume that the random variation of the observed parameter is governed by the same probability rules that produce the functions $p(S)$ and $P(S)$ or $P^*(S)$ and that it can, therefore, be predicted beyond the range of actual observation by the application of these rules.

It is generally more expedient to use the cumulative frequency and probability functions $F_i(S)$ or $F^*_i(S)$ and $P(S)$ or $P^*(S)$, respectively, than the associated distribution functions $f_i(S)$ or $p(S)$ because even for a limited number of observations n, arranged in ascending order, the ordinates of the cumulative frequency functions

$$F_m(S) = \frac{m}{n+1} \qquad (3a)$$

or

$$F^*_m(S) = 1 - \frac{m}{n+1} \qquad (3b)$$

representing the frequency of occurrence of values smaller or larger than the mth observation can be easily determined. However, the direct establishment of the associated distribution function is not possible unless many observations are made. Moreover, various types of probability paper on which—as a result of a suitable distortion of the probability scale—the respective probability function is transformed into a straight line make a simple graphical fitting of the particular $P(S)$-function to the plotted $F_m(S)$ points possible and, in most cases, sufficiently accurate.

If $P^*(y)$ denotes the probability of a value larger than y, the reciprocal

$$N(y) = \frac{1}{P^*(y)} \qquad (4)$$

defines the "return number" of observations, which is the mean number of observations expected to contain one value exceeding y or the "return period" if the observations are made at fixed time intervals.

The nature of design requires extrapolation of the fitted function because load intensities that have actually occurred during the period of observation cannot be considered rare enough to be associated with failure or, if the period of observation is relatively short, even with unserviceability. Hence, the selection of a probability function for the observed frequency function involves more than mere curve fitting; unless the probability function correctly describes the general pattern of variations, extrapolation toward the extremes will result in erroneous predictions within the extreme range of variation, which is the range relevant to design. Therefore, distribution functions that have been developed for curve fitting are useless when the main purpose of the fitted function is to guide extrapolation from the range of the observation toward the region of small probabilities. The only functions that can fulfill this purpose are those which represent a definite pattern of variation resulting from certain basic assumptions concerning its origin. Both continuous and discrete functions of this general type can be applied to the study of random variations of load intensities, depending on the formulation of the problem and on the kind of information available.

On the basis of records of observation of load intensities taken at certain time intervals, it is possible to formulate the problem in alternative ways:

a. Considering the load intensity as a continuously changing variable, a continuous probability function is fitted to the observed frequency function.

b. Dividing the range of variation of the load intensity by a suitably chosen limiting (lower) load level, the occurrence of intensities exceeding this level are considered as discrete events, and their frequencies are fitted by a suitable discrete probability distribution.

When the load intensity cannot be obtained directly by observation, as in the case of highway bridges, it is derived from information concerning the expected proportion of traffic units of various types and weight by combining the standard-load units into patterns of various probabilities of occurrence and by computing their respective gross weights.

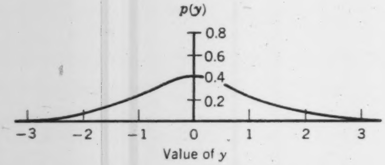

FIG. 1.—NORMAL DISTRIBUTION FUNCTION

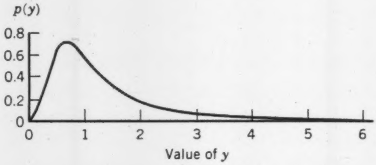

FIG. 2.—LOGARITHMIC-NORMAL DISTRIBUTION FUNCTION

Principal Types of Random Variation of Load.—Continuous distribution functions which represent distinct patterns of variation of a dimensionless random variable y are:

1. The Normal or Gauss-Laplace Distribution (Fig. 1).—

$$p(y) = \frac{1}{\sqrt{2\pi}} \exp\left(-\frac{y^2}{2}\right) \quad \ldots\ldots\ldots\ldots\ldots\ldots\ldots (5)$$

This distribution is symmetrical and expresses the fact that the random variable y is the sum of a large number of independent random variables of arbitrary distribution.

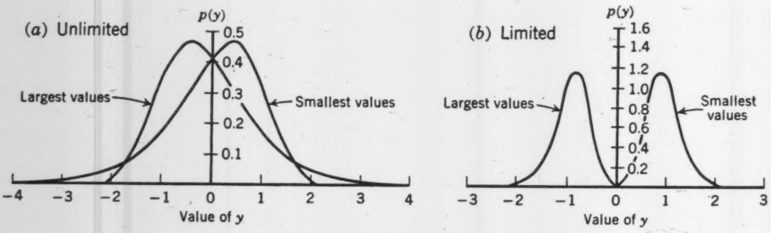

FIG. 3.—DISTRIBUTION FUNCTIONS OF LARGEST AND SMALLEST VALUES

2. The Logarithmic-Normal Distribution (Fig. 2).—

$$p(y) = \frac{1}{y\sqrt{2\pi}} \exp\left(-\frac{1}{2}(\log y)^2\right) \quad \ldots\ldots\ldots\ldots\ldots\ldots (6)$$

This distribution is skew and may be interpreted (*a*) to be the result of the fact that y is the product of a large number of independent variables or (*b*) by assuming that y depends on the consecutive operation of a large number of independent variables in such a way that the change in y is proportional to the momentary value of y—that is, to the sum of the effects of all previously operating variables.

3. The Distributions of Extreme Values in Groups of n Observations (Fig. 3).—These distributions are obtained when $(n - 1)$-values are either smaller or larger than the value of y so that y represents either the largest or the smallest value of the group. If $\bar{P}(y)$ and $\bar{p}(y)$ denote, respectively, the probability function and the distribution function of the infinite population of observations out of which finite groups of n observations each have been formed, the following expressions are obtained by the application of simple rules of combination for the probability that y is, respectively, the largest or the smallest value of the group—

$$p(y) = n\,\bar{P}(y)^{n-1}\,\bar{p}(y) \quad \text{(7a)}$$

and

$$p_1(y) = n\,[1 - \bar{P}(y)]^{n-1}\,\bar{p}(y) \quad \text{(7b)}$$

For distributions of the original population $\bar{p}(y)$ which approach zero as a negative power of e (exponential type) and for values of $n \rightarrow \infty$, the following asymptotic functions which are valid for large sample sizes n have been obtained for, respectively, the distributions of the largest and the smallest values of such a population (24)—

$$P^*(z) = \exp\,(-\,e^{-z}) \quad \text{(8a)}$$

$$p^*(z) = \exp\,[-\,z - e^{-z}] \quad \text{(8b)}$$

$$P_1(z) = 1 - \exp\,(-\,e^{z}) \quad \text{(8c)}$$

and

$$p_1(z) = \exp\,(z - e^{z}) \quad \text{(8d)}$$

in which z is a "reduced" variable given by

$$z = \alpha\,(y - v) \quad \text{(9)}$$

In Eq. 9 y is the observed variable, v represents the most probable extreme value (mode of the distribution of y), and $1/\alpha$ is a measure of dispersion proportional to the standard deviation.

Because this type of extreme-value distribution is unlimited in both directions, its application to engineering problems in which only positive values of the variable are physically possible is open to similar objections as the application of the normal distribution. This objection can be met by simple logarithmic transformation:

$$y = \ln x \quad \text{(10)}$$

and

$$v = \ln u \quad \text{(11)}$$

as a result of which Eqs. 8 are transformed into

$$P^*(x) = \exp\left[-\left(\frac{x}{u}\right)^{-\alpha}\right] \qquad (12a)$$

and

$$p^*(x) = \frac{\alpha}{u}\left(\frac{x}{u}\right)^{-\alpha-1} \exp\left[-\left(\frac{x}{u}\right)^{-\alpha}\right] \qquad (12b)$$

for the largest values, and

$$P_1(x) = 1 - \exp\left[-\left(\frac{x}{u}\right)^{\alpha}\right] \qquad (12c)$$

and

$$p_1(x) = \frac{\alpha}{u}\left(\frac{x}{u}\right)^{\alpha-1} \exp\left[-\left(\frac{x}{u}\right)^{\alpha}\right] \qquad (12d)$$

for the smallest values. These distributions are limited at $x = 0$, being valid, respectively, for $x \leqq 0$ and $x \geqq 0$ only.

The logarithmic transformation can be justified on the basis of expediency for it produces an extreme-value distribution of a desired physical limitation. The transformation can also be justified on the basis of the assumption that the variation in the original population is not the result of more or less independent additive effects but of cumulative effects, leading to a logarithmic-normal distribution for the original population.

Distributions of extreme values are of importance in engineering. Many statistical problems relevant to design can be formulated in terms of extreme values of the infinitely large "population" of the load intensities; only the relatively high intensities are representative of design loads. Hence, gusts may be considered as extreme values of randomly varying wind loads, floods as extremes of randomly varying water levels, high maneuver loads of aircraft as extremes of randomly operating flight loads. Because in the application of Eqs. 8 and 12 the actual shape of the distribution of the original population is irrelevant as long as it approaches zero exponentially in the direction of either large or small values, Eqs. 12*a* and 12*b* can be expected to represent variations of certain loads sufficiently well to permit extrapolation toward the small-probability values. This fact has been confirmed by statistical analysis of observations of gust loads, maximum wind velocities, flood levels (24), and live loads on floors (6).

Discrete probability distributions are used either (*a*) for the prediction of the frequency with which the intensity of a proportional load will exceed a limiting intensity within a given number of observations or (*b*) for the prediction of the probability of occurrence of combinations of various standard-load units in the total number of units making up a complex load. In the first case the average frequency of such an intensity, or its return number or return period, must be obtained from sufficiently extensive load records; in the second case the average proportion of various types of traffic units and the load distribution within each type must be known. If only two types of load units are considered, both problems can be dealt with by the binominal distribution, which is given by the successive terms of the expansion $[p + (1 - p)]^n$ —in which p is the probability of occurrence of an intensity belonging to one group, or of one type of load unit; $(1 - p)$ indicates the probability of its nonoccurrence or of the occurrence of the alternative load unit; and n is the total number of loading cycles or of load units involved. The mth term of this expansion is

$$p(m) = \frac{n!}{m!\,(n - m)!}\, p^m\, (1 - p)^{n-m} \ldots\ldots\ldots\ldots\ldots (13)$$

and gives the probability of m occurrences of the first alternative in n load cycles or load units. The sums,

$$P(m) = \sum_{o}^{m-1} p(m) \qquad \text{or} \sum_{o}^{m} p(m) \qquad \text{and} \sum_{m}^{n} p(m) \ldots\ldots\ldots (14)$$

give, respectively, the probabilities of less than m, not more than m, or at least m occurrences. The average number of occurrences is equal to $n\,p$. Frequency distributions of the number of trucks in the total number of vehicles on a bridge have been computed on the basis of the binomial distribution (1) (2).

The terms of the binomial distribution can be replaced by those of the Poisson distribution—

$$p(m) = (n\,p)^m \frac{\exp - n\,p}{m!} \ldots\ldots\ldots\ldots\ldots\ldots\ldots (15)$$

which can be evaluated with comparatively little effort (and for which extensive tables have been computed), when n tends toward ∞ and p toward zero and the average number of occurrences is less than five. The small values of the *a priori* probability p characterizes the occurrences governed by the Poisson distribution as rare events.

Conversely, therefore, occurrences which have the character of rare events may naturally be assumed to be governed by the Poisson distribution. Because the high load intensities relevant to design should, by definition, occur infrequently enough to be classified as rare or relatively rare events, the Poisson distribution is likely to provide a reasonable approach for their prediction. This conclusion has been confirmed, for example, with respect to flight loads (multiples $x\,g$ of the acceleration of gravity g); the frequency of occurrence of the relatively rare, large values of x is closely reproduced by a Poisson distribution (25). Thus, if $(V - g)$-records give the return period T of load intensities equal to or exceeding $x\,g$, the average number of occurrences of such a load during a certain time t is (t/T); this number replaces $n\,p$ in Eq. 15. Hence, the probability that a flight-load intensity equal to or exceeding $x\,g$ may be expected m times during an interval t is given by

$$p(m) = \left(\frac{t}{T}\right)^m \frac{\exp\,(-\,t/T)}{m!} \ldots\ldots\ldots\ldots\ldots\ldots (16)$$

The probabilities that such a load intensity will occur not more than or at least r times during T are, respectively, therefore,

$$P(r) = \exp\left(-\frac{t}{T}\right)\sum_{o}^{r}\frac{(t/T)^m}{m!}\ldots\ldots\ldots\ldots\ldots\ldots(17)$$

and

$$P^*(r) = \exp\left(-\frac{t}{T}\right)\sum_{r}^{\infty}\frac{(t/T)^m}{m!}\ldots\ldots\ldots\ldots\ldots\ldots(18)$$

For example, if it can be assumed, as in fatigue, that the $(r + 1)$th occurrence of this load intensity will produce a critical condition (failure) of the structure which has survived r repetitions of this load, Eq. 17 represents the function of survival of the structure. The associated frequency distribution $p_F(t)$ expressing the probability of failure as a function of service time t is obtained by differentiating $[1 - P(r)]$, or

$$p_F(t) = -\frac{dP(r)}{dt} = \left(\frac{t}{T}\right)^r \frac{\exp(-t/T)}{r!T}\ldots\ldots\ldots\ldots(19)$$

is valid for $t > 0$, which is known as the gamma distribution (or Type III Pearson distribution). Eq. 19 has a maximum value at $t = r\,T$ which, therefore, represents the most probable time to failure, as would be expected. The cumulative distribution

$$P_F = \int_o^t p_F(t)\,dt\ldots\ldots\ldots\ldots\ldots\ldots\ldots\ldots(20)$$

which represents the probability of failure between $t = 0$ and t is the incomplete gamma function.

A continuous distribution function can thus be derived from a problem originally formulated in terms of a discrete distribution.

The Poisson distribution can also be used to predict the distribution of the intensity of a standard load, if the problem is suitably formulated, by specifying a lower limit of this intensity as the zero level and dividing the range of load intensities above the zero level into equal load steps. The principal consideration for the specification of the zero level is the condition that the occurrences of load intensities exceeding this level should be sufficiently rare to be governed by the Poisson distribution; the number of load steps in excess of the zero level is then considered the random variable. Hence, the probability of occurrence of a load intensity exceeding the zero level by m load steps is given by

$$p(m) = \frac{K^m e^{-K}}{m!}\ldots\ldots\ldots\ldots\ldots\ldots\ldots\ldots(21)$$

in which K is the number of load steps by which the average load intensity exceeds the zero level.

It is of interest to note that in an investigation of highway-bridge loadings (15) Poisson distributions have been compared with frequency distributions of equivalent H-truck standard loads derived for short spans from a loadometer survey. Such comparison of the statistical loadometer data and the Poisson distribution on the basis of plotted cumulative functions shows that in most cases agreement is disappointing, particularly for the gross-weight distribution. Thus, extrapolation on the basis of the Poisson distribution toward high load values would lead to erroneous predictions. This is clearly illustrated for the combined data of all trucks in Fig. 4, in which the frequency functions for the equivalent H-truck loading for spans 50 ft and 100 ft long and for the gross weight are plotted on logarithmic-normal probability paper and compared with the respective, continuously plotted Poisson functions.

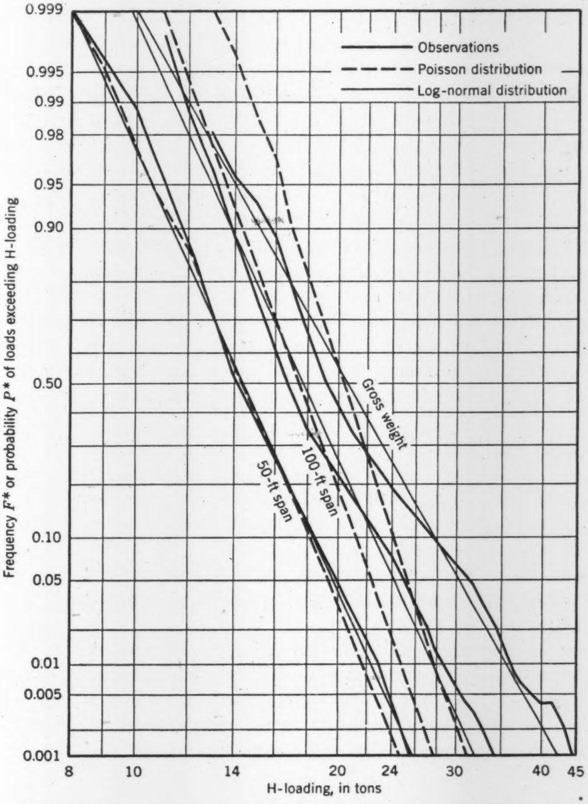

FIG. 4.—COMPARISON OF LOADOMETER SURVEY OF HEAVY TRUCKS WITH POISSON AND LOGARITHMIC-NORMAL DISTRIBUTIONS

It appears that, in this case, the definition of heavy trucks has not been narrow enough to justify analysis by the rare-event approach. Limitation of the analysis to trucks of equivalent H-loads exceeding, for example, 20 tons might have produced better agreement with the Poisson distribution than has been obtained by including the relatively frequent trucks of lighter weight; it may also be expected that the distribution of real rare events—such as strong wind and gust loads, seismic forces, and wave forces—can be predicted by the Poisson distribution with fair accuracy if the problems of variation are formulated in terms of discrete probabilities.

According to Fig. 4, the logarithmic-normal distributions fit the data much better than Poisson distributions, particularly with respect to possible extrapolation. In the only case for which the Poisson distribution provides a good fit (a 50-ft span), the logarithmic-normal and the continuously plotted Poisson distributions cannot be easily distinguished.

When a complex load simultaneously produces two independent types of structural action, as in the case of an airplane wing loaded in bending by acceleration forces and in torsion by forces resulting from speed, information concerning the variability of the loading is represented by a three-dimensional probability surface rather than by a two-dimensional probability distribution. The ordinates of this surface are a measure of the expected frequencies of occurrence of the various loading conditions defined by the points in the reference plane, the coordinates of which represent the intensities of the two component loading actions. Such surfaces can be constructed from (V-g)-records by counting the number of occurrences of various combinations in the total number of observations and tracing contour lines connecting points of equal frequency of occurrence (3). Similar problems arise in the design of long-span bridges, particularly suspension bridges, under the joint action of traffic load and wind and in other types of structures and machine parts subject to dual load action.

Time Dependence of Standard Load.—Because the properties by which failure and unserviceability of a structure are determined are not independent of time, the time dependence of the application of the standard load will significantly affect the critical operating conditions of the structure. The principal aspects of this time dependence are (*a*) the rate of load application, (*b*) the duration of the loading, and (*c*) the number, frequency, and sequence of load repetitions.

The rate of load application defines the possible "spectrum of behavior" bounded by static loading on the one side and by shock loading or impact on the other. In general, the longer the span and the larger the mass of the structure, the narrower is the range of variation in the rate of load application. In certain relatively short-span structures the full range of variation is possible; in main girders of long-span bridges the range of variation is limited because of the limitation of the variation of the speed of traffic. In cases of floor loads or of snow loads on buildings or, at the other extreme, in cases of operating loads on hammer foundations or on blast-resisting structures, the possible range of variation of the rate of load application within each of the two structural types is negligibly narrow.

The duration of the loading is significant in design only when it is long enough to produce either a significant permanent deformation or a significant reduction in the fracture strength of the material, or both. In these cases the critical operating conditions of the structure are determined with reference to the end of the expected period of service of the structure, during which the load may have been sustained continually or intermittently for long periods. Loading conditions of this type usually arise in the design of long span or prestressed concrete structures or in the design of metal structures or parts used at elevated temperatures.

The effect of the number of load repetitions on the failure condition of a structure determines their significance in the particular design; only under exceptional conditions does the effect of frequency become important, as in the case of a very low frequency of application of loads to a highly time-sensitive material at elevated temperatures. Because the fracture strength of most engineering materials decreases with an increasing number of repetitions of a load intensity exceeding a critical level (fatigue), the effect of load repetitions on the failure load of the structure must usually be analyzed when rather frequent load repetition is an integral part of the operating conditions. A reasonably close estimate of the expected number of applications of various intensities of the standard load, therefore, is an important part of the load information, particularly as these figures are also of considerable importance with respect to the specification of an acceptable probability of failure.

Although it is known that the sequence in which the loads are applied considerably affects the number of load applications that can be sustained by the structure without damage or failure ("cumulative fatigue damage"), information concerning the effect of sequence is scarce. The statistical distribution of the standard-load intensity determines the type of load sequences to be expected; statistical time series can be derived from any particular type of distribution. It is with respect to such random time series of load intensity that the fatigue life of a material should be determined. Some investigations (26) (27) have been made along these lines; preliminary results have demonstrated the inadequacy of the conventional concept of cumulative fatigue damage, which defines equality of damage at different load levels by equality of "cycle ratios" n_i/N_i in which n_i denotes the number of load cycles of a certain intensity actually applied and N_i is the number of load cycles producing fatigue fracture at the same load intensity. However, no generally valid alternative concept has been established.

STRUCTURAL ANALYSIS

Conditions of Unserviceability and Structural Failure.—

Unserviceability.—Only idealized materials are truly and invariably elastic, plastic, or viscous. The behavior of real materials changes with the state of stress and its intensity, with the applied stress rate, and with the external temperature. Therefore, terms such as brittle or ductile can only refer to the particular state of a material. With a change in the loading and external conditions, one or the other of the component types of deformation may become dominant so that the material will appear nearly elastic under one set of conditions and highly viscous under another. Thus, the question as to whether a specific method of inelastic analysis is always applicable to the design of structures of a particular material is meaningless; different conditions of loading and temperature require different methods of evaluation of the load intensities leading to unserviceability or failure. Hence, any design procedure in which these two critical limits are correctly related to the applied loading represents a limit-design procedure.

For the evaluation of the limit of serviceability, methods of elastic analysis are usually adequate. In the cases in which localized inelastic strain is considered acceptable, the relation between the intensity of the applied load and the extent of the inelastic deformation must be determined by analysis beyond the elastic range. Such cases will arise when a load considerably exceeding the elastic-limit load is accompanied by elastically constrained inelastic deformation. These cases are limited to conditions in which (*a*) a very steep elastic stress gradient exists (as in beams of sharp curvature or in thick-walled tubes); (*b*) the resisting section is of a shape that is marked by a considerable difference between the elastic and the fully plastic moment (as in diamond-shaped beams or circular beams) and, therefore, by a high so-called plastic "shape factor;" or (*c*) where both conditions occur simultaneously (as in the design of eye bars, chain links, or crane hooks). Shape factors which specify the ratio between the fully plastic moments and the elastic moments of the section vary between from 1.10 to 1.20 for wide-flanged structural sections to 2.20 for diamond-shaped sections. Therefore, little advantage is gained by permitting a small plastic deformation under service conditions in members made of structural shapes unless the stress gradient is very steep. Large increases of the service loads of crane hooks, chain links, or thick-walled tubes can, however, be obtained by permitting localized, elastically constrained plastic deformation.

Methods of analysis of structures and structural parts under conditions of elastically constrained plastic deformation are well established for relatively simple structures and shapes. The design criterion usually adopted is a limiting depth of penetration of the plastic deformation, a limiting over-all permanent deformation of the structure, or a limiting strain in the critical section (0.1% to 0.2%). Approximate methods for the evaluation of the depth of penetration as a function of the applied load have been developed (28).

For structures made of time-sensitive materials, such as concrete, plastics, or metals at elevated temperatures, the application of visco-elastic analysis may become necessary even for the evaluation of the limiting service load, as a maximum permanent deformation at the end of the expected period of service of the structure is introduced as a design criterion whenever the time-dependent component of the deformation ("creep") cannot be neglected. In visco-elastic analysis (29) this component is generally assumed to be a linear function of time and a linear or power function of stress. The acceptable design limit of permanent deformation is determined by the maximum change of shape which the structure can suffer without being affected in its proper functioning.

Failure.—Elastic analysis is, in general, inadequate for the evaluation of the failure load of metal structures unless failure occurs by general or local elastic instability of members in compression or in bending or after a large number of repetitions of stresses far below the yield stress. Elastic buckling and, to a limited extent, fatigue, represent the principal conditions for which elastic analysis leads to limit design.

Most other conditions require the application of methods of plastic analysis in the evaluation of the failure load of metal structures. These methods are generally based on the assumption that, after reaching the yield stress, the metal yields at constant stress (ideal plasticity); they represent two different types of failure—one characteristic of proportional loads, the other of complex loads. These are referred to in the literature on the subject as, respectively, total "plastic collapse" and "alternating plasticity" or "progressive collapse" (11).

Plastic collapse is produced by a proportional increase of the loads leading to the collapse of the structure as a kinematical chain (mechanism) after the formation of a sufficient number of plastic hinges. Methods of plastic-collapse analysis determine the sections in which plastic hinges can occur as well as the alternative arrangements of such hinges which might transform the considered structure into a kinematical chain, together with the respective load intensities that are necessary to produce the various arrangements. The collapse load is the lowest load intensity that can transform the structure into a mechanism; the ratio between this load and the limiting elastic load has been considered a safety factor (30), although it actually represents a plastic-load factor. Collapse analysis is usually not concerned with the order in which the plastic hinges occur nor with the local strain in them. However, it is quite probable that, before the last hinge produces the theoretical collapse, some of the previously formed hinges have undergone large plastic strains which, in real materials, may be associated with strain hardening, fracture, or local instability.

Conditions of alternating plasticity or of progressive collapse are produced by the repeated application of a complex load system as a result of which one or more sections of a structure, in consecutive loading cycles, are subject either to plastic strains of opposite direction or to plastic strain in the same direction whenever a certain loading sequence is applied. It is assumed that the alternating plastic strain gradually produces an exhaustion of the cohesion of the metal terminating in fracture; progressive plastic strain in the same direction, however, is assumed finally to produce plastic collapse.

Because alternating plasticity and progressive collapse produce failure after a relatively small number of load applications (which fact distinguishes alternating plasticity from fatigue) any sequence which results in either condition is a failure loading. If, however, under a certain sequence of application of a standard load the alternating or the progressive plastic strain tends toward a limiting value so that the plastic deformation is stabilized before failure occurs, and if the structure responds elastically to any subsequently applied arbitrary sequence of this load, the structure is said to have attained a condition of "shake-down," as a result of which failure by alternating plasticity or progressive collapse is permanently prevented (31) (32) (33). The highest intensity of the standard load for which a shake-down of the structure is still possible therefore represents the lower limit of the standard failure-load intensity. This limiting shake-down load is usually much lower than the plastic-collapse load under the same proportionally applied load pattern, sometimes even as low as the elastic-limit load. Most of the excess of the plastic-collapse load over the elastic-limit load may, therefore, be lost when the operating conditions of the structure require analysis for repeated sequences of complex loading.

As a result of discrepancies between the assumed and the real response of the structure, the indiscriminate application of plastic analysis for the evaluation of the failure load is limited, even in cases in which analysis is required only for proportional loading. The full plastic-collapse load of a redundant structure depends on the development of the full plastic carrying capacity of all plastic hinges by which the structure is transformed into a mechanism, notwithstanding the large hinge rotations associated with such transformation. The two effects which most seriously interfere with such development of the full plastic hinge moments are local lateral buckling of flanges (34) and discontinuous spread of plastic deformation along glide lines, which result in the formation of plastic wedges in advance of the isotropically spreading plastic regions (35). Separately or together, these effects tend to reduce the carrying capacity of the plastic hinges and thus the plastic-collapse load of the structure. Tests of mild-steel continuous beams have shown that only under exceptionally favorable conditions can the theoretical load be attained; in most cases not more than one half to two thirds of the excess of the plastic-collapse load over the elastic-limit load can actually be realized (36), particularly when the loads are applied at slow rates or are sustained over several hours (37).

The choice of the appropriate method for the evaluation of the failure load of reinforced concrete structures depends on the percentage of reinforcement in the critical sections, on the type of the structure, and on its operating conditions. Plastic-design methods (38) (39) (40), based on an assumed analogy with the behavior of metal structures in bending, appear to be useful for weakly reinforced sections the carrying capacities of which are exceeded by yielding of the reinforcement at relatively low compressive stresses in the concrete, with the resulting effect of a "plastic hinge"; the question as to which shape of distribution of the compressive stresses—triangular, parabolic, or any other—is more adequate has, in this case, little meaning. Any stress distribution can be fitted to the test data, provided that the ratio between the critical compressive fiber stress in bending (computed on the basis of the assumed distribution) and the compression strength of a standard uniform cylinder is accepted as the empirical parameter that it actually is.

It should, however, be realized that the apparent plasticity of concrete subject to high compressive stresses is the manifestation of a progressive internal disruption of the material beginning far below the conventional "compressive strength" obtained in the relatively high-speed standard tests, rather than plastic flow of a type occurring in metals. Hence, its effect on the failure load of the structure will be different from that of metal plasticity, particularly for repeated or sustained application of loads producing high stresses. Because almost all test results have been obtained under conditions of short-time static tests, the extrapolation of those results to the condition of failure even after a small number of load repetitions does not seem justified. With respect to failure of reinforced concrete after a large number of load repetitions, it is generally assumed (although on the basis of insufficient experimental evidence) that a load of approximately one half of the static failure load can be applied an infinite number of times to a reinforced concrete beam (15).

In the analysis of failure caused by instability (buckling) or by restraints on free expansion and contraction (temperature stresses and stresses caused by motion of the supports) of structures of reinforced concrete and of other time-sensitive materials, the time dependence of the deformation (creep) or of the stresses (relaxation) must be considered. Thus, the axial force on a column or the dead-load thrust in a long-span slender concrete arch rib will produce additional time-dependent bending moments as a result of which the failure load of the strut or rib is reduced (41) (42). Conversely, the internal moment of the prestressing force in a prestressed concrete girder gradually diminishes as a result of the relaxation of this force because of concrete creep, reducing the failure load of the beam.

Stress relaxation also prevents the full build-up of elastic temperature stresses (43) or other restraint stresses in structures or elements of time-sensitive materials, particularly metals at elevated temperatures.

Variation of Unserviceability and Failure Loads.—The variation of the critical design loads is essentially the result of the random variations of the pertinent material properties. In redundant structures a further source of variation is the development of alternative mechanisms of transformation into a state of plastic collapse.

In metal structures the load associated with unserviceability depends primarily on the yield stress; the failure load depends on either the yield stress or the fatigue strength of the material. In concrete structures either the yield stress of the steel or the compressive strength of the concrete determines the failure load, whereas a compressive concrete stress defined by an acceptable amount of inelastic strain or a tensile stress in the steel producing damaging cracks in the concrete may determine the limiting condition of unserviceability. The random variations of the yield stress, of the fatigue strength, and of the compressive strength of concrete have been investigated. The character of the frequency distributions of these properties has been reasonably well established.

The approach to the analysis of random variation of the relevant strength properties is similar to that for the analysis of the variation of load intensities. Because for design purposes predictions must be made of the probability of occurrence of strength values that are smaller than those that have actually occurred in the performed tests, extrapolation of the fitted probability function toward improbably low strength values becomes necessary. As in the case of loads, such extrapolation can be made with some confidence only if the fitted probability function represents the general pattern of variation that can reasonably be expected.

It is reasonable to assume that the lowest values obtained in tests of material samples are of particular significance in the prediction of the low range of failure loads on which a rational estimate of the probability of failure must necessarily be based. Hence, extrapolation of strength values should be based on the limited probability function of smallest values, Eqs. 12*c* and 12*d*, fitted to the test results that have been arranged and plotted in ascending order.

Attempts to fit extreme-value distributions of the type given by Eqs. 12*c* and 12*d* to strength data have generally shown that a good fit can be obtained, particularly over the range of low strength values. Whereas in the vicinity of the mean or the mode no differentiation between various distributions is possible, the range of high strength values is better fitted by the distribution function of the population itself than by that of its extreme values (6).

Instead of using two distribution functions for low and high strength values of the same test series, a reasonably good fit of strength data can usually be obtained by using the logarithmic-normal distribution. The advantage of using the logarithmic-normal distribution is that the statistical procedures developed for the normal distribution—particularly methods for the interpretation of the results of small numbers of tests—can be applied to the interpretation of strength data and to their extrapolation toward the range of the small values pertinent in design.

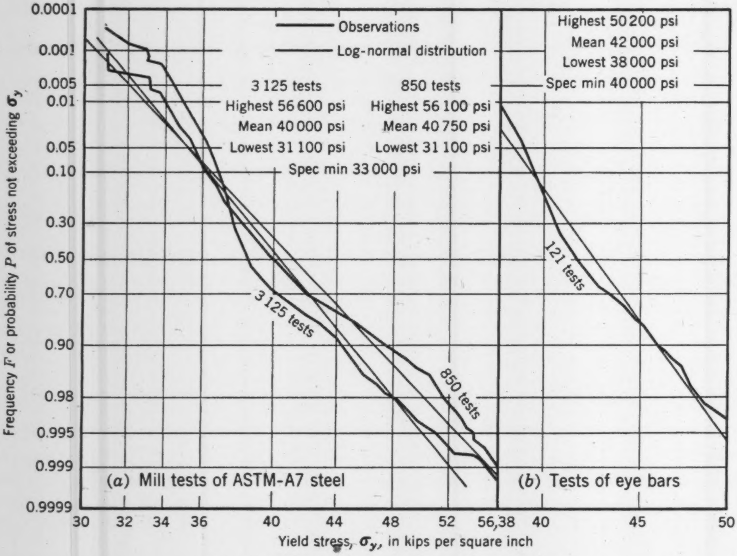

FIG. 5.—DISTRIBUTION OF YIELD STRESS

Fig. 5(*a*) represents the results of 3,125 and 850 mill tests of the yield stress of A7 structural steel plotted on logarithmic-normal probability paper with straight lines graphically fitted to the data. This presentation shows that the probability of occurrence of values lower than the specified minimum (33,000 lb per sq in.) is at least 5×10^{-3}. Considering that the results of mill tests are consistently higher than those of standard tests as a result of the higher testing speeds, it appears that the specification of a minimum of 27,000 lb per sq in. to 28,000 lb per sq in. might be more reasonable if the probability of values falling below the minimum is to be lower than 10^{-3}.

Fig. 5(*b*) represents the results of 121 tests of the yield stress of eye bars, also plotted on logarithmic-normal probability paper and fitted by a straight line. In this case the probability of occurrence of values smaller than the specified minimum is as high as 0.12.

Fig. 6(*a*) shows the results of 673 compression tests of structural concrete manufactured under reasonably good control, fitted by a logarithmic-normal distribution. Because of the fact that, in spite of a mean of 5,320 lb per sq in. the minimum has been specified as low as 3,825 lb per sq in., the probability of values lower than the minimum could be kept down to about 10^{-3}.

It appears that inadequate control produces a distribution that is closer to an extreme-value distribution over its whole range than to a logarithmic-normal distribution, as indicated by Fig. 6(*b*), in which the results of 296 compression tests of concrete manufactured under difficult control conditions have been plotted on extremal probability paper and fitted by a straight line representing Eq. 12*c*. The conclusion to be drawn from Fig. 6(*b*) is that inadequate control reduces the extremes rather than the mean value, increasing the range and number of low test results and sharply reducing the number of high values.

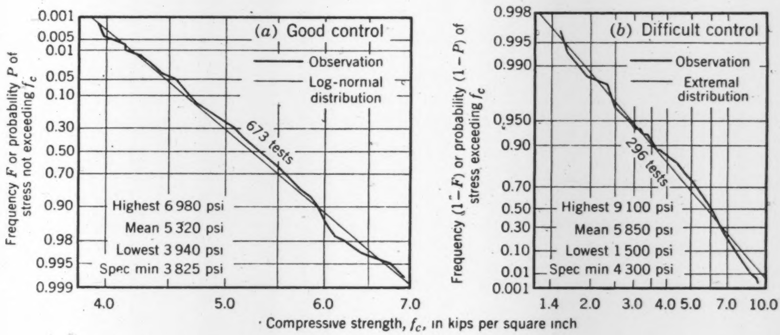

FIG. 6.—DISTRIBUTION OF COMPRESSIVE STRENGTH OF CONCRETE

The principal sources of nonrandom variation of the strength properties that determine unserviceability or failure loads are the variations of the applied rate of strain or stress and the effect of size on the strength properties. Thus, for example, the large difference in the loading rates of floor beams and of main girders in a long-span steel bridge may produce significant differences in the stresses at which the first yielding occurs in the two structural parts. Considering, as an example, that on a 300-ft-span highway bridge with floor beams spaced at 20 ft the critical floor-beam load (single or double truck axle) might travel at 60 miles per hour, whereas the critical girder load (sequence of vehicles of high load intensity) travels at approximately 12 miles per hour (2), the ratio of the loading rates of the floor beams and the girders may be as high as 75, or almost two orders of magnitude. Such differences in loading rate produce quite significant differences in yield stresses; for mild steel a yield stress of 30,000 lb per sq in. obtained under the standard test strain rate of approximately 10^{-4} in. per in. per sec is increased by 20% at a strain rate of 10^{-2} in. per in. per sec and by 50% at a strain rate of 1 in. per in. per sec.

It is also quite well known that the yield stress of steel obtained in the relatively high-speed mill tests is substantially (10% to 15%) higher than that obtained in standard tests or in low-speed structural loading. Moreover, it is common knowledge that the yield stress decreases with the size of the section or its diameter (in reinforcing bars). Even for the same structural section, it is considerably higher for specimens taken from the web than for those taken from the flanges; differences of 15% are not unusual.

These influences have to be considered in conjunction with the random variations but cannot be combined with them; rather, their effect should be considered by shifting the mean of the distribution of the random variation in accordance with the expected trend of the nonrandom variation.

PROBABILITY OF FAILURE

Choice of Decision Rule.—The acceptable probability of failure or of unserviceability can be specified arbitrarily, in relation to the expected number of load applications, or on the basis of an economic balance between the cost of increasing the safety and the cost of failure. The choice of the specification of the probability of failure depends on the importance and cost of the structure, as well as on the consequences and cost of failure. It is evident that the probability of failure of an important structure or of a structure the failure of which would endanger human life should be practically zero. It can, however, never be theoretically zero, unless the design could be based on an absolute upper limit of the load intensity and on a distribution of the significant strength parameter known to be definitely limited at a minimum value; structures designed on such a basis would, however, be inefficient and uneconomical. It is, moreover, not quite logical to attempt to design for zero probability of failure or unserviceability as other risks to a structure, such as fire or earthquake, are accepted as inevitable. Although all measures are taken to reduce their incidence or the damage associated with their occurrence, the risk remains real—however small—and its magnitude finds numerical expression in terms of insurance rates or of that part of the rates that represent the pure risk. Hence, comparison of the risk of failure or unserviceability with other risks of similar consequences may provide a first rough rule for the specification of an acceptable probability of failure or of unserviceability.

A more rational rule can be derived from the requirement that the combination of an improbably high load intensity with an improbably low carrying capacity (failure load) which would produce failure of the structure should not be expected to occur during the lifetime of the structure. Hence, the probability of its occurrence should be extremely small; the return period of such a combination should be very much longer than the life of the structure, or its return number should be much higher than the expected total number of load applications.

In the relatively simple case of the design of aircraft wings, for example, an estimate of a reasonable ratio between the return period of a failure combination of applied load and carrying capacity and the service life of the aircraft may be deduced from flight insurance rates. Considering, for example, that transatlantic flight insurance rates are roughly 0.02% for a 20-hr flight—of which 1/3 to 1/2 may represent actual risk—and assuming a service life of 10,000 flying hrs, the accident risk implied is 1/20 or 20 times the assumed life. This is much higher than the usually accepted design value of two in 10^7 flying hrs, or a return period of failure 500 times the expected service life of the aircraft; the accepted chance of an accident is, therefore, 1/500.

In the case of a railroad or highway bridge the total number of standard-load applications N for the various structural parts can be roughly estimated from the expected total traffic volume per year and the anticipated service life of the structure. The ratio of N to the return number (inverse probability of occurrence) of failure combinations of applied-load intensity and carrying capacity expresses the accepted risk of failure.

The economic approach to the specification of an acceptable failure risk (44) is based on the assumption that the cost of failure or of unserviceability can be considered as a charge against the structure equal to the capitalized total cost of failure C_F or of unserviceability C_S, multiplied by the probability of its occurrence P_F or P_S. As the cost of failure and, to a lesser extent, the cost of unserviceability are necessarily functions of the probability of failure or of unserviceability for which the structure has been designed, the optimal economic probabilities of failure or of unserviceability should make the sum of the initial cost of the structure A and the capitalized cost of failure or of unserviceability a minimum. Hence, the condition for the optimal probabilities,

$$A + P_S C_S \rightarrow \min \ldots\ldots\ldots\ldots (22a)$$

or

$$A + P_F C_F \rightarrow \min \ldots\ldots\ldots\ldots (22b)$$

and

$$\frac{dA}{dP_S} + P_S \frac{dC_S}{dP_S} + C_S = 0 \ldots\ldots\ldots\ldots (23a)$$

or

$$\frac{dA}{dP_F} + P_F \frac{dC_F}{dP_F} + C_F = 0 \ldots\ldots\ldots\ldots (23b)$$

The relation between initial cost of the structure and the design probability of failure may, in first approximation, be introduced in the form,

$$A = A_0 (1 - c \log P_F) \ldots\ldots\ldots\ldots (24)$$

Only the cost of the load-carrying part of the structure will be affected by changes of P_F. For simple reinforced concrete floors, for example, a value of $c \doteq 0.018$ has been established from comparative designs (17).

The total cost of failure is made up of two components—one which is independent of P_F and includes all direct and indirect losses resulting from the failure, as well as the cost of repair (if such repair is possible), and the other which represents the cost of reconstruction when repair is not possible and depends on P_F as does the initial cost. Hence, considering that for a long service life

$$Q \doteq \frac{q}{q-1} \qquad (25)$$

represents the factor of capitalization, in which q is the interest factor $(1 + i)$ and i is the interest rate,

$$C_F = [C_{OF} + m\,A_O\,(1 - c \log P_F)]\,Q \qquad (26)$$

in which m denotes the ratio between cost of reconstruction and initial cost; when the structure can be repaired without total reconstruction

$$C_F = Q\,C_{FO} \qquad (27)$$

The cost of unserviceability can, in first approximation, be regarded as independent of P_S; hence,

$$C_S = Q\,C_{SO} \qquad (28)$$

Introducing Eqs. 24 and 26 into Eq. 23*b*,

$$d(\log P_F)\,c\,A_0\,(1 + m\,P_F\,Q) + c\,m\,A_0\,Q \log P_F = (C_{FO} + m\,A_0)\,Q \qquad (29)$$

Because, for any reasonably small probability of failure, $m\,P_F\,Q$ can be neglected in comparison to unity:

$$\frac{1}{P_F} = \left(\frac{C_{FO} + m\,A_0}{c\,A_0} - m \log P_F\right)\frac{Q}{\log e} \doteq \frac{C_{FO} + m\,A_0}{c\,A_0}\,\frac{Q}{\log e} \qquad (30)$$

in which e is the base of the natural logarithms. For example, with $C_{FO} = 10\,A_0$, $m = 2$, $c = 0.015$, $i = 3\%$, the optimal economical probability of failure $P_F \doteq 1/6{,}300$. Similarly, the relation for the evaluation of P_S is obtained from Eq. 23*a* if it is assumed that the relation between A and P_S is of the same type as Eq. 24—

$$\frac{1}{P_S} = C_{SO}\,\frac{Q}{A_0\,c} \log e \qquad (31)$$

Because, in general, the cost of unserviceability C_S will be lower than A_0 (unless such condition can only be repaired with considerable difficulty, in which case it should be considered as failure rather than unserviceability and, therefore, $C_S = C_F$) the economically optimal probability of unserviceability $P_S > P_F$. For example, with a high value of $C_S = 0.2\,A_0$, $c = 0.015$, and $i = 3\%$ the design probability of unserviceability $P_S = 1/1{,}050$.

Thus, the economically optimal risk of failure or unserviceability for which the structure should be designed decreases with increasing ratio of cost of such failure or unserviceability to the initial cost, as well as with increasing service life and decreasing interest rate.

A reasonable estimate of the acceptable risk of failure or unserviceability combinations of applied load intensity and carrying capacity can be obtained by combining the economically optimal risk of failure with the expected total number of applications N of the standard load in the forms P_F/N and P_S/N, respectively. The number N to be used depends on the distribution of standard-load intensities on which the design of the structure is based. For example, if the standard-load distribution for a highway bridge represents only heavy trucks of gross weights exceeding 20,000 lb, their number N will be a small fraction of the total number of trucks, which has to be considered as N if the standard-load distribution represents all truck weights that might be encountered.

Analysis of Failure and Survival.—

Safety Factors.—The probabilities of failure or of survival for which structures are designed must be referred to the critical operating conditions of the structure; different values of the probabilities are necessarily associated with different operating conditions. Methods for the selection of such probabilities have been cited previously.

The simplest operating condition of a structure is defined as the joint action of dead load and service load; the action of dead load alone is not an operating condition as no important structure is built for the purpose of carrying only its own weight. The load intensity S associated with this operating condition is the sum of the dead load S_W and the live load S_P; the variation of S is therefore made up of the variation of the load components S_W and S_P. As variations of the dead load are essentially caused by unavoidable errors and inaccuracies in design and construction (1), the distribution of S_W can generally be assumed as normal. The distribution of S_P, however, will usually not be normal. Both distributions must be combined in order to obtain the distribution of their sum S; this distribution will, therefore, not be of a simple type. Because, in general, the range of variation of the dead load is much narrower than that of the service load, it may be assumed as a first approximation that the character of the distribution function of S is identical with that of S_P and that only the values of the mean and the variance are combined by superposition of S_W and S_P. Hence, if the distribution of S_P is extremal (unlimited) with mean S_{PO} and variance

$$\sigma^2{}_P = \frac{\pi^2}{6}\frac{1}{\alpha^2{}_P} \qquad (32)$$

and the distribution of S_W is normal with mean S_{WO} and variance $\sigma^2{}_W$, and if $\left[1 - \left(\frac{\sigma_W}{\sigma_P}\right)^2\right]$ does not appreciably differ from unity, the distribution of S remains approximately extremal with

$$S_O = S_{OW} + S_{OP} \qquad (33a)$$

and

$$\frac{1}{\alpha^2{}_S} = \frac{6}{\pi^2}\sigma^2{}_W + \frac{1}{\alpha^2{}_P} = \frac{6}{\pi^2}\sigma^2{}_S \qquad (33b)$$

The addition of a dead load of comparatively high intensity and low variability to the service load reduces the range of relative variation of the total load intensity S; the reduction is higher for larger (S_{OW}/S_{OP})-ratios.

When other types of load are included in the operating conditions, as, for example, wind loads acting jointly with dead load and service load, the load intensity S is obtained by combining the intensities and the variations of the three types. As a result of such combinations the total load intensity S is increased and its probable number of applications is reduced. Hence, the design for such operating conditions can be based on a smaller number N and thus on a higher probability of failure or unserviceability. In the extreme case of operating conditions defined by the occurrence of destructive forces (earthquake or blast) in addition to the other design loads, the expected number of occurrences of such conditions may be as low as 1 or 2; the ratio of the design probabilities of failure for such extreme load intensities and for the normal operating conditions may, therefore, be as high as N for normal operating conditions. Because the failure loads associated with probabilities of failure differing by a factor of N—that is, by several orders of magnitude—may differ quite considerably, relatively high intensities of very infrequent destructive loads usually require not more than a disproportionately small increase of the carrying capacity of the structure to assure its survival—however, without assuring its complete serviceability.

If S denotes the intensity of the applied loads under specified operating conditions and R is the intensity of the same type of load that would produce failure of the structure or unserviceability, the relationship—

$$r = R - S \leq 0 \ldots\ldots\ldots\ldots (34)$$

determines the conditions of failure or of unserviceability; the inequality $r > 0$ is the condition of survival. If a "factor of ignorance" $n > 1$ is introduced, Eq. 34 becomes

$$r = R - n\,S \leqq 0 \ldots\ldots\ldots\ldots (35)$$

Because the statistical variations of R and S are independent, the probability of failure P_F is the product of the probability P_S of occurrence of a load intensity exceeding S and the probability P_R of occurrence of a failure load $R \leq S$. Conversely, the probability of survival is the product of the probability P^*_S of occurrence of a load intensity less than S and the probability P^*_R of occurrence of a failure load $R > S$. Both probabilities can be defined either with respect to failure or with respect to unserviceability, provided that the "failure load" R is related to actual failure or to unserviceability of the structure, respectively.

When S and R are normally distributed with means S_O and R_O and standard deviations σ_S and σ_R and if two variables x and y are defined by

$$x = \frac{S - S_O}{\sigma_S} = \frac{\Delta S}{\sigma_S} \ldots\ldots\ldots\ldots (36a)$$

and

$$y = \frac{R_O - R}{\sigma_R} = \frac{\Delta R}{\sigma_R} \ldots\ldots\ldots\ldots (36b)$$

the distribution functions of x and y are

$$p(x) = \frac{1}{\sqrt{2\pi}} \exp\left(-\tfrac{1}{2} x^2\right) \qquad (37a)$$

and

$$p(y) = \frac{1}{\sqrt{2\pi}} \exp\left(-\tfrac{1}{2} y^2\right) \qquad (37b)$$

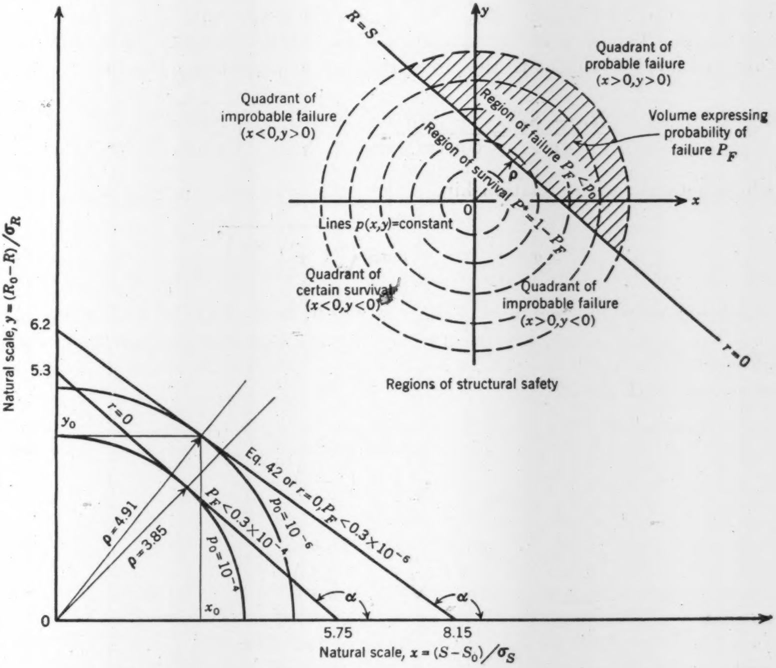
R=S
y
x
0
Quadrant of probable failure (x>0,y>0)
Quadrant of improbable failure (x<0,y>0)
Volume expressing probability of failure P_F
Region of failure $P_F<p_0$
Region of survival $P^*=1-P_F$
ρ
Lines p(x,y)=constant
Quadrant of certain survival (x<0,y<0)
Quadrant of improbable failure (x>0,y<0)
r=0
Regions of structural safety
Natural scale, $y=(R_0-R)/\sigma_R$
6.2
5.3
y_0
r=0
Eq. 42 or $r=0, P_F<0.3\times10^{-6}$
$p_0=10^{-6}$
$P_F<0.3\times10^{-4}$
$p_0=10^{-4}$
ρ=4.91
ρ=3.85
x_0
α
α
0
5.75
8.15
Natural scale, $x=(S-S_0)/\sigma_S$

Fig. 7.—Analysis of Safety for Normal Distribution of S and R

Hence, the probability of any combination of values (x, y) defining a certain value of the variable

$$r = R - S = (R_O - S_O) - (x\,\sigma_S + y\,\sigma_R) \qquad (38)$$

is given by

$$p(x)\,p(y) = \frac{1}{2\pi} \exp\left[-\tfrac{1}{2}\left(x^2 + y^2\right)\right] \qquad (39)$$

The lines of constant probability,

$$p(x, y) = p_O \qquad (40)$$

in the coordinate system (x, y) are therefore the circles,

$$x^2 + y^2 = -2 \ln (2 \pi p_O) = -4.606 \log (2 \pi p_O) \dots\dots\dots \tag{41}$$

centered at $(R_O/\sigma_R, S_O/\sigma_S)$ with radii $\rho = 2.15 \sqrt{-\log 2 \pi p_O}$. In the same coordinate system the condition $r = 0$ is represented by

$$x \sigma_S + y \sigma_R = R_O - S_O \dots\dots\dots\dots\dots\dots \tag{42}$$

which cuts off the length $(R_O - S_O)/\sigma_S$ on the x-axis and $(R_O - S_O)/\sigma_R$ on the y-axis. The slope of Eq. 42 against the x-axis is $-\sigma_S/\sigma_R$. The condition that this line be tangent to the circle of constant probability (Eq. 41) is

$$\frac{R_O - S_O}{\sigma_R} = \frac{\rho}{\cos (\pi - \alpha)} = \rho \sqrt{1 + \left(\frac{\sigma_S}{\sigma_R}\right)^2} \dots\dots\dots\dots \tag{43}$$

which determines the relationship,

$$x \sigma_S + y \sigma_R = \rho \sigma_R \sqrt{1 + \left(\frac{\sigma_S}{\sigma_R}\right)^2} \dots\dots\dots\dots\dots \tag{44}$$

which separates the region of "failure" $(r < 0)$ from the region of "survival" $(r > 0)$. On this line, the failure combination with the highest probability of occurrence, which is equal to p_O, is defined by the coordinates of the point of contact with the circle—

$$x_O = \frac{\rho}{\sqrt{1 + \left(\frac{\sigma_R}{\sigma_S}\right)^2}} \dots\dots\dots\dots\dots\dots \tag{45a}$$

$$y_O = \frac{\rho}{\sqrt{1 + \left(\frac{\sigma_S}{\sigma_R}\right)^2}} \dots\dots\dots\dots\dots\dots \tag{45b}$$

so that

$$S - S_O = x_O \sigma_S \dots\dots\dots\dots\dots\dots\dots \tag{46a}$$

and

$$R_O - R = y_O \sigma_R \dots\dots\dots\dots\dots\dots\dots \tag{46b}$$

The probability of failure P_F for all combinations (S, R) along the line $r = 0$ is given by that part of the volume under the surface of rotation $p(x, y)$ which is cut off by a plane along the line $r = 0$ perpendicular to the $(x\, y)$-plane. Because the critical failure combination (x_O, y_O) has the highest probability of occurrence along the line $r = 0$, it represents the combination to be used in design. In a hypothetical design based on the mean values $S = S_O = R = R_O$ for which the line $r = 0$ according to Eq. 42 degenerates into an arbitrary straight line of negative slope passing through the origin, the chances of failure and survival would be even and equal to 0.5 as in this case the plane along $r = 0$ bisects the volume of $p(x, y)$.

The difference $(R_O - S_O)$ represents the "margin of safety," and the ratio R_O/S_O is the factor of safety with respect to the mean values of the applied load and the failure load, associated with the design for the critical "failure combination,"

$$S = S_O + X_O \sigma_S \qquad \text{(47a)}$$

and

$$R = R_O - y_O \sigma_R \qquad \text{(47b)}$$

If S_O, σ_S, σ_R, and p_O, are given, the required mean value R_O and the associated safety factor $\nu = R_O/S_O$ can be computed from Eq. 43 (the design problem). Conversely, if either (*a*) R_O, σ_S, σ_R, and p_O or (*b*) R_O, S_O, σ_S, and σ_R are given, the permissible mean value of S_O or the probability of failure can be computed (the rating problem).

For example, with $\sigma_S = 0.2\ S_O$, $\sigma_R = 0.1\ R_O$, and $p_O = 10^{-6}$ (so that according to tables of the normal functions the probability of failure for the critical combination $P_F < 0.3 \times 10^{-6}$, which is the area of the normal curve beyond the ordinate p_O) the radius $\rho = 4.91$. Hence, from Eq. 43

$$\frac{R_O - S_O}{\sqrt{1 + 4\left(\frac{S_O}{R_O}\right)^2}} = 0.49\ R_O \qquad \text{(48)}$$

from which $S_O = 0.38\ R_O$; this represents a safety factor with respect to the means of $\nu = 2.63$. With $x_O = 2.97$ and $y_O = 3.91$, the critical limit design combination $S = 1.60\ S_O = 0.61\ R_O = R$. By increasing p_O by two orders of magnitude to $p_O = 10^{-4}$, so that $P_F < 0.3 \times 10^{-4}$, the radius is reduced to $\rho = 3.85$. Hence,

$$\frac{R_O - S_O}{\sqrt{1 + 4\left(\frac{S_O}{R_O}\right)^2}} = 0.385\ R_O \qquad \text{(49)}$$

from which $S_O = 0.47\ R_O$; this is equivalent to a decrease of the required safety factor with respect to the means to $\nu = 2.12$. The critical limit design combination $S = 1.46\ S_O = 0.695\ R_O = R$. Thus, under the specified conditions, an increase of the design probability of failure by two orders of magnitude for the same mean carrying capacity is associated with an increase of the mean (permissible) applied load of approximately 25%; conversely, for a specified mean applied load, the required mean carrying capacity of the structure can be reduced by 20%.

Eq. 43 can be rewritten so as to permit direct evaluation of the safety factor ν by solving the equation,

$$\nu^2\left[1 - \left(\frac{\rho\,\sigma_R}{R_O}\right)^2\right] - 2\,\nu + \left[1 - \left(\frac{\rho\,\sigma_S}{S_O}\right)^2\right] = 0 \qquad \text{(50)}$$

The same procedure of safety analysis can be applied if the distribution functions of S and of R are logarithmic-normal with standard deviations of the logarithms of the variables δ_S and δ_R, provided that the variables x and y are defined by

$$x = \frac{\log S - \log S_O}{\delta_S} \qquad (51a)$$

and

$$y = \frac{\log R_O - \log R}{\delta R} \qquad (51b)$$

Eqs. 39 and 41 remain valid, whereas Eq. 42, based on $R - S = 0$ or $\log (R/S) = 0$, is transformed into

$$x\,\delta_S + y\,\delta_R = \log\left(\frac{R_O}{S_O}\right) \qquad (52)$$

which is a straight line with a slope $(-\,\delta_S/\delta_R)$ against the x-axis, cutting off the length $\frac{1}{\delta_S}\log\left(\frac{R_O}{S_O}\right)$ on the x-axis and $\frac{1}{\delta_R}\log\left(\frac{R_O}{S_O}\right)$ on the y-axis. The condition that this line be tangent to the circle $p(x, y) = p_O$ with radius ρ given by Eq. 41 is

$$\frac{1}{\delta_S}\log\left(\frac{R_O}{S_O}\right) = \frac{\rho}{\sin\,(\pi - \alpha)} = \rho\left(\frac{\delta_R}{\delta_S}\right)\sqrt{1 + \left(\frac{\delta_S}{\delta_R}\right)^2} \qquad (53)$$

which again determines the straight line

$$x\,\delta_S + y\,\delta_R = \rho\,\delta_R\sqrt{1 + \left(\frac{\delta_S}{\delta_R}\right)^2} \qquad (54)$$

that separates the regions of failure and survival. The failure combination with the highest probability of occurrence is, therefore, determined by Eqs. 45 in which σ_S and σ_R are replaced by δ_S and δ_R.

Hence,

$$\log\left(\frac{S}{S_O}\right) = x_O\,\delta_S \qquad (55a)$$

and

$$\log\left(\frac{R_O}{R}\right) = y_O\,\delta_R \qquad (55b)$$

For given values of S_O, δ_S, δ_R, and p_O the required mean value R_O can be obtained by solving Eq. 53 and vice versa (Fig. 8).

For an extreme-value distribution of S and R (unlimited distribution, Eqs. 8) or of log S and log R (limited distribution, Eqs. 12) the probability of failure P_F for any combination (S, R) in which $S > S_O$, $R < R_O$ can be analytically expressed directly by the product of the probability of occurrence P_S of values $\geq S$ and the probability of occurrence P_R of values $\leq R$, whereas the probability of survival P^*_F under the same conditions is given by the product of the probability of occurrence P^*_S of values less than S and the probability of occurrence P^*_R of values greater than R. This is simpler than for a normal or logarithmic-normal distribution for which the evaluation of P_F requires the computation of the volume of $p(x, y)$ cut off by a plane along $r = 0$.

Using P^*_F in preference to P_F for reasons of expediency so as to have a three-dimensional coordinate system (x, y, P^*_F) in which all coordinates increase from the origin, and introducing the reduced variables,

$$x = \alpha_S (S - S'_O) \qquad (56a)$$

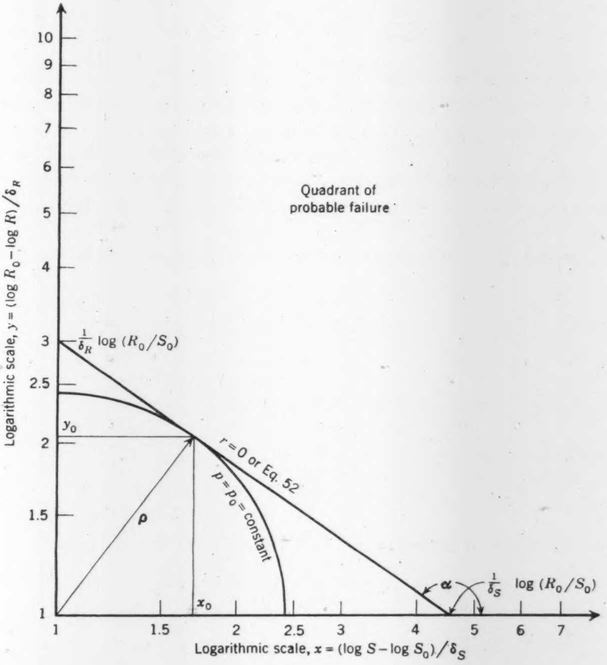

FIG. 8.—ANALYSIS OF SAFETY FOR LOGARITHMIC-NORMAL DISTRIBUTION OF S AND R

and

$$-y = \alpha_R (R'_O - R) \qquad (56b)$$

in which S'_O and R'_O denote the modes of the distributions and

$$\frac{1}{\alpha^2_S} = \frac{6\,\sigma^2_S}{\pi^2} \qquad (57a)$$

and

$$\frac{1}{\alpha^2_R} = \frac{6\,\sigma^2_R}{\pi^2} \qquad (57b)$$

denote the squares of the measure of dispersion, the probability of survival for unlimited extremal distributions is

$$P^*_F = P^*_S\, P^*_R = \exp\left[-\,(e^{-x} + e^{+y})\right] \tag{58}$$

The lines of constant probability of survival P^*_{FO} therefore, are given by

$$(e^{-x} + e^{+y}) = -\ln P^*_{FO} = -\,2.303 \log P^*_{FO} \tag{59}$$

The point of contact of the tangent $r = 0$ or

$$\frac{x}{\alpha_S} + \frac{y}{\alpha_R} = R'_O - S'_O \tag{60}$$

to any of those curves defined by different values of P^*_{FO} determines the critical failure condition (lowest probability of survival) along this tangent which separates the region of probabilities of survival $P^*_F > P^*_{FO}$ from that for which $P^*_F < P^*_{FO}$. The intercepts with the x-axis and the y-axis determine again the values of S'_O and R'_O compatible with given values of α_S, α_R, and P^*_{FO} and, thus, the safety factor with respect to the modes of the distributions.

For extremal distributions limited to positive values of the variables,

$$x = \alpha_S \log\left(\frac{S}{S'_O}\right) \tag{61a}$$

and

$$-\,y = \alpha_R \log\left(\frac{R'_O}{R}\right) \tag{61b}$$

the probability of survival

$$P^*_F = P^*_S\, P^*_R = \exp\left[-\,(x^{-\alpha_S} + y^{+\alpha_R})\right] \tag{62}$$

Therefore, the lines of constant probability of survival

$$x^{-\alpha_S} + y^{+\alpha_R} = -\,2.303 \log P^*_{FO} \tag{63}$$

the point of contact of the tangent $r = 0$ or

$$\frac{x}{\alpha_S} + \frac{y}{\alpha_R} = \log\left(\frac{R'_O}{S'_O}\right) \tag{64}$$

to any of the curves $P^*_F = P^*_{FO}$ determines the critical failure condition along this tangent, and its intercepts with the coordinate axes determine the safety factor with respect to the modes of the distribution.

It should be noted, however, that even when cumulative functions are used P^*_F is not the true probability of survival because, for reasons of expediency, it refers only to the "quadrant of probable failure" (Fig. 7) in which $S > S_O$ and $R < R_O$. Failure, however, is also possible in the "quadrants of improbable failure" in which $S < S_O$ and $R < R_O$, or $S > S_O$ and $R > R_O$, provided in both cases that $S > R$. Hence, the true probability of survival is equal to the sum of the probabilities of survival in the three quadrants, which is higher than P^*_F computed for the quadrant of probable failure alone. In the limiting cases of design for S'_O and R'_O, for which the line $r = 0$ passes through the origin, the true probability of failure is therefore twice P^*_F; for all other conditions it is larger than P^*_F and smaller than 2 P^*_F, so that P^*_F is a safe estimate of the true probability of survival.

When a logarithmic scale for P^*_F is used in a three-dimensional coordinate system, the "surface of survival" (Eq. 58) slopes down exponentially in the directions of increasing x and y measured in a natural scale. When x and y are also plotted on a logarithmic scale, the surface of survival (Eq. 62) slopes down in the direction of increasing x and y according to $x^{-\alpha_S}$ and $y^{-\alpha_R}$. The use of the extreme-value probability scale for P^*_F, as a result of which the functions $P^*_S(x)$ and $P^*_R(y)$ are transformed into straight lines, transforms both surfaces into hyperbolic paraboloids with straight-line generatrices in the directions of the coordinate axes (Fig. 9).

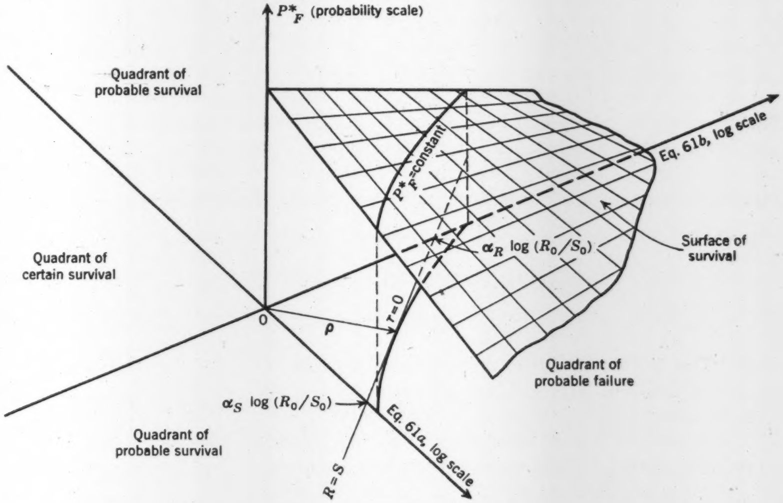
P^*_F (probability scale)
Quadrant of probable survival
P^*_F=constant
Eq. 61b, log scale
Surface of survival
α_R log (R_0/S_0)
Quadrant of certain survival
0
ρ
$r=0$
Quadrant of probable failure
α_S log (R_0/S_0)
Eq. 61a, log scale
Quadrant of probable survival
$R=S$

FIG. 9.—HYPERBOLIC PARABOLOID SURFACE OF PROBABILITY OF SURVIVAL

When the distributions of S and R cannot be analytically expressed but only plotted, a purely graphical procedure of safety analysis may be used in which the product $P^*_S\, P^*_R$ is computed for a sufficient number of points in the (x, y)-plane to make the drawing of the contour lines $P^*_F = P^*_{FO}$ by interpolation possible. The tangents to these lines inclined toward the x-axis by $(-\sigma_S/\sigma_R)$ define the critical failure combinations for limit design as well as the factors of safety with respect to the mean for various probabilities of survival.

CONCLUSIONS

In the analysis of a structure, the analyses of the applied loads as well as of the probability of failure or unserviceability are as necessary and important as the analysis of the stresses. The information required for an integrated analysis which produces a rational value for the safety of the structure related to acceptable probabilities of failure are the distribution functions of the intensity of an applied standard load and of the standard-load intensity producing, respectively, structural failure and unserviceability—both presented in a form which justifies extrapolation toward high values of the applied load and low values of the failure and unserviceability loads. Because structural failure is usually associated with or preceded by substantial inelastic deformation, inelastic analysis of the carrying capacity should replace the elastic-stress analysis in the computation of the probability of failure, whereas elastic-stress analysis is in most cases sufficient to determine the probability of unserviceability.

The existing data suggest that either the logarithmic-normal or the extreme-value distribution functions represent actual load and strength distributions fairly well so that they can be used in the analysis of the probability of failure and of the safety of structures. For either type of distribution the safety factors associated with specified probabilities of failure or of unserviceability can be rapidly computed or easily determined by a graphical procedure.

APPENDIX. BIBLIOGRAPHY

(1) **"The Safety of Structures,"** by Alfred M. Freudenthal, *Transactions*, ASCE, Vol. 112, 1947, p. 125.

(2) **"Reflections on Standard Specifications for Structural Design,"** by Alfred M. Freudenthal, *ibid.*, Vol. 113, 1948, p. 269.

(3) **"Concepts of Safety in Structural Engineering,"** by A. G. Pugsley, *Proceedings*, Inst. of C. E., London, Vol. 29, 1951.

(4) **"Conceptions Modernes Relatives à la Securité des Constructions,"** by M. Prot and R. Lévi, *Revue Générale des Chemins de Fer*, June, 1951.

(5) **"Determinacion del Coefficiente de Seguridad en las Distintas Obras,"** by A. P. Balaca and E. Torroja, Instituto Técnico de la Construcción, Madrid, 1950.

(6) **"Strength, Safety and Economical Dimensions of Structures,"** by A. I. Johnson, *Meddelanden No. 12,* Inst. of Byggnadsstatik, Royal Inst. of Technology, Stockholm, 1953.

(7) **"Preliminary Report,"** Third International Cong. of Bridge and Structural Eng., Liège, Belgium, 1948, pp. 555–653.

(8) **"Final Report,"** Third International Cong. of Bridge and Structural Eng., Liège, Belgium, 1948, pp. 635–686.

(9) **"Preliminary Report,"** Fourth International Cong. of Bridge and Structural Eng., Cambridge, England, 1952, pp. 165–176.

(10) **"Final Report,"** Fourth International Cong. of Bridge and Structural Eng., Cambridge, England, 1952, pp. 145–165.

(11) **"Recent Progress in the Plastic Methods of Structural Analysis,"** by P. S. Symonds and B. G. Neal, *Journal*, Franklin Inst., Vol. 252, 1951, p. 383. (*a*) p. 469.

(12) **"Review of Recent Investigations into the Behavior of Steel Frames in the Plastic Range,"** by A. L. Baker, *Journal*, Inst. of C. E., London, Vol. 27, 1949, p. 188. (*a*) p. 397.

(13) **"Bedeutung der Zaehigkeit des Stahles fuer die Berechnung und Bemessung von Stahlhochbauten,"** by H. Maier-Leibnitz, Preliminary Report, Second International Cong. of Bridge and Structural Eng., Berlin, 1936, p. 103.

(14) **"Theorie Statisch Unbestimmter Systeme aus Idealplastichem Baustoff,"** by E. Melan, Sitzungsberichte Akademie der Wissenschaften, Vienna, Vol. 145 (IIa), 1936, p. 195.

(15) **"Methods of Converting Heavy Motor Vehicle Loads into Equivalent Design Loads, etc.,"** by H. K. Stephenson and K. Cluninger, *Bulletin No. 127*, Texas Eng. Experiment Station, College Station, Tex., 1952.

(16) **"Gust Factors for the Design of Buildings,"** by R. H. Sherlock, *Publications*, International Assn. of Bridge and Structural Eng., Vol. 8, 1947, p. 207.

(17) **"Quality Control of Concrete, its Rational Basis and Economic Aspects,"** by N. M. Plum, *Proceedings*, Inst. of C. E., London, 1953, p. 311.

(18) **"Essais Statistiques sur Mortiers et Bétons,"** by M. Prot, Final Report, Third Cong., International Assn. of Bridge and Structural Eng., Liège, Belgium, 1948, p. 701.

(19) **"On the Statistical Interpretation of Fatigue Tests,"** by A. M. Freudenthal and E. J. Gumbel, *Proceedings*, Royal Soc. of London, Series A, Vol. 216, 1953, p. 309.

(20) **"A Statistical Representation of Fatigue Failures in Solids,"** by W. Weibull, *Transactions*, Royal Inst. of Technology, Stockholm, No. 27, 1949.

(21) **"Statistical Analysis of Behavior in the Transition Temperature Zone,"** by R. W. Vanderbeck, H. D. Wilde, R. W. Lindsay, and C. Daniel, Welding Research Supplement, *Welding Journal*, Vol. 18, 1953, p. 325.

(22) **"Floods Estimated by Probability Method,"** by E. J. Gumbel, *Engineering News-Record*, Vol. 134, 1945, p. 97.

(23) **"Forecasting Floods,"** by E. J. Gumbel, *ibid.*, Vol. 135, 1946, p. 96.

(24) **"The Statistical Theory of Extreme Values and Some Practical Applications,"** by E. J. Gumbel, *Applied Mathematics Series*, National Bureau of Standards, Washington, D. C., 1954.

(25) **"A Note on the Interpretation of V-g Records,"** by P. E. Montague, A. Robinson, and V. Fagg, *Reports and Memoranda 2097*, Ministry of Supply, London, 1945.

(26) **"Behavior of 24S-T4 Aluminum Alloy Subjected to Repeated Stress of Variable Amplitude,"** by H. F. Hardrath, *Technical Note No. 2798*, National Advisory Committee for Aeronautics, Washington, D. C., 1952.

(27) **"A Random Fatigue Testing Procedure and Machine,"** by A. M. Freudenthal, *Proceedings*, A. S. T. M., Vol. 53, 1953, p. 896.

(28) **"Advanced Mechanics of Materials,"** by F. B. Seely and J. O. Smith, John Wiley & Sons, Inc., New York, N. Y., 1952, p. 514.

(29) **"Inelastic Behavior of Engineering Materials and Structures,"** by A.M . Freudenthal, John Wiley & Sons, Inc., New York, N. Y., 1950.

(30) **"The Safety Factor of an Elastic-Plastic Body in Plane Strain,"** by D. C. Drucker, H. J. Greenberg, and W. Prager, *Journal of Applied Mechanics*, Vol. 18, 1951, p. 371.

(31) **"Die Tragfähigkeit Statisch Unbestimmter Tragwerke aus Stahl bei beliebig häufig wiederholter Belastung,"** by M. Grüning, Julius Springer, Berlin, 1926.

(32) **"Ueber die Bemessung Statisch Unbestimmter Stahltragwerke unter der Berücksichtigung des Elastisch-Plastischen Verhaltens des Baustoffes,"** by H. H. Bleich, *Bauingenieur*, Vol. 13, 1932, p. 261.

(33) **"Elastic-Plastic Analysis of Structures Subjected to Loads Varying Arbitrarily between Prescribed Limits,"** by P. S. Symonds and W. Prager, *Journal of Applied Mechanics*, Vol. 17, 1950, p. 315.

(34) **"Flange Buckling, A Limitation of Plastic Design of Beams, Frames, and Columns,"** by G. Winter, *Final Report*, Fourth International Cong. of Bridge and Structural Eng., Cambridge, England, 1953, p. 139.

(35) **"Allgemeine Plastizitätstheory, Gleitlinienfelder,"** by A. M. Freudenthal, *Preliminary Report*, Second Cong. of Bridge and Structural Eng., Berlin, 1936, p. 3.

(36) **"Beitrag zum Traglastverfahren,"** by F. Stuessi and G. F. Kollbrunner, *Bautechnik*, Vol. 13, 1953, p. 264.

(37) **"Peculiar Behavior of Steel Beams under Dead Loads that Produce Inelastic Strains,"** by H. T. Corten, M. E. Clark, and O. M. Sidebottom, *Transactions*, ASME, Vol. 74, 1952, p. 349.

(38) **"Theory of Plasticity in the Investigation of Statically Indeterminate Structures of Reinforced Concrete,"** by A. M. Freudenthal, *Publications*, International Assn. of Bridge and Structural Eng., Vol. 2, 1933–1934, p. 180.

(39) **"Plastic Theory of Reinforced Concrete Design,"** by Charles S. Whitney, *Transactions*, ASCE, Vol. 107, 1942, p. 251.

(40) **"Session on Ultimate Load Design,"** by L. H. Corning, B. G. Anderson, E. Hognestad, C. P. Siess, R. C. Reese, and T. Y. Lin, *Proceedings*, A. C. I., Vol. 48, 1952, pp. 797–900.

(41) **"Some Time Effects in Structural Analysis,"** by A. M. Freudenthal, Sixth International Cong. for Applied Mechanics, Paris, 1946.

(42) **"Theorie des Grandes Voûtes en Béton et en Béton Armé,"** by A. M. Freudenthal, *Publications*, International Assn. of Bridge and Structural Eng., Vol. 4, 1936, p. 249.

(43) **"On Inelastic Thermal Stresses,"** by A. M. Freudenthal, von Mises Memorial Volume, Academic Press, New York, N. Y., 1954.

(44) **"Sakerhets Problemet ur Principiell och Teoretisk Synpunkt,"** by W. Kjellman, *Proceedings*, Academy of Eng. Sciences, No. 156, Stockholm, 1940.

(45) **"Introduction to the Theory of Probability and Statistics,"** by Neils Arley and K. Rander Buch, John Wiley & Sons, Inc., New York, N. Y., 1950, p. 87.

(46) **"Introduction to Mathematical Statistics,"** by Paul G. Hoel, John Wiley & Sons, Inc., New York, N.Y., 1946, p. 71.

(47) **"Tables of Normal Probability Functions,"** *Applied Mathematics Series No. 23,* National Bureau of Standards, Washington, D. C., 1953.

(48) **"Tables of the Error Function and its Derivative,"** *Applied Mathematics Series No. 41,* National Bureau of Standards, Washington, D. C., 1954.

(49) **"Statistical Methods in Concrete Research",** by P. J. F. Wright, *Concrete Research Number 15,* Cement and Concrete Assn., London, March, 1954.

DISCUSSION

ANTHONY CHIBARO,[3] M. ASCE.—Although one of the most significant approaches to the application of the laws of probability to the safety of structures has been presented by Mr. Freudenthal, the most valuable result of the paper, in the writer's opinion, is that rational design has at long last received thorough logical scrutiny. How much of the design procedure suggested by the author will be adopted by the profession is open to question. Because of this work, however, engineers have gained a better understanding of the laws governing some of the most important variables involved in engineering problems. Furthermore, they have again been reminded that no single line of investigation can produce a solution of a design problem and that the elastic theory and the plastic theory are each useful in expressing the state of a structure under different intensities of load. It can be concluded from Mr. Freudenthal's exposition that, because of the random variations pertaining to values of loads and strengths, the factor of safety which engineers have used as a definite number in fact varies. It is a minimum when the incidence of the maximum service load coincides with the minimum strength of the structure, and is a maximum when the service load is minimum and the strength of the structure is maximum. The probability of occurrence of the most unsafe condition may be considered as a measure of safety.

Although the author's approach may prove to be a milestone in engineering design, it will probably be a long time before the use of the "factor of safety" concept will be supplanted by the use of the "probability of failure" concept. However, as forcibly illustrated by Mr. Freudenthal, these concepts are evidently mutually dependent, and the latter is a better measure of safety than the former. In order to use the concept of probability of failure a great mass of statistical data pertaining to load effects and strengths must be obtained and correlated. This would appear to be a time-consuming and difficult task, especially in so far as load effects are concerned. As the author notes, the frequency distribution pertaining to the strength of concrete manufactured under good control conditions is quite different from that pertaining to concrete manufactured with inadequate control. The distribution pertaining to the latter will ordinarily be skewed to a marked degree toward low strengths.

An important factor which needs considerable study is the definition of terms. What are the exact meanings of "unserviceability" and "failure"? Does failure begin where serviceability ends? If so, the terms failure and unserviceability would appear to be synonymous. Terms found in the paper such as service load, standard load, standard failure load, shake-down load, plastic-collapse load, elastic-limit load, critical design load, and maximum service oad should be clearly defined in simple language.

A significant question which has no satisfactory answer is how much nearer are engineers toward a balanced design procedure by using the laws of probability if a good part (maybe the majority) of the variables are nonrandom and baffle mathematical analysis? Designers must still be guided largely by "horse sense" and must depend on their ability to guess correctly.

---

[3] Prin. Structural Engr., Jackson & Moreland, Engrs., Boston, Mass.

In the preparation of the paper Mr. Freudenthal has done the profession a real and much needed service. This service might well be extended by the presentation of definite numerical examples pertaining to "Probability of Failure: Analysis of Failure and Survival: Safety Factors."

Lloyd S. Lawrence,[4] A. M. ASCE.—The application of the concept of probability to the study of factors of safety as presented by Mr. Freudenthal should be of great interest and benefit to the profession. This work should lead to a better understanding of the physical significance of the factor of safety even though the practical application of the results in many cases may be difficult, primarily because of inadequate knowledge of the relative frequency of many types of loads.

The relationship between the factor of safety and the probability of failure cited under the heading, "Probability of Failure: Analysis of Failure and Survival: Safety Factors," appears to be of primary importance. It is unfortunate that this section was not expanded to indicate more clearly the final conclusions.

The method of analysis leading to Figs. 7 and 8 which indicate the relation of the probability of failure P_F to the statistical parameters of the load effect S and the failure load (or load of unserviceability) R for normal and logarithmic-normal distribution is correct, and integration to obtain the volume indicated would lead to the true probability of failure. However, it should be made clear that S_O and R_O as used in the equations for logarithmic-normal distribution are the geometric mean values of S and R, respectively, and not the arithmetic mean values as implied by the definition given for the case of the normal distribution.

Although the method of attack given by Mr. Freudenthal leads to the correct evaluation of the probability of failure, it appears to be a rather devious solution as the total probability of failure can be more easily obtained directly from the usual statistical parameters without the introduction of additional frequencies, such as p_O, which require computation.

In cases in which the normal frequency function applies to both S and R, the total probability of failure P_F (including all "quadrants of failure") is merely the area under the normal frequency curve,

$$p(x) = \frac{1}{\sqrt{2\pi}} e^{-1/2(x^2)} \qquad \text{(65)}$$

from $x = \rho$ to $x = \infty$, in which S_O and R_O are the arithmetic means and σ_S and σ_R are the standard deviations of S and R, respectively, and ρ is defined from Eq. 43 as

$$\rho = \left(\frac{R_O - S_O}{\sigma_R}\right) \frac{1}{\sqrt{1 + (\sigma_S/\sigma_R)^2}} \qquad \text{(66)}$$

---

[4] Senior Structural Engr., Jackson & Moreland, Engrs., Boston, Mass.

That is,

$$P_F = \frac{1}{\sqrt{2\,\pi}} \int_{\rho}^{\infty} e^{-1/2(x^2)}\, dx \ldots\ldots\ldots\ldots\ldots\ldots (67)$$

This area can readily be obtained from tables of the normal frequency function.

The foregoing may not be evident from the paper but can easily be derived. If

$$x = \frac{S - S_O}{\sigma_S} \ldots\ldots\ldots\ldots\ldots\ldots\ldots\ldots (68)$$

the probability of the load S being such that the corresponding x-value lies within limits the difference between which is equal to dx is

$$p(x)\, dx = \frac{1}{\sqrt{2\,\pi}}\, e^{-1/2(x^2)}\, dx \ldots\ldots\ldots\ldots\ldots\ldots (69)$$

If

$$w = \frac{R - R_O}{\sigma_R} \ldots\ldots\ldots\ldots\ldots\ldots\ldots\ldots (70)$$

the probability of the failure load R being equal to $S + r$ and such that the corresponding w-value lies within limits the difference between which is equal to dr/σ_R is

$$p(w)\, \frac{dr}{\sigma_R} = \frac{1}{\sqrt{2\,\pi}\,\sigma_R}\, e^{-1/2(w^2)}\, dr \ldots\ldots\ldots\ldots\ldots\ldots (71)$$

evaluated for w obtained from $R = S + r$.

When $R = S + r$, $w = (S + r - R_O)/\sigma_R$ but

$$S = \sigma_S\, x + S_O \ldots\ldots\ldots\ldots\ldots\ldots\ldots\ldots (72)$$

which on substitution gives $w = (\sigma_S/\sigma_R)\, x - [(R_O - S_O - r)/\sigma_R]$. Substituting this value of w into the right side of Eq. 71 gives

$$p(w)\, \frac{dr}{\sigma_R} = \frac{1}{\sqrt{2\,\pi}\,\sigma_R}\, e^{-1/2\,\{(\sigma_S/\sigma_R)\, x\, -\, [(R_0 - S_0 - r)/\sigma_R]\}^2}\, dr \ldots\ldots (73)$$

for the probability of the failure load being as assumed in the foregoing.

The probability of these events occurring simultaneously is equal to the product of their probabilities. Integration with respect to x between the limits $-\infty$ to $+\infty$ of the resulting expression gives the total probability of the failure load being equal to $S + r$ and such that the corresponding w-value lies within limits the difference between which is equal to dr/σ_R. It follows that the relative frequency of R being equal to $S + r$ is

$$p(r) = \frac{1}{2\,\pi\,\sigma_R} \int_{-\infty}^{\infty} e^{-1/2(x^2)}\, e^{-1/2\,\{(\sigma_S/\sigma_R)\, x\, -\, [(R_0 - S_0 - r)/\sigma_R]\}^2}\, dx \ldots\ldots (74)$$

Integration of Eq. 74 by combining exponents and completing the square leads to

$$p(r) = \frac{1}{\sigma_R \sqrt{2\pi\,[1 + (\sigma_S/\sigma_R)]}} \, e^{-1/2\,\{(R_0 - S_0 - r)^2/[1 + (\sigma_S/\sigma_R)^2]\sigma^2_R\}} \ldots (75)$$

Therefore, the probability of r being equal to or less than zero—which is the probability of failure—is

$$P_F = \frac{1}{\sigma_R \sqrt{2\pi\,[1 + (\sigma_S/\sigma_R)^2]}} \int_{-\infty}^{0} e^{-1/2\,\{(R_0 - S_0 - r)^2/[1 + (\sigma_S/\sigma_R)^2]\sigma^2_R\}} \, dr \ldots (76)$$

Transformation of Eq. 76 gives Eq. 67.

The same conclusion could have been arrived at by application of statistical theorems (45) regarding the frequency function of the sum or difference of two variables which are normally distributed. However, the procedure used in the derivation given previously can be applied directly to cases in which the frequency function is not normal.

It is of interest to note that, for the hypothetical case in which $S_O = R_O$, the lower limit of integration in Eq. 67 becomes 0 and $P_F = 0.5$.

As noted by Mr. Freudenthal under the heading, "Load Analysis: Random Variation of Standard-Load Intensity," it is quite often expedient to take the probability of the load being S_O as unity. For this limiting case σ_S equals 0 and Eq. 67 becomes

$$P_F = \frac{1}{\sqrt{2\pi}} \int_{(R_O - S_O)/\sigma_R}^{\infty} e^{-1/2(x^2)} \, dx = \frac{1}{\sqrt{2\pi}} \int_{-\infty}^{(S_O - R_O)/\sigma_R} e^{-1/2(w^2)} \, dw \ldots (77)$$

which is obviously the probability of R being less than S_O because, when $R = S_O$, $w = (S_O - R_O)/\sigma_R$.

Although there is no possibility of there being a structure in which the failure load can be determined with certainty, it may be of mathematical interest to investigate this condition. For this limiting case σ_R equals 0 and Eq. 67 becomes

$$P_F = \frac{1}{\sqrt{2\pi}} \int_{(R_O - S_O)/\sigma_S}^{\infty} e^{-1/2(x^2)} \, dx \ldots\ldots\ldots\ldots\ldots (78)$$

which is obviously the probability of S being greater than R_O because, when $S = R_O$, $x = (R_O - S_O)/\sigma_S$.

For cases in which the logarithmic-normal frequency function applies to both S and R, the total probability of failure P_F is equal to the area under the normal frequency curve, Eq. 65, from $x = \rho$ to $x = \infty$, ρ being defined, according to Eq. 53, as

$$\rho = \frac{\log (R_{O_g}/S_{O_g})}{\log \sigma_{R_g}} \, \frac{1}{\sqrt{1 + (\log \sigma_{S_g}/\log \sigma_{R_g})^2}} \ldots\ldots\ldots\ldots (79)$$

In Eq. 79, S_{O_g} and R_{O_g} are the geometric means of S and R, respectively; or $\log S_{O_g}$ and $\log R_{O_g}$ are the arithmetic means of the logarithms of S and R, and

σ_{S_g} and σ_{R_g} are the standard geometric deviations of S and R, respectively; or $\log \sigma_{S_g}$ and $\log \sigma_{R_g}$ are the standard deviations of the logarithms of S and R.

The foregoing can be deduced from the previous derivation for the case of normal distribution for, if S and R in this derivation had been defined as the logarithms of the load and the failure load, the logic and equations would still be correct. The means and standard deviations would then refer to the logarithms, and $[(R_O - S_O)/\sigma_R][1/\sqrt{1 + (\sigma_S/\sigma_R)^2}]$ would become $[(\log R_{O_g} - \log S_{O_g})/\log \sigma_{R_g}][(1/\sqrt{1 + (\log \sigma_{S_g}/\log \sigma_{R_g})^2}]$.

Solutions for extreme-value distributions and for many other types or combinations of frequency functions could undoubtedly be derived by a similar procedure. For functions for which this procedure would involve the solution of integrals that could not be expressed simply (or at all) in terms of known functions, the solution for particular cases can be obtained fairly readily by numerical-integration methods. In these cases it appears advantageous to attack the problem in a somewhat different manner.

If $p(S)$ is the frequency function of S and $p(R)$ is the frequency function of R such that the areas under the plots of $p(S)$ versus S and $p(R)$ versus R are each unity, the probability of S being within limits the difference between which is equal to dS is $p(S)\, dS$ and the probability of R being less than this value of S is equal to $\int_{-\infty}^{S} p(R)\, dR$. The probability of both events occurring simultaneously is equal to $p(S) \left[\int_{-\infty}^{S} p(R)\, dR \right] dS$.

Therefore, the total probability of failure is

$$P_F = \int_{-\infty}^{\infty} p(S) \left[\int_{-\infty}^{S} p(R)\, dR \right] dS \ldots\ldots\ldots\ldots\ldots (80)$$

To determine P_F, a plot or tabulation of $p(S) \left[\int_{-\infty}^{S} p(R)\, dR \right]$ versus S can be made. The value of the integral appearing in Eq. 80 can ordinarily be easily obtained. The probability of failure P_F is then obtained by determining the total area under this plot by numerical integration or by the use of a planimeter.

It may be desirable to express Eq. 80 in terms of dimensionless variables, which can easily be accomplished by direct substitution. For example, if it is convenient to use the deviation in terms of the standard deviation as for the normal frequency functions,

$$p(S)\, dS = p(x)\, dx \ldots\ldots\ldots\ldots\ldots\ldots\ldots\ldots (81)$$

$$p(R)\, dR = p(w)\, dw \ldots\ldots\ldots\ldots\ldots\ldots\ldots\ldots (82)$$

and when $R = S$, $w = (\sigma_S/\sigma_R)\, x - [(R_O - S_O)/\sigma_R]$. Therefore, Eq. 80 becomes

$$P_F = \int_{-\infty}^{\infty} p(x) \int_{-\infty}^{w=(\sigma_S/\sigma_R)x-[(R_O-S_O)/\sigma_R]} p(w)\, dw\, dx \ldots\ldots\ldots (83)$$

Example.—As an illustration of the use of the foregoing equations, the solution of a hypothetical example is given herewith.

To determine the probability of failure, given that $\sigma_S = 0.25\ S_O$, $\sigma_R = 0.1\ R_O$, and the safety factor $\nu = R_O/S_O = 1.25$ (purposely taken low to illustrate the high probability of failure associated with the low factor of safety), the use of Eq. 67 will lead to

$$\frac{R_O - S_O}{\sigma_R} \frac{1}{\sqrt{1 + (\sigma_S/\sigma_R)^2}} = \frac{2}{\sqrt{5}} = 0.8944 \qquad (84)$$

From tables of the normal frequency function the area of the normal curve from $x = 0.8944$ to $x = \infty$ equals 0.1856.

Although Eq. 83 is intended for use only for frequency functions or combinations of frequency functions for which the equivalent of Eq. 67 cannot readily be obtained, the example has been solved by this method also. The use of Simpson's rule for the evaluation of the last integral, with $\Delta x = 0.5$ from $x = -1$ to $x = +4$, gives $P_F = 0.1849$ which differs from the exact result of Eq. 67 by only 0.4%.

Application of Eq. 67 to the example given by Mr. Freudenthal using the computed ratios of S_O/R_O equal to 0.38 and 0.47, gives values for the total probability of failure P_F of 0.40×10^{-6} and 0.56×10^{-4}, respectively. These values are somewhat higher than the corresponding values of 0.3×10^{-6} and 0.3×10^{-4} given by the author, which apparently include only the part contributed by the "quadrant of probable failure" as mentioned by Mr. Freudenthal subsequent to Eq. 64.

It is not made clear in the derivation why P_F is considered to be the area of the normal curve beyond the ordinate p_O as indicated parenthetically in the solution of the example given by the author. Something appears to be amiss here because, for the special case of normal distribution (when $R_O = S_O$), $\rho = 0$ from Eq. 43 and $p_O = 1/2\pi$. From tables of the normal function the area beyond the ordinate $1/2\pi = 0.0875$, whereas the true probability of failure for this case is obviously 0.5 as indicated subsequent to Eq. 46*b*. In order to obtain the correct values of P_F (including all the quadrants) the author should have multiplied his values of p_O by $\sqrt{2\pi}$ and then obtained P_F from tables using $\sqrt{2\pi}\, p_O$ for the relative frequency.

The note on Fig. 7 which indicates that $P_F < p_O$ does not appear to be valid in general, although it would be valid in most practical cases. Note that when $R_O = S_O$, P_F is more than three times p_O. In fact, when ρ, from Eq. 43, is less than approximately 2.15, $P_F > p_O$.

José M. Corso,[5] A.M. ASCE.—Congratulations must be offered Mr. Freudenthal for treating a subject little known to many engineers and on which little emphasis has been placed in the past. The realization that the factor of safety is not a fixed arbitrary quantity but that it must be gaged to the particular conditions of load, resistance, and life of a given structure is most important. The fact that present (1956) knowledge is not advanced sufficiently in many cases to permit direct application of the methods presented by the author does not by any means imply that they are not extremely valuable.

---

[5] Engr., Jackson & Moreland, Engrs., Boston, Mass.

In order to permit direct evaluation of the total probability of failure P_F, in case normal frequency functions apply to both the load effect S and the resistance R, the writer has carried Mr. Freudenthal's procedure one step further. As noted by the author, the total probability of failure is given by the part of the volume under the surface $p(x, y)$ which is cut off by a plane perpendicular to the (x, y)-plane and along the line $r = 0$ (shaded part of Fig. 7). This volume may be obtained easily if a new set of orthogonal coordinate axes (u, v) having the same origin as the axes shown, but with the u-axis parallel to the line $r = 0$, is introduced. Then the probability of failure is given by

$$P_F = \int_{r=0}^{r=-\infty} p(x, y)\, du\, dv \qquad (85)$$

in which

$$p(x, y) = \frac{1}{2\pi} e^{-\frac{1}{2}(x^2+y^2)} = \frac{1}{2\pi} e^{-\frac{1}{2}(u^2+v^2)} \qquad (86)$$

Therefore,

$$P_F = \frac{1}{2\pi} \int_\rho^\infty \int_{-\infty}^\infty e^{-\frac{1}{2}(u^2+v^2)}\, du\, dv = \frac{1}{2\pi} \int_\rho^\infty e^{-\frac{1}{2}v^2}\, dv \int_{-\infty}^\infty e^{-\frac{1}{2}u^2}\, du \qquad (87)$$

or

$$P_F = \frac{1}{\sqrt{2\pi}} \int_\rho^\infty e^{-\frac{1}{2}v^2}\, dv \qquad (88)$$

in which the value of ρ, as obtained from Eq. 43, is

$$\rho = \frac{R_O - S_O}{\sqrt{\sigma^2{}_R + \sigma^2{}_S}} \qquad (89)$$

Therefore, if ρ is known, to determine the probability of failure P_F the area of the normal distribution curve between ρ and ∞ is obtained from available tables of the normal function. Conversely, if P_F is known, ρ may be obtained from the same tables.

This result is not surprising because (as is known) if R and S are normally and independently distributed, the difference,

$$r = R - S \qquad (90a)$$

is also distributed normally with mean

$$r_O = R_O - S_O \qquad (90b)$$

and standard deviation (46)

$$\sigma_r = \sqrt{\sigma^2{}_R + \sigma^2{}_S} \qquad (90c)$$

Therefore, the relative frequency of r is

$$\rho(r) = \frac{1}{\sqrt{2\pi\sigma_r}} e^{-\frac{1}{2}(r - r_O/\sigma_r)^2} \qquad (91)$$

and the probability of failure, which is the same as the probability of $r \leq 0$, is given by

$$P_F = \frac{1}{\sqrt{2\,\pi}} \int_{-\infty}^{0} e^{-\frac{1}{2}(r - r_O/\sigma_r)^2} \frac{dr}{\sigma_r} \qquad (92)$$

Eq. 88 is obtained by introducing a new variable

$$v = \frac{r_O - r}{\sigma_r} \qquad (93a)$$

and noting that the upper limit of integration becomes

$$\frac{r_O}{\sigma_r} = \rho \qquad (93b)$$

the lower limit is $+ \infty$, and

$$dv = - \frac{dr}{\sigma_r} \qquad (93c)$$

Because no structure is safer than its foundation, the subject of safety and probability of failure is very important in the field of foundation engineering. Seldom, if ever, are enough test data available to determine the frequency distribution of the soil properties. Furthermore, in many cases the loading effect and resistance cannot be considered as independent variables, and the interrelation between the load and the resistance, including variations with time, is often so complicated as to defy rigorous analysis. Nevertheless, these very facts should make the engineer more conscious of the probability of variations of estimated properties. In many cases the range of expected values and the relative frequency of their occurrence must be estimated from past experience and by the judgment of the engineer. The desired factor of safety must then be determined from a thorough analysis of all these considerations. When this is done, the engineer is really applying the principles presented by the author, although rigorous mathematical analysis may not be feasible. However, in some simple cases, after a set of reasonable assumptions is made, direct application of the methods and formulas presented by Mr. Freudenthal is practicable.

In the case of a structure supported by clusters of point-bearing piles driven to rock or a comparable hard layer, the ultimate resistance (failure load) of a pile cluster may be assumed equal to the sum of the ultimate resistances of all the piles in the cluster. The foregoing implies that after each pile reaches its failure load it continues to carry this load until all the piles in the cluster have reached their respective failure loads. It seems logical to choose the maximum mean load per cluster in such a way that the probability of failure of each of the clusters in the foundation is the same.

It is assumed that (*a*) normal frequency functions apply to both the ultimate resistance R of each pile and the applied load per cluster S; (*b*) the value of the mean R_O and the ratio σ_R/R_O are known from pile-loading tests in the area; (*c*) the ratio σ_S/S_O between the standard deviation σ_S and the mean S_O of the applied load per cluster S is known from a study of the superstructure and foundation load; and (*d*) a probability of failure P_F to be used in the design has been determined by any of the methods proposed by the author. Using these assumptions the problem is reduced to the determination of the maximum mean applied load per cluster S_O as a function of the number of piles n in the cluster and the assumed known quantities so that the probability of failure of the cluster is P_F.

Because the ultimate resistance of each pile is normally distributed and the ultimate resistance of the pile cluster is assumed equal to the sum of the ultimate resistances of the piles, the ultimate resistance of the pile cluster will be also normally distributed with mean

$$R'_O = n\,R_O \qquad (94a)$$

and standard deviation

$$\sigma'_R = \sqrt{n\,\sigma^2_R} \qquad (94b)$$

Therefore, when applied to the probability of failure of the pile cluster, Eq. 43 becomes

$$\rho = \frac{n\,R_O - S_O}{\sqrt{n\,\sigma^2_R + \sigma^2_S}} \qquad (95)$$

Solving for S_O, the maximum mean applied load per cluster is

$$S_O = n\,R_O \left\{ \frac{1 - \rho \sqrt{\left(\frac{\sigma_S}{S_O}\right)^2 + \left(\frac{\sigma_R}{R_O}\right)^2 \frac{1}{n}\left[1 - \rho^2 \left(\frac{\sigma_S}{S_O}\right)^2\right]}}{1 - \rho^2 \left(\frac{\sigma_S}{S_O}\right)^2} \right\} \qquad (96)$$

To compare clusters of different numbers of piles, it is more convenient to use the mean allowable load per pile

$$\bar{S}_O = \frac{S_O}{n} \qquad (97)$$

which is the maximum value of the mean applied load per pile compatible with a probability of failure P_F. Then

$$\bar{S}_O = R_O \left\{ \frac{1 - \rho \sqrt{\left(\frac{\sigma_S}{S_O}\right)^2 + \left(\frac{\sigma_R}{R_O}\right)^2 \frac{1}{n}\left[1 - \rho^2 \left(\frac{\sigma_S}{S_O}\right)^2\right]}}{1 - \rho^2 \left(\frac{\sigma_S}{S_O}\right)^2} \right\} \qquad (98)$$

The results given by Eq. 98 will be examined after numerical examples are presented.

Four numerical examples have been solved. In all four, it has been assumed that $R_O = 100$ tons and $\sigma_S/S_O = 0.1$ which indicates that the probability that the applied load S exceeds by 20% the mean applied load S_O is approximately 0.023. Two values, 0.2 and 0.1, of σ_R/R_O have been used; these values indicate that approximately 15.9% and 2.3%, respectively, of the piles are expected to have an ultimate resistance of 80 tons or less. Also, two values of the probability of failure P_F were used—1×10^{-4} and 1×10^{-6}; these values represent practical limits and are used to compare the results obtained. To these values of P_F correspond values of ρ of 3.71 and 4.75, obtained, as described previously, from tables of the normal function. Numerical values of $\bar{S}_O$ computed from Eq. 98 for different values of n are plotted in Fig. 10(*a*). The corresponding values of the required minimum factor of safety with respect to the means

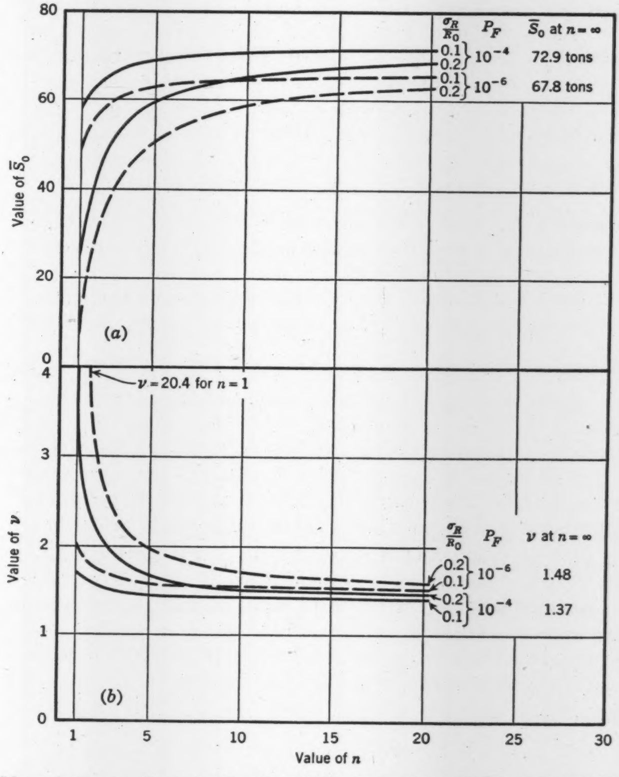

FIG. 10.—MEAN ALLOWABLE LOAD PER PILE AND MINIMUM REQUIRED FACTOR OF SAFETY RELATED TO THE NUMBER OF PILES IN A CLUSTER OF POINT-BEARING PILES WITH $\sigma_S/S_O = 0.1$ AND $R_O = 100$ TONS

$$\nu = \frac{n R_O}{S_O} = \frac{R_O}{\bar{S}_O} \qquad (99)$$

are plotted in Fig 10(*b*) for the same four numerical examples. From the plotted curves and Eq. 98, the following can be inferred:

1. For a given probability of failure the mean allowable load per pile in a cluster increases as the number of piles increases.
2. For a large number of piles in a cluster, the mean allowable load per pile is not significantly affected by the value of σ_R/R_O and depends primarily on the value of the mean R_O and the ratio σ_S/S_O.
3. As noted by the author, a relatively small decrease in the mean allowable load greatly decreases the probability of failure. For example, for $n = 10$ and $\sigma_R/R_0 = 0.1$, a reduction of the mean allowable load $\bar{S}_0$ from 71 tons to 65.5 tons decreases the probability of failure P_F from 1×10^{-4} to 1×10^{-6}.
4. If a constant minimum required factor of safety is used, the probability of failure of the clusters with a small number of piles is much larger than the probability of failure of clusters with a large number of piles.
5. For the same probability of failure, the minimum required factor of safety decreases as the number of piles per cluster increases.

Although the foregoing conclusions have been known to foundation engineers for some time, they are offered as an example of the application of the method presented by Mr. Freudenthal to a practical problem. However, it must be emphasized that these conclusions depend on the stated set of assumptions and must not be generalized because they might then lead to dangerous results. For example, in the case of friction piles, the assumption that the ultimate resistance of a cluster of piles is equal to the sum of the ultimate resistances of the piles, each considered independently, is far from true; in this case the foregoing obviously would not apply. It may also be noted that, for a small number of piles in a cluster and large values of σ_R/R_O, the mean allowable load per pile is small. Inspection of Eq. 98 shows that, for some values of the variables, negative or even complex values of $\bar{S}_O$ may be obtained. Because only positive values of $\bar{S}_O$ have practical meaning, negative or complex values involving $\sqrt{-1}$ indicate that the assumptions do not correspond to the actual conditions. In the case treated, normal distributions which are unlimited in both directions actually do not represent accurately the distributions of R or S which are limited. For some combinations of the variables in Eq. 98, the "tails" of the distributions become very important, and the error involved in assuming unlimited distribution is far from negligible. In this case Eq. 98 does not apply, and a solution based on limited distributions must be used.

Oliver G. Julian,[6] M. ASCE.—The truth of the quotation (46): "It is remarkable that a science which began with considerations of games of chance, should have become the most important object of human knowledge" is even more evident in 1956 than when it was written by Pierre Simonde Laplace in about 1800. It seems even more remarkable that "the most important object of human knowledge" has until recently been almost entirely neglected by structural engineers. So far as the writer knows (6*a*) it was not until the second decade of the twentieth century that the design of structures was first studied by Carl Forssell from a statistico-economic point of view. Even in 1956, the methods of statistics and the calculus of probability appear too conspicuous by their absence in many curricula for structural engineers.

---

[6] Head of Structural Div., Jackson & Moreland, Engrs., Boston, Mass.

In the paper Mr. Freudenthal has again brought out the obvious fact that all structural engineers should acquire a working knowledge of at least the elements of statistics and probability. An understanding of the author's work requires considerable study; however, such study is fully warranted as it will pay dividends not only to those who make the effort but also to their clients. The paper presents a broad synoptic view of the minimum the profession should know regarding the subject. For the preparation of such a view, Mr. Freudenthal has certainly earned the gratitude of the entire profession. However, his work will be of little avail until such time as engineers have acquired (*a*) a good statistical background regarding the resistances of materials and structures, including dynamic and fatigue effects; (*b*) a similar background regarding load effects, and (*c*) the necessary competence in the calculus of probability.

The author has brought out the fact (which does not appear to be generally recognized) that the factor of safety of a structure, as measured by the ratio of structural resistance to design load effects, based on averages, may be fairly high whereas the probability of failure is close to one half—that is, the odds are even that it will fail. The term "probability of failure" carries much more meaning than "factor of safety." In fact, one might well dispense with the latter term. Under the heading, "Design Procedure: The Concept of Safety," Mr. Freudenthal states

> "* * * the notion that a finite (no matter how small) probability of failure or at least of unserviceability is repulsive to a majority of engineers * * *."

Such a sentiment is unrealistic and reminiscent of an ostrich hiding his head in the sand. On the other hand, insurance underwriters having actuarial training and being realistic would be apt to disregard such terms as "factor of safety" and inquire: What is the probability of a loss? Similar remarks apply to the factor of unserviceability and probability of becoming unserviceable. A structure may be quite safe from collapse and at the same time be unserviceable because it does not satisfactorily perform the functions for which it was designed. For example, if tenants vacate a building because of what they feel is excessive or uncomfortable vibration, the building may be said to be unserviceable.

The statement under the heading, "Design Procedure: Conditions of Failure and Unserviceability," that

> "* * * the specification of the failure condition in terms of a [unit] stress cannot reflect the behavior of the structure at or close to the instant of failure"

cannot be emphasized too strongly The concept of limiting (unit) stress on which many specifications are based is valid only in case the principle of superposition and Hooke's law regarding the linear proportionality of stress to strain apply. It is far better to view the strength of a structure for given conditions than to view only the stresses. As implied by the author, the values of the latter considered alone may in many cases be devoid of objective meaning. A structure may be safe and serviceable after redundant parts have failed completely. The effect of "stress raisers" in purely statically loaded structures may be, and ordinarily is, negligible. However, the strength of a structure subjected to varying loads over an extended period of time will be governed by the fatigue strength of essential parts corresponding to the applicable range, time rate, and duration of stress application. The statement (under the heading, "Structural Analysis: Conditions of Unserviceability and Structural Failure: Unserviceability"): "For the evaluation of the limit of serviceability, methods of elastic analysis are usually adequate" should be emphasized. Methods of design which place undue emphasis on postelastic resistance of essential parts may lead to structures which are safe with respect to collapse but which prove to be unserviceable. It is at least desirable that upon removal of a load the structure regain substantially the configuration it had prior to the application of the load. Also, as stated by Mr. Freudenthal (under the heading, "Structural Analysis: Conditions of Unserviceability and Structural Failure: Failure"),

> "Most of the excess of the plastic-collapse load over the elastic-limit load may * * * be lost when the operating conditions of the structure require analysis for repeated sequences of complex loading."

Considering all factors, the postelastic region should be entered with caution.

The statement (under the heading, "Structural Analysis: Conditions of of Unserviceability and Structural Failure: Failure")—

> "* * * the apparent plasticity of concrete subject to high compressive stresses is the manifestation of a progressive internal disruption of the material beginning far below the conventional 'compressive strength' obtained in the relatively high-speed standard tests, rather than plastic flow of a type occurring in metals"

—appears reasonable and cautions one not to place undue confidence in the "plastic theory" of concrete design, especially if load repetitions are involved. The writer is inclined to disagree with the statement (under the same heading) to the effect that the relaxation of the prestressing force in a concrete beam reduces the failure load. Such relaxation, without doubt, reduces the limit of serviceability, but it is not apparent why it should reduce the failure (collapse) load.

Under the heading, "Load Analysis: Random Variation of Standard-Load Intensity," Mr. Freudenthal states that the maximum values of certain types of loads, such as floor loads in warehouses, fluid loads and pressures in storage tanks, and train loads on railroad bridges can be specified in a nonstatistical manner. Realizing that in many cases the collection and interpretation of adequate statistical data pertaining to load effects are indeed difficult if not impossible—and especially that the values may change substantially after a structure is built—and that such changes can only be anticipated by the employment of engineering judgment, the writer inclines to the view that the author's statement might well be extended to include many other types of loads such as floor loads in powerhouses, traffic loads on highway bridges, and loads on runways of airports. It is only in case adequate data, such as, for example, those pertinent to water loads on dams made from long-time records (including allowances for floods which may occur during the useful life of the structure), are available that one is warranted in using a statistical approach as to the values of loads. The analysis can be no better than the data on which it is based. Perhaps in most cases one would do as well to estimate the values of design load effects by the use of engineering judgment and consider the probability of occurrence of such values as unity. Incidently, this procedure simplifies the problem of analysis and design somewhat.

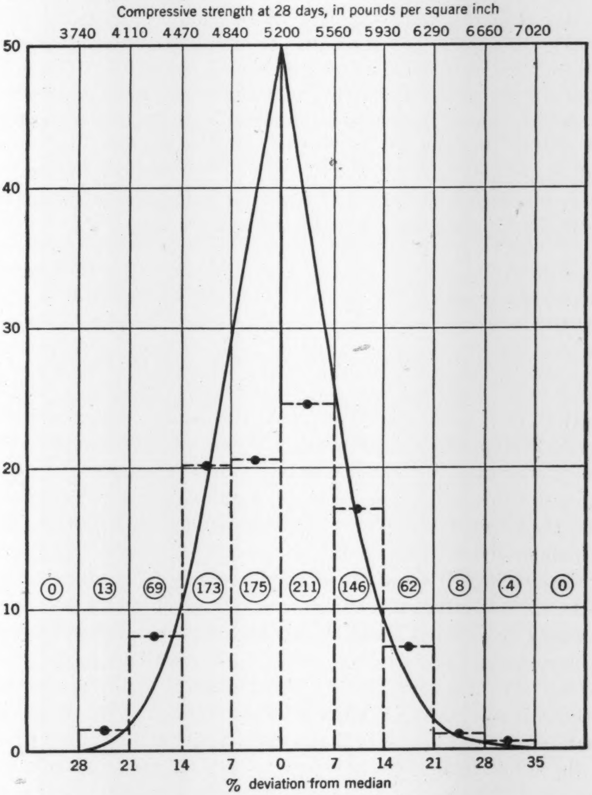

Fig. 11.—Distribution of Compressive Strength of Concrete Under Good Control on Natural Scales

The method of exhibiting the relation between strengths of materials (or magnitude of loads) and probability of occurrence on various types of probability paper has definite advantages; it greatly facilitates extrapolation beyond the range of the tests. As stated by Mr. Freudenthal, such extrapolation is of prime importance when considering extreme probabilities. However, the author's illustrations do not give one as direct and realistic an over-all view of the situation as when the same data are plotted to natural scales. Fig. 11 was made from the same data (plus 188 typical tests) as Fig. 6(*a*).

In Fig. 11 the rectangular cells, outlined with dashed lines and extending above the axis of abscissas, represent the histogram of the test results. The width of these cells has been taken as 0.6745 of a standard deviation of the compressive strength, or 0.6745 of the coefficient of variation in percentage deviation from the median. (This width was chosen because it corresponds to a probable deviation of a Gauss-Laplace distribution.) The numerals shown in circles indicate the number of test results pertaining to each cell; the corresponding relative frequencies in percentages are given as ordinates. The curve drawn in solid lines represents the probability of occurrence, expressed as percentages. The ordinates pertaining to this curve indicate (*a*) to the left of the median the percentage of total number of samples testing below the value indicated by the corresponding abscissa and (*b*) to the right of the median the percentage of total number of samples testing above the value indicated by the corresponding abscissa. Pertinent data regarding this set of tests are

Standard deviation	540 lb per sq in.
Coefficient of variation	10.4%
Highest test	6,980 lb per sq in.
Average	5,180 lb per sq in.
Lowest	3,810 lb per sq in.

The strength f'_c used in the design of the structures on which this concrete was placed was 3,825 lb per sq in. However, the control of the concrete was aimed at a minimum strength of 4,500 lb per sq in. It will be noted that approximately 10% of the test results fell below this latter figure which is midway between the median and the lowest test. The writer has found such data to be typical for cases in which special care is taken as to control.

Under the heading, "Probability of Failure: Analysis of Failure and Survival: Safety Factors," the author has all too concisely given methods for correlating factors of safety ($\nu = R_O/S_O$) and the associated probabilities of failure P_F, in terms of the coefficient of variation pertaining to resistance σ_R/R_O and loading effects σ_S/S_O. Mr. Freudenthal has also indicated how P_F can be approximated without involving ν. It should be emphasized that ν is the minimum factor of safety required to assure that a chosen probability of failure P_F is not exceeded; the actual factor of safety pertaining to an existing structure may be quite different. This part of the paper depends on a working knowledge of geometry rather than on the calculus of probability if one accepts (*a*) the expressions pertaining to the types of relative frequency functions given and (*b*) the well-known principle that if the frequencies are independent they combine by multiplication (as in Eq. 39).

It is unfortunate that the author, like many others, has used the term "probability" as a synonym for "relative frequency." It is believed that much confusion would be avoided if, when speaking about continuous functions, a sharp distinction were made between these terms. For continuous functions a relative frequency such as $f(x)$ can be represented by a line segment (such as an ordinate), a simple probability such as $\int_a^b f(x)\,dx$, by an area, and a compound probability such as $\int_c^d \int_a^b f(x)\,f(y)\,dx\,dy$, by a volume. The latter expression can usually be reduced to a single integral so as to have the appearance of representing an area, but it still represents a volume of unit depth. Fig. 7 represents a surface of revolution, the axis of which is at O where the ordinate, normal to the paper, equals $1/2\,\pi$; the circles represent contour lines of equal relative frequency. The total volume under the surface represents the probability of failure plus the probability of survival and must, of necessity, equal unity. Any section normal to the paper has the shape of a Gauss-Laplace frequency curve. Sections that include the axis of revolution can be normalized by multiplying the ordinates by $\sqrt{2\,\pi}$, thereby making the area of the section (extending from $-\infty$ to $+\infty$) equal to unity. Parts or the whole of the volume represented by these areas times unit depth (normal to radii) are compound probabilities.

It appears advisable to extend the author's notation slightly. In Fig. 7 one might designate the radial line passing through the points O and (x_O, y_O) extended as the ρ-axis and let the distance along this line from O to (x_O, y_O) be termed ρ_O. Then Eqs. 43 and 50 can be written as

$$\rho_O = \frac{R_O - S_O}{\sqrt{\sigma^2_R + \sigma^2_S}} \qquad (100)$$

and

$$\nu = \frac{1}{A}\left(1 + \sqrt{1 - A\,B}\right) \qquad (101)$$

in which $\nu = R_O/S_O$ is a real (not imaginary) number greater than unity,

$$A = 1 - \rho^2_O \left(\frac{\sigma_R}{R_O}\right)^2 \qquad (102a)$$

and

$$B = 1 - \rho^2_O \left(\frac{\sigma_S}{S_O}\right)^2 \qquad (102b)$$

It will be noted that $A\,B$ is less than unity. Special cases of Eq. 101 for a few ratios of σ_S/S_O to σ_R/R_O are as follows:

Value of $\frac{\sigma_S}{S_O}\Big/\frac{\sigma_R}{R_O}$	Minimum required factor of safety
m	$\frac{1}{A}\left\{1 + \sqrt{1 - A\,[1 - m^2\,(1 - A)]}\right\}$
0	$\frac{1}{A}\left(1 + \sqrt{1 - A}\right) = \frac{1}{1 - \rho_O \frac{\sigma_R}{R_O}}$

1.........$\frac{1}{A}\left(1+\sqrt{1-A^2}\right)$

2.........$\frac{1}{A}\left(1+\sqrt{1+3\,A-4\,A^2}\right)$

3.........$\frac{1}{A}\left(1+\sqrt{1+8\,A-9\,A^2}\right)$

It can be shown that

$$P_F=\frac{1}{\sqrt{2\,\pi}}\int_{\rho_O}^{\infty}e^{-(1/2)\rho^2}\,d\rho\ldots\ldots\ldots\ldots\ldots\ldots\ldots(103)$$

This follows from the corresponding normalized frequency function,

$$f(\rho)=\frac{1}{\sqrt{2\,\pi}}e^{-(1/2)\rho^2}\ldots\ldots\ldots\ldots\ldots\ldots\ldots(104)$$

and is obvious for limiting conditions such as $\rho_O=0$ or $\sigma_S=0$ and upon reflection appears to be almost intuitively evident in general (45).

Equation 100 or Eq. 101 together with Eq. 103 are sufficient for the correlating of ν and P_F. In practice the problem is usually posed in one of two alternative forms: (*a*) Given R_O, S_O, σ_R, and σ_S to find P_F or (*b*) given P_F, σ_R/R_O and σ_S/S_O to find ν. For case (*a*) ρ_O can be determined from Eq. 100, and the corresponding P_F-value can then be obtained from probability or error function tables (47) (48). Unfortunately, these tables do not give P_F directly in terms of ρ_O; however, conversion to the required terms is quite simple. When using error function tables one must note that $\rho_O=\sqrt{2}\,x$ and that

$$P_F=\tfrac{1}{2}\left(1-\frac{2}{\sqrt{\pi}}\int_0^x e^{-\alpha^2}\,d\alpha\right)\ldots\ldots\ldots\ldots\ldots(105)$$

in which α and x pertain to the functions tabulated. The use of tables giving P_F to at least nine decimal places greatly facilitates the work. For case (*b*), ρ_O corresponding to P_F can be obtained from such tables and ν can then be computed by Eq. 101.

Taking $P_F=0.5\times10^{-6}$, the corresponding ρ_O-value is found from tables to be 4.9; taking $P_F=0.6\times10^{-4}$, the corresponding ρ_O-value is found to be 3.85. The values of ν computed by the formulas tabulated previously, assuming that $\sigma_R=0.1\,R_O$, are

	Minimum required factor of safety	
$\frac{\sigma_S}{S_O}\Big/\frac{\sigma_R}{R_O}$	for $P_F=0.5\times10^{-6}$ $\rho_O=4.9$	for $P_F=0.6\times10^{-4}$ $\rho_O=3.85$
0	2.0	1.6
1	2.2	1.8
2	2.6	2.1
3	3.1	2.5

It will be noted that the values of ρ_O and σ_R used in the foregoing are identical with those used by the author in his numerical examples and that the values of

ν corresponding to $\frac{\sigma_S}{S_O} \Big/ \frac{\sigma_R}{R_O} = 2$ (the value used by the author) are practically identical with his values. However, although the values of P_F are of the same order of magnitude as Mr. Freudenthal's, the writer's values are considerably higher than those given as maximum estimates. The differences are believed to be caused by the author's not normalizing his p_O-function and then determining P_F from the normalized function. The effect of this normalizing process increases as ν decreases and P_F increases. In view of the foregoing, the author's comment to the effect that computed values of probabilities of failure and survival are not complete would appear to be unnecessary; Eqs. 103, 100, and 101 take account of the contributions of all quadrants toward failure. The comments made previously regarding treatment of the Gauss-Laplace frequency function and the corresponding volumes representing probabilities of failure also apply with necessary modifications as to detail to other types of functions.

It will be noted that, knowing R_O, S_O, σ_R, and σ_S, P_F can be computed easily by Eqs. 100 and 103 without involving ν and Eq. 101 which is simply another form of Eq. 100. Also, knowing P_F, σ_R, σ_S and R_O (or S_O), Eqs. 103 and 100 are sufficient for the determinations of S_O (or R_O). These procedures would simplify the labor of analysis or design. The value of the popular, but somewhat misleading, ν is obvious if R_O and S_O are known; however, knowledge as to its value adds little if anything to the evaluation of safety.

In the numerical examples outlined by Mr. Freudenthal and in this discussion, the value of $\sigma_R = 0.1\, R_O$ used may be low for many cases. The writer inclines to the view that it approximates a minimum value which should only be used provided one is assured of good control conditions. For the concrete represented by Figs. 6(*a*) and 11, $\sigma_R = 0.104\, R_O$. This value has been characterized as reflecting good control. However, for the concrete represented by Fig. 6(*b*), which was mixed, placed, and cured under "difficult conditions," $\sigma_R = 0.26\, R_O$. The latter case may be more nearly typical of common practice than the former. For the yield strength for structural steel, as represented by mill test reports, the distribution of which is shown in Fig. 5(*a*), $\sigma_R = 0.0875\, R_O$. Considering variations not reflected by mill test reports, this value for σ_R might well be 25% higher. The coefficient of variation pertaining to concrete reinforcing steel is considerably higher than that pertaining to structural steel. Considering the great mass of literature, including text and reference books published on properties of materials, the scarcity of data regarding variations in strength and other properties in such form as can be used in statistical or probability studies is remarkable. The authors' paper and that by P. J. F. Wright (49) are among the few sources known to the writer in which such data are given.

AIDEN R. GIERASCH,[7] A. M. ASCE.—The paper is a valuable addition to the several treatises that Mr. Freudenthal has contributed on the use of probability theory in evaluating the safety of structures (1)(2). The combined treatment of loads and structural capacity in a statistical analysis results in a comprehensive view of a structure's adequacy that cannot be obtained by the procedures now generally used. A design based on the method outlined would result in a structure of balanced strength, having a specified probability of survival under critical operating conditions. A building designed by this method would probably be characterized by a considerably greater economy of material than is attained by current (1956) procedures.

---

[7] Structural Engr., Jackson & Moreland, Engrs., Boston, Mass.

In the field of building design, acceptance of a new fundamental concept is particularly slow because of the necessity of superseding practices required by building codes. However, the increasing publication of technical papers dealing with statistical treatments of loads and structural materials indicates that the time is ripe for detailed development of a design procedure having as its basis the synthesis of load and strength probabilities. Full development of this design method will require compilation of existing statistical data on loads and material tests, as well as programs to fill in many areas where additional information is essential. Structural engineers have not commonly made use of statistical mathematics as a working tool, although the effectiveness of the statistical approach has long been apparent in scientific fields. In designing a building by the rational procedure outlined by the author, completion of the work with a reasonable amount of computation would require judgment in sizing the trial structure and in grouping the test conditions for which unserviceability and failure loads are to be determined. In the case of buildings, it may be that design economics will exclude consideration of the failure condition; in the usual case, the allowed probability of unserviceability will be so small that the failure probability will be almost negligible.

The basic paper is pithy, far-ranging, and almost philosophical in style. Illustrative examples would help greatly to point up the implications of the procedures outlined.

ALFRED M. FREUDENTHAL,[8] M. ASCE.—The discussion of the paper represents a significant contribution to its value by the comments made, the questions raised, and the detailed and painstaking re-evaluation of some of the concepts. There can hardly be a more gratifying response to a paper than a discussion at this level.

Mr. Chibaro is certainly correct in assuming that the day is still a long way off when the concept of "factor of safety" will be supplanted by the concept of "probability of failure." It is not the purpose of this work even to advocate such a radical change in the engineering approach to structural design and analysis. Enough will be gained if the profession is gradually reconciled to the fact that the concept of "factor of safety" is meaningless unless it is supplemented by the specification of a "probability of failure" associated with any specific value of it and that, therefore, a reasonably efficient design, even the most careful and conservative one, tacitly implies an accepted risk of failure. The difference between the "safe" and the "unsafe" design is in the degree of risk considered acceptable, not in the delusion that such risk can be completely eliminated.

---

[8] Prof. of Civ. Eng., Columbia Univ., New York, N. Y.

Mr. Chibaro's question concerning the ultimate value of probability considerations in the presence of unavoidable and significant nonrandom causes of variation has no satisfactory answer. This is especially true if probability considerations are used as an alternative to common sense rather than as a complement to it, which should reduce the range of possible error in evaluating the contribution of random effects, and thus provide a better guide to correct guessing about the effects of the mathematically untractable nonrandom variations.

It is regretted that all terms used in the paper were not clearly explained. Some of the terms, the meanings of which are questioned by Mr. Chibaro, have, however, acquired such definite connotations in the field of "plastic" or "limit design" that they have been considered as self explanatory. This refers to the concept of "shake-down load" (the maximum movable load pattern for which a condition of elastic-plastic equilibrium is possible), the "plastic-collapse load" (the minimum intensity of a steady load pattern under which the system is transformed into an unstable kinematical chain), and the "elastic-limit load" (the maximum intensity of a steady load pattern under which all deformations are reversible). With respect to the distinction between unserviceability and failure, however, it seems that the definition of these terms is still not sufficiently clarified. "Failure" and "unserviceability" are neither synonyms nor are they neighboring conditions. When serviceability ends because certain service requirements—such as a limiting maximum elastic deformation of a metal structure or the absence of visible cracks in the tension zone of a reinforced concrete beam—are no longer fulfilled, the structure is usually still very far removed from conditions of designated failure or of actual collapse. In fact, the ratio between the intensities of a certain standard load pattern associated with certain probabilities of collapse and of unserviceability can be considered as an "overload factor" characteristic of the structure; this factor will be higher the larger the difference between the two load intensities, and will depend on the probabilities selected as acceptable. These probabilities may be equal for both conditions, or the acceptable probability of failure may have to be reduced against that of unserviceability because of the more serious consequences of the former, with a consequent reduction of the "overload factor"; in either case this factor is not represented by a single value but by a probability function, specifying the probability of the structure to be able to withstand a certain ratio of "overload" in terms of the unserviceability load, without failure or collapse. The "overload factor" thus represents a characteristic that appears suitable for rating of existing structures.

Messrs. Lawrence and Corso have made a valuable contribution by proving, independently, that the writer's procedure for the evaluation of the probability of failure in the case of normal or logarithmic-normal distributions of S and R can be improved and simplified by using the fact that, in this case, the distributions of $r = (R - S)$ or $\log r = \log (R/S)$ are also normal or logarithmic-normal. In the case of extreme-value distribution, no such simplification is necessary because the distribution functions are integrable in closed form and the values of P_F are obtained directly by multiplication of the respective cumulative probabilities, as indicated in Eq. 62.

Both Messrs. Lawrence and Julian are correct in pointing out that any meridional section of the surface of revolution shown in Fig. 7 should be normalized before being used for the evaluation of probabilities of failure; the slight discrepancies in the discussed example between Mr. Lawrence's and Mr. Julian's computed values for P_F on the one hand and the writer's values on the other are caused by this omission.

Mr. Corso has made a most interesting contribution by actually applying the principles outlined in the paper to the specific problem of the safety of a cluster of piles driven to rock. The conclusions reached on the basis of this analysis are not new to experienced foundation engineers. However, the particular value of Mr. Corso's analysis is in its illustration of the fact that these conclusions can be derived by even a relatively inexperienced engineer on the basis of an objective analysis and that the results of this analysis provide numerical values of the safety factor or orders of the magnitudes of the probability of failure for different pile arrangements. These values permit a rational comparison of various arrangements without recurrence to "subjective experience."

The writer does not, however, intend to create the impression that in this way, engineering experience and common sense could be dispensed with, but rather wishes to point to Mr. Corso's analysis as an illustration of how the safety analysis can provide a guide to common-sense engineering decisions similar to those which structural analysis provides at a different stage of design. Whereas most engineers prefer to compute the maximum stresses expected in a certain structural part rather than to guess at their magnitude (even if they have sufficient experience to guess correctly), the same is not true with respect to the safety of the same part. The safety guessed on the basis of personal experience and "intuition" is widely used. By his analytical treatment of a problem of soil mechanics, Mr. Corso has illustrated a rational alternative to this procedure in a field in which most of the engineering decisions are, by necessity, based on guesses rather than on rigorous analysis.

Mr. Julian has presented a very instructive and useful extension of Eqs. 43 and 50 in the form of two tables—one for the rapid estimate of the required minimum factor of safety and the associated probability of failure and the other giving the results of such estimate under specific assumptions concerning the ratio of relative dispersion of S and R. In his general comments on the basis of his wide professional experience, he succeeds in emphasizing and reformulating several of the writer's statements in a manner which clarifies their meaning for the practicing engineer who is less interested in the methods of safety analysis themselves than in the practical implications of the results. Mr. Julian's discussion of these implications contributes greatly to the understanding of the paper.

Concerning some of Mr. Julian's more specific comments, he is only partly right in disagreeing with the writer's obviously too general statement about the effect of relaxation of prestress on the failure load of prestressed concrete beams. Although such relaxation has indeed no effect on the failure load of underreinforced beams failing primarily by yielding or fracture of the reinforcement, it actually reduces the failure load of overreinforced beams failing primarily by crushing of the concrete. With respect to the question of using the term "probability" as a synonym for "relative frequency," it is believed that this is correct. The term "probability" was used only with respect to continuous and, therefore, theoretical curves, and "frequency" was reserved for representation of actual observations. This usage is consistent with the frequency definition of probability, according to which a probability can be only the stochastic limit of an observed frequency. Hence, when mentioning continuous functions which, by their very nature, cannot be directly observed but represent the "stochastic limit" fitted to the necessarily discontinuous observations, the term "probability" alone should be used; "frequency" can refer exclusively to observations, represented by a (discontinuous) histogram or by a sequence of points.

Mr. Gierasch stresses the principal advantage gained by a rational safety analysis—the possibility of attaining a balanced strength of all structural members—with the resulting optimal compromise between safety or probability of failure and economy. This compromise is not based on intuition or "engineering judgment" but on a consciously accepted risk of failure that can be numerically specified and therefore compared with other risks. It can thus provide a measure against which the economic advantages of increasing or reducing this risk can be rationally assessed.

The writer wishes to express his sincere appreciation to all discussers for their valuable contributions.

AMERICAN SOCIETY OF CIVIL ENGINEERS
Founded November 5, 1852
TRANSACTIONS

Paper No. 2844

OUR EXCITING PROFESSION
ADDRESS AT THE SUMMER CONVENTION
KNOXVILLE, TENN., JUNE 7, 1956

BY ENOCH R. NEEDLES,[1] PRESIDENT, ASCE

The profession of civil engineering is as old as the crudest shelter built unknown centuries in the past to protect our forebears against their foes and the elements. This profession is as new as atomic fission itself, if only because of the new materials, methods, problems, and power sources which will come with the Atomic Age. For the civil engineer is a builder, a constructive builder, the provider of structures and facilities for the better living of his fellow man.

We civil engineers are members of a great and honorable profession, an exciting profession, a living profession, and a profession of great and continual change. Our American Society of Civil Engineers is now 104 years old, a venerable age by any standard of measurement for professional organizations. Yet, as an individual observer, I can speak rather intimately of the great changes which have come upon us during the past fifty years; for it will be just fifty years this July 5th, 1956, since I proudly took my first job on a surveying party and obtained my first glimpse of some of the basic principles of civil engineering.

THE PAST

One hundred years ago, the status of our profession reflected our activities in earlier canal building, then railroad building, the provision of pure water for our young but growing cities, and steps toward the disposal of the city wastes. Our highways and streets were built in keeping with the limitations of our horse-drawn vehicles.

Recently I received a book presented by a fellow consulting engineer in Scotland. Surprisingly, this volume pertains to the building of the Croton Aqueduct, which was the first major undertaking to bring fresh water to the city of New York. This Aqueduct was completed in 1842. This book was printed in 1843. On large pages, appear numerous reproductions of steel engravings pertaining to the young city and the details of the Aqueduct construction. It is an inspiring book. In finest literary style, the story is presented of the background preliminary to this Aqueduct, the fine planning and designs entering into this project, and the remarkably high standards of materials and construction which were a part of it. The masonry structures were designed for beauty as well as utility.

---

[1] Cons. Engr., Howard, Needles, Tammen & Bergendoff, New York, N.Y.

In glancing through this volume, I became very thoughtful. Once more, I became very respectful of our civil engineers of earlier generations and their fine accomplishments. I thought of a ceremony I attended last year at which a young Norwegian received an award for research. In his acceptance, he recited an old saying of his native country,

> "If we reached higher than they,
> We but stood on their shoulders."

With deep humility, we pay tribute to our pioneers and earlier leaders in civil engineering. In the same spirit of humility, we dare express the hope that we older engineers will merit the respect and appreciation of those who are following us in the profession of civil engineering; those fine young men who will be responsible for meeting the demands to be made upon the civil engineer when the impacts of the Atomic Age are fully upon us.

Thirty-four years ago I opened a one-man office for my firm in New York City. Only a short time before had I seen this city for the first time; and I had just been accepted as an Associate Member of our Society. I made it my business to attend the meetings of the Metropolitan Section of our Society; and there I was privileged to form many wonderful friendships which have grown richer through the years.

Thirty-four years ago the elevated railway system of this city was in full flower, even though some of the petals were beginning to show signs of wear and withering. The principal elements of the New York subway system were being completed; and I was privileged to know Robert Ridgway. The water supply in the Catskills was being developed, and I met J. Waldo Smith. The Grand Central Station area was a very new development. Our first airports were in the development stage. Later, there was discussion and some planning for arterial highways. The importance and complications of the engineering problems attached to the development of this great city were mounting; and I was able to count Arthur Tuttle as a friend.

As a bystander, and sometimes a doubting one, I watched the momentous and successful solution of the ventilation problems attached to the Holland Tunnel, and I have a vivid memory of our Society inspection trip and luncheon in the tunnel as the lining was being placed. And so our modern vehicular tunnel became a practicability.

Likewise as a bystander, but never doubting, I saw the tremendous George Washington Bridge come into being, setting new patterns for span length, carrying capacity, use of cables and other materials, and theory relative to stiffness and distortion of such structures; and also beauty.

The "Roaring Twenties" are years to be remembered well for something other than just flappers, jazz, and prohibition. It was then that I had the very great privilege of seeing, hearing, and often knowing men like John R. Freeman, Daniel Mead, Arthur N. Talbot, Harrison P. Eddy, Leon Moisseiff, Clifford Holland, John F. Stevens, Anson Marston, Thaddeus Merriman, and other giants of the civil engineering profession who have long since passed on. How can names such as those be mentioned without great pride in our profession and deep appreciation of their struggles and accomplishments?

THE PRESENT

The advance in civil engineering throughout the past one hundred years has increased steadily in tempo as the years have gone by. Certainly the advances of the past thirty years well exceed those of the previous seventy years. The advances of the past ten years probably equal those of the twenty years immediately previous. The coming of the motorized vehicle by land, sea, and air has motorized our entire economy. The highways and airfields cannot keep pace, build them as big and as fast as we can. Our entire transportation field, with its multitude of service facilities, has been revolutionized. Our bridges and tunnels and dams are far larger and more numerous than any could have been foreseen thirty years ago. Our facilities for water supply for manufacture, irrigation, power, and human consumption almost stagger the imagination. Our waste disposal facilities have multiplied, expanded, and improved beyond any reasonable prophesy, just as our national population has grown beyond any reasonable expectation.

Our construction methods and equipment and the materials with which we build are hard to recognize by the standards of thirty years ago. Notably, we have huge pieces of construction equipment which move earth and other materials at unit costs which compare favorably with those of fifty years ago. This equipment and the accompanying construction methods became available to our builders, engineers and contractors, just before and during World War II.

Our nation proved to have then a great resource in our constructive capacity never before known throughout the world. Camps, airfields, huge manufacturing areas, storage facilities, and highways through "uncharted wildernesses" became imperative almost over night. Our engineering and construction organizations had burdens of magnitude thrust upon them which could not be denied if our nation was to survive. Our huge pieces of construction equipment performed legendary feats in completing necessary facilities almost at once. Our manufacturers and material suppliers came up with production records never before equaled. In actual battle zones our construction men and equipment became as essential as armament and trucks, and troops to man them.

The biggest lesson out of all of this for peace-time use was the great value of coordination and cooperation and the feasibility of using ten engineering and contracting organizations to produce a completed one hundred million dollar project in the same time as one such organization could produce a completed ten million dollar project; all ten parts being integrated into one huge construction project of unprecedented proportions.

In the practice of his profession, the design methods and equipment and procedures of the civil engineer have changed and are changing notably. Without denoting the new and improved materials and the combinations materials which have come into being in relatively recent years, and without special emphasis upon our new highway designs and conceptions, our airfield developments, our soil and foundation explorations and designs, and our tremendous water supply and waste disposal arrangements, we can well give some recognition to certain factors which affect design and planning procedures and utilization of professional man power.

The uses of aerial photography have become worthy of special note. With improved techniques and controls, aerial maps provide detail, accuracy, adaptability, and brilliance of portrayal never possible previously. The development of optical viewers and plotting devices permit contour mapping of ever increasing accuracy and scope. The use of these contour maps for highway location and similar purposes, particularly in rough country and highly developed areas, saves time and labor for the engineer forces which are of inestimable value. Steadily improving techniques permit usage of these maps for geological determinations, soil and foundation investigations, and location of material deposits.

Computing devices, especially of the electronic type, are being adapted constantly and more widely to the more complicated and laborious phases of engineering calculations. Clearly we have only begun to learn of the multitude of advantageous services which are possible through this equipment. Certainly these mechanical and electrical computers will give unusual advantages in stress calculations for indeterminant and other structures, in geometric calculations for complicated highway interchanges and grade separations, and even in the age-old, back-breaking, and often depressing field of earth-work calculations.

The continued adaptation of aerial photography and computing devices to the operations of the civil engineer may well become rather revolutionary in their effects upon our profession. Instead of being over-burdened physically by the labors of field locations and investigations, and instead of being a slave to the demands of his design and long hand calculations, the professional civil engineer will become the master of both. He will be far more free to explore, inquire, think, and create. He will be much more efficient and effective in his activity, and far more productive.

As we contemplate the changing tools and equipment of the civil engineer, we can wisely recognize the improving use of our talents as professional men, particularly in our larger organizations. A definite and planned movement is underway by which the experienced professional personnel are being used more extensively on professional work and in supervisory and administrative positions. Non-professionals or engineer aides are being trained and used far more extensively than before for routine work. Over 60,000 prospective aides of all types are enrolled in 69 schools and the program appears to be growing steadily. The length of the training course generally does not exceed two years. There is no record of the number of aides now being trained by employing organizations, but the number must be very large and is growing.

One state highway department reports one professional civil engineer supervising the work of seven surveying parties, all of which are made up of non-professionals. In addition, the professionals are being taken out of real estate acquisition, personnel work, and similar positions into which they had drifted in times less demanding and are being called back to professional activity.

A story in itself was the extensive but effective and very successful usage of aides or non-professionals, under the direction of professionals, in the creation of engineering organizations to cope with our unprecedented war construction program preliminary to and during World War II. There is no evidence yet that the present and any reasonable future demand for manning our major national construction programs cannot be met adequately by the utilization of rapidly improving techniques and methods and by the wider use of aides or non-professionals under the direction of professional civil engineers such as constitute the membership of our Society. This program of proper use of professionals must make the fullest and most appropriate use of our new civil engineer graduates, our pre-professionals, and move them forward to full professional status as promptly as can be wisely accomplished.

THE FUTURE

Now, what is ahead in years to come for the civil engineer and the builder? A spirit of adventure comes upon us as we contemplate the vast possibilities of the era ahead. An unbridled imagination may prove more accurate in visualizing the future than any forecast based mainly on reason; but in any event I endeavor to avoid pure fantasy; and I may assume that human behavior and principles and motives may remain basically unchanged for the next 25 or even 50 years from what they have been for countless past generations.

What part may research have in determining our future; and in what fields may research prove most productive for builders? No dogmatic answers are possible; but we have some stubborn problems and some old conditions which have been with us in some form for generations. Transportation into and out of our major metropolitan areas is becoming increasingly difficult and almost baffling, whether we consider New York, Chicago, or Los Angeles. For generations, the gage of a standard railroad track has been 4 feet, $8\frac{1}{2}$ inches, with one basic type of road bed. Will this always be so; together with all that this track implies?

What will the answers to our fog problems be?

What will we do about smog?

When and how will we end the corrosion of structural steel?

What will the wearing surface be for our highways of the future, and will such surfaces be truly permanent?

Will our future water supplies come from sources other than rainfall?

Will there be new provisions for disposal of waste, both domestic and industrial?

Will there be drastic changes in our construction methods and procedures?

How fast will we travel? How safe will the journey be? And how quiet and dependable?

Each question we ask prompts others. I ask these questions not to baffle, but to picture in part what the brilliant future of living may become, and what a great and vital part in that future the civil engineer will occupy, as he helps to bring into being the answers to the questions we may propound.

My optimism has sound basis. When we build, we do so with men, materials, tools and harnessed power. No longer a theory, we are rapidly moving into the age of nuclear fission. So far as a variety of power sources is concerned never before has man been so wealthy. We dare not limit our thinking as to how our expanding multitude of power sources will be adapted to the use of man and how his living will be affected. The chemistry, physics, and electronics of the future will certainly be productive of new materials and processes as in the past. We can be certain that our construction equipment will be different and better, and our construction methods will be radically changed for the better. We can be very sure that our engineers and our engineering techniques will always improve. Some of our future structures may appear fantastic in terms of present concepts.

As our power sources are changing, we find our materials already changing and promising far more drastic changes. Think of the changes in metals and alloys in recent years. Most of us can remember when aluminum was sort of a laboratory specimen. As our many building materials are developed or refined, and as we witness new synthetics and plastics come into existence, we again cannot limit our imaginations in thinking of what the nuclear age will produce in materials or tools, and how these may come into the construction field.

In adapting new materials to construction, could it be possible that some day we may be using a concrete with a new type of cementing agent? We might find this concrete to be quite indestructible, have a very high degree of permanence, with full resistance to weathering, acid and alkali effects, unusual toughness and durability, and a high tensile strength as well as a very high compressive strength.

At the risk of being considered wholly irrational, I almost posed the question of a plastic type of cement as a possibility of the future. Also, I am wondering about new materials which may greatly reduce or practically eliminate expansion and contraction joints and temperature stresses in our structures.

Is it possible that glass fibers or some other form of glass may give usable structural elements of high tensile strength, complete resistance to corrosion, and other qualities of benefit to the structural engineer?

With our new materials and new construction equipment and methods, may we begin to see realized our often-dreamed-of elevated tunnels or tubular sections to carry the future rapid transportation facilities of our metropolitan areas? These tubes would be above the street level, but would pass through our buildings and cross at mid-block over our streets and avenues. They would not run lengthwise of our streets. Thus the light, air, quiet, and beauty of our cities would be conserved to the maximum, and the access to and from these tubes would be from within the buildings which they serve. The imagination of others, or even your own, may picture better for you the transportation equipment within these tubes, the power source to provide propulsion, and the accommodations which this equipment will afford for the traveler.

I am wondering what the great bridge of the future may look like, what new materials may go into its construction, and what the construction methods for this bridge may be. I am sure it will be stronger, lighter, more durable, more graceful and more beautiful than any bridge we have ever built or planned to this time.

My optimism for the future of our Society and of the civil engineering profession is unbounded. Our history, our traditions, and our services to our fellow man in past years have given us great reason to be proud. As we pursue our research and learn better how to help solve the problems of living and provide the structures and facilities of the future for our people, we will be faced with ever-changing challenges, and our solutions of those problems will enable us to be even more proud, even as our responsibilities become increasingly greater.

Education for Civil Engineers

During the past eight months, I have had the privilege of meeting with many of our Local Sections and attending quite a number of our Student Chapter Conferences. These meetings have proven most impressive and informative. Particular mention is to be made of the notably high quality of our Junior Members and our civil engineer student body. It is a deep sense of pride, yet humility, with which the older engineers, non-educators, view the fine educational facilities of today. Yet we admit no inferiority complex. We older men knew some educational giants. Many of our pioneers were giants, both as engineers and as men.

"If we reached higher than they,
We but stood on their shoulders."

What about our civil engineering curricula of today? I agree firmly with those who believe in a curriculum slanted toward the special needs of the practicing civil engineer; not a curriculum which assumes that all engineers are potential electronics experts or research physicists. I have the idea that the civil engineer student has some idea of what his work will be and what the field is in which his talents may prove most productive and he most happy.

It may be assumed that an overwhelming portion of the projects with which the civil engineer is associated has to do with direct service to and usage by his fellow men. Whether we consider bridges, tunnels, highways, water supplies, waste disposal, transportation arrangements, or the many other facilities of direct and individual use by our citizens, the civil engineer is in mind always. His studies, proposals, designs, and plans are subject to close and often critical scrutiny by the public. Frequently, important financing plans are a basic part of the project. The construction, operation, maintenance, and over-all functioning of the facility become a part of a field in which the user, the citizen, is a most expert and highly qualified judge. As smart as we may be, our facilities are only as good and as justified as they are approved and used by our fellow men. It may be possible that technically, on occasion, we are right; but psychologically and practically we may be wrong, if only because of lack of public acceptance or understanding of our favorite idea or project.

In no other field of engineering are the relations to the public so intimate and important as in civil engineering. The public is so often the qualified critic of the civil engineer.

As a part of doing his job right, the civil engineer should have reasonable facility and skill in the art of communication with the public. If we are to develop understanding of our plans, support for our proposals, and proper usage of our facilities, we must convey the proper messages to our fellow men, either by the written word, the spoken word, the adequate delineation or portrayal of ideas by plans or picturization, or other visualization, or the combination of all these means of expression. Where else can the young civil engineer student begin to improve himself in the art of expression better than during his college days? Any curriculum which does not recognize adequately the importance of this tool of the practicing civil engineer is an example of a lost opportunity for very beneficial instruction.

In every profession, certain skills are very important and even paramount in the practice of that profession. Civil engineering is no exception. Those who tend to minimize greatly the importance in the curriculum of a moderate degree of skill in drafting, surveying, and mathematical calculation, do the civil engineer student a real disservice. Reasonable facility in these skills can mean a high degree of confidence and self-respect for the new graduate as he enters his first permanent position. As he advances to a supervisory position over others using these productive skills, his own facility will contribute to the degree of respect in which he is held. A graduating civil engineer will be well served if upon receiving his diploma he can know that he has been required to obtain not less than six months of actual full time practice in these skills, preferably through summer employment and not wholly at the expense of his college hours, which are so short at the best. It is satisfying to know that the program is steadily expanding by which more and more colleges are requiring more than a four year undergraduate course to qualify for a degree.

LOOKING FOR A JOB

Nothing could be more significant of the days in which we live than the conditions confronting our graduating civil engineers. Speaking facetiously in part, strange things have really come upon us. Our young graduate may have from six to ten positions open to him. In selecting his first job, he must ponder many things.

He must consider the type of work offered, whether office or field, and its location, near home or far away.

He will be thinking about the working hours and conditions, and possibly the amount of overtime available.

He will be interested in promotion schedules and a possible bonus at the end of the year.

He will want to know about vacation and sickness provisions, possible group and health insurance, and other fringe benefits.

Of course he will want to know the basic salary, and about security. Who ever heard of a fellow remaining secure in his first position?

The other day, two fellows were overheard discussing the adequacy of the parking facilities which went with a certain job. And another was heard to tell a fellow-student that he couldn't take off for the afternoon to see a particular movie, since he had given appointments for interviews to three different personnel directors.

Finally, our young graduate settles everything, even as might you or I. He takes the job which offers the best starting salary.

More seriously, I am very sympathetic with these young graduates. Actually, they are faced with a great responsibility in selecting their position, calling for experience and judgment materially beyond their years. We older men, who had no offers of positions upon graduation, had to go out to hunt a job, any job. We took the job which was available and we froze onto it. We had to make the most of it and we were either appreciative or else. We were the fortunate ones, for we were able to learn some of the basic facts of life very early indeed. Actually we were much more fortunate than we knew.

Still seriously, the young graduate may readily get false ideas and improper perspectives by exposure to such a multitude of starting jobs at surprisingly high salaries. It is to be hoped and, in due course, anticipated that such high starting salaries may start soon a wave of increases which will roll up into the salary lists of the older men, particularly those in federal, state, and municipal service. But the major problem before our young graduate is how he will grow into his future. Will his high starting salary lull him into a complacency which could never be anything but deadly for a young man? Will he retain his ambition, his enthusiasm, his zest for work? Will he fall into a rut? The ruts are still with us, and always will be for those who are not alert and determined to avoid them. Ruts and frustration go hand in hand. It is bad enough to know frustration in our mature years without inviting it in our youth. Our late Secretary, George T. Seabury, several years ago quoted John F. Stevens, Chief Engineer of the Panama Canal, as having said "The principal difference between a grave and a rut is that the grave is shorter and deeper."

If the young civil engineer strives to grow steadily into full professional status, the other phases of his living will show wholesome orientation. If he finds himself consigned to and held indefinitely in non-professional work, or that performed equally well by engineering aides, he should take such severe measures with himself as are necessary to move into more wholesome and healthful surroundings.

SHORTAGE OF ENGINEERS

Current discussions regarding the so called "shortage of engineers" appears to pertain to industrial operations engaging the attention of mechanical, electrical, and chemical engineers, to a considerably greater extent than in the field of public works and other areas in which the civil engineer predominates. Steadily increasing salaries in all branches of engineering, including civil engineering, make it clear that there is no current over-supply of engineers.

What are a few of the statistics pertaining to civil engineering?

If we agree that the total civil engineer population of our country approximates 100,000, this figure may be compared with a total population of about 165,000,000 and a current Society membership of about 39,000. Of the 61,000 non-members of our Society, a substantial portion may be civil engineer graduates who have gone into industry and business, for which they will be unusually well prepared. Another substantial portion, even though classed as civil engineers for statistical purposes, may not be of Society membership quality.

Also for comparative purposes, it has been reported that in 1954 there were 3,955 civil engineer graduates, against a total of 292,880 college graduates of all types.

Now if we consider, as of 1955, the average small city of 16,500 population, we get the following simple determinations.

This city is receiving 29 new college graduates each year, but only 1 civil engineer graduate every 2½ years. Ten civil engineers of all types of activity reside in this city, and 4 of them are members of our American Society of Civil Engineers. Of these 4, one is a full Member, one is an Associate Member, and 2 are Junior Members. But only 1 Junior Member will advance to a higher grade of membership in our Society.

Other statistics indicate that this average city of 16,500 will have 22 medical doctors, assuming 1 physician for each 730 of our population. And other statistics indicate that we will have 33 practicing attorneys.

Those of us who have considered the professional civil engineer to be a rare and distinctive person have plenty of statistics to support our view.

When we speak of a shortage of professional civil engineers, we must not be thinking of a possible temporary short supply of engineer-aides or non-professionals. It is surprising how quickly the supply of these aides can be expanded if the demand exists, the training is intensive and adequate, and the compensation attractive. Witness the war construction activities of 1940–1942. The conditions which appear to exist now should generally result in a transfer of professional men in non-professional activity into more professional positions. When this transfer is completed, when greater advantage has been taken of our growing assembly of optical, mechanical, and electronic devices for professional usage, and when we are unable to further build up our reservoir of non-professionals, we can more realistically discuss a "shortage of engineers."

Intimate knowledge of my fellow professional civil engineer, his resource, and his capacity for technical accomplishment and administration prompts the expression of great assurance in his ability to perform and the present adequacy of the supply.

The supply of professional civil engineers cannot be regulated and turned on and off at the spigot as with water. Attractive compensation is still the greatest magnet in drawing men to any field of endeavor, professional or non-professional. Intelligence and desire to serve are equally essential and important factors in professional activity, but the adequacy of compensation will very often determine the field to which the prospective student will choose to direct his talents. There is every reason to believe that the currently increasing compensations for engineers will catch the attention of parents and students alike and that our college ranks will be filled to capacity, if we have not already begun to reach that state. In due course, maybe sooner than we expect, we may have many more civil engineer practitioners, possibly to the appropriate or reasonable limit of our nation to produce or utilize.

INTERSOCIETY RELATIONS

In a relatively few years after the formation of the American Society of Civil Engineers in 1852, there came several developments, inventions, and highly specialized engineering activities which resulted in the formation of new technical societies to serve better those highly specialized fields. The growth and strength of these societies as of today measure fully the adequacy of the service which they have rendered to their members.

During the past thirty-five years there has been a growing demand that these societies have an agency through which they could meet common problems in an effective cooperative endeavor. An excellent example of such cooperative endeavor exists in the Engineers' Council for Professional Development. The work which ECPD has done in the field of accreditation for engineering curricula during the past twenty years has been monumental, of very far reaching significance, and has established a place for ECPD which will endure.

During the past ten years there has been developing the Engineers Joint Council. The strength of EJC has become steadily greater, and its position is clearly one of permanence because of the wide-spread society representations now in its meetings and councils. EJC provides a common meeting ground on which each member society can present its views and take its appropriate position in matters calling for joint activity in behalf of the entire profession of engineering. Representation of each individual engineer in EJC through his own professional and technical society is now almost universal or approaching so. EJC is sensitive to the position and views of its constituent societies. It is an excellent stand-by forum available for quick action in the event that subjects arise demanding urgent attention.

It may be observed that in years past many comparisons between the medical and engineering professions have been drawn. Undoubtedly, the apparent economic status of the individuals in each profession had quite a bit to do with these comparisons. There was also discussion of relative professional status. The reasonableness and appropriateness of such comparisons are not now considered to exist in the minds of most engineers, and we can be satisfied this is so. Peas have never been compared with peanuts with any great effectiveness.

Unlike the engineer, all medical practitioners have many things wholly in common. Their work is with, on, and for other individuals. They are practically all "individual contractors." Their work and client relationships are personal. The diseases, troubles, aches, cures, and treatments with which they work are of very personal interest to all of their fellow men. All medical doctors must finish their education, complete their training, and acquire their skills to such a high degree that they are fully accepted as members of their profession when they start practice on their own.

Upon graduation from college, practically all engineers become employee members of engineering organizations. None of them have the skills, training, experience, and judgment to qualify as fully professional men. One feature of strength in our own Society is that all of its members, regardless of age, have served a considerable time as employees, and they share a common experience and hold a common point of view which is never wholly lost.

Certainly in the field of civil engineering, our profession is happily one of maturity. A look at our Life Members at the time they receive their certificates denoting such membership invariably shows us men who have lived full and rich lives in the constructive service of their fellow men. George Bernard Shaw could not have had the civil engineer in mind when he spoke of "The tragedy of youth; it is wasted on young people." The civil engineer, the builder, retains always his youth and his youthful point of view. Nor could Victor Hugo have had the civil engineer in mind when he said, "The misery of a child is of interest to its mother. The misery of a young man is of interest to a woman. The misery of an old man is of interest to no one." Such bitter pessimism could never pertain to the later years of the civil engineer, rich in the assets, memories, and attainments within his professional life.

The assembly of our many engineering societies under EJC and ECPD gives full recognition to the many varieties of specialized practices in which our professional engineers participate and the great variety of specialized conditions which surround the many different practices. After full professional status has been attained by the individual engineer, he undoubtedly is deeply concerned with just one or possibly two major fields of practice, and these become probably his chief interest in life thereafter. This engineer may properly expect his special, professional, and technical interests to be served best by a society which is particularly set up for and identified with technical advancement and whose membership consists of those individuals of like interests and needs. EJC and ECPD cannot hope to fill all the needs of these many different engineers, but these councils can and do function handsomely on broad general problems of vital import to the entire engineering profession. These councils have a most important and vital place to fill, but are never to be expected to accomplish all things for all engineers.

Our Society and Our Profession

Our great American Society of Civil Engineers has advanced steadily through the years in its vital service to its members and our profession. It has enabled our members to advance technically and professionally. It has remained a democratic and responsive Society. It has afforded fellowship and mutual respect within its membership. In furthering the technical advancement of our profession and its members, the spoken and written word has been used with utmost freedom, in our Section meetings, in our technical conferences, and in our technical publications. Whatever our employment or nature of service or compensation, whatever our political or social views, technical truths and technical advances provide common ties for all of us which are not to be severed. Our Society must have untold years of increasing and fruitful service ahead.

Last year I had particular reason to review again the qualities and characteristics of a profession and its members. I could find no brief definition of a profession. But all definitions covered four basic truths.

In the practice of a profession, proper education and training are most significant. Unusual and thorough preparation for practice is almost paramount.

Next is stressed the importance of ethics in the practice of a profession. We must have integrity. We must be honest with ourselves and with our fellowmen. It is unthinkable that a true professional man would be lacking in basic integrity.

Then there is the element of service; service in behalf of our fellow men rather than service primarily in our own behalf. Truly, real service must be a cardinal element in true professional practice.

Finally, there is the element of avowal. By avowal is meant the expression of a conscious determination to serve as a professional man; a form of consecration. Without positive decision or dedication on the part of the individual, service as a professional would not exist.

These four elements of professional practice are clear in definition, and without argument as to possession by the individual. We either possess them or we do not. If we as civil engineers have these qualities in our individual activities, we are professional men, we know it, and no one can take that knowledge away from us. To that degree, our professional status is for our own determination. If we have those qualities, our fellow men will know it and they will respect us and our profession and our Society without reservation. Our status starts with the individual. There can be no profession made up of non-professionals. Laws or rules or claims or shouts will not obtain for us as a group what we are unwilling to attain as individuals, a true professional status.

We civil engineers can be very proud of our Society. Our profession holds many treasures for us. We may know that as we serve our fellow men with our constructive undertakings and our facilities for finer and more complete living, and as we build well, we are also serving our God.

MEMOIRS OF DECEASED MEMBERS

ABSTRACTS

Honorary Member

Harvey Seeley Mudd 1412

Other Members

Burwell Bantz 1413
Louis Sterling Boggess 1414
George Calbraith Clarke 1414
John Williams Cleland 1415
James Lyford Davis 1416
Oswald Hewitt Dodkin 1416
George Edward Franklin 1417
David Warner Fry 1418
Charles Radcliffe Haile 1418
Frederic Francis Hall 1419
Norman Bateman Hodgkinson 1420
Carl Joseph Jacobsen 1420
Walter Johannessen 1421
Edmund Randolph Kent 1422
Max Werner King 1423
John Goulding Little 1423
Alexis McCormick 1424
Arthur Roscoe McGinness 1425
Howard Chester Means 1425
Gilbert Francis Mellin 1426
Jennings Bryan Oldham 1427
John Waller Pritchett 1427
Paul Lyon Reed 1428
Robert Bonaparte Reilly 1429
Walter Jackman Ryan 1430
Boris Michael Shimkin 1430
Carl Richard Skooglund 1431
William Sherman Tanner 1432
Engel Bert Van de Greyn 1432
Winsor Dornin Wilkinson 1433

HARVEY SEELEY MUDD, HON. M. ASCE[1]

DIED APRIL 12, 1955

Harvey Seeley Mudd, the son of Seeley W. and Della (Mulock) Mudd, was born in Leadville, Colo., on August 30, 1888. He attended Stanford University (Stanford, Calif.) from 1906 to 1908, transferring to Columbia University (New York, N. Y.). He was graduated an Engineer of Mines from Columbia in 1912.

After graduation Mr. Mudd was employed for two years as a mining engineer in Arizona and then joined his father's mining engineering company in Los Angeles (Calif.). During World War I he served as Assistant Secretary of the War Minerals Committee and as a technologist in the Bureau of Mines in Washington, D. C.

Mr. Mudd's main work was with the Cyprus Mines enterprise. In 1914, Cyprus ore bodies, unmined for centuries, were rediscovered, and after World War I operations were begun. As president and managing director of this vast enterprise he is credited with the successful operation of the mines and their related transportation features—one of Europe's greatest mining activities. He was responsible for greatly improving sanitary and living conditions of employees and raising living standards in nearby communities.

Under Mr. Mudd's leadership the Cyprus Mines Corporation acquired several mining properties in the western United States, and operations of the company were extended into iron ore production (and associated ocean transport enterprises) from a deposit 300 miles south of Lima, Peru. The corporate activities also branched into petroleum and natural gas development and production.

During the growing years of the Cyprus Mines Corporation, Mr. Mudd participated in other mining enterprises. These ventures produced ores in California, Nevada, and Mexico. He was a director of the Mesabi Iron Company.

In engineering and industrial fields detached from metal mining, Mr. Mudd served on the board of directors of the Southern Pacific Company, the Founders Insurance Company, and others; as a voting trustee of the Pacific Mutual Life Insurance Company; and as an active director on the Board of Texas Gulf Sulphur. He also directed the development and operation of the Pacific Alkali Company.

He was active in community programs in Los Angeles and was the head of fund raising campaigns and state committees for reconstruction and reemployment. He served the Rand Corporation, the California Institute of Technology, the American Heritage Foundation, and the Southwest Museum as

---

NOTE.—Complete manuscripts have been filed in the Engineering Societies' Library, 29 West 39th Street, New York, N. Y., and are available for consultation. Many of these memoirs have been considerably abbreviated for printing in *Transactions*.

[1] Abstract of memoir prepared by James L. Bruce, Cyprus Mines Corp., Los Angeles, Calif.

trustee, and the Board of Fellows of Claremont College and the Southern California Symphony Association as president.

For many years Mr. Mudd was an active member of the American Institute of Mining and Metallurgical Engineers, serving as director, vice-president, and president. He was a councilor of the Mining and Metallurgical Society of America. He was on the board of directors of the Seeley W. Mudd Memorial Fund Committee for the advancement of sciences and arts of mining and metallurgy.

Columbia University awarded him the honorary degree of Doctor of Science (1947) and the Egleston Medal for distinguished engineering achievements (1949). The honorary degrees of Doctor of Law were conferred on him by Loyola University (1943) and by the University of California (1941).

In 1913 he was married to Mildred Hardy Esterbrook. He is survived by his widow, a daughter, Caryll, and a son, Henry Thomas.

Mr. Mudd was elected an Honorary Member of the Society on September 6, 1952.

BURWELL BANTZ, M. ASCE[1]

DIED NOVEMBER 22, 1955

Burwell Bantz, the son of Clarence W. and Rebecca Jane (Blackiston) Bantz, was born at Piedmont, W. Va., on July 30, 1884. He was graduated from the University of Washington at Seattle with the degree of Bachelor of Science in Civil Engineering in 1909.

Mr. Bantz's entire engineering career was spent in the State of Washington. For three years he worked as an engineer for the City of Seattle, the Northern Pacific Railway Company, and the State Highway Department. From 1913 to 1917, he served as county engineer for Island County; from 1918 to 1929, as city engineer for Chehalis (during this period and until 1933 he also maintained a private practice at Chehalis); from 1933 to 1941, as county engineer for Lewis County; from 1941 to 1945, as director of state highways; from February, 1945, to June, 1948, as city engineer of Tacoma; and from 1952 to March, 1955, in the right-of-way division of the highway department. After his retirement from state service, he returned to Chehalis as city engineer.

In addition to serving state agencies, Mr. Bantz was an active member of the Tacoma Section of the Society.

On June 30, 1910, in Coupeville, Wash., Mr. Bantz was married to Minerva Ann Le Sourd. He is survived by his widow, three sons, and two daughters.

Mr. Bantz was elected a Member of the Society on April 10, 1944.

---

[1] Abstract of the memoir was prepared by Roy L. Greene, M. ASCE.

LOUIS STERLING BOGGESS, A.M. ASCE[1]

DIED AUGUST 18, 1947

Louis Sterling Boggess was born in Lawrenceburg, Ky., in 1886. He received the degrees of Bachelor of Science in Civil Engineering (1907) and Civil Engineer (1908) from the University of Kentucky at Lexington.

Shortly after graduation, he was employed by the Bureau of Public Works in the Philippine Islands. His first position there consisted of topographic and irrigation work. Later, he served as district engineer in charge of construction in Zambales and Bohol provinces. In 1918 he became division engineer in the eastern Visayan group with headquarters at Cebu.

Mr. Boggess left the Philippine Islands in 1919 and from 1919 to 1944 was engaged on various projects in Kentucky, Oklahoma, Indiana, and elsewhere. His last assignment in the United States was on the construction of the Indiana Ordnance Company—one of the largest explosive plants built during World War II.

From 1943 to late 1946, Mr. Boggess was engaged on road construction on the Inter-American Highway in Nicaragua. At this time he was transferred to Guatemala, also on work for the Inter-American Highway.

He is survived by his widow and one son, Louis Sterling Boggess.

Mr. Boggess was elected an Associate Member of the Society on March 14, 1916.

GEORGE CALBRAITH CLARKE, M. ASCE[2]

DIED SEPTEMBER 5, 1955

George Calbraith Clarke, the son of Robert Banks and Henrietta (Calbraith) Clarke, was born in Pittsburgh, Pa., on January 16, 1870. He was graduated from Pennsylvania State College (State College) in 1891 and returned to obtain the degree of Civil Engineer in 1902.

He entered the Engineering Department of the Pennsylvania Railroad in 1891 and rose to the position of engineer in charge of construction of the Pennsylvania terminals in New York, N. Y., and Pittsburgh. These outstanding engineering projects included construction of the Pennsylvania Railroad Station, the access tunnels under the Hudson and East rivers, and the terminal yards in New York; the Union Station and yard at Pittsburgh; and a railroad bridge over the Monongahela River at Pittsburgh.

---

[1] Abstract of the memoir prepared by Wallace C. A. Palmer, M. ASCE.

[2] Abstract of memoir prepared by Dougall C. Fraser, Treasurer, Fraser, Brace & Co., New York, N. Y.

After completion of the New York Pennsylvania terminals, he resigned to become a member of the firm of Fraser, Brace & Company in 1911. He was associated with this company until his retirement in November, 1945.

In Canada, Mr. Clarke was engaged in the construction of many industrial projects, including metallurgical plants and smelters, pulp and paper mills, and hydroelectric developments. As vice-president in charge of engineering for Fraser, Brace Engineering Company, Limited, Mr. Clarke was well known for his work on the design and construction of hydroelectric power plants at Chelsea and Farmers Rapids on the Gatineau River and at Island Falls (Saskatchewan) on the Churchill River. In addition to these Canadian projects, Mr. Clarke was actively engaged on many outstanding projects in the United States, such as the construction of the federal shipyard at Kearny, N. J., in World War I and three large government ordnance works during World War II.

On September 6, 1898, in Juniata County, Pennsylvania, he was married to Elizabeth Lloyd. He is survived by his daughter, Mrs. Nelson S. Dearmont, and four grandchildren.

Mr. Clarke was elected a Member of the Society on June 3, 1903. He became a Life Member in January, 1938.

JOHN WILLIAMS CLELAND, A. M. ASCE[1]

DIED OCTOBER 17, 1954

John Williams Cleland, the son of Thomas Louis and Elizabeth (Everbach) Cleland, was born at Louisville, Ky., on April 25, 1886. He received the degree of Bachelor of Science in Civil Engineering from the University of Southern California at Los Angeles.

Prior to 1910 he was engaged in the establishment of a system of pipelines in Mexico City (Mexico). He then became well known for his work as a civil engineer for the Southern California Gas Company in Los Angeles, serving during a period of great expansion of that company's facilities.

He was a member of the Free and Accepted Masons and the Benevolent Protective Order of Elks in Glendale, Calif.

On December 14, 1914, he was married to Lillian Jenson. He is survived by his daughters, Elizabeth Ann (Mrs. Frank Babcock) and Patricia May; two sons, Jack and Thomas; three grandchildren; and a brother, Herbert.

Mr. Cleland was elected an Associate Member of the Society on August 26, 1922.

---

[1] Abstract of the memoir prepared by A. E. Clune, Los Angeles, Calif.

JAMES LYFORD DAVIS, M. ASCE[1]

DIED JUNE 25, 1955

James Lyford Davis, the son of Benjamin Webster and Susan (Young) Davis, was born on September 18, 1870, at Fairlee, Vt. He was graduated from the University of Vermont, at Burlington, with the degree of Bachelor of Science in Civil Engineering in 1897, and in 1911 was also granted the graduate degree of Civil Engineer.

Mr. Davis was identified with important engineering projects in the fields of bridge, highway, railroad, sewer, and subway construction; laboratory and practical research in materials; water supply; and surveying.

He held various positions in the bridge engineering departments of railroad and bridge companies and later worked for the state highway departments or commissions in Vermont, New Jersey, Florida, and New York. He was engaged as inspector of steel work for the Rapid Transit Company (New York, N. Y.) during the period of its greatest construction. For a time Mr. Davis was engaged in testing concrete materials for the Jerome Park Reservoir (New York) and the New York City Board of Water Supply. He did a variety of work in New York in Dutchess and Westchester counties and in the Catskill Mountain area on the construction of reservoirs and aqueducts and entire water-supply systems. His final project was the extension of the Fairlee Water Supply system. Throughout his career he made numerous land surveys in Vermont, New Hampshire, and Florida.

He was a member of the Association of Highway Officials of the North Atlantic States, the American Road Builders' Association, the Vermont Society of Engineers, and the Board of Professional Engineers of Vermont. He was a licensed Civil Engineer and Land Surveyor in New Jersey.

In 1906 he was married to Margaret Seaver. Two years after her death he married Ethel Derby. He is survived by his widow; a daughter, Margaret (Mrs. John C. Rambeau), from his first marriage; two grandchildren, Jean and John; and a sister, Mrs. Rosalene Ordway.

Mr. Davis was elected an Associate Member of the Society on May 4, 1904, and a Member on March 12, 1918. He became a Life Member in January, 1939.

OSWALD HEWITT DODKIN, M. ASCE[2]

DIED SEPTEMBER 7, 1953

Oswald Hewitt Dodkin, the son of Alfred Thomas and Faith (Williams) Dodkin, was born at Foxboro, Mass., on June 22, 1902. He received the degree of Bachelor of Science in Mechanical Engineering in 1923 from Worcester Polytechnical Institute at Worcester, Mass.

---

[1] Abstract of memoir prepared by Frederick M. Hollister, South Duxbury, Mass.

[2] Abstract of the memoir prepared by Gordon L. Williams, M. ASCE.

In 1926 he joined the Brazilian Traction Light and Power Company in São Paulo, Brazil, as testing engineer. In 1950, after serving in several capacities, he became head of that company's Planning Department, which was organized at that time. He was very active in the conception and construction of Brazilian hydroelectric developments and directed investigations for several important projects.

For the Cubatão project, near São Paulo, he suggested and helped develop the idea of making the pumping plants reversible for peaking purposes and contributed much to water-hammer studies on the unprecedented penstocks for the project. These studies resulted in a paper[1] which is still considered a classic in engineering literature.

Mr. Dodkin was very active in civic affairs in the American community of São Paulo and was also a member of several technical societies. He helped to organize the Brazilian Section of the Society.

On November 1, 1930, he was married to Florence Winifred Dawson. He is survived by his widow and two daughters, Ray and Roberta.

Mr. Dodkin was elected a Member of the Society on August 16, 1948.

GEORGE EDWARD FRANKLIN, A. M. ASCE[2]

DIED FEBRUARY 5, 1955

George Edward Franklin, the son of William Edward and Marietta Ann (Nash) Franklin, was born in Chicago, Ill., on August 25, 1889. He received the degree of Bachelor of Science in Civil Engineering from Purdue University at Lafayette, Ind.

He was involved in railroad engineering until 1913 when he was put in charge of construction of locks and dams. After two years as division and resident engineer with the Texas Highway Department, he became superintendent of streets for the City of Dallas. He later became senior engineer for the City of Dallas and worked with consulting engineers on the original plans, specifications, and estimates for the Central Expressway. He was appointed coordinator of various interests for that and the East-West Expressway.

His spare time was devoted to church and professional activities and to tennis.

On March 10, 1914, he was married to Ida Lou Netherland. He is survived by his widow; one son, George Edward; and three daughters, Angela Ann, Frances Marietta, and Betty Jean (Mrs. Robert J. Slackney).

Mr. Franklin was elected an Associate Member of the Society on May 18, 1926.

---

[1] "High-Head Penstock Design," by A. W. K. Billings, O. H. Dodkin, F. Knapp, and A. Santos, Jr., "Symposium on Water Hammer," ASME, 1935, p. 29.

[2] Abstract of the memoir prepared by Grayson Gill, M. ASCE.

DAVID WARNER FRY, A. M. ASCE [1]

DIED MARCH 30, 1956

David Warner Fry, the son of John Webb and Nannie (Nichol) Fry, was born in Pratts, Va., on September 20, 1890. In 1910, he was graduated from Virginia Polytechnic Institute in Blacksburg with the degree of Bachelor of Science in Civil Engineering.

Following graduation he began his career with the Mexico Northwestern Railway Company which was building its line from Madera to Nogales in Mexico.

In December, 1911, Mr. Fry entered the service of the Baltimore and Ohio Railroad Company as axman in the engineering department. He advanced through many engineering positions to his appointment as senior assistant engineer in December, 1941, and principal assistant engineer on January 1, 1943. He held this position at the time of his death.

During his early years with the railroad he was engaged on reconnaissances and on location surveys for some of the branch lines serving the coal fields in Pennsylvania and West Virginia and on studies for grade and alinement improvements. He wrote numerous reports used to interest coal operators in locating in coal fields served by the railroad and also made studies and investigations concerning government projects affecting the railroad.

Mr. Fry was a member of the Engineers Club of Baltimore (Md.) and a Registered Professional Engineer and Land Surveyor in the State of Maryland.

On May 18, 1918, in Baltimore, he was married to Marguerite Mullen. He is survived by his widow; two daughters, Mrs. James R. Benner and Mrs. Frank M. McCarthy; two grandchildren; five sisters; and two brothers.

Mr. Fry was elected an Associate Member of the Society on June 1, 1920. He became a Life Member in January, 1955.

CHARLES RADCLIFFE HAILE, M. ASCE [2]

DIED MARCH 2, 1955

Charles Radcliffe Haile, the son of William A. and Helen (Foote) Haile, was born in San Antonio, Tex., on November 28, 1889. In 1912 he was graduated from the Agricultural and Mechanical College of Texas at College Station with the degree of Bachelor of Science in Civil Engineering.

After work in Mexico and Brazil and service as a Captain in the United States Corps of Engineers in France, he worked in various capacities for the

---

[1] Abstract of memoir prepared by K. J. Wagoner, M. ASCE.

[2] Abstract of the memoir prepared by Thad Spence Love, M. ASCE.

State Highway Department of Texas. In 1925 he went into private practice as a bridge contractor. Subsequently, he became assistant county engineer and county engineer for Harris County, Texas. In 1951 he incorporated his own firm as Chas. R. Haile and Associates, Inc. His career as a consultant included subdivision work, municipal utility work, federal camp work, road building, bridge building, and reclamation and reservoir work. The later years of his career were spent in study of the Gulf Coast area. His firm was selected to help in rebuilding Texas City (Tex.) after the explosion in 1947.

Mr. Haile was an active member of civic, fraternal, technical, and other organizations—he was a past-president of the Houston (Tex.) Engineers Club and the Houston Branch of the Society.

On December 23, 1919, he was married to Jennie Carr. He is survived by his widow.

Mr. Haile was elected a Member of the Society on April 25, 1932.

FREDERIC FRANCIS HALL, M. ASCE[1]

DIED MARCH 26, 1955

Frederic Francis Hall, the son of Charles and Mary (Corbett) Hall, was born on August 16, 1876, in Oakland, Calif. He received the degree of Civil Engineer from Cornell University at Ithaca, N. Y., in 1899 and the degree of Master of Science in mining from the University of California at Berkeley in 1904.

Mr. Hall was in charge of the surveys of the California Development Company for the Imperial Valley irrigation system from 1900 to 1904. He then worked in Nevada on the location and construction of a railroad and on mine surveys until 1906. The remainder of Mr. Hall's career was spent in private practice as a structural engineer in California. He was a partner in the structural engineering firms of Barker, Little and Hall, C. H. Snyder, and Hall, Pregnoff and Matheu. He participated in the structural design of more than a thousand buildings.

Mr. Hall was a member of various technical organizations, as well as fraternal and social associations.

On March 20, 1906, he was married to Katharine Johnson. He is survived by his widow; a son, Charles; a daughter, Marie (Mrs. W. B. Offutt); and two grandchildren.

Mr. Hall was elected a Member of the Society on November 14, 1938. He became a Life Member in January, 1950.

---

[1] Abstract of the memoir prepared by Michael V. Pregnoff, M. ASCE, and Robert R. Matheu.

NORMAN BATEMAN HODGKINSON, M. ASCE[1]

Died July 11, 1955

Norman Bateman Hodgkinson, the son of Oscar and Mabel (Bateman) Hodgkinson, was born in Emmetsburg, Iowa, on June 14, 1898. He attended the College of Engineering, University of California, at Berkeley, from 1917 to 1922, majoring in hydraulic engineering.

From 1922 until 1927 he was employed as a design engineer on irrigation systems and reclamation projects at Suisun Valley and Tulare Lake, and worked for light and power companies in California.

Mr. Hodgkinson entered the service of the Los Angeles County Flood Control District in 1927. In 1929 he was appointed design engineer; in 1930, chief designer for the district; in 1934, resident engineer; and in 1940, division engineer—having served as senior engineer and investigation engineer prior to this appointment. For a period during World War II, he was given the assignment of temporary assistant chief, and at the time of his death was division engineer in charge of the Project Planning Division of the district. He also served as an instructor in hydraulics at the Civic Center Division of the University of Southern California in 1932 and 1933.

Mr. Hodgkinson played a significant part in the planning and execution of the comprehensive flood-control program for Los Angeles County, which represents a capital investment of $1,000,000,000. The construction of many of the major dams and the hundreds of miles of temporarily and permanently improved flood-control channels were completed during his administration.

On January 21, 1922, in Martinez, Calif., he was married to Faith Smead. He is survived by his widow; his mother; a daughter, Janet (Mrs. R. H. Coughran); two sons, Gerald and Dave; and three sisters.

Mr. Hodgkinson was elected an Associate Member of the Society on October 26, 1931, and a Member on August 25, 1952.

CARL JOSEPH JACOBSEN, A. M. ASCE[2]

Died October 31, 1954

Carl Joseph Jacobsen, the son of Ole and Anne (Nelson) Jacobsen, was born in Walworth County, Wisconsin, on January 22, 1885. He was graduated from the University of Wisconsin at Madison in 1912 with the degree of Bachelor of Science in Mechanical Engineering.

---

[1] Abstract of memoir prepared by H. E. Hedger, M. E. Salsbury, and Paul Baumann, Members, ASCE.

[2] Abstract of the memoir prepared by Donald E. Wilson, J. M. ASCE.

After graduation he joined the Farris Bridge Company in Charleston, W. Va., and was associated with them until 1916. He then went to Pittsburgh, Pa., where he helped to organize the Farris Engineering Company, contractors and consulting engineers. On the dissolution of this company in 1940, Mr. Jacobsen practiced as an individual contractor and consulting engineer until the formation of Carl J. Jacobsen, Inc., in 1948. This firm specialized in the erection, reconstruction, and repair of highway and railroad bridges.

Mr. Jacobsen was a past-president and member of the Board of Governors of the Constructors Association of Western Pennsylvania and a member of various other technical and nontechnical organizations. He also served as an Elder of the Third Presbyterian Church in Pittsburgh.

On December 22, 1923, he was married to Helen Schlegel. He is survived by his widow. A daughter, Mary Helen, died in 1942.

Mr. Jacobsen was elected an Associate Member of the Society on September 9, 1919. He became a Life Member in January, 1954.

WALTER JOHANNESSEN, M. ASCE[1]

DIED NOVEMBER 14, 1954

Walter Johannessen, the son of Julius A. and Julia (Johnson) Johannessen, was born in Chicago, Ill., on August 31, 1891. He was graduated from George Washington University in Washington, D. C., with the degree of Bachelor of Science in Civil Engineering.

His early work included the supervision of the construction of many railroad bridges and trestles across the "quicksands" of Arizona streams; he developed the method first used to sink open caissons in quicksand which is now standard practice throughout the Southwest. He was then put in charge not only of street railway construction in Phoenix, Ariz., but also of its multi-million-dollar water supply program, its first modern disposal plant, and many of the municipal improvements of that day. From 1935 until 1942, Mr. Johannessen was involved in the municipal development of many areas in the Southwest. In 1942, he formed the consulting engineering firm of Johannessen and Girand; he was responsible for preparing plans for many of the major airfields in the southwest and was finally appointed Chairman of the Executive Committee of the Society's Air Transport Division.

Mr. Johannessen was President of the Arizona Section of the Society in 1947 and Chairman of the national spring meeting in Phoenix that year. He was also responsible for numerous reports as well as several papers published by the Society.

---

[1] Abstract of the memoir prepared by John Girand, M. ASCE.

On July 7, 1919, he was married to Zona Hildreth. He is survived by his widow; two daughters, Lucile (Mrs. David West) and Gertrude (Mrs. William Woodruff); and a son, Allyn.

Mr. Johannessen was elected an Associate Member of the Society on February 23, 1932, and a Member on December 13, 1937.

EDMUND RANDOLPH KENT, A. M. ASCE[1]

DIED OCTOBER 20, 1955

Edmund Randolph Kent, the son of Joseph Gordon and Mary (Randolph) Kent, was born on January 8, 1890, in Wythe County, Virginia. He was graduated in 1916 from the University of California (Berkeley) with the degree of Bachelor of Science in Civil Engineering. For a time he was a special student at the Massachusetts Institute of Technology (Cambridge).

He entered the United States Army in 1917 and served in France. After military service he was a student at the University of Cambridge in England. He was one of the first American exchange students.

Mr. Kent was active for many years as a consulting civil engineer, sometimes working on government projects and at other times for private concerns. His chief activities were the planning and construction of waterworks systems and bridges in New York, California, and New Mexico. He designed the water systems for Pleasantville, N. Y., and made water-supply studies of other villages in Westchester County. He was in charge of constructing the water-supply system of Stillwater, N. Y., and of one of the combination incinerator and power plants for the City of New York. Earlier in his career he was engaged on construction of the state penitentiary at Dannemora, N. Y., and the federal penitentiary at Milan, Mich. For more than two years he was the resident engineer at Mt. Vernon, Virginia (in the employ of the Mt. Vernon Association); he was in charge of all construction on the estate of George Washington. In 1951 he was in charge of the construction of large earth fill-concrete flood control dam on the Arizona-New Mexico border for the U. S. Soil Conservation Service. During the last four years of his life, Mr. Kent was engaged in the planning of land development in Pasadena, Tex.

He is survived by his sisters, Lucy Kent and Charlotte Kent, and his brother, Arthur Kent.

Mr. Kent was elected an Associate Member of the Society on January 16, 1928.

---

[1] Abstract of memoir prepared by David W. Conrey, Phillips H. Lovering, A. M. ASCE, and Roger H. Galt.

MAX WERNER KING, M. ASCE[1]

DIED JANUARY 17, 1955

Max Werner King, the son of Franklin Hiram and Carrie (Baker) King, was born on June 23, 1882, in Whitewater, Wis. He received the degree of Bachelor of Science in Civil Engineering in 1909 from the University of Wisconsin at Madison.

In 1911 he became manager of an oil pipeline company in Touapse, South Russia, for which he completed construction of a pipeline from Touapse to the Black Sea. In 1913 he began four years' work on the New York State Barge Canal and then was engaged in construction in the Buffalo (N. Y.) Harbor. Following responsibility for the Rio Mante and Rio Conchos irrigation projects in Mexico, he was employed by the International Boundary Commission as construction engineer in charge of channel rectification of the Rio Grande. He was then associated with the Mexican government in the construction of the San Juan Irrigation Project and the Marte Gomez Dam. From 1945 to 1947, he was in charge of construction of several highway and irrigation projects in Ecuador. He then returned to Mexico as consulting construction engineer for the Ministry of Hydraulic Resources.

On December 12, 1907, Mr. King was married to Estella E. Wright. He is survived by his widow; two daughters, Margaret Elizabeth (Mrs. H. J. Clifford) and Mary Ann (Mrs. T. H. Bass); and six sons, Harold, Charles, William, Robert, James, and Thomas.

Mr. King was elected a Member of the Society on May 12, 1919. He became a Life Member in January, 1953.

JOHN GOULDING LITTLE, M. ASCE[2]

DIED FEBRUARY 26, 1955

John Goulding Little, the son of George and Caroline (Doak) Little, was born on March 17, 1880, in Atlanta, Ga. He was graduated from the University of Alabama at University with the degree of Bachelor of Science in 1900 and was awarded the degree of Civil Engineer in 1902.

As a young engineer Mr. Little had varied design experience with the American Bridge Company (Pittsburgh, Pa.); the Bureau of Yards and Docks, United States Navy Department (Washington, D. C.); Post & McCord, steel contractors (New York, N. Y.); and the United States Reclamation Service (Washington, D. C., North Dakota, and Oregon).

---

[1] Abstract of the memoir prepared by John A. Focht, M. ASCE.

[2] Abstract of the memoir prepared by John C. Vandermey, A. M. ASCE.

In 1906 he went to San Francisco, Calif., where he worked with the Ferrolite Company, and later with the Board of State Harbor Commissioners.

He established his own firm of civil engineers in 1907 and from time to time served as chief structural engineer for the city architect, structural engineer for the state engineer in Sacramento, consulting structural engineer and superintendent of the Bureau of Building Inspection in San Francisco, and senior structural engineer with the Division of Architecture, State of California.

For his own company he designed and detailed numerous buildings, bridges, and other structures. He was also consulting engineer for the Golden Gate Bridge.

On April 10, 1910, in San Rafael, Calif., Mr. Little was married to Maude Bretherton. He is survived by his widow, a daughter, and four grandchildren.

Mr. Little was elected a Member of the Society on January 13, 1947.

ALEXIS McCORMICK, A. M. ASCE[1]

DIED JUNE 11, 1955

Alexis McCormick, the son of Stephen and Hattie (Simpson) McCormick, was born in Weimar, Tex., on June 19, 1886. He was graduated from the Agricultural and Mechanical College of Texas (College Station) with the degree of Bachelor of Science in Civil Engineering in 1904.

After graduation Mr. McCormick worked for railroad companies in Texas and Louisiana and for private construction companies on varied projects. In 1924–1926 he was county engineer for Madison County, Texas, and city engineer for Madisonville, Tex. Later he worked for the Texas Highway Department as division engineer and as resident engineer. From 1935 to 1940 he was resident-engineer inspector for the Public Works Administration and was in charge of designing and constructing one of the largest county highway systems in Texas. From 1940 until 1946, when Mr. McCormick formed a consulting engineering partnership, he was in charge of a highway construction project in Montgomery County, Texas, and was city engineer of Conroe, Tex. (1940–1941) and Corpus Christi, Tex. (1942–1946). As city engineer he was responsible for the design and construction of many public works. In Mr. McCormick's engineering consulting firm he continued in the field of municipal engineering. Many of the improvements in the cities of Livingston, Lake Jackson, and Beaumont (in Texas) were under his direction.

On December 23, 1913, he was married to Mattie L. Sherman. He is survived by his widow; two daughters, Mrs. C. L. Bodin and Mrs. Spencer Hays; and two grandchildren, Virginia Bodin and Christopher Hays.

Mr. McCormick was elected an Associate Member of the Society on February 24, 1931.

---

[1] Abstract of memoir prepared by John A. Focht, M. ASCE.

ARTHUR ROSCOE McGINNESS, A. M. ASCE[1]

DIED JULY 26, 1954

Arthur Roscoe McGinness, the son of Henry Monroe and Ida (Barton) McGinness, was born in Harlan, Iowa, on March 23, 1884. He was graduated from Colorado State College, at Fort Collins, in 1910, with the degree of Bachelor of Science in civil and irrigation engineering.

In April, 1912, after varied hydrographic and surveying experience, Mr. McGinness joined the Bureau of Reclamation. Following brief assignments on projects in Montana and Wyoming, he transferred to the Huntley Project in Montana. He was promoted to project manager in June, 1921, and administered the affairs of the project until his resignation in December, 1926.

In March, 1928, Mr. McGinness accepted a position as structural engineer with the City of Long Beach, Calif. He supervised the design of various structures including public buildings.

In November, 1933, he joined the Bridge Department of the Division of Highways, California Department of Public Works, as associate bridge design engineer. He terminated his connection with the State of California and returned to the Bureau of Reclamation in April, 1936, as an associate engineer in the Central Valley Project. He was promoted to assistant regional engineer in June, 1946, and to regional engineer in November, 1946. He retired in May, 1953.

On April 15, 1916, he was married to Martha Edna Montgomery. He is survived by his widow; two brothers, Raymond U. and Earl E.; two daughters, Dorothy M. (Mrs. James Bainbridge) and Olive L. (Mrs. Richard Horrell); a son, Bryce A.; and four grandchildren.

Mr. McGinness was elected an Associate Member of the Society on July 10, 1944.

HOWARD CHESTER MEANS, M. ASCE[2]

DIED MARCH 20, 1951

Howard Chester Means, the son Joseph C. and Frances Rebecca (Graves) Means, was born in Bloomington, Ill., on April 27, 1875. He was graduated from the University of Illinois at Urbana in 1898.

From 1898 to 1905, Mr. Means was in charge of locating and constructing irrigation systems in Montana. He was the superintendent of irrigation and the disbursing agent for the United States Indian Service from 1905 to 1913.

---

[1] Abstract of memoir prepared by a Committee of the Sacramento Section consisting of Arthur J. Bunas, M. ASCE, and Glenn O. Laurgaard and Robert S. Thomas, Associate Members, ASCE.

[2] Abstract of the memoir prepared by Richard R. Lyman, M. ASCE.

From 1913 to 1918, he organized a power plant corporation at Myton, Utah, and an investment company to develop the townsite of Soldier Summit, Utah. From 1921 to 1926, Mr. Means was chief engineer of the Utah State Road Commission, directing construction and maintenance of many miles of highways. Two unusual roads constructed during his administration are the Wendover Cutoff across the salt flats of Great Salt Lake and the Zion-Mt. Carmel Highway, much of which was constructed in the east wall of Zion National Park. After 1926 Mr. Means served as secretary-treasurer for a petroleum company in Wyoming, as an investigator for the purchase of power properties in the northwestern states, and as manager and engineer for a company developing natural rock asphalt deposits in eastern Utah.

Mr. Means was a Past-President of the Utah Section of the Society and was the first president of the Western Association of State Highway Officials. He was an active Rotarian and member of the F. and A. M.

In 1916 Mr. Means was married to Lillian Arnold. He is survived by his widow; a son, Howard Arnold; two grandchildren; and two sisters.

Mr. Means was elected an Associate Member of the Society on June 30, 1910, and a Member on January 19, 1923. He became a Life Member in January, 1945.

GILBERT FRANCIS MELLIN, A.M. ASCE [1]

DIED APRIL 26, 1955

Gilbert Francis Mellin, the son of Otto and Julia (Colby) Mellin, was born on October 16, 1893, in Vallejo, Calif. He was graduated from the Engineering College of the University of California at Berkeley in 1916.

In 1916 Mr. Mellin was appointed civil and hydraulic engineer and later became chief of assessment of the California State Reclamation Board in Sacramento. These positions involved design and construction work and spreading and collecting assessments in the Sacramento-San Joaquin Drainage District.

From April, 1923, to September, 1929, he was engaged in private practice—planning and designing irrigation, drainage, and flood protection works. He was also assessment commissioner for a storage district and several reclamation districts as well as appraiser for many bond issues and loans.

In September, 1929, Mr. Mellin re-entered the employ of the State of California; he classified many acres of land to determine water requirements in what is now the Central Valley Project. From 1931 to 1936, as senior hydraulic engineer, he assisted in the liquidation of assessments of the Reclamation Board and had charge of the appraisal and acquisition of many acres of flowage easements.

From April, 1936, to June, 1943, he was chief right-of-way agent of the Bureau of Reclamation on the Central Valley Project. He appraised hundreds of acres in Shasta Reservoir, Friant Reservoir, Friant-Kern Canal, and Contra Costa Canal. In July, 1943, he returned to the State Reclamation Board as assistant chief engineer and appraiser.

---

[1] Abstract of memoir prepared by William J. Stich, A. M. ASCE, J. N. Soderstrand, A. M. ASCE, and Thomas H. Means, M. ASCE.

On August 31, 1919, in Sacramento, he was married to Marion Perkins. He is survived by his widow, a daughter, and a grandson.

Mr. Mellin was elected an Associate Member of the Society on December 15, 1924.

JENNINGS BRYAN OLDHAM, A. M. ASCE[1]

Died October 5, 1954

Jennings Bryan Oldham, the son of Charles William and Ida (Lett) Oldham, was born in Fulton, Ky., on December 2, 1896. He moved to Dallas, Tex., in about 1909 and later entered the University of Texas at Austin where in 1921 he was graduated with a degree in civil engineering.

He first worked in the engineering department of the Texas and Pacific Railroad Company. From railroad work, he transferred to the Portland Cement Association as field engineer throughout most of Texas.

In September, 1924, Mr. Oldham was employed as sales engineer for the Lone Star Cement Corporation in Dallas and in July, 1927, was made sales manager for the Texas Division. In September, 1942, he was transferred from Dallas to New York, N. Y., as general sales manager for the corporation. In January, 1946, he returned to Dallas as vice-president and manager for the corporation and operated cement plants in Dallas, Houston, and Maryneal.

Mr. Oldham was a director of the Texas Manufacturer's Association, a member of the City Club and of Phi Kappa Psi Fraternity; he was also a member of the Industrial Development Committee of the State Fair of Texas and was president of the Lakewood Country Club of Dallas.

On September 15, 1922, he was married to Ingeberg Johnson of Waco, Tex. He is survived by his widow; a son, Charles William; and two daughters, Betty Jane and Patsy Jean.

Mr. Oldham was elected a Junior of the Society on May 19, 1924, and an Associate Member on April 12, 1926.

JOHN WALLER PRITCHETT, M. ASCE[2]

Died April 19, 1954

John Waller Pritchett, the son of H. Carr and Kate (Smith) Pritchett, was born in Glasgow, Mo., on May 15, 1882. In 1902 he was graduated from the

---

[1] Abstract of memoir prepared by Grayson Gill, M. ASCE.

[2] Abstract of memoir prepared by John A. Focht, M. ASCE.

Sam Houston State Teachers College, at Huntsville, Tex., receiving a teachers certificate, and in 1906 he was awarded the degree of Civil Engineer from the University of Texas at Austin.

His early engineering experiences were in the fields of railroad maintenance and surveying (Texas), municipal engineering (Monterrey, N.L., Mexico), and railroad location and construction (Mexico).

In July, 1911, he returned to Texas and was engaged on construction projects and field locations of drainage systems. From 1912 to 1918, he was employed by the General Land Office of Texas and held various positions ranging from compiling draftsman to acting chief draftsman.

Mr. Pritchett's main work was for the Texas State Board of Water Engineers; from June, 1918, until March, 1936, he was chief engineer; and from March, 1936, to November, 1949, he was a member of the Board of Water Engineers. During this long period of service he had an important part in formulating technical procedures used in analyzing hydrologic data and conducting investigations required by the board.

Mr. Pritchett was a frequent contributor to *Transactions* and *Civil Engineering* of the Society.

In 1919 he was married to Anna Louise Burnett. He is survived by his widow; two sons, William Carr and Phillip Walter; and a daughter, Kathleen Louise.

Mr. Pritchett was elected an Associate Member of the Society on May 8, 1922, and a Member on December 16, 1946. He became a Life Member in January, 1953.

PAUL LYON REED, M. ASCE[1]

DIED JUNE 30, 1955

Paul Lyon Reed, the son of the Reverend Myron and Louise (Lyon) Reed, was born in Clifton, Ill., on August 25, 1872. In 1894 he was graduated from Rensselaer Polytechnic Institute at Troy, N. Y., with the degree of Civil Engineer.

After graduation, Mr. Reed was engaged in engineering work in England, Belgium, and India. He was commissioned in the Civil Engineer Corps of the United States Navy in 1902 and served as Public Works Officer at various naval yards and stations in the United States and the Philippines. He was promoted to Captain in 1922 and was the Assistant Chief of the Bureau of Yards and Docks from 1926 to 1930. He was retired in 1936 but recalled to duty for nearly seven years prior to and during World War II.

---

[1] Abstract of the memoir prepared by DeWitt C. Webb, M. ASCE.

He was a member of Sigma Xi, the Falk Foundation, and the American Association for the Advancement of Science.

On March 24, 1898, Mr. Reed was married to Laura Van Wyck, at Liege, Belgium. He is survived by his widow; two daughters, Dorothy (Mrs. Dale Harris) and Charlotte (Mrs. Charles A. Fletcher); six grandchildren; two great grandchildren; and a brother, Ralph.

Mr. Reed was elected a Member of the Society on July 9, 1906. He became a Life Member in January, 1941.

ROBERT BONAPARTE REILLY, A. M. ASCE [1]

DIED FEBRUARY 19, 1955

Robert Bonaparte Reilly, the son of James M. and Bonnie Lou (Cain) Reilly, was born in Dallas, Tex., on April 3, 1904. He attended the Agricultural and Mechanical College of Texas (College Station), being graduated in June, 1926.

After graduation, he was employed by the Austin Brothers Structural Steel Company of Dallas; the Muskogee Iron Works in Muskogee, Okla.; the L. E. Myers Company of Chicago, Ill.; the Reilly Engineering Sales Company (self-employed) in Dallas; the Austin Road Company of Dallas; and Powell & Powell, Engineers, in Dallas.

He was appointed district engineer for the American Institute of Steel Construction in 1948 and was subsequently promoted to regional engineer for the southwest. While Mr. Reilly was employed by the institute, he conceived the idea of holding a seminar on structural shop drafting for the drafting teachers of the Dallas Independent School District. This seminar was held, and the material used, as later compiled and edited by Mr. Reilly, was widely accepted throughout the United States.

He was active in club and church work. He was a member of the Texas Society of Professional Engineers, the Society of American Military Engineers, the Technical Club of Dallas, the American Welding Society, the Dallas A and M Club (president, spring of 1947), and Kappa Tau Z, a social fraternity. He belonged to the Men's Club of the All Saints Episcopal Church and served as vestryman, senior warden, and acolyte. He also worked on the church building committee.

In March, 1928, he was married to Philo Crane. He is survived by his widow and two daughters, Bonnie and Patricia.

Mr. Reilly was elected an Associate Member of the Society on November 18, 1946.

---

[1] Abstract of memoir prepared by Grayson Gill, M. ASCE.

WALTER JACKMAN RYAN, M. ASCE[1]

Died August 12, 1951

Walter Jackman Ryan, the son of Almon J. and Lottie (Jackman) Ryan, was born on February 28, 1882, at Blair, Nebr. He was awarded the degree of Bachelor of Arts from Oberlin College (Oberlin, Ohio) in 1903 and the degree of Civil Engineer from Cornell University (Ithaca, N. Y.) in 1906.

Early in his engineering career Mr. Ryan worked for several railroad companies in Arkansas, North Dakota, and Oregon. Later he was employed by the Bureau of Reclamation and private engineering companies.

In 1914, Mr. Ryan joined the Weyerhaeuser Timber Company and remained in their service until his retirement in 1947. During this time he served as engineer for subsidiary companies and after 1923 was chief logging engineer at Tacoma, Wash. His work included development of logging programs, mapping of timber lands, developing of camps and towns, and constructing logging railroads, roads, and bridges.

Following his retirement, Mr. Ryan became a consultant. In 1950 he advised the New Zealand Forest Service on matters of logging engineering. In 1951 he worked with the Tacoma Chamber of Commerce as a consultant in industrial development.

Mr. Ryan was especially interested in the proper use of timber as a structural material and was an early user of modern timber connectors. He served on the Wooden Bridges Committee of the American Railway Engineering Association and worked with the West Coast Lumberman's Association. He was a member of the Society of American Foresters, the Forest Products Research Society, the American Society of Photogrammetry, the Western Forestry and Conservation Association, and the American Society of Military Engineers.

Mr. Ryan helped to organize the Tacoma Section of the Society and was president of the section in 1933. He served on both local and national committees and in 1950 was elected Director for District 12.

In 1913 he was married to Edith Hatch. He is survived by his widow and a son, Harrison.

Mr. Ryan was elected a Junior of the Society on May 5, 1908; an Associate Member on March 1, 1910; and a Member on March 11, 1919. He became a Life Member in January, 1945.

BORIS MICHAEL SHIMKIN, A. M. ASCE[2]

Died November 30, 1954

Boris Michael Shimkin, the son of Michael Boris and Lydia C. (Kolobov) Shimkin, was born in Omsk, Siberia, on April 13, 1888. He received the degree of Civil Engineer from the Tomsk Technological Institute of Nicholas II in 1914. In 1928 he was awarded the degree of Master of Science in Civil Engineering from the University of California at Berkeley.

---

[1] Abstract of memoir prepared by Daniel G. O'Shea, M. ASCE.

[2] Abstract of memoir prepared by Howard C. Wood, M. ASCE, and D. E. Marsh, A. M. ASCE.

During World War I, Mr. Shimkin served as a colonel in the Imperial Russian Army and was in charge of bridge and other construction on the Trans-Siberian Railway. In 1919–1920 he was chief engineer on port installations in Vladivostok. He escaped with his family to Java just before the revolution. There he worked as a consulting and designing engineer on railway, bridge, and irrigation projects. In 1923 he came to the United States with his family and in 1928 he became an American citizen.

After working in the structural engineering field in the San Francisco (Calif.) area, he was appointed associate bridge engineer in the California Division of Highways at Sacramento in October, 1933. He remained at bridge department headquarters in Sacramento until late in 1943 when he was transferred to the San Francisco-Oakland Bay Bridge engineering office.

On January 8, 1912, Mr. Shimkin was married to Lydia J. Serebrov. He is survived by his widow; two sons, Michael B. and Demitri B.; and five grandchildren.

Mr. Shimkin was elected an Associate Member of the Society on November 12, 1928.

CARL RICHARD SKOOGLUND, A. M. ASCE[1]

Died December 21, 1954

Carl Richard Skooglund, the son of John and Amanda (Skoog) Skooglund, was born in Youngstown, Ohio, on November 21, 1908. He was graduated from the University of Washington at Seattle with the degree of Bachelor of Science in Civil Engineering in 1933.

Mr. Skooglund worked for the Clark County (Washington) Highway Department until September, 1938, when he joined the Bonneville Power Administration. In August, 1942, he was engaged in laying out and detailing sewage disposal plants. From January, 1943, until January, 1945, he was employed by the United States Navy Department. In 1946 and 1947 he assisted in the layout and design of utilities for a large housing unit for the Meridian Dam project in Oregon.

From November, 1947, to December, 1948, he was a designing engineer and from December, 1948, to January, 1950, was employed by N. W. Haner and Associates as engineer. He became a partner in January, 1950, and remained with them until June, 1952, when he was appointed city engineer of Vancouver, Wash. He held this position until the time of his death.

On November 17, 1933, he was married to June McMahon. He is survived by his widow; a son, Richard; two daughters, Marylin and Karen; his parents; and a sister, Catherine Jester.

---

[1] Abstract of the memoir prepared by Orrin Stanley, M. ASCE.

Mr. Skooglund was elected an Associate Member of the Society on March 18, 1946.

WILLIAM SHERMAN TANNER, M. ASCE[1]

DIED NOVEMBER 10, 1955

William Sherman Tanner, the son of William and Anna Belle (Sherman) Tanner, was born on January 22, 1895, in Waco, Tex. He attended Southern Methodist University in Dallas, Tex.

For sixteen years he worked for the City of Dallas, ultimately being placed in charge of the sanitary sewer department and of plans for modern sewers and a sewage disposal plant. Just before World War II he joined the firm of Holmes & Narver, consulting engineers in Los Angeles, Calif.; he designed a sewage disposal plant for Camp Roberts and a water storage system and sewage disposal system on Maui, one of the Hawaiian Islands. In 1949, after service as a senior engineer in the Corps of Engineers (United States Department of the Army), he moved to Sacramento, Calif. There he again was engaged in the design of various water and sewage facilities and also in preparing plans for streets, drainage, and sewage facilities. In 1954 he began private practice in the firm of Butler & Tanner.

On January 14, 1920, he was married to Tommie Lois Davis. He is survived by his widow; a daughter, Mrs. Marguerite L. Donahue; two sons, William S. and Alvin L.; a granddaughter, Deane Donahue; and a sister, Mabel E. Stone Compton.

Mr. Tanner was elected an Associate Member of the Society on January 14, 1929, and a Member on November 17, 1947.

ENGEL BERT VAN DE GREYN, M. ASCE[2]

DIED JULY 23, 1955

Engel Bert Van de Greyn, the son of Derk and Clasina (Van Aalsberg) Van de Greyn, was born in Grand Haven, Mich., on January 25, 1882.

Before entering college he did surveying work and joined an engineering party of Waddell and Hedrick (St. Louis, Mo.) on railway construction between Mexico City and Vera Cruz. Later he became resident engineer in charge of bridge construction.

In 1904 Mr. Van de Greyn was assigned to projects in the United States for this firm, serving for a time as resident engineer on the Intercity Viaduct in

---

[1] Abstract of the memoir prepared by Drury Butler, M. ASCE.

[2] Abstract of memoir prepared by W. E. Strohm, A. M. ASCE.

Kansas City, Mo. In 1906 he established an engineering practice in Excelsior Springs, Mo., and became town engineer. In 1908 he entered the University of Illinois (Urbana), graduating in 1911 with the degree of Bachelor of Science in municipal and sanitary engineering. After graduation he became resident engineer on a large bridge project in Tacoma, Wash., and in 1912, city engineer of Denver, Colo. In 1914 Mr. Van de Greyn began a practice in structural and municipal engineering in Houston, Tex. During World War I he was chief engineer for the Beaumont Shipbuilding and Drydock Company. Shortly afterward, he became general manager and was elected to the Board of Directors.

In 1921 he retired to New Mexico for reasons of health. At first he undertook part-time work designing bridges for the New Mexico Highway Department and later, when he recovered sufficiently, he accepted full-time employement with this department. He served the State of New Mexico as bridge engineer from 1923 until his retirement from active service in 1951.

Mr. Van de Greyn also served for many years as a member of the Committee on Bridges and Structures of the American Association of State Highway Officials. He was a member of the Tau Beta Pi Association and the Masonic Orders (Scottish Rite and the Shrine).

He is survived by his sister, Mrs. Artje North; a nephew, William H. North; and a niece, Mrs. Paul R. Williams.

Mr. Van de Greyn was elected a Member of the Society on May 7, 1951.

WINSOR DORNIN WILKINSON, A. M. ASCE[1]

DIED OCTOBER 4, 1955

Winsor Dornin Wilkinson, the son of Crayton and Mary (Dornin) Wilkinson, was born in Berkeley, Calif., on May 30, 1887. He was graduated from Dartmouth College (Hanover, N. H.) in 1910 with the degree of Bachelor of Science and did postgraduate work at the University of California, School of Engineering (Berkeley).

Mr. Wilkinson was first employed by the National Park Service. In 1931 and 1932 he worked for the San Francisco (Calif.) Water Department, returning in 1947 to serve until his retirement in June, 1952. During this period he was in charge of preparation of statements for payment to contractors on several large pipeline projects. Prior to 1935 he did roadwork in Santa Barbara County (California), and for a period between 1937 and 1939, was engaged on the construction of roads for the San Francisco International Exposition on Treasure Island.

During World War I, Mr. Wilkinson was a Captain in the Field Artillery, United States Army. He remained in the Reserve Army and was recalled to active duty during World War II; he served in various camps throughout the United States.

---

[1] **Abstract of memoir prepared by C. A. Lauenstein, M. ASCE.**

He was a member of the Society of California Pioneers, the Mayflower Society, Sigma Nu Fraternity, the Masonic Lodge, and the Dartmouth Alumni Club. Mr. Wilkinson was an active member of the First Congregational Church of Berkeley and the Dartmouth Outing Club and was secretary of Boy Scout Council, Troop 5, Berkeley. He was a registered Civil Engineer in the State of California.

On February 21, 1935, in Berkeley he was married to Mabel Sutton. He is survived by his widow; four daughters, Jean, Sally, Mary, and Louisa; a son, Albert; and two sisters, Dorothy Wilkinson and Pauline Macaulay.

Mr. Wilkinson was elected an Associate Member of the Society on January 14, 1924.

TRANSACTIONS

OF THE

AMERICAN SOCIETY OF CIVIL ENGINEERS

INDEX

VOLUME 121

1956

SUBJECT INDEX, PAGE 1437
AUTHOR INDEX, PAGE 1479

Titles of papers are in quotation marks when given with the author's name.

VOLUME 121

SUBJECT INDEX

ABUTMENTS
See DAMS, ARCH (cross reference thereunder)

ACCIDENTS
See STREETS—Safety; *see also* FAILURES . . .

ACCOUNTS AND ACCOUNTING
See COSTS . . . ; *also* subheading Financing under relative subject

ADDRESSES
See AMERICAN SOCIETY OF CIVIL ENGINEERS—Addresses; *see also* under subject of address

AERATION
"Studies of Air Entrainment in Open-Channel Flows," Lorenz G. Straub and Owen P. Lamb, 30.

AERATION TANKS
See TANKS, AERATION

AERIAL . . .
See also AIR . . .

AERIAL MAPS AND MAPPING
See MAPS AND MAPPING, AERIAL

AERIAL NAVIGATION
See AIR TRANSPORT

AERIAL PHOTOGRAPHY
See SURVEYS AND SURVEYING, AERIAL

AERIAL SURVEYS AND SURVEYING
See SURVEYS AND SURVEYING, AERIAL

AERODYNAMICS
See also AIR FLOW; *also* under relative subject
"Resonant Vibration of Steel Stacks," Ernest A. Dockstader, William F. Swiger and Emory Ireland (with discussion), 1088.
"The Vibrations of Steel Stacks," Walter L. Dickey and Glenn B. Woodruff (with discussion), 1054.

AERONAUTIC MAPS
See MAPS AND MAPPING, AERIAL; SURVEYS AND SURVEYING; AERIAL

AGRICULTURE
See DRAINAGE (cross references thereunder); FLOODS; IRRIGATION; LAND . . . (cross references thereunder); SOILS

AIR . . .
See also AERIAL . . . (cross references thereunder); AERO- . . .

AIRCRAFT
See also BUCKLING; *see also* AIRPLANES
Increase in aircraft weights, 10 year periods, 1920–1950, 725.

AIR ENTRAINMENT
See WATER, FLOW OF . . .

AIRFIELDS
See AIRPORT . . .

AIR FLOW
"Resonant Vibration of Steel Stacks," Ernest A. Dockstader, William F. Swiger and Emory Ireland (with discussion), 1088.
"The Vibrations of Steel Stacks," Walter L. Dickey and Glenn B. Woodruff (with discussion), 1054.
"Wind Loads on Girder Bridges," John M Biggs, Saul Namyet and Jiro Adachi, 101.

AIRPLANES
See also AIRCRAFT
"The Effect of Jet Aircraft on Airport Pavements," Gayle McFadden, 172.

AIR POLLUTION
See AIR SANITATION

AIRPORT APPROACHES
Airport standards for current and future length of runways, 722.

AIRPORTS (structures and localities)
See also FOUNDATIONS, AIRPORT; HANGARS; PAVEMENT AND PAVING . . .
"Airport Standards," John M. Kyle, 722.
Classification of ideal subgrade soil material at Willow Run Airport, Michigan, 551, 552.
"Development of an International Airport," Earle M. Rader, 96.

AIRPORTS (*Continued*)

"The Effect of Jet Aircraft on Airport Pavements," Gayle McFadden, 172.

"Increasing the Load-Carrying Capacities of Subgrades," Charles M. Noble (with discussion), 544.

AIR SANITATION

See also COSTS, AIR SANITATION; ODORS

Behavior of aerosols in air cleaning, 94.

"Handling Atomic Energy Industry Wastes," Joseph A. Lieberman and Arthur E. Gorman, 85.

Municipal refuse incinerator stack gases and their reduction, 287, 297, 303, 309.

Smoke control program in Pittsburgh, Pennsylvania, 887.

AIR TERMINALS

See AIRPORTS

AIR TRAFFIC

See TRAFFIC, AIR

AIR TRANSPORT

See also AIR TERMINALS (cross reference thereunder)

Noise control in the vicinity of airports and air routes, 722, 727.

AIRWAYS

See AIR TRANSPORT

ALLOYS

See also under name of relative metal

"Design of Aluminum Alloy Beam-Columns," Harry N. Hill and Ernest C. Hartmann and John W. Clark (with discussion), 1.

Bibliography

Aluminum alloy beam-columns, 12.

ALLUVIATION

See BARS (alluvia); SEDIMENT AND SEDIMENTATION; SILT AND SILTING . . .

ALUMINUM

See ALLOYS; CORROSION AND PROTECTION OF METALS

AMERICAN SOCIETY OF CIVIL ENGINEERS

Addresses

1956—Address at the Summer Convention, Knoxville, Tenn., June 7, 1956, Enoch R. Needles, 1398.

Memoirs of Members. *See* name of member in Author Index. (*See also* p. 1411)

ANALOGS AND ANALOGIES

See under relative subject, e.g., EQUATIONS; STRUCTURES, THEORY OF

ANALYSIS, DESIGN

See under relative subject, e.g., CONCRETE—Design; STRUCTURES, THEORY OF

ANALYSIS OF DATA

See EQUATIONS; GRAPHICAL CHARTS (cross references thereunder); MATHEMATICS; PROBABILITY, THEORY OF; STRUCTURES, THEORY OF; *also* under relative subject

ANALYSIS, STATISTICAL

See STATISTICAL ANALYSIS (cross references thereunder)

ANALYSIS, STRUCTURAL

See EQUATIONS; STRESS AND STRAIN; STRUCTURES, THEORY OF

APPARATUS

See under relative subject, e.g., EQUATIONS; WATER, FLOW OF, IN OPEN CHANNELS; *also* INSTRUMENTS (cross references thereunder); *also* under general types of apparatus, e.g., VIBRATION RECORDING APPARATUS

APPRAISAL

See VALUATION

ARCH BRIDGES

See BRIDGES, ARCH (cross reference thereunder)

ARCH DAMS

See DAMS, ARCH (cross reference thereunder)

ARCHES

See BRIDGES, ARCH (cross reference thereunder); DAMS, ARCH (cross reference thereunder)

ARCHITECTS AND ARCHITECTURE

See under type of structure or structural part, e.g., BUILDINGS

ASPHALT PAVEMENT AND PAVING

See PAVEMENT AND PAVING, BITUMINOUS

ASSOCIATIONS

See SOCIETIES, TECHNICAL

ATMOSPHERIC POLLUTION

See AIR SANITATION

ATOMIC BLAST

"An Engineering Approach to Blast-Resistant Design," Nathan M. Newmark, 45. *Discussion:* Stephen J. Fraenkel, and Nathan M. Newmark, 62.

ATOMIC BLAST (*Continued*)
Bibliography
Blast resistant design, 60.
ATOMIC ENERGY
"Handling Atomic Energy Industry Wastes," Joseph A. Lieberman and Arthur E. Gorman, 85.
AUTOMOBILE . . .
See also MOTOR TRUCKS; TRAFFIC . . .
AUTOMOBILE ACCIDENTS
See STREETS—Safety
AUTOMOBILE PARKING
See also COSTS, AUTOMOBILE PARKING
Financing
"Private Enterprise Can Satisfy the Parking Demand," Charles T. McGavin, 165.
AUTOMOBILE TRUCKS
See MOTOR TRUCKS
BACKWATER
Application of regime theory, 870.
"Fundamental Concepts of Rectangular Settling Tanks," Alfred C. Ingersoll, Jack E. McKee and Norman H. Brooks (with discussion), 1179.
BAFFLES
See WATER, FLOW OF . . .
BANKS AND BANK PROTECTION, CHANNEL
See CHANNEL BANKS AND BANK PROTECTION (cross references thereunder)
BANKS AND BANK PROTECTION, RIVER
See RIVER BANKS AND BANK PROTECTION (cross references thereunder)
BAROMETERS
See SURVEYING INSTRUMENTS
BARS (alluvia)
"The Present Status of Research on Sediment Transport," Ning Chien (with discussion), 833.
BASINS, FLOCCULATION
See FLOCCULATION BASINS (cross references thereunder)
BASINS, SETTLING (water supply)
See SETTLING BASINS
BASINS, STILLING
See WATER, FLOW OF, OVER DAMS AND WEIRS
BEAMS (General)
See also BUCKLING; GIRDERS; STRESS AND STRAIN—Beams (General); STRUCTURES, THEORY OF—Beams and Girders (General); *see also* under material, structure or structural part
"Beam Restraints Provided by Walls with Openings," Ibrahim A. Mohammed and Egor P. Popov, 1034.
"Design of Aluminum Alloy Beam-Columns," Harry N. Hill and Ernest C. Hartmann and John W. Clark (with discussion), 1.
"Lateral Buckling of Cantilevered I-Beams under Uniform Load," Stanley Poley, 786.
"Nonuniform Torsion of Plate Girders," Gerald G. Kubo, Bruce G. Johnston and William J. Eney (with discussion), 759.
Bibliography
Aluminum alloy beam-columns, 12.
BEAMS, CONTINUOUS
See also BRIDGES; STRESS AND STRAIN—Beams, Continuous; STRUCTURES, THEORY OF—Beams and Girders, Continuous; STRUCTURES, THEORY OF—Frames, Continuous
"Continuous Prestressing," Robert B. B. Moorman (with discussion), 814.
"Numerical Analysis of Frames with Curved Girders," James Michalos (with discussion), 521.
BEARING CAPACITY (foundations, rocks, soils)
For more general interpretation *see* cross references under LOAD
"Increasing the Load-Carrying Capacities of Subgrades," Charles M. Noble (with discussion), 544.
"Pile-Loading Tests, Morganza Floodway Control Structure," Charles I. Mansur and John A. Focht, Jr. (with discussion), 555.
BED LOAD
See CANALS (cross references thereunder); CHANNELS; SILT AND SILTING . . . ; WATER, FLOW OF, IN OPEN CHANNELS
BENDING
See BUCKLING; MOMENTS; STRESS AND STRAIN; *also* under relative structure, structural part or material, e.g., BEAMS; PILES AND PILE DRIVING

BIBLIOGRAPHY
See subheading Bibliography under relative subject. (Comprehensive bibliographical footnotes existing in individual papers in which books and other material are cited)

BIOGRAPHIES OF DECEASED MEMBERS
See cross reference under MEMOIRS OF DECEASED MEMBERS. (*See also* p. 1411)

BITUMEN
See PAVEMENT AND PAVING, BITUMINOUS

BLAST, ATOMIC
See ATOMIC BLAST

BOGS
See MARSHES; PEAT

BOILERHOUSES
See POWER PLANTS

BOILER PLATE
See IRON (cross references thereunder); PLATES

BOLTED JOINTS
See JOINTS (General)

BOLTS
See JOINTS

BORINGS
See also DRILLS AND DRILLING
Geological section described for two pile driving sites, 699, 700.

BOUNDARY LAYER, THEORY OF (fluid flow)
See FLUIDS, FLOW OF (cross reference thereunder); LIQUIDS, FLOW OF; WATER, FLOW OF . . .

BRIDGE CABLES
"An Influence-Line Analysis for Suspension Bridges," David J. Peery (with discussion), 463.

BRIDGE FLOORS AND FLOORING
"Moments and Deflections in Steel-Grid Bridge Floors," Herbert J. Greenberg, 410. *Discussion:* Kuang-Han Chu, Fu-Kuei Chang, and Herbert J. Greenberg, 426.
Usable formulas for designing steel grid highway bridge floors, 410.

BRIDGES (General)
See also BEAMS . . . ; COLUMNS; GIRDERS; PILES AND PILE DRIVING; STRUCTURES, THEORY OF—Bridges; TRUSSES, STIFFENING; VIBRATION; WATER, FLOW OF, IN OPEN CHANNELS

BRIDGES, ARCH
See STRUCTURES, THEORY OF—Bridges

BRIDGES, GIRDER
"Wind Loads on Girder Bridges," John M. Biggs, Saul Namyet and Jiro Adachi, 101.

BRIDGES, SUSPENSION
"An Influence-Line Analysis for Suspension Bridges," David J. Peery, 463. *Discussion:* Nan-sze Sih, Jacob Karol, Harry M. Palmbaum, Vincenzo Franciosi, and David J. Peery, 481.

BUBBLES
See VISCOSITY

BUCKLING
"Design of Aluminum Alloy Beam-Columns," Harry N. Hill and Ernest C. Hartmann and John W. Clark (with discussion), 1.
"Lateral Buckling of Cantilevered I-Beams under Uniform Load," Stanley Poley, 786.
"Lateral Buckling of Eccentrically Loaded I-Columns," Mario G. Salvadori, 1163.
Bibliography
Failure due to specific types of buckling in aluminum alloy beam-columns, 12.

BUILDING (process)
See CONSTRUCTION

BUILDING MATERIALS
See MATERIALS OF CONSTRUCTION

BUILDINGS
See also CHIMNEY AND FLUE . . . ; COSTS . . . ; EARTHQUAKES; FAILURES . . . ; FOUNDATIONS . . . ; MATERIALS OF CONSTRUCTION; STRENGTH OF MATERIALS; STRESS AND STRAIN . . . ; STRUCTURES . . . ; VIBRATION; *also* under type of building, e.g., WAREHOUSES
"Beam Restraints Provided by Walls with Openings," Ibrahim A. Mohammed and Egor P. Popov, 1034.
Blast resistant design for diffraction type, drag type, and partly open buildings, 51, 52, 63, 64.
Pittsburgh comprehensive improvement program, 885.

BUILDINGS (*Continued*)

Financing

Financing the Pittsburgh auditorium and other structures, 895, 897.

BUSES

See MOTOR BUSES (cross reference thereunder)

BUTTRESS DAMS

See DAMS, BUTTRESS

CABLES, BRIDGE

See BRIDGE CABLES

CADASTRAL SURVEYS AND SURVEYING

See SURVEYS AND SURVEYING, GEODETIC

CANALS (General)

See IRRIGATION CANALS; SEDIMENT AND SEDIMENTATION; SILT AND SILTING, CHANNEL; WATER, FLOW OF, IN OPEN CHANNELS; WATER TRANSPORTATION (cross references thereunder); WATERWAYS (General) (cross references thereunder); WAVES

CANALS, IRRIGATION

See IRRIGATION CANALS

CANTILEVER BEAMS

See BEAMS (General)

CAPITALISM

See PRIVATE ENTERPRISE

CARRIERS

See AIRCRAFT; MOTOR . . . ; RAIL . . . (cross references thereunder); TRANSPORTATION (cross references thereunder); WATER...

CARS

See AUTOMOBILE . . . ; MOTOR . . . ; TRAFFIC . . . ; WHEEL LOADS

CARTOGRAPHY

See CHARTS (cross references thereunder); MAPS AND MAPPING . . . ; SURVEYS AND SURVEYING

CAR WHEELS

See WHEEL LOADS

CAST IRON

See CORROSION AND PROTECTION OF METALS; STEEL (cross references thereunder)

CHANNEL BANKS AND BANK PROTECTION

See WATER, FLOW OF, IN OPEN CHANNELS; WAVES

CHANNEL RECTIFICATION

See BARS (alluvia); CHANNELS; DIKES; IRRIGATION CANALS; WATER DIVERSION; WATER, FLOW OF, IN OPEN CHANNELS

CHANNELS (waterways)

See also HYDRAULIC JUMP; RIVERS; SILT AND SILTING, CHANNEL; WATER DIVERSION; WATER, FLOW OF, IN OPEN CHANNELS; WATER POLLUTION

Channel characteristics at certain river junctions and under specific conditions, 1274, 1276, 1277, 1278.

"Graphic Design of Alluvial Channels," Ning Chien, 1267. *Discussion:* Thomas Blench, Emory W. Lane, and Ning Chien, 1281.

Results of experiment with self-aerated flow in a sloping channel, 30.

"River Surveys in Unmapped Territory," Gerard H. Matthes (with discussion), 739.

"Verification of Theory for Oblique Standing Waves," Arthur T. Ippen and Donald R. F. Harleman, 678.

CHARTS

See GRAPHICAL CHARTS (cross references thereunder); HYDROGRAPHS; *see also* MAPS AND MAPPING . . . ; *also* under relative subject

CHEMISTRY

See under relative technical subject, e.g., CORROSION AND PROTECTION OF METALS; PUBLIC HEALTH

CHIMNEY AND FLUE LININGS

Damping effects of a gunite lining, 1059, 1067.

Severe cracking related to continued vibration with variance in amplitudes, assuming damping exists, 1106.

Vibrations in gunite lined and unlined stacks described, 1091, 1097, 1101, 1107.

CHIMNEYS AND FLUES

See also COSTS, CHIMNEY AND FLUE; FAILURES, CHIMNEY AND FLUE; FOUNDATIONS, CHIMNEY AND FLUE; STRESS AND STRAIN—Chimneys and Flues; STRUCTURES, THEORY OF—Chimneys and Flues

Power plant boilerhouse stack vibration problem, 266.

CHIMNEYS AND FLUES (*Continued*)

"Resonant Vibration of Steel Stacks," Ernest A. Dockstader, William F. Swiger and Emory Ireland, 1088. *Discussion:* Cedric Marsh; and Ernest A. Dockstader, William F. Swiger and Emory Ireland, 1110.

"The Vibrations of Steel Stacks," Walter L. Dickey and Glenn B. Woodruff, 1054. *Discussion:* Richard Jenney; George S. Vincent; John N. Pirok; Frederick B. Farquharson; W. Watters Pagon; Robert H. Sherlock; and Walter L. Dickey and Glenn B. Woodruff, 1071.

CHUTES, WATER FLOW THROUGH

See SPILLWAYS; WATER, FLOW OF, IN OPEN CHANNELS

CITIES

See AIRPORTS; AIR SANITATION; AUTOMOBILE PARKING; BUILDINGS; CITY PLANNING; COSTS . . . ; DOCKS AND WHARVES (cross references thereunder); EMPLOYEES AND EMPLOYMENT; FREIGHT; GAS AND GASWORKS; GOVERNMENT; INDUSTRIAL . . . ; ODORS; PARKING . . . (cross reference thereunder); PUBLIC HEALTH; REFUSE DISPOSAL; REGIONAL PLANNING; SEWAGE . . . ; STREET . . . ; TERMINALS (cross references thereunder); TRAFFIC . . . ; WATER FRONT (cross references thereunder); WATER SUPPLY (cross references thereunder); *also* geographical subheadings under relative subject, e.g., HARBORS—New York, N. Y.

CITY PLANNING (General)

See also HIGHWAYS AND ROADS; STREETS; TRAFFIC, STREET

"Metropolitan Traffic and Transportation Planning," Charles A. Blessing, 135.

CITY PLANNING (Geographical)

Pittsburgh, Pa.

"Pittsburgh's Comprehensive Improvement Program," Park H. Martin, 885.

CIVIL ENGINEERS AND ENGINEERING

See AMERICAN SOCIETY OF CIVIL ENGINEERS; ENGINEERS AND ENGINEERING (and cross references thereunder)

CLASSIFICATION OF SOILS

See SOILS—Classification

CLAY

See also SOILS

"Effect of Sample Disturbance on the Strength of a Clay," Max L. Calhoon (with discussion), 925.

"Engineering Properties of Expansive Clays," Wesley G. Holtz and Harold J. Gibbs, 641. *Discussion:* Raymond F. Dawson; William T. Altmeyer; Edward S. Barber; Lawrence A. DuBose; and Wesley G. Holtz and Harold J. Gibbs, 664.

"Pile-Loading Tests, Morganza Floodway Control Structure," Charles I. Mansur and John A. Focht, Jr. (with discussion), 555.

COAGULANTS AND COAGULATION

See SEWAGE SLUDGE

COAST

See SEACOAST (cross references thereunder)

COLUMNS

See also BUCKLING; STRESS AND STRAIN—Columns; STRUCTURES, THEORY OF—Columns

"Design of Aluminum Alloy Beam-Columns," Harry N. Hill and Ernest C. Hartmann and John W. Clark, 1. *Discussion:* Robert B. McCalley, Jr., Herbert A. Sawyer, Jr.; and Harry N. Hill, Ernest C. Hartmann, and John W. Clark, 15.

Bibliography

Aluminum alloy beam-columns, 12.

COMMERCE

See AIRPORTS; AIR TRANSPORT; CANALS (cross references thereunder); CHANNELS; CITIES (cross references thereunder); DOCKS AND WHARVES (cross references thereunder); FREIGHT; HARBORS; RAILROAD . . . (cross references thereunder); RIVERS; TERMINALS (cross references thereunder); TRANSPORTATION (cross references thereunder); and other relative subject headings

COMMUNICATION

See TRANSPORTATION (cross references thereunder)

COMPACTION

See BEARING CAPACITY

COMPRESSION

See STRESS AND STRAIN

COMPRESSION MEMBERS
See COLUMNS

COMPRESSION TESTS, SOIL
See SOILS—Tests and Testing

COMPUTERS, ELECTRONIC
See ELECTRONIC INSTRUMENTS

CONCRETE (General)
See also FAILURES, CONCRETE; PAVEMENT AND PAVING, CONCRETE; SAND; SLABS; STRESS AND STRAIN—Concrete; STRUCTURES, THEORY OF—Concrete, Reinforced; *also* under special structure or structural part, e.g., DAMS, MASONRY AND CONCRETE

Cracks and Cracking
"Economy and Safety of Concrete Dams," August E. Komendant (with discussion), 899.
"Thicknesses of Concrete Pavements for Highways," Joseph H. Moore (with discussion), 1125.

Design
"Beam Restraints Provided by Walls with Openings," Ibrahim A. Mohammed and Egor P. Popov, 1034.

Expansion and Contraction
"Thicknesses of Concrete Pavements for Highways," Joseph H. Moore (with discussion), 1125.

Placing
Method used for leaf spring shell type dams resulting in quicker filling of basin, 917, 924.

Prestressing. *See* CONCRETE, PRESTRESSED

Slabs. *See* SLABS

Temperature
"Economy and Safety of Concrete Dams," August E. Komendant (with discussion), 899.
"The Effect of Jet Aircraft on Airport Pavements," Gayle McFadden, 172.
"Thicknesses of Concrete Pavements for Highways," Joseph H. Moore (with discussion), 1125.

Tests and Testing
"Safety and the Probability of Structural Failure," Alfred M. Freudenthal (with discussion), 1337.

CONCRETE DAMS
See DAMS, MASONRY AND CONCRETE

CONCRETE HIGHWAYS AND ROADS
See HIGHWAYS AND ROADS, CONCRETE

CONCRETE—METAL
See cross reference under REINFORCED CONCRETE

CONCRETE PAVEMENT AND PAVING
See PAVEMENT AND PAVING, CONCRETE

CONCRETE, PRESTRESSED
"Continuous Prestressing," Robert B. B. Moorman, 814. *Discussion:* Abdel F. Diwan, Leopold J. Mensch, and Robert B. B. Moorman, 826.
"The Design of Two Steam Electric Plants," Walter L. Dickey, 253.

CONCRETE, REINFORCED
See CONCRETE . . .

CONDEMNATION, PROPERTY
See RIGHTS OF WAY (land strips)

CONNECTORS AND CONNECTIONS
See JOINTS . . .

CONSOLIDATION, TESTS, SOIL
See SOILS—Tests and Testing

CONSTRUCTION
See also BUILDINGS; CONTRACTORS AND CONTRACTING; COSTS . . . ; FAILURES . . . ; MATERIALS OF CONSTRUCTION; SOILS—Construction; SPECIFICATIONS (cross reference thereunder); STRESS AND STRAIN . . . ; STRUCTURES, THEORY OF . . . ; *also* under type of construction, e.g., DAMS, MASONRY AND CONCRETE; PIPE LINES
"Vertical Sand Drains for Stabilizing Muck-Peat Soils," J. C. Carpenter and Edward S. Barber (with discussion), 188.

CONSTRUCTION MATERIALS
See MATERIALS OF CONSTRUCTION

CONTAMINATION, STREAM
See WATER POLLUTION

CONTINUOUS BEAMS
See BEAMS, CONTINUOUS

CONTINUOUS FRAMES
See COSTS, FRAME; STRUCTURES, THEORY OF—Frames, Continuous; *see also* BEAMS . . . ; COLUMNS; GIRDERS

CONTINUOUS GIRDERS
See GIRDERS, CONTINUOUS (cross references thereunder)

CONTINUOUS STRUCTURES
See STRUCTURES, THEORY OF

CONTRACTION
See under relative subject, e.g., CLAY; WATER, FLOW OF, IN OPEN CHANNELS

CONTRACTORS AND CONTRACTING
See also ENGINEERS AND ENGINEERING
Maps and materials furnished by reservoir contractors, 516.

CONVENTIONS (American Society of Civil Engineers)
See AMERICAN SOCIETY OF CIVIL ENGINEERS—Addresses

CONVEYERS AND CONVEYANCE
See under usage

CORROSION AND PROTECTION OF METALS
"Corrosion and Corrosion Research," Thomas R. Camp, 791. *Discussion:* Edward W. Moore, and Thomas R. Camp, 811.

COSTS (General)
See also subheading Financing under relative subject

COSTS (of work)
See COSTS . . .

COSTS, AIR SANITATION
Smoke control costs in Pittsburgh, Pennsylvania, 888.

COSTS, AUTOMOBILE PARKING
Municipal parking costs, 170.

COSTS, CHIMNEY AND FLUE
Economical steel and concrete smokestack design procedures, 1068, 1072.

COSTS, DAM
"Economy and Safety of Concrete Dams," August E. Komendant (with discussion), 899.
Leaf spring shell type dams as related to construction costs and time required, 899, 918, 922, 923, 924.
Most economical type of arch dam, 903, 922.
Steel dam advantages and disadvantages compared with concrete dams, 923.

COSTS, FOUNDATION . . .
Usage of bent (dog leg) piles as related to savings in foundation costs, 716.

COSTS, FRAME
Multiple span frames regarded economical and efficient, 1288, 1289, 1297.

COSTS, HIGHWAY AND ROAD
Penn-Lincoln Parkway and other projects in Pittsburgh area, 894.

COSTS, INDUSTRIAL WASTE
Air filters commercially developed for use in radioactive waste treatment, 93.

COSTS, PAVEMENT AND PAVING
Slab thickness and subgrade bearing power as they relate to cost, 1148, 1151.

COSTS, PILE AND PILE DRIVING
Salvaging of dog leg (curved) steel encased and pipe piles in relation to cost and time consumed, 697, 702, 715, 716.

COSTS, PIPE LINE
Location surveys in relation to construction costs, 133.
Modern and former costs of oil transport compared, 1117.

COSTS, POWER PLANT
Cost of certain California power plants, 256.

COSTS, REFUSE DISPOSAL
Means of reducing municipal collection and treatment costs, 273.

COSTS, RESERVOIR (MULTIPURPOSE RESERVOIRS)
Planning and designing procedures economically compared, 511, 519.

COSTS, RETAINING WALL
Most economical type of wall, 271, 272.

COSTS, SPILLWAY
Morning glory type spillway in relation to cost, 314, 405.

COSTS, TRANSPORTATION
One-way and two-way street costs compared, 22, 23, 25.

COUNTY PLANNING
See REGIONAL PLANNING

CRACKS AND CRACKING
See under relative subject, e.g., CLAY; CONCRETE—Cracks and Cracking

CREEP
See STRESS AND STRAIN

CURRENT METERS
See METERS AND METERING, CURRENT

CURRENTS
See WATER . . .

CURVED GIRDERS
See GIRDERS, CONTINUOUS (cross references thereunder)

CURVES (design curves)
See relative subject of design, e.g., CHANNELS

CURVES (elastic curves)
See STRUCTURES, THEORY OF

CUTOFFS, TRANSPORTATION
See RIVERS

CYLINDRICAL SHELLS
See CHIMNEYS AND FLUES; STRESS AND STRAIN—Shell Structures; STRUCTURES, THEORY OF—Shell Structures

DAMPING
See also STRESS AND STRAIN; STRUCTURES, THEORY OF
Details of friction type damper system, 1099.
"Resonant Vibration of Steel Stacks," Ernest A. Dockstader, William F. Swiger and Emory Ireland (with discussion), 1088.

DAMS (General)
See also COSTS, DAM; MODELS, HYDRAULIC; RESERVOIRS; SPILLWAYS; STRESS AND STRAIN—Dams (General); WATER, FLOW OF, OVER DAMS AND WEIRS; WATER PRESSURE
Dam types used (1956) in the United States and foreign countries, 899.
Safety
"Economy and Safety of Concrete Dams," August E. Komendant (with discussion), 899.

DAMS, ARCH
See STRESS AND STRAIN—Dams, Arch

DAMS, BUTTRESS
Economy and safety of buttress dams for flat valleys, 918.

DAMS, CONCRETE
See DAMS, MASONRY AND CONCRETE

DAMS, GRAVITY
See DAMS, MASONRY AND CONCRETE

DAMS, MASONRY AND CONCRETE
See also STRESS AND STRAIN—Dams. Masonry and Concrete; WATER PRESSURE
"Economy and Safety of Concrete Dams," August E. Komendant, 899. *Discussion:* Jaro J. Polivka, and August E. Komendant, 922.

DEFENSE
See NATIONAL DEFENSE (cross reference thereunder)

DEFINITIONS
See TERMINOLOGY

DEFLECTION RECORDING APPARATUS
"Safe Loads on Dog-Leg Piles," James D. Parsons and Stanley D. Wilson (with discussion), 695.

DEFLECTIONS
See MOMENTS; SIDESWAY (cross reference thereunder); SLOPE DEFLECTION; STRESS AND STRAIN; STRUCTURES, THEORY OF; VIBRATION; *also* under relative structure or structural part, e.g., BRIDGE FLOORS AND FLOORING; DAMS . . .

DEFORMATION
See FAILURES . . . ; STRESS AND STRAIN; STRUCTURES, THEORY OF; *also* under specific type of stress, e.g., TORSION; *also* under type of material; *also* under type of structure

DEFORMATION INSTRUMENTS
Slope indicator described for measuring the inclination of steel piling under water, 702.

DEFORMATION, THERMAL
See TEMPERATURE (cross reference thereunder)

DESIGN
See under relative subject, e.g., ATOMIC BLAST; BEAMS . . . ; CHANNELS; STRUCTURES, THEORY OF

DESIGN ANALYSIS
See under relative subject, e.g., CONCRETE—Design; STRUCTURES, THEORY OF

DESIGN CURVES
See CURVES (design curves) (cross reference thereunder)

DIAGRAMS
See under relative subject

DIFFUSER FLOW
See WATER, FLOW OF, THROUGH ORIFICES

DIKES
See also EMBANKMENTS
"The Box Inlet Drop Spillway and Its Outlet," Fred W. Blaisdell and Charles A. Donnelly (with discussion), 955.

DISCHARGE
See METERS AND METERING, CURRENT; WATER, FLOW OF . . .

DISCHARGE COEFFICIENTS
See under relative subject, e.g., SPILLWAYS; WATER, FLOW OF . . .

DISEASE
See PUBLIC HEALTH

DISINTEGRATION OF MATERIALS
See CORROSION AND PROTECTION OF METALS; *also* under type of material

DISTORTION
See STRESS AND STRAIN; TORSION

DIVERSION
See WATER DIVERSION

DOCKS AND WHARVES
See HARBORS; PILES AND PILE DRIVING; WATER TERMINALS

DRAINAGE
See WELLS; *also* under type of drainage, e.g., HIGHWAYS AND ROADS—Drainage

DRAIN WELLS
See WELLS

DRAWINGS
See under relative subject

DRILLS AND DRILLING
See also BORINGS
"Vertical Sand Drains for Stabilizing Muck-Peat Soils," J. C. Carpenter and Edward S. Barber (with discussion), 188.

DROP-DOWN
See SPILLWAYS

DROP STRUCTURES
See DAMS

DYNAMICS OF FLUIDS
See HYDRODYNAMICS

DYNAMICS OF GASES
See AERODYNAMICS

DYNAMICS OF HEAT
See THERMODYNAMICS

DYNAMICS OF STRUCTURES
See STRUCTURAL DYNAMICS

EARTH . . .
See also GROUND . . . (cross references thereunder); LAND . . . (cross references thereunder); SOIL . . .

EARTH MOVEMENTS
See EARTHQUAKES

EARTH PRESSURE
"Engineering Properties of Expansive Clays," Wesley G. Holtz and Harold J. Gibbs (with discussion), 641.
"Safe Loads on Dog-Leg Piles," James D. Parsons and Stanley D. Wilson (with discussion), 695.

EARTHQUAKES
See also VIBRATION
Power plant design problems in areas subjected to seismic disturbances, 259, 266.

EARTHS
See SOILS

EARTHWORK
See also EMBANKMENTS; FOUNDATIONS . . .
"Engineering Properties of Expansive Clays," Wesley G. Holtz and Harold J. Gibbs (with discussion), 641.
"Increasing the Load-Carrying Capacities of Subgrades," Charles M. Noble (with discussion), 544.

ECHO SOUNDINGS AND SOUNDING INSTRUMENTS
See SOUNDINGS AND SOUNDING INSTRUMENTS

ECONOMICS
See also COSTS . . . ; VALUATION; *also* under relative subject, subheading Financing
"Pittsburgh's Comprehensive Improvement Program," Park H. Martin, 885.
"Safety and the Probability of Structural Failure," Alfred M. Freudenthal (with discussion), 1337.

EDDIES
See WATER, FLOW OF, IN OPEN CHANNELS

EDUCATION
Education for civil engineers, 1401, 1404.
Training in biological and medical sciences for engineers in environmental health work, 224.

ELASTIC CURVES
See CURVES (elastic curves) (cross reference thereunder)

ELASTICITY
See also PLASTICITY; STRESS AND STRAIN
"Constant-Segment Method for Analysis of Nonuniform Members," Walter E. Hanson and Wallace F. Wiley (with discussion), 1317.
"Safety and the Probability of Structural Failure," Alfred M. Freudenthal (with discussion), 1337.

ELASTO-PLASTIC STRUCTURES
See also STRUCTURES, THEORY OF—Elasto-Plastic Structures
"An Engineering Approach to Blast-Resistant Design," Nathan M. Newmark (with discussion), 45.

ELECTRIC POWER (General)
See POWER PLANTS

ELECTROLYSIS
"Corrosion and Corrosion Research," Thomas R. Camp (with discussion), 791.

ELECTRONIC COMPUTERS
See ELECTRONIC INSTRUMENTS

ELECTRONIC INSTRUMENTS
"Analog Computers Applied to Elasto-Plastic Systems," Leo Schenker and Gunther Martin, 728. *Discussion:* John S. Archer and Allen Lange, 736.

EMBANKMENTS
See also DIKES; FOUNDATIONS, EMBANKMENT; SOILS
"Vertical Sand Drains for Stabilizing Muck-Peat Soils," J. C. Carpenter and Edward S. Barber (with discussion), 188.

EMPLOYEES AND EMPLOYMENT
The civil engineer graduate seeking his first position, 1405.
"Engineering Biotechnology in Occupational Health," Alvin F. Meyer, Jr., 205.
Personnel and average salary in pipe line companies, 1117.
Personnel problems of river survey operations in undeveloped foreign lands, 748.
Sources of occupational disease summarized by type, 210.
Bibliography
Occupational health and the engineer, 225.

ENERGY
See AERODYNAMICS; ATOMIC ENERGY; ELECTRIC POWER (cross reference thereunder); ENGINES (cross references thereunder); POWER; STRUCTURAL DYNAMICS; THERMODYNAMICS; WATER, FLOW OF, IN OPEN CHANNELS; WIND . . .

ENERGY, KINETIC
See DYNAMICS . . . (cross references thereunder)

ENERGY, LOSS OF
See FRICTION; HYDRAULIC JUMP; WATER, FLOW OF . . .

ENGINEERING
See ENGINEERS AND ENGINEERING

ENGINEERING AND WAR
See cross references under WAR AND ENGINEERING

ENGINEERING BIBLIOGRAPHY
See BIBLIOGRAPHY (cross references thereunder)

ENGINEERING EDUCATION
See EDUCATION

ENGINEERING GLOSSARIES
See TERMINOLOGY

ENGINEERING HISTORY
See ENGINEERS AND ENGINEERING—History; *also* under relative subject, e.g., SEDIMENT AND SEDIMENTATION; TIMBER STRUCTURES

ENGINEERING MECHANICS
See MECHANICS

ENGINEERING SOCIETIES
See SOCIETIES, TECHNICAL; *see also* AMERICAN SOCIETY OF CIVIL ENGINEERS

ENGINEERS AND ENGINEERING (General)
See also AMERICAN SOCIETY OF CIVIL ENGINEERS. (For memoirs of deceased members, *see* name of member in Author Index.) (*See also* p. 1411); ARCHITECTS AND ARCHITECTURE (cross reference thereunder); CONTRACTORS . . . ; EDUCATION; EMPLOYEES AND EMPLOYMENT; RESEARCH; SOCIETIES; TECHNICAL; TERMINOLOGY
The sanitary engineers' responsibility to the community, 206, 207, 211, 220, 221.
Shortage and supply statistics for civil engineers, 1956, 1406.

ENGINEERS AND ENGINEERING (General) (*Continued*)

History

"Our Exciting Profession": Address at the Summer Convention, Knoxville, Tenn., June 7, 1956, Enoch R. Needles, 1398.

Present and Future Trends

"Our Exciting Profession": Address at the Summer Convention, Knoxville, Tenn., June 7, 1956, Enoch R. Needles, 1398.

ENGINES

See LOCOMOTIVES; TURBINES

ENTRAINMENT, AIR

See WATER, FLOW OF . . .

EQUATIONS

See also under relative subject, e.g., WATER, FLOW OF . . .

"Analog Computers Applied to Elasto-Plastic Systems," Leo Schenker and Gunther Martin (with discussion), 728.

Apparatus for solving differential equations, 153, 162.

"Design of Aluminum Alloy Beam-Columns," Harry N. Hill and Ernest C. Hartmann and John W. Clark (with discussion), 1.

"Moments and Deflections in Steel-Grid Bridge Floors," Herbert J. Greenberg (with discussion), 410.

"The Octagonal-Girder Four-Column Space Frame," Paul C. Disario, Jr., John S. Podolan and Nicholas A. Weil (with discussion), 995.

ERECTION

See CONSTRUCTION

EROSION (General)

"Fundamental Concepts of Rectangular Settling Tanks," Alfred C. Ingersoll, Jack E. McKee and Norman H. Brooks (with discussion), 1179.

EROSION, TAIL WATER

"The Box Inlet Drop Spillway and Its Outlet," Fred W. Blaisdell and Charles A. Donnelly (with discussion), 955.

EVALUATION

See VALUATION

EXCAVATION

See EARTHWORK; FOUNDATIONS . . .

EXPANSION

See under relative subject, e.g., CLAY; CONCRETE (General)—Expansion and Contraction; WATER, FLOW OF, IN OPEN CHANNELS

EXPANSION JOINTS

See JOINTS, EXPANSION AND CONTRACTION

EXPERIMENTS AND EXPERIMENTATION

See LABORATORIES (cross references thereunder); MODELS . . . ; TESTS AND TESTING (cross references thereunder); *also* under material, structure, or structural part tested, e.g., CHIMNEYS AND FLUES; SPILLWAYS; *also* under relative subject, e.g., WAVES

EXPLORATION

See BORINGS; EXCAVATION (cross references thereunder); FOUNDATIONS . . . ; PILES AND PILE DRIVING

EXPLOSION, ATOMIC

See ATOMIC BLAST

FACT FINDING

See RESEARCH

FACTOR OF SAFETY

See under relative subject, e.g., LIMIT DESIGN, THEORY OF; STRUCTURES (General)—Safety

FAILURES (General)

See also BEARING CAPACITY; SAFETY (cross references thereunder); STRENGTH OF MATERIALS; STRESS AND STRAIN; STRUCTURES, THEORY OF . . . ; *also* under relative subject

Cumulative fatigue damage to structures described, 1353.

"Safety and the Probability of Structural Failure," Alfred M. Freudenthal, 1337. *Discussion:* Anthony Chibaro, Lloyd S. Lawrence, Jose M. Corso, Oliver G. Julian, Aiden R. Gierasch, and Alfred M. Freudenthal, 1376.

FAILURES, CHIMNEY AND FLUE

Power plant boilerhouse stack failure due to wind, 266.

FAILURES, CONCRETE

"Safety and the Probability of Structural Failure," Alfred M. Freudenthal (with discussion), 1337.

"Thicknesses of Concrete Pavements for Highways," Joseph H. Moore (with discussion), 1125.

FAILURES, PAVEMENT AND PAVING

"Thicknesses of Concrete Pavements for Highways," Joseph H. Moore (with discussion), 1125.

FAILURES, PILE
"Safe Loads on Dog-Leg Piles," James D. Parsons and Stanley D. Wilson (with discussion), 695.

FAILURES, TIMBER STRUCTURE
"Examples of Timber-Structure Failures," Michael N. Salgo, 588. *Discussion:* E. George Stern, Ralph H. Gloss, and Michael N. Salgo, 601.

FAILURES, TRUSS
"Examples of Timber-Structure Failures," Michael N. Salgo (with discussion), 588.

FASTENERS AND FASTENING
See CONNECTORS AND CONNECTIONS (cross references thereunder)

FATIGUE
See under relative subject, e.g., STRESS AND STRAIN—Joints; *see also* FAILURES

FILL, SETTLEMENT OF
See SOILS—Construction

FILTERS AND FILTRATION, WATER
See SETTLING BASINS

FINANCE
See COSTS . . . ; ECONOMICS; VALUATION; *see also* subheading Financing under relative subject, e.g., AUTOMOBILE PARKING—Financing; HIGHWAYS AND ROADS—Financing

FINITE DIFFERENCES, THEORY OF
See MATHEMATICS

FLANGES
See STRESS AND STRAIN—Flanges

FLEXURE
See STRESS AND STRAIN; STRUCTURES, THEORY OF

FLOCCULATION BASINS
See SETTLING BASINS (water supply); TANKS, SEDIMENTATION (sewage)

FLOOD HYDROGRAPHS
See HYDROGRAPHS, STREAM FLOW

FLOODS (General)
See also HYDROGRAPHS, STREAM FLOW; SPILLWAYS
"Morning-Glory Shaft Spillways": A Symposium, Joseph N. Bradley, William E. Wagner, and Alvin J. Peterka (with discussion), 311.

FLOODS (Geographical)
Heart River, N. Dak.
Heart River floods of 1950 and 1951, 385, 391, 403.
Morganza, La.
"Pile-Loading Tests, Morganza Floodway Control Structure," Charles I. Mansur and John A. Focht, Jr. (with discussion), 555.

FLOODWAYS
See FLOODS

FLOOR BEAMS
See BEAMS . . .

FLOORS AND FLOORING
See BRIDGE FLOORS AND FLOORING

FLOW
See AIR FLOW; DIFFUSER FLOW (cross reference thereunder); FLOODS; LIQUIDS, FLOW OF; TURBULENCE; UNDERFLOW (cross reference thereunder); WATER, FLOW OF . . .

FLOW, LAMINAR
See AIR FLOW; WATER, FLOW OF, IN OPEN CHANNELS

FLOW METERS
See METERS AND METERING

FLOW OF FLUIDS
See GAS AND GASWORKS; LIQUIDS, FLOW OF . . . ; WATER, FLOW OF . . .

FLOW OF LIQUIDS
See LIQUIDS, FLOW OF

FLOW OF OIL
See PIPE LINES

FLOW OF SOLIDS
See SOLIDS, FLOW OF (cross references thereunder)

FLOW OF WATER
See WATER, FLOW OF . . .

FLOW, SEPARATION OF
See WATER, FLOW OF, IN OPEN CHANNELS

FLUES
See CHIMNEYS AND FLUES

FLUID MECHANICS
See WATER, FLOW OF . . .

FLUIDS, DYNAMICS OF
See HYDRODYNAMICS

FLUIDS, FLOW OF
See GAS AND GASWORKS; LIQUIDS, FLOW OF . . . ; WATER, FLOW OF . . .

FLUMES
See also WATER, FLOW OF, IN OPEN CHANNELS
"Graphic Design of Alluvial Channels," Ning Chien (with discussion), 1267.
"The Present Status of Research on Sediment Transport," Ning Chien (with discussion), 833.

FLUVIAL MODELS
See MODELS, HYDRAULIC

FORMULAS
See under relative subject, e.g., BRIDGE FLOORS AND FLOORING; PILES AND PILE DRIVING; SEDIMENT AND SEDIMENTATION; SILT AND SILTING, CHANNEL

FOUNDATIONS (General)
See also BEARING CAPACITY; BORINGS; COSTS, FOUNDATION . . . ; EARTH PRESSURE; EARTHWORK; PILES AND PILE DRIVING; SOILS
Importance of safety and probability of failure in foundation engineering, 1383.

FOUNDATIONS, AIRPORT
"Increasing the Load-Carrying Capacities of Subgrades," Charles M. Noble (with discussion), 544.

FOUNDATIONS, CHIMNEY AND FLUE
Energy dissipation source in smokestacks found to be at the foundation, 1067.

FOUNDATIONS, EMBANKMENT
"Engineering Properties of Expansive Clays," Wesley G. Holtz and Harold J. Gibbs (with discussion), 641.

FOUNDATIONS, HIGHWAY AND ROAD
"Increasing the Load-Carrying Capacities of Subgrades," Charles M. Noble (with discussion), 544.

FOUNDATIONS, PILE
See PILES AND PILE DRIVING

FOUNDATIONS, POWERHOUSE
Unusual hull type foundations of Contra Costa steam electric station at Antioch, California, 257.

FOUNDATIONS, UNDERWATER
See also PILES AND PILE DRIVING
"Engineering Properties of Expansive Clays," Wesley G. Holtz and Harold J. Gibbs (with discussion), 641.

FRAMES, CONTINUOUS
See COSTS, FRAME; STRUCTURES, THEORY OF—Frames, Continuous; *see also* BEAMS . . . ; COLUMNS; GIRDERS

FRAMES, RIGID
See STRUCTURES, THEORY OF —Frames, Rigid

FRAMEWORKS
See STRUCTURES, THEORY OF

FREE ENTERPRISE
See PRIVATE ENTERPRISE

FREIGHT
See also MOTOR TRUCKS; WAREHOUSES
"Design of General Cargo Marine Terminals," Frank W. Herring, 433.

FRICTION
See also TURBULENCE
"Continuous Prestressing," Robert B. B. Moorman (with discussion), 814.
"Pile-Loading Tests, Morganza Floodway Control Structure," Charles I. Mansur and John A. Focht, Jr. (with discussion), 555.
"The Present Status of Research on Sediment Transport," Ning Chien (with discussion), 833.
"Research on Bolted Connections," William H. Munse, 1255.
"Similarity of Distorted River Models with Movable Beds," Hans A. Einstein and Ning Chien (with discussion), 440.

FRICTION PILES
See PILES AND PILE DRIVING

FUEL
See GAS AND GASWORKS; OIL . . . (cross references thereunder)

FURNACES
See INCINERATORS AND INCINERATION (cross reference thereunder)

GABLES
See FRAMES, CONTINUOUS (cross references thereunder)

GARBAGE DISPOSAL
See REFUSE DISPOSAL

GAS AND GASWORKS
See also PIPE LINES
"Pipeline Transportation in the United States," Eldon V. Hunt, 1113.

GAS DISTRIBUTION
See GAS AND GASWORKS

GASES, DYNAMICS OF
See AERODYNAMICS

GEODESY
"A Conformal and World-Wide Military Grid System," Floyd W. Hough, 633.

GEODETIC SURVEYS AND SURVEYING
See SURVEYS AND SURVEYING, GEODETIC

GEOGRAPHY
See under relative technical subject, e.g., MAPS AND MAPPING . . .

GIRDER BRIDGES
See BRIDGES, GIRDER

GIRDERS (General)
See also BEAMS; BRIDGES; CONNECTORS AND CONNECTIONS (cross reference thereunder); FLANGES (cross reference thereunder); STRESS AND STRAIN—Girders; STRUCTURES, THEORY OF—Beams and Girders
"Nonuniform Torsion of Plate Girders," Gerald G. Kubo, Bruce G. Johnston and William J. Eney (with discussion), 759.

GIRDERS, CONTINUOUS
See BRIDGES, GIRDER; STRUCTURES, THEORY OF—Beams and Girders, Continuous

GIRDERS, CURVED
See GIRDERS, CONTINUOUS (cross references thereunder)

GLOSSARIES
See TERMINOLOGY

GOVERNMENT
See also PRIVATE ENTERPRISE; PUBLIC . . . ; *also* LAW subject heading under related topic, e.g., WATER LAW
Municipal versus private enterprise automobile parking, 165, 167, 170, 171.

GRADES
See HIGHWAYS AND ROADS—Grades

GRADES, SUB-
See SUBGRADES (cross reference thereunder)

GRADING
See EARTHWORK

GRAPHICAL CHARTS
See HYDROGRAPHS . . . ; *also* under relative subject, e.g., PAVEMENT AND PAVING, CONCRETE

GRAVITY DAMS
See DAMS, MASONRY AND CONCRETE

GRID SYSTEMS (map projection)
See MAPS AND MAPPING, LAND

GRIDWORKS
See BRIDGE FLOORS AND FLOORING

GROUND . . .
See also EARTH . . . ; LAND . . . (cross references thereunder); SOIL . . .

GROUND MOVEMENTS
See EARTHQUAKES

GROUNDWORK
See EARTHWORK; FOUNDATIONS . . .

HANGARS
See also AIRPORTS
Multiple span frames regarded economical and efficient, 1288, 1289.

HARBORS (General)
See also CHANNELS; FREIGHT; PILES AND PILE DRIVING; WAREHOUSES; WATER POLLUTION; WATER TERMINALS; WATER TRANSPORTATION (cross references thereunder); WAVES

HARBORS (Geographical)

News York, N. Y.
"Design of General Cargo Marine Terminals," Frank W. Herring, 433.

San Francisco, Calif.
"Design of General Cargo Marine Terminals," Frank W. Herring, 433.

HEAD GATES
See INTAKES

HEAD, LOSS OF
See AERATION; FRICTION; WATER, FLOW OF . . .

HEALTH, PERSONAL
See EMPLOYEES AND EMPLOYMENT

HEALTH, PUBLIC
See PUBLIC HEALTH

HEAT AND HEAT TRANSMISSION
See THERMODYNAMICS

HEAT, DYNAMICS OF
See THERMODYNAMICS

HIGHWAY BRIDGE FLOORS
See BRIDGE FLOORS AND FLOORING

HIGHWAY BRIDGES
See BRIDGES

HIGHWAY ENGINEERS AND ENGINEERING
See HIGHWAYS AND ROADS; *see also* under relative subject

HIGHWAY GRADES
See HIGHWAYS AND ROADS—Grades

HIGHWAYS AND ROADS (General)
See also BRIDGE . . . ; COSTS, HIGHWAY AND ROAD; EARTHWORK; FOUNDATIONS, HIGHWAY AND ROAD; MOTOR . . . ; PAVEMENT AND PAVING . . . ; SOILS; STREET . . . ;TRAFFIC . . . ; WHEEL LOADS

Concrete Highways and Roads. *See* HIGHWAYS AND ROADS, CONCRETE

Costs. *See* COSTS, HIGHWAY AND ROAD

Drainage
"Increasing the Load-Carrying Capacities of Subgrades," Charles M. Noble (with discussion), 544.
"Thicknesses of Concrete Pavements for Highways," Joseph H. Moore (with discussion), 1125.

Financing
Pittsburgh area highway financing, 897.

Foundations. *See* FOUNDATIONS, HIGHWAY AND ROAD

Grades
"Increasing the Load-Carrying Capacities of Subgrades," Charles M. Noble (with discussion), 544.

Roadbeds. *See* SOILS

HIGHWAYS AND ROADS (Geographical)

Pittsburgh, Pa.
Pittsburgh region highway program, 894.

HIGHWAYS AND ROADS, CONCRETE
"Thicknesses of Concrete Pavements for Highways," Joseph H. Moore (with discussion), 1125.

HINGES
See JOINTS

HISTORY, ENGINEERING
See ENGINEERS AND ENGINEERING—History; *also* under relative subject, e.g., SEDIMENT AND SEDIMENTATION; TIMBER STRUCTURES

HOSE
See under relative technical subject, e.g., WATER, FLOW OF . . .

HOUSES (places of abode)

Drainage. *See* PIPES AND PIPING (cross references thereunder)

HYDRAULIC JUMP
See also WATER, FLOW OF . . .
"Morning-Glory Shaft Spillways": A Symposium, Joseph N. Bradley, William E. Wagner, and Alvin J. Peterka (with discussion), 311.
"Verification of Theory for Oblique Standing Waves," Arthur T. Ippen and Donald R. F. Harleman, 678.

HYDRAULIC MODELS
See MODELS, HYDRAULIC

HYDRAULICS
See AERATION; CANALS (cross references thereunder); CHANNEL . . . ; COSTS . . . ;DAMS . . . ; DIKES; DOCKS AND WHARVES (cross references thereunder); DRAINAGE (cross references thereunder); EROSION . . . ; FAILURES . . . ; FILTERS AND FILTRATION . . . (cross reference thereunder); FLOOD . . . ; FLOW . . . (cross references thereunder); FLUID . . . (cross references thereunder); FLUMES; FOUNDATIONS . . . ; FRICTION . . . ; HARBORS; HEAD GATES (cross reference thereunder); HYDRAULIC . . . ; HYDRO- . . . ; INTAKES; IRRIGATION . . . ; LIQUIDS, FLOW OF; METERS AND METERING . . . ; MODELS, HYDRAULIC; PILES AND PILE DRIVING; PIPE . . . ; RESERVOIRS . . . ; RETAINING WALLS; RIVER . . . ; SEDIMENT AND SEDIMENTATION; SEWAGE . . . ; SILT AND SILTING; SPILLWAYS; SPRINKLERS AND SPRINKLING; STILLING BASINS (cross reference thereunder); STRESS AND STRAIN . . . ; TANKS . . . ; TERMINOLOGY; TURBINES, WATER; TURBULENCE; VISCOSITY; WATER . . . ; WAVES; WELLS

HYDRAULIC STRUCTURES
See also under type of structure, e.g., DAMS; SPILLWAYS

HYDRAULIC STRUCTURES (*Continued*)
"Engineering Properties of Expansive Clays," Wesley G. Holtz and Harold J. Gibbs (with discussion), 641.

HYDRAULIC TURBINES
See TURBINES, WATER

HYDRODYNAMICS
"An Experimental Study of Bubbles Moving in Liquids," William L. Haberman and Rose K. Morton, 227. *Discussion:* John A. Roberson, Charles L. Barker, and Paul F. Ruff; and William L. Haberman and Rose K. Morton, 251.
"Flow Expansion and Pressure Recovery in Fluids," Harald Tults, 65.
"A Physical Approach to Turbulent-Boundary-Layer Problems," Donald Ross (with discussion), 1219.
"Verification of Theory for Oblique Standing Waves," Arthur T. Ippen and Donald R. F. Harleman, 678.

HYDROELECTRIC POWER PLANTS
See POWER PLANTS

HYDROGRAPHS, RIVER
See HYDROGRAPHS, STREAM FLOW

HYDROGRAPHS, STREAM FLOW
Flood hydrograph for 1950, Heart River, North Dakota, 391, 393.

HYDROLOGY
See DRAINAGE; FLOODS; HYDROGRAPHS . . . ; MARSHES; RIVER . . . ; WATER . . .

HYDROMETRY
See WATER, FLOW OF . . .

INCINERATORS AND INCINERATION
See under type of disposal or type of waste, e.g., REFUSE DISPOSAL

INDUSTRIAL PLANTS
See also under specific type of plant, e.g., POWER PLANTS; WAREHOUSES; *also* cross references under WORKS
"Handling Atomic Energy Industry Wastes," Joseph A. Lieberman and Arthur E. Gorman, 85.
"Pittsburgh's Comprehensive Improvement Program," Park H. Martin, 885.

INDUSTRIAL SANITATION
"Engineering Biotechnology in Occupational Health," Alvin F. Meyer, Jr., 205.
Bibliography
Occupational health and the engineer, 225.

INDUSTRIAL WASTE
See also COSTS, INDUSTRIAL WASTE; ODORS; REFUSE DISPOSAL; SEWAGE SLUDGE; WATER POLLUTION—Industrial Waste Pollution
"Handling Atomic Energy Industry Wastes," Joseph A. Lieberman and Arthur E. Gorman, 85.

INDUSTRIAL WATER SUPPLY
See IRRIGATION; RESERVOIRS . . . ; WATER SUPPLY (cross references thereunder)

INDUSTRY
See under relative technical classification, e.g., PIPE LINES; *see also* EMPLOYEES AND EMPLOYMENT; *also* under type of industry or industrial plant, e.g., GAS AND GASWORKS; POWER PLANTS

INFILTRATION
See FLOODS

INFLUENCE CHARTS
See GRAPHICAL CHARTS (cross references thereunder)

INFLUENCE LINES
See MOMENTS

INSTRUMENTS
See METERS AND METERING . . . ; *also* under general types of instruments, e.g., DEFORMATION INSTRUMENTS; ELECTRONIC INSTRUMENTS; *also* under usage; *see also* cross references under specific type of instrument, e.g., BAROMETERS; *also* cross references under APPARATUS

INTAKES
"Morning-Glory Shaft Spillways": A Symposium, Joseph N. Bradley, William E. Wagner, and Alvin J. Peterka (with discussion), 311.

IRON
See CORROSION AND PROTECTION OF METALS; STEEL (cross references thereunder); *also* under structure or structural part

IRRIGATION (General)
See also SPRINKLERS AND SPRINKLING; WATER SUPPLY (General) (cross references thereunder)

IRRIGATION (Geographical)

California

"Unsteady Flow in Open-Type Pipe Irrigation Systems," Edward H. Taylor, Arthur F. Pillsbury, Thomas O. Ellis and George A. Bekey (with discussion), 143.

Eastern States

"Factors Influencing Irrigation in Humid Areas," Tyler H. Quackenbush, 179. *Discussion:* Alfred R. Golze, 186.

IRRIGATION CANALS

Design of irrigation canals, 1267, 1278.

IRRIGATION LAW

Status (1955) of irrigation water law, 184.

JETTIES

See WAVES

JOINTS (General)

See also STRESS AND STRAIN—Joints

"A Brief for Limit Design," George C. Ernst (with discussion), 605.

"Research on Bolted Connections," William H. Munse, 1255.

Slippage possibility and fatigue life in high strength bolted joints, 1257, 1262.

Superior behavior of high strength bolts ASTM-A 325, 1255.

Timber structure failures caused by bolt tightening operations, 592, 596, 601, 603.

JOINTS, BOLTED

See JOINTS (General)

JOINTS, EXPANSION AND CONTRACTION

"Thicknesses of Concrete Pavements for Highways," Joseph H. Moore (with discussion), 1125.

JUMP, HYDRAULIC

See HYDRAULIC JUMP

KINETIC ENERGY

See DYNAMICS . . . (cross references thereunder)

LABORATORIES

See under relative subject; *also* under material, structure or structural part tested, e.g., CLAY; SOILS; *also* under MODELS . . . ; TESTS AND TESTING (cross references thereunder)

LAMINAR FLOW

See AIR FLOW; WATER, FLOW OF, IN OPEN CHANNELS

LAND . . .

See also EARTH . . . ; GROUND . . . (cross references thereunder); MAPS AND MAPPING, LAND; MARSHES; SOIL . . . ; SURVEYS AND SURVEYING . . . ; VALUATION

LAND MAPS AND MAPPING

See MAPS AND MAPPING, LAND

LAND RECLAMATION

See IRRIGATION; MARSHES

LATERAL FORCES

See EARTHQUAKES; WIND . . .

LATERAL PRESSURE

See ATOMIC BLAST; DIKES; EARTH PRESSURE; WATER PRESSURE

LAW

See LAW subject heading under related topic, e.g., WATER LAW; *see also* GOVERNMENT

LIGHTING

See GAS AND GASWORKS

LIMIT DESIGN, THEORY OF

"A Brief for Limit Design," George C. Ernst, 605. *Discussion:* Abdel F. Diwan, and George C. Ernst, 620.

"Safety and the Probability of Structural Failure," Alfred M. Freudenthal (with discussion), 1337.

LININGS

See under relative type, e.g., CHIMNEY AND FLUE LININGS; *also* under relative subject

LIQUIDS, FLOW OF

See also VISCOSITY; WATER, FLOW OF . . .

"A Physical Approach to Turbulent-Boundary-Layer Problems," Donald Ross, 1219. *Discussion:* William D. Baines, James M. Robertson, William J. Bauer, and Donald Ross, 1241.

Bibliography

Turbulent boundary layer problems, 1238.

LOAD

See ATOMIC BLAST; BEARING CAPACITY; BUCKLING; EARTH PRESSURE; FAILURES . . . ; STRESS AND STRAIN; STRUCTURES, THEORY OF; VIBRATION; WATER PRESSURE; WHEEL LOADS; WIND PRESSURE; *also* under structure, structural member or part, e.g., BEAMS; PILES AND PILE DRIVING

LOAD, BED

See CANALS (cross references thereunder); CHANNELS; SILT AND SILTING . . . ; WATER, FLOW OF, IN OPEN CHANNELS

LOAD, SUSPENDED

See SEDIMENT AND SEDIMENTATION; SILT AND SILTING, CHANNEL

LOCOMOTIVES

Increase in locomotive weights, 25 year periods, 1829–1950, 724.

LOSS OF ENERGY

See FRICTION; HYDRAULIC JUMP; WATER, FLOW OF . . .

LOSS OF HEAD

See AERATION; FRICTION; WATER, FLOW OF . . .

LUMBER AND LUMBERING

See TIMBER AND TIMBERING

MACHINERY

See under usage, e.g., POWER PLANTS; *also* under specific type of machine, e.g., TURBINES, WATER

MAPS AND MAPPING (General)

See also SURVEYS AND SURVEYING; *also* under relative subject

Usage of topographic mapping in certain phases of reservoir planning, 511, 518.

MAPS AND MAPPING, AERIAL

"Aerial Surveys for Reservoir Planning," Francis J. Guscio (with discussion), 511.

"River Surveys in Unmapped Territory," Gerard H. Matthes (with discussion), 739.

"Surveys and Maps for Pipelines," George E. MacDonald (with discussion), 121.

MAPS AND MAPPING, LAND

"A Conformal and World-Wide Military Grid System," Floyd W. Hough, 633.

Elements of the Universal Polar Stereograph (UPS) projection reference system, 638.

United States Army adoption of standardized Universal Transverse Mercator (UTM) projection system, 633.

MARINE . . .

See WATER . . .

MARSHES

"Vertical Sand Drains for Stabilizing Muck-Peat Soils," J. C. Carpenter and Edward S. Barber (with discussion), 188.

MASONRY

See EARTHQUAKES

MATERIALS, CONVEYANCE OF

See CONVEYERS AND CONVEYANCE (cross reference thereunder)

MATERIALS OF CONSTRUCTION

See also ALUMINUM (cross references thereunder); CAST IRON (cross references thereunder); CLAY; CONCRETE; CORROSION AND PROTECTION OF METALS; COSTS . . . ; DISINTEGRATION OF MATERIALS (cross references thereunder); EARTHWORK; FAILURES . . . ; IRON (cross references thereunder); METALS (cross references thereunder); PEAT; PERMEABILITY OF MATERIALS (cross references thereunder); SAND; SOILS; STEEL (cross references thereunder); STRENGTH OF MATERIALS; STRESS AND STRAIN . . . ; STRUCTURES, THEORY OF; TIMBER . . . ; *see also* under usage, e.g., PIPE LINES

Estimating the ductility factor for blast resistant design, 59.

MATERIALS, PERMEABILITY OF

See PERMEABILITY OF MATERIALS (cross references thereunder)

MATERIALS, STRENGTH OF

See STRENGTH OF MATERIALS

MATERIALS, TESTING OF

See TESTS AND TESTING (cross references thereunder)

MATERIALS, WASTE

See cross references under WASTE DISPOSAL

MATHEMATICS

See also EQUATIONS; GRAPHICAL CHARTS (cross references thereunder); PROBABILITY, THEORY OF; *also* under relative subject

"Numerical Analysis of Frames with Curved Girders," James Michalos (with discussion), 521.

"Safety and the Probability of Structural Failure," Alfred M. Freudenthal (with discussion), 1337.

MATHEMATICS (*Continued*)

Use of theory of finite differences for solution of lateral buckling of cantilevered I-beams under uniform load, 786, 788.

MEASURING INSTRUMENTS

See METERS AND METERING; SOUNDING AND SOUNDING INSTRUMENTS; SURVEYING INSTRUMENTS; VIBRATION MEASURING INSTRUMENTS

MECHANICAL ENGINEERS AND ENGINEERING

See MECHANICS; *see also* under relative subject, e.g., AUTOMOBILE . . . ; MACHINERY (cross references thereunder); MOTOR . . . ; TURBINES, WATER

MECHANICS (General)

See also DYNAMICS . . . (cross references thereunder); FLUID . . . (cross references thereunder); HYDRAULIC . . . ; MATHEMATICS; STRENGTH OF MATERIALS; STRUCTURAL . . . ; STRUCTURES, THEORY OF; TESTS AND TESTING (cross references thereunder)

"An Experimental Study of Bubbles Moving in Liquids," William L. Haberman and Rose K. Morton (with discussion), 227.

MECHANICS, FLUID

See WATER, FLOW OF . . .

MECHANICS, SOIL

See SOILS

MEMBERS (ASCE)

See AMERICAN SOCIETY OF CIVIL ENGINEERS. (For memoirs of deceased members, *see* name of member in Author Index.) (*See also* p. 1411)

MEMBERS, COMPRESSION

See COLUMNS

MEMBERS, STRUCTURAL

See BEAMS . . . ; COLUMNS; GIRDERS . . . ; STRUCTURES, THEORY OF . . . ; *also* under name of material, e.g., CONCRETE; *also* under structure

MEMOIRS OF DECEASED MEMBERS

See name of member in Author Index. (*See also* p. 1411)

MERCHANT MARINE

See WATER TRANSPORTATION (cross references thereunder)

METAL PROTECTION

See CORROSION AND PROTECTION OF METALS

METALS

See ALLOYS; CORROSION AND PROTECTION OF METALS; MATERIALS OF CONSTRUCTION; REINFORCED CONCRETE (cross reference thereunder); STRUCTURES, THEORY OF . . . ; *also* under specific metal or its alloy, e.g., STEEL (cross references thereunder)

METERS AND METERING (General)

See also INSTRUMENTS (cross references thereunder); WEIRS (cross references thereunder)

"Studies of Air Entrainment in Open-Channel Flows," Lorenz G. Straub and Owen P. Lamb, 30.

METERS AND METERING, CURRENT

Determining river discharge measurements in absence of current meters in undeveloped regions, 741, 749, 755.

METERS AND METERING, WATER (stream velocity)

See METERS AND METERING, CURRENT

MILITARY ENGINEERS AND ENGINEERING

See under relative technical subject, e.g., AIRPORTS; MAPS AND MAPPING, LAND; SURVEYS AND SURVEYING, GEODETIC

MINERALS

See under relative technical subject, e.g., CLAY

MINES AND MINING

See BORINGS; DRILLS AND DRILLING; *also* under specific element, ore or substance, e.g., IRON (cross references thereunder)

MODELS, HYDRAULIC

"The Box Inlet Drop Spillway and Its Outlet," Fred W. Blaisdell and Charles A. Donnelly (with discussion), 955.

"Fundamental Concepts of Rectangular Settling Tanks," Alfred C. Ingersoll, Jack E. McKee and Norman H. Brooks (with discussion), 1179.

"Morning-Glory Shaft Spillways": A Symposium, Joseph N. Bradley, William E. Wagner, and Alvin J. Peterka (with discussion), 311.

MODELS, HYDRAULIC (*Continued*)
  "Similarity of Distorted River Models with Movable Beds," Hans A. Einstein and Ning Chien, 440. *Discussion:* Thomas Blench; and Hans A. Einstein and Ning Chien, 458.
  "Unsteady Flow in Open-Type Pipe Irrigation Systems," Edward H. Taylor, Arthur F. Pillsbury, Thomas O. Ellis and George A. Bekey (with discussion), 143.

MODELS, STRUCTURAL
  "The Design of Two Steam Electric Plants," Walter L. Dickey, 253.
  "Wind Loads on Girder Bridges," John M. Biggs, Saul Namyet and Jiro Adachi, 101.

MOISTURE
  See CLAY; SOILS

MOMENT DISTRIBUTION
  See MOMENTS; STRUCTURES, THEORY OF

MOMENTS
  See also STRESS AND STRAIN; STRUCTURES, THEORY OF
  "Constant-Segment Method for Analysis of Nonuniform Members," Walter E. Hanson and Wallace F. Wiley (with discussion), 1317.
  "An Influence-Line Analysis for Suspension Bridges," David J. Peery (with discussion), 463.
  "Lateral Buckling of Eccentrically Loaded I-Columns," Mario G. Salvadori, 1163.
  "Moments and Deflections in Steel-Grid Bridge Floors," Herbert J. Greenberg (with discussion), 410.
  "Numerical Analysis of Frames with Curved Girders," James Michalos (with discussion), 521.
  "The Octagonal-Girder Four-Column Space Frame," Paul C. Disario, Jr., John S. Podolan and Nicholas A. Weil (with discussion), 995.

MOMENTUM
  See WATER, FLOW OF . . .

MOTOR BUSES
  See TRAFFC . . .

MOTOR CARS
  See AUTOMOBILE . . . ; MOTOR . . . ; TRAFFIC . . . ; WHEEL LOADS

MOTOR TRAFFIC
  See TRAFFIC . . .

MOTOR TRANSPORTATION
  See STREET TRANSPORTATION

MOTOR TRUCKING
  See STREET TRANSPORTATION

MOTOR TRUCKS
  See also TRAFFIC . . . ; WHEEL LOADS
  Importance of truck development in relation to cargo water terminal design, 434, 435.

MOTOR VEHICLE ACCIDENTS
  See STREETS—Safety

MOTOR VEHICLES
  See TRAFFIC . . . ; WHEEL LOADS

MOTORWAYS
  See HIGHWAYS AND ROADS

MULTI-PURPOSE RESERVOIRS
  See RESERVOIRS, MULTI-PURPOSE

MUNICIPAL ENGINEERS AND ENGINEERING
  See ENGINEERS AND ENGINEERING; *see also* AIRPORTS; BRIDGES; CITY PLANNING; COSTS . . . ; FILTERS AND FILTRATION . . . (cross reference thereunder); HARBORS; PAVEMENT AND PAVING . . . ; POWER . . . ; SANITATION (cross references thereunder); WATER . . .

MUNICIPALITIES
  See CITIES (cross references thereunder)

NATIONAL DEFENSE
  See cross references under WAR AND ENGINEERING

NAVIGATION
  See CANALS (cross references thereunder); CHANNELS; DAMS; FLOODS; HARBORS; RIVERS; WATER TRANSPORTATION (cross references thereunder); WATERWAYS (cross references thereunder)

NAVIGATION, AIR
  See AIR TRANSPORT

NETWORKS
  See PIPE LINES

NOISE CONTROL
  See AIR TRANSPORT; POWER PLANTS

NOMENCLATURE
  See TERMINOLOGY

NONUNIFORM MEMBERS, STRUCTURAL

See MEMBERS, STRUCTURAL (cross references thereunder)

NUISANCES, ABATEMENT OF

See NOISE CONTROL (cross references thereunder); ODORS; PUBLIC HEALTH; SMOKE ABATEMENT (cross reference thereunder)

OBITUARIES OF MEMBERS

See name of member in Author Index. (*See also* p. 1411)

OCEAN . . .

See WAVES

ODORS

Odor reduction methods in refuse disposal processes, 273.

OIL, FLOW OF

See PIPE LINES

OIL STORAGE

See TANKS, OIL STORAGE

OPEN CHANNELS

See CHANNELS; WATER, FLOW OF, IN OPEN CHANNELS

ORDNANCE

See METALS (cross references thereunder)

ORGANIZATIONS

See SOCIETIES, TECHNICAL; *see also* AMERICAN SOCIETY OF CIVIL ENGINEERS

ORIFICES

See WATER, FLOW OF, THROUGH ORIFICES

OSCILLATION

See VIBRATION; WAVES

OSCILLOGRAPHS

See VIBRATION RECORDING APPARATUS

OXIDATION

See CORROSION AND PROTECTION OF METALS

PARKING REGULATIONS

See AUTOMOBILE PARKING

PAVEMENT AND PAVING (General)

See also COSTS, PAVEMENT AND PAVING; FAILURES, PAVEMENT AND PAVING; SOILS; WHEEL LOADS

"Increasing the Load-Carrying Capacities of Subgrades," Charles M. Noble, 544. *Discussion:* Eugene Y. Huang, and Charles M. Noble, 550.

PAVEMENT AND PAVING, ASPHALT

See PAVEMENT AND PAVING, BITUMINOUS

PAVEMENT AND PAVING, BITUMINOUS

"The Effect of Jet Aircraft on Airport Pavements," Gayle McFadden, 172.

PAVEMENT AND PAVING, CONCRETE

Airfield pavement strength standards, 722.

"The Effect of Jet Aircraft on Airport Pavements," Gayle McFadden, 172.

Importance of subgrade support in pavement life, 1125.

"Thicknesses of Concrete Pavements for Highways," Joseph H. Moore, 1125. *Discussion:* Lawrence A. Palmer, Earl C. Sutherland, Warner Harwood, Albert de Neufville, and Joseph H. Moore, 1143.

Usage of influence chart for aircraft loads, 726.

PEAT

"Vertical Sand Drains for Stabilizing Muck-Peat Soils," J. C. Carpenter and Edward S. Barber (with discussion), 188.

PEDOLOGY

See SOILS—Classification

PERMEABILITY OF MATERIALS

See CORROSION AND PROTECTION OF METALS; STRENGTH OF MATERIALS; *also* under type of material, e.g., CONCRETE; SOILS

PERSONNEL

See EMPLOYEES AND EMPLOYMENT

PETROLEUM

See OIL . . . (cross references thereunder)

PHOTOGRAMMETRY

See MAPS AND MAPPING, AERIAL; SURVEYS AND SURVEYING, AERIAL

PHOTOGRAPHY, AERIAL

See SURVEYS AND SURVEYING, AERIAL

PIERS (waterway structures)

See DOCKS AND WHARVES (cross references thereunder)

PILES AND PILE DRIVING

See also BEARING CAPACITY; COSTS, PILE AND PILE DRIVING; FAILURES, PILE; FOUN-

PILES AND PILE DRIVING (*Continued*)
DATIONS, UNDERWATER; STRESS AND STRAIN—Piles; TIMBER . . .
Dynamic pile driving formulas, 573, 575, 576.
Equipment devised to measure curvature underground of steel encased or pipe piles, 695.
Forces acting on a composite pile, 707.
Importance of safety and probability of failure in pile foundation engineering, 1383.
"Pile-Loading Tests, Morganza Floodway Control Structure," Charles I. Mansur and John A. Focht, Jr., 555. *Discussion:* John W. Dunham; Leroy D. Graves and James E. Binckley; James F. McNulty; and Charles I. Mansur and John A Focht, Jr., 577.
"Safe Loads on Dog-Leg Piles," James D. Parsons and Stanley D. Wilson, 695. *Discussion:* A. E. Cummings, and James D. Parsons and Stanley D. Wilson, 717.
Slope indicator for deflection measurements, 695, 702, 703.

PILLARS
See COLUMNS

PIPE LINES
See also COSTS, PIPE LINE; SPRINKLERS AND SPRINKLING; WATER, FLOW OF, IN PIPES
Early history of United States pipe line industry, 1113.
Pipe line construction materials and methods, 1122.
"Pipeline Transportation in the United States," Eldon V. Hunt, 1113.
"Surveys and Maps for Pipelines," George E. MacDonald, 121. *Discussion:* Norman E. Geuder, and George E. MacDonald, 133.
Total United States pipe line mileages, by state, for oil and gas, year 1953, 1114.
Bibliography
Pipe line industry, 1123.

PIPES AND PIPING (fluid conveyance)
See CORROSION AND PROTECTION OF METALS; PIPE LINES; WATER, FLOW OF, IN PIPES

PLANNING
See under type of planning, e.g., CITY PLANNING; *also* under relative subject, e.g., AIRPORTS; RESERVOIRS, MULTI-PURPOSE; STREETS (General)—Planning and Design

PLANTS (industrial buildings and equipment)
See INDUSTRIAL PLANTS; *see also* under type of plant, e.g., POWER PLANTS; *see also* WORKS (cross references thereunder)

PLASTICITY
See also ELASTICITY
"A Brief for Limit Design," George C. Ernst (with discussion), 605.
"Safety and the Probability of Structural Failure," Alfred M. Freudenthal (with discussion), 1337.

PLASTIC THEORY
See PLASTICITY

PLATE, BOILER
See IRON (cross references thereunder); PLATES

PLATE GIRDERS
See GIRDERS

PLATES
See also JOINTS; SLABS; STRUCTURES, THEORY OF—Plates
"Beam Restraints Provided by Walls with Openings," Ibrahim A. Mohammed and Egor P. Popov, 1034.
Formulas for simply supported plates subjected to concentrated moments and uniformly distributed moments, 1050.
Test apparatus for wall simulated by steel plate, 1039.

POLLUTION, AIR
See AIR SANITATION

POLLUTION, STREAM
See WATER POLLUTION

PORE WATER PRESSURE
See WATER PRESSURE

PORTS
See AIRPORTS; HARBORS

POWER (General)
See also DAMS; DYNA- . . . (cross references thereunder); ELECTRIC POWER (cross reference thereunder); ENGINES (cross references thereunder); FUEL (cross references thereunder); TOWERS;

POWER (General) (*Continued*)
TURBINES, WATER; WATER POWER (cross references thereunder)

POWER (Geographical)

United States

Energy consumption, with percentage statistics, in United States, in 1952, 1119.

POWERHOUSES

See POWER PLANTS

POWER PLANTS (General)

See also CHIMNEYS AND FLUES; COSTS, POWER PLANT; FOUNDATIONS, POWERHOUSE; STRUCTURES, THEORY OF—Power Plants; TURBINES, WATER

Equipment vibrations as cause of objectionable noises, 1153.

"Vibration in Hydroelectric Power Plants," Samuel Judd, 1153.

POWER PLANTS (Geographical)

California

"The Design of Steam Electric Plants," Walter L. Dickey, 253.

"Resonant Vibration of Steel Stacks," Ernest A. Dockstader, William F. Swiger and Emory Ireland (with discussion), 1088.

"The Vibrations of Steel Stacks," Walter L. Dickey and Glenn B. Woodruff (with discussion), 1054.

United States

"The Vibrations of Steel Stacks," Walter L. Dickey and Gleen B. Woodruff (with discussion), 1054.

PRESERVATION OF . . .

See CORROSION AND PROTECTION OF . . .

PRESIDENTIAL ADDRESSES (American Society of Civil Engineers)

See AMERICAN SOCIETY OF CIVIL ENGINEERS—Addresses; *see also* under subject of address

PRESSURE

See EARTH PRESSURE; LATERAL PRESSURE (cross references thereunder); STRESS AND STRAIN; WATER PRESSURE; WIND PRESSURE

PRESTRESSED CONCRETE

See CONCRETE, PRESTRESSED

PRIME MOVERS

See ENERGY (cross references thereunder); POWER

PRINCIPLE OF SUPERPOSITION

See STRUCTURES, THEORY OF

PRINCIPLE OF VIRTUAL WORK

See VIRTUAL WORK, PRINCIPLE OF

PRIVATE ENTERPRISE

See also GOVERNMENT

"Private Enterprise Can Satisfy the Parking Demand," Charles T. McGavin, 165.

PROBABILITY, THEORY OF

"Safety and the Probability of Structural Failure," Alfred M. Freudenthal (with discussion), 1337.

PROPERTY (landed property)

See LAND . . . ; RIGHTS OF WAY (land strips); STREETS (General)—Planning and Design; SURVEYS AND SURVEYING; VALUATION

PROPERTY CONDEMNATION

See RIGHTS OF WAY (land strips)

PROTOTYPES AND MODELS

See MODELS

PUBLIC HEALTH

See also EDUCATION; SANITATION (cross references thereunder); WATER SUPPLY (cross references thereunder)

Chemical hazards classified, 218.

"Engineering Biotechnology in Occupational Health," Alvin F. Meyer, Jr., 205.

"Handling Atomic Energy Industry Wastes," Joseph A. Lieberman and Arthur E. Gorman, 85.

Bibliography

Occupational health and the engineer, 225.

PUBLIC HEALTH ENGINEERS AND ENGINEERING

See PUBLIC HEALTH

PUBLIC SERVICES

See CITIES (cross references thereunder); GOVERNMENT; *see also* under type of service, e.g., REFUSE DISPOSAL

PUBLIC UTILITIES

See ELECTRIC POWER (cross reference thereunder); GAS AND GASWORKS; POWER . . . ; STEAM POWER . . . (cross reference thereunder); WATERWORKS (cross references thereunder)

PUBLIC WORKS
See COSTS . . . ; *also* under type of structure or project

PUMPING STATIONS
See PIPE LINES

PURIFICATION
See AIR SANITATION; WATER TREATMENT

RADIOACTIVE WASTE
See INDUSTRIAL WASTE

RAILROAD BRIDGES
See BRIDGES

RAILROAD TERMINALS (structures and localities)
See WATER TERMINALS

RAILROAD TRACKS
See EARTHWORK; EMBANKMENTS; PAVEMENTS AND PAVING; TIMBER . . .

RAILROAD TRAINS
See LOCOMOTIVES

RAINFALL (General)
See DRAINAGE (cross references thereunder); FLOODS

RECLAMATION, LAND
See LAND RECLAMATION (cross references thereunder)

RECORDING APPARATUS
See under general types of apparatus, e.g., DEFLECTION RECORDING APPARATUS; VIBRATION RECORDING APPARATUS; *see also* under relative subject

RECORDING INSTRUMENTS
See under general types of instruments, e.g., SOUNDING AND SOUNDING INSTRUMENTS; *see also* under relative subject

RECORD KEEPING
See HYDROGRAPHS, STREAM FLOW; *see also* cross references under RECORDING . . . ; *also* under relative subject, e.g., PAVEMENT AND PAVING, CONCRETE

REFUSE DISPOSAL
See also COSTS, REFUSE DISPOSAL; INDUSTRIAL WASTE; ODORS; SEWAGE SLUDGE
First usage and history of incineration of municipal refuse in United States and foreign countries, 279.
"Incineration and Alternative Refuse Disposal Processes," Ralph Stone and Francis R. Bowerman, 273. *Discussion:* George R. Thompson; William A. Xanten; Samuel A. Greeley; and Ralph Stone and Francis R. Bowerman, 299.
Municipal disposal systems compared, 274.
Schematic drawing of an incinerator, 285.
Bibliography
Municipal incineration and other refuse disposal processes, 298.

REGIONAL PLANNING
See also CITY PLANNING
"Pittsburgh's Comprehensive Improvement Program," Park H. Martin, 885.

REINFORCED CONCRETE
See CONCRETE . . .

RESEARCH
See also LABORATORIES (cross references thereunder); MODELS . . . ; PROBABILITY, THEORY OF; STRUCTURES, THEORY OF; SURVEYS (research data) (cross references thereunder); TESTS AND TESTING (cross references thereunder); *also* under relative subject, e.g., CORROSION AND PROTECTION OF METALS; SEDIMENT AND SEDIMENTATION
Air entrainment research studies at St. Anthony Falls Hydraulic Laboratory of University of Minnesota, 30, 44.
Data deficiency on influence of one smokestack on adjacent stacks under wind pressure, 1082, 1083, 1084, 1087.
Further structural research possibilities described in the application of analog computers, 728.
Need for research in fatigue properties of pavement slabs, 1151.
Research in timber construction during 1930's, 590.
Sediment transport and deposition problems, highly important to the engineer, needing research study, 873, 876, 881, 882.

RESERVOIRS (General)
See also DAMS; SEDIMENT AND SEDIMENTATION; SPILLWAYS; WATER DIVERSION; WAVES

RESERVOIRS, MULTI-PURPOSE
See also COSTS, RESERVOIR (MULTI-PURPOSE RESERVOIRS)

RESERVOIRS, MULTI-PURPOSE (*Continued*)

"Aerial Surveys for Reservoir Planning," Francis J. Guscio (with discussion), 511.

RESONANCE

See VIBRATION

RETAINING WALLS

See also COSTS, RETAINING WALL; EARTH PRESSURE; EMBANKMENTS

Fuel oil tank retaining walls, 271.

RIGHTS OF WAY (land strips)

See also STREETS—Planning and Design

Land acquisition for pipe line construction, 127, 133, 134.

Rights of way problems relating to pipe line construction, 1121.

RIGID FRAMES

See STRUCTURES, THEORY OF—Frames, Rigid

RIPARIAN RIGHTS

State riparian rights doctrine in the eastern United States, 184, 187.

RIVER BANKS AND BANK PROTECTION

See DIKES; FLOODS; RIPARIAN RIGHTS; SEDIMENT AND SEDIMENTATION; SILT AND SILTING, CHANNEL

RIVER BANK STABILIZATION

See RIVER BANKS AND BANK PROTECTION (cross references thereunder)

RIVER CHANNELS

See CHANNELS

RIVER DIVERSION

See WATER DIVERSION

RIVER POLLUTION

See WATER POLLUTION

RIVER REGULATION

See BARS (alluvia); DIKES; IRRIGATION CANALS; RIVERS; WATER DIVERSION; WATER, FLOW OF, IN OPEN CHANNELS

Rivers (General)

See also BARS (alluvia); BRIDGE . . . ; CHANNELS; COSTS . . . ; DIKES; FLOODS; HARBORS; HYDROGRAPHS, STREAM FLOW; MODELS, HYDRAULIC; RESERVOIRS . . . ; SEDIMENT AND SEDIMENTATION; SILT AND SILTING, CHANNEL; WATER . . . ; WATERWAYS (cross references thereunder); WAVES

Effects of cutoff on rivers in regimen and on aggrading rivers, 1277.

Planning of river works, 1270.

"River Surveys in Unmapped Territory," Gerard H. Matthes, 739. *Discussion:* Frederic T. Mavis, T. H. F. Nevins, Chesley J. Posey, Edward Kuiper, and Gerard H. Matthes, 753.

RIVERS (Geographical)

United States

Relationship between flow and width, and depth and velocity, of various American rivers, 460, 461.

RIVER TRANSPORTATION

See WATER TRANSPORTATION (cross references thereunder)

ROADBEDS

See EARTHWORK; HIGHWAYS and ROADS—Roadbeds (cross reference thereunder); RAILROAD TRACKS (cross references thereunder)

ROADS

See HIGHWAYS AND ROADS

ROLLING STOCK

See LOCOMOTIVES

ROOFS AND ROOFING

See CHIMNEYS AND FLUES

ROUGHNESS

See FRICTION

RUBBISH DISPOSAL

See REFUSE DISPOSAL

RUNWAYS

See AIRPORT APPROACHES; AIRPORTS

SAFETY (General)

See DAMS (General)—Safety; EARTHQUAKES; STREETS—Safety; STRUCTURES (General)—Safety

SAFETY FACTOR

See under relative subject, e.g., LIMIT DESIGN, THEORY OF; STRUCTURES (General)—Safety

SAFETY, PERSONAL

See EMPLOYEES AND EMPLOYMENT

SAMPLING

See under relative material, e.g., CLAY; SOILS; *also* under relative subject

SAND

See also BARS (alluvia); PILES AND PILE DRIVING; SEDIMENT AND SEDIMENTATION;

SAND (*Continued*)
SILT AND SILTING, CHANNEL; SOILS
"Pile-Loading Tests, Morganza Floodway Control Structure," Charles I. Mansur and John A. Focht, Jr. (with discussion), 555.
"Vertical Sand Drains for Stabilizing Muck-Peat Soils," J. C. Carpenter and Edward S. Barber (with discussion), 188.

SAND BARS
See BARS (alluvia)

SAND DRAINS
See WELLS

SANITARY ENGINEERS AND ENGINEERING
See ENGINEERS AND ENGINEERING; SANITATION (cross references thereunder)

SANITATION
See AIR SANITATION; COSTS . . . ; INDUSTRIAL SANITATION; INDUSTRIAL WASTE; ODORS; PIPES AND PIPING (cross references thereunder) ; PUBLIC HEALTH; REFUSE DISPOSAL; SEWAGE SLUDGE; TANKS; WATER . . .

SCALES
See under type of scales, e.g., MODELS . . .

SCIENCE
See under specific science, e.g., EDUCATION; HYDRODYNAMICS; MATHEMATICS

SCIENTIFIC SOCIETIES
See AMERICAN SOCIETY OF CIVIL ENGINEERS; SOCIETIES, TECHNICAL; *see also* ENGINEERS AND ENGINEERING

SCOUR
See EROSION . . .

SEA . . .
See WAVES

SEACOAST
See HARBORS; NATIONAL DEFENSE (cross reference thereunder) ; WAVES

SEAPLANE BASES
See AIRPORTS

SEAPORTS
See HARBORS

SEA WALLS
See WAVES

SEDIMENT AND SEDIMENTATION
See also SETTLING BASINS; SILT AND SILTING . . . ; TURBULENCE; WATER DIVERSION
"Fundamental Concepts of Rectangular Settling Tanks," Alfred C. Ingersoll, Jack E. McKee and Norman H. Brooks (with discussion), 1179.
"Graphic Design of Alluvial Channels," Ning Chien (with discussion), 1267.
Pioneering experiments in controlled sediment movement, 833.
"The Present Status of Research on Sediment Transport," Ning Chien, 833. *Discussion:* Thomas Blench; Jan M. Jordaan, Jr.; Joe M. Lara; Navinchandra L. Rupani and John B. Stall; Hsin-Kuan Liu; and Ning Chien and Hans A. Einstein, 869.
Settling of ore slimes in open and baffled tanks, 1194.

Bibliography
Sediment transport as bed load and in suspension, 861.

SEDIMENTATION TANKS (sewage)
See TANKS, SEDIMENTATION (sewage)

SEISMOLOGY
See EARTHQUAKES

SETTLEMENT OF FILL
See SOILS—Construction

SETTLEMENT OF STRUCTURES
See BEARING CAPACITY; EARTH PRESSURE; EMBANKMENTS; FOUNDATIONS . . . ; SOIL . . .

SETTLING BASINS (water supply)
See also SEDIMENT AND SEDIMENTATION; TANKS, SEDIMENTATION (sewage)
"Fundamental Concepts of Rectangular Settling Tanks," Alfred C. Ingersoll, Jack E. McKee and Norman H. Brooks (with discussion), 1179.

SETTLING TANKS (sewage)
See TANKS, SEDIMENTATION (sewage)

SEWAGE DISPOSAL (General)
See INDUSTRIAL WASTE; PIPES AND PIPING (cross references thereunder) ; SEWAGE SLUDGE; TANKS, SEDIMENTATION

SEWAGE SLUDGE
See also TANKS . . .
Factors that influence thickening of sludge, 1199.

SEWAGE SLUDGE (*Continued*)
"Fundamental Concepts of Rectangular Settling Tanks," Alfred C. Ingersoll, Jack E. McKee and Norman H. Brooks (with discussion), 1179.

SEWAGE TANKS
See cross references under TANKS, SEWAGE

SEWAGE WORKS
See TANKS, SEDIMENTATION (sewage)

SEWERS (General)
See BACKWATER; PIPES AND PIPING (cross references thereunder)

SHAFT SPILLWAYS
See SPILLWAYS

SHEAR
"Effect of Sample Disturbance on the Strength of a Clay," Max L. Calhoon (with discussion), 925.
"An Influence-Line Analysis for Suspension Bridges," David J. Peery (with discussion), 463.
"Nonuniform Torsion of Plate Girders," Gerald G. Kubo, Bruce G. Johnston and William J. Eney (with discussion), 759.
"A Physical Approach to Turbulent-Boundary-Layer Problems," Donald Ross (with discussion), 1219.
"Research on Bolted Connections," William H. Munse, 1255.

SHEARING STRESS
See SHEAR

SHELL STRUCTURES
See CHIMNEYS AND FLUES; FLUMES; PIPE LINES; STRESS AND STRAIN—Shell Structures; STRUCTURES, THEORY OF—Shell Structures

SHOCK
See ATOMIC BLAST; EARTHQUAKES

SHORES AND SHORE PROTECTION
See WAVES; *see also* cross references under RIVER BANKS AND BANK PROTECTION

SHRINKAGE, SOIL
See CLAY

SIDESWAY
See STRUCTURES, THEORY OF—Frames . . .

SIDEWALKS (General)
See CONCRETE; PAVEMENT AND PAVING; STREETS

SILT AND SILTING (General)
See also SEDIMENT AND SEDIMENTATION

SILT AND SILTING, CHANNEL
Formula for minimum radii of stable bends in alluvium, of value for river surveys in unmapped regions, 754, 758.
"The Present Status of Research on Sediment Transport," Ning Chien (with discussion), 833.
Regime theory applied to channels, 833.
"River Surveys in Unmapped Territory," Gerard H. Matthes (with discussion), 739.
"Similarity of Distorted River Models with Movable Beds," Hans A. Einstein and Ning Chien (with discussion), 440.

Bibliography
Bed load and suspended load in natural streams, 861.

SIMILARITY, THEORY OF
See MODELS

SKIN FRICTION
See FRICTION

SLABS
See also PLATES; STRUCTURES, THEORY OF—Slabs
"Moments and Deflections in Steel-Grid Bridge Floors," Herbert J. Greenberg (with discussion), 410.
"Thicknesses of Concrete Pavements for Highways," Joseph H. Moore (with discussion), 1125.

SLIPS AND SLIPPAGE (movement of surfaces)
See JOINTS, BOLTED (cross reference thereunder)

SLOPE DEFLECTION
"A Brief for Limit Design," George C. Ernst (with discussion), 605.

SLOPING CHANNELS
See CHANNELS

SLUDGE, SEWAGE
See SEWAGE SLUDGE

SMOKE ABATEMENT
See AIR SANITATION

SMOKESTACKS
See CHIMNEYS AND FLUES

SOCIETIES, TECHNICAL

See also AMERICAN SOCIETY OF CIVIL ENGINEERS; ENGINEERS AND ENGINEERING; *also* under relative subject

Intersociety relations, 1407.

SOIL . . .

See also EARTH . . . ; GROUND . . . (cross references thereunder); LAND (cross references thereunder)

SOIL CORROSION

See CORROSION AND PROTECTION OF METALS

SOIL MECHANICS

See SOILS

SOIL PRESSURE

See EARTH PRESSURE

SOILS (General)

See also BEARING CAPACITY; CLAY; DRAINAGE (cross references thereunder); EARTH PRESSURE; FOUNDATIONS . . . ; FRICTION; PAVEMENT AND PAVING . . . ; PEAT; SAND; SEDIMENT AND SEDIMENTATION; SILT AND SILTING . . . ; STRESS AND STRAIN—Soils; *also* under name of soil structure

"Factors Influencing Irrigation in Humid Areas," Tyler H. Quackenbush (with discussion), 179.

"Safe Loads on Dog-Leg Piles," James D. Parsons and Stanley D. Wilson (with discussion), 695.

Classification

Ideal pavement subgrade soil classification, 551, 552.

Compaction. *See* BEARING CAPACITY

Construction

"Vertical Sand Drains for Stabilizing Muck-Peat Soils," J. C. Carpenter and Edward S. Barber (with discussion), 188.

Tests and Testing

"Effect of Sample Disturbance on the Strength of a Clay," Max L. Calhoon, 925. *Discussion:* John H. Schmertmann, and Max L. Calhoon, 940.

"Pile-Loading Tests, Morganza Floodway Control Structure," Charles I. Mansur and John A. Focht, Jr. (with discussion), 555.

Rutledge hypothesis, its validity and need of modification for soils sensitive to remolding, 931, 932, 940, 942, 945, 949, 950.

SOIL TRANSPORTATION

See SEDIMENT AND SEDIMENTATION; SILT AND SILTING . . .

SOLIDS, FLOW OF

See SEDIMENT AND SEDIMENTATION; SILT AND SILTING . . . ; WATER, FLOW OF, IN OPEN CHANNELS; WATER, FLOW OF, IN PIPES

SOUNDINGS AND SOUNDING INSTRUMENTS

Echo sounding equipment for unmapped undeveloped areas, 749.

SPACE STRUCTURES

See STRUCTURES, THEORY OF . . . ; *also* under special type of structure, e.g., CHIMNEYS AND FLUES; TOWERS

SPECIFICATIONS

See under relative subject, e.g., BRIDGE FLOORS AND FLOORING

SPEED

See STREETS—Safety

SPILLWAYS (General)

See also COSTS, SPILLWAY; DAMS; WATER, FLOW OF, OVER DAMS AND WEIRS

Additional investigations needed relating to drop spillways, 957, 958.

Apparatus and procedure for testing box inlet drop spillways and their outlets, 959.

"The Box Inlet Drop Spillway and Its Outlet," Fred W. Blaisdell and Charles A. Donnelly, 955. *Discussion:* Neal E. Minshall; and Fred W. Blaisdell and Charles A. Donnelly, 987.

First morning glory shaft spillway, 312.

"Morning-Glory Shaft Spillways": A Symposium, Joseph N. Bradley, William E. Wagner, and Alvin J. Peterka, 311. *Discussion:* Bernard Donelan, Donald S. Walter, Fred W. Blaisdell, Rodolfo E. Ballester, John W. Ridley, and Joseph N. Bradley, Maxwell W. White and Murray B. McPherson; Fred W. Blaisdell; Ibrahim M. Mostafa, Benoyendra Chanda, and Howard P. Johnson; and William E. Wagner, and Fred W. Blaisdell, and Alvin J. Peterka, 312, 345, 385.

SPILLWAYS (Geographical)

Montana

Hungry Horse Dam morning glory shaft spillway, 311.

SPILLWAYS (Geographical) (*Continued*)

Wisconsin

Drop spillways and their outlets in a four county survey, 987, 992.

SPRINKLERS AND SPRINKLING (irrigation)

"Factors Influencing Irrigation in Humid Areas," Tyler H. Quackenbush (with discussion), 179.

STABILITY

See AERODYNAMICS; BUCKLING; HYDRODYNAMICS; MECHANICS; SOIL . . . ; STRUCTURES, THEORY OF

STACKS

See CHIMNEYS AND FLUES

STATICALLY INDETERMINATE STRUCTURES

See STRUCTURES, CONTINUOUS (cross reference thereunder); STRUCTURES, THEORY OF

STATIONS

See cross references under TERMINALS; *also* under relative subject

STATISTICAL ANALYSIS

See GRAPHICAL CHARTS (cross references thereunder); MATHEMATICS; PROBABILITY, THEORY OF

STATISTICS

See under relative subject, e.g., ENGINEERS AND ENGINEERING

STEAM POWER PLANTS

See POWER PLANTS

STEEL

See CORROSION AND PROTECTION OF METALS; REINFORCED CONCRETE (cross reference thereunder); *also* under special structure or structural part, e.g., PILES AND PILE DRIVING

STEEL PLATES

See PLATES

STIFFENING TRUSSES

See TRUSSES, STIFFENING

STIFFNESS

"Beam Restraints Provided by Walls with Openings," Ibrahim A. Mohammed and Egor P. Popov, 1034.

"Constant-Segment Method for Analysis of Nonuniform Members," Walter E. Hanson and Wallace F. Wiley (with discussion), 1317.

"Multiple-Span Gabled Frames," John D. Griffiths (with discussion), 1288.

"Numerical Analysis of Frames with Curved Girders," James Michalos (with discussion), 521.

STILLING BASINS

See WATER, FLOW OF, OVER DAMS AND WEIRS

STORAGE

See OIL STORAGE (cross reference thereunder); WAREHOUSES; WATER STORAGE (cross reference thereunder)

STRAIN

See STRESS AND STRAIN

STREAM CONTAMINATION

See WATER POLLUTION

STREAM FLOW

See WATER, FLOW OF, IN OPEN CHANNELS

STREAMS

See RIVERS and cross references thereunder

STREET CLEANING

See REFUSE DISPOSAL

STREETS (General)

See also BRIDGES; CITY PLANNING; FOUNDATIONS, HIGHWAY AND ROAD; HIGHWAYS AND ROADS; MOTOR . . . ; PAVEMENT AND PAVING; PIPES AND PIPING (cross references thereunder); PUBLIC UTILITIES (cross references thereunder); REFUSE DISPOSAL; TRAFFIC, STREET; WHEEL LOADS

Planning and Design

"Metropolitan Traffic and Transportation Planning," Charles A. Blessing, 135.

Safety

Accident reduction and movement speed on one-way streets, in Sacramento, California, 25.

STREET TRAFFIC

See TRAFFIC, STREET

STREET TRANSPORTATION

See also WATER FRONT (cross references thereunder)

"Metropolitan Traffic and Transportation Planning," Charles A. Blessing, 135.

"One-Way Street System in Sacramento, Calif.," D. Jackson Faustman, 22.

Relationship of the transit industry to general parking conditions, 169.

STRENGTH OF MATERIALS

See also FAILURES . . . ; STRESS AND STRAIN; *also* under specific material (*see* list of materials under MATERIALS OF CONSTRUCTION); *also* under fabricated structure or structural part

"Safety and the Probability of Structural Failure," Alfred M. Freudenthal (with discussion), 1337.

Bibliography

Probability of unserviceability and failure, 1372.

STRESS AND STRAIN (General)

See also CONCRETE—Temperature; DEFORMATION INSTRUMENTS; EARTH PRESSURE; EARTHQUAKES; FAILURES . . . ; MOMENTS; STIFFNESS; STRENGTH OF MATERIALS; STRUCTURES, THEORY OF; VIBRATION; WATER PRESSURE; WHEEL LOADS; WIND . . . ; *also* under specific type of stress, e.g., BUCKLING; SHEAR; TORSION

Beams (General). *See also* BUCKLING; STRESS AND STRAIN—Flanges; TORSION

"Lateral Buckling of Cantilevered I-Beams under Uniform Load," Stanley Poley, 786.

Beams, Continuous

"Continuous Prestressing," Robert B. B. Moorman (with discussion), 814.

Chimneys and Flues

"The Vibrations of Steel Stacks," Walter L. Dickey and Glenn B. Woodruff (with discussion), 1054.

Columns

"Lateral Buckling of Eccentrically Loaded I-Columns," Mario G. Salvadori, 1163.

Concrete (General)

"Thicknesses of Concrete Pavements for Highways," Joseph H. Moore (with discussion), 1125.

Dams (General)

Leaf spring shell type dam advantages, 909.

Dams, Arch

"Economy and Safety of Concrete Dams," August E. Komendant (with discussion), 899.

Dams, Masonry and Concrete

"Economy and Safety of Concrete Dams," August E. Komendant (with discussion), 899.

Flanges

"Nonuniform Torsion of Plate Girders," Gerald G. Kubo, Bruce G. Johnston and William J. Eney (with discussion), 759.

Girders. *See also* TORSION

"Nonuniform Torsion of Plate Girders," Gerald G. Kubo, Bruce G. Johnston and William J. Eney (with discussion), 759.

Joints

"Research on Bolted Connections," William H. Munse, 1255.

Piles

"Pile-Loading Tests, Morganza Floodway Control Structure," Charles I. Mansur and John A. Focht, Jr. (with discussion), 555.

"Safe Loads on Dog-Leg Piles," James D. Parsons and Stanley D. Wilson (with discussion), 695.

Shell Structures

"Economy and Safety of Concrete Dams," August E. Komendant (with discussion), 899.

Soils

"Pile-Loading Tests, Morganza Floodway Control Structure," Charles I. Mansur and John A. Focht, Jr. (with discussion), 555.

Solids. *See* EARTH PRESSURE

Structures (General)

"Safety and the Probability of Structural Failure," Alfred M. Freudenthal (with discussion), 1337.

Trusses and Trussed Structures

"Examples of Timber-Structure Failures," Michael N. Salgo (with discussion), 588.

STRESS, SHEARING

See SHEAR

STRUCTURAL ANALYSIS

See EQUATIONS; STRESS AND STRAIN; STRUCTURES, THEORY OF

STRUCTURAL DYNAMICS

See also AERODYNAMICS; EARTHQUAKES; STRUCTURES, THEORY OF; VIBRATION

"Analog Computers Applied to Elasto-Plastic Systems," Leo Schenker and Gunther Martin (with discussion), 728.

Blast resistant structures designed by approximating an equivalent static loading, 45.

STRUCTURAL ENGINEERS AND ENGINEERING
See STRUCTURES . . . ;*also* under relative structure, e.g., BRIDGES . . . ; BUILDINGS

STRUCTURAL JOINTS
See JOINTS

STRUCTURAL MATERIALS
See MATERIALS OF CONSTRUCTION; STRENGTH OF MATERIALS

STRUCTURAL MEMBERS
See MEMBERS, STRUCTURAL (cross references thereunder)

STRUCTURAL MODELS
See MODELS, STRUCTURAL

STRUCTURAL STEEL
See STEEL (cross references thereunder)

STRUCTURES (General)
See also BUILDINGS; CONSTRUCTION; FOUNDATIONS . . . ; MATERIALS OF CONSTRUCTION; MODELS, STRUCTURAL; SAFETY (cross references thereunder); STRESS AND STRAIN . . . ; STRUCTURES, THEORY OF; VIBRATION; *also* under general types of structures, e.g., ELASTO-PLASTIC STRUCTURES; *also* under specific type of structure or related subject, e.g., WATER TERMINALS
"An Engineering Approach to Blast-Resistant Design," Nathan M. Newmark (with discussion), 45.
Usage of analog computers to solve equations of motion of elasto-plastic systems, 728.

Bibliography
Blast resistant design, 60.
Safety and the probability of structural failure, 1372.

Safety
"Safety and the Probability of Structural Failure," Alfred M. Freudenthal (with discussion), 1337.

STRUCTURES, CONTINUOUS
See STRUCTURES, THEORY OF

STRUCTURES, DROP
See DAMS

STRUCTURES, ELASTO-PLASTIC
See ELASTO-PLASTIC STRUCTURES

STRUCTURES, HYDRAULIC
See HYDRAULIC STRUCTURES

STRUCTURES, SETTLEMENT OF
See BEARING CAPACITY; EARTH PRESSURE; EMBANKMENTS; FOUNDATIONS . . . ; SOIL . . .

STRUCTURES, SHELL
See SHELL STRUCTURES (cross references thereunder)

STRUCTURES, SPACE
See SPACE STRUCTURES (cross references thereunder)

STRUCTURES, STATICALLY INDETERMINATE
See STATICALLY INDETERMINATE STRUCTURES (cross references thereunder)

STRUCTURES, SUB-
See SUBSTRUCTURES (cross references thereunder)

STRUCTURES, THEORY OF (General)
See also STRESS AND STRAIN; *also* under type of structure or structural part
"Safety and the Probability of Structural Failure," Alfred M. Freudenthal (with discussion), 1337.

Bibliography
The octagonal girder, four column space frame, 1019.

Beams and Girders (General)
"Constant-Segment Method for Analysis of Nonuniform Members," Walter E. Hanson and Wallace F. Wiley, 1317. *Discussion:* Thomas F. Hickerson; Eugene J. Vayda; Jaro J. Polivka; and Walter E. Hanson and Wallace F. Wiley, 1331.
Principle of superposition usage in computation of slopes and deflections in nonuniform beams, 1318.

Beams and Girders, Continuous
Beam constants for curved members, 523, 526, 530, 531.
"A Brief for Limit Design," George C. Ernst (with discussion), 605.
"Continuous Prestressing," Robert B. B. Moorman (with discussion), 814.
"Numerical Analysis of Frames with Curved Girders," James Michalos (with discussion), 521.

Bridges
"An Influence-Line Analysis for Suspension Bridges," David J. Peery (with discussion), 463.
Principle of superposition applied to arch and suspension bridge analysis, 490.

STRUCTURES, THEORY OF (General) (*Continued*)

Chimneys and Flues

"The Vibrations of Steel Stacks," Walter L. Dickey and Glenn B. Woodruff (with discussion), 1054.

Columns

"Constant-Segment Method for Analysis of Nonuniform Members," Walter E. Hanson and Wallace F. Wiley (with discussion), 1317.

"Lateral Buckling of Eccentrically Loaded I-Columns," Mario G. Salvadori, 1163.

Concrete, Reinforced

"A Brief for Limit Design," George C. Ernst (with discussion), 605.

Elasto-Plastic Structures

"Analog Computers Applied to Elasto-Plastic Systems," Leo Schenker and Gunther Martin (with discussion), 728.

Frames, Continuous

A method of continuous frame analysis regarded accurate and not requiring solution by simultaneous equations, 1288.

"Multiple-Span Gabled Frames," John D. Griffiths, 1288. *Discussion:* Abdel F. Diwan, and John D. Griffiths, 1308.

"Numerical Analysis of Frames with Curved Girders," James Michalos, 521. *Discussion:* William A. Conwell, and James Michalos, 540.

"The Octagonal-Girder Four-Column Space Frame," Paul C. Disario, Jr., John S. Podolan and Nicholas A. Weil, 995. *Discussion:* Abdel F. Diwan; Sidney Shore and Humberto Rincon; and Paul C. Disario, Jr., John S. Podolan and Nicholas A. Weil, 1022.

Properties of gables, 1304.

Frames, Rigid

"A Brief for Limit Design," George C. Ernst (with discussion), 605.

"Multiple-Span Gabled Frames," John D. Griffiths (with discussion), 1288.

Girders (General). *See* Beams and Girders (General) (hereunder)

Girders, Continuous. *See* Beams and Girders, Continuous (hereunder)

Plates

"Beam Restraints Provided by Walls with Openings," Ibrahim A. Mohammed and Egor P. Popov, 1034.

Power Plants

"Vibration in Hydroelectric Power Plants," Samuel Judd, 1153.

Shell Structures

"Economy and Safety of Concrete Dams," August E. Komendant (with discussion), 899.

Slabs

"Moments and Deflections in Steel-Grid Bridge Floors," Herbert J. Greenberg (with discussion), 410.

Walls

"Beam Restraints Provided by Walls with Openings," Ibrahim A. Mohammed and Egor P. Popov, 1034.

STRUCTURES, TIMBER

See TIMBER STRUCTURES

STRUCTURES, UNDERGROUND

See UNDERGROUND STRUCTURES (cross references thereunder)

SUB- . . .

See also UNDER- . . .

SUBGRADES

See PAVEMENT AND PAVING . . .

SUBSTRUCTURES

See CONCRETE; EARTHWORK; FOUNDATIONS . . . ; MASONRY (cross reference thereunder); *also* under type of substructure, e.g., PIPE LINES

SUPERPOSITION, PRINCIPLE OF

See STRUCTURES, THEORY OF

SURFACES, SLIPPAGE OF

See SLIPS AND SLIPPAGE (cross reference thereunder)

SURFACING

See AIRPORTS

SURGES (water surface)

See WAVES

SURVEYING

See SURVEYS AND SURVEYING

SURVEYING INSTRUMENTS

Barometer types best suited for use in unmapped regions, 746.

Best river instruments for use in unmapped backward and undeveloped regions, 739, 748.

SURVEYS (research data)

See under relative subject, e.g., SPILLWAYS; *see also* RESEARCH

SURVEYS AND SURVEYING (General)

See also MAPS AND MAPPING; PROPERTY (landed property) (cross references thereunder)

"River Surveys in Unmapped Territory," Gerard H. Matthes (with discussion), 739.

"Surveys and Maps for Pipelines," George E. MacDonald (with discussion), 121.

SURVEYS AND SURVEYING, AERIAL

See also MAPS AND MAPPING, AERIAL

"Aerial Surveys for Reservoir Planning," Francis J. Guscio, 511. *Discussion:* Lewis A. Dickerson, and Francis J. Guscio, 518.

"River Surveys in Unmapped Territory," Gerard H. Matthes (with discussion), 739.

"Surveys and Maps for Pipelines," George E. MacDonald (with discussion), 121.

SURVEYS AND SURVEYING, CADASTRAL

See SURVEYS AND SURVEYING, GEODETIC

SURVEYS AND SURVEYING, GEODETIC

See also GEODESY

"A Conformal and World-Wide Military Grid System," Floyd W. Hough, 633.

SUSPENDED LOAD

See SEDIMENT AND SEDIMENTATION; SILT AND SILTING, CHANNEL

SUSPENSION BRIDGES

See BRIDGES, SUSPENSION

SWAMPS

See MARSHES

SWELLING

See EXPANSION (cross references thereunder)

SYMBOLS

See under relative subject, e.g., MATHEMATICS; STRUCTURES, THEORY OF

TAIL WATER EROSION

See EROSION, TAIL WATER

TANKS (General)

See also STILLING BASINS (cross reference thereunder); WATER, FLOW OF, IN OPEN CHANNELS

TANKS, AERATION

"An Experimental Study of Bubbles Moving in Liquids," William L. Haberman and Rose K. Morton (with discussion), 227.

TANKS, OIL STORAGE

"The Design of Two Steam Electric Plants," Walter L. Dickey, 253.

TANKS, SEDIMENTATION (sewage)

See also SETTLING BASINS (water supply)

"Fundamental Concepts of Rectangular Settling Tanks," Alfred C. Ingersoll, Jack E. McKee and Norman H. Brooks, 1179. *Discussion:* Thomas R. Camp; Henry L. Thackwell; and Alfred C. Ingersoll, Jack E. McKee and Norman H. Brooks, 1205.

TANKS, SETTLING (sewage)

See TANKS, SEDIMENTATION (sewage)

TANKS, SEWAGE

See TANKS, AERATION; TANKS, SEDIMENTATION (sewage)

TANKS, WATER FLOW OF, IN

See WATER, FLOW OF, IN OPEN CHANNELS

TAXIWAYS

See AIRPORTS

TECHNICAL SOCIETIES

See AMERICAN SOCIETY OF CIVIL ENGINEERS; SOCIETIES, TECHNICAL; *see also* ENGINEERS AND ENGINEERING

TEMPERATURE

See CONCRETE—Temperature

TENSILE STRESS

See STRESS AND STRAIN

TENSION

See STRESS AND STRAIN; STRUCTURES, THEORY OF

TERMINALS (structures and localities)

See AIR TERMINALS (cross reference thereunder); WATER TERMINALS (structures and localities)

TERMINOLOGY (Arranged hereunder by specific or comprehensive subject word when possible)

Channels in regime, 859.

Clay terms described, 926.

Corrosion of metals. (Polarization and other current terms as used in corrosion literature), 803.

TERMINOLOGY (*Continued*)

Earthquakes. (Tectonic earthquakes as type of tremor), 1154.

Factor of safety versus probability of failure as a term, 1387, 1394.

Failures. (Plastic collapse, alternating plasticity or progressive collapse, shake-down and other terms differentiated), 1355.

Failure terms need study to be effective in usage, 1376, 1387, 1390, 1394, 1395, 1397.

Finger pier and marginal wharf in transportation usage, 434.

Human engineering defined, 208.

Map projections. (Conformality, orthomorphic and grid as terms), 634.

Pile testing failure. (Engineers lacking in agreement on true definition), 577.

Pile "tips" in testing, 559.

The ratio of settling velocity to overflow rate named Hazen number, 1181.

Refuse varied as a term, 305.

Sanitary engineering defined, 207.

Sediment. (Suspended load, bed layer, bed material load and wash load, in sediment transport), 843, 855, 856.

Sediment transport. (Tractive force and critical tractive force in bed load movement), 848, 849.

Similarity as a term describing prototype-model relationship, 441.

Stiffness factors that include both moments and forces, 1310.

Torsion. (Usage of terms pure torsion, simple torsion and St. Venant torsion), 760.

Vibration. (Magnification factor as related to displacement), 1157.

Water flow. (Density and turbidity currents defined), 860.

Water flow. (Interface as a zone with high velocity gradient), 877.

TESTING MACHINES

See under use, material, structure or structural part tested

TESTS AND TESTING

See BUCKLING; ELASTICITY; FAILURES . . . ; LABORATORIES (cross references thereunder); MODELS . . . ; SHEAR; STRENGTH OF MATERIALS; STRESS AND STRAIN; STRUCTURES, THEORY OF; TORSION; WATER, FLOW OF . . . ; *also* under material, structure or structural part tested, e.g., PILES AND PILE DRIVING; SOILS—Tests and Testing

THEORIES

See cross references hereunder and under ANALYSIS OF DATA; *see also* STRUCTURES, THEORY OF; *see also* under relative subject or its related science, e.g., SILT AND SILTING, CHANNEL; WAVES

THEORY OF BOUNDARY LAYER (fluid flow)

See BOUNDARY LAYER, THEORY OF (fluid flow) (cross references thereunder)

THEORY OF ELASTICITY

See ELASTICITY

THEORY OF FINITE DIFFERENCES

See MATHEMATICS

THEORY OF LIMIT DESIGN

See LIMIT DESIGN, THEORY OF

THEORY OF PLASTICITY

See PLASTICITY

THEORY OF PROBABILITY

See PROBABILITY, THEORY OF

THEORY OF SIMILARITY

See MODELS

THEORY OF STRUCTURES

See STRUCTURES, THEORY OF

THEORY OF VIRTUAL WORK

See VIRTUAL WORK, PRINCIPLE OF

THEORY, PLASTIC

See PLASTICITY

THERMAL DEFORMATION

See TEMPERATURE (cross reference thereunder)

THERMODYNAMICS

"Incineration and Alternative Refuse Disposal Processes," Ralph Stone and Francis R. Bowerman (with discussion), *273*.

THRUST

See under relative structure, structural part or material, e.g., FRAMES . . . (cross references thereunder)

TIMBER AND TIMBERING

Lack of proper lumber seasoning in relation to timber structure failures, 592, 593, 596, 598, 600.

TIMBER STRUCTURES

"Example of Timber-Structure Failures," Michael N. Salgo (with discussion), 588.

History of World War II construction program, 588.

TOOLS

See under general types of tools or usage; *also* cross references under APPARATUS; INSTRUMENTS; MACHINERY

TOPOGRAPHIC MAPS AND MAPPING

See MAPS AND MAPPING (General)

TORSION

"Lateral Buckling of Eccentrically Loaded I-Columns," Mario G. Salvadori, 1163.

"Nonuniform Torsion of Plate Girders," Gerald G. Kubo, Bruce G. Johnston and William J. Eney, 759. *Discussion:* DeForest A. Matteson, Jr.; and Gerald G. Kubo, Bruce G. Johnston and William J. Eney, 781.

"Numerical Analysis of Frames with Curved Girders," James Michalos (with discussion), 521.

"The Octagonal-Girder Four-Column Space Frame," Paul C. Disario, Jr., John S. Podolan and Nicholas A. Weil (with discussion), 995.

Summary of torsion theory, 759, 760, 772, 779, 781.

Torsion testing machine for girder specimens, 760.

TOWERS

Damping characteristics of tubular aluminum towers under wind induced vibration, 1110.

"The Octagonal-Girder Four-Column Space Frame," Paul C. Disario, Jr., John S. Podolan and Nicholas A. Weil (with discussion), 995.

TRACKS

See under type of track, e.g., RAILROAD TRACKS (cross references thereunder)

TRADE WASTE

See INDUSTRIAL WASTE

TRAFFIC (General)

See STREETS—Safety; WHEEL LOADS

TRAFFIC ACCIDENTS

See STREETS—Safety

TRAFFIC, AIR

Air, rail, water traffic, in 1952, compared, 722.

Air traffic forecasts in relation to the development of international airports, 96.

TRAFFIC, BUS

See TRAFFIC, STREET

TRAFFIC, STREET

See also AUTOMOBILE PARKING

"Metropolitan Traffic and Transportation Planning," Charles A. Blessing, 135.

"One Way Street System in Sacramento, Calif.," D. Jackson Faustman, 22.

Traffic trends, 1927–1951 and plan for Sacramento, California, 23, 24.

TRAINS, RAILROAD

See cross reference under RAILROAD TRAINS

TRANSPORTATION

See AIR TRANSPORT; CANALS (cross references thereunder); COSTS, TRANSPORTATION; FREIGHT; PIPE LINES; RIVERS; ROLLING STOCK (cross reference thereunder); SOIL TRANSPORTATION (cross references thereunder); STREET TRANSPORTATION; TERMINALS (cross references thereunder); TRAFFIC; WAREHOUSES; WATER TRANSPORTATION (cross references thereunder); WATERWAYS (cross references thereunder)

TRANSPORTATION CUTOFFS

See RIVERS

TRIAXIAL SHEAR

See SHEAR

TRUCKING

See STREET TRANSPORTATION

TRUCKS

See MOTOR TRUCKS

TRUSSES (General)

See also FAILURES, TRUSS; STRESS AND STRAIN—Trusses and Trussed Structures

TRUSSES, STIFFENING

"An Influence-Line Analysis for Suspension Bridges," David J. Peery (with discussion), 463.

TUBES

See PIPE LINES; PIPES AND PIPING (cross references there-

TUBES (*Continued*)
under); SHELL STRUCTURES (cross references thereunder); STRUCTURES, THEORY OF—Shell Structures; WATER, FLOW OF, IN PIPES

TURBINES, WATER
"Vibration in Hydroelectric Power Plants," Samuel Judd, 1153.

TURBULENCE (water agitation)
See also EDDIES (cross reference thereunder); FRICTION; HYDRAULIC JUMP; WATER, FLOW OF . . .
"Flow Expansion and Pressure Recovery in Fluids," Harald Tults, 65.
"Fundamental Concepts of Rectangular Settling Tanks," Alfred C. Ingersoll, Jack E. McKee and Norman H. Brooks (with discussion), 1179.
"Unsteady Flow in Open-Type Pipe Irrigation Systems," Edward H. Taylor, Arthur F. Pillsbury, Thomas O. Ellis and George A. Bekey (with discussion), 143.

TURBULENCE, WIND
See WIND . . .

TWISTING
See TORSION; *also* under relative structure, structural part or material, e.g., FRAMES . . . (cross references thereunder)

UNDER- . . .
See also SUB- . . .

UNDERFLOW
See WELLS

UNDERGROUND CORROSION
See CORROSION AND PROTECTION OF METALS

UNDERGROUND STRUCTURES
See PIPES AND PIPING (cross references thereunder); SEWERS (cross references thereunder); *see also* under related subject, e.g., CORROSION AND PROTECTION OF METALS; SOILS

UNDERWATER FOUNDATIONS
See FOUNDATIONS, UNDERWATER

URBAN . . .
See CITIES (cross references thereunder)

UTILITIES
See PUBLIC UTILITIES (cross references thereunder)

VALUATION
See also COSTS
Pittsburgh redevelopment program and its effect on property valuations, 898.

VEHICLES
See general types of vehicles, e.g., MOTOR VEHICLE . . . (cross references thereunder); *also* under specific type of vehicle, e.g., AUTOMOBILE . . .

VEHICULAR TRAFFIC
See TRAFFIC . . .

VELOCITY
See HYDRODYNAMICS; VIBRATION; WATER, FLOW OF . . . ; WIND . . .

VELOCITY DISTRIBUTION
See WATER, FLOW OF . . .

VELOCITY METERS
See WATER VELOCITY METERS (cross reference thereunder)

VENTILATION
See AIR SANITATION

VIBRATION
See also EARTHQUAKES
"An Engineering Approach to Blast-Resistant Design," Nathan M. Newmark (with discussion), 45.
"Resonant Vibration of Steel Stacks," Ernest A. Dockstader, William F. Swiger and Emory Ireland (with discussion), 1088.
Stacks designed against possible earthquake action, 1090.
Stack vibration, 266.
"Vibration in Hydroelectric Power Plants," Samuel Judd, 1153.
"The Vibrations of Steel Stacks," Walter L. Dickey and Glenn B. Woodruff (with discussion), 1054.

VIBRATION MEASURING INSTRUMENTS
Vibration meter and vibration analyzer usage described, 1162.

VIBRATION RECORDING APPARATUS
Oscillograph records for circuit relating to elasto-plastic resistance function, 731, 734.

VIRTUAL WORK, PRINCIPLE OF
Application of principle to influence line analysis of suspension bridges, 494.
Usage of virtual work method in octagonal frame analysis, 1022, 1033.

VISCOSITY
  See also WATER, FLOW OF . . .
  "An Experimental Study of Bubbles Moving in Liquids," William L. Haberman and Rose K. Morton (with discussion), 227.
  "A Physical Approach to Turbulent-Boundary-Layer Problems." Donald Ross (with discussion), 1219.
Bibliography
  Bubble motion, 246.
WALLS
  See under relative structure or type of wall, e.g., BUILDINGS; RETAINING WALLS; SEA WALLS (cross reference thereunder); *see also* STRUCTURES, THEORY OF—Walls
WAR AND ENGINEERING
  See cross reference under MILITARY ENGINEERS AND ENGINEERING; WORLD WAR II (1941–1945) (cross reference thereunder)
WAREHOUSES
  See also BUILDINGS
  "Design of General Cargo Marine Terminals," Frank W. Herring, 433.
WASTE DISPOSAL
  See INDUSTRIAL WASTE; ODORS; REFUSE DISPOSAL; SANITATION (cross references thereunder); SEWAGE . . . ; SEWERS (cross references thereunder); WATER POLLUTION
WASTE MATERIALS
  See cross references under WASTE DISPOSAL
WASTE WATER
  See SEWERS (cross references thereunder); WATER POLLUTION
WATER . . .
  See also AERATION; BACKWATER; COSTS . . . ; DAMS; DIKES; DRAINAGE (cross references thereunder); DROP-DOWN (cross reference thereunder); EROSION . . . ; FILTERS AND FILTRATION, WATER (cross reference thereunder); FLOODS; FLUMES; FOUNDATIONS, UNDERWATER; HYDRAULIC . . . ; HYDRO- . . . ; IRRIGATION; MARSHES; METERS AND METERING . . . ; MODELS, HYDRAULIC; PIPE LINES; PIPES AND PIPING (cross references thereunder); RESERVOIRS; SANITATION (cross references thereunder); SETTLING BASINS; SEWAGE DISPOSAL (cross references thereunder); SEWERS (cross references thereunder); SPILLWAYS; SPRINKLERS AND SPRINKLING; TANKS . . . ; TERMINOLOGY; TURBULENCE; WAVES; WELLS
WATER COLLECTION
  See INFILTRATION (cross reference thereunder); INTAKES; WATERWORKS (cross references thereunder); WELLS
WATER DISTRIBUTION
  See CANALS (cross references thereunder); IRRIGATION; PIPES AND PIPING (cross references thereunder)
WATER DIVERSION
  "Graphic Design of Alluvial Channels," Ning Chien (with discussion), 1267.
WATER FILTERS AND FILTRATION
  See FILTERS AND FILTRATION, WATER (cross reference thereunder)
WATER, FLOW OF (General)
  See also FLOODS; FLUMES; FRICTION; HYDRAULIC . . . ; LIQUIDS, FLOW OF; MODELS, HYDRAULIC; SPILLWAYS; TURBULENCE; VISCOSITY; WELLS
  Experiments on two dimensional turbulent boundary layers, years 1930–1951, 1233.
  "A Physical Approach to Turbulent-Boundary-Layer Problems," Donald Ross, 1219. *Discussion:* William D. Baines, James M. Robertson, William J. Bauer, and Donald Ross, 1241.
Bibliography
  Turbulent boundary layer problems, 1238.
WATER, FLOW OF, IN FLUMES
  See WATER, FLOW OF, IN OPEN CHANNELS
WATER, FLOW OF, IN OPEN CHANNELS
  See also BACKWATER; FLOODS; HYDROGRAPHS, STREAM FLOW; INTAKES; METERS AND METERING, CURRENT; SEDIMENT AND SEDIMENTATION; SILT AND SILTING, CHANNEL; WAVES

WATER, FLOW OF, IN OPEN CHANNELS (*Continued*)
Adjustable apparatus for studying high velocity flow, 685.
Bank cutting and building up, and river widening causes, 1284.
Effect of effluent weirs on pathlines of settling particles, 1197.
Effect of turbulent eddies, 1179, 1203.
"Flow Expansion and Pressure Recovery in Fluids," Harald Tults, 65.
"Fundamental Concepts of Rectangular Settling Tanks," Alfred C. Ingersoll, Jack E. McKee and Norman H. Brooks (with discussion), 1179.
"Graphic Design of Alluvial Channels," Ning Chien (with discussion), 1267.
Hydraulics of alluvial channel flow, 834.
Overflow residual efficiency as developed theoretically, 1179, 1182, 1185, 1212.
"River Surveys in Unmapped Territory," Gerard H. Matthes (with discussion), 739.
Separation of flow as it affects the energy conversion in flow expansion, 65.
"Similarity of Distorted River Models with Movable Beds," Hans A. Einstein and Ning Chien (with discussion), 440.
"Studies of Air Entrainment in Open-Channel Flows," Lorenz G. Straub and Owen P. Lamb, 30.
"Verification of Theory for Oblique Standing Waves," Arthur T. Ippen and Donald R. F. Harleman, 678.

WATER, FLOW OF, IN PIPES
See also PIPE LINES; PIPES AND PIPING (cross references thereunder); SEWERS (cross references thereunder); SPRINKLERS AND SPRINKLING; WATER PRESSURE
"Corrosion and Corrosion Research," Thomas R. Camp (with discussion), 791.
"Unsteady Flow in Open-Type Pipe Irrigation Systems," Edward H. Taylor, Arthur F. Pillsbury, Thomas O. Ellis and George A. Bekey, 143. *Discussion:* Robert E. Glover; and Edward H. Taylor, Arthur F. Pillsbury, Thomas O. Ellis and George A. Bekey, 162.

WATER, FLOW OF, IN TANKS
See WATER, FLOW OF, IN OPEN CHANNELS

WATER, FLOW OF, OVER DAMS AND WEIRS
"The Box Inlet Drop Spillway and Its Outlet," Fred W. Blaisdell and Charles A. Donnelly (with discussion), 955.
Determining the discharge coefficient establishing the shape of the nappe of water flowing over a sharp-crested circular weir as to pressure, 345.
Stilling basin performance problems for shaft spillways, 389.

WATER, FLOW OF, THROUGH CHUTES
See SPILLWAYS; WATER, FLOW OF, IN OPEN CHANNELS

WATER, FLOW OF, THROUGH ORIFICES
"A Physical Approach to Turbulent-Boundary-Layer Problems," Donald Ross (with discussion), 1219.

WATER FRONT
See DOCKS AND WHARVES (cross references thereunder); HARBORS; JETTIES (cross reference thereunder); PILES AND PILE DRIVING; STREET TRANSPORTATION; WATER TERMINALS

WATER INSTRUMENTS
See under type of instrument, e.g., METERS AND METERING

WATER LAW
See also RIPARIAN RIGHTS
Status (1955) of irrigation water law, 184.

WATER MAINS
See PIPES AND PIPING (cross references thereunder); WATER SUPPLY (cross references thereunder)

WATER METERS AND METERING (stream velocity)
See METERS AND METERING, CURRENT

WATER PIPES AND PIPING
See PIPES AND PIPING (cross references thereunder)

WATER POLLUTION (General)
See also SEWAGE DISPOSAL (cross references thereunder); WATER TREATMENT

Industrial Waste Pollution
"Handling Atomic Energy Industry Wastes," Joseph A. Lieberman and Arthur E. Gorman, 85.

WATER POWER (General)
See DAMS; POWER PLANTS; TURBINES, WATER

WATER PRESSURE
See also WAVES
"Economy and Safety of Concrete Dams," August E. Komendant (with discussion), 899.
"Flow Expansion and Pressure Recovery in Fluids," Harald Tults, 65.
"Fundamental Concepts of Rectangular Settling Tanks," Alfred C. Ingersoll, Jack E. McKee and Norman H. Brooks (with discussion), 1179.
Pore pressure measuring devices installed on the New Jersey Turnpike, 198.
"Vertical Sand Drains for Stabilizing Muck-Peat Soils," J. C. Carpenter and Edward S. Barber (with discussion), 188.

WATERPROOFING
See CORROSION AND PROTECTION OF METALS

WATER PURIFICATION
See WATER TREATMENT

WATER RIGHTS
See RIPARIAN RIGHTS

WATER STORAGE
See RESERVOIRS . . .

WATER SUPPLY (General)
See DAMS; FLOODS; IRRIGATION; PIPE LINES; PIPES AND PIPING (cross references thereunder); RESERVOIRS . . . ; SETTLING BASINS; SILT AND SILTING . . . ; SPRINKLERS AND SPRINKLING; TANKS . . . ; WATER . . . (related subject headings thereunder); WATER, FLOW OF, IN PIPES

WATER SURFACE SURGES
See WAVES

WATER TERMINALS (structures and localities)
"Design of General Cargo Marine Terminals," Frank W. Herring, 433.

WATER TRANSPORTATION (General)
See CANALS (cross references thereunder); CHANNELS; FREIGHT; HARBORS; PIPE LINES; RIVERS; WATER TERMINALS

WATER TREATMENT
See also AERATION; FILTERS AND FILTRATION, WATER (cross reference thereunder); WATER POLLUTION
Selection of water treatment processes for corrosion control, 791.

WATER TURBINES
See TURBINES, WATER

WATER VELOCITY METERS
See METERS AND METERING, CURRENT

WATER, WASTE
See SEWERS (cross references thereunder); WATER POLLUTION

WATER WAVES
See WAVES

WATERWAYS (General)
See CANALS (cross references thereunder); CHANNELS; COSTS . . . ; DOCKS AND WHARVES (cross references thereunder); FREIGHT; HARBORS; RIPARIAN RIGHTS; RIVERS; WATER DIVERSION; WATER TRANSPORTATION (cross references thereunder)

WATERWAY TRANSPORTATION
See WATER TRANSPORTATION (cross references thereunder)

WATERWORKS (General)
See DAMS; FILTERS AND FILTRATION, WATER (cross reference thereunder); INTAKES; PIPE LINES; PIPES AND PIPING (cross references thereunder); RESERVOIRS; SEDIMENT AND SEDIMENTATION; WATER SUPPLY (cross references thereunder); WATER TREATMENT

WAVE RECORDING AND RECORDING APPARATUS
Apparatus for solving equations of motion in elasto-plastic structures, 728.

WAVES
See also ATOMIC BLAST; WATER PRESSURE
Experimental results concerning sand wave properties summarized, 881.
"Unsteady Flow in Open-Type Pipe Irrigation Systems," Edward H. Taylor, Arthur F. Pillsbury, Thomas O. Ellis and George A. Bekey (with discussion), 143.
"Verification of Theory for Oblique Standing Waves," Arthur T. Ippen and Donald R. F. Harleman, 678.

WEATHER
See FLOODS; HYDROLOGY (cross references thereunder); WIND . . .

WEATHERPROOFING
See CORROSION AND PROTECTION OF METALS

WEBS
See GIRDERS

WEIRS (General)
See WATER, FLOW OF, IN OPEN CHANNELS; WATER, FLOW OF, OVER DAMS AND WEIRS

WELLS
First usage of vertical sand drains, 200, 202.
"Vertical Sand Drains for Stabilizing Muck-Peat Soils," J. C. Carpenter and Edward S. Barber, 188. *Discussion:* Hubert M. Raedschelders, 202.

WHARVES
See DOCKS AND WHARVES (cross references thereunder)

WHEEL LOADS
"Thicknesses of Concrete Pavements for Highways," Joseph H. Moore (with discussion), 1125.

WIND . . .
See also AIR FLOW; VIBRATION

WIND PRESSURE
"Resonant Vibration of Steel Stacks," Ernest A. Dockstader, William F. Swiger and Emory Ireland (with discussion), 1088.
"The Vibrations of Steel Stacks," Walter L. Dickey and Glenn B. Woodruff (with discussion), 1054.
"Wind Loads on Girder Bridges," John M. Biggs, Saul Namyet and Jiro Adachi, 101.

WOOD
See PILES AND PILE DRIVING; TIMBER . . .

WORK, COST OF
See COSTS

WORKS (industrial buildings and equipment)
See under general types of works, e.g., PUBLIC WORKS (cross references thereunder); *also* under specific types of works, e.g., GAS AND GASWORKS; WATERWORKS (cross references thereunder); *see also* cross references under PLANTS

WORK, VIRTUAL
See VIRTUAL WORK, PRINCIPLE OF

WORLD WAR II (1941–1945)
See under relative technical subject, e.g., TIMBER STRUCTURES

WRECKS
See SAFETY (cross references thereunder); *also* under relative subject

ZONING
See CITY PLANNING; PROPERTY (landed property) (cross references thereunder); REGIONAL PLANNING; STREETS—Planning and Design

AUTHOR INDEX

(including Memoirs of deceased members)

Adachi, Jiro
"Wind Loads on Girder Bridges," 101.

Altmeyer, William T.
Expansive clays, 666.

Archer, John S.
Analog computers, 736.

Baines, William D.
Boundary layers, 1241.

Ballester, Rodolfo E.
Shaft spillways, 340.

Bantz, Burwell
Memoir of, 1413.

Barber, Edward S.
Expansive clays, 669.
"Vertical Sand Drains for Stabilizing Muck-Peat Soils," 188.

Barker, Charles L.
Bubble motion, 251.

Bauer, William J.
Boundary layers, 1250.

Bekey, George A.
"Unsteady Flow in Open-Type Pipe Irrigation Systems," 143.

Biggs, John M.
"Wind Loads on Girder Bridges," 101.

Binckley, James E.
Pile tests, 578.

Blaisdell, Fred W.
"The Box Inlet Drop Spillway and Its Outlet," 955.
Shaft spillways, 338, 374, 406.

Blench, Thomas
Alluvial channels, 1281.
Distorted river models, 458.
Sediment transport, 869.

Blessing, Charles A.
"Metropolitan Traffic and Transportation Planning," 135.

Boggess, Louis Sterling
Memoir of, 1414.

Bowerman, Francis R.
"Incineration and Alternative Refuse Disposal Processes," 273.

Bradley, Joseph N.
"Morning-Glory Shaft Spillways (symposium): Prototype Behavior," 312.

Brooks, Norman H.
"Fundamental Concepts of Rectangular Settling Tanks," 1179.

Calhoon, Max L.
"Effect of Sample Disturbance on the Strength of a Clay," 925.

Camp, Thomas R.
"Corrosion and Corrosion Research," 791.
Settling tanks, 1205.

Carpenter, J. C.
"Vertical Sand Drains for Stabilizing Muck-Peat Soils," 188.

Chanda, Benoyendra
Shaft spillways, 375.

Chang, Fu-Kuei
Grid floors, 428.

Chibaro, Anthony
Structural failure, 1376.

Chien, Ning
"Graphic Design of Alluvial Channels," 1267.
"The Present Status of Research on Sediment Transport," 833.
"Similarity of Distorted River Models with Movable Beds," 440.

Chu, Kuang-Han
Grid floors, 426.

Clark, John W.
"Design of Aluminum Alloy Beam-Columns," 1.

Clarke, George Calbraith
Memoir of, 1414.

Cleland, John Williams
Memoir of, 1415.

Conwell, William A.
Curved girders, 540.

Corso, Jose M.
Structural failure, 1381.

Cummings, A. E.
Dog leg piles, 717.

Davis, James Lyford
Memoir of, 1416.

Dawson, Raymond F.
Expansive clays, 664.

de Neufville, Albert
Concrete pavement thickness, 1150.

Dickerson, Lewis A.
Aerial surveys, 518.
Dickey, Walter L.
"The Design of Two Steam Electric Plants," 253.
"The Vibrations of Steel Stacks," 1054.
Disario, Paul C., Jr.
"The Octagonal-Girder Four-Column Space Frame," 995.
Diwan, Abdel F.
Continuous prestressing, 826.
Limit design, 620.
Multiple span frames, 1308.
Octagonal frames, 1022.
Dockstader, Ernest A.
"Resonant Vibration of Steel Stacks," 1088.
Dodkin, Oswald Hewitt
Memoir of, 1416.
Donelan, Bernard
Shaft spillways, 334.
Donnelly, Charles A.
"The Box Inlet Drop Spillway and Its Outlet," 955.
DuBose, Lawrence A.
Expansive clays, 674.
Dunham, John W.
Pile tests, 577.
Einstein, Hans A.
Sediment transport, 883.
"Similarity of Distorted River Models with Movable Beds," 440.
Ellis, Thomas O.
"Unsteady Flow in Open-Type Pipe Irrigation Systems," 143.
Eney, William J.
"Nonuniform Torsion of Plate Girders," 759.
Ernst, George C.
"A Brief for Limit Design," 605.
Farquharson, Frederick B.
Stack vibrations, 1077.
Faustman, D. Jackson
"One-Way Street System in Sacramento, Calif.," 22.
Focht, John A., Jr.
"Pile-Loading Tests, Morganza Floodway Control Sstructure," 555.
Fraenkel, Stephen J.
Blast resistant design, 62.
Franciosi, Vincenzo
Suspension bridges, 490.
Franklin, George Edward
Memoir of, 1417.
Freudenthal, Alfred M.
"Safety and the Probability of Structural Failure," 1337.
Fry, David Warner
Memoir of, 1418.
Geuder, Norman O.
Pipe line surveys, 133.
Gibbs, Harold J.
"Engineering Properties of Expansive Clays," 641.
Gierasch, Aiden R.
Structural failure, 1393.
Gloss, Ralph H.
Timber structure failures, 601.
Glover, Robert E.
Unsteady flow, 162.
Golze, Alfred R.
Irrigation in humid areas, 186.
Gorman, Arthur E.
"Handling Atomic Energy Industry Wastes," 85.
Graves, Leroy D.
Pile tests, 578.
Greeley, Samuel A.
Refuse disposal, 304.
Greenberg, Herbert J.
"Moments and Deflections in Steel-Grid Bridge Floors," 410.
Griffiths, John D.
"Multiple-Span Gabled Frames," 1288.
Guscio, Francis J.
"Aerial Surveys for Reservoir Planning," 511.
Haberman, William L.
"An Experimental Study of Bubbles Moving in Liquids," 227.
Haile, Charles Radcliffe
Memoir of, 1418.
Hall, Frederic Francis
Memoir of, 1419.
Hanson, Walter E.
"Constant-Segment Method for Analysis of Nonuniform Members," 1317.
Harleman, Donald R. F.
"Verification of Theory for Oblique Standing Waves," 678.
Hartmann, Ernest C.
"Design of Aluminum Alloy Beam-Columns," 1.
Harwood, Warner
Concrete pavement thickness, 1148.

Herring, Frank W.
"Design of General Cargo Marine Terminals," 433.

Hickerson, Thomas F.
Constant-segment method, 1331.

Hill, Harry N.
"Design of Aluminum Alloy Beam-Columns," 1.

Hodgkinson, Norman Bateman
Memoir of, 1420.

Holtz, Wesley G.
"Engineering Properties of Expansive Clays," 641.

Hough, Floyd W.
"A Conformal and World-Wide Military Grid System," 633.

Huang, Eugene Y.
Subgrades, 550.

Hunt, Eldon V.
"Pipeline Transportation in the United States," 1113.

Ingersoll, Alfred C.
"Fundamental Concepts of Rectangular Settling Tanks," 1179.

Ippen, Arthur T.
"Verification of Theory for Oblique Standing Waves," 678.

Ireland, Emory
"Resonant Vibration of Steel Stacks," 1088.

Jacobsen, Carl Joseph
Memoir of, 1420.

Jenney, Richard
Stack vibrations, 1071.

Johannessen, Walter
Memoir of, 1421.

Johnson, Howard P.
Shaft spillways, 375.

Johnston, Bruce G.
"Nonuniform Torsion of Plate Girders," 759.

Jordaan, Jan M., Jr.
Sediment transport, 870.

Judd, Samuel
"Vibration in Hydroelectric Power Plants," 1153.

Julian, Oliver G.
Structural failure, 1386.

Karol, Jacob
Suspension bridges, 483.

Kent, Edmund Randolph
Memoir of, 1422.

King, Max Werner
Memoir of, 1423.

Komendant, August E.
"Economy and Safety of Concrete Dams," 899.

Kubo, Gerald G.
"Nonuniform Torsion of Plate Girders," 759.

Kuiper, Edward
River surveys, 755.

Kyle, John M.
"Airport Standards," 722.

Lamb, Owen P.
"Studies of Air Entrainment in Open-Channel Flows," 30.

Lane, Emory W.
Alluvial channels, 1283.

Lange, Allen
Analog computers, 736.

Lara, Joe M.
Sediment transport, 871.

Lawrence, Lloyd S.
Structural failure, 1377.

Lieberman, Joseph A.
"Handling Atomic Energy Industry Wastes," 85.

Little, John Goulding
Memoir of, 1423.

Liu, Hsin-Kuan
Sediment transport, 877.

MacDonald, George E.
"Surveys and Maps for Pipelines," 121.

Mansur, Charles I.
"Pile-Loading Tests, Morganza Floodway Control Structure," 555.

Marsh, Cedric
Stack vibrations, 1110.

Martin, Gunther
"Analog Computers Applied to Elasto-Plastic Systems," 728.

Martin, Park H.
"Pittsburgh's Comprehensive Improvement Program," 885.

Matteson, DeForest A., Jr.
Nonuniform torsion, 781.

Matthes, Gerard H.
"River Surveys in Unmapped Territory," 739.

Mavis, Frederic T.
River surveys, 753.

McCalley, Robert B., Jr.
Beam-columns, 15.

McCormick, Alexis
Memoir of, 1424.
McFadden, Gayle
"The Effect of Jet Aircraft on Airport Pavements," 172.
McGavin, Charles T.
"Private Enterprise Can Satisfy the Parking Demand," 165.
McGinness, Arthur Roscoe
Memoir of, 1425.
McKee, Jack E.
"Fundamental Concepts of Rectangular Settling Tanks," 1179.
McNulty, James F.
Pile tests, 581.
McPherson, Murray B.
Shaft spillways, 369.
Means, Howard Chester
Memoir of, 1425.
Mellin, Gilbert Francis
Memoir of, 1426.
Mensch, Leopold J.
Continuous prestressing, 830.
Meyer, Alvin F., Jr.
"Engineering Biotechnology in Occupational Health," 205.
Michalos, James
"Numerical Analysis of Frames with Curved Girders," 521.
Minshall, Neal E.
Drop spillways, 987.
Mohammed, Ibrahim A.
"Beam Restraints Provided by Walls with Openings," 1034.
Moore, Edward W.
Corrosion, 811.
Moore, Joseph H.
"Thicknesses of Concrete Pavements for Highways," 1125.
Moorman, Robert B. B.
"Continuous Prestressing," 814.
Morton, Rose K.
"An Experimental Study of Bubbles Moving in Liquids," 227.
Mostafa, Ibrahim M.
Shaft spillways, 375.
Mudd, Harvey Seeley
Memoir of, 1412.
Munse, William H.
"Research on Bolted Connections," 1255.
Namyet, Saul
"Wind Loads on Girder Bridges," 101.
Needles, Enoch R.
"Our Exciting Profession": Address at the Summer Convention, Knoxville, Tenn., June 7, 1956, 1398.
Nevins, T. H. F.
River surveys, 754.
Newmark, Nathan M.
"An Engineering Approach to Blast-Resistant Design," 45.
Noble, Charles M.
"Increasing the Load-Carrying Capacities of Subgrades," 544.
Oldham, Jennings Bryan
Memoir of, 1427.
Pagon, W. Watters
Stack vibrations, 1082.
Palmbaum, Harry M.
Suspension bridges, 487.
Palmer, Lawrence A.
Concrete pavement thickness, 1143.
Parsons, James D.
"Safe Loads on Dog-Leg Piles," 695.
Peery, David J.
"An Influence-Line Analysis for Suspension Bridges," 463.
Peterka, Alvin J.
"Morning-Glory Shaft Spillways (symposium) : Performance Tests on Prototype and Model," 385.
Pillsbury, Arthur F.
"Unsteady Flow in Open-Type Pipe Irrigation Systems," 143.
Pirok, John N.
Stack vibrations, 1075.
Podolan, John S.
"The Octagonal-Girder Four-Column Space Frame," 995.
Poley, Stanley
"Lateral Buckling of Cantilevered I-Beams under Uniform Load," 786.
Polivka, Jaro J.
Concrete dams, 922.
Constant-segment method, 1334.
Popov, Egor P.
"Beam Restraints Provided by Walls with Openings," 1034.
Posey, Chesley J.
River surveys, 755.
Pritchett, John Waller
Memoir of, 1427.
Quackenbush, Tyler H.
"Factors Influencing Irrigation in Humid Areas," 179.

Rader, Earle M.
"Development of an International Airport," 96.
Raedschelders, Hubert M.
Sand drains, 202.
Reed, Paul Lyon
Memoir of, 1428.
Reilly, Robert Bonaparte
Memoir of, 1429.
Ridley, John W.
Shaft spillways, 342.
Rincon, Humberto
Octagonal frames, 1028.
Roberson, John A.
Bubble motion, 251.
Robertson, James M.
Boundary layers, 1243.
Ross, Donald
"A Physical Approach to Turbulent-Boundary-Layer Problems," 1219.
Ruff, Paul F.
Bubble motion, 251.
Rupani, Navinchandra L.
Sediment transport, 874.
Ryan, Walter Jackman
Memoir of, 1430.
Salgo, Michael N.
"Examples of Timber-Structure Failures," 588.
Salvadori, Mario G.
"Lateral Buckling of Eccentrically Loaded I-Columns," 1163.
Sawyer, Herbert A., Jr.
Beam-columns, 16.
Schenker, Leo
"Analog Computers Applied to Elasto-Plastic Systems," 728.
Schmertmann, John H.
Soil sample disturbance, 940.
Sherlock, Robert H.
Stack vibrations, 1084.
Shimkin, Boris Michael
Memoir of, 1430.
Shore, Sidney
Octagonal frames, 1028.
Sih, Nan-sze
Suspension bridges, 481.
Skooglund, Carl Richard
Memoir of, 1431.
Stall, John B.
Sediment transport, 874.
Stern, E. George
Timber structure failures, 601.
Stone, Ralph
"Incineration and Alternative Refuse Disposal Processes," 273.
Straub, Lorenz G.
"Studies of Air Entrainment in Open-Channel Flows," 30.
Sutherland, Earl C.
Concrete pavement thickness, 1144.
Swiger, William F.
"Resonant Vibration of Steel Stacks," 1088.
Tanner, William Sherman
Memoir of, 1432.
Taylor, Edward H.
"Unsteady Flow in Open-Type Pipe Irrigation Systems," 143.
Thackwell, Henry L.
Settling tanks, 1209.
Thompson, George R.
Refuse disposal, 299.
Tults, Harald
"Flow Expansion and Pressure Recovery in Fluids," 65.
Van de Greyn, Engel Bert
Memoir of, 1432.
Vayda, Eugene J.
Constant-segment method, 1332.
Vincent, George S.
Stack vibrations, 1072.
Wagner, William E.
"Morning-Glory Shaft Spillways (symposium): Determination of Pressure-Controlled Profiles," 345.
Walter, Donald S.
Shaft spillways, 334.
Weil, Nicholas A.
"The Octagonal-Girder Four-Column Space Frame," 995.
White, Maxwell W.
Shaft spillways, 369.
Wiley, Wallace F.
"Constant-Segment Method for Analysis of Nonuniform Members," 1317.
Wilkinson, Winsor Dornin
Memoir of, 1433.
Wilson, Stanley D.
"Safe Loads on Dog-Leg Piles," 695.
Woodruff, Glenn B.
"The Vibrations of Steel Stacks," 1054.
Xanten, William A.
Refuse disposal, 300.